Edited by Johannes G. de Vries and
Cornelis J. Elsevier

WILEY-VCH

Handbook of Homogeneous Hydrogenation

Volume 1

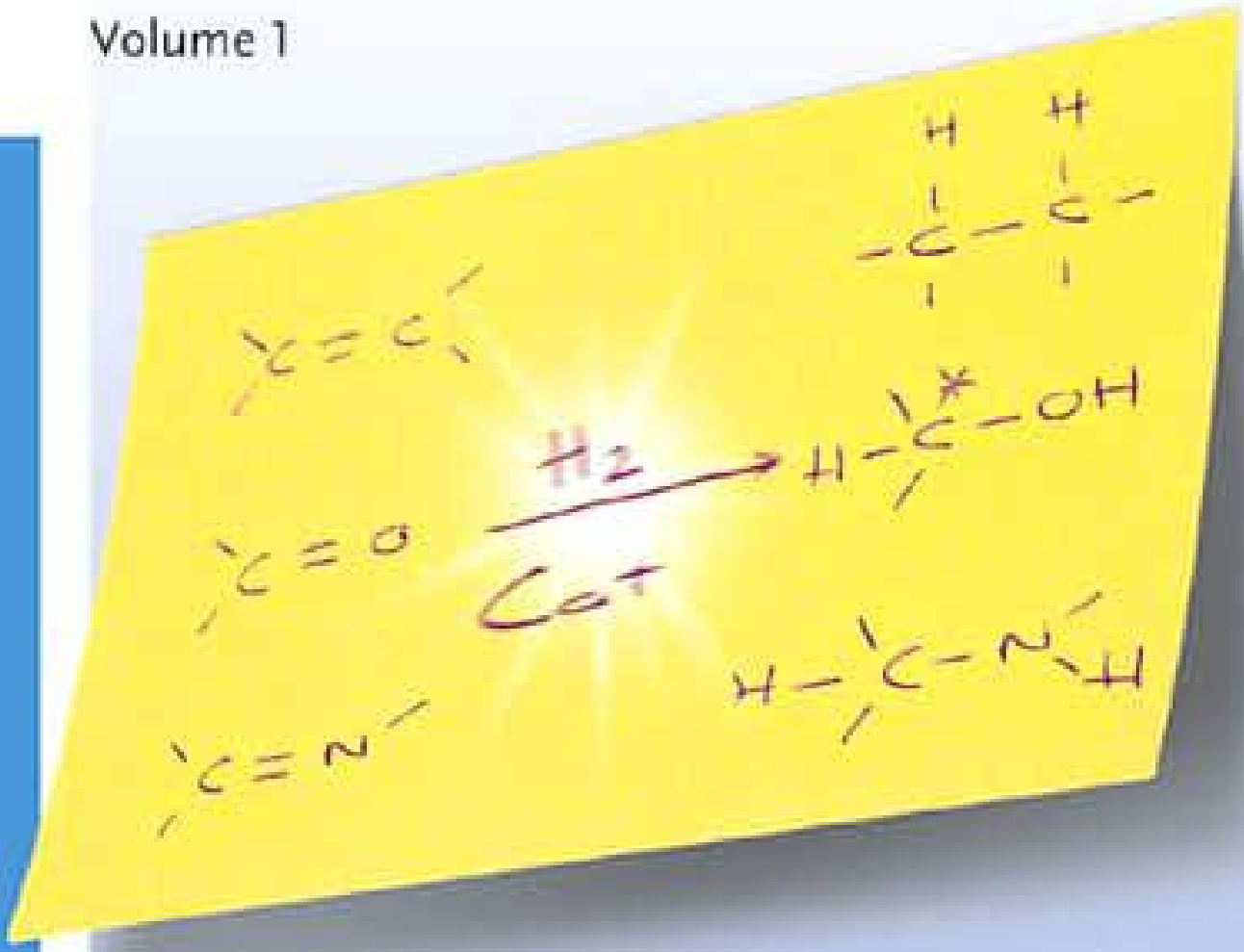

With a Foreword by Brian R. James

The Handbook of Homogeneous Hydrogenation

Edited by
Johannes G. de Vries
and Cornelis J. Elsevier

The Handbook of Homogeneous Hydrogenation.
Edited by J.G. de Vries and C.J. Elsevier
Copyright © 2007 WILEY-VCH Verlag GmbH & Co. KGaA, Weinheim
ISBN: 978-3-527-31161-3

Related Titles

Boy Cornils, Wolfgang A. Herrmann, Istvan T. Horvath, Walter Leitner, Stefan Mecking, Hélèn Olivier-Bourbigou, Dieter Vogt (eds.)

Multiphase Homogeneous Catalysis
2 volumes

2005
ISBN 3-527-30721-4

Jens Christoffers, Angelika Baro, Steven V. Ley (eds.)

Quaternary Stereocenters
Challenges and Solutions for Organic Synthesis

2005
ISBN 3-527-31107-6

1807–2007 Knowledge for Generations

Each generation has its unique needs and aspirations. When Charles Wiley first opened his small printing shop in lower Manhattan in 1807, it was a generation of boundless potential searching for an identity. And we were there, helping to define a new American literary tradition. Over half a century later, in the midst of the Second Industrial Revolution, it was a generation focused on building the future. Once again, we were there, supplying the critical scientific, technical, and engineering knowledge that helped frame the world. Throughout the 20th Century, and into the new millennium, nations began to reach out beyond their own borders and a new international community was born. Wiley was there, expanding its operations around the world to enable a global exchange of ideas, opinions, and know-how.

For 200 years, Wiley has been an integral part of each generation's journey, enabling the flow of information and understanding necessary to meet their needs and fulfill their aspirations. Today, bold new technologies are changing the way we live and learn. Wiley will be there, providing you the must-have knowledge you need to imagine new worlds, new possibilities, and new opportunities.

Generations come and go, but you can always count on Wiley to provide you the knowledge you need, when and where you need it!

William J. Pesce
President and Chief Executive Officer

Peter Booth Wiley
Chairman of the Board

The Handbook of Homogeneous Hydrogenation

Edited by
Johannes G. de Vries and Cornelis J. Elsevier

WILEY-VCH Verlag GmbH & Co. KGaA

The Editors

Prof. Dr. Johannes G. De Vries
DSM Pharmaceutical Products
Advanced Synthesis, Catalysis, and Development
P.O. Box 18
6160 MD Geleen
The Netherlands

Prof. Dr. Cornelis J. Elsevier
Universiteit van Amsterdam
HIMS
Nieuwe Achtergracht 166
1018 WV Amsterdam
The Netherlands

All books published by Wiley-VCH are carefully produced. Nevertheless, authors, editors, and publisher do not warrant the information contained in these books, including this book, to be free of errors. Readers are advised to keep in mind that statements, data, illustrations, procedural details or other items may inadvertently be inaccurate.

Library of Congress Card No.: applied for

British Library Cataloguing-in-Publication Data
A catalogue record for this book is available from the British Library.

Bibliographic information published by the Deutsche Nationalbibliothek
The Deutsche Nationalbibliothek lists this publication in the Deutsche Nationalbibliografie; detailed bibliographic data are available in the Internet at http://dnb.d-nb.de.

© 2007 WILEY-VCH Verlag GmbH & Co. KGaA, Weinheim, Germany

All rights reserved (including those of translation into other languages). No part of this book may be reproduced in any form – by photoprinting, microfilm, or any other means – nor transmitted or translated into a machine language without written permission from the publishers. Registered names, trademarks, etc. used in this book, even when not specifically marked as such, are not to be considered unprotected by law.

Printed in the Federal Republic of Germany
Printed on acid-free paper

Composition K+V Fotosatz GmbH, Beerfelden
Printing Betz-Druck GmbH, Darmstadt
Bookbinding Litges & Dopf Buchbinderei GmbH, Heppenheim

ISBN: 978-3-527-31161-3

Contents

Foreword *XIX*

Preface *XXIII*

List of Contributors *XXV*

Part I **Introduction, Organometallic Aspects and Mechanism of Homogeneous Hydrogenation**

1 **Rhodium** *3*
Luis A. Oro and Daniel Carmona
1.1 Introduction *3*
1.1.1 Monohydride Hydrogenation Catalysts *4*
1.1.2 Dihydride Hydrogenation Catalysts *4*
1.2 The Early Years (1939–1970) *5*
1.3 The $[RhH(CO)(PPh_3)_3]$ Catalyst *6*
1.4 The $[RhCl(PPh_3)_3]$ Complex and Related Catalysts *8*
1.5 The Cationic$[Rh(diene)(PR_3)_X]^+$ Catalysts *11*
1.6 Enantioselective Rhodium Catalysts *14*
1.6.1 Hydrogenation of Alkenes *14*
1.6.2 Hydrogenation of Ketones *19*
1.6.3 Hydrogenation of Imines *20*
1.6.4 Mechanism of Rhodium-Catalyzed Enantioselective Hydrogenation *21*
1.7 Some Dinuclear Catalyst Precursors *26*
1.8 Concluding Remark *26*
Abbreviations *26*
References *27*

2 **Iridium** *31*
Robert H. Crabtree
2.1 Introduction *31*
2.2 Historical Aspects *31*
2.3 Organometallic Aspects *36*

The Handbook of Homogeneous Hydrogenation.
Edited by J.G. de Vries and C.J. Elsevier
Copyright © 2007 WILEY-VCH Verlag GmbH & Co. KGaA, Weinheim
ISBN: 978-3-527-31161-3

2.4 Catalysis *39*
2.4.1 Enantioselective Versions of the Iridium Catalyst *39*
2.4.2 Mechanism *40*
2.4.3 Practical Considerations *42*
Acknowledgments *43*
Abbreviations *43*
References *43*

3 Ruthenium and Osmium *45*
Robert H. Morris
3.1 Introduction *45*
3.2 Ruthenium *46*
3.2.1 The First Catalysts for Alkene Hydrogenation: Mechanistic Considerations *46*
3.2.2 Synthesis of Ruthenium Precatalysts and Catalysts *50*
3.2.3 Dihydrogen Complexes and Non-Classical Hydrogen Bonding in Catalysis *52*
3.2.4 Toward the Reduction of Simple Ketones, Nitriles, Esters and Aromatics with Monodentate Phosphine Systems *55*
3.2.5 Enantiomeric Hydrogenation of Alkenes with Bidentate Ligand Systems *58*
3.2.6 Enantiomeric Hydrogenation of Carbonyl Compounds *60*
3.3 Osmium *64*
Acknowledgment *66*
Abbreviations *67*
References *67*

4 Palladium and Platinum *71*
Paolo Pelagatti
4.1 Introduction *71*
4.2 Palladium *72*
4.2.1 Phosphorus-Containing Catalysts *72*
4.2.2 Nitrogen-Containing Catalysts *76*
4.2.3 Other Catalysts *78*
4.2.4 Mechanistic Aspects *79*
4.3 Platinum *84*
4.3.1 Platinum Complexes Activated with Sn(II) Salts *84*
4.3.1.1 Phosphorus-Containing Catalysts *84*
4.3.1.2 Other Catalysts *85*
4.3.2 Platinum Complexes not Activated with Sn(II) Salts *86*
4.3.3 Mechanistic Aspects *87*
Abbreviations *89*
References *89*

5 Nickel *93*
Elisabeth Bouwman
5.1 Introduction *93*
5.2 Coordination Chemistry and Organometallic Aspects of Nickel *94*
5.2.1 Nickel–Hydride Complexes *94*
5.2.2 Nickel-Alkene and Nickel-Alkyl Complexes *96*
5.2.3 Mechanistic Aspects of Hydrogen Activation *97*
5.3 Hydrogenation Catalysis *98*
5.3.1 Ziegler Systems *98*
5.3.2 Nickel Complexes of Oxygen- or Nitrogen-Containing Ligands *99*
5.3.3 Nickel Complexes of Triphenylphosphane *100*
5.3.4 Nickel Complexes of Didentate Phosphane Ligands *101*
5.4 Concluding Remarks *107*
Abbreviations *108*
References *108*

6 Hydrogenation with Early Transition Metal, Lanthanide and Actinide Complexes *111*
Christophe Copéret
6.1 Introduction *111*
6.2 Mechanistic Considerations *112*
6.3 Group IV Metal Hydrogenation Catalysts *113*
6.3.1 Hydrogenation of Alkenes *113*
6.3.2 Hydrogenation of Alkynes and Dienes *114*
6.3.3 Enantioselective Hydrogenation of Alkenes *116*
6.3.4 Enantioselective Hydrogenation of Imines and Enanimes *118*
6.4 Hydrogenation Catalysts Based on Group III, Lanthanide, and Actinide Complexes *126*
6.4.1 Hydrogenation of Alkenes with Group III Metal and Lanthanide Complexes *126*
6.4.2 Hydrogenation of Dienes and Alkynes with Group III and Lanthanide Complexes *129*
6.4.3 Hydrogenation of Imines with Group III and Lanthanide Complexes *131*
6.4.4 Hydrogenation of Alkenes with Actinide Complexes *132*
6.4.5 Enantiomeric Hydrogenation of Alkenes *134*
6.5 Hydrogenation Catalysts Based on Groups V–VII Transition-Metal Complexes *136*
6.5.1 Hydrogenation of Alkenes and Dienes with Groups V–VII Transition-Metal Complexes *136*
6.5.2 Hydrogenation of Aromatics with Well-Defined Nb and Ta Aryloxide Complexes *138*
6.6 Supported Early Transition-Metal Complexes as Heterogeneous Hydrogenation Catalysts *140*
6.6.1 Supported Homogeneous Catalysts *140*

6.6.2 Heterogeneous Catalysts Prepared via Surface Organometallic Chemistry *142*
6.7 Conclusions *145*
Acknowledgments *146*
Abbreviations *146*
References *146*

7 Ionic Hydrogenations *153*
R. Morris Bullock
7.1 Introduction *153*
7.2 Stoichiometric Ionic Hydrogenations *154*
7.2.1 Stoichiometric Ionic Hydrogenations using CF_3CO_2H and $HSiEt_3$ *154*
7.2.2 Stoichiometric Ionic Hydrogenations using Transition-Metal Hydrides *157*
7.2.2.1 General Aspects *157*
7.2.2.2 Transition-Metal Hydrides as Proton Donors *157*
7.2.3 Transition Metal Hydrides as Hydride Donors *159*
7.2.4 Stoichiometric Ionic Hydrogenation of Alkenes with Metal Hydrides as the Hydride Donor *164*
7.2.5 Stoichiometric Ionic Hydrogenation of Alkynes *166*
7.2.6 Stoichiometric Ionic Hydrogenation of Ketones and Aldehydes using Metal Hydrides as Hydride Donors and Added Acids as the Proton Donor *167*
7.2.7 Stoichiometric Ionic Hydrogenation of Acyl Chlorides to Aldehydes with HOTf/Metal Hydrides *171*
7.2.8 Stoichiometric Ionic Hydrogenation of Ketones with Metal Dihydrides *173*
7.3 Catalytic Ionic Hydrogenation *174*
7.3.1 Catalytic Ionic Hydrogenation of C=C Bonds *174*
7.3.2 Catalytic Ionic Hydrogenation of Ketones by Anionic Cr, Mo, and W Complexes *174*
7.3.3 Catalytic Ionic Hydrogenation of Ketones by Molybdenocene Complexes *176*
7.3.4 Catalytic Ionic Hydrogenation of Ketones by Cationic Mo and W Complexes *178*
7.3.4.1 In Solution *178*
7.3.4.2 Solvent-free *181*
7.3.4.3 N-Heterocyclic Carbene Complexes *182*
7.3.5 Use of a Pd Hydride in Hydrogenation of C=C Bonds *184*
7.3.6 Catalytic Hydrogenation of Iminium Cations by Ru Complexes *184*
7.4 Ruthenium Complexes Having an OH Proton Donor and a RuH as Hydride Donor *186*
7.4.1 The Shvo System *186*
7.4.2 Hydrogenation of Imines by Shvo Complexes *189*

7.4.3 Dehydrogenation of Imines and Alcohols by Shvo Complexes *191*
7.4.4 Catalytic Hydrogenations with Metal–Ligand Bifunctional Catalysis *193*
7.5 Catalytic Hydrogenation of Ketones by Strong Bases *193*
7.6 Conclusion *194*
Acknowledgments *194*
Abbreviations *195*
References *195*

8 Homogeneous Hydrogenation by Defined Metal Clusters *199*
Roberto A. Sánchez-Delgado
8.1 Introduction *199*
8.1.1 Is a Cluster the Real Catalyst? Fragmentation and Aggregation Phenomena *200*
8.2 Hydrogenation of C=C Bonds *201*
8.3 Hydrogenation of C≡C Bonds *206*
8.4 Hydrogenation of Other Substrates *211*
8.5 Concluding Remarks *212*
Abbreviations *213*
References *213*

9 Homogeneous Hydrogenation: Colloids – Hydrogenation with Noble Metal Nanoparticles *217*
Alain Roucoux and Karine Philippot
9.1 Introduction *217*
9.2 Concepts *217*
9.2.1 Electrostatic Stabilization *218*
9.2.2 Steric Stabilization *219*
9.3 Hydrogenation of Compounds with C=C Bonds *220*
9.3.1 Use of Polymers as Stabilizers *220*
9.3.2 Use of Non-Usual Polymers as Stabilizers *221*
9.3.3 Use of Dendrimers as Stabilizers *225*
9.3.4 Use of Surfactants as Stabilizers *226*
9.3.5 Use of Polyoxoanions as Stabilizers *227*
9.3.6 Use of Ligands as Stabilizers *228*
9.3.7 Biomaterial as a Protective Matrix *232*
9.3.8 Ionic Liquids used as Templates for the Stabilization of Metal Nanoparticles *233*
9.3.9 Supercritical Microemulsions Used as Templates for the Stabilization of Metal Nanoparticles *236*
9.3.10 Conclusion *238*
9.4 Hydrogenation of Compounds with C≡C Bonds *238*
9.5 Arene Hydrogenation *241*
9.6 Hydrogenation of Compounds with C=O Bonds *245*
9.7 Enantioselective Hydrogenation *249*

9.8 Conclusion *252*
Abbreviations *252*
References *253*

10 Kinetics of Homogeneous Hydrogenations: Measurement and Interpretation *257*
Hans-Joachim Drexler, Angelika Preetz, Thomas Schmidt, and Detlef Heller
10.1 Introduction *257*
10.2 The Basics of Michaelis-Menten Kinetics *259*
10.3 Hydrogenation From a Kinetic Viewpoint *263*
10.3.1 Measurement of Concentration–Time Data and Possible Problems *263*
10.3.1.1 Monitoring of Hydrogenations via Hydrogen Consumption *264*
10.3.1.2 Monitoring of Hydrogenations by NMR and UV/Visible Spectroscopy *272*
10.3.2 Gross-Kinetic Measurements *277*
10.3.2.1 Derivation of Michaelis-Menten Kinetics with Various Catalyst-Substrate Complexes *277*
10.3.2.2 Data from Gross Kinetic Measurements *280*
Abbreviations *288*
References *288*

Part II Spectroscopic Methods in Homogeneous Hydrogenation

11 Nuclear Magnetic Resonance Spectroscopy in Homogeneous Hydrogenation Research *297*
N. Koen de Vries
11.1 Introduction *297*
11.1.1 Nuclear Magnetic Resonance (NMR) *297*
11.1.2 NMR in Homogeneous Hydrogenation Research *298*
11.2 NMR Methods *299*
11.2.1 General *299*
11.2.2 Chemical Shift *300*
11.2.2.1 General *300*
11.2.2.2 Chemical Shifts in Homogeneous Hydrogenation Research *300*
11.2.3 Coupling Constant *301*
11.2.4 2D-NMR *302*
11.2.4.1 General *302*
11.2.4.2 2D-NMR in Homogeneous Hydrogenation Research *302*
11.2.5 Variable Temperature and Variable Pressure Studies *307*
11.2.5.1 General *307*
11.2.5.2 Variable-Temperature Studies in Homogeneous Hydrogenation Research *307*
11.2.5.3 Variable-Pressure Studies in Homogeneous Hydrogenation Research *308*

11.2.6 PGSE NMR Diffusion Methods *309*
11.3 Outlook *309*
Abbreviations *310*
References *310*

12 Parahydrogen-Induced Polarization: Applications to Detect Intermediates of Catalytic Hydrogenations *313*
Joachim Bargon
12.1 *In-Situ* Spectroscopy *313*
12.1.1 *In-Situ* NMR Spectroscopy *313*
12.1.2 *In-Situ* PHIP-NMR Spectroscopy *314*
12.2 Ortho- and Parahydrogen *315*
12.2.1 Magnetic Field Dependence of the PHIP-Phenomenon: PASADENA and ALTADENA Conditions *316*
12.2.2 PHIP, CIDNP, and Radical Mechanisms *318*
12.2.3 Preparation of Parahydrogen *319*
12.2.3.1 Parahydrogen Enrichment *319*
12.2.3.2 High-Pressure Apparatus for Parahydrogen Enrichment *320*
12.2.3.3 Enrichment of Parahydrogen using Closed-Circuit Cryorefrigeration *321*
12.2.4 Preparation of Orthohydrogen *322*
12.2.5 Thermal Conductivity Cells for Ortho/Para Determination *322*
12.2.6 Determination of the Ortho/Para Ratio *323*
12.2.7 Enrichment of Ortho- or Paradeuterium *323*
12.3 Applications of PHIP-NMR Spectroscopy *324*
12.3.1 *In-Situ* PHIP-NMR Spectroscopy of Homogeneous Hydrogenations *324*
12.3.1.1 Activation of Dihydrogen *324*
12.3.1.2 Concepts of Reaction Mechanisms *324*
12.3.2 *In-Situ* PHIP-NMR Observation of Mono- and Binuclear Rhodium Dihydride Complexes *325*
12.3.2.1 Reactions of $[RhCl(NBD)]_2$ with Parahydrogen in the Presence of Tertiary Phosphines *325*
12.3.2.2 Formation of the Binuclear Complexes $[(H)(Cl)Rh(PMe_3)_2(\mu\text{-}Cl)(\mu\text{-}H)Rh(PMe_3)]$ and $[(H)(Cl)Rh(PMe_2Ph)_2(\mu\text{-}Cl)(\mu\text{-}H)Rh(PMe_2Ph)]$ *328*
12.3.2.3 General Procedure for the Generation of the Complexes $[Rh(H)_2ClL_3]$ (L=Phosphine) *329*
12.3.3.3 Intermediate Dihydrides of Cationic Rh Catalysts *329*
12.3.3.4 Obtaining Structural Information using ^{13}C-Labeled Substrates *332*
12.4 Catalyst-Attached Products as Observable Intermediates *335*
12.4.1 Enantioselective Substrates *336*
12.4.2 Chiral Catalysts *336*
12.4.3 Determination of Kinetic Constants *338*

12.4.4 Computer-Assisted Prediction and Analysis of the Polarization Patterns: DYPAS2 *341*
12.5 Colloidal Catalysts *342*
12.5.1 *In-Situ* PHIP-NMR Investigation of the Hydrogenation of Ethynylbenzene by $Pd_x[N(octyl)_4Cl]_y$ *342*
12.6 Transfer of Proton Polarization to Heteronuclei *344*
12.6.1 General Aspects *344*
12.6.2 Polarization Transfer to ^{13}C *346*
12.6.3 Polarization Transfer to ^{19}F *352*
12.6.4 Parahydrogen-Assisted Signal Enhancement for Magnetic Resonance Imaging *353*
12.7 Catalysts Containing other Transition Metals *354*
12.8 Summary and Conclusions *354*
Acknowledgment *355*
Abbreviations *355*
References *356*

13 A Tour Guide to Mass Spectrometric Studies of Hydrogenation Mechanisms *359*
Corbin K. Ralph, Robin J. Hamilton, and Steven H. Bergens
13.1 Introduction *359*
13.2 A General Description of ESI-MS *360*
13.3 Mechanistic Hydrogenation Studies *364*
13.4 Conclusions *369*
Acknowledgments *370*
Abbreviations *370*
References *370*

Part III Homogeneous Hydrogenation by Functional Groups

14 Homogeneous Hydrogenation of Alkynes and Dienes *375*
Alexander M. Kluwer and Cornelis J. Elsevier
14.1 Stereoselective Homogeneous Hydrogenation of Alkynes to Alkenes *375*
14.1.1 Introduction *375*
14.1.2 Chromium Catalysts *376*
14.1.3 Iron Catalysts *377*
14.1.4 Ruthenium Catalysts *378*
14.1.5 Osmium Catalysts *382*
14.1.6 Rhodium Catalysts *384*
14.1.7 Iridium Catalysts *386*
14.1.8 Palladium Catalysts *388*
14.1.9 Conclusions *394*
14.2 Homogeneous Hydrogenation of Dienes to Monoenes *394*
14.2.1 Introduction *394*

14.2.2 Zirconium Catalysts *395*
14.2.3 Chromium Catalysts *397*
14.2.4 Ruthenium Catalysts *400*
14.2.5 Cobalt Catalysts *402*
14.2.6 Rhodium Catalysts *402*
14.2.7 Palladium and Platinum Catalysts *406*
14.2.8 Conclusions *408*
Abbreviations *409*
References *409*

15 Homogeneous Hydrogenation of Aldehydes, Ketones, Imines and Carboxylic Acid Derivatives: Chemoselectivity and Catalytic Activity *413*
Matthew L. Clarke and Geoffrey J. Roff
15.1 Introduction *413*
15.2 Hydrogenation of Aldehydes *414*
15.2.1 Iridium Catalysts *414*
15.2.2 Rhodium Catalysts *417*
15.2.2.1 Rh-amine Catalysts *417*
15.2.2.2 Cationic Rhodium Phosphine Catalysts *418*
15.2.2.3 Water-Soluble Rh Catalysts *419*
15.2.3 Ruthenium Catalysts *420*
15.2.3.1 Ru-PPh_3 Catalysts *420*
15.2.3.2 Polydentate Ru Catalysts *421*
15.2.3.3 Diamine-Modified Ru Catalysts *422*
15.2.3.4 Ru-TPPMS/TPPTS Catalysts *423*
15.2.4 Other Metal Catalysts *425*
15.2.4.1 Copper *425*
15.2.4.2 Osmium *425*
15.3 Hydrogenation of Ketones *426*
15.3.1 Iridium Catalysts *426*
15.3.2 Rhodium Catalysts *428*
15.3.2.1 Rh-Phosphine Catalysts *428*
15.3.2.2 Water-Soluble Rh Catalysts *430*
15.3.3 Ruthenium Catalysts *431*
15.3.3.1 Ruthenium Carbonyl Clusters *431*
15.3.3.2 Ru–PPh_3 Complexes *431*
15.3.3.3 Diamine-Modified Ru Catalysts *433*
15.3.3.4 Other Ru Catalysts *434*
15.3.4 Other Metal Catalysts *435*
15.3.4.1 Copper *435*
15.3.4.2 Metal Carbonyls *436*
15.4 Domino-Hydroformylation-Reduction Reactions *436*
15.4.1 Cobalt Catalysts *436*
15.4.2 Rhodium Catalysts *437*

15.5 Reductive Amination of Ketones and Aldehydes *437*
15.6 Hydroaminomethylation of Alkenes (Domino Hydroformylation-Reductive Amination) *439*
15.7 Hydrogenation of Carboxylic Acid Derivatives *441*
15.7.1 Hydrogenation of Acids and Anhydrides *442*
15.7.2 Hydrogenation of Esters *445*
15.8 Summary and Outlook *450*
Abbreviations *451*
References *452*

16 Hydrogenation of Arenes and Heteroaromatics *455*
Claudio Bianchini, Andrea Meli, and Francesco Vizza
16.1 Introduction *455*
16.2 Hydrogenation of Arenes *456*
16.2.1 Molecular Catalysts in Different Phase-Variation Systems *456*
16.2.2 Molecular Catalysts Immobilized on Support Materials *466*
16.3 Hydrogenation of Heteroaromatics *470*
16.3.1 Molecular Catalysts in Different Phase-Variation Systems *470*
16.3.1.1 S-Heteroaromatics *470*
16.3.1.2 N-Heteroaromatics *474*
16.3.1.3 O-Heteroaromatics *479*
16.3.2 Molecular Catalysts Immobilized on Support Materials *479*
16.4 Stereoselective Hydrogenation of Prochiral Heteroaromatics *481*
16.4.1 Molecular Catalysts in Homogeneous Phase *481*
16.4.2 Molecular Catalysts Immobilized on Support Materials *484*
Abbreviations *484*
References *485*

17 Homogeneous Hydrogenation of Carbon Dioxide *489*
Philip G. Jessop
17.1 Introduction *489*
17.2 Reduction to Formic Acid *490*
17.2.1 Insertion Mechanisms *494*
17.2.2 Ionic Hydrogenation *497*
17.2.3 Concerted Ionic Hydrogenation *498*
17.2.4 Bicarbonate Hydrogenation *498*
17.2.5 Other Mechanisms *499*
17.3 Reduction to Oxalic Acid *499*
17.4 Reduction to Formate Esters *500*
17.4.1 In the Presence of Alcohols *500*
17.4.2 In the Presence of Alkyl Halides *502*
17.4.3 In the Presence of Epoxides *503*
17.5 Reduction to Formamides *504*
17.6 Reduction to Other Products *506*
17.7 Concluding Remarks *507*

Acknowledgments *507*
Abbreviations *508*
References *508*

18 **Dehalogenation Reactions** *513*
Attila Sisak and Ottó Balázs Simon

19 **Homogeneous Catalytic Hydrogenation of Polymers** *547*
Garry L. Rempel, Qinmin Pan, and Jialong Wu

20 **Transfer Hydrogenation Including the Meerwein-Ponndorf-Verley Reduction** *585*
Dirk Klomp, Ulf Hanefeld, and Joop A. Peters

21 **Diastereoselective Hydrogenation** *631*
Takamichi Yamagishi

22 **Hydrogen-Mediated Carbon–Carbon Bond Formation Catalyzed by Rhodium** *713*
Chang-Woo Cho and Michael J. Krische

Part IV **Asymmetric Homogeneous Hydrogenation**

23 **Enantioselective Alkene Hydrogenation: Introduction and Historic Overview** *745*
David J. Ager

24 **Enantioselective Hydrogenation: Phospholane Ligands** *773*
Christopher J. Cobley and Paul H. Moran

25 **Enantioselective Hydrogenation of Alkenes with Ferrocene-Based Ligands** *833*
Hans-Ulrich Blaser, Matthias Lotz, and Felix Spindler

26 **The other Bisphosphine Ligands for Enantioselective Alkene Hydrogenation** *853*
Yongxiang Chi, Wenjun Tang, and Xumu Zhang

27 **Bidentate Ligands Containing a Heteroatom–Phosphorus Bond** *883*
Stanton H. L. Kok, Terry T.-L. Au-Yeung, Hong Yee Cheung, Wing Sze Lam, Shu Sun Chan, and Albert S. C. Chan

28 **Enantioselective Alkene Hydrogenation: Monodentate Ligands** *995*
Michel van den Berg, Ben L. Feringa, and Adriaan J. Minnaard

29 **P,N and Non-Phosphorus Ligands** *1029*
Andreas Pfaltz and Sharon Bell

30 **Enantioselective Hydrogenation of Unfunctionalized Alkenes** *1049*
Andreas Pfaltz and Sharon Bell

31 **Mechanism of Enantioselective Hydrogenation** *1073*
John M. Brown

32 **Enantioselective Ketone and β-Keto Ester Hydrogenations (Including Mechanisms)** *1105*
Takeshi Ohkuma and Ryoji Noyori

33 **Rhodium-Catalyzed Enantioselective Hydrogenation of Functionalized Ketones** *1165*
André Mortreux and Abdallah Karim

34 **Enantioselective Hydrogenation of C=N Functions and Enamines** *1193*
Felix Spindler and Hans-Ulrich Blaser

35 **Enantioselective Transfer Hydrogenation** *1215*
A. John Blacker

36 **High-Throughput Experimentation and Ligand Libraries** *1245*
Johannes G. de Vries and Laurent Lefort

37 **Industrial Applications** *1279*
Hans-Ulrich Blaser, Felix Spindler, and Marc Thommen

Part V **Phase Separation in Homogeneous Hydrogenation**

38 **Two-Phase Aqueous Hydrogenations** *1327*
Ferenc Joó and Ágnes Kathó

39 **Supercritical and Compressed Carbon Dioxide as Reaction Medium and Mass Separating Agent for Hydrogenation Reactions using Organometallic Catalysts** *1361*
Walter Leitner

40 **Fluorous Catalysts and Fluorous Phase Catalyst Separation for Hydrogenation Catalysis** *1377*
Elwin de Wolf and Berth-Jan Deelman

41 **Catalytic Hydrogenation using Ionic Liquids as Catalyst Phase** *1389*
Peter Wasserscheid and Peter Schulz

42 **Immobilization Techniques** *1421*
Imre Tóth and Paul C. van Geem

Part VI Miscellaneous Topics in Homogeneous Hydrogenation

43 **Transition Metal-Catalyzed Regeneration of Nicotinamide Cofactors** *1471*
Stephan Lütz

44 **Catalyst Inhibition and Deactivation in Homogeneous Hydrogenation** *1483*
Detlef Heller, André H. M. de Vries, and Johannes G. de Vries

45 **Chemical Reaction Engineering Aspects of Homogeneous Hydrogenations** *1517*
Claude de Bellefon and Nathalie Pestre

Subject Index *1547*

Contents

Part I **Introduction, Organometallic Aspects and Mechanism of Homogeneous Hydrogenation**

1 **Rhodium** *3*
Luis A. Oro and Daniel Carmona

2 **Iridium** *31*
Robert H. Crabtree

3 **Ruthenium and Osmium** *45*
Robert H. Morris

4 **Palladium and Platinum** *71*
Paolo Pelagatti

5 **Nickel** *93*
Elisabeth Bouwman

6 **Hydrogenation with Early Transition Metal, Lanthanide and Actinide Complexes** *111*
Christophe Copéret

7 **Ionic Hydrogenations** *153*
R. Morris Bullock

8 **Homogeneous Hydrogenation by Defined Metal Clusters** *199*
Roberto A. Sánchez-Delgado

9 **Homogeneous Hydrogenation: Colloids – Hydrogenation with Noble Metal Nanoparticles** *217*
Alain Roucoux and Karine Philippot

The Handbook of Homogeneous Hydrogenation.
Edited by J.G. de Vries and C.J. Elsevier
Copyright © 2007 WILEY-VCH Verlag GmbH & Co. KGaA, Weinheim
ISBN: 978-3-527-31161-3

10 **Kinetics of Homogeneous Hydrogenations: Measurement and Interpretation** *257*
Hans-Joachim Drexler, Angelika Preetz, Thomas Schmidt, and Detlef Heller

Part II **Spectroscopic Methods in Homogeneous Hydrogenation**

11 **Nuclear Magnetic Resonance Spectroscopy in Homogeneous Hydrogenation Research** *297*
N. Koen de Vries

12 **Parahydrogen-Induced Polarization: Applications to Detect Intermediates of Catalytic Hydrogenations** *313*
Joachim Bargon

13 **A Tour Guide to Mass Spectrometric Studies of Hydrogenation Mechanisms** *359*
Corbin K. Ralph, Robin J. Hamilton, and Steven H. Bergens

Part III **Homogeneous Hydrogenation by Functional Groups**

14 **Homogeneous Hydrogenation of Alkynes and Dienes** *375*
Alexander M. Kluwer and Cornelis J. Elsevier

15 **Homogeneous Hydrogenation of Aldehydes, Ketones, Imines and Carboxylic Acid Derivatives: Chemoselectivity and Catalytic Activity** *413*
Matthew L. Clarke and Geoffrey J. Roff

16 **Hydrogenation of Arenes and Heteroaromatics** *455*
Claudio Bianchini, Andrea Meli, and Francesco Vizza

17 **Homogeneous Hydrogenation of Carbon Dioxide** *489*
Philip G. Jessop

18 Dehalogenation Reactions *513*
Attila Sisak and Ottó Balázs Simon
18.1 Introduction *513*
18.2 Catalytic Dehalogenation with Various Reducing Agents *517*
18.2.1 Molecular Hydrogen *517*
18.2.2 Simple and Complex Metal Hydrides *520*
18.2.3 Hydrosilanes and Hydrostannanes *524*
18.2.4 Hydrogen Donors other than Hydrides *526*
18.2.5 Biomimetic Dehalogenations *528*
18.2.6 Electrochemical Reductions *532*
18.2.7 Miscellaneous Reducing Methods *533*
18.3 Mechanistic Considerations *534*
18.3.1 Activation of the C–X Bond *535*
18.3.1.1 Oxidative Addition *535*
18.3.1.2 σ-Bond Metathesis *537*
18.3.1.3 S_N2 Attack of the Hydride Ligand *538*
18.3.1.4 1,2-Insertion *538*
18.3.2 Reaction Steps Involving the Reducing Agents *538*
18.3.3 Formation of the Product *539*
18.4 Concluding Remarks *540*
Acknowledgments *540*
Abbreviations *540*
References *541*

19 Homogeneous Catalytic Hydrogenation of Polymers *547*
Garry L. Rempel, Qinmin Pan, and Jialong Wu
19.1 General Introduction *547*
19.1.1 Diene-Based Polymers *547*
19.1.2 Hydrogenation of Diene-Based Polymers *548*
19.1.2.1 Heterogeneous Catalysts *549*
19.1.2.2 Homogeneous Catalysts *550*
19.2 Reaction Art *551*
19.2.1 Catalyst Techniques *551*
19.2.2 Hydrogenation Kinetic Mechanism *565*
19.2.2.1 Rhodium-Based Catalysts *565*
19.2.2.2 Ruthenium-Based Catalysts *568*
19.2.2.3 Osmium-Based Catalysts *571*
19.2.2.4 Palladium Complexes *572*
19.2.3 Kinetic Mechanism Discrimination *573*
19.3 Engineering Art *573*
19.3.1 Catalyst Recovery *574*
19.3.1.1 Precipitation *575*
19.3.1.2 Adsorption *575*
19.3.2 Solvent Recycling *576*
19.3.3 Reactor Technology and Catalytic Engineering Aspects *577*

19.4 A Commercial Example: Production of HNBR via a Homogeneous Hydrogenation Route *578*
19.5 Future Outlook and Perspectives *579*
Abbreviations *579*
References *579*

20 Transfer Hydrogenation Including the Meerwein-Ponndorf-Verley Reduction *585*
Dirk Klomp, Ulf Hanefeld, and Joop A. Peters
20.1 Introduction *585*
20.2 Reaction Mechanisms *587*
20.2.1 Hydrogen Transfer Reduction of Carbonyl Compounds *588*
20.2.1.1 Meerwein-Ponndorf-Verley Reduction and Oppenauer Oxidation *588*
20.2.1.2 Transition Metal-Catalyzed Reductions *590*
20.2.2 Transfer Hydrogenation Catalysts for Reduction of C–C Double and Triple Bonds *595*
20.3 Reaction Conditions *597*
20.3.1 Hydrogen Donors *597*
20.3.2 Solvents *600*
20.3.3 Catalysts and Substrates *601*
20.3.4 Selectivity *603*
20.4 Related Reactions and Side-Reactions *609*
20.4.1 Aldol Reaction *609*
20.4.2 Tishchenko Reaction *609*
20.4.3 Cannizzaro Reaction *609*
20.4.4 Decarbonylation *610*
20.4.5 Leuckart-Wallach and Eschweiler-Clarke Reactions *610*
20.4.6 Reductive Acetylation of Ketones *610*
20.4.7 Other Hydrogen Transfer Reactions *611*
20.5 Racemizations *612*
Abbreviations *627*
References *627*

21 Diastereoselective Hydrogenation *631*
Takamichi Yamagishi
21.1 Introduction *631*
21.2 Hydrogenation of Alkenes, Ketones, and Imines *631*
21.3 Substrate-Directive Diastereoselective Hydrogenation *638*
21.3.1 Hydrogenation of Cyclic Alcohols with Endo- or Exo-Cyclic Olefinic Bond *638*
21.3.2 Hydrogenation of Acyclic Allyl and Homoallyl Alcohols *653*
21.3.3 Ester Unit- or Amide-Directive Hydrogenation *667*
21.4 Hydrogenation of Dehydrooligopeptides *671*
21.5 Diastereoselective Hydrogenation of Keto-Compounds *676*

21.5.1 Substrate-Directive Hydrogenation of Keto-Compounds *681*
21.5.2 Hydrogenation of Diketo Esters and Diketones *684*
21.6 Kinetic Resolution to Selectively Afford Diastereomers and Enantiomers *691*
21.7 Kinetic Resolution of Keto- and Imino-Compounds *694*
21.8 Dynamic Kinetic Resolution *697*
21.9 Conclusions *701*
Abbreviations *708*
References *708*

22 Hydrogen-Mediated Carbon–Carbon Bond Formation Catalyzed by Rhodium *713*
Chang-Woo Cho and Michael J. Krische
22.1 Introduction and Mechanistic Considerations *713*
22.2 Reductive Coupling of Conjugated Enones and Aldehydes *716*
22.2.1 Intramolecular Reductive Aldolization *716*
22.2.2 Intermolecular Reductive Aldolization *720*
22.3 Reductive Coupling of 1,3-Cyclohexadiene and α-Ketoaldehydes *723*
22.4 Reductive Coupling of Conjugated Enynes and Diynes with Activated Aldehydes and Imines *726*
22.5 Reductive Cyclization of 1,6-Diynes and 1,6-Enynes *733*
22.6 Conclusion *736*
Acknowledgments *737*
Abbreviations *737*
References *737*

Part IV Asymmetric Homogeneous Hydrogenation

23 Enantioselective Alkene Hydrogenation: Introduction and Historic Overview *745*
David J. Ager
23.1 Introduction *745*
23.2 Development of CAMP and DIPAMP *746*
23.3 DIOP *749*
23.4 Ferrocene Ligands *753*
23.4.1 Ferrocene Hybrids *756*
23.5 Atropisomeric Systems *756*
23.6 DuPhos *758*
23.7 Variations at Phosphorus *760*
23.8 Monophosphorus Ligands *762*
23.9 A Return to Monodentate Ligands *762*
23.10 Summary *763*
References *764*

24 Enantioselective Hydrogenation: Phospholane Ligands *773*
Christopher J. Cobley and Paul H. Moran
24.1 Introduction and Extent of Review *773*
24.2 Phospholane Ligands: Synthesis and Scope *774*
24.2.1 Early Discoveries and the Breakthrough with DuPhos and BPE *774*
24.2.2 Modifications to the Backbone *778*
24.2.3 Modifications to the Phospholane Substituents *779*
24.2.4 Other Phospholane-Containing Ligands *783*
24.2.5 Related Phosphacycle-Based Ligands *786*
24.3 Enantioselective Hydrogenation of Alkenes *788*
24.3.1 Enantioselective Hydrogenation of α-Dehydroamino Acid Derivatives *788*
24.3.2 Enantioselective Hydrogenation of β-Dehydroamino Acid Derivatives *801*
24.3.3 Enantioselective Hydrogenation of Enamides *806*
24.3.4 Enantioselective Hydrogenation of Unsaturated Acid and Ester Derivatives *810*
24.3.5 Enantioselective Hydrogenation of Unsaturated Alcohol Derivatives *816*
24.3.6 Enantioselective Hydrogenation of Miscellaneous C=C Bonds *819*
24.4 Enantioselective Hydrogenation of C=O and C=N Bonds *820*
24.4.1 Enantioselective Hydrogenation of Ketones *820*
24.4.2 Enantioselective Hydrogenation of Imines and C=N–X Bonds *822*
24.5 Concluding Remarks *823*
Abbreviations *823*
References *824*

25 Enantioselective Hydrogenation of Alkenes with Ferrocene-Based Ligands *833*
Hans-Ulrich Blaser, Matthias Lotz, and Felix Spindler
25.1 Introduction *833*
25.2 Ligands with Phosphine Substituents Bound to One Cyclopentadiene Ring *835*
25.3 Ligands with Phosphine Substituents Bound to both Cyclopentadiene Rings *835*
25.3.1 Bppfa, Ferrophos, and Mandyphos Ligands *836*
25.3.2 Miscellaneous Diphosphines *837*
25.4 Ligands with Phosphine Substituents Bound to a Cyclopentadiene Ring and to a Side Chain *839*
25.4.1 Josiphos *839*
25.4.2 Immobilized Josiphos and Josiphos Analogues *841*
25.4.3 Taniaphos *842*
25.4.3 Various Ligands *843*
25.5 Ligands with Phosphine Substituents Bound only to Side Chains *844*

25.6 Major Applications of Ferrocene Diphosphine-Based Catalysts *847*
25.6.1 Hydrogenation of Substituted Alkenes *848*
25.6.2 Hydrogenation of C=O and C=N Functions *848*
Abbreviations *850*
References *850*

26 The other Bisphosphine Ligands for Enantioselective Alkene Hydrogenation *853*
Yongxiang Chi, Wenjun Tang, and Xumu Zhang
26.1 Introduction *853*
26.2 Chiral Bisphosphine Ligands *853*
26.2.1 Atropisomeric Biaryl Bisphosphine Ligands *853*
26.2.2 Chiral Bisphosphine Ligands Based on DIOP Modifications *860*
26.2.3 P-Chiral Bisphosphine Ligands *861*
26.2.4 Other Bisphosphine Ligands *862*
26.3 Applications in Enantioselective Hydrogenation of Alkenes *864*
26.3.1 Enantioselective Hydrogenation of α-Dehydroamino Acid Derivatives *864*
26.3.2 Enantioselective Hydrogenation of Enamides *866*
26.3.3 Enantioselective Hydrogenation of (β-Acylamino) Acrylates *868*
26.3.4 Enantioselective Hydrogenation of Enol Esters *870*
26.3.5 Enantioselective Hydrogenation of Unsaturated Acids and Esters *872*
26.3.5.1 α,β-Unsaturated Carboxylic Acids *872*
26.3.5.2 α,β-Unsaturated Esters, Amides, Lactones, and Ketones *874*
26.3.5.3 Itaconic Acids and Their Derivatives *874*
26.3.6 Enantioselective Hydrogenation of Unsaturated Alcohols *875*
26.4 Concluding Remarks *877*
References *877*

27 Bidentate Ligands Containing a Heteroatom–Phosphorus Bond *883*
Stanton H. L. Kok, Terry T.-L. Au-Yeung, Hong Yee Cheung, Wing Sze Lam, Shu Sun Chan, and Albert S. C. Chan
27.1 Introduction *883*
27.2 Aminophosphine-Phosphinites (AMPPs) *883*
27.3 Bisphosphinamidite Ligands *907*
27.4 Mixed Phosphine-Phosphoramidites and Phosphine-Aminophosphine Ligands *918*
27.5 Bisphosphinite Ligands (One P–O Bond) *924*
27.6 Bisphosphonite Ligands (Two P–O Bonds) *978*
27.7 Bisphosphite Ligands (Three P–O Bonds) *980*
27.8 Other Mixed-Donor Bidentate Ligands *981*
27.9 Ligands Containing Neutral S-Donors *983*
Acknowledgments *988*
Abbreviations *988*
References *988*

28 **Enantioselective Alkene Hydrogenation: Monodentate Ligands** *995*
Michel van den Berg, Ben L. Feringa, and Adriaan J. Minnaard
28.1 Introduction *995*
28.2 Monodentate Phosphines *997*
28.3 Monodentate Phosphonites *1000*
28.4 Monodentate Phosphites *1000*
28.5 Monodentate Phosphoramidites *1005*
28.6 Monodentate Phosphinites, Aminophosphinites, Diazaphospholidines and Secondary Phosphine Oxides *1010*
28.7 Hydrogenation of N-Acyl-α-Dehydroamino Acids and Esters *1011*
28.8 Hydrogenation of Unsaturated Acids and Esters *1014*
28.9 Hydrogenation of *N*-Acyl Enamides, Enol Esters and Enol Carbamates *1016*
28.10 Hydrogenation of *N*-Acyl-β-Dehydroamino Acid Esters *1020*
28.11 Hydrogenation of Ketones and Imines *1021*
28.12 Conclusions *1023*
Abbreviations *1024*
References *1024*

29 **P,N and Non-Phosphorus Ligands** *1029*
Andreas Pfaltz and Sharon Bell
29.1 Introduction *1029*
29.2 Oxazoline-Derived P,N Ligands *1030*
29.2.1 Phosphino-oxazolines *1030*
29.2.2 Phosphite and Phosphinite Oxazolines *1033*
29.2.3 Oxazoline-Derived Ligands Containing a P–N Bond *1036*
29.2.4 Structurally Related Ligands *1038*
29.3 Pyridine and Quinoline-Derived P,N Ligands *1040*
29.4 Carbenoid Imidazolylidene Ligands *1042*
29.5 Metallocenes *1043*
29.6 Other Ligands *1044*
29.7 Conclusions *1046*
Abbreviations *1046*
References *1047*

30 **Enantioselective Hydrogenation of Unfunctionalized Alkenes** *1049*
Andreas Pfaltz and Sharon Bell

31 **Mechanism of Enantioselective Hydrogenation** *1073*
John M. Brown

32 **Enantioselective Ketone and β-Keto Ester Hydrogenations (Including Mechanisms)** *1105*
Takeshi Ohkuma and Ryoji Noyori

33 **Rhodium-Catalyzed Enantioselective Hydrogenation of Functionalized Ketones** *1165*
André Mortreux and Abdallah Karim

34 **Enantioselective Hydrogenation of C=N Functions and Enamines** *1193*
Felix Spindler and Hans-Ulrich Blaser

35 **Enantioselective Transfer Hydrogenation** *1215*
A. John Blacker

36 **High-Throughput Experimentation and Ligand Libraries** *1245*
Johannes G. de Vries and Laurent Lefort

37 **Industrial Applications** *1279*
Hans-Ulrich Blaser, Felix Spindler, and Marc Thommen

Part V Phase Separation in Homogeneous Hydrogenation

38 **Two-Phase Aqueous Hydrogenations** *1327*
Ferenc Joó and Ágnes Kathó

39 **Supercritical and Compressed Carbon Dioxide as Reaction Medium and Mass Separating Agent for Hydrogenation Reactions using Organometallic Catalysts** *1361*
Walter Leitner

40 **Fluorous Catalysts and Fluorous Phase Catalyst Separation for Hydrogenation Catalysis** *1377*
Elwin de Wolf and Berth-Jan Deelman

41 **Catalytic Hydrogenation using Ionic Liquids as Catalyst Phase** *1389*
Peter Wasserscheid and Peter Schulz

42 **Immobilization Techniques** *1421*
Imre Tóth and Paul C. van Geem

Part VI **Miscellaneous Topics in Homogeneous Hydrogenation**

43 **Transition Metal-Catalyzed Regeneration of Nicotinamide Cofactors** *1471*
Stephan Lütz

44 **Catalyst Inhibition and Deactivation in Homogeneous Hydrogenation** *1483*
Detlef Heller, André H. M. de Vries, and Johannes G. de Vries

45 **Chemical Reaction Engineering Aspects of Homogeneous Hydrogenations** *1517*
Claude de Bellefon and Nathalie Pestre

Subject Index *1547*

Contents

Part I **Introduction, Organometallic Aspects and Mechanism of Homogeneous Hydrogenation**

1 **Rhodium** *3*
Luis A. Oro and Daniel Carmona

2 **Iridium** *31*
Robert H. Crabtree

3 **Ruthenium and Osmium** *45*
Robert H. Morris

4 **Palladium and Platinum** *71*
Paolo Pelagatti

5 **Nickel** *93*
Elisabeth Bouwman

6 **Hydrogenation with Early Transition Metal, Lanthanide and Actinide Complexes** *111*
Christophe Copéret

7 **Ionic Hydrogenations** *153*
R. Morris Bullock

8 **Homogeneous Hydrogenation by Defined Metal Clusters** *199*
Roberto A. Sánchez-Delgado

9 **Homogeneous Hydrogenation: Colloids – Hydrogenation with Noble Metal Nanoparticles** *217*
Alain Roucoux and Karine Philippot

The Handbook of Homogeneous Hydrogenation.
Edited by J.G. de Vries and C.J. Elsevier
Copyright © 2007 WILEY-VCH Verlag GmbH & Co. KGaA, Weinheim
ISBN: 978-3-527-31161-3

10 **Kinetics of Homogeneous Hydrogenations: Measurement and Interpretation** *257*
Hans-Joachim Drexler, Angelika Preetz, Thomas Schmidt, and Detlef Heller

Part II **Spectroscopic Methods in Homogeneous Hydrogenation**

11 **Nuclear Magnetic Resonance Spectroscopy in Homogeneous Hydrogenation Research** *297*
N. Koen de Vries

12 **Parahydrogen-Induced Polarization: Applications to Detect Intermediates of Catalytic Hydrogenations** *313*
Joachim Bargon

13 **A Tour Guide to Mass Spectrometric Studies of Hydrogenation Mechanisms** *359*
Corbin K. Ralph, Robin J. Hamilton, and Steven H. Bergens

Part III **Homogeneous Hydrogenation by Functional Groups**

14 **Homogeneous Hydrogenation of Alkynes and Dienes** *375*
Alexander M. Kluwer and Cornelis J. Elsevier

15 **Homogeneous Hydrogenation of Aldehydes, Ketones, Imines and Carboxylic Acid Derivatives: Chemoselectivity and Catalytic Activity** *413*
Matthew L. Clarke and Geoffrey J. Roff

16 **Hydrogenation of Arenes and Heteroaromatics** *455*
Claudio Bianchini, Andrea Meli, and Francesco Vizza

17 **Homogeneous Hydrogenation of Carbon Dioxide** *489*
Philip G. Jessop

18 **Dehalogenation Reactions** *513*
Attila Sisak and Ottó Balázs Simon

19 **Homogeneous Catalytic Hydrogenation of Polymers** *547*
Garry L. Rempel, Qinmin Pan, and Jialong Wu

20 **Transfer Hydrogenation Including the Meerwein-Ponndorf-Verley Reduction** *585*
Dirk Klomp, Ulf Hanefeld, and Joop A. Peters

21 **Diastereoselective Hydrogenation** *631*
Takamichi Yamagishi
References *708*

22 **Hydrogen-Mediated Carbon–Carbon Bond Formation Catalyzed by Rhodium** *713*
Chang-Woo Cho and Michael J. Krische

Part IV **Asymmetric Homogeneous Hydrogenation**

23 **Enantioselective Alkene Hydrogenation: Introduction and Historic Overview** *745*
David J. Ager

24 **Enantioselective Hydrogenation: Phospholane Ligands** *773*
Christopher J. Cobley and Paul H. Moran

25 **Enantioselective Hydrogenation of Alkenes with Ferrocene-Based Ligands** *833*
Hans-Ulrich Blaser, Matthias Lotz, and Felix Spindler

26 **The other Bisphosphine Ligands for Enantioselective Alkene Hydrogenation** *853*
Yongxiang Chi, Wenjun Tang, and Xumu Zhang

27 **Bidentate Ligands Containing a Heteroatom–Phosphorus Bond** *883*
Stanton H. L. Kok, Terry T.-L. Au-Yeung, Hong Yee Cheung, Wing Sze Lam, Shu Sun Chan, and Albert S. C. Chan

28 **Enantioselective Alkene Hydrogenation: Monodentate Ligands** *995*
Michel van den Berg, Ben L. Feringa, and Adriaan J. Minnaard

29 **P,N and Non-Phosphorus Ligands** *1029*
Andreas Pfaltz and Sharon Bell

30 Enantioselective Hydrogenation of Unfunctionalized Alkenes *1049*
Andreas Pfaltz and Sharon Bell
30.1 Introduction *1049*
30.2 Terminal Alkenes *1050*
30.2.1 2-Aryl-1-Butenes *1050*
30.2.2 Other Terminal Alkenes *1054*
30.3 Trisubstituted Alkenes *1056*
30.3.1 Introduction *1056*
30.3.2 Ir Catalysts *1057*
30.3.3 Standard Test Substrates *1057*
30.3.4 Other Substrates *1063*
30.4 Tetrasubstituted Alkenes *1066*
30.4.1 Substrates *1066*
30.5 Dienes and Trienes *1067*
30.6 Conclusions *1069*
Abbreviations *1070*
References *1070*

31 Mechanism of Enantioselective Hydrogenation *1073*
John M. Brown
31.1 Introduction *1073*
31.2 Rhodium-Catalyzed Hydrogenations *1074*
31.2.1 Background *1074*
31.2.2 More Recent Developments *1076*
31.2.3 Transient and Reactive Intermediates in Rhodium Enantioselective Hydrogenation *1078*
31.2.4 Mnemonics for the Sense of Enantioselective Hydrogenation *1082*
31.2.5 Status of the Computational Study of Rhodium-Complex-Catalyzed Enantioselective Hydrogenation *1082*
31.2.6 Monophosphines in Rhodium-Complex-Catalyzed Enantioselective Hydrogenation *1086*
31.2.7 Mechanism of Hydrogenation of β-Dehydroamino Acid Precursors *1087*
31.2.8 Current Status of Rhodium Hydrogenations *1088*
31.3 Ruthenium-Complex-Catalyzed Hydrogenations *1093*
31.3.1 Reactive Intermediates in Ruthenium-Complex-Catalyzed Hydrogenations *1093*
31.3.2 Kinetic Analysis of Ruthenium-Complex-Catalyzed Hydrogenations *1093*
31.4 Iridium-Complex-Catalyzed Hydrogenations *1094*
31.4.1 Background *1094*
31.4.2 Mechanistic and Computational Studies *1095*
31.4.3 Counter-Ion Effects *1097*
31.5 Summary and Conclusions *1098*
Acknowledgments *1099*

Abbreviations *1099*
References *1099*

32 Enantioselective Ketone and β-Keto Ester Hydrogenations (Including Mechanisms) *1105*
Takeshi Ohkuma and Ryoji Noyori
32.1 Chiral Ligands *1105*
32.2 β-Keto Esters and Analogues *1107*
32.2.1 β-Keto Esters *1107*
32.2.2 1,3-Diketones *1122*
32.2.3 β-Keto Phosphonates, Sulfonates, and Sulfones *1125*
32.2.4 Dynamic Kinetic Resolution *1127*
32.3 Simple Ketones *1131*
32.3.1 Alkyl Aryl Ketones *1131*
32.3.2 Hetero-Substituted Aromatic Ketones *1141*
32.3.3 Diaryl Ketones *1144*
32.3.4 Heteroaromatic Ketones *1144*
32.3.5 Dialkyl Ketones *1147*
32.3.6 Unsaturated Ketones *1148*
32.3.7 Kinetic Resolution and Dynamic Kinetic Resolution *1150*
32.3.8 Enantioselective Activation and Deactivation *1154*
Abbreviations *1156*
References *1156*

33 Rhodium-Catalyzed Enantioselective Hydrogenation of Functionalized Ketones *1165*
André Mortreux and Abdallah Karim
33.1 Introduction *1165*
33.2 Basic Principles of Ketone Hydrogenation on Rhodium Catalysts *1166*
33.3 Enantioselective Hydrogenation of Ketoesters *1166*
33.3.1 Enantioselective Hydrogenation of Ketopantoyllactone (KPL) *1166*
33.3.2 Hydrogenation of Ketoesters and Ketoamides *1172*
33.3.2.1 α-Ketoesters and Ketoamides *1172*
33.3.2.2 α,γ-Diketoesters *1176*
33.3.3 Hydrogenation of Amino Ketones *1177*
33.3.3.1 α-Amino Ketones *1177*
33.3.3.2 β- and γ-Amino Ketones *1184*
33.4 Enantioselective Hydrogenation of Fluoroketones *1186*
33.5 Conclusions *1188*
Abbreviations and Acronyms *1189*
References *1189*

34 Enantioselective Hydrogenation of C=N Functions and Enamines *1193*
Felix Spindler and Hans-Ulrich Blaser
34.1 Introduction *1193*
34.2 Chiral Ligands *1195*
34.3 *N*-Aryl Imines *1197*
34.4 *N*-Alkyl Imines *1200*
34.5 Cyclic Imines and Heteraromatic Substrates *1202*
34.6 Miscellaneous C=N–X Systems *1204*
34.7 Enamines *1206*
34.8 Mechanistic Aspects *1207*
34.9 Alternative Reduction Systems *1209*
34.10 Assessment of Catalysts and Conclusions *1210*
34.10.1 Iridium Complexes *1210*
34.10.2 Rhodium Complexes *1211*
34.10.3 Ruthenium Complexes *1211*
34.10.4 Titanium Complexes *1211*
Abbreviations *1212*
References *1212*

35 Enantioselective Transfer Hydrogenation *1215*
A. John Blacker
35.1 Introduction *1215*
35.2 Homogenous Metal Catalysts *1216*
35.2.1 Early studies *1216*
35.2.2 Group VIII Metal Catalysts *1217*
35.2.3 Chiral Ligands *1218*
35.2.4 Immobilized Ligands *1220*
35.2.5 Water-Soluble Ligands *1221*
35.2.6 Catalyst Selection *1221*
35.2.7 Catalyst Preparation *1222*
35.2.8 The Reaction Mechanism *1223*
35.3 Hydrogen Donors *1224*
35.3.1 The IPA System *1224*
35.3.2 The TEAF System *1225*
35.3.3 Other Hydrogen Donors *1229*
35.4 Substrates and Products *1229*
35.4.1 Aldehydes *1229*
35.4.2 Ketones *1229*
35.4.3 Aldimines *1231*
35.4.4 Ketimines *1232*
35.4.5 Alkenes *1235*
35.5 Solvents *1235*
35.6 Reaction Conditions, Optimization, and Scale-Up *1236*
35.6.1 Temperature *1236*

35.6.2 Productivity *1237*
35.6.3 Reaction Control *1238*
35.6.4 Large-Scale Processes *1239*
35.7 Discussion *1239*
Abbreviations *1240*
References *1241*

36 High-Throughput Experimentation and Ligand Libraries *1245*
Johannes G. de Vries and Laurent Lefort
36.1 Introduction *1245*
36.2 High-Throughput Experimentation *1248*
36.2.1 Serial Mode *1248*
36.2.2 Parallel Experimentation *1249*
36.2.3 Combinatorial Protocols *1249*
36.3 Generating and Testing Libraries of Catalysts and Ligands *1250*
36.3.1 Libraries of Individually Synthesized Ligands *1250*
36.3.2 Automated Synthesis of Ligand Libraries *1258*
36.3.3 Mixtures of Chiral Monodentate Ligands *1263*
36.3.4 Mixtures of Chiral Monodentate Ligands and Nonchiral Ligands *1267*
36.3.5 Supramolecular Approaches to Ligand Libraries *1270*
36.4 Methodology for Testing Catalysts *1272*
36.5 High-Throughput Analysis *1273*
36.6 Conclusions *1274*
Abbreviations *1275*
References *1275*

37 Industrial Applications *1279*
Hans-Ulrich Blaser, Felix Spindler, and Marc Thommen
37.1 Introduction and Scope of the Chapter *1279*
37.2 Requirements for Technical-Scale Applications *1280*
37.2.1 Catalyst Performance *1281*
37.2.2 Availability and Cost of the Catalyst *1281*
37.2.3 Development Time *1282*
37.3 Process Development and Equipment *1283*
37.4 Industrial Processes: General Comments *1284*
37.5 Chemo- and Diastereoselective Hydrogenations *1286*
37.6 Enantioselective Hydrogenation of C=C Bonds *1287*
37.6.1 Dehydro α-Amino Acid Derivatives *1287*
37.6.1.1 L-Dopa (Monsanto, VEB Isis-Chemie) *1288*
37.6.1.2 Aspartame (Enichem/Anic, Degussa) *1289*
37.6.1.3 Various Pilot- and Bench-Scale Processes for α-Amino Acid Derivatives *1289*
37.6.2 Dehydro β-Amino Acid Derivatives *1292*
37.6.3 Simple Enamides and Enol Acetates *1293*

37.6.4 Itaconic Acid Derivatives *1293*
37.6.5 Allylic Alcohols and α,β-Unsaturated Acids *1294*
37.6.5.1 Allylic Alcohols *1295*
37.6.5.2 α,β-Unsaturated Acids *1296*
37.6.6 Miscellaneous C=C Systems *1298*
37.6.6.1 Hydrogenation of a Biotin Intermediate (Lonza) *1299*
37.6.6.2 Synthesis of (+)-Methyl *cis*-Dihydrojasmonate (Firmenich) *1300*
37.6.6.3 Intermediate for Tipranavir (Chirotech) *1300*
37.6.6.4 Various C=C Substrates *1302*
37.7 Enantioselective Hydrogenation of C=O Bonds *1302*
37.7.1 α-Functionalized Ketones *1302*
37.7.2 β-Functionalized Ketones *1305*
37.7.3 Aromatic Ketones *1307*
37.8 Enantioselective Hydrogenation of C=N Bonds *1308*
37.9 Ligands and Metal Complexes for Large-Scale Applications *1311*
37.9.1 Companies Offering Services, Technology, Ligands and Catalysts *1312*
37.9.2 Chiral Ligands with Established Industrial Performance *1313*
37.9.3 Metal Complexes and Anions *1313*
37.9.4 Intellectual Property Aspects *1317*
37.10 Conclusions and Future Developments *1317*
Acknowledgments *1319*
Abbreviations *1319*
References *1319*

Part V Phase Separation in Homogeneous Hydrogenation

38 Two-Phase Aqueous Hydrogenations *1327*
Ferenc Joó and Ágnes Kathó
38.1 Introduction *1327*
38.2 Two-Phase Hydrogenation of Alkenes, Alkynes, and Arenes *1334*
38.3 Enantioselective Hydrogenation of Alkenes in Two-Phase Aqueous Systems *1338*
38.4 Aqueous Two-Phase Hydrogenation of Aldehydes and Ketones *1344*
38.5 Aqueous Two-Phase Hydrogenations of Nitro-Compounds, Imines, Nitriles, Oximes, and Heteroaromatics *1352*
38.6 Conclusions *1354*
Abbreviations *1355*
References *1355*

39 Supercritical and Compressed Carbon Dioxide as Reaction Medium and Mass Separating Agent for Hydrogenation Reactions using Organometallic Catalysts *1361*
Walter Leitner
39.1 Introduction *1361*
39.2 The Molecular and Reaction Engineering Basis of Organometallic-Catalyzed Hydrogenations using Compressed and $scCO_2$ *1362*
39.2.1 Control of Hydrogen Availability *1362*
39.2.2 Catalyst Recycling and Immobilization *1363*
39.2.2.1 Solubility Control for Separation *1364*
39.2.2.2 Membrane Separation *1364*
39.2.2.3 Biphasic Liquid/Supercritical Systems *1364*
39.2.2.4 Inverted Biphasic Systems *1364*
39.2.2.5 Solid-Supported Catalysts *1365*
39.2.3 Catalytic Systems for Hydrogenation using SCFs, and their Synthetic Applications *1365*
39.2.4 Mechanistic Aspects *1371*
39.3 Conclusions and Outlook *1373*
Abbreviations *1374*
References *1374*

40 Fluorous Catalysts and Fluorous Phase Catalyst Separation for Hydrogenation Catalysis *1377*
Elwin de Wolf and Berth-Jan Deelman
40.1 Introduction *1377*
40.2 Catalysts Based on Fluorous Alkylphosphines, -Phosphinites, -Phosphonites, and -Phosphites *1378*
40.3 Catalysts Based on Perfluoroalkyl-Substituted Arylphosphines *1380*
40.4 Fluorous Anions for the Separation of Cationic Hydrogenation Catalysts *1384*
40.5 Catalysts Based on Nonphosphorus Ligands *1386*
40.6 Enantioselective Hydrogenation Catalysts *1386*
40.7 Conclusions *1386*
Abbreviations *1387*
References and Notes *1387*

41 Catalytic Hydrogenation using Ionic Liquids as Catalyst Phase *1389*
Peter Wasserscheid and Peter Schulz
41.1 Introduction to Ionic Liquids *1389*
41.2 Homogeneous Catalyzed Hydrogenation in Biphasic Liquid–Liquid Systems *1394*
41.2.1 Hydrogenation of Olefins *1394*
41.2.2 Hydrogenation of Arenes *1397*

41.2.3 Hydrogenation of Polymers *1400*
41.2.4 Stereoselective Hydrogenation *1401*
41.2.5 Ketone and Imine Hydrogenation in Ionic Liquids *1407*
41.2.6 Imine Hydrogenation *1411*
41.3 Homogeneous Catalyzed Hydrogenation in Biphasic Ionic Liquid/Supercritical (sc)CO_2 System *1412*
41.4 Supported Ionic Liquid Phase Catalysis *1413*
41.5 Conclusion *1416*
Abbreviations *1417*
References *1417*

42 Immobilization Techniques *1421*
Imre Tóth and Paul C. van Geem
42.1 Introduction *1421*
42.2 Engineering and Experimental Aspects *1422*
42.3 Immobilization Methods *1424*
42.3.1 Physical Methods of Immobilization *1426*
42.3.1.1 Physisorption of Metal Complexes *1427*
42.3.1.2 Weak Chemisorption: Supported Hydrogen-Bonded (SHB) Catalysts *1427*
42.3.2 Encapsulated Homogeneous Catalysts *1430*
42.3.2.1 Synthesis of SIB Catalysts *1431*
42.3.2.2 Application of SIB Catalysts *1433*
42.3.3 Catalysts Entangled in a Polymer *1434*
42.3.4 Catalyst Dissolved in a Supported Liquid-Phase *1435*
42.3.4.1 Supported Aqueous-Phase Catalysis *1436*
42.3.4.2 Hybrid SLP Systems *1437*
42.3.5 Covalently Bound Metal Centers *1438*
42.3.6 Covalent Attachment of Ligands *1439*
42.3.6.1 Grafting to Oxide Supports *1440*
42.3.6.2 Sol–Gel Method *1441*
42.3.6.3 Anchoring with Organic Phosphonates *1442*
42.3.6.4 Attachment to Polymer Supports *1444*
42.3.6.4.1 Functionalized Polymers as Supports *1444*
42.3.6.4.2 Enzymes as Support *1448*
42.3.6.4.3 Functionalized Monomers *1448*
42.3.6.4.4 Dendrimers as Supports: Membrane Filtration *1453*
42.3.6.4.5 Grafting to Polymers *1454*
42.3.7 Ionic Bonding of Metals to Supports *1455*
42.3.7.1 Ionically Bound Metal Centers on Inorganic Supports *1455*
42.3.7.2 Ionically Bound Metal Centers on Polymer Supports *1456*
42.3.8 Attachment of Ligands via Ion Exchange *1457*
42.4 Catalyst Deactivation *1461*
42.5 Conclusions *1462*
42.6 Outlook *1462*

Abbreviations *1463*
References *1463*

Part VI Miscellaneous Topics in Homogeneous Hydrogenation

43 Transition Metal-Catalyzed Regeneration of Nicotinamide Cofactors *1471*
Stephan Lütz
43.1 Introduction *1471*
43.2 Enzymatic Cofactor Regeneration *1474*
43.3 Electrochemical Cofactor Regeneration *1475*
43.4 Chemical Cofactor Regeneration *1477*
43.5 Other Chemical Cofactor Regeneration Procedures *1479*
43.6 Conclusions and Outlook *1479*
Acknowledgments *1480*
Abbreviations *1480*
References *1480*

44 Catalyst Inhibition and Deactivation in Homogeneous Hydrogenation *1483*
Detlef Heller, André H. M. de Vries, and Johannes G. de Vries
44.1 Introduction *1483*
44.2 Mechanisms of Catalyst Inhibition *1484*
44.3 Induction Periods *1485*
44.3.1 Introduction *1485*
44.3.2 Induction Period Caused by Slow Hydrogenation of COD or NBD *1486*
44.4 Substrate and Product Inhibition *1494*
44.5 Reversible Inhibition Caused by Materials that can Function as Ligand *1499*
44.5.1 Catalyst Deactivation Caused by Solvents *1500*
44.5.2 Catalyst Inhibition Caused by Compounds Containing Heteroatoms *1503*
44.5.3 Inhibition by CO and sources of CO *1504*
44.5.4 Inhibition by Acids and Bases *1505*
44.6 Irreversible Deactivation *1507*
44.6.1 Inhibition by Anions *1507*
44.6.2 Inhibition by Oxidation and by Ligand Modification *1507*
44.6.3 Formation of Dimers, Trimers, Clusters, Colloids, and Solids *1509*
44.7 Conclusions *1512*
Abbreviations *1513*
References *1513*

45 Chemical Reaction Engineering Aspects of Homogeneous Hydrogenations *1517*
Claude de Bellefon and Nathalie Pestre
45.1 Introduction *1517*
45.2 Fundamentals *1518*
45.2.1 Basics of Mass Transfer in Gas–Liquid Systems *1518*
45.2.2 Physical and Chemical Data for Hydrogenations *1521*
45.2.2.1 Heat of Reaction *1522*
45.2.2.2 Solubility *1522*
45.2.2.3 Diffusivity *1525*
45.2.3 Coupling Between Mass Transfer and a Single Homogeneous Irreversible Reaction *1526*
45.2.4 Coupling of Reaction and Mass Transfer in Ideal Reactors *1533*
45.2.4.1 Mass Balance for a Batch Reactor *1534*
45.2.4.2 Mass Balance for a CSTR Reactor *1535*
45.2.4.2.1 Simplified Mass Balances *1535*
45.2.4.3 Mass Balance for a Plug Flow Reactor *1536*
45.3 Industrial Reactor and Scale-Up Issues *1536*
45.4 Future Developments *1541*
Nomenclature *1542*
Abbreviations *1544*
References *1544*

Subject Index *1547*

Foreword

Homogeneous hydrogenation of organic compounds catalyzed by metal complexes is undoubtedly the most studied of the entire class of homogenously catalyzed reactions. Indeed, advances in hydrogenation systems have contributed significantly to progress in homogeneous catalysis more generally, mainly because of the involvement of intermediate metal hydrides in a wider range of catalytic processes. The historical development of homogeneous hydrogenation is documented in my 1973 text on this topic, which was intended to represent an exhaustive treatise on the subject (the process, prior to the computer era, was certainly *exhausting* as over 1900 multi-language references were compiled).

Before outlining the content of *The Handbook of Homogeneous Hydrogenation*, I will briefly note here a few early facts chronologically for the appropriate context. Melvin Calvin first used the term "homogeneous hydrogenation" in 1938 for some non-aqueous, Cu-based systems, and a year later an M. Iguchi was the first to record the use of Rh species for hydrogenations in aqueous media. Jack Halpern was the first to study (in the mid-1950s) the kinetics and detailed mechanisms of such hydrogenations, while notably R. J. P. (Bob) Williams was the first (in 1960) to suggest in an equation the possibility of an $M(H_2)$ species, long before their true characterization in the early 1980s! The majority of the systems studied up to the early 1960s (for homogeneous catalysis generally, as well as hydrogenations) were in aqueous media – a fact frequently overlooked by current researchers – but developments at that time in the isolation and characterization of transition metal hydrides (pioneered especially by Joseph Chatt's group), including their stabilization by tertiary phosphines, led to increased studies in non-aqueous systems. Cleaner and "greener" aqueous systems are preferred for industrial processes, and intense interest remains in the incorporation of, for example, water-solubility enhancing, polar groups (sulfonate, carboxylate, hydroxide, etc.) into phosphine-containing ligands, protonation of N-atoms in P-N donor ligand, and more general use of cationic or anionic species for catalysis. The completion of the cycle back to aqueous systems is now in progress.

The classic 1961 paper by Halpern *et al.* (the '*al.*' being John Harrod and myself) on the catalytic hydrogenation of unsaturated acids using chlororuthenium(II) species in aqueous acid solutions certainly motivated the work of Geoffrey Wilkinson's group on Ru- and Rh-triphenylphosphine hydrogenation catalysts; these

The Handbook of Homogeneous Hydrogenation.
Edited by J. G. de Vries and C. J. Elsevier
Copyright © 2007 WILEY-VCH Verlag GmbH & Co. KGaA, Weinheim
ISBN: 978-3-527-31161-3

findings, published in the mid-1960s, are now legendary. The next highly significant step was the use of chiral phosphines with Rh precursors, first reported in 1968 by the groups of Knowles and Horner, the work providing the first examples of catalytic enantioselective hydrogenation (of unsaturated acids and α-substituted styrenes). Thousands of subsequent publications have recorded the development of catalyst systems containing chiral ligands (such as phosphines, sulfoxides, oxazolines, nitrogen-ligands, combinations of P/N/O/S-donors, carbenes, etc.) for hydrogenation of a wide range of prochiral substrates including alkenes, ketones, and ketimines. Processes reaching close to 100% enantiomeric excess (e.e.) are no longer uncommon, and, in a few cases, a remarkable degree of understanding of the mechanistic pathways has been achieved. About one dozen industrial, catalytic enantioselective homogeneous hydrogenation processes are now operating, and the potential for chiral catalyst systems within fine chemical industries (particularly for pharmaceuticals and agrochemicals) remains enormous. The first such process, that went on-line in 1970, was for the synthesis of L-dopa, a drug for treatment of Parkinson's disease; the system involved hydrogenation of a prochiral enamide using a Rh-chiral phosphine catalyst. In the production of the herbicide Metolachlor, a process that went on-line in 1996, a chiral amine is generated by hydrogenation of a ketimine using an Ir catalyst, and this currently provides the largest scale industrial process for an enantioselective synthesis of any type. The discovery and explanation of non-linear effects in enantioselective reactions, first reported by Kagan's group in 1986, are also noteworthy, and should lead to improved applications in enantioselective synthesis and, more importantly, a better understanding of the origins of enantioselectivity.

Advances thus far in experimental enantioselective hydrogenation have stemmed largely from empirical studies. More trendy and certainly more effective is high-throughput experimentation using ligand libraries, a methodology that is being increasingly promoted by researchers in the fine-chemical industries. Novel attempts to find the best catalyst by purely theoretical work that involves screening virtual catalyst libraries are also being published.

Hydrogenation catalysis in the petrochemical and related industries remains in the domain of heterogeneous systems, because of the practicality of separating and recycling the catalyst, although advances in the use of multiphase systems might find eventually use in relatively small-scale systems where a requirement is high selectivity, a vital property that can be engineered with a homogeneous catalyst. The design of supported metal complexes, including dendrimers, the use of size-exclusion filtration methodology, and the use of biphasic systems with all their ramifications (fluorous solvents, ionic liquids, and supercritical fluids), continue to be areas of intense current interest, and the findings should lead to further industrial uses of homogeneous catalysts, particularly in the small-scale synthesis of high value products.

The classic division between heterogeneous and homogeneous catalysts appears to becoming increasingly blurred and, in some cases involving colloidal/nanoparticle and metal cluster catalysts, the difference is difficult to determine experimentally. The large majority of reported homogeneous hydrogenation cat-

alysts for aromatic residues now appear to be colloidal systems; in terms of activity within a particular reaction, the true nature of a catalyst may be considered somewhat irrelevant, but this is key when catalyst separation/removal for the purposes of recycling and residual toxicity levels is considered.

The exponential increase in the homogeneous hydrogenation literature over the last three decades shows no sign of abatement, and indeed, with the "replacement" of phosphine ligands by the increasingly popular carbenes, and the use of various two- and multi-phase systems, a further endemic literature expansion in homogeneous catalysis, and especially in the most understood area of hydrogenation, is guaranteed.

There is no question that much general knowledge on homogeneous catalysis has stemmed from studies on homogeneous hydrogenation, and it is fitting that *The Handbook of Homogeneous Hydrogenation* is published about 50 years after Halpern's first reports on the mechanistic aspects of such reactions. The editors have assembled an impressive list of eighty-one international experts that review the field from several aspects noted above. The first six chapters are categorized according to the catalyst metal used (most often the more traditional group 8–10 noble metals, although data on the early transition metals are presented), and there are chapters on the use of metal clusters and nanoparticles. A separate chapter appears on the kinetics commonly observed in hydrogenation systems, and there is one chapter on ionic hydrogenations. Three well-known techniques for studying homogeneous hydrogenation are then each presented in a chapter that discuss: NMR methods in general, the PHIP (parahydrogen induced polarization) NMR method, and the application of mass spectrometry. There are chapters on hydrogenation of organic substrates that are generally assembled according to the nature of the unsaturated function present in the organic, while separate chapters describe hydrogen transfer processes, CO_2 hydrogenation, and Rh-catalyzed, hydrogen-mediated, carbon-carbon bond formation. A large number of the chapters appropriately cover the many aspects of enantioselective hydrogenation, including a synopsis of current industrial applications. The final chapters deal with the fundamental problem associated with applications of homogeneous catalysis: deactivation, separation and recovery of the catalyst, and related engineering aspects.

The editors and authors are to be congratulated on assembling what is destined to become a classic in the area of Homogeneous Hydrogenation, which over the years has earned its title in capital letters.

Brian R. James
(University of British Columbia)

Preface

It is truly astonishing that such a simple reaction as the addition of one molecule of hydrogen to a double or triple bond can have so many facets.

When we had chosen the title of Handbook of Homogeneous Hydrogenation for our book we meant it to be a comprehensive work of reference. In this respect we are quite satisfied. We only had to skip the chapter on dehydrogenations, for which we could not find an author. We are extremely grateful to the other 88 authors for dedicating so much of their valuable time to writing the 81 marvellous chapters included in these volumes. We had envisaged an average of 30 pages per chapter but in the end this was not enough, necessitating an expansion of the two projected volumes to three.

One may wonder how long this handbook remains up-to-date. Indeed many areas are continuously undergoing new developments. In addition, new topics that were hardly emerging five years ago seem to develop at a very fast pace. Colloidal hydrogenation catalysts, for instance, which until recently were seen as the Cinderella of both homogeneous and heterogeneous catalysis – too soluble to be heterogeneous and too ill-defined to be homogeneous – have become quite respectable since they were recognized to be part of nanotechnology. Reductive coupling reactions can be considered as a green method to construct carbon-carbon bonds without taking resort to leaving groups. Indeed, not only this class of reactions, but all hydrogenations are of course extremely environmentally benign. Also the number of substrates is continuously expanding; carboxylic acid derivatives and heteroarenes are good examples of substrates recently added to the existing pool.

Just when everyone thought the chiral-ligand-boom was coming to an end, extremely simple monodentate ligands turned out to be quite effective, also allowing a combinatorial approach using mixtures of ligands. There is now a bewildering choice of chiral ligands available, increasing the chances of application. Indeed, the number of industrial applications is steadily increasing; an important breakthrough in this area was the advent of high throughput experimentation, which allowed for the first time to find a chiral ligand with good performance within a matter of weeks.

Our insight into the mechanisms of hydrogenation reactions has grown tremendously, thanks to advances in spectroscopic techniques, but also thanks to the hard work of many organometallic chemists. Many authors now also recog-

The Handbook of Homogeneous Hydrogenation.
Edited by J.G. de Vries and C.J. Elsevier
Copyright © 2007 WILEY-VCH Verlag GmbH & Co. KGaA, Weinheim
ISBN: 978-3-527-31161-3

nise the importance of the rate of these reactions. Turnover frequencies of hydrogenations are listed throughout the book.

One aspect that remains underdeveloped is the insight in deactivation pathways. Our knowledge in this area is growing, but the pace is slow. We have devoted an entire chapter to this topic, since the economics of many processes could benefit a lot from more insight in ways to reduce catalyst deactivation.

So far none of the industrial processes recycle the catalyst. Yet the number of ways to do this has grown far beyond simple immobilization. Two-phase catalysis now comes in many flavours.

Looking into the future, we expect that hydrogenation reactions will also be tremendously important for the conversion of renewable resources. Going from carbohydrates to valuable chemicals will require deoxygenating reactions. Thus, hydrogenation of alcohols, aldehydes and carboxylic acids will become very important topics.

We hope the readers will appreciate as well as enjoy the contents of this book. Any comments you may have are of course very welcome.

Hans de Vries September 2006
Kees Elsevier

List of Contributors

David Ager
DSM Pharma Chemicals
9650 Strickland Road, Suite 103
Raleigh NC 27615-1937
USA

Terry T.-L. Au-Yeung
Open Laboratory of Chirotechnology
Institute of Molecular Technology
for Drug Discovery and Synthesis
Department of Applied Biology
and Chemical Technology
The Hong Kong Polytechnic
University
Hong Kong

Joachim Bargon
Institute of Physical and Theoretical
Chemistry
University of Bonn
Wegelerstraße 12
53115 Bonn
Germany

Sharon Bell
University of Basel
Department of Chemistry
St.-Johanns-Ring 19
4056 Basel
Switzerland

Claude de Bellefon
Laboratoire de Génie des Procédés
Catalytiques
CNRS-ESCPE Lyon
69616 Villeurbanne
France

Steven H. Bergens
Department of Chemistry
University of Alberta
Edmonton
Alberta
Canada T6G 2G2

Claudio Bianchini
ICCOM-CNR
Area della Ricerca CNR
Via Madonna del Piano snc
500019 Sesto Fiorentina/Firenze
Italy

A. John Blacker
Avecia Pharma (UK) Ltd.
Research and Development
Leeds Road
Huddersfield
HD1 9GA
UK

The Handbook of Homogeneous Hydrogenation.
Edited by J.G. de Vries and C.J. Elsevier
Copyright © 2007 WILEY-VCH Verlag GmbH & Co. KGaA, Weinheim
ISBN: 978-3-527-31161-3

Hans-Ulrich Blaser
Solvias AG
WRO-1055.6.28
Klybeckstrasse 191
4002 Basel
Switzerland

Elisabeth Bouwman
Leiden Institute of Chemistry
Leiden University
P.O. Box 9502
2300 RA Leiden
The Netherlands

John M. Brown
Chemical Research Laboratory
Oxford University
Oxford OX1 3TA
UK

R. Morris Bullock
Brookahven National Laboratory
Chemistry Department
Upton
New York 11973-5000
USA

Daniel Carmona
Departamento de Química Inorgánica
Instituto Universitario de Catálisis
Homogénea
Universidad de Zaragoza
Instituto de Ciencia de Materiales
de Aragón
C.S.I.C.-Universidad de Zaragoza
Zaragoza 50009
Spain

Shu Sun Chan
Open Laboratory of Chirotechnology
Institute of Molecular Technology
for Drug Discovery and Synthesis
Department of Applied Biology
and Chemical Technology
The Hong Kong Polytechnic
University
Hong Kong

Albert S.C. Chan
Open Laboratory of Chirotechnology
Institute of Molecular Technology
for Drug Discovery and Synthesis
Department of Applied Biology
and Chemical Technology
The Hong Kong Polytechnic
University
Hong Kong

Yongxiang Chi
Department of Chemistry
104 Chemistry Building
The Pennsylvania State University
University Park
PA 16802
USA

Chang-Woo Cho
University of Texas at Austin
Department of Chemistry
and Biochemistry
Austin
Texas 78712
USA

Hong Yee Cheung
Open Laboratory of Chirotechnology
Institute of Molecular Technology
for Drug Discovery and Synthesis
Department of Applied Biology
and Chemical Technology
The Hong Kong Polytechnic
University
Hong Kong

Matthew L. Clarke
School of Chemistry,
University of St. Andrews
St. Andrews
Fife KY16 9ST
UK

Christoper J. Cobley
Dowpharma
Chirotech Technology Limited
The Dow Chemical Company
321 Cambridge Science Park
Milton Road,
Cambridge CB4 0WG
UK

Christophe Copéret
Laboratoire de Chimie
Organométallique de Surface
UMR 9986 CNRS – CPE Lyon
CPE Lyon – Bât. 308
69616 Villeurbanne Cedex
France

Robert H. Crabtree
Yale University
Chemistry Department
350 Edwards Street
New Haven
CT 06520-8107
USA

Berth-Jan Deelman
Arkema Vlissingen B.V.
P.O. Box 70
4380 AB Vlissingen
The Netherlands

André H.M. de Vries
DSM Pharmaceutical Products
Advanced Synthesis, Catalysis,
and Development
P.O. 18
6160 MD
Geleen
The Netherlands

Johannes G. de Vries
DSM Pharmaceutical Products
Advanced Synthesis, Catalysis,
and Development
P.O. Box 18
6160 MD Geleen
The Netherlands

N. Koen de Vries
DSM Research Geleen
P.O. Box 18
6160 MD Geleen
The Netherlands

Elwin de Wolf
Debye Institute
Dept. of Metal-Mediated Synthesis
Utrecht University
Padualaan 8
3584 CH Utrecht
The Netherlands

Hans-Joachim Drexler
Leibniz-Institut für Organische
Katalyse an der Universität Rostock e.V.
Albert-Einstein-Str. 29 a
18059 Rostock
Germany

Cornelis J. Elsevier
Institute of Molecular Chemistry
Univeristy of Amsterdam
Niewe Achtergracht 166
1018 WV Amsterdam
The Netherlands

Ben L. Feringa
Stratingh Institute
University of Groningen
Nijenborgh 4
9747 AG Groningen
The Netherlands

Robin J. Hamilton
Department of Chemistry
University of Alberta
Edmonton
Alberta
Canada T6G 2G2

Ulf Hanefeld
Organic Chemistry
Delft University of Technology
Julianalaan 136
2628 BL Delft
The Netherlands

Detlef Heller
Leibniz-Institut für Katalyse
an der Universität Rostock
Albert-Einstein-Str. 29a
18059 Rostock
Germany

Philip G. Jessop
Department of Chemistry
Queen's University
90 Bader Lane
Kingston
Ontario
Canada K7L 3N6

Ferenc Joó
Institute of Physical Chemistry
University of Debrecen
1, Egyetem tér
4010 Debrecen
Hungary

Abdallah Karim
Laboratoire de Chimie
de Coordination
Faculté des Sciences Semlalia
Université Cadi Ayyad
BP 2390
Marrakech
Morocco

Ágnes Kathó
Institute of Physical Chemistry
University of Debrecen
1, Egyetem tér
Debrecen
4010 Debreden
Hungary

Dirk Klomp
Organic Chemistry
Delft University of Technology
Julianalaan 136
2628 BL Delft
The Netherlands

Alexander M. Kluwer
Van't Hoff Institute for Molecular
Sciences
Nieuwe Achtergracht 166
1018 WV Amsterdam
The Netherlands

Stanton H. L. Kok
Open Laboratory of Chirotechnology
Institute of Molecular Technology
for Drug Discovery and Synthesis
Department of Applied Biology
and Chemical Technology
The Hong Kong Polytechnic
University
Hong Kong

Michael J. Krische
University of Texas
Depart. of Chemistry
and Biochemistry
1 University Station A5300
Austin TX 78712-0165
USA

Wing Sze Lam
Open Laboratory of Chirotechnology
Institute of Molecular Technology
for Drug Discovery and Synthesis
Department of Applied Biology
and Chemical Technology
The Hong Kong Polytechnic
University
Hong Kong

Laurent Lefort
DSM Pharmaceutical Products
Advanced Synthesis
Catalysis & Development
P.O. Box 16
6160 MD Geleen
The Netherlands

Walter Leitner
Lehrstuhl für Technische Chemie
und Petrolchemie
Institut für Technische
und Makromolekulare Chemie
RWTH Aachen
Worringer Weg 1
52070 Aachen
Germany

Matthias Lotz
Solvias AG
P.O. Box
4002 Basel
Switzerland

Stephan Lütz
Institute of Biotechnology 2
Research Centre Jülich
52425 Jülich
Germany

Andrea Meli
ICCOM-CNR
Area della Ricerca CNR
Via Madonna del Piano snc
500019 Sesto Fiorentina/Firenze
Italy

Adriaan J. Minnaard
Stratingh Institute
University of Groningen
Nijenborgh 4
9747 AG Groningen
The Netherlands

Paul H. Moran
Dowpharma
Chirotech Technology Limited
The Dow Chemical Company
321 Cambridge Science Park
Milton Road
Cambridge CB4 0WG
UK

Robert H. Morris
Department of Chemistry
University of Toronto
80 St. George St.
Toronto M5S 3H6
Canada

André Mortreux
Laboratoire de Catalyse de Lille
UMR 8010 CNRS, USTL, ENSCL
BP 90108
59652, Villeneuve d'Ascq Cedex
France

Ryoji Noyori
Department of Chemistry
and Research Center
for Materials Science
Nagoya University Chikusa
Nagoya 464-8602
Japan

Taheshi Ohkuma
Graduate School of Engineering
Hokkaido University
Laboratory of Organic Synthesis
Division of Molecular Chemistry
Sapporo 060-8628
Japan

Luis A. Oro
Departamento de Química Inorgánica
Instituto Universitario de Catálisis Homogénea
Universidad de Zaragoza
Instituto de Ciencia de Materiales de Aragón
C.S.I.C.-Universidad de Zaragoza
Zaragoza 50009
Spain

Qinmin Pan
University of Waterloo
Department of Chemical Engineering
Waterloo
Ontario
Canada N2L 3G1

Paolo Pelagatti
Dipartimento di Chimica Generale ed Inorganica
Chimica Analitica, Chimica Fisica
Università degli Studi di Parma
Parco Area Scienze 17/A
43100 Parma
Italy

Nathalie Pestre
Laboratoire de Génie des Procédés Catalytiques
CNRS-ESCPE Lyon
69616 Villeurbanne
France

Joop A. Peters
Organic Chemistry
Delft University of Technology
Julianalaan 136
2628 BL Delft
The Netherlands

Andreas Pfaltz
University of Basel
Department of Chemistry
St.-Johanns-Ring 19
4056 Basel
Switzerland

Karine Philippot
Laboratoire de Chimie de Coordination du CNRS
UPR 8241
205, route de Narbonne
31077 Toulouse Cedex 04
France

Angelika Preetz
Leibniz-Institut für Katalyse an der Universität Rostock e.V.
Albert-Einstein-Str. 29a
18059 Rostock
Germany

Corbin K. Ralph
Department of Chemistry
University of Alberta
Edmonton
Alberta
Canada T6G 2G2

Garry L. Rempel
University of Waterloo
Department of Chemical Engineering
Waterloo
Ontario
Canada N2L 3G1

Geoffrey J. Roff
Clarke Research Group
School of Chemistry
University of St. Andrews
St. Andrews
Fife KY16 9ST
UK

Alain Roucoux
UMR CNRS 6052
Synthèses et Activations
de Biomolécules
Ecole Nationale Supérieure de Chimie
de Rennes
Institut de Chimie de Rennes
Ave. du Général Leclerc
35700 Rennes
France

Roberto A. Sánchez-Delgado
Brooklyn College and the Graduate
Center of the City University
of New York
New York
USA

Thomas Schmidt
Leibniz-Institut für Organische
Katalyse an der Universität Rostock e.V.
Albert-Einstein-Str. 29 a
18059 Rostock
Germany

P. Schulz
Lehrstuhl für Chemische
Reaktionstechnik
Universität Erlangen
Egerlandstraße 3
91058 Erlangen
Germany

Ottó Balázs Simon
Department of Organic Chemistry,
University of Veszprém
P.O. Box 158
Veszprém
Hungary

Attila Sisak
Research Group for Petrochemistry of
the Hungarian Academy of Sciences
P.O. Box 158
Veszprém
Hungary

Felix Spindler
Solvias AG
P.O. Box
4002 Basel
Switzerland

Wenjun Tang
Department of Chemistry
104 Chemistry Building
The Pennsylvania State University
University Park
PA 16802
USA

Marc Thommen
Solvias AG
P.O. Box
4002 Basel
Switzerland

Imre Toth
DSM Research
Department of Industrial Chemicals-
Chemistry and Technology
Urmonderbaan 22
6167 RD Geleen
The Netherlands

Michel van den Berg
Stratingh Institute
University of Groningen
Nijenborgh 4
9747 AG Groningen
The Netherlands

Paul C. van Geem
DSM Research
Department of Industrial Chemicals-
Chemistry and Technology
Urmonderbaan 22
6167 RD Geleen
The Netherlands

Francesco Vizza
ICCOM-CNR
Area della Ricerca CNR
Via Madonna del Piano snc
500019 Sesto Fiorentina/Firenze
Italy

Peter Wasserscheid
RWTH Aachen
Institut für Technische
und Makromolekulare Chemie
Worringer Weg 1
52056 Aachen
Germany

Jialong Wu
University of Waterloo
Department of Chemical Engineering
Waterloo
Ontario
Canada N2L 3G1

Takamichi Yamagishi
Department of Applied Chemistry
Graduate School of Engineering
Tokyo Metropolitan University
Tokyo
Japan

Xumu Zhang
Department of Chemistry
152 Davey Laboratory
University Park
Pennsylvania, PA 16802-6300
USA

Part I
Introduction, Organometallic Aspects and Mechanism of Homogeneous Hydrogenation

The Handbook of Homogeneous Hydrogenation.
Edited by J.G. de Vries and C.J. Elsevier
Copyright © 2007 WILEY-VCH Verlag GmbH & Co. KGaA, Weinheim
ISBN: 978-3-527-31161-3

1
Rhodium

Luis A. Oro and Daniel Carmona

1.1
Introduction

Homogeneous hydrogenation constitutes an important synthetic procedure and is one of the most extensively studied reactions of homogeneous catalysis. The homogeneous hydrogenation of organic unsaturated substrates is usually performed with molecular hydrogen, but it is also possible to derive hydrogen from other molecules acting as hydrogen donors, such as alcohols; these are termed hydrogen transfer reactions. The impressive developments of coordination and organometallic chemistry have allowed the preparation of a wide variety of soluble metal complexes active as homogeneous hydrogenation catalysts under very mild conditions. These complexes are usually derived from transition metals, especially late transition metals with tertiary phosphine ligands, having partially filled *d* electron shells. These transition metal complexes present the ability to stabilize a large variety of ligands with a variability of the coordination number and oxidation state. Among those ligands are unsaturated substrates containing π-electron systems, such as alkenes or alkynes, as well as key σ-bonded ligands such as hydride or alkyl groups.

Although the reaction of hydrogen with alkenes is exothermic, the high activation energy required constrains the reaction. Thus, the concerted addition of hydrogen to alkenes is a forbidden process according to orbital symmetry rules. In contrast, transition metals have the appropriate orbitals to interact readily with molecular hydrogen, forming metal hydride species, allowing the transfer of the hydride to the coordinated alkene. Rhodium is a good example of such transition metals, and has played a pivotal role in the understanding of homogeneous hydrogenation, providing clear examples of the two types of homogeneous hydrogenation catalysts that formally can be considered, namely monohydride and dihydride catalysts.

The Handbook of Homogeneous Hydrogenation.
Edited by J.G. de Vries and C.J. Elsevier
Copyright © 2007 WILEY-VCH Verlag GmbH & Co. KGaA, Weinheim
ISBN: 978-3-527-31161-3

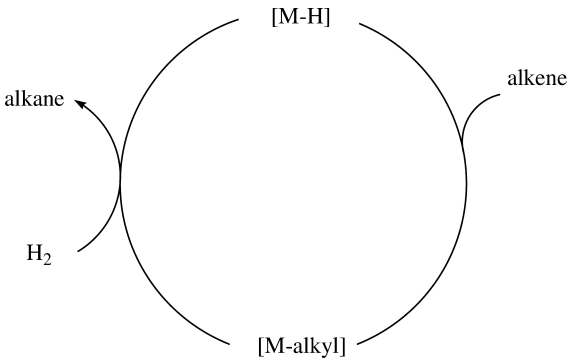

Scheme 1.1

1.1.1
Monohydride Hydrogenation Catalysts

Monohydride (MH) catalysts, such as $[RhH(CO)(PPh_3)_3]$, react with substrates such as alkenes, according to Scheme 1.1, yielding rhodium–alkyl intermediates which, by subsequent reaction with hydrogen, regenerate the initial monohydride catalyst. This mechanism is usually adopted by hydrogenation catalysts which contain an M–H bond.

1.1.2
Dihydride Hydrogenation Catalysts

Many of these catalysts are derived from metal complexes which, initially, do not contain metal hydride bonds, but can give rise to intermediate MH_2 (alkene) species. These species, after migratory insertion of the hydride to the coordinated alkene and subsequent hydrogenolysis of the metal alkyl species, yield the saturated alkane. At first glance there are two possibilities to reach MH_2 (alkene) intermediates which are related to the order of entry of the two reaction partners in the coordination sphere of the metal (Scheme 1.2).

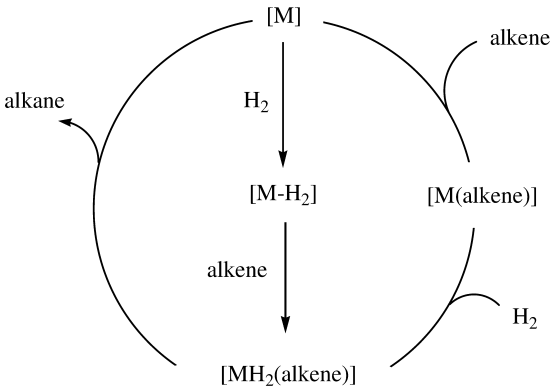

Scheme 1.2

The hydride route involves the initial reaction with hydrogen followed by coordination of the substrate; the well-known Wilkinson catalyst $[RhCl(PPh_3)_3]$ is a representative example. A second possible route is the alkene (or unsaturated) route which involves an initial coordination of the substrate followed by reaction with hydrogen. The cationic catalyst derived from $[Rh(NBD)(DIPHOS)]^+$ (NBD = 2,5-norbornadiene; DIPHOS = 1,2-bis(diphenyl)phosphinoethane) is a well-known example. The above-mentioned rhodium catalysts will be discussed, in the detail, in the following sections.

Homogeneous hydrogenation reactions by metal complexes have been investigated extensively during previous years. The first authoritative book on this subject, containing interesting and detailed historical considerations, was written by James, and appeared in 1973 [1]. Following this, other monographs [2, 3] were published, as well as several reviews and book chapters [4], reporting on the rapid and impressive development of this field.

1.2 The Early Years (1939–1970)

Calvin made the first documented example of homogeneous hydrogenation by metal compounds in 1938, reporting that quinoline solutions of copper acetate, at 100 °C, were capable of hydrogenating unsaturated substrates such as *p*-benzoquinone [5]. One year later, Iguchi reported the first example of homogeneous hydrogenation by rhodium complexes. A variety of organic and inorganic substrates were hydrogenated, at 25 °C, by aqueous acetate solutions of $RhCl_3$, $[Rh(NH_3)_5(H_2O)]Cl_3$, or $[Rh(NH_3)_4Cl_2]Cl$, whilst more inert complexes $[Rh(NH_3)_6]Cl_3$ and $[Rh(en)_3]Cl_3$, were inactive [6]. The initial hydrogen reduction of these and other related rhodium(III) complexes with nitrogen donor ligands seems to proceed via hydride rhodium intermediates formed by the heterolysis of hydrogen [1, 7]. In the case of the Iguchi rhodium(III) catalysts, however, after some time, partial autoreduction to rhodium metal occurred. Another seminal contribution of Iguchi, which appeared few years later in 1942, was the observation of the ready absorption of hydrogen by cobalt cyanide aqueous solutions; the formed cobalt hydride, $[CoH(CN)_5]^-$, was seen to be highly selective for the hydrogenation of conjugated dienes to monoenes [8].

During this period, the most significant advances in homogeneous hydrogenation catalysis have been the discovery of rhodium phosphine complexes. The hydridocarbonyltris(triphenylphosphine)rhodium(I) complex, $[RhH(CO)(PPh_3)_3]$, was reported in 1963 [9], and its catalytic activity was studied in detail by Wilkinson and coworkers a few years later [10–13]. The most important rhodium catalyst, the chlorotris(triphenylphosphine)rhodium(I) complex, was prepared during the period 1964–1965 by several groups [14]. It is easily synthesized by treating $RhCl_3 \cdot 3H_2O$ with triphenylphosphine in ethanol. It can also be prepared by displacement of the coordinated diene 1,5-cyclooctadiene from $[RhCl(diene)]_2$ complexes [15]. Wilkinson and coworkers extensively studied the remarkable catalytic properties of this complex, which is usually known as Wilkinson's catalyst. It was

the first practical hydrogenation system to be used routinely under very mild conditions – usually room temperature and atmospheric pressure of hydrogen. This compound catalyzes the chemospecific hydrogenation of alkenes in the presence of other easily reduced groups such as NO_2 or CHO, and terminal alkenes in the presence of internal alkenes [14 b, 16]. The remarkable success of this catalyst inspired the incorporation of chiral phosphines, which in turn prompted the birth of the catalytic enantioselective hydrogenation with pioneering contribution from the groups of Knowles and Horner (see [38, 39, 45 b] in Section 1.1.6).

The synthesis of cationic rhodium complexes constitutes another important contribution of the late 1960s. The preparation of cationic complexes of formula $[Rh(diene)(PR_3)_2]^+$ was reported by several laboratories in the period 1968–1970 [17, 18]. Osborn and coworkers made the important discovery that these complexes, when treated with molecular hydrogen, yield $[RhH_2(PR_3)_2(S)_2]^+$ (S = solvent). These rhodium(III) complexes function as homogeneous hydrogenation catalysts under mild conditions for the reduction of alkenes, dienes, alkynes, and ketones [17, 19]. Related complexes with chiral diphosphines have been very important in modern enantioselective catalytic hydrogenations (see Section 1.1.6).

Rhodium(II) acetate complexes of formula $[Rh_2(OAc)_4]$ have been used as hydrogenation catalysts [20, 21]. The reaction seems to proceed only at one of the rhodium atoms of the dimeric species [20]. Protonated solutions of the dimeric acetate complex in the presence of stabilizing ligands have been reported as effective catalysts for the reduction of alkenes and alkynes [21].

It is noteworthy to comment that the remarkable advances of experimental techniques made during the past few decades has allowed, in many cases, information to be obtained about key intermediates. As a consequence, detailed mechanistic studies have now firmly established reaction pathways.

1.3 The $[RhH(CO)(PPh_3)_3]$ Catalyst

This complex was first prepared by Bath and Vaska in 1963 [9], and studied in detail by Wilkinson and coworkers some years later [10] as an active catalyst for hydrogenation [11], isomerization [12], and hydroformylation [13] reactions.

The crystal structure of the $[RhH(CO)(PPh_3)_3]$ complex [22] shows a bipyramidal structure with equatorial phosphines. This coordinatively saturated 18-electron complex should be considered strictly as a precatalyst (or catalyst precursor) which, after dissociation of PPh_3 and creation of a vacant coordination site, yields the real catalytic species, $[RhH(CO)(PPh_3)_2]$. It should be remembered at this point that homogeneous mechanisms involve multistep processes, characteristic of coordination and organometallic chemistry (e.g., ligand dissociation or substitution, oxidative addition, reductive elimination), and therefore several types of intermediates are involved. The intermediates proposed by Wilkinson and coworkers in 1968 [11], based on kinetic studies, are shown in Scheme 1.3. Thus, the first step is the *ligand dissociation* of PPh_3 (step a), yielding

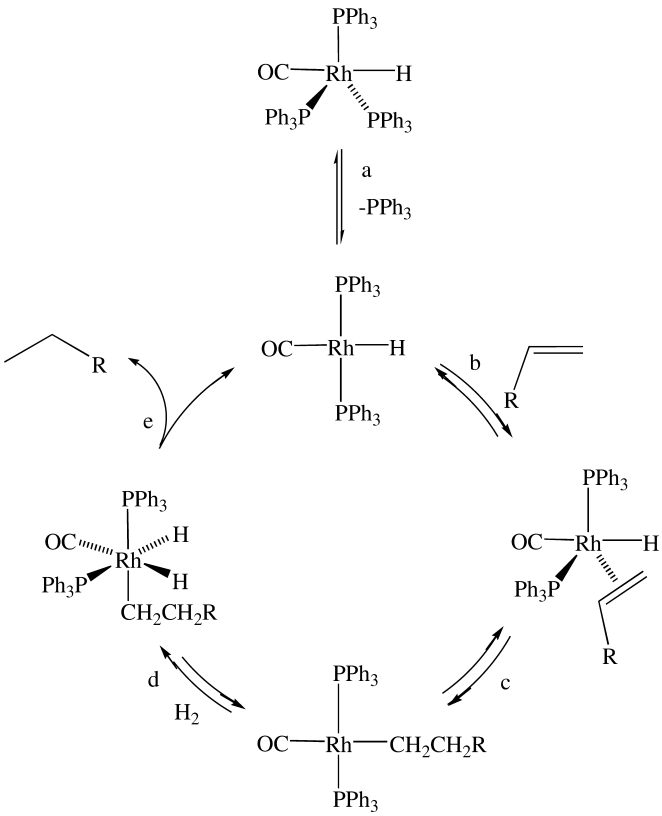

Scheme 1.3

[RhH(CO)(PPh_3)$_2$]. A vacant coordination site has been created and *coordination* of the 1-alkene substrate to the [RhH(CO)(PPh_3)$_2$] catalyst is feasible (step b). This is followed by the *migratory insertion* of the hydride to the coordinated alkene (step c), and then *hydrogenolysis* of the metal alkyl species to yield the saturated alkane. This hydrogenolysis proceeds, in this case, through two steps – *oxidative addition* of H_2 (step d), followed by *reductive elimination* to regenerate the [RhH(CO)(PPh_3)$_2$] catalyst (step e). Further support for steps c and d has been obtained by studying the reaction of [RhH(CO)(PPh_3)$_2$] with tetrafluoroethylene that yields the stable *trans*-[Rh(C_2F_2H)(CO)(PPh_3)$_2$] that, under reaction with hydrogen and in the presence of phosphine, gives $C_2F_2H_2$ and [RhH(CO)(PPh_3)$_3$] [13].

Rhodium species in oxidation states I and III are involved in the process. Rhodium-catalyzed hydrogenations generally involve oxidative addition reactions, followed by the reverse process of reductive elimination in the final step. Another common elimination process is the so-called *β-elimination*, which accounts for the frequent side reaction of isomerization of alkenes, according to Eq. (1):

$$\begin{array}{c} RCH_2CH_2CH_2 \\ | \\ M \end{array} \rightleftharpoons \begin{array}{c} RCH_2CH=CH_2 \\ | \\ MH \end{array} \rightleftharpoons \begin{array}{c} RCH_2CHMe \\ | \\ M \end{array} \rightleftharpoons \begin{array}{c} RCH=CHMe \\ | \\ MH \end{array} \quad (1)$$

This reversibility explains the frequent isomerization of alkenes by metal hydride complexes, even in the absence of hydrogen. The formation of the secondary alkyl should be unfavored when bulky ligands are present. This steric argument explains why internal alkenes are isomerized by $[RhH(CO)(PPh_3)_2]$ but are not competitively hydrogenated, as well as the high selectivity of this catalyst for the hydrogenation of terminal alkenes compared to 2-alkenes due to the lowered stability of the secondary alkyl species. The formation of the real catalyst $[RhH(CO)(PPh_3)_2]$ requires the dissociation of PPh_3 from the rhodium precatalyst. Thus, an addition of excess PPh_3 prevents the dissociation and inhibits alkene hydrogenation. On the other hand, at very low concentrations, the $RhH(CO)(PPh_3)$ intermediate, which is still more active, is formed by further dissociation of $RhH(CO)(PPh_3)_2$ according to Eq. (2).

$$[RhH(CO)(PPh_3)_3] \xrightleftharpoons{-PPh_3} [RhH(CO)(PPh_3)_2] \xrightleftharpoons{-PPh_3} [RhH(CO)(PPh_3)] \quad (2)$$

1.4 The $[RhCl(PPh_3)_3]$ Complex and Related Catalysts

The widely studied $[RhCl(PPh_3)_3]$ complex, usually known as Wilkinson's catalyst, was discovered independently in 1965 by Wilkinson (a recipient of the Nobel Prize in 1973) and other groups [14]. This compound catalyzes the chemospecific hydrogenation of alkenes in the presence of other easily reduced groups such as NO_2 or CHO, and terminal alkenes in the presence of internal alkenes [16]. The rate of hydrogenation parallels their coordination ability (Scheme 1.4), but tetrasubstituted alkenes are not reduced.

This burgundy-red compound can be easily prepared by reacting $RhCl_3 \cdot 3H_2O$ with triphenylphosphine in refluxing ethanol. In this reaction, rhodium(III) is reduced to the rhodium(I) complex $RhCl(PPh_3)_3$, whilst the phosphine is oxidized to phosphine oxide according to Eq. (3).

$$[RhCl_3(H_2O)_x] + y\,PPh_3 \xrightarrow{EtOH/78^\circ C} [RhCl(PPh_3)_3] + OPPh_3 \quad (3)$$
$$y > 4$$

The most accepted mechanism for alkene hydrogenation is mainly due to Halpern [23], and is supported by careful kinetic and spectroscopic studies of cyclo-

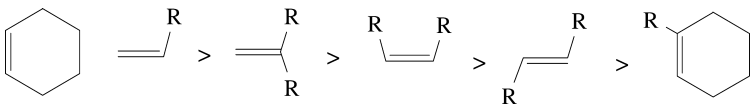

Scheme 1.4

hexene hydrogenation. This mechanism is shown in Scheme 1.5, where the route dominating the catalytic cycle is surrounded by the dotted line. According to this scheme, the predominant hydride route consists of oxidative addition of a hydrogen molecule prior to alkene coordination. Both the associative pathway *via* a 16-electron complex [RhCl(PPh$_3$)$_3$] and the dissociative pathway *via* a 14-electron species RhCl(PPh$_3$)$_2$ could function for hydrogenation, depending on the concentration of free PPh$_3$. However RhCl(PPh$_3$)$_2$ reacts with H$_2$ at least 10 000-fold faster than [RhCl(PPh$_3$)$_3$], and is therefore the active intermediate. Thus, the hydride path is much more efficient than the alkene path. However, in the absence of hydrogen, RhCl(PPh$_3$)$_2$ showed a remarkable tendency to dimerize, yielding [(PPh$_3$)$_2$Rh(μ-Cl)Rh(PPh$_3$)$_2$] species with bridging chloro ligands; the formation of alkene complexes of general formula [RhCl(alkene)(PPh$_3$)$_2$] can also be observed. The addition of small amounts of free phosphine inhibits the formation of these dimers, thereby enhancing the catalytic activity of the complex.

The rapid oxidative addition of hydrogen to RhCl(PPh$_3$)$_2$, followed by alkene coordination, affords the 18-electron octahedral dihydride alkene complex [RhH$_2$Cl(alkene)(PPh$_3$)$_2$]. The unsaturated [RhH$_2$Cl(PPh$_3$)$_2$] intermediate is also capable of ligand association with PPh$_3$, being in equilibrium with [RhH$_2$Cl(PPh$_3$)$_3$]. The rate-determining step for the whole process is the intramolecular alkene insertion into the rhodium–hydride bond of [RhH$_2$Cl(alkene)(PPh$_3$)$_2$], to produce the alkyl hydride intermediate, [RhH(alkyl)Cl(PPh$_3$)$_2$]. The next step, the reductive elimination of alkane from this alkyl hydride intermediate to regenerate RhCl(PPh$_3$)$_2$, occurs rapidly. The proposed cycle implies changes in the oxidation state (I and III) in the oxidative addition and reductive elimination

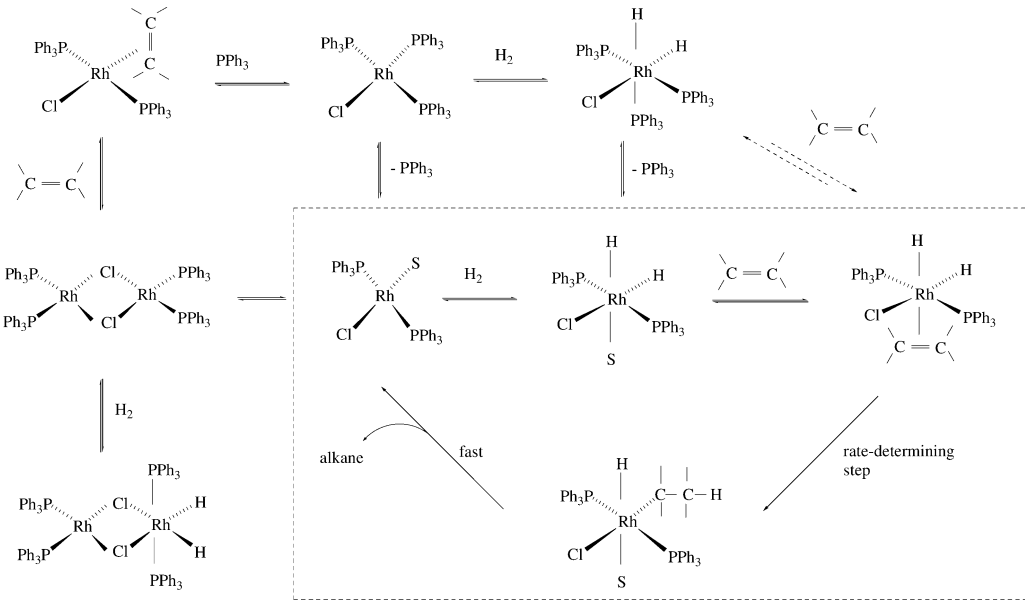

Scheme 1.5

steps, as well as changes in the electronic environment (14-, 16-, and 18-electron species) and coordination numbers, from 3 to 6. Nevertheless, in some cases, some coordination vacancies could be occupied by polar solvent molecules, such as ethanol, which are frequently added to the usual aromatic organic solvents.

This cycle was pieced together from the results of a variety of experiments. The complexes $[RhCl(PPh_3)_3]$, $[RhCl(alkene)(PPh_3)_2]$, $[RhH_2Cl(PPh_3)_3]$, $[(PPh_3)_2Rh(\mu\text{-}Cl)_2Rh(PPh_3)_2]$ and $[(PPh_3)_2Rh(\mu\text{-}Cl)_2RhH_2(PPh_3)_2]$ were directly observed, but the species of Scheme 1.5 which are inside the dashed line, and are thus responsible for the hydrogenation process, were not observable. Furthermore, when styrene was used as substrate, a further path involving the coordination of two styrene molecules was found to be operating. It seems important to remember that, in some catalytic reactions, those compounds that are readily isolable might not be the true intermediates in the catalytic cycle.

Recently [24], using parahydrogen-induced polarization (PHIP) NMR techniques, it has been possible to observe the dihydride $[Rh(H)_2Cl(styrene)(PPh_3)_2]$, which is involved in the hydrogenation process. Although traditionally it has been depicted with *trans* phosphines, this technique shows that the two phosphines are arranged in a *cis* fashion. When PHIP NMR was used to examine the reaction of $[Rh(\mu\text{-}Cl)(PPh_3)_2]_2$ with parahydrogen, the dinuclear hydride complexes $[Rh(H)_2(PPh_3)_2(\mu\text{-}Cl)_2Rh(PPh_3)_2]$ and $[Rh(H)_2(PPh_3)_2(\mu\text{-}Cl)]_2$ were detected and characterized [25]. The same reaction, when carried out in the presence of an alkene, revealed signals corresponding to new dinuclear dihydrides of the type $[Rh(H)_2(PPh_3)_2(\mu\text{-}Cl)_2Rh(PPh_3)(alkene)]$. Kinetic data showed that hydrogenation *via* this intermediate may be significant [26].

Related triarylphosphine complexes of formula $[RhCl(P(C_6H_4\text{-}4\text{-}X)_3)_3]$ are also active hydrogenation catalysts. Studies on cyclohexene hydrogenation show an increase in the relative rates when the basicity of the triarylphosphine increases: $P(C_4H_4\text{-}4\text{-}Cl)_3$ (1.8) < $P(C_6H_5)_3$ (41) < $P(C_6H_4\text{-}4\text{-}Me)_3$ (86) < $P(C_6H_4\text{-}4\text{-}OMe)_3$ (100). However, complexes with more basic tertiary phosphines, such as PEt_3 or $PPhEt_2$, are practically inactive.

A simple method for the *in-situ* preparation of Wilkinson-type catalysts consists of the addition of the appropriate amount of the triarylphosphine to the rhodium dimers, $[Rh(\mu\text{-}Cl)(diene)]_2$ or $[Rh(\mu\text{-}Cl)(cyclooctene)_2]_2$, according to Eqs. (4) and (5). The best results are usually obtained for a rhodium/phosphine ratio of 1 : 2.

$$[Rh(\mu\text{-}Cl)(COD)]_2 + 2\,n\,PPh_3 \longrightarrow 2[RhCl(PPh_3)_n] + 2\,COD \quad (4)$$
COD = 1,5-cyclooctadiene

$$[Rh(\mu\text{-}Cl)(COE)_2]_2 + 2\,n\,PPh_3 \longrightarrow 2[RhCl(PPh_3)_n] + 4\,COE \quad (5)$$
COE = cyclooctene, n = 3 or 2

The water-soluble analogue of Wilkinson's catalyst, $[RhCl(TPPMS)_3]$ [TPPMS = $PPh_2(C_6H_4SO_3Na)$], prepared *in situ* from $[Rh(\mu\text{-}Cl)(diene)]_2$ and TPPMS, reacts with hydrogen in aqueous solution to yield $[RhH(TPPMS)_3]$, instead of $[RhH_2(TPPMS)_3]$, according to Eq. (6):

$$[RhCl(TPPMS)_3] + H_2 \longrightarrow [RhH(TPPMS)_3] + Cl^- + H^+ \quad (6)$$
$$TPPMS = PPh_2(C_6H_4SO_3Na)$$

The presence of $[RhH(TPPMS)_3]$ causes substantial changes in the mechanism of hydrogenation, that most probably follows a conventional monohydride mechanism as shown in Scheme 1.1. This is also reflected in the rates and the hydrogenation selectivities [27].

1.5 The Cationic[Rh(diene)(PR$_3$)$_X$]$^+$ Catalysts

The catalytic potential of $[Rh(diene)L_n]^+$ (n = 2 or 3; L = phosphine, phosphite or arsine) complexes as hydrogenation catalysts was discovered by Osborn and coworkers during the period 1969 to 1976 [19, 28]. Under a hydrogen atmosphere the diene is hydrogenated, generating the reactive $[RhH_2S_xL_n]^+$ species which, in some cases such as in $[RhH_2(solvent)_2L_2]^+$ intermediates, can be isolated relatively easily from coordinating solvents such as acetone or ethanol. In contrast to Wilkinson's catalyst, a large number of donor ligands can be used and several easy preparative routes are available. NBD was the preferred diene for the $[Rh(diene)L_n]^+$ catalyst precursors, but other dienes such as 1,5-cyclooctadiene (COD) or tetrafluorobenzobarrelene (TFB) have also been used [28, 29]. The dihydride complexes $[RhH_2S_2L_2]^+$ (S = Me_2CO, EtOH) have two solvent molecules bound through their oxygen lone pairs in the coordination sphere. They are excellent hydrogenation catalysts, and some unusual properties seem to depend on its ionic character.

The dihydride complexes $[RhH_2S_xL_n]^+$ are in equilibrium with monohydride species according to Eq. (7).

$$[RhH_2S_xL_n]^+ \rightleftharpoons [RhHS_yL_n] + H^+ \quad (7)$$

The equilibrium can be shifted by the addition of acid or base, and is also sensitive to the nature of the ligands and solvents. Scheme 1.6 qualitatively accounts for the experimental observations involving three possible pathways by which an unsaturated substrate can be hydrogenated.

Path A involves a neutral monohydride species which both extensively isomerizes and also hydrogenates alkenes, and is favored in the presence of NEt_3 or when the catalyst contains basic phosphine ligands. In path B, which is favored in the presence of acids, cationic dihydride species are the active catalyst; they hydrogenate alkenes less efficiently, but with limited isomerization. Path C involves formation of $[RhH_2S_x(alkene)L_n]^+$ from $[RhS_xL_n]^+$ by intermediacy of $[RhS_x(alkene)L_n]^+$. In the proposed cycles the substrate enters the coordination sphere by displacing a solvent molecule. The experimental observations suggest that the neutral monohydride species $RhHS_yL_n$ are considerably more efficient hydrogenation

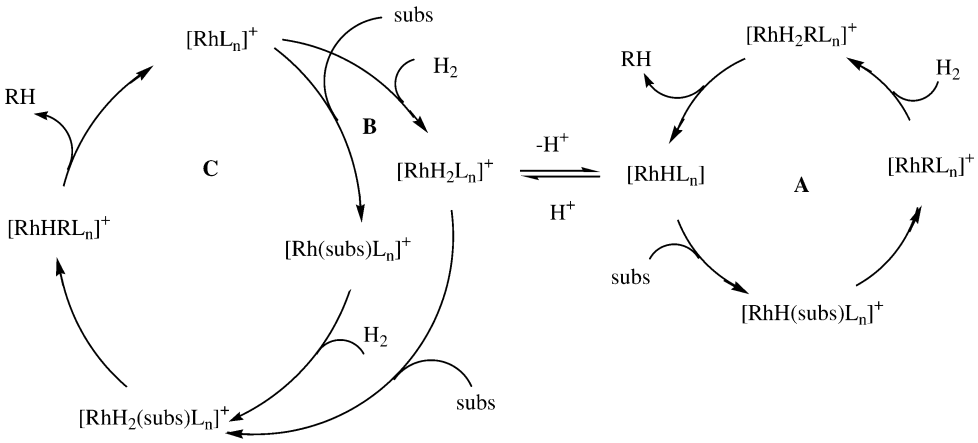

Scheme 1.6

catalysts than the dihydrides $[RhH_2S_xL_n]^+$. However, in order to hydrogenate an alkene without concomitant isomerization, path A must be suppressed; thus, hydrogenation under acidic conditions (path B) becomes operative due to the presence of the cationic $[RhH_2S_xL_n]^+$ dihydrides. The mechanism for hydrogenation via path B shows a close analogy to the proposed mechanism involving the Wilkinson catalyst (Scheme 1.5). The equilibrium illustrated in Eq. (7) offers considerable flexibility, and it is possible to identify appropriate conditions for the selective hydrogenation of alkynes to *cis* alkenes following pathways A and B. However, the rate of hydrogenation with the monohydride species is at least twice that with the dihydride species. It has been proposed that the origin of the selective reduction of 2-hexyne to *cis*-2-hexene seems to arise from the fact that the coordinated *cis*-2-hexene, formed by hydrogenation, is immediately displaced by 2-hexyne, before it can be isomerized or hydrogenated to hexane. Almost exclusive *cis*-addition of hydrogen to the alkyne was observed [28 b].

The selective hydrogenation of dienes to monoenes can also be accomplished by using these rhodium cationic catalysts with proper choice of the phosphine ligand [28 c]. Path C seems to be dominant, where the strongly coordinated dienes were hydrogenated selectively to monoenes, with hydrogen adding both 1,2 and 1,4 to conjugated dienes. The hydrogenation process follows the unsaturated route; in fact, the only detectable species are $[Rh(diene)L_2]^+$ which, after reaction with hydrogen, yield the alkyl–hydride complex. It should be noted that the latter species are common to both pathways B and C, the only difference being the sequence of substrate coordination and previous or posterior reaction with molecular hydrogen. The hydrogenation activity of catalysts derived from $[Rh(TFB)(P(C_6H_4\text{-}4\text{-}X)_3)_2]^+$ species depends on the electron-releasing ability of the X-substituent [29, 30].

Cationic $[Rh(diene)L_2]^+$ species are also catalyst precursors for the hydrogenation of ketones and aldehydes [19]. The mechanism presents some analogies

with that proposed for alkene hydrogenation, with formation of alkoxy species by insertion.

The catalytic activity of cationic rhodium precursors of formula [Rh(diene)(diphosphine)]$^+$ was also explored by Schrock and Osborn [28]. Halpern and coworkers made very detailed mechanistic studies of olefin hydrogenation by [RhS$_2$(diphos)]$^+$ species (diphos = 1,2-bis(diphenylphosphino)ethane; S = solvent) [31]. Significant differences have been observed in the reaction of the catalyst precursors [Rh(NBD)(PPh$_3$)$_2$]$^+$ and [Rh(NBD)(diphos)]$^+$ in methanol, as shown in Eqs. (8) and (9):

$$[\mathrm{Rh(NBD)(PPh_3)_2}]^+ + 3\,\mathrm{H_2} \xrightarrow{\mathrm{MeOH}} [\mathrm{RhH_2(MeOH)_2(PPh_3)_2}]^+ + \text{norbornane} \tag{8}$$

$$[\mathrm{Rh(NBD)(diphos)}]^+ + 3\,\mathrm{H_2} \xrightarrow{\mathrm{MeOH}} [\mathrm{Rh(MeOH)_2(diphos)}]^+ + \text{norbornane} \tag{9}$$

(NBD = 2,5-norbornadiene; diphos = 1,2-bis(diphenylphosphino)ethane)

Although the latter product is a solvated mononuclear [Rh(MeOH)$_2$(diphos)]$^+$ cation, in the solid state it is isolated as a binuclear complex of formula [Rh$_2$(diphos)$_2$](BF$_4$)$_2$, in which each rhodium center is bonded to two phosphorus atoms of a chelating bis(diphenylphosphino)ethane ligand, and to a phenyl ring of the bis(diphenylphosphino)ethane ligand of the other rhodium atom. This dimer reverts to a mononuclear species on redissolving. The mechanism of hydrogenation of the prochiral alkene methyl(*Z*)-*α*-acetamidocinnamate, studied in detail by Halpern [31], is depicted in Scheme 1.7.

The hydrogenation process follows the unsaturated route, the rate-determining step being the reaction of [Rh(alkene)(diphos)]$^+$ with hydrogen. The proposed mechanism corresponds to pathway C of Scheme 1.6. Analogous cationic rhodium complexes with chiral diphosphines have allowed remarkable progress to be made on the subject of enantioselective hydrogenations, as will be discussed in the following section.

Several heteroaromatic compounds can be hydrogenated by [Rh(COD)(PPh$_3$)$_2$]$^+$ species. Thus, this cationic complex has been reported to be a catalyst precursor for the homogeneous hydrogenation of heteroaromatic compounds such as quinoline [32] or benzothiophene [33]. Detailed mechanistic cycles have been proposed by Sánchez-Delgado and coworkers. The mechanism of hydrogenation of benzothiophene by the cationic rhodium(III) complex, [Rh(C$_5$Me$_5$)(MeCN)$_3$]$^{2+}$, has been elucidated by Fish and coworkers [34].

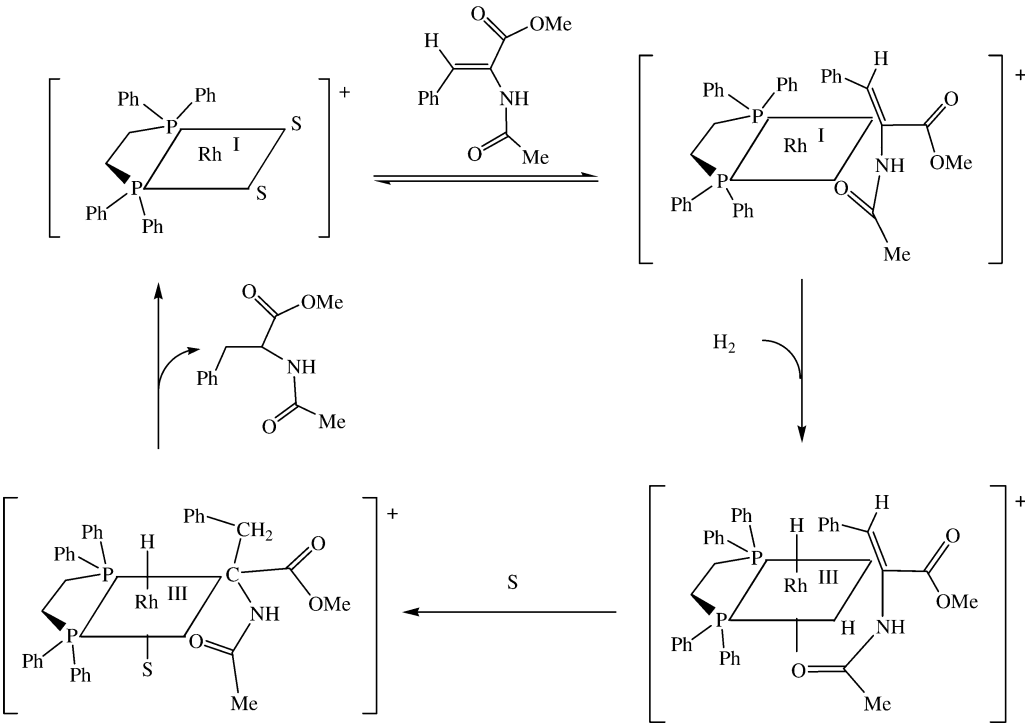

Scheme 1.7

1.6 Enantioselective Rhodium Catalysts

1.6.1 Hydrogenation of Alkenes

Following Wilkinson's discovery of $[RhCl(PPh_3)_3]$ as an homogeneous hydrogenation catalyst for unhindered alkenes [14b, 35], and the development of methods to prepare chiral phosphines by Mislow [36] and Horner [37], Knowles [38] and Horner [15, 39] each showed that, with the use of optically active tertiary phosphines as ligands in complexes of rhodium, the enantioselective asymmetric hydrogenation of prochiral C=C double bonds is possible (Scheme 1.8).

Knowles reported the hydrogenation of *α*-phenylacrylic acid and itaconic acid with 15% and 3% optical purity, respectively, by using $[RhCl_3(P^*)_3]$ [P* = (*R*)-(–)-methyl-*n*-propylphenylphosphine] as homogeneous catalyst [38]. Horner found that *α*-ethylstyrene and *α*-methoxystyrene can be hydrogenated to (*S*)-(+)-2-phenylbutane (7–8% optical purity) and (*R*)-(+)-1-methoxy-1-phenylethane (3–4% optical purity), respectively, by using the complex formed *in situ* from $[Rh(1,5\text{-hexadiene})Cl]_2$ and (*S*)-(–)-methyl-*n*-propylphenylphosphine as catalyst [39].

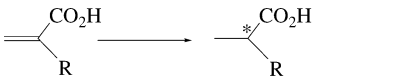

R = Ph, 15% *ee*
R = CH_2CO_2H, 3% *ee*

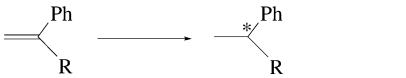

R = Et, 7 - 8% *ee*
R = OMe, 3 - 4% *ee* **Scheme 1.8**

These were the first examples of metal-catalyzed enantioselective hydrogenation. The ee-values achieved were modest [40], but they established the validity of the hydrogenation method. Furthermore, the inherent generality of the method offered enormous opportunities for optimization of the results. It is interesting to note that, in these examples, the chirality of the ligands resides in the phosphorus atom.

The degree of enantioselective bias was improved shortly after this time. In 1971, Morrison et al. reported that the rhodium(I) complex $[RhCl(NMDPP)_3]$ (NMDPP = neomethyldiphenylphosphine) reduces (*E*)-*β*-methylcinnamic and (*E*)-*α*-methylcinnamic acids with 61 and 52% ee, respectively (Scheme 1.9) [41]. NMDPP is a monodentate phosphine derived from (–)-menthol, and its asymmetry lies at carbon atoms.

An important breakthrough was the finding, by Kagan and Dang, that a rhodium complex containing the chiral diphosphine (–)-DIOP ((–)-2,3-*O*-isopropylidene-2,3-dihydroxy-1,4-bis(diphenylphosphino)butane, derived from (+)-ethyl tartrate) efficiently catalyzed the enantiomeric reduction of unsaturated prochiral acids. In particular, *α*-acetamidocinnamic acid and *α*-phenylacetamidoacrylic acid were reduced quantitatively with 72 and 68% ee, respectively (Scheme 1.10) [42]. Two assumptions were presented by Kagan as being necessary to achieve a high degree of stereoselectivity in enantioselective catalysis:

- the ligand conformations must have maximum rigidity;
- in order to avoid epimerization equilibria, ligands must stay firmly bonded to the metal.

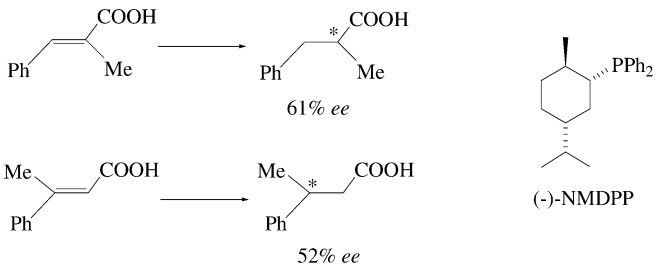

Scheme 1.9

Kagan concluded that diphosphines fulfill both of these conditions. In addition, it is desirable to avoid the possibility of geometric isomerism by choosing diphosphine having two equivalent phosphorus atoms [43]. These conditions strongly conditioned the subsequent development of the field, with the greater research effort being subsequently laid on metallic compounds with chiral diphosphines with C_2 symmetry as ligands. Additionally, Kagan introduced amino acid precursors as benchmark in enantioselective hydrogenation reactions.

At the same time, Knowles' team concentrated their efforts on the use of chiral at phosphorus ligands. Four years after the first report, these authors obtained 88% ee in the reduction of α-acylaminoacrylic acids by incorporating cyclohexyl and *ortho*-anisyl substituents [44] (Scheme 1.11).

A crucial achievement significantly stimulated the development of the investigation in the field of homogeneous enantioselective catalysis. The Knowles group established a method for the industrial synthesis of *L*-DOPA, a drug used for the treatment of Parkinson's disease. The key step of the process is the enantiomeric hydrogenation of a prochiral enamide, and this reaction is efficiently catalyzed by the air-stable rhodium complex $[Rh(COD)((R_P)\text{-}CAMP)_2]BF_4$ (Scheme 1.12).

This achievement was unique in two respects: 1) it was the first example of industrial application of a homogeneous enantioselective catalysis methodology; and 2) it represented a rare example of very quick convergence of basic knowledge into commercial application. The monophosphine ligand CAMP was shortly replaced by the related diphosphine ligand DIPAMP which improved the selectivity for the *L*-DOPA system up to 95% ee [45].

The following years witnessed the development of a plethora of new diphosphine ligands with chiral carbon backbones, and at a very impressive pace [46]. Among these, two examples were of particular interest.

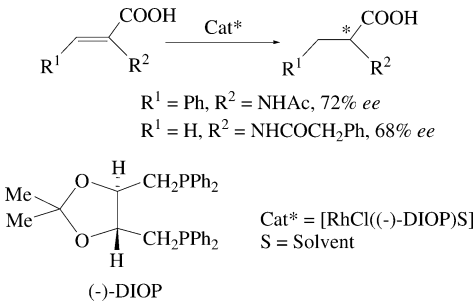

Scheme 1.10

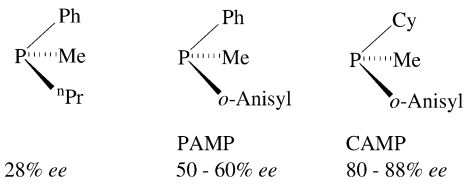

Scheme 1.11

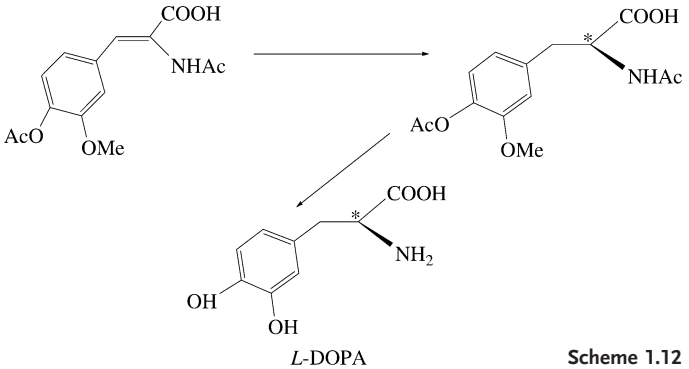

Scheme 1.12

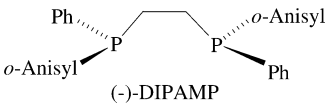

Scheme 1.13

The first example was the 2,2′-bis(diphenylphosphino)-1,1′-binaphthyl (BINAP) ligand synthesized by Noyori and Takaya in 1980 [47]. BINAP is an atropoisomeric C_2 diphosphine that forms a seven-membered chelate ring through coordination to metals. The λ or δ conformations of this chelate determine the chiral disposition of the phenyl rings and, in this way, the chirality of BINAP is transmitted to the metal environment. BINAP complexes exhibit high enantioselectivity in various catalytic reactions, including hydrogenation. Thus, BINAP rhodium complexes [48] readily catalyze the hydrogenation of prochiral α-acylaminoacrylic acids with up to 100% ee (Scheme 1.14).

The second example was the bis(phospholanyl)ethanes (BPE) and bis(phospholanyl)benzenes (DuPHOS) ligands developed by Burk some years later [49]. These ligands are electron-rich diphosphines that contain two phospholanes *trans*-substituted in the 2,5 position, and in which the phosphorus atoms are connected by 1,2-ethano or 1,2-phenylene backbones. Chirality lies in the carbon atoms adjacent to the phosphorus atoms and therefore, in the derived catalysts, it lies in the immediacy of the rhodium atoms (Scheme 1.15). By choosing the appropriate R substituent, a large variety of substrates, including α-(acylamino) acrylic acids, enamides, enol acetates, β-keto esters, unsaturated carboxylic acids and itaconic acids, are efficiently hydrogenated by cationic rhodium complexes of the type [Rh(COD)(bisphospholane)]X (X = weakly coordinating anion) with exceedingly high enantioselectivities [50].

Subsequently, it was shown that rhodium complexes derived from diphosphinites, diphosphonites, and diphosphites – as well as hybrid ligands – are similarly active and selective to diphosphines [46 i].

Enantioselective hydrogenation catalysts with chiral nitrogen ligands have been rather neglected, however. Until now, it seems that ligands containing only

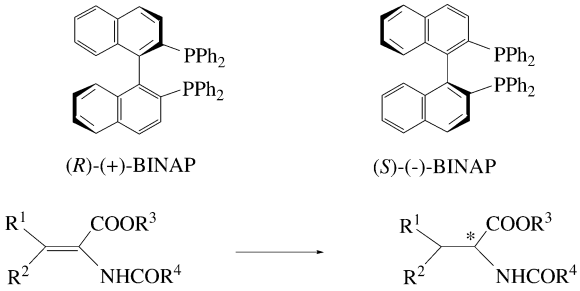

R^1	R^2	R^3	R^4	*ee* (%)
H	Ph	H	Ph	100
Ph	H	H	Ph	87
H	Ph	Me	Ph	93
H	Ph	H	Me	84
H	*m*–OMe, *p*–OH–C_6H_2	H	Ph	79
H	H	H	Ph	98

Scheme 1.14

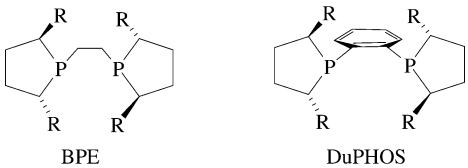

Scheme 1.15

nitrogen donor atoms are not well suited for this purpose. Nevertheless, there are some examples of rhodium-based catalysts containing mixed P,N-chiral chelating ligands active for the reduction of C=C double bonds [51].

Since 1999 [52], the potential of monophosphorus ligands in the area has been reconsidered. The commonly accepted rule that bidentate ligands are necessary to achieve high enantioselectivity in hydrogenation reactions has been countered by the discovery that enantiopure monodentate P ligands may provide optical yields comparable to those obtained with chelating diphosphines [46i, 53]. This mostly occurs when two ligands on rhodium strongly restrict each other's conformational freedom [54]. In fact, monodentate P ligands containing biaryl, spirobiindane, oxaphosphinane, or carbohydrate building blocks have been used to efficiently hydrogenate α- and β-dehydroamino acids, itaconic acid derivatives and enamides with an ee systematically greater than 99% [46j, 53]. Recently, Reetz's group has demonstrated that mixtures of two different monodentate phosphorus ligands can be used in a combinatorial approach [53d–f]. Notably it has been shown that, in several cases, monodentate catalytic

ligands induce higher enantioselectivity and lead to faster asymmetric hydrogenations than bidentate analogues [54, 55].

1.6.2
Hydrogenation of Ketones

Enantioselective hydrogenation of unfunctionalized ketones is promoted only by a limited number of transition metal catalysts. Among these, a few reports dealing with rhodium catalysts have appeared [46 a, b, e, g, i, j, m, 56]. In 1980, Markó et al. reported on the enantioselective catalytic reduction of unfunctionalized ketones, for the first time. In the presence of NEt_3, a neutral rhodium complex (prepared from $[RhCl(NBD)]_2$ and (+)-DIOP) hydrogenated methyl, *α*-naphthyl ketone to give the corresponding chiral alcohol in 84% ee [57]. Another important contribution to the field was the communication by Zhang et al. that alkyl methyl ketones can be efficiently hydrogenated by the *in-situ*-prepared catalyst from $[RhCl(COD)]_2$ and the conformational rigid chiral bisphosphines *P,P′*-1,2-phenylenebis(*endo*-2,5-dialkyl-7-phosphabicyclo[2.2.1] heptanes (PennPhos; Scheme 1.16). Enantiomeric excesses of up to 94% ee for the *tert*-butyl methyl ketone and 92% ee for cyclohexyl methyl ketone were observed, with the R = Me PennPhos ligand [58].

The hydrogenation of ketones with O or N functions in the *α*- or *β*-position is accomplished by several rhodium compounds [46 a, b, e, g, i, j, m, 56]. Many of these examples have been applied in the synthesis of biologically active chiral products [59]. One of the first examples was the asymmetric synthesis of pantothenic acid, a member of the B complex vitamins and an important constituent of coenzyme A. Ojima et al. first described this synthesis in 1978, the most significant step being the enantioselective reduction of a cyclic *α*-keto ester, dihydro-4,4-dimethyl-2,3-furandione, to *D*-(–)-pantoyl lactone. A rhodium complex derived from $[RhCl(COD)]_2$ and the chiral pyrrolidino diphosphine, (2*S*,4*S*)-*N*-*tert*-butoxycarbonyl-4-diphenylphosphino-2-diphenylphosphinomethyl-pyrrolidine ((*S*,*S*)-BPPM; Scheme 1.17) was used as catalyst [60]. The enantioselective hydrogenation of functionalized ketones was also efficiently achieved by a series of rhodium(I) aminophosphine- and amidophosphine-phosphinite complexes [61].

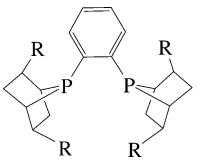

R = Me, *i*Pr

PennPhos

Scheme 1.16

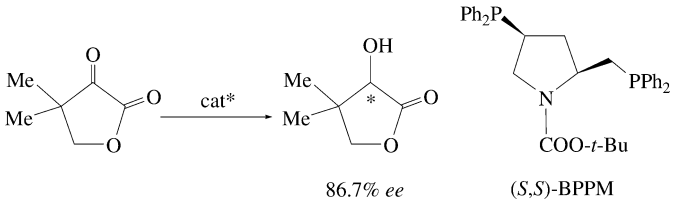

Scheme 1.17

1.6.3
Hydrogenation of Imines

To date, catalyzed enantioselective reductions of C=N double bonds have only led to relatively limited success. Currently, only a few efficient chiral catalytic systems are available for the hydrogenation of imines. Hydrogenation of functionalized C=N double bonds such as *N*-acylhydrazones, sulfonimides, and *N*-diphenylphosphinylketimines has also been attempted, with some relevant results [46 b, g, i, j, 50, 62]. The first report on enantioselective homogeneous reduction of C=N double bonds mediated by rhodium complexes appeared in 1975. Kagan et al. reported that *N*-benzyl-*α*-phenyl ethylamine was prepared by hydrosilylation with 65% optical purity, using a chiral rhodium complex with (+)-DIOP [63]. Some years later, the Markó group reported that using catalysts prepared *in situ* from $[RhCl(NBD)]_2$ and chiral phosphines of the type $Ph_2PCHRCH_2PPh_2$ (R = Ph, *i*Pr, $PhCH_2$), optical yields up to 77% were achieved, although reproducibility of the results was poor [64]. Subsequently, some rhodium complexes have shown good ee values, among which two cases are remarkable. Acyclic *N*-alkylimines $ArC(Me)=NCH_2Ph$ (Ar = Ph, 2-$MeOC_6H_4$, 3-$MeOC_6H_4$, 4-$MeOC_6H_4$) were hydrogenated in a two-phase system, with ee values up to 96%, using $[RhCl(COD)]_2$ together with sulfonated (*S*,*S*)-(–)-2,4-bis(diphenylphosphino)pentane ((*S*,*S*)-$BDPP_{sulf}$; Scheme 1.18) [65]. Similarly, the C=N group of *N*-acylhydrazones can be reduced by [Rh(COD)(DuPHOS)] (CF_3SO_3) as catalyst precursor. Enantioselectivities up to 97% were achieved (Scheme 1.19). The N–N bond of the resulting *N*-benzoylhydrazines is cleaved by SmI_2 to afford the corresponding amines [66].

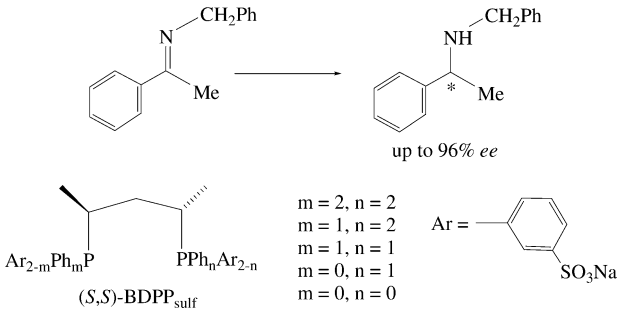

Scheme 1.18

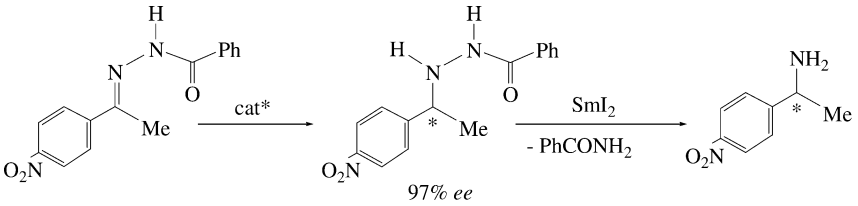

cat* = [Rh(COD)(Et-DuPHOS)](CF_3SO_3)

Scheme 1.19

1.6.4
Mechanism of Rhodium-Catalyzed Enantioselective Hydrogenation

The mechanism of rhodium-catalyzed enantioselective hydrogenation is one of the most thoroughly studied mechanisms of all metal-catalyzed processes [46 b, c, h, i, k, 23, 50, 67]. Studies have been focused on cationic rhodium chiral diphosphine complexes as catalyst precursors, and on prochiral enamides as hydrogenation substrates. Early mechanistic studies were conditioned by the case of achiral hydrogenation of alkenes by Wilkinson's catalyst. In the catalytic cycle proposed for Wilkinson's catalyst, dihydride rhodium(III) complexes [14 b, 35] are obtained by reversible oxidative addition of dihydrogen to the active species $RhCl(PPh_3)_2$ [23] (see Section 1.4). Thus, the formation of similar intermediates was expected upon hydrogenation of the catalyst precursors employed in asymmetric hydrogenation. However, Halpern et al. showed that [Rh(DIPHOS)(NBD)]$^+$ reacted with 2.0 mol of H_2/Rh yielding norbornane and the solvate complex [Rh(DIPHOS)S_2]$^+$ which was isolated as the dimer compound [Rh_2(DIPHOS)$_2$](BF_4)$_2$ (see Section 1.5) [31 a, 68]. Further investigations showed that the formation of [Rh(PP*)S_2]$^+$ (PP* = chiral diphosphine; S = solvent molecule) complexes by hydrogenation of the catalyst precursors is a general behavior of *cis*-chelating diphosphine rhodium complexes [46 c, 70]. It has been concluded that, under catalytic conditions, a molecule of the prochiral alkene coordinates to the rhodium atom, affording a bischelate catalyst–substrate complex (see Scheme 1.21). In fact, in 1978, for the first time, Brown and Chaloner provided ^{31}P-NMR-based evidence for the formation of such a type of compound [72], whilst shortly afterwards Halpern et al. reported the first X-ray molecular structure determination for a catalyst–substrate species, namely [Rh{(*S*,*S*)–CHIRAPHOS}{(*Z*)-EAC}]ClO_4 (EAC = ethyl-α-acetamidocinnamate) [73]. For C_2-symmetrical diphosphines – the most commonly used in enantioselective hydrogenation – two diastereomeric catalyst–substrate complexes can be formed, depending on the alkene enantioface that coordinates with the metal. However, only a single diastereomer of [Rh{(*S*,*S*)-CHIRAPHOS}{(*Z*)-EAC}]ClO_4 was detected in solution by NMR (Scheme 1.20); therefore, the second diastereomer must be present to the extent of less than 5%. Subsequently, numerous catalyst–substrate complexes have been described, and all have demonstrated stereodifferentiation in solution [67 d].

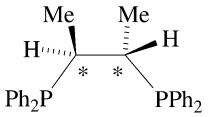

(*S*,*S*)-CHIRAPHOS

Scheme 1.20

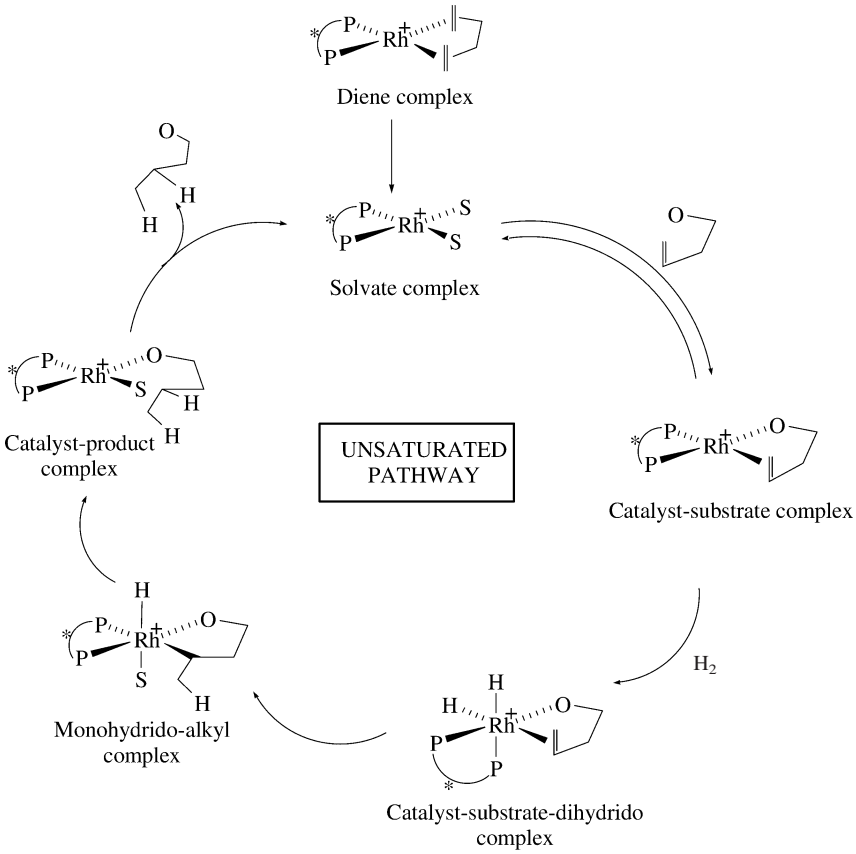

Scheme 1.21

From all the above observations, it was concluded that, for diphosphine chelate complexes, the hydrogenation stage occurs after alkene association; thus, the unsaturated pathway depicted in Scheme 1.21 was proposed [31 a, c, 74]. The monohydrido-alkyl complex is formed by addition of dihydrogen to the enamide complex, followed by transfer of a single hydride. Reductive elimination of the product regenerates the active catalysts and restarts the cycle. The monohydrido-alkyl intermediate was also observed and characterized spectroscopically [31 c, 75], but the catalyst–substrate–dihydrido complex was not detected.

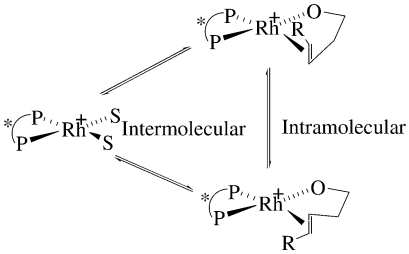

Scheme 1.22

The catalyst–substrate complexes deserve some additional comments. The two possible diastereomers for C_2-symmetrical diphosphines interconvert inter- and intramolecularly, the latter being the dominant mechanism [76] (Scheme 1.22). A second property – at least of some catalyst–substrate complexes – is that the reactivity of the minor diastereomer toward H_2 is notably higher than that of the major diastereomer.

Consequently, the stereochemistry of the hydrogenation is regulated by this relative reactivity rather than by the relative thermodynamic stability of the diastereomers [73, 75, 77]. Halpern and Landis accomplished detailed kinetic measurements on the hydrogenation of methyl-(*Z*)-*α*-acetamidocinnamate [(*Z*)-MAC] enamide catalyzed by Rh(DIPAMP) species. These authors studied the influence of temperature and pressure on the interconversion of catalyst–substrate complexes, on their reaction with H_2 and, as a consequence, on the ee achieved. The oxidative addition of H_2 is the enantio-determining and the turnover-limiting step, and it was concluded that the ee increased with decreasing temperature, because the concentration of the minor diastereomer increased, whereas it decreased with increasing pressure because hydrogenation of the major diastereomer became significant [78].

Extensive computational calculations have been performed by using molecular mechanics (MM) [79], quantum mechanics (QM) [80], or combined MM/QM methods [81]. As major contributions, these theoretical studies predict the greater stability of the major isomer, explain the higher reactivity of the minor diastereomer, introduce the formation of a dihydrogen adduct as intermediate in the oxidative addition of H_2 to the catalyst–substrate complexes, and propose the migratory insertion, instead of the oxidative addition, as a turnover-limiting step.

A new insight into the mechanism of enantioselective hydrogenation was achieved when the elusive dihydride intermediates were detected and characterized spectroscopically [82]. Bargon, Selke et al. detected, through parahydrogen-induced polarization (PHIP), NMR experiments [83, 84], the formation of a dihydride in the hydrogenation of dimethylitaconate with an enantiomerically pure bis(phosphinite)rhodium(I) catalyst (see Scheme 1.23). The structural assignment was not complete: it was not proven that the itaconate is in the coordination sphere of the metal (no ^{13}C-labeled experiments were performed) and there is a supposed *trans* $^2J_{PH}$ of only 4 Hz, far from the usual values for this coupling. However, the presence of

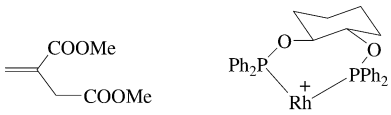

Dimethylitaconate Bis(phosphinite)rhodium complex **Scheme 1.23**

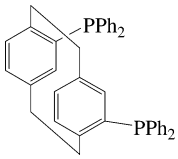

PHANEPHOS **Scheme 1.24**

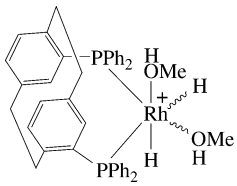

Scheme 1.25

some transient rhodium dihydride is definitive from the experimental evidences [84].

The use of the diphosphine PHANEPHOS (see Scheme 1.24) permitted Bargon, Brown and colleagues to detect and characterize a dihydrido intermediate in the hydrogenation of the enamide MAC by a rhodium-based catalyst. The PHIP NMR technique was employed, and showed one of the hydrogen atoms to be agostic between the rhodium center and the β-carbon of the substrate [85]. By using the same diphosphine and technique it was also possible to detect two diastereomers of the dihydride depicted in Scheme 1.25, which may also be detected using conventional NMR measurements [86].

Following a preparative method developed by Evans [87], Imamoto et al. prepared the C_2-symmetric electron-rich diphosphines BisP* with two stereogenic phosphorus centers [88] (Scheme 1.26). Further, Gridnev and Imamoto carried out detailed mechanistic investigations on the hydrogenation of α-dehydroamino acids and other unsaturated substrates such as enamides, (*E*)-β-dehydroamino acids or 1-benzoyloxyethenephosphonate using the rhodium complexes $[Rh(diene)(t\text{-Bu-BisP*})]^+$ (diene = COD, NBD) as catalyst precursors [46 h, 67 c, d, 89]. These authors showed that hydrogenation of the diene precursors at –20 °C gives the expected solvate complexes $[Rh(t\text{-Bu-BisP*})S_2]^+$, but at –90 °C affords two diastereomers of the catalysts–solvate dihydrido complex $[RhH_2(t\text{-Bu-BisP*})S_2]^+$. The formation of these dihydrides is reversible [89 a]. Similar dihydrides were prepared for the other BisP* ligands [89 b]. The catalysts–solvate–dihydrido reacts with α-dehydroamino acids, giving monohydride intermediates

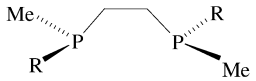

R = *t*-Bu, 1-adamantyl, 1-methylcyclohexyl, Et_3C, *c*-C_5H_9, *c*-C_6H_{11}, *i*-Pr

(*S*,*S*)-BisP*

Scheme 1.26

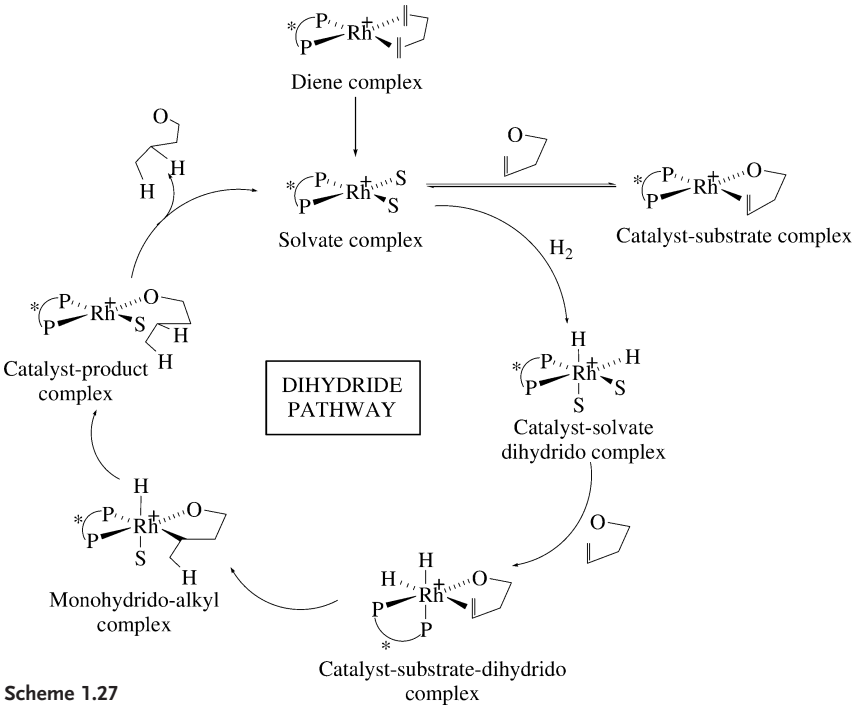

Scheme 1.27

and, eventually, the hydrogenation product with the same configuration and ee value (99%) as obtained in the catalytic reaction. On the other hand, the catalyst–substrate complexes were easily prepared by adding the substrates to the solvates. Hydrogenation of the catalyst-substrate complexes gives, in general, the hydrogenation product, but only at higher temperatures and with a lower ee. From the comparison of their results, the authors concluded that in this case the dihydride mechanism depicted in Scheme 1.27 was operating. The catalyst–substrate complexes dissociate, yielding the solvate complex that is hydrogenated to the solvate–dihydride complex. This dihydride reacts with the substrate, giving the monohydride–alkyl complex as the next observable species. The hydrogenation product is obtained after the reductive elimination step.

Notably, under catalytic conditions, reaction steps preceding catalyst–substrate–dihydrido formation are shown to be in rapid equilibrium. Therefore, stereoselec-

tion must occur at a later step in the catalytic cycle, and the authors suggested the migratory insertion as an enantio-determining and turnover-limiting irreversible step of enantioselective hydrogenation. As a major consequence, following the Gridnev and Imamoto contribution, the boundaries between unsaturated pathway and dihydride pathway are blurred. At least in some cases, both mechanisms are operating, joining in a single pathway before stereoselection occurs.

1.7
Some Dinuclear Catalyst Precursors

Several dinuclear rhodium complexes such as the above-mentioned $[Rh_2(OAc)_4]$ have been used as hydrogenation catalysts [22, 23]. Maitlis and coworkers have studied the chemistry and catalytic activity of the $[Rh(C_5Me_5)Cl_2]_2$ complex and related complexes. Kinetic studies suggested that cleavage into monomer occurs in the most active catalysts [90].

Muetterties has suggested that the dimeric hydride $[RhH(P\{OiPr\}_3)_2]_2$ catalyzes alkene and alkyne hydrogenation *via* dinuclear intermediates [91]. However, no kinetic evidence has been reported to prove the integrity of the catalysts during the reactions. On the other hand, studies of the kinetics of the hydrogenation of cyclohexene catalyzed by the heterodinuclear complexes $[H(CO)(PPh_3)_2Ru(\mu\text{-bim})M(diene)]$ (M = Rh, Ir; bim = 2,2′-biimidazolate) suggested that the full catalytic cycle involves dinuclear intermediates [92].

1.8
Concluding Remark

Throughout the history of homogeneous catalysis – and especially of homogeneous hydrogenation – rhodium complexes have played a crucial role due to the combination of excellent coordinative properties, remarkable activity and selectivity, the adequate redox characteristics of the couple Rh(I)/Rh(III) as well as NMR properties (100% abundance, spin 1/2). The selection of results presented in this chapter show that homogeneous hydrogenation by rhodium complexes represents not only a rich past, as indicated by the exponential growth of the past forty years, but also a bright future.

Abbreviations

BINAP	2,2′-bis(diphenylphosphino)-1,1′-binaphthyl
BPE	bis(phospholanyl)ethane
COD	1,5-cyclooctadiene
DIPHOS	1,2-bis(diphenyl)phosphinoethane
DuPHOS	bis(phospholanyl)benzene
MH	monohydride

MM	molecular mechanics
NBD	2,5-norbornadiene
NMDPP	neomethyldiphenylphosphine
PHIP	parahydrogen-induced polarization
QM	quantum mechanics
TFB	tetrafluorobenzobarrelene
(*Z*)-MAC	methyl-(*Z*)-*α*-acetamidocinnamate

References

1 B.R. James, *Homogeneous Hydrogenation*, Wiley, New York, **1973**.

2 P.A. Chaloner, M.A. Esteruelas, F. Joó, L.A. Oro, *Homogeneous Hydrogenation*, Kluwer Academic, Dordrecht, **1994**.

3 F.J. McQuilin, *Homogeneous Hydrogenation in Organic Chemistry*, D. Reidel, Dordrecht, **1976**.

4 (a) L.A. Oro, in: *Encyclopedia of Catalysis*, I.V. Horváth, E. Iglesia, M.T. Klein, J.A. Lercher, A.J. Russell, E.I. Stiefel (Eds.), John Wiley & Sons, **2003**, Vol. 4, p. 55; (b) R. Sánchez-Delgado, M. Rosales, *Coord. Chem. Rev.* **2000**, *196*, 249; (c) A. Spencer, in: *Comprehensive Coordination Chemistry*, G. Wilkinson, R.D. Guillard, J.A. McCleverty (Eds.), Pergamon, Oxford, **1987**, Vol. 6, Chapter 61.2, p. 229; (d) B.R. James, in: *Comprehensive Organometallic Chemistry*, G. Wilkinson, F.G.A. Stone, E.A. Abel (Eds.), Pergamon, Oxford, **1982**, vol. 8, Chapter 51, p. 285; (e) B.R. James, *Adv. Organomet. Chem.*, **1979**, *17*, 319.

5 (a) M. Calvin, *Trans. Faraday Society* **1938**, *34*, 1181; (b) M. Calvin, *J. Am. Chem. Soc.* **1939**, *61*, 2230.

6 M. Iguchi, *J. Chem. Soc. Japan* **1939**, *60*, 1287.

7 P.J. Brothers, *Progress Inorg. Chem.* **1981**, *28*, 1.

8 (a) M. Iguchi, *J. Chem. Soc. Japan* **1942**, *63*, 634; (b) M. Iguchi, *J. Chem. Soc. Japan* **1942**, *63*, 1752.

9 (a) S.S. Bath, L. Vaska, *J. Amer. Chem. Soc.* **1965**, *85*, 3500; (b) L. Vaska, *Inorg. Nucl. Chem. Lett.* **1965**, *1*, 89.

10 (a) D. Evans, G. Yagupsky, G. Wilkinson, *J. Chem. Soc. (A)* **1968**, 2660; (b) M. Yagupsky, C.K. Brown, G. Yagupsky, G. Wilkinson, *J. Chem. Soc. (A)* **1970**, 937.

11 (a) C. O'Connor, G. Yagupsky, D. Evans, G. Wilkinson, *Chem. Commun.* **1968**, 420; (b) C. O'Connor, G. Wilkinson, *J. Chem. Soc. (A)* **1968**, 2665.

12 G. Yagupsky, G. Wilkinson, *J. Chem. Soc. (A)* **1970**, 941.

13 (a) D. Evans, J.A. Osborn, G. Wilkinson, *J. Chem. Soc. (A)* **1968**, 3133; (b) G. Yagupsky, C.K. Brown, G. Wilkinson, *Chem. Commun.* **1969**, 1244; (c) G. Yagupsky, C.K. Brown, G. Wilkinson, *J. Chem. Soc. (A)* **1970**, 1392; (d) C.K. Brown, G. Wilkinson, *J. Chem. Soc. (A)* **1970**, 2753.

14 (a) J.A. Osborn, G. Wilkinson, J.F. Young, *Chem. Commun.* **1965**, 17; (b) J.A. Osborn, F.H. Jardine, J.F. Young, G. Wilkinson, *J. Chem. Soc. (A)* **1966**, 1711; (c) M.A. Bennett, P.A. Longstaff, *Chem. Ind. (London)* **1965**, 846; (d) R.S. Coffey, British Patent 1121642, **1965**; (e) L. Vaska, R.E. Rhodes, *J. Am. Chem. Soc.* **1965**, *87*, 4970.

15 L. Horner, H. Büthe, H. Siegel, *Tetrahedron Lett.* **1968**, 4023.

16 F.H. Jardine, *Progress Inorg. Chem.* **1981**, *28*, 63.

17 J.R. Shapley, R.R. Schrock, J.A. Osborn, *J. Am. Chem. Soc.* **1969**, *91*, 2816.

18 (a) B.F.G. Jonson, J. Lewis, D.A. White, *J. Am. Chem. Soc.* **1969**, *91*, 5186; (b) L.M. Haines, *Inorg. Nucl. Chem. Lett.* **1969**, *5*, 399; (c) M. Green, T.A. Kuc, S. Taylor, *Chem. Commun.* **1970**, 1553.

19 R.R. Schrock, J.A. Osborn, *Chem. Commun.* **1970**, 567.

20 B.C. Hui, G.L. Rempel, *Chem. Commun.* **1970**, 1195.

21 (a) P. Legzdins, G. Rempel, G. Wilkinson, *Chem. Commun.* **1969**, 825; (b) P. Legzdins, R.W. Mitchell, G. Rempel,

J. D. Ruddick, G. Wilkinson, *J. Chem. Soc. (A)* **1970**, 3322.
22 S. J. La Placa, J. Ibers, *Acta Cryst.* **1965**, *18*, 511.
23 J. Halpern, *Inorg. Chim. Acta* **1981**, *50*, 11, and references therein.
24 (a) S. B. Duckett, C. L. Newell, R. Eisenberg, *J. Am. Chem. Soc.* **1994**, *116*, 10548; (b) S. B. Duckett, C. L. Newell, R. Eisenberg, *J. Am. Chem. Soc.* **1997**, *119*, 2068.
25 (a) S. A. Colebrooke, S. B. Duckett, J. A. B. Lohman, *Chem. Commun.* **2000**, 695; (b) S. A. Colebrooke, S. B. Duckett, J. A. B. Lohman, R. Eisenberg, *Chem. Eur. J.* **2004**, *10*, 2459.
26 D. Blazina, S. B. Duckett, J. P. Dunne, C. Godard, *Dalton Trans.* **2004**, 2601.
27 F. Joó, P. Csiba, A. Bényei, *J. Chem. Soc., Chem. Commun.* **1993**, 1602.
28 (a) R. R. Schrock, J. A. Osborn, *J. Am. Chem. Soc.,* **1976**, *98*, 2134; (b) R. R. Schrock, J. A. Osborn, *J. Am. Chem. Soc.* **1976**, *98*, 2143; (c) R. R. Schrock, J. A. Osborn, *J. Am. Chem. Soc.* **1976**, *98*, 4450.
29 R. Usón, L. A. Oro, R. Sariego, M. Valderrama, C. Rebullida, *J. Organomet. Chem.* **1980**, *197*, 87.
30 M. A. Esteruelas, L. A. Oro, *Coord. Chem. Rev.* **1999**, *193*, 557.
31 (a) J. Halpern, D. P. Riley, A. S. C. Chan, J. J. Pluth, *J. Am. Chem. Soc.* **1977**, *98*, 8055; (b) J. Halpern, D. P. Riley, A. S. C. Chan, J. J. Pluth, *Adv. Chem. Ser.* **1977**, *173*, 16; (c) A. S. C. Chan, J. Halpern, *J. Am. Chem. Soc.* **1980**, *102*, 838.
32 R. A. Sánchez-Delgado, D. Rondón, A. Andriollo, V. Herrera, G. Martín, B. Chaudret, *Organometallics* **1993**, *12*, 4291.
33 (a) R. A. Sánchez-Delgado, V. Herrera, L. Rincón, A. Andriollo, G. Martín, *Organometallics* **1994**, *13*, 553; (b) V. Herrera, A. Fuentes, M. Rosales, R. A. Sánchez-Delgado, C. Bianchini, A. Meli, F. Vizza, *Organometallics* **1997**, *16*, 2465.
34 E. Baralt, S. J. Smith, J. Hurwitz, I. T. Horvath, R. H. Fish, *J. Am. Chem. Soc.* **1992**, *114*, 5187.
35 J. F. Young, J. A. Osborn, F. H. Jardine, G. Wilkinson, *Chem. Commun.* **1965**, 131.
36 O. Korpin, K. Mislow, *J. Am. Chem. Soc.* **1967**, *89*, 4784.
37 L. Horner, H. Winkler, A. Rapp, A. Mentrup, H. Hoffmann, P. Beck, *Tetrahedron Lett.* **1961**, 161.
38 W.S. Knowles, M. J. Sabacky, *Chem. Commun.* **1968**, 1445.
39 L. Horner, H. Siegel, H. Büthe, *Angew. Chem.* **1968**, *80*, 1034; *Angew. Chem., Int. Ed. Engl.* **1968**, *7*, 942.
40 The ee were improved up to 28% by increasing the optical purity of the phosphine (it was 69% ee at the beginning).
41 J. D. Morrison, R. E. Burnett, A. M. Aguiar, C. J. Morrow, C. Phillips, *J. Am. Chem. Soc.* **1971**, *93*, 1301.
42 T. P. Dang, H. B. Kagan, *Chem. Commun.* **1971**, 481.
43 H. B. Kagan, T.-P. Dang, *J. Am. Chem. Soc.* **1972**, *94*, 6429.
44 W. S. Kowles, M. J. Sabacky, B. D. Vineyard, *J. Chem. Soc., Chem. Commun.* **1972**, 10.
45 (a) W. S. Knowles, M. J. Sabacky, B. D. Vineyard, D. J. Weinkauff, *J. Am. Chem. Soc.* **1975**, *97*, 2567; (b) W. S. Knowles, *Acc. Chem. Res.* **1983**, *16*, 106; (c) W. S. Knowles, *Angew. Chem.* **2002**, *114*, 2096; *Angew. Chem. Int. Ed.* **2002**, *41*, 1998 (Nobel lecture).
46 (a) H. Takaya, T. Otha, R. Noyori, in: *Catalytic Asymmetric Synthesis*, I. Ojima (Ed.), VCH: New York, **1993**, p. 1; (b) R. Noyori, in: *Asymmetric Catalysis in Organic Synthesis*, Wiley: New York, **1994**, p. 16; (c) J. M. Brown, in: *Comprehensive Asymmetric Catalysis*, E. N. Jacobsen, A. Pfaltz, H. Yamamoto (Eds.), Springer: Berlin, **1999**, Vol. 1, p. 121; (d) R. L. Halterman, *Comprehensive Asymmetric Catalysis*, E. N. Jacobsen, A. Pfaltz, H. Yamamoto (Eds.), Springer: Berlin, **1999**, Vol. 1, p. 183; (e) T. Ohkuma, R. Noyori, *Comprehensive Asymmetric Catalysis*, E. N. Jacobsen, A. Pfaltz, H. Yamamoto (Eds.), Springer: Berlin, **1999**, Vol. 1, p. 199; (f) H.-U. Blaser, F. Spindler, *Comprehensive Asymmetric Catalysis*, E. N. Jacobsen, A. Pfaltz, H. Yamamoto (Eds.), Springer: Berlin, **1999**, Vol. 1, p. 247; (g) T. Okhuma, M. Kitamura, R. Noyori, in: *Catalytic Asymmetric Synthesis*, I. Ojima (Ed.), Wiley-VCH: New York, **2000**, p. 1; (h) K. V. L.

Crépy, T. Imamoto, *Adv. Synth. Catal.* **2003**, *345*, 79; (i) H.-U. Blaser, C. Malan, B. Pugin, F. Spindler, H. Steiner, M. Studer, *Adv. Synth. Catal.* **2003**, *345*, 103; (j) W. Tang, X. Zhang, *Chem. Rev.* **2003**, *103*, 3029; (k) L. Dahlenburg, *Eur. J. Inorg. Chem.* **2003**, 2733; (l) J.-P. Genet, *Acc. Chem. Res.* **2003**, *36*, 908; (m) P. Barbaro, C. Bianchini, G. Giambastiani, S.L. Parivel, *Coord. Chem. Rev.* **2004**, *248*, 2131.

47 A. Miyashita, A. Yasuda, H. Takaya, K. Toriumi, T. Ito, T. Souchi, R. Noyori, *J. Am. Chem. Soc.* **1980**, *102*, 7932.

48 The methanol complex [Rh(BINAP)$(MeOH)_2]ClO_4$ and the complex resulting from loss of MeOH from it are used as catalysts [47]. Both BINAP enantiomers were employed.

49 M.J. Burk, *J. Am. Chem. Soc.* **1991**, *113*, 8518.

50 M.J. Burk, *Acc. Chem. Res.* **2000**, *33*, 363.

51 (a) A. Togni, L.M. Venanzi, *Angew. Chem.* **1994**, *106*, 517; *Angew. Chem. Int. Ed. Engl.* **1994**, *33*, 497; (b) F. Fache, E. Schulz, M.L. Tommasino, M. Lemaire, *Chem. Rev.* **2000**, *100*, 2159.

52 F. Guillen, J. Fiaud, *Tetrahedron Lett.* **1999**, *40*, 2939.

53 (a) T. Hayashi, *Acc. Chem. Res.* **2000**, *33*, 354; (b) F. Lagasse, H.B. Kagan, *Chem. Pharm. Bull.* **2000**, *48*, 315; (c) I.V. Komarov, A. Börner, *Angew. Chem.* **2001**, *113*, 1237; *Angew. Chem. Int. Ed.* **2001**, *40*, 1197; (d) M.T. Reetz, T. Sell, A. Meiswinkel, G. Mehler, *Angew. Chem.* **2003**, *115*, 814; *Angew. Chem. Int. Ed.* **2003**, *42*, 790; (e) M.T. Reetz, G. Mehler, *Tetrahedron Lett.* **2003**, *44*, 4593; (f) M.T. Reetz, G. Mehler, A. Meiswinkel, *Tetrahedron: Asymmetry* **2004**, *15*, 2165; (g) M.T. Reetz, J.-A. Ma, R. Goddard, *Angew. Chem.* **2005**, *117*, 416; *Angew. Chem. Int. Ed.* **2005**, *44*, 412.

54 C. Claver, E. Fernández, A. Gillon, K. Heslop, D.J. Hyett, A. Martorell, A.G. Orpen, P.G. Pringle, *Chem. Commun.* **2000**, 961.

55 (a) M. van den Berg, A.J. Minnaard, E.P. Schudde, J. van Esch, A.H.M. de Vries, J.G. de Vries, B. Feringa, *J. Am. Chem. Soc.* **2000**, *122*, 11539; (b) D. Peña, A.J. Minnaard, A.H.M. de Vries, J.G. de Vries, B.L. Feringa, *Org. Lett.* **2003**, *5*, 475.

56 R. Noyori, T. Ohkuma, *Angew. Chem.* **2001**, *113*, 41; *Angew. Chem. Int. Ed. Engl.* **2001**, *40*, 40.

57 S. Törös, B. Heil, L. Kollár, L. Markó, *J. Organomet. Chem.* **1980**, *197*, 85.

58 Q. Jiang, Y. Jiang, D. Xiao, P. Cao, X. Zhang, *Angew. Chem.* **1998**, *110*, 1203; *Angew. Chem. Int. Ed. Engl.* **1998**, *37*, 1100.

59 (a) K. Inoguchi, S. Sakuraba, K. Achiwa, *Synlett* **1992**, 169; (b) H.P. Märki, Y. Crameri, R. Eigenmann, A. Krasso, H. Ramuz, K. Bernauer, M. Goodman, K.L. Melmon, *Helv. Chim. Acta* **1988**, *71*, 320; (c) S. Sakuraba, N. Nakajima, K. Achiwa, *Tetrahedron: Asymmetry* **1993**, *4*, 1457; (d) H.-U. Blaser, H.-P. Jalett, F. Spindler, *J. Mol. Catal. A: Chem.* **1996**, *107*, 85.

60 I. Ojima, T. Kogure, T. Terasaki, K. Achiwa, *J. Org. Chem.* **1978**, *43*, 3444.

61 C. Pasquier, S. Naili, A. Mortreux, F. Agbossou, L. Pélinski, J. Brocard, J. Eilers, I. Reiners, V. Peper, J. Martens, *Organometallics* **2000**, *19*, 5723 and references therein.

62 H.-U. Blaser, F. Spindler, *Comprehensive Asymmetric Catalysis*, E.N. Jacobsen, A. Pfaltz, H. Yamamoto (Eds.), Springer: Berlin, **1999**, Vol. 1, p. 247.

63 H.B. Kagan, N. Langlois, T.P. Dang, *J. Organomet. Chem.* **1975**, *90*, 353.

64 S. Vastag, J. Bakos, S. Törös, N.E. Takach, R.B. King, B. Heil, L. Markó, *J. Mol. Catal.* **1984**, *22*, 283.

65 J. Bakos, A. Orosz, B. Heil, M. Laghmari, P. Lhoste, D. Sinou, *J. Chem. Soc., Chem. Commun.* **1991**, 1684.

66 M.J. Burk, J.E. Feaster, *J. Am. Chem. Soc.* **1992**, *114*, 6266.

67 (a) J. Halpern, *Science* **1982**, *217*, 401; (b) J.M. Brown, *Chem. Soc. Rev.* **1993**, *22*, 25; (c) J.M. Brown, R. Giernoth, *Curr. Opinion Drug Discov. Devel.* **2000**, *3*, 825; (d) I.D. Gridnev, T. Imamoto, *Acc. Chem. Res.* **2004**, *37*, 633.

68 Some years later, *para*-enriched dihydrogen experiments indicated the existence of a non-detectable amount of a dihydride in equilibrium with $[RhP_2S_2]^+$ species [69].

69 J.M. Brown, L.R. Canning, A.J. Downs, A.M. Foster, *J. Organomet. Chem.* **1983**, *255*, 103.

70 At an early stage, only for diphosphine ligands capable of *trans*-coordination were detected hydride solvate intermediates [71], but a catalytic pathway based on diphosphine *trans*-chelation has not been developed to date (see [80 b]).

71 J.M. Brown, P.A. Chaloner, A.G. Kent, B.A. Murrer, P.N. Nicholson, D. Parker, P.J. Sidebottom, *J. Organomet. Chem.* **1981**, *216*, 263.

72 J.M. Brown, P.A. Chaloner, *J. Chem. Soc., Chem. Commun.* **1978**, 321.

73 J. Halpern, A.S.C. Chan, J.J. Pluth, *J. Am. Chem. Soc.* **1980**, *102*, 5952.

74 A.S.C. Chan, J.J. Pluth, J. Halpern, *Inorg. Chim. Acta* **1979**, *37*, L477.

75 J.M. Brown, P.A. Chaloner, *J. Chem. Soc., Chem. Commun.* **1980**, 344.

76 J.A. Ramsden, T.D.W. Claridge, J.M. Brown, *J. Chem. Soc., Chem. Commun.* **1995**, 2469 and references therein.

77 P.S. Chua, N.K. Roberts, B. Bosnich, S.J. Okrasinski, J. Halpern, *J. Chem. Soc., Chem. Commun.* **1981**, 1278.

78 C.R. Landis, J. Halpern, *J. Am. Chem. Soc.* **1987**, *109*, 1746.

79 J.S. Giovannetti, C.M. Kelly, C.R. Landis, *J. Am. Chem. Soc.* **1993**, *115*, 4040.

80 (a) C.R. Landis, P. Hilfenhaus, S. Feldgus, *J. Am. Chem. Soc.* **1999**, *121*, 8741; (b) A. Kless, A. Börner, D. Heller, R. Selke, *Organometallics* **1997**, *16*, 2096.

81 (a) C.R. Landis, S. Feldgus, *Angew. Chem.* **2000**, *112*, 2985; *Angew. Chem. Int. Ed.* **2000**, *39*, 2863; (b) S. Feldgus, C.R. Landis, *J. Am. Chem. Soc.* **2000**, *122*, 12714; (c) S. Feldgus, C.R. Landis, *Organometallics* **2001**, *20*, 2374.

82 K. Rosen, *Angew. Chem.* **2001**, *113*, 4747; *Angew. Chem. Int. Ed.* **2001**, *40*, 4611.

83 C. Russell Bowers, D.P. Weitekamp, *J. Am. Chem. Soc.* **1987**, *109*, 5541.

84 A. Harthun, R. Kadyrov, R. Selke, J. Bargon, *Angew. Chem.* **1997**, *109*, 1155; *Angew. Chem. Int. Ed. Engl.* **1997**, *36*, 1103.

85 R. Giernoth, H. Heinrich, N.J. Adams, R.J. Deeth, J. Bargon, J.M. Brown, *J. Am. Chem. Soc.* **2000**, *122*, 12381.

86 H. Heinrich, R. Giernoth, J. Bargon, J.M. Brown, *Chem. Commun.* **2001**, 1296.

87 A.R. Muci, K.R. Campos, D.A. Evans, *J. Am. Chem. Soc.* **1995**, *117*, 9075.

88 T. Imamoto, J. Watanabe, Y. Wada, H. Masuda, H. Yamada, H. Tsuruta, S. Matsukawa, K. Yamaguchi, *J. Am. Chem. Soc.* **1998**, *120*, 1635.

89 (a) I.D. Gridnev, N. Higashi, K. Asakura, T. Imamoto, *J. Am. Chem. Soc.* **2000**, *122*, 7183; (b) I.D. Gridnev, Y. Yamanoi, N. Higashi, H. Tsuruta, M. Yasutake, T. Imamoto, *Adv. Synth. Catal.* **2001**, *343*, 118.

90 P.M. Maitlis, *Acc. Chem. Res.* **1978**, *11*, 301.

91 (a) A.J. Sivak, E.L. Muetterties, *J. Am. Chem. Soc.* **1979**, *101*, 4878; (b) E.L. Muetterties, *Inorg. Chim. Acta* **1981**, *50*, 9.

92 (a) M.P. García, A.M. López, M.A. Esteruelas, F.J. Lahoz, L.A. Oro, *J. Chem. Soc., Chem. Commun.* **1988**, 793; (b) M.A. Esteruelas, M.P. García, A.M. López, L.A. Oro, *Organometallics* **1991**, *10*, 127.

2
Iridium

Robert H. Crabtree

2.1
Introduction

Today, iridium compounds find so many varied applications in contemporary homogeneous catalysis it is difficult to recall that, until the late 1970s, rhodium was one of only two metals considered likely to serve as useful catalysts, at that time typically for hydrogenation or hydroformylation. Indeed, catalyst/solvent combinations such as $[IrCl(PPh_3)_3]$/MeOH, which were modeled directly on what was previously successful for rhodium, failed for iridium. Although iridium was still considered potentially to be useful, this was only for the demonstration of stoichiometric reactions related to proposed catalytic cycles. Iridium tends to form stronger metal–ligand bonds (e.g., Cp(CO)Rh-CO, 46 kcal mol^{-1}; Cp(CO)Ir-CO, 57 kcal mol^{-1}), and consequently compounds which act as reactive intermediates for rhodium can sometimes be isolated in the case of iridium.

When low-coordinate iridium fragments in "non-coordinating" solvents (e.g., $\{Ir(PPh_3)_2\}^+$ in CH_2Cl_2) were found to be much more active than their rhodium analogues, it became clear that it is the *dissociation* of ligands or solvent – much slower for Ir versus Rh and for MeOH versus CH_2Cl_2 – that leads to low catalytic rates with $[IrCl(PPh_3)_3]$/MeOH. The other steps in the catalytic cycle are often very fast for Ir, so if the need for dissociation is avoided, then highly active Ir catalysts can be formed. However, a new consensus has now emerged: rhodium catalysts are often considered to be slower but more selective, whilst iridium catalysts are faster but less selective.

2.2
Historical Aspects

Iridium made its first major mark in 1965, in the arena of organometallic chemistry with the discovery of Vaska's complex, $[IrCl(CO)(PPh_3)_2]$ (**1**) [1]. Only weakly catalytic itself, Vaska's complex is nevertheless highly relevant to cataly-

The Handbook of Homogeneous Hydrogenation.
Edited by J.G. de Vries and C.J. Elsevier
Copyright © 2007 WILEY-VCH Verlag GmbH & Co. KGaA, Weinheim
ISBN: 978-3-527-31161-3

sis in providing the classic examples of oxidative addition – normally a key step in almost any catalytic cycle. Equation (1) shows how a variety of molecules X-Y can oxidatively add in a concerted manner to this Ir(I) species to form a series of Ir(III) adducts. The H_2 adduct (X = Y = H) is only very weakly catalytically active for alkene hydrogenation because all the ligands in $[IrH_2Cl(CO)(PPh_3)_2]$ are firmly bound and do not dissociate to make way for substrate alkene. Without alkene binding, hydrogen transfer from the metal to the alkene cannot occur.

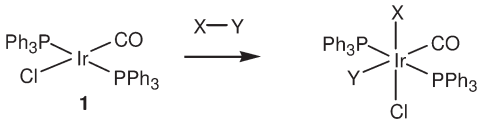

(1)

Following the discovery of Wilkinson's hydrogenation catalyst, $[RhCl(PPh_3)_3]$ (**2**) in 1964, the iridium analogue was naturally also investigated as a catalyst, but proved to be only very weakly active. Once again, the reason was that the adduct $[IrH_2Cl(PPh_3)_3]$ failed to lose PPh_3, unlike the Rh analogue, so that the alkenes were unable to bind and undergo reduction [2].

Schrock and Osborn [3] introduced the valuable idea that the reaction should be started with a PR_3 to Rh ratio of 2 : 1 in order to avoid the need for ligand dissociation. These authors used Chatt's diene-metal precursors, $[(nbd)RhCl]_2$ (nbd = norbornadiene), to form a series of very useful catalysts of the type $[(nbd)Rh(PR_3)_2]BF_4$. The nbd was shown to be lost during hydrogenation to form species based on the $\{Rh(PR_3)_2\}^+$ fragment, such as $[(MeOH)_2RhL_2]BF_4$. In the Rh series, MeOH was easily lost and catalytic alkene reduction was rapid. In the iridium analogues, however, the Ir(III) complexes $[IrH_2(solvent)_2(PPh_3)_2]^+$ (**3**, solvent = MeOH) were formed. These proved to be very much less labile and less active than the Rh series [4], and consequently attention was naturally focused on rhodium.

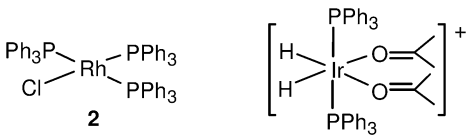

At this point, the initial intent of these investigations was to seek stable hydrides in iridium that were relevant to transient intermediates proposed in the rhodium series. With this aim in view, attention was focused on a series of complexes $[(cod)Ir(PR_3)_2]BF_4$, analogous to the Schrock-Osborn Rh catalysts; many of these had been synthesized previously, but had only been tested for catalysis in coordinating solvents and the results had been disappointing. The related mixed-ligand complexes, such as $[(cod)Ir(py)(PR_3)_2]BF_4$ (cod = 1,5-cyclooctadiene; py = pyridine), were new [5, 6]. Since solvent dissociation from **3** was needed to generate a site for alkene binding, it seemed appropriate to examine the variation of the solvent, particularly the use of CH_2Cl_2; this was considered

to be non-coordinating because, at the time, it was not known to be capable of binding to metals. Halocarbon solvents in general had been avoided for Rh catalysts, presumably because of the risk of C–Cl oxidative addition to Rh(I). The iridium complexes resisted such pathways, possibly because their resting state is Ir(III) (versus Rh(I)), and possibly also because of their cationic nature; many neutral Ir(I) species do add C–Cl bonds easily. Not only was the catalytic rate very greatly enhanced in CH_2Cl_2 but, more importantly, the substrate scope was also greatly expanded. At the time, no homogeneous hydrogenation catalysts were known which would reduce tri- and especially tetrasubstituted alkenes efficiently; even today, these are very rare. By using a low PR_3 to M ratio, a non-coordinating solvent, and Ir rather than Rh, very high activity was achieved for hindered alkenes [7].

If a PR_3 to M ratio of 2 was so good, then would a ratio of 1 be better? A catalyst of this type indeed proved to be the best of the whole series. $[Ir(cod)(PCy_3)(py)]BF_4$ (**4**, Cy = cyclohexyl) is sometimes referred to as Crabtree's catalyst, although both Hugh Felkin and George Morris were also very closely associated with its initial development [5, 6]. The rates measured for reduction of various alkenes by **4** illustrate the high activity for hindered alkenes: *t*-BuCH=CH_2, 8300; 1-hexene, 6400; cyclohexene, 4500; 1-methylcyclohexene, 3800; $Me_2C{=}CMe_2$, 4000 h^{-1}. Even at 0.1% loading, the catalyst completely reduces all but the tetrasubstituted alkene, where 400 catalytic turnovers are seen ($Me_2C{=}CMe_2$, 0 °C, CH_2Cl_2) before catalyst deactivation. The deactivation product is a hydride-bridged polynuclear complex [7], presumably formed by intermolecular reaction of the catalyst when the depleted substrate is no longer able to compete effectively for binding to the metal. Hydrogenation tends to be favored over deactivation by operating at 0 °C rather than at room temperature.

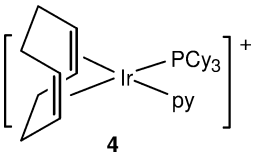

4

The above-mentioned rates can usefully be compared with those for other catalysts under similar conditions [7]: $[RhCl(PPh_3)_3]$ at 0 °C (1-hexene, 60; cyclohexene, 70; $Me_2C{=}CMe_2$, 0 h^{-1}) is far slower and $[RuHCl(PPh_3)_3]$ at 25 °C in C_6H_6 (1-hexene, 9000; cyclohexene, 7; 1-methylcyclohexene, $Me_2C{=}CMe_2$, 0) is highly selective for terminal alkenes.

The initial studies on the catalyst did not attract the attention of the organic synthetic community, partly because the details were not published in an organic chemistry journal, and the substrates used were not "real" multifunctional organic compounds. On the basis of a suggestion made by Bill Suggs, the catalyst was used for more appropriate substrates, and the results obtained published [8]. More importantly, based on a further suggestion by Sarah Danishevsky, strong (99%) directing effects were also found in which the catalyst binds to a substrate OH or

C=O group and then delivers H_2 almost exclusively from the face of the substrate that contains the binding group [9]. This property of the catalyst, which was discovered independently by Stork [10], is illustrated in Eq. (2). Any of a variety of directing groups such as ether, ketone or ester is capable of binding to the catalyst before hydrogenation takes place. This sets the stereochemistry of as many as two new stereocenters in the reduction. Since Stork is a highly respected member of the organic chemistry community, his intervention was critical in first making the catalyst known, after which time it began to be used more generally.

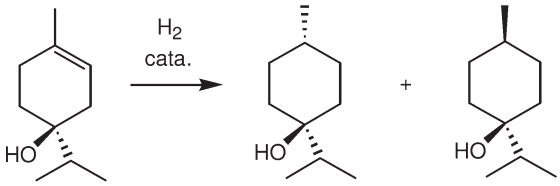

(2)

Pd/C	20%	80%
$[Ir(cod)(PCy_3)py]^+$	99.9%	0.1%

The reason that directing effects are so efficient is related to the low PR_3 to Ir ratio, which allows the directing group, the H_2 and the C=C bond all to bind to the metal at the same time. This was suggested by the detection of **5** at low temperature in the reaction of Eq. (3) [9].

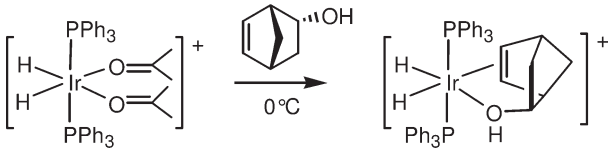

3 **5**

(3)

In the initial studies, the Ir system appeared to be less useful for enantioselective reduction because the *e.e.* values were never as high as seen for the Rh analogues. In commercial practice, however, rate can be more important than *e.e.* In this vein, Blaser [11] was able to equip the $\{(cod)Ir\}^+$ fragment with an asymmetric ligand of Togni's [12] to give a complex **6** that is used for the commercial production of the agrochemical metolachlor (Dual Magnum®). This is one of the few enantioselective hydrogenation systems that is in commercial use today.

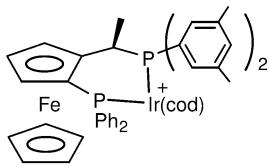

6

In a purely mechanistic experiment, the deuteration of 8-methylquinoline and related compounds by the Ir catalysts was examined, whereupon very rapid and selective isotope incorporation into the methyl CH bonds was found; once again, chelation control was operating [13]. Much later, the pharmaceutical industry developed this aspect of the catalyst for the tritiation of drug candidates, needed for metabolic studies. By introducing the radioactive tritium at the last step, a full organic synthesis involving radioactive intermediates was avoided; this also greatly minimized the production of radioactive organic waste. Catalysts **3**, **4** and $[Ir(cod)(dppb)]BF_4$ ($dppb = Ph_2P\{CH_2\}_4PPh_2$) have all proved useful in this commercially important reaction, with each catalyst having a slightly different selectivity [14]. As before, pronounced directing effects caused exchange to occur at well-defined positions on the substrate, notably those immediately adjacent to the point on the compound where the catalyst binds. This is usually an O heteroatom, such as in an amide, ester, alcohol or ketone.

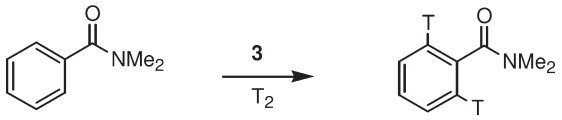

(4)

A wide variety of iridium-based hydrogenation catalysts are currently under development, notably for organic syntheses including enantioselective synthesis. Hydrogenation by hydrogen transfer is well known [15], and the reduction of C=O and C=N double bonds is also possible [16, 17].

The hydroboration of terminal and internal alkenes with pinacolborane can be carried out at room temperature in the presence of an iridium(I) catalyst (3 mol.%) formed by the addition of dppm (2 equiv.) to $[Ir(cod)Cl]_2$ ($dppm = Ph_2PCH_2PPh_2$), a mixture that presumably furnishes $[Ir(cod)(dppm)]Cl$ as the true catalyst precursor. Hydroboration results in the addition of the boron atom to the terminal carbon of 1-alkenes with more than 99% selectivity [18].

The reversal of hydrogenation is also possible, as evidenced by the many iridium catalysts for alkane dehydrogenation to alkenes or arenes, though to date this area is of mainly academic interest rather than practical importance [19].

One point of practical importance is the sensitivity of these catalysts to counterion and solvent; this is particularly the case in asymmetric hydrogenation, where significant changes in properties have been seen in several cases [20]. This implies that a range of solvents and counterions might usefully be examined in planning trials of the catalyst for a given reduction. In one case [20a], even the usually satisfactory triflate and tetrafluoroborate counterions almost completely inhibited a cationic iridium-PHOX catalyst. In that case, catalysts with $[Al\{OC(CF_3)_3\}_4]^-$, $BArF^-$, and $[B(C_6F_5)_4]^-$ counterions did not lose activity during the reaction, and even remained active after all of the substrate had been consumed. Tetraphenylborate is another undesirable anion as it tends to coordinate via an arene ring. In contrast to their sensitivity to anion and solvent, the Ir catalysts are air-stable, unlike typical Rh analogues.

2.3 Organometallic Aspects

The above-mentioned catalysts rely for their activity on losing the cod ligand via hydrogenation to give cyclooctane, thus liberating sites on the metal. The origin of cod as a ligand lies in some of Chatt's early studies [21] that were related to the development of the Dewar-Chatt model [21]. The intellectual roots of the concept go back to Langmuir and to Pauling in the 1920s and 1930s, who proposed that CO could form multiple bonds with metals such as Ni(0) [22].

Many useful iridium catalysts, such as those mentioned above, are synthetically accessible from $[Ir(cod)Cl]_2$, which is now commercially available. Treatments with PR_3 in a nonpolar solvent gives $[Ir(cod)PR_3Cl]$ for the less bulky members of the series, with PEt_3 marking the dividing line between the two types of pathway. Smaller ligands produce neutral bis-phosphine halo-complexes. In polar solvents (e.g., aqueous acetone), in contrast, the chloride ion can dissociate and ionic $[(cod)Ir(PR_3)_2]^+$ (**7**) or $[(cod)Ir(PR_3)_3]^+$ are obtained, again depending on the steric bulk, with smaller ligands yielding the tris-phosphine species. If $[IrCl(cod)PCy_3]$ is treated with pyridine in aqueous acetone, $[Ir(cod)(PCy_3)py]^+$ (**4**) is obtained. This species is not in equilibrium with $[Ir(cod)(PPh_3)_2]^+$ and $[Ir(cod)py_2]^+$ to any detectable extent (^1H- and ^{31}P-NMR spectroscopy). Variants of these routes can be made to provide chelate compounds of the type $[(cod)Ir(L\text{-}L)]^+$, where L-L are diphosphines, diamines, or mixed-donor ligands [5, 6, 23]. Typically, reactions are carried out at room temperature under N_2 or Ar.

A vast number of derivatives of these general types have been prepared by similar routes for catalytic applications, and at this point we can do no more than provide a series of recent references: some have P-donor ligands [24], some have N-heterocyclic carbenes [25], and others have mixed donors [26].

The hydrogenation product from $[Ir(cod)(PPh_3)_2]BF_4$ in various solvents is the readily isolable series $[IrH_2(solvent)_2(PPh_3)_2]BF_4$ [4], where the solvent can be Me_2CO, MeOH, and even H_2O. The acetone complex (**3**) has been characterized crystallographically [27]. These are precursors for the synthesis of a wide variety of unusual derivatives (Scheme 2.1). The first complexes of halocarbons were made by the route of Eq. (4), where L = MeI [28]. For L = H_2, the products were the first bis-dihydrogen complexes [29]. Agostic species arise from reaction with 8-methylquinoline (Scheme 2.1). Instead, benzoquinoline undergoes cyclometalation.

Styrene yields a stable η^6-arene complex (Scheme 2.1), which explains why neither **3** nor **7** is an effective hydrogenation catalyst for styrene and related substrates. The formation of such stable adducts is highly disadvantageous for rapid catalysis, but not for the exploration of organometallic chemistry. No similar stable complexes have been obtained from the catalyst **4**; the faster catalytic rates seen for **4** may correlate with the presence of less stable intermediates in this case [30].

One of the limitations of both **4** and **7** in catalysis is their ready decomposition to inactive cluster hydride complexes in the absence of substrate. If the substrate is a weak ligand (e.g., $Me_2C{=}CMe_2$), this decomposition can be competitive with cluster formation. A high concentration of substrate favors catalysis

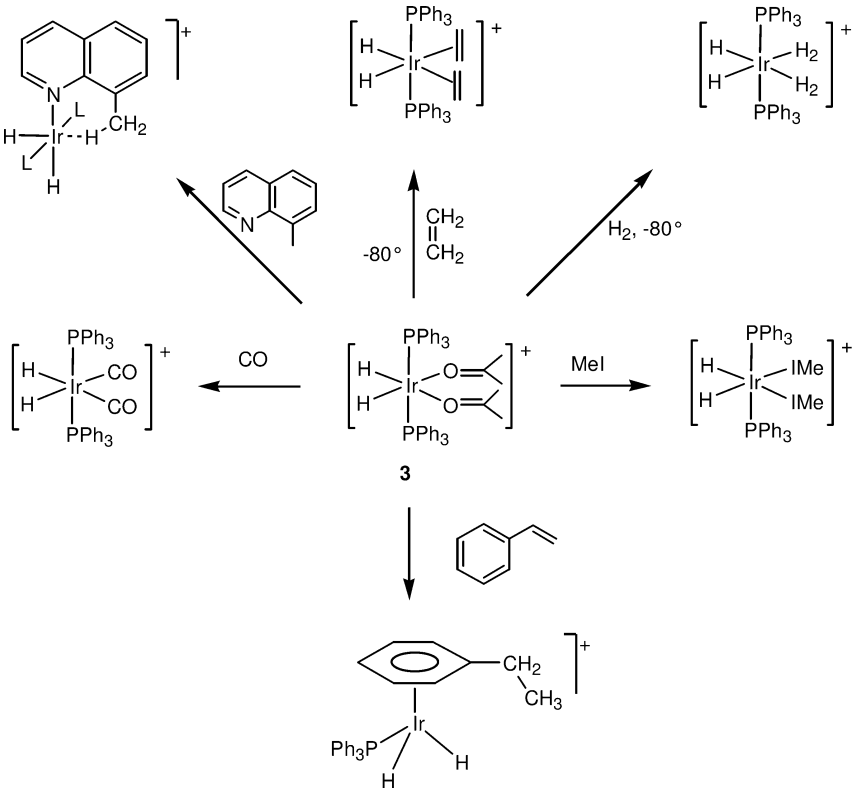

Scheme 2.1 Some reactions of $[IrH_2(Me_2CO)_2(PPh_3)_2]^+$.

by intercepting unsaturated metal-containing intermediates before they have a chance to cluster [31].

Moving to specific cases, $[Ir(cod)(PPh_3)_3]BF_4$ (**7**) yields the tris hydrogen-bridged cluster shown in Eq. (5).

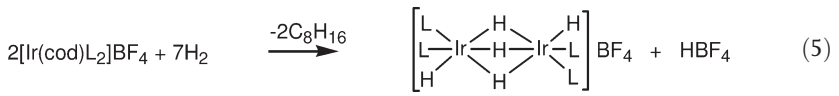

(5)

$[Ir(cod)(PCy_3)(py)]BF_4$ (**4**) forms the tri-nuclear cluster shown in Eq. (6):

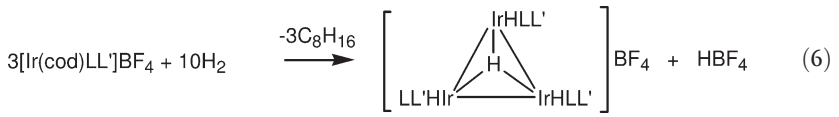

(6)

Rates of cluster formation are minimized by having the catalyst concentrations as low as possible. Successive additions of aliquots of catalyst can help in

difficult cases. None of the cluster hydrides can be converted back to catalytically active or mononuclear complexes (H_2, 1 atm, –80° to +60 °C).

The addition of H_2 at –80 °C to $[Ir(cod)(PPh_3)_2]^+$ results in complete conversion to a detectable intermediate dihydride **8** (Scheme 2.2). On warming under H_2 to about –20 °C, this produces cyclooctane and a trinuclear hydride cluster. If excess cod is present during the warming procedure, a new alkene complex (**9**) is formed. This is much more stable than species **8** and survives to room temperature. This explains why the $[Ir(cod)(PPh_3)_2]BF_4$ catalyst is ineffective for cod as substrate. The lack of reactivity of **8** can be explained by the C=C bond being coplanar with the cis hydride, allowing insertion. **9** also has C=C cis to an Ir–H, but the C=C bond is now orthogonal, forbidding insertion. **8** must be implicated in the activation of the catalyst by hydrogen. As before, catalyst **4** does not give rise to stable intermediates of similar structure, although they are assumed to be present [32].

At low temperatures (–80 °C), $[IrH_2(solvent)_2(PPh_3)_2]^+$ (**3**) also reacts with small monoolefins such as ethylene in CH_2Cl_2 solution, to give $[IrH_2(olefin)_2(PPh_3)_2]^+$. These transfer coordinated H_2 to olefin on warming to –20 °C, and so can be considered as probable intermediates in hydrogenation. Bulky alkenes such as *t*BuCH=CH produce $[IrH_2(olefin)(solvent)(PPh_3)_2]^+$.

Under similar conditions (–80 °C, CD_2Cl_2) H_2 also reacts with **3** to give bis dihydrogen complex $[IrH_2(H_2)_2(PPh_3)_2]^+$; this is detected by ^{1}H-NMR spectroscopy, including T_1 relaxation measurements. This loses H_2 at 0 °C when the H_2 is removed, to form the dinuclear hydride of Eq. (5).

These results suggest that the resting state of the catalyst is probably an $[IrH_2(L)_2(PPh_3)_2]^+$ species, where L can be solvent, substrate or H_2 depending on conditions, with L = substrate being predominant at the start of the reduction when the substrate concentration is highest.

Apparently similar Rh catalysts appear to have Rh(I) resting states of type $[Rh(PPh_3)_2L_2]^+$, which possibly accounts for their very different properties, for example their inability to reduce tri- and tetrasubstituted olefins.

Monoolefins containing coordinating groups often chelate, as in **5**. These also transfer coordinated H_2 to the C=C bond on warming to –20 °C and provide a rationalization for the directed hydrogenation mentioned earlier, in which hydrogenation occurs with almost exclusive H_2 addition from the face of the substrate that contains the coordinating group.

The presence of base such as NEt_3 in the system leads to conversion of the cationic $[IrH_2L_2(PPh_3)_2]^+$ forms to catalytically inactive neutral analogues. An ex-

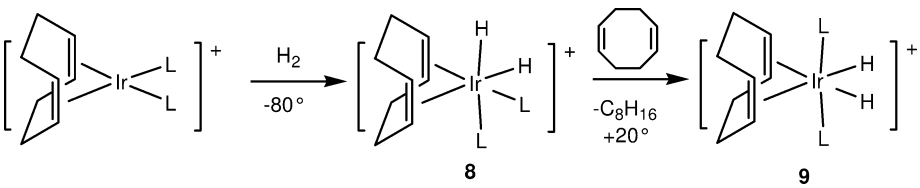

Scheme 2.2 Some intermediates in the hydrogenation of $[Ir(cod)(PPh_3)_2]BF_4$.

ample of a reaction of this type that gives an isolable neutral hydride is shown in Eq. (7):

$$[Ir(cod)(PPh_3)_2]BF_4 + NEt_3 + 6\,H_2 \rightarrow [IrH_5(PPh_3)_2] + [Et_3NH]BF_4 + C_8H_{16} \quad (7)$$

2.4 Catalysis

The above-mentioned reaction with base has relevance for catalytic chemistry in that substrates that are also bases may deactivate the catalyst by deprotonation; this can be avoided by addition of HOAc, HBF_4 or H_2SO_4 or use of the corresponding salt of the substrate. Coordinating anions react with the catalyst, again with deactivation of the catalyst, so any halide counterions should be replaced by BF_4 or PF_6. Carboxylate salts also react with the system to give inactive $[IrH_2(O_2CR)(PPh_3)_2]$, so carboxylates should be reduced in the protonated form (or as the ester). Amides bind via the carbonyl oxygen, albeit reversibly, so they can affect the rate of reaction and the stereochemistry of the product via directing effects, but are otherwise well tolerated. Esters and alcohols bind less strongly and have little effect on the rate, but still show directing effects. The Ir catalyst has been used for a wide variety of transformations in the organic synthesis of complex molecules. When attention is paid to the points mentioned above, the results have often proved very satisfactory.

2.4.1 Enantioselective Versions of the Iridium Catalyst

Despite extensive efforts, only a handful of enantioselective hydrogenations have as yet achieved the status of commercial processes. Among these is one that involves the enantiomeric reduction of imines by catalyst **6**: Syngenta's process for (*S*)-metolachlor [11]. The latter is now the largest scale industrial enantiomeric catalytic process, with annual sales of the product, Dual-Magnum®, now exceeding 10^4 tons. Imines tend to be difficult substrates because of the possibility of unproductive ligand binding via the imine lone pair. For reasons that are still not entirely clear, the Ir catalysts are less seriously affected by such binding as are the Rh analogues. It is possible that the high trans-effect of the hydrides in the Ir(III) resting state labilizes the substrate binding sites, located trans to the hydrides. Enhanced back-bonding by the third row metal may also enhance the relative stability of the η^2-bound form of the imine that leads to insertion and productive catalysis.

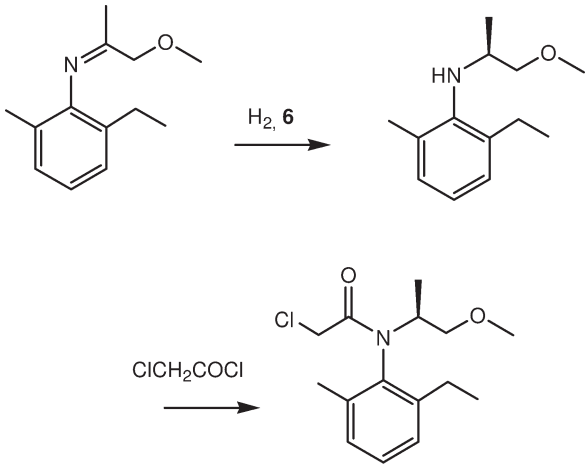

(8)

(S)-metolachlor

Bulky groups on the imine also help to disfavor η^1 binding. A ketimine is normally required for the reduction product to contain an asymmetric carbon α to nitrogen, as in the case of metolachlor (Eq. (8)). Finally, the presence of an acid of a non-coordinating anion helps to protonate the nitrogen lone pair and disfavor η^1 binding to the metal via this lone pair. The iodide additive leads to the formation of iodoiridium species that are beneficial for precatalyst **6**. Rates of up to $1.8\times10^6\ h^{-1}$ are achieved (50 °C, 80 bar) allowing substrate/catalyst ratios of 10^6. This is said to be one of the fastest homogeneous catalysts of any type known. For economic success of the process, the rate is more significant than the ee (80%), whereas in reports made by academic contributors the ee-values often dominate the discussion. A more appropriate figure of merit (FOM) [11] might be obtained by multiplying the ee by the rate; hence, an FOM value for the metolachlor catalyst system is $1.45\times10^6\ h^{-1}$.

2.4.2
Mechanism

The fastest [Ir(cod)LL′]BF_4 systems have proved difficult to study from a mechanistic standpoint because they are so active that the rates are often limited by the mass transfer of hydrogen from the gas phase into solution. This implies that efficient stirring is desirable for the most effective use of the catalyst.

Perhaps the best data are available from Brandt's study of Pfaltz's asymmetric $[Ir(cod)(P\text{-}N)]^+$ catalyst [33], bearing a chelating phosphino-oxazolidene ligand. The rate is first order in catalyst and H_2, but zero order in substrate. Taken together with the density functional theory (DFT) calculations, this is consistent with the mechanism of Scheme 2.3, shown here in its essentials only (the interested reader is urged to consult the original paper for the complete story). Surprisingly, an Ir(III)/Ir(V) cycle is proposed, rather than the M(I)/M(III) cycle

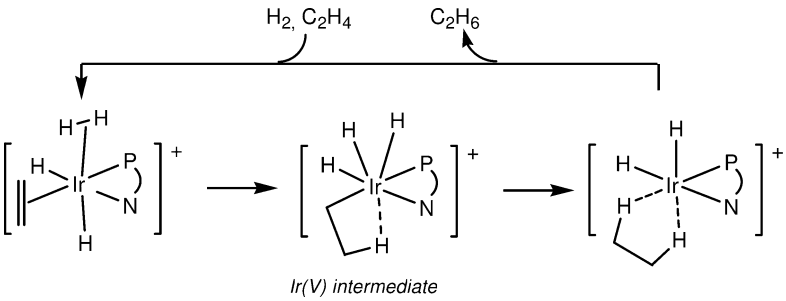

Scheme 2.3 The essential features of the Brandt mechanism for the Pfaltz catalyst [34].

that is usually considered for iridium and that is well established for rhodium. This explains the insensitivity of the iridium system to air and to oxidizing solvents, since Ir(III) and Ir(V) tend to be more stable than Ir(I) both to air and to oxidants in general. It also explains the markedly different catalytic selectivities of what are entirely analogous Rh(I) and Ir(I) catalyst precursors. It is very likely that a similar Ir(III)/Ir(V) cycle applies to typical $[(cod)IrL_2]^+$ catalysts. Related iridium species are effective alkane dehydrogenation catalysts, for which a similar reverse-hydrogenation mechanism could readily apply.

In other studies, imine reduction by $[Ir(cod)(PPh_3)_2]BF_4$ in THF has been shown to be first order in each of the catalyst, the H_2, and the substrate. Initial formation of $[IrH_2(imine)_2(PPh_3)_2]^+$ was proposed to lead to amine and $[Ir(imine)_2(PPh_3)_2]$. Oxidative addition regenerates the Ir(III) species [34].

Oro, Werner and coworkers found that alkyne reduction by the P,O chelated $[Ir(cod)(PrPr_2CH_2CH_2OMe)]BF_4$ in CH_2Cl_2 at 25 °C is also first order in each of catalyst, H_2 and substrate. Styrene is formed rapidly, whilst subsequent reduction to ethyl benzene is much slower. Stopping the reaction after the appropriate time led to essentially complete selectivity for styrene formation [35]. Surprisingly, the cod remains coordinated to Ir throughout the catalytic cycle, in contrast to every other case, where cod is proposed to be hydrogenated or the cyclooctane hydrogenation product is detected. In view of the case with which 6-alkynes rearrange to vinylidenes, such a pathway might easily be involved in 1-alkyne hydrogenation. The appropriate isotope labeling experiments seem to be carried out only rarely.

A detailed combined experimental computational mechanistic study, performed for isotope exchange in 2-dimethylamino pyridine, showed how the presence of hydrides in the Ir(III) intermediates helps to flatten the potential energy surface, accounting for the extremely high rates of exchange. In this case, carbene intermediates were also involved as a result of double C–H activation.

2.4.3 Practical Considerations

As the iridium catalysts are often somewhat thermally sensitive, synthetic procedures to prepare them should be carried out at room temperature, or below. These catalysts are normally stable to air as solids, but are somewhat air-sensitive in solution. An inert atmosphere (N_2 or Ar) is typically used for the storage of solids and to protect solutions, as the catalysts deactivate in the absence of substrate. The order of addition must be: substrate first, followed by H_2. Weakly coordinating solvents are required for optimum activity. Dichloromethane is typical, but tetrahydrofuran (THF) has also been used. $PhNO_2$, PhCl and $PhCF_3$ may also be satisfactory, but MeCN, pyridine and alcohols should be avoided. The presence of water is tolerated. Basic substrates should be neutralized by the addition of HOAc or HBF_4 in an amount equivalent to the number basic groups to be neutralized, though an excess does not seem to be detrimental. A catalyst loading of 0.1% is usually satisfactory, though very much lower loadings have been used in commercial processes. BF_4^- is the usual counterion, but PF_6^- can also be used. BPh_4^- is unsatisfactory because it tends to bind to the metal to produce catalytically inactive arene complexes. Coordinating anions such as halides are to be avoided in the substrate, but the presence of some iodide has proved beneficial in one case. In the relatively low-polarity solvents used, the complexes form tight ion pairs. In related systems, such as $[IrH_2(dipy)(PPh_3)_2]BF_4^-$, the ion pair has a definite structure, as shown by NMR spectroscopy [36]. Hydrogen is usually supplied at 1 atm pressure, although commercial applications use pressures up to 80 atm. Rates may also slow at low H_2 pressures, but the reaction still occurs. Reaction temperatures from 0 °C to 50 °C have been used successfully.

A variety of functional groups resist reduction: arene rings, NO_2, COOMe, $CONH_2$, sulfones, nitrile, and ArHal. Nitriles can bind to the metal, and the N lone pair is not effectively masked by acid addition so lower rates can be encountered if this group is present. Alkynes, alkenes, and imines are the best-studied substrates for which reduction is efficient.

The isolation of product is usually possible after evaporation of the solvent and extraction with hexane, ether, or toluene. Supported versions, for example on polystyrene grafted with PPh_2 groups, have proved unsatisfactory because the rate of deactivation is greatly enhanced under these conditions [37]. Asymmetric versions exist, but the ee-values tend to be lower than in the Rh series [38]. With acid to neutralize the basic N lone pair, imine reduction is fast. Should it be necessary to remove the catalyst from solutions in order to isolate a strictly metal-free product, a resin containing a thiol group should prove satisfactory. A thiol group in the substrate deactivates the catalyst, however.

Acknowledgments

The author thanks the U.S. Department of Energy and Johnson Matthey for the support of these studies, and also those coworkers mentioned in the references.

Abbreviations

cod	1,5-cyclooctadiene
Cy	cyclohexyl
DFT	density functional theory
ee	enantiomeric excess
FOM	figure of merit
nbd	norbornadiene
py	pyridine
THF	tetrahydrofuran

References

1 L. Vaska, D. Rhodes, *J. Am. Chem. Soc.* **1965**, *87*, 4970.
2 J.A. Osborn, F.H. Jardine, J.F. Young, G. Wilkinson, *J. Chem. Soc.* **1966**, 1711.
3 R.R. Schrock, J.A. Osborn, *J. Am. Chem. Soc.* **1976**, *98*, 2134, 2143, 4450.
4 J.R. Shapley, R.R. Schrock, J.A. Osborn, *J. Am. Chem. Soc.* **1969**, *91*, 2816.
5 R.H. Crabtree, H. Felkin, G.E. Morris, *J. Organomet. Chem.* **1977**, *141*, 205.
6 R.H. Crabtree, H. Felkin, T. Fillebeen-Khan, G.E. Morris, *J. Organomet. Chem.* **1979**, *168*, 183.
7 R.H. Crabtree, *Acc. Chem. Res.* **1979**, *12*, 331.
8 J.W. Suggs, S.D. Cox, R.H. Crabtree, J.M. Quirk, *Tetrahedron Lett.* **1981**, *22*, 303.
9 R.H. Crabtree, M.W. Davis, *Organometallics* **1983**, *2*, 681; *J. Org. Chem.* **1986**, *51*, 2655.
10 G. Stork, D.E. Kahne, *J. Am. Chem. Soc.* **1983**, *105*, 1072.
11 H.U. Blaser, H.P. Buser, K. Coers, R. Hanreich, H.P. Jalett, E. Jelsch, B. Pugin, H.D. Schneider, F. Spindler, A. Wegmann, *Chimia* **1999**, *53*, 275.
12 A. Togni, C. Breutel, A. Schnyder, F. Spindler, H. Landert, A. Tijani, *J. Am. Chem. Soc.* **1994**, *116*, 4062.
13 R.H. Crabtree, E.M. Holt, M.E. Lavin, S.M. Morehouse, *Inorg. Chem.* **1985**, *24*, 1986.
14 (a) J.S. Valsborg, L. Sorensen, C. Foged, *J. Label. Compds. Radiopharm.* **2001**, *44*, 209; (b) A.Y.L. Shu, D. Saunders, S.H. Levinson, S.W. Landvatter, A. Mahoney, S.G. Senderoff, J.F. Mack, J.R. Heys, *J. Label. Compds. Radiopharm.* **1999**, *42*, 797.
15 J.S. Chen, Y.Y. Li, Z.R. Dong, B.Z. Li, J.X. Gao, *Tetrahedron Lett.* **2004**, *45*, 8415.
16 R. Sablong, J.A. Osborn, *Tetrahedron Lett.* **1996**, *37*, 4937.
17 K. Tani, J. Onouchi, T. Yamagata, Y. Kataoka, *Chem. Lett.* **1995**, 955.
18 Y. Yamamoto, R. Fujikawa, T. Umemoto, N. Miyaura, *Tetrahedron* **2004**, *60*, 10695.
19 (a) R.H. Crabtree, C.P. Parnell, *Organometallics* **1985**, *4*, 519–523; (b) C.M. Jensen, *Chem. Commun.* **1999**, 2443; (c) P. Braunstein, Y. Chauvin, J. Nahring, A. DeCian, J. Fischer, A. Tiripicchio, F. Ugozzoli, *Organometallics* **1996**, *15*, 5551–5567; (d) F.C. Liu, A.S. Goldman, *Chem. Commun.* **1999**, 655; (e) D.M. Tellers, R.G. Bergman, *Organometallics* **2001**, *20*, 4819.

20 (a) S. P. Smidt, N. Zimmermann, M. Studer, A. Pfaltz, *Chem. Eur. J.* **2004**, *10*, 4685; (b) N. Kinoshita, K. H. Marx, K. Tanaka, K. Tsubaki, T. Kawabata, N. Yoshikai, E. Nakamura, K. Fuji, *J. Org. Chem.* **2004**, *69*, 7960 and references cited therein.

21 J. Chatt, R. G. Wilkins, *Nature* **1950**, *165*, 859; J. Chatt, L. M. Venanzi, *J. Chem. Soc.* **1957**, 4735.

22 R. H. Crabtree, *J. Organomet. Chem.* **2004**, *689*, 4083.

23 R. H. Crabtree, G. E. Morris, *J. Organomet. Chem.* **1977**, *135*, 395.

24 T. Focken, G. Raabe, C. Bolm, *Tetrahedron: Asymmetry* **2004**, *15*, 1693.

25 (a) C. Bolm, T. Focken, G. Raabe, *Tetrahedron: Asymmetry* **2003**, *14*, 1733; (b) A. C. Hillier, H. M. Lee, E. D. Stevens, S. P. Nolan, *Organometallics* **2001**, *20*, 4246.

26 (a) O. Pamies, M. Dieguez, G. Net, A. Ruiz, C. Claver, *Organometallics* **2000**, *19*, 1488; (b) X. Sava, N. Mezailles, L. Ricard, F. Mathey, P. Le Floch, *Organometallics* **1999**, *18*, 807; (c) M. Dieguez, A. Orejon, A. M. Masdeu-Bulto, R. Echarri, S. Castillon, C. Claver, A. Ruiz, *J. Chem. Soc. Dalton Trans.* **1997**, 4611; (d) C. Bianchini, L. Glendenning, M. Peruzzini, G. Purches, F. Zanobini, E. Farnetti, M. Graziani, G. Nardin, *Organometallics* **1997**, *16*, 4403.

27 R. H. Crabtree, G. G. Hlatky, C. A. Parnell, B. E. Segmuller, R. J. Uriarte, *Inorg. Chem.* **1984**, *23*, 354.

28 (a) M. J. Burk, R. H. Crabtree, E. M. Holt, *Organometallics* **1984**, *3*, 638; (b) M. J. Burk, B. Segmuller, R. H. Crabtree, *Organometallics* **1987**, *6*, 2241.

29 R. H. Crabtree, M. Lavin, *Chem. Commun.* **1985**, 1661.

30 (a) R. H. Crabtree, M. F. Mellea, J. M. Quirk, *Chem. Commun.* **1981**, 1217; (b) R. H. Crabtree, M. F. Mellea, J.M. Quirk, *J. Am. Chem. Soc.* **1984**, *106*, 2913.

31 (a) R. H. Crabtree, H. Felkin, G. E. Morris, T. J. Khan, J. A. Richards, *J. Organomet. Chem.* **1976**, *113*, C7; (b) D. F. Chodosh, R. H. Crabtree, H. Felkin, G. E. Morris, *J. Organomet. Chem.* **1978**, *161*, C67–C70; (c) D. F. Chodosh, R. H. Crabtree, H. Felkin, S. Morehouse, G. E. Morris, *Inorg. Chem.* **1982**, *21*, 1307.

32 R. H. Crabtree, H. Felkin, T. Fillebeen-Khan, G. E. Morris, *J. Organomet. Chem.* **1979**, *168*, 183.

33 (a) P. Brandt, E. Hedberg, P. G. Andersson, *Chem. Eur. J.* **2003**, *9*, 339; (b) A. Pfaltz, J. Blankenstein, R. Hilgraf, E. Hormann, S. McIntyre, F. Menges, M. Schonleber, S. P. Smidt, B. Wustenberg, N. Zimmermann, *Adv. Synth. Catal.* **2003**, *345*, 33.

34 V. Herrera, B. Munoz, V. Landaeta, N. Canudas, *J. Mol. Catal. A* **2001**, *174*, 141.

35 M. A. Esteruelas, A. M. Lopez, L. A. Oro, A. Perez, M. Schultz, H. Werner, *Organometallics* **1993**, *12*, 1823.

36 A. Macchioni; C. Zuccaccia, E. Clot, K. Gruet, R. H. Crabtree, *Organometallics* **2001**, *20*, 2367.

37 R. H. Crabtree, unpublished data.

38 P. Schnider, G. Koch, R. Pretôt, G. Z. Wang, F. M. Bohnen, C. Kruger, A. Pfaltz, *Chem. Eur. J.* **1997**, *3*, 887.

3
Ruthenium and Osmium

Robert H. Morris

3.1
Introduction

There is much current excitement and activity in the field of homogeneous hydrogenation using ruthenium catalysts. This is reflected in the recent, explosive increase in the number of research publications in this area, now rivaling those for rhodium catalysts (Fig. 3.1). Meanwhile, the price of rhodium metal has risen dramatically, becoming about ten times that of ruthenium, on a molar basis. The number of reports on the use of osmium catalysts has remained low, partly because of the higher price of osmium compounds – about ten times that of ruthenium – and partly because the activity of osmium catalysts is often lower.

During the early years of catalyst development (1960–1980), rhodium chemistry dominated the scene, led by the investigations, for example, of Wilkinson, Kagan, Osborn, and Knowles [1]. The more complex catalytic chemistry of ruthenium was slower to develop, starting with studies by Halpern [2] and Wilkinson [3] during the 1960s. This continued with an exploration of the types of ruthenium complexes that were active hydrogenation catalysts in the 1970s, as reviewed by James [4, 5]. During the 1980s the search for new chemistry for synthesis gas (CO, H_2) and coal utilization to combat petroleum shortages (the "energy crisis") shifted attention to Ru and Os complexes, and promising activity was found for the hydrogenation of difficult substrates such as arenes, simple ketones, nitriles, and esters. For both economic and scientific reasons, attention then shifted to enantioselective hydrogenations using ruthenium complexes. Japanese scientists were on the crest of this new wave, with Noyori leading the way. Noyori was awarded the Nobel prize for this work in 2001 and his lecture has subsequently been published [6, 7].

The current research areas with ruthenium chemistry include the effective asymmetric hydrogenation of other substrates such as imines and epoxides, the synthesis of more chemoselective and enantioselective catalysts, CO_2 hydrogenation and utilization, new methods for recovering and recycling homogeneous catalysts, new solvent systems, catalysis in two or three phases, and the replace-

The Handbook of Homogeneous Hydrogenation.
Edited by J.G. de Vries and C.J. Elsevier
Copyright © 2007 WILEY-VCH Verlag GmbH & Co. KGaA, Weinheim
ISBN: 978-3-527-31161-3

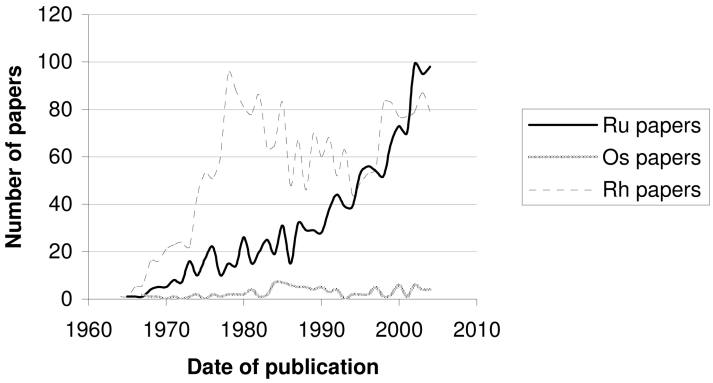

Fig. 3.1 Graphical illustration of numbers of reports per year versus date of publication. Data were obtained by searching the Chemical Abstracts Database using the term "hydrogenation catalyzed by ruthenium complexes" or osmium complexes or rhodium complexes. These are not comprehensive searches but are still representative of the activity in the field.

ment of phosphine ligands with other donors such as stable carbene and nitrogen donors.

3.2 Ruthenium

3.2.1 The First Catalysts for Alkene Hydrogenation: Mechanistic Considerations

In 1961, Halpern's group reported that the water-soluble, activated alkenes, fumaric, acrylic and maleic acid, could be catalytically hydrogenated in a solution containing chlororuthenium(II) species at 70 to 90 °C and 1 bar H_2 [2]. Interest in such chloro complexes grew out of reports about their electron-transfer behavior, a topic of interest at the time due to the extensive studies of Taube and others. Details of the hydrogenation of maleic acid are provided in Table 3.1. The kinetics of this system were thoroughly investigated by H_2 uptake measurements and spectroscopy, and the rate law was consistent with a mechanism where the alkene first binds to the metal in a pre-equilibrium followed by the turnover-limiting reaction of the alkene complex with dihydrogen where hydrogen is added *cis* on the double bond, as in Scheme 3.1.

Chatt and Hayter reported the first ruthenium and osmium hydride complexes of the type $MHCl(PR_2CH_2CH_2PR_2)_2$ in 1959, but these are not catalysts [9, 10]. Subsequently, in 1965, Wilkinson and coworkers found that the reaction of $RuCl_2(PPh_3)_3$ with hydrogen and a base gave the hydride complex $RuHCl(PPh_3)_3$, a very active hydrogenation catalyst [3]. A modern interpretation

Table 3.1 Representative conditions for the hydrogenation of alkenes.

	Precatalyst (Ru)	Substrate (S)	S:C	Solvent	$p(H_2)$ [bar]	Product	Conversion [%]	Temp [°C]	TON	TOF [h^{-1}]	Reference
1	$[RuCl_6]^{4-}$ by reduction of $[RuCl_6]^{2-}$ with $TiCl_3$	Maleic acid (*cis*-HOOCCH=CHCOOH) (0.061 M)	100	3 M HCl	1	Succinic acid	100	80	100	3	8
2	$RuHCl(PPh_3)_2$	1-Octene (1.1 M)	1400	Toluene	0.66	Heptane		25	1400	$<1\times10^{4}$ a)	12
3	$RuCl_2(PPh_3)_2$	Maleic acid	100	Dimethyl-acetamide	1	Succinic acid	100	35	100	10 b)	4
4	Ru(1,5-COD)(1,3,5-COT)	1,3,5-Cycloheptatriene	46	THF	1	Cycloheptene	90	37	46	7	39
5	$Os(\eta^2\text{-}H_2)HCl(CO)(P^iPr_3)_2$	Styrene	100	*i*PrOH	1	Ethylbenzene	100	60	100	1200	123

a) With other conditions constant as listed, the TOF varies with the alkene concentration as $TOF = 2.1\times10^4$ [octene]/(1.3+[octene]).
b) TOF varies depending on the concentration of several species; the rate law and kinetic parameters have been reported [4].

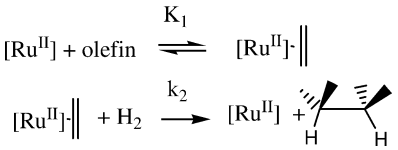

Scheme 3.1

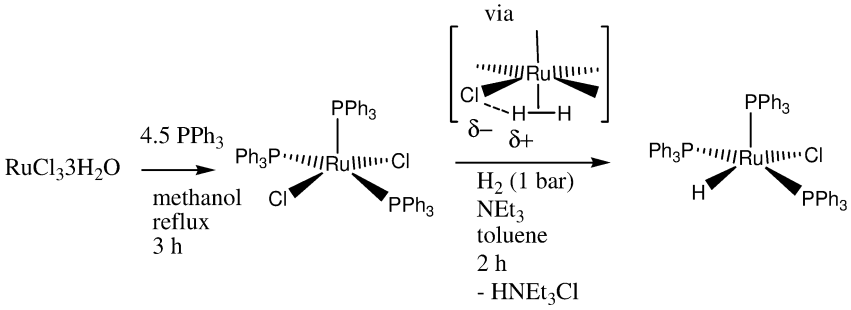

Scheme 3.2 Preparation of the alkene hydrogen catalyst $RuHCl(PPh_3)_3$.

of the formation of the hydride is that it proceeds via an acidic η^2-dihydrogen complex [11] (Scheme 3.2). This monohydride complex is an extremely active and selective catalyst for the hydrogenation of 1-alkenes in benzene at 25 °C [3, 12]. The turnover frequency (TOF) for 1-octene hydrogenation is about 10^4 h^{-1} for the mild conditions listed in Table 3.1, entry 1 (e.g., 0.66 bar H_2, 25 °C), and this changes with the alkene concentration, as listed. Disubstituted alkenes are hydrogenated about 1000-fold more slowly. The catalyst is only soluble to the extent of 10^{-4} M in toluene. It is about 20 times more active than the well-known alkene hydrogenation catalyst $RhCl(PPh_3)_3$ under similar conditions [12].

It has been a challenge to determine the mechanism of catalysis of this very oxygen-sensitive system (the current view is summarized in Scheme 3.3). $RuHCl(PPh_3)_3$ is an unusual case of a coordinatively unsaturated (5-coordinate) d^6 complex. The three bulky triphenylphosphine ligands prevent the coordination of other large ligands. In the catalytic reaction, this complex reacts with the alkene substrate to form an unstable alkyl intermediate by hydride addition to the double bond. In the turnover-limiting step, dihydrogen coordinates and becomes acidic. Proton transfer to the alkyl carbon releases the hydrogenated product with retention of configuration at carbon, and regenerates the starting hydride. The hydrogenolysis of a ruthenium–carbon bond via protonation by an acidic dihydrogen ligand *cis* to the alkyl has become a well-accepted mechanism [11, 13, 14], and would provide the observed *cis* stereochemistry of the addition of dihydrogen to the double bond. The formation of an alkyl intermediate is supported by the observation that the related complex $RuH(OC(O)CF_3)(PPh_3)_3$ reacts with ethylene in the absence of H_2 to give, reversibly, an ethyl complex $Ru(Et)(OC(O)CF_3)(PPh_3)_3$. Such a β-addition/elimination of hydride explains why such monohydride complexes are alkene isomerization catalysts. This po-

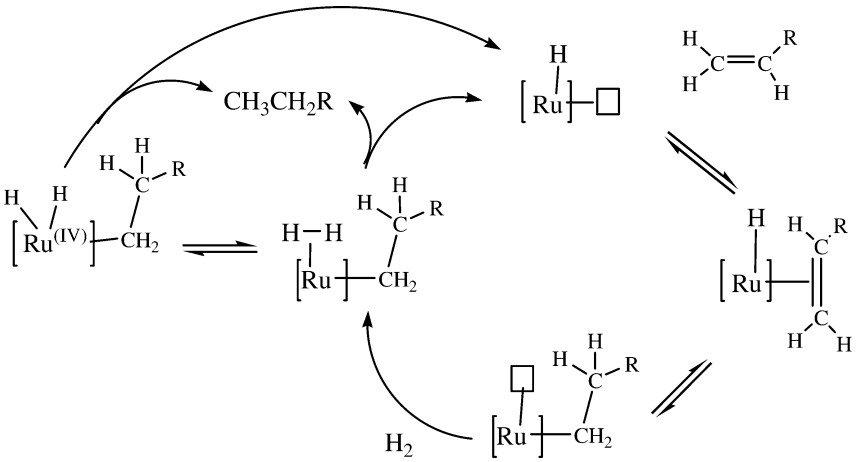

Scheme 3.3 Mechanism for the hydrogenation of 1-alkenes catalyzed by $RuHCl(PPh_3)_3$. [Ru] represents the $RuCl(PPh_3)_n$ fragment. The box represents an empty coordination site on ruthenium(II).

tentially undesirable side reaction may have been a reason why rhodium catalysts were favored over Ru(II) catalysts during the early days of these studies. Most rhodium catalysts proceed through a dihydride intermediate that hydrogenates, but does not isomerize, alkenes.

Quantitative rate measurements under a variety of conditions support such a mechanism [4, 15]. A complete kinetic analysis is available for the hydrogenation of acrylic acid derivatives using the precatalysts $RuCl_2(PPh_3)_3$ in the solvent dimethylacetamide, although the system is much less active in this more polar and coordinating solvent (e.g., entry 3, Table 3.1).

The triphenylphosphine complexes of the type $RuCl_2(PPh_3)_3$, $RuHX(PPh_3)_3$, X=Cl, O_2CR, etc., $RuH_2(PPh_3)_4$, $RuH(CO)X(PPh_3)_3$, $RuCl_2(CO)_2(PPh_3)_2$ all proved to be catalysts for a variety of reductions, although the carbonyl complexes tended to require higher temperatures [5]. For example, the last complex is a catalyst for the selective hydrogenation of 1,5,9-cyclododecatriene to cyclododecene in dimethylformamide (DMF) at 140 °C and 10 bar H_2 in the presence of PPh_3 [16]. The complex $RuCl_2(PPh_3)_3$ proved active in the hydrogenation of the C=C bond in α,β-unsaturated ketones by hydrogen transfer from formic acid or benzylalcohol [17]. Later, it was demonstrated that the addition of base greatly accelerates such transfer reactions by promoting the formation of hydride species, as reviewed elsewhere [18, 19]. Thus, $RuCl_2(PPh_3)_3$ in the presence of a base catalyzes the transfer of hydrogen to ketones or imines from *i*PrOH or formic acid [18]. Transfer hydrogenation reactions will be discussed further in Chapters 20 and 32.

3.2.2
Synthesis of Ruthenium Precatalysts and Catalysts

The modification of these precursor compounds with other ligands, including a vast array of chiral phosphorus-donors, has resulted in an ever-expanding list of useful ruthenium hydrogenation catalysts, as described in the following sections. Figure 3.2 illustrates how the PPh_3 ligands of $RuCl_2(PPh_3)_3$ are readily displaced by a wide range of ligands to produce new catalysts. The reaction with diphosphines with medium bite angles (dppb, diop, binap) (Fig. 3.3) produces complexes $RuCl_2$(diphosphine)(PPh_3) that are used as catalysts for the hydrogenation of 1,3-diketones [20], the hydrogenation of benzonitrile [21], and the hydrogenation of imines [22]. The dppb complex can be converted to the binuclear dihydrogen complex (η^2-H_2)(dppb)Ru(μ-Cl)$_3$Ru(dppb)Cl, which is a precatalyst for the hydrogenation of styrene and aldimines [23, 24]. The reactions with P-N ligands (chiral phosphinooxazolines [25] or phosphine-imines [26]) produce $RuCl_2(PPh_3)$(P-N) precatalysts for the enantioselective transfer hydrogenation of ketones. The reaction with diamines such as ethylene diamine produces $RuCl_2(PPh_3)_2$(diamine) complexes for the efficient H_2-hydrogenation of simple ketones [27] (see below). The reaction with 2 equiv. of chiral β-aminophosphine ligands produces $RuCl_2(P\text{-}NH_2)_2$, very active enantioselective hydrogenation cat-

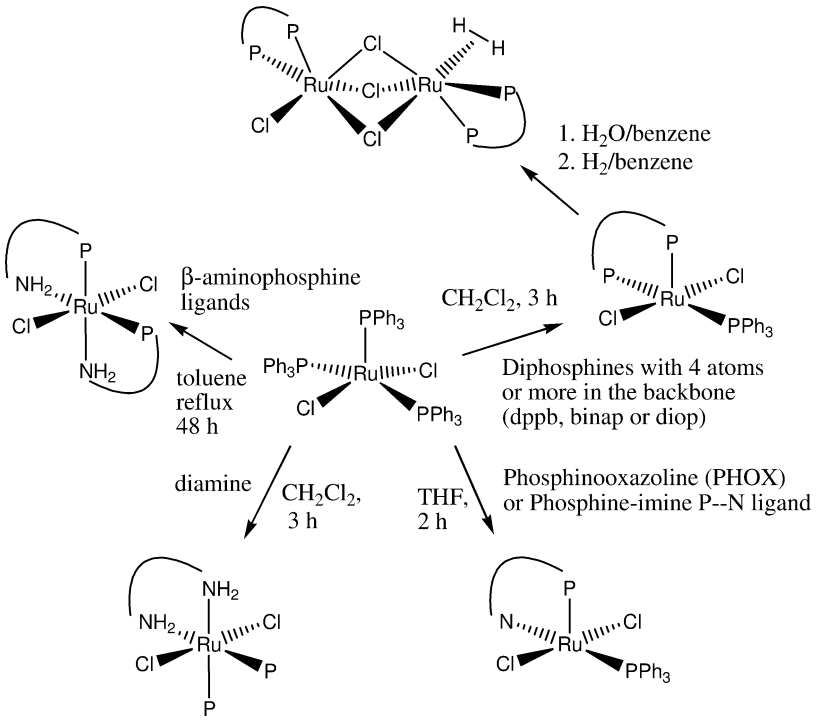

Fig. 3.2 Synthetic routes to ruthenium precatalysts starting from $RuCl_2(PPh_3)_3$.

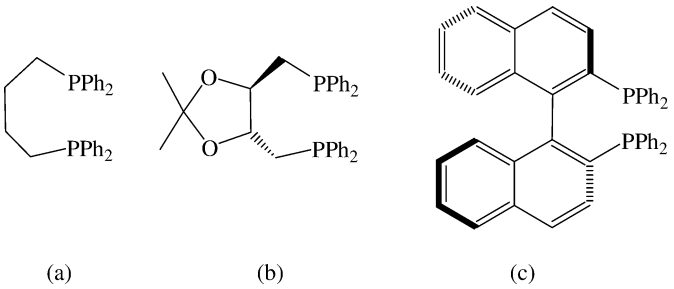

Fig. 3.3 The structures of diphosphines with four atoms in the backbone: (a) dppb; (b) (–)-(*R*,*R*)-diop; (c) (*R*)-binap.

alysts for ketones and imines [28, 29]. Finally, the reaction with water-soluble sulfonated tri-arylphosphines (not shown in Fig. 3.2) produces water-soluble complexes such as $[RuCl_2(P(C_6H_4\text{-m-}SO_3Na)_3)_2]_2$ that catalyze the H_2-hydrogenation of aldehydes in water [30] and $[RuCl_2(PPh_2(C_6H_4\text{-m-}SO_3Na))_2]_2$ which, in the presence of excess phosphine, selectively hydrogenates the C=C bond of α,β-unsaturated aldehydes at pH 3 but switches to selectively hydrogenating the aldehyde C=O at pH 9 [31].

The PPh_3 ligands in $RuHCl(PPh_3)_3$ can be displaced in a similar fashion to produce a range of analogous precatalysts such as $RuHCl(diamine)(PPh_3)_2$ and *trans*-RuHCl(diamine)(diphosphine). When the former diamine compound is activated with alkoxide base under H_2, it is an active catalyst for ketone and imine hydrogenation [32, 33], while the latter is a precatalyst for the asymmetric hydrogenation of imines and ketones under mild conditions [34, 35].

The compounds $[RuCl_2(C_6H_6)]_2$ [36] (Fig. 3.4 a), $Ru(\eta^3\text{-methylallyl})_2(COD)$ [37] (Fig. 3.4 b), COD = η^4-1,5-cyclooctadiene and $[RuCl_2(COD)]_n$ [38, 39] are also very useful starting materials that are commercially available. The complex $RuCl_2(dmso)_4$ [40] in Figure 3.4 c has relatively labile ligands. The starting material Ru(COD)(COT) [38] (Fig. 3.4 d) is a source of Ru^0 complexes and the dihydrogen complex $RuH_2(H_2)_2(PCy_3)_2$ (see Fig. 3.6). The complex Ru(COD)(COT) is also a useful catalyst for the hydrogenation of trienes to monoenes (see Table 3.1, entry 4) [39].

The structure of $[RuCl_2(COD)]_n$ is not well defined, but it is a very useful starting material to catalysts (Fig. 3.5). Its reaction with binap (see Fig. 3.3) and NEt_3 can lead to the chloride-bridged dimer $[NEt_2H_2][Ru_2Cl_5(binap)_2]$, or with sodium acetate to the excellent catalyst precursor $Ru(binap)(OAc)_2$ (see below). The former complex [41] was originally thought to be $Ru_2Cl_4(binap)_2(NEt_3)$ [42]; however, the ethyl group in NEt_3 appears to undergo an interesting fragmentation reaction. It is an excellent precatalyst for the enantioselective hydrogenation of dehydroamino acids [24, 41–43]. The reaction of the $Ru(\eta^3\text{-methylallyl})_2(COD)$ complex with enantiopure diphosphines, and then with HBr, yields catalyst solutions thought to contain a solvated form of $RuBr_2$(diphosphine) that are useful for the asymmetric hydrogenation of functionalized alkenes and ketones in-

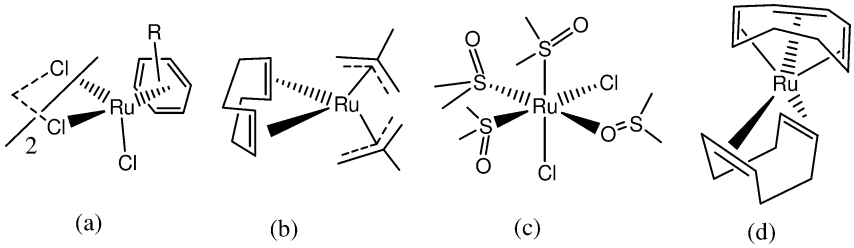

Fig. 3.4 Useful starting ruthenium complexes.

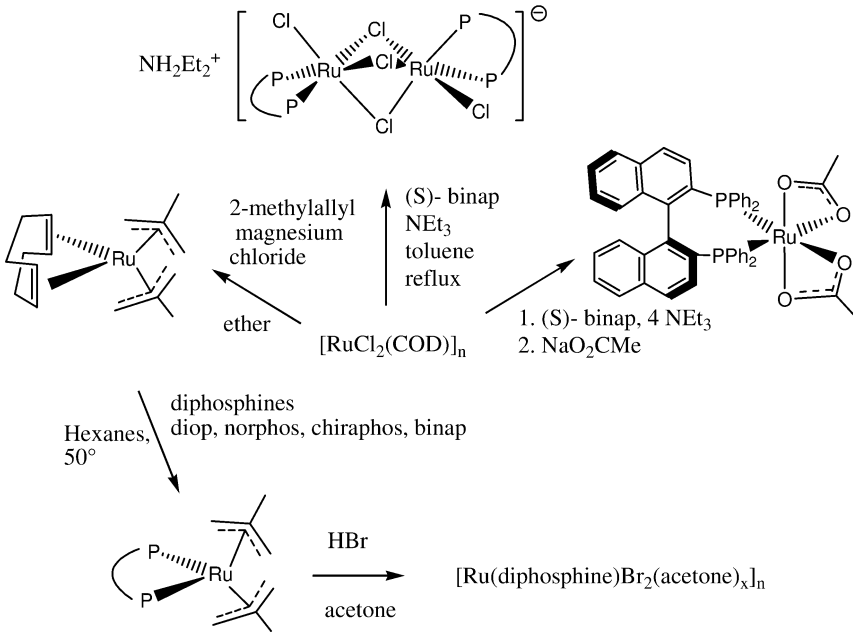

Fig. 3.5 Reactions starting with $[RuCl_2(1,5\text{-cyclooctadiene})]_n$.

cluding unsaturated acids, β-ketoesters, and allylic alcohols [44, 45]. The π-allyl complex can also be reacted with chiral diphosphines and HBF_4/BF_3 to generate a very active hydrogenation catalyst for tetrasubstituted alkenes that are precursors to fragrances [46].

3.2.3
Dihydrogen Complexes and Non-Classical Hydrogen Bonding in Catalysis

Schemes 3.2 and 3.3 show intermediates containing dihydrogen ligands with the H–H bond intact. It has only been appreciated since the discovery of the first dihydrogen complexes by Kubas and coworkers in 1984 [14] that such complexes are key intermediates in catalytic cycles [11, 13, 14].

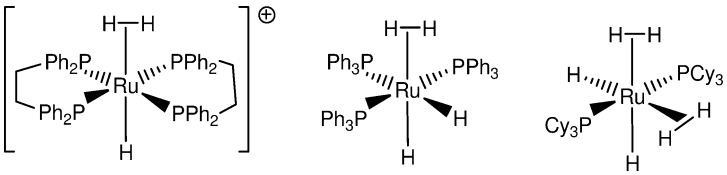

Fig. 3.6 The dihydrogen complexes $[Ru^{II}(\eta^2\text{-}H_2)H(dppe)_2]^+$, $Ru^{II}(\eta^2\text{-}H_2)(H)_2(PPh_3)_3$ and $Ru^{II}(\eta^2\text{-}H_2)_2(H)_2(PCy_3)_2$.

Before 1984, the oxidative addition of H_2 to square-planar Ru^{II} to produce octahedral Ru^{IV} ($H_2 + [Ru^{II}] \rightarrow [Ru^{IV}](H)_2$) was thought to be the turnover-limiting step in this cycle (c.f., the left equilibrium of Scheme 3.3) by analogy to rhodium systems. The discovery that the complexes $[RuH_3(diphosphine)_2]^+$ [47] and $RuH_4(PPh_3)_3$ [48] are not seven-coordinate Ru^{IV} structures but instead are octahedral, Ru^{II} complexes $[Ru(\eta^2\text{-}H_2)H(diphosphine)_2]^+$ and $Ru(\eta^2\text{-}H_2)(H)_2(PPh_3)_3$ (Fig. 3.6) supports the inner pathway of Scheme 3.3. The dihydrogen ligands in these complexes have H–H distances of 0.94 Å [49] and about 1.1 Å, respectively, longer than that of free H_2 at 0.74 Å. Even $RuH_6(PCy_3)_2$ [50, 51] retains an octahedral, Ru^{II} configuration.

Dihydrogen complexes display a wide range of acidity or, in other words, a propensity to undergo heterolytic splitting. The neutral dihydrogen complexes of Figure 3.6 have approximate pK_a^{THF} values of about 36–40 [52] (similar to cyclohexanol in THF), while the cationic complex has a value of about 14 [53]. Dicationic complexes in CH_2Cl_2 containing a π-acid ligand become very acidic; for example, *trans*-$[Ru(\eta^2\text{-}H_2)(CO)(PPh_2CH_2CH_2CH_2PPh_2)_2]^{2+}$ has a $pK^{CH_2Cl_2}$ value of –7 relative to $HPCy_3^+/PCy_3$ defined as 9 [54]. Such values are determined by measuring an equilibrium constant, usually by use of nuclear magnetic resonance (NMR), for a reaction of the dihydrogen complex with a base, the conjugate acid of which has a known pK_a value [52]. For example, the dihydrogen complex $[Ru(\eta^2\text{-}H_2)(\eta^2\text{-}C_5H_5)(dppm)]^+$, dppm = $PPh_2CH_2PPh_2$, has an approximate pK_a^{THF} of about 7.3 as determined from the equilibrium constant of Eq. (1) [52].

$$[Ru(\eta^2\text{-}H_2)(C_5H_5)(PPh_2CH_2PPh_2)]^+ + PBu_3 \rightleftharpoons RuH(C_5H_5)(PPh_2CH_2PPh_2) + HPBu_3^+ \quad (1)$$

The easy heterolytic splitting of dihydrogen in such cationic cyclopentadienyl complexes can be exploited in the hydrogenation of CO_2. Lau and coworkers found that heating solutions of $[(\eta^5,\eta^1\text{-}C_5H_4(CH_2)_3NMe_2)Ru(dppm)]BF_4$, under H_2/CO_2 (40 bar/40 bar) at 80 °C for 16 h gave formic acid in low yields (TON = 8) [55]. These authors proposed that dihydrogen undergoes heterolytic splitting into a hydride and a proton on the amine as shown in Scheme 3.4, and that the hydride and proton then react with the CO_2 to produce formic acid. This ligand-assisted splitting of dihydrogen is also observed in the enantioselective hydrogenation of tiglic acid and in the Noyori ketone hydrogenation catalysts (see below). A feature of such a reaction is that when the dihydrogen is deprotonated by the base in a

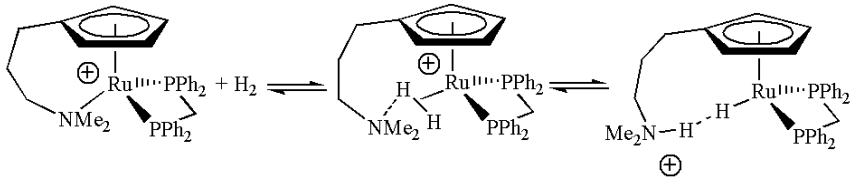

Scheme 3.4 The heterolytic splitting of dihydrogen at Ru(II) to give a hydridic-protonic bond, as proposed by Chu et al. [55] in the mechanism of the homogeneous hydrogenation of carbon dioxide.

low-dielectric solvent such as toluene or THF, the protonated base can donate a non-classical hydrogen bond (also referred to as a dihydrogen bond [56]) to the hydride, as shown in Scheme 3.4. This type of MH···HN or MH···HO hydrogen bond was discovered by Crabtree's group [58] and Morris' group [59] in 1994, and can have an energy of several kcal mol^{-1} and have an H···H distance of 1.8–2.3 Å. These are now known to be important features of mechanisms of reactions involving transition metal hydrides.

A related chiral complex $[Ru(\eta^2\text{-}H_2)(\eta^5\text{-}C_5H_5)(chiraphos)]^+$ has been used for the enantioselective outer-sphere hydrogenation of iminum salts [60].

The cationic complexes $[RuH(\eta^2\text{-}H_2)(PP_3)]BPh_4$, $PP_3 = P(CH_2CH_2PPh_2)_3$ [61] and $[RuH(L)(PMe_2Ph)_4]PF_6$, $L = PMe_2Ph$ [62] or $\eta^2\text{-}H_2$ [63], are catalysts for the selective hydrogenation of alkynes to alkenes, even in the presence of added alkenes. The PMe_2Ph compounds are sources of $[RuH(PMe_2Ph)_4]^+$ that hydrogenates terminal and internal alkynes in the presence of excess PMe_2Ph, probably as shown in Scheme 3.5. The alkyne coordinates to ruthenium and is attacked by the hydride to give an intermediate vinyl species. This is hydrogenolyzed, probably via proton transfer from an acidic η^2-dihydrogen ligand situated cis to the vinyl. However, the alternative oxidative addition of dihydrogen and reductive elimination of the hydrogenolyzed product has not been ruled out. 1-Hexyne is hydrogenated to 1-hexene with an initial TOF of 4 h^{-1} at 1 bar H_2, 30 °C. Steric effects of the phosphine ligands in $[RuHL_5]^+$ are very important. The rate is smaller, the smaller the cone angle of the phosphine used ($PMe_2Ph > PMe_3 > P(OMe)_3$) [64].

The $[RuH(\eta^2\text{-}H_2)(PP_3)]BPh_4$ complex is also thought to operate by the mechanism of Scheme 3.5, and the hydrogenolysis step is shown to be turnover-limiting [61]. A representative TOF for 94% conversion of phenylacetylene to styrene is 376 h^{-1} at 40 °C, 5 bar H_2 with a turnover number (TON) of 940 [61]. At higher pressures the TOF is reduced, probably because the dissociation of H_2 from the starting dihydrogen complex is quickly reversed. Terminal alkynes can undergo a side reaction where they couple to form other complexes that are inactive or less active as hydrogenation catalysts. This coupling is prevented in the case of the PMe_2Ph systems by adding excess PMe_2Ph. The complex $[Ru(COD)(H)(PMe_2Ph)_3]PF_6$ is, under H_2 gas, a source of $[RuH(PMe_2Ph)_3(solvent)_2]^+$; this species is a very active hydrogenation catalyst for alkynes and alkenes, although

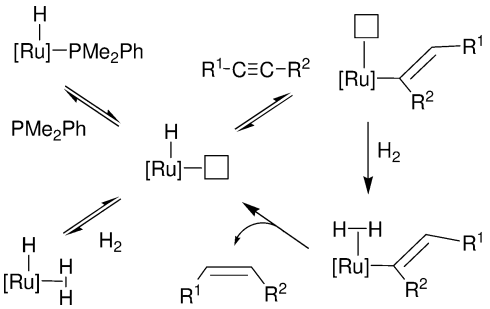

Scheme 3.5 Hydrogenation of alkynes to alkenes catalyzed by $[RuH(\eta^2\text{-}H_2)(P(CH_2CH_2PPh_2)_3)]BPh_4$ ([Ru] = $[Ru(P(CH_2CH_2PPh_2)_3)]^+$) or $[RuH(PMe_2Ph)_5]PF_6$ or $[RuH(\eta^2\text{-}H_2)(PMe_2Ph)_4]PF_6$ ([Ru] = $[Ru(PMe_2Ph)_4]^+$). The square represents a vacant site on ruthenium.

the system deactivates rapidly for terminal alkynes [64]. The rate of hydrogenation to cis alkenes increased as 1-hexyne < 2-hexyne < 3-hexyne.

3.2.4
Toward the Reduction of Simple Ketones, Nitriles, Esters and Aromatics with Monodentate Phosphine Systems

At the end of the 1970s, chemists were focusing on applying ruthenium catalysts to enantioselective hydrogenation reactions (see below), and to the hydrogenation of more difficult substrates such as simple ketones, nitriles and esters and reactions related to coal and synthesis gas (H_2/CO) chemistry. Important to the utilization of coal (and lignin [65]) is the hydrogenation of arenes and polycyclic aromatics. The very oxygen- and water-sensitive anionic hydride complexes $K[RuH_2((C_6H_4)PPh_2)(PPh_3)_2]$ and $K_2[Ru_2H_4(PPh_2)(PPh_3)_3]$ were reported by Pez and coworkers to catalyze a variety of difficult hydrogenations, including simple ketones to alcohols (e.g., acetone to *i*PrOH in toluene, 80 °C, 6 bar, TON 380, TOF 24 h^{-1}), esters activated with CF_3 groups to the alcohols (90 °C, 6 bar, toluene), nitriles to amines with selectivities up to 90% for the primary amine (acetonitrile to ethylamine in toluene, 90 °C, 6 bar, TON 150, TOF 8 h^{-1}) [66], and anthracenes to 1,2,3,4-tetrahydroanthracenes. The rate of ketone hydrogenation tripled when 18-crown-6 was added to complex the potassium.

Linn and Halpern later found that the active catalyst in the ketone and anthracene hydrogenation reactions of Pez was likely to be $Ru(\eta^2\text{-}H_2)(H)_2(PPh_3)_3$ (Fig. 3.6) [67]. For example, cyclohexanone is converted to cyclohexanol under mild conditions in toluene (see Table 3.3). The TOF depends on the substrate concentration, and the rate law for the catalytic reaction was determined to be given by Eq. (2), with $k = 1.3 \times 10^{-3}\ M^{-1}\ s^{-1}$ at 20 °C.

$$\text{Rate} = k[RuH_4(PPh_3)_3][\text{ketone}] \quad (2)$$

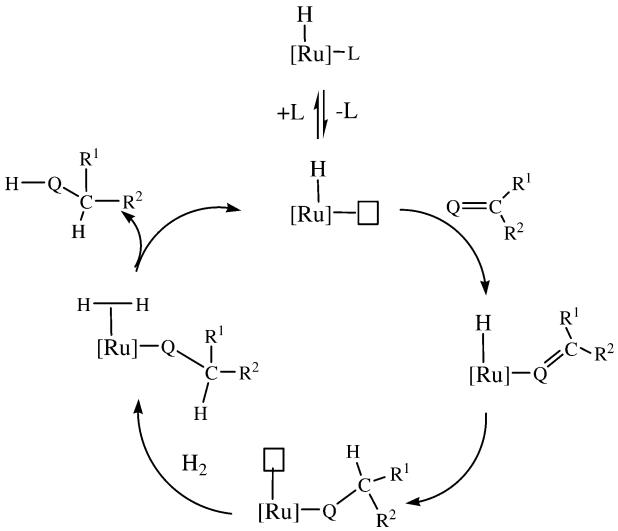

Scheme 3.6 Conventional mechanism for the H_2-hydrogenation of aldehydes, ketones (Q=O) and imines (Q=NR). Ruthenium remains as Ru^{II} throughout the cycle. The square represents a vacant site on ruthenium.

Linn and Halpern proposed a mechanism where the lack of a dihydrogen concentration dependence in the rate law of Eq. (2) was rationalized by the canceling effects of a pre-equilibrium H_2 dissociation and then rate-determining re-addition step. In this mechanism, H_2 dissociates from $RuH_4(PPh_3)_3$ when the ketone coordinates, an alkoxide intermediate $RuH(OR)(PPh_3)_3$ forms, and then H_2 re-coordinates to this intermediate in the rate-determining step. This is followed by the rapid elimination of alcohol and reaction with H_2 to reform $RuH_4(PPh_3)_3$. These steps are commonly proposed for inner-sphere hydrogenation mechanisms (HI) of carbonyl compounds (Scheme 3.6, [Ru]=$RuH(PPh_3)_3$, Q=O, L=H_2) [19]. Note the striking similarities between Schemes 3.3 and 3.6.

Directly related to the cycle shown in Scheme 3.6 is the mechanism of transfer-hydrogenation of ketones and imines catalyzed by, for example, $RuCl_2(PPh_3)_3$/base or $RuH_2(PPh_3)_4$ solutions in *i*PrOH. Here, instead of the H_2 in Scheme 3.6, the *i*PrOH solvent, formic acid or formate is the source of H^+/H^- for regeneration of the starting hydride catalyst, as shown in Scheme 3.7. In the case of dihydride catalysts, Scheme 3.8 has been proposed [18]. Note that the former mechanism involves β-hydride elimination from formate or alkoxide that maintains a Ru^{II} oxidation state, while the later mechanism involves reductive elimination of an alkoxide and hydride with a resulting reduction of the metal to Ru^0.

More recently, dihydrogen complexes have been patented for nitrile hydrogenation. For example, the complex $Ru(\eta^2\text{-}H_2)_2(H)_2(PCy_3)_2$ (Fig. 3.6) catalyzes the hydrogenation of adiponitrile to hexamethylenediamine (HMD) in toluene at 90 °C, 70 bar H_2 with TON 52, TOF 5 h^{-1} [68]. At intermediate conversions, the

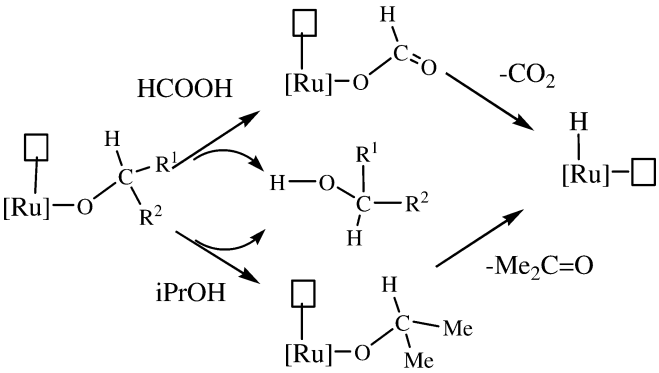

Scheme 3.7 Generation of the active hydride catalyst by hydrogen transfer from formic acid or *iso*-propanol via β-hydride elimination from formate or alkoxide intermediates. The square represents a vacant site on ruthenium.

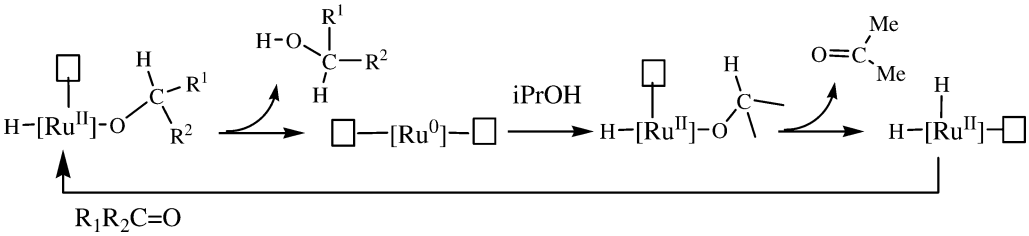

Scheme 3.8 Generation of the active dihydride catalyst by transfer hydrogenation by reductive elimination of the product to give a ruthenium(0) intermediate ([Ru] = $Ru(PPh_3)_3$).

system displays an interesting, non-statistical reduction of the two CN groups, giving a higher ratio of aminocapronitrile to HMD than expected.

Several ruthenium systems catalyze the hydrogenation of aromatic rings, and this topic is detailed in Chapter 16. An early example reported by Bennett and coworkers was that of $RuHCl(\eta^6\text{-}C_6Me_6)(PPh_3)$, which catalyzed the hydrogenation of benzene to cyclohexane at 25 °C, 1 bar H_2 [69]. Since ruthenium colloids are very active for this reaction under certain conditions, there is evidence that at least some of the reported catalysts are heterogeneous [70].

The hydrogenation of esters remains a challenge. Some recent progress has been reported by Teunissen and Elsevier [71, 72] where a mixture of $Ru(acac)_3$ and $MeC(CH_2PPh_2)_3$ was used to hydrogenate aromatic and aliphatic esters to the alcohols in MeOH at 100–120 °C with 85 bar H_2.

The use of $Ru(acac)_3$ under very high temperature (268 °C) and pressure (1300 bar of H_2/CO) in THF provides a catalyst for the hydrogenation of carbon monoxide to methanol and methyl formate [73]. The active species is derived from $Ru(CO)_5$.

3.2.5
Enantiomeric Hydrogenation of Alkenes with Bidentate Ligand Systems

More than one-half of the reports in Figure 3.1 are associated with asymmetric hydrogenation and its application in organic synthesis. The first studies from the groups of James and Bianchi in the 1970s involved Kagan's readily prepared chiral, chelating ligand (–)-diop (see Fig. 3.3), in ruthenium complexes such as $Ru_2Cl_4(diop)_3$ [74], *trans*-$RuHCl(diop)_2$ [5], and $Ru_4H_4(CO)_8(diop)_2$ [75]. The chloro complexes were moderately active and selective for the hydrogenation of acrylic acid derivatives (Table 3.2). A kinetic study revealed that the active catalyst contained only one diop ligand per ruthenium [76].

Complexes containing one binap ligand per ruthenium (Fig. 3.5) turned out to be remarkably effective for a wide range of chemical processes of industrial importance. During the 1980s, such complexes were shown to be very effective, not only for the asymmetric hydrogenation of dehydroamino acids [42] – which previously was rhodium's domain – but also of allylic alcohols [77], unsaturated acids [78], cyclic enamides [79], and functionalized ketones [80, 81] – domains where rhodium complexes were not as effective. Table 3.2 (entries 3–5) lists impressive TOF values and excellent ee-values for the products of such reactions. The catalysts were rapidly put to use in industry to prepare, for example, the perfume additive citronellol from geraniol (Table 3.2, entry 5) and alkaloids from cyclic enamides. These developments have been reviewed by Noyori and Takaya [82, 83].

Ashby and Halpern deduced the mechanism of the hydrogenation of tiglic acid catalyzed by $Ru(binap)(OAc)_2$ in MeOD [84]. This is shown in Scheme 3.9, with some modification to accommodate more recent knowledge of the heterolytic splitting of dihydrogen assisted by a ligand [57]. In the turnover-limiting addition of dihydrogen, this molecule splits into a hydride on the metal and a proton on the carboxylate ligand. The enantioselectivity of the process is directed by the binap ligand ((*S*)-binap in this case) that sets the chirality at the metal (Δ in this case) and the carbon on the C=C double bond to which the hydride adds. The difference from the classical alkene hydrogenation mechanism of Scheme 3.3 is that the alkyl intermediate is protonated by the carboxylic acid and not by a dihydrogen ligand. The evidence for this is the selective formation of (*S*)-3-deutero-2-methylbutanoic acid when MeOD is used as the solvent.

By contrast, a recent, detailed mechanism of the enantiomeric hydrogenation of α-(acylamino)acrylic esters catalyzed by $Ru((S)\text{-binap})(OAc)_2$ follows that of Scheme 3.3, where both H atoms from the dihydrogen add to the C=C double bond [85]. The high enantioselectivity of the process is produced, in part, by the chelation of the alkene substrate via the C=C double bond and by a carbonyl oxygen of the substrate [86].

Table 3.2 Representative conditions for the enantiomeric hydrogenation of alkenes.

	Precatalyst (Ru)	Substrate (S)	S:C	Solvent	$p(H_2)$ [bar]	Product	Conversion [%]	ee [%]	Time [h]	Temp. [°C]	TON	TOF [h^{-1}]	Reference
1	Ru_2Cl_4((–)-diop)$_3$	Atropic acid $H_2C{=}CPh(COOH)$ (0.2 M)	50	Dimethyl-acetamide	1	(*R*)-2-phenyl-propionic acid	100	40		60	50	8	127
2	Ru_2Cl_4((–)-diop)$_3$	2-Acetamidoacrylic acid	50	Dimethyl-acetamide	1	(*S*)-acetylalanine	100	59		60	50	1	127
3	"Ru_2Cl_4((*S*)-binap)$_2$-NEt_3" (now thought to be NEt_2H_2-[Ru_2Cl_5((*S*)-binap)$_2$])	PhHC=C(COOH) (NHCOPh)	80	EtOH/THF (NEt_3 added)	2	(*R*)-phenylalanine derivative	100	>90	<24	35	80	>3	42
4	Λ-Ru((*R*)-binap)-$(O_2CMe)_2$	Tiglic acid MeHC=C-MeCOOH (0.05 M)	500	MeOH	1	(*R*)-EtCMeH-(COOH)	100	93 (*R*)	0.3	21	500	<4000 [a)]	128
5	Δ-Ru((*S*)-binap)$(O_2CCF_3)_2$	Geraniol (5.8 M)	20000	MeOH	30	(*R*)-citronellol	100	92 (*R*)	13	20	20 000	1500	77
6	[RuH((*R*)-binap)-$(NCMe)_{3-n}$(sol.)$_n$]$^+$	(*Z*)-methyl-*R*-acetamidocinnamate (0.13 M)	50	Acetone	4	(*R*)-$PhCH_2CH$-(COOMe)(NHCOMe)	100	92 (*R*)	96	30	980	54	129

a) TOF varies with alkene concentration as TOF = 8×10^4 [alkene] h^{-1}.

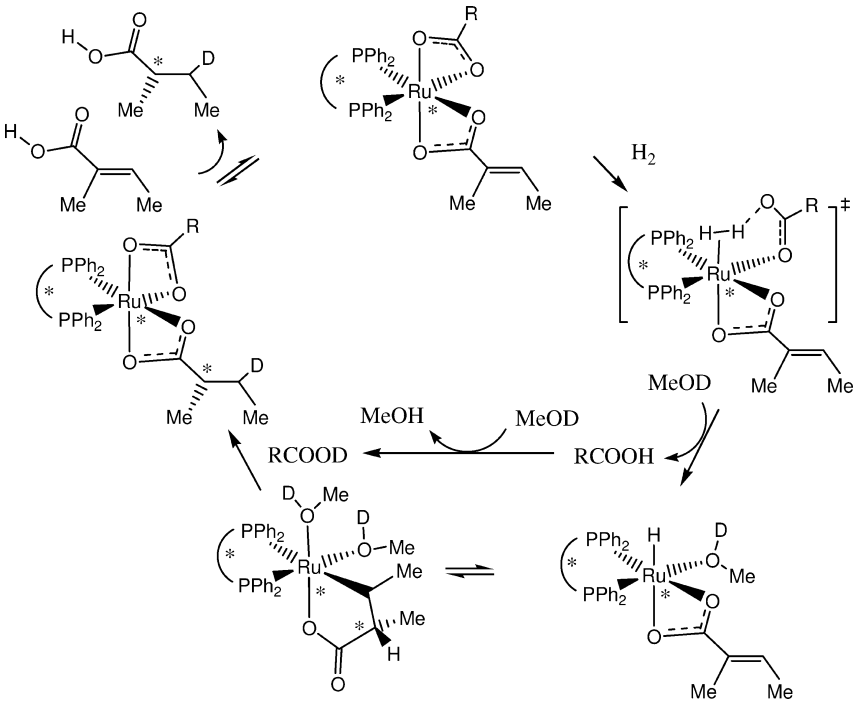

Scheme 3.9 A possible mechanism of the hydrogenation of tiglic acid catalyzed by Ru((*S*)-binap)$(OAc)_2$ (as adapted from [84]). The stereochemistry of the metal center and coordination geometries are speculative at this stage.

3.2.6
Enantiomeric Hydrogenation of Carbonyl Compounds

Complexes of the type RuX_2(diphosphine), where X is a halogen or carboxylic acid (see Fig. 3.5), are precatalysts for the hydrogenation of ketones that have a functional group such as an ester carbonyl or amino group in the vicinity of the C=O bond so that the two groups can chelate to the metal [45, 80, 81]. The mechanism is thought to involve a monohydride route (as shown in Scheme 3.6), with a step that involves an inner-sphere transfer of hydride to the carbonyl of the ketone (Scheme 3.10). Similarly, the cationic catalyst [RuH((*R*)-binap) $(NCMe)_{3\text{-}n}(sol.)_n]^+$, sol. = solvent, is very active for the hydrogenation of ketoesters (Table 3.3) and in this case, the intermediate alkoxide complex, where the hydride has added to the carbonyl group, has been completely characterized [87].

In a series of breakthroughs during the 1990s, Noyori's group discovered that simple prochiral ketones that do not contain such functional groups are hydrogenated to pure, optically active alcohols by use of extremely active ruthenium complexes containing primary or secondary amine groups [88, 89]. These cata-

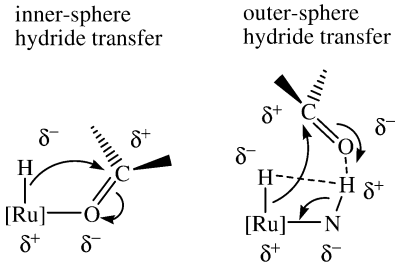

Scheme 3.10 Inner-sphere versus outer-sphere hydride transfer to the ketone.

lysts follow a fundamentally different, newly discovered mechanism, involving the outer-sphere transfer of the hydride to the carbonyl assisted by an N–H group (Scheme 3.10). Noyori has called this "metal–ligand bifunctional catalysis", where both the ruthenium and the amine are involved in the hydrogenation of the ketone and also in the dihydrogen activation (see below). First, they reported that the presence of a diamine with at least one N–H group in Ru^{II} precatalysts of the type $RuCl_2$(diamine)$(PR_3)_2$ and $RuCl_2$(diamine)(diphosphine) spectacularly increased the activity of ruthenium complexes toward the hydrogenation of simple ketones [90]. The chirality of the diamine, such as (*R,R*)-$NH_2CHPhCHPhNH_2$ ((*R,R*)-dpen), and the diphosphine, such as (*R*)-binap, must be properly matched to obtained high ee-values in the hydrogenation of a wide range of ketones [89]. The precatalysts are activated by reaction with dihydrogen and base to give the active catalyst solution. The example in Table 3.3 for the hydrogenation of acetophenone catalyzed by the $Ru(Cl)_2$((*S*)-tolbinap)((*S,S*)-dpen)/KO^{t}Bu system shows an astounding TOF of $2\times10^5\ h^{-1}$ at 30 °C, 45 bar H_2 (TOF increases as the hydrogen pressure increases). This illustrates the orders of magnitude effect of the N–H group compared to the first two entries of Table 3.3 that probably involve inner-sphere hydride transfer. Clapham et al. [19] have reviewed the mechanisms of ruthenium hydrides in catalytic hydrogenation proposed in the literature up to 2004, and have systematized them according to the inner-sphere and outer-sphere classification.

Recent mechanistic studies conducted by the present author and colleagues [32, 33, 91, 92] and Noyori and colleagues [93] suggest that a *trans*-dihydride complex and an amineamido complex are the active catalysts in the main cycle (Scheme 3.11). The dihydride forms a six-member RuH···C-O···HN ring with the aryl ketone in the transition state, while simultaneous outer-sphere hydride and proton transfer gives the alcohol and an amineamido complex with a distorted trigonal bipyramidal geometry about ruthenium. Addition of dihydrogen to the ruthenium-amido bond via an unstable dihydrogen complex regenerates the *trans*-dihydride. The amido ligand assists in the heterolytic splitting of the dihydrogen. There is evidence that the alcohol solvent also assists in this splitting process. The lack of coordination sites *cis* to the hydride means that C=C bonds cannot be hydrogenated by an inner-sphere mechanism, and so these catalysts are selective for the hydrogenation of polar bonds (C=O) or (C=N) [34] over C=C bonds.

Table 3.3 Representative conditions for the hydrogenation of carbonyl compounds including enantiomeric reactions.

	Precatalyst (Ru)	Substrate (*S*)	S:C	Solvent	$p(H_2)$ [bar]	Conversion [%]	ee [%]	Time [h]	Temp. [°C]	TOF [h^{-1}]	Reference
1	$Ru(H)_2(H_2)(PPh_3)_3$	Cyclohexanone	36	Toluene	0.6	3		1	20	1	67
2	$[RuH((R)\text{-binap})(NCMe)_{3-n}(sol.)_n]^+$	$MeOOCCMe_2C(=O)COOMe$	200	MeOH	50	100	59 (*R*)	50	50	4	87
3	$Ru(Cl)_2((S)\text{-tolbinap})((S,S)\text{-dpen})/KO^tBu$	PhMeC=O	2,400,000[a)]	*i*PrOH	45	100	80 (*R*)	48	30	2×10^5	89
4	$RuH_2((R)\text{-binap})(NH_2CMe_2CMe_2NH_2)$	PhMeC=O	400	Benzene	8	100	62–68 (*R*)	2	20	200	91
5	$OsH(NHCMe_2CMe_2NH_2)(PPh_3)_2$	PhMeC=O	346	Benzene	5	100		0.3	20	1400	125

a) Substrate: base = 100 : 1.

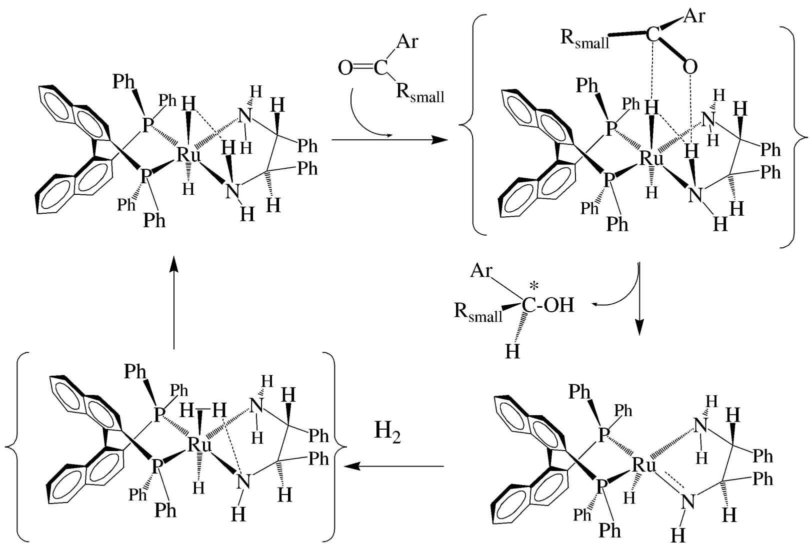

Scheme 3.11 Partial mechanistic scheme for the hydrogenation of aryl ketones to give the (*S*)-alcohol catalyzed by $RuCl_2$((*R*)-binap)((*R,R*)-dpen)/KO^tBu/H_2 as based on the observed mechanism for RuH_2((*R*)-binap)($NH_2CMe_2CMe_2NH_2$).

Noyori and coworkers reported well-defined ruthenium(II) catalyst systems of the type RuH(η^6-arene)(NH_2CHPhCHPhNTs) for the asymmetric transfer hydrogenation of ketones and imines [94]. These also act via an outer-sphere hydride transfer mechanism shown in Scheme 3.12. The hydride transfer from ruthenium and proton transfer from the amino group to the C=O bond of a ketone or C=N bond of an imine produces the alcohol or amine product, respectively. The amido complex that is produced is unreactive to H_2 (except at high pressures), but readily reacts with *i*PrOH or formate to regenerate the hydride catalyst.

An interesting catalytic ruthenium system, Ru(η^5-C_5Ar_4OH)$(CO)_2$H based on substituted cyclopentadienyl ligands was discovered by Shvo and coworkers [95–98]. This operates in a similar fashion to the Noyori system of Scheme 3.12, but transfers hydride from the ruthenium and proton from the hydroxyl group on the ring in an outer-sphere hydrogenation mechanism. The source of hydrogen can be H_2 or formic acid. Casey and coworkers have recently shown, on the basis of kinetic isotope effects, that the transfer of H^+ and H^- equivalents to the ketone for the Shvo system and the Noyori system (Scheme 3.12) is a concerted process [99, 100].

Palmer and Wills in 1999 reviewed other ruthenium catalysts for the asymmetric transfer hydrogenation of ketones and imines [101]. Gladiali and Mestroni reviewed the use of such catalysts in organic synthesis up to 1998 [102]. Review articles that include the use of ruthenium asymmetric hydrogenation catalysts cover the literature from 1981 to 1994 [103, 104], the major contributions

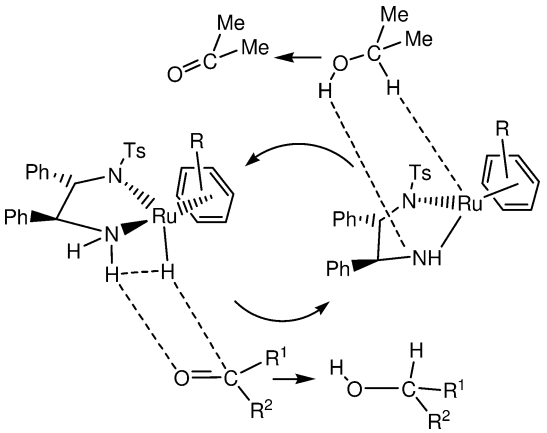

Scheme 3.12 Enantioselective hydrogenation of a ketone by transfer from *iso*-propanol catalyzed by the hydride complex RuH(η^6-arene)($NH_2CHPhCHPhNTs$) and the amido complex Ru(η^6-arene)(NHCHPhCHPhNTs) [94].

by the group of Genêt until 2003 [45], and the field from an industrial perspective to 2003 [105] (see also Chapter 25). The field of asymmetric imine hydrogenation, that includes ruthenium catalysts, has been reviewed both in 1997 [106] and 2001 [107]. The specific use of the following ligand systems in ruthenium H_2-hydrogenation catalysts has been summarized: aminophosphine-phosphinite ligands in 1998 [108], P-chirogenic diphosphine ligands in 2003 [109], chiral ferrocenyl phosphines [110], and a range of new chiral ligand systems in 2003 [111]. Much current research effort is directed at immobilizing these valuable chiral catalysts [112] or keeping them in the aqueous phase [113] so that they can be recovered and recycled. Aqueous-phase and biphasic catalysis involving ruthenium complexes is an active area that was reviewed in 2002 [31, 114].

3.3 Osmium

Complexes of Os^{II} have similar properties to those of Ru^{II}, and can often be prepared in analogous fashions. However, fewer exploratory investigations have been conducted into the starting materials for osmium chemistry than for ruthenium chemistry. In a review of the few osmium hydrogenation catalysts known up to 1995, Sanchez-Delgado et al. [115] point out that the stronger bonding of this 5d metal results in catalysts with higher thermal and oxidative stability than its 4d counterpart, ruthenium, and this – along with other interesting properties – may counter the high cost of using osmium. These authors have since discussed the mechanism of related ruthenium and osmium systems to 2000 [116]. Esteruelas and Oro have described the catalysts based on dihydro-

gen complexes of osmium [13], and specifically on the derivatives of the five-coordinate compound $OsHCl(CO)(P^iPr_3)_2$ [117].

The investigation of osmium hydrogenation catalysts began with a brief report by Vaska in 1965 that the six-coordinate trisphosphine complex $OsHCl(CO)(PPh_3)_3$ could catalyze the hydrogenation of acetylene to ethylene and ethane [118]. Activity during the 1970s and early 1980s focused mainly on the potential of osmium carbonyl clusters as catalysts for the hydrogenation of CO [119]. An interest here is whether a molecule that is made up of a well-defined multimetallic cluster could act like a metal surface found in a Fisher-Tropsch catalyst. The activity of such clusters is relatively low, even for the catalytic hydrogenation of alkenes, as reported, for example, for $Os_3(H)_2(CO)_{10}$ by Keister and Shapely in 1976 [120]. At 50 °C and 3 bar H_2, the hydrogenation of 1-hexene to *n*-hexane proceeded at a TOF of 1 h^{-1} for a TON of 31, but at the same time the isomerization of some of the hexene to internal alkenes proceeded at a TOF of 2 h^{-1} with a TON of 69. The observation of triosmium intermediates in the reaction indicated that the triangular cluster remains intact throughout the cycle. The catalyst $OsHBr(CO)(PPh_3)_3$ is somewhat less active, isomerizing hexene in the same way, but eventually hydrogenating the intermediates to hexane with a TON of about 60 and a TOF of 5 h^{-1} at 100 °C, 1 bar H_2. Under similar conditions, cyclohexene was hydrogenated to cyclohexane at a TOF of 0.5 h^{-1}, while the C=C bond of cyclohex-2-en-1-one was reduced with a TOF of 24 h^{-1} with a TON of 80. Osmium and ruthenium complexes of the type $MHX(CO)(PR_3)_3$, X = halogen, carboxylate, showed similar, low activity of about TOF 0.5 to 3 h^{-1} for the hydrogenation of propionaldehyde in toluene at 150 °C, 30 bar H_2. Acetone was hydrogenated at a slow rate at 150 °C, 65 bar H_2 [121] until the catalyst decomposed to metal, at which point the rate increased and also the solvent, toluene, was hydrogenated [122]. Several other substrates were investigated as described elsewhere [115].

The five-coordinate bisphosphine complexes $MHCl(CO)(PR_3)_2$, M = Ru, Os, $PR_3 = PMe^tBu_2$, P^iPr_3, PCy_3 and their air-stable precatalysts forms such as $OsHCl(CO)(\eta^2\text{-}O_2)(PR_3)_2$ or $RuHCl(CO)(styrene)(PR_3)_2$ are active alkene hydrogenation catalysts and ketone transfer hydrogenation catalysts in the presence of $NaBH_4$. The dihydrogen complex $OsHCl(CO)(\eta^2\text{-}H_2)(P^iPr_3)_2$, presumably a source of $OsHCl(CO)(P^iPr_3)_2$ by loss of H_2, catalyzes the H_2-hydrogenation of styrene in *i*PrOH at 60 °C, 1 bar H_2 with a TON of 100 and a TOF of 1200 h^{-1} [123]. Phenyl acetylene is hydrogenated slowly by $OsHCl(CO)(\eta^2\text{-}H_2)(P^iPr_3)_2$, first completely to styrene, because a stable styryl intermediate $OsCl(CO)(CH{=}CHPh)(P^iPr_3)_2$ ties up all of the osmium and prevents reactions with styrene (Scheme 3.13). This styryl complex is hydrogenolyzed in the turnover-limiting step. The styrene that is produced cannot be hydrogenated until this compound is consumed, after which the hydrogenation to ethylbenzene is rapid [117]. The catalyst precursor $OsHCl(CO)(\eta^2\text{-}O_2)(PCy_3)_2$ is effective, and more active than $RhCl(PPh_3)_3$, for the selective hydrogenation of the disubstituted C=C bonds instead of the C≡N triple bonds of nitrile-butadiene rubbers at 5–40 bar H_2, 130 °C in monochlorobenzene [124].

The mildest conditions for the osmium-catalyzed hydrogenation of a simple ketone (in this case acetophenone) were reported recently by Clapham and Mor-

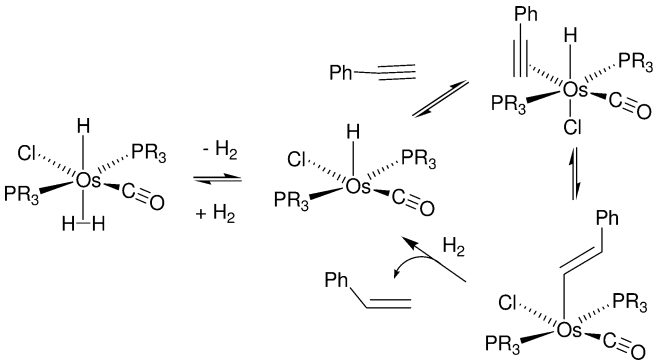

Scheme 3.13 Proposed mechanism for the hydrogenation of phenyl acetylene catalyzed by $OsHCl(CO)(P^iPr_3)_2$ [115].

ris [125] by use of the catalyst $OsH(NHCMe_2CMe_2NH_2)(PPh_3)_2$ in benzene with a maximum TOF of 1400 h^{-1} and TON of 346 at 20 °C, 5 bar H_2. This reaction is thought to proceed through a mechanism analogous to the one shown in Scheme 3.11. Here, the osmium complex appears to be as active as the ruthenium analogue.

Bianchini and coworkers [126] found a difference in the chemoselectivity between the metals Fe, Ru, and Os in the complexes $[M(H_2)H(P(CH_2CH_2PPh_2)_3)]$-$BPh_4$ in the hydrogenation of benzylideneacetone by transfer from *iso*-propanol. The Fe and Ru catalysts reduced the C=O bond to give the allyl alcohol, with Ru more active than iron (TOF 79 h^{-1} at 60 °C for Ru versus 13 h^{-1} at 80 °C for Fe), while the Os catalyst first reduced the C=O bond but then catalyzed isomerization of the allyl alcohol to give the saturated ketone (TOF 55 h^{-1} at 80 °C). The difference in reactivity was attributed to the weak binding of the alkene of the allyl alcohol to Fe and Ru relative to Os in these complexes. A variety of selectivities was noted for other unsaturated ketones, whereas unsaturated aldehydes were not hydrogenated.

In future, it will be interesting to identify a catalytic hydrogenation process that justifies the use of osmium over ruthenium, though one possibility might be a high temperature application such as that required in the hydrogenation of unsaturated rubbers.

Acknowledgment

The author wishes to thank NSERC Canada for the provision of a discovery grant.

Abbreviations

DMF	dimethylformamide
ee	enantiomeric excess
HMD	hexamethylenediamine
SCR	substrate catalyst ratio
TOF	turnover frequency
TON	turnover number

References

1 Brown, J. M., Chaloner, P. A. In: *Homogeneous Catalysis with Metal Phosphine Complexes*, Pignolet, L. H. (Ed.), Plenum Press, New York, **1983**, Chapter 4.
2 Halpern, J., Harrod, J. F., James, B. R., *J. Am. Chem. Soc.* **1961**, *83*, 753.
3 Evans, D., Osborn, J. A., Jardine, F. H., Wilkinson, G., *Nature* **1965**, *208*, 1203.
4 James, B. R., *Homogeneous Hydrogenation*, John Wiley, New York, **1973**.
5 James, B. R., *Adv. Organomet. Chem.* **1979**, *17*, 319.
6 Noyori, R., *Angew. Chem. Int. Ed. Engl.* **2002**, *41*, 2008.
7 Noyori, R., *Adv. Synth. Cat.* **2003**, *345*, 15.
8 Halpern, J., Harrod, J. F., James, B. R., *J. Am. Chem. Soc.* **1966**, *88*, 5150.
9 Chatt, J., Hayter, R. G., *Proc. Chem. Soc.* **1959**, 153.
10 Chatt, J., Hayter, R. G., *J. Chem. Soc.* **1961**, 2605.
11 Jessop, P. G., Morris, R. H., *Coord. Chem. Rev.* **1992**, *121*, 155.
12 Hallman, P. S., McGarvey, B. R., Wilkinson, G., *J. Chem. Soc. A* **1968**, 31430.
13 Esteruelas, M. A., Oro, L. A., *Chem. Rev.* **1998**, *98*, 577.
14 Kubas, G. J., *Metal Dihydrogen and Sigma-Bond Complexes*. Kluwer Academic/Plenum, New York, **2001**.
15 Rose, D., Gilbert, J. D., Richardson, R. P., Wilkinson, G., *J. Chem. Soc. A* **1969**, 2610.
16 Fahey, D. R., *J. Org. Chem.* **1973**, *38*, 80–87.
17 Blum, J., Sasson, Y., Iflah, S., *Tetrahedron Lett.* **1972**, 1015.
18 Bäckvall, J.-E., *J. Organomet. Chem.* **2002**, *652*, 105.
19 Clapham, S. E., Hadzovic, A., Morris, R. H., *Coord. Chem. Rev.* **2004**, *248*, 2201.
20 Maienza, F., Santoro, F., Spindler, F., Malan, C., Mezzetti, A., *Tetrahedron Asymm.* **2002**, *13*, 1817.
21 Joshi, A. M., MacFarlane, K. S., James, B. R., Frediani, P., *Stud. Surf. Sci. Catal.* **1992**, *73*, 143.
22 Fogg, D. E., James, B. R. In: *Catalysis of Organic Reactions of the Chemical Industry*. Dekker, **1995**, Vol. 62, pp. 435.
23 Joshi, A. M., Macfarlane, K. S., James, B. R., *J. Organomet. Chem.* **1995**, *488*, 161.
24 Macfarlane, K. S., Thorburn, I. S., Cyr, P. W., Chau, D., Rettig, S. J., James, B. R., *Inorg. Chim. Acta* **1998**, *270*, 130.
25 Langer, T., Helmchen, G., *Tetrahedron Lett.* **1996**, *37*, 1381.
26 Crochet, P., Gimeno, J., Garcia-Granda, S., Borge, J., *Organometallics* **2001**, *20*, 4369.
27 Doucet, H., Ohkuma, T., Murata, K., Yokozawa, T., Kozawa, M., Katayama, E., England, A. F., Ikariya, T., Noyori, R., *Angew. Chem. Int. Ed. Eng.* **1998**, *37*, 1703.
28 Abdur-Rashid, K., Guo, R., Lough, A. J., Morris, R. H., Song, D., *Adv. Synth. Catal.* **2005**, *347*, 571.
29 Guo, R., Lough, A. J., Morris, R. H., Song, D., *Organometallics* **2004**, *23*, 5524.
30 Fache, E., Santini, C., Senocq, F., Basset, J. M., *J. Mol. Catal.* **1992**, *72*, 337.
31 Joó, F., *Acc. Chem. Res.* **2002**, *35*, 738.
32 Abdur-Rashid, K., Lough, A. J., Morris, R. H., *Organometallics* **2000**, *19*, 2655.

33 Abbel, R., Abdur-Rashid, K., Faatz, M., Hadzovic, A., Lough, A.J., Morris, R.H., *J. Am. Chem. Soc.* **2005**, *127*, 1870.

34 Abdur-Rashid, K., Lough, A.J., Morris, R.H., *Organometallics* **2001**, *20*, 1047.

35 Guo, R., Elpelt, C., Chen, X., Song, D., Morris, R.H., *Chem. Commun.* **2005**, 3050.

36 Bennett, M.A., Smith, A.K., *J. Chem. Soc., Dalton Trans.* **1974**, 233.

37 Schrock, R.R., Johnson, B.F.G., Lewis, J., *J. Chem. Soc., Dalton Trans.* **1974**, 951.

38 Frosin, K.-M., Dahlenburg, L., *Inorg. Chim. Acta* **1990**, *167*, 83.

39 Airoldi, M., Deganello, G., Dia, G., Gennaro, G., *J. Organomet. Chem.* **1980**, *187*, 391.

40 Evans, I.P., Spencer, A., Wilkinson, G., *J. Chem. Soc., Dalton Trans.* **1973**, 204.

41 DiMichele, L., King, S.A., Douglas, A.W., *Tetrahedron Asymm.* **2003**, *14*, 3427.

42 Ikariya, T., Ishii, Y., Kawano, H., Arai, T., Saburi, M., Yoshikawa, S., Akutagawa, S., *J. Chem. Soc., Chem. Commun.* **1985**, 922.

43 Ohta, T., Tonomura, Y., Nozaki, K., Takaya, H., Mashima, K. *Organometallics* **1996**, *15*, 1521.

44 Genêt, J.-P., Pinel, C., Ratovelomanana-Vidal, V., Mallart, S., Pfister, X., Bischoff, L., Deandrade, M.C.C., Darses, S., Galopin, C., Laffitte, J.A., *Tetrahedron Asymm.* **1994**, *5*, 675.

45 Genêt, J.P., *Acc. Chem. Res.* **2003**, *36*, 908.

46 Dobbs, D.A., Vanhessche, K.P.M., Brazi, E., Rautenstrauch, V., Lenoir, J.-Y., Genêt, J.-P., Wiles, J., Bergens, S.H., *Angew. Chem. Int. Ed. Engl.* **2000**, *39*, 1992.

47 Morris, R.H., Sawyer, J.F., Shiralian, M., Zubkowski, J., *J. Am. Chem. Soc.* **1985**, *107*, 5581.

48 Crabtree, R.H., Hamilton, D.G., *J. Am. Chem. Soc.* **1986**, *108*, 3124.

49 Albinati, A., Klooster, W., Koetzle, T.F., Fortin, J.B., Ricci, J.S., Eckert, J., Fong, T.P., Lough, A.J., Morris, R.H., Golombek, A., *Inorg. Chim. Acta* **1997**, *259*, 351.

50 Arliguie, T., Chaudret, B., Morris, R.H., Sella, A., *Inorg. Chem.* **1988**, *27*, 598.

51 Sabo-Etienne, S., Chaudret, B., *Coord. Chem. Rev.* **1998**, *180*, 381.

52 Abdur-Rashid, K., Fong, T.P., Greaves, B., Gusev, D.G., Hinman, J.G., Landau, S.E., Morris, R.H., *J. Am. Chem. Soc.* **2000**, *122*, 9155.

53 Cappellani, E.P., Drouin, S.D., Jia, G., Maltby, P.A., Morris, R.H., Schweitzer, C.T., *J. Am. Chem. Soc.* **1994**, *116*, 3375.

54 Rocchini, E., Mezzetti, A., Ruegger, H., Burckhardt, U., Gramlich, V., Del Zotto, A., Martinuzzi, P., Rigo, P., *Inorg. Chem.* **1997**, *36*, 711.

55 Chu, H.S., Lau, C.P., Wong, K.Y., Wong, W.T., *Organometallics* **1998**, *17*, 2768.

56 Crabtree, R.H., Eisenstein, O., Sini, G., Peris, E., *J. Organomet. Chem.* **1998**, *567*, 7.

57 Morris, R.H. In: *Recent Advances in Hydride Chemistry.* Peruzzini, M., Poli, R. (Eds.). Elsevier, Amsterdam, **2001**, pp. 1.

58 Lee, Jr, J.C., Rheingold, A.L., Muller, B., Pregosin, P.S., Crabtree, R.H., *J. Chem. Soc. Chem. Commun.* **1994**, 1021.

59 Lough, A.J., Park, S., Ramachandran, R., Morris, R.H., *J. Am. Chem. Soc.* **1994**, *116*, 8356.

60 Guan, H.R., Iimura, M., Magee, M.P., Norton, J.R., Zhu, G., *J. Am. Chem. Soc.* **2005**, *127*, 7805.

61 Bianchini, C., Bohanna, C., Esteruelas, M.A., Frediani, P., Meli, A., Oro, L.A., Peruzzini, M., *Organometallics* **1992**, *11*, 3837.

62 Albers, M.O., Singleton, E., Viney, M.M., *J. Mol. Catal.* **1985**, *30*, 213–217.

63 Lough, A.J., Morris, R.H., Ricciuto, L., Schleis, T., *Inorg. Chim. Acta* **1998**, *270*, 238.

64 Nkosi, B.S., Coville, N.J., Albers, M.O., Gordon, C., Viney, M.M., Singleton, E., *J. Organomet. Chem.* **1990**, *386*, 111.

65 Wong, T.Y.H., Pratt, R., Leong, C.G., James, B.R., Hu, T.Q. In: *Catalysis of Organic Reactions, Chemical Industries.* Dekker, **2001**, Vol. 82, pp. 255.

66 Grey, R.A., Pez, G., Wallo, A., *J. Am. Chem. Soc.* **1981**, *103*, 7536.

67 Linn, D.E., Halpern, J., *J. Am. Chem. Soc.* **1987**, *109*, 2969.

68 Beatty, R.P., Paciello, R.A. **1998**, US Patent 5726334.

69 Bennett, M.A., Huang, T.-N., Smith, A.K., Turney, T.W., *J. Chem. Soc., Chem. Commun.* **1978**, 582.
70 Widegren, J.A., Bennett, M.A., Finke, R.G., *J. Am. Chem. Soc.* **2003**, *125*, 10301.
71 Teunissen, H.T., Elsevier, C., *J. Chem. Commun.* **1997**, 667.
72 Teunissen, H.T., Elsevier, C., *J. Chem. Commun.* **1998**, 1367.
73 Bradley, J.S., *J. Am. Chem. Soc.* **1979**, *101*, 7419.
74 James, B.R., Wang, D.K.W., Voigt, R.F., *J. Chem. Soc., Chem. Commun.* **1975**, 574.
75 Botteghi, C., Gladiali, S., Bianchi, M., Matteoli, U., Frediani, P., Vergamini, P.G., Benedetti, E., *J. Organomet. Chem.* **1977**, *140*, 221.
76 James, B.R., Wang, D.K.W., *Can. J. Chem.* **1980**, *58*, 245.
77 Takaya, H., Ohta, T., Sayo, N., Kumobayashi, H., Akutagawa, S., Inoue, S., Kasahara, I., Noyori, R., *J. Am. Chem. Soc.* **1987**, *109*, 1596.
78 Ohta, T., Takaya, H., Kitamura, M., Nagai, K., Noyori, R., *J. Org. Chem.* **1987**, *52*, 3174.
79 Noyori, R., Ohta, M., Hsiao, Y., Kitamura, M., Ohta, T., Takaya, H., *J. Am. Chem. Soc.* **1986**, *108*, 7117.
80 Kitamura, M., Ohkuma, T., Inoue, S.-I., Sayo, N., Kumobayashi, H., Akutagawa, S., Ohta, T., Takaya, H., Noyori, R., *J. Am. Chem. Soc.* **1988**, *110*, 629.
81 Noyori, R., Ohkuma, T., Kitamura, M., Takaya, H., Sayo, N., Kumobayashi, H., Akutagawa, S., *J. Am. Chem. Soc.* **1987**, *109*, 5856.
82 Noyori, R., Takaya, H., *Acc. Chem. Res.* **1990**, *23*, 345.
83 Takaya, H., Ohta, T., Mashima, K. In: *Homogeneous Transition Metal Catalyzed Reactions.* Moser, W.R., Slocum, D.W. (Eds.), American Chemical Society, Washington, **1992**, Chapter 8.
84 Ashby, M.T., Halpern, J., *J. Am. Chem. Soc.* **1991**, *113*, 589.
85 Kitamura, M., Tsukamoto, M., Bessho, Y., Yoshimura, M., Kobs, U., Widhalm, M., Noyori, R., *J. Am. Chem. Soc.* **2002**, *124*, 6649.
86 Wiles, J.A., Bergens, S.H., *Organometallics* **1999**, *18*, 3709.
87 Daley, C.J.A., Bergens, S.H., *J. Am. Chem. Soc.* **2002**, *124*, 3680.
88 Noyori, R., Hashiguchi, S., *Acc. Chem. Res.* **1997**, *30*, 97.
89 Noyori, R., Ohkuma, T., *Angew. Chem. Int. Ed. Engl.* **2001**, *40*, 40.
90 Ohkuma, T., Ooka, H., Hashiguchi, S., Ikariya, T., Noyori, R., *J. Am. Chem. Soc.* **1995**, *117*, 2675.
91 Abdur-Rashid, K., Clapham, S.E., Hadzovic, A., Harvey, J.N., Lough, A.J., Morris, R.H., *J. Am. Chem. Soc.* **2002**, *124*, 15104.
92 Abdur-Rashid, K., Faatz, M., Lough, A.J., Morris, R.H., *J. Am. Chem. Soc.* **2001**, *123*, 7473.
93 Sandoval, C.A., Ohkuma, T., Muñiz, K., Noyori, R., *J. Am. Chem. Soc.* **2003**, *125*, 13490.
94 Haack, K.J., Hashiguchi, S., Fujii, A., Ikariya, T., Noyori, R., *Angew. Chem. Int. Ed. Engl.* **1997**, *36*, 285.
95 Shvo, Y., Czarkie, D., Rahamim, Y., Chodosh, D.F., *J. Am. Chem. Soc.* **1986**, *108*, 7400.
96 Abed, M., Goldberg, I., Stein, Z., Shvo, Y., *Organometallics* **1988**, *7*, 2054.
97 Menashe, N., Shvo, Y., *Organometallics* **1991**, *10*, 3885.
98 Menashe, N., Salant, E., Shvo, Y., *J. Organomet. Chem.* **1996**, *514*, 97.
99 Casey, C.P., Johnson, J.B., *J. Org. Chem.* **2003**, *68*, 1998.
100 Casey, C.P., Singer, S.W., Powell, D.R., Hayashi, R.K., Kavana, M., *J. Am. Chem. Soc.* **2001**, *123*, 1090.
101 Palmer, M.J., Wills, M., *Tetrahedron Asymm.* **1999**, *10*, 2045.
102 Gladiali, S., Mestroni, G., *Transition Metals in Organic Synthesis.* Beller, M., Bolm, C. (Eds.), Wiley-VCH, Weinheim, **1998**, Volume 2, pp. 97.
103 Trost, B.M., Fleming, I., *Comprehensive Organic Synthesis: Selectivity, Strategy, and Efficiency in Modern Organic Chemistry.* Pergamon Press, New York, **1991**, Vol. 8.
104 Ojima, I., Eguchi, M., Tzamarioudaki, M. In: *Comprehensive Organometallic Chemistry.* Abel, E.W., Stone, F.G.A.,

Wilkinson, G. (Eds.), Pergamon, New York, **1995**, Vol. 12, pp. 9.
105 Blaser, H. U., Malan, C., Pugin, B., Spindler, F., Steiner, H., Studer, M., *Adv. Synth. Catal.* **2003**, *345*, 103.
106 James, B. R., *Catalysis Today* **1997**, *37*, 209.
107 Dai, X., Qin, Z., *Prog. Chem.* **2001**, *13*, 183.
108 Agbossou, F., Carpentier, J. F., Hapiot, F., Suisse, I., Mortreux, A., *Coord. Chem. Rev.* **1998**, *180*, 1615.
109 Crepy, K. V. L., Imamoto, T., *Adv. Synth. Catal.* **2003**, *345*, 79.
110 Barbaro, P., Bianchini, C., Giambastiani, G., Parisel, S. L., *Coord. Chem. Rev.* **2004**, *248*, 2131.
111 Tang, W., Zhang, X., *Chem. Rev.* **2003**, *103*, 3029.
112 Bianchini, C., Barbaro, P., *Top. Catal.* **2002**, *19*, 17.
113 Sinou, D., *Adv. Synth. Catal.* **2002**, *344*, 221.
114 Dwars, T., Oehme, G., *Adv. Synth. Catal.* **2002**, *344*, 239.
115 Sanchez-Delgado, R. A., Rosales, M., Esteruelas, M. A., Oro, L. A., *J. Mol. Cat. A* **1995**, *96*, 231.
116 Sanchez-Delgado, R. A., Rosales, M., *Coord. Chem. Rev.* **2000**, *196*, 249.
117 Esteruelas, M. A., Oro, L. A., *Adv. Organomet. Chem.* **2001**, *47*, 1.
118 Vaska, L., *Inorg. Nucl. Chem. Lett.* **1965**, *1*, 89.
119 Choi, H. W., Muetterties, E. L., *Inorg. Chem.* **1981**, *20*, 2664.
120 Keister, J. B., Shapely, J. R., *J. Am. Chem. Soc.* **1976**, *98*, 1056.
121 Sanchez-Delgado, R. A., Andriollo, A., Gonzalez, E., Valencia, N., Leon, V., Espidel, J., *J. Chem. Soc., Dalton Trans.* **1985**, 1859.
122 Sanchez-Delgado, R. A., Valencia, N., Marquez-Silva, R., Andriollo, A., Medina, M., *Inorg. Chem.* **1986**, *25*, 1106.
123 Esteruelas, M. A., Sola, E., Oro, L. A., Meyer, U., Werner, H., *Angew. Chem.* **1988**, *100*, 1621.
124 Parent, J. S., McManus, N. T., Rempel, G. L., *J. Appl. Polymer Sci.* **2001**, *79*, 1618.
125 Clapham, S. E., Morris, R. H., *Organometallics* **2005**, *24*, 479.
126 Bianchini, C., Farnetti, E., Graziani, M., Peruzzini, M., Polo, A., *Organometallics* **1993**, *12*, 3753.
127 James, B. R., McMillan, R. S., Morris, R. H., Wang, D. K. W. In: *Advances in Chemistry Series*. Bau, R. (Ed.), American Chemical Society, Washington, DC, **1978**, Vol. 167, pp. 122.
128 Ashby, M. T., Halpern, J., *J. Am. Chem. Soc.* **1991**, *113*, 589.
129 Wiles, J. A., Bergens, S. H., *Organometallics* **1998**, *17*, 2228.

4
Palladium and Platinum

Paolo Pelagatti

4.1
Introduction

Studies of homogeneous hydrogenation catalyzed by soluble palladium (Pd) or platinum (Pt) catalysts first began when the process of heterogeneous hydrogenation was already known. The reduction of $[Pt(C_2H_4)Cl_2]_2$ with H_2 to produce Pt(0), C_2H_6 and HCl was first reported in 1954, and can be considered as one of the events to have opened up the field of homogeneous hydrogenation [1]. The homogeneity of the reaction appeared to be dependent upon the temperature and on the amount of hydrogen employed [2]. The discovery that H_2 could be homogeneously activated by Pd(II) was first observed by Halpern's group in the 1950s and 1960s, as part of a series of hydrometallurgical investigations involving the precipitation of metals from solution with H_2 [3]. The first reports relating to homogeneous catalysts appeared in the literature during the 1960s, their aim being mainly to identify the reaction mechanisms of heterogeneous hydrogenations [2]. The use of Pd(II) as a hydrogenation catalyst was retarded by its instability under H_2 atmosphere, as demonstrated during alkene isomerization reactions [4, 5], in favor of the more stable catalyst, Pt(II). However, interest towards Pd- and Pt-catalyzed homogeneous reductions of unsaturated functions was renewed when it was found that the selectivities were usually higher than those obtained under heterogeneous conditions [6]. Today, the use of soluble Pd and Pt hydrogenating catalysts remains the subject of intense academic and industrial research, as evidenced by the numerous publications on the subject, and the many deposited patents.

An analysis of the most significant homogeneous catalytic systems reported in the literature reveals a structural variety for Pd which is not found for Pt. In fact, although in most cases Pd is incorporated into the (pre)catalyst as divalent ion, active Pd(0)-catalysts have also been reported. By contrast, Pt(0)-catalysts are a rarity. Moreover, Pd complexes containing mono-, di-, tri-, and even tetradentate ligands have found application as hydrogenation catalysts, and often their activity and selectivity is governed by the steric and electronic features of

The Handbook of Homogeneous Hydrogenation.
Edited by J.G. de Vries and C.J. Elsevier
Copyright © 2007 WILEY-VCH Verlag GmbH & Co. KGaA, Weinheim
ISBN: 978-3-527-31161-3

the chelating systems. The most thoroughly studied Pt-catalysts are instead simple phosphine-containing Pt(II) complexes, usually activated with stannous chloride, $SnCl_2$. Tin(II) salts have instead found scarce application with Pd, and in some cases have turned out to be poisons of the catalytic processes. Another important aspect which differentiates the two metals has practical consequences: the well-known higher reactivity of Pd with respect to Pt [7] allows the Pd-promoted hydrogenations to be carried out under much milder conditions (room temperature and atmospheric pressure of H_2) than those usually required for activating Pt-catalysts. However, Pd-based catalysts are usually more subject to decomposition than are Pt-based catalysts.

As unsaturated C–C bonds have certainly been the most thoroughly investigated substrates, this chapter focuses on the hydrogenation of alkenes and alkynes, and the hydrogenation of other functional groups such as nitro, nitrile, and carbonyl will be excluded. Particular emphasis will be given to those catalytic systems for which a mechanistic study has been carried out. Where possible, a brief discussion of the homogeneous character of the catalytic processes will be given.

4.2 Palladium

4.2.1 Phosphorus-Containing Catalysts

In 1963, in a report which focused mainly on the use of first-row transition-metal catalysts combined with organoaluminum compounds, the hydrogenating activity of the catalytic system $[PdCl_2(Pn\text{-}Bu_3)_2/Al(i\text{-}Bu)_3]$ towards 1-hexene under mild conditions (heptane, 25 °C, 3.5–3.7 atm of H_2 pressure, Pd : alkene ratio ~1 : 80) was briefly addressed [8]. After 19 h of reaction, a 25.5% conversion to hexane was obtained (TOF ~1.1 h^{-1}). In 1967, several Pd(II) complexes of the general formula $[PdX_2(Ph_3Q)_2]$ (Q = P or As, X = Cl or CN) were used to homogeneously hydrogenate soybean oil Me-ester in the presence or absence of co-catalysts, such as $SnCl_2$ or $GeCl_2$ [9]. *Cis-trans* double-bond isomerization, migration of isolated double bonds to conjugated dienes, and selective hydrogenation of polyenes to monoenes without further reduction were observed. The most active system was found to be $PdCl_2(PPh_3)_2/SnCl_2 \cdot 2H_2O$ which, after 3 h, converted both linoleate and linolenate to monoenes almost completely, but not at all to stearate (benzene/methanol, 90 °C, 39.1 atm H_2 pressure); Me-oleate was selectively converted to the corresponding monoene under the same experimental conditions and reaction time. In both cases high catalyst loadings were applied. Traces of Pd black were observed at the end of the reaction. Lowering of the temperature precluded the formation of Pd black, but slowed down the hydrogenations.

By the end of the 1970s, $PdCl_2(PPh_3)_2$ was being used to hydrogenate 1,5-cyclooctadiene [10]. The substrate isomerization to 1,3-cyclooctadiene preceded its

reduction to cyclooctene. For example, after 5 h of reaction (CH_2Cl_2/MeOH, 90 °C, 51 atm H_2 pressure, alkene : Pd ratio = 1 : 15) the products distribution was 4% of 1,3-cyclooctadiene, 93% of cyclooctene, and 3% of cyclooctane. The reactivity and selectivity remained quite high up to an alkene : Pd ratio of 250. However, under the same experimental conditions, $SnCl_2$ proved to be a poison of the reaction. The π-allylic reaction intermediate [PdCl(π-cyclooctenyl)(PPh_3)] was isolated from the reactant solutions and resulted in a much more active catalyst than its precursor $PdCl_2(PPh_3)_2$, although it was less selective. After 3 h of reaction, under 34 atm H_2 pressure, the product distribution was 10% of 1,3-cyclooctadiene, 83% of cyclooctene, and 6% of cyclooctane. During the same period, other π-allyl-Pd(II) complexes that were effective in the selective hydrogenation of allene to propene (THF, 15 °C, 1 atm total pressure) were reported [11]. Turnover numbers (TONs) ranging from 18 to 75 were obtained with [(η^3-allyl)-PdCl(PR_3)] (allyl = C_3H_5, 1-Me-C_3H_4, 2-Me-C_3H_4; R = PPh_3, PPh_2Me, Pt-Bu_3) or [Pd(η^3-$C_3H_5)_2$] ([Pd(η^3-$C_3H_5)_2$] was used at 0 °C). The TOFs ranged from 0.19 to 75 h^{-1}, the highest being obtained with the bis-allene complex [Pd($C_3H_5)_2$], though this was significantly decomposed. Since the stability of the complexes under H_2 atmosphere were shown to differ, a comparison of the catalytic results was possible only for the strictly similar allyl-complexes [(η^3-C_3H_5)PdCl(PPh_3)], [(η^3-1-Me-C_3H_4)PdCl(PPh_3)] and [(η^3-2-Me-C_3H_4)PdCl(PPh_3)]. These showed similar turnover frequency (TOF) values of 0.21, 0.23, and 0.19 h^{-1}, respectively, and comparable stability. The same complexes slowly catalyzed the selective hydrogenation of 1,5-cyclooctadiene and 1,3-cyclooctadiene to the corresponding monoenes (Pd : diene ratio = 1 : 31) [12]; 1,5-cyclooctadiene was first isomerized to 1,3-cyclooctadiene and then hydrogenated to cyclooctene. In several cases, however, Pd-black was detected at the end of the catalytic reactions.

The catalytic activity of other Pd-complexes containing mono- or chelating phosphines was studied by Stern and Maples [13]. In the hydrogenation of butadiene (toluene, r.t., 6.8 atm H_2 pressure), the dinuclear Pd(0) complex $Pd_2(dppm)_3$ showed the highest TOF (0.25 h^{-1}), leading to an excess of 1-butene with respect to *cis*- or *trans*-2-butene. (Since the complex was handled in plain air, caution must be taken about its nature.) The Pd(II) complexes [$PdCl_2$(dppm)], [$PdCl_2$(1,1-dppe)] and [$PdCl_2$(dppe)], although not completely soluble in toluene, also promoted the hydrogenation, albeit with lower TOF values and selectivities. $PdCl_2(PhCN)_2$ was practically inactive. The hydrogenating activity of $Pd_2(dppm)_3$ towards a variety of other unsaturated substrates (alkenes, dienes, trienes, and acetylenes) was reported in the same work. The nature of the substrate appeared to regulate the catalyst activity, in the sense that complexing substrates led to faster reactions. For example, the TOFs varied in the following order: 0.012 h^{-1} (1,9-decadiene), 0.014 h^{-1} (1,5-hexadiene), 0.16 h^{-1} (1,4-pentadiene), 0.25 h^{-1} (butadiene), 0.44 h^{-1} (*cis*-1,3-pentadiene), 0.58 h^{-1} (1,3-cyclohexadiene), 0.80 h^{-1} (*trans*-1,3-pentadiene), and 1.3 h^{-1} (norbornadiene). Studies on the catalyst pretreatment showed that a dissociation equilibrium in solution is necessary in order to enable a coordinatively unsaturated species to bind the substrate, according to Eqs. (1) and (2) (L = ligand, S = solvent, ol = alkene).

$$PdL_4 + S \leftrightarrow PdL_3S + L \quad (1)$$

$$PdL_3S + ol \leftrightarrow PdL_3ol + S \quad (2)$$

Treatment of the precatalytic solutions with oxygen brought about a remarkable enhancement of the catalysis, and an improved selectivity. The effect of oxygen was tentatively rationalized in terms of oxidation of a phosphine ligand with subsequent dissociation of the so-formed phosphine oxide or, alternatively, with formation of oxygen complexes able to promote the substrate/hydrogen activation via hydroperoxide intermediates or the formation of either hydrogen or substrate complexes. The effect of the activating oxygen pretreatment was, at least partially, clarified by Alper et al. for the dinuclear Pd(II) complex $[\{(t\text{-Bu})_2HP\}PdP(t\text{-Bu})_2]_2$. This alone was a completely inactive hydrogenating catalyst towards α,β-unsaturated compounds. Once exposed to oxygen for some minutes, it transformed into the mononuclear species $[Pd\{O_2P(t\text{-Bu})_2\}\{OP(t\text{-Bu})_2\}\{OHP(t\text{-Bu})_2\}]$ [14] containing a η^2-phosphinate ligand. This species was an active pre-catalyst for the selective reduction of the double C–C bond of several α,β-unsaturated ketones and aldehydes under mild conditions (THF, r.t., 1 atm H_2 pressure, 1–2% catalyst loading) [15]. A TOF $\approx 5\ h^{-1}$ was achieved in the hydrogenation of 3-nonen-2-one. The same system was applied in the chemoselective hydrogenation of several substrates, such as α,β-unsaturated sulfones and phosphonates [16], simple and functionalized conjugated dienes [17], and vinyl epoxides [18]. In all cases good catalytic activities and selectivities were obtained (TOFs up to $100\ h^{-1}$).

In recent years, a number of other polynuclear complexes have been investigated in addition to $[Pd_2(dppm)_3]$. In 1989, Eisenberg reported that the reaction between $Pd_2Cl_2(dppm)_2$ with an excess of $NaBH_4$ led to the formation of a palladium hydride species of approximate stoichiometry $[Pd_2H_x(dppm)_2]$ [19]. This hydride was effective in small-scale hydrogenations of alkynes and alkenes. Parahydrogen-induced polarization was observed in styrene formed during the hydrogenation of phenylacetylene, indicating that the transfer of hydrogen to the substrate occurred pairwise and rapidly relative to proton relaxation. In 1998, the structure of $[Pd_2H_x(dppm)_2]$ was inferred by using a variety of spectroscopic tools [20], and revealed to be a cluster of formula $[Pd_4(dppm)_4(H_2)]^{2+}$. The hydrogenating capability of this material was further investigated quite recently [21]. The $[Pd_4(dppm)_4(H_2)](BPh_4)_2$ cluster catalyzed the homogeneous hydrogenation of phenylacetylene, diphenylethyne and 1-phenyl-1-propyne (THF, 20 °C, 1 atm H_2 pressure), with TOFs of 500, 200, and $500\ h^{-1}$, respectively. The products distribution was seen to be time-dependent; after 3 h the *cis*-alkenes were in the range 75–90%, whereas after 24 h the over-reduced products were predominant, at least with phenylacetylene and diphenylethyne. Strongly coordinating solvents such as dimethylformamide (DMF) led to high TOFs (up to $1800\ h^{-1}$ under 41 atm H_2 pressure), while less-coordinating solvents such as tetrahydrofuran (THF), acetone (Me_2CO), and acetonitrile (MeCN) led to lower TOF values (1240, 1130, and $1060\ h^{-1}$, respectively, under the same pressure); pyridine inhibited the reaction (TOF = $660\ h^{-1}$), most likely due to the presence

of reactivity with $[Pd_4(dppm)_4(H_2)]^{2+}$. The polymeric low-valent complex $[Pd_5(PPh_2)]_n$ ($n \approx 4$) was also reported to be a highly active catalyst in the semi-hydrogenation of phenylacetylene and 1,3-pentadiene, as well as in the hydrogenation of 1- and 2-pentene (DMF, 20 °C, 1 atm H_2 pressure) [22]. The TOFs reached with the different substrates were 7200, 60 000, and 6000 (for both simple alkenes) h^{-1}, respectively.

Palladium(II) complexes containing tridentate PNP ligands first appeared during the late 1980s. A complex of general formula [Pd(PNP)Cl]Cl containing the pincer ligand N,N′-bis(diphenylphosphino)-2,6-diaminopyridine was briefly mentioned in 1987 as a catalyst for styrene hydrogenation (ethanol, 60 °C, 10 atm H_2 pressure) [23]; the platinum version was also active. In 1988, a kinetic analysis of the hydrogenation of cyclohexene catalyzed by different [Pd(PNP)Cl]Cl complexes (PNP = bis-2-(diphenylphosphino)ethyl benzylamine [24], bis-2-(diphenylphosphino)ethyl amine [25] or tris-2-(diphenylphosphino)ethyl amine [25]) under mild conditions (ethanol, 10–40 °C, 0.1–1 atm H_2 pressure) was reported (see Section 4.2.4).

During the 1990s, [Pd(PNO)X] (X = OAc, Cl, I) complexes derived from protic HPNO acyl-hydrazones (**1** in Scheme 4.1) were reported to be effective in the homogeneous hydrogenation of styrene and phenylacetylene under mild conditions (MeOH, r.t. or 40 °C, 1 atm H_2 pressure, 1% catalyst loading) [26–28]. With styrene, the acetate-complexes showed appreciable activity (TOFs up to 67 h^{-1}), the chloride-complexes reacted sluggishly (complete conversion after 48 h), and the iodide-complexes were completely inactive. With phenylacetylene as the substrate, the hydrogenations catalyzed by the chloride-complexes proceeded slowly (conversions not complete after 24 h), although with good selectivity to styrene, whilst the iodide complexes were, again, not active. With the acetate complexes, hydrogenation of the alkyne was poisoned by the precipitation of phenylethynyl palladium(II) complexes of the type [Pd(PNO)(C≡C–Ph)], which formed by the elimination of acetic acid. The formation of these organometallic species is independent of the catalytic conditions, as shown by the possibility of synthesizing them by reaction between the acetate complexes [Pd(PNO)(OAc)] and an excess of alkyne in methanol. Catalytic hydrogenations promoted by the phenylethynyl palladium(II) complexes in solvents in which these are completely soluble (CH_2Cl_2 or THF), led to much lower conversions than those reached with the acetate precursors, which exemplifies the pollutant nature of this *in-situ*-formed species.

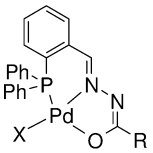

X = OAc, Cl, I

R = Me, C_6H_5, *p*-Me-C_6H_4
p-Br-C_6H_4, *p*-NO_2-C_6H_4, py

1

Scheme 4.1 The Pd(II) complexes containing acyl-hydrazone ligands, Pd(PNO)X.

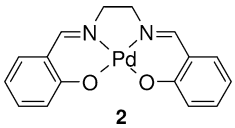

2

Scheme 4.2 The Pd-Salen complex.

4.2.2
Nitrogen-Containing Catalysts

Nitrogen ligand-containing complexes were first reported in the literature during the 1970s. Pd-Salen (**2** in Scheme 4.2) was reported as being a suitable catalyst for the hydrogenation of 1-hexene, and a good enzyme hydrogenase model [29, 30]. The complex was active in heterogeneous as well as homogeneous conditions, depending on the solvent employed (ethanol or DMF, respectively). Modified versions of the present catalyst appeared later in the literature [31, 32]; low reactivities and selectivities were observed in the hydrogenations of 1-hexene and phenylacetylene.

Ferrocenyl sulfide palladium(II) complexes of formula $[(\eta^5\text{-}C_5H_5)Fe(\eta^5\text{-}C_5H_3\text{-}1\text{-}CHRNR'_2\text{-}2\text{-}SR'')PdCl_2]$ or $[(R''S)(\eta^5\text{-}C_5H_4)Fe(\eta^5\text{-}C_5H_3\text{-}1\text{-}CHRNR'_2\text{-}2\text{-}SR'')PdCl_2]$ were employed in the selective hydrogenation of conjugated dienes to monoenes and in the hydrogenation of styrene derivatives [33–38]. The speed and selectivity were governed mainly by the nature of the R″ group, with 4-Cl-C_6H_4 leading to the best results in both series of complexes (TOFs up to 722 h^{-1} and almost complete selectivity to cyclooctene were achieved in the hydrogenation of 1,3-cyclooctadiene conducted at r.t. under 7 atm H_2 pressure). The solvent of choice was acetone, while dichloromethane, THF, and DMF led to much poorer results. Replacement of the Pd–S bond with a Pd–Se bond, or substitution of Pd with Pt, led to inactive systems. On the basis of these observations the authors argued that rupture of the Pd–S bond was a necessary prerequisite to form the active species. Nevertheless, induction times observed in some catalytic reactions (up to 49.7 h) cannot completely rule out – at least in those cases – a heterogeneous contribution to the reaction. Systems containing two sulfide moieties were almost inactive under the same experimental conditions [38].

Orthometallated dimer palladium(II) complexes $[Pd(NC)X]_2$ (**3** in Scheme 4.3) were reported by Saha as effective catalysts for the hydrogenation of alkenes and alkynes under mild conditions (25 °C, 1 atm H_2 pressure) [39, 40]. The reactions were efficient in either DMF or DMSO, reaching initial TOFs higher than 10 000 h^{-1} in the case of styrene, while in less-coordinating or non-coordinating solvents no activity was observed. Selectivity was never obtained, and the over-reduced products (or a mixture of different isomers) were always obtained. This, and the fact that the authors reported for a set of experiments that "... the yellow DMF solution of the catalyst turned deep greenish brown within 10 min on stirring under hydrogen at 20 °C" before the addition of the substrate [40], cast serious doubt on the homogeneous character of the reaction.

In 1991, Elsevier reported other nitrogen ligand-containing complexes as active hydrogenating catalysts. Palladium(0) complexes containing the Ar-bian bis-imine

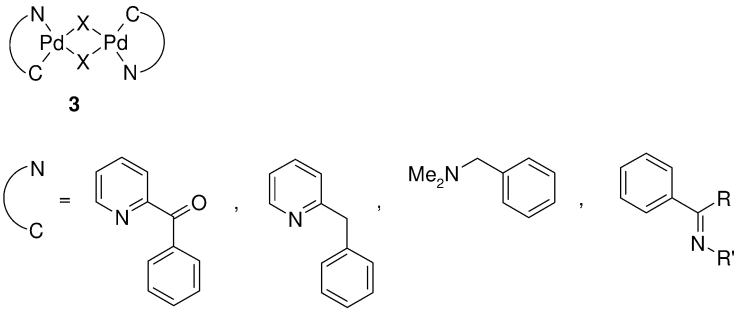

X = OAc or Cl; R = H or Me; R' = Me or aryl

Scheme 4.3 The orthometallated Pd(II) complexes, $[Pd(NC)_2X]_2$.

Ar = C_6H_5, *p*-Me-C_6H_4, *p*-MeO-C_6H_4
E = CO_2Me, CN, C(O)–O–C(O)

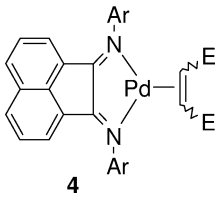

Scheme 4.4 The [Pd(Ar-bian)(dmf)] complexes.

ligand bis(arylimino)acenaphthene (**4** in Scheme 4.4), were successful in the reduction of electron-deficient alkenes [41]. The hydrogenations proceed under mild conditions (THF, 20 °C, 1–1.5 atm H_2 pressure, 1% catalyst loading, complete conversion within 8–16 h), with high chemoselectivity for C=C double bonds. Thus, nitro and cyano groups were not reduced to the corresponding amines, and the alkene functions of unsaturated esters, ketones and anhydrides were selectively hydrogenated. High selectivity (up to 90%) was also observed in the hydrogenation of *α*,*β*-unsaturated aldehydes. In the case of alkenes not containing electron-withdrawing substituents, the hydrogenations began only after an induction period, and for these instances a heterogeneous contribution was evidenced. [Pd(Ar-bian)(dmf)] (dmf = dimethylfumarate) complexes were also efficient in the highly selective hydrogenation of alkynes to the corresponding *Z*-alkenes [42]. The complex with Ar = *p*-Me-C_6H_4 was able to hydrogenate several linear and cyclic alkynes with selectivity up to 99% to the corresponding alkenes, and with high tolerance towards different functional groups. Substitution of the Ar-bian ligand with other nitrogen (bipy or dab = *p*-anisyldiazabutadiene) or phosphine (dppe) ligands led to poorer catalysts. More recently, other bis-imine ligands containing Pd(0) complexes of the general formula 6-R″-C_5H_3N-(C(R′)=NR)-2 (R″ = H, Me; R′ = H, Me; R = alkyl, aryl) were used in the stereoselective hydrogenation of 1-phenyl-1-propyne to *Z*-1-phenyl-1-propene [43]. The experimental conditions were identical to those applied with the [Pd(Ar-bian)(dmf)] complexes. The stability and behavior of the complexes under H_2 atmosphere were strongly dependent on the substitu-

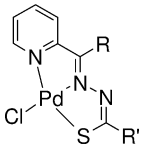

5

R = Me or Ph
R' = NH_2 or Ph

Scheme 4.5 The Pd(II) complexes with thiosemicarbazone or thiobenzoylhydrazone ligands, Pd(NN′S)Cl.

ents R, R′, and R″. Moderately bulky, σ-donating substituents were necessary in order to have hydrogenating activity without loss of palladium. The best compromise was reached with R″ = H, R′ = H and R = *i*-Pr, which led to complete consumption of the alkyne within 2 h of reaction, and with the following products distribution: 87% *Z*-alkene, 3% *E*-alkene, and 10% alkane. Water-soluble bis-imine Pd(0) complexes of the general formula 6-R′-C_5H_3N-(C(H)=NR)-2 (R′ = H, Me; R = 2,3,4,6-tetra-*O*-acetyl-β-D-glucopyranose residue) were used to hydrogenate unsaturated nitriles in water (r.t., 1 atm H_2 pressure, Pd : substrate ratio = 1 : 50) [44]. The complexes displayed high activity in distilled water, but the reactions were substantially heterogeneous. In 0.1 M KOH solution, the hydrogenations of acrylonitrile, methacrylonitrile, and crotonitrile were homogeneous and proceeded fairly rapidly (after 2 h the yields of the saturated products were 70, 50, and 50%, respectively); however, undesired side reactions also occurred. In 0.25 M KOH solution only the hydrogenation of acrylonitrile was homogeneous and complete within 2 h. No enantioselectivity was observed in the hydrogenation of α-ethylacrylonitrile.

High chemoselectivities (up to 96%) were reached in the hydrogenation of phenylacetylene to styrene (DMF, 30 °C, 1 atm H_2 pressure, 1% catalyst loading, TOFs up to 4.2 h^{-1}) catalyzed by chloride Pd(II) complexes [Pd(NN′S)Cl] containing thiosemicarbazone or thiobenzoylhydrazone ligands (**5** in Scheme 4.5) [45]. Instead, minor reactivities and selectivities were obtained with NN′N″ pyridyl-hydrazone-containing Pd(II) complexes in the hydrogenation of phenylacetylene [46].

4.2.3
Other Catalysts

$Pd(acac)_2$ has been reported to be an active catalyst in soybean oil hydrogenation [47]. The reactions were conducted in bulk with low catalyst loadings (1–60 ppm) and without any co-catalyst. Under 10 atm H_2 pressure and at 80–120 °C, optimum linolenate selectivity and high *trans*-isomers content were obtained. Decomposition of the catalyst occurred at temperatures above 120 °C.

Simple inorganic salts, such as $PdCl_2$, were also studied. $PdCl_2/SnCl_2 \cdot 2H_2O$ and $K_2PdCl_4/SnCl_2 \cdot 2H_2O$ turned out to be completely inactive in the hydrogenation of soybean oil methylester [9], while $PdCl_2$ in DMF was active towards conjugated dienes and alkynes (DMF, 25 °C, 25 atm H_2 pressure, 0.31–0.5% cat-

alyst loading) [48]. 1-Heptyne and 2-pentyne were selectively reduced to the corresponding alkenes within 25 minutes, while the hydrogenation of dienes was slower. $PdCl_2$ dissolved in a CH_2Cl_2-polyethylene glycol (PEG) mixture was employed in the hydrogenation of diphenylacetylene (10 °C, 1 atm H_2 pressure, Pd : substrate ratio $\approx$1 : 10) [49]. The rate and selectivity of the reaction were dependent on the PEG molecular weight; with PEG-400, 90% conversion was achieved after 80 minutes, with 80% of *cis*-stilbene.

4.2.4 Mechanistic Aspects

Reaction mechanisms based on kinetic studies have been proposed for most of the aforementioned catalytic hydrogenations. For the Pd(II)-catalysts, the heterolytic activation of molecular hydrogen results generally favored compared to oxidative addition which, in contrast, is common for low-valent Pd-catalysts. For example, a molecular orbital analysis of the hydrogenation of styrene catalyzed by the $[PdCl_4]^{2-}$ anion [50] showed that H_2 was activated by heterolytic splitting (in these experiments the catalyst was supported on a solid, but no profound differences were believed to exist between the homogeneous and heterogeneous cases). The four successive steps depicted in Eqs. (3) to (6) were defined as:

- Splitting of H_2 with formation of the palladium hydride $[HPdCl_3]^{2-}$ and HCl (Eq. (3)).
- π-coordination of styrene through a pentacoordinate intermediate (Eq. (4)).
- Alkene insertion into the Pd–H bond with formation of an alkyl intermediate (Eq. (5)).
- Reaction with HCl to eliminate ethylbenzene and re-form the anion $[PdCl_4]^{2-}$ (Eq. (6)).

$$[PdCl_4]^{2-} + H_2 \leftrightarrow [HPdCl_3]^{2-} + HCl \tag{3}$$

$$[HPdCl_3]^{2-} + C_6H_5\text{-}CH = CH_2 \leftrightarrow [HPdCl_3(C_6H_5\text{-}CH = CH_2)]^{2-} \tag{4}$$

$$[HPdCl_3(C_6H_5\text{-}CH = CH_2)]^{2-} \leftrightarrow [(C_6H_5\text{-}CH_2\text{-}CH_2)PdCl_3]^{2-} \tag{5}$$

$$[(C_6H_5\text{-}CH_2\text{-}CH_2)PdCl_3]^{2-} + HCl \rightarrow [PdCl_4]^{2-} + C_6H_5CH_2CH_3 \tag{6}$$

The elimination of HCl was proposed to occur also during the H_2 activation with the [Pd(PNP)Cl]Cl complexes (PNP = bis-2-(diphenylphosphino)ethyl benzylamine, bis-2-(diphenylphosphino)ethyl amine or tris-2-(diphenylphosphino)ethyl amine) [24, 25]. Based on the findings of $^{31}P\{^1H\}$- and ^1H-NMR investigations, the hydride [HPd(PNP)]Cl was detected under H_2 atmosphere. The alternative mechanism which involves the oxidative addition of H_2 with formation of a Pd(IV)-dihydride intermediate, appeared less likely on the basis of thermodynamic considerations.

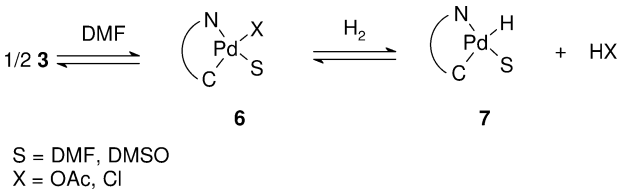

Scheme 4.6 Heterolytic splitting of H_2 with $[Pd(NC)_2X]_2$ complexes.

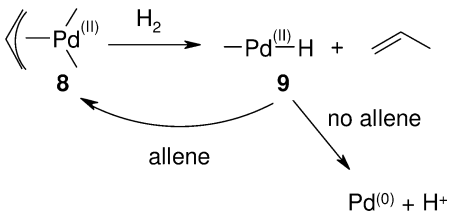

Scheme 4.7 Hydrogenation of allene catalyzed by $[(\eta^3\text{-allyl})Pd(PR_3)Cl]$ complexes.

The efficiency of the orthometallated Pd(II) complexes $[Pd(NC)X]_2$ [39, 40] (**3** in Scheme 4.3) in coordinating solvents such as DMF or DMSO was considered to be in favor of the initial dissociation of the dimers **3** into the mononuclear species **6** (Scheme 4.6). The heterolytic splitting of H_2 leads to the formation of the hydride **7** plus HCl or AcOH. The solvato-hydride intermediate **7** was characterized spectroscopically and its elemental analysis furnished [39]; regrettably, no data regarding its catalytic activity were reported.

The dissociation of a coordinated allene by hydrogen was evidenced for $[(\eta^3\text{-allyl})Pd(PR_3)Cl]$ complexes [11]. The hydrogenation of allene to propene was then invoked to follow the pathway depicted in Scheme 4.7:

- H_2 activation by protonation of the coordinated allene in **8** with formation of the palladium hydride intermediate **9** and propene.
- Insertion of an allene molecule into the Pd–H bond, with regeneration of the starting allene complex **8** which then re-enters the catalytic cycle. In the absence of allene, extensive Pd black formation was observed.

In the hydrogenation of styrene catalyzed by the [Pd(PNO)(OAc)] complexes (**1** in Scheme 4.1) [26–28], a clear correlation between the activity of the complexes and the basicity of the hydrazonic ligand, in turn governed by the nature of the R group, was established [28]. Indeed, the higher the ligand basicity, the faster the hydrogenation reactions. This result, combined with a kinetic analysis, led to the mechanism depicted in Scheme 4.8. The first step is the heterolytic activation of H_2 with protonation of the hydrazonic arm in **1** and formation of the hydride intermediate **10**; **10** can be considered at equilibrium with **11**, where the acetate anion re-enters in the coordination sphere by displacement of the C=O amide group of the ligand. By rupture of the Pd-O(amide) (**10**) or Pd-O-

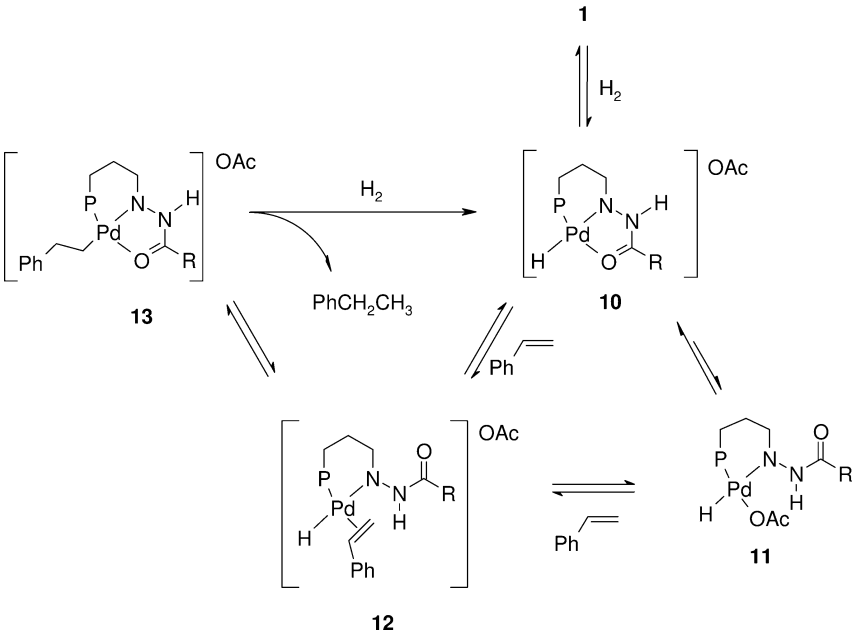

Scheme 4.8 Proposed pathway for the hydrogenation of styrene catalyzed by Pd(PNO)(OAc) complexes.

(acetate) (**11**) bond, a styrene molecule coordinates to palladium with formation of **12**, and after the alkene insertion into the Pd–H bond the alkyl-intermediate **13** forms. The involvement of **10** in the catalytic cycle appeared more likely than that of **11**, on the basis of the inertness shown by the acetate complex [Pd(PNS)(OAc)] (PNS = 2-(diphenylphosphino)benzaldehyde thiosemicarbazone), where the two soft donors P and S make the complex too stable [27]. The cycle closes with the intervention of a H_2 molecule, which leads to the restoration of **10** (or alternatively **11**) and elimination of ethylbenzene.

A similar H_2 activation mechanism was proposed for the [Pd(NN′S)Cl] complexes (**5** in Scheme 4.5) in the semi-hydrogenation of phenylacetylene [45]; after formation of the hydride **14** (Scheme 4.9), coordination of the alkyne occurs by displacement of the chloride ligand from Pd (**15**). The observed chemoselectivity (up to 96% to styrene) was indeed ascribed to the chloride anion, which can be removed from the coordination sphere by phenylacetylene, but not by the poorer coordinating styrene. This was substantiated by the lower chemoselectivities observed in the presence of halogen scavengers, or in the hydrogenations catalyzed by acetate complexes of formula [Pd(NN′S)(OAc)]. Here, the acetate anion can be easily removed by either phenylacetylene or styrene.

A net heterolytic H_2 cleavage was evidenced for [Pd(Salen)] (**2** in Scheme 4.2) [29, 30]. Its catalytic activity was pH-dependent; namely, it was inhibited by acids and enhanced by bases. A kinetic study of the hydrogenation of 1-hexene in DMF led to the definition of the following mechanism (Scheme 4.10):

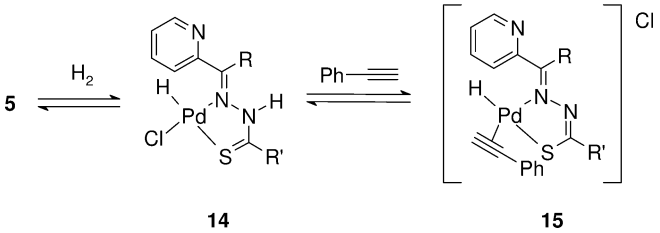

Scheme 4.9 Heterolytic splitting of H_2 and coordination of phenylacetylene in Pd(NN′S)Cl complexes.

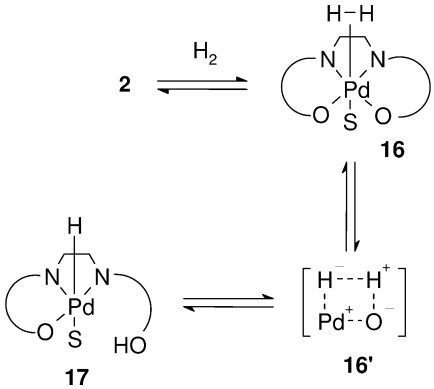

Scheme 4.10 Heterolytic H_2 splitting promoted by Pd–Salen complex; S = DMF.

- solvent-assisted hydrogen coordination to the metal (**16**);
- heterolytic activation of the molecular hydrogen through a highly polarized, four-center transition state (**16′**) which involves a coordinate phenolate group. The so-formed OH group leaves a vacant coordination site on the metal (**17**), which can now accommodate the entering alkene, the subsequent alkene insertion into the Pd–H bond forming an alkyl intermediate. Finally, hydrogen transfer from the OH group of the ligand to the coordinated alkyl group gives the final alkane, with restoration of **2**.

Oxidative addition of molecular hydrogen was considered to be involved in the alkyne hydrogenations catalyzed by [Pd(Ar-bian)(dmf)] complexes (**4** in Scheme 4.4) [41, 42]. Although the mechanism was not completely addressed, **4** was considered to be the pre-catalyst, the real catalyst most likely being the [Pd(Ar-bian)(alkyne)] complex **18** in Scheme 4.11. Alkyne complex **18** was then invoked to undergo oxidative addition of H_2 followed by insertion/elimination or pairwise transfer of hydrogen atoms, giving rise to the alkene-complex **19**.

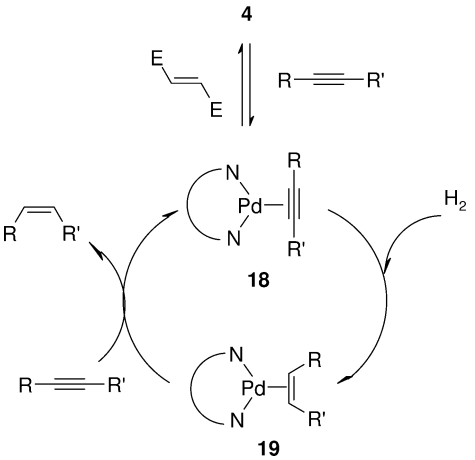

Scheme 4.11 Proposed catalytic cycle for the hydrogenation of alkynes promoted by Pd(Ar-bian)(dmf) complexes.

Displacement of the alkene by an incoming alkyne molecule leads to the elimination of the product and restoration of **18** (see also chapter 14).

The higher catalytic activity of the cluster compound $[Pd_4(dppm)_4(H_2)](BPh_4)_2$ [21] (**20** in Scheme 4.12) in DMF with respect to less coordinating solvents (e.g., THF, acetone, acetonitrile), combined with a kinetic analysis, led to the mechanism depicted in Scheme 4.12. Initially, **20** dissociates into the less sterically demanding d^9-d^9 solvento-dimer **21**, which is the active catalyst. An alkyne molecule then inserts into the Pd–Pd bond to yield **22** and, after migratory insertion into the Pd–H bond, the d^9-d^9 intermediate **23** forms. Now, H_2 can oxidatively add to **23** giving rise to **24** which, upon reductive elimination, results in the formation of the alkene and regenerates **21**.

The high activity of the polymeric compound $[Pd_5(PPh_2)]_n$ ($n \approx 4$) [22] in the hydrogenation of alkenes and alkynes was ascribed to the initial DMF-assisted dissociation of the polymer (Eq. (7)); the resulting $[Pd_5(PPh)_2]$ species forms an adduct with the substrate molecule (Sub) (Eq. (8)) which, after reaction with H_2, leads to the hydrogenation product and gives back $[Pd_5(PPh)_2]$ (Eq. (9)), which re-enters the catalytic cycle.

$$[Pd_5(PPh)_2]_n \leftrightarrow n[Pd_5(PPh)_2] \tag{7}$$

$$[Pd_5(PPh)_2] + Sub \leftrightarrow [Pd_5(PPh)_2](Sub) \tag{8}$$

$$[Pd_5(PPh)_2](Sub) + H_2 \leftrightarrow [Pd_5(PPh)_2] + SubH_2 \tag{9}$$

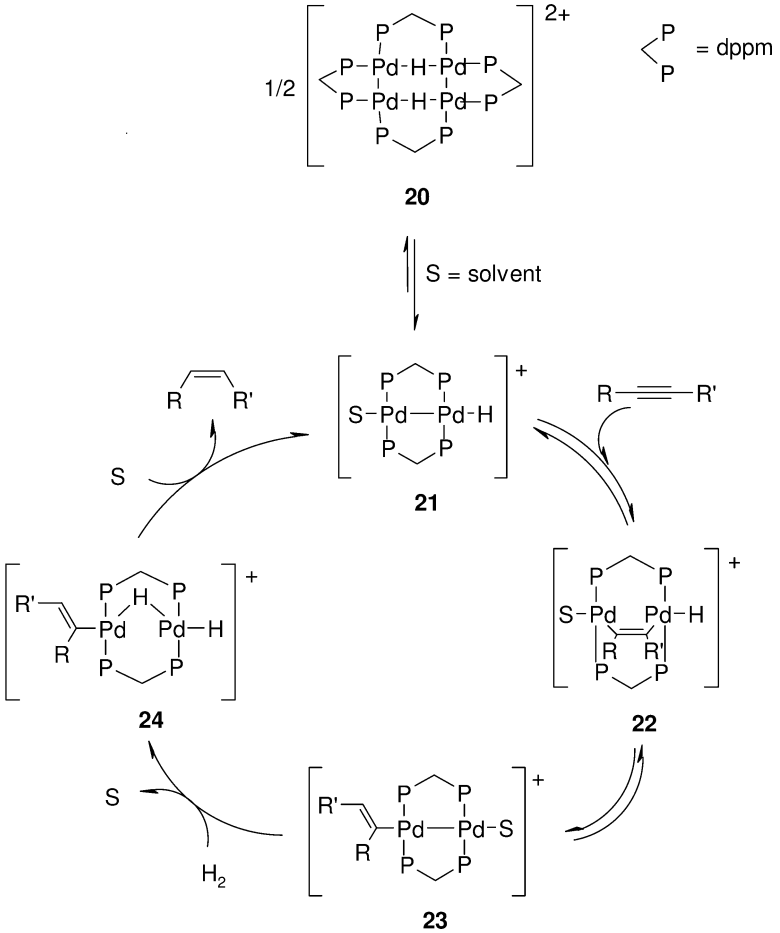

Scheme 4.12 Proposed mechanism for the hydrogenation of alkynes catalyzed by $[Pd_4(dppm)_4(H_2)]^{2+}$.

4.3 Platinum

4.3.1 Platinum Complexes Activated with Sn(II) Salts

4.3.1.1 Phosphorus-Containing Catalysts

The catalytic activity of $[PtX_2(QPh_3)_2]/SnCl_2$ complexes (Q = P or As, X = halogen or pseudo-halogen) was intensively studied, starting during the late 1960s. Such catalytic systems promoted the isomerization and hydrogenation of methyl oleate [51], methyl linolenate [52], and polyenes [53], as well as short-chain alkenes

[54]. The Pt : substrate ratios ranged from 1 : 10 to 1 : 180. The formation of conjugated isomers which were slowly hydrogenated to the corresponding monoene was observed (see Section 4.3.3). *Cis*-$[PtCl_2L(PR_3)]/SnCl_2$ complexes ($L = SR'_2$, p-$X\text{-}C_6H_4NH_2$; R = aryl) also showed activity in the hydrogenation of alkenes, such as styrene (acetone, 60 °C, 41 atm H_2 pressure) [55]. TOF values up to 4400 h^{-1} were reached, depending on the nature of ligands L and PR_3. These complexes resulted in more active catalysts than the parent complexes *cis*-$[PtCl_2L_2]/SnCl_2$ or *cis*-$[PtCl_2(PR_3)_2]/SnCl_2$, which brought about a maximum TOF of 910 h^{-1}. Rationalization of the results, in terms of a plausible reaction mechanism, was far from straightforward because of the contemporary presence, under catalytic conditions, of several Pt and Pt-Sn species, both neutral and ionic, all of which played a catalytic role. Indeed, the authors reported that the multicomponent system was necessary to establish the catalytic cycle, as evidenced by catalytic runs involving isolated species. Dimeric versions of the aforementioned complexes of the type $[Pt_2(\mu\text{-}Cl)_2(PR_3)_2]/SnCl_2$ [55] or *cis*-$[Pt_2(\mu\text{-}SR')(\mu\text{-}Cl)Cl_2(PR_3)_2]$ [56] led to reactivities similar to those observed with the mononuclear parents, thus indicating the necessity of dimer dissociation to bring about the formation of active mononuclear species.

4.3.1.2 **Other Catalysts**

In 1963, the hydrogenation of ethylene and acetylene under mild conditions (methanol, r.t., 1 atm total pressure) was readily carried out with the catalytic system $H_2PtCl_6/SnCl_2$ (Pt/Sn ratio = 1 : 10) [57]. With higher Pt/Sn ratios and higher alcohols, the hydrogenation of higher alkenes became feasible. For example, the hydrogenation of cyclohexene in *i*-PrOH proceeded with a TOF of 5 h^{-1} [58]. The addition of chloride or bromide ions and water strongly increased the hydrogenation rate (TOFs up to 94 h^{-1}). Carboxylic acids or esters also turned out to be suitable solvents: with a Pt/Sn ratio of 1 : 5, the hydrogenation of 1-hexene in glacial acetic acid led, after 2 h of reaction, to a mixture of hexane ($\approx$50%), 2-*trans*-hexene ($\approx$25%), 3-*trans*-hexene ($\approx$5%), traces of 2-*cis*- and 3-*cis*-hexene, and unreacted 1-hexene [59]. As expected, the hydrogenation of 2-hexene proceeded somewhat sluggishly, whilst in the hydrogenation of soybean oil a remarkable preference for the reduction of linoleic acid was observed. Again, $H_2PtCl_6/SnCl_2$ was employed in the hydrogenation of Dewar-benzene derivatives, such as dimethyl tetramethylbicyclo[2.2.0]hexa-2,5-diene-2,3-dicarboxylate (**25** in Scheme 4.13) and its di-*tert*-Bu-ester under mild conditions (*i*-PrOH, 25 °C, 1 atm H_2 pressure, Pt : substrate ratio 1 : 10) [60]. Contrary to heterogeneous systems, the hydrogenation of **25** was restricted to the ester-substituted double bond, giving rise to dimethyl tetramethylbicyclo[2.2.0]hex-5-ene-2-endo, 3-endo-dicarboxylate (**26**); the exo,endo hydrogenation (**27**) was involved for 16%. In 1972, Parshall showed that $PtCl_2$ could be used as hydrogenation catalyst for alkenes in molten $[R_4N][SnCl_3]$ [61]. With $PtCl_2/[Et_4N][SnCl_3]$, a 50% conversion was obtained in the hydrogenation of ethylene after 5 h of reaction (100 °C, 1.7 atm total pressure, Pt : ethylene ratio 1 : 13). At higher temperatures

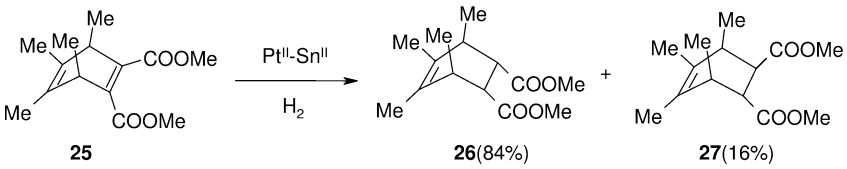

Scheme 4.13 Hydrogenation of Dewar-benzene derivatives.

and pressures, 1,5,9-cyclododecatriene was hydrogenated to cyclododecene with considerable selectivity: 87% monoene, 10% diene, 2% of unreacted triene, and traces of over-reduced product were obtained at 160 °C and 100 atm H_2 pressure after 8 h of reaction (Pt : substrate ratio = 1 : 15).

4.3.2
Platinum Complexes not Activated with Sn(II) Salts

Platinum complexes that display hydrogenating activity without the addition of Sn(II) salts are scarce in the literature. The dihydride Pt(II) complex $[PtH_2\{(t\text{-}Bu)_2PCH_2CH_2P(t\text{-}Bu)_2\}]$ hydrogenated cyclohexene to cyclohexane only under drastic conditions (benzene, 100 °C, 77.4 atm H_2 pressure, 1% catalyst loading), with a TOF of 0.26 h^{-1} [62]. The chloro-bridged complex $[PtCl_2(2,4,6\text{-}Me_3\text{-pyridine})]_2$ was active at r.t. and 1 atm H_2 pressure toward mono- and dienes (a TOF of 270 h^{-1} was obtained with styrene) [63]; however, when racemization was possible all the isomers were detected in the final solutions. The hydride complex *trans*-$[PtH(NO_3)(PEt_3)_2]$ [64] was active towards both internal and terminal alkenes, but was inactive toward alkenes bearing electron-withdrawing substituents. The hydrogenation rate was dependent on the solvent employed, with methanol leading to the highest TOF values. With styrene as substrate, a TOF of 115 h^{-1} was reached at 60 °C and 41 atm H_2 pressure. The methoxide intermediate $PtH(OMe)(PEt_3)_2$ was considered to be involved in the reaction mechanism. The activity towards internal alkenes was slower.

Pt(0) complexes of the type $[Pt(P\text{-}P)(C_2H_4)]$ (P-P = dppb, 1,2-bis[(diphenylphosphino)methyl]benzene (dpmb) and (+)-2,3-*O*-isopropylidene-2,3-dihydroxy-1,4-bis(diphenylphosphino)butane ((+)-diop)) were used in the hydrogenation of several alkenes in combination with CH_3SO_3H (toluene, 80 °C, 50 atm H_2 pressure, Pt : substrate ratio 1 : 320) [65]. With the dppb-containing complex, the reduction of terminal alkenes was accompanied by extensive isomerization, and the resulting internal alkenes underwent very little hydrogenation (1-hexene led to 29.3% yield of hexane and 68.8% yield of hexenes after 22 h). Alkenes bearing electron-withdrawing substituents were hydrogenated much more easily (3-buten-2-one and 2-cyclohexen-1-one were reduced to the corresponding saturated ketones with TOFs of 68 and 282 h^{-1}, respectively). The activity of $[Pt(dppb)(C_2H_4)]$ was usually higher than that of $[Pt(dpmb)(C_2H_4)]$, both with simple olefins (styrene, TOFs of 6.2 and 3.7 h^{-1}, respectively) and unsaturated ketones (2-cyclohexen-1-one, TOFs of 80 and 48 h^{-1}, respectively). Poor chiral in-

duction (8% *ee*, *R*-isomer) was observed in the hydrogenation of α-ethylstyrene catalyzed by [Pt((+)-diop)(C_2H_4)].

Finally, the only example of a polynuclear homogeneous catalyst is the dinuclear complex $[Pt_2(P_2O_5H_2)_4]^{4-}$ [66], which catalyzed the hydrogenation of styrene, phenylacetylene, 1-octyne, and 1-hexyne (*i*-PrOH, 60 °C, 20.7 atm H_2 pressure, Pd : substrate ratio 1 : 1800) to the corresponding alkanes within 10 h of reaction.

4.3.3
Mechanistic Aspects

Because of its industrial importance, many studies have conducted in order to establish the mechanism which regulates the hydrogenation of polyunsaturated fatty acid derivatives catalyzed by the $[PtX_2(QPh_3)_2]/SnCl_2$ complexes (Q = P or As, X = halogen or pseudo-halogen) [51, 52]. The following observations were made:

- Initial, rapid step-wise migration of double bonds takes place to give a conjugated isomer [67], which is then reduced more slowly to the corresponding monoene. The necessary formation of conjugated isomers was highlighted by the inertness of polyenes where the double bonds are separated by several methylene groups [52]. Isomerization occurred before, as well as after, the hydrogenation. *Cis-trans* isomerization also occurred. High H_2 pressures (usually higher than 30 atm) were required, otherwise only isomerization was observed.
- Hydride formation was a fundamental step in the mechanism, and indeed $PtHCl(PPh_3)_2$ species were isolated from the reactant solutions. However, their formation was not the rate-determining step, since the same rate of hydrogenation was observed with either $PtCl_2(PPh_3)_2$ or $PtHCl(PPh_3)_2$ complexes.
- Metal–alkene complex formation was also necessary, but again was not rate-determining.
- The formation of hydride-Pt(II)-alkene complexes was thought to be the rate-determining step, as evidenced by the isolation of a number of such species.
- The addition of an excess of $SnCl_2$ (a Pt : Sn ratio of 1 : 5 was found to be the best) was necessary as co-catalyst; $SnCl_2$ reacts with chloride ions to give the poor σ-donor and strong π-acceptor $SnCl_3^-$ ligand [68] that, decreasing the electron density on Pt, favors the formation of Pt–H or Pt–alkene bonds.
- Triphenylphosphine and related ligands stabilized the hydride intermediate once formed, besides rendering Pt soluble in non-polar organic solvents. These observations have been condensed in the mechanism depicted in Scheme 4.14.

Penta-coordinate Pt–Sn anions of the type $[Pt(SnCl_3)_5]^{3-}$ [69] appeared also to be involved in the hydrogenations catalyzed by the phosphine-free $H_2PtCl_6/SnCl_2$ [57] and $PtCl_2/[R_4N][SnCl_3]$ [61] systems. The anion $[Pt(SnCl_3)_5]^{3-}$ transforms into the active species $[PtH(SnCl_3)_3]^{2-}$ upon heterolytic hydrogen activation and loss of two $SnCl_3^-$ ligands (Eqs. (10) to (12)).

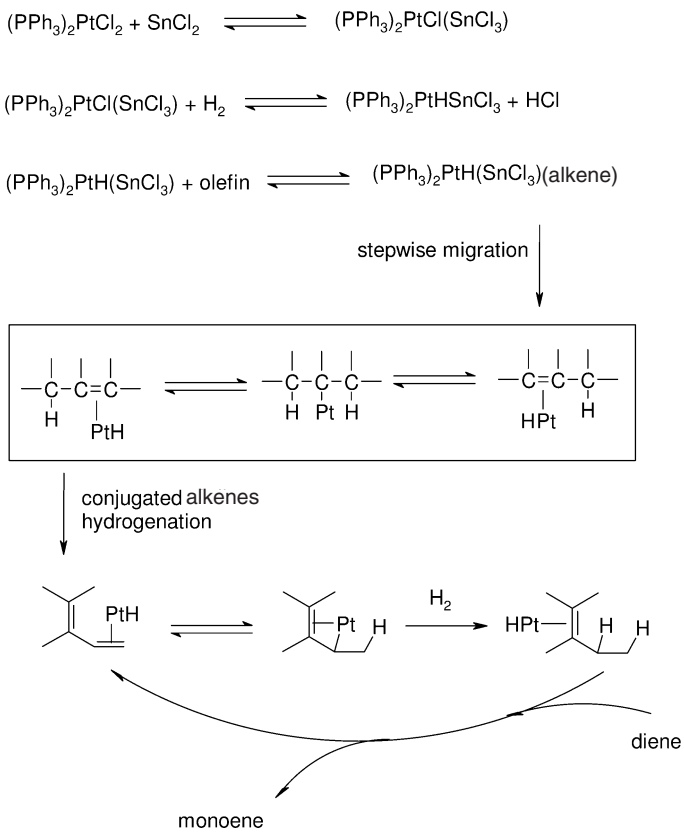

Scheme 4.14 Pathway for the selective hydrogenation of polyenes to monoenes catalyzed by $PtX_2(QPh_3)_2/SnCl_2$; Q = P or As, X = halogen or pseudo-halogen.

$$[Pt(SnCl_3)_5]^{3-} \leftrightarrow [Pt(SnCl_3)_4]^{2-} + SnCl_3^- \tag{10}$$

$$[Pt(SnCl_3)_4]^{2-} + H_2 \leftrightarrow [PtH(SnCl_3)_4]^{3-} + H^+ \tag{11}$$

$$[PtH(SnCl_3)_4]^{3-} \leftrightarrow [PtH(SnCl_3)_3]^{2-} + SnCl_3^- \tag{12}$$

In the case of ethylene hydrogenation, the mechanism proposed by Parshall [61] involves the coordination of an alkene molecule through a five-coordinate intermediate (Eq. (13)); the subsequent alkene insertion into the Pt–H bond (Eq. (14)) and intervention of a second molecule of H_2 (Eq. (15)) leads to the elimination of ethane and restoration of the catalytic active species $[PtH(SnCl_3)]^{2-}$. However, in 1976 Yasumori and coworkers reported a kinetic analysis conducted on the hydrogenation of ethylene catalyzed by the Pt–Sn complex $[(Me)_4N]_3[Pt(SnCl_3)_5]$ [70], under much milder conditions than those

applied by Parshall (acetone, 0–15 °C, partial H_2 pressure up to 0.13 atm). The collected data were in agreement with the formation of Pt_n clusters of different sizes (n = 1 to 6, depending on Pt concentration), which were invoked as being responsible for the observed catalytic activity. The possibility that the catalyses described by Parshall might have a heterogeneous character is further supported by the well-known ability of tetraalkylammonium salts to stabilize metal-clusters, and by the harsh experimental conditions applied [71].

$$[PtH(SnCl_3)_3]^{2-} + C_2H_4 \leftrightarrow [PtH(C_2H_4)(SnCl_3)_3]^{2-} \quad (13)$$

$$[PtH(C_2H_4)(SnCl_3)_3]^{2-} \leftrightarrow [Pt(C_2H_5)(SnCl_3)_3]^{2-} \quad (14)$$

$$[Pt(C_2H_5)(SnCl_3)_3]^{2-} + H_2 \rightarrow [PtH(SnCl_3)_3]^{2-} + C_2H_6 \quad (15)$$

A kinetic analysis of the styrene hydrogenation catalyzed by $[Pt_2(P_2O_5H_2)_4]^{4-}$ [66] was indicative of the fact that the dinuclear core of the catalyst was maintained during hydrogenation. However, three speculative mechanisms were in agreement with the kinetic data, which mainly differ in the H_2 activation step. This in fact can occur through the formation of two Pt–monohydrides, still connected by a Pt–Pt bond, or through the formation of two independent Pt–monohydrides. The third mechanism involves the dissociation of a phosphine from one Pt center, with subsequent oxidative addition of H_2 to produce a Pt–dihydride intermediate.

Abbreviations

dmf	dimethylfumarate
DMF	dimethylformamide
DMSO	dimethylsulfoxide
PEG	polyethylene glycol
THF	tetrahydrofuran
TOF	turnover frequency
TON	turnover number

References

1 J.H. Flynn, H.M. Hulburt, *J. Am. Chem. Soc.* **1954**, *76*, 3393.
2 A.S. Gow, H. Heinemann, *J. Phys. Chem.* **1960**, *64*, 1574.
3 J. Halpern, *J. Organomet. Chem.* **1980**, *200*, 133.
4 J.F. Harrod, A.J. Chalk, *J. Am. Chem. Soc.* **1964**, *86*, 1776.
5 R. Cramer, R.V. Lindsey, *J. Am. Chem. Soc.* **1966**, *88*, 3534.
6 B.R. James, *Homogeneous Hydrogenation*, Wiley, New York, **1975**.
7 F. Basolo, H.B. Gary, R.G. Pearson, *J. Am. Chem. Soc.* **1960**, *82*, 4200.
8 M.F. Sloan, A.S. Matlack, D.S. Breslow, *J. Am. Chem. Soc.* **1963**, *85*, 4014.

9 H. Itatani, J.C. Bailar Jr., *J. Am. Oil Chemists' Soc.* **1967**, *44*, 147.
10 Y. Fujii, J.C. Bailar Jr., *J. Catal.* **1978**, *55*, 146.
11 G. Carturan, G. Strukul, *J. Organomet. Chem.* **1978**, *157*, 475.
12 G. Strukul, G. Carturan, *Inorg. Chim. Acta* **1979**, *35*, 99.
13 E.W. Stern, P.K. Maples, *J. Catal.* **1972**, *27*, 120.
14 P. Leoni, F. Marchetti, M. Pasquali, *J. Organomet. Chem.* **1993**, *451*, C25.
15 M. Sommovigo, H. Alper, *Tetrahedron Lett.* **1993**, *34*, 59.
16 I.S. Cho, H. Alper, *J. Org. Chem.* **1994**, *59*, 4027.
17 I.S. Cho, H. Alper, *Tetrahedron Lett.* **1995**, *36*, 5673.
18 I.S. Cho, B. Lee, H. Alper, *Tetrahedron Lett.* **1995**, *36*, 6009.
19 R.U. Kirss, R. Eisenberg, *Inorg. Chem.* **1989**, *28*, 3372.
20 I. Gauthron, J. Gagnon, T. Zhang, D. Rivard, D. Lucas, Y. Mugnier, P.D. Harvey, *Inorg. Chem.* **1998**, *37*, 1112.
21 D. Evrard, K. Groison, Y. Mugnier, P.D. Harvey, *Inorg. Chem.* **2004**, *43*, 790.
22 I.I. Moiseev, M.N. Vargaftic, *New J. Chem.* **1998**, 1217.
23 W. Schirmer, U. Flörke, H.-J. Haupt, *Z. Anorg. Allg. Chem.* **1987**, *545*, 83.
24 V.V.S. Reddy, *J. Mol. Catal.* **1988**, *45*, 73.
25 M.M. Taqui Khan, B. Taqui Khan, S. Begum, *J. Mol. Catal.* **1988**, *45*, 305.
26 A. Bacchi, M. Carcelli, M. Costa, P. Pelagatti, C. Pelizzi, G. Pelizzi, *Gazz. Chim. Ital.* **1994**, *124*, 429.
27 A. Bacchi, M. Carcelli, M. Costa, A. Leporati, E. Leporati, P. Pelagatti, C. Pelizzi, G. Pelizzi, *J. Organomet. Chem.* **1997**, *535*, 107.
28 P. Pelagatti, A. Bacchi, M. Carcelli, M. Costa, A. Fochi, P. Ghidini, E. Leporati, M. Masi, C. Pelizzi, G. Pelizzi, *J. Organomet. Chem.* **1999**, *583*, 94.
29 G.H. Olivé, S. Olivé, *Angew. Chem. Int. Ed. Engl.* **1974**, *13*, 549.
30 G.H. Olivé, S. Olivé, *J. Mol. Catal.* **1975/76**, *1*, 121.
31 A. El-M.M. Ramadan, *Transition Met. Chem.* **1996**, *21*, 536.
32 A. Bacchi, M. Carcelli, L. Gabba, S. Ianelli, P. Pelagatti, G. Pelizzi, D. Rogolino, *Inorg. Chim. Acta* **2003**, *342*, 229.
33 R.V. Honeychuck, M.O. Okoroafor, L.-H. Shen, C.H. Brubaker, Jr., *Organometallics* **1986**, *5*, 482.
34 M.O. Okoroafor, L.-H. Shen, R.V. Honeychuck, C.H. Brubaker, Jr., *Organometallics* **1988**, *7*, 1297.
35 C.-K. Lai, A.A. Naiini, C.H. Brubaker, Jr., *Inorg. Chim. Acta* **1989**, *164*, 205.
36 A.A. Naiini, C.-K. Lai, D.L. Ward, C.H. Brubaker, Jr., *J. Organomet. Chem.* **1990**, *390*, 73.
37 A.A. Naiini, H.M. Ali, C.H. Brubaker, Jr., *J. Mol. Catal.* **1991**, *67*, 47.
38 C.-H. Wang, C.H. Brubaker, Jr., *J. Mol. Catal.* **1992**, *75*, 221.
39 A. Bose, C.R. Saha, *Indian J. Chem.* **1990**, *29A*, 461.
40 D.K. Mukherjee, B.K. Palit, C.R. Saha, *Indian J. Chem.* **1992**, *31A*, 243.
41 R. van Asselt, C.J. Elsevier, *J. Mol. Catal.* **1991**, *65*, L13.
42 M.W. van Laren, C.J. Elsevier, *Angew. Chem. Int. Ed. Engl.* **1999**, *38*, 3715.
43 M.W. van Laren, M.A. Duin, C. Klerk, M. Naglia, D. Rogolino, P. Pelagatti, A. Bacchi, C. Pelizzi, C.J. Elsevier, *Organometallics* **2002**, *21*, 1546.
44 C. Borriello, M.L. Ferrara, I. Orabona, A. Panunzi, F. Ruffo, *J. Chem. Soc., Dalton Trans.* **2000**, 2545.
45 P. Pelagatti, A. Venturini, A. Leporati, M. Carcelli, M. Costa, A. Bacchi, G. Pelizzi, C. Pelizzi, *J. Chem. Soc., Dalton Trans.* **1998**, 2715.
46 M. Costa, P. Pelagatti, C. Pelizzi, D. Rogolino, *J. Mol. Catal. A: Chem.* **2002**, *178*, 21.
47 S. Koritala, *J. Am. Oil Chemist's Soc.* **1985**, *62*, 517.
48 A. Sisak, F. Ungváry, *Chem. Ber.* **1976**, *109*, 531.
49 N. Suzuki, Y. Ayaguchi, Y. Izawa, *Chem. Ind.* **1983**, *4*, 166.
50 D.R. Armstrong, O. Novaro, M.E. Ruiz-Vizcaya, R. Linarte, *J. Catal.* **1977**, *48*, 8.
51 J.C. Bailar, Jr., H. Itatani, *J. Am. Chem. Soc.* **1967**, *89*, 1592.
52 E.N. Frankel, E.A. Emken, H. Itatani, J.C. Bailar, Jr., *J. Org. Chem.* **1967**, *32*, 1447.
53 H.A. Tayim, J.C. Bailar, Jr., *J. Am. Chem. Soc.* **1967**, *89*, 4330.
54 R.W. Adams, G.E. Batley, J.C. Bailar, Jr., *J. Am. Chem. Soc.* **1968**, *90*, 6051.

55 G. K. Anderson, C. Billard, H. C. Clark, J. A. Davies, C. S. Wong, *Inorg. Chem.* **1983**, *22*, 439.

56 V. K. Jain, G. S. Rao, *Inorg. Chim. Acta* **1987**, *127*, 161.

57 R. D. Cramer, E. L. Jenner, R. V. Lindsey, Jr., U. G. Stolberg, *J. Am. Chem. Soc.* **1963**, *85*, 1691.

58 H. van Bekkum, J. van Gogh, G. van Minnen-Pathuis, *J. Catal.* **1967**, *7*, 292.

59 L. P. van 't Hoff, B. G. Linsen, *J. Catal.* **1967**, *7*, 295.

60 F. van Rantwijk, G. J. Timmermans, H. van Bekkum, *Recl. Trav. Chim. Pays-Bas* **1976**, *95*, 39.

61 G. W. Parshall, *J. Am. Chem. Soc.* **1972**, *94*, 8716.

62 T. Yoshida, T. Yamagata, T. H. Tulip, J. A. Ibers, S. Otsuka, *J. Am. Chem. Soc.* **1978**, *100*, 2063.

63 R. Rumin, *J. Organomet. Chem.* **1983**, *247*, 351.

64 H. C. Clark, C. Billard, C. S. Wong, *J. Organomet. Chem.* **1979**, *173*, 341.

65 S. Paganelli, U. Matteoli, A. Scrivanti, C. Botteghi, *J. Organomet. Chem.* **1990**, *397*, 375.

66 J. Lin, C. U. Pittman, Jr., *J. Organomet. Chem.* **1996**, *512*, 69.

67 H. A. Tayim, J. C. Bailar, Jr., *J. Am. Chem. Soc.* **1967**, *89*, 3420.

68 G. W. Parshall, *J. Am. Chem. Soc.* **1966**, *88*, 704.

69 R. D. Cramer, R. V. Lindsey, Jr., C. T. Prewitt, U. G. Stolberg, *J. Am. Chem. Soc.* **1965**, *87*, 658.

70 H. Nowatary, K. Hirabayashi, I. Yasumori, *J. Chem. Soc., Faraday Trans.* **1976**, *72*, 2785.

71 J. A. Widegren, R. G. Finke, *J. Mol. Catal. A: Chem.* **2003**, *198*, 317.

5
Nickel

Elisabeth Bouwman

5.1
Introduction

Nickel is frequently used in industrial homogeneous catalysis. Many carbon–carbon bond-formation reactions can be carried out with high selectivity when catalyzed by organonickel complexes. Such reactions include linear and cyclic oligomerization and polymerization reactions of monoenes and dienes, and hydrocyanation reactions [1]. Many of the complexes that are active catalysts for oligomerization and isomerization reactions are supposed also to be active as hydrogenation catalysts.

The choice of nickel as a homogeneous hydrogenation catalyst is self-evident if one considers Nature. The hydrogenase enzymes make use of the abundantly available transition metals nickel and iron for the activation of dihydrogen or the reduction of protons. The nickel-containing hydrogenase enzyme is not able to hydrogenate organic substrates, but it can activate dihydrogen at atmospheric pressure and ambient temperatures [2]. Dihydrogen oxidation in living cells is coupled to the reduction of electron acceptors such as oxygen, nitrate, sulfate, carbon dioxide and fumarate, whereas proton reduction (dihydrogen evolution) is an essential element of pyruvate fermentation or the disposal of excess electrons. Studies of either *para*- to *ortho*-hydrogen conversion or H_2/D^+ (or D_2/H^+) exchange reactions indicate that in the hydrogenase active site dihydrogen is activated *via* a heterolytic pathway, forming a hydride and a proton, as shown schematically in Scheme 5.1 [2]. The rational design and synthesis of structural and functional models for hydrogenases [3], as well as their characterization and reactivity studies, might contribute to the development of new catalysts for practical use in, for example, fuel cells, as has been expertly described by Cammack et al. [4]. The advantage of the use of inexpensive nickel over costly metals such as rhodium or ruthenium is evident.

Despite the fact that Nature uses nickel for the activation of dihydrogen, and that Raney-Ni is one of the oldest and the most important heterogeneous hydrogenation catalysts, very few nickel complexes are known to catalyze the homoge-

The Handbook of Homogeneous Hydrogenation.
Edited by J.G. de Vries and C.J. Elsevier
Copyright © 2007 WILEY-VCH Verlag GmbH & Co. KGaA, Weinheim
ISBN: 978-3-527-31161-3

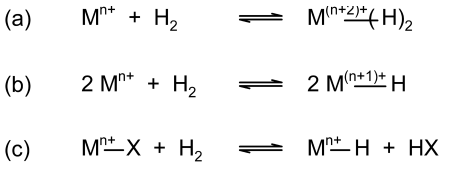

Scheme 5.1 Different modes of dihydrogen activation. (a) Oxidative addition, forming a metal dihydride species; (b) homolytic activation, forming two metal monohydride species; (c) heterolytic splitting, forming a metal hydride species and a proton.

neous hydrogenation reaction. In this section, a brief overview will be provided of mononuclear nickel complexes, which have been reported to catalyze homogeneously the hydrogenation of various olefins. Many of the reported nickel-containing hydrogenation catalysts are of the Ziegler type (i.e., a nickel salt in combination with a reducing agent such as trialkylaluminum), and in many cases it is questionable whether the reported complexes yield really homogeneous hydrogenation catalysts or that the observed catalytic hydrogenation activity is due to formation of colloidal (heterogeneous) nickel particles [5].

5.2 Coordination Chemistry and Organometallic Aspects of Nickel

5.2.1 Nickel–Hydride Complexes

The existence of hydride complexes of nickel has long been recognized, with the first reports of these compounds relying mainly on the evidence of ^{1}H-NMR investigations. The number of X-ray structures containing at least one nickel–hydride bond is rather limited, and the reported structures include a relatively large number of organometallic clusters. Only a limited number of mononuclear or dinuclear structures possibly relevant for hydrogenation catalysis have been reported. These complexes typically contain electron-donating phosphane ligands with cyclohexyl, isopropyl or tertiary-butyl groups at phosphorus. The synthesis of the nickel hydride complexes is usually achieved by reaction of nickel(II) halide complexes with the mild reducing agents such as $HBMe_3^-$ and BH_4^-, or by addition of H^+ to a nickel(0) complex.

An interesting nickel–hydride complex with a biologically relevant ligand arising from enzyme modeling has been reported by the group of Holm [6]. Reaction of the complex $[Ni(NS_3)Cl]^+$ (NS_3 = tris(*t*-butylsulfanylethyl)amine) with $NaBH_4$ results in the trigonal bipyramidal complex $[Ni(NS_3)H]^+$; the presence of the hydride was confirmed by a high-field ^{1}H-NMR resonance at –37.75 ppm. The latter complex reacts reversibly with ethene to form the ethyl complex, and it catalyzes the isomerization of 1-hexene [6]. A similar complex has been reported with the tripo-

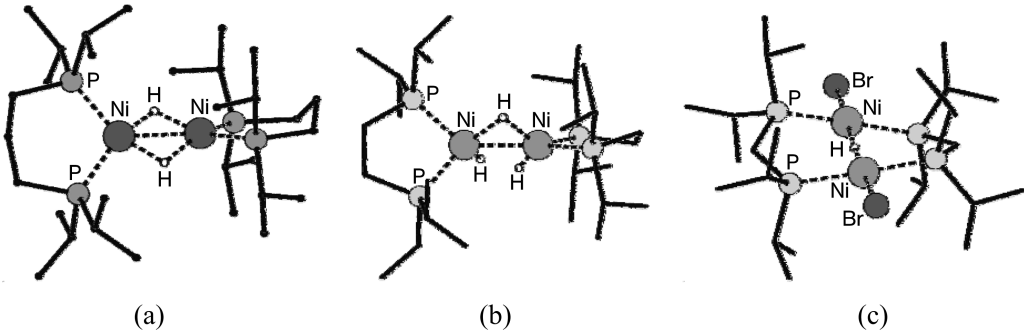

Fig. 5.1 Projection of hydride complexes:
(a) $[Ni(dippp)(\mu\text{-}H)]_2$ [15]; (b) $[\{HNi(dippe)\}_2(\mu\text{-}H)]^+$ [16];
(c) $[Ni_2Br_2(dippm)_2(\mu\text{-}H)]$ [17].

dal phosphorus ligand tris(2-diphenylphosphanylethyl)amine, but in this case substoichiometric amounts of hydride were found to be present in the complex [7].

Using monodentate phosphane ligands, only a few square-planar nickel(II) complexes have been reported, containing a hydride coordinated *trans* to a halide ion (based only on NMR evidence) [8], a phenolate group [9], an imine nitrogen [10], or a tetrahydridoborate anion [11]. The structures show significant distortion from the ideal square-planar geometry due to the bulky phosphane ligands. The hydride is visible in the ^{1}H-NMR spectra around –25 ppm as a triplet resulting from the coupling with two *cis* phosphane donors.

The use of chelating didentate phosphane ligands with an ethyl or propyl bridge often results in the formation of dinuclear nickel complexes with two bridging hydrides [12–15]. The complexes are readily formed by the reaction of the corresponding mononuclear nickel dichloride complex with mild reducing agents such as $HBMe_3^-$ or $HBEt_3^-$. In the resulting complexes of general formula $[P_2Ni(\mu\text{-}H)]_2$, the metal ion is formally nickel(I) with a nickel–nickel bond length of 2.4 Å. A projection of the structure of $[Ni(dippp)(\mu\text{-}H)]_2$ is shown in Figure 5.1 (a) (dippp = 1,3-bis(diisopropylphosphanyl)propane). Despite earlier predictions and theoretical calculations, the dinuclear core is nonplanar; the complexes are diamagnetic, showing the hydride resonance as a quintet around –10 ppm [12–15]. Bach et al. have studied the reactivity of the complex $[(dbpe)\text{-}Ni(\mu\text{-}H)]_2$ (dbpe = tBu$_2$PCH$_2$CH$_2$PtBu$_2$) with deuterium gas; scrambling was observed resulting in the formation of the monodeuteride and dideuteride complexes [14]. The ^{31}P-NMR spectrum of the complex $[(dbpe)Ni(\mu\text{-}H)]_2$ shows a singlet at +94.6 ppm; when a spectrum is recorded in an H_2 atmosphere it shows an additional singlet at +108 ppm which has been tentatively ascribed to a mononuclear nickel(II) dihydride complex, or to a nickel(IV) tetrahydride complex as a result of oxidative addition of dihydrogen, and which would be intermediates in the scrambling process [14].

The reaction of $[Ni(dippe)Br_2]$ (dippe = 1,2-bis(diisopropylphosphanyl)ethane) with $NaBH_4$ results in the formation of a dinuclear trihydride complex [{HNi-

(dippe)}$_2$(μ-H)]$^+$ (see Fig. 5.1 b) [16]. The structure shows a bridging hydride at a bent angle as well as a Ni–Ni bond with a distance of 2.3 Å. The complex is diamagnetic and displays one quintet at –13.4 ppm, indicating rapid interconversion of the bridging hydride with the terminal hydrides. The structure can be regarded as a protonated form of the dihydrides described above, but attempts to deprotonate the complex have failed, even using a strong base [16].

The small bite-angle ligands dcpm (bis(dicyclohexylphosphanyl)methane) or dippm (bis(diisopropylphosphanyl)methane) yield dinuclear nickel complexes of formula [Ni_2X_2(μ-P_2)$_2$(μ-H)] (X = halide) with one hydride bridging the two nickel centers [17, 18]. The ligands in these complexes are not chelating, but are binding two nickel ions. The compounds are mixed-valent, containing a nickel(I) and a nickel(II) ion. The complexes are therefore paramagnetic and for [Ni_2Cl_2(μ-dcpm)$_2$(μ-H)] a *g*-value of 2.139 at room temperature was reported [18]. The complex [Ni_2Cl_2(μ-dcpm)$_2$(μ-H)] is bent, with a Ni–H–Ni angle of 128° and a Ni–Ni distance of 2.9 Å [18], whereas the complex [Ni_2Br_2(μ-dippm)$_2$-(μ-H)] (see Fig. 5.1 c) is nearly planar with a Ni–H–Ni angle of 178° and a Ni–Ni distance of 3.2 Å [17].

A mononuclear nickel hydride complex with three N-heterocyclic carbene ligands has been reported; the compound was formed by oxidative addition of an imidazolium salt to the Ni(0) bis(carbene) complex [19]. The hydride signal of this nickel(II) complex appears at –15 ppm.

Recently, the crystal structure of a nickel(II) complex with a tridentate silyl ligand has been reported [20]. The structure in the solid state shows an η^2-(Si–H) binding to nickel, with a Ni–H distance of 1.47 Å; NMR spectra of the complex in solution at –80 °C suggest the formation of a nickel(IV) hydride species through oxidative addition of the silyl-hydrogen to nickel [20].

5.2.2
Nickel–Alkene and Nickel–Alkyl Complexes

A large number of (mostly zero-valent) nickel–alkene complexes has been reported. Although these complexes have not been recently reviewed, their general properties and structures were expertly described in 1982 [21]. A complete overview of the reported nickel–alkene and nickel–alkyl complexes is beyond the scope of this section, in which a selection of nickel–alkene and nickel–alkyl complexes is described, mostly related to possible intermediates in hydrogenation catalysis.

The reaction of [Ni(ethene)$_3$] with a hydride donor such as trialkyl(hydrido)-aluminate results in the formation of the dinuclear anionic complex [{Ni(ethene)$_2$}$_2$H]$^-$ [22]. The nickel(0) centers in this complex are in a trigonal planar environment of two ethene molecules and a bridging hydride ion, with the ethene carbons in the plane of coordination. The two planes of coordination within the dinuclear complex are almost perpendicular to each other, and the Ni–H–Ni unit is significantly bent, with an angle of 125° and a Ni–Ni distance of 2.6 Å [22].

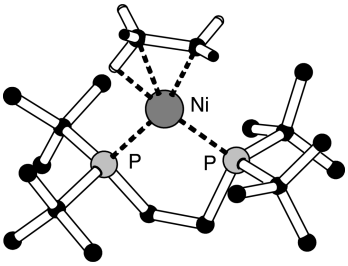

Fig. 5.2 Projection of [Ni(dbpe)(ethyl)] [23].

Protonation of (diphosphane)nickel(0)–ethene complexes with $HBF_4 \cdot OEt_2$ results in the formation of the corresponding cationic three-coordinate nickel(II)–alkyl complexes, in which a β-agostic hydrogen is present [23]. Figure 5.2 illustrates the structure of [Ni(dbpe)(ethyl)] with an agostic Ni–H distance of 1.64 Å [23]. For these nickel complexes, β-elimination and alkene rotation appeared to be slow on the NMR timescale at temperatures below 27 °C. NMR spectroscopy at 20 °C revealed a multiplet at –1.24 ppm for the three protons at the β-carbon, whereas at –100 °C a broad signal at –5.8 ppm is assigned to the agostic hydrogen [23].

In contrast, the fluxionality of neutral three-coordinate nickel(II)–alkyl complexes with β-diketiminato ligands is described in a recent publication [24]. The β-agostic complexes undergo facile β-elimination and reinsertion resulting in a mixture of primary and secondary nickel(II)–propyl complexes [24]. The corresponding four-coordinate, square-planar complexes with an additional nitrogen-donor ligand do not show β-agostic interactions in the solid state. In solution, however, dissociation of the nitrogen-donor ligand readily occurs and in the NMR spectra resonances are observed that are due to a β-agostic hydrogen interaction of the coordinated alkyl group [25]. Similarly, the neutral (acetylacetonato)(triphenylphosphane)nickel(II)–ethyl complex does not show agostic interactions in the square-planar solid-state structure, whereas in solution scrambling of the alkyl protons is observed [26]. In another recent report a remarkably stable dinuclear nickel(II)–hexyl complex has been reported; the compound does not show any agostic interactions, neither in the solid state nor in solution [27].

5.2.3
Mechanistic Aspects of Hydrogen Activation

For catalytic hydrogenation the activation of a dihydrogen molecule, the binding of an alkene, and the formation of a metal–alkyl intermediate are the most crucial aspects of a plausible catalytic mechanism. Support for a nickel–hydride mechanism in the oligomerization of ethene by nickel complexes with a chelating phosphorus–oxygen ligand was obtained through the crystallization of a complex trapped with triphenylphosphane [28]. The proton NMR spectrum of this complex shows the hydride resonance at –24.85 ppm as a double doublet due to the two *cis* phosphorus atoms [28].

Protonation mechanisms of nickel complexes and the relevance to hydrogenases, as well as to industrial catalysts, have recently been reviewed [29]. The huge interest in the possibilities of a hydrogen economy, based on the cheap and sustainable generation of H_2, and the clean and efficient oxidation of H_2 in fuel cells has given impetus to the research for functional models of hydrogenases. In the search for active functional models for [NiFe] hydrogenases, nickel complexes are tested on hydrogenase activity and three types of reactivity can be distinguished: 1) H_2/D^+ exchange (scrambling); 2) activation of H_2 (oxidation to H^+); and 3) reduction of H^+ to H_2. For functional models of the [NiFe] hydrogenases the first two activities are of importance.

Bis(diphosphane)nickel complexes have been reported to show heterolytic splitting of dihydrogen [30]. The complex $[Ni(PNP)_2](BF_4)_2$, in which PNP is the ligand $Et_2PCH_2N(Me)CH_2PEt_2$, possesses both hydride and proton acceptor sites. When dihydrogen gas is passed through a solution of $[Ni(PNP)_2]^{2+}$ in acetonitrile or dichloromethane, the solution bleaches during formation of the hydride species $[HNi(PNHP)(PNP)]^{2+}$, in which one of the central nitrogen atoms of the ligands is protonated. In the ^{1}H-NMR of the complex $[HNi(PNHP)(PNP)]^{2+}$ at low temperatures, two resonances are observed at –15.2 and 7.4 ppm, that have been assigned to the hydride and the NH-proton, respectively. The hydride and the NH-proton undergo rapid intramolecular exchange with each other and with protons in solution [30].

The structures and reactivity of the nickel complexes described above seem to indicate that, for nickel-containing hydrogenation catalysts, heterolytic activation of dihydrogen may be the most likely mechanistic pathway. The nickel–hydride complexes are stabilized by the presence of electron-donating phosphane ligands, making the nickel complexes with these ligands the most likely candidates for active homogeneous hydrogenation catalysts.

5.3 Hydrogenation Catalysis

5.3.1 Ziegler Systems

The so-called Ziegler-type catalysts have been studied rather extensively. This type of catalyst is formed by treating a transition-metal salt with a reducing agent. The most frequently used reducing agents include trialkylaluminum, alkylaluminum chlorides, alkali metals, $LiAlH_4$, and $NaBH_4$. The mixtures yield dark, air-sensitive solutions that appear homogeneous to the eye, but most likely contain colloidal metal [5]. Ziegler-type catalysts made from cobalt or nickel salts with triethylaluminum can be used for the hydrogenation of benzene to cyclohexane under rather mild conditions (155 °C, 10 bar). In a typical patent example, benzene is hydrogenated to cyclohexane (99% conversion) with more than 2500 turnovers after 1 h, using a catalyst prepared from a mixture of nickel and

zinc octoates and excess triethylaluminum [31]. A process has been developed by Institut Français du Petrole [32].

Ziegler-type hydrogenation catalysts have been used for the hydrogenation of vegetable oils [33, 34], cyclohexadienes [35], and butadiene rubbers [36–38]. Under rather mild (1 bar H_2, 40 °C) conditions (substituted) 1,4-cyclohexadienes can be hydrogenated selectively to the cyclohexenes in yields of up to 80%; trace amounts of benzene were detected as a result of disproportionation reactions [35]. The active catalyst was prepared from $[Ni(acac)_2]$ (Hacac = acetylacetone), $Et_3Al_2Cl_3$ (10 equiv. to Ni) and PPh_3. The activity is rather low, and with a substrate : catalyst ratio (SCR) of 100 complete conversion is reached after 6 to 28 h. Isomerization of the substituted cyclohexadienes occurred, and a mechanistic pathway involving η^3-allyl coordination of the substrate was proposed. Dihydrogen activation was proposed to occur via oxidative addition [35].

Recent investigations into the hydrogenation of rubbers include catalytic systems prepared from nickel(II) 2-ethylhexanoate or nickel(II) acetylacetonate activated with triisobutylaluminum [36], triethylaluminum [38], or butyl lithium [37, 38]. Large amounts of co-catalysts (initiator) are necessary. Hydroxyl-containing polybutadienes were hydrogenated at low H_2 pressures, affording the saturated polymers with full retention of the OH functionality [38]. Again, the activity of the catalysts is rather low, with SCRs of approximately 20 having been used.

5.3.2
Nickel Complexes of Oxygen- or Nitrogen-Containing Ligands

Catalytic homogeneous hydrogenation of cyclohexene has been claimed for simple systems such as nickel(II) acetylacetonate [39] or a nickel–chloride complex with two monodentate amines [40]. The latter complex was used as comparison for a heterogeneous catalyst obtained by impregnation of the complex on γ-alumina [40]. SCRs of 100 were used at 30 atm. H_2 and temperatures up to 100 °C, resulting in conversions of only 20–35% after 1 h.

Nickel complexes of simple tetradentate ligands containing nitrogen- and oxygen-donor atoms have also been investigated for their catalytic activity in homogeneous hydrogenation [41–43]. The complex [Ni(saloph)] (saloph = bis(salicylidene)phenylenediamine) has been reported to catalyze the hydrogenation of cyclohexene to cyclohexane and cyclooctene to cyclooctane at a moderately high dihydrogen pressure of 60 bar and a temperature of 50 °C [42]. The catalyst is more reactive in the hydrogenation of cyclohexene than in the hydrogenation of cyclooctene, the turnover frequency (TOF) being 13 h^{-1} and 7 h^{-1}, respectively (SCR 100, t = 5 h, in ethanol). The reaction is suggested to proceed *via* the high-valent $[Ni^{IV}(saloph)(H)_2]$ species, which supposedly is formed through the oxidative addition of dihydrogen to the divalent [Ni(saloph)] complex [42]. It has been claimed that encapsulation of the analogous nickel complex [Ni(salen)] (salen = bis(salicylidene)ethylenediamine) in zeolite Y also results in a homogeneous catalyst for hydrogenation reactions [44]. The hydrogenation of 1,5,9-cyclododde-

catriene has been investigated using similar salen-type nickel complexes under rather harsh conditions (150 °C, 50 bar), but giving rather low activities (TOF $<14\ h^{-1}$) [41]. In a recent study, nickel complexes of similar tetradentate ligands derived from pyrrole 2-carboxaldehyde and various diamines were used as catalysts in the hydrogenation of phenylacetylene [43]. The activity of these systems is also rather low, and complete conversion was not even reached after 24 h (SCR 150, at 40 °C and 1 bar). Also in this case activation of dihydrogen is believed to proceed via oxidative addition to give a Ni(IV) dihydride intermediate [43].

$[Ni(acac)_2]$ has been reported to be an active catalyst for the hydrogenation of cyclohexene to cyclohexane in methanol at moderate pressures and high temperature. At 100 °C and a H_2 pressure of 30 bar, a TOF of $450\ h^{-1}$ is reported (SCR 1000, t = 1 h, in methanol). From a study including pretreatment of the catalyst under a nitrogen atmosphere, it was concluded that alkene coordination precedes hydrogen activation [39]. $[Ni\text{-}(acac)_3]$ has been used for the catalytic hydrogenation of unsaturated fatty acids and esters [45]. No hydrogenation activity is observed at temperatures below 100 °C. After an induction period of 3 h, methyl linolenate can be hydrogenated with a TOF of $10\ h^{-1}$ (SCR 10, t = 1 h, 100 °C, 7 bar, in methanol). It is quite likely that the actual catalyst is heterogeneous, as an induction period is needed and black precipitates are formed during the hydrogenation reaction.

5.3.3
Nickel Complexes of Triphenylphosphane

The tetrahedral nickel complexes $[NiX_2(PPh_3)_2]$ (X = Cl, Br, or I) have been reported to show catalytic activity in the hydrogenation of linear, cyclic, terminal, and sterically hindered olefins; a summary of the reported activities in the hydrogenation of various substrates is provided in Table 5.1 [46–50]. The catalytic activity of the different halide complexes in the hydrogenation of methyl linoleate decreases in the order I > Br > Cl, but also when the iodide complex is used the activities remain extremely low, even at elevated temperatures and pressures [46]. Selective hydrogenation of polyunsaturated compounds to monounsaturated compounds is observed, as well as migration of the double bond and the isomerization of *cis*- to *trans*-alkenes. Nonconjugated dienes are assumed to be converted into conjugated dienes through migration of the double bonds. Subsequently, these conjugated dienes are hydrogenated to monoenes. Monoolefins are hardly further hydrogenated. The isomerization reaction was found not to occur in the absence of dihydrogen. Therefore, it was suggested that both the hydrogenation and isomerization reaction proceed *via* a monohydride species and that dihydrogen is activated via a heterolytic pathway [46].

Similar low activities were found in the hydrogenation of 1-octene [47]. The use of $[Ni(PPh_3)_2I_2]$ in the hydrogenation of norbornadiene resulted in considerable amounts of nortricyclene, *via* transannular ring closure, whereas 1,5-cyclooctadiene yielded bis-cyclo-[3.3.0]oct-2-ene. According to these authors, the re-

Table 5.1 Hydrogenation of several substrates in the presence of the nickel complex $[Ni(PPh_3)_2I_2]$.[a])

Entry	Substrate	pH_2 [bar]	T [°C]	TOF[b)]	Main product	Reference
1	1,5,9-cyclododecatriene	78.5	175	165	cyclododecene	50
2	1,5,9-cyclododecatriene	50	100	1	cyclododecene	49
3	methyl linoleate	40	90	2	methyl oleate	46
4	1,3-cyclooctadiene	50	100	8	cyclooctene	49
5	1,5-cyclooctadiene	50	100	9	cyclooctene[c)]	49
6	2,5-dimethyl-1,5-hexadiene	50	100	7	2,5-dimethyl-2-hexene	49
7	2,5-dimethyl-2,4-hexadiene	50	100	8	2,5-dimethyl-2-hexene	49
8	isoprene	50	100	0		49
9	norbornadiene	50	100	29	nortricyclene[d]	49
10	methyl oleate	40	90	0		46
11	methyl *cis*-9,*cis*-15-octadecadienoate	40	90	trace	monoene	48
12	1-octene	1	20	trace	*n*-octane	47

a) Reaction conditions for entry 1: SCR = 100, t = 30 min, no solvent added; entries 2, 4–9: SCR = 15 (59 for entry 8), t = 1 h (30 min for entry 9), in acetic acid; entries 3, 10, 11: SCR = 5 (9 for entry 11), t = 3 h, in benzene.
b) Turnover frequency in mol converted substrate per mol Ni per hour, calculated from data in [46–50].
c) Transannular ring closure was also observed.
d) *Via* transannular ring closure, nortricyclene is further hydrogenated to norbornane.

sults suggested the involvement of a η^3-allyl-nickel intermediate in the catalytic cycle [49]. Kinetic studies have been undertaken for the hydrogenation of 1,5,9-cyclododecatriene to cyclododecene, using the catalyst $[Ni(PPh_3)_2I_2]$ under rather harsh conditions (155–175 °C, 80 bar) [50]. It was proposed that a monohydride–nickel complex is the active species, and dihydrogen activation was proposed to proceed via oxidative addition [50].

5.3.4
Nickel Complexes of Didentate Phosphane Ligands

The catalytic activity of nickel(II) acetate in combination with a number of chelating phosphane ligands in the hydrogenation of 1-octene has been studied extensively during the past decade [51–56]. It was found that *in-situ*-prepared mixtures of nickel(II) acetate with the electron-donating ligands *o*-MeO-dppe, *o*-MeO-dppp, dcpe, or dcpp (see Scheme 5.2) achieved quite high activities in the hydrogenation of 1-octene, the nonoptimized catalytic systems showing turnover numbers (TONs) of up to 460 per hour at 25 °C and 50 bar [51]. In

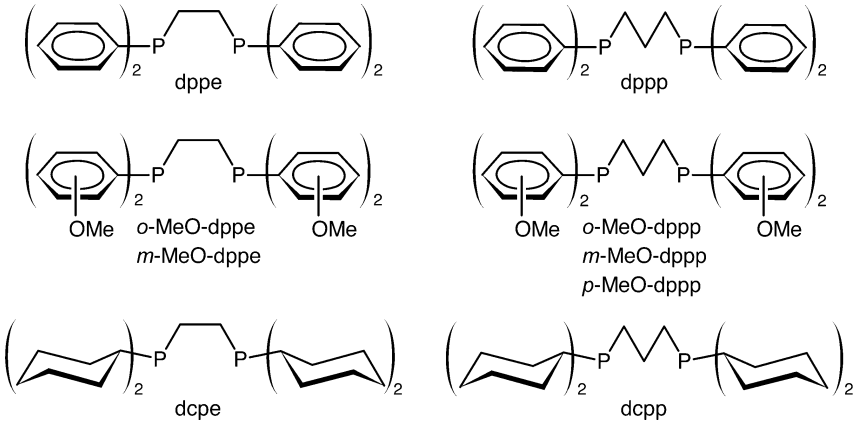

Scheme 5.2 Structure of the ligands used. dppe: 1,2-*bis*(diphenylphosphanyl)ethane; *o*-MeO-dppe: 1,2-*bis*(di(*o*-methoxyphenyl) phosphanyl)ethane; dcpe: 1,2-*bis*(dicyclohexylphosphanyl)ethane; *m*-MeO-dppe: 1,2-*bis* (di(*m*-methoxyphenyl)phosphanyl)ethane; dppp: 1,3-*bis*(diphenylphosphanyl)propane; *o*-MeO-dppp: 1,3-*bis*(di-*o*-methoxyphenylphosphanyl)propane; dcpp: 1,3-*bis*(dicyclohexylphosphanyl)propane; *m*-MeO-dppp: 1,3-*bis*(di(*m*-methoxyphenyl)phosphanyl)propane; *p*-MeO-dppp: 1,3-*bis*(di(*p*-methoxyphenyl)phosphanyl)propane.

contrast, use of the simple ligands dppe or dppp resulted in inactive systems; the results are summarized in Table 5.2 [51].

In a first attempt to separate electronic from steric effects of the *ortho*-methoxy group, the *meta* and *para* analogues of the methoxy-substituted ligands were also tested for hydrogenation activity. None of these showed any hydrogenation activity, however, seemingly indicating that the positive effect of the *ortho*-methoxy group should be attributed mainly to steric effects [51].

In order to explain the differences in catalytic activity of nickel compounds containing the various ligands, the behavior of the nickel complexes in solution was investigated in more detail, for which NMR spectroscopy appeared to be a valuable tool [54]. Using ^{1}H- and ^{31}P{^{1}H}-NMR spectroscopy, the behavior of the complexes has been studied in several solvents. It appeared that, in solutions, the nickel complexes of the ligand *o*-MeO-dppe are involved in ligand-exchange reactions; the mono(ligand) complexes [Ni(*o*-MeO-dppe)X_2] are in equilibrium with bis(ligand) complexes $[Ni(o\text{-MeO-dppe})_2]^{2+}$ and "naked" (solvated) nickel ions $[\text{“}NiX_4\text{”}]^{2-}$ (see Scheme 5.3) [54]. The exact nature of the species "NiX_4^{2-}" is dependent on the solvent and the anions; in coordinating solvents it may exist as $[Ni(solvent)_6]^{2+}$. The position of the equilibrium appeared to be highly dependent on the anion X and the solvent used. In a polar solvent in combination with weakly coordinating anions, only the bis(ligand) complex was observed, whereas in an apolar solvent in combination with coordinating anions only the mono(ligand) complex was present. From these studies it appeared that the differences in catalytic hydrogenation activity of nickel(II) acetate in combi-

Table 5.2 Nickel-catalyzed hydrogenation of 1-octene.[a)]

Entry	Ligand	$TOF_{1\text{-octene}}$[b)]	$S_{n\text{-octane}}$[c)]	[Ni] [mM]	SCR
At 25 °C					
1	dppe	0		1.8	1000
2	dppp	2	100	1.8	1000
3	*o*-MeO-dppe	8	100	1.4	2000
4	*o*-MeO-dppp	500	100	1.4	2000
5	dcpe	2000[d)]	98	3.6	500
6	dcpe	1740	80	1.4	2000
7	dcpp	360	97	3.6	500
At 50 °C					
8	dppe	0		1.8	1000
9	dppp	0		1.8	1000
10	*o*-MeO-dppe	400	94	1.4	2000
11	*o*-MeO-dppp	1160	99	1.4	2000
12	dcpe	1990	83	1.4	2000
13	*m*-MeO-dppe[e)]	0		3.6	500
14	*m*-MeO-dppp[e, f)]	0		3.6	500
15	*p*-MeO-dppp[f)]	10	0	3.6	500

a) Reaction conditions: Ni:ligand ratio = 1, t = 1 h, pH_2 = 50 bar, in 20 mL methanol.
b) Turnover number in mol converted 1-octene per mol $Ni(OAc)_2$ after 1 h.
c) Selectivity towards *n*-octane (mol *n*-octane per mol converted 1-octene).
d) Complete conversion after 15 min.
e) No clear solution could be obtained after mixing nickel(II) acetate and the ligand.
f) Reaction performed in ethanol.
All data taken from [57].

nation with dppe or *o*-MeO-dppe could not be rationalized by the assumption that the bulkier ligand would prevent the formation of inactive bis(ligand) complexes. A comparison of the behavior of the nickel complexes of the ligand *o*-MeO-dppe with the unsubstituted analogue dppe showed that the latter ligand was more readily oxidized [54]. The source of the oxygen was unknown; as the experiments were carried out in an inert atmosphere the oxidation seemed to be related to the nickel(II) center, as observed previously [58]. It has been reported earlier that $Pd(OAc)_2$ is able to oxidize tertiary phosphanes [59]. This possibility of oxidation was found to play a major role in the case of the nickel complexes of the propane-bridged ligands *o*-MeO-dppp and dppp, as for both of these ligands the formation of bis(ligand) complexes is not possible, but only the substituted ligand *o*-MeO-dppp yields an active catalyst [53]. Prevention of oxidation of the phosphorus atom by the *ortho*-methoxy group is most likely due to steric effects; nickel(II) acetate in combination with *p*-MeO-dppp did not

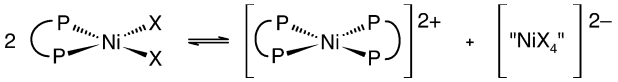

Scheme 5.3 Schematic representation of the ligand-exchange equilibrium.

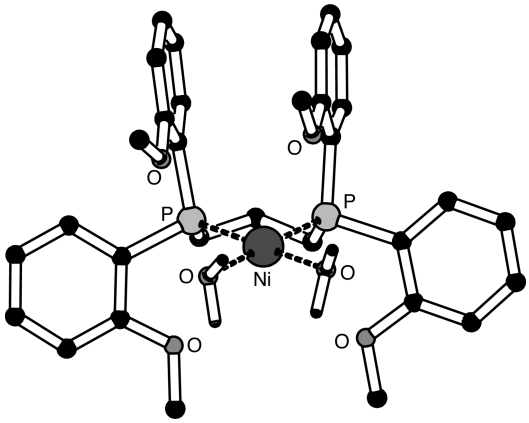

Fig. 5.3 Projection of $[Ni(o\text{-MeO-dppp})(H_2O)_2]^{2+}$.

yield an active hydrogenation catalyst [51], and $^{31}P\{^1H\}$-NMR spectroscopy showed that also in this case the ligand is rapidly oxidized [54].

The inability to form a *bis*(ligand) complex with the ligand *o*-MeO-dppp is most likely due to a combination of the large bite angle caused by the propylene-bridge in the ligand, and the rather small ionic radius of the nickel(II) ion. Attempts to synthesize a *bis*(ligand) complex using the ligand *o*-MeO-dppp were unsuccessful. Instead, an unprecedented low-spin nickel complex containing two coordinated water molecules was formed – that is the complex $[Ni(o\text{-MeO-dppp})(H_2O)_2](PF_6)_2$ (Fig. 5.3) [53]. This complex yields a highly active and selective hydrogenation catalyst, with a TOF of 2800 h^{-1} in the hydrogenation of 1-octene [55]. The impossibility to form a *bis*(ligand) complex might be the most important reason for the considerably higher hydrogenation activity of catalysts based on this ligand, compared to those based on *o*-MeO-dppe [53].

The catalytic activity of nickel(II) complexes of didentate phosphane ligands containing *ortho*-methoxy phenyl, *ortho*-ethoxy phenyl or cyclohexyl groups in the hydrogenation of 1-octene has been studied in more detail [55, 56]. The only observed side reaction in the hydrogenation of 1-octene is the isomerization to internal alkenes. The factors which influence the availability and accessibility of the coordination sites in the catalytically active species are solvent, anion, and amount and nature of ligand. The influence of these factors has been investigated using catalysts containing *o*-MeO-dppp, as these are not prone to ligand-exchange equilibria [55]. The presence of a solvent that is both polar and protic has been found to be essential in order to observe catalytic activity. This catalytic

activity is furthermore inversely related to the coordination ability of the anion. In the case of *o*-MeO-dppe, the catalyst is not active at all at a ligand-to-metal ratio higher than 2. In the case of *o*-MeO-dppp, the catalytic activity gradually decreases with increasing ligand-to-metal ratio. At a ratio of 5 : 1 an activity of 77 turnovers after 1 h is still observed, though the selectivity for hydrogenation has fallen considerably (70%). Although the ligand-exchange equilibrium occurs, the nickel complexes containing the ligands *o*-MeO-dppe and *o*-EtO-dppe still yield active hydrogenation catalysts. The presence of the more bulky ethoxy groups instead of the methoxy groups increases the hydrogenation activity by a factor of three, with the TOF rising from 400 h^{-1} to 1200 h^{-1}; the selectivity for *n*-octane, however, is decreased from 99 to 65% [55]. The type of ligand merely influences the accessibility of the axial or equatorial coordination sites for the reactants, and hence the selectivity towards the hydrogenated product *n*-octane [55]. With the ligand dcpe, very active hydrogenation catalysts are obtained; at 50 °C and 50 bar H_2, TONs of up to 3000 h^{-1} have been reached, although also in this case the selectivity was decreased to 88% [56].

The kinetics of the nickel-catalyzed hydrogenation of 1-octene have been studied using nickel(II) acetate in combination with the ligand *o*-MeO-dppp [52]. The effects of temperature and dihydrogen pressure, as well as the influence of nickel and substrate concentrations have been studied (T = 30–60 °C, pH_2 = 30–60 bar, [Ni] = 0.35–2.81 mM, [1-octene] = 0.98–3.91 M, ligand : Ni ratio = 1.1 in a mixture of dichloromethane and methanol). The kinetic study resulted in the surprisingly simple rate law: $r = k_{cat}[Ni][1\text{-octene}]pH_2$. These kinetic data are consistent with a mechanism in which the terminating hydrogenolysis step of the nickel–alkyl complex is the rate-determining step of the catalytic cycle with all preceding steps at equilibrium. The first-order dependence in the nickel concentration indicates that dinuclear nickel complexes with bridging hydrides are not present during catalysis, and that thus only mononuclear nickel complexes are present [52]. This absence of dinuclear species is remarkable, as these dinuclear complexes are known for a number of didentate phosphane ligands (see Section 5.2.1). The first-order dependence of the substrate was confirmed by the results with other substrates, as the hydrogenation rate was seen to depend strongly on the nature of the substrate. The results for some different substrates are listed in Table 5.3 [52]. The rate of hydrogenation of the internal alkene cyclooctene was much lower than that of the terminal alkene 1-octene. The hydrogenation of ethene was found to be very rapid, with an estimated TOF of 9000 h^{-1}; this is quite unusual, as ethene is not hydrogenated by the generally very active Wilkinson's catalyst [60].

The homogeneous nature of the catalysts is confirmed by the linear dependence of the catalytic activity on the concentration of nickel(II). Only in the case of a truly homogeneous catalyst is the activity expected to be directly proportional to the catalyst concentration. In the case of the formation of nanoclusters, larger agglomerates – and, therefore, a comparatively lower number of active sites – will be formed at higher concentrations of the nickel salt. Furthermore, a sigmoidal curve for the rate of consumption of substrate has been proposed

Table 5.3 Different substrates in the homogeneous hydrogenation catalyzed by *in-situ* mixtures of $Ni(OAc)_2$ and *o*-MeO-dppp.[a)]

Entry	Substrate	TOF[b)]	SCR	Main product
1	1-octene	1480	2000	*n*-octane
2	ethene[c)]	9000	2000	ethane
3	cyclooctene	30	400	cyclooctane
4	1,7-octadiene	30	1000	1-octene
5	styrene	0	200	
6	1-octyne	0	250	

a) Reaction conditions: [Ni] = 2.5 mM (before substrate is added), t = 1 h, pH_2 = 50 bar, T = 50 °C, in 20 mL dichloromethane/methanol (1 : 1, v/v).
b) Turnover is mol converted substrate per mol nickel in 1 h.
c) T = 40 °C and t = 10 min.
All data taken from [52].

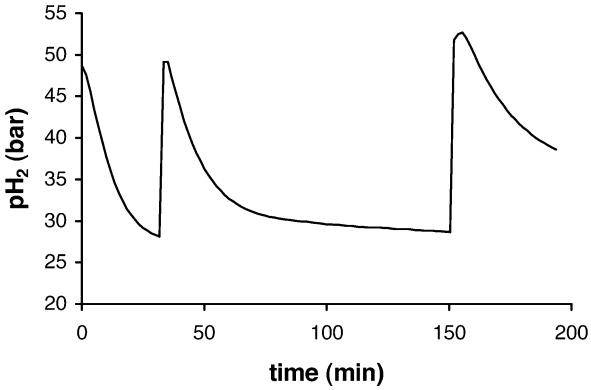

Fig. 5.4 Dihydrogen pressure drop of the hydrogenation of 1-octene using an *in-situ*-formed catalyst containing $Ni(OAc)_2$ and the ligand *o*-MeO-dppe. After 30 and 150 min, fresh 1-octene is added to the reaction mixture and the H_2 pressure is reset to 50 bar. (Reproduced from [57])

as being characteristic for the nanocluster formation reaction [5]. For the nickel(II) catalysts with didentate phosphane ligands the hydrogenation reaction starts immediately without any induction period (Fig. 5.4) [57]. In addition, it is possible to regenerate the catalysts from the reaction mixtures after the hydrogenation experiments. These results – in combination with the observation that pure nickel(II) acetate does not lead to an active catalyst under the applied reaction conditions (50 °C) and the excellent reproducibility of the results – lead to conclusion that the reported nickel(II) complexes of didentate phosphane ligands yield truly homogeneous hydrogenation catalysts.

5.4 Concluding Remarks

Many Ziegler-type catalytic systems, in addition to a few mononuclear nickel complexes of nitrogen- or oxygen-containing ligands, have been reported as being homogeneous hydrogenation catalysts for a number of substrates. In most of these cases, it is doubtful whether the reported nickel complexes really yield homogeneous hydrogenation catalysts; it is more likely that catalytic hydrogenation activity is due to formation of colloidal (heterogeneous) nickel particles. Despite the recent report of a nickel(IV) hydride species [20], the assumption that dihydrogen activation in these catalytic systems would proceed via oxidative addition remains dubious.

Nickel(II) complexes with the correct choice of a didentate phosphane ligand do yield very active homogeneous hydrogenation catalysts. It has been found that nickel complexes with chelating diphosphane ligands may be involved in three different processes, namely ligand-exchange reactions, ligand oxidation, and the actual hydrogenation reaction (see Scheme 5.4).

The larger bite angles of the C_3-bridged ligands preclude the ligand-exchange equilibrium, the ionic radius of the nickel(II) ion being too small to accommo-

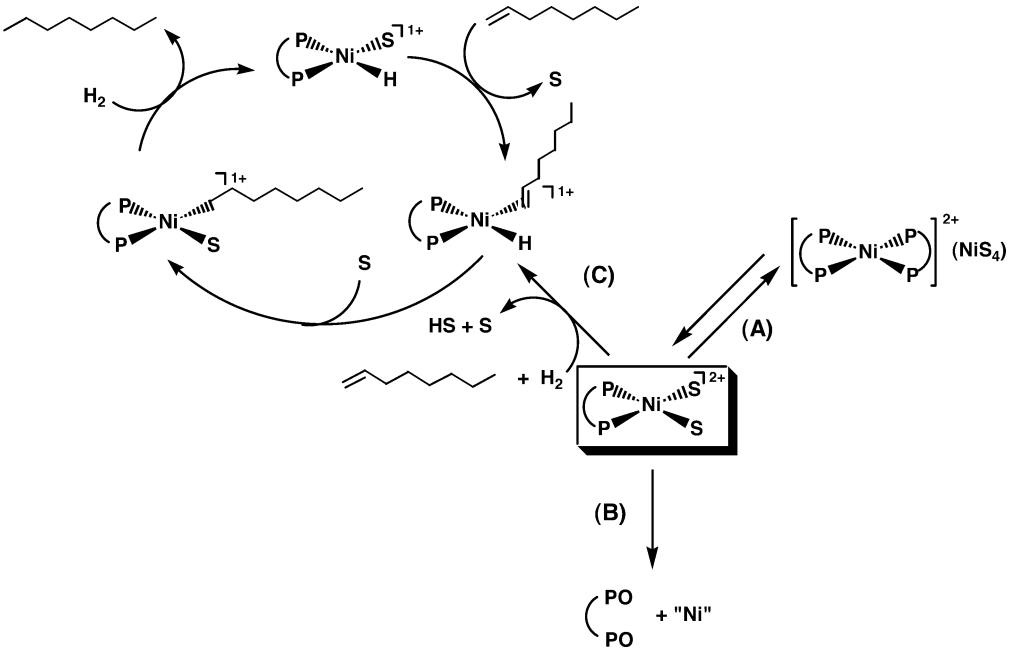

Scheme 5.4 Three processes in which nickel diphosphane complexes can be involved under catalytic hydrogenation conditions. (A) ligand exchange; (B) oxidation; and (C) hydrogenation of 1-octene. For simplicity, the reaction steps are not depicted as equilibria and the isomerization reaction has been omitted. In this scheme, S depicts a solvent molecule, but it might also be an anion.

date two of these didentate ligands in a square-planar geometry. Considering the C_2-bridged ligands, only dcpe (see Scheme 5.2) has a ligand cone that is large enough to prevent coordination of a second didentate ligand. It is assumed that the nickel(II) ion catalyzes the oxidation of tertiary phosphane ligands. This oxidation appeared to be very rapid in the case of the unsubstituted ligands dppe and dppp, whereas it is relatively slow for *o*-MeO-dppe and *o*-MeO-dppp. Most probably, the electronic properties of the ligand influence the oxidation sensitivity of the ligand in the presence of nickel.

If the ligand-exchange reaction, as well as oxidation of the ligand, could be prevented, then the formation of highly active hydrogenation catalysts with simple diphosphane ligands might be possible. Consequently, the bulk application of inexpensive, nickel-containing homogeneous hydrogenation catalysts might come within reach.

Abbreviations

SCR substrate : catalyst ratio
TOF turnover frequency
TON turnover number

References

1 W. Keim, *Angew. Chem., Int. Ed. Engl.* **1990**, *29*, 235.
2 R. Cammack, P. van Vliet. In: *Bioinorganic Catalysis*, 2nd edn. J. Reedijk, E. Bouwman (Eds.), Marcel Dekker, Inc., New York, **1999**.
3 E. Bouwman, J. Reedijk, *Coord. Chem. Rev.* **2005**, *249*, 1555.
4 R. Cammack, M. Frey, R. Robson, *Hydrogen as a Fuel: Learning from Nature*. Taylor & Francis, London and New York, **2001**.
5 J.A. Widegren, R.G. Finke, *J. Mol. Catal.* **2003**, *198*, 317.
6 P. Stavropoulos, M.C. Muetterties, M. Carrié, R.H. Holm, *J. Am. Chem. Soc.* **1991**, *113*, 8485.
7 L. Sacconi, A. Orlandini, S. Midollini, *Inorg. Chem.* **1974**, *13*, 2850.
8 K. Jonas, G. Wilke, *Angew. Chem., Int. Ed. Engl.* **1969**, *8*, 519.
9 A.L. Seligson, R.L. Cowan, W.C. Trogler, *Inorg. Chem.* **1991**, *30*, 3371.
10 M. Aresta, E. Quaranta, A. Dibenedetto, P. Giannoccaro, I. Tommasi, M. Lanfranchi, A. Tiripicchio, *Organometallics* **1997**, *16*, 834.
11 T. Saito, M. Nakajima, A. Kobayashi, Y. Sasaki, *J. Chem. Soc., Dalton Trans.* **1978**, 482.
12 K. Jonas, G. Wilke, *Angew. Chem.* **1970**, *82*, 295.
13 B.L. Barnett, C. Kruger, Y.H. Tsay, R.H. Summerville, R. Hoffmann, *Chem. Ber.* **1977**, *110*, 3900.
14 I. Bach, R. Goddard, C. Kopiske, K. Seevogel, K.R. Pörschke, *Organometallics* **1999**, *18*, 10.
15 M.D. Fryzuk, G.K.B. Clentsmith, D.B. Leznoff, S.J. Rettig, S.J. Geib, *Inorg. Chim. Acta* **1997**, *265*, 169.
16 M. Jiménez Tenorio, M.C. Puerta, P. Valerga, *J. Chem. Soc., Dalton Trans.* **1996**, 1305.
17 D.A. Vicic, T.J. Anderson, J.A. Cowan, A.J. Schultz, *J. Am. Chem. Soc.* **2004**, *126*, 8132.
18 C.E. Kriley, C.J. Woolley, M.K. Krepps, E.M. Popa, P.E. Fanwick, I.P. Rothwell, *Inorg. Chim. Acta* **2000**, *300*, 200.

19 N. D. Clement, K. J. Cavell, C. Jones, C. J. Elsevier, *Angew. Chem. Int. Ed.* **2004**, *43*, 1277.
20 W. Z. Chen, S. Shimada, M. Tanaka, Y. Kobayashi, K. Saigo, *J. Am. Chem. Soc.* **2004**, *126*, 8072.
21 P. W. Jolly. In: *Comprehensive Organometallic Chemistry*, Vol. 8. G. Wilkinson, F. G. A. Stone, E. W. Abel (Eds.), Pergamon Press, Oxford, **1982**, Section 56.2.
22 K. R. Pörschke, W. Kleimann, G. Wilke, K. H. Claus, C. Krüger, *Angew. Chem., Int. Ed. Engl.* **1983**, *22*, 991.
23 F. M. Conroy-Lewis, L. Mole, A. D. Redhouse, S. A. Litster, J. L. Spencer, *J. Chem. Soc., Chem. Commun.* **1991**, 1601.
24 E. Kogut, A. Zeller, T. H. Warren, T. Strassner, *J. Am. Chem. Soc.* **2004**, *126*, 11984.
25 H. L. Wiencko, E. Kogut, T. H. Warren, *Inorg. Chim. Acta* **2003**, *345*, 199.
26 F. A. Cotton, B. A. Frenz, D. L. Hunter, *J. Am. Chem. Soc.* **1974**, *96*, 4820.
27 M. Stollenz, M. Rudolph, H. Görls, D. Walther, *J. Organometal. Chem.* **2003**, *687*, 153.
28 U. Müller, W. Keim, C. Krüger, P. Betz, *Angew. Chem., Int. Ed. Engl.* **1989**, *28*, 1011.
29 R. A. Henderson, *J. Chem. Research (S)* **2002**, 407.
30 C. J. Curtis, A. Miedaner, R. Ciancanelli, W. W. Ellis, B. C. Noll, M. R. DuBois, D. L. DuBois, *Inorg. Chem.* **2003**, *42*, 216.
31 D. Durand, G. Hillion, C. Lassau, L. Sajus, US Patent 4271323, **1981**.
32 B. Cornils, W. A. Herrmann, *Applied Homogeneous Catalysis with Organometallic Compounds.* VCH, Weinheim, **1996**.
33 A. G. Hinze, D. J. Frost, *J. Catal.* **1972**, *24*, 541.
34 P. Abley, F. J. McQuillin, *J. Catal.* **1972**, *24*, 536.
35 M. Sakai, N. Hirano, F. Harada, Y. Sakakibara, N. Uchino, *Bull. Chem. Soc. Jpn.* **1987**, *60*, 2923.
36 S. N. Gan, N. Subramaniam, R. Yahya, *J. Appl. Polym. Sci.* **1996**, *59*, 63.
37 V. A. Escobar Barrios, R. Herrera Nájera, A. Petit, F. Pla, *Eur. Polym. J.* **2000**, *36*, 1817.
38 S. Sabata, J. Hetflejs, *J. Appl. Polym. Sci.* **2002**, *85*, 1185.
39 T. Thangaraj, S. Vancheesan, J. Rajaram, J. C. Kuriacose, *Indian J. Chem. Sect A-Inorg. Phys. Theor. Anal. Chem.* **1980**, *19*, 404.
40 P. C. L'Argentière, E. A. Cagnola, M. G. Canon, D. A. Liprandi, D. V. Marconetti, *J. Chem. Technol. Biotechnol.* **1998**, *71*, 285.
41 T. E. Zhesko, N. S. Barinov, A. G. Nikitina, I. Y. Kvitko, L. V. Alam, N. P. Smirnova, *Zhurnal Obshchei Khimii* **1980**, *50*, 2301.
42 D. Chatterjee, H. C. Bajaj, S. B. Halligudi, K. N. Bhatt, *J. Mol. Catal.* **1993**, *84*, L1.
43 A. Bacchi, M. Carcelli, L. Gabba, S. Ianelli, P. Pelagatti, G. Pelizzi, D. Rogolino, *Inorg. Chim. Acta* **2003**, *342*, 229.
44 D. Chatterjee, H. C. Bajaj, A. Das, K. Bhatt, *J. Mol. Catal.* **1994**, *92*, L235.
45 E. A. Emken, E. N. Frankel, R. O. Butterfield, *J. Am. Oil Chemists Soc.* **1966**, *43*, 14.
46 H. Itatani, J. C. Bailar, *J. Am. Chem. Soc.* **1967**, *89*, 1600.
47 P. Abley, F. J. McQuillin, *Discuss. Faraday Soc.* **1968**, 31.
48 E. N. Frankel, H. Itatani, J. C. Bailar, *J. Am. Oil Chemists Soc.* **1972**, *49*, 132.
49 H. Itatani, J. C. Bailar, *Ind. Eng. Chem. Prod. Res. Develop.* **1972**, *11*, 146.
50 T. E. Zhesko, Y. N. Kukushkin, A. G. Nikitina, V. P. Kotelnikov, N.S. Barinov, *Zhurnal Obshchei Khimii* **1979**, *49*, 2254.
51 I. M. Angulo, A. M. Kluwer, E. Bouwman, *Chem. Commun.* **1998**, 2689.
52 I. M. Angulo, E. Bouwman, *J. Mol. Catal.* **2001**, *175*, 65.
53 I. M. Angulo, E. Bouwman, S. M. Lok, M. Lutz, W. P. Mul, A. L. Spek, *Eur. J. Inorg. Chem.* **2001**, 1465.
54 I. M. Angulo, E. Bouwman, M. Lutz, W. P. Mul, A. L. Spek, *Inorg. Chem.* **2001**, *40*, 2073.
55 Angulo, S. M. Lok, V. F. Q. Norambuena, M. Lutz, A. L. Spek, E. Bouwman, *J. Mol. Catal.* **2002**, *187*, 55.
56 I. M. Angulo, E. Bouwman, R. van Gorkum, S. M. Lok, M. Lutz, A. L. Spek, *J. Mol. Catal.* **2003**, *202*, 97.
57 I. M. Angulo, PhD Thesis, Leiden University, Leiden, The Netherlands, **2001**.
58 P. S. Jarrett, P. J. Sadler, *Inorg. Chem.* **1991**, *30*, 2098.
59 C. Amatore, E. Carré, A. Jutland, M. A. M'Barki, *Organometallics* **1995**, *14*, 1818.
60 J. A. Osborn, F. H. Jardine, J. F. Young, G. Wilkinson, *J. Chem. Soc. A* **1966**, 1711.

6
Hydrogenation with Early Transition Metal, Lanthanide and Actinide Complexes

Christophe Copéret

6.1
Introduction

Homogeneous hydrogenation catalysts have been mainly based on late transition-metal complexes since the discovery of Wilkinson's catalyst, $[(Ph_3P)_3RhCl]$ [1]. Nonetheless, some of the first homogeneous catalysts to emerge were based on early transition metals. In fact, soon after the discovery of metallocene complexes [2, 3], which were rapidly exploited as the soluble equivalent of Ziegler-Natta olefin polymerization catalysts [4], these systems were introduced as homogeneous hydrogenation catalysts [5–11]. Other Ziegler-Natta-type olefin polymerization catalysts, $[L_nMX_n/M'R]$ {M = Ti, Zr, V, Cr, Mo, Mn, Fe, Co, Ni, Pd, Ru; X = Cl, OR; M′ = Al or Li, R = H, Et, Bu or *i*Bu} were also investigated, and the results obtained showed that all metals could indeed activate H_2 and hydrogenate olefins. This pioneering chemistry most likely formed the basis for the discovery of most homogeneous catalyzed processes known to date, and has led to the development of well-defined systems and to the success of molecular organometallic chemistry and homogeneous catalysis [12, 13].

In hydrogenation, early transition-metal catalysts are mainly based on metallocene complexes, and particularly the Group IV metallocenes. Nonetheless, Group III, lanthanide and even actinide complexes as well as later metals (Groups V–VII) have also been used. The active species can be stabilized by other bulky ligands such as those derived from 2,6-disubstituted phenols (aryloxy) or silica (siloxy) (*vide infra*). Moreover, the catalytic activity of these systems is not limited to the hydrogenation of alkenes, but can be used for the hydrogenation of aromatics, alkynes and imines. These systems have also been developed very successfully into their enantioselective versions.

This chapter will provide an overview of the development and use of early transition-metal complexes in hydrogenation, and in consequence has been divided into several sections. Section 6.2 will focus on the mechanistic differences in the hydrogenation reaction between early and late transition metals. The following three sections will describe the various systems based on Group IV (Sec-

The Handbook of Homogeneous Hydrogenation.
Edited by J.G. de Vries and C.J. Elsevier
Copyright © 2007 WILEY-VCH Verlag GmbH & Co. KGaA, Weinheim
ISBN: 978-3-527-31161-3

tion 6.3), earlier (Section 6.4: Group III, lanthanides and actinides) and later metals (Section 6.5: Groups V–VII). In each section, the hydrogenation of alkenes, dienes, alkynes, aromatics and imines will be described, and the development of enantioselective hydrogenation catalysts will be discussed. Section 6.6 will be devoted to their heterogeneous equivalents. Finally, Section 6.7 will provide a brief conclusion of the current state of the art in this area, its scope, and its limitations.

6.2 Mechanistic Considerations

For late transition metals, one of the key elementary steps is the oxidative addition of H_2 (see Chapter 1) [12, 13], and therefore the process requires transition-metal complexes which can readily undergo oxido-reduction processes (low oxidation state, d^n configuration). In contrast, most early transition-metal hydrogenation catalysts are based on d^0 metal complexes, having ligands, which often excludes the possibility to change the oxidation of the metal center. Therefore, the activation of H_2 and formation of the alkane must proceed through elementary steps other than oxidative addition and reductive elimination. Additionally, because these metal complexes have a d^0 configuration, they cannot generate stable π-alkene complexes. Three types of catalyst precursors can be used: L_nM-R, L_nM-H, or L_nM-X, the latter being used in combination with an alkylated agent or a metal hydride to generate the L_nM-R or the L_nM-H catalytically active species (Scheme 6.1).

Starting from L_nM-H, the first step is insertion of the alkene in the M–H bond to generate the corresponding alkyl complex [12]. Note that successive insertion and β-H transfer steps allow the starting alkene to be isomerized, and it can be

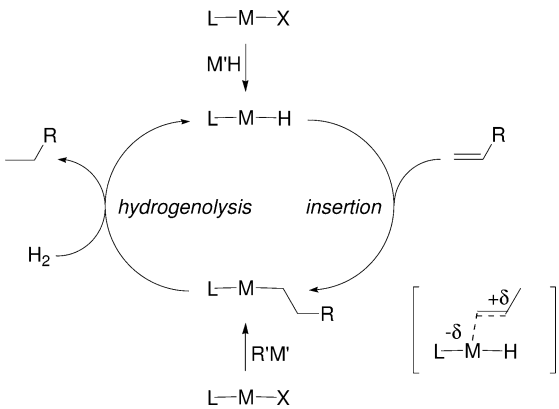

Scheme 6.1 Elementary steps for the hydrogenation of olefins with d^0 transition-metal complexes.

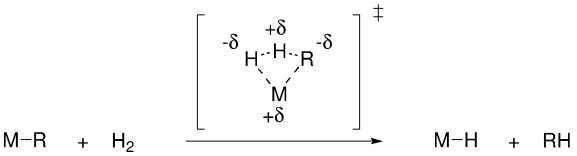

Scheme 6.2 σ-Bond metathesis transition state.

observed when hydrogenation is carried out under H_2-limiting conditions (low pressure, diffusion control experiments, poor stirring, etc.). The insertion step is probably preceded by a polarization of the alkene by the metal complex. While such types of intermediates have not been observed on d^0 L_nM-H complexes, they have been found on the corresponding d^0 L_nM-X complexes (X = Cl, OR, CH_2R) [14–28]. The following step is the direct hydrogenolysis of the metal–carbon bond by H_2 through a four-centered σ-bond metathesis transition state [29–34] which does not require a change of oxidation state, thereby regenerating the M–H species. While this step corresponds to an exchange of four atoms between two molecules, the geometry of this transition state does not have a kite-shape geometry, but rather a triangular shape, where three atoms are almost co-linear. Overall, it corresponds to a transfer of a proton between the H_2 molecule coordinated to the metal center and an alkyl ligand (Scheme 6.2). The reverse step, which is usually slightly endothermic for early transition metals, corresponds to a C–H activation on a metal–hydride. Successive C–H bond activation and hydrogenolysis will be responsible for H-scrambling, which can be possible under H_2-deprived conditions and can be observed by using D_2 in place of H_2.

Finally, the hydrogenation of other substrates such as imines involve similar elementary steps.

6.3 Group IV Metal Hydrogenation Catalysts

6.3.1 Hydrogenation of Alkenes

In Group IV metal complexes, metallocene complexes are the main catalyst precursors for hydrogenation. Two major catalytic systems have been used: 1) Cp_2MR_2 (R = H, Alkyl, Aryl); and 2) Cp_2MX_2 in combination with alkylating agent or an hydride (Table 6.1). The catalytic tests are typically run with 50 equiv. of substrate per metal, but in some cases turnover numbers (TONs) exceeding 1000 can be achieved [35].

The hydrogenation is usually limited to nonpolar alkenes (terminal and internal cyclic and acyclic alkenes), even though Ti systems have been used to hydrogenate alkenes containing ether and ester functionalities such as vinyl ethers or methyl oleate [42, 45, 59, 62].

Table 6.1 Catalytic systems based on Group IV dicyclopentadienyl complexes.

Ti Catalytic systems	Reference(s)	Zr and Hf catalytic systems	Reference(s)
$Ti(OiPr)_4/R_3Al$	5	$Cp_2ZrCl_2/BuLi$ (Cp_2Zr-olefin)	36, 37
$Ti(OiPr)_4/RLi$	5	Cp_2ZrCl_2/R_3Al	5
$Cp_2TiCl_2/BuLi$	6	$(RC_5H_4)_2ZrH_2$ R = H, Me, *i*Pr, Bn	7, 38, 39
$AnsaCp_2TiCl_2/EtLi$	40	$(RC_5H_4)_2HfH_2$ R = Me, *i*Pr, Bn	38, 39
$Cp_2TiCl_2/PhMgBr$	6	$[Cp^*(carboranyl)HfH]_2$	25
$Cp_2TiCl_2/RMgBr$	6, 41, 42		
Cp_2TiCl_2/R_2Mg	43		
$Cp_2Ti(CO)_2$	44		
Cp_2TiCl_2/Mg	45, 46		
$Cp_2Ti(CO)(Ph_2C_2)$	10, 11		
$CpCp'Ti(PMe_3)(Ph_2C_2)$ $Cp' = Cp^*$, MeC_5H_4	47		
$Cp_2Ti(Ph_2C_2)$	48, 49		
$Cp_2Ti(AlH_4)_2$	50–52		
Cp_2TiCl_2/NaH	35, 53–57		
Cp_2TiPh_2	9, 58		
$Cp_2TiR_2 + h\nu$ R = Me, CH_2Ph, Ph	59		
$Cp_2TiMe_2/RSiH_3$	60, 61		

In the Cp_2Ti system, Brintzinger et al. have shown that the angle between the two cyclopentadienyl ligands is important. For example, the activity in the hydrogenation of cyclohexene varies as follows: $[(CH_2)_2(C_5H_4)_2TiCl_2]$ (turnover frequency (TOF) = 266 000 mol H_2 cons. $mol^{-1}\ h^{-1}$) > $[(CH_2)_3(C_5H_4)_2TiCl_2]$ (TOF = 223 000 mol H_2 cons. $mol^{-1}\ h^{-1}$) > $[(CH_2)(C_5H_4)_2TiCl_2]$ (TOF = 118 000 mol H_2 cons. $mol^{-1}\ h^{-1}$) > $[(C_5H_5)_2TiCl_2]$ (TOF = 90 000 mol H_2 cons. $mol^{-1}\ h^{-1}$) [40].

This field is still active today: numerous recent patents [46, 63–89] and several reports [90–92] have detailed the efficiency of such types of systems for the hydrogenation of unsaturated polymers resulting from the polymerization of dienes (butadiene, isoprene, 1,3-cyclohexadiene) or the co-polymerization of dienes and styrenes (block co-polymers of butadiene and styrene: SB, SBS, SBSB polymers).

6.3.2
Hydrogenation of Alkynes and Dienes

Alkynes are hydrogenated to *cis* olefins with the same catalytic systems, and subsequently undergo hydrogenation to yield the corresponding alkanes [7, 42, 45, 47, 49, 59, 93]. For example, Jordan et al. reported the selective hydrogenation of 3-hexyne into *cis* 3-hexene with a TOF of 25 h^{-1} [25], and *cis* 3-hexene is

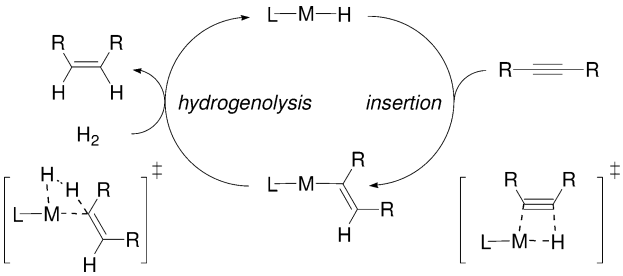

Scheme 6.3

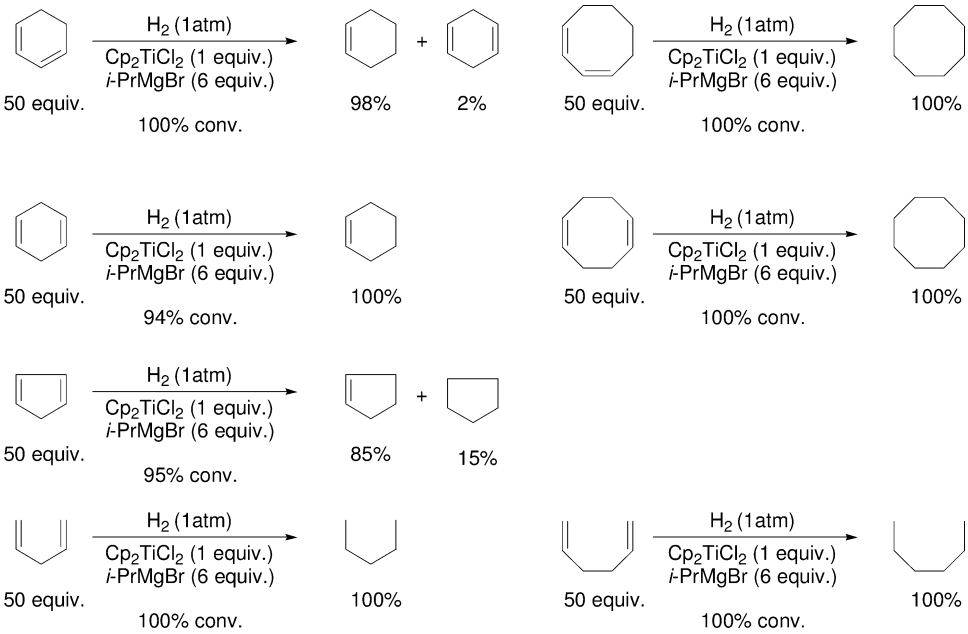

Scheme 6.4

subsequently hydrogenated at 12 h^{-1} (Scheme 6.3). Typically, the hydrogenation of alkynes is slower than that of alkenes (hydrogenolysis is probably rate determining in this case), but because alkynes react more rapidly with the metal hydride intermediate than alkenes do, they can be hydrogenated selectively, especially at low conversions (*vide infra* for a thorough study of reaction rates with lanthanide and actinide complexes).

Similarly, in some cases, dienes can be selectively hydrogenated into the corresponding alkenes, but they usually provide the corresponding alkane or a mixture of alkanes and alkenes [6, 45, 49, 59]. For example, the hydrogenation of 50 equiv. of 1,3- or 1,4-cyclohexadiene in the presence of $[Cp_2TiCl_2]$-*i*PrMgBr

(1:6 ratio) gives selectively cyclohexene (>98%; Scheme 6.4) [42]. On the other hand, using the same experimental procedure, cyclopentadiene is converted (95% conv.) into a mixture of cyclopentene (85%) and cyclopentane (15%), and 1,3- or 1,5-cyclooctadienes give only cyclooctane. Additionally, linear nonconjugated dienes such as 1,4-pentadiene and 1,5-hexadiene are directly converted into the corresponding alkanes.

6.3.3
Enantioselective Hydrogenation of Olefins

Kagan et al. were the first to report the corresponding enantioselective catalytic hydrogenation using chiral metallocene derivatives [94, 95]. By using menthyl- and neomenthyl-substituted cyclopentadienyl titanium derivatives in the presence of activators (Scheme 6.5) [96], these authors observed low ee-values (7–14.9%) for the catalytic hydrogenation of 2-phenyl-1-butene into 2-phenylbutane. In contrast, no enantiomeric excess was obtained with the corresponding zirconocene derivatives.

The use of other simple chiral cyclopentadienyl systems proved to be unsuccessful [39]. The design of better catalysts was directed first at preparing bulkier chiral cyclopentadienyl ligands. The chirality was introduced by preparing substituted cyclopentadienes derived from pinene and camphor (Scheme 6.6), but the ee-values were still low (<35%) [97, 98]. The ee-values have been improved to 61–69% by introducing more steric bulk in the system (Scheme 6.6; R=H versus Me) [99]. The first high ee-values were obtained using a C_2 symmetric cyclopentadienyl ligand, for which both enantiomers are accessible in an enantiomerically pure form [100]. This system hydrogenates 2-phenyl-1-butene at –78 °C with enantiomeric excess up to 96%, albeit with a low TON (e.g., 10). It should be noted that *ansa* titanocene derivatives prepared by White et al. give low ee-values compared to the Group III and lanthanide derivatives developed by Marks et al. (*vide infra*, Section 6.4.1) [101].

The best results were obtained with the Brintzinger indenyl zirconene and titanocene derivatives [(EBTHI)MX_2], developed earlier for the stereocontrolled po-

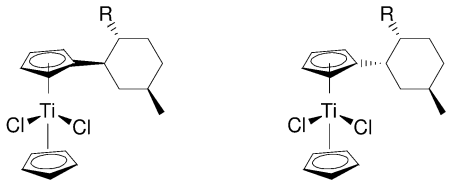

R = CMe_2Ph, $CHMe_2$ (menthyl) R = CMe_2Ph, $CHMe_2$ (neomenthyl)

Scheme 6.5 First enantioselective hydrogenation by a Group IV metallocene catalysts.

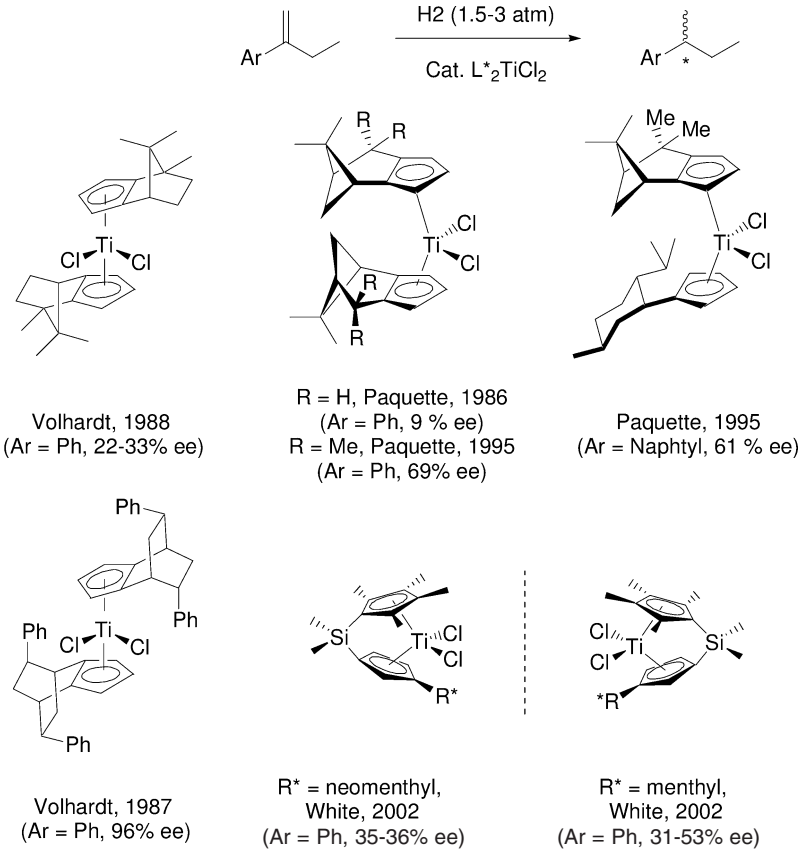

Scheme 6.6

lymerization of propene (Scheme 6.7) [102, 103]. When 2-phenyl-1-butene is used as the standard test substrates, low ee% are still obtained, despite high activity [104, 105]. However, tri-substituted [106] and tetra-substituted [107] alkenes are hydrogenated with very high enantioselectivities. In the case of tri-substituted alkenes [106], the catalytic system is generated by the treatment of [(EBTHI)TiX_2] (5 mol.%) (X_2 = binolate) with BuLi in the presence of 2.5 equiv. $PhSiH_3$, which is used to stabilize the catalytic system. The active species is probably [(EBTHI)$Ti^{III}H$]. Acyclic and cyclic tri-substituted alkenes are hydrogenated in typically 70–90% yields, with enantiomeric excesses ranging from 83% to >99% (Table 6.2). The favored enantiomer is formed through the pathway in which the substituent R points as far away as possible from the indenyl ligand (Scheme 6.7).

When the hydrogenation of (*E*)-1,2-diphenylpropene is performed under D_2, 1,2-diphenylpropane is selectively deuterated in positions 1 and 2, which shows that no isomerization of the alken takes place under these conditions. Noteworthy, the reaction rate is highly dependent on the substrate, and typically

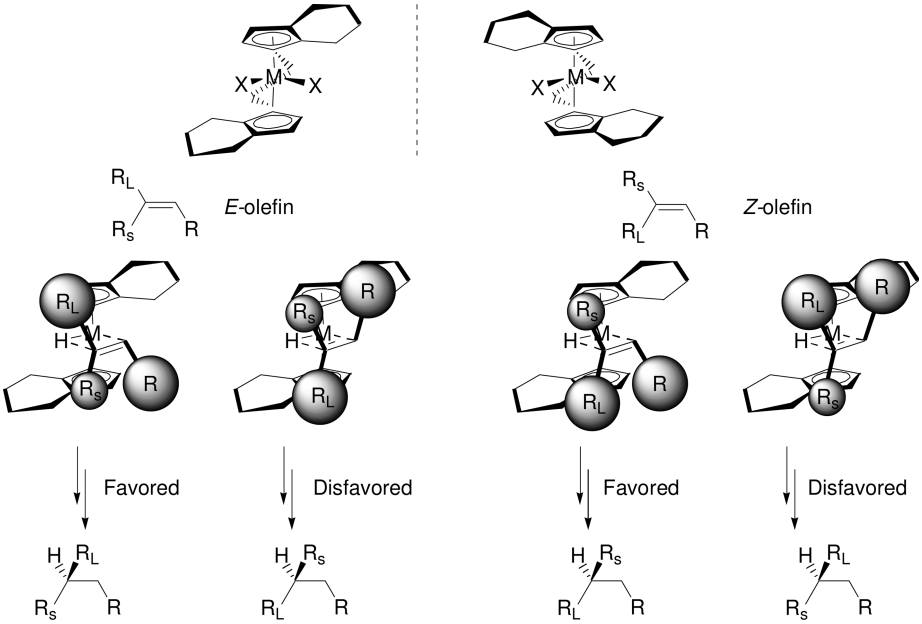

Scheme 6.7

Z-alkenes are reduced much more slowly than are *E*-isomers. For instance, the (*E*)-(1,2)-diphenylpropene is reduced in 9 h at 65 °C under 5.3 bar, while the *Z*-isomer reaches only 3% conversion after 48 h at 70 °C under 133 bar of H_2. These data are fully consistent with the model proposed to predict the stereochemical outcome of the reaction (see Scheme 6.7), which shows that, for the *Z*-isomers, the R_L substituent points towards the indenyl ligands in the favored pathway, thus decreasing the reaction rate.

For tetra-substituted alkenes [107], it was necessary to rely on the more reactive cationic Zr equivalent generated from [(EBTHI)$ZrMe_2$] and either methylaluminoxane or $[PhMe_2NH]^+[Co(C_2B_9H_{11})_2]^-$ developed earlier by Waymouth et al. [104]. Using H_2 pressure ranging between 5 and 133 bar, it was possible to obtain the hydrogenated products with 80–98% ee in most cases (Table 6.3).

6.3.4
Enantioselective Hydrogenation of Imines and Enanimes

One of the best enantioselective olefin hydrogenation catalysts, (EBTHI)TiH, was originally developed for the enantioselective hydrogenation of imines [108, 109]. The catalytic system is generated by the treatment of [(EBTHI)TiX_2] (5 mol%, X = binolate) with BuLi in the presence of 2.5 equiv. $PhSiH_3$, and the hydrogenation is typically performed with 5 mol% of catalyst at 65 °C under 133 bar H_2. High pressure is usually required to obtain high ee-values with this

Table 6.2 Enantioselective hydrogenation of tri-substituted alkenes catalyzed by [(*S*,*S*,*S*)-(EBTHI)TiX_2]. [a)]

Substrate	Product [b)]	Time [h]	Yield [%]	ee [%]
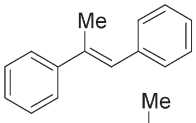	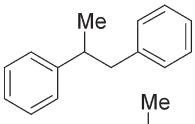	48	91	99
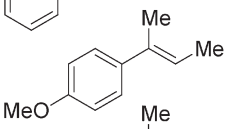	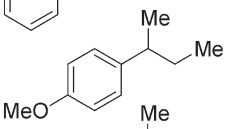	48	79	95
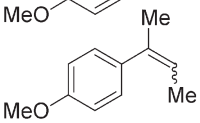	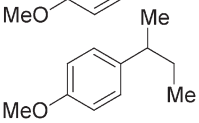	146	80	31
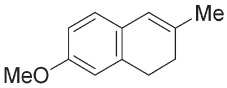	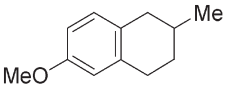	44	77	92
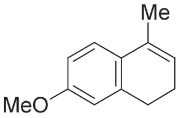	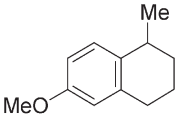	132	70	93
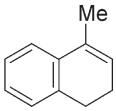	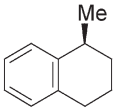	184	70	83
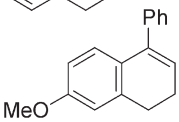	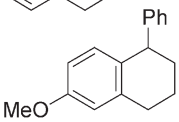	169	87	83
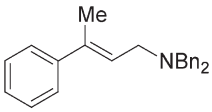	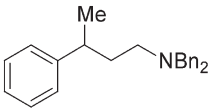	43	75	95
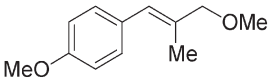	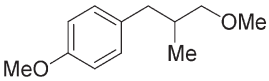	48	80–86	93–94

a) Reaction conditions: 65 °C, 133 bar H_2 in THF with 5 mol% [(*S*,*S*,*S*)-(EBTHI)TiX_2].
b) No absolute configuration given when unknown.

system. Acyclic benzyl protected imines, used as mixture of diastereomers, are converted to their corresponding amines in good yields (66–93%) and moderate enantioselectivities (58–85% ee). Better results are obtained for cyclic imines, which are hydrogenated in 97–99% ee (Tables 6.4 and 6.5). The absolute configuration of the amine can be predicted using the following model and rules

Table 6.3 Enantioselective hydrogenation of tetra-substituted alkenes catalyzed by $[(S,S)\text{-(EBTHI)ZrMe}_2]/[\text{PhMe}_2\text{NH}^+\text{B}(\text{C}_6\text{F}_5)_4^-]$.[a)]

Substrate	Product	P_{H2} [bar] (% cat)	Yield [%]	ee [%] (*cis*:*trans*)
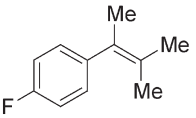	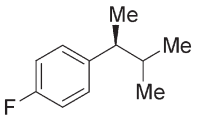	5.3 (8) 110 (8)	79 77	84 96
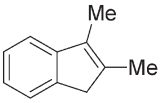	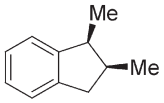	5.3 (5) 110 (8)	76 87	86 (95:5) 93 (>99:1)
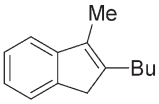	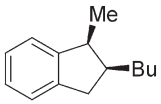	5.3 (8)	96	92 (99:1)
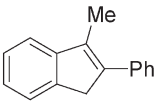	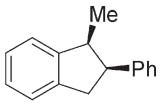	5.3 (5) 67 (8)	34 89	97 98 (>99:1)
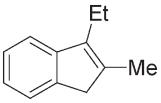	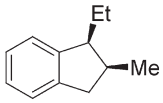	5.3 (5) 110 (8)	57 95	5 (9:1) 52 (95:5)
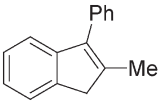	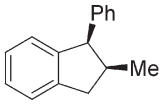	5.3 (5) 133 (8)	44 94	29 (>99:1) 78 (>99:1)
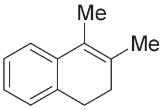	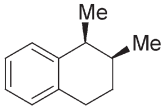	133 (5)	91	92 (>99:1)

a) Reaction conditions: 25 °C, 5.3–133 bar H_2 with 5–8 mol% $[(S,S,S)\text{-(EBTHI)ZrMe}_2]$.

(Scheme 6.8): the substituent (R) on the nitrogen should point as far away as possible from the indenyl ligand. This model predicts that hydrogenation of *syn*- and *anti*-imines give rise to enantiomers of opposite stereochemistry as observed experimentally. The model also predicts that if one takes into consideration the influence of R_s and R_L substituents, the energy difference of the two possible pathways should be lower for the *syn* imines, giving rise to lower enantioselectivities.

As illustrated in the hydrogenation of cyclic imines, the system is compatible with a wide range of functional groups, such as olefins, protected or unpro-

Table 6.4 Enantioselective hydrogenation of imines catalyzed by [(*R*,*R*,*R*)-(EBTHI)TiX_2] [108, 109].[a)]

Substrate	Product[k)]	Yield [%][a)]	ee [%]
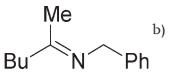 b)	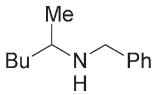	68	56
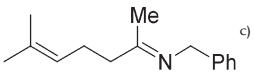 c)	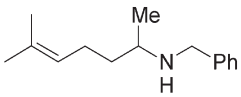	64	62
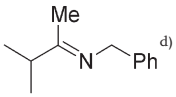 d)	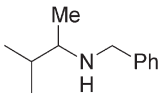	66	75
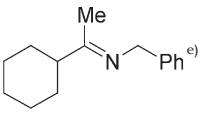 e)	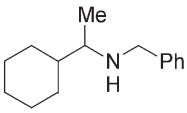	93	76
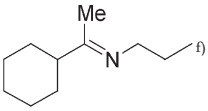 f)	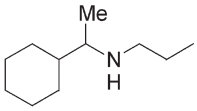	70	79
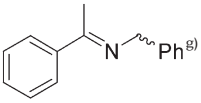 g)	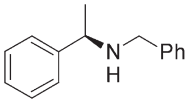	93	85
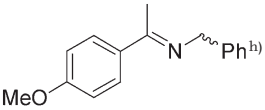 h)	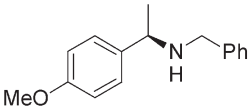	86	86
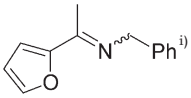 i)	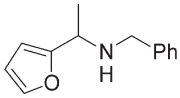	70	83
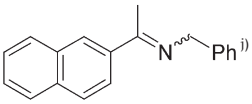 j)	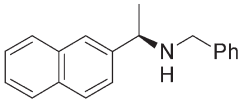	82	70

a) Reaction conditions: 65 °C, 133 bar H_2 in THF with 5 mol.% [(*R*,*R*,*R*)-(EBTHI)TiX_2].
b) *anti*/*syn* = 3.3.
c) *anti*/*syn* = 3.
d) *anti*/*syn* = 13.
e) *anti*/*syn* = 9.
f) *anti*/*syn* = 17.
g) *anti*/*syn* = 17.
h) *anti*/*syn* = 17.
i) *anti*/*syn* = 10.
j) *anti*/*syn* = 3.3.
k) No absolute configuration given when unknown.

Table 6.5 Enantioselective hydrogenation of cyclic imines catalyzed by [(*R*,*R*,*R*)-(EBTHI)TiX_2].

Substrate	Product [b)]	Conditions [P/T/t] [a)]	Yield [%]	ee [%]
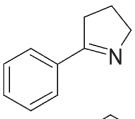	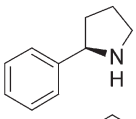	5.3/65/42	83	99
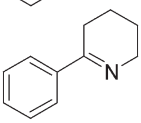	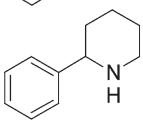	33/65/24	70	97
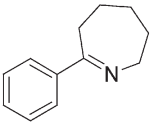	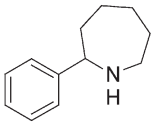	5.3/65/30	74	97
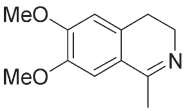	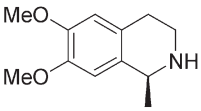	5.3/65/50	79–82	98
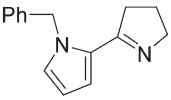	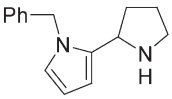	5.3/65/6	72	99
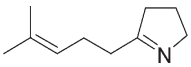	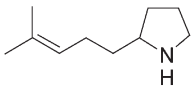	5.3/50/23	79	99
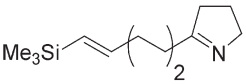	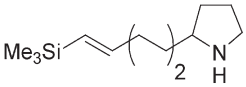	5.3/50/27	73	99
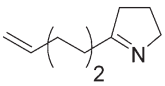	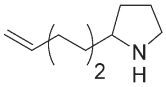	5.3/45/23	72	99
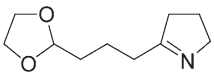	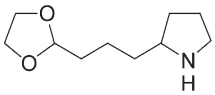	5.3/65/16	82	99
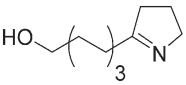	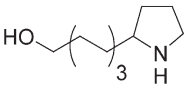	5.3/65/8	84	99
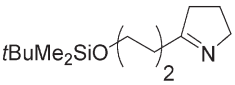	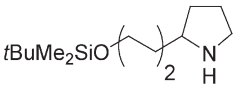	5.3/65/10	72	99

a) P = pressure (bar); T = temperature (°C); t = time (h).
b) No absolute configuration given when unknown.

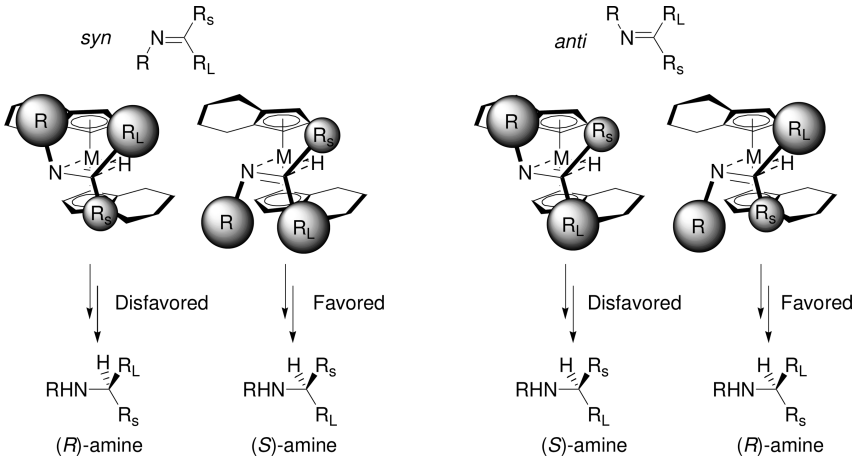

Scheme 6.8

Table 6.6 Kinetic resolution of di-substituted 1-pyrrolines catalyzed by [(*R*,*R*,*R*)-(EBTHI)TiX_2] [111].[a)]

Substrate	Yield [% recovered S]	ee [%]	Yield [% product]	ee [%]
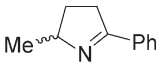	37	99	34	99
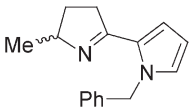	42	96	44	98
	43	98	41	98
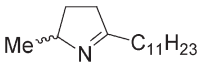	41	>95	41	>95
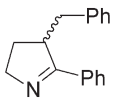	–	75	42	>95
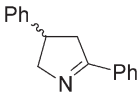	33	49	44	99

a) 5 mol% cat., THF, 65–75 °C, 5.3 bar H_2, reaction run to 50% completion.

Table 6.7 Enantioselective hydrogenation of enamines catalyzed by [(*R*,*R*,*R*)-(EBTHI)TiX_2] [112].[a)]

Substrate	Product[b)]	Pressure [bar]	Yield [%][a)]	ee [%]
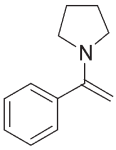	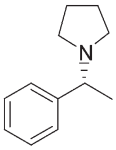	1	75	92
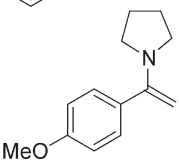	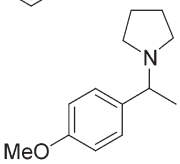	1	72	92
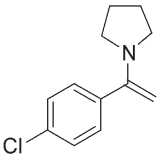	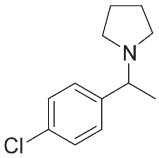	1	89	89
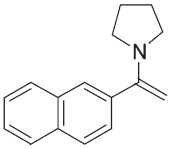	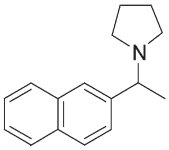	1	77	96
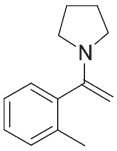	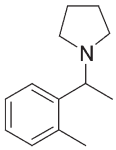	5.3	87	98
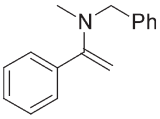	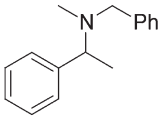	5.3	83	96
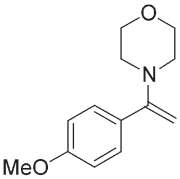	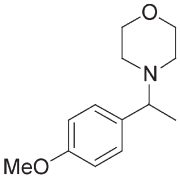	5.3	88	91

Table 6.7 (contributed)

Substrate	Product	Pressure [bar]	Yield [%][a)]	ee [%]
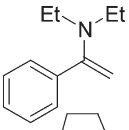	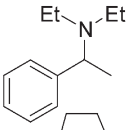	5.3	72	99
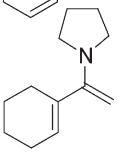	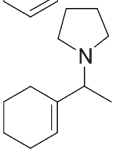	5.3	72	95

a) Using 5 mol% of catalyst.
b) No absolute configuration given when unknown.

tected alcohols, acetals and aromatic groups [109, 110]. The same model can be used to predict the absolute stereochemistry of the amine product – that is, formation of the *S*-amine from the (*R,R,R*)-catalyst (Scheme 6.8).

This catalytic system can be used for the kinetic resolution of di-substituted 1-pyrrolines, for which high ee-values are achieved for both the amine and the recovered materials, especially when they are substituted in positions 2 and 5 (Table 6.6) [111]. Moreover, it should be noted that acyclic enamines are converted with high ee-values into their corresponding amines (89–98% ee; Table 6.7), which is in sharp contrast to what is obtained for acyclic imines (*vide supra*) [112].

Hydrogenation is not limited to the use of (EBTHI)MX_2-type catalysts. In polymerization, linked amido-cyclopentadienyl ligands have emerged as very important systems, and the corresponding chiral derivatives have been prepared (Scheme 6.9) [113–116]. Nonetheless, whilst high TON can be achieved (500–1000), the ee-values are quite low (<25%).

Finally, Brintzinger et al. have reported a different type of *ansa*-metallocene, which can be readily prepared enantiomerically pure, and which catalyzes the

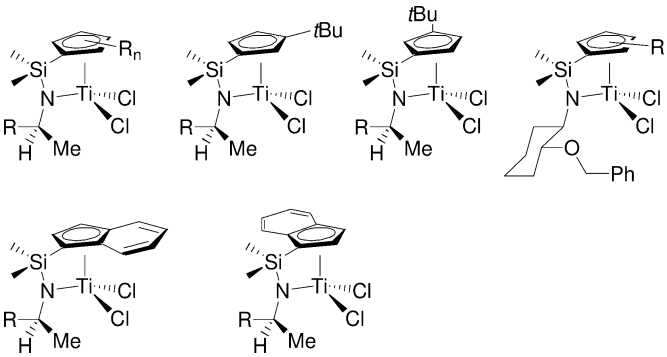

Scheme 6.9

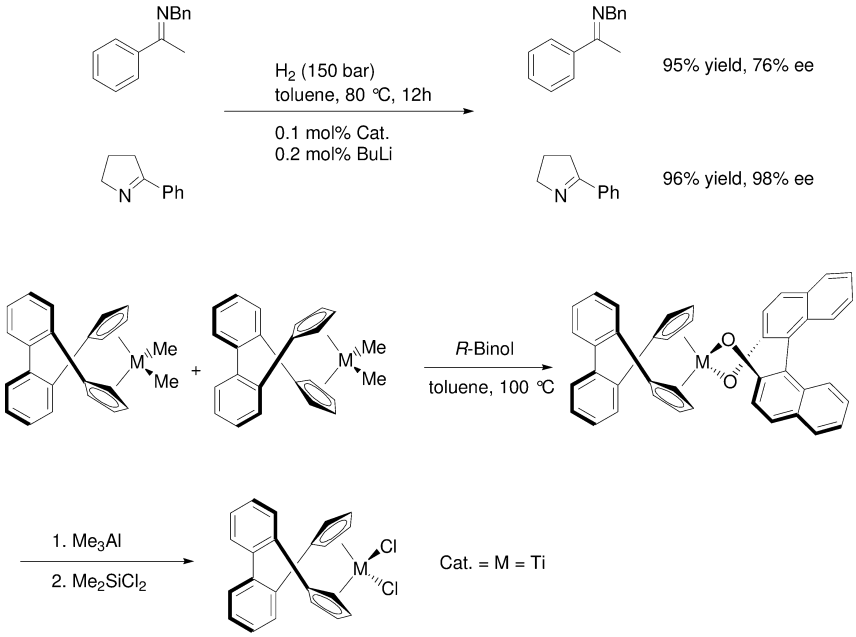

Scheme 6.10

hydrogenation of imines very efficiently (TON of 1000) with enantiomeric excesses comparable to those reported with (EBTHI)MX_2 [117, 118]. The synthesis of the enantiomerically pure catalyst is noteworthy because it relies on the preparation of a racemate. After reaction of this racemate with pure (*R*)-binol, two diastereomers are formed, but after heating at 100 °C a single diastereomer is obtained. This single diastereomer is converted into the enantiomerically pure dichloro complex by treatment of the binolate complex with Me_3Al and then Me_3SiCl (Scheme 6.10).

6.4 Hydrogenation Catalysts Based on Group III, Lanthanide, and Actinide Complexes

6.4.1 Hydrogenation of Alkenes with Group III Metal and Lanthanide Complexes

The hydrogenation of unfunctionalized alkenes is readily performed by Group III and lanthanide cyclopentadienyl hydride derivatives, one key feature being the high TOFs of these systems (up to 120 000 h^{-1} for hydrogenations catalyzed by Lu, Tables 6.8 and 6.9) [119, 120]. The reaction rate depends heavily on the metal and the ligands. It is inversely proportional to the metal radius (Lu > Sm > Nd > La), and it is faster for the Cp^*_2M derivatives than for the *ansa* di-

Table 6.8 Rate constants for the catalytic hydrogenation of alkenes catalyzed by Group III and lanthanide complexes.[a)]

	$[Cp^*_2LaH]_2$	$[Cp^*_2NdH]_2$	$[Cp^*_2SmH]_2$	$[Cp^*_2LuH]_2$
1-Hexene	6.2	21.6	23.8	34.5
(*E*) 2-Hexene	1.7	7.1	7.9	9.0
(*E*) 3-Hexene	7.3	33.4	51	240
(*Z*) 2-Hexene	–	6.6[b)]	–	13.4[c)]
(*Z*) 3-Hexene	–	2.2[b)]	3.8[b)]	8.1[c)]
Cyclohexene	0.015[b)]	0.014[b)]	0.005[b)]	0.023[c)]

a) Based on $r = k[M][H_2]$ unless otherwise specified, in units of $atm^{-1}\ s^{-1}$ (multiply by 224 to convert to $M^{-1}\ s^{-1}$).
b) $r = k[M]^{1/2}[alkene]$, in units of $M^{-1/2}\ s^{-1}$.
c) $r = k[M][alkene]$, in units of $M^{-1}\ s^{-1}$.

Table 6.9 Hydrogenation of alkenes catalyzed by Group III and lanthanide complexes.

	$[Me_2SiCp''_2NdH]_n$	$[Me_2SiCp''_2SmH]_n$	$[Me_2SiCp''_2LuH]_n$
1-Hexene	21.6[a)]	23.8[a)]	34.5[a)]
Cyclohexene	0.014[b)]	0.005[b)]	0.023[b)]

a) Based on $r = k[M][H_2]$ unless otherwise specified, in units of $atm^{-1}\ s^{-1}$ (multiply by 224 to convert to $M^{-1}\ s^{-1}$).
b) $r = k[M]^{1/2}[alkene]$, in units of $M^{-1/2}\ s^{-1}$.

$Me_2SiCp''_2M\text{-}X =$ 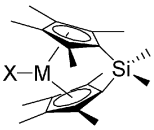

cyclopentadienyl derivatives, $Me_2SiCp''_2MR$ (Tables 6.8 and 6.9). Kinetic studies show that the rate-determining step depends on the alkene. In terms of elementary steps, these hydrides are dimers, and need to dissociate (Eq. (1)) prior to insertion of the alkenes (Eq. (2)). Hydrogenolysis subsequently liberates the alkane and re-forms the hydride (Eq. (3)).

$$(LMH)_2 \underset{k_{-1}}{\overset{k_1}{\rightleftharpoons}} 2\ LMH \tag{1}$$

$$LM\text{-}H + alkene \underset{k_{-2}}{\overset{k_2}{\rightleftharpoons}} LM\text{-}R \tag{2}$$

$$LM\text{-}R + H_2 \xrightarrow{k_3} LM\text{-}H + RH \tag{3}$$

For 1-hexene, the rate can be expressed as: $r = k[L_nM][H_2]$, which is consistent with hydrogenolysis being rate-determining (Eq. (3)). In contrast, for bulkier alkenes the rate law is as follows: $k[L_nM]^{1/2}[olefin]$, which is consistent with inser-

tion being rate-determining (Eq. (2); cyclohexene and internal *cis* acyclic alkenes). In the case of Lu, the dimer readily dissociates, and therefore the rate law is independent of the mechanism and the substrate, as observed experimentally $\{k[L_nM][\text{alkene}]\}$. Moreover, independently of the catalyst, hydrogenation of 1-hexene under D_2 generates 1,2-d_2-hexane, along with small amount of d_1-2-hexene, suggesting that β-H elimination can be competitive (the reverse step of insertion, Eq. (2)). In the case of cyclohexene however, Lu-based catalysts generate large quantities of various polydeuterated cyclohexane, suggesting that successive β-H elimination–insertion processes occur. Finally, when operating under deprived D_2 conditions, the amount of polydeuterated compounds increases, suggesting that the β-H elimination process becomes competitive with hydrogenolysis.

It should be noted that, in the case of [(R)(Me)SiCp$''_2$YR], the TOF of the hydrogenation of 1-hexene decreases dramatically, from 11 100 h^{-1} (R = Me) to 200 h^{-1} when an ether functional group is bound on the *ansa* bridge (R = $(CH_2)_5OMe$), which shows the sensitivity of Group III metal complexes towards polar functionalities [121].

These types of catalysts, [$Cp^*_2LnCH(SiMe_3)_2$], are also used to hydrogenate substituted methylenecyclopentenes and cyclohexenes in good to very good diastereoselectivities, especially when the substituent is in the α-position to the alkene (Tables 6.10 and 6.11). However, the presence of functional groups such as amine or ether is detrimental to catalysis.

Table 6.10 Hydrogenation of substituted methylenecyclopentene catalyzed by $Cp^*_2LnCH(SiMe_3)_2$ [122].

Substrate	Catalyst	SCR (temp., °C)	Product	Yield [%] (dr, %)
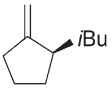	Ln = Sm	10 (25)	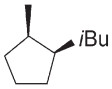	84 (> 99/1)
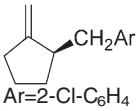 Ar=2-Cl-C_6H_4	Ln = Sm	10 (25)	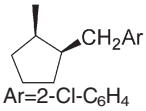 Ar=2-Cl-C_6H_4	32 (> 99/1)
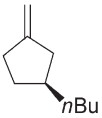	Ln = Sm	33 (0)	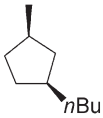	32 (60/40)

dr = diastereomeric ratio; SCR = substrate : catalyst ratio.

Table 6.11 Hydrogenation of mono-substituted methylenecyclohexene catalyzed by $Cp^*_2LnCH(SiMe_3)_2$ [122].

Substrate	Catalyst	SCR (temp., °C)	Product	Yield [%] (dr, %)
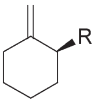			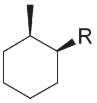	
R = Me	Ln = Sm	33 (–20)	R = Me	77 (93/7)
R = *i*Bu	Ln = Sm	33 (–20)	R = *i*Bu	90 (95/5)
R = *t*Bu	Ln = Sm	20 (25)	R = *t*Bu	95 (>99/1)
R = CH_2Ph	Ln = Sm	33 (–20)	R = CH_2Ph	95 (93/7)
R = $(CH_2)_3NMe_2$	Ln = Sm	33 (50)	$(CH_2)_3NMe_2$	76 (91/9)
R = OMe	Ln = Sm	20 (70)	R = OMe	0 (–)
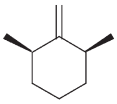	Ln = Sm	20 (70)	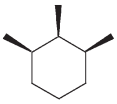	0 (–)
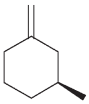	Ln = Yb	33 (–20)	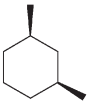	73 (61/39)
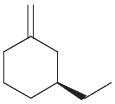	Ln = Yb	33 (–20)	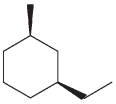	79 (73/27)
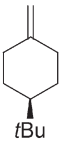	Ln = Yb	33 (–20)	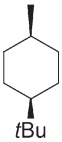	73 (77/23)

dr = diastereomeric ratio; SCR = substrate : catalyst ratio.

6.4.2
Hydrogenation of Dienes and Alkynes with Group III and Lanthanide Complexes

It is possible to selectively hydrogenate dienes into monoolefins when there is a large difference in reactivity between the two olefins. For example, vinylcyclohexene and 4-vinylnorbornene undergo a selective hydrogenation of the acyclic olefins in the presence of catalytic amount of [Cp^*_2YMe] (Table 6.12). Note that *α*-allylmethylenecyclohexene gives a mixture of *α*-propylmethylenecyclohexene and the reductive cyclization product, which shows that the intramolecular insertion of a second alkene can be competitive with hydrogenolysis (Table 6.12).

Table 6.12 Hydrogenation of dienes catalyzed by Cp^*_2YMe [123].

Substrate	SCR (time, h)	Product	Yield [%]	Byproduct [%]
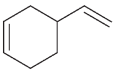	100 (2)	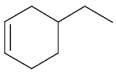	70	–
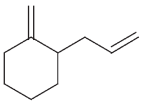	25 (1)	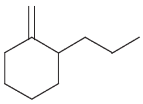	67	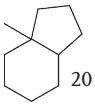 20
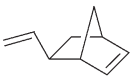	100 (1)	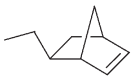	72	–

SCR = substrate : catalyst ratio.

Similarly, when a diene is constituted of both terminal and tri-substituted olefins, the terminal olefin is selectively hydrogenated. Note that ether substituted systems could be hydrogenated in these cases. Moreover, for 3-substituted 1,5-hexadienes, the less-hindered olefins can be selectively hydrogenated into the corresponding 2-substituted 1-hexene, especially when the substituent in position 2 is large (Table 6.13). However, when no substituent is present on the alkyl chain, 1,5-dienes undergo reductive cyclization in the presence of *ansa* Cp derivatives of Y and Lu to give the corresponding cyclic alkanes in quantitative yields (Table 6.14) [124]. Note that no conversion is observed when an ether group is present in the starting material.

An original report by Evans reports the catalytic hydrogenation of 3-hexyne and diphenylacetylene into the corresponding alkanes by generating *in situ* [Cp^*_2SmH] from [Cp^*_2Sm] [120, 125]. Later, Evans showed that *cis*-3-hexene was formed selectively at the beginning of the reaction [126]. In a comprehensive study, Marks et al. have shown that the reaction rate of hydrogenation of alkynes, namely 3-hexyne, is slower (Table 6.15) than that of olefins (*vide supra*) [120, 125]. The rate law is as follows: $r = k[L_nMH][H_2]$, and it is fully consistent with hydrogenolysis being rate-determining. Since the rate of hydrogenation is faster for *cis* alkenes in the absence of alkynes, it shows that alkynes react faster with the hydride than alkenes.

Table 6.13 Hydrogenation of acyclic dienes catalyzed by Cp_2^*YMe [123].

Substrate	SCR (time, h)	Product	Yield [%]	Byproduct [%]
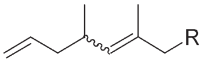 R = $OSiMe_2tBu$	50 (1)	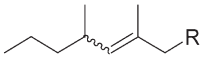 R = $OSiMe_2tBu$	98	–
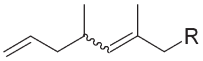 R = OMe	50 (2)	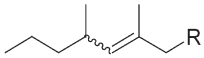 R = OMe	74	–
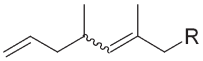 R = OCH_2Ph	50 (2)	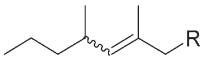 R = OCH_2Ph	99	–
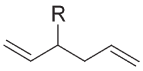 R = $OSiMe_2tBu$	33 (1)	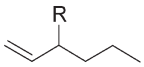	85	10 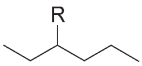
R = $OSiMe_2tBu$	25 (1.5)	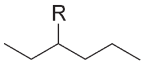	99	–
R = Ph	33 (1)	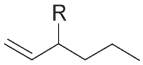	64	23 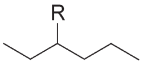
R = Ph	25 (1.5)	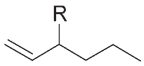	92	–
*i*Pr	33 (1.1)	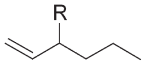	70	16 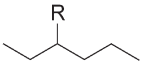
R = $OCPh_3$	33 (1)	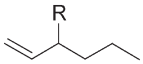	96	1 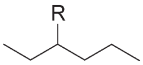
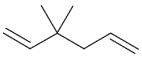	33 (1)	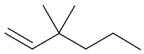	42	20 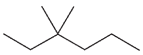

SCR = substrate : catalyst ratio.

6.4.3
Hydrogenation of Imines with Group III and Lanthanide Complexes

The hydrogenation of imines is typically carried out with 1 mol% of the lanthanocene catalyst under an H_2 pressure of 13 bar at 90 °C [127]. The best catalysts are based on Sm having Cp* ligands, the *ansa* systems being unreactive. The rate and the total conversion are improved by the addition of $PhSiH_3$, probably because it stabilizes the system (Table 6.16), and both are very sensitive to the

Table 6.14 Reductive cyclization of dienes catalyzed by $Me_2SiCp^*CpLnCH(SiMe_3)_2$ [124].

Substrate	Ln	SCR (P_{H_2}, atm)	Product	Yield [%]
	Y	200 (1)		100
	Lu	200 (1)		100
	Y	200 (1)		100
	Lu	200 (1)		100
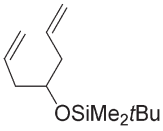	Y Lu	200 (1) 200 (1)	– –	0 0

SCR = substrate : catalyst ratio.

Table 6.15 Rate constants for the catalytic hydrogenation of olefins catalyzed by Group III and lanthanide complexes. [a)]

	$[Cp^*_2LaH]_2$	$[Cp^*_2NdH]_2$	$[Cp^*_2SmH]_2$	$[Cp^*_2LuH]_2$
3-Hexyne	0.2	0.46	0.82	2.3

a) Based on $r = k[M][H_2]$, in units of $bar^{-1}\,s^{-1}$ (multiply by 224 to convert to $M^{-1}\,s^{-1}$).

substituents on the imine. Acyclic imines are fully converted into the corresponding amines under these conditions, while the cyclic ones do not react. Additionally, di-substituted imines at the carbon atom are less reactive than their mono-substituted counterparts. Finally, substitution at the nitrogen atom is also important, with their reactivity varying as follows: =N-Alkyl >= N-Aryl >= N-SiR_3.

6.4.4
Hydrogenation of Alkenes with Actinide Complexes

Biscyclopentadienyl actinide complexes catalyze the hydrogenation of alkenes. In the hydrogenation of 1-hexene, $[Cp^*_2UH_2]$ is more efficient (higher TOF) than the corresponding Th complex, and up to 812 TON can be achieved with the U complex (Table 6.17) [128]. Using cationic Th complexes improves the rate by an order of magnitude [129], but the strongest positive effect is obtained when Cp* ligands are replaced by a Si-tethered *ansa* dicyclopentadienyl ligand,

Table 6.16 Hydrogenation of imines catalyzed by Group III and lanthanide complexes.

Substrate	Product	Catalyst	Conditions [R/P/T/t][a)]	Conv. [%][a)]	Rate [h^{-1}]
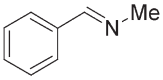	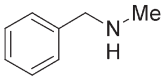	Cp^*_2SmR	100/13/90/92	83	1.0
		Cp^*_2SmR	100/13/50/122	57	0.5
		Cp^*_2SmR	100/14/25/51	4	0.04
		$Cp^*_2SmR + PhSiH_3$	100/13/90/44	98	2.2
		Cp^*_2LaR	100/10/25/50	11	0.05
		Cp^*_2LuR	100/13/25/90	51	0.60
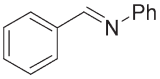	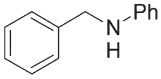	Cp^*_2SmR	100/13/90/120	16	0.10
		$Cp^*_2SmR + PhSiH_3$	100/13/90/120	10	–
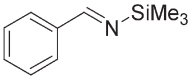	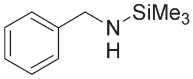	Cp^*_2SmR	100/13/90/58	21	0.40
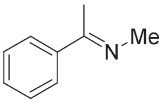	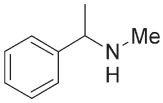	Cp^*_2SmR	100/13/90/144	26	0.20
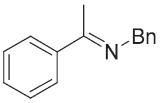	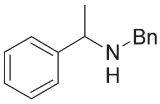	$Cp^*_2SmR + PhSiH_3$	100/13/90/134	98	0.70

a) SCR = substrate : catalyst ratio; P = pressure (bar); T = temperature (°C); t = time (h).

Table 6.17 Hydrogenation of alkenes catalyzed by actinide complexes.

Catalyst	Substrate	SCR (P_{H_2})[a)]	TOF [h^{-1}]
$[Cp^*_2ThH_2]$	1-hexene	14 (1)	0.5
$[Cp^*_2UH_2]$	1-hexene	14 (1)	70
$[Cp^*_2ThMe^+B(C_6F_5)_4^-]$	1-hexene	330 (1)	5.2
$[Cp^*_2ThMe_2]$/ $\{tBuCH[B(C_6F_5)_2]_2HNBu_3\}$	1-hexene	330 (1)	6
$[Me_2SiCp''_2ThH_2]$	1-hexene	– (1)	610
$[Cp^*_2ThH_2]$	*E* 2-hexene	14 (1)	0.086
$[Me_2SiCp''_2ThH_2]$	*E* 2-hexene	– (1)	2.45

a) SCR = substrate : catalyst ratio; $P_{H_2} = H_2$ pressure (bar).

$Me_2SiCp''_2MX_2 =$ 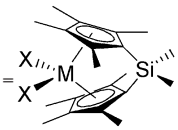

for which TOFs up to 610 h^{-1} are obtained [130]. For all these systems, the rate of hydrogenation decreases sharply (10- to 100-fold) in going from 1-hexene to *trans*-2-hexene, showing that the insertion step is highly sensitive to the substitution on the olefin [128, 130].

6.4.5
Enantiomeric Hydrogenation of Alkenes

Enantiomeric hydrogenation of alkenes can be performed with chiral lanthanide complexes. The design of an enantiomerically pure catalyst has been based on the introduction of the chirality (*R**) through the preparation of menthyl- or neomenthyl-substituted cyclopentadienyl derivatives [*R**$CpSiMe_2(C_5Me_4)$] (Scheme 6.11) [131]. Formation of the *ansa* dichloro lanthanide complexes generates two diastereomers, usually with a high level of diastereoselection, and these can be separated by simple crystallization. Access to two enantiomorphous families as pure diastereomers is possible by using the menthyl and neomenthyl derivatives, respectively [121, 124, 132]. The catalyst precursor is then formed by a simple alkylation step, which takes place with retention of configuration.

In the Sm series, the two diastereomers of one enantiomorphous family give rise to very different ee-values (Table 6.18). For example, the hydrogenation of

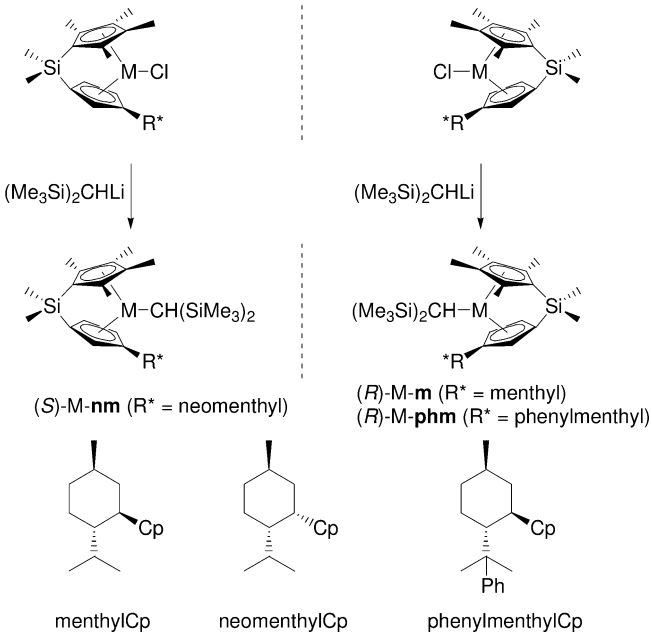

Scheme 6.11 Enantioselective hydrogenation Group III and lanthanide metallocene catalysts.

Table 6.18 Enantioselective hydrogenation of alkenes catalyzed by Group III and lanthanide complexes.

Catalyst [a)]	Substrate	SCR (P_{H2}) [b)]	Temp. [°C]	ee [%]
(*R*)-[$Me_2SiCp'Cp^{nm}SmH]_2$	2-phenyl-1-butene	100–500 (1)	25	71 (–)
(*S*)-[$Me_2SiCp'Cp^{nm}SmH]_2$	2-phenyl-1-butene	100–500 (1)	25	19 (+)
(*R*)-[$Me_2SiCp'Cp^{nm}SmH]_2$	Styrene [c)]	100 (1)	25	43 (–)
(*R*)-[$Me_2SiCp'Cp^{nm}SmR$]	2-phenyl-1-butene	100–1000 (1)	25	71 (–)
(*S*)-[$Me_2SiCp'Cp^{nm}SmR$]	2-phenyl-1-butene	100–1000 (1)	25	19 (+)
(*R*)-[$Me_2SiCp'Cp^{m}SmR$]	2-phenyl-1-butene	100–1000 (1)	25	8 (–)
(*S*)-[$Me_2SiCp'Cp^{m}SmR$]	2-phenyl-1-butene	100–1000 (1)	25	19 (–)
(*R*)-[$Me_2SiCp'Cp^{m}SmR$]	2-phenyl-1-butene	100–1000 (1)	25	43 (–)
(*S*)-[$Me_2SiCp'Cp^{m}YR$]	2-phenyl-1-butene	100–1000 (1)	25	3 (–)
(*S*)-[$Me_2SiCp'Cp^{m}YR$]	2-phenyl-1-butene	100–1000 (1)	25	3 (–)

a) nm = neomenthyl, M-**nm**; m = menthyl, M-**m**.

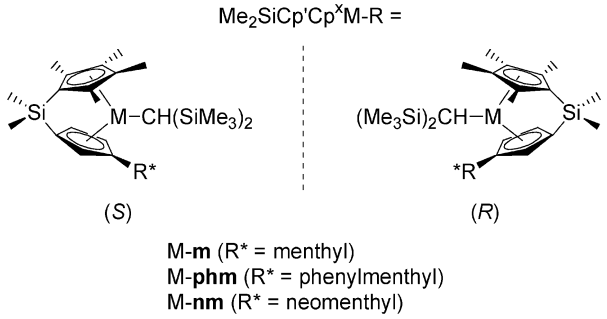

b) SCR = substrate : catalyst ratio; $P_{H2} = H_2$ pressure (bar).
c) Using D_2 instead of H_2.

2-phenyl-1-butene at 25 °C gives (*R*)-(–)-2-phenylbutane in 70% ee with the (*R*)-Sm-**nm**, while it is (*S*)-(+)-2-phenylbutane in 19% ee with the (*S*)-Sm-**nm**. When using the other enantiomorphous family, opposite enantioselection is usually observed: the (*S*)-Sm-**m** gives the (*R*)-(–)-2-phenylbutane in 8% ee under the same conditions. Moreover, when a 70/30 mixture of the (*S*) and (*R*)-Sm-**m** is used, 64% ee in (*S*)-(+)-2-phenylbutane is observed. Reducing the temperature of the reaction to –78 °C increases the level of enantioselection to 96% e.e. Finally, using D_2 instead of H_2 provides exclusively the corresponding deuterated product, arising from a *cis*-addition. The best model to explain the observed stereochemistry corresponds to a frontal approach of the alkene towards the metal center (Scheme 6.12).

Kinetic studies show that insertion (the enantioselection step) is very rapid, and that the rate-determining step is the hydrogenolysis of the M–C bond. Nonetheless, under H_2-starving conditions, there is evidence that β-H elimination can be competitive with hydrogenolysis. β-H elimination of the alkyl intermediate gives back the starting alkene and, through an equilibration process, it

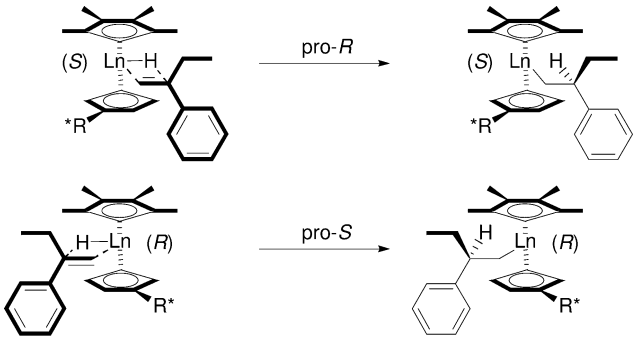

Scheme 6.12

induces an erosion of the enantioselectivity [132]. Noteworthy is the finding that, when Sm is replaced by Group III or other lanthanide metals, the following trend for ee-values is observed: La > Nd > Sm > Y > Lu, which parallels the decrease in ionic radius on going from La to Lu [132]. Other *ansa* dicyclopentadienyl systems have been designed, but this was only applicable to Y and Lu. Whilst the catalysts could be prepared as stable enantiomers, they show only low ee-values in the hydrogenation of styrene derivatives [124].

6.5
Hydrogenation Catalysts Based on Groups V–VII Transition-Metal Complexes

6.5.1
Hydrogenation of Alkenes and Dienes with Groups V–VII Transition-Metal Complexes

As shown by Breslow et al. during the mid-1960s, most transition-metal alkoxide or acetylacetonate complexes catalyze the hydrogenation of alkenes in the presence of an activator (Table 6.19) [5]. Other precursors have been used such as $[CpCr(CO)_3]_2$, but it is more difficult to understand how the active species are formed [133].

Moreover, systems based on Group V and VI transition metals can be used to selectively hydrogenate dienes into mono-enes. For example, Cp_2VCl_2 in combination with 2 equiv. BuLi or PhMgBr selectively hydrogenate butadiene into butenes, while the system based on $[Cp_2TiCl_2]/R'M$ gives butane [6]. Similarly, the V system hydrogenates isopropene selectively into 2-methyl-2-butene (92–93% selectivity), along with the other branched pentene isomers as well as traces of 2-methylbutane. Similarly, a catalytic amount of $[Cp_2MoH_2]$ (0.2 mol%) converts dienes and trienes selectively into the corresponding mono-enes in 50–90% yields at 180 °C (Scheme 6.13) [134, 135]. It has been reported that methyl acrylate, methyl crotonate, crotonaldehyde, and mesityl oxide can be hydrogenated under the same

Table 6.19 Hydrogenation catalysts based on Group V–VII transition-metal complexes activated with Al*i*Bu$_3$.

M complex	Activator [a)]	Temp. [°C]	Olefin (SCR) [b)]	Conv. [%] (time, h)
[VO(O*i*Pr)$_3$]	*i*Bu$_3$Al (3.9)	40	Cyclohexene (52)	100 (<20)
[VO(O*i*Pr)$_3$]	*i*Bu$_3$Al (3.9)	40	1-Octene (52)	100 (<20)
[Cr(acac)$_3$]	*i*Bu$_3$Al (6.0)	30	Cyclohexene (105)	100 (2)
[Cr(acac)$_3$]	*i*Bu$_3$Al (6.0)	30	1-Octene (105)	55 (1.2)
[MoO$_2$(acac)$_2$]	*i*Bu$_3$Al (7.1)	30	Cyclohexene (63)	100 (<16)
[MoO$_2$(acac)$_2$]	*i*Bu$_3$Al (7.1)	30	1-Octene (67)	100 (<21)
[Mn(acac)$_2$]	*i*Bu$_3$Al (6.0)	30	Cyclohexene (63)	100 (<16)

a) Values in parentheses correspond to the number of equivalents of activator per transition-metal complex.
b) SCR = substrate : catalyst ratio.

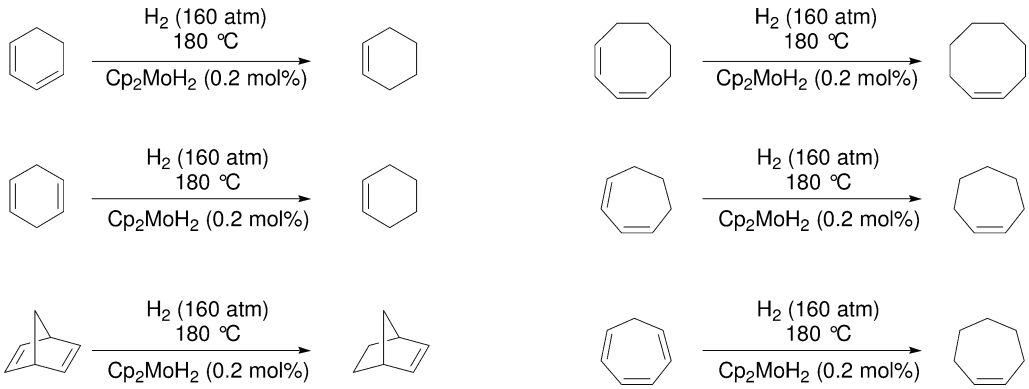

Scheme 6.13

reaction conditions, but no yields were reported. In sharp contrast, [Cp$_2$Cr, Cp$_2$WH$_2$] and [Cp$_2$ReH] are completely inactive under the same reaction conditions.

Finally, whilst rhenium hydride complexes have not been reported to hydrogenate alkenes, there are several reports of the dehydrogenation of alkanes in the presence of *t*BuCH=CH$_2$ as an hydrogen acceptor (Scheme 6.14) [136–142]. For example, cycloalkanes are transformed catalytically into the corresponding cyclic alkene, which shows that, in principle, a Re-based catalyst could be designed.

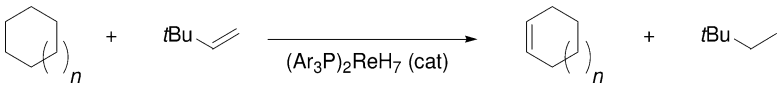

Scheme 6.14

6.5.2
Hydrogenation of Aromatics with Well-Defined Nb and Ta Aryloxide Complexes

Treatment under H_2 of $[(2,6\text{-diPhC}_6H_3O)_2Ta(CH_2R)_3]$ ($R = CH_2Ar$) in the presence of different arylphosphine ligands generated well-defined monomeric Ta hydride complexes, $[(2,6\text{-diCyC}_6H_3O)_2Ta(H_3)(PCy_3)_2$ (Scheme 6.15) [143, 144]. During this treatment, the four phenyl substituents of the aryloxide ligands are hydrogenated into cyclohexyl units, which demonstrates the catalytic potential of these systems for the hydrogenation of aromatics.

In fact, this Ta complex catalyzes the hydrogenation of naphthalene into tetraline, and that of anthracene into 1,2,3,4-decahydroanthracene [145]. The corresponding dihydride, $[(2,6\text{-di-}i\text{PrC}_6H_3O)_3Ta(H_2)(PMe_2Ph)_2]$, prepared by treatment under H_2 of $[(2,6\text{-di-}i\text{PrC}_6H_3O)_3Ta(CH_2Ar)_2]$ in the presence of PMe_2Ph, is an efficient hydrogenation catalyst of aromatics such as naphthalene [146].

Similarly, $[(2,6\text{-diPhC}_6H_3O)_2NbR_3]$ ($R = CH_2Ph\text{-}4\text{-}Me$) is an hydrogenation catalyst precursor for aromatics. It catalyzes the hydrogenation of naphthalenes into the corresponding tetraline, giving selectively the product of hydrogenation of the nonsubstituted ring (Table 6.20). It is noteworthy that anthracene is converted exclusively into 1,2,3,4,5,6,7,8-octahydroanthracene, with no trace of 9,10-dihydroanthracene, whilst phenanthrene yields 9,10-dihydroanthracene (78%) along

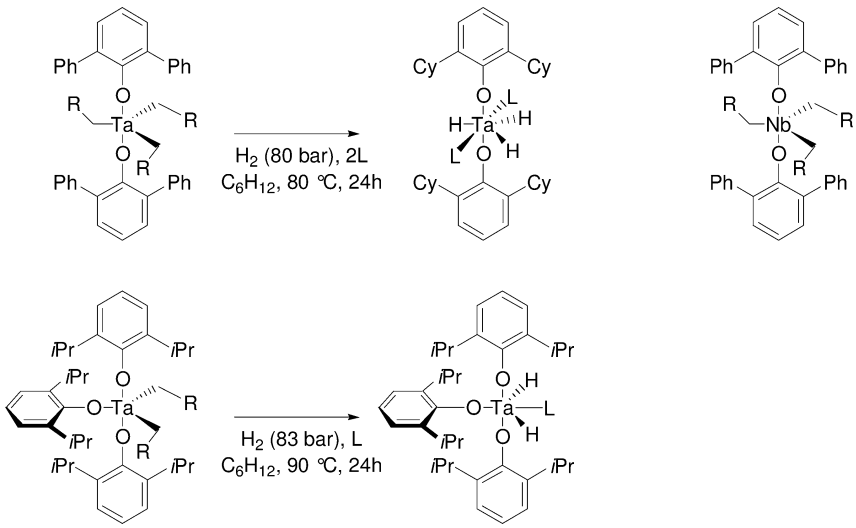

Scheme 6.15

Table 6.20 Hydrogenation of aromatics catalyzed by $[(2,6\text{-diPhC}_6H_3O)_2NbR_3]$ and $[(2,6\text{-diCyC}_6H_3O)_2Ta(H)_3(PCy_3)_2]$ [145].

Substrate	Catalyst	SCR (P) [a)]	Product	Yield [%]	Byproduct [%]
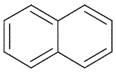	Nb Ta	20 (80) 20 (80)	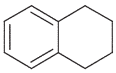	>95 >95	– –
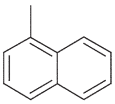	Nb	20 (80)	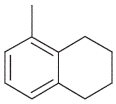	>95	–
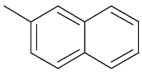	Nb	20 (80)	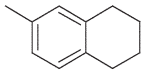	>95	–
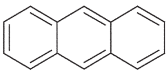	Nb	20 (80)	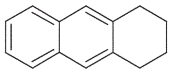	>95	–
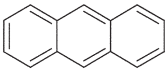	Ta	20 (80)	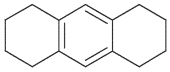	>95	–
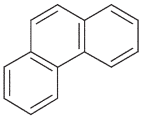	Nb	20 (80)	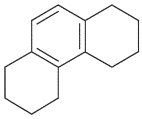	78	22 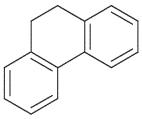
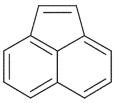	Nb	20 (80)	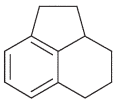	>95	–
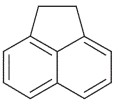	Nb	20 (80)	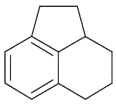	>95	–

a) SCR = substrate : catalyst ratio; P = pressure (bar).

with 1,2,3,4,5,6,7,8-octahydroanthracene (22%) [143–156]. Both, acenaphthylene and anthracene are transformed into 1,2,2a,3,4,5-hexahydronaphthalene. For both catalyst precursors, the hydrogenation of perdeuterated naphthalene gives exclusively the tetraline product with six hydrogens *cis*, all on one face.

Moreover, the Nb complex hydrogenates catalytically aryl- and benzyl-substituted phosphine under similar conditions (Scheme 6.16) [149]. Kinetic studies show that the hydrogenation of triphenylphosphine into the monocyclohexyl, dicyclohexyl, and tricyclohexylphosphine are successive reactions, and the rate of hydrogenation of the arylphosphine decreases as the number of cyclohexyl substituents increases [153].

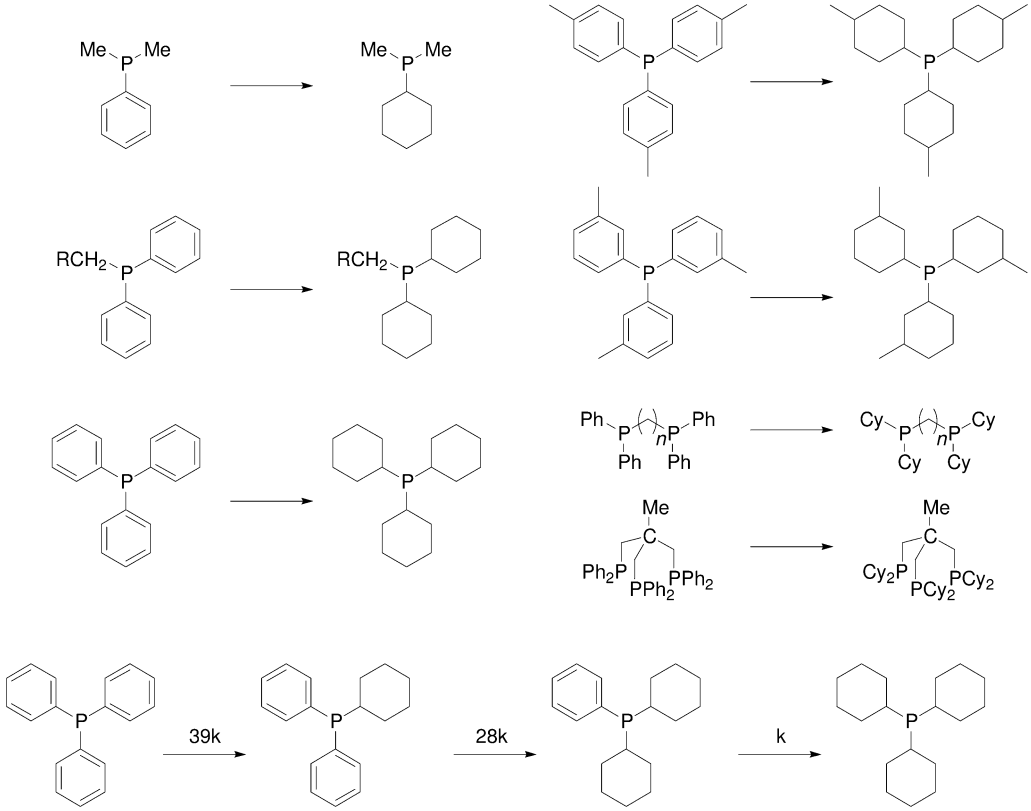

Scheme 6.16 Relative rates indicated above arrows.

6.6 Supported Early Transition-Metal Complexes as Heterogeneous Hydrogenation Catalysts

6.6.1 Supported Homogeneous Catalysts

Several strategies have been adopted to prepare the heterogeneous equivalents of the metallocene hydrogenation catalysts. One approach centers on the preparation of cyclopentadienyl-containing polymers based on either co-polymers of styrene and divinylbenzene (PSDVB) [157–164] or poly(phenylene oxide) (PPO) (Scheme 6.17) [165]. For the PSDVB system, the rate of hydrogenation of the supported systems is much greater than the molecular complex. For example, the TOF for the hydrogenation of cyclohexene for the polymer-supported Ti complex and [Cp_2TiCl_2] activated by BuLi are 1900 and 18 h^{-1}, respectively [160]. Note that critical factors are low metal loadings and small particle sizes (grind-

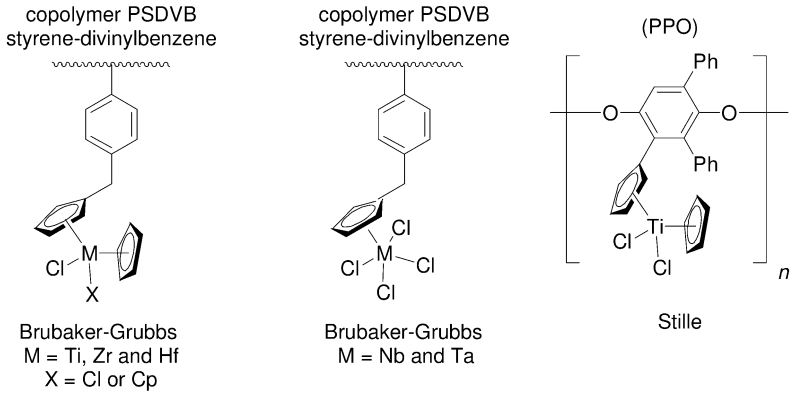

Scheme 6.17

ing of the polymer-supported catalysts prior to activation with BuLi is necessary for good activities). This system hydrogenates 1-hexene, styrene, 1,3- and 1,5-cyclooctadienes with comparable TOF, while tri-, tetra-substituted and functionalized alkenes do not undergo hydrogenation [158]. Several other metals have been used, but Ti is by far the most active [159, 163, 164]. Similarly, PPO-supported Ti complexes are more active (e.g., 10- to 70-fold) than their molecular equivalents [165].

Another approach has consisted of preparing a cyclopentadiene having an alkoxy silane substituent, which is grafted onto a silica support and then transformed into the corresponding metal cyclopentadiene complex (Scheme 6.18) [166]. After activation with BuLi or PrMgBr, their performances in the hydrogenation of 1-octene are about three- to five-fold better than the corresponding homogeneous catalysts (0.24–0.4 versus 0.08 h^{-1}, [$CpTiCl_3$]). Finally, a cyclopentadiene-containing silica has been prepared by sol-gel condensation of trisalkoxysilyl-substituted cyclopentadiene and then used to anchor the Ti center [167]. This system catalyzes the hydrogenation of 1-octene in the presence of BuLi,

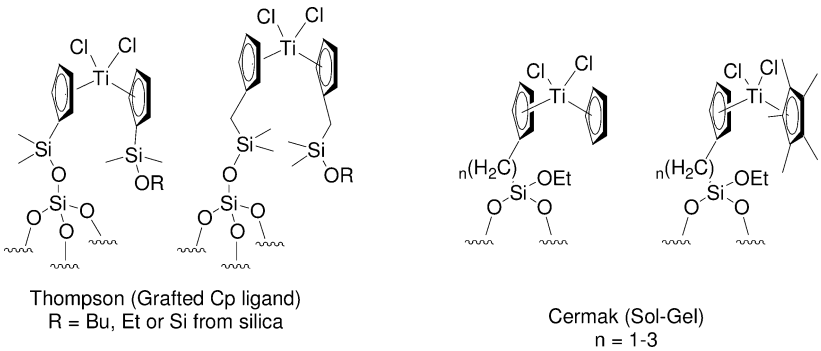

Scheme 6.18

with activities comparable to those of the homogeneous systems (2 mol% Ti): $[CpTiCl_3]$ (5640 h^{-1}) > $[(\equiv SiO\text{-}(CH_2)_nC_5H_4)Cp^*TiCl_2]$ (1730 h^{-1}) > $[Cp^*TiCl_3]$ (1300 h^{-1}) > $[(\equiv SiO\text{-}(CH_2)_nC_5H_4)CpTiCl_2]$ (865 h^{-1}).

6.6.2
Heterogeneous Catalysts Prepared via Surface Organometallic Chemistry

In contrast to supported homogeneous catalysis, surface organometallic chemistry (SOMC) uses an inorganic oxide (E_xO_y) as a solid ligand, on which the metal is directly attached by at least a bond with a surface atom, usually an oxygen, through a M–OE bond.

During the late 1960s, polymer chemists were interested in developing well-defined equivalents of the Ziegler-Natta catalysts [168, 169], and prepared supported Group IV complexes by reacting organometallic complexes with oxide supports. Yermakov et al. showed that, under treatment under H_2, these systems evolved into the corresponding hydrides. All of these systems are efficient polymerization catalysts [169–172]. Moreover, the Ti- and Zr- hydrides have turned out to be efficient hydrogenation catalysts of alkenes and aromatics (TOF = 3600 to 360 000 h^{-1} for the hydrogenation of cyclohexene or benzene) [173–176]. The structure of these systems has required a detailed understanding of the surface chemistry. In short, as a general rule, the structure of the surface organometallic complex depends on the temperature of pretreatment of silica [177]. When silica is treated at a low temperature under vacuum (e.g., 200 °C), the reaction with an organometallic complex yields a bis(siloxy) surface complex. On the other hand, when silica is treated at a high temperature under vacuum (e.g., 700 °C), a mono(siloxy) surface complex is formed (Scheme 6.19). Under H_2, Group IV and V surface complexes generate well-defined surface metal hydrides (Ti [178], Zr [179, 180], Hf [181], and Ta [182]).

The hydrogenation catalysts can be prepared *in situ*, starting from the surface alkyl complex. In terms of catalytic performances, these catalysts are highly effective (Table 6.21) [150]. The best hydrogenation systems are based on silica supported dinuclear complexes, for which the structures of the active sites have not been investigated. Hydrogenation of toluene and xylenes can be achieved under similar conditions.

Similarly, the cyclopentadienyl Zr derivatives supported on alumina are highly active olefin hydrogenation catalysts [183, 184]. The initial rates of propene hydrogenation depending on the cyclopentadienyl derivatives and the level of dehydroxylation of alumina are as follows: $[Cp^*ZrMe_3]/Al_2O_{3\text{-}(1000)}$ (3960 h^{-1}) > $[Cp^*ZrMe_3]/Al_2O_{3\text{-}(500)}$ (1080 h^{-1}) ≈ $[Cp_2ZrMe_2]/Al_2O_{3\text{-}(1000)}$ (1080 h^{-1}) > $[Cp^*CpZrMe_2]/Al_2O_{3\text{-}(1000)}$ (720 h^{-1}) > $[Cp_2ZrMe_2]/Al_2O_{3\text{-}(500)}$ (360 h^{-1}) > $[Cp^*CpZrMe_2]/Al_2O_{3\text{-}(500)}$ (216 h^{-1}) [185]. Typically, highly dehydroxylated alumina ($Al_2O_{3\text{-}(1000)}$) is a better support, and it has been associated with the formation of cationic surface species.

Several other supports have been used in order to generate more-electrophilic Zr systems, including sulfated zirconia [186], sulfated alumina [187], or other sulfated oxide supports [188], though the surface species are quite complex for these sys-

tems. The catalytic activities in the hydrogenation of benzene are as follows: $[Cp^*Zr(CH_3)_3]/ZrO_{2\text{-sulfated}}$ (970 h^{-1}) > $[Cp^*Zr(CH_3)_3]/Al_2O_{3\text{-sulfated}}$ (360 h^{-1}) > $[Cp^*Zr(CH_3)_3]/SnO_{2\text{-sulfated}}$ (10 h^{-1}) > $[Cp^*Zr(CH_3)_3]/SnO_{2\text{-sulfated}}$ (5 h^{-1}) > $[Cp^*Zr(CH_3)_3]/TiO_{2\text{-sulfated}}$ (< 3 h^{-1}), and they are correlated with the surface Brönsted acidity [188].

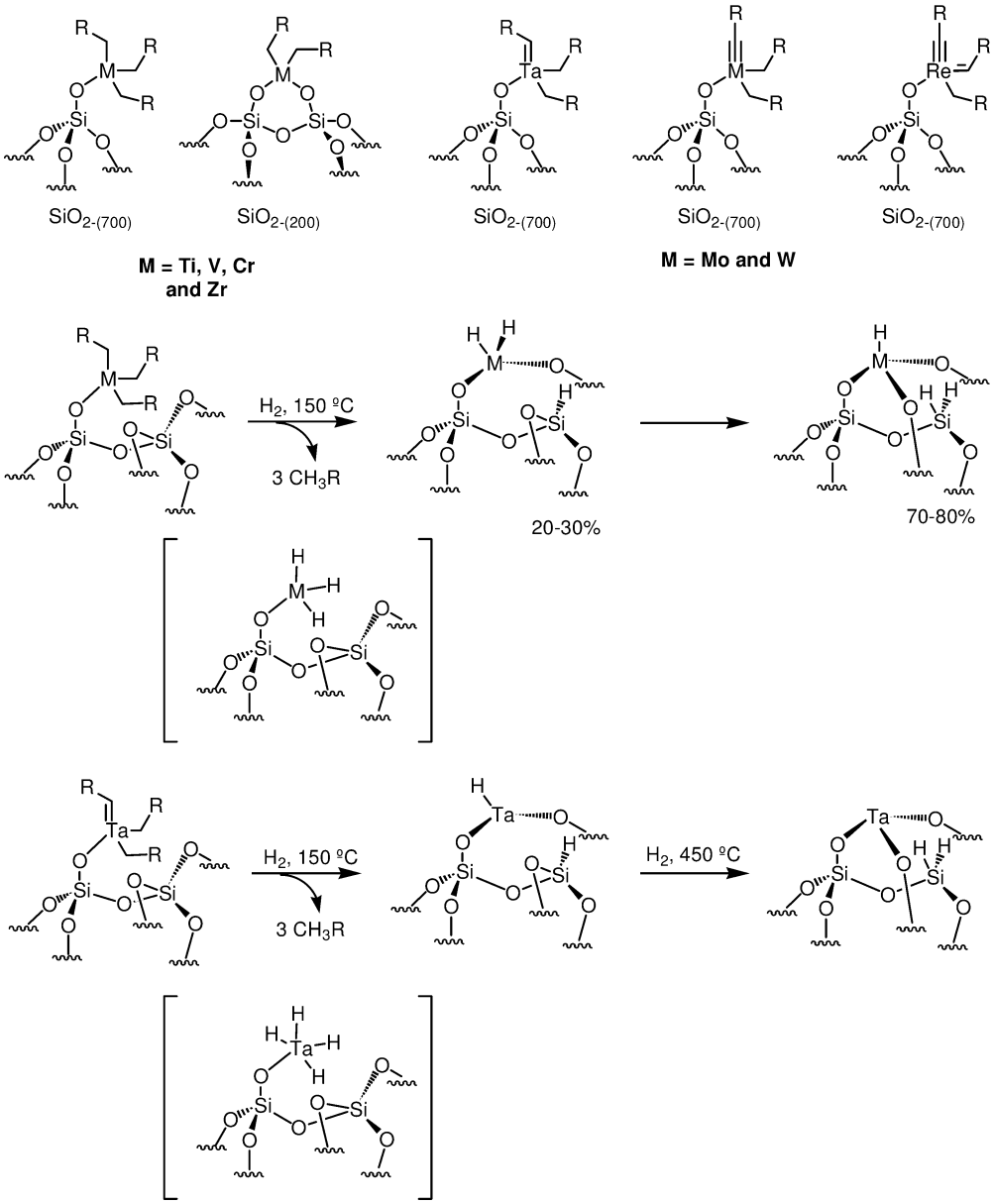

Scheme 6.19

Table 6.21 Hydrogenation of benzene and naphthalene catalyzed by silica-supported Group IV–VI transition-metal complexes.

Catalytic system	Substrate	Time [min]	Conversion [%]	Selectivity [%]
$Ti(CH_2SiMe_3)_4/SiO_2$	Benzene [a)]	360	39	100
	Naphthalene [b)]	150	100	55:45 [d)]
$Zr(CH_2Ph)_4/SiO_2$	Benzene [a)]	240	100	100
	Naphthalene [b)]	30	100	25:75 [d)]
$Hf(CH_2Ph)_4/SiO_2$	Benzene [a)]	600	100	100
	Naphthalene [b)]	60	100	19:81 [d)]
$Ta(CH_2Ar)_5/SiO_2$	Benzene [a)]	24 h	100	100
Ar = 4-Me-C_6H_4	Naphthalene [b)]	160	100	20:80 [d)]
$[Nb(CSiMe_3)(CH_2SiMe_3)_2]_2/SiO_2$	Benzene [a)]	300	100	100
	Naphthalene [b)]	20	100	15:85 [d)]
	Benzene [c)]	25	100	100
	Toluene [c)]	33	100	100
	o-Xylene [c)]	30	100	57:43 [d)]
	m-Xylene [c)]	20	100	78:22 [d)]
	p-Xylene [c)]	25	100	57:43 [d)]
$[Ta(CSiMe_3)(CH_2SiMe_3)_2]_2/SiO_2$	Benzene [a)]	720	100	100
	Naphthalene [b)]	70	100	20:80 [d)]
	Benzene [c)]	55	100	100
	Toluene [c)]	64	100	100
	o-Xylene [c)]	75	100	91:9 [d)]
	m-Xylene [c)]	70	100	92:8 [d)]
	p-Xylene [c)]	65	100	82:18 [d)]
$[Mo_2(CH_2SiMe_3)_6]/SiO_2$	Benzene [a)]	720	100	100
	Naphthalene [b)]	70	100	20:80 [d)]

a) 0.056 mmol M loaded on 5 g silica treated at 200 °C under vacuum, 17.5 g C_6H_6 (4000 equiv.), 80–100 bar H_2 at 120 °C.
b) 0.056 mmol M loaded on 5 g silica treated at 200 °C under vacuum, 2.0 g naphthalene (280 equiv.), 25 mL hexane, 100 bar H_2 at 120 °C.
c) 0.056 mmol M loaded on 5 g silica treated at 200 °C under vacuum, 26 mmol substrate (280 equiv.), 80–100 bar H_2 at 120 °C.
d) *cis/trans* ratio.

Soon after the discovery that dimeric actinide hydride complexes were active hydrogenation catalysts, Marks et al. investigated the formation of monomeric actinide active species by supporting them on an oxide support [184, 189]. The supported complexes on alumina are much more active than the corresponding molecular complexes. For comparison, the rate of hydrogenation of propene at 25 °C can be ranked as follows: $[Cp^*_2U(CH_3)_2]/Al_2O_{3\text{-}(1000)}$ (1080 h^{-1}) > $[Cp^*_2Th(CH_3)_2]/Al_2O_{3\text{-}(1000)}$ (580 h^{-1}) > $[Cp^*_2U(CH_3)_2]$ (68 h^{-1}) > $[Cp^*_2Th(CH_3)_2]$ (0.54 h^{-1}). Using partially dehydroxylated silica or an alumina dehydroxylated at a lower tempera-

ture as supports produces poorer catalysts [190]. Other supports have been used, but highly dehydroxylated alumina remains the best available to date. For example, the TOFs for the hydrogenation of propene at 25 °C are: $[Cp^*_2Th(CH_3)_2]/Al_2O_{3\text{-}(1000)}$ (580 h^{-1}) > $[Cp^*_2Th(CH_3)_2]/SiO_2\text{-}Al_2O_3$ (160–230 h^{-1}) > $[Cp^*_2Th(CH_3)_2]/MgCl_2$ (25–43 h^{-1}) > $[Cp^*_2Th(CH_3)_2]/SiO_2\text{-}MgO$ (0 h^{-1}) [191]. Note also that the TOF depends on the alkenes as measured by the hydrogenation at –45 °C: *cis*-butene (3960 h^{-1}) > *trans*-2-butene (2900 h^{-1}) ≫ propene (470 h^{-1}) ≫ isobutene (13 h^{-1}). Finally, some of these systems are highly active aromatic hydrogenation catalysts. At 90 °C and 13 bar, the TOF of hydrogenation is as follows: $[Th(allyl)_4]/Al_2O_{3\text{-}(1000)}$ (1970 h^{-1}) ≫ $[Th(CH_2Ar)_4]/Al_2O_{3\text{-}(1000)}$ (825 h^{-1}) > $[Cp^*Th(CH_2Ar)_3]$ (765 h^{-1}) [192, 193]. Noteworthy, the TOF for the hydrogenation of benzene with $[Th(allyl)_4]/Al_2O_{3\text{-}(1000)}$ is comparable to Rh or Pt heterogeneous catalysts. The hydrogenation TOF is also function of the aromatic compounds: benzene (6850 k) > toluene (4100 k) > xylene (1450 k) ≫ naphthalene (1 k). Using D_2 in place of H_2 shows that hydrogenation corresponds to a random 1,2-*cis* addition of H_2.

6.7 Conclusions

Early transition-metal complexes have been some of the first well-defined catalyst precursors used in the homogeneous hydrogenation of alkenes. Of the various systems developed, the biscyclopentadienyl Group IV metal complexes are probably the most effective, especially those based on Ti. The most recent development in this field has shown that enantiomerically pure *ansa* zirconene and titanocene derivatives are highly effective enantioselective hydrogenation catalysts for alkenes, imines, and enamines (up to 99% ee in all cases), whilst in some cases TON of up to 1000 have been achieved.

Moreover, Group III, lanthanide and actinide biscyclopentadienyl complexes are efficient hydrogenation catalysts exhibiting a very rapid rate of hydrogenation. These catalysts are, nonetheless, somewhat more sensitive to the presence of functional groups, even though they can be used to hydrogenate imines. Enantiomerically pure chiral catalysts have also been developed for the enantiomeric hydrogenation of olefins in good enantiomeric excess (up to 71% ee).

Hydrogenation with Group V–VII transition metals has not yet been investigated in detail, despite the early discoveries of Breslow et al. Nonetheless, the findings of Rothwell et al. are noteworthy as Group V aryloxy systems can hydrogenate aromatics, including triphenylphosphine.

Finally, some of these systems have been supported on polymers or oxides, and these are typically more active than their homogeneous equivalents.

In general, the rate of alkene hydrogenation is typically ordered as follows: terminal > di-substituted > tri-substituted ≫ tetra-substituted. In fact, this allows terminal or di-substituted olefins to be hydrogenated selectively in the presence of tri- or tetra-substituted ones. Additionally, the rate of hydrogenation of alkynes is much slower than that of alkenes, although the *cis*-alkene intermediate

can be observed and in some cases formed selectively, before its hydrogenation into the corresponding alkanes.

Whilst hydrogenation catalysts based on early transition metals are as active and selective as those based on late transition metals, they are usually not as compatible with functional groups, and this represents the major difficulty for their use in organic synthesis. Nonetheless, titanocene derivatives have been used in industry to hydrogenate unsaturated polymers.

Undoubtedly, further studies in this area are required, and it is most likely that, based on such investigations, new systems based on Group III–VII metals will emerge during the coming years.

Acknowledgments

These studies are dedicated to I.P. Rothwell for his pioneering contributions towards the development of early transition-metal hydrogenation catalysts. The author thanks the CNRS for financial support.

Abbreviations

ee	enantiomeric excess
PPO	poly(phenylene oxide)
PSDVB	co-polymers of styrene and divinylbenzene
SOMC	surface organometallic chemistry
TOF	turnover frequency
TON	turnover number

References

1 J.F. Young, J.A. Osborn, F.H. Jardine, G. Wilkinson, *J. Chem. Soc., Chem. Commun.* **1965**, 131.
2 G. Wilkinson, P.L. Pauson, J.M. Birmingham, F.A. Cotton, *J. Am. Chem. Soc.* **1953**, *75*, 1011.
3 G. Wilkinson, J.M. Birmingham, *J. Am. Chem. Soc.* **1954**, *76*, 4281.
4 D.S. Breslow, N.R. Newburg, *J. Am. Chem. Soc.* **1959**, *81*, 81.
5 M.F. Sloan, A.S. Matlack, D.S. Breslow, *J. Am. Chem. Soc.* **1963**, *85*, 4014.
6 Y. Tajima, E. Kunioka, *J. Org. Chem.* **1968**, *33*, 1689.
7 P.C. Wailes, H. Weigold, A.P. Bell, *J. Organometal. Chem.* **1972**, *43*, C32.
8 E.E. Van Tamelen, W. Cretney, N. Klaentschi, J.S. Miller, *J. Chem. Soc., Chem. Soc.* **1972**, 481.
9 J.E. Bercaw, R.H. Marvich, L.G. Bell, H.H. Brintzinger, *J. Am. Chem. Soc.* **1972**, *94*, 1219.
10 G. Fachinetti, C. Floriani, *J. Chem. Soc., Chem. Soc.* **1974**, 66.
11 C. Floriani, G.F. Fachinetti (Snamprogetti SpA, Italy), De2449257, **1975**.
12 G.W. Parshall, S.D. Ittel. The Applications and Chemistry of Catalysis by Soluble Transition Metal Complexes. In: *Homogeneous Catalysis*, 2nd edn., Wiley-VCH, Weinheim, **2000**.

13 D. Astruc. In: *Chimie Organométallique*, PUF, Grenoble, **2001**.
14 C.P. Casey, S.L. Hallenbeck, D.W. Pollock, C.R. Landis, *J. Am. Chem. Soc.* **1995**, *117*, 9770.
15 C.P. Casey, S.L. Hallenbeck, J.M. Wright, C.R. Landis, *J. Am. Chem. Soc.* **1997**, *119*, 9680.
16 C.P. Casey, J.J. Fisher, *Inorg. Chim. Act.* **1998**, *270*, 5.
17 C.P. Casey, M.A. Fagan, S.L. Hallenbeck, *Organometallics* **1998**, *17*, 287.
18 C.P. Casey, D.W. Carpenetti, II, H. Sakurai, *J. Am. Chem. Soc.* **1999**, *121*, 9483.
19 C.P. Casey, D.W. Carpenetti, II, *Organometallics* **2000**, *19*, 3970.
20 C.P. Casey, J.F. Klein, M.A. Fagan, *J. Am. Chem. Soc.* **2000**, *122*, 4320.
21 C.P. Casey, T.-Y. Lee, J.A. Tunge, D.W. Carpenetti, II, *J. Am. Chem. Soc.* **2001**, *123*, 10762.
22 C.P. Casey, D.W. Carpenetti, II, H. Sakurai, *Organometallics* **2001**, *20*, 4262.
23 C.P. Casey, J.A. Tunge, T.-Y. Lee, M.A. Fagan, *J. Am. Chem. Soc.* **2003**, *125*, 2641.
24 Z. Wu, R.F. Jordan, J.L. Petersen, *J. Am. Chem. Soc.* **1995**, *117*, 5867.
25 M. Yoshida, D.J. Crowther, R.F. Jordan, *Organometallics* **1997**, *16*, 1349.
26 J.-F. Carpentier, Z. Wu, C.W. Lee, S. Stroemberg, J.N. Christopher, R.F. Jordan, *J. Am. Chem. Soc.* **2000**, *122*, 7750.
27 E.J. Stoebenau, III, R.F. Jordan, *J. Am. Chem. Soc.* **2003**, *125*, 3222.
28 E.J. Stoebenau, III, R.F. Jordan, *J. Am. Chem. Soc.* **2004**, *126*, 11170.
29 P.L. Watson, *J. Am. Chem. Soc.* **1983**, *105*, 6491.
30 P.L. Watson, *J. Chem. Soc., Chem. Soc.* **1983**, 276.
31 M.E. Thompson, S.M. Baxter, A.R. Bulls, B.J. Burger, M.C. Nolan, B.D. Santarsiero, W.P. Schaefer, J.E. Bercaw, *J. Am. Chem. Soc.* **1987**, *109*, 203.
32 B.-J. Deelman, J.H. Teuben, S.A. MacGregor, O. Eisenstein, *New J. Chem.* **1995**, *19*, 691.
33 L. Maron, L. Perrin, O. Eisenstein, *J. Chem. Soc., Dalton Trans.* **2002**, 534.
34 C. Copéret, A. Grouiller, M. Basset, H. Chermette, *Chem. Phys. Chem.* **2003**, *4*, 608.
35 Y.-H. Fan, S.-J. Liao, J. Xu, F.-D. Wang, Y.-L. Qian, J.-L. Huang, *J. Catal.* **2002**, *205*, 294.
36 T. Takahashi, N. Suzuki, M. Kageyama, Y. Nitto, M. Saburi, E. Negishi, *Chem. Lett.* **1991**, 1579.
37 S.J. Liao, Y. Xu, Y.P. Zhang, Q. Sun, R.A. Sun, R.W. Yang, *Chin. Chem. Lett.* **1994**, *5*, 689.
38 S. Couturier, B. Gautheron, *J. Organometal. Chem.* **1978**, *157*, C61.
39 S. Couturier, G. Tainturier, B. Gautheron, *J. Organometal. Chem.* **1980**, *195*, 291.
40 J.A. Smith, H.H. Brintzinger, *J. Organometal. Chem.* **1981**, *218*, 159.
41 K. Shikata, K. Nishino, K. Azuma, Y. Takegami, *Kogyo Kagaku Zasshi* **1965**, *68*, 358.
42 Y. Qian, G. Li, Y. Huang, *J. Mol. Cat.* **1989**, *54*, L19.
43 F. Masi, R. Santi, G. Longhini, A. Vallieri (Enichem S.p.A., Italy), Ep908234, **1999**.
44 K. Sonogashira, N. Hagihara, *Bull. Chem. Soc. Jap.* **1966**, *39*, 1178.
45 F. Scott, H.G. Raubenheimer, G. Pretorius, A.M. Hamese, *J. Organometal. Chem.* **1990**, *384*, C17.
46 K. Iwase, K. Kato, G. Yamamoto (Asahi Chemical Ind, Japan), Jp08041081, **1996**.
47 B. Demerseman, P. Le Coupanec, P.H. Dixneuf, *J. Organometal. Chem.* **1985**, *287*, C35.
48 V.B. Shur, V.V. Burlakov, M.E. Vol'pin, *Izv. Akad. Nauk SSSR, Ser. Khim.* **1986**, 728.
49 V.B. Shur, V.V. Burlakov, M.E. Vol'pin, *J. Organometal. Chem.* **1992**, *439*, 303.
50 E.B. Lobkovskii, L. Soloveichik, A.I. Sizov, B.M. Bulychev, *J. Organometal. Chem.* **1985**, *280*, 53.
51 V.K. Bel'skii, A.I. Sizov, B.M. Bulychev, G.L. Soloveichik, *J. Organometal. Chem.* **1985**, *280*, 67.
52 A.I. Sizov, T.M. Zvukova, V.K. Bel'sky, B.M. Bulychev, *Russ. Chem. Bull.* (Translation of Izvestiya Akademii Nauk, Seriya Khimicheskaya) **1998**, *47*, 1186.
53 Y. Zhang, S. Liao, Y. Xu, S. Chen, *J. Organometal. Chem.* **1990**, *382*, 69.
54 Q. Sun, S. Liao, Y. Xu, Y. Qian, J. Huang, *Cuihua Xuebao* **1996**, *17*, 495.
55 Y.-H. Fan, S.-J. Liao, J. Xu, Y.-L. Qian, J.-L. Huang, *Gaodeng Xuexiao Huaxue Xuebao* **1997**, *18*, 1683.

56 M. Zhang, Y. Fan, S. Liao, Y. Qian, *Huadong Ligong Daxue Xuebao* **1998**, *24*, 580.

57 Y. Fan, S. Liao, Y. Xu, Y. Qian, J. Huang, *Cuihua Xuebao* **1998**, *19*, 389.

58 J.-G. Lee, H.Y. Jeong, Y.H. Ko, J.H. Jang, H. Lee, *J. Am. Chem. Soc.* **2000**, *122*, 6476.

59 E. Samuel, *J. Organometal. Chem.* **1980**, *198*, C65.

60 J.F. Harrod, S.S. Yun, *Organometallics* **1987**, *6*, 1381.

61 J.F. Harrod, R. Shu, H.-G. Woo, E. Samuel, *Can. J. Chem.* **2001**, *79*, 1075.

62 Y. Tajima, E. Kunioka, *J. Am. Oil Chem. Soc.* **1968**, 45, 478.

63 F. Hayano, Y. Nakafutami, Y. Kishimoto (Asahi Chemical Industry Co., Ltd., Japan), Jp61034050, **1986**.

64 T. Masubuchi, Y. Kishimoto (Asahi Chemical Industry Co., Ltd., Japan), Jp61033132, **1986**.

65 T. Masubuchi, Y. Kishimoto (Asahi Chemical Industry Co., Ltd., Japan), Jp61057524, **1986**.

66 T. Teramoto, K. Goshima, M. Takeuchi (Japan Synthetic Rubber Co., Ltd., Japan), Ep339986, **1989**.

67 I. Hattori, A. Takashima, T. Imamura (Japan Synthetic Rubber Co., Ltd., Japan), Jp02272004, **1990**.

68 Y. Hashiguchi, H. Katsumata, K. Goshima, T. Teramoto, Y. Takemura (Japan Synthetic Rubber Co., Ltd., Japan), Ep434469, **1991**.

69 L.R. Chamberlain, C.J. Gibler (Shell Oil Co., USA), US5039755, **1991**.

70 L.R. Chamberlain, C.J. Gibler, R.A. Kemp, S.E. Wilson (Shell International Research Maatschappij B.V., Neth.), Ep471415, **1992**.

71 L.R. Chamberlain, C.J. Gibler, R.A. Kemp, S.E. Wilson, T.F. Brownscombe (Shell Oil Co., USA), US5177155, **1993**.

72 K. Kato, G. Yamamoto (Asahi Chemical Ind., Japan; Asahi Kasei Chemical Corporation), Jp08033846, **1996**.

73 H. Nakafutami, K. Kato (Asahi Chemical Ind, Japan), Jp08027216, **1996**.

74 H. Nakafutami, K. Kato (Asahi Chemical Ind, Japan), Jp08027231, **1996**.

75 K. Iwase, K. Kato, K. Miyamoto (Asahi Chemical Industry Co., Ltd., Japan), Jp09278677, **1997**.

76 E.J.M. de Boer, B. Hessen, A.A. van der Huizen, W. de Jong, A.J. van der Linden, B.J. Ruisch, L. Schoon, H.J.A. de Smet, F.H. van der Steen, H.C.T.L. van Strien, A. Villena, J.J.B. Walhof (Shell Internationale Research Maatschappij BV, Neth.), Ep801079, **1997**.

77 E.J.M. de Boer, B. Hessen, A.A. van der Huizen, W. de Jong, A.J. van der Linden, B.J. Ruisch, L. Schoon, H.J.A. de Smet, F.H. van der Steen, H.C.T. van Strien, A. Villena, J.J.B. Walhof (Shell Internationale Research Maatschappij BV, Neth.), Ep795564, **1997**.

78 K. Kato, Y. Kusanose (Asahi Chemical Industry Co., Ltd., Japan), Jp10259221, **1998**.

79 A. Vallieri, C. Cavallo, G.T. Viola (Enichem S.P.A., Italy), Ep816382, **1998**.

80 J. Yonezawa, K. Kato, E. Sasaya, T. Sato (Asahi Kasei Kogyo K.K., Japan), De19815895, **1998**.

81 J.A. Barrio Calle, M.D. Parellada Ferrer, M.J. Espinosa Soriano (Repsol Quimica S.A., Spain), Ep885905, **1998**.

82 K. Miyamoto, Y. Kitagawa, S. Sasaki (Asahi Kasei Kogyo Kabushiki Kaisha, Japan), Ep889057, **1999**.

83 S. Sasaki, M. Kamatani, H. Shinjo (Asahi Chemical Industry Co., Ltd., Japan), Jp2000095804, **2000**.

84 S. Sasaki, M. Kamatani, H. Shinjo (Asahi Chemical Industry Co., Ltd., Japan), Jp2000095814, **2000**.

85 J. Cai, W. Zhang, Y. Zhao, C. Huang, H. Xiao, Z. Zhu (Inst. of Industrial Technology, Financial Group, Peop. Rep. China; Qimei Industrial Co., Ltd.), Cn1324867, **2001**.

86 J.-C. Tsai, W.-S. Chang, Y.-S. Chao, C.-N. Chu, C.-P. Huang, H.-Y. Hsiao (Industrial Technology Research Institute, Taiwan; Chi Mei Corporation), Us6313230, **2001**.

87 H. Zhang, W. Li, H. Liang, J. Zhang, X. Peng, H. Fang, H. Luo (Yueyang Petrochemical General Plant, Baling Petrochemical Corp., Peop. Rep. China), Cn1332183, **2002**.

88 S. Sasaki, T. Kasai, Y. Kusanose (Asahi Kasei Chemical Corporation, Japan), Jp2004269665, **2004**.

89 A. J. Calle Barrio, M. D. Ferrer Parellada, M. J. E. Soriano (Epsol Quimica S.A., Spain), Ro115527, **2000**.
90 R. C.-C. Tsiang, W.-S. Yang, M.-D. Tsai, *Polymer* **1999**, *40*, 6351.
91 R. C.-C. Tsiang, W.-S. Yang, M.-D. Tsai, *ACS Symp. Ser.* **2000**, *760*, 108.
92 S.-s. Xu, L. Yang, K. Yuan, B.-q. Wang, X.-z. Zhou, W. Li, X.-j. He, *Gaodeng Xuexiao Huaxue Xuebao* **2001**, *22*, 2022.
93 P. Meunier, B. Gautheron, S. Couturier, *J. Organometal. Chem.* **1982**, *231*, C1.
94 V. E. Cesarotti, R. Ugo, H. B. Kagan, *Angew. Chem. Int. Ed.* **1979**, *18*, 779.
95 E. Cesarotti, R. Ugo, R. Vitiello, *J. Mol. Cat.* **1981**, *12*, 63.
96 E. Cesarotti, H. B. Kagan, R. Goddard, C. Krueger, *J. Organometal. Chem.* **1978**, *162*, 297.
97 L. A. Paquette, J. A. McKinney, M. L. McLaughlin, A. L. Rheingold, *Tetrahedron Lett.* **1986**, *27*, 5599.
98 R. L. Halterman, K. P. C. Vollhardt, *Organometallics* **1988**, *7*, 883.
99 L. A. Paquette, M. R. Sivik, E. I. Bzowej, K. J. Stanton, *Organometallics* **1995**, *14*, 4865.
100 R. L. Halterman, K. P. C. Vollhardt, M. E. Welker, D. Blaeser, R. Boese, *J. Am. Chem. Soc.* **1987**, *109*, 8105.
101 P. Beagley, P. J. Davies, A. J. Blacker, C. White, *Organometallics* **2002**, *21*, 5852.
102 F. R. W. P. Wild, L. Zsolnai, G. Huttner, H. H. Brintzinger, *J. Organometal. Chem.* **1982**, *232*, 233.
103 F. R. W. P. Wild, M. Wasiucionek, G. Huttner, H. H. Brintzinger, *J. Organometal. Chem.* **1985**, *288*, 63.
104 R. Waymouth, P. Pino, *J. Am. Chem. Soc.* **1990**, *112*, 4911.
105 R. B. Grossman, R. A. Doyle, S. L. Buchwald, *Organometallics* **1991**, *10*, 1501.
106 R. D. Broene, S. L. Buchwald, *J. Am. Chem. Soc.* **1993**, *115*, 12569.
107 M. V. Troutman, D. H. Appella, S. L. Buchwald, *J. Am. Chem. Soc.* **1999**, *121*, 4916.
108 C. A. Willoughby, S. L. Buchwald, *J. Am. Chem. Soc.* **1992**, *114*, 7562.
109 C. A. Willoughby, S. L. Buchwald, *J. Am. Chem. Soc.* **1994**, *116*, 8952.
110 C. A. Willoughby, S. L. Buchwald, *J. Org. Chem.* **1993**, *58*, 7627.
111 A. Viso, N. E. Lee, S. L. Buchwald, *J. Am. Chem. Soc.* **1994**, *116*, 9373.
112 N. E. Lee, S. L. Buchwald, *J. Am. Chem. Soc.* **1994**, *116*, 5985.
113 J. Okuda, S. Verch, T. P. Spaniol, R. Stuermer, *Chem. Ber.* **1996**, *129*, 1429.
114 R. Stürmer, J. Okuda, K. Ritter (BASF AG, Germany), De19622271, **1997**.
115 J. Okuda, S. Verch, R. Stürmer, T. P. Spaniol, *J. Organometal. Chem.* **2000**, *605*, 55.
116 J. Okuda, S. Verch, R. Stürmer, T. P. Spaniol, *Chirality* **2000**, *12*, 472.
117 M. Ringwald, R. Stürmer, H. H. Brintzinger, *J. Am. Chem. Soc.* **1999**, *121*, 1524.
118 M. Ringwald, R. Stuermer, H. H. Brintzinger, *J. Am. Chem. Soc.* **1999**, *121*, 7278.
119 H. Mauermann, P. N. Swepston, T. J. Marks, *Organometallics* **1985**, *4*, 200.
120 G. Jeske, H. Lauke, H. Mauermann, H. Schumann, T. J. Marks, *J. Am. Chem. Soc.* **1985**, *107*, 8111.
121 P. W. Roesky, C. L. Stern, T. J. Marks, *Organometallics* **1997**, *16*, 4705.
122 G. A. Molander, J. Winterfeld, *J. Organometal. Chem.* **1996**, *524*, 275.
123 G. A. Molander, J. O. Hoberg, *J. Org. Chem.* **1992**, *57*, 3266.
124 C. M. Haar, C. L. Stern, T. J. Marks, *Organometallics* **1996**, *15*, 1765.
125 W. J. Evans, I. Bloom, W. E. Hunter, J. L. Atwood, *J. Am. Chem. Soc.* **1983**, *105*, 1401.
126 W. J. Evans, J. H. Meadows, W. E. Hunter, J.L. Atwood, *J. Am. Chem. Soc.* **1984**, *106*, 1291.
127 Y. Obora, T. Ohta, C. L. Stern, T. J. Marks, *J. Am. Chem. Soc.* **1997**, *119*, 3745.
128 P. J. Fagan, J. M. Manriquez, E. A. Maatta, A. M. Seyam, T. J. Marks, *J. Am. Chem. Soc.* **1981**, *103*, 6650.
129 L. Jia, X. Yang, C. Stern, T. J. Marks, *Organometallics* **1994**, *13*, 3755.
130 C. M. Fendrick, L. D. Schertz, V. W. Day, T. J. Marks, *Organometallics* **1988**, *7*, 1828.
131 V. P. Conticello, L. Brard, M. A. Giardello, Y. Tsuji, M. Sabat, C. L. Stern, T. J. Marks, *J. Am. Chem. Soc.* **1992**, *114*, 2761.
132 M. A. Giardello, V. P. Conticello, L. Brard, M. R. Gagne, T. J. Marks, *J. Am. Chem. Soc.* **1994**, *116*, 10241.

133 A. Miyake, H. Kondo, *Angew. Chem. Int. Ed.* **1968**, *7*, 631.

134 A. Nakamura, S. Otsuka, *J. Am. Chem. Soc.* **1973**, *95*, 7262.

135 A. Nakamura, S. Otsuka, *Tetrahedron Lett.* **1973**, 4529.

136 D. Baudry, M. Ephritikhine, H. Felkin, *J. Chem. Soc., Chem. Soc.* **1980**, 1243.

137 D. Baudry, M. Ephritikhine, H. Felkin, Y. Jeannin, F. Robert, *J. Organometal. Chem.* **1981**, *220*, C7.

138 D. Baudry, M. Ephritikhine, H. Felkin, J. Zakrzewski, *J. Chem. Soc., Chem. Soc.* **1982**, 1235.

139 D. Baudry, M. Ephritikhine, H. Felkin, *J. Chem. Soc., Chem. Soc.* **1982**, 606.

140 D. Baudry, M. Ephritikhine, H. Felkin, *J. Organometal. Chem.* **1982**, *224*, 363.

141 D. Baudry, M. Ephritikhine, H. Felkin, R. Holmes-Smith, *J. Chem. Soc., Chem. Soc.* **1983**, 788.

142 T. Burchard, H. Felkin, *New J. Chem.* **1986**, *10*, 673.

143 B.C. Ankianiec, P.E. Fanwick, I.P. Rothwell, *J. Am. Chem. Soc.* **1991**, *113*, 4710.

144 I.P. Rothwell, *Chem. Commun.* **1997**, 1331.

145 J.S. Yu, B.C. Ankianiec, I.P. Rothwell, M.T. Nguyen, *J. Am. Chem. Soc.* **1992**, *114*, 1927.

146 V.M. Visciglio, P.E. Fanwick, I.P. Rothwell, *J. Chem. Soc., Chem. Soc.* **1992**, 1505.

147 D.R. Mulford, J.R. Clark, S.W. Schweiger, P.E. Fanwick, I.P. Rothwell, *Organometallics* **1999**, *18*, 4448.

148 R.W. Chesnut, B.D. Steffey, I.P. Rothwell, *Polyhedron* **1989**, *8*, 1607.

149 J.S. Yu, I.P. Rothwell, *J. Chem. Soc., Chem. Soc.* **1992**, 632.

150 R.D. Profilet, A.P. Rothwell, I.P. Rothwell, *J. Chem. Soc., Chem. Soc.* **1993**, 42.

151 I.P. Rothwell, S.J. Yu (Research Corp. Technologies, Inc., USA), Wo9321192, **1993**.

152 M.A. Lockwood, M.C. Potyen, B.D. Steffey, P.E. Fanwick, I.P. Rothwell, *Polyhedron* **1995**, *14*, 3293.

153 M.C. Potyen, I.P. Rothwell, *J. Chem. Soc., Chem. Soc.* **1995**, 849.

154 B.C. Parkin, J.R. Clark, V.M. Visciglio, P.E. Fanwick, I.P. Rothwell, *Organometallics* **1995**, *14*, 3002.

155 V.M. Visciglio, M.T. Nguyen, J.R. Clark, P.E. Fanwick, I.P. Rothwell, *Polyhedron* **1996**, *15*, 551.

156 V.M. Visciglio, J.R. Clark, M.T. Nguyen, D.R. Mulford, P.E. Fanwick, I.P. Rothwell, *J. Am. Chem. Soc.* **1997**, *119*, 3490.

157 R.H. Grubbs, C. Gibbons, L.C. Kroll, W.D. Bonds, Jr., C.H. Brubaker, Jr., *J. Am. Chem. Soc.* **1973**, *95*, 2373.

158 W.D. Bonds, Jr., C.H. Brubaker, Jr., E.S. Chandrasekaran, C. Gibbons, R.H. Grubbs, L.C. Kroll, *J. Am. Chem. Soc.* **1975**, *97*, 2128.

159 E.S. Chandrasekaran, R.H. Grubbs, C.H. Brubaker, Jr., *J. Organometal. Chem.* **1976**, *120*, 49.

160 R. Grubbs, C.P. Lau, R. Cukier, C. Brubaker, Jr., *J. Am. Chem. Soc.* **1977**, *99*, 4517.

161 J.G.-S. Lee, C.H. Brubaker, Jr., *J. Organometal. Chem.* **1977**, *135*, 115.

162 C.-P. Lau, B.-H. Chang, R.H. Grubbs, C.H. Brubaker, Jr., *J. Organometal. Chem.* **1981**, *214*, 325.

163 B.H. Chang, R.H. Grubbs, C.H. Brubaker, Jr., *J. Organometal. Chem.* **1985**, *280*, 365.

164 B.H. Chang, C.P. Lau, R.H. Grubbs, C.H. Brubaker, Jr., *J. Organometal. Chem.* **1985**, *281*, 213.

165 L. Verdet, J.K. Stille, *Organometallics* **1982**, *1*, 380.

166 R. Jackson, J. Ruddlesden, D.J. Thompson, R. Whelan, *J. Organometal. Chem.* **1977**, *125*, 57.

167 J. Cermak, M. Kvicalova, V. Blechta, M. Capka, Z. Bastl, *J. Organometal. Chem.* **1996**, *509*, 77.

168 D.G.H. Ballard, *Adv. Catal.* **1973**, *23*, 263.

169 Y.I. Yermakov, B.N. Kuznetsov, V.A. Zakharov, *Stud. Surf. Sci. Catal.* **1981**, *8*, 1.

170 C.W. Tullock, F.N. Tebbe, R. Mulhaupt, D.W. Ovenall, R.A. Setterquist, S.D. Ittel, *J. Polym. Sci., A: Polym. Chem.* **1989**, *27*, 3063.

171 C. W. Tullock, R. Mulhaupt, S. D. Ittel, *Makromol. Chem., Rapid Commun.* **1989**, *10*, 19.
172 S. D. Ittel, *J. Macromol. Sci., Chem.* **1990**, *A27*, 1133.
173 J. Schwartz, M. D. Ward, *J. Mol. Cat.* **1980**, *8*, 465.
174 S. A. King, J. Schwartz, *Inorg. Chem.* **1991**, *30*, 3771.
175 Y. I. Yermakov, Y. A. Ryndin, O. S. Alekseev, D. I. Kochubei, V. A. Shmachkov, N. I. Gergert, *J. Mol. Cat.* **1989**, *49*, 121.
176 V. A. Zakharov, Y. A. Ryndin, *J. Mol. Cat.* **1989**, *56*, 183.
177 C. Copéret, M. Chabanas, R. P. Saint-Arroman, J.-M. Basset, *Angew. Chem. Int. Ed.* **2003**, *42*, 156.
178 C. Rosier, G. P. Niccolai, J.-M. Basset, *J. Am. Chem. Soc.* **1997**, *119*, 12408.
179 J. Corker, F. Lefebvre, C. Lecuyer, V. Dufaud, F. Quignard, A. Choplin, J. Evans, J.-M. Basset, *Science* **1996**, *271*, 966.
180 F. Rataboul, A. Baudouin, C. Thieuleux, L. Veyre, C. Copéret, J. Thivolle-Cazat, J.-M. Basset, A. Lesage, L. Emsley, *J. Am. Chem. Soc.* **2004**, *126*, 12541.
181 L. d'Ornelas, S. Reyes, F. Quignard, A. Choplin, J. M. Basset, *Chem. Lett.* **1993**, 1931.
182 V. Vidal, A. Theolier, J. Thivolle-Cazat, J. M. Basset, J. Corker, *J. Am. Chem. Soc.* **1996**, *118*, 4595.
183 R. L. Burwell, Jr., T. J. Marks, *Chem. Ind.* **1985**, *22*, 207.
184 T. J. Marks, *Acc. Chem. Res.* **1992**, *25*, 57.
185 K. H. Dahmen, D. Hedden, R. L. Burwell, Jr., T. J. Marks, *Langmuir* **1988**, *4*, 1212.
186 H. Ahn, C. P. Nicholas, T. J. Marks, *Organometallics* **2002**, *21*, 1788.
187 C. P. Nicholas, H. Ahn, T. J. Marks, *J. Am. Chem. Soc.* **2003**, *125*, 4325.
188 C. P. Nicholas, T. J. Marks, *Langmuir* **2004**, *20*, 9456.
189 R. G. Bowman, R. Nakamura, P. J. Fagan, R. L. Burwell, Jr., T. J. Marks, *J. Chem. Soc., Chem. Soc.* **1981**, 257.
190 M. Y. He, G. Xiong, P. J. Toscano, R. L. Burwell, Jr., T. J. Marks, *J. Am. Chem. Soc.* **1985**, *107*, 641.
191 R. D. Gillespie, R. L. Burwell, Jr., T. J. Marks, *Langmuir* **1990**, *6*, 1465.
192 M. S. Eisen, T. J. Marks, *J. Am. Chem. Soc.* **1992**, *114*, 10358.
193 M. S. Eisen, T. J. Marks, *J. Mol. Cat.* **1994**, *86*, 23.

7
Ionic Hydrogenations

R. Morris Bullock

7.1
Introduction

One pervasive mechanistic feature of many of the hydrogenations described in other chapters of this handbook concerns the bonding of the unsaturated substrate to a metal center. As illustrated in generalized form in Eq. (1) for the hydrogenation of a ketone, a key step in the traditional mechanism of hydrogenation is migratory insertion of the bound substrate into a metal hydride bond (M–H).

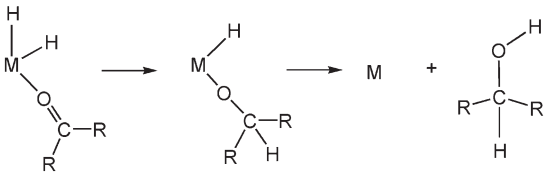

(1)

Since this can formally be viewed as an addition of M–H to C=O, the bond order is reduced in this case to a C–O single bond. Reductive elimination generates the hydrogenated product and an unsaturated metal complex that subsequently re-enters the catalytic cycle. Many subtleties of this mechanism have been delineated in studies of hydrogenations of C=C and C=O bonds, and catalysts that follow this mechanism have been very successful.

Most homogeneous catalysts that proceed by traditional insertion mechanisms use precious metals. If the requirement for substrate binding and insertion is removed, then alternative mechanisms would be possible. Such alternative mechanisms could exploit other reactivity patterns accessible to metal hydrides, thus removing the requirement for precious metals. The use of inexpensive metals potentially offers several advantages, if catalysts containing them could be developed with sufficient turnover frequencies (TOFs) and lifetimes. A substantially lower cost of the metal is an obvious advantage, though it is recognized that many factors influence the overall costs of a process, and phosphines or

The Handbook of Homogeneous Hydrogenation.
Edited by J.G. de Vries and C.J. Elsevier
Copyright © 2007 WILEY-VCH Verlag GmbH & Co. KGaA, Weinheim
ISBN: 978-3-527-31161-3

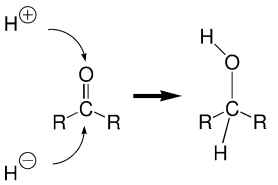

$$H_2 \rightleftharpoons H^+ + H^-$$

Scheme 7.1

other ligands can substantially add to the cost of synthesis of an organometallic catalyst precursor. In addition to the initial cost of the metal, other considerations include less stringent requirements for recovery of the catalyst in an industrial process. For processes that might be used in the manufacture of pharmaceutical products, catalysts using abundant metals might be permitted at a higher residual level than other metals, owing to toxicity considerations. The premise of using "Cheap Metals for Noble Tasks" thus has appeal despite these caveats; fundamentally new mechanistic information and novel reactivity patterns have resulted from research directed towards this long-term goal.

Ionic hydrogenations involve addition of H_2 in the form of H^+ followed by H^-, as shown in Scheme 7.1; the proton and hydride transfers may be either sequential or concerted. A potential advantage of ionic hydrogenations is that the nature of the mechanism would tend to favor hydrogenation of polar bonds such as C=O over less-polar C=C bonds. Kinetic and mechanistic studies have played a key role in the development of ionic hydrogenations. In many cases to be discussed in this chapter, the individual proton-transfer and hydride-transfer steps that comprise the key steps in catalytic cycles can be separately studied in stoichiometric reactions. Mechanistic information can then be used to guide the rational design of new catalysts or the improvement and optimization of initially discovered ionic hydrogenation catalysts.

7.2 Stoichiometric Ionic Hydrogenations

7.2.1 Stoichiometric Ionic Hydrogenations using CF_3CO_2H and $HSiEt_3$

Ionic hydrogenations of C=C and C=O bonds were reported prior to the development of ionic hydrogenations mediated or catalyzed by transition metals. Trifluoroacetic acid (CF_3CO_2H) as the proton donor and triethylsilane ($HSiEt_3$) as the hydride donor are most commonly used, though a variety of other acids and several other hydride donors have also been shown to be effective. A review [1] by Kursanov et al. of the applications of ionic hydrogenations in organic synthe-

sis documents the early progress in this field; a book gives further details [2]. As shown in Eq. (2), proton transfer to the alkene generates a carbenium ion, and hydride transfer from the hydrosilane generates the product.

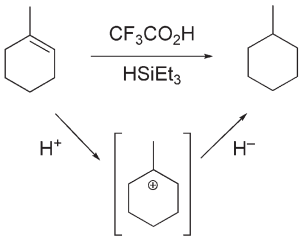

(2)

Ionic hydrogenations of C=C bonds generally work well only in cases where a tertiary or aryl-substituted carbenium ion can be formed through protonation of the C=C bond. Alkenes that give a tertiary carbenium ion upon protonation include 1,1-disubstituted, tri-substituted and tetra-substituted alkenes, and each of these are usually hydrogenated by ionic hydrogenation methods in high yields.

The success of stoichiometric ionic hydrogenations is due to achieving a fine balance that favors the intended reactivity rather than any of several possible alternative reactions. The acid must be strong enough to protonate the unsaturated substrate, yet the reaction of the acid and the hydride should avoid producing H_2 too quickly under the reaction conditions. The commonly used pair of CF_3CO_2H and $HSiEt_3$ meets all these criteria.

The very strong acid, CF_3SO_3H (triflic acid, abbreviated as HOTf) can be used in conjunction with $HSiEt_3$ for the hydrogenation of certain alkenes [3]. These reactions proceed cleanly in 5 minutes at –50 °C. This discovery was surprising, since a review of the use of CF_3CO_2H and $HSiEt_3$ had stated that "... stronger acids cannot be used in conjunction with silanes because they react" [1]. Indeed, rapid evolution of H_2 does occur when HOTf is added to $HSiEt_3$ in the absence of an alkene. The order of addition is important in the use of HOTf/$HSiEt_3$ for hydrogenation of C=C bonds, to ensure that acid-induced formation of H_2 is minimized. The addition of HOTf to a solution containing the alkene and the hydrosilane results in rapid and clean hydrogenation, but the reaction is still subject to the limitation of forming a tertiary carbenium ion.

Another potential mechanistic complication is capture of the intermediate carbenium ion by the conjugate base of the acid. When CF_3CO_2H is used as the acid, this would lead to trifluoroacetate esters. Kursanov et al. showed that, under the reaction conditions for ionic hydrogenations, trifluoroacetate esters can be converted to the hydrocarbon product (Eq. (3)).

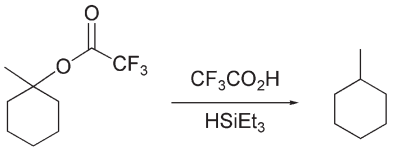

(3)

The intermediacy of the trifluoroacetate ester does not undermine the efficacy of the overall hydrogenation reaction, since the ionizing solvent CF_3CO_2H converts the ester back to the carbenium ion under the reaction conditions, resulting in its ultimate conversion to the hydrogenation product.

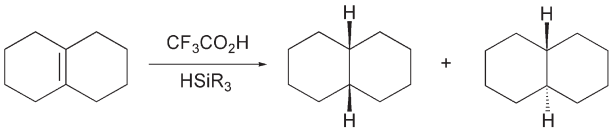

(4)

Studies of the ionic hydrogenation of $\Delta^{9(10)}$-octalin using CF_3CO_2H and a variety of hydrosilanes demonstrated that a considerable degree of stereoselectivity can be obtained (Eq. (4)) [4]. Use of $^{n}BuSiH_3$ as the hydride donor led to a 22:78 ratio of *cis*:*trans* decalin. Hydrogenation using the sterically demanding hydrosilane tBu_3SiH, in contrast, led to predominant formation of the opposite isomer, with 93% of the decahydronaphthalene product being the *cis* isomer. Steric factors of the silane hydride donor appear to dominate the stereoselectivity in this example, though in other examples the effect is much less, suggesting that additional factors can influence the product distribution. Ionic hydrogenation of 4-*tert*-butylmethylenecyclohexane with the same series of hydrosilanes invariably produced a predominance of the *trans* isomer [4].

Ionic hydrogenation of benzophenone using CF_3CO_2H and $HSiEt_3$ proceeds at room temperature and gives high yields of diphenylmethane (Eq. (5)) [1, 5]. This reaction presumably proceeds through the alcohol, as indicated in Eq. (5), but deoxygenation of the alcohol proceeds faster than hydrogenation of the C=O function, so the alcohol is not detected. Similar hydrogenations of the C=O group to CH_2 were found for aryl alkyl ketones. Dialkyl ketones react with CF_3CO_2H and $HSiEt_3$ to produce trifluoroacetate esters of the secondary alcohols, so conversion to the alcohol requires a subsequent hydrolysis reaction [1].

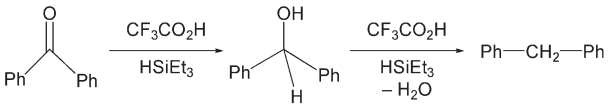

(5)

The hydrogenation of aldehydes by $CF_3CO_2H/HSiEt_3$ is often complicated by the formation of ethers. Doyle et al. found that the use of aqueous acids such as H_2SO_4, together with nonreactive solvents (CH_3CN), allowed some aldehydes and dialkyl ketones to be reduced to alcohols using $HSiEt_3$ [6].

7.2.2 Stoichiometric Ionic Hydrogenations using Transition-Metal Hydrides

7.2.2.1 General Aspects

While stoichiometric ionic hydrogenations using CF_3CO_2H and $HSiEt_3$ have enjoyed significant utility in organic synthetic reactions, they require stoichiometric quantities of both the hydrosilane and an acid. One of the principles of Green Chemistry [7] is that catalytic reactions are preferred over stoichiometric reagents. The development of a catalytic route to ionic hydrogenations would be environmentally attractive. In addition to the requirement of delivering a proton and a hydride to the substrate, catalytic methods additionally require a metal complex that is capable of reacting with H_2 to regenerate the proton and hydride sources. The following sections will demonstrate how kinetic and mechanistic studies separately documented the proton-transfer and hydride-transfer capabilities of transition-metal hydrides. These studies provided a firm mechanistic basis for the development and understanding of catalytic ionic hydrogenations.

7.2.2.2 Transition-Metal Hydrides as Proton Donors

The fact that metal hydrides can be acidic may seem paradoxical in view of the nomenclature that insists that all complexes with a M–H bond be referred to as "hydrides" regardless of whether their reactivity is hydridic or not. Not only can some metal hydrides donate a proton, but some can be remarkably acidic. Some cationic dihydrogen complexes are sufficiently acidic to protonate Et_2O [8], and some dicationic ruthenium complexes have an acidity comparable to or exceeding that of HOTf [9].

Systematic studies of the thermodynamic and kinetic acidity of metal hydrides in acetonitrile were carried out by Norton et al. [10, 11]. A review of the acidity of metal hydrides presents extensive tabulations of pK_a data [12]; only a few of the trends will be mentioned here. Metal hydrides span a wide range of pK_a values; considering only metal carbonyl hydrides shown in Table 7.1, the range exceeds 20 pK_a units. As expected, a substantial decrease in acidity is

Table 7.1 pK_a values of neutral metal carbonyl hydrides in CH_3CN.

Metal hydride	pK_a	Reference
$(CO)_4CoH$	8.3	11
$Cp(CO)_3MoH$	13.9	11
$(CO)_5MnH$	14.2	12
$(CO)_3(PPh_3)CoH$	15.4	11
$Cp(CO)_3WH$	16.1	11
$Cp^*(CO)_3MoH$	17.1	11
$(CO)_5ReH$	21.1	11
$Cp(CO)_2(PMe_3)WH$	26.6	11

found when an electron-accepting CO ligand is replaced by an electron-donating phosphine. The cobalt hydride $[(CO)_4CoH]$ is quite acidic, being of comparable acidity in CH_3CN to that of HCl ($pK_a = 8.9$ in CH_3CN); substitution of one CO by PPh_3 to give $[(CO)_3(PPh_3)CoH]$ reduces the acidity by about seven pK_a units. The stronger electron donor, PMe_3, has an even larger effect, as exemplified by the acidity of $[Cp(CO)_2(PMe_3)WH]$ ($Cp = \eta^5\text{-}C_5H_5$) being less than that of $[Cp(CO)_3WH]$ by about 10 pK_a units. Replacement of a Cp by Cp* [($Cp^* = \eta^5\text{-}C_5Me_5$)] also decreases the acidity, by about three pK_a units in the case of $[Cp(CO)_3MoH]$ versus $[Cp^*(CO)_3MoH]$. Third-row metals are less acidic than their first- or second-row analogues, as shown by $[Cp(CO)_3MoH]$ being two pK_a units less acidic than $[Cp(CO)_3WH]$. A larger difference of about seven pK_a units was found between first-row $[(CO)_5MnH]$ and third-row $[(CO)_5ReH]$.

DuBois and coworkers have studied a wide range of metal hydrides, concentrating on those with two diphosphine ligands [13–19]. Measurements of pK_a values for a series of cobalt hydrides (Table 7.2, upper part) showed that the cationic dihydride $[(H)_2Co(dppe)_2]^+$ has a pK_a of 22.8, while the neutral cobalt hydride $[HCo(dppe)_2]$ is far less acidic ($pK_a = 38.1$). Oxidation of this neutral hydride gives the paramagnetic Co(II) hydride, $[HCo(dppe)_2]^+$, which is much more acidic ($pK_a = 23.6$). The dicationic hydride $[HCo(dppe)_2(NCCH_3)]^{2+}$ ($pK_a = 11.3$) is by far the most acidic of this series. This remarkable series of complexes, all containing a $Co(dppe)_2$ core, span about 27 pK_a units as the oxidation states and formal charges are varied. The series of $[HM(diphosphine)_2]^+$ complexes in the lower part of Table 7.2 show that altering the electronic properties of substituents on the diphosphine ligand can have a profound effect on acidity. Complexes with two dmpe ligand (with methyl groups on the phosphorus) are six to ten pK_a units less acidic than corresponding complexes with a dppe ligand (with phenyl groups on the phosphorus). As was found for the metal carbonyl complexes discussed above, hydrides of the third row metal are

Table 7.2 pK_a values of metal bis(diphosphine) hydrides in CH_3CN.

Metal hydride [a)]	pK_a	Reference
$[(H)_2Co(dppe)_2]^+$	22.8	16
$[HCo(dppe)_2]^+$	23.6	16
$HCo(dppe)_2$	38.1	16
$[HCo(dppe)_2(NCCH_3)]^{+2}$	11.3	16
$[HNi(dppe)_2]^+$	14.2	13
$[HPt(dppe)_2]^+$	22.0	13
$[HNi(dmpe)_2]^+$	24.3 [b)]	13
$[HPt(dmpe)_2]^+$	31.1 [b)]	15

a) dmpe = 1,2-bis(dimethylphosphino)ethane; dppe = 1,2-bis(diphenylphosphino)ethane.

b) Value determined in PhCN, though these values are usually similar to those found in CH_3CN, typically differing by less than 1 pK_a unit between the two solvents.

significantly less acidic than those of the first-row metal (Ni versus Pt in the examples shown in Table 7.2).

Morris et al. carried out extensive studies [20] of the acidity of metal hydrides in tetrahydrofuran (THF), including metal hydrides of very low acidity as well as dihydrogen complexes that are reactive with CH_3CN. The dielectric constant of THF is low compared to that of CH_3CN, so ion-pairing issues must be taken into account [21], though these measurements in THF provide useful comparisons to data in CH_3CN and other solvents.

7.2.3
Transition Metal Hydrides as Hydride Donors

An understanding of the factors that influence the propensity of metal hydrides to function as hydride donors is important in the use of such hydrides in ionic hydrogenations. Thermodynamic hydricities are immensely useful in considering the viability of potential hydride transfer reactions in stoichiometric or catalytic reactions. Since catalysis is a kinetic phenomenon, it is also necessary to understand the factors influencing the kinetics of hydride transfer reactions. Systematic studies that provided quantitative values for the thermodynamic and kinetic hydricity of a wide series of hydrides occurred after studies had been conducted that identified the factors influencing proton-transfer reactions of metal hydrides. A complicating factor in considering tests for hydricity is that removal of H^- from M–H produces a cationic species M^+ [22]. When the starting hydride M–H is an 18-electron complex, the M^+ that initially results will be an unsaturated 16-electron species. In most cases these 16-electron metal cations will not be stable but will voraciously seek an additional ligand. Since the overall reaction may involve ligand capture as well as the hydride transfer, comparisons of hydricity may be complicated by the subsequent reactivity of M^+ following the hydride transfer reaction.

It has long been recognized that the hydricity of a metal hydride can vary according to its position in the Periodic Table. Labinger and Komadina found evidence for this trend from an examination of the reactivity of a series of metallocene hydrides [23]. The Group 4 zirconium dihydride $[Cp_2ZrH_2]_n$ reacts quickly at room temperature with acetone to give $[Cp_2Zr(OCHMe_2)_2]$, which releases isopropyl alcohol upon hydrolysis. The Group 5 complex $[Cp_2NbH_3]$ reacts slowly with acetone, but quickly with the more electrophilic ketone $(CF_3)(CH_3)C{=}O$. The Group 6 dihydride, $[Cp_2MoH_2]$, did not react with acetone at 78 °C, but did react slowly at 25 °C with $(CF_3)(CH_3)C{=}O$. The Group 7 hydride $[Cp_2ReH]$ did not react with either acetone or with $(CF_3)(CH_3)C{=}O$. This study provided evidence that hydricity is higher for metals to the left side of the Periodic Table, though if the ketone coordinates to the metal prior to hydride transfer, these measurements may reflect a combination of factors, rather than measuring only hydricity.

Darensbourg et al. have conducted extensive studies of the nucleophilic reactivity of a series of anionic metal carbonyl hydrides [24], which have been used for the reduction of alkyl halides [25], acyl chlorides [26], and ketones [27]. The

Table 7.3 Rate constants for reaction of anionic metal hydrides with *n*-BuBr (THF solvent at 26 °C) [25].

Metal hydride	$10^3 \times k_H$ [M^{-1} s^{-1}]
$[HW(CO)_4P(OCH_3)_3]^-$	50
$[HCr(CO)_4P(OCH_3)_3]^-$	30
$[HW(CO)_5]^-$	3.3
$[HV(CO)_3Cp]^-$	2.2
$[HCr(CO)_5]^-$	1.8
$[HRu(CO)_5]^-$	1.0

kinetics of bromide displacement from *n*-BuBr by a series of anionic hydrides (Eq. (6)) gave the results shown in Table 7.3.

$$MH^{\ominus} + Bu - Br \quad \rightarrow \quad MBr^{\ominus} + Bu - H \tag{6}$$

Although the range of rate constants observed is only about a factor of 50, there is a clear trend indicating that the replacement of one CO by a phosphite ligand increases the kinetic hydricity. The third-row tungsten hydrides are faster hydride donors compared to the first-row chromium analogues. Whilst direct displacement of the bromide by hydride is the prevalent mechanism in the reaction of this primary alkyl bromide, a radical chain mechanism involving hydrogen atom transfer from the metal hydride is also operative. This radical chain mechanism (S_H2 pathway) is the predominant pathway in reactions of these same anionic hydrides with sterically encumbered alkyl halides, where the S_N2 hydride displacement pathway is disfavored [28].

DuBois et al. carried out extensive studies on the thermodynamic hydricity of a series of metal hydrides [13, 15–19]. The determination of thermodynamic hydricity generally requires several measurements (coupled with known thermochemical data) to constitute a complete thermochemical cycle. As with other thermodynamic cycles, obtaining reliable values in an appropriate solvent can be a difficult challenge, and this is sometimes coupled with problems in obtaining reversible electrochemical data. Scheme 7.2 illustrates an example in which the hydricity of cationic monohydrides have been determined.

Thus, the thermodynamic hydricity shown in Eq. (10) is determined by evaluating the values for Eqs. (7) to (9). Equation (7) is the pK_a of the hydride, and

$$L_nMH^+ \rightarrow L_nM + H^+ \tag{7}$$

$$L_nM \rightarrow L_nM^{2+} + 2e^- \tag{8}$$

$$H^+ + 2e^- \rightarrow H^- \tag{9}$$

$$L_nMH^+ \rightarrow L_nM^{2+} + H^- \tag{10}$$

$(\Delta G^{\circ}_{H^-})$

Scheme 7.2 Thermodynamic cycle for determination of the hydricity of cationic metal hydrides.

$$L_nMH^+ + BH^+ \rightarrow L_nM^{2+} + H_2^{\ +} + B \qquad (11)$$

$$B + H^+ \rightarrow BH^+ \qquad (12)$$

$$H_2 \rightarrow H^+ + H^- \qquad (13)$$

$$L_nMH^+ \rightarrow L_nM^{2+} + H^- \qquad (\Delta G^\circ_{H^-}) \quad (14)$$

Scheme 7.3 Thermodynamic cycle for determination of the hydricity using heterolytic cleavage of hydrogen.

Eq. (8) requires determination of the two-electron oxidation potential of L_nM by electrochemical methods. When combined with the two-electron reduction of protons in Eq. (9), the sum provides Eq. (10), the $\Delta G^0_{H^-}$ values of which can be compared for a series of metal hydrides. Another way to determine the $\Delta G^0_{H^-}$ entails the thermochemical cycle is shown in Scheme 7.3. This method requires measurement of the K_{eq} of Eq. (11) for a metal complex capable of heterolytic cleavage of H_2, using a base (B), where the pK_a of BH^+ must be known in the solvent in which the other measurements are conducted. In several cases, DuBois et al. were able to demonstrate that the two methods gave the same results. The thermodynamic hydricity data ($\Delta G^0_{H^-}$ in CH_3CN) for a series of metal hydrides are listed in Table 7.4. Transition metal hydrides exhibit a remarkably large range of thermodynamic hydricity, spanning some 30 kcal mol^{-1}.

Several trends are revealed by these data. For example, third-row metal hydrides are much more hydridic compared to their first-row analogues, so the trend of higher hydricity for third-row hydrides holds for both kinetic and thermodynamic hydricity. The hydricity of $[HPt(depe)_2]^+$ exceeds that of $[HNi(depe)_2]^+$ by 15 kcal mol^{-1}, and other Pt hydrides reflect the same trend, by 11–14 kcal mol^{-1} [13]. The second-row hydride $[HRh(dppb)_2]$ is a very powerful hydride donor, and its hydricity exceeds that of the first-row Co analogue by 14 kcal mol^{-1} [17]. Changing the ligands on a metal can also cause a profound change in thermodynamic hydricity. The chelating diphosphine ligand dmpe is much more electron-donating than dppe, with the Pt complex $[HPt(dmpe)_2]^+$ having a hydricity that exceeds that of $[HPt(dppe)_2]^+$ by 10 kcal mol^{-1} [13, 15]. The same conclusion is reached for comparisons of Ni complexes with different diphosphine ligands. Replacement of one of the electron-withdrawing CO ligands of $[HW(CO)_5]^-$ with PPh_3 leads to an increase of 4 kcal mol^{-1} in the hydricity of $[HW(CO)_4(PPh_3)]^-$ [18]. DuBois et al. found a dramatic dependence of hydricity on the bite angle of a series of Pd hydrides [19]. A variation of the bite angle of 33° results in tuning of the hydricity over a range of 27 kcal mol^{-1}, with smaller bite angles of the diphosphine leading to higher hydricity. Overall, DuBois et al. have concluded that, for isoelectronic complexes, the order of hydricity is second row > third row > first row [17]. The charge on a metal complex can affect its hydricity. For a series of cobalt complexes, the neutral complex $[HCo(dppe)_2]$ is a stronger hydride donor than the cationic, paramagnetic complex $[HCo(dppe)_2]^+$ [16]. While this follows the expected trend, it is clear from the data in Table 7.4 that the overall charge is just one factor influencing

Table 7.4 ΔG^0 for hydride transfer from metal hydrides in CH_3CN.

Hydride donor [a)]	ΔG^0 [kcal mol^{-1}] [b)]	Reference
$HRh(dppb)_2$	34	17
$HW(CO)_4(PPh_3)^-$	36	18
$[HPt(dmpe)_2]^+$	42	15
$HW(CO)_5^-$	40	18
$[HPt(depe)_2]^+$	44	15
$[HPt(dmpp)_2]^+$	51	15
$HCo(dppe)_2$	49	16
$HCo(dppb)_2$	48	17
$[HNi(dmpe)_2]^+$	51	13
$[HPt(dppe)_2]^+$	52	15
$HMo(CO)_2(PMe_3)Cp$	55	91
$[HNi(depe)_2]^+$	56	13
$[HCo(dppe)_2]^+$	60	16
$[HNi(dmpp)_2]^+$	61	13
$[HNi(dppe)_2]^+$	63	13
$[(H)_2Co(dppe)_2]^+$	65	16
$[HPd(EtXantphos)_2]^+$	70	19
H_2	76	15
$HCPh_3$	99	92

a) dmpe and dppe as defined in Table 7.2; dmpp = 1,3-bis(dimethylphosphino)propane; depe = 1,2-bis(diethylphosphino)ethane; dppe = 1,2-bis(diphenylphosphino)ethane; depp = 1,2-bis(diethylphosphino)propane; EtXantphos = 9,9-dimethyl-4,5-bis(diethylphosphino)xanthene.

b) Estimated uncertainties on ΔG^0 values are typically ±2 kcal mol^{-1}.

the hydricity, as many of the cationic hydrides are stronger hydride donors than neutral hydrides. For the series of $[HM(diphosphine)_2]^+$ complexes that have been the focus of much of the research by DuBois and colleagues, the high stability of the square-planar products, $[M(diphosphine)_2]^{+2}$, which result from hydride transfer, helps to explain the high hydricity of $[HM(diphosphine)_2]^+$.

The kinetics of hydride transfer from a series of neutral metal carbonyl hydrides have been determined by studying hydride transfer to $Ph_3C^+BF_4^-$ (Eq. (15)). In CH_2Cl_2 solvent, the M^+ cation resulting from hydride transfer from the metal hydride is captured by the BF_4^- anion, forming complexes with weakly bound FBF_3 ligands. A wide range of M–FBF_3 complexes have been studied by Beck and Sünkel [29]. The second-order rate constants for the hydride transfer reaction in Eq. (15) are listed in Table 7.5. The range of rate constants spans a factor of over 10^6, documenting a considerable range of kinetic hydricity.

$$\text{M-H} + Ph_3C^+BF_4^- \xrightarrow{k_{H^-}} \text{M-F-}BF_3 + Ph_3\text{C-H} \qquad (15)$$

Table 7.5 Rate constants for hydride transfer from metal hydrides to Ph_3C^+ BF_4^- (CH_2Cl_2 solvent at 25 °C) [58, 93].

Metal hydride	k_H [M^{-1} s^{-1}]
$HRu(CO)_2Cp^*$	$>5 \times 10^6$
trans-$HMo(CO)_2(PMe_3)Cp$	4.6×10^6
$HFe(CO)_2Cp^*$	1.1×10^6
trans-$HMo(CO)_2(PPh_3)Cp$	5.7×10^5
trans-$HMo(CO)_2(PCy_3)Cp$	4.3×10^5
$HOs(CO)_2Cp^*$	3.2×10^5
$HW(NO)_2Cp$	1.9×10^4
cis-$HRe(CO)_4(PPh_3)$	1.2×10^4
$HMo(CO)_3Cp^*$	6.5×10^3
$HRe(CO)_5$	2.0×10^3
$HW(CO)_3(\eta^5$-indenyl)	2.0×10^3
$HW(CO)_3Cp^*$	1.9×10^3
$HMo(CO)_3Cp$	3.8×10^2
$HW(CO)_3(C_5H_4Me)$	2.5×10^2
cis-$HMn(CO)_4(PPh_3)$	2.3×10^2
$HSiEt_3$	1.5×10^2
$HW(CO)_3Cp$	7.6×10^1
$HCr(CO)_3Cp^*$	5.7×10^1
$HMn(CO)_5$	5.0×10^1
$W(CO)_3(C_5H_4CO_2Me)$	7.2×10^{-1}

This systematic study reveals how changes in the metal and both steric and electronic changes of the ligand can alter the hydricity. Third-row metal hydrides are substantially more kinetically hydridic than their first-row analogues, with $[Cp^*(CO)_3WH]$ being about 33-fold faster at hydride transfer than $[Cp^*(CO)_3CrH]$, and a factor of about 40–50 being found for Re versus Mn hydrides. The second-row hydrides of Mo are about three- to five-fold faster than those of the third-row W hydrides. Changes in ligands cause an even more dramatic change in the kinetic hydricity. When a Cp ligand in $[CpM(CO)_3H]$ is replaced by Cp*, the kinetic hydricity increases by a factor of 25 for M = W and a factor of 17 for M = Mo. Compared to Cp, the Cp* ligand is much larger, so steric effects would predict a lower reactivity of the Cp* compared to the Cp complex. Since Cp* is a much better electron donor than Cp, the higher rate constant for the Cp* complex makes it clear that electronic effects dominate over steric effects in these reactions. Even a single methyl group has a small, but measurable, effect on the hydricity, as indicated by the larger rate constant for $[(C_5H_4Me)(CO)_3WH]$ compared to $[Cp(CO)_3WH]$. An even more prominent effect upon substitution of a single substituent on the Cp ligand was found for the compound containing an electron-withdrawing group on the Cp ligand, with the hydricity of $[Cp(CO)_3WH]$ exceeding that of $[(C_5H_4CO_2Me)(CO)_3WH]$ by about a factor of 100. Replacement of one CO by a phosphine ligand has an even larger effect in enhancing the kinetic hydricity of metal hydrides. The

PMe_3-substituted Mo hydride *trans*-[$Cp(CO)_2(PMe_3)MoH$] is about 10^4 times as hydridic as [$Cp(CO)_3MoH$]. Some evidence for steric effects is apparent from the kinetic hydricity of *trans*-[$Cp(CO)_2(PCy_3)MoH$]. The PCy_3 is similar to PMe_3 electronically, but it is much more sterically demanding. The hydricity of *trans*-[$Cp(CO)_2(PCy_3)MoH$] is about 10 times less than that of *trans*-[$Cp(CO)_2(PMe_3)$-MoH], presumably due to steric effects. Yet even with this large ligand, the hydricity of *trans*-[$Cp(CO)_2(PCy_3)MoH$] exceeds that of $Cp(CO)_3MoH$ by about three orders of magnitude, again providing strong evidence of the predominance of electronic over steric effects in these kinetic hydricity studies.

7.2.4
Stoichiometric Ionic Hydrogenation of Alkenes with Metal Hydrides as the Hydride Donor

As discussed earlier, Kursanov et al. showed that some alkenes can be hydrogenated using acids in conjunction with $HSiEt_3$ as the hydride donor. Compared with silanes, transition-metal hydrides as hydride donors offer substantial advantages, if their hydride donor capability can be coupled into a catalytic cycle that regenerates the M–H bond through reaction with H_2. Additionally, the versatile reactivity patterns of metal hydrides reveal another benefit. Whilst silanes generally react with acids to immediately evolve H_2, many transition-metal hydrides can be protonated (Scheme 7.4) to give dihydrogen complexes [30] or dihydrides. Protonation at the M–H to produce a dihydrogen complex is often kinetically preferred [31] over direct protonation at the metal to generate a dihydride; in many cases, the dihydrogen and dihydride forms are in equilibrium with each other. For the purposes of hydrogenation, it may not make much difference which form is predominant, as long as the complex is sufficiently acidic to transfer a proton to the substrate that is to be hydrogenated. Thus, the possibility of protonation of a metal hydride provides an alternate mechanistic pathway for stoichiometric ionic hydrogenations. Proton transfer from an external acid may occur to the substrate directly, or may involve protonation of a metal hydride, with subsequent delivery of the proton to the substrate. Deprotonation of a cationic dihydride or dihydrogen complex will generate a neutral metal hy-

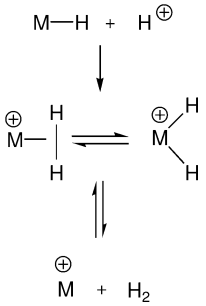

Scheme 7.4

dride, which can then serve as a hydride donor. Failures can occur if irreversible loss of H_2 from the metal occurs more quickly than proton transfer to the unsaturated substrate.

Ionic hydrogenation of certain C=C double bonds is readily accomplished through reaction with HOTf and transition-metal hydrides (Eq. (16)). These reactions proceed in high yield (>90%) in less than 5 minutes at 22 °C, and were shown in some cases to occur at temperatures as low as –50 °C. The limitations on the olefin substrate are the same as those encountered in the stoichiometric ionic hydrogenations using $HSiEt_3$ as the hydride donor – the alkene starting material must be able to be protonated to give a tertiary carbenium ion, which essentially limits the starting materials to 1,1-disubstituted, tri-substituted, and tetra-substituted alkenes. Styrene, stilbene and related phenyl-substituted C=C bonds were hydrogenated by this method also, but the yields were lower (46–57%).

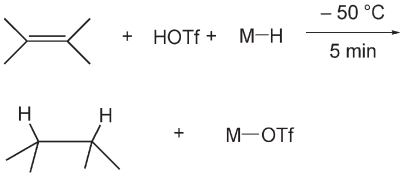

(16)

Metal hydrides that were shown to be suitable hydride donors for this reaction included [$Cp(CO)_3WH$, $Cp^*(CO)_3WH$], [$Cp(CO)_3MoH$], [$(CO)_5MnH$], [$(CO)_5ReH$] and [$Cp^*(CO)_2OsH$]. As discussed above, a metal hydride may fail if it loses hydrogen too quickly after protonation (see Scheme 7.4). The failure of [$Cp^*(CO)_2FeH$], [$Cp^*(CO)_3MoH$], and [$Cp(PPh_3)(CO)_2MoH$] in the ionic hydrogenation of olefins is attributed to thermal decomposition occurring instead of proton transfer following protonation of these hydrides. Insufficient acidity of the protonated form (a cationic dihydride or dihydrogen complex) was found as the reason for failure of [$Cp(PMe_3)(CO)_2WH$] and [$Cp(PMe_3)(CO)RuH$]. These stoichiometric studies revealed the required characteristics of metal hydrides for them to be suitable for ionic hydrogenations. They must be able to function as hydride donors in the presence of acids. Protonation of the metal hydride is not required, but if it is protonated, it must be able to transfer the proton to the unsaturated substrate, and this requires both sufficient kinetic acidity and thermal stability to overcome alternate pathways that could thwart the desired reactivity.

Stoichiometric ionic hydrogenation of the C=C bond of α,β-unsaturated ketones by HOTf and [$Cp(CO)_3WH$] results in the formation of η^1-ketone complexes of tungsten [32]. As exemplified in Eq. (17), hydrogenation of methyl vinyl ketone gives a 2-butanone complex of tungsten. The bound ketone is displaced by the triflate counterion, giving the free ketone. Similar reactions were reported for hydrogenation of the C=C bond of α,β-unsaturated aldehydes.

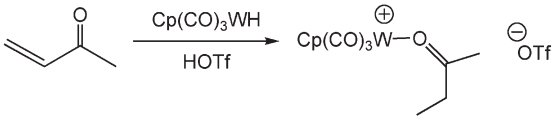

(17)

7.2.5
Stoichiometric Ionic Hydrogenation of Alkynes

Ionic hydrogenations of C≡C bonds of alkynes has only been studied in a few cases. Kursanov et al. reported that low yields were obtained upon attempted hydrogenation of aryl alkynes using CF_3CO_2H and $HSiEt_3$ [2]. In contrast, ionic hydrogenation of phenylacetylene by HOTf and $[Cp(CO)_3WH]$ produced ethylbenzene as the product of double ionic hydrogenation of the C≡C bond [33]. In addition to the ethylbenzene that was promptly formed, the vinyl triflate and the geminal ditriflate shown in Scheme 7.5 were also observed; these organic triflates are formed by the addition of one or two equivalents of HOTf to the C≡C bond.

In the presence of HOTf and $[Cp(CO)_3WH]$, these organic intermediates were slowly consumed, with more ethylbenzene being produced, the yield of which reached 92% after 28 h. Reaction of $PhC{\equiv}CCH_3$ with HOTf and $[Cp(CO)_3WH]$ also led to the observation of vinyl triflates as intermediates. In addition to these organic intermediates, both *cis*- and *trans*-isomers of the *β*-methylstyrene complex $[Cp(CO)_3W(\eta^2\text{-}PhHC{=}CHCH_3)]^+OTf^-$ were observed, with this tungsten alkene complex reaching a maximum yield of 40% during the reaction. Ultimately, this complex as well as the vinyl triflates were converted to propylbenzene, which was observed in 91% yield. Ionic hydrogenation of BuC≡CH by HOTf and $[Cp(CO)_3WH]$ led to vinyl triflate intermediates, but conversion to *n*-hexane was slow, requiring several days in the presence of excess HOTf. Since ionic hydrogenation of alkynes is so much slower than that of ionic hydrogenation of alkenes, the requirements of a suitable hydride donor are much more stringent. The ability of $[Cp(CO)_3WH]$ to function as a hydride donor in the presence of acid is a key characteristic of this metal hydride that distinguishes it from $HSiEt_3$. Reaction of this tungsten hydride with HOTf leads to partial formation of the cationic dihydride $[Cp(CO)_3W(H)_2]^+OTf^-$ [34], but formation of H_2

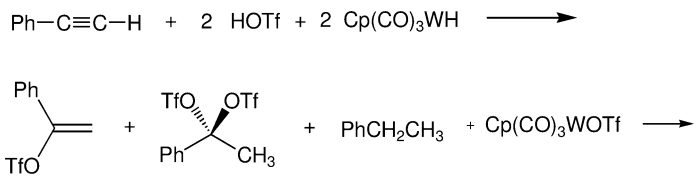

Scheme 7.5 $PhCH_2CH_3$ (92%)

from this dihydride is very slow, occurring over a time scale of weeks at room temperature.

7.2.6
Stoichiometric Ionic Hydrogenation of Ketones and Aldehydes using Metal Hydrides as Hydride Donors and Added Acids as the Proton Donor

Several systems have been reported involving stoichiometric hydrogenation of ketones or aldehydes by metal hydrides in the presence of acids. An ionic hydrogenation mechanism accounts for most of these hydrogenations, though in some examples alternative mechanisms involving the insertion of a ketone into a M–H bond are also plausible.

An early example came from the report in 1985 by Darensbourg et al. on the reactions of $[HCr(CO)_5]^-$ and $[HCr(CO)_4P(OMe_3)_3]^-$ with aldehydes and ketones, in the presence and absence of acids [27]. Paraformaldehyde reacts readily with $PPN^+[HCr(CO)_5]^-$ $\{PPN^+ = N(PPh_3)_2^+\}$ giving the alkoxide complex $[(CO)_5CrOCH_3]^-$ through insertion of formaldehyde into the Cr–H bond (Eq. (18)). The addition of HOAc produced methanol (Eq. (19)).

$$[(CO)_5CrH]^- + (CH_2O)_n \quad \rightarrow \quad [(CO)_5Cr\text{-}OCH_3]^- \tag{18}$$

$$[(CO)_5Cr\text{-}OCH_3]^- + HOAc \quad \rightarrow \quad CH_3OH + [(CO)_5Cr\text{-}OAc]^- \tag{19}$$

In contrast, only a sluggish reaction between propionaldehyde and $[HCr(CO)_5]^-$ was observed over several days, though addition of HOAc led to a 98% yield of *n*-propanol within 1 h. This striking change in reactivity between the two aldehydes suggests that propionaldehyde is hydrogenated to propanol not by an insertion mechanism, but rather through an ionic hydrogenation which protonation of the aldehyde activates it toward hydride transfer (Scheme 7.6). The phosphite-substituted anionic hydride $[HW(CO)_4P(OMe_3)_3]^-$ was more reactive with propionaldehyde in the absence of acids, providing evidence for a tungsten alkoxide complex that subsequently reacted with HOAc to produce a high yield of propanol. In the absence of acids, cyclohexanone showed little reactivity with any of the anionic hydrides $[HM(CO)_4L]^-$ (M = Cr or W, L = CO or $P(OMe_3)_3$).

As was found for aldehydes, however, the addition of HOAc led to the alcohol product. For less-reactive ketones, lower yields were found in some cases, and loss of some of the metal hydride occurs through formation of H_2 from reaction

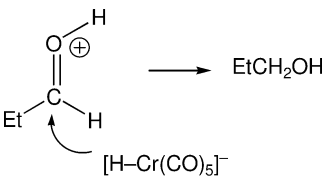

Scheme 7.6

of HOAc with $[HCr(CO)_5]^-$. In some cases, the weaker acid phenol could be used instead of HOAc.

In contrast to the lack of reactivity of ketones with $PPN^+[HCr(CO)_5]^-$, Brunet et al. reported different reactivity with K^+ rather than PPN^+ as the counterion. They found that $K^+[HCr(CO)_5]^-$ reacts with cyclohexanone in the absence of acid [35]. Hydrolysis with acid led to a 50% yield of cyclohexanol. These results suggest assistance from the K^+ cation; ion-pairing in metal anions has been studied in detail by Darensbourg [36].

Gibson and El-Omrani found that aldehydes were hydrogenated in refluxing THF by the bimetallic Mo hydride $[(\mu\text{-H})Mo_2(CO)_{10}]^-$ in the presence of HOAc [37]. These reactions most likely proceed through generation of the mononuclear hydride $[HMo(CO)_5]^-$, in analogy to the results discussed above for the Cr and W analogues.

Ito et al. found that hydrogenation of acetaldehyde, acetone, or cyclohexanone occurs at room temperature using $[Cp_2MoH_2]$ and HOAc [38]. An ionic hydrogenation pathway was favored, in which protonation of the ketone or aldehyde was followed by hydride transfer from the metal, though a mechanism involving insertion of the C=O into the Mo–H bond was also considered possible. Both of the Mo–H bonds are active for this reaction. For example, in stoichiometric reactions using HOAc as the acid, the first hydride transfer occurs from $[Cp_2MoH_2]$, which produces $[Cp_2MoH(OAc)]$, and this complex functions as a hydride donor for the second equivalent. The reactivity of Cp_2MoH_2 is greater than that of $[Cp_2MoH(OAc)]$, so that the first step is faster than the second. Using $[Cp_2MoH(OTs)]$ (Ts = *p*-$CH_3C_6H_4SO_2$) as the hydride donor, a very high diastereoselectivity was found for hydrogenation of the C=O bond of 4-*tert*-butylcyclohexanone, which gave only the *cis* isomer of 4-*tert*-butylcyclohexanol. Hydrogenation of the C=N bond of imines is also accomplished using $[Cp_2MoH_2]$ and HOAc; good yields of imines were obtained from reactions carried out at room temperature from 18 to 92 h. While most of these hydrogenations used protic acids, hydrogenation of N-cyclohexylidenecyclohexylamine was carried out using $[Cp_2MoH_2]$ and the Lewis acid $[Yb(OTf)_3]$, giving a 90% yield of the amine in 24 h at 50 °C (Eq. (20)).

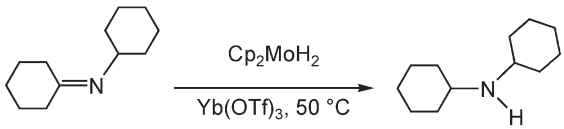

(20)

Hydride transfer from $[(bipy)_2(CO)RuH]^+$ occurs in the hydrogenation of acetone when the reaction is carried out in buffered aqueous solutions (Eq. (21)) [39]. The kinetics of the reaction showed that it was a first-order in $[(bipy)_2(CO)RuH]^+$ and also first-order in acetone. The reaction proceeds faster at lower pH. The proposed mechanism involved general acid catalysis, with a fast pre-equilibrium protonation of the ketone followed by hydride transfer from $[(bipy)_2(CO)RuH]^+$.

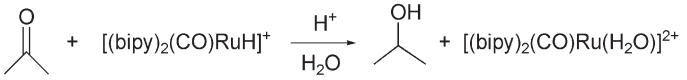

(21)

Harman and Taube found that the diamagnetic dihydrogen complex $[(NH_3)_5Os(\eta^2\text{-}H_2)]^{+2}$ does not react with acetone [40]. Oxidation gives the Os^{III} complex $[(NH_3)_5Os(\eta^2\text{-}H_2)]^{+3}$, which hydrogenates acetone to isopropyl alcohol. The reaction is slow, taking place over two days at room temperature. These results suggest that proton transfer to the ketone occurs from the acidic dihydrogen complex $[(NH_3)_5Os(\eta^2\text{-}H_2)]^{+3}$, and that hydride transfer from $[(NH_3)_5OsH]^{+2}$ to the protonated acetone generates the alcohol.

Extensive studies on stoichiometric hydrogenations of ketones have been carried out using HOTf as an acid, and metal carbonyl hydrides such as $[Cp(CO)_3WH]$ as the hydride donor [41, 42]. The addition of HOTf to a solution containing acetone and the tungsten hydride $[Cp(CO)_3WH]$ at 22 °C results in hydrogenation of the C=O bond to the alcohol, with the kinetically stabilized product having an alcohol ligand bound to the metal (Scheme 7.7) [41, 42]. Most previously reported alcohol complexes had been prepared by adding an alcohol to a metal complex with a weakly bound ligand, but in this case the alcohol ligand is formed in the reaction, without leaving the metal. The OH of the alcohol ligand is strongly hydrogen bonded to the triflate counterion, as shown by the short O···O distance of 2.63(1) Å found in the crystal structure of $[Cp(CO)_3W(HO^iPr)]^+OTf^-$. Evidence that the hydrogen bonding is maintained in solution comes from the appearance of the OH of the bound alcohol ligand at δ 7.34 (d, J = 7.4 Hz) in the ^{1}H-NMR spectrum, a chemical shift substantially downfield of

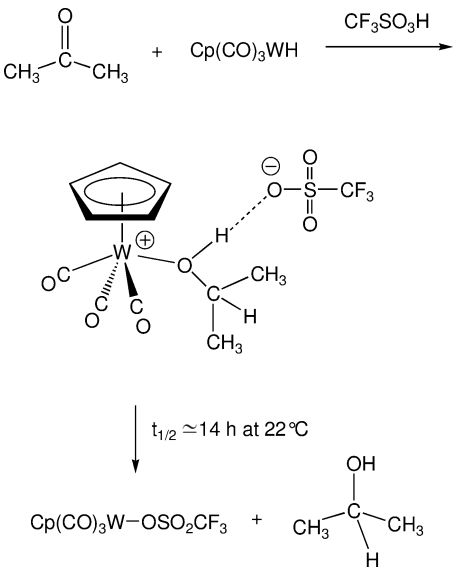

Scheme 7.7

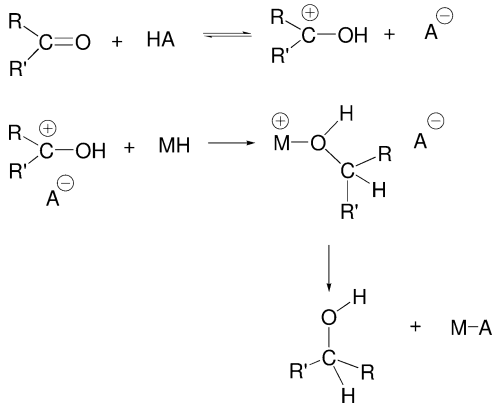

Scheme 7.8

that found for free alcohols. The bound alcohol is displaced by the triflate counterion, producing free alcohol and $[Cp(CO)_3WOTf]$. Other substrates that are readily hydrogenated by HOTf and $[Cp(CO)_3WH]$ include propionaldehyde, cyclohexanone, 2-adamantanone; in all of these cases fully characterized W(alcohol) complexes were isolated.

The kinetics of the ionic hydrogenation of isobutyraldehyde were studied using $[CpMo(CO)_3H]$ as the hydride and CF_3CO_2H as the acid [41]. The apparent rate decreases as the reaction proceeds, since the acid is consumed. However, when the acidity is held constant by a buffered solution in the presence of excess metal hydride, the reaction is first-order in acid. The reaction is also first-order in metal hydride concentration. A mechanism consistent with these kinetics results is shown in Scheme 7.8. Pre-equilibrium protonation of the aldehyde is followed by rate-determining hydride transfer.

Ionic hydrogenation of acetophenone by HOTf (1 equiv.) and $[Cp(CO)_3WH]$ (1 equiv.) consumes only half of the ketone, and generates ethylbenzene (Eq. (22)) and $[Cp(CO)_3WOTf]$ [42].

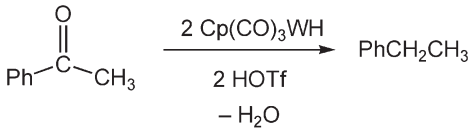

(22)

No intermediate tungsten complexes were observed in this reaction. The alcohol, *sec*-phenethylalcohol, is consumed at a rate which is much faster than that of its formation. It was shown separately to be converted to ethylbenzene (Eq. (23)) by HOTf and $[Cp(CO)_3WH]$. This reaction presumably proceeds through loss of water from the protonated alcohol, followed by hydride transfer from $[Cp(CO)_3WH]$ to give ethylbenzene.

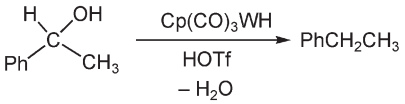

(23)

A competition between stoichiometric hydrogenation of acetone and acetophenone resulted in hydrogenation of the acetone [42]. Competitions of this type could be influenced by both the basicity of the ketone, as well as by the kinetics of hydride transfer to the protonated ketone. An intramolecular competition between an aliphatic and aromatic ketone resulted in preferential hydrogenation of the aliphatic ketone, with the product shown in Eq. (24) being isolated and fully characterized by spectroscopy and crystallography. Selective ionic hydrogenation of an aldehyde over a ketone was also found with HOTf and [Cp(CO)$_3$WH].

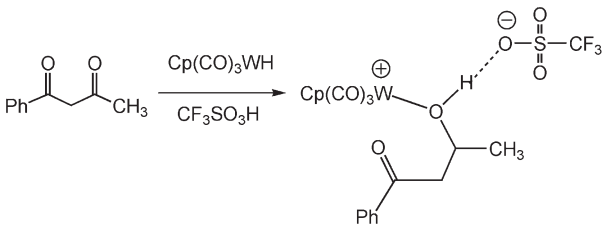

(24)

Bakhmutov et al. reported the ionic hydrogenation of acetone or benzaldehyde by [ReH$_2$(CO)(NO)(PR$_3$)$_2$], (R = *i*Pr, CH$_3$, O*i*Pr) and CF$_3$CO$_2$H [43]. The resultant alcohol complexes were characterized by low-temperature NMR, and the OH protons had downfield chemical shifts. For example, the OH of the bound isopropyl alcohol in [ReH(CO)(NO)(PMe$_3$)$_2$(HO^{i}Pr)]$^+$CF$_3$CO$_2^-$ appears as a doublet at δ 8.17. The alcohol is subsequently released through displacement by the counterion, giving [ReH(CO)(NO)(PR$_3$)$_2$(O$_2$CCF$_3$)]. A significant kinetic preference was found for hydrogenation of benzaldehyde over acetone. Protonation of the dihydride [ReH$_2$(CO)(NO)(PR$_3$)$_2$] produces the cationic dihydrogen complexes [ReH(H$_2$)(CO)(NO)(PR$_3$)$_2$]$^+$, so protonation of the aldehyde or ketone can occur from these observable species, prior to hydride transfer to generate the alcohol. Whilst these hydrogenations produced alcohol complexes at low temperature, carrying out the reactions at room temperature gave mostly H$_2$ elimination, and only 10–15% yields of the alcohol as the hydrogenation product.

7.2.7
Stoichiometric Ionic Hydrogenation of Acyl Chlorides to Aldehydes with HOTf/Metal Hydrides

Conversion of acyl chlorides to aldehydes occurs upon reaction with HOTf and [Cp(CO)$_3$WH] [32]. The reaction of HOTf with benzoyl chloride and [Cp(CO)$_3$WH] led to the isolation of [Cp(CO)$_3$W(PhCHO)]$^+$OTf$^-$ (Eq. (25)), in which the aldehyde is bound to the metal [32]. The spectroscopic properties and

crystal structure of this aldehyde complex revealed that it was bound through the oxygen, as an η^1-aldehyde. As was found in the case of the alcohol complexes, the aldehyde complex is kinetically stabilized. The triflate counterion displaces the bound aldehyde in a first-order process ($k = 3.6 \times 10^{-4}$ s^{-1}, $t_{1/2} \approx 33$ min at 25 °C), releasing the free aldehyde and generating [Cp(CO)$_3$WOTf].

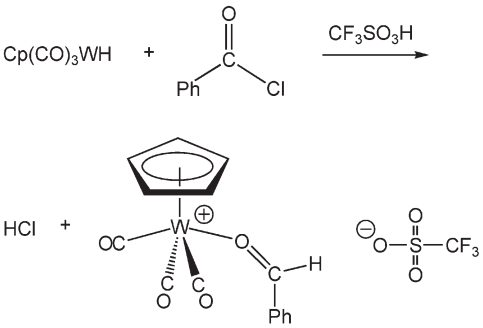

(25)

An analogous reaction occurs when $CH_3(C{=}O)Cl$ is reacted with HOTf and [Cp(CO)$_3$WH], with the acetaldehyde complex $[Cp(CO)_3W(CH_3CHO)]^+OTf^-$ being isolated [32]. Reaction with >1 equiv. each of HOTf and Cp(CO)$_3$WH led to subsequent hydrogenation of the CH_3CHO to ethanol, which was initially present as a bound ethanol ligand. It is possible that the mechanism of formation of the aldehyde complex involves protonation of the acyl chloride and hydride transfer from the metal, leading to a bound chlorohydrin complex, $[Cp(CO)_3W(CH_3C(Cl)(H)OH)]^+OTf^-$, which could expel HCl to produce $[Cp(CO)_3W(CH_3CHO)]^+OTf^-$. Since acyl chlorides are known to react with HOTf to produce acyl triflates, an alternative mechanism is formation of $CH_3C(=O)OTf$ followed by reaction with [Cp(CO)$_3$WH]. The acyl triflate $CH_3C(=O)OTf$ was prepared and shown to react with [Cp(CO)$_3$WH] to give $[Cp(CO)_3W(CH_3CHO)]^+OTf^-$, documenting the viability of this mechanistic pathway. It has not been established which of the two pathways is operative for these reactions.

Several anionic metal carbonyl hydrides stoichiometrically convert acyl chlorides to aldehydes. The anionic vanadium complex $[Cp(CO)_3VH]^-$ reacts quickly with acyl chlorides, converting them to aldehydes [44]. Although no further reduction of the aldehyde to alcohol was observed, the aldehydes reacted further under the reaction conditions in some cases, so a general procedure for isolation of the aldehydes was not developed.

Darensbourg et al. found that $HCr(CO)_5^-$ converts acyl chlorides to aldehydes rapidly at 25 °C (Eq. (26)) [26]. Yields >90% were detected by gas chromatography (GC) for preparation of CH_3CHO, *n*-BuCHO, PhCHO, and $PhCH_2CHO$. Since CH_3OD converts $HCr(CO)_5^-$ to $DCr(CO)_5^-$, the reaction of $[HCr(CO)_5]^-$ with PhCOCl in the presence of CH_3OD provided a convenient synthesis of the deuterated aldehyde, PhCDO.

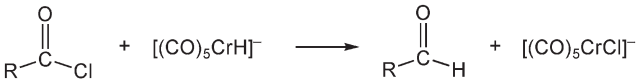

(26)

As noted earlier, $[HCr(CO)_5]^-$ also converts alkyl halides to alkanes, but the reactivity of the acyl chloride is much higher, such that it was possible to selectively convert the acyl chloride to an aldehyde in one step, without interference from the alkyl bromide functionality. A second equivalent of $[HCr(CO)_5]^-$ further reduced the alkyl bromide (Eq. (27)).

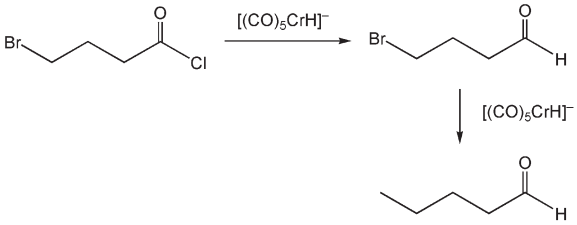

(27)

7.2.8
Stoichiometric Ionic Hydrogenation of Ketones with Metal Dihydrides

Many examples of stoichiometric ionic hydrogenation discussed above involved hydride transfer from metal hydrides, following proton transfer from an *external* acid source. Achieving a catalytic system still requires the hydride transfer step, but will additionally require a source of protons from a metal complex. In many cases the proton source will be an acidic M–H bond, so examples of stoichiometric hydrogenation involving a metal-based proton and hydride source are an important step in documenting the viability of catalytic ionic hydrogenation methodology.

The cationic tantalum dihydride $Cp_2(CO)Ta(H)_2]^+$ reacts at room temperature with acetone to generate the alcohol complex $[Cp_2(CO)Ta(HO^iPr)]^+$, which was isolated and characterized [45]. The mechanism appears to involve protonation of the ketone by the dihydride, followed by hydride transfer from the neutral hydride. The OH of the coordinated alcohol in the cationic tantalum alcohol complex can be deprotonated to produce the tantalum alkoxide complex $[Cp_2(CO)Ta(O^iPr)]$. Attempts to make the reaction catalytic by carrying out the reaction under H_2 at 60 °C were unsuccessful. The strong bond between oxygen and an early transition metal such as Ta appears to preclude catalytic reactivity in this example.

The cationic tungsten dihydride $[Cp(CO)_2(PMe_3)W(H)_2]^+$ hydrogenates the C=O bond of propionaldehyde within minutes at 22 °C, leading to the formation of *cis* and *trans* isomers of $[Cp(CO)_3W(HO^nPr)]^+OTf^-$ (Eq. (28)) [42]. The *cis* isomer of the alcohol complex released the free alcohol faster than the *trans* isomer. A similar stoichiometric ionic hydrogenation of acetone was also observed using $[Cp(CO)_2(PMe_3)W(H)_2]^+$.

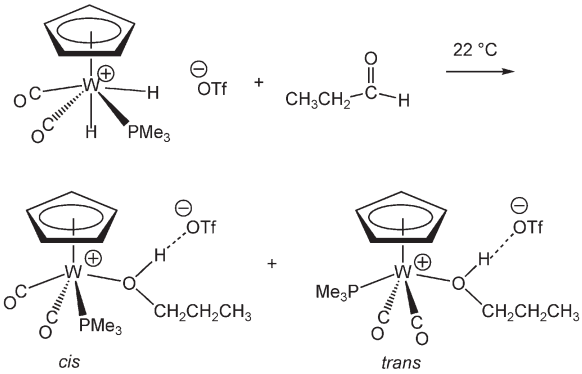

(28)

7.3 Catalytic Ionic Hydrogenation

7.3.1 Catalytic Ionic Hydrogenation of C=C Bonds

A series of cationic cobalt and rhodium complexes with a tetradentate chelating phosphine ligand have been reported [46]. These complexes were initially formulated as dihydrogen complexes, $[(PP_3)Co(H_2)]^+$ $\{PP_3 = P(CH_2CH_2PPh_2)_3\}$, but subsequent NMR studies conducted by Heinekey et al. showed that they were dihydride complexes $[(PP_3)Co(H)_2]^+$ [47]. Bianchini et al. found that, under an argon atmosphere, $[(PP_3)Co(H)_2]^+$ hydrogenates the C=C bond of dimethyl maleate in 3 h at room temperature [46]. When the reaction is conducted under H_2, catalytic hydrogenation of the C=C bond is observed, with a TOF of 1.5 h^{-1}. This reaction was suggested to proceed by an ionic mechanism, in which the cationic dihydride transfers a proton to the electron-deficient alkene, followed by hydride transfer from the neutral cobalt hydride complex. The acidity of Bianchini's $[(PP_3)Co(H)_2]^+$ would be expected to be roughly similar to that of $[(dppe)_2Co(H)_2]^+$, for which a pK_a of 22.8 was determined in CH_3CN (see Table 7.2). The low acidity of the dihydride raises questions about the likelihood of a proton-transfer mechanism for the initial step.

7.3.2 Catalytic Ionic Hydrogenation of Ketones by Anionic Cr, Mo, and W Complexes

Extensive studies on the hydride transfer reactivity of metal carbonyl anions such as $[HCr(CO)_5]^-$ presaged the development of anionic catalysts using Cr, Mo, and W. Darensbourg and coworkers found that 5 mol.% $[(CO)_5M(OAc)]^-$ (M = Cr, Mo, W) catalyzed the hydrogenation of cyclohexanone to cyclohexanol at 125 °C in THF using 36 bar H_2 (Eq. (29)) [48]. Under these conditions, TON determined after 24 h were 10 for W, 3.5 for Mo, and 18 for Cr.

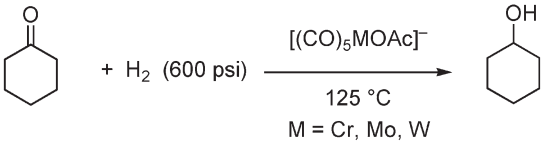

(29)

The organometallic products included recovered $[(CO)_5M(OAc)]^-$, along with $M(CO)_6$ and the bimetallic bridging hydride complex $[(\mu\text{-}H)M_2(CO)_{10}]^-$. It was proposed that, under the reaction conditions, $[(CO)_5MH]^-$ and HOAc were produced, and that insertion of the ketone into the M–H bond gave a metal alkoxide that reacted with HOAc to produce the alcohol.

Catalytic hydrogenations of cyclohexanone and benzaldehyde were also reported by Darensbourg et al. using 5% $[(\mu\text{-}H)M_2(CO)_{10}]^-$ (M = Cr, Mo, W) at 125 °C for 24 h; between four and 18 turnovers were observed under these conditions [48]. Related observations were made by Markó, who found that ketones (acetophenone, cyclohexanone, acetone, isobutyl methyl ketone) and aldehydes (benzaldehyde, butyraldehyde) could be catalytically hydrogenated at 160 °C under 100 bar of CO + H_2 [49]. Their experiments used 5 mol.% $[Cr(CO)_6]$ as the catalyst precursor, together with $NaOCH_3$ in methanol solution; under these conditions $[(CO)_5CrH]^-$ and $[(\mu\text{-}H)Cr_2(CO)_{10}]^-$ are formed. Similar hydrogenations were carried out starting with $[W(CO)_6]$ and with $[Mo(CO)_6]$. For the molybdenum example, milder conditions were used, with 91% hydrogenation of acetophenone being found after 3 h at 70 °C starting with 5 mol.% $Mo(CO)_6$ in methanol with added $NaOCH_3$. Fuchikami et al. found that $[(\mu\text{-}H)Cr_2(CO)_{10}]^-$ is much more active as a catalyst in dimethoxyethane (DME) than in THF [50]. Hydrogenation (50 bar H_2) of benzaldehyde at 100 °C using 1 mol.% $[(\mu\text{-}H)Cr_2(CO)_{10}]^-PPN^+$ produced 100 turnovers of benzyl alcohol after 13 h in DME, whereas using THF for 24 h at 125 °C gave only 14 turnovers.

Brunet et al. developed a transfer hydrogenation catalyst based on chromium, using 20% $K^+[(CO)_5CrH]^-$ as the catalyst precursor in THF solution, together with 5 equiv. each of HCO_2H and NEt_3 (Eq. (30)) [35, 51].

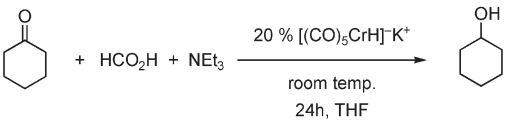

(30)

In reactions carried out for 24 h at room temperature, a 95% yield of cyclohexanol from cyclohexanone was obtained. Other ketones and aldehydes were also hydrogenated under identical conditions, but with slower rates (38% conversion for hydrogenation of 2-hexanone, 25% conversion of acetophenone, 45% for 3-methyl-2-butanone). Insertion of the C=O bond of the ketone or aldehyde into the Cr–H bond was proposed as the first step, producing a chromium alkoxide complex that reacts with acid to generate the alcohol product. The anionic chromium hydride $[(CO)_5CrH]^-$ is regenerated from the formate complex by

decarboxylation (Eq. (31)). The role of the triethylamine is to moderate the strength of the formic acid, since formic acid alone is too strong of an acid, converting $[(CO)_5CrH]^-$ into $[(\mu\text{-}H)Cr_2(CO)_{10}]^-$.

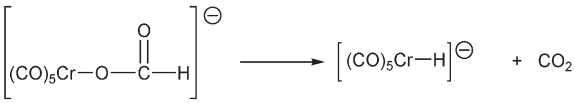

(31)

7.3.3
Catalytic Ionic Hydrogenation of Ketones by Molybdenocene Complexes

Hydride transfer reactions from $[Cp_2MoH_2]$ were discussed above in studies by Ito et al. [38], where this molybdenum dihydride was used in conjunction with acids for stoichiometric ionic hydrogenations of ketones. Tyler and coworkers have extensively developed the chemistry of related molybdenocene complexes in aqueous solution [52–54]. The dimeric bis-hydroxide bridged dication dissolves in water to produce the monomeric complex shown in Eq. (32) [53]. In D_2O solution at 80 °C, this bimetallic complex catalyzes the H/D exchange of the α-protons of alcohols such as benzyl alcohol and ethanol [52, 54].

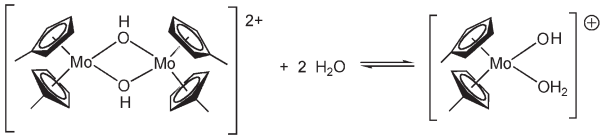

(32)

The proposed mechanism for this H/D exchange is shown in Scheme 7.9. The formation of the alkoxide complex likely proceeds by displacement of the water ligand by the alcohol, forming an unobserved alcohol complex that transfers D^+ to the OD ligand, producing an OD_2 ligand.

The key step involves C–H bond activation, and produces a molybdenum complex with hydride and ketone ligands from the alkoxide ligand. Subsequent

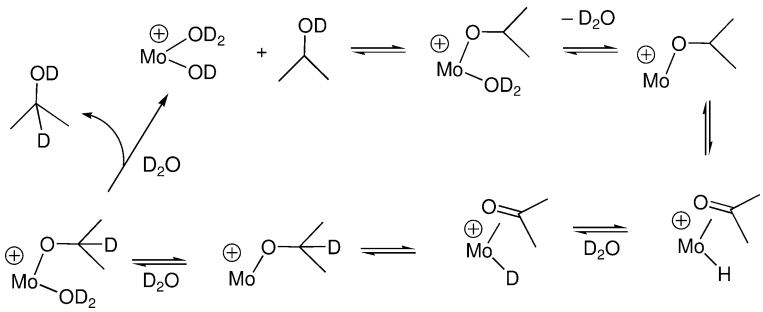

Scheme 7.9

H/D exchange leads to deuterium incorporation into the α-position of the alcohol.

Heating the bimetallic complex in D_2O solution also results in deuteration of the CH_3 sites on the cyclopentadienyl ring, through a mechanism involving oxidative addition of a C–H bond of the CH_3 group, followed by deuterium incorporation into the methyl group [54]. Heating of a mixture of the molybdenum complex with isopropyl alcohol and 2-butanone led to hydrogenation of the ketone, producing 2-butanol, and dehydrogenation of the isopropyl alcohol, generating acetone [52, 54]. Kuo et al. carried out further studies on these hydrogenations [55, 56]. Acetone is hydrogenated to isopropyl alcohol by $[Cp_2MoH(OTf)]$ in water. The rates are faster in acidic solution than when the solution is buffered at pH 7, consistent with a general acid-catalyzed pathway in which the ketone is protonated prior to hydride transfer from the molybdenum hydride [55]. An alternative mechanism would involve insertion of the ketone into a Mo–H bond to give a metal alkoxide, which could then generate the alcohol by hydrolysis with water. The transfer hydrogenation of acetophenone by isopropyl alcohol in water is catalyzed by $[Cp_2Mo(\mu\text{-}OH)_2MoCp_2]^{2+}(OTs^-)_2$ [56]. At 75 °C, the TOF is about 0.1 h^{-1}. Scheme 7.10 shows the proposed mechanism for this transfer hydrogenation; several of these steps have precedent in Tyler's H/D exchange reactions shown in Scheme 7.9 [52].

The catalytic ketone hydrogenation reaction is accelerated by addition of KOH. In the presence of 25 equiv. KOH, 1 mol.% of the molybdenum complex completely hydrogenated acetophenone overnight in refluxing 2-propanol

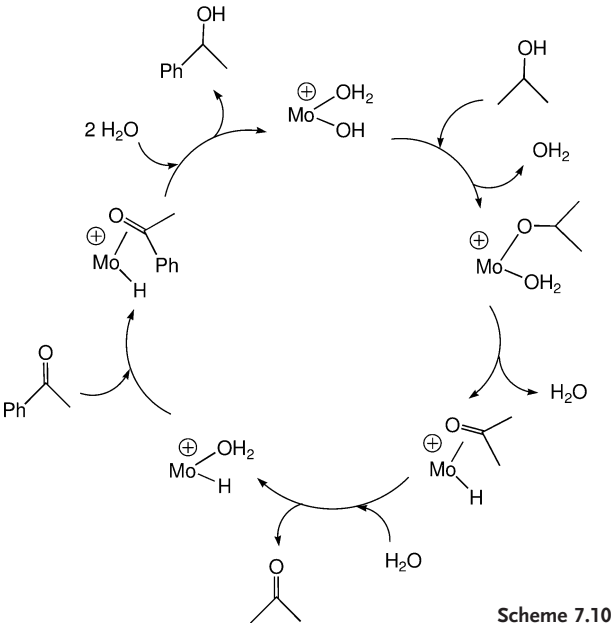

Scheme 7.10

(82 °C). The exact role of the base is not clear, but it may accelerate the formation of the molybdenum alkoxide complex from a bound alcohol ligand.

7.3.4
Catalytic Ionic Hydrogenation of Ketones by Cationic Mo and W Complexes

7.3.4.1 In Solution

Molybdenum and tungsten carbonyl hydride complexes were shown (Eqs. (16), (17), (22), (23), (24); see Schemes 7.5 and 7.7) to function as hydride donors in the presence of acids. Tungsten dihydrides are capable of carrying out stoichiometric ionic hydrogenation of aldehydes and ketones (Eq. (28)). These stoichiometric reactions provided evidence that the proton and hydride transfer steps necessary for a catalytic cycle were viable, but closing of the cycle requires that the metal hydride bonds be regenerated from reaction with H_2.

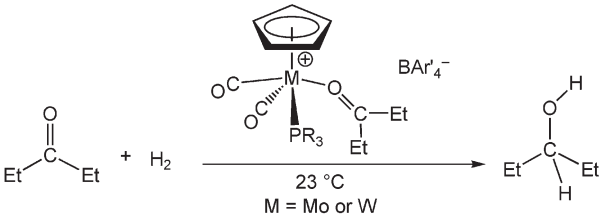

(33)

Tungsten and molybdenum ketone complexes, $[Cp(CO)_2(PR_3)M(O{=}CEt_2)]^+$-$BAr'_4^-$ [Ar′ = 3,5-bis(trifluoromethyl)phenyl], could be isolated for $PR_3 = PMe_3$ and PPh_3 but were prepared *in situ* for the PCy_3 (Cy = cyclohexyl) complexes [57]. A series of experiments were carried out in CD_2Cl_2 solvent at 23 °C under 4 bar H_2, with about 10 equiv. $Et_2C{=}O$ (Eq. (33)). Formation of the alcohol (Et_2CH-OH) was accompanied at later times by small amounts of the ether, $(Et_2CH)_2O$, which arises from condensation of the alcohol. Under these reaction conditions, since the ketone substrate was not present in large excess, it was possible to monitor simultaneously the progress of the hydrogenation, as well as to detect the organometallic species present under catalytic hydrogenation conditions. As the reaction proceeds, the concentration of the ketone complex decreases, with concomitant formation of the alcohol complex. For example, in the case of the W complexes with a PPh_3 ligand, NMR evidence indicated the formation of *trans*-$[CpW(CO)_2(PPh_3)(Et_2CHOH)]^+$, with the concentration of this alcohol complex exceeding that of the ketone complex at later reaction times. As discussed earlier, alcohol complexes were previously found to be the kinetic product of stoichiometric ionic hydrogenation of ketones, so the observation under catalytic conditions indicates that the stoichiometric reactivity provides a good model in this case for the catalytic reactivity, even with some changes in ligands and counterions between the stoichiometric and catalytic reactions.

The proposed mechanism shown in Scheme 7.11 is supported by stoichiometric proton- and hydride-transfer reactions of metal hydrides that were dis-

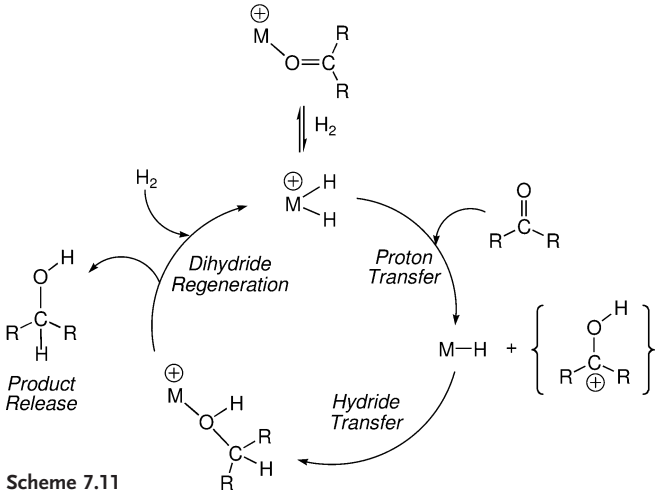

Scheme 7.11

cussed earlier. The key step to closure of the cycle, regeneration of the M–H bonds by H_2, is accomplished by reaction of the ketone complex with H_2. Tungsten dihydride complexes were sufficiently stable to be isolated and fully characterized [34], but molybdenum analogues were not directly observed. Evidence for the intermediacy of molybdenum dihydrides (or dihydrogen complexes) comes from heterolytic cleavage of H_2 by a molybdenum ketone complex in the presence of a hindered amine base (Eq. (34)). When H_2 is added to $[CpW(CO)_2(PPh_3)(Et_2C{=}O)]^+$ (with no added ketone), the dihydride $[CpW(CO)_2(PPh_3)(H)_2]^+$ is formed, providing further support for the operation of this step under catalytic conditions.

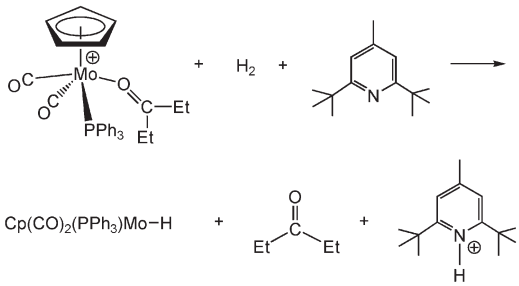

(34)

Conversion of $[CpW(CO)_2(PPh_3)(Et_2C{=}O)]^+$ to *trans*-$[CpW(CO)_2(PPh_3)(Et_2CHOH)]^+$ was observed when $Et_2C{=}O$ was hydrogenated under high pressure (65 bar) of H_2 for 17 h at 22 °C. Hydride transfer from $[CpW(CO)_2(PPh_3)H]$ to $Ph_3C^+BAr'_4{}^-$, followed by addition of the alcohol Et_2CHOH, led to the isolation of the *cis* isomer of $[CpW(CO)_2(PPh_3)(Et_2CHOH)]^+$. The studies of kinetic hydricity of metal hydrides had shown that hydride transfer from *trans*-$[Cp(CO)_2(PCy_3)MoH]$ to $Ph_3C^+BF_4{}^-$ occurs much faster than hydride transfer

from the *cis* isomer of the hydride, *cis*-$[Cp(CO)_2(PCy_3)MoH]$ [58]. Since the *trans* isomer of the alcohol complex is observed under catalytic conditions, the alcohol binds to the metal at the site from which hydride transfer took place. The studies of stoichiometric ionic hydrogenation of ketones had previously provided evidence that some amount of W–O bond formation is taking place in the transition state, before W–H bond cleavage is complete [41, 42].

Comparison of the rates of hydrogenation in these systematic studies of ionic hydrogenation of ketones by $[Cp(CO)_2(PR_3)M(O{=}CEt_2)]^+$ indicated the trends in metal and phosphine ligand [57]. For comparisons involving the same PR_3 ligand, the Mo complexes are invariably faster catalysts compared to the W analogue. The initial rate of hydrogenation is about eight-fold faster for Mo than for W for the PPh_3 complexes, and the difference is roughly two orders of magnitude for the PCy_3 complexes. For the Mo catalysts, the rate varies substantially with different phosphine ligands, in the order $PCy_3 > PPh_3 > PMe_3$. The approximate initial rate was about two turnovers per hour for the Mo–PCy_3 complex. For the W complexes, the same order was found, though the range of relative rates was smaller for W than for Mo. The phosphines PCy_3 and PMe_3 are similar electronically, so the much higher rate of catalysis found with the PCy_3 complexes makes it clear that steric effects predominate over electronic effects.

For the PPh_3 and PMe_3 complexes, the ketone or alcohol complexes were observed spectroscopically during the hydrogenation reaction, and those species are the resting states. Formation of the dihydride complexes under catalytic conditions is proposed to involve dissociation of the ketone or alcohol followed by addition of H_2. The higher rate of catalysis with the PCy_3 complexes suggests that the steric bulk of this ligand promotes ketone dissociation more than in the case of the PPh_3 or PMe_3 complexes. In contrast to the PPh_3 and PMe_3 complexes, the predominant tungsten complex observed during hydrogenation with the PCy_3 complex was $[Cp(CO)_2(PCy_3)W(H)_2]^+$. In this case, proton transfer from the metal to the ketone is slow and has become the turnover-limiting step of the catalytic cycle. Ketone binding to the metal is destabilized by steric factors for the PCy_3 complex, compared to analogues with PMe_3. In addition, the steric effects of the bulky PCy_3 ligand likely disfavor proton transfer from the metal to the free ketone. Norton et al. reported a pK_a of 5.6 in CH_3CN for $[CpW(CO)_2(PMe_3)(H)_2]^+$ [31]. The pK_a of protonated acetone in CH_3CN is about –0.1 [59, 60]. Presuming that there is not a large change in relative pK_a values in CH_3CN (in which the pK_a measurements were made) and CD_2Cl_2 (in which the hydrogenations were carried out), the thermodynamics of proton transfer from the dihydride to the ketone are uphill in all of these cases. The tungsten dihydride $[CpW(CO)_2(PMe_3)(H)_2]^+$ (for which pK_a data are available) is the one that leads to the slowest hydrogenation, so it is likely that this represents the least thermodynamically favorable example for proton transfer. Based on the trends in acidity identified above, $[CpW(CO)_2(PPh_3)(H)_2]^+$ is expected to be more acidic than $[CpW(CO)_2(PMe_3)(H)_2]^+$; similarly, Mo hydrides are more acidic than W hydrides. Rate constants for hydride transfer to protonated ketones have not been as extensively studied as those for hydride transfer to Ph_3C^+ (see Table 7.5), but

hydride transfer from $Cp(CO)_2(PPh_3)MoH$ to protonated acetone occurs in CH_3CN with a reported rate constant of $1.2\times10^4\ M^{-1}\ s^{-1}$ at 25 °C [60]. Proton transfer from the dihydride to the ketone is thermodynamically uphill, but this does not prevent catalytic ionic hydrogenations with these W and Mo complexes from proceeding smoothly, since rapid hydride transfer from the neutral hydride follows the proton transfer.

Evidence for a major mode of catalyst deactivation in this system came from the observation of phosphonium cations (HPR_3^+) in the reaction mixture, which could form through the protonation of free PR_3 by the acidic dihydride complex. It is not known which species decomposes to release free PR_3, but the decomposition pathway is exacerbated by the subsequent reactivity in which protonation of phosphine removes a proton from the metal dihydride, effectively removing a second metal species from the cycle.

Knowledge of the pathway for catalyst deactivation suggested that catalysts with longer lifetimes might result if phosphine dissociation could be suppressed. A series of Mo complexes was prepared that had a two-carbon chain chelating the cyclopentadienyl ligand to the phosphine [61]. Hydride abstraction from $[HMo(CO)_2\{\eta^5:\eta^1\text{-}C_5H_4(CH_2)_2PR_2\}]$ (R = Cy, *t*Bu, and Ph) using $Ph_3C^+BAr'_4{}^-$ in the presence of $Et_2C{=}O$ led to ketone hydrogenation catalysts (Eq. (35)) that exhibited several advantages over the unbridged complexes.

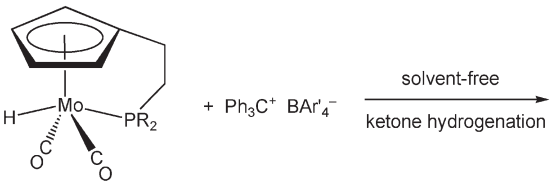

(35)

Comparisons of catalysis of these C_2-tethered P,C chelate complexes with the non-chelate analogues in CD_2Cl_2 solvent showed that the former were somewhat slower catalysts than the latter, but the compelling advantage of the chelate complexes is that they had much longer lifetimes.

7.3.4.2 **Solvent-free**

Environmental concerns have caused an intense emphasis on the development of chemical reactions that reduce waste. Solvents are used on a huge scale, with more than 15 billion kilograms of organic solvents being produced each year [62]. One of the Principles of Green Chemistry [7] indicates that the use of a solvent should be avoided whenever possible, and it has been found that the hydrides $[HMo(CO)_2\{\eta^5:\eta^1\text{-}C_5H_4(CH_2)_2PR_2\}]$ can be used as catalyst precursors for the solvent-free [62,63] hydrogenation of $Et_2C{=}O$. Hydrogenations can be carried out at higher temperatures, since the C_2–PR_2 complexes have significantly improved stability compared to the unbridged complexes. Another attractive feature of these bridged catalysts is that they can be used at low catalyst loading,

less than 1 mol.% typically, and as low as 0.09 mol.% in one example. Solvent-free hydrogenation of $Et_2C{=}O$ using $[HMo(CO)_2\{\eta^5:\eta^1\text{-}C_5H_4(CH_2)_2PCy_2\}]$ (0.35 mol.%) as the catalyst precursor (activated by hydride removal using $Ph_3C^+BAr'^-_4$) was carried out under 4 bar H_2 at 50 °C for 10 days, and 132 turnovers were observed (Eq. (35)). Only 62 turnovers were found when the analogous C_2–PPh_2 complex was employed under identical conditions, indicating that the performance of the catalyst with R = Cy was superior to that found with R = Ph, the same trend that was found for the unbridged complexes. Although the steric bulk of the Cy group on the phosphines was recognized as an advantage, the use of the C_2–P*t*Bu_2 complex (82 turnovers under identical conditions) was superior to that of the C_2–PPh_2 complex but not as high as the C_2–PCy_2 complex. Higher pressure of H_2 led to faster rates of catalysis – complete hydrogenation of $Et_2C{=}O$ was accomplished using $[HMo(CO)_2\{\eta^5:\eta^1\text{-}C_5H_4(CH_2)_2PCy_2\}]$ (0.35 mol.%) as the catalyst precursor at 50 °C under 55 bar H_2 for 8 days.

Most of the studies of these Mo catalysts were carried out with BAr'^-_4 as the counterion; catalysis is also observed using BF^-_4 or PF_6^- as the counterion, albeit with lower turnover numbers [61]. Triflate is an attractive counterion; it offers advantages of lower cost compared to BAr'^-_4, but may be slightly different mechanistically since it coordinates to the metal. Protonation of $[HMo(CO)_2\{\eta^5:\eta^1\text{-}C_5H_4(CH_2)_2PCy_2\}]$ with HOTf leads to the formation of the triflate complex $[Mo(CO)_2\{\eta^5:\eta^1\text{-}C_5H_4(CH_2)_2PR_2\}OTf]$, presumably through an unobserved dihydride or dihydrogen complex. Solvent-free hydrogenation (4 bar H_2) of $Et_2C{=}O$ using 0.35 mol.% $[Mo(CO)_2\{\eta^5:\eta^1\text{-}C_5H_4(CH_2)_2PCy_2\}OTf]$ (50 °C, 10 days) gave 120 turnovers, only slightly less than the 132 turnovers found under identical conditions using the BAr'^-_4 counterion. Even lower catalyst loading was successfully carried out with $[Mo(CO)_2\{\eta^5:\eta^1\text{-}C_5H_4(CH_2)_2PCy_2\}OTF]$: 0.09 mol.% catalyst loading at 75 °C for 10 days provided 462 turnovers in the hydrogenation of $Et_2C{=}O$ under solvent-free conditions.

These Mo catalysts with a C_2-tether connecting the phosphine and cyclopentadienyl ligand provide an example of the use of mechanistic principles in the rational design of improved catalysts, in this case based on information about a decomposition pathway for the prior generation of catalysts. The new catalysts offer improved lifetimes, higher thermal stability, and low catalyst loading. The successful use of a triflate counterion and solvent-free conditions for the hydrogenation are additional features that move these catalysts closer to practical utility.

7.3.4.3 **N-Heterocyclic Carbene Complexes**

N-heterocyclic carbenes have recently been used as alternatives to phosphines in many catalytic reactions, owing in part to a decreased propensity to dissociate from the metal [64]. Hydride abstraction from the tungsten hydride $[Cp(CO)_2(IMes)WH]$ (IMes = the carbene ligand 1,3-bis(2,4,6-trimethylphenyl)-imidazol-2-ylidene) using $Ph_3C^+B(C_6F_5)^-_4$ leads to the formation of an unusual complex in which one C=C of a mesityl ring has a weak bonding interaction with the tungsten (Eq. (36)) [65].

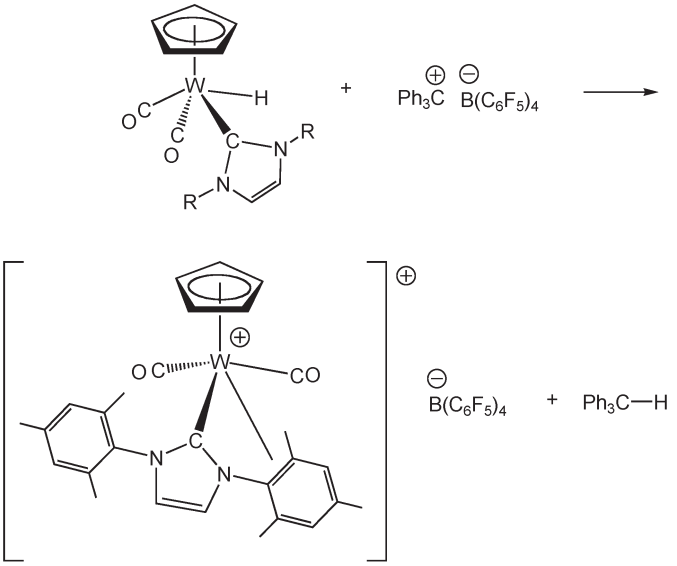

(36)

This complex can be used as a catalyst precursor for hydrogenation of ketones, though only two turnovers occurred in one day for solvent-free hydrogenation of $Et_2C{=}O$ at 23 °C using 0.34 mol.% catalyst at 4 bar H_2. At the same catalyst loading, 61 turnovers occurred in 7 days at higher temperature (50 °C) and higher H_2 pressure (54 bar), though some decomposition of the catalyst is also observed. These catalysts are thought to operate by a mechanism analogous to that shown above (see Scheme 7.11) for the related phosphine complexes.

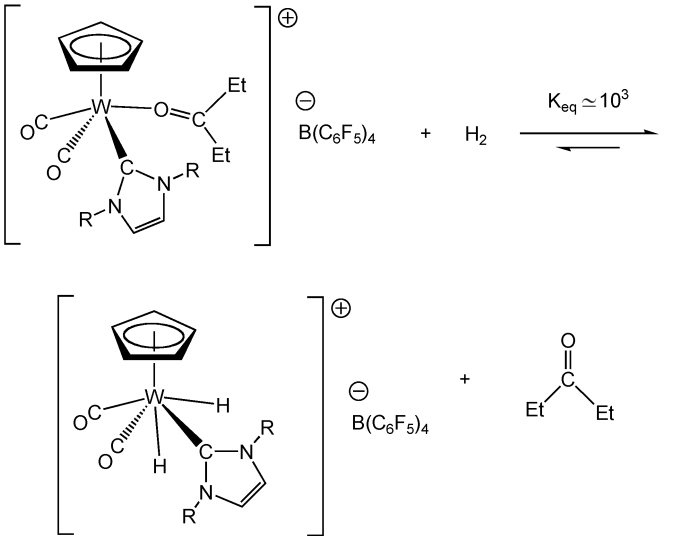

(37)

Displacement of the bound ketone by H_2 was directly observed by NMR (Eq. (37)), and an approximate equilibrium constant was determined. The cationic tungsten complex can also be used for catalytic hydrosilylation of ketones. In the case of catalytic hydrosilylation of aliphatic substrates using $HSiEt_3$, the catalyst precipitates at the end of the reaction, facilitating recycle and reuse [66].

7.3.5
Use of a Pd Hydride in Hydrogenation of C=C Bonds

DuBois et al. reported extensive studies on the thermodynamics of acidic and hydridic reactivity of a large series of complexes $[HM(diphosphine)_2]^+$. Aresta et al. found that protonation of the Pd complex $[Pd(dppe)_2]$ leads to the cationic hydride $[HPd(dppe)_2]^+$ [67]. The Pd–H bond can be cleaved as either a proton or as a hydride. Solutions of $[HPd(dppe)_2]^+$ decompose to give H_2, $[Pd(dppe)_2]$ and $[Pd(dppe)_2]^{2+}$. Reaction of $[HPd(dppe)_2]^+$ with methyl acrylate at 20 °C resulted in hydrogenation of the C=C bond, producing methyl propionate (Eq. (38)). In contrast to the previously discussed examples of ionic hydrogenation, two equivalents of the same palladium hydride complex are thought to furnish both the proton and the hydride in this case. Computations suggested that hydride transfer occurs first, producing a carbanionic intermediate that is then protonated by a second equivalent of the metal hydride. Catalytic hydrogenation of the C=C bond of cyclohexene-2-one was observed when $[HPd(dppe)_2]^+BF_4^-$ was used as the catalyst precursor under H_2 (4 MPa). A maximum TOF of about 16 h^{-1} was found at 50 °C. At higher temperatures (67 °C), higher TOF values were found, but decomposition of the Pd complex was observed, producing decomposition products (Pd black) that are also catalytically active.

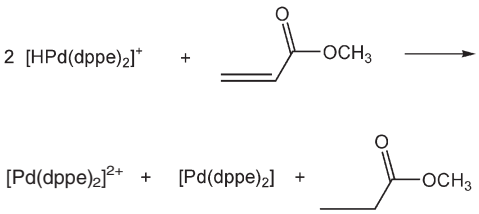

(38)

7.3.6
Catalytic Hydrogenation of Iminium Cations by Ru Complexes

Norton and coworkers found that catalytic enantioselective hydrogenation of the C=N bond of iminium cations can be accomplished using a series of Ru complexes with chiral diphosphine ligands such as Chiraphos and Norphos [68]. Even tetra-alkyl-substituted iminium cations can be hydrogenated by this method. These reactions were carried out with 2 mol.% Ru catalyst and 3.4–3.8 bar H_2 at room temperature in CH_2Cl_2 solvent (Eq. (39)).

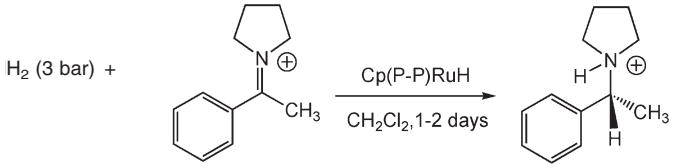

(39)

The enantiomeric excess (ee) obtained under catalytic conditions was similar to that found when the hydride transfer was carried out in a stoichiometric reaction (Eq. (40)); these stoichiometric reactions were carried out in the presence of excess CH_3CN, which captures the 16-electron cationic Ru complex following hydride transfer.

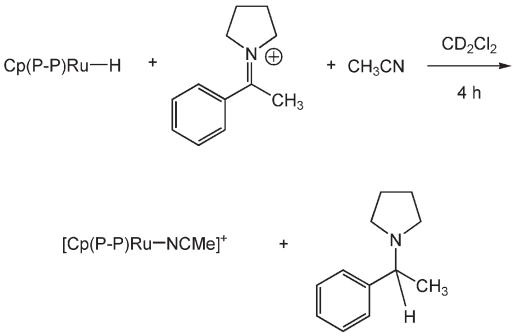

(40)

No change in the rate or ee of the catalytic reaction was observed when the pressure of H_2 was varied, indicating that H_2 does not play a role in the turnover-limiting step or in the determination of enantioselectivity. When the catalytic reaction was monitored by NMR under H_2 (5 bar), the neutral hydride was observed. All of these observations support the proposed mechanism shown in Scheme 7.12. This

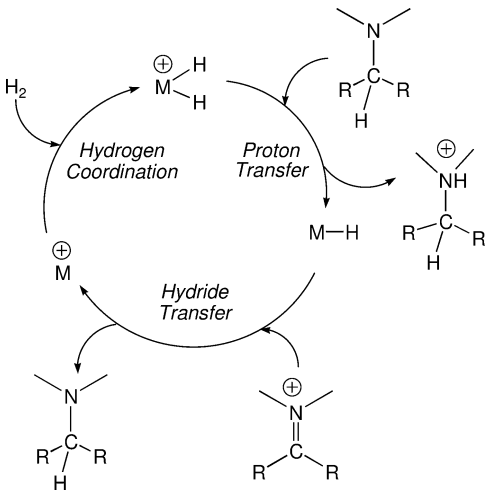

Scheme 7.12

mechanism is similar to the mechanism for ionic hydrogenation of ketones (Scheme 7.11), except that in the hydrogenation of iminium cations the hydride transfer occurs first, whereas proton transfer from cationic dihydrides to the ketone occurs first in Scheme 7.11. Hydride transfer to the iminium cation is the turnover-limiting and enantioselectivity-determining step of the mechanism.

The kinetics of hydride transfer (Eq. (40)) were determined for a series of chelating diphosphines. The rate constant of hydride transfer was found to be highly dependent on the bite angle of the diphosphine, increasing as the bite angle decreases [69]. The rate constant for [Cp(dppm)RuH] (dppm = $Ph_2PCH_2PPh_2$; bite angle 72°) was about 200 times higher than that for [Cp(dppp)RuH] (dppp = $Ph_2P(CH_2)_3PPh_2$; bite angle 92°). The rate constant for the Ru complex of the diphosphine with a C_2 bridge, [Cp(dppe)RuH] (dppe = $Ph_2P(CH_2)_2PPh_2$; bite angle 85°) was intermediate between the two. The increased *kinetic* hydricity resulting from a decreased bite angle parallels the observations of DuBois and colleagues, who found the same trend for *thermodynamic* hydricity [19].

7.4 Ruthenium Complexes Having an OH Proton Donor and a RuH as Hydride Donor

7.4.1 The Shvo System

Shvo and coworkers prepared a bimetallic complex in which the two metals are joined by a bridging hydride as well as by an O–H–O hydrogen bond joining the two substituted Cp ligands [70]. Shvo used this versatile catalyst precursor for hydrogenation of C=C and C=O bonds at 145 °C under 34 bar H_2 (Eq. (41)) [71].

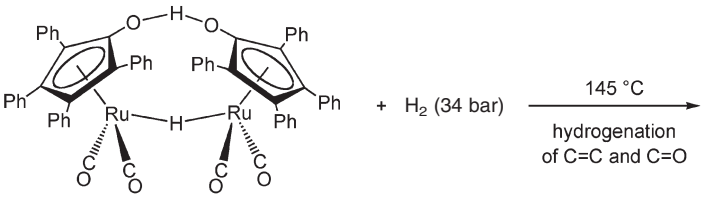

Shvo Catalyst

(41)

Under these conditions, the bimetallic complex is cleaved into an 18-electron complex that performs the hydrogenations, and an unsaturated 16-electron complex. Addition of H_2 to the 16-electron complex produces the 18-electron complex that has an acidic OH and a hydridic RuH (Eq. (42)).

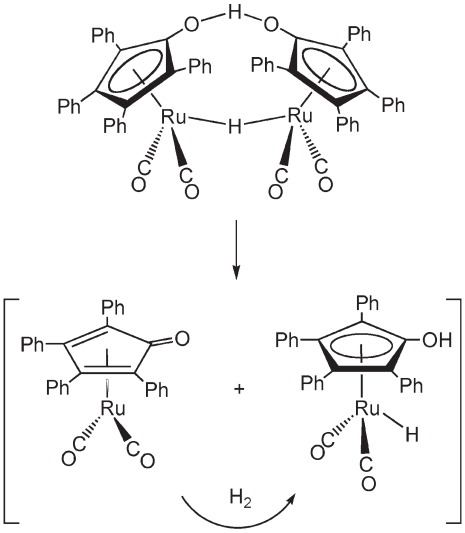

(42)

Solvent-free hydrogenations of 1-octene, 2-pentene, cyclohexene, and styrene were carried out with catalyst loadings as low as 0.05 mol.% of the dimer, in some cases with TOF values as high as 6000 h^{-1} [71]. Total turnover numbers of almost 2000 were obtained in most of these cases. Solvent-free hydrogenation of ketones such as $Et_2C{=}O$, cyclohexanone, and diisopropyl ketone were also reported at the same temperature and H_2 pressure, but with somewhat lower TOFs for the hydrogenation of C=O compared to C=C hydrogenations.

Kinetic and mechanistic studies by Casey et al. provided further insight into the mechanistic details of the hydrogenation of ketones and aldehydes, using a more soluble analogue of Shvo's catalyst (with *p*-tolyl groups instead of two of the Ph groups) [72]. The kinetics of hydrogenation of benzaldehyde by the Ru complex shown in Eq. (43) were first order in aldehyde and first order in the Ru complex; the

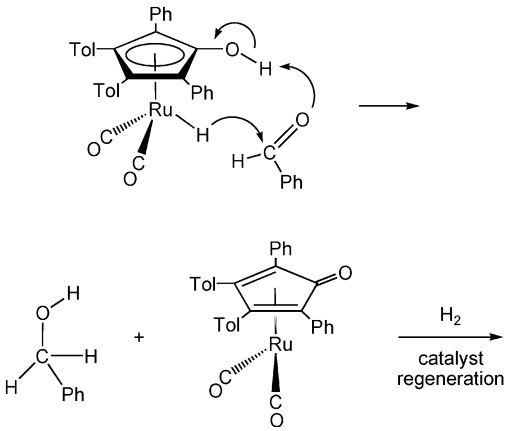

(43)

second-order rate constant at –10 °C was determined to be $k = (3.0 \pm 0.2) \times 10^{-4}$ M^{-1} s^{-1}. The activation enthalpy was $\Delta H^{\ddagger} = 12.0 \pm 1.5$ kcal mol^{-1}, and the very negative entropy of activation ($\Delta S^{\ddagger} = -28 \pm 5$ cal K^{-1} mol^{-1}) further supports a highly ordered transition state.

Isotope effects have been very useful in understanding the detailed mechanisms of many organometallic reactions [73], and have been used extensively in studies of Shvo complexes. Separate kinetic isotope effects were measured for hydrogenation of PhCHO at 0 °C (Eq. (43)); deuteration at the RuH(D) and OH(D) positions gave values of $k_{RuH}/k_{RuD} = 1.5 \pm 0.2$ and $k_{OH}/k_{OD} = 2.2 \pm 0.1$. Deuteration of both the RuH and OH sites gave a combined kinetic isotope effect of $k_{RuHOH}/\ k_{RuDOD} = 3.6 \pm 0.3$. The proposed mechanism involves concerted proton transfer from the OH site and hydride transfer from the Ru hydride, and is supported by the product of the two individual isotope effects ($1.5 \times 2.2 = 3.3$) being within experimental uncertainty of the combined isotope effect of 3.6. Since the actual hydrogenation step (Eq. (43)) occurs at low temperatures, the elevated temperature required for the catalytic reaction starting with the bimetallic complex as the catalyst precursor (see Eq. (41)) is necessary to generate the active mononuclear species. A pK_a of 17.5 was determined in CH_3CN for the OH of [[2,5-Ph_2-3,4-Tol_2(η^5-C_4COH)]Ru$(CO)_2$H], so this OH is significantly more acidic than either phenol ($pK_a = 26.6$ in CH_3CN) or benzoic acid ($pK_a = 20.7$ in CH_3CN). As shown in Table 7.5, [Cp*Ru$(CO)_2$H] has high kinetic hydricity, so this remarkable combination of acidity of an OH site and hydricity of the RuH combine to make the concerted proton- and hydride-transfer mechanism feasible in this type of complex.

A variety of ketones were hydrogenated using Shvo's catalyst at 100 °C using excess formic acid rather than H_2 as the source of hydrogen [74]. Excellent yields (>90%) of alcohols were generally obtained in 6 h or less, with total turnovers in the range of 6000–8000. The unsaturated 16-electron Ru complex that results after hydrogen is delivered to the substrate is proposed to react with for-

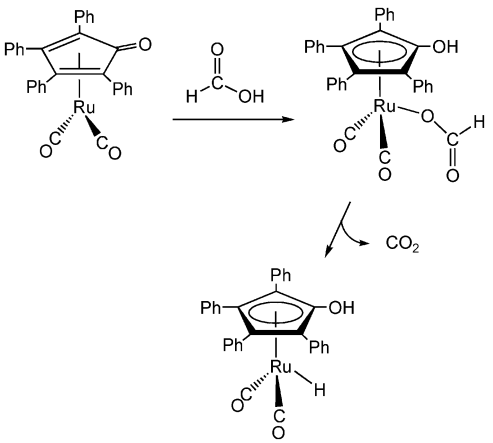

(44)

mic acid to produce a formate complex that expels CO_2, regenerating the metal hydride (Eq. (44)). Subsequent studies by Casey et al. showed that the formate complex is formed upon reaction of excess formic acid (HCO_2H) with Shvo's catalyst at low temperature [75]. This formate complex loses CO_2 above 0 °C, but the formate complex does not hydrogenate benzaldehyde directly.

Casey has suggested that the hydrogenation of alkenes by Shvo's catalyst may proceed by a mechanism involving loss of CO from the Ru–hydride complex, and coordination of the alkene. Insertion of the alkene into the Ru–H bond would give a ruthenium alkyl complex that can be cleaved by H_2 to produce the alkane [75]. If this is correct, it adds further to the remarkable chemistry of this series of Shvo complexes, if the same complex hydrogenates ketones by an ionic mechanism but hydrogenates alkenes by a conventional insertion pathway.

7.4.2
Hydrogenation of Imines by Shvo Complexes

Samec and Bäckvall found that the dinuclear Shvo complex catalyzes the transfer hydrogenation of imines using benzene as solvent and isopropanol as the hydrogen source (Eq. (45)) [76]. These catalytic hydrogenations were typically carried out at 70 °C, and gave >90% yields of the amine in 4 h or less.

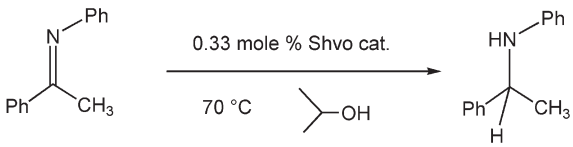

(45)

Ketimines were hydrogenated faster than aldimines, and electron-donating groups accelerated the rate of hydrogenation. The OH and RuH bonds are regenerated by hydrogen transfer to the unsaturated 16-electron Ru complex from isopropanol, generating acetone (Scheme 7.13).

Kinetic studies were carried out by Bäckvall and coworkers at –54 °C on the hydrogenation of a ketimine, which produces a ruthenium complex with a bound amine (Eq. (46)) [77].

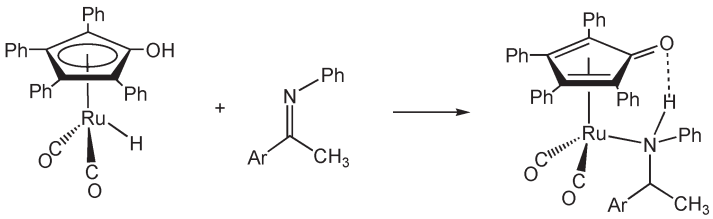

(46)

The crystal structure of an isopropylamine complex of Ru of this type has been reported [78]. Surprisingly, a negligible kinetic isotope effect (k_{RuHOH}/k_{RuDOD} = 1.05 ± 0.14) was found when D labels on both the OH and RuH sites were used,

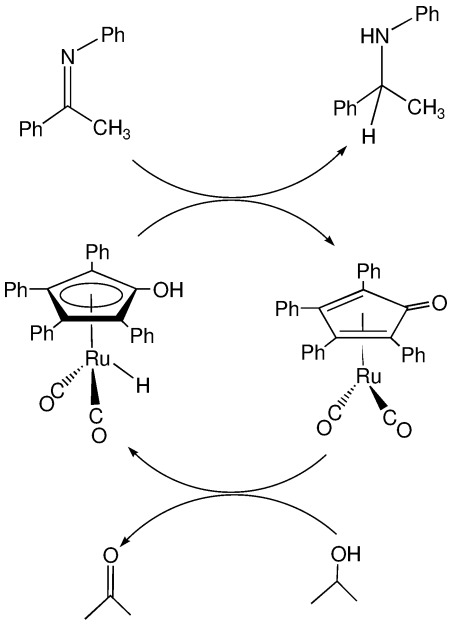

Scheme 7.13

indicating that the rate-determining step does not involve hydrogen transfer. The reaction is first order in amine and also first order in ruthenium. Bäckvall proposed a mechanism involving a ring slip ($\eta^5 \rightarrow \eta^3$) followed by coordination of the imine. Proton transfer from the OH concerted with hydride transfer from the RuH to an η^2-coordinated imine would give the coordinated amine, then rearrangement of the substituted cyclopentadiene ligand to η^4 was proposed to generate the observed product. An alternative mechanism consistent with the data was proposed by Casey and Johnson [79].

Casey and Johnson also reported kinetics and isotope effects for the hydrogenation of imines [79]. Hydrogenation of an electron-deficient imine, *N*-benzilidenepentafluoroaniline, gave the free amine as the organic product. Deuteration of the RuH site gave $k_{RuH}/k_{RuD} = 1.99 \pm 0.13$ at 11 °C, and deuteration of the acidic OH site gave a kinetic isotope effect of $k_{OH}/k_{OD} = 1.57 \pm 0.07$. The experimentally determined combined isotope effect ($k_{RuHOH}/k_{RuDOD} = 3.32 \pm 0.17$) is within experimental uncertainty of the product of the two individual isotope effects ($1.99 \times 1.57 = 3.12$). These observations are similar to those for hydrogenation of the C=O bond discussed above, and the data are consistent with the proposed concerted proton and hydride transfer for this imine hydrogenation.

Examination of a series of imines of differing electronic properties showed that a change in the rate-determining step of this stoichiometric C=N hydrogenation occurs as the imine becomes more electron-rich. Hydrogenation of *N*-isopropyl-(4-methyl)benzilidene amine led to an amine complex of ruthenium. In addition, the C=N hydrogenation was accompanied by isomerization of the imine to a ketimine (Eq. (47)).

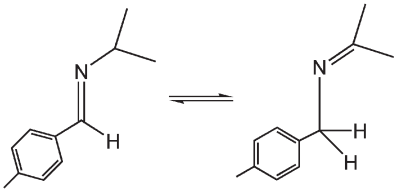

(47)

When the hydrogenation was carried out with RuD labels, scrambling of D into the starting material and product was observed, indicating reversible hydrogen transfer. Hydrogenation of N-benzilidene-*tert*-butylamine was studied; this substrate has no β-hydrogens, so its reactions are not complicated by isomerization or exchange reactivity. Hydrogenation of this imine produces an amine complex (cf. Eq. (46)), and the kinetics at –48 °C were first order in imine and first order in Ru. In contrast to the normal kinetic isotope effects discussed above for the hydrogenation of aldehydes or other imines, inverse isotope effects were observed for the hydrogenation of this electron-rich *tert*-butyl imine. Deuteration of the RuH site resulted in $k_{RuH}/k_{RuD} = 0.64 \pm 0.05$, and this is thought to be due to an inverse equilibrium isotope effect that favors deuterium on the carbon in the reversible transfer between ruthenium and carbon. Deuteration of the acidic OH site gave a kinetic isotope effect of $k_{OH}/k_{OD} = 0.90 \pm 0.07$. The rate-determining step of the reaction is proposed to be coordination of the nitrogen of the amine to the ruthenium. Since the proton and hydride transfers occur prior to the amine coordination, the mechanistic information does not distinguish between concerted or stepwise proton and hydride transfer in this ionic mechanism.

7.4.3
Dehydrogenation of Imines and Alcohols by Shvo Complexes

Remarkably, the same Shvo complex can be used for the catalytic transfer *de*hydrogenation of aromatic amines to give imines (Scheme 7.14) [80]. This reaction produces high yields when carried out for 2–6 h in refluxing toluene with 2 mol.% catalyst. A quinone is used as the hydrogen acceptor, giving the corresponding hydroquinone.

The reaction can be made catalytic in 2,6-dimethoxy-1,4-benzoquinone (20 mol.%) by the addition of 1.5 equiv. MnO_2 to regenerate the quinone from the hydroquinone. Dehydrogenation is the slow step in this reaction; separate experiments had documented that conversion of the benzoquinone to the hydroquinone has a TOF of $> 4000\ h^{-1}$ [81]. Kinetic isotope effects showed that the rate-limiting step was cleavage of the C–H bond, and that the transfer of the two hydrogens is not concerted [82]. The proposed mechanism involved slow β-elimination from a coordinated amine followed by proton transfer to the oxygen of the cyclopentadienone ligand.

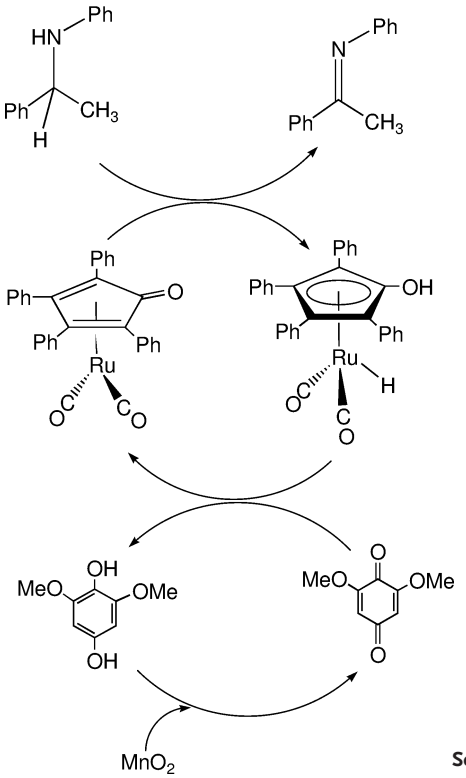

Scheme 7.14

Johnson and Bäckvall reported that the bimetallic Shvo catalyst can also catalyze the transfer dehydrogenation of alcohols (Eq. (48)) [83].

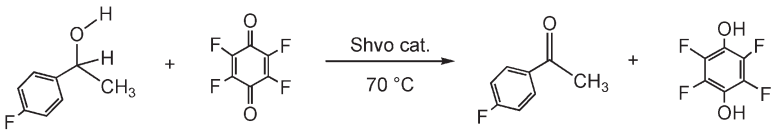

(48)

Using tetrafluorobenzoquinone as the hydrogen acceptor, the kinetics at 70 °C showed that the reaction was first order in alcohol, zero order in the quinone, and half-order in the Ru_2 catalyst. The half-order in bimetallic catalyst is expected in cases where a bimetallic species must dissociate into a monomeric active species. Proton and hydride transfer outside of the coordination sphere of the ruthenium is a possible mechanism, and this is essentially the reverse of the reaction shown in Eq. (42). An alternative mechanism favored by Bäckvall and colleagues [81, 83] and by Menashe and Shvo [84] involves the formation of an alcohol complex which undergoes proton transfer from the alcohol's OH to the oxygen of the ligand, together with β-hydride elimination to form the RuH

bond. Kinetic isotope effects found with deuteration of the OH and CD sites of the alcohol were $k_{CHOH}/k_{CHOD} = 1.87 \pm 0.17$ and $k_{CHOH}/k_{CDOH} = 2.57 \pm 0.26$. This provides evidence for a concerted ionic mechanism, since the experimentally observed isotope effect with both sites labeled ($k_{CHOH}/k_{CDOD} = 4.61 \pm 0.37$) is within experimental uncertainty of the product of the individual isotope effects ($1.87 \times 2.57 = 4.80$). The ability of the Shvo and other ruthenium catalysts to reversibly dehydrogenate alcohols has been used by Bäckvall and coworkers to accomplish the dynamic kinetic resolution of secondary alcohols, where the metal catalyst is used in conjunction with enzymes [85].

7.4.4
Catalytic Hydrogenations with Metal–Ligand Bifunctional Catalysis

The concerted delivery of protons from OH and hydride from RuH found in these Shvo systems is related to the proposed mechanism of hydrogenation of ketones (Scheme 7.15) by a series of ruthenium systems that operate by metal–ligand bifunctional catalysis [86]. A series of Ru complexes reported by Noyori, Ohkuma and coworkers exhibit extraordinary reactivity in the enantioselective hydrogenation of ketones. These systems are described in detail in Chapters 20 and 31, and mechanistic issues of these hydrogenations by ruthenium complexes have been reviewed [87].

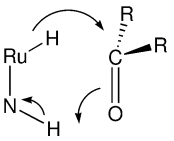

Scheme 7.15

7.5
Catalytic Hydrogenation of Ketones by Strong Bases

As documented throughout this handbook, the diversity of reaction patterns of transition-metal complexes leads to a remarkably rich chemistry, with a tremendous mechanistic diversity in the details of how H_2 is added to unsaturated substrates. Over forty years ago, Walling and Bollyky reported a catalytic hydrogenation of benzophenone that required no transition metal at all! They found that the C=O bond of benzophenone can be catalytically hydrogenated using KO*t*Bu as a base [88], but harsh conditions (200 °C, 100 bar H_2) were used (Eq. (49)). Berkessel et al. recently examined details of this reaction and provided evidence that it was first order in ketone, first order in hydrogen, and first order in base [89].

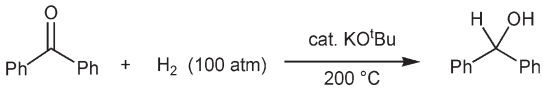

(49)

This ketone hydrogenation is limited to non-enolizable ketones; hydrogenation rates are similar for benzophenone and Ph(C=O)*t*Bu, slower for $(tBu)_2C{=}O$, and still slower for 2,2,5,5-tetramethylcyclopentanone. The relative initial rates as the alkali metal was changed were the same for K^+ and Rb^+ (relative initial rate = 100), slightly faster for Cs^+ (relative initial rate = 105), slower for Na^+ (relative initial rate = 50), and much slower for Li^+ (relative initial rate = 7). The proposed six-membered cyclic transition state is shown in Scheme 7.16. Recent molecular orbital calculations on a simplified model of this system (hydrogenation of formaldehyde by $NaOCH_3$) suggest that the slow rates are due in large part to high entropic barriers to properly assemble and orient the highly ordered transition state required [90].

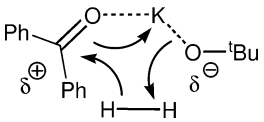

Scheme 7.16

7.6 Conclusion

Ionic hydrogenations are far less developed than hydrogenations that proceed by traditional insertion mechanisms. Despite this later historical development, recent developments have shown that ionic hydrogenations have become more widely recognized, and the prevalence of this area is expected to continue to expand. The development of ionic hydrogenations has benefited immensely from mechanistic experiments on model organometallic complexes. Fundamental studies of the acidity and hydricity of metal hydrides have – and will continue – to play an important role in helping the rational design of ionic hydrogenation catalysts. Both thermodynamic and kinetic studies of acidity and hydricity of metal hydrides are helpful in assessing the specific combinations of ligands and metals that may be suitable for consideration as catalysts. Despite being less extensively developed than other hydrogenation methods, there is burgeoning interest in ionic hydrogenations, and there are numerous promising avenues for future research into this area.

Acknowledgments

Research studies at the Brookhaven National Laboratory were carried out under contract DE-AC02-98CH10886 with the U.S. Department of Energy, and were supported by its Division of Chemical Sciences, Office of Basic Energy Sciences. The author thanks those dedicated postdoctorate scientists who have worked at Brookhaven on ionic hydrogenations, namely Drs. Jeong-Sup Song, Li Luan, Mark Voges, Marcel Schlaf, Prasenjit Ghosh, Barbara Kimmich, and Vladimir Dioumaev.

Abbreviations

DME	dimethoxyethane
HOTf	triflic acid
THF	tetrahydrofuran
TOF	turn over frequency
TON	turn over number

References

1 D.N. Kursanov, Z.N. Parnes, N.M. Loim, *Synthesis* **1974**, 633.
2 D.N. Kursanov, Z.N. Parnes, M.I. Kalinkin, N.M. Loim, *Ionic Hydrogenation and Related Reactions*, Harwood Academic Publishers, New York, **1985**.
3 R.M. Bullock, J.-S. Song, *J. Am. Chem. Soc.* **1994**, *116*, 8602.
4 M.P. Doyle, C.C. McOsker, *J. Org. Chem.* **1978**, *43*, 693.
5 C.T. West, S.J. Donnelly, D.A. Kooistra, M.P. Doyle, *J. Org. Chem.* **1973**, *38*, 2675.
6 M.P. Doyle, D.J. DeBruyn, S.J. Donnelly, D.A. Kooistra, A.A. Odubela, C.T. West, S.M. Zonnebelt, *J. Org. Chem.* **1974**, *39*, 2740.
7 P.T. Anastas, M.M. Kirchhoff, *Acc. Chem. Res.* **2002**, *35*, 686.
8 (a) M.S. Chinn, D.M. Heinekey, N.G. Payne, C.D. Sofield, *Organometallics* **1989**, *8*, 1824–1826; (b) M. Schlaf, A.J. Lough, P.A. Maltby, R.H. Morris, *Organometallics* **1996**, *15*, 2270.
9 T.P. Fong, C.E. Forde, A.J. Lough, R.H. Morris, P. Rigo, E. Rocchini, T. Stephan, *J. Chem. Soc., Dalton Trans.* **1999**, 4475.
10 (a) R.F. Jordan, J.R. Norton, *J. Am. Chem. Soc.* **1982**, *104*, 1255; (b) R.T. Edidin, J.M. Sullivan, J.R. Norton, *J. Am. Chem. Soc.* **1987**, *109*, 3945; (c) S.S. Kristjánsdóttir, A.E. Moody, R.T. Weberg, J.R. Norton, *Organometallics* **1988**, *7*, 1983.
11 E.J. Moore, J.M. Sullivan, J.R. Norton, *J. Am. Chem. Soc.* **1986**, *108*, 2257.
12 S.S. Kristjánsdóttir, J.R. Norton. In: *Transition Metal Hydrides*, A. Dedieu (Ed.), VCH, New York, **1991**, Chapter 9, p. 309.
13 D.E. Berning, B.C. Noll, D.L. DuBois, *J. Am. Chem. Soc.* **1999**, *121*, 11432.
14 (a) D.E. Berning, A. Miedaner, C.J. Curtis, B.C. Noll, M.C. Rakowski DuBois, D.L. DuBois, *Organometallics* **2001**, *20*, 1832; (b) A. Miedaner, J.W. Raebiger, C.J. Curtis, S.M. Miller, D.L. DuBois, *Organometallics* **2004**, *23*, 2670.
15 C.J. Curtis, A. Miedaner, W.W. Ellis, D.L. DuBois, *J. Am. Chem. Soc.* **2002**, *124*, 1918.
16 R. Ciancanelli, B.C. Noll, D.L. DuBois, M.C. Rakowski DuBois, *J. Am. Chem. Soc.* **2002**, 2984.
17 A.J. Price, R. Ciancanelli, B.C. Noll, C.J. Curtis, D.L. DuBois, M.R. DuBois, *Organometallics* **2002**, *21*, 4833.
18 W.W. Ellis, R. Ciancanelli, S.M. Miller, J.W. Raebiger, M.R. DuBois, D.L. DuBois, *J. Am. Chem. Soc.* **2003**, *125*, 12230.
19 J.W. Raebiger, A. Miedaner, C.J. Curtis, S.M. Miller, O.P. Anderson, D.L. DuBois, *J. Am. Chem. Soc.* **2004**, *126*, 5502.
20 K. Abdur-Rashid, T.P. Fong, B. Greaves, D.G. Gusev, J.G. Hinman, S.E. Landau, A.J. Lough, R.H. Morris, *J. Am. Chem. Soc.* **2000**, *122*, 9155.
21 A. Streitwieser, Y.-J. Kim, *J. Am. Chem. Soc.* **2000**, *122*, 11783.
22 J.A. Labinger. In: *Transition Metal Hydrides*, A. Dedieu (Ed.), VCH, New York, **1991**, Chapter 10, p. 361.
23 J.A. Labinger, K.H. Komadina, *J. Organomet. Chem.* **1978**, *155*, C25.
24 M.Y. Darensbourg, C.E. Ash, *Adv. Organomet. Chem.* **1987**, *27*, 1.
25 S.C. Kao, M.Y. Darensbourg, *Organometallics* **1984**, *3*, 646.

26 S.C. Kao, P.L. Gaus, K. Youngdahl, M.Y. Darensbourg, *Organometallics* **1984**, *3*, 1601.
27 P.L. Gaus, S.C. Kao, K. Youngdahl, M.Y. Darensbourg, *J. Am. Chem. Soc.* **1985**, *107*, 2428.
28 C.E. Ash, P.W. Hurd, M.Y. Darensbourg, M. Newcomb, *J. Am. Chem. Soc.* **1987**, *109*, 3313.
29 W. Beck, K. Sünkel, *Chem. Rev.* **1988**, *88*, 1405.
30 (a) G.J. Kubas, *Metal Dihydrogen and σ-Bond Complexes: Structure, Theory, and Reactivity*, Kluwer Academic/Plenum Publishers, New York, **2001**; (b) D.M. Heinekey, W.J. Oldham, Jr., *Chem. Rev.* **1993**, *93*, 913; (c) P.G. Jessop, R.H. Morris, *Coord. Chem. Rev.* **1992**, *121*, 155.
31 E.T. Papish, F.C. Rix, N. Spetseris, J.R. Norton, R.D. Williams, *J. Am. Chem. Soc.* **2000**, *122*, 12235.
32 J.-S. Song, D.J. Szalda, R.M. Bullock, *Inorg. Chim. Acta* **1997**, *259*, 161.
33 L. Luan, J.-S. Song, R.M. Bullock, *J. Org. Chem.* **1995**, *60*, 7170.
34 R.M. Bullock, J.-S. Song, D.J. Szalda, *Organometallics* **1996**, *15*, 2504.
35 J.-J. Brunet, R. Chauvin, P. Leglaye, *Eur. J. Inorg. Chem.* **1999**, 713.
36 M.Y. Darensbourg, *Prog. Inorg. Chem.* **1985**, *33*, 221.
37 D.H. Gibson, Y.S. El-Omrani, *Organometallics* **1985**, *4*, 1473.
38 (a) T. Ito, M. Koga, S. Kurishima, M. Natori, N. Sekizuka, K. Yoshioka, *J. Chem. Soc., Chem. Commun.* **1990**, 988; (b) M. Minato, Y. Fujiwara, M. Koga, N. Matsumoto, S. Kurishima, M. Natori, N. Sekizuka, K. Yoshioka, T. Ito, *J. Organomet. Chem.* **1998**, *569*, 139.
39 S.M. Geraty, P. Harkin, J.G. Vos, *Inorg. Chim. Acta* **1987**, *131*, 217.
40 W.D. Harman, H. Taube, *J. Am. Chem. Soc.* **1990**, *112*, 2261.
41 J.-S. Song, D.J. Szalda, R.M. Bullock, C.J.C. Lawrie, M.A. Rodkin, J.R. Norton, *Angew. Chem., Int. Ed. Engl.* **1992**, *31*, 1233.
42 J.-S. Song, D.J. Szalda, R.M. Bullock, *Organometallics* **2001**, *20*, 3337.
43 V.I. Bakhmutov, E.V. Vorontsov, D.Y. Antonov, *Inorg. Chim. Acta* **1998**, *278*, 122.
44 R.J. Kinney, W.D. Jones, R.G. Bergman, *J. Am. Chem. Soc.* **1978**, *100*, 7902.
45 J.-F. Reynoud, J.-F. Leboeuf, J.-C. Leblanc, C. Moïse, *Organometallics* **1986**, *5*, 1863.
46 C. Bianchini, C. Mealli, A. Meli, M. Peruzzini, F. Zanobini, *J. Am. Chem. Soc.* **1988**, *110*, 8725.
47 (a) D.M. Heinekey, A. Liegeois, M. van Roon, *J. Am. Chem. Soc.* **1994**, *116*, 8388; (b) D.M. Heinekey, M. van Roon, *J. Am. Chem. Soc.* **1996**, *118*, 12134.
48 P.A. Tooley, C. Ovalles, S.C. Kao, D.J. Darensbourg, M.Y. Darensbourg, *J. Am. Chem. Soc.* **1986**, *108*, 5465.
49 L. Markó, Z. Nagy-Magos, *J. Organomet. Chem.* **1985**, *285*, 193.
50 T. Fuchikami, Y. Ubukata, Y. Tanaka, *Tetrahedron Lett.* **1991**, *32*, 1199.
51 J.-J. Brunet, *Eur. J. Inorg. Chem.* **2000**, 1377.
52 C. Balzarek, T.J.R. Weakley, D.R. Tyler, *J. Am. Chem. Soc.* **2000**, *122*, 9427.
53 C. Balzarek, T.J.R. Weakley, L.Y. Kuo, D.R. Tyler, *Organometallics* **2000**, *19*, 2927.
54 C. Balzarek, D.R. Tyler, *Angew. Chem., Int. Ed.* **1999**, *38*, 2406.
55 L.Y. Kuo, T.J.R. Weakley, K. Awana, C. Hsia, *Organometallics* **2001**, *20*, 4969.
56 L.Y. Kuo, D.M. Finigan, N.N. Tadros, *Organometallics* **2003**, *22*, 2422.
57 (a) R.M. Bullock, M.H. Voges, *J. Am. Chem. Soc.* **2000**, *122*, 12594; (b) M.H. Voges, R.M. Bullock, *J. Chem. Soc., Dalton Trans.* **2002**, 759.
58 T.-Y. Cheng, B.S. Brunschwig, R.M. Bullock, *J. Am. Chem. Soc.* **1998**, *120*, 13121.
59 I.M. Kolthoff, M.K. Chantooni, Jr., *J. Am. Chem. Soc.* **1973**, *95*, 8539.
60 K.-T. Smith, J.R. Norton, M. Tilset, *Organometallics* **1996**, *15*, 4515.
61 (a) B.F.M. Kimmich, P.J. Fagan, E. Hauptman, R.M. Bullock, *Chem. Commun.* **2004**, 1014; (b) B.F.M. Kimmich, P.J. Fagan, E. Hauptman, W.J. Marshall, R.M. Bullock, *Organometallics* **2005**, *24*, 6220.
62 J.M. DeSimone, *Science* **2002**, *297*, 799.
63 (a) G.W.V. Cave, C.L. Raston, J.L. Scott, *J. Chem. Soc., Chem. Commun.* **2001**, 2159; (b) J.M. Thomas, R. Raja,

G. Sankar, B. F. G. Johnson, D. W. Lewis, *Chem. Eur. J.* **2001**, *7*, 2973.

64 (a) A. J. Arduengo, III, *Acc. Chem. Res.* **1999**, *32*, 913; (b) D. Bourissou, O. Guerret, F. P. Gabbaï, G. Bertrand, *Chem. Rev.* **2000**, *100*, 39; (c) W. A. Herrmann, *Angew. Chem., Int. Ed.* **2002**, *41*, 1290; (d) C. M. Crudden, D. P. Allen, *Coord. Chem. Rev.* **2004**, *248*, 2247.

65 V. K. Dioumaev, D. J. Szalda, J. Hanson, J. A. Franz, R. M. Bullock, *Chem. Commun.* **2003**, 1670.

66 V. K. Dioumaev, R. M. Bullock, *Nature* **2003**, *424*, 530.

67 M. Aresta, A. Dibenedetto, I. Pápai, G. Schubert, A. Macchioni, D. Zuccaccia, *Chem. Eur. J.* **2004**, *10*, 3708.

68 (a) M. P. Magee, J. R. Norton, *J. Am. Chem. Soc.* **2001**, *123*, 1778; (b) H. Guan, M. Imura, M. P. Magee, J. R. Norton, G. Zhu, *J. Am. Chem. Soc.* **2005**, *127*, 7805.

69 H. Guan, M. Iimura, M. P. Magee, J. R. Norton, K. E. Janak, *Organometallics* **2003**, 4084.

70 Y. Shvo, D. Czarkie, Y. Rahamim, D. F. Chodosh, *J. Am. Chem. Soc.* **1986**, *108*, 7400.

71 Y. Blum, D. Czarkie, Y. Rahamim, Y. Shvo, *Organometallics* **1985**, *4*, 1459.

72 C. P. Casey, S. W. Singer, D. R. Powell, R. K. Hayashi, M. Kavana, *J. Am. Chem. Soc.* **2001**, *123*, 1090.

73 (a) R. M. Bullock, B. R. Bender. In: *Encyclopedia of Catalysis*, I. Horváth (Ed.), Wiley, New York, **2002**; (b) R. M. Bullock. In: *Transition Metal Hydrides*, A. Dedieu (Ed.), VCH, New York, **1991**, Chapter 8, p. 263.

74 N. Menashe, E. Salant, Y. Shvo, *J. Organomet. Chem.* **1996**, *514*, 97.

75 C. P. Casey, S. W. Singer, D. R. Powell, *Can. J. Chem.* **2001**, *79*, 1002.

76 J. S. M. Samec, J.-E. Bäckvall, *Chem. Eur. J.* **2002**, *8*, 2955.

77 J. S. M. Samec, A. H. Éll, J.-E. Bäckvall, *Chem. Commun.* **2004**, 2748.

78 C. P. Casey, G. A. Bikzhanova, J.-E. Bäckvall, L. Johansson, J. Park, Y. H. Kim, *Organometallics* **2002**, *21*, 1955.

79 C. P. Casey, J. B. Johnson, *J. Am. Chem. Soc.* **2005**, *127*, 1883.

80 A. H. Éll, J. S. M. Samec, C. Brasse, J.-E. Bäckvall, *Chem. Commun.* **2002**, 1144.

81 G. Csjernyik, A. H. Éll, L. Fadini, B. Pugin, J.-E. Bäckvall, *J. Org. Chem.* **2002**, *67*, 1657.

82 A. H. Éll, J. B. Johnson, J.-E. Bäckvall, *Chem. Commun.* **2003**, 1652.

83 J. B. Johnson, J.-E. Bäckvall, *J. Org. Chem.* **2003**, *68*, 7681.

84 N. Menashe, Y. Shvo, *Organometallics* **1991**, *10*, 3885.

85 F. F. Huerta, A. B. E. Minidis, J.-E. Bäckvall, *Chem. Soc. Rev.* **2001**, *30*, 321.

86 R. Noyori, M. Yamakawa, S. Hashiguchi, *J. Org. Chem.* **2001**, *66*, 7931.

87 S. E. Clapham, A. Hadzovic, R. H. Morris, *Coord. Chem. Rev.* **2004**, *248*, 2201.

88 (a) C. Walling, L. Bollyky, *J. Am. Chem. Soc.* **1961**, *83*, 2968; (b) C. Walling, L. Bollyky, *J. Am. Chem. Soc.* **1964**, *86*, 3750.

89 A. Berkessel, T. J. S. Schubert, T. N. Müller, *J. Am. Chem. Soc.* **2002**, *124*, 8693.

90 B. Chan, L. Radom, *J. Am. Chem. Soc.* **2005**, *127*, 2443.

91 W. W. Ellis, J. W. Raebiger, C. J. Curtis, J. W. Bruno, D. L. DuBois, *J. Am. Chem. Soc.* **2004**, *126*, 2738.

92 X.-M. Zhang, J. W. Bruno, E. Enyinnaya, *J. Org. Chem.* **1998**, *63*, 4671.

93 T.-Y. Cheng, R. M. Bullock, *Organometallics* **2002**, *21*, 2325.

8
Homogeneous Hydrogenation by Defined Metal Clusters

Roberto A. Sánchez-Delgado

8.1
Introduction

The catalytic potential of well-defined transition-metal clusters in homogeneous reactions has attracted a great deal of attention over the years, as they represent a natural bridge between mononuclear complexes, metal nanoparticles, and metal-oxide, -sulfide and related surfaces used in heterogeneous catalysis. The molecular nature of metal clusters, together with their solubility properties, provides the advantages of classical mononuclear homogeneous catalysts (high activity, high selectivity, moderate operating conditions, possibility of catalyst design and modification), while the polynuclear framework can offer the possibility of multi-metallic cooperative effects often identified as a key element in the desirable properties of solid heterogeneous catalysts. Therefore, metal clusters can be expected, in principle, to combine the positive aspects of homogeneous and heterogeneous catalytic reactions and, perhaps more importantly, they may react through unique pathways associated with the cluster structures and thereby catalyze reactions not accessible by mononuclear or heterogeneous catalysts. Nevertheless, despite the impressive amount of work that has been devoted to develop these concepts over several decades, the great expectations first advanced during the mid-1970s have not yet been fully accomplished [1–6].

From a different perspective, well-defined metal clusters have served as useful models for discerning the complex mechanisms of heterogeneous catalytic systems. The structural trends for metal clusters are now well understood, and their reactions in solution can be studied in detail by relatively simple chemical and spectroscopic methods, thereby producing important information at the molecular level – something that is very difficult to achieve on solid catalysts. The knowledge thus gained from studying metal cluster chemistry can be extrapolated, with adequate caution, to heterogeneous reactions [1–6].

Another trend that has received considerable recent attention is the decomposition of metal clusters under controlled conditions on solid supports or on liquid suspensions, which generates small metallic particles of specific size, struc-

The Handbook of Homogeneous Hydrogenation.
Edited by J.G. de Vries and C.J. Elsevier
Copyright © 2007 WILEY-VCH Verlag GmbH & Co. KGaA, Weinheim
ISBN: 978-3-527-31161-3

ture or composition, displaying interesting catalytic features [7]. Although this is perhaps the area in which cluster chemistry has had the highest impact, such methods lead unambiguously to *heterogeneous* systems, and therefore it falls beyond the scope of this book.

Homogeneous hydrogenation has been one of the most frequently studied classes of reactions in an effort to demonstrate the principles of cluster catalysis and its links to heterogeneous catalysis. A good number of well-defined metal clusters have been claimed to promote hydrogen addition to C=C, C≡C, C=O bonds and aromatic rings, and a number of detailed mechanistic studies have been conducted. Many of these catalysts have later been shown to be mononuclear or heterogeneous in nature, but some others have proved to induce truly homogeneous cluster-catalyzed reactions. For the purpose of the discussion that follows, the classical definition of a cluster as a compound containing at least three metal atoms [8] will be adopted. Also, the concept of *cluster catalysis* is associated here to reaction mechanisms involving only polynuclear intermediates, regardless of whether the important interactions take place at only one or at several metal atoms.

8.1.1
Is a Cluster the Real Catalyst? Fragmentation and Aggregation Phenomena

One of the key points in discussing cluster catalysis is to determine whether a cluster is actually catalyzing the hydrogenation reaction, or if instead a mononuclear entity derived from cluster fragmentation, or metallic nanoparticles resulting from decomposition and aggregation are responsible for the catalytic transformation. An ideal model reaction would involve bonding of the substrate to more than one metal atom, so that if the cluster becomes degraded in the process, the catalytic activity would be lost. Nevertheless, sensible hydrogenation cycles have been proposed in which the cluster framework is maintained but the substrate does not need to bind to more than one metal atom in order to be transformed. In such cases it is difficult to ascertain which is the true catalytically active species. Several methods have been used to address the two questions that need to be answered:

- Is the catalyst truly homogeneous?
- If so, is the catalyst really a cluster?

Finke and coworkers have extensively addressed the question of homogeneous versus heterogeneous catalysis, and have provided a rather complex (but extremely reliable) set of experiments that allow the distinction of a molecular catalyst in solution from a suspended nanostructured metallic material [9]. The generation of metallic particles from metal complexes under a highly reducing hydrogen atmosphere is now recognized as a frequent phenomenon, particularly in arene hydrogenation studies [9, 10].

Once the homogeneity of a reaction has been established, it is never easy to determine the precise nuclearity of the active species, and a series of indicators or qualitative tests has been proposed [11]. Many publications provide as evi-

dence for cluster catalysis simple statements such as "… the cluster was quantitatively recovered at the end of the reaction" or "… the cluster was the only species observed by IR or NMR spectroscopy". This type of assumption can be very misleading; it suffices to have 1% or less of the cluster transform into highly active mononuclear fragments or metallic particles in order to develop a high hydrogenation activity. Such small amounts of very reactive species easily go unnoticed in *in-situ* spectroscopic studies, and would certainly not be accounted for in a "quantitative" recovery of the cluster at the end of the reaction.

In order to establish the participation of a cluster, the best approach is to use a combination of experiments:

- Kinetic measurements, particularly the study of the rate-dependence on *cluster* concentration can be very informative; cluster-catalyzed reactions often display a first-order rate dependence on *cluster* concentration, whereas fractional or complex orders of reaction are associated with fragmentation processes.
- Reactions that are much faster than the analogous one catalyzed by a mononuclear complex, or that lead to different products or selectivities, are more likely to involve cluster intermediates.
- Heterobimetallic complexes that induce reactions at significantly faster rates than (or notably different product selectivities from) monometallic derivatives are probably genuine cluster catalysts.
- Edge- and face-capping chelating ligands have been proposed as a method to guarantee the stability of the cluster framework.
- Another interesting idea that has been explored without much success so far is the use of clusters with a chiral metal framework as catalysts for asymmetric hydrogenation, since only the intact cluster would induce enantioselectivity.
- NMR studies involving *para*-hydrogen has recently been introduced as a powerful tool to obtain direct evidence for cluster catalysis (*vide infra*).

This chapter reviews the literature involving well-defined molecular metal clusters as hydrogenation catalysts or catalyst precursors, with particular emphasis being placed on those systems that are likely to involve only or predominantly cluster intermediates throughout the hydrogenation cycle. The mechanisms in cases where cluster catalysis is strongly supported by experimental evidence are discussed in more detail.

8.2 Hydrogenation of C=C Bonds

Early investigations by Shapley [12], Basset [13], and Gladfelter [14] provided the first convincing examples of C=C bond hydrogenation cycles involving metal clusters; these are shown in Schemes 8.1–8.3. Shapley's mechanisms for [$Os_3H_2(CO)_{10}$] was based on experiments performed under noncatalytic conditions, involving the isolation and/or NMR observation of all the species implicated in the cycle depicted in Scheme 8.1, as well as the pathways for their interconversion.

Basset's proposal for the silica-supported cluster $[Os_3(CO)_{10}(\mu\text{-}H)(\mu\text{-}OSi\equiv)]$ was made on the basis of surface IR spectroscopy studies, kinetic and gas uptake measurements, and reactions of the soluble analogue $[Os_3\ (CO)_{10}(\mu\text{-}H)(\mu\text{-}OSi\text{-}Ph)]$; the supported catalyst hydrogenated ethylene at 90 °C and atmospheric pressure in a flow reactor at a TOF of 144 h^{-1} for extended periods of time, achieving up to 24 000 turnovers overall. Gladfelter also used kinetic measurements and IR spectroscopy to deduce the mechanism of alkene hydrogenation by anionic clusters containing isocyanate ligands $[Ru_3(\mu\text{-}NCO)\ (CO)_{10}]^-$; this catalyst reduced 3,3-dimethylbutene at rates of about 300 to 360 turnovers h^{-1} under ambient conditions. The same group also characterized intermediates and individual reactions of the more stable, but catalytically less active, osmium analogue $[Os_3(\mu\text{-}NCO)(CO)_{10}]^-$ (eight turnovers after 24 h at 78 °C and 3.3 bar H_2 for 3,3-dimethylbutene hydrogenation). Although these are important pioneering cases from a fundamental point of view, they are of no practical use because catalytic activities were low and the scope of the reactions was limited.

Sánchez-Delgado et al. reported a comparative study of the hydrogenation of 1-hexene by use of $[Ru_3(CO)_{12}]$ in solution and supported on silica; IR evidence pointed to cluster catalysis in solution [turnover frequency (TOF) ca. 200 h^{-1} at 90 °C and 40 bar H_2] and to the formation of mononuclear species on the silica surface (TOF ca. 600 h^{-1} at 90 °C and 40 bar H_2) [15]. Another early proposal for a cluster-catalyzed reaction was provided by Doi et al. for $[H_4Ru_4(CO)_{12}]$ in the

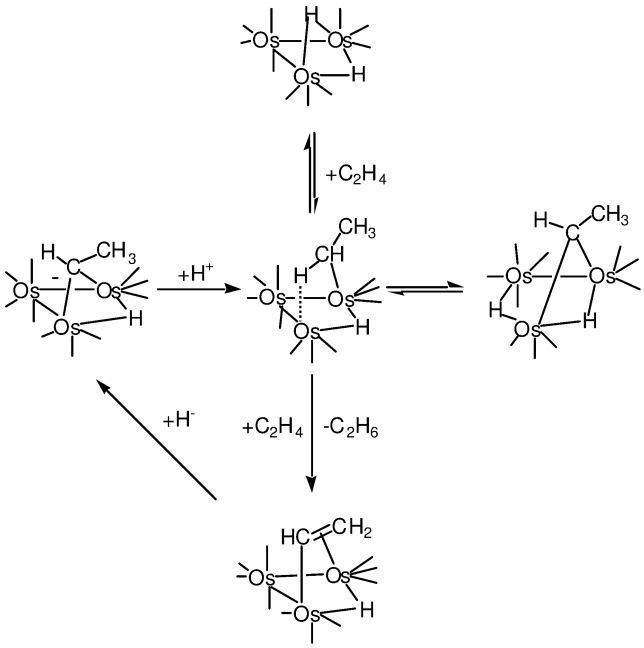

Scheme 8.1 Mechanism for the hydrogenation of alkenes catalyzed by $[Os_3H_2(CO)_{10}]$ (CO ligands omitted for clarity).

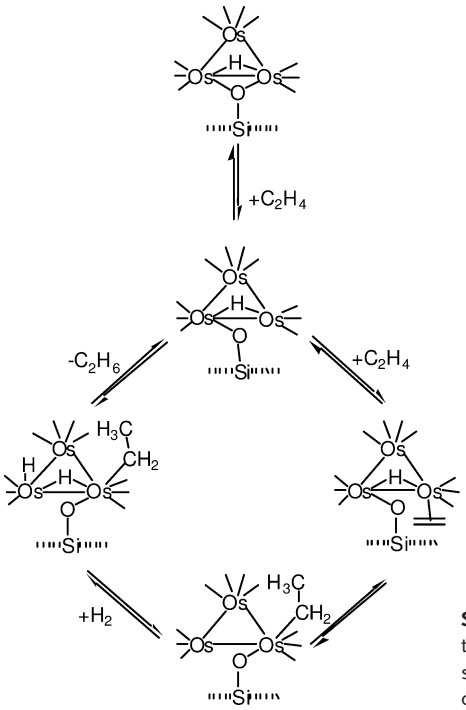

Scheme 8.2 Mechanism for the hydrogenation of ethylene catalyzed by silica-supported osmium clusters (CO ligands omitted for clarity).

hydrogenation of ethylene (TOF 40 h^{-1} at 72 °C, 0.13 bar H_2, and 0.26 atm ethylene). Kinetic measurements were in agreement with a mechanism involving Eqs. (1)–(3); in particular, a first-order dependence of the reaction rate on cluster concentration was taken as evidence of cluster catalysis, although the hydrogenation cycle involved a single Ru atom [16].

$$H_4Ru_4(CO)_{11} + H_2 \rightleftharpoons H_6Ru_4(CO)_{11} \quad (1)$$

$$H_4Ru_4(CO)_{11} + C_2H_4 \rightleftharpoons H_3Ru_4(CO)_{11}(C_2H_5) \quad (2)$$

$$H_3Ru_4(CO)_{11}(C_2H_5) + H_2 \rightleftharpoons H_4Ru_4(CO)_{11} + C_2H_6 \quad (3)$$

Related studies by Sánchez-Delgado and coworkers on the kinetics of the hydrogenation of styrene (140 °C, 1.05 bar H_2) catalyzed by the tetranuclear Os clusters $[H_4Os_4(CO)_{12}]$ (TOF 87 h^{-1}), $[H_3Os_4(CO)_{12}]^-$ (TOF 52 h^{-1}), $[H_3Os_4(CO)_{12}I]$ (TOF 583 h^{-1}), and $[H_2Os_4(CO)_{12}I]^-$ (TOF 63 h^{-1}), pointed to cluster fragmentation as being responsible for the catalytic activity of these systems, which conclusion was based on a complex rate-dependence on cluster concentration and the similarity of the hydrogenation rate when a mononuclear Os complex was employed [17].

Phosphine-substituted complexes have shown promise for cluster catalysis, especially in the case of chelating ligands, because of the added stability that might help avoid cluster fragmentation. Bergounhou et al. reported a detailed study of the hy-

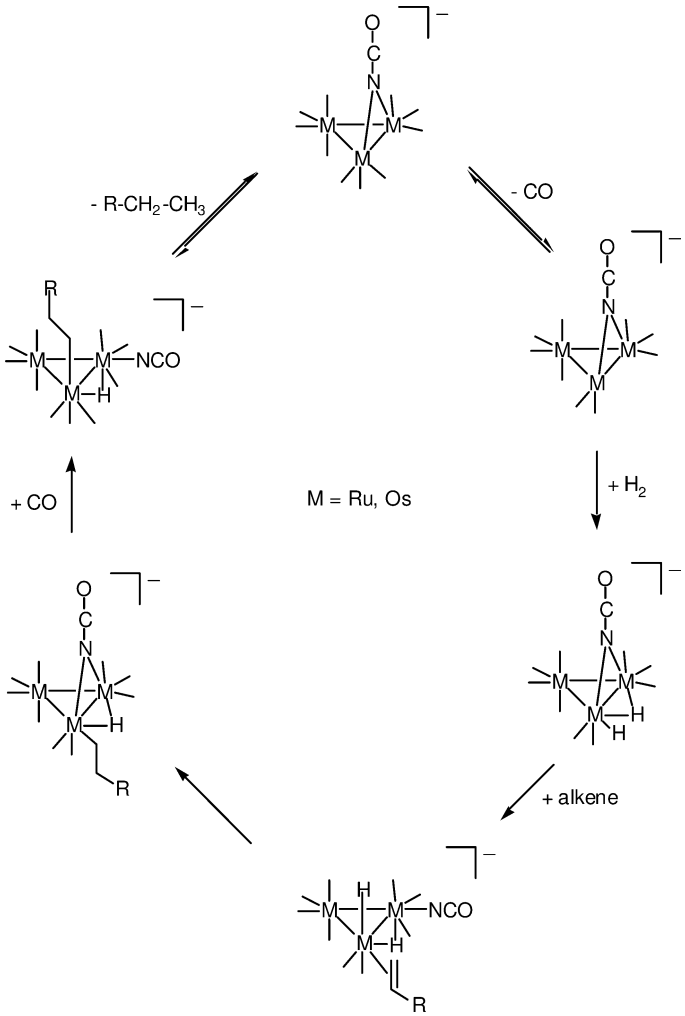

Scheme 8.3 Mechanism for the hydrogenation of alkenes catalyzed by anion-promoted osmium clusters (CO ligands omitted for clarity).

drogenation of 1-hexene by $[Ru_3(\mu\text{-}H)_2(\mu^3\text{-}O)(CO)_5(dppm)_2]$ (TOF ca. 25 200 h^{-1}), and provided kinetic and spectroscopic evidence for the cycle depicted in Scheme 8.4, in which a Ru–Ru bond is broken but the cluster integrity is maintained by the oxo and diphosphine ligands [18]. Further catalytic studies with $[Ru_3(CO)_{12}]$ substituted with chelating diphosphines were provided by Fontal et al. [19], and with PPh_3 by Dallmann and Buffon [20]. The suggestion was that the reactions proceed through cluster intermediates, although C=C bond hydrogenation was accompanied by extensive isomerization and no details of reaction mechanisms were provided. Clusters derived from $[H_4Ru_4(CO)_{12}]$ by substitution with *chiral* dipho-

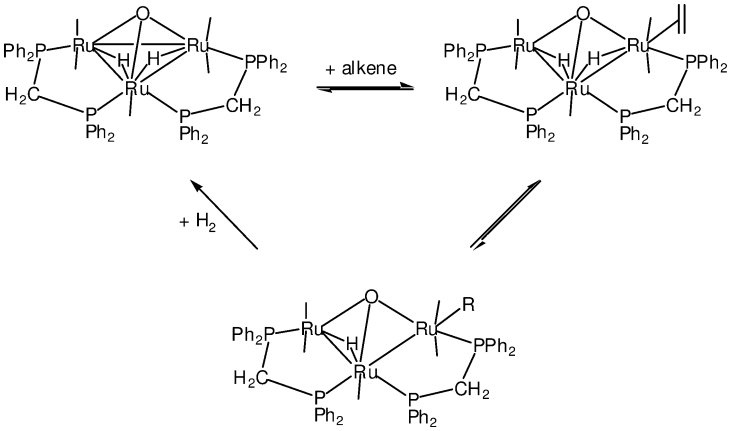

Scheme 8.4 Mechanism for the hydrogenation of alkenes catalyzed by ruthenium clusters stabilized by edge-bridging diphosphine ligands (CO ligands omitted for clarity).

sphines exhibited reasonable activities (TOF up to 60 000 h^{-1}) and moderate enantioselectivities (6 to 46% ee) in the hydrogenation of α,β-unsaturated carboxylic acids. Although the clusters were generally "recovered intact" at the end of the reactions, the participation of mononuclear species cannot be ruled out [21, 22].

Moura et al. recently reported the first example of the use of Ir clusters in homogeneous diene hydrogenation [23]. $[Ir_4(CO)_{11}(PPh_2H)]$, $[Ir_4(CO)_8(\mu^3\text{-}\eta^2\text{-}HCCPh)(\mu\text{-}PPh_2)_2]$, $[Ir_4(CO)_9(\mu^3\text{-}\eta^3\text{-}Ph_2PC(H)CPh)(\mu\text{-}PPh_2)]$, and $[Ir_4(CO)_{12}]$ selectively reduce 1,5-cyclooctadiene to cyclooctene with high activities [average turnover number (TON) 2816], in contrast with mononuclear or metallic Ir catalysts, which quickly yielded the fully reduced product cyclooctane; this is strongly indicative of a cluster-catalyzed reaction. All the complexes lose the phosphine ligands during the course of the reactions to produce a common active species likely related to $[Ir_4(CO)_5(C_8H_{12})_2(C_8H_{10})]$; an "anchor-type" interaction between the two C=C bonds of the diene to one Ir atom allows the activation and hydrogenation of only one of those bonds by the cluster.

Much emphasis has been placed in recent times on easily recoverable liquid biphasic catalysts, including metal clusters in nonconventional solvents. For instance, aqueous solutions of the complexes $[Ru_3(CO)_{12\text{-}x}(TPPTS)_x]$ (x = 1, 2, 3; TPPTS = triphenylphosphine-trisulfonate, $P(m\text{-}C_6H_4SO_3Na)_3$) catalyze the hydrogenation of simple alkenes (1-octene, cyclohexene, styrene) at 60 °C and 60 bar H_2 at TOF up to 500 h^{-1} [24], while $[Ru_3(CO)_9(TPPMS)_3]$ (TPPMS = triphenylphosphine-monosulfonate, $PPh_2(m\text{-}C_6H_4SO_3Na)$ is an efficient catalyst precursor for the aqueous hydrogenation of the C=C bond of acrylic acid (TOF 780 h^{-1} at 40 °C and 3 bar H_2) and other activated alkenes [25]. The same catalysts proved to be poorly active in room temperature ionic liquids such as $[bmim][BF_4]$ (bmim = 1-butyl-3-methylimidazolium). No details about the active species involved are known at this point.

Well-known anionic clusters such as $[HFe_3(CO)_{11}]^-$, $[HWOs_3(CO)_{14}]^-$, $[H_3Os_4(CO)_{12}]^-$, and $[Ru_6C(CO)_{16}]^{2-}$ have also been tested as catalyst precursors in the hydrogenation of styrene in [bmim][BF_4], and in organic solvents such as octane and methanol [26]. The activity of the Fe cluster is the lowest of the series, and that for Ru is the highest, but the robust Ru_6 cluster was found to decompose under the reaction conditions to metallic particles, which are responsible for the catalytic activity. The WOs_3 and Os_4 clusters are much more active in the ionic liquid than in octane or methanol, and the improvement in activities (TOF 30 000 h^{-1}) was associated with increased stability of the clusters in the ionic medium, although no detailed mechanistic studies were conducted.

8.3 Hydrogenation of C≡C Bonds

The hydrogenation of alkynes is a very interesting reaction, since the selectivity toward the partially or the fully reduced product allows the *in-situ* comparison of the ability of a catalyst to reduce C≡C versus C=C bonds. This is perhaps the area in which cluster catalysis has been most extensively developed, as recently reviewed by Cabeza [27], Adams and Captain [4], and Dyson [28]. A good number of metal clusters have been employed as catalyst precursors in alkyne hydrogenation, the majority of them containing ruthenium.

Early studies by Valle and coworkers showed that $[Ru_3(CO)_{12}]$ [29], $[H_4Ru_4(CO)_{12}]$ [30], and the phosphine- and phosphite-substituted derivatives $[H_4Ru_4(CO)_{12-n}(PR_3)_n]$ (R = Bu^n, Ph, OEt, OPh) (n = 1–3) [31] hydrogenate 1-pentyne and 2-pentyne efficiently at 80 °C and 1 atm H_2 to the corresponding alkenes; the internal C≡C bond is reduced more rapidly than the terminal one. Reaction rates increased with increasing number of P-donor ligands for the hydrogenation of 1-pentyne and decreased for 2-pentyne; rates were also increased with increasing basicity of the phosphine or phosphite. The complexes also promote C=C bond migration, and therefore 1-pentene, *cis*-2-pentene and *trans*-2-pentene are observed during the course of the reaction. Consecutive hydrogenation of the alkenes to *n*-pentane takes place only after the alkyne has been completely consumed. No attempt was made then to identify reaction intermediates or the catalytic mechanism, although common pathways were presumed for both complexes. The same clusters $[Ru_3(CO)_{12}]$, $[H_4Ru_4(CO)_{12}]$ [32], the related complex $[H_2Ru_4(CO)_{13}]$ [33, 34], and the diphenylphosphine and diphenylphosphido derivatives $[H_4Ru_4(CO)_{12-n}(PPh_2H)_n]$ (n = 1–3), $[Ru_3(\mu\text{-}H)(\mu\text{-}PPh_2)_n(CO)_{11-n}]$ (n = 1, 3), $[Ru_3(\mu\text{-}H)_{2-n}(\mu\text{-}PPh_2)_{2+n}(CO)_{8-n}]$ (n = 0, 1), and $[Ru_4(\mu^3\text{-}PPh)(CO)_{13}]$ [33–38] were evaluated by the group of Sappa and found to hydrogenate *tert*-butylacetylene and diphenylacetylene at 120 °C and 1 atm H_2 (TOF 200–400 h^{-1}) to a mixture of *cis*- and *trans*-stilbene; complete hydrogenation to the alkane was not observed in this case, and the dihydride displayed the slowest rate. The direct participation of cluster structures in the catalytic cycle was suggested by the isolation of some intermediates that could be used as catalyst precursors with essentially the same activity.

Long-awaited direct evidence for cluster catalysis has recently been provided using *para* hydrogen induced polarization (PHIP) NMR techniques (see Chapter 12); hydride transfer to coordinated organic fragments and fluxional processes were shown to occur on metal clusters [39, 40]. When such methods were applied to the hydrogenation of alkenes and alkynes by $[Os_3(\mu\text{-}H)_2(CO)_{10}]$, $Ru_3(CO)_{10}L_2$ ($L = PPh_3$, PMe_2Ph, dppe), several active intermediates could be identified, including clusters and mononuclear species. It was further demonstrated that the catalytic route is dependent on the solvent; cluster catalysis is preferred in polar media and in that case, the active species are produced either by CO dissociation or, more slowly, by phosphine dissociation, which generates the vacant coordination site required for the alkene or alkyne to bind. In nonpolar media, fragmentation to a mononuclear complex was observed, and this complex actually competes with the clusters in the hydrogenation cycle (Scheme 8.5). Interestingly, for the phosphido-bridged cluster $[Ru_3(CO)_9(\mu\text{-}H)(\mu\text{-}PPh_2)]$, similar experiments show that, independently of the solvent used, only cluster catalysis takes place, according to Scheme 8.6 [41].

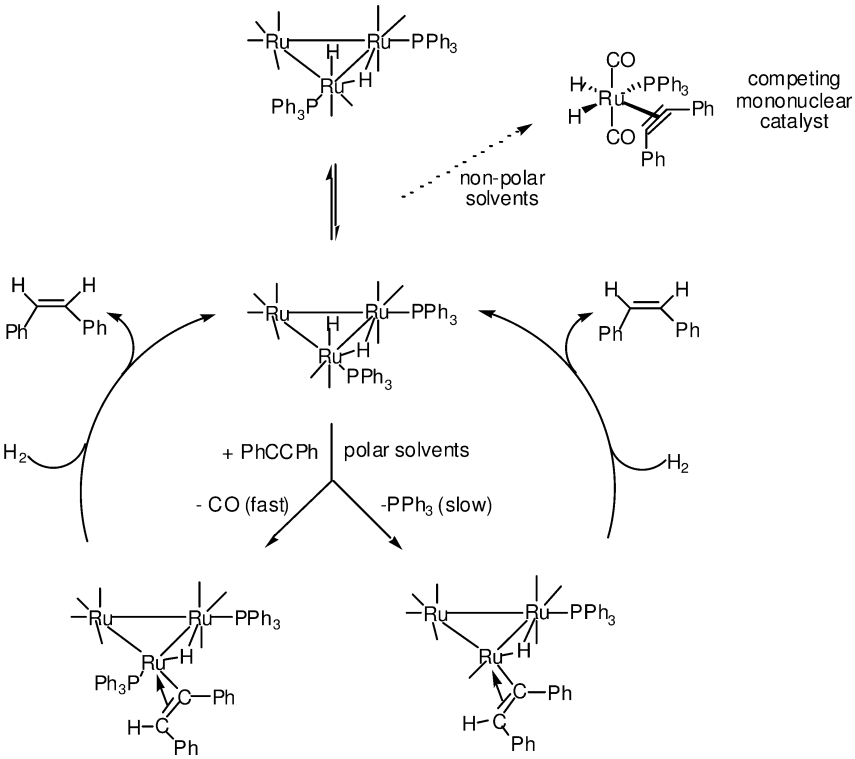

Scheme 8.5 Main species involved in the hydrogenation of diphenylacetylene catalyzed by ruthenium clusters, as determined by PHIP methods (CO ligands omitted for clarity).

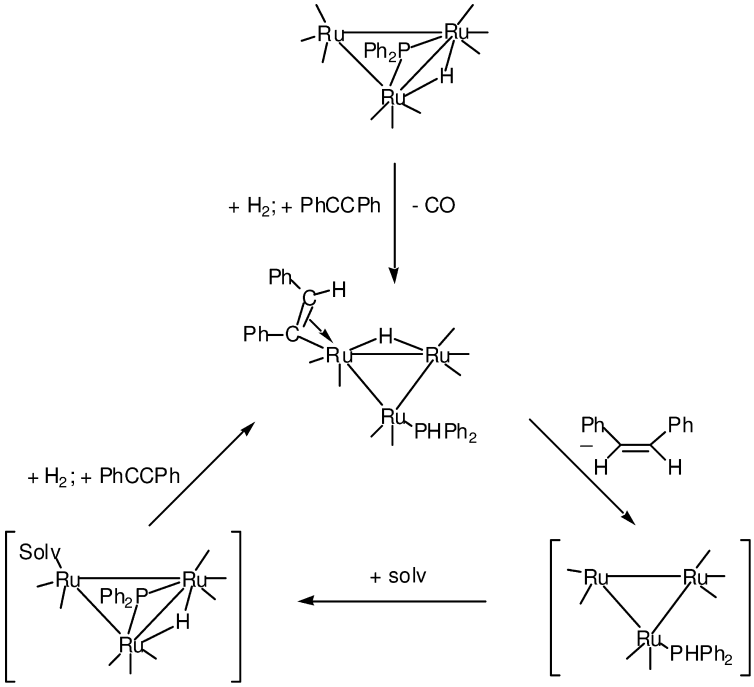

Scheme 8.6 Mechanism for the hydrogenation of diphenylacetylene catalyzed by ruthenium clusters containing phosphido bridging ligands, as determined by PHIP methods (CO ligands omitted for clarity).

The Cp derivative $[Ru_3Cp_2(\mu^3\text{-}Ph_2C_2)(CO)_5]$ [42] also hydrogenates diphenylacetylene and 3-hexyne, but fragmentation probably takes place in this case to an important extent.

Cabeza and coworkers have extensively investigated the catalytic hydrogenation of alkynes by metal clusters substituted with N-donor ligands. Diphenylacetylene hydrogenation is induced by $[Ru_3(\mu\text{-}H)(\mu\text{-dmdab})(CO)_9]$ (Hdmdab = 3,5-dimethyl-1,2-diaminobenzene), but the catalytic activity is thought to be due to an unidentified mononuclear fragment [43]. This indicates that edge-bridging bidentate N-donor ligands do not stabilize the cluster structure sufficiently to avoid fragmentation. On the other hand, face-bridging N-donor ligands derived from 2-amino-6-methylpyridine (Hampy) do seem to stabilize clusters enough to maintain the polynuclear structure throughout a catalytic cycle. The complexes $[Ru_3(\mu\text{-}H)(\mu_3\text{-ampy})(CO)_9]$, $[Ru_6(\mu\text{-}H)_6(\mu^3\text{-ampy})(CO)_{14}]$, and their acetylene and phosphine derivatives [44–50], hydrogenate diphenylacetylene selectively to mixtures of *E*- and *Z*-stilbene readily at 80 °C and sub-atmospheric H_2 pressure (TOF 27 h^{-1}), as well as phenylacetylene to styrene under more forcing conditions (100 °C, 15 bar H_2). A related cluster containing the 2-anilinopyridine ligand has also been reported to hydrogenate phenyl-1-propyne [51]. Scheme 8.7

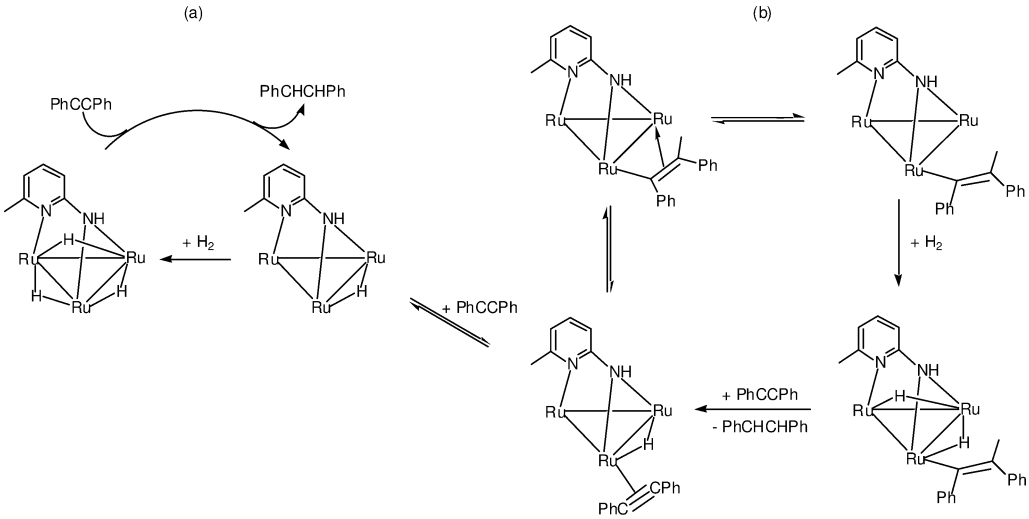

Scheme 8.7 Mechanism for the hydrogenation of diphenylacetylene catalyzed by ruthenium clusters containing face-capping ampy ligands at: (a) low [substrate]:[cat] ratios; and (b) high [substrate]:[cat] ratios (CO ligands omitted for clarity).

shows the main features of the diphenylacetylene hydrogenation mechanism for $[Ru_3(\mu\text{-}H)(_{\mu_3}\text{-ampy})(CO)_9]$, where the active species is the alkenyl derivative $[Ru_3(\mu_3\text{-ampy})(\mu\text{-PhC}{=}\text{CHPh})(CO)_8]$, readily formed by reaction of the hydride with the alkyne. If the latter complex is used as the catalyst precursor, the activity of diphenylacetylene hydrogenation is increased to TOF ca. 40 h^{-1} at 60 °C and 0.8 bar H_2. The catalytic cycle in Scheme 8.7 is supported by detailed kinetic studies, together with isolation and identification of a number of intermediates, and the independent study of various elementary steps included in the cycle. Phosphine-substituted ampy clusters also catalyze the hydrogenation of alkynes, albeit at lower rates (TOF < 11 h^{-1} at 80 °C and 0.8 bar H_2), but probably through very similar mechanisms.

Heteronuclear clusters have also been used in homogeneous hydrogenation with some success. Early studies by Ugo and Braunstein led to low-activity bimetallic catalysts [52]. $[RuFe_2(CO)_{12}]$, $[Ru_2Fe(CO)_{12}]$ and $[Ru_3FeH_2(CO)_{13}]$ were studied by Giordano and Sappa [32]; these promote the hydrogenation of diphenylacetylene at lower rates than the homonuclear Ru clusters, and the nature of the active species was not established. Süss-Fink and coworkers reported the use of $[IrRu_3(CO)_{13}(\mu\text{-}H)]$ in the hydrogenation of diphenylacetylene, curiously to *E*-stilbene (TOF 3900 h^{-1}), and proposed a cycle involving cluster intermediates [53].

More recently, Adams and coworkers have provided a very interesting case of heteronuclear clusters that are very active for the hydrogenation of alkynes [4, 54, 55]. The high-nuclearity layer-segregated Pt–Ru complex $[Pt_3Ru_6(CO)_{21}(\mu^3\text{-}H)(\mu\text{-}H)_3]$, consisting of three stacked triangular layers of metal atoms with an

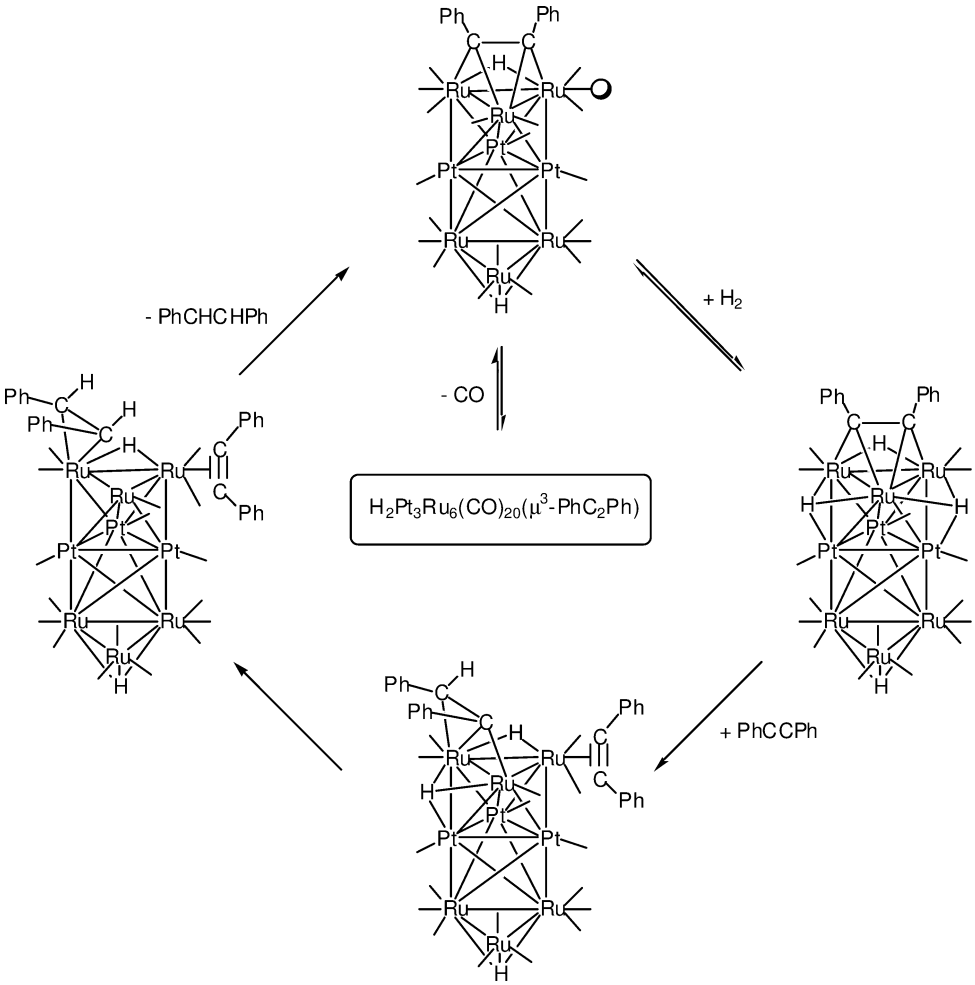

Scheme 8.8 Mechanism for the hydrogenation of diphenylacetylene catalyzed by layer-segregated Pt_3Ru_6 clusters (CO ligands omitted for clarity).

alternating arrangement $Ru_3Pt_3Ru_3$, readily reacts with diphenylacetylene to yield an alkyne complex, according to Eq. (4). In the process, two of the hydrides are transferred to a second diphenylacetylene molecule to yield 1 equiv. *Z*-stilbene, and one CO ligand is lost.

The resulting alkyne complex is capable of catalytically hydrogenating diphenylacetylene at 50 °C and 1 bar of H_2 with TOF close to 50 h^{-1}. The hydrogenation rate is first order in cluster concentration, indicating the participation of polynuclear species in the cycle, and it is also first order in substrate and hydrogen concentrations, while it is inhibited by CO. Labeling studies involving D_2

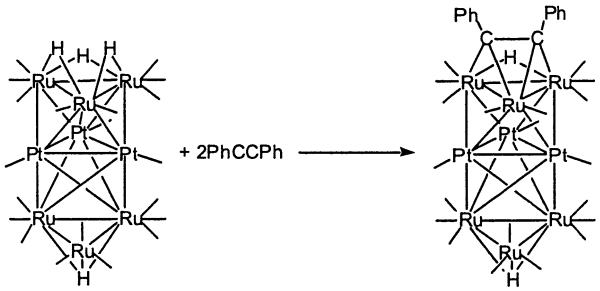

(4)

and TolC≡CTol further pointed to cluster catalysis, according to the mechanism depicted in Scheme 8.8. The catalytic activity is high, but catalyst life is short, the cluster being degraded into various species after a few hundred turnovers. A related homonuclear cluster $[Ru_3(CO)_9(\mu^3\text{-PhCCPh})(\mu\text{-H})_2]$ was shown to hydrogenate the alkyne at considerably lower rates than those observed for the heteronuclear complex, showing that the presence of platinum in the vicinity of the "working" ruthenium triangle enhances the catalytic activity. Even though there is no evidence for any direct participation of platinum in the catalytic cycle, the activation of H_2 is thought to occur on Ru_2Pt triangular units (see Scheme 8.8). The same Pt_3Ru_6 cluster has also been found to catalyze the hydrosilylation of diphenylacetylene with triethylsilane [56].

8.4 Hydrogenation of Other Substrates

The anionic cluster $[Ru_4H_3(CO)_{12}]^-$ is a catalyst precursor for the transfer hydrogenation of simple and α,β-unsaturated ketones in boiling Pr^iOH, with reasonable rates (TOF up to 100 h^{-1}) and, in the latter case, with moderate diastereoselectivity (up to 77%). Although a detailed kinetic modeling was performed, the identity or nuclearity of the active species could not be ascertained, and a radical mechanism was proposed [57]. $[Ru_3(CO)_{12}]$, in combination with chiral tetradentate diimino phosphines (P_2N_2), catalyzes the transfer hydrogenation of prochiral ketones in boiling $Pr^iOH/KOPr^i$, with enantioselectivities up to 81% at 91% yield (TOF ca. 40 h^{-1}). Evidence pointing to a cluster-catalyzed reaction include the fact that an anionic cluster $[HRu_3(CO)_{12}(P_2N_2)]^-$ could be isolated at the end of the hydrogenation runs, and it was shown to catalyze the reaction in the absence of added base. The reaction rate was also first order in cluster concentration, and a related mononuclear complex containing the same ligand was inactive [58].

The ligand-stabilized cluster $[Ru_3(CO)_7(\mu^3, \eta^5:\eta^5\text{-4,6,8-trimethylazulene})]$ reacts with $PhMe_2Si\text{-}H$ to yield a new cluster containing a partially hydrogenated azulene ligand $[Ru_3(CO)_7(\mu^3, \eta^5:\eta^5\text{-4,5-dihydro-4,6,8-trimethylazulene})]$. Both of these complexes are efficient catalyst precursors for the hydrosilylation of aceto-

phenone with moderate activities (TOF ca. 10 h^{-1}). Cluster participation is proposed on the basis of observed intermediates by NMR, and the fact that lower nuclearity-related complexes were not active in catalysis [59].

A series of tri- and tetra-nuclear Ru clusters previously reported by the groups of Süss-Fink [60] and of Dyson [61] as catalysts for the hydrogenation of benzene and other simple aromatics in biphasic media have later been shown to consist predominantly of active metallic particles [9, 10, 62].

8.5 Concluding Remarks

Despite the fact that the great expectations produced by cluster chemistry over two decades ago as a means of discovering novel catalysts with unique properties have not yet been realized, cluster catalysis continues to attract attention both as a conceptual issue and as a potential method to achieve unusual catalytic features. A number of catalysts originally thought to operate through cluster intermediates have subsequently been shown to owe their activity to the formation of mononuclear complexes or of metallic aggregates. Other systems do provide strong cases for catalytic cycles involving well-defined polynuclear intermediates, and a number of thorough kinetic and mechanistic studies have been performed which shed light on this fundamental question. The introduction of PHIP as a means of obtaining direct evidence for cluster catalysis is a most welcome development, and it is expected that further studies involving this technique will either corroborate or contradict the participation of polynuclear species in other catalytic systems. Although it is difficult to predict accurately whether fragmentation will occur when a given cluster is placed under catalytic hydrogenation conditions, some indicators are available to orient the search for polynuclear active species; in particular, the use of polydentate edge-bridging or face-capping ligands provides a good probability of obtaining cluster catalysis.

To date, there are no examples available of well-defined clusters that are of practical use, or that offer any advantages over mononuclear complexes in homogeneous hydrogenation reactions. The promising approach to enantioselective hydrogenation by use of chiral metal frameworks or of chiral polydentate ligands on clusters has been explored with limited success, but developments of possible utility are yet to be realized; continued efforts in that direction are certainly worthwhile. Heterobimetallic clusters appear as good candidates for promoting reactions not catalyzed by a single metal through synergistic enhancement of the properties of individual components; some interesting examples are now available where bimetallic high-nuclearity cluster catalysis has been demonstrated, and applications to unusual reactions are to be expected [4, 53–56]. The use of defined clusters as precursors of nanostructured materials is also of great interest, even if it falls outside the field of homogeneous hydrogenation. For example, applications to the synthesis of active catalysts for the important arene hydrogenation reaction are very appealing.

Until now, most studies on homogeneous hydrogenation by clusters have concentrated on alkenes and alkynes, though hopefully other substrates such as aldehydes, ketones, imines, and others will be further investigated, particularly using those systems that are now known to be genuine cluster catalysts.

Although the field of homogeneous hydrogenation by use of well-defined metal clusters has risen and fallen in popularity over the years, it has never been abandoned, most likely because the basic concept of a limited number of metal atoms in a well-defined structural and electronic molecular unit performing unique catalytic reactions still appears very seductive, and its realization poses exciting challenges in molecular design and synthetic chemistry. Hopefully, the expected breakthroughs toward distinctive catalytic properties in hydrogenation reactions by metal clusters will "see the light" before too long.

Abbreviations

bmim	1-butyl-3-methylimidazolium
ee	enantiomeric excess
IR	infra-red
NMR	nuclear magnetic resonance
PHIP	*para* hydrogen-induced polarization
TOF	turnover frequency
TON	turnover number
TPPMS	triphenylphosphine-monosulfonate
TPPTS	triphenylphosphine-trisulfonate

References

1 Adams, R.D., Cotton, F.A. (Eds.), *Catalysis by Di- and Poly-nuclear Metal Cluster Complexes*. Wiley-VCH: New York, **1998**.

2 Braunstein, P., Oro, L.A., Raithby, P.R. (Eds.), *Metal Clusters in Chemistry*. Wiley-VCH: New York, **1999**.

3 Dyson, P.J., *Coord. Chem. Rev.* **2004**, *248*, 2443.

4 Adams, R.D., Captain, B., *J. Organomet. Chem.* **2004**, *689*, 4521.

5 Dyson, P.J., McIndoe, J.S. (Eds.), *Transition Metal Carbonyl Chemistry*. Gordon and Breach: Amsterdam, **2000**.

6 Süss-Fink, G., Meister, G., *Adv. Organomet. Chem.* **1993**, *35*, 41.

7 Gates, B.C., *J. Mol. Catal.* **2000**, *163*, 55; Argo, A.M., Odzak, J.F., Lai, F.S., Gates, B.C., *Nature* **2002**, *415*, 623.

8 Johnson, B.F.G. (Ed.), *Transition Metal Clusters*. Wiley: Chichester, **1980**.

9 Widegreen, J.A., Finke, R.G., *J. Mol. Catal. A: Chem.* **2003**, *198*, 317.

10 Dyson, P.J., *Dalton Trans.* **2003**, 2964.

11 Rosenberg, E., Laine, R. In: Adams, R.D., Cotton, F.A. (Eds.), *Catalysis by Di- and Poly-nuclear Metal Cluster Complexes*. Wiley-VCH: New York, **1998**, p. 1.

12 Cree-Uchiyama, M., Shapley, J.R., St. George, G.M., *J. Am. Chem. Soc.* **1986**, *108*, 1316.

13 Choplin, A., Besson, B., D'Ornelas, L.D., Sánchez-Delgado, R., Basset, J.M., *J. Am. Chem. Soc.* **1988**, *100*, 2783.

14 Zuffa, J.L., Blohm, M.L., Gladfelter, W.L., *J. Am. Chem. Soc.* **1986**, *108*, 552;

Zuffa, J.L., Gladfelter, W.L., *J. Am. Chem. Soc.* **1986**, *108*, 4669.
15 Sánchez-Delgado, R.A., Durán, I., Monfort, J., Rodríguez, E., *J. Mol. Catal.*, **1981**, *11*, 193–203.
16 Doi, Y., Koshizuka, K., Keii, T., *Inorg. Chem.* **1982**, *21*, 2732.
17 Sánchez-Delgado, R.A., Andriollo, A., Puga, J., Martín, G., *Inorg. Chem.* **1987**, *26*, 1867.
18 Bregounhou, G., Fompegrine, P., Commenges, G., Bonnett, J.J., *J. Mol. Catal.* **1988**, *48*, 285.
19 Fontal, B., Reyes, M., Suárez, T., Bellandi, F., Díaz, J.C., *J. Mol. Catal. A: Chem.* **1999**, *149*, 75; Fontal, B., Reyes, M., Suárez, T., Bellandi, F., Ruiz, N., *J. Mol. Catal. A: Chem.* **1999**, *149*, 87.
20 Dallmann, K., Buffon, R., *J. Mol. Catal. A: Chem.* **2001**, *172*, 81.
21 Matteoli, U., Menchi, V., Frediani, P., Bianchi, M. Piacenti, F., *J. Organomet. Chem.* **1985**, *285*, 281; Matteoli, U., Beghetto, V., Scrivanti, A., *J. Mol. Catal. (A): Chem.* **1996**, *109*, 45; Salvini, A., Frediani, P. Bianchi, M., Piacenti, F., Pistolesi, L., Rosi, L., *J. Organomet. Chem.* **1999**, *582*, 218.
22 Homanen, P., Persson, R., Haukka, M., Pakkanen, T.A. Nordlander, E., *Organometallics* **2000**, *19*, 5568.
23 Moura, F.C.C., dos Santos, E.N., Lago, R.M., Vargas, M.D., Araujo, M.H., *J. Mol. Catal. A: Chem.* **2005**, *226*, 243.
24 Dyson, P.J., Ellis, D.J., Parker, D.G., Welton, T., *J. Mol. Catal. A: Chem.* **1999**, *150*, 71.
25 Gao, J.-X., Xu, P.-P., Yi, X.-D., Wan, H.-L., Tsai, K.-R., *J. Mol. Catal. A: Chem.* **1999**, *147*, 99.
26 Zhao, D., Dyson, P.J., Laurenczy, G., McIndoe, J.S., *J. Mol. Catal. A: Chem.* **2004**, *214*, 19.
27 Cabeza, J.A. In: Braunstein, P., Oro, L.A., Raithby, P.R. (Eds.), *Metal Clusters in Chemistry.* Wiley-VCH: New York, **1999**, Vol. 2, p. 715.
28 Dyson, P.J., *Coord. Chem. Rev.* **2004**, *248*, 2443.
29 Michelin-Lausarot, P., Vaglio, G.A., Valle, M., *J. Organomet. Chem.* **1984**, *275*, 233.
30 Michelin-Lausarot, P., Vaglio, G.A., Valle, M., *Inorg. Chim. Acta* **1977**, *25*, L107.
31 Michelin-Lausarot, P., Vaglio, G.A., Valle, M., *Inorg. Chim. Acta* **1979**, *36*, 213.
32 Giordano, R., Sappa, E., *J. Organomet. Chem.* **1993**, *448*, 157.
33 Cauzzi, D., Giordano, R., Sappa, E., Tiripicchio, A., Tiripicchio-Camellini, M., *J. Cluster Sci.* **1993**, *4*, 279.
34 Castiglioni, M., Giordano, R., Sappa, E., *J. Organomet. Chem.* **1983**, *258*, 217.
35 Castiglioni, M., Giordano, R., Sappa, E., *J. Organomet. Chem.* **1988**, *342*, 97.
36 Castiglioni, M., Giordano, R., Sappa, E., *J. Organomet. Chem.* **1989**, *362*, 399.
37 Castiglioni, M., Giordano, R., Sappa, E., *J. Organomet. Chem.* **1989**, *369*, 419.
38 Castiglioni, M., Giordano, R., Sappa, E., *J. Organomet. Chem.* **1991**, *407*, 377.
39 Aime, S., Gobetto, R., Canet, D., *J. Am. Chem. Soc.* **1998**, *120*, 6770; Aime, S., Dastru, W., Gobetto, R., Russo, A., Viale, D., Canet, D., *J. Phys. Chem.* **1999**, *103*, 9702; Bergman, B., Rosenberg, E., Gobetto, R., Aime, S., Milone, L., Reineri, F., *Organometallics* **2002**, *21*, 1508.
40 Gobetto, R., Milone, L., Reineri, F., Salassa, L., Viale, A., Rosenberg, E., *Organometallics* **2002**, *21*, 1919.
41 Blazina, D., Duckett, S.B., Dyson, P.J., Lohman, J.A.B., *Angew. Chem. Int. Ed. Engl.* **2001**, *40*, 3874; Blazina, D., Duckett, S.B., Dyson, P.J., Johnson, B.F.G., Lohman, J.A.B., Sleigh, C.J., *J. Am. Chem. Soc.* **2001**, *123*, 9760; Blazina, D., Duckett, S.B., Dyson, P.J., Lohman, J.A.B., *Chem. Eur. J.* **2003**, *9*, 1045; Blazina, D., Duckett, S.B., Dyson, P.J., Lohman, J.A.B., *Dalton Trans.* **2004**, 2108. Prestwich, T.G., Blazina, D., Ducket, S.B., Dyson, P.J., *Eur. J. Inorg. Chem.* **2004**, 4381.
42 Giordano, R., Sappa, E., Knox, S.A.R., *J. Cluster Sci.* **1996**, *7*, 179.
43 Cabeza, J.A., Fernández-Colinas J.M., Llamazares, A., Riera, V., *Organometallics* **1992**, *11*, 4355.
44 Cabeza, J.A., Fernández-Colinas, J.M., Llamazares, A., Riera, V., *J. Mol. Catal.* **1992**, *71*, L7.
45 Cabeza, J.A., Fernández-Colinas, J.M., Llamazares, A., Riera, V., *J. Organomet. Chem.* **1995**, *494*, 169.
46 Cabeza, J.A., Fernández-Colinas, J.M., Llamazares, A., Riera, V., García-Granda,

S., van der Maelen, J. F., *Organometallics* **1994**, *13*, 4352; Cabeza, J. A., Fernández-Colinas, J. M., Llamazares, A., Riera, V., García-Granda, S., van der Maelen, J. F., *Organometallics* **1994**, *13*, 3120.

47 Cabeza, J. A., del Rio, I., Fernández-Colinas J. M., Riera, V., *Organometallics* **1996**, *15*, 449.

48 Cabeza, J. A., Fernández-Colinas J. M., Llamazares, A., Riera, V., *Organometallics* **1993**, *12*, 4141.

49 Alvarez, S., Briard, P., Cabeza, J. A., del Rio, I., Fernández-Colinas, J. M., Mulla, F., Ouahab, L., Riera, V., *Organometallics* **1994**, *13*, 4360.

50 Cabeza, J. A., Llamazares, A., Riera, V., Briard, P., Ouahab, L., *J. Organomet. Chem.* **1994**, *480*, 205.

51 Lugan, N., Laurent, F., Lavigne, G., Newcomb, T. P., Liimatta, E. W., Bonnet, J. J., *J. Am. Chem. Soc.* **1990**, *112*, 8607.

52 Fusi, A., Ugo, R., Psaro, R., Braunstein, P., Dehand, J., *Philos. Trans. R. Soc. London A* **1982**, *308*, 125.

53 Ferrand, V., Süss-Fink, G., Neels, A., Stoeckli-Evans, H., *J. Chem. Soc. Dalton Trans.* **1998**, 3825.

54 Adams, R. D., Barnard, T. S., Li, Z., Wu, W., Yamamoto, J. H., *Organometallics* **1994**, *13*, 2357.

55 Adams, R. D., Barnard, T. S., Li, Z., Wu, W., Yamamoto, J. H., *J. Am. Chem. Soc.* **1994**, *116*, 9103.

56 Adams, R. D., Barnard, T. S., *Organometallics* **1998**, *17*, 2567.

57 Bhaduri, S., Sharma, K., Mukesh, D., *J. Chem. Soc. Dalton Trans.* **1993**, 1191.

58 Zhang, H., Yang, Ch.-B., Li, Y.-Y., Donga, Zh.-R., Gao, J.-X., Nakamura, H., Murata, K., Ikariya, T., *Chem. Commun.* **2003**, 142.

59 Matsubara, K., Ryu, K., Maki, T., Iura, T., Nagashima, H., *Organometallics* **2002**, *21*, 3023.

60 Plasseraud, L., Süss-Fink, G., *J. Organomet. Chem.* **1997**, *539*, 163; Süss-Fink, G., Faure, M., Ward, T. R., *Angew. Chem. Int. Ed.* **2002**, *41*, 99; Vielle-Petit, L., Therrien, B., Süss-Fink, G., Ward, T. R., *J. Organomet. Chem.* **2003**, *684*, 117; Süss-Fink, G., Therrien, B., Vielle-Petit, L., Tschan, M., Romack, V. B., Ward, T. R., Dadras, M., Laurenczy, G., *J. Organomet. Chem.* **2004**, *689*, 1362.

61 Dyson, P. J., Ellis, D. J., Welton, T., Parker, D. G., *Chem. Commun.* **1999**, 25; Dyson, P. J., Russel, K., Welton, T., *Inorg. Chem. Commun.* **2001**, *4*, 571.

62 Hagen, C. M., Vielle-Petit, L., Laurenczy, G., Süss-Fink, G., Finke, R. G., *Organometallics* **2005**, *24*, 1819.

9
Homogeneous Hydrogenation: Colloids – Hydrogenation with Noble Metal Nanoparticles

Alain Roucoux and Karine Philippot

9.1
Introduction

Today, metal nanoparticle science is a strategic research area in material development due to their particular physical and chemical properties. Catalysis is a traditional application of metal nanoparticles, but they also find application in diverse fields such as photochemistry, electronics, optics or magnetism [1, 2]. Metal nanocatalysts, defined as particles between 1 and 10 nm in size, can be obtained by a variety of methods according to the "organic" or "aqueous" nature of the media and the stabilizers used: polymers, ligands or surfactants [3]. During the past five years, the use of nanoparticles in this active research area has received increased attention since some homogeneous catalysts have been shown to be "nanoheterogeneous" [4–6]. Since that time, modern methods to distinguish the true nature of the catalysts have been described. From today onwards, soluble noble metal nanoparticles are to be considered as an unavoidable family of catalysts for hydrogenation under mild conditions at the border between homogeneous and heterogeneous chemistry. This chapter reviews recent progress in the hydrogenation of unsaturated compounds by noble metal nanoparticles in various liquid media.

9.2
Concepts

In materials chemistry, nanoparticles of noble metals are an original family of compounds. Well-defined in terms of their size, structure and composition, zerovalent transition-metal colloids provide considerable current interest in a variety of applications. Here, the main interest is their application in catalysis. Zerovalent nanocatalysts can be generated in various media (aqueous, organic, or mixture) from two strategic approaches according to the nature of the precursor, namely: (i) mild chemical reduction of transition-metal salt solutions; and (ii) metal atom

The Handbook of Homogeneous Hydrogenation.
Edited by J.G. de Vries and C.J. Elsevier
Copyright © 2007 WILEY-VCH Verlag GmbH & Co. KGaA, Weinheim
ISBN: 978-3-527-31161-3

extrusion starting from organometallic compounds able to decompose in solution under mild conditions [7]. To date, the key goal is the reproducible synthesis of nanoparticles in opposition to larger ones (nanopowders) and bulk materials. Consequently, nanostructured particles should have at least: (i) a specific size (1–10 nm); (ii) a well-defined surface composition; (iii) constant properties related to reproducible syntheses; and (iv) be isolable and redissolvable. In this respect, several synthetic methods have been described, including:

- chemical or electrochemical reduction;
- thermal, photochemical or sonochemical decomposition; and
- metal vapor synthesis.

Whichever method is followed, a protective agent able to induce a repulsive force opposed to the van der Waals forces is generally necessary to prevent agglomeration of the formed particles and their coalescence into bulk material. Since aggregation leads to the loss of the properties associated with the colloidal state, stabilization of metallic colloids – and therefore the means to preserve their finely dispersed state – is a crucial aspect for consideration during their synthesis.

The stabilization mechanisms of colloidal materials have been described in Derjaguin-Landau-Verway-Overbeek (DLVO) theory [8, 9]. Colloids stabilization is usually discussed in terms of two main categories, namely charge stabilization and steric stabilization.

9.2.1
Electrostatic Stabilization

Various anionic compounds such as halides, carboxylates or polyoxoanions, generally dissolved in aqueous solution, can establish electrostatic stabilization. Adsorption of these compounds onto the metallic surface and the associated countercations necessary for charge balance produces an electrical double-layer around the particles (Scheme 9.1). The result is a coulombic repulsion between the particles. At short interparticle distances, if the electric potential associated with the double layer is sufficiently high, repulsive forces opposed to the van der Waals forces will be significant to prevent particle aggregation.

Colloidal suspensions stabilized by electrostatic repulsion are highly sensitive to any phenomenon able to disrupt the double layer, such as ionic strength or thermal motion.

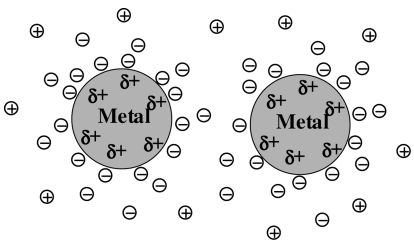

Scheme 9.1 Schematic representation of electrostatic stabilization: a coulombic repulsion between metal colloid particles.

9.2.2
Steric Stabilization

Nanoparticulate metal colloids can also be prevented from agglomeration by using protecting macromolecules such as polymers or oligomers [10, 11] or related stabilizers such as cyclodextrins [12] or cellulose derivatives [13]. The adsorption of these molecules at the surface of the particles provides a protective layer. In the interparticle space, the sterical environment of the adsorbed macromolecules reduces their mobility (Scheme 9.2). The result is an osmotic repulsion to restore the equilibrium by diluting the macromolecules, thereby separating the particles. By contrast with electrostatic stabilization, which is mainly used in aqueous media, steric stabilization can be used in either an organic or aqueous phase. Nevertheless, the length and/or nature of the adsorbed macromolecules can influence the thickness of the protective layer and thus modify the stability of the colloidal metal particles.

The electrostatic and steric effects can be combined to stabilize nanoparticles in solution. This type of stabilization is generally provided by means of ionic surfactants such as alkylammonium cations (Scheme 9.3). These compounds bear both a polar head group which is able to generate an electrical double layer, and a lipophilic side chain which is able to provide steric repulsion [14, 15].

Electrosteric stabilization can be also obtained from the couple ammonium (Bu_4N^+)/polyoxoanion ($P_2W_{15}Nb_3O_{62}^{9-}$). The significant steric repulsion of the bulky Bu_4N^+ countercation, when associated with the highly charged polyoxoanion (coulombic repulsion), provides efficient electrosterical stability towards agglomeration in solution of the resultant nanocatalysts [2, 5, 6].

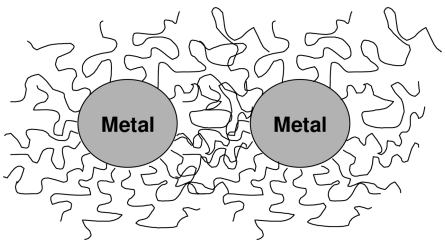

Scheme 9.2 Schematic representation of steric stabilization.

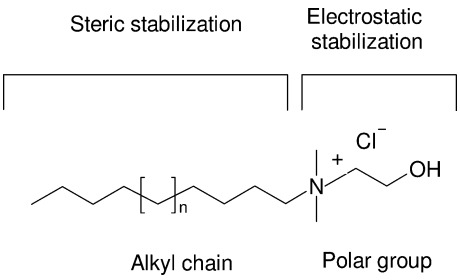

Scheme 9.3 *N*-alkyl-*N*,*N*-dimethyl-*N*-(2-hydroxyethyl)-ammonium chloride salt, a typical cationic surfactant which combines electrostatic and steric stabilizations (electrosteric stabilization).

The term "steric stabilization" may also be used to describe protective transition-metal colloids with traditional ligands or solvents. This stabilization occurs by: (i) the strong coordination of various metal nanoparticles with ligands such as phosphines [16–18], thiols [19–22], amines [21, 23–26], oxazolines [27] or carbon monoxide [18]; or (ii) weak interactions with solvents such as tetrahydrofuran (THF) or various alcohols [18, 28–31].

Finally, the development of modified nanoparticles having better stability and a longer lifetime has involved interesting results in diverse catalytic reactions. Efficient activities are obtained with these transition-metal colloids used as catalysts for the hydrogenation of various unsaturated substrates. Consequently, several recent investigations in total, partial or selective hydrogenation have received significant attention.

9.3
Hydrogenation of Compounds with C=C Bonds

Alkene hydrogenation is a common field of catalytic application for metal nanoparticles. Various approaches have been utilized to obtain stable and active nanocatalysts in hydrogenation reactions. The main approaches are described in the following sections, and are classified according to the stabilizing mode retained for the nanoparticles.

9.3.1
Use of Polymers as Stabilizers

Organic polymers are very often used for the stabilization of metal nanoparticles by providing a steric stabilizing effect. Due to this embedding effect, it is generally considered that the diffusion of substrates through the polymer matrix can be limited. Nevertheless, some interesting results have been obtained.

Hirai and Toshima have published several reports on the synthesis of transition-metal nanoparticles by alcoholic reduction of metal salts in the presence of a polymer such as polyvinylalcohol (PVA) or polyvinylpyrrolidone (PVP). This simple and reproducible process can be applied for the preparation of monometallic [32, 33] or bimetallic [34–39] nanoparticles. In this series of articles, the nanoparticles are characterized by different techniques such as transmission electronic microscopy (TEM), UV-visible spectroscopy, electron diffraction (EDX), powder X-ray diffraction (XRD), X-ray photoelectron spectroscopy (XPS) or extended X-ray absorption fine structure (EXAFS, bimetallic systems). The great majority of the particles have a uniform size between 1 and 3 nm. These nanomaterials are efficient catalysts for olefin or diene hydrogenation under mild conditions (30 °C, P_{H_2} = 1 bar). In the case of bimetallic catalysts, the catalytic activity was seen to depend on their metal composition, and this may also have an influence on the selectivity of the partial hydrogenation of dienes.

Delmas et al. produced PVP-stabilized rhodium nanoparticles using the method reported by Hirai [32] to perform catalytic hydrogenation of oct-1-ene in a two-liquid-phase system [40]. These authors investigated the effect of various parameters on nanoparticle stability and activity under more or less severe conditions. It was also shown that PVP/Rh colloids could be reused twice or more, without any loss of activity.

9.3.2
Use of Non-Usual Polymers as Stabilizers

Several groups have developed the use of non-usual polymers for the stabilization of colloids for hydrogenation catalysis. Mayer reported the use of various nonionic polymers and cationic polyelectrolytes as stabilizers for the synthesis of metal nanoparticles [41]; poly(1-vinylpyrrolidone-*co*-acrylic) and poly(2-ethyl-2-oxazoline) can be cited as examples here. Stable palladium and platinum colloids were prepared by the reduction of noble metal salts by refluxing the alcoholic solutions containing the polymers [42, 43]. Depending on the polymer used, a range of particle sizes and narrow size distributions were obtained. It appeared that a hydrophobic backbone and hydrophilic side chains are required for the nonionic polymers to become well stabilized and to provide controlled-size particles. Cationic polyelectrolytes also provided interesting results. With regard to catalysis, cyclohexene hydrogenation in MeOH was performed with Pd and Pt colloids, and conversions of 100% could be obtained in many cases. These authors also compared the activities of the nanocatalysts for this reaction depending on their protective polymer, polyelectrolyte or nonionic polymers [44]. In the same context, the ability of amphiphilic block copolymers, namely poly(dimethylsiloxane)-*b*-poly(ethylene oxide) (PDMS-*b*-PEO), polystyrene-*b*-poly-(methacrylic acid) (PS-*b*-PMAA) and poly-styrene-*b*-poly(ethylene oxide) (PS-*b*-PEO), to stabilize colloidal palladium, platinum, silver and gold nanoparticles has been investigated [45, 46]. Transmission electron microscopy (TEM) revealed randomly distributed nanoparticles with narrow size distributions in the range of 1 to 10 nm. In the case of Pd and Pt, cyclohexene hydrogenation has been chosen as model reaction for evaluation of the nanocatalysts. The influence of the precursor type, the polymer nature and also the preparation conditions on the catalytic activities have also been studied [46].

Liu et al. prepared palladium nanoparticles in water-dispersible poly(acrylic acid) (PAA)-lined channels of diblock copolymer microspheres [47]. The diblock microspheres (mean diameter 0.5 μm) were prepared using an oil-in-water emulsion process. The diblock used was poly(*t*-butylacrylate)-*block*-poly(2-cinnamoyloxyethyl) methacrylate (P*t*BA-*b*-PCEMA). Synthesis of the nanoparticles inside the PAA-lined channels of the microspheres was achieved using hydrazine for the reduction of $PdCl_2$, and the nanoparticle formation was confirmed from TEM analysis and electron diffraction study (Fig. 9.1). The Pd-loaded microspheres catalyzed the hydrogenation of methylacrylate to methyl-propionate. The catalytic reactions were carried out in methanol as solvent under dihydro-

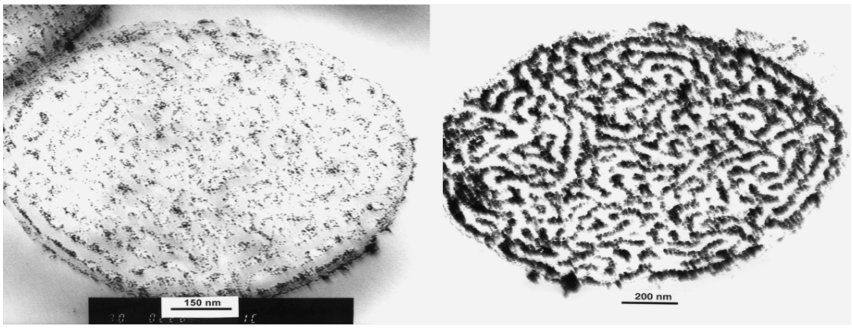

Fig. 9.1 Transmission electron microscopy images of Pd-loaded PCEMA-*b*-PAA microspheres containing 27% Pd (left) and 63% Pd (right). (Adapted from [47])

gen bubbling. The catalysts were recovered by centrifugation and methanol washing, and recovery efficiency was 100%.

Bronstein et al. also used block copolymer micelles for the preparation of noble-metal monometallic or bimetallic colloids (Pd, Pd/Au) [48]. These colloids were characterized by electron microscopy and wide-angle X-ray scattering (WAXS) and studied in the hydrogenation of cyclohexene, 1,3-cyclooctadiene, and 1,3-cyclohexadiene. The catalytic reactions were carried out in toluene at 30 °C with [catalyst]/[substrate] molar ratios of 1 : 250 and 1 : 500 in the case of cyclohexene, and 1 : 500 and 1 : 10 000 for 1,3-cyclohexadiene. High catalytic activities were obtained in the hydrogenation reactions, which were found to depend strongly on a number of parameters such as colloid morphology and reducing agent residues at the colloid surface. In fact, the strength of the reducing agent determines the rate of nucleation and growth of the colloids inside the micelle core and, consequently, a number of different architectures can be tailor-made. The second effect of the reducing agent used is provided by its residues or reaction products after reduction of the metal colloids that can influence the catalytic properties. Finally, Pd colloids could selectively hydrogenate 1,3-cyclohexadiene in cyclohexene with rates of between 10 to 1230 (Table 9.1). Nevertheless, it was observed that the hydrogenation of 1,3-cyclohexadiene is accompanied by the disproportionation of 1,3-cyclohexadiene to cyclohexene and benzene as a side reaction.

Akashi and coworkers prepared small platinum nanoparticles by ethanol reduction of $PtCl_6^{2-}$ in the presence of various vinyl polymers with amide side chains [49]. These authors studied the effects of molecular weight and molar ratio [monomeric unit]/[Pt] on the particle sizes and size distributions by electron microscopy, and in some cases by the dispersion stability of the Pt colloids. The hydrogenation in aqueous phase of allyl alcohol was used as a model reaction to examine the change in catalytic activity of polymer-stabilized Pt colloids upon addition of Na_2SO_4 to the reaction solution. The catalytic tests were performed in water or in Na_2SO_4 aqueous solution at 25 °C under atmospheric pressure of

Table 9.1 Activity of block copolymer-stabilized Pd colloids in selective hydrogenation of 1,3-cyclohexadiene. (Adapted from [48])

Catalyst [a)]	Reducing agent	Substrate/ catalyst ratio [mol]	t [min]	substrate conversion [%]	Selectivity [%]			Rate [c)]
					Cyclohexene	Cyclohexane	Benzene	
PS-1,2; Na_2PdCl_4	superhydride [b)]	500:1	10	100	71.3	0.1	28.6	40
PS-3,4; $Pd(CH_3COO)_2$	superhydride	750:1	5	100	58.5	0.0	41.5	90
PS-3,4; $Pd(CH_3COO)_2$	$NaBH_4$	10000:1	5	100	65.9	0.0	34.1	1230
PS-3,4; $Pd(CH_3COO)_2$	no reduction	500:1	25	100	60.1	5.4	34.5	10
Pd on activated carbon (Aldrich, 1 wt% Pd)	–	5000:1	7	100	54.7	0.7	44.6	420

a) PS-1,2 and PS-3,4 are the two different chosen PS-*b*-P4VP block copolymers.
b) Superhydride = 1 M solution of $LiB(C_2H_5)_3H$ in THF.
c) Rate: mol cyclohexene min^{-1} g^{-1} atom metal as a total for both hydrogenation and disproportionation.

dihydrogen. 1-Propanol was the only product. The PNVF-Pt (PNVF = poly(*N*-vinylformamide)) colloid did not show any critical flocculation point, and was very stable in 0.8 M Na_2SO_4 solution. Moreover, it provided the same activity as that obtained in pure water, while the other polymer-stabilized colloids showed markedly different behavior. The same authors described the synthesis of poly(*N*-isopropylacrylamide)-protected Au/Pt nanoparticles (mean diameter = 1.9 nm), their characterization by UV-visible spectroscopy, electron microscopy and X-ray diffraction, and their temperature-dependent catalytic activity in the aqueous hydrogenation of allyl alcohol [50]. The Au/Pt bimetallic colloids were found to have an alloy structure, the two metals being fully mixed, and were more active than the Pt monometallic colloids for the hydrogenation of allyl alcohol in water at room temperature. The hydrogenation rate was also seen to depend on the molar ratio of the Au/Pt in the bimetallic nanoparticles.

Recently, Liew et al. reported the use of chitosan-stabilized Pt and Pd colloidal particles as catalysts for olefin hydrogenation [51]. The nanocatalysts with a diameter ca. 2 nm were produced from $PdCl_2$ and K_2PtCl_4 upon reduction with sodium borohydride in the presence of chitosan, a commercial biopolymer, under various molar ratios. These colloids were used for the hydrogenation of oct-1-ene and cyclooctene in methanol at atmospheric pressure and 30 °C. The catalytic activities in term of turnover frequency (TOF; mol. product mol. $metal^{-1}$ h^{-1})

Table 9.2 Selective reduction of conjugated aromatic alkenes catalyzed by "Pd-PMHS" nanocomposites. (Reprinted with the permission of the American Chemical Society [52])

Substrate	Reaction conditions	Product	Yield [%]
Styrene	4 h/benzene/RT	Ethylbenzene	95 [a)]
4-Methoxystyrene	3 h/benzene/RT	1-Ethyl-4-methoxybenzene	95
2-Allylphenol	4 h/benzene/RT	2-Propylphenol	96
Cinnamonitrile	5 h/benzene/RT	3-Phenylpropionitrile	90
2-Chlorostyrene	6 h/benzene/RT	(2-Chloroethyl)benzene	85
1,2-Diphenylethene	4 h/benzene/RT	1,2-Diphenylethane	94
2-Vinylnaphthalene	4 h/benzene/RT	2-Ethylnaphthalene	96 [b)]
9-Vinylanthracene	6 h/benzene/RT	9-Ethylanthracene	92

a) All reactions performed with 2:1 molar equivalents of colloid:alkene and stirred under argon or nitrogen atmosphere. Reaction progress was monitored by ^{1}H-NMR and/or FT-IR spectroscopy.
b) Isolated yields.
RT = room temperature.

ranged from 10^4 h^{-1} to 10^5 h^{-1}. Chitosan-stabilized Pt and Pd colloids had similar catalytic properties for the hydrogenation of cyclooctene, which led to cyclooctane in both cases. By contrast, they showed different properties for the hydrogenation of oct-1-ene, in which Pd isomerized octene, giving rise to oct-2-ene and oct-3-ene. The activity of the nanocatalysts decreased with increasing concentration of chitosan.

The group of Chauhan has reported the preparation of polysiloxane-encapsulated Pd nanoclusters [52]. These colloids were synthesized by the reduction of $Pd(OAc)_2$ with polymethylhydrosiloxane, which functions as a reducing agent as well as a capping material. Chemoselective hydrogenation of functional conjugated alkenes was achieved by these polysiloxane-stabilized particles under mild conditions in high yields (Table 9.2). These authors also investigated the nature of the true catalyst by performing several experiments such as UV-visible studies of the precursor transformation in nanoclusters, TEM studies during catalysis, quantitative poisoning studies, and recyclability and reproducibility studies of the nanoclusters. All of the results obtained confirmed Pd-nanoclusters as the active catalytic species.

As a final example of catalytic hydrogenation activity with polymer-stabilized colloids, the studies of Cohen et al. should be mentioned [53]. Palladium nanoclusters were synthesized within microphase-separated diblock copolymer films. The organometallic repeat-units contained in the polymer were reduced by exposing the films to hydrogen at 100 °C, leading to the formation of nearly monodisperse Pd nanoclusters that were active in the gas phase hydrogenation of butadiene.

9.3.3
Use of Dendrimers as Stabilizers

The use of dendrimers constitutes an attractive stabilization mode for the synthesis of metal nanoparticles for several reasons:

- Due to their specific structure, which contains cavities with functional groups, they can act both as template and stabilizer for the nanoparticles.
- Dendrimers can also act as selective gates controlling the access of small molecules to the encapsulated nanoparticles.
- Tailoring of their terminal groups can enhance their solubility.

Dendrimer interior functional groups and cavities can retain guest molecules selectively, depending on the nature of the guest and the dendritic endoreceptors, the cavity size, the structure, and the chemical composition of the peripheric groups. Two main methods are known for the synthesis of metal nanoparticles inside dendrimers. The first method consists of the direct reduction of dendrimer-encapsulated metal ions (Scheme 9.4); the second method corresponds to the displacement of less-noble metal clusters with more noble elements [54].

The team of Crooks is involved in the synthesis and the use of dendrimers and, more particularly, poly(amidoamine) dendrimers (PAMAM), for the preparation of dendrimer-encapsulated mono- or bimetallic nanoparticles of various metals (Pt, Pd, Cu, Au, Ag, Ni, etc.) [55, 56]. The dendrimers were used as nanocatalysts for the hydrogenation of allyl alcohol and *N*-isopropylacrylamide or other alkenes under different reaction conditions (water, organic solvents, biphasic fluorous/organic solvents or supercritical CO_2). The hydrogenation reaction rate is dependent on dendrimer generation, as higher-generation dendrimers are more sterically

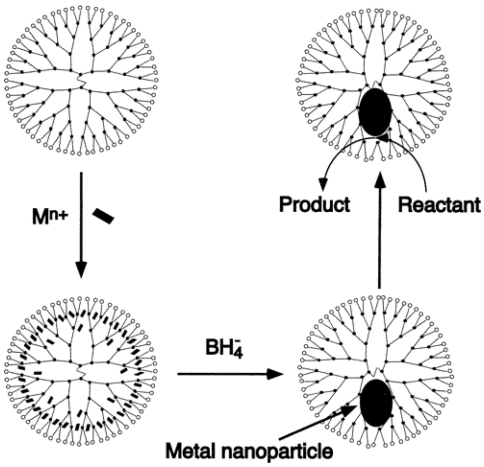

Scheme 9.4 Schematic of metal nanoparticles synthesis within dendrimer templates. (Reprinted from [54]; copyright 2002, Marcel Dekker.)

Table 9.3 Hydrogenation of alkenes using dendrimer-encapsulated Pd nanoparticles.[a)] (Reprinted with permission of the American Chemical Society [59])

Initial rate [mL H_2 $min^{-1} \times 10$]				
Substrate	**Pd(0)/G_3-TEBA**	**Pd(0)/G_4-TEBA**	**Pd(0)/G_5-TEBA**	**Pd/C**
1,3-Cyclooctadiene	5.4	4.1	2.9	12.0
1,3-Cyclohexadiene	9.8	8.7	7.2	11.8
1,3-Cyclopentadiene	9.2	9.0	8.3	10.3
1-Heptene[b)]	0.98	0.90	0.88	0.0
Cyclohexene	0.92	0.80	0.70	2.8
Methylacrylate	9.5	9.0	7.6	10.0
Tert-Butylacrylate	5.5	4.5	3.1	9.1
Allyl alcohol	12.1	11.5	11.2	11.6
2-Methyl-3-buten-2-ol	5.8	4.2	3.8	9.3

a) Reaction conditions: catalyst 5.0 μmol Pd, substrate 1.0 mmol, toluene 12.5 mL, H_2 1 atm, 30 °C.
b) After 15 min, the reaction mixture contained *n*-hexane, 1-hexene, 2-hexene and 3-hexene.

crowded on their periphery and thus less porous and less likely to admit substrates to interior metal nanoparticles than those of lower generations. Another advantage of dendrimer-encapsulated nanoparticles is that they can be recycled.

Rhee and coworkers published the synthesis of bimetallic Pt-Pd nanoparticles [57] or Pd-Rh nanoparticles [58] within dendrimers as nanoreactors. These nanocatalysts showed a promising catalytic activity in the partial hydrogenation of 1,3-cyclooctadiene. The reaction was carried out in an ethanol/water mixture at 20 °C under dihydrogen at atmospheric pressure. The dendrimer-encapsulated nanoclusters could be reused, without significant loss of activity.

Kaneda et al. reported substrate-specific hydrogenation of olefins using the tri-ethoxybenzamide-terminated poly(propylene imine) dendrimers (PPI) as nanoreactors encapsulating Pd nanoparticles (mean diameter 2–3 nm) [59]. The catalytic tests were performed in toluene at 30 °C under dihydrogen at atmospheric pressure (Table 9.3). The hydrogenation rates were seen to decrease with increasing generation of dendrimers, from G_3 to G_5.

9.3.4
Use of Surfactants as Stabilizers

Surfactants are well known as stabilizers in the preparation of metal nanoparticles for catalysis in water. Micelles constitute interesting nanoreactors for the synthesis of controlled-size nanoparticles from metal salts due to the confinement of the particles inside the micelle cores. Aqueous colloidal solutions are then obtained which can be easily used as catalysts.

Toshima et al. obtained colloidal dispersions of platinum by hydrogen- and photo-reduction of chloroplatinic acid in an aqueous solution in the presence of various types of surfactants such as dodecyltrimethylammonium (DTAC) and sodium dodecylsulfate (SDS) [60]. The nanoparticles produced by hydrogen reduction are bigger and more widely distributed in size than those resulting from the photo-irradiation method. Hydrogenation of vinylacetate was chosen as a catalytic reaction to test the activity of these surfactant-stabilized colloids. The reaction was performed in water under atmospheric pressure of hydrogen at 30 °C. The photo-reduced colloidal platinum catalysts proved to be best in terms of activity, a fact explained by their higher surface area as a consequence of their smaller size.

Larpent and coworkers were interested in biphasic liquid–liquid hydrogenation catalysis [61], and studied catalytic systems based on aqueous suspensions of metallic rhodium particles stabilized by highly water-soluble trisulfonated molecules as protective agent. These colloidal rhodium suspensions catalyzed octene hydrogenation in liquid–liquid medium with TOF values up to 78 h^{-1}. Moreover, it has been established that high activity and possible recycling of the catalyst could be achieved by control of the interfacial tension.

Gedanken et al. have reported the preparation of palladium nanoscale particles by sonochemical reduction of palladium acetate at room temperature in THF or methanol solution and in the presence of myristyltrimethylammonium bromide ($CH_3(CH_2)_{13}N(CH_3)_3Br$) as stabilizing agent [62]. XRD and TEM with selected area electron diffraction (SAED) techniques confirmed that the stabilized-Pd nanoclusters were nanocrystalline and composed of aggregates of spherical particles of size 10–20 nm. Cyclohexene hydrogenation reactions were carried out in diethyl ether under a hydrogen atmosphere (ca. 0.2 MPa) at room temperature. The formation of cyclohexane could be observed with a conversion of 64%, which was higher than that obtained using a commercial Pd/C catalyst.

9.3.5
Use of Polyoxoanions as Stabilizers

An original method for the stabilization of metal nanoparticles destined for catalytic applications was developed by Finke et al., who produced polyoxoanion- and tetrabutylammonium-stabilized iridium and rhodium nanoparticles (Scheme 9.5) [63, 64]. The synthesis method consists of the hydrogen reduction, in acetone, of the polyoxoanion-supported Ir(I) or Rh(I) complex $[(n\text{-}C_4H_9)_4N]_5\text{-}Na_3[(1,5\text{-COD})Rh \cdot P_2W_{15}Nb_3O_{62}]$. The resultant Rh(0) nanoclusters are near-monodisperse with a mean size of 4±0.6 nm, and can be isolated as a black powder and redispersed in non-aqueous solvents such as acetonitrile. The particles have been characterized by a variety of techniques, including TEM, energy-dispersive spectroscopy, electron diffraction, UV-visible spectroscopy and elemental analysis. Ion-exchange chromatography revealed that the Rh(0) nanoclusters are stabilized by the adsorption of the polyoxoanion onto their outer surface. These nanoclusters were active in cyclohexene hydrogenation at room

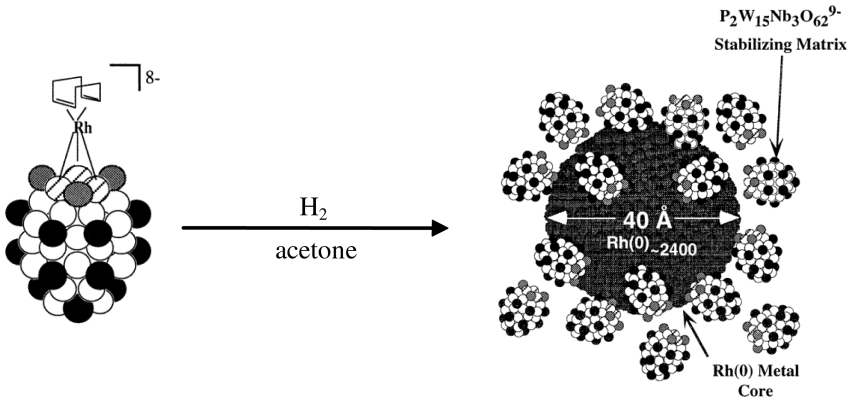

Scheme 9.5 Synthesis of Rh(0) nanoclusters from (1,5-COD)$RhP_2W_{15}Nb_3O_{62}^{9-}$ polyoxoanion-supported nanocluster-forming precatalyst (space-filling representation). (Adapted from [63].)

temperature and under dihydrogen pressure, with TOF of 3650 h^{-1}. In another report, the same group studied the in-solution lifetimes of Rh(0) nanocatalysts; these were found to approach those of a solid-oxide-supported Rh(0) catalyst, with values higher than were previously reported [65].

9.3.6
Use of Ligands as Stabilizers

The use of ligands as protective agents for metal nanoparticle synthesis has become increasingly common during the past few years. The main advantage of this stabilizing mode for nanocatalysts is the possibility of modulating the surface state of the particles by chemical influence of the ligand. Nevertheless, it is necessary to identify ligands that give rise to stable, but active, nanocatalysts. Until now, the ligands used have been generally simple organic ligands (thiols, amines, carboxylic acids, phosphines), though on occasion more sophisticated ligands are used such as phenanthroline, β-cyclodextrins or ferritines.

As an initial example, Sastry et al. [66] described a single-step procedure for the synthesis of catalytically active, hydrophobic platinum nanoparticles involved in the spontaneous reduction of aqueous $PtCl_6^{2-}$ ions by hexadecylaniline (HDA) at a liquid–liquid interface. HDA acts simultaneously as phase-transfer molecule, reducing agent and nanoparticle capping agent. The HDA chloroform solution of nanoparticles could be isolated as a black powder after solvent evaporation, while any uncoordinated HDA was removed by ethanol washing. The nanoparticles could then be redispersed in organic solvents (benzene, toluene, hexane). UV-visible, TEM and XRD measurements confirmed the formation of Pt nanoparticles of mean size 15.5±0.7 nm and with a face-centered cubic structure, while TGA analysis showed desorption of the HDA molecule (a weight

loss of 30% at 270 °C) and ^{1}H-NMR spectra proved close contact of the ligand with the metal surface. These Pt nanoparticles were investigated in styrene hydrogenation under H_2 pressure (14 bar) at 60 °C, and showed complete conversion into ethylbenzene with a TOF of 655 h^{-1}. They were also active in cyclohexene hydrogenation, allowing complete conversion into cyclohexane with 100% selectivity and a TOF of 2112 h^{-1}.

Vargaftik and Moiseev have obtained near-spherical palladium nanoclusters with an average size of 1.8 nm by reduction of palladium carboxylates $Pd_3(OCOR)_6$ (R = Me, Et, $CHMe_2$, CMe_3) with hydrogen in alcohol solutions containing 1,10-phenanthroline as ligand [67]. Based on elemental analysis, NMR, X-ray photoelectron spectroscopy and EXAFS investigations, these nanoclusters were described by the idealized formula $Pd_{147}phen_{32}O_{60}(OCOR)_{30}$. These nanocatalysts were used in the hydrogenation of alkynes and alkenes, the reduction of nitriles with formic acid, and the oxidation of aliphatic and benzylic alcohols. For alkene hydrogenation, styrene was used as substrate, the catalytic reaction being performed in alcohol at temperatures up to 70 °C. The results revealed that Pd-147 nanoclusters were much more active than the giant Pd-561 clusters or the traditional Pd/C catalyst. By comparison, ethylbenzene has been produced using all three catalysts, with respective TOF values of 242, 155, and 25 h^{-1}, respectively, at 20 °C.

Sahle-Demessie and Pillai studied the catalytic activity of phenanthroline-stabilized palladium nanoparticles in polyethylene glycol (PEG) as a recyclable catalyst system for the selective hydrogenation of olefins using molecular hydrogen under mild reaction conditions [68]. PEG acts not only as a reducing agent but also as a dispersing medium for the ligand-stabilized nanoparticles. The phenanthroline-stabilized Pd nanoparticles are well defined, with a mean size of 2–6 nm. Hydrogenation of various olefins (cyclohexene, then aliphatic, alicyclic and aromatic olefins) was performed in liquid phase under hydrogen at atmospheric pressure; some results are presented in Table 9.4. The catalyst system was found to be active and selective for the hydrogenation of a variety of olefins, with good to excellent conversion. In the case of 1,5-cyclooctadiene, cyclooctene is formed, but the selectivity of the di-hydrogenated product was enhanced with an increase in reaction time. The hydrogenation of unsaturated alcohols, aldehydes and ketones, such as cinnamyl alcohol and citral, formed the C=C hydrogenated product selectively without affecting the C=O group. However, the selectivity of the di-hydrogenated product also increased with reaction time. The catalyst system was easily separable from the reaction mixture by extraction of the products with diethyl ether, and could be reused several times (six cycles) without any loss of activity or selectivity. These authors demonstrated that phenanthroline stabilizes the palladium nanoparticles in PEG, which may act as a mobile supporting phase, thereby achieving high stability and high activity for the catalyst system.

Kaifer and coworkers showed interest in the modification of metal nanoparticles with organic monolayers prepared with suitable molecular hosts. They reported the preparation of water-soluble platinum and palladium nanoparticles modified with thiolated β-cyclodextrin (β-CD) [69]. Nanoparticle synthesis was

Table 9.4 Phenanthroline-stabilized palladium nanoparticles in PEG for the hydrogenation of alkenes.[a] (Adapted from [68])

Substrate	Product	Temp. [°C]	Time [h]	Conversion [%]	Selectivity [%]	TON
Cyclopentene	Cyclopentane	30	20	100	100	448
1-Hexene	*n*-Hexane	50	8	100	100	448
Cyclohexene	Cyclohexane	30	8	100	100	448
1-Methyl Cyclohexene	Methyl cyclohexane	50	20	54	100	242
1-Phenyl Cyclohexene	Phenyl cyclohexane	50	20	100	94[b]	448
1-Octene	*n*-Octane	50	8	100	100	448
2-Octene	*n*-Octane	50	20	100	100	448
Cyclooctene	Cyclooctane	50	8	100	100	448
1,5-Cyclooctadiene	Cyclooctene	40	20	100	38[c]	448
Styrene	Ethyl benzene	30	20	100	100	448
Stilbene	Dibenzyl	50	4	100	100	448
Norbornylene	Norborane	40	4	100	100	448
Cinnamyl alcohol	3-Phenyl propanol	40	20	100	100	448
Citral	Citronellal	50	20	100	15[d]	448
3-Methyl-2-butenal	3-Methyl butyraldehyde	40	8	94	100	422
Mesityl oxide	4-Methyl-2-pentanone	40	8	94	100	422
Cyclohexenone	Cyclohexanone	40	8	51	100	229
3-Methyl cyclohexene-1-ol	3-Methyl cyclohexanol	40	20	100	100	448

a) Reaction conditions: 10 mmol substrate, 5 mg Pd acetate, 1.5–3.0 mg 1,10-phenanthroline, 4 g PEG (400), stir, H_2 balloon.
b) Remaining biphenyl.
c) Remaining cyclooctane.
d) Remaining hydrocitronellal.
TON: calculated as the number of moles product formed per mol palladium.

realized by the reduction of a DMSO-water solution of Na_2PtCl_4 (or Na_2PdCl_4) by $NaBH_4$ in the presence of HS-β-cyclodextrin at room temperature. The nanoparticles were isolated as a dark precipitate after the addition of ethanol. Centrifugation and washing with DMSO and ethanol, followed by drying at 60 °C, provided dried powders containing Pt or Pd nanoparticles with a respective mean size of 14.1±2.2 and 15.6±1.3 nm. These Pt and Pd nanoparticles could be redispersed in water, and were tested for catalytic allylamine hydrogenation under atmospheric pressure of H_2 and room temperature (Table 9.5). Both types of CD-modified metal nanoparticles were soluble in the reaction media and could be easily recovered at the end of the reaction by precipitation with ethanol.

Table 9.5 Percentage conversion from allylamine (1.8 mmol) to propylamine obtained with cyclodextrin (CD)-modified Pt and Pd nanoparticles under 1.0 atm H_2(g) at room temperature in D_2O solution (2.0 mL). (Reprinted with permission of the Royal Society of Chemistry [69])

Catalyst	Quantity [mg]	Time [h]	Conversion [%]
CD-mod. Pt	10	6	>95
CD-mod. Pd	10	6	100
None	–	6	0
CD-mod. Pt	5	1	10
CD-mod. Pd	5	1	30

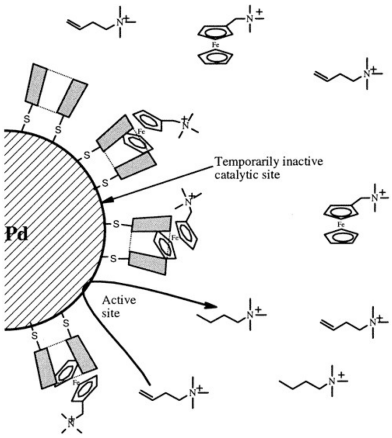

Scheme 9.6 Deactivation of active catalytic sites by binding ferrocene derivatives to the CD hosts on the Pd nanoparticles. (Reprinted with permission of the American Chemical Society [70].)

Following the same procedure, these authors also reported [70] water-soluble Pd nanoparticles (diameter 3.5±1.0 nm) which were modified with covalently attached cyclodextrin receptors and obtained by $NaBH_4$ reduction of $PdCl_4^{2-}$ in dimethylformamide solution containing perthiolated β-CD. After characterization by usual methods (TEM, UV-visible, NMR), hydrogenation of 1-butenyl(trimethyl)ammonium bromide under H_2 (1 atm) in D_2O at 25 °C gave a TOF of 320 h^{-1}. Since these Pd nanoparticles behave as active catalyst for the hydrogenation of alkenes in aqueous media, the group investigated whether this catalytic activity could be modulated through binding of guests to the surface-immobilized CD hosts. Since it is well known that ferrocene derivatives form stable inclusion complexes with β-CD, ferrocene compounds were added to the reaction mixture (Scheme 9.6). Under these circumstances, a substantial reduction in the rate of hydrogenation, dependent upon the ferrocene concentration, was noted. In addition, the catalytic ability of such a system for the hydrogenation of an olefin bearing a ferrocenyl group was compared. The inhibitory effect was lower in this case, probably because of the affinity of the olefin through its ferrocene moiety for the

CD-modified nanoparticles sites. These studies afford an interesting example of "tunable catalyst" design at the molecular level. Manipulation of the surface of catalytically active metal nanoparticles seems possible, and can be used to modulate the catalytic activity on demand.

9.3.7
Biomaterial as a Protective Matrix

Ueno et al. have published results relating to olefin hydrogenation by a Pd nanocluster confined in an apo-ferritin cage [71]. Ferritin, an iron-storage protein, comprises 24 subunits that assemble to form a hollow cage-like structure with a diameter of 12 nm and an internal cavity of 8 nm. These authors used ferritin as a stabilizing agent for the synthesis of Pd nanoparticles and their use in hydrogenation catalysis. The aqueous synthesis was realized by reduction of K_2PdCl_4 with $NaBH_4$ in the presence of apo-ferritin, giving rise to a clear brown solution containing monodispersed spherical Pd nanoparticles with a mean size of

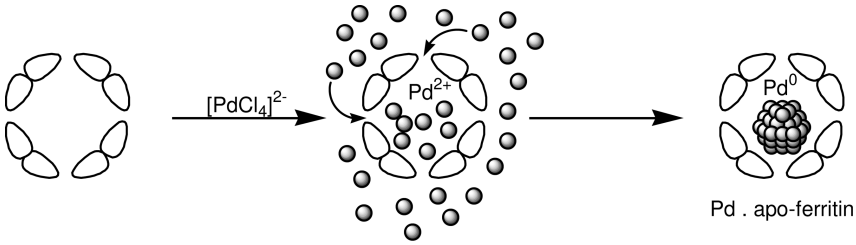

Scheme 9.7 Schematic synthesis of apo-ferritin stabilized-Pd nanoparticles. (Reprinted with permission of Wiley [71].)

Table 9.6 Hydrogenation activity of Pd-apo-ferritin nanoparticles in water. (Reprinted with permission of Wiley [71].)

Olefin	TOF [h^{-1}] for Pd apo-ferritin[a), b)]	TOF [h^{-1}] for Pd particles[b), c)]
CH_2=CHCONH$_2$ (1)	72 ± 0.7	58 ± 5.9
CH_2=CHCOOH (2)	6.3 ± 1.1	12 ± 2.6
CH_2=CHCONH-*i*Pr (3)	51 ± 6.5	15 ± 0.3
CH_2=CHCONH-*t*Bu (4)	31 ± 5.9	6.1 ± 0.6
CH_2=CHCO-Gly-OMe (5)	6.3 ± 3.8	28 ± 2.6
CH_2=CHCO-D,L-Ala-OMe (6)	Not detected	23 ± 0.3

a) Hydrogenation reactions catalyzed by Pd apo-ferritin carried out at 7 °C (pH 7.5) with 30 μM Pd.
b) TOF = [product(mol)] per atom Pd per hour.
c) The same conditions were used, but apo-ferritin was omitted.

2.0±0.3 nm (Scheme 9.7). The catalytic hydrogenation of olefins (acrylamide derivatives) by Pd apo-ferritin nanoparticles was evaluated in aqueous medium (Table 9.6). Since the observed TOFs are dependent upon substrate size, it could be concluded that Pd-apo-ferritin particles induce size-selective olefin hydrogenation.

9.3.8
Ionic Liquids used as Templates for the Stabilization of Metal Nanoparticles

More efficient catalytic systems that might combine the advantages of both homogeneous (catalyst modulation) and heterogeneous catalysis (catalyst recycling) are the subjects of great attention by the scientific community working on catalysis. For such purpose, ionic liquids are interesting systems as they can provide simple product separation and catalyst recycling.

The group of Dupont has developed the synthesis of metal nanoparticles in ionic liquids for use as catalysts. The group has published several reports relating to ionic liquid-stabilized nanoparticles of various metals, including iridium [72], platinum [73] and ruthenium [74]. Mostly, the nanoparticles are synthesized from organometallic precursors such as $[Ir\ COD\ Cl]_2$, $Pt_2(dba)_3$ or Ru COD COT (COD = cycloocta-1,5-diene; COT = cycloocta-1,3,5-triene; dba = dibenzylydeneacetone). The decomposition of these complexes is accomplished under molecular hydrogen (4 atm) at 75 °C in the chosen ionic liquid such as 1-*n*-butyl-3-methylimidazolium hexafluorophosphate (BMI PF_6) or 1-*n*-butyl-3-methylimidazolium tetrafluoroborate (BMI BF_4). These reaction conditions lead to well-dispersed nano-

Table 9.7 Catalytic performance of Pt(0) nanoparticles in solventless, homogeneous, and biphasic conditions.[a)] (Reprinted with permission of the American Chemical Society [73].)

Medium	Substrate	Product	Time [h]	Conversion [%][b)]	TOF [h^{-1}][c)]
Solventless	Hex-1-ene	Hexane	0.25	100	1000
Acetone	Hex-1-ene	Hexane	0.25	100	1000
BMI PF_6	Hex-1-ene	Hexane	0.4	100	625
BMI PF_6	Cyclohexene	Cyclohexane	1.6	100	156
Solventless	Cyclohexene	Cyclohexane	0.3	100	833
Acetone	Cyclohexene	Cyclohexane	0.3	100	833
BMI PF_6	2,3-Dimethyl-1-butene	2,3-Dimethyl-butane	3	82	68
Solventless	2,3-Dimethyl-1-butene	2,3-Dimethyl-butane	0.6	100	417
Solventless	1,3-Cyclohexadiene	Cyclohexane	0.3	100	833

a) Reaction conditions: [substrate]/[Pt] = 250 at 75 °C and under 4 atm H_2 (constant pressure).
b) Substrate conversion.
c) [mol product] [mol Pt]$^{-1}$ [h].

Table 9.8 Hydrogenation of alkenes by Ru(0) nanoparticles under multiphase and solventless conditions (75 °C and constant pressure of 4 atm, substrate/Ru = 500). (Adapted from [74])

Medium	Substrate	Time [h]	Conversion [%]	TON [a)]	TOF [h^{-1}] [b)]
Solventless	1-hexene	0.7	>99	500	714
BMI BF_4	1-hexene	0.6	>99	500	833
BMI PF_6	1-hexene	0.5	>99	500	1000
Solventless	cyclohexene	0.5	>99	500	1000
BMI BF_4	cyclohexene	5.0	>99	500	100
BMI PF_6	cyclohexene	8.0	>99	500	62
Solventless	2,3-dimethyl-2-butene	1.2	76	380	316

a) Turnover number (TON) = mol hydrogenated product mol^{-1} Ru.
b) Turnover frequency (TOF) = TON h^{-1}.

metric particles (d_m = 2–3 nm) in the ionic liquid. The thus-obtained nanoparticles are stable and isolable by centrifugation and acetone washing, and were characterized using a variety of techniques such as TEM, XRD, EDX, or XPS. The isolated nanoparticles can be redispersed in the ionic liquid, acetone, or used in solventless conditions for respectively, liquid–liquid biphasic, homogeneous or heterogeneous hydrogenation of alkenes and arenes under mild conditions (75 °C, 4 atm). Various olefins were used as substrates for the catalytic experiments, and results obtained with the Pt and Ru nanoparticles are listed in Tables 9.7 and 9.8, respectively. In general, the best results were obtained in solventless conditions. The recovered catalysts could be reused as solids or redispersed in the ionic liquid several times, without significant loss in catalytic activity.

In order to avoid the problem of aggregation, some research groups have studied the addition of a stabilizer (ligand or polymer) to increase stability of the nanocatalysts in ionic liquid. Han and coworkers reported the use of ligand-stabilized palladium nanoparticles for the hydrogenation of olefins in an ionic liquid [75]. These authors prepared phenanthroline-stabilized Pd nanoparticles (2–5 nm) in BMIM PF_6 and tested them directly as catalyst for olefin hydrogenation at 40 °C. The catalytic system showed high activity, with TOFs up to 234 h^{-1}, and the catalyst could be recycled (Table 9.9). The authors proposed that the ligand protected the Pd nanoparticles while the ionic liquid acted as a mobile support for the nanocatalyst and enhanced their stability.

Similarly, Kou et al. published the synthesis of PVP-stabilized noble-metal nanoparticles in ionic liquids BMI PF_6 at room temperature [76]. The metal nanoparticles (Pt, Pd, Rh) were produced by reduction of the corresponding metal halide salts in the presence of PVP into a refluxing ethanol-water solution. After evaporation to dryness the residue was redissolved in methanol and the solution added to the ionic liquid. The methanol was then removed by evaporation to give the ionic liquid-immobilized nanoparticles. These nanoparticles were very stable. TEM ob-

Table 9.9 Hydrogenation of olefins catalyzed by Phen-protected Pd nanoparticles in [BMIM][PF_6].[a)] (Adapted from [75])

Olefin	Olefin/Pd [mol mol^{-1}]	Temperature [°C]	Time [h]	Conversion [%]
Cyclohexene	2000	40	2.0	35
Cyclohexene	500	40	5.0	100
Cyclohexene	500	30	7.0	100
Cyclohexene	500	50	4.0	100
Cyclohexene	500	60	3.5	100
1-Hexene	500	20	3.0	100
1-Hexene	500	40	1.5	100
1,3-Cyclohexadiene	500	40	2.0	95[b)]
1,3-Cyclohexadiene	500	40	7.0	100[c)]

a) 1 bar H_2 (constant pressure).
b) Product is cyclohexene; no cyclohexane was detected.
c) Product is cyclohexane.

servations indicated that the distribution of particles size in the range 2–5 nm were similar before and after their immobilization in the ionic liquid. The catalytic performance was evaluated in the hydrogenation of olefins at 40 °C under hydrogen pressure (1 atm) in biphasic conditions (Table 9.10). The results showed that nanoparticles were highly active catalysts for the hydrogenation of olefins under very mild conditions. The ionic liquid-immobilized nanoparticles were easily separated from the product mixture by simple decantation or reduced pressure distillation, and could be reused several times, without loss of activity. TEM analysis carried out after several catalytic experiments showed that the particles did not aggregate; thus, the combination of PVP and ionic liquid appeared to be successful in inhibiting particle aggregation.

Table 9.10 Hydrogenation of alkenes catalyzed by PVP-stabilized noble-metal nanoparticles in [BMI][PF_6]. (Adapted from [76])

Substrate	Metal	Substrate/metal [mol mol^{-1}]	Time [h]	Conversion [%][a)]	TOF [h^{-1}][b)]
Cyclohexene	Pt	2000	16	100	125
1-Hexene	Pt	1000	1	100	1000
1-Dodecene	Pt	1000	1	100	1000
Cyclohexene	Pd	250	1	100	250
Cyclohexene	Rh	250	2	100	125

a) Substrate conversion.
b) Turnover frequency (TOF) = [mol product] [mol metal]$^{-1}$ h^{-1}.

Table 9.11 Hydrogenation reactions with Pd nanocatalysts in methanol, toluene or [BMIM][PF_6].[a] (Adapted from [77])

Substrate	Time [h]	Product	Yield [%]
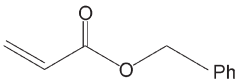	20	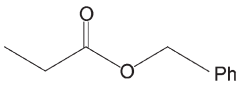	97
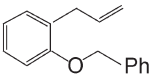	22	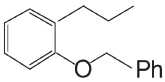	98
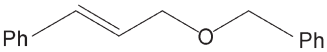	20	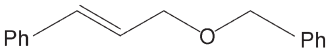 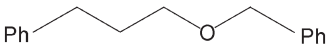	82 17
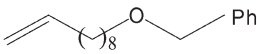	40	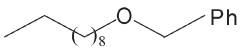	92

a) Reactions carried out at room temperature using a balloon filled with H_2 and 0.001 equiv. Pd_{OAc} as catalyst in [BMIM][PF_6] as solvent. Substrate/metal ratio = 100.

Recently, tetrabutylammonium bromide-stabilized Pd nanoparticles have been described for the hydrogenation of carbon-carbon double bonds bearing benzyloxy groups in [BMIM][PF_6] under 1 bar of hydrogen and at room temperature [77]. Some results are summarized in Table 9.11. The nanoparticles were synthesized from $PdCl_2$ or $Pd(OAc)_2$ precursors. These metal salts were mixed with tetrabutylammonium bromide and heated under vacuum at 120 °C before addition of tri-*n*-butylamine (*n*-Bu_3N) and an additional treatment at 120 °C for 3 h. The black powders formed could be isolated and characterized by a variety of techniques (IR, NMR, elemental analysis, TEM). TEM analysis revealed dispersed nanoparticles (d_m = 4.1±1.0 nm) in the case of $Pd(OAc)_2$ as precursor, but agglomerated particles (d_m = 7.5±1.7 nm) with $PdCl_2$. It appeared that the hydrogenation of double bonds was chemoselective. Recycling of the system [BMIM][PF_6]/palladium nanoparticles has been carried out, without noticeable modification of the chemoselectivity and yield.

9.3.9
Supercritical Microemulsions Used as Templates for the Stabilization of Metal Nanoparticles

In recent years, supercritical fluids such as $scCO_2$ were considered to be modern "green" solvents: they were non-toxic, readily available, inexpensive, and environmentally benign. They are studied as a reaction medium for catalytic applications because of their interest in product separation and catalyst recovery, and

several reports have described the use of metal nanoparticles in supercritical fluids.

Wai et al. used water-in-CO_2 microemulsions as a medium for synthesizing metallic Pd nanoparticles [78]. The water-in-CO_2 microemulsion was prepared by mixing an aqueous $PdCl_2$ solution with a mixture of bis(2-ethylhexyl)sulfosuccinate (AOT) as surfactant and perfluoropolyetherphosphate (PFPE-PO_4) as co-surfactant into CO_2 at 80 atm to ensure the formation of an optically transparent microemulsion. Injection of dihydrogen into the microemulsion allowed the formation of Pd nanoparticles in the size range 5–10 nm, as confirmed by UV-visible spectroscopy and TEM analysis. The hydrogenation of 4-methoxy-cinnamic acid to 4-methoxyhydrocinnamic acid was performed first in liquid CO_2 and then in supercritical CO_2 at 35 °C and 50 °C. The hydrogenation process is much faster in the $scCO_2$ phase (35 and 50 °C) compared with that in the liquid CO_2 phase (20 °C), probably due to a better diffusion of the reactant from bulk CO_2 to the Pd nanoparticles surface, the diffusion coefficient of CO_2 dramatically changing at the critical point (31 °C). *Trans*-stilbene and maleic acid hydrogenations were also performed, undergoing the production of 1,2-diphenylethane and succinic acid respectively, as determined by NMR investigation.

The same authors also reported the dispersion of palladium nanoparticles in a water/AOT/*n*-hexane microemulsion by hydrogen gas reduction of $PdCl_4^{2-}$ and its efficiency for hydrogenation of alkenes in organic solvents [79]. UV-visible spectroscopy and TEM analysis revealed the formation of Pd nanoparticles with diameters in the range of 4 to 10 nm. Three olefins (1-phenyl-1-cyclohexene, methyl *trans*-cinnamate, and *trans*-stilbene) were used as substrates for the catalytic hydrogenation experiments under 1 atm of H_2 (Table 9.12). All of the start-

Table 9.12 Catalytic hydrogenation of olefins with Pd nanoparticles in a water-in-hexane microemulsion. (Reprinted with the permission of the American Chemical Society [79])

Olefin	Catalyst	Reaction time [min]	Conversion [%]	Product
	Pd/ME[a)]	5	>97	
	Pd/C[b)]	20	50	
	Pd/C[b)]	40	>97	
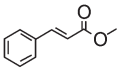	Pd/ME[a)]	6	>97	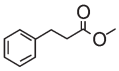
	Pd/C[b)]	25	60	
	Pd/C[b)]	45	>97	
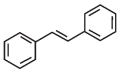	Pd/ME[a)]	7	>97	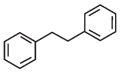
	Pd/C[b)]	40	68	
	Pd/C[b)]	60	>97	

a) Molar ratio of alkene/AOT/Na_2PdCl_4 = 1/1/0.01 and 10 mL of *n*-hexane used as solvent (W = 15) at 30 °C.

b) 1.7 mg Pd/C (0.17 mg or 1.6 μmol Pd) in 10 mL *n*-hexane.

ing alkenes were converted into the saturated hydrocarbons within 6–7 min, while the Pd nanoparticles dispersed in the microemulsion proved to be more efficient catalysts than the Pd/C catalyst tested for comparison.

9.3.10 Conclusion

A variety of approaches has been explored for the synthesis of metal nanoparticles, with the objective of using them as catalysts for alkenes hydrogenation. It appears, clearly, that whichever the chosen stabilizing mode, it is possible to obtain active nanoparticles for olefin hydrogenation. Nevertheless, the activities obtained are difficult to compare as the experimental conditions are, by necessity, different. Even if the tested catalytic reaction is for most of the time the hydrogenation of simple olefins, other colloidal systems have permitted the hydrogenation of more interesting alkenes. Recycling of the nanocatalysts is also of major interest, as colloidal catalysts may be considered to be pseudo-homogeneous catalysts (soluble nanocatalysts) with clear advantages over their heterogeneous counterparts. Indeed, colloidal nanoparticles represent highly interesting systems for the future development of catalysis in terms of both activity and selectivity.

9.4 Hydrogenation of Compounds with C≡C Bonds

The use of dispersed or immobilized transition metals as catalysts for partial hydrogenation reactions of alkynes has been widely studied. Traditionally, alkyne hydrogenations for the preparation of fine chemicals and biologically active compounds were only performed with heterogeneous catalysts [80–82]. Palladium is the most selective metal catalyst for the semihydrogenation of monosubstituted acetylenes and for the transformation of alkynes to *cis*-alkenes. Commonly, such selectivity is due to stronger chemisorption of the triple bond on the active center.

The liquid-phase hydrogenation of various terminal and internal alkynes under mild conditions was largely described with metal nanoparticles deposited/incorporated in inorganic materials [83, 84], although several examples of selective reduction achieved by stabilized palladium, platinum or rhodium colloids have been reported in the literature.

The selective hydrogenation of hex-2-yne into *cis*-hex-2-ene with Pd colloids stabilized by 1,10-phenanthroline and derivatives has been reported by Schmid. Selectivity in alkenes up to 99% was obtained [25]. The use of PVP-stabilized Pt colloids with an average particle size of 1.4 nm dispersed in a propanol mixture prepared from $Pt_2(dba)_3$ provided 81% and 62% selectivity to *cis*-hexene at 50% and 90% hex-2-yne conversion, respectively. Bradley has shown that selectivity up to 89% in *cis*-hex-2-ene could be obtained with colloids supported in an

amorphous microporous mixed oxides [85]. Following the adapted procedure, Bönnemann performed the hydrogenation of hex-3-yn-1-ol into *cis*-hex-3-en-1-ol with previously synthesized Pd colloids and immobilized on $CaCO_3$; the obtained selectivity was about 98% [86].

Partial hydrogenation of acetylenic compounds bearing a functional group such as a double bond has also been studied in relation to the preparation of important vitamins and fragrances. For example, selective hydrogenation of the triple bond of acetylenic alcohols and the double bond of olefin alcohols (linalol, isophytol) was performed with Pd colloids, as well as with bimetallic nanoparticles Pd/Au, Pd/Pt or Pd/Zn stabilized by a block copolymer (polystyrene-poly-4-vinylpyridine) (Scheme 9.8). The best activity (TOF 49.2 s^{-1}) and selectivity (>99.5%) were obtained in toluene with Pd/Pt bimetallic catalyst due to the influence of the modifying metal [87, 88].

Recently, Chaudhari compared the activity of dispersed nanosized metal particles prepared by chemical or radiolytic reduction and stabilized by various polymers (PVP, PVA or poly(methylvinyl ether)) with the one of conventional supported metal catalysts in the partial hydrogenation of 2-butyne-1,4-diol. Several transition metals (e.g., Pd, Pt, Rh, Ru, Ni) were prepared according to conventional methods and subsequently investigated [89]. In general, the catalysts prepared by chemical reduction methods were more active than those prepared by radiolysis, and in all cases aqueous colloids showed a higher catalytic activity (up to 40-fold) in comparison with corresponding conventional catalysts. The best results were obtained with cubic Pd nanosized particles obtained by chemical reduction (Table 9.13).

Catalytic studies and kinetic investigations of rhodium nanoparticles embedded in PVP in the hydrogenation of phenylacetylene were performed by Choukroun and Chaudret [90]. Nanoparticles of rhodium were used as heterogeneous catalysts (solventless conditions) at 60 °C under a hydrogen pressure of 7 bar with a [catalyst]/[substrate] ratio of 3800. Total hydrogenation to ethylbenzene was observed after 6 h of reaction, giving rise to a TOF of 630 h^{-1}. The kinetics of the hydrogenation was found to be zero-order with respect to the alkyne compound, while the reduction of styrene to ethylbenzene depended on the concentration of phenylacetylene still present in solution. Additional experi-

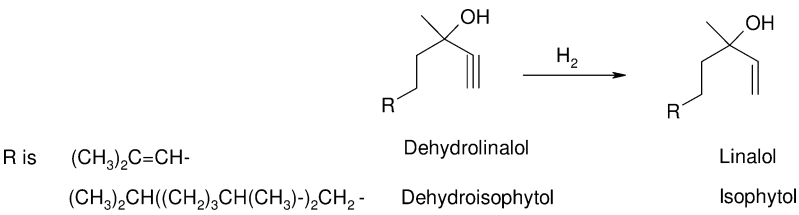

Scheme 9.8 Semihydrogenation of olefin alcohols with Pd colloids stabilized by a block copolymer polystyrene-poly-4-vinylpyridine.

Table 9.13 Comparison of colloidal and heterogeneous catalysts in the hydrogenation of 2-butyne-1,4-diol. (Adapted from [89])

Catalyst	Size [nm]	Selectivity [%]	TOF [$\times 10^{-5}$ h^{-1}]	$TOF_{Mt\text{-}PVP}$/ $TOF_{Mt\text{-}CaCO_3}$
Pt/PVP	5.1	96	5.5	
Pt/$CaCO_3$	–	83	0.2	27
Rh/PVP	5	96	4.2	
Rh/$CaCO_3$	–	85	0.1	42
Ru/PVP	4.8	95.2	5.1	
Ru/$CaCO_3$	–	75	0.14	36
Ni/PVP	9.4	99	0.1	
Ni/C	–	65	0.01	10
Pd/PVA	5.7	99	5	–
Pd/PMVE	5.4	89.2	5.2	–
Pd/PVP	5	91.1	5.7	
Pd/$CaCO_3$	–	83	0.15	38

ments conducted in the presence of phosphine showed that the amount of styrene increased while the formation of ethylbenzene versus styrene decreased.

Colloidal catalysts in alkyne hydrogenation are widely used in conventional solvents, but their reactivity and high efficiency were very attractive for application in $scCO_2$. This method, which is based on colloidal catalyst dispersed in $scCO_2$, yields products of high purity at very high reactions rates. Bimetallic Pd/Au nanoparticles (Pd exclusively at the surface, while Au forms the cores) embedded in block copolymer micelles of polystyrene-block-poly-4-vinylpyridine

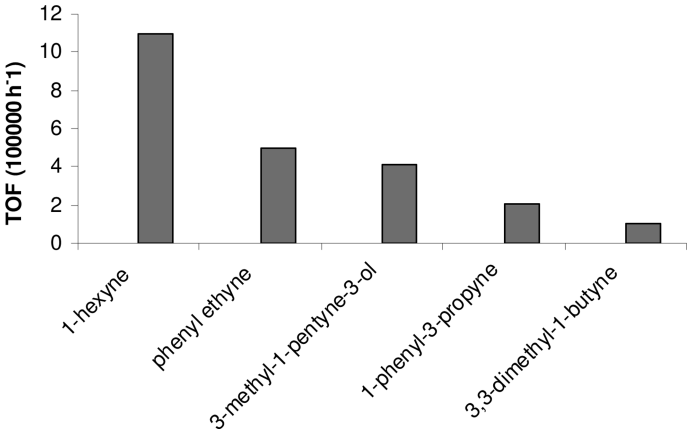

Fig. 9.2 TOF-values calculated at 50% conversion in the hydrogenation of various alkynes with a [substrate]/[Pd] ratio near 6500. (Adapted from [91])

were reported in highly efficient single-phase hydrogenation of alkynes in $scCO_2$ [91]. Several substrates, including 1-hexyne, 3-methyl-1-pentyne-3-ol, 3,3-dimethyl-1-butyne, phenyl ethyne and 1-phenyl-3-propyne, were investigated at a hydrogen pressure of 15 bar, 50 °C and a CO_2 pressure of 150 bar (Fig. 9.2).

According to the hydrogen pressure and substrate/Pd ratio, a TOF up to 4×10^6 h^{-1} was observed for the hydrogenation of 1-hexyne, this being the highest TOF ever reported for alkyne hydrogenation.

9.5 Arene Hydrogenation

In most cases, the industrial hydrogenation of benzene and derivative compounds is performed using heterogeneous catalysis [92, 93]. In many cases (if not the majority) these systems require drastic conditions (high hydrogen pressure and/or temperature), but the use of nanoparticles under mild conditions has received an increasing amount of attention since some homogeneous catalysts were shown to be micro- or nano-heterogeneous [4–6]. Recent progress [94, 95] in the complete catalytic hydrogenation of monocyclic aromatic compounds by noble metal (0) nanoparticles such as Pt, Rh, Ru or Ir in various liquid media has been described in the literature (Scheme 9.9).

In this strategic research area, significant results based on a critical combination of various parameters were obtained by several catalytic systems [94]. Three parameters seem to be highly important:

- the stabilizing agent, which may be either one of PVP, polyoxoanion, surfactant or ionic liquids;
- the nature of the precursor: metal salts or organometallic compounds; and
- the type of the catalytic system: monophasic (organic) or biphasic liquid–liquid (organic/organic and water/organic) media.

Ammonium salts are commonly used to stabilize aqueous colloidal suspensions of nanoparticles. The first such example was reported in 1983–84 by Januszkiewicz and Alper [96, 97], who described the hydrogenation of several benzene derivatives under 1 bar H_2 and biphasic conditions starting with $[RhCl(1,5\text{-hexadiene})]_2$ as the metal source and with tetraalkylammonium bromide as a stabilizing agent. Some ten years later, Lemaire and coworkers investigated the *cis*/

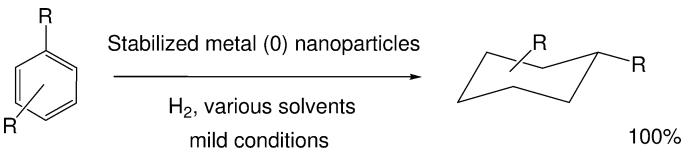

Scheme 9.9 Total hydrogenation of monocyclic arene compounds by various zerovalent noble-metal nanoparticles.

trans selectivity in the hydrogenation of methylanisole and cresol derivatives. Rhodium colloids in the 2- to 3-nm size range were obtained from rhodium trichloride in the presence of tricaprylylmethylammonium chloride salt or trioctylamine. A Total Turn Over (TTO) of 40 in 24 h was reported for the hydrogenation of 2-methylanisole, and the *cis* compound was formed with selectivities exceeding 97% [98]. These authors also observed a partial hydrogenolysis of the methoxy group (10%). Similarly, James and coworkers used tetrabutylammonium salts to stabilize rhodium and ruthenium nanoparticles. Several substrates containing the 4-propylphenol fragment were hydrogenated in biphasic media and under various conditions (20–100 °C, 1–50 bar H_2). The best results were obtained for the hydrogenation of 2-methoxy-4-propylphenol by ruthenium nanoparticles with a TTO of 300 in 24 h [99–101].

In 1999, the group of Roucoux succeeded in the synthesis of aqueous suspensions of rhodium(0) colloids by reducing $RhCl_3 \cdot 3H_2O$ with $NaBH_4$ in the presence of surfactants which provide an electrosterical stabilization. Nanoparticles stabilized by *N,N*-dimethyl-*N*-cetyl-*N*-(2-hydroxyethyl)ammonium salts (counteranion: Br, Cl, I, CH_3SO_3, BF_4) are well-defined with a mean size of 2–3 nm. Various mono-, di-substituted and/or functionalized arene derivatives are hydrogenated, with TOFs up to 200 h^{-1}, in pure biphasic liquid–liquid (water/substrate) media at 20 °C and 1 bar H_2. The hydrogenation of anisole is observed with a TOF of 4000 h^{-1} under 40 bar H_2. The nanocatalyst could be separated by simple decantation and reused in successive hydrogenation reactions. Significant results have been obtained in the hydrogenation of anisole, with 2000 TTO in 37 h [14,15]. In the same manner, the efficient hydrogenation of various benzene compounds in aqueous media at room temperature and under 40 bar H_2 has also been described by using similar reusable surfactant-protected iridium(0) nanoparticles [102]. In all cases, the conversion is complete after a few hours. A TTO of 3000 was obtained for anisole hydrogenation in 45 h. TEM observations showed the particles to be monodispersed, with an average diameter of 1.9±0.7 nm (Scheme 9.10). Selective hydrogenation of di-substituted benzenes such as xylene, methylanisole, and cresol was also observed with these aqueous suspensions of rhodium(0) and iridium(0) nanoparticles. In all cases, the *cis*-compound is the major product (>80%). The *cis/trans* ratio decreases with the position of the substituents *ortho* > *meta* > *para*, but the nature of the metal does not seem important with this surfactant-stabilized system [14, 102].

Similar surfactant-stabilized colloidal systems have been reported by Albach and Jautelat, who prepared aqueous suspensions of Ru, Rh, Pd, Ni nanoparticles and bimetallic mixtures stabilized by dodecyldimethylammonium propanesulfonate [103]. Benzene, cumene and isopropylbenzene were reduced in biphasic conditions under various conditions at 100–150 °C and 60 bar H_2, and TTO up to 250 were obtained.

The immobilization of metal nanoparticles with a water-soluble polymeric material such as PVP has also been described. The groups of Choukroun and Chaudret have described the hydrogenation of benzene in a biphasic mixture with PVP-protected native Rh nanoparticles synthesized from the organometal-

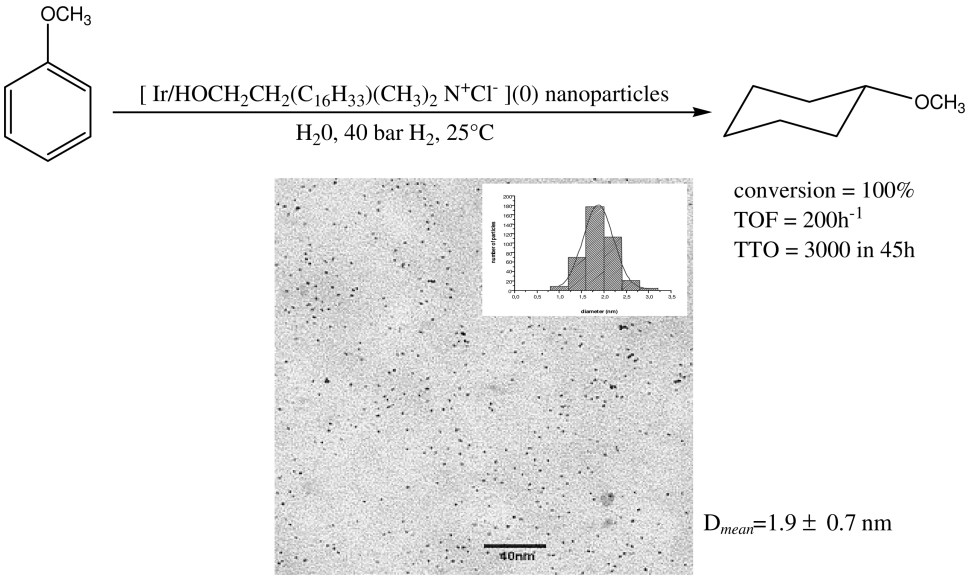

Scheme 9.10 Hydrogenation of anisole by reusable surfactant-stabilized Ir(0) colloids in water. TEM micrograph and size distribution of Ir(0). (Adapted from [102].)

lic complex $[RhCl(C_2H_4)_2]_2$ [90]. The presence of soluble Rh nanoparticles with sizes in the 2- to 3-nm range was confirmed by TEM. In water/benzene biphasic conditions at 30 °C and under 7 bar H_2, complete benzene hydrogenation is observed at a substrate : catalyst ratio of 2000 after 8 h, giving rise to a TOF of 675 h^{-1} (related to H_2 consumed).

Details of a similar polymer-stabilized colloidal system were published by James and coworkers [104]. Rhodium colloids are produced by reducing $RhCl_3 \cdot 3H_2O$ with ethanol in the presence of PVP. The monophasic hydrogenation of various substrates such as benzyl acetone and 4-propylphenol and benzene derivatives was performed under mild conditions (25 °C, 1 bar H_2). The nanoparticles are poorly characterized and benzyl acetone is reduced, with 50 TTO in 43 h.

Recently, Dupont and coworkers described the use of room-temperature imidazolium ionic liquids for the formation and stabilization of transition-metal nanoparticles. The potential interest in the use of ionic liquids is to promote a biphasic organic–organic catalytic system for a recycling process. The mixture forms a two-phase system consisting of a lower phase which contains the nanocatalyst in the ionic liquid, and an upper phase which contains the organic products. Rhodium and iridium [105], platinum [73] or ruthenium [74] nanoparticles were prepared from various salts or organometallic precursors in dry 1-butyl-3-methylimidazolium hexafluorophosphate (BMI PF_6) ionic liquid under hydrogen pressure (4 bar) at 75 °C. Nanoparticles with a mean diameter of 2–3 nm

were isolated by centrifugation. The isolated colloids could be used as solids (heterogeneous catalyst), in acetone solution (homogeneous catalyst), or re-dispersed in BMI PF_6 (biphasic system) for benzene hydrogenation studies. Iridium and rhodium nanoparticles have also been studied in the hydrogenation of various aromatic compounds [105]. In all cases, total conversions were not observed in BMI PF_6. A comparison between Ir(0) and Rh(0) nanoparticles shows that iridium colloids are much more active for the benzene hydrogenation in biphasic conditions, with TOFs of 50 h^{-1} and 11 h^{-1}, respectively, and 24 h^{-1} and 5 h^{-1} for *p*-xylene reduction at 75 °C and under 4 bar H_2. The best results were obtained with platinum nanoparticles prepared from simple decomposition of $Pt_2(dba)_3$ in heterogeneous (solventless) conditions with a TOF of 28 h^{-1} for 100% conversion. The authors reported that the TOF dramatically decreased in biphasic liquid–liquid condition (BMI PF_6) to 11 h^{-1} at 46% conversion, justifying the absence of recycling studies with this substrate [73]. Finally, Dupont and coworkers have described the preparation of Ru(0) nanoparticles by H_2 reduction of the organometallic precursor Ru(COD)(COT) in BMI PF_6, a room-temperature ionic liquid, with hydrogen pressure [74]. These nanoparticles are efficient catalysts for the complete hydrogenation of benzene (TOF = 125 h^{-1}) under solventless conditions (heterogeneous catalyst). In a biphasic system, the authors observed a partial conversion in BMI PF_6 with a modest TOF of 20 h^{-1} at 73% conversion in the benzene hydrogenation.

More recently, Dupont and coworkers studied the impact of the steric effect in the hydrogenation of monoalkylbenzenes by zerovalent nanoparticles (Ir, Rh, Ru) in the ionic liquid BMI PF_6. The results, when compared with those obtained with the classical supported heterogeneous catalysts, showed a relationship between the reaction constants and the steric factors [106].

Finally, these particles generated in ionic liquids are efficient nanocatalysts for the hydrogenation of arenes, although the best performances were not obtained in biphasic liquid–liquid conditions. The main importance of this system should be seen in terms of product separation and catalyst recycling. An interesting alternative is proposed by Kou and coworkers [107], who described the synthesis of a rhodium colloidal suspension in BMI BF_4 in the presence of the ionic copolymer poly[(*N*-vinyl-2-pyrrolidone)-*co*-(1-vinyl-3-butylimidazolium chloride)] as protective agent. The authors reported nanoparticles with a mean diameter of ca. 2.9 nm and a TOF of 250 h^{-1} in the hydrogenation of benzene at 75 °C and under 40 bar H_2. An impressive TTO of 20 000 is claimed after five total recycles.

An alternative approach to stabilize nanoparticles is to use polyoxoanions (see Scheme 9.5). Finke and coworkers described polyoxoanion- and ammonium-stabilized rhodium zerovalent nanoclusters for the hydrogenation of classical benzene compounds [95, 108]. This organometallic approach allows reproducible preparation of stable nanoparticles starting from a well-defined complex in terms of composition and structure (see Section 9.3.5).

The polyoxoanion-stabilized Rh(0) nanoclusters were investigated in anisole hydrogenation [6,95]. The catalytic reactions were carried out in a single phase

using a propylene carbonate solution under mild conditions (22 °C, 3.7 bar H_2). Under these standard conditions, anisole hydrogenation with a substrate : catalyst (S : Rh) ratio of 2600 was performed in 120 h, giving rise to a TTO of 1500 ± 100. The authors observed that the addition of proton donors such as HBF_4 Et_2O or H_2O increased the catalytic activity, and reported 2600 TTO for complete hydrogenation in 144 h at 22 °C and 3.7 bar H_2 with a ratio HBF_4 Et_2O : Rh of 10. A black precipitate of bulk Rh(0) is visible at the end of the reaction as a result of the destabilization of nanoclusters due to the interaction of H^+ or H_2O with the basic $P_2W_{15}Nb_3O_{62}^{9-}$ polyoxoanion.

During the past decade, a variety of stabilized systems based on transition-metal nanoparticles has been seriously investigated, and better lifetimes and activities for the total hydrogenation of monocyclic arene derivatives under mild conditions have been reported. New catalytic systems have been described in various media such as supercritical fluids [109], and these represent a promising area of future research. Several recent investigations have shown modest, but promising, results in partial or selective arene hydrogenation with well-defined colloids [94]. In the future, the partial hydrogenation of arene derivatives into cyclohexene or cyclohexadiene compounds should be highlighted as they are key intermediates in organic synthesis.

The process developed by Asahi Chemical Industry in Japan [110], and performed in a tetraphasic system combining gas, oil, water and ruthenium particles with an average diameter of 20 nm, is a significant milestone in this area. The selectivity is very high and a yield of 60% in cyclohexene is obtained with this "bulk" ruthenium catalyst in the presence of zinc as co-catalyst at 150 °C and under 50.4 bar of H_2. The cyclohexene produced by this process is used as a feedstock for caprolactam.

At present, the efficient partial hydrogenation of benzene and its derivatives has been rarely described with well-defined soluble nanoparticles catalysts. Nonetheless, this remains an interesting area for research, with promising future applications.

9.6 Hydrogenation of Compounds with C=O Bonds

Several reports have been made of the hydrogenation of compounds bearing C=O bonds by colloidal catalytic systems.

In 1996, Liu et al. reported the selective hydrogenation of cinnamaldehyde, an α,β-unsaturated aldehyde, to cinnamyl alcohol, an α,β-unsaturated alcohol, by means of PVP-protected Pt/Co bimetallic colloids prepared by the polyol process [111]. The colloids were obtained as a dark-brown homogeneous dispersion in a mixture of ethylene glycol and diethylene glycol, and characterized by TEM and XRD. These authors prepared different samples of nanoparticles with Pt : Co ratios of 3 : 1 and 1 : 1, the mean diameters of which measured 1.7 and 2.2 nm, respectively. These colloidal systems were also compared with the single metal-

based colloids Pt/PVP and Co/PVP. The catalytic tests were carried out under a H_2 pressure of 4 MPa at 333 K in EtOH. While Pt/PVP and Co/PVP colloids gave low activity and selectivity, bimetallic colloids exhibited interesting behavior, with the Pt:Co/PVP (3:1) system being the most interesting. Selectivity in cinnamyl alcohol up to 99.8% was indeed obtained with colloid Pt:Co (3:1) with very good conversions (up to 96.2%). It was observed that activity and selectivity could be affected by the presence of added water or NaOH in the reaction mixture. These results are of interest as it is a difficult task to reduce only the C=O bond when it is conjugated to a C=C double bond, with almost all metal catalysts readily reducing the C=C double bond. These results also showed that the colloids were stable enough for catalytic hydrogenation reaction at elevated temperature and pressure.

Another example from Liu's team in this field concerns the selective hydrogenation of citronellal to citronellol by using a Ru/PVP colloid obtained by $NaBH_4$ reduction method [112]. This colloid contains relatively small particles with a narrow size distribution (1.3 to 1.8 nm by TEM), whereas the metallic state of Ru was confirmed by XPS investigation. This colloid exhibited a selectivity to citronellol of 95.2% with a yield of 84.2% (total conversion 88.4%), which represented a good result for a monometallic catalyst.

Gin and coworkers have presented an original strategy for the synthesis of Pd nanoparticles with both good stability and catalytic activity in benzaldehyde hydrogenation by using a cross-linked lyotropic liquid crystal (LLC) assembly as an organic template (Fig. 9.3) [113]. Incorporation of Pd atoms has been performed by ion exchange on the cross-linked inverted hexagonal phase of the sodium salt with an acetonitrile solution of dichloro(1,5-cyclooctadiene)palladium II complex. The Pd-(II)-LLC composite was treated with dihydrogen to afford spherical Pd nanoparticles of 4–7 nm mean size dispersed in the polymer ma-

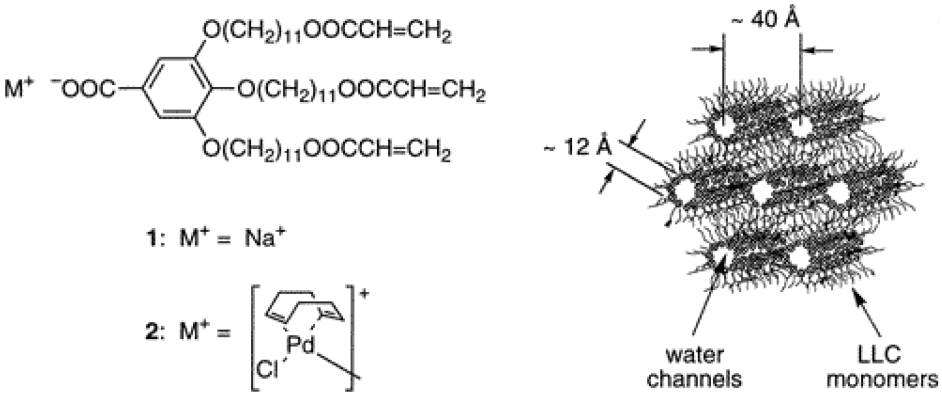

Fig. 9.3 The structure of LLC monomers, 1 and 2, and the inverted hexagonal phase. (Reprinted with the permission of the American Chemical Society [113])

trix. The benzaldehyde hydrogenation was carried out under 1 bar H_2 and 60 °C, and a 98% yield of benzylalcohol was observed after 3 h of reaction.

Pertici et al. described the synthesis of ruthenium nanoparticles on polyorganophosphazenes (PDMP) as stabilizing polymers [114]. The synthesis method consisted of the decomposition of a THF solution of the organometallic Ru(η^4-COD)(η^6-COT) complex at 45 °C under dihydrogen atmosphere in the presence of various polyorganophosphazenes. This procedure gave rise to new materials in which small ruthenium clusters were bound to the arene groups of the polymers. High-resolution TEM analysis revealed well-dispersed and very small nanoparticles of 1.55±0.5 nm mean size in the polymer matrix. These materials could be purified as fine powders containing 5 wt.% of Ru, the dispersion of which could be easily obtained in organic solvent such as ethanol or THF, or in water, allowing their use as homogeneous catalysts. The catalytic experiments were carried out under mild conditions (25 °C, 1 bar H_2) in ethanol, THF or water as solvent. Olefin and ketone hydrogenations were performed. A wide range of carbonyl compounds has been tested such as cyclohexanone, ethyl

Table 9.14 Hydrogenation of ketones with Ru/PDMP at atmospheric hydrogen pressure and 25 °C. (Reprinted with the permission of Elsevier [114])

Substrate [a)]	Solvent	Phase [b)]	Time [h]	Product [c)] [%]	TOF [d)]
Cyclohexanone	Ethanol	Hom	10	Cyclohexanol (100)	10
Ethyl acetoacetate	Ethanol	Hom	24	Ethyl 3-hydroxybutyrate (100)	4.2
Ethyl pyruvate	Ethanol	Hom	6	Ethyl lactate (100)	16.6
Pyruvic acid	Ethanol	Hom	8	Lactic acid (100) [e)]	12.5
Acetophenone	Ethanol	Hom	96	1-Phenylethanol (100)	1
Pyruvic acid	Water	Hom	7	Lactic acid (100) [e)]	14.3
Cyclohexanone [f)]	Ethanol	Hom	30	Cyclohexanol (100)	10
Ethyl acetoacetate [f)]	Ethanol	Hom	6	Ethyl 3-hydroxybutyrate (100)	3.3
Ethyl pyruvate [f)]	Ethanol	Hom	10	Ethyl lactate (100)	16.6
Pyruvic acid [f)]	Ethanol	Hom	8	Lactic acid (100) [e)]	12.5
Acetophenone [f)]	Ethanol	Hom	96	1-Phenylethanol (100)	1
Pyruvic acid [f)]	Water	Hom	7	Lactic acid (100) [e)]	14.3
Cyclohexanone	THF	Het	10	Cyclohexanol (30)	3
Ethyl acetoacetate	THF	Het	30	Ethyl 3-hydroxybutyrate (20)	0.7
Ethyl pyruvate	THF	Het	6	Ethyl lactate (20)	3
Acetophenone	THF	Het	96	1-Phenylethanol (20)	0.2

a) Substrate (13 mmol); catalyst Ru on PDMP (5 wt.% Ru), 0.26 g (0.13 mg atoms Ru); solvent, 15 mL.
b) Hom: homogeneous phase; Het: heterogeneous phase.
c) Composition determined by GLC analysis.
d) Moles converted substrate per gram-atom ruthenium h^{-1}.
e) Composition determined by ^{1}H-NMR spectroscopy.
f) Catalyst recovered from runs 1–6, respectively, and reused.

acetoacetate, ethyl pyruvate and pyruvic acid as examples of aliphatic carbonyl compounds, and acetophenone as an example of ketone bearing an aryl group. All carbonyl compounds were quantitatively reduced to the corresponding alcohols (Table 9.14). The catalysts could be reused after precipitation with a non-solvent.

A HRTEM study showed these catalysts to be more resistant towards agglomeration, as only a low degree of aggregation was noted after dissolution and precipitation of the catalysts. However, this slight agglomeration did not lead to catalyst deactivation. Finally, a catalytic study of a Ru/poly[bis(aryloxy)]phosphazene system indicated that the structure of the side chain of the support had considerable influence on the activity of the deposited metal, providing the possibility of modifying the catalytic activity by changing the support structure [114].

The group of Dupont has described the use of ionic liquids for the formation and stabilization of various metal nanoparticles and their application in hydrogenation reactions. In a report concerning the use of Ir(0) nanoparticles (mean diameter 2.1±0.3 nm) prepared by reduction with molecular hydrogen (4 bar) of $[Ir(COD)Cl]_2$ (COD = 1,5-cyclooctadiene) dissolved in BMI PF_6 ionic liquid at 75 °C, it was mentioned that the solvent, acetone, used for the "homogeneous" hydrogenation reaction of benzene (75 °C, 4 bar H_2) is also hydrogenated, even in the early stages of the reaction [115]. These nanoparticles could be isolated by centrifugation and characterized by TEM and XRD. The authors also reported the hydrogenation of acetophenone. Under "solventless" conditions, they observed the formation not only of 1-cyclohexylethanol but also of ethylcyclohexane, the hydrogenolysis product in a high yield (up to 42%). It was concluded that this result suggested a "heterogeneous" behavior of the Ir(0) nanoparticles in terms of active sites. On pursuing these investigations, it was found that such Ir(0) nanoparticles constitute an efficient and recyclable catalyst for the "solventless" or biphasic hydrogenation of various cyclic and acyclic ketones un-

Table 9.15 Hydrogenation of various carbonyl compounds by Ir(0) nanoparticles in solventless conditions ([substrate]/[Ir] ratio = 250, 75 °C, 4 bar). (Adapted from [116])

Substrate	Product	Time [h]	Yield [%][a)]	TOF[b)] [h^{-1}]
Benzaldehyde	Phenylmethanol	15	100	17
Cyclopentanone	Cyclopentanol	4	100[c)]	62.5
2-Pentanone	2-Pentanol	2.5	96	96
4-Methyl-2-pentanone	4-Methyl-2-pentanol	2.5	96	96
3-Pentanone	3-Pentanol	3.7	100	68
Ethylpyruvate	Ethyl-lactate	2.5	98	98
Acetone	2-Propanol	2.0	95	119

a) Conversions determined by GLC.
b) Mol ketone mol^{-1} iridium h^{-1}.
c) Products obtained were cyclopentanol and bicyclopentyl ether (12%).

der mild conditions (Table 9.15) after optimization of the reaction conditions with cyclohexanone [116]. In the case of ketones containing aromatic cycles, a tendency for the selective hydrogenation of the aromatic ring was observed. The method was also applied to the hydrogenation of benzaldehyde.

9.7 Enantioselective Hydrogenation

The enantioselective hydrogenation of prochiral substances bearing an activated group, such as an ester, an acid or an amide, is often an important step in the industrial synthesis of fine and pharmaceutical products. In addition to the hydrogenation of β-ketoesters into optically pure products with Raney nickel modified by tartaric acid [117], the asymmetric reduction of α-ketoesters on heterogeneous platinum catalysts modified by cinchona alkaloids (cinchonidine and cinchonine) was reported for the first time by Orito and coworkers [118–121]. Asymmetric catalysis on solid surfaces remains a very important research area for a better mechanistic understanding of the interaction between the substrate, the modifier and the catalyst [122–125], although excellent results in terms of enantiomeric excesses (up to 97%) have been obtained in the reduction of ethyl pyruvate under optimum reaction conditions with these Pt/cinchona systems [126–128].

Supported palladium and platinum modified by chiral compounds are largely used as pure heterogeneous hydrogenation catalysts. However, recent studies have been performed starting with catalysts of colloidal nature and particles with dimensions of only a few nanometers. Their development continues to attract substantial interest for three main reasons:

- The elimination of the support such as Al_2O_3, SiO_2, TiO_2, zeoliths and of its influences.
- The possibility of obtaining size- and shape-controlled nanoparticles, thereby giving efficient activities.
- The possibility of adapting chiral molecules as inducer or stabilizer (form and amount) for better selectivities.

The concept of using colloids stabilized with chiral ligands was first applied by Bönnemann to hydrogenate ethyl pyruvate to ethyl lactate with Pt colloids. The nanoparticles were stabilized by the addition of dihydrocinchonidine salt (DHCin, HX) and were used in the liquid phase or adsorbed onto activated charcoal and silica [129, 130]. The molar ratio of platinum to dihydrocinchonidine, which ranged from 0.5 to 3.5 during the synthesis, determines the particle size from 1.5 to 4 nm and contributes to a slight decrease in activity (TOF = 1 s^{-1}). In an acetic acid/MeOH mixture and under a hydrogen pressure up to 100 bar, the (*R*)-ethyl lactate was obtained with optical yields of 75–80% (Scheme 9.11).

Several mechanistic investigations concerning the hydrogenation of pyruvate derivatives (ethyl or methyl esters) were performed with platinum, rhodium and

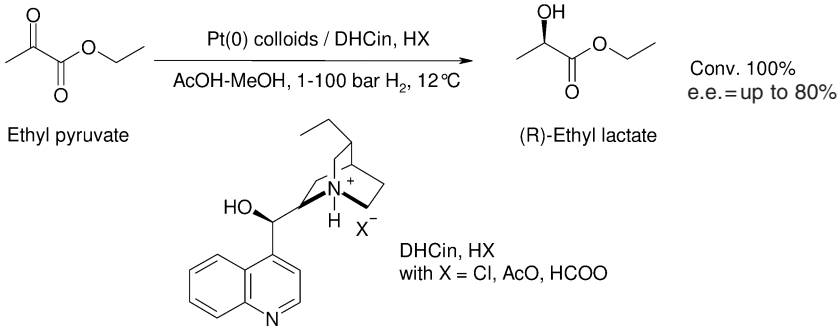

Scheme 9.11 Enantioselective hydrogenation of ethyl pyruvate with platinum colloids stabilized by protonated-dihydrocinchonidine.

iridium nanoparticles stabilized by PVP. In all cases, nanoparticles of size range 2 to 4 nm were modified by cinchonidine or quinine [127, 131–135]. The Pt/PVP catalyst hydrogenated ethyl pyruvate, with ee-values up to 92%, and methyl pyruvate with ee-values up to 98%, depending upon the nanoparticle size. The best results were obtained in acetic acid. The asymmetric hydrogenation of trifluoroacetophenone and α-diketones such as 2,3-butanedione and 3,4-hexanedione was also investigated using finely dispersed PVP-stabilized Pt nanoparticles modified with cinchonidine, and ee-values of up to 30% were reported, according to the solvent [136, 137]. Similar results (ee 30%) were described with solvent-stabilized Pt and Pd nanoparticles prepared by the metal vapor synthesis route for the enantioselective hydrogenation of ethyl pyruvate [138].

Recently, platinum nanoparticles protected by *N,N*-dimethyl-*N*-cetyl-*N*-(2-hydroxyethyl)ammonium chloride salt and modified with cinchonidine were investigated in the enantiomeric hydrogenation of ethyl pyruvate in pure biphasic liquid–liquid (water/substrate) media at room temperature [139]. For the first time, the aqueous phase containing Pt(0) nanocatalysts with an average size of 2.5 nm could be reused for successive hydrogenations, and with a total conversion of activity and enantioselectivity in (*R*)-(+)-ethyl lactate up to 55% (Scheme 9.12).

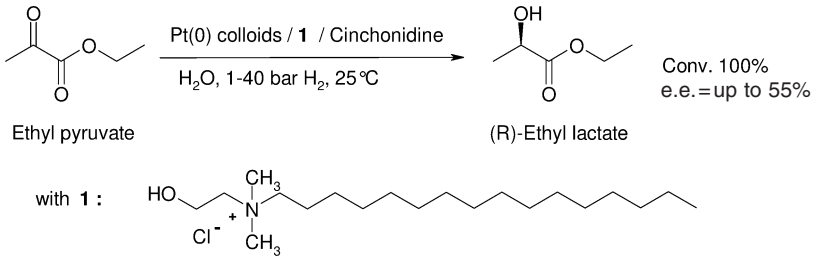

Scheme 9.12 Reusable aqueous suspension of Pt nanoparticles for enantioselective hydrogenation of ethyl pyruvate.

Table 9.16 Comparison of stabilized nanoparticle systems modified with cinchonidine for the hydrogenation of various α-ketoesters and α-diketones.

Catalyst	Substrate	Solvent	Conversion [%]	Temp. [°C]	PH_2 [bar]	ee [%] (config.)	Reference(s)
Pt-PVP	Methyl pyruvate [a)]	AcOH	100	25	40	97.6 (*R*)	127, 135
Pt-PVP	Ethyl pyruvate [b)]	AcOH	100	25	40	93.8 (*R*)	127, 135
Pt-PVP	*n*-propyl pyruvate [b)]	AcOH	100	25	40	95.6 (*R*)	135
Pt-PVP	*Iso*-propyl pyruvate [b)]	AcOH	58.5	25	40	77.1 (*R*)	135
Pt-PVP	*n*-butyl pyruvate [b)]	AcOH	86.7	25	40	90.5 (*R*)	135
Pt-PVP	*Iso*-butyl pyruvate [b)]	AcOH	95.5	25	40	93.1 (*R*)	135
Pt-PVP	Methyl pyruvate [c)]	EtOH	61.3	25	40	84.7 (*R*)	127
Pt-DHCin,HX	Ethyl pyruvate [d)]	AcOH/MeOH	100	19	1–100	75–80 (*R*)	129, 130
Pt-MEK	Ethyl pyruvate [e)]	MEK	100	25	70	25 (*R*)	138
Pt-MMK	Ethyl pyruvate [f)]	MMK-H_2O	100	25	70	36 (*S*)	138
Pt-HEA16Cl	Ethyl pyruvate [g)]	H_2O	100	25	40	55 (*R*)	139
Pt/PVP	2,3-Butanedione [h)]	EtOH	95.5	25	40	27.9 (*R*)	136
Pt/PVP	2,3-Butanedione [h)]	AcOH	92.9	25	40	22.6 (*R*)	136
Ir-PVP	2,3-Butanedione [h)]	AcOH	80.5	25	40	20.4 (*R*)	136
Pt/PVP	3,4-Hexanedione [h)]	EtOH	94.9	25	40	18.0 (*R*)	136
Pt/PVP	3,4-Hexanedione [h)]	AcOH	87.8	25	40	20.6 (*R*)	136
Pd-MEK-KD1	Ethyl pyruvate [i)]	MEK	13	25	70	29 (*R*)	138
Rh-PVP	Ethyl pyruvate [j)]	EtOH/THF	100	25	50	42.2 (*R*)	133
Ir-PVP	Methyl pyruvate [k)]	EtOH	85	20	25	17.0 (*R*)	134

a) TOF = 1.21 s^{-1}.
b) [substrate]/[Pt] ratio = 1600.
c) TOF = 0.76 s^{-1}.
d) TOF $\approx$ 1 s^{-1}.
e) Initial rate = 1025 mmol s^{-1} mol_{metal}^{-1}.
f) Cinchonine is used as modifier, initial rate = 2253 mmol s^{-1} mol_{metal}^{-1}.
g) [substrate]/[Pt] ratio = 400.
h) [substrate]/[Pt] ratio = 1765.
i) Initial rate = 47 mmol s^{-1} mol_{metal}^{-1}.
j) TOF = 941 h^{-1}.
k) Average rate = 838 mmol h^{-1} g_{metal}^{-1}.

Although several noble-metal nanoparticles have been investigated for the enantiomeric catalysis of prochiral substrates, platinum colloids remain the most widely studied. PVP-stabilized platinum modified with cinchonidine showed ee-values >95%. Several stabilizers have been also investigated such as surfactants, cinchonidinium salts and solvents, and promising ee-values have been observed. Details of a comparison of various catalytic systems are listed in Table 9.16; in one case, the colloid suspension was reused without any loss in enantioselectivity. Clearly, the development of convenient two-phase liquid–liquid systems for the recycling of chiral colloids remains a future challenge.

9.8 Conclusion

This chapter provides a non-exhaustive overview of the hydrogenation of carbon-carbon double or triple bonds, carbonyl groups and aromatic compounds with colloids as soluble catalysts. The subject, while of crucial importance, is generally not covered in detail in books on homogeneous catalysis, despite several efficient molecular homogeneous complexes having been shown to be precursors of "nanoheterogeneous" catalysts. Such materials, when correctly characterized, constitute an interesting class of both homogeneous and/or heterogeneous catalysts, and the use of colloids is generally seen as being compatible with a variety of reaction media according to the organic- or water-soluble nature of the stabilizers. Colloids can also be adapted for use in biphasic conditions, thereby allowing recovery of the nanocatalysts by simple decantation/filtration, and subsequent recycling. Although stabilized colloids are neither "traditional" nor "routine" catalysts, their performances in some cases – and their potential role as catalysts – is now clearly recognized by the scientific community, and nanoparticle systems represent an interesting compromise between homogeneous and heterogeneous catalytic systems, both in terms of activity and selectivity. Finally, the number of reports related to the use of colloids in catalysis has increased significantly, with interest in colloidal systems limited not only to current hydrogenation reactions but also being indicative of future processes.

Abbreviations

β-CD	*β*-cyclodextrin
BMI PF_6	1-*n*-butyl-3-methylimidazolium hexafluorophosphate
COD	cycloocta-1,5-diene
COT	cycloocta-1,3,5-triene
DLVO	Derjaguin-Landau-Verway-Overbeek
DTAC	dodecyltrimethylammonium
EDX	electron diffraction X-ray
EXAFS	extended X-ray absorption fine structure
HDA	hexadecylaniline
HRTEM	high-resolution TEM
LLC	lyotropic liquid crystal
NMR	nuclear magnetic resonance
PAA	poly(acrylic acid)
PAMAM	poly(amidoamine)
PDMS-*b*-PEO	poly(dimethylsiloxane)-*b*-poly(ethylene oxide)
PEG	polyethylene glycol
PPI	poly(propylene imine)
PS-*b*-PEO	polystyrene-*b*-poly(ethylene oxide)
PS-*b*-PMAA	polystyrene-*b*-poly(methacrylic acid)

P*t*BA-*b*-PCEMA	poly(*t*-butyl acrylate)-*block*-poly(2-cinnamoyloxyethyl) methacrylate
PVA	polyvinylalcohol
PVP	polyvinylpyrrolidone
SAED	selected area electron diffraction
SDS	sodium dodecylsulfate
TEM	transmission electronic microscopy
TGA	thermogravimetric analysis
TOF	turnover frequency
THF	tetrahydrofuran
TTO	total turnover
WAXS	wide-angle X-ray scattering
XPS	X-ray photoelectron spectroscopy
XRD	X-ray diffraction

References

1 G. Schmid (Ed.), *Nanoparticles. From theory to application*. Wiley-VCH, Weinheim, **2004**.
2 D.L. Feldheim, C.A. Foss, Jr. (Eds.), *Metal Nanoparticles: Synthesis, Characterization and Applications*. Marcel Dekker, New York, **2002**.
3 A. Roucoux, J. Schulz, H. Patin, *Chem. Rev.* **2002**, *102*, 3757.
4 P.J. Dyson, *Dalton Trans.* **2003**, 2964.
5 J.A. Widegren, R.G. Finke, *J. Mol. Catal. A Chem.* **2003**, *198*, 317.
6 M.C. Hagen, L. Vieille-Petit, G. Laurenczy, G. Suss-Fink, R. Finke, *Organometallics* **2005**, *24*, 1819.
7 K. Philippot, B. Chaudret, *C. R. Chimie* **2003**, *6*, 1019.
8 J.T.G. Overbeek, in: Goodwin, J.W. (Ed.), *Colloidal Dispersions*. Royal Society of Chemistry, London **1981**, pp. 1–23.
9 D.F. Evans, H. Wennerström, in: *The Colloidal Domain*, 2nd edn. Wiley-VCH, New York, **1999**.
10 R.J. Hunter, in: *Foundations of Colloid Science*. Oxford University Press, New York **1987**, vol. 1, pp. 316.
11 D.H. Napper, in: *Polymeric Stabilization of Colloidal Dispersions*. Academic Press, London, **1983**.
12 M. Komiyama, H. Hirai, *Bull. Chem. Soc. Mater.* **1993**, *56*, 2833.
13 A. Duteil, R. Queau, B. Chaudret, C. Roucau, J.S. Bradley, *Chem. Mater.* **1993**, *5*, 341.
14 J. Schulz, A. Roucoux, H. Patin, *Chem. Eur. J.* **2000**, *6*, 618.
15 A. Roucoux, J. Schulz, H. Patin, *Adv. Synth. Catal.* **2002**, *345*, 222.
16 L. Manna, S.C. Scher, A.P. Alivisatos, *J. Am. Chem. Soc.* **2000**, *122*, 12700.
17 A. Duteil, G. Schmid, W. Meyer-Zaika, *J. Chem. Soc. Chem. Commun.* **1995**, 31.
18 A. Rodriguez, C. Amiens, B. Chaudret, M.J. Casanove, P. Lecante, J.S. Bradley, *Chem. Mater.* **1996**, *8*, 1978.
19 F. Dassenoy, K. Philippot, T. Ould Ely, C. Amiens, P. Lecante, E. Snoeck, A. Mosset, M.J. Casanove, B. Chaudret, *New J. Chem.* **1998**, *22*, 703.
20 S. Chen, K. Kimura, *J. Phys. Chem. B* **2001**, *105*, 5397.
21 C. Pan, K. Pelzer, K. Philippot, B. Chaudret, F. Dassenoy, P. Lecante, M.J. Casanove, *J. Am. Chem. Soc.* **2001**, *123*, 7584.
22 C.J. Kiely, J. Fink, M. Brust, D. Bethell, D.J. Schiffrin, *Nature* **1998**, *396*, 444.
23 G. Schmid, V. Maihack, F. Lantermann, S. Peschel, *J. Chem. Soc. Dalton Trans.* **1996**, 589.
24 N. Cordente, M. Respaud, F. Senocq, M.J. Casanove, C. Amiens, B. Chaudret, *Nano Lett.* **2001**, *1*, 565.

25 G. Schmid, S. Emde, V. Maihack, W. Meyer-Zaika, S. Peschel, *J. Mol. Catal. A Chem.* **1996**, *107*, 95.
26 K. Soulantica, A. Maisonnat, M.C. Fromen, M.J. Casanove, P. Lecante, B. Chaudret, *Angew. Chem. Int. Ed.* **2001**, *38*, 3736.
27 M. Gomez, K. Philippot, V. Collière, P. Lecante, G. Muller, B. Chaudret, *New J. Chem.* **2003**, *27*, 114.
28 O. Vidoni, K. Philippot, C. Amiens, B. Chaudret, O. Balmes, J.O. Malm, J.aO. Bovin, F. Senocq, M.J. Casanove, *Angew. Chem. Int. Ed.* **1999**, *38*, 3736.
29 K. Pelzer, K. Philippot, B. Chaudret, *Z. Phys. Chem.* **2003**, *217*, 1539.
30 K. Pelzer, O. Vidoni, K. Philippot, B. Chaudret, V. Colliere, *Adv. Funct. Mater.* **2003**, *13*, 118.
31 Y. Wang, J. Ren, K. Deng, L. Gui, Y. Tang, *Chem. Mater.* **2000**, *12*, 1622.
32 H. Hirai, *J. Macromol. Sci. Chem.* **1979**, *A13*(5), 633.
33 Y. Shiraishi, M. Nakayama, E. Takagi, T. Tominaga, N. Toshima, *Inorg. Chim. Acta* **2000**, *300–302*, 964.
34 N. Toshima, K. Kushihashi, T. Yonezawa, H. Hirai, *Chem. Lett.* **1989**, 1769.
35 N. Toshima, T. Yonezawa, M. Harada, K. Asakura, Y. Iwasawa, *Chem. Lett.* **1990**, 815.
36 N. Toshima, T. Yonezawa, K. Kushihashi, *J. Chem. Soc. Faraday Trans.* **1993**, *89*(14), 2537.
37 M. Harada, K. Asakura, N. Toshima, *J. Phys. Chem.* **1993**, *97*, 5103.
38 N. Toshima, Y. Wang, *Langmuir* **1994**, *10*, 4574.
39 N. Toshima, *Fine Particles Science and Technology* **1996**, 371.
40 A. Borsla, A.M. Wilhelm, H. Delmas, *Catal. Today* **2001**, *66*, 389.
41 A.B.R. Mayer, J.E. Mark, *Polym. Mater. Sci. Eng.* **1995**, *73*, 220.
42 A.B.R. Mayer, J.E. Mark, *Polymer Bulletin* **1996**, *37*, 683.
43 A.B.R. Mayer, J.E. Mark, *Macromol. Rep.* **1996**, *A33*(suppl. 7/8), 451.
44 A.B.R. Mayer, J.E. Mark, *J. Polym. Sci. Part A: Polym. Chem.* **1997**, *35*(15), 3151.
45 A.B.R. Mayer, J.E. Mark, *Polymers Preprints* **1996**, *37*(1), 459.
46 A.B.R. Mayer, J.E. Mark, R.E. Morris, *Polym. J.* **1998**, *30*(3), 197.
47 Z. Lu, G. Liu, H. Phillips, J.M. Hill, J. Chang, R.A. Kydd, *Nano Lett.* **2001**, *1*(12), 683.
48 M.V. Seregina, L.M. Bronstein, O.A. Platonova, D.M. Chernyshov, P.M. Valetsky, *Chem. Mater.* **1997**, *9*, 923.
49 C.-W. Chen, D. Tano, M. Akashi, *J. Colloid Interface Sci.* **2000**, *225*, 349.
50 C.-W. Chen, M. Akashi, *Polym. Adv. Technol.* **1999**, *10*, 127.
51 M. Adlim, M.A. Bakar, K.Y. Liew, J. Ismail, *J. Mol. Catal. A: Chem.* **2004**, *212*, 141.
52 B.P.S. Chauhan, J.S. Rathore, T. Bandoo, *J. Am. Chem. Soc.* **2004**, *126*, 8493.
53 J.F. Cieben, R.E. Cohen, A. Duran, *Mater. Sci. Eng.* **1999**, *C7*, 45.
54 R.M. Crooks, V. Chechik, B.I. Lemon, III, L. Sun, L.K. Yeung, M. Zhao, in: D.L. Feldheim, C.A. Foss, Jr. (Eds.), *Metal Nanoparticles: Synthesis, Characterization and Applications.* Marcel Dekker, New York, **2002**, pp. 262.
55 R.M. Crooks, M. Zhao, L. Sun, V. Chechik, L.K. Yeung, *Acc. Chem. Res.* **2001**, *34*(3), 181.
56 R.M. Crooks, Y. Niu, *C.R. Chimie* **2003**, *6*, 1049.
57 Y.-M. Chung, H.-K. Rhee, *Catal. Lett.* **2003**, *85*(3/4), 159.
58 Y.-M. Chung, H.-K. Rhee, *J. Mol. Catal. A: Chem.* **2003**, *206*, 291.
59 M. Ooe, M. Murata, T. Mizugaki, K. Ebitani, K. Kaneda, *NanoLett.* **2002**, *2*(9), 999.
60 N. Toshima, T. Takahashi, H. Hirai, *Chemistry Lett.* **1985**, 1245.
61 C. Larpent, E. Bernard, F. Brisse-le-Menn, H. Patin, *J. Mol. Catal. A: Chem.* **1997**, *116*, 277.
62 N.A. Dhas, A. Gedanken, *J. Mater. Chem.* **1999**, *8*(2), 445.
63 J.D. Aiken, III, R.G. Finke, *J. Mol. Catal. A: Chem.* **1996**, *114*, 29.
64 J.D. Aiken, III, R.G. Finke, *Chem. Mater.* **1999**, *11*, 1035.
65 J.D. Aiken, III, R.G. Finke, *J. Am. Chem. Soc.* **1999**, *121*, 8803.
66 S. Mandal, P.R. Selvakannan, D. Roy, R.V. Chaudhari, M. Sastry, *Chem. Commun.* **2002**, 3002.

67 I.P. Stoolyarov, Y.V. Gaugash, G.N. Kryukova, M.N. Vargaftik, I.I. Moiseev, *Russ. Chem. Bull., Int. Ed.* **2004**, *53*(6), 1194.

68 U.R. Pillai, E. Sahle-Demessie, *J. Mol. Catal. A: Chem.* **2004**, *222*, 153.

69 J. Alvarez, J. Liu, E. Román, A.E. Kaifer, *Chem. Commun.* **2000**, 1151.

70 J. Liu, J. Alvarez, W. Ong, E. Román, A.E. Kaifer, *Langmuir* **2001**, *17*, 6762.

71 T. Ueno, M. Suzuki, T. Goto, T. Matsumoto, K. Nagayama, Y. Watanabe, *Angew. Chem. Int. Ed.* **2004**, *43*, 2527.

72 J. Dupont, G.S. Fonseca, A.P. Umpierre, P.F.P. Fichtner, S.R. Teixera, *J. Am. Chem. Soc.* **2002**, *124*, 4228.

73 C.W. Scheeren, G. Machado, J. Dupont, P.F.P. Fichtner, S.R. Texeira, *Inorg. Chem.* **2003**, *42*, 4738.

74 E.T. Silveira, A.P. Umpierre, L.M. Rossi, G. Machado, J. Morais, G.V. Soares, I.J.R. Baumvol, S.R. Teixeira, P.F.P. Fichtner, J. Dupont, *Chem. Eur. J.* **2004**, *10*, 3734.

75 J. Huang, T. Jiang, B. Han, H. Gao, Y. Chang, G. Zhao, W. Wu, *Chem. Commun.* **2003**, 1654.

76 X.-D. Mu, D.G. Evans, Y. Kou, *Catal. Lett.* **2004**, *97*(3-4), 151.

77 J. Le Bras, D.K. Mukherjee, S. González, M. Tristany, B. Ganchegui, M. Moreno-Maas, R. Pleixats, F. Hénin, J. Muzart, *New J. Chem.* **2004**, *28*, 1550.

78 H. Ohde, C.M. Wai, H. Kim, J. Kim, M. Ohde, *J. Am. Chem. Soc.* **2002**, *124*, 4540.

79 B. Yoon, H. Kim, C.M. Wai, *Chem. Commun.* **2003**, *9*, 1040.

80 H. Lindlar, *Helv. Chim. Acta* **1952**, *35*, 446.

81 M. Bartok, J. Czombos, K. Felfoldi, L. Gera, G. Göndos, A. Molnar, F. Notheisz, I. Palinko, G. Wittmann, A.G. Zsigmond, *Stereochemistry of Heterogeneous Metal Catalysis.* John Wiley & Sons, New York, **1985**.

82 S. Bailey, F. King, in: R.A. Sheldon, H. van Bekkum (Eds.), *Fine Chemicals through Heterogeneous Catalysis.* Wiley, New York, **2001**, p. 351.

83 For recent examples, see A. Mastalir, Z. Kiraly, *J. Catal.* **2003**, *220*, 372.

84 A. Mastalir, Z. Kiraly, Gy. Szöllosi, M. Bartok, *Appl. Catal. A* **2001**, *213*, 133.

85 C. Lange, D. De Caro, A. Gamez, S. Stork , J.S. Bradley, W.F. Maier, *Langmuir* **1999**, *15*, 5333.

86 H. Bönnemann, W. Brijoux, K. Siepen, J. Hormes, R. Franke, J. Pollmann, J. Rothe, *Appl. Organomet. Chem.* **1997**, *11*, 783.

87 L.M. Bronstein, D.M. Chernyshov, I.O. Volkov, M.G. Ezernitskaya, P.M. Valetsky, V.G. Matveeva, E.M. Sulman, *J. Catal.* **2000**, *196*, 302.

88 E. Sulman, V. Matveeva, A. Usanov, Y. Kosivtov, G. Demidenko, L. Bronstein, D. Chernyshov, P. Valetsky, *J. Mol. Catal. A: Chem.* **1999**, *146*, 265.

89 M.M. Telkar, C.V. Rode, R.V. Chaudhari, S.S. Joshi, A.M. Nalawade, *Appl. Catal. A* **2004**, *273*, 11.

90 J.L. Pellagatta, C. Blandy, V. Collière, R. Choukroun, B. Chaudret, P. Cheng, K. Philippot, *J. Mol. Catal. A: Chem.*, **2002**, *178*, 55.

91 H.G. Niessen, A. Eichhorn, K. Woelk, J. Bargon, *J. Mol. Catal. A: Chem.* **2002**, *182-183*, 463.

92 K. Weissermel, H.J. Arpe, *Industrial Organic Chemistry*, 2nd edn. VCH, New York, **1993**, p. 343.

93 J.A. Moulijn, P.W.N.M. van Leeuwen, R.A. van Santen (Eds.), *An Integrated Approach to Homogeneous, Heterogeneous and Industrial Catalysis.* Elsevier, Amsterdam, **1995**.

94 A. Roucoux, Stabilized noble metal nanoparticles: An unavoidable family of catalysts for arene derivatives hydrogenation, in: C. Copéret, B. Chaudret (Eds.), *Topics in Organometallic Chemistry.* Springer, **2005**, Vol. 16, p. 261.

95 J.A. Widegren, R.G. Finke, *J. Mol. Catal. A: Chemical* **2003**, *187*, 207.

96 K.R. Januszkiewicz, H. Alper, *Organometallics* **1983**, *2*, 1055.

97 K.R. Januszkiewicz, H. Alper, *Can. J. Chem.* **1984**, *62*, 1031.

98 K. Nasar, F. Fache, M. Lemaire, J.C. Beziat, M. Besson, P. Gallezot, *J. Mol. Catal.* **1993**, *78*, 257.

99 T.Q. Hu, B.R. James, S.J. Rettig, C.L. Lee, *Can. J. Chem.* **1997**, *75*, 1234.

100 T.Q. Hu, B.R. James, S.J. Rettig, C.L. Lee, *J. Pulp. Pap. Sci.* **1997**, *23*, 153.

101 B.R. James, Y. Wang, C.S. Alexander, T.Q. Hu, *Chem. Ind.* **1998**, *75*, 233.

102 V. Mévellec, A. Roucoux, E. Ramirez, K. Philippot, B. Chaudret, *Adv. Synth. Catal.* **2004**, *346*, 72.

103 R.W. Albach, M. Jautelat, German Patent DE 19807995, Bayer AG **1999**.

104 T.Q. Hu, B.R. James, C.L Lee, *J. Pulp. Pap. Sci.* **1997**, *23*, 200.

105 G.S. Fonseca, A.P. Umpierre, P.F.P. Fichtner, S.R. Teixeira, J. Dupont, *Chem. Eur. J.* **2003**, *9*, 3263.

106 G.S. Fonseca, E.T. Silveira, M.A. Gelesky, J. Dupont, *Adv. Synth. Catal.* **2005**, *347*, 847.

107 X.D. Mu, J.Q. Meng, Z.C. Li, Y. Kou, *J. Am. Chem. Soc.* **2005**, *27*, 127.

108 R.G. Finke, in: D.L. Feldheim, C.A. Foss, Jr. (Eds.), *Metal Nanoparticles: Synthesis, Characterization and Applications.* Marcel Dekker, New York, **2002**, Chapter 2, pp. 17.

109 R.J. Bonilla, P.G. Jessop, B.R. James, *Chem. Commun.* **2000**, 941.

110 H. Nagahara, M. Ono, M. Konishi, Fukuoka, *Appl. Surf. Sci.* **1997**, *121/122*, 448.

111 W. Yu, Y. Wang, H. Liu, W. Zheng, *J. Mol. Catal. A: Chemical* **1996**, *112*, 105.

112 W. Yu, M. Liu, H. Liu, X. Ma, Z. Liu, *J. Colloid Interface Sci.* **1998**, *238*, 439.

113 H.D. Ding, D.L. Gin, *Chem. Mater.* **2000**, *12*, 22.

114 A. Spitaleri, P. Pertici, N. Scalera, G. Vitulli, M. Hoang, T.W. Turney, M. Gleria, *Inorg. Chim. Acta* **2003**, 61.

115 G.S. Fonseca, A.P. Umpierre, P.F.P. Fichtner, S.R. Teixeira, J. Dupont, *Chem. Eur.* **2003**, *9*, 3263.

116 G.S. Fonseca, J.D. Scholten, J. Dupont, *Synlett* **2004**, *9*, 1525.

117 Y. Izumi, *Adv. Catal.* **1983**, *32*, 215.

118 Y. Orito, S. Imai, S. Niwa, G.-H. Nguyen, *J. Synth. Org. Chem. Jpn.* **1979**, *37*, 173.

119 Y. Orito, S. Imai, S. Niwa, *J. Chem. Soc. Jpn.* **1979**, 1118.

120 Y. Orito, S. Imai, S. Niwa, *J. Chem. Soc. Jpn.* **1980**, 670.

121 S. Niwa, S. Imai, Y. Orito, *J. Chem. Soc. Jpn.* **1982**, 137.

122 A. Baiker, in: D.E. De Vos, I.F.J. Vankelecom, P.A. Jacobs (Eds.), *Chiral Catalyst Immobilization and Recycling.* Wiley-VCH, Weinheim, **2000**, pp. 155.

123 P.B. Wells, R.P.K. Wells, in: D.E. De Vos, I.F.J. Vankelecom, P.A. Jacobs (Eds.), *Chiral Catalyst Immobilization and Recycling.* Wiley-VCH, Weinheim, **2000**, pp. 123.

124 M. Studer, H.-U. Blaser, C. Exner, *Adv. Synth. Catal*, **2003**, *345*, 45 and references cited therein.

125 P.B. Wells, K.E. Simons, J.A. Slipszenko, S.P. Griffiths, D.F. Ewing, *J. Mol. Catal.* **1999**, *146*, 159.

126 H.U. Blaser, H.P. Jallet, *J. Mol. Catal.* **1991**, *68*, 215.

127 X. Zuo, H. Liu, M. Liu, *Tetrahedron Lett.* **1998**, *39*, 1941.

128 B. Torok, K. Felfoldi, G. Szakonyi, K. Balazsik, M. Bartok, *Catal. Lett.* **1998**, *52*, 81.

129 H. Bönnemann, G.A. Braun, *Angew. Chem. Int. Ed. Engl.* **1996**, *35*, 1992.

130 H. Bönnemann, G.A. Braun, *Chem. Eur. J.* **1997**, *3*, 1200.

131 J.U. Köhler, J.S. Bradley, *Catal. Lett.* **1997**, *45*, 203.

132 J.U. Köhler, J.S. Bradley, *Langmuir* **1998**, *14*, 2730.

133 Y. Huang, J. Chen, H. Chen, R. Li, Y. Li, L. Min, X. Li, *J. Mol. Catal.* **2001**, *170*, 143.

134 X. Zuo, H. Liu, C. Yue, *J. Mol. Catal.* **1999**, *147*, 63.

135 X. Zuo, H. Liu, D. Guo, X. Yang, *Tetrahedron* **1999**, *55*, 7787.

136 X. Zuo, H. Liu, J. Tian, *J. Mol. Catal.* **2000**, *157*, 217.

137 J. Zhang, X. Yan, H. Liu, *J. Mol. Catal.* **2001**, *175*, 125.

138 P.J. Collier, J.A. Iggo, R. Whyman, *J. Mol. Catal.* **1999**, *146*, 149.

139 V. Mévellec, C. Mattioda, J. Schulz, J.P. Rolland, A. Roucoux, *J. Catal.* **2004**, *225*, 1.

10
Kinetics of Homogeneous Hydrogenations: Measurement and Interpretation

Hans-Joachim Drexler, Angelika Preetz, Thomas Schmidt, and Detlef Heller

10.1
Introduction

Recently, the results of kinetic measurements have been summarized for homogeneous hydrogenations with transition metal complexes in a review [1]. Essential new results of kinetic investigations leading to the completion of hitherto existing ideas regarding the reaction mechanism of particular catalyses are represented in the respective chapters of this book, and shall not be repeated here. Rather, this chapter will introduce the kinetic treatment of reaction sequences with pre-equilibria typical for catalyses, together with the analysis and interpretation of Michaelis-Menten kinetics, the monitoring of hydrogenations, and a discussion of possible problems, with selected examples.

Kinetic investigations deliver quantitative correlations regarding the concentration–time dependence of the participating reactants, and therefore serve as the major methodical approach in the elucidation of reaction mechanisms. A knowledge of funded mechanistic ideas opens the possibility of an aimed manipulation of activity and selectivity, respectively, which are important parameters of catalyses. As "operating values", pressure and temperature – as well as the concentration of particular reaction partners – are available. However, when scaling-up from a laboratory standard to an industrial application, kinetic results are indispensable. Moreover, kinetics provides essential indications about the nature of the actual catalyst and the distinction between homogeneous and heterogeneous catalysis. This objective has been investigated more intensively during the past few years, partly with surprising results, and naturally plays an important role when transition-metal complexes meet with hydrogen as reducing agent [2]. Thereby, the problem does not lie in the kinetics as the method. ("In the kinetic approach no frontiers exist today between homogeneous, enzymatic, and heterogeneous catalysis. There is a consistent science which permits the definition of useful and efficient rate laws describing sequences of elementary steps." [3])

In spite of these capabilities of kinetics it is necessary to emphasize here that, in principle, it is not possible to *prove* that a reaction mechanism occurs only by

The Handbook of Homogeneous Hydrogenation.
Edited by J.G. de Vries and C.J. Elsevier
Copyright © 2007 WILEY-VCH Verlag GmbH & Co. KGaA, Weinheim
ISBN: 978-3-527-31161-3

using kinetic investigations! Rather, it is the nature of kinetics to describe quantitative dependences between reaction partners and thus to exclude specific reaction sequences. This model discrimination, however, does not principally allow the favoring of one reaction mechanism among a few remaining possibilities [4]. Furthermore, it is possible that formal-kinetically equivalent reaction sequences are chemically different and hence are not to be distinguished by merely applying kinetic methods [5]. Only additional findings such as the detection (or rather the isolation) of intermediates, the interpretation of isotope labeling studies, as well as computational chemistry, allow descriptions to be made of experimental results which are consistent in the form of a closed catalytic cycle – the reaction mechanism most probable on the basis of the existing indications.

There is, however, no doubt about the significance of kinetics for catalysis as the following statements indicate:

- "Kinetic measurements are essential for the elucidation of any catalytic mechanism since catalysis, by definition and significance, is purely a kinetic phenomenon" [6].
- "Asymmetric catalysis is four-dimensional chemistry. Simple stereochemical scrutiny of the substrate or reagent is not enough. The high efficiency that the reactions provide can only be achieved through a combination of both an ideal three-dimensional structure (x,y,z) and suitable kinetics (t)" [7].
- "Carefully determined conversion–time diagrams, *in-situ* spectroscopic studies and, if possible, kinetic time laws belong to the fundamentals of catalysis research and are prerequisites for a mechanistic understanding" [8].

Although the outstanding relevance of kinetics is clear, very few publications relate to in-depth kinetic analyses. The reasons for this are complex, and some of these are detailed below:

- The field of homogeneous catalysis deals primarily with the organometallic complex catalysis, besides organocatalysis, which is at present experiencing a renaissance [9]. One problem of most of the transition-metal complexes used today is a need for anaerobic reaction conditions, and this is why many conventional possibilities of kinetic investigations are restricted in their application.
- A further problem results from the catalysis itself. Only the permanent repetition of a catalytic cycle demonstrates clearly the advantage of catalysis over a simple stoichiometric reaction. A good catalyst must be very effective, leading to a desired product with a high turnover number (TON, defined as moles of substrate per mole of catalyst) and turnover frequency (TOF, defined as TON per unit time) [10–12]. Because of the large substrate : catalyst ratio, however, detailed kinetic investigations are complicated as the interesting intermediates of the catalytic cycle must be detected and quantified, beside large quantities of substrate and/or product. In addition, in a catalytic cycle, the amount of transition-metal complex is shared by several intermediates. In the case of stereoselective catalyses, the number of relevant intermediates might also easily be multiplied [13]. Furthermore, one condition of catalytic reaction se-

quences with transition-metal complexes must not be neglected, namely that intermediates can relatively easily be transposed into one another, mostly reversibly. Due to disadvantageous equilibrium positions, the intermediates might not be detectable, even under stationary catalytic conditions [14].

- In almost every case differential equations for the quantitative description of the time dependence of particular species resulting from a catalytic cycle cannot be solved directly. This requires approximate solutions to be made, such as the equilibrium approximation [15], the Bodenstein principle [16], or the more generally valid steady-state approach [17]. A discussion of differences and similarities of different approximations can be found in [18].
- Another problem arises from the fact that good kinetic studies in the field of homogeneous catalysis require not only complex-chemical and methodical experience, but also a solid knowledge of physical chemistry. Yet, this additional requirement is seldom requested at a time when financial pressure on research is steadily growing [19].

10.2 The Basics of Michaelis-Menten Kinetics

Most catalytic cycles are characterized by the fact that, prior to the rate-determining step [18], intermediates are coupled by equilibria in the catalytic cycle. For that reason Michaelis-Menten kinetics, which originally were published in the field of enzyme catalysis at the start of the last century, are of fundamental importance for homogeneous catalysis. As shown in the reaction sequence of Scheme 10.1, the active catalyst first reacts with the substrate in a pre-equilibrium to give the catalyst–substrate complex [20]. In the rate-determining step, this complex finally reacts to form the product, releasing the catalyst.

Under isobaric conditions ($k_2 = k_2' \cdot [H_2]$), many hydrogenations exactly follow this model. The classical example is the asymmetric hydrogenation of prochiral dehydroamino acid derivatives with Rh or Ru catalysts [21].

The so-called Michaelis-Menten equation (Eq. 1) [22] follows independently of the approximation chosen to solve the differential equation resulting from Scheme 10.1. Its derivation in detail can, for example, be found in [23].

$$V = \frac{dP}{dt} = \frac{k_2 \cdot [E]_0 \cdot [S]}{K_M + [S]} = \frac{V_{sat} \cdot [S]}{K_M + [S]} \tag{1}$$

with (a) $K_M = \frac{k_{-1}}{k_1} = \frac{[E] \cdot [S]}{[ES]}$, (b) $K_M = \frac{k_{-1} + k_2}{k_1} = \frac{[E] \cdot [S]}{[ES]}$,

(c) $K_M = \frac{k_2}{k_1} = \frac{[E] \cdot [S]}{[ES]}$

where (a) is the equilibrium approximation; (b) is the steady-state approach; and (c) is the irreversible formation of the substrate complex ($k_{-1}=0$).

$$E + S \underset{k_{-1}}{\overset{k_1}{\rightleftharpoons}} ES \xrightarrow{k_2} P + (E)$$

Scheme 10.1 Reaction sequence of the simplest case of Michaelis-Menten kinetics. E = catalyst; S = substrate; ES = catalyst–substrate complex; P = product; k_i = rate constants.

The Michaelis-Menten equation is characterized by two constants:

- the rate constant for the reaction of the catalyst–substrate complex to the product (k_2); and
- the Michaelis constant (K_M).

A more detailed examination shows that, in case of equilibrium approximation, the value of K_M corresponds to the inverse stability constant of the catalyst–substrate complex, whereas in the case of the steady-state approach the rate constant of the (irreversible) product formation is additionally included. As one cannot at first decide whether or not the equilibrium approximation is reasonable for a concrete system, care should be taken in interpreting K_M-values as inverse stability constants. At best, the reciprocal of K_M represents a lower limit of a "stability constant"! In other words, the stability constant quantifying the pre-equilibrium can never be smaller than the reciprocal of the Michaelis constant, but can well be significantly higher.

The Michaelis constant has the dimension of a concentration and characterizes – independently of the method of approximation – the substrate concentration at which the ratio of free catalyst to catalyst–substrate complex equals unity. At this point, exactly one-half of the catalyst is complexed by the substrate. Likewise, one finds that at a value of $[S] = 10\ K_M$, the ratio of [E]/[ES]

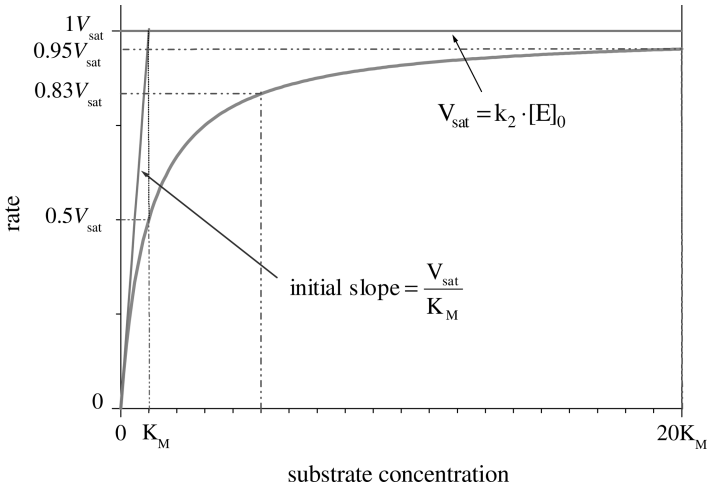

Fig. 10.1 Product formation rate as a function of substrate concentration (Eq. (1)).

equals 0.1, which means that virtually 91% of the initial catalyst ($[E_0]$) is present as substrate complex. The product formation rate is shown schematically as a function of substrate concentration in Figure 10.1.

Because of the complexity of biological systems, Eq. (1) as the differential form of Michaelis-Menten kinetics is often analyzed using the initial rate method. Due to the restriction of the initial range of conversion, unwanted influences such as reversible product formation, effects due to enzyme inhibition, or side reactions are reduced to a minimum. The major disadvantage of this procedure is that a relatively large number of experiments must be conducted in order to determine the desired rate constants.

An analysis of the product formation is, in principle, not limited to the initial range of rates, however. Laidler investigated the problem of the validity range of the Michaelis-Menten equation as a function of time under the assumption of steady-state conditions for the catalyst–substrate complex [24]. As long as either condition shown in Eq. (2) is fulfilled – by choice of experimental conditions it is usually $[S]_0 >> [E]_0$ – Eq. (3) applies up to high conversions for hydrogenations, which corresponds to Eq. (1) [23]. In fact, each point of a hydrogenation curve can be understood as an "initial rate experiment". By analyzing a hydrogenation over a wide range of conversion, a large number of initial rate experiments can be omitted. "Reaction progress kinetic analysis" as a powerful methodology was very recently described by Blackmond in a highly recommended review [25].

$$[S]_0 \gg [E]_0 \;\; [E]_0 \gg [S]_0 \;\; k_{-1} + k_2 \gg k_1 \cdot [E]_0 \;\; k_{-1} + k_2 \gg k_1 \cdot [S]_0 \tag{2}$$

$$\frac{d[P]}{dt} = \frac{k_2 \cdot [E]_0 \cdot ([S]_0 - n_{H_2})}{K_M + ([S]_0 - n_{H_2})} \quad (n_{H_2} = \text{hydrogen consumption}) \tag{3}$$

There are two limiting cases of Michaelis-Menten kinetics. Beginning from Eq. (1) at high substrate excesses (or very small Michaelis constants) Eq. (4a) results. This corresponds to a zero-order reaction with respect to the substrate, the rate of product formation being independent of the substrate concentration. In contrast, very low substrate concentrations [26] (or large Michaelis constants) give the limiting case of first-order reactions with respect to the substrate, Eq. (4b):

$$\text{(a)}\; V = \frac{d[P]}{dt} = k_2 \cdot [E]_0 = V_{sat}\,[27] \quad \text{(b)}\; V = \frac{d[P]}{dt} = \frac{k_2 \cdot [E]_0}{K_M} \cdot [S] = k_{obs} \cdot [S] \tag{4}$$

In Figure 10.1, it can be seen that even with substrate excesses of $[S] = 20\ K_M$, the saturation range is not yet reached. Conversely, the data in Figure 10.2 indicate that even for very small substrate concentrations ($[S] = 0.05\ K_M$) the limiting case for the first-order reaction – when the rate is directly proportional to the substrate concentration – is not identical with the values from Eq. (1).

Since methods to analyze Michaelis-Menten kinetics have been sufficiently described in the literature [23, 28], this problem is discussed only briefly at this point.

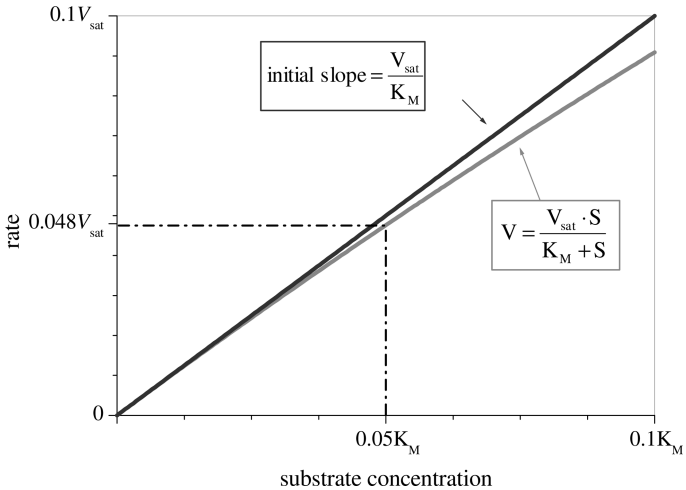

Fig. 10.2 Comparison of Eq. (1) (upper line) with the limiting case of a first-order reaction Eq. (4b) (lower line) for very low substrate concentrations.

In principle, the differential form (Eq. (1)), as well as the integrated form (Eq. (8)), can be used. The differential form of the Michaelis-Menten equation is applied in many cases, since differential values (e.g., flow meter or heat flow data) are often available; by contrast, time-dependent substrate or product concentrations (or proportional quantities) can easily be differentiated numerically.

Initial values for a non-linear fit of Eq. (1) can be achieved by linearizations. Most conventional linearizations result from the transformation of the Michaelis-Menten equation, and are plotted according to:

$$\text{Lineweaver-Burk [29]:} \quad \frac{1}{V} = \frac{K_M}{V_{sat}} \cdot \frac{1}{[S]} + \frac{1}{V_{sat}} \quad \text{plot}: 1/V \text{ versus } 1/[S] \tag{5}$$

$$\text{Eadie-Hofstee [30]:} \quad V = V_{sat} - \frac{V}{[S]} \cdot K_M \quad \text{plot}: V \text{ versus } V/[S] \tag{6}$$

$$\text{Hanes [31]:} \quad \frac{[S]}{V} = \frac{K_M}{V_{sat}} + \frac{1}{V_{sat}} \cdot [S] \quad \text{plot}: [S]/V \text{ versus } [S] \tag{7}$$

An analysis of the influence of errors shows clearly that the double-reciprocal plot according to Lineweaver-Burk [32] is the least suitable. "Although it is by far the most widely used plot in enzyme kinetics, it cannot be recommended, because it gives a grossly misleading impression of the experimental error: for small values of v small errors in v lead to enormous errors in $1/v$; but for large values of v the same small errors in v lead to barely noticeable errors in $1/v$" [23]. Due to the error distribution, that is much more uniform, the plot according to Hanes (Eq. (7)), is the most favored.

The integrated form of the simple Michaelis-Menten kinetics (Eq. (8)), is most suitable to analyze the time-dependent progressive substrate conversion or the corresponding product formation.

$$\frac{1}{t} \cdot \ln \frac{[S]_0}{[S]_t} = -\frac{[P]_t}{K_M \cdot t} + \frac{V_{sat}}{K_M} \tag{8}$$

A more detailed discussion of further possibilities for the analysis of Eq. (1) can be found in [23].

In homogeneous catalysis, the quantification of catalyst activities is commonly carried out by way of TOF or half-life. From a kinetic point of view, the comparison of different catalyst systems is only reasonable if, by giving a TOF, the reaction is zero order or, by giving a half-time, it is a first-order reaction. Only in those cases is the quantification of activity independent of the substrate concentration utilized!

As derived above, there are two limiting cases of Michaelis-Menten kinetics, which is often the basis of homogeneous catalysis. Depending upon the substrate concentration, a reaction of either first or zero order is possible as a limiting case. For hydrogenations of various substrates involving pre-equilibria, reaction orders of unity or zero have been reported for the substrate. Data relating to the kinetics of homogeneous hydrogenations with transition metal complexes before the year 2000 can be found in reference [1], and more recent examples in reference [33] (olefins: [21 c, 33 a–h]; ketones: [33 i–k]; imines: [33 l]; alkynes: [33 m]; nitro groups: [33 m]; N-hetero aromatic compounds: [33 n, o]; CO_2: [33 p]).

If a reaction that must be investigated follows a reaction sequence as in Scheme 10.1, and if the reaction order for the substrate equals unity, it means that (with reference to Eq. (4 b)), the observed rate constant (k_{obs}) is a complex term. Without further information, a conclusion about the single constants k_2 and K_M is not possible. Conversely, from the limiting case of a zero-order reaction, the Michaelis constant cannot be determined for the substrate. For particular questions such as the reliable comparison of activity of various catalytic systems, however, both parameters are necessary. If they are not known, the comparison of catalyst activities for given experimental conditions can produce totally false results. This problem is described in more detail for an example of asymmetric hydrogenation (see below).

10.3 Hydrogenation From a Kinetic Viewpoint

10.3.1 Measurement of Concentration–Time Data and Possible Problems

There exists a multitude of possibilities to monitor hydrogenations in various pressure ranges. In principle, isochoric and isobaric techniques are feasible. In the latter case, the kinetics allows simplification because the concentration of

the reaction partner, hydrogen, is constant. The classical method for measuring concentration–time data is to take samples from the reaction vessel during the hydrogenation, and then to analyze those samples via common methods such as gas chromatography (GC), high-performance liquid chromatography (HPLC), and nuclear magnetic resonance (NMR). In so doing, the sampling over various temperature and pressure ranges can be automated, as can the analysis. The advantage of this method is that any eventually occurring intermediates are detected individually as a function of time, and thus are accessible for kinetic interpretation. The disadvantage, however, is the major analytical effort required. For rapid reactions this method is also hardly appropriate. Moreover, it is sometimes difficult to stop the reaction immediately after sampling, this being a problem which is often underestimated.

A significantly more elegant solution is an *in-situ* monitoring of hydrogenations, as this advantageously provides a large amount of data available for analyses.

Both integrally and differentially measured values can be detected *in situ*. In the first case, substrate- or product-specific signals, or directly proportional quantities, are suitable. Hence, Noyori describes the monitoring of a ketone hydrogenation via the intensity of the infra-red (IR) carbonyl stretching band at $1750\,cm^{-1}$ [21 c]. To register the hydrogen consumption of a hydrogenation, a product-proportional concentration as a function of time is monitored. However, the measurement of rates – for example using flow meters or via a heat flow with a calorimeter – represents a typical differential method.

In those cases where concentrations are not measured directly, the problem of "calibration" of the *in-situ* technique becomes apparent. An assurance must be made that no additional effects are registered as systematic errors. Thus, for an isothermal reaction, calorimetry as a tool for kinetic analysis, heat of mixing and/or heat of phase transfer can systematically falsify the measurement. A detailed discussion of the method and possible error sources can be found in [34].

High-throughput methods for catalyst screening and optimization, as described in the literature even for hydrogenations [35], are not suitable for kinetic analyses in most cases.

10.3.1.1 **Monitoring of Hydrogenations via Hydrogen Consumption**

One method, which is still used frequently to follow hydrogenations *in situ*, is the registration of hydrogen consumption. There is a multitude of solutions that can be simply subdivided into normal-pressure and high-pressure measurements. Due to common isobaric reaction conditions the hydrogen concentration is constant, which simplifies kinetics. An isochoric mode of operation is not advisable because of the complexity of the measurement. In fact, the decreasing hydrogen concentration in solution during the course of the hydrogenation must also be taken into account.

For hydrogen, deviations from the ideal gas law must be considered only at higher pressures [36]. Nonetheless, the virial equation allows the amount of hydrogen to be calculated, for example in a reservoir of known volume, by apply-

ing Eq. (9). By using mass balances – based on the initial pressure or cumulatively on the previous value – hydrogen consumption can be determined with accuracy [37]. The problem of such measurements rather lies in a possible temperature gradient between the reservoir and the reaction vessel.

$$n_{H_2} = \frac{\text{reservoir volume}}{\text{real molar volume}} \quad \text{real molar volume} = \frac{R \cdot T}{p} + B + \left(\frac{C - B^2}{R \cdot T}\right) \tag{9}$$

where R=gas constant, T=temperature, p=pressure, and B and C=virial coefficients.

For flow rate measurements the volume or, more conveniently, the mass flow is suitable. In the first case a pressure- and temperature-dependent calibration is necessary if the gas does not show ideal behavior. This also applies for heat conductivity as the measured quantity often used in flow meters. Currently, real pressure- and temperature-independent measurement of a hydrogen mass flow of a hydrogenation remains problematic on the laboratory scale, at least for low substrate concentrations.

By contrast, the measurement of the hydrogen consumption under normal pressure is relatively simple. The elementary structure of many such measuring devices is similar, and is based principally on the fact that the pressure drop is balanced by reduction in the reaction volume or by supply of the consumed gas, thus ensuring isobaric conditions. An appropriate device for monitoring major gas consumptions is described in [38].

For hydrogenations under normal pressure and isobaric conditions, we use a device which registers gas consumption automatically (Fig. 10.3). Possible error sources resulting from such gas consumption measurements and possibilities of their minimization will be discussed.

The basic principle to realize isobaric conditions for the hydrogenation apparatus shown in Figure 10.3 is to change the volume of the closed reaction space via a (not commercially available) gas-tight syringe in order to ensure a permanent atmospheric pressure as the reference. For this purpose, a sensible pressure sensor registers the pressure drop caused by hydrogen consumption in the closed reaction system. Using a processor-controlled stepping motor axis, the piston of the syringe is depressed until the initial pressure is reached. At this point the position of the piston is registered as a function of time and finally visualized as the hydrogenation curve. (The same arrangement also allows the automatic registration of gas formation.)

This method, although being used analogously in other devices, incorporates a number of principal error sources. These result substantially from transport phenomena, vapor pressure of the solvent, gas solubility, and tempering problems. Particular points, together with possible means of their minimization, will be discussed in the following section.

One problem encountered when monitoring gas-consuming reactions is the influence of transport phenomena. The reaction partner hydrogen must be transported to the catalyst, and thereby it should penetrate the gas–liquid inter-

Fig. 10.3 Normal pressure hydrogenation device for the automatic registration of hydrogen consumption under isobaric conditions.

face at a distinctly higher rate than it is consumed by the hydrogenation. Only if such a regime holds it can be guaranteed that the detected effect can be interpreted as being exclusively kinetic.

Blackmond et al. investigated the influence of gas-liquid mass transfer on the selectivity of various hydrogenations [39]. It could be shown – somewhat impressively – that even the pressure-dependence of enantioselectivity of the asymmetric hydrogenation of α-dehydroamino acid derivatives with Rh-catalysts (as described elsewhere [21 b]) can be simulated under conditions of varying influence of diffusion! These results demonstrate the importance of knowing the role of transport phenomena while monitoring hydrogenations.

Several possibilities exist to determine the influence of transport phenomena. The measurement of gas consumption in dependence on the interfacial area, the physical absorption coefficient, the rate of a chemical reaction following the absorption, and the concentration gradient (as the driving force of the absorption) allows decisions to be made on which regime is, in fact, in existence [40].

For the rate of physical absorption of a gas into a liquid without subsequent chemical reaction, Eq. (10) is valid.

$$\frac{d[C]}{dt} = k_L \cdot a \cdot ([C^*] - [C]) \quad \text{or} \quad [C] = [C^*] \cdot (1 - e^{-k_L \cdot a \cdot t}) \tag{10}$$

where k_L = physical mass-transfer coefficient (liquid side), a = interfacial area, $[C^*]$ = gas concentration in solution at time $t\infty$ (gas solubility), and $[C]$ = gas concentration in solution at time t.

The analysis of gas absorption proceeding exponentially under experimental conditions provides the gas solubility $[C^*]$ and the value of $k_L \cdot a$. As a rule of thumb, this value should be approximately ten-fold larger than the rate of a subsequent chemical reaction in order to eliminate diffusion influences on the latter reaction [41].

The often-applied method of determining the dependence of initial rate on stirring speed must be treated with caution, for two reasons. On the one hand, the initial rate can be lower than at higher conversions due to induction periods [42], and on the other hand an increase in stirring speed does not enforce a proportionally higher interfacial area.

The following procedure has been approved as being straightforward (also see [43]). A zero-order dependence is achieved by monitoring a reaction in the range of diffusion control. The rate is determined only by the constant concentration gradient in the interfacial area. The systematic investigation of whether diffusion influences hydrogenations is appropriate only if they also follow zero order, but in the range of kinetic control. An example of this is the catalytic hydrogenation of dienes as COD (cycloocta-1,5-diene) or NBD (norborna-2,5-diene) with cationic rhodium(I) chelates. Up to high conversions this reaction proceeds in the saturation range of Michaelis-Menten kinetics, and hence as a zero-order reaction. The pseudo-rate constant $k_{obs} = k_2' \cdot [H_2] \cdot [E]_0$ is a linear function of the initial catalyst concentration. A continuous increase of the employed catalyst concentration ($[E]_0$) under given experimental conditions (reactor geometry, stirring speed, stirrer size) leads to a straight line, and the hydrogen consumption is independent of the predominating regime (kinetics versus diffusion). Plotting the slopes of the straight lines as a function of the catalyst concentration provides information about the limitations of the regime, which is exclusively controlled by kinetics. Figure 10.4 illustrates the hydrogenation curves of the catalytic hydrogenation of NBD with $[Rh(Ph\text{-}\beta\text{-glup-OH})NBD]BF_4$ (Ph-β-glup-OH = phenyl 2,3-bis(*O*-diphenylphosphino)-β-D-glyco-pyranoside).

The plot of measured rates as a function of the initial catalyst concentration is shown in Figure 10.5. For the range from 0 to ca. 12 mL min^{-1} the straight line passing through the origin proves the direct proportionality between rate and catalyst concentration. In other words, the hydrogen concentration in solution (gas solubility) for the mentioned range of rates is constant, and it is measured in the kinetically controlled range. As the figure indicates, rates of hydrogen consumption of 30 mL min^{-1} are indeed nonproblematic with regard to the registration. However, for rates greater than 12 mL min^{-1}, gas consumption under the given experimental conditions is increasingly determined by transport phenomena. Because of the rising influence of diffusion, the bulk concentration of hydrogen in solution continuously decreases below the value of the hydrogen solubility. The hydrogenations are slower than would be expected for the kinetically controlled range.

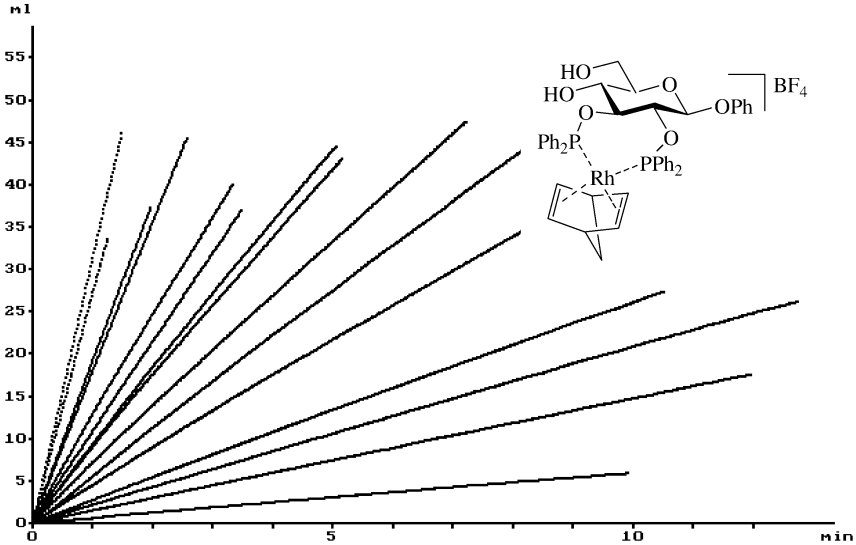

Fig. 10.4 Hydrogenation curves of catalytic NBD hydrogenations (each at least 2.0 mmol) with [Rh(Ph-β-glup-OH)NBD]BF_4 at varying catalyst concentrations (0.0025, 0.005, 0.0075, 0.01, 0.015, 0.02, 0.025, 0.03, 0.035, 0.04, 0.05, 0.08, 0.1, 0.15, and 0.2 mmol) each in 15.0 mL MeOH at 25.0 °C and 1.013 bar total pressure.

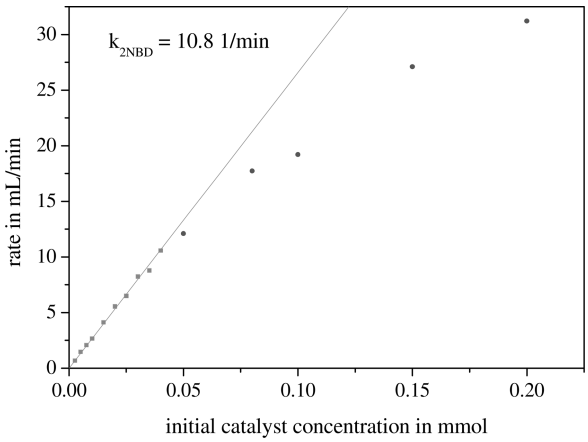

Fig. 10.5 Rate of gas consumption from Figure 10.4 as a function of initial catalyst concentration $[E]_0$.

One further source of error is that of vapor pressure of the solvent. Whilst this plays only a minor role at higher hydrogen pressures, its neglect for hydrogenations under normal pressure is a problem that is often underestimated. Figure 10.6 illustrates the vapor pressure of various solvents often used in hydrogenations as a function of temperature [44].

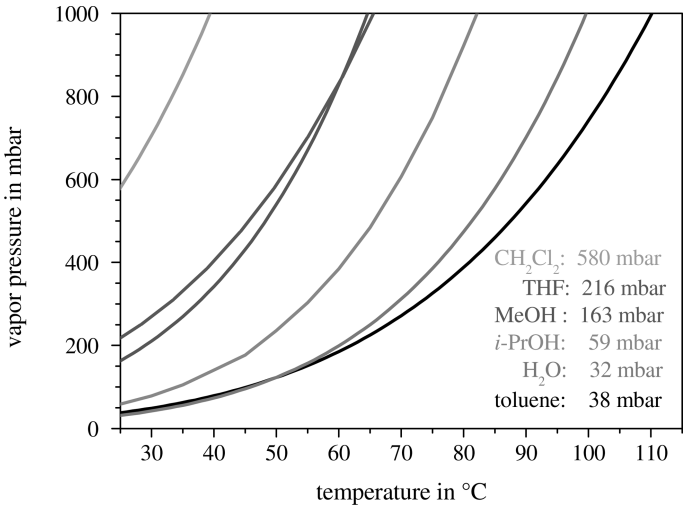

Fig. 10.6 Vapor pressure of CH_2Cl_2, THF, MeOH, *i*-PrOH, H_2O and toluene as a function of temperature. The concrete values refer to 25.0 °C.

Although in the case of methylene chloride under normal pressure more than one-half of the gas phase consists of solvent vapor (57%), in the case of toluene and water this share amounts to only ca. 3–4% of the total pressure. In order to compare activities in various solvents at the same hydrogen pressure above the reaction solution, besides a different gas solubility for the solvents (i.e., the hydrogen concentration in solution), a different partial pressure of hydrogen must be taken into account.

Another problem results from high vapor pressures of relatively low-boiling solvents. With regard to the dependence on reactor geometry, it can take some time for the vapor pressure of the solvent to become established in the gas phase of the closed system. As this equilibration of vapor pressure provides a positive volume contribution (the pressure above the reaction solution increases in a closed system), measured gas consumptions can be considerably falsified not only as a function of time but also in respect of the overall balance! One way to avoid this problem is to separate the gas phase above the reaction solution from the gas in the measuring burette by using a tempered bubble counter (cf. Fig. 10.3).

A further problem is constituted by the different solubilities of hydrogen in the conventional solvents used for hydrogenations. In Table 10.1 (column 2), data are listed of gas solubility (expressed as mole fraction) $[x_{H_2} = n_{H_2}/(n_{solvent} + n_{H_2})]$ of various solvents at 25.0 °C and 1.013 bar H_2 partial pressure [45].

Because very small mole fraction solubilities correspond in practice to the molar ratio [45 a], the values can (considering the molar volume and density of the solvent) be easily transformed into hydrogen concentrations (see Table 10.1,

Table 10.1 Hydrogen solubilities in various solvents at 25.0 °C [46].

Solvent	H_2-solubility [mole fraction x at 1.013 bar]	Mol H_2 in 1 L solvent [1.013 bar H_2]	Mol H_2 "effective" in 1 L solvent [1.013 bar total pressure]
THF	0.000270	3.3291×10^{-3}	2.62×10^{-3}
MeOH	0.000161	3.9752×10^{-3}	3.33×10^{-3}
i-PrOH	0.000266	3.4742×10^{-3}	3.27×10^{-3}
H_2O	0.0000141	7.80576×10^{-4}	7.56×10^{-4}
Toluene	0.000317	2.9576×10^{-3}	2.85×10^{-3}

column 3). In hydrogenations under normal pressure, however, the different vapor pressure of the solvent, by which the relevant hydrogen partial pressure is reduced, must be taken into account (Fig. 10.6). Consideration of the vapor pressure of the solvent at a total pressure of 1.013 bar above the reaction solution leads to an "effective" gas solubility – that is the actually interesting hydrogen concentration in solution (see Table 10.1, column 4). The results show that under equal conditions (25.0 °C and 1.013 bar total pressure above the reaction solution), the hydrogen concentration in solution differs markedly for different solvents. The solvents THF and *i*-PrOH indeed show a similar hydrogen solubility (Table 10.1, column 2), despite differing in the "effective" hydrogen concentration (Table 10.1, column 4) by ca. 20%. In contrast, the solvents H_2O and toluene exhibit approximately the same vapor pressure above the reaction solution (Fig. 10.6), yet the "effective" hydrogen concentration in solution differs by a factor of 3.7. In the first case, variation in vapor pressure is the cause for such behavior, but in the second case it is the variation in gas solubility.

For meaningful comparisons of the activity of catalysts in various solvents under seemingly equal conditions these factors must, of course, be considered.

In order to determine the reaction order in hydrogen of a homogeneously catalyzed hydrogenation under isobaric conditions, the variation of partial pressure is an essential precondition. Commonly, hydrogen/inert gas mixtures are used, yet the change in composition of the gas mixture (the share of H_2 is reduced due to consumption in the hydrogenation) is generally neglected. However, this may lead to a dependence on the volume of the gas phase and, potentially, to a major systematic error. By contrast, the method described in the following section permits the use of isobaric conditions by varying the partial pressure.

While the gas phase above the reaction solution contains the reactive gas at a chosen concentration (obtained by dissolution with an inert gas such as argon; H_2/Ar gas mixtures are available commercially), pure hydrogen is arranged in the gas burette. Mixing of the gas phases, each of which has a different hydrogen concentration, is prevented by a bubble counter. After beginning the hydrogenation, hydrogen is delivered exclusively from the gas burette in order to obtain pressure equalization. The main problem with this type of measurement is that a concentration gradient (caused by the higher concentration of gas streaming into the

Fig. 10.7 An apparatus used to monitor hydrogenations at different hydrogen partial pressures.

gas space above the reaction solution) must be avoided. In addition to thorough mixing of the gas phase above the reaction solution, this problem could be solved by including an arrangement whereby the bubble counter between the gas volume above the reaction solution and the gas burette is located directly above the reaction solution in the gas phase of the hydrogenation vessel (cf. Fig. 10.7).

The result of the described methodical solution to monitor gas-consuming reactions at reduced partial pressure under isobaric conditions is shown in Figure 10.8 for the catalytic hydrogenation of COD with a cationic Rh-complex. The slope of the measured straight lines corresponds to the maximally obtainable rate ($V_{sat} = k_2 \cdot [E]_0 = k'_2 \cdot [H_2] \cdot [E]_0$) [42 b], which is directly proportional to the hydrogen concentration in solution and at validity of Henry's law to the hydrogen partial pressure above the reaction solution. The experiments prove that the "dilution factor" of the gas phase can adequately be found in the rate constant. (Further examples can be found in [47].)

Besides the above-mentioned errors, further difficulties may arise in the *in-situ* monitoring of hydrogenations. For example, in order to start a hydrogenation it is necessary to exchange inert gas and hydrogen by evacuation. In fact, this procedure leads to a cooling of the solution caused by the evaporation enthalpy of the solvent. The time taken to reach the equilibrium value of the vapor pressure of the solvent above the reaction solution must also be taken into account. In order to avoid such problems, it has been proven of value to seal the catalyst (or the substrate) in a glass ampoule under argon (cf. Fig. 10.3), and to start the hydrogena-

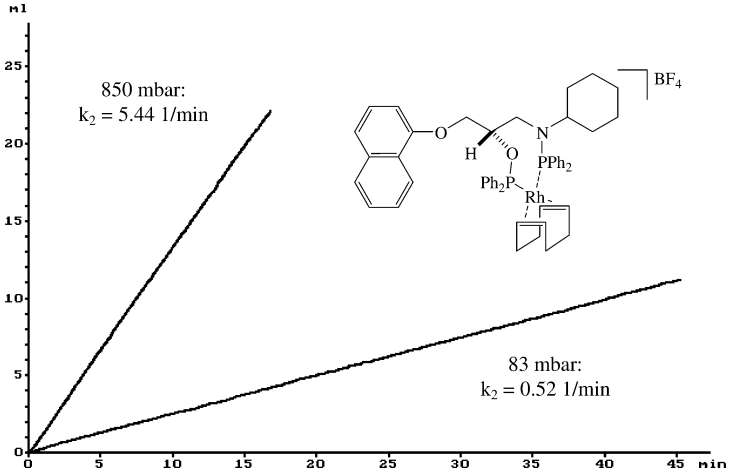

Fig. 10.8 Rate constant k_2 for the catalytic COD-hydrogenation with [Rh(cyclohexyl-PROPRAPHOS)COD]BF_4 as catalyst at various hydrogen partial pressures (normal pressure and commercial argon/hydrogen mixtures (AGA) which contain 9.71% H_2). Reaction mixture: 15.0 mL MeOH; 0.01 mmol catalyst; 1.0 mmol COD.

tion by destroying the ampoule only when the thermal equilibria have been established. It must be borne in mind, however, that it is extremely difficult to exclude all error sources, and at best a minimization of the problem is possible for a concrete case. However, it is important to assess – and at least report – the expected relative importance of those errors that have been neglected.

10.3.1.2 Monitoring of Hydrogenations by NMR and UV/Visible Spectroscopy

The details of a series of *in-situ* methods and appropriate investigations have been described concerning NMR spectroscopic monitoring of catalytic reactions with gases in various pressure ranges [42 e, 48]. However, disadvantages might include the reactive gas not being supplied, that isobaric conditions during the gas consumption are not possible, that thorough mixing of the reaction solution is insufficient (diffusion problems), or that special NMR probe heads are necessary. A very interesting solution has been described by Iggo et al. [48 d], in which the NMR flow cell for the *in-situ* study of homogeneous catalysis allows measurements up to 190 bar (!), but requires the use of a standard wide-bore NMR probe. Details of state-of-the-art methods for the *in-situ* monitoring of reactions using NMR spectroscopy can be found in [49].

An improvement of the possibility for experiments under normal pressure (as described in [42 e]) is shown in Figure 10.9 [50]. During registration of the spectrum, the reactive gas is continuously bubbled into the reaction solution below the NMR-active sample volume; thus, diffusion problems can be excluded for mod-

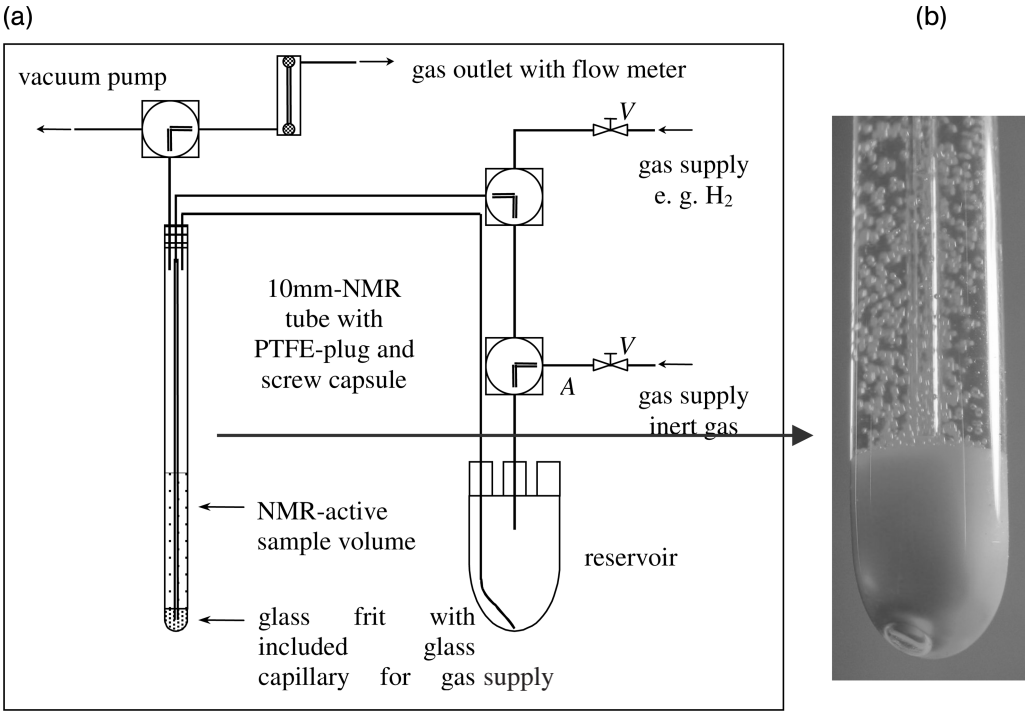

Fig. 10.9 (a) Schematic arrangement for the NMR-spectroscopic monitoring of gas-consuming reactions under catalytic conditions according to [50]. (b) Gas flow during the measurement (a – argon, b – hydrogen).

erately fast reactions. In spite of the introduction of gas during the measurement (cf. Fig. 10.9 b) and hence a deterioration in the homogeneity of the magnetic field, sufficiently good spectra (^{1}H, ^{13}C, ^{31}P) can be obtained under *in-situ* catalytic conditions using the non-rotating NMR tube. One disadvantage of this arrangement is that the gas excess is withdrawn from the device and disappears. For this reason, it is not economical to employ expensive, isotopically labeled gaseous reaction partners such as $^{2}H_2$ and ^{13}CO. Moreover, because of the permanent loss of gas – especially in long-term measurements – the solvent is also discharged.

An application of the arrangement shown in Figure 10.9 is depicted in Figure 10.10. For the hydrogenation of (*Z*)-*N*-acetylamino methyl cinnamate (AMe) with [Rh(DIPAMP)(solvent)$_2$]anion (DIPAMP = 1,2-bis-(*o*-methoxy-phenyl-phenyl phosphino)ethane) in isopropyl alcohol at 25 °C and under normal pressure, the ^{31}P-NMR spectrum shown in Figure 10.10 b was measured during hydrogenation under steady-state conditions. The comparison with the spectrum taken under argon (Fig. 10.10 a) proves that the ratio major/minor catalyst–substrate complex is higher during the hydrogenation than under thermodynamic conditions (argon). The measurement of a similar spectrum after termination of hydrogen supply and in-

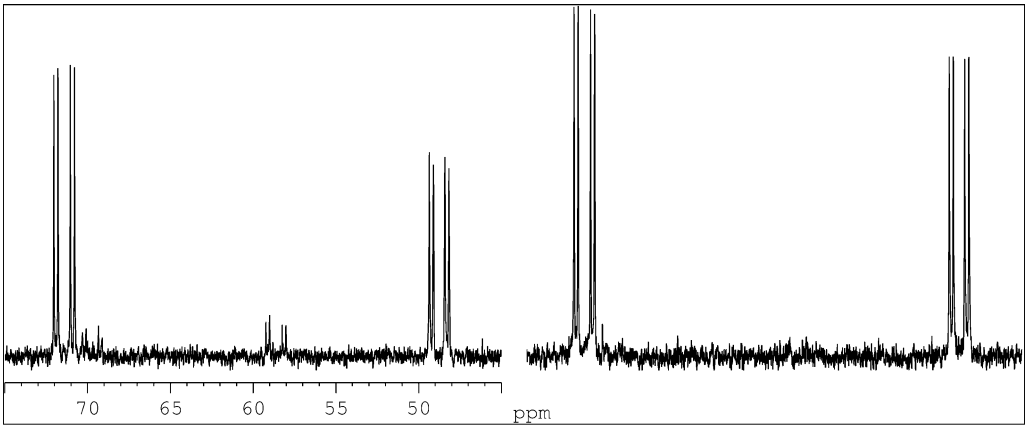

Fig. 10.10 ^{31}P-NMR spectra of $[Rh(DIPAMP)(MeOH)_2]^+$ and 1.0 mmol AMe in 5.0 mL iso-propyl alcohol-d_8 at 25 °C with the arrangement shown in Figure 10.9. Spectrum (a) is registered under argon; spectrum (b) is accumulated during a reaction time of 30 min (1200 pulses).

troduction of argon virtually congruently leads to the initial spectrum. Thus, it could clearly be proven that the change in the phosphorus spectra should be exclusively attributed to the reaction with hydrogen.

Recently, a new (and now commercially available) methodology was reported for measuring *in-situ* high pressure NMR spectra up to 50 bar under stationary conditions. The instrument uses a modified sapphire NMR tube, and gas saturation of the sample solution and exact pressure control is guaranteed throughout the overall measurement, even at variable temperatures. For this purpose, a special gas cycling system is positioned outside the magnet in the routine NMR laboratory [51].

Today, stirring inside UV/visible cells, cell tempering, the use of flow-through cells, and the detection of smallest amounts of samples in microcells are all possible, without problems. However, a complete gas exchange (e.g., argon for hydrogen) is still difficult. Moreover, because of the disadvantageous geometry of a cell in terms of the ratio of surface to volume, it is generally only possible to trace relatively slow reactions with gases in the kinetically controlled regime. After all, the realization of isobaric conditions for the gaseous reaction partner in case of a cell represents high requirements to the pressure adjustment since the gas consumptions are relatively small. For such problems, the application of immersion probes (known also as "fiber-optical probes") represents a good alternative. Due to the arbitrary dimensioning of the reaction vessel and the immersion probe (an example for analyses under normal pressure is shown in Fig. 10.11), hydrogenations can be monitored *in situ* over a variety of pressure and temperature ranges, and in an elegant manner.

The "external" measurement of UV/visible spectra principally allows the tracing of other quantities at the same time, such as conductivity, pH, and gas con-

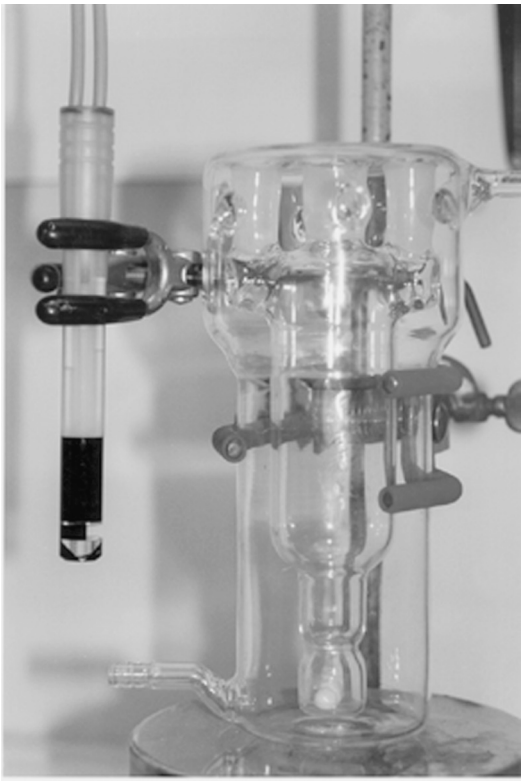

Fig. 10.11 Immersion probe with standard ground joint and reaction vessel for UV/visible spectroscopic analyses under normal pressure.

sumption under catalytic conditions. Monitoring of the time-dependent change of extinction at the maximum (441 nm) of [Rh(DIOP)(COD)]BF_4 (DIOP = 4,5-bis(diphenyl-phosphino-methyl)-2,2-dimethyl-1,3-dioxolane)] for the catalytic hydrogenation of COD and the simultaneous registration of hydrogen consumption is shown graphically in Figure 10.12.

The rate constant can be obtained directly from the slope of the graph [42f]. Furthermore, it can clearly be seen that the concentration of [Rh(DIOP)(COD)]BF_4, both under argon and during the hydrogenation, is the same until depletion of the substrate COD. This confirms that hydrogenation proceeds in the range of saturation kinetics of the underlying Michaelis-Menten kinetics. Thus, the experimental procedure provides information regarding the catalyst via UV/visible spectroscopy; subsequently, the rate of product formation can be quantified from the hydrogen consumption of the very same reaction solution [52].

In addition to the above-mentioned possibilities for the *in-situ* monitoring of hydrogenations, there are, of course, also techniques involving calorimetry and IR spectroscopy [34, 35c, 39, 41, 53, 54].

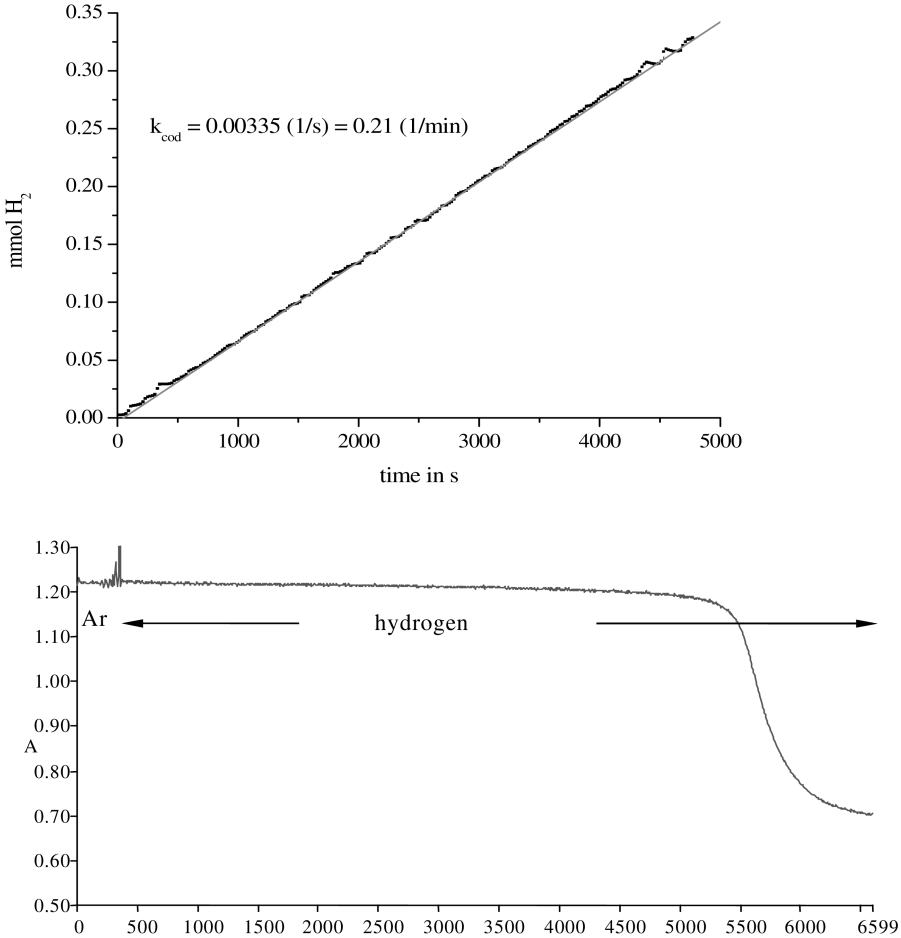

Fig. 10.12 Simultaneous monitoring of the time-dependent UV/visible spectrum at 441 nm (maximum of the catalyst extinction) and hydrogen consumption for the hydrogenation of COD with [Rh(DIOP)COD]BF_4. Conditions: 0.02 mmol precatalyst; 0.33 mmol COD; 20.0 mL methanol; 25.0 °C; 1.013 bar total pressure.

10.3.2 Gross-Kinetic Measurements

10.3.2.1 Derivation of Michaelis-Menten Kinetics with Various Catalyst-Substrate Complexes

The catalytic asymmetric hydrogenation with cationic Rh(I)-complexes is one of the best-understood selection processes, the reaction sequence having been elucidated by Halpern, Landis and colleagues [21 a, b], as well as by Brown et al. [55]. Diastereomeric substrate complexes are formed in pre-equilibria from the solvent complex, as the active species, and the prochiral olefin. They react in a series of elementary steps – oxidative addition of hydrogen, insertion, and reductive elimination – to yield the enantiomeric products (cf. Scheme 10.2) [56].

The rate law for two diastereomeric catalyst–substrate complexes (C_2-symmetric ligands) resulting from Michaelis-Menten kinetics (Eq. (11)) has already been utilized by Halpern et al. for the kinetic analysis of hydrogenations according to Scheme 10.2, and corresponds to Eq. (3) of this study.

$$\frac{d[H_2]}{dt} = \frac{d[R]}{dt} + \frac{d[S]}{dt} = \frac{\left(\frac{(k_{2min} \cdot K_{ESmin}) + (k_{2maj} \cdot K_{ESmaj})}{K_{ESmin} + K_{ESmaj}}\right) \cdot [Rh]_0 \cdot [olefine]}{\left(\frac{1}{K_{ESmin} + K_{ESmaj}}\right) + [olefine]}$$

with

$$K_{ESmin} = \frac{k_{1min}}{k_{-1min} + (k_{2min} \cdot [H_2])} \quad K_{ESmaj} = \frac{k_{1maj}}{k_{-1maj} + (k_{2maj} \cdot [H_2])} \tag{11}$$

In answer to the question, "why are there not much more kinetic analyses of selection processes in analogy to these classic works?", it should be realized that particular prerequisites are necessary. In the concrete case, such prerequisites included a major stability of the substrate complexes, a convenient ratio of the diastereomeric substrate complexes, and a pressure-dependence of the enantioselectivities.

The following section deals with kinetic equations for the simple Michaelis-Menten kinetics with more than two intermediates; subsequently, their application for the interpretation of hydrogenations in practical examples is discussed.

If C_1-symmetric ligands are employed in asymmetric hydrogenation instead of the corresponding C_2-symmetric ligands, there coexist principally four stereoisomeric substrate complexes, namely two pairs of each diastereomeric substrate complex. Furthermore, it has been shown that, for particular catalytic systems, intramolecular exchange processes between the diastereomeric substrate complexes should in principle be taken into account [57]. Finally, the possibility of non-established pre-equilibria must be considered [58]. The consideration of four intermediates, with possible intramolecular equilibria and disturbed pre-equilibria, results in the reaction sequence shown in Scheme 10.3. This is an example of the asymmetric hydrogenation of dimethyl itaconate with a Rh-complex, which contains a C_1-symmetrical aminophosphine phosphinite as the chiral ligand.

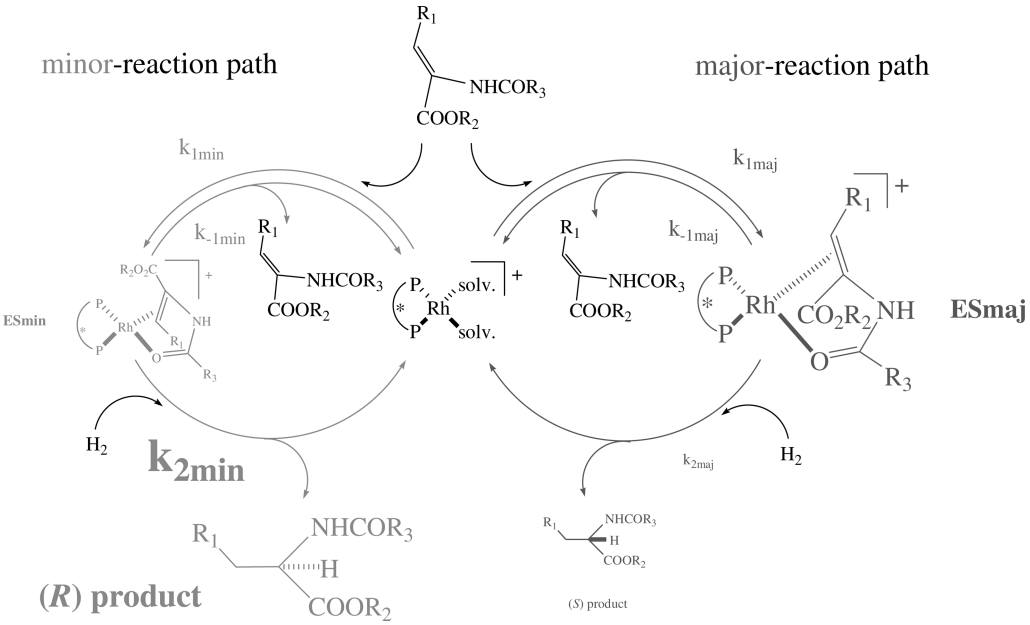

Scheme 10.2 Selection model of the Rh(I)-complex-catalyzed asymmetric hydrogenation to the (*R*)-amino acid derivative (according to [21a, b, 55]). ES_{maj} and ES_{min} correspond to the diastereomeric catalyst–substrate complexes.

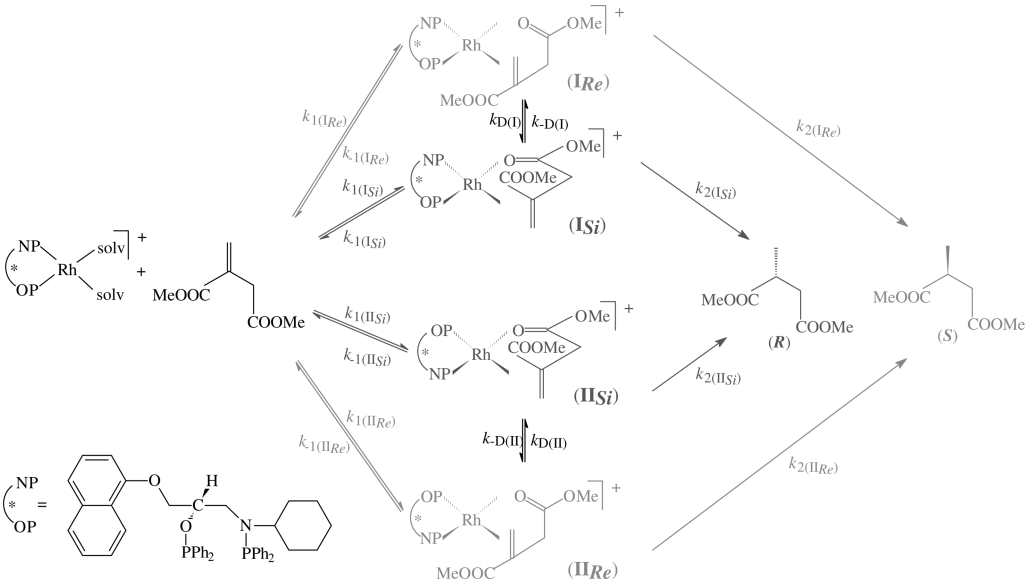

Scheme 10.3 Reaction sequence for the asymmetric hydrogenation of dimethyl itaconate with a C_1-symmetric ligand under consideration of intramolecular exchange processes between the intermediates and of disturbed pre-equilibria.

For the time-dependent change of the particular concentrations, Eqs. (12a) and (12b) result.

$$\text{(a)}\ \frac{\mathrm{d}[S]}{\mathrm{d}t} = k_{2(\mathrm{I_{Re}})} \cdot [\mathrm{I_{Re}}] + k_{2(\mathrm{II_{Re}})} \cdot [\mathrm{II_{Re}}] \quad \text{(b)}\ \frac{\mathrm{d}[R]}{\mathrm{d}t} = k_{2(\mathrm{I_{Si}})} \cdot [\mathrm{I_{Si}}] + k_{2(\mathrm{II_{Si}})} \cdot [\mathrm{II_{Si}}] \tag{12}$$

The common further treatment of the approach – assumption of steady-state conditions for the intermediate substrate complexes, consideration of the catalyst balance ($[\text{catalyst}]_0 = [\text{solvent complex}] + [\mathrm{I_{Re}}] + [\mathrm{I_{Si}}] + [\mathrm{II_{Re}}] + [\mathrm{II_{Si}}]$) and of the stoichiometry of the hydrogenation – provides the rate of hydrogen consumption under isobaric conditions (Eq. (13)) [57f]. A more general derivation can be found in [59].

$$\begin{aligned} -\frac{\mathrm{d}[\mathrm{H_2}]}{\mathrm{d}t} &= \frac{\mathrm{d}[S]}{\mathrm{d}t} + \frac{\mathrm{d}[R]}{\mathrm{d}t} \\ &= \frac{\dfrac{(k_{2(\mathrm{I_{Re}})} \cdot K_{\mathrm{I_{Re}}} + k_{2(\mathrm{II_{Re}})} \cdot K_{\mathrm{II_{Re}}} + k_{2(\mathrm{I_{Si}})} \cdot K_{\mathrm{I_{Si}}} + k_{2(\mathrm{II_{Si}})} \cdot K_{\mathrm{II_{Si}}})}{(K_{\mathrm{I_{Re}}} + K_{\mathrm{I_{Si}}} + K_{\mathrm{II_{Re}}} + K_{\mathrm{II_{Si}}})} \cdot [\mathrm{cat}]_0 \cdot [\mathrm{S}]}{\dfrac{1}{(K_{\mathrm{I_{Re}}} + K_{\mathrm{I_{Si}}} + K_{\mathrm{II_{Re}}} + K_{\mathrm{II_{Si}}})} + [\mathrm{S}]} \\ &= \frac{k_{\mathrm{obs}} \cdot [\mathrm{cat}]_0 \cdot ([\mathrm{S}]_0 - n_{\mathrm{H_2}})}{K_{\mathrm{M}} + ([\mathrm{S}]_0 - n_{\mathrm{H_2}})} \end{aligned} \tag{13}$$

This relationship corresponds to the simplest Michaelis-Menten kinetics (Eq. (3)). In addition to the equation derived earlier by Halpern et al. for the simplest model case of a C_2-symmetric ligand without intramolecular exchange [21b], every other possibility of reaction sequence corresponding to Scheme 10.3 can be reduced to Eq. (13). Only the physical content of the values of k_{obs} and K_{M}, which must be determined macroscopically, differs depending upon the approach (see [59] for details). Nonetheless, the constants k_{obs} and K_{M} allow conclusions to be made about the catalyses:

- The value $1/K_{\mathrm{M}}$ corresponds to the ratio of concentrations of the sum of all catalyst–substrate complexes to the product {[solvent complex]·[substrate]}, and thus is a measure of how much catalyst–substrate complex is present [60].
- The k_{obs}-values are all to be interpreted as the sum of all rate constants for the oxidative addition of hydrogen, each multiplied by the mole fraction of the corresponding catalyst–substrate complex. Hence this "gross-rate constant" is dependent only on the ratio of intermediates, and not on their absolute concentrations.

Clearly, a comprehensive description of catalytic systems is not possible from the hydrogen consumption alone. The reaction sequence represented in Scheme 10.3 already contains 16 rate constants. However, valuable data regarding the catalysis can be obtained from an analysis of the gross hydrogen consumption on the basis of Eq. (13), for various catalytic systems. Some practical examples of this are described in the following section.

10.3.2.2 Data from Gross Kinetic Measurements

The hydrogen consumption and enantioselectivities for the asymmetric hydrogenation of dimethyl itaconate with various substituted catalysts of the basic type [Rh(PROPRAPHOS)COD]BF_4 are illustrated in Figure 10.13 [61]. The systems are especially suitable for kinetic measurements because of the rapid hydrogenation of COD in the precatalyst. There are, in practice, no disturbances due to the occurrence of induction periods.

NMR-analyses suggest that the hydrogenation runs corresponding to Scheme 10.3. Three of the four possible catalyst–substrate complexes are detectable in the ^{31}P-NMR-spectrum [57f].

A comparison of the activities for various catalyst derivatives shown in Figure 10.13 seems to prove that the ligand with the cyclohexyl residue leads to the most active catalyst for the hydrogenation of dimethyl itaconate. The catalyst containing the methyl derivative apparently exhibits the lowest activity.

A more detailed analysis, however, shows that such comparisons of activity can be completely misleading, because Michaelis-Menten kinetics are principally described by two constants. The Michaelis constant contains information regarding the pre-equilibria, the rate constants quantify the product formation from the intermediates.

An analysis of the hydrogenation curves shown in Figure 10.13 indicates, for those precatalysts with R = 2-propyl, 3-pentyl and cyclopentyl, that they can be described quantitatively as first-order reactions. The comparison between experimental and calculated data (the latter being determined by least-squares regres-

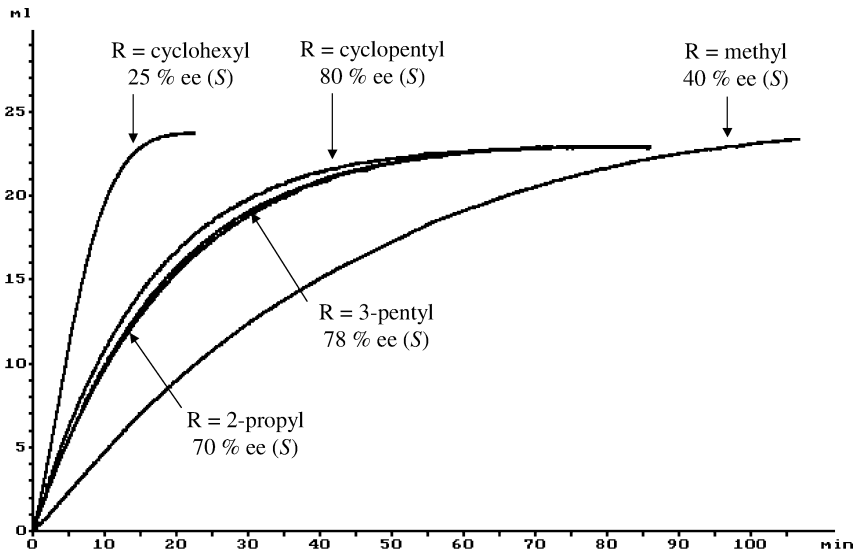

Fig. 10.13 Catalytic asymmetric hydrogenation of 1.0 mmol dimethyl itaconate with 0.01 mmol [Rh(PROPRAPHOS)COD]BF_4-precatalysts ((*S*)-PROPRAPHOS: R = 2-propyl) in 15.0 mL MeOH at 1.013 bar total pressure and 25 °C.

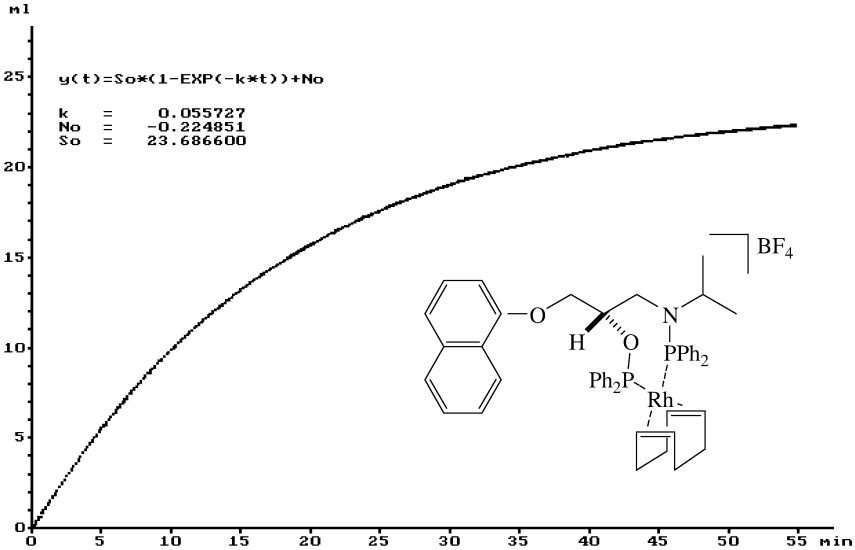

Fig. 10.14 Comparison of the experimental hydrogenation curve and first-order calculated values for the asymmetric hydrogenation of the PROPRAPHOS-precatalyst with dimethyl itaconate.

sion analysis) is shown in Figure 10.14. Due to the excellent conformity, these curves lie on top of each other.

If the ligands containing R = methyl and R = cyclohexyl are employed, the hydrogenations describe not only the initial range of the Michaelis-Menten equation, but also a range which cannot be assigned to the limiting case of the first-order reaction (cf. Figs. 10.1 and 10.2). Determination of the sought constants is carried out using nonlinear regression, with the initial values determined by linearization of Eq. (7). The comparison between experimental and calculated values corresponding to Eq. (13) for the ligand containing the methyl residue is shown in Figure 10.15. The results prove a good correspondence between the experiment and the model. For the initial quantity of substrate (1.0 mmol), the range of half-saturation concentration is reached almost at the start of the hydrogenation (Fig. 10.15).

The results of the kinetic analysis for the investigated systems are summarized in Table 10.2, the substrate concentration used being the same for all trials. In the case of methyl- and cyclohexyl-substituted ligands the Michaelis constant is smaller than the initial substrate concentration of $[S]_0 = 0.06666$ mol L^{-1} (Table 10.2). However, a description of the hydrogenations with other catalyst ligands as first-order reactions shows that in each of these cases the Michaelis constant must be much greater than the experimentally chosen substrate concentration.

Even at a rather higher substrate concentration, the limiting value of a concentration-independent rate is not reached in these cases. This is illustrated for the example of the PROPRAPHOS-type catalyst in Figure 10.16. It is, further-

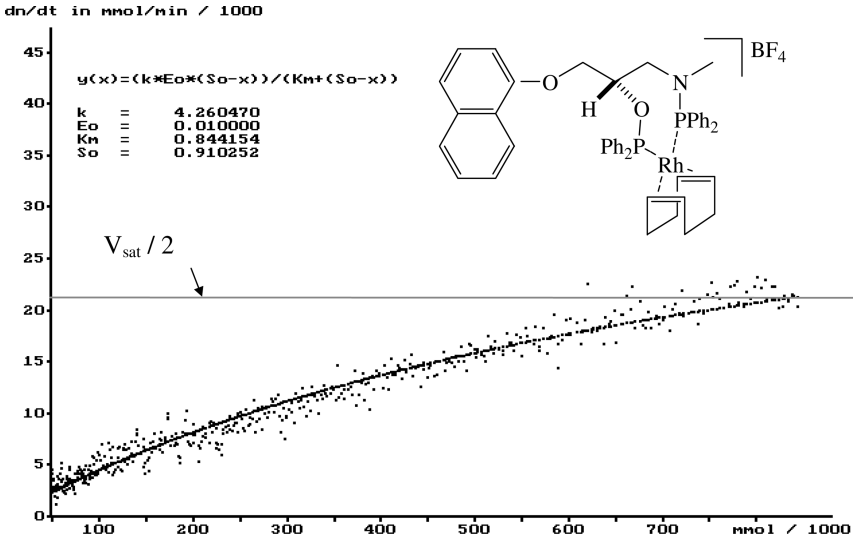

Fig. 10.15 Comparison of experimental and calculated values for the asymmetric hydrogenation of dimethyl itaconate with the methyl substituted ligand of the PROPRAPHOS precatalyst. Specifications of concentration refer to 15.0 mL of solvent.

Table 10.2 Kinetic analysis of the asymmetric hydrogenation of dimethyl itaconate with derivatives of [Rh(PROPRAPHOS)-COD]BF_4 (see Fig. 10.13).

Ligand	% ee	k (1st order) [1 s^{-1}]	K_M [mol L^{-1}]	$1/K_M$ [L mol^{-1}]	k_{obs} (Eq. (13)) [1 s^{-1}]	V_{sat} [mol L^{-1} s]
R=cyclohexyl	25	7.27×10^{-3}	0.0286	35	3.12×10^{-1}	2.08×10^{-4}
R=methyl	40	8.42×10^{-4}	0.0562	18	7.10×10^{-2}	4.73×10^{-5}
R=2-propyl	70	9.28×10^{-4}	–	–	–	–
R=3-pentyl	78	8.50×10^{-4}	–	–	–	–
R=cyclopentyl	80	1.07×10^{-3}	–	–	–	–

more, remarkable that at an increase in the substrate/catalyst ratio from 100 (standard conditions) to 1000 the PROPRAPHOS catalyst already shows an initial rate which is more than twice the maximum reachable rate with the cyclohexyl derivative (4.2×10^{-4} mol L^{-1} s versus 2.1×10^{-4} mol L^{-1} s). Indeed, PROPRAPHOS is still not used optimally with regard to its activity (see Fig. 10.16).

Interpretation of the reciprocals of the Michaelis constants allows the following conclusions to be made regarding hydrogenations under specified experimental conditions. In the case of the methyl and cyclohexyl ligand, the prevailing form of the catalyst in solution is the catalyst–substrate complex. However, for the other examples of first-order reactions, large Michaelis constants (or very

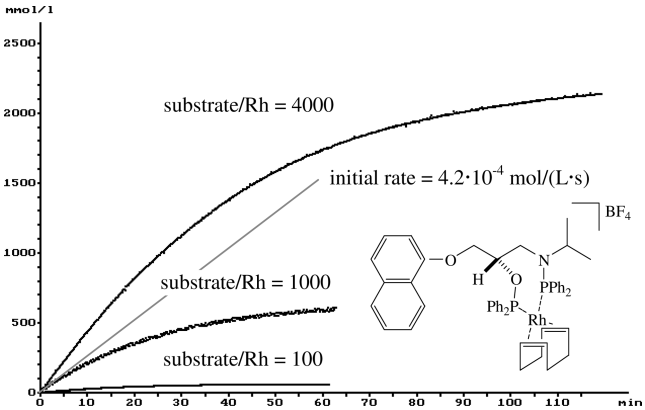

Fig. 10.16 Variation of the concentration of dimethyl itaconate for the hydrogenation with [Rh((*S*)-PROPRAPHOS)COD]BF_4.

small reciprocals of the same) prove that in these cases the equilibrium between solvent complex and the diastereomeric catalyst–substrate complexes is shifted to the side of the solvent complex.

These results, obtained from the gross-hydrogen consumption under normal conditions on the basis of the model developed above, make it clear that even catalysts of the same basic type can give rise to considerably different pre-equilibria. As a consequence, comparison of activities of various catalytic systems under "standard conditions" can provide the wrong picture. Hence, the cyclohexyl precatalyst with dimethyl itaconate seems to be the most active one (by reference to Fig. 10.13). Nonetheless, an increase in the initial substrate concentration by a factor of ten already leads to a different order in activity.

In addition to comparisons of activity of various catalysts, the choice of an appropriate solvent represents yet another problem in catalysis. The choice is usually made by direct comparison of the activity of a catalyst in various solvents. Nonetheless, analogous problems as mentioned above must be considered. Variable substrate concentrations can lead to seemingly different orders in the activity of solvents. The reason for this is based on the fact that macroscopic activity is caused by different amounts of catalyst–substrate complex.

These results underline the fact that "gross-activities" based on TOFs or half-lives only are not appropriate to compare catalytic systems that are characterized by pre-equilibria. Rather, only an analysis of gross-kinetics on the basis of suitable models can provide detailed information concerning the catalysis.

As explained earlier, the pre-equilibria are characterized by the limiting values of Michaelis-Menten kinetics. In the case of first-order reactions with respect to the substrate, we have: $K_M >> [S]_0$. Since the pre-equilibria are shifted to the side of educts during hydrogenation, only the solvent complex is detectable. In contrast, in the case of zero-order reactions only catalyst–substrate complexes are expected under stationary hydrogenation conditions in solution. These consequences resulting from Michaelis-Menten kinetics can easily be proven by var-

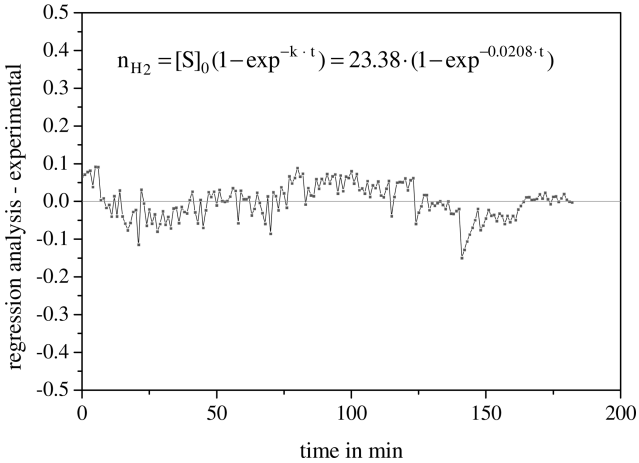

Fig. 10.17 Asymmetric hydrogenation of dimethyl itaconate with [Rh(Ph-β-glup-OH)(MeOH)$_2$]BF$_4$; comparison between first-order fit (x-axis) and experimental values. Conditions: 0.01 mmol catalyst; 1.0 mmol substrate; 15.0 mL MeOH; 1.013 bar total pressure.

ious methods such as NMR- and UV/visible spectroscopy, and this is demonstrated by some examples in the following section.

The asymmetric hydrogenation of dimethyl itaconate with [Rh(Ph-β-glup-OH-MeOH)$_2$]BF$_4$ runs as a first-order reaction. The deviation of experimental values from the hydrogen consumption calculated from parameters of nonlinear regression analysis (x-axis) is shown in Figure 10.17. In solution, only the solvent complex should be detectable during hydrogenation. In order to monitor hydrogenation via UV/visible spectroscopy, a 100-fold excess of the prochiral olefin is added to the solvent complex. The exchange of argon for hydrogen starts the hydrogenation, which is then monitored by cyclic measurement of the spectra (Fig. 10.18).

Although the substrate complexes absorb in the range of measurement (see Fig. 10.18, inset), the spectra observed during hydrogenation do not differ from the spectrum of the pure solvent complex. On completion of the reaction, gas chromatographic analysis proves that hydrogenation has occurred and that the usual values for conversion and selectivity have resulted. Thus, only solvent complex is present during the hydrogenation, and this corresponds to expectations from kinetic interpretations of the hydrogen consumption curve.

NMR spectroscopy provides analogue results. Inspection of hydrogen consumption curves following the hydrogenation of *Z*- or *E*-methyl 3-acetamidobutenoate with [Rh(Et-DuPHOS)(MeOH)$_2$]BF$_4$ (Et-DuPHOS = 1,2-bis(2,5-diethylphospholanyl)benzene)) showed the reaction to exhibit first-order kinetics (Fig. 10.19).

For both cases in these examples only the solvent complex is detectable, besides traces of non-hydrogenated COD-precatalyst (cf. Fig. 10.20).

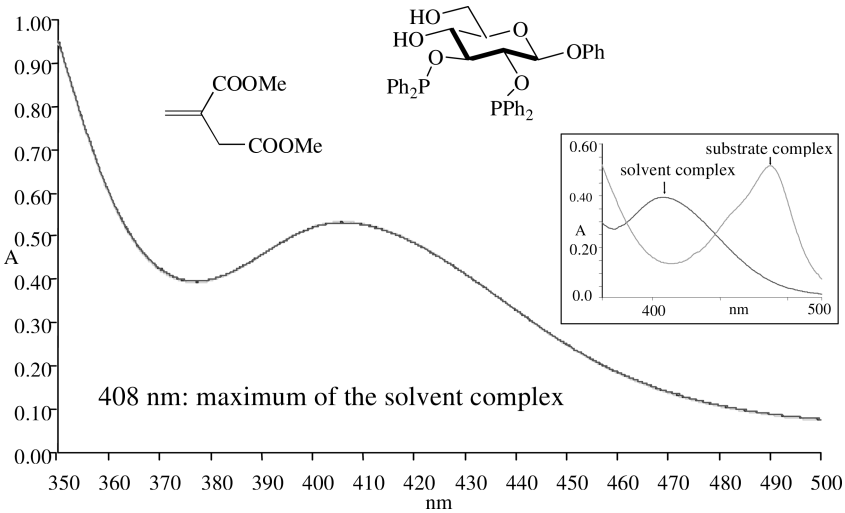

Fig. 10.18 UV/visible spectrum of 0.02 mmol [Rh(Ph-*β*-glup-OH)(MeOH)$_2$]BF$_4$ in 35.0 mL MeOH under Ar, and five spectra (cyclic, monitored at 6.0 min intervals) after addition of a 100-fold excess of dimethyl itaconate and exchange of Ar for H_2. Inset: the spectrum of the catalyst–substrate complex. GC analysis after 30 min hydrogenation: 45% conversion, 78% ee (*R*), which agrees well with corresponding hydrogenations.

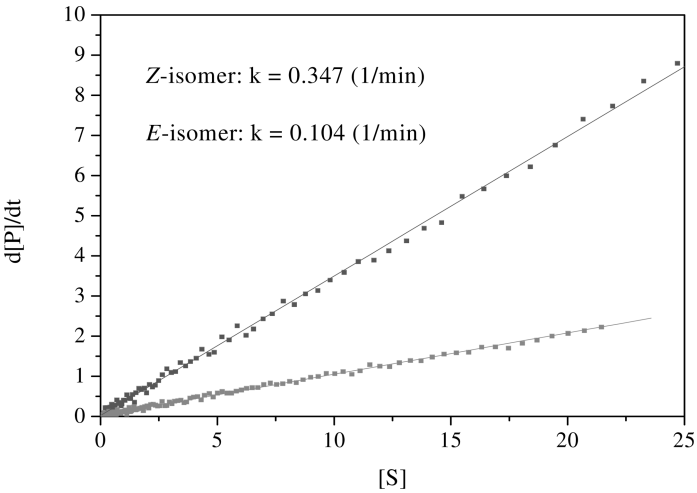

Fig. 10.19 Asymmetric hydrogenation of *E*- and *Z*-methyl 3-acetamidobutenoate with [Rh(Et-DuHOS)MeOH$_2$)BF$_4$ as first-order reactions; d[P]/d*t* versus [S] (Eq. (4b)).

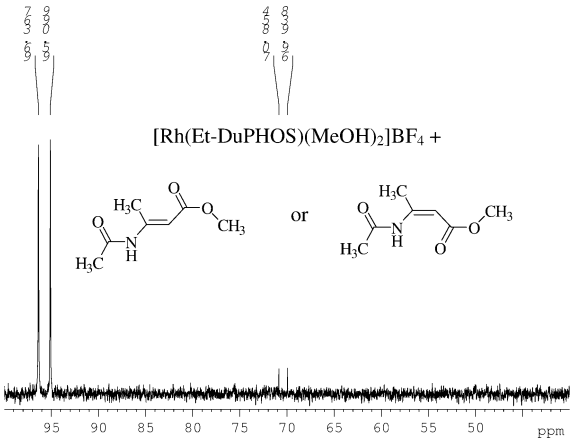

Fig. 10.20 ^{31}P-NMR spectrum of a solution of 0.01 mM [Rh(Et-DuPHOS)(MeOH)$_2$]BF$_4$ and 0.1 mM *E*- or *Z*-methyl 3-acetamidobutenoate.

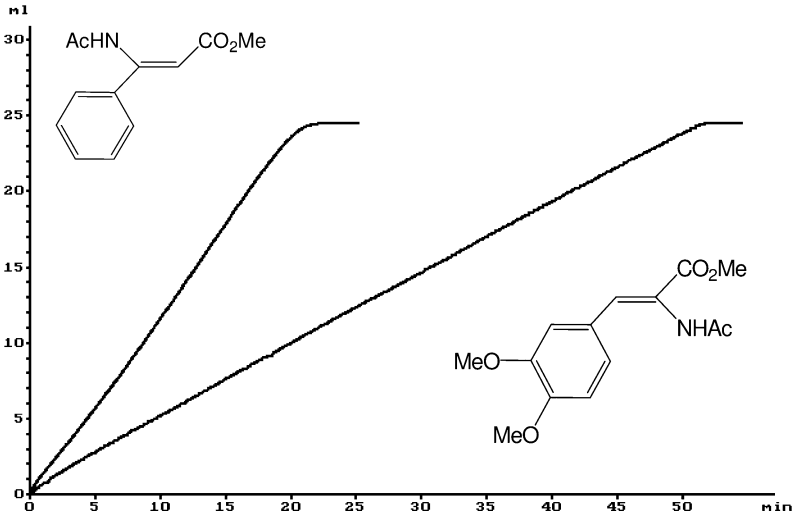

Fig. 10.21 Hydrogen consumption for the hydrogenation of (*Z*)-3-*N*-acetylamino-3-(phenyl)-methyl propenoate with [Rh((*R*,*R*)-Et-DuPHOS)(MeOH)$_2$]BF$_4$ in *i*-PrOH (59% ee) and (*Z*)-2-benzoylamino-3-(3,4-dimethoxy phenyl)-methyl acrylate with [Rh((*S*,*S*)-DIPAMP)(MeOH)$_2$]BF$_4$ in MeOH (98% ee). Conditions: 0.01 mmol catalyst; 1.0 mmol substrate; 15.0 mL solvent; 1.013 bar total pressure.

Nonetheless, if zero-order reactions are analyzed in terms of the validity of Michaelis-Menten kinetics, all of the catalyst is present in solution as catalyst–substrate complex up to high conversions. The hydrogenation rate is independent of the substrate concentration; two such examples are provided in Figure 10.21.

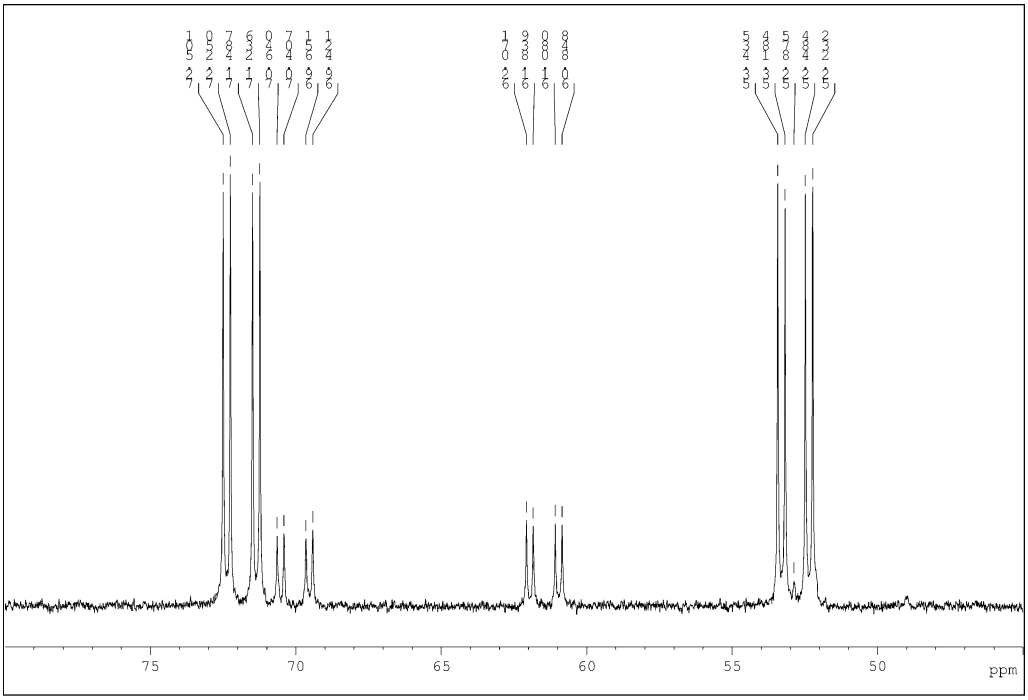

Fig. 10.22 ^{31}P-NMR spectrum of a solution of 0.02 mM [Rh((*S*,*S*)-DIPAMP)(MeOH)$_2$]BF$_4$ and 0.1 mM (*Z*)-2-benzoylamino-3-(3,4-dimethoxyphenyl)-methyl acrylate.

In these cases, the ^{31}P-NMR spectrum exhibits only signals of substrate complexes; there is almost no solvent complex visible. This is illustrated for (*Z*)-2-benzoylamino-3-(3,4-dimethoxyphenyl)-methyl acrylate with [Rh((*S*,*S*)-DIPAMP)(MeOH)$_2$]BF$_4$ in Figure 10.22.

Thus, if information is being sought about intermediates for this type of catalysis, it does not make sense to analyze systems that lead to first-order reactions! Rather, systems in which the hydrogenation rate is independent of the substrate concentration would be more appropriate. Indeed, for both catalytic systems shown in Figure 10.21, in each case one of the catalyst–substrate complexes could be isolated and characterized by crystal structure analysis (Fig. 10.23).

In the case of the α-dehydroamino acid (Fig. 10.23, right), it could be shown by using low-temperature NMR spectroscopy that the isolated crystals correspond to the major substrate complex in solution. However, according to the major–minor concept (see Scheme 10.2), it does not lead to the main enantiomer [63]. On the contrary, it could be proven unequivocally for various substrate complexes with β-dehydroamino acids that the isolated substrate complexes are major-substrate complexes. Surprisingly, they also gave the main enantiomer of the asymmetric hydrogenation, which would not be expected on the basis of

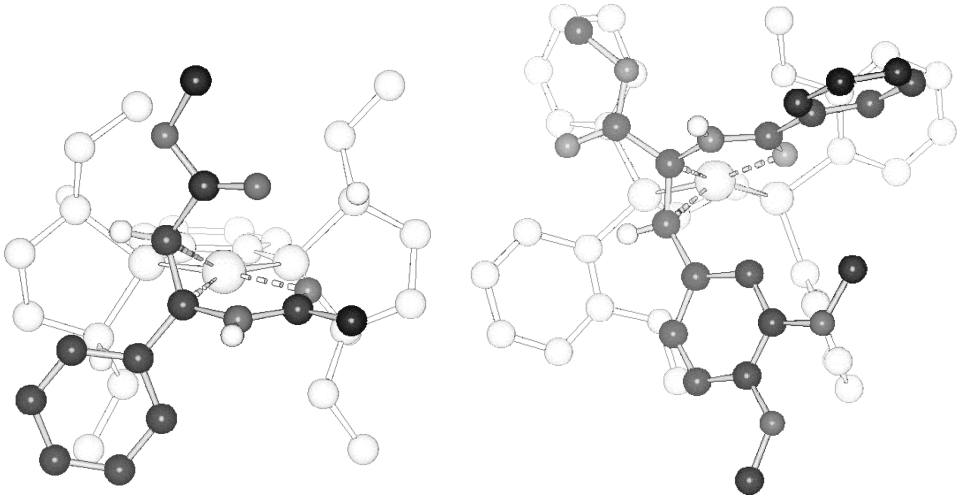

Fig. 10.23 X-ray structure of [Rh((*R*,*R*)-Et-DuPHOS)((*Z*)-3-*N*-acetylamino-3-(phenyl)-methyl propenoate)]$^+$ and of [Rh((*S*,*S*)-DIPAMP)((*Z*)-2-benzoylamino-3-(3,4-dimethoxyphenyl)-methyl acrylate)]$^+$ [62].

classical ideas [62 a]. In these cases the major-substrate complex determines the selectivity, in analogy to the well known lock-and-key concept of enzyme catalysis proposed by Emil Fischer. This result could only be gained by quantitative monitoring of the hydrogenation and the subsequent interpretation of kinetic findings within the frame of Michaelis-Menten kinetics.

Abbreviations

COD	cycloocta-1,5-diene
NBD	norborna-2,5-diene
TOF	turnover frequency
TON	turnover number

References

1 R.A. Sanchez-Delgado, M. Rosales, *Coord. Chem. Rev.* **2000**, *196*, 249.
2 J.A. Widegren, R.G. Finke, *J. Mol. Cat. A: Chemical* **2003**, *198*, 317.
3 G. Djéga-Mariadassou, M. Boudart, *J. Catal.* **2003**, *216*, 89.
4 The number of reaction possibilities that fulfill particular limiting conditions can be surprisingly high. This is shown by mechanisms of various catalyzed reactions generated by computer programs such as ChemNet or MECHEM. (a) R.E. Valdes-Perez, A.V. Zeigarnik, *J. Chem. Inf. Comput. Sci.* **2000**, *40*, 833; (b) L.G. Bruk, S.N. Gorodskii, A.V. Zeigarnik, R.E. Valdes-Perez, O.N. Temkin, *J. Mol. Catal. A: Chem.* **1998**, *130*, 29; (c) A.V. Zeigarnik, R.E. Valdes-Perez, O.N. Tem-

kin, L.G. Bruk, S.I. Shalgunov, *Organometallics* **1997**, *16*, 3114.

5 According to Chen et al., alkali cation co-catalysis kinetics cannot be distinguished from classic ideas (proton instead of alkali) for the asymmetric hydrogenation of acetophenone with the Noyori-catalyst (*trans*-$RuCl_2$[(*S*)-BINAP] [(*S*,*S*)DPEN]) (see [43b]).

6 J. Halpern, *Science* **1982**, *217*, 401.

7 R. Noyori, *Asymmetric catalysis in organic synthesis*. John Wiley & Sons, Inc., New York, **1994**.

8 W.A. Herrmann, B. Cornils, *Angew. Chem. Int. Ed.* **1997**, *36*, 1049.

9 (a) P.I. Dalko, L. Moisan, *Angew. Chem. Int. Ed.* **2004**, *43*, 5138; (b) Special edition *Accounts Chem. Res.* **2004**, *37*, 8, 487.

10 We point out that in enzyme kinetics TON is understood as TOF! "It is also sometimes called the turnover *number*, because it is a reciprocal time and defines the number of catalytic cycles (or "turnovers") that the enzyme can undergo in unit time, or the number of molecules of substrate that one molecule of enzyme can convert into products in one unit of time." Quotation from [23].

11 For the hydrogenation of acetophenone with the Ru-BINAP-DPEN system by Noyori, for example, in the course of 48 h 2.4 million conversions at the catalyst are reached (H. Doucet, T. Ohkuma, K. Murata, T. Yokozawa, M. Kozawa, E. Katayama, A.F. England, T. Ikariya, R. Noyori, *Angew. Chem. Int. Ed.* **1998**, *37*, 1703). Rautenstrauch could – under slightly changed conditions – reach a TOF of 333 000 h^{-1} (V. Rautenstrauch, X. Hoang-Cong, R. Churlaud, K. Abdur-Rashid, R.H. Morris, *Chem. Eur. J.* **2003**, *9*, 4954). The best results as concerns the activity of transfer hydrogenations were reported by Mathey, according to who cyclohexanone can, during the course of 15 h, be completely converted with a substrate/catalyst ratio of 20 million by a catalyst containing a P/N-ligand (C. Thoumazet, M. Melaimi, L. Ricard, F. Mathey, P. Le Floch, *Organometallics* **2003**, *22*, 1580).

12 The following TON and TOF specifications refer to minimum quantities for technically relevant processes: H.U. Blaser, B. Pugin, F. Spindler, *Enantioselective Synthesis, Applied Homogeneous Catalysis by Organometallic Complexes*, 2nd edn, Volume 3, B. Cornils, W.A. Herrmann (Eds.), Wiley-CH, Weinheim, **2002**, pp. 1131. "Catalyst productivity, given as substrate/catalyst ratio (*s/c*) or turnover number (TON), determines catalyst costs. These *s/c* ratios ought to be >1000 for small-scale, high-value products and >50 000 for large-scale or less-expensive products (catalyst re-use increases the productivity)" and "Catalyst activity, given as turnover frequency for >95% conversion (TOF_{av}, h^{-1}), determines the production capacity. TOF_{av} ought to be >500 h^{-1} for small-scale and >10 000 h^{-1} for large-scale products" (p. 1133).

13 Due to *re*- and *si*-coordination of prochiral substrates at a catalyst with C_2-symmetric chiral ligands two diastereomeric catalyst-substrate complexes emerge. In the case of C_1-symmetric ligands already four stereoisomer intermediates result.

14 The so-called "minor-substrate complexes" of asymmetric hydrogenations are not detectable in many cases, even though they determine the stereochemical course of the hydrogenation due to their high reactivity according to classical ideas.

15 L. Michaelis, M.L. Menten, *Biochem. Z.* **1913**, *49*, 333.

16 M. Bodenstein, *Z. Phys. Chem.* **1913**, *85*, 329.

17 G.E. Briggs, J.B.S. Haldane, *Biochem. J.* **1925**, *19*, 338.

18 (a) F.G. Helfferich, *Kinetics of Homogeneous Multistep Reactions, Comprehensive Chemical Kinetics*, Volume 38, Elsevier, Amsterdam, **2001**; (b) K.A. Connors, *Chemical Kinetics. The Study of Reaction Rates in Solution*, VCH Publishers Inc., New York, **1990**.

19 "Quite often, kinetic studies are not performed because it appears time-consuming, expensive (with respect to the price or availability of most of chiral ligands) and not rewarding") (see [35a]).

20 An irreversible formation of the catalyst–substrate complex is described in: D.D.

van Slyke, G. E. Cullen, *J. Biol. Chem.* **1914**, *19*, 141.

21 (a) A. S. C. Chan, J. J. Pluth, J. Halpern, *J. Am. Chem. Soc.* **1980**, *102*, 5952; (b) C. R. Landis, J. Halpern, *J. Am. Chem. Soc.* **1987**, *109*, 1746; (c) M. Kitamura, M. Tsukamoto, Y. Bessho, M. Yoshimura, U. Kobs, M. Widhalm, R. Noyori, *J. Am. Chem. Soc.* **2002**, *124*, 6649.

22 Today, this synonym is used for the more common steady-state approach by Briggs and Haldane (see [17]).

23 A. Cornish-Bowden, *Fundamentals of Enzyme Kinetics*, 3rd edn, Portland Press Ltd., London, **2004**.

24 K. J. Laidler, *Can. J. Chem.* **1955**, *33*, 1614.

25 D. G. Blackmond, *Angew. Chem. Int. Ed.* **2005**, *44*, 4302.

26 At the end of a hydrogenation the substrate concentration is naturally also low.

27 The term for the saturation rate (V_{sat}) in earlier works commonly employed as "maximum rate" (V_{max}) should not – according to the recommendation of the International Union of Biochemistry – be used any more because it does not describe a real maximum, but a limit.

28 (a) A. G. Marongoni, *Enzyme Kinetics – A Modern Approach*, Wiley-Interscience, **2003**; (b) R. A. Copeland, *Enzymes – A Practical Introduction to Structure, Mechanism, and Data Analysis*, VCH Publishers, Inc., New York, **1996**; (c) H. Bisswanger, *Enzymkinetik*, VCH Verlagsgesellschaft mbH, Weinheim, **1994**; (d) A. Cornish-Bowden, *Principles of Enzyme Kinetics*, Butterworth & Co. Ltd., London, **1976**; (e) H.J. Fromm, *Initial Rate Enzyme Kinetics*, Springer, Berlin, **1975**; (f) I.H. Segel, *Enzyme kinetics*, Wiley & Sons, New York, **1975**.

29 H. Lineweaver, D. Burk, *J. Am. Chem. Soc.* **1934**, *56*, 658.

30 (a) G. S. Eady, *J. Biol. Chem.* **1942**, *146*, 85; (b) B. H. J. Hofstee, *J. Biol. Chem.* **1952**, *199*, 357; (c) B. H. J. Hofstee, *Nature* **1959**, *184*, 1296.

31 C. S. Hanes, *Biochem. J.* **1932**, *26*, 1406.

32 The original work of Lineweaver and Burk [29] is the most cited one in *J. Am. Chem. Soc.* (according to *Chem. Eng. News* **2003**, *81*, 27).

33 (a) Y. Fu, X.-X. Guo, S.-F. Zhu, A.-G. Hu, J.-H. Xie, Q.-L. Zhou, *J. Org. Chem.* **2004**, *69*, 4648; (b) H.-J. Drexler, J. You, S. Zhang, C. Fischer, W. Baumann, A. Spannenberg, D. Heller, *Org. Process Res. Dev.* **2003**, *7*, 355; (c) D. Heller, H.-J. Drexler, J. You, W. Baumann, K. Drauz, H.-P. Krimmer, A. Börner, *Chemistry – A European Journal* **2002**, *8*, 5196; (d) D. Heller, H.-J. Drexler, A. Spannenberg, B. Heller, J. You, W. Baumann, *Angew. Chem. Int. Ed.* **2002**, *41*, 777; (e) O. Pàmies, M. Diéguez, G. Net, A. Ruiz, C. Claver, *J. Org. Chem.* **2001**, *66*, 8364; (f) I. M. Angulo, E. Bouman, *J. Mol. Catal. A: Chemical* **2001**, *175*, 65; (g) N. Tanchoux, C. de Bellefon, *Eur. J. Inorg. Chem.* **2000**, 1495; (h) O. Pàmies, G. Net, A. Ruiz, C. Claver, *Eur. J. Inorg. Chem.* **2000**, 1287; (i) M. Rosales, A. González, M. Mora, N. Nader, J. Navarro, L. Sánchez, H. Soscín, *Trans. Met. Chem.* **2004**, *29*, 205; (j) C. A. Sandoval, T. Ohkuma, K. Muniz, R. Noyori, *J. Am. Chem. Soc.* **2003**, *125*, 13490; (k) A. Salvini, P. Frediani, S. Gallerini, *Appl. Organometal. Chem.* **2000**, *14*, 570; (l) V. Herrera, B. Munoz, V. Landaeta, N. Canudas, *J. Mol. Catal. A: Chemical* **2001**, *174*, 141; (m) P. K. Santra, P. Sagar, *J. Mol. Catal. A: Chemical* **2003**, *197*, 37; (n) M. Rosales, J. Castillo, A. González, L. González, K. Molina, J. Navarro, I. Pacheco, H. Pérez, *Trans. Met. Chem.* **2004**, *29*, 221; (o) M. Rosales, F. Arrieta, J. Castillo, A. Gonzàlez, J. Navarro, R. Vallejo, *Stud. Surf. Sci. Catal.* **2000**, *130*, 3357; (p) C. A. Thomas, R.J. Bonilla, Y. Huang, P.G. Jessop, *Can. J. Chem.* **2001**, *79*, 719.

34 A. Zogg, F. Stoessel, U. Fischer, K. Hungerbühler, *Thermochim. Acta* **2004**, *419*, 1.

35 (a) C. deBellefon, N. Pestre, T. Lamouille, P. Grenouillet, V. Hessel, *Adv. Synth. Catal.* **2003**, *345*, 190; (b) C. deBellefon, R. Abdallah, T. Lamouille, N. Pestre, S. Caravieilhes, P. Grenouillet, *Chimia* **2002**, 621; (c) J.L. Bars, T. Häußner, J. Lang, A. Pfaltz, D. G. Blackmond, *Adv. Synth. Catal.* **2001**, *343*, 207; (d) C. deBellefon, N. Tanchoux, S. Caravieilhes, P. Grenouillet, V. Hessel, *Angew. Chem. Int. Ed.* **2000**, *39*, 3442.

36 The real molar volume of hydrogen amounts to 24.48 cm^3 mol^{-1} at 25.0 °C and 1.013 bar (ideal gas: 24.46 cm^3 mol^{-1}). Due to non-linear compressibility, pV/p-isotherms at 100 bar deviate from ideal gas behavior by a few per cent.

37 Virial coefficients of hydrogen can, for example, be found in: J. H. Dymond, E. B. Smith, *The Virial Coefficients of Pure Gases and Mixtures*, Clarendon Press, Oxford, **1980**. By interpolation (e.g., with cubic spline functions), virial coefficients can be determined for any temperature.

38 B. Bogdanovic, B. Spliethhoff, *Chem.-Ing.-Tech.* **1983**, *55*, 156.

39 (a) Y. Sun, J. Wang, C. Le Blond, R.N. Landau, J. Laquidara, J. R. Sowa, Jr., D. G. Blackmond, *J. Mol. Catal. A: Chemical* **1997**, *115*, 495; (b) Y. Sun, R. N. Landau, J. Wang, C. LeBlond, D. G. Blackmond, *J. Am. Chem. Soc.* **1996**, *118*, 1348.

40 (a) J.-C. Charpentier, Mass-transfer rates in gas-liquid absorbers and reactors. In: *Advances in Chemical Engineering*, T. B. Drew, G. R. Cokeleit, J. W. Hoopes, Jr., T. Vermeulen (Eds.), Academic Press Inc., New York, **1981**, Volume 11, pp. 1; (b) G. Astarita, *Mass transfer with chemical reaction*, Elsevier Publishing Company, Amsterdam, **1967**.

41 Y. Sun, J. Wang, C. Le Blond, R. A. Reamer, J. Laquidara, J. R. Sowa, Jr., D. G. Blackmond, *J. Organomet. Chem.* **1997**, *548*, 65.

42 Such induction periods can, for example, result from transferring a precatalyst into the active species. For the asymmetric hydrogenation this is described in detail in: (a) W. Braun, A. Salzer, H.-J. Drexler, A. Spannenberg, D. Heller, *Dalton Trans.* **2003**, 1606; (b) H.-J. Drexler, W. Baumann, A. Spannenberg, C. Fischer, D. Heller, *J. Organomet. Chem.* **2001**, *621*, 89; (c) C. J. Cobley, I. C. Lennon, R. McCague, J. A. Ramsden, A. Zanotti-Gerosa, *Tetrahedron Lett.* **2001**, *42*, 7481; (d) A. Börner, D. Heller, *Tetrahedron Lett.* **2001**, *42*, 223; (e) W. Baumann, S. Mansel, D. Heller, S. Borns, *Magn. Res. Chem.* **1997**, *35*, 701; (f) D. Heller, S. Borns, W. Baumann, R. Selke, *Chem. Ber.* **1996**, *129*, 85.

43 (a) L. Greiner, M. B. Ternbach, *Adv. Synth. Catal.* **2004**, *346*, 1392 (supplementary information); (b) R. Hartmann, P. Chen, *Adv. Synth. Catal.* **2003**, *345*, 1353.

44 (a) A. G. Osborn, D. R. Douslin, *J. Chem. Eng. Data* **1974**, *19*, 114; (b) T. Boublik, K. Aim, *Collect. Czech. Chem. Comm.* **1972**, *11*, 3513; (c) D. W. Scott, *J. Chem. Thermodynamics* **1970**, *2*, 833; (d) T. E. Jordan, *Vapor pressure of Organic Compounds*, Interscience Publishers, Inc. New York, **1954**.

45 (a) P. G. T. Fogg, W. Gerrard, *Solubility of Gases in Liquids*, John Wiley & Sons, Chichester, **1991**; (b) E. Brunner, *J. Chem. Eng. Data* **1985**, *30*, 269.

46 To the best of our knowledge there are no experimental data available for CH_2Cl_2.

47 D. Heller, J. Holz, S. Borns, A. Spannenberg, R. Kempe, U. Schmidt, A. Börner, *Tetrahedron: Asymmetry* **1997**, *8*, 213.

48 (a) A. Aghmiz, A. Orejón, M. Dieguez, M. D. Miquel-Serrano, C. Claver, A. M. Masdeu-Bultó, D. Sinou, G. Laurenczy, *J. Mol. Catal. A: Chemical* **2003**, *195*, 113; (b) H. G. Niessen, P. Trautner, S. Wiemann, J. Bargon, K. Woelk, *Rev. Sci. Instrum.* **2002**, *73*, 1259; (c) S. Gaemers, H. Luyten, J. M. Ernsting, C. J. Elsevier, *Magn. Res. Chem.* **1999**, *37*, 25; (d) J. A. Iggo, D. Shirley, N. D. Tong, *New J. Chem.* **1998**, 1043; (e) A. Cusanelli, U. Frey, D. Marek, A. E. Merbach, *Spectr. Eur.* **1997**, *9*, 22; (f) S. Mansel, D. Thomas, C. Lefeber, D. Heller, R. Kempe, W. Baumann, U. Rosenthal, *Organometallics* **1997**, *16*, 2886; (g) W. Baumann, S. Mansel, D. Heller, S. Borns, *Magn. Reson. Chem.* **1997**, *35*, 701; (h) P. M. Kating, P. J. Krusic, D. C. Roe, B. E. Smart, *J. Am. Chem. Soc.* **1996**, *118*, 10000; (i) M. Haake, J. Natterer, J. Bargon, *J. Am. Chem. Soc.* **1996**, *118*, 8688; (j) K. Woelk, J. Bargon, *Rev. Sci. Instrum.* **1992**, *63*, 3307; (k) D. C. Roe, *J. Magn. Res.* **1985**, *63*, 388.

49 (a) L. Damoense, M. Datt, M. Green, C. Steenkamp, *Coord. Chem. Rev.* **2004**, *248*, 2393; (b) E. M. Vincente, P. S. Pregosin, D. Schott, *Mechanism in Homogeneous Catalysis – A Spectroscopic Approach*. B. Heaton (Ed.), Wiley-VCH,

2005, Chapter 1, pp. 1–80; (c) G. Laurenczy, L. Helm, *Mechanism in Homogeneous Catalysis – A Spectroscopic Approach*. B. Heaton (Ed.), Wiley-VCH, **2005**, Chapter 2, pp. 81.

50 D. Heller, W. Baumann, DE 102 02 173 C2, **2003**.

51 (a) D. Selent, W. Baumann, A. Börner, DE 10333143.A1 (3.3.**2005**); (b) D. Selent, W. Baumann, K.-D. Wiese, D. Ortmann, A. Börner, 14th International Symposium on Homogeneous Catalysis, Munich, 5.–9.7. **2004**, poster no. 0044.

52 Analogue trials in a cell are not practicable. To monitor hydrogen consumption accurately (ca. 8 mL in the example), an absolute quantity of COD is necessary. With equal catalyst/substrate ratios (as in the example), the resultant intracellular high catalyst concentration could only be compensated by a very small cell thickness, which would in turn considerably restrict intracellular mixing.

53 (a) S. Richards, M. Ropic, D. Blackmond, A. Walmsley, *Analytica Chim. Acta* **2004**, *519*, 1; (b) C. LeBlond, J. Wang, R. Larsen, C. Orella, Y.-K. Sun, *Topics Catal.* **1998**, 149; (c) C. LeBlond, J. Wang, R.D. Larsen, C.J. Orella, A.L. Forman, R.N. Landau, J. Laquidara, J.R. Sowa, D.G. Blackmond, Y.-K. Sun, *Thermochim. Acta* **1996**, *289*, 189.

54 A. Haynes, *Mechanism in Homogeneous Catalysis – A Spectroscopic Approach*. B. Heaton (Ed.), Wiley-VCH, **2005**, Chapter 3, pp. 107.

55 (a) J.M. Brown, P.A. Chaloner, *J. Chem. Soc., Chem. Commun.* **1980**, 344; (b) J.M. Brown, P.A. Chaloner, *Homogeneous Catalysis with Metal Phosphine Complexes*. L.H. Pignolet (Ed.), Plenum Press, New York, **1983**, pp. 137; (c) J.M. Brown, *Chem. Soc. Rev.* **1993**, *22*, 25.

56 A review regarding experimental findings, which seemingly speak for the alternatively discussed dihydride mechanism, can be found in: I.D. Gridnev, T. Imamoto, *Acc. Chem. Res.* **2004**, *37*, 633. However, it must be stressed that verified results such as the pressure dependence of enantioselectivity cannot be described by this model. Models related to the dihydride mechanism and developed substantially on the basis of low-temperature NMR spectroscopy have not yet been investigated in terms of kinetic consequences.

57 (a) J.M. Brown, P.A. Chaloner, G.A. Morris, *J. Chem. Soc., Chem. Commun.* **1983**, 664; (b) J.M. Brown, P.A. Chaloner, G.A. Morris, *J. Chem. Soc., Perkin Trans. II* **1987**, 1583; (c) H. Bircher, B.R. Bender, W. von Philipsborn, *Magn. Reson. Chem.* **1993**, *31*, 293; (d) R. Kadyrov, T. Freier, D. Heller, M. Michalik, R. Selke, *J. Chem. Soc., Chem. Commun.* **1995**, 1745; (e) J.A. Ramsden, T.D.W. Claridge, J.M. Brown, *J. Chem. Soc., Chem. Commun.* **1995**, 2469; (f) D. Heller, R. Kadyrov, M. Michalik, T. Freier, U. Schmidt, H.W. Krause, *Tetrahedron: Asymmetry* **1996**, *7*, 3025; (g) A. Kless, A. Börner, D. Heller, R. Selke, *Organometallics* **1997**, *16*, 2096.

58 In case of the asymmetric hydrogenation with Rh complexes this disturbance in the equilibrium establishment is shown in pressure-dependent e.e. values (see [21 b]). Djega-Mariadassou and Boudart [3] describe this phenomenon as "kinetic coupling"; see also G. Djega-Mariadassou, *Catal. Lett.* **1994**, 7. In this context, we point out that under "kinetic coupling" conditions it is principally not possible experimentally to determine a partial order of 1 with respect to hydrogen.

59 D. Heller, R. Thede, D. Haberland, *J. Mol. Cat. A: Chemical* **1997**, *115*, 273.

60 This statement also applies if intermolecular pre-equilibria are not established. In case of established intermolecular pre-equilibria the value of $1/K_M$ corresponds to the sum of all stability constants.

61 (a) H.W. Krause, H. Foken, H. Pracejus, *New J. Chem.* **1989**, *13*, 615; (b) H.W. Krause, U. Schmidt, S. Taudien, B. Costisella, M. Michalik, *J. Mol. Catal. A: Chemical* **1995**, *104*, 147; (c) C. Döbler, H.-J. Kreuzfeld, M. Michalik, H.W. Krause, *Tetrahedron: Asymmetry* **1996**, *7*, 117; (d) H.J. Kreuzfeld, C. Döbler, U. Schmidt, H.W. Krause, *Amino Acids* **1996**, *11*, 269; (e) U. Schmidt, H.W. Krause, G. Oehme, M. Michalik, C. Fischer, *Chirality* **1998**, *10*, 564;

(f) C. Döbler, H.-J. Kreuzfeld, C. Fischer, M. Michalik, *Amino Acids* **1999**, *16*, 391; (g) T. Dwars, U. Schmidt, C. Fischer, I. Grassert, H.W. Krause, M. Michallik, G. Oehme, *Phosphorus, Sulfur, and Silicon* **2000**, *158*, 209.

62 (a) H.-J. Drexler, W. Baumann, T. Schmidt, S. Zhang, A. Sun, A. Spannenberg, C. Fischer, H. Buschmann, D. Heller, *Angew. Chem. Int. Ed.* **2005**, *44*, 1184; (b) H.-J. Drexler, S. Zhang, A. Sun, A. Spannenberg, A. Arrieta, A. Preetz, D. Heller, *Tetrahedron: Asymmetry* **2004**, *15*, 2139.

63 T. Schmidt, W. Baumann, H.-J. Drexler, A. Arrieta, D. Heller, H. Buschmann, *Organometallics* **2005**, *24*, 3842.

Part II
Spectroscopic Methods in Homogeneous Hydrogenation

The Handbook of Homogeneous Hydrogenation.
Edited by J.G. de Vries and C.J. Elsevier
Copyright © 2007 WILEY-VCH Verlag GmbH & Co. KGaA, Weinheim
ISBN: 978-3-527-31161-3

11
Nuclear Magnetic Resonance Spectroscopy in Homogeneous Hydrogenation Research

N. Koen de Vries

11.1
Introduction

11.1.1
Nuclear Magnetic Resonance (NMR)

NMR spectroscopy is a very powerful tool for structural characterization purposes. Following the discovery of the technique, organic chemists were quick to recognize its potential and as soon as commercial instruments came on the market they began to use NMR to elucidate the structures of their synthetic efforts. During the late 1960s and early 1970s, some very important developments took place that made the technique what it is today. The first development was that of the so-called Fourier transform (or FT-NMR) measurement [1]. Until then, the magnetic field was varied, and as it swept through the whole frequency range a recorder noted the moment when a nucleus was on resonance. In the FT-mode, all frequencies are excited at the same time by a short pulse, and the response in time of all the nuclei together is recorded as they relax back to equilibrium. The Fourier transformation converts this time-dependent signal to a frequency-dependent signal, which is the NMR-spectrum. As in all FT-techniques, the major advantage is that one can acquire more than one scan. This improves the signal-to-noise ratio because it increases with the square root of the number of scans. From then on, insensitive nuclei such as ^{13}C-NMR could also be measured routinely. This nucleus has a much larger chemical shift range and thus allows a better resolution.

The second development that has revolutionized the practice of NMR was the introduction of multidimensional spectroscopy. This was initialized by Jeener [2], who showed that, by introducing a second pulse and varying the time between them, a second "time-axis" could be constructed. A double Fourier transformation yields the familiar two-dimensional spectrum, nowadays known by everyone as the COSY spectrum. Ernst, already involved in the development of FT-NMR, showed that the concept was more generally applicable [3], and paved

The Handbook of Homogeneous Hydrogenation.
Edited by J.G. de Vries and C.J. Elsevier
Copyright © 2007 WILEY-VCH Verlag GmbH & Co. KGaA, Weinheim
ISBN: 978-3-527-31161-3

the way for the whole variety (hundreds, if not thousands) of multidimensional experiments that exist today. A typical and well-known example of what can be achieved is the complete three-dimensional structure elucidation of peptides consisting of hundreds of amino acids.

NMR continued to develop during the 1980s and 1990s with techniques such as inverse NMR [4] and gradient pulses [5]. It would also be valuable to mention here the various instrumental improvements such as cryo-probes and the ever-increasing magnetic-field strength (with commercial 1000-MHz spectrometers almost in reach), all aimed at improving resolution and sensitivity.

It is this relative insensitivity that is usually considered as the major drawback of NMR spectroscopy. However, the flexibility of the NMR technique, with the ability to obtain structural information, quantitative data (e.g. kinetic parameters), as well as an indication of molecular volume, using pulsed gradient spin echo (PGSE) NMR diffusion methods [6], makes NMR a most valuable tool.

11.1.2
NMR in Homogeneous Hydrogenation Research

On the subject of NMR spectroscopy in homogeneous hydrogenation research, we can recognize that most developments have found their way into this research area, albeit with some delay. For example, the PGSE methods had been used for over twenty years to determine diffusion coefficients of organic molecules before their potential in organometallic chemistry was investigated [7]. Pioneering studies were also conducted by von Philipsborn who, during the early 1980s, was already performing transition metal NMR spectroscopy in order to probe structures of organometallic compounds and their reactivity. For further information, the reader is referred to an excellent review on this topic [8].

In this chapter, we will provide an introduction into the application of NMR in the area of homogeneous hydrogenation research, and suggest further reading for those who wish to obtain more information on the subject. The principles of NMR spectroscopy have been covered thoroughly by Ernst [9], and numerous books and review articles have appeared on all aspects of the application of NMR in homogeneous hydrogenation research. Typical reviews include "NMR and homogeneous catalysis" in general [10], "NMR at elevated gas pressures and its application to homogeneous catalysis" [11], the measurement of transition metals by NMR [12] and, more recently, "^{103}Rh NMR spectroscopy and its application to rhodium chemistry" [13].

Other important topics, such as the use of *para*-hydrogen-induced polarization (PHIP) NMR, are discussed in more detail elsewhere in this book. Basically, this approach enhances the NMR signal one thousandfold, thus allowing the detection of intermediates that go unnoticed when using "classical" NMR techniques. PHIP is particularly suited for homogeneous hydrogenation research because a prerequisite of the method is that both former *para*-hydrogen nuclei must be present (and J-coupled) in the molecule of interest.

In summary, NMR in homogeneous hydrogenation research is used for:

- Structure elucidation of various species present in the reaction mixtures; typical tools used for this purpose include chemical shifts, coupling constants, PHIP-NMR, and 2D-NMR.
- Determination of reaction mechanisms by combining the observed intermediates in a catalytic cycle. To do this, it is often necessary to measure under different conditions – that is, variable temperature NMR. The use of high-pressure NMR cells is crucial in order to measure under the real catalytic conditions. The EXSY experiment helps to unravel exchange pathways, both intra- and intermolecular.
- Determination of the reaction kinetics if the reaction is slow enough to record a series of NMR spectra. This can be done with standard 1D-NMR measurements if the concentrations are high enough, and if not, by making use of sensitivity enhancement through *para*-hydrogen. NMR experiments designed for kinetic investigations in combination with PHIP techniques include ROCHESTER (Rates Of Catalytic Hydrogenation Estimated Spectroscopically Through Enhanced Resonances) [14] and DYPAS. An example of the investigation of kinetics of homogeneous hydrogenation reactions using both experiments can be found in [15].

11.2 NMR Methods

11.2.1 General

In order to perform the various tasks mentioned in Section 11.1.2, it is necessary to use one or several methods to gather information by NMR spectroscopy. Typically, chemical shift and coupling constant information, 2D-NMR measurements, variable temperature or pressure studies are used. If appropriate, specific examples of the particular topic as applied in homogeneous hydrogenation research are detailed below.

The most popular nucleus for NMR measurements is the proton, and this is obviously related to its high sensitivity. As a rotating charged particle, a proton will generate a magnetic moment. Because, for a proton, the spin quantum number $I=1/2$, there are two possible spin states. In the absence of a field these states have the same energy, but in a strong magnetic field they are no longer equivalent. The population of the lower level is slightly higher than that of the upper level, according to the Boltzmann distribution. This results in a small excess magnetization vector along the z-axis. By applying a radiofrequency field for a short time, this vector can be moved and ends up in the x-y-plane (90° pulse), where it will rotate. This time-response is registered by a radiofrequency coil aligned along the x-axis. This oscillatory decay (or FID) is transformed to a frequency response spectrum by the FT calculation.

11.2.2 Chemical Shift

11.2.2.1 General

The chemical shift is caused by shielding of the proton due to a local field, generated by circulations of electrons. It is this local effect that makes it possible to use NMR as a structural characterization tool. For ^{1}H-NMR there is a relatively straightforward correlation between chemical shift and electron density, because only diamagnetic contributions play a role, but for most other nuclei a paramagnetic term also contributes to the shielding. This makes it difficult to relate, for example, the geometry around a metal with its chemical shift [13]. For qualitative discussions of chemical shifts, the following simplified expression can be used:

$$\delta = -\mathrm{A} + \mathrm{B} \times (k^2 \langle r^{-3} \rangle)(\Delta E)^{-1}$$

where r is the valence shell radius and ΔE the ligand field-splitting energy.

If either one of the terms dominates, it is sometimes possible to observe correlations. For example, a linear dependence of ^{195}Pt chemical shift with UV-visible data for a series of octahedral platinum complexes has been identified [16].

Another example is the linear correlation of the ^{59}Co chemical shifts of the catalyst with the regioselectivity of a trimerization reaction of acetylenes [15].

Despite the difficulties in explaining the metal NMR shifts, it is still worthwhile measuring them because the huge chemical shift range makes it easy to observe the different species present, for example diastereoisomers [18].

Bender et al. [19] used ^{103}Rh-NMR chemical shift differences to demonstrate an electronic difference at rhodium between two diastereoisomers, and suggested that this might influence the crucial hydrogen addition step.

Another popular NMR nucleus is ^{31}P; this is because it is quite sensitive, it already has a large chemical shift range (as compared to ^{1}H-NMR), the phosphorus atom is usually coupled directly to the metal atom, and phosphorus is often present in ligands of homogeneous hydrogenation complexes. Verkade [20] has reviewed aspects of ^{31}P-NMR including chemical shifts, coupling constants and 2D-NMR experiments involving ^{31}P.

11.2.2.2 Chemical Shifts in Homogeneous Hydrogenation Research

In the context of ^{1}H chemical shifts and determination of the reaction mechanism of homogeneous hydrogenation catalysts, one usually tries to observe hydride-intermediates that typically resonate at high field (–5 to –30 ppm). Agostic bonds (see Fig. 11.1) also tend to have a hydride-like proton chemical shift.

Similarly, bridging hydrides have negative chemical shifts (e.g., at –11.18 ppm for the bridging hydride in Figure 11.2 [21]).

An excellent example of the use of ^{31}P chemical shifts, in combination with ^{1}H-NMR and ^{103}Rh-NMR data as well as coupling constants information, can be found in the report by Duckett et al. [21] on the activation of

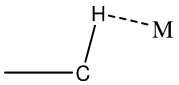

Fig. 11.1 An agostic bond.

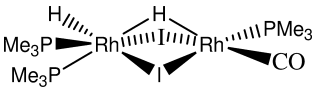

Fig. 11.2 A bridging hydride.

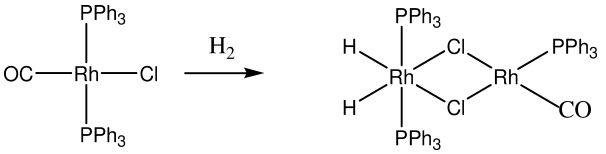

Fig. 11.3 Activation of $RhCl(CO)(PPh_3)_2$.

$RhX(CO)(PPh_3)_2$ [X=halogen] complexes with hydrogen. The reaction for X=Cl is shown in Figure 11.3.

The resulting product showed a single ^{31}P chemical shift at 40 ppm with a ^{1}J coupling to rhodium of 118 Hz, indicative of a rhodium (III) center. As this rhodium atom was shown to couple to two phosphorus atoms, it could be concluded that the phosphorus atoms are in a symmetrical position, as shown in Figure 11.3. The other Rh atom couples only to a phosphorus atom with a $^{1}J_{RhP}$ of 196 Hz, indicative of a rhodium (I) center.

When the smaller $P(Me)_3$ ligand was used, not only the halogens but also a hydride were found in the bridging position, as was concluded from the fact that the phosphorus atom connected to the rhodium (I) center was now coupled to a hydride.

11.2.3
Coupling Constant

A second aspect that is important for the structural characterization, as mentioned above, is that of the coupling constant. Both the magnitude of the coupling constant and the multiplicity (which reflects the number of (equivalent) nuclei that couple) are important. For example, the magnitude of the $^{1}J_{RhH}$ coupling constant provides information about the degree of s-character of the bond [13].

In general, in square-planar and octahedral complexes $^{1}J_{ML}$ depends on the *trans*-ligand: stronger donors reduce the $^{1}J_{ML}$-value [10]. Similarly, $^{2}J_{L1,M,L2}$-values are usually greater for *trans*-interactions than for *cis*-interactions [10], which is clearly an important tool for structural characterization (see Fig. 11.4).

The binuclear Rh-complex in Figure 11.2 contains two hydride resonances at –11.18 and –14.75 ppm [21]. The former has two smaller phosphorus couplings

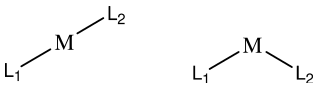

Fig. 11.4 *Trans* (left) and *cis* (right) interactions.

($^2J_{PH}$ = 21 Hz and 16 Hz) and one large coupling ($^2J_{PH}$ = 99.5 Hz), indicative of a *trans* arrangement, as mentioned above. In addition, two essentially equal couplings to the two rhodium centers were found, which is consistent with the bridge position.

Gridnev et al. showed in their study of the asymmetric hydrogenation of enamides by Rh-catalysts another useful application of coupling constant patterns. By selectively labeling certain atoms, for example with ^{13}C or ^2D, additional couplings appear (as compared to the non-labeled product) and this will provide information about the exact structure [22].

11.2.4 2D-NMR

11.2.4.1 General

As mentioned above, 2D-NMR (or more generally multidimensional NMR) is based on the transfer of magnetization during the evolution/mixing period.

The transfer of magnetization is not restricted to protons as in the ^1H–^1H COSY experiment, but can also be applied between other nuclei (i.e., ^1H–^{13}C-correlation or ^{31}P–^{31}P correlation experiments).

A major advance in the field has been the reverse or inverse detected NMR experiment [4]. Originally, signals were enhanced by transferring magnetization from protons to insensitive nuclei that were consequently detected, as in the INEPT sequence. By reversing this process and detecting the more abundant and receptive nucleus (mostly ^1H, but it can also be ^{19}F or ^{31}P), the sensitivity of the experiment was greatly enhanced. An additional advantage is that the relaxation delay between the pulses is now governed by the ^1H relaxation time, which is usually relatively short compared to relaxation time of other nuclei.

Technically, the inverse experiment used to be very demanding because the excess of protons not coupled to the nucleus of interest (e.g., protons coupled to the almost hundred-fold excess of ^{12}C instead of ^{13}C) needed to be suppressed. Originally, this was achieved by the use of elaborate phase-cycling schemes, but today the coherence pathway selection by gradient pulses facilitates this process.

11.2.4.2 2D-NMR in Homogeneous Hydrogenation Research

A variety of examples of 2D-NMR experiments is provided in reference [21]. The structure elucidation of the di-rhodium compound shown in Figure 11.3 was mostly carried out in this way. For example, 2D ^1H–^{31}P heteronuclear multiple quantum correlation (HMQC) experiments were used to show that two rhodium-coupled hydride resonances are connected to a single type of ^{31}P nucleus.

A 2D ^{1}H–^{103}Rh HMQC experiment was used to show that both the hydrides are connected to a Rh center that resonates at 925 ppm and is coupled to two ^{31}P-nuclei. A ^{1}H–^{1}H COSY experiment shows that the two hydrides are coupled.

An example of a ^{103}Rh–^{31}P correlation experiment of $Rh(MonoPhos)_2$-$(COD)BF_4$ is shown in Figure 11.5. Here also, two inequivalent ^{31}P atoms are connected to the same Rh center [23].

A second class of multidimensional experiments uses through-space interactions; perhaps the best-known example is the NOESY sequence, which is as follows:

$$90^\circ\ (+x) - \text{evolution time} - 90^\circ\ (-x) - \text{mixing time} - 90^\circ\ (+x) - \text{acquisition}$$

As with the COSY experiment, the sequence starts with a pulse followed by an evolution period, but now the mechanism that couples the two spins (which must be in close proximity, typically <6 Å) is the Nuclear Overhauser Effect (NOE). The second pulse converts magnetization into population disturbances, and cross-relaxation is allowed during the mixing time. Finally, the third pulse transfers the spins back to the x-y-plane, where detection takes place. The spectrum will resemble a COSY spectrum, but the off-diagonal peaks now indicate through-space rather than through-bond interactions.

Just as in the COSY type of experiments this cross-relaxation effect is not restricted to protons, but can also involve heteronuclei; the acronym HOESY (heteronuclear Overhauser effect) is used in these cases. This can be used, for example, to show that an anion such as BF_4^- is in close proximity to the ligands of the organometallic compound, as was carried out by Macchioni et al. with a ^{19}F-^{1}H HOESY experiment [24].

Another important experiment here is that of EXSY (exchange spectroscopy). Here, the pulse sequence is identical to the NOESY sequence, but during the mixing time the spins physically migrate to another site due to slow chemical exchange [25]. This exchange can be both intra- and intermolecular. An example of a ^{31}P–^{31}P EXSY spectrum of the hydrogenation catalyst $Rh(MonoPhos)_2$-$(COD)BF_4$ is shown in Figure 11.6.

This molecule exists of isomers of the complex shown in Figure 11.7 that inter-convert rapidly, even at temperatures below 200 K, as shown by the off-diagonal peaks between the double doublets of one structure and the broad doublet of the other structure [23]. The isomeric structures are caused by the relative positions of the two ligands with respect to each other (i.e., parallel or anti-parallel orientation of the NMe_2 groups).

By recording EXSY spectra at different temperatures, information can be obtained about exchange rates and activation parameters. Duckett et al. [21] used 2D-EXSY experiments to show that, for the dihydride shown in Figure 11.3, the hydride exchange process is intramolecular. The only observable off-diagonal peaks are between the two hydride resonances. Because of a negative entropy of activation of –61 J K^{-1} mol^{-1} it was concluded that a step with a degree of ordering is required: an additional rotation step around a Rh–halogen bond (see Fig. 11.8).

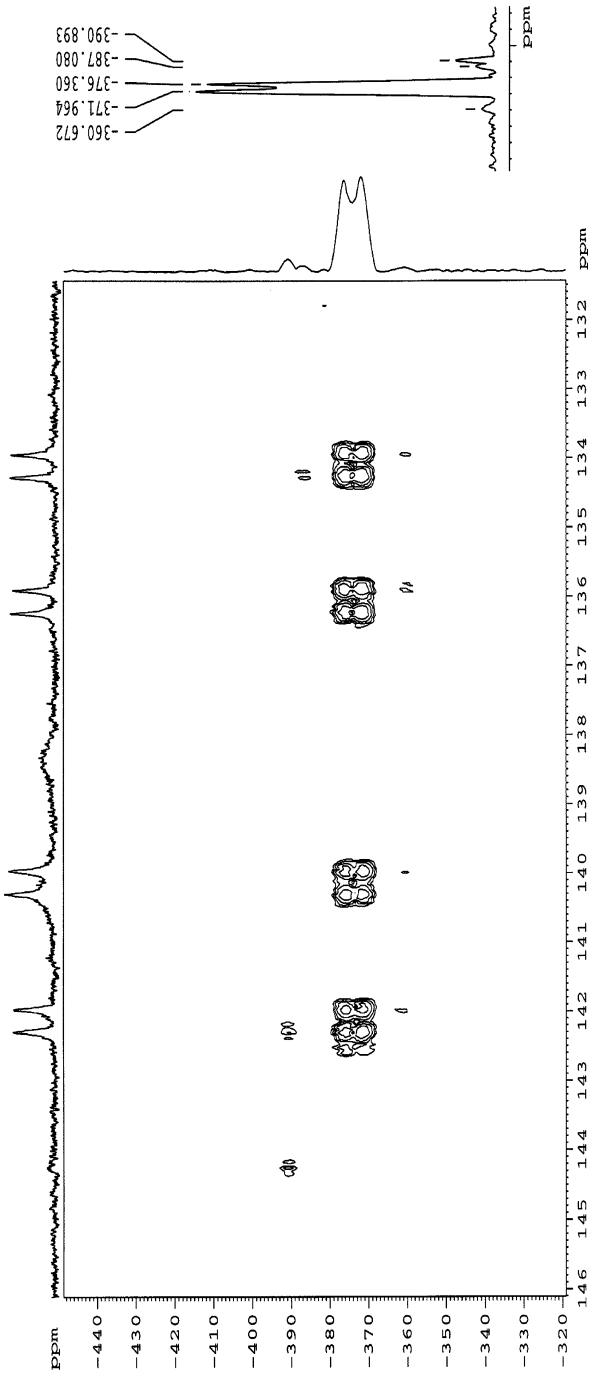

Fig. 11.5 $^{103}Rh-^{31}P$ correlation experiment of $Rh(MonoPhos)_2(COD)BF_4$ in CD_2Cl_2 at 211 K.

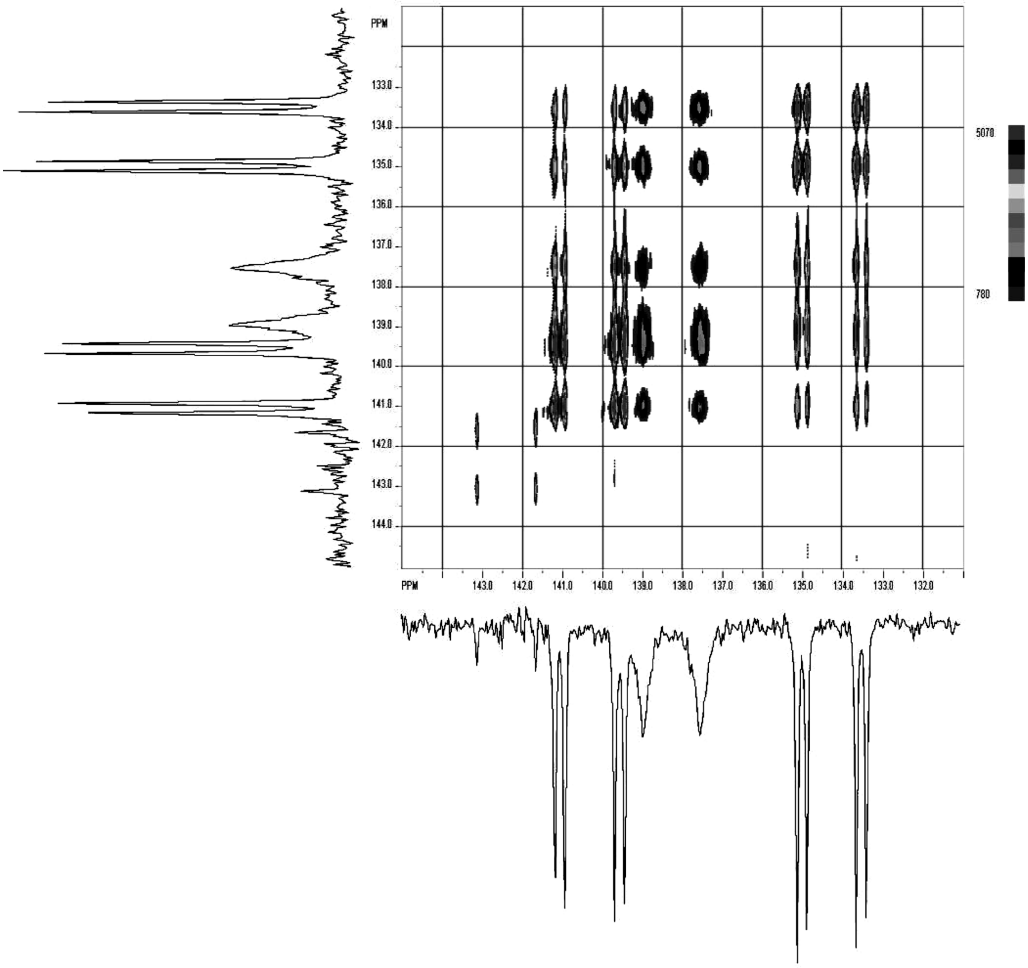

Fig. 11.6 ^{31}P–^{31}P EXSY spectrum of Rh(MonoPhos)$_2$(COD)BF$_4$ in $C_2D_2Cl_2$.

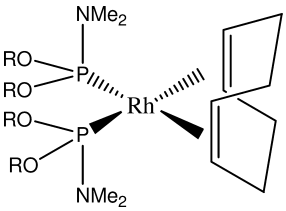

Fig. 11.7 Rh(MonoPhos)$_2$(COD)BF$_4$.

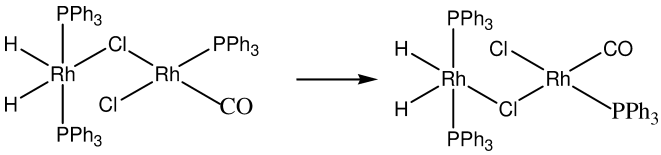

Fig. 11.8 Rotation about the Rh–Cl bond.

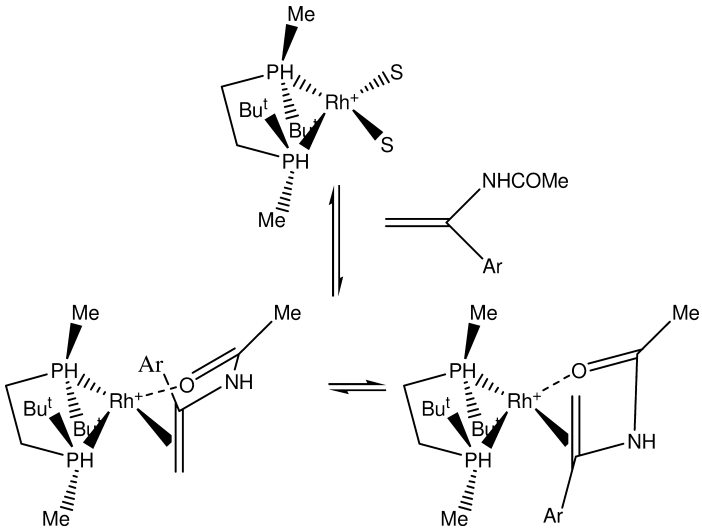

Fig. 11.9 Intermolecular exchange of Rh–*t*-Bu-BisP* complex at 348 K.

Gridnev et al. studied the mechanism of the enantioselective hydrogenation of enamides with Rh–BisP* and Rh–MiniPHOS catalysts [22].

By using EXSY measurements, it was shown that at 323 K there is only intramolecular exchange, whereas at 348 K intermolecular exchange also occurs via complete dissociation of the complex, producing a free substrate and a solvate complex (Fig. 11.9).

One example of the use of 2D-NMR experiments in conformational analysis is the study of molecular interactions between cinchonidine and acetic acid [26]. These alkaloids are used as chiral auxiliaries in enantioselective hydrogenations, and the enantiomeric excess is dependent on solvent polarity, acetic acid being a good solvent. This suggests that protonation and a preferred conformation play a role in achieving high enantioselectivities. With a combination of COSY-experiments, ^3J coupling constants and NOESY experiments, it was shown that one conformer is preferred in acidic solutions.

11.2.5 Variable Temperature and Variable Pressure Studies

11.2.5.1 General

Both temperature and pressure are important parameters/variables in NMR measurements of homogeneous hydrogenation catalysts. Usually, a certain hydrogen pressure is needed to form the active catalyst. The temperature controls the rate of reactions. Sometimes, temperatures above room temperature are needed; for example, the reaction shown in Figure 11.3 occurs at a hydrogen pressure of 3 atmos and temperatures above 318 K. In other cases, intermediates can only be observed at temperatures below room temperature. Modern NMR instruments routinely allow measurements to be made in the range of, for example 170 to 410 K, but this range can easily be extended by the use of special NMR probes.

As mentioned above, variable-temperature measurements are also used to obtain exchange rates and activation parameters. In the slow exchange regime, the average lifetime of a spin is long enough to observe individual lines for the various states. By increasing the exchange rate (e.g., by raising the temperature), the individual lines broaden and shift to each other until they merge into one single line. This is termed the "coalescence phenomenon" (for background information, see [27]).

11.2.5.2 Variable-Temperature Studies in Homogeneous Hydrogenation Research

Figure 11.10 illustrates an example of a ^{31}P-NMR variable-temperature measurement, in this case of the isomeric complexes of $Rh(MonoPhos)_2(COD)BF_4$ (see

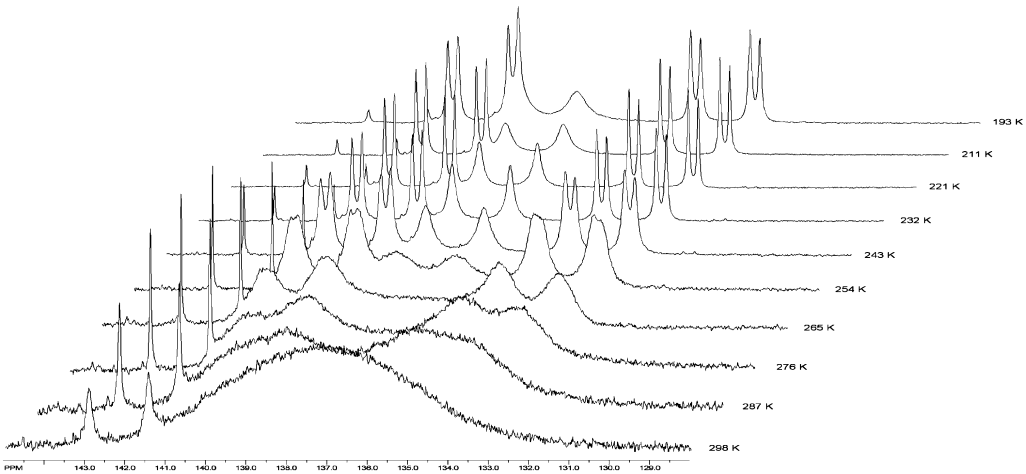

Fig. 11.10 Temperature-dependency of ^{31}P-NMR spectra of $Rh(MonoPhos)_2(COD)BF_4$ in CD_2Cl_2.

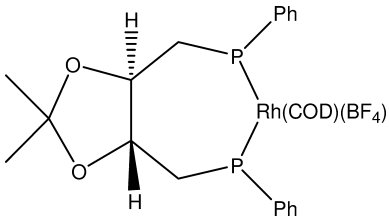

Fig. 11.11 Hydrogenation catalyst showing temperature-dependent ^{31}P-NMR spectra.

Fig. 11.7) [23]. This measurement shows clearly the broadening and merging of the peaks as the temperature is increased.

Another example is the temperature-dependent study of the ^{31}P-NMR spectra of the hydrogenation catalyst shown in Figure 11.11 [28]. At 240 K the ^{31}P-NMR signals are equivalent, whereas at 123 K two sets of signals are observed which are attributed to a seven-membered ring in a twist-chair and a distorted boat conformation.

11.2.5.3 **Variable-Pressure Studies in Homogeneous Hydrogenation Research**

The use of high-pressure cells and probes has been reviewed recently [29]. For homogeneous hydrogenation reactions, there is no requirement for very high pressures, and in these cases the popular sapphire tubes designed by Roe [30] will do well. In fact, the present author's group has used this type of tube in the laboratory to carry out hydrogenations, carbonylations and hydroformylations, and they have been found to be very convenient to work with. They can be pressurized in a safety hood and transported to the NMR in a transport cylinder [11]. Moreover, since the sapphire tube is transparent, color changes can also be observed.

When the tube has been placed inside the NMR spectrometer, the procedure used is exactly as for a standard NMR tube.

An example of these pressure studies is provided by the studies of Elsevier et al. [31], who investigated the dependence of the hydrogenation rate of 4-octyne by a Pd-catalyst on the dihydrogen pressure, which was varied between 0 and 40 bar. The hydrogenation rate was shown to depend linearly on the dihydrogen pressure. In order to elucidate the reaction mechanism, the dependence of the reaction rate on substrate and catalyst concentration, and on the temperature, was also measured. NMR experiments with deuterium gas as well as PHIP-experiments were also carried out.

Another interesting application of high-pressure tubes is the *in-situ* investigation of reactions in supercritical solvents such as carbon dioxide. For example, the iridium-catalyzed enantioselective hydrogenation of imines was investigated in a sapphire tube at 313 K [32].

Despite the advantages and ease of use of sapphire tubes, great care must be taken. It is very important that protective measurements are put in place when a pressurized tube is handled outside the spectrometer, because the tube's abil-

ity to cope with high pressure can be diminished if the sapphire surface is scratched. Another potentially weak point is the glue that is used to fix the titanium head to the sapphire tube. In the author's laboratory, on one occasion the head separated from the tube and was launched to the ceiling when operating close to the tube's design limits (for both temperature and pressure). Consequently, it is advised that the transport cylinder be left on top of the magnet when the tube is in the spectrometer.

11.2.6
PGSE NMR Diffusion Methods

Pulsed-field gradient NMR methods are relatively new in homogeneous hydrogenation research. They allow the investigation of the diffusion of a molecule in solution by applying a defocusing and refocusing gradient pulse and measuring the decrease in intensity of the NMR signals belonging to this molecule. By carrying out a series of measurements with increasing gradient strengths, a diffusion coefficient can be calculated. If the technique is applied to a mixture of compounds and the resulting diffusion coefficients are plotted against the chemical shifts in a "2D-like fashion", the experiment is named DOSY (diffusion-ordered spectroscopy).

An example of the use of PGSE NMR spectroscopy can be found in the studies of Selke et al. [33], who investigated the dependence of enantioselectivity on the distribution of a chiral hydrogenation catalyst between aqueous and micellar phases. When a compound is incorporated into a micelle, its mobility is much lower compared to its mobility in solution. This effect is exactly what is probed with PGSE NMR. The calculated diffusion coefficient is a time-averaged value of the lower diffusion coefficient of the catalyst incorporated into the micelles, and of the diffusion coefficient of the free catalyst. An increased amount of micelle-embedded catalyst was found to lead to an increased enantioselectivity.

11.3
Outlook

The use of NMR continues to improve existing methods, and to develop new concepts. By cleverly combining existing pulse-sequences, new sequences are formed with improved properties. An example is the combination of the COSY and DOSY sequence to a new 3D-NMR COSY-IDOSY sequence with improved sensitivity, a 32-fold decrease in experiment time, and an improved resolution resulting in better data analysis [34].

Other developments are based on a completely new concept, for example the possibility of recording multi-dimensional NMR spectra with a single scan which, in theory, will allow the elucidation of structures to be made in seconds [35].

In time, all of these developments will be used in future chemical research studies, making NMR an even more useful tool than it is today.

Abbreviations

DOSY	diffusion-ordered spectroscopy
EXSY	exchange spectroscopy
FT	Fourier transform
HMQC	heteronuclear multiple quantum correlation
HOESY	heteronuclear Overhauser effect
NMR	nuclear magnetic resonance
NOE	nuclear Overhauser effect
PGSE	pulsed-gradient spin echo
PHIP	*para*-hydrogen-induced polarization
ROCHESTER	Rates Of Catalytic Hydrogenation Estimated Spectroscopically Through Enhanced Resonances

References

1 R. R. Ernst, W. A. Anderson, *Rev. Sci. Instr.* **1966**, *37*, 93.
2 J. Jeener, Ampere International Summer School, Basko Polje, Yugoslavia, **1971**.
3 W. P. Aue, E. Bartholdi, R. R. Ernst, *J. Chem. Phys.* **1976**, *64*, 2229.
4 L. Müller, *J. Am. Chem. Soc.* **1979**, *101*, 4481.
5 (a) R. E. Hurd, *J. Magn. Reson.* **1990**, *87*, 422; (b) A. Bax, P. G. de Jong, A. F. Mehlkopf, J. Schmidt, *Chem. Phys. Lett.* **1978**, *55*, 9.
6 E. O. Stejskal, J. E. Tanner, *J. Chem. Phys.* **1965**, *42*, 288.
7 M. Valentini, P. S. Pregosin, H. Ruegger, *Organometallics* **2000**, *19*, 2551.
8 W. von Philipsborn, *Chem. Soc. Rev.* **1999**, *28*, 95.
9 R. R. Ernst, G. Bodenhausen, A. Wokaun, *Principles of Nuclear Magnetic Resonance in One and Two Dimensions*, Oxford University Press, Oxford, **1987**.
10 E. M. Viviente, P. S. Pregosin, D. Scott. In: B. Heaton (Ed.), *Mechanisms in Homogeneous Catalysis. A Spectroscopic Approach*. Wiley-VCH, Weinheim, **2005**.
11 C. J. Elsevier, *J. Mol. Catal.* **1994**, *92*, 285.
12 P. S. Pregosin (Ed.), *Transition Metal Nuclear Magnetic Resonance*, Elsevier, Amsterdam, **1991**.
13 J. M. Ernsting, S. Gaemers, C.J. Elsevier, *Magn. Reson. Chem.* **2004**, *42*, 721.
14 M. S. Chinn, R. J. Eisenberg, *J. Am. Chem. Soc.* **1992**, *114*, 1908.
15 P. Hübler, R. Giernoth, G. Kümmerle, J. Bargon, *J. Am. Chem. Soc.* **1999**, *121*, 5311.
16 W. Juranic, *J. Chem. Soc., Dalton Trans.* **1984**, 1537.
17 W. von Philipsborn, *Pure Appl. Chem.* **1986**, *58*, 513.
18 C. Weidemann, W. Priebsch, D. Rehder, *Chem. Ber.* **1989**, *122*, 235.
19 B. R. Bender, M. Koller, D. Nanz, W. von Philipsborn, *J. Am. Chem. Soc.* **1993**, *115*, 5889.
20 L. D. Quin, J. G. Verkade (Eds.), *Phosphorus-31 NMR Spectral Properties in Compound Characterization and Structural Analysis*, VCH Publishers, New York, **1994**.
21 P. D. Morran, S. B. Duckett, P. R. Howe, J. E. McGrady, S. A. Colebrooke, R. Eisenberg, M. G. Partridge, J. A. B. Lohman, *J. Chem. Soc., Dalton Trans.* **1999**, 3949.
22 I. D. Gridnev, M. Yasutake, N. Higashi, T. Imamoto, *J. Am. Chem. Soc.* **2001**, *123*, 5268.
23 M. van den Berg, Dissertation, University of Groningen, The Netherlands, **2006**.
24 B. Binotti, C. Carfagna, E. Foresti, A. Macchioni, P. Sabatino, C. Zuccaccia, D. Zuccaccia, *J. Organomet. Chem.* **2004**, *689*, 647.

25 S. Schaeublin, A. Hoehener, R. R. Ernst, *J. Magn. Reson.* **1974**, *13*, 196.
26 D. Ferri, T. Bürgi, A. Baiker, *J. Chem. Soc., Perkin Trans. 2,* **1999**, 1305.
27 J. J. Delpuech (Ed.), *Dynamics of Solutions and Fluid Mixtures by NMR*, John Wiley & Sons Ltd, Chichester, **1995**.
28 R. Kadyrov, A. Borner, R. Selke, *Eur. J. Inorg. Chem.* **1999**, 705.
29 G. Laurenczy, L. Helm. In: B. Heaton (Ed.), *Mechanisms in Homogeneous Catalysis. A Spectroscopic Approach*, Wiley-VCH, Weinheim, **2005**.
30 D. C. Roe, *J. Magn. Reson.* **1985**, *63*, 388.
31 A. M. Kluwer, T. S. Koblenz, Th. Jonischkeit, K. Woelk, C. J. Elsevier, *J. Am. Chem. Soc.* **2005**, *127*, 15470.
32 S. Kainz, A. Brinkmann, W. Leitner, A. Pfaltz, *J. Am. Chem. Soc.* **1999**, *121*, 6421.
33 M. Ludwig, R. Kadyrov, H. Fiedler, K. Haage, R. Selke, *Chem. Eur. J.* **2001**, *7*(15), 3298.
34 M. Nilsson, A. M. Gil, I. Degadillo, G. Morris, *Chem. Commun.* **2005**, 1737.
35 L. Frydman, L. Lupulescu, *Proc. Natl. Acad. Sci. USA* **2002**, *99*, 15858.

12
Parahydrogen-Induced Polarization: Applications to Detect Intermediates of Catalytic Hydrogenations

Joachim Bargon

12.1
In-Situ Spectroscopy

The level of understanding the mechanisms of homogeneously catalyzed reactions correlates with information about reactive intermediates. Therefore, *in-situ* methods – that is, investigations based upon physical techniques conducted *during* the reactions – are highly desirable and important. For this purpose, a considerable scope of *in-situ* techniques based upon time-proven classical types of spectroscopy has been developed. Since many of the industrially important catalyzed reactions require the use of high pressures and high temperatures for optimum performance, ideally, these techniques should accommodate such conditions. Contemporary *in-situ* methods include specialized forms of optical or magnetic resonance spectroscopy, in particular vibration and rotation spectroscopy, such as infrared or Raman spectroscopy, or nuclear magnetic resonance (NMR) [1, 2]. This chapter will focus on the latter technique.

12.1.1
In-Situ NMR Spectroscopy

For the elucidation of chemical reaction mechanisms, *in-situ* NMR spectroscopy is an established technique. For investigations at high pressure either sample tubes from sapphire [3] or metallic reactors [4] permitting high pressures and elevated temperatures are used. The latter represent autoclaves, typically machined from copper-beryllium or titanium-aluminum alloys. An earlier version thereof employs separate torus-shaped coils that are imbedded into these reactors permitting *in-situ* probing of the reactions within their interior. However, in this case certain drawbacks of this concept limit the filling factor of such NMR probes; consequently, their sensitivity is relatively low, and so is their resolution. As a superior alternative, the metallic reactor itself may function as the resonator of the NMR probe, in which case no additional coils are required. In this way gas/liquid reactions or reactions within supercritical fluids can be studied

The Handbook of Homogeneous Hydrogenation.
Edited by J.G. de Vries and C.J. Elsevier
Copyright © 2007 WILEY-VCH Verlag GmbH & Co. KGaA, Weinheim
ISBN: 978-3-527-31161-3

conveniently at high pressure and elevated temperatures with much higher sensitivity [4].

12.1.2
In-Situ PHIP-NMR Spectroscopy

A number of years ago, an additional *in-situ* method to investigate hydrogenation reactions via NMR spectroscopy was introduced, which gives rise to a significant signal enhancement primarily of the proton NMR spectra; consequently, the intermediates and minor reaction products of homogeneous hydrogenations can be identified much more readily. This signal enhancement is due to proton spin polarization originally derived from separating the spin isomers of dihydrogen, which can readily be achieved at low temperatures. Using only one of these spin isomers for the hydrogenation – namely parahydrogen – NMR spectra recorded during homogeneous hydrogenations of various substrates in the presence of suitable organometallic catalysts exhibit considerable signal enhancement in the form of intense emission or absorption lines. In principle, either one of the two spin isomers – that is, ortho- or parahydrogen – may be used instead of ordinary dihydrogen (H_2), though typically parahydrogen is employed. This phenomenon was originally observed experimentally by chance [5], but it has later been independently thought of theoretically, and has been attributed to symmetry breaking during the hydrogenation reaction [6].

This concept has originally been named PASADENA (*P*arahydrogen *A*nd *S*ynthesis *A*llow *D*ramatically *E*nhanced *N*uclear *A*lignment) [6], but the spectroscopic method based on this phenomenon has subsequently also been called PHIP (*P*ara-*H*ydrogen *I*nduced *P*olarization) [7]. In this chapter the abbreviation PHIP will be used throughout.

The signal enhancement due to this approach can, in principle, be as high as 10^5-fold – that is, equal to the reciprocal Boltzmann factor; however, the experimentally achievable enhancement factors typically range between 10 and 10^3. Thanks to this increase in sensitivity, the PHIP phenomenon, therefore, provides for a powerful tool to investigate the fate of the dihydrogen, the catalysts, and of the substrates during hydrogenation reactions.

The observed polarization is primarily associated with the former parahydrogen protons. However, other protons may also experience a drastic signal enhancement due to nuclear spin polarization transferred to these nuclei via the nuclear Overhauser effect (NOE) or similar processes, both in the final reaction products as well as in their precursor intermediates.

Likewise, the original proton polarization can be transferred to other magnetically active heteronuclei, notably to ^{13}C, ^{15}N, ^{19}F, ^{29}Si, ^{31}P or appropriate isotopes of various transition metals. This is especially attractive because of the frequently low sensitivity of many heteronuclei, in particular of those with low magnetic moments [8].

Furthermore, in favorable cases, (para-)hydrogenation-derived spin polarization may be carried on to subsequent follow-up reactions, where it can serve to

boost the notoriously low sensitivity of NMR spectroscopy in general. For this purpose, the follow-up reactions have to be reasonably fast, such as the bromination of alkenes, for example [51].

The polarization patterns are dependent upon the strength of the magnetic field, in which the reactions are carried out. If the reactions are carried out at high fields (i.e., notably within the NMR spectrometer), the resonances appear in "antiphase" – that is, there is an equal number of absorption and emission lines and no net polarization. At low field however (i.e., when the reaction is carried out at zero or a very low field and then transferred into the high field of the NMR spectrometer for subsequent investigation), the resonances display net polarization, as has been outlined by Pravica and Weitekamp [9].

Initially in this chapter, the various features of the PHIP phenomenon, of the apparatus to enrich parahydrogen and orthodeuterium, and of the computer-based analysis or simulations of the PHIP spectra to be observed under specific assumptions will be outlined. In the following sections, comparisons of the experimentally obtained and of the simulated spectra reveal interesting details and mechanistic information about the hydrogenation reactions and their products.

12.2 Ortho- and Parahydrogen

H_2 consists of two nuclear spin isomers, namely p-H_2 with antiparallel proton spins, and o-H_2 with parallel arrangement. Whereas p-H_2 is diamagnetic (i.e., it represents a singlet state (S)), o-H_2 shows nuclear paramagnetism with a resulting nuclear spin of one (Fig. 12.1). Its three allowed alignments relative to an external magnetic field – namely with, against, or orthogonal to the field – are labeled T_{+1}, T_{-1} or T_0, respectively (Fig. 12.2). Accordingly, in the absence of a magnetic field, o-H_2 is degenerate threefold, and in thermal equilibrium at room temperature, n-H_2 consists of 25.1% p-H_2 and of 74.9% o-H_2; that is, the ratio is approximately 1 : 3 [10].

Due to symmetry requirements, only specific quantum states of the spin and of the rotational states of H_2 are mutually compatible. Therefore, the energeti-

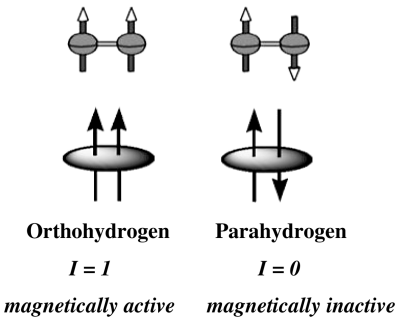

Fig. 12.1 The spin isomers of molecular hydrogen ("dihydrogen").

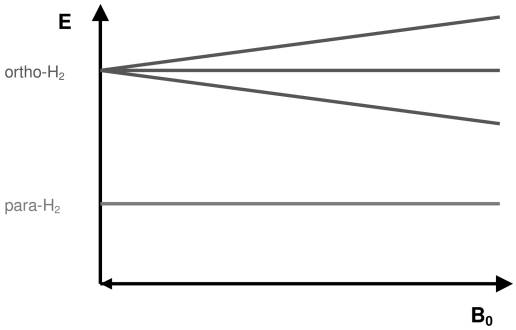

Figure 12.2 Magnetic field dependence of the energy levels of ortho- and para-H_2. Parahydrogen (p-H_2) is a singlet that is unaffected by the magnetic field, whereas orthohydrogen (o-H_2) is a triplet. Its energy levels split, showing the Zeeman effect.

cally lowest state of H_2 corresponds to p-H_2, which prevails at cryogenic temperatures. This fact is used to enrich fractions in p-H_2. Even though both spin isomers, p-H_2 and o-H_2, can even be separated completely, the ~50% enrichment of p-H_2 achieved at 77 K using liquid nitrogen as a coolant is sufficient for conducting parahydrogen labeling experiments [11].

12.2.1
Magnetic Field Dependence of the PHIP-Phenomenon: PASADENA and ALTADENA Conditions

According to Bowers and Weitekamp [6], ^{1}H spin polarization occurs in the hydrogenation products of p-H_2, if a chemical reaction breaks its initial symmetry. Pure p-H_2 itself is NMR-inactive (i.e., it cannot be detected via ^{1}H-NMR). Correspondingly, since hydrogenation of an asymmetrically substituted acetylene yields an olefin with chemically inequivalent protons, the use of p-H_2 give rise to two resonances, typically consisting of doublets with one component in emission and one in absorption each ("antiphase doublets") [6]. Bowers and Weitekamp named this phenomenon PASADENA, which applies to reactions carried out within the high magnetic field of a NMR spectrometer.

Figure 12.3 outlines the essential features of the PASADENA/PHIP concept for a two-spin system. If the symmetry of the p-H_2 protons is broken, the reaction product exhibits a PHIP spectrum (Fig. 12.3, lower). If the reaction is carried out within the high magnetic field of the NMR spectrometer, the PHIP spectrum of the product consists of an alternating sequence of enhanced absorption and emission lines of equal intensity. This is also true for an AB spin system due to a compensating balance between the individual transition probabilities and the population rates of the corresponding energy levels under PHIP conditions. The NMR spectrum after the product has achieved thermal equilibrium exhibits intensities much lower than that of the intermediate PHIP spectrum.

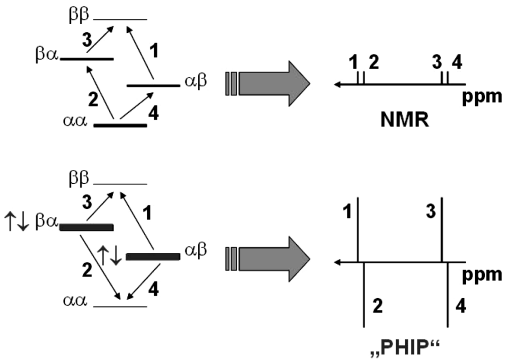

Fig. 12.3 Regular NMR (upper) and high-field PHIP-NMR spectrum (lower) of a two-spin AX system.

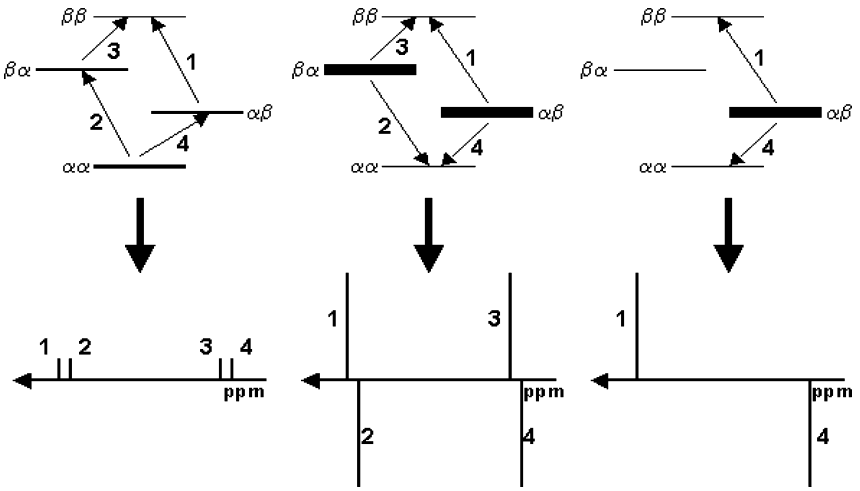

Fig. 12.4 Normal NMR, high-field (PASADENA) and low-field (ALTADENA) PHIP.

A related phenomenon occurs if the reactions are carried out at low field outside, but where the samples are transferred immediately thereafter into the spectrometer for subsequent NMR analysis. This variety has been termed ALTADENA (*A*diabatic *L*ongitudinal *T*ransport *A*fter *D*issociation *E*ngenders *N*et *A*lignment) [9]. Other authors [7] have since used the acronym PHIP as an alternative for the same phenomenon.

An essential requirement for the occurrence of PHIP is that the rates of the reactions compete favorably with the relaxation of the nuclear spins in the products; therefore, the reaction rates must be faster than the relaxation rates, and the polarization must be detected during the reactions – that is, *in situ*.

Today, many examples have been reported which demonstrate the potential of the PHIP technique as a powerful analytical tool to investigate the reaction mechanisms of homogeneously catalyzed hydrogenations [12].

For more complex spin systems, a computer program PHIP$^+$ has been developed [13, 45] which allows the expected PHIP spectra to be calculated from the chemical shifts and coupling constants of the products. Depending upon which proton pair in the product molecule stems from p-H_2, different – but characteristic – polarization patterns result [14]. The patterns also depend on the sign of the coupling constants. Simple "sign rules" governing the relative sequence of the emission and absorption lines in the PHIP spectra (i.e., their "phase") can be formulated in similar manner to the "Kaptein Rules" of chemically induced dynamic nuclear polarization (CIDNP) [15].

12.2.2
PHIP, CIDNP, and Radical Mechanisms

In appearance, the PHIP phenomenon closely resembles those due to CIDNP [16], another phenomenon, which also gives rise to emission and enhanced absorption lines in NMR spectra. However, CIDNP is the consequence of the occurrence of free radicals, and previously has frequently been considered unequivocal proof for free radical reactions.

The fact that two entirely different phenomena can both yield nuclear spin polarization may cause confusion; therefore, the appearance of intense emission and absorption lines during *in-situ* NMR investigations of hydrogenation reactions is not necessarily proof for free radical intermediates, and examples of erroneous conclusions do exist [5].

For the mechanisms of homogeneous catalysis this may seem irrelevant, but as early as 1977 – long before the discovery of PHIP – Halpern [16e] had used "…the observation of CIDNP…" to "…establish a radical reaction path…" during the hydrogenation of styrene with an organometallic catalyst. Given the fact that even at room temperature (i.e., without any cooling of dihydrogen) there is a slight excess of parahydrogen, which is well capable of giving rise to "CIDNP-like phenomena" in the ^{1}H-NMR spectra, observations of emission and enhanced absorption lines alone are no longer a reliable proof of the occurrence of free radicals, if H_2 is involved. Therefore, caution is recommended, especially when exploiting the results of earlier investigations. Today, it is easy to err on the safe side, since a reliable discrimination exists between the alternatives CIDNP and PHIP, using both enriched ortho- and parahydrogen in independent runs [17]. In this way it should be possible to ascertain, whether a "…radical reaction pathway in homogeneous hydrogenation" [16e] really exists by using both para- and orthohydrogen in subsequent experiments.

12.2.3
Preparation of Parahydrogen

Molecular hydrogen or dihydrogen (H_2) occurs in two isomeric forms, namely with its two proton spins aligned either parallel (orthohydrogen) or antiparallel (parahydrogen) (see Fig. 12.1). Parahydrogen was first prepared during the 1920s by Bonhoeffer and Harteck [18]. The separation of both spin isomers [10] has also been possible for many years, even though orthohydrogen – the energetically less favorable form – is occasionally still described in the literature as "obtainable only in theory" [20 a], especially in older text books [20 b].

12.2.3.1 **Parahydrogen Enrichment**

As stated earlier, in the state of thermal equilibrium at room temperature, dihydrogen (H_2) contains 25.1% parahydrogen (nuclear singlet state) and 74.9% orthohydrogen (nuclear triplet state) [19]. This behavior reflects the three-fold degeneracy of the triplet state and the almost equal population of the energy levels, as demanded by the Maxwell-Boltzmann distribution. At lower temperatures, different ratios prevail (Fig. 12.5) due to the different symmetry of the singlet and the triplet state [19].

Since interconversions between different states of symmetry (i.e., between ortho- and parahydrogen) are forbidden, the adjustment of the relative ratios of the two spin isomers to the values corresponding to the thermal equilibrium at an arbitrary temperature is normally very slow and, therefore, must be catalyzed. In the absence of a catalyst, dihydrogen samples retain their once achieved ratio and, accordingly, they can be stored in their enriched or separated forms for rather long periods (a few weeks or even a few years in favorable cases).

In spite of the fact that ortho- or parahydrogen, once separated, last for a long time, they are normally not available commercially; therefore, they must be prepared as needed. A time-proven process for the enrichment of parahydrogen follows a procedure first described by Bonhoeffer and Harteck [18]. This is based upon the fact that, at low temperature, the energetically more favorable isomer

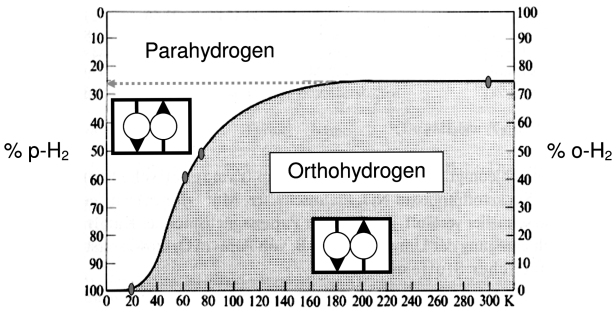

Fig. 12.5 Fraction of spin isomers at thermal equilibrium between o-H_2 and p-H_2.

(i.e., parahydrogen) becomes enriched, provided that a suitable catalyst renders the conversion possible. In this respect, activated charcoal functions as a convenient catalyst.

12.2.3.2 High-Pressure Apparatus for Parahydrogen Enrichment

The apparatus used (Fig. 12.6) follows the Bonhoeffer and Harteck concept [18]. Using liquid nitrogen as a coolant, it produces a constant flow of a mixture of 51% parahydrogen and 49% orthohydrogen (i.e., 51% enriched parahydrogen), at pressures up to 20 bar. As such it is especially suited for NMR investigations at elevated pressures using recently developed NMR probes [4]. The U-shaped charcoal reactor A shown in Figure 12.7 is manufactured from brass tubing, 4 cm in diameter and 30 cm in height, and capable of withstanding pressures of 20 bar and more. Copper tubing (3 mm) is used throughout to connect the reactor with the pressure relief valve (P) and the other components of the apparatus. The reactor is filled up to two-thirds of its height with coarse-grained charcoal, which is topped off with glass wool to constrain the filling. It is not advantageous to use powdered charcoal, as this tends to restrict the flow of the hydrogen through the reactor. Furthermore, tiny particles of charcoal are then carried along by the gas and drift into other parts of the apparatus.

In order to prime the apparatus, the charcoal-filled reactor is initially heated to 400 °C and maintained at this temperature for 10 h while operating the vacuum pump. This procedure must be repeated subsequently at regular intervals in order to regenerate the charcoal filling. The so-activated charcoal removes contaminants from the hydrogen stream, and thereby also serves as a gas cleaner.

Upon appropriate priming, the activated charcoal reactor A must be evacuated and is subsequently chilled in a liquid nitrogen bath. After an induction period, which depends on the operating pressure, 51% enriched parahydrogen is avail-

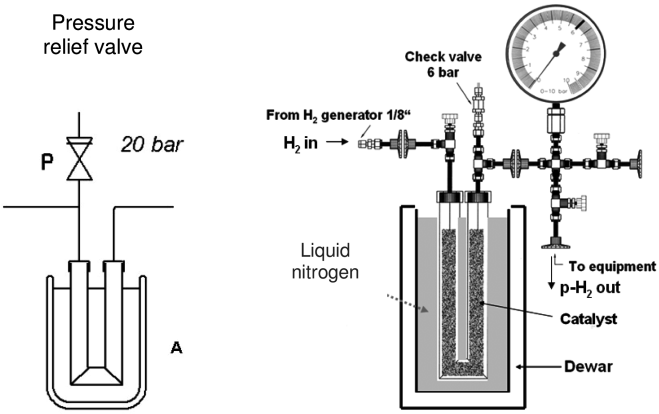

Fig. 12.6 Apparatus for the enrichment of parahydrogen at high pressure; principle and details.

able and can be supplied continuously. Typical induction periods are 30 min at 1 bar hydrogen pressure and 60 min at 10 bar. Flow rates of 50 mL min^{-1} have been achieved and tested in this mode, without any loss of parahydrogen enrichment during a prolonged flow period.

Upon termination of the experiment, all parts of the apparatus should be evacuated once again, before the liquid nitrogen bath is removed. The same precaution should also be maintained during removal of the bath, in order to safeguard against pressure surges caused by thermal expansion of the residual hydrogen or due to sudden desorption from the charcoal.

Integrated thermal conductivity cells (see Fig. 12.8) allow a quantitative determination of the corresponding ortho/para ratios of the dihydrogen. The enriched parahydrogen is well-suited for *in-situ* NMR studies of hydrogenation reactions that yield nuclear spin polarization due to symmetry breaking during the reaction. The same apparatus has also been used successfully to enrich ortho- and paradeuterium mixtures.

12.2.3.3 Enrichment of Parahydrogen using Closed-Circuit Cryorefrigeration

Virtually pure parahydrogen can conveniently be obtained upon cooling molecular hydrogen to temperatures between 20 and 30 K. For this purpose, commercially manufactured systems are available, and details have been described elsewhere [52]. It is advantageous (for thermodynamic considerations) and preferable (for safety reasons) to maintain the cooling temperature above the boiling point of dihydrogen at the corresponding pressure; therefore, the cryo-system should be operated at ca. 30 K. The level of enrichment for parahydrogen at 1.5 bar and flow rates of 10 to 30 mL min^{-1} for the two systems operating at 30 or 77 K, respectively, is illustrated in Figure 12.7.

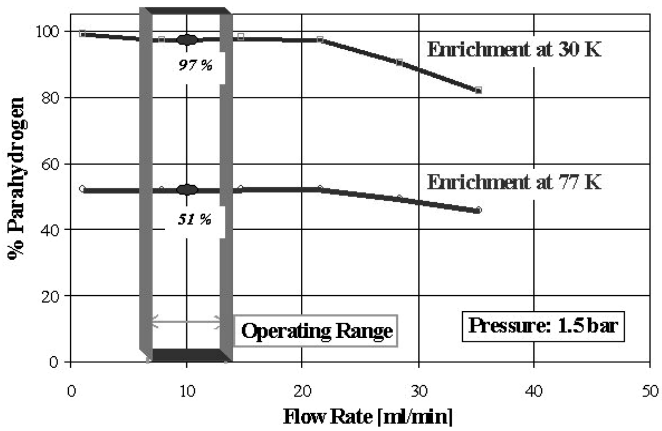

Fig. 12.7 Enrichment of parahydrogen as a function of temperature and flow rate.

12.2.4
Preparation of Orthohydrogen

During the 1950s, the enrichment or isolation of orthohydrogen was occasionally assumed to be impossible [19], until Sandler [10] described a procedure based on the preferential adsorption of the ortho form of dihydrogen on diamagnetic surfaces at low temperatures. The energy difference of orthohydrogen between its free and adsorbed state can be explained using the model of the hindered rotator [53]. Cunningham et al. [54] have presented an apparatus for the enrichment of orthohydrogen up to 99% using carefully selected γ- alumina in a cascade of selective desorption at 20.4 K. The present author's group have used single-stage separation of orthohydrogen on γ-alumina at 77 K (liquid nitrogen), and routinely obtained a mixture of 15% parahydrogen and 85% orthohydrogen (i.e., 85% enriched orthohydrogen), which is sufficient for most purposes [17]. Since the enrichment of orthohydrogen is carried out at ambient pressure, it is superfluous to design this apparatus for higher pressures. The alumina adsorption cell (B in Fig. 12.8) forms the core of the low-pressure apparatus. This cell is designed as a glass tube helix, and is fabricated from 150 cm of 20-mm diameter glass tubing. The helix provides for a rapid and homogeneous temperature change using a Dewar flask containing liquid nitrogen. This helix is charged with 260 g of γ-alumina that must not contain paramagnetic impurities (E. Merck, Darmstadt, Germany, Art. # 1095) [55]. The helix is terminated with fritted glass, through which it is connected to the remainder of the all-glass apparatus. Prior to the first orthohydrogen enrichment the γ-alumina filling is activated and degassed at 400 °C for 10 h, similar to the process described for the activated charcoal filling. Batches of orthohydrogen enriched to 85% can be prepared in this low-pressure apparatus, and the degree of enrichment can be determined accurately using thermal conductivity cells.

12.2.5
Thermal Conductivity Cells for Ortho/Para Determination

A pair of thermal conductivity cells (C in Fig. 12.8) according to Grilly [56] is used to determine the ortho/para ratio. Each cell is constructed from 120 mm of 10-mm diameter glass tubing, whereby two VACON pins lead into the interior carrying a tungsten filament, which is aligned along the center axis of the cell. Electrically, the filaments of the two cells form a bridge circuit together with appropriate resistors, which can be balanced externally. For maximum sensitivity reasons their resistance should be of the same order of magnitude as the filament resistance. The bridge voltage (here 25 V) is chosen such that the filaments heat up to 250 K, since under these conditions the resulting temperature gradient between the filaments and the walls of the liquid nitrogen-chilled cells is appropriately within the range of optimum sensitivity and performance.

The thermal conductivity cells are connected to their respective valves V1 and V2, using U-shaped glass tubing. This design has been found advantageous, as it minimizes any unavoidable convection of hydrogen within the cells.

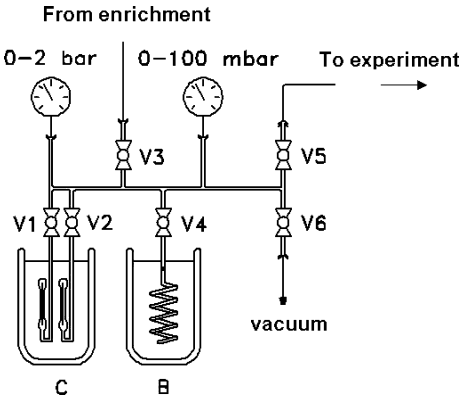

Fig. 12.8 Apparatus for orthohydrogen enrichment at low pressure, and integrated thermal conductivity cells.

12.2.6
Determination of the Ortho/Para Ratio

The specific heats of ortho- and parahydrogen differ one from another, whereby the difference reaches a maximum at temperatures in between 140 and 170 K. Within this temperature range the difference between heat capacities is sufficient and suitable to determine the ortho/para ratio of H_2 using thermal conductivity cells. Typically, the setup according to Grilly is used; this consists of two conductivity cells, whereby one functions as a reference to eliminate long-term thermal drift [56]. The resistance of the tungsten filament in these cells is almost proportional to the orthohydrogen concentration [57]; therefore, it can be used as a measure for the ortho/para ratio.

12.2.7
Enrichment of Ortho- or Paradeuterium

Using the same apparatus, molecular deuterium (D_2) can also be enriched in its ortho- or para-forms. It must be noted, however, that in the case of D_2 the ortho-form is the energetically more favorable and hence easier to prepare [19]. Therefore, it is orthodeuterium which becomes enriched when using an appropriately cooled charcoal cell. The achievable degree of enrichment at the temperature of liquid nitrogen (77 K) is considerably lower than in the case of H_2, but nonetheless the apparatus has been used successfully for the enrichment of the D_2 spin isomers, albeit with appropriate modifications of the procedure. Essentially, in this case the Dewar flask to be filled with liquid nitrogen should tolerate a partial vacuum (underpressure) because, by lowering the pressure of the boiling nitrogen, the temperature falls, and eventually the nitrogen solidifies somewhere at around 60 K. This temperature suffices to achieve an adequate enrichment to observe orthodeuterium-induced polarization (ODIP) [46].

Far superior results have been obtained, however, using closed-circuit cryorefrigeration for the required cooling of the D_2, as this allows the temperature to

be lowered to 20–30 K. In this case, when determining the enrichment the resistors of the bridge circuit and the operating temperature of the thermal conductivity cells must be optimized for D_2, due to the different physical parameters of its individual spin isomers [52].

12.3 Applications of PHIP-NMR Spectroscopy

12.3.1 *In-Situ* PHIP-NMR Spectroscopy of Homogeneous Hydrogenations

12.3.1.1 Activation of Dihydrogen

Dihydrogen shows a weak tendency to undergo chemical reactions, unless it is activated by certain types of transition-metal compounds. Buntkowsky et al. [21] have investigated the early stages of activation of H_2 using parahydrogen, and the results and conclusions derived thereof have been reported.

In general, the activation of dihydrogen by transition-metal complexes has been investigated intensely since the 1960s, when Wilkinson and colleagues discovered the first successful homogeneous hydrogenation catalyst $RhCl(PPh_3)_3$ [22]. Herewith, terminal alkenes and alkynes can be readily hydrogenated at 25 °C at a hydrogen pressure of 1 bar. The mechanism and kinetics thereof have since been extensively studied. Some intermediate dihydrides such as $Rh(H)_2Cl(PPh_3)_3$ and $Rh(H)_2Cl_2(PPh_3)_4$ have been previously observed and characterized using NMR spectroscopy [23], and even PHIP-NMR spectroscopy [24].

The data available in the literature, however, are typically restricted to those containing PPh_3 as the phosphine ligands. In general, the spectroscopic observation of such dihydride species is rather difficult. Due to their intermediate character they have a short lifetime, and hence they typically occur only at rather low concentrations. Whereas conventional NMR spectroscopy frequently fails to identify their existence, PHIP has allowed the detection of several new dihydride products, even at these low concentrations. If hydrogenation with parahydrogen is carried out *in situ* using a spectrometer-activated apparatus, the kinetic constants of the reactions of the formation and disappearance of intermediates may be determined; details of this method are outlined in the following section.

12.3.1.2 Concepts of Reaction Mechanisms

Time-proven concepts for the reaction mechanisms of homogeneous hydrogenations follow two approaches which, according to Halpern's step-wise analysis of hydrogenations using "Wilkinson's catalyst" [25] and the cationic catalyst DIPHOS [26], respectively, can be grouped into the so-called "dihydride" or "unsaturate" routes [27] (Fig. 12.9).

Due to these alternatives, the detection of intermediates is of considerable interest, as this would allow differentiation to be made between these two principal al-

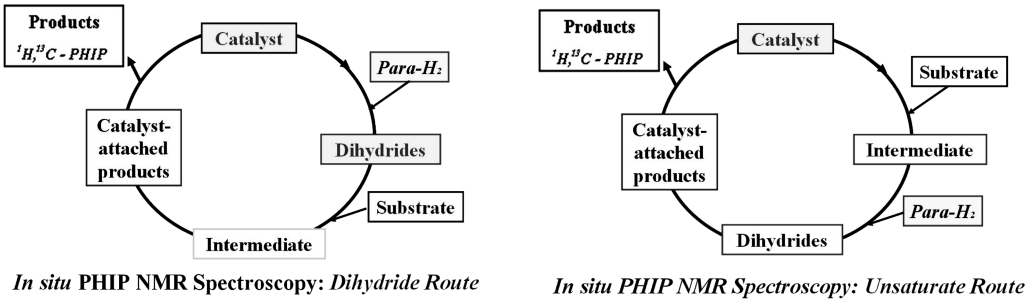

Fig. 12.9 Alternative approaches to the sequence of events during the catalytic activation of dihydrogen.

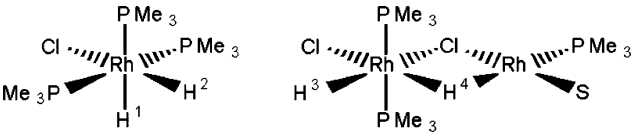

Fig. 12.10 Mono- and binuclear rhodium dihydride complexes.

ternatives. Evidence in favor of one or the other route has been accumulated and associated with the nature of the catalysts – that is, whether they are cationic or neutral – and extensive accounts of this have been published. Within the scope of this chapter, a number of special cases will be discussed that provide evidence for the existence of different intermediates, including a number of dihydrides.

12.3.2 *In-Situ* PHIP-NMR Observation of Mono- and Binuclear Rhodium Dihydride Complexes

PHIP can also be used to identify and characterize mono- and binuclear rhodium dihydride complexes such as $[RhH_2ClL_3]$ (L = PMe_3, PMe_2Ph, $PMePh_2$, PEt_3, PEt_2Ph, $PEtPh_2$, or P(*n*-butyl)$_3$, $[(H)(Cl)Rh(PMe_3)_2(\mu\text{-}Cl)(\mu\text{-}H)Rh(PMe_3)]$, and $[(H)(Cl)Rh(PMe_2Ph)_2(\mu\text{-}Cl)(\mu\text{-}H)Rh(PMe_2Ph)]$ (Fig. 12.10) obtained from the binuclear complex $[RhCl(2,5\text{-norbornadiene})]_2$ when treated with the corresponding phosphine and parahydrogen. By substituting chloride with trifluoroacetate, the complexes $[RhH_2(CF_3COO)L_3]$ (L = PPh_3, PEt_2Ph, PEt_3, and P(*n*-butyl)$_3$) are analogously generated [58].

12.3.2.1 Reactions of $[RhCl(NBD)]_2$ with Parahydrogen in the Presence of Tertiary Phosphines

The binuclear precursor (di-μ-chloro-bis-[η^4-2,5-norbornadiene]-rhodium(I)) = $[(Rh(NBD)Cl]_2$ is well suited for the *in-situ* preparation of a variety of homogeneous hydrogenation catalysts, if tertiary phosphines (here: PMe_3, PMe_2Ph,

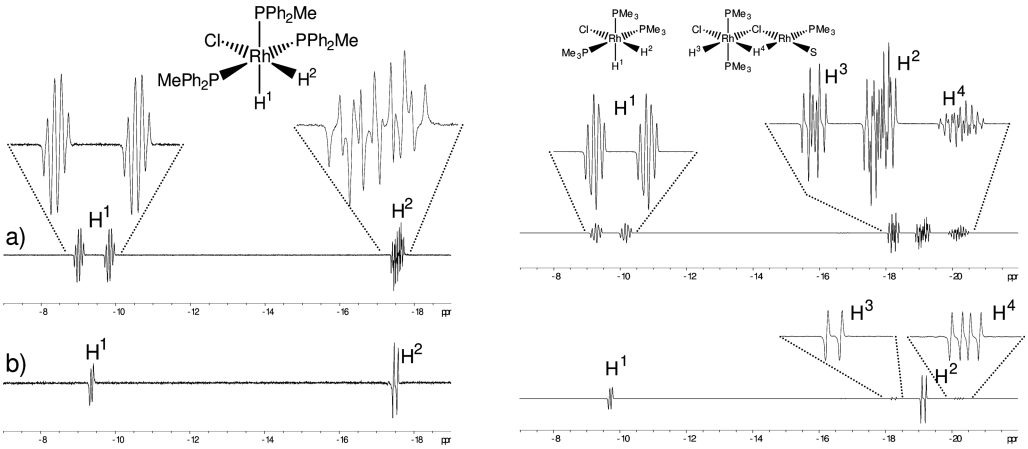

Fig. 12.11 PHIP-NMR spectra of some mono- (left) and binuclear Rh-complexes (right).

$PMePh_2$, PEt_3, PEt_2Ph, $PEtPh_2$, or P(*n*-butyl)$_3$) are added. Upon the addition of dihydrogen to solutions of these mixtures, NBD is hydrogenated off, and mononuclear dihydride species $[Rh(H)_2ClL_3]$ are generated, most likely via the complexes $[RhClL_3]$ as intermediates. These dihydride complexes play a key role as intermediates in any subsequent catalytic hydrogenation.

As characteristic examples, Figure 12.11 (left) shows the results obtained upon addition of parahydrogen to a solution of 10 mg $[Rh(NBD)Cl]_2$ and 19 μL $PMePh_2$ in acetone-d_6 (Rh : P = 1 : 3). Strongly enhanced resonances of the dihydride protons of the complex $[Rh(H)_2Cl(PMePh_2)_3]$ are observed in the ^{1}H-NMR spectrum, whereby the hydride *trans* to a $PMePh_2$ ligand occurs at $\delta_H = -9.4$ ppm, whereas the hydride *trans* to the chloride has a higher chemical shift and appears at $\delta_{H'} = 17.6$ ppm. The latter is characteristic for hydride protons in the *trans* position to such an electronegative ligand. The hydride resonance at lower field shows a large coupling to one *trans* phosphorus ($J_{HP(trans)} = 178.6$ Hz), an additional coupling to two equivalent *cis* phosphorus nuclei ($J_{HP(cis)} = 14.1$ Hz), a coupling to the central rhodium ($J_{HRh} = 13$ Hz), and a coupling to the upfield hydride proton ($J_{HH'} = -7.7$ Hz).

The coupling between the two former parahydrogen protons causes the antiphase character of this resonance, exhibiting emission and absorption maxima, accordingly. The second hydride resonance at higher field is a complex multiplet with couplings to rhodium ($J_{HRh} = 22$ Hz), one equatorial and two axial phosphorus nuclei ($J_{HP(ax.)} = 16.5$ Hz, $J_{HP(eq.)} = 11$ Hz), and the lower field hydride proton ($J_{HH'} = -7.7$ Hz). These data have been tested by simulating the resulting multiplet and its polarization pattern using the computer program PHIP^{++}, upon which very good agreement has been obtained [28].

If the ^{1}H-NMR spectrum is recorded with complete ^{31}P decoupling, both hydride resonance at –9.4 ppm and –17.6 ppm collapse into a doublet of antiphase doublets. The remaining 13-Hz and 22-Hz couplings correspond to J_{HRh} and $J_{HRh'}$,

Table 12.1 ^{1}H-NMR data of the observed hydrides.

No.	Complex	^{1}H chemical shifts δ [ppm] in acetone-d$_6$ and coupling constants J [Hz]
1	$[Rh(H)_2Cl(PMe_3)_3]$	–9.7 ($^1J_{HRh}$=15, $^2J_{HP(trans)}$=178.6, $^2J_{HP(cis)}$=20, $^2J_{HH}$=–7.5) –19.0 ($^1J_{HRh}$=27, $^2J_{HP(ax.)}$=19, $^2J_{HP(eq.)}$=13, $^2J_{HH}$=–7.5)
2	$[Rh(H)_2Cl(PMe_2Ph)_3]$	–9.6 ($^1J_{HRh}$=18, $^2J_{HP(trans)}$=172.5, $^2J_{HP(cis)}$=18, $^2J_{HH}$=–7.2) –18.2 ($^1J_{HRh}$=24.7, $^2J_{HP(ax.)}$=16.5, $^2J_{HP(eq.)}$=11, $^2J_{HH}$=–7.2)
3	$[Rh(H)_2Cl(PMePh_2)_3]$	–9.4 ($^1J_{HRh}$=13, $^2J_{HP(trans)}$=164, $^2J_{HP(cis)}$=14.1, $^2J_{HH}$=–7.7) –17.6 ($^1J_{HRh}$=22, $^2J_{HP(ax.)}$=15, $^2J_{HP(eq.)}$=10, $^2J_{HH}$=–7.7)
4	$[Rh(H)_2Cl(PEt_3)_3]$	–10.7 ($^1J_{HRh}$=14.7, $^2J_{HP(trans)}$=161.7, $^2J_{HP(cis)}$=16, $^2J_{HH}$=–7.9) –19.8 ($^1J_{HRh}$=24.1, $^2J_{HP(ax.)}$=16, $^2J_{HP(eq.)}$=13, $^2J_{HH}$=–7.9)
5	$[Rh(H)_2Cl(PEt_2Ph)_3]$	–10.1 ($^1J_{HRh}$=15.4, $^2J_{HP(trans)}$=162, $^2J_{HP(cis)}$=16.3, $^2J_{HH}$=–7.3) –19.3 ($^1J_{HRh}$=24.6, $^2J_{HP(ax.)}$=17, $^2J_{HP(eq.)}$=15.1, $^2J_{HH}$=–7.3)
6	$[Rh(H)_2Cl(PEtPh_2)_3]$	–9.9 ($^1J_{HRh}$=12.5, $^2J_{HP(trans)}$=155, $^2J_{HP(cis)}$=13.3, $^2J_{HH}$=–7.9) –18.3 ($^1J_{HRh}$=20, $^2J_{HP(ax.)}$=12.5, $^2J_{HP(eq.)}$=13.5, $^2J_{HH}$=–7.9)
7	$[Rh(H)_2Cl(P(n\text{-butyl})_3)_3]$	–10.7 ($^1J_{HRh}$=13.5, $^2J_{HP(trans)}$=163, $^2J_{HP(cis)}$=16.7, $^2J_{HH}$=–7.8) –19.8 ($^1J_{HRh}$=23, $^2J_{HP(ax.)}$=15.8, $^2J_{HP(eq.)}$=13.1, $^2J_{HH}$=–7.8)
8	$[(H)(Cl)Rh(PMe_3)_2(\mu\text{-}Cl)(\mu\text{-}H)\text{-}Rh(PMe_3)]$	–18.2 ($^1J_{HRh}$=25, $^2J_{HP(cis)}$=17.3, $^2J_{HH}$=–4.2) –20.2 ($^1J_{HRh}$=30.3, 20, $^2J_{HP(tans)}$=29, $^2J_{HP(cis)}$=14.6, $^2J_{HH}$=–4.2)
9	$[(H)(Cl)Rh(PMe_2Ph)_2(\mu\text{-}Cl)\text{-}(\mu\text{-}H)Rh(PMe_2Ph)]$	–17.3 ($^1J_{HRh}$=23, $^2J_{HP(cis)}$=15.4, $^2J_{HH}$=–4.2) –20.0 ($^1J_{HRh}$=30, 21.4, $^2J_{HP(trans)}$=29, $^2J_{HP(cis)}$=15.5 $^2J_{HH}$=–4.2)
10	$[Rh(H)_2(CF_3COO)(PPh_3)_3]$	–8.9 ($^1J_{HRh}$=6, $^2J_{HP(trans)}$=161, $^2J_{HP(cis)}$=12, $^2J_{HH}$=–9.5) –19.1 ($^1J_{HRh}$=18, $^2J_{HP(ax.)}$=17, $^2J_{HP(eq.)}$=17, $^2J_{HH}$=–9.5)
11	$[Rh(H)_2(CF_3COO)(PEt_3)_3]$	–10.1 ($^1J_{HRh}$=14.8, $^2J_{HP(trans)}$=160, $^2J_{HP(cis)}$=16, $^2J_{HH}$=–8.7) –22.5 ($^1J_{HRh}$=13, $^2J_{HP(ax.)}$=17, $^2J_{HP(eq.)}$=17, $^2J_{HH}$=–8.7)
12	$[Rh(H)_2(CF_3COO)(PEt_2Ph)_3]$	–9.5 ($^1J_{HRh}$=15.5, $^2J_{HP(trans)}$=161, $^2J_{HP(cis)}$=16.8, $^2J_{HH}$=–8.6) –21.9 ($^1J_{HRh}$=26.8, $^2J_{HP(ax.)}$=16.7, $^2J_{HP(eq.)}$=16.7, $^2J_{HH}$=–8.6)
13	$[Rh(H)_2(CF_3COO)(P(n\text{-butyl})_3)_3]$	–9.5 ($^1J_{HRh}$=15.5, $^2J_{HP(trans)}$=161.5, $^2J_{HP(cis)}$=16.7, $^2J_{HH}$=–7.1) –21.9 ($^1J_{HRh}$=28.8, $^2J_{HP(ax.)}$=17.5, $^2J_{HP(eq.)}$=17.5, $^2J_{HH}$=–7.1)

respectively (Fig. 12.11). Analogous complexes with other phosphine ligands have also been observed (Table 12.1). If the temperature is elevated, the intensities of the polarized hydride resonances increase significantly. The spectrum displayed in Figure 12.11 was recorded at 315 K. Experiments in acetone-d$_6$ can be carried out up to about 330 K, since above this value, boiling and associated evaporation of the solvent becomes so significant that this badly interferes with the quality of the spectra. Furthermore, the resolution of the corresponding hydride resonances deteriorates with increasing temperature. Therefore, a lower temperature is advantageous for better resolution, since the rate of phosphine dissociation slows down with decreasing temperature, upon which the resonances sharpen.

The rate of the observed exchange reaction of the phosphine ligands in the dihydrides increases in the above-listed series of phosphines from PMe_3 to $P(n\text{-butyl})_3$ (Table 12.1), which in turn correlates with the activity of the corresponding complexes as hydrogenation catalysts.

Furthermore, the intensities of the polarized hydride resonances increase with temperature. Since these intensities correlate with the rate of the oxidative addi-

tion of parahydrogen to the corresponding Rh complexes and with the subsequent decay of the so-formed dihydrides, both the rates of their formation as well as the rates of their decay seem to increase with temperature.

12.3.2.2 Formation of the Binuclear Complexes $[(H)(Cl)Rh(PMe_3)_2(\mu\text{-}Cl)(\mu\text{-}H)Rh(PMe_3)]$ and $[(H)(Cl)Rh(PMe_2Ph)_2(\mu\text{-}Cl)(\mu\text{-}H)Rh(PMe_2Ph)]$

Upon the addition of parahydrogen to a solution of $[RhCl(NBD)]_2$ and PMe_3 (ratio of Rh : P = 1 : 3) in acetone-d_6 at 315 K, intense polarization signals of the dihydride complex $[Rh(H)_2Cl(PMe_3)_3]$ (**1**) can be observed, together with strongly polarized resonances in the aliphatic region due to hydrogenation of the NBD ligand. This complex **1** has also been investigated by others using PHIP-NMR spectroscopy [29]. In the later stages of the reaction, however, two new resonances emerge at –18.2 ppm and –20.2 ppm, respectively (Fig. 12.11, right), which can be assigned to the hydride protons of the complex **8** (Scheme 12.1). These signals also have antiphase character due to coupling between the two parahydrogen protons ($J_{HH'}$ = -4.2 Hz). Thereby, the hydride resonance at –18.2 ppm exhibits a coupling to Rh (J_{HRh} = 25 Hz) and the *cis* phosphorus ($J_{HP(cis)}$ = 17.3 Hz). The second hydride resonance consists of a complex multiplet with couplings to the two inequivalent Rh atoms (J_{HRh} = 30.3 Hz and $J_{Rh'H}$ = 20 Hz, respectively), as well as to the *trans* ($J_{HP(trans)}$ = 29 Hz) and the two *cis* phosphorus nuclei ($J_{HP(cis)}$ = 14.6 Hz). This assignment is confirmed upon ^{31}P decoupling of the hydride protons: In the $^{1}H\{^{31}P\}$ NMR spectrum (see Fig. 12.11) the signal at –18.2 ppm has collapsed into a doublet of antiphase doublets with the 25-Hz coupling corresponding to J_{HRh}. The second hydride resonance has simplified to a doublet of doublet of antiphase doublets, with couplings of 30.3 Hz and 20 Hz corresponding to J_{HRh} and $J_{HRh'}$, respectively.

Complexes of the type $[(H)(Cl)Rh(PMe_3)_2(\mu\text{-}Cl)(\mu\text{-}H)Rh(CO)(PMe_3)]$ and $[(H)(Cl)Rh(PMe_3)_2(\mu\text{-}I)(\mu\text{-}H)Rh(CO)(PMe_3)]$, with NMR data corresponding to our results, have also been observed before by Duckett, Eisenberg, and coworkers, using PHIP-NMR spectroscopy [30, 31].

In these earlier studies the phosphine ligand at the rhodium(I) center has been shown to be *trans* to the μ-hydride with a phosphorus coupling of $J_{HP(trans)}$ = 30 Hz and 32 Hz, respectively. Therefore, we assign to complex **8** the structure as outlined in Scheme 12.1.

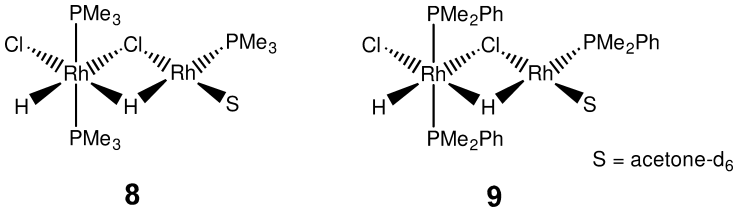

8 **9**

Scheme 12.1

In their study of Wilkinson's catalyst, Duckett and Eisenberg postulated binuclear complexes containing an alkene at the rhodium(I) center [24].

Additional dihydride complexes can be obtained using PEt_3, PEt_2Ph, or P(*n*-butyl)$_3$ as the phosphine ligands. However, in the case of PEt_2Ph or P(*n*-butyl)$_3$ the resonances of the dihydrides are broadened due to a rapid exchange of these phosphine ligands, which blurs the resonances of the hydride protons. Upon cooling the sample, the rate of this exchange process can be slowed down resulting in improved resolution.

Upon using either acetic acid or tetrafluoroboronic acid instead of trifluoroacetic acid, however, no analogous rhodium-containing dihydrides could be observed. A few similar Rh-containing complexes have been described before by other authors [32].

12.3.2.3 General Procedure for the Generation of the Complexes $[Rh(H)_2ClL_3]$ (L = Phosphine)

In a typical experiment, the rhodium complex $[RhCl(NBD)]_2$ (10 mg) and the corresponding amount of phosphine ligand (Rh : P = 1 : 3) are placed into an NMR tube together with 700 μL of degassed acetone-d_6 (Scheme 12.2). p-H_2 is then bubbled *in situ* through the solution within the magnetic field of the spectrometer, using a thin capillary that can be lowered into the spinning NMR tube. This lowering is synchronized by the NMR spectrometer, whereby the spectra are recorded not until the capillary is raised again and the p-H_2 bubbles have vanished.

Likewise, the complex [Rh(NBD)(acac)] (10 mg), together with trifluoroacetic acid (1 μL) and a corresponding amount of phosphine ligand (Rh : P = 1 : 3) is dissolved in 700 μL acetone-d_6 and treated as described above to obtain the complexes $[Rh(H)_2(CF_3COO)L_3]$ (L = phosphine).

12.3.3.3 Intermediate Dihydrides of Cationic Rh Catalysts

NMR evidence for intermediate dihydrides of cationic Rh catalysts remained elusive for a long time, ever since the first demonstrations [33] of effective enantioselective catalysis, for example in the homogeneous hydrogenation of dehydroamino acid derivatives for the synthesis of L-DOPA.

Para-enriched hydrogen offers considerable advantages for the NMR identification of transient intermediates [12d, 34]. PHIP experiments carried out *in situ* under PASADENA conditions are especially powerful in this regard. The PHANEPHOS [MM]-derived Rh catalyst is unusually reactive, with turnover possible even at –40 °C. This high reactivity, coupled with good enantioselectivity, provides an ideal case for characterizing the elusive Rh dihydrides.

Upon displacement of the NBD ligand with parahydrogen according to Scheme 12.3, the ^{1}H-PHIP-NMR spectra displayed in Figure 12.12 were observed, whereby the details of their parameters depended on the type and polarity of the solvent.

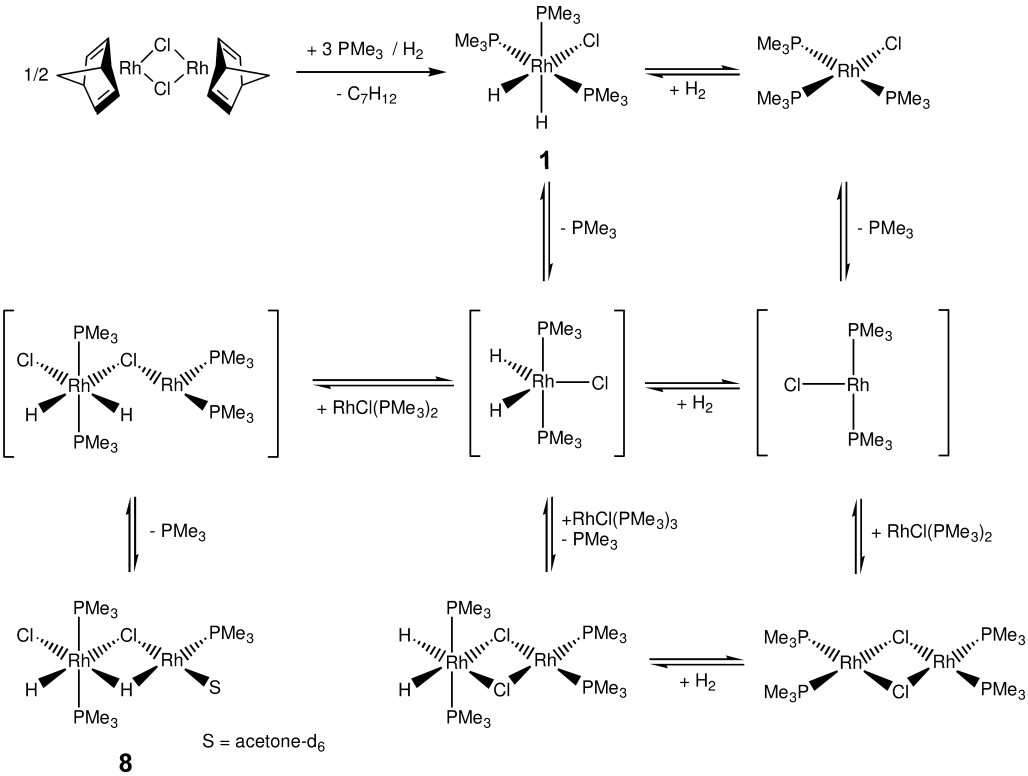

Scheme 12.2 The sequence of reactions leading to the observed intermediates.

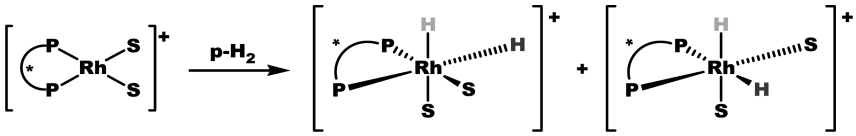

Scheme 12.3 Formation of dihydride intermediates of a cationic Rh complex via displacement of the NMD ligand in the DIPHOS-derived catalyst (S = solvent).

Upon addition of dehydroamino acid esters, the Rh complexes from the above-illustrated NBD-precursor formed *in situ* with displacement of the solvents even at –40 °C. Using differently substituted substrates and mixtures thereof, the spectra shown in Figure 12.13 were observed.

The relative shift of the resonances of the dihydride nuclei listed in Table 12.2 follow a free energy correlation, as is outlined in the Hammett plots shown in Figure 12.14.

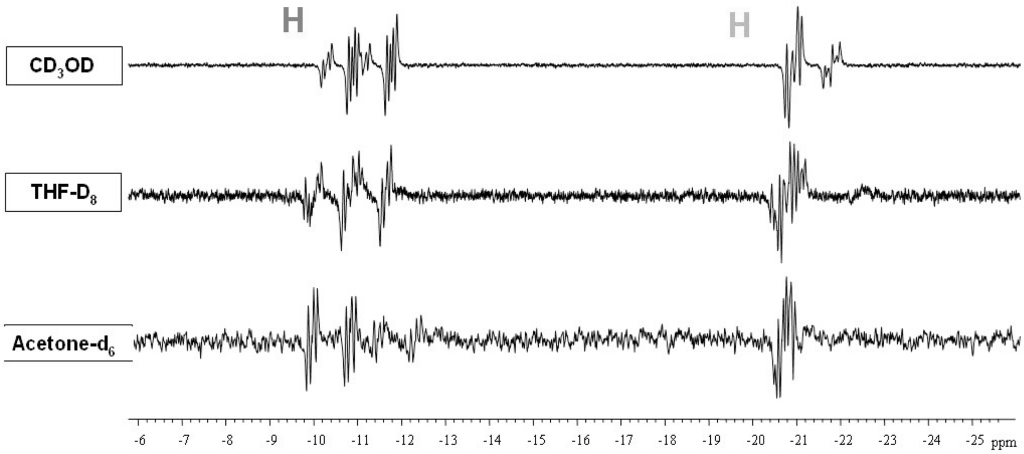

Fig. 12.12 Cationic Rh-dihydrides derived from $[Rh(NBD)(DIPHOS)]^+$.

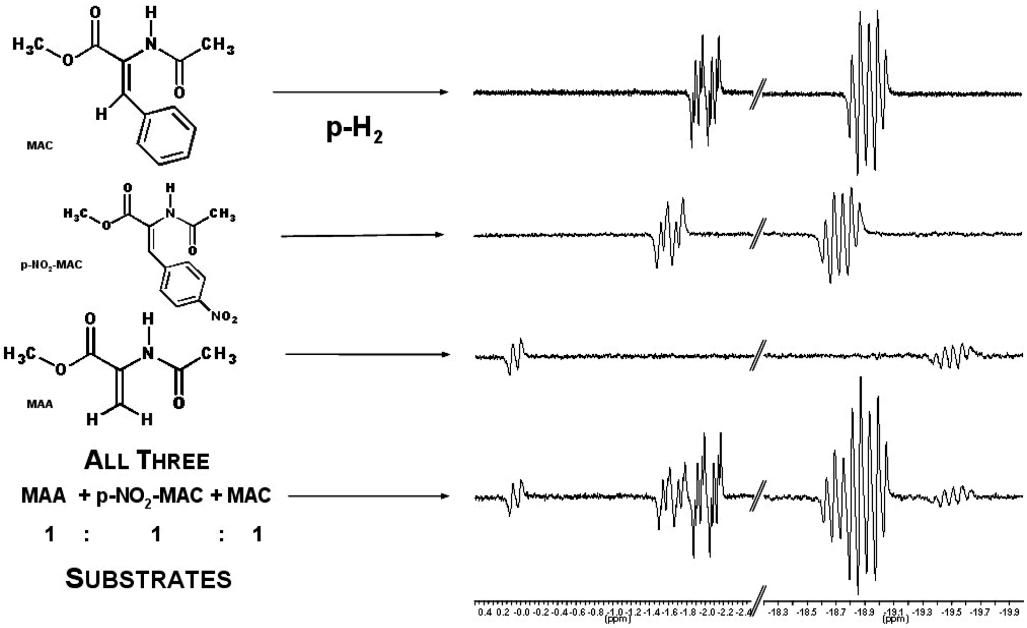

Fig. 12.13 Simultaneous ^{1}H-PHIP-NMR spectra of dihydrides from enamide complexes of the DIPHOS-containing Rh-catalyst.

Table 12.2 NMR data and substituent effects of the observed dihydride intermediates.

R	H	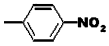		
δ_H	+0.07 ppm	–1.60 ppm	–1.93 ppm	–1.97 ppm
$^2J_{HH}$	–1.0 Hz	–3.0 Hz	–4.3 Hz	–4.3 Hz
$^1J_{HRh}$	1.0 Hz	14.2 Hz	15 Hz	13.4 Hz
$^2J_{HP}$	17.5 Hz	32.8 Hz	36.0 Hz	34.0 Hz
	1.0 Hz	5.25 Hz	6.5 Hz	5.8 Hz

$^1J_{H^{13}C}$=85.8 Hz

Substituent	σ^0	$\Delta\delta_{LF}$ [ppm]	$\Delta\delta_{HF}$ [ppm]
p-OMe	-0.14	+0.052	+0.061
p-F	+0.15	-0.038	-0.028
p-NO_2	+0.81	-0.366	-0.190

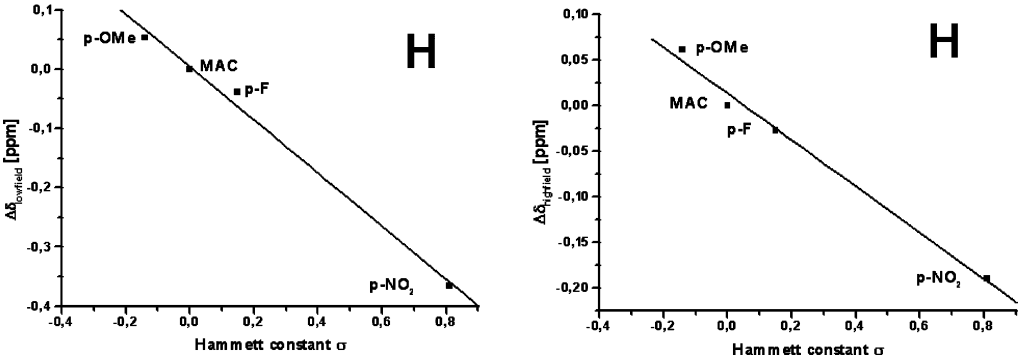

Fig. 12.14 Free energy correlation and Hammett plot of chemical shift data of the intermediate dihydrides.

12.3.3.4 Obtaining Structural Information using ^{13}C-Labeled Substrates

By conducting experiments with the β-^{13}C-labeled ester outlined in Figure 12.15, an additional ^{13}C coupling of 86 Hz to the low-field Rh hydride can be detected. In addition to the expected polarization transfer to the $^{13}CH_2Ph$ of the product at 38 ppm, a strong reactant signal appears in the ^{13}C INEPT(+π/4) spectrum at 135 ppm, implying reversibility of enamide complexation in the observed transient. With the α-^{13}C-labeled enamide, however, weak ^{13}C coupling (ca. 3 Hz) to the low-field hydride is observed [35].

The experimental result and the simulated spectrum are shown in Figure 12.16. The spectroscopic data of this intermediate allows the structure and geo-

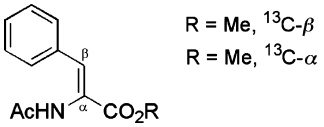

Fig. 12.15 β-^{13}C-labeled esters used as substrates.

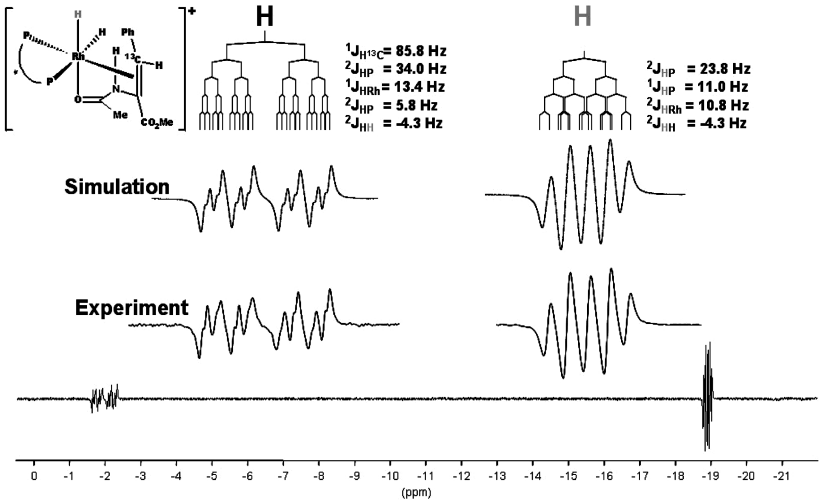

Fig. 12.16 ^{1}H-NMR spectrum of the dihydride of the enamide Rh complex.

metric details of this intermediate to be predicted. These postulates agree well with the results of high-level density functional theory (DFT) calculations. According to such calculations on the simple $[Rh(PH_3)_2]$ complex [36], the reaction proceeds through a η^2-dihydrogen complex to a classical dihydride. The thermodynamically favored Rh diastereomer of this dihydride has a low energy pathway to an agostic species closely resembling the agostic dihydride intermediate outlined in Figure 12.17, although this is not on the computationally preferred pathway of hydrogenation. More specific DFT calculations [36] on the model dehydroamino ester indicate that the structure outlined in Figure 12.17 represents a significant minimum, with a computed Rh–H bond length of 1.76 Å [35, 36].

Whereas, from all of these informative ^{1}H-PHIP-NMR spectra, the structure of the dihydride intermediate (including geometric details about peculiar bonding therein) can be determined rather exactly and reliably, a degree of uncertainty remains as to whether this intermediate represents the "major" or the "minor" diastereomer according to the nomenclature of Halpern [27]. This is the consequence of different kinetic constants associated with the two alternative cycles with different stereochemistry, and which accounts for the "major" and "minor" reaction product (Fig. 12.18). In fact, it is the difference in the rate

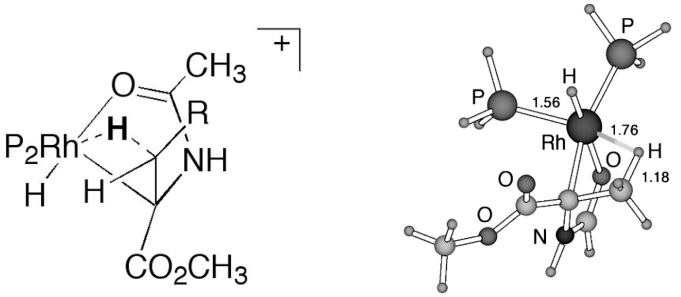

Fig. 12.17 Agostic dihydride intermediate derived from a dehydroamino ester substrate.

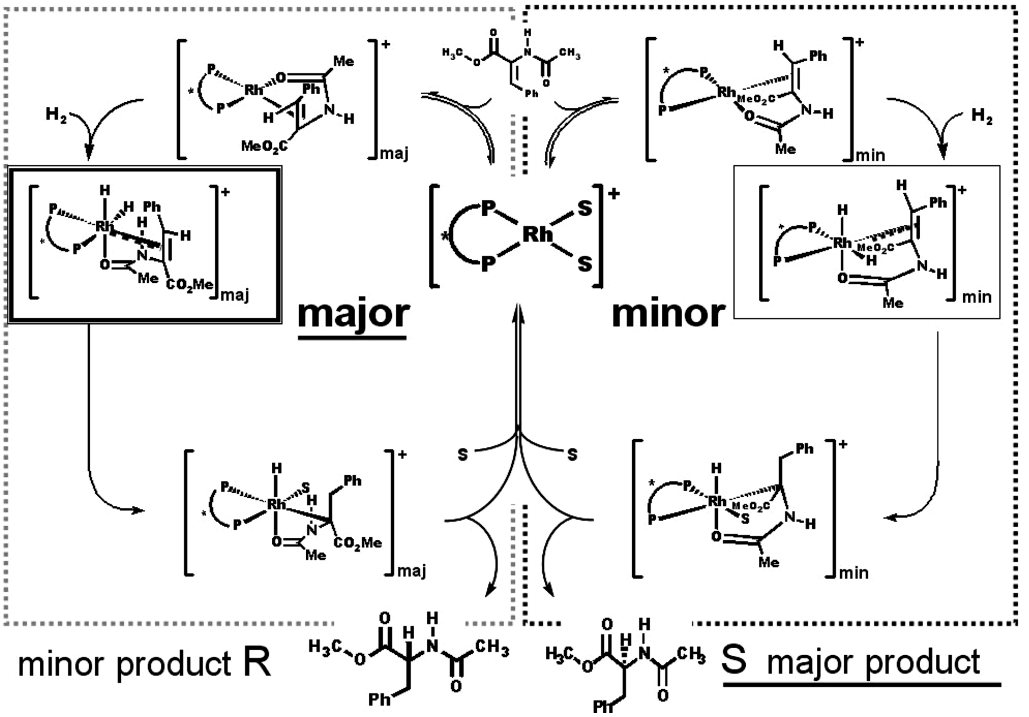

Fig. 12.18 The two equivalent but stereochemically different reaction cycles of homogeneous hydrogenation correlating the "minor" intermediate with the "major" reaction product, and vice-versa (according to [27]).

of generation and the rate of decay of the two respective intermediates that accounts for their respective lifetimes and concentrations.

In consequence, the "major" intermediate (which, in principle, is easier to detect because it should occur at a somewhat higher concentration) correlates with the "minor" reaction product, which is the irrelevant one for most synthetic purposes. The opposite is true for the "minor" intermediates, which correlate with

the "major" reaction product. Although of course the latter two are of more importance, it remains unclear as to which intermediate is seen here – the "minor", more difficult to detect, or (more likely) the "major" intermediate [35].

12.4
Catalyst-Attached Products as Observable Intermediates

During the homogeneous hydrogenation of a variety of substrates – and in particular of those containing aryl groups – "satellites" appear in addition to the "expected" PHIP-NMR spectra of the usual para-hydrogenated products, typically shifted upfield relative to those of the authentic parent compounds [37].

The shift correlates in magnitude with the separation of each particular group distance-wise from the aromatic moiety of the substrate or product; this points to the formation of an intermediate π-complex, for which the rate of formation and the rate of decay can be determined. The ^{1}H-PHIP-NMR spectrum, as well as the anticipated intermediate product–catalyst-π-complex observed during the hydrogenation of styrene, is outlined in Figure 12.19.

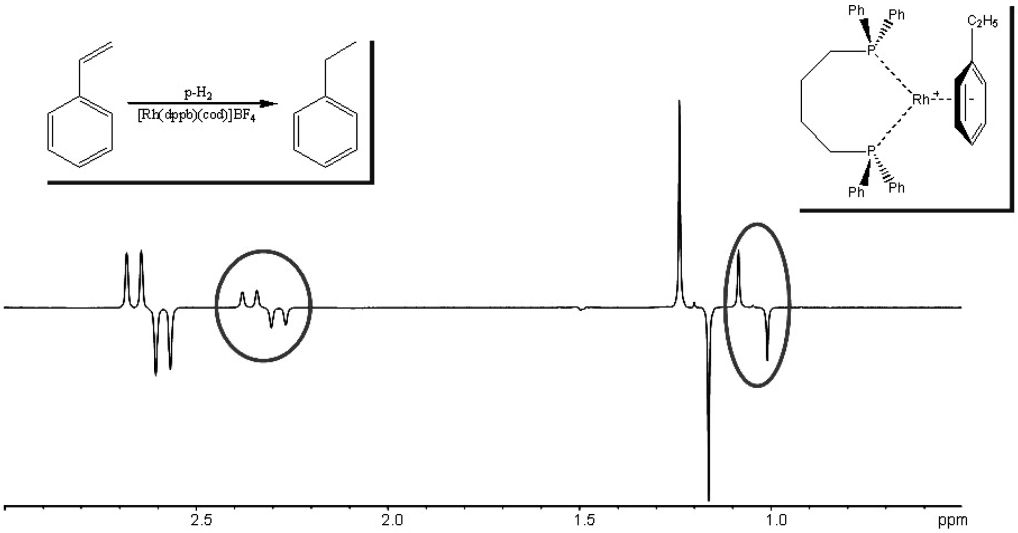

Fig. 12.19 The ^{1}H-PHIP-NMR spectrum and the anticipated intermediate product–catalyst-π-complex observed during the hydrogenation of styrene.

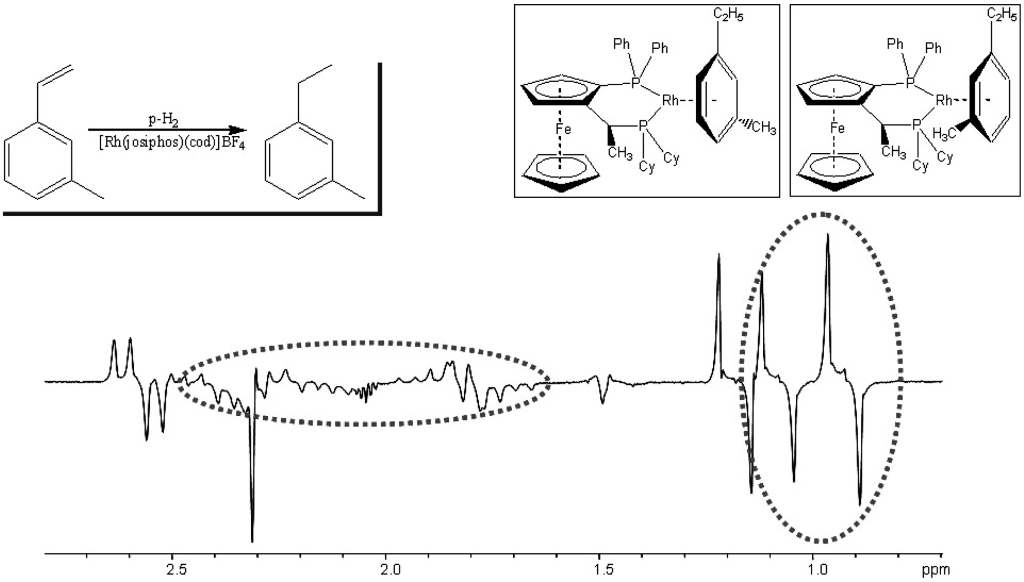

Fig. 12.20 The ^{1}H-PHIP-NMR spectrum and the anticipated two-intermediate product–catalyst–complexes observed during the hydrogenation of *meta*-methylstyrene.

12.4.1
Enantioselective Substrates

If the substrate is enantioselective, as for example *meta*-methylstyrene, the "satellites" split into (at least) two separate resonances, respectively, for the CH_2- and the CH_3-resonances of the resulting product *meta*-methyl-ethylbenzene (Fig. 12.20).

12.4.2
Chiral Catalysts

As opposed to the *meso* forms of catalyst, their chiral counterparts give rise to more complex ^{1}H-PHIP-NMR spectra of the catalyst-attached intermediates. This fact is outlined for the selection of precatalysts and catalysts derived from those listed in Figure 12.21.

Figure 12.22 shows the CH_2-resonance of the catalyst-attached intermediates observed during the hydrogenation of styrene using an achiral catalyst, whilst Figure 12.23 depicts the same region of the spectrum of the intermediate when employing a chiral catalyst. In the latter case the more complex splitting pattern is clear. Finally, Figure 12.24 depicts the CH_2- and CH_3-resonances observed in the ^{1}H-PHIP-NMR spectrum of the catalyst-attached intermediates observed during the hydrogenation of styrene, using the catalysts listed in Figure 12.21.

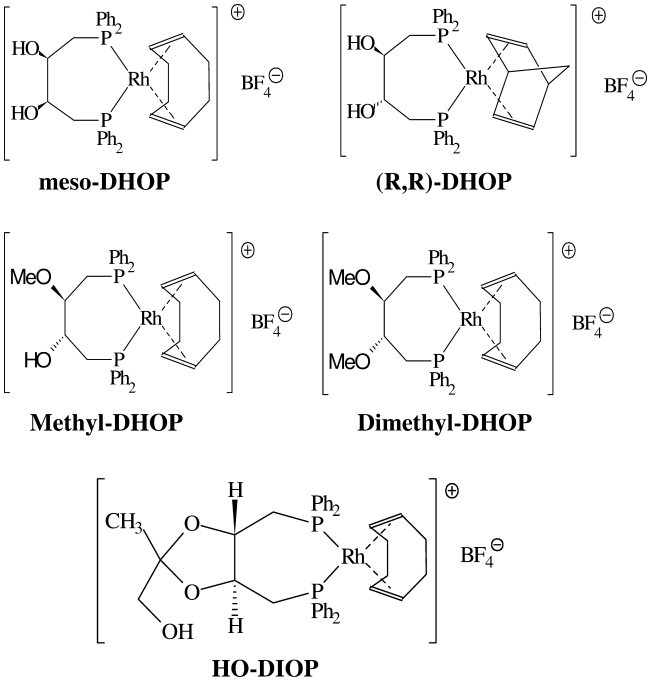

Fig. 12.21 Chiral and achiral Rh-catalysts employed for the hydrogenation of styrene.

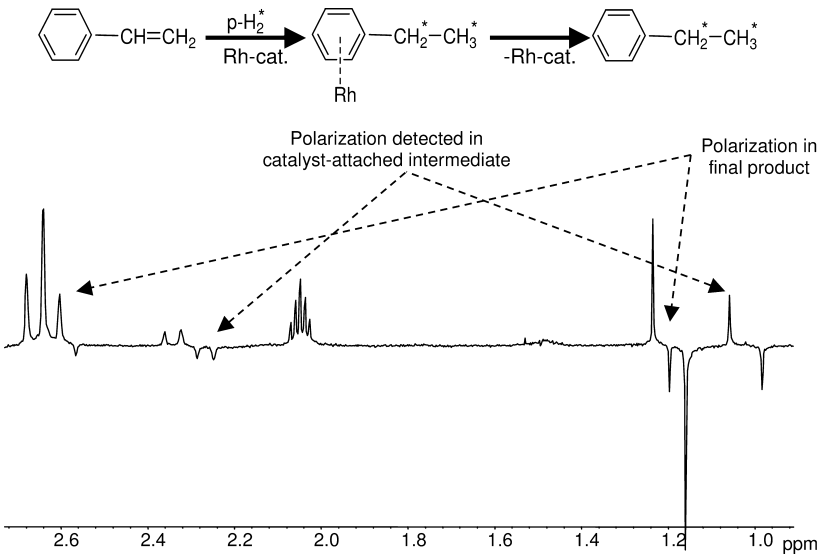

Fig. 12.22 CH_2- and CH_3-resonances observed in the ^{1}H-PHIP-NMR spectrum of the intermediate attached to an achiral catalyst during the hydrogenation of styrene.

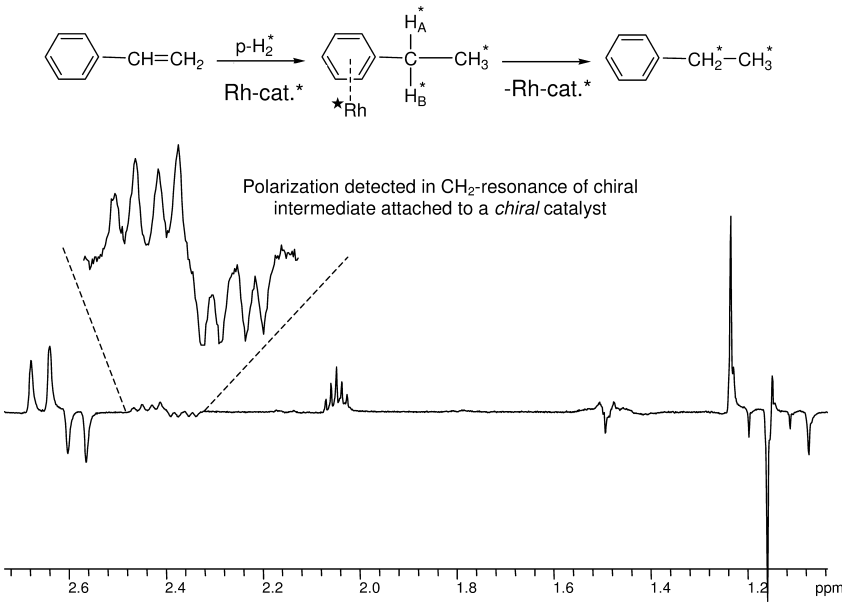

Fig. 12.23 CH_2- and CH_3-resonances observed in the ^{1}H-PHIP-NMR spectrum of the intermediate attached to a chiral catalyst during the hydrogenation of styrene.

12.4.3
Determination of Kinetic Constants

The formation and decay of these product–catalyst-π-complexes are expected to occur according to the sequence of reactions as outlined in Scheme 12.4. The kinetic constants associated with the occurrence of k_{HYD} and the decay of k_{OFF}, respectively, can both be determined by PHIP-NMR using a process termed dynamic PASADENA (DYPAS) spectroscopy, as has been outlined previously [37]. For this purpose the addition of parahydrogen to the reaction is synchronized with the pulse sequences of the NMR spectrometer, whereby the time for acquiring the NMR spectra is delayed by variable amounts. The results thereof are listed in Table 12.3. A variety of kinetic constants can be determined, and the method is reasonably accurate; the margins of error are also indicated in Table 12.3 [37].

The data reveal that electron-donating groups such as amino- or alkoxy-groups increase the rate of formation of k_{HYD} according to their donor strength; for the rate of decay, such a correlation is more likely opposite – that is, they decrease the rate of decay of k_{OFF}. Similar observations have been made for electron-withdrawing substituents, which decrease the rate of formation of k_{HYD} according to their acceptor strength, but increase the rate of decay of k_{OFF}. Again, a free-energy correlation appears to be possible (unpublished results). One clear consequence of this correlation is a variable relative intensity of "satellite" resonances

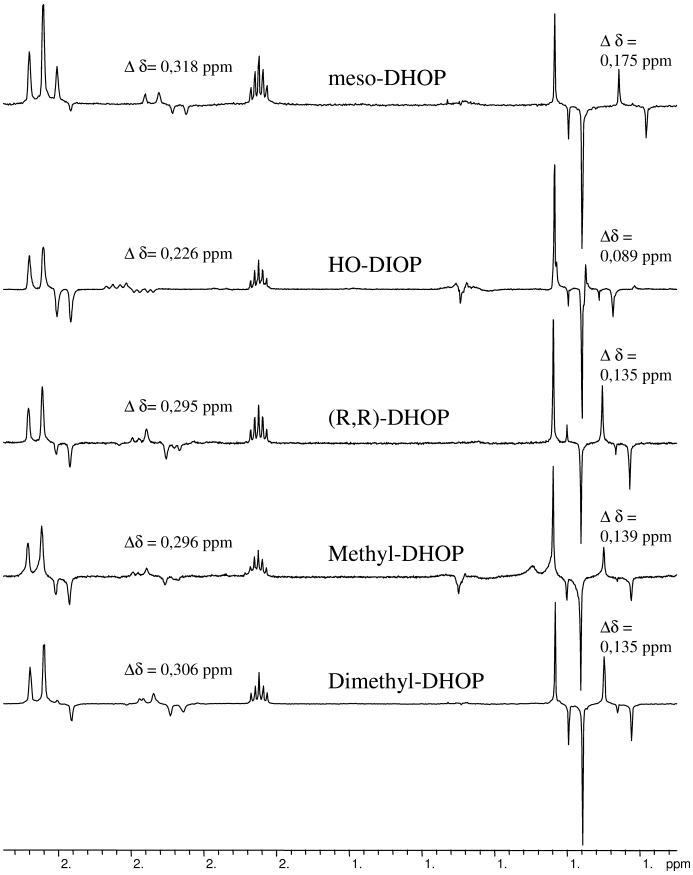

Fig. 12.24 CH_2- and CH_3-resonances observed in the ^{1}H-PHIP-NMR spectrum of the intermediate attached to the selection of various catalysts during the hydrogenation of styrene.

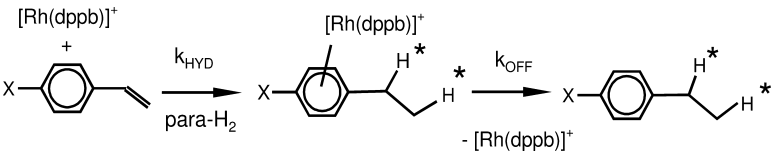

Scheme 12.4

and those of the final hydrogenation products. In cases where the rate of formation k_{HYD} is high, but the rate of decay of k_{OFF} is low, the intensity of the satellites can exceed those of the final hydrogenation products.

The principle of the DYPAS experiment is outlined in Figure 12.25. The results derived from the DYPAS experiments (see Table 12.3) of reactions following Scheme 12.4 may be represented pictorially as the time-dependence of the

Table 12.3 Rates of formation and of decay of the interim product–catalyst-π-complexes [44].

X-	K_{HYD} [s^{-1}]	k_{OFF} [s^{-1}]
-H	0.111 ± 0.009	0.35 ± 0.03
-OMe	0.138 ± 0.010	0.45 ± 0.04
-OEt	(0.40)	0.273 ± 0.024
-NH_2	(0.84)	0.113 ± 0.036

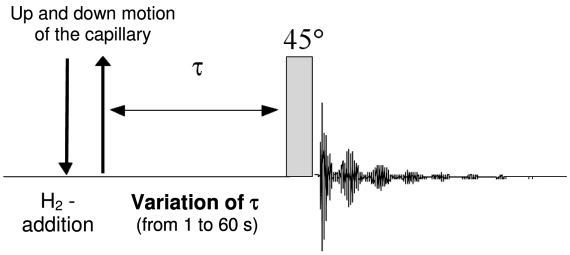

Fig. 12.25 The principle of the DYPAS experiment.

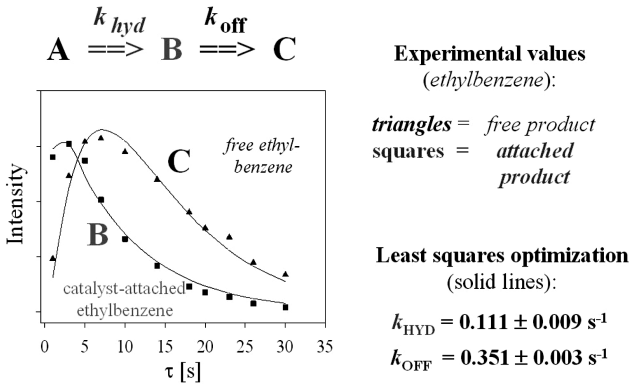

Fig. 12.26 Plots of the time-dependence of concentrations of the intermediates and products of the hydrogenation of styrene.

intermediate and the final product of two consecutive reactions (Fig. 12.26). Unlike the standard appearance of a plot of time-dependence of final product for two consecutive reactions, which typically shows asymptotic saturation behavior, the curve for the signal intensity of C also decays, due to relaxation of the PHIP-derived signal enhancement of this product. The DYPAS method is not restricted to the determination of the kinetic constants listed in Table 12.3, but may also be used to determine other rates of formation and decay (Table 12.4).

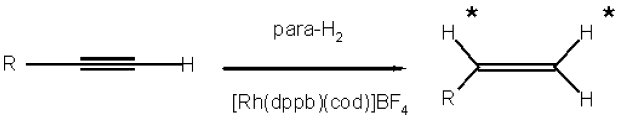

Scheme 12.5 Hydrogenation of differently substituted ethynylbenzenes.

Table 12.4 Rates of hydrogenation of differently substituted ethynylbenzenes.

Substrate	R-	K_{HYD} [s^{-1}]
1	Ph-	0.140 ± 0.005
2	$(CH_3)_3C$-	0.085 ± 0.002
3	$(CH_3)Si$-	0.064 ± 0.004
4	$(Ph)_3Si$-	0.085 ± 0.003

As a further example, the hydrogenation of differently substituted ethynylbenzenes have been investigated using the catalyst [Rh(dppb)(cod)]BF_4. The reaction is outlined in Scheme 12.5 and the results are listed in Table 12.4.

12.4.4
Computer-Assisted Prediction and Analysis of the Polarization Patterns: DYPAS2

For *in-situ* studies of reaction mechanisms using parahydrogen it is desirable to compare experimentally recorded NMR spectra with those expected theoretically. Likewise, it is advantageous to know, how the individual intensities of the intermediates and reaction products depend on time. For this purpose a computer simulation program DYPAS2 [45] has been developed, which is based on the density matrix formalism using superoperators, implemented under the C^{++} class library GAMMA.

DYPAS2 [45] offers a large variety of simulation modes and allows the calculation of polarization patterns of the expected NMR spectra derived either from parahydrogen or orthodeuterium. Furthermore, the individual boundary conditions can be taken into account, under which the hydrogenations take place. Accordingly, the magnetic field dependence of the resulting polarization patterns can be predicted, for example in spectra based on the PASADENA or ALTADENA effect, respectively.

The kinetics of hydrogenation transfer is covered by the use of an exchange superoperator assuming a pseudo first-order reaction. Thereby, competing hydrogenations of the substrate to more than one product can also be accommodated. In addition, the consequences of relaxation effects or NOEs can be included into the simulations if desired. Furthermore, it is possible to simulate the consequences of different types of pulse sequences, such as PH-INEPT or INEPT+, which have previously been developed for the transfer of polarization from the parahydrogen-derived protons to heteronuclei such as ^{13}C or ^{15}N. The

individual delays required in these pulse sequences are critical parameters for the associated magnitude of the transferred polarization, but it is not trivial to estimate their optimal values. Therefore – and in particular for large spin systems – it is desirable to obtain access to intensity plots, which display the calculated intensities of the polarization-enhanced NMR spectra of the heteronuclei as a function of the individual delay times. DYPAS2 contains this option and provides an even greater variety of other possibilities [45].

12.5 Colloidal Catalysts

12.5.1 *In-Situ* PHIP-NMR Investigation of the Hydrogenation of Ethynylbenzene by $Pd_x[N(octyl)_4Cl]_y$

It is recognized that some colloidal catalysts show "homogeneous"-like behavior, though for the most part it is unclear which parameters define the borderline between heterogeneous- (i.e., surface reactions) and homogeneous-type catalysis of colloidal systems. The reaction of ethynylbenzene (phenylacetylene) with parahydrogen using the colloidal palladium catalyst $Pd_x[N(octyl)_4Cl]_y$ leads to nuclear spin polarization in the hydrogenation products [38]. Heterogeneous catalysts are not expected to give rise to the PHIP effect, as the spin correlation in the adsorbed p-H_2 is considered to be lost once the dihydrogen molecules interact with a catalytically active surface. Therefore, most likely hydrogen atoms transferred in such fashion would stem from different p-H_2 molecules. However, it has been shown that the colloidal transition-metal catalyst system $Pd_x[N(octyl)_4Cl]_y$ gives rise to the PHIP phenomenon, thereby implying a homogeneous reaction pathway and proving that the two transferred hydrogen atoms stem from the same dihydrogen molecule (Scheme 12.6).

For this purpose, standard 5-mm NMR tubes were charged with 100 μL ethynylbenzene, 6 mg of the catalyst $Pd_x[N(octyl)_4Cl]_y$, and 0.7 mL acetone-d_6 and placed into a 200-MHz spectrometer. Charges of 51%-enriched p-H_2 were prepared as previously outlined via catalytic equilibration over charcoal at 77 K and injected repeatedly in synchronization with the pulsed NMR-experiment via an electromechanically lowered glass capillary mechanism.

The PHIP-NMR spectra shown in Figure 12.27 were obtained during the hydrogenation of 4-chlorostyrene with p-H_2 parahydrogen [38]. In order to elimi-

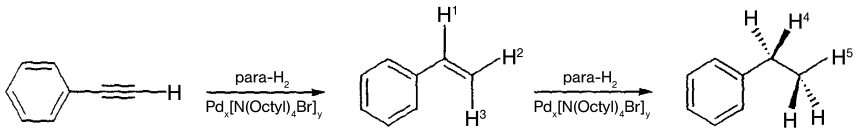

Scheme 12.6 Hydrogenation of phenylacetylene using a colloidal Pd-catalyst system.

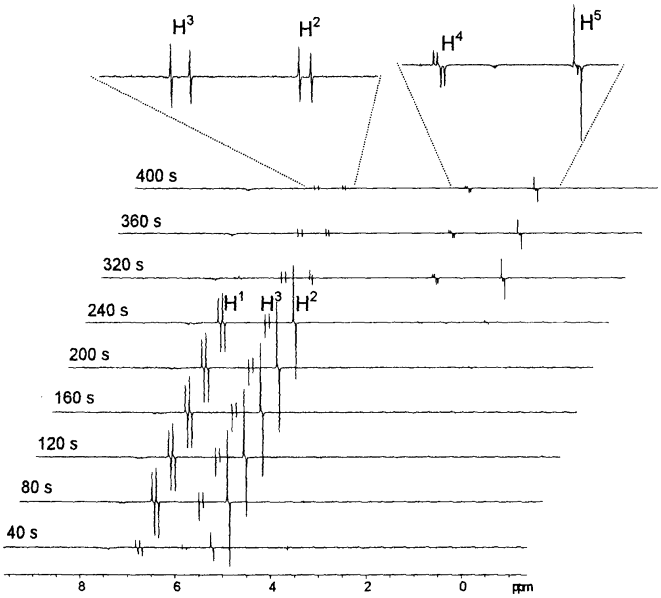

Fig. 12.27 200 MHz ^{1}H-PHIP-NMR spectra recorded during the hydrogenation of phenylacetylene using a colloidal Pd catalyst.

nate interfering signals originating from spins in thermal equilibrium (i.e., "non-PHIP signals"), the NMR spectra were acquired after a hydrogenation time of 10 s accumulating the responses to different pulse angles.

The maximum signal intensity for ^{1}H-PHIP signals occurs at a flip angle of 45°, in contrast to the usual "90° pulse" used for substrates in thermal equilibrium. Therefore, by alternately adding and subtracting scans acquired using pulse angles of –45° and 135°, respectively, it is possible to minimize or even suppress the signal intensity of the "unpolarized", so-called "thermal" proton spins, whereas the signals of the proton spins in polarization then display the maximum of their signal intensity. Less than perfect elimination of the thermal signals may occur, nevertheless, in part because of a slight drift of the external magnetic field (B_0), or because of changes of the homogeneity. Each spectrum shown in Figure 12.27 is the result of four accumulated scans and 40 s of hydrogenation time each.

Cis hydrogenation of ethynylbenzene leads to polarization signals in the respective positions H^1 and H^2 of styrene (Scheme 12.6), as is detected. Furthermore, polarization also occurs in position H^3. This signal shows an anti-phase coupling of 1 Hz with its geminal hydrogen. In order to distinguish whether this is a result of geminal transfer of p-H_2 parahydrogen to the positions H^2 and H^3, or the consequence of a NOE, the use of deuterated ethynylbenzene is required.

With proceeding hydrogenation, the concentration of ethynylbenzene decreases; therefore, the positions H^1 and H^2 show increasingly less polarization.

Subsequently, the polarization signals H^4 and H^5 of ethylbenzene (i.e., the hydrogenation product of styrene) appear. Accordingly, ethylbenzene is also formed via homogeneous catalysis as well – that is, two more p-H_2 protons are transferred simultaneously.

The hydrogenation of ethynylbenzene to styrene (as well as that of styrene to ethylbenzene) mediated by the colloidal catalyst $Pd_x[N(octyl)_4Cl]_y$ occurs in a "pairwise" fashion – that is, the two hydrogen atoms of dihydrogen are transferred simultaneously, which is otherwise characteristic of a homogeneous hydrogenation. This *in-situ* NMR experiment convincingly demonstrates the unique power of PHIP for the investigation of hydrogenations mediated by colloidal systems.

12.6 Transfer of Proton Polarization to Heteronuclei

12.6.1 General Aspects

Homogeneously catalyzed hydrogenations of unsaturated substrates with parahydrogen leading to strong polarization signals in ^{1}H-NMR spectra also give rise to strong heteronuclear polarization, especially if the hydrogenations are carried out at low magnetic fields. The mechanisms underlying the process of PHIP transfer to heteronuclei, however, are still not fully understood, and different mechanisms have been discussed. The polarization transfer from protons to carbon nuclei during the hydrogenation of alkynes may serve as a typical example, which has been investigated for several substrates. It could be shown that in systems containing easily accessible triple bonds (Table 12.5) (e.g., ethynylbenzene or 2,2-dimethylbutyne), a polarization transfer takes place to all carbon nuclei in the molecule. Accordingly, all ^{13}C resonances can be observed in NMR spectra recorded *in situ* with good to excellent signal-to-noise ratios (SNRs) using only a single transient [42]. This technique has made it possible to identify a Ru-based catalyst system, which yields *E*-alkenes via homogeneous hydrogenations of alkynes with central triple bonds, as opposed to the more conventional *Z*-alkenes that result from hydrogenation with Rh-based catalysts [47].

PHIP studies together with polarization transfer permit elucidation of the structure (i.e., the carbon skeleton of compounds) in a fashion which is far superior to the conventional ^{1}H-PHIP technique outlined above.

Furthermore, the qualitative influence of substituents on the symmetry and electronic structure of the substrate and its hydrogenation product on the efficiency of the transfer of polarization to the ^{13}C-nuclei have been discussed, as well as the feasibility of a polarization transfer to other heteronuclei. Evidence in the form of a shift of the aromatic ^{13}C resonances has been found for an initial attachment of hydrogenation products containing aromatic segments to the metal center of the cationic hydrogenation catalyst – probably in the form of a π-complex.

Table 12.5 Reactions studied using ^{13}C-PHIP-NMR spectroscopy.

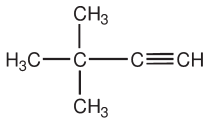	p-H_2 → Cat. / Acetone-d_6	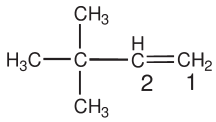
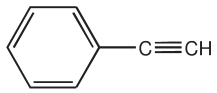	p-H_2 → Cat. / Acetone-d_6	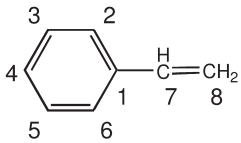
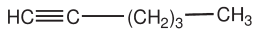	p-H_2 → Cat. / Acetone-d_6	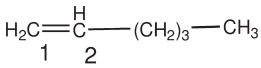
	p-H_2 → Cat. / Acetone-d_6	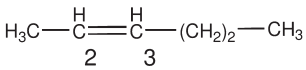
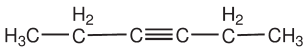	p-H_2 → Cat. / Acetone-d_6	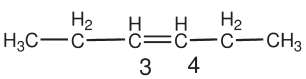
	p-H_2 → Cat. / Acetone-d_6	
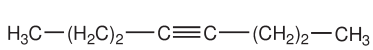	p-H_2 → Cat. / Acetone-d_6	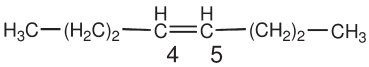

It has been postulated [39] and demonstrated previously that "Hetero-PHIP" for nuclei such as ^{13}C, ^{29}Si, and ^{31}P can result in a signal enhancement (SE) >10 [8, 40, 41], particularly if the reactions are carried out at low magnetic fields (i.e., under ALTADENA conditions). ^{31}P INEPT($+\pi/4$) experiments have also been carried out to transfer the initial proton polarization to ^{31}P [8].

Barkemeyer et al. [8a] showed previously that high enhancement can also be achieved at high magnetic fields when hydrogenating symmetric systems, where the breakdown of symmetry is caused by the naturally abundant ^{13}C nuclei occurring individually in the two other equivalent carbon atoms of the double bond of the substrate (see Scheme 12.8) [8a].

Although this phenomenon provides a powerful tool for the NMR investigation of low-γ nuclei, the full potential of this sizeable polarization transfer from parahydrogen to other nuclei has not been applied very much as compared to ^{1}H-PHIP-NMR spectroscopy. In particular, the use of the PHIP effect to en-

hance and correspondingly simplify the detection of carbon nuclei is a powerful tool for investigating the structure of organic molecules.

12.6.2
Polarization Transfer to ^{13}C

The PHIP phenomenon may be used to label specifically individual, naturally occurring ^{13}C nuclei magnetically via specific enhancement of their corresponding resonances. This frequently simplifies the assignment, thereby facilitating the interpretation of ^{13}C-NMR spectra of more complex molecules. The polarization phenomena occurring in the ^{13}C-PHIP-NMR spectra during the *in-situ* hydrogenation of various alkynes using the catalyst $[Rh(cod)(dppb)]^+$ in $CDCl_3$ at 5 bar of parahydrogen may serve as a characteristic example [42].

The spectra depicted in Figure 12.28 were recorded during the hydrogenation of 3,3-dimethylbut-1-yne to 3,3-dimethylbut-1-ene, and occur according to Scheme 12.7. As is apparent from Figure 12.28, signals from all carbon atoms are visible and nearly all expected couplings can be determined accordingly.

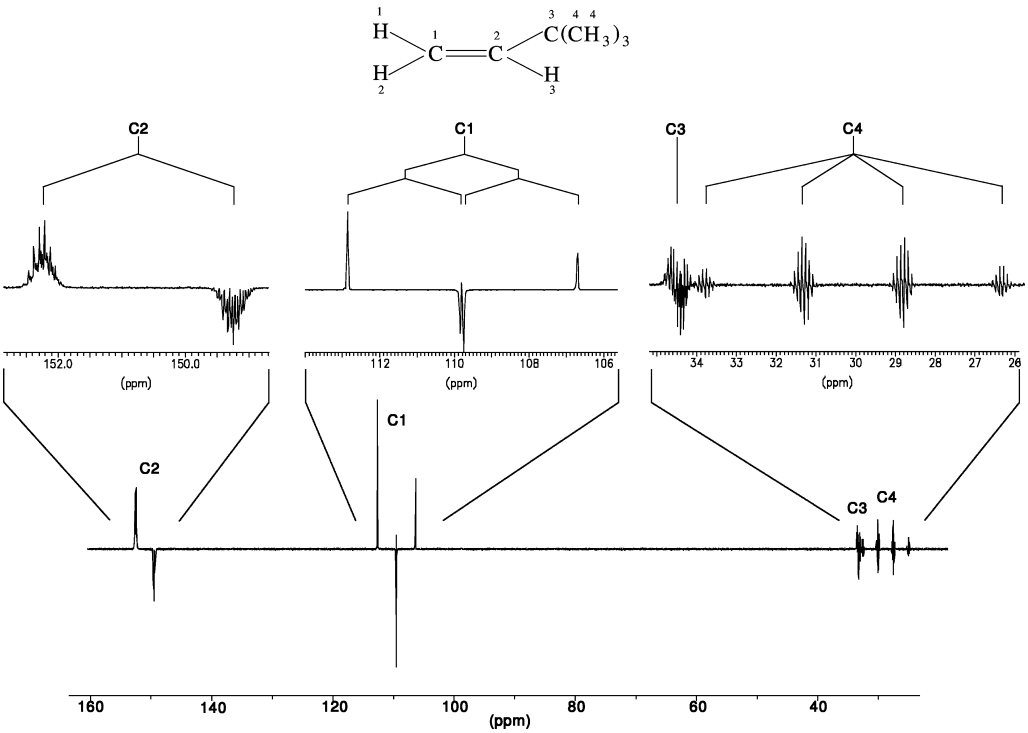

Fig. 12.28 ^{13}C-PHIP spectrum of the hydrogenation of 3,3-dimethylbut-1-yne to 3,3-dimethylbut-1-ene.

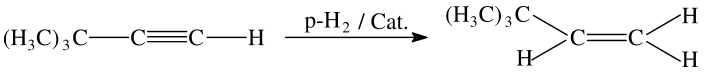

Scheme 12.7 Hydrogenation of 3,3-dimethylbut-1-yne to 3,3-dimethylbut-1-ene.

Other alkynes investigated include ethynylbenzene, 1-hexyne, 2-hexyne, 3-hexyne, and 4-octyne (Table 12.5). These substrates have in common that the triple bond is rather accessible. The substituents cover a wide range of different electronic structures and steric requirements, and in addition, they provide for symmetric and asymmetric substrates. Within this selection of hexynes the electronic structure and accessibility of the individual triple bonds are almost the same, but the symmetry of the bond is different. Furthermore, 1-hexyne, 3,3-dimethylbutyne, and ethynylbenzene all have terminal triple bonds, but the electronic structure and accessibility of the π-system of these triple bonds are influenced differently by the catalyst, depending on the group adjacent to the triple bond. Within this series it could be shown how +M and +I effects or steric hindrance influence the hydrogenation and polarization transfer from the protons to the carbon atoms [42]. The six reactions investigated are outlined in Table 12.5 – that is, the starting materials and the corresponding reaction products, together with the numeration of the individual carbon atoms following IUPAC nomenclature.

The corresponding signal enhancements, as well as the magnitude of the polarization transfer from the former parahydrogen atoms to the directly adjacent former acetylenic carbon, and also to other carbon atoms in the product molecules, have been compared, whereby the polarization spectra were measured under ALTADENA conditions. This means that the hydrogenation was conducted within the Earth's magnetic field, upon which the reaction solution was transferred into the high magnetic field of the superconducting magnet of the NMR spectrometer (corresponding to a proton resonance frequency of 200 MHz or $\sim$50 MHz for the ^{13}C nuclei, respectively) to detect the PHIP spectra. By means of this procedure, polarization is transferred to all magnetically active nuclei in the following way. The resonance frequencies of all nuclei in this very low magnetic field of the Earth (or less) are all virtually the same. Therefore, a highly coupled spin system of a high order is obtained – that is, the differences of resonance frequencies between the carbons (^{13}C) and the protons are small compared to their coupling constants. This is essential for the polarization transfer from protons to a large number of carbons.

By contrast, in the high field of a superconducting magnet, polarization transfer to heteronuclei is less efficient, because now the difference in resonance frequency of ^{1}H and ^{13}C is significant and exceeds the magnitude of the coupling constants between the carbons and the protons. In this latter case, polarization transfer can be achieved most effectively by appropriate pulse sequences (e.g., via cross-polarization).

For these experiments, standard 5-mm NMR tubes equipped with a screw cap and a septum were charged with 200 μL of the substrate, 6 mg of the catalyst [Rh(cod)(dppb)]BF_4 (Cat.), 0.7 mL of degassed chloroform-d_1, and 5 bar of 50%-

enriched parahydrogen. This degree of enrichment was achieved via catalytic equilibration over charcoal at 77 K. Higher levels of enrichment, namely >97%, have also been achieved using a closed-cycle cooler cryostat.

In this fashion, ^{13}C-PHIP-NMR spectra were obtained using the six substrates 3,3-dimethylbut-1-yne, ethynylbenzene, 1-hexyne, 2-hexyne, 3-hexyne, and 4-octyne, respectively. The relevant spectroscopic data for these substrates were obtained from a database [43]. All ^{13}C spectra could be recorded using only a single transient, as they exhibited a higher SNR than expected. The enhanced SNR is due to the PHIP effect, and results from a transfer of the initial proton polarization of the parahydrogen to the carbon atoms. Because of the strong signal enhancement caused by the PHIP effect, no signals were visible for the carbon atoms of the starting material. In general, it is not possible to obtain carbon spectra using just a single transient, at least not with such a high SNR.

Normally in ^{13}C-NMR spectra, the solvent gives rise to the strongest signal of the spectrum; therefore, it frequently must be suppressed via an appropriate pulse sequence. In ^{13}C-PHIP-NMR spectroscopy as outlined here, however, this is not necessary; rather, the signal due to the solvent $CDCl_3$ (normally occurring as a triplet at $\delta = 77.7$ ppm) is not even visible, at least not in the more favorable cases. In all reactions investigated, the signals of all carbon atoms in the products could be detected exploiting only a single transient, which yields a good to excellent SNR.

Although a polarization transfer to all carbon atoms in the corresponding substrates is observed universally, the associated SNR is quite different for the individual substrates. By contrast to the ^{1}H-PHIP-NMR spectra, namely, the ^{13}C-PHIP-NMR spectra observed exhibit much more significant differences depending on the individual substrates. In general, in the ^{1}H-NMR the SNR is much higher; therefore, small differences cannot be distinguished so easily, whereas for ^{13}C-NMR and accordingly for ^{13}C-PHIP-NMR this is much easier. In addition, in ^{1}H-PHIP-NMR the polarization is only transferred to the adjacent protons not further away than approximately corresponding to a ^{3}J coupling. For ^{13}C, however, transfers of the polarization to carbon nuclei as far away as six bonds have been detected.

It is worthwhile pointing out that it is desirable to acquire all spectra under identical conditions, such as hydrogen pressure, elapsed time prior to the acquisition of the spectrum, temperature, and amount of catalyst used. For this reason it is desirable to use a set-up which permits the spectra to be recorded in totally standardized fashion, which does not depend on any individual "human factor". Such a system would allow the reaction to be conducted at a low magnetic field and would thereafter transfer the solution automatically (notably quickly and "adiabatically") into the NMR spectrometer for subsequent analysis.

In addition to the transfer of some degree of polarization to all carbon atoms in the product molecule, a slight low field shift of the ^{13}C resonances in the aromatic region of the PHIP-NMR spectrum of the product recorded during the hydrogenation of ethynylbenzene can be observed. A similar effect has been observed before in the ^{1}H-PHIP-NMR spectra recorded during the hydrogenation of styrene derivatives using cationic rhodium catalysts. This phenomenon has

been termed "product attachment" (see Section 12.4), implying that the hydrogenation product binds to the catalyst's metal center via the phenyl ring in the form of a π-complex. The strength of this attachment depends on the electronic structure of the product and the catalyst, and it can either lead to a shift to high or low frequencies in the ^{1}H-NMR spectrum. By contrast to the ^{1}H-PHIP-NMR investigations of this product attachment (as reported earlier), the effect as observed here in ^{13}C-PHIP-NMR spectra is more pronounced. For ^{1}H-NMR the magnitude of this shift is about 0.5 ppm, whereas for ^{13}C-NMR a shift of about 4 ppm was observed. However, considering the wider range of ^{13}C-shifts compared to those of ^{1}H-nuclei, this is to be expected.

These ^{13}C-PHIP-NMR investigations show clearly that it is possible to effectively transfer polarization from parahydrogen to ^{13}C atoms, especially when conducting the hydrogenations at low magnetic fields. This polarization transfer clearly depends on the electronic and steric features of the groups adjacent to the triple bond. The strongest ^{13}C-PHIP-NMR signals have been observed using either 3,3-dimethylbutyne or ethynylbenzene as the substrate, whereby a transfer of the polarization has been observed for all carbon atoms in the molecule, associated with an excellent SNR. Furthermore, the hydrogenation of 1-hexyne also shows polarization and signal enhancement for all carbon nuclei, but the SNR is not as good as it is for 3,3-dimethylbutyne or ethynylbenzene. With 2-hexyne as the substrate, polarization transfer is observed for all carbon nuclei likewise. Finally, during the hydrogenation of 3-hexyne to 3-hexene, and of 4-octyne to 4-octene, respectively, polarization signals are also observed, with good intensity for the two carbons of the olefinic group and of all aliphatic carbon nuclei. This is consistent with previous studies of other symmetrically substituted alkynes showing strong ^{13}C-PHIP-NMR signals, and it is especially true for symmetrically substituted alkynes carrying electron-poor substituents (e.g., acetylene dicarboxylic acid and its esters). This finding has now been extended to electron-rich alkyne substrates.

When acquiring NMR spectra under ALTADENA conditions, polarization is transferred to all magnetically active nuclei in the substrate. This means that the initial polarization of the parahydrogen is distributed over the number of atoms present in the substrate. This "sharing of the polarization" permits an explanation of the observed decrease in intensity from 3,3-dimethylbut-1-yne or ethynylbenzene to the hexynes, and 4-octyne. In the latter two cases there are more nuclei participating in this sharing. Additionally, the good accessibility of the terminal triple bond of 3,3-dimethylbut-1-yne, ethynylbenzene, and 1-hexyne implies an easy hydrogenation of these substrates, yielding a higher SNR in contrast to the SNR of 2- and 3-hexyne carrying a more central and hence less-accessible triple bond. Finally, the electron-richness of 3,3-dimethylbut-1-yne or ethynylbenzene facilitates the coordination of these substrates to the metal center of the catalyst, thereby resulting in a slightly better SNR, than is the case for 1-hexyne.

Because of the low natural abundance of ^{13}C nuclei (1.1%), practically all observed product molecules contain only one ^{13}C nucleus. Accordingly, the polarization signals in the ^{13}C NMR spectrum clearly do not originate from one and

the same product molecule, but rather stem from different, singly labeled molecules. Since the fraction of the product molecules that contain two or even more ^{13}C nuclei are practically negligible, the observed ^{13}C-NMR spectra are the result of a superimposition of the spectra stemming from product molecules which contain only a single ^{13}C nucleus at the respective position. Therefore, a transfer of polarization from the former parahydrogen atoms to an individual ^{13}C nucleus cannot occur via transfer along the backbone (i.e., not along the carbon chain of the molecules), but it is caused by direct or indirect coupling, either scalar or dipolar, between the former parahydrogen nuclei, other protons, and the corresponding ^{13}C nucleus.

In these experiments it was shown possible to transfer polarization, induced by the PHIP effect, to almost any given carbon in the hydrogenation product of an alkyne, and that certain asymmetrical and electronically activated substrates give rise to the strongest polarization transfer to ^{13}C nuclei. In the cases of 3,3-dimethylbutyne or ethynylbenzene, all carbon atoms were detected using only a single transient, and thereby yielding an excellent SNR [42]. Even with substrates that yield only a weaker polarization transfer (i.e., 1-, 2-, 3-hexyne, and 4-octyne) the SNR was significantly better than was obtained using conventional ^{13}C-NMR without accumulation. In favorable cases, the normally dominating ^{13}C signals of the solvent (e.g., $CDCl_3$) are barely visible in the PHIP-enhanced spectra.

Because of large coupling constants between ^{13}C and ^{1}H (as compared to the coupling constants between ^{1}H nuclei), polarization transfer to ^{13}C nuclei is more effective than among protons. It appears that the maximum distance for transfer of polarization between protons (i.e., in ^{1}H-PHIP-NMR) is about three bonds, whereas it is five for ^{13}C-PHIP-NMR.

In addition to the observed polarization transfer, attachment of the hydrogenated product to the catalyst – most likely in the form of a π-complex between the aromatic portion of a product and the cationic catalyst – has also been observed in the ^{13}C-PHIP-NMR spectra. The associated larger shift range of the affected ^{13}C will make it possible to characterize the nature of this attachment as well as the associated binding energies of the hydrogenation product to the catalyst's metal center more precisely and effectively.

Figure 12.29 illustrates the ^{13}C-PHIP spectrum obtained when hydrogenating 4-fluoro-1-ethynylbenzene under ALTADENA conditions in the Earth's magnetic field. The reaction proceeds according to Scheme 12.5 and the catalyst used is outlined there. This system and the other isomers thereof, namely the hydrogenation of 2-, 3-, and 4-fluoro-1-ethynylbenzene, have also been studied using ^{1}H- and ^{19}F-PHIP-NMR, and the results of the latter will be outlined in the following section (Fig. 12.30).

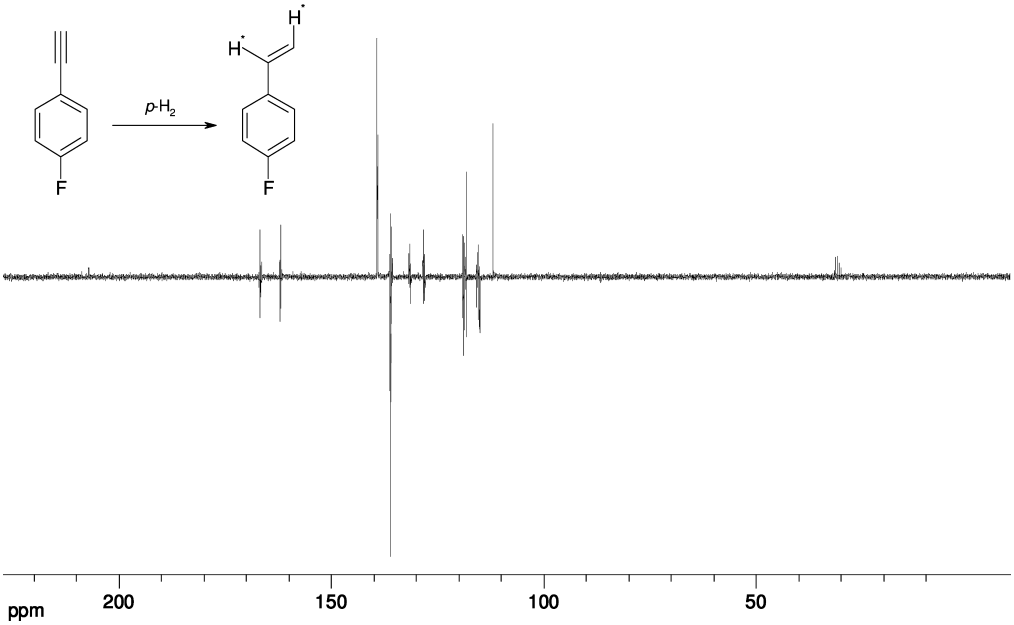

Fig. 12.29 ^{13}C-PHIP spectrum of the hydrogenation of 4-fluoro-1-ethynylbenzene.

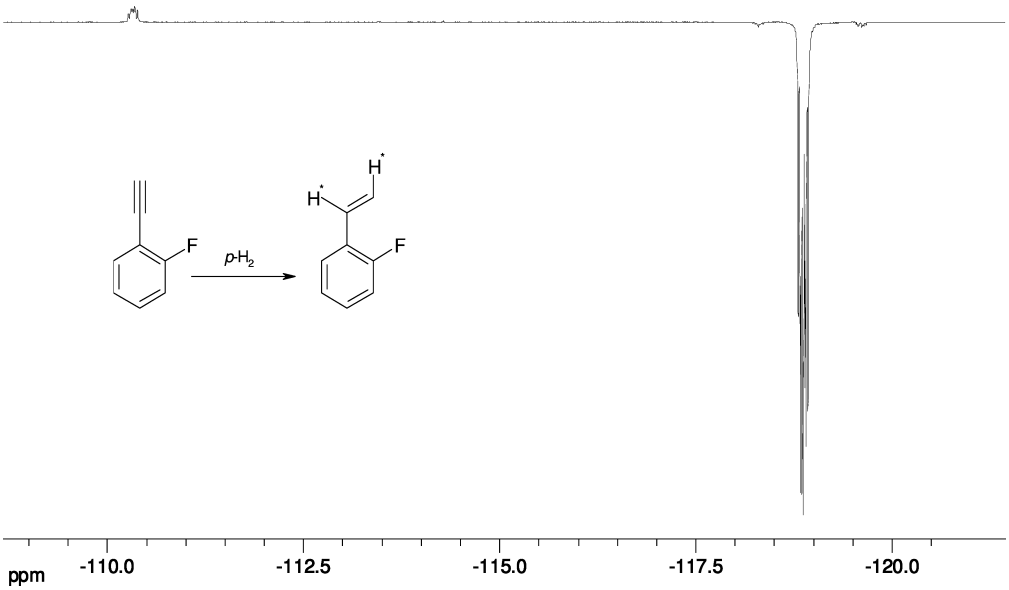

Fig. 12.30 ALTADENA-^{19}F-PHIP-spectrum of the hydrogenation of 2-fluoro-1-ethynylbenzene.

12.6.3
Polarization Transfer to ^{19}F

Transfer of the initial proton polarization is not confined to other protons or ^{13}C, but the signals of other heteronuclei (^{2}H, ^{15}N, ^{29}Si, ^{31}P) in the hydrogenation products can also become substantially enhanced, thereby also increasing their receptivity. Accordingly, the transfer of the PHIP-derived high spin order to ^{19}F has been accomplished using a set of chemically similar fluorinated styrene and ethynylbenzene derivatives.

Additionally, the transfer to ^{19}F occurs not only when the hydrogenation is initiated in the Earth's magnetic field (ALTADENA condition) but also when the whole reaction is carried out in the presence of the strong field of the NMR spectrometer (PASADENA). Both through-bond and through-space interactions are responsible for this process, termed parahydrogen-aided resonance transfer (PART). The high-field and low-field PHIP transfer mechanisms must be strictly distinguished, because they give rise to different phenomena [48].

The best results are obtained when using substrates associated with high hydrogenation rates and long spin-lattice relaxation time for all nuclei of interest, and if the reactions are carried out in the absence of the strong field of the NMR spectrometer. Therefore, in order to study the consequences of polarization transfer to ^{19}F, the hydrogenations of ^{19}F-containing ethynylbenzenes and

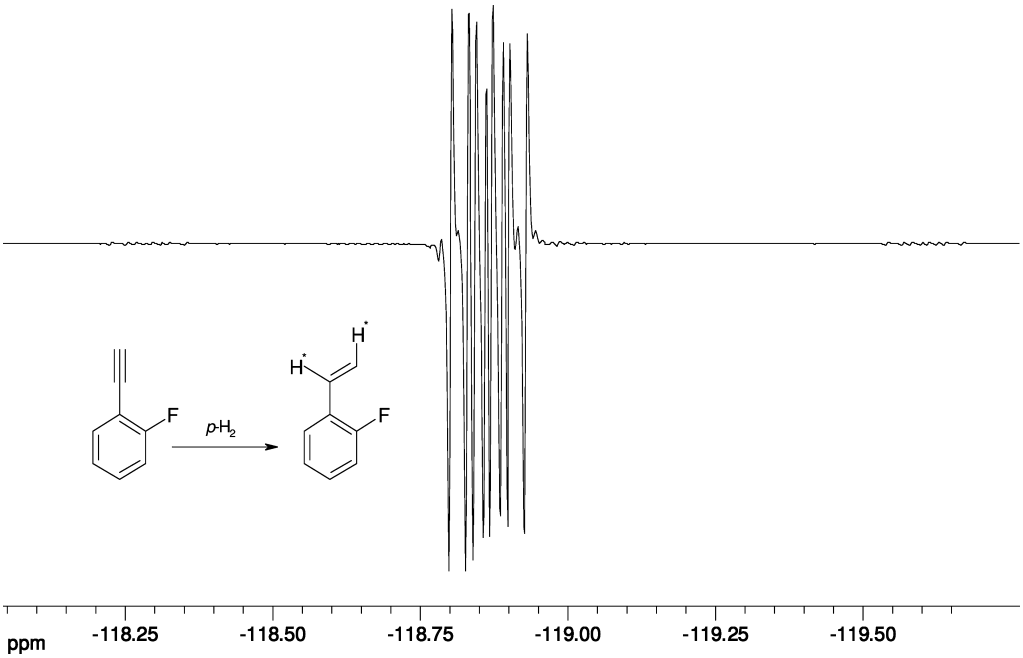

Fig. 12.31 PASADENA-^{19}F-PHIP of the hydrogenation of 2-fluoro-1-ethynylbenzene.

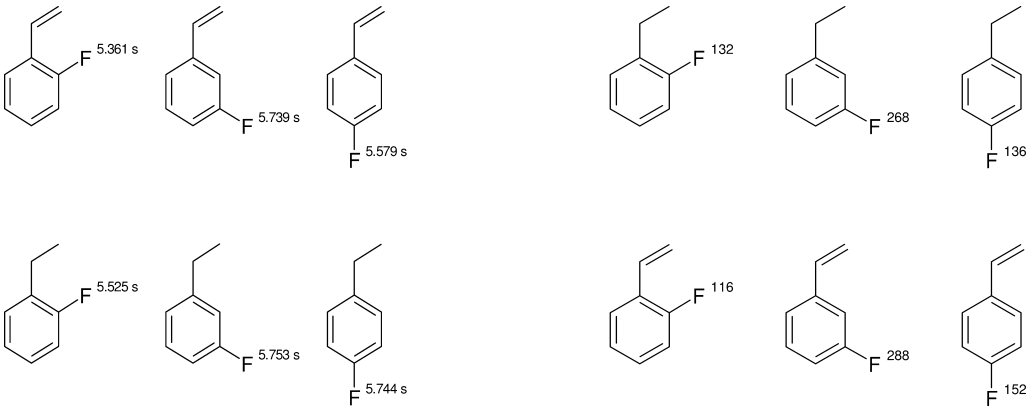

Fig. 12.32 ^{19}F-NMR T_1-spin relaxation times (left) and ^{19}F-PHIP ALTADENA enhancement factors (right) for the hydrogenation products shown.

styrenes have been investigated. It might be expected that if the chemical reaction occurred at high field (i.e., within a MRI or NMR magnet), the signal enhancement would be confined to certain protons only. Instead, if the reaction occurs at low field, the polarization might be transferred to heteronuclei such as ^{31}P, ^{13}C, or ^{19}F, without requiring any special pulse sequences. It transpires, however, that in these systems the ^{19}F nuclei become spin polarized both at low field (Fig. 12.30) and at high field (Fig. 12.31), which opens up new possibilities.

The pentafluorophenyl derivatives are particularly revealing, since the polarization transferred to the individual ^{19}F positions can be compared and correlated with different concepts of their interactions with the primarily spin polarized protons [48]. The enhancement factors achieved in the hydrogenation products of monosubstituted compounds at low field under ALTADENA conditions are given in Figure 12.32.

Likewise, the initial proton polarization may be transferred to other magnetically active heteronuclei, most attractively to those associated with a low γ-value of their nucleus (i.e., to ^{15}N, ^{29}Si), and similarly "difficult" ones, using heteroatom PHIP at low magnetic fields [8, 45].

12.6.4
Parahydrogen-Assisted Signal Enhancement for Magnetic Resonance Imaging

The initial observation of a significant PHIP-derived enhancement factor of >2500 for ^{13}C has rendered this approach attractive for heteronuclear magnetic resonance imaging (MRI) [49]. Using the system as outlined in Scheme 12.8 that is associated with an enhancement factor for ^{13}C of 2500 [8 a], Golman et al. [49] have demonstrated the feasibility of heteronuclear MRI originally in the form of ^{13}C angiography investigations.

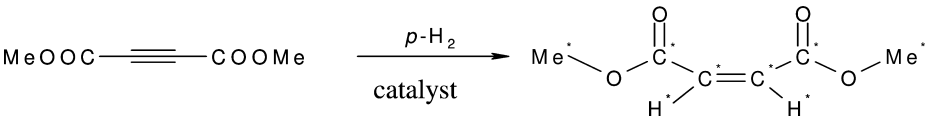

Scheme 12.8 Hydrogenation of acetylene dicarboxylic acid dimethylester to the corresponding maleate [8a].

This initial system, though not optimized for this particular application in medicine, has since been superseded by more appropriate systems with other choices of the components [48]. Finally, possible applications for using selectively hyperpolarized fluorine-containing molecules as contrast agents for medical imaging techniques appear especially attractive; however, this subject matter is discussed elsewhere [50].

12.7
Catalysts Containing other Transition Metals

Over the years, a considerable number of systems have been investigated, comprising catalysts that contain a variety of transition metals, including Co [5], Pd [59, 60], Pt [60, 61], Ru [47, 62], and Ta [63], although the most detailed studies have been conducted on systems containing either Rh or Ir (including some rather exotic ones [64]) as the transition metals. Even investigations on the surfaces of ZnO have been conducted successfully [59]. Further details have also been reported in earlier reviews [12d, 34c, 65].

12.8
Summary and Conclusions

PHIP-NMR spectroscopy is an *in-situ* method, which is associated with a significant signal enhancement of both the protons as well as of various heteronuclei. On the basis of an associated increase in sensitivity, this approach and method allows the identification of unstable intermediates and previously elusive minor reaction products of homogeneous hydrogenations and other reactions. It brings about strong signal enhancement (factor $\cong 1000$ for protons and even higher for heteronuclei such as ^{13}C). This increase in sensitivity renders it possible to detect and analyze crucial reaction intermediates. Therefore, structural and geometric conclusions can be made, and even the rate of formation and of the decay of the intermediates can be determined. The initial proton polarization can be transferred to heteronuclei and to yield enhancement factors for ^{13}C nuclei of more than 2500. The method has interesting applications in MRI, especially in medicinal imaging and molecular spectroscopy.

The method yields unique mechanistic information, it permits the determination of kinetic parameters, it allows the determination of the degree of reversi-

bility of various homogeneous hydrogenations, it yields information about simultaneous (i.e., "pairwise" hydrogen transfer versus asynchronous transfer of individual hydrogens in subsequent events), and it also promises attractive applications to boost the normally low sensitivity of ^{1}H-MRI and, in particular, of heteronuclear MRI.

By using PHIP-NMR studies, various intermediates such as the previously elusive dihydrides of neutral and cationic hydrogenation catalysts, as well as hydrogenation product/catalyst complexes, have already been detected during the hydrogenation of styrene derivatives using cationic Rh catalysts. Information about the substituent effect on chemical shifts and kinetic constants has been obtained via time-resolved PASADENA NMR spectroscopy (DYPAS).

Acknowledgment

The financial support of the Deutsche Forschungsgemeinschaft (DFG), Bonn, Germany, and of the Fonds der Chemischen Industrie, Frankfurt/M., Germany, is gratefully acknowledged.

Abbreviations

ALTADENA	Adiabatic Longitudinal Transport After Dissociation Engenders Net Alignment
CIDNP	chemically induced dynamic nuclear polarization
DFT	density functional theory
MRI	magnetic resonance imaging
NOE	nuclear Overhauser effect
ODIP	orthodeuterium-induced polarization
PART	parahydrogen-aided resonance transfer
PASADENA	Parahydrogen And Synthesis Allow Dramatically Enhanced Nuclear Alignment
PHIP	Para-Hydrogen Induced Polarization
SE	signal enhancement
SNR	signal-to-noise ratio

References

1 Moser, W. R., Reaction Monitoring by High-Pressure Cylindrical Internal-Reflectance and Optical-Fiber Coupled Reactors. In: Moser, W. R., Slocum, D. W. (Eds.), *Homogeneous Transition Metal-Catalyzed Reactions*, American Chemical Society, Washington DC, **1992**, Advanced Chemistry Series 230, p. 5.

2 Whyman, R., *In Situ Spectroscopic Studies in Homogeneous Catalysis*. In: Moser, W. R., Slocum, D.W. (Eds.), *Homogeneous Transition Metal-Catalyzed Reactions*, American Chemical Society, Washington DC, **1992**, Advanced Chemistry Series 230, p. 19 and references therein.

3 (a) Roe, D. C., *Adv. Chem. Ser.* **1992**, *230*, 33; (b) Elsevier, C. J., *J. Mol. Catal.* **1994**, *92*, 258.

4 (a) Rathke, J. W., Klingler, R. J., Chen, M. J., Woelk, K., *Trends Organomet. Chem.* **1994**, *1*, 117; (b) Woelk, K., Bargon, J., *Rev. Sci. Instrum.* **1992**, *63*, 33070; (c) Trautner, P., Woelk, K., Bargon, J., et al., *J. Magn. Reson.* **2001**, *151*, 284; (d) Niessen, H. P., Trautner, P., Wiemann, S., Bargon, J., Woelk, K., *Rev. Sci. Inst.* **2002**, *73* Part 1, 1259.

5 (a) Bryndza, H. E., Thesis, Berkeley, **1981**; (b) Seidler, P. F., Bryndza, H. E., Frommer, J. E., Stuhl, L. S., Bergman, R.G., *Organometallics* **1983**, *2*, 1701.

6 (a) Bowers, C. R., Weitekamp, D. P., *Phys. Rev. Lett.* **1986**, *57*, 2645; (b) Bowers, C. R., Weitekamp, D. P., *J. Am. Chem. Soc.* **1987**, *109*, 5541.

7 Eisenschmid, T. C., Kirrs, R. U., Deutsch, P. P., Hommeltoft, S. I., Eisenberg, R., Bargon, J., Lawler, R. G., Balch, A. L., *J. Am. Chem. Soc.* **1987**, *109*, 8089.

8 (a) Barkemeyer, J., Haake, M., Bargon, J., *J. Am. Chem. Soc.* **1995**, *117*, 2927; (b) Haake, M., Natterer, J., Bargon, J., *J. Am. Chem. Soc.* **1996**, *118*, 8688, and references therein.

9 Pravica, M. G., Weitekamp, D. P., *Chem. Phys. Lett.* **1988**, *145*, 255.

10 (a) Sandler, Y. L., *J. Phys. Chem.* **1954**, *58*, 54–57; (b) Sandler, Y. L., *J. Chem. Phys.* **1958**, *29*, 97.

11 Depatie, D. A., Mills, R. L., *Rev. Sci. Instr.* **1968**, *39*, 105.

12 (a) Bowers, C. R., Jones, D. H., Kurur, N. D., Labinger, J. A., Pravica, M. G., Weitekamp, D.P., *Adv. Mag. Res.* **1990**, *14*, 269; (b) Eisenberg, R., *Acc. Chem. Res.* **1991**, *24*, 110; (c) Bargon, J., Kandels, J., Woelk, K., *Z. Phys. Chem.* **1993**, *180*, 65.

13 Greve, T., Bargon, J., unpublished results.

14 Bargon, J., Kandels, J., Kating, P., *J. Chem. Phys.* **1993**, *98*, 6150.

15 Kaptein, R., *J. Chem. Soc. Chem. Commun.* **1972**, 872.

16 (a) Lepley, A. R., Closs, G. L., *Chemically Induced Magnetic Polarization*, J. Wiley and Sons, New York, **1973**; (b) Pine, S. H., *J. Chem. Edu.* **1972**, *49*, 664, and references therein; (c) Carey, F. A., Sundberg, R. J., *Advanced Organic Chemistry*, Plenum Press, New York, **1984**, 2nd edn, Part A, p. 623; (d) Buchachenko, A. L., Frankevich, E. F., *Chemical Generation and Reception of Radio- and Microwaves*, VCH Publishers, New York, **1994**, p. 33; (e) Sweany, R.L., Halpern, J., *J. Am. Chem. Soc.* **1977**, *99*, 8335.

17 Bargon, J., Kandels, J., Woelk, K., *Angew. Chem. Int. Ed.* **1990**, *29*, 58; *Angew. Chemie* **1990**, *102*, 70.

18 Bonhoeffer, K. F., Harteck, P., *Z. Phys. Chem.* **1929**, *B4*, 113.

19 (a) Sandler, Y. S., *J. Phys. Chem.* **1954**, *58*, 58; (b) Sandler, Y. S., *J. Chem. Phys.* **1958**, *29*, 97.

20 (a) Steinfeld, J. I., *Molecules and Radiation*, The MIT Press, Cambridge, Massachusetts, London, Third Printing, **1981**, p. 98; (b) Sidgwick, N. V., *The Chemical Elements and Their Compounds*, Vol. I, Oxford University Press, Oxford, **1951**; (c) Driesen, A., van der Poll, E., Silvera, I. F., *Phys. Rev.* **1984**, *B30*, 2317.

21 Buntkowsky, G., Bargon, J., Limbach, H. H., *J. Am. Chem. Soc.* **1996**, *118*, 8677.

22 (a) Young, J. F., Osborn, J. A., Jardine, F. H., Wilkinson, G., *J. Chem. Soc., Chem. Commun.* **1965**, 131; (b) Osborn, J. A., Jardine, F. H., Young, J. F., Wilkinson, G., *J. Chem. Soc.* A **1966**, 1711

23 Tolman, C. A., Meakin, P. Z., Lindner, D. L., Jesson, J. P., *J. Am. Chem. Soc.* **1974**, *96*, 2762.

24 Duckett, S. B., Newell, C. L., Eisenberg, R., *J. Am. Chem. Soc.* **1994**, *116*, 10548.

25 (a) Halpern, J., Okamoto, T., Zakhariev, A., *J. Mol. Catal.* **1976**, *2*, 65; (b) Dawans, F., Morel, D., *J. Mol. Catal.* **1977–78**, *3*, 403.

26 Schrock, R. R., Osborn, J. A., *J. Am. Chem. Soc.* **1976**, *98*, 2134.

27 (a) Halpern, J., Riley, D. P., Chan, A. S. C., Pluth, J. J., *J. Am. Chem. Soc.* **1977**, *99*, 8055; (b) Chan, A. S. C., Halpern, J., *J. Am. Chem. Soc.* **1980**, *102*, 838; (c) Halpern, J., *Inorg. Chim. Acta.* **1981**, *50*, 11; (d) Halpern, J., *Science* **1982**, *217*, 401; (e) Collman, J. P., Hegedus, L. S., Norton, J. R., Finke, R. G., *Principles and Applications of Organotransition Metal Chemistry,* University Science Books, Mill Valley, California, **1987**, p. 529.

28 Greve, T., PhD Thesis, Faculty of Sciences/Physics, University of Bonn, **1996**.

29 Duckett, S. B., Eisenberg, R., Goldman, A. S., *J. Chem. Soc., Chem. Commun.* **1993**, 1185.

30 Duckett, S. B., Eisenberg, R., *J. Am. Chem. Soc.* **1993**, *115*, 5292.

31 D., Colebrooke, S. A., Duckett, S. B., Lohman, J. A. B., Eisenberg, R., *J. Chem. Soc., Dalton Trans.* **1998**, 3363.

32 Esteruelas, M. A., Lahuerta, O., Modrego, J., Nürnberg, O., Oro, L. A., Rodriguez, L., Sola, E., Werner, H., *Organometallics* **1993**, *12*, 266.

33 (a) Dang, T. P., Kagan, H. B., *Chem. Commun.* **1971**, 481; (b) Knowles, W. S., Sabacky, M. J., Vineyard, B. D., *Chem. Commun.* **1972**, 10.

34 (a) Harthun, A., Selke, R., Bargon, J., *Angew. Chem. Int. Ed.* **1996**, *35*, 2505; (b) Harthun, A., Barkemeyer, J., Selke, R., Bargon, J., *Tetrahedron Lett.* **1995**, *36*, 7423; (c) Natterer, J., Bargon, J., *Progr. NMR Spectr.* **1997**, *31*, 293; (d) Duckett, S. B., Sleigh, C. J., *Prog. NMR Spect.* **1999**, *34*, 71.

35 (a) Heinrich, H., Giernoth, R., Bargon, J., Brown, J. M., *Chem. Commun.* **2001**, 1296; (b) Giernoth, R., Heinrich, H., Adams, N. J., Bargon, J., Brown, J. M., *J. Am. Chem. Soc.* **2000**, *122*, 12381; (c) Giernoth, R., Hydrogenation. In: *Mechanisms in Homogeneous Catalysis: A Spectroscopic Approach*, B. Heaton (Ed.), John Wiley & Sons Inc., **2005**, p. 359.

36 (a) Landis, C. R., Feldgus, S., *Angew. Chem. Int. Ed.* **2000**, *39*, 2863; (b) Landis, C. R., Hilfenhaus, P., Feldgus, S., *J. Am. Chem. Soc.* **1999**, *121*, 8741; (c) Kless, A., Börner, A., Heller, D., Selke, R., *Organometallics* **1997**, *16*, 2096; (d) Bray, M. R., Deeth, R. J., Paget, V. J., Sheen, P. D., *Int. J. Quant. Chem.* **1997**, *61*, 85.

37 Giernoth, R., Hübler, P., Bargon, J., *Angew. Chem. Int. Edit.* **1998**, *37*, 2473.

38 Eichhorn, A., Koch, A., Bargon, J., *J. Mol. Catal. A – Chem.* **2001**, *174*, 293.

39 Bowers, C. R., Jones, D. H., Kurur, N. D., Labinger, J. A., Pravica, M. G., Weitekamp, D. P., *Adv. Magn. Reson.* **1990**, *14*, 269 and references therein.

40 Eisenberg, R., Eisenschmid, T. C., Chinn, M. S., Kirss, R. U., *Homogenous Transition Metal Catalyzed Reactions.* Moser, W.R., Slocum, D.W. (Eds.), Advances in Chemistry 230, Washington DC, **1992**, p. 45 and references therein.

41 Duckett, S. B., Newell, C. L., Eisenberg, R., *J. Am. Chem. Soc.* **1993**, *11*, 1156.

42 Stephan, M., Kohlmann, O., Niessen, H. G., Eichhorn, A., Bargon, J., *Magn. Reson. Chem.* **2002**, *40*, 157.

43 Aldrich/ACD Library of FT NMR SpectrA Pro, V 1.7, **1998**.

44 Wildschütz, S., Hübler, P., Bargon, J., *Chem. Phys. Chem.* **2001**, *2*, 328.

45 (a) Schmidt, T., Bargon, J., unpublished results; (b) Schmidt, T., PhD Thesis, Bonn University, **2003**, http://hss.ulb.uni-bonn.de/diss_online/math_nat_fak/2003/schmidt_thorsten/index.htm.

46 (a) Limbacher, A., Jonischkeit, T., Bargon, J., to be published; (b) Limbacher, A., PhD Thesis, Bonn University, **2004**. http://hss.ulb.uni-bonn.de/diss_online/math_-nat_fak/2004/limbacher_arndt/index.htm; (c) Jonischkeit, T., PhD Thesis, Bonn University, **2004**. http://hss.ulb.uni-bonn.de/diss_online/math_nat_fak/2004/jonischkeit_thorsten/index.htm.

47 (a) Niessen, H. G., Schleyer, D., Wiemann, S., Bargon, J., et al., *Magn. Reson. Chem.* **2000**, *38*, 747; (b) Schleyer, D., Niessen, H. G., Bargon, J., *New. J. Chem.*

2001, *25*, 423; (c) Schleyer, D., PhD Thesis, Bonn University, **2000**. http://hss.ulb.uni-bonn.de/diss_online/math_nat_-fak/2000/schleyer_dana/index.htm.

48 (a) Kuhn, L.T., Fligg, R., Bargon, J., unpublished results; (b) Kuhn, L.T., Bommerich, U., Bargon, J., submitted; (c) Bommerich, U., PhD Thesis, Bonn University, **2005**. http://hss.ulb.uni-bonn.de/diss_online/math_nat_fak/2005/bommerich_ute/index.htm.

49 (a) Golman, K., Axelsson, O., Jóhannesson, H., Månsson, S., Olofsson, C., Petersson, J.S., *Magn. Reson. Med.* **2001**, *46*, 1; (b) Golman, K., Ardenkjaer-Larsen, J.H., Svensson, J., Axelsson, O., Hansson, G., Hansson, L., Jóhannesson, H., Leunbach, I., Månsson, S., Petersson, J.S., et al., *Acad. Radiol.* **2002**, *9* (Suppl. 2), S507; (c) Ardenkjær-Larsen, J.H., Fridlund, B., Gram, A., Hansson, G., Hansson, L., Lerche, M.H., Servin, R., Thaning, M., Golman, K., *Proc. Natl. Acad. Sci. USA* **2003**, *100*, 10158; (d) Mansson, S., Johansson, E., Magnusson, P., Chai, C.M., Hansson, G., Petersson, J.S., Stahlberg, F., Golman, K., *Eur. Radiol.* **2005**, June 14 [Epub ahead of print]. *http://www.ncbi.nlm.nih.gov/entrez/query.fcgi?cmd=Retrieve&db=PubMed&list_uids=15954020 &dopt=Citation* (November 15, 2005).

50 Bargon, J., to be published.

51 Koch, A., Bargon, J., *Magn. Reson. Chem.* **2000**, *38*, 216.

52 Fligg, R., Bargon, J., Enrichment of parahydrogen using the Oxford closed cycle cooler cryostat. *Research Matters*, **2000**, 12, Oxford Instruments, Oxford, UK.

53 (a) Evett, A.A., *J. Chem. Phys.* **1959**, *31*, 565; (b) White, D., Lassettre, E.N., *J. Chem. Phys.* **1960**, *32*, 72; (c) Freeman, M.P., Hagyard, M.J., *J. Chem. Phys.* **1969**, *49*, 4020.

54 Cunningham, C.M., Chapin, D.S., Johnston, H.L., *J. Am. Chem. Soc.* **1958**, *80*, 2382.

55 Dosiere, M., *J. Chem. Edu.* **1985**, *62*, 891.

56 Grilly, E.R., *Rev. Sci. Instrum.* **1953**, *24*, 72.

57 Bradshaw, T.W., Norris, J.O.W., *Rev. Sci. Instr.* **1987**, *58*, 83.

58 Koch, A., Bargon, J., *Inorg. Chem.* **2001**, *40*, 533.

59 Carson, P.J., Bowers, C.R., Weitekamp, D.P., *J. Am. Chem. Soc.* **2001**, *123*, 11821.

60 Sulman, E., Deibele, C., Bargon, J., *React. Kinet. Catal.* **1999**, *L67* (1), 117.

61 Jang, M., Duckett, S.B., Eisenberg, R., *Organometallics* **1996**, *15*, 2863.

62 Duckett, S.B., Mawby, R.J., Partridge, M.G., *Chem. Commun.* **1996**, 383.

63 Millar, S.P., Zubris, D.L., Bercaw, J.E., Eisenberg, R., *J. Am. Chem. Soc.* **1998**, *120*, 5329.

64 Suardi, G., Cleary, B.P., Duckett, S.B., Sleigh, C., Rau, M., Reed, E.W., Lohman, J.A.B., Eisenberg, R., *J. Am. Chem. Soc.* **1997**, *119*, 7716.

65 Bowers, C.R., Sensitivity enhancement utilizing parahydrogen. In: Grant, D.M., Harris, R.K. (Eds.), *Encyclopedia of Nuclear Magnetic Resonance*, Volume 9, **2002**, p. 1.

13
A Tour Guide to Mass Spectrometric Studies of Hydrogenation Mechanisms

Corbin K. Ralph, Robin J. Hamilton, and Steven H. Bergens

13.1
Introduction

The ability of electrospray ionization (ESI) to generate intact complex organometallic ions in the gas phase has revolutionized the application of mass spectrometry (MS) to the study of reactions catalyzed by organometallic compounds [1]. To date, the catalytic reactions studied using ESI-MS include oxy transfer reactions with manganese-oxo-salen complexes [2], Ziegler-Natta polymerizations of alkenes [3], alkene metathesis using ruthenium-alkylidene catalysts [4], C–H activation by iridium complexes [5], Suzuki couplings [6], nickel-catalyzed coupling reactions [7], chiral catalysts for allylations [8], and catalytic hydrogenations [9]. The objectives of these studies have ranged from understanding elementary reactions between substrates and coordinatively unsaturated catalytic intermediates in the gas phase, to rapid screening of one-pot, complex catalyst mixtures for activity towards various reactions. Although MS studies of alkene hydrogenations have been carried out using other ionization techniques [10], for example to characterize product isotopomers or organometallic species present in solution, the focus of this chapter will be on ESI-MS studies.

The reported ESI-MS studies of catalytic reactions can roughly be divided into two categories: 1) characterization of species present in catalytically active solutions; and 2) application of tandem ESI-MS systems to study the chemistry of complex organometallic ions in the gas phase [1]. It is the study of reactivity of ions in the gas phase that has provided the most mechanistic information about catalytic hydrogenations using MS. A paramount concern which attends such studies from a solution-phase chemist's point of view is the relevance of gas-phase ion chemistry to a reaction of interest carried out in solution under a given set of conditions (temperature, pressure, concentrations, solvent, etc.). A number of factors come into play when making such comparisons. Ionic species in the gas phase can induce polarizations in neutral reagent molecules, for example, causing an electrostatic attraction between the reactants, and thereby resulting in substantially larger Arrhenius frequency factors and different activa-

The Handbook of Homogeneous Hydrogenation.
Edited by J.G. de Vries and C.J. Elsevier
Copyright © 2007 WILEY-VCH Verlag GmbH & Co. KGaA, Weinheim
ISBN: 978-3-527-31161-3

tion energies in the gas phase than in solution [3a, 4a, 11]. Further, the concentrations and contact times between reagents are smaller in the gas phase than in solution. Also, a large component of activation energies for reactions carried out in solution can involve solvent effects [12]. Various steps in reactions catalyzed by transition-metal complexes in solution involve changes in coordination number, and thereby are accompanied by coordination or dissociation of solvent molecules. These and other factors are involved when comparing the reactivity of organometallic ions in solution to the gas phase, and no rigorous mechanistic theories or studies currently exist that specifically address these concerns [13]. The approach adopted for the present chapter is to provide a tour guide-level description and an understanding of the methods used to carry out such experiments. The studies of catalytic hydrogenation are then discussed in some detail, with the discussions being accompanied by relevant information and perspective from the other reactions and systems studied by ESI-MS. The objective of this tour guide is to provide chemists studying catalytic hydrogenations with sufficient perspective and information to determine if ESI-MS can provide experimental data relevant to a catalytic hydrogenation of interest. As with all tour guides, more detailed and insightful information can be obtained from the locals. Therefore, the interested hydrogenation tourist is encouraged to "step off the bus", to study the source literature in more detail, and perhaps to contact the researchers involved to discuss a reaction of interest.

13.2
A General Description of ESI-MS

Perhaps of high interest to the hydrogenation chemist are the pertinent details of how gas-phase ions of organometallic catalysts are prepared. Of specific interest are the types of fragmentation events that can occur during the preparation of the gas phase ions, and what forms coordinatively unsaturated organometallic ions adopt in the gas phase.

ESI was first developed for MS by Fenn et al. in the mid-1980s [14]. ESI is the mildest method to generate ions in the gas phase from species dissolved in solution. Species with high molecular masses, such as synthetic polymers, DNA fragments, and proteins can be transferred to the gas phase without fragmentation. ESI has been applied to a wide variety of organometallic species [11]. The application of ESI has allowed the production of various organometallic ions in the gas phase with control over the number of solvent molecules associated with the ion, and control over gas-phase ligand dissociation reactions that generate coordinatively unsaturated ions for study [15]. Of note, however, is that ESI does not, in the strictest sense, generate charged molecules. Rather, it separates the charged species from each other, and from the neutral species in solution. In fact, ESI cannot easily be applied to neutral molecules unless they have, for example, basic groups that can associate with charged species also present in solution (e.g., protons or sodium ions). An interesting illustration of the ability of ESI-MS to detect

and separate minute amounts of charged species in solution is the study by Chen et al. of a mixture containing a variety of neutral alkene metathesis catalyst precursors with the general formula [$RuCl_2$(alkylidene)(diphosphane)] [4 c]. When dissolved in solution, these neutral catalyst precursors are in equilibrium with small amounts of the cationic catalysts, [RuCl(alkylidene)(diphosphane)]$^+$, formed by chloride dissociation. The application of ESI-MS to these mixtures allowed the detection of trace amounts of cationic catalysts, which could also be separated in the gas phase on the basis of their m/z ratio. The separated catalysts were then individually screened for activity towards the ring-opening olefin metathesis of norbornene in the gas phase. It was found that the cationic catalysts with the highest activities towards norbornene in the gas phase also had the highest activities in solution.

ESI operates in stages (Fig. 13.1) [1, 14]. A typical sequence is as follows. The organometallic ion is introduced as a salt dissolved in a sprayable solvent through a capillary into the electrospray chamber. Polar solvents such as dichloromethane, acetonitrile, and alcohols are easily sprayed, whilst nonpolar solvents can be sprayed as mixtures with polar solvents. The concentration of the organometallic complex typically ranges from 0.001 to 10 mM, which is similar to the concentration range used in homogeneous catalysts. The electrospray chamber often contains a nitrogen "bath" gas at or near atmospheric pressure when used to transfer organometallic ions to the gas phase. The capillary contains an electrode which is in contact with the sample solution. A large potential difference (typically 4–6 kV) is applied between this electrode and the walls of the chamber. The electric field is intensified at the tip of the capillary, causing ion separation and formation of charged droplets in the atmosphere of the chamber. The droplets contain an excess of either negative or positive ions, depending on whether the capillary tip is negative relative to the chamber walls, or positive. Solvent evaporation occurs as the charged droplets containing the ions are accelerated towards the chamber walls by the potential difference. Rapid solvent evaporation leads to a decrease in the droplet diameter. The droplet diameter decreases until the coloumbic repulsions between the ions near the surface exceed the surface tension of the solvent. The droplet will then undergo fission into smaller droplets containing fewer ions than the parent, and/or expulsion of the ions from the surface of the droplet into the gas phase. This sequence repeats itself until all the ions in the gas phase are free from solvent. In practice, desolvation occurs over several stages of the process (*vide infra*). The charged ions or solvated ions are driven by a pressure differential through a heated capillary (held typically at temperatures ranging from 150 to 200 °C) into the first vacuum chamber that is typically maintained at 0.5–1 Torr. The ions are essentially pulled through the capillary by the viscous drag forces of the nitrogen gas escaping into the first vacuum chamber to emerge as a supersonic stream. The outlet of the capillary is sheathed in a metal tube, and a potential is applied between this tube and a skimmer at the other end of the chamber. This "skimmer-" or "tube potential" accelerates the ions in the expanding stream towards the skimmer. The skimmer potential typically ranges from 35 to 100 V. The first

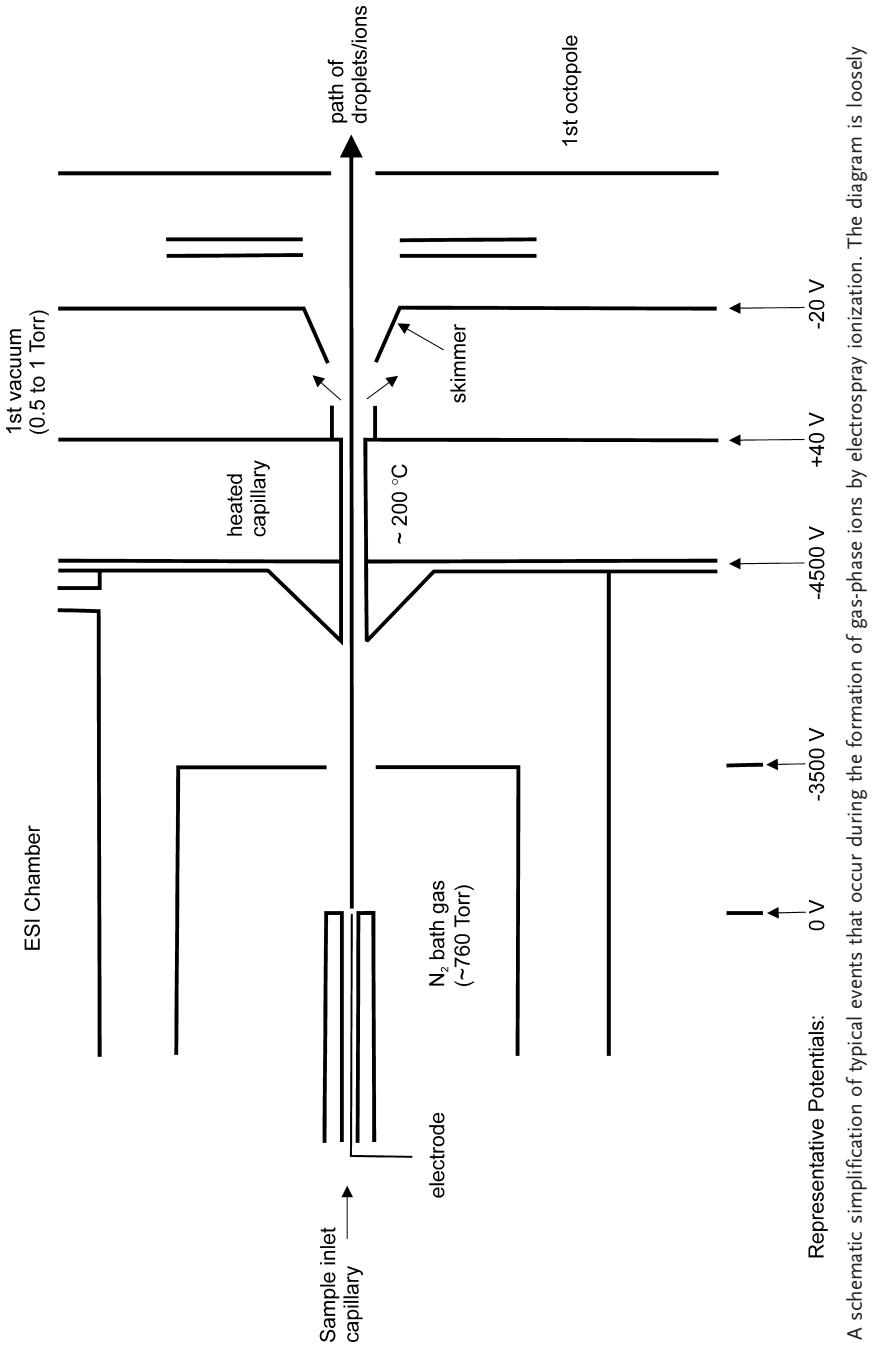

Fig. 13.1 A schematic simplification of typical events that occur during the formation of gas-phase ions by electrospray ionization. The diagram is loosely based upon those found elsewhere [1b, c, 12].

pumping chamber typically serves three functions. First, it completes desolvation of the ions. Second, it imparts translational kinetic energy to the ions via the skimmer potential before the ions pass into the next chamber (either an octopole or quadrupole). Third, collisions occur between the background gas in the chamber and the ions as they are accelerated towards the skimmer. The energy of these collisions is in part controlled by the magnitude of the skimmer potential. At higher voltages, the collisions with the remaining background gas can induce ligand dissociation from the parent organometallic ion. The skimmer potential is thereby used as an adjustable parameter to control the translational kinetic energy of the ions before they pass into the next chamber, and if desired, to control collision-induced dissociation (CID) of ligands from the parent organometallic ions before they leave the skimmer chamber.

A point of interest at this stop in our tour is that fragmentation of organometallic ions in ESI-MS often proceeds via ligand dissociation (e.g., phosphane loss) to generate coordinatively unsaturated organometallic ions [1–9]. One of the strengths of this technique is that such unsaturated ions are typically proposed as reactive intermediates in catalytic reactions carried out in solution (*vide infra*), allowing ESI-tandem-MS systems to study directly the gas-phase reactivity of such species.

For the published ESI-MS mechanistic hydrogenation studies, the ions pass through the skimmer into the first octopole [9]. The longitudinal kinetic energy of the ions entering the first octopole is determined in part by the skimmer potential. The octopole serves several functions. The first is as an ion guide in which any neutral molecules remaining in the ion stream are removed by vacuum. A radiofrequency is applied to the poles that functions, in effect, to contain the ions in the region near the radial center of the octopole without imparting significant kinetic energy upon them as they move longitudinally through the unit. The second function of the octopole is to act as a gas-phase reactor. The octopole is typically held at moderate temperatures (e.g., 70 °C) and it contains a neutral inert or reagent gas at pressures up to ~ 0.1 Torr. The organometallic ions interact with the neutral gas molecules as they move through the octopole via collisions and/or reactions. One experimental concern is to keep the energy distribution of the gas molecules as near as possible to thermal equilibrium inside the octopole. The process is called "thermalization", and it occurs via collisions between the ions that have been accelerated by the skimmer potential and the neutral gas present in the octopole. One incentive for establishing and maintaining thermal equilibrium among the ions in the octopoles is that the system then better represents ions in solution. Another incentive is that Maxwell-Boltzmann statistics can then be applied to model the distribution of vibrational, rotational, and kinetic energies among the molecules in the gas phase. Models have been developed that incorporate Maxwell–Boltzmann statistics as well as certain experimental parameters (e.g., temperature, pressure, and longitudinal velocity) [1 b, c]. These models provide information such as the number of collisions between an ion and the neutral gas molecules as it travels through the octopole, or information about the kinetic energies of the collisions, or in

some cases, bond dissociation energies can be obtained through CID studies. Reaction probabilities can be obtained by comparing product yields to the number of calculated collisions between an organometallic ion and the reagent gas in the octopole. Apart from thermalization, collisions between the ions and the background gas can induce either CID (at high skimmer potentials) or reactions with reagent gases such as hydrogen [1 b, c, 16].

The resulting mixture of organometallic ions leaves the octopole and is then separated on the basis of m/z using the first quadrupole, typically at 10^{-6} Torr. The quadrupole allows ions of only one m/z ratio to pass through. The separated organometallic ions are characterized as much as possible by subsequent CID and gas-phase reactivity studies, and by isotopic labeling (*vide infra*). After leaving the first quadrupole, the separated organometallic ions are then driven into a second octopole containing a neutral or reagent gas *via* another potential difference. The magnitude of this potential difference determines the kinetic energy of the organometallic ions entering the second octopole. The product ions leaving the second octopole (or gas-phase reactor) are analyzed with a second quadrupole and detector. The experimental strategy typically applied to mechanistic studies with ESI-MS is thereby to vary the operating parameters of the ESI, the first octopole, and quadrapole to generate an organometallic ion of interest. The ion of interest is fragmented or reacted with a reagent molecule in the second octopole, and the products characterized in the last quadrupole and detector. It is the gas-phase reactions of the organometallic ions in the octopoles that are used to model the solution chemistry of the reaction. A point of interest at this part of our tour is that one-pot catalyst mixtures have been screened with ESI-MS systems by separating out the ions using the first octopole-quadrupole and then studying their individual gas-phase reactivity in the second octopole [1 c, 4 c, 8].

13.3 Mechanistic Hydrogenation Studies

Although a number of reactions catalyzed by organometallic complexes have been studied using ESI-MS (*vide supra*), the number of reports detailing ESI-MS mechanistic studies of alkene hydrogenation is small [9]. The first was carried out by Chen et al. using cationic rhodium(I)-phosphine complexes as catalyst systems. A number of cationic Rh(I) precursors were sprayed, including $[Rh(P(CD_3)_3)_4(H)_2]^+$ (**1**), $[Rh(P(CH_3)_3)_3(nbd)]^+$ (**2**, nbd = norbornadiene), $[Rh(PPh_3)_2(nbd)]^+$ (**3**), [Rh((*S*, *S*)-chiraphos)(nbd)]$^+$ (**4**, (*S*, *S*)-chiraphos = (2*S*, 3*S*)-(–)-*bis*(diphenylphosphino)butane), and $[Rh((R)\text{-BINAP})(MeOH)_2]^+$ (**5**, BINAP = 2,2′-*bis*(diphenylphosphino)-1,1′-binaphthyl). As discussed in the previous section, the tube lens potential was adjusted to control successively the amount of desolvation to produce gas phase ions of the parent rhodium compound, or to induce ligand and/or hydrogen loss by CID. The mixture of ions leaving the first octopole were separated by the first quadrupole, and then studied by CID or reactions with reagent gases in the second octopole.

Spraying dichloromethane solutions of **1** and using N_2 gas in the first octopole allowed mass selection at the first quadrupole of either $[Rh(P(CD_3)_3)_4]^+$ (**6**), from loss of hydrogen from **1**; $[Rh(P(CD_3)_3)_3]^+$ (**7**), from subsequent loss of $P(CD_3)_3$; and $[Rh(P(CD_3)_3)_2]^+$ (**8**), from further loss of $P(CD_3)_3$ (Scheme 13.1). Compound **8** is a gas-phase mimic of catalyst species that have been observed in solution such as *trans*-$[Rh(PPh_3)_2(MeOH)_2]^+$ (**9**), that contain extremely labile solvento ligands, and that are proposed to be catalytic intermediates in hydrogenations of alkenes using cationic rhodium-$(PR_3)_2$ complexes as catalysts [17]. One immediate difference between **9** in methanol solvent, and **8** in the gas phase is the absence of coordinating solvent molecules, making **8** an extremely reactive, coordinatively-unsaturated species. This difference is not unique to this system and warrents further discussion here. Most fundamental steps of catalytic cycles such as oxidative additions, reductive eliminations, and insertions involve changes in the ligands coordinating and changes in coordination number, and are thereby influenced by solvent molecules that act as ligands. The empirical observation can be made that organometallic ions in the gas phase tend to relieve coordination unsaturation by intramolecular bonding or activation. For example, gas-phase reactivity, CID, and deuterium-labeling experiments indicate that the formally 12-electron species **8** exists in equilibrium with the mono- and di-C–D activated species **10** and **11** (Scheme 13.1).

As another example, studies of the catalytic activity of the gas-phase ions [Ru-Cl(alkylidene)(diphosphane)]$^+$ toward ring-opening olefin metathesis of norbornene show that an alkene group in the growing polymer chain reaches back to oc-

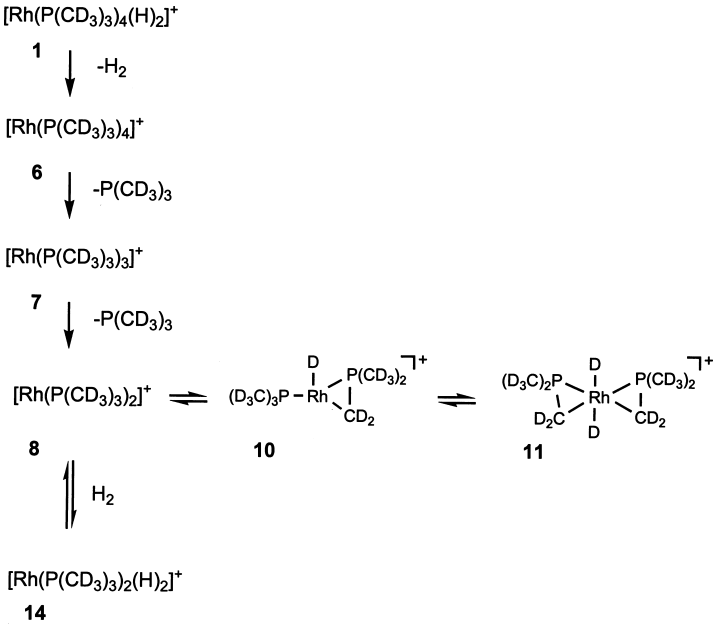

Scheme 13.1

cupy a vacant coordination site on ruthenium [4d]. In some cases, this tendency towards intramolecular bonding or activation has led to new discoveries that have borne true in the corresponding solution-phase chemistry. For example, an ESI-MS study of the gas-phase chemistry of the unsaturated, formally 16-electron cation $[(\eta^5\text{-}C_5Me_5)Ir(CH_3)(P(CH_3)_3)]^+$ (**12**) showed that it undergoes C–H activation down a P–CH_3 group, followed by elimination of methane to generate $[(\eta^5\text{-}C_5Me_5)Ir(CH_3)(\eta^2\text{-}CH_2P(CH_3)_2)]^+$ (**13**) [5]. Further study in the gas phase showed that **13** is substantially more active towards intermolecular C–H activation than **12**. Subsequent solution-phase chemistry by another group confirmed that $[(\eta^5\text{-}C_5Me_5)Ir(CH_3)(\eta^2\text{-}CH_2P(CH_3)_2)(OTf)]$ (**13′**, OTf = triflate, a weakly coordinating anion) is substantially more active towards intermolecular C–H activation in solution than is $[(C_5Me_5)Ir(CH_3)(P(CH_3)_3)(OTf)]$ (**12′**) [18].

Organometallic ions that undergo reversible intramolecular activation or bonding are more likely to provide gas-phase analogues to reactions of catalytic intermediates in solution containing labile solvento ligands. Returning to hydrogenation for an example, the mass-selected compound **8**, which likely exists as a mixture with **10** and **11**, reacts with H_2 gas in the second octopole to give the dihydride $[Rh(P(CD_3)_3)_2(H)_2]^+$ (**14**) (see Scheme 13.1). The reaction can be reversed without H–D exchange with the CD_3 groups, showing that it was **8**, not **10** or **11**, that reacted with the H_2 gas. The reversible activation of the methyl groups to form **10** and **11** thereby functions partially to relieve the coordination unsaturation of **8**, as do the methanol solvento ligands in solutions of **9**. In this sense, reaction of **8** with H_2 gas to generate the dihydride **14** provides a gas-phase analogue to the known oxidative addition of H_2 to **9** in methanol solution to generate *trans*-$[Rh(H)_2(PPh_3)_2(MeOH)_2]^+$ (**15**) [17b].

Intramolecular bonding or activation to alleviate coordination unsaturation in the gas phase does fail, at times, to mimic the behavior of labile solvento complexes in solution. For example, the gas-phase ion $[Rh(PPh_3)_2]^+$ (**16**), which is the solvent-free, direct analogue of **9**, failed to add H_2 or D_2 in the second octopole. The authors attributed this lack of analogous reactivity for **16** in the gas phase to the proposed formation of an intramolecular η^6-arene complex with one of the phosphines. The formation of such an 18-electron arene complex is presumably irreversible on the timescale that the ion resides in the second octopole. Consistent with this behavior, the gas-phase ions [Rh((*S*, *S*)-chiraphos)]$^+$ (**17**) and [Rh((*R*)-BINAP)]$^+$ (**18**) also failed to react with H_2 in the second octopole. Worthy of mention, however, is that the analogues of complexes **17** and **18** in methanol solution react reversibly, but only to a small extent with hydrogen to generate traces of $[Rh(diphosphane)(H)_2(MeOH)_2]^+$ [19]. One therefore cannot rule out, on the bases of the data in the literature, that the gas-phase ions **17** and **18** did not mimic the behavior of their solvento analogues in methanol solution. The authors also reported that **17** reacts, at very low collision energies, with methyl acrylate to generate the adduct [Rh((*S*, *S*)-chiraphos)(methyl acrylate)]$^+$ (**19**). Although the authors did not pursue this avenue further, formation of the adduct **19** does provide an analogue to the known reactions between $[Rh((S, S)\text{-chiraphos})(CH_3OH)_2]^+$ and $[Rh((R)\text{-BINAP})(MeOH)_2]^+$ and various

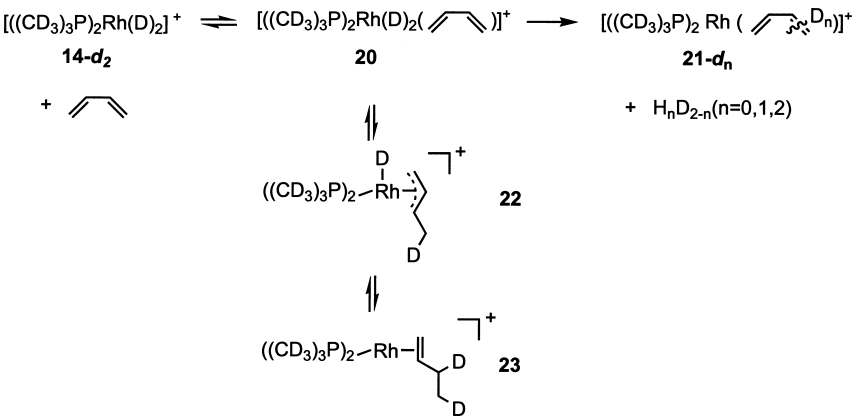

Scheme 13.2

unsaturated organic carbonyl compounds to form adducts similar to **19** in methanol solution [19].

Further studies using butadiene and isotopic labeling established the reaction pathway shown in Scheme 13.2. Complex **14**-d_2 was shown to react with butadiene to generate the observed diene adduct **20**. Compound **20** then reacted further to lose H_nD_{2-n} (n = 0, 1, 2) and generate the observed butadiene compound **21**-d_n (n = 0, 1, 2). The observation of H–D exchange between the deuterides and butadiene-hydrogen atoms in **20** is evidence for the reversible formation of the allyl-deuteride **22** and perhaps for the butene complex **23** (both not observed). This pathway thereby provides a gas-phase analogue for the following plausible sequence of steps in a catalytic alkene hydrogenation: oxidative addition of H_2, alkene coordination, and alkene-hydride insertion. In support of this sequence in the gas phase, reaction of $[Rh(P(CD_3)_3)_2]^+$ (**8**) with 1-butene leads to the butadiene-dihydride isotopomer of **20**, presumably via the protio isotopomers of **22** and **23**.

Noyori et al. recently used ESI-MS to characterize species present in catalytically active solutions during the hydrogenation of aryl-alkyl ketones using their base-free catalyst precursors *trans*-[Ru((*R*)-tol-BINAP)((*R*, *R*)-dpen)(H)(η^1-BH_4)] (tol-BINAP = 2,2′-bis(ditolylphosphino)-1,1′-binaphthyl; dpen = 1,2-diphenylethylenediamine) in 2-propanol [9b]. Based upon ESI-MS observations, deuterium-labeling studies, kinetics, NMR observations, and other results, the authors proposed that the cationic dihydrogen complex *trans*-[Ru((*R*)-tol-BINAP)((*R*, *R*)-dpen)(H)(η^2-H_2)]$^+$ is an intermediate in hydrogenations carried out in the absence of base.

The mechanism for hydrogenation of styrene using the iridium-phosphanyloxazoline compound [(PHOX)Ir(COD)]$^+$ (**24**, Scheme 13.3) as catalyst precursor has also been studied using ESI-MS [9c]. Catalytically active solutions were prepared by reacting the catalyst precursor and substrate dissolved in methylene chloride with hydrogen gas until all the cyclooctadiene-containing iridium species were consumed. To minimize loss of H_2 during spraying, the mixture was forced into the spray chamber using the pressure of hydrogen in the reactor (6 bar H_2). Three

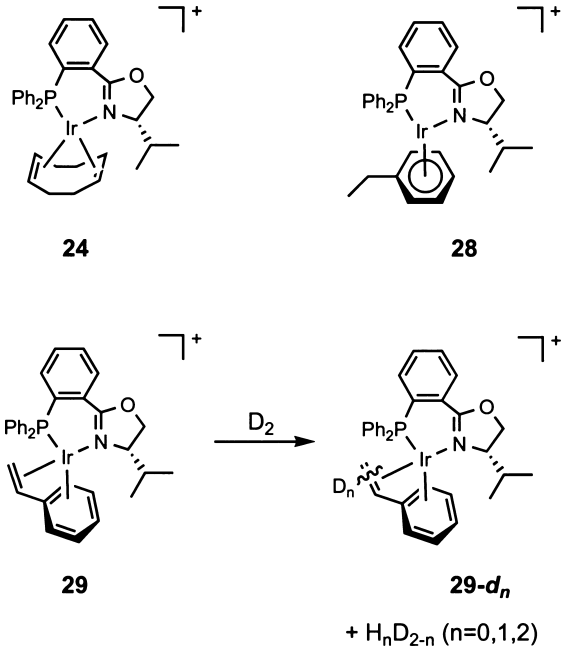

Scheme 13.3

species were observed at low tube potentials: one with a *m/z* ratio corresponding to the sum of $[(PHOX)Ir]^+$, styrene, and H_2 (**25**); the second with a *m/z* ratio corresponding to the sum of $[(PHOX)Ir]^+$, styrene, and $2 \times H_2$ (**26**); and the third with a *m/z* ratio corresponding to the sum of $[(PHOX)Ir]^+$ and styrene (**27**). Further, the gas-phase reaction of $[(PHOX)Ir(H)_2]^+$ and ethylbenzene formed a mixture from which a species $[(PHOX)Ir(ethylbenzene)]^+$ (**28**) was separated in the gas phase by its *m/z* ratio at the first quadrupole. Although precise structural determinations are not possible with MS data, the authors quite reasonably proposed that **28** is an 18-electron compound with ethylbenzene acting as η^6-arene ligand (Scheme 13.3). Based upon this proposal, it is possible that **25**, the species isolated from the active catalytic solution, and **28** are the same compound.

The ion **28** loses H_2 by CID with argon to form $[(PHOX)Ir(styrene)]^+$ (**29**). Compound **29** then undergoes H–D exchange with D_2 gas to form the mixture of isotopomers **29**, **29**-d_1, and **29**-d_2 (Scheme 13.3). When combined, these observations show that the oxidative addition of H_2 to **29** is followed by alkene hydride insertion, and that both these steps occur rapidly and reversibly in the gas phase. These results thereby provide gas-phase analogues for catalytic elementary steps that are proposed to occur in solution. Support for this proposed sequence of steps was obtained from a solution-phase catalytic deuteration of styrene. Analysis showed no deuterium incorporation in the unreacted styrene at various conversions, and clean formation of dideuterio ethylbenzene as sole product.

Based upon their data and upon results in the literature, the authors concluded that hydrogenations using **24** or related species as catalyst precursor proceed in solution by mechanisms involving iridium(I)/(III) formal oxidation states. During the course of their discussions, the authors made the interesting observation that the rate of gas-phase collisions between the thermalized iridium organometallic ions and D_2 under their experimental conditions in the octopole were similar to the rate of diffusion-controlled encounters between iridium species and D_2 in solution.

13.4 Conclusions

ESI represents a powerful method by which to transfer organometallic ions from catalytically active solutions into the gas phase. ESI-MS systems allow the characterization of the gas-phase ions using CID, reactivity, and isotope-labeling studies. The application of ESI-tandem-MS systems allows gas-phase preparations and isolation of desired organometallic ions in the first ESI-octopole-quadrupole, followed by characterization or reactivity studies in the second octopole-quadrupole.

ESI-MS study of gas-phase chemistry is a relative young area of interest in organometallic chemistry. ESI-MS mechanistic investigations have shown that organometallic reactions occurring as part of catalytic reactions in solution – including oxidative additions, insertions, metathesis, and eliminations – also occur in the gas phase. The extent to which such gas-phase analogues are relevant to reactions that occur in solution has not, to date, been addressed by a rigorous theoretical and experimental investigation. However, we end this tour by pointing out that a number of examples now exist where the gas-phase organometallic reactivity has been shown experimentally to be relevant to solution-phase catalytic reactions. In some cases, the gas-phase organometallic reactions have provided successful new leads to solution-phase studies. We predict that with careful gas-phase experimentation, combined with confirmation by experiments carried out in solution, ESI-MS studies will continue to discover and explore hydrogenation systems for which the gas-phase organometallic chemistry is relevant to the analogous reactions carried out in solution. Finally, there are a number of hydrogenations catalyzed by cationic catalyst systems that have not yet been studied using ESI-MS [20]. Further, hydrogenations using non-ionic catalyst systems can, in principle, be modified for ESI-MS studies by substituting neutral for ionic groups in the ancillary ligands. Recent advances in the use of ESI-tandem-MS systems to evaluate chiral catalysts for enantioselective allylations can perhaps also be modified for enantioselective catalytic hydrogenations [8].

Acknowledgments

The production of this chapter was supported by the University of Alberta. The authors are very grateful to Professor Paul Kebarle for many useful discussions, and for his kind patience.

Abbreviations

CID collision-induced dissociation
ESI electrospray ionization
MS mass spectrometry

References

1 Reviews: (a) R. Colton, A. D'Agostino, J.C. Traeger, *Mass Spectrom. Rev.* **1995**, *14*, 79; (b) D.A. Plattner, *Int. J. Mass. Spec.* **2001**, *207*, 125; (c) P. Chen, *Angew. Chem. Int. Ed.* **2003**, *42*, 2832.
2 (a) D. Feichtinger, D.A. Plattner, *Angew. Chem. Int. Ed.* **1997**, *36*, 1718; (b) D.A. Plattner, D. Feichtinger, J. El-Bahraoui, O. Wiest, *Int. J. Mass. Spec.* **2000**, *195/196*, 351; (c) D. Feichtinger, D.A. Plattner, *J. Chem. Soc., Perkin Trans. 2* **2000**, 1023; (d) D. Feichtinger, D.A. Plattner, *Chem. Eur. J.* **2001**, *7*, 591.
3 (a) D. Feichtinger, D.A. Plattner, P. Chen, *J. Am. Chem. Soc.* **1998**, *120*, 7125; (b) C. Hinderling, P. Chen, *Int. J. Mass. Spec.* **2000**, *195/196*, 377.
4 (a) C. Hinderling, C. Adlhart, P. Chen, *Angew. Chem. Int. Ed.* **1998**, *37*, 2685; (b) C. Adlhart, C. Hinderling, H. Baumann, P. Chen, *J. Am. Chem. Soc.* **2000**, *122*, 8204; (c) C. Adlhart, P. Chen, *Helv. Chim. Acta* **2000**, *83*, 2192; (d) M.A.O. Volland, C. Adlhart, C.A. Kiener, P. Chen, P. Hofmann, *Chem. Eur. J.* **2001**, *7*, 4621.
5 (a) C. Hinderling, D. A. Plattner, P. Chen, *Angew. Chem. Int. Ed.* **1997**, *36*, 243; (b) C. Hinderling, D. Feichtinger, D. A. Plattner, P. Chen, *J. Am. Chem. Soc.* **1997**, *119*, 10793.
6 O. Aliprantis, J.W. Canary, *J. Am. Chem. Soc.* **1994**, *116*, 6985.
7 S.R. Wilson, Y. Wu, *Organometallics* **1993**, *12*, 1478.
8 C. Markert, A. Pfaltz, *Angew. Chem. Int. Ed.* **2004**, *43*, 2498.
9 (a) Y.-M. Kim, P. Chen, *Int. J. Mass. Spec.* **1998**, *185/186/187*, 871; (b) C.A. Sandoval, T. Ohkuma, K. Muniz, R. Noyori, *J. Am. Chem. Soc.* **2003**, *125*, 13490; (c) R. Dietiker, P. Chen, *Angew. Chem. Int. Ed.* **2004**, *43*, 5513.
10 Examples: (a) J.R. Morandi, H.B. Jensen, *J. Org. Chem.* **1969**, *34*, 1889; (b) M. Castiglioni, R. Giordano, E. Sappa, *J. Organomet. Chem.* **1995**, *491*, 111; (c) X.-Y. Wang, Z.-Y. Hou, W.-M. Lu, F. Chen, X.-M. Zheng, *J. Chromatogr. A* **1999**, *855*, 341.
11 For example, see: (a) W.E. Farneth, J.I. Brauman, *J. Am. Chem. Soc.* **1976**, *98*, 7891; (b) T.B. McMahon, T. Heinis, G. Nicol, J.K. Hovey, P. Kebarle, *J. Am. Chem. Soc.* **1988**, *110*, 7591.
12 R.B. Jordan, *Reaction Mechanisms of Inorganic and Organometallic Systems*, 2nd edn. Oxford University Press, New York, **1998**.
13 See [1b,c] and references cited therein for discussions of these factors.
14 (a) M. Yamashita, J.B. Fenn, *J. Phys. Chem.* **1984**, *88*, 4451; (b) C.M. Whitehouse, R.N. Dreyer, M. Yamashita, J.B. Fenn, *Anal. Chem.* **1985**, *57*, 675.
15 The first example, V. Katta, S.K. Chowdhury, B.T. Chait, *J. Am. Chem. Soc.* **1990**, *112*, 5348.
16 Y.-M. Kim, P. Chen, *Int. J. Mass. Spec.* **2000**, *202*, 1.

17 (a) R.R. Schrock, J.A. Osborn, *J. Am. Chem. Soc.* **1976**, *98*, 2134; (b) J. Halpern, D.P. Riley, A.S.C. Chan, J.J. Pluth, *J. Am. Chem. Soc.* **1977**, *99*, 8055; (c) J.M. Brown, P.A. Chaloner, P.N. Nicholson, *J. Chem. Soc., Chem. Comm.* **1978**, 646.

18 H.F. Luecke, R.G. Bergman, *J. Am. Chem. Soc.* **1997**, *119*, 11538.

19 For examples, see: (a) J.M. Brown, P.A. Chaloner, *J. Chem. Soc., Chem. Commun.* **1978**, 321; (b) A.S.C. Chan, J. Halpern, *J. Am. Chem. Soc.* **1980**, *102*, 838; (c) A.S.C. Chan, J.J. Pluth, J. Halpern, *J. Am. Chem. Soc.* **1980**, *102*, 5952; J. Halpern, *Science* **1982**, *217*, 401; (d) A. Miyashita, H. Takaya, T. Souchi, R. Noyori, *Tetrahedron* **1984**, *40*, 1245; reference [15b]; and references cited therein.

20 For examples, see: (a) J.A. Wiles, S.H. Bergens, *Organometallics* **1999**, *18*, 3709; (b) D.A. Dobbs, K.P.M. Vanhessche, E. Brazi, V. Rautenstrauch, J.-V. Lenoir, J.-P. Genêt, J. Wiles, S.H. Bergens, *Angew. Chem. Int. Ed.* **2000**, *39*, 1992.

Part III
Homogeneous Hydrogenation by Functional Groups

The Handbook of Homogeneous Hydrogenation.
Edited by J.G. de Vries and C.J. Elsevier
Copyright © 2007 WILEY-VCH Verlag GmbH & Co. KGaA, Weinheim
ISBN: 978-3-527-31161-3

14
Homogeneous Hydrogenation of Alkynes and Dienes

Alexander M. Kluwer and Cornelis J. Elsevier

14.1
Stereoselective Homogeneous Hydrogenation of Alkynes to Alkenes

14.1.1
Introduction

The reduction of carbon-carbon double and triple bonds is a very important transformation in synthetic organic chemistry. In this context, the conversion of alkynes into alkenes (i.e., semihydrogenation) is particularly useful, especially the stereoselective addition of one molar equivalent of hydrogen to the triple bond. This allows for the selective preparation of the corresponding (*E*)- or (*Z*)-alkenes depending on the choice of reaction conditions during the reduction. The classical catalytic hydrogenation using a heterogeneous transition-metal catalyst and molecular hydrogen constitutes the most general method for the selective reduction of carbon-carbon triple bonds. However, other pathways involving for instance organoaluminum and organoboron intermediates or hydride-transfer reagents in combination with metal salts have also been successfully applied [1, 2].

The most widely used catalytic procedures for the catalytic hydrogenation of alkynes to afford (*Z*)-alkenes generally employ palladium or nickel as the catalytically active transition metal. The Lindlar catalyst (lead-poisoned Pd on $CaCO_3$) and the P2-Ni catalyst are among the most prominent members of this group [1–3]. These systems show considerable selectivity for a variety of alkynes; however, substrates with triple bonds conjugated to other unsaturated moieties or electron-poor alkynes display low selectivity due to overreduction or other side reactions [1]. The complex nature of the surface of the Lindlar catalyst, containing different domains each of which contributes to the product distribution, makes the outcome of the stereoselective hydrogenation unpredictable. Thus, the yields and selectivity will generally vary, even for identical compounds under identical conditions [2, 4].

A large number of homogeneous transition-metal complexes have been reported as catalysts for the stereoselective hydrogenation of alkynes, although the

The Handbook of Homogeneous Hydrogenation.
Edited by J.G. de Vries and C.J. Elsevier
Copyright © 2007 WILEY-VCH Verlag GmbH & Co. KGaA, Weinheim
ISBN: 978-3-527-31161-3

details of this apparently simple reaction remain mostly obscure. Only a few homogeneous catalysts have been investigated in more detail, and some of these show a remarkable selectivity towards a variety of alkynes containing various functional groups. The origin of the stereoselectivity of these catalysts in the semihydrogenation of alkynes can often be ascribed to kinetic factors and sometimes to the lack of interaction of the catalyst with the product alkene, which is consequently not further reduced. The exhaustive reduction of alkynes to alkanes, which can in synthetic terms be useful, is very similar to alkene hydrogenation and will, therefore, not be treated here. This chapter will mainly focus on the homogeneous catalytic semihydrogenation of alkynes using molecular hydrogen. Supported catalysts and cluster-catalyzed hydrogenations will not be treated here. The performance of the catalysts has been the major criterion for selecting the homogeneous catalytic systems discussed in this chapter. Special attention will be given to the mechanistic details of selected systems.

14.1.2
Chromium Catalysts

One of the most selective semihydrogenation catalysts reported concerns a class of chromium tricarbonyl compounds with the generic formula $[Cr(CO)_3(arene)]$ (**1**) [5]. This catalyst is able to hydrogenate a wide variety of polyunsaturated compounds, and has been successfully applied in, for example, the 1,4-hydrogenation of conjugated dienes and α,β-unsaturated carbonyl compounds [6]. The outstanding performance of this catalyst in alkyne hydrogenation has been attributed to its complete inactivity towards compounds containing isolated carbon-carbon double bonds (i.e., neither isomerization nor over-reduction is observed). The (*Z*)-alkene is the sole product, which is isolated in very high yields (87–100%; see Table 14.1). Generally, the hydrogenation only proceeds under rather forcing reaction conditions, although, less strongly coordinated arenes (e.g., naphthalene or methyl benzoate) allow for milder conditions while maintaining the high stereoselectivity (see Table 14.1). Details about the reaction mechanism have not been revealed, but the similarity with the $[Cr(CO)_3]$-catalyzed 1,4-hydrogenation of conjugated dienes suggests that $[Cr(CO)_3(S)_3]$ (S = solvent) species is the catalytically active complex.

The applicability of the $[Cr(CO)_3(arene)]$ 1,2-*syn*-hydrogenation has been demonstrated in the syntheses of pheromones where the hydrogenation of the alkyne to the (*Z*)-isomer is a key step in the synthetic scheme [5, 7]. For such compounds, obtaining the correct the stereo- and regio-isomer is essential for its biological activity. In these cases, selectivities up to 100% have been reported. Special attention has been given to conjugated alkyne-diene systems of which the stereo- and regio-chemical outcome can be precisely predicted based on the specific chemistry of the $[Cr(CO)_3(arene)]$ catalyst towards alkynes and conjugated dienes.

Table 14.1 Hydrogenation of alkynes using $[Cr(CO)_3(arene)]$ (**1**) [5].

Entry	Alkyne	Catalyst	Time [h]	H_2 pressure [bar]	(*Z*) alkene [%] [c)]
1	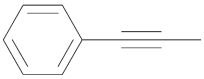	$[Cr(CO)_3(mbz)]$ [a)]	23	69	92
2	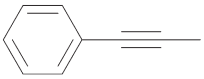	$[Cr(CO)_3(nap)]$ [b)]	24	20	92
3	C_6H_{13}—≡—C_6H_{13}	$[Cr(CO)_3(nap)]$ [b)]	15	69	100
4	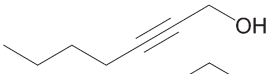	$[Cr(CO)_3(mbz)]$ [a)]	8	69	95
5	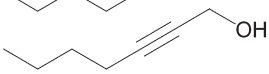	$[Cr(CO)_3(nap)]$ [b)]	8	49	87

a) $[Cr(CO)_3(mbz)] = [Cr(CO)_3(\text{methyl benzoate})]$ (**1a**). Reaction conditions: solvent acetone, reaction temp. 120 °C, substrate : catalyst ratio = 5 : 1.
b) $[Cr(CO)_3(nap)] = [Cr(CO)_3(\text{naphthalene})]$ (**1b**). Reaction conditions: solvent THF, reaction temp. 45 °C, substrate : catalyst ratio = 5 : 1.
c) Determined by GC analysis relative to internal standard.

14.1.3
Iron Catalysts

Terminal alkynes are selectively hydrogenated to alkenes by the iron(II) catalyst precursors $[(PP_3)FeH(N_2)]BPh_4$ (**2**) and $[(PP_3)FeH(H_2)]BPh_4$ (**3**) ($PP_3 = P(CH_2CH_2PPh_2)_3$) in tetrahydrofuran (THF) under mild conditions (1 bar H_2) [8]. The hydrogenation rates when using complexes **2** and **3** were found to be low at ambient temperature, but increased with increasing reaction temperature. The turnover frequency (TOF) ranges from 8 to 20 mol mol^{-1} h^{-1} at 66 °C for various substrates. Under these conditions, alkynes are converted chemoselectively into alkenes, regardless of the reaction temperature. The only exception is ethynyltrimethylsilane $HC{\equiv}CSiMe_3$, which mainly produces the dimeric product 1,4-bis(trimethylsilyl)butadiene by a reductive coupling reaction [9]. A thorough kinetic study of the hydrogenation of phenyl acetylene employing **2** has provided more insight into the mechanistic details of this reaction.

The mechanism is dominated by the remarkable stability of the $Fe(\eta^2\text{-}H_2)$ bond, which is one of the most stable $\eta^2\text{-}H_2$ complexes reported in the literature [8, 10]. Remarkably, the free coordination site for the incoming alkyne is provided by the reversible dissociation of one of the phosphine moieties of the PP_3 ligand rather than dissociation of the dihydrogen ligand (see Scheme 14.1). The coordinated alkyne subsequently inserts into the Fe–H bond and the emerging Fe–vinyl bond is

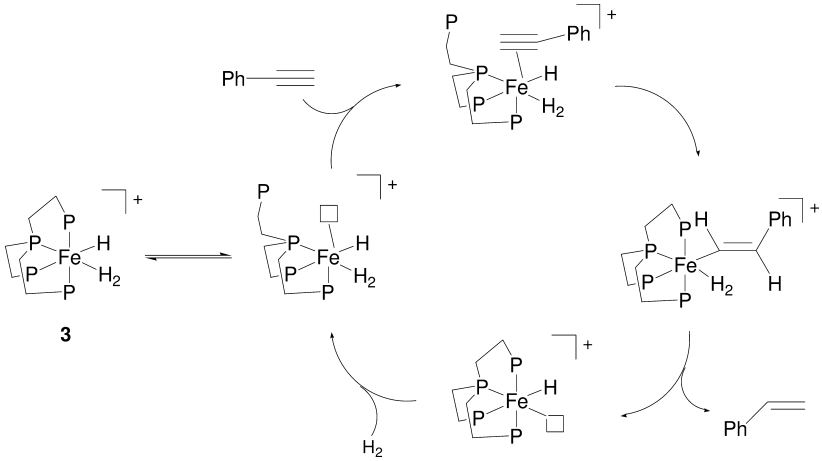

Scheme 14.1 Proposed mechanism for the hydrogenation of phenyl acetylene catalyzed by $[(PP_3)FeH(H_2)]^+BPh_4^-$ (**3**); the anion is BPh_4^- throughout in this scheme.

then cleaved *via* an intramolecular protonolysis (i.e., heterolytic splitting of the dihydrogen molecule occurs). The binding of the alkyne to the metal center appears to be the rate-determining step as it is supported by the zero-order in dihydrogen gas and a first-order in phenyl acetylene. The activation parameters for this reaction are $\Delta H^{\ddagger} = 11 \pm 1$ kJ mol^{-1}, $\Delta S^{\ddagger} = -27 \pm 3$ J K^{-1}, and $\Delta G^{\ddagger} = 19 \pm 4$ kJ mol^{-1}.

The cationic complex $[FeH(\eta^2\text{-}H_2)(PP_3)]^+$ (**3**; $PP_3 = P(CH_2CH_2PPh_2)_3$) displays an identical octahedral structure as the comparable ruthenium complex $[RuH(\eta^2\text{-}H_2)(PP_3)]^+$ (**4**; $PP_3 = P(CH_2CH_2PPh_2)_3$) [11]. Both complexes have been found to be selective catalysts for the hydrogenation of alkynes. Despite their structural similarities, the chemistry of compounds **3** and **4** in the semihydrogenation of alkynes is dominated by the difference in metal–dihydrogen bond strength, which decreases in the order Fe > Ru and has been attributed to a stronger back-donation from iron into the antibonding $\sigma^*(H_2)$ orbital compared to ruthenium [12].

14.1.4
Ruthenium Catalysts

Numerous compounds containing ruthenium are found to be active catalysts for the semihydrogenation of alkynes. Much attention has been devoted to the class of ruthenium carbonyl clusters, and it has been demonstrated that both internal and terminal alkynes can be effectively hydrogenated using such compounds, affording the corresponding alkenes [13]. However, the activities of these catalysts are generally lower than those of the mononuclear complexes and their stereoselectivity is also significantly lower due to extensive isomerization of the (primary) reaction products.

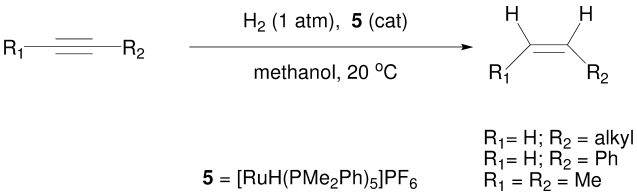

Scheme 14.2 Hydrogenation of terminal and internal alkynes by $[RuH(PMe_2Ph)_5]PF_6$ (**5**) [14].

Mononuclear ruthenium complexes, particularly ruthenium–phosphine complexes, are among the best-characterized catalytic systems. A particular active catalyst for this reaction is based on the sterically crowded complex $[RuH(PMe_2Ph)_5]PF_6$ (**5**) which, in the presence of 25 equiv. PMe_2Ph in methanol, has been shown to be an extremely active catalyst system for the selective hydrogenation of alkynes to alkenes [14] (Scheme 14.2). The rates of hydrogenation were limited by mass transfer processes in this case – that is, by diffusion of hydrogen into the solution. Thus, under these conditions, the TOF reported amounts to 130 mol mol^{-1} h^{-1}. The reaction proceeds affording the corresponding (*Z*)-alkenes without subsequent isomerization or further hydrogenation of the products. In addition, at high phosphine concentrations, the catalyst is completely inactive in the hydrogenation of alkenes to alkanes. In order to prevent catalyst deactivation, a large excess of PMe_2Ph is needed and the reaction temperature should be kept below 20 °C.

A related cationic ruthenium catalyst precursor, $[RuH(cod)(PMe_2Ph)_3]PF_6$ (**6**; cod = cyclooctadiene), was studied in the semihydrogenation of alkynes, and the results demonstrate a distinctly different catalyst behavior and chemoselectivity compared to $[RuH(PMe_2Ph)_5]PF_6$ (**5**) [15]. Under 1 bar H_2, **6** reacts to produce a complex, regarded as $[RuH(PMe_2Ph)_3(solvent)_2]^+$, which is a very active hydrogenation catalyst for alkynes as well as alkenes. The catalyst reveals an unusual order of reactivity – that is, the rate of hydrogenation to *cis*-alkenes increased in the order 1-hexyne < 2-hexyne < 3-hexyne, which has been attributed to the lower tendency of 3-hexyne to form the alleged catalytically inactive ruthenium-bis(alkyne) complexes. The activity of the catalyst for alkene hydrogenation could be significantly suppressed by the addition of 1 equiv. PMe_2Ph, and **6** becomes completely inactive towards alkenes by the addition of 2 equiv. PMe_2Ph. This addition will effectively lead to the more saturated, less-active ruthenium complex ions $[RuH(PMe_2Ph)_4]^+$ (**8**) and $[RuH(PMe_2Ph)_5]^+$ (**5**), respectively.

The two ruthenium complexes $[RuH(PMe_2Ph)_5]PF_6$ (**5**) and $[RuH(cod)PMe_2Ph)_3]PF_6$ (**6**) are considered to be related by Scheme 14.3. Since the cationic catalyst precursors **5** and **6** are both 18-electron species, hydrogenation of cyclooctadiene in **6** and phosphine dissociation from **5** will produce the catalytically active intermediate ions $[RuHL_4]^+$ (**8**) and $[RuHL_3]^+$ (**7**) (L = PMe_2Ph), respectively. It has thus been proposed that **7** is active for the hydrogenation of alkenes as well as alkynes, whereas **8** only hydrogenates alkynes. This scheme

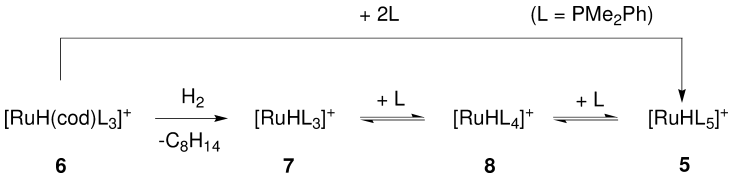

Scheme 14.3 Proposed relationship between different ruthenium–phosphine complexes. The anion has been omitted and is PF_6^+ throughout.

can be further extended to include the ruthenium complex $[Ru(H)(H_2)(PMe_2Ph)_4]^+$ (not shown in Scheme 14.3), which is formed by a reaction of **8** with hydrogen [16]. In the absence of additional phosphine, **8** shows rapid deactivation in the hydrogenation of 1-alkynes and in the isomerization of internal alkenes. However, under similar phosphine-deficient conditions, $[RuH(PMe_2Ph)_5]PF_6$ (**5**) remains active as a hydrogenation catalyst, but it displays a lower rate and a higher selectivity towards (*Z*)-alkenes.

The related cationic complex $[RuH(\eta^2\text{-}H_2)(PP_3)]^+$ (**4**; $PP_3 = P(CH_2CH_2PPh_2)_3$) is a non-classical trihydride complex where the metal is coordinated by the four phosphorus atoms, by a dihydrogen ligand, and a terminal hydride ligand. Although this complex is generally less active than, for instance, $[RuH(PMe_2Ph)_5]^+$ (**5**), it has a better defined chemistry [11]. The kinetic study of the selective hydrogenation of phenyl acetylene employing **4** reveals a first-order dependence on the catalyst concentration and second-order in hydrogen. The order in substrate changes from apparently first-order to zero-order with increasing substrate concentration. This catalytic behavior has been attributed to the formation of $[Ru(\eta^3\text{-1,4-diphenylbutenynyl})(PP_3)]$ (**9**) complexes by coupling of two substrate molecules. Complex **9** was found to be equally active in the hydrogenation of phenyl acetylene as compared to complex **4** (Scheme 14.4).

The proposed reaction mechanism follows a sequence of reaction steps usually adopted for a monohydride-metal hydrogenation catalyst, although other, more complex ruthenium intermediates contribute to the overall hydrogenation [11, 16]. Here, the η^2-coordinated dihydrogen serves merely as a stabilizing ligand and the formally unsaturated species $[RuH(PP_3)]^+$ (**10**) is the actual, reactive intermediate. Possibly, such a species must be thought of as labile, transient solvento species. Coordination of phenyl acetylene, insertion into the Ru–H bond followed by reaction of dihydrogen will eventually generate styrene and the ruthenium-monohydride species.

A particularly interesting hydrogenation catalyst for the semihydrogenation of alkynes concerns the ruthenium complex $[Cp^*Ru(\eta^4\text{-}CH_3CH{=}CHCH{=}CHCO_2H)][CF_3SO_3]$ (**11**) [17]. This ruthenium complex represents one of the few homogeneous catalysts that allow for the direct *trans*-hydrogenation of internal alkynes, yielding the (*E*)-alkene stereoselectively. Generally, internal alkynes can be transformed selectively into *E*-alkenes using different homogeneous and heterogeneous methods (e.g., dissolving metal reduction). However, under these

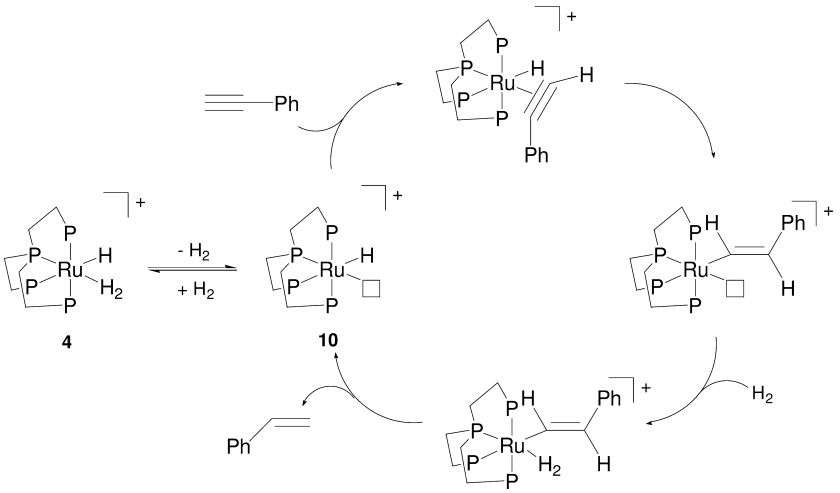

Scheme 14.4 Proposed mechanism for the hydrogenation of phenyl acetylene catalyzed by $[RuH(\eta^2\text{-}H_2)(PP_3)]^+$ (**4**) [11].

reaction conditions other functional groups will be affected and, hence, low chemoselectivities are obtained in these cases.

The $[Cp^*Ru]^+$-catalyzed semihydrogenation of alkynes has been studied in more detail using PHIP-NMR (PHIP = *Para*-Hydrogen Induced Polarization; see Chapter 12). With this method the initially formed hydrogenation products can be identified and characterized, even at very low concentrations and low conversions. Different types of alkynes were probed, and it was found that the reaction is not influenced greatly by the functional groups present in the substrate. However, internal alkynes readily produced polarized signals in the hydrogenation product (i.e., the *E*-isomer), even at low temperature. This finding indicates that the hydrogen is transferred in a *pair-wise* manner and it confirms that the *E*-isomer emerges as the primary reaction product. No polarized signals were detected for terminal alkynes, which has been ascribed to an allegedly inactive vinylidene complex that has been formed *via* a 1,2-hydrogen shift [17].

The remarkable stereoselectivity of this catalyst – that is, the *trans*-addition of the two hydrogen atoms – has been explained by the involvement of a dimeric ruthenium complex. In the proposed reaction mechanism (Scheme 14.5) the intermediates are assumed to be alkyne-bridged dinuclear ruthenium complexes (**13**, **14** and **15**). It has been suggested that the hydrogenation should be fast and without total separation of the two *para*hydrogen atoms – that is, without loss of the spin correlation between the two hydrogen atoms. Only under these conditions can *para*-hydrogen polarized signals be observed. The observation of these polarized signals reveals that the hydrogen atoms transferred to the alkyne stem from the same hydrogen molecule and supports the mechanism depicted in Scheme 14.5.

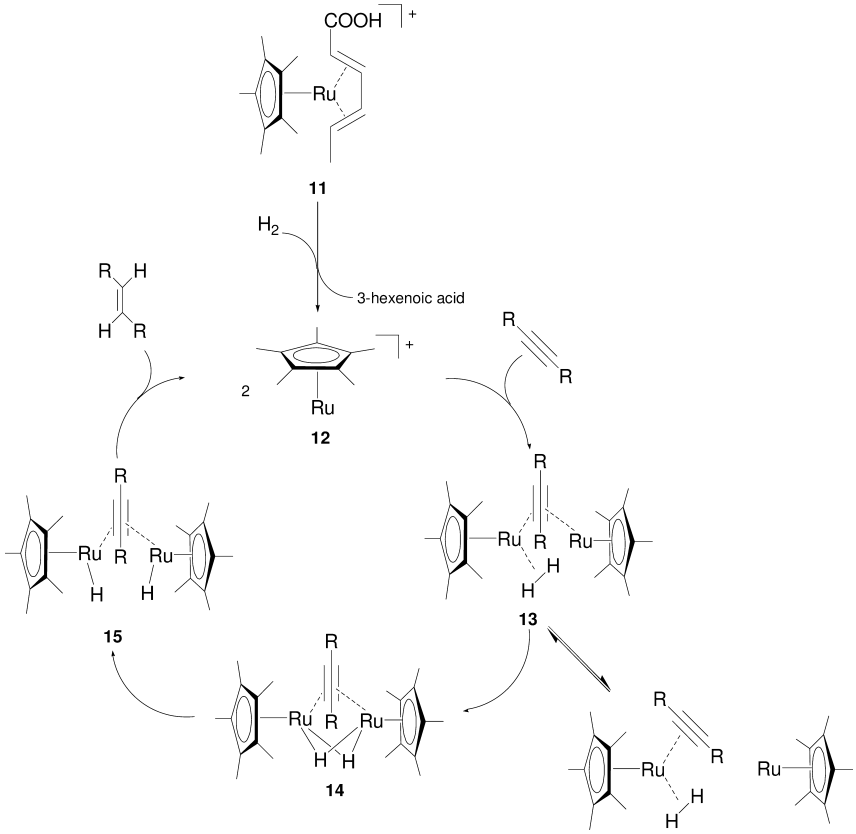

Scheme 14.5 Stereoselective hydrogenation of internal alkynes by complex [$Cp^*Ru(\eta^4$-$CH_3CH{=}CHCH{=}CHCOOH)$][CF_3SO_3] (**11**); the anion is CF_3SO3^- throughout [17].

14.1.5
Osmium Catalysts

An interesting example of the alkyne hydrogenation by homogeneous transition-metal catalysts is provided by the complexes [$OsH(Cl)(CO)(PR_3)_2$] (**16**; $PR_3 = PMeBu^t_2$, PPr^i_3), which catalyze the hydrogenation of phenyl acetylene at 1 bar H_2 in 2-propanol solution at 60 °C [18]. These complexes react rapidly with phenyl acetylene to produce the respective stable 16-electron alkenyl-osmium compounds [$Os((E)$-$CH{=}CHPh)Cl(CO)(PR_3)_2$] (**17**) almost quantitatively. Subsequent reaction with dihydrogen produces styrene, ethylbenzene and the dihydrogen complex [$OsH(Cl)(\eta^2$-$H_2)(CO)(PR_3)_2$] (**18**). These reactions constitute a catalytic cycle for the reduction of alkynes affording the corresponding alkenes with selectivities close to 100%.

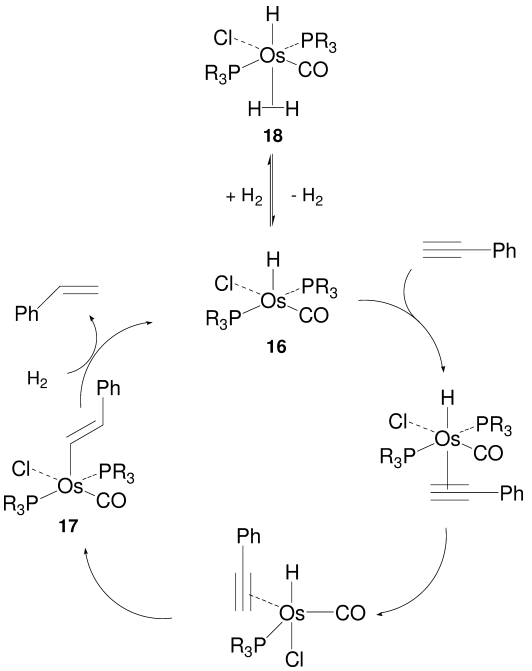

Scheme 14.6 Proposed mechanism for the hydrogenation of phenyl acetylene catalyzed by $[OsHCl(CO)(PR_3)_2]$ (**16**).

The kinetic investigation of this reaction reveals the reaction is first-order in substrate, catalyst and hydrogen concentration, and thus yields the rate law: $r = k_{cat}[Os][alkyne][H_2]$. The proposed mechanism as given in Scheme 14.6 is based on the rate law and the coordination chemistry observed with these osmium complexes.

In the absence of phenyl acetylene, these Os-complexes catalyze the hydrogenation of styrene to ethyl benzene at rates about ten-fold faster than those observed for the C≡C bond reduction. The authors concluded that the styrene hydrogenation is kinetically favored, so the observed selectivity must originate from a thermodynamic difference. This difference is established by the formation of the very stable vinyl-osmium intermediates, which forms a thermodynamic sink that causes all the osmium present to be tied up in this form; consequently the kinetically unfavorable pathway becomes essentially the only one available in the presence of alkyne. Furthermore, it has been shown that the hydrogenation of phenyl acetylene to styrene by $[OsHCl(CO)(PPr^i_3)_2]$ can also be performed under hydrogen-transfer conditions using 2-propanol as the hydrogen donor [19, 20].

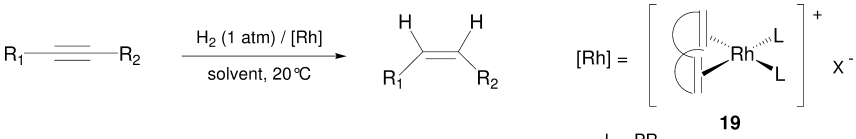

R_1	R_2	Selectivity
Ph	H	>95%
Ph	COOEt	95%
CH_3	C_3H_7	99%
$Me_2C(OH)$	CH_3	n.d.

Scheme 14.7 Hydrogenation of various alkynes using complex $[Rh(nbd)L_n]^+X^-$ (**19**) [21].

14.1.6
Rhodium Catalysts

The Schrock/Osborn cationic Rh-catalyst with the general formula $[Rh(nbd)L_n]^+X^-$ (**19**; wherein nbd is norbornadiene, L is a phosphine ligand and X^- is a – weakly coordinating – anion) is counted among the most successful and most widely applied catalysts for the semihydrogenation of alkynes [21]. The reaction proceeds well in coordinating solvents (such as acetone, ethanol, or 2-methoxyethanol), and under these conditions internal alkynes are reduced efficiently affording the corresponding (*Z*)-alkene in yields as high as 99% (see Scheme 14.7). This catalyst system is a moderately active hydrogenation catalyst with TOF (determined at 50% conversion) ranging between 20 and 80 mol mol^{-1} h^{-1} [21–23]. However, the reduction of terminal alkynes by these systems is less successful since the fairly acidic character of the alkyne destroys the active species (such as $[RhH(L_n)S_y]$) by formation of an alkynyl-rhodium derivative [21].

The mechanism of the semihydrogenation of alkynes in coordinating solvents is assumed to be analogous to the alkene hydrogenation – that is, a catalytic scheme consisting of a mono-hydride route (*via* $RhH(L)_n(solvent)_y$) and a dihydride route (*via* $Rh(H)_2(L)_n(solvent)_y$) (see Scheme 14.8) [21, 24]. The active rhodium(solvento) species are formed by a reaction of **19** with molecular hydrogen. Generally, the cationic rhodium mono-hydride $RhH(L)_n(solvent)_y$ is an extremely active isomerization and hydrogenation catalyst, whereas the rhodium dihydride $[Rh(H)_2(L)_n(solvent)_y]^+$ is a less active hydrogenation catalyst but displays very little isomerization activity [21]. Under catalytic conditions, the mono-hydride and the dihydrido-rhodium(solvento) species are in equilibrium; the amount of each species – and thus the contribution of each route to the product formation – can be shifted by the addition of acid or base. Therefore, performing the semihydrogenation under acidic conditions will generate a highly selective hydrogenation system for the reduction of alkynes to (*Z*)-alkenes. Another method of generating related rhodium species involves protonation of the acetate of a neutral Rh(I) or Rh(II) complex in the presence of a phosphine ligand (such as $[Rh(OAc)(PPh_3)_3]$ or $[Rh_2(OAc)_4/PR_3]$) [20, 25]. Catalytic hydrogenation systems prepared by this method behave in many respects similarly to the systems based on $[Rh(diene)L_2]^+A^-$.

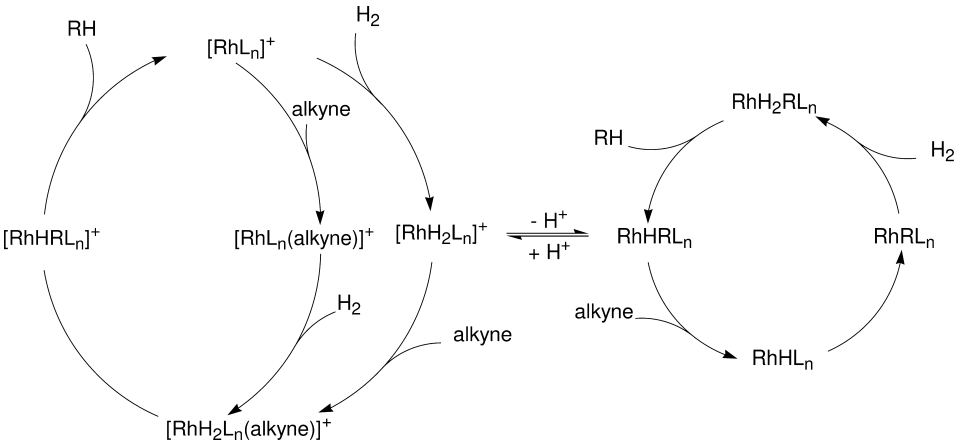

Scheme 14.8 General hydrogenation mechanism catalyzed by cationic $[Rh(nbd)L_n]^+$ species (**19**) [21].

Recovery of the precious Rh-catalyst has been successfully developed by using various strategies. One of the approaches concerns the use of highly fluorous Rh-catalysts for selective hydrogenation of terminal and internal alkynes under fluorous biphasic conditions yielding catalyst retentions of >99.92% (for FC-75/hexanes, 1:3 v/v) [23]. Furthermore, the immobilization of the rhodium catalyst on a solid support has been reported as a feasible approach, which shows only little leaching of the rhodium, while maintaining a high selectivity and activity [26].

In less-coordinating solvents such as dichloromethane or benzene, most of the cationic rhodium catalysts $[Rh(nbd)(PR_3)_n]^+A^-$ (**19**) are less effective as alkyne hydrogenation catalysts [21, 27]. However, in such solvents, a few related cationic and neutral rhodium complexes can efficiently hydrogenate 1-alkynes to the corresponding alkene [27–29]. A kinetic study revealed that a different mechanism operates in dichloromethane, since the rate law for the hydrogenation of phenyl acetylene by $[Rh(nbd)(PPh_3)_2]^+BF_4^-$ is given by: $r = k[\text{catalyst}][\text{alkyne}][pH_2]^2$ [29].

$$[Rh(nbd)(PPh_3)_2]BF_4 + H_2 \rightleftharpoons [RhH_2(nbd)(PPh_3)_2]BF_4 \tag{1}$$

$$[RhH_2(nbd)(PPh_3)_2]BF_4 \rightleftharpoons [RhH_2(nbd)(PPh_3)]BF_4 + PPh_3 \tag{2}$$

$$[RhH_2(nbd)(PPh_3)]BF_4 + PhC{\equiv}CH \rightleftharpoons [RhH(CH = CHPh)(nbd)(PPh_3)]BF_4 \tag{3}$$

$$[RhH(CH{=}CHPh)(nbd)(PPh_3)]BF_4 + H_2 \rightarrow [RhH_2(nbd)(PPh_3)]BF_4 + CH_2{=}CHPh \tag{4}$$

$$[RhH_2(nbd)(PPh_3)]BF_4 + PPh_3 \rightarrow [RhH_2(nbd)(PPh_3)_2]BF_4 \tag{5}$$

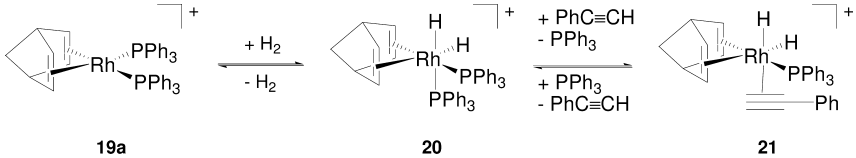

Scheme 14.9 Reaction of $[Rh(nbd)(PPh_3)_2]^+BF_4^-$ (**19**) with H_2 to give *cis,cis*-$[RhH_2(nbd)(PPh_3)_2]^+BF_4^-$ (**20**) and the subsequent formation of $[RhH_2(nbd)(PPh_3)(alkyne)]^+BF_4^-$ (**21**).

The proposed mechanism for this case is summarized by Eqs (1) to (5). Note that norbornadiene is *not* hydrogenated under the reaction conditions and remains coordinated to the metal center during the hydrogenation process. This feature has been observed for both rhodium and iridium systems of the general formula $[M(diene)(L)_2]^+X^-$ [28–31]. In the first step of the catalytic sequence, $[Rh(nbd)(PPh_3)_2]^+BF_4^-$ (**19**) reacts with dihydrogen to form the coordinatively saturated intermediate *cis,cis*-$[RhH_2(nbd)(PPh_3)_2]^+BF_4^-$ (**20**), which must then dissociate a phosphine ligand in order to create a vacant coordination site for the incoming alkyne, to give the corresponding alkyne complex $[RhH_2(nbd)(PPh_3)(PhC_2H)]^+$ BF_4^- (**21**) (see Scheme 14.9). Most likely, the phosphine *trans* to the hydride would be most labile due to the large *trans*-influence of the hydride ligand. The alkyne would then arrive *cis* to one hydride but *trans* to the other, and migratory insertion will thus lead to the *trans*-hydrido-vinyl species. If the metal center in **21** is stereochemically integer under the hydrogenation conditions, this complex would not facilitate the reductive elimination. Therefore, a subsequent reaction with dihydrogen is required for the formation of the alkene, rationalizing the second-order in hydrogen.

14.1.7
Iridium Catalysts

The iridium complex $[Ir(cod)(\eta^2\text{-}^i PrPCH_2CH_2OMe)]^+BF_4^-$ (**22**) in dichloromethane at 25 °C at 1 bar H_2 is a particularly active catalyst for the hydrogenation of phenyl acetylene to styrene [29]. In a typical experiment, an average TOF of 50 mol mol^{-1} h^{-1} was obtained (calculated from a turnover number, TON, of 125) with a selectivity close to 100%. The mechanism of this reaction has been elucidated by a combination of kinetic, chemical and spectroscopic data (Scheme 14.10).

The main species in solution has been identified to be the hydrido-alkynyl complex $[IrH(C_2Ph)(cod)(\eta^2\text{-}^i PrPCH_2CH_2OMe)]^+BF4^-$ (**23**). This is, however, only a sink that results from direct reaction of **22** with the 1-alkyne, draining the active catalyst from the system. The catalysis proceeds *via* the dihydrido-diene intermediate $[IrH_2(cod)(\eta^2\text{-}^i PrPCH_2CH_2OMe)]^+$ BF_4^- (**24**), which reacts reversibly with the alkyne to yield the hydrido-iridium-styryl complex **25**, followed by a rate-determining reaction of this hydrido-vinyl species with hydrogen to re-

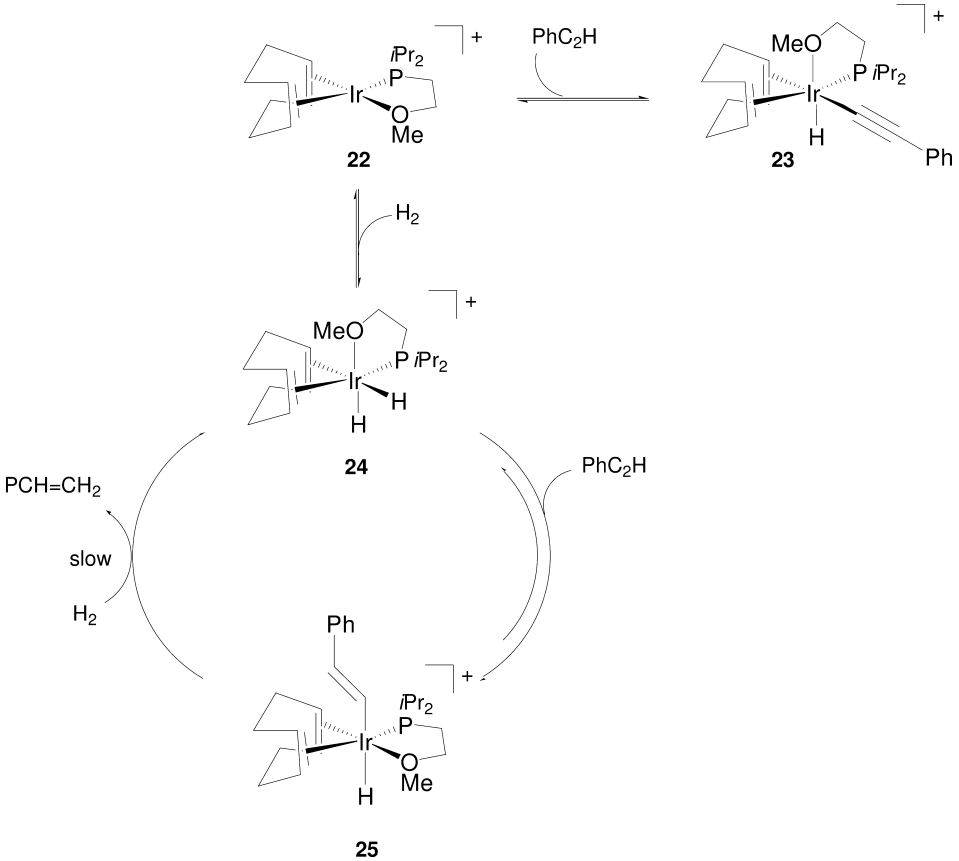

Scheme 14.10 Proposed mechanism for the hydrogenation of phenyl acetylene catalyzed by [Ir(cod)(η^2-^{i}PrPCH$_2$CH$_2$O-Me)]$^+$BF$_4^-$ (**22**); the anion is BF$_4^-$ throughout [29].

generate the dihydrido-diene complex **24** and liberate the alkene. This mechanism is in agreement with the observed rate law $r = k[\mathrm{Ir}][\mathrm{pH_2}]$. As in the case of the hydrogenation of phenyl acetylene by [Rh(nbd)(PPh$_3$)$_2$]$^+$BF$_4^-$ in dichloromethane, the diene is not hydrogenated under these reaction conditions and remains coordinated to the iridium. Furthermore, the origin of the selectivity has been ascribed to kinetic reasons – that is, the alkyne competes more effectively for the position liberated by displacement of the methoxy group of the ether-phosphine ligand than the alkene [29].

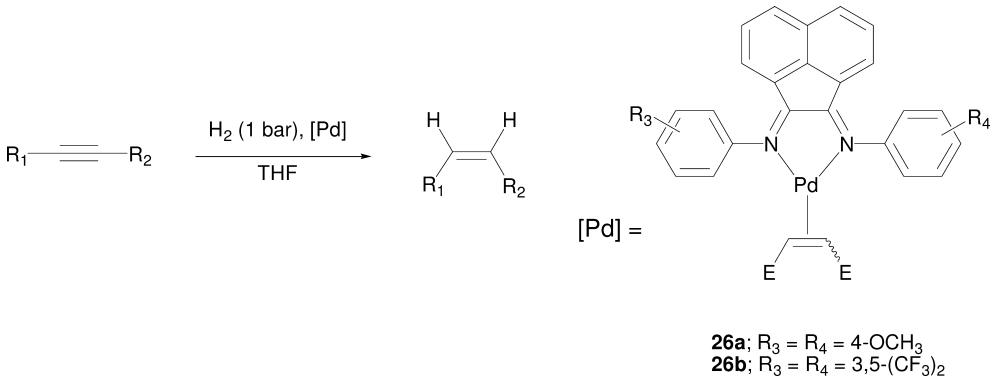

Scheme 14.11 Stereoselective hydrogenation of alkynes to alkenes by [Pd(Ar-bian)(alkene)] (**26**). In compound **26a** the electron-poor alkene is dimethyl fumarate, E = CO_2Me; in **26b** the electron-poor alkene is maleic anhydride, E = C(O)OC(O).

14.1.8
Palladium Catalysts

As mentioned earlier, the Lindlar catalyst has been the most widely used heterogeneous hydrogenation catalyst for the semihydrogenation of alkynes. However, the surface of these catalysts is a rather complex assembly of various domains, each of which contributes to the product distribution in its own way, often resulting in unpredictable overall results. In order to circumvent the presence of different palladium species, much attention has been devoted to the application of homogeneous mononuclear palladium complexes; either in the form of a Pd(II) complex [32, 33] or a Pd(0) compound [34–36]. In most of the reported cases, these mononuclear palladium complexes display a higher chemo- and (sometimes) higher stereoselectivity than the heterogeneous counterparts.

An important advantage of a heterogeneous catalyst over a homogeneous one concerns the ease of catalyst separation from the products. Therefore, much research effort in this field has been directed towards immobilized palladium complexes, where the palladium is coordinated to a ligand attached to a polymer, a clay, or another inorganic support [37–43]. Assuming that a single type of palladium species is formed, these heterogenized palladium catalysts are potentially very important and might compete with the Lindlar catalysts in certain applications. For the sake of completeness, it should be noted that palladium-clusters have been found to be active, with some showing extremely high activities and very good selectivities in the hydrogenation of alkynes to alkenes [44–46]. These Pd-clusters will not be treated here, however.

Elsevier et al. have reported the stereoselective hydrogenation of alkynes by zerovalent palladium catalysts bearing a bidentate nitrogen ligand, which are able homogeneously to hydrogenate a wide variety of alkynes to the corresponding (*Z*)-alkenes (see Scheme 14.11). The semihydrogenation occurs under very

mild conditions (25 °C, 1 bar H_2), and the observed selectivity towards the (*Z*)-alkene for the various alkynes is very high indeed [35]. The precatalysts employed are isolable [Pd(Ar-bian)(alkene)] compounds (**26**), which have previously been used in the homogeneous hydrogenation of electron-poor alkenes [47] and in carbon–element bond-formation reactions [48]. With respect to most other diimine ligands, Ar-bian derivatives are rigid, which imposes the correct geometry for coordination and imparts a high chemical stability. The ease of modifying the electronic as well as the steric properties of these ligands make them ideal to study their complexes in a variety of catalytic reactions.

Using [Pd(*p*-MeO-C_6H_4-bian)(dmfu)] (**26a**; dmfu = dimethyl fumarate), the observed selectivity towards semihydrogenation to the (*Z*)-isomer for the various alkynes is very high (> 99%) at 25 °C and 1 bar H_2 [35]. Typically, TOFs of 100 to 200 mol mol^{-1} h^{-1} have been obtained with this catalyst. The high selectivity, which is in many cases superior to that obtained with Lindlar catalyst, is maintained until full conversion of the alkyne; the selectivity has been determined at > 99.5% conversion. As can be seen from Table 14.2, internal as well as terminal alkynes are reduced to the corresponding (*Z*)-alkenes with great ease and selectivity. Besides the high stereoselectivity, the chemoselectivity is also remarkably high, as was demonstrated by the presence of other reducible functional groups in various substrates, such as carboalkoxy, nitro-groups, or even alkene moieties in conjugated enynes.

The complex [Pd{(*m,m'*-$(CF_3)_2C_6H_3$)bian}(ma)] (**26b**; ma = maleic anhydride) displays an unprecedented high reaction rate, while maintaining the high stereo- and chemoselectivity, which is typical for the [Pd(Ar-bian)] systems. In a detailed kinetic study [49] the catalyst behavior was investigated in the hydrogenation of 4-octyne. Under the reaction conditions (7 bar H_2, 21 °C) an average TOF of 16 000 (calculated from TON of 1600) can be reached, though hydrogen diffusion limitations prevent higher rates. The reaction rate is given by the equation: $r = k[\mathrm{Pd}][\mathrm{H_2}][\mathrm{alkyne}]^{0.65}$. Thus, the reaction is first-order in palladium and dihydrogen, confirming that mononuclear species are involved in the catalysis. The broken reaction order for the substrate suggests that an equilibrium between palladium complexes containing the substrate and the reaction product is operative under the reaction conditions. High-level density functional theory (DFT) calculations and *para*hydrogen induced polarization (PHIP) NMR measurements support a mechanism consisting of the following consecutive steps: alkyne coordination, heterolytic dihydrogen activation (hydrogenolysis of one Pd–N bond). Subsequently, hydropalladation of the alkyne, followed by addition of N–H to palladium, reductive coupling of the vinyl and hydride, and finally, substitution of the product alkene by the alkyne substrate (see Scheme 14.12) [49].

At high substrate, or low hydrogen concentration, the semihydrogenation of 4-octyne is inhibited by the formation of catalytically inactive palladacycle species. These species are formed by oxidative coupling of two substrate molecules. In addition, careful kinetic measurements and product analysis has revealed that the activation of the catalyst precursor **26b** during the induction period occurs by hydrogenation of the coordinated maleic anhydride to succinic anhy-

Table 14.2 Product distribution in the hydrogenation of alkynes using [Pd(*p*-MeO-C_6H_4-bian)(dmfu)] (**26a**) [35].[a)]

Entry	Substrate	Product distribution [%][b)]		
		(*Z*)-alkene	(*E*)-alkene	alkane
1	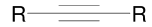 R = alkyl, CO_2Me	>98	–	–
2		>99	–	–
3	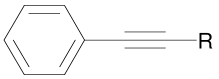 R = H, Me, *n*-Bu, CO_2H	>99 (R=H)[c)] 91 (R=Me) 92 (R=*n*-Bu) 95 (R=COOMe)	– 2 6 5	– 6 3 –
4	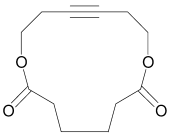	95	5	–
5	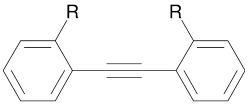 R = H, NO_2	87 (R=H) 97 ($R=NO_2$)	– 3	13 –
6	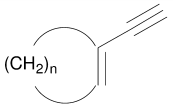	n=4, ethenylcyclohexene exclusively[c)] n=6, ethenylcyclooctene exclusively		

a) Reaction conditions: 80 mM substrate and 0.8 mM using [Pd(*p*-MeO Ar-bian)(dmfu)] (**26a**) in THF at 20 °C and 1 bar H_2.
b) Product distribution determined by GC and ^{1}H-NMR at >99.5% conversion of alkyne.
c) Determined by reaction with D_2.

dride, concurrently producing the catalytically active [Pd(Ar-bian)(alkyne)] complex [49].

It was concluded that the high selectivity observed in the hydrogenation experiments using **26b** is explained by the relatively strong coordination of the alkyne to the palladium center, which only allows for the presence of small amounts of alkene complexes. Only the latter are responsible for the observed minor amounts of (*E*)-alkene, which was shown to be a secondary reaction product formed by a subsequent palladium-catalyzed, hydrogen-assisted isomerization reaction. Since no *n*-octane was detected in the reaction mixture, only a tiny

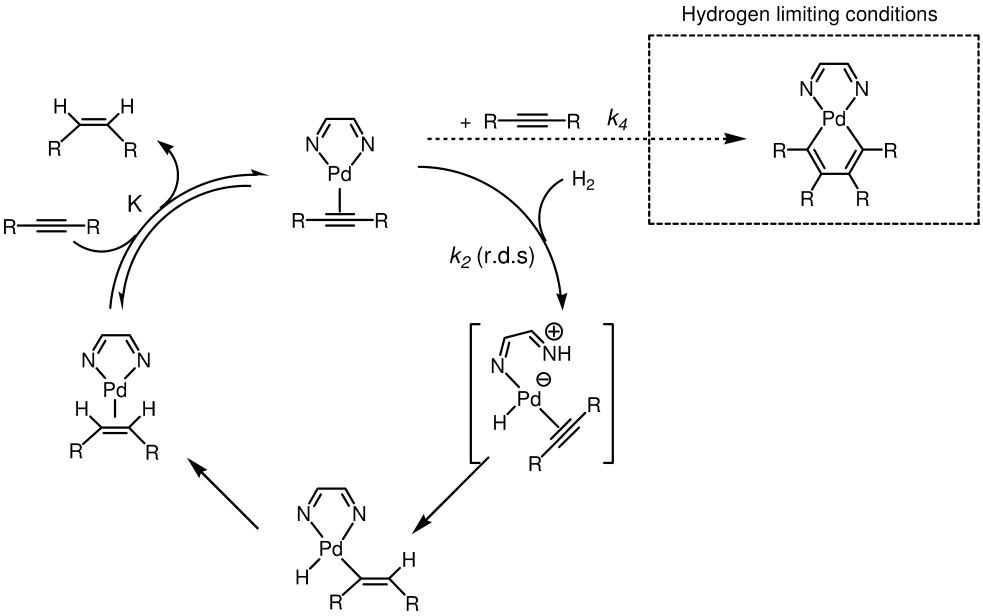

Scheme 14.12 Mechanism for the selective hydrogenation of alkynes by [Pd{(*m*,*m*′-$(CF_3)_2C_6H_3$)bian}(ma)] (**26b**) [49].

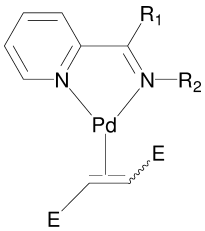

27

Fig. 14.1 Zerovalent [Pd(pyca)(alkene)] (**27**) precatalyst complex.

amount of the intermediate Pd(hydrido)(alkyl) species will reductively eliminate to form the alkane.

Zerovalent [palladium(alkene)] complexes **27** containing pyca ligands (pyca = pyridine-2-carbaldimine; Fig. 14.1) have been investigated in the stereoselective hydrogenation reaction of 1-phenyl-1-propyne in THF [34]. Most of the obtained inherently high *cis*-selectivities in the semihydrogenation of 1-phenyl-1-propyne are comparable to each other and to the results of the [Pd(Ar-bian)] system. However, the stability of the [Pd(pyca)] systems is generally lower and decomposition occurs in several cases before full consumption of the alkyne has taken place. It was concluded that the nature of the substituents on the imine nitrogen atom seems to be the most important factor determining the stability of the various catalysts precursors under hydrogenation conditions. It appeared

that more donating capacity of the N-substituent results in a more stable catalyst, whereas increased steric bulk reduces its stability.

Members of the Parma group have shown that a large variety of divalent palladium complexes, with the generic formula [Pd(L)X] (X = OAc^- or Cl^-) bearing a hydrazinato-based tridentate ligand L (containing different donor atoms), are able to hydrogenate alkynes to the corresponding alkenes with different degrees of success [32, 50–52]. Considerable mechanistic details have been reported for this reaction employing the catalysts [Pd(thiosemicarbazonato)X] (**28**) and [Pd(thiobenzoylhydrazonato)X] (**29**) (see Fig. 14.2) [32]. The hemilability of these ligands plays an intricate role in the catalysis with such compounds. Under the reaction conditions used (1 bar H_2, 30 °C, substrate : catalyst ratio = 100), the chloro-analogue [Pd(NNS)Cl] (**28a**) exhibits a full conversion in 24 h with 92% selectivity for styrene. The overall reaction rate is low, and TOFs around 4 mol · mol^{-1} h^{-1} have been reported. Although these catalysts are completely unreactive towards styrene present in solution, the ethylbenzene formed during the reaction was proposed to be the result from a second, consecutive hydrogenation step of the primary reaction product – that is, styrene which remains coordinated to the palladium (see Scheme 14.13). The stereoselectivity of the reaction could be tailored by changing the counter ion of the Pd(II) complex.

A kinetic investigation was performed using the [Pd(methyl-2-pyridylketone-thiosemicarbazonato)Cl] (**29a**) complex at 50 °C, and this yielded the experimentally obtained rate law; $r = k$[catalyst][alkyne][pH_2] [32]. Based on this rate law and the activity data, a catalytic cycle as depicted in Scheme 14.13 was postulated. The first step of the mechanism is the activation of molecular hydrogen *via* heterolytic hydrogen splitting to generate a palladium hydride species (**30**) and accommodating the proton on one of the basic sites of the ligand (the hydrazone nitrogen). It is assumed that the pyridine moiety acts as a hemilabile ligand, creating the coordination site for the hydride. After hydrogen activation, the incoming alkyne replaces the counterion X^- from the first coordination sphere and generates the [Pd(NNS)(alkyne)] species (**32**). This step appears to be the predominant factor in driving the chemoselectivity of the hydrogenation reaction. It was shown that the weakly bonded acetate anion is easily replaced by both phenyl acetylene and the reaction product styrene, hence displaying low chemoselectivity, while tightly associated anions such as iodide show no hydrogenation activity under the reaction conditions used. The chloride ion appears to take an intermediate position, allowing it to be replaced by phenyl acetylene but not by the reaction product styrene; thus it forms a basis for discriminating between these potential substrates. Subsequently, the hydride is transferred to the coordinated phenyl acetylene forming a $[Pd(NNS)(alkenyl)]^+X^-$ species (**32**) which then reacts with molecular hydrogen, leading to the $[Pd(NNS)(H)(styrene)]^+X^-$ complex (**33**). Either the chloride anion or the phenyl acetylene then displaces the coordinated styrene resulting in complex **30** or **31**, respectively.

In addition, the related divalent palladium complexes [Pd(PNO)X] (**35**) (PNO = *N′*-(2-(diphenylphosphino)benzylidene)acetohydrazonato and related ligands) [50, 51] and [Pd(NNN)X] (**36**) (NNN = *N*-pyridin-2-yl-*N′*-pyridin-2-ylmethy-

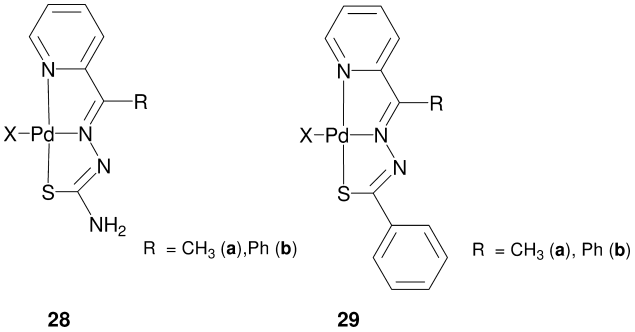

Fig. 14.2 Structure of the precursor catalysts [Pd(thiosemicarbazonato)X] (**28**) and [Pd(thiobenzoylhydrazonato)X] (**29**).

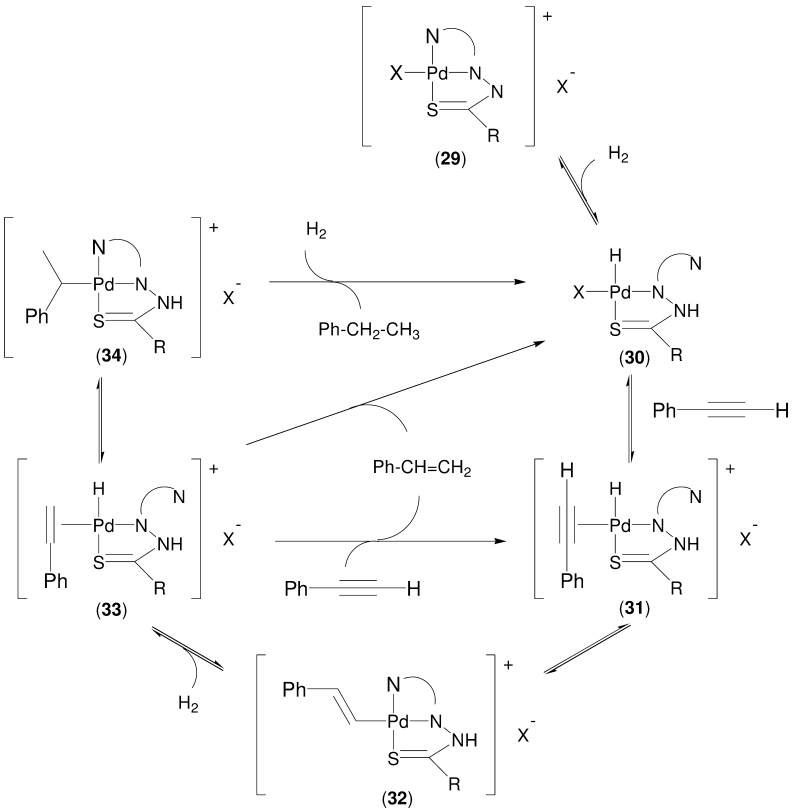

Scheme 14.13 Proposed mechanism for the hydrogenation of phenyl acetylene by [Pd(methyl 2-pyridyl ketone thiosemicarbazonato)Cl] (**29a**).

lene hydrazinato) (X = Cl^- or OAc^-) [52] have been reported to be able to hydrogenate alkynes to the corresponding alkenes. For these systems, a heterolytic hydrogen activation similar to catalysts **28** and **29** is suggested. The hemilability of the ligand and the nature of the anion is important feature of the catalytic activity. The rate of phenyl acetylene hydrogenation employing **36** appears similar to the rate reported for **28** and **29**, while **35** displays a distinctively lower reaction rate. Furthermore, no further mechanistic details concerning the chemo- or stereoselectivity of these catalytic systems have been reported.

14.1.9
Conclusions

The stereoselective hydrogenation of alkynes to alkenes can be effected by a wide variety of homogeneous catalysts. The appropriate choice of catalyst and reaction conditions allows the selective formation of either the (*Z*)- or the (*E*)-alkene. Most of the catalysts display a very high chemoselectivity, as they are not reactive towards reducible functional groups such as carbonyl, ester, and double bonds. Many of the details related to catalyst behavior and intricate mechanistic details concerning semihydrogenation of alkynes have often not been unraveled, and will remain a topic of research for the coming years.

14.2
Homogeneous Hydrogenation of Dienes to Monoenes

14.2.1
Introduction

The hydrogenation of polyenes is a research topic that has attracted substantial attention over the past three decades. Especially, the removal of diene constituents from (light) hydrocarbon fractions, polydiene rubbers and fatty acids has been a major focus in the research effort. Although the importance of this reduction is generally recognized, there are only a small number of homogeneous catalysts that have been reported to be active in the diene hydrogenation reaction. Details about the catalytic behavior and mechanism are often very scarce, or these have not been explored at all. Frequently, a distinction is made between the hydrogenation of conjugated and non-conjugated dienes. The latter type is often considered as consisting of two single, isolated double bonds, which are thus fairly easily reduced by most hydrogenation catalysts. Substrates containing conjugated double bonds (either present in the substrate or formed by prior isomerization reactions of non-conjugated double bonds) often pose more difficulty in a hydrogenation reaction. Especially, the formation of stable diene- or allyl complexes often inhibits the reaction and, hence, the selective hydrogenation of conjugated dienes to monoenes forms a particular challenge.

Selectivity in the hydrogenation reaction of dienes to monoenes can be achieved by two types of catalytic system: (i) those which are completely inert with respect to the hydrogenation of the resulting monoenes; and (ii) those for which the selectivity is due to the discrimination based on thermodynamic and/or kinetic factors that suppress the rate of formation of the saturated hydrocarbon. The latter approach is the most common way of achieving selectivity for these hydrogenations.

In this section, an overview will be provided of reported catalysts that can perform the hydrogenation of conjugated dienes to monoenes with a considerable degree of selectivity using molecular hydrogen as a hydrogen source. Most attention will be given to those catalytic systems that show remarkable (high) selectivities, high reaction rates, or which have demonstrated their value in organic synthesis. Furthermore, special attention will be given to the mechanistic details of these homogeneous hydrogenation systems.

14.2.2
Zirconium Catalysts

The oligomeric hydrido-zirconium complexes $[Cp_2Zr(H)(CH_2PPh_2)]_n$ (**37**) constitute selective systems for the hydrogenation of dienes [53]. The reaction is performed at 80 °C at hydrogen pressures between 10 and 40 bar; under these conditions the linear dienes (e.g., 1,3-pentadiene) are hydrogenated consecutively to the corresponding alkanes. The monoene *E*-2-pentene is detected only as intermediate in the reaction mixture. Remarkably, cyclic olefins such as cycloheptatriene, 1,3- and 1,5-cyclooctadiene are selectively hydrogenated to the cycloheptene and cyclooctene, respectively (>98% selectivity). In contrast to linear dienes, cyclic dienes are not fully hydrogenated to the alkane and the hydrogenation stops at the monoene stage.

In order to understand the unusual reactivity of $[Cp_2Zr(H)(CH_2PPh_2)]_n$ towards cyclic dienes, the reaction mechanism was studied using 1,3-cyclooctadiene and butadiene as substrate. It appears that the first step, the activation of the initial zirconium precursor catalyst **37**, is achieved by a sequence of decomposition steps consisting of the reductive elimination of the phosphine PPh_2Me and the simultaneous formation of the zirconocene intermediate $[Cp_2Zr]$. This intermediate will then be trapped, either by the diene, producing $[Cp_2Zr(diene)]$ (**44**) or by **37** to give the homometallic hydride bridged complex $[Cp_2Zr(\mu\text{-}H)(\mu\text{-}CH_2PPh_2)ZrCp_2]$ (**38**) (see Scheme 14.14) [54]. The complexes **44** and **38** are related species. From detailed stoichiometric reactions, using the less sterically demanding butadiene as substrate, it has been shown that the reaction of intermediate **44** with starting material **37** and the reaction of compound **38** with butadiene are viable and produce a common intermediate. This common intermediate has been identified as a dinuclear Zr(IV)–Zr(II) complex in which the butenyl fragment bridges between the two zirconium centers in a μ^1-η^1:1,2-η^2-fashion, structurally similar to compound **39** (Scheme 14.14) [55].

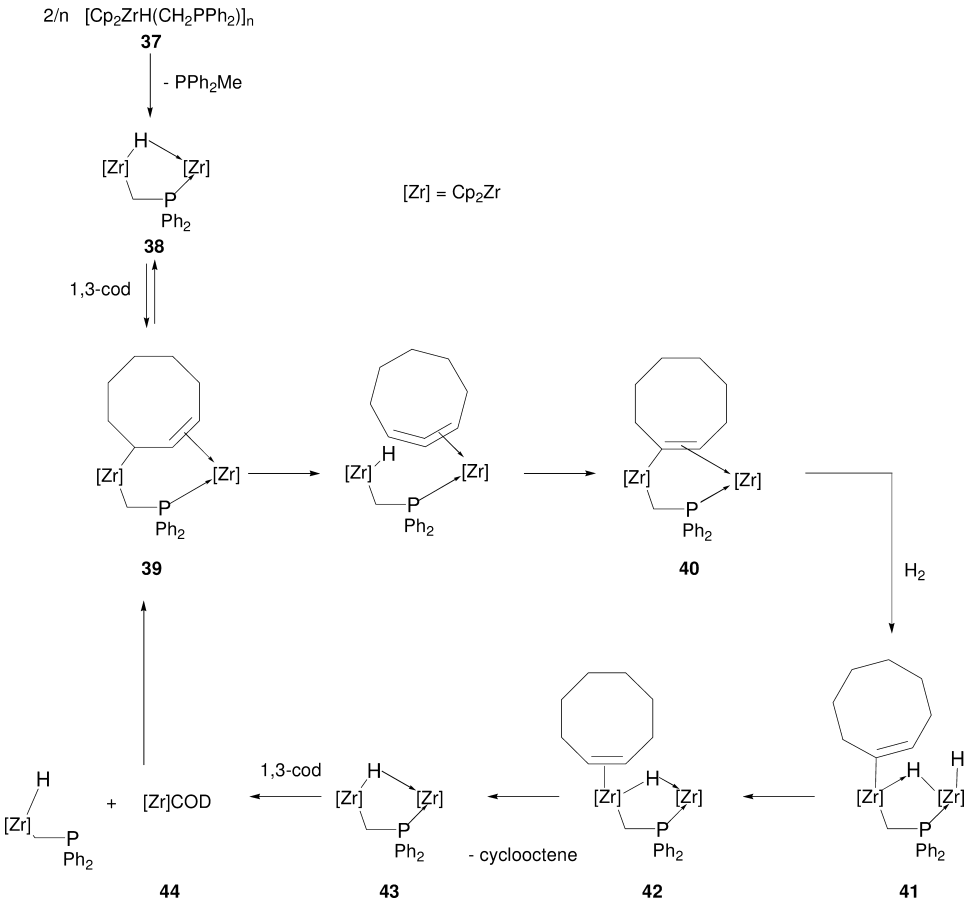

Scheme 14.14 Proposed mechanism for the hydrogenation of 1,3-cyclooctadiene catalyzed by $[Cp_2Zr(H)(CH_2PPh_2)]_n$ (**37**) [53].

Kinetic studies revealed that the order of reaction with respect to the zirconium is a half, reflecting the dissociation of active catalytic species [53]. Since the order in substrate is zero and one in hydrogen, the addition of H_2 is the rate-limiting step in the reaction mechanism. The rate of the reaction, expressed in average TOFs, ranges between 180 and 750 mol mol^{-1} h^{-1}, and the activation energy of the hydrogenation of 1,3-cyclooctadiene was determined to be 29 kJ mol^{-1}. The proposed catalytic cycle, as is depicted in Scheme 14.14, consists of the formation of the initial Zr(IV)–Zr(II) bimetallic complex **39** in which a cyclooctenyl ligand is bridging between the two zirconium centers. Compound **39** then isomerizes to the μ-alkenyl zirconium(IV)/zirconium(II) intermediate **40**, which is considered the key intermediate in the reaction mechanism. Formation of complex **40** is proposed to explain the effective protection of the remaining C=C double bond in the catalytic cycle. This species then reacts with

molecular hydrogen in an oxidative addition manner to form the dinuclear Zr(IV)–Zr(IV) dihydride complex (**41**), having one bridging and one terminal hydride. Reductive elimination of the alkenyl and one of the hydrides yields the dinuclear-monohydride bridged complex (**42**) which then loses the cyclooctene. The unusual selectivity is ascribed to the cooperative effect of two zirconium centers, stabilized and held together by the bridging CH_2PPh_2-ligand, to combine the action of a zirconium(IV) and a zirconium(II) centre, bringing about rapid mono-hydrogenation and at the same time effective protection of the remaining C=C double bond.

14.2.3
Chromium Catalysts

Group VI metal carbonyls and their derivatives, especially chromium carbonyl compounds, are able to hydrogenate a variety of substrates (e.g., alkynes, enones) with high stereospecificity [6]. The regio- and stereospecific 1,4-hydrogenation of conjugated dienes to (*Z*)-monoenes catalyzed by $[Cr(CO)_3(arene)]$ complexes (**45**) was first reported in 1968 by the groups of Cais et al. [56] and of Frankel et al. [57]. The catalysts $[Cr(CO)_3(benzene)]$, and similar ones containing a benzene derivative that were initially explored, required rigorous reaction conditions (150–160 °C and 50 bar H_2) in order for the stereoselective 1,4-hydrogenation to proceed. However, the activity depends on the substituents attached to the benzene ligand – that is, the presence of more electron-withdrawing substituents and more coordinating solvents allowed milder reaction conditions (Table 14.3).

Spectroscopic studies have revealed that $[Cr(CO)_3(S)_3]$ (S = solvent) is the active species for the hydrogenation, and the formation of these species is promoted either by less strongly coordinated ligands (electron-poor benzene or polyaromatic compounds) or by more strongly coordinating solvents. The use of polyaromatic compounds such as naphthalene, anthracene and phenanthrene as ligands combined with polar coordinating solvents (THF or acetone) has proven to be particular effective for constructing a highly active catalytic system under mild conditions [58]. Whereas several mechanistic schemes have been suggested for the chromium-catalyzed diene hydrogenation, they all share a common feature: the active metal fragment $[Cr(CO)_3]$ is generated *in situ* by thermal or photochemical activation of a coordinatively saturated $[Cr(CO)_3(L)_3]$ complex ($(L)_3$ = arene; L = CH_3CN or CO) [58–60].

At ambient reaction temperatures and hydrogen pressures, kinetic studies employing $[Cr(CO)_3(nap)]$ (nap = naphthalene) (**45a**) as catalyst revealed that two reaction mechanisms operate simultaneously, namely a hydride route and a diene route (Scheme 14.15) [61]. After the initial step, in which $[Cr(CO)_3(nap)]$ reacts with the solvent to generate the active catalyst $[Cr(CO)_3(S)_3]$ (**46**), this solvent complex can then subsequently react either with hydrogen or the conjugated diene. In the hydride route, $[Cr(CO)_3(S)_3]$ undergoes oxidative addition of dihydrogen to give complex **48**, which still has two labile coordination sites nec-

Table 14.3 Hydrogenation of methyl sorbate to 3-hexenoic acid methyl ester with $[Cr(CO)_3(arene)]$ (**45**) catalysts.

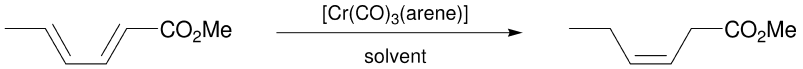

Entry	Catalyst arene (mol.%)	Solvent	Reaction temp. [°C]	H_2 pressure [bar]	Induction period [min]	10^{-5} k_{obs} [s^{-1}]	TOF [mol mol^{-1} h^{-1}] a)	Selectivity [mol.%]
1	Benzene (5)	Cyclohexane	165	48	285	39.6	14	94.3
2	Benzene (5)	Acetone	165	48	–	246	84	92.2
3	Methyl benzoate (5)	Cyclohexane	120	48	45	56.0	20	99.3
4	Chlorobenzene (5)	Cyclohexane	120	48	15	61.5	21	96.1
5	Phenanthrene (2)	Decalin	120	4	14.3	340	294	–
6	Phenanthrene (3)	THF	40	4	100	53	29	–
7	Phenanthrene (3)	Acetone	40	4	29	361	29	–
8	Naphthalene (2)	Decalin	120	4	1	963	832	–
9	Naphthalene (3)	THF	40	4	8	385	208	–
10	Naphthalene (3)	Acetone	~27	4	4	963	520	–

a) TOF determined at 50% conversion using first-order kinetics.
TOF = 0.5 k_{obs}[substrate]/[catalyst].

essary to accommodate the diene in a η^4-fashion. After coordination of the conjugated diene producing complex **49**, the two hydrides are rapidly transferred, producing a (*Z*)-monoene. The diene route is established by initial coordination of the diene to the solvento complex **46** to produce $[Cr(CO)_3(diene)(S)]$ **47** prior to the hydrogen activation. Although both hydrogenation routes are active under the typical hydrogenation conditions, additional kinetic studies performed at high temperatures and elevated hydrogen pressures employing $[Cr(CO)_3(arene)]$ (arene = substituted benzene derivative) show that, under these conditions, only the hydride route is operative. The oxidative addition of molecular hydrogen is the rate-determining step for this hydrogenation route [62, 63].

The $[Cr(CO)_3(arene)]$-catalyzed 1,4-hydrogenation of conjugated dienes has become an established route for the stereocontrolled synthesis of alkenes in organic synthesis [6, 7]. The potential of this method has been clearly demonstrated in the synthesis of olfactory compounds (fragrances and insect pheromones), where the 1,4-hydrogenation of dienes was employed in a key step of the synthesis. For such compounds, the stereo- and regio control of the double-bond geometry is extremely important for maintaining its biological activity. Furthermore, the $[Cr(CO)_3(arene)]$-catalyzed hydrogenation displays a remarkably high chemoselectivity, and the outcome of the reaction is not affected by the presence of other functional groups such as non-conjugated carbon-carbon double bonds, esters, ketones, carboxylic acids, epoxides, phosphonate esters, sulfonamides, or even cyano groups [6].

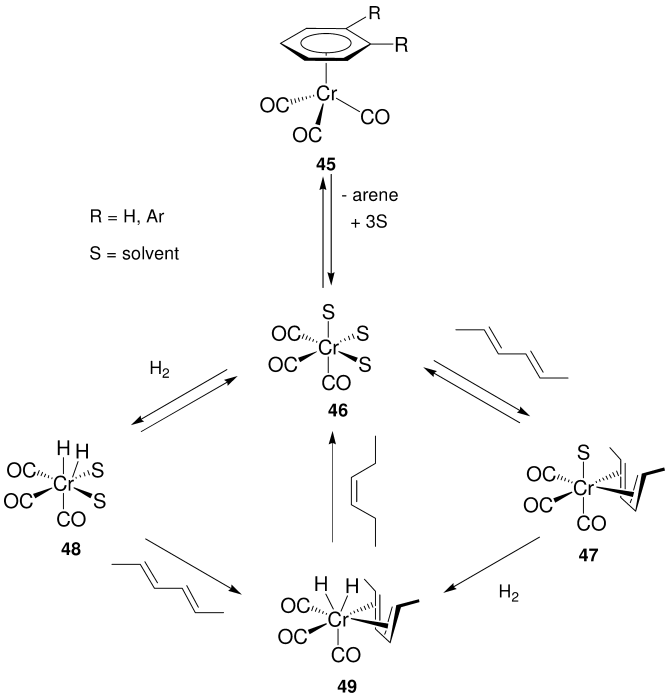

Scheme 14.15 Proposed hydrogenation mechanism for the 1,4-hydrogenation of dienes by $[Cr(CO)_3(arene)]$ (**45**).

An interesting feature of the $[Cr(CO)_3]$-catalyzed 1,4-hydrogenation is the predetermined outcome of the stereocontrolled reaction; the diene must coordinate in a η^4-s-*cis* fashion to the chromium, allowing only one conformationally rigid and predisposed intermediate [6]. The presence of only one accessible catalyst–substrate intermediate structure invokes the 1,4-hydrogenation to proceed with complete regio- and stereocontrol, regardless of the thermodynamic stability of the hydrogenation products. This was demonstrated in the stereocontrolled synthesis of carbacyclin analogues for the production of the exclusively (*E*)-exocyclic isomer (Scheme 14.16). The chromium–diene intermediate, in conjunction with the 1,4-addition, dictates the formation of the exocyclic isomer, and since the chromium catalyst is inactive in the isolated double-bond isomerization reaction, the (*E*)-isomer is obtained solely as the reaction product.

Apart from Cr(0) carbonyl complexes, similar Mo, W and Co complexes also catalyze 1,4-*cis*-hydrogenation of dienes, though the selectivity of these catalysts is relatively low [63].

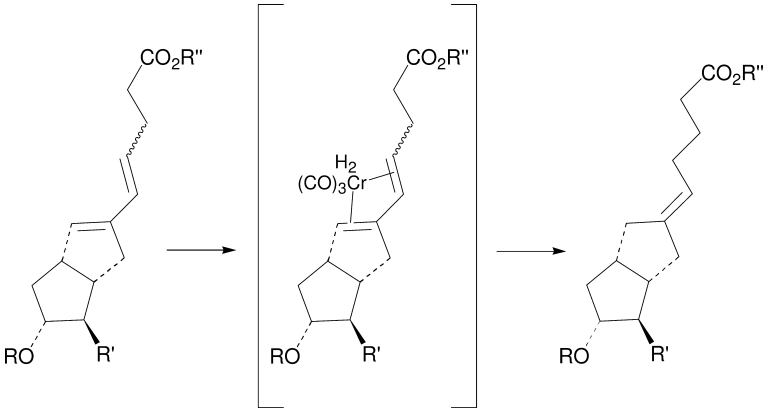

Scheme 14.16 Stereocontrolled 1,4-hydrogenation of a carbacyclin analogue using $[Cr(CO)_3(arene)]$ (**45**) complexes.

14.2.4
Ruthenium Catalysts

Ruthenium complexes are active hydrogenation catalysts for the reduction of dienes to monoenes. Both zerovalent and divalent ruthenium complexes containing various (alkene, diene and phosphine) ligands have been employed as catalysts that have met with different degrees of success.

Ruthenium(0) complexes containing cyclic polyenes such as Ru(cod)(η^6-triene) (**50**) (cod = 1,5-cyclooctadiene; triene = 1,3,5-cyclooctatriene or 1,3,5-cycloheptatriene) have proven to be selective hydrogenation catalysts for the reduction of cycloheptatriene and cyclooctadiene to the corresponding cyclic monoenes [64, 65]. The [Ru(cod)] fragment is maintained as the catalytic unit throughout the hydrogenation reaction and the η^6-coordinated triene (e.g., cyclooctatriene) is hydrogenated to the monoene during the induction period.

For instance, cycloheptatriene has been selectively hydrogenated at 1 bar H_2 pressure at 20 °C, yielding cycloheptene. The selectivity depended largely on the solvent used, ranging from 100% when *n*-hexane was used, or 99.5% in THF, to very low values when ethanol was employed. The conversion is quantitative in THF and ethanol, but in *n*-hexane it did not exceed 65%; consequently, the authors concluded that THF gives the best combination of selectivity and conversion. In this case, the formation of cycloheptane was observed only after the substrate cycloheptatriene had completely been consumed.

Cyclooctadiene isomers (i.e., 1,5-cod or 1,3-cod) are selectively hydrogenated by $[Ru(\eta^4\text{-cod})(\eta^6\text{-}C_8H_{10})]$ (**51**) to produce exclusively cyclooctene in THF, under ambient temperature (20 °C) and 1 bar H_2 pressure [64]. Again, cyclooctane is only detected when the diene substrate is completely transformed to the monoene. The rate of hydrogenation is higher in case of the conjugated 1,3-cyclooctadiene substrate, whereas isomerization of the non-conjugated 1,5-cyclooctadiene

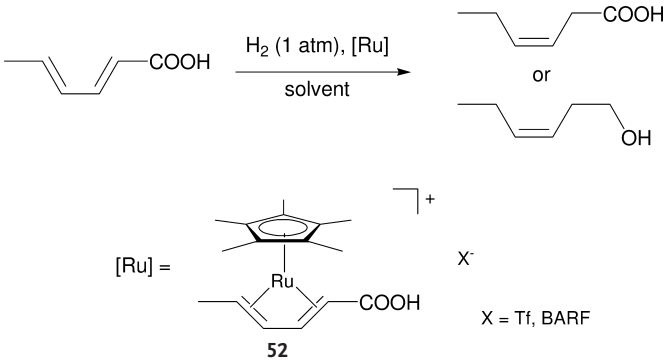

Scheme 14.17 Hydrogenation of sorbic acid by [Cp*Ru(η^4-sorbic acid)]$^+$X$^-$ (**52**). X$^-$ = $CF_3SO_3^-$ or BARF$^-$.

to 1,3-cyclooctadiene has been proposed. This isomerization appeared to be necessary for the catalytic hydrogenation of 1,5-cod.

Cationic ruthenium complexes containing the fragment [Cp*Ru] (**52a**) can stereoselectively hydrogenate sorbic acid or sorbic alcohol to *cis*-3-hexenoic acid or *cis*-3-hexen-1-ol, respectively (Scheme 14.17). The highest rate and stereoselectivity have been obtained with the "naked" [Cp*Ru] – that is, a monocyclopentadiene–ruthenium complex without any additional, inhibiting ligands and [Cp*Ru(η^4-sorbic acid)]$^+$X$^-$ (**52**) (sorbic acid = (2*E*,4*E*)-MeCH=CHCH=CHCO$_2$H and X = $CF_3SO_3^-$ or BARF$^-$) displays the best results. These ionic ruthenium catalysts have been used successfully in a single phase as well as liquid two-phase systems (such as liquid–liquid, ionic liquid–liquid solvent systems) [66, 67]. The activity of these catalysts depends strongly on the solvent or solvent mixtures used, with the rate of hydrogenation of sorbic acid (in TOF) ranging from 92 to 1057 mol mol^{-1} h^{-1}. The highest rate and selectivity have been reported for the solvent methyl-*tert*-butyl ether (TOF = 1057, *cis*:*trans* ratio 96 : 3). In general, the hydrogenation of sorbic alcohol proceeds with higher activity and almost complete selectivity when using **52** as the catalyst.

Mechanistic studies employing the PHIP phenomenon showed that the homogeneous hydrogenation of sorbic acid (in acetone under 1 bar H_2) proceeds by concerted 1,4-hydrogenation of the diene moiety [68]. Both atoms of the same dihydrogen molecule are transferred to the substrate in a synchronous fashion, yielding *cis*-3-hexenoic acid as the primary reaction product. Furthermore, it was found that the *trans*-isomer is formed by subsequent rearrangement of the *cis*-3-hexenoic acid, and is not the result of direct hydrogenation of sorbic acid.

14.2.5
Cobalt Catalysts

In spite of the number of disadvantages, considerable interest has been given to the hydrogenation of dienes by the water-soluble catalyst $K_3[Co(CN)_5H]$ (**53**) [69, 70]. The catalyst shows a high chemoselectivity towards conjugated carbon-carbon double bonds; that is, isolated carbon-carbon double bonds or carbonyl functional groups will not be affected by the catalyst under the hydrogenation conditions. However, the hydrogenation reaction suffers from short catalyst lifetime, substrate inhibition, low hydrogenation rate (generally TOF ≤ 2) and low regioselectivity of the monoene products [71]. The addition of phase-transfer reagents (e.g., ammonium salts [71], β-cyclodextrin [72]) or surfactants [73, 74] largely overcomes these complications, but the rate of the reaction remains low. In general, the product ratios are dominated by the overall 1,4-addition of hydrogen under the phase-transfer conditions, although in some cases 1,2-addition has been observed [73, 75]. Several modified versions of this catalyst are known where one or more cyanides are replaced by diamines such as ethylenediamine, bipy or phen [75].

14.2.6
Rhodium Catalysts

The well-known cationic Osborn catalyst $[Rh(nbd)L_n]^+A^-$ (**54**), which has been an extremely useful catalyst for the reduction of alkenes and alkynes, also facilitates the rapid and selective hydrogenation of dienes in polar solvents, affording the corresponding monoenes [76]. In order to probe this reaction, various substrates such as norbornadiene, substituted butadienes and conjugated and non-conjugated cyclic dienes have been tested. The TOF depends strongly on the reaction conditions (i.e., solvent), the catalyst employed, and on the structure of the substrate. Hence, the rate of hydrogenation typically ranges from 140 to 250 mol mol^{-1} h^{-1}. More sterically encumbered substrates such as 2,5-dimethylhexa-2,4-diene show very low hydrogenation rates (~6 mol mol^{-1} h^{-1}), while 1,3-cyclooctadiene is rapidly hydrogenated to the monoene (330 mol mol^{-1} h^{-1}). The product monoenes, which are formed almost quantitatively (up to 99% yield), result from overall 1,2- and 1,4-addition of H_2 onto the diene moiety [25, 76, 77]. The ratio of the two addition modes depends strongly on the structure of the substrate and on the nature of the ligand, L. For the diene reduction, chelating diphosphines or diarsines are preferred as stabilizing ligands, as catalysts derived from monodentate ligands tend to become easily deactivated due to the formation of an unsaturated $[Rh(diene)_2L]^+$ fragment (**55**).

The proposed hydrogenation mechanism for (conjugated) dienes by the cationic rhodium catalyst $[P_2Rh(nbd)]^+X^-$ (**54**) is depicted in Scheme 14.18. Activation of the precursor catalyst **54** has been studied in considerable detail, and reveals that the hydrogenation of the initially coordinated norbornadiene is fast and complete for most investigated systems (contrary to the often-used $[P_2Rh(cod)]^+X^-$ analogues) [78–80]. In contrast to the reported hydrogenation mechanisms for mono-

enes and alkynes, the hydrogenation of dienes does not depend on the addition of acid and, therefore, it is assumed to proceed by a different catalytic route (Scheme 14.18) [21, 76, 81]. The proposal of an "unsaturated" mechanism, in which the diene coordinates to form $[P_2Rh(diene)]^+$ (**57**), prior to hydrogen activation, can be rationalized by the high coordination constant of the *cis*-s-coordinated (chelating) diene to the rhodium. The hydrogenation mechanism shows a zero order in diene, and it has been suggested that the rate-determining step involves the reaction of H_2 with the cationic $[P_2Rh(diene)]^+$ species (**57**). Detailed *in-situ* NMR studies employing deuterium and *para*-hydrogen-enriched molecular hydrogen has allowed the proposal of the structure of the $[P_2Rh(diene)(H)_2]$ (**58**) intermediate, which was revealed by the cross-relaxation transfer, originating from the enhanced magnetization inflicted by the *para*-hydrogen adducts [78]. In addition, these studies demonstrated that the hydrogenation of norbornadiene and 1,4-cyclooctadiene occurs successively and confirms the mechanism presented in Scheme 14.18 [82]. To date, many details of the hydrogenation of 1,3-dienes have not been resolved, such as the true nature of the $[P_2Rh(R)(H)]$ intermediate between complex **58** and **59** (not shown in Scheme 14.18), possibly being either a [Rh(alkenyl)] or a [Rh(allyl)] species. The first species would lead to 1,2-addition, and the latter one to either 1,2- or 1,4-addition.

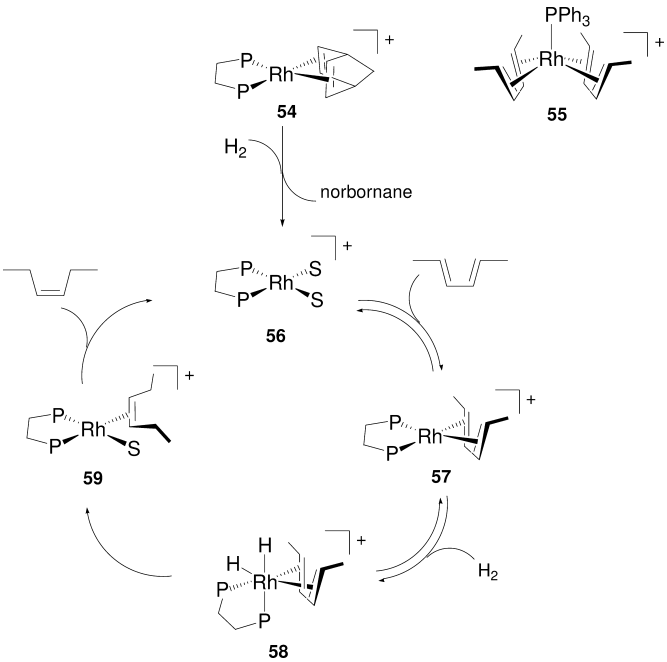

Scheme 14.18 Proposed 1,4-hydrogenation mechanism for the hydrogenation of dienes by cationic rhodium complexes $[P_2Rh(diene)]^+A^-$ (**54**).

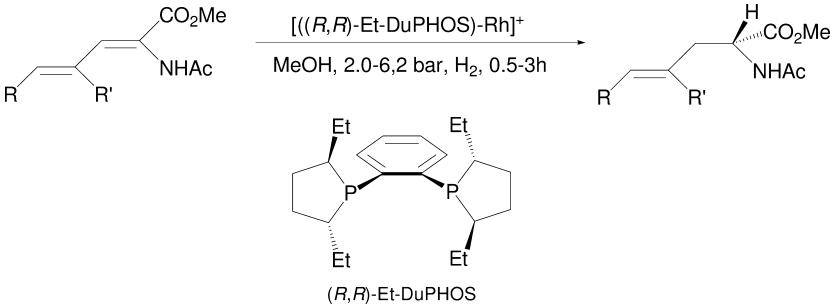

Scheme 14.19 Hydrogenation of conjugated α,γ-dienamide esters by [((*R*,*R*)-Et-DuPHOS)-Rh(cod)]OTf (**54b**) (OTf = triflate) [83].

The characteristics of the hydrogenation of norbornadiene, substituted butadienes and conjugated and cyclic dienes are all very similar. In the case of conjugated dienes, there appears to be hardly any isomerization activity, while in the case of 1,4-dienes an isomerization step to form the corresponding 1,3-diene is assumed prior to hydrogenation. The catalyst behavior changes after the diene has been completely converted to the monoene, whereupon the rhodium catalyst resumes its "normal" monoene hydrogenation behavior.

An interesting example of the use of $[Rh(nbd)L_n]^+A^-$ (**54**) in organic synthesis is provided by the cationic rhodium complex [((*R*,*R*)-Et-DuPHOS)-Rh(cod)]OTf (**54b**), which appears to be particularly effective in the enantiomeric hydrogenation of conjugated α,γ-dienamide esters [83]. Full conversion to the corresponding γ,δ-unsaturated amino acids could be obtained using the Et-DuPHOS-Rh catalyst system, yielding very high regio- and enantioselectivity (>95% and 99% ee, respectively; see Scheme 14.19) with over-reductions as low as <0.5%. The rate of the reaction (expressed as average TOFs, determined at full conversion) for different substrates ranged from 160 to 1000 mol mol^{-1} h^{-1}. Either enantiomer of the γ,δ-unsaturated amino acid could be obtained by the use of (*R*,*R*)- or (*S*,*S*)-Et-DuPHOS. Interestingly, the reaction proceeds by hydrogenation of the enamide C=C double bond, with complete regioselectivity over the distal C=C double bond. Effectively, only 1,2-addition is observed, which can be explained by the chelating effect of the enamide group to the metal center and preventing over-reduction, even after the enamide double bond has been completely converted.

The selective diene hydrogenation of monoterpenes such as myrcene, which contain both isolated monoene and diene moieties, forms a particular challenge [84]. The catalyst $[RhH(CO)(PPh_3)_3]$ (**60**) has been reported to perform remarkably well for such hydrogenation reactions, and the diene moiety was shown to be selectively reduced to the monoene, while the isolated double bond remained unaffected under the reaction conditions used (Scheme 14.20). The rates of reaction expressed as average TOF (determined at ca. 80% conversion) ranged from ca. 640 (in benzene, 20 atm H_2 at 100 °C) to 7600 mol mol^{-1} h^{-1} (in cyclohexane, 20 atm H_2 at 80 °C). The hydrogenation in benzene solution resulted in

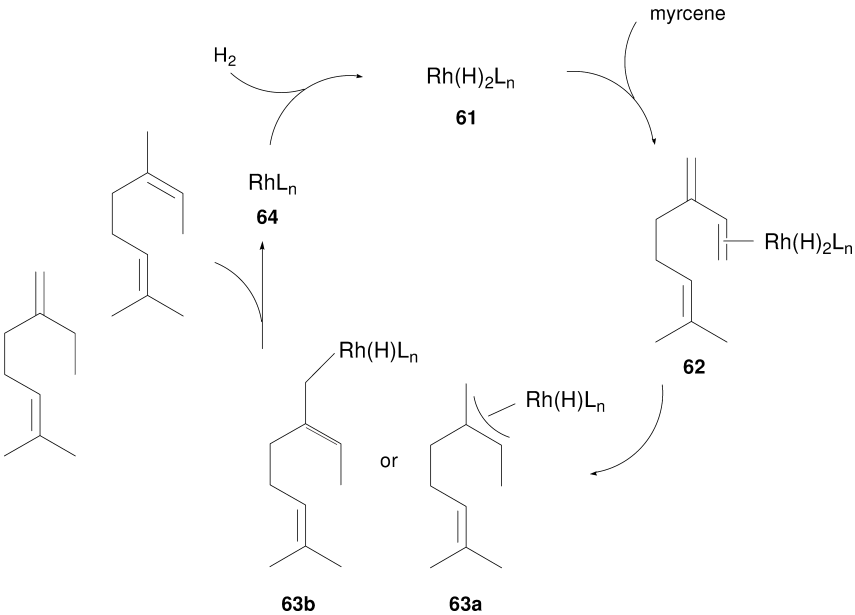

Scheme 14.20 Proposed mechanism for the hydrogenation of myrcene by [RhH(CO)(PPh$_3$)$_3$] (**60**) and the formation of the major reaction products [84].

the highest chemoselectivity of the reduction of the conjugated diene to the corresponding monoene (98% selectivity). The products arise from overall 1,2- and 1,4-addition onto the diene moiety.

The proposed reaction mechanism differs from the mechanism reported for the cationic rhodium complexes [Rh(nbd)L$_n$]$^+$A$^-$ (**54**); that is, in the present case a "dihydride route" is favored by the authors, implying that first molecular hydrogen is activated to yield the rhodium dihydride species [Rh(H)$_2$L$_n$] (**61**). This species subsequently reacts with the substrate's conjugated diene fragment. However, formation of the proposed rhodium(dihydride) species from the precursor catalyst [RhH(CO)(PPh$_3$)$_3$] **60** has not been disclosed. Based on the product distribution, the authors suggest that the diene initially coordinates in an η^2-fashion (complex **62**), showing preference for the least-substituted double bond (Scheme 14.20). The presence of [Rh(η^4-diene)] complexes has not been ruled out as possible intermediates in the product formation, and could be the bias for the observed chemoselectivity. After transfer of the first hydride to the substrate, either a [Rh(η^3-allyl)] complex (**63 a**) or the [Rh(η^1-allyl)] complex (**63 b**) is formed; the latter species leads to overall 1,2-addition, while [Rh(η^3-allyl)] leads to both 1,2- as well as 1,4-addition. Although the dihydride route is the favored mechanism, a catalytic cycle based on a rhodium-monohydride has not been excluded.

Finally, other rhodium catalysts for the selective diene hydrogenation worth mentioning include [RhCl(PPh$_3$)$_3$] (**64**), [RhCl(nbd)]$_2$ (**65**), and the catalytic sys-

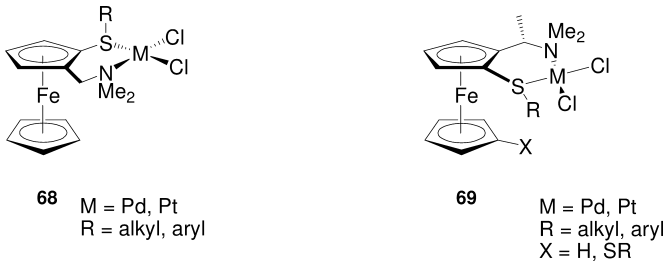

Fig. 14.3 General structures of compounds **68** and **69**.

tems resulting from protonation of $[Rh(CO_2Me)_2(PPh_3)_2]$ (**66**) or $[Rh(CO_2Me)(PPh_3)_3]$ (**67**) precursors [25, 77]. Generally, these complexes show chemoselectivity that is similar to or lower than that of the cationic rhodium complexes $[Rh(nbd)L_n]^+A^-$ (**54**), with comparable reaction rates. The observed selectivity for these systems is attributed principally to the much higher coordinating power of dienes compared with monoenes. Catalysts **64**, **65**, **66** and **67** reduce conjugated dienes by 1,2- as well as 1,4-addition of hydrogen, yielding mixtures of monoenes.

14.2.7
Palladium and Platinum Catalysts

Palladium has been frequently used to reduce conjugated dienes to monoenes. Most of the catalysts based on palladium consist of palladium species – that is, mononuclear complexes and Pd nanoparticles that are heterogenized on a solid support. Both mineral and organic supports have been successfully employed in these systems and, in addition, various hydrogen donors can be used, namely dihydrogen, Group XIII or XIV metal hydrides, and various formate salts. The number of homogeneous palladium complexes able to hydrogenate conjugated dienes to monoenes using molecular hydrogen is very limited. The majority of the accounts reported in the open literature concerning these homogeneous palladium catalysts merely state the observed activity and, hence, the mechanistic details mostly remain obscure.

A large variety of palladium complexes of the general type **68** and **69** (Fig. 14.3), containing ferrocenyl-amine-sulfide or -selenide ligands, are active catalysts for the selective hydrogenation of conjugated dienes to monoenes [85, 86]. The best results (at H_2 pressure of 4–7 bar and room temperature) have been obtained with cyclic substrates. 1,3-Cyclooctadiene is converted into cyclooctene, with the most efficient catalyst reported for this transformation being $[\eta^2\text{-}\{FeCpC_5H_3(CH_2NMe_2)(S(t\text{-}Bu)\}PdCl_2]$, with a TOF of 345 mol mol^{-1} h^{-1} and a selectivity of 97.2% [87]. Higher activities are accompanied by lower selectivities due to a higher degree of over-reduction to cyclooctane. Acyclic dienes yielded less satisfactory results, although these substrates are selectively hydro-

Table 14.4 Selective hydrogenation of 1,3-cyclooctadiene to cyclooctene with various palladium complexes.

	Catalyst	Induction time [h]	Conversion [%]	TOF [mol mol^{-1} h^{-1}]	Selectivity [%]	Reference
1	[{$FeCpC_5H_3(CH_2NMe_2)(SMe)$}$PdCl_2$] [a)]	49.7	100	14	94.1	87
2	[{$FeCpC_5H_3(CH_2NMe_2)(SEt)$}$PdCl_2$] [a)]	42.3	100	15	98.4	87
3	[{$FeCpC_5H_3(CH_2NMe_2)(S(n\text{-}Pr))$}$PdCl_2$] [a)]	37.5	100	16	90.9	87
4	[{$FeCpC_5H_3(CH_2NMe_2)(S(t\text{-}Bu))$}$PdCl_2$] [a)]	0.0	100	345	97.2	87
5	[{$FeCpC_5H_3(CH_2NMe_2)(S(4\text{-tolyl}))$}$PdCl_2$] [a)]	0.0	100	691	78.5	87
6	[{$FeCpC_5H_3(CHMeNMe_2)(SMe)$}$PdCl_2$	42.5	100	17	96.7	85
7	[{$FeCpC_5H_3(CHMeNMe_2)(S(4\text{-tolyl}))$}$PdCl_2$]	0	98.6	465	91.9	85
8	[{$FeCpC_5H_3(CHMeNMe_2)(S(4\text{-ClPh})$}$PdCl_2$]	0	100	684	96.8	85

a) 9.0 mL acetone, 2.0×10^{-5} mol, 7.45×10^{-3} mol substrate, room temperature, 4 bar H_2.
b) 9.0 mL acetone, 2.0×10^{-5} mol, 7.45×10^{-3} mol substrate, room temperature, 7 bar H_2.

genated by 1,4-addition to give the monoenes. A subsequent isomerization reaction leads to product mixtures and, hence, lower stereoselectivities.

The testing of a wide variety of substituted palladium complexes with ferrocene-based diphosphines has revealed several trends. One of the most apparent trends is that increasing the steric bulk on both the amine and the sulfide substituents increases the rate of the reaction, while the monoene selectivity is retained (Table 14.4). The hydrogenation reaction is strongly dependent on the solvent used, and the best results are obtained in acetone. It has been suggested that the solvent is involved in dissociation of the thioether ligand to create a free coordination site, to accommodate the diene [87]. In line with this observation, it appears that neither the platinum aminothioether complexes nor the palladium or platinum complexes of the homologous amino-selenide ligands are active hydrogenation catalysts. Apparently, the Pt–S, Pt–Se and the Pd–Se bonds are too strong, which prevents the required ligand dissociation needed to form an active catalyst. In addition, some catalysts display an induction period before the active catalyst is formed. No further mechanistic details about these catalytic systems have been reported.

Palladium-allyl complexes in combination with stabilizing ligands (e.g., phosphine, halide, allyl, and dienes) are able to hydrogenate conjugated dienes and non-conjugated dienes to the corresponding monoenes under relatively mild reaction conditions [88]. One of the most effective catalytic systems concerns [Pd(L)(PPh_3)Cl] (**70a**, L=allyl; **70b**, L=1-Me-allyl) in *N,N*-dimethylformamide. Hydrogenation reactions performed at 55 °C and 1 bar H_2 using **70b** show a moderate rate ($\sim$10 mol mol^{-1} h^{-1} determined at 50% conversion) in the hydrogenation of 1,5- and 1,3-cyclooctadiene. However, these catalysts appear to be completely inactive towards the hydrogenation of monoenes (cyclooctene, cyclohexene and 1-octene), thereby corroborating the proposal that the catalysis is

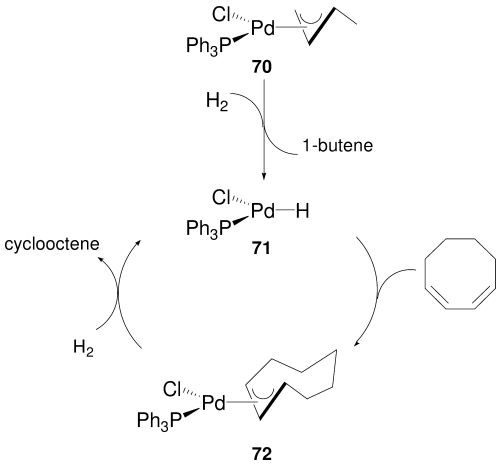

Scheme 14.21 Selective hydrogenation of 1,3-cyclooctadiene catalyzed by [Pd(1-Me-allyl)PPh_3Cl] (**70**) [88].

performed by the mononuclear palladium species. In case of hydrogenation of non-conjugated dienes, the substrate is isomerized to the corresponding conjugated diene prior to hydrogenation.

The influence of hydrogen pressure, substrate and catalyst concentration has briefly been mentioned. The reaction rate is dependent upon the catalyst concentration and hydrogen pressure, but appears to be independent of substrate concentration. The mechanism is proposed to involve the activation of the parent [Pd(allyl)] species producing an unstable hydrido-Pd(II) species (**71**), ensued by a fast reaction with the diene to restore the [Pd(allyl)] moiety (**72**) (Scheme 14.21). The observation that most of the starting material is isolated after the reaction suggests that only a small portion of the catalyst is active under the reaction conditions. Although a complete selectivity for the monoene is observed (even after full conversion), the presence of catalytically active colloidal palladium has not been completely excluded.

14.2.8
Conclusions

The homogeneous hydrogenation of dienes, especially of conjugated dienes remains a challenge, and only a few catalysts have been reported that show good chemo- and stereoselectivity. Until now, the most widely and best explored catalyst for this reaction is constituted by the group of [$Cr(CO)_3$(arene)] (**45**) and [$Rh(nbd)L_n]^+A^-$ (**54**) complexes. Clearly, this is a research area that has received relatively little attention in the past, and several of the catalytic systems discussed seem to be promising candidates for future investigations.

Abbreviations

DFT	density functional theory
PHIP	*para*hydrogen induced polarization
THF	tetrahydrofuran
TOF	turnover frequency
TON	turnover number

References

1 Hutchins, R.O., Hutchins, M.G.K., in: Patai, S., Rappoport, Z. (Eds.), *Reduction of Triple-Bonded Groups, The Chemistry of Functional Groups*. John Wiley & Sons Ltd, New York, **1983**; Vol. 1, pp. 571.

2 Schlögl, R., Noack, K., Zbinden, H., Reller, A., *Helv. Chim. Acta* **1987**, *70*, 627.

3 Molnár, A., Sárkány, A., Varga, M., *J. Mol. Catal. A* **2001**, *173*, 185.

4 Ulan, J.G., Maier, W.F., Smith, D.A., *J. Org. Chem.* **1987**, *52*, 3132.

5 Sodeoka, M., Shibasaki, M., *J. Org. Chem.* **1985**, *50*, 1147.

6 Sodeoka, M., Shibasaki, M., *Synthesis* **1993**, 643.

7 Vasil'ev, A.A., Serebryakov, E.P., *Russ. Chem. Bull.* **2002**, *51*, 1341.

8 Bianchini, C., Meli, A., Peruzzini, M., Frediani, P., Bohanna, C., Esteruelas, M.A., Oro, L.A., *Organometallics* **1992**, *11*, 138.

9 Bianchini, C., Meli, A., Peruzzini, M., Vizza, F., Zanobini, F., *Organometallics* **1989**, *8*, 2080.

10 Esteruelas, M.A., Oro, L.A., *Chem. Rev.* **1998**, *98*, 577.

11 Bianchini, C., Bohanna, C., Esteruelas, M.A., Frediani, P., Meli, A., Oro, L.A., Peruzzini, M., *Organometallics* **1992**, *11*, 3837.

12 Eckert, J., Albinati, A., White, R.P., Bianchini, C., Peruzzini, M., *Inorg. Chem.* **1992**, *31*, 4241.

13 Cabeza, J.A., in: Braunstein, P., Oro, L.A., Raithby, P.R. (Eds.), *Homogeneous Catalysis with Ruthenium Carbonyl Cluster Complexes: Metal Clusters in Chemistry*, Vol. 2. Wiley-VCH GmbH, Weinheim, **1999**, pp. 715.

14 Albers, M.O., Singleton, E., Viney, M.M., *J. Mol. Cat.* **1985**, *30*, 213.

15 Nkosi, B.S., Coville, N.J., Albers, M.O., Singleton, E., *J. Mol. Cat.* **1987**, *39*, 313.

16 Lough, A.J., Morris, R.H., Ricciuto, L., Schleis, T., *Inorg. Chim. Acta* **1998**, *270*, 238.

17 Schleyer, D., Niessen, H.G., Bargon, J., *New J. Chem.* **2001**, *25*, 423.

18 Andriollo, A., Esteruelas, M.A., Meyer, U., Oro, L.A., Sanchez-Delgado, R.A., Sola, E., Valero, C., Werner, H., *J. Am. Chem. Soc.* **1989**, *111*, 7431.

19 Werner, H., Meyer, U., Esteruelas, M.A., Sola, E., Oro, L.A., *J. Organomet. Chem.* **1989**, *366*, 187.

20 Espuelas, J., Esteruelas, M.A., Lahoz, F.J., Oro, L.A., Valero, C., *Organometallics* **1993**, *12*, 663.

21 Schrock, R.R., Osborn, J.A., *J. Am. Chem. Soc.* **1976**, *98*, 2143.

22 Dickson, R.D., in: *Homogeneous Catalysis with Compounds of Rhodium and Iridium, Catalysis by Metal Complexes*. D. Reidel Publishing Co., Dordrecht, **1985**, pp. 40.

23 de Wolf, E., Spek, A.L., Kuipers, B.W.M., Philipse, A.P., Meeldijk, J.D., Bomans, P.H.H., Frederik, P.M., Deelman, B.-J., van Koten, G., *Tetrahedron* **2002**, *58*, 3911.

24 Chaloner, P.A., Esteruelas, M.A., Joó, F., Oro, L.A., in: *Homogeneous Hydrogenation*. Kluwer Academic Publishers, Dordrecht, **1993**.

25 Spencer, A., *J. Organomet. Chem.* **1975**, *93*, 389.

26 Burk, M.J., Gerlach, A., Semmeril, D., *J. Org. Chem.* **2000**, *65*, 8933.

27 Crabtree, R. H., Gautier, A., Giordano, G., Khan, T., *J. Organomet. Chem.* **1977**, *141*, 113.
28 Usón, R., Oro, L. A., Sariego, R., Valderrama, M., Rebullida, C., *J. Organomet. Chem.* **1980**, *197*, 87.
29 Esteruelas, M. A., González, I., Herrero, J., Oro, L. A., *J. Organomet. Chem.* **1998**, *551*, 49.
30 Esteruelas, M. A., López, A. M., Oro, L. A., Pérez, A., Schulz, M., Werner, H., *Organometallics* **1993**, *12*, 1823.
31 Chen, W., Esteruelas, M. A., Herrero, J., Lahoz, F. J., Martín, M., Oñate, E., Oro, L. A., *Organometallics* **1997**, *16*, 6010.
32 Pelagatti, P., Venturini, A., Leporati, A., Carcelli, M., Costa, M., Bacchi, A., Pelizzi, G., Pelizzi, C., *J. Chem. Soc., Dalton Trans.* **1998**, 2715.
33 Costa, M., Pelagatti, P., Pelizzi, C., Rogolino, D., *J. Mol. Catal. A* **2002**, *178*, 21.
34 van Laren, M. W., Duin, M. A., Klerk, C., Naglia, M., Rogolino, D., Pelagatti, P., Bacchi, A., Pelizzi, C., Elsevier, C. J., *Organometallics* **2002**, *21*, 1546.
35 van Laren, M. W., Elsevier, C. J., *Angew. Chem., Int. Ed.* **1999**, *38*, 3715.
36 Sulman, E., Deibele, C., Bargon, J., *React. Kinet. Catal. Lett.* **1999**, *67*, 117.
37 Choudary, B. M., Sharma, G. V. M., Bharathi, P., *Angew. Chem.* **1989**, *101*, 506.
38 Elman, B., Moberg, C., *J. Organomet. Chem.* **1985**, *294*, 117.
39 Ferrari, C., Predieri, G., Tiripicchio, A., Costa, M., *Chem. Mater.* **1992**, *4*, 243.
40 Holy, N. L., Shelton, S. R., *Tetrahedron* **1981**, *37*, 25.
41 Islam, M., Bose, A., Mal, D., Saha, C. R., *J. Chem. Res., Synop.* **1998**, 44.
42 Moberg, C., Rakos, L., *J. Organomet. Chem.* **1987**, *335*, 125.
43 Sobczak, J. W., Lesiak, B., Jablonski, A., Kosinski, A., Palczewska, W., *Pol. J. Chem.* **1995**, *69*, 1732.
44 Stern, E. W., Maples, P. K., *J. Catal.* **1972**, *27*, 120.
45 Evrard, D., Groison, K., Mugnier, Y., Harvey, P. D., *Inorg. Chem.* **2004**, *43*, 790.
46 Niessen, H. G., Eichhorn, A., Woelk, K., Bargon, J., *J. Mol. Catal. A* **2002**, *182*, 463.
47 van Asselt, R., Elsevier, C. J., *J. Mol Catal. A* **1991**, *65*, L13.
48 Elsevier, C. J., *Coord. Chem. Rev.* **1999**, *185*, 809.
49 Kluwer, A. M., Koblenz, T. S., Jonischkeit, T., Woelk, K., Elsevier, C. J., *J. Am. Chem. Soc.* **2005**, *127*, 15470.
50 Bacchi, A., Carcelli, M., Costa, M., Leporati, A., Leporati, E., Pelagatti, P., Pelizzi, C., Pelizzi, G., *J. Organomet. Chem.* **1997**, *535*, 107.
51 Pelagatti, P., Bacchi, A., Carcelli, M., Costa, M., Fochi, A., Ghidini, P., Leporati, E., Masi, M., Pelizzi, C., Pelizzi, G., *J. Organomet. Chem.* **1999**, *583*, 94.
52 Costa, M., Pelagatti, P., Pelizzi, C., Rogolino, D., *J. Mol. Catal. A* **2002**, *178*, 21.
53 Raoult, Y., Choukroun, R., Basso-Bert, M., Gervais, D., *J. Mol. Cat.* **1992**, *72*, 47.
54 Raoult, Y., Choukroun, R., Blandy, C., *Organometallics* **1992**, *11*, 2443.
55 Raoult, Y., Choukroun, R., Gervais, D., *J. Organomet. Chem.* **1990**, *399*, C1.
56 Cais, M., Frankel, E. N., Rejoan, A., *Tetrahedron Lett.* **1968**, *9*, 1919.
57 Frankel, E. N., Selke, E., Grass, C. A., *J. Am. Chem. Soc.* **1968**, *90*, 2446.
58 Yagupsky, G., Cais, M., *Inorg. Chim. Acta* **1975**, *12*, L27.
59 Wrighton, M. S., Schroeder, M. A., *J. Am. Chem. Soc.* **1973**, *95*, 5764.
60 Schroeder, M. A., Wrighton, M. S., *J. Organomet. Chem.* **1974**, *74*, C29.
61 Chandiran, T., Vancheesan, S., *J. Mol. Cat.* **1992**, *71*, 291.
62 Chandiran, T., Vancheesan, S., *J. Mol Cat.* **1994**, *88*, 31.
63 Frankel, E. N., Butterfield, R. O., *J. Org. Chem.* **1969**, *34*, 3930.
64 Airoldi, M., Deganello, G., Dia, G., Gennaro, G., *Inorg. Chem. Acta* **1983**, *68*, 179.
65 Airoldi, M., Deganello, G., Dia, G., Gennaro, G., *J. Organomet. Chem.* **1980**, *187*, 391.
66 Steines, S., Engelert, U., Drießen-Hölscher, B., *Chem. Commun.* **2000**, 217.
67 Steines, S., Wasserscheid, P., Drießen-Hölscher, B., *J. Prakt. Chem.* **2000**, *342*, 348.
68 Niessen, H. G., Schleyer, D., Wiemann, S., Bargon, J., Steines, S., Drießen-Hölscher, B., *Magn. Reson. Chem.* **2000**, *38*, 747.

69 Funabiki, T., Matsumoto, M., Tarama, K., *Bull. Chem. Soc. Jpn.* **1972**, *45*, 2723.
70 Funabiki, T., Kasaoka, S., Matsumoto, M., Tarama, K., *J. Chem. Soc., Dalton Trans.* **1974**, 2043.
71 Reger, D. L., Habib, M. M., Fauth, D. J., *J. Org. Chem.* **1980**, *45*, 3860.
72 Lee, J. T., Alper, H., *J. Org. Chem.* **1990**, *55*, 1854.
73 Reger, D. L., Habib, M. M., *J. Mol. Cat.* **1978**, *4*, 315.
74 Reger, D. L., Habib, M. M., *J. Mol. Cat.* **1980**, *7*, 365.
75 Reger, D. L., Gabrielli, A., *J. Mol. Cat.* **1981**, *12*, 173.
76 Schrock, R. R., Osborn, J. A., *J. Am. Chem. Soc.* **1976**, *98*, 4450.
77 Heldal, J. A., Frankel, E. N., *J. Am. Oil Chem. Soc.* **1985**, *62*, 1117.
78 Aimé, S., Canet, D., Dastrù, W., Gobetto, R., Reineri, F., Viale, A., *J. Phys. Chem. A* **2001**, *105*, 6305.
79 Drexler, H. J., Baumann, W., Spannenberg, A., Fischer, C., Heller, D., *J. Organomet. Chem.* **2001**, *621*, 89.
80 Cobley, C. J., Lennon, I. C., McCague, R., Ramsden, J. A., Zanotti-Gerosa, A., in: H. U. Blaser, E. Schmidt (Eds.), *Asymmetric Catalysis on Industrial Scale*. Wiley-VCH, Weinheim, Germany, **2004**, p. 269.
81 Schrock, R. R., Osborn, J. A., *J. Am. Chem. Soc.* **1976**, *98*, 2134.
82 Bargon, J., Kandels, J., Kating, P., Thomas, A., Woelk, K., *Tetrahedron Lett.* **1990**, *31*, 5721.
83 Burk, M.J., Allen, J. G., Kiesman, W.F., *J. Am. Chem. Soc.* **1998**, *120*, 657.
84 Speziali, M. G., Moura, F. C. C., Robles-Dutenhefner, P. A., Araujo, M. H., Gusevskaya, E. V., dos Santos, E. N., *J. Mol. Cat. A* **2005**, *239*, 10.
85 Naiini, A. A., Lai, C. K., Ward, D. L., Brubaker, C. H., Jr., *J. Organomet. Chem.* **1990**, *390*, 73.
86 Lai, C. K., Naiini, A. A., Brubaker, C. H., Jr., *Inorg. Chim. Acta* **1989**, *164*, 205.
87 Okoroafor, M. O., Shen, L. H., Honeychuck, R. V., Brubaker, C. H., Jr., *Organometallics* **1988**, *7*, 1297.
88 Strukul, G., Carturan, G., *Inorg. Chim. Acta* **1979**, *35*, 99.

15
Homogeneous Hydrogenation of Aldehydes, Ketones, Imines and Carboxylic Acid Derivatives: Chemoselectivity and Catalytic Activity

Matthew L. Clarke and Geoffrey J. Roff

15.1
Introduction

The reduction of aldehydes, ketones, esters, acids, and anhydrides to alcohols is one of the most fundamental and widely employed reactions in synthetic chemistry. Sodium borohydride, lithium aluminum hydride and other stoichiometric reducing agents are often perfectly adequate reagents for laboratory-scale syntheses. In an industrial setting, however, the increased demands for atom economy, cleaner synthesis and straightforward work-up procedures make the use of these reagents disadvantageous. Reduction procedures that make use of molecular hydrogen show better ecology, are more cost-effective, and are potentially easier to operate than those that require the clean-up of boron or aluminum waste at the end of the reaction. The hydrogenation of C=O (and C=N) bonds is therefore the preferred method for their reduction.

Heterogeneous catalysts such as Pd/C and Pt/C are widely used for this purpose, and often represent the most economical method to carry out these reductions. However, in cases where milder conditions, functional group tolerance and chemoselectivity are required, heterogeneous catalysts can be unsuitable for the task. There has therefore been a substantial research effort aimed towards developing homogeneous catalysts for this purpose.

This chapter aims to provide an overview of the current state of the art in homogeneous catalytic hydrogenation of C=O and C=N bonds. Diastereoselective or enantioselective processes are discussed elsewhere. The chapter is divided into sections detailing the hydrogenation of aldehydes, the hydrogenation of ketones, domino-hydroformylation-reduction, reductive amination, domino hydroformylation-reductive amination, and ester, acid and anhydride hydrogenation.

The Handbook of Homogeneous Hydrogenation.
Edited by J.G. de Vries and C.J. Elsevier
Copyright © 2007 WILEY-VCH Verlag GmbH & Co. KGaA, Weinheim
ISBN: 978-3-527-31161-3

15.2 Hydrogenation of Aldehydes

15.2.1 Iridium Catalysts

The first report of a catalytic system for the effective homogeneous hydrogenation of an aldehyde to an alcohol was published during the late 1960s [1]. Coffey reported that the use of a catalyst prepared *in situ* by the reaction of $[Ir(H)_3(PPh_3)_3]$ with acetic acid was effective for the hydrogenation of *n*-butyraldehyde to *n*-butanol at 50 °C and at 1 bar (Scheme 15.1). The reaction was found to be first order in both substrate and catalyst concentration, and to be highly dependent upon the solvent. No hydrogenation occurred in undiluted aldehyde or in toluene, but the addition of acetic acid initiated gas uptake. The active catalytic species was thought to be $[Ir(H)_2(CH_3COO)(PPh_3)_3]$.

This catalytic system was further studied by Strohmeier and Steigerwald, who performed reactions at 10 bar without solvent to achieve hydrogenation of a series of aldehydes (Table 15.1) [2]. Turnover numbers (TON) of up to 8000 were achieved in the case of the hydrogenation of benzaldehyde. The chemoselectivity of this catalyst towards carbonyl hydrogenation over alkene hydrogenation was

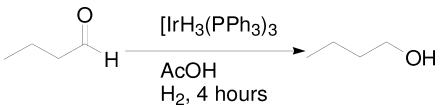

Scheme 15.1 Hydrogenation of *n*-butyraldehyde.

Table 15.1 Hydrogenation of aldehydes with $[IrH_3(PPh_3)_3]$ in acetic acid.

Substrate	Catalyst [mol.%]	Temperature [°C]	Yield [%]	TON	TOF [h^{-1}]
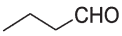	0.022	80	73	3280	492
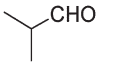	0.023	110	82	3540	177
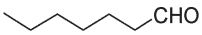	0.032	90	64	2000	89
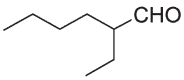	0.039	110	80	2030	81
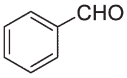	0.013	110	98	7780	259

examined for α,β-unsaturated aldehydes (Scheme 15.2). Using the $[IrH_3(PPh_3)_3]$ complex in acetic acid for the hydrogenation of crotonaldehyde resulted in the formation of the saturated alcohol (Scheme 15.3). It was also noted that this catalyst did not allow for ketone hydrogenation at 10 bar.

Other attempts to use iridium PPh_3 complexes such as $[IrCl(PPh_3)_3]$, $[IrCl(CO)(PPh_3)_2]$, $[Ir(ClO_4)(CO)(PPh_3)_2]$ and $[Ir(CO)(PPh_3)_3]ClO_4$ to hydrogenate unsaturated aldehydes did not yield great results [3], mainly because these catalysts suffered from low activity and selectivity.

The catalytic system of $[Ir(COD)Cl]_2$ with an excess of the bulky phosphine $P(o\text{-}MeOPh)_3$ under transfer hydrogenation conditions of propan-2-ol and KOH was used successfully in the selective hydrogenation of cinnamaldehyde (Scheme 15.4) [4]. Selectivity and activity were found to increase with increasing P/Ir ratios, and complete conversion was achieved in as little as 5 minutes (turnover frequency (TOF) $\sim 6000\ h^{-1}$).

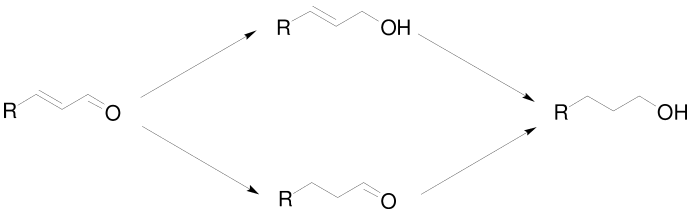

Scheme 15.2 Distribution of products in the hydrogenation of α,β-unsaturated aldehydes.

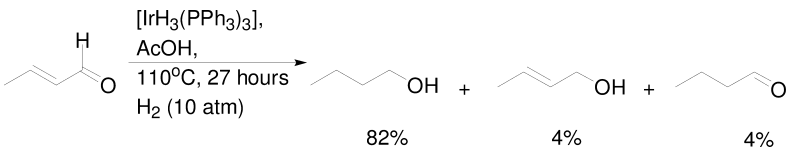

Scheme 15.3 Hydrogenation of crotonaldehyde with $[IrH_3(PPh_3)_3]$ in acetic acid.

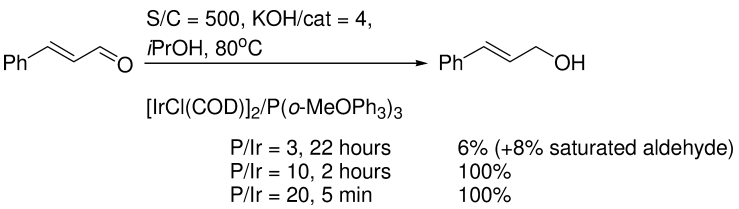

Scheme 15.4 Transfer hydrogenation of cinnamaldehyde.

Using molecular hydrogen as the reducing agent, $[Ir(COD)(OCH_3)]_2$ with an excess of tertiary phosphine was better than $[Ir(COD)Cl]_2$ for the selective hydrogenation of cinnamaldehyde [5]. In these studies, a great dependence on solvent and ligand was reported. A variety of different phosphines, which were markedly different in their steric and electronic properties, were examined in this reaction. In propan-2-ol the most effective phosphine was PCy_2Ph which gave 94% yield (TOF 235 h^{-1}) of the unsaturated alcohol in a 2 h reaction under 30 bar H_2 at 100 °C. Phosphines such as $PCyPh_2$, $PPhPr^i_2$, PPh_2Pr^i and $PEtPh_2$ were also effective in giving over 95% selectivity. The less-effective phosphines were PEt_2Ph, $PMePh_2$, PBu^i_3 and PMe_2Ph. Reactions that were performed in toluene were generally less effective.

More recent advances in iridium-catalyzed aldehyde hydrogenation have been through the use of bidentate ligands [6]. In the hydrogenation of citral and cinnamaldehyde, replacing two triphenylphosphines in $[IrH(CO)(PPh_3)_3]$ with bidentate phosphines BDNA, BDPX, BPPB, BISBI and PCP (Fig. 15.1) led to an increase in catalytic activity.

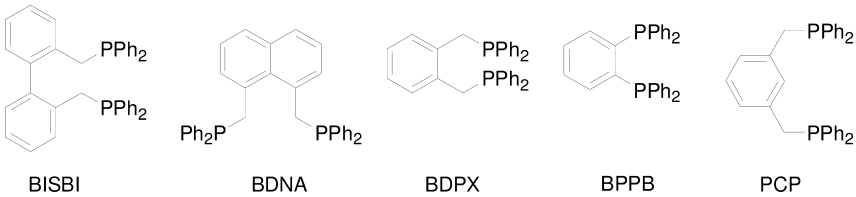

Fig. 15.1 Bidentate ligands employed in Ir-catalyzed hydrogenation.

Table 15.2 Bidentate ligands used for the hydrogenation of citral and cinnamaldehyde under 50 bar H_2 at 100 °C.

Complex	Substrate	Conversion [%]	Selectivity [%] a)	TOF [h^{-1}] b)
$[IrH(CO)(PPh_3)_3]$	Citral	3.1	70.5	7
	Cinnamaldehyde	11.4	35.0	61
$[IrH(CO)(PPh_3)(BPPB)]$	Citral	7.7	61.2	18
	Cinnamaldehyde	27.3	19.3	146
$[IrH(CO)(PPh_3)(BISBI)]$	Citral	11.6	92.2	28
	Cinnamaldehyde	44.6	13.1	238
$[IrH(CO)(PPh_3)(BDNA)]$	Citral	19.3	95.8	46
	Cinnamaldehyde	20.6	77.4	110
$[IrH(CO)(PPh_3)(BDPX)]$	Citral	58.8	96.4	141
	Cinnamaldehyde	58.1	9.0	310
$[IrHCl(CO)(PCP)]$	Citral	13.9	42.5	33
	Cinnamaldehyde	52.0	1.3	277

a) Selectivity of allylic alcohol formed as a percentage of total hydrogenation products.
b) TOF (h^{-1}) expressed for conversion of starting material.

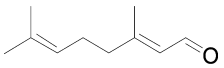

Fig. 15.2 Citral.

Even though the activity was better than the PPh_3 analogue (Table 15.2), the conversion was still low. Of the ligands tested, BDPX showed the greatest promise in selectivity for citral (Fig. 15.2).

The selectivities in forming cinnamyl alcohol from cinnamaldehyde using these catalysts were poor, and generally resulted in the formation of the saturated aldehyde. This could be overcome by the use of a large excess of phosphine, though at the expense of yield. The same group have demonstrated that ruthenium analogues of the BDNA complex are more active and selective [7].

15.2.2 Rhodium Catalysts

Wilkinson's catalyst $[RhCl(PPh_3)_3]$ [8], a convenient catalyst for the hydrogenation of olefins, was found to be deactivated by aldehydes to give the catalytically non-active complex $[RhCl(CO)(PPh_3)_2]$ as a result of the competing decarbonylation reaction. Despite the lack of activity of this catalyst, extensive investigations have been made into rhodium catalysis for aldehyde hydrogenation, and these have led to the development of some highly efficient catalysts.

15.2.2.1 Rh-amine Catalysts

The first report of rhodium catalysts for aldehyde reduction came from Marko who reported the use of $RhCl_3 \cdot 3H_2O$ under hydroformylation conditions [9]. It was suggested that the active species were rhodium carbonyls, and the catalyst system was successfully utilized in the hydrogenation of ethanal, propanal, and benzaldehyde.

In the presence of strongly basic amines, $RhCl_3 \cdot 3H_2O$ was effective in catalyzing the hydrogenation of cinnamaldehyde [10]. In the absence of carbon monoxide or triethylamine, however, only small amounts of hydrogenated products were obtained. Under hydroformylation conditions with increasing concentrations of triethylamine, catalytic activity and selectivity to cinnamyl alcohol were increased. The effect of the amines was found to be very important. Primary or secondary amines were ineffective in producing hydrogenation products. Strongly basic tertiary amines such as triethylamine and *N*-methylpyrolidine were more effective for activity and selectivity. The addition of triphenylphosphine increased hydrogenation of the carbon–carbon double bond, giving dihydrocinnamaldehyde. The activity of $RhCl_3 \cdot 3H_2O$ at lower temperatures can be increased by the pretreatment with CO giving $RhCl_2(CO)_4$ and allowing hydrogenations to occur at 60 °C with up to 94% yield and 85% selectivity in a 1-h reaction (TOF = 289 h^{-1}).

The rhodium carbonyl cluster $[Rh_6(CO)_{16}]$, in combination with the diamine *N,N,N′*,N′-tetramethyl-1,3-propanediamine is an effective catalytic system for the

hydrogenation of saturated and unsaturated aldehydes in water under a pressure of carbon monoxide and hydrogen [11]. In reactions lasting only a few hours, and using a substrate catalyst ratio of 300, simple aldehydes are converted in quantitative yields. The unsaturated aldehydes take longer to react, but the selectivity favors the formation of unsaturated alcohols in high yields.

15.2.2.2 **Cationic Rhodium Phosphine Catalysts**

The effect of the phosphines has been further studied by the hydrogenation of aldehydes and ketones in the presence of the cationic species $[Rh(nbd)(PR_3)_2]ClO_4$ [12]. Both, triethylphosphine and trimethylphosphine complexes showed the greatest activity (triethylphosphine being preferred), whereas triphenylphosphine-based catalysts showed little or no activity and the diphosphine (dppe) complex inhibited the reaction completely. At 30 °C and under 1 bar H_2, the triethylphosphine catalyst could complete the hydrogenation of benzaldehyde in 24 h, whereas under the same conditions it could only manage 80% and 41% hydrogenation for phenylacetaldehyde and *n*-butyraldehyde, respectively. The presence of propane and propene in the reaction mixture of *n*-butyraldehyde hydrogenation suggests the occurrence of a certain degree of decarbonylation, which leads to deactivation of the catalyst.

An alternative air-stable cationic rhodium complex [(COD)Rh(DiPFc)]OTf is an efficient catalyst precursor for the hydrogenation of aldehydes and ketones [13]. This is the first useful diphosphine-based catalyst, possibly due to backbone rigidity and strong electron-donating alkyl-substituted phosphorus atoms. Using this commercially available catalytic system, benzaldehyde can be converted to benzyl alcohol under mild conditions. Using a substrate : catalyst ratio (SCR) of 500 : 1, a quantitative yield was obtained in 3 h at 25 °C and under only 4 bar hydrogen (TOF $\sim 165\ h^{-1}$). Unlike some alternative catalysts, there was no deactivation of the catalyst through decarbonylation, and a range of saturated aldehydes have been successfully hydrogenated in the presence of this catalyst (Fig. 15.3).

The hydrogenations were active either with the isolated catalyst or *in situ* generation of the catalyst by the reaction of DiPFc with $[(COD)_2Rh]OTf$ in methanol (Scheme 15.5). Both, the components and the isolated catalysts are available from Strem Chemicals.

The solid catalyst is stable to oxygen and moisture, showing no loss of activity when exposed to the atmosphere for several days. However, the catalyst reacts fairly rapidly with oxygen when in solution and this leads to catalyst deactivation, a problem which is easily overcome by simply degassing the reaction solvent.

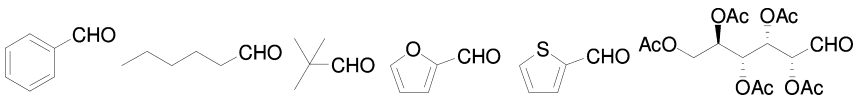

Fig. 15.3 Substrates hydrogenated using $[Rh(dippf)(COD)]^+OTf^-$.

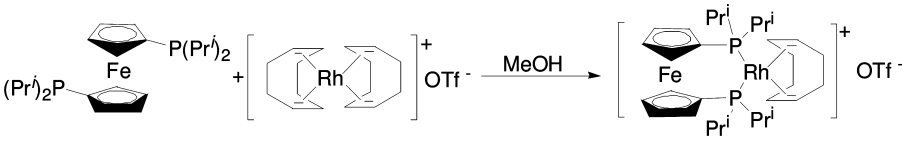

Scheme 15.5 Preparation of cationic DiPFc catalyst.

The Rh-DiPFc catalyst has recently been immobilized on modified alumina essentially to provide an immobilized homogeneous catalyst [14]. Although in this form it is strictly a heterogeneous catalyst, it provides the best of both worlds. These catalysts may be superior to the traditional heterogeneous catalysts in terms of reactivity and selectivity, but benefit over homogeneous catalysts in their ease of removal and re-use. Similar immobilizations have involved the binding of rhodium carbonyl clusters to polymers [15, 16]. Generally high selectivity was observed in the hydrogenation of a series of unsaturated aldehydes either under hydrogen and carbon monoxide or formic acid transfer hydrogenations.

15.2.2.3 **Water-Soluble Rh Catalysts**

Water-soluble complexes constitute an important class of rhodium catalysts as they permit hydrogenation using either molecular hydrogen or transfer hydrogenation with formic acid or propan-2-ol. The advantages of these catalysts are that they combine high reactivity and selectivity with an ability to perform the reactions in a biphasic system. This allows the product to be kept separate from the catalyst and allows for an ease of work-up and cost-effective catalyst recycling. The water-soluble Rh-TPPTS catalysts can easily be prepared *in situ* from the reaction of $[RhCl(COD)]_2$ with the sulfonated phosphine (Fig. 15.4) in water [17].

In the reduction of benzaldehyde performed in water in the presence of Na_2CO_3 and *i*-PrOH, the yields were generally very high. This system was highly effective in 2 h with complete conversion when H_2 was used as the hydrogen donor. Using *i*-PrOH as the hydrogen donor, yields were well above 90% even after recycling of the catalyst several times. Sodium formate could also provide efficient hydrogenation, with over 90% yield. Using iridium analogues resulted in very poor yields. Several other aldehydes were reduced with good yields using the transfer hydrogenation protocol (Fig. 15.5).

This catalyst is chemoselective in the reduction of α,β-unsaturated aldehydes, without any decarbonylation [18]. However, the resulting product was the saturated aldehyde. Generally, at pressures <20 bar H_2 and temperatures between 30 and 80 °C, selectivities exceeding 95% can be achieved in 1 h. Recycling posed no problem with successive runs, showing the same selectivity and activity.

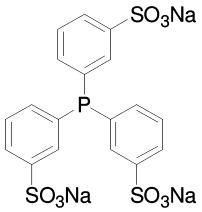

Fig. 15.4 TPPTS.

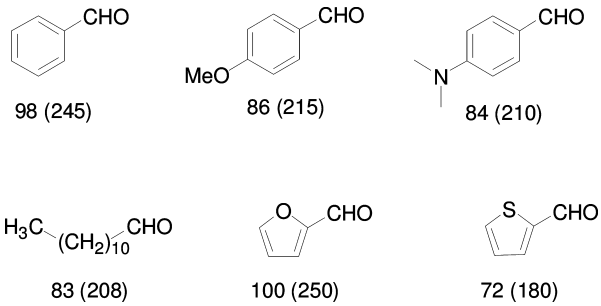

Fig. 15.5 Transfer hydrogenation of aldehydes using $[Rh(COD)Cl]_2$/TPPTS at 80 °C using *i*-PrOH as hydrogen donor. Values shown are yields (TOF, h^{-1}).

15.2.3 Ruthenium Catalysts

15.2.3.1 Ru-PPh_3 Catalysts

The most common carbonyl hydrogenation catalysts are derived from ruthenium species. In early studies, these were generally based on the phosphine-coordinated ruthenium carbonyls that are more commonly used for hydroformylation reactions. Thus, the hydroformylation catalyst $[Ru(CO)_3(PPh_3)_2]$ was shown to be effective in the hydrogenation of propionaldehyde under 20 bar H_2 and at 120 °C [19]. Increasing the temperature and pressure led to an increase in reaction time. Tsuji and Suzuki used the complex $[RuCl_2(PPh_3)_3]$ to hydrogenate a series of aliphatic and aromatic aldehydes [20]. Under 10 bar H_2 the reactions were found to be sluggish at room temperatures, but proceeded smoothly above 70 °C. Hydrogenation of aldehydes in the presence of ketones showed selectivity exclusively for the aldehydes. Benzaldehyde was also exclusively reduced in the presence of nitrobenzene, a substrate which is known to be reduced to aniline under harsh conditions by this catalyst [21]. Strohmeier and Weigelt used the catalyst $[RuCl_2(CO)_2(PPh_3)_2]$ to hydrogenate a series of aldehydes at 15 bar H_2 and at 160–180 °C, with generally high yield and turnover numbers (Table 15.3) [22]. Although these are amongst the highest turnover numbers reported for aldehyde hydrogenation, the reactions were carried out at relatively high temperatures.

Table 15.3 Hydrogenation of simple aldehydes using $RuCl_2(CO)_2(PPh_3)_2$.

Substrate	Catalyst [mol %]	Temperature [°C]	Time [h]	Yield [%]	TON
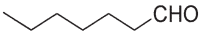	0.0083	180	4	90	10 800
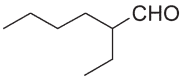	0.0033	160	11	98	29 400
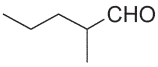	0.0017	160	12	99	59 400
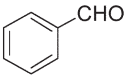	0.0017	180	14	93	56 000

Sanchez-Delgado and De Ochoa achieved excellent conversion of linear aldehydes by introducing chloride ligands [23]. The catalyst precursors $[RuHCl(CO)(PPh_3)_3]$, $[RuHCl(PPh_3)_3]$ and $[RuCl_2(PPh_3)_3]$ were used to reduce both aliphatic and aromatic aldehydes, although benzaldehyde reduction was less efficient than with the previously mentioned $[RuCl_2(CO)_2(PPh_3)_2]$ catalyst. Although $[RuHCl(PPh_3)_3]$ was found to be the more active catalyst, it required inert conditions and promoted decarbonylation of the aldehyde. Evidence of this comes from the presence of metal carbonyl species at the end of reaction. Having carbonyl ligands appears to solve this problem, and $[RuHCl(CO)(PPh_3)_3]$ was found to be the most convenient catalyst. Using propionaldehyde with a SCR of 50 000, turnover numbers of up to 32 000 were achieved after 50 h of continuous reaction at 140 °C under 30 bar H_2 [24]. Using this same catalyst in the reduction of crotonaldehyde, the favored product was the fully saturated alcohol [25].

Hotta, using $[RuHCl(PPh_3)_3]$ and HCl, allowed for highly selective reduction of citral [26]. Using 2.5 mol% $[RuHCl(PPh_3)_3]$ in toluene under 50 bar H_2 at 30 °C, the selectivity achieved was 66%. The addition of 12.5% HCl, and performing the reaction in toluene : ethanol (27 : 3) further increased selectivity to 98%, with 99% conversion. The desirable mild conditions were offset by the relatively low turnover numbers.

15.2.3.2 **Polydentate Ru Catalysts**

The use of polydentate ligands is rare for aldehyde hydrogenation. The ruthenium complex $[RuCl_2(TRIPHOS)]$ $(TRIPHOS = PhP(CH_2CH_2PPh_2)_2$ catalyzes the hydrogenation and isomerization of alkenes, as well as the hydrogenation of aldehydes, ketones, and nitriles [27]. For simple aldehydes such as *n*-propanol, *n*-butanol, and *n*-hexanol, reasonable conversions can be achieved in 2 h under 34 bar H_2 at 100 °C, with turnover numbers of around 1000. In the hydrogenation of crotonaldehyde and cinnamaldehyde, it is the olefinic bond that is reduced favorably, although some unsaturated alcohol is also produced.

Table 15.4 Ru-BDNA-catalyzed hydrogenations of citral and cinnamaldehyde.

Catalyst	Substrate	Conversion [%] a)	Selectivity [%] b)	TOF [h^{-1}] c)
$[RuCl_2(PPh_3)_3]$	Citral	35	36	141
	Cinnamaldehyde	40	62	212
$[RuHCl(CO)(PPh_3)(BDNA)]$	Citral	93	96	371
	Cinnamaldehyde	86	94	461
$[RuH_2(CO)(PPh_3)(BDNA)]$	Citral	64	>99	255
	Cinnamaldehyde	62	95	328

a) 50 bar H_2, 70–80 °C, toluene, SCR 1200 (citral) or 1600 (cinnamaldehyde).
b) Selectivity of allylic alcohol formed as a percentage of total hydrogenation products.
c) TOF expressed for conversion of starting material.

The bidentate ligand BDNA shows good conversions and selectivity in the hydrogenation of citral and cinnamaldehyde [7]. These crystalline complexes are easily prepared by the replacement of triphenylphosphines in several Ru–PPh_3 complexes with BDNA by refluxing for several hours in toluene. In comparison with $[RuCl_2(PPh_3)_3]$, the most promising complexes were $[RuHCl(CO)(PPh_3)(BDNA)]$ and $[RuH_2(CO)(PPh_3)(BDNA)]$ (Table 15.4).

Another bidentate ligand which shows improvements over triphenylphosphine is that of BISBI [28]. The complex $[RuCl_2(PPh_3)(BISBI)]$ shows selectivities over 80%, but the yields are only 40–50% [28]. The analogous iridium complexes are less active, but show similar selectivity [6].

15.2.3.3 **Diamine-Modified Ru Catalysts**

$RuCl_2(PPh_3)_3$ has been shown to catalyze the reduction of several aldehydes, but does not have widespread scope. This catalyst is not chemoselective and, in the presence of alkenes, would favor olefin reduction over that of the aldehyde. Noyori and coworkers showed that chemoselectivity is easily introduced by the addition of ethylene-diamine as a ligand (Scheme 15.6) [29, 30]. This system requires the presence of co-catalytic KOH/*i*-PrOH as an activator.

Using an easily prepared stock solution of $[RuCl_2(PPh_3)_3]/NH_2(CH_2)_2NH_2$ and KOH in *i*-PrOH, unsaturated aldehydes are quantitatively reduced exclusively to unsaturated alcohols (Scheme 15.7).

Direct comparisons of the diamine system against the parent complex led to the conclusion that the effect of the diamine and KOH/*i*-PrOH activator decelerate olefin hydrogenation and in turn accelerate carbonyl hydrogenation. In the published report, there were no attempts to optimize turnover numbers or TOF for aldehyde hydrogenation. However, the catalyst has been shown to hydrogenate ketones with a SCR of 10 000 at room temperature, which suggests that these catalysts represent the current state of the art in terms of activity and selectivity.

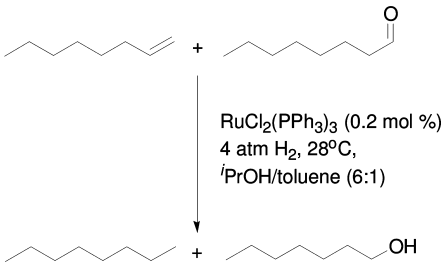

No additive, 150 mins	250	1
$H_2N(CH_2)_2NH_2$ + KOH, 10 Mins (Ru:en:KOH = 1:1:2)	1	1500

Scheme 15.6 Direct comparison of aldehyde and alkene hydrogenation.

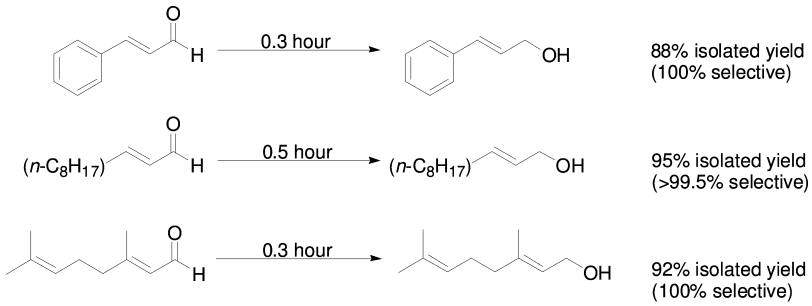

Conditions: 28°C in 6:1 propanol-toluene under 4 atm H_2; Substrate:Ru:en:KOH = 500:1:1:2

Scheme 15.7 Hydrogenation of unsaturated aldehydes using Noyori's system.

15.2.3.4 **Ru-TPPMS/TPPTS Catalysts**

It has been shown previously how water-soluble rhodium Rh-TPPTS catalysts allow for efficient aldehyde reduction, although chemoselectivity favors the olefinic bond in the case of unsaturated aldehydes [17]. The analogous ruthenium complex shows selectivity towards the unsaturated alcohol in the case of crotonaldehyde and cinnamaldehyde [31].

The biphasic reduction of 3-methyl-2-butenal under a pressure of hydrogen demonstrated a non-dependence on solvent (Table 15.5) [18]. Good conversions and selectivities were achieved in a selection of immiscible solvents in just over an hour, using a SCR of 200 : 1. No phase-transfer agents were needed as the slight solubility of the substrate in water ensured a rapid reaction. Under the same conditions, the catalyst was recycled three times with no loss of activity or selectivity: in fact, the reactions were faster than the initial reaction [18]. This was due to the initial run requiring an induction period for formation of the active catalyst. The analogous rhodium catalysts could cleanly reduce unsaturated aldehydes, but the high selectivity was towards the saturated aldehyde.

Table 15.5 Biphasic reduction of 3-methyl-2-butenal.

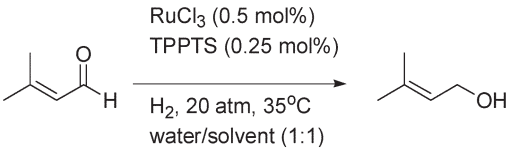

Solvent	Time [min]	Conversion [%]	Selectivity [%]
Cyclohexane	80	99	92
Chloroform	70	84	96
Ethyl acetate	75	93	96
Toluene (fresh catalyst)	60	100	96
Toluene (1st recycle)	30	99	97
Toluene (2nd recycle)	30	99	97

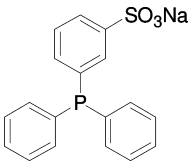

Fig. 15.6 TPPMS.

Table 15.6 Hydrogenation of α,β-unsaturated aldehydes using $[(PPh_3)CuH]_6$ (5 mol% Cu) and $PhPMe_2$ (30 mol%) at room temperature.

Substrate	Pressure [bar]	Conversion [%]	Selectivity [%]	TOF [h^{-1}]
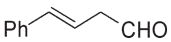	5	94	97	5
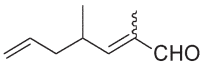	28	91	94	<1
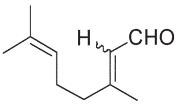	34	90	92	1
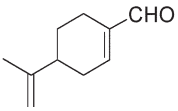	34	95	97	1

The ruthenium complex of the mono-sulfonated TPPMS (Fig. 15.6) is not only good for the transfer hydrogenation of simple substituted benzaldehydes with yields over 90% and with over 98% selectivity [32], but it is also chemoselective in the transfer hydrogenation of *α,β*-unsaturated aldehydes without the aid of phase-transfer agents [33]. The $RuCl_2$/(TPPMS) catalyst was far more effective than either rhodium or iridium TPPMS catalysts [32]. The solution of the catalyst is air-stable in the presence of $HCOO^-$, and the reactions and workups are very simple. In a direct comparison of homogeneous and biphasic reductions of cinnamaldehyde using Ru-PPh_3 catalysts against Ru-TPPMS/TPPTS, the homogeneous Ru-PPh_3 systems were found to favor complete reduction of both the carbonyl and the olefinic bond. In contrast, if aqueous biphasic systems were employed, selectivity was restricted to the carbonyl bond [34].

15.2.4 Other Metal Catalysts

15.2.4.1 Copper

Phenyldimethylphosphine-stabilized copper(I) hydrides catalyze a highly chemoselective hydrogenation of unsaturated aldehydes and ketones [35]. The reaction tolerates the use of either benzene or tetrahydrofuran (THF) as solvent, but requires a high concentration of *tert*-butanol as co-solvent to ensure high turnover and reaction homogeneity. Although high pressures are not required, they must exceed 1 bar in order to obtain complete conversion. In the reduction of *α,β*-unsaturated aldehydes using $[(PPh_3)CuH]_6$ and $PhPMe_2$, chemoselectivity was high, in most cases giving greater than 90% yields although the TOF was very low in all cases (Table 15.6). The minor byproducts were the saturated alcohols that arise from complete reduction.

As allylic alcohols are unaffected by use of this catalyst it is proposed that the complete reduction occurs through competitive conjugate reduction, followed by subsequent reduction of the carbonyl. Although this catalyst is slower in action and results in low turnover numbers compared to some catalysts, it is inexpensive and provides good selectivity at room temperature.

15.2.4.2 Osmium

The Osmium cluster $Os_3(CO)_{12}$ and clusters in the presence of various phosphines and triphenylphosphite have been utilized for the hydrogenation of cinnamaldehyde and crotonaldehyde (Table 15.7) [36]. The results show that good yields of unsaturated alcohols can be obtained by using a large excess of phosphine at elevated hydrogenation temperatures.

In such reactions, a temperature exceeding 130 °C has a dramatic effect on the catalytic activity. The pressure of hydrogen has a similar effect, with a large increase in activity above 30 bar. These catalysts did not exhibit the same selectivity for ketones. Osmium triphenylphosphine systems have been briefly exam-

Table 15.7 Hydrogenation of crotonaldehyde and cinnamaldehyde under 45 bar H_2 at 140 °C for 9 h.

Catalytic system	Substrate	Conversion [%]	Unsaturated alcohol [%]	Saturated aldehyde [%]	Saturated alcohol [%]
$[Os_3(CO)_{12}]$	Crotonaldehyde	18	13	5	0
	Cinnamaldehyde	15	7	6	2
$[Os_3(CO)_{12}]/P^nBu_3$	Crotonaldehyde	93	89	0	4
(15 : 1)	Cinnamaldehyde	97	86	0	11
$[Os_3(CO)_{12}]/PPh_3$	Crotonaldehyde	47	35	4	8
(15 : 1)	Cinnamaldehyde	98	91	1	6
$[Os_3(CO)_{12}]/P(OPh)_3$	Crotonaldehyde	28	9	0	19
(15 : 1)	Cinnamaldehyde	81	79	1	1

ined as potential catalysts for hydrogenation. However, in the reduction of crotonaldehyde, it is generally the unsaturated aldehyde which is produced [25].

The use of water-soluble ligands was referred to previously for both ruthenium and rhodium complexes. As in the case of ruthenium complexes, the use of an aqueous biphasic system leads to a clear enhancement of selectivity towards the unsaturated alcohol [34]. Among the series of systems tested, the most convenient catalysts were obtained from mixtures of $OsCl_3 \cdot 3H_2O$ with TPPMS (or better still TPPTS) as they are easily prepared and provide reasonable activities and modest selectivities. As with their ruthenium and rhodium analogues, the main advantage is the ease of catalyst recycling with no loss of activity or selectivity. However, the ruthenium-based catalysts are far superior.

15.3 Hydrogenation of Ketones

15.3.1 Iridium Catalysts

The cyclometallated iridium complex $[Ir(H)_2(P,C\text{-}Ph_2PC_6H_4N(Me)CH_2)(P,N\text{-}Ph_2PC_6H_4NMe_2)]$ (Fig. 15.7) is formed from the reaction of $[Ir(COD)(OMe)]_2$ with *o*-(diphenylphosphino)-*N,N*-dimethylaniline [37].

The product, although sensitive to light and air, was an effective catalyst for the transfer hydrogenation of several ketones in propan-2-ol. Unsaturated ketones were used with a SCR of 500 : 1, and mostly gave high selectivity and modest yields (Table 15.8).

This was the first example of catalytic chemoselective reduction of *α,β*-unsaturated ketones to allylic alcohols by hydrogen transfer and, unusually, did not require the use of a basic co-catalyst.

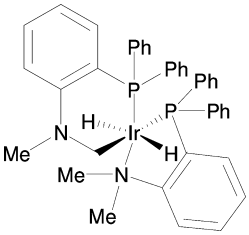

Fig. 15.7 $[Ir(H)_2(P,C\text{-}Ph_2PC_6H_4N(Me)CH_2)(P,N\text{-}Ph_2PC_6H_4NMe_2)]$.

Table 15.8 Hydrogenation of unsaturated ketones in propan-2-ol at 83 °C (SCR = 500).

Substrate	Conversion [%]	Saturated ketone [%]	Saturated alcohol [%]	Unsaturated alcohol [%]	Selectivity [%]
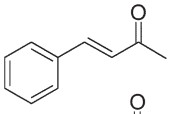	99 (1 h)	1	6	92	93
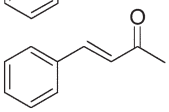	94 (1 h)	13	14	67	71
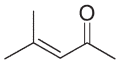	65 (7 h)	2	1	62	95
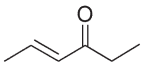	35 (7 h)	23	0	12	34

In the selective hydrogenation of benzylideneacetone (PhCH=CHCOMe) using an iridium phosphine system generated *in situ* from $[Ir(COD)(OMe)]_2$ and the appropriate phosphine [38], a heavy dependence was found on the nature and amount of phosphine used. Both of these factors are important in the activity and selectivity of the catalyst. Using PMe_2Ph as the model phosphine in a two-fold excess, the C=C bond was hydrogenated and the saturated ketone further hydrogenated to the saturated alcohol. However, increasing the excess of phosphine led to a switch in selectivity towards the carbonyl, although a loss of catalytic activity was reported. The cone angle of the phosphine is also important. Regardless of the solvent used, selectivity is raised above 90% when the cone angle is between 135 and 150°. The selectivity falls to zero at cone angles above and below this range.

These results suggest that, depending on the cone angle and relative concentration of the phosphines, different catalytic species are formed, and only catalysts formed from a large excess of relatively small phosphines are selective.

Generally, the selective reactions were complete in less than 24 h (SCR = 500, 30 bar H_2, 100 °C; TOF ~20 h^{-1}).

The mixed donor polydentate ligands Pr^n-$N(CH_2CH_2PPh_2)_2$ (PNP) and $Et_2NCH_2CH_2N(CH_2CH_2PPh_2)_2$ (P_2N_2) have been reacted with $[Ir(COD)(OMe)]_2$ to produce complexes that were active in the reduction of PhCH=CHCOMe [39]. Conversions of 90% with modest selectivity were achieved in 2–4 h in propan-2-ol at 83 °C. At 140 °C in cyclopentanol, similar results are obtained in less than 30 min.

15.3.2 Rhodium Catalysts

15.3.2.1 Rh-Phosphine Catalysts

The cationic species $[RhH_2(PPh_3)_2L_2]^+$ (L = solvent) has been used by Schrock and coworkers to catalyze the hydrogenation of alkenes, dienes and allynes [40]. These authors discovered that when the triphenylphosphine groups are replaced with more basic phosphines, ketones were reduced under mild conditions [41]. Using the $[RhH_2(PPhMe_2)_2L_2]^+X^-$ ($X^- = PF_6^-$ or ClO_4^-), acetone was reduced under atmospheric pressure of H_2 at 25 °C in the presence of 1% water. Under identical conditions, cyclohexanone, acetophenone and butan-2-one were also successfully reduced. Benzophenone was not hydrogenated, and it is thought that it may have formed a stable Rh complex. The addition of water was vital for activity, with the maximum rate achieved when 1% water is used. This addition of water also inhibited the reduction of alkenes. When the same catalysts were used for aldehyde reduction they proved to be effective initially, but their activity fell rapidly.

Rossi and coworkers successfully hydrogenated a series of simple ketones, with over 96% yields, using the complex $[Rh_2H_2Cl_2(COD)(PPh_2)_3]$ in the presence of a strong base [42].

$[Rh(bpy)_2]^+$, obtained by the *in-situ* reduction of $[Rh(bpy)_2Cl_2]Cl$ with hydrogen in methanolic sodium hydroxide [43], can reduce a series of simple ketones under 1 bar H_2 and at 30 °C [44]. Yields of over 98% were obtained in all cases with a SCR of up to 680 : 1. When a mixture of ketones and aldehydes was placed under such conditions, the ketones were found to be reduced preferentially, although unsaturated ketones were generally reduced to saturated ketones.

Although the complex $[RhCl(PPh_3)_3]$ is inactive towards the hydrogenation of ketones, the addition of triethylamine dramatically increases the rate. Yields were increased from only 0.5% to over 98% for the reduction of acetophenone at 50 °C under 71 bar H_2 in a 1 : 1 mixture of methanol and benzene [45]. Several other ketones have been reduced this manner, including benzophenone, which has proved difficult (see above; Fig. 15.8).

The catalyst derived from $[Rh(NBD)Cl]_2$ and PPh_3 showed the same enhancement with triethylamine [45]. Later studies [46] showed that increasing the amount of methanol increased the rate, although some benzene must be retained to dissolve the catalyst. The presence of triethylamine as co-catalyst must be at least 5 equivalents relative to the rhodium in order to obtain a maximum

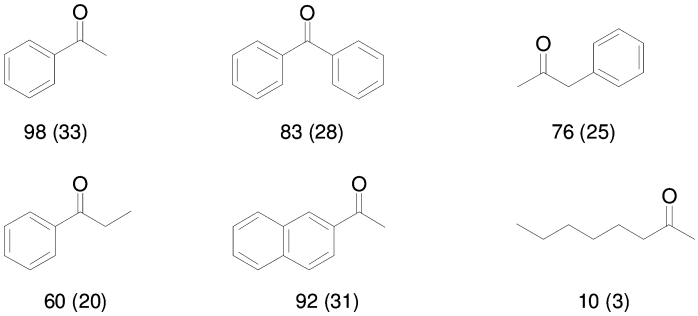

Fig. 15.8 Hydrogenation of ketones using $RhCl(PPh_3)_3$ + $5Et_3N$. Values shown are yields (TOF, h^{-1}).

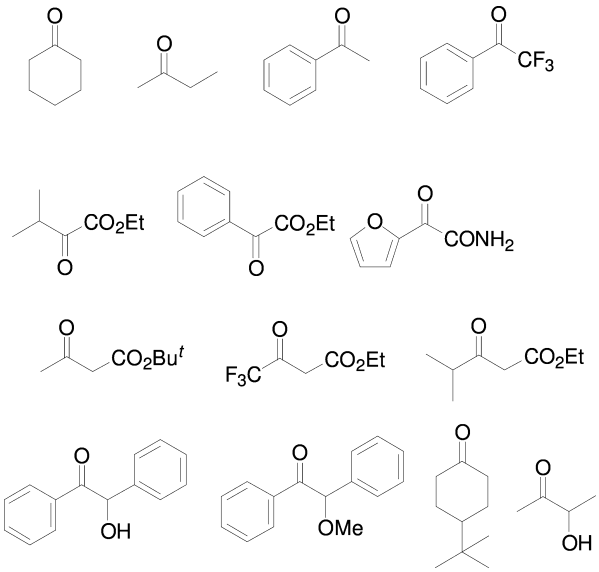

Fig. 15.9 The range of ketones hydrogenated using [Rh(DiPFc)(COD)]OTf.

rate. Coupled with this, an increase of triphenylphosphine from 2 to 4 equivalents also increases the activity. Combining all of these factors provides an idealized catalytic system of $[Rh(NBD)Cl]_2$ (2.5 mol%) with PPh_3 (8 mol%) and NEt_3 (12.5 mol%). With a SCR of 40:1, this system was used to reduce a vast range of ketones in benzene:methanol (30:70) at 50 °C under 1 bar H_2, with yields that were still below 80%.

The cationic complex [Rh(DiPFc)(COD)]OTf was discussed earlier as being an excellent catalyst for the hydrogenation of aldehydes under mild conditions. Under similarly mild conditions (25 °C, 4 bar H_2, SCR 450, 4 h, TOF $\sim 110\ h^{-1}$), a range of ketones was hydrogenated quantitatively (Fig. 15.9) [13].

In optimizing the conditions for such a reduction, protic solvents such as methanol and ethanol are required over dichloromethane (DCM), ethyl acetate (EtOAc), and THF which deactivate the catalyst. High substrate concentrations were also required, presumably due to dimerization of the catalyst that can occur in the absence of ketone or olefinic substrates. Finally, increasing the hydrogen pressure also gave an increase in yield. When this catalyst is used for the hydrogenation of unsaturated ketones, the C=C bond is first reduced very rapidly to give the saturated ketone. A slower reduction of the carbonyl group then occurs to yield the saturated alcohol.

15.3.2.2 **Water-Soluble Rh Catalysts**

The water-soluble ligand (TPPTS) was discussed earlier with regard to aldehyde reduction [17]. Similarly, in ketone transfer hydrogenation, high yields are obtained for a variety of substrates with the ability for efficient catalyst recycling at no expense of activity or selectivity (Fig. 15.10).

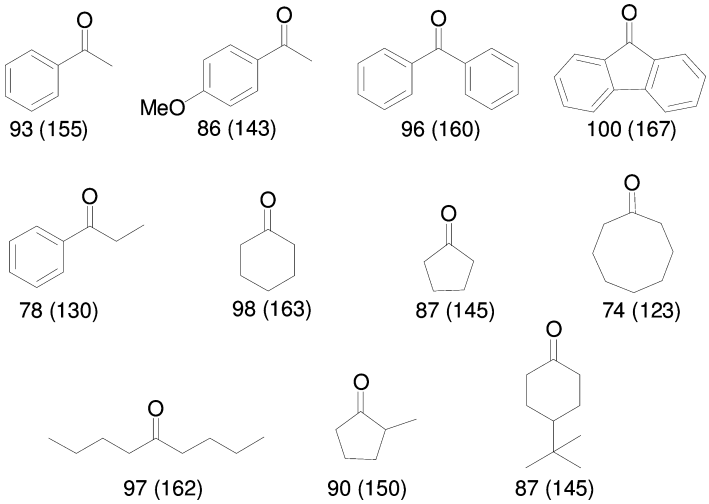

Fig. 15.10 Transfer hydrogenation of ketones at 80 °C catalyzed by $[RhCl(COD)]_2$/TPPTS. Values shown in brackets are yields (TOF, h^{-1}).

15.3.3 Ruthenium Catalysts

15.3.3.1 Ruthenium Carbonyl Clusters

Early efforts into ruthenium-catalyzed ketone hydrogenation experiments were performed using ruthenium-carbonyl clusters [47]. With cyclohexanone as a substrate and $[H_4Ru_4(CO)_{12}]$ as the catalyst, a range of solvents was tested for applicability. The greater reaction rates were achieved using alcohols, although the use of primary or secondary alcohols led to a decrease in selectivity due to the formation of ethers. The catalyst could be recovered at the end of the reaction. Partial displacement of the carbonyls with phosphines led to a decrease in activity, but further replacement of carbonyls with phosphines increased activity. By modifying such complexes with chiral bidentate phosphines, the first example of enantioselective transfer hydrogenation using $[H_4Ru_4(CO)_8[(-)\text{-DIOP})]_2]$ was realized, although optical yields were less than 10% [48].

15.3.3.2 Ru–PPh_3 Complexes

Mononuclear ruthenium complexes were found to be superior to carbonyl clusters during a comprehensive comparison of a variety of catalysts in the reduction of acetone [49]. Without solvent, most catalysts were highly selective, although the activity was quite low. The addition of water to the system vastly increased yields, in agreement with Schrock and Osborn's observations into rhodium-catalyzed hydrogenations (Table 15.9) [41].

The addition of aqueous NaOH or acetic acid resulted in an increase in rate, but the selectivity was reduced – perhaps due to the formation of aldol condensation products. This is in contrast to the findings of Rossi with rhodium systems [42] and Strohmeier, who claimed that the addition of acid or base also increased selectivity when using $RuCl_2(PPh_3)_3$ and $Ru(CF_3CO_2)_2(CO)(PPh_3)_2$ as catalyst [50]. It was found that catalysts possessing carbonyl ligands or nitrosyl ligands were

Table 15.9 Hydrogenation of acetone. Conditions: SCR = 1300, 150 °C, 69 bar, 4 h.

Complex	Conversion (2.5% H_2O) [%]	Selectivity (2.5% H_2O) [%]	Conversion (dry) [%]	Selectivity (dry) [%]
$[RuHCl(CO)(PPh_3)_3]$	95	95	25	93
$[RuH(NO)(PPh_3)_3]$	97	95	22	95
$[RuCl_2(CO)_2(PPh_3)_2]$	90	92	26	87
$[Ru(H)_2(CO)(PPh_3)_3]$	69	94	67	100
$[Ru(H)_2(PPh_3)_4]$	39	82	56	98
$[RuCl_2(PPh_3)_3]$	33	83	18	82
$[RuH_4(PPh_3)_3]$	30	86	78	100
$[RuHCl(PPh_3)_3]$	13	70	6	70
$[Ru_3(CO)_{12}]$	3	41	6	69

higher in activity and selectivity. This was attributed to the complexes of general formula $[RuX_2(PPh_3)_n]$ (X = H, Cl; n = 3, 4) having a competing decarbonylation reaction, as demonstrated by the presence of metal carbonyl complexes in the reaction mixture after completion. In the hydrogenation of acetone under 69 bar H_2 at 150 °C with a SCR of 100 000, turnover numbers of up to 15 000 h^{-1} could be achieved over three days, using $[RuHCl(CO)(PPh_3)_3]$ and a little water. These were similar findings to the hydrogenation of aldehydes under the same conditions.

Table 15.10 Hydrogenation of unsaturated ketone at 28 °C and 4 bar H_2 (ketone : $RuCl_2(PPh_3)_3$: $H_2N(CH_2)_2NH_2$: KOH = 500 : 1 : 1 : 2).

Substrate	Yield [%]	Unsaturated alcohol [%]	Saturated alcohol [%]	TON	TOF [h^{-1}]
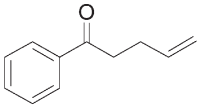	100	98.2	1.8	491	714
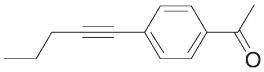	99.5	100	0	498	332
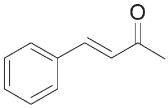	100	99.9	0	10 000	555 [a)]
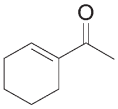	98.2	99.6	0.4	489	327
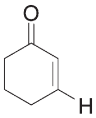	100	70	30	350	500
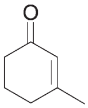	99.8	99.9	0.1	499	333 [b)]
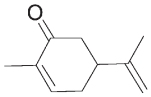	100	92.8	7.2	464	71
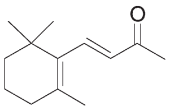	99	100	0	495	495

Yields of saturated ketone are < 0.1% in all cases.

a) Reaction performed with ketone : Ru = 10 000 : 1.

b) H_2 pressure of 8 bar used.

The $[RuCl_2(PPh_3)_3]$ catalysts can be used more effectively to hydrogenate ketones using formic acid as the hydrogen source [51]. In solvent-free reactions, the formic acid completely decomposes and the products are easily obtained from the reaction mixture. Thus, in reactions carried out at 125 °C with a SCR of 800:1, simple ketones and aldehydes are reduced with excellent yields. Applying formic acid as a hydrogen source to the Ru cluster catalysts and other Ru phosphine catalysts gave less favorable results.

15.3.3.3 **Diamine-Modified Ru Catalysts**

Noyori and coworkers discovered that the activity of $[RuCl_2(PPh_3)_3]$ could be enhanced by the addition of ethylenediamine (en) and KOH/*i*-PrOH [52]. Using the system for acetophenone hydrogenation (Ru:en:KOH, 1:1:20, SCR 5000 at 28 °C under 3 bar H_2), TOFs of 6700 h^{-1} were obtained. The pressure of hydrogen is important, as demonstrated by a TOF of 880 h^{-1} under 1 bar H_2 (SCR = 500). By increasing the pressure to 50 bar and using a SCR of 10 000, TOFs in excess of 23 000 were obtained. The reaction was even shown to work at –20 °C, showing just how mild the conditions employed can be. In order for the catalytic system to work, both the organic and inorganic bases are required with at least one primary amine end to the diamine. Applying this catalytic system to unsaturated ketones shows a remarkable selectivity towards the unsaturated alcohol (Table 15.10) [29]. Reaction times vary from substrate to substrate between 1 and 18 h, with yields and selectivities of over 99% easily achieved. The catalyst will even reduce the acetylenic ketones without the alkyne group being affected. The catalyst shows great scope and, with ligand modification, a highly enantioselective catalyst can be produced. The mechanism of this unique catalyst is described in Chapters 20 and 32.

An alternative variation to this catalyst, *trans*-$[RuCl_2[P(C_6H_4\text{-}4\text{-}CH_3)_3]_2(H_2NCH_2CH_2NH_2)]$ and KOtBu in isopropanol, is excellent for the selective hydrogenation of benzophenones (Scheme 15.8) [53].

The products of such reactions can be useful intermediates in the synthesis of commercial drugs. The nature of the substituents within the benzophenones has an effect on rate, with electron-withdrawing groups favoring the reaction more than electron-donating groups. For example, kinetic studies showed that *p*-trifluoromethylbenzophenone was hydrogenated 11-fold faster than the *p*-

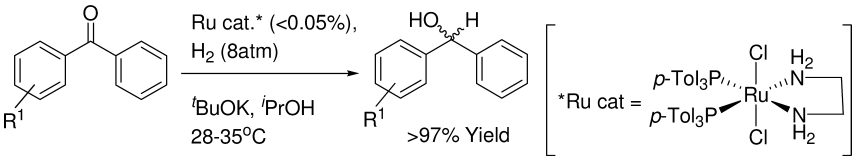

Scheme 15.8 Hydrogenation of benzophenones.

Table 15.11 Hydrogenation of benzophenones with *trans*-[$RuCl_2\{P(C_6H_4\text{-}4\text{-}CH_3)_3\}_2(H_2NCH_2CH_2NH_2)$] and KO*t*Bu in *i*PrOH under 8 bar H_2 at 28–35 °C.

R^1	SCR	Concentration [M]	Yield [%]	TON	TOF [h^{-1}]
H	20 000	2.7	99	19 800	413
o-CH_3	3000	1.5	99	2970	165
p-CH_3O	3000	1.5	99	2970	165
p-Cl	3000	1.3	100	3000	375
p-CF_3	2000	0.4	99	1980	1980

methoxy derivative. However, a range of benzophenones was reduced smoothly at 30 °C (Table 15.11). In an optimized experiment demonstrating the practicability of the method, a slurry of 200 g benzophenone in 200 mL *i*-PrOH was hydrogenated with an SCR of 20 000 within 48 h at 30 °C.

Recently, several catalysts based on ligands containing an NH_2 or NH grouping within the phosphine ligand, such as $Ph_2PCH_2CH_2NH_2$, have been shown to have considerable activity and chemoselectivity for ketone hydrogenation [54–56].

15.3.3.4 **Other Ru Catalysts**

As for some of the monodentate phosphine-based catalysts, *cis*-[Ru(6,6′-Cl_2bpy)$_2(OH_2)_2][CF_3SO_3]_2$ was found to require water for the best catalytic activity in the reduction of aldehydes and ketones [57]. Aldehydes and ketones were found to be hydrogenated, with reasonable yields. Unsaturated aldehydes were reduced with selectivity towards the unsaturated alcohol, whereas unsaturated ketones showed selectivity towards the saturated ketones.

The water-soluble ruthenium TPPTS system which functioned well for saturated and unsaturated aldehydes has also been tested for the hydrogenation of ketones [31]. Although good yields for simple ketones could be obtained depending on the substrate, the selectivity when used for unsaturated ketones was in favor of the C=C bond. The polyphosphine catalysts $RuHCl(CO)(PPh_3)$(dppe) (dppe = $Ph_2PCH_2CH_2PPh_2$) and RuHCl(CO)(tdpme) (tdpme = $CH_3C(CH_2PPh_2)_3$) show greater activity than $RuHCl(CO)(PPh_3)_3$ in the hydrogenation of cyclohexanone [58]. Turnover numbers of 450 and 625 are achieved, respectively, for the polydentate complexes, compared to 82 for the triphenylphosphine complex.

Highly efficient transfer hydrogenation of ketones can be achieved by the use of the transfer hydrogenation catalyst *trans,cis,cis*-[$RuX_2(CNR)_2$(dppf)] (X = Cl or Br; R = CH_2Ph, cy, *t*-Bu, 2,6-$C_6H_3Me_2$) [59]. These are the first examples of isocyanide–ruthenium species being used for the transfer hydrogenation of ketones. The complexes are prepared by the reaction of bis(allyl)-ruthenium(II) complex [Ru(η^3-2-$C_3H_4Me)_2$(dppf)] with HX acid in the presence of the isocyanide. All the catalysts were effective in the hydrogenation of acetophenone, giving quanti-

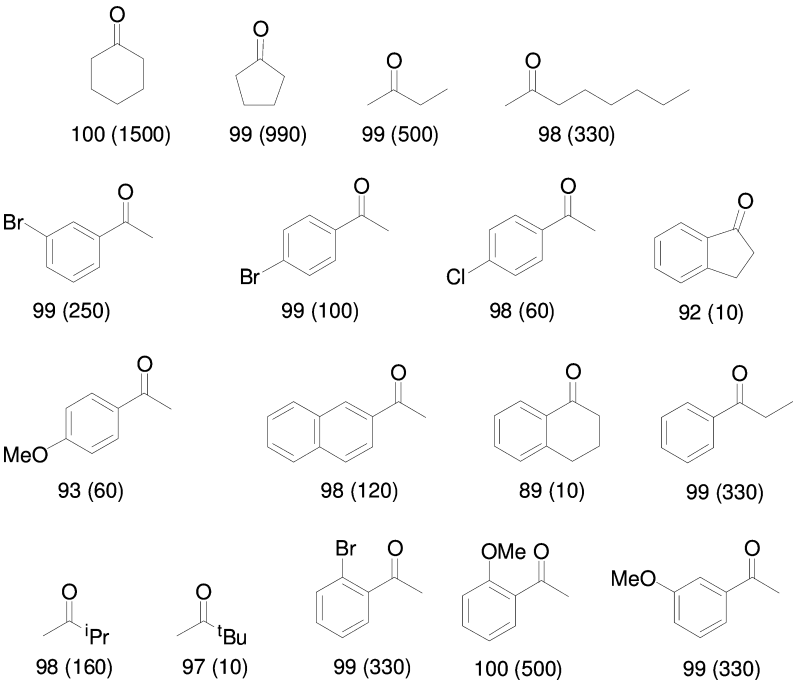

Fig. 15.11 *trans,cis,cis*-[$RuCl_2(CNCH_2Ph)_2$(dppf)] catalysed hydrogenation of ketones. Values shown are yields (TOF, h^{-1}).

tative yields between 0.5 and 8 h. *trans,cis,cis*-[$RuCl_2(CNCH_2Ph)_2$(dppf)] proved to be the most active, and was further utilized in the transfer hydrogenation of a series of ketones at 82 °C using a ketone : Ru : NaOH ratio of 250 : 1 : 24 (Fig. 15.11).

15.3.4 Other Metal Catalysts

15.3.4.1 Copper

The use of phosphine-stabilized copper complexes as hydrogenation catalyst was discussed previously for aldehydes. The same catalysts have been used in the hydrogenation of simple ketones, with high yields achieved in reactions lasting for up to 48 h [35]. Several unsaturated ketones were hydrogenated, with high chemoselectivity, to the unsaturated alcohol. These catalysts are sensitive to the structure of the phosphine ligand. In the hydrogenation of 4-phenyl-3-butan-2-one, it is possible to obtain any of the three possible products by varying the phosphine (Fig. 15.12) [60].

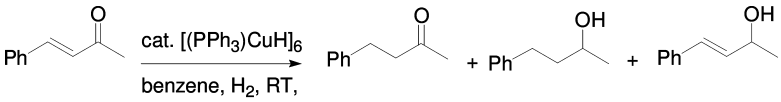

No phosphine, 70 atm H_2	91	:	9	:	0	89% (3)
PPh_3, 117 atm H_2	0	:	92	:	8	95% (1.5)
Me_2PPh, 34 atm H_2	0	:	8	:	92	91% (6)

Fig. 15.12 Effect of phosphine on selectivity. Values shown are yields (TOF, h^{-1}).

15.3.4.2 **Metal Carbonyls**

The metal carbonyls $Cr(CO)_6$, $Mo(CO)_6$, $W(CO)_6$ and $Fe(CO)_5$ have all been tested in the hydrogenation of acetophenone in the presence of a strong base [61, 62]. In reactions performed in either triethylamine of sodium methoxide in methanol using 5 mol% of catalyst, the Mo and Cr complexes proved to be superior. The different bases had an effect on the yield that was further demonstrated when $Cr(CO)_6$ was used in the hydrogenation of a series of ketones under the same conditions. In most cases, the reactions were found to be better in the methoxide system, with over 98% yields obtained in reactions lasting 3 h at 120 °C.

15.4 Domino-Hydroformylation-Reduction Reactions

15.4.1 Cobalt Catalysts

Cobalt-catalyzed hydroformylation of terminal alkenes using $[Co(H)(CO)_4]$ as catalyst delivers mixtures of branched and linear aldehydes under elevated pressures and high temperatures (160–200 °C). In 1968, it was found that adding a trialkylphosphine to the cobalt catalyst reduces activity, but stabilizes the catalyst for use under 100 bar syngas pressure [63]. The use of phosphine ligands increases the hydrogenation activity such that the aldehydes are directly hydrogenated to alcohols as the only oxygenated products isolated. This is a desirable process, since linear alcohols are often the target products from many hydroformylation processes. Tributylphosphine can serve as a ligand for this purpose, but the ligands which provide the best catalyst stability are those that have a bicyclic structure such as the "phobane" ligand [64] and, more recently, the limonene-derived phosphines shown below [65]. Recent studies of the hydroformylation of dodecene at 170 °C, 85 bar syngas pressure using 1000 ppm $[Co(H)(CO)_4]$ show that 70% linear alcohols can be formed, with relatively small amounts of branched alcohol ($n:iso=4.9$) and alkane (6%) as the side products. Under these typical conditions, aldehyde hydrogenation appears to be the most facile step in the process, as aldehydes are not observed.

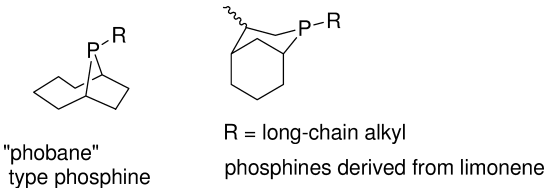

Fig. 15.13 Bicyclic phosphines used in cobalt-catalyzed hydroformylation.

15.4.2
Rhodium Catalysts

Rhodium-catalyzed hydroformylation can be carried out under much milder conditions (5–50 bar H_2/CO, $T = 20–120\,^{\circ}C$), shows higher TOFs, fewer alkane byproducts, and can be manipulated to give very high selectivity towards the linear aldehydes [66]. Given that linear alcohols are frequently the desired products, several investigations have been made on the use of Rh catalysts to hydrogenate aldehydes under the reaction conditions. This has indeed been observed in several cases, using strongly electron-donating phosphines [67–69] or amines [70, 71] as ligands. The most detailed studies on this topic have been carried out by Cole-Hamilton and coworkers, who used $[Rh_2(OAc)_4]/PEt_3$ as a catalyst [72–74]. In the hydroformylation of hex-1-ene in aprotic solvents, hydrogenation of the initially formed heptanal and 2-methylhexanal products to the corresponding alcohols occurs as the reactions proceeds. High TOFs were observed at 120 °C (40 bar syngas) with modest linear-to-branched regioselectivity: low linear selectivity is often observed using alkyl phosphine ligands in hydroformylation. Pure heptan-1-al is also readily hydrogenated under similar reaction conditions using the same catalysts. However, when the reactions were carried out in alcoholic solvents, mechanistic investigations established that alcohols are actually the initial reaction products with no aldehyde intermediates being formed.

More recently, during research aimed at supporting the highly linear selective hydroformylation catalyst $[Rh(H)(Xantphos)(CO)_2]$ onto a silica support, the presence of a cationic rhodium precursor in equilibrium with the desired rhodium hydride hydroformylation catalyst was observed. The presence of this complex gave the resulting catalyst considerable hydrogenation activity such that high yields of linear nonanol could be obtained from oct-1-ene by domino hydroformylation-reduction reaction [75].

15.5
Reductive Amination of Ketones and Aldehydes

Although imine hydrogenation is discussed in greater detail in Chapter 34, it seems appropriate at this point to describe one-pot reductive amination of aldehydes and ketones. The reductive amination of aldehydes and ketones using so-

dium borohydride or sodium cyanoborohydride is well established. However, a more environmentally benign and economical method to carry out this reaction is to use molecular hydrogen. Several heterogeneous catalysts have been shown to be effective in this transformation, but interest has been expressed in the use of more controllable homogeneous catalysts for this purpose.

The first example of this type of transformation was reported in 1974 [76]. Three catalysts were investigated, namely $[Co_2(CO)_8]$, $[Co(CO)_8/PBu^n_3]$, and $[Rh_6(CO)_{16}]$. The $[Co(CO)_8/PBu^n_3]$ catalyst showed activity for reductive amination using ammonia and aromatic amines. The $[Rh_6(CO)_{16}]$ catalyst could be used for reductive amination using the more basic aliphatic amines that were found to poison the cobalt catalyst. This early report pointed out that the successful reductive amination of *iso*-butanal (Me_2CCHO) with piperidine involves selective enamine hydrogenation, that reductive amination of cyclohexanone with isopropylamine probably involves imine hydrogenation, and that reductive amination of benzaldehyde with piperidine would presumably involve the reduction of a carbinolamine.

Although this report establishes some of the principles of this class of reaction, no turnover numbers or SCRs were reported, and harsh reaction conditions (100–300 bar H_2/CO, 110–200 °C) were employed. Subsequently, this process received sporadic attention, except as a process combined with a hydroformylation stage. In 1997, Knifton found that amination of linear aldehydes using ammonia could be achieved, and showed that the related domino hydroformylation-amination process was also possible [77]. In 2000, Borner and coworkers released preliminary results describing a more practical catalyst system for these reactions [78]. Benzaldehyde and piperidine could be reductively aminated using $[Rh(dppb)(COD)]BF_4$ or [Rh(1,2-bis-diphenylphosphinitoethane)(COD)]BF_4 under mild conditions (50 bar H_2, room temperature). A total of 500 catalytic turnovers could be achieved within a few hours, with the reaction being hampered by only moderate selectivity towards the tertiary amine (Scheme 15.9).

Selectivities of about 2 : 1 are the best found for this type of hydrogenation and are highly dependent on the secondary amine used: they seem to correlate with the nucleophilicity of the amine. Reductive amination of PhCHO with benzylamine can proceed through an imine intermediate, and thus gave better selectivities (12 : 1) but was found to be sluggish using this catalyst system.

Beller and coworkers recently realized a more practical system for reductive amination of aromatic aldehydes using ammonia [79]. Their preferred conditions, which require the addition of an acidic additive, are shown in Scheme 15.10. Without extensive optimization, turnover numbers of 1700 could be

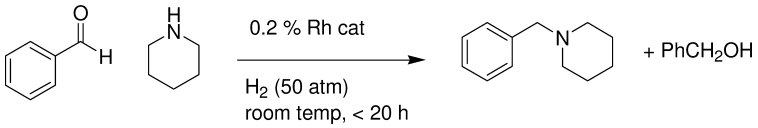

Scheme 15.9 Reductive amination of benzaldehyde.

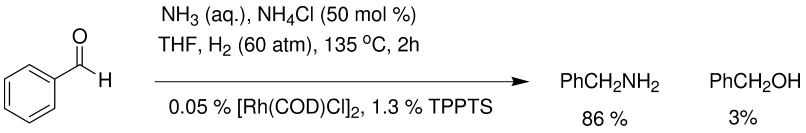

Scheme 15.10 Reductive amination using ammonia.

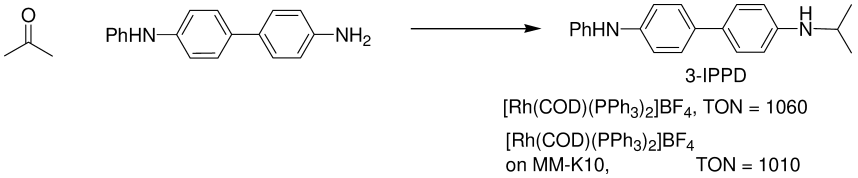

Scheme 15.11 Reductive amination of acetone.

achieved. A biphasic system is required in order to make use of aqueous ammonia. However, preliminary data show a second advantage in that the Rh-containing aqueous phase can be recovered by phase separation and re-used. Aliphatic aldehydes remain a problem for which further research is required.

$[Rh(COD)(PPh_3)_2]BF_4$ has been shown to be a good catalyst for reductive amination of acetone with 4-anilino-aniline to give the commercial product 3-IPPD. In laboratory-scale comparative experiments, this catalyst – both in homogeneous phase or immobilized on Montmorillonite K10 clay – was found to be superior to the commercially applied Pt/C catalyst (Scheme 15.11) [80].

In recent years there has been emerging interest in one-pot asymmetric amination of ketones, but this subject is beyond the scope of this chapter. However, an interesting observation by Borner and coworkers is that different catalysts seem to be required to carry out this process compared to those used for hydrogenation of the corresponding imines or enamines [81, 82].

15.6 Hydroaminomethylation of Alkenes (Domino Hydroformylation-Reductive Amination)

Given the previous discussion on reductive amination, it is surprising that the potentially more complicated domino hydroformylation-reductive amination reactions have been more thoroughly developed. The first example of hydroaminomethylation was reported as early as 1943 [83]. The most synthetically useful procedures utilize rhodium [84–87], ruthenium [88], or dual-metal (Rh/Ir) catalysts [87, 89, 90]. This area was reviewed extensively by one of the leading research groups in 1999 [91], and so is only briefly outlined here as the second step in the domino process is reductive amination of aldehydes. Eilbracht's group have shown that linear selective hydroaminomethylation of 1,2-disubstituted alkenes

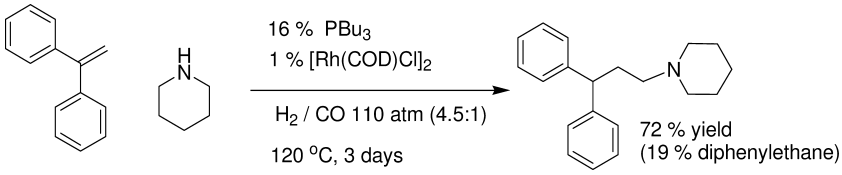

Scheme 15.12 Synthesis of fenpiprane using hydroaminomethylation of diphenylethene.

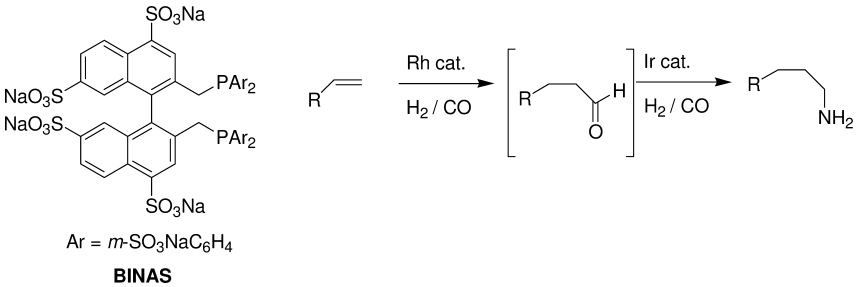

Scheme 15.13 Hydroaminomethylation of terminal alkenes to linear amines.

such as diphenylethene can give access to a series of compounds of pharmaceutical interest such as fenpiprane, diisopromine, tolpropamine, fendiline, prozapine [92], penfluridol [93], and fluspirilene [93]. An example of one of their procedures is shown in Scheme 15.12. The use of a relatively large amount of phosphine is required to suppress competing alkene hydrogenation reactions.

Eilbracht's group has done much to demonstrate the synthetic possibilities of using this reaction. However, the most recent developments in this field have also shown that the reaction could be applied as a practical method to prepare linear amines. Beller and coworkers have shown that linear selective hydroaminomethylation of propene, but-1-ene, and pent-1-ene with aqueous ammonia can be realized in a two-phase solvent system (water : methyl *tert*-butylether), using $[Rh(COD)Cl]_2$/$[Ir(COD)Cl]_2$ and water-soluble diphosphine ligand, BINAS as catalyst. If excess ammonia is used, primary amines can be produced with good primary : secondary selectivity and near-perfect linear-to-branched selectivity (Scheme 15.13, Table 15.12). Running the reaction with excess alkene allows for secondary amines to be synthesized with excellent chemo- and regioselectivity. The catalyst displays up to 4000 turnovers with respect to rhodium, although relatively high concentrations of phosphine ligand seem to be required [90].

This group subsequently invented a domino reaction consisting of isomerization of internal to terminal alkenes, followed by linear selective hydroformylation and reductive amination (Scheme 15.14) [89].

A more recent report thoroughly investigates hydroaminomethylation of terminal alkenes to give high yields of linear (linear : branched = 99 : 1) tertiary amines from secondary amines and terminal alkenes or linear secondary

Table 15.12 Hydroaminomethylation of terminal alkenes to linear primary and secondary amines.[a)]

Alkene	NH_3/alkene	Yield (amine)	*n*:*iso*	Primary:secondary
Propene	8:1	90	99:1	77:23
Propene	0.5:1	90	99:1	1:99
Pent-1-ene	8:1	75	99:1	87:13
Pent-1-ene	0.5:1	90	99:1	10:90

a) Conditions: temperature = 130 °C; 79 bar H_2/CO (5:1); time = 10 h; 0.026% Rh; 0.21% Ir; ligand:Rh ratio = 140.

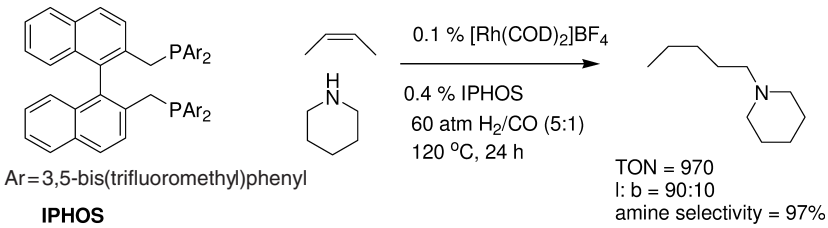

Scheme 15.14 Domino isomerization hydroaminomethylation.

amines from primary amines and alkenes. Reactions were conducted at 125 °C with TOF of ca. 160 h^{-1} [87].

The recent improvements described above suggest that hydroaminomethylation is approaching use as a practical process for preparing a range of amines with good linear selectivity, and good catalytic activity.

15.7 Hydrogenation of Carboxylic Acid Derivatives

The hydrogenation of acids, esters and anhydrides using molecular hydrogen is a neglected and difficult challenge. Lithium aluminum hydride ($LiAlH_4$) and certain boron hydrides are traditionally used for this reduction. However, a stoichiometric aluminum reagent is not atom-efficient and requires the separation and disposal of aluminum reagents at the end of the reaction. Catalytic hydrogenation using molecular hydrogen is potentially the ideal "green" alternative to any of the stoichiometric procedures, and would attract industrial attention if a catalyst were sufficiently active. Heterogeneous catalysts (especially copper-chromite) can carry out this process, albeit under severe conditions (200–250 °C; 14 000–20 000 kPa), which limits their application.

15.7.1
Hydrogenation of Acids and Anhydrides

The first examples of a homogeneous reduction of this type were reported in 1971. Cobalt carbonyl was found to reduce anhydrides such as acetic anhydride, succinic anhydride and propionic anhydride to mixtures of aldehydes and acids. However, scant experimental details were recorded [94]. In 1975, Lyons reported that $[Ru(PPh_3)_3Cl_2]$ catalyzes the reduction of succinic and phthalic anhydrides to the lactones γ-butyrolactone and phthalide, respectively [95]. The proposed reaction sequence for phthalic anhydride is shown in Scheme 15.15. Conversion of phthalic anhydride was complete in 21 h at 90 °C, but yielded an equal mixture of the lactone, phthalide (TON = 100; TOF $\sim$ 5) and *o*-phthalic acid, which is presumably formed by hydrolysis of the anhydride by water during lactonization. Neither acid or lactone were further hydrogenated to any extent using this catalyst system, under these conditions.

This catalyst was subsequently applied in the regioselective hydrogenation of 2,2-dimethylsuccinic anhydride [96]. An interesting reversal of regioselectivity towards the isomer B was found when switching from $LiAlH_4$ reduction to the catalytic method. Quite good isolated yields and selectivity were recorded, though no data on catalytic turnover were reported (Scheme 15.16).

Mitsubishi have reported several processes based on Ru-catalyzed hydrogenation of anhydrides and acids. Succinic anhydride can be converted into mixtures of 1,4-butane-diol and γ-butyrolactone using $[Ru(acac)_3]$/trioctylphosphine and an activator (often a phosphonic acid) [97]. Relatively high temperatures are required ($\sim$200 °C) for this reaction. The lactone can be prepared selectively under the appropriate reaction conditions, and a process has been developed for isolating the products and recycling the ruthenium catalyst [98–100].

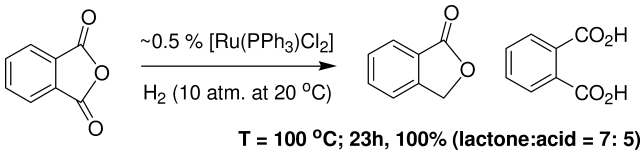

Scheme 15.15 Hydrogenation of *o*-phthalic acid.

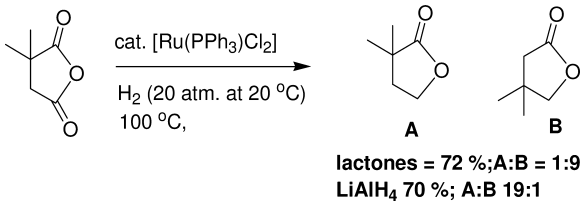

Scheme 15.16 Regioselective hydrogenation of an unsymmetrical succinic acid derivative.

Table 15.13 Hydrogenation of succinic acid and anhydride using $[Ru_4H_4(CO)_8(P^nBu_3)_4]$. [a)]

Substrate	Temperature [°C]	Time [h]	Conversion [%]	Yield of γ-butyrolactone [%] [b)]
Succinic acid	150	20	11	11
Succinic acid	180	22	83	83
Succinic acid	180	48	100	100
Succinic anhydride	100	22	40	16
Succinic anhydride	100	48	78	36
Succinic anhydride	170	40	100	100

a) TON were not reported but, based on the 100 mg of catalyst reported, are approximately 300.
b) The remaining mass is succinic acid.

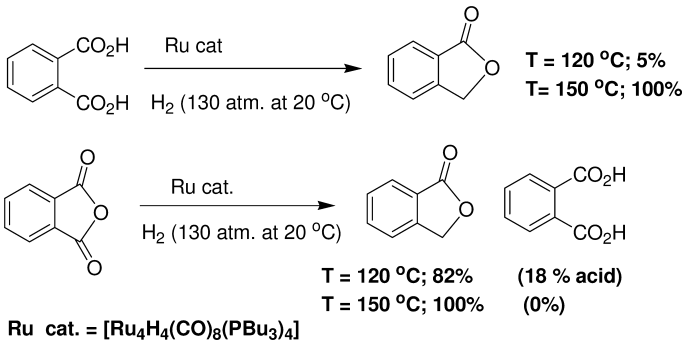

Scheme 15.17 Hydrogenation of *o*-phthalic acid and anhydride.

The first example of carboxylic acid hydrogenation was reported as a side product in the hydrogenation of citraconnic acid using the chiral catalyst $[RuH_4(CO)_8\{(-)\text{-DIOP})\}]$ [101]. This research team subsequently investigated acid, ester, and anhydride hydrogenation in some detail in studies which exclusively used Ru carbonyl clusters with monodentate trialkylphosphine ligands as catalysts. The reduction of succinic acid, $(CH_2CO_2H)_2$ with succinic anhydride, is compared in Table 15.13 [102].

Succinic anhydride is clearly hydrogenated more readily than the acid, as was the case with phthalic acid (Scheme 15.17), but faster absolute rates were observed in the hydrogenation of *o*-phthalic acid and phthalic anhydride to phthalide. In these reactions, the problem of anhydride hydrolysis is less significant as the acid can also be reduced to the same lactone product.

The effect of carboxylic acid structure was also investigated. Oxalic acid and malonic acids were found to decompose, while glutaric acid $HO_2C(CH_2)_3CO_2H$ was hydrogenated, though with poor selectivity. Although the glutaric acid results were not synthetically useful, the products included 1,5-pentane-diol and 2-hydroxy-tetrahydropyran, which showed that ester hydrogenation was a possibility. Adi-

pic acid ($HO_2C(CH_2)_4CO_2H$) was only 25% converted to ε-caprolactone, while azelaic acid ($HO_2C(CH_2)_7CO_2H$) was not reduced under similar conditions. The importance of a neighboring carboxylate group was therefore demonstrated, although it is not clear from these results whether the origin of this effect is the formation of stable lactones, secondary coordination to the ruthenium catalyst, or the presence of an electron-withdrawing substituent. Benzoic and phenyl acetic acids are not reduced under the conditions shown in Table 15.13, and are only slowly hydrogenated at 200 °C (9% in 48 h for benzoic acid). Although this study provides some important information regarding the feasibility of acid and anhydride hydrogenation, a number of questions remain unanswered. The effect of different ligands on ruthenium, and the importance of the cluster species on catalytic activity were not investigated. It would therefore be unwise to conclude that hydrogenation of a certain acid substrate is impractically difficult. In particular, a rough comparison of the results in Table 15.13 for succinic anhydride hydrogenation (Entry 4) with those previously described with $[Ru(PPh_3)_3Cl_2]$ for succinic anhydride (90 °C, 100% conversion in 21 h, 50 : 50 mix of lactone : acid) does not suggest that the cluster catalysts used by this group are necessarily the most reactive catalysts possible. Davy Process and Technology have recently developed a useful catalyst for hydrogenation of acids, whereby unactivated propionic acid can be hydrogenated to propanol at 240 °C with good productivity and selectivity using a catalyst derived from a ruthenium (III) salt such as $[Ru(acac)_3]$ and the tridentate phosphine, triphos (see also Table 15.17). The choice of ligand is essential for high catalytic activity [103].

An investigation of several transition-metal catalysts – including those that could be considered heterogeneous – were investigated in the hydrogenation of pentadecanoic acid. A strong promotional effect of metal carbonyls such as $Re_2(CO)_{10}$ and $Mo(CO)_6$ on catalysts such as $M(acac)_3$ (M = Ru, Rh), increasing yields of pentadecanol from 2% to 97% (TON = 97) at 160 °C and 100 bar H_2 pressure. A chemoselective reduction of pentadecanedioic acid monomethyl ester was also reported using these catalysts. The authors note that these reactions gave alcohols relatively cleanly, without ester side products [104].

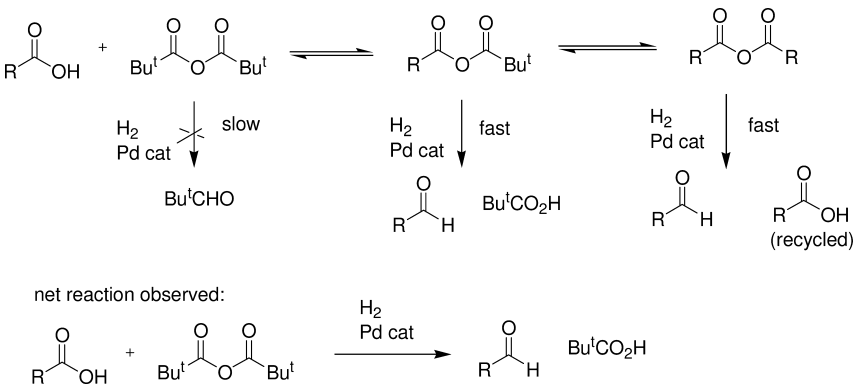

Scheme 15.18 Hydrogenation of acids *via* anhydride intermediates.

The hydrogenation of cyclic anhydrides using $[Pd(PPh_3)_4]$ as catalyst was reported by Yamamoto and coworkers. The reaction proceeds by oxidative addition of the anhydride followed by hydrogenolysis, and proceeds well in THF at 80 °C (~100 turnovers, unoptimized). However, aldehyde productivity is limited to 50% by the reaction mechanism that involves hydrogenolysis of Pd-acyl and Pd-carboxylato groups in $[Pd(PPh_3)_2(C(O)R)(O_2CR)]$ to give an equal mixture of aldehydes and acids [105]. Very bulky anhydrides were significantly more difficult to reduce, which led this group to design a process for converting carboxylic acids into aldehydes in the presence of bulky anhydrides [105–107]. Thus, heating a wide range of less sterically demanding acids in the presence of $[Pd(PPh_3)_4]$ (~1%), $(t\text{BuCO})_2O$ (3 equiv.) and H_2 (~30 bar) delivers both $t\text{BuCO}_2H$ and aldehyde in high yield. The reaction is proposed to occur via transesterification between acid, (RCO_2H) and $(t\text{BuCO})_2O$ to give mixed anhydride $RC(O)OC(O)t\text{Bu}$ and new anhydride $(RCO)_2O$. These anhydrides are hydrogenated much more rapidly than $(t\text{BuCO})_2O$ and the oxidative addition of the mixed anhydride is regioselective, giving the acyl complexes of type $[Pd(L)_2(C(O)R)(OC(O)t\text{Bu}]$, which hydrogenate to RCHO and $t\text{BuCO}_2H$.

The reaction tolerates ketone, chloride, internal C=C bonds, esters, nitriles, and ether functional groups. Given that the DIBAL-H reduction of acid derivatives often suffers from over-reduction to alcohols, these catalytic procedures are of synthetic value for laboratory-scale syntheses. However, it is likely that the requirement for excess $(t\text{BuCO})_2O$ will prevent this reaction from ever being used in commercial production.

15.7.2
Hydrogenation of Esters

The first examples of a clean hydrogenation of an ester to an alcohol was reported by Grey et al. [108]. A catalyst prepared by potassium naphthalide reduction of $[RuH(PPh_3)_2Cl]_2$, formulated as $K_2[Ru_2(PPh_3)_3(PPh_2)H_4]_2$. Diglyme hydrogenated methyl trifluoroacetate (MTFA) to trifluoroethanol and methanol at 90 °C (6 bar H_2). The 88% yield obtained corresponds to 290 turnovers. Trifluoroethyl trifluoroacetate (TFETFA) was hydrogenated more readily using the same catalyst system, while methyl acetate could be hydrogenated for the first time (TON = 35), but with considerable difficulty. Formate esters decompose with the liberation of carbon monoxide under these reaction conditions. The anionic catalysts used by this group were compared with $[RuH(PPh_3)_3Cl]$, and found to be significantly more active (Table 15.14).

In addition to the successful hydrogenation of the two fluorinated esters, this report describes the hydrogenation of dimethyl oxalate. Using the reactive anionic ruthenium catalyst, a 70% conversion to methyl glycolate could be achieved (TON = 235; TOF ~12 h^{-1}) (Scheme 15.19, Table 15.14, final entry).

The results suggest a pronounced electronic effect on ester hydrogenations. This substrate effect has not been studied exhaustively by any means, but led to

Table 15.14 Hydrogenation of esters using ruthenium catalysts.[a)]

Substrate	Catalyst	Conversion [%]	Remarks
MeOAc	$[RuH(PPh_3)_3Cl]$	0	–
MeOAc	$K_2[Ru_2(PPh_3)_3(PPh_2)H_4]$	22	Toluene, 13% EtOAc product (by transesterification) and EtOH (9%)
MeOAc	$K_2[Ru_2(PPh_3)_3(PPh_2)H_4]$	5	THF
MTFA	$[RuH(PPh_3)_3Cl]$	0	Toluene
MTFA	$K_2[Ru_2(PPh_3)_3(PPh_2)H_4]$	88	Toluene
TFETFA	$[RuH(PPh_3)_3Cl]$	20	Toluene
TFETFA	$K_2[Ru_2(PPh_3)_3(PPh_2)H_4]$	100	Toluene, 4 h
DMO	$K_2[Ru_2(PPh_3)_3(PPh_2)H_4]$	70	Toluene, 70% MG, 0% EG

a) Conditions: 5.7 mmol ester, 0.017 mmol $K_2[Ru_2(PPh_3)_3(PPh_2)H_4]_2$ diglyme, 0.045 mmol $[RuH(PPh_3)_3Cl]$; reaction time = 20 h; temperature = 90 °C; P = 620 kPa H_2.

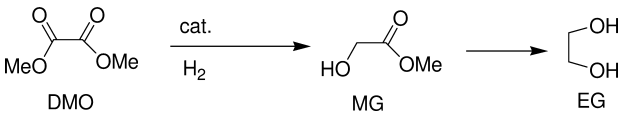

Scheme 15.19 Dimethyl oxalate hydrogenation.

a considerable research effort aimed at reducing dimethyl oxalate (DMO) to either methyl glycolate (MG) or ethylene glycol (EG).

By using the $[Ru_4H_4(CO)_8(PnBu_3)_4]$ catalyst system reported for acid hydrogenation of acids [102], Matteoli and coworkers investigated the hydrogenation of dicarboxylic acid ester derivatives at 130 bar pressure and 180 °C [109]. Using relatively high catalyst loadings (maximum TON ~ 150), DMO could be converted cleanly into the hydroxyl-ester, MG. The hydrogenations of various dicarboxylate esters under similar conditions are listed in Table 15.15. No TOF were reported, though these data do show the relative reactivity of several substrates. Consistent with Grey's observation regarding the activating effect of electron-withdrawing substituents, striking differences in hydrogenation rates were seen, depending on the proximity of the second carboxylate ester group in the substrate.

As can be seen from the data in Table 15.15, increasing the tether length results in significantly less hydrogenation. The results obtained with the C_4 esters, dimethyl-*o*-phthalate, dimethyl-*cis*-cyclohexane-1,2-carboxylate and dimethyl succinate are informative (Table 15.15, Entries 4–6, respectively). The close proximity of the second carboxylate ester in the substrates that are readily hydrogenated suggests two possibilities: an electronic effect, or a chelate effect. It can be envisaged that the electron-withdrawing effects of the ester group are more readily

Table 15.15 Hydrogenation of dicarboxylic esters under similar conditions.[a)]

Entry	Substrate	Conversion [%]	Product(s)[b)]
1	$(CO_2Me)_2$	51	Methylglycolate (MG) (51)
2	$CH_2(CO_2Me)_2$	38	$HOCH_2CH_2CO_2Et$ (17) $CH_3CH_2CO_2Et$ (10) Ethyl acetate and transesterification products (11)
3	$(CH_2CO_2Me)_2$	7	γ-Butyrolactone (7)
4	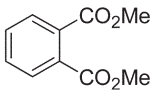	21	Phthalide (11) Methyl benzoate (10)
5	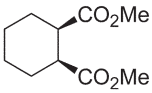	1	–
6	$CH_2(CH_2CO_2Me)_2$	0	–
7	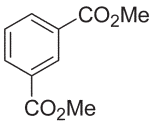	0	–

a) Conditions: 144 h; 25 mg $[Ru_4H_4(CO)_8(PnBu_3)_4]$; 6 g substrate, 130 bar H_2; 180 °C.
b) Values in brackets are product yields (%).

transmitted through the aromatic system in dimethyl-*o*-phthalate than in dimethyl succinate. If chelate coordination of the substrate was primarily responsible for the high reaction rates, then dimethyl-*cis*-cyclohexane-1,2-carboxylate and dimethyl-*o*-phthalate should give similar yields. Since this is not the case it seems that, for ester hydrogenations – at least using this type of catalytic system – reactivity is primarily controlled by electronic effects within the ester substrate.

In 1986, the same research group reported an improved pre-catalyst, $[Ru(CO)_2(CO_2CH_3)_2(PnBu_3)_2]$ [110]. Using this catalyst system in hydroxylated solvents, the hydrogenation of DMO produced ethylene glycol in addition to methyl glycolate, therefore inferring the hydrogenation of the less-activated ester methyl glycolate. When this system was studied in detail under standard conditions, the gradual conversion of DMO to MG then to EG is clear to see (t=1 h: DMO 48%, MG 52%, EG 0%, t=2.5 h: DMO 0%, MG 100%, EG 0%, t=72 h: DMO 0%; MG 78.4%; EG 21.6%). The DMO hydrogenation shows half-order reliance on DMO concentration, whereas the MG hydrogenation does not fit any steady-

Table 15.16 Hydrogenation of dimethyl oxalate using $[Ru(CO)_2(CO_2CH_3)_2(PnBu_3)_2]$.

Pressure [bar]	Catalyst concentration [mmol L^{-1}]	Temperature [°C]	Methyl glycolate [%]	Ethylene glycol [%]
10	4.9	180	96.2	3.8
90	4.9	180	81.2	18.8
130	4.9	180	78.4	21.6
130	2.45	180	90.8	9.2
130	9.70	180	69.2	30.8
130	4.9	120	51.4	0

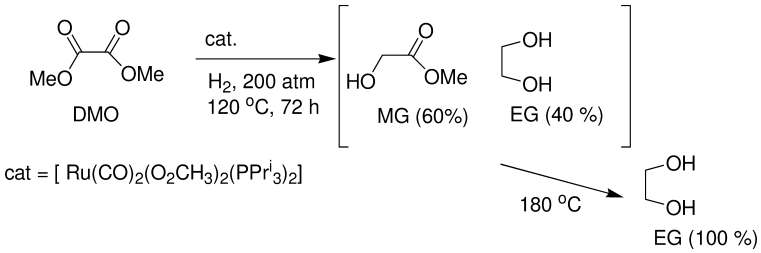

Scheme 15.20 Two-stage hydrogenation of esters giving ethylene glycol (EG), without decomposition products. MG = methyl glycolate.

rate laws. The conversion did not surpass 31%, inferring a decomposition pathway for the catalyst – not surprisingly, after many days at 180 °C. A careful set of optimization experiments were carried out focused on increasing the yields of EG from DMO. Increasing hydrogen pressures, catalyst loading, and temperature all have beneficial effects on the hydrogenation. Informative results from these experiments are in Table 15.16. Finally, a pronounced improvement on conversion was realized by the interesting – but not entirely satisfactory – addition of ~1 equiv. of product in 0.5 mL benzene as additive. A 95% conversion to EG after 144 h at 180 °C (200 bar H_2) was observed.

In a subsequent report, the authors compared the more bulky triisopropylphosphine-based catalyst in DMO hydrogenation [111]. This initially appeared worse than the first system, as it produced considerable decomposition products (65%). However, the rates for hydrogenation of isolated MG using this system are superior to those with $[Ru(CO)_2(CO_2CH_3)_2(PnBu_3)_2]$, and do not produce decomposition products, which were proven to come only from DMO. A two-stage (two-temperature) procedure using the $PiPr_3$-based catalyst was therefore developed, which uses a lower initial temperature to suppress substrate decomposition (Scheme 15.20).

Table 15.17 Hydrogenation of dimethyl oxalate using bi-, tri-, and tetra-dentate ligands.[a)]

Ligand	Catalyst [μmol]	L:Ru ratio	Conversion [%]	MG [%]	EG [%]	TON [h^{-1}]
dppe	16.1	3	18	11	0	6
PPh_3	9.6	5.9	73	36	0	18
$PhP(C_2H_4PPh_2)_2$	20.1	1.7	76	67	0	38
$MeC(CH_2PPh_2)_3$	21.1	1.4	100	1	95	160
$(CH_2P(Ph)C_2H_4PPh_2)_2$	22.8	1.0	91	85	0	36

a) Conditions: MeOH solvent, 80 bar H_2; 120 °C; 0.3% Zn as additive.

There has been one further, recent development in this area. Elsevier and co-workers studied DMO hydrogenation using a broader range of catalysts, and under milder conditions than those used by Matteoli et al. [112, 113]. Elsevier and colleagues showed that tetra- and tri-dentate phosphines, when used in combination with $[Ru(acac)_3]$, are very promising pre-catalysts for this class of reaction (Table 15.17). Although no direct comparisons to Matteoli's or Grey's system were reported, a comparison of the preceding discussion with the data in Table 15.16 suggests that, at present, this catalyst system is the most active one known.

The data in Table 15.17 clearly show the improved activity of all three multidentate ligands, and more strikingly, the selective formation of EG using the TRIPHOS ligand. The most significant difference between triphos ($MeC(CH_2PPh_2)_3$) and $PhP(CH_2CH_2PPh_2)_2$ is that triphos is a facially coordinating ligand to octahedral ruthenium complexes. This type of coordination chemistry could therefore prove a key to further improved ester hydrogenation catalysts.

The Elsevier system has since been shown to carry out several ester hydrogenations that were previously deemed impossible [114]. The hydrogenation of dimethyl phthalate to phthalide with ruthenium cluster catalysts has already been discussed (Table 15.15, Entry 4). The application of $[Ru(acac)_3]$ and triphos – this time with a 20-fold excess of Et_3N as additive – delivers good yields of phthalide. However, the use of isopropanol (IPA) as solvent and 24% HBF_4 allows further hydrogenation to 1,2,-bis-hydroxylmethyl benzene for the first time. Both of these reactions were carried out under milder conditions (100 °C, 85 bar H_2, 16 h) than those reported previously.

A striking improvement in catalytic activity was observed when hydrogenating the esters benzyl benzoate (BZB) and methyl palmitate (MP; $C_{15}H_{31}CO_2Me$). An increase from the TON of ~100 observed in IPA to ~2000 (BZB hydrogenation) and 600 (MP hydrogenation) were found by using hexafluoroisopropanol as solvent with 9 mol% Et_3N as additive. Although this solvent is rather expensive, these are high turnover numbers for the hydrogenation of substrates that previously could not be hydrogenated at all using homogeneous catalysts. Hopefully, these two reports will lead the way towards developing practical ester

hydrogenation in the not too distant future. Indeed, a recent patent from Davy Process and Technology has explored this type of catalyst system in the hydrogenation of unactivated esters such as methyl propionate and dimethylmaleate. In methyl propionate hydrogenation at $\sim 190\,^{\circ}C$, good conversions to the propanol can be achieved, provided that water is present in the reaction vessel. The role of the water is to regenerate the catalyst which is deactivated during the reaction. This was proven by an experiment in which a catalyst that was no longer active for hydrogenation was reactivated by heating in the presence of water [103]. This catalyst system also hydrogenates anhydrides and acids. In these cases, the water produced by the hydrogenation is sufficient to allow the reaction to be run without any added water. Another patent on effective solutions for ester hydrogenation has also recently appeared [115].

The field of ester hydrogenation is significantly less developed in comparison with the hydrogenation of other double bonds. Many of the studies are limited to DMO hydrogenation, and the full scope of the reaction needs to be evaluated. At present, the research findings suggest that electron-withdrawing substituents activate substrates considerably, but the breakthrough by Elsevier's group suggest that a more broadly applicable procedure for ester hydrogenation might become reality.

Catalyst development has also been relatively unexplored. It is noteworthy that two of the most significant developments were made when the effect of different phosphine ligands were being investigated in more detail for the first time [111, 114]. At present, it is difficult to predict the future for ester hydrogenation, but if the "catalysis community" invests time into the development of the process it could prove to be an environmentally benign method for carrying out reductions in the fine chemical and pharmaceutical industries. Indeed, recent developments in industry suggest that the reaction could be viable for production-scale synthesis, and that the discovery of more active catalysts would be of considerable value.

15.8 Summary and Outlook

Since the first report of a homogeneously catalyzed reduction of a C=O bond, various research groups have endeavored to develop catalysts that show sufficient activity and high chemoselectivity to be used as a viable alternative to heterogeneous catalysts in the production of primary and racemic/achiral secondary alcohols. Much of this research effort has been conducted side-by-side with, and informed developments in, the diastereoselective and enantioselective hydrogenation of polar bonds, since activity and chemoselectivity are also key issues for these catalysts. This research effort has brought some catalysts to a level of development that suggests they might be applied in commercial production.

The ruthenium-phosphine-diamine catalysts exhibit high turnover numbers and frequencies, and near-perfect chemoselectivity for ketone/aldehyde over

C=C reduction. The achiral catalysts are relatively cheap, easy to prepare/handle, and sufficiently active to set SCRs near the threshold for Ru content in pharma products. This suggests that these catalysts could certainly be competitive, easy to operate in hydrogenations in which heterogeneous catalysts are less effective, and thereby also worthy of investigation in other cases.

The improvements made in hydroaminomethylation technology suggest that certain variants of this reaction are sufficiently developed for the potential production of amines. The synthesis of linear tertiary and secondary amines from terminal alkenes shows promise in this regard. Beller's recent contributions towards hydroaminomethylation using ammonia to produce linear primary amines, which are of industrial significance due to their abundance, suggest a bright future for this reaction. Branched selective hydroaminomethylation remains relatively underdeveloped and needs further study.

The hydrogenation of carboxylic acid derivatives using molecular hydrogen represents a major challenge, but has considerable importance from a "green chemistry" point of view. The heterogeneous catalysts capable of achieving this transformation function under energy-consuming and harsh conditions, and homogeneous catalysts for ester hydrogenation would clearly attract industrial interest if they were adequately efficient. Given that only a handful of reports have appeared on this subject, and that both substrate scope and catalyst structure–activity relationships have barely been defined, considerable further research is required in this area.

In summary, the research effort aimed towards active, chemoselective hydrogenations of certain C=O and C=N bonds have delivered several catalysts that approach the level of activity required for use in the synthesis of alcohols and amines. However, other classes of substrate require considerable additional investigations to be conducted before homogeneous catalysts may be considered for this purpose.

Abbreviations

DCM	dichloromethane
DMO	dimethyl oxalate
EG	ethylene glycol
EtOAc	ethyl acetate
MG	methyl glycolate
MTFA	methyl trifluoroacetate
SCR	substrate-catalyst-ratio
TFETFA	trifluoroethyl trifluoroacetate
THF	tetrahydrofuran
TOF	turnover frequency
TON	turnover number
TPPMS	triphenylphosphine, mono-sulfonated
TPPTS	3,3′,3″-phosphinidynetris-, trisodium salt

References

1 R. S. Coffey, *J. Chem. Soc. Chem. Commun.* **1967**, 923.
2 W. Strohmeier, H. Steigerwald, *J. Organomet. Chem.* **1977**, *129*, C43.
3 C. S. Chin, B. Lee, S. C. Park, *J. Organomet. Chem.* **1990**, *393*, 131.
4 M. Visintin, R. Spogliarich, J. Kaspar, M. Graziani, *J. Mol. Catal.* **1985**, *32*, 349.
5 E. Farnetti, M. Pesce, J. Kaspar, R. Spogliarich, M. Graziani, *J. Mol. Catal.* **1987**, *43*, 35.
6 R.-X. Li, X.-J. Li, N.-B. Wong, K.-C. Tin, Z.-Y. Zhou, T. C. W. Mak, *J. Mol. Catal. Sect. A* **2002**, *178*, 181.
7 R.-X. Li, N.-B. Wong, X.-J. Li, T. C. W. Mak, Q.-C. Yang, K.-C. Tin, *J. Organomet. Chem.* **1998**, *571*, 223.
8 J. A. Osborn, F. M. Jardine, J. F. Young, G. Wilkinson, *J. Chem. Soc. Sect. A* **1966**, 1711.
9 B. Heil, L. Marko, *Chem. Abstr.* **1969**, *71*, 286.
10 T. Mizoroki, K. Seki, S.-I. Meguro, A. Ozaki, *Bull. Chem. Soc. Jpn.* **1977**, *50*, 2148.
11 K. Kaneda, M. Yasumura, T. Imanaka, S. Teranishi, *J. Chem. Soc. Chem. Commun.* **1982**, 935.
12 H. Fujitsu, E. Matsumura, K. Takeshita, I. Mochida, *J. Org. Chem.* **1981**, *46*, 5353.
13 M. J. Burk, T. G. P. Harper, J. R. Lee, C. Kalberg, *Tetrahedron Lett.* **1994**, *35*, 4963.
14 M. J. Burk, A. Gerlach, D. Semmeril, *J. Org. Chem.* **2000**, *65*, 8933.
15 K. Kaneda, T. Mizugaki, *Organometallics* **1996**, *15*, 3247.
16 T. Mizugaki, Y. Kanayama, K. Ebitani, K. Kaneda, *J. Org. Chem.* **1998**, *63*, 2378.
17 A. N. Ajjou, J.-L. Pinet, *J. Mol. Catal. Sect. A.* **2004**, *214*, 203.
18 J. M. Grosselin, C. Mercier, G. Allmang, F. Grass, *Organometallics* **1991**, *10*, 2126.
19 R. A. Sanchez-Delgado, J. S. Bradley, G. Wilkinson, *J. Chem. Soc. Dalton Trans.* **1976**, 399.
20 J. Tsuji, H. Suzuki, *Chem. Lett.* **1977**, 1085.
21 J. F. Knifton, *Tetrahedron Lett.* **1975**, *16*, 2163.
22 W. Strohmeier, L. Weigelt, *J. Organomet. Chem.* **1978**, *145*, 189.
23 R. A. Sanchez-Delgado, O. L. De Ochoa, *J. Mol. Catal.* **1979**, *6*, 303.
24 R. A. Sanchez-Delgado, A. Andriollo, O. L. De Ochoa, T. Suarez, N. Valencia, *J. Organomet. Chem.* **1981**, *209*, 77.
25 R. A. Sanchez-Delgado, A. Andriollo, N. Valencia, *J. Mol. Catal.* **1984**, *24*, 217.
26 K. Hotta, *J. Mol. Catal.* **1985**, *29*, 105.
27 T. Suarez, B. Fontal, *J. Mol. Catal.* **1988**, *45*, 335.
28 R.-X. Li, K.-C. Tin, N.-B. Wong, T. C. W. Mak, Z.-Y. Zhang, X.-J. Li, *J. Organomet. Chem.* **1998**, *557*, 207.
29 T. Ohkuma, H. Ooka, T. Ikariya, R. Noyori, *J. Am. Chem. Soc.* **1995**, *117*, 10417.
30 R. Noyori, T. Ohkuma, *Angew. Chem. Int. Ed.* **2001**, *40*, 40.
31 M. Hernandez, P. Kalck, *J. Mol. Catal. Sect. A.* **1997**, *116*, 131.
32 A. Benyei, F. Joo, *J. Mol. Catal.* **1990**, *58*, 151.
33 F. Joo, A. Benyei, *J. Organomet. Chem.* **1989**, *363*, C19.
34 R. A. Sanchez-Delgado, M. Medina, F. Lopez-Linares, A. Fuentes, *J. Mol. Catal. Sect. A* **1997**, *116*, 167.
35 J.-X. Chen, J. F. Daeuble, D. M. Brestensky, J. M. Stryker, *Tetrahedron* **2000**, *56*, 2153.
36 C. P. Lau, C. Y. Ren, C. H. Yeung, M. T. Chu, *Inorg. Chim. Acta* **1992**, *191*, 21.
37 E. Farnetti, G. Nardin, M. Graziani, *J. Chem. Soc. Chem. Commun.* **1988**, 1264.
38 E. Farnetti, J. Kaspar, R. Spogliarich, M. Graziani, *J. Chem. Soc., Dalton Trans.* **1988**, 947.
39 C. Bianchini, E. Farnetti, M. Graziani, G. Nardin, A. Vacca, F. Zanobini, *J. Am. Chem. Soc.* **1990**, *112*, 9190.
40 J. R. Shapely, R. R. Schrock, J. A. Osborn, *J. Am. Chem. Soc.* **1969**, *91*, 2816.
41 R. R. Schrock, J. A. Osborn, *J. Chem. Soc. Chem. Commun.* **1970**, 567.
42 M. Gargano, P. Giannoccaro, M. Rossi, *J. Organomet. Chem.* **1977**, *129*, 239.
43 G. Mestroni, G. Zassinovich, A. Camus, *J. Organomet. Chem.* **1977**, *140*, 63.
44 G. Mestroni, R. Spogliarich, A. Camus, F. Martinelli, G. Zassinovich, *J. Organomet. Chem.* **1978**, *157*, 345.

45 B. Heil, S. Toros, J. Bakos, L. Marko, *J. Organomet. Chem.* **1979**, *175*, 229.
46 S. Toros, L. Kollar, B. Heil, L. Marko, *J. Organomet. Chem.* **1983**, *253*, 375.
47 P. Frediani, U. Matteoli, *J. Organomet. Chem.* **1978**, *150*, 273.
48 M. Bianchi, U. Matteoli, G. Menchi, P. Frediani, S. Pratesi, F. Piacenti, C. Botteghi, *J. Organomet. Chem.* **1980**, *198*, 73.
49 R.A. Sanchez-Delgado, O.L. Ochoa, *J. Organomet. Chem.* **1980**, *202*, 427.
50 W. Strohmeier, L. Weigelt, *J. Organomet. Chem.* **1979**, *171*, 121.
51 Y. Watanabe, T. Ohta, Y. Tsuji, *Bull. Chem. Soc. Jpn.* **1982**, *55*, 2441.
52 T. Ohkuma, H. Ooka, S. Hashiguchi, T. Ikariya, R. Noyori, *J. Am. Chem. Soc.* **1995**, *117*, 2675.
53 T. Ohkuma, M. Koizumi, H. Ikehira, T. Yokozawa, R. Noyori, *Org. Lett.* **2000**, *2*, 659.
54 M.L. Clarke, M.B. Diaz-Valenzuela, unpublished results.
55 V. Rautenstrauch, X. Hoang-Cong, R. Churlaud, K. Abdur-Rashid, R.H. Morris, *Chem. Eur. J.* **2003**, *9*, 4954.
56 L. Dahlenburg, C. Kuhnlein, *J. Organomet. Chem.* **2005**, *690*, 1.
57 C.P. Lau, L. Cheng, *Inorg. Chim. Acta* **1992**, *195*, 133.
58 K.-M. Sung, S. Huh, M.-J. Jun, *Polyhedron* **1999**, *18*, 469.
59 V. Cadierno, P. Crochet, J. Diez, S.E. Garcia-Garrido, J. Gimeno, *Organometallics* **2004**, *23*, 4836.
60 W.S. Mahoney, J.M. Stryker, *J. Am. Chem. Soc.* **1989**, *111*, 8818.
61 L. Marko, Z. Nagy-Magos, *J. Organomet. Chem.* **1985**, *285*, 193.
62 L. Marko, J. Palagyi, *Trans. Met. Chem.* **1983**, *8*, 207.
63 L.H. Slaugh, R.D. Mullineaux, *J. Organomet. Chem.* **1968**, *13*, 469.
64 J.L. van Winkle, S. Lorenzo, R.C. Morris, R.F. Mason, US3420898, **1969**.
65 C. Crause, L. Bennie, L. Damoense, C.L. Dwyer, C. Grove, N. Grimmer, W.J. van Rensburg, M.M. Kirk, K.M. Mokheseng, S. Otto, P.J. Steynberg, *J. Chem. Soc. Dalton Trans.* **2003**, 2036.
66 P.C.J. Kamer, P.W.N. van Leeuwen, J.N.H. Reek, *Acc. Chem. Res.* **2001**, *34*, 895.
67 E. Drent, European Patent 151822, **1985**.
68 M.J. Lawrenson, G. Foster, Ger. Offen 1901145, **1969**.
69 M.J. Lawrenson, UK Patent 1284615, **1972**.
70 B. Fell, A. Guerts, *Chem. Ing. Tech.* **1972**, *44*, 708.
71 L.D. Jurewicz, L.D. Rollman, D.D. Whitehurst, *Adv. Chem. Ser.* **1974**, *132*, 240.
72 P. Cheliatsidou, D.F.S. White, D.J. Cole-Hamilton, *J. Chem. Soc. Dalton Trans.* **2004**, 3425.
73 J.K. MacDougall, M.C. Simpson, M.J. Green, D.J. Cole-Hamilton, *J. Chem. Soc. Dalton Trans.* **1996**, 1161.
74 M.C. Simpson, K. Porteous, J.K. MacDougall, D.J. Cole-Hamilton, *Polyhedron* **1993**, *12*, 2883.
75 A.J. Sandee, J.N.H. Reek, P.C.J. Kamer, P.W.N.M. van Leeuwen, *J. Am. Chem. Soc.* **2001**, *123*, 8468.
76 L. Marko, J. Bakos, *J. Organomet. Chem.* **1974**, *81*, 411.
77 J.F. Knifton, *Catal. Today* **1997**, *36*, 305.
78 V.I. Tararov, R. Kadyrov, T.H. Riermeier, A. Borner, *J. Chem. Soc. Chem. Commun.* **2000**, 1867.
79 T. Gross, A.M. Seayad, M. Ahmad, M. Beller, *Org. Lett.* **2002**, *4*, 2055.
80 R. Margalef-Catala, C. Claver, P. Salagre, E. Fernandez, *Tetrahedron Lett.* **2000**, *41*, 6583.
81 V.I. Tararov, R. Kadyrov, T.H. Riermeier, A. Borner, *Adv. Synth. Catal.* **2002**, *344*, 200.
82 V.I. Tararov, R. Kadyrov, K.H. Riermeier, C. Fischer, A. Borner, *Adv. Synth. Catal.* **2004**, *346*, 561.
83 W. Reppe, *Experientia* **1949**, *5*, 93.
84 F. Jachimowicz, J.W. Raksis, *J. Org. Chem.* **1982**, *47*, 445.
85 T. Baig, P. Kalck, *J. Chem. Soc. Chem. Commun.* **1992**, 1373.
86 T. Baig, J. Molinier, P. Kalck, *J. Organomet. Chem.* **1993**, *455*, 219.
87 M. Ahmed, A.M. Seayad, R. Jackstell, M. Beller, *J. Am. Chem. Soc.* **2003**, *125*, 10311.
88 H. Schaffrath, W. Keim, *J. Mol. Catal. Sect. A* **1999**, *140*, 107.
89 A. Seayad, M. Ahmed, H. Klein, R. Jackstell, T. Gross, M. Beller, *Science* **2002**, *297*, 1676.

90 B. Zimmermann, J. Herwig, M. Beller, *Angew. Chem. Int. Ed.* **1999**, *38*, 2372.

91 P. Eilbracht, L. Barfacker, C. Buss, C. Hollmann, B. E. Kitsos-Rzychon, C. L. Kranemann, T. Rische, R. Roggenbuck, A. Schmidt, *Chem. Rev.* **1999**, *99*, 3329.

92 T. Rische, P. Eilbracht, *Tetrahedron* **1999**, *55*, 1915.

93 A. Schmidt, M. Marchetti, P. Eilbracht, *Tetrahedron* **2004**, *60*, 11487.

94 H. Wakamatsu, J. Furukawa, N. Yamakami, *Bull. Chem. Soc. Jpn.* **1971**, *44*, 288.

95 J. E. Lyons, *J. Chem. Soc. Chem. Commun.* **1975**, 412.

96 P. Morand, M. Kayser, *J. Chem. Soc. Chem. Commun.* **1976**, 314.

97 H. Yoshinori, I. Hiroko, US5077442, **1991**.

98 W. Keisure, H. Yoshinori, K. Sasaki, US5079372, **1992**.

99 M. Chihiro, T. Kazunari, K. Hiroshi, I. Shinji, O. Masayuki, US5047561, **1991**.

100 S. Hitoshi, T. Kazunari, K. Haruhiko, US5580991, **1996**.

101 M. Pianchi, F. Piacenti, P. Frediani, U. Matteoli, C. Botteghi, S. Gladiali, E. Benedetti, *J. Organomet. Chem.* **1977**, *141*, 107.

102 M. Bianchi, G. Menchi, F. Francalanci, F. Piacenti, U. Matteoli, P. Frediani, C. Botteghi, *J. Organomet. Chem.* **1980**, *188*, 109.

103 D. V. Tyers, M. Kilner, S. P. Crabtree, M. A. Wood, WO0309308, **2003**.

104 D. He, N. Wakasa, T. Fuchikami, *Tetrahedron Lett.* **1995**, *36*, 1059.

105 A. Yamamoto, Y. Kayaki, K. Nagayama, I. Shimizu, *Synlett* **2000**, 925.

106 K. Nagayama, I. Shimizu, A. Yamamoto, *Chem. Lett.* **1998**, 1143.

107 K. Nagayama, I. Shimizu, A. Yamamoto, *Bull. Chem. Soc. Jpn.* **2001**, *74*, 1803.

108 R. A. Grey, G. P. Pez, A. Wallo, *J. Am. Chem. Soc.* **1981**, *103*, 7536.

109 U. Matteoli, M. Bianchi, G. Menchi, P. Frediani, F. Piacenti, *J. Mol. Catal.* **1984**, *22*, 353.

110 U. Matteoli, G. Menchi, M. Bianchi, F. Piacenti, *J. Organomet. Chem.* **1986**, *299*, 233.

111 U. Matteoli, G. Menchi, M. Bianchi, F. Piacenti, *J. Mol. Catal.* **1991**, *64*, 257.

112 H. T. Teunissen, C. J. Elsevier, *J. Chem. Soc. Chem. Commun.* **1997**, 667.

113 M. C. van Engelen, H. T. Teunissen, J. G. de Vries, C. J. Elsevier, *J. Mol. Catal. Sect. A*, **2003**, 206, 185.

114 H. T. Teunissen, C. J. Elsevier, *J. Chem. Soc. Chem. Commun.* **1998**, 1367.

115 K. Yamamoto, T. Watanabe, T. Abe, JP2004300131, **2004**.

16
Hydrogenation of Arenes and Heteroaromatics

Claudio Bianchini, Andrea Meli, and Francesco Vizza

16.1
Introduction

The hydrogenation of arenes and heteroaromatics to partially or fully saturated cyclic hydrocarbons is a reaction of paramount industrial importance, typically catalyzed in heterogeneous phase by a number of transition metals [1]. Just to mention a few huge applications, each year a million tons of benzene are hydrogenated on Raney nickel to cyclohexane for the production of nylon *via* adipic acid [2], and much larger amounts of liquid fossil fuels are hydrotreated in refineries to remove sulfur, nitrogen, and oxygen from various heteroaromatics – the hydrodesulfurization (HDS), hydrodenitrogenation (HDN), and hydrodeoxygenation (HDO) processes [3]. The hydrogenation of aromatics and heteroaromatics will become increasingly important if coal, which contains a huge amount of such compounds, continues to be used for the production of petrochemicals.

Aromatic hydrogenation reactions in homogeneous phase are much less numerous, and also much less efficient than in heterogeneous phase, especially in terms of turnover frequencies and catalyst stability [4]. On the other hand, soluble metal complexes still provide a better regio- and stereo-control in the reduction of heteroaromatics, although this supremacy over heterogeneous catalysis is being threatened by the development of increasingly efficient chiral phase-transfer reagents and chiral auxiliaries adsorbed onto the support materials [5]. There is little doubt, however, that organometallic compounds will always play an irreplaceable role as models systems to gain insight into the mechanisms of substrate binding and activation as well as hydrogen adsorption, activation, and transfer. The origin of the chemo-, regio-, and stereoselectivity is another issue that can be better addressed at the molecular level than using a supported metal particle.

The scarce number of metal complexes capable of catalyzing the hydrogenation of arenes is a direct consequence of the tendency of these substrates to use all the available π-electrons for coordination, and hence to occupy three contigu-

The Handbook of Homogeneous Hydrogenation.
Edited by J.G. de Vries and C.J. Elsevier
Copyright © 2007 WILEY-VCH Verlag GmbH & Co. KGaA, Weinheim
ISBN: 978-3-527-31161-3

ous coordination sites [6]. Indeed, the barrier to disruption of the aromaticity is generally very high and other bonding modes, such as the η^2 and the η^4, which would allow a more facile metal coordination and a lower barrier to reduction (H_2 activation and transfer), are extremely difficult to accomplish, even with highly energetic metal fragments [7]. Just the presence of the heteroatom, with suitable lone pairs for σ-bonding to the metal, is the main reason for the relatively large number of homogeneous catalysts capable of hydrogenating sulfur-, oxygen-, and nitrogen-heteroaromatics [8]. The most effective molecular catalysts for the hydrogenation of arenes and heteroaromatics are complexes consisting of a central metal ion (generally ruthenium, rhodium, or iridium), one or more ligands, and anions. The ensemble of these three components is responsible for the activation of hydrogen (either heterolytic or homolytic) and its selective transfer to an acceptor substrate. Experience has shown that low-valent metal complexes stabilized by ligands with phosphorus and/or nitrogen donor atoms constitute the most active and versatile catalysts [2, 8, 9].

The aim of this chapter is to provide the reader with a survey of the molecular catalysts that are able to hydrogenate aromatics, and to demonstrate the advantages and limits of the homogeneous approach. This review includes hydrogenation reactions performed in aqueous-biphasic systems, while the many structural and mechanistic analogies between molecular catalysts and heterogenized single-site metal catalysts induced us to comment also about aromatic hydrogenation by metal complexes tethered to both inorganic and organic support materials.

Several excellent reviews on the selective hydrogenation of arenes and heteroaromatics by single-site metal catalysts have been published over the past few years [8–10]. Consequently, the reader is advised to become acquainted with these accounts in order to obtain a deeper insight into the subject.

16.2 Hydrogenation of Arenes

16.2.1 Molecular Catalysts in Different Phase-Variation Systems

Very few metal complexes have been reported to generate effective catalysts for the hydrogenation of carbocyclic aromatic rings in homogeneous phase. Moreover, even the reported cases are not completely convincing, as black metal often precipitates during the catalysis. In fact, the reduction of arenes is the domain of heterogeneous catalysts, especially those based on noble metals among which rhodium, ruthenium, and platinum generate the most active systems [11]. The chemoselectivity is generally low, as most of the functional groups are hydrogenated prior to the aromatic ring. In contrast, several regioselective examples of *cis* hydrogen addition have been reported [12], while no example of asymmetric hydrogenation of prochiral arenes in homogeneous phase has been reported so far.

Table 16.1 Homogeneous catalysts, tethered single-site catalysts, and biphase catalysts for the hydrogenation of aromatic hydrocarbons.

Catalyst	Substrate	T [°C]	pH_2 [bar]	Reference(s)
$M(OAr)(H)_3L_2$ (M = Ta, Nb; L = PM_2Ph, $PMePh_2$)	benzenes, polyaromatics	80–100	3–100	30
$[Ru(\eta^6\text{-}C_{10}H_{14})(\eta^2\text{-triphos})Cl]PF_6$	benzenes [a)]	90	60	19
$RuH_2(H_2)_2(PCy_3)_2$	benzenes, polyaromatics	80	3–20	18
$[Ru_3(\eta^6\text{-}C_6Me_6)_2(\eta^6\text{-}C_6H_6)(\mu_3\text{-}O)(\mu_2\text{-}OH)(\mu_2\text{-}H)_2]BF_4$	benzenes [a)]	20	40	22
$RuCl_2(PTA)(\eta^6\text{-}C_{10}H_{14})$; $RuCl(PTA)_2(\eta^6\text{-}C_{10}H_{14})$	benzenes	90	60	21
$Co(\eta^3\text{-}C_3H_5)\{P(OR_3)_3\}$	benzenes, polyaromatics	25	1	13
$Ni(\eta^6\text{-}CH_3C_6H_5)(C_6F_5)_2$	benzene		35	45
Metal alkoxides, acac, or carboxylates + AlR_3	benzenes, polyaromatics	150–210	70	34, 35
$Co(Cy_2PC_8H_{11})(\eta^5\text{-}C_8H_{13})$	benzene	25	1	46
$[Cp^*RhCl_2]_2$	benzenes, anthracene	50	50	25
$L_2RhH(\mu\text{-}H)_3RhL_2$ (L = $P(O^iPr)_3$)	benzenes	25	1	14
$Rh(acac)\{P(OPh)_3\}_2$	benzenes	80	10	47
$RhH\{P(NC_4H_4)_3\}_4$; $RhH(CO)\{P(NC_4H_4)_3\}_4$	benzenes	25	5	48
$[Rh(diphos)(MeOH)_2]BF_4$	anthracenes	50–75	1	17
$[RhCl(diene)]_2^+[NR_4]X$	benzenes [b)], naphthalene	25	1	49
$Rh(cod)(sulphos)/Pd^0/SiO_2$	benzenes [c)]	40	30	42
Rh or Pt complexes on SiO_2-supported metals (Pd, Pt, Ru)	benzenes, naphthalene [c)]	40	1	38, 40
$Ru(\eta^6\text{-}C_6Me_6)(\eta^4\text{-}C_6Me_6)$	benzenes	90	2–3	50
$[Ru(\eta^6\text{-}C_6Me_6)_2(\mu\text{-}H)_2(\mu\text{-}Cl)]Cl_2$	benzenes	50	50	25
$Ru(H)_3(PPh_3)_3$; $Ru(H)_2(H_2)(PPh_3)_3$	anthracenes	50–100	5	23
$Ru_4H_4(\eta^6\text{-}C_6Me_6)$; $Ru_2Cl_4(\eta^6\text{-}C_6Me_6)$	benzenes [a)]	90	60	20, 52
Fe, Co, Mn, Rh, Ru, W, Mo, Cr carbonyls	polyaromatics [d), e)]	180	25	24
$Fe(CO)_5$ + ammonium salt	anthracene	150	35	51
Early metal complexes on oxides (Th, U, Nb, Ta, Zr)	benzenes, polyaromatics [c)]	100–120	70–90	44
$Co_2(CO)_8$	polyaromatics [e)]	135–185	230–270	36

a) Liquid biphasic catalysis.
b) Phase transfer catalysis.
c) Supported metal complexes.
d) CO/H_2O as reducing agent.
e) Syngas as reducing agent.

As a general trend in both homogeneous and heterogeneous phase, the hydrogenation of arenes requires higher H_2 pressures and higher temperature as compared to the hydrogenation of olefins. Naphthalenes are extremely difficult to reduce, while higher polynuclear arenes are hydrogenated more easily than benzenes, especially at the outer rings, the resonance-stabilization of which is not as efficacious as that of the inner benzene ring.

A list of the metal complexes that have been claimed to generate catalysts for the hydrogenation of carbocyclic aromatic rings is provided in Table 16.1. This list includes homogeneous catalysts, biphase catalysts, and tethered single-site catalysts.

Ruthenium (Ru), rhodium (Rh), and cobalt (Co) form the most active and versatile catalysts, with a prevalence for Ru; effective catalysts have been reported also for other metals such as Ni, Pd, Pt, Cr, W, Mo, Mn, Nb, and Ta, some of which, however, are selective for the partial reduction of polynuclear aromatics.

The first well-documented case of homogeneous catalytic hydrogenation of a carbocyclic aromatic ring was reported by Muetterties and coworkers, who employed allyl cobalt complexes of the general formula (η^3-C_3H_5)Co(PR_3)$_3$ (PR_3 = phosphite, phosphine) to hydrogenate benzene, alkylbenzenes, anisole, naphthalene, anthracene, and phenanthrene under mild conditions (25 °C, 1–3 bar H_2) [13]. The catalytic activity was found to increase with the size of the phosphite/phosphine ligand in the order $P(OMe)_3 < P(OEt)_3 < PMe_3 < P(OiPr)_3$. Remarkably, the hydrogenation of benzene to cyclohexane could be achieved already at 25 °C and 1 bar H_2, yet only 25 turnovers were observed prior to catalyst deactivation. Alkyl substituents on the benzene ring were also found to inhibit the reduction. In contrast to what is generally observed in both homogeneous and heterogeneous phase, the cobalt catalysts proved more active for benzene than for polyaromatics. The monohydride Co^I fragment $CoH(PR_3)_2$, generated by hydrogenation of the precursor, was proposed as the catalytically active species. This unsaturated 14-electron fragment reacts with further phosphite/phosphine, yielding $CoH(PR_3)_n$ (n = 3, 4) and with H_2 yielding the trihydride $CoH_3(PR_3)_3$ (Scheme 16.1). As both these species are catalytically inactive, their unavoidable formation during the catalysis was suggested to be the main factor for catalyst deactivation.

Scheme 16.2 illustrates the catalytic mechanism proposed by Muetterties and coworkers [13]. Salient features of this mechanism are the coordination of benzene in the η^4-fashion, to give a transient $CoH(\eta^4\text{-}C_6H_6)(PR_3)_2$ complex, and the intramolecular hydride transfer to form the allylic intermediate $Co(\eta^3\text{-}C_3H_7)(PR_3)_2$. Hydrogen addition would give an η^4-1,3-cyclohexadiene complex that ultimately releases cyclohexane *via* H_2 addition/hydride migration steps. Complete *cis* stereoselectivity of hydrogen addition was demonstrated by replacing H_2 with D_2.

A mechanism similar to that shown in Scheme 16.2 has also been proposed to rationalize the arene hydrogenation activity of the triply-bridged dirhodium complex $L_2HRh(\mu\text{-}H_3)RhL_2$ (L = P(O*i*Pr)$_3$) [14].

Some steps of the mechanism proposed by Muetterties have been proved experimentally by Bianchini and coworkers [15]. These authors synthesized the η^4-benzene Ir^I complex $[Ir(triphos)(\eta^4\text{-}C_6H_6)]^+$(triphos = $CH_3C(CH_2PPh_2)_3$), and studied

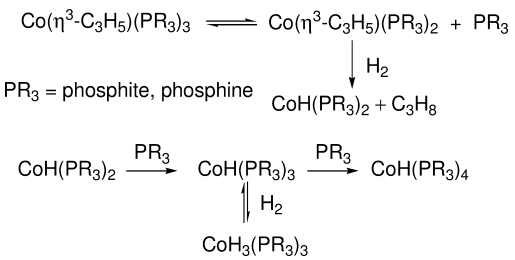

Scheme 16.1

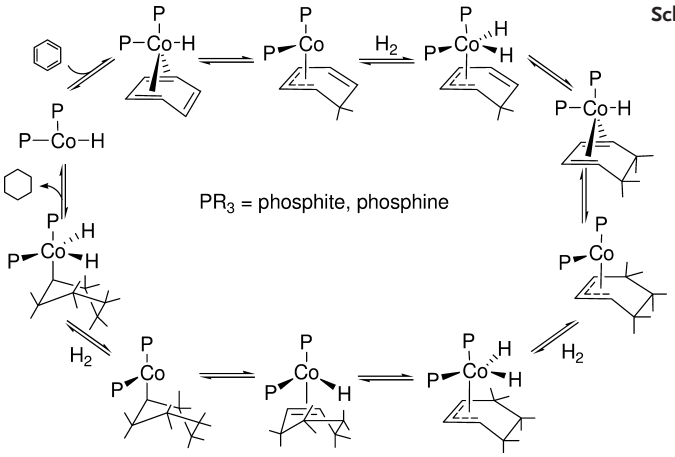

Scheme 16.2

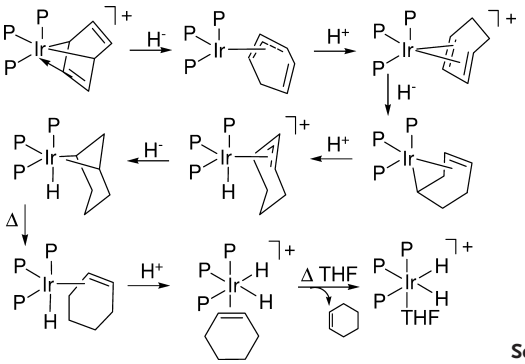

Scheme 16.3

in detail each reduction step down to the conversion of benzene to cyclohexene by sequential addition of H^- and H^+. The overall reaction sequence is illustrated in Scheme 16.3. All the metal intermediates along the conversion of benzene to cyclohexene were unambiguously characterized and the region/stereochemistry of each "H" addition was determined.

It is noteworthy that the starting η^4-benzene complex was prepared by cyclotrimerization of acetylene by $IrCl(C_2H_4)$(triphos) [16]. All of the attempts to react the fragment $[Ir(triphos)]^+$ with benzene were unsuccessful, which reflects the difficulty met by a transition-metal fragment to overcome the energy barrier to η^4-benzene coordination.

The complex $[Rh(MeOH)_2(diphos)]^+$ (diphos = 1,2-bis(diphenylphosphino)ethane) has been reported to hydrogenate polynuclear aromatic hydrocarbons under mild conditions (60 °C, 1 bar H_2) [17]. A kinetic study of the hydrogenation of 9-CF_3CO-anthracene to the corresponding 1,2,3,4-tetrahydroanthracene was consistent with a rapid conversion of the precursor to $[Rh(\eta^6\text{-anthracene})(diphos)]^+$ and a rate-determining step involving the reaction of the latter complex with H_2

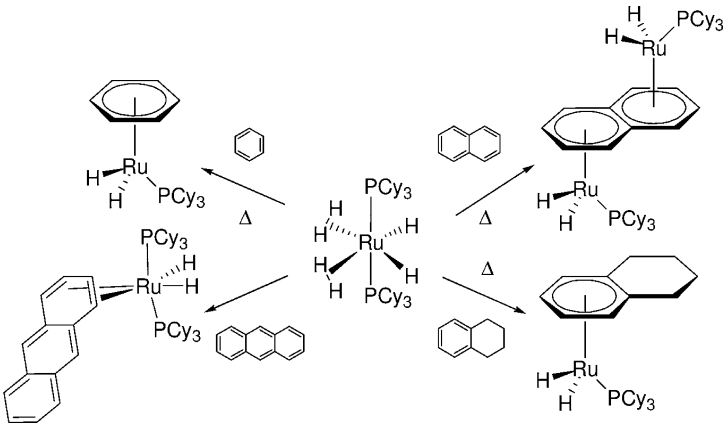

Scheme 16.4

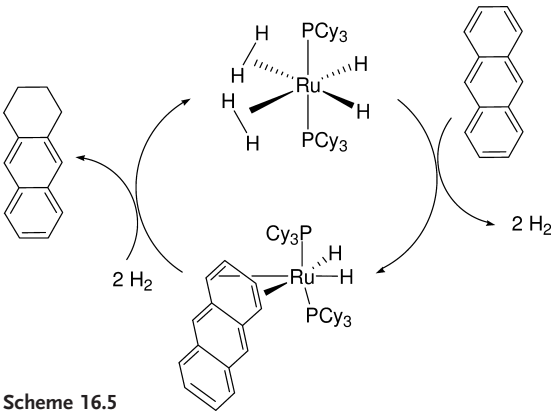

Scheme 16.5

to give 1,2-dihydroanthracene. A second-order rate kinetic law (–d[anthracene]/dt = k [Rh] [H_2]) was determined with $k(59.7\,^{\circ}C) = (9.0 \pm 1.0) \times 10^{-2}\ M^{-1}\ s^{-1}$.

Whilst the metals of the cobalt group have provided valuable mechanistic information on the mechanism of homogeneous hydrogenation of arenes, there is little doubt that ruthenium forms the most active and versatile catalysts.

Borowski and coworkers have reported that benzene, naphthalene, and anthracene are reduced to cyclohexane, tetralin and a mixture of 1,2,3,4-tetrahydroanthracene (4H-An) and 1,2,3,4,5,6,7,8-octahydroanthracene (8H-An), respectively, in the presence of the dihydride bishydrogen complex $RuH_2(H_2)_2(PCy_3)_2$ (80 °C, 3–30 bar H_2) [18]. Notably, the latter was found to react at 80 °C with neat benzene or with cyclohexane solutions of naphthalene or tetralin to form the corresponding η^6-adducts (Scheme 16.4). These products were also isolated from the final catalytic mixtures.

Unlike the previous arenes, anthracene reacted with $RuH_2(H_2)_2(PCy_3)_2$ already at room temperature to form an η^4-anthracene adduct which was found to be an

effective catalyst for anthracene hydrogenation. It was suggested, therefore, that all these arene adducts may have an active role in the catalytic cycle. A simplified cycle for the hydrogenation of anthracene to 4H-An by $RuH_2(H_2)_2(PCy_3)_2$ is shown in Scheme 16.5. This involves the preliminary dissociation of two H_2 molecules to generate a coordination vacancy for the incoming molecule that ultimately binds the metal in η^4 fashion. The occurrence of this step was supported by evidence that the reaction rate decreased by increasing the H_2 pressure. The reduction of the second external ring of 4H-An to 8H-An would follow a similar mechanism as it appreciably started only when most – if not all – anthracene was consumed. 9,10-Dihydroanthracene – a typical product of catalysis proceeding through a radical mechanism – was not detected.

It is worth noting, however, that the real homogeneous character of the reactions catalyzed by the hexahydride $RuH_2(H_2)_2(PCy_3)_2$ remains questionable, as elemental mercury was found to inhibit the hydrogenation reaction, which may indicate the formation of catalytically active ruthenium metal. In contrast, a truly homogeneous ruthenium catalyst for the hydrogenation of benzenes seems to be generated by the precursor $[RuCl(\eta^2\text{-triphos})(\eta^6\text{-}p\text{-cymene})]PF_6$, recently described by Dyson and coworkers (Scheme 16.6) [19]. The catalytic activity of this complex was evaluated at 90 °C and 60 bar H_2 either in dichloromethane or in a biphasic system comprising the substrate and 1-butyl-3-methylimidazolium tetrafluoroborate. Due to its solubility in the ionic liquid (IL), the catalyst could be recovered and recycled after use. Interestingly, 1-alkenyl-substituted arenes, such as styrene and 1,3-divinylbenzene, were not hydrogenated, whereas allylbenzene was selectively converted to allylcyclohexane with a turnover frequency (TOF; mol. product mol^{-1} catalyst h^{-1}) of 329 and complete regioselectivity.

The catalytic hydrogenation of various benzene derivatives by the ruthenium tetrahydride clusters $[Ru_4H_4(\eta^6\text{-}C_6H_6)_4]^{2+}$ was investigated by Süss-Fink in both

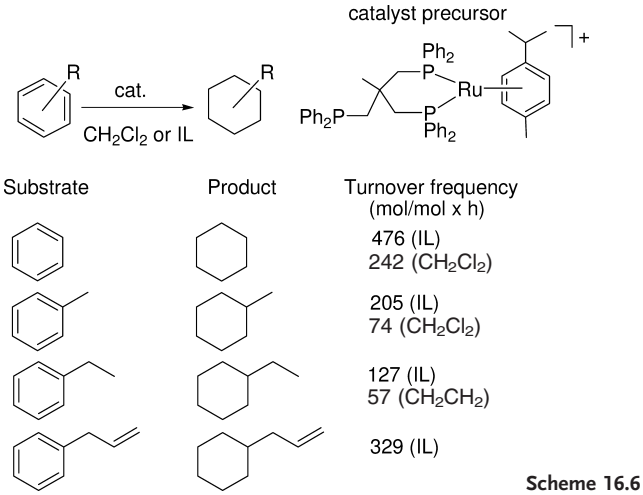

Scheme 16.6

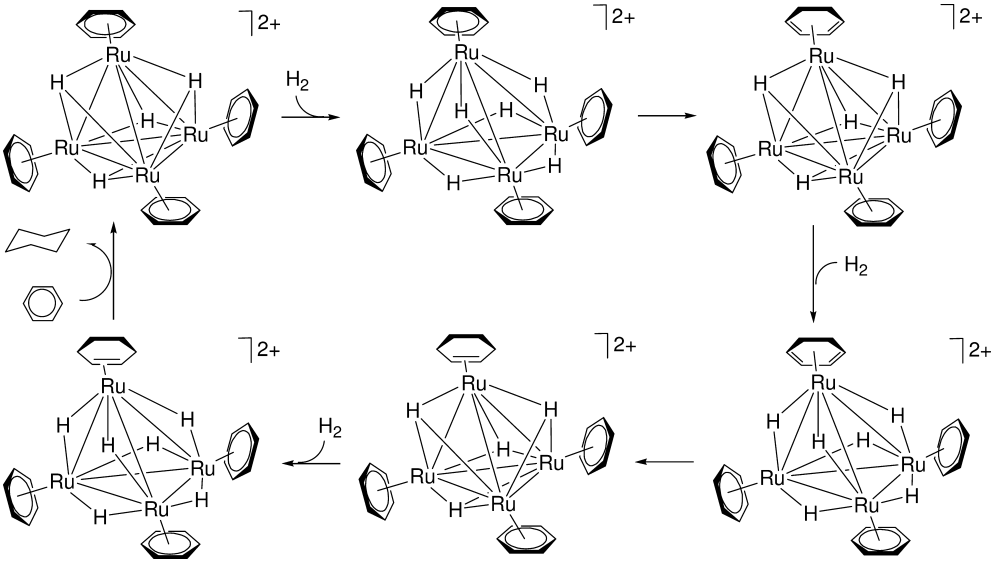

Scheme 16.7

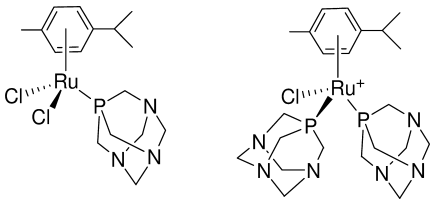

Fig. 16.1 Sketches of $Ru(PTA)Cl_2(\eta^6\text{-}C_{10}H_{14})$ and $[RuCl(PTA)_2(\eta^6\text{-}C_{10}H_{14})]^+$ (PTA = 1,3,5-triaza-7-phosphadamantane).

biphasic and aqueous systems [20]. Under aqueous biphasic conditions, cyclohexanes were produced with TOFs varying from 20 to 2000, depending on the substrate. On a quite speculative basis, a hydrogenation mechanism was proposed involving $\eta^6 \rightarrow \eta^4 \rightarrow \eta^2$ arene intermediates (Scheme 16.7). However, the only proven step was the hydrogenation of the starting $[Ru_4H_4(\eta^6\text{-}C_6H_6)_4]^{2+}$ cluster to $[Ru_4H_6(\eta^6\text{-}C_6H_6)_4]^{2+}$.

The ruthenium cluster $[Ru_4H_4(\eta^6\text{-}C_6H_6)_4]^{2+}$ was also employed for the hydrogenation of arenes in a biphasic water/1-butyl-3-methylimidazolium tetrafluoroborate biphasic system. At 90 °C and 60 bar H_2, benzene was reduced to cyclohexane with a TOF of 364.

The two water-soluble complexes $Ru(PTA)Cl_2(\eta^6\text{-}C_{10}H_{14})$ and $[RuCl(PTA)_2(\eta^6\text{-}C_{10}H_{14})]^+$ (PTA = 1,3,5-triaza-7-phosphadamantane) (Fig. 16.1) have been tested as catalyst precursors for the hydrogenation of benzenes at 90 °C and 60 bar H_2 [21]. After catalysis, the former complex was converted to a triruthenium cluster

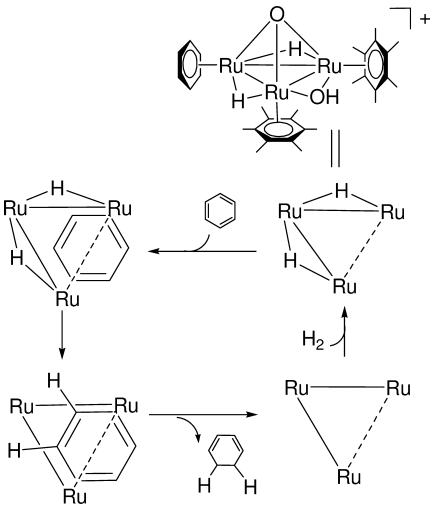

Scheme 16.8

with no coordinated PTA (NMR and electrospray mass spectrometry). In contrast, the starting complex with two PTAs gave a termination-metal product containing these ligands.

It is worth highlighting a very particular case of arene hydrogenation involving a triruthenium cluster [22]. In contrast to any other previous report, the hydrogenation of benzene was suggested by Süss-Fink to involve a direct H-transfer without substrate coordination to the metal. The proposed mechanism is shown in Scheme 16.8. The salient feature of this mechanism is adsorption of the arene in the hydrophobic pocket formed by the three arene ligands of the trimetallic precursor. The lack of substrate exchange with the originally coordinated arenes and the mass-spectrometry detection of a benzene adduct of the starting cluster were brought forward as substantial evidence for the proposed mechanism.

Many other mononuclear and binuclear Ru^{II} complexes stabilized by phosphine, cyclopentadienyl or arene ligands – for example $Ru(H)_2(H_2)(PPh_3)_3$ [23], $RuCl_2(CO)_2(PPh_3)_3$ [24], $[Ru(\mu\text{-}H_2)(\mu\text{-}Cl)(\eta^6\text{-}C_6H_6)_2]Cl_2$ [25], $[Rh(\eta^5\text{-}C_5Me_5)Cl_2]_2$ [26], and $Ru(\eta^6\text{-}C_6Me_6)(O_2CMe)_2$ [27] – have been claimed to catalyze the hydrogenation of polynuclear aromatic hydrocarbons in homogeneous fashion. Later evidence has suggested and, in some cases proved, that most of these systems are heterogeneous [28]. A paradigmatic case is the binuclear complex $[Rh(\eta^5\text{-}C_5Me_5)Cl_2]_2$ that was reported to hydrogenate benzene and substituted benzenes to cyclohexanes under relatively mild conditions (50 °C, 50 bar H_2) in the presence of a base that would promote the heterolytic splitting of H_2 as well as tie up the evolved HCl. Based on light-scattering experiments and on the good *cis* stereospecificity of hydrogen addition (e.g., *o*-xylene gave *cis*- and *trans*-1,2-dimethylcyclohexanes in a 62 : 1 ratio and *m*-xylene gave 1,3-dimethylcyclohexanes in *cis* : *trans* 38 : 1 ratio), this catalyst was thought to be homogeneous. However, later studies suggested that the true catalyst is likely heterogeneous [29].

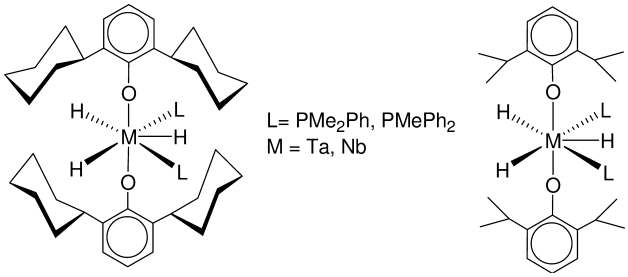

Fig. 16.2 The Nb^V and Ta^V hydride complexes containing bulky aryloxide ligands (as described by Rothwell).

Arene hydrogenation catalysts based on other metals than late transition ones are less numerous. Of particular relevance are the results reported by Rothwell, who found that Nb^V and Ta^V hydride complexes containing bulky aryloxide ligands (Fig. 16.2) are active for the homogeneous hydrogenation of arenes [30].

These catalytic systems demonstrated high regio- and stereoselectivity in the hydrogenation of benzene and of polynuclear aromatic hydrocarbons. For instance, the isolated tantalum trihydrides $Ta\{OC_6H_3(C_6H_{11})_2\text{-}2,6\}_2(H_3)(PMe_2Ph)_2$ and $Ta\{OC_6H_3\text{-}Pr^i_2\text{-}2,6)\}_2(H_3)(PMe_2Ph)_2$ catalyzed the hydrogenation of naphthalene and anthracene at 80 °C and 3–100 bar H_2. The former substrate was converted to tetralin, while anthracene was reduced to 1,2,3,4,5,6,7,8-octahydroanthracene *via* 1,2,3,4-tetrahydroanthracene. Since no trace of 9,10-dihydroanthracene was observed, the occurrence of either a radical reaction [31] or a Birch-type reduction was ruled out [32].

As shown in Scheme 16.9, the intermolecular hydrogenation of $[^2H_8]$toluene, $[^2H_{10}]$acenaphthene, $[^2H_8]$naphthalene, and $[^2H_{10}]$anthracene produced single isotopomers. The ^1H- and $^{13}C\{^1H\}$-NMR spectra confirmed a high selectivity: all-*cis* hydrogenation occurred without H/D scrambling between unreacted substrates and products. The all-*cis* nature of $[^2H_8]$tetralin was also proved using mass-spectrometry techniques. A unique characteristic of the niobium compound is its ability to rapidly hydrogenate arylphosphine ligands, thereby providing a new interesting procedure for the synthesis of cyclohexylphosphine ligands [33].

The only "homogeneous or substantially homogeneous" system which seems to offer a viable alternative to heterogeneous catalysis for the large-scale hydrogenation of arenes remains the IFP process [34]. This process utilizes Ziegler-type catalysts obtained by reacting at least two different metal salts (e.g., nickel and cobalt alkoxides, acetylacetonates or carboxylates), and a metal, selected among iron, zinc, and molybdenum, with trialkylaluminum as reducing agent. The hydrogenation of aromatic hydrocarbons is carried out under relatively mild conditions (155–180 °C, 10–30 bar H_2) in a solvent or in neat substrate. Bis-phenol A, phenol and benzene are hydrogenated to propane-dicyclohexanol, cyclohexanol and cyclohexane, respectively (Table 16.2).

cat = Ta or Nb trihydrides

Scheme 16.9

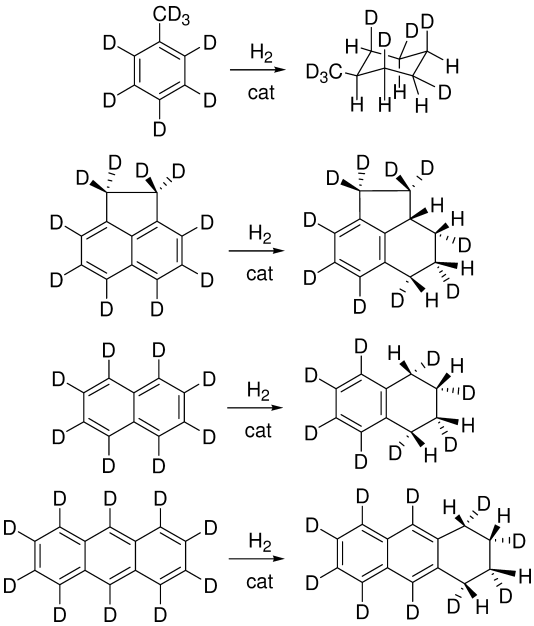

Table 16.2 Hydrogenation of aromatic hydrocarbons with the IFP process.[a)]

Catalyst	Substrate	Substrate/M ratio	% Conversion (TOF)[b)] product
1	bis-phenol A	250	99 (62) propane-dicyclohexanol
2	benzene	1829	99 (3621) cyclohexane
3	phenol	708	99 (2805) cyclohexanol

a) Experimental conditions: **1** (nickel octoate 0.35 mmol, iron octoate 0.35 mmol, triethylaluminum 5.6 mmol, solvent = 100 g cyclohexanol, 30 bar H_2, 4 h, 180 °C); **2** (cobalt stearate 2.2 mmol, iron stearate 0.2 mmol, triisobutylaluminum 2 mmol, 10 bar H_2, 30 min, 155 °C); **3** (nickel octoate 0.25 mmol, zinc octoate 0.25 mmol, triethylaluminum 2.1 mmol, 30 bar H_2, 15 min, 155 °C).

b) Mol of product (mol M × h)$^{-1}$.

Other examples of arene hydrogenation by Ziegler-type catalysts have been reported [35]. However, none of them is discussed at this point as they are generally poorly defined. Likewise, some hydrogenation catalytic systems in either oxo or water-gas-shift conditions are only reported in the list of references for sake of information [24, 36].

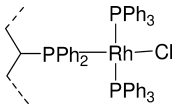

Fig. 16.3 Heterogenization of $RhCl(PPh_3)_2$ by grafting to a cross-linked phosphinated styrene/divinylbenzene resin.

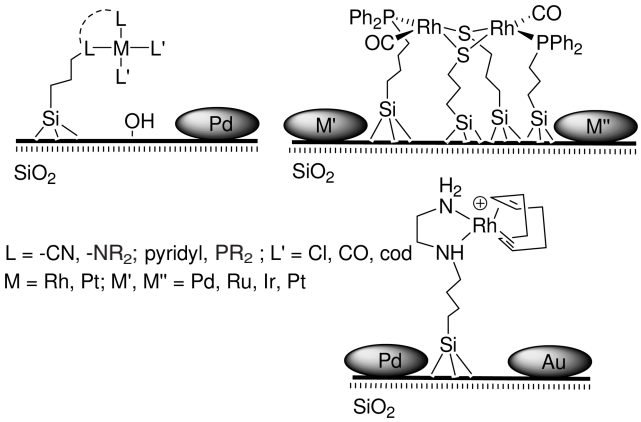

Fig. 16.4 Some examples of tethered complexes on supported metals (as described by Angelici).

16.2.2
Molecular Catalysts Immobilized on Support Materials

One of the very first attempts to hydrogenate aromatic compounds by means of a single-site metal catalyst was reported by Fish and coworkers, who were able to tether "$RhCl(PPh_3)_2$" moieties to a cross-linked phosphinated styrene/divinylbenzene (DVB) resin ($RhCl(PPh_3)_2$/P) (Fig. 16.3).

The resulting catalyst proved active for the hydrogenation of pyrene, tetralin, *p*-cresol, and methylnaphthalene [37]. A rate-enhancement effect was observed which was attributed to the ability of some substrates (especially *p*-cresol) to stabilize unsaturated rhodium species formed during the course of the catalysis. Since then, no remarkable progress in arene hydrogenation by single-site metal catalysts has been made, until a new class of catalysts emerged from the combination on the same support of both molecular complexes and metal particles. These systems, known under the name of tethered complexes on supported metals (TCSM), were introduced by Angelici [38 a] and developed independently by Angelici [38 b, c] and Bianchini [39].

Angelici's approach to heterogenization involves the functionalization of a ligand, either monodentate or bidentate, with a tail bearing a reactive group capable of forming covalent bonds to silica (e.g., alkyl-$Si(OR)_3$). Three TCSM catalysts, among several Rh/Pd, Pt/Pd and Rh/Pd : Au examples reported by Angelici, are shown in Figure 16.4 [38].

It has been found that the complexed metal and the supported metal(s) act synergistically, to provide enhanced results, superior to those of the component catalysts, in various reactions that include the hydrogenation of arenes. Typical tethered complexes contain Rh^I, while the silica-grafted ligands can be either monodentate with N and P donors or chelating with P-N and N-N donors (diamines, pyridylphosphines). Benzenes bearing a variety of functional groups (ester, ether, hydroxy, acyl, vinyl) have been hydrogenated with TOFs much higher than those of the single components which in some cases are completely inactive. To report one such example, the hydrogenation of phenol to cyclohexanol occurs with a TOF of 3400 with a Rh(N-N)/Pd-SiO_2 catalyst, whereas both Pd-SiO_2 and unsupported Rh(N-N) are inactive (N-N = bipyridyl) [40].

Angelici has proposed that the enhanced activity might be due to a hydrogen-spillover process, promoted by the supported metallic phase, that would enhance specifically the hydrogenation activity of the molecular catalyst [40]. A later study of the hydrogenation of arenes with a catalyst obtained by silica sol-gel co-entrapment of metallic palladium and $[Rh(cod)(\mu\text{-}Cl)]_2$ (cod = cyclohexa-1,5-diene) disagreed with the hydrogen spillover hypothesis and suggested that the action of both metals is caused by a type of synergistic effect [41]; however, no clear-cut explanation was provided.

A synergistic effect operating at the level of the first H_2 addition (e.g., conversion of benzene to cyclohexadiene) was demonstrated by Bianchini and co-workers for the hydrogenation of various benzenes to cyclohexanes by means of a different class of TCSM catalysts [42]. These differ substantially from Angelici's catalysts for the bonding interaction of the molecular complexes to the support material. The ligands of the molecular complexes were functionalized with sulfonate tails capable of forming robust hydrogen bonds to the isolated silanols of silica (Fig. 16.5 a) [42, 43].

For this reason, these catalysts are also known under the name of supported hydrogen-bonded (SHB) catalysts and, in conjunction with Pd^0 particles on the same support material, have contributed to generate active heterogeneous systems for the hydrogenation of benzenes in aprotic solvents. Irrespective of the substrate, the combined single-site/dispersed-metal catalyst Rh^I-Pd^0/SiO_2 shown in Figure 16.5 a was from four- to six-fold more active than supported palladium

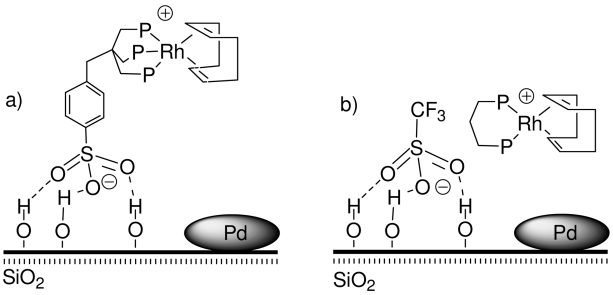

Fig. 16.5 Some examples of supported hydrogen-bonded catalysts (as described by Bianchini).

Table 16.3 Hydrogenation of benzenes with Pd^0/SiO_2, Rh^I/SiO_2 or Rh^I-Pd^0/SiO_2.[a)]

Catalyst	Temp. [°C]	Substrate	Substrate/M ratio	% Conversion[b)] (TOF, M)[c)] product
Pd^0/SiO_2	40	benzene	525	4 (11) cyclohexane
Rh^I/SiO_2	40	benzene	9200	0
Rh^I-Pd^0/SiO_2	40	benzene	525/9200	15 (39, Pd) cyclohexane
Pd^0/SiO_2[d)]	40	toluene	426	4 (8) methylcyclohexane
Rh^I/SiO_2[e)]	40	toluene	7520	0
Rh^I-Pd^0/SiO_2[f)]	40	toluene	426/7520	16 (32, Pd) methylcyclohexane
Pd^0/SiO_2	60	styrene	400	97 (194) ethylbenzene; 3 (6) ethylcyclohexane
Rh^I/SiO_2	60	styrene	8750	98 (4287) ethylbenzene
Rh^I-Pd^0/SiO_2	60	styrene	400/8750	81 (162, Pd) ethylbenzene; 19 (38, Pd) ethylcyclohexane
Pd^0/SiO_2	60	ethylbenzene	400	3 (6) ethylcyclohexane
Rh^I/SiO_2	60	ethylbenzene	8750	0
Rh^I-Pd^0/SiO_2	60	ethylbenzene	400/8750	20 (40, Pd) ethylcyclohexane

a) Experimental conditions: Pd^0/SiO_2 (9.86 wt.% Pd), 0.044 mmol Pd; Rh^I/SiO_2 (0.56 wt.% Rh), 0.0025 mmol Rh; Rh^I-Pd^0/SiO_2 (0.56 wt.% Rh, 9.86 wt.% Pd), 0.044 mmol Pd, 0.0025 mmol Rh; 30 bar H_2; 30 mL *n*-pentane, 2 h, 1500 rpm.
b) Average values over at least three runs.
c) Mol product (mol M × h)$^{-1}$ (M = Pd, Rh).
d) 0.088 mmol Pd.
e) 0.005 mmol Rh.
f) 0.088 mmol Pd, 0.005 mmol Rh.

alone (Pd^0/SiO_2), while the tethered Rh^I complex alone (Rh^I/SiO_2) proved to be totally inactive (Table 16.3).

Separate experiments with cyclohexadienes and cyclohexenes showed that 1,3-cyclohexadienes are more rapidly reduced to cyclohexenes at rhodium, while the latter are predominantly reduced at palladium. It was also found that the 1,3-cyclohexadiene disproportionation, occurring on palladium, is inhibited by the grafted rhodium complex. Based on this information, as well as a number of experiments (including the isolation of relevant intermediates), the authors concluded that the enhanced activity of the Rh^I-Pd^0/SiO_2 catalyst is not due to hydrogen spillover, but to the fact that the rate-limiting hydrogenation of benzenes to cyclohexa-1,3-dienes is assisted by both palladium and rhodium, the concerted action of which, besides preventing the competitive diene disproportionation to benzene and cyclohexene, speeds up the reduction of the first double bond (Scheme 16.10).

The intimate mechanism by which the single rhodium sites and the neighboring palladium particles interact with benzene to accelerate its reduction to cyclohexadiene remains somewhat obscure.

A variation of the SHB technology to immobilize cationic molecular catalysts on silica is shown in Figure 16.5 b. This involves SHB immobilization of the counter-

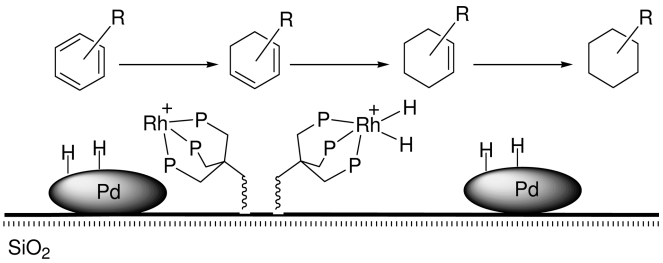

Scheme 16.10

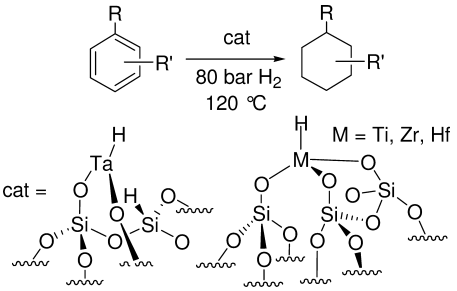

Scheme 16.11

anion, provided that the latter is capable of forming robust hydrogen bonds to the surface silanols, as is the case of the triflate counter-anion. Clearly, only aprotic solvents are viable for the successful use in catalysis of this SHB technique. It has been shown, using ^{31}P- and ^{19}F-NMR spectroscopy in CD_2Cl_2, that the metal cations reside close to the silica surface by electrostatic interaction with the SHB triflate. Therefore, only the counter-anions are truly immobilized on the support, whereas the cationic catalysts can interact freely with the substrate and H_2 as if they were in solution. Following this protocol, several chiral catalysts, for example [Rh((+)-DIOP)(nbd)](SO_3CF_3) and [Rh((*S*)-BINAP)(nbd)](SO_3CF_3) (nbd = norbornadiene), have been immobilized and successfully employed for the enantioselective hydrogenation of prochiral alkenes [39 c]. Recently, this SHB approach was successfully extended to arene hydrogenation through the immobilization of cationic catalysts, such as [Rh(diphos)(cod)] (SO_3CF_3), on silica containing supported palladium particles [39 c]. Enhanced conversions to saturated cyclic hydrocarbons, as compared to the single components, were observed for the hydrogenation of benzenes and anthracenes [43].

A distinct class of single-site metal catalysts for arene hydrogenation is known under the name of surface organometallics. The surface organometallic technique has been introduced and largely developed by Basset and Marks, and is currently utilized in a number of catalytic processes [44]. Silica- or alumina-supported Ta, Ti, Zr and Hf hydrides, generated *in situ* by hydrogenation of alkyl derivatives, have been found capable of catalyzing the reduction of benzene and alkyl-substituted benzenes with TOFs as high as 1000 (Scheme 16.11) [44 b, c].

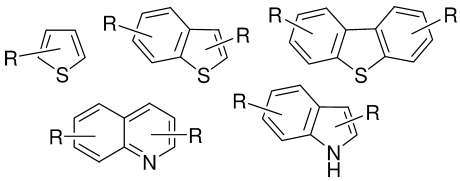

Fig. 16.6 Common *S*- and *N*-heterocycles contained in fossil fuels.

16.3 Hydrogenation of Heteroaromatics

16.3.1 Molecular Catalysts in Different Phase-Variation Systems

The number of homogeneous catalysts available for the hydrogenation of *N*-, *S*- and *O*-heteroaromatics is exceedingly greater than that of the catalysts for arenes. A crucial role in making the reduction of heteroaromatics easier than that of carbocyclic aromatic rings is just played by the heteroatom that possesses at least one σ-lone pair for occupying a coordination vacancy at the metal center. The heteroatom also has the effect of decreasing the overall aromatic character of the molecule, favoring the localization of electron density on the proximal X=C bond, hence allowing for the coordination of the substrate in the easily reducible olefin-like η^2-C-X mode (X=heteroatom) [8, 9].

A great impulse to design homogeneous catalysts for the hydrogenation heteroaromatics stems from the need to understand the mechanisms of the HDS, HDN, and HDO reactions [3]. These three processes form the heart of fossil fuels hydrotreatments, and have a vast commercial and environmental importance. It is not surprising, therefore, that most studies have been centered on the development of molecular catalysts for the hydrogenation of thiophenes, quinolines, and indoles (Fig. 16.6), as these substrates are largely abundant in crude oils and their degradation remains incomplete, even with the most efficient heterogeneous catalysts [3, 8, 9].

16.3.1.1 S-Heteroaromatics

The homogeneous hydrogenation of thiophenes and benzothiophenes to the corresponding cyclic thioethers is a reaction which is catalyzed, under relatively mild experimental conditions, by a number of metal complexes, generally comprising noble metals modified with phosphine ligands: $RuCl_2(PPh_3)_3$ [53], $RuHCl(CO)(PPh_3)_3$ [53], $RuH_2(\eta^2\text{-}H_2)(PCy_3)_2$ [54], $OsHCl(CO)(PPh_3)_3$ [53], $RhCl(PPh_3)_3$ [53], $[Rh(MeCN)_3(Cp^*)](BF_4)_2$ [55], $[Rh(PPh_3)_2(cod)]PF_6$ [53, 56], $[Ir(PPh_3)_2(cod)]PF_6$ [53, 57, 58], and $[Ru(MeCN)_3(triphos)](SO_3CF_3)_2$ [39b, 59, 60]. In contrast, no metal complex has been ever reported to hydrogenate diben-

zo[*b,d*]thiophene (DBT) to either tetrahydrodibenzothiophenes or hexahydrodibenzothiophenes, which reflects the strong aromatic character of this substrate.

A common feature of all hydrogenation catalysts for thiophene (T) and benzo[*b*]thiophene (BT) is apparently a d^6 electronic configuration of the metal ion, which favors the η^2-*C,C* coordination of the thiophenic molecule over the alternative η^1-*S* bonding mode. The latter is more frequent for low-valent metal fragment and is precursor to C-S insertion, hence to hydrogenolysis rather than to hydrogenation [8, 9a]. As a general trend, the hydrogenation activity decreases in the order $Ru^{II} > Rh^{III} > Os^{II} > Ir^{III}$ as well as with increasing nucleophilicity of the solvent that may compete with the substrate for coordination.

The highest activity for BT hydrogenation to dihydrobenzo[*b*]thiophene (DHBT) has been reported for the Ru^{II} catalyst $[(triphos)RuH]^+$ obtained by hydrogenation of the precursor $[Ru(NCMe)_3(triphos)](SO_3CF_3)_2$ in basic solvents capable of promoting the heterolytic splitting of H_2 (Scheme 16.12) [59]. Interestingly, the hydrogenation of $[Ru(NCMe)_3(triphos)](SO_3CF_3)_2$ in apolar or non-basic solvents (e.g., CH_2Cl_2) produced the 16-electron system $[Ru(H)_2(triphos)]^+$, which was slightly less active than the monohydride fragment (TOF = 1340) [39b, 60].

The hydrogenation mechanism of BT has been widely studied using a variety of techniques, including operando HP-NMR, kinetic studies, and deuterium labeling. A unique mechanism has been proposed, irrespective of the metal catalyst: η^2-*C,C* coordination of the substrate (eventually in equilibrium with η^1-*S* coordination), addition of H_2 in either oxidative $[M(H)_2]$ or intact form $[M(H_2)]$ (this step may also precede the previous one), hydride transfer to form dihydrobenzothienyl, and elimination of DHBT by hydride/dihydrobenzothienyl reductive coupling. Scheme 16.13 exemplifies this mechanism for a model catalyst bearing one hydride ligand, as is the case of the 14-electron fragment $[RuH(triphos)]^+$ [39b, 59, 60].

Kinetic studies of the hydrogenations of BT to DHBT catalyzed by $[Rh(PPh_3)_2(cod)]PF_6$ [56] and $[Ir(PPh_3)_2(cod)]PF_6$ [57] indicated the hydride migration yielding the dihydrobenzothienyl intermediate as the rate-determining step. In contrast, the rate-determining step of the reaction catalyzed by $[RuH(triphos)]^+$ was shown to be the reversible dissociation of DHBT from the metal center [59].

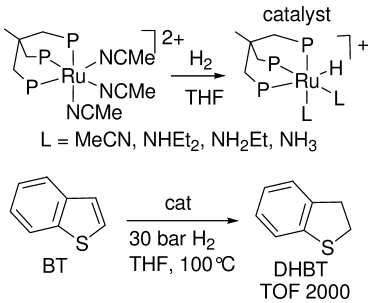

Scheme 16.12

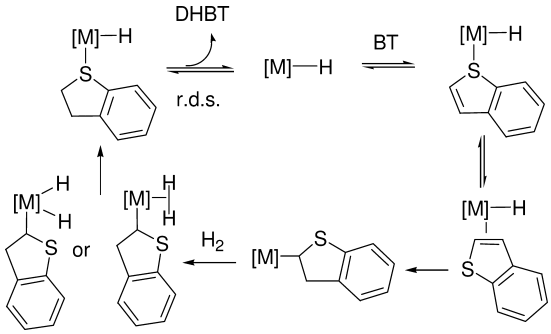

Scheme 16.13

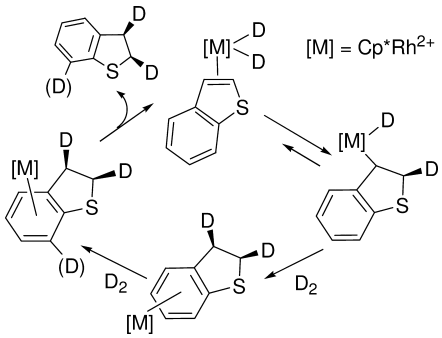

Scheme 16.14

Substituting deuterium for hydrogen gas in the reduction of BT to DHBT with the catalyst precursor $[Rh(NCMe)_3(Cp^*)](BF_4)_2$ has shown that the stereoselective *cis*-deuteration of the double bond is kinetically controlled by the η^2-*C,C* coordination of BT. The incorporation of deuterium in the 2- and 3-positions of unreacted substrate and in the 7-position of DHBT has been interpreted in terms of reversible double-bond reduction and arene-ring activation, respectively (Scheme 16.14) [55].

Overall, the hydrogenation of thiophene to tetrahydrothiophene (THT) is quite similar to that of BT, the only remarkable difference being the formation of a thioallyl complex via regio- and stereospecific hydride migration (*endo* migration). Scheme 16.15 shows the catalytic mechanism proposed for $IrH_2(\eta^1\text{-}S\text{-}T)(PPh_3)_2]PF_6$ [58]. Upon hydride addition, the thioallyl intermediate formed a 2,3-dihydrothiophene ligand which was then hydrogenated like any other alkene. The substitution of either 2,3- or 2,5-dihydrothiophene for thiophene showed that only the 2,3-isomer was hydrogenated to THT.

The use of water-soluble metal catalysts for the hydrogenation of thiophenes in aqueous biphasic systems has been primarily introduced by Sanchez-Delgado and coworkers at INTEVEP S.A. [61]. The precursors $RuHCl(TPPTS)_2(L_2)$ (TPPTS = triphenylphosphine trisulfonate; L = aniline, 1,2,3,4-tetrahydroquinoline) and $RuHCl(TPPMS)_2(L_2)$ (TPPMS = triphenylphosphine monosulfonate) were

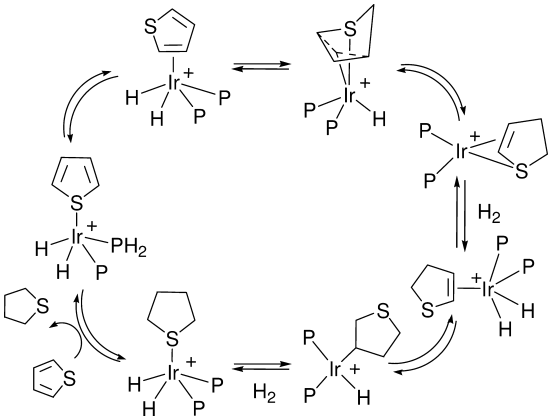

Scheme 16.15

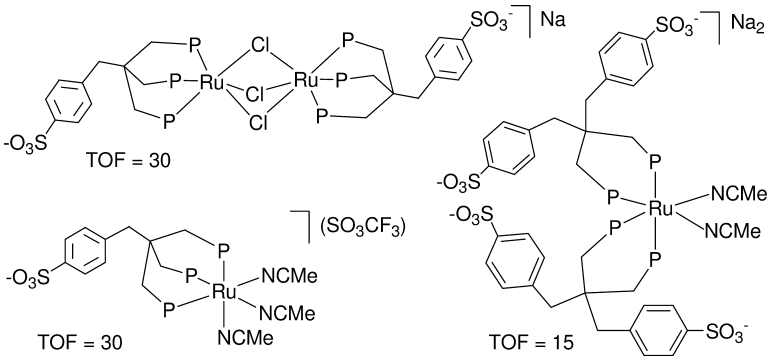

Fig. 16.7 Water-soluble polyphosphine metal catalysts used to hydrogenate thiophenes.

employed to hydrogenate BT to DHBT in water-decaline under relatively harsh experimental conditions (130–170 °C, 70–110 bar H_2). It was observed that nitrogen compounds did not inhibit the hydrogenation; on the contrary, a promoting effect was observed. Later, rhodium and ruthenium catalysts with the polydentate water-soluble ligands $(NaO_3S(C_6H_4)CH_2)_2C(CH_2PPh_2)_2$ (Na_2DPPPDS) [62] and $NaO_3S(C_6H_4)CH_2C(CH_2PPh_2)_3$ (Nasulphos) [63], which differ from traditional water-soluble phosphines for the presence of the hydrophilic groups in the ligand backbone were successfully employed to hydrogenate BT under biphasic conditions (Fig. 16.7) [39 b, 59, 60, 64, 65].

The aqueous-biphase hydrogenation reactions of thiophenes to the corresponding cyclic thioethers have been shown to be mechanistically similar to those in truly homogenous phase.

16.3.1.2 *N*-Heteroaromatics

As a general trend, six-membered mononuclear *N*-heteroaromatics such as pyridine and derivatives are much less prone to undergo hydrogenation than bi- and trinuclear *N*-ring compounds (e.g., quinolines, benzoquinolines, acridines) due to their higher resonance stabilization energy.

The first examples of selective hydrogenation of pyridine to piperidine and of quinoline to 1,2,3,4-tetrahydroquinoline (THQ) by a homogeneous metal catalyst ($Rh(PY)_3Cl_3/NaBH_4$ in DMF under 1 bar H_2) were reported in 1970 by Jardine and McQuillin [66]. The first mechanistic studies appeared much later, when Fish employed the Rh^{I} and Ru^{II} precatalysts $RhCl(PPh_3)_3$ [67] and $RuHCl(PPh_3)_3$ [68] to hydrogenate various *N*-polyaromatics (85 °C, 20 bar H_2, benzene). The hydrogenation rates decreased in the order phenanthridine > acridine > quinoline >5,6-benzoquinoline (5,6-BQ) >7,8-BQ, which reflects the influence of both steric and electronic effects. All substrates were hydrogenated regioselectively at the heteroaromatic ring; only acridine was converted to a mixture of 9,10-dihydroacridine and 1,2,3,4-tetrahydroacridine. The hydrogenation of quinoline was found to be inhibited by the presence of pyridines and of THQ in the reaction mixture, due to competing coordination to the metal center, while all the other substrates had no appreciable effect on the hydrogenation rate.

The substitution of D_2 for H_2 in the reduction of quinoline catalyzed by either $RhCl(PPh_3)_3$ [67] or $RuHCl(PPh_3)_3$ [68] showed that: 1) hydrogenation of the C=N bond is reversible; 2) the C_3–C_4 double bond is irreversibly hydrogenated in stereoselective *cis* manner; and 3) the C_8–H bond in the carbocyclic ring is activated, likely *via* cyclometalation. Later, Fish studied the hydrogenation of 2-methylpyridine to 2-methylpiperidine catalyzed by $[Rh(NCMe)_3Cp^*]^{2+}$, again by means of deuterium labeling experiments [55]. The rate-limiting step of the reaction was identified as being the initial C=N bond hydrogenation, which actually disrupts the aromaticity of the molecule. It was also proposed that the reversible reduction of the C=N and C=C bonds was promoted by the allylic nature of the reduction product, NH-CH_2-C=C, which is highly activated toward re-aromatization of the N-ring.

The reduction of 1,2,5,6-tetrahydropyridine (THPY) with D_2 in the presence of $[Rh(NCMe)_3Cp^*]^{2+}$, yielding exclusive deuterium incorporation in the C_3 and C_4 carbon atoms, and the independent synthesis of $[Rh(\eta^1(N)\text{-THPY}(NCMe)_2Cp^*]^{2+}$ showed that: 1) η^1(N)-THPY complexes are not intermediate to piperidine production; and 2) partially hydrogenated N-heterocycles are easily dehydrogenated to their aromatic precursors [55].

Deuterium gas experiments, continuous NMR and GC/MS analysis, *in situ* high-pressure NMR spectra and the isolation of some intermediates provided Fish with sufficient information to propose the mechanism shown in Scheme 16.16 for the hydrogenation of quinoline to THQ, catalyzed by $[Rh(NCMe)_3Cp^*]^{2+}$ (40 °C, 33 bar H_2, CH_2Cl_2) [55].

The salient features of this mechanism are:

- η^1(N) bonding of quinoline to rhodium with loss of complexed MeCN, followed by the formation of a hydride.

- Reversible 1,2-N=C bond hydrogenation, likely *via* η^2(N,C) coordination.
- Migration of Cp*Rh from nitrogen to the C_3–C_4 double bond.
- Reversible C_3–C_4 double bond reduction.
- Cp*Rh complexation to the carbocyclic ring, followed by C_6–H and C_8–H bond activation.
- η^6(πC) coordination of THQ, followed by ligand exchange with quinoline to continue the catalytic cycle.

In this mechanistic picture, the rhodium center goes through the catalysis with the unusual III → V → III oxidation/reduction cycle.

Various late transition-metal carbonyls, alone or modified by phosphine ligands, have been found to hydrogenate pyridine and polyaromatic heterocycles such as quinoline, 5,6-BQ, 7,8-BQ, acridine, and isoquinoline (IQ) using either H_2 obtained from water-gas-shift (WGS) or syngas (SG) [69, 70]. Selective hydrogenation of the heterocyclic ring has been achieved with $Fe(CO)_5$, $Mn_2(CO)_8(PBu_3)_2$ and $Co_2(CO)_6(PPh_3)_2$ [24a]. The cobalt catalyst was the most active for the hydrogenation of both acridine to 9,10-dihydroacridine (TOF = 10) and quinoline to THQ (TOF = 14). The iron and manganese catalysts converted appreciably only acridine, with TOFs of 5 and 2 (or 10 under SG conditions), respectively. Under WGS conditions, $RuCl_2(CO)_2(PPh_3)_2$ and $Ru_4H_4(CO)_{12}$ proved to be inactive due to competitive coordination of CO, while efficient regioselective hydrogenation of the substrate was achieved using H_2 gas ($TOF_{acridine/9,10\text{-}dihydroacridine} = TOF_{quinoline/THQ} = 5$) [24a]. In all cases, however, high temperatures (180–200 °C) were required for appreciable conversions.

Using as catalyst precursors the clusters $Os_3H_2(CO)_{10}$ and $Os_3(CO)_{12}$ [71, 72], Laine and coworkers found a deuteration pattern of quinoline hydrogenation similar to that shown in Scheme 16.16, except for the presence of more deuterium in the 4-position and less in the 2-position, which has been interpreted in terms of the occurrence of oxidative addition of the osmium cluster to C–H bonds in quinoline, and also 1,4-hydrogenation (Scheme 16.17).

In an attempt to correlate the catalytic performance of comparable precursors with the nature of the metal center, Sánchez-Delgado and Gonzáles have investigated the selective hydrogenation of quinoline to THQ (150 °C, 30 bar H_2, toluene) by $RuCl_2(PPh_3)_3$ (TOF = 63), $RhCl(PPh_3)_3$ (TOF = 52), $RuHCl(CO)(PPh_3)_3$ (TOF = 29), $OsHCl(CO)(PPh_3)_3$ (TOF = 5), $[Rh(PPh_3)_2(cod)]^+$ (TOF = 199), and $[Ir(PPh_3)_2(cod)]^+$ (TOF = 17) [73]. The cationic rhodium complex was by far the most active.

Several ruthenium complexes have been found capable of hydrogenating *N*-heteroaromatics (acridine, quinoline, 5,6-BQ, 7,8-BQ, indole, IQ, for example: $[Ru(NCMe)_3(triphos)](SO_3CF_3)_2$ ($TOF_{indole/indoline} = 17$) in conjunction with protic acids [59, 65a, 74–76], $[RuH(CO)(NCMe)_2(PPh_3)_2]BF_4$ ($TOF_{quinoline/THQ} = 16$) [77,78], and $RuH_2(\eta^2\text{-}H_2)_2(PCy_3)_2$ ($TOF_{quinoline/5,6,7,8\text{-}THQ} = 2$; $TOF_{indole/indoline} < 1$) [79]. The latter complex also led to saturation of the aromatic ring, which has been proposed to involve the coordination of the substrate through the aromatic ring, in a manner similar to that reported for η^4-arene complexes (see Scheme

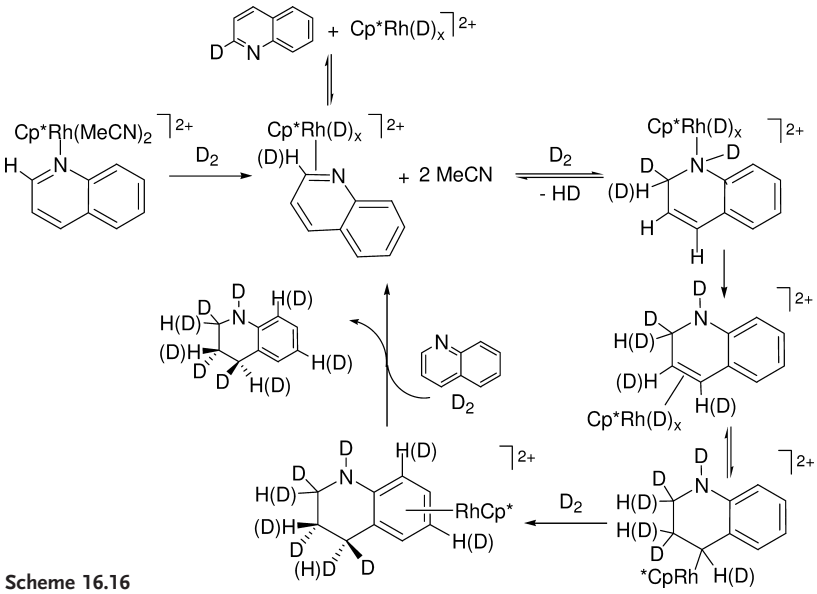

Scheme 16.16

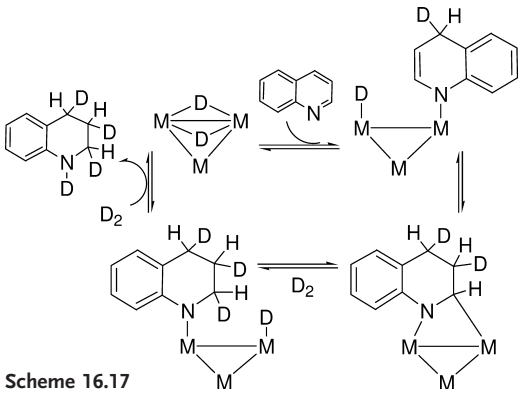

Scheme 16.17

16.4). However, it must be remembered that the true homogeneous nature of this system remains a matter of debate.

Kinetic studies of the hydrogenation of *N*-heteroaromatics have been reported wherein quinoline is the most studied substrate. Sánchez-Delgado and co-workers have identified the experimental rate law $r_i = k_{cat}\ [Rh][H_2]^2$, with $k_{cat} = 50 \pm 6\ M^{-2}\ s^{-1}$ at 370 K for the hydrogenation of quinoline by $[Rh(PPh_3)_2(cod)]PF_6$ [80]. Kinetic studies for quinoline reduction to THQ have also been reported by Rosales for the reactions catalyzed by $[RuH(CO)(MeCN)(PPh_3)_2]BF_4$ [77]. At low hydrogen pressure, the experimental rate law was $r_i = k_{cat}\ [Ru_0][H_2]^2$ ($k_{cat} = 28.5\ M^{-2}\ s^{-1}$ at 398 K), while a first-order dependence of the reaction rate with respect to the hydrogen concentration was ob-

served at high H_2 pressure. The proposed mechanism involves a rapid and reversible partial hydrogenation of bonded quinoline, followed by a rate-determining second hydrogenation of dihydroquinoline.

A much more complex kinetic law has been reported by Bianchini and coworkers for the hydrogenation of quinoline catalyzed by the Rh^I complex $[Rh(DMAD)(triphos)]PF_6$ (DMAD = dimethyl acetylenedicarboxylate) [74, 75]. The rate was first order with respect to both H_2 in the pressure range from 4 to 30 bar, and in the catalyst concentration range from 36 to 110 mM, while the hydrogenation rate showed an inverse dependence with respect to quinoline concentration. The empiric rate law $r = k''$ $[Rh][H_2][Q]^2$, where $k'' = k$ $(a + b[Q] + c[Q]^2)^{-1}$, was proposed to account for the inhibiting effect of quinoline (Q) concentration and the experimental observation that the rate tends to be second order for very low quinoline concentrations (< 30 mM) and zero-order for very high quinoline concentrations (> 70 mM). On the basis of the kinetic study, deuterium labeling and high-pressure NMR experiments under catalytic conditions, as well as the identification of catalytically relevant intermediates, a mechanism was proposed (Scheme 6.18) which essentially differs from that proposed by Sánchez-Delgado for the rate-limiting step (i.e., reversible reduction of the C=N bond instead of the irreversible one of the C_3=C_4 bond). The overall hydrogenation of the C=N bond, which actually disrupts the aromaticity of quinoline, was proposed as the rate-determining step, which was consistent with the fact that 2,3-dihydroquinoline was reduced faster than quinoline, while the lack of deuterium incorporation into the carbocyclic ring of both THQ and quinoline ruled out the formation of η^6-quinoline or η^6-THQ intermediates [74, 75].

The reduction of acridine to 9,10-dihydroacridine by the precursor $[RuH(CO)(NCMe)_2(PPh_3)_2]BF_4$ has been found to occur with the experimental rate law $r = k_{cat}$ $[Ru][H_2]$ and the postulated mechanism involves, as the determining

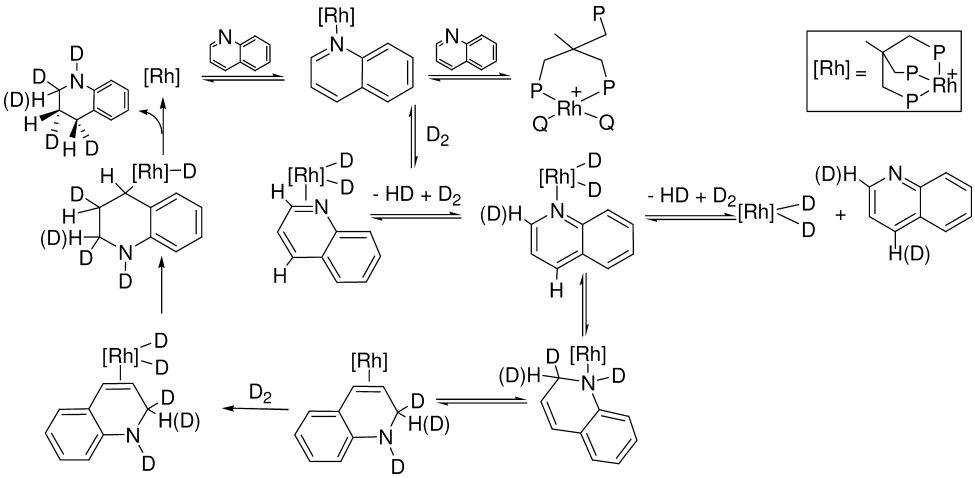

Scheme 16.18

step, the hydrogenation of coordinated acridine in $[RuH(CO)(\eta^1(N)\text{-AC})(NCMe)(PPh_3)_2]^+$ to yield 9,10-dihydroacridine and the coordinatively unsaturated complex $[RuH(CO)(NCMe)(PPh_3)_2]^+$ [78].

In homogeneous phase, indole is much more difficult to reduce than quinoline, as shown by the limited number of known catalysts (e.g., $RuHCl(PPh_3)_3$ [68] and $[RuH(CO)(NCMe)(PPh_3)_2]BF_4$ [78]) as well as their very scarce activity (TOFs ≤ 1). Indeed, the $\eta^1(N)$ coordination, which is critical for selective nitrogen ring reduction in quinoline, is virtually unknown for indole, which prefers to bind metal centers using the carbocyclic ring. In the latter coordination mode, the C=N bond is not activated and the many occupied coordination sites at the metal center make oxidative addition of H_2 very difficult to accomplish. Consistently, the hydrogenation of indole is generally inhibited when the reaction mixture contains basic substrates such as quinoline, THQ, and pyridine. The only catalysts that have proved able to regioselectively hydrogenate indole to indoline with an acceptable TOF are $[Rh(DMAD)(triphos)]PF_6$ and $[Ru(NCMe)_3(triphos)](SO_3CF_3)_2$, though on condition that a protic acid is added to the catalytic mixture [74, 76]. The rhodium catalyst was more efficient than the ruthenium catalyst, and allowed for hydrogenation of the substrate even at 60 °C and 30 bar H_2, with TOFs as high as 100. It was shown experimentally that indoline was actually formed by reduction of the protonated form of indole, the 3H-indolium cation which possesses a localized C=N bond.

The selective hydrogenation of N-heterocycles has been achieved with the use of water-soluble Ru^{II} catalysts prepared *in situ* by reacting an excess of either triphenylphosphine trisulfonate (TPPTS) or triphenylphosphine monosulfonate (TPPMS) with $RuCl_3 \cdot 3H_2O$. The resulting solutions were added to a hydrocarbon solution containing various N-heteroaromatics such as quinoline, acridine, and IQ. The biphasic reactions were performed under relatively drastic experimental conditions (130–170 °C, 70–110 bar H_2) and led to selective reduction of the heterocyclic ring [61, 81].

The regioselective reduction of quinoline to THQ in water/hydrocarbon has also been achieved with bidentate and tridentate water-soluble ligands. The Rh^I complex $[Rh(H_2O)_2(DPPPDS)]Na$ was employed in water/*n*-octane to hydrogenate 1 : 1 mixtures of quinoline and BT at high temperature (160 °C). Only the N-heterocycle was efficiently reduced (TOF = 50), with BT hydrogenation to DHBT being only marginal (TOF = 2) [8c]. A similar selectivity has been reported for the catalytic system $RuCl_3 \cdot H_2O/2Na_2DPPPDS$ prepared *in situ*. In contrast, the individual hydrogenation rates for quinoline and BT have been reported to be similar (TOF = 30 at 140 °C, 30 bar H_2, water/*n*-heptane) and independent of the presence of either substrate by using the binuclear precursor $Na[\{(sulphos)Ru\}_2(\mu\text{-}Cl)_3]$ (sulphos = $(PPh_2CH_2)_3CCH_2(C_6H_4)SO_3^-$) [8c, 82].

Under biphasic conditions, the zwitterionic Rh^I complex Rh(cod)(sulphos) proved to be very efficient for the hydrogenation of quinoline to THQ (TOF = 20 at 160 °C, 30 bar H_2, water/*n*-heptane) [8c].

16.3.1.3 O-Heteroaromatics

Very few examples of hydrogenation of O-heteroaromatics with molecular metal catalysts have appeared in the literature to date. Besides some cases of enantioselective catalysis (see Section 16.4), there is only one example reported by Fish dealing with the homogeneous hydrogenation of benzofuran to 2,3-dihydrobenzofuran using $[Rh(NCMe)_3(Cp^*)](BF_4)_2$ as the catalyst precursor [55]. As for the hydrogenation of BT performed by the same catalyst, the hydrogenation of benzofuran has been proposed to involve coordination of the substrate through the 2,3 double bond to a Rh–H species, followed by hydrogen transfer to yield 2,3-dihydrobenzofuran.

16.3.2 Molecular Catalysts Immobilized on Support Materials

$Rh(PPh_3)_3Cl$ tethered to 2% cross-linked phosphinated polystyrene-divinylbenzene was the first heterogenized single-site metal catalyst to be used in the hydrogenation of N- and S-heteroaromatics (see Fig. 16.3) [37]. This catalyst was able to hydrogenate quinoline, acridine, 5,6-BQ and 7,8-BQ in benzene solution (85 °C, 20 bar H_2) with an order of activity (acridine > quinoline > 5,6-BQ > 7,8-BQ) that is identical to that in homogeneous phase with the unsupported catalysts, except for the initial rates that were from 10- to 20-fold faster than in homogeneous phase [67]. This remarkable rate enhancement was attributed to steric requirements surrounding the active metal center in the tethered complex, which apparently would favor the coordination of the N-heterocycles by disfavoring that of PPh_3. The regioselectivity of hydrogenation was even higher than that in homogeneous phase as no formation of 1,2,3,4-tetrahydroacridine was observed. The deuteration pattern of the heteroaromatic ring after a catalytic reaction with D_2 was identical to that observed in homogeneous phase, except for the absence of deuterium incorporation at position 8 of the carbocyclic ring. The tethered catalyst proved able also to hydrogenate BT to DHBT (benzene, 85 °C, 20 bar H_2) with rates three-fold faster than those observed in homogeneous phase with the parent precursor $RhCl(PPh_3)_3$ [37].

The most active and fully recyclable single-site catalyst for the hydrogenation of thiophenes is still that generated by the SHB precursor $[Ru(NCMe)_3(sulphos)](OSO_2CF_3)/SiO_2$ (Ru^{II}/SiO_2), obtained by tethering $[Ru(NCMe)_3(sulphos)](OSO_2CF_3)$ to silica (Scheme 16.19). In this case, immobilization of the molecular catalyst involves the formation of hydrogen-bonds to the surface silanols by SO_3^- groups from both the sulphos ligand and the triflate counter-anion [39 b]. Upon hydrogenation (30 bar H_2), Ru^{II}/SiO_2 has been found to generate a very active, recyclable and stable catalyst for the selective hydrogenation of BT to DHBT, with TOFs as high as 2000. The TOF with Ru^{II}/SiO_2 did not practically change even when a new feed containing 2000 equiv. BT in *n*-octane was injected into the reactor after 1 h reaction, which means that DHBT does not compete with BT for coordination to the Ru^{II} center.

All attempts to hydrogenate thiophenes by using TCSM catalysts of the types shown in Figures 16.4 and 16.5 have, so far, been unsuccessful. Rh^{I}-Pd^{0}/SiO_2

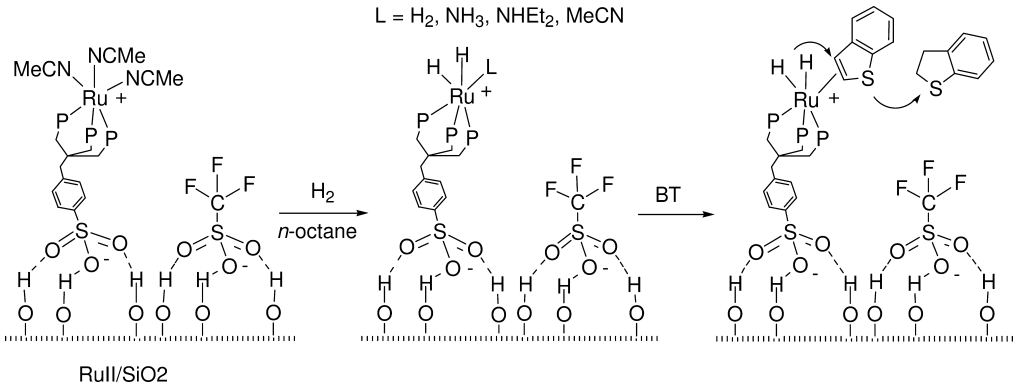

Scheme 16.19

was tested in the hydrogenation (30 bar H_2) of BT in *n*-octane under 30 bar at 100–170 °C, but the production of a DHBT was the same as that obtained with silica-supported Pd^0 nanoparticles alone (TOF = 8–10) [43]. Apparently, no synergistic effect between the isolated rhodium sites and the surface palladium atoms takes place for the hydrogenation of thiophenes. This was not totally unexpected, as neither silica-supported Rh(cod)(sulphos)/SiO_2 in *n*-octane [43] nor free Rh(cod)(sulphos) [83] in MeOH or [Rh(cod)(triphos)]PF_6 [83] in THF proved able to hydrogenate appreciably BT and thiophene below 150–170 °C. In fact, at these high temperatures hydrogenolysis to the corresponding thiol occurred [83 b, c]. In contrast, the SHB rhodium complexes Rh(cod)(sulphos)/SiO_2 and [Ru(NCMe)$_3$(sulphos)](SO_3CF_3)/SiO_2 have been used successfully to hydrogenate quinoline in *n*-octane (100 °C, 30 bar H_2), yielding selectively THQ with TOFs as high as 100 [43]. In line with the behavior of the Fish catalyst RhCl(PPh_3)$_3$/P [37], both Rh(cod)(sulphos)/SiO_2 and [(sulphos)Ru(NCMe)$_3$] (SO_3CF_3)/SiO_2 have been found to be more efficient catalysts than the homogeneous and aqueous-biphasic counterparts with triphos or sulphos ligands. The rate enhancement observed for the heterogeneous reactions has been attributed to the fact that, unlike in fluid solution systems, the heterogenized complexes do not undergo dimerization to give catalytically inactive species.

The supported complex [Rh(cod)(POLYDIPHOS)]PF_6, obtained by stirring a CH_2Cl_2 solution of [RhCl(cod)]$_2$ and Bu_4NPF_6 in the presence of a diphenylphosphinopropane-like ligand tethered to a cross-linked styrene/divinylbenzene matrix (POLYDIPHOS), forms an effective catalyst for the hydrogenation of quinoline (Fig. 16.8) [84]. Under relatively mild experimental conditions (80 °C, 30 bar H_2), quinoline was mainly converted to THQ, though appreciable formation of both 5,6,7,8-THQ and decahydroquinoline also occurred (Scheme 16.20).

An effective catalyst recycling with no loss of catalytic activity was accomplished by removing the liquid phase via the liquid sampling valve and re-charging the autoclave with a solution containing the substrate. In all cases, no rhodium leaching occurred. Remarkably, the hydrogenation activity of the 1,3-bis-

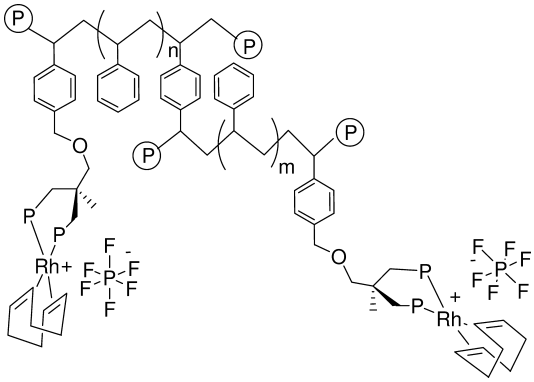

Fig. 16.8 Schematic of a diphosphine rhodium complex covalently tethered to a cross-linked styrene/divinylbenzene matrix, used for the hydrogenation of quinoline.

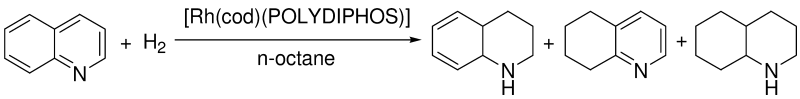

Scheme 16.20

diphenylphosphinopropane complex [Rh(dppp)(cod)]PF_6 in THF was much lower, as well as being selective, for THQ.

16.4 Stereoselective Hydrogenation of Prochiral Heteroaromatics

16.4.1 Molecular Catalysts in Homogeneous Phase

The enantioselective hydrogenation of prochiral heteroaromatics is of major relevance for the synthesis of biologically active compounds, some of which are difficult to access via stereoselective organic synthesis [4]. This is the case for substituted N-heterocycles such as piperazines, pyridines, indoles, and quinoxalines. The hydrogenation of these substrates by supported metal particles generally leads to diastereoselective products [4], while molecular catalysts turn out to be more efficient in enantioselective processes. Rhodium and chiral chelating diphosphines constitute the ingredients of the vast majority of the known molecular catalysts.

Relevant examples of enantioselective hydrogenation of aromatic N-heterocycles are given below. Scheme 16.21 shows the hydrogenation of a 2-ester substituted piperazine to the corresponding 2-substituted pyrazine with a catalyst

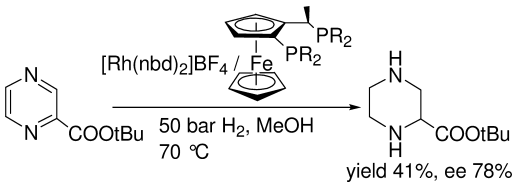

Scheme 16.21

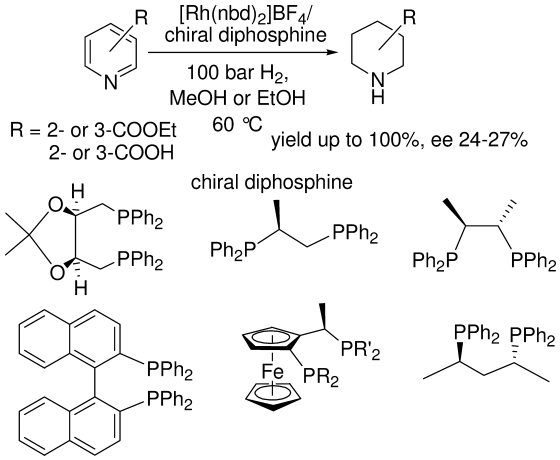

Scheme 16.22

prepared *in situ* by mixing $[Rh(nbd)_2Cl]_2$ with a *Josiphos*-type ferrocenyldiphosphine, preferentially 1-[1(*R*)-(dicyclohexylphosphino)ethyl]-2(*S*)-(diphenylphosphino)ferrocene [85]. Under relatively mild conditions, the conversions were low, but the ee-values were quite satisfactory.

Josiphos-rhodium systems have been also used to hydrogenate 2- or 3-substituted pyridines and furans, yet both the activities (TOF = 1–2) and enantioselectivities were rather low (Scheme 16.22) [86, 87]. Comparable results were obtained with a number of chiral chelating diphosphines of various symmetries.

The diphosphines leading to the formation of six- or seven-membered metallarings have been found to give higher ee-values as compared to 1,2-diphosphines. With most ligands, the 2- or 3-substituted furans were hydrogenated with much lower enantioselectivity (ee 1–7%). Only the *Josiphos* ligand with R = *t*-Bu gave a significant ee (24%) for the reduction of substituted furans, yet the activity was almost negligible (3%) [85]. It is worth noting that black precipitates were observed in some experiments, which may indicate catalyst decomposition.

Excellent ee-values (up to 94%) have been obtained for the hydrogenation of various 2-substituted *N*-acetyl indoles with an *in-situ* prepared rhodium catalyst modified with the *trans*-chelating diphosphine (*S*,*S*)-(*R*,*R*)-2,2″-bis[1-(diphenylphosphino)ethyl]-1,1″-biferrocene (Scheme 16.23) [88]. A strong base was required as co-reagent to observe both high conversion (TOFs of 50–100) and en-

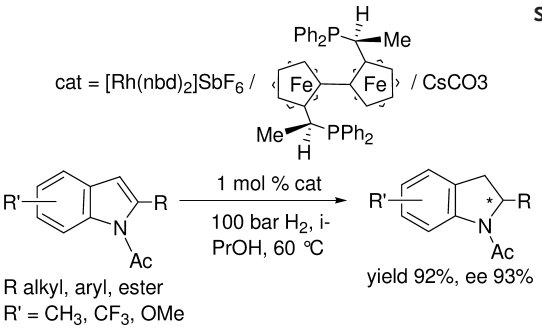

Scheme 16.23

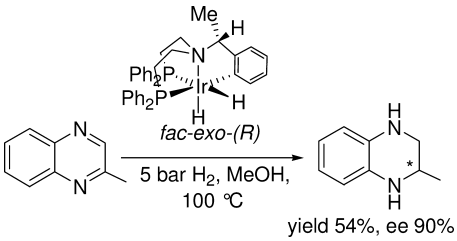

Scheme 16.24

antioselectivity. Best results were achieved with catalytic systems comprising $CsCO_3$ and $[Rh(nbd)_2]SbF_6$.

A quite different ligand system has been found to generate a selective iridium catalyst for the hydrogenation of 2-methylquinoxaline to (–)-(2*S*)-2-methyl-1,2,3,4-tetrahydroquinoxaline (Scheme 16.24) [89]. Unlike all previous examples of enantiomeric hydrogenation, an isolated catalyst precursor, namely the Ir^{III} *o*-metalated dihydride *fac-exo*-(*R*)-$[IrH_2\{C_6H_4C^*H(Me)N(CH_2CH_2PPh_2)_2\}]$, was employed. Under quite mild experimental conditions, ee-values of up to 90% were obtained at 50% conversion, while at 100% conversion the ee decreased to 75%. An *operando* high-pressure NMR study showed that the catalytically active species was generated by de-orthometalation rather than by H_2-reductive elimination. It was also shown that the two C=N moieties of 2-methylquinoxaline were reduced at comparable rates. Notably, the use of the *fac-exo*-(*S*) dihydride precursor gave the product with opposite configuration, that is (+)-(2*R*)-2-methyl-1,2,3,4-tetrahydroquinoxaline [89].

The only other example of enantioselective hydrogenation of 2-methylquinoxaline has been reported by Murata and coworkers, who used a [(+)-(DIOP)RhH] catalyst to produce 2-methyl-1,2,3,4-tetrahydroquinoxaline, albeit in 3% ee [90].

Scheme 16.25

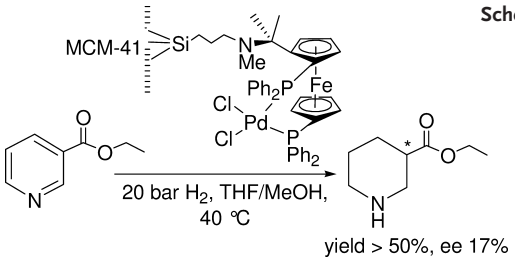

16.4.2
Molecular Catalysts Immobilized on Support Materials

The enantioselective hydrogenation of ethyl nicotinate to ethyl nipecotinate is a difficult process of which only a few heterogeneous examples are known, generally catalyzed by Pd/C modified with supported chiral auxiliaries [91]. No example in homogeneous phase has been reported to date. Palladium(II) complexes with the chelating ligand (*S*)-1-[(*R*)-1,2′-bis(diphenylphosphino)ferrocene are equally inactive, but their immobilization onto the inner walls of MCM-41 has surprisingly generated an effective catalyst, albeit with a modest ee (Scheme 16.25) [92]. Nonetheless, this reaction deserves to be highlighted for the elegant approach to heterogenization as well as for developing the concept of catalyst confinement as an innovative method to magnify both the catalytic activity and the asymmetric induction [92, 93].

Abbreviations

4H-An	1,2,3,4-tetrahydroanthracene
8H-An	1,2,3,4,5,6,7,8-octahydroanthracene
BQ	benzoquinoline
BT	benzo[*b*]thiophene
DBT	dibenzo[*b,d*]thiophene
DHBT	dihydrobenzo[*b*]thiophene
DVB	divinylbenzene
ee	enantiomeric excess
HDN	hydrodenitrogenation
HDO	hydrodeoxygenation
HDS	hydrodesulfurization
IQ	isoquinoline
PTA	1,3,5-triaza-7-phosphadamantane
SG	syngas
SHB	supported hydrogen-bonded
TCSM	tethered complexes on supported metals
THPY	1,2,5,6-tetrahydropyridine

THQ	1,2,3,4-tetrahydroquinoline
THT	tetrahydrothiophene
TOF	turnover frequency
TPPMS	triphenylphosphine monosulfonate
TPPTS	triphenylphosphine trisulfonate
WGS	water-gas-shift

References

1 S. Siegel. In: B.M. Trost, I. Fleming (Eds.), *Comprehensive Organic Synthesis*. Volume 9. Pergamon Press, New York, **1991**.

2 A.F. Noels, A.J. Hubert. In: A. Montreux, F. Petit (Eds.), *Industrial Applications of Homogeneous Catalysis*. Riedel Publishing Company, Dordrecht, Netherlands, **1988**.

3 (a) T. Kabe, A. Ishihara, W. Qian, *Hydrodesulfurization and Hydrodenitrogenation*, Wiley-VCH, Tokyo, Japan, **1999**; (b) H. Topsøe, B.S. Clausen, F.E. Massoth, *Hydrotreating Catalysis*, Springer, Heidelberg, Germany, **1996**.

4 T.J. Donohoe, R. Garg, C.A. Stevenson, *Tetrahedron: Asymmetry* **1996**, *7*, 317.

5 H.-U. Blaser, C. Malan, B. Pugin, F. Spindler, H. Steiner, M. Studer, *Adv. Synth. Catal.* **2003**, *345*, 103.

6 M.F. Semmelhack. In: E.W. Abel, F.G.A. Stone, G. Wilkinson (Eds.), *Comprehensive Organometallics Chemistry II*. Pergamon, New York, **1995**, Volume 12, p. 979.

7 P.A. Chaloner, M.A. Esteruelas, F. Joo, L.A. Oro, *Homogeneous Hydrogenation*, Kluwer Academic Publishers, Dordrecht, Netherlands, **1993**.

8 (a) C. Bianchini, A. Meli, F. Vizza, *J. Organomet. Chem.* **2004**, *689*, 4277; (b) C. Bianchini, A. Meli, F. Vizza. In: B. Cornils, W.A. Herrmann (Eds.), *Applied Homogeneous Catalysis with Organometallic Compounds*. Wiley-VCH, New York, **2002**, Volume 3, p. 1099; (c) C. Bianchini, A. Meli, F. Vizza, *Eur. J. Inorg. Chem.* **2001**, 43.

9 (a) R.A. Sánchez-Delgado, *Organometallic Modeling of the Hydrodesulfurization and Hydrodenitrogenation Reactions*, Kluwer Academic, Dordrecht, Netherlands, **2002**; (b) R.H. Fish. In: R. Ugo (Ed.), *Aspects of Homogeneous Catalysis*. Kluwer Academic Publishers, Dordrecht, Netherlands, **1990**, Volume 7, p. 65.

10 (a) B.R. James, *Homogeneous Hydrogenation*, Wiley, New York **1973**; (b) B.R. James. In: G. Wilkinson, F.G.A. Stone, E. Abel (Eds.), *Comprehensive Organometallic Chemistry*. Pergamon Press, Oxford, **1982**, Volume 8, Chapter 51.

11 (a) P.N. Rylander, *Hydrogenation Methods*, Academic Press, New York, **1990**; (b) S. Nishimur, *Hand-book of Heterogeneous Catalytic Hydrogenation for Organic Synthesis*, Wiley, New York, **2001**; (c) J.G. Donkervoort, E.G.M. Kuijpers. In: R.A. Sheldon, H. van Bekkum (Eds.), *Fine Chemicals through Heterogeneous Catalysis*. Wiley-VCH, Weinheim, **2001**.

12 (a) R. Burmeister, A. Freund, P. Panster, T. Tacke, S. Wieland, *Stud. Surf. Sci. Catal.* **1995**, *92*, 343; (b) T.Q. Hu, B.R. James, J.S. Retting, C.-L. Lee, *Can. J. Chem.* **1977**, *75*, 1234.

13 (a) E.L. Muetterties, F.J. Hirsekorn, *J. Am. Chem. Soc.* **1974**, *96*, 4063; (b) E.L. Muetterties, F.J. Hirsekorn, *J. Am. Chem. Soc.* **1974**, *96*, 7920; (c) E.L. Muetterties, M.C. Rakowski, F.J. Hirsekorn, W.D. Larson, V.J. Bauss, F.A.L. Anet, *J. Am. Chem. Soc.* **1975**, *97*, 1266; (d) M.C. Rakowski, F.J. Hirsekorn, L.S. Stuhl, E.L. Muetterties, *Inorg. Chem.* **1976**, *15*, 2379; (e) L.S. Stuhl, M.C. Rakowski, A. Du Bois, F.J. Hirsekorn, J.R. Bleeke, A.E. Stevens, E.L. Muetterties, *J. Am. Chem. Soc.* **1978**, *100*, 2405; (f) J.R. Bleeke, E.L. Muetterties, *J. Am. Chem. Soc.* **1981**, *103*, 556.

14 A.J. Sivak, E.L. Muetterties, *J. Am. Chem. Soc.* **1979**, *101*, 4878.

15 C. Bianchini, K.G. Caulton, K. Folting, A. Meli, M. Peruzzini, A. Polo, F. Vizza, *J. Am. Chem. Soc.* **1992**, *114*, 7290.

16 C. Bianchini, K.G. Caulton, C. Chardon, M.L. Doublet, O. Eisenstein, S.A. Jackson, T.J. Johonson, A. Meli, M. Peruzzini, W.E. Streib, A. Vacca, F. Vizza, *Organometallics* **1994**, *13*, 2010.

17 C.R. Landis, J. Halpern, *Organometallics* **1983**, *2*, 840.

18 A.F. Borowski, S. Sabo-Etienne, B. Chaudret, *J. Mol. Catal. A: Chem.* **2001**, *174*, 69.

19 C.J. Boxwell, P.J. Dyson, D.J. Ellis, T. Welton, *J. Am. Chem. Soc.* **2002**, *124*, 9334.

20 (a) L. Plasseraud, G. Süss-Fink, *J. Organomet. Chem.* **1997**, *539*, 163; (b) E.G. Fidalgo, L. Plasseraud, G. Süss-Fink, *J. Mol. Cat. A: Chem.* **1998**, 132, 5; (c) M. Faure, A.T. Vallina, H. Stoeckli-Evans, G. Süss-Fink, *J. Organomet. Chem.* **2001**, *621*, 103.

21 P.J. Dyson, D.J. Ellis, G. Laurenczy, *Adv. Synth. Catal.* **2003**, 345.

22 G. Süss-Fink, M. Faure, T.R. Ward, *Angew. Chem. Int. Ed.* **2002**, *41*, 99.

23 (a) R.A. Grey, G.P. Pez, A. Wallo, *J. Am. Chem. Soc.* **1980**, *102*, 5949; (b) R. Wilczynski, W.A. Fordyce, J. Halpern, *J. Am. Chem. Soc.* **1983**, *105*, 2066; (c) D.E. Linn, J. Halpern, J. *Am. Chem. Soc.* **1987**, *109*, 2969.

24 (a) R.H. Fish, A.D. Thormodsen, G.A. Cremer, *J. Am. Chem. Soc.* **1982**, *104*, 5234; (b) R.H. Fish, *Ann. N. Y. Acad. Sci.* **1983**, *415*, 292.

25 M.A. Bennet, T.-N. Huang, T.W. Turney, *J. Chem. Soc. Chem. Commun.* **1979**, 312.

26 M.J. Russell, C. White, P.M. Maitlis, *J. Chem. Soc. Chem. Commun.* **1977**, 427.

27 D.A. Tocker, R.O. Gould, T.A. Stephenson, M.A. Bennett, J.P. Ennett, T.W. Matheson, L. Sawyer, V.K. Shah, *J. Chem. Soc., Dalton Trans.* **1983**, 1571.

28 A. Widegren, R.G. Finke, *J. Mol. Catal. A: Chem.* **2003**, *198*, 317.

29 J.P. Collman, K.M. Kosydar, M. Bressan, W. Lamanna, T. Garrett, *J. Am. Chem. Soc.* **1984**, *106*, 7228.

30 (a) J.S. Yu, B.C. Ankianiec, M.T. Nguyen, I.P. Rothwell, *J. Am. Chem. Soc.* **1992**, *114*, 1927; (b) B.C. Ankianiec, P.E. Fanwick, I.P. Rothwell, *J. Am. Chem. Soc.* **1991**, *113*, 4710; (c) V.M. Visciglio, J.R. Clark, M.T. Nguyen, D.R. Mulford, P.E. Fanwick, I.P. Rothwell, *J. Am. Chem. Soc.* **1997**, *119*, 3490; (d) I.P. Rothwell, *J. Chem. Soc. Chem. Commun.* **1997**, 1331; (e) J.R. Clark, P.E. Fanwick, I.P. Rothwell, *J. Chem. Soc. Chem. Commun.* **1995**, 553.

31 M. Feder, J. Halpern, *J. Am. Chem. Soc.* **1975**, *97*, 7186.

32 J. Birch, *Quart. Rev.* **1950**, *4*, 69.

33 J.S. Yu, I.P. Rothwell *J. Chem. Soc. Chem. Commun.* **1992**, 632.

34 D. Durand, G. Hillion, C. Lassau, C. Sajus, US Patent 4.271.323, **1981**.

35 (a) A. Alvanipour, L.D. Kispert, *J. Mol. Cat.* **1998**, *48*, 277; (b) M.F. Sloan, A.S. Matlack, D.S. Breslow, *J. Am. Chem. Soc.* **1963**, *85*, 4014; (c) S.J. Lapporte, W.R. Schuett *J. Org. Chem.* **1963**, *28*, 1947; (d) S.J. Lapporte, *Ann. N.Y. Acad. Sci.* **1969**, *158*, 510.

36 I. Wender, R. Levine, M. Orchin, *J. Am. Chem. Soc.* **1950**, *72*, 4375.

37 R.H. Fish, A.D. Thormodsen, H. Heinemann, *J. Mol. Catal.* **1985**, *31*, 191.

38 (a) H. Gao, R.J. Angelici, *J. Am. Chem. Soc.* **1997**, *119*, 6937; (b) H. Gao, R.J. Angelici, *Organometallics* **1999**, *18*, 989; (c) H. Gao, R.J. Angelici, *J. Mol. Catal. A: Chem.* **1999**, *145*, 83.

39 (a) C. Bianchini, D.G. Burnaby, J. Evans, P. Frediani, A. Meli, W. Oberhauser, R. Psaro, L. Sordelli, F. Vizza, *J. Am. Chem. Soc.* **1999**, *121*, 5961; (b) C. Bianchini, V. Dal Santo, A. Meli, W. Oberhauser, R. Psaro, F. Vizza, *Organometallics* **2000**, *19*, 2433; (c) C. Bianchini, P. Barbaro, V. Dal Santo, R. Gobetto, A. Meli, W. Oberhauser, R. Psaro, F. Vizza, *Adv. Synth. Catal.* **2001**, *343*, 41.

40 H. Yang, H. Gao, R.J. Angelici, *Organometallics* **2000**, *19*, 622.

41 R. Abu-Reziq, D. Avnir, I. Miloslavski, H. Schumann, J. Blum, *J. Mol. Catal. A* **2002**, *185*, 179.

42 C. Bianchini, V. Dal Santo, A. Meli, S. Moneti, M. Moreno, W. Oberhauser, R. Psaro, L. Sordelli, F. Vizza, *Angew. Chem. Int. Ed.* **2003**, *42*, 2636.

43 C. Bianchini, F. Vizza (manuscript in preparation).

44 (a) M.S. Eisen, T.J. Marks, *J. Am. Chem. Soc.* **1992**, *114*, 10358; (b) H. Ahn,

C. P. Nicholas, T. J. Marks, *J. Am. Chem. Soc.* **2003**, *125*, 4325; (c) C. Coperet, M. Chabanas, R. P. Saint-Arroman, J. M. Basset, *Angew. Chem. Int. Ed.* **2003**, *42*, 157.

45 K. J. Klabunde, B. B. Anderson, M. Bader, L. J. Radonovich, *J. Am. Chem. Soc.* **1978**, *100*, 1313.

46 K. Jonas, *Angew. Chem. Int. Ed. Engl.* **1985**, *24*, 295.

47 D. Pieta, A. M. Trzeciak, J. J. Ziolkowiski, *J. Mol. Cat.* **1983**, *18*, 193.

48 M. Trzeciak, T. Glowiak J. Ziolkowiski, *J. Organomet. Chem.* **1998**, *552*, 159.

49 K. R. Januszklewicz, H. Alper, *Organometallics,* **1983**, *2*, 1055.

50 (a) J. W. Johnson, E. L. Muetterties, *J. Am. Chem. Soc.* **1977**, *99*, 7395; (b) M. Y. Darensburg, E. L. Muetterties *J. Am. Chem. Soc.* **1978**, *100*, 7425.

51 T. J. Lynch, M. Banah, H. D. Kaesz, C. R. Porter, *J. Org. Chem.* **1984**, *49*, 1266.

52 P. J. Dyson, D. J. Ellis, D. G. Parker, T. Welton *J. Chem. Soc. Chem. Commun.* **1999**, 25.

53 R. A. Sánchez-Delgado, E. González, *Polyhedron* **1989**, *8*, 1431.

54 A. F. Borowski, S. Sabo-Etienne, B. Domadieu, B. Chaudret, *Organometallics* **2003**, *22*, 4803.

55 E. Baralt, S. J. Smith, I. Hurwitz, I. T. Horváth, R. H. Fish, *J. Am. Chem. Soc.* **1992**, *114*, 5187.

56 R. A. Sánchez-Delgado, V. Herrera, L. Rincón, A. Andriollo, G. Martín, *Organometallics* **1994**, *13*, 553.

57 V. Herrera, A. Fuentes, M. Rosales, R. A. Sánchez-Delgado, C. Bianchini, A. Meli, F. Vizza, *Organometallics* **1997**, *163*, 2465.

58 C. Bianchini, A. Meli, M. Peruzzini, F. Vizza, V. Herrera, R. A. Sánchez-Delgado, *Organometallics* **1994**, *13*, 721.

59 C. Bianchini, A. Meli, S. Moneti, W. Oberhauser, F. Vizza, V. Herrera, A. Fuentes, R. A. Sánchez-Delgado, *J. Am. Chem. Soc.* **1999**, *121*, 7071.

60 C. Bianchini, V. Dal Santo, A. Meli, S. Moneti, M. Moreno, W. Oberhauser, R. Psaro, L. Sordelli, F. Vizza, *J. Catal.* **2003**, *213*, 47.

61 (a) INTEVEP S. A. (D. E. Páez, A. Andriollo, R. A. Sánchez-Delgado, N. Valencia, R. E. Galiasso, F. A. López), US Patent 5,753,584, **1998**; (b) INTEVEP S. A. (D. E. Páez, A. Andriollo, R. A. Sánchez-Delgado, N. Valencia, R. E. Galiasso, F. A. López), **1999**, US Patent 5,958,223; (c) INTEVEP S. A. (D. E. Páez, A. Andriollo, R. A. Sánchez-Delgado, N. Valencia, R. E. Galiasso, F. A. López), US Patent 5,981,421, **1999**; (d) M. A. Busolo, F. Lopez-Linares, A. Andriollo, D. E. Páez, *J. Mol. Catal. A.* **2002**, *189*, 211.

62 (a) CNR (C. Bianchini, A. Meli, F. Vizza), **1999**, PCT/EP97/06493; (b) CNR (C. Bianchini, A. Meli, F. Vizza), **1996**, IT FI96A000272.

63 C. Bianchini, P. Frediani, V. Sernau, *Organometallics* **1995**, *14*, 5458.

64 I. Rojas, F. López-Linares, N. Valencia, C. Bianchini, *J. Mol. Catal. A* **1999**, *144*, 1.

65 (a) C. Bianchini, A. Meli, S. Moneti, F. Vizza, , *Organometallics* **1998**, *17*, 2636; (b) C. Bianchini, D. Masi, A. Meli, M. Peruzzini, F. Vizza, F. Zanobini, *Organometallics* **1998**, *17*, 2495.

66 I. Jardine, F. J. McQuillin, *J. Chem. Soc. D* **1970**, 626.

67 R. H. Fish, J. L. Tan, A. Thormodsen, *J. Org. Chem.* **1984**, *49*, 4500.

68 R. H. Fish, J. L. Tan, A. Thormodsen, *Organometallics* **1985**, *4*, 1743.

69 R. M. Laine, D. W. Thomas, L. W. Cary, *J. Org. Chem.* **1979**, *44*, 4964.

70 K. Kindler, D. Mathies, *Chem. Abstr.* **1960**, *54*, 19731b.

71 R. M. Laine, *New J. Chem.* **1987**, *11*, 543.

72 A. Eisenstadt, C. M. Giandomenico, M. F. Frederick, R. M. Laine, *Organometallics* **1985**, *4*, 2033.

73 R. A. Sánchez-Delgado, E. Gonzalez, *Polyhedron* **1989**, *8*, 1431.

74 M. Macchi, PhD Dissertation, Università di Trieste (Italy), **1999**.

75 C. Bianchini, P. Barbaro, M. Macchi, A. Meli, F. Vizza, *Helv. Chim. Acta* **2001**, *84*, 2895.

76 P. Barbaro, C. Bianchini, A. Meli, M. Moreno, F. Vizza, *Organometallics* **2002**, *21*, 1430.

77 M. Rosales, Y. Alvarado, M. Boves, R. Rubio, H. Soscun, R. Sánchez-Delgado, *Trans. Met. Chem.* **1995**, *20*, 246.

78 M. Rosales, J. Navarro, L. Sanchez, A. Gonzales, Y. Alvarado, R. Rubio,

C. De la Cruz, T. Rajmankina, *Trans. Met. Chem.* **1996**, *21*, 11.

79 A. F. Borowski, S. Sabo-Etienne, B. Domadieu, B. Chaudret, *Organometallics* **2003**, *22*, 1630.

80 R. A. Sánchez-Delgado, D. Rondón, A. Andriollo, V. Herrera, G. Martin, B. Chaudret, *Organometallics* **1993**, *12*, 4291.

81 D. E. Páez, A. Andriollo, F. López-Linares, R. E. Galiasso, J. A. Revete, R. A. Sánchez-Delgado, A. Fuentes, *Am. Chem. Soc. Div. Fuel Chem. Symp. Prepr.* **1998**, *43*, 563.

82 I. Rojas, F. López-Linares, N. Valencia, C. Bianchini, *J. Mol. Cat. A* **1999**, *144*, 1.

83 (a) C. Bianchini, A. Meli, V. Patinec, V. Sernau, F. Vizza, *J. Am. Chem. Soc.* **1997**, *119*, 4945; (b) C. Bianchini, J. Casares, A. Meli, V. Sernau, F. Vizza, R. A. Sánchez-Delgado, *Polyhedron* **1997**, *16*, 3099; (c) C. Bianchini, V. Herrera, M. V. Jiménez, A. Meli, R. A. Sánchez-Delgado, F. Vizza, *J. Am. Chem. Soc.* **1995**, *117*, 8567.

84 C. Bianchini, M. Frediani, G. Mantovani, F. Vizza, *Organometallics* **2001**, *20*, 2660.

85 Lonza AG (R. Fuchs) EP 0803502 A2, **1997**.

86 C. Bianchini, P. Barbaro, G. Giambastiani, S. Parisel, *Coord. Chem. Rev.* **2004**, *248*, 2131.

87 M. Studer, C. Wedemeyer-Exl, F. Spindler, H.-U. Blaser, *Monatsh. Chem.* **2000**, *131*, 1335.

88 R. Kuwano, K. Sato, T. Kurosawa, D. Karube, Y. Ito, *J. Am. Chem. Soc.* **2000**, *122*, 7614.

89 C. Bianchini, P. Barbaro, G. Scapacci, E. Farnetti, M. Graziani, *Organometallics* **1998**, *17*, 3308.

90 S. Murata, T. Sugimoto, S. Matsuura, *Heterocycles* **1987**, *26*, 883.

91 H.-U. Blaser, H. Konig, M. Studer, C. Wedemeyer-Exl, *J. Mol. Catal. A: Chem.* **1999**, *139*, 253.

92 S. A. Raynor, J. M. Thomas, R. Raja, B. F. G. Johnson, R. G. Bell, M. D. Mantle, *Chem. Commun.* **2000**, 1925.

93 B. F. G. Johnson, S. A. Raynor, D. S. Shephard, T. Mashmayer, J. M. Thomas, G. Sankar, S. Bromley, R. Oldroyd, L. Gladden, M. D. Mantle, *Chem. Commun.* **1999**, 1167.

17
Homogeneous Hydrogenation of Carbon Dioxide

Philip G. Jessop

17.1
Introduction

Carbon dioxide (CO_2) fixation for synthetic purposes requires either reduction or coupling reactions. Reduction of CO_2 by catalytic hydrogenation has been extensively studied. Industrial application at present is minor; CO_2 is included with CO in the feed for the currently-practiced heterogeneous hydrogenation to methanol, while Lurgi Öl-Gas-Chemie has explored the hydrogenation of CO_2 without CO as an alternative process [1, 2]. Homogeneously catalyzed hydrogenation of CO_2 is not in production at this time, although it has been 35 years since the first catalysts for the production of formamides were discovered by Haynes and coworkers [3, 4]. During the past 15 years, much more efficient catalysts have been developed; before 1990, the only system to give high yields of formic acid (>1 000 TON) operated at 160 °C [5], but now a catalyst giving 32 000 TON at only 50 °C is known [6]. Even greater improvements have been observed for the synthesis of formamides by CO_2 reduction. Unfortunately, the same progress has not been observed for homogeneously catalyzed hydrogenation of CO_2 to other products such as methanol or oxalic acid.

This chapter presents an overview of the primary findings from 1970 to the present. Hydrogenation using H_2 as the reductant will be described, although there are examples of the electrocatalytic reduction of CO_2 [7–10] and the use of other reductants [11]. More detailed reviews on homogeneous hydrogenation of CO_2 have been published, covering the years up to 1994 [12, 13] and from 1995 to 2003 [14].

The motivation for studying or contemplating industrial applications of CO_2 hydrogenation does not stem from a desire to use up excess CO_2 in order to lessen global warming. If the H_2 that is used in the reduction is derived from either the water-gas shift reaction (WGSR) or from steam reforming of methane, then 1 or 0.25 equivalents of CO_2, respectively, were produced per molecule of H_2. Thus, the hydrogenation of CO_2 to formic acid, using H_2 from WGSR, results in neither a net consumption nor a net production of CO_2. Hy-

The Handbook of Homogeneous Hydrogenation.
Edited by J.G. de Vries and C.J. Elsevier
Copyright © 2007 WILEY-VCH Verlag GmbH & Co. KGaA, Weinheim
ISBN: 978-3-527-31161-3

			ΔG° (kJ/mol)	ΔH° (kJ/mol)	ΔS° J/(mol•K)
$CO_2(g) + H_2(g)$	$\rightleftharpoons$	$HCO_2H(l)$	32.8	-31.5	-216
$CO_2(g) + H_2(g) + NH_3(aq)$	$\rightleftharpoons$	$HCO_2^-(aq) + NH_4^+(aq)$	-9.5	-84.3	-250
$CO_2(g) + H_2(g) + NHMe_2(liq)$	$\rightleftharpoons$	$HC(O)NMe_2(liq) + H_2O(l)$	na	-239	na
$CO_2(g) + 3H_2(g)$	$\rightleftharpoons$	$CH_3OH(l) + H_2O(l)$	-9.5	-131	-409

Scheme 17.1 The thermodynamics of CO_2 reductions.

drogenation of CO_2 to formic acid using H_2 from methane does result in the net consumption of CO_2, but in order to consume a significant portion of the excess CO_2 one would have to synthesize a ridiculously large amount of formic acid!

Multiple products are possible from CO_2 hydrogenation, but all of the products are entropically disfavored compared to CO_2 and H_2 (Scheme 17.1). As a result, the reactions must be driven by enthalpy, which explains why formic acid is usually prepared in the presence of a base or another reagent with which formic acid has an exothermic reaction. Of the many reduction products that are theoretically possible, including formic acid, formates, formamides, oxalic acid, methanol, CO, and methane, only formic acid and its derivatives are readily prepared by homogeneous catalysis.

17.2 Reduction to Formic Acid

Formic acid, a synthetic precursor and a commercial product for use in the leather, agriculture and dye industries, is traditionally prepared by carbonylation of NaOH at elevated pressure and temperature [15, 16]. The use of toxic CO begs the question; can a competitive route be found using CO_2 instead? Given that CO and H_2 are roughly interchangeable thanks to the WGSR and that CO_2 in the post-Kyoto world is essentially free, CO_2/H_2 should be competitive with CO if sufficiently active and inexpensive catalysts can be identified. Of course, the economics are considerably more complicated than that simple analysis: complicating factors include the costs of water addition or removal and the costs of the bases used. Nevertheless, the homogeneous hydrogenation of CO_2 as an alternative route to formic acid has been the subject of a large number of studies, starting with the first reports in the mid-1970s [17, 18].

Hydrogenation of CO_2 to formic acid (Eq. (1)) is thermodynamically unfavorable unless a base is present (see Scheme 17.1); the proton transfer to the base drives the reaction. In the absence of a base, the reaction usually fails completely or provides only small yields [19, 20], even though the initial rate of reaction was high in one case [21]. For the reaction in water, NaOH, bicarbonates, carbonates and even dialkylamines [22] are used as the base. For the reaction in or-

ganic solvents, amines are most commonly used, but some amines are decidedly superior to others in this respect. Whilst NEt_3 is most often used because it is inexpensive, far greater rates are observed (at least for the RuCl(OAc)$(PMe_3)_4$-catalyzed hydrogenation) if an amidine or guanidine base such as 1,8-diazabicyclo-[5.4.0]-undec-7-ene (DBU) is used instead [6]. The increase in rate with some bases has never been satisfactorily explained, but could be related to a base-assisted step in the mechanism (e.g., a hydrogen-bonding interaction between metal-bound H_2 and base during hydrogenolysis of a metal formate; see Section 17.2.1) or possibly to the ability of amidine bases to solubilize CO_2 in the form of bicarbonate in wet organic solvents [23]. Whichever base is used, there remains the question of how to separate the base from the formic acid product. The addition of an acid to the raw amine/formic acid mixture would liberate the formic acid and leave the amine in the form of a salt [24]. A base-exchange [25, 26] with a high-boiling amine such as imidazole would allow for thermal decomposition of the salt to give free formic acid and recyclable amine [27, 28].

$$CO_2 + H_2 \rightleftharpoons HCO_2H \tag{1}$$

The equilibrium yield of formic acid is limited by the amount of base. Many reports describing the hydrogenation in aqueous solution indicate yields of up to 1 mol formic acid per mol base, although Karakhanov was able to obtain 1.34 mol per mol $NHEt_2$ in water at 155 °C [29]. Higher yields of 1.6 to 1.9 are found for the reaction in organic solvents [18] and in supercritical CO_2 ($scCO_2$) [30, 31]. Because the reaction in the absence of base is thermodynamically unfavorable, added base must still stabilize the formic acid product, even after 1 equiv. acid has been produced and essentially all of the base is protonated. In fact, HCO_2H and NEt_3 are known [32–34] to exist in relatively stable adducts of various ratios, including 1:1, 2:1, and 3:1, plus unprotonated amine (even at 3:1 acid:amine ratios) and oligomeric chains of formic acid molecules ending with an amine. It is not clear, given that these higher ratios are possible, why the yield in practice is limited to a ratio of 1.9:1, or lower.

Solvent choice is important for optimizing the rate of this reaction. One of the most active catalysts to date, $RhCl(TPPTS)_3$, is used in water, despite the very poor solubility of H_2 in that medium. For the hydrophobic catalysts, the best solvents so far have been $scCO_2$ and polar aprotic solvents. The supercritical medium is highly effective because of the enormous concentrations of CO_2 and H_2 in the same phase as the catalyst, and also the elimination of mass-transfer limitations on the transfer of these reagent gases into traditional liquid solvents. These advantages are particularly important for the $RuH_2(PMe_3)_4$ and RuCl(OAc)$(PMe_3)_4$ catalyst precursors [30, 31, 35] because the hydrogenation rate is first order with respect to both H_2 and CO_2 [36]. For the same catalysts in conventional liquid solvents, the rate was found to decrease in the order DMSO > MeOH > MeCN > THF > H_2O. Performing the reaction in MeOH/NEt_3 and diluting the solvent with hexane causes the rate to decrease, a result which was attributed to the

decrease in the dielectric constant of the medium [36]. Similarly, dissolving large amounts of ethane or fluoroform (CHF_3) into the $MeOH/NEt_3$ mixture causes the rate to drop or rise, respectively [36]. Rhodium(I) catalyst precursors [20, 37] have similar dependence of rate on solvent polarity, with DMSO always being excellent and less-polar aprotic solvents such as acetone, THF, or benzene being inferior. However, methanol was found to be better than DMSO for $RhCl(PPh_3)_3$ [37] and decidedly inferior for $[RhCl(COD)]_2$/dppb [20]. The overall need for a highly polar solvent is not related to gas solubility (H_2 is more soluble in the nonpolar solvents), but may be related to the ability of polar solvents such as DMSO to increase the entropy of the formic acid product by disrupting hydrogen bonding [20].

Even in aprotic solvents, the hydrogenation with most catalysts requires at least a small quantity of water or an alcohol as a co-catalyst or promoter; using thoroughly dried solvents leads to poor rates of reaction. This phenomenon was first observed by Inoue et al. [18] for $Pd(dppe)_2$, but has since been found to exist also for many of the Rh- and Ru-based catalysts. However, for the catalyst precursor $[RhCl(COD)]_2$/dppb, added water was found to inhibit the hydrogenation, and added molecular sieves to remove trace water were found to help the rate [20]. For those systems which require water, the amount needed is typically very small; on the order of a few equivalents per catalyst [6, 18]. There are so many possible roles for water in a hydrogenation mechanism that it is very difficult to demonstrate conclusively how the water may be helping. Possibilities include hydrogen bonding during CO_2 insertion, hydrolysis of formate ligands, capturing CO_2 in the form of bicarbonate, or even supplying protons in an ionic hydrogenation. Some alcohols can be more effective than water at promoting the reaction. Munshi et al. [6] surveyed a large number of alcohols as co-catalysts for the $RuCl(OAc)(PMe_3)_4$ and found the most effective alcohols to be those that have an aqueous-scale pK_a below that of the protonated amine (10.7 for $HNEt_3^+$) and that have a potentially coordinating conjugate base. Thus, 3,5-$(CF_3)_2C_6H_3OH$ and triflic acid, which fulfill both requirements, are particularly effective, whereas MeOH and water are only moderately active because they are insufficiently acidic, and 2,6-tBu$_2C_6H_3OH$ and HBF_4 have no activity because their conjugate bases are too sterically encumbered or insufficiently nucleophilic to have any coordinating ability.

A large number of catalysts or catalyst precursors for the reaction in Eq. (1) have been identified (Table 17.1). Almost all of these are complexes of Rh and Ru, although there are a few, less active, examples of Ir, Pd, Ni, Fe, Ti, and Mo. The most active catalysts are $RhCl(TPPTS)_3$, Rh(hfacac)(dcpb) and $RuCl(OAc)(PMe_3)_4$, with little difference between them after rough correction of the turnover frequencies (TOF) for pressure and temperature differences [38]. Musashi and Sakaki [39] argue that the barrier to CO_2 insertion into M–H bonds increases in the order Rh(I) < Ru(II) < Rh(III) because Rh(III)–formate bonds are too weak and Ru(II)–H bonds are too strong compared to the case of Rh(I).

Table 17.1 Homogeneous catalyst precursors for the hydrogenation of CO_2 to formic acid.

Catalyst precursor	Base	$P_{H2,CO2}$ [a] [atm]	Temperature [°C]	Time [h]	TON	TOF [b] [h^{-1}]	Reference(s)
Ruthenium							
$Ru_2(CO)_5(dppm)_2$	NEt_3	38, 38	RT	21	2160	103	40
$RuCl_3$, PPh_3	NEt_3	60, 60	60	5	200	40	41
$RuH_2(PPh_3)_4$	NEt_3	25, 25	RT	20	87	4	18
$RuH_2(PPh_3)_4$	Na_2CO_3	25, 25	100	4	169	42	42
$RuH_2(PMe_3)_4$	NEt_3	85, 120	50	1	1400	1400	30
$RuCl_2(PMe_3)_4$	NEt_3	80, 140	50	47	7200	153	31
$RuCl(OAc)(PMe_3)_4$	NEt_3	70, 120	50	0.3	32 000	95 000	6
$TpRuH(PPh_3)(CH_3CN)$	NEt_3	25, 25	100	16	1815	113	43, 44
$[Ru(Cl_2bpy)_2(H_2O)_2][O_3SCF_3]_2$	NEt_3	30, 30	150	8	5000	625	45
$[(C_5H_4(CH_2)_3NMe_2)Ru(dppm)]BF_4$	None	40, 40	80	16	8	0.5	46
$[RuCl_2(CO)_2]_n$	NEt_3	81, 27	80	0.3	400	1300	24
K[RuCl(EDTA-H)]	None	3, 17	40	0.5	na	250	21
$[RuCl_2(TPPMS)_2]_2$	$NaHCO_3$	60, 35	80	0.03	320	9600	**47**
$[RuCl(C_6Me_6)(DHphen)]Cl$	KOH	30, 30	120	24	15 400	642	48
$CpRu(CO)(\mu\text{-dppm})Mo(CO)_2Cp$	NEt_3	30, 30	120	45	43	1	49
Rhodium							
$[RhCl(COD)]_2$+dppb	NEt_3	20, 20	RT	22	1150	52	25
$[RhCl(COD)]_2$+dippe	NEt_3	40 total	24	18	205	11	50
$[RhH(COD)]_4$+dppb	NEt_3	40 total	RT	18	2200	122	20
$RhCl(PPh_3)_3$	Na_2CO_3	60, 55	100	3	173	58	51
$RhCl(PPh_3)_3$	NEt_3	20, 40	25	20	2700	125	37
$RhCl(TPPTS)_3$	$NHMe_2$	20, 20	81	0.5		7260	22, 52
$[RhCl(\eta^2\text{-CYPO})_2]BPh_4$	NEt_3	25, 25	55	4.2	420	100	53
Rh(hfacac)(dcpb)	NEt_3	20, 20	25	–	–	1335	54
$[Rh(NBD)(PMe_2Ph)_3]BF_4$	None	48, 48	40	48	128	3	19
$RhCl_3$+PPh_3	$NHMe_2$	10, 10	50	10	2150	215	29
Palladium							
$Pd(dppe)_2$	NEt_3	25, 25	110	20	62	3	18
$Pd(dppe)_2$	NaOH	24, 24	RT	20	17	0.9	55
$PdCl_2$	KOH	110, na	160	3	1580	530	5
$PdCl_2(PPh_3)_2$	NEt_3	50, 50	RT	na	15	na	26

Table 17.1 (continued)

Catalyst precursor	Base	$P_{H2,CO2}$ [a] [atm]	Temperature [°C]	Time [h]	TON	TOF [b] [h^{-1}]	Reference(s)
Other metals							
$TiCl_4$/Mg	None	1, 1	RT	na	15	na	17
$Ni(dppe)_2$	NEt_3	25, 25	RT	20	7	0.4	18
$NiCl_2$(dcpe)	DBU	40, 160	50	216	4400	20	56
$FeCl_3$/dcpe	DBU	40, 60	50	7.5	113	15	56
$MoCl_3$/dcpe	DBU	40, 60	50	7.5	63	8	56
[Cp*IrCl(DHphen)]Cl	KOH	30, 30	120	10	21 000	2100	48

a) In some cases, the pressure of CO_2 was not given and was calculated from the total stated pressure minus the pressure of H_2.
b) The TOF values are not directly comparable to each other because some are at complete conversion and some are at partial conversion. They can, however, give an order of magnitude indication. Initial TOF values will be even higher.
na = data not available; RT = room temperature.

17.2.1
Insertion Mechanisms

Carbon dioxide is known to readily insert into a metal–hydride bond to give a metal formate [57, 58]; this forms the first step in insertion mechanisms of CO_2 hydrogenation (Scheme 17.2). Both this insertion step and the return path from the formate complex to the hydride, generating formic acid, have a number of possible variations.

Insertion of CO_2 into a metal–hydride bond normally requires the prior dissociation of an ancillary ligand to generate a coordinatively unsaturated complex, because CO_2 coordination to the metal usually precedes the formal insertion (Scheme 17.3, lower pathway). *Ab initio* calculations [59] support this mechanism for the insertion of CO_2 into the Ru–H bond of $RuH_2(PH_3)_4$, a model for the catalyst $RuH_2(PMe_3)_4$. However, it is theoretically possible for CO_2 insertion to take place without prior CO_2 coordination (Scheme 17.3, upper pathway) [60, 61]. The

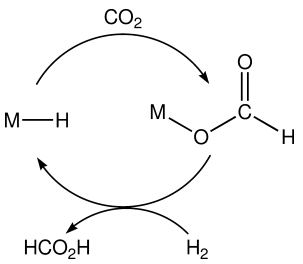

Scheme 17.2 Simplified insertion mechanism.

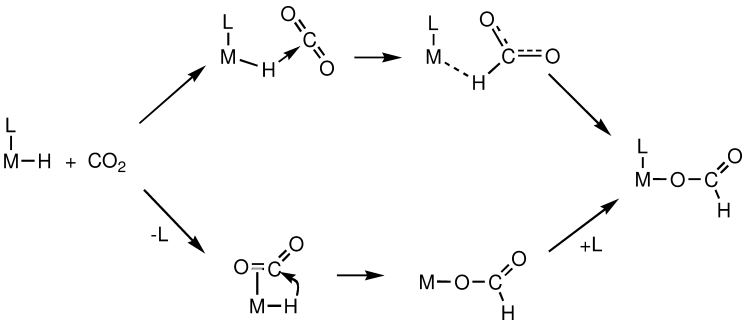

Scheme 17.3 Mechanisms of CO_2 insertion into a metal-hydrogen bond. "L" represents a potentially dissociable ligand. Ancillary ligands are not shown.

upper pathway of Scheme 17.3 was supported for the CO_2 insertion step of the catalyst in Eq. (2) by hybrid density functional calculations [62, 63].

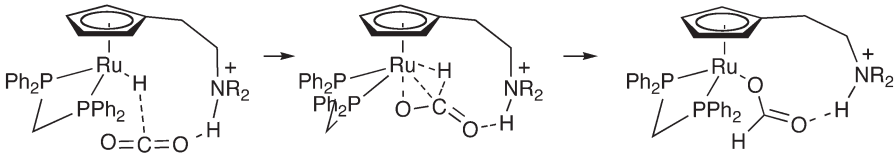

(2)

Hydrogen-bonding during the CO_2 insertion step may bring down the kinetic barrier and thereby explain the promoting effect of water and alcohols. Tsai and Nicholas [19] first proposed this for their system based on the catalyst precursor $[Rh(nbd)(PMe_2Ph)_3]BF_4$ (Scheme 17.4a). However, for the insertion of CO_2 into the Rh–H bonds of $[RhH_2(PH_3)_2(H_2O)]^+$ and $[RhH_2(PH_3)_3]^+$, proposed to be models of the actual catalyst in Tsai and Nicholas' system, Musashi and Sakaki's calculations [39] show that for this particular system the barrier-lowering effect of water during the attack of CO_2 is due not to hydrogen-bonding but to differing trans effects present in the complexes with and without water. In contrast, for the $TpRuH(PPh_3)(MeCN)$ system, hydrogen-bonding to external water was proposed (Scheme 17.4b). Density functional theory (DFT) calculations suggest that this interaction reduces the transition state energy by only 23 kJ mol^{-1} [43].

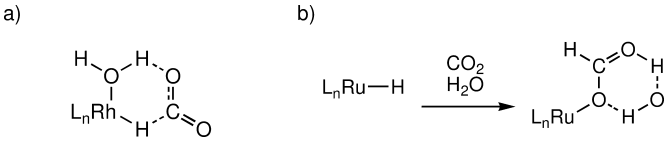

Scheme 17.4 Possible hydrogen-bonding interactions assisting in the insertion of CO_2 for the (a) $[Rh(nbd)(PMe_2Ph)_3]BF_4$ [19] and (b) $TpRuH(PPh_3)(MeCN)$ systems.

The hydrogen-bonding interaction in Eq. (2) greatly decreases the activation energy for CO_2 insertion [62, 63].

The formate complex that results from CO_2 insertion can liberate formic acid and return to the starting hydride species by one of three return pathways, the most obvious of which is hydrogenolysis (path A of Scheme 17.5). Hydrogenolysis involves either oxidative addition of H_2 or coordination of H_2 as a molecular hydrogen ligand, followed by elimination of formic acid, although technically it is possible for hydrogenolysis via a "sigma-bond metathesis" mechanism without prior H_2 coordination. Evidence for the hydrogenolysis mechanism for the intermediate $[M(O_2CH)(CO)_5]^-$ (M = Cr, W) was the fact that the related carboxylate species $[M(O_2CMe)(CO)_5]^-$ reacts with MeOH to form $MeCO_2Me$ only when H_2 is present [64]. In that system, H_2 was believed to bind to a site made available by prior dissociation of a carbonyl ligand. The hydrogenolysis pathway was also proposed for the catalytic intermediate $Rh(O_2CH)(dppb)$; the dihydride formed by H_2 oxidative addition was calculated to be lower in energy than the molecular hydrogen complex, but the latter was more reactive and therefore was the dominant pathway [65, 66]. The reaction between the bound H_2 ligand and formate was facilitated by a hydrogen-bonding interaction with external base (Scheme 17.6 b). For some systems, the H atom from the H_2 ligand might transfer to the free carbonyl oxygen atom by a six-center transition state (Scheme 17.6 c) rather than to the metal-bound oxygen via a four-center transition state (Scheme 17.6 a). The six-membered transition state was shown, by calculation, to be preferred for the Ru intermediate $[RuH(O_2CH)(H_2)(PR_3)_3]^+$ [59].

Path B in Scheme 17.5 involves hydrolysis or alcoholysis of the formate complex, yielding formic acid and a hydroxide or alkoxide complex, which then undergoes hydrogenolysis. This pathway would explain the observations that water

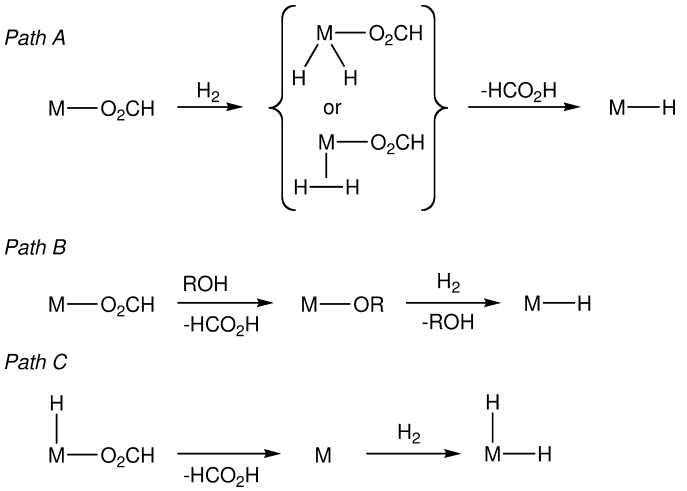

Scheme 17.5 Return pathways from the formate intermediate to the starting hydride.

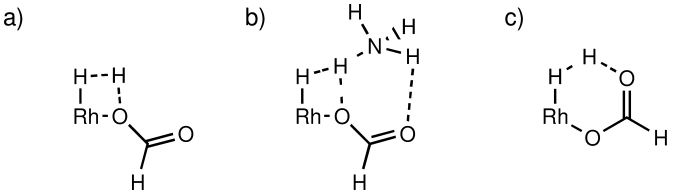

Scheme 17.6 Transition states for the transfer of a hydrogen atom from a molecular hydrogen ligand to a formate ligand: a) four-centered; b) four-centered and base-assisted [66]; and c) six-centered [59].

and alcohols increase the rate of reaction for many catalysts. Inoue et al. [18] proposed this mechanism for the reaction catalyzed by $Pd(dppe)_2$ for precisely this reason. Further, it has been observed for the $RuCl(OAc)(PMe_3)_4$ catalyst precursor that the most effective alcohols are those for which the conjugate bases are not sterically encumbered (and therefore are potentially coordinating) [6], although none of these arguments can be considered to be more than circumstantial.

Path C (Scheme 17.5), which involves reductive elimination of formic acid before reaction with H_2, is only possible for dihydride and polyhydride catalysts. This pathway was proposed for the catalyst precursor $[Rh(nbd)(PMe_2Ph)_3]^+$ by Tsai and Nicholas [19], who observed the intermediates $[RhH_2(PMe_2Ph)_3L]^+$ and $[RhH(\eta^2\text{-}O_2CH)(PMe_2Ph)_2L]^+$ ($L = H_2O$ or solvent).

17.2.2
Ionic Hydrogenation

Ionic hydrogenation mechanisms involve the sequential transfer of hydride and proton to the substrate [67]. This was suggested by the Leitner group for the hydrogenation of CO_2 with the catalyst precursor $RhH(dppp)_2$ (Scheme 17.7) [50]. Spectroscopic evidence for each of the three intermediates was obtained by studying the steps as stoichiometric reactions. However, catalyst precursors that generate the highly active RhH(diphosphine) species in solution were subsequently found to operate by a more conventional insertion mechanism [20].

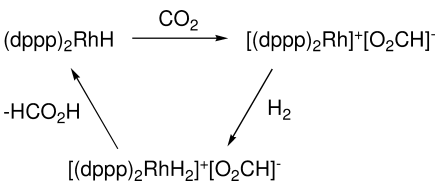

Scheme 17.7 An ionic hydrogenation mechanism for CO_2 hydrogenation [50].

17.2.3
Concerted Ionic Hydrogenation

The Noyori mechanism for the concerted ionic hydrogenation of ketones involves the simultaneous donation of a hydride ion from a metal hydride complex and a proton from an acidic ligand bound to the same metal (Scheme 17.8 a). There is no reason why this mechanism should not also be possible for CO_2 hydrogenation (Scheme 17.8 b) [6, 43, 68], although it has not yet been possible to demonstrate that this mechanism operates for any of the catalysts shown in Table 17.1. The mechanism does not require the ketone or CO_2 to bind to the metal or to insert into the M–H bond, as is required in more conventional mechanisms. Pomelli et al. [68] evaluated the possibility that bound formic acid could serve as the proton source in such a mechanism for RhH(diphosphine) catalyst, but found that the energy of the intermediates in the conventional insertion pathway were lower. The concerted mechanism for CO_2 hydrogenation was more recently suggested by Lau's group [43, 44] to explain the catalytic activity of the complex TpRuH(MeCN)(PPh_3) in the presence of water, methanol and the acidic alcohol CF_3CH_2OH, the last of which offers the greatest rates of reaction. NMR spectroscopy detected TpRu(OCH_2CF_3)(PPh_3)(MeCN) and possibly TpRu($O_2COCH_2CF_3$)(PPh_3)(MeCN). The ionic hydrogenation mechanism does not necessarily require an inner-sphere alcohol ligand. The alcohol could merely be outer-sphere, bound by an unconventional hydrogen bond to the metal hydride (i.e., M–H···HOR). Hybrid density functional calculations have shown that the transfer of H_2 from an unconventional hydrogen bond to CO_2 is energetically feasible [63].

17.2.4
Bicarbonate Hydrogenation

In basic aqueous solutions, CO_2 exists primarily in the bicarbonate or carbonate forms. Thus, the hydrogenation of either CO_2 or bicarbonate salts in such solutions could conceivably proceed by hydrogenation of the bicarbonate anion. Pd

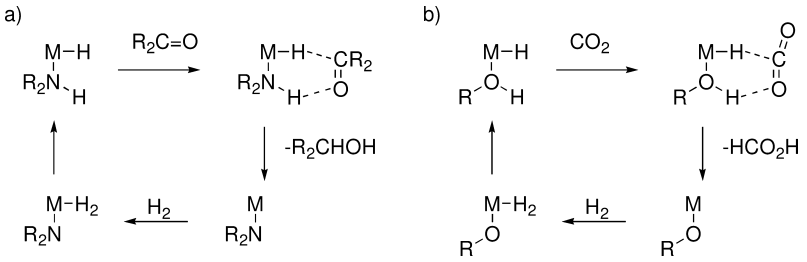

Scheme 17.8 Concerted ionic hydrogenation mechanisms for the hydrogenation of (a) ketones and (b) CO_2. The acidic ligand is shown as an alcohol in Scheme 17.7 b, but could equally well be water, a secondary amine, or a carboxylic acid.

complexes are known [5, 18] to catalyze the hydrogenation of bicarbonates and carbonates, although the mechanism is unknown. This mechanism has been proposed for the catalyst precursors $PdCl_2$/KOH [5, 69], $RuCl_2(PTA)_4$ [70], and $[RuCl_2(TPPMS)_2]_2$ [47]. The complex $RuCl_2(PTA)_4$ hydrogenates CO_2 rapidly in basic aqueous solutions but not in the absence of base, although this may be due to thermodynamics rather than evidence of a bicarbonate hydrogenation mechanism. Reaction of $RuCl_2(TPPMS)_2$ with $NaHCO_3$ gives $Ru(O_3CH)_2(TPPMS)_2$, which reacts stoichiometrically with H_2 to produce HCO_2^-.

It must keep be borne in mind that insertion and other pathways for CO_2 hydrogenation are not only possible but are believed to operate for some catalyst precursors, such as $RhCl(TPPTS)_3$, even in aqueous solutions [52].

17.2.5
Other Mechanisms

Hydrogenation of CO_2 to formic acid could potentially proceed first by reduction to CO, followed by a reaction between CO and water to give formic acid, a reaction which is known (Eq. (3)). It is unlikely that this pathway to formic acid is common because very few homogeneous catalysts (primarily homoleptic carbonyl complexes) [71–73] have been reported for the hydrogenation of CO_2 to CO, and because the few CO_2 hydrogenation catalysts that have deliberately been exposed to CO, in order to check whether this pathway is operating, have been poisoned as a result [18, 19, 31, 74].

$$CO_2 + H_2 \rightleftharpoons CO + H_2O \rightleftharpoons HCO_2H \tag{3}$$

17.3
Reduction to Oxalic Acid

Hydrogenation of CO_2 could also generate oxalic acid (Eq. (4)); the electrochemical reduction of CO_2 to oxalate dianion has been well studied [75–77]. However, there have been almost no reports of oxalic acid or its esters being detected among the products of homogeneous CO_2 hydrogenation. Denise and Sneeden [78] reported the detection of traces of diethyloxalate (0.002 TON) in a similar reaction in ethanol solvent at 120 °C. The lack of other reports may not necessarily be evidence that oxalic acid is not formed; the conventional methods for detecting formic acid (especially ^{1}H-NMR spectroscopy) are not effective for oxalic acid. Therefore, oxalic acid – were it formed – would go undetected by many researchers studying the hydrogenation of CO_2 to formic acid. In order to determine whether oxalic acid is a co-product of formic acid production, a method was developed in the Jessop group which used dimethylsulfate to methylate the oxalate anion. The dimethyloxalate was then detectable by gas chromatography. By using this assay method, it was possible to show that catalysts having

high activity for the hydrogenation of CO_2 to formate anion do not simultaneously produce detectable quantities of oxalate anion [79].

$$2CO_2 + H_2 \rightleftharpoons HO_2CCO_2H \tag{4}$$

It may not be that surprising that an effective homogeneous catalyst for the reaction shown by Eq. (4) has not been found; it is difficult to imagine a facile mechanism by which oxalate anion or oxalic acid could be generated at a metal center.

17.4 Reduction to Formate Esters

17.4.1 In the Presence of Alcohols

Formate esters can be synthesized by the hydrogenation of CO_2 in the presence of alcohols in addition to the usual base (Eq. (5) and Table 17.2). The alcohol used is typically methanol or ethanol, giving methyl- or ethylformate; the yield decreases with increasing length of the alkyl chain [80, 81]. Most typically, the pathway is catalytic hydrogenation of CO_2 to formic acid followed by an uncatalyzed thermal esterification (Eq. (6)). The formic acid intermediate, which has been observed spectroscopically for the $RhCl(PPh_3)_3$ [80] and $RuCl_2(PMe_3)_4$ [82] systems, builds up to a concentration somewhat lower than 1 : 1 with the base. The thermal esterification is slow because the reaction is performed in the presence of excess base. Tests of thermal esterification under basic conditions have been performed separately; acetic acid is esterified, in 25% yield after 44 h at 100 °C, by an excess of methanol in the presence of 1 equiv. NEt_3 [31]. The yield of methyl formate from CO_2 is optimum at a temperature which is sufficiently high to allow substantial esterification, but not so high that the hydrogenation catalyst is deactivated. This optimum temperature is ~80 °C for the $RuCl_2(PMe_3)_4$ catalyst precursor [31, 82] and 100–125 °C for the $RhCl(PPh_3)_3$ [80]. Selectivity, on the other hand, is poor at the optimum temperature but greater at higher temperatures, where the yield is poor instead [31, 82]. Complete selectivity is not obtained in the presence of base, although Lodge and Smith [83] showed that the liquid products obtained after the reaction in the presence of basic Al_2O_3 contained only the ester and no formic acid; presumably the acid was captured by the solid base.

$$CO_2 + H_2 + ROH \rightleftharpoons HCO_2R + H_2O \tag{5}$$

$$CO_2 + H_2 \overset{\text{catalyst}}{\rightleftharpoons} HCO_2H \underset{\Delta}{\overset{ROH}{\rightleftharpoons}} HCO_2R + H_2O \tag{6}$$

Formate ester synthesis by CO_2 hydrogenation in the absence of base has also been observed [45, 64, 74, 84]. As one might expect, the selectivity is much

Table 17.2 Homogeneous catalyst precursors for the hydrogenation of CO_2, in the presence of methanol or ethanol, to the corresponding formate esters.

Catalyst precursor	Base	$P_{H2,CO2}$ [a] [atm]	Temperature [°C]	Time [h]	TON	TOF [b] [h^{-1}]	Reference(s)
Ruthenium							
$Ru_4H_3(CO)_{12}^-$	None	17, 17	125	24	7	0.3	74
$RuHCl(PPh_3)_3/BF_3$	None	30, 30	100	na	17	na	86
$RuCl_2(PPh_3)_3$	Al_2O_3	60, 20	100	64	470	7.3	83
$RuCl_2(PMe_3)_4$	NEt_3	80, 125	80	64	3500	55	82
$[Ru(Cl_2bpy)_2(H_2O)_2][O_3SCF_3]_2$	NEt_3	30, 30	100	8	160	20	45
$*RuCl_2(dppe)_2$	NEt_3	85, 130	100	16	12 900	830	87
$TpRuH(PPh_3)(MeCN)$	NEt_3	25, 25	100	16	75	4.7	44
Rhodium							
$RhCl(PPh_3)_3$	NEt_3	25, 25	140	21	30	1.4	81
$RhCl(PPh_3)_3$	NaOMe	68, 29	140	21	27	1.3	55
$RhCl(PPh_3)_3$	TED	>200, 48	100	5	120	24	80
Palladium							
$Pd(dppe)_2$	NEt_3	25, 25	140	21	24	1.1	81
$Pd(dppm)_2$	NEt_3	70, 30	160	21	58	2.8	88
$Pd(dppm)_2$	NEt_3	15, 15	120	24	9	0.4	89, 90
$MnPdBr(CO_3)(dppm)_2$	NEt_3	6, 6	130	na	na	7	91
Other metals							
$Fe_3H(CO)_{11}^-$	None	20, 20	175	96	6	0.06	84
$W(O_2CH)(CO)_5^-$	None	17, 17	125	24	16	0.7	64
$IrH_3(PPh_3)_3/BF_3$	None	30, 30	100	na	38	na	86

a) In some cases, the pressure of CO_2 was not given and was calculated from the total stated pressure minus the pressure of H_2.
b) The TOF values are not directly comparable to each other because some are at complete conversion and some are at partial conversion. They can, however, give an order of magnitude indication. Initial TOF values will be even higher.
na = data not available.

greater by this method because there is no base to interfere with the esterification or to stabilize the formic acid intermediate. Although there have not yet been reports of very high TON by this method, the value of 160 obtained by Lau and Chen using the $[Ru(Cl_2bpy)_2(H_2O)_2][O_3SCF_3]_2$ precursor is the most impressive [45].

Other mechanisms for the synthesis of alkylformates, not via formic acid esterification, are possible. Hydrogenation of CO_2 to CO, followed by catalytic carbonylation of alcohol, would produce alkyl formate. This mechanism seems more likely for the anionic metal carbonyls because they are known catalysts for alcohol carbonylation. However, Darensbourg and colleagues [64, 74, 85] showed

that $[W(O_2CH)(^{13}CO)_5]^-$ gives $H^{12}CO_2H$ as a product, and they proposed that formic acid was again the intermediate for the $[MH(CO)_5]^-$ (M = Cr, W) system, even though formic acid was not directly observed in the presence of alcohol. Another possible mechanism is the hydrogenation of alkyl carbonate anion formed by the reaction of alcohol, amine, and CO_2, although to date there are no known examples of this mechanism. Finally, alcoholysis of a metal formate complex to give a metal hydroxide and alkyl formate (Eq. (7), in contrast to path B in Scheme 17.5), was proposed by Kolomnikov et al. [86]. However, Darensbourg showed that this mechanism could be ruled out for $[M(O_2CH)(CO)_5]^-$ because that complex does not react with alcohol [64].

$$MO_2CH + ROH \rightleftharpoons MOH + RO_2CH \tag{7}$$

17.4.2
In the Presence of Alkyl Halides

Given the lack of reactivity of higher alcohols in this reaction, alternative means of producing alkylformates have been explored using more reactive reagents instead of alcohols. Alkyl halides have been known, since Kolomnikov's 1972 study [86], to produce alkyl formates when they are present during CO_2 hydrogenation (Eq. (8)). That study described the production of methyl formate from methyl iodide in very low yield and only 5 TON using Ru, Ir, and Os phosphine complexes. Better yields (up to 64% but only 15 TON) were obtained by Darensbourg and Ovalles [92] using $[Cr_2H(CO)_{10}]^-$ or $[WCl(CO)_5]^-$ catalyst precursors and NaO_2COH or NaOMe as base. The base was necessary to trap the HX acid. The proposed mechanism is shown in Scheme 17.9. The last step of the mechanism, the reaction of bound RCl with a formate ligand, was investigated kinetically and is proposed to proceed by oxidative addition of the RCl followed by reductive elimination of the formate ester. Alkyl chlorides were found to be more reactive than the bromides or iodides because the heavier halides led to excessive stability of the catalytic intermediate $[MX(CO)_5]^-$. Bulky alkyl halides react

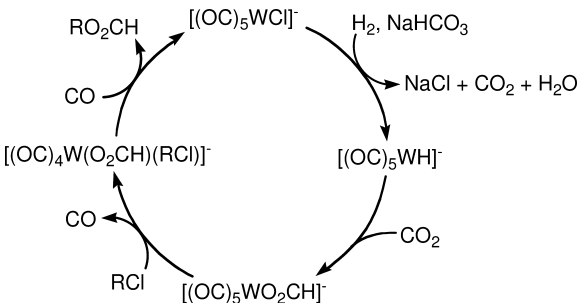

Scheme 17.9 Proposed mechanism for the preparation of formate esters using alkyl halides [92].

slowly, or not at all. Yields would have been better had there not been production of alcohol by formate ester hydrolysis and production of alkane by a side reaction (Eq. (9)).

$$H_2 + CO_2 + RX \rightleftharpoons RO_2CH + HX \tag{8}$$

$$[MH(CO)_5]^- + RX \rightleftharpoons [MX(CO)_5]^- + RH \tag{9}$$

17.4.3
In the Presence of Epoxides

Hydrogenation of carbon dioxide in the presence of an epoxide generates a mixture of the diol, its formate esters, and the cyclic carbonate. While the reaction has been shown to operate in high yield (1300 TON for the cyclic carbonate; Eq. (10)) [93], the fact that a mixture is generated and that the cyclic carbonate could be made more cleanly in the absence of H_2 makes the reaction uninteresting for synthesis. Sasaki's group showed that this reaction in the presence of an amine base gives CO rather than cyclic carbonate (Eq. (11)) [94]. The epoxide then serves as a trap for the water.

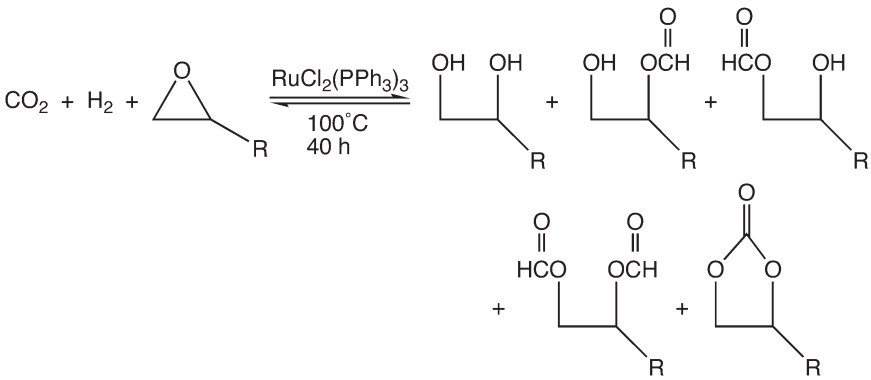

(10)

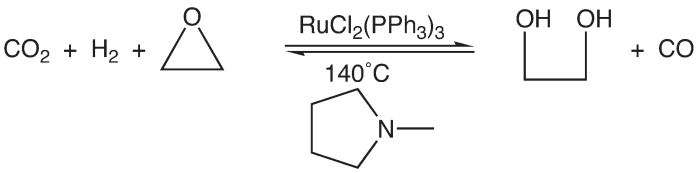

(11)

17.5 Reduction to Formamides

Formamides have applications as solvents (particularly dimethylformamide (DMF) and formamide itself), as intermediates for insecticides and pharmaceuticals, and (for formanilide, PhNHC(O)H) as an antioxidant [95]. Formamides are prepared either from CO or from methylformate or formamide, which are themselves prepared from CO.

Preparation of formamides from CO_2 and a non-tertiary amine by homogeneous hydrogenation has been well studied and is extremely efficient (Eq. (12)). Essentially complete conversions and complete selectivity can be obtained (Table 17.3). This process seems more likely to be industrialized than the syntheses of formic acid or formate esters by CO_2 hydrogenation. The selectivity is excellent, in contrast to the case for alkyl formates, because the amine base which would stabilize the formic acid is used up in the synthesis of the formamide; consequently little or no formic acid contaminates the product. The only byproducts that are likely to crop up in industrial application are the methylamines by overreduction of the formamide. This has been observed [96], but not with such high conversion that it could constitute a synthetic route to methylamines.

$$CO_2 + H_2 + NHR_2 \rightleftharpoons HC(O)NR_2 + H_2O \tag{12}$$

The formamide that has most often been synthesized in studies of this reaction is DMF. The first report of the reaction was by Haynes et al. in 1970 [3]. By far the most active catalyst precursors are the Ru(II) complexes $RuCl_2(PMe_3)_4$ [31, 97] and $RuCl_2(dppe)_2$ [87], although $RuCl_3$ and dppe or PPh_3 can be combined to make an active catalyst [98]. The mechanism, at least for $RuCl_2(PMe_3)_4$, is believed to be hydrogenation of CO_2 to formic acid by the usual insertion mechanism followed by uncatalyzed thermal condensation between the formic acid and the dimethylamine (Eq. (13)). The formic acid/formate salt intermediate is observed spectroscopically [31, 97]. Fortunately, the condensation step seems to be essentially irreversible.

$$CO_2 + H_2 + NHR_2 \xrightleftharpoons{\text{catalyst}} [NH_2R_2][O_2CH] \xrightarrow[2]{} HC(O)NR_2 + H_2O \tag{13}$$

Three alternative mechanisms have been mentioned in the literature. Reduction of CO_2 to CO followed by carbonylation of dimethylamine was ruled out by Haynes et al. [3] for $RhCl(PPh_3)_3$ because no carbonyl complexes were detected. Aminolysis of formate complexes (Eq. (14)) was proposed by Kudo et al. [69], but strong evidence has not been obtained. Finally, CO_2 is known to react with the amine to produce a carbamate salt (Eq. (15)), and it is possible that the pathway to the formamide is by hydrogenation of the carbamate rather than of the CO_2.

$$MO_2CH + NHR_2 \rightarrow MOH + HC(O)NR_2 \quad (14)$$

$$CO_2 + 2NHR_2 \rightleftharpoons [NH_2R_2][O_2CNR_2] \quad (15)$$

For longer-chain or more bulky amines, yields and conversions are often significantly lower, possibly because the carbamate formed (Eq. (15)) is solid [99], but some successful syntheses have been reported. Süss-Fink et al. were able to prepare the formamides of piperidine and pyrrolidine at 140 °C using

Table 17.3 Homogeneous catalyst precursors for the hydrogenation of CO_2, in the presence of dimethylamine, to dimethylformamide.

Catalyst precursor	$P_{H2,CO2}$ a) [atm]	Temperature [°C]	Time [h]	TON	TOF b) [h^{-1}]	Yield c) [%]	Reference(s)
Ruthenium							
$RuCl_3$/dppe/$AlEt_3$	29, 29	130	6	3400	570	73	105
$RuCl_2(PPh_3)_3$	29, 29	130	6	2650	440	51	105
$RuCl_2(PMe_3)_4$	80, 130	100	70	420 000	6000	71	31, 97
$RuCl_2(PMe_3)_4$	80, 130	100	19	62 000	3000	99	31, 97
$RuCl_2(dppe)_2$	85, 130	100	2	740 000	360 000	18	87
$RuCl_2PH(CH_2OH)_{22}P(CH_2OH)_{32}$	85, 133	100	48	10 000	210	100	106
Rhodium							
$RhCl(PPh_3)_3$	28, 28	100	17	43	2.5	11	3
$RhCl(PPh_3)_3$	80, 40	150	5	36	7	65	107
Palladium							
$Pd(CO_3)(PPh_3)_2$	28, 28	100	17	120	7	60	3
$PdCl_2/KHCO_3$	80, 40	170	1.5	34	23	99	69
Other metals							
$CdCl_2(PPh_3)_2$	28, 28	125	17	10.5	0.6	4	4
$Pt(CO_3)(PPh_3)_2$	28, 28	100	17	104	6	47	3
$Pt_2(dppm)_3$	67–94, 10–12	75	24	1460	61	na	96
$Pt_2(dppm)_3$	114 total	100	24	1375	57	na	108
$IrCl(CO)(PPh_3)_2$ d	50–68, 13–17	125	240	1145	5	na	109

a) In some cases, the pressure of CO_2 was not given and was calculated from the total stated pressure minus the pressure of H_2.
b) The TOF values are not directly comparable to each other because some are at complete conversion and some are at partial conversion. They can, however, give an order of magnitude indication. Initial TOF values will be even higher.
c) Data in this column may be either isolated yield or % conversion, depending on data available.
d) Using NH_3 to produce formamide.
na = data not available.

$Na[Ru_3H(CO)_{11}]$ catalyst precursor [100]. Tumas' group [101] obtained 100% conversion to di(*n*-propyl)formamide from di(*n*-propyl)amine by performing the reaction in an ionic liquid at 80 °C. Jessop's group [102] found that adding C_6F_5OH to the $RuCl_2(PMe_3)_4$ catalyst precursor allows one to obtain 96–100% conversion to a variety of bulky formamides, including those from heptylamine, piperidine, and benzylamine, at 100 °C (3 μmol Ru, 100 μmol C_6F_5OH, 5 mmol amine). For less basic amines such as aniline [103], no formamide is obtained unless an additional base is added such as DBU instead of, and not in addition to, the C_6F_5OH. Baiker's group [99, 104] used $RuCl_2(dppe)_2$ catalyst precursor and water as a promoter to prepare a range of formamides from aliphatic amines in very high TON at 100 °C.

17.6 Reduction to Other Products

Reduction of CO_2 past formic acid generates formaldehyde, methanol or methane (Eqs. (16–18)), and ethanol can be produced by homologation of the methanol. The liberation of water makes these reactions thermodynamically favorable but economically less favorable. The reductions typically require much higher temperatures than does the reduction to formic acid, and consequently few homogeneous catalysts are both kinetically capable and able to withstand the operating conditions.

$$CO_2 + H_2 \rightarrow HC(O)H + H_2O \tag{16}$$

$$CO_2 + 3H_2 \rightarrow CH_3OH + H_2O \tag{17}$$

$$CO_2 + 4H_2 \rightarrow CH_4 + 2H_2O \tag{18}$$

The hydrogenation of CO_2 to CO is the reverse water-gas shift reaction, which has been reviewed elsewhere [110, 111].

Hydrogenation to both formaldehyde and formic acid is catalyzed by K[RuCl(EDTA-H)] [21, 112, 113], but the proposed mechanism involved a highly unlikely reverse insertion of CO_2 (Eq. (19)).

$$MH + CO_2 \rightarrow MCO_2H \tag{19}$$

Methane production by CO_2 hydrogenation has been catalyzed by $[PdCl(dppm)]_2$ (1.5 TON at 120 °C) [78, 89] and $Ru_3(CO)_{12}/I_2$ (76 TON at 240 °C) [72, 73, 114]. The inclusion of KI in the latter system shifted the selectivity over to methanol production (95 TON) by preventing deposition of Ru metal which would have catalyzed methane production. The mechanism was believed [114] to be reduction of CO_2 to CO followed by hydrogenation of the CO to CH_3OH via Dombek's [115] mechanism.

Ethanol production by homologation of methanol can be achieved by hydrogenation of CO_2 (Eq. (20)) [116]. Sasaki's group showed that both Ru and Co car-

bonyl catalysts are required, as is an iodide salt; in the absence of iodide, methyl formate is obtained. The high-boiling solvent 1,3-dimethyl-2-imidazolidinone (DMI) was required for the reaction, which was typically performed at 180 °C. In a separate study [71], the same group showed that hydrogenation of CO_2 to methanol by these same catalysts also produces ethanol (up to TON 17, TOF 1 h^{-1}) because of the *in-situ* homologation of the methanol product.

$$CH_3OH + CO_2 + 3H_2 \xrightarrow[\text{LiI, DMI}]{\substack{Ru_3(CO)_{12} \\ Co_2(CO)_8}} CH_3CH_2OH + 2H_2O \tag{20}$$

Carboxylic acids have been prepared by CO_2 hydrogenation in the presence of alkyl iodides and catalyzed by the $Ru_3(CO)_{12}/Co_2(CO)_8$ combination (Eq. (21)). Although the yield was not high (2.5 TON, mol acetic acid per mol Co), the reaction is an interesting variation [117].

$$CH_3I + CO_2 + H_2 \xrightarrow[\text{150 pC}]{\substack{Ru_3(CO)_{12} \\ Co_2(CO)_8}} CH_3CO_2H + HI \tag{21}$$

17.7 Concluding Remarks

Highly efficient catalysts have been developed for the hydrogenation of CO_2 to formic acid and formamides, to the point where industrialization could be considered. Researchers have been far less successful in developing efficient homogeneous catalysts and optimum conditions for the hydrogenation of CO_2 to alkyl formates, methanol, methane, and especially oxalic acid. These are the areas in which research efforts are most needed.

Great progress has been made in the understanding of the insertion mechanism of CO_2 hydrogenation to formic acid. However, the evidence for other mechanisms remains circumstantial. Strong evidence for exciting new mechanisms, such as concerted ionic hydrogenation, is unavailable. Because research in this area has progressed far more rapidly during the past decade than in earlier decades, one can anticipate many more new results in the near future and look forward to a greater clarification on the subject of mechanism.

Acknowledgments

The author acknowledges support from the Division of Chemical Sciences, Office of Basic Energy Sciences, Office of Science, U.S. Department of Energy (grant number DE-FG03-99ER14986) and the support of the Canada Research Chair program (http://www.chairs.gc.ca).

Abbreviations

Cl_2bpy	6,6′-dichloro-2,2′-bipyridine
COD	1,5-cyclooctadiene
CYPO	$Cy_2PCH_2CH_2OCH_3$
DBU	1,8-diazabicyclo[5.4.0]undec-7-ene
dcpb	1,4-bis(dicyclohexylphosphino)butane
dcpe	1,2-bis(dicyclohexylphosphino)ethane
DFT	density functional theory
DHphen	4,7-dihydroxy-1,10-phenanthroline
dippe	1,2-bis(diisopropylphosphino)ethane
DMF	dimethylformamide
DMI	1,3-dimethyl-2-imidazolidinone
DMSO	dimethylsulfoxide
dppb	1,4-bis(diphenylphosphino)butane
dppe	1,2-bis(diphenylphosphino)ethane
dppp	1,3-bis(diphenylphosphino)propane
dppm	1,1-bis(diphenylphosphino)methane
EDTA-H	protonated ethylenediaminetetraacetic acid
hfacac	1,1,1,5,5,5-hexafluoroacetylacetonate
NBD	norbornadiene
PTA	1,3,5-triaza-7-phosphaadamantane
$scCO_2$	supercritical CO_2
TED	triethylenediamine
THF	tetrahydrofuran
TOF	turnover frequency (TON per h)
TON	turnover number (mol product per mol catalyst)
Tp	tris(pyrazolyl)borate
TPPMS	sodium triphenylphosphine monosulfonate
TPPTS	sodium triphenylphosphine trisulfonate
WGSR	water-gas shift reaction

References

1 J. Haggin, *Chem. Eng. News* **1994**, 29.
2 H. Goehna, P. Koenig, *ChemTech* **1994**, 36.
3 P. Haynes, L.H. Slaugh, J.F. Kohnle, *Tetrahedron Lett.* **1970**, 365.
4 P. Haynes, J.F. Kohnle, L.H. Slaugh, U.S. Patent 3530182, **1970**.
5 K. Kudo, N. Sugita, Y. Takezaki, *Nihon Kagaku Kaishi* **1977**, 302.
6 P. Munshi, A.D. Main, J. Linehan, C.C. Tai, P.G. Jessop, *J. Am. Chem. Soc.* **2002**, *124*, 7963.
7 B.P. Sullivan, K. Krist, H.E. Guard (Eds.), *Electrochemical and Electrocatalytic Reactions of Carbon Dioxide*. Elsevier, Amsterdam, **1993**.
8 A. Miedaner, C.J. Curtis, R.M. Barkley, D.L. DuBois, *Inorg. Chem.* **1994**, *33*, 5482.
9 I. Bhugun, D. Lexa, J.-M. Savéant, *J. Am. Chem. Soc.* **1994**, *116*, 5015.
10 I. Bhugun, D. Lexa, J.-M. Savéant, *J. Am. Chem. Soc.* **1996**, *118*, 1769.

11 H. Hayashi, S. Ogo, T. Abura, S. Fukuzumi, *J. Am. Chem. Soc.* **2003**, *125*, 14266.
12 P.G. Jessop, T. Ikariya, R. Noyori, *Chem. Rev.* **1995**, *95*, 259.
13 W. Leitner, *Angew. Chem., Int. Ed. Engl.* **1995**, *34*, 2207.
14 P.G. Jessop, F. Joo, C.-C. Tai, *Coord. Chem. Rev.* **2004**, *248*, 2425.
15 E.B. Reid. In: *McGraw-Hill Encyclopedia of Science and Technology*, Volume 5. McGraw-Hill Book Co., New York, **1982**, p. 670.
16 W. Reutemann, H. Kieczka. In: B. Elvers, S. Hawkins, M. Ravenscroft, J.F. Rounsaville, G. Schulz (Eds.), *Ullmann's Encyclopedia of Industrial Chemistry*, Volume A12, 5th edn. VCH, Weinheim, **1989**, p. 13.
17 B. Jezowska-Trzebiatowska, P. Sobota, *J. Organomet. Chem.* **1974**, *80*, C27.
18 Y. Inoue, H. Izumida, Y. Sasaki, H. Hashimoto, *Chem. Lett.* **1976**, 863.
19 J.-C. Tsai, K.M. Nicholas, *J. Am. Chem. Soc.* **1992**, *114*, 5117.
20 W. Leitner, E. Dinjus, F. Gaßner, *J. Organomet. Chem.* **1994**, *475*, 257.
21 M.M.T. Khan, S.B. Halligudi, S. Shukla, *J. Mol. Catal.* **1989**, *57*, 47.
22 F. Gassner, W. Leitner, *J. Chem. Soc., Chem. Commun.* **1993**, 1465.
23 D.J. Heldebrant, P.G. Jessop, C.A. Thomas, C.A. Eckert, C.L. Liotta, *J. Org. Chem.* **2005**, *70*, 5335.
24 D.J. Drury, J.E. Hamlin, European Patent Application 0095321, **1983**.
25 E. Graf, W. Leitner, *J. Chem. Soc., Chem. Commun.* **1992**, 623.
26 M. Sakamoto, I. Shimizu, A. Yamamoto, *Organometallics* **1994**, *13*, 407.
27 J.J. Anderson, J.E. Hamlin, European Patent Appl. 0126524, **1984**.
28 J.J. Anderson, D.J. Drury, J.E. Hamlin, A.G. Kent, European Patent Application 0181078, **1985**.
29 E.A. Karakhanov, S.V. Egazar'yants, S.V. Kardashev, A.L. Maksimov, S.S. Minos'yants, A.D. Sedykh, *Petroleum Chem.* **2001**, *41*, 268.
30 P.G. Jessop, T. Ikariya, R. Noyori, *Nature* **1994**, *368*, 231.
31 P.G. Jessop, Y. Hsiao, T. Ikariya, R. Noyori, *J. Am. Chem. Soc.* **1996**, *118*, 344.
32 F. Kohler, H. Atrops, H. Kalali, E. Liebermann, E. Wilhelm, F. Ratkovics, T. Salamon, *J. Phys. Chem.* **1981**, *85*, 2520.
33 K. Wagner, *Angew. Chem., Int. Ed. Engl.* **1970**, *9*, 50.
34 F. Kohler, R. Gopal, G. Goetze, H. Atrops, M.A. Demeriz, E. Liebermann, E. Wilhelm, F. Ratkovics, B. Palagyi, *J. Phys. Chem.* **1981**, *85*, 2524.
35 T. Ikariya, P.G. Jessop, R. Noyori, Japan Tokkai 5-274721, **1993**.
36 C.A. Thomas, R.J. Bonilla, Y. Huang, P.G. Jessop, *Can. J. Chem.* **2001**, *79*, 719.
37 N.N. Ezhova, N.V. Kolesnichenko, A.V. Bulygin, E.V. Slivinskii, S. Han, *Russ. Chem. Bull., Int. Ed.* **2002**, *51*, 2165.
38 The TOF data from the table were corrected to 20 °C by assuming that every 10° rise doubled the rate. The TOF data were corrected to 1 atm each of H_2 and CO_2 by assuming that the rates were first order with respect to both H_2 and CO_2, but switched to 0 order above 80 atm due to saturation kinetics. The same sequence was obtained if saturation kinetics were not assumed.
39 Y. Musashi, S. Sakaki, *J. Am. Chem. Soc.* **2002**, *124*, 7588.
40 Y. Gao, J.K. Kuncheria, H.A. Jenkins, R.J. Puddephatt, G.P.A. Yap, *J. Chem. Soc., Dalton Trans.* **2000**, 3212.
41 J.Z. Zhang, Z. Li, H. Wang, C.Y. Wang, *J. Mol. Catal. A: Chem.* **1996**, *112*, 9.
42 T. Yamaji, Japan Kokai Tokkyo Koho 140948, **1981**.
43 C. Yin, Z. Xu, S.-Y. Yang, S.M. Ng, K.Y. Wong, Z. Lin, C.P. Lau, *Organometallics* **2001**, *20*, 1216.
44 S.M. Ng, C. Yin, C.H. Yeung, T.C. Chan, C.P. Lau, *Eur. J. Inorg. Chem.* **2004**, 1788.
45 C.P. Lau, Y.Z. Chen, *J. Mol. Catal. A: Chem.* **1995**, *101*, 33.
46 H.S. Chu, C.P. Lau, K.Y. Wong, *Organometallics* **1998**, *17*, 2768.
47 J. Elek, L. Nádasdi, G. Papp, G. Laurenczy, F. Joó, *Appl. Catal. A: General* **2003**, *255*, 59.
48 Y. Himeda, N. Onozawa-Komatsuzaki, H. Sugihara, H. Arakawa, K. Kasuga. In: *50th Symposium on Organometallic Chemistry*, Osaka, Japan, **2003**.
49 M.L. Man, Z. Zhou, S.M. Ng, C.P. Lau, *J. Chem. Soc., Dalton Trans.* **2003**, 3727.

50 T. Burgemeister, F. Kastner, W. Leitner, *Angew. Chem., Int. Ed. Engl.* **1993**, *32*, 739.
51 T. Yamaji, Teijin Ltd., Japan Kokai Tokkyo Koho, 166.146, **1981**.
52 W. Leitner, E. Dinjus, F. Gassner. In: B. Cornils, W.A. Herrmann (Eds.), *Aqueous-Phase Organometallic Catalysis*. Wiley-VCH, Weinheim, **1998**, p. 486.
53 E. Lindner, B. Keppeler, P. Wegner, *Inorg. Chim. Acta* **1997**, *258*, 97.
54 R. Fornika, H. Görls, B. Seemann, W. Leitner, *J. Chem. Soc., Chem. Commun.* **1995**, 1479.
55 H. Hashimoto, S. Inoue, Japanese Patent 07.612, **1978**.
56 C.C. Tai, T. Chang, B. Roller, P.G. Jessop, *Inorg. Chem.* **2003**, *42*, 7340.
57 T. Ito, A. Yamamoto. In: S. Inoue, N. Yamazaki (Eds.), *Organic and Bioorganic Chemistry of Carbon Dioxide*. Kodansha Ltd., Tokyo, **1982**, p. 79.
58 A. Behr. In: W. Keim (Ed.), *Catalysis in C1 Chemistry*. D. Reidel Publishing Co., Dordrecht, **1983**, p. 169.
59 Y. Musashi, S. Sakaki, *J. Am. Chem. Soc.* **2000**, *122*, 3867.
60 C. Bo, A. Dedieu, *Inorg. Chem.* **1989**, *28*, 304.
61 S. Sakaki, K. Ohkubo, *Inorg. Chem.* **1989**, *28*, 2583.
62 T. Matsubara, K. Hirao, *Organometallics* **2001**, *20*, 5759.
63 T. Matsubara, *Organometallics* **2001**, *20*, 19.
64 D.J. Darensbourg, C. Ovalles, *J. Am. Chem. Soc.* **1984**, *106*, 3750.
65 F. Hutschka, A. Dedieu, W. Leitner, *Angew. Chem., Int. Ed. Engl.* **1995**, *34*, 1742.
66 F. Hutschka, A. Dedieu, M. Eichberger, R. Fornika, W. Leitner, *J. Am. Chem. Soc.* **1997**, *119*, 4432.
67 D.N. Kursanov, Z.N. Parnes, M.I. Kalinkin, N. Loim, *Ionic Hydrogenation and Related Reactions*, Harwood Academic Publishers, New York, **1985**.
68 C.S. Pomelli, J. Tomasi, M. Sola, *Organometallics* **1998**, *17*, 3164.
69 K. Kudo, H. Phala, N. Sugita, Y. Takezaki, *Chem. Lett.* **1977**, 1495.
70 G. Laurenczy, F. Joó, L. Nádasdi, *Inorg. Chem.* **2000**, *39*, 5083.
71 K.-I. Tominaga, Y. Sasaki, M. Saito, K. Hagihara, T. Watanabe, *J. Mol. Catal.* **1994**, *89*, 51.
72 K. Tominaga, Y. Sasaki, M. Kawai, T. Watanabe, M. Saito, *J. Chem. Soc., Chem. Commun.* **1993**, 629.
73 K. Tominaga, Y. Sasaki, K. Hagihara, T. Watanabe, M. Saito, *Chem. Lett.* **1994**, 1391.
74 D.J. Darensbourg, C. Ovalles, M. Pala, *J. Am. Chem. Soc.* **1983**, *105*, 5937.
75 L. Skarlos, U.S. Patent 3720591, **1973**.
76 F.R. Keene, B.P. Sullivan. In: B.P. Sullivan (Ed.), *Electrochemical and Electrocatalytic Reactions of Carbon Dioxide*. Elsevier, Amsterdam, **1993**, p. 118.
77 M.M. Ali, H. Sato, T. Mizukawa, K. Tsuge, M. Haga, K. Tanaka, *Chem. Commun.* **1998**, 249.
78 B. Denise, R.P.A. Sneeden, *J. Organomet. Chem.* **1981**, *221*, 111.
79 C.-C. Tai, P. G. Jessop, unpublished material, **2002**.
80 H. Phala, K. Kudo, S. Mori, N. Sugita, *Bull. Inst. Chem. Res., Kyoto Univ.* **1985**, *63*, 63.
81 Y. Inoue, Y. Sasaki, H. Hashimoto, *J. Chem. Soc., Chem. Commun.* **1975**, 718.
82 P.G. Jessop, Y. Hsiao, T. Ikariya, R. Noyori, *J. Chem. Soc., Chem. Commun.* **1995**, 707.
83 P.G. Lodge, D.J.H. Smith, European Patent Application 0 094 785, **1983**.
84 G.O. Evans, C.J. Newell, *Inorg. Chim. Acta* **1978**, *31*, L387.
85 D.J. Darensbourg, C. Ovalles, *CHEMTECH* **1985**, *15*, 636.
86 I.S. Kolomnikov, T.S. Lobeeva, M.E. Vol'pin, *Izv. Akad. Nauk SSSR, Ser. Khim.* **1972**, 2329.
87 O. Kröcher, R.A. Köppel, A. Baiker, *Chem. Commun.* **1997**, 453.
88 H. Hashimoto, S. Inoue, Japanese Patent 138614, **1976**.
89 B. Denise, R.P.A. Sneeden, *CHEMTECH* **1982**, February, 108.
90 B. Beguin, B. Denise, R.P.A. Sneeden, *J. Organomet. Chem.* **1981**, *208*, C18.
91 B.F. Hoskins, R.J. Steen, T.W. Turney, *Inorg. Chim. Acta* **1983**, *77*, L69.
92 D.J. Darensbourg, C. Ovalles, *J. Am. Chem. Soc.* **1987**, *109*, 3330.

93 H. Koinuma, H. Kato, H. Hirai, *Chem. Lett.* **1977**, 517.
94 K.-I. Tominaga, Y. Sasaki, T. Watanabe, M. Saito, *J. Chem. Soc., Chem. Commun.* **1995**, 1489.
95 H. Bipp, H. Kieczka. In: B. Elvers, S. Hawkins, M. Ravenscroft, J.F. Rounsaville, G. Schulz (Eds.), *Ullmann's Encyclopedia of Industrial Chemistry*, Volume A12, 5th edn. VCH, Weinheim, **1989**, p. 1.
96 S. Schreiner, J.Y. Yu, L. Vaska, *Inorg. Chim. Acta* **1988**, *147*, 139.
97 P.G. Jessop, Y. Hsiao, T. Ikariya, R. Noyori, *J. Am. Chem. Soc.* **1994**, *116*, 8851.
98 M. Rohr, J.-D. Grunwaldt, A. Baiker, *J. Mol. Catal. A: Chem.* **2005**, *226*, 253.
99 L. Schmid, M.S. Schneider, D. Engel, A. Baiker, *Catal. Lett.* **2003**, *88*, 105.
100 G. Süss-Fink, M. Langenbahn, T. Jenke, *J. Organomet. Chem.* **1989**, *368*, 103.
101 F.C. Liu, M.B. Abrams, R.T. Baker, W. Tumas, *Chem. Commun.* **2001**, 433.
102 P. Munshi, P.G. Jessop, E. McKoon, unpublished material, **2002**.
103 P. Munshi, D. Heldebrant, E. McKoon, P.A. Kelly, C.-C. Tai, P.G. Jessop, *Tetrahedron Lett.* **2003**, *44*, 2725.
104 L. Schmid, A. Canonica, A. Baiker, *Applied Catalysis A: General* **2003**, *255*, 23.
105 Y. Kiso, K. Saeki, Vol. 22 March, Japan Kokai 36617, **1977**, p. 9.
106 Y. Kayaki, T. Suzuki, T. Ikariya, *Chem. Lett.* **2001**, 1016.
107 H. Phala, K. Kudo, N. Sugita, *Bull. Inst. Chem. Res., Kyoto Univ.* **1981**, *59*, 88.
108 S. Schreiner, J.Y. Yu, L. Vaska, *J. Chem. Soc., Chem. Commun.* **1988**, 602.
109 L. Vaska, S. Schreiner, R.A. Felty, J.Y. Yu, *J. Mol. Catal.* **1989**, *52*, L11.
110 P. Ford. In: B.P. Sullivan, K. Krist, H.E. Guard (Eds.), *Electrochemical and electrocatalytic reactions of carbon dioxide.* Elsevier, Amsterdam, **1993**, Chapter 3.
111 M. Torrent, M. Sola, G. Frenking, *Chem. Rev.* **2000**, *100*, 439.
112 M.M.T. Khan, S.B. Halligudi, S. Shukla, *J. Mol. Catal.* **1989**, *53*, 305.
113 M.M.T. Khan, S.B. Halligudi, N.N. Rao, S. Shukla, *J. Mol. Catal.* **1989**, *51*, 161.
114 K. Tominaga, Y. Sasaki, T. Watanabe, M. Saito, *Bull. Chem. Soc. Jpn.* **1995**, *68*, 2837.
115 B.D. Dombek, *J. Organometal. Chem.* **1983**, *250*, 467.
116 K.-I. Tominaga, Y. Sasaki, T. Watanabe, M. Saito. In: T. Inui, M. Anpo, K. Izui, S. Yanagida, T. Yamaguchi (Eds.), *Advances in Chemical Conversions for Mitigating Carbon Dioxide.* Elsevier, Amsterdam, **1998**, p. 495.
117 A. Fukuoka, N. Gotoh, N. Kobayashi, M. Hirano, S. Komiya, *Chem. Lett.* **1995**, 567.

18
Dehalogenation Reactions

Attila Sisak and Ottó Balázs Simon

18.1
Introduction

Reductive dehalogenation – one of the earliest reactions described in the organic chemical literature – has achieved special significance since the 1980s when the harmful properties of numerous halogenated (chiefly chlorinated) hydrocarbons became clear. The identification of methods capable of neutralizing or, at least, diminishing these dangers, remains a major challenge for chemistry. It is reasonable to convert stocks of the prohibited chemicals (e.g., polychlorobiphenyls, PCBs; chlorofluorocarbons, CFCs) to valuable products as far as possible. At the same time, the halogen-containing wastes should be detoxified by degradation. During the past two decades, the mainly heterogeneous (but also homogeneous) catalytic dehalogenation provided a major share towards solving these problems. Within this period, substantial progress was also made in the application of these reactions in organic syntheses.

Hydrodehalogenation – that is, hydrogenolysis of the carbon–halogen bond – involves the displacement of a halogen bound to carbon by a hydrogen atom. This chapter is devoted to dehalogenations mediated by transition-metal complexes (Eq. (1)):

$$-\overset{|}{\underset{|}{C}}-X \xrightarrow[{[L_nM]|}]{\text{reducing agent}} -\overset{|}{\underset{|}{C}}-H\,, \qquad (1)$$

where X = F, Cl, Br, I, and $[L_nM]$ = a transition metal complex. The use of a wide variety of reducing agents (H_2, hydrides of metals and metalloids, organic reductants, etc.) under the most diverse reaction conditions (e.g., one- or two-phase systems) has been reported. Organic halides have also been reduced by electrochemical and photochemical methods in the presence of compounds of the type $[L_nM]$. Reductive transformations of organic halides not relevant to Eq. (1) (e.g., coupling reactions) and dehalogenation of acyl halides will not be included here.

The Handbook of Homogeneous Hydrogenation.
Edited by J.G. de Vries and C.J. Elsevier
Copyright © 2007 WILEY-VCH Verlag GmbH & Co. KGaA, Weinheim
ISBN: 978-3-527-31161-3

The reactivity of the carbon–halogen bond in Eq. (1) depends on several factors:

- the nature of the halogen atom;
- the environment of the halogen atom in the molecule; and
- the reagents and conditions used in Eq. (1) [1].

The order of reactivity of the C–X bond (generally: I > Br > Cl > F) is consistent with its strength. For instance, the experimentally found dissociation energies for phenyl halides (D_{Ph-X}) are 528, 402, 339, and 272 kJ mol^{-1} at 298 K for X = F, Cl, Br, and I, respectively [2]. Consequently, catalytic defluorination in the literature is comparatively rare. The different reactivity of the C–X bonds renders possible the selective dehalogenation of compounds containing two dissimilar halides, leaving intact the stronger C–X bond.

Table 18.1 Catalytic hydrodechlorination of chlorobenzene. [a)]

Catalyst/Reductant(s)	Solvent	Temperature [K]	TON [b)]	TOF [c)] [h^{-1}]	Reference
$[py_3RhCl_3]/NaBH_4/H_2$	DMF	298	9.9 [d)]	0.76 [d)]	11
$[(1,5\text{-hexadiene})RhCl]_2/H_2/Et_2NH$	*p*-Xylene/H_2O	323	>64 [d)]	–	12
$[(Cy_3P)_2Rh(H)Cl_2]/H_2/PhCH_2NEt_3^+Cl^-/NaOH$	Toluene	298	19.4 [d)]	0.81 [d)]	13
$[Cp^*RhCl_2]_2/H_2/NEt_3$	*i*-PrOH	348	≥16.6 [d, e)]	5.55 [d)]	16
$[(COD)RuCl_2]/2PCy_3/H_2/NaOH$	2-BuOH	353	39.6 [d)]	39.6 [d)]	20
$RhCl_3$/Aliquat 336/H_2	CH_2Cl_2	353	≥48.8 [d, e)]	2.71 [d)]	21
$[(PPh_3)_4Ni]/MgH_2$	THF	298	13.3 [d)]	0.74 [d)]	33
$NiCl_2/MgH_2$	THF	298	≥50 [d)]	2.5 [d)]	34
$[Cp_3Ln]/NaH$	THF	319	5.6 [d)]	0.12 [d)]	35
$Ni(OAc)_2/[Cp_2TiCl_2]/NaH$	THF	339	≥16.7 [d)]	8.33 [d)]	37
$[(PPh_3)_3Ni]/NaBH_4$	DMF	343	5.40 [d)]	0.23 [d)]	43
$[(PhCH_2CN)PdCl_2]/NaAlH_2(OCH_2CH_2OMe)_3$	Benzene	343	43.3 [d)]	9.63 [d)]	53
$Pd(OAc)_2$/Polymethylhydrosiloxane/KF	THF/H_2O	298	19.0 [d)]	66.7 [d)]	77
$PdCl_2$/indoline	MeOH	413	6.79 [d)]	1.70 [d)]	92
$Pd(OAc)_2$/2dippp [f)]/MeOH/NaOH	MeOH	373	90 [d)]	4.5 [d)]	100
$Pd(OAc)_2$/2dippp [f)]/HCO_2Na	MeOH	373	≥100 [d)]	≈5 [d)]	100
$[Pd(dba)_2]$/3L/*i*-PrOH/K_2CO_3 [g)]	*i*-PrOH	353	1019	46.3 [d)]	103
$[Cp^*Rh(OAc)_2]$ H_2O/2-BuOH/KOH	2-BuOH	371	38.4 [d, i)]	2.26 [d)]	106
[(IPr)Pd(allyl)Cl] [h)]/*t*-BuONa	*i*-PrOH	333	≥380 [d, i)]	109 [d)]	108
Ni(0)/IMes HCl [f)]/*i*-PrONa	THF	338	3.2 [d)]	3.2 [d)]	109
$[Cp_2TiCl_2]$/BuMgCl	THF	298	7.4 [d)]	0.15 [d)]	116

a) Benzene product unless otherwise stated.
b) Mol converted substrate/mol catalyst.
c) Mol converted substrate/(mol catalyst × h).
d) Calculated from the experimental data of the author(s).
e) Cyclohexane product.
f) See text.
g) L = Dicyclohexyl-{(2,4,6-triisopropyl)phenyl}phosphine; 4-chloro-*α*-methylstyrene substrate, methylstyrene product.
h) IPr: *N,N′*-bis(2,6-diisopropyl-phenyl)imidazol-2-ylidene.
i) 4-Chlorotoluene substrate, toluene product.

Table 18.2 Hydrodechlorination of PCBs and related compounds.[a)]

Catalysts/Reductant(s)	Substrate	Solvent	Temperature [K]	Dechlorination [%][b)]	TOF[c)] [h^{-1}]	Reference
$[(Et_3P)_2NiCl_2]/NaBH_2(OCH_2CH_2OMe)_2$	3,3′,4,4′-tetrachlorobiphenyl	THF	341	>99[d)]	–	31
$[(Et_3P)_2NiCl_2]/NaBH_2(OCH_2CH_2OMe)_2$	Arochlor 1232[e)]	THF	341	75[d, f)]	–	31
$[Cp_2TiCl_2]/NaBH_4$/py	Octachlorodibenzofuran	Bis(2-methoxyethyl)ether	398	100[g)]	1.4×10^{-2}[h)]	48
$Ni(acac)_2/NaAlH_2(OCH_2CH_2OMe)_2$	Delor 103[i)]	Toluene	383	>99[j)]	19.7[h)]	56
$Co(acac)_2/NaAlH_2(OCH_2CH_2OMe)_2$	Delor 103[i)]	Toluene	383	>99[j)]	56.9[h)]	56
$[(dppf)PdCl_2]$[k)]$/NaBH_4$	4,4′-dibromobiphenyl	THF/TMEDA[i)]	298	100[l)]	22.8[h)]	67
$Pd(OAc)_2/2PPh_3/i$-PrOH/NaOH	Kanechlor 600[m)]	i-PrOH	355	50[d, f)]	0.24[h)]	94
[ZnPc][j, n)]	Arochlor 1232[e)]	DDAB[o)]/dodecane/H_2O (microemulsion)	298	>99.8	–	167
[ZnPc][j, n)]	Arochlor 1260[m)]	DDAB[o)]/dodecane/H_2O (microemulsion)	298	94[f)]	–	167
$CeCl_3/LiAlH_4$	4,4′-dichlorobiphenyl	DME	358	>99	0.22[h)]	214
$NiCl_2/NaBH_2(OCH_2CH_2OMe)_2$	Arochlor 1016[p)]	THF	341	90[f, r)]	3.3×10^{-2}[h)]	215

a) Biphenyl product unless otherwise stated.
b) Conversion of PCB in % (w/w) unless otherwise stated.
c) mol converted substrate/(mol catalyst×h).
d) Determined by analysis of the Cl-content of the product.
e) Refined compound of mono- to tetrachlorobiphenyls with a majority of mono-, di-, and trichlorobiphenyls.
f) The product is a mixture.
g) Dibenzofuran product.
h) Calculated from the experimental data of the author(s).
i) Refined compound of di- to pentachlorobiphenyls with a majority of trichlorobiphenyls.
j) Determined by GC analysis.
k) See text.
l) Debromination % (w/w).
m) Refined compound of penta- to enneachlorobiphenyls with a majority of hexachlorobiphenyls.
n) Electrolysis: 1.07 mA cm^{-2} on lead cathode.
o) Didodecyldimethylammonium bromide.
p) Refined compound of mono- to pentachlorobiphenyls with a majority of trichlorobiphenyls.
r) mol.%.

Table 18.3 Hydrodechlorination of carbon tetrachloride. [a)]

Catalyst/Reductant(s)	Solvent	Temperature [K]	TON [b)]	TOF [c)] [h^{-1}]	Reference
$[(PPh)_3RuCl_2]/H_2/(CH_2OH)_2$	Xylene	298	81	–	24
$[(PPh)_3RuCl_2]H_2/Et_3N$	Xylene	298	69	–	24
$[(PPh)_3RuCl_2]/Et_3SiH$	–	353	778 [d)]	156 [d)]	74
$[(PN)PtMeCl]/HSiMe_2Ph$	Benzene	333	≥50 [d)]	11.1 [d)]	82
$[(PTA)_3Ru(H_2O)_3](tosylate)_2$ [e)]/ HCOONa	H_2O	353	478	–	111
$[RuCl_2(TPPMS)_2]$ [f)]/HCOONa	H_2O	353	≈480 [d, g)]	≈160 [d)]	111
$[RuCl_2(TPPMS)_2]$ [f)]/$HCOONH_4$	H_2O	353	416 [d)]	139 [d)]	111
CoTMPyP-SG [g)]	Phosphate buffer (pH = 7.5)	298	–	37.3	121
CoPcTs [h)]	Phosphate buffer (pH = 7.5)	298	–	35.8	121
Vitamin B_{12}/Ti(III)-citrate	MeOH	298	> 48 [d, g)]	> 2.66 [d)]	130
Cobinamide-dicyanide/Ti(III)-citrate	MeOH	298	> 48 [d, g)]	> 2.66 [d)]	130
Fe-porphyrin/cysteine	Phosphate buffer (pH = 7.0)	298	≈0.8 [d, j)]	–	136
$Na_4[W_{10}O_{32}]$ [k)]	DMF/*i*-PrOH [f)]	295	≈49 [d)]	–	173
$[Bu_4N][W_{10}O_{32}]$ [k, l)]	DMF	295	40 [d, g)]	5 [d)]	173

a) Chloroform product unless otherwise stated.
b) Mol converted substrate/mol catalyst.
c) Mol converted substrate/(mol catalyst × h).
d) Calculated from the experimental data of the author(s).
e) PTA: 1,3,5-triaza-7-phosphaadamantane.
f) See text.
g) Mixture of products.
h) 5,10,15,20-tetrakis(1-methyl-4-pyridino)porphinecobalt(II) tetrachloride supported on silica gel.
i) Cobalt(II) phthalocyanine-tetrasulfonic acid, tetrasodium salt.
j) Complete degradation.
k) Irradiation with 1000-W high-pressure Hg lamp.
l) Under pure O_2.

The diversity of the substrates, catalysts, and reducing methods made it difficult to organize the material of this chapter. Thus, we have chosen an arrangement related to that used by Kaesz and Saillant [3] in their review on transition-metal hydrides – that is, we have classified the subject according to the applied reducing agents. Additional sections were devoted to the newer biomimetic and electrochemical reductions. Special attention was paid mainly to those methods which are of preparative value. Stoichiometric hydrogenations and model reactions will be discussed only in connection with the mechanisms.

In order to facilitate the comparison of the effectiveness of the very diverse methods, turnover numbers (TON), and/or turnover frequencies (TOF) (if they were given by the author or could be calculated based on their data) are sum-

marized in the tables. The limited space available for this chapter allowed results to be compiled only for the dehalogenation of chlorobenzene (Table 18.1), for polychlorinated biphenyls and related compounds (Table 18.2), and for carbon tetrachloride (Table 18.3). To emphasize the environmental concerns, two of the three chosen compounds are common pollutants.

Despite catalytic hydrodehalogenation having been reviewed on several occasions, even when such reports contained data for homogeneous catalysis it was the information for heterogeneous which generally dominated [1, 2, 4–6]. The only comprehensive volume discussing only homogeneous hydrogenolysis, the classical handbook of James [7], was published more than 30 years ago.

18.2 Catalytic Dehalogenation with Various Reducing Agents

18.2.1 Molecular Hydrogen

This type of hydrodehalogenation has been performed generally in the presence of organic or inorganic bases to neutralize the hydrogen halides formed. Among published results, the use of rhodium complexes as catalysts dominates, but palladium and ruthenium complexes have also been applied on a frequent basis.

Although relatively few investigations have been published on the use of homogeneous hydrogenolysis of organic halides with molecular hydrogen, the first examples are rather old. During the 1960s, Kwiatek and coworkers [8] reduced a number of halogenated alkanes, alkenes, and alkynes with alkaline solutions of pentacyanocobaltate(II) under atmospheric hydrogen at 25 °C. The catalytic results, as well as their mechanistic interpretation, have been exhaustively reviewed [8, 9].

Roček and coworkers [10] attempted to compare the activity of various transition-metal complexes in the hydrodehalogenation of 5-iodouracil with atmospheric H_2 at 70–80 °C. The majority of the examined complexes decomposed to metal, but $[(PPh_3)_2CoCl_2]$, and $[(PPh_3)_3RuCl_2]$ in DMA (*N,N*-dimethyl-acetamide) remained homogeneous. The more active Ru complex catalyzed also the preparation of [5-2H]uracil using D_2 instead of H_2.

Love and McQuillin [11] have shown that the catalyst system $[py_3RhCl_3]/NaBH_4$ (1 : 1) in DMF (py = pyridine, DMF = *N,N*-dimethylformamide) is active in halogen/hydrogen exchange concerning several alkyl and aryl halides with atmospheric H_2. Interestingly, the reactivity orders $ClC_6H_5 > BrC_6H_5$, and $PhCH_2Cl > PhCH_2Br$ have been found. (–)-2-Chloro-2-phenylpropanoic acid and its methyl ester were dechlorinated to produce almost totally racemic products.

Markó and coworkers [12] dehalogenated several alkyl and benzyl halides as well as halobenzenes (X = Cl, Br, I) with $[(1,5\text{-hexadiene})RhCl]_2/PPh_3$ in the presence of Et_2NH using a medium of *p*-xylene/water at 50 °C and atmospheric H_2 pressure. Grushin and Alper [13] elaborated a similar (but more effective)

method for the hydrogenolysis of chloroarenes using $[L_2Rh(H)Cl_2]$ (**1**) (L = PCy_3, P*i*-Pr_3) as catalysts in a toluene/40% NaOH solvent system with benzyltriethylammonium chloride as a phase-transfer agent. The reaction occurred under mild conditions (25–100 °C, 0.1 MPa), and many functional groups (e.g., R, OR, CF_3, COAr, COOH, NH_2) were compatible with the C–Cl bond cleavage. Some chloro-substituted heterocycles were also readily dehalogenated. Hydrogenolysis of the C–F bond of 1-fluoronaphthalene with a similar catalytic system (**1**, L = PCy_3) could be performed at 95 °C and 0.5 MPa [14]. The use of the two-phase system improved the chance for the recovery of the catalysts [13, 14].

Setti and Mascaretti [15] realized the highly chemoselective and stereocontrolled hydrodehalogenation of the carbon-6-halogen bond of (pivaloyloxy)-methyl-6,6-dihalopenicillanate by $[(PPh_3)_3RhCl]$ in EtOAc and/or MeOH solvent systems with atmospheric H_2. For the diiodo derivative (Eq. (2)):

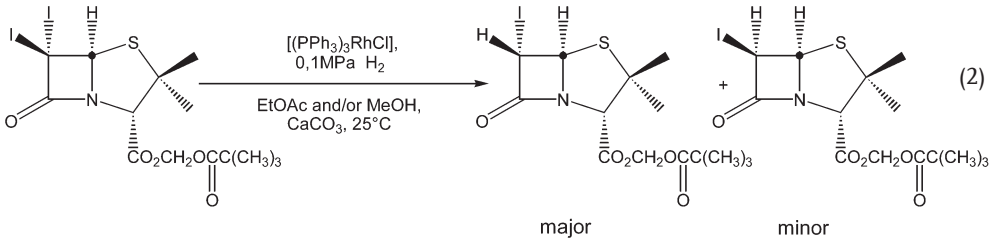

(2)

Ferrughelli and Horváth [16] converted chloroaromatics into the corresponding saturated hydrocarbons by a system generated from $[Cp_2RhCl_2]_2$ (Cp = η^5-cyclopentadienyl) in the presence of Et_3N and 2-propanol under 4.1 MPa H_2 at 75 °C. For example, 1 mmol 1,2,4-trichlorobenzene was successively reduced to cyclohexane within 6 h using 0.03 mmol of catalyst. Aizenberg and Milstein [17] have reported on the effective and selective hydrogenolysis of some polyfluorinated arenes. Heating $[L_3RhY]$ (L = PMe_3, Y = C_6F_5 or H) at 95–100 °C in C_6F_6 or C_6F_5H in the presence of a base under 0.6 MPa of H_2 led to the displacement of one of the F atoms by H with selectivities > 92%. Jones' group realized a quasicatalytic hydrogenolysis of hexafluorobenzene: heating the solution of $[Cp^*Rh(H)_2PMe_3]$ (Cp* = 1,2,3,4,5-pentamethylcyclopentadienyl) and C_6F_6 at 135 °C for 25 days under 0.1 MPa of H_2, they produced 1.4 equiv. of C_6F_5H based on the starting rhodium complex [18].

Angeloff, Brunet and colleagues [19] have found $[(PPh_3)_4Pd]$ to be an efficient catalyst for the selective conversion of 2,3-dichloronitrobenzene into 3-chloronitrobenzene at 120 °C under atmospheric H_2. The reaction could be stopped at the maximum selectivity (> 90%). Nolan, Grubbs, and associates [20] have described that $[(PCy_3)_2RuH_2(H_2)_2]$ and *in-situ*-generated $[L_2Ru(H)Cl(H_2)_2]$ (from $[(COD)RuCl_2]_x$ (COD = 1,5-cyclooctadiene) and 2L, L = PCy_3 or P*i*-Pr_3) hydrogenolyze aryl chlorides completely in alcohols as solvents at 80 °C under 0.3 MPa of H_2 within 1 h. $[(PCy_3)_2Ru(H)Cl(H_2)_2]$ was very active also in the transfer hydrogenolysis of

chloroarenes in *sec*-butyl alcohol. The systems exhibited significant functional group tolerance.

The heterogenization as a method for recycling of organotransition metal catalysts has also been studied in the case of haloarene hydrogenolysis. Blum's group [21] reported that the SiO_2 sol-gel entrapped ion pair $[(C_8H_{17})_3NMe]^+[RhCl_4 \cdot nH_2O]^-$, generated from $RCl_3 \cdot 3H_2O$, Aliquat 336, and $Si(OMe)_4$ catalyzes the hydrogenation of aryl fluorides and chlorides to give cyclohexane derivatives at 80 °C and 1.6 MPa of H_2. Fluorobenzenes, however, were proved to lose HF in a noncatalytic process. The catalyst was leach-proof and recyclable, with little or no loss in activity. Angelici and coworkers [22] have developed a process using the complexes $[(COD)Rh(\mathbf{2})]BF_4$ and $[(COD)Rh(\mathbf{3})]BF_4$ tethered on a heterogeneous catalyst, Pd/SiO_2. Fluorobenzene and 1,2-difluorobenzene were reduced under very mild conditions (0.4 MPa H_2, 70 °C) in the presence of NaOAc. The supported catalyst was more active than Pd/SiO_2 or the starting rhodium complexes alone.

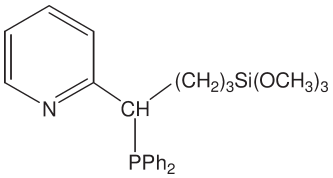

(**2**)

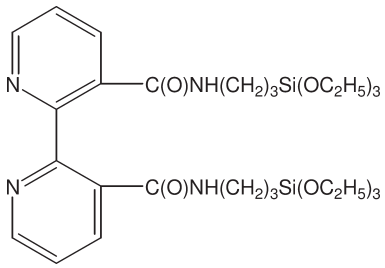

(**3**)

It has not been shown unambiguously, however, whether the rhodium remains coordinated to the ligands **2** and **3** during the catalysis. Kantam and associates [23] have used a Pd(II) catalyst anchored onto MCM-41/silylamine (MCM-41: a molecular-sieve) for hydrodehalogenation of aryl halides by atmospheric hydrogen. The catalyst was reused for several cycles with constant activity.

During the past ten years, several research groups have attempted to catalyze homogeneously the dechlorination of chlorofluorocarbon (CFC) and hydrochlorofluorocarbon (HCFC) compounds. Roundhill and associates [24] have studied the transformation of CCl_4 to $CHCl_3$, and that of $CFCl_3$ to $CHFCl_2$ in the presence of $[(PPh_3)_3RuCl_2]$ and $[(dppe)_2RuCl_2]$ (dppe = 1,2-bis(diphenylphosphino) ethane) at 25 °C and 0.11 MPa. The first transformation occurred more easily

than the second (TONs up to 90 could be reached in 5–14 days in the former case; see Table 18.3). Lee and colleagues [25, 26] achieved efficient and selective hydrodechlorination of CF_3CCl_3 to CF_3CHCl_2, as well as $CF_2ClCFCl_2$ to $CF_2ClCHClF$ and $CFCl{=}CCl_2$, by the use of Group VIII transition metal complexes at 80–150 °C and about 1 MPa H_2 pressure. In the case of the most effective catalyst, $[RhCl(PPh_3)_3]$, a slightly polar solvent such as tetrahydrofuran (THF) was found to be appropriate for selective hydrogenolysis of CFCs. Mingos and Vilar [27, 28] synthesized the novel methylidyne cluster compounds $[(Pt\text{-}Bu_3)_4Pd_4(\mu_3\text{-}CY)(\mu\text{-}Cl)_3]$ (**4**) from $[Pd_2(dba)_3]$ (dba = dibenzylideneacetone) and $Pt\text{-}Bu_3$ in the presence of the halides $CYCl_3$ (Y = H, F). In toluene/Et_3N, **4** catalyzed the transformation of $CFCl_3$ into CH_3F and $CHFCl_2$ with atmospheric H_2. Under similar conditions with $[(Pt\text{-}Bu_3)_2Pd]$, $CFCl_2H$ was the only hydrogenation product. Recently, Sisak and coworkers [29] have found that $[py_3RhCl_3]$ – in the presence of pyridine as a base – and *in-situ*-generated $[(Pi\text{-}Pr_3)_3Pd]$, surpassed Pd/Al_2O_3, the most active heterogeneous catalyst tested in the selective conversion of CF_3CHFCl into CF_3CH_2F at 120 °C and 8–10 MPa H_2 pressure. The dechlorination of $CHFCl_2$ and CF_2Cl_2 with the same catalysts, however, could be performed only at higher temperatures, and hydrodefluorination of the substrates also occurred.

18.2.2
Simple and Complex Metal Hydrides

Simple and complex metal hydrides are capable of reducing organic halides due to their nucleophilic character. The efficiency of these reducing agents can be increased considerably by adding stoichiometric or catalytic amounts of various transition-metal compounds. Initially, hydrides and simple metal salts (without any stabilizing ligands) were combined, and although these catalytic systems were qualified only rarely as definitely *heterogeneous* (for example, see [30]), it is questionable whether they are in fact *homogeneous*, or not (see [31, 32]). Similar problems arose in the case of the application of simple metal salts together with other reducing agents (vide infra).

Carfagna and coworkers [33] found that Ni(0) and Pd(0) tertiary phosphine complexes activate MgH_2 and MgD_2 in the reduction of organic halides. The more active $[(PPh_3)_4Ni]$ promoted the reduction of chlorobenzene, whereas $[(PPh_3)_4Pd]$ promoted only that of bromo- and iodobenzene to benzene (deuterobenzene) at room temperature or at 67 °C, respectively, in THF. The same authors [34] also tested several transition-metal salts as promoters in the hydrodehalogenation of halobenzenes with MgH_2. $NiCl_2$ proved to be the most active, hydrogenolyzing even the C–F bond at 67 °C. A $[Cp_3Ln]$/NaH/THF system has been reported to dehalogenate aryl halides with moderate activity at 45–65 °C [35]. Bromochlorobenzenes gave chlorobenzene selectively. The dimeric organolanthanide hydrides, $[O(CH_2CH_2C_5H_4)_2LaH]_2$ hydrogenolyzed *p*-bromoanisole and 1-bromohexadecane catalytically under similar conditions [36].

Aromatic halides such as chlorobenzene and *p*-fluorotoluene were rapidly hydrogenolyzed in 100% conversion by NaH of nanometric size in the presence of homogeneous catalysts. One- or two-component (e.g., $Ni(OAc)_2/TiCl_4$) systems were effective. The combination of ytterbium chloride and a transition-metal chloride showed a remarkable synergistic effect [37, 38].

Dzhemilev and associates [39–41] prepared monohalocyclopropanes and cyclopropanes by the reductive dehalogenation of alkyl- and aryl-substituted *gem*-dihalocyclopropanes with *i*-Bu_2AlH in the presence of catalytic amounts of titanium and zirconium complexes. The stereochemistry of the reductions has been also studied. Very recently, Knight and coworkers [42] hydrogenolyzed racemic bromoalkanes using *i*-Bu_2AlH or *i*-PrMgCl in stoichiometric, and chiral, single-enantiomer titanium complexes in catalytic amounts at 0 to 110 °C. There was no detectable difference in the reduction rate between the two enantiomers of the alkyl halide. An enantiomerically pure secondary bromide was reduced under the same conditions without racemization during the course of the reaction.

As early as 1979, Roth's group [43] reported that aryl bromides could be reduced with a homogeneous system generated from $[(PPh_3)_2NiCl_2]$ and $NaBH_4$ in DMF at 70 °C. The same group [44] later studied the reduction of a series of pure PCB congeners with $NaBH_4$. Extensive hydrogenolysis occurred in the presence of a Ni(0) triphenylphosphine complex at ambient temperatures in DMF. High selectivity for 2-, 3-, and 4-chloro displacement from di- and trichlorobiphenyls has been found. The solvent properties determined the catalytic efficiency in the transformation of 1,2,3-trichlorobenzene with a related system at 70 °C: using ethanol/pyridine solvent mixtures, benzene was produced a high rate [45].

The $[Cp_2TiCl_2]/NaBH_4$ system has been studied by several groups. Meunier [46] observed that the dehalogenation of iodobenzenes in DMF at 70 °C requires the presence of molecular oxygen. In a later and more exhaustive study, Schwartz and coworkers [47, 48] found the reaction scope and mechanism of the haloarene reduction by this system to be solvent-dependent. At 85–93 °C in DMF, halogen/hydrogen exchange and the formation of dimethylamino-substituted byproducts were observed. In DMA or in ethers, however, only dechlorinated products resulted. The $[Cp_2TiCl_2]/NaBH_4$/amine systems reduced catalytically pollutants such as PCBs and DDT (1,1-bis(4-chlorophenyl)-2,2,2-trichloroethane) [49]. Kim and coworkers [50, 51] reported that $[Cp'_2MCl_2]$ (Cp′ = Cp or Cp*; M = Ti, Zr, Hf) in the presence of several metal hydrides or alkyls catalyzes the conversion of monohalopyridines to give pyridine at room temperature. The effectiveness decreased as follows: Ti > Zr > Hf. The order of the aryl halide reactivity was surprising: C–F > C–Cl > C–Br. The reaction rate was boosted by adding 4 Å molecular sieves. Very recently, monofluoroaromatics have been reduced to the corresponding aromatic hydrocarbons when treated with the $NbCl_5/LiAlH_4$ system [52].

Several Czech research groups have studied the dehalogenation with $NaAlH_2(OCH_2CH_2OCH_3)_2$ (**5**). Hydrogenolysis of haloarenes with this hydride was accelerated by transition-metal species formed *in situ* from $[(RCN)_2PdCl_2]$ (R = Ph, $PhCH_2$) [53] or from 2,4-pentanedionates [54–56]. In the latter case, the efficiency decreased in the order Co ≈ Ni ≈ Pd > Cu ≫ Mn > Fe [54]. Complete

conversion of the PCB liquid Delor 103 (42.6% Cl) to biphenyl has been effected in toluene with **5** and catalytic amounts of Ni(II) and Co(II) 2,4-pentanedionates at elevated temperatures [56].

Sharf's group [57–59] has investigated Rh and Ru complexes with various ligands immobilized on the surface of silica gels modified with, for example, γ-aminopropyl groups (γ-AMPS), or polymers containing 3(5)-methyl-pyrazole and imidazole groups. $[Rh_2(OAc)_4]$ immobilized on γ-AMPS dehalogenated *p*-bromotoluene by transfer of hydrogen from $NaBH_4$ and 2-propanol [57]. The immobilized binuclear Ru(II)-Ru(III) tetraacetate exhibited higher catalytic activity in the hydrogenolysis of *p*-bromotoluene than the heterogenized mononuclear systems [58]. The same authors [59] hydrogenolyzed *gem*-dihalocyclopropanes partially in the presence of the system Rh(I)-γ-AMPS/$NaBH_4$/CaO/2-propanol.

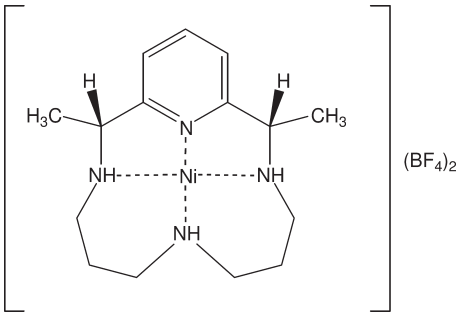

(6)

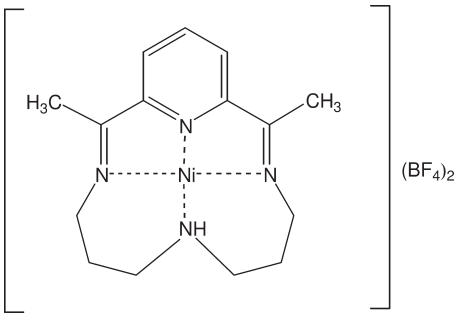

(7)

The Ni(II) complexes **6** and **7** have been found by Stiles [60] to be soluble catalysts for reductive dehalogenation when combined with $NaBH_4$ or hydrazine at 25–45 °C in protic solvents. Reactivity toward the reducing system increased with the halogen content of the substrate. Aryl bromides were converted much faster than chlorides, polychlorobenzenes, however, reacted readily with stepwise loss of chlorine.

The dehalogenation of several types of polyhalogenated arenes has been studied by Hor's group [61–67]. Brominated thiophenes and bithiophenes were re-

duced regioselectively using $NaBH_4$ in the presence of numerous Ni and Pd complexes as catalysts (e.g., 2,3,5-tribromothiophene afforded isomerically pure 2,3- or 2,4-dibromothiophene depending on the catalyst). The extent of debromination was controlled by the stoichiometry and substrate quantity. Pd-containing catalysts produced greater regioselectivity [61–63]. A variety of catalysts hydrogenolyzed 4,4′-dibromobiphenyl [64] as well as polybromobenzenes [65, 66] at room temperature, and complete conversions to biphenyl and benzene, respectively, has been achieved. The most satisfactory catalysts were generated *in situ* from the complexes $[(dppf)PdCl_2]$ or $[(dppf)_2Pd]$ (dppf = 1,1′-bis(diphenylphosphino)ferrocene), $NaBH_4$ as a hydrogen source, and TMEDA (*N*,*N*,*N*′,*N*′-tetramethylethylenediamine) as a supporting base and THF as a solvent (the addition sequence of the reactants was critical) [64, 65] (Eq. (3)):

$$\mathrm{ArX} + \mathrm{NaBH_4} + {}^{1}/_{2}\,\mathrm{TMEDA} \xrightarrow[\mathrm{THF}]{\text{“Pd(dppf)”}} \mathrm{ArH} + \mathrm{NaX} + {}^{1}/_{2}\,\mathrm{TMEDA} \cdot 2\mathrm{BH_3} \tag{3}$$

A convenient one-pot system was developed also for the conversion of highly chlorinated benzenes to less chlorinated ones at room temperature, with reasonable conversion rates using the system $[(dppf)PdCl_2]/NaBH_4/TMEDA/THF$ [67]. Degradation to benzene could not be achieved. Removal of chlorines in *meta*-position was preferred over those in *ortho*- or *para*-positions. The effectiveness of the method has been tested on the PCB mixtures Aroclor 1242, 1248, and 1254 at 67 °C.

King and coworkers [31] have used homogeneous organophosphorus–nickel complexes to detoxify PCBs by catalyzed hydrodechlorination using $NaBH_2(OCH_2CH_2OCH_3)_2$ in boiling THF. In model experiments with decachlorobiphenyl, the cone angle of the organophosphorus ligand was shown to be a key factor controlling the magnitude and position of chlorine displacement. Significantly, the highly toxic, coplanar dioxin precursor 3,3′,4,4′-tetrachlorobiphenyl, a *meta-para* chlorine-substituted congener, was dechlorinated quantitatively with a PEt_3-containing catalyst system.

Organic analogues of metal hydrides have been applied recently as reductants in homogeneous hydrodehalogenations. Treatment of aryl halides containing other functional groups with catalytic amounts of $[(PPh_3)_2NiCl_2]/PPh_3$ in the presence of 1 equiv. $Me_2NH \cdot BH_3$ and a base under mild conditions resulted in halogen/hydrogen exchange products. Noteworthy was the clean dehalogenation of densely functionalized haloperidol benzoate (Eq. (4)), attesting to the functional group compatibility offered by this combination of reagents [68].

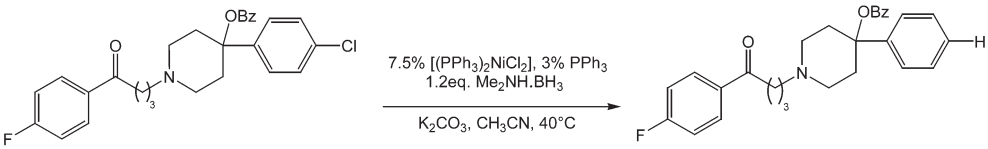

(4)

The novel, low-melting-point salt [*N*-pentylpyridinium][*closo*-$CB_{11}H_{12}$] has been used as solvent in several dehalogenations of mono- and polychlorides and -bromides, catalyzed by several Pd phosphine complexes [69]. The debromination of hexabromo- and 1,2,4,5-tetrabromobenzene was accomplished quite rapidly, whereas the dechlorination of 1,2,4-trichlorobenzene proceeded more slowly, but with excellent selectivity to 1,2-dichlorobenzene. The system could be recycled at least seven times without noticeable decrease of activity.

18.2.3
Hydrosilanes and Hydrostannanes

Hydrosilanes have a low ability to donate hydride or a hydrogen atom (cf. Section 18.2.2), but they are also useful reducing agents in combination with transition-metal complexes (Eq. (5)) [70]:

$$R'X + R_3SiH \xrightarrow[{[L_nM]}]{} R'H + R_3SiX \tag{5}$$

The problem of *homogeneity-heterogeneity* mentioned in Section 18.2.2 arises also here in the cases of using a simple metal salt instead of a ligand-stabilized salt (see [70, 71]).

Freidlina and coworkers [72, 73] were the first to use hydrosilanes for reducing organochlorine derivatives catalyzed by transition-metal complexes. For example, 1,1,1,5-tetrachloropentane was transformed into 1,1,5-trichloropentane by [$Fe_2(CO)_9$], and 1,3,3,5-tetrachlorodecane into 1,3,5-trichlorodecane by [$Mn_2(CO)_{10}$], respectively. Kono's group [74] has described the dechlorination of polychloroalkanes by silicon hydrides and in the presence of Ru(II) phosphine complexes as catalysts. CCl_4, CH_3CCl_3 and 1,1,1,3-tetrachloroalkanes have been reduced selectively to give $CHCl_3$, CH_3CHCl_2 and 1,1,3-trichloroalkanes with high turnovers at 80–100 °C (see Table 18.3). Pri-Bar and Buchman [75] hydrodehalogenated aryl iodides and bromides by polymethylhydrosiloxane (PHMS) using [$(PPh_3)_4Pd$] as a catalyst and Bz_3N as a base in Me_2SO/MeCN solvent mixtures at 60–110 °C. The debromination took place with a notable functional group tolerance. Recently, Maleczka and coworkers [76] developed a similar, but more powerful, method by fluoride activation of PMHS. In this case, the hydrodehalogenations of bromo- and iodoarenes were carried out in an amine-free system using THF as a solvent with relatively low loads of [$(PPh_3)_2PdCl_2$] catalyst. The same authors [77] reduced chloroarenes using catalytic amounts of $Pd(OAc)_2$ in combination with PMHS and aqueous KF at room temperature. The mildness of these methods was demonstrated by its functional group tolerance.

Aizenberg and Milstein [78] have found rhodium complex-catalyzed reactions between polyfluorobenzenes and hydrosilanes which resulted in the substitution of fluorine atoms by hydrogen and were both chemoselective and regioselective (Eq. (6):

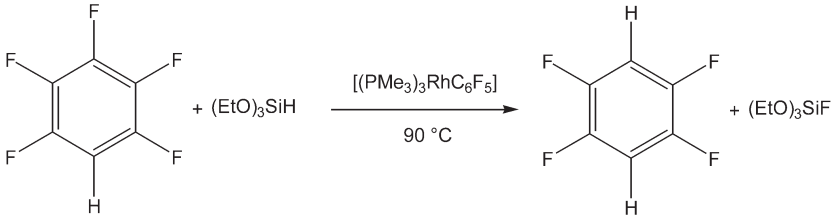

(6)

Esteruelas, Herrero and associates [79–81] have studied the simultaneous dechlorination of polychlorinated substrates and chlorination of Et_3SiH catalyzed by several complexes of Group VIII. The Os and Ir derivatives were less effective catalysts than those of Ru and Rh, and the former ones underwent deactivation during polychloroarene hydrogenolysis [79, 80]. Very recently, the same group showed that hexachlorocyclohexanes and Et_3SiH in the presence of various Rh and Ru complexes (e.g., $[(PPh_3)_3RhCl]$, $[(P\mathit{i}\text{-}Pr_3)_2RhH_2Cl]$, $[(PPh_3)_3Ru(H)Cl]$, and $[(P\mathit{i}\text{-}Pr_3)_2Ru(H)Cl(H_2)]$), afford cyclohexane/cyclohexene/benzene mixtures and Et_3SiCl. The reactivities of the substrates decreased in the order γ->α->δ-hexachlorocyclohexane [81].

Schubert's group [82, 83] has discovered that the reactivity of Pt(II) complexes is enhanced towards organosilanes by employing hemilabile chelating ligands such as $Me_2NCH_2CH_2PPh_2$ ($P\cap N$). Thus, the complex $[(P\cap N)PtMeCl]$ catalyzed the hydrogenolysis of R–Cl compounds by Me_2PhSiH to give R–H and $Me_2PhSiCl$ at 60 °C in benzene [82].

The dehalogenation of organic halides by organotin hydrides takes place in most cases with a free-radical mechanism [1, 84, 85]. The stereospecific reduction of 1,1-dibromo-1-alkenes with Bu_3SnH discovered by Uenishi and coworkers [86–89], however, did not occur in the absence of palladium complexes and did not involve radicals. For the synthesis of (*Z*)-1-bromo-1-alkenes, $[(PPh_3)_4Pd]$ proved to be the most effective catalyst which could also be generated *in situ*. The reaction in Eq. (7) proceeded at room temperature and a wide range of solvents could be used.

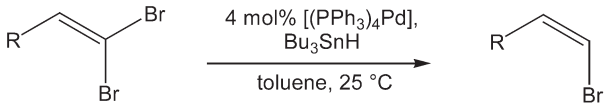

(7)

The authors determined the optimal reaction conditions and illustrated the scope of the method with 32 different starting compounds including alkenyl-, alkynyl-conjugated and 2,2-disubstituted 1,1-dibromo-1-alkenes.

18.2.4
Hydrogen Donors other than Hydrides

Various reagents have been found to be capable of donating hydrogen to transition metals in low valent state (e.g., formates, cyclic amines, alcohols in the presence of ligands and/or in basic medium). The reduction of transition-metal salts with metal alkyls (e.g., Grignard reagents with alkyl groups having β-hydrogen) may be regarded in close relation to their reactions with alcohol/base systems. The hydrogen transfer takes place from a metal-coordinated group both for alcoholates and for metal alkyls [3].

The dehalogenation of activated organic halides (e.g., benzyl halides and α-haloketones) was first published with various non-hydridic hydrogen donors. Grigg and coworkers [90] hydrogenolyzed activated organic halides with some noble metal chlorides (e.g., $RhCl_3 \cdot 3H_2O$) as catalysts in the presence of an alcohol and an excess of PPh_3. A very intriguing reducing agent, *N*-benzyl-1,4-dihydronicotinamide (BNAH) as a NAD(P)H model has been applied by Yasui and associates [91]. Aryl iodides and activated alkyl halides were reduced with the system $[(PPh_3)_3RhCl]$/BNAH in good yields at 70 °C in MeCN. Secondary cyclic amines proved to be useful reducing agents for the transfer hydrogenolysis of aryl halides with $PdCl_2$ as a catalyst in methanol at 140 °C. Indoline had the highest hydrogen-donating ability, and various bases (e.g., KOH) promoted the reaction [92].

Cortese and Heck [93] were first to report the application of palladium(0) triaryl phosphine complexes for homogeneous catalytic halogen/hydrogen exchange. The $Pd(OAc)_2/PAr_3/HCOOH/Et_3N$ (Ar = Ph, *o*-tolyl, 2,5-*i*-$Pr_2C_6H_3$) systems reduced bromoarenes at 50 °C, and the P(*o*-tolyl)$_3$-containing catalyst converted *m*-bromonitrobenzene selectively to nitrobenzene. Okamoto and Oka [94] dehalogenated aryl bromides by heating them with NaOH in alcoholic solvents in the presence of $RhCl_3$ or $Pd(OAc)_2$ and PPh_3. The method was suitable for destroying aromatic polyhalides. For example, $(C_6Br_5)_2O$ was transformed into $(C_6H_5)_2O$ in 2-propanol with more than 80 turnovers when treated for 5 h at 82 °C. Helquist has applied sodium methoxide [95] and formate [96] as reducing agents for the hydrogenolysis of haloarenes with 5 mol.% of $[(PPh_3)_4Pd]$ in DMF at 100 °C. In the case of formate, the debromination was really compatible with various functional groups.

Sasson and Rempel [97] showed that the system $[(PPh_3)_3RuCl_2]$/secondary alcohol is suitable for the selective transformation of 1,1,1,3-tetrachloro into 1,1,3-trichloro compounds. Similarly, Blum and coworkers [98, 99] employed $[(PPh_3)_3RuCl_2]$ as well as polystyrene-anchored Rh, Ru and Ir complexes for the hydrogen transfer from alcohols to trihalomethyl compounds, leading to dihalomethyl derivatives. For example, one of the Cl atoms of 2,2,2-trichloro-1-phenylethanol was displaced by H at 140–160 °C in 2-propanol. The polymer-anchored catalysts proved to be resistant to leaching [99].

Milstein and colleagues [100] have developed very efficient methods using basic, chelating phosphine ligands. Even aryl chlorides underwent reductive dechlorination to the corresponding arenes with $[(dippp)_2Pd]$ as catalyst (dippp,

dippe, dippb = 1,3-bis(diisopropylphosphino)propane, -ethane, -butane) with high yields. The systems exhibited high functional group tolerance. Base-sensitive groups (e.g., CHO, CN) did not survive the conditions of the NaOH/MeOH reducing system, but remained unaffected when treated with HCO_2Na in MeOH or DMF. Dippp homologues were also effective ligands (reactivity order: dippp > dippb > dippe). Beletskaya and associates [101] have reported that using the system $[Pd(dba)_2]$/dppf/NaO*t*-Bu/dioxane the formation of dialkyl anilines from *m*- and *p*-dibromobenzenes and secondary amines – that is, the exchange of one of the Br atoms to H became the main process. $[(PPh_3)_2PdCl_2]$ or $[(PPh_3)_4Pd]$ catalyzed the deiodination of 5-iodopyrrole-2-carboxylates with HCOONa to give the corresponding 5-unsubstituted pyrrole-2-carboxylates in good yields [102]. Very recently, the C–Cl bond of various chloroarenes was reduced by $[Pd(dba)_2]$/phosphine/K_2CO_3/*i*-PrOH systems at 80 °C with very remarkable turnovers (see Table 18.1) [103].

Dicyclohexyl-{(2,4,6-triisopropyl)phenyl}-phosphine proved to be the most suitable ligand for the functional group-friendly hydrogenolysis. Rapid and specific deuterium labeling has been achieved through the microwave-enhanced dehalogenation of a number of *N*-4-picolyl-4-halogenobenzamides using deuterated formate as solid deuterium donor and $Pd(OAc)_2$, $RhCl_3$ or $[(PPh_3)_3RhCl]$ as catalysts in dimethyl sulfoxide (DMSO) [104]. Polychloroarenes could be dehalogenated with HCOONa in 2-propanol using $[(PPh_3)_3RhCl]$ catalyst. For example, the hydrogenolysis of 1,2,4-trichlorobenzene proved selective for 1,2-dichlorobenzene [105]. Fujita and colleagues [106] have achieved effective transfer hydrodechlorination of aryl chlorides catalyzed by $[Cp^*RhCl_2]_2$ and related complexes using refluxing 2-butanol as solvent and hydrogen source in the presence of bases. The system showed high compatibility with functional groups.

Intriguing transition-metal complex/NHC/alkoxide systems (NHC = *N*-heterocyclic carbene) have been applied recently for haloarene reduction. Nolan and coworkers [107] have found that SIMes · HCl ((2,4,6-trimethylphenyl)dihydroimidazolium chloride) is the most effective of the NHC precursors when combined with $[Pd(dba)_2]$ for the dehalogenation of mono- and polyhalogenated arenes at 100 °C in dioxane. Strong bases having β-hydrogens both performed deprotonation of the imidazolium salt and behaved as hydrogen sources. Very recently, these authors have used a series of air- and moisture-stable [(NHC)Pd(allyl)Cl] complexes for dehalogenation processes with microwave assistance (120 °C) or with conventional heating (60 °C) affording very high yields in both cases [108]. In related studies, Fort and associates [109] have applied $[Ni(acac)_2]$ as a catalyst. The complex associated to IMes · HCl (1,3-bis(2,4,6-trimethylphenyl)imidazolium chloride) and *in-situ*-generated *i*-PrONa in refluxing THF proved to have high efficiency and functional group tolerance in the reduction of various mono- and polyhalogenated arenes.

Water-soluble transition-metal complexes have been used recently for transfer hydrogenolysis of halocarbons. Paetzold and Oehme [110] have realized the reductive dehalogenation of allyl or benzyl halides in the presence of $[(phosphine)_2PdCl_2]$ complexes with sulfonated phosphines as ligands (e.g., $Ph_2P(CH_2)_3SO_3K$) by

means of formates in a biphasic water/heptane system at 90 °C. This reaction could be promoted by addition of polyethers of different types as phase-transfer agents, the best results being obtained with triethylene glycol. Joó and associates [111] catalyzed the transformation of C–X bonds into C–H bonds by water-soluble Ru(II) phosphine complexes. CCl_4 was converted into $CHCl_3$ and CH_2Cl_2. Excellent TOFs up to 1000 h^{-1} could be achieved at 80 °C when, for example, an aqueous solution of HCOONa was the hydrogen donor and $[(TPPMS)_2RuCl_2]$ the catalyst (TPPMS = *m*-sulfophenyldiphenylphosphine Na salt) (see Table 18.3). Ogo, Watanabe and colleagues [112] have reported a pH-dependent transfer dehalogenation of water-soluble substrates with organoiridium(III) aqua complexes such as $[Cp^*Ir(bpy)(H_2O)]^{2+}$ (**8**) as catalyst precursors and formates as hydrogen donors. For example, **8** reacted with the formate ions at pH 5.0 to form the hydride $[Cp^*Ir(bpy)(H)]^+$, which acted as active catalysts in the hydrogenolysis of 2- and 3-halopropanoic acids.

Perfluoroaromatic Grignard reagents (R_FMgBr) were formed from alkylmagnesium bromides and perfluoroarenes in the presence of transition-metal halides (mainly $CoCl_2$) as catalysts in THF at about 0 °C, as had been reported during the late 1960s. Hydrolysis of the reaction mixtures resulted in the formation of R_FH [113]. Colomer and Corriu have applied the system $[Cp_2TiCl_2]$/*i*-PrMgBr in Et_2O for debromination, and *p*-BrC_6H_4Cl gave chlorobenzene selectively [114]. Deiodination and debromination of aromatic halides proceeded smoothly with high yields when treated with RMgX (where R groups have β-hydrogens) and a catalytic amount of $[Cp_2ZrCl_2]$ [115]. From $[Cp_2TiCl_2]$ and the above type of Grignard reagents, an effective catalyst system was obtained even for dechlorination [116]. Addition of $[(dppf)PdCl_2]$ or [(dppf)Pd] markedly accelerated the reduction of alkyl halides with Grignard reagents in Et_2O, but in THF the reduction was independent of palladium [117]. Benzyl halides underwent halogen/hydrogen exchange with equimolar amounts of Et_2Zn in DMF at room temperature using $[(PPh_3)_4Pd]$ as a catalyst. The method tolerated a variety of functional groups [118]. Very recently, Kotora and coworkers [119] have developed iron- and ruthenium-containing catalytic systems capable of reductive dehalogenation of 2-chloro-α,ω-dienes when combined with trialkylaluminum reagents.

18.2.5
Biomimetic Dehalogenations

Halocarbons are common soil, sediment, and groundwater pollutants, many of them being toxic, mutagenic materials [6, 120]. Although certain anaerobic microorganisms are capable of reductively degrading halocarbons, these processes are often slow, and high pollutant concentrations may be toxic, even for the bacteria. Thus, the problem of toxicity may be eliminated rather by biomimetic catalysis than by biocatalysis [121]. Reduction of organic halides has been investigated in the presence of transition metal-containing coenzymes vitamin B_{12} (Co, **9**), F_{430} (Ni, **10**), hematin (Fe, **11**), and related complexes. In the most cases, corrinoids have been applied (for earlier results, see [122]).

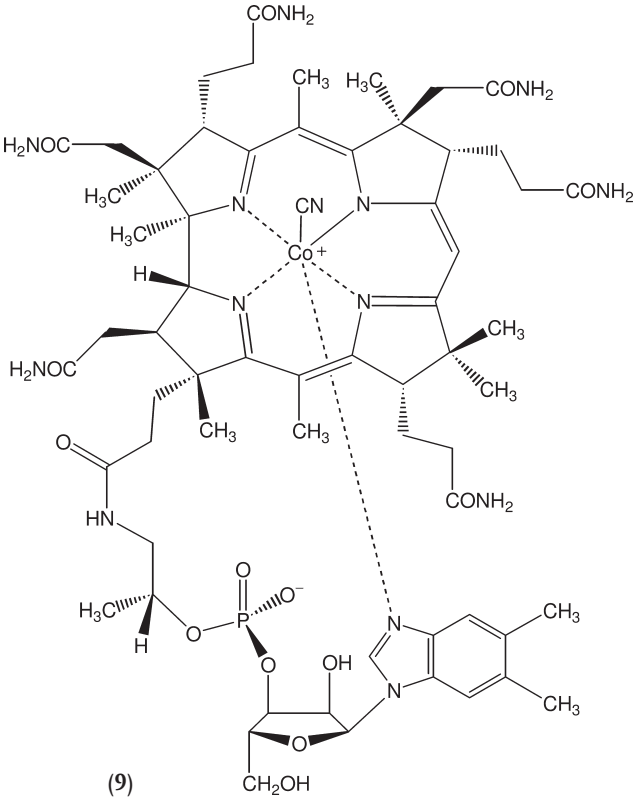
CONH2
CH3
H3C
CONH2
H2NOC
CONH2
H3C
N
CN
N
H3C
Co+
H
N
N
CH3
H2NOC
CH3
CH3
CH3
O
CONH2
HN
O
H3C
O−
P
H
O
N
CH3
O
OH
N
CH3
O
CH2OH

(**9**)

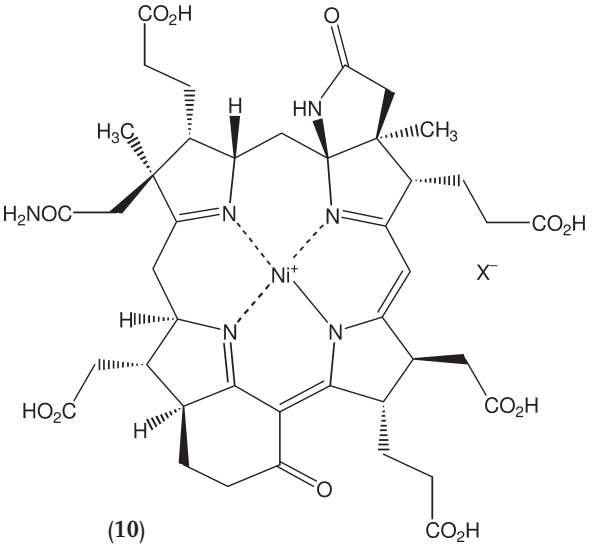
CO2H
O
H
HN
H3C
CH3
H2NOC
N
N
CO2H
Ni+
X−
H
N
N
HO2C
CO2H
H
O
CO2H

(**10**)

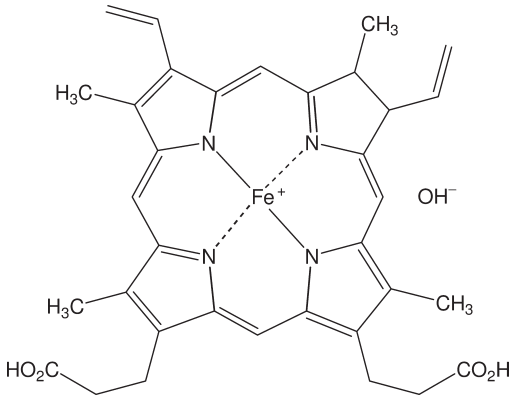

(**11**)

It should be emphasized that the aim of the great part of these biomimetic studies was *degradation* of the substrate and not the halogen/hydrogen exchange resulting in one or more product(s). This concerns above all the detoxification of polyhalogenated methanes and related pollutants (cf. [123–127]). The product composition depends strongly on the reducing agents: Ti(III) citrate [121, 128–131], dithiothreitol [121, 130], cysteine, and sulfides [130, 132, 133] have been used most frequently. The results of Morra and colleagues [130] may serve as an example. They catalyzed the dehalogenation of CCl_4 with corrins (vitamin B_{12}, cobinamide dicyanide, or aquocobalamin). Products in the presence of Ti(III) citrate were mostly hydrogenolytic and included predominantly CH_3Cl and CH_4, whereas they were CH_2Cl_2, CO and formate in the case of dithiothreitol. Sulfide/cysteine reductants were least reactive against CCl_4, giving the major products $CHCl_3$, CS_2, 2-oxothiazolidine carboxylic acid, and 2-thioxo-4-thiazolidinecarboxylic acid. In addition to cobalt complexes, a pyridine-2,6-bis(thiocarboxylic acid)-Cu(II) complex [134], and an iron porphyrin in the presence of cysteine [135, 136] have been found to be active in the degradation of CCl_4 and related compounds.

Vitamin B_{12} catalyzed also the dechlorination of tetrachloroethene (PCE) to trichloroethene (TCE) and 1,2-dichloroethene (DCE) in the presence of dithiothreitol or Ti(III) citrate [137–141], but zero-valent metals have also been used as bulk electron donors [142, 143]. With vitamin B_{12}, carbon mass recoveries were 81–84% for PCE reduction and 89% for TCE reduction; *cis*-1,2-DCE, ethene, and ethyne were the main products [138, 139]. Using Ni(II) humic acid complexes, TCE reduction was more rapid, leading to ethane and ethene as the primary products [144, 145]. Angst, Schwarzenbach and colleagues [140, 141] have shown that the corrinoid-catalyzed dechlorinations of the DCE isomers and vinyl chloride (VC) to ethene and ethyne were pH-dependent, and showed the reactivity order: 1,1-DCE > VC > *trans*-DCE > *cis*-DCE. Similar results have been obtained by Lesage and colleagues [146]. Dror and Schlautmann [147, 148] have demonstrated the importance of specific core metals and their solubility for the reactivity of a porphyrin complex.

Several research groups have investigated catalytic systems related to F_{430}. Gantzer and Wackett [149] have found different reactivity orders for the substrates examined: in the case of vitamin B_{12} (**9**) and coenzyme F_{430} (**10**), $CCl_4 > C_2Cl_4 > C_6Cl_6$, for hematin (**11**), $CCl_4 > C_6Cl_6 > C_2Cl_4$. TCE was dechlorinated stereoselectively to *cis*-1,2-dichloroethene with **9–11**. Arai and colleagues [150] catalyzed efficiently the hydrodehalogenation of cycloalkyl halides yielding cycloalkanes by [Ni(tmtaa)] (**12**; tmtaa = dianion of 6,8,15,17-tetramethyl-5,14-dihydro-dibenzo[b,i][1,4,8,11]tetraaza-cyclotetradecine) in combination with $NaBH_4$ or $NaBH(OMe)_3$ under mild conditions.

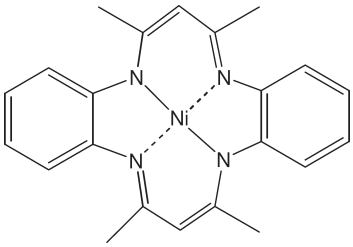

(**12**)

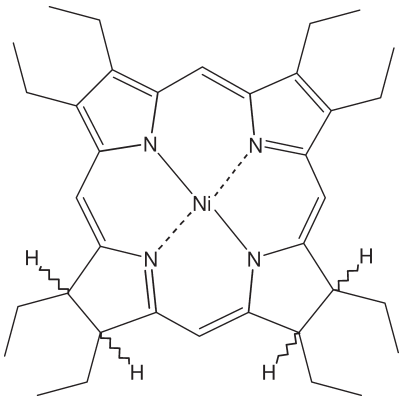

(**13**)

Stolzenberg's group [151–153] has studied the ability of various nickel(II) macrocycle and coordination complexes (e.g., **7**, **10**, and [Ni(OEiBC)] (**13**; OEiBC = octaethylisobacteriochlorin, mixture of isomers)). The facility of catalytic reduction of cyclohexyl bromide by $NaBH_4$ varied markedly with the structure of the ligands and the solvent composition. The highest TOFs (up to 70 h^{-1}) were obtained by the complex **7** (see Section 18.2.2) in diglyme/ethanol. Morra and coworkers [154] have shown that a combination of aquocobalamin or **10** and Fe(0) may effectively promote dehalogenation.

18.2.6
Electrochemical Reductions

Electrochemical methods are available for the direct dehalogenation of organic halides to a limited extent: fluorides and monochlorides are generally not reducible [1]. In the presence of transition-metal complexes as mediators (Med), however, the electrolysis of halocarbons (RX) can be performed more effectively and selectively under various conditions [155–158]. Mediated electroreduction is most efficient when the electron transfer step E° (Med/Med$^{\bullet-}$) is more negative than E° (RX/RX$^{\bullet-}$) [157] (cf. Section 18.4.1).

Pletcher and associates [155, 159, 160] have studied the electrochemical reduction of alkyl bromides in the presence of a wide variety of macrocyclic Ni(II) complexes. Depending on the substrate, the mediator, and the reaction conditions, mixtures of the dimer and the disproportionation products of the alkyl radical intermediate were formed (cf. Section 18.4.1). The same group [161] reported that traces of metal ions (e.g., Cu^{2+}) in the catholyte improved the current density and selectivity for several cathodic processes, and thus the conversion of trichloroacetic acid to chloroacetic acid. Electrochemical reductive coupling of organic halides was accompanied several times by hydrodehalogenation, especially when Ni complexes were used as mediators. In many of the reactions examined, dehalogenation of the substrate predominated over coupling [162–165].

The use of electrochemical methods for the destruction of aromatic organochlorine wastes has been reviewed [157]. Rusling, Zhang and associates [166, 167] have examined a stable, conductive, bicontinuous surfactant/soil/water microemulsion as a medium for the catalytic reduction of different pollutants. In soils contaminated with Arochlor 1260, 94% dechlorination was achieved by [Zn(pc)] (H_2pc = phthalocyanine) as a mediator with a current efficiency of 50% during a 12-h electrolysis. Conductive microemulsions have also been employed for the destruction of aliphatic halides and DDT in the presence of $[Co(bpy)_3]^{2+}$ (bpy = 2,2′-bipyridine) [168] or metal phthalocyanine tetrasulfonates [169].

Nünnecke and Voss [158] reduced aryl chlorides electrochemically in methanol using $[(bpy)NiCl_2]$ and $[(cyclam)NiCl_2]$ (cyclam = 1,4,8,11-tetraazacyclotetradecane) as mediators. More highly chlorinated benzenes were converted to chlorobenzene, whereas chlorodibenzofurans gave unsubstituted dibenzofuran as the major product. Due to the mediators, higher selectivities could be achieved, and the formation of hydrogenated products was completely suppressed. Peters and associates [170–174] have applied electrogenerated Co(I) salen (H_2salen = bis(salicylidene)ethylenediamine) or Co(I) salophen (H_2salophen = bis(salicylidene)-1,2-phenylenediamine) for the catalytic reduction of various halogenated substrates. In the case of 1,1,2-trichloro-1,2,2-trifluoroethane, cyclic voltammetry and controlled-potential electrolysis resulted in the formation of $CFCl{=}CF_2$ and CF_3CH_2F as main products, respectively, using DMF as a solvent and Bu_4NBF_4 as a supporting electrolyte [174]. Mugnier, Harwey and coworkers [175, 176] activated the C–Br and the C–I bonds by the cluster $[(dppm)_3Pd_3(CO)]^{2+}$ (dppm = bis(diphenylphosphino)-

methane). Catalytic dehalogenation of 2,3,4-tri-*O*-acetyl-5-thioxylopyranosyl bromide (Xyl-Br, both α- and β-isomers) provided Xyl-H as the major organic product at the potential of –0.9 V (versus SCE).

18.2.7
Miscellaneous Reducing Methods

Martin and associates [124, 125] have studied the dehalogenation of $CHCl_3$ in boiling methanol by Schiff-base complexes of some transition metals in the presence of TMEDA. The kinetics of chloride ion formation has been measured without characterizing the organic products. Nahar and Mukhedkar [126, 127] found that the reactivities of related Schiff-base complexes in the above reaction decreased in the order Pd > Pt > Ni > Cu > Zn.

Several researchers hydrogenolyzed – mostly activated – alkyl halides under carbonylation conditions and/or in the presence of metal carbonyls. Alper and coworkers debrominated bromomethyl ketones with $[Co_2(CO)_8]$ as a catalyst under phase-transfer conditions [177]. Brunet and Taillefer [178, 179] catalyzed the reduction of aryl iodides by *in-situ*-generated $K[HFe(CO)_5]$ in methanol (up to 18 cycles) under 0.1 MPa CO pressure at 60 °C; several functional groups were tolerated. An intriguing method has been developed by Cavinato and Toniolo [180] for the synthesis of γ-keto acids of the type $ArC(O)CH_2CH_2COOH$ via carbonylation-decarboxylation of $ArC(O)CH_2CHClCOOH$. The reactions were carried out in the presence of Pd(II) phosphine complexes, typically at 2–3 MPa CO and 100–120 °C in acetone/H_2O. When the same authors [181] attempted the carbonylation of 2-chlorocyclohexanone with the system $[(PPh_3)_2PdCl_2]/PPh_3/EtOH/H_2O$ (at 100 °C and 10 MPa CO, P/Pd = 2.5), a hydrogen transfer occurred leading to halogen/hydrogen exchange. Trabuco and Ford [182] have shown that homogeneous catalysts prepared from $RhCl_3$ in aqueous aromatic amines reduce C–Cl bonds under mild water gas shift conditions (100 °C and 0.1 MPa CO). In a 4-picoline/H_2O solvent mixture, 1,2-dichloroethane was transformed to ethene and ethane. An ambient temperature liquid carbonylmetallate, $[bmim][Co(CO)_4]$ ($[bmim]^+$ = 1-butyl-3-methylimidazolium cation), has been prepared by Dyson and coworkers [183]. The mixture of the ionic liquid and NaOH catalyzed the debromination of 2-bromoketones.

An interesting new homogeneous catalytic process was developed by Buijs [184] for the reductive dehalogenation of polychlorinated and -brominated aromatic hydrocarbons and ethers. Cu(I) benzoate catalyzed the reaction under Dow-Phenol conditions in the absence of air at 235 °C (Eq. (8)):

$$Ar'COOH + ArX + H_2O \xrightarrow[Cu(I)]{} Ar'OH + ArH + HX + CO_2 \,. \qquad (8)$$

Starichenko and colleagues [185–187] have studied the hydrogenolysis of polychloro- and polyfluoroaromatic compounds with the $[(N \cap N)NiCl_2]/Zn$ reducing system ($N \cap N$ = bpy or phen (phen = 1,10-phenanthroline)). Using DMF or DMA

solvents in the presence of water or NH_4Cl, the displacement of the Cl or F atoms by H took place at 50–70 °C. Interestingly, the systems catalyzed the regioselective *ortho*-hydrodefluorination of pentafluorobenzoic acid to 2,3,4,5-tetrafluorobenzoic and 3,4,5-trifluorobenzoic acids in high yields [187].

The applications of polyoxometalates in catalytic dehalogenation of halocarbons have been succinctly reviewed by Hill and coworkers [188]. This reaction involves the photocatalytic transformation of organic halides coupled with the oxidation of sacrificial organic reductants (secondary alcohols or tertiary amides) (Eq. (9)) [189, 190]:

$$3CCl_4 + 3\,(CH_3)_2CHOH + W_{10}O_{32}^{4-} \xrightarrow[hv]{} CHCl_3 + C_2Cl_6 + 3(CH_3)_2CO + H_2W_{10}O_{32}^{4-} \tag{9}$$

Very recently, Gkika and colleagues [191] realized the degradation of diversified pesticides (e.g., lindane) to CO_2, H_2O and the corresponding inorganic anions by photolysis in the presence of polyoxotungstates. A stable "hydrophobic vitamin B_{12}", heptamethyl cobyrinate perchlorate catalyzed efficiently the reduction of DDT using a visible light irradiation system containing a $[Ru(bpy)_3]Cl_2$ photosensitizer [192].

18.3 Mechanistic Considerations

The mechanisms of the homogeneous catalytic hydrodehalogenation have been examined by the following methods:

- spectroscopic investigations to detect intermediates in the reaction mixtures;
- isolation and characterization of possible intermediates or related model compounds;
- qualitative and quantitative analysis of the organic products;
- kinetic measurements; and
- systematic variation of the structure of the substrate and/or the catalyst. Theoretical investigations (e.g., MO calculations) have also been made.

In spite of the wide variety of substrates, hydrogen sources, and catalysts applied in the hydrodehalogenations of organic halides, some general statements can be made on the reaction pathways. We shall examine the following crucial steps of the dehalogenations: activation of the C–X bond, steps involving the reducing agents, and formation of the products.

18.3.1 Activation of the C–X Bond

18.3.1.1 Oxidative Addition

This type of activation may proceed by various mechanisms, which have been discussed exhaustively [2, 193, 194].

S_N2 and S_NAr Reactions In these reactions the metal atom attacks aliphatic or aromatic carbon bonded to X, respectively. A stronger nucleophilic metal as well as a better leaving group X (I > Br > Cl > F) facilitates, whereas steric hindrance in R slows these types of oxidative addition [193, 194]. S_NAr reactions are favored by electron-withdrawing substituents Y in the case of the substrates 4-YC_6H_4X [2]. S_N2 [27, 29, 89, 117, 180, 181] and S_NAr [31, 33, 62–67, 95, 100, 107–109] mechanisms have been suggested frequently for zerovalent d^{10} complexes such as $[L_nM]$ (M = Ni, Pd, Pt; L = tertiary phosphine; n = 2,3,4). For example:

$$[(PPh_3)_3Pd] + Ar - X \longrightarrow [(PPh_3)_2Pd(X)Ar] + PPh_3 \tag{10}$$

Products of S_NAr-type oxidative additions in some active Pd- or Ni-containing hydrodehalogenating systems have been isolated and characterized structurally (e.g., $[(PEt_3)_2NiCl(p\text{-}C_6Cl_5C_6Cl_4)]$ [31], $[(PPh_3)_2PdBr(3,4,5\text{-tribromo-2-thienyl})]$ [62]). The reactivity order Ni > Pd > Pt has been found for the oxidative addition of aryl halides. Steric and electronic properties, and the numbers of L as well as chelate effects, play an important role [65, 194–196]. For example, Pd(0) complexes of basic chelating phosphines react substantially more easily with chlorobenzenes than their nonchelating analogues (see Section 18.2.4) [2, 100, 196]. In contrast to $[L_nPd]$, oxidative addition of aryl halides on $[L_nNi]$ often proceed by single electron transfer mechanism [2, 197]. S_N2 and S_NAr types of oxidative addition as a step of the catalytic dehalogenation have also been proposed in the literature for low-valent Ti [40, 114], Zr(II) [115], Ru(II) [20, 74, 81, 98], Rh(I) [18, 29, 68, 81, 91] and Pt(II) [82, 83] complexes.

Atom Transfer Atom Transfer (AT) takes place typically in the case of d^7 complexes, which abstract the halogen atom from RX. The radical formed combines then with a second metal [193, 194]. A "classical" example of this mechanism is the hydrodehalogenation with cyanocobaltates(II) (see Section 18.2.1) [8, 9], but an analogous pathway was suggested recently for the Co(II) corrin-catalyzed dechlorination of CCl_4 in the presence of S^{2-}/cysteine as reductant (Eqs. (11)–(12)) [130]:

$$BCo^{II} + CCl_4 \rightarrow BCo^{III}Cl + CCl_3^{\bullet} \tag{11}$$

$$BCo^{II} + CCl_3^{\bullet} \rightleftarrows BCo^{III}CCl_3 \ldots \tag{12}$$

Single Electron Transfer A single electron transfer (SET) mechanism is often difficult to distinguish from an S_N2 reaction because the principal product of these two pathways is the same, apart from the stereochemistry at carbon (racemization instead of inversion). The radicals formed can recombine rapidly in a solvent cage (*inner-sphere ET*) [2, 193, 194]. The $[HFe(CO)_5]^-$-catalyzed deiodination of iodobenzene may serve as an example [179] (Eq. (13)).

$$[HFe(CO)_5]^- + PhI \rightarrow [HFe(CO)_5^{\bullet},\ PhI^{\bullet -}] \rightarrow [HFe(CO)_5^{\bullet},\ Ph^{\bullet}, I^-] \rightarrow [HFePh(CO)_5,\ I^-] \quad (13)$$

Coordinatively unsaturated complexes and those giving easily such species by ligand dissociation favor pathways related to that described in Eqs. (10) and (13). Coordinatively saturated complexes reduce halocarbons via *outer-sphere ET* [193, 194]. In cases of electrochemical dehalogenations, the species formed by one-electron reduction of the mediators on the cathode often react in this way [156, 157, 198]. For example (Eq. (14)) [157, 166]:

$$[Zn(pc)]^{\bullet -} + ArX \rightarrow [Zn(pc)] + [ArX]^{\bullet -} \rightarrow [Zn(pc)] + Ar^{\bullet} + X^- \quad (14)$$

A SET process has been postulated between Rh(III) oxidative adducts and an NAD(P)H model compound (cf. Section 18.2.4) [91]. Oxidative adducts formed by S_N2, S_NAr, or inner-sphere SET pathways may produce radicals by homolytic M–C bond cleavage [130, 155, 176, 199].

The transformation of the radical ($R^{\bullet}$) (which may escape also from the solvent cage) affords several products. Usually, RH is formed by hydrogen abstraction from the reducing agent or the solvent [36, 91, 150, 157, 169, 173, 179, 198], but dimerization [173, 194, 198], disproportionation (formation of RH and R(–H) simultaneously) [155, 158–160, 170], or rearrangement [43, 49, 55, 165, 194] can also take place. For example, the formation of the cyclized product in the reaction of Eq. (15) requires the intermediacy of an aryl radical [49, 55]:

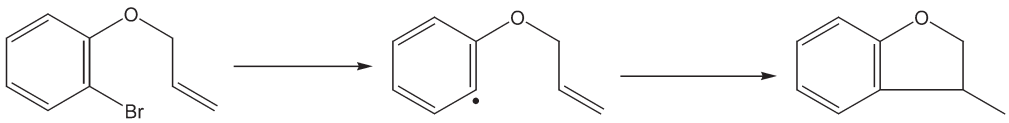

(15)

The C–F bond activations in C_6F_6 and related compounds with ruthenium [200, 201] and rhodium [17, 78, 201] complexes, for which an S_NAr mechanism is energetically unfavorable, have been explained by SET pathways. Both S_N2 [128, 129, 131, 170–174, 199, 202] and SET [130, 132, 199] mechanisms have been proposed for the reaction of Co(I) complexes with alkyl and vinyl halides.

Carbanions may be formed in the electrochemical reductions of aryl halides [157, 158] (Eq. (16)):

$$Ar^{\bullet} + Med^{\bullet -} \rightarrow Ar^{-} + Med\,, \tag{16}$$

and of *gem*-di- or trihaloaliphatics [174, 198], as well as in the hydrogenolysis of the latter type of substrates with corrinoids and related complexes [130, 199, 203]. The cleavage of a halide ion from a polyhalocarbanion (or from its complex) affords (di)halocarbene (or its complex) which will be transformed depending on the reaction conditions [130, 203, 204]. Equation (17) shows some of the possible transformations of CCl_4 in the presence of corrins [130]:

$$CCl_4 \xrightarrow[\text{-}Cl^-]{2e^-} : CCl_3^- \xrightarrow[\text{-}Cl^-]{} : CCl_2 \xrightarrow{H_2O} CO + 2HCl \ldots \tag{17}$$

Radical Chain Mechanism This mechanism also requires a coordinatively unsaturated metal and the presence of a radical initiator $Q^{\bullet}$ (trace of O_2, hν, etc.). Such a pathway has been proposed for a Ni(II) complex-catalyzed dehalogenation of polyhaloarenes [60], and it occurs frequently in the stoichiometric C–X activations with early transition-metal complexes (see [205–207]).

$$Q^{\bullet} + [Cp_2^{*}ZrH_2] \rightarrow [Cp_2^{*}Zr^{\bullet}H_2] + QH \tag{18}$$

$$[Cp_2^{*}Zr^{\bullet}H_2] + RF \rightarrow [Cp_2^{*}ZrHF] + R^{\bullet} \tag{19}$$

$$[Cp_2^{*}ZrH_2] + R^{\bullet} \rightarrow [Cp_2^{*}Zr^{\bullet}H_2] + RH \tag{20}$$

In addition to initiation (Eq. (18)) and propagation (Eqs. (19) and (20)), termination steps are also possible (resulting in, for example, dimers of $R^{\bullet}$). Radical traps inhibit this type of oxidative addition [194].

18.3.1.2 *σ*-Bond Metathesis

This is the simultaneous breaking and formation of bonds to the metal with a four-membered ring transition state (Eq. (21)):

(21)

This concerted process may operate in the case of d^0 early metal complexes where the oxidative addition is forbidden [194]. Nevertheless, it was postulated also in the interaction of a dihalo-ruthenium(II) intermediate and a hydrosilane [74].

18.3.1.3 S_N2 Attack of the Hydride Ligand

Another route not involving an M–C bond formation has been suggested recently for some water-soluble Ir(III) complexes [112]. The hydride pushes the halide from the carbon atom directly by an S_N2 way with the **14** transition state.

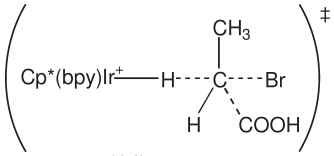

(**14**)

18.3.1.4 1,2-Insertion

1,2-Insertion of the C=C bond into an M–H bond precedes frequently the C–X bond activation in halogenated alkenes. Such a pathway has been suggested for the cobalamin-mediated dechlorinations of *cis*- and *trans*-DCE, as well as VC with Ti(III) citrate as a reducing agent [141].

18.3.2 Reaction Steps Involving the Reducing Agents

The double role of the reducing agents in homogeneous hydrodehalogenations is:

(i) transformation of the transition-metal complex into a state capable of the activation of the substrate;
(ii) formation of the M–H bond to cleave – directly or indirectly – the C–X bond of the substrate [3, 208].

Processes corresponding to both of these roles are not involved by all means in each catalytic cycle. They may also take place in one step [24, 74]. Process (i) is needed generally to transfer – mostly to reduce – the precursor complex into a catalytically active form. Reactions related to that of Eq. (22) (L = PCy_3, P*i*-Pr_3 [13]) are promoted by the addition of bases [2, 20, 24, 28, 29, 45, 47, 65, 106, 108]:

$$[L_2Rh(H)Cl_2] + H_2 + NaOH \rightarrow [L_2Rh(H)_2Cl] + NaCl + H_2O \qquad (22)$$

In outer-sphere SET reductions (e.g., in electrochemical dehalogenations), hydrogen abstraction by $R^{\bullet}$ leads to the product RH (i.e., no step related to (ii) is required to occur). Process (ii) follows generally the activation of the substrate in the proposed hydrodehalogenation cycles, but we know also of opposite examples [77, 82, 106, 112].

The nature of the M–H bond-forming step, (ii), in a given catalytic cycle depends strongly on the reducing agent used. Dihydrogen [13, 14, 17, 20, 24, 29] and hydrosilane [78, 81, 82] react mostly by *oxidative addition* [193, 209, 210]. For example, the product of the reaction in Eq. (23) – which is involved in an

actual "working" catalytic cycle – has been isolated and characterized by its X-ray structure (L = PMe_3) [78]:

$$[L_3RhC_6F_5] + (EtO)_3SiH \rightarrow [L_3RhH(C_6F_5)Si(OEt)_3] \tag{23}$$

The *heterolytic activation* of H_2 has been considered in systems containing basic ligands such as pyridine [18, 29, 209]. *Transmetalation* proposed for Bu_3SnH as a reductant resulted in the transformation of the Pd–Br bond into Pd–H [89].

Simple and complex metal hydrides as strong nucleophiles easily displace the halide bound to the central atom of the catalyst by *hydride transfer* [40, 45, 62–67]. Alcoholates [97, 98, 100, 106, 108], formates [93, 96, 100, 112], and metal alkyls [114, 115, 117] also substitute the halogen atom on the transition metal, after which the hydrogen transfer takes place from the alkoxy, formato and alkyl ligands formed [3, 211]. A good model for the halobenzene reduction catalyzed by the $[L_nPd]/HCOO^-$ system [98, 100, 112] has been found by Alper and coworkers [211]. Decomposition of the organopalladium formato complex, $[(PPh_3)_2PdPh(HCOO)]$, gave benzene, indicating the intermediacy of a Pd–H species (Eq. (24), L = PPh_3) [211]:

$$[L_2PdPh(HCOO)] \xrightarrow[-CO_2]{\Delta} [L_2PdPh(H)] \xrightarrow[-RH]{} [L_2Pd] \tag{24}$$

18.3.3
Formation of the Product

The product-forming steps of dehalogenations by free radical pathways were discussed earlier (see Section 18.3.1.1). In non-radical mechanisms, the dehalogenated products (RH) will be formed mostly by reductive elimination [193, 194]; however, concerted processes lead directly from RX to RH (see Sections 18.3.1.2 and 18.3.1.3).

Catalytic dehalogenation cycles with a binuclear reductive elimination step have not yet been reported, but many examples are known with a single metal. The RH product eliminates easily from d^8 metals (Ni(II), Pd(II)) or d^6 metals (Ru(II), Rh(III)) (Eq. (25)) [196]. This reaction is believed to go by a three-center transition state [193, 194, 212]:

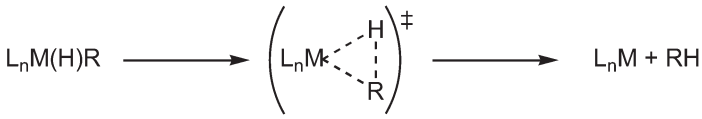

(25)

In the case of R = aryl with electron-withdrawing substituents, however, kinetic measurements indicated a rapid, reversible η^2-arene complex formation followed by the rate-determining loss of the arene [213].

Since the reaction in Eq. (26) is generally the last step of the catalytic cycle, the [L_nM] fragment should survive long enough to react with the substrate again. The presence of an excess of phosphine ligand can facilitate the reductive elimination and can also stabilize the [L_nM] species [3, 194].

18.4 Concluding Remarks

Our knowledge regarding transition metal-mediated (catalytic and stoichiometric) hydrodehalogenation has advanced significantly during the past two decades. One favorable aspect of this progress is that such progress has been achieved mainly in the activation of the more stable C–Cl and C–F bonds. In the former case, environmental concerns have dominated, including the detoxification of chlorocarbon pollutants by biomimetic, electrochemical and other methods in solving problems caused by chemical industrial processes. From the synthetic viewpoint, the most intriguing results have been achieved in fluorine/hydrogen exchange, as in addition to stoichiometric transformations a number of catalytic processes have also been developed. In the near future, a step-up in the efficiency of the homogeneous hydrodehalogenation – that is, increasing the turnovers under the mildest possible reaction conditions – appears to be a real possibility, both in environmental and synthetic applications.

Acknowledgments

The authors gratefully acknowledge the Hungarian Academy of Sciences (Grant nos. OTKA T 031934/2000, T 037817/2002) for financial support of these studies. O. B. S. also thanks the Ministry of Education (Hungary) for a PhD fellowship.

Abbreviations

γ-AMP	γ-aminopropyl
BNAH	*N*-benzyl-1,4-dihydronicotinamide
CFC	chlorofluorocarbon
DCE	1,2-dichloroethene
DMF	dimethylformamide
DMSO	dimethyl sulfoxide
HCFC	hydrochlorofluorocarbon
NHC	*N*-heterocyclic carbene
OEiBC	octaethylisobacteriochlorin
PCB	polychlorinated biphenyl
PCE	tetrachloroethene

PHMS	polymethylhydrosiloxane
SCE	standard calomel electrode
SET	single electron transfer
TCE	trichloroethene
TMEDA	*N,N,N′,N′*-tetramethylethylenediamine
TOF	turnover frequency
TON	turnover number
TPPMS	*m*-sulfophenyldiphenylphosphine
VC	vinyl chloride

References

1 A. R. Pinder, *Synthesis* **1980**, *6*, 425.
2 V. V. Grushin, H. Alper, *Chem. Rev.* **1994**, *94*, 1047.
3 H. D. Kaesz, R. B. Saillant, *Chem. Rev.* **1972**, *72*, 231.
4 B. R. James, *Homogeneous Hydrogenation*, John Wiley & Sons, New York, **1973**.
5 M. Hudlicky, In: B. M. Trost, I. E. Fleming (Eds.), *Comprehensive Organic Synthesis, Volume 8*, Pergamon, Oxford, **1991**, p. 895.
6 O. Hutzinger, S. Safe, V. Zitko, *The Chemistry of PCBs*, CRC Press, Cleveland, OH, **1974**.
7 Z. Ainbinder, L. E. Manzer, M. J. Nappa, in: G. Ertl, H. Knözinger (Eds.) *Handbook of Heterogeneous Catalysis, Vol. 4*, VCH, Weinheim, **1997**, p. 1677.
8 J. Kwiatek, J. K. Seyler, *Adv. Chem.* **1968**, *70*, 207.
9 B. R. James, *Homogeneous Hydrogenation*, John Wiley & Sons, New York, **1973**, p. 139.
10 J. Rocek, V. Svata, L. Leseticky, *Collection Czechoslov. Chem. Commun.* **1985**, *50*, 1244.
11 C. J. Love, F. J. McQuillin, *J. Chem. Soc., Perkin I Trans.* **1973**, 2509.
12 P. Kvintovics, B. Heil, J. Palágyi, L. Markó, *J. Organomet. Chem.* **1978**, *148*, 311.
13 V. V. Grushin, H. Alper, *Organometallics* **1991**, *10*, 1620.
14 R. J. Young, V. V. Grushin, *Organometallics* **1999**, *18*, 294.
15 E. L. Setti, O. A. Mascaretti, *J. Org. Chem.* **1989**, *54*, 2233.
16 D. T. Ferrughelli, I. T. Horváth, *J. Chem. Soc. Chem. Commun.* **1992**, 806.
17 M. Aizenberg, D. Milstein, *J. Am. Chem. Soc.* **1995**, *117*, 8674.
18 B. L. Edelbach, W. D. Jones, *J. Am. Chem. Soc.* **1997**, *119*, 7734.
19 A. Angeloff, J. J. Brunet, P. Legars, D. Neibecker, D. Souyri, *Tetrahedron Lett.* **2001**, *42*, 2301.
20 M. E. Cucullu, S. P. Nolan, T. R. Belderrain, R. H. Grubbs, *Organometallics* **1999**, *18*, 1299.
21 J. Blum, A. Rosenfeld, F. Gelman, H. Schumann, D. Avnir, *J. Mol. Catal. A-Chem.* **1999**, *146*, 117.
22 H. Yang, H. R. Gao, R. J. Angelici, *Organometallics* **1999**, *18*, 2285.
23 M. L. Kantam, A. Rahman, T. Bandyopadhyay, Y. Haritha, *Synth. Commun.* **1999**, *29*, 691.
24 S. Xie, E. M. Georgiev, D. M. Roundhill, *J. Organomet. Chem.* **1994**, *482*, 39.
25 O. J. Cho, I. M. Lee, K. Y. Park, H. S. Kim, *J. Fluorine Chem.* **1995**, *71*, 107.
26 H. S. Kim, O. J. Cho, I.M. Lee, S. P. Hong, C. Y. Kwag, B. S. Ahn, *J. Mol. Catal. A-Chem.* **1996**, *111*, 49.
27 R. Vilar, S. E. Lawrence, D. M. P. Mingos, D. J. Williams, *J. Chem. Soc. Chem. Commun.* **1997**, 285.
28 R. Vilar, D. M. P. Mingos, *J. Organomet. Chem.* **1998**, *557*, 131.
29 A. Sisak, O. B. Simon, K. Nyíri, *J. Mol. Catal. A-Chem.* **2004**, *213*, 163.
30 R. A. Egli, *Helv. Chim. Acta* **1968**, *51*, 2090.
31 C. M. King, R. B. King, N. K. Bhattacharyya, M. G. Newton, *J. Organomet. Chem.* **2000**, *600*, 63, and references therein.

32 J. P. Collman, L. S. Hegedus, J. R. Norton, R. G. Finke, *Principles and Applications of Organotransition Metal Chemistry*, University Science Books, Mill Valley, CA, **1987**, p. 673, and references therein.
33 C. Carfagna, A. Musco, R. Pontellini, *J. Mol. Catal.* **1989**, *54*, L23.
34 C. Carfagna, A. Musco, R. Pontellini, *J. Mol. Catal.* **1989**, *57*, 23.
35 C. Qian, D. Zhu, Y. Gu, *J. Mol. Catal.* **1990**, *63*, L1.
36 Z. W. Xie, C. T. Qian, Y. Z. Huang, *J. Organomet. Chem.* **1991**, *412*, 61.
37 H. Q. Li, S. J. Liao, Y. Xu, *Chem. Lett.* **1996**, 1059.
38 Y. K. Zhang, S. J. Liao, Y. Xu, D. R. Yu, Q. Shen, *Synth. Commun.* **1997**, *27*, 4327.
39 U. M. Dzhemilev, R. L. Gaisin, *Bull. Acad. Sci. USSR Div. Chem. Sci.* **1988**, *37*, 2332.
40 U. M. Dzhemilev, R. L. Gaisin, A. A. Turchin, N. R. Khalikova, I. P. Baikova, G. A. Tolstikov, *Bull. Acad. Sci. USSR Div. Chem. Sci.* **1990**, *39*, 967.
41 U. M. Dzhemilev, R. L. Gaisin, A. A. Turchin, G. A. Tolstikov, *Bull. Acad. Sci. USSR Div. Chem. Sci.* **1991**, *40*, 2084.
42 A. R. Abbott, J. Thompson, L. C. Thompson, K. S. Knight, *Transition Met. Chem.* **2003**, *28*, 305.
43 S. T. Lin, J. A. Roth, *J. Org. Chem.* **1979**, *44*, 309.
44 J. A. Roth, S. R. Dakoji, R. C. Hughes, R. E. Carmody, *Environ. Sci. Technol.* **1994**, *28*, 80.
45 A. Scrivanti, B. Vicentini, V. Beghetto, G. Chessa, U. Matteoli, *Inorg. Chem. Commun.* **1998**, *1*, 246.
46 B. Meunier, *J. Organomet. Chem.* **1981**, *204*, 345.
47 Y. M. Liu, J. Schwartz, *J. Org. Chem.* **1994**, *59*, 940.
48 C. L. Cavallaro, Y. M. Liu, J. Schwartz, P. Smith, *New J. Chem.* **1996**, *20*, 253–257.
49 Y. M. Liu, J. Schwartz, *Tetrahedron* **1995**, *51*, 4471.
50 H. G. Woo, B. H. Kim, S. J. Song, *Bull. Korean Chem. Soc.* **1999**, *20*, 865.
51 B. H. Kim, H. G. Woo, W. G. Kim, S. S. Yun, T. S. Hwang, *Bull. Korean Chem. Soc.* **2000**, *21*, 211.
52 K. Fuchibe, T. Akiyama, *Synlett* **2004**, 1282.
53 I. Simunek, M. Kraus, *Collection Czechoslov. Chem. Commun.* **1973**, *38*, 1786.
54 J. Vcelák, J. Hetflejs, *Collection Czechoslov. Chem. Commun.* **1994**, *59*, 1645.
55 M. Czakóová, J. Hetflejs, J. Vcelák, *React. Kinet. Catal. Lett.* **2001**, *72*, 277.
56 J. Hetflejs, M. Czakoova, R. Rericha, J. Vcelák, *Chemosphere* **2001**, *44*, 1521.
57 V. I. Isaeva, Z. L. Dykh, L. I. Lafer, V. I. Yakerson, V. Z. Sharf, *Bull. Russ. Acad. Sci. Div. Chem. Sci.* **1992**, *41*, 49.
58 V. Z. Sharf, V. I. Isaeva, Y. V. Smirnova, Z. L. Dykh, G. N. Baeva, A. N. Zhilyaev, T. A. Fomina, I. B. Baranovskii, *Russ. Chem. Bull.* **1995**, *44*, 64.
59 V. F. Dovganyuk, V. Z. Sharf, L. G. Saginova, I. I. Antokolskaya, L. I. Bolshakova, *Bull. Acad. Sci. USSR Div. Chem. Sci.* **1989**, *38*, 777.
60 M. Stiles, *J. Org. Chem.* **1994**, *59*, 5381.
61 Y. Xie, S. C. Ng, T. S. A. Hor, H. S. O. Chan, *J. Chem. Res. (S)* **1996**, *3*, 150.
62 Y. Xie, S. C. Ng, B. M. Wu, F. Xue, T. C. W. Mak, T. S. A. Hor, *J. Organomet. Chem.* **1997**, *531*, 175.
63 Y. Xie, B.M. Wu, F. Xue, S. C. Ng, T. C. W. Mak, T. S. A. Hor, *Organometallics* **1998**, *17*, 3988.
64 B. Wei, S. H. Li, H. K. Lee, T. S. A. Hor, *J. Mol. Catal. A-Chem.* **1997**, *126*, L83.
65 B. Wei, T. S. A. Hor, *J. Mol. Catal. A-Chem.* **1998**, *132*, 223.
66 S. H. Li, H. S. Ngew, S. O. H. Chan, S. C. Ng, H. K. Lee, T. S. A. Hor, *Environ. Monitor. Assess.* **1997**, *44*, 481.
67 L. Lassova, H. K. Lee, T. S. A. Hor, *J. Org. Chem.* **1998**, *63*, 3538.
68 B. H. Lipshutz, T. Tomioka, S. S. Pfeiffer, *Tetrahedron Lett.* **2001**, *42*, 7737.
69 Y. H. Zhu, C. B. Ching, K. Carpenter, R. Xu, S. Selvaratnam, N. S. Hosmane, J. A. Maguire, *Appl. Organomet. Chem.* **2003**, *17*, 346.
70 R. Boukherroub, C. Chatgilialoglu, G. Manuel, *Organometallics* **1996**, *15*, 1508.
71 D. Villemin, B. Nechab, *J. Chem. Res. (S)* **2000**, *9*, 432.
72 E. C. Chukovskaia, N. A. Kuzmina, R. K. Freidlina, *Bull. Acad. Sci. USSR Div. Chem. Sci.* **1967**, *16*, 1031.
73 L. N. Kiseleva, N. A. Rybakova, R. K. Freidlina, *Bull. Acad. Sci. USSR Div. Chem. Sci.* **1986**, *35*, 10302.

74 H. Kono, H. Matsumoto, Y. Nagai, *J. Organomet. Chem.* **1978**, *148*, 267.
75 I. Pri-Bar, O. Buchman, *J. Org. Chem.* **1986**, *51*, 734.
76 R.E. Maleczka, R.J. Rahaim, R.R. Teixeira, *Tetrahedron Lett.* **2002**, *43*, 7087.
77 R.J. Rahaim, R.E. Maleczka, *Tetrahedron Lett.* **2002**, *43*, 8823.
78 M. Aizenberg, D. Milstein, *Science* **1994**, *265*, 359.
79 M.A. Esteruelas, J. Herrero, F.M. Lopez, M. Martin, L.A. Oro, *Organometallics* **1999**, *18*, 1110.
80 J. Diaz, M.A. Esteruelas, J. Herrero, L. Moralejo, M. Olivan, *J. Catal.* **2000**, *195*, 187.
81 M.A. Esteruelas, J. Herrero, M. Olivan, *Organometallics* **2004**, *23*, 3891.
82 F. Stöhr, D. Sturmayr, U. Schubert, *Chem. Commun.* **2002**, 2222.
83 U. Schubert, J. Pfeiffer, F. Stöhr, D. Sturmayr, S. Thompson, *J. Organomet. Chem.* **2002**, *646*, 53.
84 I. Terstiege, R.E. Maleczka, *J. Org. Chem.* **1999**, *64*, 342.
85 D.P. Curran, *Synthesis* **1988**, 417.
86 J. Uenishi, R. Kawahama, O. Yonemitsu, *J. Org. Chem.* **1996**, *61*, 5716.
87 J. Uenishi, R. Kawahama, Y. Shiga, O. Yonemitsu, J. Tsuji, *Tetrahedron Lett.* **1996**, *37*, 6759.
88 J. Uenishi, R. Kawahama, A. Tanio, S. Wakabayashi, O. Yonemitsu, *Tetrahedron* **1997**, *53*, 2439.
89 J. Uenishi, R. Kawahama, O. Yonemitsu, *J. Org. Chem.* **1998**, *63*, 8965.
90 R. Grigg, T.R.B. Mitchell, S. Sutthivaiyakit, *Tetrahedron Lett.* **1979**, *12*, 1067.
91 S. Yasui, K. Nakamura, M. Fujii, A. Ohno, *J. Org. Chem.* **1985**, *50*, 3283.
92 H. Imai, T. Nishiguchi, M. Tanaka, K. Fukuzumi, *J. Org. Chem.* **1977**, *42*, 2309.
93 N.A. Cortese, R.F. Heck, *J. Org. Chem.* **1977**, *42*, 3491.
94 T. Okamoto, S. Oka, *Bull. Chem. Soc. Jpn.* **1981**, *54*, 1265.
95 A. Zask, P. Helquist, *J. Org. Chem.* **1978**, *43*, 1619.
96 P. Helquist, *Tetrahedron* **1978**, *22*, 1913.
97 Y. Sasson, G.L. Rempel, *Synthesis* **1975**, 448.
98 J. Blum, S. Shtelzer, P. Albin, *J. Mol. Catal.* **1982**, *16*, 167.
99 Y. Migron, J. Blum, *J. Mol. Catal.* **1983**, *22*, 187.
100 Y. Ben-David, M. Gozin, M. Portnoy, D. Milstein, *J. Mol. Catal.* **1992**, *73*, 173.
101 I.P. Beletskaya, A.G. Bessmertnykh, R. Guilard, *Tetrahedron Lett.* **1999**, *40*, 6393.
102 S.H. Leung, D.G. Edington, T.E. Griffith, J.J. James, *Tetrahedron Lett.* **1999**, *40*, 7189.
103 X. Bei, A. Hagemayer, A. Volpe, R. Saxton, H. Turner, A.S. Guram, *J. Org. Chem.* **2004**, *69*, 8626.
104 J.R. Jones, W.J.S. Lockley, S.Y. Lu, S.P. Thompson, *Tetrahedron Lett.* **2001**, *42*, 331.
105 M.A. Atienza, M.A. Esteruelas, M. Fernandez, J. Herrero, M. Olivan, *New J. Chem.* **2001**, *25*, 775.
106 K. Fujita, M. Owaki, R. Yamaguchi, *J. Chem. Soc. Chem. Commun.* **2002**, 2964.
107 M.S. Viciu, G.A. Grasa, S.P. Nolan, *Organometallics* **2001**, *20*, 3607.
108 O. Navarro, H. Kaur, P. Mahjoor, S.P. Nolan, *J. Org. Chem.* **2004**, *69*, 3173.
109 C. Desmarets, S. Kuhl, R. Schneider, Y. Fort, *Organometallics* **2002**, *21*, 1554.
110 E. Paetzold, G. Oehme, *J. Prakt. Chem.* **1993**, *335*, 181.
111 A.C. Bényei, S. Lehel, F. Joó, *J. Mol. Catal. A-Chem.* **1997**, *116*, 349 and references therein.
112 S. Ogo, N. Makihara, Y. Kaneko, Y. Watanabe, *Organometallics* **2001**, *20*, 4903.
113 W.L. Respess, C. Tamborski, *J. Organomet. Chem.* **1969**, *18*, 263.
114 E. Colomer, R. Corriu, *J. Organomet. Chem.* **1974**, *82*, 367.
115 R. Hara, W.H. Sun, Y. Nishihara, T. Takahashi, *Chem. Lett.* **1997**, 1251.
116 R. Hara, K. Sato, W.H. Sun, T. Takahashi, *J. Chem. Soc. Chem. Commun.* **1999**, 845.
117 K. Yuan, W.J. Scott, *J. Org. Chem.* **1990**, *55*, 6188.
118 K.A. Agrios, M. Srebnik, *J. Org. Chem.* **1993**, *58*, 6908.
119 D. Necas, M. Kotora, I. Cisarova, *Eur. J. Org. Chem.* **2004**, 1280.
120 L.N. Zanaveskin, V.A. Averyanov, Y.A. Treger, *Uspekhi Khimii* **1996**, *65*, 667.

121 L. Ukrainczyk, M. Chibwe, T. J. Pinnavaia, S. A. Boyd, *Environ. Sci. Technol.* **1995**, *29*, 439.
122 B. R. James, *Homogeneous Hydrogenation*, John Wiley & Sons, New York, **1973**, p. 193, and references therein.
123 L. Wilputte-Steinert, *Transition Met. Chem.* **1978**, *3*, 172.
124 D. F. Martin, *J. Inorg. Nucl. Chem.* **1975**, *37*, 1941.
125 D. F. Martin, K. A. Hewes, S. G. Maybury, B. B. Martin, *Inorg. Chim. Acta* **1986**, *111*, 5.
126 C. T. Nahar, A. J. Mukhedkar, *J. Indian Chem. Soc.* **1980**, *57*, 961.
127 C. T. Nahar, A. J. Mukhedkar, *J. Indian Chem. Soc.* **1981**, *58*, 343.
128 U. E. Krone, R. K. Thauer, H. P. C. Hogenkamp, *Biochemistry* **1989**, *28*, 4908.
129 U. E. Krone, R. K. Thauer, H. P. C. Hogenkamp, K. Steinbach, *Biochemistry* **1991**, *30*, 2713.
130 T. A. Lewis, M. J. Morra, P. D. Brown, *Environ. Sci. Technol.* **1996**, *30*, 292.
131 P. C. Chiu, M. Reinhard, *Environ. Sci. Technol.* **1995**, *29*, 595.
132 N. Assaf-Anid, K. Y. Lin, *J. Environ. Engineering-ASCE* **2002**, *128*, 94.
133 P. C. Chiu, M. Reinhard, *Environ. Sci. Technol.* **1996**, 30, 1882.
134 T. A. Lewis, A. Paszczynski, S. W. Gordon-Wylie, S. Jeedigunta, C. H. Lee, R. L. Crawford, *Environ. Sci. Technol.* **2001**, *35*, 552.
135 J. A. Perlinger, J. Bushmann, W. Angst, R. P. Schwarzenbach, *Environ. Sci. Technol.* **1998**, *32*, 2431.
136 J. Buschmann, W. Angst, R. P. Schwarzenbach, *Environ. Sci. Technol.* **1999**, *33*, 1015.
137 B. D. Habeck, K. L. Sublette, *Appl. Biochem. Biotechnol.* **1995**, *51/52*, 747.
138 D. R. Burris, C. A. Delcomyn, M. H. Smith, A. L. Roberts, *Environ. Sci. Technol.* **1996**, *30*, 3047.
139 D. R. Burris, C. A. Delcomyn, B. L. Deng, L. E. Buck, K. Hatfield, *Environ. Toxicol. Chem.* **1998**, *17*, 1681.
140 G. Glod, W. Angst, C. Holliger, R. P. Schwarzenbach, *Environ. Sci. Technol.* **1997**, *31*, 253.
141 G. Glod, U. Brodmann, W. Angst, C. Holliger, R. P. Schwarzenbach, *Environ. Sci. Technol.* **1997**, *31*, 3154.
142 Y. H. Kim, E. R. Carraway, *Environ. Technol.* **2002**, *23*, 1135.
143 J. K. Gotpagar, E. A. Grulke, D. Bhattacharyya, *J. Hazardous Materials* **1998**, *62*, 243.
144 E. J. O'Loughlin, D. R. Burris, C. A. Delcomyn, *Environ. Sci. Technol.* **1999**, *33*, 1145.
145 H. Ma, E. J. O'Loughlin, D. R. Burris, *Environ. Sci. Technol.* **2001**, *35*, 717.
146 S. Lesage, S. Brown, K. Millar, *Environ. Sci. Technol.* **1998**, *32*, 2264.
147 I. Dror, M. A. Schlautman, *Environ. Toxicol. Chem.* **2003**, *22*, 525.
148 I. Dror, M. A. Schlautman, *Environ. Toxicol. Chem.* **2004**, *23*, 252.
149 C. J. Gantzer, L. P. Wackett, *Environ. Sci. Technol.* **1991**, *25*, 715.
150 T. Arai, K. Kashitani, H. Kondo, S. Sakari, *Bull. Chem. Soc. Jpn.* **1994**, *67*, 705.
151 G. K. Lahiri, L. J. Schussel, A. M. Stolzenberg, *Inorg. Chem.* **1992**, *31*, 4991.
152 G. K. Lahiri, A. M. Stolzenberg, *Inorg. Chem.* **1993**, *32*, 4409.
153 M. Stolzenberg, Z. Zhang, *Inorg. Chem.* **1997**, *36*, 593.
154 M. J. Morra, V. Borek, J. Koolpe, *J. Environ. Quality* **2000**, *29*, 706.
155 J. Y. Becker, J. B. Kerr, D. Pletcher, R. Rosas, *J. Electroanal. Chem.* **1981**, *117*, 87.
156 C. P. Andrieux, A. Merz, J. M. Saveant, R. Tomabogh, *J. Am. Chem. Soc.* **1984**, *106*, 1957.
157 N. J. Bunce, S. G. Serica, J. Lipkowski, *Chemosphere* **1997**, *35*, 2719.
158 D. Nünnecke, J. Voss, *Acta Chem. Scand.* **1999**, *53*, 824.
159 C. Gosden, D. Pletcher, *J. Organomet. Chem.* **1980**, *186*, 401.
160 C. Gosden, J. B. Kerr, D. Pletcher, R. Rosas, *J. Electroanal. Chem.* **1981**, *117*, 101.
161 D. Pletcher, A. J. Sheridan, *Electrochim. Acta* **1998**, *43*, 3105.
162 M. Troupel, Y. Rollin, S. Sibille, J. Perichon, *J. Organomet. Chem.* **1980**, *202*, 435.

163 Y. Rollin, M. Troupel, D.G. Tuck, J. Perichon, *J. Organomet. Chem.* **1986**, *303*, 131.

164 A. Bakac, J.H. Espenson, *J. Am. Chem. Soc.* **1986**, *108*, 719.

165 M.A. Fox, D.A. Chandler, C. Lee, *J. Org. Chem.* **1991**, *56*, 3246.

166 S.P. Zhang, J.F. Rusling, *Environ. Sci. Technol.* **1993**, *27*, 1375.

167 S.P. Zhang, J.F. Rusling, *Environ. Sci. Technol.* **1995**, *29*, 1195.

168 J.F. Rusling, G.N. Kamau, *J. Electroanal. Chem.* **1985**, *187*, 355.

169 J.F. Rusling, S. Schweizer, S. Zhang, G.N. Kamau, *Colloids and Surfaces A: Physicochemical and Engineering Aspects* **1994**, *88*, 41.

170 K.S. Alleman, D.G. Peters, *J. Electroanal. Chem.* **1998**, *451*, 121.

171 K.S. Alleman, D.G. Peters, *J. Electroanal. Chem.* **1999**, *460*, 207.

172 C. Ji, D.G. Peters, J.A. Karty, J.P. Reilly, M.S. Mubarak, *J. Electroanal. Chem.* **2001**, *516*, 50.

173 A.J. Moad, L.J. Klein, D.G. Peters, J.A. Karty, J.P. Reilly, *J. Electroanal. Chem.* **2002**, *531*, 163.

174 J.D. Persinger, J.L. Hayes, L.J. Klein, D.G. Peters, J.A. Karty, J.P. Reilly, *J. Electroanal. Chem.* **2004**, *568*, 157.

175 D. Brevet, D. Lucas, H. Cattey, F. Lemaitre, Y. Mugnier, P.D. Harvey, *J. Am. Chem. Soc.* **2001**, *123*, 4340.

176 D. Brevet, Y. Mugnier, F. Lemaitre, D. Lucas, S. Samreth, P.D. Harvey, *Inorg. Chem.* **2003**, *42*, 4909.

177 H. Alper, K.D. Logbo, H. des Abbayes, *Tetrahedron Lett.* **1977**, *33*, 2861.

178 J.J. Brunet, M. Taillefer, *J. Organomet. Chem.* **1988**, *348*, C5.

179 J.J. Brunet, D. Demontauzon, M. Taillefer, *Organometallics* **1991**, *10*, 341.

180 G. Cavinato, L. Toniolo, *J. Mol. Catal.* **1993**, *78*, 121.

181 G. Cavinato, L. Toniolo, *J. Mol. Catal. A-Chem.* **1999**, *143*, 325.

182 E. Trabuco, P.C. Ford, *J. Mol. Catal. A-Chem.* **1999**, *148*, 1.

183 R.J.C. Brown, P.J. Dyson, D.J. Ellis, T. Welton, *J. Chem. Soc. Chem. Commun.* **2001**, 1862.

184 W. Buijs, *Catal. Today* **1996**, *27*, 159.

185 N.Y. Adonin, V.F. Starichenko, *Mendeleev Commun.* **2000**, *2*, 60.

186 D.V. Trukhin, N.Y. Adonin, V.F. Starichenko, *Russ. J. Org. Chem.* **2000**, *36*, 1227.

187 N.Y. Adonin, V.F. Starichenko, *J. Fluor. Chem.* **2000**, *101*, 65.

188 C.L. Hill, M. Kozik, J. Winkler, Y.Q. Hou, C.M. Prosser-McCartha, *Adv. Chem. Ser.* **1993**, *238*, 243.

189 D. Sattari, C.L. Hill, *J. Chem. Soc. Chem. Commun.* **1990**, 634.

190 D. Sattari, C.L. Hill, *J. Am. Chem. Soc.* **1993**, *115*, 4649.

191 E. Gkika, P. Kormali, S. Antonaraki, D. Dimoticali, E. Papaconstantinou, A. Hiskia, *Int. J. Photoenergy* **2004**, *6*, 227.

192 H. Shimakoshi, M. Tokunaga, T. Baba, Y. Hisaeda, *J. Chem. Soc. Chem. Commun.* **2004**, *16*, 1806.

193 J.P. Collman, L.S. Hegedus, J.R. Norton, R.G. Finke, *Principles and Applications of Organotransition Metal Chemistry*, University Science Books, Mill Valley, CA, **1987**, p. 278.

194 R.H. Crabtree, *The Organometallic Chemistry of the Transition Metals*, 2nd edn. John Wiley & Sons, New York, **1994**, p. 140.

195 C. Amatore, E. Carré, A. Jutand, M.A. M'Barki, *Organometallics* **1995**, *14*, 1818.

196 M. Portnoy, D. Milstein, *Organometallics* **1993**, *12*, 1665.

197 T.T. Tsou, J.K. Kochi, *J. Am. Chem. Soc.* **1979**, *101*, 6319.

198 L. Eberson, M. Ekström, *Acta Chem. Scand. B* **1987**, *41*, 41.

199 K.M. McCauley, S.R. Wilson, W.A. van der Donk, *Inorg. Chem.* **2002**, *41*, 393.

200 M.K. Whittlesey, R.N. Perutz, M.H. Moore, *J. Chem. Soc. Chem. Commun.* **1996**, 787.

201 J. Burdeniuc, B. Jedlicka, R.H. Crabtree, *Chem. Ber./Recueil* **1997**, *130*, 145.

202 G.N. Schrauzer, E. Deutsch, *J. Am. Chem. Soc.* **1969**, *91*, 3341.

203 K.L. Brown, X. Zou, M. Richardson, W.P. Henry, *Inorg. Chem.* **1991**, *30*, 4834.

204 K.L. Brown, G.Z. Wu, *Organometallics* **1993**, *12*, 496.

205 R. J. Kinney, W. D. Jones, R. G. Bergman, *J. Am. Chem. Soc.* **1978**, *100*, 7902.

206 S. C. Kao, M. Y. Darensbourg, *Organometallics* **1984**, *3*, 646.

207 W. D. Jones, *J. Chem. Soc. Dalton Trans.* **2003**, *21*, 3991 and references therein.

208 J. P. Collman, L. S. Hegedus, J. R. Norton, R. G. Finke, *Principles and Applications of Organotransition Metal Chemistry*, University Science Books, Mill Valley, CA, **1987**, p. 89.

209 J. P. Collman, L. S. Hegedus, J. R. Norton, R. G. Finke, *Principles and Applications of Organotransition Metal Chemistry*, University Science Books, Mill Valley, CA, **1987**, p. 286.

210 R. H. Crabtree, *The Organometallic Chemistry of the Transition Metals*, 2nd edn. John Wiley & Sons, New York, **1994**, p. 229.

211 V. V. Grushin, C. Bensimon, H. Alper, *Organometallics* **1995**, *14*, 3259.

212 R. A. Michelin, S. Faglia, P. Uguagliati, *Inorg. Chem.* **1983**, *22*, 1831.

213 A. D. Selmeczy, W. D. Jones, R. Osman, R. N. Perutz, *Organometallics* **1995**, *14*, 5677

214 T. Imamoto, T. Takeyama, T. Kusumoto, *Chem. Lett.* **1985**, 1491.

215 S. M. H. Tabaei, C. U. Pittman, Jr., K. T. Mead, *J. Org. Chem.* **1992**, *57*, 6669.

19
Homogeneous Catalytic Hydrogenation of Polymers

Garry L. Rempel, Qinmin Pan, and Jialong Wu

19.1
General Introduction

Chemical modification of polymers via catalysis is of great importance as it provides an efficient synthetic route for the production of novel polymers with desirable physical properties. It also allows the introduction of functional groups that are often inaccessible by conventional polymerization techniques. One of the most important chemical modifications is the hydrogenation of unsaturated carbon-carbon double bonds in polymers. Basically, there are two technical routes for the hydrogenation of polymers: homogeneous and heterogeneous. This chapter reviews research and process development with respect to homogeneous catalytic hydrogenation of diene-based polymers.

19.1.1
Diene-Based Polymers

Diene polymers refer to polymers synthesized from monomers that contain two carbon-carbon double bonds (i.e., diene monomers). Butadiene and isoprene are typical diene monomers (see Scheme 19.1). Butadiene monomers can link to each other in three ways to produce *cis*-1,4-polybutadiene, *trans*-1,4-polybutadiene and 1,2-polybutadiene, while isoprene monomers can link to each other in four ways. These dienes are the fundamental monomers which are used to synthesize most synthetic rubbers. Typical diene polymers include polyisoprene, polybutadiene and polychloroprene. Diene-based polymers usually refer to diene polymers as well as to those copolymers of which at least one monomer is a diene. They include various copolymers of diene monomers with other monomers, such as poly(butadiene-styrene) and nitrile butadiene rubbers. Except for natural polyisoprene, which is derived from the sap of the rubber tree, *Hevea brasiliensis*, all other diene-based polymers are prepared synthetically by polymerization methods.

The Handbook of Homogeneous Hydrogenation.
Edited by J.G. de Vries and C.J. Elsevier
Copyright © 2007 WILEY-VCH Verlag GmbH & Co. KGaA, Weinheim
ISBN: 978-3-527-31161-3

Scheme 19.1 The monomers butadiene and isoprene.

19.1.2
Hydrogenation of Diene-Based Polymers

Polymers obtained by polymerizing or copolymerizing conjugated dienes are widely utilized for commercial purposes. These polymers have residual double bonds in their polymer chains. A limited amount of these residual double bonds are advantageously utilized for vulcanization, yet the residual double bonds have a disadvantage in that they lack the stability to resist weather conditions, oxidation, and ozone. Such disadvantages are more severe for block copolymers of conjugated dienes and vinyl aromatic hydrocarbons when used as thermoplastic elastomers. Moreover, the disadvantages are even more severe when the polymers are used as modifiers and transparent impact-resistant materials for styrenic resins and olefinic resins, or when they are used to make parts of equipment for utilization in solvent/oily/high-temperature environments. This deficiency in stability can be notably improved by hydrogenating the conjugated diene polymers in order to eliminate the residual double bonds that persist within the polymer chains.

With the availability of a large number of unsaturated polymers of differing microstructures, the selective reduction of carbon-carbon double bonds offers a means of producing a wide variety of specialty polymers. By reducing the unsaturation level of the polymers, their physical properties – such as tensile strength, elongation, thermal stability, light stability and solvent resistance – may be optimized. For example, the removal of the C=C unsaturation in polybutadiene (PB) provides a tough semi-crystalline polymer similar to linear polyethylene or an elastomer such as poly(ethylene-*co*-butylene), depending on the relative levels of units with 1,2 or 1,4 structure (Scheme 19.2 a). Hydrogenation of a styrene-butadiene-styrene triblock copolymer (SBS) with a moderate amount of 1,2-addition units in the center block yields a copolymer with a poly(ethylene-*co*-butylene) center segment (Scheme 19.2 b). This modified polymer has greatly increased thermal and oxidative stability, together with processability and serviceability at higher temperature, by virtue of its poly(ethylene-*co*-butylene) center block. The catalytic hydrogenation of acrylonitrile-butadiene rubber (NBR) (Scheme 19.2 c) is an especially important commercial example, resulting in its tougher and more stable derivative, hydrogenated nitrile butadiene rubber (HNBR), which has been widely used in the automotive industry.

Numerous methods have been employed for hydrogenating conjugated diene-based polymers in the presence of suitable and effective hydrogenation catalysts. Typical hydrogenation catalysts can be classified into two types: heterogeneous and homogeneous catalysts.

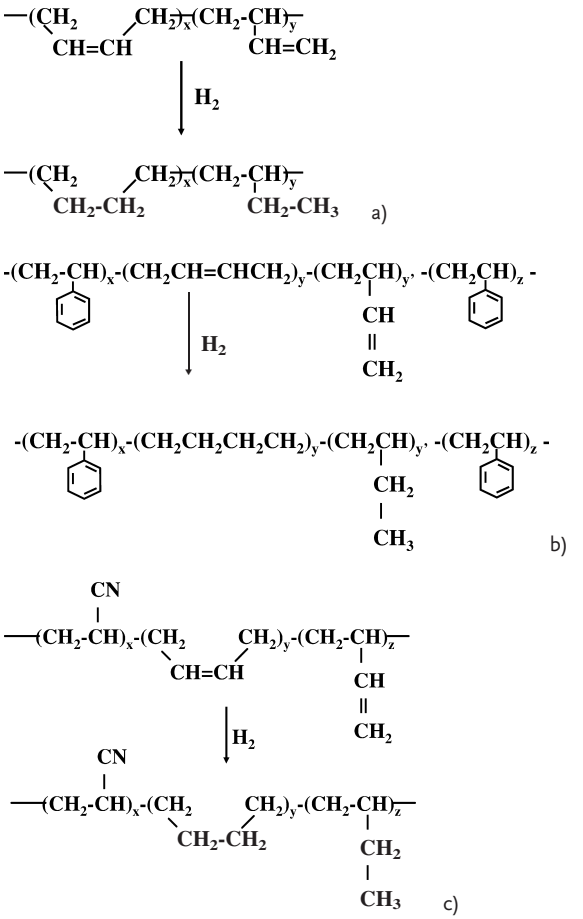

Scheme 19.2 (a) Hydrogenation of polybutadiene.
(b) Hydrogenation of the copolymer of butadiene and styrene.
(c) Hydrogenation of acrylonitrile butadiene rubber.

19.1.2.1 **Heterogeneous Catalysts**

Heterogeneous catalysts, which are not soluble in the diene-based polymers to be hydrogenated, have involved metals such as nickel, platinum, or palladium deposited onto supports such as activated carbon, silica, alumina, or calcium carbonate. Hydrogenation using a heterogeneous catalyst is described as follows. First, the polymer to be hydrogenated is dissolved in a suitable solvent, after which the polymer is brought into contact with hydrogen in the presence of a heterogeneous catalyst. During hydrogenation of the polymer, contact between the polymer and catalyst is difficult due to the influence of the high viscosity of the reaction system and the influence of steric hindrance of the polymer chain. In addition the polymer, once hydrogenated, tends to remain on the

surface of the catalyst and to interfere with subsequent access to active centers of the catalyst with the non-hydrogenated polymer.

The hydrogenation also requires higher temperature and pressure, and hence decomposition of the polymer and gelation of the reaction system often tends to occur. For the hydrogenation of a copolymer of a conjugated diene with a vinyl aromatic hydrocarbon, even hydrogenation of the aromatic ring portion may take place to some extent due to the high temperature and hydrogen pressure. Thus, it is often difficult to selectively hydrogenate only the double bonds in the conjugated diene portion of the polymer. Although widely used in industry, heterogeneous catalysts generally have lower activity than homogeneous catalysts, and usually a larger amount of heterogeneous catalyst is required. Furthermore, since the polymer may be strongly adsorbed onto the heterogeneous catalyst, it is impossible to completely remove the catalyst from the hydrogenated polymer solution, although the separation of catalyst from heterogeneous catalytic systems is usually easier than from homogeneous ones.

19.1.2.2 **Homogeneous Catalysts**

Homogeneous catalysts, which are soluble in the solutions of the diene-based polymers to be hydrogenated, include:

- Ziegler-type catalysts obtained from an organic acid salt or acetylacetone salt of nickel, cobalt, iron, or chromium which reacts with a reducing agent such as an organic aluminum compound.
- Metallocene complexes.
- Organometallic catalysts containing Ru-, Rh-, Os-, Ir-, Pd-complexes, etc.

The reaction operation using a homogeneous catalyst is similar to that using heterogeneous catalysts, except for the nature of the contact between the catalyst and the polymer. First, the polymer to be hydrogenated is dissolved in a suitable solvent. The catalyst can be prepared in a solution or solid form. Then, the catalyst is mixed with the polymer solution in the presence of hydrogen. During hydrogenation of the polymer, contact between the polymer and catalyst is much more effective compared to a heterogeneous catalyst system. Therefore, compared to the heterogeneous catalyst, the homogeneous catalyst generally shows higher activity, and only a small amount of catalyst enables hydrogenation to be effected at mild temperature and low pressure. In addition, homogeneous catalysts usually have high selectivity. When appropriate hydrogenation conditions are selected, it is possible to preferentially hydrogenate the conjugated diene portion of a copolymer of a conjugated diene with a vinyl aromatic hydrocarbon, while not hydrogenating the aromatic ring portion. Compared to heterogeneous catalysis, the disadvantage of homogeneous catalysis is that the catalyst recovery from a homogeneous system is often much more difficult than from a heterogeneous system. Therefore, in recent years, a new class of catalysts termed “heterogenized homogeneous catalysts” have received significant attention and have become an area of extensive research interest.

This chapter provides a review of the progress in reaction art, reactor techniques and process technology with respect to homogeneous catalytic hydrogenation of diene-based polymers, in accordance with the homogeneous hydrogenation theme of this handbook.

19.2 Reaction Art

19.2.1 Catalyst Techniques

Although the overall polymer hydrogenation reaction is exothermic, a high activation energy prevents it from taking place under normal conditions in the absence of a catalyst. An efficient catalyst is needed to circumvent this restriction and it is in fact the key in realizing a successful homogeneous hydrogenation. Metals from Group VIIIB (e.g., platinum, palladium, nickel, rhodium, ruthenium, iridium, osmium) and from Group IV (e.g., titanium) are among the most widely used hydrogenation catalysts, and they usually can be activated for hydrogenation at a temperature of less than 200 °C.

An early US Patent [1] disclosed that the catalyst $RhHCO(PPh_3)_3$ was effective for a limited degree of hydrogenation of PB. However, because of the very low reaction temperature and hydrogen pressure employed (25 °C, 2 atm, 3 h), the concentration of catalyst used was about 1100 μM, which was very high compared to the level now used in industrial polymer hydrogenation processes. Moreover, the hydrogenation degree was very low where mainly some of the vinyl C=Cs were hydrogenated. However, it indicated there was some degree of efficacy of the rhodium catalyst in hydrogenating PB. The low hydrogenation efficiency was successfully overcome for the hydrogenation of diene-based polymers by increasing the hydrogenation temperature to 110 °C or higher [2], in which a much lower catalyst concentration was used and a hydrogenation degree of 99.95% was achieved.

Research in this area over the past 30 years has focused on the design of efficient catalytic systems and on improving the hydrogenation operations. Besides rhodium-based species, a variety of catalysts has been investigated for the homogeneous hydrogenation of diene-based polymers, including Os-, Ru-, Ir-, Ni- and Ti-based catalysts. The patents most relevant to the hydrogenation technology of diene-based polymers are summarized in Table 19.1.

Two critical reviews with respect to polymer hydrogenation have been published [63, 64]. Among the investigated catalysts, Wilkinson's catalyst ($RhCl(PPh_3)_3$) is still considered as the most preferable for the hydrogenation of diene-based polymers as it provides high selectivity towards the olefin double bonds with minimized crosslinking problems. The only concern for using the rhodium catalyst is its relatively high cost.

In order to overcome the catalyst recovery problem in homogeneous hydrogenation operations, the significant enhancement of catalyst activity has been pur-

Table 19.1 Outline of major patents with respect to catalysts for diene-based polymer hydrogenation.

Catalyst	Polymer	Representative example [a)]	Assignee	Reference (Year)
$RhHCO(PPh_3)_3$; $RuHCl(PPh_3)_3$	PB	PB in toluene (2.3 wt.%); $RhHCO(PPh_3)_3$: 5 g per 100 g PB; P_{H2}: 0.2 MPa; *T*: 25 °C; *t*: 3 h; Conversion: 10.4%	The Firestone Tire & Rubber Company (Akron, USA)	1 (1976)
$RhH(PPh_3)_4$; $RhCl(PPh_3)_3$/epoxidized soybean oil ($R^1OCH_2CH(OR^2)CH_2)R^3$)	NBR, SBS, methacrylic acid-acrylonitrile – butadiene copolymer	NBR in chlorobenzene (2.5 wt.%); $RhH(PPh_3)_4$: 1 g per 100 g NBR; PPh_3: 10 g per 100 g NBR; P_{H2}: 2.8 MPa; *T*: 160 °C; *t*: 1 h; Conversion: >99%	Polysar Limited/Bayer Inc. (Sarnia, Canada)	2 (1984) 3 (1985) 4 (2004)
$OsHX(CO)(L)(PR_3)_2$, where X: Cl, BH_4 or CH_3COO; L: O_2 or no ligand; R: cyclohexyl or isopropyl	NBR, styrene butadiene random copolymer (SBR), methacrylic acid-acrylonitrile – butadiene copolymer	NBR in chlorobenzene (2.4 wt.%); $OsHCl(CO)(P(cyclohexyl)_3)_2$: 0.25 g per 100 g NBR; P_{H2}: 2.07 MPa; *T*: 130 °C; *t*: 1 h; Conversion: 99.3%	University of Waterloo (Waterloo, Canada)	5 (1996)
$RuX_m(L^1)(L^2)_n$, where X: H, Halogen or $SnCl_3$, etc.; L^1: H, Halogen or substituted indenyl, etc.; L^2: phosphane or arsane, etc.	NBR	NBR in butanone (9.7 wt.%); $RuCl_2(PPh_3)_3$: 0.16 g per 100 g NBR; P_{H2}: 14 MPa; *T*: 130 °C; *t*: 4 h; Conversion: 99.7%	Bayer Aktiengesellschaft (Leverkusen, Germany)	6 (1986) 7 (1989) 8 (1991)

Table 19.1 (continued)

Catalyst	Polymer	Representative example [a)]	Assignee	Reference (Year)
$HRuCl(CO)(PPh_3)_3$; $RuCl_2(PPh_3)_3$; $RuH_2(CO)(PPh_3)_3$, etc.	NBR, SBS, styrene butadiene diblock copolymer (SB), acrylonitrile-isoprene copolymer	NBR in chlorobenzene (1.7 wt.%); $HRuCl(CO)(PPh_3)_3$: 0.8 g per 100 g NBR; C_2H_5COOH: 0.2 g per 100 g NBR; P_{H2}: 4.1 MPa; *T*: 140 °C; *t*: 1.8 h; Conversion: >99%	University of Waterloo (Waterloo, Canada)	9 (1989) 10 (1989) 11 (1991)
$HRuCl(CO)(PCy_3)_3$, etc./ Amine(RNH_2)	NBR	NBR in chlorobenzene (1.7 wt.%); $HRuCl(CO)(PCy_3)_3$: 0.05 g per 100 g NBR; octylamine: 0.39 g per 100 g NBR; P_{H2}: 5.5 MPa; *T*: 145 °C; *t*: 5 h; Conversion: >99%	University of Waterloo (Waterloo, Canada)	12 (1991)
$HRuCl(CO)(PPh_3)_3$, etc.	Ring-opening polymers	Poly(8-methyl-8-methoxy-carbonyltetracyclo-3-dodecene) in toluene (20 wt.%); $HRuCl(CO)(PPh_3)_3$: 0.01 g per 100 g polymer; P_{H2}: 4.0 MPa; *T*: 160 °C; *t*: 4 h; Conversion: 99.7%	Japan Synthetic Rubber Co., Ltd. (Tokyo, Japan)	13 (1993)
$RuCl_2(PPh_3)_4$, etc.	Ring-opening metathesis polymers	Polymer in tetrahydrofuran (11.4 g L^{-1}); $RuCl_2(PPh_3)_4$: 0.05 g per 100 g polymer; Et_3N: 0.021 g per 100 g polymer; P_{H2}: 8.3 MPa; *T*: 165 °C; *t*: 5 h; Conversion: 100%	Mitsui Chemicals Inc. (Tokyo, Japan)	14 (1999)

Table 19.1 (continued)

Catalyst	Polymer	Representative example [a)]	Assignee	Reference (Year)
Bimetallic complexes, Rh/Ru ($RhCl(PPh_3)_3/RuCl_2(PPh_3)_3$), etc.	NBR	NBR in xylene (7 g per 100 mL); $RhCl(PPh_3)_3/RuCl_2(PPh_3)_3$ (Rh : Ru = 3 : 1, mole ratio): 0.4 g per 100 g NBR, PPh_3: 2 g per g catalyst; P_{H2}: 0.8 MPa; *T*: 145 °C; *t*: 4 h; Conversion: 98.5%	Nantex Industry Co., Ltd., (Taiwan)	15 (2000)
Nickel acetylacetonate ($(CH_3COCH{=}C(O\text{-})CH_3)_2Ni$)/ *p*-nonylphenol ($C_9H_{19}C_6H_4OH$)/ *n*-butyllithium ($CH_3(CH_2)_3Li$)	Polyisoprene, EPDM	Polyisoprene in hexane (2.5 wt.%); Catalyst (Nickel acetylacetonate: *p*-nonylphenol: *n*-butyllithium = 8 : 8 : 25, mol ratio): 4 mmol nickel per 100 mL solution; P_{H2}: 0.34 MPa; *T*: room temperature; *t*: 0.8 h; Conversion: 78%	Uniroyal Inc. (New York, USA)	16 (1976)
Cobalt or nickelbenzohydroxamic acid ($(C_6H_5CONH\text{-}O\text{-})_2M$, M = Co, Ni)/ organoaluminum (R_3Al, R = alkyl)	PB, SBR	SBR in hexane (10 wt.%); Catalyst (nickel benzohydroxamic acid : triisobutyl aluminum = 1 : 3, mol ratio): 0.01 mmol Ni per g SBR; P_{H2}: 1.4 MPa; *T*: 180 °C; *t*: 2 h; Conversion: 99%	The Firestone Tire & Rubber Company (Akron, USA)	17 (1976)

Table 19.1 (continued)

Catalyst	Polymer	Representative example [a)]	Assignee	Reference (Year)
Nickel-2-ethylhexanoate ($(CH_3(CH_2)_3CH(C_2H_5)CO_2)_2Ni$)/ alkylaluminum ($R_3Al$, R = alkyl) or alkylalumoxane ($(\text{-}Al(R)O\text{-})_n$) or hydrocarbyl-substituted silicon alumoxane $(Et_2AlO)_2SiO_2$, etc.)	SBS, Styrene-butadiene-isoprene copolymers	SBS in cyclohexane (18 wt.%); Catalyst (nickel-2-ethylhexanoate/triethyl aluminum, Al : Ni = 2.2 : 1, atomic ratio): 0.05 g Ni per 90 g SBS; P_{H2}: 6.2 MPa; *T*: 90 °C; *t*: 3 h; Conversion: 93.4%	Shell Oil Company (Houston, USA)	18 (1991) 19 (1991) 20 (1991) 21 (1989) 22 (1991)
Nickel acetylacetonate ($(CH_3COCH{=}C(O\text{-})CH_3)_2Ni$)/alkylaluminum ($R_3Al$, R = alkyl)	SBR	SBR (0.9 L BD + 0.5 L ST anionic polymerization) in 4.8 L cyclohexane; Catalyst: 0.3 g nickel acetylacetonate (in 9 mL toluene) + 11 mL aluminum triisobutyl solution (10% in hexane); H_2O: 14 mol per mol Ni; P_{H2}: 1 MPa; *T*: 25–30 °C; *t*: 1 h; Conversion: 93.4%	BASF Aktiengesellschaft (Germany)	23 (1980)
Nickel bis(acetylacetonate) or 2-ethylhexanoic acid nickel ($(CH_3COCH{=}C(O\text{-})CH_3)_2Ni$ or $(CH_3(CH_2)_3CH(C_2H_5)CO_2)_2Ni$)/ alkylaluminum ($R_3Al$, R = alkyl)	Styrene-isoprene-styrene block copolymer (SIS), polyisoprene, PB	PB in cyclohexane (20 wt.%); Catalyst (2-ethylhexanoic acid nickel/triisobutyl aluminum, Ni : Al = 1 : 3): 0.74 mol Ni per 100 g PB; P_{H2}: 0.98 MPa; *T*: 70–80 °C; *t*: 6 h; Conversion: 97%	Kuraray Co., Ltd. (Tokyo, Japan)	24 (2002) 25 (2002) 26 (2003)

Table 19.1 (continued)

Catalyst	Polymer	Representative example [a)]	Assignee	Reference (Year)
Nickel or Cobalt acetylacetonate ($(CH_3COCH{=}C(O\text{-})CH_3)_nM$, n = 2,3; M = Ni, Co)/alkylaluminum (R_3Al, R = alkyl); titanium compounds (Cp_2TiCl_2, etc.)/organoaluminum (R_3Al, etc., R = alkyl) or organolithium (RLi, R = alkyl)	Metathesis polymers	Poly(dicyclopentadiene) in cyclohexane (7.6 wt.%); Catalyst (cobalt(III) acetylacetonate: triisobutyl-aluminum = 1.9 : 4.2, weight ratio): 0.2 g per g polymer; P_{H2}: 0.98 MPa; *T*: 60 °C; *t*: 0.5 h; Conversion: 99.9%	Nippon Zeon Co., Ltd (Tokyo, Japan)	27 (1996)
Cobalt-2-ethylhexanoate ($(CH_3(CH_2)_3CH(C_2H_5)CO_2)_2Co$)/ alkylaluminum ($R_3Al$, R = alkyl)	Polymers containing ketone groups	SBS (include ketone groups) in cyclohexane (~5 wt.%); Catalyst (cobalt-2-ethylhexanoate: triethyl aluminum = 1 : 3.9, weight ratio): [Co] = 880 ppm (added in increments); P_{H2}: 3.45 MPa; *T*: 70–90 °C; *t*: 6 h; Conversion: 78%	Shell Oil Company (Houston, USA)	28 (1996) 29 (1997)
Palladium-2-ethylhexanoate ($(CH_3(CH_2)_3CH(C_2H_5)CO_2)_2Pd$)/ organoaluminum ($(\text{-}Al(CH_3)O\text{-})_n$)	NBR	NBR in methylethyl ketone (5 wt.%); Catalyst (palladium-2-ethylhexanoate/methyl alumoxane, Al : Pd = 0.7 : 1, atomic ratio): 8.5 mmol Pd per lb NBR; P_{H2}: 6.2 MPa; *T*: 60 °C; *t*: 2 h; Conversion: 90%	Shell Oil Company (Houston, USA)	30 (1989) 31 (1989)

Table 19.1 (continued)

Catalyst	Polymer	Representative example [a)]	Assignee	Reference (Year)
Titanocene ($Cp_2Ti(C_6H_2(R^1)(R^2)(R^3))C_6H_2(R^4)(R^5)(R^6)$, $R^1 \sim R^6$: alkyls or hydrogen atoms)	PB, polyisoprene, styrene/isoprene or butadiene copolymers	SBS in cyclohexane (5 wt.%); Catalyst (di-*p*-tolyl-bis(η-cyclopentadienyl) titanium): 4 μM; P_{H2}: 0.49 MPa; *T*: 90 °C; *t*: 2 h; Conversion: 99%	Asahi Kase Kogyo Kabushiki Kaisha (Osaka, Japan)	32 (1987)
Titanocene ($Cp_2Ti(R^1)R^2$, R^1 and R^2: halogen atoms, aryloxy groups, etc.)/alkyloxy lithium (R^3OLi, R^3: a hydrocarbon group, etc.); Titanocene or zirconocene $Cp_2M^1(R^1)R^2$, M^1: Ti or Zr; R^1 and R^2: halogen atoms, aryloxy groups, etc.)/organoalkali (M^2OR^4, M^2: alkali metal, R^4: alkyl group, etc.)/organoaluminum or organomagnesium ($M^2M^3R^5_n$, M^2: alkali metal; M^3: Al or Mg; n: 3, 4; R^5: halogen, alkyl, aryl or alkoxy group, etc.)	SB, SBS, SIS	SB in cyclohexane (20 wt.%); Catalyst (bis(cyclopentadienyl) titanium dichloride: 2,6-di-butyl-4-methylphenoxylithium = 1 : 6, mole ratio): 25 μmol Ti per 100 g SB; P_{H2}: 0.98 MPa; *T*: 70 °C; *t*: 1 h; Conversion: 99%	Japan Synthetic Rubber Co. Ltd. (Tokyo, Japan)	33 (1990) 34 (1992)
Titanocene ($Cp_2Ti(R^1)R^2$, etc., R^1 and R^2: halogen atoms, aryloxy groups, etc.) or Tebbe's reagent 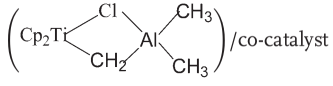 and/or promoter (LiR, R: alkyl, etc.)	Styrene, butadiene and/or isoprene living copolymers	SBS in cyclohexane (18 wt.%); Catalyst (2,5-diphenylphospholyl (cyclopentadienyl) titanium dichloride): 0.5 mg per g SBS; P_{H2}: 1 MPa; *T*: 70 °C; *t*: 3 h; Conversion: 100%	Shell Oil Company (Houston, USA)	35 (1992) 36 (1992) 37 (1992) 38 (1992) 39 (1993) 40 (1994) 41 (1998) 42 (1999) 43 (1999) 44 (2002)

Table 19.1 (continued)

Catalyst	Polymer	Representative example [a)]	Assignee	Reference (Year)
Titanocene or Zirconocene ($(A)(E)M(R^4)^+$, A and E represent: 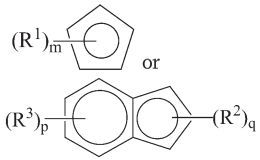 R^1–R^4: halogens, hydrocarbonyl groups, etc.)/non-coordinating stable anion ($B(Ar)_4^-$, Ar: C_6F_5, etc.)	Polyisoprene	Polyisoprene in bromobenzene (8 wt.%); Catalyst ($Cp^*Cp(tBu)ZrMe_2$: $(Ph_3C)(B(C_6F_5)_4$ = 1.1 : 1, mole ratio): 60 μmol per g polymer; P_{H2}: 0.1 MPa; *T*: not available; *t*: 0.75 h; Conversion: 100%	Shell Oil Company (Houston, USA)	45 (1999)
Rare earth (Sm) metallocene (Cp_2SmR)/organolithium (LiR, etc.)	SBS	SBS in cyclohexane (5 wt.%); Catalyst (*sec*-butyllithium: $(Cp^*_2SmH)_2$ = 7.5 : 1, mole ratio): 2.6 mmol per 100 g SBS; P_{H2}: 3.45 MPa; *T*: 40–66 °C; *t*: 3 h; Conversion: 81%	Shell Oil Company (Houston, USA)	46 (1992)
Rare earth (Sm) metallocene ($(C_5R_5)_2SmX$, X is an inert substituent capable of replacement by hydrogen)	PB	PB in cyclohexane (1.4 wt.%); Catalyst (bis(pentamethylcyclopentadienyl) (bis(trimethylsilyl)methyl) samarium: 0.018 g per g PB; P_{H2}: 2.8 MPa; *T*: 90 °C; *t*: 3 h; Conversion: 99.5%	The Dow Chemical Company (Midland, USA)	47 (1990)

Table 19.1 (continued)

Catalyst	Polymer	Representative example [a)]	Assignee	Reference (Year)
Monocyclopentadienyl titanium compound (R_nCpSmL_m, R: anion or dianion non-Cp group; L: neutral ligand)	SBR, PB	PB in cyclohexane (~10 wt.%); Catalyst (pentamethylcyclopenta-dienyl tribenzyl titanium): 0.66 mmol per 100 g PB; P_{H2}: 2.1 MPa; *T*: 55 °C; *t*: 24.6 h; Conversion: 71%	The Dow Chemical Company (Midland, USA)	48 (1998)
Metallocene (CpCp′MD, M: metal; D: conjugated, neutral diene)	Unsaturated polymers		The Dow Chemical Company (Midland, USA)	49 (2002)
Monocyclopentadienyl titanium compound ($CpTi(R^1)(R^2)R^3$, $R^1 \sim R^3$: non-Cp groups)	SBS, SBR, PB, SIS	SBS in cyclohexane (12.5 wt.%); Catalyst ($CpTiCl_2(\text{-}OC_5NH_4)$): 0.4 mmol per 100 g SBS; P_{H2}: 0.98 MPa; *T*: 80 °C; *t*: 3 h; Conversion: 99.4%	Korea Kumho Petrochemical Co., Ltd. (Seoul, Rep. of Korea)	50 (1999) 51 (1999) 52 (2000) 53 (2002)
Titanocene ($Cp_2Ti(PhOR)_2$ or Cp_2TiR_2)	PB, SBS, SB	SBS in cyclohexane (2 wt.%); Catalyst ($Cp_2Ti(4\text{-}CH_3OPh)_2$): 4 mmol per 100 g SBS; P_{H2}: 0.59 MPa; *T*: 85 °C; *t*: 2 h; Conversion: 91%	Repsol Quimica S.A. (Madrid, Spain)	54 (1996)
Zirconocene (Cp_2ZrR_2, R: halogen or alkyl group, etc.)/ alumoxane ($(\text{-}Al(CH_3)O\text{-})_n$, etc.)	SBS (star-form)	SBS in toluene (5.5 wt%); Catalyst (Cp_2ZrCl_2/methylalumoxane, Zr:Al = 1:118, atomic ratio): 3.08 mmol Zr per 100 g SBS; P_{H2}: 2 MPa; *T*: 90 °C; *t*: 0.65 h; Conversion: 80%	Neste Oy (Provoo, Finland)	55 (1998)

Table 19.1 (continued)

Catalyst	Polymer	Representative example[a)]	Assignee	Reference (Year)
Cobaltocene or Nickellocene (Cp_2MR_2, M: metal)/Organic lithium (LiR, etc.)	SBS	SBS in cyclohexane (5.8 wt.%); Catalyst (bis(cyclopentadienyl) cobalt(II)/butyllithium): 4.1 mmol Co per 100 g SBS; P_{H2}: 2.45 MPa; *T*: 80 °C; *t*: 2 h; Conversion: 99.2%	Taiwan Synthetic Rubber Corporation (Taiwan)	56 (1998)
Titanocene (Cp_2TiR_2)/silyl hydride ($RSiO\text{-}(SiH(R)O\text{-})_nSiR_3$, etc.)	SBS	SBS in cyclohexane (13 wt.%); Catalyst (Cp_2TiMe_2 : ethylhydrocyclosiloxane = 1 : 1.5, mole ratio): 0.08 mmol per 100 g SBS; P_{H2}: 1.4 MPa; *T*: 60 °C; *t*: 1 h; Conversion: 99%	Industrial Technology Research Institute (Taiwan), Chi Mei Co. (Taiwan)	57 (2001)
Titanocene (Cp_2TiR_2)/organoderivate (MR_2, M: Mg or Zn)/modifier (ROR, etc.) or another organoderivate (AlR_3)	Styrene, butadiene and/or isoprene copolymers	SBS in cyclohexane (12.5 wt.%); Catalyst (bis-cyclopentadienyltitanium dichloride: 1,2-di-*n*-butoxy-ethane: diisobutyl magnesium = 1 : 0.1 : 0.25, mole ratio): 0.19 mmol per 100 g SBS; P_{H2}: 0.49 MPa; *T*: 70 °C; *t*: 1 h; Conversion: >98%	Enichem S.p.A. (Milan, Italy)	58 (1999) 59 (2001)
Titanocene (Cp_2TiR_2)	SBS, SIS	SBS in cyclohexane (12.5 wt.%); Catalyst ($Cp_2Ti((C_5H_8)_2C_4H_9)$): 0.2 mmol Ti per 100 g SBS; P_{H2}: 0.8 MPa; *T*: 100 °C; *t*: 0.5 h; Conversion: >98%	Enichem S.p.A. (Rome, Italy); Polimeri Europa S.p.A. (Brindisi, Italy)	60 (2004)

Table 19.1 (continued)

Catalyst	Polymer	Representative example [a)]	Assignee	Reference (Year)
Titanocene (Cp_2TiR_2)/titanium alkoxide (R_3TiOR)/trialkylaluminum (AlR_3)	SBS	SBS in cyclohexane (9.7 wt.%); Catalyst (titanium(IV) isopropoxide: bis(cyclopentadienyl) titanium dichloride: triisobutyl aluminum = 1 : 0.5 : 3, mole ratio): 0.17 mmol Ti per 100 g SBS; P_{H2}: 2.5 MPa; *T*: 80 °C; *t*: 1 h; Conversion: 97%	TSRC Corporation (Taiwan)	61 (2005)
Titanocene (Cp_2TiR_2)/alkyllithium (LiR)	Styrene, butadiene or isoprene copolymers	PB in cyclohexane and toluene (5 wt.%); Catalyst (bis(cyclopentadienyl) titanium dichloride): 0.4 mmol per 100 g PB; P_{H2}: 0.49 MPa; *T*: 40 °C; *t*: 2 h; Conversion: 97%	Asahi Kasei Kogyo Kabushiki Kaisha (Osaka, Japan)	62 (1985)

P_{H2}: pressure of hydrogen; *T*: temperature; *t*: time.

sued such that the amount of catalyst required may be significantly reduced. Parent et al. [65] described the selective hydrogenation of C=C within NBR using the homogeneous catalyst precursor, $OsHCl(CO)(O_2)(PCy_3)_2$ in solution, which has a high hydrogenation activity for hydrogenation of NBR as well as poly-isoprene [66]. However, this catalyst is not as effective as Wilkinson's catalyst in suppressing the polymer crosslinking problem, which tends to occur during the later stages of hydrogenation. Pan and Rempel [67] described an efficient catalytic system for the hydrogenation of styrene-butadiene rubber (SBR) in solution using a ruthenium complex ($Ru(CH{=}CHPh)Cl(CO)(PCy_3)_2$, where Ph = phenyl, Cy = cyclohexyl). Because of the high efficiency of the ruthenium catalyst, the catalyst required to realize the hydrogenation is used at a very low level. Indeed, even if all of the catalyst were to be retained in the final products the metal residue would still be less than 7 ppm. Ruthenium-based catalysts have also been used for the hydrogenation of NBR [6–12, 15, 68], polyisoprene [68, 69] and PB [68, 70]. As with the osmium-based catalyst, the ruthenium-based catalysts are efficient but more susceptible with respect to causing crosslinking in NBR during hydrogenation. The mechanism of crosslinking is not well understood. Although a Michael-type addition mechanism (see Scheme 19.3) was speculated to account for this problem, and there were some signs to support this mechanism (e.g., the hydrogenation of NBR catalyzed by ruthenium-based catalysts in the presence of an amine helped to suppress crosslinking [12]), this mechanism has not been substantiated by definitive experimental results [71].

Hsu et al. [15] applied a bimetallic catalyst comprising rhodium and ruthenium for the hydrogenation to combine the high selectivity of the rhodium complex with the lower cost of the ruthenium complex. When the amount of each metal is identical, the catalytic activity of the bimetallic complex catalyst system was similar to that of the single rhodium-complex catalyst, containing

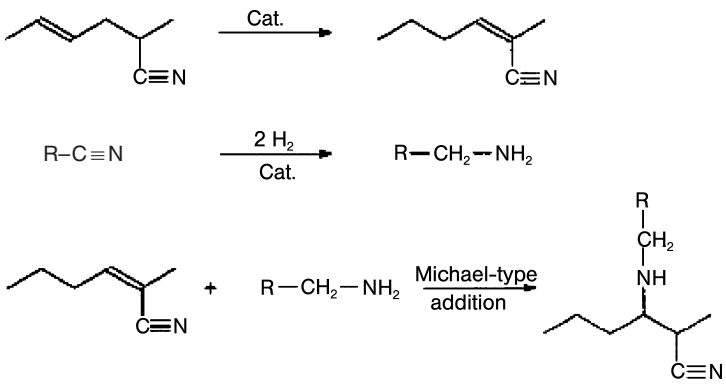

Scheme 19.3 Michael-type addition mechanism for nitrile butadiene rubber (NBR) crosslinking [71].

the same total amount of metal. However, since part of the rhodium is substituted by ruthenium, the bimetallic catalyst becomes less expensive.

Few reports have been published on the hydrogenation of diene polymers using iridium complexes. Gilliom [72] and Gilliom and Honnell [73] described the use of $[Ir(COD)L_2]PF_6$, where COD = cyclooctadiene and L = a phosphine, for the hydrogenation of bulk PB. It was found that $[Ir(COD)(PMePh_2)_2]PF_6$, where Me = methyl and Ph = phenyl, when compared with Wilkinson's catalyst, resulted in a faster hydrogenation than the rhodium complex in the early stages of the reaction; however, the degree of hydrogenation achieved was less than that with the Wilkinson's catalyst. This study presented a rare example of polymer hydrogenation occurring in a pure polymer matrix. In this case an organic solvent was used initially to disperse the catalyst into the polymer matrix, with subsequent removal of the solvent before the hydrogenation operation.

Some examples of the hydrogenation of unsaturated rubber catalyzed by palladium complexes have been reported by Bhattacharjee et al. [74–78]. When palladium acetate ($(CH_3CO_2)_2Pd$) was used as a catalyst for the hydrogenation of NBR [74] and styrene-isoprene-styrene triblock copolymer (SIS) [75], the catalyst showed good selectivity. However the observed maximum conversion was 96% for NBR and 90% for SIS. This catalyst also showed activity for the hydrogenation of natural rubber and epoxidized natural rubber [76]. The results showed that the catalyst was highly selective in reducing olefinic unsaturation in the presence of epoxy groups, and an increase in the epoxy content of the rubber resulted in a decrease in hydrogenation rate and a decrease in the maximum attainable hydrogenation level. Another palladium complex, namely, a six-membered cyclopalladate complex of 2-benzoyl pyridine ($(Pd(CH_3COO)(C_6H_5COC_5H_4N))_2$), was used as catalyst for the selective hydrogenation of NBR, carboxylated nitrile rubber (XNBR) and PB [77, 78]. The reported maximum conversion of C=C using this complex was lower than that obtained with palladium acetate. The main drawback of the palladium complex catalysts is that the degree of hydrogenation achieved cannot satisfy the commercial requirement.

One type of Ziegler-catalyst system, used for polymer hydrogenation, consisted of an organic acid salt or acetylacetone salt of Ni, Co, Pd, etc. and a reducing agent such as an organoaluminum compound. Nickel-based catalysts, such as nickel 2-ethyl hexanoate ($(CH_3(CH_2)_3CH(C_2H_5)CO_2)_2Ni$)/triisobutyl aluminum ($((CH_3)_3CH)_3Al$), nickel acetylacetonate ($(CH_3COCH{=}C(O\text{-})CH_3)_2Ni$)/triisobutyl aluminum, and nickel benzohydroxamic acid ($(C_6H_5CONH\text{-}O\text{-})_2M$, M = Co, Ni)/triisobutyl aluminum, demonstrated activities for the hydrogenation of PB, SBR, and polyisoprene [16, 17, 79]. The Shell Oil Company (Houston, Texas) has filed a series of patents for the application of a Ni/Al catalyst system [18–22]. Besides nickel, cobalt [27–29] and palladium [30, 31] salts together with alkylaluminum compounds or alkylalumoxane have also been used as catalyst systems for polymer hydrogenation. The chief benefit of these systems is that they are relatively inexpensive in terms of the cost of metals used. However, these types of catalysts and co-catalysts need to be used at relatively high concentration in order to achieve favorable reaction rates at the chosen reaction

conditions due to their relative lower activities compared with organometallic catalysts containing Pt-group metals. The high metal concentration in the solution is also a major obstacle when removal of the metal is necessary, as the residual catalyst adversely affects the stability of the hydrogenated product and is detrimental to various applications. Another drawback of these types of catalysts is their poor selectivity as hydrogenation of both ethylenic and aromatic unsaturation may occur, though under certain conditions they show some degree of selectivity for the hydrogenation of ethylenic unsaturations as a result of steric hindrance [21, 22].

Another type of Ziegler-catalyst, which was investigated for polymer hydrogenation, is that of metallocene catalysts. These catalysts consist mainly of halides or aryls of cyclopentadienyl Group III or IV metals (e.g., $RMX^1X^2X^3$, where R is an unsubstituted or substituted cycopentadienyl group; M is metal; X^1, X^2 and X^3 may be either the same or different selected from halogen atoms, aryl groups, aryloxy groups or carbonyl groups, etc., and one of them may be an unsubstituted or substituted cyclopentadienyl group) which are often treated with organolithium reducing agents, and have been applied for homogeneous polymer hydrogenation [32–62, 80]. The most widely used of these catalysts are substituted or unsubstituted bis(cyclopentadienyl)-titanium compounds; however, zirconium and hafnium complexes have also been reported for the purpose of polymer hydrogenation [34, 45, 55]. When these titanocene-based catalysts are used for the hydrogenation of unsaturated living polymers, the hydrocarbon lithium or lithium hydride compounds which are produced from the termination reactions of the hydrocarbon or hydrogen with the alkyllithium initiator serve as a reducing agent for the hydrogenation catalyst. In this case, the addition of an organolithium compound which is necessary for reduction of the complex during the hydrogenation process can be omitted [35–38, 41–44]. In this catalyst system, when the alkyllithium complex (lithium hydride generated *in situ*) or the alkoxy lithium compound is used to activate the bis(cyclopentadienyl) titanium catalyst for effective hydrogenation of polymers, an excess amount of the lithium species may also induce reduction of the titanium compounds, resulting in decomposition of the catalyst component as well as a reduction in catalyst activity. In this case some reagents such as ethanol or difluorodiphenyl silane can be added to the system to adjust the ratio of lithium hydride to titanium [37, 44]. Some of these catalysts may be used without the addition of Group I, II, IIIA alkyl compounds such as substituted titanocene biaryl compounds, etc. [32, 54].

Related to these catalysts are the systems based on lanthanide metal systems or rare earth metal complexes [46, 47]. The main problem with these catalyst systems is their instability. When the catalyst solution is prepared by reacting a metallocene with an organolithium compound in a polar solvent, the prepared catalyst solution is unstable and decomposes quickly, even under a nitrogen atmosphere. The activity of these catalysts can be high only if the catalyst is added to the polymer solution immediately after preparation. Attempts have been made to overcome the stability problem by using an additive in the system to improve the stability and the activity of the catalyst [33–35, 41, 57, 58, 61]. Re-

cently, it was also found that monocyclopentadienyl titanium compounds are more stable and less sensitive to the extra lithium hydride [50–53] than bis(cyclopentadienyl) titanium compounds. Another disadvantage of the above catalysts is that the Group III and IV metal halides (as well as the lithium halides) formed from the catalyst system tend to corrode the metal reactors used in the hydrogenation process. This results in increased investment costs to provide expensive, corrosion-resistant metal alloy reactor systems. It may be possible to overcome such a problem by replacing the titanium with a Group VIIIB metal such as cobalt or nickel [56], as no corrosion of the reactor system was observed when a bis(cyclopentadienyl) cobalt (or nickel) complex and an organolithium compound were used as a catalyst system for the hydrogenation of polymers. Furthermore, this cobalt or nickel catalyst system showed much higher stability than the titanocene catalysts. In fact, the bis(cyclopentadienyl) cobalt(II)/*n*-butyllithium catalyst still had high activity for the hydrogenation of the polymer two weeks after it was prepared and stored under nitrogen.

The metallocene catalysts have good selectivity and high activity under mild reaction conditions. Given these advantages, it is to be expected that these systems would show promise for the homogeneous hydrogenation of polymers on a commercial scale. However, there is no report on the application of this catalyst for the hydrogenation of NBR. One possible reason for this is that the polar (CN) groups in NBR may bond to the active metal center and deactivate the catalyst.

19.2.2
Hydrogenation Kinetic Mechanism

An understanding of the kinetics and catalytic mechanism of polymer hydrogenation is essential in order to optimize the reaction conditions, to control the reaction systems, and to design commercial production processes. Catalytic kinetic mechanisms for Rh-, Os- and Ru-complex polymer hydrogenation systems have been extensively investigated, and are summarized in the following sections.

19.2.2.1 **Rhodium-Based Catalysts**

$RhCl(PPh_3)_3$ has been used for the homogeneous hydrogenation of various diene-based polymers, and its catalytic mechanism is understood to a considerable extent. Parent et al. [81] proposed a mechanism which has been found to be consistent with the kinetic data for various diene-based polymer hydrogenation systems and an understanding of the coordination chemistry of $RhCl(PPh_3)_3$ in solution. The main points comprising the mechanism are outlined as follows:

- $RhCl(PPh_3)_3$ oxidatively adds molecular hydrogen to form a five-coordinate dihydride complex which is consistent with the previous understanding [82] for olefin hydrogenation. This was also confirmed by experiments conducted by Mohammadi and Rempel [83] for NBR hydrogenation, where at 65 °C under 1 bar H_2 the reaction is quantitative towards formation of the dihydride:

$$RhCl(PPh_3)_3 + H_2 \leftrightarrows RhClH_2(PPh_3)_3 \quad (1)$$

- The dissociation of phosphine from $RhClH_2(PPh_3)_3$, whilst limited at room temperature, increases at higher hydrogenation temperatures:

$$RhClH_2(PPh_3)_3 \leftrightarrows RhClH_2(PPh_3)_2 + PPh_3 \quad (2)$$

- The initial coordination of the substrate is rate-limiting; however, the reductive elimination of the alkane is considered to be rapid:

$$RhClH_2(PPh_3)_2 + C{=}C \rightarrow RhClH_2(C{=}C)(PPh_3)_2 \quad (3)$$

$$RhClH_2(C{=}C)(PPh_3)_2 \rightarrow RhCl(PPh_3)_2 + C{-}C \quad (4)$$

- A potential ligand such as the nitrile present in a nitrile-butadiene copolymer may inhibit the catalytic hydrogenation cycle:

$$RhClH_2(PPh_3)_2 + \wedge\wedge\wedge\, CNR \leftrightarrows RhClH_2(CNR)(PPh_3)_2 \quad (5)$$

$$RhCl(PPh_3)_2 + \wedge\wedge\wedge\, CNR \leftrightarrows RhCl(CNR)(PPh_3)_2 \quad (6)$$

$[Rh(CO)(MeCN)(PPh_3)_2]ClO_4$ has been prepared [84] and $[Rh(PPh_3)_3(MeCN)][BF_4]$ analyzed crystallographically by Pimblett et al. [85]. Schrock and Osborn [86] report that the use of acetonitrile as a solvent has a deleterious effect on the hydrogenation activity of $[Rh(diene)(PPh_3)_2]A$ ($A = ClO_4$, BF_4 or PF_6). To date, a detailed study of the propensity of nitrile to associate with complexes derived from $RhCl(PPh_3)_3$ is lacking, although Ohtani, Yamagishi and Fujimoto [87] have presented some spectrophotometric data on the system. As nitrile likely coordinates by donation of its lone pair of electrons, it experiences little of the steric hindrance which affects coordination of the olefin. It may therefore compete effectively with olefin for coordination to coordinatively unsaturated metal complexes.

Based on the above reactions, an overall mechanism for the hydrogenation of NBR catalyzed by Wilkinson's catalyst was proposed (see Scheme 19.4), which is also applicable to the kinetic performance of the homogeneous hydrogenation of PB [88] and styrene-butadiene *copoly*mers [89], where K_2 and K_5 vanish.

Based on Scheme 19.4, the following mathematical equation can be derived for calculating the hydrogenation rate:

$$R_H = \frac{k'K'KK_1[H_2][Rh][C{=}C]}{KK_1 + K'[PPh_3] + KK'[H_2][PPh_3] + KK_1K'[H_2] + KK_1K_5[CN] + KK_1K_2K'[H_2][CN]} \quad (7)$$

The investigated experimental ranges and experimental estimations of the kinetic parameters for various hydrogenation systems are listed in Table 19.2,

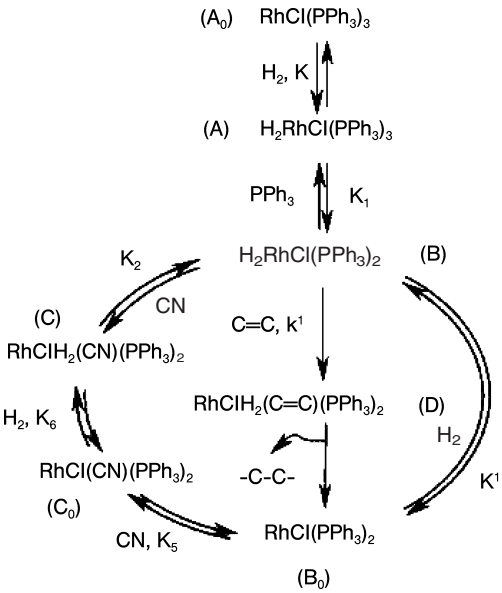

Scheme 19.4 The proposed reaction mechanism for the $RhCl(PPh_3)_3$/NBR system [90].

Table 19.2 Kinetic parameters for homogeneous hydrogenation of diene-based polymers.

Polymer (solvent)	K [mM^{-1}]	K_1 [mM]	K' [mM^{-1}]	K_2 [mM^{-1}]	K_5 [mM^{-1}]	k' [mMs^{-1}]	E [kJ mol^{-1}]	Reference
NBR (chlorobenzene)	∞	1.44	3.41×10^{-3}	3.98×10^{-2}	2.71×10^{-2}	1.19	73.5	81
NBR (butanone)	∞	0.198	0.276	6.5×10^{-2}	0	4.23×10^{-4}	87.3	83
1,4-PB (*o*-di-cholorobenzene)	0.60	4.45	0.59	0	0	1.28×10^{-3}	98.5	88
SBS (*o*-di-cholorobenzene)	0.31	3.13	0.63	0	0	3.26×10^{-4}	78.8	89
SB (toluene)	1.23	4.70	0.72	0	0	4.77×10^{-4}	60.8	89

with typical reaction conditions provided in Table 19.3. These parameters are consistent with the observed experimental results. For the hydrogenation of NBR in chlorobenzene using $RhCl(PPh_3)_3$, Bhattacharjee et al. [91] reported a value of 22 kJ mol^{-1} for the apparent activation energy, though this was not consistent with the normal range of reaction activation energy and also quite different from the value shown in Table 19.2. However, these authors did not provide sufficient data to account for the discrepancy. It would appear from this value of activation energy that Bhattacharjee et al.'s catalytic hydrogenation study was possibly mass transfer-controlled.

Table 19.3 Typical reaction conditions for the hydrogenation of polybutadiene (PB), styrene-butadiene diblock copolymer (SB), styrene-butadiene-styrene triblock copolymer (SBS) and nitrile butadiene rubber (NBR).

Polymer	[Rh] [mM]	[PPh_3] [mM]	Temperature [K]	H_2 [mM] (P_{H2} [MPa])	Solvent	Reference
NBR	0.080	4.0	418.2	101 (2.37)	Chlorobenzene	81
NBR	1.958	0	313.2	3.142 (0.10)	Butanone	83
1,4-PB	1.99	7.40	338.2	3.90 (0.10)	*o*-Dichlorobenzene	88
SBS	1.99	7.40	338.2	3.90 (0.10)	*o*-Dichlorobenzene	89
SB	2.04	0	324.2	3.17 (0.10)	Toluene	89

19.2.2.2 **Ruthenium-Based Catalysts**

Ruthenium catalysts, such as $Ru(CHCH(Ph))Cl(CO)(PCy_3)_2$, have been found to be active for catalyzing the hydrogenation of various diene-based polymers. The catalytic mechanism for the hydrogenation of NBR, SBR and PB has been investigated [68].

Kinetic results show that the hydrogenation reaction rate exhibits a first-order dependence on both hydrogen concentration, $[H_2]$, and the total ruthenium concentration, $[Ru]_T$ and an inverse dependence on the nitrile concentration, [CN]. The catalytic mechanism proposed for polymer hydrogenation is illustrated in Scheme 19.5 and the main points of the mechanism are outlined below:

- Rapid hydrogenation of the styryl group in $Ru(CH{=}CH(Ph))Cl(CO)(PCy_3)_2$, to give the active species $RuHCl(CO)(PCy_3)_2$, and styrene, which is subsequently rapidly hydrogenated to ethyl benzene.

$$Ru(CH{=}CH(Ph))Cl(CO)(PCy_3)_2 + H_2 \rightarrow RuHCl(CO)(PCy_3)_2 + \text{styrene} \quad (8)$$

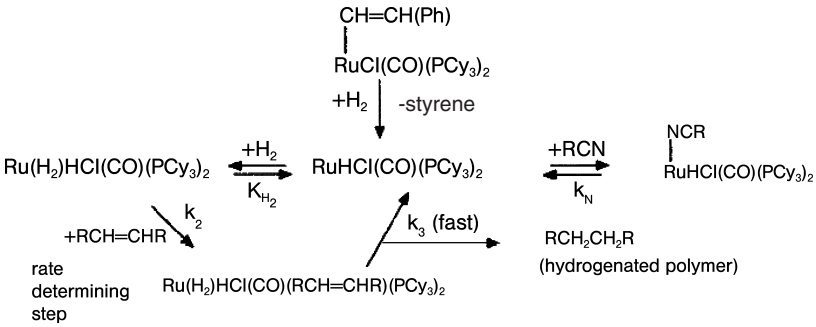

Scheme 19.5 Mechanism of nitrile butadiene rubber (NBR) hydrogenation catalyzed by $Ru(CH{=}CH(Ph))Cl(CO)(PCy_3)_2$.

- The coordination of H_2 to $RuHCl(CO)(PCy_3)_2$ is the initial step in the catalytic cycle.

$$RuHCl(CO)(PCy_3)_2 + H_2 \leftrightarrows Ru(H_2)HCl(CO)(PCy_3)_2 \tag{9}$$

- The coordination of olefin before the final rapid elimination of products and regeneration of $RuHCl(CO)(PCy_3)_2$, which is assumed to be the rate-determining step:

$$Ru(H_2)HCl(CO)(PCy_3)_2 + C{=}C \rightarrow Ru(H_2)HCl(CO)(C{=}C)(PCy_3)_2 \tag{10}$$

$$Ru(H_2)HCl(CO)(C{=}C)(PCy_3)_2 \rightarrow RuHCl(CO)(PCy_3)_2 + \text{-}C{-}C\text{-} \tag{11}$$

- A potential ligand such as a nitrile may inhibit the hydrogenation cycle:

$$RuHCl(CO)(PCy_3)_2 + CNR \leftrightarrows Ru(CNR)HCl(CO)(PCy_3)_2 \tag{12}$$

Based on the above reaction mechanism, and with some reasonable simplification, the hydrogenation rate can be expressed as:

$$R_H = \frac{k_1[H_2][Ru]_T[C{=}C]}{1 + K_N[RCN]} \tag{13}$$

The mechanism for this catalyst for the hydrogenation of *cis*-1,4-polyisoprene (CPIP) is slightly different [69]. As there was no clear evidence that coordination of hydrogen occurs prior to the coordination of C=C to the $RuHCl(CO)(PCy_3)_2$, there may be two possible pathways for the hydrogenation of CPIP in the presence of $Ru(CH{=}CH(Ph))Cl(CO)(PCy_3)_2$, namely an unsaturated path and a hydride path. The catalytic mechanism for these two pathways is represented in Scheme 19.6.

Based on this mechanism, if the unsaturated pathway ($A_0 \rightarrow B \rightarrow D$) is undertaken, with the reaction of the alkyl complex with hydrogen serving as the rate-limiting step, the hydrogenation rate can be expressed as:

$$R_H = \frac{k_3 K_{C=C}[H_2][Ru]_T[C{=}C]}{1 + K_{C=C}[C{=}C]} \tag{14}$$

If the hydride pathway ($A_0 \rightarrow B' \rightarrow C' \rightarrow D$) is undertaken, the hydrogenation rate can be expressed as:

$$R_H = \frac{K_2 K_{H_2}[H_2][Ru]_T[C{=}C]}{1 + K_{H_2}[H_2]} \tag{15}$$

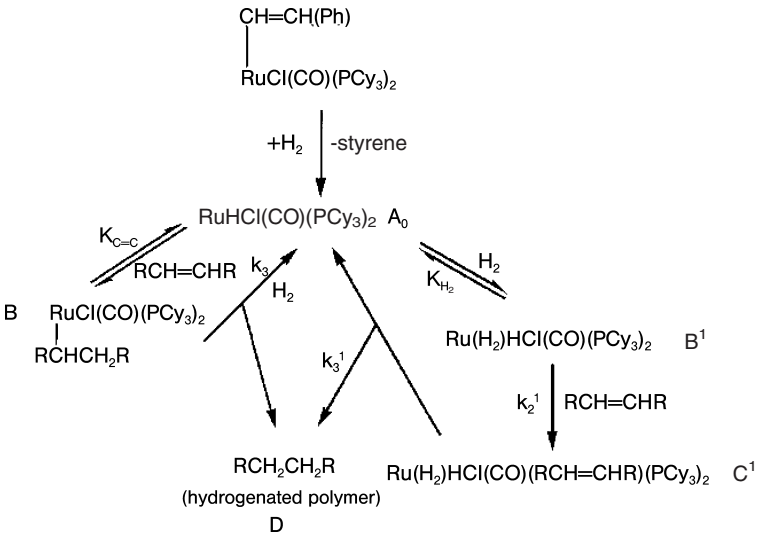

Scheme 19.6 Proposed mechanism of *cis*-1,4-polyisoprene (CPIP) hydrogenation using $Ru(CH{=}CH(Ph))Cl(CO)(PCy_3)_2$.

If both K_{H2} and $K_{C=C}$ are assumed to be very small, depending on which pathway is considered, then both equations will reduce to

$$R_H = k[H_2][Ru]_T[C{=}C] \tag{16}$$

which is consistent with the observed experimental kinetics.

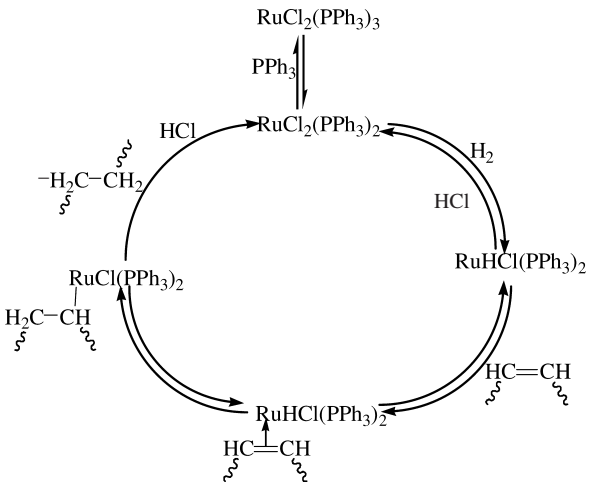

Scheme 19.7 Proposed mechanism for polybutadiene (PB) hydrogenation using $RuCl_2(PPh_3)_3$.

Rao et al. [70] investigated the hydrogenation of PB catalyzed by $RuCl_2(PPh_3)_3$, and showed a degree of hydrogenation >99% to be obtained within 6 h using 0.3 mol.% catalyst at 100 °C and under 50 bar H_2 pressure. These authors proposed the possible mechanism shown in Scheme 19.7, but provided no detailed kinetic data to check the reliability of the above mechanism.

19.2.2.3 **Osmium-Based Catalysts**

For the hydrogenation of NBR, osmium complexes such as $OsHCl(CO)(O_2)(PCy_3)_2$ have shown distinctive performance which permits their discrimination from Rh- and Ru-based catalysts [65]. A somewhat difficult element of the kinetic NBR hydrogenation data is the apparent second-to-zero-order dependence of the reaction rate with respect to $[H_2]$. A second-order behavior requires 2 molecules of H_2 either to produce an active complex or to participate in the rate-determining step. Bakhmutov et al. [92] identified an exchange between the apical hydride and the *trans*-coordinated dihydrogen ligand, but concluded that the trihydride could at most be a reactive intermediate. The addition of a second molecule of H_2 to the catalyst intermediate had not been observed. Another distinguishing characteristic in the Os catalytic system is that of severe inhibition of hydrogenation activity when additional PCy_3 is present. Based on these phenomena, two possible hydrogenation mechanisms have been proposed (Schemes 19.8 a and b).

A rate expression, as shown in Eq. (17), may be obtained from Scheme 19.8 a:

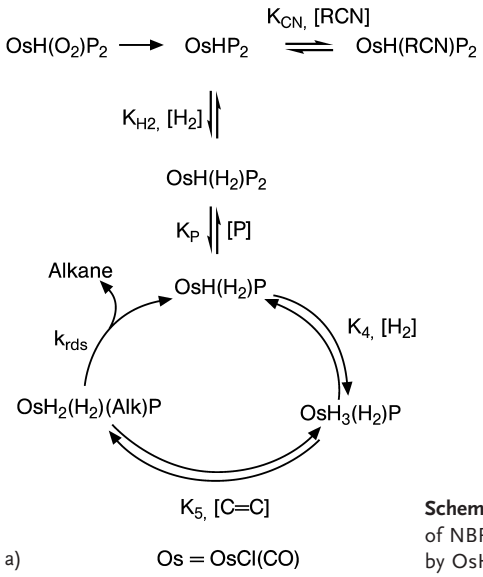

Scheme 19.8 (a, b) Alternative mechanisms of NBR hydrogenation catalyzed by $OsHCl(CO)(O_2)(PCy_3)_2$.

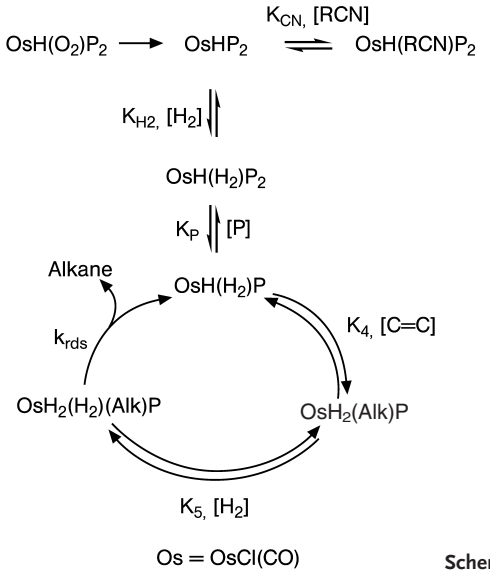

Scheme 19.8 b

$$R_H = \frac{k_{rds} K_{H_2} K_p K_4 K_5 [Os]_T [H_2]^2 [C{=}C]}{[P](1 + K_{CN}[CN] + K_{H_2}[H_2]) + K_{H_2} K_p [H_2] + K_{H_2} K_p K_4 [H_2]^2 (1 + K_5 [C{=}C]))} \quad (17)$$

The rate expression is consistent with the observed kinetic data. A similar mechanism was also proposed for the hydrogenation of polyisoprene catalyzed by $OsHCl(CO)(O_2)(PCy_3)_2$ [93].

Scheme 19.8 b illustrates a more conventional mechanism, which results in a rate expression as shown in Eq. (18):

$$R_H = \frac{k_{rds} A [Os]_T [H_2]^2 [C{=}C]}{[P](1 + K_{CN}[CN] + K_{H_2}[H_2]) + K_{H_2} K_p [H_2] + B[C{=}C][H_2](1 + C[H_2]))} \quad (18)$$

While this mechanism involves lower formal coordination numbers than that of Scheme 19.8 a, its shortcoming is a zero-order dependence on $[H_2]$ that must be accompanied by a zero-order reaction dependence on [C=C].

19.2.2.4 **Palladium Complexes**

Palladium acetate has an unusual structure that comprises three palladium atoms in a triangular arrangement, held together by six bridging acetate groups. Details of the structure of the complex have been reported [75]. The catalyst has been used for the hydrogenation of both nitrile rubber and natural rubber [74–76].

Another palladium complex, namely, a six-membered cyclopalladate complex of 2-benzoyl pyridine, has also been used for the hydrogenation of polymers [77, 78]. Possible catalytic mechanisms for the hydrogenation of natural rubber [76] and NBR [77] catalyzed by these two complexes were proposed, but unfortunately the authors did not provide sufficient evidence to support their proposed mechanisms.

Although Ziegler-type catalysts have been widely investigated for the homogeneous hydrogenation of polymers, their catalytic mechanism remains unknown. One possible reason for this may be the complexity of the coordination catalysis and the instability of the catalysts. Metallocene catalysts are highly sensitive to impurities, and consequently it is very difficult to obtain reproducible experimental data providing reliable kinetic and mechanistic information.

19.2.3
Kinetic Mechanism Discrimination

Modeling and analysis of the kinetics represent powerful tools by which a better understanding of the catalysis involved in polymer hydrogenation may be obtained. These approaches also form the basis for a more thorough design of chemical reactors, and for a better insight into the behavior of existing reactors. In homogeneous catalytic systems, in the presence of organometallic catalysts, complicated equilibrium reaction cycles often exist and in general the networks composed of the elementary reactions are highly complex. Thus, model discrimination, selection on the basis of experiment of the best rate equation among a set of rivals, is very important. Fortunately, on the basis that overall catalytic intermediates can be considered to be reasonably constant, model discrimination may be significantly simplified, and a generalized method has quite recently been proposed for the hydrogenation of diene-based polymers [94].

19.3
Engineering Art

Homogeneous polymer hydrogenation operation involves a number of unit operations, and some typical procedures are shown in Figure 19.1 with respect to NBR hydrogenation. The major unit operations include homogeneous catalytic hydrogenation, catalyst recovery and solvent recycling, in addition to emulsion polymerization before the hydrogenation stage. Because of the high exothermicity in the initial stage of the hydrogenation reaction, and because gaseous hydrogen is used, heat transfer and mass transfer are major concerns for hydrogenation reactors. As a high degree of hydrogenation is usually required for high-performance hydrogenated elastomers, a suitable flow pattern in the reactor is also required for a continuous operation, besides a need for superior mass transfer and heat transfer. Because of the high price of the catalyst used, and also because of potential catalyst toxicity, catalyst recovery is a critical stage for

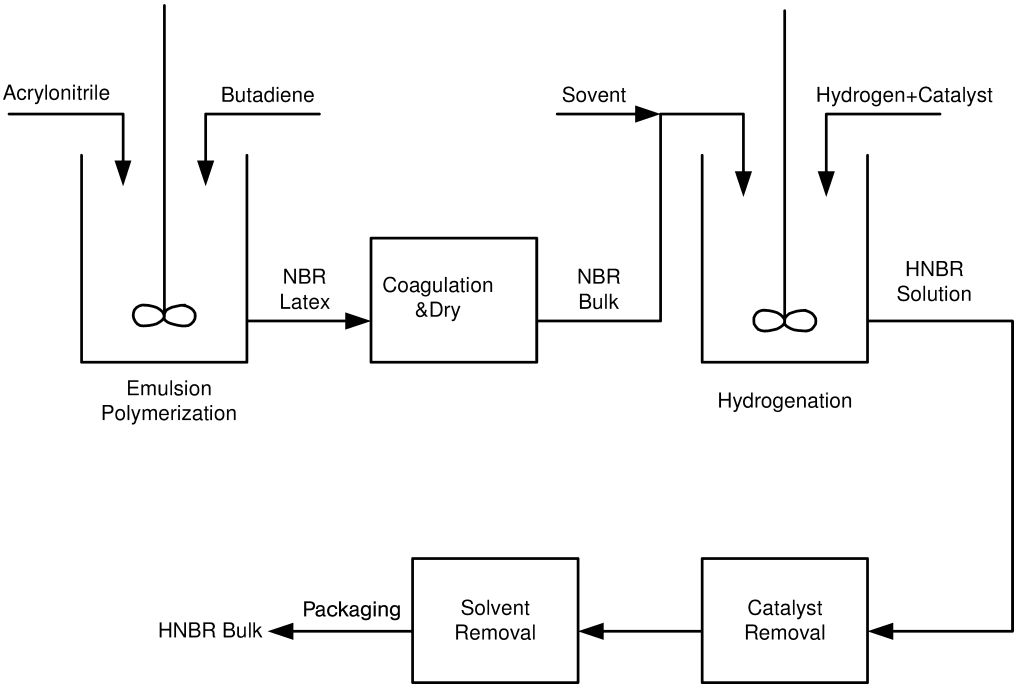

Fig. 19.1 Schematic process for the production of hydrogenated nitrile butadiene rubber (HNBR).

both batch and continuous operations. Likewise, as large amounts of organic solvent are required to realize homogeneous hydrogenation, an efficient design for solvent removal and recycle is necessary. Together, these three aspects determine the commercial feasibility of the hydrogenation process.

19.3.1
Catalyst Recovery

Catalyst recovery is a universal problem in the field of homogeneous catalysis. For the homogeneous hydrogenation of unsaturated polymers, the incentives of catalyst removal dwell on both improving the quality of the polymer product and on reducing the high costs of the process that relate mainly to the expensive noble metals often used as catalysts. Catalyst removal is especially difficult from polymer solutions because of the high viscosity and the good compatibility between the catalysts and the functionalized polymers. In general, two main methods are used for the removal of metal catalysts. The first method is to precipitate the catalyst from the polymer solution and then to separate it by filtration or gravity settling. The second method is to adsorb the catalyst from the polymer solution by ion-exchange resins or other absorbents which have an affinity for the spent catalyst.

19.3.1.1 **Precipitation**

Precipitation of the catalyst can be effected by treating the polymer solution with acid/base and/or oxidants. Poloso and Murray [95] proposed a method to recycle the nickel octanoate ($(CH_3(CH_2)_6CO_2)_2Ni$)/triethylaluminum($(C_2H_5)_3Al$) catalyst from a styrene-butadiene polymer solution. The polymer solution containing the catalysts was refluxed with 4 wt.% glacial acetic acid (relative to polymer) for 4 h, followed by treatment with 1.4 wt.% anhydrous ammonia. The solution was then filtered through a diatomaceous earth. The nickel content in the polymer was decreased from 310 ppm to 5.6 ppm.

In a method developed by Kang [96], 2 equiv. dimethylglyoxime (based on nickel content) was used to treat a butadiene-styrene polymer solution. The reddish bis(dimethylglyoximato) nickel complex was precipitated and then removed by filtration. By using this method, the nickel content in the polymer was reduced to less than 1 ppm. Alternatively, Hoxmeier [97] mixed the polymer solution with azelaic acid or adipic acid (50 wt.% excess based on the metals) in organic solvents, after which a phase separation was realized by gravity settling. Subsequently, it was claimed that nickel levels within the polymers were reduced to 2 ppm. The process was later improved by using hydrogen peroxide to oxidize the nickel catalyst in the polymer solution initially, and then by adding azelaic acid or adipic acid as an aqueous solution to precipitate the catalyst [98]. Nickel-based catalysts have also been removed by contacting the polymer solution with molecular oxygen with subsequent treatment with activated carbon [99]. Other similar methods to precipitate catalysts from the polymer solutions include contacting the polymer solution with a trialkylaluminum compound in the presence of water [100], treating the polymer solution with a chelating resin which is comprised of iminodiacetate ions [101], bubbling oxygen/nitrogen in the presence of an aqueous solution of an acid [102], reacting with an aqueous solution of ammonia and carbon dioxide [103], and contacting with an aqueous solution of a weak acid followed by contacting with an aqueous solution of a weak base [104]. In selecting a suitable agent to remove metallic catalyst residues from hydrogenated polymer solutions, the following criteria should be considered: (i) the agent should be substantially inert toward the polymer and the polymer solvent; and (ii) it should be capable of turning the catalyst into an insoluble compound, efficiently. Contamination of the polymer by the catalyst recovery procedure must also be considered.

19.3.1.2 **Adsorption**

Adsorption is commonly used for catalyst removal/recovery. The process involves treating the polymer solution with suitable materials which adsorb the catalyst residue and are then removed by filtration. Panster et al. [105] proposed a method involving adsorbers made from organosiloxane copolycondensates to recover rhodium and ruthenium catalysts from solutions of HNBR. These authors claimed that the residual rhodium could be reduced to less than 5 ppm, based on the HNBR content which had a hydrogenation conversion of over

99%. Silicates, including calcium silicate, magnesium silicate and diatomaceous earth, have also been used as adsorbers [106]. When these were applied to a hydrogenated SBS solution containing a nickel-based catalyst, the nickel content of the polymer was reduced to less than 1 ppm. Rhodium-based catalyst residues from HNBR solution can also be removed by using an ion-exchange resin with thiourea functional groups present on a resin which is both macroporous and monodispersed [107]. The criterion for selecting adsorbers is similar to that for selecting a precipitating agent: an efficient catalyst adsorber should be inert to both the polymer and the solvent.

19.3.2
Solvent Recycling

Solvent recycling is an important post-treatment stage of the homogeneous catalytic hydrogenation of polymers, for both economical and environmental reasons. This topic has not been widely investigated for homogeneous polymer hydrogenation operations, but in present-day processes the organic solvents used are stripped by steam, which is itself an energy-intensive operation.

In other related areas, such as solution polymerization and bulk polymerization, the removal/recycling of solvents or unreacted monomer has been extensively investigated [108–112]. The methods used are based on lateral heat-dependent operations such as evaporation and steam-stripping, or non-lateral heat-dependent operations that include a variety of extraction procedures.

Many types of equipment have been developed to improve the evaporation of solvent in order to provide energy savings. The most widely used techniques for devolatilization are the falling strand devolatilizer (FSD), the thin-film evaporator and the vented extruder [113].

The FSD is a flash evaporator, whereby the preheated polymer solution/melt falls within the vessel primarily by gravity, while the volatiles evaporate during falling. This method is normally used with process streams that are not exceptionally temperature-sensitive and where the concentration of volatiles is relatively high.

Thin-film and surface renewal evaporators are mostly applied to materials with medium to high viscosity, or to high-boiling contaminated mixtures. A typical thin-film evaporator employs a unique rotor with an array of discrete, plow-like blades attached to the rotor core. The blades transport the viscous concentrate or melt through the evaporator while simultaneously forming films to facilitate heat and mass transfer.

Single-screw and double-screw extruders are normally used for polymer melts to accomplish the deaeration or devolatilization of residual volatiles. Devolatilization in an extruder is effected through formation of the venting zone inside the chamber by carefully designed upstream and downstream screw sections.

Many techniques have also been developed to improve devolatilization efficiency, including steam stripping [114], second fluid-assisted devolatilization [115], supercritical fluid devolatilization [116], and a variety of specially designed

devolatilizers. Some of the above methods can also be used for solvent recycling in polymer hydrogenation processes.

19.3.3
Reactor Technology and Catalytic Engineering Aspects

There are many commercial advantages to hydrogenating relatively inexpensive polymers in order to create new, more valuable materials. Polymer hydrogenation is not widely developed today on a commercial scale, however, mainly because of the high production costs associated with catalyst and reactor technologies. The development of an efficient reactor for homogeneous hydrogenation of diene-based polymers remains a major challenge for several reasons:

- In order to reduce production costs, high polymer concentrations are preferred in hydrogenation operations. However, the viscosity of polymer solutions rises rapidly as the polymer concentration increases. In present-day commercial processes, polymer concentrations do not normally exceed 15 wt.%.
- The hydrogenation operation involves hydrogen transfer from the gas phase into the viscous polymer solution phase. If the mass transfer capacity is not sufficiently superior, the hydrogenation could be significantly retarded and product quality adversely affected.
- The hydrogenation reaction is highly exothermic. Thus, heat release during the initial hydrogenation may be a serious problem, and a reactor with a superior heat transfer capacity tunability will be required.
- Due to the viscous and highly exothermic characteristics of the hydrogenation reactions, the reactor should have superior mixing capabilities in order to avoid possible crosslinking induced by hot spots in the reactor.
- As high hydrogenation conversion is usually desired, and crosslinking of the polymer should be avoided, correct control of the reaction conditions is very important.

Among present-day commercial processes for the homogeneous hydrogenation of polymers, a semi-batch operation system prevails where the hydrogen gas supply is provided continuously and the liquid phase is operated batchwise. A semi-batch operation is suitable for relatively small volume production, but it is not economical for high-production yields. Such semi-batch reactor systems cannot meet the needs of the growing demand for hydrogenated polymers, and the development of more efficient reactor systems is needed. A Japanese Patent [117] disclosed a production process for hydrogenated polymer wherein a polymer solution containing olefinic unsaturated groups, hydrogen gas, and a hydrogenation catalyst are continuously supplied to a stirred-tank reactor and the reaction product is continuously removed. Another Japanese Patent [118] disclosed a continuous production process of a hydrogenated polymer containing olefinic unsaturated groups wherein plural reactors are connected in series and hydrogen is supplied to at least one of the reactors from the lower portion

thereof. An improved method was proposed [119] to obtain a polymer having a desirable degree of hydrogenation steadily for a long period in the above continuous reactors by recycling one part of the hydrogenated polymer solution. Pan and Rempel et al. [120–122] investigated the effect of various reactor performances on the hydrogenation of diene-based polymers via modeling and simulation, and proposed that an optimal reactor for diene-based polymer hydrogenation would be a plug flow reactor with an instantaneous mixing component in the inlet zone. These studies provide useful information for commercial continuous hydrogenation process development.

19.4 A Commercial Example: Production of HNBR via a Homogeneous Hydrogenation Route

HNBR has an intriguing combination of properties [123], including high tensile strength, low permanent set (especially at high temperatures), very good abrasion resistance and high elasticity. HNBR also shows excellent stability towards heat, being able to resist temperatures of up to ca. 150 °C (NBR under the same conditions is stable up to only ca. 120 °C); it also demonstrates better properties at low temperatures (lower brittle point) than other heat- and oil-resistant elastomers. This combination of properties is opening up a broad range of applications for these materials, particularly in the automotive industry. HNBR is now widely used for timing belts in cars, due to its good static as well as dynamic properties at under-the-hood operation temperatures, and it also exhibits good retention of properties under continuous heat exposure. In addition, new grades of the material with improved low-temperature flexibility are extending the HNBR service temperature range, allowing new applications in seals and mounts. For example, HNBR is also proving useful for seals and moldings of motor car engines that run on new fuels such as rapeseed oil methyl ester. Seal applications also include air conditioner O-rings, shock absorbers, power steering systems and water pumps. HNBR has also been widely used in industrial seals for oil field exploration and processing, as well as rolls for steel and paper mills.

There are two major commercial producers of HNBR worldwide. Nippon Zeon Corporation manufactures HNBR (heterogeneous hydrogenation) under the tradename Zetpol®, while Lanxess Inc. produces HNBR (homogeneous hydrogenation) in Orange, Texas, and in Leverkusen, Germany under the tradename Therban®. The manufacturing process of HNBR is shown schematically in Figure 19.1. The process begins with the production of an emulsion-polymerized NBR which is then dissolved in an appropriate solvent (chlorobenzene). When dissolution is complete, the addition of hydrogen gas, in conjunction with a precious-metal catalyst at a designated temperature and pressure, brings about a selective hydrogenation to produce the hydrogenated polymer. The solvent and catalyst are then recovered and the remaining polymer crumb is dried. After vulcanization, the HNBR is ready for industrial use.

19.5
Future Outlook and Perspectives

Hydrogenated polymers have many desirable properties over their parent polymers, although the high cost of hydrogenated products still restricts their widespread application. The following aspects should be considered for the sustainable development of the hydrogenated polymer industry:

- The development of highly efficient and easily recoverable catalyst systems. Today, the high cost of hydrogenated polymers is due mainly to the cost of the metal catalyst and its recovery operation.
- A reduction in the amounts of organic solvent used in the hydrogenation process. Considerable energy costs result from solvent recycling. Investigations into the hydrogenation of NBR in supercritical fluid media have been carried out, and positive results obtained [124, 125]. Considerable cost savings could be realized if an efficient catalyst system were to be developed for the hydrogenation of polymers in aqueous latex form [126, 127].
- The development of high-efficiency reactors (e.g., continuous/flexible systems) for the hydrogenation process [117–122].
- The extension of new applications for hydrogenated polymers.
- An overall improvement on the hydrogenation process to reduce production costs is required.

Abbreviations

CPIP	*cis*-1,4-polyisoprene
FSD	falling strand devolatilizer
HNBR	hydrogenated nitrile butadiene rubber
NBR	acrylonitrile-butadiene rubber
PB	polybutadiene
SBR	styrene-butadiene rubber
SBS	styrene-butadiene-styrene triblock copolymer
SIS	styrene-isoprene-styrene triblock copolymer
XNBR	carboxylated nitrile rubber

References

1 Kang, J. US Patent 3,993,855, **1976** (to The Firestone Tire & Rubber Company, Akron, OH).

2 Rempel, G. L., Azizian, H., US Patent 4,464,515, **1984** (to Polysar Limited, Sarnia, CA).

3 Rempel, G. L., Azizian, H., US Patent 4,503,196, **1985** (to Polysar Limited, Sarnia, CA).

4 Guo, S., Nguyen, P., US Patent 6,683,136, **2004** (to Bayer Inc., Sarnia, CA)

5 Rempel, G. L., McManus, N. T., Parent, J. S., US Patent 5,561,197,**1996** (to University of Waterloo, CA),

6 Buding, H., Fiedler, P., Konigshofen, H., Thormer, J., US Patent 4,631,315, **1986** (to Bayer Aktiengesellschaft, Leverkusen, DE).

7 Himmler, T., Fiedler, P., Braden, R., Buding, H., US Patent 4,795,788, **1989** (to Bayer Aktiengesellschaft, Leverkusen, DE).

8 Buding, H., Thormer, J., Nolte, W., Hohn, J., Fiedler, P., Himmler, T., US Patent 5,034,469, **1991** (to Bayer Aktiengesellschaft, Leverkusen, DE).

9 Rempel, G. L., Mohammadi, N. A., Farwaha, R., US Patent 4,812,528, **1989** (to University of Waterloo, CA).

10 Rempel, G. L., Mohammadi, N. A., Farwaha, R., US Patent 4,816,525, **1989** (to University of Waterloo, CA).

11 Rempel, G. L., McManus, N. T., Mohammadi, N. A., US Patent 5,057,581, **1991** (to University of Waterloo, CA).

12 Rempel, G. L., McManus, N. T., US Patent 5,075,388, **1991** (to University of Waterloo, CA).

13 Iio, A., Oshima, N., Ohira, Y., Sakamoto, M., Oka, H., US Patent 5,202,388, **1993** (to Japan Synthetic Rubber Co. Ltd., Tokyo, Japan).

14 Tadahiro, S., Masutada, O., Tadashi, A., Japanese Patent 11-193,323, **1999** (to Mitsui Chemicals Inc., Japan).

15 Hsu, K., Wu, G., Xu, R., Yue, D., Zhou, S., US Patent 6,084,033, **2000** (to Nantex Industry Co., Ltd., Taiwan).

16 Loveless, F. C., Miller, D. H., US Patent 3,932,308, **1976** (to Uniroyal Inc., New York, NY).

17 Halasa, A. F., US Patent 3,988,504, **1976** (to The Firestone Tire & Rubber Company, Akron, OH).

18 Hoxmeier, R. J., Slaugh, L. H., US Patent 5,013,798, **1991** (to Shell Oil Company, Houston, TX).

19 Hoxmeier, R. J., Slaugh, L. H., US Patent 5,030,799, **1991** (to Shell Oil Company, Houston, TX).

20 Hoxmeier, R. J., Slaugh, L. H., US Patent 5,061,668, **1991** (to Shell Oil Company, Houston, TX).

21 Hoxmeier, R. J., US Patent 4,879,349, **1989** (to Shell Oil Company, Houston, TX).

22 Hoxmeier, R. J., US Patent 5,001,199, **1991** (to Shell Oil Company, Houston, TX).

23 Ladenberger, V., Bronstert, K., Fahrbach, G., Grog, W., US Patent 4,207,409, **1980** (to BASF Aktiengesellschaft, DE).

24 Mizuho, M., Kenichi, T., Japanese Patent 14-308,905, **2002** (to Kuraray Co Ltd, Japan).

25 Mizuho, M., Kenichi, T., Japanese Patent 14-317,008, **2002** (to Kuraray Co Ltd, Japan).

26 Kazuya, O., Mizuho, M., Kenichi, T., Japanese Patent 15-002,917, **2003** (to Kuraray Co Ltd, Japan).

27 Tsungae, Y., Mizuno, H., Kohara, T., Natsuume, T., US Patent 5,539,060, **1996** (to Nippon Zeon Co., Ltd., Tokyo, Japan).

28 Willis, C., US Patent 5,521,254, **1996** (to Shell Oil Company, Houston, TX).

29 Willis, C., US Patent 5,597,872, **1997** (to Shell Oil Company, Houston, TX).

30 Hoxmeier, R. J., Slaugh, L. H., US Patent 4,876,314, **1989** (to Shell Oil Company, Houston, TX).

31 Hoxmeier, R. J., US Patent 4,892,928, **1989** (to Shell Oil Company, Houston, TX).

32 Kishimoto, Y., Masubuchi, T., US Patent 4,673,714, **1987** (to Asahi Kase Kogyo Kabushiki Kaisha, Osaka, Japan).

33 Teramoto, T., Goshima, K., Takeuchi, M., US Patent 4,980,421, **1990** (to Japan Synthetic Rubber Co., Ltd., Tokyo, Japan).

34 Hashiguchi, Y., Katsumata, H., Goshima, K., Termoto, T., Takemura, Y., US Patent 5,169,905 **1992** (to Japan Synthetic Rubber Co., Ltd., Tokyo, Japan).

35 Chamberlain, L. R., Gibler, C. J., US Patent 5,132,372, **1992** (to Shell Oil Company, Houston, TX).

36 Chamberlain, L. R., Gibler, C. J., Kemp, R. A., Wilson, S. E., US Patent 5,141,997, **1992** (to Shell Oil Company, Houston, TX).

37 Chamberlain, L. R., Gibler, C. J., US Patent 5,173,537, **1992** (to Shell Oil Company, Houston, TX).

38 Gibler, C. J., Chamberlain, L. R., Hoxmeier, R. J., US Patent 5,242,986, **1992** (to Shell Oil Company, Houston, TX).

39 Gibler, C.J., Wilson, S.E., US Patent 5,244,980, **1993** (to Shell Oil Company, Houston, TX).

40 Gibler, C.J., Wilson, S.E., US Patent 5,334,566, **1994** (to Shell Oil Company, Houston, TX).

41 De Boer, E.J.M., Hessen, B., Van Der Huizen, A.A., De Jong, W., Van Der Linden, A.J., Ruisch, B.J., Schoon L., De Smet, H.J.A., Van Der Steen, F.H., Van Strien, H.C.T.L., Villena, A., Walhof, J.J.B., US Patent 5,814,709, **1998** (to Shell Oil Company, Houston, TX).

42 De Boer, E.J.M., Hessen, B., Van Der Huizen, A.A., De Jong, W., Van Der Linden, A.J., Ruisch, B.J., Schoon L., De Smet, H.J.A., Van Der Steen, F.H., Van Strien, H.C.T.L., Villena, A., Walhof, J.J.B., US Patent 5,886,107, **1999** (to Shell Oil Company, Houston, TX).

43 De Boer, E.J.M., Hessen, B., Van Der Huizen, A.A., De Jong, W., Van Der Linden, A.J., Ruisch, B.J., Schoon L., De Smet, H.J.A., Van Der Steen, F.H., Van Strien, H.C.T.L., Villena, A., Walhof, J.J.B., US Patent 5,925,717, **1999** (to Shell Oil Company, Houston, TX).

44 Van Der Heijden, H., Van De Weg, H., US Patent 6,461,993, **2002** (to Shell Oil Company, Houston, TX).

45 Van Der Heijden, H., Van De Weg, H., US Patent 5,592,430, **1999** (to Shell Oil Company, Houston, TX).

46 Chamberlain, L.R., Gibler, C.J., Kemp, R.A., Wilson, S.E., Brownscombe, T.F., US Patent 5,177,155, **1992** (to Shell Oil Company, Houston, TX).

47 Wilson, D.R., Stevens, J.C., US Patent 4,929,699, **1990** (to The Dow Chemical Company, Midland, MI).

48 Hahn, S.F., Wilson, D.R., US Patent 5,789,638, **1998** (to The Dow Chemical Company, Midland, MI).

49 Devore, D.D., Stevens, J.C., Hahn, S.F., Timmers, F.J., Wilson, D.R., US Patent 6,476,283, **2002** (The Dow Chemical Company, Midland, MI).

50 Ko, Y.H., Kim, J.Y., Hwang, J.M., US Patent 5,910,566, **1999** (to Korea Kumho Petrochemical Co., Ltd., Seoul, Rep. of Korea).

51 Ko, Y.H., Kim, H.C., US Patent 5,994,477, **1999** (to Korea Kumho Petrochemical Co., Ltd., Seoul, Rep. of Korea).

52 Ko, Y.H., Kim, H.C., US Patent 6,020,439, **2000** (to Korea Kumho Petrochemical Co., Ltd., Seoul, Rep. of Korea).

53 Ko, Y.H., Kim, H.C., Kim, J.Y., Hwang, J.M., US Patent 6,410,657, **2002** (to Korea Kumho Petrochemical Co., Ltd., Seoul, Rep. of Korea).

54 Parellada Ferrer, M.D., Barrio Calle, J.A., US Patent 5,583,185, **1996** (to Repsol Quimica S.A., Madrid, Spain).

55 Rekonen, P., Kopola, N., Koskimies, S., Andell, O., Oksman, M., US Patent 5,814,710, **1998** (to Neste Oy, Provoo, FI).

56 Tsiang, R.C., Hsien, H.C., Yang, W., US Patent 5,705,571, **1998** (to Taiwan Synthetic Rubber Corporation, Taipei, Taiwan).

57 Tsai, J., Chang, W., Chao, Y., Chu, C., Huang, C., Hsiao, H., US Patent 6,313,230, **2001** (to Industrial Technology Research, Hsinchu, Taiwan; Chi Mei Co., Tainan, Taiwan).

58 Vallieri, A., Cavallo, C., Viola, G.T., US Patent 5,948,869, **1999** (to Enichem S.p.A., Milan, Italy).

59 Viola, G.T., Vallieri, A., Cavallo, C., US Patent 6,228,952, **2001** (to Enichem S.p.A., Milan, Italy).

60 Masi, F., Sommazzi, A., Santi, R., US Patent 6,831,135, **2004** (to Enichem S.p.A., Roma, IT; Polimeri Europa S.p.A., Brindisi, Italy).

61 Lin, F., Tsai, C., Liu, S., US Patent 6,881,797, **2005** (to TSRC Corporation, Kaohsiung, Taiwan).

62 Kishimoto, Y., Morita, H., US Patent 4,501,857, **1985** (to Asai Kasei Kogyo Kabushiki Kaisha, Osaka, Japan).

63 McManus, N.T., Rempel, G.L., *J. Macromol. Chem. Physics* **1995**, *35*(2), 239–285.

64 Singha, N.K., Bhattacharjee, S., Sivaram, S., *Rubber Chem. Technol.* **1997**, *70*(3), 309.

65 Parent, J.S., McManus, N.T., Rempel, G.L., *Ind. Eng. Chem. Res.* **1998**, *37*, 4253.

66 Charmondusit, K., Prasassarakich, P., McManus, N.T., Rempel, G.L., *J. Appl. Polym. Sci.* **2003**, *89*, 142.

67 Pan, Q., Rempel, G. L., *Macromolec. Rapid Commun.* **2004**, *25*, 843.
68 Martin, P., McManus, N. T., Rempel, G. L., *J. Mol. Catal. A: Chemical* **1997**, *126*, 115.
69 Tangthongkul, R., Prasassarakich, P., McManus, N. T., Rempel, G. L., *J. Appl. Polym. Sci.* **2004**, *91*(5), 3259.
70 Rao, P. V. C., Upadhyay, V. K., Pillai, S. M., *Eur. Polym. J.* **2001**, *37*, 1159.
71 Parent, J. S., McManus, N. T., Rempel, G. L., *J. Appl. Polym. Sci.* **2001**, *79*, 1618.
72 Gilliom, L. R., *Macromolecules* **1989**, *22*, 662.
73 Gilliom, L. R., Honnell, K. G., *Macromolecules*, **1992**, *25*, 6066.
74 Bhattacharjee, S., Bhowmick, A. K., Avasthi, B. N., *J. Polym. Sci., Polym. Chem.* **1992**, *30*, 471.
75 Bhattacharjee, S., Rajagopalan, P., Bhowmick, A. K., Avasthi, B. N., *J. Appl. Polym. Sci.* **1993**, *49*, 19717.
76 Bhattacharjee, S., Bhowmick, A. K., Avasthi, B. N., *Polymer* **1993**, *34*, 5168.
77 Bhattacharjee, S., Bhowmick, A. K., Avasthi, B. N., *J. Appl. Polym. Sci.* **1990**, *41*, 1357.
78 Bhattacharjee, S., Bhowmick, A. K., Avasthi, B. N., *J. Polym. Sci., Polym. Chem.* **1992**, *30*, 1961.
79 Velichkova, R., Toncheva, V., Antonov, V., Alexandrov, V., Pavlova, S., Dubrovina, L., Cadkova, E., *J. Appl. Polym. Sci.* **1991**, *42*, 3083.
80 Yang, W., Hsieh, H. C., Tsiang, R. C., *J. Appl. Polym. Sci.* **1999**, *72*, 1807.
81 Parent, J. S., McManus, N. T., Rempel, G. L., *Ind. Eng. Chem. Res.* **1996**, *35*, 4417.
82 Halpern, J., *J. Chem. Soc. Chem. Commun.* **1973**, 629.
83 Mohammadi, N. A., Rempel, G. L., *Macromolecules* **1987**, *20*, 2362.
84 Booth, B. L., Haszeldine, R. N., Holmes, R. G.G., *J. Chem. Soc. Chem. Commun.* **1976**, *13*, 489.
85 Pimblett, B., Garner, C. D., Clegg, W., *J. Chem. Soc., Dalton Trans.* **1985**, 1977.
86 Schrock, R. R., Osborn, J. A., *J. Am. Chem. Soc.* **1976**, *98*, 2134.
87 Ohtani, Y., Yamagishi, A., Fujimoto, M., *Bull. Chem. Soc. Jpn.* **1979**, *52*, 2149.
88 Guo, X., Rempel, G. L., *J. Mol. Catal.* **1990**, *63*, 279.
89 Guo, X., Parent, J. S., Rempel, G. L., *J. Mol. Catal.* **1992**, *72*, 193.
90 Pan, Q., Rempel, G. L., *Ind. Eng. Chem. Res.* **2000**, *39*, 277.
91 Bhattacharjee, S., Bhowmick, A. K., Avasthi, B. N., *Ind. Eng. Chem. Res.* **1991**, *30*, 1086.
92 Bakhmutov, V. I., Bertran, J., Esteruelas, M. A., Lledos, A., Maseras, F., Modrego, J., Oro, L. A., Sola, E., *Chem. Eur. J.* **1996**, *2(7)*, 815.
93 Charmondusit, K., Prasassarakich, P., McManus, N. T., Rempel, G. L., *J. Appl. Polym. Sci.* **2003**, *89*, 142.
94 Pan, Q., Rempel, G. L. *Computer-Aided Modeling and Analysis of Complex Catalysis Kinetics*, October, 49th CSChE, Saskatoon, October **1999**.
95 Poloso, A., Murray, J. G., US Patent 4,028,485, **1977** (to Mobil Oil Corporation, New York, NY).
96 Kang, J., US Patent 4,098,991, **1978** (to The Firestone Tire & Rubber Company, Akron, OH).
97 Hoxmeier, R. J., US Patent 4,595,749, **1986** (to Shell Oil Company, Houston, TX).
98 Tsiang, R. C., US Patent 5,073,621, **1991** (to Shell Oil Company, Houston, TX).
99 Madgavkar, A. M., Daum, D. W., Gibler, C. J., US Patent 5,089,541, **1992** (to Shell Oil Company, Houston, TX).
100 Gibler, C. J., US Patent 5,821,696, **1994** (to Shell Oil Company, Houston, TX).
101 Diaz, Z., Gibler, C. J., US Patent 5,212,285, **1993** (to Shell Oil Company, Houston, TX).
102 Gibler, C. J., Austgen, Jr., D. M., Parker, R. A., US Patent 6,177,521, **2001** (to Shell Oil Company, Houston, TX).
103 Wilkey, J. D., US Patent 6,207,795, **2001** (to Shell Oil Company, Houston, TX).
104 Hofman, A. H., De Smet, H. J. A., Villena, A., Wirts, A. G. C., US Patent 6,800,725, **2004** (to KRATON Polymers U. S. LLC, Houston, TX).
105 Panster, P., Wieland, S., Buding, H., Obrecht, W., US Patent 5,403,566, **1995** (to Bayer AG, Leverkusen, DE).
106 Madgavkar, A. M., Gibler, C. J., Daum, D. W., US Patent 5,104,972, **1992** (to Shell Oil Company, Houston, TX).

107 Nguyen, P., Bender, H., Arsenault, G., Spadola, I., Mersmann, F.-J., US Patent 6,646,059, **2003** (to Bayer Inc., Sarnia, CA).

108 Biesenberger, J.A., Sebastian, D.H., *Principles of Polymerization Engineering*, Chapter 6, John Wiley Interscience, New York, NY, **1983**.

109 Pan, Q., Liu, Q., Sun, J., Li, C., Liang, A., Xie, F. Zhang, T., Chinese Patent ZL 97110481 (**1997**).

110 Pan, Q., Liu, Q., Sun, J., Li, C., Xie, F., Zhang, S., Chinese Patent, ZL 97113303 (**1997**).

111 Pan, Q., Zhou, X., Song, H., Feng, L., Xie, F., Jin, F., Chinese Patent, ZL 97219386 (**1997**).

112 Nauman, E.B., Flash devolatilization, in: *Encyclopedia of Polymer Science and Engineering*, Supplement Volume, Wiley, New York, **1989**, p. 317.

113 Biesenberger, J.A., *Devolatilization of Polymers: Fundamentals, Equipment, Applications*. Hanser Publishers, Munich, Vienna, New York, **1983**.

114 Flock, J.W., Matson, S.L., US Patent 4,408,040, **1983** (to General Electric Company, Schenectady, NY).

115 Houslay, R.J.G., US Patent 4,049,897, **1977** (to Imperial Chemical Industries Limited, London, UK).

116 Alsoy, S., Duda, J.L., *Aiche J.*, **1998**, *44(3)*, 582.

117 Hiroshi, Y., Shigeru, S., Japanese Patent 08-109,219, **1996** (to Asahi Chem. Ind. Co. Ltd, Japan).

118 Taizo, K., Tomohiro, Y., Yoshihiro, M., Kazumi, N., Japanese Patent 11-286,513, **1999** (to JSR CORP, Japan).

119 Miyamot, K., Yamakoshi, Y., Shiraki, T., US Patent 6,815,509, **2004** (to Asahi Kasei Kabushiki Kaisha, Osaka, Japan).

120 Pan, Q., Rempel, G.L., Ng, F.T.T., *Polymer Eng. Sci.* **2002**, *42*(5), 899.

121 Pan, Q., Kehl, A., Rempel, G.L., *Ind. Eng. Chem. Res.* **2002**, *41*(15), 3505.

122 Pan, Q., Rempel, G.L., *Int. J. Chemical Reactor Eng.* **2003**, *1*, A59.

123 Kempermann, T., Koch, S., Sumner, J., *Manual for the Rubber Industry*. Bayer AG, **1993**.

124 Rempel, G.L., Li, G.H., Pan, Q., Ng, F.T.T., *Macromol. Symp.* **2002**, *186*, 23.

125 Li, G., Pan, Q., Rempel, G.L., Ng, F.T.T., *Macromol. Symp.* **2003**, *204*, 141.

126 Rempel, G.L., Guo, X., US Patent 5,208,296, **1993** (to Polysar Rubber Corporation, Sarnia, CA).

127 Rempel, G.L., Guo, X., US Patent 5,210,151, **1993** (to Polysar Rubber Corporation, Sarnia, CA).

20
Transfer Hydrogenation Including the Meerwein-Ponndorf-Verley Reduction

Dirk Klomp, Ulf Hanefeld, and Joop A. Peters

20.1
Introduction

The first homogeneous transfer hydrogenation was reported in 1925 when Meerwein and Schmidt described the reduction of ketones and aldehydes using alcohols as reductants and aluminum alkoxides as the catalysts (Scheme 20.1) [1]. The major difference from previous studies was the hydrogen source; instead of molecular hydrogen, a small organic molecule was utilized to provide the hydrogen necessary to reduce the carbonyl compound. The scope of the reaction was independently investigated by Verley [2], Ponndorf [3], and Lund [4]. Some 12 years later, Oppenauer recognized the possibility of reversing the reaction into an oxidation procedure [5]. Ever since that time, the Meerwein-Ponndorf-Verley (MPV) reduction and the Oppenauer oxidation have been taken as textbook examples of highly selective and efficient reactions under mild conditions.

More recently, Ln^{III} alkoxides were shown to have much higher catalytic activity in this reaction, which allowed their use in only catalytic amounts [6, 7]. Later, however, much higher reactivities for Al^{III}-catalyzed Meerwein-Ponndorf-Verley and Oppenauer (MPVO) reactions have also been achieved with dinuclear Al^{III} complexes [8,9] and with Al^{III} alkoxides generated *in situ* [10]. Several reviews on the MPVO reactions have been published [11–14].

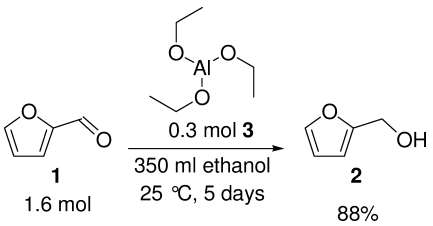

Scheme 20.1 The first homogeneous transfer hydrogenation reduction of furfural (**1**) to furfurylalcohol (**2**), described by Meerwein and Schmidt, using 0.18 equiv. aluminum ethoxide (**3**) [1].

The Handbook of Homogeneous Hydrogenation.
Edited by J.G. de Vries and C.J. Elsevier
Copyright © 2007 WILEY-VCH Verlag GmbH & Co. KGaA, Weinheim
ISBN: 978-3-527-31161-3

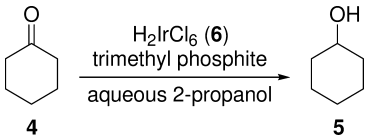

Scheme 20.2 A new approach towards the transfer hydrogenation of ketones, performed in 1964.

Pioneering studies on a different class of transfer hydrogenation catalysts were carried out by Henbest et al. in 1964 [15]. These authors reported the reduction of cyclohexanone (**4**) to cyclohexanol (**5**) in aqueous 2-propanol using chloroiridic acid (H_2IrCl_6) (**6**) as catalyst (Scheme 20.2). In the initial experiments, turnover frequencies (TOF) of 200 h^{-1} were reported.

A major step forward at this time was the introduction of the Wilkinson catalyst ($RhCl(PPh_3)_3$) (**7**) for hydrogen transfer reactions [16]. Although actually designed for hydrogenation with molecular hydrogen, this catalyst has been intensively used in transfer hydrogenation catalysis. Ever since, iridium, rhodium and also ruthenium complexes have been widely used in reductive transfer hydrogenations. The main advantage of these catalysts over the MPVO catalysts known until then was their comparatively higher catalytic activity. The TOFs of the transition-metal catalysts could be improved even further by the use of a base as additive, which deprotonates the substrate, facilitating complexation of the substrate to the metal ion in the intermediate complex [17–21]. Numerous reviews have been published on the topic of transition metal-catalyzed transfer hydrogenations [22–28].

The scope of hydrogen transfer reactions is not limited to ketones. Imines, carbon–carbon double and triple bonds have also been reduced in this way, although homogeneous and heterogeneous catalyzed reductions using molecular hydrogen are generally preferred for the latter compounds.

The advantages of hydrogen transfer over other methods of hydrogenation comprise the use of readily available hydrogen donors such as 2-propanol, the very mild reaction conditions, and the high selectivity. High concentrations of the reductant can be applied and the hydrogen donor is often used as the solvent, which means that mass transfer limitations cannot occur in these reactions. The uncatalyzed reduction of ketones requires temperatures of 300 °C [29].

Hydrogen transfer reactions are reversible, and recently this has been exploited extensively in racemization reactions in combination with kinetic resolutions of racemic alcohols. This resulted in dynamic kinetic resolutions, kinetic resolutions of 100% yield of the desired enantiopure compound [30]. The kinetic resolution is typically performed with an enzyme that converts one of the enantiomers of the racemic substrate and a hydrogen transfer catalyst that racemizes the remaining substrate (see also Scheme 20.31). Some 80 years after the first reports on transfer hydrogenations, these processes are well established in synthesis and are employed in ever-new fields of chemistry.

20.2
Reaction Mechanisms

Since the first use of catalyzed hydrogen transfer, speculations about, and studies on, the mechanism(s) involved have been extensively published. Especially in recent years, several investigations have been conducted to elucidate the reaction pathways, and with better analytical methods and computational chemistry the catalytic cycles of many systems have now been clarified. The mechanism of transfer hydrogenations depends on the metal used and on the substrate. Here, attention is focused on the mechanisms of hydrogen transfer reactions with the most frequently used catalysts. Two main mechanisms can be distinguished: (i) a direct transfer mechanism by which a hydride is transferred directly from the donor to the acceptor molecule; and (ii) an indirect mechanism by which the hydride is transferred from the donor to the acceptor molecule via a metal hydride intermediate (Scheme 20.3).

In the direct transfer mechanism, the metal ion coordinates both reactants enabling an intramolecular reaction, and activates them via polarization. Consequently, strong Lewis acids including Al^{III} and the Ln^{III} ions are the most suitable catalysts in this type of reactions. In the hydride mechanism, a hydride is transferred from a donor molecule to the metal of the catalyst, hence forming a metal hydride. Subsequently, the hydride is transferred from the metal to the acceptor molecule. Metals that have a high affinity for hydrides, such as Ru, Rh and Ir, are therefore the catalysts of choice. The Lewis acidity of these metals is too weak to catalyze a direct hydride transfer and, vice versa, the affinity of Al^{III} and Ln^{III} to hydride-ions is too low to catalyze the indirect hydrogen transfer. Two distinct pathways are possible for the hydride mechanism: one in which the catalyst takes up two hydrides from the donor molecule; and another in which the catalyst facilitates the transfer of a single hydride.

All hydrogen transfer reactions are equilibrium reactions. Consequently, both a reduction and an oxidation can be catalyzed under similar conditions. The balance of the reaction is determined by the thermodynamic stabilities of the spe-

direct transfer mechanism

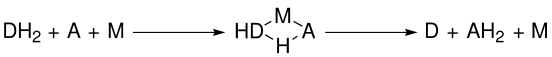

hydride mechanisms

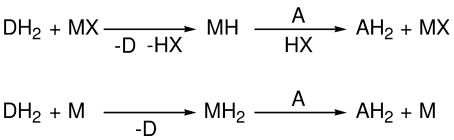

Scheme 20.3 Schematic representation of the two different hydrogen transfer mechanisms (D = donor molecule; A = acceptor molecule; M = metal).

cies in the redox equilibrium involved and by the concentrations of the hydride donors and acceptors.

20.2.1
Hydrogen Transfer Reduction of Carbonyl Compounds

Transfer hydrogenations of carbonyl compounds are often conducted using 2-propanol as the hydrogen donor. One advantage of this compound is that it can be used simultaneously as a solvent. A large excess of the hydrogen donor shifts the redox equilibrium towards the desired product (see also Section 20.3.1).

Studies aimed at the elucidation of reaction mechanisms have been performed by many groups, notably by those of Bäckvall [28]. In test reactions, typically enantiopure 1-phenylethanol labeled with deuterium at the 1-position (**8**) is used. The compound is racemized with acetophenone (**9**) under the influence of the catalyst and after complete racemization of the alcohol, the deuterium content of the racemic alcohol is determined. If deuterium transfer proceeds from the α-carbon atom of the donor to the carbonyl carbon atom of the acceptor the deuterium is retained, but if it is transferred to the oxygen atom of the acceptor it is lost due to subsequent exchange with alcohols in the reaction mixture (Scheme 20.4).

20.2.1.1 **Meerwein-Ponndorf-Verley Reduction and Oppenauer Oxidation**

The most common catalysts for the Meerwein-Ponndorf-Verley reduction and Oppenauer oxidation are Al^{III} and Ln^{III} isopropoxides, often in combination with 2-propanol as hydride donor and solvent. These alkoxide ligands are readily exchanged under formation of 2-propanol and the metal complexes of the substrate (Scheme 20.5). Therefore, the catalytic species is in fact a mixture of metal alkoxides.

The catalytic cycle of the reaction is depicted in Scheme 20.6 [31]. After the initial ligand exchange, the ketone (**10**) is coordinated to the metal ion of **11** (a), yielding complex **12**. A direct hydride transfer from the alkoxide to the ketone takes place via a six-membered transition state (b) in which one alkoxy group is oxidized (**13**). The acetone (**14**) and the newly formed alcohol (**15**) are released

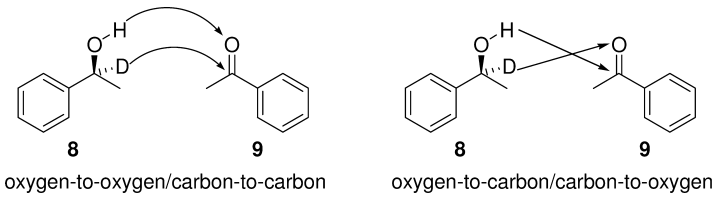

Scheme 20.4 Possible pathways of hydrogen transfer during the racemizations of alcohols using the corresponding carbonyl compound and a hydrogen transfer catalyst.

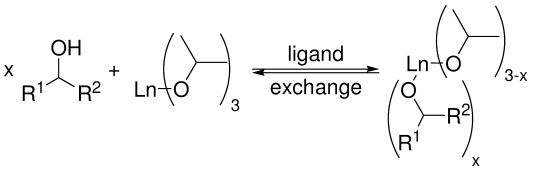

Scheme 20.5 Ligand exchange in MPVO reactions.

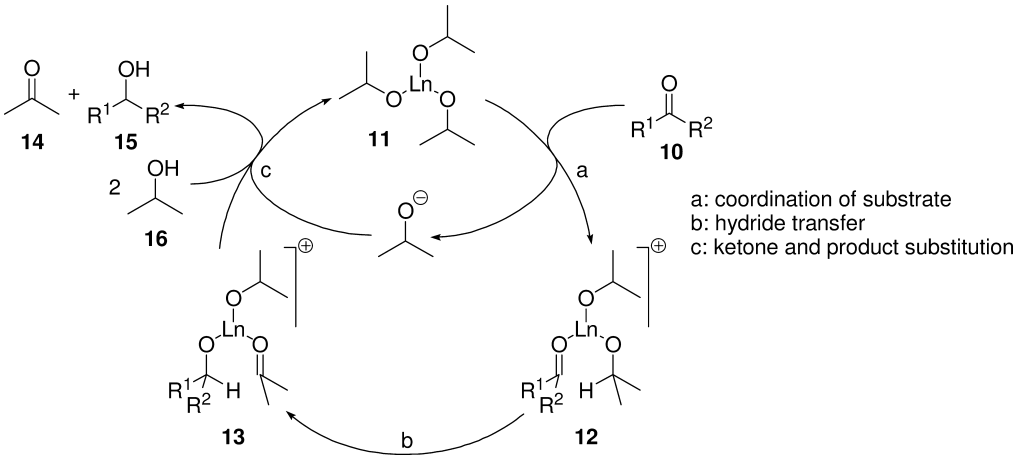

Scheme 20.6 Mechanism of the Meerwein-Ponndorf-Verley-Oppenauer reaction.

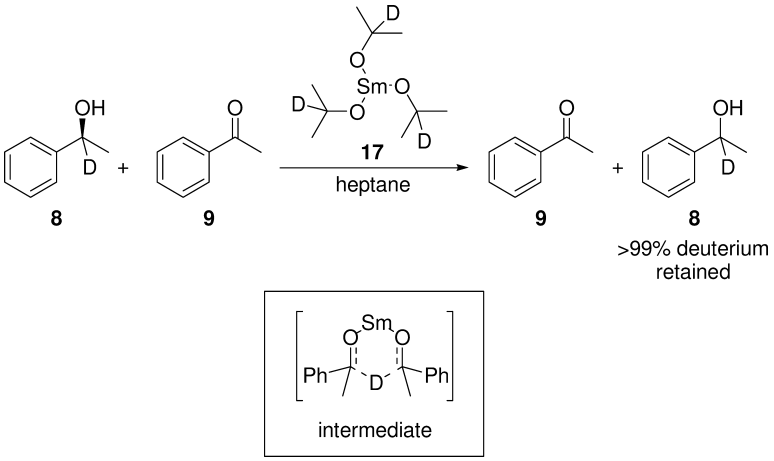

Scheme 20.7 Racemization of (*S*)-1-deutero-1-phenylethanol (**9**) with deuterated samarium(III) isopropoxide (**17**).

from the metal center by substitution for new donor molecules (**16**) (c) completing the cycle.

The mechanism of the MPVO reactions has been investigated and questioned on several occasions, and a variety of direct hydrogen-transfer pathways have been suggested (see Scheme 20.4) [31–35]. Recently, racemization of D-labeled 1-phenylethanol with deuterated samarium(III) isopropoxide (**17**) proved that the MPVO reaction occurs via a direct hydrogen transfer from the α-position of the isopropoxide to the carbonyl carbon of the substrate (Scheme 20.7) [31].

The selectivity of the hydrogen transfer is excellent. When employing a catalyst with deuterium at the α-positions of the isopropoxide ligands (**17**), complete retention of the deuterium was observed. A computational study using the density functional theory comparing the six-membered transition state (as in Scheme 20.3, the direct transfer mechanism) with the hydride mechanism (Scheme 20.3, the hydride mechanism) supported the experimental results obtained [36]. A similar mechanism has been proposed for the MPV alkynylations [37] and cyanations [38].

20.2.1.2 **Transition Metal-Catalyzed Reductions**

The Wilkinson catalyst, ($RhCl(PPh_3)_3$) (**7**), is not only an excellent hydrogenation catalyst when using molecular hydrogen as hydrogen donor, but can also be employed as a hydrogen transfer catalyst. It is a square-planar, 16-electron complex, which catalyzes these reactions via different pathways depending on the hydrogen donor. The intermediate rhodium complexes tend to retain a four-coordinated square-planar configuration, whereas the molecular hydrogen pathway proceeds through an octahedral state [35, 39–42] (Scheme 20.8).

In transfer hydrogenation with 2-propanol, the chloride ion in a Wilkinson-type catalyst (**18**) is rapidly replaced by an alkoxide (Scheme 20.9). β-Elimination then yields the reactive 16-electron metal monohydride species (**20**). The ketone substrate (**10**) substitutes one of the ligands and coordinates to the catalytic center to give complex **21** upon which an insertion into the metal hydride bond takes place. The formed metal alkoxide (**22**) can undergo a ligand exchange with the hydride donor present in the reaction mixture, liberating the product (**15**).

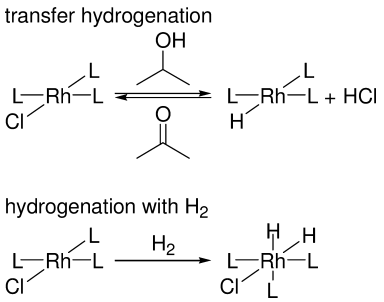

Scheme 20.8 Different behavior of the Wilkinson catalyst (**7**) for transfer hydrogenation and hydrogenation using molecular hydrogen.

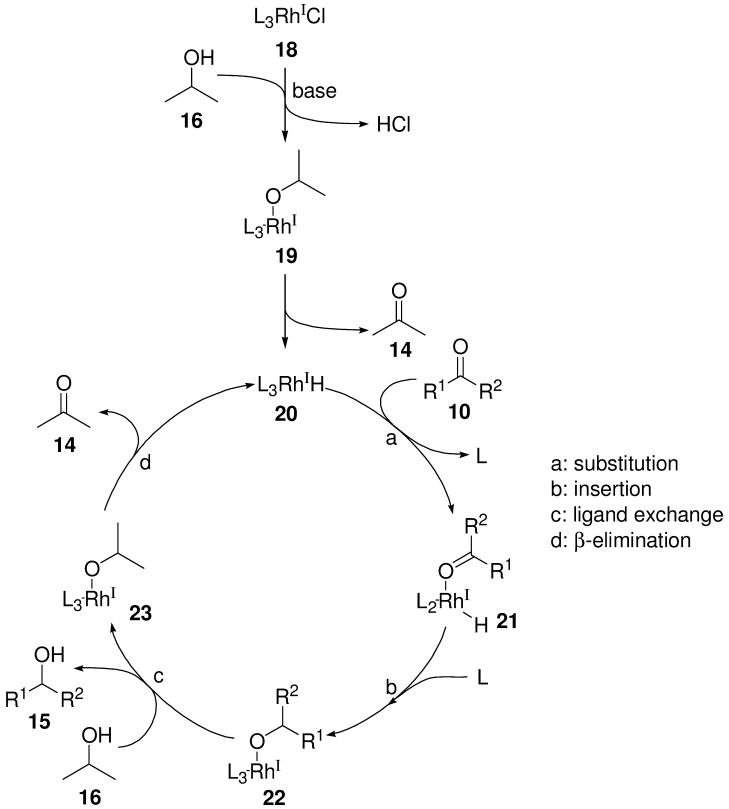

Scheme 20.9 Transition metal alkoxide mechanism.

After *β*-elimination, acetone is released and the metal monohydride (**20**) is obtained again from **23**, closing the catalytic cycle.

Mechanistic studies show that the extent of deuterium-labeling at the *α*-position of (*S*)-1-deutero-1-phenylethanol remains almost unchanged during a racemization reaction with this system (Scheme 20.10) [35]. This indicates that a single hydride is transferred from the *α*-position of the donor to the *α*-position of the acceptor. Only a slight decrease in deuterium content occurs (5%), which may be attributed to exchange with traces of water. In catalysts bearing phenyl phosphine ligands, the loss of deuterium can also be explained by orthometalation [43], leading to H/D exchange. Several other catalysts have been shown to operate via the same mechanism as the Wilkinson catalyst (Fig. 20.1).

A different mechanism is operative with the 16-electron complex $RuCl_2(PPh_3)_3$ (**24**) (Scheme 20.11). Here, the dichloride complex (**25**) is rapidly converted into a dihydride species (**26**) by substitution of both chloride ligands with alkoxides and subsequent eliminations similar to the conversion of **18** to **20** described above [46, 47]. Subsequently, the ruthenium dihydride species **26**

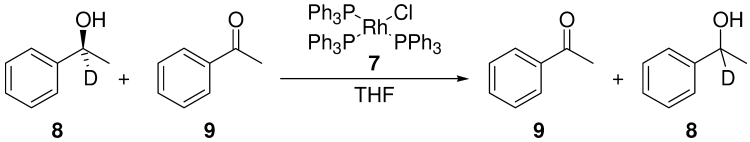

Scheme 20.10 Racemization of (*S*)-1-deutero-1-phenylethanol (**8**) with the Wilkinson catalyst (**7**).

Fig. 20.1 Examples of catalysts operating via the same mechanism as the Wilkinson catalyst (bipy = bipyridine; dppp = 1,3-bis(diphenylphosphinopropane) [35, 44, 45].

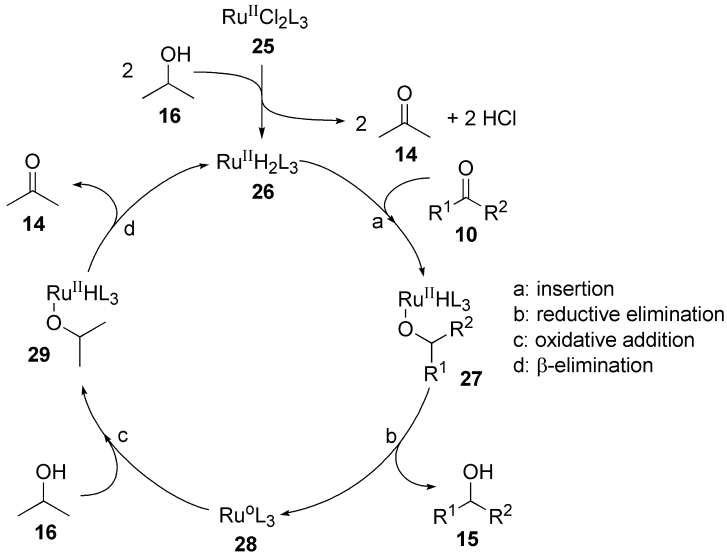

Scheme 20.11 Transition metal dihydride mechanism.

reacts (a) with a substrate molecule (**10**) to give the monohydride alkoxide complex (**27**). Reductive elimination (b) liberates the product (**15**) and a Ru^0 species (**28**). Oxidative addition (c) of an alcohol (**16**) yields a new monohydride alkoxide complex (**29**). After a β-elimination step (d), Ru^{II} dihydride (**26**) is formed again. This mechanism is supported by the fact that the racemization of (*S*)-1-deutero-1-phenylethanol (**8**), catalyzed by this and similar catalysts, decreased to about 40% [35]. In theory, the mechanism depicted in Scheme 20.11 leads to an equal distribution of the deuterium-label over the α-position of the alcohol and its hy-

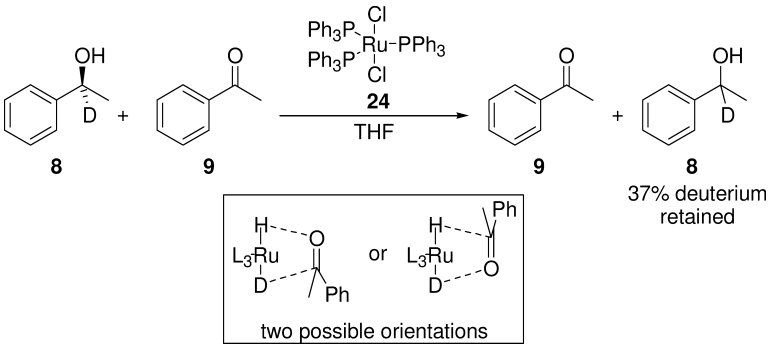

Scheme 20.12 Racemization of (*S*)-1-deutero-1-phenylethanol (**8**) with $RuCl_2(PPh_3)_3$ (**24**).

droxyl function (Scheme 20.12). The deuterium content of the product is probably somewhat lower due to H/D exchange between the alcohol function and traces of water and other alcohols in the reaction mixture.

In the transition metal-catalyzed reactions described above, the addition of a small quantity of base dramatically increases the reaction rate [17–21]. A more elegant approach is to include a basic site into the catalysts, as is depicted in Scheme 20.13. Noyori and others proposed a mechanism for reactions catalyzed with these 16-electron ruthenium complexes (**30**) that involves a six-membered transition state (**31**) [48–50]. The basic nitrogen atom of the ligand abstracts the hydroxyl proton from the hydrogen donor (**16**) and, in a concerted manner, a hydride shift takes place from the α-position of the alcohol to ruthenium (a), re-

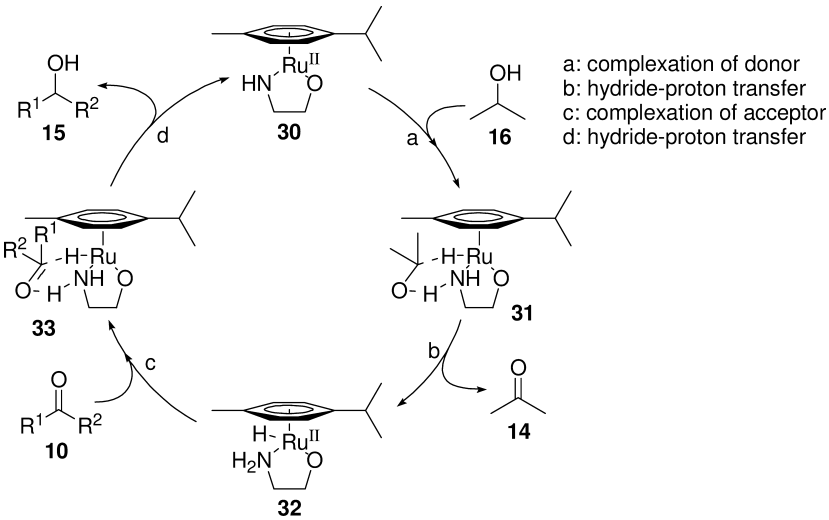

Scheme 20.13 Concerted hydride-proton transfer mechanism.

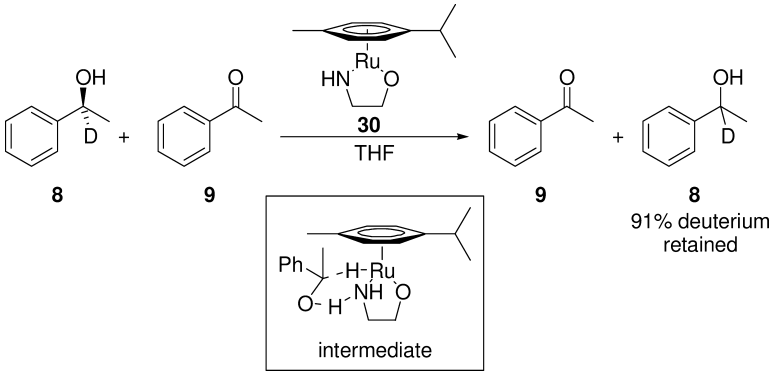

Scheme 20.14 Racemization of (*S*)-1-deutero-1-phenylethanol (**8**) with $Ru(OC_2H_4NH)$(cymene) (**30**).

leasing a ketone (**14**) (b). The Ru^{II} monohydride (**32**) formed is now able to bind to the substrate ketone (**10**) (c) and, in another concerted reaction, the alcohol (**15**) is formed together with the 16-electron ruthenium complex (**30**) (d).

Formation of the Ru^{II} hydride species is supported by the findings of deuterium-labeling studies (Scheme 20.14) [35]. The deuterium label remains at the *α*-position of the alcohol during racemizations; this is due to the orientation of the alcohol when it coordinates to the Ru-complex. Once again, some deuterium

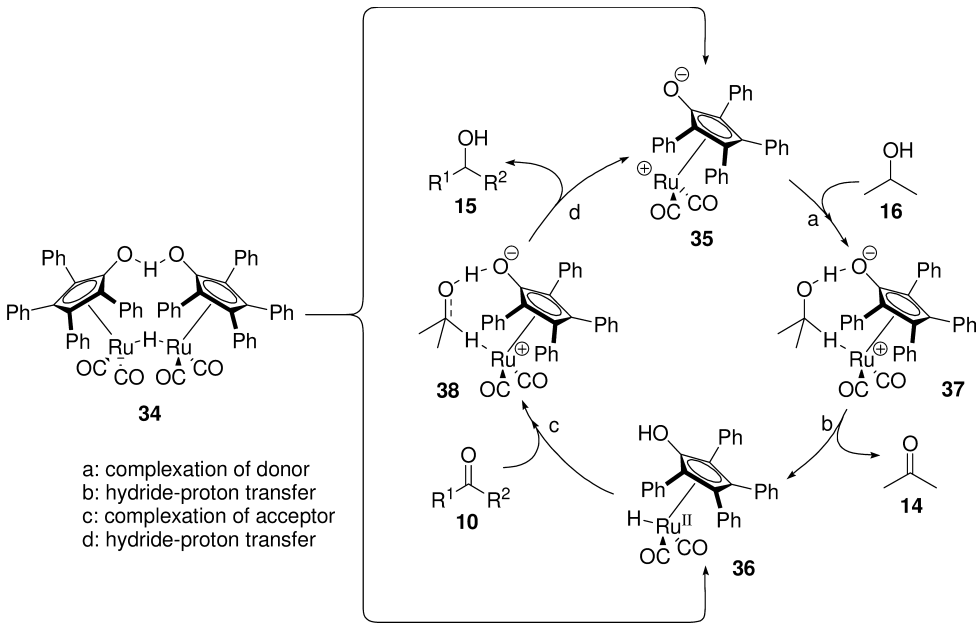

Scheme 20.15 The catalytic cycle of the Shvo catalyst (**34**).

is probably lost due to H/D exchange with traces of water or alcohol in the reaction mixture.

The most reactive transition metal transfer hydrogenation catalysts identified to date have bidentate ligands. Studies towards active catalysts are mainly directed towards the size and nature of the bridge in the ligand [51] and towards the nature of coordinating atoms to the metal [52–54]. It seems that ligands containing both a phosphorus and a nitrogen atom possess the best properties for these types of reactions (see also Section 20.3.3).

Of particular interest is the dinuclear Ru complex **34**, the so-called Shvo catalyst [55, 56]. It has been established that, under the reaction conditions, this complex is in equilibrium with two monometal complexes (**35** and **36**) [57–59]. Both of these resemble catalytic intermediates in the concerted proton-hydride transfer pathway (Scheme 20.13), and will react in a similar way (Scheme 20.15) involving the six-membered transition state **37** and the reduction of the substrate via **38**.

20.2.2
Transfer Hydrogenation Catalysts for Reduction of C–C Double and Triple Bonds

The reduction of C–C double and triple bonds using molecular hydrogen is generally preferred over transfer hydrogenation. However, some interesting examples of transfer hydrogenations of alkenes and alkynes are known. As an illustration of the mechanism of a typical transfer hydrogenation, the reduction of an alkene with dioxane as the hydride donor and the Wilkinson catalyst (**7**) is discussed. The reduction does not necessarily have to be performed with dioxane, but this hydride donor is rather common in these reductions. The use of hydrogen donors and their distinct advantages and disadvantages are discussed in Section 20.3.1.

The first step consists of the substitution of one of the ligands (L) of **18** by dioxane (**39**) in an oxidative addition (a) (Scheme 20.16). β-Elimination of **40** releases 2,3-dihydro-dioxine (**41**) and the 16-electron dihydrogen rhodium complex (**42**) (b). Alkene **43** coordinates to the vacant site of **42** (c) to give complex **44**. A hydride insertion then takes place (d), affording complex **45**. After a reductive elimination (e) of the product **46**, the coordination of a ligand reconstitutes the Wilkinson-type catalyst (**18**).

The coordination of dioxane and subsequent oxidative addition to the catalytic species (step (a) in Scheme 20.16) probably proceeds after the oxygen atom coordinates to the rhodium (**47**), followed by abstraction of a hydrogen atom. The cationic species (**48**) then rearranges to a complex in which the dioxane is bound to the rhodium via the carbon atom (**40**) (Scheme 20.17) [60].

Transfer hydrogenations are typically equilibrium reactions; however, when formic acid (**49**) is utilized as the hydrogen donor, carbon dioxide (**50**) is formed which escapes from the reaction mixture [61–64].

Here, an example is given for the reduction of itaconic acid (**51**) with a rhodium catalyst precursor (**52**) and a phosphine ligand (**53**) (Scheme 20.18). The

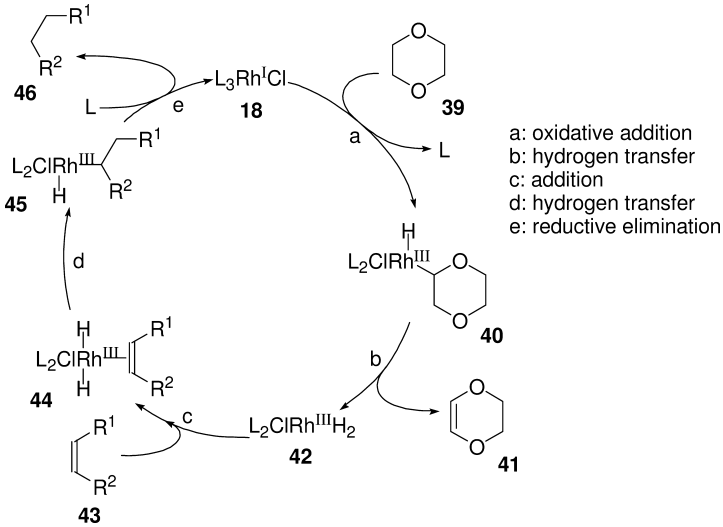

Scheme 20.16 Alkene reduction with dioxane (**39**) as hydride donor and a Wilkinson-type catalyst (**18**).

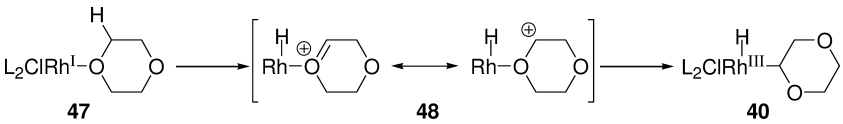

Scheme 20.17 Step (a) of Scheme 20.16: the coordination and oxidative addition of dioxane.

itaconic acid (**51**) is a good chelating ligand for the catalyst, and when the 16-electron Rh^{I} active species **54** is formed, an oxidative addition of formic acid (**49**) takes place (a). Decarboxylation (b) of **55** liberates CO_2 (**50**), forming a Rh^{III}-dihydride (**56**). A hydride transfer (c) leading to a pentacoordinated metal (**57**) and subsequent reductive elimination (d), in which the product (**58**) is liberated and a new substrate (**51**) is coordinated, closes the cycle.

This system is very selective towards the reduction of C–C double bonds, and the oxygen of the acid group that coordinates to the metal is important for good catalytic properties. In the reaction mixture, triethylamine is added in a ratio of formic acid : triethylamine of 5 : 2, which is the commercially available azeotropic mixture of these compounds.

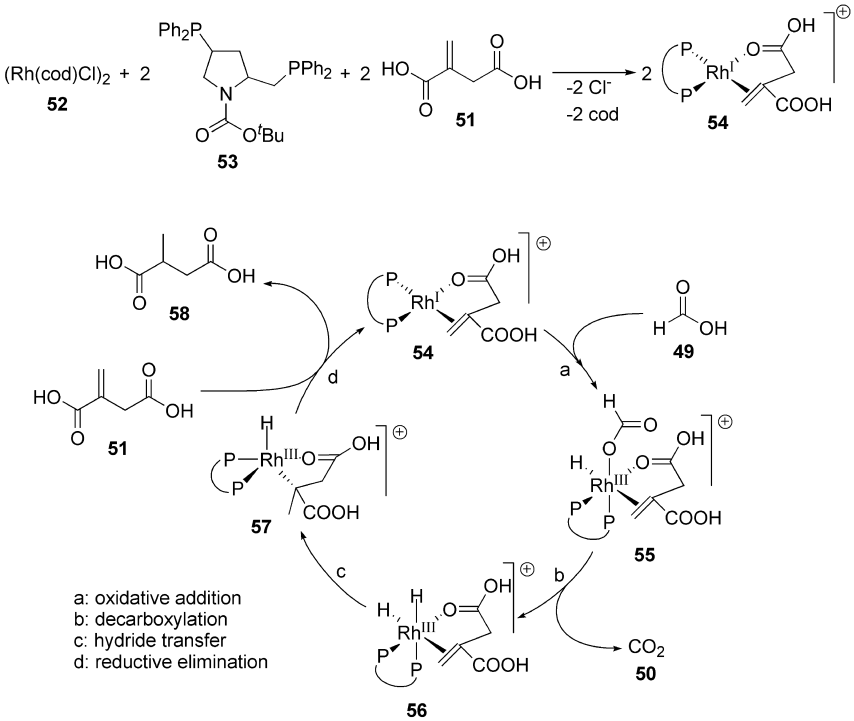

Scheme 20.18 Reduction of the C–C double bond of itaconic acid (**51**) utilizing a rhodium catalyst (**54**) and formic acid (**49**) as hydrogen donor.

20.3 Reaction Conditions

20.3.1 Hydrogen Donors

By definition, hydrogen transfer is a reaction during which hydrogen is transferred from a source other than molecular hydrogen. In theory, the donor can be any compound that has an oxidation potential which is low enough to allow hydrogen abstraction under influence of a catalyst under mild conditions. Another requirement is that the donor is able to coordinate to the catalytic center and does not bind tightly after donation of the hydrogen.

The hydrogen donors vary widely from heteroatom-containing compounds such as alcohols, amines, acids and cyclic ethers to hydrocarbons such as alkanes (Table 20.1). The choice of donor is largely dependent on several issues:

- the *type* of reaction: MPVO or transition metal-catalyzed;
- the *affinity* of the substrate for the metal concerned;

- the *exchange rates* of the substrate between the metal-bound and the free form;
- its *solubility* in the reaction medium or its ability to *dissolve* all other reaction ingredients;
- its influence on the *equilibrium* of the reaction;
- the *temperature* at which the reaction is taking place;
- its ability to avoid harmful *side products*; and
- the *nature* of the functional group to be reduced.

Alcohols have always been the major group of hydrogen donors. Indeed, they are the only hydrogen donors that can be used in Meerwein-Ponndorf-Verley (MPV) reductions. 2-Propanol (**16**) is most commonly used both in MPV reductions and in transition metal-catalyzed transfer hydrogenations. It is generally available and cheap, and its oxidation product, acetone (**14**), is nontoxic and can usually be removed readily from the reaction mixture by distillation. This may have the additional advantage that the redox equilibrium is shifted even more into the direction of the alcohol. As a result of sigma inductive electronic ef-

Table 20.1 Hydrogen donors and their oxidized products.

Entry	Donor	Acceptor
1 [a)]		
2 [b)]	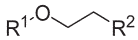	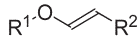
3		
4	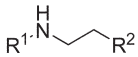	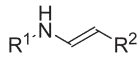
5 [c)]		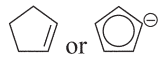
6 [d)]		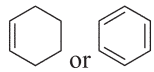
7		CO_2

a) Both primary and secondary alcohols.
b) Typically cyclic ethers as dioxane and THF; only one pair of hydrogens is abstracted.
c) The cyclopentadienyl ring coordinates to the catalyst.
d) The reaction preferably stops at cyclohexene.

fects, secondary alcohols are generally better hydrogen donors than primary ones. However, many examples of the use of primary alcohols have been reported. Ethanol, as already pointed out by Meerwein and Schmidt [1], yields acetaldehyde which, even at room temperature, leaves the reaction mixture and results in irreversible reductions. Unfortunately, the aldehydes resulting from primary alcohols as donors are known to act as catalyst poisons. Furthermore, they may decarbonylate, forming CO, which may modify the catalysts and consequently change their activity [65, 66].

Other alcohols, such as diols [67–69], polyols such as furanoses, pyranoses [70, 71] and polyvinyl alcohol [72] have been reported to enable the reduction of ketones to alcohols.

Heterocyclic compounds are frequently used as hydrogen donors in the reduction of C–C double and triple bonds catalyzed by complexes of transition metals. Cyclic ethers such as [1,4]dioxane (**39**) and 2,3-dihydrofuran are known to donate a pair of hydrogen atoms to this type of compound. 2,3-Dihydro-[1,4]dioxine (**41**), the product of dioxane (**39**), is not able to donate another pair of hydrogen atoms [46, 60, 73, 74]. These heterocyclic compounds are in general also very good solvents for both the catalyst and the substrates.

Nitrogen-containing heterocyclic compounds, including 1,2,3,4-tetrahydroquinoline, piperidine, pyrrolidine and indoline, are also popular hydrogen donors for the reduction of aldehydes, alkenes, and alkynes [75, 76]. With piperidine as hydrogen donor, the highly reactive 1-piperidene intermediate undergoes trimerization or, in the presence of amines, an addition reaction [77]. Pyridine was not observed as a reaction product.

Hydrocarbons are also able to donate hydrogen atoms. In particular, indan and tetralin, which are able to form conjugated double bonds or a fully aromatic system, are used [74].

Once again, use of these donors as solvent may shift the reaction equilibrium towards the desired product. Since the reactivity of olefins is lower than that of carbonyl compounds, higher reaction temperatures are usually required to achieve acceptable TOFs, and then the relatively higher boiling hydrogen donating solvents mentioned above may be the best choice.

Henbest and Mitchell [78] have shown that water can be used as hydrogen source with chloroiridic acid (**6**) as the catalyst through oxidation of phosphorous acid (**59**) to phosphoric acid (**60**) in aqueous 2-propanol. Under these conditions, no hydrogen transfer occurs from 2-propanol. However, iridium complexes with sulfoxide or phosphine ligands show the usual transfer from 2-propanol [79–81].

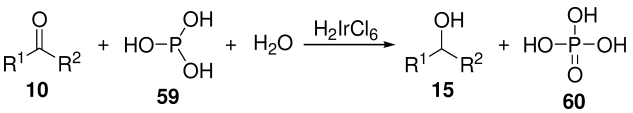

Scheme 20.19 Transfer hydrogenation with the Henbest system.

Hydrogen transfer reactions are highly selective and usually no side products are formed. However, a major problem is that such reactions are in redox equilibrium and high TOFs can often only be reached when the equilibria involved are shifted towards the product side. As stated above, this can be achieved by adding an excess of the hydrogen donor. (For a comparison, see Table 20.2, entry 8 and Table 20.7, entry 3, in which a 10-fold increase in TOF, from 6 to 60, can be observed for the reaction catalyzed by neodymium isopropoxide upon changing the amount of hydrogen donor from an equimolar amount to a solvent. Removal of the oxidation product by distillation also increases the reaction rate. When formic acid (**49**) is employed, the reduction is a truly irreversible reaction [82]. This acid is mainly used for the reduction of C–C double bonds. As the proton and the hydride are removed from the acid, carbon dioxide is formed, which leaves the reaction mixture. Typically, the reaction is performed in an azeotropic mixture of formic acid and triethylamine in the molar ratio 5 : 2 [83].

In summary, the most popular hydrogen donors for the reduction of ketones, aldehydes and imines are alcohols and amines, while cyclic ethers or hydroaromatic compounds are the best choice for the reduction of alkenes and alkynes.

20.3.2 Solvents

As mentioned above, the hydrogen donor is the solvent of choice in hydrogen-transfer reactions. However, if for any reason another solvent is needed, it is important to select one that does not compete with the substrate or the ligands of

Table 20.2 Racemization of (*S*)-1-phenylethanol (**61**) in different solvents (Scheme 20.20).[a)]

Entry	Solvent	Time [h]	ee [%][b)]	TOF [h^{-1}][c)]
1	Acetonitrile	>48	>99	0
2	Dioxane	5	28	2
3	THF	3.5	0	4
4	Diisopropyl ether	3.5	0	4
5	MTBE	3.5	0	4
6	Toluene	3	0	5
7	Hexane	2	0	6
8	Heptane	2	0	6

a) Solvent (12 mL), zeolite NaA (30 mg, dried at 400 °C), (*S*)-1-phenylethanol (**61**) (0.24 mL, 2 mmol), acetone (**14**) (0.15 mL, 2 mmol, 1 equiv.), 1,3,5-triisopropylbenzene (int. std.) (0.2 mL) and neodymium(III) isopropoxide (120 mg, 0.37 mmol, 0.185 equiv.) were stirred at 50 °C.
b) ee (starting material) >99%.
c) As determined in the first 15 min of the reaction; in this period predominantly oxidation takes place.

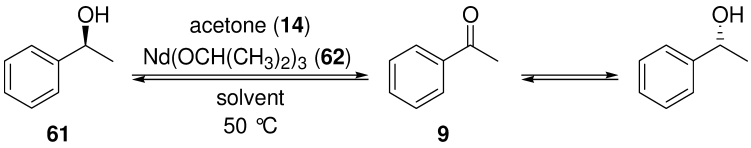

Scheme 20.20 Racemization of **61** with 19% neodymium(III) isopropoxide (**62**) and 1 equiv. acetone (**14**).

the catalyst. By replacing ligands of the catalyst, the electron density of the metal changes, and this may have a detrimental effect on the activity of the catalyst.

As an example, Table 20.2 lists the rate of the racemization of **61** via an MPVO procedure utilizing the catalyst neodymium(III) isopropoxide (**62**) as a function of the solvent. In this case, an equimolar amount of acetone was applied as the oxidant. The best results were obtained with hydrocarbons such as hexane (entry 7) and heptane (entry 8) as solvents, while the reaction rates in dioxane (entry 2) and acetonitrile (entry 1) were much lower due to inactivation of the catalyst by coordination of the solvent to the metallic center (Table 20.2) [84].

20.3.3
Catalysts and Substrates

Meerwein-Ponndorf-Verley-Oppenauer catalysts typically are aluminum alkoxides or lanthanide alkoxides (see above). The application of catalysts based on metals such as ytterbium (see Table 20.7, entries 6 and 20) and zirconium [85, 86] has been reported.

Lanthanide(III) isopropoxides show higher activities in MPV reductions than $Al(O\mathit{i}Pr)_3$, enabling their use in truly catalytic quantities (see Table 20.7; compare entry 2 with entries 3 to 6). Aluminum-catalyzed MPVO reactions can be enhanced by the use of TFA as additive (Table 20.7, entry 11) [87, 88], by utilizing bidentate ligands (Table 20.7, entry 14) [89] or by using binuclear catalysts (Table 20.7, entries 15 and 16) [8, 9]. With bidentate ligands, the aluminum catalyst does not form large clusters as it does in aluminum(III) isopropoxide. This increase in availability per aluminum ion increases the catalytic activity. Lanthanide-catalyzed reactions have been improved by the *in-situ* preparation of the catalyst; the metal is treated with iodide in 2-propanol as the solvent (Table 20.7, entries 17–20) [90]. Lanthanide triflates have also been reported to possess excellent catalytic properties [91].

One drawback of all these catalysts is their extreme sensitivity to water. To avoid this problem, reactions should be carried out under an inert atmosphere and, if possible, in the presence of molecular sieves [92]. The molecular sieves also suppress aldol reactions, as will be discussed in Section 20.4.

For the reduction of carbonyl groups or the oxidation of alcohols in the presence of C–C double and triple bonds, MPVO catalysts seem to be the best choice with respect to selectivity for the carbonyl group, as reductions with com-

plexes of transition metals are less selective (see Section 20.3.4). In the vast majority of syntheses, aluminum(III) isopropoxide is used as the catalyst. From a catalytic point of view, this is not the best choice, since it typically must be added in equimolar amounts. Probably due to its availability in the laboratory and ease of handling, it is the most frequently used MPVO-catalyst, despite the development of the more convenient lanthanide(III)isopropoxides. An advantage of the aluminum catalyst in industrial processes is the possibility to distil off the products while the catalyst remains active in the production vessel.

In recent years, many active transition-metal catalysts have been developed (see Table 20.7, entries 21–53). Careful design of the ligands of the transition-metal complexes has led to the development of catalysts with high activities. Mixed chelate ligands containing both a phosphorus- and a nitrogen-binding site were employed to prepare catalysts with unusual electronic properties (Table 20.7, entries 24–29, 40–42, 44). In particular, the catalyst in entry 44 shows a very high TOF for the reduction of acetophenone ($10^6\ h^{-1}$). Other very good catalysts have bidentate phosphine ligands and TOFs of up to $2300\ h^{-1}$ (entries 34 and 35), contain both nitrogen and phosphorus ligands and TOFs of up to $900\ h^{-1}$ (entries 45–47), or have different bidentate moieties (entries 48 and 50–52) and TOFs of up to $14\,700\ h^{-1}$.

Neutral mixed chelate ligands containing both phosphorus- and nitrogen-binding sites often show a hemilabile character (they are able to bind via one or two atoms to the metal; Fig. 20.2), which allows for the temporary protection and easy generation of reactive sites in the complexes.

Furthermore, the acidity of PCH_2 protons in oxazoline ligands (**63**) enables easy deprotonation of the chelate, giving rise to a static (non-dissociating) anionic four-electron-donating ligand (**64**). These properties give rise to a high activity (Fig. 20.2) [52].

Transition-metal catalysts are, in general, more active than the MPVO catalysts in the reduction of ketones via hydrogen transfer. Especially, upon the introduction of a small amount of base into the reaction mixture, TOFs of transition-metal catalysts are typically five- to 10-fold higher than those of MPVO catalysts (see Table 20.7, MPVO catalysts: entries 1–20, transition-metal catalysts: entries 21–53). The transition-metal catalysts are less sensitive to moisture than MPVO catalysts. Transition metal-catalyzed reactions are frequently carried out in 2-propanol/water mixtures. Successful transition-metal catalysts for transfer hydrogenations are based not only on iridium, rhodium or ruthenium ions but also on nickel [93], rhenium [94] and osmium [95]. It has been reported that

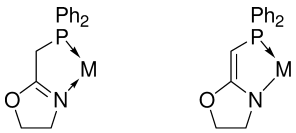

63 **64**

Fig. 20.2 The neutral PCH_2-oxazoline ligand (**63**) and the anionic PCH-oxazoline ligand (**64**).

MPV reductions with aluminum(III) isopropoxide as the catalyst can be hugely enhanced by microwave irradiation [96].

In summary, the reduction of ketones and aldehydes can both be performed with MPV and transition-metal complexes as catalysts. Reductions of alkenes, alkynes, and imines require transition-metal catalysts; MPV reductions with these substrates are not possible.

Hydrogen transfer towards imines is in general slower than towards the corresponding carbonyls. Nonetheless, the reduction can be performed using the same catalysts, although harsher reaction conditions may have to be applied [97]. This is probably a result of the relative stability of imines with respect to carbonyls. In general, the hydrogen transfer of imines proceeds faster with aldimines than with ketimines. The Shvo catalyst (**34**), however, is slightly more reactive towards the latter [56].

In general, the activity of transition-metal catalysts is higher in hydrogenation reactions than in hydrogen transfer reactions. In the few cases where both hydrogenation methods were performed with the same catalyst, it has been shown that reaction rates are lower for transfer hydrogenations. Some examples are known in which transfer hydrogenation is faster than hydrogenation with H_2 [98–100]. The simplicity of the transfer hydrogenation protocol and the abundance of selective and active catalysts make this method very competitive with hydrogenations utilizing H_2, and it is often the preferred reaction.

20.3.4
Selectivity

As mentioned above, MPVO catalysts are very selective towards carbonyl compounds. Alkenes, alkynes or other heteroatom-containing double bonds are not affected by these catalysts, while they can be reduced by transition-metal catalysts. Examples of the reduction of α,β-unsaturated ketones and other multifunctional group compounds are compiled in Table 20.3.

Transition metals can display selectivities for either carbonyls or olefins (Table 20.3). $RuCl_2(PPh_3)_3$ (**24**) catalyzes reduction of the C–C double bond function in the presence of a ketone function (Table 20.3, entries 1–3). With this catalyst, reaction rates of the reduction of alkenes are usually higher than for ketones. This is also the case with various iridium catalysts (entries 6–14) and a ruthenium catalyst (entry 15). One of the few transition-metal catalysts that shows good selectivity towards the ketone or aldehyde function is the nickel catalyst (entries 4 and 5). Many other catalysts have never been tested for their selectivity for one particular functional group.

In total syntheses where a homogeneously catalyzed transfer hydrogenation is applied, almost exclusively aluminum(III) isopropoxide is utilized as the catalyst. At an early stage in the total synthesis of (–)-reserpine (**65**) by Woodward [106], an intermediate with two ketone groups and two C–C double bonds is formed (**66**) by a Diels-Alder reaction of *para*-benzoquinone (**67**) and vinylacrylate (**68**). The two ketone groups were reduced with aluminum(III) isopropoxide

Table 20.3 Selectivity towards functional groups.

Entry	Catalyst	Substrate ([S]/[C]) [a)]	Product	Reductant	Temperature (time) [°C, h] [b)]	Conversion ratio [%]	TOF [h^{-1}]	Reference
1	$RuCl_2(PPh_3)_3$	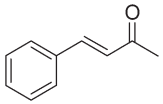 (400)	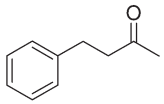	1-phenylethanol	180 (1)	95	380	101
2	$RuCl_2(PPh_3)_3$	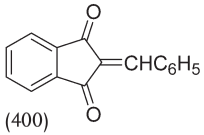 (400)	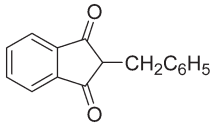	1-phenylethanol	180 (1)	45	180	101
3	$RuCl_2(PPh_3)_3$	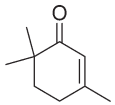 (400)	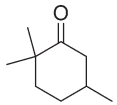	1-phenylethanol	180 (1)	54	216	101
4	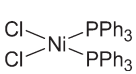	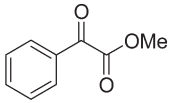 (7)	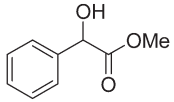	2-propanol	82 (36)	65	0.12	102
5	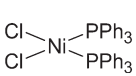	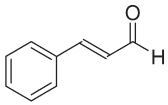 (7)	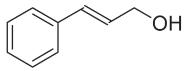	2-propanol	82 (30)	51	0.11	102

Table 20.3 (continued)

Entry	Catalyst	Substrate ([S]/[C]) [a)]	Product	Reductant	Temperature (time) [°C, h] [b)]	Conversion ratio [%]	TOF [h^{-1}]	Reference
6	$[Ir(cod)Cl]_2$	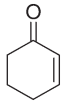 (500)	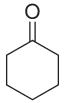	2-propanol	80 (4)	99	12.0	103
7	$[Ir(cod)Cl]_2$	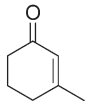 (500)	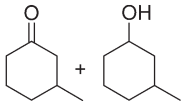	2-propanol	80 (4)	91 (3:1)	23.0	103
8	$[Ir(cod)Cl]_2$	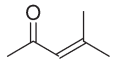 (500)	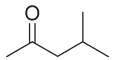	2-propanol	80 (4)	99	12.0	103
9	$[Ir(cod)Cl]_2$	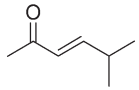 (500)	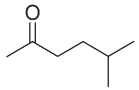	2-propanol	80 (4)	90	6.0	103
10	$[Ir(cod)Cl]_2$	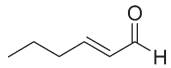 (500)	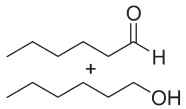	2-propanol	80 (4)	75 (10:1)	9.0	103

Table 20.3 (continued)

Entry	Catalyst	Substrate ([S]/[C]) [a)]	Product	Reductant	Temperature (time) [°C, h] [b)]	Conversion ratio [%]	TOF [h^{-1}]	Reference
11	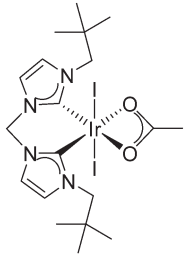	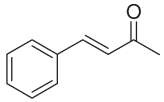 (1000)	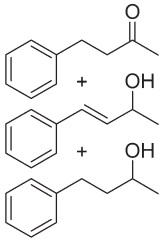	2-propanol	82 (20)	92 (9:3:2)	1.0	104
12	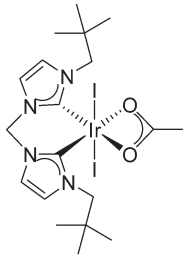	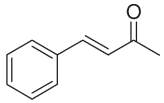 (200)	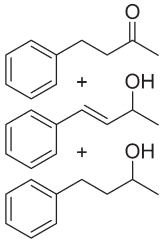	2-propanol	82 (4)	>98 (0:0:1)	1.0	104
13	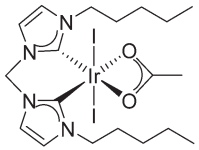	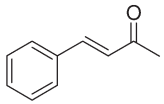 (1000)	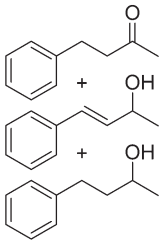	2-propanol	82 (20)	66 (7:1:0)	0.7	104

Table 20.3 (continued)

Entry	Catalyst	Substrate ([S]/[C]) [a]	Product	Reductant	Temperature (time) [°C, h] [b]	Conversion ratio [%]	TOF [h^{-1}]	Reference
14	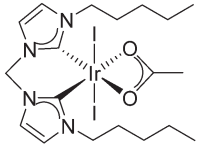	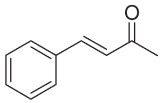 (200)	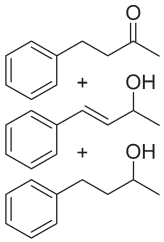	2-propanol	82 (7)	100 (1:0:5)	0.6	104
15	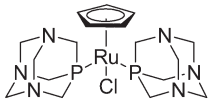	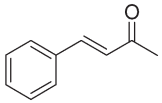 (100)	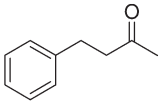	$HCO_2Na/MeOH/H_2O$	90 (6)	97	16.0	105

a) Substrate : catalyst ratio shown in parentheses.
b) Reaction temperature (reaction time in parentheses).

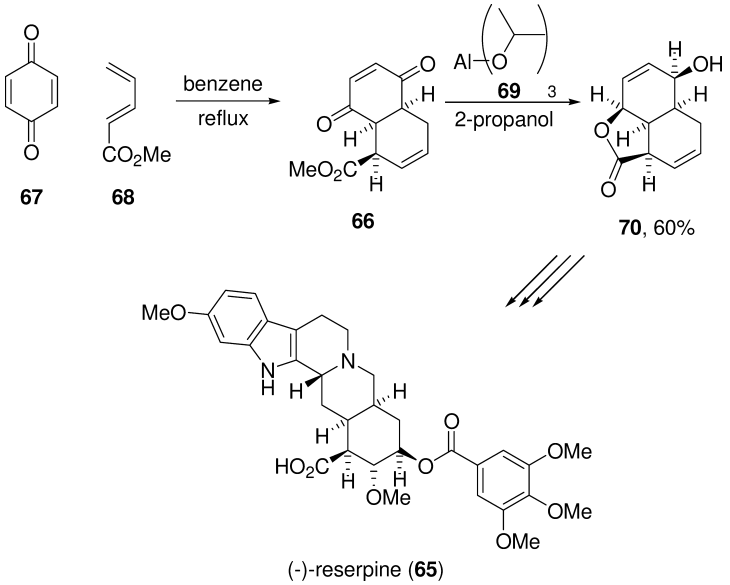

Scheme 20.21 Woodward's total synthesis of (–)-reserpine (**65**).

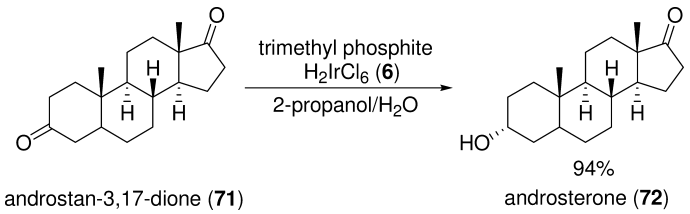

Scheme 20.22 The reduction of androstan-3,17-dione (**71**) using an iridium catalyst.

(**69**) while leaving the remainder of the molecule unaltered. The resulting dialcohol is immediately lactonized to the tricyclic compound **70** (Scheme 20.21).

One of the very few examples of a practical application of a transition-metal catalyst in total synthesis is shown in Scheme 20.22 [107]. The chloroiridic acid catalyst (H_2IrCl_6) (**6**) reduces **71** to androsterone (**72**) by selective attack of the sterically less hindered ketone in the 3-position of **71**.

20.4 Related Reactions and Side-Reactions

20.4.1 Aldol Reaction

In the MPVO reaction, several side-reactions can occur (Scheme 20.23). For example, an aldol reaction can occur between two molecules of acetone, which then leads to the formation of diacetone alcohol. The latter acts as a good ligand for the metal of the MPVO catalyst, rendering it inactive. Moreover, the aldol product may subsequently eliminate water, which hydrolyzes the catalyst. The aldol reaction can be suppressed by adding zeolite NaA [84, 92].

20.4.2 Tishchenko Reaction

When aldehydes are reduced, the Tishchenko reaction may be a side-reaction. It is the result of an attack of the oxygen atom of the alkoxide on the carbonyl function of the aldehyde. In particular, aldehydes lacking an α-hydrogen atom such as benzaldehyde are prone to form esters (Scheme 20.24) [108]. It has been reported that many aldehydes can be converted into Tishchenko esters at room temperature, almost quantitatively and with high turnovers, using SmI_2 catalysts [109] or a bi-aluminum catalyst [8].

20.4.3 Cannizzaro Reaction

In the Cannizzaro reaction [110, 111] two aldehyde functionalities disproportionate into the corresponding hydroxyl and carboxyl functions, either as separate compounds or as an ester (Scheme 20.25). The reaction conditions needed are rather harsh, except when R^1 or R^2 is a phenyl group. Typically, an excess of so-

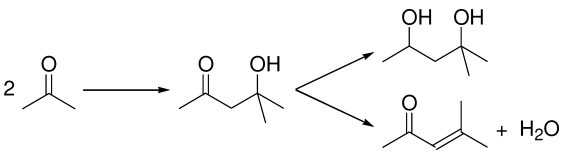

Scheme 20.23 The aldol reaction.

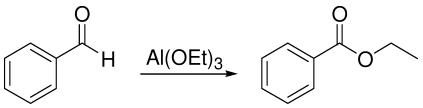

Scheme 20.24 The original Tishchenko reaction.

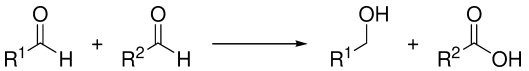

Scheme 20.25 The Cannizzaro reaction.

dium or potassium hydroxide is needed. Therefore, in general, during MPVO reactions only traces of Cannizzaro products are formed.

20.4.4
Decarbonylation

Aldehydes may sometimes pose a problem in transfer hydrogenations catalyzed by transition metals. They can poison the catalyst or decarbonylate, forming CO, which may coordinate to the metal complex and result in a change in activity (Scheme 20.26) [65, 66].

20.4.5
Leuckart-Wallach and Eschweiler-Clarke Reactions

The reductive alkylation of amines is called the Leuckart-Wallach reaction [112–115]. The primary or secondary amine reacts with the ketone or aldehyde. The formed imine is then reduced with formic acid as hydrogen donor (Scheme 20.27). When amines are reductively methylated with formaldehyde and formic acid, the process is termed the Eschweiler-Clarke procedure [116, 117].

20.4.6
Reductive Acetylation of Ketones

In the presence of an active acyl donor such as isopropenyl acetate, a reductive acetylation of a ketone can be performed in the presence of MPVO catalysts

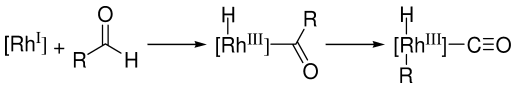

Scheme 20.26 Decarbonylation of an aldehyde under influence of a transition-metal catalyst.

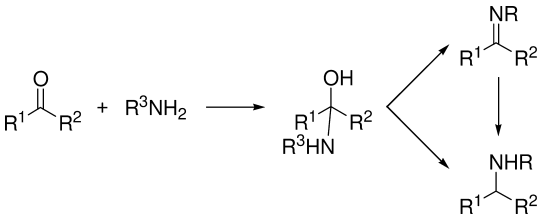

Scheme 20.27 The Leuckart-Wallach reaction.

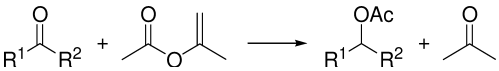

Scheme 20.28 Reductive acetylation of ketones.

(Scheme 20.28) [84, 118]. The first step in this procedure is reduction of the ketone, followed by the acetylation of the formed alkoxide. It may be noted that aluminum(III) isopropoxide and zirconium(IV) isopropoxide do not catalyze the acetylation. With these catalysts, the alcohol is obtained.

20.4.7
Other Hydrogen Transfer Reactions

A few remarkable, but rather uncommon, transfer hydrogenations also deserve mention within the context of this chapter: namely, the reduction of alkynes to alkenes using a chromium catalyst, and the reduction of double bonds using diimines.

In the reduction of C–C triple bonds with chromous sulfate in water, the key intermediate consists of a dichromium complex with the alkyne (Scheme 20.29) [119]. This configuration assures the selective formation of *trans* double bonds. Various substrates have been reduced in excellent yields without the occurrence of isomerizations or byproduct formation (Table 20.4).

One very fast and reliable method for the reduction of double bonds is that of transfer hydrogenation with diimine (Scheme 20.30). Under the influence of traces of copper ion and oxygen from air, hydrazine is rapidly transformed into diimine. This compound is able to hydrogenate double bonds with great success under the formation of nitrogen [120].

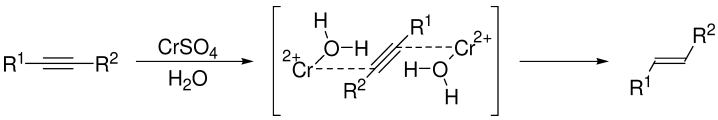

Scheme 20.29 Reduction of alkynes to *trans*-alkenes by chromous sulfate.

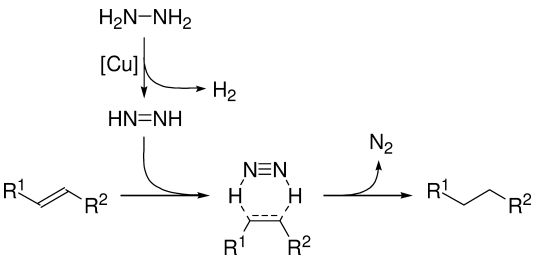

Scheme 20.30 Reduction of alkenes with hydrazine.

Table 20.4 Reduction of alkynes to *trans*-alkenes by chromous sulfate.

Entry	Substrate	Product	Reaction time [h]	Yield [%]	TOF [h^{-1}]
1	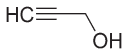	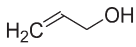	0.08	89	5.0
2	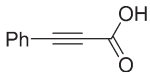	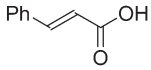	0.25	91	2.5
3	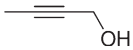	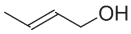	2	84	0.4
4	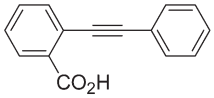	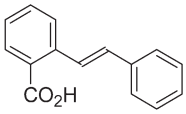	24	85	0.02

20.5 Racemizations

Since transfer hydrogenation reactions of carbonyls are always equilibrium reactions, it is possible to perform both a reduction and an oxidation of a substrate simultaneously. In this way, these reactions can be utilized for both racemizations and epimerizations.

In the contemporary production of enantiopure compounds this feature is highly appreciated. Currently, kinetic resolution of racemates is the most important method for the industrial production of enantiomerically pure compounds. This procedure is based on chiral catalysts or enzymes, which catalyze conversion of the enantiomers at different rates. The theoretical yield of this type of reaction is only 50%, because the unwanted enantiomer is discarded. This generates a huge waste stream, and is an undesirable situation from both environmental and economic points of view. Efficient racemization catalysts that enable recycling of the undesired enantiomer are, therefore, of great importance.

In order to accomplish a racemization rather than an oxidation of an alcohol, the hydrogen acceptor should be added in an equimolar or lower concentration. This is illustrated in Table 20.5 [84]. In order to achieve acceptable reaction times and yields, the amount of hydrogen donor must be adjusted to meet every single reactant.

Racemizations are not limited to alcohols; indeed, some racemizations of amines have also been reported [121].

The next step in the use of transfer hydrogenation catalysts for recycling of the unwanted enantiomer is the dynamic kinetic resolution. This is a combination of two reaction systems: (i) the continuous racemization of the alcohol via hydrogen transfer; and (ii) the enantioselective protection of the alcohol using a

Table 20.5 Racemization of a conjugated and a non-conjugated ketone.

Entry	Substrate	Acetone [equiv.]	Time [h] [a)]	Ketone formed [%]
1	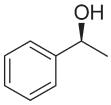	1	1.5	50
2	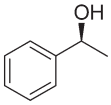	0.1	3	10
3	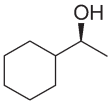	1	2.5	25
4	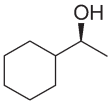	0.1	>7	9

a) Time needed for complete racemization.

stereoselective catalyst, typically an enzyme [122–127]. As was first demonstrated by Williams and colleagues [30], a dynamic kinetic resolution of racemic alcohols by the combination of two catalysts provides a mild and effective means of obtaining enantiomerically pure alcohols in high yields and selectivities (Scheme 20.31).

It is important that the catalysts are stable in each other's presence. Typically, kinetic resolution of the reaction is performed with an enzyme, which always will contain traces of water. Hence, MPVO catalysts and water-sensitive transition-metal catalysts cannot be used in these systems. The influence of the amount of the hydrogen acceptor in the reaction mixture during a dynamic kinetic resolution is less pronounced than in a racemization, since the equilibrium of the reaction is shifted towards the alcohol side.

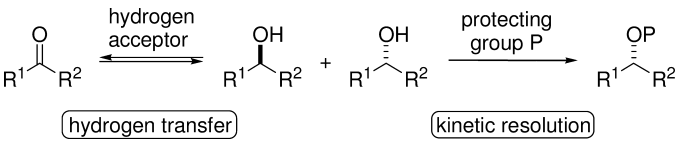

Scheme 20.31 The dynamic kinetic resolution of a racemic alcohol.

Table 20.6 Recent examples of successful dynamic kinetic resolutions.

Entry	Substrate	Product	Racemization catalyst [a)]	SCR [b)]	Time [h]	Temperature [°C]	Yield [%]	ee [%]	Reference
1	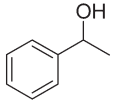	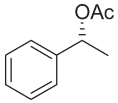	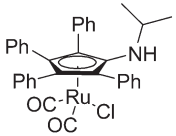	25	31	25	95	>99	128
2	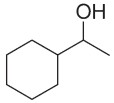	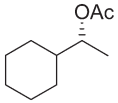	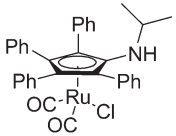	25	48	25	86	>99	128
3	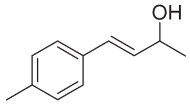	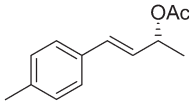	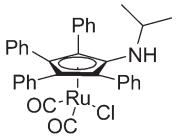	25	96	25	92	>99	128
4	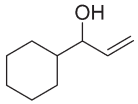	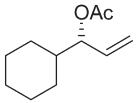	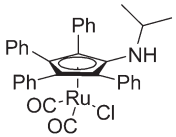	25	96	25	90	>99	128
5	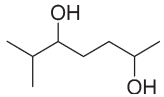	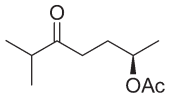	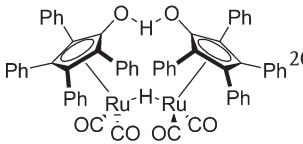	20	18	70	77	89	129

Table 20.6 (continued)

Entry	Substrate	Product	Racemization catalyst [a)]	SCR [b)]	Time [h]	Temperature [°C]	Yield [%]	ee [%]	Reference
6	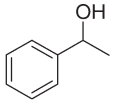	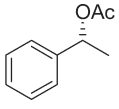	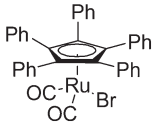	25	3	25	98	>99	130
7	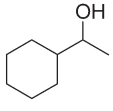	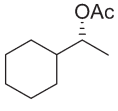	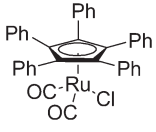	20	17	25	98	>99	130
8	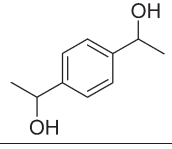	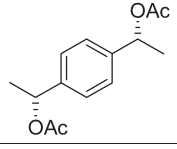	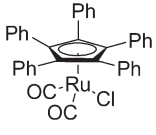	20	10	25	94	>99 (99:1 d.r.)	130

a) The catalyst for the kinetic resolution is in all cases *Candida antarctica* Lipase B.
b) SCR = substrate:catalyst ratio between the racemic alcohol and the hydrogen transfer catalyst.

Table 20.7 A short overview of the reduction of acetophenone with MPVO catalysts and transition metal catalysts developed during the past five years.

Entry	Catalyst	Reducing agent [a)]	Additive/Solvent [a)]	Temperature [°C]	SCR	Conversion [%]	Reaction time [h]	TOF [h^{-1}]	Reference
1	tBuOSmI$_2$	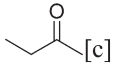	THF	65	10	98	24	0.4	131
2	$Al(OCH(CH_3)_2)_3$			50	10	1	1	0.1	7
3	$Nd(OCH(CH_3)_2)_3$			50	100	57	1	60	7
4	$Gd(OCH(CH_3)_2)_3$			50	100	58	1	60	7
5	$Er(OCH(CH_3)_2)_3$			50	100	22	1	20	7
6	$Yb(OCH(CH_3)_2)_3$			50	100	5	1	5	7
7	$La(OCH(CH_3)_2)_3$	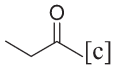		80	20	75	60	0.3	132
8	$Ce(OCH(CH_3)_2)_3$	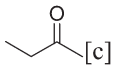		80	20	15	48	0.1	132

Table 20.7 (continued)

Entry	Catalyst	Reducing agent [a)]	Additive/Solvent [a)]	Temperature [°C]	SCR	Conversion [%]	Reaction time [h]	TOF [h^{-1}]	Reference
9	$Sm(OCH(CH_3)_2)_3$	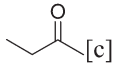		80	20	70	24	0.6	132
10	$Yb(OCH(CH_3)_2)_3$	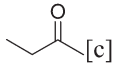		80	20	98	24	0.8	132
11	$Al(OCH(CH_3)_2)_3$		TFA (1)	25	12	44	22	0.3	88
12	$Pu(N(Si(CH_3)_3)_2)_3$			25	20	91	24	0.8	133
13	$Al(CH_3)_3$			65	10	80	12	0.7	10
14	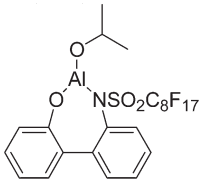	(10)	CH_2Cl_2	25	10	85	5	1.5	84

Table 20.7 (continued)

Entry	Catalyst	Reducing agent[a)]	Additive/Solvent[a)]	Temperature [°C]	SCR	Conversion [%]	Reaction time [h]	TOF [h^{-1}]	Reference
15	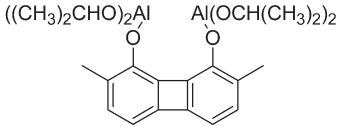	(3)	CH_2Cl_2	25	20	96	1	20	8
16	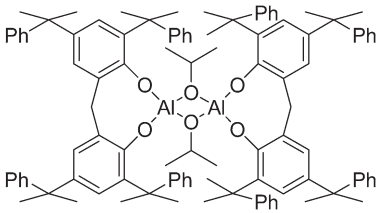	(100)	Toluene	111	40	93	1	40	9
17	La + 5% I_2			25	1	48	20	0.048	90
18	Ce + 5% I_2			25	1	34	20	0.039	90
19	Sm + 5% I_2			25	1	96	20	0.05	90
20	Yb + 5% I_2			25	1	24	20	0.036	90

Table 20.7 (continued)

Entry	Catalyst	Reducing agent[a)]	Additive/Solvent[a)]	Temperature [°C]	SCR	Conversion [%]	Reaction time [h]	TOF [h^{-1}]	Reference
21	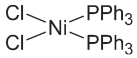		NaOH (0.33)	82	7	82	30	0.2	102
22	$NiBr_2$		NaOH (85)	95	250	60	4	10	134
23	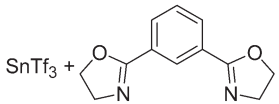		MeOH	25	10	98	12	0.8	135
24	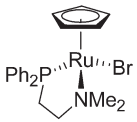		(0.02)	82	200	>99	48	5	136
25	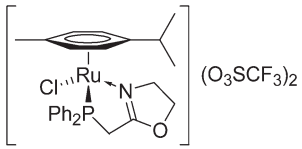		(0.025)	82	200	61	1	120	52

Table 20.7 (continued)

Entry	Catalyst	Reducing agent[a)]	Additive/Solvent[a)]	Temperature [°C]	SCR	Conversion [%]	Reaction time [h]	TOF [h^{-1}]	Reference
26	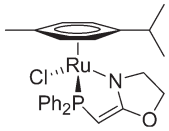		(0.025)	82	200	25	0.25	200	52
27	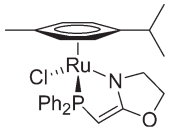		(0.025)	82	200	94	6	30	52
28	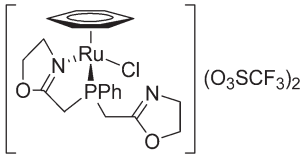		(0.12)	82	200	54	1	110	52
29	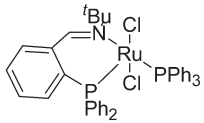		NaOH (0.5)	90	5	91	0.5	910	137
30	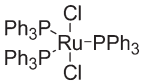		NaOH (0.024)	82	500	50	2	2.0	138

Table 20.7 (continued)

Entry	Catalyst	Reducing agent[a)]	Additive/Solvent[a)]	Temperature [°C]	SCR	Conversion [%]	Reaction time [h]	TOF [h^{-1}]	Reference
31	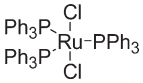		NaOH (0.024) $Yb(OTf)_3$ (0.004)	82	500	86	2	3.5	138
32	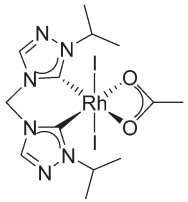		KOH (0.5)	82	1000	>98	10	100	139
33	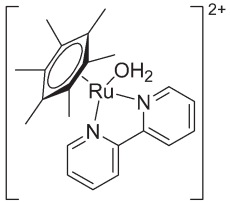	 (30)	H_2O	70	200	98	4	50	140
34	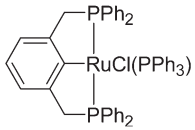			82	1000	50	0.22	2300	141

Table 20.7 (continued)

Entry	Catalyst	Reducing agent[a)]	Additive/Solvent[a)]	Temperature [°C]	SCR	Conversion [%]	Reaction time [h]	TOF [h^{-1}]	Reference
35	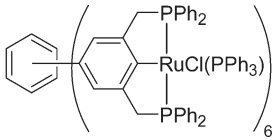			82	1000	50	0.23	2200	141
36	$[Cp^*Ir_{III}(bpy)(H_2O)]^{2+}$	(5)	H_2O	70	200	97	1	194	142
37	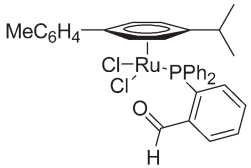		NaOH (0.048)	82	500	98	10	50	143
38	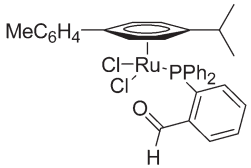		NaOH (0.048)	82	500	97	9	55	143

Table 20.7 (continued)

Entry	Catalyst	Reducing agent[a)]	Additive/Solvent[a)]	Temperature [°C]	SCR	Conversion [%]	Reaction time [h]	TOF [h^{-1}]	Reference
39	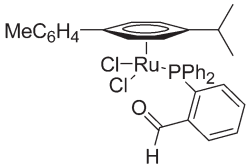		NaOH (0.048)	82	500	96	6	80	143
40	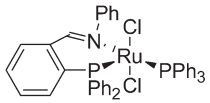		NaOH (0.048)	82	500	98	1	485	144
41	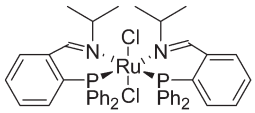		NaOH (0.048)	82	500	97	1	240	144
42	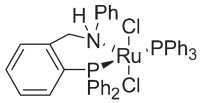		NaOH (0.048)	82	500	96	2	240	144
43	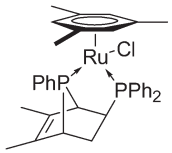		KOH (0.025)	82	200	>99	0.5	400	145

Table 20.7 (continued)

Entry	Catalyst	Reducing agent [a)]	Additive/Solvent [a)]	Temperature [°C]	SCR	Conversion [%]	Reaction time [h]	TOF [h^{-1}]	Reference
44	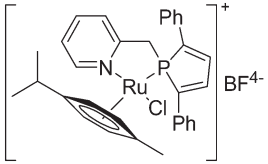		KOH (0.5)	90	$60 \cdot 10^6$	>99	60	$1 \cdot 10^6$	53
45	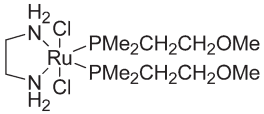		KOH (0.1)	82	500	93	0.5	935	146
46	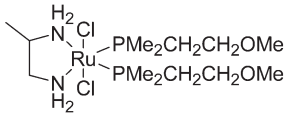		KOH (0.1)	82	500	82	0.5	815	146
47	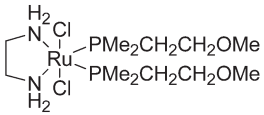		KOH (0.1)	82	500	90	0.5	900	146

Table 20.7 (continued)

Entry	Catalyst	Reducing agent[a)]	Additive/Solvent[a)]	Temperature [°C]	SCR	Conversion [%]	Reaction time [h]	TOF [h^{-1}]	Reference
48	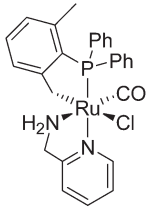		NaOH (0.02)	82	400	98	0.08	4700	54
49	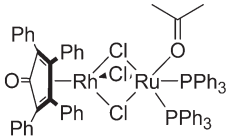		K_2CO_3 (1)	RT	1000	70	6	60	147
50	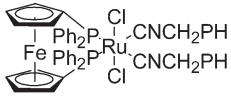		NaOH (0.096)	250	250	84	0.17	1260	148
51	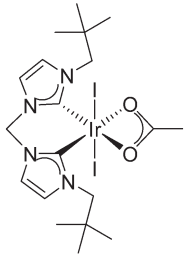		KOH (0.005)	82	1000	98	0.07	14700	51

Table 20.7 (continued)

Entry	Catalyst	Reducing agent[a)]	Additive/Solvent[a)]	Temperature [°C]	SCR	Conversion [%]	Reaction time [h]	TOF [h^{-1}]	Reference
52	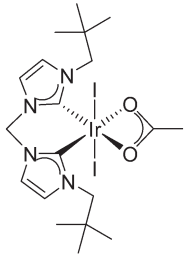		K_2CO_3 (0.5)	82	1000	97	0.67	1455	51
53	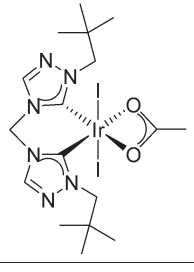		KOH (0.005)	82	1000	80	2	400	51

a) The number in parentheses denotes the number of equivalents used. If no number is given, the donor/additive is used as solvent.
b) TOF = [substrate]/[catalyst] h^{-1}, calculated from the yield and stated reaction time.
c) Oxidation of 1-phenylethanol.
SCR = substrate : catalyst ratio.

Several groups have been active in the field of dynamic kinetic resolution since its introduction, and products have been obtained at almost quantitative yields and with excellent enantiomeric excesses (Table 20.6) [128–130].

Abbreviations

MPV	Meerwein-Ponndorf-Verley
MPVO	Meerwein-Ponndorf-Verley and Oppenauer
TFA	trifluoroacetic acid
TOF	turnover frequency
TON	turnover number

References

1 H. Meerwein, R. Schmidt, *Justus Liebigs Ann. Chem.* **1925**, *444*, 221.
2 A. Verley, *Bull. Soc. Chim. Fr.* **1925**, *37*, 537.
3 W. Ponndorf, *Angew. Chem.* **1926**, *29*, 138.
4 H. Lund, *Ber. Dtsch. Chem. Ges.* **1937**, *70*, 1520.
5 R.V. Oppenauer, *Recl. Trav. Chim. Pays-Bas* **1937**, *56*, 137.
6 J.L. Namy, J. Souppe, J. Collin, H.B. Kagan, *J. Org. Chem.* **1984**, *49*, 2045.
7 T. Okano, M. Matsuoka, H. Konishi, J. Kiji, *Chem. Lett.* **1987**, 181.
8 T. Ooi, T. Miura, Y. Itagaki, H. Ichikawa, K. Maruoka, *Synthesis* **2002**, 279.
9 Y.-C. Liu, B.-T. Ko, B.-H. Huang, C.-C. Lin, *Organometallics* **2002**, *21*, 2066.
10 E.J. Campbell, H. Zhou, S.T. Nguyen, *Org. Lett.* **2001**, *3*, 2391.
11 A.L. Wilds, *Org. React.* **1944**, *2*, 178.
12 C. Djerassi, *Org. React.* **1953**, *6*, 207.
13 C.F. de Graauw, J.A. Peters, H. van Bekkum, J. Huskens, *Synthesis* **1994**, 1007.
14 K. Nishide, M. Node, *Chirality* **2002**, *14*, 759.
15 Y.M.Y. Haddad, H.B. Henbest, J. Husbands, T.R.B. Mitchell, *Proc. Chem. Soc.* **1964**, 361.
16 J.A. Osborn, F.H. Jardine, J.F. Young, G. Wilkinson, *J. Chem. Soc. A* **1966**, 1711.
17 R. Uson, L.A. Oro, R. Sariego, M.A. Esteruelas, *J. Organomet. Chem.* **1981**, *214*, 399.
18 P. Kvintovics, B.R. James, B. Heil, *Chem. Commun.* **1986**, 1810.
19 S. Gladiali, G. Chelucci, G. Chessa, G. Delogu, F. Soccolini, *J. Organomet. Chem.* **1987**, *327*, C15.
20 S. Gladiali, L. Pinna, G. Delogu, S. De Martin, G. Zassinovich, G. Mestroni, *Tetrahedron. Asymm.* **1990**, *1*, 635.
21 R.L. Chowdhury, J.-E. Bäckvall, *Chem. Commun.* **1991**, 1063.
22 N.C. Deno, H.J. Peterson, G.S. Saines, *Chem. Rev.* **1960**, *60*, 7.
23 G. Brieger, T.J. Nestrick, *Chem. Rev.* **1974**, *74*, 567.
24 R.A.W. Johnstone, A.H. Wilby, I.D. Entwistle, *Chem. Rev.* **1985**, *85*, 129.
25 P.A. Chaloner, M.A. Esteruelas, F. Joó, L.A. Oro, *Homogeneous hydrogenation*. Kluwer Academic Publishers, Dordrecht, Boston, London, **1994**, Chapter 3, p. 87.
26 P.A. Chaloner, M.A. Esteruelas, F. Joó, L.A. Oro, *Homogeneous hydrogenation*. Kluwer Academic Publishers, Dordrecht, Boston, London, **1994**, Chapter 5, p. 183.
27 S. Gladiali, G. Mestroni, Transfer hydrogenations. In: M. Beller, C. Bolm (Eds.), *Transition Metals for Organic Synthesis*. Wiley-VCH, Weinheim, New York, Chichester, Brisbane, Singapore, Toronto, **1998**, Chapter 3, p. 97.

28 J.-E. Bäckvall, *J. Organomet. Chem.* **2002**, *652*, 105.
29 L. Sominsky, E. Rozental, H. Gottlieb, A. Gedanken, S. Hoz, *J. Org. Chem.* **2004**, *69*, 1492.
30 P.M. Dinh, J.A. Howarth, A.R. Hudnott, J.M.J. Williams, W. Harris, *Tetrahedron Lett.* **1996**, *37*, 7623.
31 D. Klomp, T. Maschmeyer, U. Hanefeld, J.A. Peters, *Chem. Eur. J.* **2004**, *10*, 2088.
32 E.D. Williams, K.A. Krieger, A.R. Day, *J. Am. Chem. Soc.* **1953**, *75*, 2404.
33 W.N. Moulton, R.E. van Atta, R.R. Ruch, *J. Org. Chem.* **1961**, *26*, 290.
34 E.C. Ashby, J.N. Argyropoulos, *J. Org. Chem.* **1986**, *51*, 3593.
35 O. Pàmies, J.-E. Bäckvall, *Chem. Eur. J.* **2001**, *7*, 5052.
36 R. Cohen, C.R. Graves, S.T. Nguyen, J.M.L. Martin, M.A. Ratner, *J. Am. Chem. Soc.* **2004**, *126*, 14796.
37 T. Ooi, T. Miura, K. Maruoka, *J. Am. Chem. Soc.* **1998**, *120*, 10790.
38 T. Ooi, T. Miura, K. Takaya, H. Ichikawa, K. Maruoka, *Tetrahedron* **2001**, *57*, 867.
39 H. Imai, T. Nishiguchi, K. Fukuzumi, *J. Org. Chem.* **1974**, *39*, 1622.
40 T. Nishiguchi, K. Tachi, K. Fukuzumi, *J. Org. Chem.* **1975**, *40*, 240.
41 J. Halpern, *Inorg. Chim. Acta* **1981**, *50*, 11.
42 H.A. Brune, J. Unsin, R. Hemmer, M. Reichhardt, *J. Organomet. Chem.* **1989**, *369*, 3352.
43 M.A. Bennett, S.K. Bhargava, M. Ke, A.C. Willis, *J. Chem. Soc., Dalton Trans.* **2000**, 3537.
44 L.Y. Kuo, D.M. Finigan, N.N. Tadros, *Organometallics* **2003**, *22*, 2422.
45 G. Mestroni, G. Zassinovich, A. Camus, F. Martinelli, *J. Organomet. Chem.* **1980**, *198*, 87.
46 H. Imai, T. Nishiguchi, K. Fukuzumi, *J. Org. Chem.* **1976**, *41*, 2688.
47 A. Aranyos, G. Csjernyik, K. J. Szabó, J.-E. Bäckvall, *Chem. Commun.* **1999**, 351.
48 K.-J. Haack, S. Hashiguchi, A. Fujii, T. Ikariya, R. Noyori, *Angew. Chem. Int. Ed. Engl.* **1997**, *36*, 285.
49 M. Yamakawa, H. Ito, R. Noyori, *J. Am. Chem. Soc.* **2000**, *122*, 1466.
50 J.-W. Handgraaf, J.N.H. Reek, E.J. Meijer, *Organometallics* **2003**, *22*, 3150.
51 J.R. Miecznikowski, R.H. Crabtree, *Polyhedron* **2004**, *23*, 2857.
52 P. Braunstein, F. Naud, S.J. Rettig, *New J. Chem.* **2001**, *25*, 32.
53 C. Thoumazet, M. Melaimi, L. Ricard, F. Mathey, P. le Floch, *Organometallics* **2003**, *22*, 1580.
54 W. Baratta, P. Da Ros, A. Del Zotto, A. Sechi, E. Zangrando, P. Rigo, *Angew. Chem. Int. Ed. Engl.* **2004**, *43*, 3584.
55 Y. Shvo, D. Czarkie, Y. Rahamim, D.F. Chodosh, *J. Am. Chem. Soc.* **1986**, *108*, 7400.
56 J.S.M. Samec, J.-E. Bäckvall, *Chem. Eur. J.* **2002**, *8*, 2955.
57 H.M. Jung, S.T. Shin, Y.H. Kim, M.-J. Kim, J. Park, *Organometallics* **2001**, *20*, 3370.
58 C.P. Casey, S.W. Singer, D.R. Powell, R.K. Hayashi, M. Kavana, *J. Am. Chem. Soc.* **2001**, *123*, 1090.
59 J.B. Johnson, J.-E. Bäckvall, *J. Org. Chem.* **2003**, *68*, 7681.
60 T. Nishiguchi, K. Fukuzumi, *J. Am. Chem. Soc.* **1974**, *96*, 1893.
61 W. Leitner, J. Brown, H. Brunner, *J. Am. Chem. Soc.* **1993**, *115*, 152.
62 A. Bucsai, J. Bakos, M. Laghmari, D. Sinou, *J. Mol. Catal. A: Chemical* **1997**, *116*, 335.
63 D. Heller, R. Kadyrov, M. Michalik, T. Freier, U. Schmidt, H.W. Krause, *Tetrahedron Asymmetry* **1996**, *7*, 3025.
64 A. Harthun, R. Kadyrov, R. Selke, J. Bargon, *Angew. Chem. Int. Ed. Engl.* **1997**, *36*, 1103.
65 M.C. Baird, C.J. Nyman, G. Wilkinson, *J. Chem. Soc. A* **1968**, 348.
66 K. Ohno, J. Tsuji, *J. Am. Chem. Soc.* **1968**, *90*, 99.
67 Y. Sasson, M. Cohen, J. Blum, *Synthesis* **1973**, 359.
68 Y. Sasson, J. Blum, E. Dunkelblum, *Tetrahedron Lett.* **1973**, *14*, 3199.
69 S. Mukhopadhyay, A. Yaghmur, A. Benichou, Y. Sasson, *Org. Proc. Res. Dev.* **2000**, *4*, 571.
70 G. Descotes, D. Sinou, J.-P. Praly, *Carbohydr. Res.* **1980**, *78*, 25.
71 G. Descotes, D. Sinou, *Tetrahedron Lett.* **1976**, *17*, 4083.
72 G. Descotes, J. Sabadie, *Bull. Soc. Chim. Fr.* **1978**, *II*, 158.

73 T. Nishiguchi, K. Tachi, K. Fukuzumi, *J. Am. Chem. Soc.* **1972**, *94*, 8916.
74 H. Imai, T. Nishiguchi, K. Fukuzumi, *J. Org. Chem.* **1976**, *41*, 665.
75 H. Imai, T. Nishiguchi, K. Fukuzumi, *J. Org. Chem.* **1977**, *42*, 431.
76 H. Imai, T. Nishiguchi, M. Tanaka, K. Fukuzumi, *J. Org. Chem.* **1977**, *42*, 2309.
77 T. Nishiguchi, K. Tachi, K. Fukuzumi, *J. Org. Chem.* **1975**, *40*, 237.
78 H.B. Henbest, T.R.B. Mitchell, *J. Chem. Soc. C* **1970**, 785.
79 M. Gullotti, R. Ugo, S. Colonna, *J. Chem. Soc. C* **1971**, 2652.
80 Y.M.Y. Haddad, H.B. Henbest, J. Trocha-Grimshaw, *J. Chem. Soc. Perkin Trans. I* **1974**, 592.
81 Y.M.Y. Haddad, H.B. Henbest, J. Husbands, T.R.B. Mitchell, J. Trocha-Grimshaw, *J. Chem. Soc. Perkin Trans. I* **1974**, 596.
82 M.E. Vol'pin, V.P. Kukolev, V.O. Chernyshev, I.S. Kolomnikov, *Tetrahedron Lett.* **1971**, *12*, 4435.
83 H. Brunner, E. Graf, W. Leitner, K. Wutz, *Synthesis* **1989**, 743.
84 D. Klomp, K. Djanashvili, N. Cianfanelli Svennum, N. Chantapariyavat, C.-S. Wong, F. Vilela, T. Maschmeyer, J.A. Peters, U. Hanefeld, *Org. Biomol. Chem.* **2005**, *3*, 483.
85 Y. Ishii, T. Nakano, A. Inada, Y. Kishigami, K. Sakurai, M. Ogawa, *J. Org. Chem.* **1986**, *51*, 240.
86 B. Knaver, K. Krohn, *Liebigs Ann.* **1995**, 677.
87 K.G. Akamanchi, N.R. Varalakshmy, *Tetrahedron Lett.* **1995**, *36*, 3571.
88 K.G. Akamanchi, N.R. Varalakshmy, *Tetrahedron Lett.* **1995**, *36*, 5085.
89 T. Ooi, H. Ichikawa, K. Maruoka, *Angew. Chem. Int. Ed. Engl.* **2001**, *40*, 3610.
90 S. Fukuzawa, N. Nakano, T. Saitoh, Eur. *J. Org. Chem.* **2004**, 2863.
91 C. Bisi Castellani, O. Carugo, A. Perotti, D. Sacchi, *J. Mol Catal.* **1993**, *85*, 65.
92 A. Lebrun, J.L. Namy, H.B. Kagan, *Tetrahedron Lett.* **1991**, *32*, 2355.
93 M.D. le Plage, D. Poon, B.R. James, *Catalysis of Organic Reactions.* Marcel Dekker, Inc., New York, Basel, Chapter 6, p. 61.
94 D. Baudry, M. Ephritikhine, H. Felkin, R. Holmes-Smith, *J. Chem. Soc. Chem. Commun.* **1983**, 788.
95 M. Aracama, M.A. Esteruelas, F.J. Lahoz, J.A. Lopez, U. Meyer, L.A. Oro, H. Werner, *Inorg. Chem.* **1991**, *30*, 288.
96 D. Barbry, S. Torchy, *Tetrahedron Lett.* **1997**, *38*, 2959.
97 G.-Z. Wang, J.-E. Bäckvall, *Chem. Commun.* **1992**, 980.
98 T. Ohkuma, H. Ooka, S. Hashiguchi, T. Ikariya, R. Noyori, *J. Am. Chem. Soc.* **1995**, *117*, 2675.
99 M. Ito, M. Hirakawa, K. Murata, T. Ikariya, *Organometallics* **2001**, *20*, 379.
100 V. Rautenstrauch, X. Hoang-Cong, R. Churlaud, K. Abdur-Rashid, R.H. Morris, *Chem. Eur. J.* **2003**, *9*, 4954.
101 Y. Sasson, J. Blum, *J. Org. Chem.* **1975**, *40*, 1887.
102 S. Iyer, J. P. Varghese, *J. Chem. Soc. Chem. Commun.* **1995**, 465.
103 S. Sakaguchi, T. Yamaga, Y. Ishii, *J. Org. Chem.* **2001**, *66*, 4710.
104 M. Albrecht, J. R. Miecznikowski, A. Samuel, J.W. Faller, R.H. Crabtree, *Organometallics* **2002**, *21*, 35964.
105 S. Bolaño, L. Gonsalvi, F. Zanobini, F. Vizza, V. Bertolasi, A. Romerosa, M. Peruzzini, *J. Mol. Catal. A* **2004**, *224*, 61.
106 R.B. Woodward, F.E. Bader, H. Bickel, A.J. Frey, R.W. Kierstead, *Tetrahedron* **1958**, *2*, 1.
107 P.A. Browne, D.N. Kirk, *J. Chem. Soc. C* **1969**, 1653.
108 W. Tischtschenko, *Chem. Zentralbl.* **1906**, *77*, 1309.
109 J. Collin, J.L. Namy, H.B. Kagan, *Nouv. J. Chim.* **1986**, *10*, 229.
110 S. Cannizzaro, *Liebigs Ann.* **1853**, *88*, 129.
111 T.A. Geissman, *Org. React.* **1944**, *2*, 94.
112 R. Leuckart, *Ber. Dtsch. Chem. Ges.* **1885**, *18*, 2341.
113 O. Wallach, *Ber. Dtsch. Chem. Ges.* **1891**, *24*, 3992.
114 M.L. Moore, *Org. React.* **1949**, *5*, 301.
115 M. Kitamura, D. Lee, S. Hayashi, S. Tanaka, M. Yoshimura, *J. Org. Chem.* **2002**, *67*, 8685.
116 W. Eschweiler, *Ber. Dtsch. Chem. Ges.* **1905**, *38*, 880.

117 H.T. Clarke, H.B. Gillespie, S.Z. Weisshaus, *J. Am. Chem. Soc.* **1933**, *55*, 4571.

118 Y. Nakano, S. Sakaguchi, Y. Ishii, *Tetrahedron Lett.* **2000**, *41*, 1565.

119 C.E. Castro, R.D. Stephens, *J. Am. Chem. Soc.* **1964**, *86*, 4358.

120 D.J. Pasto, D.M. Chipman, *J. Am. Chem. Soc.* **1979**, *101*, 2290.

121 O. Pàmies, A.H. Éll, J.S.M. Samec, N. Hermanns, J.-E. Bäckvall, *Tetrahedron Lett.* **2002**, *43*, 4699.

122 K. Faber, *Chem. Eur. J.* **2001**, *7*, 5005.

123 F.F. Huerta, A.B.E. Minidis, J.-E. Bäckvall, *Chem. Soc. Rev.* **2001**, *30*, 321.

124 M.-J. Kim, Y. Ahn, J. Park, *Curr. Opin. Biotechnol.* **2002**, *13*, 578.

125 M.T. El Gihani, J.M.J. Williams, *Curr. Opin. Biotechnol.* **1999**, *3*, 11.

126 O. Pàmies, J.-E. Bäckvall, *Chem. Rev.* **2003**, *103*, 3247.

127 O. Pàmies, J.-E. Bäckvall, *Trends Biotechnol.* **2004**, *22*, 130.

128 J.H. Choi, Y.K. Choi, Y.H. Kim, E.S. Park, E.J. Kim, M.-J. Kim, J. Park, *J. Org. Chem.* **2004**, *69*, 1972.

129 B. Mártin-Matute, J.-E. Bäckvall, *J. Org. Chem.* **2004**, *69*, 9191.

130 B. Mártin-Matute, M. Edin, K. Bogár, J.-E. Bäckvall, *Angew. Chem. Int. Ed. Engl.* **2004**, *43*, 6535.

131 J.L. Namy, J. Souppe, J. Collin, H.B. Kagan, *J. Org. Chem.* **1984**, *49*, 2045.

132 A. Lebrun, J.-L. Namy, H.B. Kagan, *Tetrahedron Lett.* **1991**, *32*, 2355.

133 B.P. Warner, J.A. D'Alessio, A.N. Morgan, III, C.J. Burns, A.R. Schake, J.G. Watkin, *Inorg. Chim. Acta* **2000**, *309*, 45.

134 M.D. Le Page, B.R. James, *Chem. Commun.* **2000**, 1647.

135 N.J. Lawrence, S.M. Bushell, *Tetrahedron Lett.* **2000**, *41*, 4507.

136 C. Standfest-Hauser, C. Slugovc, K. Mereiter, R. Schmid, K. Kirchner, L. Xiao, W. Weissensteiner, *J. Chem. Soc., Dalton Trans.* **2001**, 2989.

137 P. Crochet, J. Gimeno, S. García-Granda, J. Borge, *Organometallics* **2001**, *20*, 4369.

138 H. Matsunaga, N. Yoshioka, T. Kunieda, *Tetrahedron Lett.* **2001**, *42*, 8857.

139 M. Albrecht, R.H. Crabtree, J. Mata, E. Peris, *Chem. Commun.* **2002**, 32.

140 S. Ogo, T. Abura, Y. Watanabe, *Organometallics* **2002**, *21*, 2964.

141 H.P. Dijkstra, M. Albrecht, S. Medici, G.P.M. van Klink, G. van Koten, *Adv. Synth. Catal.* **2002**, *344*, 1135.

142 T. Abura, S. Ogo, Y. Watanabe, S. Fukuzumi, *J. Am. Chem. Soc.* **2003**, *125*, 4149.

143 P. Crochet, M.A. Fernández-Zumel, C. Beauquis, J. Gimeno, *Inorg. Chim. Acta* **2003**, *356*, 114.

144 P. Crochet, J. Gimeno, J. Borge, S. García-Granda, *New. J. Chem.* **2003**, *27*, 414.

145 K.Y. Ghebreyessus, J.H. Nelson, *J. Organomet. Chem.* **2003**, *669*, 48.

146 Z.-L. Lu, K. Eichele, I. Warad, H.A. Mayer, E. Lindner, Z.-J. Jiang, V. Schurig, *Z. Anorg. Allg. Chem.* **2003**, *629*, 1308.

147 S. Gauthier, R. Scopelliti, K. Severin, *Organometallics* **2004**, *23*, 3769.

148 V. Cadierno, P. Crochet, J. Díez, S.E. García-Garrido, J. Gimeno, *Organometallics* **2004**, *23*, 4836.

21
Diastereoselective Hydrogenation

Takamichi Yamagishi

21.1
Introduction

The stereochemical control of a reaction is a continuing challenge in the synthesis of complex organic compounds, especially those with stereogenic center(s) or molecular chirality. Homogeneous catalytic hydrogenation is a simple and widely applicable method for the construction of stereogenic centers and enantioselective hydrogenation using chiral transition metal complexes. It has undergone striking development during the past two decades [1]. In enantioselective hydrogenation, prochiral substrates with unsaturated linkages are converted to chiral compounds by using chirally modified transition metal complexes based on rhodium, iridium, ruthenium, cobalt, and lanthanide metals, etc. In enantioselective hydrogenation, stereochemical control is performed through the selection of one diastereomeric intermediate composed of a prochiral (achiral) substrate and a chiral metal complex. For this purpose, many chiral ligands (representatives of which include chiral diphosphine ligands) have been developed to realize the production of almost homochiral products with stereogenic center(s). In the hydrogenation of compounds with a stereogenic center, an achiral metal complex can induce a new stereogenic center selectively, by utilizing the steric factor of the stereogenic center in the substrate to afford compounds with two or more stereogenic centers. These diastereoselective hydrogenations also go through the selection of diastereomeric intermediates by differentiating the reaction face of unsaturated bonds. This is termed "intramolecular asymmetric induction".

21.2
Hydrogenation of Alkenes, Ketones, and Imines

In the hydrogenation of alkenes, rhodium–, ruthenium– and iridium–phosphine catalysts are typically used [2–4]. Rhodium–phosphine complexes, such as Wilkinson's catalyst, are effective for obtaining alkanes under atmospheric pres-

The Handbook of Homogeneous Hydrogenation.
Edited by J.G. de Vries and C.J. Elsevier
Copyright © 2007 WILEY-VCH Verlag GmbH & Co. KGaA, Weinheim
ISBN: 978-3-527-31161-3

Table 21.1 Diastereoselective hydrogenation of olefinic bonds.

Substrate	Major diastereomer	Catalyst	mol%	P_{H_2}	Solvent	Temp. [°C]	Diastereo-meric ratio	TOF	Reference
1	R = *i*-Bu	Sm	10	1 atm	c-C_5H_{10}	r.t.	100:0	1.7	6
2	R = Me	Sm	3	1 atm	c-C_5H_{10}	–20	93:7	5.1	6
	R = *t*-Bu	Sm	5	1 atm	c-C_5H_{10}	r.t.	100:0	6.3	6
	R = Ph	Sm	5	1 atm	c-C_5H_{10}	50	100:0	6.4	6
	R = $(CH_2)_3NMe_2$	Sm	3	1 atm	c-C_5H_{10}	50	91:9	6.4	6
3 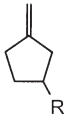	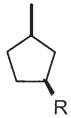 R = *n*-Bu	Sm	3	1 atm	c-C_5H_{10}	0	60:40	5.6	6
4 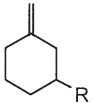	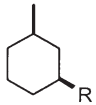 R = Me	Yb	3	1 atm	c-C_5H_{10}	–20	61:39	4.9	6
	R = Et	Yb	3	1 atm	c-C_5H_{10}	–20	73:27	5.3	6
5 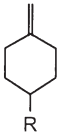	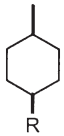 R = *t*-Bu	Yb	3	1 atm	c-C_5H_{10}	–20	77:23	4.9	6
		Cat: $Cp^*_2LnCH(SiMe_3)_2$ (Ln = Sm, Yb)							

Table 21.1 (continued)

	Substrate	Major diastereomer	Catalyst	mol%	P_{H_2}	Solvent	Temp. [°C]	Diastereo-meric ratio	TOF	Reference
6	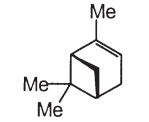 (1*S*,5*S*)-α-pinene	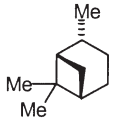 (1*S*,2*R*,5*S*)-*cis*-pinane	$Ru_2(CO)_4(OAc)_2(PPh_3)_2$	0.9	50 bar	THF	90	98.3:1.7	2.7	7
7	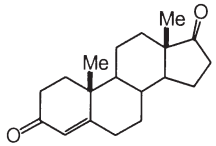	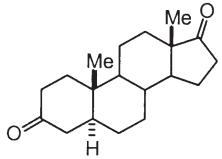	$[Ir(PCy_3)(py)(nbd)]^+$	20	1 atm	CH_2Cl_2	r.t.	100:0	0.87	8
8	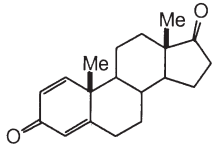	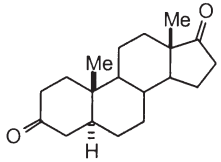	$[Ir(PCy_3)(py)(nbd)]^+$	15	1 atm	CH_2Cl_2	r.t.	100:0	0.27	8
9	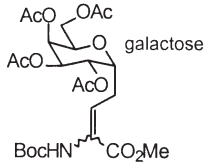	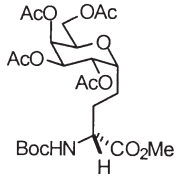	[Rh(diphos-4)]$^+$ [Rh((*R*,*R*)-Me-Du-phos)]$^+$ [Rh((*R*,*R*)-Et-Duphos)]$^+$ [Rh((*R*,*R*)-Pr-Du-phos)]$^+$		90 psi 90 psi 90 psi 90 psi	MeOH MeOH MeOH MeOH		50:50 79:21 91:9 88.5:11.5		9

Table 21.1 (continued)

	Substrate	Major diastereomer	Catalyst	mol%	P_{H_2}	Solvent	Temp. [°C]	Diastereomeric ratio	TOF	Reference
10	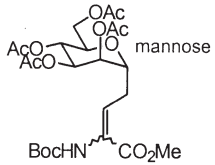	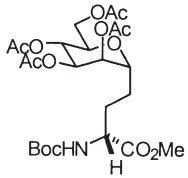	[Rh(diphos-4)]$^+$ [Rh((*R*,*R*)-Me-Duphos)]$^+$ [Rh((*R*,*R*)-Et-Duphos)]$^+$ [Rh((*R*,*R*)-Pr-Duphos)]$^+$		90 psi 90 psi 90 psi 90 psi	MeOH MeOH MeOH MeOH		50:50 87:13 >97.5:2.5 >97.5:2.5		9
11	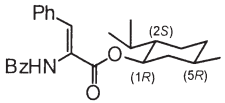	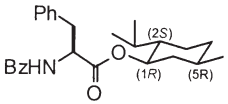	[Rh(Ph-*β*-glup-OH)]$^+$ [Rh(Ph-*β*-glup-OH)]$^+$ [Rh(Me-*α*-glu)]$^+$ [Rh(Me-*α*-glu)]$^+$	1 1 1 1	0.1 MPa 0.1 MPa 0.1 MPa 0.1 MPa	MeOH benzene acetone benzene		96.3:3.7 91:9 86:14 75:25		10
12	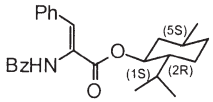	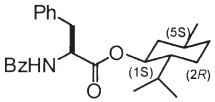	[Rh(Ph-*β*-glup-OH)]$^+$ [Rh(Ph-*β*-glup-OH)]$^+$ [Rh(Me-*α*-glu)]$^+$ [Rh(Me-*α*-glu)]$^+$	1 1 1 1	0.1 MPa 0.1 MPa 0.1 MPa 0.1 MPa	MeOH benzene MeOH benzene		97.4:2.6 79:21 66:34 14:86		10
13	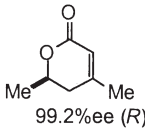 99.2%ee (*R*)	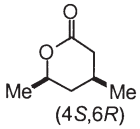 (4*S*,6*R*)	Ru(OAc)$_2$((*S*)-3,5-xylyl-biphep)	0.2	60 bar	*i*-PrOH		80:20		11
14	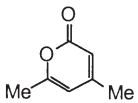	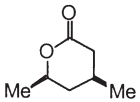	Ru(OAc)$_2$((*S*)-3,5-xylyl-biphep)	0.2	60 bar	*i*-PrOH		92:8	25	11

Table 21.2 Diastereoselective hydrogenation of ketones and imines.

	Substrate	Major diastereomer		Catalyst	mol%	P_{H_2}	Solvent	Temp. [°C]	Diastereo-selectivity	TOF	Reference
1	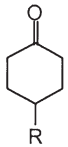	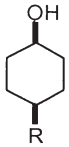	R = Me	Ru	0.2	4 atm	*i*-PrOH	28	92:8	485	12
			R = Ph	Ru	0.2	4 atm	*i*-PrOH	28	96:4	500	12
			R = *t*-Bu	Ru	0.2	4 atm	*i*-PrOH	28	98.4:1.6	500	12
2	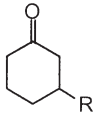	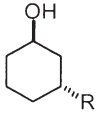	R = Me	Ru	0.2	4 atm	*i*-PrOH	28	96:4	500	12
3	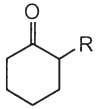	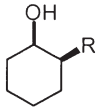	R = Me	Ru	0.2	4 atm	*i*-PrOH	28	98:2	475	12
			R = *t*-Bu	Ru	0.2	4 atm	*i*-PrOH	28	>99.8:0.2	500	12
4			R = Me	Ru	0.2	4 atm	*i*-PrOH	28	99:1	500	12
5	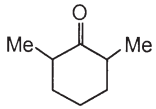	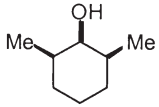		Ru	0.2	4 atm	*i*-PrOH	28	98.7: 1.1:0.2		12

Table 21.2 (continued)

Substrate	Major diastereomer	Catalyst	mol%	P_{H_2}	Solvent	Temp. [°C]	Diastereo-selectivity	TOF	Reference
6 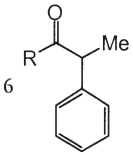	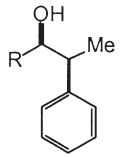 *syn*	R = Me Ru-a	0.2	4 atm	*i*-PrOH	28	96:4		12
		R = Me Ru-b	0.2	4 atm	*i*-PrOH	28	95:5		12
		R = Me Ru	0.2	4 atm	*i*-PrOH	28	86:14	480	12
		R = *n*-Bu Ru	0.2	4 atm	*i*-PrOH	28	93:7	480	12
		R = Ph Ru	0.2	4 atm	*i*-PrOH	28	98:2	480	12
7 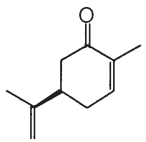 (*R*)-carvone	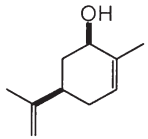	Ru	0.2	4 atm	*i*-PrOH	28	81:19	66.4	13
		$RuCl_2$((*S*)-binap)(dmf)m-(*R*,*R*)-DPEN-KOH/*i*-PrOH	0.2	4 atm	*i*-PrOH	28	100:0	143	13
		$RuCl_2$((*R*)-binap)(dmf)m-(*S*,*S*)-DPEN-KOH/*i*-PrOH	0.2	8 atm	*i*-PrOH	28	34:66	29.4	13
8 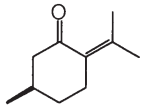 (*R*)-pulegone	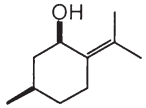	$RuCl_2$((*S*)-binap)(dmf)m-(*S*,*S*)-DPEN-KOH/*i*-PrOH	0.4	8 atm	*i*-PrOH	28	98:2	15.1	13
		$RuCl_2$((*R*)-binap)(dmf)m-(*R*,*R*)-DPEN-KOH/*i*-PrOH	0.4	8 atm	*i*-PrOH	28	95:5	14	13
9 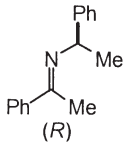 (*R*)	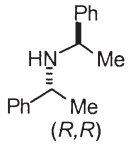 (*R*,*R*)	[RhCl(diphos-3)]Cl	2	1000 psi	MeOH	r.t.	91:9		14
		[RhCl((*S*,*S*)-bdpp)]Cl	2	1000 psi	MeOH	r.t.	99.7:0.3		
		[RhCl((–)-diop]Cl	2	1000 psi	MeOH	r.t.	93:7		

Table 21.2 (continued)

	Substrate	Major diastereomer	Catalyst	mol%	P_{H_2}	Solvent	Temp. [°C]	Diastereo-selectivity	TOF	Reference
10	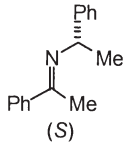	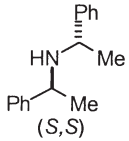	[RhCl((*S*,*S*)-bdpp)]Cl	2	1000 psi	MeOH	r.t.	93.8:6.2		14
11	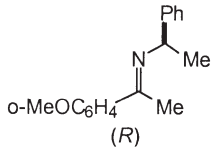	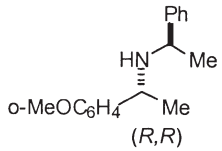	[RhCl((*S*,*S*)-bdpp)]Cl	2	1000 psi	MeOH	r.t.	98.1:1.9		14
12	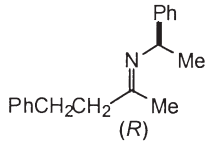	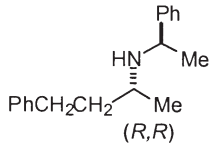	[RhCl(diphos-3)]Cl	2	1000 psi	MeOH	r.t.	67:33		
			[RhCl((*S*,*S*)-bdpp)]Cl	2	1000 psi	MeOH	r.t.	84:16		14

Ru = $RuCl_2(PPh_3)_3$-EN-KOH; Ru-a = $RuCl_2(P(C_6H_4\text{-p-OMe})_3)_3$-EN-KOH; Ru-b = $RuCl_2(P(C_6H_4\text{-p-Me})_3)_3$-EN-KOH

sure. The reactivity of rhodium complexes in homogeneous hydrogenation is sensitive to the degree of substitution on the olefinic bond, and trisubstituted or tetrasubstituted alkenes are intact in the hydrogenation, whereas iridium catalysts can hydrogenate the multi-substituted olefins under atmospheric hydrogen pressure. The unreactivity of trisubstituted alkenes towards rhodium complexes is overcome by increasing the hydrogen pressure, and the selectivity is comparable to (or a little better than) that obtained with iridium catalysts under atmospheric pressure [5]. The results of the hydrogenation of alkenes with lanthanide, ruthenium and iridium catalysts are listed in Table 21.1 [6–8]. In these reductions, the catalyst approaches the face of the double bond from the less-hindered side, and selection of the diastereoface of the substrate is straightforward when the stereogenic center is disposed adjacent to the double bond [6]. In the hydrogenation of double bonds in steroidal compounds, diastereoselectivity induced by iridium catalysts is very high [8]. In the reduction of dehydroamino acid derivatives with a chiral unit, an achiral rhodium catalyst resulted in stereorandom products (Table 21.1, entries 9 and 10) [9]. In the reaction of pyrone, the hydrogenation does not stop at the dihydropyrone stage, and *cis*-lactone is obtained in high diastereoselectivity, whereas hydrogenation of (*R*)-dihydropyrone afforded *cis*-lactone in lower diastereoselectivity, suggesting the complex character of the second hydrogenation step (Table 21.1, entries 13 and 14) [11]. Ruthenium–phosphine complexes combined with a diamine ligand effectively reduced ketones with a stereogenic center, and high diastereoselectivities are obtained (Table 21.2, entries 1–6) [12, 13]. The apparent effect of an adjacent stereogenic center was also observed in the reduction of imines [14]. For high stereoinduction, the proximity of the aromatic ring to the C=N bond seems to be essential.

21.3
Substrate-Directive Diastereoselective Hydrogenation

21.3.1
Hydrogenation of Cyclic Alcohols with Endo- or Exo-Cyclic Olefinic Bond

In the diastereoselective hydrogenation of olefinic, keto or imino double bonds, enhanced diastereoface differentiation will be possible by utilizing the interaction of functional groups in the substrates with the metal or with the ligand of the complex. Heteroatom(s) in the functional group would ligate to the metal and serve to fix the coordination mode of the substrate onto the catalyst. The key factor in the enantioselective hydrogenation of dehydroamino acids and esters is the formation of the rhodium–enamide chelate complex in which olefinic and amidocarbonyl units ligate to the metal [15]. Also in the diastereoselective hydrogenation, chelation of the substrate would serve to control the course of the hydrogenation. This potentiality of functional group-directed hydrogenation was first disclosed by Thompson and McPherson in 1974. In the hydrogenation

of a cyclic homoallyl alcohol derivative by $RhCl(PPh_3)_3$, the reaction did not even proceed under forced conditions (100 psi at 50 °C), but the substrate was hydrogenated by converting the alcohol to the potassium alkoxide **1** to afford the *cis*-product predominantly [Eq. (1)] [16].

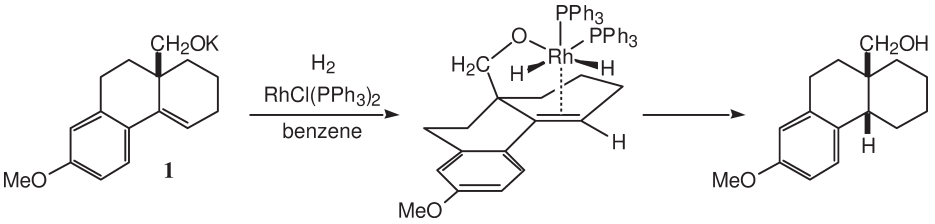

(1)

It was proposed that the chloride ion is displaced by the alkoxide ion from the coordination sphere of the dihydride complex, while delivery of the hydride to the unsaturated bond is controlled to afford the *cis*-product. In the case of the alcohol form, the chloride ion is not displaced, and the substrate is strongly resistant to hydrogenation by $RhCl(PPh_3)_3$. The heteroatom-directive hydrogenation would generally require vacant sites on the metal complex for the binding of H_2, the olefin unit and the directing heteroatom to the metal under hydrogenation conditions; thus, an active catalyst would be of 12-electron structure. Cationic $[Rh(diphosphine)(cod)]^+$ complex and cationic iridium complex (e.g., $[Ir(PCy_3)(py)(nbd)]^+$: Crabtree's catalyst [18]) and ruthenium complexes (e.g., $Ru(binap)(OAc)_2$) could hydrogenate the olefinic substrate with a directing heteroatom moiety to cause diastereoselective hydrogenation. Using $[Rh(diphosphine)(cod)]^+$ or $[Ir(PCy_3)(py)(nbd)]^+$ complexes, coordinating dienes are easily reduced by treatment with H_2, and 12-electron species are easily formed in a non-coordinating solvent such as dichloromethane (DCM). Brown reported the selective hydrogenation of acyclic allylic alcohols to produce chiral acyclic alcohols diastereoselectively using $[Rh(diphos\text{-}4)]^+$ catalyst in 1982 [19, 20]. Crabtree and Stork reported the highly diastereoselective hydrogenation of diverse types of cyclic alcohols in 1983 (allyl and homoallyl alcohols), using the cationic iridium complex ($[Ir(PCy_3)(py)(nbd)]PF_6$: Ir^+) [21, 22]. The data provided in Tables 21.3, 21.4 and 21.5 indicate the hydrogenation of diverse types of cyclic allylic and homoallylic alcohols.

In these reactions, the major diastereomer is formed by the addition of hydrogen *syn* to the hydroxyl group in the substrate. The cationic iridium catalyst $[Ir(PCy_3)(py)(nbd)]^+$ is very effective in hydroxy-directive hydrogenation of cyclic alcohols to afford high diastereoselectivity, even in the case of bishomoallyl alcohols (Table 21.4, entries 10–13) [5, 34, 35]. An intermediary dihydride species is not observed in the case of rhodium complexes, but iridium dihydride species are observed and the interaction of the hydroxyl unit of an unsaturated alcohol with iridium is detected spectrometrically through the presence of diastereotopic hydrides using NMR spectroscopy [21].

Table 21.3 Diastereoselective hydrogenation of cyclic allyl alcohols.

	Substrate	Major diastereomer	Catalyst	mol%	P_{H_2}	Solvent	Temp. [°C]	Diastereo-meric ratio	TOF	Reference(s)
1	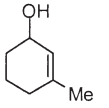	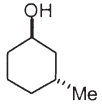	Rh^+	3.5	375 psi			290:1	28	23
			Ir^+	20	15 psi	CH_2Cl_2	r.t.	98.5:1.5	>2.5	22
				20	15 psi	CH_2Cl_2	r.t.	98:2	>2.5	24
				2.5	15 psi	CH_2Cl_2	r.t.	140 ~ 150:1	20, 80	24, 25
2	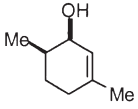	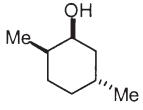	Ir^+	2.5	1 atm	CH_2Cl_2	r.t.	99:1	80	25
3	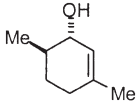	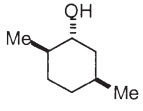	Ir^+	2.5	1 atm	CH_2Cl_2	r.t.	940:1	80	25
4	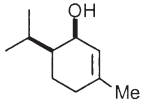	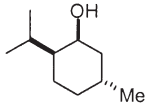	Ir^+	2.5	1 atm	CH_2Cl_2	r.t.	98.5:1.5	80	25
5	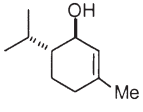	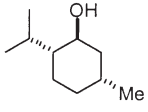	Ir^+	2.5	1 atm	CH_2Cl_2	r.t.	96:4	80	25
6	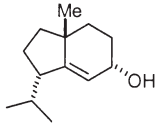	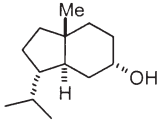	Rh^+	5	800 psi	THF		98.6:1.4		5
			Ir^+	30	1 atm	CH_2Cl_2		highly selective		26

Table 21.3 (continued)

	Substrate	Major diastereomer	Catalyst	mol%	P_{H_2}	Solvent	Temp. [°C]	Diastereo-meric ratio	TOF	Reference(s)
7	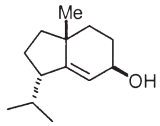	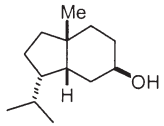	Ir^+	20	1 atm	CH_2Cl_2		100:0		26
8	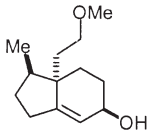	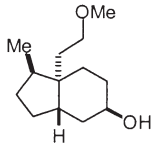	Rh^+	5	55 atm	THF		95:5	8	27
9	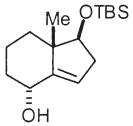	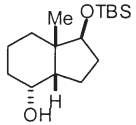	Ir^+	20	40 psi	CH_2Cl_2		highly selective	0.16	28
10	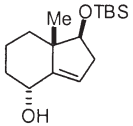	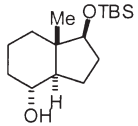	Rh	25	40 psi	benzene		75:25	0.15	28
11	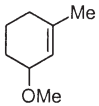	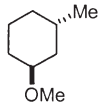	Ir^+	2.5	1 atm	CH_2Cl_2		>99.9:0.1	80	25

Table 21.3 (continued)

	Substrate	Major diastereomer	Catalyst	mol%	P_{H_2}	Solvent	Temp. [°C]	Diastereo-meric ratio	TOF	Reference(s)
12	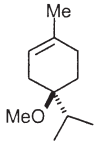	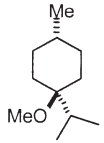	Ir^+	2.5	1 atm	CH_2Cl_2		>99.9:0.1	80	25
13	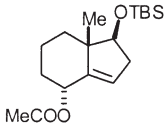	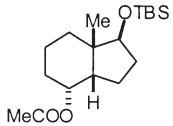	Ir^+	20	40 psi	CH_2Cl_2		100:0	0.13	28
14	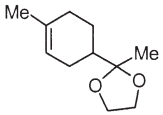	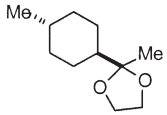	Ir^+	2.5	15 psi	CH_2Cl_2		62:38	36	25
15	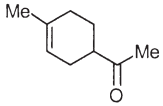	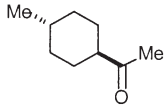	Ir^+	2.5	15 psi	CH_2Cl_2		99:1	80	25

$Rh = RhCl(PPh_3)_3$; $Rh^+ = [Rh(diphos\text{-}4)(cod)]^+$; $Ir^+ = [Ir(PCy_3)(py)(nbd)]^+$

Table 21.4 Diastereoselective hydrogenation of cyclic homoallyl and bishomoallyl alcohols.

	Substrate	Major diastereomer		Catalyst	mol%	P_{H_2}	Solvent	Temp. [°C]	Diastereo-meric ratio	TOF	Reference
1	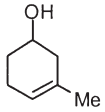	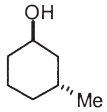		Ir^+	20	15 psi	CH_2Cl_2	r.t.	96.5:3.5	>2.5	22
2	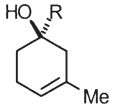	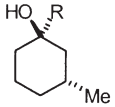	R = Me	Ir^+	20	15 psi	CH_2Cl_2	r.t.	>100:1	>2.5	22
			R = ^{i}Pr	Ir^+	2.3	1 atm	CH_2Cl_2	0	1000:1	28.7	21
3	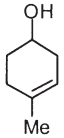	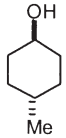		Rh^+	10	640 psi	CH_2Cl_2	r.t.	98.5:1.5	10	5
				Ir^+	20	15 psi	CH_2Cl_2	r.t.	97:3	>2.5	24
					2.5	15 psi	CH_2Cl_2	r.t.	98.1:1.9	20	24
4	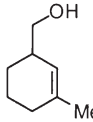	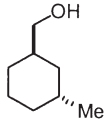		Ir^+	20	15 psi	CH_2Cl_2	r.t.	86:14	>2.5	22
5	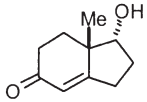	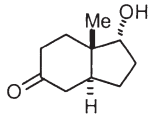		Ir^+	20	15 psi	CH_2Cl_2		96:4	<0.21	22

Table 21.4 (continued)

	Substrate	Major diastereomer	Catalyst	mol%	P_{H_2}	Solvent	Temp. [°C]	Diastereo-meric ratio	TOF	Reference
6	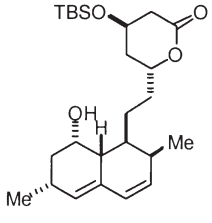	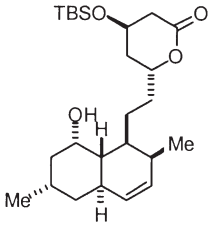	Ir^+	2.5	1 atm	CH_2Cl_2/ ^iPrOH		highly selective	1.9	30
7	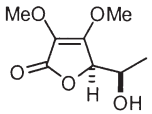	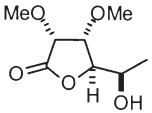	Rh^+	20	1850 psi	CH_2Cl_2		100:0		31
8	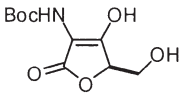	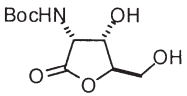	Rh^+	20	130 atm	CH_2Cl_2	r.t.	91:9	0.25	32
9	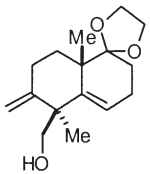	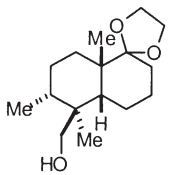	Ir^+	0.11	1000 psi	CH_2Cl_2		100:0	6.3	33

Table 21.4 (continued)

	Substrate	Major diastereomer	Catalyst	mol%	P_{H_2}	Solvent	Temp. [°C]	Diastereo-meric ratio	TOF	Reference
10	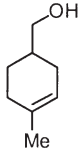	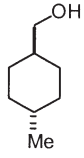	Rh^+	10	1000 psi	CH_2Cl_2	r.t.	95:5	10	5
			Ir^+	20	15 psi	CH_2Cl_2	r.t.	96.2:3.8	>2.5	5
11	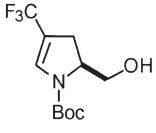	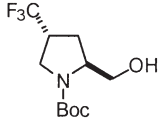	Ir^+	15	15 psi	CH_2Cl_2	r.t.	95:5		34
				2	15 psi	CH_2Cl_2	r.t.	99.4:0.6	12.5	34
12	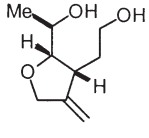	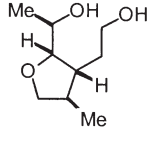	Ir^+	1	15 psi	CH_2Cl_2		>99:1		35
			Rh^+	6		CH_2Cl_2		90:10		
			Rh	100		toluene		6:94		
13	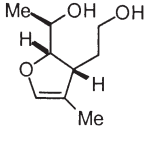	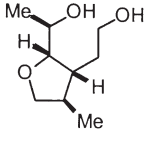	Ir^+	0.5	15 psi	CH_2Cl_2		>99:1		35

$Rh = RhCl(PPh_3)_3$; $Rh^+ = [Rh(diphos\text{-}4)(cod)]^+$; $Ir^+ = [Ir(PCy_3)(py)(nbd)]^+$

Table 21.5 Diastereoselective hydrogenation of alcohols with exocyclic double bond.

	Substrate	Major diastereomer	Catalyst	mol%	P_{H_2}	Solvent	Temp. [°C]	Diastereomeric ratio	TOF	Reference
1	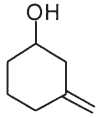	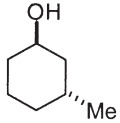	Rh^+	2	15 psi			>98:2		36
2	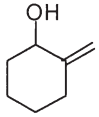	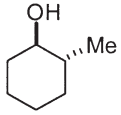	Rh^+ Rh^+	3.5 2	500 psi 15 psi			75:25 45:55		23 36
3	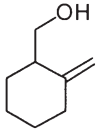	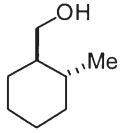	Rh^+	2	15 psi			47:53		36
4	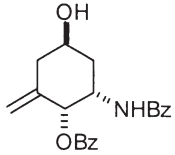	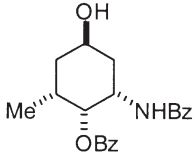	Rh^+ Ir^+	35 17.5	15 psi 15 psi	CH_2Cl_2 CH_2Cl_2	r.t. r.t.	100:0 72:28	0.12	37 37

Table 21.5 (continued)

	Substrate	Major diastereomer	Catalyst	mol%	P_{H_2}	Solvent	Temp. [°C]	Diastereo-meric ratio	TOF	Reference
5	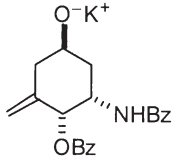	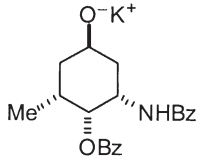	Rh	100 3.6	15 psi 15 psi	CH_2Cl_2 CH_2Cl_2	r.t. r.t.	95:5 no reaction		37 37
6	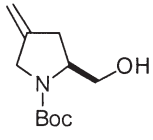	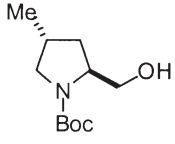	Ir^+	3	15 psi	CH_2Cl_2	r.t.	>97.5:2.5	1.67	38
7	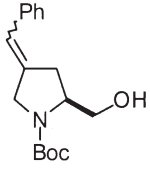	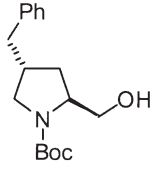	Ir^+	3	15 psi	CH_2Cl_2	r.t.	>97.5:2.5	1.7	38
8	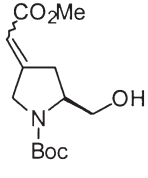	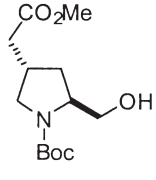	Ir^+	3	15 psi	CH_2Cl_2	r.t.	94:6	1.85	38

Table 21.5 (continued)

	Substrate	Major diastereomer	Catalyst	mol%	P_{H_2}	Solvent	Temp. [°C]	Diastereo-meric ratio	TOF	Reference
9	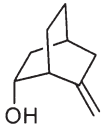	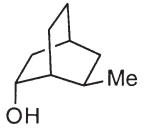	Rh^+	2	15 psi	CH_2Cl_2		95:5	10	29
			Ir^+	2	15 psi	CH_2Cl_2		99.7:0.3	1500	39
						CH_2Cl_2		99.7:0.3	6000	29
10	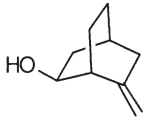	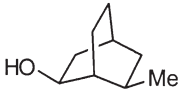	Ir^+	2	15 psi	CH_2Cl_2		55:45	16.7	29
11	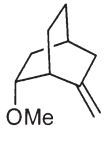	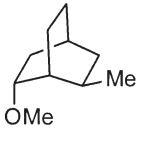	Rh^+	2	15 psi	CH_2Cl_2		86.5:14.5	600	29
			Ir^+	2	15 psi	CH_2Cl_2		97.4:2.6	1000	29

$Rh = RhCl(PPh_3)_3$; $Rh^+ = [Rh(diphos\text{-}4)(cod)]^+$; $Ir^+ = [Ir(PCy_3)(py)(nbd)]^+$

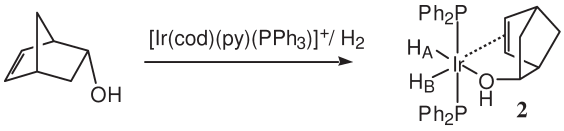

$\delta(H_A) = -29.4$, $\delta(H_B) = -9.6$ ppm (2)

Thus, coordination of the OH-group controls the selection of the face to be reduced, and in some cases may also induce higher reactivity compared with the simple olefins not bearing OH-groups. Even in the presence of exceptional levels of steric congestion which are disposed to override the directivity of hydroxyl group, the addition of hydrogen occurs predominantly on the diastereoface bearing the hydroxyl group (Table 21.3, entry 6) [5, 26]. The concentration of the iridium catalyst strongly affects the stereoselectivity: a low concentration of the iridium complex is necessary to effect high diastereoselectivity; the decreases in stereoselectivity at a higher iridium concentration is ascribed to the formation of more than one complex, including trinuclear cluster complexes [24] in solution (Table 21.3, entry 1 and Table 21.4, entries 2 and 3). Cationic rhodium complexes such as $[Rh(nbd)(diphos\text{-}4)]^+$ are also effective for directive-hydrogenation of cyclic unsaturated alcohols, although in terms of selectivity they are somewhat inferior to the iridium catalysts. In entry 9 of Table 21.3, an attempt to obtain the *trans*-hydroindane product using a cationic iridium catalyst (Crabtree's catalyst) unexpectedly produced *cis*-hydroindanol highly selectively [28]. This suggests direction by the ether linkage of the TBSO unit. In contrast, hydrogenation by 25 mol.% of Wilkinson's catalyst in benzene (entry 10) afforded the *trans*-hydroindanol as a 3 : 1 mixture by the approach of rhodium catalyst from the less-hindered face of the double bond [28]. Even an exocyclic hydroxyl group can direct high diastereoselectivity with a rhodium or iridium catalyst in entries 7 and 9 of Table 21.4 [31, 33], though in entry 8 the directivity of the hydroxyl group is depressed by competition with the carbamate unit [32]. The hydroxyl group in bishomoallyl type alcohols also serves to direct the hydrogenation course to afford high diastereoselectivity. In entries 10–13 of Table 21.4, a cationic iridium complex can induce high diastereoselectivity by adding hydrogen from the face bearing the hydroxyl group [5, 34, 35]. With the Wilkinson catalyst, however, the reversed diastereoselectivity was again observed by the approach of the complex from the less-hindered side of the double bond without interaction with a hydroxyl unit (Table 21.4, entry 12).

Cationic iridium and rhodium catalysts are also effective for the hydrogenation of exocyclic olefinic alcohols (see Table 21.5), except for 2-exomethylenecyclohexanol and 2-methylenecyclohexanemethanol (entries 2 and 3). In entry 4, a cationic rhodium catalyst gave a single product whilst a cationic iridium catalyst induced only modest selectivity (72 : 28).

This lowering of the selectivity may be attributed to competitive binding between the hydroxyl and amide groups to iridium [37]. In entries 6, 7 and 8, the directivity of the hydroxyl group at the bishomoallylic position effectively overrides the effect of the carbamate unit [38]. In the hydrogenation of methylenebi-

cyclo[2.2.2]octan-2-ol, the exo hydroxyl group does not serve as a directive group, and stereorandom hydrogenation proceeds contrary to the hydrogenation of methylenebicyclo[2.2.2]octan-2-ol with an endo hydroxyl group (entries 9 and 10) [29]. In entry 11 of Table 21.5, the methylenebicyclo[2.2.2]octane compound is hydrogenated in lower selectivity but at a higher rate than the parent alcohol with rhodium catalyst [29].

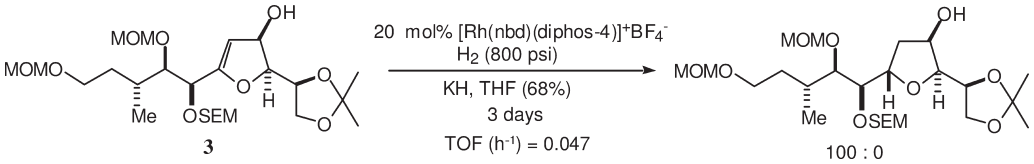

(3)

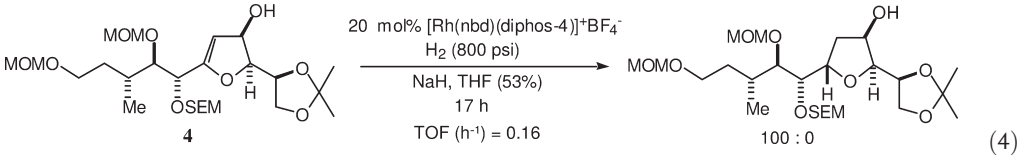

(4)

As exemplified by Thompson for the case of tricyclic alcohol **1** [Eq. (1)], alkoxide has a strong coordinative ability to the metal, and high diastereoselectivity is realized in spite of the presence of a proximal bulky substituent in dihydrofuran derivatives [Eqs. (3) and (4)] [17].

Other functional groups which have a heteroatom rather than a hydroxyl group capable of directing the hydrogenation include alkoxyl, alkoxycarbonyl, carboxylate, amide, carbamate, and sulfoxide. The alkoxy unit efficiently coordinates to cationic iridium or rhodium complexes, and high diastereoselectivity is induced in the reactions of cyclic substrates (Table 21.3, entries 11–13) [25, 28]. An acetal affords much lower selectivity than the corresponding unsaturated ketone (Table 21.3, entries 14 and 15) [25].

Table 21.6 indicates the hydrogenation results of substrates with ester and carboxyl functionalities. An ester functionality also serves well as a directive unit, and high selectivity is reported for β,γ-unsaturated esters with both rhodium and iridium catalysts (Table 21.6, entries 1 and 2) [40, 41]. Directivity of the alkoxycarbonyl unit of an γ,δ-unsaturated ester is slightly diminished (entry 3) [25, 40, 41], and an acyloxy unit in the homoallylic position does not direct apparent stereoselectivity (entry 4) [41]. In the Wilkinson catalyst, hydroxyl, ether, esters or amide units cannot displace chloride ion from the metal, but carboxylate – being a better nucleophile – may be able to replace the chloride ion. In the hydrogenation of β,γ-carboxylic acids (Table 21.6, entries 8 and 9), the carboxylates are generated *in situ* by the addition of triethylamine, and the hydrogenation proceeds cleanly under 60 psi. As a consequence, one diastereoisomer is formed predominantly with a high selectivity of more than 99% diastereomeric

Table 21.6 Diastereoselective hydrogenation of double bond in cyclic esters and carboxylic acids.

	Substrate	Major diastereomer	Catalyst	mol%	P_{H_2}	Solvent	Temp. [°C]	Diastereo-meric ratio	TOF	Reference
1	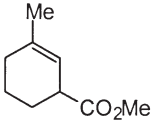	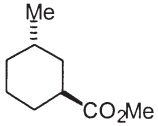	Rh^+	2	1 atm	CH_2Cl_2	r.t.	97:3	>1.8	40
			Ir^+	2	1 atm	CH_2Cl_2	r.t.	99.9:0.1	300	40
2	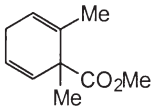	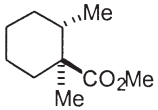	Ir^+	5	1 atm	CH_2Cl_2	r.t.	99:1	4.5 ~ 9	41
3	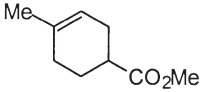	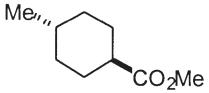	Rh^+	2	1 atm	CH_2Cl_2	r.t.	88:12	<0.23	40
			Ir^+	2	1 atm	CH_2Cl_2	r.t.	89:11	200	40
			Ir^+	2.5	1 atm	CH_2Cl_2	r.t.	95:5	77	25
			Ir^+	5	1 atm	CH_2Cl_2	r.t.	97.6:2.4	4.5–9	41
4	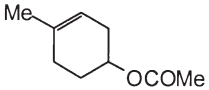	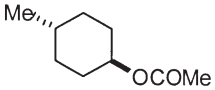	Ir^+	5	1 atm	CH_2Cl_2	r.t.	50:50		41
5	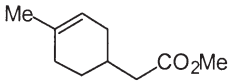	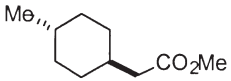	Ir^+	5	1 atm	CH_2Cl_2	r.t.	54.5:45.5		41
6	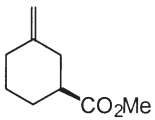	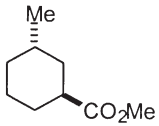	Rh^+	2	1 atm	CH_2Cl_2	r.t.	90:10	0.88	40
			Ir^+	2	1 atm	CH_2Cl_2	r.t.	81:19	300	40

Table 21.6 (continued)

	Substrate	Major diastereomer	Catalyst	mol%	P_{H_2}	Solvent	Temp. [°C]	Diastereomeric ratio	TOF	Reference
7	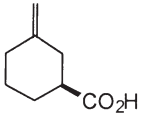	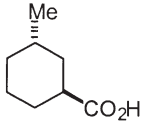	Rh^+	2	1 atm	CH_2Cl_2	r.t.	50:50	<0.33	40
			Ir^+	2	1 atm	CH_2Cl_2	r.t.	88:12	8.3	40
8	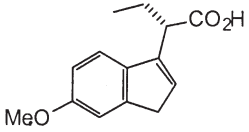	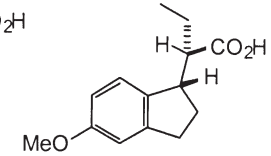	Rh	5	60 psi	THF/EtOH(1/9) (1.5 eq TEA)		>99.5:0.5	1.7	42
			Rh	5	60 psi	THF/EtOH(1/9) (0 eq TEA)		94:6	1.0	42
9	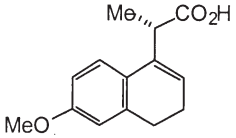	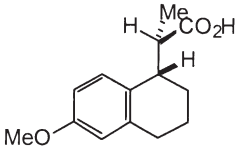	Rh	5	60 psi	THF/EtOH(1/9) (1.5 eq TEA)		>99.5:0.5		42

Rh = $RhCl(PPh_3)_3$; $Rh^+ = [Rh(diphos\text{-}4)(cod)]^+$; $Ir^+ = [Ir(PCy_3)(py)(nbd)]^+$

excess (d.e.). The carboxylate anion binds to the rhodium complex, and discrimination of the diastereoface is caused by minimizing interaction of the stereogenic center with the peri-aromatic proton [42]. Even in the absence of amine, hydrogenation using the Wilkinson catalyst induces moderate reactivity and selectivity (88% d.e.) (entry 8), because part of the carboxylic acid undergoes dissociation to afford carboxylate in polar tetrahydrofuran (THF)/EtOH solution. In entry 7, the hydrogenation proceeds incompletely in DCM under the standard conditions. This implies the formation of inactive carboxylate complex in dichloromethane.

The amide group shows a prominent directivity in the hydrogenation of cyclic unsaturated amides by a cationic iridium catalyst, and much higher diastereoselectivity is realized than in the corresponding ester substrates (Table 21.7). In the case of β,γ-unsaturated bicyclic amide (entry 3), the stereoselectivity surpasses 1000 : 1 [41]. An increase of the distance between the amide carbonyl and olefinic bond causes little decrease in the selectivity (δ,ε-unsaturated amide, entry 6) compared with the case of the less-basic ester functionality (Table 21.6, entry 5).

In the case of cyclopentenyl carbamate in which a directive group is present at the homoallyl position, the cationic rhodium $[Rh(diphos\text{-}4)]^+$ or iridium $[Ir(PCy_3)(py)(nbd)]^+$ catalyst cannot interact with the carbamate carbonyl, and thus approaches the double bond from the less-hindered side. This affords a *cis*-product preferentially, whereas with the chiral rhodium–duphos catalyst, directivity of the carbamate unit is observed (Table 21.7, entry 7). The presence of a hydroxyl group at the allyl position induced hydroxy-directive hydrogenation, and higher diastereoselectivity was obtained (entry 8) [44].

21.3.2
Hydrogenation of Acyclic Allyl and Homoallyl Alcohols

The hydrogenation of acyclic allyl alcohols with a 1,1-disubstituted olefinic bond are listed as entries 1 to 5 of Table 21.8. The reduction of (α-hydroxyalkyl)acrylates proceeds stereoselectively with the cationic rhodium catalyst $[Rh(diphos\text{-}4)(nbd)]^+$, and 1,2-*anti*-compounds are obtained as the major product by the direction of the hydroxyl group. Under these reaction conditions, isomerization of the olefinic unit occurs to afford about 20% of the corresponding methyl ketone. If the isomerization occurs prior to the hydrogenation, diminished stereoselectivity would be observed, even if the individual reduction mode were to occur discriminately [5]. With a cationic iridium catalyst, the degree of isomerization is greater than with the rhodium catalyst, and the hydrogenation occurs with lower diastereoselectivity (Table 21.8, entries 5–7). This is in contrast to the high stereoinduction ability of iridium catalysts for cyclic unsaturated compounds, but the isomerization can be suppressed by increasing the hydrogen pressure. The concentration of iridium catalyst strongly affects the stereoselectivity, and at higher concentration stereorandom hydrogenation almost occurs

Table 21.7 Amido-directive diastereoselective hydrogenation.

	Substrate	Major diastereomer	Catalyst	mol%	P_{H_2}	Solvent	Diastereo-meric ratio	TOF	Reference
1	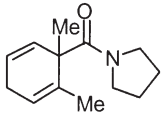	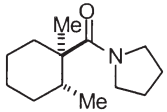	Ir^+	5	1 atm	CH_2Cl_2	170:1	4 ~ 8	41
2	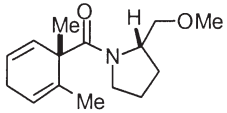	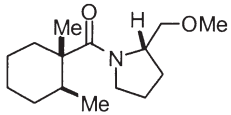	Ir^+	5	1 atm	CH_2Cl_2	530:1	4.5 ~ 9	41
3	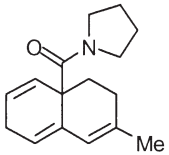	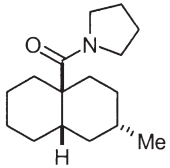	Ir^+	5	1 atm	CH_2Cl_2	>1000:1	4.5 ~ 9	41
4	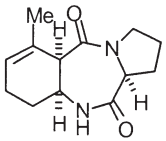	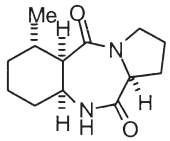	Ir^+ Ir^+	5 5	1 atm 1 atm	CH_2Cl_2 CH_2Cl_2	>99:1 >99:1	4.5 ~ 9 3.3	41 43
5	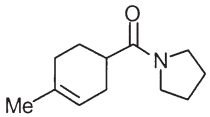	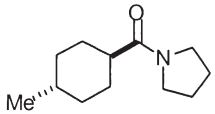	Ir^+	5	1 atm	CH_2Cl_2	130:1	4.5 ~ 9	41

Table 21.7 (continued)

	Substrate	Major diastereomer	Catalyst	mol%	P_{H_2}	Solvent	Diastereomeric ratio	TOF	Reference
6	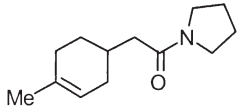	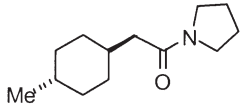	Ir^+	5	1 atm	CH_2Cl_2	>100:1	4.5 ~ 9	41
7	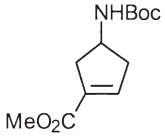	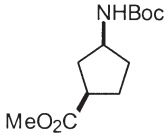	Ir^+	1	5 atm	CH_2Cl_2	92.5:7.5	7.1	44
			Rh^+	1	5 atm	MeOH	78.5:21.5	7.1	44
			[Rh((*R*,*R*)-Me-Duphos)]$^+$	1	5 atm	MeOH	20:80	7.1	44
			[Rh((*S*,*S*)-Me-Duphos)]$^+$	1	5 atm	MeOH	9:91	7.1	44
8	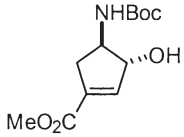	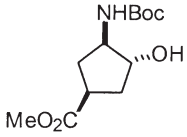	Ir^+	1	5 atm	CH_2Cl_2	97:3	7.1	44
			Rh^+	1	5 atm	MeOH	80:20	7.1	44
			[Rh((*R*,*R*)-Me-Duphos)]$^+$	1	5 atm	MeOH	4:96	7.1	44
			[Rh((*S*,*S*)-Me-Duphos)]$^+$	1	5 atm	MeOH	33.5:66.5	7.1	44

$Rh^+ = [Rh(diphos\text{-}4)(cod)]^+$; $Ir^+ = [Ir(PCy_3)(py)(nbd)]^+$

Table 21.8 Hydroxy-directed hydrogenation of acyclic allyl aclohols.

	Substrate	Major diastereomer	Catalyst	mol%	P_{H_2}	Solvent	Temp. [°C]	Diastereo-meric ratio	TOF	Reference
1	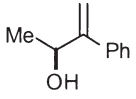	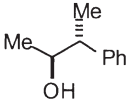	Rh^+	2	15 psi	CH_2Cl_2	0	97:3		19
2	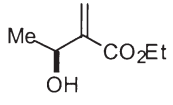	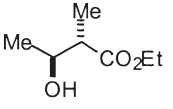	Rh^+	1	15 psi	CH_2Cl_2 MeOH		100:1 100:1	50 50	45 45
3	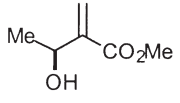	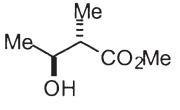	$Rh(OAc)_2$((*S*)-binap) $Rh(OAc)_2$((*R*)-binap)	4 atm 4 atm	MeOH MeOH	25 25	>23:1 >23:1		46 46
4	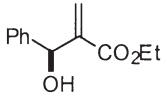	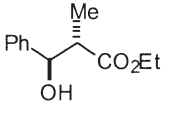	Rh^+	1	15 psi	CH_2Cl_2 MeOH	20 20	100:1 97.5:2.5	50	45
5	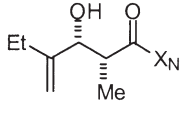	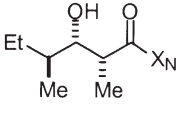	Rh^+ Ir^+ Ir^+	17.5 20 2.5	640 psi 15 psi 15 psi	CH_2Cl_2 CH_2Cl_2 CH_2Cl_2	25 25 25	93:7 57:43 85:15	>2.8 >2.5 >20	5 24 24
6	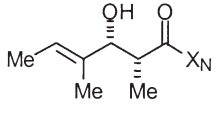	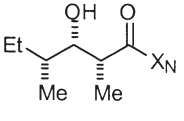	Rh^+ Ir^+ Ir^+	17.5 20 2.5	640 psi 15 psi 15 psi	CH_2Cl_2 CH_2Cl_2 CH_2Cl_2	25 25 25	91:9 43:57 73:27	>2.8 >2.5 >20	5 24 24

Table 21.8 (continued)

	Substrate	Major diastereomer	Catalyst	mol%	P_{H_2}	Solvent	Temp. [°C]	Diastereo-meric ratio	TOF	Reference
7	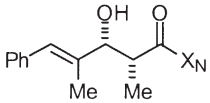	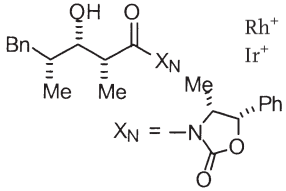	Rh^+	17.5	640 psi	CH_2Cl_2	25	94:6	>2.8	24
			Ir^+	2.5	15 psi	CH_2Cl_2	25	48:52	<0.4	24
8	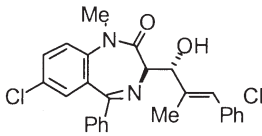	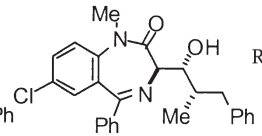	Rh^+	10	45 bar	CH_2Cl_2		75:25	1.1	47
9	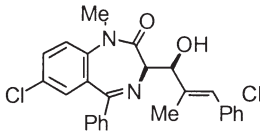	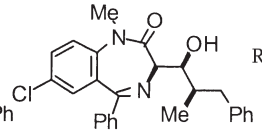	Rh^+	10	45 bar	CH_2Cl_2		80:20	1.3	47
10	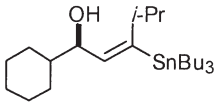	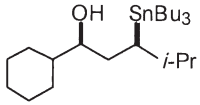	Rh^+	5	1500 psi	CH_2Cl_2	r.t.	300:1	0.47	48

Table 21.8 (continued)

	Substrate	Major diastereomer	Catalyst	mol%	P_{H_2}	Solvent	Temp. [°C]	Diastereo-meric ratio	TOF	Reference
11	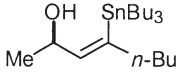	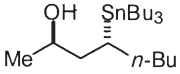	Rh^+	5	1500 psi	CH_2Cl_2	r.t.	>100:1	0.2	48
12	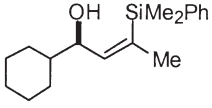	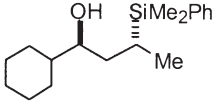	Rh^+	5	1500 psi	CH_2Cl_2	r.t.	>500:1	0.4	48
13	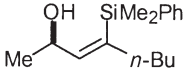	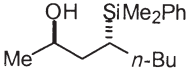	Rh^+	5	1500 psi	CH_2Cl_2	r.t.	>500:1	0.4	48
14	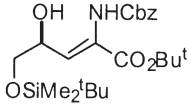	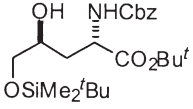	$[Rh((R,R)\text{-dipamp})]^+$ 0.7		3 bar	MeOH		highly selective	11.8	49

$Rh^+ = [Rh(diphos\text{-}4)(cod)]^+$; $Ir^+ = [Ir(PCy_3)(py)(nbd)]^+$

(Table 21.8, entries 5 and 6) [5, 24], similarly to the reduction of cyclic compounds.

The configuration of the product in diastereoselective hydrogenation – whether 1,2-*syn* or 1,2-*anti* – is related to the substitution pattern of the starting alkene. The allyl alcohol with a 1,1-disubstituted olefin unit affords the *anti*-product, while the *syn*-product is formed from the allyl alcohol with a trisubstituted olefinic bond (Table 21.8, entries 6–9). The complementarity in diastereoselective hydrogenation of di- and tri-substituted olefins may be rationalized based on the conformation analysis of the intermediary complex (Scheme 21.1) [23].

In entries 10–13 (Table 21.8) of trisubstituted alkenes, very high diastereoselectivity is realized by the use of a cationic rhodium catalyst under high hydrogen pressure, and the 1,3-*syn*- or 1,3-*anti*-configuration naturally corresponds to the (*E*)- or (*Z*)-geometry of the trisubstituted olefin unit [48, 49]. The facial selectivity is rationalized to be controlled by the A(1,3)-allylic strain at the intermediary complex stage (Scheme 21.2) [48].

Entries 8–13 in Table 21.9 illustrate the effect of S–O coordination on the hydrogenation of allyl alcohols. The hydrogenation of (α-hydroxyalkyl)vinyl sulfones follows the same stereochemical course as the corresponding acrylate via HO coordination (entries 8 and 9). However, the hydrogenation of (α-hydroxyalkyl)vinyl sulfoxides is directed by S–O coordination, which overrides the HO-participation in the stereochemical course (entries 10–13) [56]. The directing power of S–O may be limited to vinylic examples, as compounds having the S–O and double bond in an allylic relationship failed to reduce under the standard conditions.

The hydrogenation of acyclic homoallylic alcohols with a 1,1-disubstituted olefinic bond by cationic $[Rh(diphos\text{-}4)]^+$ catalyst proceeds in modest to moderate stereoselectivity, generally forming 1,3-*anti* compounds (Table 21.10, entries 1, 4 and 5), and the effect of the stereogenic center at the allylic position overrides the directivity of hydroxyl group. The 1,3-*syn* product is then observed though in poor selectivity (entry 3) [19, 57, 58]. Inspection of the hydrogenation prod-

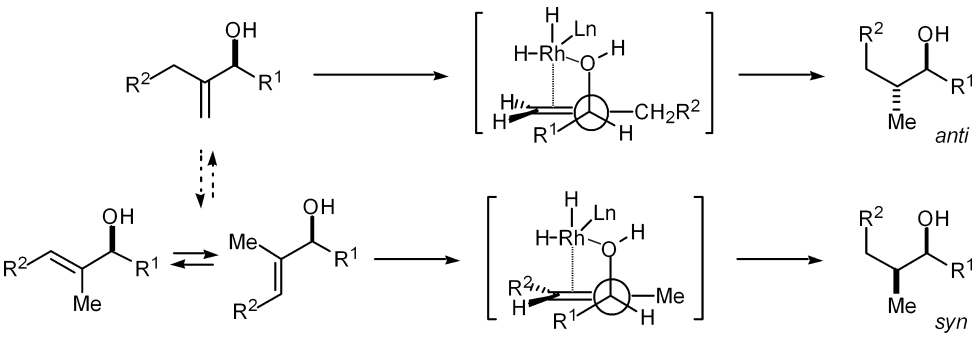

Scheme 21.1

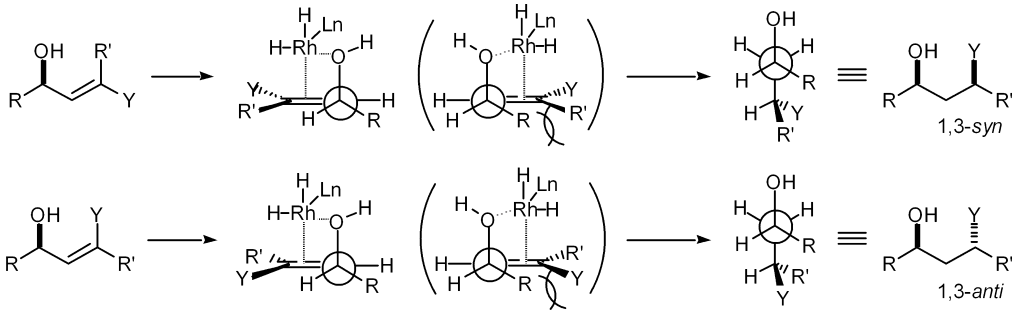

Scheme 21.2

ucts indicates that the substituent at the allylic position dictates the stereochemistry to afford the 1,2-*syn* product preferentially. The observed stereochemistry in 1,1-disubstituted homoallylic alcohols can be explained by considering the conformational analysis of the alkene complexes (Scheme 21.3). In conformation A, unfavorable A(1,2) interactions between R and R^1 are minimized and through A and C the 1,3-*anti* product will be formed. In the case of homoallylic alcohols without an allylic substituent, the group at the homoallylic carbon will adapt the pseudoequatorial orientation to afford the 1,3-*anti* product. In homoallylic alcohols with a stereogenic center at the allyl position, the group in the allylic position will also prefer the pseudoequatorial orientation so that the A(1,2) strain will be minimized [23, 57].

In the case of tri-substituted alkenes, the 1,3-*syn* products are formed in moderate to high diastereoselectivities (Table 21.10, entries 6~12). The stereochemistry of hydrogenation of homoallylic alcohols with a trisubstituted olefin unit is governed by the stereochemistry of the homoallylic hydroxy group, the stereogenic center at the allyl position, and the geometry of the double bond (Scheme 21.4). In entries 8 to 10 of Table 21.10, the product of 1,3-*syn* structure is formed in more than 90% d.e. with a cationic rhodium catalyst. The stereochemistry of the products in entries 10 to 12 shows that it is the stereogenic center at the allylic position which dictates the sense of asymmetric induction

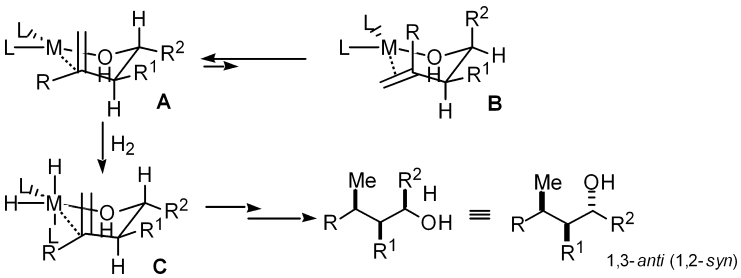

Scheme 21.3 Conformation of 1,1-disubstituted alkenes in the hydrogenation.

Table 21.9 Functinoal group-directed hydrogenation.

	Substrate	Major diastereomer	Catalyst	mol%	P_{H_2}	Solvent	Diastereomeric ratio	TOF	Reference
1	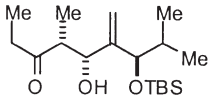	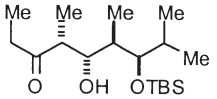	$[RhCl(PPh_3)_3]$		50 bar	benzene	99:1		50
2	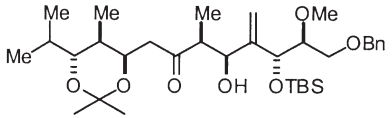	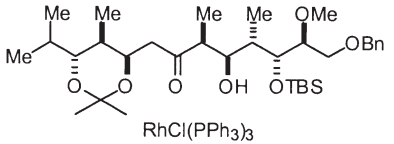	$RhCl(PPh_3)_3$		15 bar	benzene	>99:1		51
3	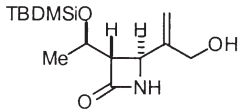	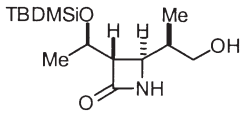	$Ru(OAc)_2((R)$-tol-binap) $Ru(OAc)_2((S)$-tol-binap) $RuBr_2((R)$-MeO-biphep)	0.2 0.2	1 atm 1 atm 15 bar	MeOH MeOH	99.9:0.1 22:78 >99:1	10.4 10.4	52 52 53
4	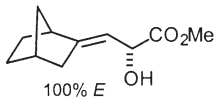	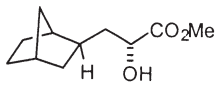	$[RuCl((R)$-binap$)]_2NEt_3$	2	70 atm	MeOH	99:1	1.07	54
5	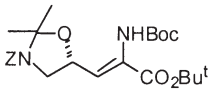	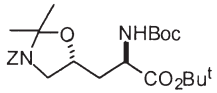	$[Rh((S,S)$-dipamp$))]^+$ $[Rh((R,R)$-dipamp$)]^+$	0.23 0.23	3 bar 3 bar	MeOH MeOH	80:20 20:80	28.6	49 49

Table 21.9 (continued)

	Substrate	Major diastereomer	Catalyst	mol%	P_{H_2}	Solvent	Diastereomeric ratio	TOF	Reference
6	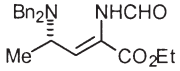	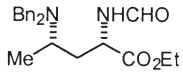	$[Rh(diphos\text{-}2)]^+$	10	25 atm	MeOH	88:12	0.25	55
7	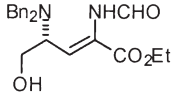	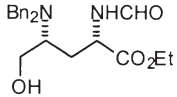	$[Rh(diphos\text{-}2)]^+$	10	85 atm	MeOH rt	90:10	0.24	55
8	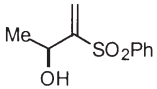	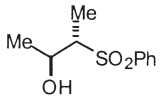	Rh^+	1	15 psi	CH_2Cl_2 MeOH	99.85:0.15 99.5:0.5		56
9	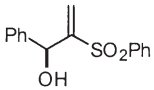	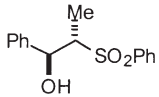	Rh^+	1	15 psi	CH_2Cl_2 MeOH	99.85:0.15 400:1		56
10	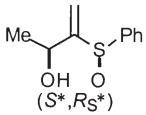 (S^*,R_S^*)	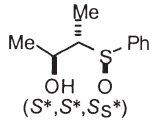 (S^*,S^*,S_S^*)	Rh^+	1	15 psi	$Cl(CH_2)_2Cl$ MeOH	99.5:0.5 97.5:2.5		56
11	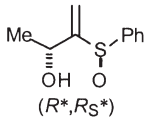 (R^*,R_S^*)	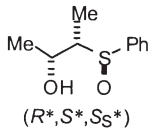 (R^*,S^*,S_S^*)	Rh^+	1	15 psi	$Cl(CH_2)_2Cl$ MeOH	99:1 80:20		56

Table 21.9 (continued)

	Substrate	Major diastereomer	Catalyst	mol%	P_{H_2}	Solvent	Diastereomeric ratio	TOF	Reference
12	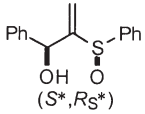 (S*,RS*)	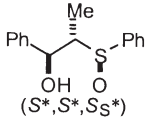 (S*,S*,SS*)	Rh^+	1	15 psi	CH_2Cl_2 MeOH	99.5:0.5 92.5:7.5		56
13	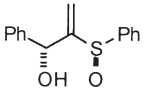 (R*,RS*)	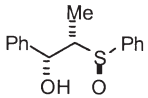 (R*,S*,SS*)	Rh^+	1	15 psi	CH_2Cl_2 MeOH	98.5:1.5 90.5:9.5		56

$Rh^+ = [Rh(diphos.4)(cod)]^+$; $Ir^+ = [Ir(PCy_3)(py)(nbd)]^+$

Table 21.10 Hydroxy-directed hydrogenation of acyclic homoallyl alcohols.

	Substrate	Major diastereomer	Catalyst	mol%	P_{H_2}	Solvent	Diastereo-selectivity	TOF	Reference
1	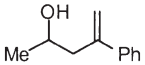	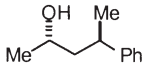	Rh^+	2	15 psi	THF	88:12		19
2	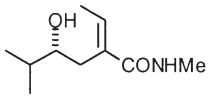	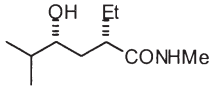	Rh^+	5	15 psi	MeOH	89:11	1	57
3	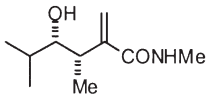	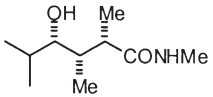	Rh^+	5	15 psi	MeOH	67:33	1	57
4	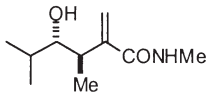	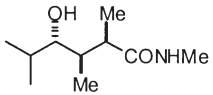	Rh^+	5	15 psi	MeOH	91:9	1	57
5	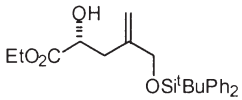	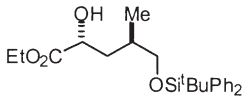	Rh^+		1000 psi	CH_2Cl_2	60:40		58
			[Rh((*S*,*S*)-Et-Duphos)]$^+$		1000 psi	CH_2Cl_2	95:5		58
			[Rh((*R*,*R*)-Et-Duphos)]$^+$		1000 psi	CH_2Cl_2	40:60		58
			[Rh(*R*)-phanephos)]$^+$		1000 psi	CH_2Cl_2	25:75		58
			Ir^+		1000 psi	CH_2Cl_2	35:65		58
6	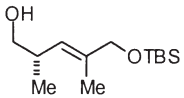	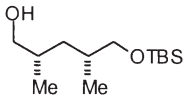	Rh^+	5	15 psi	CH_2Cl_2	95:5		59
			Ir^+	2.5	15 psi	CH_2Cl_2	73:27		59

Table 21.10 (continued)

	Substrate	Major diastereomer	Catalyst	mol%	P_{H_2}	Solvent	Diastereo-selectivity	TOF	Reference
7	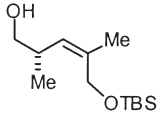	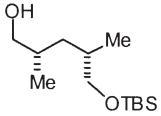	Rh^+	5	15 psi	CH_2Cl_2	91:9		59
8	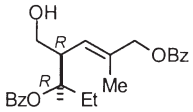	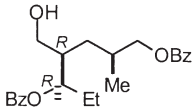	Rh^+ Ir^+	20 2.5	15 psi 15 psi	CH_2Cl_2 CH_2Cl_2	97:3 97:3		59 59
9	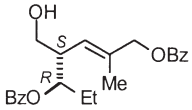	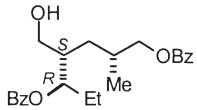	Rh^+ Ir^+	20 2.5	15 psi 15 psi	CH_2Cl_2 CH_2Cl_2	99:1 97:3		59 59
10	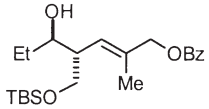	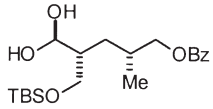	Rh^+ Ir^+	20 2.5	15 psi	CH_2Cl_2 CH_2Cl_2	97:3 94:6		59 59
11	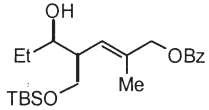	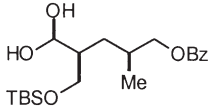	Rh^+ $[Rh((+)\text{-binap})]^+$ $[Rh((-)\text{-binap})]^+$	20	15 psi 1000 psi 1000 psi	CH_2Cl_2 CH_2Cl_2 CH_2Cl_2	89:11 97:3 92:8		59 59 59

Table 21.10 (continued)

	Substrate	Major diastereomer	Catalyst	mol%	P_{H_2}	Solvent	Diastereo-selectivity	TOF	Reference
12	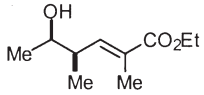	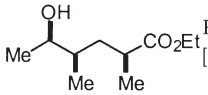	Rh^+		1000 psi	CH_2Cl_2	85:15		60
			$[Rh((+)\text{-binap})]^+$		1000 psi	CH_2Cl_2	98:2		59
13	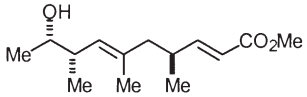	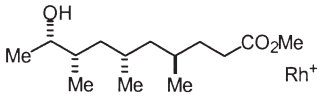							
			Rh^+	5	15 psi	CH_2Cl_2	94:6	1.6	61
14	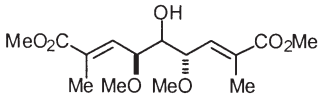	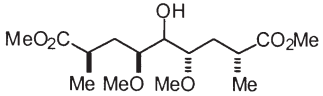							
			$[Rh(diphos\text{-}4)(nbd)]^+$	16	1000 psi	CH_2Cl_2	19:2.2:1	1.56	62
15	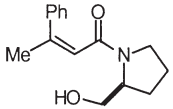	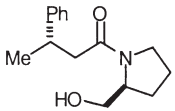	$[Rh(diphos\text{-}4)(nbd)]^+$	8	640 psi	1,5-asymmetric induction	80:20		23

$Rh^+ = [Rh(diphos\text{-}4)]^+$; $Ir^+ = [Ir(PCy_3)(py)(nbd)]^+$

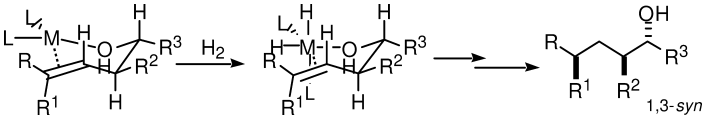

Scheme 21.4 Conformation of trisubstituted alkenes in the hydrogenation.

in combination with the direction by the hydroxyl group [59, 60]. In entries 6 and 7 of Table 21.10, the alkyl group at the allylic stereogenic center is small and the diastereoselectivity is ca. 80 ∼ 90% d.e. In the directive hydrogenation of a 5-hydroxy-4,6-dimethoxy-2,7-nonadienedioic acid derivative, which was part of the synthesis of the C_{10}-C_{19} fragment of the immunosuppressive agent FK-506 (entry 14), the diastereoselectivity is controlled by the methoxy units at the allylic positions, and not by the hydroxy group, to afford a product with two 1,3-*syn* disposition in the structure [62].

In some cases of enantioselective hydrogenation of dehydroamino acids with a chiral cationic rhodium catalyst, the less-stable substrate–metal complex (minor species) reacts with hydrogen far more rapidly (∼1000-fold faster) than the more stable complex (major species), and the stereochemistry of the predominant enantiomer is determined by the reaction of the minor species [63]. In these cases, the stereochemical outcome is not related to the initial equilibrium of the substrate–metal complex, and a higher hydrogen pressure and rise in reaction temperature suppress the enantioselectivity. In contrast to the enantioselective hydrogenation of dehydroamino acids, olefinic alcohols are hydrogenated with higher diastereoselectivity at higher hydrogen pressure and at lower reaction temperature [24, 48]. This implies that the major substrate–metal complex determines the stereochemical outcome of the hydrogenation.

In entry 15 of Table 21.10, it is noted that even a remote hydroxyl group directed hydrogenation by the cationic $[Rh(diphos\text{-}4)(nbd)]^+$ catalyst to afford a moderate diastereoselectivity (80 : 20) [23]. This is an interesting example of long-range 1,5-asymmetric induction.

21.3.3
Ester Unit- or Amide-Directive Hydrogenation

The diastereoselective hydrogenation of itaconate derivatives by cationic rhodium catalysts are listed in Table 21.11. The observed high diastereoselectivity indicates a strong directivity by the alkoxycarbonyl unit in the reduction of acyclic systems (entries 1 and 2). Decrease of stereoselectivity in entry 3 indicates the definite effect of the ether functionality on the sense of asymmetric induction, competing with the directivity exerted by the alkoxycarbonyl group [64]. An amide or a carbamate group also serves as an admirable directing group in acrylic acid derivatives (entries 4–6) [65–67], although the hydrogenation of an amine or its corresponding trifluoroacetate salt was quite unselective (entry 7) [65].

Table 21.11 Directive hydrogenation of acrylic acid derivatives.

	Substrate	Major diastereomer	Catalyst	mol%	P_{H_2}	Solvent	Diastereomeric ratio	TOF	Reference
1	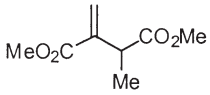	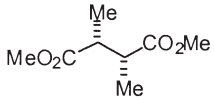	Rh^+	2	1 atm	MeOH	99.6:0.4	50	64
2	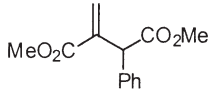	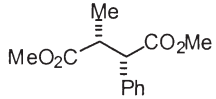	Rh^+	2	1 atm	MeOH	99.5:0.5		64
3	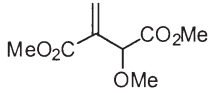	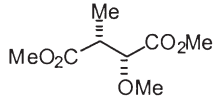	Rh^+	2	1 atm	MeOH	98:2		64
4	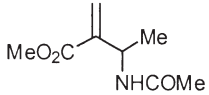	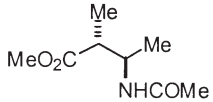	Rh^+ Rh^+	5 5	 1 atm	CH_2Cl_2 MeOH	99:1 100:0		65 65
5	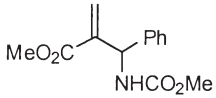	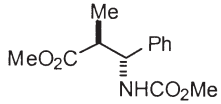	[Rh(diphos-2)]$^+$ [Rh(diphos-2)]$^+$ $Ru(TFA)_2(PPh_3)_2$ $Ru(TFA)_2(PPh_3)_2$ [Rh((*S*)-skewphos)]$^+$ [Rh((*S*)-chiraphos)]$^+$ [Rh((*R*)-binap)]$^+$	1 1 1 1 1 1 1	30 atm 30 atm 30 atm 75 atm 30 atm 30 atm 30 atm	THF MeOH THF MeOH MeOH MeOH MeOH	95:5 98:2 58:42 99:1:0.9 93:7 96:4 71:29	2.1 2.1 0.8 2.5 28.3 5.9 5.7	66 66 66 66 67 67 67

Table 21.11 Directive hydrogenation of acrylic acid derivatives.

	Substrate	Major diastereomer	Catalyst	mol%	P_{H_2}	Solvent	Diastereomeric ratio	TOF	Reference
6	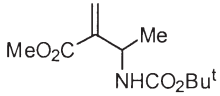	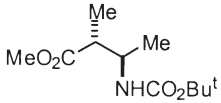	Rh^+	5		CH_2Cl_2	99:1		65
			Rh^+	5	1 atm	MeOH	100:0		65
7	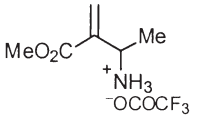	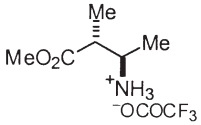	Rh^+	5		CH_2Cl_2	50:50		65
8	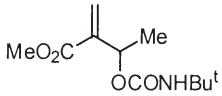	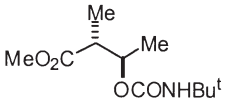	Rh^+	5		CH_2Cl_2	94:6		65

$Rh^+ = [Rh(diphos\text{-}4)(cod)]^+$

As described hitherto, diastereoselectivity is controlled by the stereogenic center present in the starting material (intramolecular chiral induction). If these chiral substrates are hydrogenated with a chiral catalyst, which exerts chiral induction intermolecularly, then the hydrogenation stereoselectivity will be controlled both by the substrate (substrate-controlled) and by the chiral catalyst (catalyst-controlled). On occasion, this will amplify the stereoselectivity, or suppress the selectivity, and is termed "double stereo-differentiation" or "double asymmetric induction" [68]. If the directions of substrate-control and catalyst-control are the same this is a matched pair, but if the directions of the two types of control are opposite then it is a mismatched pair.

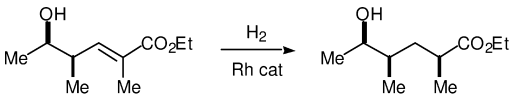

cat	mol%	P_{H_2}	solvent	diastereo. ratio
$RhCl(PPh_3)_3$	20	15 psi	CH_2Cl_2	83 : 15
$[Rh((+)\text{-binap})]^+$		1000 psi	CH_2Cl_2	98 : 2
$[Rh((-)\text{-binap})]^+$		1000 psi	CH_2Cl_2	67 : 33

(5) [60]

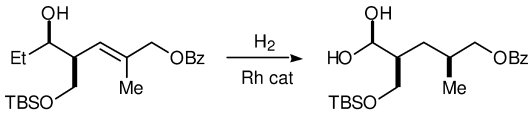

$[Rh((+)\text{-binap})]^+$	1000 psi	CH_2Cl_2	97 : 3
$[Rh((-)\text{-binap})]^+$	1000 psi	CH_2Cl_2	92 : 8

(6) [59]

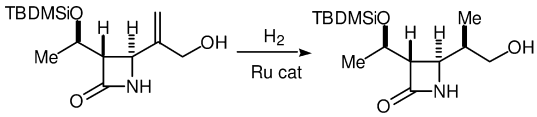

$Ru(OAc)_2((R)\text{-tol-binap})$	0.2	1 atm	MeOH	99.9 : 0.1
$Ru(OAc)_2((S)\text{-tol-binap})$	0.2	1 atm	MeOH	22 : 78

(7) [52]

Striking examples of this phenomenon are presented for allyl and homoallyl alcohols in Eqs. (5) to (7). The stereodirection in Eq. (5) is improved by a chiral (+)-binap catalyst and decreased by using the antipodal catalyst [60]. In contrast, in Eq. (6) both antipode catalysts induced almost the same stereodirection, indicating that the effect of catalyst-control is negligible when compared with the directivity exerted by the substrate [59]. In Eq. (7), the sense of asymmetric induction was inversed by using the antipode catalysts, where the directivity by chiral catalyst overrides the directivity of substrate [52]. In the case of chiral dehydroamino acids, where both double bond and amide coordinate to the metal, the effect of the stereogenic center of the substrate is negligibly small and diastereoface discrimination is unsuccessful with an achiral rhodium catalyst (see Table 21.1, entries 9 and 10) [9].

21.4
Hydrogenation of Dehydrooligopeptides

The hydrogenation of dehydrodipeptides and -tripeptides is a versatile method for the synthesis of oligopeptides of various compositions. In the homogeneous hydrogenation of dehydrodipeptide derivatives, coordination of the olefin and the amidocarbonyl oxygen to the metal is also anticipated (similar to the reduction of dehydroamino acid derivatives), and this presents the question of whether the reaction proceeds by substrate-control or by catalyst-control. In general, the chiral center in the dehydrodipeptide was found to have little influence on the stereoselectivity, and this small degree of substrate-control enables the synthesis of dipeptides or tripeptides having a desired configuration at will, with the newly forming chiral center being controlled by the external effect of the chiral catalysts [70, 71, 77, 78]. The structure of dehydrodipeptides also influences stereoselectivity, and dehydrodipeptides of the RCO-ΔAA-AA-OR′ type can be hydrogenated with high stereoselectivities, while those of the RCO-Gly-ΔAA-OR′ type could be converted with only moderate to good stereoselectivities. Ojima conducted the diastereoselective hydrogenation of various dehydrodipeptides and -tripeptides, and succeeded in preparing Leu-enkephalin analogues in high diastereoselectivity by coupling the dipeptide and tripeptide formed via hydrogenation using Rh-(*R*,*R*)-dipamp and Rh-Ph-CAPP catalysts [70, 73]. In these hydrogenations of dehydrodipeptides, the direction of asymmetric induction generally turned out to be the same as that observed in the asymmetric hydrogenation of (*Z*)-*α*-acylaminocinnamic acid. Kagan reported the diastereoselective synthesis of Leu-enkephalin analogues by the Rh-catalyzed hydrogenation of dehydroenkephalins Cbz-(O)Bn-(*S*)Tyr-(Gly)2-ΔPhe-(*S*)Leu-OMe **8** or Cbz-(O)Bn-ΔTyr-$(Gly)_2$-(*S*)Phe-(*S*)Leu-OMe **9**, with a diastereoselectivity up to 98 : 2 ((*S*,*S*,*S*) : (*S*,*R*,*S*)) using $[Rh((R,R)\text{-dipamp})]^+$ [79] [Eqs. (8) and (9)]. The substitution of a glycyl residue by (*R*)alanyl in the above dehydropentapeptide had minimal effect on the stereochemical course of the hydrogenation (diastereoselectivity was 89 : 11).

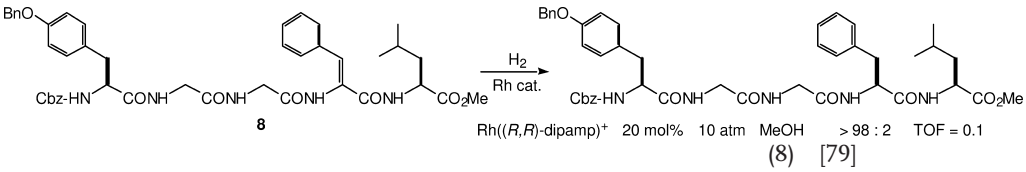

(8) [79]

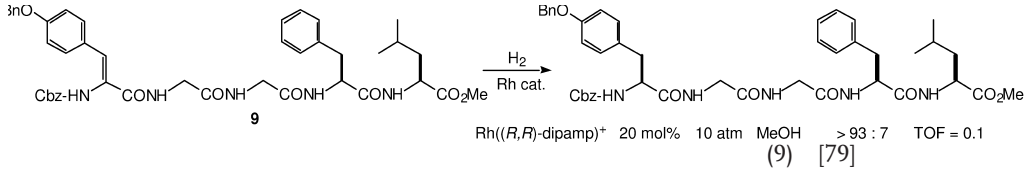

(9) [79]

In the enantioselective hydrogenation of dehydroamino acids, many diphosphine ligands are reported to give high enantioselectivity (often >95% ee). However, in the diastereoselective hydrogenation of dehydrodipeptides, many ligands – with very few exceptions – induce a somewhat lower stereoselectivity, especially in the case of mismatched pairs. Dipamp and Et-Duphos ligands retain their high chiral induction ability in the reduction of dehydrodipeptides [69, 70, 73, 76, 86, 87] (Table 21.12).

In the hydrogenation of dehydrodipeptides possessing a free carboxyl unit, the chiral ligands with an amine moiety would form an ion pair with the substrate which is expected to amplify the stereodifferentiation in the hydrogenation. Yamagishi realized high stereoinduction between 90 and 98% d.e. in the hydrogenation of dehydrodipeptides of the Ac-ΔPhe-AA-OH type in ethanol, using chiral diphosphinite ligands containing a dimethylamino moiety ((*S*,*S*)-POP-AEs) (Eq. (10)) [80]. In these systems, the chiral induction is governed by the chiral center of the substrate (substrate-control) and (*S*,*S*)- and (*R*,*R*)-products are formed highly selectively (Eq. (11)) [81].

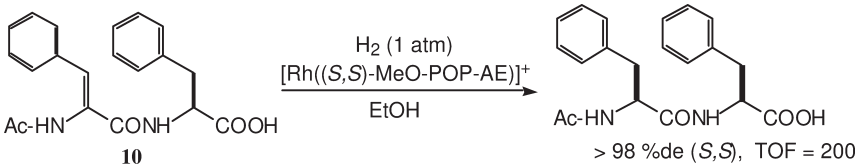

(10)

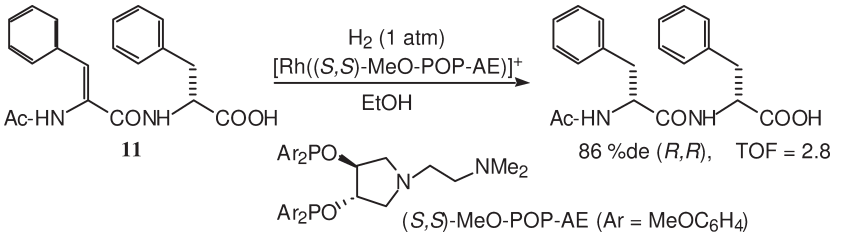

(11)

These diphosphinite ligands are not effective for the hydrogenation of Ac-ΔPhe-AA-OR-type substrates. This striking substrate-controlled behavior is also observed in the hydrogenation of RCO-ΔPhe-AA-OH-type substrates using an *achiral* diphos-3 ligand with a 2-dimethylaminoethyl unit at the 2-position (DPP-AE ligand). The $[Rh(I)(DPP\text{-}AE)]^+$ catalyst induced high diastereoselectivity (up to 96% d.e.) in the hydrogenation of Ac-ΔPhe-AA-OH in alcoholic solvents [82]. The kinetic parameters ($\Delta\Delta S^{\ddagger}$ and $\Delta\Delta H^{\ddagger}$) indicate that $\Delta\Delta G^{\ddagger}$ is governed by the $T\Delta\Delta S^{\ddagger}$ term, and not by the $\Delta\Delta H^{\ddagger}$ in the reactions where electrostatic interaction is possible. Moreover, the effect of solvent polarity and of the added amine on stereoselectivity also support the contribution of the attractive electrostatic interaction to the stereodifferentiation. NMR and circular dichroism spec-

Table 21.12 Diastereoselective hydrogenation of dehydrodipeptides.

	Substrate	Major diastereomer	Catalyst	mol%	P_{H_2}	Solvent	Diastereomeric ratio	TOF	Reference
1	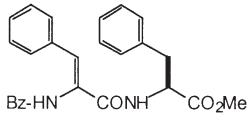	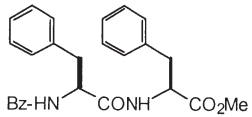	[Rh(diphos-4)]$^+$	1	1 atm	EtOH	62.2:37.8	17	69
			[Rh((*R*,*R*)-dipamp)]$^+$	1	10 atm	EtOH	97.8:2.2	6.7	70
			[Rh((+)-diop)]$^+$	1	5 atm	EtOH	83.6:16.4	6.7	70
			[Rh((–)-diop)]$^+$	1	5 atm	EtOH	84.1:15.9	6.7	70
			[Rh(Br-Ph-CAPP)]$^+$	1	1 atm	EtOH	0.8:99.2	33	69
2	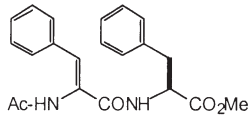	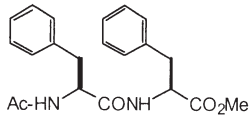	[Rh((+)-diop)]$^+$	1	5 atm	EtOH	92.7:7.3	4.2	70
			RhCl((+)-diop)	1	1 atm	MeOH	95:5		71
			RhCl((–)-diop)	1	1 atm	MeOH	10:90		71
			[Rh(Br-Ph-CAPP)]$^+$	1	5 atm	EtOH	2:98	4.2	70
3	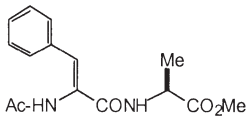	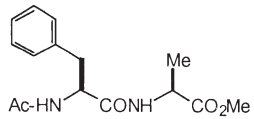	[Rh(Br-Ph-CAPP)]$^+$	1	5 atm	EtOH	1:99	5.5	70
			[Rh((+)-diop))$^+$	1	5 atm	EtOH	91.4:8.6	10.6	70
			[RhCl((+)-diop)]	3.5	1 atm	MeOH	85.6:14.4		72
			[RhCl((–)-diop)]	3.5	1 atm	MeOH	10.2:89.8		72
4	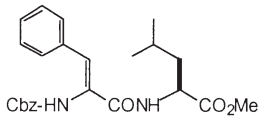	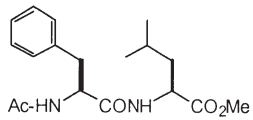	[Rh((*R*,*R*)-dipamp)]$^+$	2	20 atm	EtOH	97.8:2.2	2.5	73
5	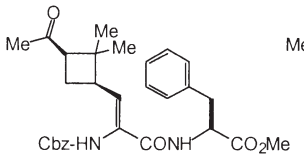	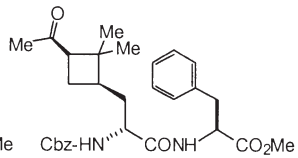	[Rh((*R*,*R*)-Et-Duphos))$^+$	4	2 atm	MeOH	>99.5:0.5	0.9	74
			[Rh((*S*,*S*)-Et-Duphos)]$^+$	4	2 atm	MeOH	5:95	0.4	74

Table 21.12 (continued)

	Substrate	Major diastereomer	Catalyst	mol%	P_{H_2}	Solvent	Diastereomeric ratio	TOF	Reference
6	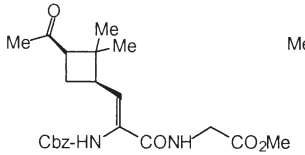	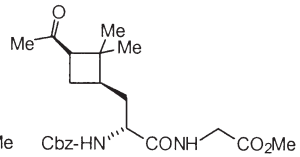	[Rh((*R*,*R*)-Et-Duphos)]$^+$	4	2 atm	MeOH	91:9	1	74
			[Rh((*S*,*S*)-Et-Duphos)]$^+$	4	2 atm	MeOH	11:89	0.9	74
7	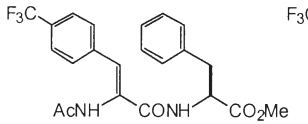	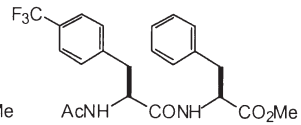	[Rh((*S*)-Pindophos)]$^+$		0.1 MPa	MeOH	95.5:4.5		75
8	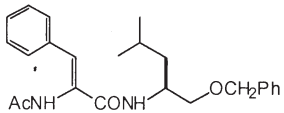	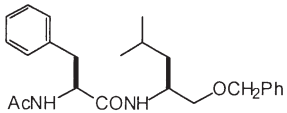	[Rh(diphos-4)]$^+$	0.33	5 atm	EtOH	58.7:41.3	7.6	76
			[Rh((+)-BPPM)]$^+$	1	5 atm		99.1:0.9	2.5	76
			[Rh(Ph-CAPP)]$^+$	1	5 atm		1.3:98.7	2.4	76
9	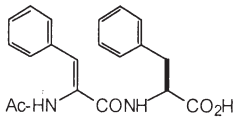	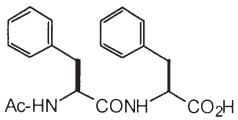	[Rh(diphos-4)]$^+$	1	10 atm	EtOH	65.9:34.1	5.9	69
			[Rh((*R*,*R*)-dipamp)]$^+$	1	5 atm	EtOH	98.6:1.4	4.5	69
			[Rh((*R*,*R*)-bppm)]$^+$	1	10 atm	EtOH	99.4:0.6	4.9	69
			[Rh(DIOXOP)]$^+$	4	1 atm	EtOH	93:7	1	77
			[Rh((*S*,*S*)-Chiraphos)]$^+$	1	10 atm	EtOH	39.1:60.9	1	69
			[Rh((*S*,*S*)-MeO-POP-AE)]$^+$	2	1 atm	EtOH	>99:1	200	80
			[Rh(DPP-AE)]$^+$	2	1 atm	MeOH	97:3	100	82

Table 21.12 (continued)

	Substrate	Major diastereomer	Catalyst	mol%	P_{H_2}	Solvent	Diastereomeric ratio	TOF	Reference
10	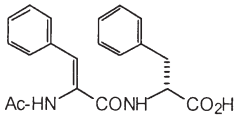	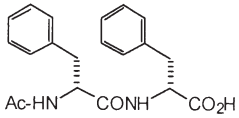	[Rh((*S*,*S*)-MeO-POP-AE)]$^+$	2	1 atm	EtOH	93:7	2.8	81
			[Rh((*S*,*S*)-POP-AE)]$^+$	2	1 atm	EtOH	93:7	2.8	81
11	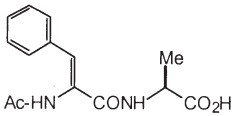	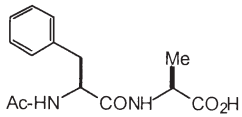	[Rh((*S*,*S*)-MeO-POP-AE)]$^+$	2	1 atm	EtOH	98:2	100	80
			[Rh(DIOXOP)]$^+$	4	1 atm	EtOH	86:14	1	77
			[Rh(DPP-AE)]$^+$	2	1 atm	MeOH	94:6	63	82
			[Rh((–)-diop)]$^+$	1	1 atm	EtOH/ C_6H_6	9:91		78
12	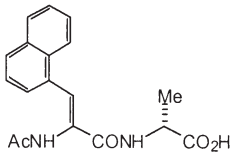	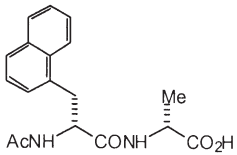	[Rh(DPP-AE)]$^+$	2	1 atm	MeOH	94.5:5.5	50	83
			[Rh((–)-bppm)]$^+$	2	1 atm	MeOH	>99:1	50	83
13	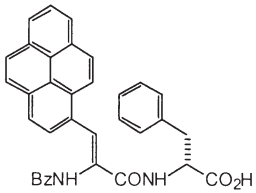	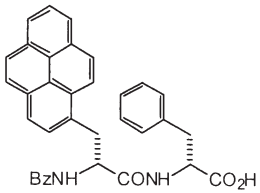	[Rh(diphos-3)]$^+$	2	1 atm	MeOH	59:41	>1.7	83
			[Rh(DPP-AE)]$^+$	2	1 atm	MeOH	94.5:5.5	150	83
			[Rh((–)-bppm)]$^+$	2	1 atm	MeOH	94.5:5.5	5	83

troscopy suggest that the change of catalyst conformation occurs by electrostatic interaction between the (*S*)-substrate and the achiral ligand (induced fitting) to form a complex of the λ-conformation preferentially. Without electrostatic interaction, the rhodium complex exists as a 1 : 1 mixture of δ- and λ-conformations [82]. The effect of attractive electrostatic interactions on chiral induction was also reported by Hayashi, for the enantioselective hydrogenation of acrylic acid derivatives. A ferrocenyldiphosphine ligand having a dimethylaminoalkyl moiety induced a high enantioselectivity of more than 95% by utilizing electrostatic interactions with the substrate [84].

Kagan reported tandem asymmetric syntheses from achiral bisdehydrodipeptides by the sequential hydrogenation of two prochiral units [85]. With the $[Rh((R,R)\text{-dipamp})]^+$ catalyst, a high diastereoselectivity ratio of 98 : 2 ((*RR* and *SS*)/(*RS* and *SR*) ratio) was reported (Table 21.13, entries 1–3). In this case, the major diastereomer has a high ee-value (97.6% (*S*,*S*)), and the minor diastereomer has a negligible ee (15% (*S*,*R*)). This result indicates that, in each step of the reaction, the same stereoselectivity is realized. In the symmetrical bis(dehydroamino acid) derivatives, similar high diastereo-differentiation of 95–99% d.e. is realized using dipamp or duphos ligands, and in some cases the enantioselectivity of the major diastereomer reaches 100% (Table 21.13, entries 7 and 8) [86, 87]. Because of the high chiral induction ability of the catalyst, almost all of the minor monohydrogenated enantiomer is converted to the *meso*-product in the second hydrogenation step, and this results in an extremely high enantioselectivity of the major product.

Several attempts towards the asymmetric reduction of *N*-(α-ketoacyl)-α-amino acid derivatives by rhodium catalysts are reported to give chiral depsipeptide building blocks, *N*-(α-hydroxyacyl)-α-amino acid derivatives (Table 21.14). Using rhodium catalysts containing an electron-rich chiral diphosphine (Cydiop) or a chiral diphosphinite (Cy-POP-AE) ligand, the hydrogenation proceeds under atmospheric hydrogen pressure affording moderate to good diastereoselectivity (entries 2, 3 and 6) [89, 90], while the catalysts based on diop or bppm required high hydrogen pressure and only low selectivity is obtained [88].

21.5
Diastereoselective Hydrogenation of Keto-Compounds

For the hydrogenation of keto-compounds, ruthenium–phosphine catalysts are efficient in obtaining compounds with a stereogenic hydroxyl unit, though the reduction usually requires high hydrogen pressure. Ruthenium–diphosphine–diamine catalyst plus strong base, as was first reported by Noyori, functions well at lower pressures in the hydrogenation of keto-compounds [91, 92]. For enantio- and diastereoselective hydrogenation of keto-compounds, atropisomeric diphosphines such as binap [93], bichep [94], biphemp or biphep [95] are used effectively.

Table 21.13 Tandem asymmetric hydrogenation of didehydrodipeptides with two double bonds.

	Substrate	Major diastereomer	Catalyst	mol%	P_{H_2}	Solvent	Diastereomeric ratio	%ee of major diastereomer	TOF	Reference
1	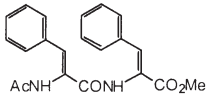	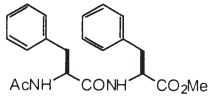	[Rh((*R*,*R*)-dipamp)]$^+$	3.5	1 atm	MeOH	98:2	99 (*S*,*S*)		85
			[Rh((*S*,*S*)-bppm)]$^+$	3.5	1 atm	MeOH	74.8:25.2	85 (*R*,*R*)		85
			[Rh(+)-(*R*,*R*)-diop)]$^+$	3.5	1 atm	MeOH	55:45	60 (*R*,*R*)		85
2	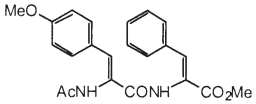	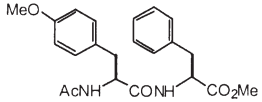	[Rh((*R*)-dipamp)]$^+$	3.5	1 atm	MeOH	98:2	97.6 (*S*,*S*)		85
3	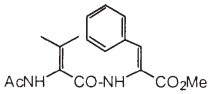	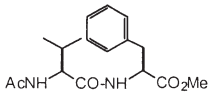	[Rh((*R*,*R*)-dipamp)]$^+$	3.5	79 atm	MeOH	68:32	90.9 (*S*,*S*)	0.71	85
4	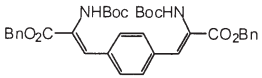	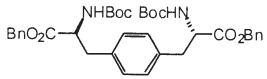	[Rh(cod)((*R*,*R*)-dipamp)]$^+$	2	2.8 atm	MeOH	>99:1	>98 (*S*,*S*)	0.52	86
5	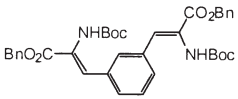	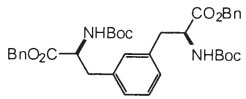	[Rh(cod)(*S*,*S*)-Me-Duphos)]$^+$	1.8	2.7 atm	MeOH	>99:1	>98 (*S*,*S*)	12.3	86

Table 21.13 (continued)

	Substrate	Major diastereomer	Catalyst	mol%	P_{H_2}	Solvent	Diastereomeric ratio	%ee of major diastereomer	TOF	Reference
6	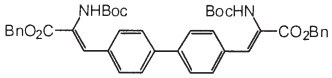	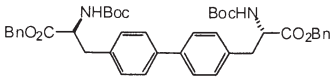	[Rh(cod)((*R*,*R*)-dipamp)]$^+$	3.6	3.5 atm	MeOH/THF	>99:1	>98 (*S*,*S*)	0.31	86
7	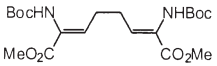	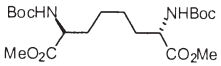	[Rh(cod)((*S*,*S*)-Et-Duphos)]$^+$	0.84	60 psi		99.5:0.5	100 (*S*,*S*)	6.6	87
			[Rh(cod)((*S*,*S*)-Me-Duphos)]$^+$		60 psi		98.5:1.5	100 (*S*,*S*)		87
			[Rh(cod)((*R*,*R*)-dipamp)]$^+$		60 psi		97.5:2.5	100 (*S*,*S*)		87
			[$RuCl_2$(binap)]$_2$ (TEA)		60 psi		85:15			87
			[Rh(cod)((*R*,*R*)-Chiraphos)]$^+$	0.84	60 psi		69.4:30.6	86 (*R*,*R*)	6.6	87
8	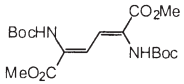	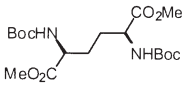	[Rh(cod)((*S*,*S*)-Et-Duphos)]$^+$	0.84	60 psi		98.5:1.5	100 (*S*,*S*)	6.6	87

Table 21.14 Diastereoselective hydrogenation of dehydrodepsipeptide.

	Substrate	Major diastereomer	Catalyst	mol%	P_{H_2}	Solvent	Diastereomeric ratio	TOF	Reference
1	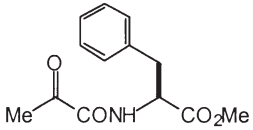	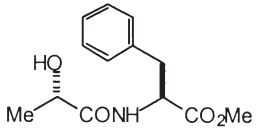	$RhCl(PPh_3)_3$	1	50 atm	C_6H_6	60:40	5	88
			RhCl((+)-diop)	1	50 atm	C_6H_6	63:37	5	88
			RhCl((+)-bppm)	1	50 atm	C_6H_6	64:36	5	88
			RhCl((–)-cydiop)	5	1 atm	THF	73:27	0.8	89
			RhCl((+)-Cydiop)	5	1 atm	THF	26:74	0.7	89
2	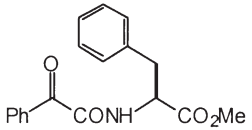	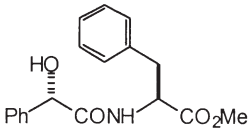	RhCl((–)-Cydiop)	5	1 atm	THF	86:14	1	89
			RhCl((+)-Cydiop)	5	1 atm	THF	16:84	1	89
3	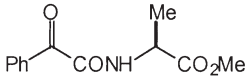	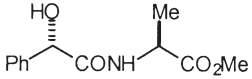	RhCl((–)-Cydiop)	5	1 atm	THF	83:17	1	89
			RhCl((+)-Cydiop	5	1 atm	THF	18:82	1	89
			RhCl((*S*,*S*)-Cy-POP-AE)	2	1 atm	MeOH	33.5:66.5	2.1	90
4	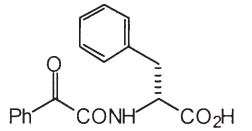	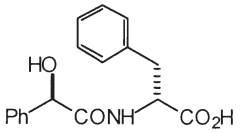	RhCl((*S*,*S*)-Cy-POP-AE)	2	1 atm	MeOH	75:25	2.1	90
			$[Rh((S,S)\text{-Cy-POP-AE})]^+$	2	1 atm	MeOH	76.5:23.5	2.1	90

Table 21.14 (continued)

	Substrate	Major diastereomer	Catalyst	mol%	P_{H_2}	Solvent	Diastereomeric ratio	TOF	Reference
5	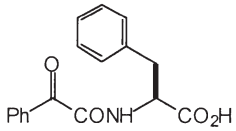	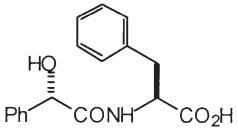	[Rh((*S*,*S*)-Cy-POP-AE)]$^+$	2	1 atm	MeOH	73.5:26.5	2.1	90
6	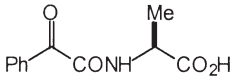	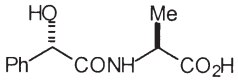	RhCl((*S*,*S*)-Cy-POP-AE)	2	1 atm	MeOH	83.5:16.5	2.1	90

21.5.1
Substrate-Directive Hydrogenation of Keto-Compounds

Several examples of substrate-directive reduction (hydroxyl, alkoxyl, carbamate or sulfoxide groups) have been reported in the hydrogenation of keto-compounds with ruthenium catalysts. In the reduction of β-keto ester derivatives, the γ- or δ-stereogenic center in the substrates significantly affects the degree of diastereoselection (Table 21.15). The hydrogenation of a β-keto ester with a carbamate unit at the γ-position ((*S*)-substrate) in the presence of Ru–(*R*)-binap (matched pair) exclusively afforded the *threo* product with the (3*S*,4*S*) configuration, whereas in the presence of Ru–(*S*)-binap (mismatched pair) the (3*R*,4*S*)-product was formed preferentially (Table 21.15, entry 1) [96]. The β-keto esters with a pyrrolidine unit showed similar behavior (entry 4) [97]. A silyloxy group at the δ-position could dictate the sense of asymmetric induction, and high diastereoselectivity is induced by using an achiral ruthenium catalyst, whereas the chiral ruthenium (*R*)-binap catalyst and the (*S*)-binap catalyst (matched and mismatched pairs, respectively) afford the same diastereomer, albeit in different selectivity (entry 7). On the other hand, the directivity of a hydroxy group was overwhelmed by the chirality of the catalyst, and a different diastereomer was formed preferentially by the antipode ruthenium catalysts (entry 8) [99].

In the hydrogenation of chiral sulfoxide **12**, the sulfoxide unit exerts strong stereodirectivity and, with axially stereogenic diphosphine ligands, high diastereoselectivity is realized whilst the antipode ligand affords lower diastereoselectivity (Scheme 21.5) [100]. The sense of asymmetric induction is rationalized by the favored conformation **E**, where the *p*-tolyl unit is disposed at a quasiequatorial position with a sulfoxide oxygen ligating to ruthenium [100].

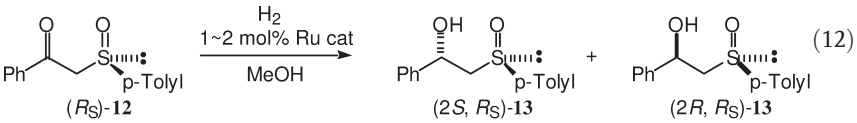

Catalyst	H_2(bar)	temp(ÞC)	time(h)	yield	(2*S*, R_S) : (2*R*, R_S)	TOF
$RuBr_2$(diphos-4)	50	50	24	12	78 : 22	0.25
$RuBr_2(PPh_3)_3$	50	20	64	99	80 : 20	1.6
$RuBr_2$((*S*)-MeO-biphep)	50	20	63	70	> 99 : 1	0.55
$RuBr_2$((*R*)-MeO-biphep)	50	20	63	95	10 : 90	0.75

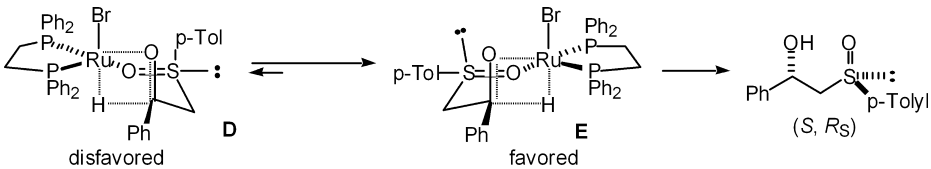

Scheme 21.5

Table 21.15 Hydroxy-directed hydrogenation of β-keto esters.

	Substrate	Major diastereomer	R	Catalyst	mol%	P_{H_2}	Solvent	Diastereomeric ratio	%ee (*syn*)	TOF	Reference
1	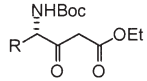	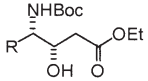	$PhCH_2$	$RuBr_2((R)$-binap)	0.2	100 atm	EtOH	>99:1	99	3.6	96
				$RuBr_2((S)$-binap)	0.2	100 atm	EtOH	9:91	>99		96
			CH_2CHMe_2	$RuBr_2((R)$-binap)	0.2	100 atm	EtOH	>99:1	97		96
			$c\text{-}C_6H_{11}CH_2$	$RuBr_2((R)$-binap)	0.2	100 atm	EtOH	>99:1	100		96
2	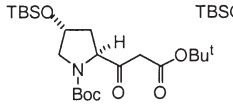	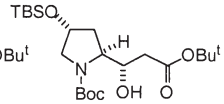		$RuCl_2((R)$-binap)$1/2NEt_3$	0.1	5 atm	THF/MeOH	96:4		19.2	97
				$RuCl_2((S)$-binap)$1/2NEt_3$	0.1	5 atm	THF/MeOH	ca 1:1		<2	97
3	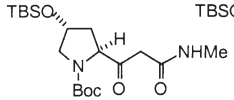	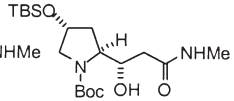		$RuCl_2((S)$-binap)$1/2NEt_3$	0.1	5 atm	THF/MeOH	34.5:65.5		32.9	97
4	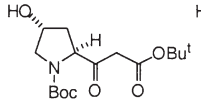	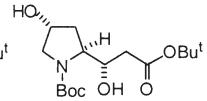		$RuCl_2((R)$-binap)Et_2NH	0.25	150 psi	MeOH 0.75 mol% HCl	>99:<1			97
				$RuCl_2((S)$-binap)Et_2NH	0.25	150 psi	MeOH 0.75 mol% HCl	12:88			97
5	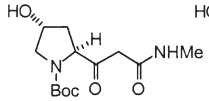	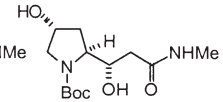		$RuCl_2((S)$-binap)$1/2NEt_3$	0.1	5 atm	THF/MeOH	23.5:76.5		5.5	98

Table 21.15 (continued)

	Substrate	Major diastereomer	R	Catalyst	mol%	P_{H_2}	Solvent	Diastereomeric ratio	%ee (*syn*)	TOF	Reference
6	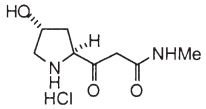	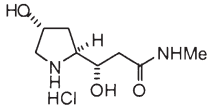		$RuCl_2$((*S*)-binap)1/2NEt_3	0.1	5 atm	THF/MeOH	1:99		35.4	98
7	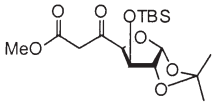	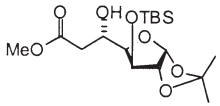		$RuBr_2$(diphos-2)	2	1 atm	MeOH	95:5		0.5	99
				$RuBr_2$((*R*)-binap)	2	1 atm	MeOH	>99:1		2.1	99
				$RuBr_2$((*S*)-binap)	2	1 atm	MeOH	82:18		1.5	99
8	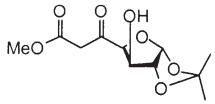	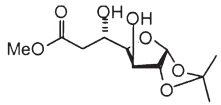		$RuBr_2$((*R*)-binap)	2	1 atm	MeOH	85:15		2.1	99
				$RuBr_2$((*S*)-binap)	2	1 atm	MeOH	10:90		1.0	99
9	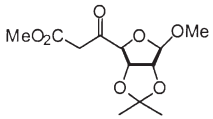	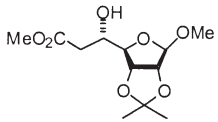		$RuBr_2$((*R*)-binap)	2	1 atm	MeOH	90:10		2.1	99
				$RuBr_2$((*S*)-binap)	2	1 atm	MeOH	5:95		2.1	99

21.5.2
Hydrogenation of Diketo Esters and Diketones

Reduction of β,δ-diketo esters using various atropisomeric diphosphine ligands afforded generally the *anti*-3,5-dihydroxy products in moderate to good diastereoselectivity, and in high enantioselectivity (Table 21.16) [101–104]. This suggests that stereocontrol in the hydrogenation of diketo esters is, in general, very similar to that found in the hydrogenation of diketones with Ru–binap (*vide infra*) [105, 106].

In these cases, using an (*S*)-axially chiral ligand, (3*R*)-3-hydroxy-5-oxoalkanoate is exclusively formed as monohydrogenation product, while the second hydrogenation step is a hydroxy-directed reduction by the Ru–catalyst bearing an (*S*)-axially chiral ligand to afford the (3*R*,5*S*)-dihydroxy product preferentially (Scheme 21.6) [103a]. With Ru–(*R*)-binap, this (3*R*)-3-hydroxy-5-oxoalkanoate is mainly converted to the (3*R*,5*R*)-*syn* dihydroxy compound. Formation of the 3-hydroxy-5-oxoalkanoate intermediate is also supported by the reduction experiment of (5*R*)-5-hydroxy-3-oxoalkanoate by Ru–(*R*)-binap to afford the (3*R*,5*R*)-*syn* diol as the major product [102]. There is a competitive ligation of functionalities to the Ru atom (Scheme 21.7). Because of the intervention of an enolic structure in **14** and the high final *anti*-selectivity, it is plausibly assumed that hydrogenation of the C-3 carbonyl unit of **14** arises mainly from a β-diketone chelated intermediate, which gives preferentially the (3*R*)-enantiomer using Ru–(*S*)-binap as catalyst. This is in contrast to the results with simple β-keto esters, which afford the (3*S*)-hydroxy product upon use of a Ru–(*S*)-axially chiral diphosphine catalyst [106, 107, 109].

In the consecutive hydrogenation of β,δ-diketo esters (Table 21.16), selection of the chiral ligand can determine the sense of diastereoselection, and the 3,5-*syn* dihydroxy product was formed predominantly upon use of a Ru–(*S*)-aminophosphinephosphinite-((*S*)-AMPP) catalyst, although the enantioselectivity of the *syn*-product is poor (Table 21.16, entry 7) [103a]. *Syn* 3,5-diol formation

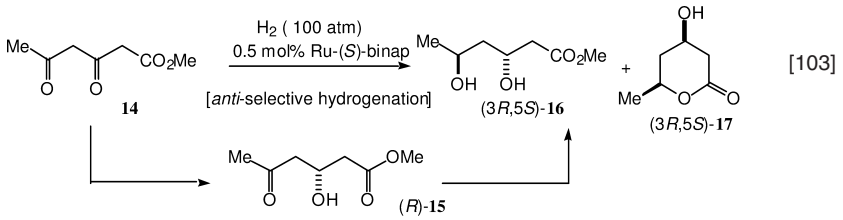

cat	mol%	P_{H2}	solvent	temp (ºC)	**15** selec.	**16 + 17** selec.	*anti* : *syn*	%ee(*anti*)	TOF(h^{-1})
$RuBr_2$((*S*)-tol-binap)	0.5	100 atm	CH_2Cl_2	60	27	73	87 : 13	93 (3*R*,5*S*)	1.1
$RuBr_2$((*S*)-MeO-biphep)	0.5	100 atm	CH_2Cl_2	60	7	86	89 : 11	95 (3*R*,5*S*)	1.8
$RuBr_2$((*S*)-tol-binap)	0.5	100 atm	CH_2Cl_2	40	96	4	nd		5
$RuBr_2$((*S*)-MeO-biphep)	0.5	100 atm	CH_2Cl_2	40	96	4	nd		4.2

Scheme 21.6

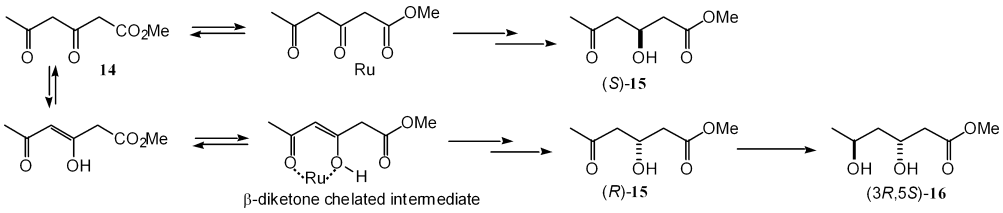

Scheme 21.7 Competitive chelation mode onto a Ru-(*S*)-binap type catalyst.

would lead to the synthesis of inhibitors of HMG-coenzyme A reductase [102]. In this case, an almost complete reversal of the diastereoselectivity was observed by changing the solvent from DCM to a polar solvent consisting of 1 : 1 DCM-methanol. In pure DCM, the Ru–(*S*)-AMPP catalyst induces the *syn*-rich diol (max. 92% d.e.), while in the DCM-methanol mixture the same catalyst leads to the formation of *anti*-rich product (72–84% d.e.). This reversal of diastereoselectivity was also observed in the reduction of *β*-diketones (Table 21.17, entry 13) [103 b].

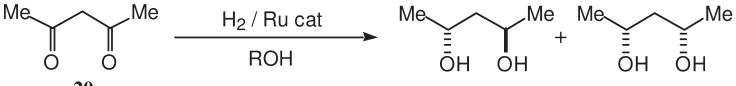

(13)

cat	mol%	P_{H2}	*anti* : *syn*	ee%(*anti*-)	TOF	
Ru_2Cl_4((*R*)-binap)$_2$(NEt_3)	0.2	50 atm	99 : 1	> 99 (*R,R*)	25	[105]
$RuCl_2$((*R*)-binap)	0.05	72 atm	99 : 1	100 (*R,R*)	22.5	[106]
$RuBr_2$((*S*)-MeO-biphep)	2	20 atm	> 99.5 : 0.5	> 99 (*S,S*)	0.8	[110]

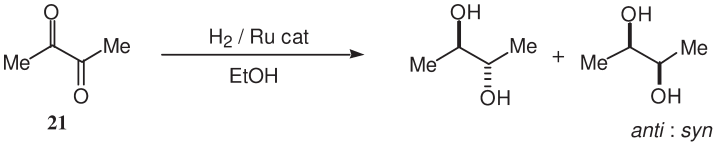

(14)

			anti : *syn*	ee%(*anti*-)	TOF	
$RuBr_2$((*S*)-binap)	0.15	80 atm	26 : 74	92 (*S,S*)	11.1	[106]

In the hydrogenation of diketones by Ru–binap-type catalysts, the degree of *anti*-selectivity is different between *α*-diketones and *β*-diketones [Eqs (13) and (14)]. A variety of *β*-diketones are reduced by Ru-atropisomeric diphosphine catalysts to indicate admirable *anti*-selectivity, and the enantiopurity of the obtained *anti*-diol is almost 100% (Table 21.17) [105, 106, 110–112]. In this two-step consecutive hydrogenation of diketones, the overall stereochemical outcome is determined by both the efficiency of the chirality transfer by the catalyst (catalyst-control) and the structure of the initially formed hydroxyketones having a stereogenic center (substrate-control). The hydrogenation of monohydrogenated product ((*R*)-hydroxy ketone) with the antipode catalyst ((*S*)-binap catalyst) (mis-

Table 21.16 Diastereoselective hydrogenation of β,δ-diketo esters.

	Substrate	Major diastereomer	Catalyst	mol%	P_{H_2}	Solvent	Diastereomeric ratio anti : syn	%e.e. of major diastereomer	TOF	Reference
1	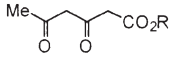	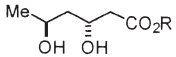	$RuCl_2(PPh_3)_3$	0.5	100 atm	CH_2Cl_2	73:27	0	2.6	101
			$[RuCl_2((S)\text{-binap})]_2NEt_3$	0.5	100 atm	CH_2Cl_2	83:17	94 (3*R*,5*S*)	8.7	101
			$[RuCl_2((S)\text{-binap})]_2NEt_3$	0.5	100 atm	MeOH	76:24	96 (3*R*,5*S*)	8.7	103
			$RuBr_2((S)\text{-Tolbinap})$	0.5	100 atm	CH_2Cl_2	83:17	94 (3*R*,5*S*)	9.5	101
			$RuBr_2((S)\text{-MeO-biphep})$	0.5	100 atm	CH_2Cl_2	84:16	98 (3*R*,5*S*)	5.1	101
			$[RuCl_2((S)\text{-binap})]_2NEt_3$	0.1	100 atm	MeOH	81:19	78 (3*R*,5*S*)	10.4	102
			$[RuCl_2((R)\text{-binap})]_2\text{-}NEt_3$	0.1	100 atm	MeOH	80:20	77 (3*S*,5*R*)	10.4	102
2	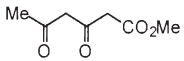	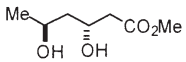	RhCl((*S*)-MeO-biphep)	0.5	50 atm	toluene	54:$6	79 (3*R*,5*S*)	0.26	101
			RhCl((*S*,*S*)-bppm)	0.5	50 atm	toluene	54:46	58 (3*R*,5*S*)	0.78	101
			RhCl((*S*)-Cy,Cy-oxoProNOP)	0.5	50 atm	toluene	65:35	80 (3*R*,5*S*)	0.43	101
			RhCl((*R*,*R*)-Me-Duphos)	0.5	50 atm	toluene	46:54		0.07	101
3	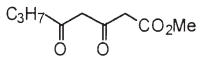	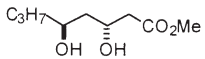	$[RuCl_2((S)\text{-binap})]_2(NEt_3)$	0.1	100 atm	MeOH	76:24	78 (3*R*,5*S*)	10.4	102
			$[RuCl_2((R)\text{-binap})]_2(NEt_3)$	0.1	100 atm	MeOH	78:22	77 (3*S*,5*R*)	10.4	102
4	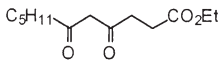	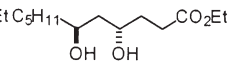	[RuCl((*S*)-binap)(p-cymene)]Cl		40 atm	MeOH	95:5 ~ 99:1	93 ~ 95 (4*S*,6*S*)		104

Table 21.16 (continued)

	Substrate	Major diastereomer		Catalyst	mol%	P_{H_2}	Solvent	Diastereo-meric ratio	%ee of major diastereomer *anti*:*syn*	TOF	Reference
5	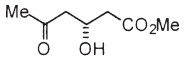 (*R*)-**15**	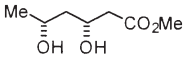	15 ee (%)								
			66 (*R*)	$Ru(TFA)_2$((*R*)-binap)	2	100 atm	CH_2Cl_2	10:90	75 (3*R*,5*R*)	2.4	103
			67 (*R*)	$Ru(TFA)_2$((*R*)-toalbinap)	2	100 atm	CH_2Cl_2	19:81	67 (3*R*,5*R*)	2.4	103
			67 (*R*)	$Ru(TFA)_2$((*R*)-MeO-biphep)	2	100 atm	CH_2Cl_2	14:86	72 (3*R*,5*R*)	2.2	103
6	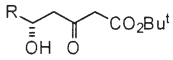 (*R*)-**18**	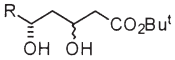 (*S*,*R*) or (*R*,*R*)	R = Me	Ru_2Cl_4((*S*)-binap)$_2$(Et_3)	0.2	100 atm	MeOH	95:5			102
			R = C_3H_7	Ru_2Cl_4((*R*)-binap)$_2$(Et_3)	0.2	100 atm	MeOH	40:60			102
				Ru_2Cl_4((*S*)-binap)$_2$(Et_3)	0.2	100 atm	MeOH	78:22			102
				Ru_2Cl_4((*R*)-binap)$_2$(Et_3)	0.2	100 atm	MeOH	43:57			102

Table 21.16 (continued)

	Substrate	Major diastereomer	Catalyst	mol%	P_{H_2}	Solvent	Diastereomeric ratio	%ee of major diastereomer *anti*:*syn*	TOF	Reference
7	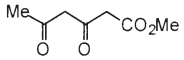	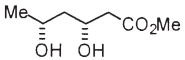	Ru((*S*)-AMPP)(methallyl)$_2$	0.5	100 atm	CH_2Cl_2	13:87	14 (3*R*,5*R*)	0.85	103
			Ru((*S*)-AMPP)(TFA)$_2$	0.5		CH_2Cl_2	28:72	40 (3*R*,5*R*)	1.4	103
			Ru((*S*)-AMPP)((*R*)-MTPA)$_2$	0.5		CH_2Cl_2	4:96	<5 (3*R*,5*R*)	11.1	103
			Ru((*S*)-AMPP)((*S*)-MTPA)$_2$	0.5		CH_2Cl_2	8:92	5 (3*R*,5*R*)	2.9	103
			Ru((*S*)-AMPP)(TFA)$_2$	0.5		CH_2Cl_2/MeOH (1/1)	86:14	12 (3*S*,5*R*)	1.9	103
			Ru((*S*)-AMPP)((*R*)-MTPA)$_2$	0.5		CH_2Cl_2/MeOH (1/1)	92:8	5 (3*S*,5*R*)	0.85	103
			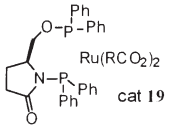 cat **19**							

Table 21.17 Consecutive hydrogenation of diketones.

	Substrate	Diastereome	Catalyst	mol%	P_{H_2}	Solvent	Temp. [°C]	Diastereomeric ratio *anti*:*syn*	%ee *anti*	TOF	Reference
1	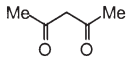	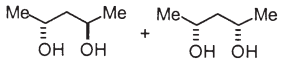	$RuCl_2$((*R*)-binap)	0.05	72 atm	EtOH		99:1	>99 (*R*,*R*)	22.5	106
2	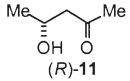 (*R*)-**11**	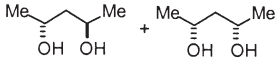	$RuCl_2$((*S*)-binap)	0.05	72 atm	EtOH		15:85			106
	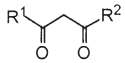	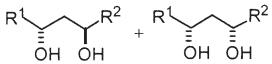									
3		R^1 R^2: Me Me	Ru_2Cl_4((*R*)-binap)$_2$(NEt_3)	0.2	50 atm	MeOH		99:1	>99 (*R*,*R*)	25	105
4		Me Et				MeOH		94:6	94 (*R*,*R*)	22	105
5		Me *i*Pr				MeOH		97:3	98 (*S*,*R*)	23	105
6		Me *i*Bu				MeOH		91:9	98 (*S*,*R*)	21	105
7		Et Et				MeOH		98:2	96 (*R*,*R*)	23	105
8		Me Me	$RuBr_2$((*R*,*R*)-Me-duphos)	2	70 atm	MeOH	80	97:3	93 (*R*,*R*)	0.8	110
9		C_6H_{11} C_6H_{11}	$RuBr_2$((*R*)-MeO-biphep)	2	100 atm	MeOH	r.t.	>99.5:0.5	>99 (*S*,*S*)	2.1	110
10		Bn Bn		2	30 atm	MeOH	r.t.	>97.5:2.5	>95 (*R*,*R*)	1.25	110
11	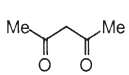	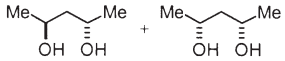	$RuBr_2$((*S*)-MeO-biphep)	2	20	MeOH	r.t.	>99.5:0.5	>99 (*S*,*S*)	0.8	110
			$RuCl_2(PPh_3)$((*S*)-biphep)	0.05	100 atm	MeOH	50	94:6	>99 (*S*,*S*)	133	111
					100 atm	EtOH	50	99.4:0.6	>99 (*S*,*S*)	83.3	112

Table 21.17 (continued)

	Substrate	Diastereome	Catalyst	mol%	P_{H_2}	Solvent	Temp. [°C]	Diastereomeric ratio *anti*:*syn*	%ee *anti*	TOF	Reference
12	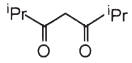	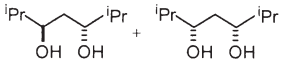	$RuBr_2$((*S*)-MeO-biphep)	2	20 atm	MeOH	r.t.	>99.5:0.5	>99 (*R*,*R*)	0.8	110
13	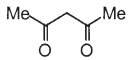	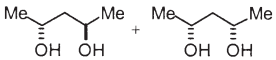 (*R*,*R*)-*anti* *meso*	**19 a** (R = CF_3)	0.5	100 atm	CH_2Cl_2		40:60	93 (*R*,*R*)	8.3	103
				0.5	100 atm	CH_2Cl_2/MeOH (1/1)		88:12	20 (*R*,*R*)	8.3	103
			19 b(R = (*R*)-PhC(CF_3)(OMe))	0.5	100 atm	CH_2Cl_2		8:92	86 (*R*,*R*)	2	103
				0.5	100 atm	CH_2Cl_2/MeOH (1/1)		92:8	14 (*R*,*R*)	3.5	103
			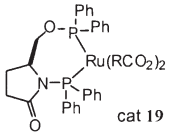 cat **19**								
14	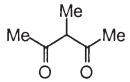	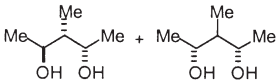	$RuCl_2$((*S*)-(binap)	0.05	94 atm	EtOH		99:1	>99 (*R*,*R*)	35.5	106

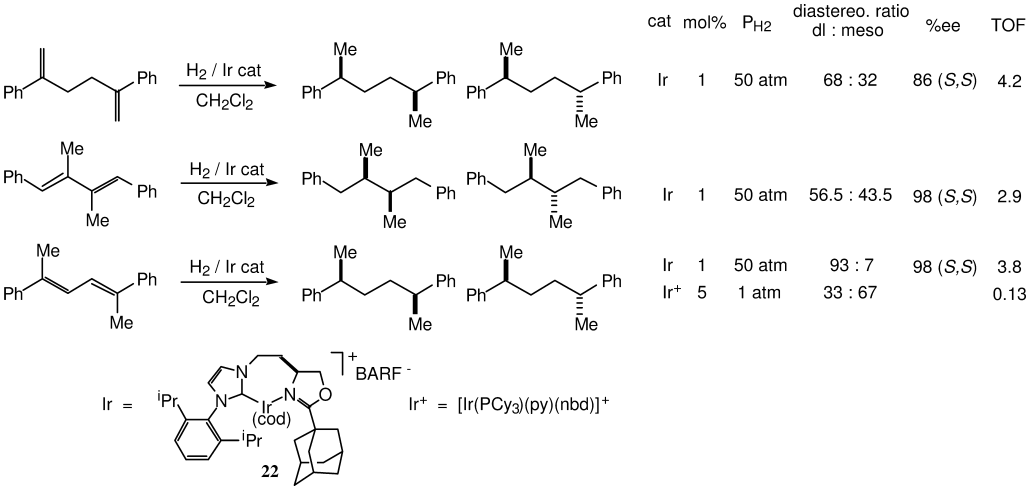

Scheme 21.8 Consecutive hydrogenation of symmetrical dienes [111].

matched pair) affords a *meso*-diol exclusively (Table 21.17, entry 1). This indicates that the catalyst-control in the second step is much more dominant over the substrate-control favoring *anti*-diol formation; thus, the high enantiomeric purity of the *anti*-diol is the result of a double stereodifferentiation [68]. In the reaction of α-diketones, substrate-control in the second hydrogenation step favors *meso*-diol formation, while minor *anti*-diol is obtained with high enantiomeric purities [Eq. (14)] [106]. This *dl*- and *meso*-products formation is also observed in the hydrogenation of symmetrical dienes [113] by an iridium carbene catalyst **22** (Scheme 21.8), or in the symmetrical bis(dehydroamino acids) by rhodium diphosphine catalysts (see Table 21.13, entries 4–8) [86, 87].

21.6
Kinetic Resolution to Selectively Afford Diastereomers and Enantiomers

In the hydrogenation of a compound with a stereogenic center by a chiral catalyst, the two possible stereocombinations – the matched pair and the mismatched pair – often afford different degrees of stereoinduction. The reaction rate of the hydrogenation is different for these two combinations (k_R and k_S, $k_R \neq k_S$), and kinetic chemical resolution is possible starting from racemic substrate using chiral catalyst by controlling the chemical conversion [114]. Kinetic resolution is now recognized as a viable tool for obtaining certain optically active compounds. In the homogeneous hydrogenation of unsaturated alcohols with a stereogenic center, various chiral catalysts were applied for their kinetic resolution. Using Rh–(*R*,*R*)-dipamp, racemic methyl (α-hydroxyethyl)acrylate **23** was resolved in THF at 0 °C to afford the (*S*)-substrate in 93% ee and the *anti*-product as the major product with a $k_R : k_S$ ratio of 6.5 : 1 at 75% conversion [Eq.

(15)] [45]. With an increase of conversion, the enantiopurity of unreacted (*S*)-substrate increases and the diastereoselectivity of the product decreases. Using Ru–((*S*)-binap)$(OAc)_2$, unreacted (*S*)-substrate was obtained in more than 99% ee and a 49 : 1 mixture of *anti*-product (37% ee (2*R*,3*R*)) at 76% conversion with a higher $k_R : k_S$ ratio of 16 : 1 [46]. In the case of a racemic cyclic allyl alcohol **24**, high enantiopurity of the unreacted alcohol was obtained using Ru–binap catalyst with a high $k_R : k_S$ ratio of more than 70 : 1 [Eq. (16)] [46]. In these two cases, the transition state structure is considered to be different since the sense of diastereoface selection with the (*S*)- or the (*R*)-catalysts is opposite if a similar OH/C=C bond spatial relationship is assumed.

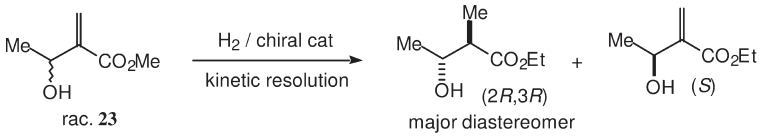

(15)

cat.	mol%	P_{H2}	solvent	temp (°C)	conv.	diastereo. ratio	recov. **23**	$k_R : k_S$	
$[Rh(dipamp)]^+$		1 atm	THF	0	75%		93 (*S*)	6.5 : 1	[45]
$[Ru(OAc)_2((S))\text{-binap})]$	0.06	4 atm	MeOH	25	76%	98 : 2	> 99 (*S*)	16 : 1	[46]
$[Ru(OAc)_2((S))\text{-binap})]$	0.1	50 atm	MeOH	20	63%	96.9 : 3.1	97 (*S*)	14 : 1	

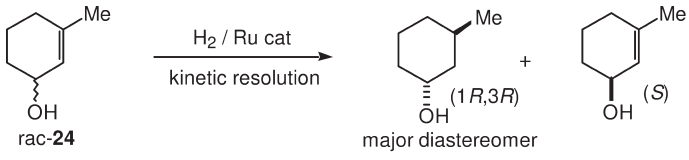

(16)

							recov. **24**		
$[Ru(OAc)_2((R))\text{-binap})]$	0.17	4 atm	MeOH	26	54%	300 : 1	> 99 (*S*)	74 : 1	[46]
$[Ru(OAc)_2((R))\text{-binap})]$	0.055	100 atm	MeOH	26	51%	98.5 : 1.5	95 (*S*)	76 : 1	

In the case of (*α*-acylaminoethyl)acrylate or (*α*-carbamoylethyl)acrylate, amido or carbamate functional groups work well in the direction of the kinetic resolution (Table 21.18). Reduction proceeded rapidly but then slowed markedly after consumption of 55–60% of the theoretical amount of H_2, indicating the large difference between the values of k_R and k_S (entries 1–3) [115]. The degree of enantiomer differentiation is considerably influenced by the hydrogen pressure, and higher k_f/k_s values were obtained at lower pressure with many substrates. The high selectivity should be noted, since binding of the substrate to rhodium through the olefin and amido units gives a fairly flexible chelate complex. In contrast, the reduction of (*α*-methoxyethyl)acrylate by the rhodium catalyst indicated a poor kinetic resolution (entry 4), in contrast to the effective OMe-directed hydrogenation with the iridium catalyst (see Table 21.3, entries 11 and 12) [25].

Table 21.18 Kinetic resolution of acrylic acid derivatives.

	Substrate	Major product	Recovered substrate	Catalyst	mol%	P_{H_2}	Solvent	Conversion [%]	Diastereomeric ratio	%ee recov.	k_f/k_s	TOF	Reference
1	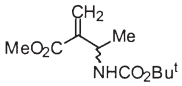	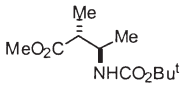	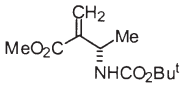	[Rh(nbd)(*R*,*R*)-dipamp)]$^+$	4	1 atm	MeOH	56	highly sel.	87 (*S*)	15	14	115
2	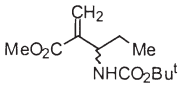	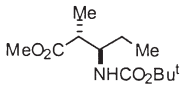	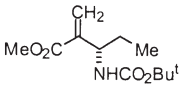	[Rh(nbd)(*R*,*R*)-dipamp)]$^+$	4	1 atm	MeOH	60	highly sel.	98 (*S*)	22	10	115
3	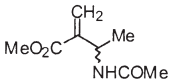	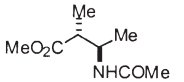	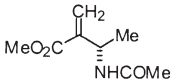	[Rh(nbd)(*R*,*R*)-dipamp)]$^+$	4	1 atm	MeOH	56	highly sel.	96 (*S*)	21	17.4	115
4	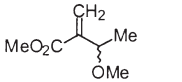	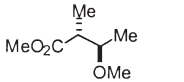	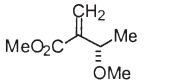	[Rh(nbd)(*R*,*R*)-dipamp)]$^+$	4	1 atm	MeOH	50	80:20	16 (*S*)	1.5	0.3	115
5	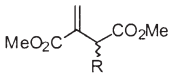	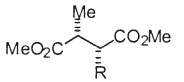	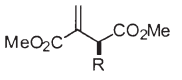										
			R = Et	[Rh((nbd)(*R*,*R*)-dipamp)]$^+$	2	1 atm	MeOH	52.7		81 (*S*)	16		64
			R = Ph		2								
			R = OMe	[Rh((nbd)(*R*,*R*)-dipamp)]$^+$	2	1 atm	MeOH	62.3		82 (*S*)	7.2		64
				[Rh((nbd)(*R*,*R*)-dipamp)]$^+$		1 atm	MeOH	62.2		93 (*S*)	11.5		64

In the hydrogenation of 3-substituted itaconate ester derivatives by rhodium–dipamp, the alkoxycarbonyl group at the stereogenic center also exerts a powerful directing effect, comparable to that induced by OH in the kinetic resolution of (*α*-hydroxyethyl)acrylate, leading to a high enantiomer-discriminating ability up to $k_R : k_S = 16:1$ (Table 21.18, entry 5) [64].

21.7
Kinetic Resolution of Keto- and Imino-Compounds

Kinetic resolution results of ketone and imine derivatives are indicated in Table 21.19. In the kinetic resolution of cyclic ketones or keto esters, ruthenium atropisomeric diphosphine catalysts **25** induced high enantiomer-discriminating ability, and high enantiopurity is realized at near 50% conversion [116, 117]. In the case of a bicyclic keto ester, the presence of hydrogen chloride in methanol served to raise the enantiomer-discriminating ability of the Ru–binap catalyst (entry 1) [116].

Racemic 2,5-disubstituted 1-pyrrolines were kinetically resolved effectively by hydrogenation with a chiral titanocene catalyst **26** at 50% conversion, which indicates a large difference in the reaction rate of the enantiomers (Table 21.19, entries 4 and 5), while 2,3- or 2,4-disubstituted 1-pyrrolines showed moderate selectivity in the kinetic resolution (entries 6 and 7) [118]. The enantioselectivity of the major product with *cis*-configuration was very high for all disubstituted pyrrolidines. The high selectivity obtained with 2,5-disubstituted pyrrolines can be explained by the interaction of the substituent at C5 with the tetrahydroindenyl moieties of the catalyst [Eq. (17)].

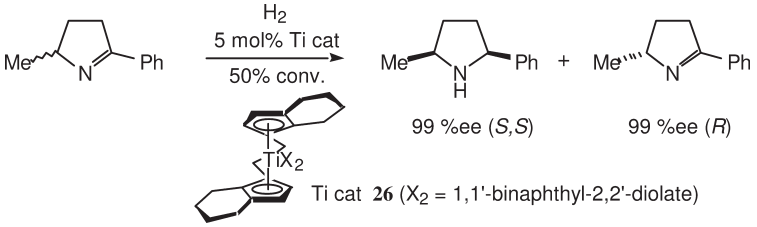

(17)

In the kinetic resolution of acyclic chiral imines derived from *α*-methylbenzylamine and acetophenone derivatives, Rh(I)–(2*S*,4*S*)-bdpp catalyst forming a six-membered chelate ring exerted good kinetic resolution results. Catalysts with 2-carbon bridged diphosphines resulted in low reactivity and low selectivity (Table 21.19, entry 8). The hydrogenation of (*R*)-**27** by Rh(I)–(2*S*,4*S*)-bdpp gives an extremely high diastereomeric ratio of $RR:SR = 333:1$ with *threo* stereochemistry, while in the reduction of (*S*)-**27** by Rh(I)–(2*S*,4*S*)-bdpp, the *threo* product is also formed in $SS:RS = 15.2:1$ ratio, indicating strong substrate-controlled selectivity [14]. Under kinetic resolution conditions, however, the Rh–bdpp catalyst re-

Table 21.19 Kinetic resolution of ketones and imines.

	Substrate	Major diastereomer	Recovered substrate	Catalyst	mol%	HCl (mol%)	P_{H_2}	Solvent	Conversion [%]	Diastereomeric ratio	%ee recov.	k_R/k_S	TOF	Reference
1	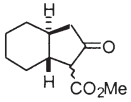	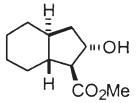	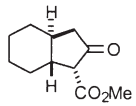	$RuCl_2$((*S*)-binap)	1.2	13.0 9.5 8.1	52 psi	MeOH	98.4 43.5 33.0	72:28 98:2 100:0				116
2		 (1*R*,2*R*)	 (2*S*)	(*S*,*SS*)-**25**	0.05		8 atm	*i*-PrOH	53	highly sel. 91 (*S*)		28		117
3	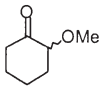	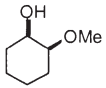 (1*R*,2*S*)	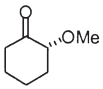 (2*R*)	(*S*,*SS*)-**25** 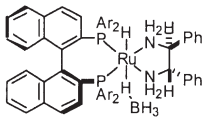 (*S*,*SS*)-**25** Ar = 3,5-$(CH_3)_2C_6H_3$	0.05		8 atm	*i*-PrOH	53	highly sel. 94 (*R*)		38		117
4	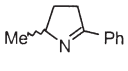	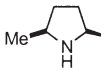	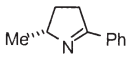	Titanocene cat **26**	5		80 psi	THF	50	highly sel. 99 (*R*) 99% ee				118

Table 21.19 (continued)

	Substrate	Major diastereomer	Recovered substrate	Catalyst	mol%	HCl (mol%)	P_{H_2}	Solvent	Conversion [%]	Diastereomeric ratio	%ee recov.	k_R/k_S	TOF	Reference
5	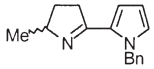	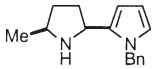 +	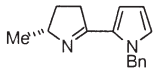	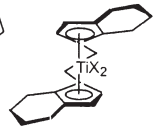 Titanocene cat **26**	5		80 psi	THF	50	highly sel. 98% ee	96 (*R*)			118
6		+		Titanocene cat	5		80 psi	THF	50	85:15 >95% ee	75 (*R*)			118
7	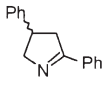	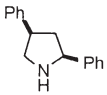 +	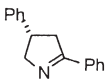	Titanocene cat	5		80 psi	THF	50	75:25 99% ee	49 (*R*)			118
8	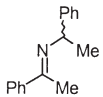 rac-**27**	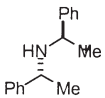 (*R*,*R*)-**28** +	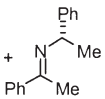 (*S*)-**27**	[RhCl((*S*,*S*)-bdpp)]Cl [RhCl((*S*,*S*)-chiraphos)]Cl	2 2		1000 psi 1000 psi	MeOH MeOH	67 82		83 (*S*) 7 (*S*)	5.7		14 14
9	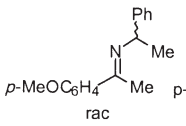 rac	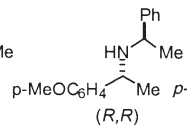 (*R*,*R*) +	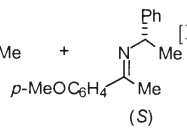 (*S*)	[RhCl((*S*,*S*)-bdpp)]Cl	2		1000 psi	MeOH	72		98 (*S*)			14

quired relatively high conversion in order to obtain (*S*)-chiral imine of high enantiomeric excess (entries 8 and 9) [14].

21.8 Dynamic Kinetic Resolution

In the kinetic resolution, the yield of desired optically active product cannot exceed 50% based on the racemic substrate, even if the chiral-discriminating ability of the chiral catalyst is extremely high. In order to obtain one diastereomer selectively, the conversion must be suppressed to less than 50%, while in order to obtain one enantiomer of the starting material selectively, a higher than 50% conversion is required. If the stereogenic center is labile in the racemic substrate, one can convert the substrate completely to gain almost 100% yield of the diastereomer formation by utilizing dynamic stereomutation.

In 1989, Noyori reported the first example of dynamic kinetic resolution in the enantioselective hydrogenation of α-substituted β-keto esters [119]. If the racemization of enantiomeric keto esters is rapid enough with respect to hydrogenation of the β-keto unit and the chiral discriminating ratio ($k_R : k_S$) is high, the hydrogenation will afford only one diastereomer out of four possible stereoisomeric hydroxy esters. The efficiency of the dynamic kinetic resolution and the sense of diastereoselection and enantioselection are strongly dependent on the structure of the substrate and the reaction conditions, including the solvent. The results of the dynamic kinetic resolution of β-keto esters are presented in Tables 21.20 to 21.22.

In the hydrogenation of cyclic β-keto esters (ketones substituted with an alkoxycarbonyl moiety), Ru(II)–binap reduced a racemic substrate in DCM with high *anti*-diastereoselectivity to give a 99 : 1 mixture of the *trans*-hydroxy ester (92% ee) and the *cis*-hydroxy ester (92% ee), quantitatively [Eq. (18)] [119, 120].

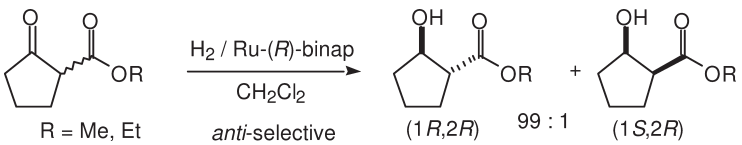

(18)

On the other hand, racemic β-keto esters with an amide or carbamate group in the α-position were reduced with high *syn*-diastereoselectivity (99:1) and with high enantioselectivity, leading to threonine-type products [Eq. (19)]. In polar methanol solution, the diastereoselectivity diminished to 71 : 29 (Table 21.20, entry 1) [123]. Results obtained using isotope-labeling experiments suggest that the hydrogenation proceeds via the ketone, and not via the enol [64]. The origin of the *syn* selectivity directed by an amide or a carbamate group was explained by a transition state stabilized by hydrogen bonding between the CONH and ester OR units [119]. *Anti*-selectivity in the case of cyclic β-keto esters is rationalized by the steric constraint of the cyclic ketone moiety (Scheme 21.10).

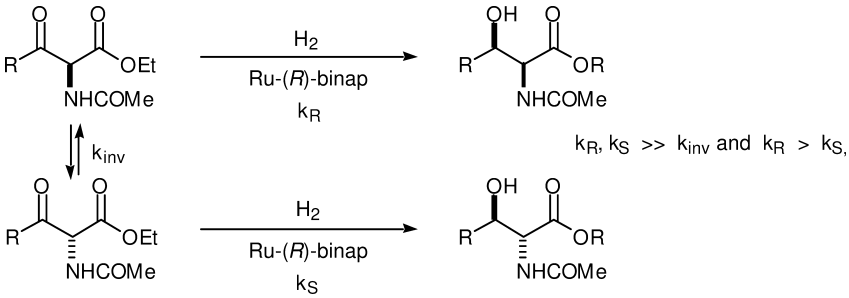

Scheme 21.9 Dynamic kinetic resolution of β-keto ester.

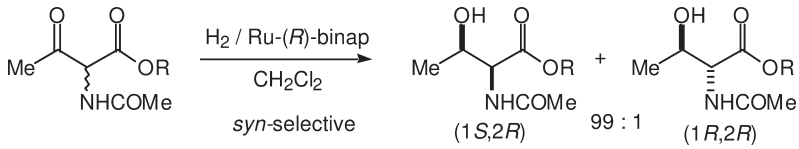

(19)

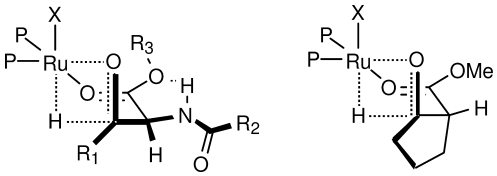

Scheme 21.10

Genêt also reported the dynamic kinetic resolution of α-substituted β-keto esters using several atropisomeric diphosphine ligands [121, 122, 124, 125] with high diastereo- and enantioselectivity. The *syn*:*anti* preference is lower using 10 mol.% of catalyst than in the presence of 1 mol.% of catalyst in MeOH [120]. This supported the fact that the hydrogenation needs to be slower than the racemization of the chiral center in order to achieve high stereoselectivities. For effective dynamic kinetic resolution, high hydrogen pressure should generally be avoided. With a rhodium catalyst, β-keto esters were reduced in moderate to good diastereoselectivities, but with low enantioselectivities [121].

The sense of diastereoselectivity in the dynamic kinetic resolution of 2-substituted β-keto esters depends on the structure of the keto ester. The ruthenium catalyst with atropisomeric diphosphine ligands (binap, MeO-biphep, synphos, etc.) induced *syn*-products in high diastereomeric and enantiomeric selectivity in the dynamic kinetic resolution of β-keto esters with an α-amido or carbamate moiety (Table 21.21) [119–121, 123, 125–127]. In contrast to the above examples of α-amido-β-keto esters, the TsOH or HCl salt of β-keto esters with an α-amino unit were hydrogenated with excellent *anti*-selectivity using ruthenium-atropiso-

Table 21.20 Dynamic kinetic resolution of β-keto esters.

	Substrate	Major diastereomer	Minor diastereomer	Catalyst	mol%	P_{H_2}	Solvent	Temp. [°C]	Diastereomeric ratio [*anti* : *syn*]	%ee (*anti*)	TOF	Reference
1	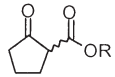	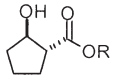 (2*R*,3*R*)	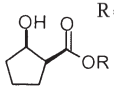	R = Et [RuCl(C_6H_6)((*R*)-binap)]Cl	0.085	100 atm	CH_2Cl_2	50	99:1	92 (2*R*,3*R*)	16.7	119
				$RuBr_{2(}$(*R*)-binap)	1	20 atm	MeOH	80	97:3	94 (2*R*,3*R*)	25	122
				$RuBr_2$((*R*)-binap)	1	100 atm	EtOH	80	96:4	85 (2*R*,3*R*)	2.1	133
				R = Me [RuC((C_6H_6)((*R*)-binap)]Cl	0.085	100 atm	CH_2Cl_2	50	99:1	92 (2*R*,3*R*)	16.7	120
2	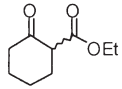	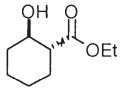 (2*R*,3*R*)	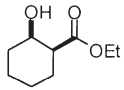	[Rucl(C_6H_6)((*R*)-binap)]Cl	0.085	100 atm	CH_2Cl_2	50	95:5	90 (2*R*,3*R*)	16.7	120
					1	20 atm	CH_2Cl_2	80	76.5:23.5	91 (2*R*,3*R*)	33	122
				$RuBr_2$((*R*)-binap)	1		MeOH		46:54	88 (2*R*,3*R*)	50	122
				$RuBr_2$((*S*)-binap)	1	20 atm	EtOH	80	73.5:26.5	91 (2*S*,3*S*)	33	133
3	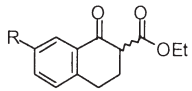	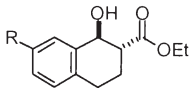 (2*R*,3*R*)	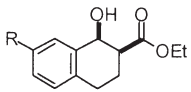									
				R = H $RuBr_2$((*R*)-MeO-biphep)		10 atm	EtOH	80	98.5:1.5	95 (2*R*,3*R*)	1.2	133
				R = OMe $RuBr_2$((*R*)-binap)	3	10 atm	CH_2Cl_2	80	98.5:1.5	96 (2*R*,3*R*)	0.7	122
				$RuBr_2$((*R*)-MeO-biphep)	3	10 atm	MeOH	80	98.5:1.5	95 (2*R*,3*R*)	0.6	122
4	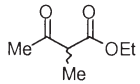	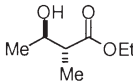	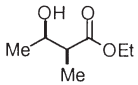	$RuBr_2$((*R*)-binap)	0.083	100 atm	EtOH	25	49:51	97 (2*R*,3*R*)	30	120
				[RuCl(C_6H_6)((*R*)-binap)]Cl	0.085	100 atm	CH_2Cl_2	50	68:32	94 (2*R*,3*R*)	20	107

Table 21.20 (continued)

	Substrate	Major diastereomer	Minor diastereomer	Catalyst	mol%	P_{H_2}	Solvent	Temp. [°C]	Diastereomeric ratio [*anti* : *syn*]	%ee (*anti*)	TOF	Reference
5	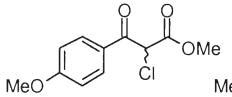	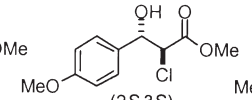 (2*S*,3*S*)	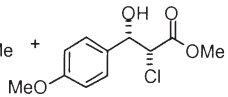									
				Ru(allyl)$_2$((*S*)-binap)	1	80 atm	CH_2Cl_2	80	96:4	94 (2*S*,3*S*)	5.3	124
				Ru(allyl)$_2$((*R*-binap)	0.5	5atm	MeOH	50	8.5:91.5	77 (2*R*,3*R*)	12.5	124
				[Ru((*S*)-MeO-biphep)]	1	60 bar	CH_2Cl_2	80	97.5:2.5	94 (2*S*,3*S*)	2.0	134
6	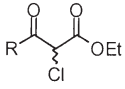	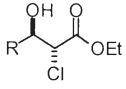 (2*R*,3*R*)	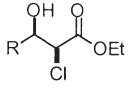									
			R = Me	Ru(allyl)$_2$((*R*)-binap)	0.5	90 atm	CH_2Cl_2	80	99:1	99 (2*R*,3*R*)	20	124
					1	30 atm	EtOH	27	52:48	93 (2*R*,3*R*)	5	124
				[Ru((*R*)-MeO-biphep)]	1	80 bar	CH_2Cl_2	80	99.5:0.5	98 (2*R*,3*R*)		133
			P = Rh	[Ru((*S*)-binap)]	0.5	86 atm	CH_2Cl_2	80	96:4	83 (2*S*,3*S*)	42.7	124
				$RuBr_2$((*R*)-binap)	1	30 atm	EtOH	27	9.5:90.5	31 (2*R*,3*R*)	5	124

meric diphosphine catalysts to afford *anti*-β-hydroxy-α-amino acids (Table 21.22, entries 1–4) [128–131]. In this case, a five-membered transition state is envisioned. High *anti*-selectivity was also observed in the reaction of an α-phthalimido-β-keto ester in methanol (Table 21.22, entry 5) [132], and in the reduction of keto esters having an α-chloro group (Table 21.20, entries 5 and 6) [124, 133, 134]. β-Keto esters with a cyclic keto unit also afforded *anti*-products selectively, as described [53, 119, 120, 122, 123, 133].

Dynamic kinetic resolution of β-keto phosphonic esters containing an α-amido group was examined using Ru–(*R*)-binap, and resulted in a phosphonate analogue of α-amino acids with (*R*,*R*)-*syn* configuration and very high selectivity ($k_R/k_S = 39$; $k_{inv}/k_S = 31$) [135]. The overall stereochemical outcome was explained on the basis of the Felkin-Anh model (Scheme 21.11), wherein β-keto phosphonic esters with α-bromo substituent were hydrogenated with high *syn*-selectivity [136].

In the hydrogenation of simple 2-alkyl-3-oxobutanoates, the interconversion between the enantiomers is relatively slow, and very poor resolution results are observed (see Table 21.20, entry 4) [107, 119, 120, 123]. Efficient dynamic kinetic resolution of 2-alkyl β-keto esters was first observed in the asymmetric hydrogenation of α-alkyl-β-keto esters which are derived from (*S*)-proline bearing a stereogenic center at the γ-position. The type of *N*-protecting group played a dramatic role, and the *N*-Boc substrate **29b** afforded naturally occurring (2*R*,3*R*)-dolaproine with *syn*-configuration, while β-keto esters *N*-protected as an amine hydrogen chloride salt **29a** afforded an *anti*-adduct in moderate to high diastereoselectivity (Scheme 21.12) [137, 138].

Dynamic kinetic resolution is possible for α-alkyl or α-alkoxy cyclic ketones in the presence of KOH, which causes mutation of the stereogenic center; *syn*-alcohols were obtained selectively with high enantioselectivity using ruthenium–3,5-xyl-binap. Dynamic kinetic resolution of 2-arylcycloalkanones also proceeded with extremely high *syn*-selectivity and with high enantioselectivity using ruthenium–binap-diamine as catalyst (Table 21.23) [12, 139, 140].

21.9 Conclusions

By linking the steric factor of the stereogenic center of substrates with the chiral-inducing ability of properly designed ligands, homogeneous diastereoselective hydrogenation can attain levels of stereoselectivity that will enable the industrial

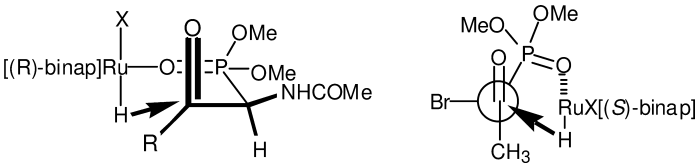

Scheme 21.11 Felkin-Anh model for the hydrogenation of keto phosphate.

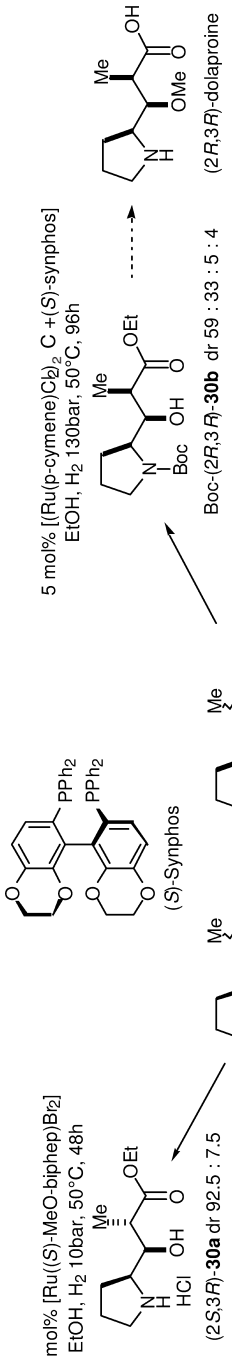

Scheme 21.12 Effect of *N*-protecting groups on the dynamic kinetic resolution.

Table 21.21 Dynamic kinetic resolution of α-subsituted β-keto esters.

	Substrate	Major diastereomer	Minor diastereomer	Catalyst	mol%	P_{H_2}	Solvent	Diastereomeric ratio [*anti* : *syn*]	%ee (*syn*)	TOF	Reference
1	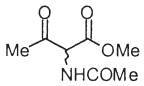	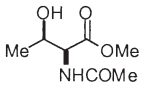 (2*S*,3*R*)	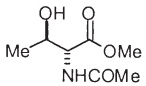	$Ru(O_2CCF_3)_2$[(*R*)-binap]	1	90 atm	CH_2Cl_2	95:5	51	0.43	121
				$RuBr_2$[(–)-chiraphos]	1	90 atm	CH_2Cl_2	97:3	85	0.83	121
				$[Rh(nbd)((–)\text{-dipamp})]^+$	1	70 atm	THF	94:6	39	1.0	121
				$RuBr_2$[(*R*)-binap]	0.4	100 atm	CH_2Cl_2	99:1	98	5	119
				$RuBr_2$[(*R*)-binap]	0.4	100 atm	MeOH	71:29	90		123
2	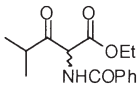	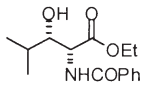 (2*R*,3*S*)	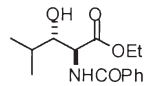	$RuCl_2$((*S*)-binap)$(dmf)_m$	2	100 atm	CH_2Cl_2	100:0	99	1.0	131
				$RuBr_2$((*S*)-synphos)	2	130 bar	CH_2Cl_2	99.5:0.5	97	0.5	127
3	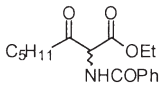	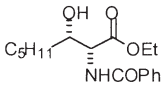 (2*R*,3*S*)	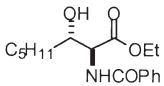	$RuBr_2$((*S*)-synphos)	2	130 bar	CH_2Cl_2	99:1	99	0.4	131
4	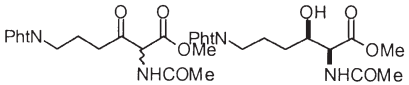 (2*S*,3*R*) (major)			$RuBr_2$((*R*)-MeO-biphep)	0.5	100 bar	CH_2Cl_2	>99:1		1.85	125
				$RuBr_2$((*R*)-MeO-biphep)	1	100 bar	MeOH	65:35		1.1	125
5	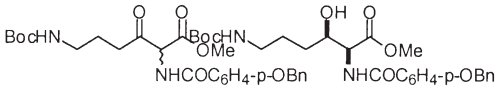 (2*S*,3*R*) (major)			$RuBr_2$((*R*)-MeO-biphep)	1	130 bar	CH_2Cl_2	96:5:3.5	94	1.1	126

Table 21.21 (continued)

	Substrate	Major diastereomer	Minor diastereomer	Catalyst	mol%	P_{H_2}	Solvent	Diastereomeric ratio [*anti* : *syn*]	%ee (*syn*)	TOF	Reference
6	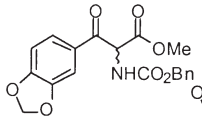	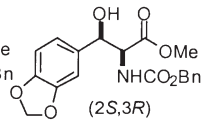 (2*S*,3*R*)	+ 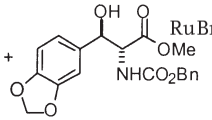	$RuBr_2$[(*R*)-binap]	0.4	100 atm	CH_2Cl_2	99:1	92	2.4	119
7	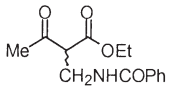	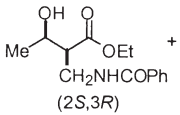 (2*S*,3*R*)	+ 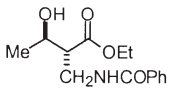	$[RuCl_2((R)\text{-binap})]_2NEt_3$	1	100 atm	CH_2Cl_2	94:6	98	5	119
				[RuCl((*R*)-3,5-Bu^t_2-binap)(*p*-cymene)]	0.1	50 atm	CH_2Cl_2/MeOH	99:1	99	13.8	123
				[RuBr((*R*)-binap)(benzene)]Br	1	50 atm	CH_2Cl_2/H_2O	89.5:10.5	98	2.3	123
				[RuBr((*R*)-binap)(benzene]Br	1	50 atm	MeOH	54.5:45.5	80	2.4	123
8	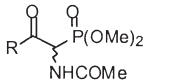	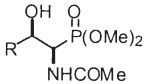 (1*S*,2*R*)	+ 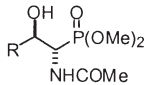								
				R = Ph [$RuCl_2$(*R*)-binap](dmf)$_n$	1	4 atm	MeOH	98:2	95	0.8	135
				R = Me [$RuCl_2$(*R*)-binap](dmf)$_n$	0.17	4 atm	MeOH	97:3	>98	9.0	135
								$k_R/k_S = 39$ and $k_{inv}/k_S = 31$			
9	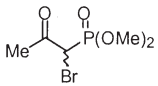	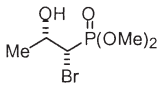 (1*R*,2*S*)	+ 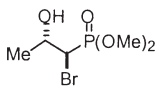	[$RuCl_2$(*S*)-binap](dmf)$_n$	0.05	4 atm	MeOH	90:10	98	0.8	136
								$k_R/k_S = 13$ and $k_{inv}/k_S = 11.5$			

Table 21.22 Dynamic kinetic resolution of α-substituted β-keto esters.

	Substrate	Major diastereomer	Minor diastereomer	Catalyst	mol%	P_{H_2}	Solvent	Diastereomeric ratio [*anti*:*syn*]	%ee (*anti*)	TOF	Reference
1	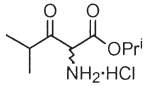	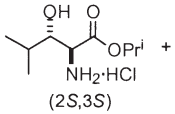 (2*S*,3*S*)	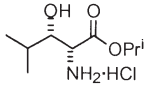	$[RuCl_2(S)\text{-binap}](dmf)_n$	4	100 atm	CH_2Cl_2	98:2	92	0.5	128
				$RuBr_2((S)\text{-MeO-biphep})$	1	12 bar	EtOH	99:1	87	4.2	131
				$RuBr_2((S)\text{-synphos})$	2	12 bar	CH_2Cl_2/2-PrOH	99.5:0.5	97	1.9	130
2	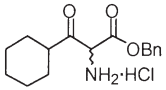	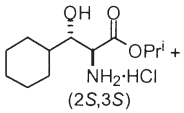 (2*S*,3*S*)	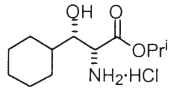	$[Rucl(S)\text{-binap}](dmf)_n$	4	100 atm	CH_2Cl_2	>99:1	97	0.44	128
3	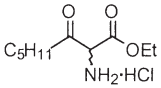	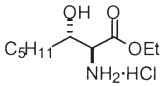	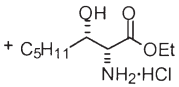	$RuBr_2((S)\text{-synphos})$	2	12 bar	CH_2Cl_2 (EtOH)	96.5:3.5	91	1.8	130
4	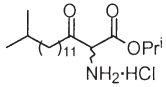	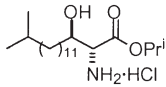	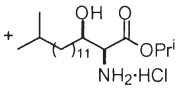	$RuBr_2((R)\text{-MeO-biphep})$	2	20 bar	MeOH	98:2	41	0.7	129
				$RuBr_2((R)\text{-MeO-biphep})$	2	20 bar	CH_2Cl_2	90:10	88	0.7	129
				$RuBr_2((R)\text{-synphos})$	2	12 bar	CH_2Cl_2/MeOH	96:4	92	1.7	129
5	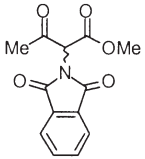	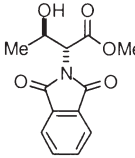	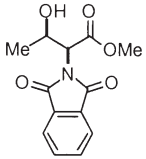	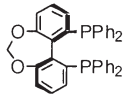 (*R*)-C_3-Tunephos [Ru(*S*)-C_3-Tunephos]	2	100 bar	MeOH	>97:3	>99	0.7	132

Table 21.23 Dynamic kinetic resolution of ketones.

	Substrate	Diastereomers	Catalyst	mol%	P_{H_2}	Solvent	Diastereomeric ratio [*syn*:*anti*]	%ee (*syn*)	TOF	Reference
1	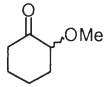	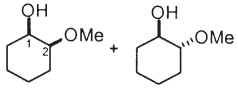 (1*R*,2*S*)	$[RuCl_2((S)\text{-binap})]_2(NEt_3)$ -(*S*,*S*)-DPEN-KOH	0.1	50 atm	*i*-PrOH	98.5:1.5	92 (*R*,*S*)	1000	139
			$[RuCl_2((S)\text{-3,5-xylyl-binap})]_2(NEt_3)$ -(*S*,*S*)-DPEN-KOH	0.1	50 atm	*i*-PrOH	99.5:0.5	99 (*R*,*R*)	50	139
2		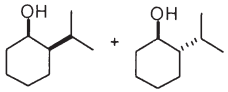	$RuCl_2((S)\text{-binap})(dmf)_m$ -(*R*,*R*)-DPEN-KOH	0.2	4 atm	*i*-PrOH	99.8:0.2	93 (*R*,*R*)	45.5	12
3	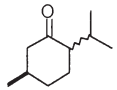	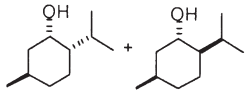	$RuCl_2((R)\text{-binap})(dmf)_m$ -(*S*,*S*)-DPEN-KOH	0.2	4 atm	*i*-PrOH	highly selective			12
4		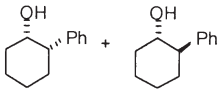	$RuCl_2((R)\text{-tol-binap})(dmf)_m$ -(*S*,*S*)-DPEN-^{t}BuOK	0.05	8 atm	*i*-PrOH	100:0	97 (*S*,*S*)	500	140
5	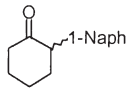	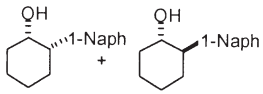	$RuCl_2((R)\text{-tol-binap})(dmf)_m$ -(*R*,*R*)-DPEN-^{t}BuOK	0.05	8 atm	*i*-PrOH	98:2	93 (*S*,*S*)	125	140

Table 21.23 (continued)

	Substrate	Diastereomers	Catalyst	mol%	P_{H_2}	Solvent	Diastereomeric ratio [*syn*:*anti*]	%ee (*syn*)	TOF	Reference
6	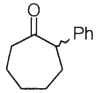	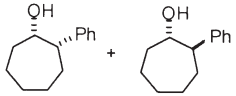	$RuCl_2$((*R*)-tol-binap)(dmf)m -(*S*,*S*)-DPEN-^{t}BuOK	0.05	8 atm	*i*-PrOH	100:0	95 (*S*,*S*)	83	140
7	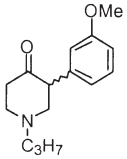	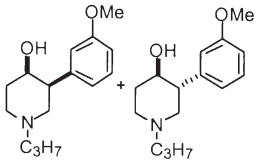	$RuCl_2$((*S*)-tol-binap)(dmf)m -(*S*,*S*)-DPEN-^{t}BuOK	0.2	8 atm	*i*-PrOH	>99:1	97 (*S*,*R*)	20.8	140

preparation of optically active compounds with several stereogenic centers. Functional group-directed hydrogenation led to good results *via* the interaction of a heteroatom in the substrate with the metal or with the ligand, whilst by selecting the catalyst, diastereoselective hydrogenation can induce excellent stereoselectivity *via* double stereo-differentiation (matched pair). However, in general the activity of hydrogenation catalysts remains poor, especially for those substrates with bulky groups proximal to the reaction site. Consequently, it will be necessary to develop more efficient catalysts to produce higher turnover frequencies.

Abbreviations

d.e.	diastereomeric excess
DCM	dichloromethane
ee	enantiomeric excess
TBSO	tert-butyldimethylsilyloxy
THF	tetrahydrofuran

References

1 (a) Knowles, W. S., Sabacky, M. J., *J. Chem. Soc., Chem. Commun.* **1968**, 1445; (b) Horner, L., Siegel, H., Buthe, H., *Angew. Chem., Int. Ed. Engl.* **1968**, *7*, 942; (c) Kagan, H. B., Chiral Ligands for Asymmetric Catalysis, in: Morrison, J. D. (Ed.), *Asymmetric Synthesis*, Academic Press, Inc.: Orlando, FL, **1985**, Vol. 5, p. 1; (d) Koenig, K. E., The Applicability of Asymmetric Homogeneous Catalytic Hydrogenation, in: *Asymmetric Synthesis*; Morrison, J. D. (Ed.), Academic Press, Inc., Orlando, FL, **1985**, Vol. 5, p. 71; (e) Brunner, H., *Top. Stereochem.* **1988**, *18*, 129; (f) Arntz, D., Schaefer, A., Asymmetric Hydrogenation, in: Noels, A. F., Graziani, M., Hubert, A. J. (Eds.), *Metal Promoted Selectivity in Organic Synthesis*, Kluwer Academic, Dordrecht, **1991**, p. 161; (g) Takaya, H., Ohta, T., Noyori, R., Asymmetric Hydrogenation, in: Ojima, I. (Ed.), *Catalytic Asymmetric Synthesis*, VCH Publishers, Inc., New York, NY, **1993**, p. 1.

2 Jardine, F.H., *Prog. Inorg. Chem.* **1984**, *431*, 265.

3 Halpern, J., Harrod, J. F., James, B. R., *J. Am. Chem. Soc.* **1961**, *83*, 753.

4 Crabtree, R. H., Felkin, H., Morris, G. E., *J. Organomet. Chem.* **1977**, *141*, 205.

5 Evans, D. A., Morrissey, M. M., *J. Am. Chem. Soc.* **1984**, *106*, 3866.

6 (a) Molander, G. A., Winterfeld, J., *J. Organomet. Chem.* **1996**, 524, 275; (b) Molander, G. A., Dowdy, E. D., *Top. Organomet. Chem.* **1999**, *2*, 119.

7 Jenke, T., Süss-Fink, G., *J. Organomet. Chem.* **1991**, *405*, 383.

8 Suggs, J. W., Cox, S. D., Crabtree, R. H., Quirk, J. M., *Tetrahedron Lett.* **1981**, *22*, 303.

9 Debenham, S. D., Debenham, J. S., Burk, M. J., Toone, E. J., *J. Am. Chem. Soc.* **1997**, *119*, 9897.

10 Berens, U., Fischer, C., Selke, R., *Tetrahedron: Asymm.* **1995**, *6*(5), 1105.

11 Fehr, M. J., Consiglio, G., Scalone, M., Schmid, R., *New J. Chem.* **1998**, 1499.

12 Ohkuma, T., Ooka, H., Yamakawa, M., Ikariya, T., Noyori, R., *J. Org. Chem.* **1996**, *61*, 4872.

13 Ohkuma, T., Ikehira, H., Ikariya, T., Noyori, R., *Synlett* **1997**, 467.

14 Lensink, C., de Vries, J. G., *Tetrahedron: Asymm.* **1993**, *4*, 215.

15 Morrison, J.D. (Ed.), *Asymmetric Synthesis*, Vol. 5, Academic Press, New York, **1985**.
16 Thompson, H.W., McPherson, E., *J. Am. Chem. Soc.* **1974**, *96*, 6232.
17 (a) Paquette, L.A., Peng, X., Bondar, D., *Org. Lett.* **2002**, *4*(6), 937; (b) Peng, X., Bondar, D., Paquette, L.A., *Tetrahedron* **2004**, *60*, 9589.
18 Crabtree, R.H., Demou, P.C., Eden, D., Mihelcic, J.M., Parnell, C.A., Quirk, J.M., Morris, G.E., *J. Am. Chem. Soc.* **1982**, *104*, 6994.
19 Brown, J.M., Naik, R.G., *J. Chem. Soc., Chem. Commun.* **1982**, 348.
20 Brown, J.M., *Angew. Chem. Int. Ed. Engl.* **1987**, *26*, 190.
21 Crabtree, R.H., Davis, M.W., *Organometallics* **1983**, *2*, 681.
22 Stork, G., Kahne, D.E., *J. Am. Chem. Soc.* **1983**, *105*, 1072.
23 Hoveyda, A.H., Evans, D.A., Fu, G.C., *Chem. Rev.* **1993**, *93*, 1307.
24 Evans, D.A., Morrissey, M.M., *Tetrahedron Lett.* **1984**, *25*(41), 4637.
25 Crabtree, R.H., Davis, M.W., *J. Org. Chem.* **1986**, *51*, 2655.
26 Corey, E.J., Engler, T.A., *Tetrahedron Lett.* **1984**, *25*, 149.
27 Sakurai, K., Kitahara, T., Morñi, K., *Tetrahedron* **1990**, *46*(3), 761.
28 Fernández, B., Martínez Pérez, J.A., Granja, J.R., Castedo, L., Mouriño, A., *J. Org. Chem.* **1992**, *57*, 3173.
29 Brown, J.M., Hall, S.A., *Tetrahedron* **1985**, *41*, 4639.
30 DeCamp, A.E., Verhoeven, T.R., Shinkai, I., *J. Org. Chem.* **1989**, *54*, 3207.
31 Poss, A.J., Smyth, M.S., *Tetrahedron Lett.* **1988**, *29*(45), 5723.
32 Kawai, A., Hara, O., Hamada, Y., Shioiri, T., *Tetrahedron Lett.* **1988**, *29*(48), 6331.
33 Watson, A.T., Park, K., Wiemer, D.F., *J. Org. Chem.* **1995**, *60*, 5102.
34 Del Valle, J.R., Goodman, M., *Angew. Chem. Int. Ed. Engl.* **2002**, *41*, 1600.
35 Bueno, J.M., Coterón, J.M., Chiara, J.L., Fernández-Moyaralas, A., Fiandor, J.M., Valle, N., *Tetrahedron Lett.* **2000**, *41*, 4379.
36 Brown, J.M., Hall, S.A., *Tetrahedron Lett.* **1984**, *25*, 1393.
37 Machado, A.S., Olesker, A., Castillon, S., Lukacs, G., *J. Chem. Soc., Chem. Commun.* **1985**, 330.
38 Del Valle, J.R., Goodman, M., *J. Org. Chem.* **2003**, *68*, 3923.
39 Brown, J.M., Derome, A.E., Hall, S.A., *Tetrahedron* **1985**, *41*, 4647.
40 Brown, J.M., Hall, S.A., *J. Organomet. Chem.* **1985**, *285*, 333.
41 Schultz, A.G., McCloskey, P.J., *J. Org. Chem.* **1985**, *50*, 5905.
42 (a) Zhang, M., Zhu, L., Ma, X., *Tetrahedron: Asymm.* **2003**, *14*, 3447; (b) Zhang, M., Zhu, L., Ma, X., Dai, M., Lowe, D., *Org. Lett.* **2003**, *5*(9), 1587.
43 Schultz, A.G., McCloskey, P.J., Court, J.J., *J. Am. Chem. Soc.* **1987**, *109*, 6493.
44 Smith, M.E.B., Derrien, N., Lloyd, M.C., Taylor, S.J.C., Chaplin, D.A., McCague, R., *Tetrahedron Lett.* **2001**, *42*, 1347.
45 Brown, J.M., Cutting, I., *J. Chem. Soc., Chem. Commun.* **1985**, 578.
46 Kitamura, M., Kasahara, I., Manabe, K., Noyori, R., Takaya, H., *J. Org. Chem.* **1988**, *53*, 708.
47 Hameršak, Z., Gašo, D., Kovač, S., Hergold-Brundić, A., Vicković, I., Šunjić, V., *Helv. Chim. Acta* **2003**, *86*(6), 2247.
48 (a) Lautens, M., Zhang, C.H., Crudden, C.M., *Angew. Chem. Int. Ed. Engl.* **1992**, *31*(2), 232; (b) Lautens, M., Zhang, C.H., Goh, B.J., Crudden, C.M., Johnson, M.J.A., *J. Org. Chem.* **1994**, *59*, 6208.
49 Schmidt, U., Stäbler, F., Lieberknecht, A., *Synthesis* **1992**, 482.
50 Paterson, I., Bower, S., Tillyer, R.D., *Tetrahedron Lett.* **1993**, *34*(27), 4393.
51 Paterson, I., Bower, S., McLeod, M.D., *Tetrahedron Lett.* **1995**, *36*, 175.
52 Kitamura, M., Nagai, K., Hsiao, Y., Noyori, R., *Tetrahedron Lett.* **1990**, *31*, 549.
53 Genêt, J.-P., *ACS Symposium Series* **1996**, *641* (Reductions in Organic Synthesis), 31.
54 Terada, M., Sayo, N., Mikami, K., *Synlett* **1995**, 411.
55 Reetz, M.T., Kayser, F., *Tetrahedron: Asymm.* **1992**, *3*, 1377.
56 Ando, D., Bevan, C., Brown, J.M., Price, D.W., *J. Chem. Soc., Chem. Commun.* **1992**, 592.
57 Birtwistle, D.H., Brown, J.M., Herbert, R.H., James, A.P., Lee, K.-F., Taylor,

R.J., *J. Chem. Soc., Chem. Commun.* **1989**, 194.
58 Wehn, P.M., Du Bois, J., *J. Am. Chem. Soc.* **2002**, *124*, 12950.
59 Evans, D.A., Morrissey, M.M., Dow, R.L., *Tetrahedron Lett.* **1985**, *26*(49), 6005.
60 Evans, D.A., DiMare, M., *J. Am. Chem. Soc.* **1986**, *108*, 2476.
61 Evans, D.A., Dow, R.L., *Tetrahedron Lett.* **1986**, *27*(9), 1007.
62 Villalobos, A., Danishefsky, S.J., *J. Org. Chem.* **1990**, *55*, 2776.
63 Landis, C.R., Halpern, J., *J. Am. Chem. Soc.* **1987**, *109*, 1746.
64 Brown, J.M., James, A.P., *J. Chem. Soc., Chem. Commun.* **1987**, 181.
65 Brown, J.M., Cutting, I., James, A.P., *Bull. Soc. Chim. Fr.* **1988**, (2), 211.
66 (a) Yamamoto, K., Takagi, M., Tsuji, J., *Bull. Chem. Soc. Jpn.* **1988**, *61*, 319; (b) Yamamoto, K., *Yuki Gousei Kagaku Kyokaishi* **1989**, *47*(2), 123.
67 Takagi, M., Yamamoto, K., *Tetrahedron* **1991**, *47*(2), 8869.
68 Masamune, S., Choy, W., Petersen, J.S., Sita, L.R., *Angew. Chem. Int. Ed. Engl.* **1985**, *24*, 1.
69 Ojima, I., Kogure, T., Yoda, N., Suzuki, T., Yatabe, M., Tanaka, T., *J. Org. Chem.* **1982**, *47*, 1329.
70 Ojima, I., Suzuki, T., *Tetrahedron Lett.* **1980**, *21*, 1239.
71 Meyer, D., Poulin, J.-C., Kagan, H.B., Levin-Pinto, H., Morgat, J.-L., Fromageot, P., *J. Org. Chem.* **1980**, *45*, 4680.
72 El-Baba, S., Poulin, J.-C., Kagan, H.B., *Tetrahedron* **1984**, *40*, 4275.
73 (a) Ojima, I., Yoda, N., Yatabe, M., *Tetrahedron Lett.* **1982**, *23*, 3917; (b) Ojima, I., Yoda, N., Yatabe, M., Tanaka, T., Kogure, T., *Tetrahedron* **1984**, *40*, 1255.
74 Aguado, G.P., Moglioni, A.G., Brousse, B.N., Ortuño, R.M., *Tetrahedron: Asymm.* **2003**, *14*, 2445; Aguado, G.P., Moglioni, A.G., García-Expósito, E., Branchadell, V., Ortuño, R.M., *J. Org. Chem.* **2004**, *69*, 7971.
75 Kreuzfeld, H.-J., Döbler, C., Schmidt, U., Krause, H.W., *Chirality* **1998**, *10*, 535.
76 Ojima, I., Yatabe, M., *Chem. Lett.* **1982**, 1335.
77 Sinou, D., Lafont, D., Descotes, G., *J. Organomet. Chem.* **1981**, *217*, 119.
78 Onuma, K., Ito, T., Nakamura, A., *Chem. Lett.* **1980**, 481.
79 Hammadi, A., Nuzillard, J.M., Poulin, J.C., Kagan, H.B., *Tetrahedron: Asymm.* **1992**, *3*(10), 1247.
80 (a) Yatagai, M., Zama, M., Yamagishi, T., Hida, M., *Chem. Lett.* **1983**, 12036; (b) Yatagai, M., Zama, M., Yamagishi, T., Hida, M., *Bull. Chem. Soc. Jpn.* **1984**, *57*, 739.
81 Yatagai, M., Yamagishi, T., Hida, M., *Bull. Chem. Soc. Jpn.* **1984**, *57*, 823.
82 Yamagishi, T., Ikeda, S., Yatagai, M., Yamaguchi, M., Hida, M., *J. Chem. Soc., Perkin Trans. 1* **1988**, 1787.
83 Ikeda, S., Yamagishi, T., Yamaguchi, M., Hida, M., *Chemistry Express* **1990**, *5*(1), 29.
84 Hayashi, T., Kawamura, N., Ito, Y., *J. Am. Chem. Soc.* **1987**, *109*, 7876.
85 (a) Poulin, J.-C., Kagan, H.B., *J. Chem. Soc., Chem. Commun.* **1982**, 1261; (b) El-Baba, S., Poulin, J.-C., Kagan, H.B., *Bull. Soc. Chim. Fr.* **1994**, *131*, 525.
86 Ritzén, A., Basu, B., Chattopadhyay, S.K., Dossa, F., Frejd, T., *Tetrahedron: Asymm.* **1998**, *9*, 503.
87 Hiebl, J., Kollmann, H., Rovenszky, F., Winkler, K., *J. Org. Chem.* **1999**, *64*, 1947.
88 Ojima, I., Tanaka, T., Kogure, T., *Chem. Lett.* **1981**, 823.
89 Tani, K., Tanigawa, E., Tatsuno, Y., Otsuka, S., *Chem. Lett.* **1986**, 737.
90 Yamagishi, T., Ikeda, S., Egawa, T., Yamaguchi, M., Hida, M., *Bull. Chem. Soc. Jpn.* **1990**, *63*, 281.
91 (a) Ohkuma, T., Ooka, H., Hashiguchi, S., Ikariya, T., Noyori, R., *J. Am. Chem. Soc.* **1995**, *117*, 2675; (b) Ohkuma, T., Ooka, H., Ikariya, T., Noyori, R., *J. Am. Chem. Soc.* **1995**, *117*, 10417; (c) Doucet, H., Ohkuma, T., Murata, K., Yokozawa, T., Kozawa, M., Katayama, E., England, A.F., Ikariya, T., Noyori, R., *Angew. Chem., Int. Ed.* **1998**, *37*(12), 1703.
92 Abdur-Rashid, K., Lough, A.J., Morris, R.H., *Organometallics* **2001**, *20*, 1047.
93 Miyashita, A., Takaya, H., Souchi, T., Noyori, R., *Tetrahedron* **1984**, *40*(8), 1245.
94 Miyashita, A., Karino, H., Shimamura, J., Chiba, T., Nagano, K., Nohira, H., Takaya, H., *Chem. Lett.* **1989**, 1849.

95 Schmid, R., Cereghetti, M., Heiser, B., Schönholzer, P., Hansen, H.-J., *Helv. Chim. Acta* **1988**, *71*(4), 897; Schmid, R., Foricher, J., Cereghetti, M., Schönholzer, P., *Helv. Chim. Acta* **1991**, *74*(2), 370.

96 Nishi, T., Kitamura, M., Ohkuma, T., Noyori, R., *Tetrahedron Lett.* **1988**, *29*(48), 6327.

97 Armstrong, III, J.D., Keller, J.L., Lynch, J., Liu, T., Hartner, Jr., F.W., Ohtake, N., Okada, S., Imai, Y., Okamoto, O., Ushijima, R., Nakagawa, S., Volante, R.P., *Tetrahedron Lett.* **1997**, *38*(18), 3203.

98 Ohtake, N., Jona, H., Okada, S., Okamoto, O., Imai, Y., Ushijima, R., Nakagawa, S., *Tetrahedron: Asymm.* **1997**, *8*(17), 2939.

99 (a) Drouillat, B., Poupardin, O., Bourdreux, Y., Greck, C., *Tetrahedron Lett.* **2003**, *44*, 2781; (b) Thomassigny, C., Greck, C., *Tetrahedron: Asymm.* **2004**, *15*, 199.

100 Duprat De Paule, S., Piombo, L., Ratovelomanana-Vidal, V., Greck, C., Genêt, J.-P., *Eur. J. Org. Chem.* **2000**, 1535.

101 Blandin, V., Carpentier, J.-F., Mortreux, A., *Eur. J. Org. Chem.* **1999**, 1787.

102 Shao, L., Kawano, H., Saburi, M., Uchida, Y., *Tetrahedron* **1993**, *49*, 1997.

103 (a) Blandin, V., Carpentier, J.-F., Mortreux, A., *Eur. J. Org. Chem.* **1999**, 3421; (b) Blandin, V., Carpentier, J.-F., Mortreux, A., *New. J. Chem.* **2000**, *24*, 309.

104 Schulz, S., *Chem. Commun.* **1999**, 1239.

105 Kawano, H., Ishii, Y., Saburi, M., Uchida, Y., *J. Chem. Soc., Chem. Commun.* **1988**, 87.

106 Kitamura, M., Ohkuma, T., Inoue, S., Sayo, N., Kumobayashi, H., Akutagawa, S., Ohta, T., Takaya, H., Noyori, R., *J. Am. Chem. Soc.* **1988**, *110*, 629.

107 Noyori, R., Ohkuma, T., Kitamura, M., Takaya, H., Sayo, N., Kumobayashi, H., Akutagawa, S., *J. Am. Chem. Soc.* **1987**, *109*, 5856.

108 Burk, M.J., Harper, T.G.P., Kalberg, C.S., *J. Am. Chem. Soc.* **1995**, *117*, 4423.

109 Genêt, J.-P., Pinel, C., Ratovelomanana-Vidal, V., Mallart, S., Pfister, X., Bischoff, L., Caño de Andrade, M.C., Darses, S., Galopin, C., Laffitte, J.A., *Tetrahedron: Asymm.* **1994**, *5*, 675.

110 Blanc, D., Ratovelomanana-Vidal, V., Marinetti, A., Genêt, J.-P., *Synlett* **1999**, (4), 480.

111 Mezzetti, A., Consiglio, G., *J. Chem. Soc., Chem. Commun.* **1991**, 1675.

112 Mezzetti, A., Tschumper, A., Consiglio, G., *J. Chem. Soc., Dalton Trans.* **1995**, 49.

113 Cui, X., Ogle, J.W., Burgess, K., *Chem. Commun.* **2005**, 672.

114 Kagan, H.B., Fiaud, J.C., *Top. Stereochem.* **1988**, *18*, 249.

115 Brown, J.M., James, A.P., Prior, L.M., *Tetrahedron Lett.* **1987**, *28*, 2179.

116 Taber, D.F., Wang, Y., *J. Am. Chem. Soc.* **1997**, *119*, 22.

117 Ohkuma, T., Koizumi, M., Muñiz, K., Hilt, G., Kabuto, C., Noyori, R., *J. Am. Chem. Soc.* **2002**, *124*, 6508.

118 Viso, A., Lee, N.E., Buchwald, S.L., *J. Am. Chem. Soc.* **1994**, *116*, 9373.

119 Noyori, R., Ikeda, T., Ohkuma, T., Widhalm, M., Kitamura, M., Takaya, H., Akutagawa, S., Sayo, N., Saito, T., Taketomi, T., Kumobayashi, H., *J. Am. Chem. Soc.* **1989**, *111*, 9134.

120 Kitamura, M., Ohkuma, T., Tokunaga, M., Noyori, R., *Tetrahedron: Asymm.* **1990**, *1*, 1.

121 Genêt, J.-P., Pinel, C., Mallart, S., Juge, S., Thorimbert, S., Laffitte, J.A., *Tetrahedron: Asymm.* **1991**, *2*(7), 555.

122 Genêt, J.-P., Pfister, X., Ratovelomanana-Vidal, V., Pinel, C., Laffitte, J.A., *Tetrahedron Lett.* **1994**, *35*, 4559.

123 (a) Mashima, K., Matsumura, Y., Kusano, K., Kumobayashi, H., Sayo, N., Hori, Y., Ishizaki, T., Akutagawa, S., Takaya, H., *J. Chem. Soc., Chem. Commun.* **1991**, 609; (b) Takaya, H., Ohta, T., Mashima, K., *Advances in Chemistry Series* **1992**, *230*, 123.

124 Genêt, J.-P., Caño de Andrade, M.C., Ratovelomanana-Vidal, V., *Tetrahedron Lett.* **1995**, *36*, 2063.

125 Coulon, E., Caño de Andrade, M.C., Ratovelomanana-Vidal, V., Genêt, J.-P., *Tetrahedron Lett.* **1998**, *39*, 6467.

126 Phansavath, P., Duprat de Paule, S., Ratovelomanana-Vidal, V., Genêt, J.-P., *Eur. J. Org. Chem.* **2000**, 3903.

127 Makino, K., Okamoto, N., Hara, O., Hamada, Y., *Tetrahedron: Asymm.* **2001**, *12*, 1757.

128 Makino, K., Goto, T., Hiroki, Y., Hamada, Y., *Angew. Chem. Int. Ed. Engl.* **2004**, *43*, 882.

129 Labeeuw, O., Phansavath, P., Genêt, J.-P., *Tetrahedron: Asymm.* **2004**, *15*, 1899.

130 Mordant, C., Dünkelmann, P., Ratovelomanana-Vidal, V., Genêt, J.-P., *Chem. Commun.* **2004**, 1296.

131 Mordant, C., Dünkelmann, P., Ratovelomanana-Vidal, V., Genêt, J.-P., *Eur. J. Org. Chem.* **2004**, 3017.

132 Lei, A., Wu, S., He, M., Zhang, X., *J. Am. Chem. Soc.* **2004**, *126*, 1626.

133 Ratovelomanana-Vidal, V., Genêt, J.-P., *J. Organomet. Chem.* **1998**, *567*, 163.

134 Mordant, C., Caño de Andrade, C., Touati, R., Ratovelomanana-Vidal, V., Hassine, B. B., Genêt, J.-P., *Synthesis* **2003**, (15), 2405.

135 Kitamura, M., Tokunaga, M., Pham, T., Lubell, W. D., Noyori, R., *Tetrahedron Lett.* **1995**, *36*(32), 5769.

136 Kitamura, M., Tokunaga, M., Noyori, R., *J. Am. Chem. Soc.* **1995**, *117*, 2931.

137 Genêt, J.-P. *Pure Appl. Chem.* **2002**, *74*, 77.

138 Mordant, C., Reymond, S., Ratovelomanana-Vidal, V., Genêt, J.-P., *Tetrahedron* **2004**, *60*, 9715.

139 Matsumonto, T., Murayama, T., Mitsuhashi, S., Miura, T., *Tetrahedron Lett.* **1999**, *40*, 5043.

140 Ohkuma, T., Li, J., Noyori, R., *Synlett* **2004**, (8), 1383.

22
Hydrogen-Mediated Carbon–Carbon Bond Formation Catalyzed by Rhodium

Chang-Woo Cho and Michael J. Krische

22.1
Introduction and Mechanistic Considerations

The development of direct catalytic methods for reductive carbon–carbon bond formation has emerged as the subject of intensive investigation [1–10]. The catalytic hydrometallative reductive coupling of alkenes [1], alkynes [2, 3], allenes [4], conjugated enones [5–7], conjugated dienes [8–10] and conjugated enynes [11] to carbonyl partners and imines has been achieved using silanes, stannanes, boranes and alanes as terminal reductant. The use of such terminal reductants mandates stoichiometric byproduct generation. Related hydrogen-mediated transformations would proceed with complete levels of atom economy [12]. However, while metal catalysts capable of reversible transfer hydrogenation have been applied to the development of C–C bond formations predicated on dehydrogenation-trapping-rehydrogenation [13], true hydrogen-mediated reductive C–C bond formations only have been achieved for processes involving migratory insertion of carbon monoxide, for example, alkene hydroformylation and the Fischer-Tropsch reaction [14, 15].

The question persists as to whether the organometallic intermediates that appear transiently during the course of catalytic hydrogenation can be intercepted and re-routed to products of C–C bond formation. In the case of rhodium-catalyzed alkene hydroformylation, a key feature appears to be the involvement of mono-hydride-based catalytic cycles, wherein the formation of (alkyl)(hydrido)metal intermediates occurs *subsequent* to C–C bond formation. In contrast, conventional dihydride-based hydrogenation cycles generally afford (alkyl)(hydrido)metal intermediates in *advance* of potential C–C bond formation. For such dihydride-based hydrogenation cycles, the capture of hydrogenation intermediates is likely untenable due to rapid C–H reductive elimination. This may account, in part, for the exceptional rarity of hydrogen-mediated C–C bond formation in the absence of carbon monoxide [15].

Recent studies from our laboratory demonstrate the feasibility of hydrogen-mediated C–C bond formation under "CO-free conditions." Here, at least two

The Handbook of Homogeneous Hydrogenation.
Edited by J.G. de Vries and C.J. Elsevier
Copyright © 2007 WILEY-VCH Verlag GmbH & Co. KGaA, Weinheim
ISBN: 978-3-527-31161-3

distinct mechanistic pathways potentially operate. Initial studies on hydrogen-mediated reductive aldol coupling demonstrate that conventional hydrogenation pathways are suppressed through the use of cationic rhodium precatalysts in the presence of a mild base. Such conditions are believed to promote heterolytic hydrogen activation (H_2+M–X → M–H+HX) [16, 20]. Monohydride-mediated hydrometallation should furnish organometallic species that do not possess hydride ligands, disabling direct C–H reductive elimination manifolds and extending the lifetimes of the organometallic intermediates obtained upon hydrometallation to facilitate their capture. Hence, one strategy for hydrogen-mediated C–C bond formation involves the hydrogenation of reactants using catalysts that operate *via* monohydride-based catalytic cycles. A second strategy for hydrogen-mediated C–C bond formations takes advantage of the fact that hydrogen activation can be quite slow for certain conventional hydrogenation catalysts. Here, oxidative coupling of the reacting partners prior to hydrogenation activation becomes feasible [17] (Scheme 22.1).

Among homogeneous hydrogenation catalysts, those based on rhodium are especially well studied [18–20, 28]. Whereas neutral rhodium(I)-complexes such as Wilkinson's catalyst induce *homolytic* hydrogen activation [18, 19], the use of cationic rhodium(I) complexes in conjunction with basic additives is believed to promote *heterolytic* activation pathways [20]. Heterolytic hydrogen activation by cationic rhodium complexes presumably is owed to the enhanced acidity of the cationic dihydrides that result upon oxidative addition in comparison to their neutral counterparts [21]. Thus, heterolytic hydrogen activation is believed to occur through a two-stage process involving hydrogen oxidative addition followed by base-induced H–X reductive elimination [22] (Scheme 22.2).

Hydrogen activation is rate-determining for enantioselective hydrogenations employing cationic rhodium catalysts [28]. This observation is significant given that closely related cationic rhodium(I) complexes are known to catalyze a variety of C–C bond formations believed to proceed through the initial oxidative coupling of π-unsaturated partners to furnish metallocyclic intermediates [17]. Accordingly, tandem oxidative coupling-metallocycle hydrogenolysis strategies toward hydrogen-mediated C–C bond formation have proven fruitful (*vide supra*).

Here, a comprehensive overview of hydrogen-mediated C–C bond formation under CO-free conditions is presented [23]. This emergent family of reductive couplings now encompasses:

- the intra- and intermolecular reductive coupling of enone and enal pronucleophiles with aldehyde and ketone partners [24];
- the intermolecular reductive coupling of 1,3-cyclohexadiene with α-ketoaldehydes [25];
- the intermolecular reductive coupling of 1,3-enynes and 1,3-diynes with α-ketoaldehydes and iminoacetates [26]; and
- the reductive cyclization of 1,6-diynes and 1,6-enynes [27].

These results establish catalytic hydrogenation as a powerful and mechanistically novel means of catalytic C–C bond formation, and support the feasibility

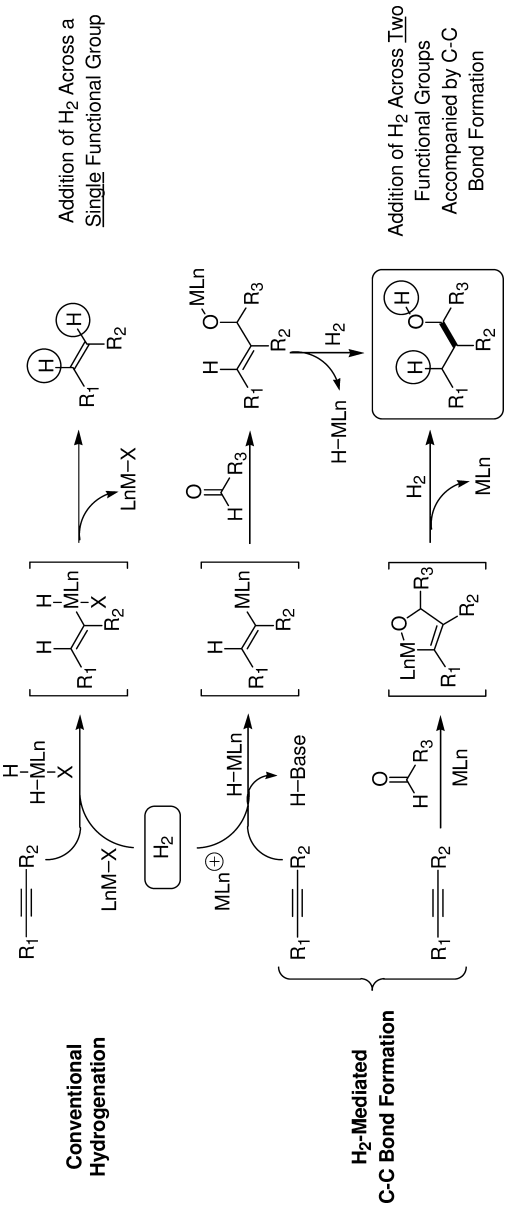

Scheme 22.1 Potential mechanistic pathways for hydrogen-mediated C–C bond formation.

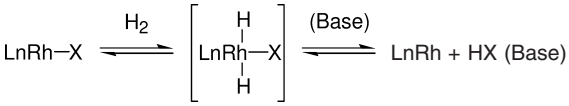

Scheme 22.2 Formal heterolytic hydrogen activation *via* deprotonation of a dihydride intermediate.

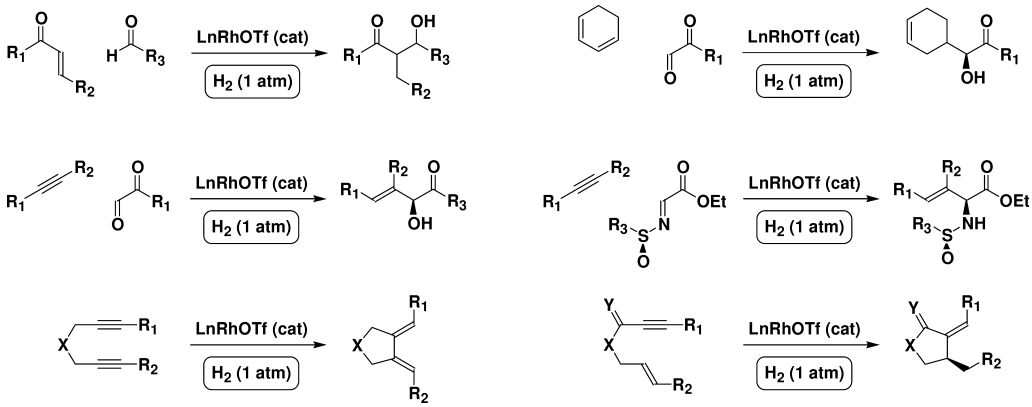

Scheme 22.3 Hydrogen-mediated C–C bond formations catalyzed by rhodium.

of developing a broad new class of catalytic reductive C–C bond formations (Scheme 22.3).

22.2
Reductive Coupling of Conjugated Enones and Aldehydes

22.2.1
Intramolecular Reductive Aldolization

Initial studies pertaining to the Rh-catalyzed aldol cycloreduction under hydrogenation conditions are consistent with the bifurcated catalytic mechanism depicted in Schemes 22.1 and 22.4 [24 a]. Catalytic hydrogenation of the indicated enone-aldehyde using the neutral complex $Rh(PPh_3)_3Cl$ provides only trace quantities of the aldol product due to competitive 1,4-reduction via conventional hydrogenation. In contrast, rhodium salts that embody increased cationic character, such as $Rh^I(COD)_2OTf$, provide almost equal proportions of aldol and 1,4-reduction products. Finally, when $Rh^I(COD)_2OTf$ is used in conjunction with substoichiometric quantities of the mildly basic additive potassium acetate, the proportion of aldol product is increased such that simple 1,4-reduction manifolds are nearly fully suppressed. The observed *syn*-diastereoselectivity suggests intermediacy of a *Z*-enolate and a Zimmerman-Traxler-type transition state. These optimized conditions

Table 22.1 Partitioning of aldolization and 1,4-reduction pathways depends critically on the use of cationic Rh-complexes and mildly basic additives.[a)]

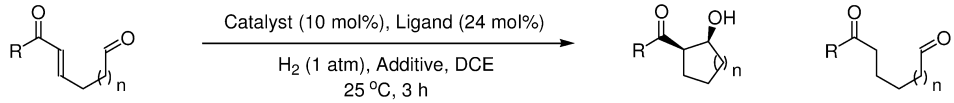

Substrate	Catalyst	Ligand	Additive (mol%)	Yield Aldol (Syn-Anti)	Yield 1,4-Reduction
n=2, R=Ph	$Rh(PPh_3)Cl$	–	–	1% (99:1)	95%
n=2, R=Ph	$Rh(COD)_2OTf$	PPh_3	–	21% (99:1)	25%
n=2, R=Ph	$Rh(COD)_2OTf$	PPh_3	KOAc (30%)	59% (58:1)	21%
n=2, R=Ph	$Rh(COD)_2OTf$	$(p\text{-}CF_3Ph)_3P$	–	57% (14:1)	22%
n=2, R=Ph	**$Rh(COD)_2OTf$**	**$(p\text{-}CF_3Ph)_3P$**	**KOAc (30%)**	**89% (10:1)**	**0.1%**
n=2, R=*p*-MeOPh	$Rh(COD)_2OTf$	$(p\text{-}CF_3Ph)_3P$	KOAc (30%)	74% (5:1)	3%
n=2, R=2-Naphthyl	$Rh(COD)_2OTf$	$(p\text{-}CF_3Ph)_3P$	KOAc (30%)	90% (10:1)	1%
n=2, R=2-thiophenyl	$Rh(COD)_2OTf$	$(p\text{-}CF_3Ph)_3P$	KOAc (30%)	76% (19:1)	2%
n=2, R=2-Furyl	$Rh(COD)_2OTf$	$(p\text{-}CF_3Ph)_3P$	KOAc (30%)	70% (6:1)	10%
n=1, R=Ph	$Rh(COD)_2OTf$	$(p\text{-}CF_3Ph)_3P$	KOAc (30%)	71% (24:1)	1%
n=2, R=CH_3	$Rh(COD)_2OTf$	$(p\text{-}CF_3Ph)_3P$	KOAc (30%)	65% (1:5)	–

a) As product ratios were found to vary with surface to volume ratio of the reaction mixture, all transformations were conducted on 1.48 mmol scale in 50 mL round bottomed flasks.

proved general for the cycloreduction of aromatic, heteroaromatic and aliphatic enone substrates to form five- and six-membered ring products (Table 22.1).

The pronounced effect of basic additives on partitioning of the aldolization and 1,4-reduction manifolds suggests that enolate-hydrogen reductive elimination pathways are disabled through deprotonation of the (hydrido)metal intermediates $LnRh^{III}X(H)_2$ or (enolato)$Rh^{III}X(H)Ln$. Thus, as proposed by Osborn and Schrock [20], deprotonation shifts the catalytic mechanism from a dihydride-based cycle to a monohydride-based cycle. In the former case, 1,4-reduction products would predominate. In the latter case, owing to the absence of (alkyl)(hydrido)rhodium intermediates, capture of the rhodium enolate through its addition to the appendant aldehyde is facilitated. The following control experiments were performed. Exposure of the simple 1,4-reduction product to the reaction conditions does not result in aldolization. Conversely, re-exposure of the aldol product to the reaction conditions does not result in retroaldolization. Finally, exposure of the substrate to standard reaction conditions in the *absence* of hydrogen does not afford products of Morita-Baylis-Hillman cyclization. For the sake of clarity, the catalytic mechanism indicated in Scheme 22.4 has been simplified. For example, equilibria involving association of the substrate to the catalyst prior to hydrogen activation are omitted, although such equilibria are known to be an important feature of the enantioselective hydrogenation of dehydroamino acids employing cationic rhodium catalysts [28] (Scheme 22.4).

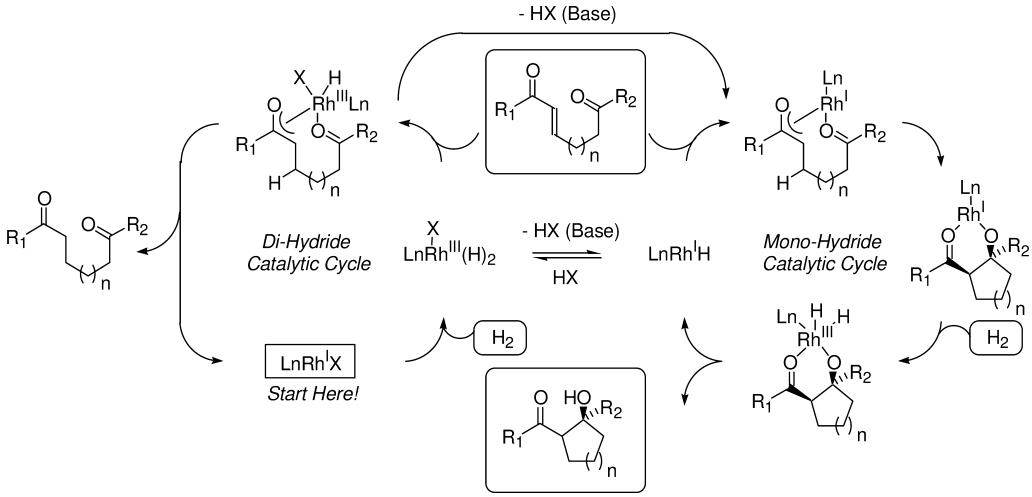

Scheme 22.4 A bifurcated mechanism accounting for the effect of basic additives.

In order to explore the scope of this hydrogen-mediated aldol addition methodology, additions to ketone acceptors were explored. Because ketones are less electrophilic than aldehydes, competitive conventional hydrogenation was anticipated to be problematic. Indeed, upon exposure of keto-enones to basic hydrogenation conditions, the formation of five- and six-membered ring aldol products is accompanied by substantial quantities of conventional hydrogenation products. As retro-aldolization does not occur upon resubmission of the aldol products to the reaction conditions, enone hydrogenation must occur prior to carbonyl addition. Nevertheless, serviceable yields of the ketone aldol products are obtained. Moreover, very high levels of *syn*-diastereoselectivity are observed, which again are attributed to the intermediacy of a *Z*-enolate and a Zimmerman-Traxler-type transition state. While aldolization proceeds readily at ambient temperature, more reproducible ratios of aldol and 1,4-reduction product are observed at 80 °C [24 b] (Table 22.2).

In order to gain further insight into the reaction mechanism, the indicated oxygen-tethered keto-enone was subjected to basic hydrogenation conditions under 1 atmos. elemental deuterium. Deuterium incorporation is observed at the former enone β-position exclusively. In addition to mono-deuterated material (81% composition), doubly-deuterated (8% composition) and non-deuterated materials (11% composition) are observed. These data suggest reversible hydrometallation in the case of keto-enone substrates. Consistent with the mechanism depicted in Scheme 22.4, deuterium is not incorporated at the α-position of the aldol product [24 b] (Scheme 22.5).

For the cycloreduction of keto-enones, competitive 1,4-reduction in response to the reduced electrophilicity of the carbonyl partner is observed. Diones are more susceptible to addition by viture of inductive effects and the relief of di-

Table 22.2 Catalytic hydrogen-mediated reductive aldol cyclization of keto-enones.

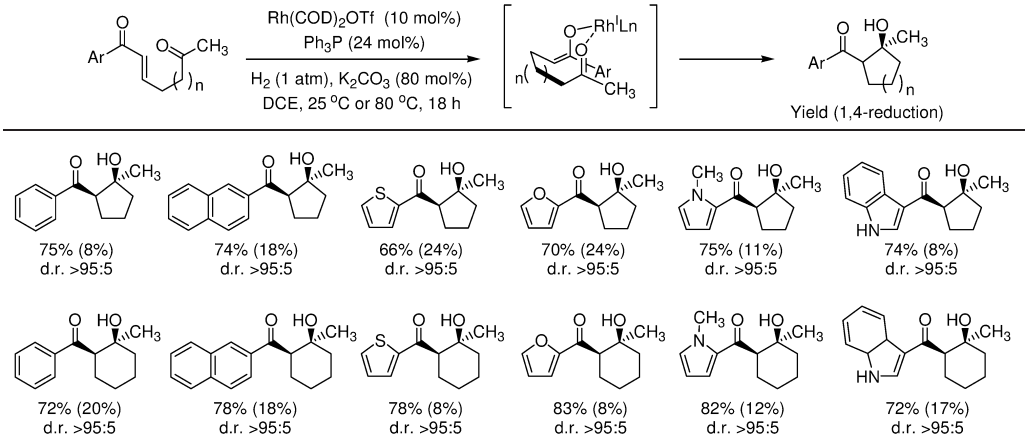

a) As product ratios were found to vary with surface-to-volume ratio of the reaction mixture, all transformations were conducted on 1.48 mmol scale in 13×100-mm sealed test tubes.

pole-dipole interactions. Accordingly, catalytic hydrogenation of dione-containing substrates affords the corresponding aldol products in good yield and with excellent *syn*-diastereoselectivity for both benzoyl- and acetyl-containing enones. Simple 1,4-reduction only accompanies formation of the strained *cis*-decalone ring system [24b] (Scheme 22.6).

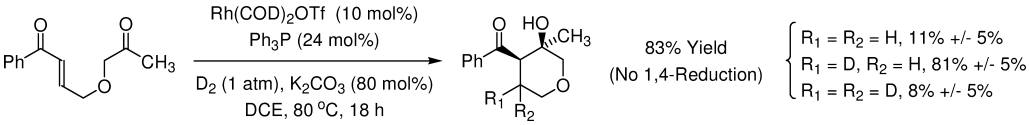

Scheme 22.5 Deuterium-labeling studies suggest reversible hydrometallation for keto-enone substrates.

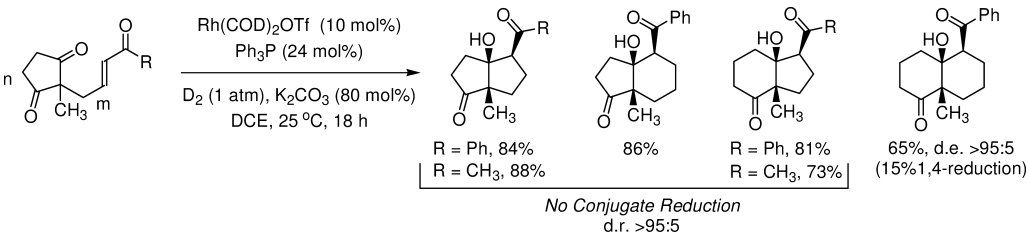

Scheme 22.6 Catalytic hydrogen-mediated reductive aldol cyclization of enone-diones.

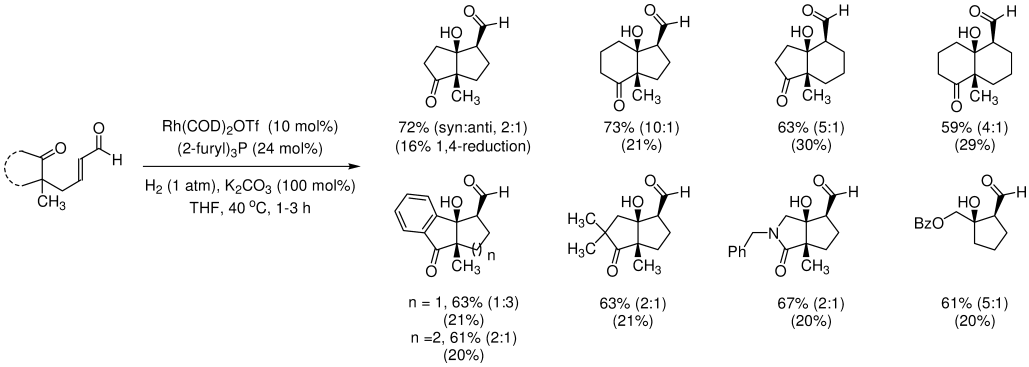

Scheme 22.7 Catalytic addition of metallo-aldehyde enolates to ketones.

Perhaps the most elusive variant of the aldol reaction involves the addition of metallo-aldehyde enolates to ketones. A single stoichiometric variant of this transformation is known [29]. As aldolization is driven by chelation, intramolecular addition to afford a robust transition metal aldolate should bias the enolate-aldolate equilibria toward the latter [30, 31]. Indeed, upon exposure to basic hydrogenation conditions, keto-enal substrates provide the corresponding cycloaldol products, though competitive 1,4-reduction is observed (Scheme 22.7) [24 d].

22.2.2
Intermolecular Reductive Aldolization

In principle, the presumed rhodium(I) enolates that occur transiently during the course of enone hydrogenation may: (i) engage in aldolization; or (ii) hydrogenolytically cleave *via* oxidative addition of hydrogen followed by reductive elimination. In principle, intermolecular capture of such hydrogenation intermediates should suffer due to increasingly competitive conventional hydrogenation. In practice, only a modest excess of vinyl ketone is required to offset conventional hydrogenation manifolds. For example, hydrogenation of phenyl vinyl ketone (PVK) (150 mol%) in the presence of aromatic and heteroaromatic aldehydes (100 mol%) provides good yields of the corresponding aldol products. As PVK is prone toward anionic polymerization, these results are especially noteworthy. Consistent with the bifurcated mechanism depicted in Scheme 22.4, the addition of potassium acetate significantly increases the yield of aldol product (Table 22.3) [24 a].

In the case of methyl vinyl ketone (MVK), similar reactivity is observed. Exposure of MVK (150 mol%) and *p*-nitrobenzaldehyde to basic hydrogenation conditions provides the corresponding aldol product in good yield, though poor diastereoselectivity is observed [24 a]. Remarkably, upon use of *tris*(2-furyl)phosphine as ligand and Li_2CO_3 as basic additive, the same aldol product is formed with high levels of *syn*-selectivity [24 e]. Addition of MVK to activated ketones such as 1-(3-bromophenyl)propane-1,2-dione is accomplished under similar con-

Table 22.3 Use of phenyl vinyl ketone (PVK) in intermolecular hydrogen-mediated reductive aldol coupling.

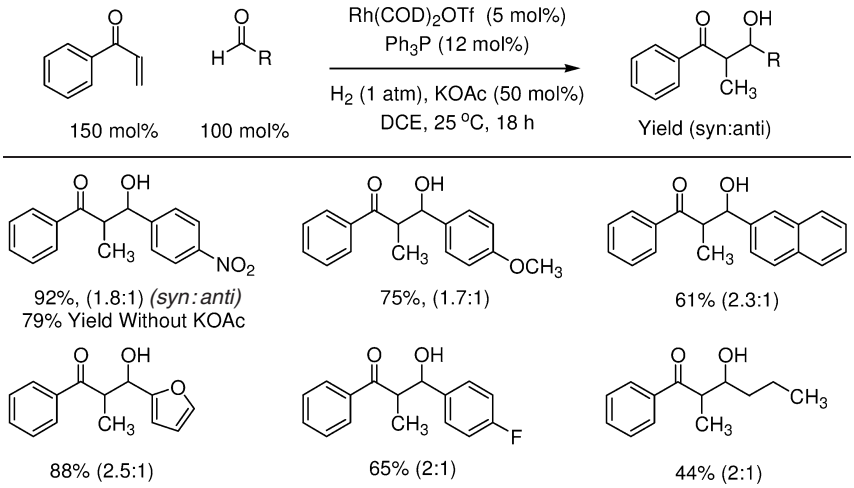

a) As product ratios were found to vary with surface-to-volume ratio of the reaction mixture, all transformations were conducted on 1.0 mmol scale in 50-mL round-bottomed flasks.

ditions [24e]. Notably, neither reduction of the nitro group or aryl bromide is observed (Scheme 22.8).]

Intermolecular cross aldolization of metallo-aldehyde enolates typically suffers from polyaldolization, product dehydration and competitive Tishchenko-type processes [32]. While such cross-aldolizations have been achieved through amine catalysis and the use of aldehyde-derived enol silanes [33], the use of aldehyde enolates in this capacity is otherwise undeveloped. Under hydrogenation conditions, acrolein and crotonaldehyde serve as metallo-aldehyde enolate precursors, participating in selective cross-aldolization with α-ketoaldehydes [24c]. The resulting β-hydroxy-γ-ketoaldehydes are highly unstable, but may be trapped *in situ* through the addition of methanolic hydrazine to afford 3,5-disubstituted pyridazines (Table 22.4).

To corroborate the proposed mechanism, the catalytic reductive aldol coupling of acrolein with phenyl glyoxal monohydrate was performed under 1 atmos. elemental deuterium. Exposure of the aldol product to excess hydrazine *in situ* results in formation of the pyridazine, which incorporates precisely one deuterium atom in a manner consistent with the general mechanism proposed in Scheme 22.4 (Scheme 22.9).

Thus far, the use of acrylates and related acyl derivatives as nucleophilic partners in hydrogen-mediated reductive aldol coupling has been unsuccessful due to competitive conventional hydrogenation. Although the mechanistic basis of these results remains unclear, it may be speculated that for acrylates and struc-

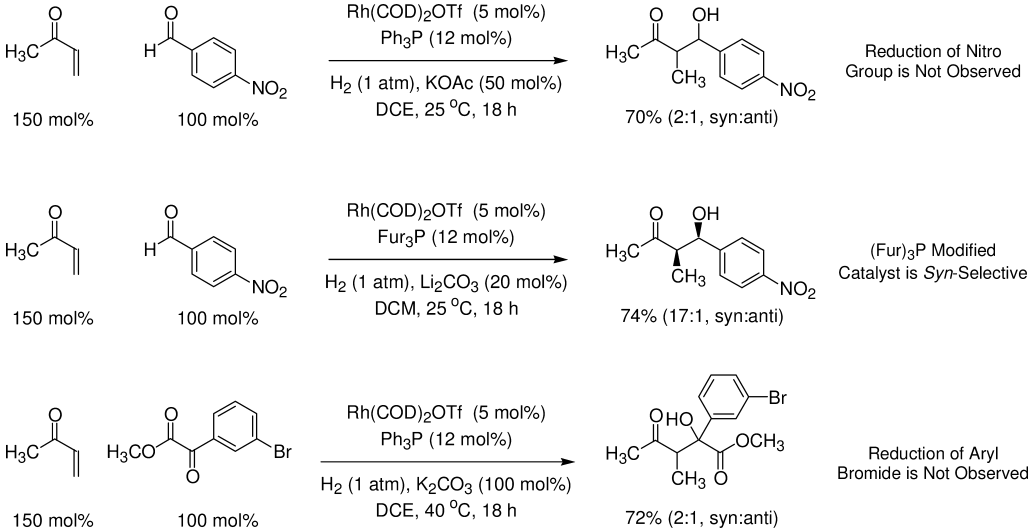

a) As product ratios were found to vary with surface-to-volume ratio of the reaction mixture, all transformations were conducted on 1.0 mmol scale in 50-mL round-bottomed flasks.

Scheme 22.8 Use of methyl vinyl ketone (MVK) in intermolecular hydrogen-mediated reductive aldol coupling.[a)]

Table 22.4 Use of acrolein and crotonaldehyde in intermolecular hydrogen-mediated reductive aldol coupling.

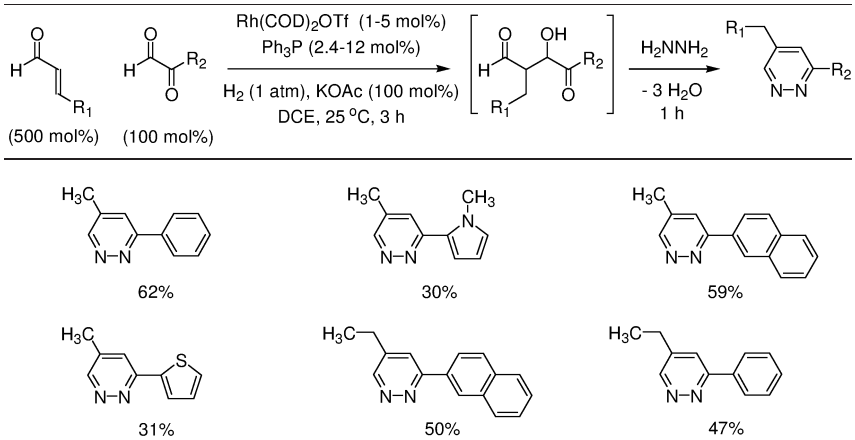

a) As product ratios were found to vary with surface-to-volume ratio of the reaction mixture, all transformations were conducted on 1.0 mmol scale in 50-mL round-bottomed flasks.

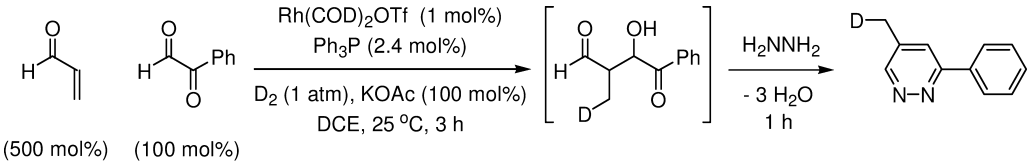

a) As product ratios were found to vary with surface-to-volume ratio of the reaction mixture, all transformations were conducted on 1.0 mmol scale in 50-mL round-bottomed flasks.

Scheme 22.9 Intermolecular reductive aldol coupling of acrolein and phenyl glyoxal under a D_2 atmosphere.[a)]

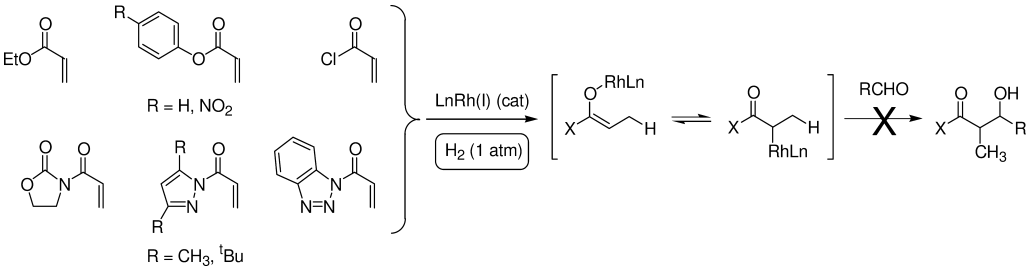

Scheme 22.10 Attempted reductive aldol coupling of ethyl acrylate and related acyl derivatives.

tural relatives possessing heteroatom substitution at the acyl position, the haptomeric equilibrium pertaining to the *O*-bound and *C*-bound forms of the rhodium(I) enolate is biased toward the latter. As aldol addition should occur by way of the *O*-bound enolate in accordance with the Zimmerman-Traxler model, the intervention of a *C*-bound enolate may diminish the rate of aldolization to the point that competitive conventional hydrogenation predominates.

22.3
Reductive Coupling of 1,3-Cyclohexadiene and α-Ketoaldehydes

Given the structural homology of conjugated enones and 1,3-dienes, the reductive coupling of 1,3-cyclohexadiene and phenyl glyoxal was examined under hydrogenation conditions [22]. Optimization studies again reveal the requirement of cationic rhodium catalysts. Whereas hydrogenation of 1,3-cyclohexadiene and phenyl glyoxal using Wilkinson's catalyst provides products of simple reduction, a 61% yield of reductive coupling product is obtained using $Rh(COD)_2OTf$ with PPh_3 as ligand. When $(p\text{-}CH_3OPh)_3P$ is employed as ligand, the yield of coupling product increases to 77%. Related cationic complexes, such as $Rh(COD)_2BF_4$, exhibit similar efficiencies when used in conjunction with $(p\text{-}CH_3OPh)_3P$. Under optimized conditions, the catalytic reductive coupling of 1,3-cyclohexadiene with di-

Table 22.5 Catalytic reductive coupling of 1,3-cyclohexadiene with alkyl, aryl and heteroaryl α-ketoaldehydes.

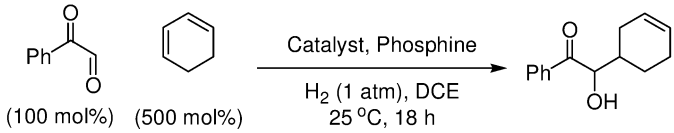

Entry	Catalyst (mol%)	Ligand (mol%)	Yiedl (%)
1	$Rh(PPh_3)_3Cl$ (10%)	–	–
2	$Rh(COD)_2OTf$ (10%)	Ph_3P (20%)	61
3	$Rh(COD)_2OTf$ (10%)	$(p\text{-}CF_3Ph)_3P$ (20%)	24
4	$Rh(COD)_2OTf$ (10%)	$(p\text{-}CH_3OPh)_3P$ (20%)	77
5	$Rh(COD)_2BF_4$ (10%)	$(p\text{-}CH_3OPh)_3P$ (20%)	79
6	**$Rh(COD)_2OTf_4$ (5%)**	**$(p\text{-}CH_3OPh)_3P$ (10%)**	**76**

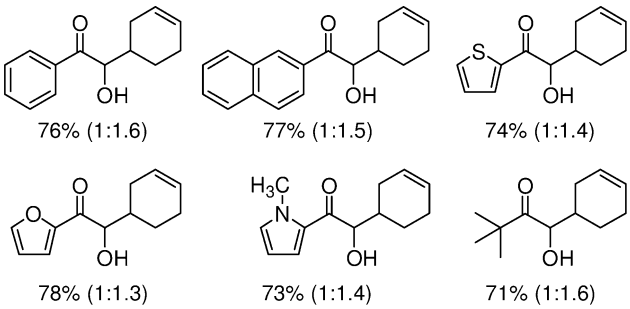

verse α-ketoaldehydes was examined. Aryl, heteroaryl and aliphatic α-ketoaldehydes provide reductive coupling products in good yield. Notably, basic additives are not required, suggesting that heterolytic hydrogen activation may not be operative (Table 22.5).

Deuterium-labeling studies reveal that the reductive coupling of 1,3-cyclohexadiene with α-ketoaldehydes occurs through a mechanism very different than that postulated for related enone-aldehyde couplings. Reductive coupling of 1,3-cyclohexadiene with 2-naphthyl glyoxal under an atmosphere of D_2(g) results in the incorporation of precisely two deuterium atoms as an equimolar distribution of 1,2- and 1,4-regioisomers. The relative stereochemistry of the deuterated materials could not be assigned (Scheme 22.11).

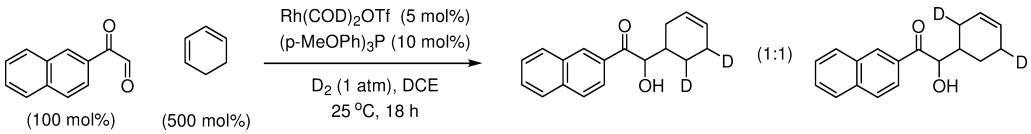

Scheme 22.11 Reductive coupling of 1,3-cyclohexadiene and 2-naphthyl glyoxal under an atmosphere of D_2(g).

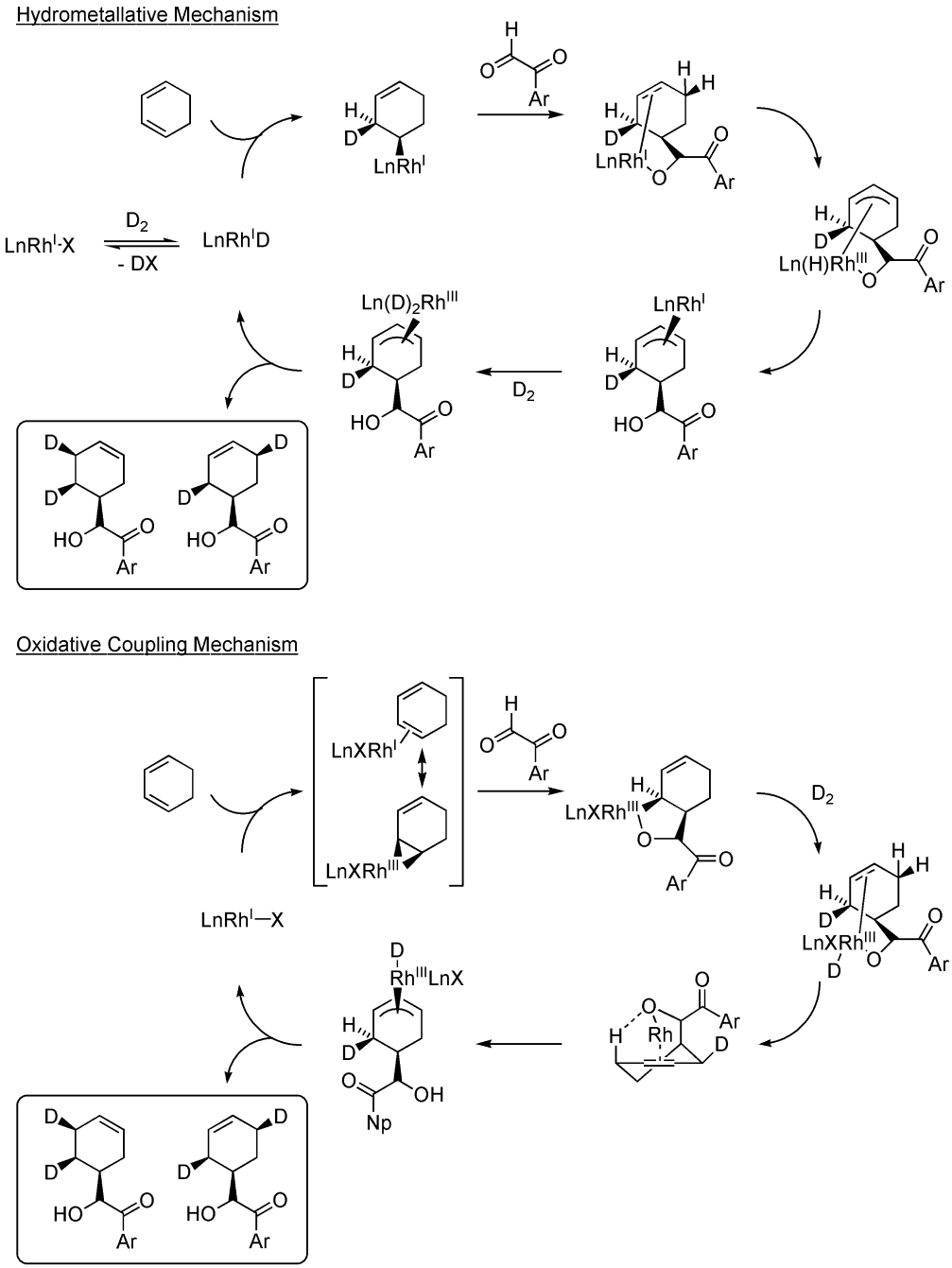

Scheme 22.12 Possible mechanisms for the reductive coupling of 1,3-cyclohexadiene and 2-naphthyl glyoxal under an atmosphere of D_2(g).

The mechanism initially proposed involves diene hydrometallation from a monohydride derived via heterolytic hydrogen activation (Scheme 22.12, upper). Here, diene deuterometallation gives rise to a homo-allyl rhodium intermediate, which engages in carbonyl addition to afford a rhodium alkoxide. The indicated regiochemistry of C–C bond formation is consistent with that observed by Loh in the nickel-catalyzed reductive coupling of 1,3-cyclohexadiene with aldehydes [9e]. Additionally, as observed by Mori, the presence of 1,3-cyclohexadiene induces 1,4-regiochemistry in nickel-promoted diene-aldehyde cyclizations [8b]. Allylic C–H insertion provides a rhodium(III) π-allyl, which upon O–H reductive elimination gives rise to a rhodium(I) π-allyl. Similar allylic C–H insertions are observed in metal-catalyzed alkene isomerization [34]. Finally, oxidative addition of elemental deuterium followed by C–D reductive elimination completes the catalytic cycle. The intermediacy of rhodium a π-allyl is required to account for the incorporation of precisely two deuterium atoms as an equimolar distribution of 1,2- and 1,4-regioisomers (Scheme 22.12, upper).

A related mechanistic proposal involves diene-glyoxal oxidative coupling (Scheme 22.12, lower). Here, complexation by low-valent rhodium(I) confers nucleophilic character to the bound diene *via* backbonding, as suggested by the Dewar-Chatt-Duncanson model for alkene coordination [35]. For low-valent *early* transition metals, such "back-bonding" is driven by the stability associated with a d^0-electronic configuration. For example, as demonstrated by the Kulinkovich reaction, complexation of olefins by Ti(II) causes them to behave as vicinal dianions: Ti(II)(olefin) $\leftrightarrow$ Ti(IV)(metallocyclopropane) [36]. For *late* transition metals, the driving force associated with attaining a noble gas electronic configuration is absent, perhaps accounting for the requirement of highly activated electrophilic partners such as α-ketoaldehydes. In any case, addition of the diene to the glyoxal provides the formal product of oxidative coupling. This oxarhodacycle may react with deuterium via sigma bond metathesis to afford a rhodium alkoxide, which abstracts an allylic hydrogen to provide a rhodium π-allyl complex. Subsequent C–D reductive elimination delivers the dideuterated products as an equimolar distribution of regioisomers (Scheme 22.12, lower). Recently, this diene-glyoxal coupling was performed under an atmosphere of HD(g) as the terminal reductant. The coupling product was found to incorporate a single molecule of deuterium, distributed over the same three carbons found when D_2(g) was used as reductant. These data disqualify the initially disclosed hydrometallative mechanism, and strongly support the latter mechanism involving direct oxidative coupling.

22.4 Reductive Coupling of Conjugated Enynes and Diynes with Activated Aldehydes and Imines

The reductive coupling of 1,3-cyclohexadiene and α-ketoaldehydes, which occurs without over-reduction of the olefinic product, suggests the feasibility of utilizing more highly unsaturated pronucleophiles in the form of 1,3-enynes. In the

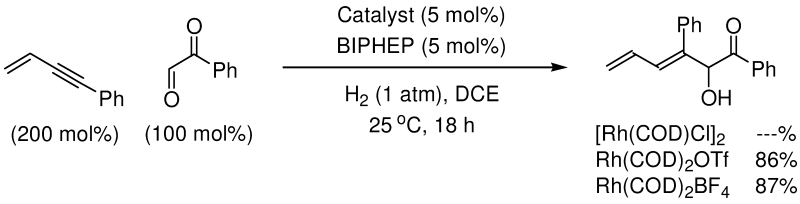

Scheme 22.13 Reductive coupling of 1-phenyl but-3-en-1-yne with phenyl glyoxal.

event, the reaction conditions optimized for the cyclohexadiene-α-ketoaldehyde couplings, which employ (p-MeOPh)$_3$P as ligand, proved ineffective at promoting the coupling of 1-phenylbut-3-en-1-yne and phenyl glyoxal. However, under otherwise identical conditions, the use of bidentate ligands such as BIPHEP provides the products of reductive coupling in excellent yield. Under optimized conditions, the coupling proceeds smoothly to afford diene-containing products as single regio- and stereoisomers. Over-reduction of the diene-containing products is not observed. Presumably, upon complete consumption of glyoxal, excess enyne nonproductively coordinates rhodium, dramatically retarding the rate of any further reduction. As for the diene couplings, basic additives are not required. Additionally, reductive coupling fails upon use of neutral Rh(I) precatalysts, such as [Rh(COD)Cl]$_2$ (Scheme 22.13, Table 22.6).

Catalytic reductive coupling of 1-phenyl but-3-en-1-yne with phenyl glyoxal conducted under 1 atmos. elemental deuterium provides the *mono*-deuterated product in 85% yield. It is instructive to compare hydrometallative and oxidative coupling mechanisms involving both heterolytic and homolytic deuterium activation. For the hydrometallative mechanism involving heterolytic deuterium activation, direct alkyne deuterometallation to afford the vinyl rhodium intermediate is followed by carbonyl addition and hydrogenolytic cleavage of the resulting

Table 22.6 Reductive coupling of assorted 1,3-enynes with alkyl, aryl and heteroaryl α-ketoaldehydes.

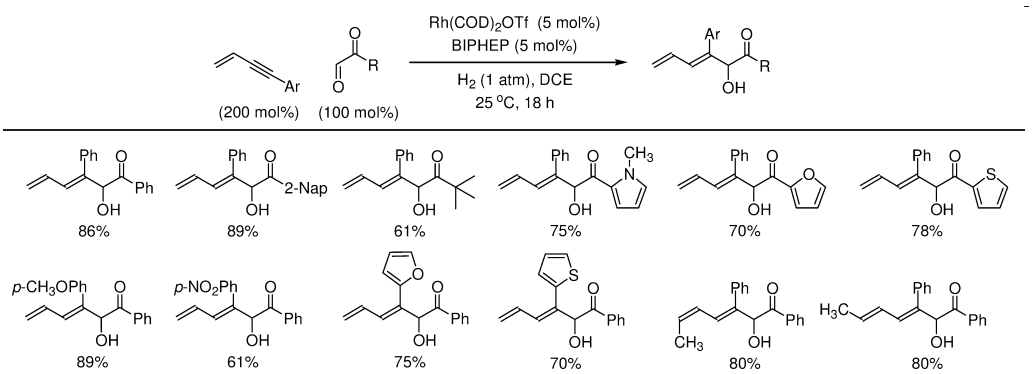

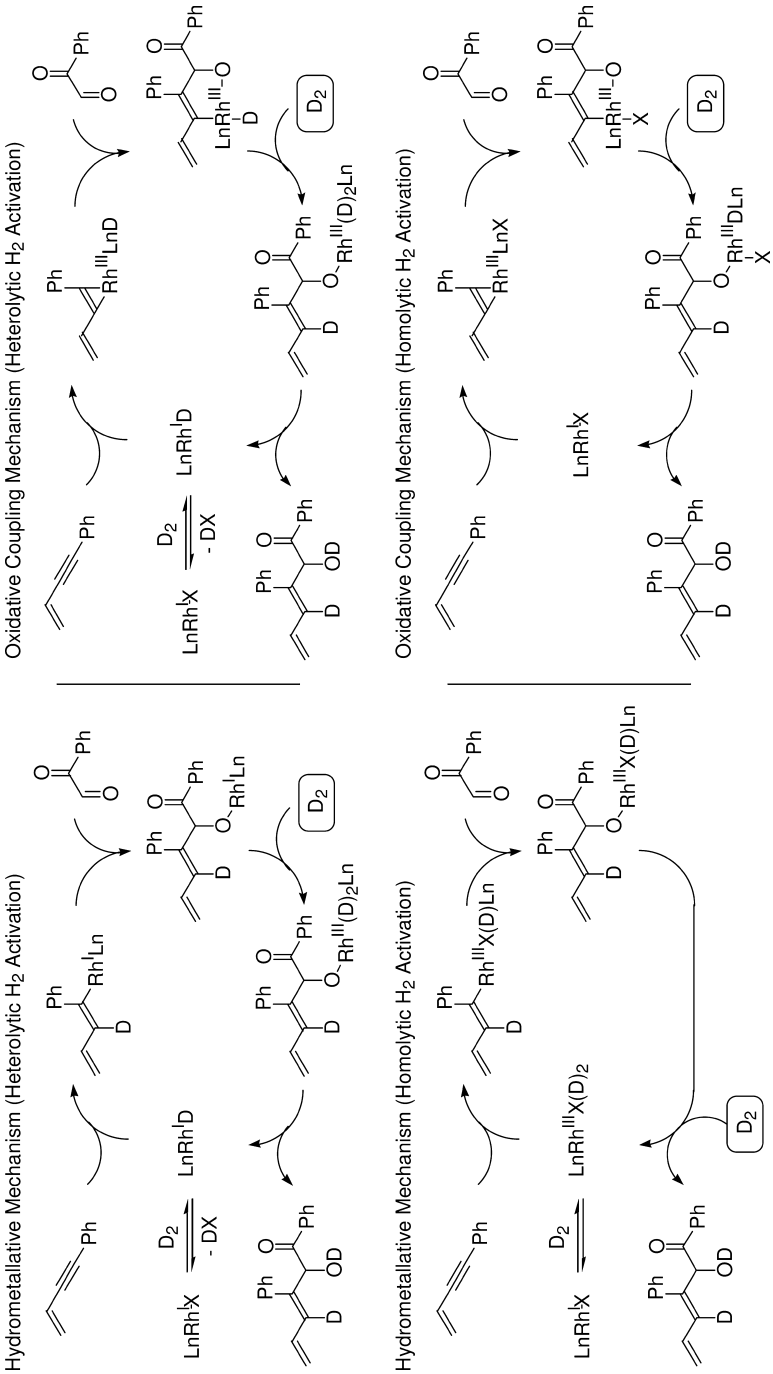

Scheme 22.14 Plausible mechanisms for the reductive coupling of 1-phenyl but-3-en-1-yne with phenyl glyoxal under an atmosphere of D_2(g).

Rh(I)-alkoxide. Notably, this mechanism requires deuterometallation to occur with complete regioselection (Scheme 22.14, top-left). The corresponding hydrometallative mechanism involving homolytic deuterium activation also requires completely regioselective deuterometallation. Moreover, carbonyl addition must compete favorably with C–D reductive elimination (Scheme 22.14, bottom-left). A mechanism involving heterolytic hydrogen activation followed by oxidative coupling of the reactants is plausible. Here, C–D reductive elimination of the resulting (hydrido)Rh(III)-oxametallocyclopentene followed by hydrogenolytic cleavage of rhodium alkoxide completes the catalytic cycle (Scheme 22.14, top-right). Finally, direct oxidative coupling of the reactants with subsequent hydrogenolytic cleavage of the resulting metallocycle may be envisaged. This latter mechanism requires deuterium activation by a rhodium(III) intermediate. An increasing body of evidence supports participation of organorhodium(III) complexes in σ-bond metathesis pathways [37], including reactions with hydrogen [37c]. In the case of the hydrometallative mechanisms, C–H bond formation precedes C–C bond formation. In the case of the oxidative coupling mechanisms, the converse is true. The oxidative coupling mechanism better accounts for the regiochemistry of reductive coupling and is preferred on the basis of related mechanistic studies (*vide supra*). In principle, it should be possible to discriminate between heterolytic and homolytic hydrogen activation modes *via* H_2–D_2 and HD isotope crossover experiments. However, rapid exchange of the hydroxylic protons and deuterons under the reaction conditions renders this prospect untenable (Scheme 22.14).

1,3-Diynes also participate in highly regio- and stereoselective reductive couplings to aryl, heteroaryl and aliphatic glyoxals under catalytic hydrogenation conditions [26b]. Unlike the corresponding reaction of 1,3-enynes, both *mono*- and *bis*(phosphines) may serve as ligands. Consistent with the requirement of cationic rhodium(I) catalysts, $Rh(COD)_2OTf$ and $Rh(COD)_2BF_4$ are viable catalysts, while $Rh(PPh_3)_3Cl$ is not. Remarkably, formation of the highly unsaturated 1,3-enyne products is not accompanied by over-reduction. As previously stated, it would appear that upon complete consumption of glyoxal, excess enyne nonproductively coordinates rhodium, retarding the rate of further reduction. Reductive coupling performed under an atmosphere of D_2 provides the indicated mono-deuterated product. This result may be interpreted on the basis of the mechanisms outlined in Scheme 22.14 (Scheme 22.15).

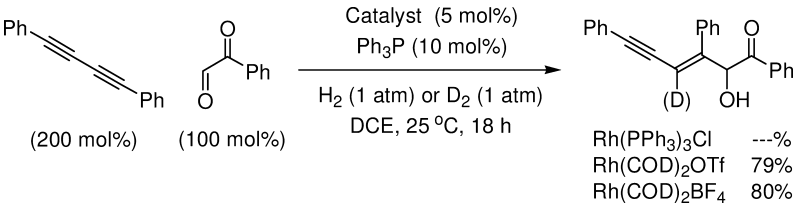

Scheme 22.15 Reductive coupling of diphenylbutadiyne with phenyl glyoxal.

A highly enantioselective variant of this transformation has been developed using the commercially available chiral *bis*(phosphine) (*R*)-Cl-MeO-BIPHEP. Optimization studies pertaining to the enantioselective transformation reveal that high levels of asymmetric induction are critically dependent upon the dihedral angle of the diphenylphosphino moieties of the ligand. Under optimized conditions, coupling products are produced in 71–77% yield and 86–95% enantiomeric excess. Notably, highly enantioselective C–C bond formation is achieved at ambient temperature and pressure (Table 22.7).

Under optimum conditions identified for enantioselective coupling, non-symmetric 1,3-diynes react with marked levels of regioselectivity. Specifically, for 1-phenyl-4-alkyl 1,3-diynes, coupling occurs preferentially at the aromatic terminus (Table 22.8). Competition experiments provide some insight into the mechanistic basis for such regioselectivity. Catalytic hydrogenation of phenyl glyoxal in the presence of equimolar quantities of 1,4-diphenylbutadiene and 1,4-diphenylbut-3-en-1-yne results in coupling to the more highly unsaturated enyne partner. Similarly, catalytic hydrogenation of phenyl glyoxal in the presence of equimolar quantities of 1,4-diphenylbut-3-en-1-yne and 1,4-diphenylbutadiyne

Table 22.7 Enantioselective catalytic reductive coupling of 1,3-diynes with alkyl, aryl and heteroaryl α-ketoaldehydes.

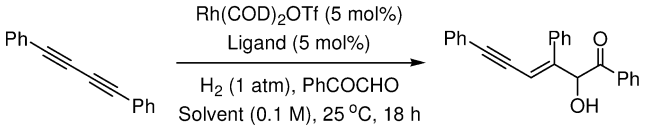

Entry	Ligand	Solvent	Yield (%)	e.e. (%)
1	(*R*)-BINAP	DCE	72	47
2	(*R*)-Phanephos	DCE	79	67
3	(*R*)-Cl-OMe-BIPHEP	DCE	74	76
4	(*R*)-Cl-OMe-BIPHEP	EtOH	69	80
5	(*R*)-Cl-OMe-BIPHEP	THF	67	82
6	**(*R*)-Cl-OMe-BIPHEP**	**PhH**	**74**	**91**

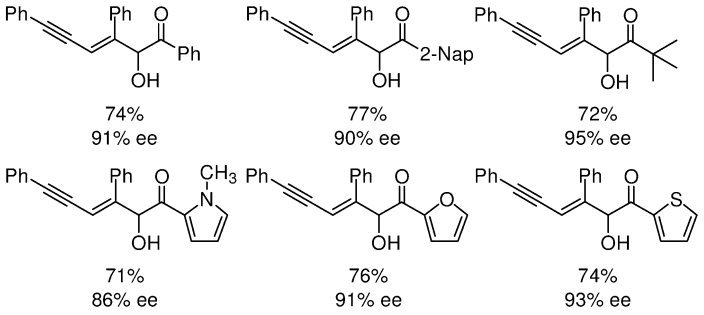

Table 22.8 Regioselective reductive coupling of non-symmetric 1,3-diynes to various α-ketoaldehydes.

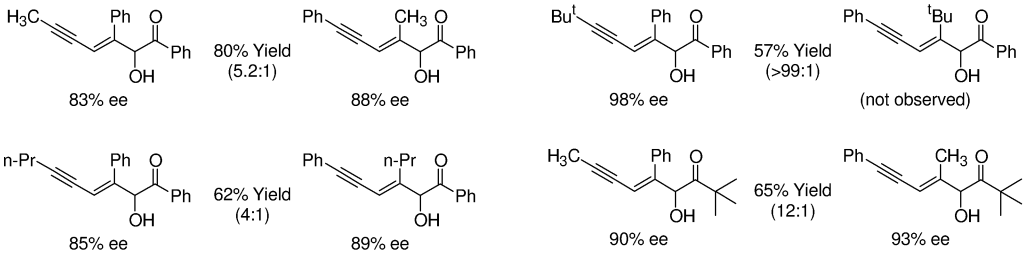

results in coupling to the more highly unsaturated diyne partner. Chemoselective coupling to the more highly unsaturated pronucleophile suggests preferential coordination of low-valent rhodium to the most π-acidic reactant. Moreover, for non-symmetric 1,3-diynes, regioselective C–C bond formation occurs at the terminus of the diyne that embodies the lowest LUMO energy. Hence, the chemo- and regioselectivity of reductive coupling may be explained by the Dewar-Chatt-Duncanson model for alkyne coordination [35] – that is, coordination of low-valent rhodium is driven by backbonding, with nucleophilic character developing at positions where backbonding occurs most effectively (Scheme 22.16).

Rhodium-catalyzed hydrogenation of 1,3-enynes and 1,3-diynes in the presence of ethyl (*N*-*tert*-butanesulfinyl)iminoacetate and ethyl (*N*-2,4,6-triisopropylbenzenesulfinyl)iminoacetate, respectively, results in reductive coupling to afford unsaturated α-amino acid esters in good to excellent yields with exceptional levels of stereocontrol [26 c] (Tables 22.9 and 22.10). Remarkably, the reductive coupling of non-symmetric 1,3-diynes to iminoacetates occurs with complete levels of regioselectivity. Further hydrogenation of the diene side chain using Wilkinson's catalyst provides the corresponding β,γ-unsaturated amino acid esters. Exhaustive hydrogenation of both the diene- and enyne-containing side chains

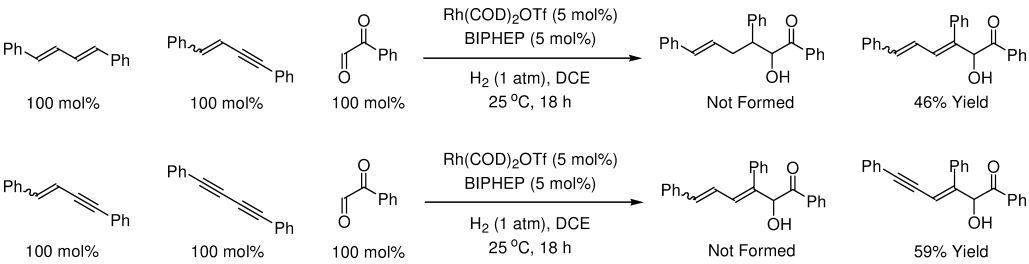

Scheme 22.16 Competition experiments reveal reductive coupling occurs chemoselectively with the strongest π-acid.

Table 22.9 Reductive coupling of 1,3-enynes with ethyl (*N-tert*-butanesulfinyl)iminoacetate.

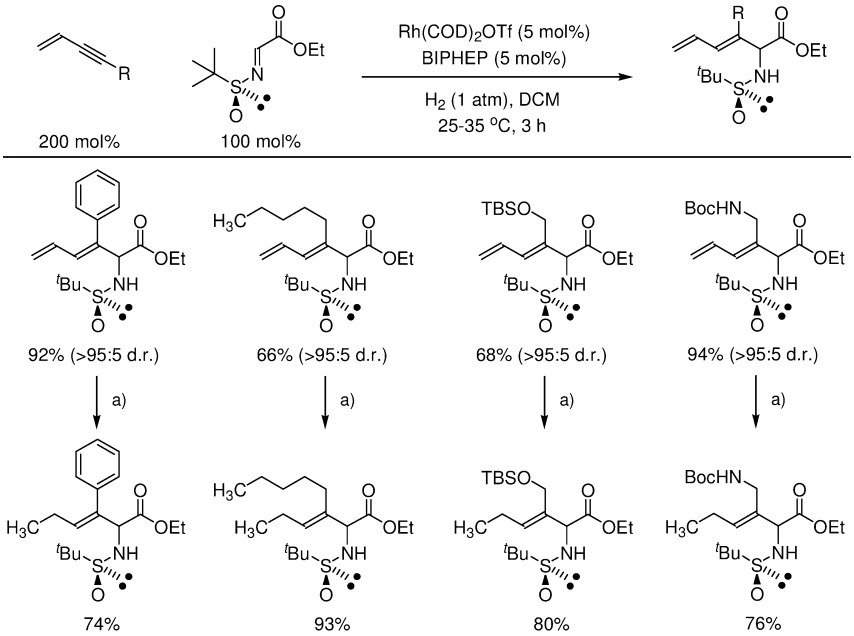

a) $Rh(PPh_3)_3Cl$ (10 mol%), H_2 (1 atm), toluene, 25 °C, 18 h.

Table 22.10 Reductive coupling of 1,3-diynes with ethyl (*N*-2,4,6-triisopropylbenzenesulfinyl)iminoacetate.

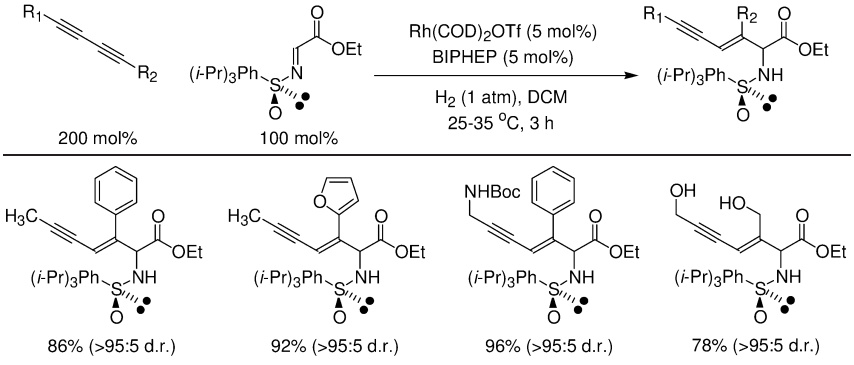

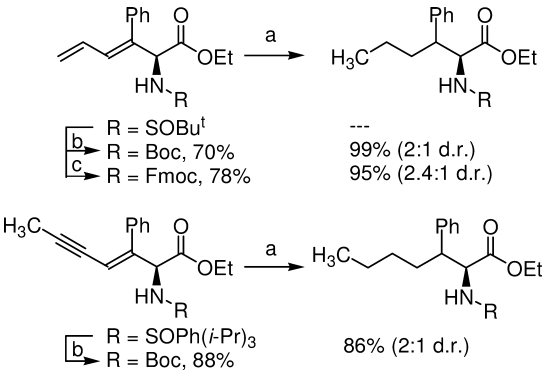

Scheme 22.17 Exhaustive hydrogenation of diene- and enyne-containing reductive coupling products using Crabtree's catalyst.

using Crabtree's catalyst also proceeds readily. However, the *N-tert*-butanesulfinyl residue must be exchanged for a carbamate protecting group (Scheme 22.17).

22.5 Reductive Cyclization of 1,6-Diynes and 1,6-Enynes

Hydrogenation of 1,6-diynes using cationic rhodium precatalysts promotes reductive cyclization to afford 1,2-dialkylidenecycloalkane products. As for all hydrogen-mediated C–C bond formations described in this account, cationic rhodium precatalysts are required. Whereas reductive cyclization proceeds readily using $Rh(COD)_2OTf$ and $Rh(COD)_2BF_4$, the neutral precatalyst $[Rh(COD)Cl]_2$ is ineffective (Scheme 22.18) [27, 38]. Under optimized conditions, reductive cyclization proceeds smoothly across a range of 1,6-diynes. Near-identical hydrogenation conditions are effective for the reductive cyclization of 1,6-enynes [39, 40]. Notably, conformationally predisposed substrates possessing geminal substitution in the tether are not necessary (Table 22.11).

Enantioselective hydrogenation of 1,6-enynes using chirally modified cationic rhodium precatalysts enables enantioselective reductive cyclization to afford alkylidene-substituted carbocycles and heterocycles [27b, 41, 42]. Good to excellent yields and exceptional levels of asymmetric induction are observed across a structurally diverse set of substrates. For systems that embody 1,2-disubstituted alkenes, competitive β-hydride elimination *en route* to products of cycloisomerization is observed. However, related enone-containing substrates cannot engage in β-hydride elimination, and undergo reductive cyclization in good yield (Table 22.12).

The products of reductive cyclization incorporate two non-exchangeable hydrogen atoms. Homolytic and heterolytic hydrogen activation pathways may now be discriminated on the basis of hydrogen-deuterium crossover experiments. Reductive cyclization of the indicated nitrogen-tethered enyne under a mixed atmosphere

Table 22.11 Reductive cyclization of assorted 1,6-diynes and 1,6-enynes.

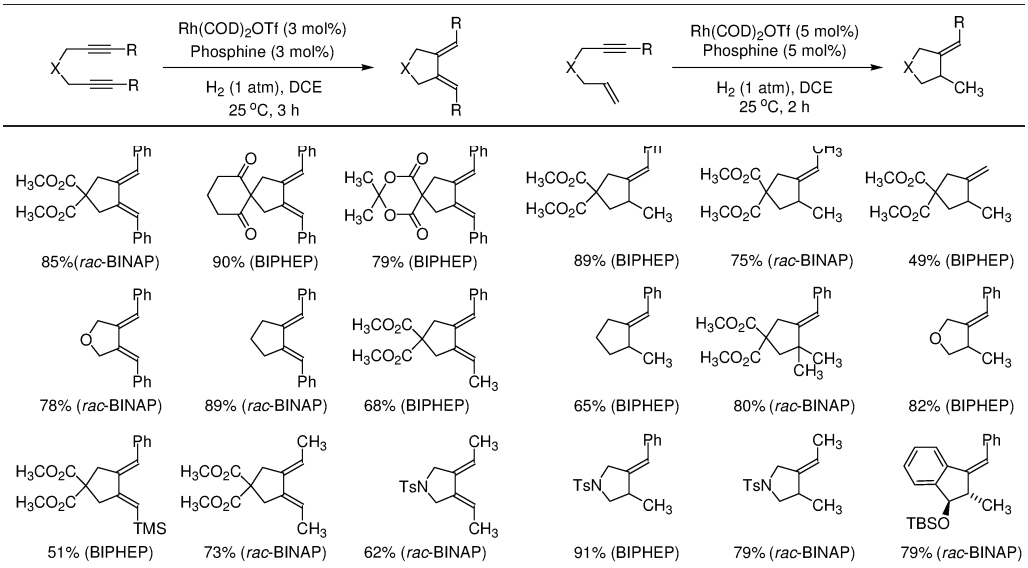

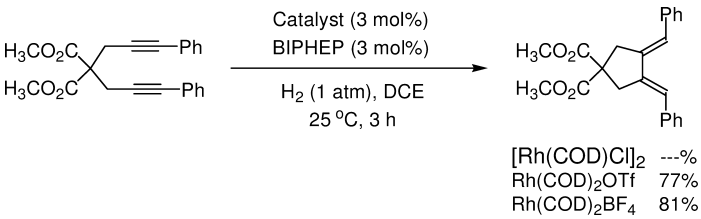

Scheme 22.18 Reductive cyclization of 1,6-diynes.

of H_2 and D_2 or under an atmosphere of DH does not provide crossover products, in accordance with homolytic hydrogen activation. Interestingly, exposure of related systems incorporating a *cis*-1,2-disubstituted alkene to identical conditions under a D_2 atmosphere does not induce reductive cyclization. Rather, products of cycloisomerization are formed. A hydrometallative mechanism for cycloisomerization would be initiated by D_2 oxidative addition and propagated by rhodium hydrides derived upon β-hydride elimination from intermediate **A**. Deuterium incorporation should occur in the first turnover of the catalytic cycle, yet deuterium incorporation is not observed, even at stoichiometric catalyst loadings. The extent of deuterium incorporation for the isotopically labeled reaction products is determined by electrospray ionization-mass spectrometry (ESI-MS) analysis with isotopic correction and is corroborated by ^{1}H-NMR analysis (Scheme 22.19).

The acquisition of cycloisomerization products without deuterium incorporation is inconsistent with a hydrometallative mechanism. Furthermore, the ab-

Table 22.12 Enantioselective reductive cyclization of 1,6-enynes.

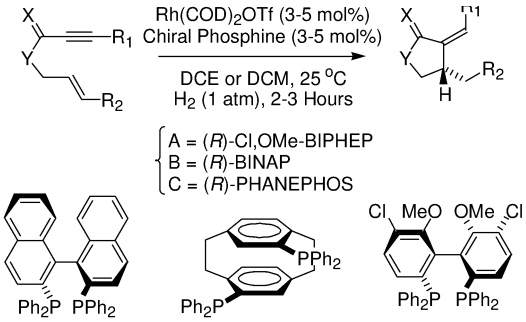

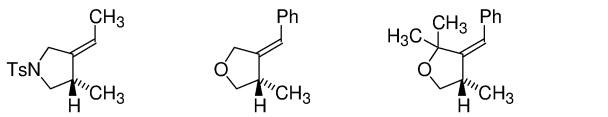

A: 69%, 94% e.e.
B: 79%, 93% e.e.
C: multiple products

A: 84%, 95% e.e.
B: 80%, 97% e.e.
C: multiple products

A: 85%, 84% e.e.
B: 76%, 82% e.e.
C: multiple products

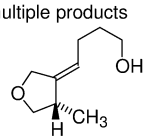

A: 77%, 95% e.e.
B: 75%, 95% e.e.
C: multiple products

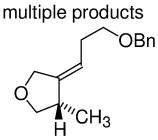

A: 75%, 98% e.e.
B: 77%, 98% e.e.
C: multiple products

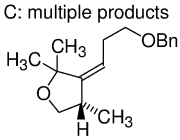

A: 82%, 98% e.e.
B: 64%, 98% e.e.
C: multiple products

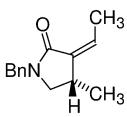

A: 40%, 26% e.e.
B: 24%, 10% e.e.
C: 73%, 91% e.e.

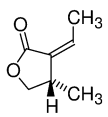

A: 89%, 6% e.e.
B: 79%, 20% e.e.
C: 73%, 94% e.e.

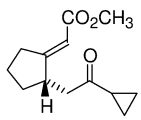

A: 68%, 98% e.e.
B: 63%, 90% e.e.
C: complete reduction

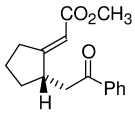

A: 78%, 88% e.e.
B: 66%, 96% e.e.
C: complete reduction

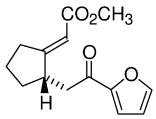

A: 65%, 95% e.e.
B: 72%, 96% e.e.
C: complete reduction

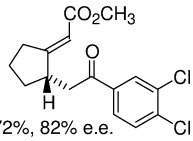

A: 72%, 82% e.e.
B: 63%, 94% e.e.
C: complete reduction

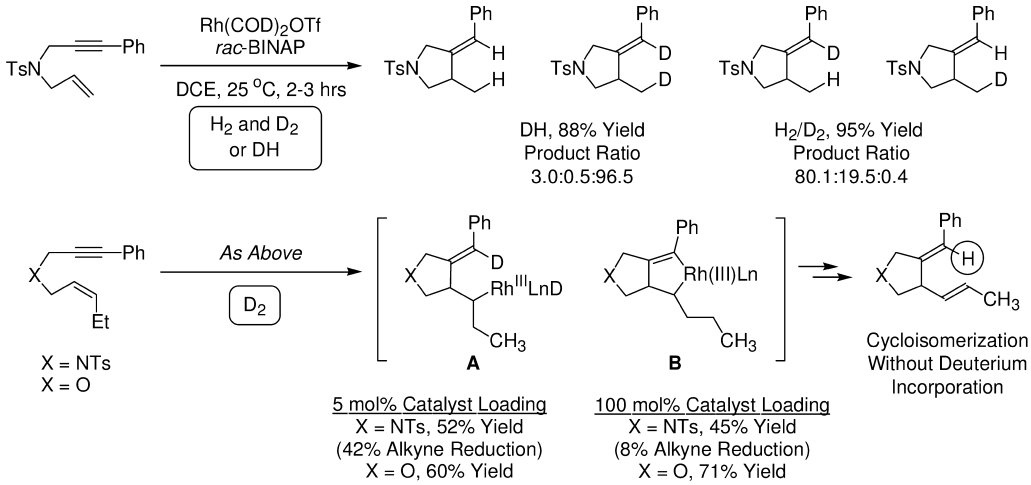

Scheme 22.19 Mechanistic studies involving hydrogen-deuterium crossover experiments, along with the observance of non-conjugated cycloisomerization products, suggest that rhodium(III) metallocyclopentene formation occurs in advance of hydrogen activation.

sence of conjugated cycloisomerization products suggests β-hydride elimination from metallocycle **B**. If indeed oxidative cyclization occurs initially to form metallocycle **B** [17], subsequent hydrogenolytic cleavage must occur via: (i) hydrogen oxidative addition or (ii) hydrogen activation via σ-bond metathesis [37c]. Whereas hydrogen oxidative addition to a Rh(III) metallocycle would afford a Rh(V) intermediate, hydrogen activation via σ-bond metathesis would not. In either case, it would appear that C–C bond formation occurs in advance of hydrogen activation. Hydrogen oxidative addition followed by rhodium(V) metallocycle formation is unlikely and, to our knowledge, without precedent. Finally, it is worth noting that hydrogen oxidative addition is rate-determining for asymmetric hydrogenations catalyzed by cationic rhodium complexes, which suggests that the oxidative cyclization manifold may compete favorably with hydrogen oxidative addition [28].

22.6 Conclusion

From the seminal studies of Sabatier [43] and Adams [44] to the more recent studies of Knowles [45] and Noyori [46], catalytic hydrogenation has been regarded as a method of reduction. The results herein demonstrate the feasibility of transforming catalytic hydrogenation into a powerful and atom-economical method for reductive C–C bond formation. Given the profound socioeconomic impact of alkene hydroformylation, the development of catalysts for the hydrogen-mediated

coupling of basic feedstocks, such as α-olefins and styrenes with aldehyde partners, represents a paramount scientific challenge. The mechanistic underpinnings of these transformations have begun to unfold. Hydrogen-mediated enone couplings require mild basic additives and, hence, likely involve heterolytic hydrogen activation by way of an intermediate dihydride. In contrast, the mechanistic data linked to the reductive coupling of conjugated dienes, enynes, and diynes to α-ketoaldehydes and related iminoacetates, along with data pertaining to the reductive cyclizations of 1,6-diynes and 1,6-enynes, suggest oxidative coupling to form metallacyclic intermediates which are then hydrogenolytically cleaved. This oxidative coupling-hydrogenolysis motif should play a key role in the design of related hydrogen-mediated couplings. It is the authors hope that the emergent mechanistic principles gleaned from these initial studies will ultimately spawn a broad new class of hydrogen-mediated C–C couplings.

Acknowledgments

The authors acknowledge the Robert A. Welch Foundation (F-1466), the Research Corporation Cottrell Scholar Award, the National Science Foundation CAREER Award, the Alfred P. Sloan Foundation, the Camille and Henry Dreyfus Foundation, Eli Lilly, and Merck.

Abbreviations

MVK methyl vinyl ketone
PVK phenyl vinyl ketone

References

1 For use of alkenes as nucleophilic partners in catalytic reductive couplings, see: (a) N.M. Kablaoui, S.L. Buchwald, *J. Am. Chem. Soc.* **1995**, *117*, 6785; (b) W.E. Crowe, M.J. Rachita, *J. Am. Chem. Soc.* **1995**, *117*, 6787; (c) N.M. Kablaoui, S.L. Buchwald, *J. Am. Chem. Soc.* **1996**, *118*, 3182.

2 For use of alkynes as nucleophilic partners in catalytic hydrometallative reductive couplings to aldehydes, see: (a) E. Oblinger, J. Montgomery, *J. Am. Chem. Soc.* **1997**, *119*, 9065; (b) X.Q. Tang, J. Montgomery, *J. Am. Chem. Soc.* **1999**, *121*, 6098; (c) W.-S. Huang, J. Chen, T.F. Jamison, *Org. Lett.* **2000**, *2*, 4221; (d) E.A. Colby, T.F. Jamison, *J. Org. Chem.* **2003**, *68*, 156; (e) K.M. Miller, W.-S. Huang, T.F. Jamison, *J. Am. Chem. Soc.* **2003**, *125*, 3442; (f) K. Takai, S. Sakamoto, T. Isshiki, *Org. Lett.* **2003**, *5*, 653; (g) J. Chan, T.F. Jamison, *J. Am. Chem. Soc.* **2003**, *125*, 11514; (h) E.A. Colby, K.C. O'Brien, T.F. Jamison, *J. Am. Chem. Soc.* **2004**, *126*, 998; (i) J. Chan, T.F. Jamison, *J. Am. Chem. Soc.* **2004**, *126*, 10682; (j) K.M. Miller, T.F. Jamison, *J. Am. Chem. Soc.* **2004**, *126*, 15342.

3 For use of alkynes as nucleophilic partners in catalytic hydrometallative reductive couplings to imines, see: S.J. Patel,

T.F. Jamison, *Angew. Chem. Int. Ed.* **2003**, *42*, 1364.

4 For use of alkynes as nucleophilic partners in catalytic hydrometallative reductive couplings to imines, see: (a) M.V. Chevliakov, J. Montgomery, *J. Am. Chem. Soc.* **1999**, *121*, 11139; (b) J. Montgomery, M. Song, *Org. Lett.* **2002**, *4*, 4009; (c) K.K.D. Amarasinghe, J. Montgomery, *J. Am. Chem. Soc.* **2002**, *124*, 9366.

5 For use of conjugated enones as nucleophilic partners in catalytic intermolecular reductive couplings to aldehydes, see: (a) A. Revis, T.K. Hilty, *Tetrahedron Lett.* **1987**, *28*, 4809; (b) S. Isayama, T. Mukaiyama, *Chem. Lett.* **1989**, 2005; (c) I. Matsuda, K. Takahashi, S. Sato, *Tetrahedron Lett.* **1990**, *31*, 5331; (d) S. Kiyooka, A. Shimizu, S. Torii, *Tetrahedron Lett.* **1998**, *39*, 5237; (e) T. Ooi, K. Doda, D. Sakai, K. Maruoka, *Tetrahedron Lett.* **1999**, *40*, 2133; (f) S.J. Taylor, J.P. Morken, *J. Am. Chem. Soc.* **1999**, *121*, 12202; (g) S.J. Taylor, M.O. Duffey, J.P. Morken, *J. Am. Chem. Soc.* **2000**, *122*, 4528; (h) C.-X. Zhao, M.O. Duffey, S.J. Taylor, J.P. Morken, *Org. Lett.* **2001**, *3*, 1829; (i) C.-X. Zhao, J. Bass, J.P. Morken, *Org. Lett.* **2001**, *3*, 2839.

6 For use of conjugated enones as nucleophilic partners in catalytic intramolecular reductive couplings to aldehydes, see: (a) T.-G. Baik, A.L. Luis, L.-C. Wang, M.J. Krische, *J. Am. Chem. Soc.* **2001**, *123*, 5112; (b) D. Emiabata-Smith, A. McKillop, C. Mills, W.B. Motherwell, A.J. Whitehead, *Synlett* **2001**, 1302; (c) L.-C. Wang, H.-Y. Jang, Y. Roh, V. Lynch, A.J. Schultz, X. Wang, M.J. Krische, *J. Am. Chem. Soc.* **2002**, *124*, 9448; (d) R.R. Huddleston, D.F. Cauble, M.J. Krische, *J. Org. Chem.* **2003**, *68*, 11; (e) M. Freiria, A.J. Whitehead, D.A. Tocher, W.B. Motherwell, *Tetrahedron* **2004**, *60*, 2673.

7 For use of conjugated enones as nucleophilic partners in catalytic intermolecular reductive couplings to aldimines, see: (a) J.A. Townes, M.A. Evans, J. Queffelec, S.J. Taylor, J.P. Morken, *Org. Lett.* **2002**, *4*, 2537; (b) T. Muraoka, S.-I. Kamiya, I. Matsuda, K. Itoh, *Chem. Commun.* **2002**, 1284.

8 For use of conjugated dienes as nucleophilic partners in catalytic intramolecular reductive couplings to aldehydes, see: (a) Y. Sato, M. Takimoto, K. Hayashi, T. Katsuhara, K. Tagaki, M. Mori, *J. Am. Chem. Soc.* **1994**, *116*, 9771; (b) Y. Sato, Y. Takimoto, M. Mori, *Tetrahedron Lett.* **1996**, *37*, 887; (c) Y. Sato, T. Takanashi, M. Hoshiba, M. Mori, *Tetrahedron Lett.* **1998**, *39*, 5579; (d) Y. Sato, N. Saito, M. Mori, *J. Am. Chem. Soc.* **2000**, *122*, 2371; (e) K. Shibata, M. Kimura, M. Shimizu, Y. Tamaru, *Org. Lett.* **2001**, *3*, 2181; (f) Y. Sato, N. Saito, M. Mori, *J. Org. Chem.* **2002**, *67*, 9310; (g) Y. Sato, T. Takanishi, M. Hoshiba, M. Mori, *J. Organomet. Chem.* **2003**, *688*, 36.

9 For use of conjugated dienes as nucleophilic partners in catalytic intermolecular reductive couplings to aldehydes, see: (a) M. Kimura, A. Ezoe, K. Shibata, Y. Tamaru, *J. Am. Chem. Soc.* **1998**, *120*, 4033; (b) M. Kimura, H. Fujimatsu, A. Ezoe, K. Shibata, M. Shimizu, S. Matsumoto, Y. Tamaru, *Angew. Chem. Int. Ed.* **1999**, *38*, 397; (c) M. Kimura, K. Shibata, Y. Koudahashi, Y. Tamaru, *Tetrahedron Lett.* **2000**, *41*, 6789; (d) M. Kimura, A. Ezoe, S. Tanaka, Y. Tamaru, *Angew. Chem. Int. Ed.* **2001**, *40*, 3600; (e) T.-P. Loh, H.-Y. Song, Y. Zhou, *Org. Lett.* **2002**, *4*, 2715; (f) Y. Sato, R. Sawaki, N. Saito, M. Mori, *J. Org. Chem.* **2002**, *67*, 656; (g) L. Bareille, P. Le Gendre, C. Moise, *Chem. Commun.* **2005**, 775.

10 For use of conjugated dienes as nucleophilic partners in catalytic intermolecular reductive couplings to aldimines, see: M. Kimura, A. Miyachi, K. Kojima, S. Tanaka, Y. Tamaru, *J. Am. Chem. Soc.* **2004**, *126*, 14360.

11 For use of conjugated enynes as nucleophilic partners in catalytic intermolecular reductive couplings to aldehydes, see: K.M. Miller, T. Luanphaisarnnont, C. Molinaro, T.F. Jamison, *J. Am. Chem. Soc.* **2004**, *126*, 4130.

12 For reviews on atom economy, see: (a) B.M. Trost, *Science* **1991**, *254*, 1471; (b) B.M. Trost, *Angew. Chem. Int. Ed. Engl.* **1995**, *34*, 259.

13 (a) P.J. Black, M.G. Edwards, J.M.J. Williams, *Tetrahedron* **2005**, *61*, 1363;

(b) M.G. Edwards, R.F.R. Jazzar, B.M. Paine, D.J. Shermer, M.K. Whittlesey, J.M.J. Williams, D.D. Edney, *Chem. Commun.* **2004**, 90; (c) G. Cami-Kobeci, J.M.J. Williams, *Chem. Commun.* **2004**, 1072; (d) M.G. Edwards, J.M.J. Williams, *Angew. Chem. Int. Ed.* **2002**, *41*, 4740; (e) P.J. Black, W. Harris, J.M.J. Williams, *Angew. Chem. Int. Ed.* **2001**, *40*, 4475.

14 For recent reviews on alkene hydroformylation and the Fischer-Tropsch reaction, see: (a) B. Breit, *Acc. Chem. Res.* **2003**, *36*, 264; (b) B. Breit, W. Seiche, *Synthesis* **2001**, 1; (c) W.A. Herrmann, *Angew. Chem. Int. Ed. Engl.* **1982**, *21*, 117; (d) C.-K. Rofer-Depoorter, *Chem. Rev.* **1981**, *81*, 447.

15 Prior to our work, two examples of hydrogen-mediated C–C bond formation under CO-free conditions are reported: (a) G.A. Molander, J.O. Hoberg *J. Am. Chem. Soc.* **1992**, *114*, 3123; (b) K. Kokubo, M. Miura, M. Nomura, *Organometallics* **1995**, *14*, 4521.

16 For reviews on the heterolytic activation of elemental hydrogen, see: (a) P.J. Brothers, *Prog. Inorg. Chem.* **1981**, *28*, 1; (b) G. Jeske, H. Lauke, H. Mauermann, H. Schumann, T.J. Marks, *J. Am. Chem. Soc.* **1985**, *107*, 8111.

17 Rh(III)-metallocycles derived from 1,6-enynes are postulated as reactive intermediates in catalytic [4+2] and [5+2] cycloadditions, Pauson-Khand reactions and cycloisomerizations: P. Cao, B. Wang, X. Zhang, *J. Am. Chem. Soc.* **2000**, *122*, 64901 and references cited therein.

18 (a) C.A. Tolman, P.Z. Meakin, D.L. Lindner, J.P. Jesson, *J. Am. Chem. Soc.* **1974**, *96*, 2762; (b) J. Halpern, T. Okamoto, A. Zakhariev, *J. Mol. Catal.* **1976**, *2*, 65.

19 For a review, see: L. Marko, *Pure Appl. Chem.* **1979**, *51*, 2211.

20 Monohydride formation by deprotonation of a dihydride intermediate is known for cationic Rh-complexes: (a) R.R. Schrock, J.A. Osborn, *J. Am. Chem. Soc.* **1976**, *98*, 2134; (b) R.R. Schrock, J.A. Osborn, *J. Am. Chem. Soc.* **1976**, *98*, 2143; (c) R.R. Schrock, J.A. Osborn, *J. Am. Chem. Soc.* **1976**, *98*, 4450.

21 For a review of the acidity of metal hydrides, see: J.R. Norton, in: A. Dedieu (Ed.), *Transition Metal Hydrides*. New York, **1992**, pp. 309.

22 Direct heterolytic activation of hydrogen by $RhCl(CO)(PPh_3)_2$ has been suggested, but likely involves an intermediate dihydride: D. Evans, J.A. Osborn, G. Wilkinson, *J. Chem. Soc. A* **1968**, 3133.

23 For earlier reviews encompassing aspects of this work, see: (a) H.-Y. Jang, M.J. Krische, *Eur. J. Org. Chem.* **2004**, 3953; (b) H.-Y. Jang, M.J. Krische, *Acc. Chem. Res.* **2004**, *37*, 653; (c) H.-Y. Jang, R.R. Huddleston, M.J. Krische, *Chemtracts* **2003**, *16*, 554.

24 (a) H.-Y. Jang, R.R. Huddleston, M.J. Krische, *J. Am. Chem. Soc.* **2002**, *124*, 15156; (b) R.R. Huddleston, M.J. Krische, *Org. Lett.* **2003**, *5*, 1143; (c) G.A. Marriner, S.A. Garner, H.-Y. Jang, M.J. Krische, *J. Org. Chem.* **2004**, *69*, 1380; (d) P.K. Koech, M.J. Krische, *Org. Lett.* **2004**, *6*, 691; (e) S.A. Garner, C.-K. Jung, M.J. Krische, *Org. Lett.* **2006**, *8*, 519.

25 H.-Y. Jang, R.R. Huddleston, M.J. Krische, *Angew. Chem. Int. Ed.* **2003**, *42*, 4074.

26 (a) H.-Y. Jang, R.R. Huddleston, M.J. Krische, *J. Am. Chem. Soc.* **2004**, *126*, 4664; (b) R.R. Huddleston, H.-Y. Jang, M.J. Krische, *J. Am. Chem. Soc.* **2003**, *125*, 11488; (c) J.-R. Kong, C.-W. Cho, M.J. Krische, *J. Am. Chem. Soc.* **2005**, *127*, 11269.

27 (a) H.-Y. Jang, M.J. Krische, *J. Am. Chem. Soc.* **2004**, *126*, 7875; (b) H.-Y. Jang, F.W. Hughes, H. Gong, J. Zhang, J.S. Brodbelt, M.J. Krische, *J. Am. Chem. Soc.* **2004**, *127, 6174.*

28 For excellent reviews, see: (a) J. Halpern, *Asymm. Synth.* **1985**, *5*, 41; (b) C.R. Landis, T.W. Brauch, *Inorg. Chim. Acta* **1998**, *270*, 285; (c) I. Gridnev, T. Imamoto, *Acc. Chem. Res.* **2004**, *37*, 633.

29 A method for the stoichiometric addition of metallo-aldehyde enolates to ketones has recently been reported: K. Yachi, H. Shinokubo, K. Oshima, *J. Am. Chem. Soc.* **1999**, *121*, 9465.

30 E.M. Arnett, F.J. Fisher, M.A. Nichols, A.A. Ribeiro, *J. Am. Chem. Soc.* **1989**, *111*, 748.

31 The failure of *tris*(dialkylamino)sulfonium enolates to react with aldehydes is

attributed to unfavorable enolate-aldolate equilibria: (a) R. Noyori, J. Sakata, M. Nishizawa, *J. Am. Chem. Soc.* **1980**, *102*, 1223; (b) R. Noyori, I. Nishida, J. Sakata, *J. Am. Chem. Soc.* **1981**, *103*, 2106; (c) R. Noyori, I. Nishida, J. Sakata, *J. Am. Chem. Soc.* **1983**, *105*, 1598.

32 (a) C. H. Heathcock, in: B. M. Trost, I. Fleming, C. H. Heathcock (Eds.), *Comprehensive Organic Synthesis: Additions to C-X Bonds Part 2*. Pergamon Press, New York, pp. 181; (b) B. Alcaide, P. Almendros, *Angew. Chem. Int. Ed.* **2003**, *42*, 858.

33 (a) S. Denmark, S. K. Ghosh, *Angew. Chem. Int. Ed.* **2001**, *40*, 4759; (b) A. B. Northrup, D. W. C. MacMillan, *J. Am. Chem. Soc.* **2002**, *124*, 6798; (c) C. Pidathala, L. Hoang, N. Vignola, B. List, *Angew. Chem. Int. Ed.* **2003**, *42*, 2785.

34 For a recent discussion, see: T. C. Morrill, C. A. D'Souza, *Organometallics* **2003**, *22*, 1626 and references therein.

35 (a) M. J. S. Dewar, *Bull. Soc. Chim. Fr.* **1951**, *18*, C71; (b) J. Chatt, L. A. Duncanson, *J. Chem. Soc.* **1953**, 2939.

36 For a review, see: F. Sato, H. Urable, S. Okamoto, *Chem. Rev.* **2000**, *100*, 2835.

37 For σ-bond metathesis involving Rh(III) intermediates, see: (a) J. F. Hartwig, K. S. Cook, M. Hapke, C. D. Incarvito, Y. Fan, C. E. Webster, M. B. Hall, *J. Am. Chem. Soc.* **2005**, *127*, 2538; (b) C. Liu, R. A. Widenhoefer, *Organometallics* **2002**, *21*, 5666; (c) F. Hutschka, A. Dedieu, W. Leitner, *Angew. Chem. Int. Ed. Engl.* **1995**, *34*, 1742.

38 For metal-catalyzed cyclization of 1,6- and 1,7-diynes, see: (a) B. M. Trost, D.C. Lee, *J. Am. Chem. Soc.* **1988**, *110*, 7255; (b) K. Tamao, K. Kobayashi, Y. Ito, *J. Am. Chem. Soc.* **1989**, *111*, 6478; (c) B. M. Trost, F. J. Fleitz, W. J. Watkins, *J. Am. Chem. Soc.* **1996**, *110*, 5146; (d) M. Lautens, N. D. Smith, D. Ostrovsky, *J. Org. Chem.* **1997**, *62*, 8970; (e) S.-Y. Onozawa, Y. Hatanaka, M. Tanaka, *Chem. Commun.* **1997**, 1229; (f) S.-Y. Onozawa, Y. Hatanaka, N. Choi, M. Tanaka, *Organometallics* **1997**, *16*, 5389; (g) I. Ojima, J. Zhu, E. S. Vidal, D. F. Kass, *J. Am. Chem. Soc.* **1998**, *120*, 6690; (h) T. Muraoka, I. Matsuda, K. Itoh, *Tetrahedron Lett.* **1998**, *39*, 7325; (i) S. Gréau, B. Radetich, T. V. RajanBabu, *J. Am. Chem. Soc.* **2000**, *122*, 8579; (j) J. W. Madine, X. Wang, R. A. Widenhoefer, *Org. Lett.* **2001**, *3*, 385; (k) X. Wang, H. Chakrapani, J. W. Madine, M. A. Keyerleber, R.A. Widenhoefer, *J. Org. Chem.* **2002**, *67*, 2778; (l) T. Muraoka, I. Matsuda, K. Itoh, *Organometallics* **2002**, *21*, 3650; (m) C. Liu, R. A. Widenhoefer, *Organometallics* **2002**, *21*, 5666; (n) T. Uno, S. Wakayanagi, Y. Sonoda, K. Yamamoto, *Synlett* **2003**, 1997; (o) B. M. Trost, M. T. Rudd, *J. Am. Chem. Soc.* **2003**, *125*, 11516.

39 For reviews encompassing the Pd-catalyzed cycloisomerization and reductive cyclization of 1,6-enynes, see: (a) B. M. Trost, *Acc. Chem. Res.* **1990**, *23*, 34; (b) I. Ojima, M. Tzamarioudaki, Z. Li, R.J. Donovan, *Chem. Rev.* **1996**, *96*, 635; (c) B. M. Trost, M. J. Krische, *Synlett* **1998**, 1; (d) C. Aubert, O. Buisine, M. Malacria, *Chem. Rev.* **2002**, *102*, 813.

40 For selected examples of the cycloisomerization of 1,6-enynes catalyzed by metals other than palladium, see: (a) Titanium: S.J. Sturla, N. M. Kablaoui, S. L. Buchwald, *J. Am. Chem. Soc.* **1999**, *121*, 1976; (b) Rhodium: P. Cao, B. Wang, X. Zhang, *J. Am. Chem. Soc.* **2000**, *122*, 6490; (c) Nickel-Chromium: B. M. Trost, J. M. Tour, *J. Am. Chem. Soc.* **1987**, *109*, 5268; (d) Ruthenium: M. Nishida, N. Adachi, K. Onozuka, H. Matsumura, M. Mori, *J. Org. Chem.* **1998**, *63*, 9158; (e) B. M. Trost, F. D. Toste, *J. Am. Chem. Soc.* **2000**, *122*, 714; (f) J. LaPaih, D. C. Rodriguez, S. Derien, P. H. Dixneuf, *Synlett* **2000**, 95; (g) Cobalt: A. Ajamian, J. L. Gleason, *Org. Lett.* **2003**, *5*, 2409; (h) Iridium: N. Chatani, H. Inoue, T. Morimoto, T. Muto, S. Muria, *J. Org. Chem.* **2001**, *66*, 4433.

41 For an excellent review covering enantioselective metal-catalyzed cycloisomerization of 1,6- and 1,7-enynes, see: I. J. S. Fairlamb, *Angew. Chem. Int. Ed.* **2004**, *43*, 1048.

42 For rhodium-catalyzed enantioselective enyne cycloisomerization and hydrosilylation-cyclization, see: (a) C. Ping, X. Zhang, *Angew. Chem. Int. Ed.* **2000**, *39*, 4104; (b) A. Lei, M. He, S. Wu, X.

Zhang, *Angew. Chem. Int. Ed.* **2002**, *41*, 3457–3460; (c) A. Lei, J. P. Waldkirch, M. He, X. Zhang, *Angew. Chem. Int. Ed.* **2002**, *41*, 4526; (d) A. Lei, M. He, X. Zhang, *J. Am. Chem. Soc.* **2003**, *125*, 11472; (e) H. Chakrapani, C. Liu, R. A. Widenhoefer, *Org. Lett.* **2003**, *5*, 157.

43 For a biographical sketch of Paul Sabatier, see: A. Lattes, *C. R. Acad. Sci. Ser. IIC: Chemie* **2000**, *3*, 705.

44 For a biographical sketch of Roger Adams, see: D.S. Tarbell, A.T. Tarbell, *J. Chem. Ed.* **1979**, *56*, 163.

45 (a) W. S. Knowles, *Prix Nobel* **2001**, *2002*, 160; (b) W. S. Knowles, *Angew. Chem. Int. Ed.* **2002**, *41*, 1998; (c) W. S. Knowles, *Adv. Synth. Catal.* **2003**, *345*, 3.

46 (a) R. Noyori, *Prix Nobel* **2001**, *2002*, 186; (b) R. Noyori, *Angew. Chem. Int. Ed.* **2002**, *41*, 2008; (c) R. Noyori, *Adv. Synth. Catal.* **2003**, *345*, 15.

Part IV
Asymmetric Homogeneous Hydrogenation

The Handbook of Homogeneous Hydrogenation.
Edited by J.G. de Vries and C.J. Elsevier
Copyright © 2007 WILEY-VCH Verlag GmbH & Co. KGaA, Weinheim
ISBN: 978-3-527-31161-3

23
Enantioselective Alkene Hydrogenation: Introduction and Historic Overview

David J. Ager

23.1
Introduction

This chapter describes, from an historic perspective, the development of ligands and catalysts for enantioselective hydrogenations of alkenes. There is no in-depth discussion of the many ligands available as the following chapters describe many of these, as well as their specific applications. The purpose here is to provide an overall summary and perspective of the area. By necessity, a large number of catalyst systems have not been mentioned. The discussion is also limited to the reductions of carbon–carbon unsaturation. In almost all cases, rhodium is the transition metal to catalyze this type of reduction. In order to help the reader, the year of the first publication in a journal has been included in parentheses under each structure.

Before 1968, attempts to perform enantioselective hydrogenations had either used a chiral auxiliary attached to the substrate [1] or a heterogeneous catalyst that was on a chiral support, usually derived from Nature [2]. Since the disclosure of chiral phosphine ligands to bring about enantioselective induction in a hydrogenation, many systems have been developed, as evidenced in this book. The evolution of these transition-metal catalysts has been discussed in a number of reviews [3–12].

In addition to academic curiosity, enantioselective hydrogenation catalysts have enjoyed an extra impetus for their development. The early commercial successes of Knowles with the Dopa process (*vide infra*), followed by the related applications of BINAP-based catalysts, have led many companies to develop their own ligand systems if not based on a completely new scaffold, then at least sufficiently different to allow patent protection and freedom to operate. This has resulted in a wide range of catalysts and ligand systems to perform the same, or very similar, reactions. In this chapter, ligands have been included if they have a familiar name. Acronyms are given in upper case, while the names of ligands that are not based on acronyms are given lower case with the parts of the name denoted by an upper-case letter.

The Handbook of Homogeneous Hydrogenation.
Edited by J.G. de Vries and C.J. Elsevier
Copyright © 2007 WILEY-VCH Verlag GmbH & Co. KGaA, Weinheim
ISBN: 978-3-527-31161-3

23.2 Development of CAMP and DIPAMP

During the late 1960s, Horner et al. [13] and Knowles and Sabacky [14] independently found that a chiral monodentate tertiary phosphine, in the presence of a rhodium complex, could provide enantioselective induction for a hydrogenation, although the amount of induction was small [15–20]. The chiral phosphine ligand replaced the triphenylphosphine in a Wilkinson-type catalyst [10, 21, 22]. At about this time, it was also found that $[Rh(COD)_2]^+$ or $[Rh(NBD)_2]^+$ could be used as catalyst precursors, without the need to perform ligand exchange reactions [23].

Knowles found that the monophosphine CAMP (**1a**) could provide an ee-value of up to 88% for the reduction of dehydroamino acids. CAMP was an extension of PAMP (**1b**) that provides ee-values of 50–60% in analogous reactions [24]. At this time, Kagan showed that DIOP (**2**) (*vide infra*), where the stereogenic centers are not at phosphorus, could also provide enantioselective induction in an hydrogenation. DIOP also showed that a bisphosphine need not have the chirality at phosphorus, and that good stereoselectivity might result from a C_2-symmetric ligand. Knowles then developed the C_2-symmetric ligand DIPAMP (**3**) [22, 25]. The use of Rh-DIPAMP for the synthesis of L-Dopa is well known and is still practiced today [12, 22, 27]. A number of variations of the DIPAMP structure were investigated for the synthesis of this important pharmaceutical, but the parent remains the best ligand in this class [22].

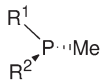

1 (1972)

a R^1 = Ph, R^2 = *o*-An (PAMP)
b R^1 = *c*-C_6H_{11}, R^2 = *o*-An (CAMP)

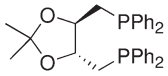

2 (DIOP) (1971)

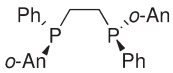

3 (DIPAMP) (1977)

It is interesting to note that a few "rules of thumb" and myths came out of these early studies. Many of these have been perpetuated for decades, and the myths are only just being put to rest. Knowles showed that only two phosphorus ligands were needed on the metal to achieve reduction, and not three as in Wilkinson's catalyst [10]. The success of DIPAMP and DIOP led to the belief

that bisphosphine ligands were required for high enantioselective induction, and that C_2-symmetry was also desirable. These hypotheses molded the design of new ligands for many years. We now know that monodentate ligands, as well as asymmetric bidentate ligands, can provide high ee-values.

Another trend that arose from Knowles' results was that a wide range of enamides (dehydroamino acids) could be reduced to amino acids [22, 25, 27, 29]. This was in contrast to the enzymatic reactions known then, where enzymes were believed to be very substrate specific. As we now know, there is no general catalytic system to perform asymmetric hydrogenations and even within a small class of substrates, some ligand variation is required to achieve optimal results.

The results obtained with the Knowles' catalyst system have led to a number of useful tools that have helped with the development of other ligand families. The low ee-values obtained with simple unsaturated acids as compared to the enamides of dehydroamino acid derivatives show that the oxygen atoms of the amide is a key to complex formation with the metal center. Knowles also proposed a quadrant model that has been adapted for many reactions [5, 22]. The mechanism of the reaction has been investigated, and it is known that the addition of the substrate to the metal is regioselective and that competing catalytic cycles can occur [5, 10, 22, 25, 27, 30–46].

Perhaps the one major drawback with DIPAMP is the long synthetic sequence required for its preparation, though shorter and cheaper methods are now available [12]. The ligand continues to be a player for the synthesis of amino acid derivatives at scale, including L-Dopa, as mentioned above [12, 25, 27–29]. Its continued use is a testament to the power of the initial discoveries, as well as showing that a chemical catalyst can achieve selectivities only previously seen with enzymes.

The difficulty in preparing *P*-chiral ligands is a large barrier to entry for this class of ligand. It has taken over twenty years to see new, useful ligands of this class appear. BisP* (**4**) provides good selectivity for the reductions of dehydroamino acids [47, 48], enamides [49], *E*-β-acylaminoacrylates [50], and α,β-unsaturated-α-acyloxyphosphonates [51], but rates can be slow. Other ligands of this type are MiniPhos (**5**) [47, 48, 52] and the unsymmetrical **6** [53, 54], TangPhos (**7**) is also a member of the class [55–58], as are BIPNOR (**8**) [59, 60] and ^{i}Pr-BeePhos (**9**) [61]. Mention should also be made of the DuPhos-type hybrid **10** that works well for the reductions of itaconic acids [62]. A recent addition to the general class is trichickenfootphos (**11**); this has been developed for the reduction of enamides, dehydroamino acids and α,β-unsaturated nitriles [63, 64]. (Throughout this chapter, R in generic structures denotes an alkyl group unless otherwise stated.)

4 R = *t*-Bu (BisP*)
(1998)

5 R = *t*-Bu (MiniPhos)
(1998)

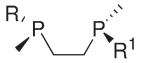

6 R =Ad, R^1 = *t*-Bu (unsymmetrical BisP*)
(2001)

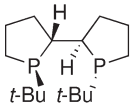

7 (TangPhos)
(2002)

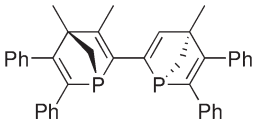

8 (BIPNOR) (1997)

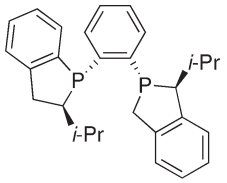

9 (^{i}Pr-BeePHOS) (1997)

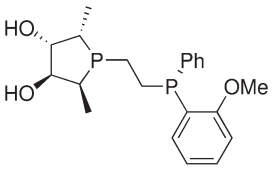

10 (2003)

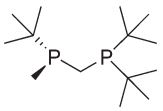

11 (Trichickenfootphos)
(2003)

23.3 DIOP

Kagan and colleagues found that DIOP (**2**) could provide significant enantioselective induction in a hydrogenation, and this finding led to Knowles' development of the DIPAMP system [65–67]. Certainly, at the time when the results were reported the ee-values were considered high, though this would not be the case today. DIOP is prepared from tartaric acid, and has the stereogenic centers in the carbon backbone rather than at the phosphorus atoms. The use of two phosphorus groups within the same molecule provided the move to the current plethora of bisphosphine ligands. The second key finding was the use of stereogenic centers in the backbone, as these are much easier to introduce than obtaining a chiral phosphorus with high enantiopurity.

DIOP has not found widespread usage after the initial investigations, presumably due to the lower selectivity.

During the 1980s, Achiwa and colleagues examined a number of derivatives of DIOP, and found that MOD-DIOP (**12c**) allowed for the enantioselective hydrogenation of itaconic acid derivatives with >96% ee [68–75].

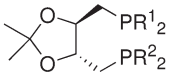

12 (1987)

a $R^1 = R^2 = Cy$ (Cy-DIOP)
b $R^1 = Cy$. $R^2 = Ph$ (DIOCP)
c $R^1 = R^2 = 3,5\text{-}Me_2\text{-}4\text{-}MeOC_6H_2$ (MOD-DIOP)

At the turn of the millennium, Zhang and RajanBabu have independently returned to derivatives of DIOP and found that the introduction of α-methyl groups as in DIOP* (**13**) greatly increases enantioselectivity [76–79]. Zhang attributes this improvement to a reduction in the conformational flexibility of the backbone within the metal complex [3, 76]. It is interesting to note that Kagan himself prepared the *S,S,S,S*-isomer of DIOP*, but enantioselectivities were lower than with DIOP itself [80].

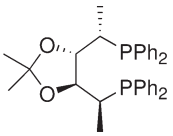

13 (DIOP*)
(2000)

The system can also be made rigid by modification of the ketal portion, as illustrated by **14** and SK-Phos (**15**). These ligands provided high stereoselection for reductions of enamides and MOM-protected β-hydroxy enamides [81].

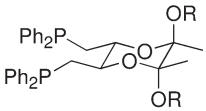

14 (2002)

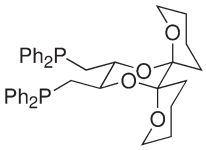

15 (SK-Phos) (2002)

As already stated, DIOP led the way for a number of ligand systems that were built on a carbon framework containing stereogenic centers. Some of these ligands followed closely on the heels of DIOP, such as ChiraPhos (**16**) where the chelate ring is five-membered [82, 83]. Even one stereogenic center in the backbone, as in ProPhos (**17**), provides reasonable selectivity [83, 84]. The main problem with these systems is that of slow reactions.

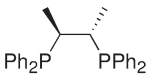

16 (ChiraPhos) (1977)

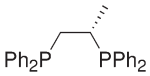

17 (ProPhos) (1977)

Other early variations on the theme led to BPPM (**18a**) [85] and CBD (**19**) [86].

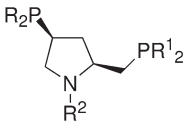

18 (1976)

a R = R^1 = Ph, R^2 = Boc (BPPM)
b R = R^1 = Ph, R^2 = H (PPM)
c R = R^1 = Ph, R^2 = CO-*t*-Bu (PPPM)
d R = R^1 = 3,5-Me_2-4-$MeOC_6H_2$, R^2 = Boc (MOD-BPPM)
e R = Cy, R^1 = Ph, R^2 = CO_2-*t*-Bu (BCPM)
f R = Cy, R^1 = 3,5-Me_2-4-$MeOC_6H_2$, R^2 = CO_2-*t*-Bu (MOD-BCPM)
g R = Cy, R^1 = Ph, R^2 = CONHMe (MCCPM)

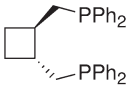

19 (CBD)
(1980)

BPPM is derived from 4-hydroxyproline [85]. As "unnatural" amino acids are often the target product for enantioselective reductions, Knowles' comment in his 1983 review is interesting: "BPPM, like DIOP, is a seven-membered chelator derived from natural (2*R*,4*R*)-hydroxyproline. It can give high efficiency at very fast rates. Unfortunately, it gives unwanted D-amino acids…" [22]. Although this may not be seen as a shortfall today, derivatives (**18**) of BPPM have been developed, mainly through different nitrogen substituents, and derivatives such as PPPM (**18c**) still give D-amino acids [85, 87–98]. The ligands are also useful for the reduction of itaconic acid derivatives [3].

One of the branches in ligand design was provided by Kumada and his introduction of the ferrocene backbone for BPPFA [99–101] (**20a**) and BPPOH [102] (**20b**). This development leads us to the next class of ligands – ferrocene-based. Other variations for development include changes in the backbone and incorporation of the phosphorus into a phospholane (see Section 23.6).

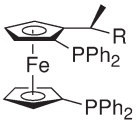

20 (1976)
a R = NMe_2 (BPPFA)
b R = OH (BPPOH)

The electronic properties around the phosphorus atom can be varied by manipulation of the groups on that atom. MOD-DIOP (**12c**) was developed by Achiwa and used to reduce itaconic acids [68–72, 75, 103]. Some variations built on BCPM (**18e**), itself a variant of BPPM, such as the MOD-BCPM (**18f**) and MCCPM (**18g**) [88–93, 95–98, 104]. Other variants are PYRPHOS (**21a**; also called DeguPHOS) [105, 106], DPCP (**22**) [107], NorPhos (**23**) [108], BDPP (**24a**) (also called SkewPHOS) [109–111], and PPCP (**25**) [112].

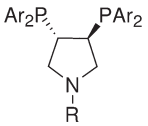

21 (1984)
a Ar = Ph, R = CH_2Ph (PYRPHOS, DeguPHOS)
b Ar = 3,5-Me_2-4-$MeOC_6H_2$, R = CH_2Ph (MOD-DeguPHOS)

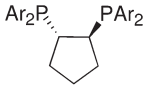

22 (DPCP)
(1983)

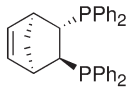

23 (NorPhos)
(1981)

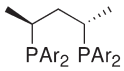

24 (1981)

a Ar = Ph (BDPP, SkewPhos)
b Ar = 3,5-Me_2-4-$MeOC_6H_2$ (MOD-BDPP)

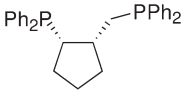

25 (PPCP)
(1991)

One ligand system which was developed during the late 1990s, and has proven quite versatile for the reduction of a wide variety of unsaturations, including α-and β-dehydroamino acids, arylenamides and MOM-protected β-hydroxy enamides, is the rigid BICP (**26**) [113–118].

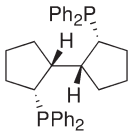

26 (BICP)
(1997)

The BDPMI (**27**) system can also be considered to be a DIOP variant, as an imidazole ring forms the rigid backbone [119–121]. Excellent stereoselectivity is seen with this system for the reductions of arylenamides.

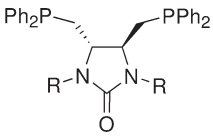

27 (BDPMI)
(2002)

An aromatic system can also provide a rigid backbone, as seen with PhanePhos (**28a**) [122–124].

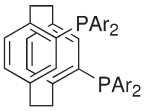

28 (1997)

a, Ar = Ph (PhanePhos)
b, Ar = 3,5-$Me_2C_6H_3$ (Xyl-PhanePhos)

23.4 Ferrocene Ligands

Kumada's use of a ferrocene moved away from the C_2-symmetrical motive, as planar chirality can result from the two ferrocene rings having different substituents. The development of this class of ligand is well documented [5, 125–127]. The best-known uses of these ligands are for reductions of carbon–heteroatom multiple bonds, as in the synthesis of the herbicide, Metolachlor™ [128, 129].

The key access compound to the early members of the class, and indeed some later ones, is the Ugi amine (**29**) and its relationship to PPFA (**30**) and BPPFA (**20a**) can be clearly seen [100, 130, 131].

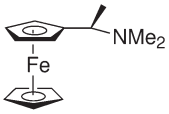

29

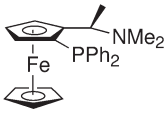

30 (PPFA)
(1980)

Analogues of BPPFA and BPPFOH have been prepared, but for many applications these two ligands still prove to be the best for enantioselective hydrogenations [125]. The introduction of another functional group into the side chain, as in **31**, provided the first catalysts capable of hydrogenating the tetra-substituted α,β-unsaturated acids with high enantioselectivity, even though the activity was very low (turnover frequency, TOF, $\sim 2\ h^{-1}$) [132, 133].

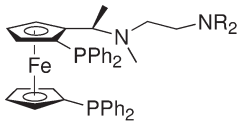

31 (1987)

a $R_2 = (CH_2)_4$
b R = Bu

Developments after these Ugi derivatives have taken a number of pathways. The MandyPhos family of ligands (**32**) have been used to reduce enamides to *α*-amino acids as well as an enol acetate to produce an *α*-hydroxy ester [134–140]. The substituents R and R^1 can be used for the fine-tuning of a specific substrate. Many of the family have R^1 as a secondary amine, relating the family back to PPFA. For confusion, MandyPhos has also been called FerriPhos, while the derivative **32** ($R = R^1 = Et$) is known as FerroPhos.

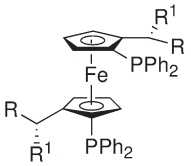

32 (MandyPhos) (1989)
$R = R^1 = Et$ (FerroPhos)

Perhaps the first successful variation of the PPFA framework was the development of the JosiPhos family of ligands (**33**) [125, 131, 141, 142]. Here, the two phosphorus groups are attached to the same cyclopentenyl ring rather than one to each of the rings. The C_2-symmetry model is now a distant memory for these ligand families.

The *R,S*-family **33**, and of course its enantiomer, provide high enantioselectivities and activities for the reductions of itaconic and dehydroamino acid derivatives as well as imines [141]. The JosiPhos ligands have found industrial applications for reductions of the carbon–carbon unsaturation within *α,β*-unsaturated carbonyl substrates [125, 127, 131, 143–149]. In contrast, the *R,R*-diastereoisomer of **30** does not provide high stereoselection in enantioselective hydrogenations [125, 141].

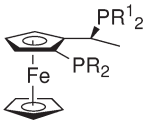

33 (JosiPhos)
(1994)

The recent introduction of the TaniaPhos ligands (**34**) provides another excellent catalyst system for the reduction of dehydroamino acid derivatives and enol

acetates [150–153]. One surprise is that the sense of induction in the product is opposite that observed with a JosiPhos-derived catalyst [125].

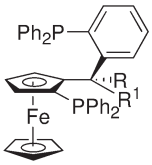

34 (TaniaPhos)
(1999)

Another ligand, the potential of which has only recently been exploited, is BoPhoz (**35**). This ligand is an aminophosphine as well as a phosphine (see also Section 23.7). It has shown high selectivities and activities with enamides and itaconates [154, 155].

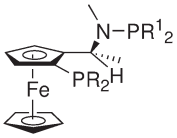

With ferrocenes, an alternative approach has been to attach the phosphorus moieties only to side chains. The WalPhos family (**36**) forms an eight-membered chelate with the metal. Members of this family provide good selectivity and reactivity for the reductions of dehydroamino and itaconic acid derivatives as well as α,β-unsaturated carboxylic acids [145, 156].

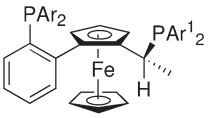

36 (WalPhos)
(2001)

A different variation on this theme has been developed by Ito, where the TRAP ligands (**37**) form a nine-membered metallocycle [157–162]. The ruthenium catalysts seem to function best at low pressures, but highly functionalized dehydroamino esters can be reduced with high degrees of asymmetric induction [157, 159–164], as well as indoles [165].

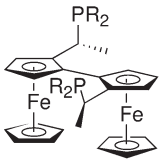

37 (TRAP)
(1995)

where R = alkyl or aryl

It is possible to use other metallocenes as the backbone, as illustrated by the rhenium complex (**38**) [166].

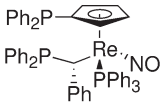

38 (2002)

23.4.1
Ferrocene Hybrids

The rhodium complexes of the ferrocene derivatives **39** have shown useful characteristics for the reduction of itaconates as well as dehydroamino acid derivatives [15, 167–170]. These compounds are hybrids between ferrocene-based ligands and the various other types. The *P*-chiral compounds, which in some ways are DIPAMP hybrids, showed tolerance for the reduction of *N*-methyl enamides to produce *N*-methyl-*α*-amino acid derivatives [169–171].

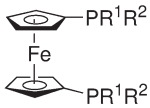

39 (1998)

where PR^1R^2 =

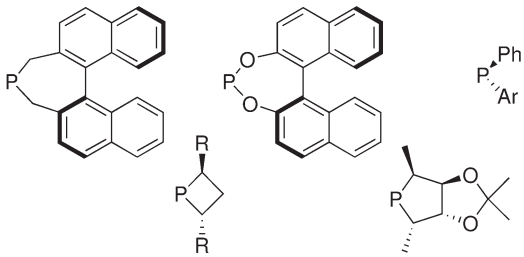

(FerroTANE)

23.5
Atropisomeric Systems

BINAP (**40a**) was first reported as a ligand in an enantioselective hydrogenation in 1980 [172], and provides good selectivity for the reductions of dehydroamino acid derivatives [173], enamides, allylic alcohols and amines, and *α*,*β*-unsaturated acids [4, 9, 11, 12, 174, 175]. The fame of the ligand system really came with the reduction of carbonyl groups with ruthenium as the metal [11, 176]. The Rh-BINAP systems is best known for the enantioselective isomerizations

used for the industrial-scale synthesis of menthol and other terpenes [12, 177–181], rather than enantioselective hydrogenations.

The use of atropisomeric ligands for carbon–carbon bond reductions was, however, the jumping-off point for variations such as BICHEP (**41a**) [182–185], BIPHEP (**41b**) [127, 186, 187], MeO-BIPHEP (**41c**) [179, 187, 188], and Cl-MeOBIPHEP (**41d**) [189]. A slightly different approach was taken by Achiwa with the BIMOP (**41e**) [190], FUPMOP (**41f**) [191], and MOC-BIMOP (**41g**) [192], with more substituents on the aryl rings. Again, most of the applications and high reactivities are seen for carbon–heteroatom unsaturation hydrogenations [12].

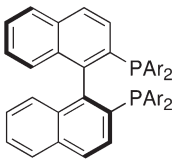

40 (1980)

a Ar = Ph (BINAP)
b Ar = *p*-MeC_6H_4 (TolBINAP)
c Ar = 3,5-$(Me)_2C_6H_3$ (XylBINAP)

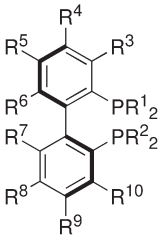

41 (1988)

where	R^1	R^2	R^3	R^4	R^5	R^6	R^7	R^8	R^9	R^{10}	
a	Cy	Cy	H	H	H	Me	Me	H	H	H	(BICHEP)
b	Ph	Ph	H	H	H	Me	Me	H	H	H	(BIPHEP)
c	Ph	Ph	H	H	H	OMe	OMe	H	H	H	(MeO-BIPHEP)
d	Ph	Ph	H	H	Cl	OMe	OMe	Cl	H	H	(Cl-MeOBIPHEP)
e	Ph	Ph	H	Me	OMe	Me	Me	OMe	Me	H	(BIMOP)
f	Ph	Ph	H	CF_3	H	CF_3	Me	OMe	Me	H	(FUPMOP)
g	Cy	Cy	H	Me	OMe	Me	Me	OMe	Me	H	(MOC-BIMOP)
h	Ph	Ph	Ph	OMe	OMe	OMe	OMe	OMe	OMe	Ph	(*o*-Ph-HexaMeO-BIPHEP)

The success of BINAP and the associated ligands families has led to many variations, and most have shown improved properties for specific applications (Fig. 23.1). Examples include derivatives of the naphthyl system of BINAP, as well as those derived from BIPHEP.

BINAP itself has been shown to be effective for the reduction of α,β-unsaturated carboxylic acids [8, 36, 177, 215–220], but H_8-BINAP often provides higher ee-values [193, 194]. The ruthenium complex with P-Phos provides high selectiv-

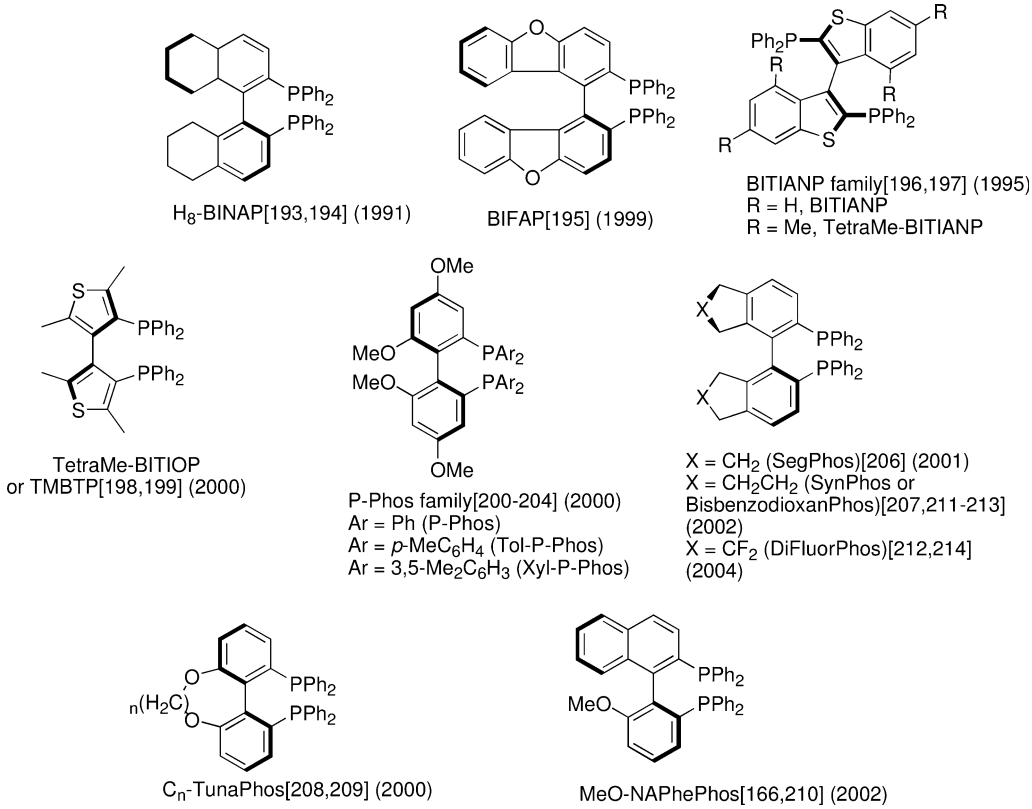

Fig. 23.1 Ligands based on atropisomeric systems.

ities and reactivities with α-arylacrylic acids [200–202]. The rhodium complex with *o*-Ph-HexaMeO-BIPHEP works well with cyclic enamides [205].

Many of these ligands have been modified to make them water-soluble, usually by the addition of a sulfate group, or attached to a support [3, 221].

23.6 DuPhos

The development of the next major class of ligands occurred during the 1990s, with Burk's DuPhos (**42**) family of phospholane ligands [222, 223]. (An individual member of the family is named after the substituent R; in Me-DuPhos, R = Me.) This structure could be considered an improvement on the DIOP-derived ligands, where the stereogenic centers are now closer to phosphorus. In addition to the aromatic spacer of DuPhos, there is also the related BPE (**43**) family, where the spacer between the two phosphorus atoms is less rigid. In both series the phosphorus is

now part of a five-membered ring that has adjacent stereogenic centers [224, 225]. DuPhos has been shown to be useful for the preparation of α-amino acid derivatives [222, 226–241], including β-branched examples that are not accessible with DIPAMP [222, 242, 243]. The catalyst system is also successful with enamides, enol acetates, unsaturated carboxylic, and itaconic acids [7, 115, 222, 244–250].

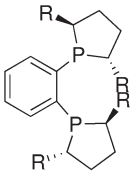

42 (DuPhos) (1990)

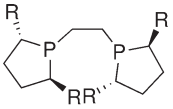

43 (BPE) (1990)

As the chirality with the DuPhos ligands is within the phospholane rings, a wide variety of backbones can be used ranging from ferrocene to heterocycles [61, 62, 77, 222, 251–262].

Variations have also been made on the DuPhos theme by changing the nature of the phospholane ring (Fig. 23.2). These ligands retain the high selectivity of

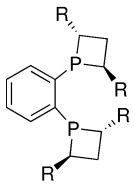

CnrPhos[168,264-268] (1997)

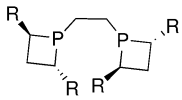

BPE-4[168,264-268] (1997)

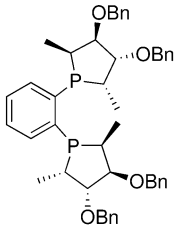

RoPhos[256,271] (1998)

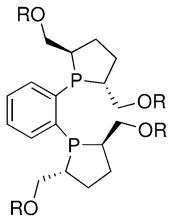

BasPhos[271,272] (1999)

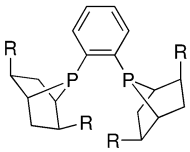

PennPhos[269,270] (1999)

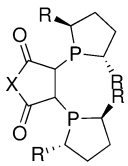

CatASium family[260] (2003)
X = O (MalPhos)
X = $(CH_2)_0$
X = NMe
X = NMeNMe

Fig. 23.2 DuPhos-derived ligands.

DuPhos. The exception for rhodium-catalyzed reductions are CnrPhos and BPE-4 [168, 264–268]. MalPhos has proven useful for the reductions of β-acylamino-acrylates [260]. The ferrocene hybrid (FerroTANE) was referred to earlier (see Section 23.4.1) [167, 222]. The PennPhos ligand is useful for the reductions of cyclic enamides and enol acetates; both classes of compounds are difficult for DuPhos itself to reduce with high selectivity [269, 270].

Neither of the phosphorus atoms needs not be in an asymmetric phospholane ring, as illustrated by both Saito and Pringle with UCAPs (**44**) [273, 274].

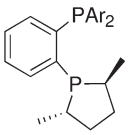

44 (UCAPs)

23.7 Variations at Phosphorus

In addition to the use of a phosphine ligands, other types of phosphorus moieties have also been used. In some cases, carbohydrates have formed the basis of the backbone, as illustrated by CarboPhos [275–280]. Some of these ligands have been available for almost twenty years. The electronic effects of the ligands can be very important with this class of compound. Other ligands of this class are variations on backbones established for bisphosphane ligands (Fig. 23.3). Most of these ligands have been employed for the reductions of dehydroamino acids; for example, the Phenyl-β-Glup ligand has been employed in a process involving L-Dopa [275–277].

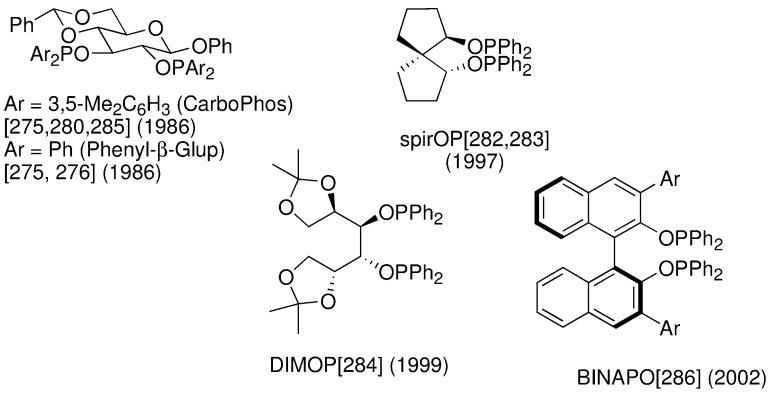

Fig. 23.3 Bisphosphites as ligands.

In addition to oxygen, the phosphorus can be tied to the backbone through nitrogen. Indeed, this was one of the earliest variations of the DIOP family (see Section 23.3) with PNNP (**45**) [22, 280, 287]. Care must be taken to avoid hydrolysis of the labile P–N bonds [22, 288]. Other examples of nitrogen-linked compounds are BDPAB (**46** and **47**) and its derivatives (Fig. 23.4). These ligands are clearly variations of the BINAP series [289–291].

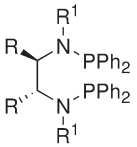

45
R = Ph, R^1 = H (PNNP)
(1979)

46 (1998)
Ar = Ph (BDPAB)
Ar = 3,5-$Me_2C_6H_3$ (Xyl-BDPAB)

47 (H_8-BDPAB) (1998)

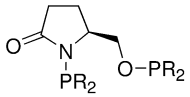

oxoProNOP family[293-300] (1993)
R = Cy (Cy,Cy-oxoProNOP)
R = Cp (Cp,Cp-oxoProNOP)

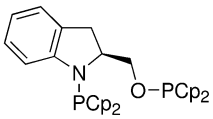

Cp,Cp-IndoNOP[301]
(1996)

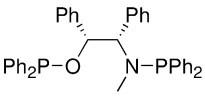

DPAMPP[302,303]
(2000)

where Cp = cyclopentadienyl

Fig. 23.4 Ligands with phosphorus attached to the backbone through oxygen and nitrogen.

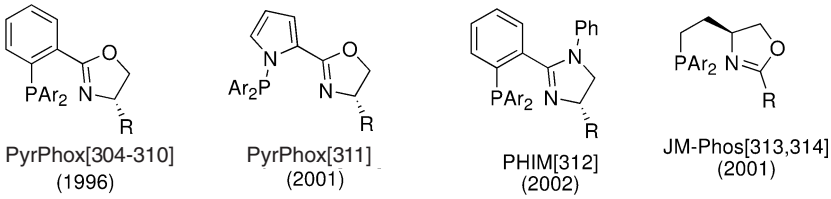

Fig. 23.5 Monophosphorus ligands.

The linkers may be nitrogen and carbon, as in BoPhoz – that is, a ferrocene-type ligand, as has already been mentioned. An example of a phosphine–phosphoramidite is provided by QuinaPhos (**48**) [292].

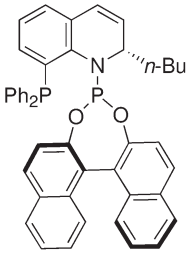

48 (*n*-Bu-QuinaPhos)
(2000)

In some cases, oxygen and nitrogen have been used as linkers to the backbones that are variations of those described previously (Fig. 23.4).

23.8
Monophosphorus Ligands

Just as Wilkinson's catalyst gave rise to the bisphosphine ligands, Crabtree's catalyst [304] spawned the family of phosphorus–nitrogen ligands for simple alkenes. Subsequently, Pfaltz developed the Phox family, which provides high ee-values with nonfunctionalized alkenes [305–310]. Other analogues are also illustrated in Figure 23.5.

23.9
A Return to Monodentate Ligands

The observation by Knowles that bisphosphines gave better selectivity for asymmetric hydrogenations resulted in a gap of over twenty-five years before monodentate ligands were investigated in detail and became useful ligands. There are several classes of these monodentate ligands (Fig. 23.6), all of which were introduced within a surprisingly short time period [314]. BINOL has proven to be a very successful backbone with this class of ligand, and covers phosphites (**49**),

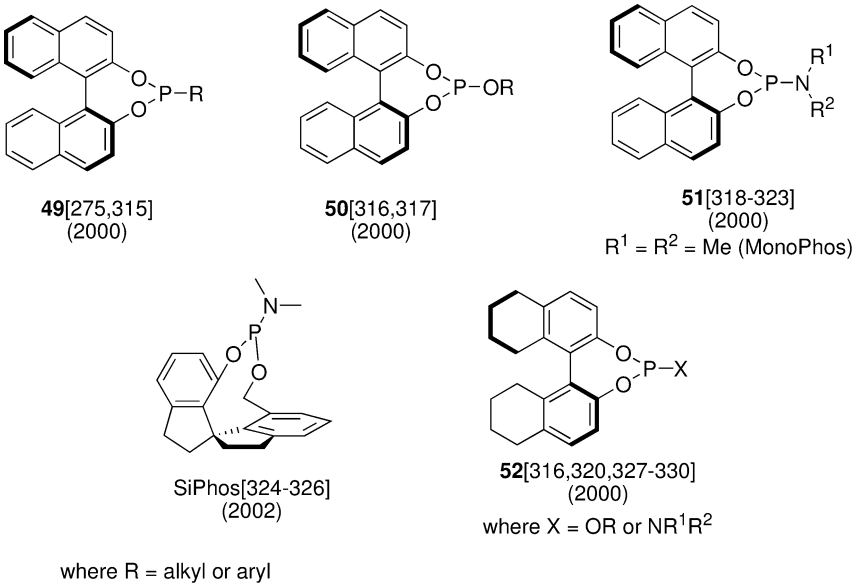

Fig. 23.6 Examples of monodentate ligands.

phosphinites (**50**), and phosphoramidites (**51**). Other variations include SiPhos, as well as reduced aromatic systems (**52**).

These ligands can be used to reduce a wide variety of carbon–carbon unsaturations, and have the advantage that their simple preparation can be used for rapid ligand library synthesis and screening [314, 318, 319, 330, 331].

23.10 Summary

The development of ligands and catalytic systems for the enantioselective hydrogenation of carbon–carbon unsaturation has been rapid, but was given an astounding start by the studies of Knowles, followed by the key findings of Kagan and colleagues. Many derivatives of these ligands have since found a place in the arsenal of the synthetic chemist. Both, Togni's ferrocene-based ligands and Burk's DuPhos family, have expanded the substrate potential of the approach as well as providing for higher selectivities and reactivities. However, recent studies have seen a return to *P*-chiral ligands, while another fairly recent contribution has come from the monodentate ligands of Pringle, Reetz, Feringa, Minnaard, and de Vries. With studies in other areas also beginning to bear fruit, it is possible that we will shortly see ligands based on alkenes making a significant impact. Although there is no "general" catalyst, there is still room for improvement with many potential substrate classes; clearly, the number of ligands appearing in the literature will continue to increase.

References

1 Harada, K. Asymmetric heterogeneous catalytic hydrogenation. In: Morrison, J.D. (Ed.), *Asymmetric Synthesis*. Academic Press, Inc., Orlando, FL, **1985**, *Vol. 5*, p. 345.
2 Blaser, H. *Tetrahedron: Asymmetry* **1991**, *2*, 843.
3 Tang, W., Zhang, Z. *Chem. Rev.* **2003**, *103*, 3029.
4 Takaya, H., Ohta, T., Noyori, R. Asymmetric hydrogenation. In: Ojima, I. (Ed.), *Catalytic Asymmetric Synthesis*. VCH Publishers, Inc., New York, NY, **1993**, p. 1.
5 Koenig, K.E. The applicability of asymmetric homogeneous catalytic hydrogenation. In: Morrison, J.D. (Ed.), *Asymmetric Synthesis*. Academic Press, Inc., Orlando, FL, **1985**; *Vol. 5*, p. 71.
6 Ojima, I., Clos, N., Bastos, C. *Tetrahedron* **1989**, *45*, 6901.
7 Nugent, W.A., RajanBabu, T.V., Burk, M.J. *Science* **1993**, *259*, 479.
8 Noyori, R. *Science* **1990**, *248*, 1194.
9 Noyori, R. *Tetrahedron* **1994**, *50*, 4259.
10 Knowles, W.S. *Angew. Chem., Int. Ed.* **2002**, *41*, **1998**.
11 Noyori, R. *Angew. Chem., Int. Ed.* **2002**, *41*, 2008.
12 Laneman, S.A. In: Ager, D.J. (Ed.), *Handbook of Chiral Fine Chemicals*, 2nd edition. CRC, Taylor Francis, Boca Raton, **2005**, p. 186.
13 Horner, L., Siegel, H., Buthe, H. *Angew. Chem., Int. Ed.* **1968**, *7*, 942.
14 Knowles, W.S., Sabacky, M.J. *J. Chem. Soc., Chem. Commun.* **1968**, 1445.
15 Marinetti, A., Carmichael, D. *Chem. Rev.* **2002**, *102*, 201.
16 Kagan, H.B. Chiral ligands for asymmetric catalysis. In: Morrison, J.D. (Ed.), *Asymmetric Synthesis*. Academic Press, Inc., Orlando, FL, **1985**, *Vol. 5*, p. 1.
17 Pietrusiewicz, K.M., Zablocka, M. *Chem. Rev.* **1994**, *94*, 1375.
18 Holz, J., Quirmbach, M., Börner, A. *Synthesis* **1997**, 983.
19 Ohff, M., Holz, J., Quirmbach, M., Börner, A. *Synthesis* **1998**, 1391.
20 Laurenti, D., Santelli, M. *Org. Prep. Proc. Int.* **1999**, *31*, 245.
21 Osborn, J.A., Jardine, F.H., Young, J.F., Wilkinson, G. *J. Chem. Soc. A* **1966**, 1711.
22 Knowles, W.S. *Acc. Chem. Res.* **1983**, *16*, 106.
23 Green, M., Kuc, T.A., Taylor, S.H. *J. Chem. Soc., Chem. Commun.* **1970**, 1553.
24 Knowles, W.S., Sabacky, M.J., Vineyard, B.D. *J. Chem. Soc., Chem. Commun.* **1972**, 10.
25 Vineyard, B.D., Knowles, W.S., Sabacky, M.J., Bachman, G.L., Weinkauff, D.J. *J. Am. Chem. Soc.* **1977**, *99*, 5946.
26 Knowles, W.S. *J. Chem. Ed.* **1986**, *63*, 222.
27 Knowles, W.S. Asymmetric hydrogenations — The Monsanto L-Dopa process. In: Blaser, H.-U., Schmidt, E. (Eds.), *Asymmetric Catalysis on Industrial Scale*. Wiley-VCH, Weinheim, **2004**, p. 23.
28 Ager, D.J., Laneman, S.A. The synthesis of unnatural amino acids. In: Blaser, H.-U., Schmidt, E. (Eds.), *Asymmetric Catalysis on Industrial Scale*. Wiley-VCH, Weinheim, **2004**, p. 259.
29 Laneman, S.A., Froen, D.E., Ager, D.J. The preparation of amino acids via Rh(DIPAMP)-catalyzed asymmetric hydrogenations. In: Herkes, F.E. (Ed.), *Catalysis of Organic Reactions*. Marcel Dekker, New York, **1998**, p. 525.
30 Chan, A.S.C., Pluth, J.J., Halpern, J. *J. Am. Chem. Soc.*, **1980**, *102*, 5953.
31 Halpern, J., Riley, D.P., Chan, A.S.C., Pluth, J.J. *J. Am. Chem. Soc.* **1977**, *99*, 8055.
32 Chan, A.S.C., Halpern, J. *J. Am. Chem. Soc.* **1980**, *102*, 838.
33 Chan, A.S.C., Pluth, J.J., Halpern, J. *J. Am. Chem. Soc.* **1980**, *102*, 5952.
34 Halpern, J. *Science* **1982**, *217*, 401.
35 Landis, C.R., Halpern, J. *J. Am. Chem. Soc.* **1987**, *109*, 1746.
36 Ashby, M.T., Halpern, J. *J. Am. Chem. Soc.* **1991**, *113*, 589.
37 Brown, J.M., Chaloner, P.A. *J. Chem. Soc., Chem. Commun.* **1978**, 321.
38 Brown, J.M., Chaloner, P.A. *Tetrahedron Lett.* **1978**, *19*, 1877.
39 Brown, J.M., Chaloner, P.A. *J. Chem. Soc., Chem. Commun.* **1979**, 613.

40 Brown, J.M., Chaloner, P.A. *J. Chem. Soc., Chem. Commun.* **1980**, 344.
41 Brown, J.M., Chaloner, P.A., Glaser, R., Geresh, S. *Tetrahedron* **1980**, *36*, 815.
42 Alcock, N.W., Brown, J.M., Derome, A., Lucy, A.R. *J. Chem. Soc., Chem. Commun.* **1985**, 575.
43 Brown, J.M., Chaloner, P.A., Morris, G.A. *J. Chem. Soc., Perkin Trans. II* **1987**, 1583.
44 Brown, J.M. *Chem. Soc. Rev.* **1993**, *22*, 25.
45 Halpern, J. Asymmetric catalytic hydrogenation: Mechanism and origin of enantioselection. In: Morrison, J.D. (Ed.), *Asymmetric Synthesis.* Academic Press, Orlando, **1985**, *Vol. 5*, p. 41.
46 Koenig, K.E., Sabacky, M.J., Bachman, G.L., Christopfel, W.C., Barnstorff, H.D., Friedman, R.B., Knowles, W.S., Stults, B.R., Vineyard, B.D., Weinkauff, D.J. *Ann. N. Y. Acad. Sci.* **1980**, *333*, 16.
47 Imamoto, T., Watanabe, J., Wada, Y., Masuda, H., Yamada, H., Tsuruta, H., Matsukawa, S., Yamaguchi, K. *J. Am. Chem. Soc.* **1998**, *120*, 1635.
48 Gridnev, I.D., Yamanoi, Y., Higashi, N., Tsuruta, H., Yasutake, M., Imamoto, T. *Adv. Synth. Catal.* **2001**, *343*, 118.
49 Gridnev, I.D., Yasutake, M., Higashi, N., Imamoto, T. *J. Am. Chem. Soc.* **2001**, *123*, 5268.
50 Yasutake, M., Gridnev, I.D., Higashi, N., Imamoto, T. *Org. Lett.* **2001**, *3*, 1701.
51 Gridnev, I.D., Higashi, N., Imamoto, T. *J. Am. Chem. Soc.* **2001**, *123*, 4631.
52 Yamanoi, Y., Imamoto, T. *J. Org. Chem.* **1999**, *64*, 2988.
53 Ohashi, A., Imamoto, T. *Org. Lett.* **2001**, *3*, 373.
54 Ohashi, A., Kikuchi, S.-I., Yasutake, M., Imamoto, T. *Eur. J. Org. Chem.* **2002**, 2535.
55 Tang, W., Zhang, X. *Angew. Chem., Int. Ed.* **2002**, *41*, 1612.
56 Tang, W., Zhang, X. *Org. Lett.* **2002**, *4*, 4159.
57 Tang, W., Liu, D., Zhang, X. *Org. Lett.* **2003**, *5*, 205.
58 Cong-Dung Le, J., Pagxenkopf, B.L. *J. Org. Chem.* **2004**, *69*, 4177.
59 Robin, F., Mercier, F., Ricard, L., Mathey, F., Spagnol, M. *Chem. Eur. J.* **1997**, *3*, 1365.
60 Mathey, F., Mercier, F., Robin, F., Ricard, L. *J. Organometal. Chem.* **1998**, *577*, 117.
61 Shimizu, H., Saito, T., Kumobayashi, H. *Adv. Synth. Catal.* **2003**, *345*, 185.
62 Carmichael, D., Doucet, H., Brown, J.M. *J. Chem. Soc., Chem. Commun.* **1999**, 261.
63 Hoge, G., Wu, H.-P., Kissel, W.S., Pflum, D.A., Greene, D.J., Bao, J. *J. Am. Chem. Soc.* **2004**, *126*, 5966.
64 Burk, M.J., De Konig, P.D., Grote, T.M., Hoekstra, M.S., Hoge, G., Jennings, R.A., Kissel, W.S., Le, T.V., Lennon, I.C., Mulhern, T.A., Ramsden, J.A., Wade, R.A. *J. Org. Chem.* **2003**, *68*, 5731.
65 Kagan, H.B., Langlois, N., Dang, T.P. *J. Organometal. Chem.* **1975**, *90*, 353.
66 Kagan, H.B., Dang, T.P. *J. Chem. Soc., Chem. Commun.* **1971**, 481.
67 Kagan, H.B., Dang, T.P. *J. Am. Chem. Soc.* **1972**, *94*, 6429.
68 Chiba, M., Takahashi, H., Takahashi, H., Morimoto, T., Achiwa, K. *Tetrahedron Lett.* **1987**, *28*, 3675.
69 Morimoto, T., Chiba, M., Achiwa, K. *Tetrahedron Lett.* **1988**, *29*, 4755.
70 Morimoto, T., Chiba, M., Achiwa, K. *Tetrahedron Lett.* **1989**, *30*, 735.
71 Morimoto, T., Chiba, M., Achiwa, K. *Chem. Pharm. Bull.* **1989**, *37*, 3161.
72 Morimoto, T., Chiba, M., Achiwa, K. *Heterocycles* **1990**, *30*, 363.
73 Yoshikawa, K., Inoguchi, K., Morimoto, T., Achiwa, K. *Heterocycles* **1990**, *31*, 261.
74 Morimoto, T., Chiba, M., Achiwa, K. *Tetrahedron Lett.* **1990**, *31*, 261.
75 Morimoto, T., Chiba, M., Achiwa, K. *Chem. Pharm. Bull.* **1993**, *41*, 1149.
76 Li, W., Zhang, X. *J. Org. Chem.* **2000**, *65*, 5871.
77 Yan, Y.-Y., RajanBabu, T.V. *J. Org. Chem.* **2000**, *65*, 900.
78 Yan, Y.-Y., RajanBabu, T.V. *Org. Lett.* **2000**, *2*, 199.
79 Yan, Y.-Y., RajanBabu, T.V. *Org. Lett.* **2000**, *2*, 4137.
80 Kagan, H.B., Fiaud, J.C., Hoornaert, C., Meyer, D., Poulin, J.C. *Bull. Soc. Chim. Belg.* **1979**, *88*, 923.
81 Li, W., Waldkirch, J.P., Zhang, X. *J. Org. Chem.* **2002**, 7618.
82 Fryzuk, M.B., Bosnich, B. *J. Am. Chem. Soc.* **1979**, *101*, 3043.

83 Fryzuk, M. B., Bosnich, B. *J. Am. Chem. Soc.* **1977**, *99*, 6262.
84 Fryzuk, M. D., Bosnich, B. *J. Am. Chem. Soc.* **1978**, *100*, 5491.
85 Achima, K. *J. Am. Chem. Soc.* **1976**, *98*, 8265.
86 Glaser, R., Geresh, S., Twaik, M. *Isr. J. Chem.* **1980**, *20*, 102.
87 Ojima, I., Kogure, T., Yoda, N. *J. Org. Chem.* **1980**, *45*, 4728.
88 Takahashi, H., Hattori, M., Chiba, M., Morimoto, T., Achiwa, K. *Tetrahedron Lett.* **1986**, *27*, 4477.
89 Takahashi, H., Morimoto, T., Achiwa, K. *Chem. Lett.* **1987**, 855.
90 Takahashi, H., Achiwa, K. *Chem. Lett.* **1987**, 1921.
91 Inoguchi, K., Morimoto, T., Achiwa, K. *J. Organomet. Chem.* **1989**, *370*, C9.
92 Takahashi, H., Yamamoto, N., Takeda, H., Achiwa, K. *Chem. Lett.* **1989**, 559.
93 Takahashi, H., Sakuraba, S., Takeda, H., Achiwa, K. *J. Am. Chem. Soc.* **1990**, *112*, 5876.
94 Sakuraba, S., Achiwa, K. *Synlett* **1991**, 689.
95 Sakuraba, S., Nakajima, N., Achiwa, K. *Synlett* **1992**, 829.
96 Sakuraba, S., Nakajima, N., Achiwa, K. *Tetrahedron: Asymmetry* **1993**, *7*, 1457.
97 Sakuraba, S., Takahashi, H., Takeda, H., Achiwa, K. *Chem. Pharm. Bull.* **1995**, *43*, 738.
98 Takeda, H., Hosokawa, S., Aburatani, M., Achiwa, K. *Synlett*, **1991**, 193.
99 Hayashi, T., Mise, T., Mitachi, S., Yamamoto, K., Kumada, M. *Tetrahedron Lett.* **1976**, 1133.
100 Hayashi, T., Mise, T., Fukushima, M., Kagotani, M., Nagashima, N., Hamada, Y., Matsumoto, A., Kawakami, S., Monishi, M., Yamomoto, K., Kumada, M. *Bull. Chem. Soc. Jpn.* **1980**, *53*, 1138.
101 Hayashi, T., Kumada, M. *Acc. Chem. Res.* **1982**, *15*, 395.
102 Hayashi, T., Mise, T., Kumada, M. *Tetrahedron Lett.* **1976**, 4351.
103 Yoshikawa, K., Inoguchi, K., Morimoto, T., Achiwa, K. *Heterocycles* **1990**, *31*, 261.
104 Sakuraba, S., Achiwa, K. *Synlett* **1991**, 689.
105 Andrade, J. G., Prescher, G., Schaefer, A., Nagel, U. In: *Chem. Ind.*, Kosik, J. (Ed.), Marcel Dekker, **1990**, p. 33.
106 Nagel, U. *Angew. Chem., Int. Ed. Engl.* **1984**, *23*, 435.
107 Allen, D. L., Gibson, V. C., Green, M. L. H., Skinner, J. F., Bashkin, J., Grebenik, P. D. *J. Chem. Soc., Chem. Commun.* **1983**, 895.
108 Brunner, H., Pieronczyk, W., Schönhammer, B., Streng, K., Bernal, I., Korp, J. *Chem. Ber.* **1981**, *114*, 1137.
109 Bakos, J., Toth, I., Markó, L. *J. Org. Chem.* **1981**, *46*, 5427.
110 NacNeil, P. A., Roberts, N. K., Bosnich, B. *J. Am. Chem. Soc.* **1981**, *103*, 2273.
111 Bakos, J., Tóth, I., Heil, B., Markó, L. *J. Organometal. Chem.* **1985**, *279*, 23.
112 Inoguchi, K., Achiwa, K. *Synlett* **1991**, 49.
113 Zhu, G., Cao, P., Jiang, Q., Zhang, X. *J. Am. Chem. Soc.* **1997**, *119*, 1799.
114 Zhu, G., Zhang, X. *J. Org. Chem.* **1998**, *63*, 9590.
115 Zhu, G., Casalnuovo, A. L., Zhang, X. *J. Org. Chem.* **1998**, *63*, 8100.
116 Zhu, G., Zhang, X. *Tetrahedron: Asymmetry* **1998**, *9*, 2415.
117 Zhu, G., Chen, Z., Zhang, X. *J. Org. Chem.* **1999**, *64*, 6907.
118 Cao, P., Zhang, X. *J. Org. Chem.* **1999**, *64*, 2127.
119 Lee, S.-G., Zhang, Y. J., Song, C. E., Lee, J. K., Choi, J. H. *Angew. Chem., Int. Ed.* **2002**, *41*, 847.
120 Lee, S.-G., Zhang, Y. J. *Org. Lett.* **2002**, *4*, 2429.
121 Lee, S.-G., Zhang, Y. J. *Tetrahedron: Asymmetry* **2002**, *13*, 1039.
122 Pye, P. J., Rossen, K., Reamer, R. A., Tsou, N. N., Volante, R. P., Reider, P. J. *J. Am. Chem. Soc.* **1997**, *119*, 6207.
123 Pye, P. J., Rossen, K., Reamer, R. A., Volante, R. P., Reider, P. J. *Tetrahedron Lett.* **1998**, *39*, 4441.
124 Burk, M. J., Hems, W., Herzberg, D., Malan, C., Zanotti-Gerosa, A. *Org. Lett.* **2000**, *2*, 4173.
125 Blaser, H.-U., Lotz, M., Spindler, F. In: *Handbook of Chiral Fine Chemicals*, 2nd edition. Ager, D. J. (Ed.), CRC: Taylor Francis, Boca Raton, **2005**, p. 287.
126 Colacot, T. J. *Chem. Rev.* **2003**, *103*, 3101.
127 Blaser, H.-U., Malan, C., Pugin, B., Spindler, F., Steiner, H., Studer, M. *Adv. Synth. Catal.* **2003**, *345*, 103.

128 Spindler, F., Pugin, B., Jalett, H.-P., Buser, H.-P., Pittelkow, U., Blaser, H.-U. Catalysis of Organic Reactions. In *Chem. Ind.*, Malz, J. (Ed.), Dekker: New York, **1996**; *Vol. 68*, p. 153.

129 Blaser, H.-U., Spindler, F. *Chimia* **1997**, *51*, 297.

130 Hayashi T. In: *Ferrocenes*. Togni, A., Hayashi T. (Eds.), VCH, Weinheim, **1995**, p. 105.

131 Togni, A., Breutel, C., Schnyder, A., Spindler, F., Landert, H., Tijani, A. *J. Am. Chem. Soc.* **1994**, *116*, 4062.

132 Hayashi, T., Kawamura, N., Ito, Y. *Tetrahedron Lett.* **1988**, *29*, 5969.

133 Hayashi, T., Kawamura, N., Ito, Y. *J. Am. Chem. Soc.* **1987**, *109*, 7876.

134 Almena Perea, J., Lotz, M., Knochel, P. *Tetrahedron: Asymmetry* **1999**, *10*, 375.

135 Hayashi, T., Yamamoto, A., Hojo, M., Ito, Y. *J. Chem. Soc., Chem. Commun.* **1989**, 495.

136 Schwink, L. *Tetrahedron Lett.* **1996**, *37*, 25.

137 Kang, J., Lee, J.H., Ahn, S.H., Choi, J.S. *Tetrahedron Lett.* **1998**, *39*, 5523.

138 Kang, J., Lee, J.H., Kim, J.B., Kim, G.J. *Chirality* **2000**, *12*, 378.

139 Almena Perea, J., Börner, A., Knochel, P. *Tetrahedron Lett.* **1998**, *39*, 8073.

140 Lotz, M., Ireland, T., Almena Perea, J., Knochel, P. *Tetrahedron: Asymmetry* **1999**, *10*, 1839.

141 Blaser, H.U., Brieden, W., Pugin, B., Spindler, F., Studer, M., Togni, A. *Topics in Catalysis* **2002**, *19*, 3.

142 Blaser, H.U., Buser, H.P., Coers, K., Hanreich, R., Jalett, H.P., Jelsch, E., Pugin, B., Schneider, H.D., Spindler, F., Wegmann, A. *Chimia* **1999**, *53*, 275.

143 Blaser, H.U., Spindler, F., Studer, M. *Appl. Catal. A: General* **2001**, *221*, 119.

144 Blaser, H.U. *Adv. Synth. Catal.* **2002**, *344*, 17.

145 Sturm, T., Xiao, L., Weissensteiner, W. *Chimia* **2001**, *55*, 688.

146 Sturm, T., Weissensteiner, W., Spindler, F., Mereiter, K., López-Agenjo, A.M., Manzano, B.R., Jalón, F.A. *Organometallics* **2002**, *21*, 1766.

147 Bader, R.R., Baumeister, P., Blaser, H.U. *Chimia* **1996**, *30*, 9.

148 Imwinkelried, R. *Chimia* **1997**, *51*, 300.

149 McGarrity, J.F., Brieden, W., Fuchs, R., Mettler, H.-P., Schmidt, B., Werbitzky, O. Liberties and constraints in the development of asymmetric hydrogenations on a technical scale. In: *Asymmetric Catalysis on Industrial Scale*. Blaser, H.U., Schmidt, E. (Eds.), Wiley-VCH, Weinheim, **2004**, Chapter III.3, p. 283.

150 Ireland, T., Tappe, K., Grossheimann, G., Knochel, P. *Chem. Eur. J.* **2002**, *8*, 843.

151 Lotz, M., Polborn, K., Knochel, P. *Angew. Chem., Int. Ed.* **2002**, *41*, 4708.

152 Ireland, T., Grossheimann, G., Wieser-Jeunesse, C., Knochel, P. *Angew. Chem., Int. Ed.* **1999**, *38*, 3212.

153 Tappe, K., Knochel, P. *Tetrahedron: Asymmetry* **2004**, *15*, 91.

154 Boaz, N.W., Debenham, S.D., Mackenzie, E.B., Large, S.E. *Org. Lett.* **2002**, *14*, 2421.

155 Boaz, N.W., Debenham, S.D., Large, S.E., Moore, M.K. *Tetrahedron: Asymmetry* **2003**, *14*, 3575.

156 Sturm, T., Weissensteiner, W., Spindler, F. *Adv. Synth. Catal.* **2003**, *345*, 160.

157 Kuwano, R., Sato, K., Kurokawa, T., Karube, D., Ito, Y. *J. Am. Chem. Soc.* **2000**, *122*, 7614.

158 Kuwano, R., Sawamura, M., Ito, Y. *Bull. Chem. Soc. Jpn.* **2000**, *73*, 2571.

159 Kuwano, R., Sawamura, M., Ito, Y. *Tetrahedron: Asymmetry* **1995**, *6*, 2521.

160 Kuwano, R., Ito, Y. *J. Org. Chem.* **1999**, *64*, 1232.

161 Kuwano, R., Okuda, S., Ito, Y. *J. Org. Chem.* **1998**, *63*, 3499.

162 Kuwano, R., Okuda, S., Ito, Y. *Tetrahedron: Asymmetry* **1998**, *9*, 2773.

163 Sawamura, M., Hamashima, H., Sugawara, M., Kuwano, N., Ito, Y. *Organometallics* **1995**, *14*, 4549.

164 Sawamura, M., Kuwano, R., Ito, Y. *J. Am. Chem. Soc.* **1995**, *117*, 9602.

165 Kuwano, R., Sato, K., Kurokawa, T., Karube, D. Ito, Y. *J. Am. Chem. Soc.*, **2000**, *122*, 7614.

166 Kromm, K., Osburn, P.L., Gladysz, J.A. *Organometallics* **2002**, *21*, 4275.

167 Berens, U., Burk, M.J., Gerlach, A., Hems, W. *Angew. Chem., Int. Ed.* **2000**, *39*, 1981.

168 Marinetti, A., Genet, J.-P., Jus, S., Blanc, D., Ratovelamanana-Vidal, V. *Chem. Eur. J.* **1999**, *5*, 1160.

169 Stoop, R.M., Mezzetti, A., Spindler, F. *Organometallics* **1998**, *17*, 668.

170 Maienza, F., Wörle, M., Steffanut, P., Mezzetti, A., Spindler, F. *Organometallics* **1999**, *18*, 1041.

171 Nettekoven, U., Kamer, P.C.J., van Leeuwen, P.W.N.M., Widhalm, M., Spek, A.L., Lutz, M. *J. Org. Chem.* **1999**, *64*, 3996.

172 Miyashita, A., Yasuda, A., Takaya, H., Toriumi, K., Ito. T., Souchi, T., Noyori, R. *J. Am. Chem. Soc.* **1980**, *102*, 7932.

173 Miyashita, A., Takaya, H., Souchi, T., Noyori, R. *Tetrahedron* **1984**, *40*, 1245.

174 Chan, A.S.C. *CHEMTECH* **1993**, *March*, 46.

175 Takaya, H., Ohta, T., Sayo, N., Kumobayashi, H., Akutagawa, S., Inoue, S., Kasahara, I., Noyori, R. *J. Am. Chem. Soc.* **1987**, *109*, 1596.

176 Noyori, R., Ohkuma, T. *Angew. Chem., Int. Ed.* **2001**, *40*, 40.

177 Noyori, R., Takaya, H. *Acc. Chem. Res.* **1990**, *23*, 345.

178 Akutagawa, S., Tani, K. Asymmetric isomerization of allylamines. In: *Catalytic Asymmetric Synthesis.* Ojima, I. (Ed.), VCH Publishers, Inc.: New York, **1993**, p. 41.

179 Noyori, R., Hasiguchi, S., Yamano, T. Asymmetric synthesis. In: *Applied Homogeneous Catalysis with Organic Compounds.* Herrmann, B.C.W.A. (Ed.), Wiley-VCH: Weinheim, **2002**; Vol. 1, p. 557.

180 Otsuka, S., Tani, K. In: *Asymmetric Catalytic Isomerization of Functionalized Olefins.* Morrison, J.D. (Ed.), Academic Press, Inc.: Orlando, FL, **1985**; Vol. 5, p. 171.

181 Kagan, H.B. *Bull. Soc. Chim. Fr.* **1988**, 846.

182 Miyashita, A., Karino, H., Shimamura, J., Chiba, T., Nagano, K., Nohira, H., Takaya, H. *Chem. Lett.* **1989**, 1007.

183 Miyashita, A., Karino, H., Shimamura, J., Chiba, T., Nagano, K., Nohira, H., Takaya, H. *Chem. Lett.* **1989**, 1849.

184 Chiba, T., Miyashita, A., Nohira, H. *Tetrahedron Lett.* **1991**, *32*, 4745.

185 Chiba, T., Miyashita, A., Nohira, H., Takaya H. *Tetrahedron Lett.* **1993**, *34*, 2351.

186 Schmid, R., Cereghetti, M., Heiser, B., Schönholzer, P., Hansen, H.-J. *Helv. Chim. Acta* **1988**, *71*, 897.

187 Schmid, R., Foricher, J., Cereghetti, M., Schonholzer, P. *Helv. Chim. Acta* **1991**, *74*, 370.

188 Gautier, I., Ratovelomanana-Vidal, V., Savignac, P., Genet, J.-P. *Tetrahedron Lett.* **1996**, *37*, 7721.

189 Gerlach, A., Scholz, U. *Spec. Chem. Magazine* **2004**, 37.

190 Yamamoto, N., Murata, M., Morimoto, T., Achiwa, K. *Chem. Pharm. Bull.* **1991**, *39*, 1085.

191 Murata, M., Morimoto, T., Achiwa, K. *Synlett* **1991**, 827.

192 Yoshikawa, K., Yamamoto, N., Murata, M., Awano, K., Morimoto, T., Achiwa, K. *Tetrahedron: Asymmetry* **1992**, *3*, 13.

193 Zhang, X., Mashima, K., Koyano, K., Sayo, N., Kumobayashi, H., Akutagawa, S., Takaya, H. *Tetrahedron Lett.* **1991**, *32*, 7283.

194 Zhang, X., Mashima, K., Koyano, K., Sayo, N., Kumobayashi, H., Akutagawa, S., Takaya, H. *J. Chem. Soc., Perkin Trans. I* **1994**, 2309.

195 Sollewijn Gelpke, A.E., Kooijman, H., Spek, A.L., Hiemstra, H. *Chem. Eur. J.* **1999**, *5*, 2472.

196 Benincori, T., Brenna, E., Sannicolò, F., Trimarco, L., Antognazza, P., Cesarotti, E. *J. Chem. Soc., Chem. Commun.* **1995**, 685.

197 Benincori, T., Brenna, E., Sannicolò, F., Trimarco, L., Antognazza, P., Cesarotti, E. Demartin, F., Pilati, T. *J. Org. Chem.* **1996**, *61*, 6244.

198 Beninicori, T., Cesarotti, E., Piccolo, O., Sannicolò, F. *J. Org. Chem.* **2000**, *65*, 2043.

199 Banzinger, M., Cercus, J., Hirt, H., Laumen, K., Malan, C., Spindler, F., Struber, F., Troxler, T. *Tetrahedron: Asymmetry* **2003**, *14*, 3469.

200 Pai, C.-C., Lin, C.-W., Lin, C.-C., Chen, C.-C., Chan, A.S.C. *J. Am. Chem. Soc.* **2000**, *122*, 11513.

201 Wu, J., Wai, H.K., Kim, H.L., Zhong, Y.Z., Yeung, C.H., Chan, A.S.C. *Tetrahedron Lett.* **2002**, 1539.

202 Wu, J., Chen, X., Guo, R., Yeung, C.H., Chan, A.S.C. *J. Org. Chem.* **2003**, *68*, 2490.

203 Wu, J., Chen, H., Zhou, Z.-Y., Yeung, C.H., Chan, A.S.C. *Synlett* **2001**, 1050.

204 Wu, J., Pai, C.-C., Kwok, W., Guo, R., Au-Yeung, T.T.-L., Yeung, C.H., Chan, A.S.C. *Tetrahedron: Asymmetry* **2003**, *14*, 987.

205 Tang, W., Chi, Y., Zhang, X. *Org. Lett.* **2002**, *4*, 1695.

206 Saito, T., Yokozawa, T., Ishizaki, T., Moroi, T., Sayo, N., Miura, T., Kumobayashi, H. *Adv. Synth. Catal.* **2001**, *343*, 264.

207 Pai, C.-C., Li, Y.-M., Zhong, Y.Z., Chan, A.S.C. *Tetrahedron Lett.* **2002**, *43*, 2789.

208 Zhang, Z., Qian, H., Longmire, J., Zhang, X. *J. Org. Chem.* **2000**, *65*, 6223.

209 Wu, S., Wang, W., Tang, W., Lin, M., Zhang, X. *Org. Lett.* **2002**, *4*, 4495.

210 Michaud, G., Bulliard, M., Ricard, L., Genêt, J.-P., Marinetti, A. *Chem. Eur. J.* **2002**, *8*, 3327.

211 Duprat de Paule, S., Jeulin, S., Ratovelomanana-Vidal, V., Genêt, J.-P., Champion, N., Dellis, P. *Tetrahedron Lett.* **2003**, *44*, 823.

212 Jeulin, S., Duprat de Paul, S., Ratovelomanana-Vidal, V., Genêt, J.-P., Champion, N., Dellis, P. *Proc. Nat. Acad. Sci. USA* **2004**, *101*, 5799.

213 Duprat de Paul, S., Jeulin, S., Ratovelomanana-Vidal, V., Genêt, J.-P., Champion, N., Dellis, P. *Eur. J. Org. Chem.* **2003**, 1931.

214 Jeulin, S., Duprat de Paul, S., Ratovelomanana-Vidal, V., Genêt, J.-P., Champion, N., Dellis, P. *Angew. Chem., Int. Ed.* **2004**, *43*, 320.

215 Ager, D.J., Babler, S., Froen, D.E., Laneman, S.A., Pantaleone, D.P., Prakash, I., Zhi, B. *Org. Proc. Research. Develop.* **2003**, *7*, 369.

216 Mashima, K., Kusano, K., Ohta, T., Noyori, R., Takaya, H. *J. Chem. Soc., Chem. Commun.* **1989**, 1208.

217 Noyori, R. *Chem. Soc. Rev.* **1989**, 187.

218 Takaya, H., Ohta, T., Mashima, K., Noyori, R. *Pure Appl. Chem.* **1990**, *62*, 1135.

219 Uemura, T., Zhang, X., Matsumura, K., Sayo, N., Kumobayashi, H., Ohta, T., Nozaki, K., Takaya, H. *J. Org. Chem.* **1996**, *61*, 5510.

220 Zhang, X., Uemura, T., Matsumura, K., Sayo, N., Kumobayashi, H., Tayaya, H. *Synlett* **1994**, 501.

221 Wan, K.T., Davis, M.E. *Nature* **1994**, *370*, 449.

222 Burk, M.J., Ramsden, J.A. In: *Handbook of Chiral Fine Chemicals*, 2nd edition. Ager, D.J. (Ed.), CRC: Taylor Francis, Boca Raton, **2005**, p. 249.

223 Cobley, C.J., Johnson, N.B., Lennon, I.C., McCague, R., Ramsden, J.A., Zanotti-Gerosa, A. In: *Asymmetric Catalysis on Industrial Scale*. Blaser, H.U., Schmidt, E. (Eds.), Wiley-VCH, Weinheim, **2004**, Chapter III.2, p. 269.

224 Burk, M.J., Feaster, J.E., Harlow, R.L. *Organometallics* **1990**, *9*, 2653.

225 Burk, M.J., Harlow, R.L., *Angew. Chem., Int. Ed.* **1990**, *29*, 1462.

226 Burk, M.J., Feaster, J.E., Nugent, W.A., Harlow, R.L. *J. Am. Chem. Soc.* **1993**, *115*, 10125.

227 Burk, M.J., Bienewald, F. In: *Transition Metals for Organic Synthesis and Fine Chemicals*. Bolm, C., Beller, M. (Eds.), VCH Publishers: Weinheim, Germany, **1998**, Vol. 2, p. 13.

228 Stammers, T.A., Burk, M.J. *Tetrahedron Lett.* **1999**, *40*, 3325.

229 Masquelin, T., Broger, E., Mueller, K., Schmid, R., Obrecht, D. *Helv. Chim. Acta* **1994**, *77*, 1395.

230 Jones, S.W., Palmer, C.F., Paul, J.M., Tiffin, P.D. *Tetrahedron Lett.* **1999**, *40*, 1211.

231 Debenham, S.D., Debenham, J.S., Burk, M.J., Toone, E.J. *J. Am. Chem. Soc.* **1997**, *119*, 9897.

232 Debenham S.D., Cossrow, J., Toone, E.J. *J. Org. Chem.* **1999**, *64*, 9153.

233 Xu, X., Fakha, G., Sinou, D. *Tetrahedron* **2002**, *58*, 7539.

234 Rizen, A., Basu, B., Chattopadhyay, S.K., Dossa, F., Frejd, T. *Tetrahedron: Asymmetry* **1998**, *9*, 503.

235 Hiebl, J., Kollmann, H., Rovenszky, F., Winkler, K. *J. Org. Chem.* **1999**, *64*, 1947.

236 Maricic, S., Ritzén, A., Berg, U., Frejd, T. *Tetrahedron*, **2001**, *57*, 6523.

237 Shieh, W.-C., Xue, S., Reel, N., Wu, R., Fitt, J., Repic, O. *Tetrahedron: Asymmetry* **2001**, *12*, 2421.

238 Wang, W., Yang, J., Ying, J., Xiong, C., Zhang, J., Cai, C., Hruby, V.J. *J. Org. Chem.* **2002**, *67*, 6353.

239 Wang, W., Cai, M., Xiong, C., Zhang, J., Trivedi, D., Hruby, V.J. *Tetrahedron* **2002**, *58*, 7365.

240 Burk, M.J., Allen, J.G., Kiesman, W.F. *J. Am. Chem. Soc.* **1998**, *120*, 657.

241 Teoh, E., Campi, E.M., Jackson, W.R., Robinson, A.J. *J. Chem. Soc., Chem. Commun.* **2002**, 978.

242 Hoerrner, R.S., Askin, D., Volante, R.P., Reider, P.J. *Tetrahedron Lett.* **1998**, *39*, 3455.

243 Burk, M.J., Gross, M.F., Martinez, J.P. *J. Am. Chem. Soc.* **1995**, *117*, 9375.

244 Burk, M.J. *Acc. Chem. Res.* **2000**, *33*, 363.

245 Burk, M.J., Wang, Y.M., Lee, J.R. *J. Am. Chem. Soc.* **1996**, *118*, 5142.

246 Burk, M.J. *J. Am. Chem. Soc.* **1991**, *113*, 8518.

247 Boaz, N.W. *Tetrahedron Lett.* **1998**, *39*, 5505.

248 Burk, M.J., Stammers, T.A., Straub, J.A. *Org. Lett.* **1999**, *1*, 387.

249 Burk, M. J., Kalberg, C.S., Pizzano, A. *J. Am. Chem. Soc.* **1998**, *120*, 4345.

250 Burk, M.J., Bienewald, F., Harris, M., Zanotti-Gerosa, A. *Angew. Chem., Int. Ed.* **1998**, *37*, 1931.

251 Morimoto, T., Ando, N., Achiwa, K. *Synlett* **1996**, 1211.

252 Dierkes, P., Ramdeehul, S., Barloy, L., De Cian, A., Fischer, J., Kamer, P.C.J., van Leeuwen, P.W.N.M., Osborn, J.A. *Angew. Chem., Int. Ed.* **1998**, *37*, 3116.

253 Schmid, R., Broger, E.A., Cereghetti, M., Crameri, Y., Foricher, J., Lalonde, M., Muller, R.K., Scalone, M., Schoettel, G., Zutter, U. *Pure Appl. Chem.* **1996**, *68*, 131.

254 Burk, M.J., Pizzano, A., Martin, J.A., Liable-Sands, L., Rheingold, A.L. *Organometallics* **2000**, *19*, 250.

255 Burk, M.J., Gross, M.F. *Tetrahedron Lett.* **1994**, *35*, 9363.

256 Holz, J., Quirmbach, M., Schmidt, U., Heller, D., Stürmer, R., Börner, A. *J. Org. Chem.* **1998**, *63*, 8031.

257 RajanBabu, T.V., Yan, Y.-Y., Shin, S. *J. Am. Chem. Soc.* **2001**, *123*, 10207.

258 Li, W., Zhang, Z., Zhang, X. *J. Org. Chem.* **2000**, *65*, 3489.

259 Holz, J., Stürmer, R., Schmidt, U., Drexler, H.-J., Heller, D., Krimmer, H.-P., Börner, A. *Eur. J. Org. Chem.* **2001**, 4615.

260 Holz, J., Monsees, A., Jiao, H., You, J., Komarov, I.V., Fischer, C., Drauz, K., Borner, A. *J. Org. Chem.* **2003**, *68*, 1701.

261 Fernandez, E., Gillon, A., Heslop, K., Horwood, E., Hyett, D.J., Orpen, A.G., Pringle, P.G. *J. Chem. Soc., Chem. Commun.* **2000**, 1663.

262 Landis, C.R., Wiechang, J., Owen, J.S., Clark, T.P. *Angew. Chem., Int. Ed.* **2001**, *40*, 3432.

263 Matsumura, K., Shimizu, H., Saito, T., Kumobayashi, H. *Adv. Synth. Catal.* **2003**, *345*, 180.

264 Marinetti, A., Kruger, V., Buzin, F.-X. *Tetrahedron Lett.* **1997**, *38*, 2947.

265 Marinetti, A., Labrue, F., Genêt, J.-P. *Synlett* **1999**, 1975.

266 Marinetti, A., Jus, S., Genêt, J.-P. *Tetrahedron Lett.* **1999**, *40*, 8365.

267 Marinetti, A., Jus, S., Genêt, J.-P., Ricard, L. *Tetrahedron* **2000**, *56*, 95.

268 Marinnetti, A., Jus, S., Genêt, J.-P., Ricard, L. *J. Organometal. Chem.* **2001**, *624*, 162.

269 Zhang, Z., Zhu, G., Jiang, Q., Xiao, D., Zhang, X. *J. Org. Chem.* **1999**, *64*, 1774.

270 Jiang, Q., Xiao, D., Zhang, Z., Cao, P., Zhang, X. *Angew. Chem., Int. Ed.* **1999**, *38*, 516.

271 Holz, J., Stürmer, R., Schmidt, U., Drexler, H.-J., Heller, D., Krimmer, H.-P., Börner, A. *Eur. J. Org. Chem.* **2000**, 4615.

272 Holz, J., Heller, D., Stürmer, R., Börner, A. *Tetrahedron Lett.* **1999**, *40*, 7059.

273 Matsumura, K., Shimizu, H., Saito, T., Kumobayashi, H. *Adv. Synth. Catal.* **2003**, *345*, 180.

274 Claver, C., Fernandez, E., Gillon, A., Heslop, K., Hyett, D.J., Martorell, A., Orpen, A.G., Pringle, P.G. *J. Chem. Soc., Chem. Commun.* **2000**, 961.

275 Selke, R., Pracejus, H. *J. Mol. Catal.* **1986**, *37*, 213.
276 Vocke, W., Hanel, R., Flother, F.-U. *Chem. Technol.* **1987**, *39*, 123.
277 de Vies, J.G. In: *Encyclopedia of Catalysis.* Horvath, I. (Ed.), Wiley, New York, **2003**, Vol. 3, p. 295.
278 Selke, R. *J. Organometal. Chem.* **1989**, *370*, 249.
279 Selke, R., Facklam, C., Foken, H., Heller, D. *Tetrahedron: Asymmetry* **1993**, *4*, 369.
280 RajanBabu, T.V., Ayers, T.A., Casalnuovo, A.L. *J. Am. Chem. Soc.* **1994**, *116*, 4101.
281 RajanBabu, T.V., Ayers, T.A., Halliday, G.A., You, K.K., Calabrese, J.C. *J. Org. Chem.* **1997**, *62*, 6012.
282 Chan, A.S.C., Hu, W., Pai, C.-C., Lau, C.-P., Jiang, Y., Mi, A., Yan, M., Sun, J., Lou, R., Deng, J. *J. Am. Chem. Soc.* **1997**, *119*, 9570.
283 Hu, W., Yan, M., Lau, C.-P., Yang, S.M., Chan, A.S.C., Jiang, Y., Mi, A. *Tetrahedron Lett.* **1999**, *40*, 973.
284 Chen, Y., Li, X., Tong, S.-K., Choi, M.C.K., Chan, A.S.C. *Tetrahedron Lett.* **1999**, *40*, 957.
285 Selke, R. *J. Organometal. Chem.* **1989**, *370*, 249.
286 Zhou, Y.-G., Zhang, X. *Chem. Commun.* **2002**, 1124.
287 Fiorini, M., Giongo, G.M. *J. Mol. Catal.* **1979**, *5*, 303.
288 Pracejus, G., Pracejus, H. *Tetrahedron Lett.* **1977**, *39*, 3497.
289 Zhang, F.-Y., Pai, C.-C., Chan, A.S.C. *J. Am. Chem. Soc.* **1998**, *120*, 5808.
290 Zhang, F.-Y., Kwok, W.H., Chan, A.S.C. *Tetrahedron: Asymmetry* **2001**, *12*, 2337.
291 Guo, R., Li, X., Wu, J., Kwok, W.H., Chen, J., Choi, M.C.K., Chan, A.S.C. *Tetrahedron Lett.* **2002**, *43*, 6803.
292 Franciò, G., Faraone, F., Leitner, W. *Angew. Chem., Int. Ed.* **2000**, *39*, 1428.
293 Roucoux, A., Agbossou, F., Mortreux, A., Petit, F. *Tetrahedron: Asymmetry* **1993**, *4*, 2279.
294 Agbossou, F., Carpentier, J.-F., Hatat, C., Kokel, N., Mortreux, A. *Organometallics* **1995**, *14*, 2480.
295 Roucoux, A., Devocelle, M., Carpentier, J.-F., Agbossou, F., Mortreux, A. *Synlett.* **1995**, 358.
296 Roucoux, A., Thieffry, L., Carpentier, J.-F., Devocelle, M., Méliet, C., Agbossou, F., Mortreux, A. *Organometallics* **1996**, *15*, 2440.
297 Devocelle, M., Agbossou, F., Mortreux, A. *Synlett* **1997**, 1306.
298 Carpentier, J.-F., Mortreux, A. *Tetrahedron Asymmetry* **1997**, *8*, 1083.
299 Pasquier, C., Naili, S., Pelinski, L., Brocard, J., Mortreux, A., Agbossou, F. *Tetrahedron: Asymmetry* **1998**, *9*, 193.
300 Agbossou, F., Carpentier, J.-F., Hapiot, F., Suisse, I., Mortreux, A. *Coord. Chem. Rev.* **1998**, *178–180*, 1615.
301 Kreuzfeld, H.-J., Schmidt, U., Döbler, C., Krause, H.W. *Tetrahedron: Asymmetry* **1996**, *7*, 1011.
302 Xie, Y., Lou, R., Li, Z., Mi, A., Jiang, Y. *Tetrahedron: Asymmetry* **2000**, *11*, 1487.
303 Lou, R., Mi, A., Jiang, Y., Qin, Y., Li, Z., Fu, F., Chan, A.S.C. *Tetrahedron* **2000**, *56*, 5857.
304 Crabtree, R.H. *Acc. Chem. Res.* 1979, *12*, 331.
305 Helmchen, G., Kudis, S., Sennhenn, P., Steinhagen, H. *Pure Appl. Chem.* **1997**, *69*, 513.
306 Pfaltz, A. *Acta Chem. Scand. B* **1996**, *50*, 189.
307 Helmchen, G., Pfaltz, A. *Acc. Chem. Res.* **2000**, *33*, 336.
308 Lightfoot, A., Schnider, P., Pfaltz, A. *Angew. Chem., Int. Ed.* **1998**, *37*, 2897.
309 Blackmond, D.G., Lightfoot, A., Pfaltz, A., Rosner, T., Schnider, P., Zimmermann, N. *Chirality* **2000**, *12*, 442.
310 Pfaltz, A., Blankenstein, J., Hilgraf, R., Hörmann, E., McIntyre, S., Menges, F., Schönleber, M., Smidt, S.P., Wüstenberg, B., Zimmermann, N. *Adv. Synth. Catal.* **2003**, *345*, 33.
311 Cozzi, P.G., Zimmermann, N., Hilgraf, R., Schaffner, S., Pfaltz, A. *Adv. Synth. Catal.* **2001**, *343*, 450.
312 Menges, F., Neuburger, M., Pfaltz, A. *Org. Lett.* **2002**, *4*, 4713.
313 Hou, D.-R., Reibenspies, J., Colacot, T.J., Burgess, K. *Chem. Eur. J.* **2001**, *7*, 5391.

314 de Vries, J.G. In: *Handbook of Chiral Fine Chemicals*, 2nd edition. Ager, D.J. (Ed.), CRC: Taylor Francis, Boca Raton, **2005**, p. 269.

315 Reetz, M.T., Sell, T. *Tetrahedron Lett.* **2000**, *41*, 6333.

316 Reetz, M.T., Mehler, G. *Angew. Chem., Int. Ed.* **2000**, *39*, 3889.

317 Reetz, M.T., Mehler, G., Meiswinkel, A., Sell, T. *Tetrahedron Lett.* **2002**, *43*, 7941.

318 de Vries, J.G., de Vries, A.H.M. *Eur. J. Org. Chem.* **2003**, 799.

319 van den Berg, M., Minnaard, A.J., Schudde, E.P., van Esch, J., de Vries, A.H.M., de Vries, J.G., Feringa, B.L. *J. Am. Chem. Soc.* **2000**, *122*, 11539.

320 van den Berg, M., Minnaard, A.J., Haak, R.M., Leeman, M., Schudde, E.P., Meetsma, A., Feringa, B.L., de Vries, A.H.M., Maljaars, C.E.P., Willans, C.E., Hyett, D., Boogers, J.A.F., Henderickx, H.J.W., de Vries, J.G. *Adv. Synth. Catal.* **2003**, *345*, 308.

321 Jia, X., Guo, R., Li, X., Yao, X., Chan, A.S.C. *Tetrahedron Lett.* **2002**, *43*, 5541.

322 van den Berg, M., Haak, R.M., Minnaard, A.J., de Vries, A.H.M., de Vries, J.G., Feringa, B.L. *Adv. Synth. Catal.* **2002**, *344*, 1003.

323 Ager, D., van den Berg, M., Minnaard, A.J., Feringa, B.L., de Vries, A.H.M., Willans, C.E., Boogers, J.A.F., de Vries, J.G. An affordable catalyst for the production of amino acids. In: *Methodologies in Asymmetric Catalysis.* Malhotra, S.V. (Ed.), ACS Symposium Series 880, American Chemical Society, Washington DC, **2004**, pp. 115.

324 Fu, Y., Xie, J.-H., Hu, A.-G., Zhou, H., Wang, L.-X., Zhou, Q.-L. *J. Chem. Soc., Chem. Commun.* **2002**, 480.

325 Hu, A.-G., Fu, Y., Xie, J.-H., Zhou, H., Wang, L.-X., Zhou, Q.-L. *Angew. Chem., Int. Ed.* **2002**, *41*, 2348.

326 Zhu, S.-F., Fu, Y., Xie, J.-H., Liu, B., Xing, L., Zhou, Q.-L. *Tetrahedron: Asymmetry* **2003**, *14*, 3219.

327 Gergely, I., Hegedüs, C; Gulyás, H., Szöllősy, Á., Monsees, A., Riermeier, T., Bakos, J., *Tetrahedron: Asymmetry* **2003**, *14*, 1087.

328 Hannen, P., Millitzer, H.-C., Vogl, E.M., Rampf, F.A. *J. Chem. Soc., Chem. Commun.* **2003**, 2210.

329 Zeng, Q., Liu, H., Cui, X., Mi, A., Jiang, Y., Li, X., Choi, M.C.K., Chan, A.S.C. *Tetrahedron: Asymmetry* **2002**, *13*, 115.

330 Lefort, L., Boogers, J.A.F., de Vries, A.H.M., de Vries, J.G. *Org. Lett.* **2004**, *6*, 1733.

331 Peña, D., Minnaard, A.J., Boogers, J.A.F., de Vries, A.H.M., de Vries J.G., Feringa, B.L. *Org. Biomol. Chem.* **2003**, *1*, 1087.

24
Enantioselective Hydrogenation: Phospholane Ligands

Christopher J. Cobley and Paul H. Moran

24.1
Introduction and Extent of Review

The ability to efficiently synthesize enantiomerically enriched materials is of key importance to the pharmaceutical, flavor and fragrance, animal health, agrochemicals, and functional materials industries [1]. An enantiomeric catalytic approach potentially offers a cost-effective and environmentally responsible solution, and the assessment of chiral technologies applied to date shows enantioselective hydrogenation to be one of the most industrially applicable [2]. This is not least due to the ability to systematically modify chiral ligands, within an appropriate catalyst system, to obtain the desired reactivity and selectivity. With respect to this, phosphorus(III)-based ligands have proven to be the most effective.

Amongst the hundreds of chiral phosphorus-based ligands developed since the seminal studies of Knowles and Horner [3], only a select few ligand families have had a revolutionary impact on the field. The highly modular chiral C_2-symmetric phospholane ligands (DuPhos^{TM} and BPE), developed by Burk and coworkers at DuPont, are one such example. As a result, much effort has been directed towards building on this breakthrough discovery and extending both the design and application of this ligand class.

In this chapter, we review the growing family of phospholane-based chiral ligands, and specifically examine their applications in the field of enantioselective hydrogenation. In general, this ligand class has found its broadest applicability in the reduction of prochiral olefins and, to a significantly lesser extent, ketones and imines; this is reflected in the composition of the chapter. Several analogous phosphacycle systems have also been included, where appropriate.

Whilst trying to be comprehensive, we have also intended to introduce a strong applied flavor to this summary. In the industrial case, catalyst performance is critically judged on overall efficiency, namely catalyst productivity and activity as well as enantioselectivity. As a result, turnover numbers (TONs) and turnover frequencies (TOFs) have been included or calculated whenever possible and meaningful.

The Handbook of Homogeneous Hydrogenation.
Edited by J.G. de Vries and C.J. Elsevier
Copyright © 2007 WILEY-VCH Verlag GmbH & Co. KGaA, Weinheim
ISBN: 978-3-527-31161-3

However, the reader should be aware of the danger of comparing systems tested under nonequivalent conditions (e.g., *in situ* versus preformed catalysts or alternative solvents). It is also worth noting that as this chapter is dedicated to applications in enantioselective hydrogenation, there may be many examples of phospholane-containing ligands that do not feature. Since this is by no means the first review of this type [2, 4], hopefully those reviews dealing with more general enantioselective applications will capture these aspects [5].

24.2 Phospholane Ligands: Synthesis and Scope

24.2.1 Early Discoveries and the Breakthrough with DuPhos and BPE

The first reported application of phospholane-based ligands for enantiomeric hydrogenation was described by Brunner and Sievi in 1987 [6]. Unfortunately, these *trans*-3,4-disubstituted phospholanes (**1**–**3**) were derived from tartaric acid, and proved to be relatively unselective for the rhodium-catalyzed hydrogenation of (*Z*)-*α*-(*N*-acetamido)cinnamic acid (6.6–16.8% ee). This was, presumably, due to the remoteness of the chiral centers from the metal coordination sphere failing to impart a significant influence. This was also found to be the case with several other bi- and tridentate analogues [7].

The fundamental discovery by Burk et al. that the analogous *trans*-2,5-disubstituted phospholanes formed a more rigid steric environment led to the introduction of the DuPhos and BPE ligand classes (Fig. 24.1) [8–13]. Subsequently, these ligands have been successfully employed in numerous enantiomeric catalytic systems [4a, 5], the most fruitful and prolific being Rh-catalyzed hydrogenations. The reduction of *N*-substituted *α*- and *β*-dehydroamino acid derivatives,

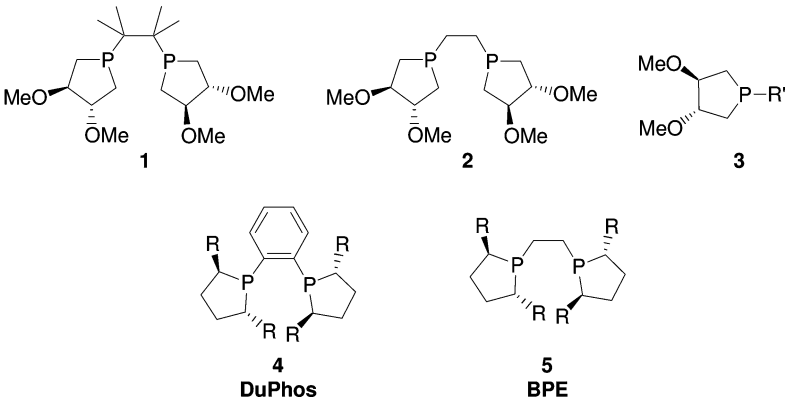

Fig. 24.1 The first phospholanes to be used for enantiomeric hydrogenation.

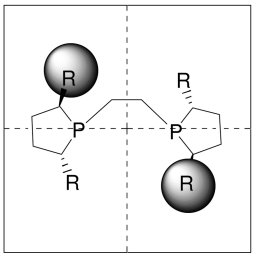

Fig. 24.2 The steric quadrant model for 2,5-disubstituted phospholanes.

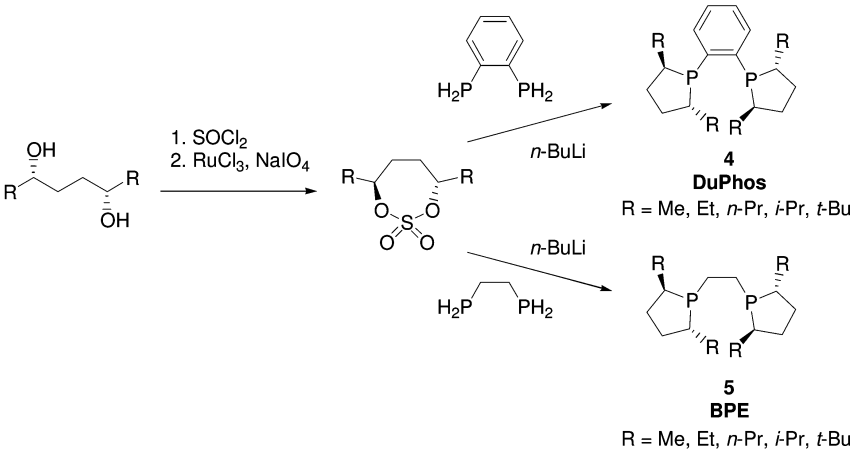

Scheme 24.1 The synthesis of *trans*-2,5-dialkyl-phospholanes, DuPhos.

β-dehydroamino alcohols, *N*-acylhydrazones, *N*-substituted enamides, enol esters, *α*,*β*-unsaturated acid and *β*-keto ester derivatives have all been achieved in exceptionally high enantioselectivity [4a, 14–21]. Furthermore, the combination of robustness, high activity, and excellent selectivity has rendered these ligands suitable for commercial-scale industrial applications [2d, 4b, 22, 23]. A simplistic, qualitative guide to explaining the high degree of selectivity observed has been provided in part by the quadrant model (Fig. 24.2) [4a]. By having two of the four phospholane substituents project into the open coordination plane of the metal, steric interactions influence the reaction pathway, though some dispute as to the validity of this model has recently been raised [24].

The conventional synthesis of *trans*-2,5-dialkyl phospholanes starting from a chiral 1,4-diol is shown in Scheme 24.1. Originally, these 1,4-diols were obtained via electrochemical Kolbe coupling of single enantiomer *α*-hydroxy acids [25], but this method proved to be commercially impracticable and has since been replaced by more viable biocatalytic routes [26]. Reaction of the chiral 1,4-diol with thionyl chloride followed by ruthenium-catalyzed oxidation with so-

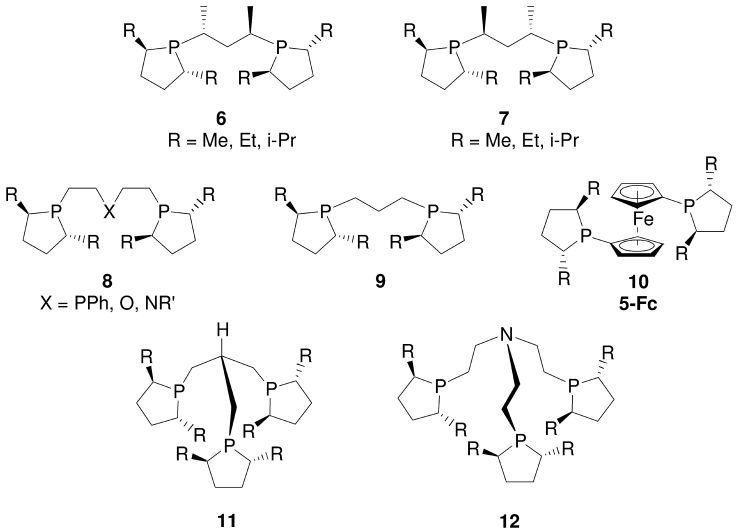

Fig. 24.3 Multidentate 2,5-disubstituted phospholanes displaying wide backbone diversity.

dium periodate yields the cyclic sulfate [27]. Treatment with 2 equiv. of a strong base, such as BuLi, and addition of a primary phosphine affords the tertiary phospholane with net inversion of stereochemistry. Practical methods have been developed for the large-scale manufacture of these ligands [28]. An alternative method via lithium phosphides was originally applied, but this was handicapped by excessive P–P bond formation [8], in addition to partial racemization of the phospholane chiral centers [11, 29]. Clearly, multidentate ligands may be obtained if a moiety containing more than one primary phosphine is used, and indeed numerous examples with a wide diversity of backbones were reported by Burk et al. (Fig. 24.3) [8, 10, 11, 29, 30].

Unfortunately, *trans*-2,5-diaryl phospholanes cannot be prepared using the traditional method described above for the alkyl derivatives; the basic conditions employed tend to induce elimination reactions with the corresponding cyclic aryl sulfate or dimesylate [31]. In 1991, Fiaud and co-workers reported a route to single enantiomer *trans*-1,2,5-triphenylphospholane oxide via epimerization of the previously reported *cis*-isomer and liquid chromatographic separation of the racemate [32]. Later, an alternative approach was developed using a chelotropic reaction between 1,4-diphenylbuta-1,3-diene and a dichloroaminophosphine (Scheme 24.2) [31]. After reduction, epimerization and hydrolysis, a diastereomeric salt resolution of the resulting racemic *trans*-2,5-diphenyl phospholanic acid could now be achieved, yielding the enantiomerically pure phospholane synthon **13**. This was ultimately converted to a series of monodentate 2,5-triphenylphospholane ligands (**14**), and shown to give reasonable to high enantioselectivities for the hydrogenation of (*Z*)-methyl-2-acetamidocinnamate (MAC), itaconic acid and esters, and *N*-acetyl enamides [31, 33]. This procedure has since

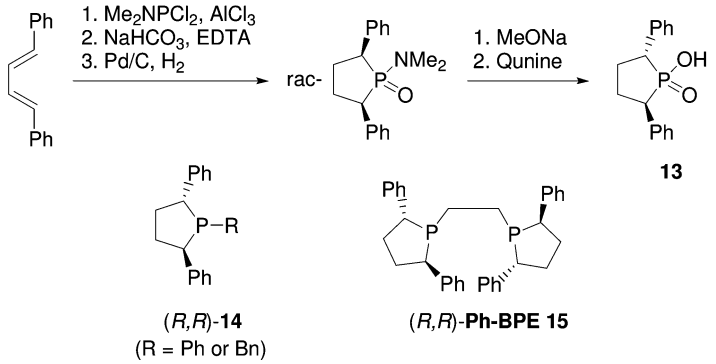

Scheme 24.2 Preparation, resolution and resulting ligands from 2,5-diaryl phospholanic acid.

been used to prepare the bidentate bisphospholane, Ph-BPE **15** (Scheme 24.2) [34]. This has been shown to have excellent levels of selectivity and activity for the hydrogenation of a range of olefinic substrates when compared to the dialkyl analogues [34, 35].

Although the DuPhos and BPE family of ligands have been shown to form active asymmetric hydrogenation catalysts with a range of transition metals (namely Ru, Ir, Pt, Pd and Au), none has shown the high degrees of selectivity and activity typically reported for the Rh-based catalysts. On the whole, the most successful results have been obtained with preformed mononuclear, cationic complexes employing the diolefin co-ligands 1,5-cyclooctadiene (COD) or norbornadiene (NBD). There has been some debate regarding COD precatalysts being uneconomic for use in industrial processes when compared with the NBD analogues [36]. A study performed at high catalyst loadings (molar substrate to catalyst ratio (SCR) = 100) showed there to be a rate difference for some substrates due to the NBD precatalyst forming the active species faster, but with no difference in enantioselectivity. However, when more industrially practical conditions were applied (SCR 2000 to 10 000), this effect became insignificant to the catalyst's overall productivity; furthermore, it was shown to be substrate-dependent [37]. In fact, the experimental conditions (e.g., stirring rate) were found to have a far more dramatic effect than the choice of precatalyst. For this class of reaction, hydrogen mass transfer into solution is the most important individual process parameter to affect the overall reaction rate [38].

In general, the choice of counteranion has a minor effect on catalyst performance, with typical examples being selected from BF_4^-, OTf^-, PF_6^-, or $BARF^-$. In one example, however, it was noted that [(*R,R*)-Et-DuPhos Rh COD]OTf gave superior selectivity for the reduction of β-βdisubstituted α-dehydroamino acid derivatives than the corresponding BARF complex when performed in a range of solvents, including supercritical carbon dioxide [39].

In recent years, considerable effort has been made to immobilize homogeneous hydrogenation catalysts because of the obvious potential advantages, such as improved separation and catalytic performance [4b, 40]. Although beyond the

remit of this chapter, it is worth mentioning that significant success has been achieved with several examples involving catalysts based on phospholane ligands [41].

Unsurprisingly, the immense success of DuPhos and BPE has created considerable interest in this ligand class, resulting in a vast number of variants appearing over the past few years. This has partly been driven by a desire to circumvent the original patents, but also by others in an attempt to explore certain mechanistic or design theories. On the whole, these ligands display similar properties to DuPhos and BPE with variable degrees of selectivity and activity when applied to enantioselective hydrogenation. This expansion has been partly facilitated by the modular nature of these ligands [4a], with modifications to the backbones, phospholane substituents, and second chelating site. A summary of these ligands concludes this section.

24.2.2
Modifications to the Backbone

The structures depicted in Figure 24.4 all display alterations to the original DuPhos and BPE backbones, and a concomitant variation in the ligand bite angle. In general, these have been prepared using the traditional cyclic sulfate method with the corresponding primary diphosphine. Pringle et al. have successfully applied a chiral *trans*-1,2-diphosphinocyclopentane to the synthesis of matching and mis-matching bidentate phospholanes **16** [24]. Hydrogenation of MAC was achieved with 77% to 98% ee, depending on the relative chirality of the backbone and 2,5-positions of the phospholane rings, with the overall stereochemis-

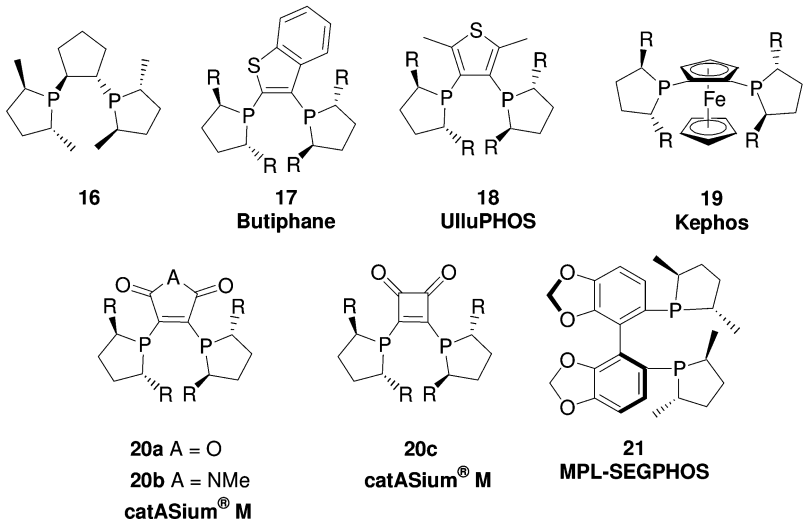

Fig. 24.4 DuPhos and BPE analogues with modified backbones.

try of the product being determined by the phospholane moieties. The sulfur heterocycle-based ligands, Butiphane (**17**) [42, 43] and UlluPHOS (**18**) [43, 44], have both been reported to be applicable for the Rh-catalyzed enantiomeric reduction of simple α-dehydroamino acid and itaconate derivatives, giving comparable results to Me-DuPhos in each case. Interestingly, the synthesis of Butiphane, together with that of several other benzo[b]thiophene-based ligands, was facilitated by the use of *N*,*N*-dialkyl-aminophosphine-containing intermediates acting as directing groups in the *ortho*-lithiation of the backbone. Several ferrocenyl-1,2-diphosphines, including Kephos (**19**), have also recently been reported to be effective for the reduction of several standard model substrates [45].

One exception to the use of primary phosphines is in the reported syntheses of the catASium® M class of ligands **20** [46–49]. In one report, reaction of the cyclic sulfate with $P(TMS)_3$ yields the TMS-protected secondary phospholane, which could then be reacted with the appropriate 1,2-dichloro species [46]. An alternative procedure to the same intermediate involves preparation of 1-phenylphospholane via the bismesylate, subsequent lithium-induced P–Ph cleavage, and quenching with TMSCl [49]. The ligand based on 2,3-dichloromaleic anhydride (**20a**; originally referred to as MalPHOS [46]) has been shown to be effective for the chiral reduction of α- and β-dehydroamino acid derivatives and itaconate derivatives.

An interesting approach to investigating the relationship between the position of enantiodescriminating sites in a number of chiral ligands and enantioselectivity in enantioselective hydrogenation has been proposed by Saito et al. [50]. In this report, (aS,S,S)-MPL-SEGPHOS (**21**) was used for the reduction of MAC, albeit in 75% ee.

24.2.3
Modifications to the Phospholane Substituents

In recent years, numerous DuPhos and BPE analogues have been introduced that contain structural variations at the 2,5-positions of the phospholane segments and/or additional stereogenic centers (Fig. 24.5).

Several groups have independently reported the synthesis of D-mannitol-derived phospholanes with either ketal, ether or hydroxy substituents in the 3,4-positions. The earliest ligand class, Rophos containing either a 1,2-benzene (**22**) or 1,2-ethane backbone (**23**), was introduced by Börner, Holz and co-workers in 1998 [51]. By taking advantage of the difference in reactivity between the primary and secondary alcohols, the mannitol framework could be manipulated to prepare the cyclic sulfate and, ultimately, the desired diphosphine. These were applied to the Rh-catalyzed hydrogenation of a range of olefinic substrates, all with excellent enantioselectivity. The research groups of Zhang [52] and Rajan-Babu [53] have both reported the synthesis of the *iso*-propylidene ketal bisphospholane **24** (R = Me or Et) and the tetrahydroxy bisphospholane **25** (R = Me or Et). Surprisingly, whilst ligand **24** (KetalPhos) was described as being inactive for the hydrogenation of dehydroamino acid derivatives when the catalyst was

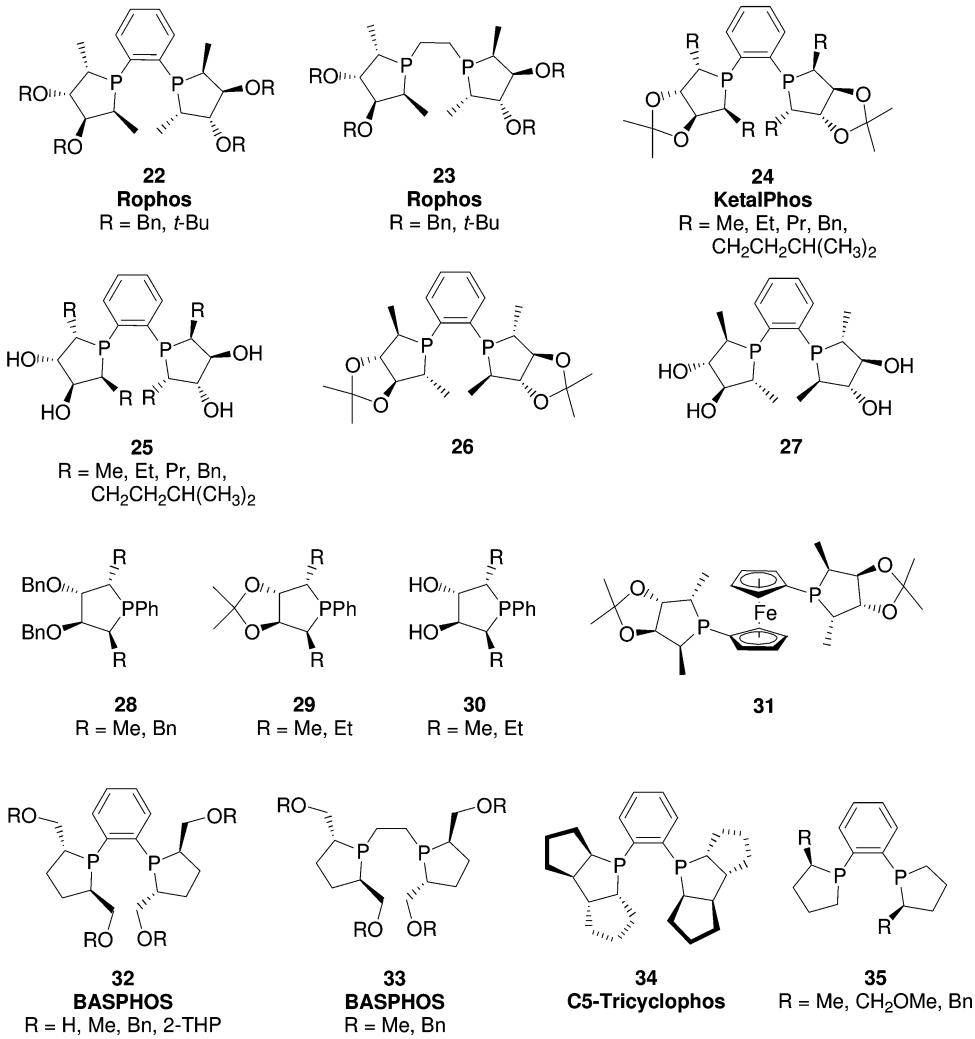

Fig. 24.5 Ligands with modifications to the phospholane substituents.

prepared *in situ* with $[Rh(COD)_2]X$ ($X = BF_4$, SbF_6, PF_6 and OTf) [52a, b], the isolated precatalyst, [(**24**) Rh(COD)]BF_4, was shown to be active and very selective (>90% ee) [53b]. A mannitol-derived cyclic sulfate has also been employed in the synthesis of monodentate phospholanes **28–30** [52a, b] and the ferrocenyl-based diphosphine **31** [54]. Although enantioselective hydrogenation with **28–30** has not been reported, **31** has been shown to be extremely active (TON 10000; TOF >800 h^{-1}) and selective (89.8–99.9% ee) for the Rh-catalyzed reduction of a range of functionalized olefins. By preparing a diasteromeric bisepoxide pair from D-mannitol (Scheme 24.3), RajanBabu and Yan have also accessed the dia-

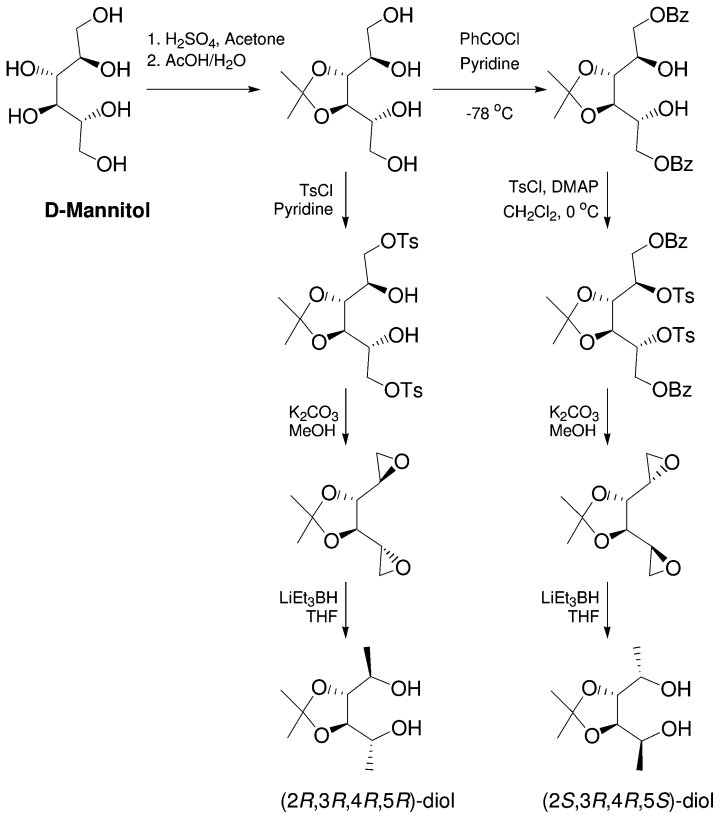

Scheme 24.3 The preparation of diastereomeric diols from D-mannitol.

stereomeric 3,4-disubstituted phospholanes **26** and **27** [53 a]. When comparing **24** (R = Me) with **26**, as expected the opposite enantiomer was obtained for the hydrogenation of methyl 2-acetamidoacrylate (MAA), but interestingly **26** gave a slight improvement on the level of selectivity [97.4% ee (*R*) versus 90.5% ee (*S*)] [53 b]. Rieger et al. extended the range of substituents at the 2,5-positions of ligands **24** and **25** (R = Et, *n*-Pr, isoamyl and Bn) by means of copper-catalyzed coupling of the appropriate Grignard reagent to the mannitol-derived bisepoxide [55]. Testing this series of ligands against the hydrogenation of *α*-methylcinnamic acid and itaconic acid showed high selectivity in every case (96–99% ee).

Several methods have been described to liberate the hydroxyl groups from **24** to produce the water-soluble, tetrahydroxyl bidentate ligand **25** [52, 53 b]. Water-soluble ligands are of interest due to the prospect of recycling the catalyst into an aqueous phase, ideally without loss of performance. The enantiomeric hydrogenation of itaconic acid was performed in aqueous methanol over a range of solvent compositions (MeOH: H_2O, 9 : 1 to 3 : 97), with consistently excellent levels of performance (100% conversion, 99% ee, SCR 100, 12 h) [52 b]. Interest-

ingly, when applied to the reduction of MAA under comparable conditions, an increase in the percentage of water was found to have a deleterious effect on selectivity [53 b]. However, at equal volumes of methanol and water, Rh complexes of **25** and analogous tetrahydroxy phospholanes could be recycled (up to five runs at SCR 100) by extracting the product into ether, with no significant losses in enantioselectivity.

Another family of mannitol-derived bisphospholanes was introduced by Holz and Börner. Removal of the hydroxy groups at the 3 and 4 positions leads to a key intermediate that ultimately produces 2,5-disubstituted phospholanes BASPHOS **32** and **33**. The water-soluble, tetrahydroxyl-substituted variant **32** (R = H) displayed excellent selectivities for the Rh-catalyzed hydrogenation of 2-acetamido acrylic acid and the corresponding methyl ester in water (99.6% and 93.6% ee, respectively) [56 a]. RajanBabu and co-workers confirmed this and showed that the catalyst could be recycled up to four times, with no loss in selectivity (SCR 100) [53 b]. An interesting feature of the synthesis of this ligand is the protection of the air-sensitive phosphine groups as the rhodium complex prior to liberation of the hydroxyl groups (tetrahydropyranyl group removal), saving two borane protection–deprotection steps. The corresponding 2,5-bis(alkoxymethylene)-substituted ligands **32** and **33** (R = Me, Bn) have also been tested for the Rh-catalyzed hydrogenation of α- and β-dehydroamino acid derivatives, itaconates and an unsaturated phosphonate, together with Ru-catalyzed reduction of prochiral β-keto esters [56 b–e]. The wide range of enantioselectivities obtained (8 to 99% ee) was found to depend strongly on both the phospholane substituent and the backbone used.

A unique tricyclic bisphospholane ligand, C5-Tricyclophos (**34**), has been described in a patent by Zhang [57]. Derived from resolved bicyclopentyl-2,2′-diol (originally used in the preparation of the chiral diphosphine, BICP [58]), this li-

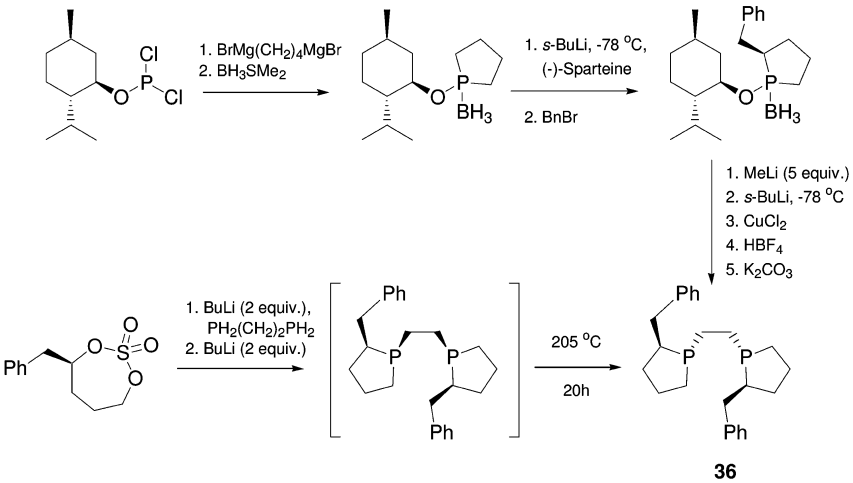

Scheme 24.4 Alternative syntheses of the BPE analogue **36**.

gand has shown moderate enantioselectivity for the reduction of α-acetamidocinnamate (53% ee) and MAC (78% ee). An interesting class of P-chirogenic monosubstituted phospholanes, **35** and **36**, has recently been introduced by Hoge [59]. Originally, the 1,2-ethane variant **36** was prepared using menthol as a chiral auxiliary for the directed selective benzylation of the phospholane ring and subsequent phosphorus methylation with stereochemical retention (Scheme 24.4) [59 a]. Oxidative homo-coupling and deboronation completed the synthesis. A more versatile method was subsequently published, via the traditional cyclic sulfate route, for the preparation of BPE, DuPhos and monodentate analogues with alternative phospholane substituents (R = Me and CH_2OMe) [59 b]. These ligands have been successfully applied to the hydrogenation of α- and β-dehydroamino acid derivatives and a pharmaceutically important precursor to Pregabalin [59 a, b, d], giving results comparable to BPE and DuPhos [60, 61].

24.2.4
Other Phospholane-Containing Ligands

In addition to direct DuPhos and BPE analogues, several other ligands containing five-membered phosphacycles have been reported (Fig. 24.6). As early as 1991, non-C_2-symmetric phospholane-containing phosphines **37–39** were reported by Brunner and Limmer [7]. These were prepared by base-induced addition of the secondary phospholane to the appropriate diphenylphosphino-substituted olefin. As for the symmetrical 3,4-disubstituted bisphospholanes, enantioselectivities for the Rh-catalyzed reduction of α-acetamidocinnamate were poor.

Brown et al. [62] prepared a family of unsymmetrical diphosphine ligands **40** by the conjugate addition of racemic borane-protected *o*-anisylphenyl phosphide to diethylvinylphosphonate followed by deprotection, reduction and phospholane formation with the appropriate cyclic sulfate (2,5-hexanediol- or L-mannitol-derived). The diastereomers of the mannitol-derived phosphines could be separated chromatographically and converted to their dihydroxyl analogue, whereas the disubstituted-phospholane required medium-pressure liquid (flash) chromatography (MPLC). Rh-catalyzed hydrogenations with these ligands gave moderate enantioselectivities for several standard substrates and, whilst some significant matching and mis-matching effects were observed, the chirality of the product was determined primarily by the phospholane moiety.

Since this report, several research groups have replaced one phospholane ring of Me-DuPhos with a diaryl phosphine group. Stelzer et al. [63] described the synthesis of ligand **41** (R = Me, Ar = Ph) by treating the standard cyclic sulfate with a mixed primary-tertiary diphosphine. The ligand was purified via its dihydrochloride salt, liberating the free diphosphine quantitatively by treatment with $NaHCO_3$. Independently, Saito [64] and Pringle [65] reported the use of **41** (R = Me, Ar = Ph) in Rh-catalyzed asymmetric hydrogenation of a range of olefins, with particularly good results being obtained for prochiral enamides. Saito and co-workers made a small family of this class of ligand, UCAPs, and demonstrated that adjusting the diaryl-substituted phosphine could lead to higher se-

lectivities than Me-DuPhos for a trisubstituted enamide [64]. The structurally related P,N ligand, DuPHAMIN **42** has also been prepared by Brauer and coworkers [66]. Remarkably, large matching and mis-matching effects were observed for the Rh-catalyzed hydrogenation of MAC, with the (*R*,*R*,*R*) ligand giving complete conversion at 20 °C (96% ee), but the (*S*,*R*,*R*) ligand being inactive. Pringle also synthesized the ferrocenyl-based **43** [65], but showed this to be less efficient than the phenylene-linked analogue.

The sterically bulky and conformationally rigid bicyclic ligand PennPhos (**44**) was developed by Zhang [57, 67]. The synthesis uses chiral 1,4-cyclohexanediols, converting them to the dimesylate to enable cyclization with 1,2-diphosphinobenzene under basic conditions. This has given high selectivity in Rh-catalyzed hydrogenation of both aryl and alkyl methyl ketones [57, 67 b], cyclic enol acetates [67 c, d], enol ethers [67 d], cyclic enamides [67 d, e] and *α*-dehydroamino acid derivatives [57]. Under certain conditions, the selectivities obtained for cyclic enamides are superior to those achieved with Me-DuPhos, but inferior for acyclic enamides. The bulky monodentate ligand **45** has been described in a patent by Börner, but gave poor enantioselectivities for *α*- and *β*-amino acid derivates, dimethylitaconate (DMI) and itaconic acid [68].

The research group of Zhang has also introduced two rigid P-chiral bisphospholane ligands, TangPhos **46** and DuanPhos **47** (Scheme 24.5), both of which contain two chiral phosphorus centers and two chiral carbon centers. Since the synthesis of TangPhos employs an enantioselective deprotonation of 1-*t*-butylphospholane sulfide with a butyllithium–sparteine complex, only one enantiomer is readily accessible [69]. On the other hand, either enantiomer of DuanPhos can be obtained enantiomerically pure by resolution of the corresponding bisoxide with either L- or D-dibenzoyl tartaric acid [70] (Scheme 24.5). Both ligands have been found to be very efficient in the Rh-catalyzed hydrogenation of a range of olefinic substrates such as *α*-acetamidoacrylate derivatives, *α*-arylenamides [69, 70], *β*-acetamidoacrylates [69 b, 70, 71], itaconic acids, and enol acetates [69 b, 70, 72]. DuanPhos has also been reported to give high rates (TON 4500; TOF 375 h^{-1}) and excellent enantioselectivities (93–99% ee) for a range of *β*-secondary-amino ketone salts [73].

The 1-*t*-butylphospholane sulfide intermediate to TangPhos was also used to prepare the P,N ligands **48** by reacting the lithium complex with CO_2 and then oxazoline formation with a range of chiral amino alcohols [69 b, 74]. The Ir complexes of these ligands have been successfully used in the reduction of *β*-methylcinnamic esters (80–99% ee) and methylstilbene derivatives (75–95% ee), a particularly challenging class of unfunctionalized olefins [4 c].

The BeePHOS (**49**) and mBeePHOS (**50**) classes of ligands introduced by Saito [75] are prepared by reacting the appropriate primary phosphine with a mesylated alkylalcohol-substituted aryl halide. Although a single diastereomer is obtained, the absolute configuration is unknown. Whilst trials of Ru-catalyzed hydrogenation of MAC and methyl *α*-hydroxymethylacrylate were disappointing, the Rh-catalyzed reactions were more active. On the whole, selectivities were lower than those obtained with Me-DuPhos under the same conditions. Ligand

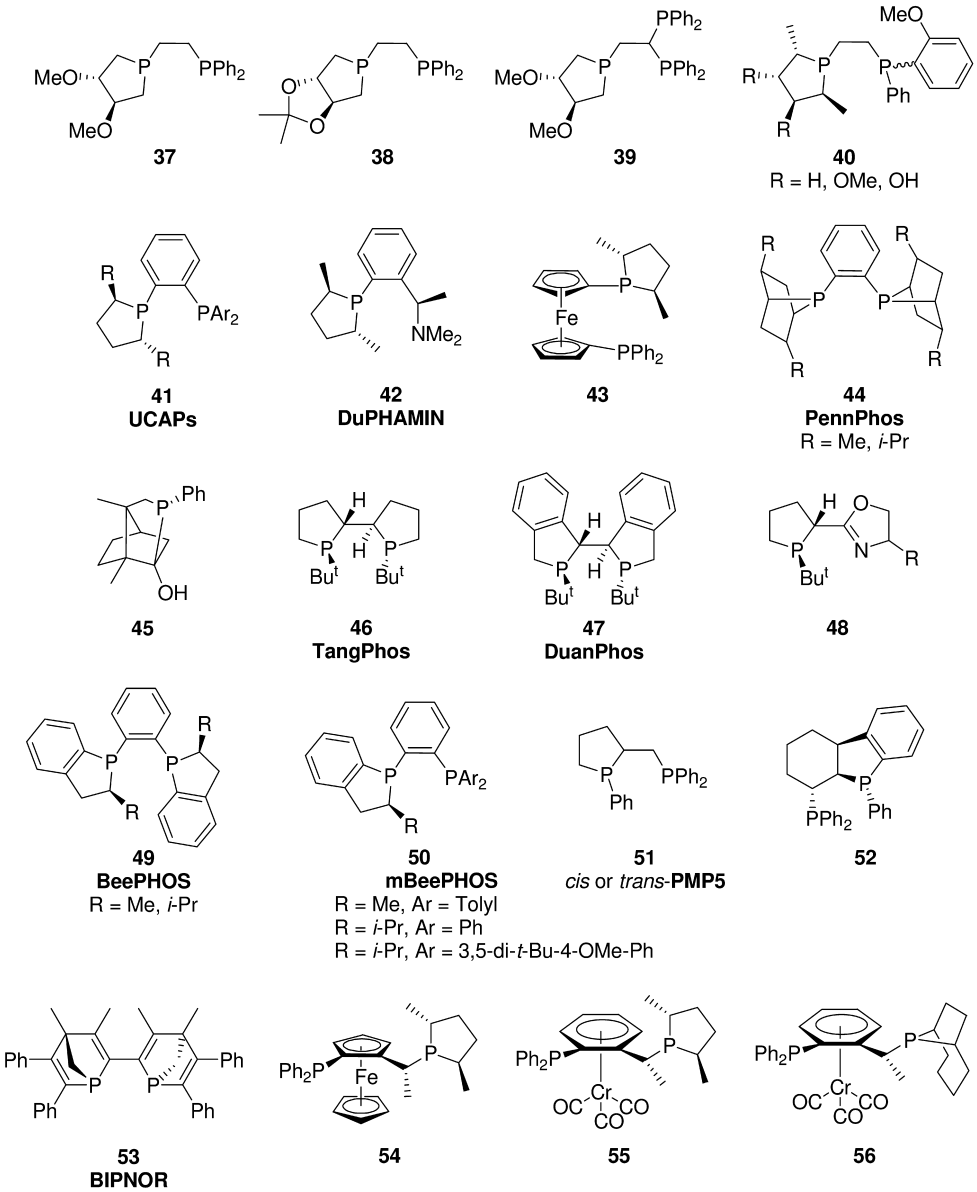

Fig. 24.6 Alternative ligands containing five-membered phosphacycles.

51 has recently appeared in separate patents from both Kobayashi and Schmid [76]. Given the name *cis* and *trans*-PMP5 by Schmid et al., the Rh complexes have been reported to be active catalysts for the reduction of several standard substrates, α-enol acetates and β-ketoacid derivatives, with variable enantioselectivities [76 b]. In general, the *cis* isomer is more selective than the *trans*.

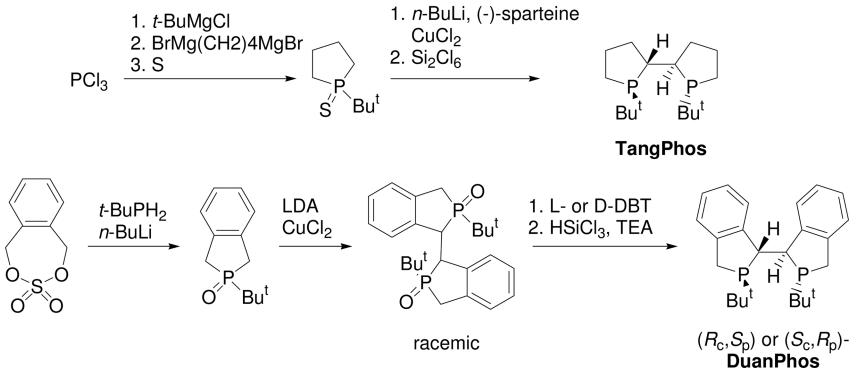

Scheme 24.5 The syntheses of TangPhos and DuanPhos.

The rigid bicyclic diphosphine **52** was prepared by Knochel and co-workers by the radical cyclization of a bromophosphine oxide, itself obtained from a double [2,3]-sigmatropic shift of an intermediate phosphinite [77]. Unfortunately, this ligand only gave moderate enantioselectivity (21–58% ee) against standard model substrates under normal screening conditions (MeOH, room temperature, 10 atm, SCR 100). The P-chiral diphosphine BIPNOR (**53**) was synthesized by Mathey et al. via a [4+2] cycloaddition of tetramethyl-1,1′-bisphospholyl and tolan, the crucial intermediate arising from a double [1,5] shift of each phosphole around the ring [78]. With the phosphorus atoms being located at the bridgehead of a bicyclic system, none of the usual racemization pathways potentially observed for P-homochiral phosphines can occur (Berry pseudorotation and edge inversion). Both *meso* and *rac* diastereomers and the resulting racemic mixture are separated by chromatography of their Pd complexes. Enantioselectivities for the Rh-catalyzed hydrogenation of α-acetamidocinnamic acid and itaconic acid are comparable to those achieved with DuPhos-based catalysts.

The group of Salzer has recently reported phospholanes **54–56** based on chiral half-sandwich complexes [79]. These were obtained by treatment of the appropriately substituted complex with a secondary phospholane, itself accessed via the cyclic sulfate or dimesylate and PH_3. These were tested against a range of substrates with C=C, C=O and C=N bonds, with variable results [80].

24.2.5
Related Phosphacycle-Based Ligands

Although strictly not phospholanes, several other noteworthy P-heterocycle-containing ligands have been applied to asymmetric hydrogenation (Fig. 24.7). The first optically active phosphetanes to be used in catalysis were described by Marinetti and Ricard [81]. Although active in Pd-catalyzed hydrosilylation, these monodentate ligands (**57**) proved to be very poor for the hydrogenation of MAC [81 b, c]. More recently, Burk and co-workers [82] and the groups of Marinetti and Genêt

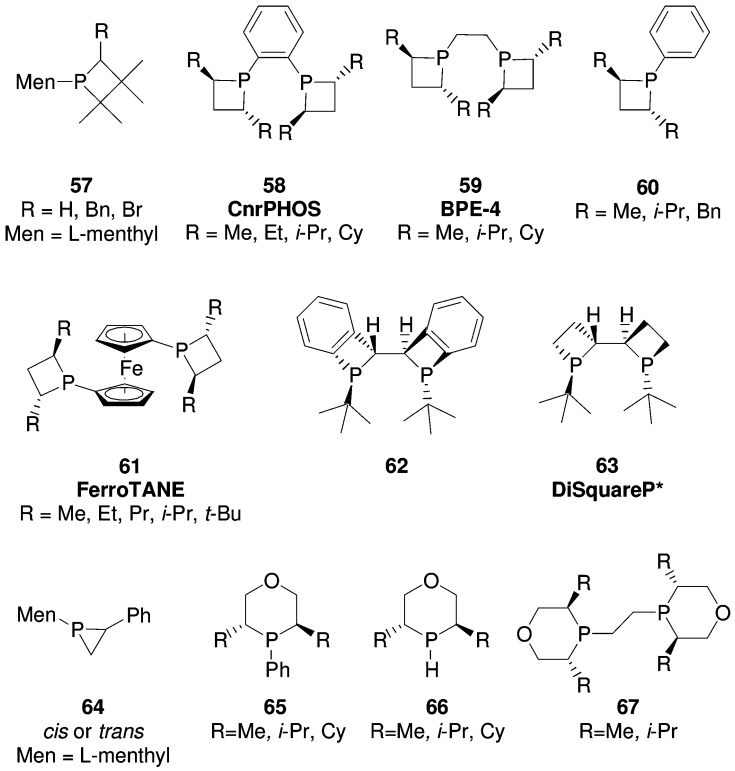

Fig. 24.7 Related P-heterocyclic ligands.

[83] have independently prepared and examined several enantiomerically pure ferrocenyl-based 2,4-disubstituted phosphetanes as ligands for asymmetric hydrogenation. These ligands were prepared from the appropriate primary phosphines and a range of chiral 2,4-diols using the traditional cyclic sulfate methodology (*vide supra*). Although not as enantioselective as their bisphospholane analogues in reducing dehydroamino acid derivatives [83 a, d], Genêt's CnrPHOS (**58**) and BPE-4 (**59**) are reported to be extremely selective in the Ru-catalyzed hydrogenation of several β-ketoesters (73–98% ee) [83 d, e]. Interestingly, reasonable levels of enantioselectivity were achievable with the monodentate ligands **60** against α-acetamidocinnamic acid (10 to 86% ee) [83 f]. The ferrocenyl-based bisphosphetanes, FerroTANE (**61**), have been shown to be exceptional for the Rh-catalyzed reduction of (*E*)-β-dehydroamino acids [56 c, 84] as well as a number of itaconic and succinamide derivatives [82 a, 85, 86], outperforming DuPhos in both cases. Albeit less selective, FerroTANE has also been examined for Ru-catalyzed hydrogenation of β-ketoesters [83 d] and Rh-catalyzed hydrogenation of α-dehydroamino acids [83 c], and is a precursor to the potent anticonvulsant (*S*)-Pregabalin [61].

In recent years, the research group of Imamoto has been very active in the area of C_2-symmetric P-stereogenic phosphine ligands [87]. Two such ligands,

62 and DiSquareP* **63**, were prepared using the same strategy, the key being an oxidative homocoupling of the corresponding benzophosphetene or phosphetane, respectively [87]. Both ligands have been applied to the Rh-catalyzed hydrogenation of MAC, but in particular DiSquareP* has displayed excellent activity (TON 50 000; TOF $\sim 1100\,h^{-1}$) and selectivity (99% ee) for this and other α-dehydroamino acid derivatives. Interestingly, **63** is also an extremely selective ligand for the reduction of α-substituted enamides, but does not perform well on either substrate class when β,β-disubstitution is present.

The three-membered phosphirane **64** was studied by Marinetti et al. for the Rh-catalyzed hydrogenation of MAA, MAC, and itaconic acid with, in general, poor enantioselectivities [88]. Since ring-opened oxidized phosphorus species were observed at the end of the reactions, some doubt was voiced as to the exact nature of the catalytic species. The oxaphosphinanes **65**, were synthesized by Helmchen via reaction of the diol ether mesylates with dilithiophenylphosphine [89]. Since these showed poor performance for the Rh-catalyzed reduction of α-dehydroamino acids and itaconate derivatives, the corresponding secondary phosphinanes **66** were prepared by cleavage of the P–Ph bond with lithium. These were then converted through to the bidentate analogue **67**. Interestingly, both **66** and **67** performed well against these standard substrates (80–98% ee), but gave the opposite sense of stereochemical induction for a number of products [89].

24.3 Enantioselective Hydrogenation of Alkenes

24.3.1 Enantioselective Hydrogenation of α-Dehydroamino Acid Derivatives

The pivotal role of natural α-amino acids among a myriad of biologically active molecules is widely appreciated, and is of particular importance in the pharmaceutical industry. Unnatural α-amino acids also have a prominent position in the development of new pharmaceutical products. It has been shown that substitution of natural α-amino acids for unnatural amino acids can often impart significant improvements in physical, chemical and biological properties such as resistance to proteolytic breakdown, stability, bioavailability, and efficacy. One of the many synthetic methods available for the production of enantiomerically enriched α-amino acids is the metal-catalyzed enantioselective reduction of α-dehydroamino acid derivatives [90].

The parent DuPhos and BPE ligands exhibit excellent enantioselectivities routinely in excess of 95% with the majority of model α-dehydroamino acid substrates (Table 24.1) [4a, 8, 12, 13, 20, 90]. High molar SCRs (in the order of $>1000:1$), as well as TOFs in excess of $1000\,h^{-1}$, are indicative of the high catalyst activity and productivity typically found with DuPhos and BPE systems with these simple substrates. Burk reported that in the enantiomeric hydrogenation

of MAA and MAC, with alkyl-DuPhos–Rh catalysts, optimal enantioselectivity could be achieved with the *n*-Pr-DuPhos ligand over other alkyl DuPhos or BPE ligands [13]. Cationic rhodium catalysts derived from Ph-BPE, the first aryl member of the diphospholane ligand class, are reported to be significantly more reactive and selective than the analogous alkyl-BPE ligands in the hydrogenation of various model substrates [34]. Experimental and computational mechanistic studies using Me-DuPhos-Ir and Me-DuPhos–Rh respectively revealed that an "anti-lock and key" reaction pathway also operates with DuPhos; consequently, the facial selectivity of the more reactive minor diastereoisomer is the source of enantioselectivity in the final product [91–93]. A small number of experimental and theoretical investigations of the use of DuPhos–Rh catalysts in supercritical CO_2 have been reported, with some notable differences with standard substrates being observed [39, 94].

The mannitol-derived phospholane systems from Zhang, Rajanbabu and Börner (ligands **22**–**27**, **31**–**33**) have been extensively tested with model substrates. In general, these ligands have been shown to hydrogenate a similar range of simple α-dehydroamino acid substrates to DuPhos and BPE, and are able to replicate their high enantioselectivities and reactivities. Furthermore, despite the further elaboration of the phospholane ring systems of several of the mannitol ligands, the stereochemical outcome of the reported reactions is identical to that of DuPhos and BPE ligands with the same spatial arrangement. As expected, the diastereomeric hydroxylated ligands (*S*,*S*,*S*,*S*)-**25** and (*R*,*S*,*S*,*R*)-**27** gave the opposite sense of stereoinduction in the hydrogenation of MAA with ee-values of >99% (*S*) and 97% (*R*) respectively. This indicates that the spatial orientation of the 2,5-positions of the phospholane is the principal factor in defining the stereochemical outcome of MAA hydrogenation. Interestingly, the ketal variants (*S*,*S*,*S*,*S*)-**24** and (*R*,*S*,*S*,*R*)-**26** showed a more marked difference in the hydrogenation of MAA, with ee-values of 90.5% (*S*) and 97.4% (*R*), respectively [53 b]. Zhang's mannitol-derived ferrocenyl phospholane Me-f-KetalPhos system facilitates the hydrogenation of MAA in 99.4% ee [54], whereas the parent Me- and Et-5-Fc ligands achieve only 64 and 83% ee, respectively [30]. Zhang has gone on to show that the hydrogenation of an extensive range of simple aromatic, substituted aromatic and heteroaromatic β-substituted α-dehydroamino acid systems can be achieved with his mannitol-derived systems with excellent enantioselectivity, albeit it under standard screening conditions and typically with high catalyst loadings [52 b]. Börner and co-workers noted that the significant degree of structural variation possible within the BASPHOS ligand family imparts a greater degree of substrate sensitivity than their DuPhos and BPE counterparts, and thus results in more variable enantioselectivities over a wide range of simple substrates [56 b].

UlluPHOS [43, 44], catASium M [48, 95], Kephos [45, 96] and Butiphane [97] – four ligand systems which possess larger P–Rh–P bite angles than DuPhos [44, 46, 97] – all achieved enantioselectivities >95% when used in the hydrogenation of some model substrates. Much importance has been attached to P–Rh–P bite angles larger than the parent DuPhos system. It is believed that the pos-

Table 24.1 Phospholanes reported to hydrogenate model α-dehydroamino acid derivatives in >95% ee.

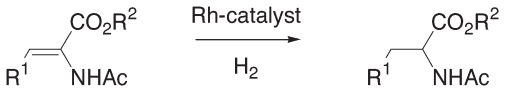

68 $R^1 = H$, $R^2 = Me$ **69** $R^1 = H$, $R^2 = H$
70 $R^1 = Ph$, $R^2 = Me$ **71** $R^1 = Ph$, $R^2 = H$

Substrate	Ligand	SCR	Reaction conditions [a)]	TON	TOF [h^{-1}]	% ee (config.)	Reference(s)
68	(*S*,*S*)-Me-DuPhos [b)]	1000	MeOH, 20 °C, 2 atm, 1 h	1 000	>1000	99	13, 27
68	(*S*,*S*)-Et-BPE [b)]	1000	MeOH, 20 °C, 2 atm, 1 h	1 000	>1000	98	13 ,27
68	(*R*,*R*)-Ph-BPE	5000	MeOH, 25 °C, 9.9 atm, 1 h	5 000	–	>99	34
68	(*R*,*R*)-Me–**16**	1000	MeOH, rt, 2 atm, 1–16 h	1 000	–	95	24
68	(*R*,S_p,S_p,*R*)-Bn-**35** [b)]	100	MeOH, rt, 2 atm, 15 min	100	>400	98 (*S*)	59 b
68	(*R*,*R*)-UlluPHOS	1000	MeOH, 27 °C, 2.8 atm, 1 h	1 000	>1000	98 (*S*)	43, 44
68	(*S*,*S*,*S*,*S*)-Me-**25** [b)]	100	MeOH, rt, 3 atm, 9 h	100	–	98 (*S*)	52 a, b
68	(*R*,*S*,*S*,*R*)-**26**	100	MeOH, rt, 2.8 atm, 7 h [c]	–	–	97 (*R*)	53 b
68	(*S*,*S*,*S*,*S*)-Me-f-Ketal-Phos	10 000	THF, rt, 3 atm, 12 h	10 000	833	99 (*S*)	54
68	(*R*,*R*,*S*,*S*)-DuanPhos	10 000	MeOH, rt, 1.4 atm, 2 h	10 000	5000	99 (*R*)	70
68	(*S*,*S*)-DiSquareP*	100	MeOH, rt, 1 atm, 1 h	100	100	99	87 b
69	(*R*,*R*)-H-Ph-BASPHOS	–	H_2O	–	–	>99 (*S*)	56 a
69	(*R*,S_p,S_p,*R*)-Bn-**35** [b)]	100	MeOH, rt, 2 atm, 15 min	100	>400	97 (*S*)	59 b
69	(*S*,*S*,*S*,*S*)-Me-**25**	100	MeOH, rt, 3 atm, 9 h	100	–	>99 (*S*)	52 a, b
69	(*R*,*R*)-Me-**67**	1 000	MeOH, 20 °C, 1.1 atm, 24 h	1 000	–	97 (*R*)	89
70	(*R*,*R*)-Ph-BPE	3 000	MeOH, 28 °C, 10 atm, 1.25 h	3 000	>2400	99	34
70	(*R*,*R*)-*n*-Pr-DuPhos [b)]	1 000	MeOH, 20 °C, 2 atm, 1 h	1 000	>1000	99	13, 27
70	(*R*,*R*)-Me–**16**	1 000	MeOH, rt, 2 atm, 1–16 h	1 000	–	98	24
70	(+)-*i*-Pr-BeePHOS	200	MeOH, 30 °C, 4 atm, 14–16 h	200	–	98	75
70	(*R*,*R*,*R*)-DuPHAMIN	100	Toluene, 20 °C, 5 atm, 12 h [f)]	95	7.9	96	66
70	(*R*,*R*)-Me-Ph-BASPHOS [b)]	100	MeOH, 25 °C, 1 atm, 15 min	100	400	99 (*S*)	56 b, e

Table 24.1 (continued)

Substrate	Ligand	SCR	Reaction conditions [a)]	TON	TOF [h^{-1}]	% ee (config.)	Reference(s)
70	(*R*,*R*)-Bn-Et-BASPHOS	100	MeOH, 25 °C, 1 atm, 5 h	100	20	96 (*S*)	56 b
70	(*R*,S_p,S_p,*R*)-Bn-**35** [b)]	100	MeOH, rt, 2 atm, 15 min	100	>400	95 (*S*)	59 b
70	(*R*,*R*)-*cis*-PMP5	1 000	MeOH, rt, 1.5 atm, 2 h [e)]	750	375	98 (*S*)	76 b
70	(*S*,*S*,*S*,*S*)-Me-**25**	100	MeOH, rt, 3 atm, 12 h	100	–	>99 (*S*)	52 a
70	(*S*,*S*,*S*,*S*)-Et-**25**	100	MeOH, rt, 3 atm, 12 h	100	–	>99 (*S*)	52 b
70	(*S*,*S*,*S*,*S*)-*t*-Bu-Rophos **23** [b)]	100	MeOH, rt, 1 atm, 2 h [d)]	50	25	98 (*S*)	53 b
70	(*S*,*S*,*S*,*S*)-Bn-Rophos **22**	100	MeOH, rt, 1 atm, 48 min [d)]	50	63	96 (*S*)	53 b
70	(*S*,*S*,*S*,*S*)-Me-f-Ketal-Phos	100	THF, rt, 1 atm, 1 h	100	–	99 (*S*)	54
70	[(*R*,*R*)-catASium M	200	THF, 25 °C, 1.5 atm, 2 h	200	100	96 (*R*)	48, 95
70	(*S*,*S*)-Me-Kephos	1 000	MeOH, rt, 1 atm	1 000	300	97	45, 96
70	(*R*,*R*)-Et-Butiphane	1 000	MeOH, rt, 1 atm	1 000	550	99	97
70	(*R*,*R*)-**14**	100	MeOH, 20 °C, 1 atm, 24 min	100	250	93 (*S*)	33
70	(*S*,*S*,*R*,*R*)-TangPhos	10 000	MeOH, rt, 1.4 atm	10 000	–	>99 (*R*)	69
70	(*R*,*R*,*S*,*S*)-DuanPhos	100	MeOH, rt, 1.4 atm, 12 h	100	–	99 (*R*)	70
70	(*S*,*S*)-**62**	1 000	MeOH, 20 °C, 2 atm, 1 h [c)]	–	–	96	87 a
70	(*R*,*R*)-Me-FerroTANE	100	MeOH, 50 °C, 1 atm, 24 h [c)]	–	–	96 (*R*)	83 d
70	(*S*,*S*)-DiSquareP*	50 000	MeOH, rt, 6 atm, 43 h	50 000	1163	99	87 b
71	(*R*,*R*)-Me-DuPhos	1 000	EtOH, 27 °C, 2 atm, 1 h	1 000	>1000	95 (*S*)	44
71	(*R*,S_p,S_p,*R*)-Bn-**35**	100	MeOH, rt, 2 atm, 15 min	100	>400	96 (*S*)	59 b
71	(*R*,*R*)-UlluPHOS	1 000	EtOH, 27 °C, 2 atm, 1 h	1 000	>1000	99 (*S*)	43, 44
71	(*S*,*S*,*S*,*S*)-Me-**25** [b)]	244	MeOH, rt, 1.3 atm, 20 h	244	–	99 (*S*)	52, 55
71	(*S*,*S*,*S*,*S*)-Et-**25**	100	MeOH, rt, 3 atm, 12 h	100	–	>99 (*S*)	52 b, 55

Table 24.1 (continued)

Substrate	Ligand	SCR	Reaction conditions [a)]	TON	TOF [h^{-1}]	% ee (config.)	Reference(s)
71	(*S*,*S*,*S*,*S*)-*t*-Bu-Rophos **23** [b)]	100	MeOH, rt, 1 atm, 2 h [d)]	50	26	97 (*S*)	51
71	(*S*,*S*,*R*,*R*)-TangPhos	100	MeOH, rt, 1.4 atm, 12 h [c)]	–	–	99 (*R*)	69

a) Complete conversion unless otherwise stated.
b) Similar high enantioselectivities have also been obtained with several other ligands of this class.
c) No conversion given.
d) 50% conversion.
e) 75% conversion.
f) 95% conversion.

session of a wider P–Rh–P angle places the substrate in closer proximity to the metal, resulting in a more intimate contact between the substrate and catalyst, which could impart a greater degree of selectivity. However, this potentially oversimplifies the differences in performance of certain ligands in enantioselective hydrogenations. It is likely that the outcome of enantiomeric hydrogenations is governed by a variety of stereoelectronic factors, as well as reaction parameters such as pressure, temperature, and solvent. Sannicolo et al. have studied the reaction rates of Me-DuPhos and UlluPHOS in the hydrogenation of 2-acetamidocinnamic acid under identical conditions. The resulting kinetic rate data revealed that the UlluPHOS–Rh catalyst hydrogenated the substrate more quickly than the Me-DuPhos catalyst, with $k_{\mathrm{UlluPHOS}}/k_{\mathrm{Me\text{-}DuPhos}}=7.73$; this was in part attributed to the greater electron density of the thiophene-based ligand [44]. Et-Butiphane and Me-Kephos both hydrogenated MAC in high enantioselectivity, with SCRs of 1000:1; however, the respective TOFs of 550 and 300 h^{-1} were somewhat lower than the value of >2400 h^{-1} reported for the Ph-BPE ligand at a SCR of 3000:1 and with the same substrate under near-identical conditions [35, 96, 97]. Pringle's 1,2-diphospholano-cyclopentane ligand **16** can be synthesized as both λ and δ conformers, though only the δ conformer is reported to achieve high enantioselectivities [24]. The corresponding λ conformer achieves enantioselectivities approximately 20% lower than the δ conformer, indicating a strong matching/mismatching effect between the chirality of the phospholane rings and chiral backbone.

The non-*trans*-2,5-disubstituted phospholanes from Hoge (**35**), Takasago (BeePHOS family) and Zhang (TangPhos and DuanPhos) are all capable of achieving high enantioselectivities with standard α-dehydroamino acid substrates (see Table 24.1) Hoge's 1,2-phenylene system (**35**) generally gave higher enantioselectivities with model substrates than its related 1,2-ethylene system (**36**) [59c]. Takasago's BeePHOS family showed variable performance when hydrogenating MAC in that the ee-values ranged from 47 to 98% [75]. Zhang demonstrated

that both the TangPhos and DuanPhos systems are able of performing hydrogenations with high enantioselectivities at economical catalyst loadings [69, 70]. In comparison to other non-*trans*-2,5-disubstituted phospholanes, only TangPhos so far has shown broad applicability akin to DuPhos and BPE. Moreover, Hoge's mono-substituted **35** and Takasago's BeePHOS show better utility with other substrate classes.

Monophospholanes or bidentate ligands containing a single phospholane moiety have also been successfully applied in the hydrogenation of standard α-dehydroamino acid substrates, though they have not yet been shown to be useful beyond the standard substrates. Remarkably, Fiaud's monophospholane **14** achieves 93% ee with MAC, whereas the bidentate monophospholano ligands (*R*,*R*,*R*)-DuPHAMIN (**42**) [66] and (*R*,*R*)-*cis*-PMP5 (**51**) [76 b] hydrogenate MAC in 96% and 98% ee, respectively. Unsurprisingly, the TOFs for DuPHAMIN are too low to be of industrial use. Other related bidentate-monophospholane systems (**37–41**, **43**, **52**, **54–56**) have generally been found to give moderate to low ee-values with model substrates under normal screening conditions [7, 62, 65, 75, 77, 80].

Standard α-dehydroamino acid substrates have been hydrogenated in high enantioselectivities by phosphetanes and phosphinanes. Imamoto's phosphetanes **62** and DiSquareP* (**63**) achieve excellent enantioselectivities; furthermore, DiSquareP*achieves a SCR of 50 000 : 1 with MAC, indicating exceptional catalyst productivity and stability [87]. The ferrocenyl system (*R*,*R*)-Me-FerroTANE hydrogenates MAC in 96% ee [83 d]. Other phosphetanes, such as Genêt's Cy-BPE-4, *i*-Pr-CnrPHOS [83 a], Berens' monophosphetanes [82 b] or Takasago's IPT-SEGPHOS [50] have to date been found to give only moderate enantioselectivities with model substrates. Helmchen's bidentate oxa-phosphinane **67**, remarkably hydrogenates 2-acetamidoacrylic acid in 97.4% ee, while several analogous mono-oxa-phosphinanes have demonstrated high enantioselectivity (> 90% ee) in the reduction of MAC and are currently the only reported examples of chiral phosphinanes which are highly selective [89].

β-Substituted α-dehydroamino acids are frequently synthesized as mixtures of (*E*/*Z*)-isomers [90], and several studies have shown that the geometry of β-substituted α-dehydroamino acid substrates can have a profound effect on both enantioselectivity and hydrogenation rates [98]. In some exceptional cases the opposite enantiomer can be produced when hydrogenating the (*E*) or (*Z*)-olefin with a single catalyst enantiomer [99]. Burk demonstrated, in a series of experiments using *n*-Pr-DuPhos–Rh with the isomerically pure (*E*) and (*Z*)-methyl-2-acetamido-2-butenoate, that both geometrical isomers of the alkene could be hydrogenated with almost identical high enantioselectivity and the same sense of facial selectivity regardless of the alkene geometry (see Scheme 24.6). Deuterium-labeling studies of the reduction of methyl 2-acetamido-2-pentenoate showed that the origin of the DuPhos–Rh catalysts' high enantioselectivity with (*E*/*Z*)-α-dehydroamino acid mixtures was not the result of alkene isomerization [13]. Reduction of (*E*) and (*Z*)-isomers of methyl 2-acetamido-2-pentenoate with D_2 and *n*-Pr-DuPhos–Rh gave rise to diastereomerically pure isotopomers

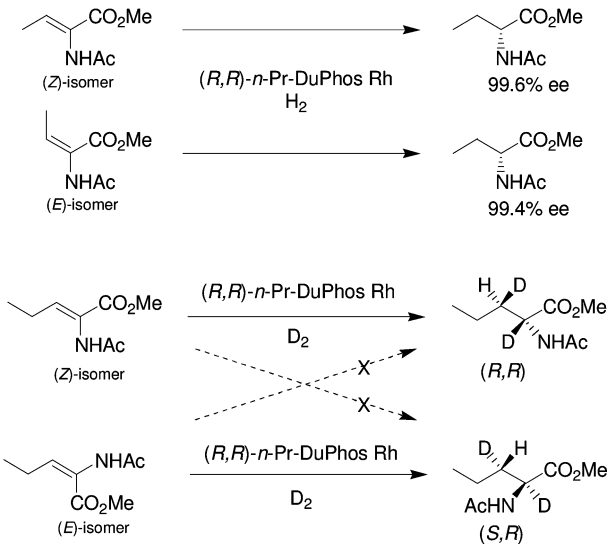

Scheme 24.6 Hydrogenation of (*E*) and (*Z*)-α-dehydroamino acid derivatives.

which, together with a 1 : 1 ratio of deuterium incorporation in the α and β-positions, excludes an (*E*/*Z*)-isomerization mechanism.

The synthetic utility of phospholane-derived catalysts has been directly extended to a broad range of simple, non-standard α-dehydroamino acid substrates, with enantioselectivities in excess of >95% ee being readily achieved [20, 100–107] (Scheme 24.7). The commercially available anti-fungicide (*R*)-metalaxyl has a MAA-related structure, and in a study by Blaser et al. conducted to assess the viability of an enantioselective hydrogenation approach to the active ingredient, the Me-DuPhos–Rh system produced the desired α-amino acid in high enantioselectivity (95.6% ee) and with extremely high productivity and activity (TON 50 000; TOF 5200 h^{-1}) [108, 109]. Some simple phenoxycarbonyl-protected cyclic α-dehydroamino acid substrates have been hydrogenated. In the case of five- and six-membered systems only low or modest enantioselectivities could be obtained, whereas seven-, eight-, nine-, thirteen-, and sixteen-atom ring systems gave 86 to 97% ee [110]. It has also been shown that even a polymer-supported dehydrophenylalanine substrate is readily hydrogenated by Me-DuPhos–Rh with high ee and de values [111].

Tandem processes consisting of enantioselective hydrogenation and cross-coupling have been shown to provide a useful approach for generating a diverse range of substituted aromatic α-amino acids, the corresponding α-dehydroamino acid precursors of which are not easily prepared (Scheme 24.8). Burk and Hruby have exploited the ability of DuPhos–Rh catalysts to hydrogenate various halogen- and boronic acid-substituted β-aromatic and β-heteroaromatic α-dehydroamino acids with high enantiomeric excesses. The resulting aromatic halides or boronic acids can be coupled with a variety of vinyl, aryl, and heteroaryl-groups

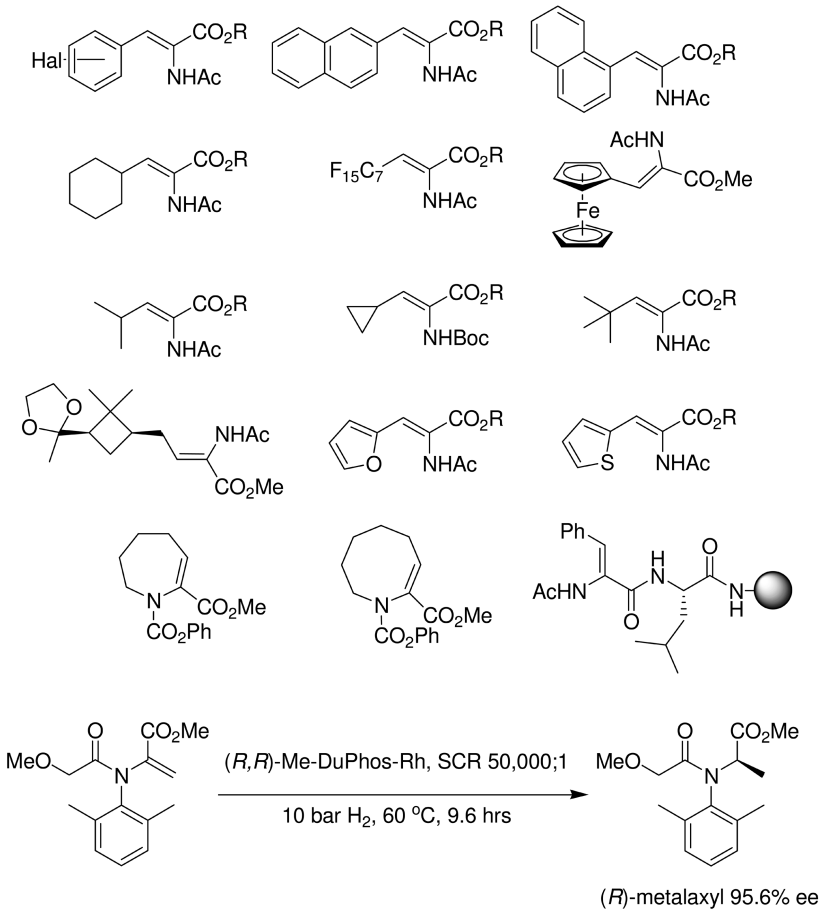

Scheme 24.7 Non-standard α-dehydroamino acid derivatives reduced by Rh-phospholane-based catalysts.

to produce a diverse range of new unnatural α-amino acids [20, 90, 100, 112–114]. Hruby has used this approach to great effect to generate a number of novel χ^2-constrained α-amino acids [112, 114].

A further key factor in the success of phospholane-derived catalysts is their ability to hydrogenate a variety of α-dehydroamino acids possessing functional groups, which in theory could either inhibit or adversely interfere with the selectivity of a hydrogenation process or, indeed, themselves be hydrogenated. These include strongly donating groups (e.g., heteroatoms, heterocycles, sulfides) or unsaturated groups (e.g., olefinic, ketonic and nitro groups). A large number of heteroaryl-α-amino acids have been prepared via asymmetric hydrogenation with chiral phospholane-modified catalysts. Zhang et al. reported that TangPhos and Et-**25** have been used in the preparation of a 2-thiophenylalanine

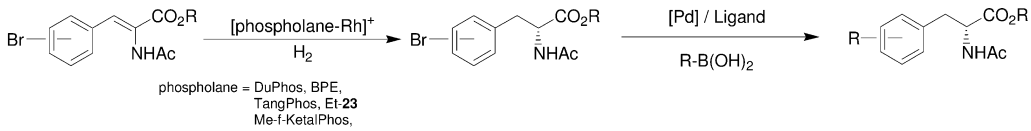

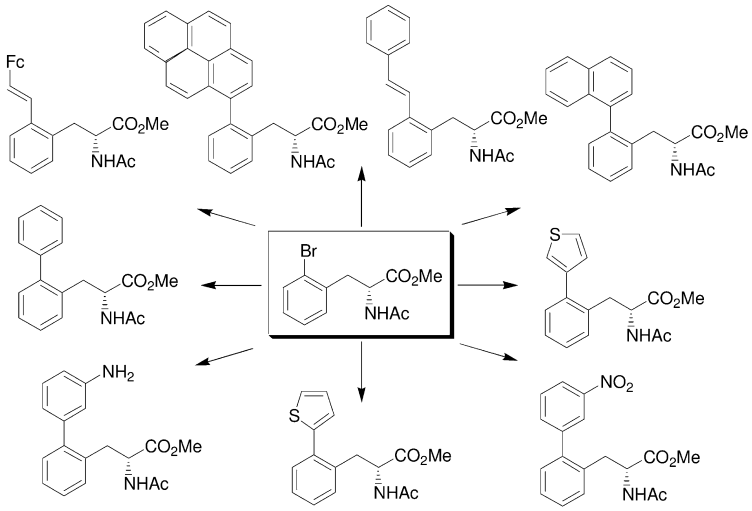

Scheme 24.8 Unnatural amino-acid derivatives accessed via tandem catalysis.

derivative in >99% ee at low pressure, without interference from the thiophene moiety [52b, 69a]. However, DuPhos, in particular, has been applied most extensively in this field. Simple thiophenyl [4a, 13, 20, 100, 115], furanyl [4a, 20, 100, 115], pyrroyl [115], pyrrolidyl [116], coumaryl [117] and a diverse range of tryptophanyl-α-amino acids [113, 114, 118–120] have all been synthesized with high enantioselectivities by means of enantiomeric hydrogenation of the requisite α-dehydroamino acids (see Fig. 24.8). In a number of cases, prolonged reaction times and molar catalysts loadings in the range of 1 to 3% were required to effect complete conversion. Moody generated di- and tri-peptide fragments of stephanotic acid using Et-DuPhos–Rh in the key asymmetric step [119]. In a remarkable piece of work, Carlier demonstrated that all five unnatural regioisomers of tryptophan derivatives could be accessed via enantioselective hydrogenation of the requisite α-dehydroamino acids with Et-DuPhos–Rh, and in no less than 96.7% ee in each case [118]. Substantially more complex and highly functionalized tryptophanyl-substrates have been prepared by Feldman et al. (Fig. 24.8), albeit with low enantioselectivities [121].

Pyridyl- and quinolyl-substrates are significantly more challenging to hydrogenate, due to the greater donating power of the nitrogen in these systems and, in general, modified hydrogenation protocols are necessary. A 2-quinolyl-alanine derivative was prepared by enantioselective hydrogenation with [Et-DuPhos–Rh]$^+$, in the presence of HBF_4, as the N-protonated species in 94% ee (see

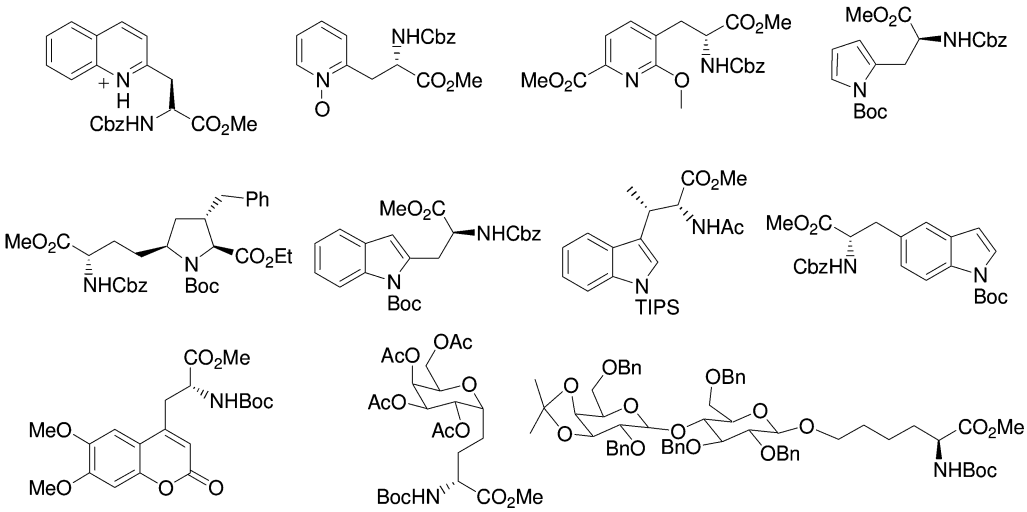

Fig. 24.8 Heteroalanines, tryptophan derivatives and glycosylated α-amino acid derivatives.

Fig. 24.8) [122]. Whilst this protocol can be used to prepare 3-pyridyl-alanine derivatives [22], the corresponding 2-pyridyl-alanine cannot be made [122]. However, Adamczyk has prepared several 2-pyridyl-alanine analogues through hydrogenation of the pyridine-*N*-oxide substrates in 80–83% ee (see Fig. 24.8) [123]. In general, only when the 2- and 6-positions of the pyridine ring are occupied can 2-, 3- or 4-pyridyl-alanine derivatives be prepared, without nitrogen modification, via hydrogenation with [phospholane–Rh]$^+$ catalysts [122–124].

Numerous examples exist of simple heteroatom-substituted substrates which have been hydrogenated by [phospholane–Rh]$^+$ including, amongst others, sulfide substrates [13,14], (*E*/*Z*)-isomers of *N*,*N*′-protected 2,3-diaminopropanoic and 2,3-diaminobutanoic acid derivatives [125], ε-NO_2-substituted α-dehydroamino acid [126], 4-piperidinylglycine precursor [127], and a ketonic substrate [14]. Heavily functionalized glycosylated α-amino acid derivatives have also been prepared using DuPhos–Rh catalysts [128]. Diastereoisomers of structurally complex and functionalized dipeptides have been prepared by Ortuño; a matching/mismatching effect is clear between the chiral substrate and the respective catalyst enantiomers, where (*R*,*R*)-Et-DuPhos–Rh gave >99% de and (*S*,*S*)-Et-DuPhos–Rh resulted in only 90% de, though the distal ketone moiety was not reduced [129].

A number of di- and tri-α-dehydroamino acid substrates have been shown to be hydrogenated in high ee and de with DuPhos–Rh catalysts, despite the potential for the initial chiral centers formed to interfere in subsequent stereodiscriminating steps [122,130] (Fig. 24.9). Interestingly, a number of these substrates are orthogonally protected at the acid or the amide functional groups, which is apparently not a barrier to high ee- and de-values [130a–d]. Hruby used this approach to synthesize a series of novel rigid dipeptide β-turn mimetics via the reduction of symmetrical di-α-dehydroamino acids [131].

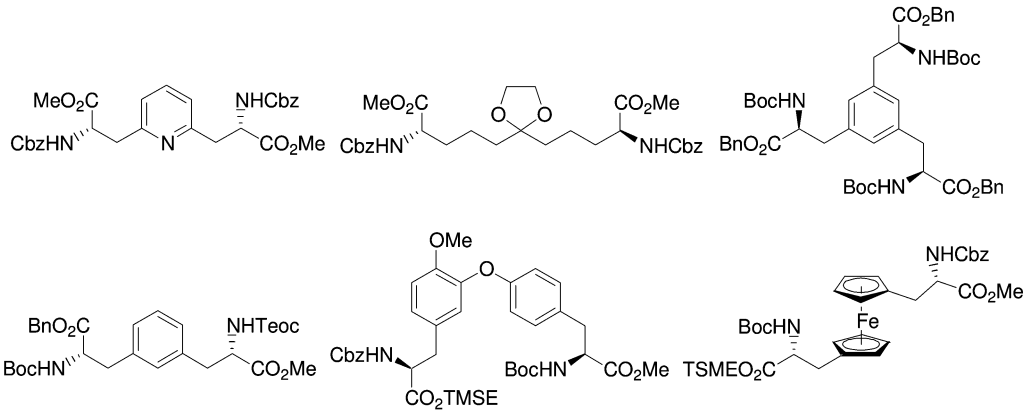

Fig. 24.9 Di and tri α-amino acid derivatives.

Phospholane-modified catalysts have shown the ability to discriminate between olefinic bonds in conjugated/nonconjugated β- and β,β-disubstituted α-didehydroamino acids, in both a highly regio- and enantioselective fashion [13, 90, 132, 133] (Scheme 24.9). The latter group involves the hydrogenation of tetrasubstituted alkenes with concomitant formation of two stereogenic centers. In general, the more reactive functionalized enamide bond is selectively reduced over simple unfunctionalized bonds. However, over-reduction can be observed, particularly when the reaction times are prolonged, as in the case of highly substituted olefins or in reactions near completion and the reduction of the distal bond becomes more favorable [132]. Over-reduction can be tempered by careful monitoring of the hydrogen uptake, solvent screening, lowering the hydrogen pressure, and reducing catalyst loadings [132, 133].

The choice of catalyst can have a significant effect on enantioselectivity and, in certain cases, the regioselectivity and activity. With nonconjugated α-didehydroamino acids, such as 2-acetamido-trideca-2,7-dienoic acid methyl ester or 2-acetamido-tetradeca-2,13-dienoic acid methyl ester, the proximal olefin is easily reduced at low catalyst loading with *n*-Pr-DuPhos–Rh in >99% ee and essentially complete regioselectivity [13]. However, in the case of conjugated α-didehydroamino acids, such as the 2-acetamido-6-(*tert*-butyl-dimethyl-silanyloxy)-hexa-2,4-dienoic acid methyl ester, the wrong choice of catalyst can lead to significant undesired over-reduction. 2-Acetamido-6-(*tert*-butyl-dimethyl-silanyloxy)-hexa-2,4-dienoic acid methyl ester can be hydrogenated in high ee and regioselectivity with Et-DuPhos–Rh (>99% ee and <0.5% over-reduction), whereas *i*-Pr-DuPhos–Rh gives only 87.8% ee and demonstrated little or no regioselectivity [133]. It has generally been observed that the DuPhos– and BPE–Rh systems can reduce tri-substituted $\alpha,\beta,\gamma.\delta$-didehydroamino acids with a remarkable degree of chemoselectivity in all but a few cases studied. Where the distal C=C bond is also activated to a certain extent, as in the case of styryl-dienamides, the degree of over-reduction is routinely <2%.

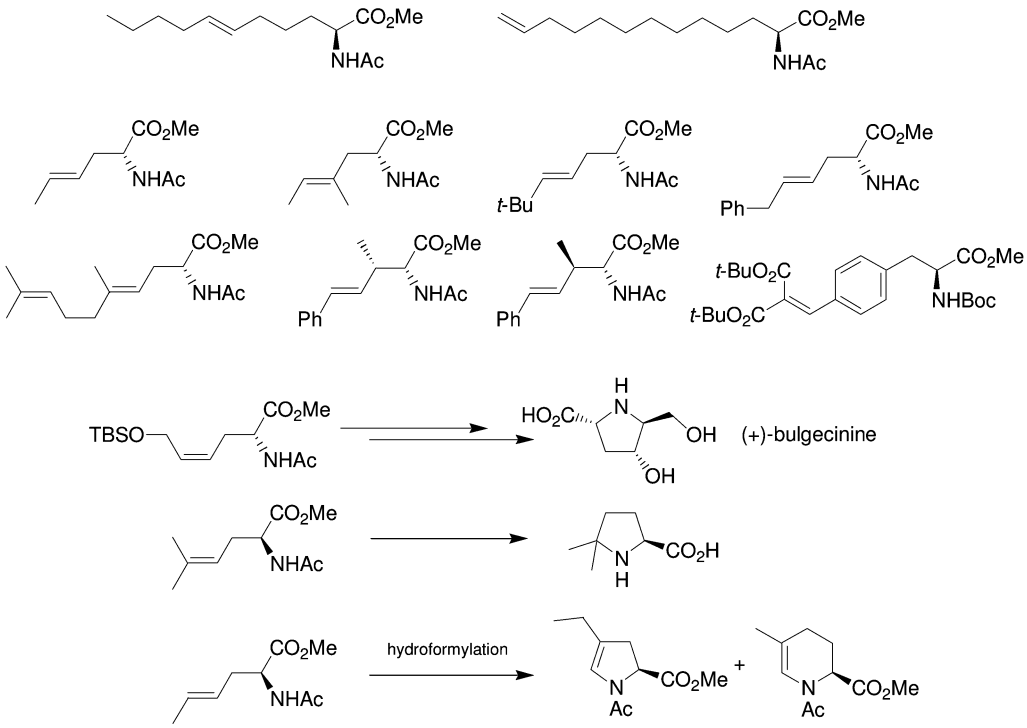

Scheme 24.9 Unsaturated α-amino acid derivatives prepared via chemoselective asymmetric hydrogenation.

In cases where the proximal double bond is highly substituted, such as tetra-substituted α-didehydroamino acids, selective reduction of the proximal double bond becomes increasingly difficult. Burk found, with a series of β,β-disubstituted $\alpha,\beta,\gamma,\delta$-didehydroamino acids, that only the smaller, sterically less-congested catalysts Me-BPE–Rh and Me-DuPhos–Rh were able to achieve high reactivity and selectivities [132]. The overall lower reactivity of these highly substituted systems generally requires higher catalyst loadings and more forcing conditions to achieve high or full conversions. In many cases complete conversion could not be achieved, and over-reduction approached 10%. Reduction of the (2*Z*,4*E*)-isomers in comparison to the (2*E*,4*E*)-dienamides has also been studied; unsurprisingly, the (2*Z*,4*E*)-isomer is more readily reduced in contrast to the (2*E*,4*E*)-dienamides.

The reduction of dienamides with [phospholane–Rh]$^+$ catalysts has been applied in the synthesis of a number of biologically interesting targets (Scheme 24.9). Burk and co-workers synthesized (+)-bulgecinine from 2-acetamido-6-(*tert*-butyl-dimethyl-silanyloxy)-hexa-2,4-dienoic acid methyl ester utilizing [(*R*,*R*)-Et-DuPhos–Rh]$^+$ [133], while Boehringer Ingelheim used (*R*,*R*,*S*,*S*)-TangPhos–Rh and (*S*,*S*)-Et-DuPhos–Rh to generate key intermediates in protease inhibitors [134], and 5,5-dimethylproline has been generated using (*S*,*S*)-Et-DuPhos–Rh

[135]. Garbay reported the chemoselective reduction of a α-dehydrophenylalanine substrate bearing a *p*-acrylate moiety [105]. Robinson et al. have also used a tandem, one-pot asymmetric hydrogenation-hydroformylation-cyclization approach to generate six- to eight-membered cyclic α-amino acids [136].

The enantioselective hydrogenation of β,β-disubstituted α-dehydroamino acids by means of [diphosphine-Metal]$^+$ catalysts is challenging in terms of enantioselectivity, chemoselectivity (*vide supra*), and reactivity. Few ligand systems have been tested with β,β-disubstituted substrates, and the reported results indicate that variable ee-values and high catalyst loadings are commonplace for many of the [diphosphine-Metal]$^+$ systems with tetrasubstituted olefins [137]. However, DuPhos and BPE catalysts demonstrate the capacity to consistently hydrogenate a wide range of β,β-disubstituted α-dehydroamino acid substrates with excellent ee-values and industrially applicable loadings [14, 20, 39, 90, 125, 138] (Fig. 24.10). Furthermore, the ability to hydrogenate (*E*) or (*Z*) α-dehydroamino acids with high enantioselectivity means that, with dissimilar substituents, two stereogenic centers can be created with high enantio- and diastereoselectivity when the (*E*) and (*Z*) α-dehydroamino acid is hydrogenated with both catalyst enantiomers.

In the majority of cases reported, optimal stereoselectivity and reactivity in sterically congested tetrasubstituted alkenes can be achieved with sterically less cumbersome Me-DuPhos and Me-BPE ligands. This is most graphically highlighted with the model substrate 2-acetamido-3-methyl-but-2-enoic acid methyl ester, where both Me-BPE and Me-DuPhos–Rh catalysts hydrogenate the substrate in >95% ee, whereas Et-DuPhos achieves 74% ee, *n*-Pr-DuPhos 45% ee, and *i*-Pr-DuPhos merely 14% ee [14]. This trend has been found over a broad range of substrates [14, 132], although there are some exceptional cases where Et-DuPhos–Rh achieves high enantio- and diastereoselectivity [39, 138]. Burk also made the observation that benzene was the optimal solvent for the majority of cases, however supercritical CO_2 ($scCO_2$) has also been shown to be a suitable medium for the enantioselective hydrogenation of β,β-disubstituted α-dehydroamino acids [39]. Zhang's phospholane catalyst Me-f-KetalPhos–Rh hydrogenated the model substrate 2-acetamido-3-methyl-but-2-enoic acid methyl

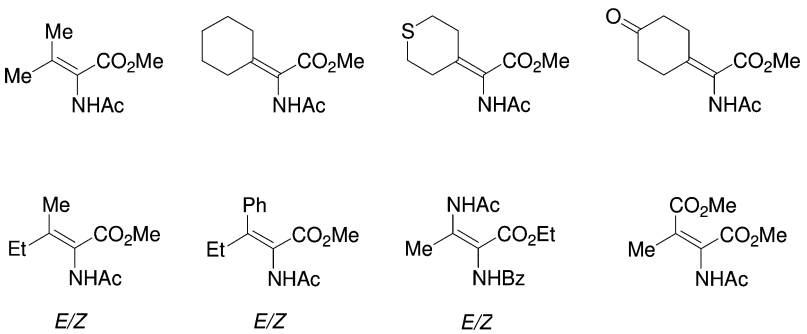

Fig. 24.10 β,β-disubstituted α-dehydroamino acid derivatives.

ester in 87.3% ee, whereas the phosphetanes DiSquareP* [87 b], *i*-Pr-CnrPHOS, and Cy-BPE-4 [83 a] have been shown to give only low to moderate ee-values with a few model substrates. (*S*,*S*)-*i*-Pr-CnrPHOS–Rh demonstrated a remarkable inversion of facial selectivity with 2-acetamido-3-phenyl-but-2-enoic acid methyl ester, giving the (2*S*,3*R*)-product in 38% ee at 10 bar H_2 and the (2*R*,3*S*)-isomer in 80% ee at 100 bar H_2.

Several biologically interesting targets have been synthesized via phospholane–Rh catalyzed hydrogenation of *β*,*β*-disubstituted *α*-dehydroamino acid substrates, including all four diastereoisomers of *N*,*N′*-protected 2,3-diaminobutanoic acid derivatives [125] (*vide supra*), a 4-piperidinylglycine derivative used as metalloproteinase and thrombin inhibitors (*vide supra*) [127 a], as well as a sterically congested *β*-methyltryptophan derivative [120].

24.3.2
Enantioselective Hydrogenation of *β*-Dehydroamino Acid Derivatives

Enantiomerically pure *β*-amino acids and their derivatives are an important class of compounds due to of their use as chiral building blocks in the synthesis of both biologically active molecules [139] and novel peptidomimetics [140]. Their incorporation is partly a result of the unusual secondary structures they can create, and also because they are frequently resistant to proteolysis. Currently, the principal methods used for their preparation involve chiral auxiliaries in stoichiometric reactions and to a lesser extent enantioselective catalysis [141]. One of the most promising and industrially viable methodologies involves the enantiomeric hydrogenation of an appropriate *β*-dehydroamino acid derivative with a homogeneous metal catalyst [142]. Owing to its simplicity, this approach has seen rapid development in recent years, with the most successful catalysts typically being Rh and Ru complexes containing phosphorus-based ligands, including several diphospholanes. The most selective examples (>95% ee), achieved with the most commonly used *β*-dehydroamino acid-derived substrates (R^1 = Me or Ph), are collected in Table 24.2, together with several results useful for comparison purposes.

As can be seen from Table 24.2, these rhodium catalysts are in general extremely active under very mild reaction conditions (H_2 pressure 1–20 atm, room temperature), albeit at catalyst loadings typical of screening studies (SCR 100). Although rare exceptions are known [143], the hydrogenation of (*E*)-*β*-dehydroamino acid esters generally proceeds with considerably higher enantioselectivity than the corresponding (*Z*)-isomers. It is worth mentioning, however, that Rh-TangPhos is reported to perform remarkably well against either stereoisomer [69 b, 71]. This is important since in the synthesis of dehydroamino acids, the (*E*/*Z*)-isomeric mixtures obtained can be difficult to separate, especially in the case of *β*-aryl substitution [71, 143, 148]. Furthermore, the (*Z*)-isomer is predominantly formed due to stabilizing hydrogen bonds [149]. Whether or not this additional bonding retards coordination to the metal center and concomitantly lowers selectivity is arguable, especially in protic media. However, use of the

Table 24.2 Phospholanes reported to hydrogenate model β-dehydroamino acid derivatives in >95% ee.

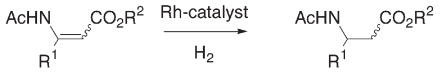

72 R^1 = Me, R^2 = Et
73 R^1 = Me, R^2 = Me
74 R^1 = Ph, R^2 = Et
75 R^1 = Ph, R^2 = Me

Substrate	Ligand	SCR	Reaction conditions [a)]	TON	TOF [h^{-1}]	% ee (config.)	Reference(s)
(*E*)-**72**	(*R*,*R*)-Me-DuPhos	100	Toluene, rt, 2.7 atm, 24 h[c]	100	–	99	143
(*Z*)-**72**	(*R*,*R*)-Me-DuPhos	100	Toluene, rt, 20 atm, 24 h[c]	100	–	88	143
(*E*)-**72**	(*S*,*S*)-Et-DuPhos	100	THF, 25 °C, 2 atm, 1 h[c]	100	–	99	144
(*Z*)-**72**	(*S*,*S*)-Et-DuPhos	100	THF, 25 °C, 2 atm, 1 h[c]	100	–	89	144
(*E*)-**72**	(*R*,*R*)-*i*-Pr-DuPhos	100	TFE, rt, 9.7 atm, <2 min	100	>3000	99	145
(Z)-**72**	(*R*,*R*)-*i*-Pr-DuPhos	100	TFE, rt, 9.7 atm, <2 min	100	>3000	92	145
(*E*/*Z*)-**72**	(*R*,*R*)-*i*-Pr-DuPhos	1000	TFE, rt, 9.7 atm, 40 min	1000	1500	95	145
(*E*)-**72**	(*R*,*R*)-Et-BPE	100	THF, 40 °C, 2 atm, 1 h[c)]	100	–	99	144
(*Z*)-**72**	(*R*,*R*)-Et-BPE	100	THF, 40 °C, 2 atm, 1 h[c)]	100	–	90	144
(*E*)-**72**	(*R*,*R*,*S*,*S*)-DuanPhos	100	MeOH, rt, 1.4 atm[b)]	–	–	99 (*R*)	70
(*Z*)-**72**	(*R*,*R*,*S*,*S*)-DuanPhos	100	MeOH, rt, 1.4 atm[b)]	–	–	97 (*R*)	70
(*E*)-**73**	(*R*,*R*)-Me-DuPhos	100	Toluene, rt, 2.7 atm, 24 h[c)]	100	–	99	143
(*Z*)-**73**	(*R*,*R*)-Me-DuPhos	100	Toluene, rt, 2.7 atm, 24 h[c)]	100	–	64	143
(*E*)-**73**	(*S*,*S*)-Me-DuPhos	100	MeOH, 25 °C, 1 atm, 1 h[c)]	100	–	98	146 a
(*Z*)-**73**	(*S*,*S*)-Me-DuPhos	100	MeOH, 25 °C, 1 atm, 1 h[c)]	100	–	88	146 a
(*E*)-**73**	(*S*,*S*)-Et-DuPhos	100	MeOH, 25 °C, 1 atm[b)]	100	–	98	146
(*Z*)-**73**	(*S*,*S*)-Et-DuPhos	100	MeOH, 25 °C, 1 atm[b)]	100	–	88	146
(*E*/*Z*)-**73**	(*S*,*S*)-Et-DuPhos	100	MeOH, 25 °C, 1 atm[b)]	100	–	92	146
(*E*)-**73**	(*R*,*R*)-Et-DuPhos	100	THF, 40 °C, 2 atm, 1 h[c)]	100	–	95	144
(*Z*)-**73**	(*R*,*R*)-Et-DuPhos	100	THF, 40 °C, 2 atm, 1 h[c)]	100	–	86	144

Table 24.2 (continued)

Substrate	Ligand	SCR	Reaction conditions [a)]	TON	TOF [h^{-1}]	% ee (config.)	Reference(s)
(*E*)-**73**	(*R*,*R*)-Et-BPE	100	THF, 40 °C, 2 atm, 1 h [c)]	100	–	98	144
(*Z*)-**73**	(*R*,*R*)-Et-BPE	100	THF, 40 °C, 2 atm, 1 h [c)]	100	–	82	144
(*E*)-**73**	(*R*,*R*)-Me-Ph-BASPHOS	100	MeOH, 25 °C, 1 atm [b)]	100	–	99 (*S*)	56 b
(*Z*)-**73**	(*R*,*R*)-Me-Ph-BASPHOS	100	MeOH, 25 °C, 1 atm [b)]	100	–	70 (*S*)	56 b
(*E*)-**73**	(*S*,R_p,*S*,R_p)-**36**	100	THF, rt, 1.4 atm, 5 min	100	1200	96 (*R*)	59 c
(*Z*)-**73**	(*S*,R_p,*S*,R_p)-**36**	100	THF, rt, 1.4 atm, 45 min	100	133	89 (*R*)	59 c
(*E*)-**73**	(*R*,S_p,S_p,*R*)-**35**	100	THF, rt, 1.4 atm, 15 min	100	400	96 (*S*)	59 c
(*Z*)-**73**	(*R*,S_p,S_p,*R*)-**35**	100	THF, rt, 1.4 atm, 1 h 15 min	100	80	83 (*S*)	59 c
(*E*)-**73**	(*R*,*R*)-catASium M	100	MeOH, 25 °C, 1 atm, 3 h [c)]	100	–	98 (*R*)	95
(*Z*)-**73**	(*R*,*R*)-catASium M	100	MeOH, 25 °C, 1 atm, 3 h [c)]	100	–	83 (*R*)	95
(*E*)-**73**	(*R*,*R*)-Et-FerroTANE	100	MeOH, 25 °C, 1 atm [b)]	100	–	99 (*S*)	56 d, 147
(*Z*)-**73**	(*R*,*R*)-Et-FerroTANE	100	MeOH, 25 °C, 1 atm [b)]	100	–	28 (*S*)	56 d, 147
(*E*)-**73**	(*S*,*S*,*R*,*R*)-TangPhos	200	THF, rt, 1.4 atm, 24 h [c)]	200	–	>99	69 b, 71
(*Z*)-**73**	(*S*,*S*,*R*,*R*)-TangPhos	200	THF, rt, 1.4 atm, 24 h [c)]	200	–	99	69 b, 71
(*E*/*Z*)-**73**	(*S*,*S*,*R*,*R*)-TangPhos	200	THF, rt, 1.4 atm, 24 h [c)]	200	–	>99	69 b, 71
(*Z*)-**73**	(*S*)-Me-Butiphane	200	MeOH, 25 °C, 5 atm [b)]	200	–	98	42
(*E*)-**74**	(*R*,*R*)-Et-FerroTANE	100	MeOH, 25 °C, 1 atm [b)]	100	–	99 (*S*)	56 d, 147
(*E*)-**75**	(*R*,*R*)-Et-FerroTANE	100	MeOH, 25 °C, 1 atm [b)]	100	–	99 (*S*)	56 d, 147
(*E*/*Z*)-**75**	(*S*,*S*,*R*,*R*)-TangPhos	200	THF, rt, 1.4 atm, 24 h [c)]	–	–	94 (*S*)	69 b, 71

a) Complete conversion unless otherwise stated.
b) No reaction time given.
c) No conversion given

strongly polar solvent 2,2,2-trifluoroethanol (TFE) had a beneficial effect on enantioselectivities when a Rh-*i*-Pr-DuPhos catalyst was applied [145]. Limited solvent studies have been performed with a number of phospholane-based ligand systems [65, 71, 143, 146 a], but in general alcoholic solvents are the most suitable, together with tetrahydrofuran (THF) and dichloromethane (CH_2Cl_2).

Several accounts have described (*Z*)-dehydroamino acid esters as being less active than the corresponding (*E*)-isomer [59 c, 143–145]. In fact, Bruneau and Demonchaux reported that when reduction of an (*E*/*Z*)-mixture of **73** with Rh-Et-DuPhos in THF was not complete, only unreacted (*Z*)-**73** was detected. These findings conflict, however, with results obtained in MeOH [56 d], where the ligand structure was also found to be significant to the relative reactivity of each stereoisomer. As for *α*-dehydroamino acid derivatives, preformed metal–diphosphine complexes generally perform in superior fashion to those prepared *in situ* [56 d].

Zhang et al. reported that for Rh-catalyzed enantiomeric hydrogenation with either BICP or Me-DuPhos, the (*Z*)-isomers were generally less reactive, and required higher pressures for complete conversion [143]. Enantioselectivities for the (*E*)-isomer were shown to be unaffected by increased pressure. On the other hand, Heller and co-workers showed that operating at low hydrogen pressures in a polar solvent had a significantly beneficial effect on enantioselectivities when hydrogenating (*Z*)-**73** with [Et-DuPhos Rh(COD)]BF_4 (e.g., 35% ee at 45 atm and 87% ee at 1 atm), albeit at the expense of reaction rates [146 a]. This was also found to be the case with several other ligand systems [56 d]. In light of these findings, a tentative mechanistic concept has been proposed which provides evidence that the reaction proceeds via an "unsaturated route" with the prochiral olefin coordinating to the metal center prior to oxidative addition of hydrogen [150].

In general, the same sense of chiral induction is obtained with either geometrical stereoisomer, which facilitates the use of (*E*/*Z*)-isomeric mixtures. An exception to this was recently reported by Heller and Börner [56 d]. Remarkably, hydrogenation of methyl (*Z*)-*β*-acetylamino pentenoate with [(*S*,*S*)-Et-DuPhosRh (COD)]BF_4 at 1 bar gave the (*R*)-enantiomer of product in 31% ee, whereas the same reaction at 30 bar resulted in an inversion of configuration and the (*S*)-product in 77% ee.

The effects of temperature on enantioselectivities have been examined using a Rh-Et-DuPhos catalyst in both MeOH [56d] and THF [144]. With *β*-dehydroamino acid derivative **73** in MeOH, an increase in temperature was found to have a slight beneficial effect for both (*E*) and (*Z*)-isomers over a 70 °C range, with maximum values being observed between 0 °C and 25 °C. In THF, however, the effect is much more pronounced, especially for the (*Z*)-isomer which varies in selectivity from 65% ee at 10 °C to 86% ee at 25 °C. Interestingly, when substrate **72** was reduced with a Rh-Et-BPE catalyst in THF, this temperature dependence on enantioselectivity for the (*Z*)-isomer was most apparent, the selectivities varying from 43% ee (10 °C) to 90% ee (40 °C). Examination of these results also seemed to indicate that the hydrogenation of *β*-dehydroamino acid derivatives follows an unsaturated pathway (*vide supra*) [144].

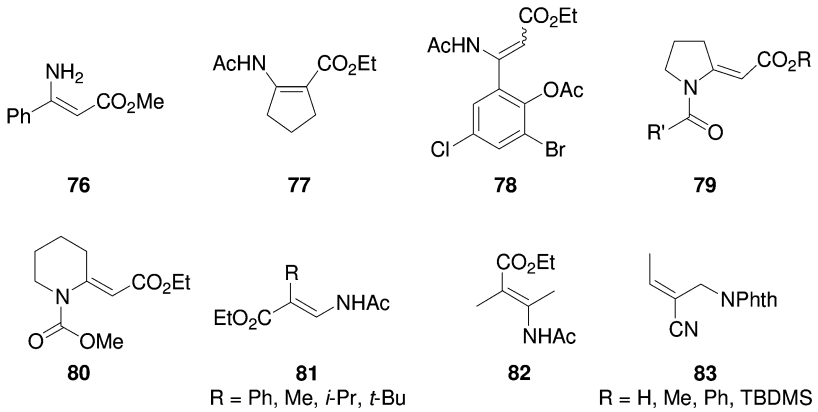

Fig. 24.11 Unusual β-dehydroamino acid derivatives to have been reduced with phospholane-based catalysts.

Several phospholane-based ligands have shown a wide substrate scope beyond the standard examples represented in Table 24.2. Both Et-FerroTANE **61** [147] and TangPhos **46** [69 b, 71] have been successfully applied to a diverse range of methyl and ethyl β-aryl-dehydroamino acids containing various aromatic substituents, whilst catASium M **20a** [95] has been used for the reduction of numerous β-alkyl-dehydroamino acid esters.

In addition to the standard substrates described above, the enantioselective hydrogenations of several other β-dehydroamino acid derivatives using phospholane-based or related ligands are worthy of note (Fig. 24.11). Using TFE as solvent, a screen of commercially available catalysts showed that the unprotected β-dehydroamino acid ester (*Z*)-**76** could be partially reduced (77% conversion) in 88% ee with [(*R*,*R*)-Et-FerroTANE Rh(COD)]BF_4, but ultimately, an *in-situ*-prepared Rh-Josiphos-type catalyst gave superior results [151]. Interestingly, preliminary deuterium-labeling studies suggested that the hydrogenation of (*Z*)-**76** proceeds through the imine tautomer in an analogous fashion to β-ketoester hydrogenations. Enantioselective reduction of the tetrasubstituted cyclic β-dehydroamino acid ester (*E*)-**77** was recently reported by Zhang et al., and although both *in-situ*-prepared Ru catalysts of Me-DuPhos and TangPhos were found to give complete conversion (SCR 20) in moderate enantioselectivities (71% ee and 57% ee, respectively), atropisomeric biaryl-based ligands were more selective (e.g., C2- to C5-TunePhos all gave 99% ee) [152].

As one of several routes investigated for the preparation of a key intermediate for a $\alpha_v\beta_3$ integrin antagonist, the enantiomeric hydrogenation of olefin **78** was examined [153]. Despite investigating several different catalysts under multiple reaction conditions on various derivatives of **78**, a viable method was not forthcoming. The best result obtained was 70% ee with [(*S*,*S*)-Et-DuPhos Rh(COD)]OTf in CH_2Cl_2 at 5 atm H_2. Lee and co-workers examined the enantioselective synthesis of homoproline derivatives via Rh-catalyzed reduction of the cyclic substrate (*E*)-**79**

with a range of different ligands [154]. Although, (*R*,*R*)-Me-DuPhos was the most selective (>99% ee (*R*)), the conversion was only 37%. The chiral bidentate phosphine Me-BDMI proved to be the overall ligand of choice. Reduction of the structurally related *β*-dehydroamino acid ester (*E*)-**80** was recently described in a patent by Solvay, with [(*R*,*R*)-Me-DuPhos Rh(COD)]OTf giving complete conversion to the (*R*)-product in 95.5% ee (5 atm H_2, 25 °C, SCR 100) [155].

Finally, an interesting variation on the standard substitution pattern shown above is the regioisomeric β^2-amino acids, the substituent being *α* to the carboxylic functionality. Two approaches for their synthesis, which adopts enantiomeric hydrogenation with a phospholane-based ligand, have been described. Robinson, Jackson and colleagues reported the preparation of a range of substrates of type (*E*)-**81** and subsequent Rh-catalyzed enantioselective hydrogenation with either Me or Et-DuPhos and Me-BPE. Through modification of the amide group, the ligand and the solvent, moderate enantioselectivities up to 67% ee where attainable [156]. The *α*,*β*-disubstituted *β*-dehydroamino acid ester (*E*)-**82** was also examined with BPE and DuPhos catalyst systems; Rh-Me-BPE was the most selective, giving complete conversion in 65% ee over 72 h in benzene (4 atm, room temperature). An alternative approach to β^2-amino acids was also explored through the reduction of *α*,*β*-unsaturated nitriles **83**, again using Rh-Me-BPE or Rh-Et-DuPhos catalysts (up to 48% ee), and the amino acids being obtained after hydrolysis and phthalimide deprotection [157]. Conversion of the nitrile to the corresponding methyl ester and switching to a Ru-BINAP-based system increased the enantioselectivities to 84% ee.

24.3.3
Enantioselective Hydrogenation of Enamides

Chiral amines constitute an important class of compounds that have been extensively employed as resolving agents, chiral auxiliaries, and pharmaceutical intermediates. Traditionally, classical resolution or biocatalysis have been typically chosen as the preferred methods for industrial manufacturing, though the enantioselective hydrogenation of enamides or imines (*vide infra*) has recently received much attention, with several phospholane-based ligands proving to be applicable. Table 24.3 details the most selective phospholanes (≥95% ee) to have been used in the Rh-catalyzed hydrogenation of frequently used simple enamides, namely *N*-(1-phenyl-vinyl)-acetamide **84** and *N*-(1-phenyl-propenyl)-acetamide **85**. In general, the conditions employed are mild, with high reactivities being observed at low temperatures and pressures. For example, TONs as high as 5000 to 10 000 have been achieved with Ph-BPE **15** [34] or the P-chiral phospholane, TangPhos **46** [69]. In the case of the *β*-branched enamide **85**, (*S*,*S*,*R*,*R*)-DiSquareP* **63** has been reported to be extremely selective for reduction of the (*E*)-isomer (>99% ee), but with the enantioselectivity being much lower for the corresponding (*Z*)-isomer (37% ee) [87 b]. However, this is not the case for the diphospholanes BPE and TangPhos, with excellent levels of selectivity being obtained even when an (*E*/*Z*)-isomeric mixture is applied.

Table 24.3 Phospholanes reported to hydrogenate model enamide substrates in >95% ee.

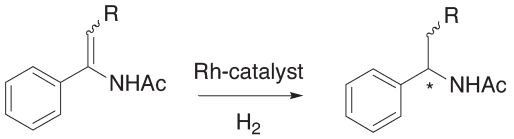

84 R = H
85 R = Me

Substrate	Ligand	SCR	Reaction conditions [a)]	TON	TOF [h^{-1}]	% ee (config.)	Reference(s)
84	(*S*,*S*,*R*,*R*)-DiSquareP*	100	MeOH, rt, 1 atm, 1 h	100	>100	>99 (*R*)	87 b
84	(*S*,*S*,*S*,*S*)-Et-**16**	100	MeOH, rt, 10 atm, 24 h	100	–	96 (*S*)	52 b, c
84	(*R*,*R*)-Me-Ph-UCAP	100	MeOH, rt, 5 atm, 3 h	100	>33	94 (*R*)	65, 67
84	(*S*,*S*,*R*,*R*)-TangPhos	10 000	MeOH, rt, 1.4 atm [d)]	10 000	–	99 (*R*)	69
84	(*R*,*R*,*S*,*S*)-DuanPhos	100	MeOH, rt, 1.4 atm [d)]	10 000	–	>99 (*R*)	70
84	(*R*,*R*)-Ph-BPE	5 000	MeOH, 25 °C, 10 atm [d]	5 000	–	99	34
84	(*R*,*R*)-Me-BPE	500	MeOH, 22 °C, 4 atm, 15 h	500	>33	95	17
(*E*)-**85**	(*S*,*S*,*R*,*R*)-DiSquareP*	100	MeOH, rt, 1 atm, 1 h	100	>100	>99 (*R*)	87 b
(*Z*)-**85**	(*S*,*S*,*R*,*R*)-DiSquareP*	100	MeOH, rt, 2 atm, 1 h	100	>100	37 (*R*)	87 b
(*Z*)-**85** [c)]	(*S*,*S*)-Me-DTBM-UCAP	500	MeOH, 30 °C, 4 atm, 15 h	500	>33	99 (*S*)	64
(*E*/*Z*)-**85**	(*S*,*S*,*R*,*R*)-TangPhos	100	MeOH, rt, 1.4 atm, 12 h	100	–	98 (*R*)	69
(*E*/*Z*)-**85**	(*R*,*R*)-Me-BPE	100	MeOH, rt, 1.4 atm, 12 h	100	–	95 (*R*)	17

a) Complete conversion unless otherwise stated.
b) Similar high enantioselectivities have also been obtained with several other ligands of this class.
c) *N*-benzoyl instead of *N*-acetyl.
d) No reaction time given.

In addition to these simple model substrates, several phospholane-containing ligands have shown broad functional group tolerance when applied to the Rh-catalyzed hydrogenation of aromatically substituted α-arylenamides. Burk et al. reported the use of DuPhos and BPE ligands for the reduction of α-arylenamides containing alkyl, halogen, thio, alkoxy, aromatic, and heteroaromatic substituents, commenting that the enantioselectivities tended to increase with decreasing steric demand of the phospholane moiety at the 2,5-positions [17]. This was later extended to include esters, ketones and cyano groups, showing that these systems are also chemoselective [35]. Similar levels of tolerance have been demonstrated, with several phospholanic ligands originating from the group of Zhang, including the tetrahydroxy diphosphine **25** (R = Me) [52 b, 53 b], TangPhos [69] and, to a lesser

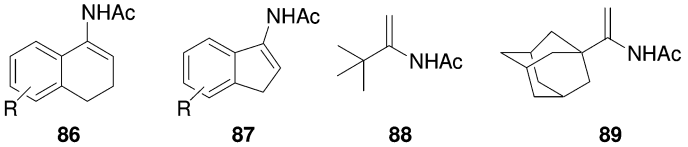

Fig. 24.12 General enamide classes to have been reduced with phospholane-based catalysts.

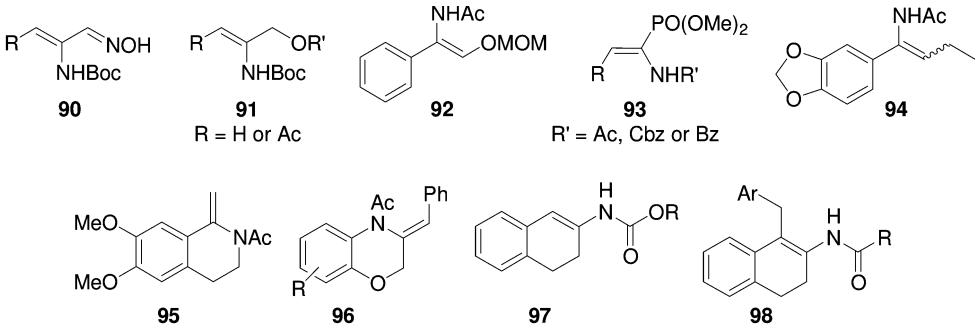

Fig. 24.13 Unusual enamides to have been reduced with phospholane-based catalysts.

extent, DuanPhos [70]. The effective hydrogenation of (*Z*)-**85** and the *N*-benzoyl analogue were independently reported by Pringle [65] and Saito [64] respectively, using a range of unsymmetrical diphosphines, UCAPs **41**.

Both (*S*,*S*)-Me-BPE [19] and (*R*,*S*,*R*,*S*)-Me-PennPhos **44** [67 d, e] have been successfully applied to the Rh-catalyzed hydrogenation of a range of cyclic enamides derived from α-tetralones and α-indolones (**86** and **87**). Under mild conditions, both ligands achieved good to excellent enantioselectivities (71–99% ee), with PennPhos giving reasonable levels of catalyst reactivity (TON up to 2000; TOF $\sim 100\ h^{-1}$), even for tetra-substituted enamides. Interestingly, PennPhos gives lower selectivities for acyclic enamides when compared to BPE catalysts, whereas BPE requires lower temperatures to attain high enantioselectivities with cyclic enamides (e.g., 71% ee at 20 °C and 92% ee at 0 °C for unsubstituted **86**).

Alkyl enamides, such as *N*-(1-*tert*-butyl-vinyl)-acetamide **88** and *N*-(1-adamantyl-vinyl)-acetamide **89**, can also be hydrogenated in high enantioselectivity (>99% ee) and activity (TON 5000; TOF >625 h^{-1}) with Rh-Me-DuPhos [19]. Remarkably, these bulky alkyl enamides are reduced with the opposite sense of induction, a phenomenon also observed when the bisphospholane DiSquareP* **63** was applied [87 b]. A computational modeling study by Landis and Feldgus suggested that the reduction of α-alkyl and α-arylenamides involves different coordination pathways [93, 158].

In addition to standard cyclic and acyclic enamides, the effective hydrogenation of several more unusual enamides has been reported (Fig. 24.13). A concise method for the synthesis of chiral β-amino alcohols, amino oximes and chiral 1,2-diamines has been described by Burk et al. via the enantioselective hydroge-

nation of **90** or **91** using Rh catalysts of Me or Et-DuPhos [18]. In general, the enantioselectivities were high (91–99% ee), with reactions proceeding smoothly to completion within 12 h at SCR 1000. Zhang and co-workers have reported the hydrogenation of a series of MOM-protected *β*-hydroxy-*α*-arylenamides **92** as a mixture of (*E*/*Z*) isomers [159]. Although BICP–Rh and Me-DuPhos–Rh complexes were both found to be excellent catalysts for this transformation (90–99% ee), Rh-Me-DuPhos displayed higher enantioselectivity over a broader substrate range. Ultimately, the products could be converted to chiral *α*-arylglycinols by *O*-MOM and *N*-acetyl deprotection under acidic conditions. By screening a range of diphosphines, including five phospholane-based ligands, Pagenkopf et al. extended the scope of this reaction to include *o*-alkoxy-substituted enamides [160]. Me-BPE and Me-DuPhos were found to be the most selective ligands (92–98% ee), with better results being achieved with the isolated [(P-P) Rh COD]OTf precatalysts over *in-situ* preparation. The size of the *o*-substituent was not found to have any significant effect on selectivity.

By using a Rh-catalyst containing a ligand from either the DuPhos or BPE family, Burk and co-workers successfully hydrogenated a range of phosphonated enamides **93** (R′ = Ac or Cbz) in moderate to high enantioselectivities (57–95% ee), with aryl-substituted examples giving lower selectivity than alkyl analogues [161]. In contrast to the reduction of several other substrate classes with Rh-DuPhos or Rh-BPE complexes [12, 13, 15, 18, 21], a strong dependence on olefin geometry was observed, with (*E*)-isomers being significantly more selective. Börner and Holz also reported the Rh-catalyzed reduction of a phosphonated enamide **93** (R = Ph, R′ = Bz) with two DuPhos/BPE type ligand systems, Rophos (**22** and **23**) [51a] and BASPHOS (**32** and **33**) [56e]. Although enantioselectivities with Rophos were generally higher than with BASPHOS (up to 99% ee versus 79% ee), activities were slightly lower (TOF 6 h^{-1} versus 25 h^{-1}). The enantioselective hydrogenation of enamide **94** using [(*R*,*R*)-Me-DuPhos Rh(COD)]BF_4 was reported by Storace et al. [162]. This intermediate to the leukocyte elastase inhibitor, DMP 777, was prepared quantitatively in 96.5% ee at SCR 1800 under mild conditions (2 atm, room temperature) in MeOH. Although a single crystallization afforded the optically pure amide in 86% yield and >99% ee, ultimately enantiomeric hydrogenation was not chosen as the preferred method for manufacturing.

As well as endo-cyclic enamides (*vide supra*), phospholane-based Rh catalysts have also been applied to the enantiomeric reduction of exo-cyclic enamides. Zhang reported TangPhos to hydrogenate **95** in 97% ee [69], while Zhou showed Me-DuPhos to be extremely efficient for a broad range of substituted dihydrobenzoxazines **96** (92–99% ee) [163]. Finally, the hydrogenation of a series of trisubstituted ene carbamates **97** and tetrasubstituted enamides **98** was found to be catalyzed by Ru complexes of either Me-DuPhos and Me-BPE [164]. The catalysts were formed *in situ* by reacting the diphosphine with [Ru(COD)(methallyl)$_2$] in the presence of HBF_4 or triflic acid. Notably, the use of atropisomeric ligands, BINAP and BIPHEMP, led to no activity and similarly, hydrogenation did not occur with the more commonly used [(diphosphine)Rh(COD)]BF_4 precatalysts.

24.3.4
Enantioselective Hydrogenation of Unsaturated Acid and Ester Derivatives

The enantioselective hydrogenation of α,β- or β,γ-unsaturated acid derivatives and ester substrates including itaconic acids, acrylic acid derivatives, butenolides, and dehydrojasmonates, is a practical and efficient methodology for accessing, amongst others, chiral acids, chiral α-hydroxy acids, chiral lactones and chiral amides. These are of particular importance across the pharmaceutical and the "flavors and fragrances" industries.

The enantioselective hydrogenation of itaconic acid derivatives in particular has received much interest; one area of significance is the generation of succinate compounds for use as peptidomimetics [82a]. As indicated in Table 24.4, a variety of phospholanes are suitable ligands for hydrogenating the commonly used model substrates, itaconic acid and its dimethyl ester (DMI), with high enantioselectivities. Moreover, phosphetanes and phosphinanes have demonstrated high enantioselectivities with both substrates. In several cases exceptionally high catalyst activity has been demonstrated; Ph-BPE and catASium M are reported to hydrogenate DMI with TOFs of 60 000 and 40 000 h^{-1}, respectively [34, 47]. Although high enantioselectivities are also reported for the parent itaconic acid substrate, catalyst activities are substantially lower with this substrate in comparison to DMI. Surprisingly, the parent Me-DuPhos ligand is neither particularly selective nor active with the diacid [44], and a number of ligands are reported with superior selectivity and activity. BASPHOS ligands have demonstrated a significant degree of substrate sensitivity with DMI and itaconic acid; enantioselectivities ranging from 8.1% to 97.9% are reported for (*R*,*R*)-Me-Et-BASPHOS (**33**) and (*R*,*R*)-Me-Ph-BASPHOS (**32**), respectively [56b]. Pressure and solvent effects have been observed in the hydrogenation of DMI using a catASium M ligand, where higher pressures (7.9 atm) and CH_2Cl_2 as solvent gave superior results [46–48]. Itaconic acid has been hydrogenated by **25** in various $MeOH/H_2O$ mixtures, ranging from 9 : 1 to 3 : 97, without variance or loss of enantioselectivity. The three-carbon bridged tridentate ligand (*S*,*S*)-Me-**11** hydrogenated DMI in 94% ee, albeit with protracted reaction times, whereas the related bidentate ligand (*R*,*R*)-Me-**7** surprisingly gave only 78% ee [11]. Remarkably, Corma et al. have reported the first use Me-DuPhos-based Pt and Au catalysts for the reduction of simple itaconic acid derivatives in high enantioselectivity (3 to 95% ee) and extremely high rates (TOF up to 10 200 h^{-1}) [166]. Unfortunately, these high activities were achieved at the expense of selectivity.

β-Substituted and β,β-disubstituted itaconic acid substrates, generated via the Stobbe condensation and resulting in mono 1-esters, provide a more structurally diverse and challenging set of substrates. Currently, only DuPhos, BPE and – to a lesser extent TangPhos and catASium M – have been shown to achieve high enantioselectivities across this broad range of itaconate substrates (Fig. 24.14). The (*E*/*Z*)-mixtures typically formed in Stobbe condensations can be tolerated by phospholane-based catalysts without loss of performance [21, 72]. Performing itaconate hydrogenations at temperatures of around 0 °C has been found to be

Table 24.4 Phospholanes reported to hydrogenate model itaconic acid substrates in >95% ee.

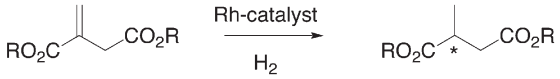

99 R = Me
100 R = H

Substrate	Ligand	SCR	Reaction conditions [a)]	TON	TOF [h^{-1}]	% ee (config.)	Reference(s)
99	(*S*,*S*)-Et-DuPhos	1000	MeOH, 20 °C, 5.4 atm, 2.8 h	1000	– [b)]	>97 (*R*)	21
99	(*R*,*R*)-Et-BPE	1000	MeOH, 20 °C, 5.4 atm, 1 h	1000	1000	97 (*R*)	34
99	(*R*,*R*)-Ph-BPE	10000	MeOH, 28 °C, 9.9 atm, 10 min	10000	60000	99 (*R*)	34
99	(*R*,*R*)-Me-Ph-BASPHOS	100	MeOH, 28 °C, 1 atm, 3 h	100	33.3	97 (*R*)	56b
99	(*R*,*R*)-UlluPHOS	1000	MeOH, 27 °C, 2 atm, 2.8 h	1000	–	>99 (*S*)	44
99	(*R*,*R*)-Me-DuPhos	1000	MeOH, 27 °C, 2 atm, 2.8 h	1000	–	>99 (*S*)	44
99	(*S*,*S*,*S*,*S*)-*t*-Bu-**23**	100	MeOH, rt, 1 atm, 8 min	50 [c)]	375	99 (*R*)	51
99	(*S*,*S*,*S*,*S*)-Bn-**22**	100	MeOH, rt, 1 atm, 28 min	50 [c)]	107	98 (*R*)	51
99	catASium M	– [a)]	CH_2Cl_2, 25 °C, 7.9 atm, 15 min	10000	40000	99	47
99	(*S*,*S*,*R*,*R*)-TangPhos	5000	THF, rt, 1.4 atm	5000	– [b)]	99 (*S*)	72
99	(*R*,*R*,*S*,*S*)-DuanPhos	100	THF, rt, 1.4 atm	–	– [b)]	99 (*S*)	70
99	(*Rp*,*Rc*,*R*,*R*)-**54**	100	MeOH, 25 °C, 1 atm, 1 h	100	100	>99 (*S*)	80
99	(*R*,*R*)-Et-FerroTANE	200	MeOH, 25 °C, 5.4 atm, 1 h	200	>200	98 (*S*)	82, 83
99	(*S*,*S*)-*n*-Pr-FerroTANE	200	MeOH, 20 °C, 5.4 atm, 1 h	200	>200	97 (*R*)	82, 83
100	(*S*,*S*)-Et-DuPhos	100	MeOH, rt, 17.8 atm, 2 h	95 [d)]	47.5	96 (*R*)	165
100	(*R*,*R*)-Me-Ph-BASPHOS	100	MeOH, 25 °C, 1 atm, 20 min	100	300	97 (*R*)	56b
100	(*R*,*R*)-*cis*-PMP5	1000	MeOH, rt, 1.5 atm, 2 h	998 [c)]	499	97 (*R*)	76b
100	(*S*,*S*,*S*,*S*)-Me-**25**	192	MeOH, rt, 1.3 atm, 20 h	192	–	>99 (*R*)	55
100	(*S*,*S*,*S*,*S*)-Bn-**23**	100	MeOH, rt, 1 atm, 24 min	50	125	98 (*R*)	51
100	(*S*,*S*,*S*,*S*)- Bn-**22**	100	MeOH, rt, 1 atm, 10 min	50	300	98 (*R*)	51
100	(*S*,*S*,*S*,*S*)-**31**	100	MeOH, rt, 5.4 atm, 12 h	100	8.3	>99 (*R*)	54

Table 24.4 (continued)

Substrate	Ligand	SCR	Reaction conditions [a)]	TON	TOF [h^{-1}]	% ee (config.)	Reference(s)
100	catASium M	–[a)]	MeOH, 25 °C, 3.9 atm, 3 h	500	–[b)]	97	47
100	(*S*,*S*,*R*,*R*)-TangPhos	200	THF, rt, 1.4 atm	–	–[b)]	99 (*S*)	72
100	(*R*,*R*)-*ent*-Cy-**66**	500	*i*-PrOH, 20 °C, 1 atm, 24 h	–	–[b)]	96 (*S*)	89

a) No catalyst loading given.
b) Insufficient data on loading, time or yield to calculate TOF.
c) Reaction not gone to completion.

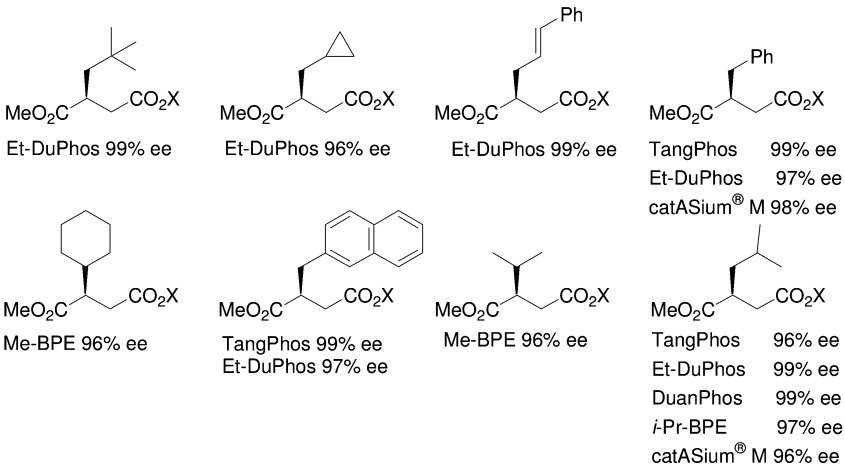

Fig. 24.14 Succinic acid derivatives produced by phospholane–Rh-catalyzed hydrogenation (X = H, Na or R_3NH).

beneficial in terms of enantioselectivity. The nature of the secondary binding group can play a critical role in terms of reaction rates and enantioselectivity with this substrate class; the hydrogenation of 2-isopropylidenesuccinic acid 1-methyl ester with (*R*,*R*)-Me-BPE at SCR 300 : 1 gave only 33% conversion and 88% ee, whereas the *tert*-butylamine salt of the acid gave complete conversion at SCR 500 : 1 with 95% ee under comparable conditions [167]. The use of a salt form is reported to enhance both reactivity and selectivity, enabling industrially viable catalyst loadings of SCR > 4000 : 1 to be readily achieved [21]. Amine and alkali metal salts of itaconic acid are generally employed, though optimal results seem to be best achieved with preformed and purified amine salts [168]. The enhanced performance of the itaconate acid salts is possibly a result of both the enhanced binding ability of the carboxylate group and higher substrate purity.

β,β-Disubstituted itaconic acid substrates require higher catalyst loadings and hydrogen pressures to achieve reasonable reaction rates, which is unsurprising given the level of steric congestion around the olefinic bond. The most effective hydrogenation was attained when using the sterically less cumbersome Me-BPE ligand; indeed, when used in conjunction with substrates as the amine salt, enantioselectivities of 96% could be realized [21].

Inverse itaconate derivatives (4-itaconic acid derivatives) have been studied to a lesser extent than the 1-itaconic acid derivatives. In the limited number of reported hydrogenations of itaconic acid 4-esters, the parent DuPhos ligands have performed poorly with model substrates. For example, in the hydrogenation of itaconic acid 4-methyl ester in MeOH, both Me- and Et-DuPhos gave less than 3% yield and poor to moderate ee-values (41 to 74%) [82 c]. However, catASium M is reported to achieve 99% ee and a TOF of 8000 h^{-1} in CH_2Cl_2 with itaconic acid 4-methyl ester [47]. The related Me- and Et-5-Fc ferrocenyl phospholanes hydrogenate itaconic acid 4-methyl ester with complete conversion at SCR 2000 : 1, though the enantioselectivities remain low at <45% [82 c]. FerroTANE based catalysts reduce itaconic acid 4-methyl ester and 2-pentylidene-succinic acid 4-methyl ester in >94% ee at SCRs of between 1000 : 1 and 2000 : 1 [82 c]. Moreover, a series of 2-alkylsuccinic acids 4-*tert*-butyl ester targets have been generated in high ee using Et-FerroTANE and Et-DuPhos. This approach has been used in synthesizing the MMP-3 inhibitor UK-370,106 101 [169] (Scheme 24.10).

Inverse amido-itaconates also proved to be challenging substrates for phospholane-based catalysts, and only limited success has been achieved to date. 2-Methylenesuccinamic acid (**102**) has been reported to be reduced by Et-DuPhos–Rh in 96% ee at SCR 100 000 : 1, with an average TOF of 13 000 h^{-1}. The removal of a trace chloride-containing contaminant was found to be crucial in obtaining high enantioselectivities and reaction rates [85]. An isoquinuclidine containing inverse amido-itaconate **103**, which is currently being evaluated in preparations for the treatment of diabetes, has been prepared using Rh-Et-DuPhos in 98.7% ee [170]. Whilst phospholane systems have achieved only moderate success in this substrate class, the FerroTANE family of ligands has been reported broadly to outperform all ligand classes, with superior enantioselectivities

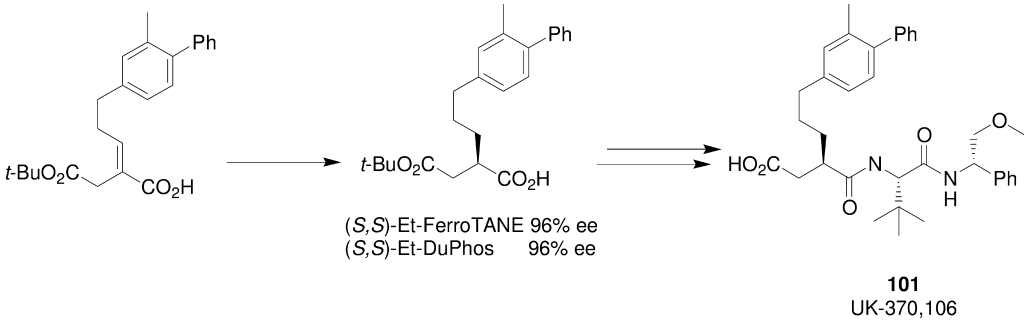

Scheme 24.10 Inverse itaconate approach to a protease inhibitor.

and industrially viable catalyst activities. Burk tested an array of inverse amido-itaconates (e.g., **104**) where both the amide fragment and β-substitution on the olefin were varied, and found most enantioselectivities to be >95% with TOFs in the range of 1000 to 6000 h^{-1} when Et-FerroTANE was used as the chiral ligand [82 a, c].

Although the efficient enantioselective reduction of α,β-unsaturated acids and lactones is typically achieved using ruthenium-biaryldiphosphine-based catalysts [2], several reports have been made of phospholane-ruthenium, -rhodium and -iridium systems that perform this hydrogenation with comparably high enantioselectivities. Burk has reported that the ubiquitous model substrate for Ru-biarylphosphine catalysts, tiglic acid, can been reduced with up to 94% ee with a Ru-*i*-Pr-DuPhos catalyst [27, 171 a, 172 a]. However, the array of substrate structures reported for this class is diverse and bears little similarity to the model substrates (Fig. 24.15). Simple acrylic acid derivatives such as methyl α-hydroxymethacrylate and 2-[[(phenylmethoxy)amino]methyl]-2-hexenoic acid methyl ester **105** have been hydrogenated by both Me-DuPhos and TangPhos–Rh catalysts in 90% and 96–98% ee [75, 173]. (*E*)-β-methylcinnamates **106** have been reduced using Zhang's mixed phospholane-oxazoline catalyst Ir-**48**, giving results comparable to Pfaltz's established iridium phosphonite-oxazoline systems [74]. Trisubstituted aryl/heteroaryl-sulfonylated acrylic acid derivatives (e.g., **107**) have been hydrogenated in remarkably high enantioselectivities with Me-DuPhos–Rh [174]. A challenging α-(γ-amino)-β-imidazolyl-acrylic acid substrate **108** was reduced using *i*-Pr-5-Fc–Rh in the presence of quinidine to give the target product in high ee using a combined enantioselective hydrogen/classical resolution approach [175]. A series of diastereomeric scaffolds (e.g., **109**) were synthesized from functionalized chiral

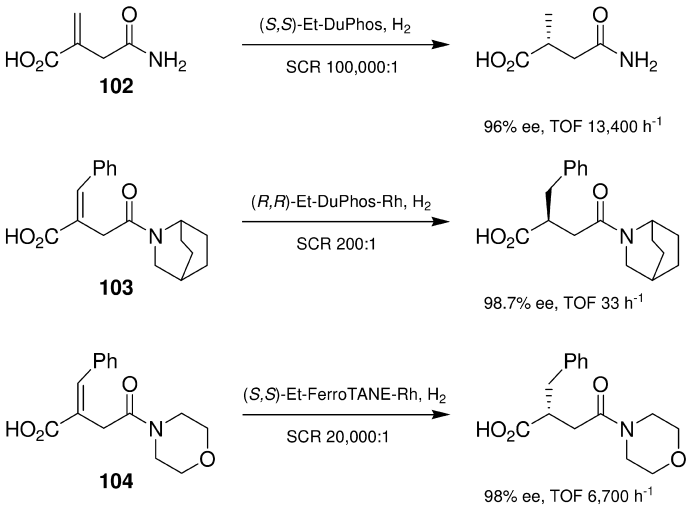

Scheme 24.11 Enantioselective reduction of inverse amido-itaconates.

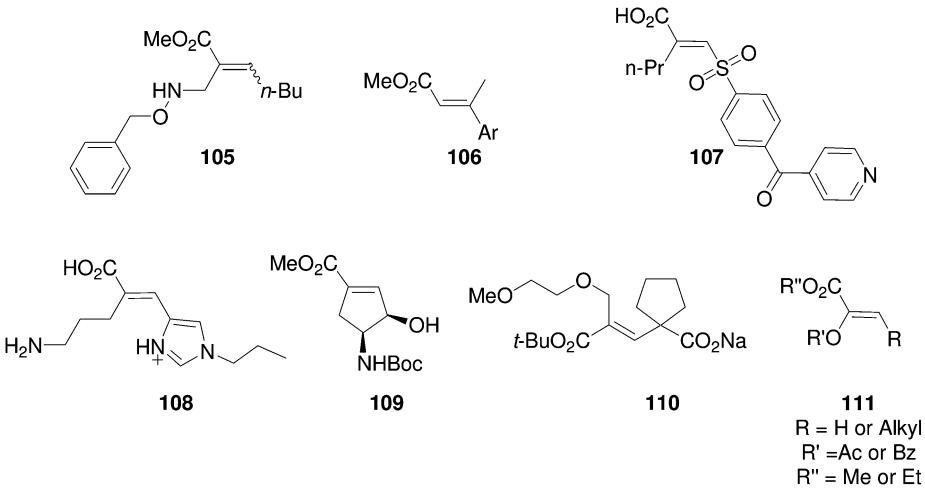

Fig. 24.15 Diverse α,β-unsaturated acid derivatives reduced with phospholane catalysts.

cyclopentene rings bearing an acrylate substructure, while facial selectivity could be controlled via the judicious use of DuPhos or BPE–Rh catalysts or Crabtree's catalyst [176]. Sterically congested α,β-unsaturated lactone substrates (butenolides) bearing potentially inhibiting heterocycles have been hydrogenated with Me-DuPhos–Rh in 80% ee [177]. A key glutarate component **110** in the atrial natriuretic factor (ANF) potentiator Candoxatril has been synthesized in high ee using both a MeDuPhos–Rh and Ph-BPE–Rh catalyst [34, 178]. The use of a Rh-phospholane catalyst circumvented the problem of the generation of unreactive enol ethers as side products, which was a major issue when Ru-BINAP was used [178]. A PennPhos–Ru species reduced 3-(*p*-fluorobenzylidene) valerolactam in 70% ee, a target molecule for producing 3-alkylpiperidines as pharmacophores; however, BDPP-Ir was found to be a better system for reducing the *exo*-cyclic olefin [179].

A wide range of α-(acetyloxy)- and α-(benzoyloxy)acrylates **111**, with both alkyl and aryl β-substituents, have been successfully hydrogenated with cationic Rh-DuPhos complexes [180]. In particular, the reduction could be performed on an (*E*/*Z*)-isomeric mixture, with selectivities generally being greater than 97% ee. A brief solvent study showed MeOH, *i*-PrOH, or CH_2Cl_2 to be the best solvents in terms of both catalyst activity and selectivity, and benzene to inhibit the reaction by formation of a stable adduct. Increased hydrogen pressure had a negligible influence on selectivity. Ultimately, the hydrogenation products were converted to enantiomerically enriched α-hydroxy esters and 1,2-diols, without any loss in optical purity. An example of a (*Z*)-α-(phenoxy)-β-alkyl-acrylate has been reported to have been reduced in 86 and 89% ee using Et-FerroTANE–Ru and *i*-Pr-DuPhos–Ru catalysts; Me-f-KetalPhos–Ru, whilst catalytically active, produced an essentially racemic product, and a SynPhos–Ru catalyst proved to be the optimal catalyst screened [181].

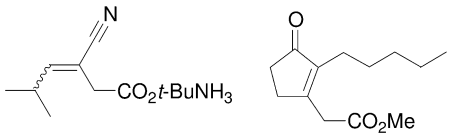

112 **113**

Fig. 24.16 β,γ-unsaturated acids reduced with MeDuPhos–Rh and Ru catalysts.

The hydrogenation of a β,γ-unsaturated acid **112** has been key to the enantioselective synthesis of a potent anticonvulsant (*S*)-(+)-3-aminomethyl-5 methylhexanoic acid, Pregabalin [60, 61] (see Fig. 24.16). (*E*/*Z*)-mixtures of three possible precursors were examined for reactivity and selectivity. The ester substrate was found to be not particularly useful in terms of both reactivity and selectivity towards a number of DuPhos, BPE and FerroTANE catalysts; remarkably, using (*R*,*R*)-Me-DuPhos at room temperature or at 55 °C resulted in a reversal of facial selectivity, albeit with modest enantioselectivities in each case. The *t*-$BuNH_3^+$ and K^+ salts of the acid were found to be superior in both reactivity and enantioselectivity, and whilst both salts performed comparably well, the hydrogenation was optimized using the *t*-$BuNH_3^+$ salt as a result of substrate quality concerns [60]. An optimized procedure using (*R*,*R*)-Me-DuPhos–Rh has been used at the kilogram scale to give the desired product in 97.7% ee at SCR 2700 : 1 and 4.4 atm. Hoge's C_1-symmetric phospholanes (**35** and **36**) are also selective towards this substrate: at low pressure (2 atm) and SCR 100 : 1, **35** was moderately more selective than **36**, giving 96% and 92% ee, respectively. Hoge demonstrated with **36** that high enantioselectivities at lower catalyst loadings could only be achieved with a concomitant increase in H_2 pressure; subsequently, 97% ee could be achieved at 13.5 atm [59a, b, d]. Jasmonoid compounds have indicated numerous phtyobiological activities and olfactory properties, the *cis*-jasmonate compounds being of particular interest to the perfume industry (Fig. 24.16). Direct reduction of the olefinic double bond of dehydrojasmonate **113** via *syn*-addition of H_2 is the most direct route to the *cis*-isomers. However, traditional cationic Rh-phospholanes are not electrophilic enough to hydrogenate the tetrasubstituted double bond. Bergens developed a more electrophilic, coordinatively unsaturated 16-electron cationic ruthenium-hydride-phosphine system that was not only capable of hydrogenating the double bond but, when modified with Me-DuPhos and provided with enantiomeric excesses up to 60% and a >99 : 1 *cis*/*trans* ratio, furnished the desired enantiomerically enriched *cis*-isomer. However, a Josiphos variant operated with better enantioselectivity [182]. It is not clear whether the pendant ester group plays a secondary binding role during the hydrogenation.

24.3.5
Enantioselective Hydrogenation of Unsaturated Alcohol Derivatives

One method of accessing chiral alcohols is through the enantioselective hydrogenation of the corresponding enol acetates. Despite this substrate class having similar structures to enamides, far fewer successful examples of this reaction

have been reported. It has been argued that this may be in part due to the enol acetate having a weaker binding acyl group than the analogous enamide [4c]. Notwithstanding this, Burk was successful in hydrogenating a range of simple α-substituted enol acetates **114** in good to excellent enantioselectivities (89–99% ee) with either Rh-DuPhos or Rh-BPE catalysts [12]. High enantioselectivities have also been obtained when applying Rh-Me-DuPhos for the reduction of 1-alkenyl or 1-alkynyl enol acetates, **115** and **116** [183]. In the case of **116**, the triple bond is reduced to a double bond with (*Z*)-configuration after reduction of the enol acetate. Interestingly, the judicious choice of **115** or **116** as substrate allows access to either (*E*) or (*Z*)-α,β-unsaturated acetates. The analogous saturated straight-chain derivatives were found to hydrogenate smoothly, but with only moderate selectivity (64–77% ee). [Me-DuPhos Rh(COD)]OTf has also been reported to catalyze the hydrogenation of 2-acetyloxy-1,1,1-trifluorododec-2-ene in 92% ee, but higher selectivities were obtained with Ru-based catalysts of atropisomeric biaryl ligands, BINAP and BIPHEMP.

Burk et al. also showed the Rh-complexes of Me and Et-DuPhos to be effective catalysts for the enantioselective reduction of several phosphonated enol acetates of type **117** (86–96% ee with TOF $\sim 10\ h^{-1}$ at 25 °C, 4 atm), providing an efficient route to enantiomerically enriched alkyl-substituted α-hydroxy phosphonites [161]. Remarkably, these catalysts were inactive against an aryl-substituted analogue, and although partial conversion could be obtained with Me-BPE, both the selectivity and reactivity were much lower (70% ee, TOF $1.5\ h^{-1}$). Recently, the research group of Zhang has reported several phospholane-based ligands to be effective for the Rh-catalyzed reduction of acyclic, α-aryl substituted enol esters of type **118** (PennPhos [67c,d], TangPhos [69b, 72], DuanPhos [70] and **48** (R = Me) [52b]). In general, high to excellent enantioselectivities are achieved (81–99% ee) under mild reaction conditions, albeit at high catalyst loadings (SCR 100). The *in-situ*-prepared Rh-PennPhos catalyst [67c,d] has also been applied to the reduction of five- and six-membered cyclic enol acetates, **119** and **120**, derived from substituted 1-indanone and 1-tetralone, respectively.

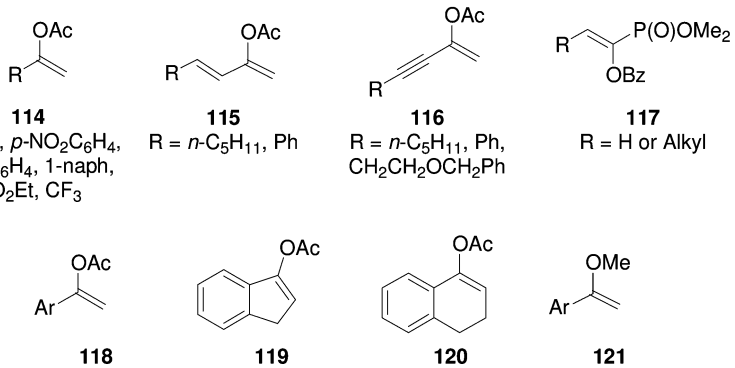

Fig. 24.17 Unsaturated alcohol derivatives to have been reduced by phospholane ligands.

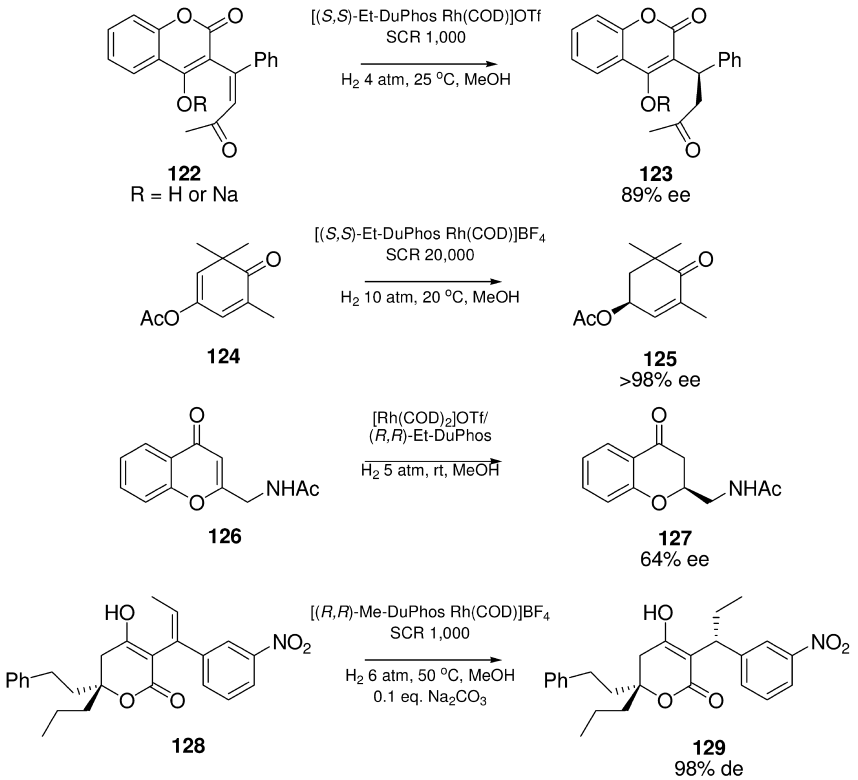

Scheme 24.12 Several pharmaceutically active compounds to have been synthesized via Rh-phospholane-mediated asymmetric hydrogenation.

Catalyst performance was far superior to the corresponding BINAP or Me-DuPhos systems, with both conversions and selectivities being higher. The hydrogenation of enol ethers using Rh-PennPhos catalysts has been reported in a patent by Zhang [67 d]. Under mild conditions, high enantioselectivities were obtained (73–94% ee) for 1-aryl-1-methoxy-ethene derivatives **121**, compared to Me-DuPhos (40–73% ee) and BINAP (46–48% ee).

The enantioselective reduction of unsaturated alcohol derivatives has been applied to the synthesis of several biologically active compounds (Scheme 24.12). Warfarin (**123**, R = H) is an important anticoagulant that is normally prescribed as the racemate, despite the enantiomers having dissimilar pharmacological profiles. One of the earliest reported uses of DuPhos was in the development of a chiral switch for this bioactive molecule, facilitating the preparation of (*R*)- and (*S*)-warfarin [184]. Although attempted reduction of the parent hydroxycoumarin **122** (R = H) led to formation of an unreactive cyclic hemiketal, hydrogenation of the sodium salt proceeded smoothly with Rh-Et-DuPhos in 86–89% ee.

Hoffman la Roche have reported the synthesis of an intermediate to zeaxanthin via the enantioselective reduction of cyclic enolacetate **124** [185]. Using a Rh-Et-DuPhos catalyst, excellent levels of selectivity (98% ee) could be obtained at extremely low catalyst loadings (TON 20 000; TOF 5000 h^{-1}). Chroman derivatives, such as **127**, have been reported by Merck to affect the central nervous system [186]. As part of a wide ligand screen, an *in-situ*-prepared Rh-Et-DuPhos complex has been reported to be amongst the most selective for the preparation of **127**, albeit in 64% ee. Finally, an enantioselective approach to **129**, a key intermediate to the HIV protease inhibitor tipranavir (PNU-140710), was developed by Chirotech for Pharmacia & Upjohn [187]. The use of [(*R*,*R*)-Me-DuPhos–Rh(COD)]BF_4 and Na_2CO_3 as a co-catalyst gave quantitative conversion in 93% de (SCR 1000, 6 atm, 50–60 °C). Once again, (*E*/*Z*)-mixtures could be tolerated together with high chemoselectivity with regards to over-reduction of the nitro functional group. Both UlluPHOS **18** [43, 44] and catASium M **20a** (A = O, R = Me) [188] have also been applied to this reaction.

24.3.6
Enantioselective Hydrogenation of Miscellaneous C=C Bonds

Through continued exploration of the applicability of enantiomeric hydrogenation, phospholane-based catalysts have been reported to be efficient for the reduction of several atypical olefinic substrates (Fig. 24.18).

Due to the lack of an ordered chelate complex provided by the substrate containing a secondary binding site, the enantioselective reduction of unfunctionalized olefins remains a challenging area where only limited success has been achieved. Noyori et al. reported Me-DuPhos–Ru catalysts to be effective for the hydrogenation of α-ethylstyrenes **130** [189]. By activating the precatalyst with an alkoxide base in 2-propanol, respectable enantioselectivities (71–89% ee) and activity (TON up to 2600; TOF 160 h^{-1}) could be obtained under mild reaction conditions. Using the cationic iridium complexes of a class of phospholane-oxazoline ligands, **48**, Zhang and co-workers successfully reduced methylstilbene derivatives **131** in 75–91% ee [74]. These selectivities are comparable to those obtained with the best ligand systems for this substrate class [4b,c, 190]. Although outperformed by biaryl-based ligands such as BINAP, Me-DuPhos has

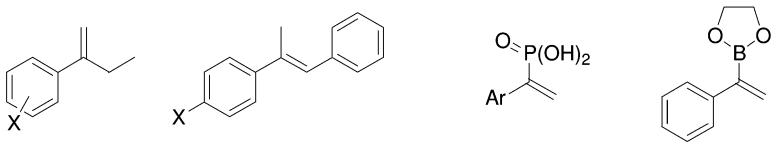

130 X = H, *p*-Me, *p*-F, *p*-Cl, *p*-Br, *p*-CF_3, *m*-Cl, *m*-Br, *o*-Br

131 X = H, OMe, Cl

132 Ar = Ph, *p*-Me-C_6H_4, 1-Np, *p*-Cl-C_6H_4

133

Fig. 24.18 Unusual olefins to have been reduced with phospholane-based catalysts.

also shown to be active in the Ru-catalyzed reduction of α-aryl-substituted ethylphosphonates **132** (16–37% ee) [191] and ethanediol 1-phenylethenylboronic ester **133** (42% ee) [192].

24.4 Enantioselective Hydrogenation of C=O and C=N Bonds

24.4.1 Enantioselective Hydrogenation of Ketones

The enantioselective hydrogenation of ketones using Rh or Ru diphosphine catalysts is the most efficient method for the synthesis of chiral alcohols. Although in general, atropisomeric biaryl-based chiral ligands have proven to be the most versatile for this substrate class [2, 4b,c], significant success has been achieved with phospholane-containing systems (Fig. 24.19). As early as 1991, Burk et al. reported the use of Rh-phospholane **7** catalysts for the reduction of methyl acetoacetate [11], albeit with poor enantioselectivity (20–27% ee). Switching to a Ru-based precatalyst greatly enhanced both the activities and selectivities obtained [172], with [*i*-Pr-BPE $RuBr_2$] being found to be broadly effective for a range of β-keto esters **134** (76–99% ee, TON 500, TOF >15 h^{-1}) at low hydrogen pressures [172a]. Interestingly, amongst other applications, this was used for the preparation of enantiomerically pure 1,4-dicyclohexyl-1,4-butanediol and, ultimately, the synthesis of a new phospholane ligand, Cy-BPE; a rare case of "ligand self-generation". In general, the DuPhos class of phospholanes (and analogues [43, 44]) shows much lower activities for the reduction of β-keto esters than the more basic BPE ligands, with higher pressures, temperatures and reaction times being required [193]. Despite these harsher conditions, excellent enantioselectivities (96–99% ee) were obtained for the reduction of **134** (R = Me or $MeO_2C(CH_2)_2$, R′ = Me or Et) with the tetramethoxy ligand, BASPHOS **32** (R = Me) [56b].

The groups of Marinetti and Genêt have shown that several bisphosphetane-derived ligands (**58**, **59**, **61**) form effective Ru-based catalysts for the hydrogena-

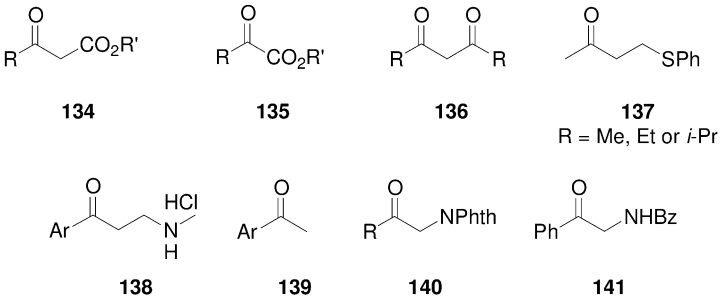

Fig. 24.19 General ketone classes to have been reduced with phospholane-based catalysts.

tion of β-keto esters, but once again, higher temperatures and pressures were generally required for reasonable activity [83 b–e]. Overall, moderate to high enantioselectivities were observed, with the bulkier 2,4-disubstituted phosphetanes (*i*-Pr > Et > Me) being more selective [83 d, e]. The bisphosphetanes CnrPHOS **58** (R = *i*-Pr or Cy) have also been applied to the Ru-catalyzed enantiomeric reduction of α-keto ester **135** (R = Ph, R′ = Et), β-diketones **136**, and β-thioketone **137**. In the case of substrates **135** and **136**, excellent selectivities were observed (98% and 97% ee, respectively), despite the high temperatures employed, with **136** also being obtained with high diastereoselectivity (94%). Cy-BPE-4 **59** has also been shown to be extremely selective for the Ru-catalyzed reduction of β-diketone **136** (R = Me), giving 98% ee and 95% de [83 b].

One application of phospholane-containing ligands for the enantiomeric reduction of a ketone recently appeared in a patent application from Lonza [194]. In the presence of NaOMe, both Me-DuPhos and Me-KetalPhos (**24**) gave reasonable selectivities (71.3% and 79.8% ee, respectively) for the Rh-catalyzed reduction of a β-amino ketone **138** (Ar = 2-thienyl), an intermediate for the pharmaceutically active drug duloxetine. Zhang and co-workers have also demonstrated the use of Rh-DuanPhos (**47**) for the reduction of a range of β-secondary-amino ketone hydrochlorides, including precursors to the drugs (*S*)-fluoxetine and (*S*)-duloxetine [73]. In general, remarkably high enantioselectivities were obtained (93–99% ee) with high TONs (> 4500) and TOF (375 h^{-1}) when using the secondary amino group, whilst the corresponding tertiary amine was unreactive.

The Rh-catalyzed hydrogenation of methyl pyruvate, **135** (R,R′ = Me), was studied by Burk et al. with bisphospholanes containing a chiral backbone, **6** and **7** (Fig. 24.20). Significant matching and mismatching effects were observed (43% versus 75% ee), with the matched system being ligand **7** [29]. Genêt also studied the reduction of α-keto esters, showing Me-DuPhos to form an effective Ru-catalyst when tested against **135** (R = Ph, R′ = Me) (80% ee) [172 b].

As for unfunctionalized olefinic substrates, the enantioselective hydrogenation of unfunctionalized ketones is considerably more challenging due to the absence of a secondary chelating moiety. Undoubtedly, until now the catalyst of choice for this substrate class is the *trans*-[$RuCl_2$(diphosphine)(diamine)] catalyst developed by Noyori [195], with numerous examples being reported with high enantioselectivities (> 95% ee) and activities (TON up to 2 400 000; TOF 259 000 h^{-1}) [196]. Although far less active (TOF < 50 h^{-1}), Zhang has reported significant selectivities with a Rh-PennPhos (**44**) system [57, 67 b]. When com-

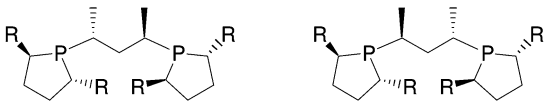

6 R = Me, Et, i-Pr

7 R = Me, Et, i-Pr

Fig. 24.20 Matching and mismatching bisphospholanes.

bined with either 2,6-lutidine or KBr additives, moderate to high enantioselectivities (55–99% ee) are achieved for a range of simple ketones, including dialkyl-substituted ketones (up to 92% ee), a class against which the Noyori system is much less effective. A ruthenium complex of the P-chiral diphosphine BIPNOR (**53**) has also been reported to reduce unfunctionalized ketones of class **139** with moderate enantioselectivity (57–81% ee) [78 b, d].

Finally, the group of Zhou has recently published the first Pd-catalyzed enantiomeric reduction of ketones using Me-DuPhos [197]. By performing the reaction in TFE, a series of α-phthalimido ketones **140** were reduced in high yield and 75–92% ee, albeit at high catalyst loadings (SCR 50), reaction times (12 h) and pressures (13.7 atm). This procedure was extended to include ketones **134** (R = Ph, R′ = Et), **139** (Ar = Ph), and **141**.

24.4.2
Enantioselective Hydrogenation of Imines and C=N–X Bonds

Enantiomerically pure amines are extremely important building blocks for biologically active molecules, and whilst numerous methods are available for their preparation, the catalytic enantioselective hydrogenation of a C=N bond potentially offers a cheap and industrially viable process. The multi-ton synthesis of (*S*)-metolachlor fully demonstrates this [108]. Although phospholane-based ligands have not proven to be the ligands of choice for this substrate class, several examples of their effective use have been reported.

Indeed, the imine intermediate **142** in the synthesis of metolachlor has been reduced in 97% ee using an iridium complex of the phospholane-containing ligand **55** [80].

A *trans*-[$RuCl_2$(diphosphine)(1,2-diamine)] complex with (*R*,*R*)-Et-DuPhos and (*R*,*R*)-1,2-diaminocyclohexane as the ligand combination has been found to be effective for the hydrogenation of imine **143**, with up to 94% ee being obtained under the standard basic conditions employed for this catalytic system [198]. Unfortunately, the optimum combination of chiral diphosphine and diamine was found to be substrate-dependent, with only 40% ee being obtained for 2-methylquinoxaline **144** with Et-DuPhos.

Corma et al. have recently demonstrated the hydrogenation of **145** using a binuclear gold complex of (*R*,*R*)-Me-DuPhos [166]. Reasonable rates were observed (TOF 1005 h^{-1}), with the enantioselectivity being higher (75% ee) than that obtained with Pt- and Ir-based catalysts (15% ee in each case).

Burk et al. showed the enantioselective hydrogenation of a broad range of *N*-acylhydrazones **146** to occur readily with [Et-DuPhos Rh(COD)]OTf [14]. The reaction was found to be extremely chemoselective, with little or no reduction of alkenes, alkynes, ketones, aldehydes, esters, nitriles, imines, carbon-halogen, or nitro groups occurring. Excellent enantioselectivities were achieved (88–97% ee) at reasonable rates (TOF up to 500 h^{-1}) under very mild conditions (4 bar H_2, 20 °C). The products from these reactions could be easily converted into chiral amines or α-amino acids by cleavage of the N–N bond with samarium diiodide.

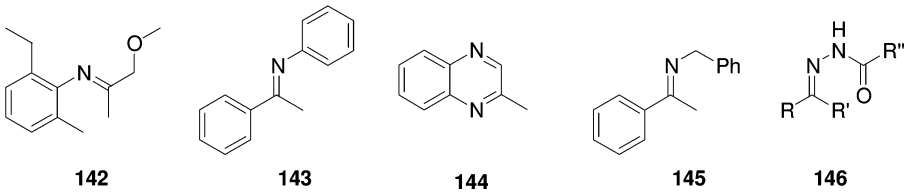

Fig. 24.21 C=N bonds to have been reduced with phospholane-based catalysts.

24.5 Concluding Remarks

Since the breakthrough introduction of the DuPhos and BPE family of ligands by Burk, the use of phospholanes in asymmetric hydrogenation has witnessed an explosion of interest, with many new and imaginative analogues emerging. This intense activity has extended the applicability of this important class of ligands beyond the standard substrates and towards the synthesis of a diverse range of chiral intermediates. This in turn has led to the realization of their commercial potential with multi-kilogram catalyst sales and applications on the industrial scale. We are only now beginning to witness the true synthetic utility of this technology and, with its increased adoption, it is anticipated that many more large-scale applications will be reported in the future.

Abbreviations

ANF	atrial natriuretic factor
BPE	1,2-bis(trans-2,5-dialkylphospholano)ethane
COD	1,5-cyclooctadiene
de	diastereomeric excess
DMI	dimethylitaconate
DuPhos	1,2-bis(trans-2,5-dialkylphospholano)benzene
ee	enantiomeric excess
LC	liquid chromatography
MAA	methyl 2-acetamidoacrylate
MAC	(*Z*)-methyl-2-acetamidocinnamate
MPLC	medium-pressure liquid (flash) chromatography
NBD	norbornadiene
SCR	substrate:catalyst ratio
TFE	2,2,2-trifluoroethanol
THF	tetrahydrofuran
TOF	turnover frequency
TON	turnover number

References

1 (a) R.A. Sheldon, *Chiral Technologies*, Marcel Dekker Inc., New York, **1993**; (b) A.N. Collins, G.N. Sheldrake, J. Crosby, *Chirality in Industry*, John Wiley & Sons, New York, **1992**.

2 (a) I. Ojima, *Catalytic Asymmetric Synthesis*, VCH, New York, **2000**; (b) R. Noyori, *Asymmetric Catalysis in Organic Synthesis*, Wiley, New York, **1994**; (c) E.N. Jacobsen, A. Pfaltz, H. Yamamoto, *Comprehensive Asymmetric Catalysis*, Springer, Heidelberg, Volumes 1–3, **1999**; (d) H.-U. Blaser, F. Spindler, M. Studer, *App. Catal. A: General*, **2001**, *221*, 119.

3 For a historical account, see H.B. Kagan, in: *Comprehensive Asymmetric Catalysis*, Springer, Heidelberg, vol. 1, **1999**, chapter 2, p. 14.

4 (a) M.J. Burk, *Acc. Chem. Res.*, **2000**, *33*, 363–372; (b) H.-U. Blaser, C. Malan, B. Pugin, F. Spindler, H. Steiner, M. Studer, *Adv. Synth. Catal.*, **2003**, *345*, 103; (c) W. Tang, X. Zhang, *Chem. Rev.*, **2003**, *103*, 3029.

5 T.P. Clark, C.R. Landis, *Tetrahedron: Asymm.*, **2004**, *15*, 2123.

6 H. Brunner, R. Sievi, *J. Organomet. Chem.*, **1987**, *328*, 71.

7 H. Brunner, S. Limmer, *J. Organomet. Chem.*, **1991**, *413*, 55.

8 M.J. Burk, J.E. Feaster, R.L. Harlow, *Organometallics*, **1990**, *9*, 2653.

9 M.J. Burk (E.I. du Pont de Nemours and Company), US 5008457, **1991**.

10 M.J. Burk, R.L. Harlow, *Angew, Chem. Int. Ed. Engl.*, **1990**, *29*, 1462.

11 M.J. Burk, J.E. Feaster, R.L. Harlow, *Tetrahedron: Asymm.*, **1991**, *2*, 569.

12 M.J. Burk, *J. Am. Chem. Soc.*, **1991**, *113*, 8518.

13 M.J. Burk, J.E. Feaster, W.A. Nugent, R.L. Harlow, *J. Am. Chem. Soc.*, **1993**, *115*, 10125.

14 M.J. Burk, M.F. Gross, J.P. Martinez, *J. Am. Chem. Soc.*, **1995**, *117*, 9375.

15 (a) M.J. Burk, J.E. Feaster, *J. Am. Chem. Soc.*, **1992**, *114*, 6266; (b) M.J. Burk (E.I. du Pont de Nemours and Company), US 5250731, **1993**; (c) M.J. Burk, J.P. Martinez, J.E. Feaster, N. Cosford, *Tetrahedron*, **1994**, *50*, 4399.

16 M.J. Burk, *Chemtracts-Org. Chem.*, **1998**, *11*, 787.

17 M.J. Burk, Y.M. Wang, J.R. Lee, *J. Am. Chem. Soc.*, **1996**, *118*, 5142.

18 M.J. Burk, N.B. Johnson, J.R. Lee, *Tetrahedron Lett.*, **1999**, *40*, 6685.

19 (a) M.J. Burk, G. Casy, N.B. Johnson, *J. Org. Chem.*, **1998**, *63*, 6804; (b) N.B. Johnson, M.J. Burk, G. Casy (Chirotech Technology Ltd.), WO 99/18065, **1999**.

20 M.J. Burk, M.F. Gross, T.G.P. Harper, C.S. Kalberg, J.R. Lee, J.P. Martinez, *Pure & Appl. Chem.*, **1996**, *68*, 37.

21 M.J. Burk, F. Bienewald, M. Harris, A. Zanotti-Gerosa, *Angew. Chem. Int. Ed.*, **1998**, *37*, 1931.

22 C.J. Cobley, N.B. Johnson, I.C. Lennon, R. McCague, J.A. Ramsden, A. Zanotti-Gerosa, in: H.-U. Blaser, E. Schmidt (Eds.), *Asymmetric Catalysis on an Industrial Scale: Challenges, Approaches and Solutions*. Wiley-VCH, Weinheim, **2004**.

23 G. Casy, N.B. Johnson, I.C. Lennon, *Chim. Oggi, Chem. Today*, **2003**, *21*, 63.

24 E. Fernandez, A. Gillon, K. Heslop, E. Horwood, D.J. Hyett, A.G. Orpen, P.G. Pringle, *Chem. Commun.*, **2000**, 1663.

25 M.J. Burk (E.I. du Pont de Nemours and Company), US 5021131, **1991**.

26 For a historical account, see M.J. Burk, *ChemTracs-Org. Chem. I*, **1998**, *11*, 787.

27 M.J. Burk (E.I. du Pont de Nemours and Company), US 5171892, **1992**.

28 U. Berens (Chirotech Technology Ltd), US 6545183 B1, **2003**.

29 M.J. Burk, A. Pizzano, J.A. Martin, L.M. Liable-Sands, A.L. Rheingold, *Organometallics*, **2000**, *19*, 250.

30 M.J. Burk, M.F. Gross, *Tetrahedron Lett.*, **1994**, *35*, 9363.

31 F. Guillen, J.-C. Fiaud, *Tetrahedron Lett.*, **1999**, *40*, 2939.

32 J.-C. Fiaud, J.-Y. Legros, *Tetrahedron Lett.*, **1991**, *32*, 5089.

33 F. Guillen, M. Rivard, M. Toffano, J.-Y. Legros, J.-C. Darran, J.-C. Fiaud, *Tetrahedron*, **2002**, *58*, 5895.

34 C.J. Pilkington, A. Zanotti-Gerosa, *Org. Lett.*, **2003**, *5*, 1273.

35 P. Harrison, G. Meek, *Tetrahedron Lett.*, **2004**, *45*, 9277.

36 A. Börner, D. Heller, *Tetrahedron Lett.*, **2001**, *42*, 223.

37 (a) C. J. Cobley, I. C. Lennon, R. McCague, J. A. Ramsden, A. Zanotti-Gerosa, *Tetrahedon Lett.*, **2001**, *42*, 7481; (b) C. J. Cobley, I. C. Lennon, R. McCague, J. A. Ramsden, A. Zanotti-Gerosa, in: *Catalysis of Organic Reactions*. Marcel Dekker, New York, chapter 24, **2002**, p. 329.

38 Y. Sun, R. N. Landau, J. Wang, C. LeBlond, D. G. Blackmond. *J. Am. Chem. Soc.*, **1996**, *118*, 1348.

39 M. J. Burk, S. Feng, M. F. Gross, W. Tumas, *J. Am. Chem. Soc.*, **1995**, *117*, 8277.

40 H.-U. Blaser, B. Pugin, M. Studer, in: D. E. De Vos, I. F. J. Vankelecom, P. A. Jacobs (Eds.), *Chiral Catalyst Immobilization and Recycling*. Wiley-VCH, Weinheim, **2000**, p. 1.

41 For examples involving DuPhos-based catalysts, see (a) A. Crosman, W. F. Hoelderich, *J. Catal.*, **2005**, *232*, 43; (b) W. P. Hems, P. McMorn, S. Riddel, S. Watson, F. E. Hancock, G. J. Hutchings, *Org. Bio. Chem.* **2005**, *3*, 1547; (c) C. Simons, U. Hanefeld, I. Arends, R. A. Sheldon, *Chem. Eur. J.*, **2004**, *10*, 5829; (d) R. L. Augustine, P. Goel, N. Mahata, C. Reyes, S. K. Tanielyan, *J. Mol. Catal. A: Chem.* **2004**, *216*, 189; (e) R. L. Augustine, S. K. Tanielyan, N. Mahata, Y. Gao, A. Zsigmond, H. Yang, *App. Catal. A: General*, **2003**, *256*, 69; (f) J. A. M. Brandts, P. H. Berben, *Org. Proc. Res. Dev.*, **2003**, *7*, 393; (g) H. H. Wagner, H. Hausmann, W. F. Hoelderich, *J. Cat.*, **2001**, *203*, 150; (h) F. M. de Rege, D. K. Morita, K. C. Ott, W. Tumas, R. D. Broene, *Chem. Commun.*, **2000**, 1797; (i) I. F. J. Vankelecom, A. Wolfson, S. Geresh, M. Landau, M. Gottlieb, H. M. Moshe, *Chem. Commun.* **1999**, 2407; (j) R. Augustine, S. Tanielyan, S. Anderson, *Chem. Commun.*, **1999**, 1257; (k) K. De Smet, S. Aerts, E. Ceulemans, I. F. J. Vankelecom, P. A. Jacobs, *Chem. Commun.*, **2001**, 597.

42 U. Berens (Solvias AG), WO 03/031456, **2003**.

43 F. Sannicol, O. Piccolo, T. Benincori, M. Sada, A. Verrazzani, S. Tollis, E. Ullucci, L. de Ferra, S. Rizzo (Chemi S.P.A.), WO 03/074169 A2, **2003**.

44 T. Benincori, T. Pilati, S. Rizzo, F. Sannicol, M. J. Burk, L. de Ferra, E. Ullucci, O. Piccolo, *J. Org. Chem.*, **2005**, *70*, 5436.

45 M. Lotz, M. Kesselgruber, M. Thommen, B. Pugin (Solvias AG), WO 2005/056568, **2005**.

46 J. Holz, A. Monsees, H. Jiao, J. You, I. V. Komarov, C. Fischer, K. Drauz, A. Börner, *J. Org. Chem.*, **2003**, *68*, 1701.

47 J. Almena, A. Monsees, R. Kadyrov, T. H. Riermeier, B. Gotov, J. Holz, A. Börner, *Adv. Synth. Catal.*, **2004**, *346*, 1263.

48 A. Börner, J. Holz, A. Monsees, T. Riermeier, R. Kadyrov, C. A. Schneider, U. Dingerdissen, K. Drauz (Degussa AG), WO 03/084971 A1, **2003**.

49 T. Riermeier, A. Monsees, J. J. Almena Perea, R. Kadyrov, B. Gotov, W. Zeiss, N. Iris, A. Börner, J. Holz, K. Drauz (Degussa AG), WO 2005/049629 A1, **2005**.

50 H. Shimizu, T. Ishizaki, T. Fujiwara, T. Saito, *Tetrahedron Asymm.*, **2004**, *15*, 2169.

51 (a) J. Holz, M. Quirmbach, U. Schmidt, D. Heller, R. Stürmer, A. Börner, *J. Org. Chem.*, **1998**, *63*, 8031; (b) R. Stürmer, A. Börner, J. Holz (BASF AG), DE 19725796, **1998**.

52 (a) W. Li, Z. Zhang, D. Xiao, X. Zhang, *Tetrahedron Lett.*, **1999**, *40*, 6701; (b) W. Li, Z. Zhang, D. Xiao, X. Zhang, *J. Org. Chem.*, **2000**, *65*, 3489; (c) X. Zhang (The Penn State Research Foundation), WO 00/11008, **2000**.

53 (a) Y.-Y. Yan, T. V. RajanBabu, *J. Org. Chem.*, **2000**, *65*, 900; (b) T. V. RajanBabu, Y.-Y. Yan, S. Shin, *J. Am. Chem. Soc.*, **2001**, *123*, 10207.

54 (a) D. Liu, W. Li, X. Zhang, *Org. Lett.*, **2002**, *4*, 4471–4474; (b) X. Zhang (The Penn State Research Foundation), US 2003/0040629, **2003**.

55 A. Bayer, P. Murszat, U. Thewalt, B. Rieger, *Eur. J. Inorg. Chem.*, **2002**, 2614.

56 (a) J. Holz, D. Heller, R. Stürmer, A. Börner , *Tetrahedron Lett.*, **1999**, *40*, 7059; (b) J. Holz, R. Stürmer, U. Schmidt, H.-J. Drexler, D. Heller, H.-P. Krimmer, A. Börner, *Eur. J. Org. Chem.*, **2001**, 4615; (c) D. Heller, H.-J. Drexler, J. You, W. Baumann, K. Drauz, H.-P. Krimmer, A. Börner, *Chem. Eur. J.*, **2002**, *8*, 5196; (d) D. Heller, J. Holz, I. Komarov, H.-J. Drexler, J. You, K. Drauz, A. Börner,

Tetrahedron Asymm., **2002**, *13*, 2735; (e) R. Stürmer, A. Börner, J. Holz (BASF AG), DE19824121, **1999**.

57 X. Zhang (The Penn State Research Foundation), US 6037500, **2000**.

58 G. Zhu, P. Cao, Q. Jiang, X. Zhang, *J. Am. Chem. Soc.*, **1997**, *119*, 1799.

59 (a) G. Hoge, *J. Am. Chem. Soc.*, **2003**, *125*, 10219; (b) H. Hoge, *J. Am. Chem. Soc.*, **2004**, *126*, 9920; (c) G. Hoge, B. Samas, *Tetrahedron: Asymm.*, **2004**, *15*, 2155; (d) G. S. Hoge, O. P. Goel (Warner-Lambert Company), WO 02/48161, **2002**.

60 M. J. Burk, O. M. Prakash, M. S. Hoekstra, T. F. Mich, T. A. Mulhern, J. A. Ramsden (Warner-Lambert Company), US 2003/0212290 A1, **2003**.

61 M. J. Burk, P. D. de Koning, T. M. Grote, M. S. Hoekstra, G. Hoge, R. A. Jennings, W. S. Kissel, T. V. Le, I. C. Lennon, T. A. Mulhern, J. A. Ramsden, R. A. Wade, *J. Org. Chem.*, **2003**, *68*, 5731.

62 (a) D. Carmichael, H. Doucet, J. M. Brown, *Chem. Commun.*, **1999**, 261; (b) J. M. Brown, D. Carmichael, H. Doucet (ISIS Innovation Ltd.), WO 00/26220, **2000**.

63 K. W. Kottsiper, U. Kuehner, O. Stelzer, *Tetrahedron Asymm.*, **2001**, *12*, 1159.

64 (a) K. Matsumura, H. Shimizu, T. Saito, H. Kumobayashi, *Adv. Synth. Catal.*, **2003**, *345*, 180; (b) K. Matsumura, T. Saito (Takasago International Corporation), EP 1318156 A1, **2003**; (c) K. Matsumura, T. Saito (Takasago International Corporation), EP 1318155 A1, **2003**.

65 S. Basra, J. G. de Vries, D. J. Hyett, G. Harrison, K. M. Heslop, A. G. Orpen, P. G. Pringle, K. von der Luehe, *Dalton Trans.*, **2004**, 1901.

66 D. J. Brauer, K. W. Kottsieper, S. Roßenbach, O. Stelzer, *Eur. J. Inorg. Chem.*, **2003**, 1748.

67 (a) Z. Chen, Q. Jiang, G. Zhu, D. Xiao, P. Cao, X. Zhang, *J. Org. Chem.*, **1997**, *62*, 4521; (b) Q. Jiang, Y. Jiang, D. Xiao, P. Cao, X. Zhang, *Angew. Chem. Int. Ed.*, **1998**, *37*, 1100; (c) Q. Jiang, D. Xiao, Z. Zhang, P. Cao, X. Zhang, *Angew. Chem. Int. Ed.*, **1999**, *38*, 516; (d) X. Zhang (The Penn State Research Foundation), WO 99/59721, **1999**; (e) Z. Zhang, G. Zhu, Q. Jiang, D. Xiao, X. Zhang, *J. Org. Chem.*, **1999**, *64*, 1774.

68 I. Komarov, A. Börner (Institut für Organische Katalyseforschung an der Universität Rostock), DE 10223442 A1, **2002**.

69 (a) W. Tang, X. Zhang, *Angew. Chem. Int. Ed.*, **2002**, *41*, 1612; (b) X. Zhang, W. Tang (The Penn State Research Institute), WO 03/042135, **2003**.

70 (a) D. Liu, X. Zhang, *Eur. J. Org. Chem.*, **2005**, 646–649; (b) X. Zhang, W. Tang (The Penn State Research Foundation), US 2004/0229846 A1, **2004**.

71 W. Tang, X. Zhang, *Org. Lett.*, **2002**, *4*, 4159.

72 W. Tang, D. Liu, X. Zhang, *Org. Lett.*, **2003**, *5*, 205.

73 D. Liu, W. Gao, C. Wang, X. Zhang, *Angew. Chem. Int. Ed.*, **2005**, *44*, 1687.

74 W. Tang, W. Wang, X. Zhang, *Angew. Chem. Int. Ed.*, **2003**, *42*, 943.

75 (a) H. Shimizu, T. Saito, H. Kumobayashi, *Adv. Synth. Catal.*, **2003**, *345*, 185; (b) H. Shimizu, T. Saito (Takasago International Corp.), US2003/0144139 A1, **2003**.

76 (a) O. Kobayashi, JP 2002069086 A2, **2002**; (b) P. Osinski, K. M. Piertrusiewicz, R. Schmid (Hoffmann-La Roche Inc.), US 2004/0110975 A1, **2004**.

77 S. Demay, M. Lotz, K. Polborn, P. Knochel, *Tetrahedron Asymm.*, **2001**, *12*, 909.

78 (a) S. Lelièvre, F. Mercier, F. Matthey, *J. Org. Chem.*, **1996**, *61*, 3531; (b) F. Matthey, F. Mercier, F. Robin, L. Ricard, *J. Organomet. Chem.*, **1998**, *577*, 117; (c) M. Spagnol, F. Dallemer, F. Matthey, F. Mercier, V. Mouries (Rhodia Chimie), WO 99/47530, **1999**; (d) F. Matthey, F. Robin, F. Mercier, M. Spagnol (Rhone-Poulenc Chimie), WO 98/00375, **1998**.

79 W. Braun, B. Calmuschi, J. Haberland, W. Hummel, A. Liese, T. Nickel, O. Stelzer, A. Salzer, *Eur. J. Inorg. Chem.*, **2004**, 2235.

80 W. Braun, A. Salzer, F. Spindler, E. Alberico, *App. Catal. A: General*, **2004**, *274*, 191.

81 (a) A. Marinetti, L. Ricard, *Tetrahedron*, **1993**, *49*, 10291; (b) A. Marinetti, *Tetrahedron Lett.*, **1994**, *35*, 5861; (c) A. Marinetti, L. Ricard, *Organometallics*, **1994**, *13*, 3956.

82 (a) U. Berens, M. J. Burk, A. Gerlach, W. Hems, *Angew. Chem. Int. Ed.*, **2000**, *39*, 1981; (b) U. Berens (Chirotech Technology

Ltd.), US 6545183, **2003**; (c) U. Berens, M. J. Burk, A. Gerlach (Chirotech Technology Ltd.), US 6172249, **2001**.

83 (a) A. Marinetti, S. Jus, J.-P. Genêt, *Tetrahedron Lett.*, **1999**, *40*, 8365; (b) A. Marinetti, S. Jus, J.-P. Genêt, L. Ricard, *J. Organomet. Chem.*, **2001**, *624*, 162; (c) A. Marinetti, F. Labrue, J.-P. Genêt, *Synlett*, **1999**, *12*, 1975; (d) A. Marinetti, F. Labrue, B. Pons, S. Jus, L. Ricard, J.-P. Genêt, *Eur. J. Inorg. Chem.*, **2003**, 2583; (e) A. Marinetti, J.-P. Genêt, S. Jus, D. Blanc, V. Ratovelomanana-Vidal, *Chem. Eur. J.*, **1999**, *5*, 1160; (f) A. Marinetti, S. Jus, F. Labrue, A. Lemarchand, J.-P. Genêt, L. Ricard, *Synlett*, **2001**, *14*, 2095.

84 J. You, H.-J. Drexler, S. Zhang, C. Fischer, D. Heller, *Angew. Chem. Int. Ed.*, **2003**, *42*, 913.

85 C. J. Cobley, I. C. Lennon, C. Praquin, A. Zanotti-Gerosa, R. A. Appell, C. T. Goralski, A. C. Sutterer, *Org. Proc. Res. Dev.*, **2003**, *7*, 407.

86 A. M. Derrick, N. M. Thomson (Pfizer Ltd.), EP 1199301 A1, **2002**.

87 (a) T. Imamoto, K. V. L. Crépy, K. Katagiri, *Tetrahedron Asymm.*, **2004**, *15*, 2213; (b) T. Imamoto, N. Oohara, H. Takahashi, *Synthesis*, **2004**, *9*, 1353.

88 A. Marinetti, F. Mathey, L. Ricard, *Organometallics*, **1993**, *12*, 1207.

89 M. Ostermeier, J. Prieß, G. Helmchen, *Angew. Chem. Int. Ed.*, **2002**, *41*, 612.

90 M. J. Burk, F. Bienewald, in: *Transition Metals for Organic Synthesis*. Wiley-VCH, Weinheim, **1998**, chapter 2, p. 13.

91 S. K. Armstrong, J. M. Brown, M. J. Burk, *Tetrahedron Lett.*, **1993**, *34*, 879.

92 S. Feldgus, C. R. Landis, *J. Am. Chem. Soc.*, **2000**, *122*, 12714.

93 S. Feldgus, C. R. Landis, *Organometallics*, **2001**, *20*, 2374.

94 B. Guzel, M. A. Omary, J. P. Fackler, A. Akgerman, *Inorg. Chim. Acta*, **2002**, *35*, 45.

95 J. Holz, A. Monsees, H. Jiao, J. You, I. V. Kamarov, C. Fischer, K. Drauz, A. Börner, *J. Org. Chem.*, **2003**, *68*, 1701.

96 M. Kesselgruber, F. Spindler (Solvias AG), personal communication.

97 H-U. Blaser (Solvias AG), personal communication.

98 (a) J. W. Scott, D. D. Keith, G. Nix, D. R. Parrish, S. Remington, G. R. Roth, J. M. Townsend, D. Valentine, R. Yang, *J. Org. Chem.*, **1981**, *46*, 5086; (b) B. D. Vineyard, W. S. Knowles, M. J. Sabacky, G. L. Bachman, D. J. Weinkauff, *J. Am. Chem. Soc.*, **1977**, *99*, 5946.

99 A. Miyashita, H. Takaya, T. Souchi, R. Noyori, *Tetrahedron*, **1984**, *40*, 1245.

100 M. J. Burk, J. R. Lee, J. P. Martinez, *J. Am. Chem. Soc.*, **1994**, *116*, 10847.

101 T. A. Stammers, M. J. Burk, *Tetrahedron Lett.*, **1999**, *40*, 3325.

102 (a) G. P. Aguado, A. Alvarez-Larena, O. Illa, A. G. Moglioni, R. M. Ortuño, *Tetrahedron Asymm.*, **2001**, *12*, 25; (b) G. P. Aguado, A. G. Moglioni, E. García-Expósito, V. Branchadell, R. M. Ortuño, *J. Org. Chem.*, **2004**, *69*, 7971.

103 (a) N. W. Boaz, S. D. Debenham, S. E. Large, M.K. Moore, *Tetrahedron Asymm.*, **2003**, *14*, 3575; (b) S. D. Debenham, N. W. Boaz (Eastman Chemical Company), WO 02/26695 A2, **2002**.

104 X. Li, C. Yeung, A. S. C. Chan, D.-S. Lee, T.-K. Yang, *Tetrahedron Asymm.*, **1999**, *10*, 3863.

105 H. Chen, J.-P. Luzy, C. Garbay, *Tetrahedron Lett.*, **2005**, *46*, 3319.

106 L. Chen, J. W. Tilley, R. W. Guthrie, F. Mennona, T.-N. Huang, G. Kaplan, R. Trilles, D. Miklowski, N. Huby, V. Schwinge, B. Wolitzky, K. Rowan, *Bioorg. Med. Chem. Lett.*, **2000**, *10*, 729.

107 Y. Lee, R. B. Silvermann, *Tetrahedron*, **2001**, *57*, 5339.

108 H.-U. Blaser, F. Spindler, *Topics in Catalysis*, **1997**, *4*, 275.

109 F. Spindler, B. Pugin, H. Buser, H.-P. Jalett, U. Pittelkow, H.-U. Blaser, *Pesticide Science*, **1998**, *54*, 302.

110 (a) K. C. Nicolaou, G.-Q. Shi, K. Namoto, F. Bernal, *Chem. Commun.*, **1998**, 1757; (b) S. H. Lim, S. Ma, P. Beak, *J. Org. Chem.*, **2001**, *66*, 9056.

111 T. Doi, N. Fujimoto, J. Watanabe, T. Takakashi, *Tetrahedron Lett.*, **2003**, *44*, 2161.

112 W. Wang, J. Zhang, C. Xiong, V. J. Hruby, *Tetrahedron Lett.*, **2002**, *43*, 2137.

113 W. Wang, C. Xiong, J. Yang, V. J. Hruby, *Tetrahedron Lett.*, **2001**, *42*, 7717.

114 W. Wang, C. Xiong, J. Zhang, V.J. Hruby, *Tetrahedron*, **2002**, *58*, 3101.

115 T. Masquelin, E. Broger, K. Mueller, R. Schmid, D. Obrecht, *Helv. Chim. Acta*, **1994**, *77*, 1395.

116 W. Wang, J. Yang, J. Ying, C. Xiong, J. Zhang, C. Cai, V.J. Hruby, *J. Org. Chem.*, **2002**, *67*, 6353.

117 W. Wang, H. Li, *Tetrahedron Lett.*, **2004**, *45*, 8479.

118 P.R. Carlier, P.C.-H. Lam, D.M. Wong, *J. Org. Chem.*, **2002**, *65*, 6256.

119 D.J. Bentley, C.J. Moody, *Org. Biomol. Chem.*, **2004**, *2*, 3545.

120 R.S. Hoerner, D. Askin, R.P. Volante, P.J. Reider, *Tetrahedron Lett.*, **1998**, *39*, 3455.

121 K.S. Feldman, K.J. Eastman, G. Lessene, *Org. Lett.*, **2002**, *4*, 3525.

122 S.W. Jones, C.F. Palmer, J.M. Paul, P.D. Tiffin, *Tetrahedron Lett.*, **1999**, *40*, 1211.

123 M. Adamczyk, S.R. Akireddy, R.E. Reddy, *Org. Lett.*, **2002**, *3*, 3157.

124 (a) M. Adamczyk, S.R. Akireddy, R.E. Reddy, *Tetrahedron Asymm.*, **2001**, *12*, 2385–2387; (b) M. Adamczyk, S.R. Akireddy, R.E. Reddy, *Tetrahedron Lett.*, **2002**, *58*, 6951.

125 (a) A.J. Robinson, C.Y. Lim, L. He, P. Ma, H.-Y. Li, *J. Org. Chem.*, **2001**, *66*, 4141; (b) A.J. Robinson, P. Stanislawski, D. Mulholland, L. He, H.-Y. Li, *J. Org. Chem.*, **2001**, *66*, 4148.

126 J. Singh, D.R. Kronenthal, M. Schwinden, J.D. Godfrey, R. Fox, E.J. Vawter, B. Zhang, T.P. Kissick, B. Patel, O. Mneimne, M. Humora, C.G. Papaioannou, W. Szymanski, M.K.Y. Wong, C.K. Chen, J.E. Heikes, J.D. DiMarco, J. Qiu, R.P. Deshpande, J.Z. Gougoutas, R.H. Mueller, *Org. Lett.*, **2003**, *5*, 3155.

127 (a) W.-C. Shieh, S. Xue, N.M. Reel, J.J. Fitt (Novartis Corporation), US**2002**/0133014, **2002**.; (b) W.-C. Shieh, S. Xue, N. Reel, R. Wu, J. Fitt, O. Repiè, *Tetrahedron Asymm.*, **2001**, *12*, 2421.

128 (a) S.D. Debenham, J.S. Debenham, M.J. Burk, E.J. Toone, *J. Am. Chem. Soc.*, **1997**, *119*, 9897; (b) S.D. Debenham, J. Cossrow, E.J. Toone, *J. Org. Chem.*, **1999**, *64*, 9153; (c) J.R. Allen, C.R. Harris, S.J. Danishefsky, *J. Am. Chem. Soc.*, **2001**, *123*, 1890; (d) J.R. Allen, S.J. Danishefsky, *J. Prakt. Chem.*, **2000**, *342*, 736; (e) X. Xu, G. Fakha, D. Sinou, *Tetrahedron*, **2002**, *58*, 7539; (f) S. Liu, R.N. Ben, *Org. Lett.*, **2005**, *7*, 2385.

129 G.P. Aguado, A.G. Moglioni, B.N. Brousse, R.M. Ortuño, *Tetrahedron Asymm.*, **2003**, *12*, 2445.

130 (a) A. Ritzén, B. Basu, S.K. Chattopadhyay, F. Dossa, T. Frejd, *Tetrahedron Asymm.*, **1998**, *8*, 503; (b) K.B. Jørgensen, O.R. Gautun, *Tetrahedron*, **1999**, *55*, 10527; (c) S. Maricic, A. Ritzén, U. Berg, T. Frejd, *Tetrahedron*, **2001**, *57*, 6523; (d) J.M. Travins, F.A. Etzkorn, *J. Org. Chem.*, **1997**, *62*, 8387; (e) A. Ritzén, B. Basu, A. Wllberg, T. Frejd, *Tetrahedron Asymm.*, **1998**, *9*, 3491; (f) S. Maricic, U. Berg, T. Frejd, *Tetrahedron*, **2002**, *58*, 3085; (g) J. Hiebl, H. Kollmann, F. Rovensky, K. Winkler, *J. Org. Chem.*, **1999**, *64*, 1947.

131 W. Wang, C. Xiong, V.J. Hruby, *Tetrahedron Lett.*, **2001**, *42*, 3159.

132 M.J. Burk, K.M. Bedingfield, W.F. Kiesman, J.G. Allen, *Tetrahedron Lett.*, **1999**, *40*, 3093.

133 M.J. Burk, J.G. Allen, W.F. Kiesman, *J. Am. Chem. Soc.*, **1998**, *120*, 657.

134 (a) C.A. Busacca, N. Haddad, S.R. Kapadia, L. Smith Keenan, J.C. Lorenz, C.H. Senanayake (Boehringer Ingelheim Pharmaceuticals Inc.), WO 2005/044799 A1, **2005**; (b) A.-M. Faucher, M.D. Bailey, P.L. Beaulieu, C. Brochu, J.-S. Duceppe, J.-M. Ferland, E. Ghiro, V. Gorys, T. Halmos, S.H. Kawai, M. Poirier, B. Simoneau, Y.S. Tsantrizos, M. Llinás-Brunet, *Org. Lett.*, **2004**, *6*, 2901.

135 J. Elaridi, W.R. Jackson, A.J. Robinson, *Tetrahedron Asymm.*, **2005**, *16*, 2025.

136 (a) E. Teoh, E.M. Campi, W.R. Jackson, A.J. Robinson, *Chem. Commun.*, **2002**, 978; (b) E. Teoh, E.M. Campi, W.R. Jackson, A.J. Robinson, *New J. Chem.*, **2003**, *27*, 387; (c) E. Teoh, W.R. Jackson, A.J. Robinson, *Aus. J. Chem.*, **2005**, *58*, 63.

137 (a) M. Sawamura, R. Kuwano, Y. Ito, *J. Am. Chem. Soc.*, **1995**, *117*, 9602; (b) T. Imamoto, J. Watanabe, Y. Wada, H. Masuda, H. Yamada, H. Tsuruta,

S. Matsukawa, K. Yamaguchi, *J. Am. Chem. Soc.*, **1998**, *120*, 1635; (c) A. Ohashi, T. Imamoto, *Org. Lett.*, **2001**, *3*, 373; (d) D.A. Evans, F.E. Michael, J.S. Tedrow, K.R. Campos, *J. Am. Chem. Soc.*, **2003**, *125*, 3534; (e) X. Jiang, M. van den Berg, A.J. Minnaard, B.L. Feringa, J.G. de Vries, *Tetrahedron Asymm.*, **2004**, *15*, 2223.

138 G.J. Roff, R.C. Lloyd, N.J. Turner, *J. Am. Chem. Soc.*, **2004**, *126*, 4098.

139 For examples, see (a) V. Wehner, H. Blum, M. Kurz, H.U. Stilz, *Synthesis*, **2002**, *14*, 2032; (b) S.D. Bull, S.G. Davies, D.J. Fox, M. Gianotti, P.M. Kelly, C. Pierres, E.D. Savory, A.D. Smith, *J. Chem. Soc., Perkin Trans I*, **2002**, 1858; (c) E. Juaristi, H. Lopez-Ruiz, *Curr. Med. Chem.*, **1999**, *6*, 983; (d) I. Ojima, S. Lin, T. Wang, *Curr. Med. Chem.*, **1999**, *6*, 927; (e) G. Cardillo, C. Tomasini, *Chem. Soc. Rev.*, **1996**, 117.

140 For examples, see (a) K. Gadermann, T. Hintermann, J.V. Schreiber, *Curr. Med. Chem.*, **1999**, *6*, 905; (b) D. Seebach, S. Abele, K. Gadermann, G. Guichard, T. Hintermann, B. Jaun, J.L. Matthews, J.V. Schreiber, *Helv. Chim. Acta*, **1998**, *81*, 932; (c) S.H. Gellman, *Acc. Chem. Res.*, **1998**, *31*, 173; (d) D. Seebach, J.L. Matthews, *Chem. Commun.*, **1997**, 2015.

141 E. Juaristi, *Enantioselective Synthesis of Amino Acids*. Wiley-VCH, New York, **1997**.

142 For an excellent review of this area, see H.-J. Drexler, J. You, S. Zhang, C. Fischer, W. Baumann, A. Spannanberg, D. Heller, *Org. Proc. Res. Dev.*, **2003**, *7*, 355.

143 G. Zhu, Z. Chen, X. Zhang, *J. Org. Chem.*, **1999**, *64*, 6907.

144 T. Jerphagnon, J.-L. Renaud, P. Demonchaux, A. Ferreira, C. Bruneau, *Tetrahedron Asymm.*, **2003**, *14*, 1973.

145 C.J. Cobley, C.G. Malan (The Dow Chemical Company), WO 0316264A1, **2003**.

146 (a) D. Heller, J. Holz, H.-J. Drexler, J. Lang, K. Drauz, H.-P. Krimmer, A. Börner, *J. Org. Chem.*, **2001**, *66*, 6816; (b) H.-P. Krimmer, K. Drauz, J. Lang, A. Börner, D. Heller, J. Holz (Degussa AG), DE 10100971 A1, **2001**.

147 J. You, H.-J. Drexler, S. Zhang, C. Fischer, D. Heller, *Angew. Chem. Int. Ed.*, **2003**, *42*, 913.

148 (a) Y.G. Zhou, W. Tang, W.-B. Wang, W. Li, X. Zhang, *J. Am. Chem. Soc.*, **2002**, *124*, 4952; (b) S. Lee, Y.J. Zhang, *Org. Lett.*, **2002**, *4*, 2429.

149 W.D. Lubell, M. Kitamura, R. Noyori, *Tetrahedron Asymm.*, **1991**, *2*, 543.

150 H.-J. Drexler, W. Baumann, T. Schmidt, S. Zhang, A. Sun, A. Spannenberg, C. Fischer, H. Buschmann, D. Heller, *Angew. Chem. Int. Ed.*, **2005**, *44*, 1184.

151 Y. Hisao, N.R. Rivera, T. Rosner, S.W. Krska, E. Njolito, F. Wang, Y. Sun, J.D. Armstrong, E.J.J. Grabowski, R.D. Tillyer, F. Spindler, C. Malan, *J. Am. Chem. Soc.*, **2004**, *126*, 9918.

152 W. Tang, S. Wu, X. Zhang, *J. Am. Chem. Soc.*, **2003**, *125*, 9570.

153 J.D. Clark, G.A. Weisenburger, D.K. Anderson, P.-J. Colson, A.D. Edney, D.J. Gallagher, H.P. Kleine, C.M. Knable, M.K. Lantz, C.M.V. Moore, J.B. Murphy, T.E. Rogers, P.G. Ruminski, A.S. Shah, N. Storer, B.E. Wise, *Org. Proc. Res. Dev.*, **2004**, *8*, 51.

154 Y.J. Zhang, J.H. Park, S. Lee, *Tetrahedron Asymm.*, **2004**, *15*, 2209.

155 R. Callens, M. Larcheveque, C. Pousset (Solvay SA), FR 2853316 A1, **2003**.

156 J. Elaridi, A. Thaqi, A. Prosser, W.R. Jackson, A.J. Robinson, *Tetrahedron Asymm.*, **2005**, *16*, 1309.

157 D. Saylik, E.M. Campi, A.C. Donohue, W.R. Jackson, A.J. Robinson, *Tetrahedron Asymm.*, **2001**, *12*, 657.

158 The same effect has been observed and studied with the diphosphine *t*Bu-BisP*: I.D. Gridnev, M. Yasutake, N. Higashi, T. Imamoto, *J. Am. Chem. Soc.*, **2001**, *123*, 5268.

159 G. Zhu, A.L. Casalnuovo, X. Zhang, *J. Org. Chem.*, **1998**, *63*, 8100.

160 J. Cong-Dung Le, B.L. Pagenkopf, *J. Org. Chem.*, **2004**, *69*, 4177.

161 M.J. Burk, T.A. Stammers, J.A. Straub, *Org. Lett.*, **1999**, *1*, 387.

162 L. Storace, L. Anzalone, P.N. Confalone, W.P. Davis, J.M. Fortunak,

M. Giangiorano, J.J. Haley, K. Kamholz, H.-Y. Li, P. Ma, W.A. Nugent, R.L. Parsons, P.J. Sheeran, C.E. Silverman, R.E. Waltermire, C.C. Wood, *Org. Proc. Res. Dev.*, **2002**, *6*, 54.

163 Y.-G. Zhou, P.-Y. Yang, X.-W. Han, *J. Org. Chem.*, **2005**, *70*, 1679.

164 (a) P. Dupau, A.-E. Hay, C. Bruneau, P.H. Dixneuf, *Tetrahedron Asymm.*, **2001**, *12*, 863; (b) P. Dupau, C. Bruneau, P.H. Dixneuf, *Adv. Synth. Catal.*, **2001**, *343*, 331.

165 P.M. Donate, D. Frederico, R. da Silva, M.G. Constantino, G. Del Ponte, P.S. Bonatto, *Tetrahedron Asymm.*, **2003**, 3253.

166 C. González-Arellano, A. Corma, M. Iglesias, F. Sánchez, *Chem. Commun.*, **2005**, 3451.

167 M.J. Burk, F. Bienewald, M.E. Fox, A. Zanotti-Gerosa (Chirotech Technology Limited), WO 99/31041.

168 M.J. Burk, F. Bienewald, A. Zanotti-Gerosa (Chirotech Technology Limited), WO 99/52852.

169 (a) A.M. Derrick, N.M. Thomson (Pfizer Ltd. and Pfizer Inc.), EP 1199301 A1; (b) C.P. Ashcroft, S. Challenger, A.M Derrick, R. Storey, N.M. Thomson, *Org. Proc. Res. Dev.*, **2003**, *7*, 362.

170 (a) Y. Toyama, A. Noda, F. Yamamoto, T. Toyama (Kotobuki Pharmaceutical Company Ltd.), JP 2003212874 A2; (b) H. Tomiyama, Y. Kobayashi, A. Noda (Kotobuki Pharmaceutical Company Ltd.), WO2002076981 A1.

171 (a) W.A. Nugent, T.V. Rajanbabu, M.J. Burk, *Science*, **1993**, *259*, 479; (b) O.M. Akotsi, K. Metera, R.D. Reid, R. McDonald, S.H. Bergens, *Chirality*, **2000**, *12*, 514.

172 (a) M.J. Burk, G.P. Harper, C.S. Kalberg, *J. Am. Chem. Soc.*, **1995**, *117*, 4423; (b) J.-P. Gent, C. Pinel, V. Ratovelomanana-Vidal, S. Mallart, X. Pfister, L. Bischoff, M.C. Caño de Andrade, S. Darses, C. Galopin, J.A. Laffitte, *Tetrahedron Asymm.*, **1994**, *5*, 675; (c) J.-P. Gent, V. Ratovelomanana-Vidal, M.C. Caño de Andrade, X. Pfister, P. Guerreiro, J.Y. Lenoir, *Tetrahedron Lett.*, **1995**, *36*, 4801.

173 M. Prashad, H.-Y. Kim, B. Hu. J. Slade, P.K. Kapa (Novartis AG), WO 2004/076053 A2.

174 J.P. Paul, C. Palmer (Darwin Discovery Ltd.), WO 99/15481.

175 I. Appleby, L.T. Boulton, C.J. Cobley, C. Hill, M.L. Hughes, P.D. de Koning, I.C. Lennon, C. Praquin, J.A. Ramsden, H.J. Samuel, N. Willis, *Org. Lett*, **2005**, *7*, 1931.

176 M.E.B. Smith, N. Derrien, M.C. Lloyd, S.J.C. Taylor, D.A. Chaplin, R. McCague, *Tetrahedron Lett.*, **2001**, *42*, 1347.

177 M. Scalone, U. Zutter (F. Hoffman-La Roche AG), EP 0974590 A1, **2000**.

178 M.J. Burk, F. Bienewald, S. Challenger, A. Derrick, J.A. Ramsden, *J. Org. Chem.*, **1999**, *64*, 3290.

179 T.-Y. Yue, W.A. Nugent, *J. Am. Chem. Soc.*, **2002**, *124*, 13692.

180 M.J. Burk, C.S. Kalberg, A. Pizzano, *J. Am. Chem. Soc.*, **1998**, *120*, 4345.

181 P.E. Maligres, S.H. Krska, G.R. Humphrey, *Org. Lett*, **2004**, *6*, 3147.

182 (a) D.A. Dobbs, K.P.M Vanhessche, E. Brazi, V. Rautenstrauch, J.-Y. Lenoir, J.-P. Genet, J. Wiles, S.H. Bergens, *Angew. Chem. Int. Ed.*, **2000**, *39*, 1992; (b) J.A. Wiles, S.H. Bergens, K.P.M. Vanhessche, D.A. Dobbs, V. Rautenstrauch, *Angew. Chem. Int. Ed.*, **2001**, *40*, 914; (c) D.A. Dobbs, K.P.M. Vanhessche, V. Rautenstrauch (Firmenich SA), US 6,455,460 B1.

183 (a) N.W. Boaz, *Tetrahedron Lett.*, **1998**, *39*, 5505; (b) N.W. Boaz (Eastman Chemical Company), EP 0872467 B1, **2003**.

184 A. Robinson, H.-Y. Li, J. Feaster, *Tetrahedron Lett.*, **1996**, *37*, 8321; (b) H.-Y. Li, A.J. Robinson (The DuPont Merck Pharmaceutical Company), US 5686631, **1997**.

185 (a) E.A. Broger, Y. Crameri, R. Schmid, T. Siegfried (F. Hoffman-La Roche AG), EP 691325, **1996**; (b) M. Scalone, R. Schmid, E.A. Broger, W. Burkart, M. Cereghetti, Y. Crameri, J. Foricher, M. Henning, F. Kienzie, F. Montavon, G. Schoettel, D. Tesauro, S. Wang, R. Zell, U. Zutter, Proceedings of the ChiraTech'97 Symposium, The Catalyst Group, Spring House, USA, **1997**.

186 H.-H Bokel, P. Mackert, C. Mürmann, N. Schweickert (Merck), WO 00/35901, **2000**.

187 (a) B.D. Hewitt, M.J. Burk, N.B. Johnson (Pharmacia & Upjohn Company), WO 00/55150, **2000**. (b) K.S. Fors, J.R. Gage, R.F. Heier, R.C. Kelly, W.R. Perrault, N. Wicnienski, *J. Org. Chem. Soc.*, **1998**, *63*, 7248; (c) J.R. Gage, R.C. Kelly, B.D. Hewitt (Pharmacia & Upjohn), WO 9912919, **1999**.

188 F.D. Klingler, M. Steigerwald, R. Ehlenz (Boehringer Ingelheim International GmbH), WO 2004/085427 A1, **2004**.

189 G.S. Forman, T. Ohkuma, W.P. Hems, R. Noyori, *Tetrahedron Lett.*, **2000**, *41*, 9471.

190 For examples, see (a) A. Pfaltz, J. Blankenstein, R. Hilgraf, E. Hormann, S. McIntyre, F. Menges, M. Schönleber, S.P. Smidt, B. Wüstenberg, N. Zimmermann, *Adv. Synth. Catal.*, **2003**, *345*, 33; (b) M.C. Perry, X. Cui, M.T. Powell, D.-. Hou, J.H. Reibenspies, K. Burgess, *J. Am. Chem. Soc.*, **2003**, *125*, 113.

191 (a) J.-C. Henry, D. Lavergne, V. Ratovelomanana-Vidal, J.-P. Gent, I.P. Beletskaya, T.M. Dolgina, *Tetrahedron Lett.*, **1998**, *39*, 3473; (b) N.S. Goulioukina, T.M. Dolgina, J.-C. Henry, D. Lavergne, V. Ratovelomanana-Vidal, J.-P. Gent, *Tetrahedron Asymm.* **2001**, *12*, 319.

192 M. Ueda, A. Saitoh, N. Miyaura, *J. Organomet. Chem.*, **2002**, *642*, 145.

193 J. Madec, X. Pfister, V. Ratovelomanana-Vidal, J.-P. Gent, *Tetrahedron*, **2001**, *57*, 2563.

194 Inventors unknown (Lonza AG), EP 1510517 A1, **2005**.

195 T. Ohkuma, H. Ooka, S. Hashiguchi, T. Ikariya, R. Noyori, *J. Am. Chem. Soc.*, **1995**, *117*, 2675.

196 R. Noyori, T. Ohkuma, *Angew. Chem. Int. Ed.*, **2001**, *40*, 40 and references therein.

197 Y.-Q. Wang, S.-M. Lu, Y.-G. Zhou, *Org. Lett.*, **2005**, *7*, 3235.

198 (a) C.J. Cobley, J.P. Henschke, *Adv. Synth. Catal.*, **2003**, *345*, 195;
b) C.J. Cobley, J.P. Henschke, J.A. Ramsden, WO 0208169 A1, **2002**.

25
Enantioselective Hydrogenation of Alkenes with Ferrocene-Based Ligands

Hans-Ulrich Blaser, Matthias Lotz, and Felix Spindler

25.1
Introduction

Ferrocene as a (at the time rather exotic) backbone for chiral ligands was introduced by Kumada and Hayashi [1] based on Ugi's pioneering studies related to the synthesis of enantiopure ferrocenes (Fig. 25.1). Ppfa, as well as bppfa and bppfoh, proved to be effective ligands for a variety of asymmetric transformations. From this starting point, several ligand families with a range of structural variations have been developed during the past few years. In this chapter we will describe effective ligand structures developed over time, the main focus being on diphosphine derivatives (Fig. 25.2) and their application to the hydrogenation of alkenes. Three recently published reviews cover some of the same area, but from slightly different points of view. Colacot and Barbaro et al. [2] presented general overviews on ferrocene-based chiral ligands and their application to various asymmetric transformations, while Blaser et al. [3] and Tang and Zhang [4] reviewed the recent progress in the application of diphosphines for the enantioselective hydrogenation. These reviews can serve to put the present account into a broader perspective.

This chapter is organized according to the position of the phosphine groups **P**, as depicted in Fig. 25.2. It is important to realize that many of the ligands described here have both planar (C_p ring with two different substituents) as well

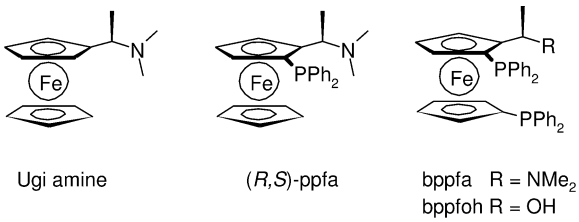

Fig. 25.1 Structures of Ugi's amine and the first ferrocene-based chiral phosphine ligands.

The Handbook of Homogeneous Hydrogenation.
Edited by J.G. de Vries and C.J. Elsevier
Copyright © 2007 WILEY-VCH Verlag GmbH & Co. KGaA, Weinheim
ISBN: 978-3-527-31161-3

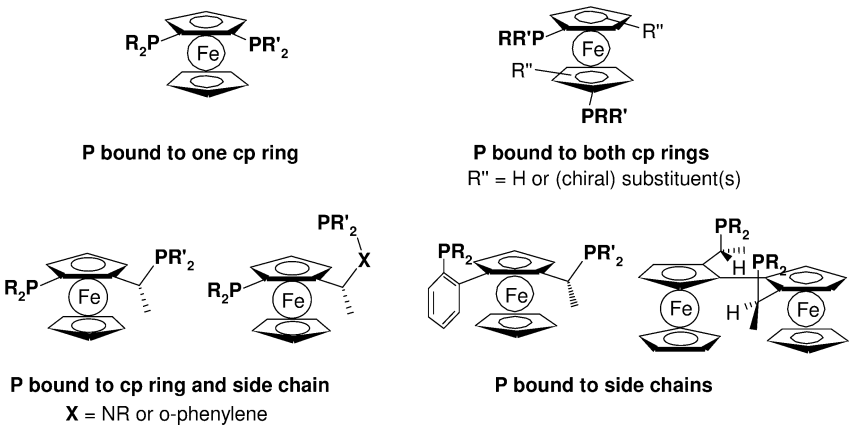

Fig. 25.2 Subclasses of ferrocenyl diphosphines.

as central (in the side chain) chirality. In most cases, the central chirality dominates the sense of induction, but strong matched-mismatched effects are very common. Except for selected cases we will not include the absolute configuration in the ligand names, but as a rule the central chirality is given first, followed by the planar and (if applicable) the axial chirality (e.g., see ppfa in Fig. 25.1).

When assessing catalytic results reported for new ligands, one must bear in mind that their quality and relevance differ widely. For most new ligands only experiments with selected model test substrates carried out under standard conditions are available, and very few have already been applied to industrially relevant problems. The test substrates for alkenes used most frequently are Acetamido Cinnamic Acid (ACA) or its methyl ester (MAC), Methyl Acetamido Acrylate (MAA), ITaconic Acid or DiMethyl ITaconate (ITA, DMIT) and selected aryl enamides (Fig. 25.3).

Especially for new ligands, reaction conditions are usually optimized for enantioselectivity, whereas catalyst productivity (given as turnover number, TON, or substrate/catalyst ratio, SCR) and catalyst activity (given as turnover frequency, TOF (h^{-1}), at high conversion) are often only a first indication of the potential of the ligand. The decisive test – namely the application of a new ligand to "real world problems" which will tell about the scope and limitations of a ligand (family) concerning tolerance to changes in the substrate structure and/or the presence of functional groups – will often come much later.

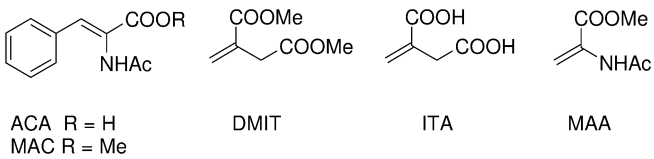

Fig. 25.3 Structures and abbreviations of frequently used model test substrates.

25.2
Ligands with Phosphine Substituents Bound to One Cyclopentadiene Ring

Until now, only a few effective ligands of this type have been identified (Fig. 25.4). Kagan and co-workers [5] prepared one of the few chiral diphosphines with only planar chirality and obtained 95% ee for the hydrogenation of DMIT with **L1** (Table 25.1, entry 1.1.), but enantioselectivities for several enamide derivatives were below 82% ee (the best results were with the cyclohexyl analogue of **L1**). For the reactions with DMIT or MAC, the cationic Rh-kephos complex showed comparable or better performance than corresponding duphos catalysts.

25.3
Ligands with Phosphine Substituents Bound to both Cyclopentadiene Rings

As noted earlier, the first effective ligands were prepared by Kumada and Hayashi during the 1970s, starting from Ugi's amine. Depending on the reaction conditions, phosphine substituents were introduced either on one or on both cyclopentadiene rings. It transpired that only the diphosphines bppfa and bppfoh were useful for hydrogenation reactions. Only recently, new, usually C_2 symmetrical, ligand families were prepared with excellent catalytic properties for a variety of hydrogenation reactions (Fig. 25.5).

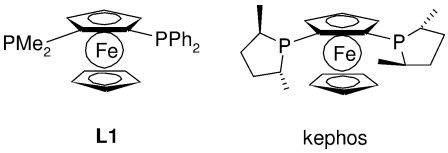

Fig. 25.4 Structures and abbreviations of diphosphines with P bound to one C_p ring.

Table 25.1 Selected results for Rh-catalyzed hydrogenations using diphosphines having both P bound to one C_p ring (for structures, see Fig. 25.4).

Entry	Ligand	Substrate	$p(H_2)$ [bar]	SCR	TOF [h^{-1}]	ee [%]	Comments	Reference
1.1	**L1**	DMIT	1	100	n.a.	95		5
1.2	kephos	DMIT	10	1000	1000	99.5	ee > 99.9% at SCR 200	6
1.3	kephos	MAC	10	1000	300	96	ee 98% at SCR 200	6

SCR = substrate:catalyst ratio; n.a. = not available.

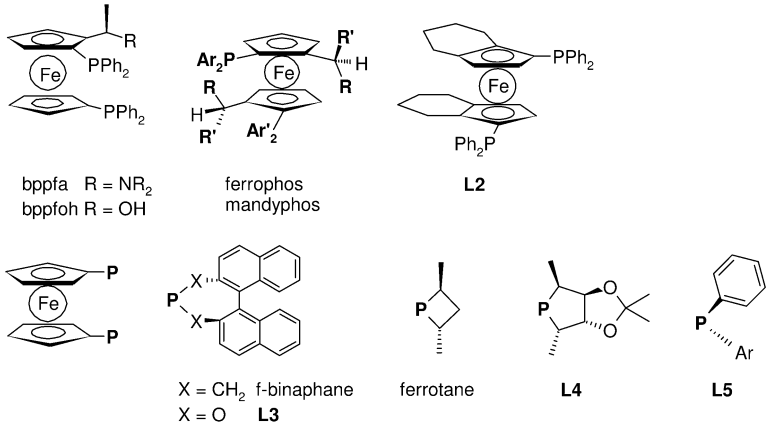

Fig. 25.5 Generic structures and names or numbers of ferrocene-based diphosphines with P bound to both C_p rings.

25.3.1
Bppfa, Ferrophos, and Mandyphos Ligands

Bppfoh and bppfa derivatives have been applied most successfully for the Rh-catalyzed hydrogenation of dehydro amino acid derivatives such as MAC (ee 97%) and of functionalized ketones [7]. The nature of the amino group has a significant effect on enantioselectivity and often also on activity, and is used to tailor the ligand for a particular substrate. Rh-bppfa complexes were among the first catalysts able to hydrogenate tetrasubstituted C=C bonds, albeit with relatively low activity (Table 25.2, entries 2.1–2.3). Ferrophos, one of the very few li-

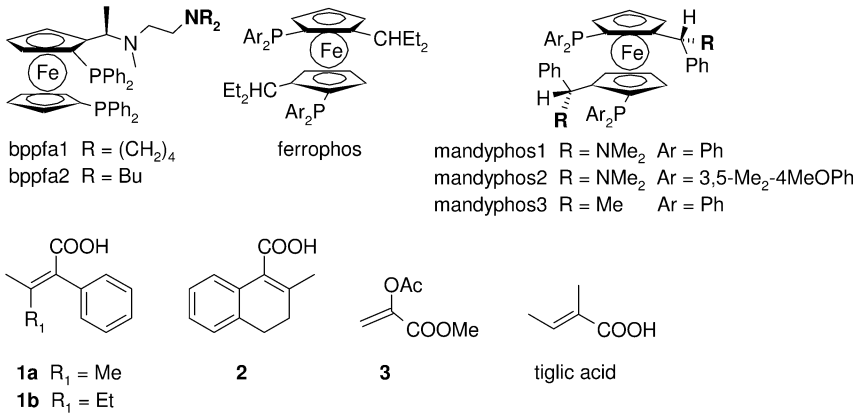

Fig. 25.6 Structures of specific bppfa, ferrophos, and mandyphos ligands and of test substrates.

Table 25.2 Selected results for Rh-catalyzed hydrogenations using bppf, ferrophos, and mandyphos derivatives (for structures, see Figs. 25.5 and 25.6)

Entry	Ligand	Substrate	$p(H_2)$ [bar]	SCR	TOF [h^{-1}]	ee [%]	Comments	Reference
2.1	bppfa1	**1a**	50	200 [a)]	7 [a)]	98.4		7
2.2	bppfa1	**1b**	50	200 [a)]	2 [a)]	97	*cis/trans* 97/3	7
2.3	bppfa2	**2**	50	100 [a)]	2 [a)]	87	*cis/trans* >99/1	7
2.4	ferrophos	ACA	2	100 [a)]	~10–30	98.9	97.6% ee for MAC	8
2.5	Mandyphos1	pCl-MAC	1	100 [a)]	n.a.	>99	98% ee for MAC	9c
2.6	Mandyphos2	MAC	1	20000	~3000	98.7	>99% ee at SCR 200	9d
2.7	Mandyphos2	tiglic acid	5	200 [a)]	11 [a)]	97	Ru complex	9d
2.8	Mandyphos3	MAC	1	100 [a)]	≥600 [a)]	98.6	97.9% ee for MAA	9b
2.9	Mandyphos3	**3**	1	100 [a)]	8 [a)]	95		9a

a) Standard test results, not optimized.

gands with only planar chirality, shows good ee-values but low activity for dehydroamino acid derivatives (Table 25.2, entry 2.4).

Mandyphos ligands [9] are highly modular bidentate analogues of ppfa where not only the phosphine moieties but also the R substituent have been used for fine-tuning purposes. Both C_2 (Ar = Ar′) as well as C_1 (Ar ≠ Ar′) symmetrical ligands have been prepared and tested in an extended screening [9d]. Even though the scope of this family is not yet fully explored, these test results indicate high enantioselectivities as well as high activity for the Rh-catalyzed hydrogenation of dehydroamino acid derivatives (Table 25.2, entries 2.5, 2.6, 2.8), tiglic acid (Ru complex, entry 2.7) and enol acetate **3** (entry 2.9). Mandyphos2 was shown to be the most versatile ligand, leading to very high TON and TOF for the MAC hydrogenation (entry 2.6). Both enantiomers of the mandyphos family are equally well accessible, and selected derivatives are now commercialized by Solvias in collaboration with Umicore (formerly OMG) [10].

25.3.2
Miscellaneous Diphosphines

A variety of C_2 symmetrical diphosphine ligands with a ferrocenyl backbone (see Fig. 25.5) have recently been described and tested, with sometimes quite impressive results. Interesting examples are f-binaphane [11], ferrotane [12], **L2**

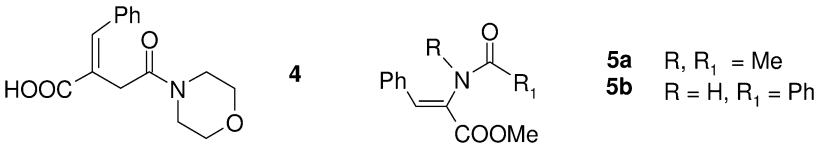

Fig. 25.7 Structures of substrates listed in Table 25.3.

Table 25.3 Selected results for Rh-catalyzed hydrogenations using miscellaneous diphosphines (for structures of ligands, see Fig. 25.5; for structures of substrates, see Fig. 25.7).

Entry	Ligand	Substrate	$p(H_2)$ [bar]	SCR	TOF [h^{-1}]	ee [%]	Comments	Reference
3.1	Ferrotane [a)]	4	5	20 000	~7000	98–99	98% ee for DMIT	12
3.2	**L2**	MAC	1	1 000 [b)]	40 [b)]	97	96% for MAA	13
3.3	**L3**	DMIT	1.3	5 400	270	>99.5		14
3.4	**L4**	ITA	5	100 [b)]	<10 [b)]	99.5	ee 90% for DMIT	15
3.5	**L4**	MAA	3	10 000	850	99.9	best solvent THF	15
3.6	**L4**	MAC [c)]	1	100 [b)]	100 [b)]	>99.9	best solvent THF	15
3.7	**L5**	5a	1	200 [b)]	15 [b)]	97	Ar 2-anisyl	16b
3.8	**L5**	5b	2	100 [b)]	15 [b)]	98.5	Ar 9-phenanthryl	16c

a) Et-ferrotane.
b) Standard test results, not optimized.
c) Various substituted analogues were tested.

with only planar chirality [13], bisphosphonite **L3** [14], the sugar-based phospholane **L4** [15] and the P-chiral phosphines **L5** [16].

Rh complexes of ferrotanes showed very good performance for various amido itaconates, and achieved very high TONs and TOFs for substrate **4** (Table 25.3, entry 3.1). The planar chiral Rh-**L2** complex achieved up to 97% ee for MAC (entry 3.2) and bisphosphonite **L3** based on a binol or related moiety achieved very high ee-values and respectable TONs for the hydrogenation of itaconates (entry 3.3). The sugar-based ligand **L4** is excellent for dehydroamino and itaconic acid derivatives, with good TONs and very high ee-values (entries 3.4–3.6). Rh-**L5** complexes (with Ar = 2-anisyl, 1-naphthyl or 9-phenanthryl) reduce MAC and ACA with ee-values of 95–99% (results not shown). In contrast to many other ligands, Rh-**L5** catalysts are quite tolerant towards changes in the structure of the amide moiety, showing high ee-values for N-methyl (**5a**, entry 3.7) or benzoyl derivatives (**5b**, entry 3.8).

25.4
Ligands with Phosphine Substituents Bound to a Cyclopentadiene Ring and to a Side Chain

The first successful variation of the ppfa structure was carried out by Togni and Spindler, who replaced the amino group at the stereogenic center of the side chain by a second phosphino moiety. Later, very effective ligands were also obtained when a further bridging group was introduced between the stereogenic center and the second phosphino group, as in bophoz or **L7** (Fig. 25.8).

25.4.1
Josiphos

The josiphos ligands arguably constitute the most versatile and successful ferrocenyl ligand family. Because the two phosphine groups are introduced in consecutive steps with very high yields (as shown in Scheme 25.1), a variety of ligands is readily available with widely differing steric and electronic properties. A comprehensive review on the catalytic performance of josiphos ligands has recently been published [17]. Until now, only the (*R*, *S*)-family (and its enantiomers) but not the (*R*, *R*) diastereomers have led to high enantioselectivities (the first descriptor stands for the stereogenic center, the second for the planar chirality). The ligands are technically developed, and available in commercial quanti-

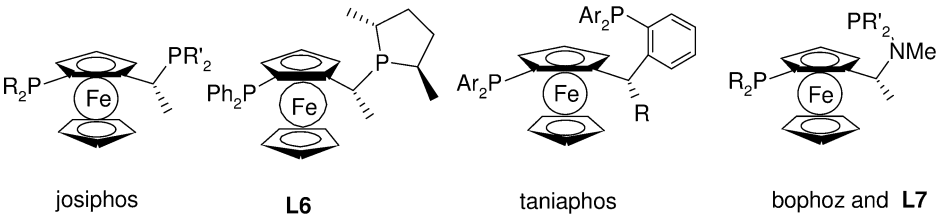

Fig. 25.8 Structures and names of the most important diphosphines with P bound to a C_p ring and a chiral side chain.

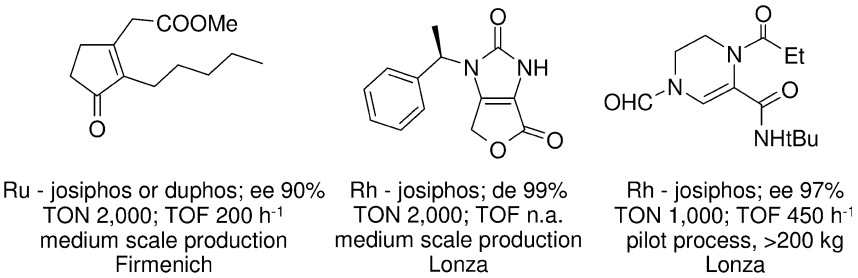

Fig. 25.9 Industrial applications of josiphos ligands for (for further information, see [19]).

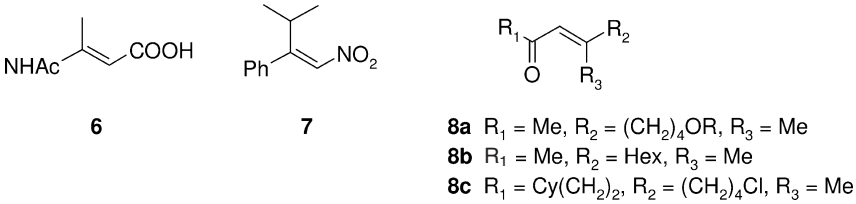

Fig. 25.10 Structures of substrates listed in Table 25.4.

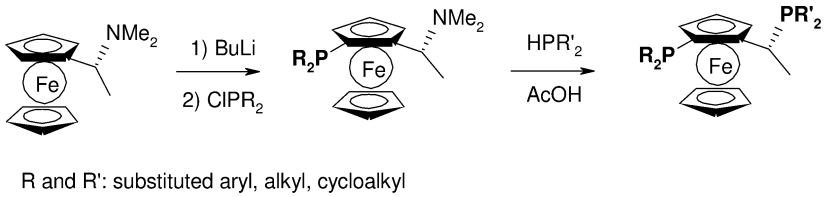

Scheme 25.1 Preparation of josiphos ligands starting from the Ugi amine.

ties from Solvias [10]. The most important application is undoubtedly the hydrogenation of C=N functions where the largest enantioselective process has been realized for the enantioselective production of the herbicide (*S*)-metolachlor [18] and of highly substituted C=C bonds. Several smaller productions and some pilot processes use josiphos ligands and important examples are shown in Fig. 25.9.

Table 25.4 Selected results for the Rh- and Cu-catalyzed hydrogenation using josiphos ligands (for structures, see Figs. 25.8 and 25.10).

Entry	Substrate	Metal-ligand (R, R′) [a]	p(H_2) [bar]	SCR	TOF [h^{-1}]	ee [%]	Reference
4.1	ACA	Rh-(3,5-$(CF_3)_2$Ph, Cy)	1	600	>600	99	6
4.2	MAA	Rh-(3,5-$(CF_3)_2$Ph, Cy)	1	600	>600	98	6
4.3	MAA	Rh-(Ph, Cy)	1	100 [b]	330 [b]	97	17
4.4	DMIT	Rh-(Ph, Cy)	1	100 [b]	200 [b]	99.9	17
4.5	DMIT	Rh-**L6**	1	200 [b]	200 [b]	99.5	20
4.6	**6**	Rh-(3,5-$(CF_3)_2$Ph, Cy)	1	100 [b]	90 [b]	92	4
4.7	**7**	Cu-(Ph, Cy)	[c]	100 [b]	~16 [b]	94	21
4.8	**8a**	Cu-(Ph, Cy)	[c]	1640	~75	98	22
4.9	**8b**	Cu-(Ph, Cy)	[c]	100 [b]	>10 [b]	99	22
4.10	**8c**	Cu-(Ph, Cy)	[c]	100 [b]	>10 [b]	99	22

a) See Fig. 25.8, Cy = cyclohexyl.
b) Standard test results, not optimized.
c) Reducing agent: polymethylhydrosiloxane/NaO*t*Bu.

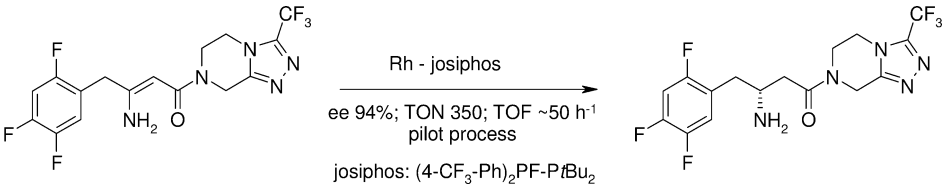

Scheme 25.2 Hydrogenation of the β-dehydro amino acid amide intermediate for MK-0431.

As can be seen from Table 25.4, several Rh-josiphos complexes are excellent catalysts for the hydrogenation of α-dehydro amino acid derivatives and DMIT with ee-values of 97–99.9% (entries 4.1–4.5). While the reactions have not been optimized, satisfactory TONs and TOFs have been observed. Good ee-values are also obtained for a β-dehydro amino acid derivative (entry 4.6) and for the Cu-catalyzed reduction with PMHS of activated C=C bonds (entries 4.7–4.10), albeit with relatively low TOFs. Interestingly, in all cases the best ligands have unsubstituted or electron-deficient aryl groups on the ring phosphorus and a PCy_2 group at the side chain.

Recently, Merck chemists reported the Rh-josiphos-catalyzed hydrogenation of unprotected dehydro β-amino acids with ee-values up to 97%, but relatively low activity [23]. It was also shown that not only simple derivatives but also the complex intermediate for MK-0431 depicted in Scheme 25.2 can be hydrogenated successfully, and this has been produced on a >50 kg scale with ee-values up to 98%, albeit with low to medium TONs and TOFs [24].

25.4.2
Immobilized Josiphos and Josiphos Analogues

Several josiphos ligands were functionalized at the lower C_p ring and grafted to silica gel or a water-soluble group [25a] to give very active catalysts for the Ir-catalyzed MEA imine reduction; a Rh-josiphos complex grafted to several dendrimers (e.g., see Fig. 25.11) hydrogenated DMIT with ee-values up to 98.6% with similar activities as the mononuclear catalyst [25b]. Salzer and co-workers [20] prepared a number of josiphos analogues based on an arene chromium tricarbonyl scaffold (**L8**) and tested their Rh complexes on several alkenic substrates. With few exceptions, relatively low ee-values and catalyst activities were observed: ≤79% ee for DMIT, ≤87% for MAC, ≤91% for MAA, and ≤85% for the β-dehydro amino acid derivative **6**. Weissensteiner and co-workers [26] described two josiphos analogues **L9** and **L10** with restricted rotation of the side chain, and observed a strong decrease in enantioselectivity (best ee ≤91% for DMIT with **L10**, R′ = Cy).

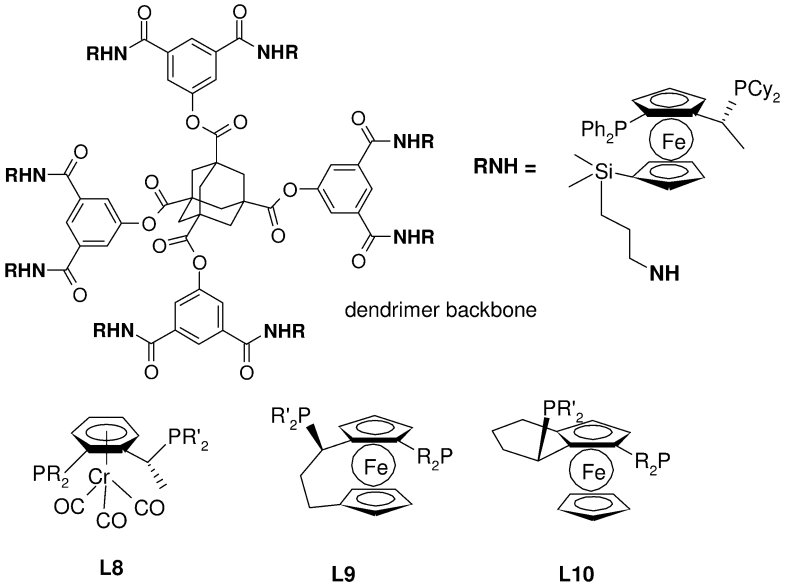

Fig. 25.11 Structure of immobilized josiphos and josiphos analogues.

25.4.3
Taniaphos

Compared to the josiphos ligands, taniaphos ligands have an additional phenyl ring inserted at the side chain of the Ugi amine. Whereas the effect of changing the two phosphine moieties has only been investigated with a few derivatives (Table 25.5, entries 5.3, 5.4, 5.5, 5.8–5.10), the nature of the substituent at the stereogenic center has a strong effect on the induction of stereochemistry for the Rh-catalyzed hydrogenation of MAC and DMIT. Rather surprisingly, a change of the substituent can even lead to a different sense of induction. For MAC, methyl or methoxy substituents lead to the opposite absolute configuration of the product compared to R = NMe_2, *i*-Pr or H (entries 5.1–5.4). Similar effects are also observed for DMIT (entries 5.7– 5.11) and for the hydrogenation of enol acetate **9** where ee-values up to 98% but low activities are achieved (entry 5.13). Interestingly, changing the absolute configuration of the stereogenic center only has an effect on the level of the ee but not on the sense of induction (compare entries 3/4 and 7/8). Enamides **10** are hydrogenated with high ee-values but low TOFs (entries 5.14 and 5.15). Currently, several taniaphos ligands are being marketed by Solvias in collaboration with Umicore (formerly OMG) [10].

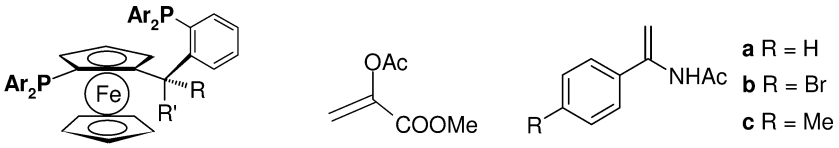

taniaphos 9 10

Fig. 25.12 Structure of taniaphos derivatives and substrates listed in Table 25.5.

Table 25.5 Selected results for Rh-catalyzed hydrogenations using taniaphos (Ar = Ph, pH_2 1 bar) (for structures, see Fig. 25.12).

Entry	Ligand (R, R′)	Substrate	$p(H_2)$ [bar]	TON [a)]	TOF [a)] [h^{-1}]	ee [%]	Comments	Reference(s)
5.1	(H, *i*Pr)	MAC	1	100	25	97 (*R*)	52% (*S*) for R′ = Me!	27a
5.2	(H, NMe_2)	MAC	1	100	200	95 (*R*)	77% (*R*) for R′ = H	27a
5.3	(H, OMe)	MAC	1	100	50	94 (*S*)	92% (*S*) for Ar = Xyl	27b
5.4	(OMe, H)	MAC	1	100	67	99 (*S*)	99% (*S*) for Ar = Xyl	27b
5.5	(H, NMe_2)	MAC	1	200	>200	99.5 (*S*)	Ar = 3,5-Me_2-4-MeOPh	6, 27c
5.6	(H, NMe_2)	MAA	1	200	106	97	Ar = 3,5-Me_2-4-MeOPh	6, 27c
5.7	(H, *i*Pr)	DMIT	1	100	25	98 (*S*)	19% (*R*) for R′ = Me!	27a
5.8	(H, NMe_2)	DMIT	1	100	7	91 (*S*)	75% (*S*) for R′ = H [b]	27a
5.9	(H, NMe_2)	DMIT	1	200	>200	99.5 (*S*)	Ar = 3,5-Me_2-4-MeOPh	6, 27c
5.10	(OMe, H)	DMIT	1	100	200	98 (*R*)	90% (*R*) for Ar = Xyl	27b
5.11	(H, OMe)	DMIT	1	100	40	95 (*R*)		27b
5.12	(H, NMe_2)	**6**	1	100	27	99.5 (*S*)	Ar = 3,5-Me_2-4-OMePh	6, 27c
5.13	(OMe, H)	**9**	1	100	5	98 (*S*)	80% (*S*) for (O, OMe)	27b
5.14	(OMe, H)	**10a**	1	100	7	96	97% ee for **10b**	27b
5.15	(OMe, H) [c]	**10a**	1	100	67	92	95% ee for **10c**	27b

a) Standard test results, not optimized.
b) At 10 bar, low conversion at 1 bar.
c) Ar = Xyl.

25.4.3 Various Ligands

Bophoz [28] and **L11** [29] are modular ligands with a PR_2 group on the C_p ring and an aminophosphine or a phosphoramidite, respectively, at the side chain. Bophoz ligands are air-stable and effective for the Rh-catalyzed hydrogenation of a variety of enamides and itaconates with high ee-values, TONs and TOFs (Table 25.6, entries 6.1–6.3); depending on the solvent the stability of the N–PR_2 bond might be a critical issue. As observed for several ligands forming seven-membered chelates, high activities can be reached (maximum TOFs up 68 000 h^{-1}) and TONs up to 10 000 have been achieved [28c]. A feasibility study for the

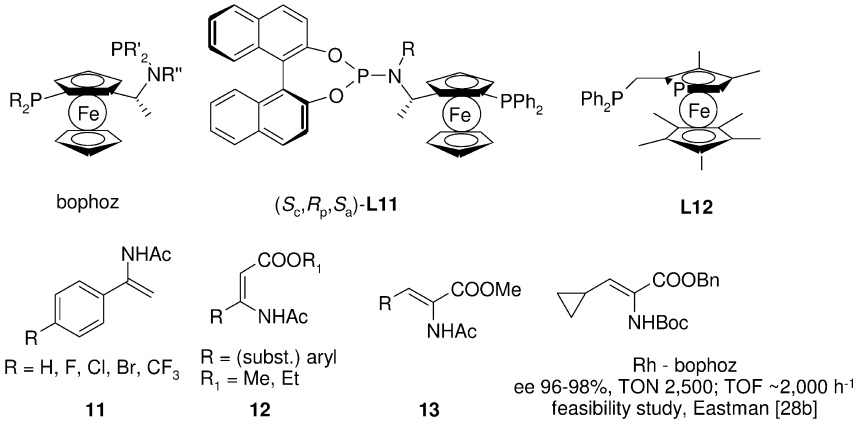

Fig. 25.13 Structures of bophoz, **L11**, **L12** and of substrates listed in Table 25.6.

preparation of enantiopure cyclopropylalanine has been reported (Fig. 25.13). Ligands of the type **L11** have three elements of chirality (central, planar, and axial), and all combinations were actually prepared and tested for enamides **11**. As can be seen comparing entries 6.4–6.7 in Table 25.6, the absolute configuration of the binaphthol moiety determines the absolute configuration of the product; the relative configurations of the other chiral elements have a variable but usually very strong effect on the magnitude of the ee. Best results were achieved for the (S_c,R_p,S_a)-**L11** diastereomer shown in Fig. 25.13 (entry 6.8), which also shows very high enantioselectivities and very good TONs and TOFs for DMIT (entry 6.9). MAC was also hydrogenated very effectively, but only when 2 equiv. of ligand were added (entry 6.10); β-dehydroamino esters **12** are also good substrates for Rh/**L11** catalysts (entries 6.11, 6.12). Ligand **L12** with only planar chirality does not quite fit in this category since one of the P atoms is not attached to but is part of the C_p ring. The corresponding Rh complexes achieve respectable ee-values for several dehydroamino esters, but have very low activity (entry 6.13).

25.5
Ligands with Phosphine Substituents Bound only to Side Chains

Until now, only two families of ligands have been realized where both P groups are attached to side chains, probably because the resulting metal complexes have relatively large chelate rings which usually are not suitable for enantioselective catalysis. A cursory inspection of the ligands depicted in Fig. 25.14 shows that, due to steric bulk of the ferrocene backbone, both diphosphines probably have sufficiently restricted flexibility so that good stereocontrol is still possible.

The starting point for walphos was also the Ugi amine. Like josiphos, walphos ligands are modular but form eight-membered metallocycles due to the

Table 25.6 Selected results for Rh-catalyzed hydrogenation using bophoz, **L11**, and **L12** (for structures, see Fig. 25.13).

Entry	Ligand	Substrate	p(H_2) [bar]	SCR	TOF [h^{-1}]	ee [%]	Comments	Reference
6.1	bophoz[a]	MAC	~1	10000	10000	97	99.4% ee for MAA	28c
6.2	bophoz[a]	subst MAC	~1	100[b)]	~100[b)]	97–99	various derivatives	28c
6.3	bophoz[c]	subst ITA	~3	2500	n.a.	94–99	various derivatives	28c
6.4	(S_c,R_p,S_b)-**L11**	**11** (R=H)	10	100[b]	100[b)]	99.6	(*R*)-product	29a
6.5	(S_c,R_p,R_b)-**L11**	**11** (R=H)	10	100[b)]	100[b)]	11	(*S*)-product	29a
6.6	(S_c,S_p,R_b)-**L11**	**11** (R=H)	10	100[b)]	100[b)]	99.6	(*S*)-product	29a
6.7	(S_c,S_p,S_b)-**L11**	**11** (R=H)	10	100[b)]	100[b)]	83	(*R*)-product	29a
6.8	(S_c,R_p,S_b)-**L11**	**11** (R=H)	10	5000	5000	99.3	for other R ee ~99%	29a
6.9	(S_c,R_p,S_b)-**L11**	DMIT	10	10000	20000	>99		29a
6.10	(S_c,R_p,S_b)-**L11**	MAC	10	10000	10000	>99	2 equiv. ligand	29a
6.11	(S_c,R_p,S_b)-**L11**	**12**	10	100[b)]	~80[b)]	97–>99	ee >99% for R=H	29b
6.12	(S_c,R_p,S_b)-**L11**	**12** (R=H)	10	5000	~4000	97	ee 98% at S/C 1000	29b
6.13	**L12**	**13** (R=Et)	1	20[b)]	<2[b)]	96	MAC 87% ee	30

a) R, R'=Ph, R''=H or Me at SCR 100, ee 99.1%.
b) Standard test results, not optimized.
c) R, R'=Ph, R''=H or Me.

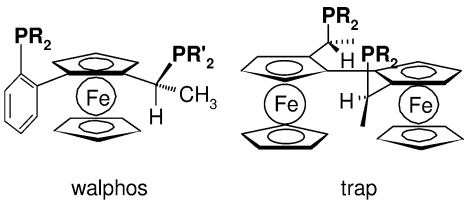

Fig. 25.14 Structures and names of walphos and trap ligands.

Table 25.7 Selected results for Rh- and Cu-catalyzed hydrogenation using (R,R′)-walphos and R-trap ligands (for ligand and substrates structures, see Figs. 25.14 and 25.16, respectively).

Entry	M – (R, R′)	Substrate	$p(H_2)$ [bar]	SCR[a]	TOF [h^{-1}][a]	ee [%]	Comments	Reference(s)
7.1	Rh-(Ph, Ar_1)[b]	MAC	1	200[b]	≥10 b[b]	95	ee 94% for Ar′ = Ph	31 b
7.2	Rh-(Ph, Ar_1)[b]	DMIT	1	200[b]	≥10 b[b]	92		31 b
7.3	Cu-(Ph, Ar_2)[c]	**8**	[c]	100	>10	97	R_1 Me, R_2 $(CH_4)_2OR$, R_3 Et	22
7.4	Cu-(Ph, Ar_2)[c]	**8**	[c]	100	>10	97	R_1 *t*Bu, R_2 Bu, R_3 Me	22
7.5	Rh-Ph-trap[d]	**14a**	50	100	50[c]	94 (*R*)	ee 7% (*S*) without Cs_2CO_3	33 a
7.6	Rh-Ph-trap[d]	**14b**	50	100	200	95	ee 78% for Boc derivative	33 a
7.7	Rh-Et-trap[f]	MAA	0.5	100	50[e]	96 (*R*)	ee 70/2%(!) at 1/100 bar	33 b
7.8	Rh-*i*Bu-trap	MAC	1	100	4	92 (*S*)	R = Et[f] ee 77% (*R*)!	33 b
7.9	Rh-Et-trap[g]	ITA	1	200	30	96	ee 68% for DMIT	33 c
7.10	Rh-Pr-trap	**15**, **16a**	1	100	4	97	ee 82% for **16b**	33 e, f
7.11	Rh-*i*Bu-trap	**17**	1	100	5	97	intermediate for indinavir	33 d

a) Standard test results, not optimized.
b) Ar_1 = 3,5-Me_2-4-MeO-Ph.
c) Ar_2 = 3,5-$(CF_3)_2$-Ph, reducing agent PMHS/NaO*t*Bu.
d) In presence of Cs_2CO_3.
e) At 60 °C.
f) For R = Pr/Ph/*i*Pr, ee = 85% (*R*)/21% (*S*)/5% (*S*), respectively.
g) For R = *i*Bu, ee = 17%.

additional phenyl ring attached to the cyclopentadiene ring [31]. They also show promise for the enantioselective hydrogenation of dehydroamino and itaconic acid derivatives (Table 25.7, entries 7.1 and 7.2), and the Cu-catalyzed enantioselective reduction of *α*,*β*-unsaturated ketones **8** (entries 7.3 and 7.4). There are noticeable electronic effects, but the scope of this ligand family is still under investigation; several derivatives are available from Solvias on a technical scale [10]. The first industrial application has just been realized in collaboration with Speedel/Novartis for the hydrogenation of SPP100-SyA, a sterically demanding *α*,*β*-unsaturated acid intermediate of the renin inhibitor SPP100 (Fig. 25.15). The process has already been operated on a multi-100 kg scale.

The trap (*trans*-chelating phosphines) ligands developed by Ito and co-workers [33] form nine-membered metallocycles where trans-chelation is possible. However, it is not clear whether the *cis* isomer which has been shown to be present in small amounts or the major *trans* isomer is responsible for the catalytic activ-

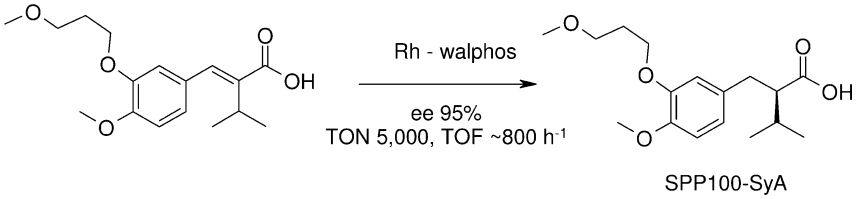

Fig. 25.15 Pilot-scale application of the walphos ligand ($R = Ph$, $R' = 3,5\text{-}(CF_3)_2\text{-}Ph$) [32].

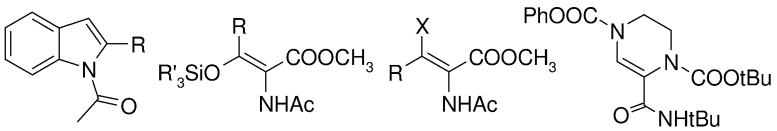

14a R = Me
14b R = COOEt
15
16a X = OOC*t*Bu
16b X = NHCbz
17

Fig. 25.16 Substrate structures listed in Table 25.7.

ity. Until now, only a few different PR_2 fragments have been tested, but it is clear that the choice of R strongly affects the level of enantioselectivity and sometimes even the sense of induction (e.g., see Table 25.7, entries 7.7 and 7.8). The Rh complexes function best at very low pressures of 0.5–1 bar, but often need elevated temperatures (e.g., entry 7.7). Effectively reduced are indole-derivatives **14** (entries 7.5, 7.6, the first examples of heteroaromatic substrates with high ee-values), dehydroamino (entries 7.7, 7.8; best ligand PEt_2-trap, unusual p and T effects), and itaconic acid derivatives (entry 7.9). β-Hydroxy–α-amino acids and α,β-diamino acids can be prepared via asymmetric hydrogenation of tetrasubstituted alkenes **14–16** with respectable de-values of 99–100% and ee-values of 97% and 82%, respectively, but low catalyst activities (entry 7.10). Also described was the hydrogenation of an indinavir intermediate **17** (entry 7.11).

25.6
Major Applications of Ferrocene Diphosphine-Based Catalysts

As can be seen in the preceding section, ferrocene-based complexes are very versatile ligands for the enantioselective hydrogenation of a variety of alkenes. One reason for this is undoubtedly the modularity of most of the described ligand families which allows them to influence the activity and enantioselectivity in an extraordinarily broad range. In the following section a short overview is provided of substrates where ferrocene-based ligands define the state of the art not only for alkene hydrogenation but also for the enantioselective reduction of C=O and C=N groups. A comparison with other classes of ligands can be found in an above-mentioned review [3].

25.6.1
Hydrogenation of Substituted Alkenes

Rh complexes of ferrocene-based ligands are very effective for the hydrogenation of several types of α- and β-dehydroamino (Fig. 25.17, structures **18–22**), enamides (**23**) and enol acetates (**24**), as well as for itaconic acid derivatives (**25**, **26**) and α,β-unsaturated acids (**27**). Of particular interest are substrates which have unusual substituents (**19**, **21**) at the C=C moiety or are more sterically hindered than the usual model compounds (**20**, **27**). Cu complexes of ferrocenyl diphosphines are very effective for the reduction of nitroalkenes **28** and α,β-unsaturated ketones **29** with high chemoselectivity. Effective metal/ligand combinations with very high ee-values and often respectable TONs and TOFs are listed in Table 25.8. Several industrial applications have already been reported using Rh-josiphos and Ru-josiphos (see Fig. 25.10), as well as for Rh-bophoz (see Fig. 25.13) and Rh-walphos (see Fig. 25.14).

25.6.2
Hydrogenation of C=O and C=N Functions

Ferrocene-based complexes have some potential for the enantioselective reduction of ketones, but compared to other ligand classes this is relatively limited [3]. Rh complexes of bppfa, bophoz and josiphos are among the most selective catalysts for the hydrogenation of α-functionalized ketones (Table 25.9; Fig. 25.18, **30–32**). Ru complexes of walphos and ferrotane are quite effective for

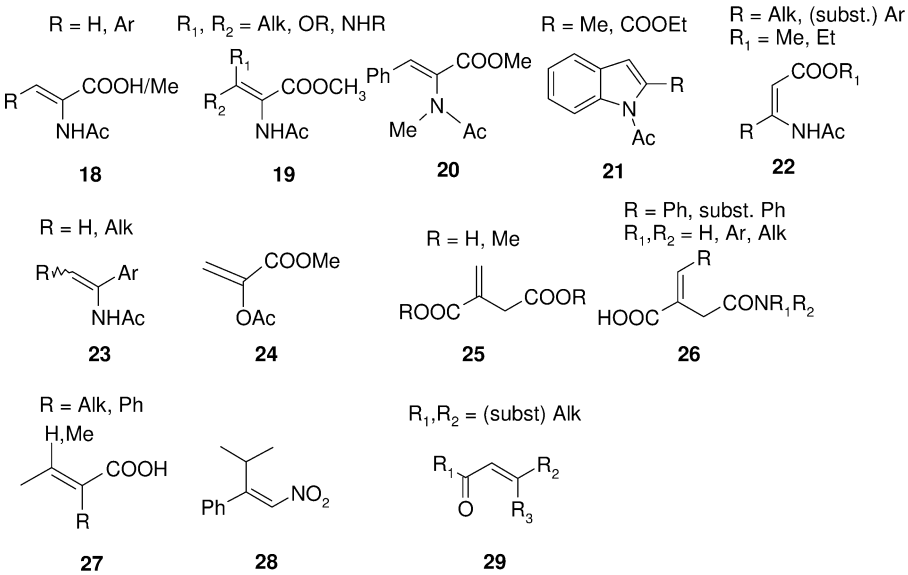

Fig. 25.17 Structures of substrates listed in Table 25.8.

Table 25.8 Best SCRs, TOF and ee-values for the reduction of selected functionalized alkenes (for substrates, see Fig. 25.17).

Substrate	Metal-ligand	TON	TOF [h^{-1}]	ee [%]
18	Rh-bophoz, Rh-josiphos, Rh-mandyphos, Rh-taniaphos, Rh-**L2**, Rh-**L4**	Up to 20 000	Up to 10 000	98–>99
19	Rh-trap	100 [a)]	4 [a)]	97
20	Rh-**L5**	200 [a)]	15 [a)]	96–98
21	Ru-taniaphos, Rh-trap	100–200 [a)]	25–200 [a)]	94–96
22	Rh-josiphos, Rh-taniaphos, Rh-**L11**	Up to 5000	Up to ~4000	92–>99
23	Rh-**L3**, Rh-taniaphos, Rh-**L11**	Up to 5000	Up to 6000	92–98
24	Rh-mandyphos, Rh-taniaphos, Rh-**L11**	Up to 10 000	Up to 20 000	95–98
25	Rh-josiphos, Rh-taniaphos, Rh-**L3**, Rh-**L4**	200 [a)]	>200 [a)]	97–99.9
26	Rh-ferrotane	Up to 20 000	Up to 7000	98–99
27	Rh-bppfa, Rh-mandyphos, Rh-walphos	Up to 5000	Up to ~800	95
28	Cu-josiphos	100 [a)]	~16 [b)]	94
29	Cu-josiphos, Cu-walphos	1640	10–80 [a)]	97–98

a) Standard test results, not optimized.

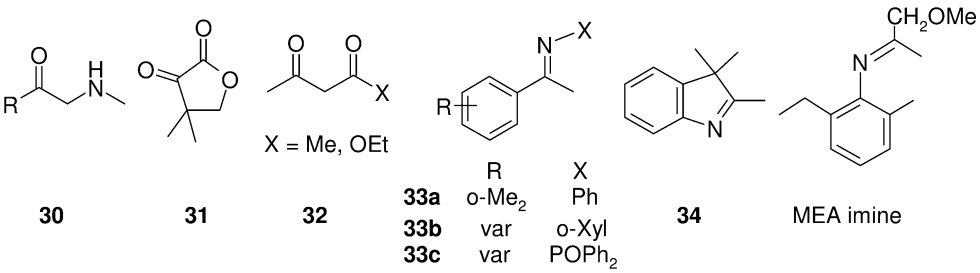

Fig. 25.18 Structures of ketone and imine substrates listed in Table 25.9.

β-keto esters and diketones **32**, though this is usually the domain of Ru-binap-type catalysts. Josiphos and f-binaphane however are the ligands of choice for the Ir-catalyzed hydrogenation of N-aryl imines such as **33** and **34**. Special mention should be made of the Ir-josiphos catalyst system which is able to hydrogenate MEA imine with TONs up to 2×10^6 [18].

Table 25.9 Best catalysts for the hydrogenation of C=O and C=N functions (for substrates, see Fig. 25.18).

Substrate	Metal-ligand (additive)	TON	TOF [h^{-1}]	ee [%]
30	Rh-bppfoh, bppfsh	200–2000	2–125	95–>99
31	Rh-bophoz, josiphos	100–200 [a)]	1 [a)]–>1000	97–99
32	Ru-walphos, ferrotane	5–200 [a)]	<1–25 [a]	95–99
33a	Ir-josiphos/I^-/H^+	200 [a)]	n.a.	96
33b	Ir-f-binaphane/I_2	100 [a)]	2 [a)]	>99
33c	Rh-josiphos	500	500	99
34	Ir-josiphos/I^-/H^+	250 [a)]	56 [a)]	93
MEA imine	Ir-josiphos/I^-/H^+	2 000 000	>400 000	80

a) Standard test results, not optimized.
n.a. = data not available.

Abbreviations

ACA acetamido cinnamic acid
DMIT dimethyl itaconate
ee enantiomeric excess
ITA itaconic acid
MAA methyl acetamido acrylate
MAC methyl esters of acetamido cinnamic acid
SCR substrate:catalyst ratio
TOF turnover frequency
TON turnover number

References

1 For an account, see T. Hayashi, in: A. Togni, T. Hayashi (Eds.), *Ferrocenes*. VCH, Weinheim, **1995**, p. 105.
2 (a) T. J. Colacot, *Chem. Rev.* **2003**, *103*, 3101; (b) P. Barbaro, C. Bianchini, G. Giambastiani, S.L. Parisel, *Coord. Chem. Rev.* **2004**, *248*, 2131.
3 H. U. Blaser, Ch. Malan, B. Pugin, F. Spindler, H. Steiner, M. Studer, *Adv. Synth. Catal.* **2003**, *345*, 103.
4 W. Tang, X. Zhang, *Chem. Rev.* **2003**, *103*, 3029.
5 G. Argouarch, O. Samuel, O. Riant, J.-C. Daran, H. B. Kagan, *Eur. J. Org. Chem.* **2000**, 2893.
6 M. Kesselgruber, C. Malan, B. Pugin, F. Spindler (Solvias AG), unpublished results.
7 T. Hayashi, N. Kawamura, Y. Ito, *J. Am. Chem. Soc.* **1987**, 1, 7876; T. Hayashi, N. Kawamura, Y. Ito, *Tetrahedron Lett.* **1988**, *29*, 5969.
8 J. Kang, J. H. Lee, S. H. Ahn, J. S. Choi, *Tetrahedron Lett.* **1998**, *39*, 5523.
9 (a) M. Lotz, T. Ireland, J. Almena Perea, P. Knochel, *Tetrahedron: Asymmetry* **1999**, *10*, 1839; (b) J. Almena Perea, A. Börner, P. Knochel, *Tetrahedron Lett.* **1998**, *39*, 8073; (c) J. Almena Perea, M. Lotz, P. Knochel, *Tetrahedron: Asymmetry* **1999**, *10*, 375; d) F. Spindler, C. Malan,

M. Lotz, M. Kesselgruber, U. Pittelkow, A. Rivas-Nass, O. Briel, H.U. Blaser, *Tetrahedron: Asymmetry* **2004**, *15*, 2299.

10 For more information see www.solvias.-com/ligands. M. Thommen, H.U. Blaser, *PharmaChem*, July/August, **2002**, 33.

11 D. Xiao, X. Zhang, *Angew. Chem.* **2001**, *113*, 3533.

12 (a) U. Berens, M.J. Burk, A. Gerlach, W. Hems, *Angew. Chem.* **2000**, *112*, 2057; (b) A. Marinetti, J.-P. Genet, S. Jus, D. Blanc, V. Ratovelamanana-Vidal, *Chem. Eur. J.* **1999**, *5*, 1160; (c). A. Marinetti, D. Carmichael, *Chem. Rev.* **2002**, *102*, 201.

13 M.F. Reetz, E.W. Beuttenmüller, R. Goddard, M. Pasto, *Tetrahedron Lett.* **1999**, *40*, 4977.

14 M.T. Reetz, A. Gosberg, R. Goddard, S.-H. Kyung, *Chem. Commun.* **1998**, 2077; M. T. Reetz, A. Gosberg, WO 0014096, **1998** (assigned to Studiengesellschaft Kohle MBH).

15 D. Liu, W. Li, X. Zhang, *Org. Lett.* **2002**, *4*, 4471.

16 (a) For overviews, see M. Ohff, J. Holz, M. Quirmbach, A. Börner, *Synthesis*, **1998**, 1391; F. Maienza, F. Spindler, M. Thommen, B. Pugin, A. Mezzetti, *Chimia* **2001**, *55*, 694; (b) F. Maienza, M. Wörle, P. Steffanut, A. Mezzetti, F. Spindler, *Organometallics* **1999**, *18*, 1041; (c) U. Nettekoven, P.C.J. Kamer, P.W.N.M. van Leeuwen, M. Widhalm, A.L. Spek, M. Lutz, *J. Org. Chem.* **1999**, *64*, 3996.

17 For an overview, see H.U. Blaser, W. Brieden, B. Pugin, F. Spindler, M. Studer, A. Togni, *Topics in Catalysis* **2002**, *19*, 3.

18 H.U. Blaser, H.P. Buser, K. Coers, R. Hanreich, H.P. Jalett, E. Jelsch, B. Pugin, H.D. Schneider, F. Spindler, A. Wegmann, *Chimia* **1999**, *53*, 275.

19 H.U. Blaser, F. Spindler, M. Studer, *Applied Catal. A: General* **2001**, *221*, 119.

20 W. Braun, A. Salzer, F. Spindler, E. Alberico, *Appl. Catal. A: General* **2004**, *274*, 191.

21 C. Czekelius, E.M. Carreira, *Angew. Chem. Int. Ed.* **2003**, *42*, 4793; C. Czekelius, E.M. Carreira, *Org. Lett.* **2004**, *6*, 4575.

22 B.H. Lipshutz, J.M. Servesko, *Angew. Chem. Int. Ed.* **2003**, *42*, 4789.

23 Y. Hsiao, N.R. Rivera, T. Rosner, S.W. Krska, E. Njolito, F. Wang, Y. Sun, J.D. Armstrong, E.J.J. Grabowski, R.D. Tillyer, F. Spindler, C. Malan, *J. Am. Chem. Soc.* **2004**, *126*, 9918.

24 M. Rouhi, *Chem. Eng. News* **2004**, *82*(37), 28.

25 (a) B. Pugin, H. Landert, F. *Spindler*, H.-U. Blaser, *Adv. Synth. Catal.* **2002**, *344*, 974; (b) C. Köllner, B. Pugin, A. Togni, *J. Am. Chem. Soc.* **1998**, *120*, 10274.

26 T. Sturm, W. Weissensteiner, F. Spindler, K. Mereiter, A.M. Lopez-Agenjo, F.A. Jalon, *Organometallics* **2002**, *21*, 1766.

27 (a) T. Ireland, K. Tappe, G. Grossheimann, P. Knochel, *Chem. Eur. J.* **2002**, *8*, 843; (b) M. Lotz, K. Polborn, P. Knochel, *Angew. Chem. Int. Ed.* **2002**, *41*, 4708; (c) F. Spindler, C. Malan, M. Lotz, M. Kesselgruber, U. Pittelkow, A. Rivas-Nass, O. Briel, H.U. Blaser, *Tetrahedron: Asymmetry* **2004**, *15*, 2299.

28 (a) N.W. Boaz, S.D. Debenham, E.B. Mackenzie, S.E. Large, *Org. Lett.* **2002**, *4*, 2421; (b) N.W. Boaz, S.D. Debenham, S.E. Large, M.K. Moore, *Tetrahedron: Asymmetry* **2003**, *14*, 3575; (c) N.W. Boaz, E.B. Mackenzie, S.D. Debenham, S.E. Large, J.A. Ponasik, *J. Org. Chem.* **2005**, *70*, 1872.

29 (a) X-P. Hu, Z. Zheng, *Org. Lett.* **2004**, *6*, 3585; (b) X-P. Hu, Z. Zheng, *Org. Lett.* **2005**, *7*, 419.

30 S. Qiao, G.C. Fu, *J. Org. Chem.* **1998**, *63*, 4168.

31 (a) T. Sturm, L. Xiao, W. Weissensteiner, *Chimia* **2001**, *55*, 688; (b) W. Weissensteiner, T. Sturm, F. Spindler, *Adv. Synth. Catal.* **2003**, *345*, 160.

32 P. Herold, S. Stutz, T. Sturm, W. Weissensteiner, F. Spindler, WO 02/02500, **2002** (assigned to Speedel Pharma AG).

33 (a) R. Kuwano, K. Sato, T. Kurokawa, D. Karube, Y. Ito, *J. Am. Chem. Soc.* **2000**, *122*, 7614; (b) R. Kuwano, M. Sawamura, Y. Ito, *Bull. Chem. Soc. Jpn.* **2000**, *73*, 2571; (c) R. Kuwano, M. Sawamura, Y. Ito, *Tetrahedron: Asymmetry* **1995**, *6*, 2521; (d) R. Kuwano, Y. Ito, *J. Org. Chem.* **1999**, *64*, 1232; (e) R. Kuwano, S. Okuda, Y. Ito, *J. Org. Chem.* **1998**, *63*, 3499; (f) R. Kuwano, S. Okuda, Y. Ito, *Tetrahedron: Asymmetry* **1998**, *9*, 2773.

26
The other Bisphosphine Ligands for Enantioselective Alkene Hydrogenation

Yongxiang Chi, Wenjun Tang, and Xumu Zhang

26.1
Introduction

This chapter describes atropisomeric biaryl bisphosphine ligands; modified DIOP-type ligands; P-chiral bisphosphane ligands; other bisphosphane ligands; and their applications in the enantioselective hydrogenation of olefins.

26.2
Chiral Bisphosphine Ligands

26.2.1
Atropisomeric Biaryl Bisphosphine Ligands

In 1980, Noyori and Takaya reported an atropisomeric C_2-symmetric bisphosphine ligand, BINAP [1]. This ligand was first used in Rh-catalyzed enantioselective hydrogenation of α-(acylamino)acrylic acids, and high selectivities were reported for some substrates [2]. However, the significant impact of BINAP in asymmetric hydrogenation did not gain very much attention until it was applied in ruthenium chemistry. In 1986, Noyori and Takaya prepared a BINAP–Ru dicarboxylate complex for the asymmetric hydrogenation of various functionalized alkenes [3]. Subsequently, these authors discovered that the halogen-containing BINAP–Ru complexes were also efficient catalysts for enantioselective hydrogenation of a range of functionalized ketones [4]. During the mid-1990s, another major breakthrough was made on BINAP–Ru chemistry when Noyori discovered that the Ru–BINAP/diamine complexes were efficient catalysts for the enantioselective hydrogenation of some unfunctionalized ketones [5]. This advance addressed a long-standing challenging problem in enantioselective hydrogenation. Importantly, the catalytic system can selectively reduce ketones in the presence of carbon–carbon double or triple bonds [6]. Inspired by Noyori's studies on the BINAP chemistry, other research groups developed many excellent atropisomeric biaryl bisphosphine ligands. For example, Miyashima reported a BI-

The Handbook of Homogeneous Hydrogenation.
Edited by J.G. de Vries and C.J. Elsevier
Copyright © 2007 WILEY-VCH Verlag GmbH & Co. KGaA, Weinheim
ISBN: 978-3-527-31161-3

CHEP ligand, which was successfully applied in both Rh- and Ru-catalyzed enantioselective hydrogenation [7]. Schmid et al. reported BIPHEMP [8] and MeO-BIPHEP [9] ligands, both of which were successfully applied in many Ru-catalyzed hydrogenations. Achiwa also developed several atropisomeric ligands such as BIMOP [10], FUPMOP [11], and MOC-BIMOP (Fig. 26.1) [12].

Modification of the electronic and steric properties of BINAP, BIPHEMP, and MeO-BIPHEP can lead to the development of new efficient atropisomeric ligands (Fig. 26.1). In fact, Takaya has found that a modified BINAP ligand, H_8-BINAP, provides better enantioselectivity than BINAP in the Ru-catalyzed hydrogenation of unsaturated carboxylic acids [13]. Mohr has developed a bis-steroidal bisphosphine **1**, which has shown similar catalytic results to BINAP in the Ru-catalyzed enantioselective hydrogenation [14]. Hiemstra has developed a dibenzofuran-based bisphosphine BIFAP, which has shown excellent enantioselectivity in the Ru-catalyzed hydrogenation of methyl acetoacetate [15]. The dihedral angle of the biaryl backbone is expected to have a strong influence on the enantioselectivity. Another chiral biaryl bisphosphine ligand, SEGPHOS, was developed in Takasago. The ligand, which possesses a narrower dihedral angle than BINAP, has provided greater enantioselectivity than BINAP in the Ru-catalyzed hydrogenation of a wide variety of carbonyl compounds [16]. Chan [17 a] and Genêt [17 b, c] have reported a closely related ligand bisbenzodioxanPhos (SYNPHOS) independently. In order systematically to investigate the influence of the dihedral angle of biaryl ligands on enantioselectivity, Zhang has developed a series of TunePhos ligands with tunable dihedral angles. When the TunePhos ligands are applied in the Ru-catalyzed enantiomeric hydrogenation of β-keto esters, the ee-values obtained fluctuate with the different dihedral angles of the TunePhos ligands [18]. C4-TunePhos shows comparable or superior enantioselectivity to BINAP in Ru-catalyzed hydrogenation of β-keto esters. More applications of the TunePhos ligands have shown that different asymmetric catalytic reactions may require a different TunePhos ligand with a different dihedral angle. When TunePhos ligands are applied in the Ru-catalyzed hydrogenation of enol acetates, C2-TunePhos is the best ligand in terms of enantioselectivity [19]. However, C3-TunePhos provided the best enantioselectivities for the synthesis of cyclic β-amino acids [20], and the hydrogenation of α-phathalimide ketones [21]. Genêt and Marinetti have developed a non-C_2 symmetric biaryl bisphosphine, MeO-NAPhePHOS, which has shown comparable results to C_2-symmetric biaryl bisphosphine in Ru-catalyzed hydrogenation [22].

Structural variation of BINAP or MeO-BIPHEP can also be made on the aromatic rings of the biaryl backbone (Fig. 26.1). For example, the aromatic rings can be replaced by five- or six-membered heteroaromatic rings. Sannicolò et al. have discovered a series of biheteroaryl bisphosphines such as BITIANP, TetraMe-BITIANP [23], and TetraMe-BITIOP [24]. These ligands have shown comparably good results to BINAP in Ru-catalyzed enantioselective hydrogenation. Chan has reported a dipyridylphosphine ligand P-Phos for Ru-catalyzed enantioselective hydrogenation, and high enantioselectivities and reactivities have been obtained in the hydrogenation of β-keto esters, α-arylacrylic acids, and simple ketones [25].

An *ortho*-substituted BIPHEP ligand, *o*-Ph-HexaMeO-BIPHEP, has been recently developed by Zhang [26]. With two phenyl groups at the *ortho* positions of two diphenylphosphino groups, *o*-Ph-HexaMeO-BIPHEP is specially designed to restrict the rotation of the P-phenyl groups, which is considered to be detrimental for some enantioselective reactions. The design is effective when *o*-Ph-HexaMeO-BIPHEP is employed in the Rh-catalyzed enantioselective hydrogenation of cyclic enamides. While chiral ligands without *ortho*-substituents such as BINAP, BIPHEP, and HexaMeO-BIPHEP provide very poor selectivities, *o*-Ph-HexaMeO-BIPHEP shows excellent enantioselectivity in the hydrogenation of a series of cyclic enamides [26]. Zhang also reported another *ortho*-substituted BIPHEP type ligand – *o*-Ph-MeO-BIPHEP – which afforded excellent enantioselectivities in the hydrogenation of α-dehydroamino acids [27].

Henschke and Casy prepared a biaryl bisphosphine ligand, HexaPhemp, which performed as well as, or better than, the corresponding BINAP ligands [28]. Dellis and Genêt have developed a new electron-deficient atropisomeric ligand based on a SEGPHOS backbone, difluorphos, which has a narrow dihedral angle and electronic-withdrawing substituents. The electron-deficiency was shown to be crucial to reach high levels of enantioselectivity in hydrogenation of some challenging β-keto ester substrates [29].

Chan has discovered a completely atropdiasteroselective synthesis of a biaryl diphosphine based on an enantioselective intramolecular Ullmann coupling or a Fe(III)-promoted oxidative coupling. A chiral atropisomeric biaryl bisphosphine ligand **2** was synthesized through this central-to-axial chirality transfer [30]. Recently, a xylyl-biaryl bisphosphine ligand, Xyl-TetraPHEMP was introduced by Moran, and found to be effective for the Ru-catalyzed hydrogenation of aryl ketones [31].

A family of tunable 4,4′-substituted BINAP was reported by Lin: 4,4-$[SiMe_3]_2$-BINAP **3** and polar 4,4-$[P(O)OH_2]_2$-BINAP **4** have shown high enantioselectivities (up to 99.6% ee) in the hydrogenation of a variety of β-aryl ketoesters [32]. 4,4-$[SiMe_3]_2$-BINAP **3** is also effective for the asymmetric hydrogenation of α-phthalimide ketones and 1,3-diaryl diketones [33]. The 4,4′-bulky groups were shown to be responsible for the enhancement of enantioselectivity and diastereoselectivity in these reactions. Lemaire prepared 4,4′- or 5,5′-diamBINAP, with a 4,4′- or 5,5′-diaminomethyl substituent; the hydrosoluble HBr salt of the Ru complex based on these ligands afforded high enantioselectivity (>97% ee) in the water/organic solvent biphasic hydrogenation of β-keto esters [34]. Lemaire also reported 4,4′- or 5,5′-perfluoroalkylated BINAP, **5** and **6**, which showed the same activities and enantioselectivities as 4,4′- or 5,5′-diamBINAP in the hydrogenation of β-keto esters (Fig. 26.1) [35].

As with most chiral atropisomeric ligands, resolution or enantioselective synthesis is requisite. Mikami developed a novel ligand-accelerated hydrogenation catalyst in which the chirality of an atropos but achiral triphos–Ru complex could be controlled by chiral diamines. Using (*S*)-dm-dabn as controller, a single diastereomeric triphos–Ru complex was obtained through isomerization of the (*R*)-triphos–Ru complex in dichloroethane at 80 °C (Scheme 26.1) [36].

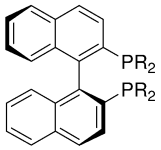

(*S*)-BINAP: R = Ph
(*S*)-TolBINAP: R = 4-MePh
(*S*)-XylBINAP: R = 3,5-$(Me)_2Ph$

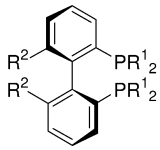

(*S*)-BICHEP: R^1 = Cy; R^2 = CH_3
(*S*)-BIPHEMP: R^1 = Ph; R^2 = CH_3
(*S*)-MeO-BIPHEP: R^1 = Ph; R^2 = OCH_3

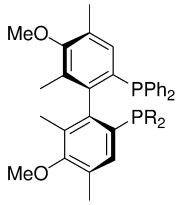

(*S*)-BIMOP: R = Ph
(*S*)-MOC-BIMOP: R = Cy

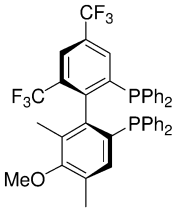

(*S*)-FUPMOP

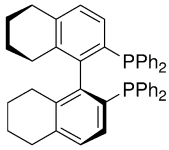

(*S*)-H_8-BINAP

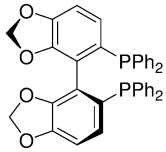

(*S*)-SEGPHOS

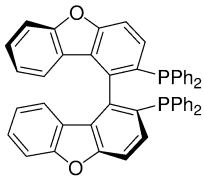

(*S*)-BIFAP

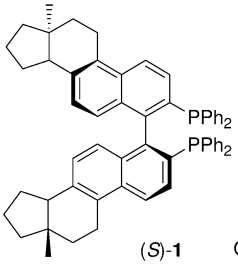

(*S*)-**1**

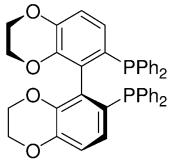

(*S*)-BisbenzodioxanPhos
(SYNPHOS)

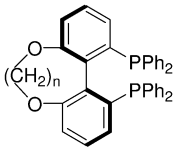

(*S*)-Cn-TunePhos
n = 1-6

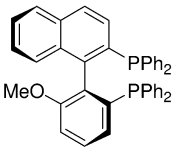

(*S*)-MeO-NAPhePHOS

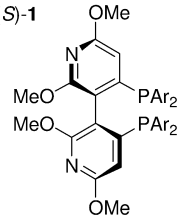

(*S*)-P-Phos: Ar = Ph
(*S*)-Tol-P-Phos: Ar = 4-MePh
(*S*)-Xyl-P-Phos: Ar = 3,5-$(Me)_2Ph$

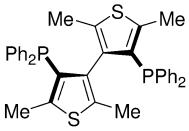

(*R*)-TetraMe-BITIOP

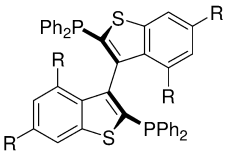

(*R*)-TetraMe-BITIANP: R = Me
(*R*)-BITIANP: R = H

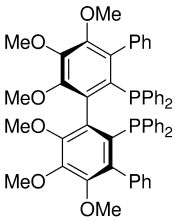

(*S*)-*o*-Ph-HexaMeO-BIPHEP

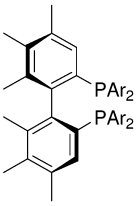

(*S*)-HexaPhemp, Ar=Ph
(*S*)-Xyl-HexaPhemp, Ar=Xyl

Fig. 26.1 Atropisomeric biaryl bisphosphine ligands.

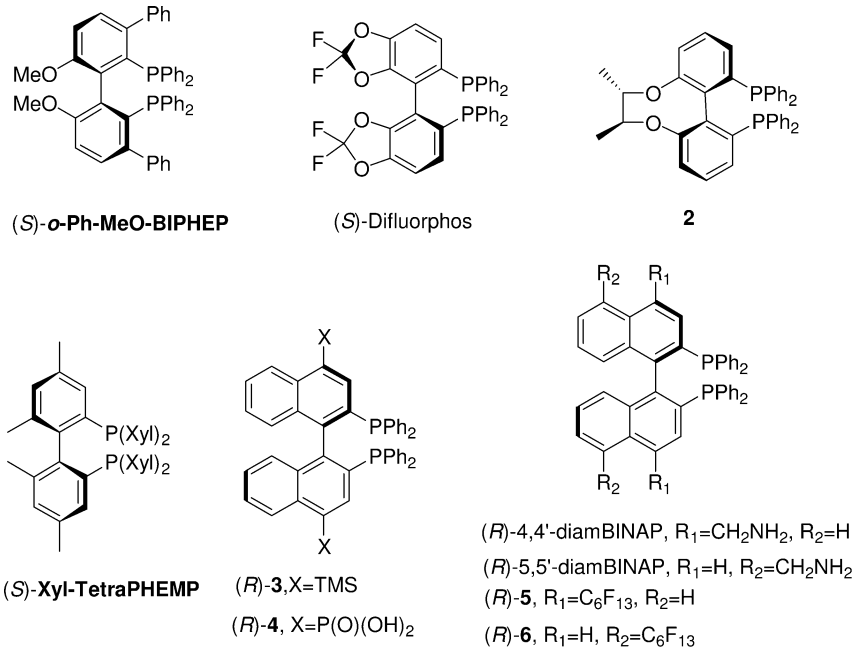

Fig. 26.1 (continued)

Some BINAP or BIPHEP derivatives have also been made in order to make the catalysts water-soluble or recyclable (Fig. 26.2). The literature on supported homogeneous catalysts in the field of asymmetric hydrogenation using BINAP derivatives has recently been reviewed [37]. Davis et al. reported a sulfonated BINAP ligand, BINAP-4-SO_3Na, and found that its water-soluble Ru complex has comparable catalytic properties to the unmodified BINAP-Ru catalyst for hydrogenation of 2-acetamidoacrylic acid [38]. Schmid et al. have developed a water-soluble MeO-BIPHEP type ligand, MeOBIPHEP-S. The ligand has the sulfonato group attached at the *para* position of each P-phenyl group to minimize the possible steric interactions of the sulfonato groups with the inner ligand sphere of a coordinated metal, and thus to retain the high enantioselectivity of the non-sulfonated catalyst. Indeed, MeOBIPHEP-S has shown similarly high enantioselectivity and reactivity to MeO-BIPHEP in the Ru-catalyzed hydrogenation of unsaturated carboxylic acids [39]. Genêt has recently reported some recyclable BINAP ligands such as *Digm*-BINAP and PEG-*Am*-BINAP, which were obtained by tethering BINAP with guanidine and PEG groups, respectively. The Ru catalysts of these ligands maintained high enantioselectivity after three or four recycles [40]. Many polymer-supported BINAP ligands have been developed. For instance, Bayston incorporated the BINAP framework onto an insoluble polymer (polystyrene). The resulting polymer-bound BINAP, after treatment with $[Ru(cod)(2\text{-methylallyl})_2]_2$ and HBr, induces high ee-values in the hydrogenation of β-keto esters and acrylic acids [41]. The polymer can be recycled as the cata-

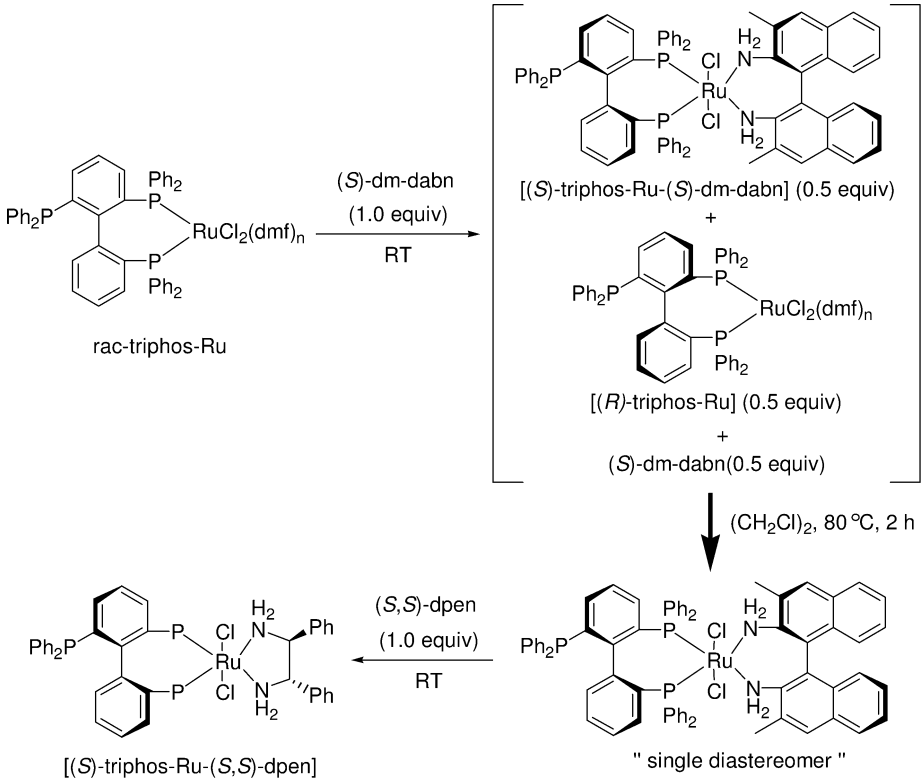

Scheme 26.1

lyst several times, while high ee-values are maintained. Noyori used the same polymer-bound BINAP to create a polymer-bound BINAP/diamine Ru catalyst, which has furnished high ee-values and turnover numbers (TONs) in the hydrogenation of simple ketones [42]. Chan has developed a highly effective polyester-supported BINAP ligand through copolymerization of chiral 5,5′-diaminoBINAP, chiral pentanediol, and terephthaloyl chloride [43]. The ligand has been successfully applied repeatedly in the Ru-catalyzed enantioselective hydrogenation of 2-(6′-methoxy-2-naphthyl)acrylic acid. A dendrimer-supported BINAP ligand has also been reported [44]. Pu has developed several polymer-based chiral ligands such as poly(BINAP) and BINOL-BINAP. These ligands have been applied successfully in the Rh-catalyzed hydrogenation of (*Z*)-methyl *α*-(benzamido)cinnamate and in the Ru-catalyzed hydrogenation of simple ketones [45]. Lemaire et al. have reported a poly-NAP Ru complex, which provides 99% ee in the hydrogenation of methyl acetoacetate, even after four recycles of the catalyst [46].

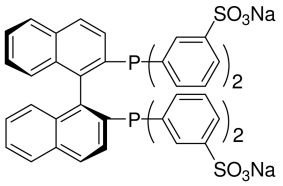

BINAP-4SO_3Na

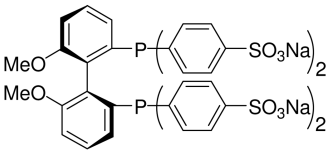

MeOBIPHEP-S

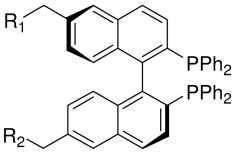

Digm-BINAP: $R_1 = R_2 =$

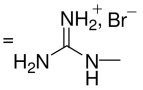

PEG-*Am*-BINAP: $R_1 =$ $MeO(CH_2CH_2O)n\text{-}CO(CH_2)_3CONH$, $R_2 = NH_2$

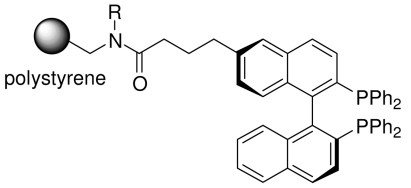

polystyrene-supported BINAP

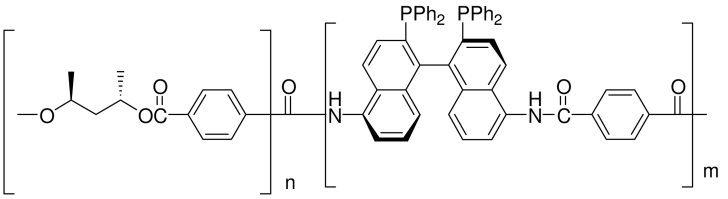

polyester-supported BINAP

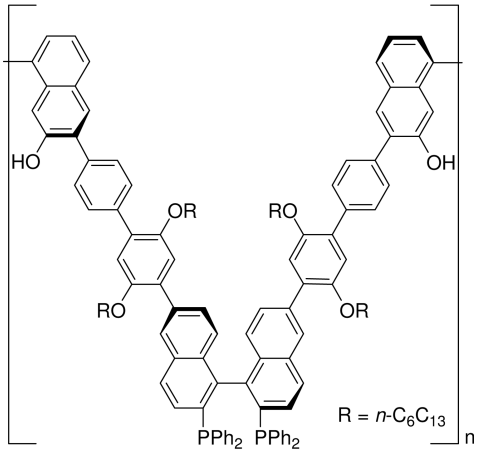

BINOL-BINAP

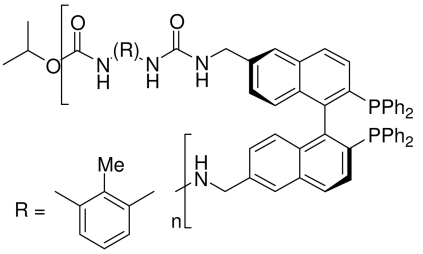

poly-BINAP

Fig. 26.2 Water-soluble or recyclable BINAP or BIPHEP derivative catalysts.

26.2.2
Chiral Bisphosphine Ligands Based on DIOP Modifications

Kagan's pioneering studies on the development of DIOP has had significant impact on the design of new efficient chiral ligands for enantioselective hydrogenation [47]. However, DIOP itself provides only moderate to good enantioselectivity in the enantioselective hydrogenation of dehydroamino acid derivatives, and its application in highly enantioselective hydrogenation has rarely been disclosed. A possible reason for this is that the seven-membered chelate ring of the DIOP metal complex is conformationally flexible. These conformational ambiguities, as depicted in Figure 26.3, may be responsible for its low efficiency.

Achiwa successfully developed several modified DIOP ligands by varying the electronic and steric properties of DIOP. MOD-DIOP was applied in the rhodium-catalyzed enantioselective hydrogenation of itaconic acid derivatives, and up to 96% ee was obtained [48]. In order to rigidify the conformational flexibility of DIOP, Zhang has introduced a rigid 1,4-diphosphane ligand BICP with two five-membered carbon rings on its backbone (Fig. 26.4). BICP was found to be an efficient ligand for the hydrogenation of α-dehydroamino acids, β-dehydroamino acids, arylenamides, and MOM-protected β-hydroxy enamides [49]. Genov introduced several BICP family ligands, and developed a new catalytic system comprising Ru–**7** or Ru–**8** complexes in combination with a nonchiral 2-(alkylthio)amine or 1,2-diamine and an alkoxide as a base for the highly enantioselective hydrogenation of aryl ketones [50]. Several rigidified DIOP-type ligands have been developed. Zhang [51] and RajanBabu [52] have independently reported the development of DIOP* by introducing two alkyl substituents at the α-positions of the diphenylphosphine groups. The (*S*,*R*,*R*,*S*)-DIOP* was found to provide excellent enantioselectivity in the Rh-catalyzed hydrogenation of arylenamides and MOM-protected β-hydroxy enamides [51]. However, its isomeric ligand (*S*,*S*,*S*,*S*)-DIOP*, which was first synthesized by Kagan [53], provided much lower enantioselectivity. It is believed that the two methyl groups of (*S*,*R*,*R*,*S*)-DIOP* orientate at pseudoequatorial positions in the "effective" conformer of the DIOP* metal complex, thereby stabilizing the "effective" conformer to promote high enantioselectivity. On the other hand, its isomeric ligand (*S*,*S*,*S*,*S*)-DIOP* has two methyl groups at pseudoaxial positions, which destabilize the "effective" conformer and lead to diminished ee-values. Lee has developed 1,4-diphosphane ligands BDPMI, **9** and **10**, with an imidazolidin-2-one backbone [54]. The *gauche* steric interaction between the *N*-substituents and

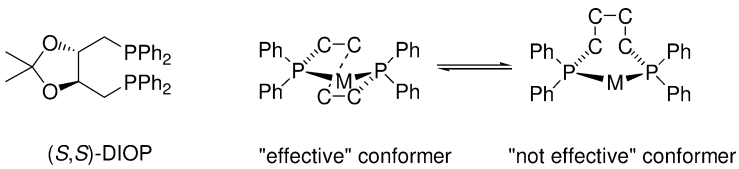

Fig. 26.3 Conformation analysis of DIOP metal complex.

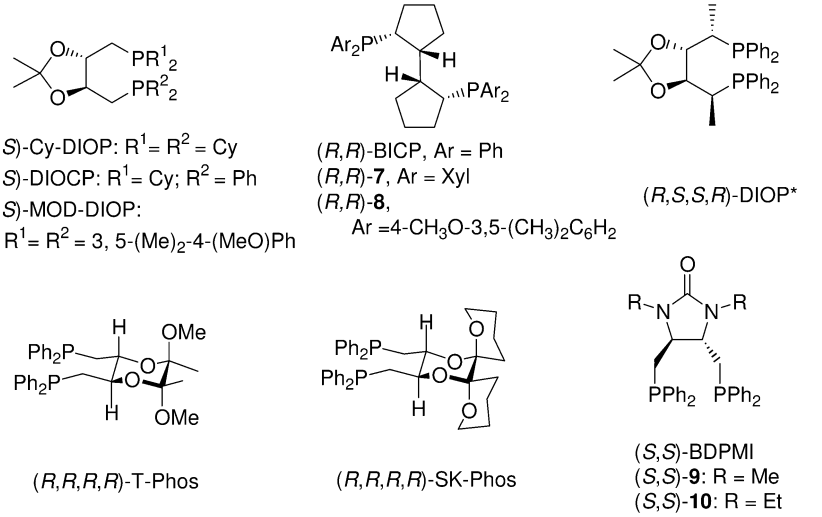

Fig. 26.4 Chiral bisphosphane ligands based on DIOP modifications.

phosphanylmethyl group of the ligands may restrict the conformational flexibility of the seven-membered metal chelate ring. The BDPMI ligands have been successfully applied in the Rh-catalyzed hydrogenation of arylenamides, and up to 99% ee-values have been obtained. A series of 1,4-diphosphane ligands with a conformationally rigid 1,4-dioxane backbone such as T-Phos, and SK-Phos have been developed by Zhang and found to be efficient (up to 99% ee) in the rhodium-catalyzed asymmetric hydrogenation of arylenamides and MOM-protected β-hydroxyl enamides [55].

26.2.3
P-Chiral Bisphosphine Ligands

Knowles made the important discovery of the first C_2-symmetric chelating bisphosphine ligand, DIPAMP, which performed much better than the monomeric PAMP [56]. Due to its high catalytic efficiency in the Rh-catalyzed enantioselective hydrogenation of dehydroamino acids, the first P-chiral bisphosphane DIPAMP was quickly employed in the industrial production of L-Dopa [57]. However the development of new efficient P-chiral bisphosphanes was slow, partly because of the difficulties in the ligand synthesis. It was not until Imamoto [58] discovered a series of efficient P-chiral ligands such as BisP* that the development of P-chiral phosphorus ligands regained attention (Fig. 26.5). The BisP* ligands have induced high activity and enantioselectivity in the rhodium-catalyzed hydrogenation of α-dehydroamino acids, enamides [59], (*E*)-β-(acylamino)-acrylates [60], and α,β-unsaturated-α-acyloxyphosphonates [61]. Mechanistic studies on enantioselective hydrogenation with ^{t}Bu-BisP* as the ligand by Gridnev and Imamoto provided evidence that the Rh-catalyzed hydrogenation can proceed by a different mechanism

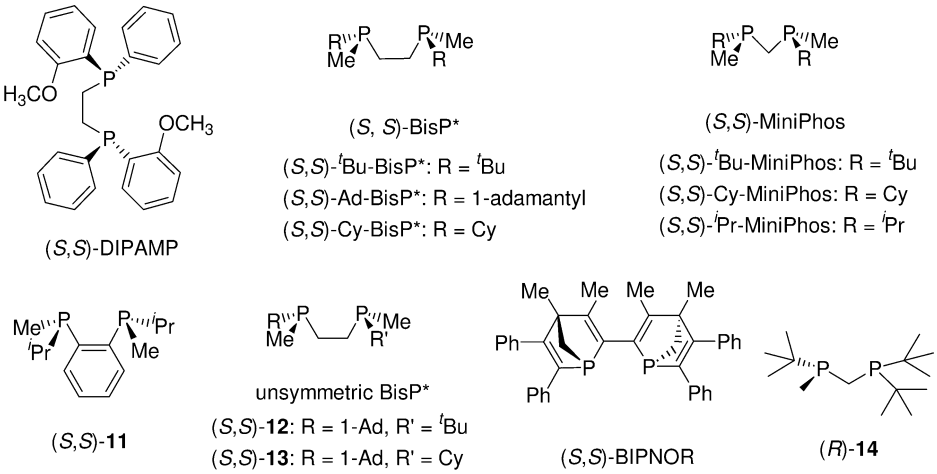

Fig. 26.5 P-chiral ligands.

with an electron-rich phosphorus ligand. A dihydride pathway [62] was suggested, which is different from the classic unsaturated pathway [63, 64] proposed by Halpern and Brown. In addition to Bisp*, several other P-chiral bisphosphanes such as MiniPhos [65], 1,2-bis(isopropylmethylphosphino)benzene (**11**) [66], and unsymmetrical P-chiral BisP* (such as **12** and **13**) [67] have been developed by Imamoto. Imamoto has also developed the P-chirogenic trialkylphosphonium salts derived from Bisp* and MiniPhos. These air-stable salts were conveniently applied in the Rh-catalyzed enantioselective hydrogenation of enamides [68].

Mathey has reported a bisphosphane ligand BIPNOR which contains two chiral bridgehead phosphorus centers [69]. BIPNOR has shown high enantioselectivity in the rhodium-catalyzed hydrogenation of α-(acetomido)cinnamic acid and itaconic acid. Recently, a three-hindered quadrant P-chirogenic ligand (*R*)-**14** was also reported by Hoge (Fig. 26.5) [70]. Using (*R*)-**14**–Rh as catalyst, both *E*- and *Z*-(β-acylamino) acrylates have been hydrogenated with high enantioselectivities (up to 99% ee) [71].

26.2.4
Other Bisphosphine Ligands

Some other efficient chiral bisphosphane ligands are illustrated in Figure 26.6. These include Bosnich's CHIRAPHOS [72] and PROPHOS [73], Achiwa's BPPM [74], and Rhône-Poulenc's TBPC [75]. A series of modified BPPM ligands such as BCPM and MOD-BPPM were also developed by Achiwa [76]. Some excellent chiral 1,2-bisphosphane ligands such as NORPHOS [77], PYRPHOS (DEGUPHOS) [78], and DPCP [79] for Rh-catalyzed enantioselective hydrogenation were also developed during this period. A few 1,3-bisphosphine ligands such as BDPP (SKEWPHOS) [80] and PPCP [81] were also prepared.

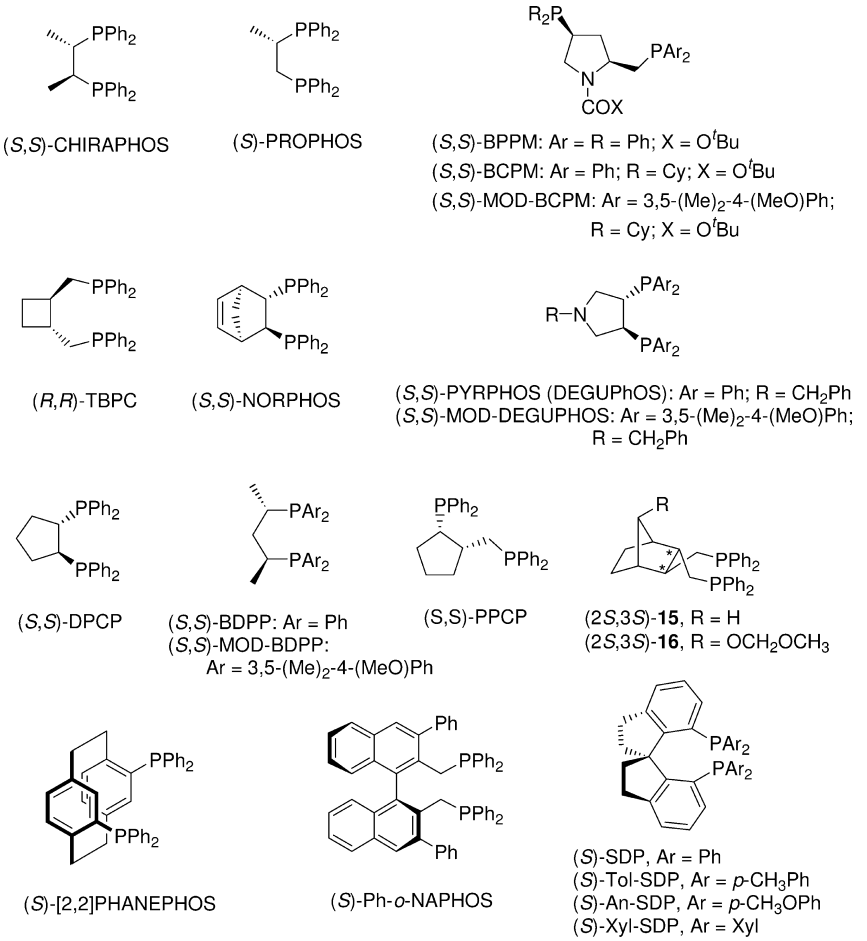

Fig. 26.6 Other efficient chiral bisphosphane ligands.

Pye and Rossen have developed a planar chiral bisphosphine ligand, [2.2] PHANEPHOS, based on a paracyclophane backbone [82]. The ligand has shown excellent enantioselectivity in Rh- or Ru-catalyzed hydrogenations. An *ortho*-phenyl substituted NAPHOS ligand, Ph-*o*-NAPHOS, has been applied successfully in the Rh-catalyzed hydrogenation of α-dehydroamino acid derivatives [83]. Compared to NAPHOS, Ph-*o*-NAPHOS has a more rigid structure and provides higher enantioselectivities. The chiral norbornane diphosphine ligands, **15** and **16**, were reported by Morimoto, and applied in Rh-catalyzed enantioselective hydrogenation [84]. Zhou reported a family of chiral spirodiphosphine ligands such as SDP, containing 1,1′-spirobi-indane as a new scaffold, which are effective for the hydrogenation of simple ketones (Fig. 26.6) [85].

26.3
Applications in Enantioselective Hydrogenation of Alkenes

26.3.1
Enantioselective Hydrogenation of α-Dehydroamino Acid Derivatives

Hydrogenation of α-dehydroamino acid derivatives has been a typical reaction to test the efficiency of new chiral phosphorus ligands. Indeed, a large number of chiral phosphorus ligands with great structural diversity are found to be effective for the Rh-catalyzed hydrogenation of α-dehydroamino acid derivatives. Since (*Z*)-2-(acetamido) cinnamic acid, 2-(acetamido) acrylic acid and their methyl esters are the most frequently applied substrates, and some efficient examples (>95% ee) of hydrogenation of these substrates with different chiral ligands are listed in Table 26.1. Generally, cationic Rh complexes and low hydrogenation pressure are applied in these hydrogenation reactions.

Table 26.1 Enantioselective hydrogenation of α-dehydroamino acid derivatives.

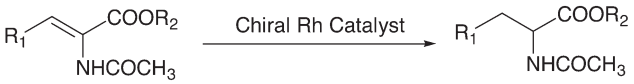

A: R_1 = H, R_2 = H B: R_1 = H, R_2 = CH_3
C: R_1 = Ph, R_2 = H D: R_1 = Ph, R_2 = CH_3

Ligand	Substrate	SCR	Reaction conditions	% ee of product (config.)	Reference
(*S*)-BINAP	D [a)]	100	EtOH, rt, 3 atm H_2	100 (*S*)	1
(*R*)-BICHEP	D [b)]	1000	EtOH, rt, 1 atm H_2	95 (*S*)	7c
(*S*)-*o*-Ph-MeO-BIPHEP	A	100	CH_2Cl_2, rt, 1.7 atm H_2	>99 (*S*)	27
(*R*,*R*)-BICP	A	100	THF, Et_3N, rt, 1 atm H_2	97.5 (*S*)	49a
(*R*,*R*)-DIPAMP	D	900	MeOH, 50 °C, 3 atm H_2	96 (*S*)	56a
(*S*,*S*)-^{t}Bu-BisP*	D	500	MeOH, rt, 2 atm H_2	99.9 (*R*)	58a
(*S*,*S*)-^{t}Bu-MiniPhos	B	500	MeOH, rt, 2 atm H_2	99.9 (*R*)	65
(*S*,*S*)-**11**	B	500	0 °C, 2 atm H_2	97 (*S*)	66
(*S*,*S*)-**12**	D	500	MeOH, rt, 2 atm H_2	99.2 (*R*)	67a
(-)-BIPNOR	C	100	EtOH, rt, 3 atm H_2	>98 (*S*)	69a
(*R*)-**14**	A	100	MeOH, rt, 3.4 atm H_2	>99 (*R*)	70
(*R*)-**14**	C	100	MeOH, rt, 3.4 atm H_2	>99 (*R*)	70
(*R*,*R*)-NORPHOS	C	95	MeOH, rt, 1.1 atm H_2	96 (*R*)	77
(*R*,*R*)-PYRPHOS	D	50000	MeOH, rt, 61 atm H_2	96.5 (*S*)	78b
(*R*)-PHANEPHOS	B	100	MeOH, rt, 1 atm H_2	99.6 (*R*)	82a
(*S*)-Ph-o-NAPHOS	B	100	MeOH, rt, 3 atm H_2	98.7 (*S*)	83

a) Benzoyl derivative.
b) Ethyl ester.
SCR: substrate:catalyst ratio.

Several chiral ligands, such as PYRPHOS [78b], have been shown to be very efficient ligands for the hydrogenation of α-dehydroamino acid derivatives in terms of both high enantioselectivity and reactivity.

In contrast to the high enantioselectivity achieved for the *Z*-isomeric substrates, hydrogenation of the *E*-isomeric substrates usually proceeds at a much lower rate and gives poor enantioselectivities [86]. With the Rh–BINAP system as the catalyst and tetrahydrofuran (THF) as solvent, hydrogenation of the *Z*- and *E*-isomeric substrates generates products with different configurations [2].

Many synthetic applications of Rh-catalyzed hydrogenation of α-dehydroamino acid derivatives have recently been explored (Scheme 26.2). Takahashi has reported a one-pot sequential enantioselective hydrogenation utilizing a BINAP–Rh and a BINAP–Ru catalyst to synthesize 4-amino-3-hydroxy-5-phenylpentanoic acids in over 95% ee. The process involves a first step in which the dehydroamino acid unit is hydrogenated with the BINAP–Rh catalyst, followed by hydrogenation of the β-keto ester unit with the BINAP–Ru catalyst [87]. A hindered pyridine substituted α-dehydroamino acid derivative has been hydrogenated by a

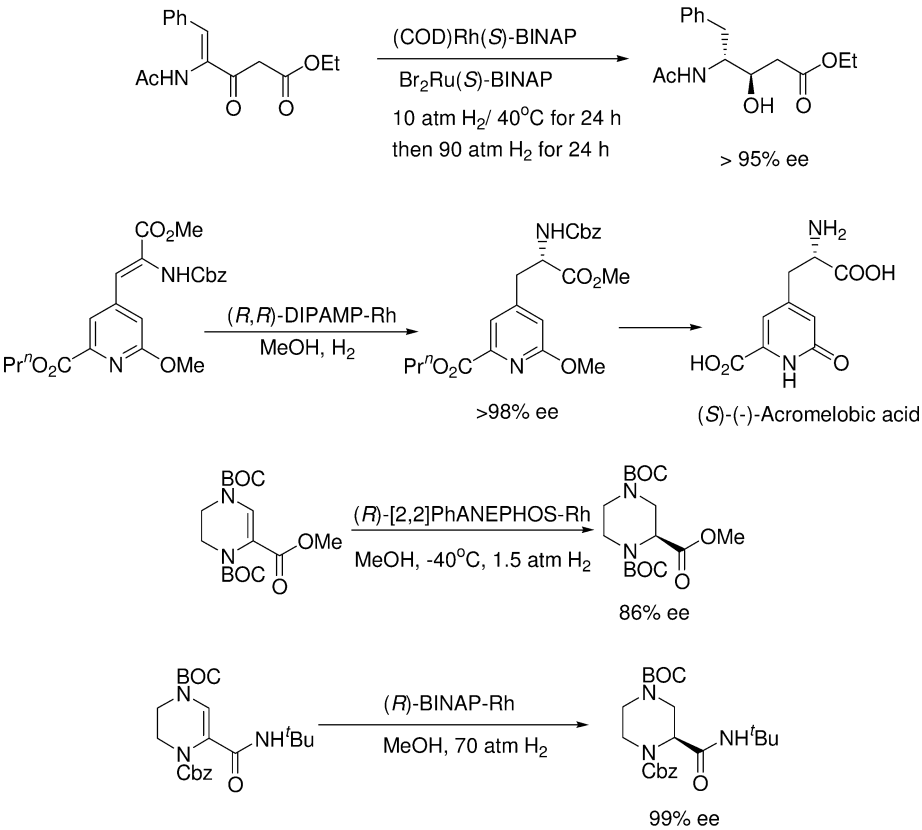

Scheme 26.2

Table 26.2 Enantioselective hydrogenation of β,β-dimethyl α-dehydroamino acid esters.

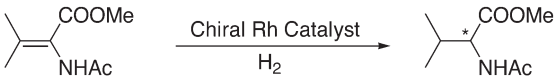

Ligand	SCR	Reaction conditions	% ee of product (config.)	Reference
(*S*,*S*)-Cy-BisP*	500	MeOH, rt, 6 atm H_2	90.9 (*R*)	58a
(*S*,*S*)-^{t}Bu-MiniPhos	500	MeOH, rt, 6 atm H_2	87 (*R*)	65
(*S*,*S*)-**11**	500	rt, 6 atm H_2	87 (*S*)	66
(*S*,*S*)-**13**	100	MeOH, rt, 20 atm H_2	96.1 (*R*)	67b

SCR: substrate:catalyst ratio.

DIPAMP–Rh complex to give the corresponding chiral α-amino acid derivative in over 98% ee. The chiral product has been used for the synthesis of (*S*)-(–)-acromelobic acid [88]. Hydrogenation of a tetrahydropyrazine derivative catalyzed by a PHANEPHOS–Rh complex at –40 °C gives an intermediate for the synthesis of Crixivan in 86% ee [82a]. Hydrogenation of another tetrahydropyrazine carboxamide derivative catalyzed by an (*R*)-BINAP–Rh catalyst leads to the chiral product in 99% ee [89].

The hydrogenation of β,β-disubstituted α-dehydroamino acids remains a relatively challenging problem. The Rh complexes of chiral ligands such as Cy-BisP* [58a], MiniPhos [65], and unsymmetrical BisP* **13** [67b] have shown high efficiencies for some β,β-disubstituted α-dehydroamino acid substrates. Some efficient examples of hydrogenation of β,β-dimethyl α-dehydroamino acid esters with different chiral phosphorus ligands are listed in Table 26.2.

26.3.2
Enantioselective Hydrogenation of Enamides

Rh-catalyzed hydrogenation of simple enamides has attracted much attention recently. With the development of increasingly efficient chiral phosphorus ligands, extremely high ee-values can be obtained in the Rh-catalyzed hydrogenation of α-aryl enamides. *E*/*Z*-isomeric mixtures of β-substituted enamides can also be hydrogenated, with excellent ee-values. Some efficient examples (>95% ee) of hydrogenation of α-phenylenamide and *E*/*Z*-isomeric mixtures of β-methyl-α-phenylenamide are listed in Table 26.3.

Some alkyl enamides such as *tert*-butylenamide or 1-adamantylenamide can also be hydrogenated with a ^{t}Bu-BisP*–Rh catalyst in 99% ee. Notably, the configurations of the hydrogenation products of these bulky alkyl enamides are opposite to those of aryl enamides. A mechanistic study [90] by Gridnev and Imamoto [59] using nuclear magnetic resonance (NMR) techniques indicates that the hydrogenations of bulky alkyl enamides and aryl enamides involve different

Table 26.3 Enantioselective hydrogenation of enamides.

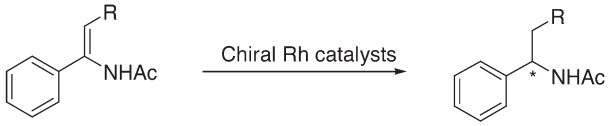

A: R = H B: R = CH_3 (*E*/*Z*)

Ligand	Substrate	SCR	Reaction conditions	% ee of product (config.)	Reference
(*R*,*R*)-BICP	B	100	Toluene, rt, 2.7 atm H_2	95.0 (*R*)	49b
(*R*,*S*,*S*,*R*)-DIOP*	A	50	MeOH, rt, 10 atm H_2	98.8 (*R*)	51
	B	50	MeOH, rt, 10 atm H_2	97.3 (*R*)	51
(*S*,*S*)-**9**	A	100	CH_2Cl_2, rt, 1 atm H_2	98.5 (*R*)	54a
	B	100	CH_2Cl_2, rt, 1 atm H_2	>99 (*R*)	54a
(*R*,*R*,*R*,*R*)-T-Phos	B	100	MeOH, rt, 3.1 atm H_2	98 (*S*)	55
(*R*,*R*,*R*,*R*)-SK-Phos	B	100	MeOH, rt, 3.1 atm H_2	97 (*S*)	55
(*S*,*S*)-^{t}Bu-BisP*	A	100	MeOH, rt, 3 atm H_2	98 (*R*)	59

SCR: substrate:catalyst ratio.

coordination pathways. *o*-Ph-HexaMeO-BIPHEP [26] has shown high efficiency in the Rh-catalyzed hydrogenation of cyclic enamides. A racemic cyclic enecarbamate has been hydrogenated with an *o*-Ph-HexaMeO-BIPHEP–Rh catalyst to yield the *cis* chiral carbamate in 96% ee [26]. The chiral product can be used directly for the synthesis of sertraline, an anti-depressant. Hydrogenation of some tetra-substituted enamides has also been reported. ^{t}Bu-BisP* and ^{t}Bu-MiniPhos have provided excellent ee-values in the Rh-catalyzed hydrogenation of a β,β-dimethyl-α-phenyl enamide derivatives (Scheme 26.3). Using an *o*-Ph-BIPHEP–Rh catalyst [26], tetra-substituted enamides derived from 1-indanone and 1-tetralone have been hydrogenated with excellent enantioselectivities.

The hydrogenation of a series of *E*/*Z*-isomeric mixtures of α-arylenamides with a MOM-protected β-hydroxyl group catalyzed by a Rh-complex of 1,4-diphosphane T-Phos with a rigid 1,4-dioxane backbone led to chiral β-amino alcohol derivatives in excellent enantioselectivities (Scheme 26.4) [55]. DIOP*–Rh is also effective for this transformation [51b].

In addition to the Rh chemistry, the Ru–BINAP system has shown excellent enantioselectivity in the hydrogenation of (*Z*)-*N*-acyl-1-alkylidenetetrahydroisoquinolines. Thus, a series of chiral isoquinoline products can be efficiently synthesized [3a, b, 91]. Using Ru–BINAP, the cyclic enamides, 6-bromotetralone-eneacetamide [92] and 7-methyltetralone-eneacetamide [93] are hydrogenated to give the corresponding chiral amide in 97% and 94% ee, respectively (Scheme 26.5). Ru–Biphemp also provided good selectivity (92% ee) in the enantiomeric hydrogenation of a cyclic enamide derived from 3-chromanone (Scheme 26.5) [93].

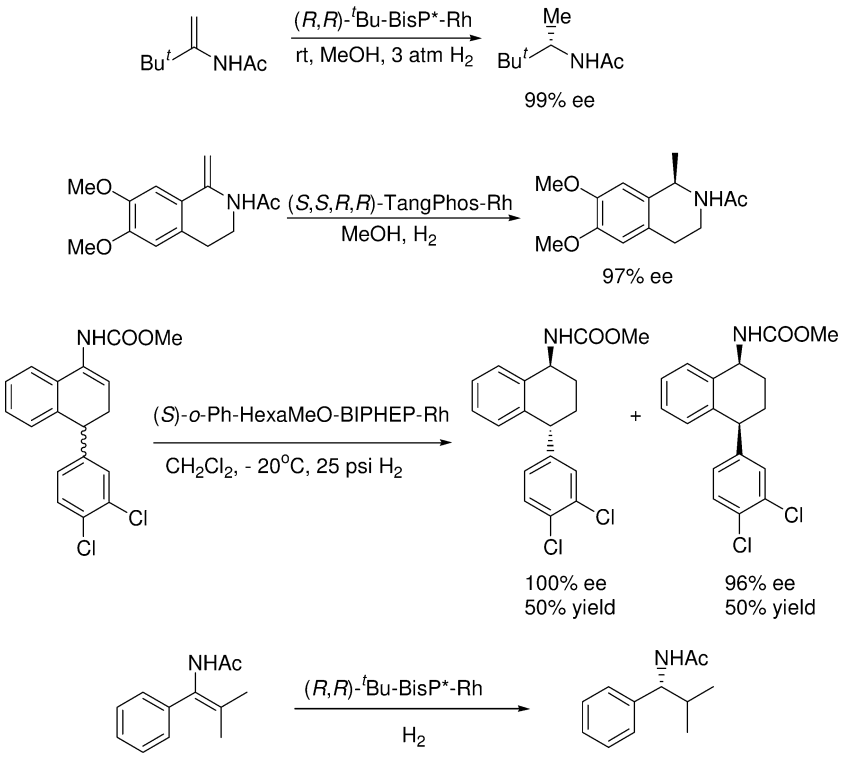

Scheme 26.3

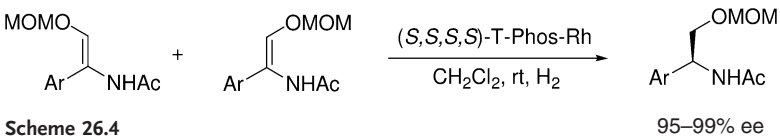

Scheme 26.4

26.3.3
Enantioselective Hydrogenation of (β-Acylamino) Acrylates

Enantioselective hydrogenation of (β-acylamino) acrylates has gained much attention recently because the β-amino acid products are important building blocks for chiral drugs [94]. Since most synthetic methods produce mixtures of *Z*- and *E*-isomeric substrates, it is important that both isomers can be hydrogenated with high enantioselectivity for the practical synthesis of β-amino acid derivatives via enantioselective hydrogenation. Some Rh and Ru complexes with chiral phosphorus ligands such as BINAP [95], BICP [49e], BDPMI [54b], ligand **4** [30], ^{t}Bu-BisP* [60], (*R*)-**14** [71], and Xyl-P-Phos [25c] are found to be effective for hydrogenation of (*E*)-alkyl (β-acylamino) acrylates. However, only a

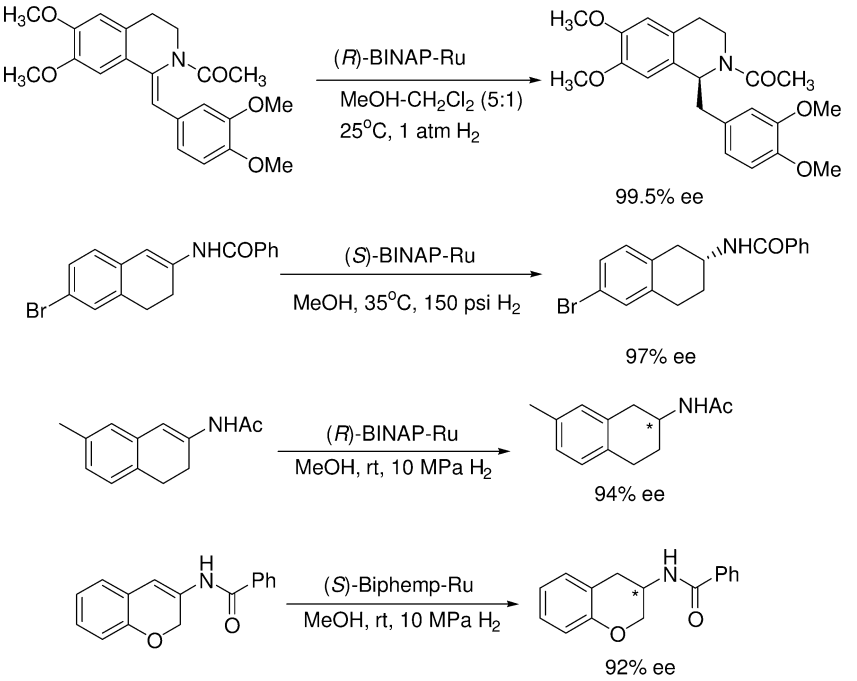

Scheme 26.5

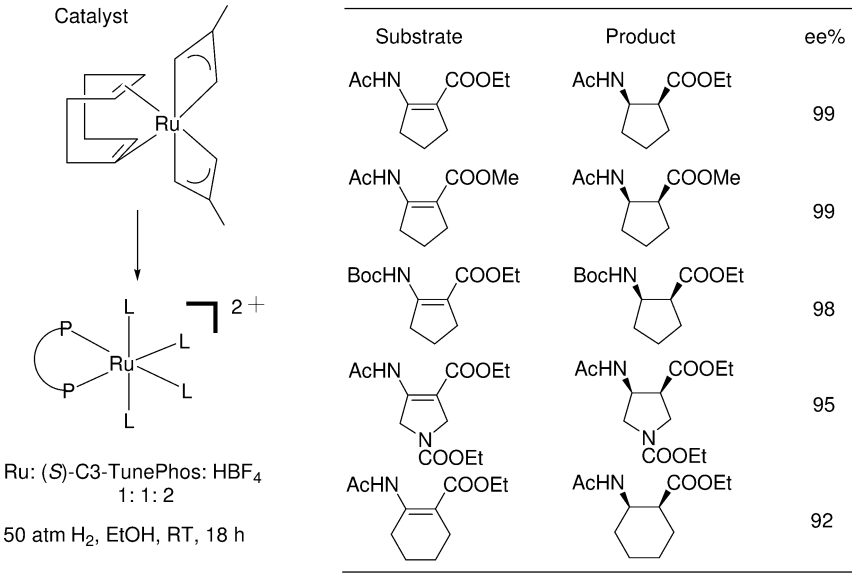

Scheme 26.6

Table 26.4 Enantioselective hydrogenation of (*β*-acylamino) acrylates.

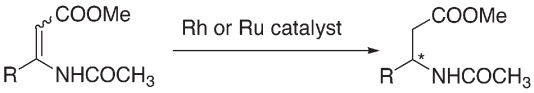

Ligand	R	Geometry	Reaction conditions	% ee of product (config.)	Reference
(*R*)-BINAP–Ru	CH_3	*E*	MeOH, 25 °C, 1 atm H_2	96 (*S*)	95
(*R*)-Xyl-P-Phos–Ru	CH_3	*E*	MeOH, 0 °C, 8 atm H_2	98.1 (*S*)	25c
(*S*)-HexaPHEMP–Rh	CH_3	*E*	MeOH, rt, 9.5 atm H_2	95 (*R*)	28
2–Rh	CH_3	*E*	MeOH, 0 °C, 17 atm H_2	97.7 (*S*)	30
2–Rh	^iPr	*E*	MeOH, 0 °C, 17 atm H_2	98.8 (*S*)	30
(*R*,*R*)-BICP–Rh	CH_3	*E*	Toluene, rt, 2.7 atm H_2	96.1 (*R*)	49e
(*S*,*S*)-**9**–Rh	CH_3 [a)]	*E*	CH_2Cl_2, rt, 1 atm H_2	94.6 (*R*)	54b
(*S*,*S*)-^{t}Bu-BisP*–Rh	CH_3	*E*	THF, rt, 3 atm H_2	98.7 (*R*)	60
(*S*,*S*)-MiniPhos–Rh	CH_3	*E*	THF, rt, 3 atm H_2	96.4 (*R*)	60
(*R*)-**14**–Rh	CH_3	*E*	MeOH, rt, 1.4 atm H_2	99 (*R*)	71
(*S*,*S*)-**9**–Rh	CH_3 [a)]	*Z*	CH_2Cl_2, rt, 6.8 atm $_{H2}$	95 (*R*)	54b
(*R*)-**14**–Rh	CH_3	*Z*	EtOAc, rt, 1.4 atm H_2	98 (*R*)	71
(*R*)-**14**–Rh	CH_3	*E*/*Z* [b)]	THF, rt, 1.4 atm H_2	98 (*R*)	71

a) Ethyl ester.
b) *E*:*Z* ratio = 1 : 1.

few chiral ligands such as BDPMI [54b] and (*R*)-**14** [71] can provide over 95% ee hydrogenation for hydrogenation of (*Z*)-alkyl (*β*-acylamino) acrylates (Table 26.4). With (*R*)-**14**–Rh catalyst, an *E*/*Z*-isomeric mixtures of methyl 3-acetamido-2-butenoate was hydrogenated in THF to give (*R*)-methyl 3-acetamidobutanoate in 98% ee [71].

By employing a Ru catalyst generated *in situ* from Ru(COD)(methallyl)$_2$, (*S*)-C3-TunePhos, and HBF_4, a series of cyclic *β*-(acylamino) acrylates were hydrogenated with excellent ee-values. As shown in Scheme 26.6, 99% ee was obtained in the hydrogenation of both 2-acetylamino-cyclopent-1-enecarboxylic acid methyl ester and ethyl ester. A heterocyclic *β*-(acylamino) acrylate is also hydrogenated to give the *cis*-product in excellent enantioselectivity (95% ee). Hydrogenation of a cyclohexenyl substrate provided the corresponding *cis* product in 92% ee [20].

26.3.4
Enantioselective Hydrogenation of Enol Esters

Enol esters have a similar structure as enamides. However, in contrast to many highly enantioselective examples on enantioselective hydrogenation of enamides, only a few successful results have been reported for the hydrogenation of

Table 26.5 Enantioselective hydrogenation of enol esters.

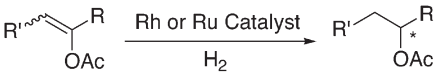

Catalyst	R	R′	Geometry	Reaction conditions	% ee of product (config.)	Reference
(*R*,*R*)-DIPAMP–Rh	CO_2Et	^iPr	*E*/*Z*[a)]	MeOH, rt, 3 atm H_2	92 (*S*)	97
(*R*)-BINAP–Ru	CO_2Et	^iPr	*E*/*Z*[a)]	MeOH, 50 °C, 50 atm H_2	98 (*S*)	97
(*R*,*R*)-DIPAMP–Rh	CO_2Et	Ph	*Z*	MeOH, rt, 3 atm H_2	88 (*S*)	97
(*S*)-C2-TunePhos–Ru	1-Np	H	N/A	EtOH/CH_2Cl_2, rt, 3 atm H_2	97.7 (*S*)	19
2–Rh	1-Np	H	N/A	EtOH/CH_2Cl_2, rt, 3.4 atm H_2	96.7 (*R*)	30
2–Rh	*p*-F-C_6H_4	H	N/A	EtOH/CH_2Cl_2, rt, 3.4 atm H_2	97.1 (*R*)	30

a) *E*:*Z* ratio = 70 : 30.
N/A: not applicable.

enol esters. One possible reason is that the acyl group of an enol ester has a weaker coordinating ability to the metal catalyst than that of the corresponding enamide substrate. Some Rh and Ru complexes associated with chiral phosphorus ligands such as DIPAMP [96,97] and BINAP [97] are effective for the enantioselective hydrogenation of *α*-(acyloxy) acrylates. Some chiral phosphorus ligands such as BINAP [98] and TunePhos [19] have been applied to the Rh- or Ru-catalyzed enantioselective hydrogenation of aryl enol acetates without other functionalities (Table 26.5). C2-TunePhos–Ru [19] and **2**-Ru [30] catalysts are found to be equally effective for this transformation.

Enantioselective hydrogenation of a series of enol phosphates with a ^{t}Bu-MiniPhos–Rh or a ^{t}Bu-BisP*–Rh catalyst provides moderate to excellent ee-values (Scheme 26.7) [99].

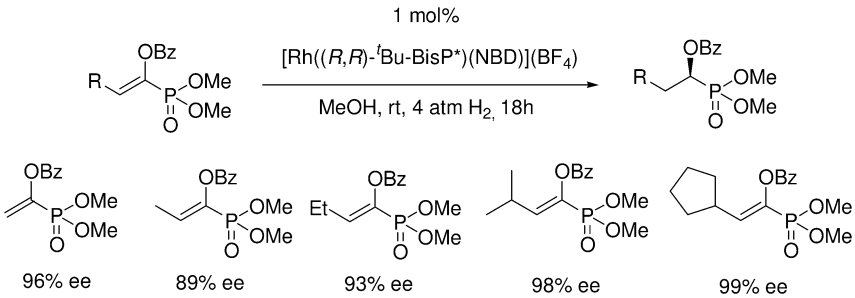

Scheme 26.7

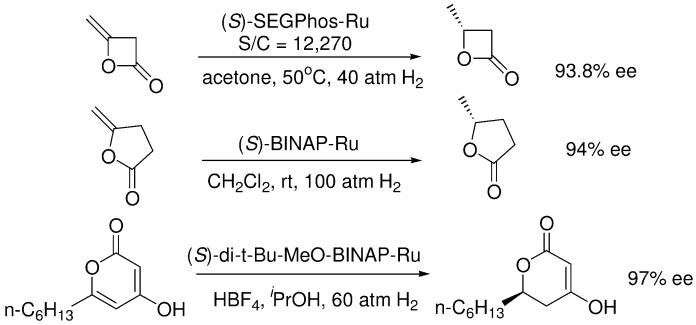

Scheme 26.8

Although high hydrogen pressure is required, BINAP and its analogous ligands gave superior results in the Ru-catalyzed hydrogenation of four- and five-membered cyclic lactones or carbonates bearing an exocyclic methylene group (Scheme 26.8) [98]. A (*S*)-SEGPHOS–Ru catalyst provided 93.8% ee in the hydrogenation of a diketene with high turnover numbers (TONs) [100]. With a (*S*)-BINAP–Ru catalyst, 94% ee was obtained in the hydrogenation of 4-methylene-γ-butyrolactone. In the presence of a small amount of HBF_4, a di-*t*-Bu-MeOBIPHEP–Ru catalyst allows the hydrogenation of a 2-pyrone substrate with 97% ee [101].

26.3.5
Enantioselective Hydrogenation of Unsaturated Acids and Esters

26.3.5.1 *α,β*-Unsaturated Carboxylic Acids

Significant advance has been achieved in the enantiomeric hydrogenation of *α,β*-unsaturated carboxylic acids with chiral Ru catalysts. The Ru–BINAP-dicarboxylate complex has shown excellent enantioselectivities in the hydrogenation of some *α,β*-unsaturated carboxylic acids, although the catalytic efficiencies are still highly sensitive to the substrates, reaction temperature, and hydrogen pressure [3 d]. Other atropisomeric ligands, such as H_8-BINAP [102], MeO-BIPHEP [103], BIPHEMP [103], P-Phos [25], TetraMe-BITIANP [23 b], and TetraMe-BITIOP [24] are also effective for this transformation. Ru complexes prepared in different forms may exhibit slightly different efficiencies. Some examples of the hydrogenation of tiglic acid with different metal–ligand complexes are listed in Table 26.6. The H_8-BINAP ligand with a larger dihedral angle gives superior results compared to the BINAP ligand.

With a BINAP–Ru [3 d,104], H_8-BINAP–Ru [102], or P-Phos–Ru [25] catalyst, the anti-inflammatory drugs (*S*)-ibuprofen and (*S*)-naproxen could be efficiently synthesized via enantioselective hydrogenation (Scheme 26.9). In these cases, high hydrogenation pressure and low temperature are required to achieve good enantioselectivity. With an (*R*)-BIPHEMP–Ru catalyst, (*S*)-2-(4-fluorophenyl)-3-methylbutanoic acid, a key intermediate for the synthesis of the calcium antago-

Table 26.6 Enantioselective hydrogenation of tiglic acid.

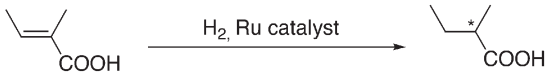

Catalyst	SCR	Reaction conditions	% ee of product (config.)	Reference
$Ru(OAc)_2$[(*R*)-BINAP]	100	MeOH, 15–30 °C, 4 atm H_2	91 (*R*)	3d
Ru[(*R*)-BINAP](2-methallyl)$_2$	100	MeOH, 20 °C, 4 atm H_2	90 (*R*)	103
$Ru(OAc)_2$[(*S*)-H8-BINAP]	200	MeOH, 10–25 °C, 1.5 atm H_2	97 (*S*)	102
[(*R*)-MeO-BIPHEP]$RuBr_2$	100	MeOH, 20 °C, 1.4 atm H_2	92 (*R*)	103
$[NH_2Et_2][\{RuCl[(S)\text{-BIPHEMP}]\}_2(\mu\text{-}Cl)_3]$	100	MeOH, 20 °C, 4 atm H_2	98 (*S*)	103
Ru(*p*-cymene)[(–)-TetraMe-BITIANP]I_2]	500	MeOH, 25 °C, 10 atm H_2	92 (*S*)	23b
[Ru(–)-TetraMe-BITIOP](2-methally)$_2$]	3000	MeOH, 25 °C, 10 atm H_2	94 (*R*)	24

SCR: substrate:catalyst ratio.

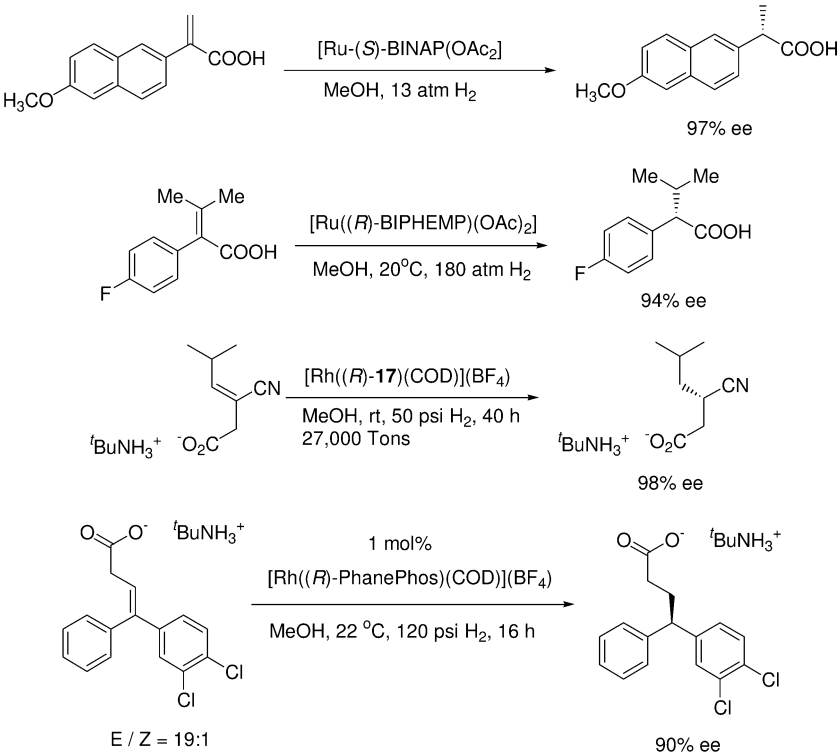

Scheme 26.9

nist mibefradil, could be reduced in 94% ee [105]. Using (*R*)-**14**–Rh as catalyst, enantioselective hydrogenation of *tert*-butylammonium (3*Z*)-3-cyano-5-methyl-3-hexenoate produced the precursor to CI-1008 (pregabalin, indicated for psychotic disorder, seizure disorder and pain) with a TON of 27 000 and 98% ee (Scheme 26.9) [70]. Using PhanePhos–Rh as catalyst, an isomeric mixture (*E*/*Z* = 19:1) of 4,4′-diaryl-3-butenoate was hydrogenated to provide a chiral intermediate for the antidepressant sertraline, with 90% ee (Scheme 26.9) [106].

26.3.5.2 *α,β*-Unsaturated Esters, Amides, Lactones, and Ketones

Limited progress has been achieved in the enantioselective hydrogenation of *α,β*-unsaturated carboxylic acid esters, amides, lactones, and ketones (Scheme 26.10). The Ru–BINAP system is efficient for the hydrogenation of 2-methylene-*γ*-butyrolactone, and 2-methylene-cyclopentanone [98]. With a dicationic (*S*)-di-*t*-Bu-MeOBIPHEP–Ru complex under a high hydrogen pressure, 3-ethoxy pyrrolidinone could be hydrogenated in isopropanol to give (*R*)-4-ethoxy-*γ*-lactam in 98% ee [39].

26.3.5.3 Itaconic Acids and Their Derivatives

Many chiral phosphorus ligands have shown excellent reactivities and enantioselectivities in the Rh-catalyzed hydrogenation of itaconic acids or esters. Some successful (>95% ee) hydrogenations of itaconic acid or its dimethyl ester with different chiral phosphorus ligands are listed in Table 26.7. High reactivity is observed with electron-rich phosphane ligands such as BICHEP [7c].

In contrast to the many successful examples of hydrogenation of the parent itaconic acid or its dimethyl ester, only a few ligands have been reported to be

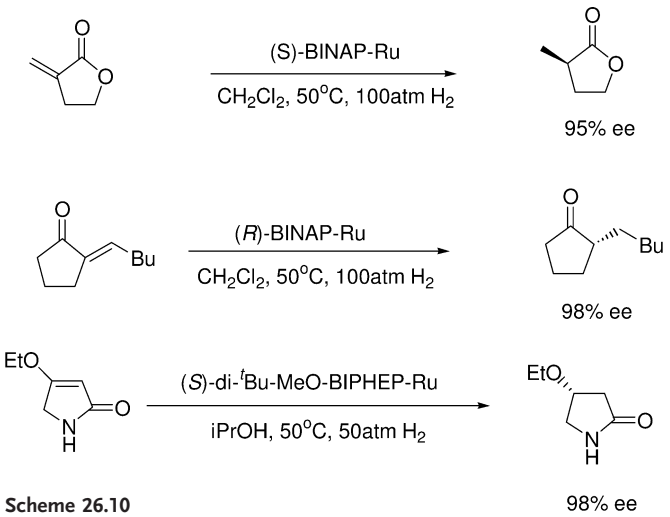

Scheme 26.10

Table 26.7 Enantioselective hydrogenation of itaconic acid derivatives.

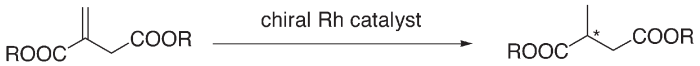

Ligand	R	SCR	Reaction conditions	% ee of product (config.)	Reference
(*R*)-BICHEP	H	1000	EtOH, 25 °C, 1 atm H_2	96 (*R*)	7c
(*S*,*S*)-Ad-BisP*	Me	500	MeOH, rt, 1.6 atm H_2	99.6	58b

SCR: substrate:catalyst ratio.

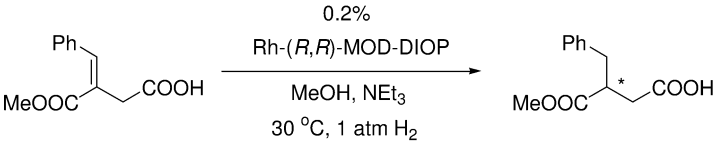

Scheme 26.11

96% ee

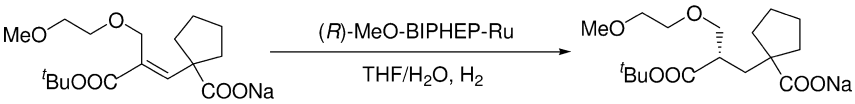

Scheme 26.12

97% ee

efficient for the hydrogenation of β-substituted itaconic acid derivatives. Rh complexed with MOD-DIOP [48] is efficient for the hydrogenation of several β-substituted itaconic acid derivatives (Scheme 26.11).

A PYRPHOS ligand was found to be effective for the hydrogenation of a β-aryl- or alkyl-substituted monoamido itaconate [107]. A MeO-BIPHEP–Ru catalyst was successfully applied for the enantioselective hydrogenation of an intermediate for the drug candoxatril in a mixed solvent (THF/H_2O) (Scheme 26.12) [108].

26.3.6
Enantioselective Hydrogenation of Unsaturated Alcohols

Enantioselective hydrogenation of unsaturated alcohols such as allylic and homoallylic alcohols was not very efficient until the discovery of the BINAP–Ru catalyst. With Ru(BINAP)$(OAc)_2$ as the catalyst, geraniol and nerol are successfully hydrogenated to give (*S*)- or (*R*)-citronellol in near-quantitative yield and with 96–99% ee [3c]. A substrate:catalyst ratio (SCR) of up to 48 500 can be applied, and the other double bond at the C6 and C7 positions of the substrate is not reduced. A high hydrogen pressure is required to obtain high enantioselec-

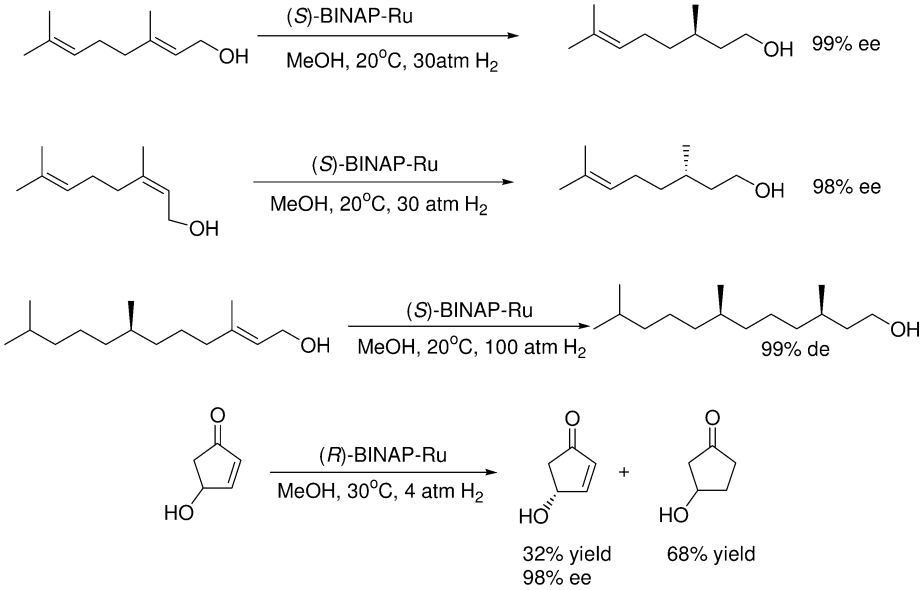

Scheme 26.13

tivity in the hydrogenation of geraniol. Low hydrogen pressure facilitates the isomerization of geraniol to γ-geraniol, which leads to the hydrogenation product with the opposite configuration, resulting in a decreased ee-value [109]. In addition to BINAP, other chiral atropisomeric ligands such as MeO-BIPHEP [9], TetraMe-BITIANP [23b], and TetraMe-BITIOP [24] are also effective for this transformation. The catalytic efficiency of the BINAP–Ru catalyst is strongly sensitive to the substitution patterns of the allylic alcohols. Homoallylic alcohols can also be hydrogenated in high ee-value with the BINAP–Ru catalyst. Its application in the synthesis of (3*R*, 7*R*)-3,7,11-trimethyldodecarol, an intermediate for the synthesis of α-tocopherol, is shown in Scheme 26.13. When racemic

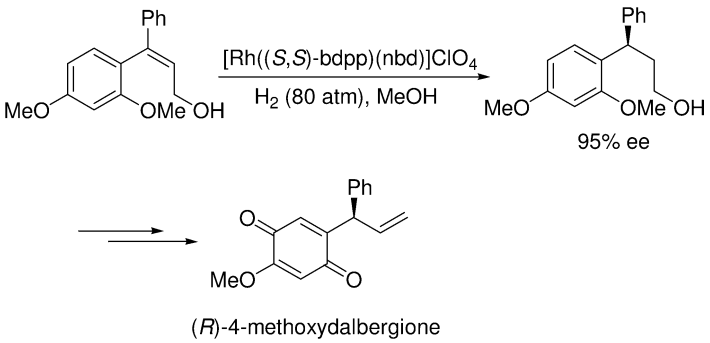

Scheme 26.14

allylic alcohols were subjected to enantioselective hydrogenation with a BINAP–Ru complex, highly efficient kinetic resolutions were achieved [4c]. A racemic 4-hydroxy-2-cyclopentenone was hydrogenated with a (*S*)-BINAP–Ru catalyst to leave unreacted starting material in 98% ee at 68% conversion. The chiral starting material serves as an important building block for three-component coupling prostaglandin synthesis.

A chiral BDPP–Rh complex is an efficient catalyst for the hydrogenation of 3-(2′,4′-dimethoxyphenyl)-3-phenyl-2-propenol. The chiral alcohol product, which was obtained in up to 95% ee, has been used for the synthesis of chiral 4-methoxydalbergione (Scheme 26.14) [110].

26.4 Concluding Remarks

The development of chiral phosphorus ligands has undoubtedly had an enormous impact on the area of enantioselective hydrogenation. Transition-metal catalysts with efficient chiral phosphorus ligands have enabled the synthesis of a variety of chiral products in a very efficient manner, and many practical hydrogenation processes have been exploited in industry for the synthesis of chiral drugs and fine chemicals. However, many challenges remain in the field of enantioselective hydrogenation, and further effort in the quest for new efficient chiral phosphorus ligands, as well as new applications in enantioselective hydrogenation, are needed.

References

1 Miyashita, A., Yasuda, A., Takaya, H., Toriumi, K., Ito, T., Souchi, T., Noyori, R. *J. Am. Chem. Soc.* **1980**, *102*, 7932.

2 Miyashita, A., Takaya, H., Souchi, T., Noyori, R. *Tetrahedron* **1984**, *40*, 1245.

3 (a) Noyori, R., Ohta, M., Hsiao, Y., Kitamura, M., Ohta, T., Takaya, H. *J. Am. Chem. Soc.* **1986**, *108*, 7117; (b) Hitamura, M., Hsiao, Y., Noyori, R., Takaya, H. *Tetrahedron Lett.* **1987**, *28*, 4829; (c) Takaya, H., Ohta, T., Sayo, N., Kumobayashi, H., Akutagawa, S., Inoue, S.-I., Kasahara, I., Noyori, R. *J. Am. Chem. Soc.* **1987**, *109*, 1596; (d) Ohta, T., Takaya, H., Kitamura, M., Nagai, K., Noyori, R. *J. Org. Chem.* **1987**, *52*, 3174.

4 (a) Noyori, R., Ohkuma, T., Kitamura, M., Takaya, H., Sayo, N., Kumobayashi, H., Akutagawa, S. *J. Am. Chem. Soc.* **1987**, *109*, 5856; (b) Kitamura, M., Ohkuma, T., Inoue, S., Sayo, N., Kumobayashi, H., Akutagawa, S., Ohta, T., Takaya, H., Noyori, R. *J. Am. Chem. Soc.* **1988**, *110*, 629; (c) Kitamura, M., Kasahara, I., Manabe, K., Noyori, R., Takaya, H. *J. Org. Chem.* **1988**, *53*, 708; (d) Noyori, R., Ikeda, T., Ohkuma, T., Widhalm, M., Kitamura, M., Takaya, H., Akutagawa, S., Sayo, N., Saito, T., Taketomi, T., Kumobayashi, H. *J. Am. Chem. Soc.* **1989**, *111*, 9134.

5 Ohkuma, T., Ooka, H., Hashiguchi, S., Ikariya, T., Noyori, R. *J. Am. Chem. Soc.* **1995**, *117*, 2675.

6 Ohkuma, T., Ooka, H., Ikariya, T., Noyori, R. *J. Am. Chem. Soc.* **1995**, *117*, 10417.

7 (a) Miyashita, A., Karino, H., Shimamura, J., Chiba, T., Nagano, K., Nohira, H., Takaya, H. *Chem. Lett.* **1989**, 1007;

(b) Miyashita, A., Karino, H., Shimamura, J., Chiba, T., Nagano, K., Nohira, H., Takaya, H. *Chem. Lett.* **1989**, 1849; (c) Chiba, T., Miyashita, A., Nohira, H. *Tetrahedron Lett.* **1991**, *32*, 4745; (d) Chiba, T., Miyashita, A., Nohira, H., Takaya H. *Tetrahedron Lett.* **1993**, *34*, 2351.

8 Schmid, R., Cereghetti, M., Heiser, B., Schönholzer, P., Hansen, H.-J. *Helv. Chim. Acta* **1988**, *71*, 897.

9 Schmid, R., Foricher, J., Cereghetti, M., Schönholzer, P. *Helv. Chim. Acta.* **1991**, *74*, 870.

10 Yamamoto, N., Murata, M., Morimoto, T., Achiwa, K. *Chem. Pharm. Bull.* **1991**, *39*, 1085.

11 Murata, M., Morimoto, T., Achiwa, K. *Synlett* **1991**, 827.

12 Yoshikawa, K., Yamamoto, N., Murata, M., Awano, K., Morimoto, T., Achiwa, K. *Tetrahedron: Asymmetry* **1992**, *3*, 13.

13 (a) Zhang, X., Mashima, K., Koyano, K., Sayo, N., Kumobayashi, H., Akutagawa, S., Takaya, H. *Tetrahedron Lett.* **1991**, *32*, 7283; (b) Zhang, X., Mashima, K., Koyano, K., Sayo, N., Kumobayashi, H., Akutagawa, S., Takaya, H. *J. Chem. Soc., Perkin Trans. 1* **1994**, 2309.

14 Enev, V., Ewers, Ch. L.J., Harre, M., Nickisch, K., Mohr, J.T. *J. Org. Chem.* **1997**, *62*, 7092.

15 Sollewijn Gelpke A.E., Kooijman, H., Spek, A.L., Hiemstra, H. *Chem. Eur. J.* **1999**, *5*, 2472.

16 (a) Saito, T., Yokozawa, T., Zhang, X., Sayo, N. (Takasago International Corporation), U.S. Patent 5 872 273, **1999**; (b) Saito, T., Yokozawa, T., Ishizaki, T., Moroi, T., Sayo, N., Miura, T., Kumobayashi, H. *Adv. Synth. Catal.* **2001**, *343*, 264.

17 (a) Pai, C.-C., Li, Y.-M., Zhou, Z.-Y., Chan, A.S.C. *Tetrahedron Lett.* **2002**, *43*, 2789; (b) de Paule, S.D., Jeulin, S., Ratovelomanana-Vidal, V., Genêt, J.P., Champion, N., Dellis, P. *Tetrahedron Lett.* **2003**, *44*, 823; (c) de Paule, S.D., Jeulin, S., Ratovelomanana-Vidal, V., Genêt, J.P., Champion, N., Dellis, P. *Eur. J. Org. Chem.* **2003**, 1931.

18 Zhang, Z., Qian, H., Longmire, J., Zhang, X. *J. Org. Chem.* **2000**, *65*, 6223.

19 Wu, S., Wang, W., Tang, W., Lin, M., Zhang, X. *Org. Lett.* **2002**, *4*, 4495.

20 Tang, W., Wu, S., Zhang, X *J. Am. Chem. Soc.* **2003**, *125*, 9570.

21 Lei, A., Wu, S., He, M., Zhang, X. *J. Am. Chem. Soc.* **2004**, *126*, 1626.

22 Michaud, G., Bulliard, M., Ricard, L., Genêt, J.-P., Marinetti, A. *Chem. Eur. J.* **2002**, *8*, 3327.

23 (a) Benincori, T., Brenna, E., Sannicolò, F., Trimarco, L., Antognazza, P., Cesarotti, E. *J. Chem. Soc., Chem. Commun.* **1995**, 685; (b) Benincori, T., Brenna, E., Sannicol, F., Trimarco, L., Antognazza, P., Cesarotti, E. Demartin, F., Pilati, T. *J. Org. Chem.* **1996**, *61*, 6244; (c) Benincori, T., Rizzo, S., Pilati, T., Ponti, A., Sada, M., Pagliarini, E., Ratti, S., Giuseppe, C., de Ferra, L., Sannicolò, F. *Tetrahedron: Asymmetry* **2004**, *15*, 2289.

24 Benincori, T., Cesarotti, E., Piccolo, O., Sannicolò, F. *J. Org. Chem.* **2000**, *65*, 2043.

25 (a) Pai C.-C., Lin, C.-W., Lin, C.-C., Chen, C.-C., Chan, A.S.C. *J. Am. Chem. Soc.* **2000**, *122*, 11513; (b) Wu, J., Chen, H., Kwok, W.H., Lam, K.H., Zhou, Z.Y., Yeung, C.H., Chan, A.S.C. *Tetrahedron Lett.* **2002**, *43*, 1539; (c) Wu, J., Pai C.C., Kwok, W.H., Guo, R.W., Au-Yeung, T.T.L., Yeung, C.H., Chan, A.S.C. *Tetrahedron: Asymmetry* **2003**, *14*, 987; (d) Wu, J., Ji, J.-X., Guo, R., Yeung, C.-H., Chan, A.S.C. *Chem. Eur. J.* **2003**, *9*, 2963.

26 Tang, W., Chi, Y., Zhang, X. *Org. Lett.* **2002**, *4*, 1695.

27 Wu, S., He, M., Zhang, X. *Tetrahedron: Asymmetry* **2004**, *15*, 2177.

28 Henschke, J.P., Burk, M.J., Malan, C.G., Herzberg, D., Peterson, J.A., Wildsmith, A.J., Cobley, C.J., Casy, G. *Adv. Synth. Catal.* **2003**, *345*, 300.

29 Jeulin, S., de Paule, S.D., Ratovelomanana-Vidal, V., Genêt, J.P., Champion, N., Dellis, P. *Angew. Chem. Int. Ed. Engl.* **2004**, *43*, 320.

30 Qiu, L., Wu, J., Chan, S., Au-Yeung, T.T.-L., Ji, J.-X., Guo, R., Pai, C.-C., Zhou, Z., Li, X., Fan, Q., Chan, A.S.C. *Proc. Natl. Acad Sci. USA* **2004**, *101*, 5815.

31 Henschke, J.P., Zanotti-Gerosa, A., Moran, P., Harrison, P., Mullen, B., Casy,

G., Lennon, I.C. *Tetrahedron Lett.* **2003**, *44*, 4379.
32 Hu, A., Ngo, H.L., Lin, W. *Angew. Chem. Int. Ed. Engl.* **2004**, *43*, 2501.
33 Hu, A., Lin, W. *Org. Lett.* **2005**, *7*, 455.
34 Berthod, M., Saluzzo, C., Mignani, G., Lemaire, M. *Tetrahedron: Asymmetry* **2004**, *15*, 639.
35 Berthod, M., Mignani, G., Lemaire, M. *Tetrahedron: Asymmetry* **2004**, *15*, 1121.
36 Aikawa, K., Mikami, K. *Angew. Chem. Int. Ed. Engl.* **2003**, *42*, 5455.
37 Saluzzo, C., Lemaire, M. *Adv. Synth. Catal.* **2002**, *344*, 915.
38 (a) Wan, K.T., Davis, M.E. *J. Chem. Soc., Chem. Commun.* **1993**, 1262; (b) Wan, K.T., Davis, M.E. *Tetrahedron: Asymmetry* **1993**, *4*, 2461; (c) Wan, K.T., Davies, M.E. *J. Catalysis* **1994**, *148*, 1.
39 Schmid, R., Broger, E.A., Cereghetti, M., Crameri, Y., Foricher, J., Lalonde, M., Müller, R.K., Scalone, M., Schoettel, G., Zutter, U. *Pure Appl. Chem.* **1996**, *68*, 131.
40 Guerreiro, P., Ratovelomanana-Vidal, V., Genêt, J.-P., Dellis, P. *Tetrahedron Lett.* **2001**, *42*, 3423.
41 Bayston, D.J., Fraser, J.L., Ashton, M.R., Baxter, A.D., Polywka, M.E.C., Moses, E. *J. Org. Chem.* **1998**, *63*, 3137.
42 Ohkuma, T., Takeno, H., Honda, Y., Noyori, R. *Adv. Synth. Catal.* **2001**, *343*, 369.
43 (a) Fan, Q.-H., Deng, G.-J., Lin, C.-C., Chan, A.S.C. *J. Am. Chem. Soc.* **1999**, *121*, 7407; (b) Fan, Q.-H., Ren, C.-Y., Yeung, C.-H., Hu, W.-H., Chan, A.S.C. *Tetrahedron: Asymmetry* **2001**, *12*, 1241.
44 Fan, Q.-H., Chen, Y.-M., Chen, X.-M., Jiang, D.-Z., Xi, F., Chan, A.S.C. *Chem. Commun.* **2000**, 789.
45 (a) Yu, H.-B., Hu, Q.-S., Pu, L. *Tetrahedron Lett.* **2000**, *41*, 1681; (b) Yu, H.-B., Hu, Q.-S., Pu, L. *J. Am. Chem. Soc.* **2000**, *122*, 6500.
46 a) Lemaire, M., Halle, R. ter, Schulz, E., Colasson, B., Spagnol, M. (CNRS-Rhodia), *Fr. Patent* 99 02119, **1999**; (b) Lemaire, M., Halle, R. ter, Schulz, E., Colasson, B., Spagno, M., Saluzzo, C., Lamouille, T. (CNRS-Rhodia), *Fr. Patent* 99 02510, **1999**; PCT Int. Appl. 2000, WO 0052081.
47 (a) Kagan, H.B., Dang, T.P. *Chem. Commun.* **1971**, 481; (b) Kagan, H.B., Dang, T.P. *J. Am. Chem. Soc.* **1972**, *94*, 6429; (c) Kagan, H.B., Langlois, N., Dang, T.P. *J. Organomet. Chem.* **1975**, *90*, 353.
48 (a) Chiba, M., Takahashi, H., Takahashi, H., Morimoto, T., Achiwa, K. *Tetrahedron Lett.* **1987**, *28*, 3675; (b) Morimoto, T., Chiba, M., Achiwa, K. *Tetrahedron Lett.* **1988**, *29*, 4755; (c) Morimoto, T., Chiba, M., Achiwa, K. *Tetrahedron Lett.* **1989**, *30*, 735; (d) Morimoto, T., Chiba, M., Achiwa, K. *Chem. Pharm. Bull.* **1989**, *37*, 3161; (e) Morimoto, T., Chiba, M., Achiwa, K. *Heterocycles* **1990**, *30*, 363; (f) Morimoto, T., Chiba, M., Achiwa, K. *Tetrahedron Lett.* **1990**, *31*, 261; (g) Yoshikawa, K., Inoguchi, K., Morimoto, T., Achiwa, K. *Heterocycles*, **1990**, *31*, 261; (h) Morimoto, T., Chiba, M., Achiwa, K. *Chem. Pharm. Bull.* **1993**, *41*, 1149.
49 (a) Zhu, G., Cao, P., Jiang, Q., Zhang, X. *J. Am. Chem. Soc.* **1997**, *119*, 1799; (b) Zhu, G., Zhang, X. *J. Org. Chem.* **1998**, *63*, 9590; (c) Zhu, G., Casalnuovo, A.L., Zhang, X. *J. Org. Chem.* **1998**, *63*, 8100; (d) Zhu, G., Zhang, X. *Tetrahedron: Asymmetry* **1998**, *9*, 2415; (e) Zhu, G., Chen, Z., Zhang, X. *J. Org. Chem.* **1999**, *64*, 6907; (f) Cao, P., Zhang, X. *J. Org. Chem.* **1999**, *64*, 2127.
50 Genov, D.G., Ager, D. *Angew. Chem. Int. Ed. Engl.* **2004**, *43*, 2816.
51 (a) Li, W., Zhang, X. *J. Org. Chem.* **2000**, *65*, 5871; (b) Liu, D., Li, W., Zhang, X. *Tetrahedron: Asymmetry* **2004**, *15*, 2181.
52 (a) Yan, Y.-Y., RajanBabu, T.V. *J. Org. Chem.* **2000**, *65*, 900; (b) Yan, Y.-Y., RajanBabu, T.V. *Org. Lett.* **2000**, *2*, 199; (c) Yan, Y.-Y., RajanBabu, T.V. *Org. Lett.* **2000**, *2*, 4137.
53 Kagan, H.B., Fiaud, J.C., Hoornaert, C., Meyer, D., Poulin, J.C. *Bull. Soc. Chim, Belg.* **1979**, *88*, 923.
54 (a) Lee, S.-g., Zhang, Y.J., Song, C.E., Lee, J.K., Choi, J.H. *Angew. Chem. Int. Ed.* **2002**, *41*, 847; (b) Lee, S.-g., Zhang, Y.J. *Org. Lett.* **2002**, *4*, 2429; (c) Lee, S.-g., Zhang, Y.J. *Tetrahedron: Asymmetry* **2002**, *13*, 1039.
55 Li, W., Waldkirch, J.P., Zhang, X. *J. Org. Chem.* **2002**, 7618.

56 (a) Vineyard, B.D., Knowles, W.S., Sabacky, M.J., Bachman, G.L., Weinkauff, O.J. *J. Am. Chem. Soc.* **1977**, *99*, 5946; (b) Knowles, W.S. *Acc. Chem. Res.* **1983**, *16*, 106.

57 Knowles, W.S. *J. Chem. Educ.* **1986**, *63*, 222.

58 (a) Imamoto, T., Watanabe, J., Wada, Y., Masuda, H., Yamada, H., Tsuruta, H., Matsukawa, S., Yamaguchi, K. *J. Am. Chem. Soc.* **1998**, *120*, 1635; (b) Gridnev, I.D., Yamanoi, Y., Higashi, N., Tsuruta, H., Yasutake, M., Imamoto, T. *Adv. Synth. Catal.* **2001**, *343*, 118.

59 Gridnev, I.D., Yasutake, M., Higashi, N., Imamoto, T. *J. Am. Chem. Soc.* **2001**, *123*, 5268.

60 Yasutake, M., Gridnev, I.D., Higashi, N., Imamoto, T. *Org. Lett.* **2001**, *3*, 1701.

61 Gridnev, I.D., Higashi, N., Imamoto, T. *J. Am. Chem. Soc.* **2001**, *123*, 4631.

62. (a) Gridnev, I.D., Higashi, N., Asakura, K., Imamoto, T. *J. Am. Chem. Soc.* **2000**, *122*, 7183; (b) Gridnev, I.D., Higashi, N., Imamoto, T. *J. Am. Chem. Soc.* **2000**, *122*, 10486; (c) Gridnev, I.D., Imamoto, T. *Organometallics* **2001**, *20*, 545.

63 (a) Halpern, J., Riley, D.P., Chan, A.S.C., Pluth, J.J. *J. Am. Chem. Soc.* **1977**, *99*, 8055; (b) Chan, A.S.C., Halpern, J. *J. Am. Chem. Soc.* **1980**, *102*, 838; (c) Chan, A.S.C., Pluth, J.J., Halpern, J. *J. Am. Chem. Soc.* **1980**, *102*, 5952; (d) Halpern, J. *Science* **1982**, *217*, 401; (e) Landis, C.R., Halpern, J. *J. Am. Chem. Soc.* **1987**, *109*, 1746; (f) Ashby, M.T., Halpern, J. *J. Am. Chem. Soc.* **1991**, *113*, 589.

64 (a) Brown, J.M., Chaloner, P.A. *J. Chem. Soc., Chem. Commun.* **1978**, 321; (b) Brown, J.M., Chaloner, P.A. *Tetrahedron Lett.* **1978**, *19*, 1877; (c) Brown, J.M., Chaloner, P.A. *J. Chem. Soc., Chem. Commun.* **1979**, 613; (d) Brown, J.M., Chaloner, P.A. *J. Chem. Soc., Chem. Commun.* **1980**, 344; (e) Brown, J.M., Chaloner, P.A., Glaser, R., Geresh, S. *Tetrahedron* **1980**, *36*, 815; (f) Alcock, N.W., Brown, J.M., Derome, A., Lucy, A.R. *J. Chem. Soc., Chem. Commun.* **1985**, 575; (g) Brown, J.M., Chaloner, P.A., Morris, G.A. *J. Chem. Soc., Perkin Trans.* 2, **1987**, 1583; (h) Brown, J.M. *Chem. Soc. Rev.* **1993**, *22*, 25.

65 Yamanoi, Y., Imamoto, T. *J. Org. Chem.* **1999**, *64*, 2988.

66 Miura, T., Imamoto, T. *Tetrahedron Lett.* **1999**, *40*, 4833.

67 (a) Ohashi, A., Imamoto, T. *Org. Lett.* **2001**, *3*, 373; (b) Ohashi, A., Kikuchi, S.-I., Yasutake, M., Imamoto, T. *Eur. J. Org. Chem.* **2002**, 2535.

68 Danjo, H., Sasaki, W., Miyazaki, T., Imamoto, T. *Tetrahedron Lett.* **2003**, *44*, 3467.

69 (a) Robin, F., Mercier, F., Ricard, L., Mathey, F., Spagnol, M. *Chem. Eur. J.* **1997**, *3*, 1365; (b) Mathey, F., Mercier, F., Robin, F., Ricard, L. *J. Organometallic Chem.* **1998**, *577*, 117.

70 Hoge, G., Wu, H.-P., Kissel, W.S., Pflum, D.A., Greene, D.J., Bao, J. *J. Am. Chem. Soc.* **2004**, *126*, 5966.

71 Wu, H.-P., Hoge, G. *Org. Lett.* **2004**, *6*, 3645.

72. (a) Fryzuk, M.B., Bosnich, B. *J. Am. Chem. Soc.* **1977**, *99*, 6262; (b) Fryzuk, M.B., Bosnich, B. *J. Am. Chem. Soc.* **1979**, *101*, 3043.

73 Fryzuk, M.D., Bosnich, B. *J. Am. Chem. Soc.* **1978**, *100*, 5491.

74 Achima, K. *J. Am. Chem. Soc.* **1976**, *98*, 8265.

75 (a) Phone Poulenc S.A. *Fr. Patent* 2230654, **1974**; (b) Glaser, R., Geresh, S., Twaik, M. *Isr. J. Chem.* **1980**, *20*, 102.

76 (a) Takahashi, H., Hattori, M., Chiba, M., Morimoto, T., Achiwa, K. *Tetrahedron Lett.* **1986**, *27*, 4477; (b) Takahashi, H., Morimoto, T., Achiwa, K. *Chem. Lett.* **1987**, 855; (c) Takahashi, H., Achiwa, K. *Chem. Lett.* **1987**, 1921; (d) Inoguchi, K., Morimoto, T., Achiwa, K. *J. Organomet. Chem.* **1989**, *370*, C9; (e) Takahashi, H., Yamamoto, N., Takeda, H., Achiwa, K. *Chem. Lett.* **1989**, 559; (f) Takahashi, H., Sakuraba, S., Takeda, H., Achiwa, K. *J. Am. Chem. Soc.* **1990**, *112*, 5876; (g) Takeda, H., Hosokawa, S., Aburatani, M., Achiwa, K. *Synlett*, **1991**, 193; (h) Sakuraba, S., Achiwa, K. *Synlett* **1991**, 689; (i) Sakuraba, S., Nakajima, N., Achiwa, K. *Synlett* **1992**, 829; (j) Sakuraba, S., Nakajima, N., Achiwa, K. *Tetrahedron: Asymmetry* **1993**, *7*, 1457; (k) Sakuraba, S., Takahashi, H., Takeda, H., Achiwa, K. *Chem. Pharm. Bull.* **1995**, *43*, 738.

77 Brunner, H., Pieronczyk, W., Schönhammer, B., Streng, K., Bernal, I., Korp, J. *Chem. Ber.* **1981**, *114*, 1137.

78 (a) Nagel, U. *Angew. Chem. Int. Ed.* **1984**, *23*, 435; (b) Nagel, U., Kinzel, E., Andrade, J., Prescher, G. *Chem. Ber.* **1986**, *119*, 3326; (c) Inoguchi, K., Achiwa, K. *Chem. Pharm. Bull.* **1990**. *38*, 818.

79 Allen, D.L., Gibson, V.C., Green, M.L.H., Skinner, J.F., Bashkin, J., Grebenik, P.D. *J. Chem. Soc., Chem. Commun.* **1983**, 895.

80 (a) Bakos, J., Toth, I., Markó, L. *J. Org. Chem.* **1981**, *46*, 5427; (b) NacNeil, P.A., Roberts, N.K., Bosnich, B. *J. Am. Chem. Soc.* **1981**, *103*, 2273; (c) Bakos, J., Tóth, I., Heil, B., Markó, L. *J. Organomet. Chem.* **1985**, *279*, 23.

81 Inoguchi, K., Achiwa, K. *Synlett* **1991**, 49.

82 (a) Pye, P.J., Rossen, K., Reamer, R.A., Tsou, N.N., Volante, R.P., Reider, P.J. *J. Am. Chem. Soc.* **1997**, *119*, 6207; (b) Pye, P.J., Rossen, K., Reamer, R.A., Volante, R.P., Reider, P.J. *Tetrahedron Lett.* **1998**, *39*, 4441; (c) Burk, M.J., Hems, W., Herzberg, D., Malan, C., Zanotti-Gerosa, A. *Org. Lett.* **2000**, *2*, 4173.

83 Zhou, Y.-G., Zhang, X. *Chem. Commun.* **2002**, 1124.

84 Morimoto, T., Yamazaki, A., Achiwa, K. *Chem. Pharm. Bull.* **2004**, *52*, 1367.

85 Xie, J.-H., Wang, L.-X., Fu, Y., Zhu, S.-F., Fan, B.-M., Duan, H.-F., Zhou, Q.-L. *J. Am. Chem. Soc.* **2003**, *125*, 4404.

86 (a) Scott, J.W., Kieth, D.D., Nix, G., Jr., Parrish, D.R., Remington, S., Roth, G.P., Townsend, J.M., Valentine, D., Jr., Yang, R. *J. Org. Chem.* **1981**, *46*, 5086; (b) Vineyard, B.D., Knowles, W.S., Sabacky, M.J., Bachman, G.L., Weinkauff, D.J. *J. Am. Chem. Soc.* **1977**, *99*, 5946.

87 Doi, T., Kokubo, M., Yamamoto, K., Takahashi, T. *J. Org. Chem.* **1998**, *63*, 428.

88 Adamczyk, M., Akireddy, S.R., Reddy, R.E. *Tetrahedron* **2002**, *58*, 6951.

89 Rossen, K., Weissman, S.A., Sager, J., Reamer, R.A., Askin, D., Valante, R.P., Reider, P.J. *Tetrahedron Lett.* **1995**, *36*, 6419.

90 Mechanistic study via a computational approach, see: Feldgus, S., Landis, C.R. *Organometallics* **2001**, *20*, 2374.

91 Kitamura, M., Hsiao, Y., Ohta, M., Tsukamoto, M., Ohta, T., Takaya, H., Noyori, R. *J. Org. Chem.* **1994**, *59*, 297.

92 Tschaen, D.M., Abramson, L., Cai, D., Desmond, R., Dolling, U.-H., Frey, L., Karady, S., Shi, Y.-J., Verhoeven, T.R. *J. Org. Chem.* **1995**, *60*, 4324.

93 Renaud, J.L., Dupau, P., Hay, A.-E., Guingouain , M., Dixneuf, P.H., Bruneau, C. *Adv. Synth. Catal.* **2003**, *345*, 230.

94 (a) Tang, T., Ellman, J.A. *J. Org. Chem.* **1999**, *64*, 12; (b) Sibi, M.P., Shay, H.J., Liu, M., Jasperse, C.P. *J. Am. Chem. Soc.* **1998**, *120*, 6615; (c) Kobayashi, S., Ishitani, H., Ueno, M. *J. Am. Chem. Soc.* **1998**, *120*, 431; (d) Boesch, H., Cesco-Cancian, S., Hecker, L.R., Hoekstra, W.J., Justus, M., Maryanoff, C.A., Scott, L., Shah, R.D., Solms, G., Sorgi, K.L., Stefanick, S.M., Thurnheer, U., Villani, F.J., Jr., Walker, D.G. *Org. Process Res. Dev.* **2001**, *5*, 23; (e) Hoekstra, W.J., Maryanoff, B.E., Damiano, B.P., Andrade-Gordon, P., Cohen, J.H., Costanzo, M.J., Haertlein, B.J., Hecker, L.R., Hulshizer, B.L., Kauffman, J.A., Keane, P., McComsey, D.F., Mitchell, J.A., Scott, L., Shah, R.D., Yabut, S.C. *J. Med. Chem.* **1999**, *42*, 5254; (f) Zhong, H.M., Cohen, J.H., Abdel-Magid, A.F., Kenney, B.D., Maryanoff, C.A., Shah, R.D., Villani, F.J., Jr., Zhang, F., Zhang, X. *Tetrahedron Lett.* **1999**, *40*, 7721; (g) Shankar, B.B., Kirkup, M.P., McCombie, S.W., Clader, J.W., Ganguly, A.K. *Tetrahedron Lett.* **1996**, *37*, 4095; (h) Burnett, D.A., Caplen, M.A., Davis, H.R., Jr., Burrier, R.E., Clader, J.W. *J. Med. Chem.* **1994**, *59*, 1733.

95 Lubell, W.D., Kitamura, M., Noyori, R. *Tetrahedron: Asymmetry* **1991**, *2*, 543.

96 Koenig, K.E., Bachman, G.L., Vineyard, B.D. *J. Org. Chem.* **1980**, *45*, 2362.

97 Schmidt, U., Langner, J., Kirschbaum, B., Braun, C. *Synthesis* **1994**, 1138.

98 Ohta, T., Miyake, T., Seido, N., Kumobayashi, H., Takaya, H. *J. Org. Chem.* **1995**, *60*, 357.

99 Gridnev, I.D., Yasutake, M., Imamoto, T., Beletskaya, I.P. *Proc. Natl. Acad. Sci. USA* **2004**, *101*, 5385.

100 Saito, T., Yokozawa, T., Ishizaki, T., Moroi, T., Sumi, K., Sayo, N. *Chirasource 2000*, Lisbon, Portugal, October 2, **2000**.

101 Fehr, M. J., Consiglio, G., Scalone, M., Schmid, R. *J. Org. Chem.* **1999**, *64*, 5768.

102 (a) Zhang, X., Uemura, T., Matsumura, K., Sayo, N., Kumobayashi, H., Takaya, H. *Synlett* **1994**, 501; (b) Uemura, T., Zhang, X., Matsumura, K., Sayo, N., Kumobayashi, H., Ohta, T., Nozaki, K., Takaya, H. *J. Org. Chem.* **1996**, *61*, 5510.

103 Genêt, J. P., Pinel, C., Ratovelomanana-Vidal, V., Mallart, S., Pfister, X., Bischoff, L., Cano De Andrade, M.C., Darses, S., Galopin, C., Laffitte, J. A. *Tetrahedron: Asymmetry* **1994**, *5*, 675.

104 Manimaran, T., Wu, T.-C., Klobucar, W. D., Kolich, C. H., Stahly, G. P. *Organometallics* **1993**, *12*, 1467.

105 Crameri, Y., Foricher, J., Scalone, M., Schmid, R. *Tetrahedron: Asymmetry* **1997**, *8*, 3617.

106 Boulton, L.T., Lennon, I. C., McCague, R. *Org. Biomol. Chem.* **2003**, *1*, 1094.

107 Jendralla, H., Henning, R., Seuring, B., Herchen, J., Kulitzscher, B., Wunner, J. *Synlett* **1993**, 155.

108 Bulliard, M., Laboue, B., Lastennet, J., Roussiasse, S. *Org. Proc. Res. Dev.* **2001**, *5*, 438.

109 (a) Sun, Y., LeBlond, C., Wang, J., Blackmond, D. G. *J. Am. Chem. Soc.* **1995**, *117*, 12647; (b) Sun, Y., Landau, R. N., Wang, J., LeBlond, C., Blackmond, D. G. *J. Am. Chem. Soc.* **1996**, *118*, 1348; (c) Sun, Y., Wang, J., LeBlond, C., Landau, R. N., Blackmond, D. G. *J. Catal.* **1996**, *161*, 756.

110 (a) Bissel, P., Sablong, R., Lepoittevin, J.-P. *Tetrahedron: Asymmetry* **1995**, *6*, 835; (b) Bissel, P., Nazih, A., Sablong, R., Lepoittevin, J.-P. *Org. Lett.* **1999**, *1*, 1283.

27
Bidentate Ligands Containing a Heteroatom–Phosphorus Bond

Stanton H. L. Kok, Terry T.-L. Au-Yeung, Hong Yee Cheung, Wing Sze Lam, Shu Sun Chan, and Albert S. C. Chan

27.1
Introduction

Bidentate phosphorus ligands containing one or more heteroatom-phosphorus bonds are of high interest because they are relatively easy to prepare, and because a huge multitude of inexpensive, commercially available chiral diols, diamines, amino alcohols and amino acids can serve as the scaffold. Although the heteroatoms in these scaffolds are usually electronegative in nature, the reactivity and enantioselectivity of the metal complexes based on some of these ligands are quite remarkable, and sometimes even surpass those of the complexes based on electron-rich phosphines. This chapter compiles the comprehensive data concerning the asymmetric hydrogenation of various prochiral olefins mediated by the rhodium(I) complexes of this class of chiral ligands.

27.2
Aminophosphine-Phosphinites (AMPPs)

The ease of synthesis from chiral amino alcohols with a wide array of derivatives in one step established its good potential in the field of asymmetric catalysis. The general preparation of "semi-symmetrical" AMPPs involves the nucleophilic attack of two equivalents of chlorophosphine in the presence of a base (Fig. 27.1). A "mixed" AMPP can also be prepared by virtue of the fact that phosphorus-based electrophiles have a strong preference for hydroxy over secondary amine or amide. Clearly, this synthetic method allows the preparation of a large variety of AMPP ligands with adjustable electronic and steric properties. Agbossou recently reviewed the state of the art of AMPPs [1]. In consideration to the modern high-throughput methods, this approach allowed a rapid combinatorial screening of various catalysts and reactions.

In general, applications of AMPP have concentrated on the asymmetric hydrogenation of functionalized olefins, especially dehydroamino acids. Among

The Handbook of Homogeneous Hydrogenation.
Edited by J. G. de Vries and C. J. Elsevier
Copyright © 2007 WILEY-VCH Verlag GmbH & Co. KGaA, Weinheim
ISBN: 978-3-527-31161-3

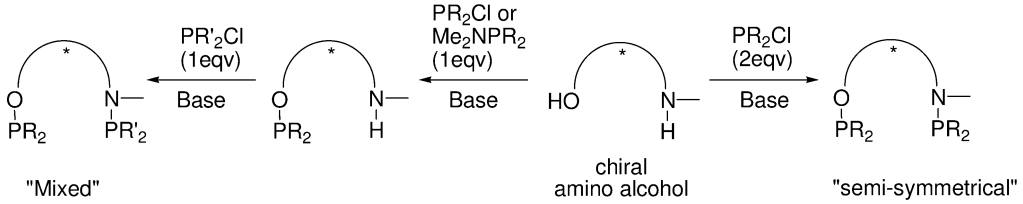

Fig. 27.1 The preparation of AMPPs.

these substrates, (*Z*)-methyl *α*-acetamidocinnamate was the most frequently used benchmark substrate. A strong influence of the solvent on catalytic activity and enantioselectivity was a common phenomenon, and protic solvents were found to be the most effective. However, to avoid the problem of solvolysis of the ligands, polar aprotic solvents were commonly used to obtain the best results. Although the *in-situ* preparation of cationic rhodium complexes was frequently used, no significant dependence of their catalytic performance on the manner of their preparation could be observed. Most Rh complexes allowed the use of atmospheric pressure for hydrogenation with high reaction rate at room temperature. In all cases, the ligands formed a chelation ring with the metal.

Many structurally diverse ephedrine-derived AMPP ligands (Fig. 27.2) have been prepared, and most of these were applied to the asymmetric hydrogenation of olefins. Cesarotti was one of the earliest pioneers in the development of aminophosphine-phosphinite **1** based on (*S*)-2-(ethylamino)butan-1-ol as a starting material. However, the results were only moderate to good [2]. Almost simultaneously with Cesarotti in 1982, Pracejus reported a similar approach [3]. Ephedrine-based Propraphos and its derivatives occupied the major area of this research field. The chiral Rh–Propraphos systems were widely applied in the enantiomeric hydrogenation of *α*-dehydroamino acids, with 31 to 95% e.e. The products included (*S*) and (*R*)-aromatic [4–6] and heteroaromatic alanine derivatives [7–16], and usually have a configuration which is opposite to that of the ligand. 2-Acetamido-cinnamic acid derivatives carrying an electron-withdrawing group at the *para*-position of the phenyl ring could be hydrogenated with relatively high enantioselectivities. In most cases, turnover frequencies (TOFs) could be obtained of up to 3000 h^{-1}, and up to 11 515 h^{-1} for a special case (Table 27.1, entry 392). The use of Rh-**15** in the hydrogenation of dimethyl itaconate gave the product with 80% ee (Table 27.1, entry 432). Structural analogues of Propraphos, Pindophos and Caraphos [7, 17] led to similar ee-values; however, a longer reaction time was required with the Caraphos–Rh complex. Use of (*R*)-Pindophos–Rh in the diastereoselective hydrogenation of dehydrodipetides produced good selectivity (up to 91% ee in the case of *para*-trifluoromethyl-phenylalanyl-phenylalanine [7] (Table 27.2, entry 10). A series of novel ephedrine-based ligands have been shown to be highly effective in the Rh-catalyzed hydrogenation of dehydroamino acids, giving the products with 95–99% ee [18, 19]. The hydrogenation of (*Z*)-acetamidocinnamate with a substrate:catalyst ratio (SCR) of

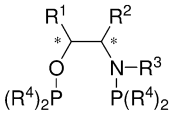

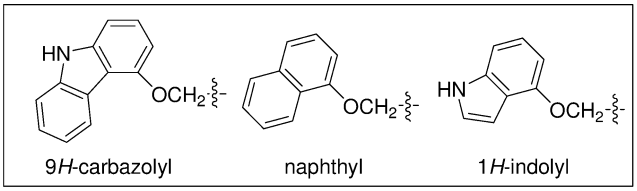

(*S*)-**1** (Butaphos) R^1 = H; R^2 = Et; R^3 = Et; R^4 = Ph
(*S*)-**2** (NEtAlaNOP) R^1 = H; R^2 = Me; R^3 = Et; R^4 = Ph
(1*R*,2*S*)-**3** R^1 = Ph; R^2 = Me; R^3 = Me; R^4 = Ph
(1*R*)-**4** R^1 = Ph; R^2 = H; R^3 = Me; R^4 = Ph
(1*R*,2*R*)-**5** R^1 = Ph; R^2 = Me; R^3 = Me; R^4 = Ph
(2*R*)-**6** R^1 = H; R^2 = Ph; R^3 = Me; R^4 = Ph
(1*R*,2*S*)-**7** (DPAMPP) R^1 = R^2 = Ph; R^3 = Me; R^4 = Ph
(1*S*,2*S*)-**7** (DPAMPP) R^1 = R^2 = Ph; R^3 = Me; R^4 = Ph
(1*S*,2*R*)-**7** (DPAMPP) R^1 = R^2 = Ph; R^3 = Me; R^4 = Ph
(*R*)-**8** R^1 = naphthyl; R^2 = H; R^3 = *i*Pr; R^4 = Cy

(*S*)-**9** (Propraphos) R^1 = naphthyl; R^2 = H; R^3 = *i*Pr, R^4 = Ph
(*R*)-**9** (Propraphos) R^1 = naphthyl; R^2 = H; R^3 = *i*Pr, R^4 = Ph
(*S*)-**10** (Pindophos) R^1 = 1*H*-indolyl; R^2 = H; R^3 = *i*Pr, R^4 = Ph
(*R*)-**10** (Pindophos) R^1 = 1*H*-indolyl; R^2 = H; R^3 = *i*Pr, R^4 = Ph
(*R*)-**11** (Caraphos) R^1 = 9*H*-carbazolyl; R^2 = H; R^3 = *i*Pr, R^4 = Ph
(*S*)-**12** R^1 = naphthyl; R^2 = H; R^3 = H, R^4 = Ph
(*S*)-**13** R^1 = naphthyl; R^2 = H; R^3 = Me, R^4 = Ph
(*S*)-**14** R^1 = naphthyl; R^2 = H; R^3 = $CHEt_2$, R^4 = Ph
(*S*)-**15** R^1 = naphthyl; R^2 = H; R^3 = Cyclopentyl, R^4 = Ph
(*S*)-**16** R^1 = naphthyl; R^2 = H; R^3 = Cyclohexyl, R^4 = Ph

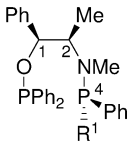

(1*S*,2*R*)-**17** (EPHOS) R^1 = Ph
(1*S*,3*R*,4S)-**18** R^1 = Me
(1*S*,2*R*,4*R*)-**19** R^1 = *o*-An
(1*S*,2*R*,4*R*)-**20** R^1 = 1-Np
(1*S*,2*R*,4*R*)-**21** R^1 = 2-Np
(1*S*,2*R*,4*S*)-**22** R^1 = *t*Bu

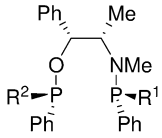

(1*S*,2*R*,4*R*)-**23** R^1 = Ph; R^2 = *o*-An
(1*S*,3*S*,4*R*,6*R*)-**24** R^1 = R^2 = *o*-An

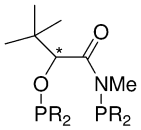

(*R*)-**25** (Ph-tLANOP) R = Ph
(*S*)-**26** (Cy-tLANO) R = Cy
(*S*)-**27** (2-Furyl-tLANOP) R = 2-furyl

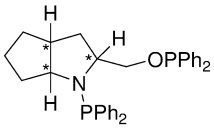

(1*R*,3*R*,5*R*)-**28**
(1*S*,3*S*,5*S*)-**28**

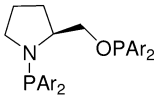

29 (ProNOP/prolophos) Ar = Ph
30 (Cy-ProNOP) Ar = Cy
31 (Bu-ProNOP) Ar = Bu

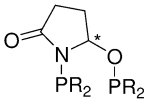

(*S*)-**32** (Ph-oxoProNOP) R = Ph
(*S*)-**33** (Cy-oxoProNOP) R = Cy
(*S*)-**34** ((2-Furyl)-oxoProNOP) R = 2-furyl

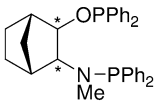

(+)-(2*S*,3S)-**35**
(–)-(2*R*,3*R*)-**35**

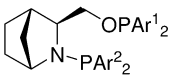

(1*R*,3*S*,4*S*)-**36** Ar^1 = Ar^2 = Ph
(1*R*,3*S*,4*S*)-**37** Ar^1 = Ar^2 = *p*-Tol
(1*R*,3*S*,4*S*)-**38** Ar^1 = Ph; Ar^2 = *p*-Tol
(1*R*,3*S*,4*S*)-**39** Ar^1 = *p*-Tol; Ar^2 = Ph

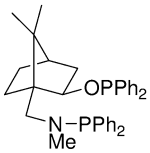

exo-**40**

Fig. 27.2 AMPP chiral ligands.

Table 27.1 Enantiomeric hydrogenation using aminophosphine–phosphinites (AMPP).

Entry	Substrate			Catalyst	Conditions				TON	TOF [h^{-1}]	Conv. [%]	ee [%]	Reference(s)
	R^1	R^2	R^3		P[H_2] [bar]	Solvent	Temp. [°C]	Time [h]					
1	H	CO_2H	NHAc	[Rh(COD)(*S*)-**1**]ClO_4	1	EtOH	20	–	200	–	100	55 (*S*) [a)]	2a, b
2	H	CO_2H	NHAc	[Rh(COD)(1*S*,2*R*)-**7**]BF_4	50	MeOH	25	1	100	100	100	95.2 (*R*)	18
3	H	CO_2H	NHAc	[Rh(COD)(*S*)-**29**]ClO_4	1	EtOH	20	–	200	–	100	80 (*S*) [a)]	2a, b
4	H	CO_2H	NHAc	RhCl(COD)(1*S*,2*S*)-**35**	1	MeOH	25	–	100	–	100	89 (*R*)	37
5	H	CO_2H	NHAc	[Rh(COD) (1*S*,2*S*)-**35**]BF_4	1	MeOH	25	–	100	–	100	86 (*R*)	37
6	H	CO_2H	NHAc	RhCl(COD)(1*R*,2*R*)-**35**	1	MeOH	25	–	100	–	100	89 (*S*)	37
7	H	CO_2H	NHBz	[Rh(COD)(1*S*,2*R*)-**7**]BF_4	50	MeOH	25	1	100	100	100	94.8 (*R*)	18
8	H	CO_2Me	NHAc	[Rh(COD)(*S*)-**2**]ClO_4	1	EtOH/ PhH	20	–	200	–	100	66 (*R*)	32
9	H	CO_2Me	NHAc	[Rh(COD)(*S*)- **29**]ClO_4	1	EtOH/ PhH	20	–	200	–	100	67 (*S*)	32
10	H	CO_2Me	NHAc	[Rh(COD)(*S*)-**29**]BF_4	1	MeOH	r.t.	–	2500	–	–	79 (*S*)	41
11	H	CO_2Me	NHAc	[Rh(COD)(*S*)-**29**]BF_4	1	DCM	r.t.	–	1500	–	–	69 (*S*)	41
12	H	CO_2Me	NHAc	[Rh(COD)(1*R*,3*S*,4*S*)-**36**]BF_4	1	MeOH	r.t.	–	3500	–	–	85 (*S*)	41
13	H	CO_2Me	NHAc	[Rh(COD)(1*R*,3*S*,4*S*)-**36**]BF_4	1	DCM	r.t.	–	1500	–	–	70 (*S*)	41
14	H	CO_2Me	NHAc	[Rh(COD)(1*R*,3*S*,4*S*)-**37**]BF_4	1	MeOH	r.t.	–	4000	–	–	80 (*S*)	41
15	H	CO_2Me	NHAc	[Rh(COD)(1*R*,3*S*,4*S*)-**37**]BF_4	1	DCM	r.t.	–	2000	–	–	61 (*S*)	41
16	H	CO_2Me	NHAc	[Rh(COD)(1*R*,3*S*,4*S*)-**38**]BF_4	1	MeOH	r.t.	–	3600	–	–	80 (*S*)	41
17	H	CO_2Me	NHAc	[Rh(COD)(1*R*,3*S*,4*S*)-**38**]BF_4	1	DCM	r.t.	–	1200	–	–	63 (*S*)	41
18	H	CO_2Me	NHAc	[Rh(COD)(1*R*,3*S*,4*S*)-**39**]BF_4	1	MeOH	r.t.	–	4500	–	–	77 (*S*)	41
19	H	CO_2Me	NHAc	[Rh(COD)(1*R*,3*S*,4*S*)-**39**]BF_4	1	DCM	r.t.	–	2500	–	–	59 (*S*)	41
20	H	OAc	Ph	[Rh(COD)(1*R*,2*S*)-**3**]BF_4	1	Dioxane	25	–	–	–	–	24 (*R*)	36
21	H	OAc	Ph	[Rh(COD) (1*R*,2*R*)-**5**]BF_4	1	Dioxane	25	–	–	–	–	13 (*R*)	36

22	$(CH_3)_2CH$	CO_2H	NHAc	[Rh(COD)(*S*)-**29**]BF_4	1	EtOH	20	–	200	–	100	96 (*S*)	2 b
23	$(CH_3)_2CH$	CO_2H	NHAc	[Rh(COD)(*S*)-**1**]BF_4	1	EtOH	20	–	200	–	100	64 (*S*)	2 b
24	$(CH_3)_2CH$	CO_2H	NHBz	[Rh(COD)(*S*)-**1**]ClO_4	1	EtOH	20	–	200	–	100	57 (*S*)	2 b
25	$(CH_3)_2CH$	CO_2H	NHBz	[Rh(COD)(*S*)-**29**]ClO_4	1	EtOH	20	–	200	–	100	45 (*S*)	2 b
26	Ph	CO_2H	NHAc	[Rh(COD)(*S*)-**1**] ClO_4	1	EtOH	20	–	–	–	–	23 (*S*) [a)]	2 a, b
27	Ph	CO_2H	NHAc	[Rh(COD)(1*R*,2*S*)-**3**]BF_4	1	Dioxane	25	–	–	–	–	80 (*R*)	36
28	Ph	CO_2H	NHAc	[Rh(COD)(1*R*,2*S*)-**3**]BF_4	1	MeOH	25	–	–	–	–	12 (*R*)	36
29	Ph	CO_2H	NHAc	[Rh(COD)(*R*)-**4**]BF_4	1	Dioxane	25	–	–	–	–	56 (*R*)	36
30	Ph	CO_2H	NHAc	[Rh(COD)(*R*)-**4**]BF_4	1	MeOH	25	–	–	–	–	5 (*R*)	36
31	Ph	CO_2H	NHAc	[Rh(COD) (1*R*,2*R*)-**5**]BF_4	1	Dioxane	25	–	–	–	–	3 (*S*)	36
32	Ph	CO_2H	NHAc	[Rh(COD) (1*R*,2*R*)-**5**]BF_4	1	MeOH	25	–	–	–	–	9 (*R*)	36
33	Ph	CO_2H	NHAc	[Rh(COD)(2*R*)-**6**]BF_4	1	Dioxane	25	–	–	–	–	24 (*R*)	36
34	Ph	CO_2H	NHAc	[Rh(COD)(2*R*)-**6**]BF_4	1	MeOH	25	–	–	–	–	0.5 (*S*)	36
35	Ph	CO_2H	NHAc	[Rh(COD)(1*S*,2*R*)-**7**]BF_4	50	MeOH	25	1	100	100	100	96.5 (*R*)	18
36	Ph	CO_2H	NHAc	[Rh(COD)(*S*)-**9**]BF_4	1	MeOH	25	0.03 [b)]	50	1667	50	87 (*R*)	8
37	Ph	CO_2H	NHAc	RhCl(COD)(*S*)-**9**	1	MeOH	25	0.12 [b)]	50	417	50	88 (*R*)	8
38	Ph	CO_2H	NHAc	[Rh(COD)(*R*)-**9**]BF_4	1	MeOH	25	0.092 [b)]	1000	10870	50	86 (*S*)	9
39	Ph	CO_2H	NHAc	[Rh(COD)(*R*)-**9**]BF_4	1	MeOH	25	0.343 [b)]	1500	4373	50	85 (*S*)	9
40	Ph	CO_2H	NHAc	Rh(COD)(*S*)-**9**	1	MeOH	25	0.12 [b)]	50	417	50	88 (*R*)	15
41	Ph	CO_2H	NHAc	Rh(COD)(*S*)-**9**	1	MeOH	25	0.58 [b)]	500	862	50	85 (*R*) [l)]	15
42	Ph	CO_2H	NHAc	[Rh(COD)(*S*)-**9**]BF_4	1	MeOH	25	0.02 [b)]	50	2500	50	87 (*R*) [m)]	15
43	Ph	CO_2H	NHAc	[Rh(COD)(*S*)-**9**]BF_4	1	MeOH	25	0.15 [b)]	500	3333	50	84 (*R*) [m)]	15
44	Ph	CO_2H	NHAc	[Rh(COD)(*S*)-**9**]BF_4	1	MeOH	25	0.22 [b)]	500	2273	50	89 (*R*)	15
45	Ph	CO_2H	NHAc	[Rh(COD)(*S*)-**9**]BF_4	1	MeOH	25	0.03 [b)]	50	1667	50	85 (*R*) [m,n)]	15
46	Ph	CO_2H	NHAc	[Rh(COD)(*S*)-**9**]BF_4	1	MeOH	25	0.58 [b)]	50	86	50	82 (*R*) [m,o)]	15
47	Ph	CO_2H	NHAc	[Rh(COD)(*R*)-**9**]BF_4	1	PhH	25	1.33 [b)]	50	38	50	69 (*S*)	15
48	Ph	CO_2H	NHAc	[(*R*)-**9**+CuCl]/$[Ru(COD)Cl]_2$	1	MeOH	25	0.02 [b)]	50	2500	50	88 (*S*)	15
49	Ph	CO_2H	NHAc	[(*R*)-**9**+CuCl]/$[Ru(COD)Cl]_2$	1	MeOH	25	0.12 [b)]	500	4167	50	88 (*S*)	15
50	Ph	CO_2H	NHAc	[Rh(COD)(*R*)-**10**]BF_4	1	MeOH	25	0.058 [b)]	500	8621	50	91 (*S*)	9
51	Ph	CO_2H	NHAc	[Rh(COD)(*R*)-**10**]BF_4	1	MeOH	25	0.117 [b)]	1000	8547	50	90 (*S*)	9

Table 27.1 (continued)

Entry	Substrate			Catalyst	Conditions				TON	TOF [h^{-1}]	Conv. [%]	ee [%]	Reference(s)
	R^1	R^2	R^3		$P[H_2]$ [bar]	Solvent	Temp. [°C]	Time [h]					
52	Ph	CO_2H	NHAc	[Rh(COD)(*R*)-**10**]BF_4	1	MeOH	25	0.267 [b)]	1500	5618	50	90 (*S*)	9
53	Ph	CO_2H	NHAc	[Rh(COD)(*S*)-**12**]BF_4	1	MeOH	25	0.2 [b)]	50	250	50	2 (*S*)	8
54	Ph	CO_2H	NHAc	[Rh(COD)(*S*)-**13**]BF_4	1	MeOH	25	0.032 [b)]	50	1563	50	45 (*R*)	8
55	Ph	CO_2H	NHAc	[Rh(COD)(*S*)-**13**]BF_4	1	MeOH	25	0.67 [b)]	500	746	50	9 (*R*)	8
56	Ph	CO_2H	NHAc	RhCl(COD)(*S*)-**13**	1	MeOH	25	0.25 [b)]	50	200	50	20 (*R*)	8
57	Ph	CO_2H	NHAc	[Rh(COD)(*S*)-**14**]BF_4	1	MeOH	25	0.03 [b)]	50	1667	50	87 (*R*)	8
58	Ph	CO_2H	NHAc	[Rh(COD)(*S*)-**15**]BF_4	1	MeOH	25	0.03 [b)]	50	1667	50	91 (*R*)	8
59	Ph	CO_2H	NHAc	[Rh(COD)(*S*)-**16**]BF_4	1	MeOH	25	0.03 [b)]	50	1667	50	89 (*R*)	8
60	Ph	CO_2H	NHAc	[Rh(COD)(1*S*,3*S*,5*S*)-**28**]BF_4	1	MeOH	25	0.017 [b)]	50	2941	50	57 (*S*) [m)]	40
61	Ph	CO_2H	NHAc	[Rh(COD)(1*R*,3*R*,5*R*)-**28**]BF_4	1	MeOH	25	0.017 [b)]	50	2941	50	54 (*R*) [m)]	40
62	Ph	CO_2H	NHAc	[Rh(COD)(*S*)-**29**] ClO_4	1	EtOH	20	–	–	–	–	78 (*S*) [a)]	2 b
63	Ph	CO_2H	NHAc	[Rh(COD)(*S*)-**29**]BF_4	1	MeOH	r.t.	–	–	250	–	80 (*S*) [c)]	41
64	Ph	CO_2H	NHAc	[Rh(COD)(*S*)-**29**]BF_4	1	DCM	r.t.	–	–	2000	–	65 (*S*) [c)]	41
65	Ph	CO_2H	NHAc	RhCl(COD)(1*S*,2*S*)-**35**	1	MeOH	25	–	100	–	100	85 (*R*)	37
66	Ph	CO_2H	NHAc	[Rh(COD)(1*S*,2*S*)-**35**]BF_4	1	MeOH	25	–	100	–	100	83 (*R*)	37
67	Ph	CO_2H	NHAc	[Rh(COD)(1*R*,2*R*)-**35**]Cl	1	MeOH	25	–	100	–	100	85 (*S*)	37
68	Ph	CO_2H	NHAc	[Rh(COD)(1*R*,3*S*,4*S*)-**36**]BF_4	1	MeOH	r.t.	–	–	3100	–	90 (*S*) [c)]	41
69	Ph	CO_2H	NHAc	[Rh(COD)(1*R*,3*S*,4*S*)-**36**]BF_4	1	DCM	r.t.	–	–	600	–	83 (*S*) [c)]	41
70	Ph	CO_2H	NHAc	[Rh(COD)(1*R*,3*S*,4*S*)-**37**]BF_4	1	MeOH	r.t.	–	–	2400	–	86 (*S*) [c)]	41
71	Ph	CO_2H	NHAc	[Rh(COD)(1*R*,3*S*,4*S*)-**37**]BF_4	1	DCM	r.t.	–	–	300	–	66 (*S*) [c)]	41
72	Ph	CO_2H	NHAc	[Rh(COD)(1*R*,3*S*,4*S*)-**38**]BF_4	1	MeOH	r.t.	–	–	2000	–	82 (*S*) [c)]	41
73	Ph	CO_2H	NHAc	[Rh(COD)(1*R*,3*S*,4*S*)-**38**]BF_4	1	DCM	r.t.	–	–	300	–	67 (*S*) [c)]	41
74	Ph	CO_2H	NHAc	[Rh(COD)(1*R*,3*S*,4*S*)-**39**]BF_4	1	MeOH	r.t.	–	–	2400	–	80 (*S*) [c)]	41

75	Ph	CO_2H	NHAc	[Rh(COD)(1*R*,3*S*,4*S*)-**39**]BF_4	1	DCM	r.t.	–	–	300	–	65 (*S*)[c]	41
76	Ph	CO_2H	NHBz	[Rh(COD)(*S*)-**1**]ClO_4	1	EtOH	20	–	200	–	100	49 (*S*)	2 b
77	Ph	CO_2H	NHBz	[Rh(COD)(1*S*,2*R*)-**7**]BF_4	50	MeOH	25	1	100	100	100	96.4 (*R*)	18, 19
78	Ph	CO_2H	NHBz	[Rh(COD)(*S*)-**9**]BF_4	1	MeOH	25	0.017[b]	50	2941	50	89 (*R*)	8
79	Ph	CO_2H	NHBz	RhCl(*S*)-**9**	1	MeOH	25	0.25[b]	500	2000	50	89 (*R*)	8
80	Ph	CO_2H	NHBz	[(*R*)-**9**+CuCl]/$[Ru(COD)Cl]_2$	1	MeOH	25	0.5[b]	1500	3000	50	89 (*S*)	15
81	Ph	CO_2H	NHBz	[Rh(COD)(*R*)-**9**]BF_4	1	MeOH	25	0.72[b]	500	694	50	79 (*S*)	15
82	Ph	CO_2H	NHBz	RhCl(*R*)-**9**	1	MeOH	25	0.25[b]	500	200	50	89 (*S*)	15
83	Ph	CO_2H	NHBz	[Rh(COD)(*R*)-**9**]$^+$	1	MeOH	25	0.72[b]	500	694	50	79 (*S*)	42
84	Ph	CO_2H	NHBz	[Rh(COD)(*S*)-**12**]BF_4	1	MeOH	25	0.27[b]	50	185	50	8 (*S*)	8
85	Ph	CO_2H	NHBz	[Rh(COD)(*S*)-**13**]BF_4	1	MeOH	25	0.04[b]	50	1250	50	41 (*R*)	8
86	Ph	CO_2H	NHBz	[Rh(COD)(*S*)-**13**]BF_4	1	MeOH	25	0.67[b]	500	746	50	3 (*R*)	8
87	Ph	CO_2H	NHBz	RhCl(*S*)-**13**	1	MeOH	25	0.2[b]	50	250	50	24 (*R*)	8
88	Ph	CO_2H	NHBz	[Rh(COD)(*S*)-**14**]BF_4	1	MeOH	25	0.07[b]	50	714	50	88 (*R*)	8
89	Ph	CO_2H	NHBz	[Rh(COD)(*S*)-**15**]BF_4	1	MeOH	25	0.03[b]	50	1667	50	94 (*R*)	8
90	Ph	CO_2H	NHBz	[Rh(COD)(*S*)-**16**]BF_4	1	MeOH	25	0.03[b]	50	1667	50	92 (*R*)	8
91	Ph	CO_2H	NHBz	[Rh(COD)(1*S*,3*S*,5*S*)-**28**]BF_4	1	MeOH	25	0.017[b]	50	2941	50	62 (*S*)	40
92	Ph	CO_2H	NHBz	[Rh(COD)(1*R*,3*R*,5*R*)-**28**]BF_4	1	MeOH	25	0.017[b]	50	2941	50	58 (*R*)	40
93	Ph	CO_2H	NHBz	[Rh(COD)(*S*)-**29**]ClO_4	1	EtOH	20	–	200	–	100	62 (*S*)	2b
94	Ph	CO_2Me	NHAc	[Rh(COD)(1*R*,2*S*)-**3**]BF_4	1	Dioxane	25	–	–	–	–	75 (*R*)	36
95	Ph	CO_2Me	NHAc	[Rh(COD)(1*R*,2*S*)-**3**]BF_4	1	MeOH	25	–	–	–	–	12 (*R*)	36
96	Ph	CO_2Me	NHAc	[Rh(COD)(1*R*)-**4**]BF_4	1	Dioxane	25	–	–	–	–	55 (*R*)	36
97	Ph	CO_2Me	NHAc	[Rh(COD)(1*R*)-**4**]BF_4	1	MeOH	25	–	–	–	–	5 (*R*)	36
98	Ph	CO_2Me	NHAc	[Rh(COD)(1*R*,2*R*)-**5**]BF_4	1	Dioxane	25	–	–	–	–	10 (*R*)	36
99	Ph	CO_2Me	NHAc	[Rh(COD)(1*R*,2*R*)-**5**]BF_4	1	MeOH	25	–	–	–	–	2 (S)	36
100	Ph	CO_2Me	NHAc	[Rh(COD)(2*R*)-**6**]BF_4	1	Dioxane	25	–	–	–	–	14 (R)	36
101	Ph	CO_2Me	NHAc	[Rh(COD)(2*R*)-**6**]BF_4	1	MeOH	25	–	–	–	–	6 (*R*)	36
102	Ph	CO_2Me	NHAc	[Rh(COD)(1*R*,2*S*)-**7**]Cl	50	MeOH	r.t.	17	31.3	1.84	31.3	27 (*S*)	18
103	Ph	CO_2Me	NHAc	[Rh(COD)(1*R*,2*S*)-**7**]BF_4	50	MeOH	r.t.	1	100	100	100	96.9 (*S*)	18
104	Ph	CO_2Me	NHAc	[Rh(COD)(1*S*,2*R*)-**7**]BF_4	50	MeOH	r.t.	1	100	100	100	98.3 (*R*)	18

Table 27.1 (continued)

Entry	Substrate			Catalyst	Conditions				TON	TOF [h^{-1}]	Conv. [%]	ee [%]	Reference(s)
	R^1	R^2	R^3		$P[H_2]$ [bar]	Solvent	Temp. [°C]	Time [h]					
105	Ph	CO_2Me	NHAc	[Rh(COD)(1*S*,2*S*)-**7**]BF_4	50	MeOH	r.t.	1	100	100	100	40.6 (*R*)	18
106	Ph	CO_2Me	NHAc	[Rh(COD)(1*R*,2*S*)-**7**]BF_4	10	MeOH	r.t.	1	100	100	100	97.0 (*S*)	18
107	Ph	CO_2Me	NHAc	[Rh(COD)(1*R*,2*S*)-**7**]BF_4	10	Acetone	r.t.	1	–	100	100	95.1 (*S*)	18
108	Ph	CO_2Me	NHAc	[Rh(COD)(1*R*,2*S*)-**7**]BF_4	10	THF	r.t.	1	–	100	100	94.8 (*S*)	18
109	Ph	CO_2Me	NHAc	[Rh(COD)(1*R*,2*S*)-**7**]BF_4	10	IPA	r.t.	1	–	100	100	92.7 (*S*)	18
110	Ph	CO_2Me	NHAc	[Rh(COD)(1*R*,2*S*)-**7**]BF_4	80	MeOH	25	0.5	100	200	100	96.8 (*S*)	18
111	Ph	CO_2Me	NHAc	[Rh(COD)(1*R*,2*S*)-**7**]BF_4	50	MeOH	25	1	100	100	100	96.9 (*S*)	18
112	Ph	CO_2Me	NHAc	[Rh(COD)(1*R*,2*S*)-**7**]BF_4	20	MeOH	25	1	100	100	100	96.4 (*S*)	18
113	Ph	CO_2Me	NHAc	[Rh(COD)(1*R*,2*S*)-**7**]BF_4	1	MeOH	25	4	100	25	100	97.2 (*S*)	18
114	Ph	CO_2Me	NHAc	[Rh(COD)(1*R*,2*S*)-**7**]BF_4	10	Acetone	25	–	100	–	100	96.2 (*S*)	18
115	Ph	CO_2Me	NHAc	[Rh(COD)(1*R*,2*S*)-**7**]BF_4	10	Acetone	25	–	100	–	100	95.8 (*S*)	18
116	Ph	CO_2Me	NHAc	[Rh(COD)(1*R*,2*S*)-**7**]BF_4	10	Acetone	25	–	100	–	100	94.5 (*S*)	18
117	Ph	CO_2Me	NHAc	[Rh(COD)(1*R*,2*S*)-**7**]BF_4	10	Acetone	25	–	100	–	100	93.8 (*S*)	18
118	Ph	CO_2Me	NHAc	[Rh(COD)(1*S*,2*R*)-**7**]BF_4	50	MeOH	25	1	100	100	100	98.3 (*R*)	18
119	Ph	CO_2Me	NHAc	[Rh(COD)(1*S*,2*R*)-**7**]BF_4	50	MeOH	25	4	1 000	250	100	97.5 (*R*)	18
120	Ph	CO_2Me	NHAc	[Rh(COD)(1*S*,2*R*)-**7**]BF_4	50	MeOH	25	16	10 000	625	100	97.0 (*R*)	18
121	Ph	CO_2Me	NHAc	[Rh(COD)(1*S*,2*R*)-**7**]BF_4	50	MeOH	25	64	41 350	646	82.7	97.0 (*R*)	18
122	Ph	CO_2Me	NHAc	[Rh(COD)(1*S*,2*R*)-**7**]BF_4	50	MeOH	25	64	41 700	652	41.7	93.0 (*R*)	18
123	Ph	CO_2Me	NHAc	[Rh(COD)(*R*)-**8**]BF_4	1	MeOH	25	1.5 [b)]	50	33	50	13 (*R*)	15
124	Ph	CO_2Me	NHAc	Rh(COD)(*R*)-**9**	1	MeOH	25	0.23 [b)]	50	217	50	86 (*S*) [m)]	15
125	Ph	CO_2Me	NHAc	Rh(COD)(*R*)-**9**	1	MeOH	25	0.33 [b)]	50	152	50	85 (*S*) [k)]	15
126	Ph	CO_2Me	NHAc	Rh(COD)(*S*)-**9**	1	MeOH	25	0.58 [b)]	500	862	50	82 (*R*) [l)]	15
127	Ph	CO_2Me	NHAc	[Rh(COD)(*R*)-**9**]BF_4	1	MeOH	25	0.03 [b)]	50	1 667	50	87 (*S*)	15

128	Ph	CO_2Me	NHAc	[Rh(COD)(*S*)-**9**]BF_4	1	MeOH	25	0.6 [b]	500	833	50	85 (*R*)	15
129	Ph	CO_2Me	NHAc	[Rh(COD)(*R*)-**9**]BF_4	1	MeOH	25	0.03 [b]	50	1667	50	88 (*S*)	15
130	Ph	CO_2Me	NHAc	[Rh(COD)(*R*)-**9**]BF_4	1	MeOH	25	0.03 [b]	50	1667	50	88 (*S*)[q]	15
131	Ph	CO_2Me	NHAc	[(*R*)-**9**+CuCl]/[Ru(COD)Cl]$_2$	1	MeOH	25	0.2 [b]	500	2500	50	85 (*S*)	15
132	Ph	CO_2Me	NHAc	[Rh(COD)(*R*)-**10**]BF_4	1	MeOH	25	0.067 [b]	500	7463	50	90 (*S*)	9
133	Ph	CO_2Me	NHAc	[Rh(COD)(*R*)-**10**]BF_4	1	MeOH	25	0.062 [b]	1000	16129	50	89 (*S*)	9
134	Ph	CO_2Me	NHAc	[Rh(COD)(*R*)-**11**]BF_4	1	MeOH	25	0.017 [b]	50	2941	50	78 (*S*)	17
135	Ph	CO_2Me	NHAc	[Rh(COD)(*S*)-**11**]BF_4	1	MeOH	25	0.017 [b]	50	2941	50	76 (*R*)	17
136	Ph	CO_2Me	NHAc	[Rh(COD)(*S*)-**12**]BF_4	1	MeOH	25	0.18 [b]	50	278	50	35 (*R*)	8
137	Ph	CO_2Me	NHAc	[Rh(COD)(*S*)-**13**]BF_4	1	MeOH	25	0.03 [b]	50	1667	50	47 (*R*)	8
138	Ph	CO_2Me	NHAc	[Rh(COD)(*S*)-**13**]BF_4	1	MeOH	25	0.12 [b]	50	417	50	40 (*R*)	8
139	Ph	CO_2Me	NHAc	RhCl(*S*)-**13**	1	MeOH	25	0.33 [b]	50	152	50	47 (*R*)	8
140	Ph	CO_2Me	NHAc	[Rh(COD)(*S*)-**14**]BF_4	1	MeOH	25	0.03 [b]	50	1667	50	85 (*R*)	8
141	Ph	CO_2Me	NHAc	[Rh(COD)(*S*)-**15**]BF_4	1	MeOH	25	0.03 [b]	50	1667	50	89 (*R*)	8
142	Ph	CO_2Me	NHAc	[Rh(COD)(*S*)-**16**]BF_4	1	MeOH	25	0.03 [b]	50	1667	50	86 (*R*)	8
143	Ph	CO_2Me	NHAc	[Rh(COD)(1*R*,2*S*)-**17**]BF_4	15	DCM	r.t.	18	30	1.7	98	11 (*S*)	31
144	Ph	CO_2Me	NHAc	[Rh(COD)(1*R*,2*S*)-**17**]BF_4	15	PhH	r.t.	22	30	1.4	95	46 (*S*)	31
145	Ph	CO_2Me	NHAc	[Rh(COD)(1*S*,3*R*,4*S*)-**18**]BF_4	15	DCM	r.t.	3	30	10	95	22 (*R*)	31
146	Ph	CO_2Me	NHAc	[Rh(COD)(1*R*,3*R*,4*S*)-**19**]BF_4	15	DCM	r.t.	10.5	30	2.9	99	89 (*S*)	31
147	Ph	CO_2Me	NHAc	[Rh(COD)(1*R*,3*R*,4*S*)-**19**]BF_4	15	PhH	r.t.	20	30	1.5	98	99 (*S*)	31
148	Ph	CO_2Me	NHAc	[Rh(COD)(1*R*,3*R*,4*S*)-**20**]BF_4	15	DCM	r.t.	4	30	7.5	99	88 (*S*)	31
149	Ph	CO_2Me	NHAc	[Rh(COD)(1*R*,3*R*,4*S*)-**20**]BF_4	15	PhH	r.t.	17	30	1.8	98	95 (*S*)	31
150	Ph	CO_2Me	NHAc	[Rh(COD)(1*R*,3*R*,4*S*)-**21**]BF_4	15	DCM	r.t.	4.5	30	6.7	96	16 (*S*)	31
151	Ph	CO_2Me	NHAc	[Rh(COD)(1*S*,3*R*,4*S*)-**22**]BF_4	15	DCM	r.t.	4	30	7.5	95	2 (*S*)	31
152	Ph	CO_2Me	NHAc	[Rh(COD)(1*S*,2*R*,4*R*)-**23**]BF_4	15	DCM	r.t.	13	30	2.3	98	80 (*S*)	31
153	Ph	CO_2Me	NHAc	[Rh(COD)(1*S*,3*S*,4*R*,6*R*)-**24**]BF_4	15	DCM	r.t.	12	30	2.5	94	1 (*S*)	31
154	Ph	CO_2Me	NHAc	[Rh(COD)(1*S*,3*S*,5*S*)-**28**]BF_4	1	MeOH	25	0.017 [b]	50	2941	50	70 (*S*)	40
155	Ph	CO_2Me	NHAc	[Rh(COD)(1*R*,3*R*,5*R*)-**28**]BF_4	1	MeOH	25	0.017 [b]	50	2941	50	69 (*R*)	40
156	Ph	CO_2Me	NHAc	[Rh(COD)(*S*)-**29**]BF_4	1	MeOH	r.t.	–	–	1100	–	80 (*S*)	41
157	Ph	CO_2Me	NHAc	[Rh(COD)(*S*)-**29**]BF_4	1	DCM	r.t.	–	–	2000	–	79 (*S*)	41

Table 27.1 (continued)

Entry	Substrate			Catalyst	Conditions				TON	TOF [h^{-1}]	Conv. [%]	ee [%]	Reference(s)
	R^1	R^2	R^3		$P[H_2]$ [bar]	Solvent	Temp. [°C]	Time [h]					
158	Ph	CO_2Me	NHAc	[Rh(COD)(*S*)-**29**]BF_4	1	EtOAc	r.t.	–	–	500	–	74 (*S*)	41
159	Ph	CO_2Me	NHAc	RhCl(COD)(1*S*,2*S*)-**35**	1	MeOH	25	–	100	–	100	87 (*R*)	37
160	Ph	CO_2Me	NHAc	[Rh(COD)(1*S*,2*S*)-**35**]BF_4	1	MeOH	25	–	100	–	100	87 (*R*)	37
161	Ph	CO_2Me	NHAc	RhCl(COD)(1*R*,2*R*)-**35**	1	MeOH	25	–	100	–	100	87 (*S*)	37
162	Ph	CO_2Me	NHAc	[Rh(COD)(1*R*,3*S*,4*S*)-**36**]BF_4	1	MeOH	r.t.	–	–	3500	–	91 (*S*)	41
163	Ph	CO_2Me	NHAc	[Rh(COD)(1*R*,3*S*,4*S*)-**36**]BF_4	1	DCM	r.t.	–	–	1600	–	88 (*S*)	41
164	Ph	CO_2Me	NHAc	[Rh(COD)(1*R*,3*S*,4*S*)-**36**]BF_4	1	EtOAc	r.t.	–	–	2000	–	83 (*S*)	41
165	Ph	CO_2Me	NHAc	[Rh(COD)(1*R*,3*S*,4*S*)-**36**]BF_4	1	THF	r.t.	–	–	1700	–	84 (*S*)	41
166	Ph	CO_2Me	NHAc	[Rh(COD)(1*R*,3*S*,4*S*)-**37**]BF_4	1	MeOH	r.t.	–	–	2700	–	85 (*S*)	41
167	Ph	CO_2Me	NHAc	[Rh(COD)(1*R*,3*S*,4*S*)-**37**]BF_4	1	DCM	r.t.	–	–	1300	–	82 (*S*)	41
168	Ph	CO_2Me	NHAc	[Rh(COD)(1*R*,3*S*,4*S*)-**37**]BF_4	1	EtOAc	r.t.	–	–	2400	–	78 (*S*)	41
169	Ph	CO_2Me	NHAc	[Rh(COD)(1*R*,3*S*,4*S*)-**37**]BF_4	1	THF	r.t.	–	–	1500	–	78 (*S*)	41
170	Ph	CO_2Me	NHAc	[Rh(COD)(1*R*,3*S*,4*S*)-**38**]BF_4	1	MeOH	r.t.	–	–	2700	–	71 (*S*)	41
171	Ph	CO_2Me	NHAc	[Rh(COD)(1*R*,3*S*,4*S*)-**38**]BF_4	1	DCM	r.t.	–	–	1200	–	78 (*S*)	41
172	Ph	CO_2Me	NHAc	[Rh(COD)(1*R*,3*S*,4*S*)-**38**]BF_4	1	EtOAc	r.t.	–	–	2000	–	76 (*S*)	41
173	Ph	CO_2Me	NHAc	[Rh(COD)(1*R*,3*S*,4*S*)-**39**]BF_4	1	MeOH	r.t.	–	–	3000	–	74 (*S*)	41
174	Ph	CO_2Me	NHAc	[Rh(COD)(1*R*,3*S*,4*S*)-**39**]BF_4	1	DCM	r.t.	–	–	1500	–	78 (*S*)	41
175	Ph	CO_2Me	NHAc	[Rh(COD)(*exo*-**40**)]BF_4	34.5	Acetone	0	7	100	14	100	79.0 (*R*)	39
176	Ph	CO_2Me	NHAc	[Rh(COD)(*exo*-**40**)]BF_4	34.5	Acetone	25	7	100	14	100	77.0 (*R*)	39
177	Ph	CO_2Me	NHAc	[Rh(COD)(*exo*-**40**)]BF_4	17.2	Acetone	25	7	100	14	100	78.0 (*R*)	39
178	Ph	CO_2Me	NHAc	[Rh(COD)(*exo*-**40**)]BF_4	34.5	MeOH	25	7	100	14	100	74.0 (*R*)	39
179	Ph	CO_2Me	NHAc	[Rh(COD)(*exo*-**40**)]BF_4	34.5	THF	25	7	100	14	100	62.0 (*R*)	39
180	Ph	CO_2Me	NHAc	[Rh(COD)(*exo*-**40**)]BF_4	34.5	DCM	25	7	100	14	100	72.0 (*R*)	39
181	Ph	CO_2Me	NHBz	[Rh(COD)(1*S*,2*R*)-**7**]BF_4	50	MeOH	25	1	100	100	100	97.1 (*R*)	18, 19

182	Ph	CO_2Me	NHBz	[Rh(COD)(*S*)-**9**]BF_4	1	MeOH	25	0.67 [b]	50	75	50	81 (*R*)	8
183	Ph	CO_2Me	NHBz	[Rh(COD)(*S*)-**9**]BF_4	1	MeOH	25	0.016 [b]	50	3 125	50	89 (*R*)	8, 10
184	Ph	CO_2Me	NHBz	[Rh(COD)(*R*)-**9**]BF_4	1	MeOH	25	0.67 [b]	500	746	50	81 (*S*)	15
185	Ph	CO_2Me	NHBz	Rh(COD)(*R*)-**9**	1	MeOH	25	0.28 [b]	500	1 786	50	87 (*S*)	15
186	Ph	CO_2Me	NHBz	[Rh(COD)(*S*)-**12**]BF_4	1	MeOH	25	0.033 [b]	50	1 515	50	27 (*R*)	8
187	Ph	CO_2Me	NHBz	[Rh(COD)(*S*)-**13**]BF_4	1	MeOH	25	0.063 [b]	50	794	50	40 (*R*)	8
188	Ph	CO_2Me	NHBz	RhCl(*S*)-**13**	1	MeOH	25	0.35 [b]	50	143	50	41 (*R*)	8
189	Ph	CO_2Me	NHBz	[Rh(COD)(*S*)-**14**]BF_4	1	MeOH	25	0.033 [b]	50	1 515	50	87 (*R*)	8
190	Ph	CO_2Me	NHBz	[Rh(COD)(*S*)-**15**]BF_4	1	MeOH	25	0.033 [b]	50	1515	50	92 (*R*)	8
191	Ph	CO_2Me	NHBz	[Rh(COD)(*S*)-**16**]BF_4	1	MeOH	25	0.033 [b]	50	1515	50	88 (*R*)	8
192	Ph	CO_2Me	NHBz	[Rh(COD)(1*S*,3*S*,5*S*)-**28**]BF_4	1	MeOH	25	0.017 [b]	50	2941	50	73 (*S*)	40
193	Ph	CO_2Me	NHBz	[Rh(COD)(1*R*,3*R*,5*R*)-**28**]BF_4	1	MeOH	25	0.017 [b]	50	2941	50	71 (*R*)	40
194	Ph	CO_2Me	NHCbz	[Rh(COD)(*S*)-**9**]BF_4	1	MeOH	25	2 [b]	50	25	50	88 (*R*)	10
195	Ph	CO_2Me	NHBoc	[Rh(COD)(*S*)-**9**]BF_4	1	MeOH	25	0.83 [b]	50	60	50	93 (*R*)	10
196	Ph	NHCOMe	CO_2H	[Rh(COD)(*S*)-**2**]ClO_4	1	EtOH/ PhH (2:1)	20	0.17–0.5	200	400–1176	100	70 (*R*)	32
197	Ph	NHCOMe	CO_2H	[Rh(COD)(*S*)-**29**]ClO_4	1	EtOH/ PhH (2:1)	20	0.17–0.5	200	400–1176	100	86 (*S*)	32
198	Ph	NHCOMe	CO_2Me	[Rh(COD)(*S*)-**2**]ClO_4	1	EtOH/ PhH (2:1)	20	0.17–0.5	200	400–1176	100	48 (*R*)	32
199	Ph	NHBz	CO_2H	[Rh(COD)(*S*)-**2**]ClO_4	1	EtOH/ PhH (2:1)	20	0.17–0.5	200	400–1176	100	53 (*R*)	32
200	Ph	NHBz	CO_2H	[Rh(COD)(*S*)-**29**]ClO_4	1	EtOH/ PhH (2:1)	20	0.17–0.5	200	400–1176	100	61 (*S*)	32
201	Ph	$MePO_2Et$	NHBz	[Rh(COD)(*S*)-**9**]BF_4	1	MeOH	25	0.33 [b]	25	76	50	77 (*Sc*) [g]	12, 16
202	Ph	$PhPO_2H$	NHBz	[Rh(COD)(*S*)-**9**]BF_4	1	MeOH	25	0.23 [b]	25	109	50	56 (*Sc*) [g]	12
203	Ph	$PhPO_2H$	NHBz	[Rh(COD)(*S*)-**9**]BF_4	1	MeOH	25	0.33	95	288	95	65 (*Sc*) [g]	16
204	Ph	$PhPO_2Me$	NHBz	[Rh(COD)(*S*)-**9**]BF_4	1	MeOH	25	0.63 [b]	25	40	50	76 (*Sc*) [g]	12

Table 27.1 (continued)

Entry	Substrate			Catalyst	Conditions				TON	TOF [h^{-1}]	Conv. [%]	ee [%]	Reference(s)
	R^1	R^2	R^3		$P[H_2]$ [bar]	Solvent	Temp. [°C]	Time [h]					
205	Ph	$PhPO_2Me$	NHBz	[Rh(COD)(*S*)-**9**]BF_4	1	MeOH	25	0.93	96	103	96	69 (*Sc*)[g]	16
206	Ph	$PhPO_2Et$	NHBz	[Rh(COD)(*S*)-**9**]BF_4	1	MeOH	25	1.17[b]	25	21	50	75 (*Sc*)[g]	12
207	Ph	$PhPO_2Et$	NHBz	[Rh(COD)(*S*)-**9**]BF_4	1	MeOH	25	2.18[b]	50	23	50	71 (*Sc*)[g]	12
208	Ph	$PhPO_2Et$	NHBz	[Rh(COD)(*S*)-**9**]BF_4	1	MeOH	25	0.67[b]	25	37	50	31 (*Sc*)[g]	12
209	Ph	$PhPO_2Et$	NHBz	[Rh(COD)(*S*)-**9**]BF_4	1	MeOH	25	0.67[b]	25	37	50	79 (*Sc*)[g]	12
210	Ph	$PhPO_2Et$	NHBz	[Rh(COD)(*S*)-**9**]BF_4	1	MeOH	25	2.18	–	–	–	71 (*Sc*)[g]	16
211	Ph	$PO(OMe)_2$	NHBz	[Rh(COD)(*S*)-**9**]BF_4	1	MeOH	25	0.23[i]	95	413	95[h]	90 (*S*)[j]	14
212	Ph	$PO(OMe)_2$	NHBz	[Rh(COD)(*R*)-**9**]BF_4	1	MeOH	25	0.23[i]	94	409	94[h]	89 (*R*)[j]	14
213	Ph	$PO(OMe)_2$	NHBz	[Rh(COD) (*S*)-**9**]BF_4	1	MeOH	25	2.33[i]	950	408	95[h]	89 (*S*)[j]	14
214	Ph	$PO(OMe)_2$	NHBz	[Rh(COD)(*S*)-**9**]BF_4	1	PhH	25	1.33[i]	95	71	95[h]	82 (*S*)[j]	14
215	Ph	$PO(OMe)_2$	NHBz	[Rh(COD)(*S*)-**9**]BF_4	1	THF	25	0.6[i]	94	157	94[h]	83 (*S*)[j]	14
216	Ph	$PO(OMe)_2$	NHBz	[Rh(COD)(*S*)-**15**]BF_4	1	MeOH	25	0.2[i]	97	485	97[h]	91 (*S*)[j]	14
217	Ph	$PO(OEt)_2$	NHBz	[Rh(COD)(*S*)-**9**]BF_4	1	MeOH	25	0.23[i]	96	417	96[h]	92 (*S*)[j]	14
218	Ph	$PO(O^iPr)_2$	NHBz	[Rh(COD)(*S*)-**9**]BF_4	1	MeOH	25	1.03[i]	95	92	95[h]	91 (*S*)[j]	14
219	C_6F_5	CO_2H	NHBz	[Rh(COD)(*R*)-**9**]$^+$	1	MeOH	25	0.17[b]	50	294	50	86 (*S*)	42
220	*o*-Cl-Ph	CO_2Me	NHAc	[Rh(COD)(1*S*,2*R*)-**7**]BF_4	50	MeOH	25	1	100	100	100	92.3 (*R*)	18
221	*o*-Cl-Ph	CO_2Me	NHAc	[Rh(COD)(1*S*,2*R*)-**7**]BF_4	50	Acetone	25	1	100	100	100	98.4 (*R*)	18
222	*o*-Cl-Ph	CO_2Me	NHAc	[Rh(COD)(*exo*-**40**)]BF_4	34.5	Acetone	25	7	95–100	13.6–14.3	95–100	42 (*R*)	39
223	*m*-Cl-Ph	CO_2Me	NHAc	[Rh(COD)(1*S*,2*R*)-**7**]BF_4	50	MeOH	25	1	100	100	100	95.1(*R*)	18
224	*m*-Cl-Ph	CO_2Me	NHAc	[Rh(COD)(*exo*-**40**)]BF_4	34.5	Acetone	25	7	95–100	13.6–14.3	95–100	85 (*R*)	39
225	*p*-Cl-Ph	CO_2H	NHBz	[Rh(COD)(*S*)-**9**]BF_4	1	MeOH	25	0.05[b]	100	2000	50	90 (*R*)	11
226	*p*-Cl-Ph	CO_2Me	NHAc	[Rh(COD)(1*S*,2*R*)-**7**]BF_4	50	MeOH	25	1	100	100	100	97.8 (*R*)	18, 19

227	*p*-Cl-Ph	CO_2Me	NHBz	[Rh(COD)(1*S*,2*R*)-**7**]BF_4	50	MeOH	25	1	100	100	100	97.0 (*R*)	18, 19
228	*p*-Cl-Ph	CO_2Me	NHBz	[Rh(COD)(*S*)-**9**]BF_4	1	MeOH	25	0.05 [b)]	100	2000	50	89 (*R*)	11
229	*p*-Cl-Ph	CO_2Me	NHBz	[Rh(COD)(*exo*-**40**)]BF_4	34.5	Acetone	25	7	95–100	13.6–14.3	95–100	84 (*R*)	39
230	*p*-Cl-Ph	$PO(OMe)_2$	NHBz	[Rh(COD)(*S*)-**9**]BF_4	1	MeOH	25	0.17 [i)]	96	565	96 [h)]	90 (*S*) [j)]	14
231	*p*-Br-Ph	CO_2Me	NHAc	[Rh(COD)(1*S*,2*R*)-**7**]BF_4	50	MeOH	25	1	100	100	100	98.0 (*R*)	18, 19
232	*p*-Br-Ph	CO_2Me	NHBz	[Rh(COD)(1*S*,2*R*)-**7**]BF_4	50	MeOH	25	1	100	100	100	96.5 (*R*)	18, 19
233	*o*-F-Ph	CO_2H	NHBz	[Rh(COD)(*S*)-**9**]$^+$	1	MeOH	25	0.022 [b)]	100	4545	50	91 (*R*)	42
234	*o*-F-Ph	CO_2H	NHBz	[Rh(COD)(*R*)-**9**]$^+$	1	MeOH	25	0.017 [b)]	100	5882	50	91 (*S*)	42
235	*o*-F-Ph	CO_2H	NHBz	[(2*S*,3*S*)-**35**-CuCl]/[Ru(-COD)Cl]$_2$ (2 : 1)	1	MeOH	25	0.17	100	588	50	75 (*R*)	42
236	*o*-F-Ph	CO_2Me	NHBz	[Rh(COD)(*R*)-**9**]$^+$	1	MeOH	25	0.018	50	2778	50	90.4 (*S*)	42
237	*o*-F-Ph	CO_2Me	NHBz	[Rh(COD)(*R*)-**9**]$^+$	1	MeOH	25	0.018	100	5556	50	89 (*S*)	42
238	*o*-F-Ph	CO_2Me	NHBz	[Rh(COD)(*S*)-**9**]$^+$	1	MeOH	25	0.025	50	2000	50	86.4 (*R*)	42
239	*o*-F-Ph	CO_2Me	NHBz	[Rh(COD)(*S*)-**9**]$^+$	1	MeOH	25	0.022	100	4545	50	88 (*R*)	42
240	*o*-F-Ph	$PO(OMe)_2$	NHBz	[Rh(COD)(*S*)-**9**]BF_4	1	MeOH	25	0.23 [i)]	97	421	97 [h)]	92 (*S*) [j)]	14
241	*m*-F-Ph	CO_2H	NHBz	[(1*S*,2*S*)-**35**-CuCl] /[Ru(COD)Cl]$_2$ (2 : 1)	1	MeOH	25	0.22	100	455	50	71 (*R*)	42
242	*m*-F-Ph	CO_2H	NHBz	[Rh(COD)(*S*)-**9**]$^+$	1	MeOH	25	0.022	100	4545	50	88 (*R*)	42
243	*m*-F-Ph	CO_2H	NHBz	[Rh(COD)(*R*)-**9**]$^+$	1	MeOH	25	0.017	100	5882	50	90 (*S*)	42
244	*m*-F-Ph	CO_2H	NHBz	[Rh(COD)(*R*)-**9**]$^+$	1	MeOH	25	0.33	500	1515	50	89 (*S*)	42
245	*m*-F-Ph	CO_2Me	NHBz	[Rh(COD)(*S*)-**9**]$^+$	1	MeOH	25	0.028	100	3571	50	89 (*R*)	42
246	*m*-F-Ph	CO_2Me	NHBz	[Rh(COD)(*R*)-**9**]$^+$	1	MeOH	25	0.027	100	3703	50	88 (*S*)	42
247	*m*-F-Ph	$PO(OMe)_2$	NHBz	[Rh(COD)(*S*)-**9**]BF_4	1	MeOH	25	0.27 [i)]	96	356	96 [h)]	90 (*S*) [j)]	14
248	*p*-F-Ph	CO_2H	NHBz	[Rh(COD)(*S*)-**9**]$^+$	1	MeOH	25	0.017	100	5882	50	88 (*R*)	42
249	*p*-F-Ph	CO_2H	NHBz	[Rh(COD)(*R*)-**9**]$^+$	1	MeOH	25	0.017	100	5882	50	88 (*S*)	42
250	*p*-F-Ph	CO_2H	NHBz	[Rh(COD)(*S*)-**9**]$^+$	1	MeOH	25	0.28	1000	3571	50	90 (*R*)	42
251	*p*-F-Ph	CO_2H	NHBz	[Rh(COD)(*S*)-**9**]$^+$	1	MeOH	25	2.67	1500	562	50	86 (*R*)	42
252	*p*-F-Ph	CO_2H	NHBz	[Rh(COD)(*S*)-**9**]$^+$ Deuteration	1	MeOH	25	0.017	25	1471	50	90 (*R*)	42
253	*p*-F-Ph	CO_2H	NHBz	[(1*S*,2*S*)-**35**-CuCl]/[Ru(-COD)Cl]$_2$ (2 : 1)	1	MeOH	25	0.15	100	667	50	75 (*R*)	42

Table 27.1 (continued)

Entry	Substrate			Catalyst	Conditions				TON	TOF [h^{-1}]	Conv. [%]	ee [%]	Reference(s)
	R^1	R^2	R^3		$P[H_2]$ [bar]	Solvent	Temp. [°C]	Time [h]					
254	*p*-F-Ph	CO_2Me	NHAc	[Rh(COD)(1*S*,2*R*)-**7**]BF_4	50	MeOH	25	1	100	100	100	97.2 (*R*)	18, 19
255	*p*-F-Ph	CO_2Me	NHAc	[Rh(COD)(*exo*-**40**)]BF_4	34.5	Acetone	25	7	95–100	13.6–14.3	95–100	80 (*R*)	39
256	*p*-F-Ph	CO_2Me	NHBz	[Rh(COD)(*S*)-**9**]$^+$	1	MeOH	25	0.043 [b)]	100	2326	50	89 (*R*)	42
257	*p*-F-Ph	CO_2Me	NHBz	[Rh(COD)(*R*)-**9**]$^+$	1	MeOH	25	0.038 [b)]	100	2632	50	90 (*S*)	42
258	*p*-F-Ph	CO_2Me	NHBoc	[Rh(COD)(*S*)-**9**]BF_4	1	MeOH	25	0.15 [b)]	50	333	50	92 (*R*)	7, 9
259	*p*-F-Ph	CO_2Me	NHBoc	[Rh(COD)(*S*)-**10**]BF_4	1	MeOH	25	0.07 [b)]	50	714	50	94 (*R*)	7, 9
260	*p*-F-Ph	CO_2Me	NHBoc	[Rh(COD)(*R*)-**10**]BF_4	1	MeOH	25	0.07 [b)]	50	714	50	94 (*S*)	7, 9
261	*p*-F-Ph	CO_2Me	NHBoc	[Rh(COD)(*R*)-**11**]BF_4	1	MeOH	25	0.13 [b)]	50	385	50	87 (*S*)	7, 17
262	*p*-F-Ph	CO_2Me	NHBoc	[Rh(COD)(*S*)-**11**]BF_4	1	MeOH	25	0.13 [b)]	50	385	50	86 (*R*)	17
263	*p*-F-Ph	$PhPO_2Et$	NHBz	[Rh(COD)(*S*)-**9**]BF_4	1	MeOH	25	1 [b)]	25	25	50	64 (*Sc*) [g)]	12
264	*p*-F-Ph	$PhPO_2Et$	NHBz	[Rh(COD)(*S*)-**9**]BF_4	1	MeOH	25	1	95	95	95	64 (*Sc*) [g)]	16
265	*p*-F-Ph	$PO(OMe)_2$	NHBz	[Rh(COD)(*S*)-**9**]BF_4	1	MeOH	25	0.23 [i)]	96	417	96 [h)]	89 (*S*) [j)]	14
266	*p*-CF_3-Ph	CO_2H	NHBz	[Rh(COD)(*S*)-**9**]$^+$	1	MeOH	25	0.017 [b)]	100	5882	50	90 (*R*)	42
267	*p*-CF_3-Ph	CO_2Me	NHBoc	[Rh(COD)(*S*)-**10**]BF_4	1	MeOH	25	0.1 [b)]	50	500	50	93 (*R*)	7, 9
268	*p*-CF_3-Ph	CO_2Me	NHBoc	[Rh(COD)(*S*)-**10**]BF_4	1	MeOH	25	0.07 [b)]	50	714	50	95 (*R*)	7, 9
269	*p*-CF_3-Ph	CO_2Me	NHBoc	[Rh(COD)(*R*)-**10**]BF_4	1	MeOH	25	0.08 [b)]	50	625	50	94 (*S*)	7, 9, 17
270	*p*-CF_3-Ph	CO_2Me	NHBoc	[Rh(COD)(*R*)-**11**]BF_4	1	MeOH	25	0.17 [b)]	50	294	50	86 (*S*)	7
271	*p*-CF_3-Ph	CO_2Me	NHBoc	[Rh(COD)(*S*)-**11**]BF_4	1	MeOH	25	0.17 [b)]	50	294	50	85 (*R*)	17
272	*p*-CF_3-Ph	$PO(OMe)_2$	NHBz	[Rh(COD)(*S*)-**9**]BF_4	1	MeOH	25	0.17 [i)]	95	559	95 [h)]	90 (*S*) [j)]	14
273	*p*-CN-Ph	CO_2H	NHBz	[Rh(COD)(*S*)-**9**]BF_4	1	MeOH	25	0.05 [b)]	100	2000	50	95 (*R*)	11
274	*p*-NO_2-Ph	CO_2H	NHBz	[Rh(COD)(1*S*,2*R*)-**7**]BF_4	50	MeOH	25	1	100	100	100	97.4 (*R*)	18, 19
275	*p*-NO_2-Ph	CO_2H	NHBz	[Rh(COD)(*S*)-**9**]BF_4	1	MeOH	25	0.05 [b)]	100	2000	50	91 (*R*)	11

276	*p*-NO_2-Ph	CO_2H	NHBz	[Rh(COD)(*R*)-**9**]BF_4	1	MeOH	25	0.05 [b]	100	2000	50	90 (*S*)	11
277	*p*-NO_2-Ph	CO_2Me	NHAc	[Rh(COD)(1*S*,2*R*)-**7**]BF_4	50	MeOH	25	1	100	100	100	97.5 (*R*)	18, 19
278	*p*-NO_2-Ph	CO_2Me	NHAc	[Rh(COD)(*exo*-**40**)]BF_4	34.5	Acetone	25	7	95–100	13.6–14.3	95–100	90 (*R*)	39
279	*p*-NO_2-Ph	CO_2Me	NHBz	[Rh(COD)(*S*)-**9**]BF_4	1	MeOH	25	0.05 [b]	100	2000	50	80 (*R*)	11
280	*p*-NO_2-Ph	CO_2Me	NHBoc	[Rh(COD)(*S*)-**9**]BF_4	1	MeOH	25	0.1 [b]	50	500	50	92 (*R*)	7, 9
281	*p*-NO_2-Ph	CO_2Me	NHBoc	[Rh(COD)(*S*)-**10**]BF_4	1	MeOH	25	0.08 [b]	50	625	50	93 (*R*)	7, 9
282	*p*-NO_2-Ph	CO_2Me	NHBoc	[Rh(COD)(*R*)-**10**]BF_4	1	MeOH	25	0.1 [b]	50	500	50	94 (*S*)	7, 9, 17
283	*p*-NO_2-Ph	CO_2Me	NHBoc	[Rh(COD)(*R*)-**11**]BF_4	1	MeOH	25	0.15 [b]	50	385	50	85 (*S*)	7, 17
284	*p*-NO_2-Ph	CO_2Me	NHBoc	[Rh(COD)(*S*)-**11**]BF_4	1	MeOH	25	0.15 [b]	50	333	50	85 (*R*)	17
285	*p*-NO_2-Ph	$PO(OMe)_2$	NHBz	[Rh(COD)(*S*)-**9**]BF_4	1	MeOH	25	0.17 [i]	95	559	95 [h]	91 (*S*) [j]	14
286	*p*-NO_2-Ph	$PhPO_2Et$	NHBz	[Rh(COD)(*S*)-**9**]BF_4	1	MeOH	25	0.75	95	127	95	60 (*S*c) [g]	16
287	*o*-HO-Ph	CO_2Me	NHBz	[Rh(COD)(1*S*,2*R*)-**7**]BF_4	50	MeOH	25	1	100	100	100	96.3 (*R*)	18, 19
288	*p*-MeO-Ph	CO_2H	NHBz	[Rh(COD)(*S*)-**9**]BF_4	1	MeOH	25	0.05 [b]	100	2000	50	90 (*R*)	11
289	*p*-MeO-Ph	CO_2H	NHBz	[Rh(COD)(*R*)-**9**]BF_4	1	MeOH	25	0.05 [b]	100	2000	50	92 (*S*)	11
290	*p*-MeO-Ph	CO_2Me	NHBz	[Rh(COD)(*S*)-**9**]BF_4	1	MeOH	25	0.05 [b]	100	2000	50	88 (*R*)	11
291	*p*-MeO-Ph	CO_2Me	NHBz	[Rh(COD)(*R*)-**9**]BF_4	1	MeOH	25	0.05 [b]	100	2000	50	91 (*S*)	11
292	*p*-MeO-Ph	CO_2Me	NHAc	[Rh(COD)(1*S*,2*R*)-**7**]BF_4	50	MeOH	25	1	100	100	100	97.3 (*R*)	18, 19
293	*p*-MeO-Ph	CO_2Me	NHAc	[Rh(COD)(*exo*-**40**)]BF_4	34.5	Acetone	25	7	95–100	13.6–14.3	95–100	82 (*R*)	39
294	*p*-AcO-Ph	CO_2Me	NHAc	[Rh(COD)(1*S*,2*R*)-**7**]BF_4	50	MeOH	25	1	100	100	100	95.6 (*R*)	18, 19
295	*p*-AcO-Ph	CO_2Me	NHAc	[Rh(COD)(*exo*-**40**)]BF_4	34.5	Acetone	25	7	95–100	13.6–14.3	95–100	80 (*R*)	39
296	*p*-NMe_2-Ph	CO_2H	NHBz	[Rh(COD)(*R*)-**9**]BF_4	1	MeOH	25	0.05 [b]	50	1000	50	72 (*S*)	11
297	*p*-NMe_2-Ph	CO_2Me	NHBz	[Rh(COD)(*R*)-**9**]BF_4	1	MeOH	25	0.05 [b]	100	2000	50	85 (*S*)	11
298	*o*-Me-Ph	CO_2H	NHBz	[Rh(COD)(*S*)-**9**]BF_4	1	MeOH	25	0.05 [b]	100	2000	50	86 (*S*)	11
299	*p*-Me-Ph	CO_2H	NHBz	[Rh(COD)(*S*)-**9**]BF_4	1	MeOH	25	0.05 [b]	100	2000	50	89 (*S*)	11
300	*p*-Me-Ph	CO_2Me	NHAc	[Rh(COD)(1*S*,2*R*)-**7**]BF_4	50	MeOH	25	1	100	100	100	97.3 (*R*)	18, 19
301	*p*-Me-Ph	CO_2Me	NHAc	[Rh(COD)(*exo*-**40**)]BF_4	34.5	Acetone	25	7	95–100	13.6–14.3	95–100	62 (*R*)	39

Table 27.1 (continued)

Entry	Substrate			Catalyst	Conditions				TON	TOF [h^{-1}]	Conv. [%]	ee [%]	Reference(s)
	R^1	R^2	R^3		$P[H_2]$ [bar]	Solvent	Temp. [°C]	Time [h]					
302	*p*-Me-Ph	CO_2Me	NHBoc	[Rh(COD)(*S*)-**10**]BF_4	1	MeOH	25	0.12 [b)]	50	417	50	93 (*R*)	7, 9
303	*p*-Me-Ph	CO_2Me	NHBoc	[Rh(COD)(*R*)-**11**]BF_4	1	MeOH	25	0.18	50	278	50	85 (*S*)	7, 17
304	*p*-Me-Ph	CO_2Me	NHBoc	[Rh(COD)(*S*)-**11**]BF_4	1	MeOH	25	0.16 [b)]	50	313	50	84 (*R*)	17
305	4-^{i}Pr-Ph	CO_2H	NHBz	[Rh(COD)(*S*)-**9**]BF_4	1	MeOH	25	0.05 [b)]	100	2000	50	92 (*R*)	11
306	4-^{i}Pr-Ph	CO_2Me	NHBz	[Rh(COD)(*R*)-**9**]BF_4	1	MeOH	25	0.05 [b)]	100	2000	50	89 (*S*)	11
307	4-^{i}Pr-Ph	$PhPO_2Et$	NHBz	[Rh(COD)(*S*)-**9**]BF_4	1	MeOH	25	2.35 [b)]	25	11	50	60 (*Sc*) [g)]	12
308	4-^{i}Pr-Ph	$PhPO_2Et$	NHBz	[Rh(COD)(*S*)-**9**]BF_4	1	MeOH	25	4.5	95	21	95	60 (*Sc*) [g)]	16
309	4-^{i}Pr-Ph	$PO(OMe)_2$	NHBz	[Rh(COD)(*S*)-**9**]BF_4	1	MeOH	25	0.4 [i)]	95	238	95 [h)]	87 (*S*) [j)]	14
310	*p*-^{t}Bu-Ph	CO_2Me	NHBoc	[Rh(COD)(*S*)-**10**]BF_4	1	MeOH	25	0.12 [b)]	50	417	50	92 (*R*)	7, 9
311	*p*-^{t}Bu-Ph	CO_2Me	NHBoc	[Rh(COD)(*R*)-**11**]BF_4	1	MeOH	25	0.25 [b)]	50	200	50	86 (*S*)	7, 17
312	*p*-^{t}Bu-Ph	CO_2Me	NHBoc	[Rh(COD)(*S*)-**11**]BF_4	1	MeOH	25	0.25 [b)]	50	200	50	85 (*R*)	17
313	2,4-dimethyl-Ph	CO_2H	NHBz	[Rh(COD)(*S*)-**9**]BF_4	1	MeOH	25	0.05 [b)]	100	2000	50	79 (*R*)	11
314	2,4-dimethyl-Ph	CO_2Me	NHBz	[Rh(COD)(*R*)-**9**]BF_4	1	MeOH	25	0.05 [b)]	100	2000	50	82 (*S*)	11
315	1-naphthyl	CO_2H	NHBz	[Rh(COD)(*S*)-**9**]BF_4	1	MeOH	25	0.05 [b)]	100	2000	50	86 (*R*)	11
316	1-naphthyl	CO_2H	NHBz	[Rh(COD)(*R*)-**9**]BF_4	1	MeOH	25	0.05 [b)]	100	2000	50	88 (*S*)	11
317	2-naphthyl	CO_2H	NHBz	[Rh(COD)(*S*)-**9**]BF_4	1	MeOH	25	0.05 [b)]	100	2000	50	87 (*R*)	11
318	2-naphthyl	CO_2H	NHBz	[Rh(COD)(*R*)-**9**]BF_4	1	MeOH	25	0.05 [b)]	100	2000	50	92 (*S*)	11
319	2-naphthyl	CO_2Me	NHBz	[Rh(COD)(*S*)-**9**]BF_4	1	MeOH	25	0.05 [b)]	100	2000	50	89 (*R*)	11
320	2-naphthyl	CO_2Me	NHBz	[Rh(COD)(*S*)-**9**]BF_4	1	MeOH	25	0.05 [b)]	100	2000	50	89 (*S*) [e)]	11
321	9-phenanthryl	CO_2H	NHBz	[Rh(COD)(*S*)-**9**]BF_4	1	MeOH	25	0.05 [b)]	50	000	50	65 (*R*)	11
322	9-phenanthryl	CO_2H	NHBz	[Rh(COD)(*R*)-**9**]BF_4	1	MeOH	25	0.05 [b)]	25	500	50	63 (*S*)	11
323	3-OMe-4-OAc-Ph	CO_2Me	NHAc	[Rh(COD)(1*S*,2*R*)-**7**]BF_4	50	MeOH	25	1	50	100	100	98.1 (*R*)	18, 19
324	3-OAc-4-OMe-Ph	CO_2Me	NHAc	[Rh(COD)(1*R*,2*S*)-**7**]BF_4	50	MeOH	25	1	100	100	100	97.4 (*S*)	18

325	3-Me-4-OAc-Ph	CO_2Me	NHAc	[Rh(COD)(*exo*-**40**)]BF_4	34.5	Acetone	25	7	95–100	13.6–14.3	95–100	75 (*R*)	39
326	3-OH-4-OMe-Ph	CO_2H	NHBz	Rh(COD)(*S*)-**9**	1	MeOH	25	0.083 [b)]	50	602	50	83 (*R*)	15
327	3,4-$(OMe)_2$Ph	CO_2H	NHAc	[Rh(COD)(*S*)-**9**]BF_4	1	MeOH	25	0.05 [b)]	50	1000	50	90 (*R*)	15
328	3,4-$(OMe)_2$Ph	CO_2H	NHBz	Rh(COD)(*S*)-**9**	1	MeOH	25	0.12 [b)]	50	417	50	82 (*R*)	15
329	3,4-$(OMe)_2$Ph	CO_2H	NHBz	[(*R*)-**9**+CuCl]/[Ru(COD)Cl]$_2$	1	MeOH	25	0.45 [b)]	250	556	50	87 (*S*)	15
330	3,4-$(OMe)_2$Ph	CO_2Me	NHAc	[Rh(COD)(*R*)-**9**]BF_4	1	MeOH	25	0.067 [b)]	50	746	50	87 (*S*)	15
331	3,4-$(OMe)_2$Ph	CO_2Me	NHAc	[Rh(COD)(*S*)-**9**]BF_4	1	MeOH	25	0.5 [b)]	500	1000	50	81 (*R*) [m,p)]	15
332	3,4-$(OMe)_2$Ph	CO_2Me	NHBz	Rh(COD)(*S*)-**9**	1	MeOH	25	0.2 [b)]	50	250	50	84 (*R*)	15
333	3,4-$(OMe)_2$Ph	CO_2Me	NHBz	Rh(COD)(*S*)-**9**	1	PhH	25	1.75 [b)]	50	29	50	8 (*R*)	15
334	2-Cl-3-OAc-4-OMe-Ph	CO_2Me	NHBz	[Rh(COD)(1*S*,2*R*)-**7**]BF_4	50	MeOH	25	1	100	100	100	98.0 (*R*)	18
335	4-OMe-3-OAc-Ph	NHCOMe	CO_2H	[Rh(COD)(*S*)-**2**]ClO_4	1	EtOH/PhH (2:1)	20	0.17-0.5	200	400-1176	100	83 (*R*)	32
336	4-OMe-3-OAc-Ph	NHCOMe	CO_2H	[Rh(COD)(*S*)-**29**]ClO_4	1	EtOH/PhH (2:1)	20	0.17-0.5	200	400-1176	100	82 (*S*)	32
337	3,4-methylene-dioxyphenyl	CO_2H	NHAc	Rh(COD)(*S*)-**9**	1	PhH	25	0.12 [b)]	50	417	50	67 (*R*)	15
338	3,4-methylene-dioxyphenyl	CO_2Me	NHAc	[Rh(COD)(1*S*,2*R*)-**7**]BF_4	50	MeOH	25	1	100	100	100	97.5 (*R*)	18
339	3,4-methylene-dioxyphenyl	CO_2Me	NHAc	[Rh(COD)(*exo*-**40**)]BF_4	34.5	Acetone	25	7	95–100	13.6–14.3	95–100	76 (*R*)	39
340	3,4-methylene-dioxyphenyl	NHCOMe	CO_2H	[Rh(COD)(*S*)-**2**]ClO_4	1	EtOH/PhH (2:1)	20	0.17–0.5	200	400–1176	100	78 (*R*)	32
341	3,4-methylene-dioxyphenyl	NHCOMe	CO_2H	[Rh(COD)(*S*)-**29**]ClO_4	1	EtOH/PhH (2:1)	20	0.17–0.5	200	400–1176	100	81 (*S*)	32
342	2-furyl	CO_2Me	NHAc	[Rh(COD)(1*S*,2*R*)-**7**]BF_4	50	MeOH	25	1	100	100	100	91.1 (*R*)	18
343	2-furyl	CO_2Me	NHAc	[Rh(COD)(*exo*-**40**)]BF_4	34.5	Acetone	25	7	95–100	13.6–14.3	5–100	83 (*R*)	39

Table 27.1 (continued)

Entry	Substrate			Catalyst	Conditions				TON	TOF [h^{-1}]	Conv. [%]	ee [%]	Reference(s)
	R^1	R^2	R^3		$P[H_2]$ [bar]	Solvent	Temp. [°C]	Time [h]					
344	Thiophen-2-yl	CO_2H	NHAc	[Rh(COD)(*S*)-**9**]$^+$	1	MeOH	25	0.033 [b)]	50	1515	50	90 (*R*)	4
345	Thiophen-2-yl	CO_2H	NHAc	[Rh(COD)(*S*)-**9**]$^+$	1	MeOH	25	0.43 [b)]	500	1163	50	89 (*R*)	4
346	Thiophen-2-yl	CO_2H	NHAc	[Rh(COD)(*R*)-**9**]$^+$	1	MeOH	25	0.033 [b)]	50	1515	50	90 (*S*)	4
347	Thiophen-2-yl	CO_2H	NHAc	[Rh(COD)(1*S*,2*S*)-**35**]$^+$	1	MeOH	25	0.058 [b)]	50	862	50	78 (*R*)	4
348	Thiophen-2-yl	CO_2H	NHBz	[Rh(COD)(1*S*,2*S*)-**35**]$^+$	1	MeOH	25	0.067 [b)]	50	746	50	80 (*R*)	4
349	Thiophen-2-yl	CO_2H	NHBz	[Rh(COD)(*R*)-**9**)]$^+$	1	MeOH	25	0.042 [b)]	50	1190	50	90 (*S*)	4
350	Thiophen-2-yl	CO_2Me	NHAc	[Rh(COD(*S*)-**9**)]$^+$	1	MeOH	25	0.05 [b)]	50	1000	50	88 (*R*)	4
351	Thiophen-2-yl	CO_2Me	NHAc	[Rh(COD(*S*)-**9**)]$^+$	1	MeOH	25	0.33 [b)]	250	758	50	86 (*R*)	4
352	Thiophen-2-yl	CO_2Me	NHAc	[Rh(COD)(1*R*,3*R*,5*R*)-**28**]BF_4	1	MeOH	25	0.1 [b)]	50	500	50	63 (*R*)	40
353	Thiophen-2-yl	CO_2Me	NHAc	[Rh(COD) (+)(1*S*,2*S*)-**35**]$^+$	1	MeOH	25	0.067 [b)]	50	746	50	77 (*R*)	4
354	Thiophen-2-yl	CO_2Me	NHBz	[Rh(COD)(1*S*,2*S*)-**35**]$^+$	1	MeOH	25	0.083	50	602	50	75 (*R*)	4
355	Thiophen-2-yl	CO_2Me	NHBz	[Rh(COD)(*R*)-**9**)]$^+$	1	MeOH	25	0.67 [b)]	50	746	50	90 (*S*)	4
356	Thiophen-3-yl	CO_2H	NHAc	[Rh(COD)(*S*)-**9**]$^+$	1	MeOH	25	0.017 [b)]	50	2941	50	88 (*R*)	4
357	Thiophen-3-yl	CO_2H	NHAc	[Rh(COD)(*S*)-**9**]$^+$	1	MeOH	25	0.13 [b)]	500	3846	50	84 (*R*)	4
358	Thiophen-3-yl	CO_2H	NHAc	[Rh(COD)(1*S*,2*S*)-**35**]$^+$	1	MeOH	25	0.042 [b)]	50	1190	50	70 (*R*)	4
359	Thiophen-3-yl	CO_2H	NHBz	[Rh(COD)(*S*)-**9**]$^+$	1	MeOH	25	0.017 [b)]	50	2941	50	85 (*R*)	4
360	Thiophen-3-yl	CO_2H	NHBz	[Rh(COD)(*S*)-**9**]$^+$	1	MeOH	25	0.058 [b)]	250	4310	50	84 (*R*)	4
361	Thiophen-3-yl	CO_2H	NHBz	[Rh(COD)(+)(1*S*,2*S*)-**35**]$^+$	1	MeOH	25	0.042 [b)]	50	1190	50	65 (*R*)	4
362	Thiophen-3-yl	CO_2Me	NHAc	[Rh(COD)(*S*)-**9**)]$^+$	1	MeOH	25	0.02 [b)]	50	2500	50	86 (*R*)	4
363	Thiophen-3-yl	CO_2Me	NHAc	[Rh(COD)(*S*)-**9**)]$^+$	1	MeOH	25	0.25 [b)]	250	1000	50	83 (*R*)	4
364	Thiophen-3-yl	CO_2Me	NHAc	[Rh(COD)(1*R*,3*R*,5*R*)**28**]BF_4	1	MeOH	25	0.017 [b)]	50	2941	50	64 (*R*)	40
365	Thiophen-3-yl	CO_2Me	NHAc	[Rh(COD)(1*S*,2*S*)-**35**]$^+$	1	MeOH	25	0.033 [b)]	50	1515	50	72 (*R*)	4

366	Thiophen-3-yl	CO_2Me	NHBz	[Rh(COD)(*S*-**9**)]$^+$	1	MeOH	25	0.025 [b]	50	2000	50	85 (*R*)	4
367	Thiophen-3-yl	CO_2Me	NHBz	[Rh(COD)(1*R*,3*R*,5*R*)-**28**]BF_4	1	MeOH	25	0.05 [b]	50	1000	50	64 (*R*)	40
368	Thiophen-3-yl	CO_2Me	NHBz	[Rh(COD)(+)(1*S*,2*S*)-**35**]$^+$	1	MeOH	25	0.042 [b]	50	1190	50	70 (*R*)	4
369	Pyridin-3-yl	CO_2H	NHAc	[Rh(COD)(*S*)-**9**]BF_4 [d]	1	MeOH	25	0.033 [b]	50	1515	50	89 (*R*)	5
370	Pyridin-3-yl	CO_2H	NHAc	[Rh(COD)(*R*)-**9**]BF_4 [d]	1	MeOH	25	0.05 [b]	50	1000	50	90 (*S*)	6
371	Pyridin-3-yl	CO_2H	NHAc	[Rh(COD)(*S*)-**9**]BF_4 [d]	1	MeOH	25	0.27 [b]	250	926	50	85 (*R*)	5, 6
372	Pyridin-3-yl	CO_2H	NHAc	[Rh(COD)(*S*)-**9**]BF_4 [d]	1	MeOH	25	0.45 [b]	500	1111	50	78 (*R*)	5, 6
373	Pyridin-3-yl	CO_2H	NHAc	[Rh(COD)(+)(1*S*,2*S*)-**35**] BF_4 [d]	1	MeOH	25	0.083 [b]	50	602	50	86 (*R*)	5
374	Pyridin-3-yl	CO_2H	NHBz	[Rh(COD)(*S*)-**9**]BF_4 [d]	1	MeOH	25	0.67 [b]	50	746	50	86 (*R*) [f]	5, 6
375	Pyridin-3-yl	CO_2H	NHBz	[Rh(COD)(*R*)-**9**]BF_4 [d]	1	MeOH	25	0.05 [b]	50	1000	50	86 (*S*)	6
376	Pyridin-3-yl	CO_2H	NHBz	[Rh(COD)(*S*)-**9**]BF_4 [d]	1	MeOH	25	0.18 [b]	50	1389	50	87 (*R*)	6
377	Pyridin-3-yl	CO_2H	NHBz	[Rh(COD)(1*S*,2*S*)-**35**]BF_4 [d]	1	MeOH	25	0.1 [b]	50	500	50	60 (*R*)	6
378	Pyridin-3-yl	CO_2Me	NHAc	[Rh(COD)(*S*)-**9**]BF_4 [d]	1	MeOH	25	0.05 [b]	50	1000	50	90 (*R*)	6
379	Pyridin-3-yl	CO_2Me	NHAc	[Rh(COD)(*R*)-**9**]BF_4 [d]	1	MeOH	25	0.033 [b]	50	1515	50	89 (*S*)	5, 6
380	Pyridin-3-yl	CO_2Me	NHAc	[Rh(COD)(*S*)-**9**]BF_4 [d]	1	MeOH	25	0.5 [b]	500	1000	50	83 (*R*)	5, 6
381	Pyridin-3-yl	CO_2Me	NHAc	[Rh(COD)(1*S*,2*S*)-**35**] BF_4 [d]	1	MeOH	25	0.067 [b]	50	746	50	84 (*R*)	5
382	Pyridin-3-yl	CO_2Me	NHBz	[Rh(COD)(*S*)-**9**]BF_4 [d]	1	MeOH	25	0.1 [b]	50	500	50	88 (*R*)	5, 6
383	Pyridin-3-yl	CO_2Me	NHBz	[Rh(COD)(*S*)-**9**]BF_4 [d]	1	MeOH	25	0.42 [b]	250	595	50	84 (*R*)	5, 6
384	Pyridin-3-yl	CO_2Me	NHBz	[Rh(COD)(*S*)-**9**]BF_4 [d]	1	MeOH	25	0.67 [b]	500	746	50	81 (*R*)	5, 6
385	Pyridin-3-yl	CO_2Me	NHBz	[Rh(COD)(1*R*,3*R*,5*R*)-**28**]BF_4 [d]	1	MeOH	25	0.12 [b]	50	417	50	59 (*R*)	40
386	Pyridin-3-yl	CO_2Me	NHBz	[Rh(COD)(1*S*,2*S*)-**35**] BF_4	1	MeOH	25	0.18 [b]	50	278	50	70 (*R*)	5
387	Pyridin-4-yl	CO_2H	NHAc	[Rh(COD)(*S*)-**9**]BF_4 [d]	1	MeOH	25	0.033 [b]	50	1515	50	89 (*S*)	5, 6
388	Pyridin-4-yl	CO_2H	NHAc	[Rh(COD)(*S*)-**9**]BF_4 [d]	1	MeOH	25	0.25 [b]	250	1000	50	84 (*R*)	5, 6
389	Pyridin-4-yl	CO_2H	NHAc	[Rh(COD)(1*S*,2*S*)-**35**] BF_4 [d]	1	MeOH	25	0.1 [b]	50	500	50	82 (*R*)	5
390	Pyridin-4-yl	CO_2H	NHBz	[Rh(COD)(*S*)-**9**]BF_4 [d]	1	MeOH	25	0.05 [b]	50	1000	50	87 (*R*)	5, 6
391	Pyridin-4-yl	CO_2H	NHBz	Rh(COD)(1*S*,2*S*)-**35**]BF_4 [d]	1	MeOH	25	0.083 [b]	50	602	50	74 (*R*)	5, 6
392	Pyridin-4-yl	CO_2Me	NHAc	[Rh(COD)(*S*)-**9**]BF_4 [d]	1	MeOH	25	0.033 [b]	50	11515	50	89 (*R*)	5, 6
393	Pyridin-4-yl	CO_2Me	NHAc	[Rh(COD)(*S*)-**9**]BF_4 [d]	1	MeOH	25	0.42 [b]	500	1190	50	86 (*R*)	5, 6

Table 27.1 (continued)

Entry	Substrate			Catalyst	Conditions				TON	TOF [h^{-1}]	Conv. [%]	ee [%]	Reference(s)
	R^1	R^2	R^3		$P[H_2]$ [bar]	Solvent	Temp. [°C]	Time [h]					
394	Pyridin-4-yl	CO_2Me	NHAc	[Rh(COD)(1*S*,2*S*)-**35**]BF_4 [d)]	1	MeOH	25	0.067 [b)]	50	746	50	74 (*R*)	5
395	Pyridin-4-yl	CO_2Me	NHBz	[Rh(COD)(*R*)-**9**]BF_4 [d)]	1	MeOH	25	0.05 [b)]	50	1000	50	90 (*S*)	5, 6
396	Pyridin-4-yl	CO_2Me	NHBz	[Rh(COD)(*S*)-**9**]BF_4 [d)]	1	MeOH	25	0.42 [b)]	500	1190	50	86 (*R*)	5
397	Pyridin-4-yl	CO_2Me	NHBz	[Rh(COD)(1*R*,3*R*,5*R*)-**28**]BF_4 [d)]	1	MeOH	25	0.12 [b)]	50	417	50	59 (*R*)	40
398	Pyridin-4-yl	CO_2Me	NHBz	[Rh(COD)(1*S*,2*S*)-**35**] BF_4	1	MeOH	25	0.1 [b)]	50	500	50	72 (*R*)	6
399	$PhCH_2$	CO_2H	NHAc	[Rh(COD)(1*R*,2*S*)-**7**]ClO_4	50	MeOH	r.t.	4	81	20.3	81	2.9 (*S*) [c)]	30
400	$PhCH_2$	CO_2Et	NHAc	[Rh(COD)(1*S*,2*R*)-**7**]BF_4	50	MeOH	25	1	100	100	100	93.1 (*R*)	18
401	$PhCH_2$	CO_2Et	NHAc	[Rh(COD)(1*R*,2*S*)-**7**]BF_4	50	MeOH	25	1	100	100	100	92.5 (*S*)	18, 30
402	$PhCH_2$	CO_2Et	NHAc	[Rh(COD)(1*R*,2*S*)-**7**]ClO_4	50	EtOH	r.t.	1	100	100	100	77.1 (*S*)	30
403	$PhCH_2$	CO_2Et	NHAc	[Rh(COD)(1*R*,2*S*)-**7**]ClO_4	50	IPA	r.t.	1	100	100	100	83.9 (*S*)	30
404	$PhCH_2$	CO_2Et	NHAc	[Rh(COD)(1*R*,2*S*)-**7**]ClO_4	50	THF	r.t.	1	100	100	100	88.3 (*S*)	30
405	$PhCH_2$	CO_2Et	NHAc	[Rh(COD)(1*R*,2*S*)-**7**]ClO_4	50	CH_2Cl_2	r.t.	1	76.1	76.1	76.1	52.4 (*S*)	30
406	$PhCH_2$	CO_2Et	NHAc	[Rh(COD)(1*R*,2*S*)-**7**]ClO_4	50	Acetone	r.t.	1	89.3	89.3	89.3	79.0 (*S*)	30
407	$PhCH_2$	CO_2Et	NHAc	[Rh(COD)(1*R*,2*S*)-**7**]ClO_4	50	PhH	r.t.	1	100	100	100	80.2 (*S*)	30
408	$PhCH_2$	CO_2Et	NHAc	[Rh(COD)(1*R*,2*S*)-**7**]ClO_4	3	MeOH	r.t.	5	100	20	100	94.6 (*S*)	30
409	$PhCH_2$	CO_2Et	NHAc	[Rh(COD)(1*R*,2*S*)-**7**]ClO_4	20	MeOH	r.t.	3	100	33	100	95.2 (*S*)	30
410	$PhCH_2$	CO_2Et	NHAc	[Rh(COD)(1*R*,2*S*)-**7**]ClO_4	50	MeOH	r.t.	1	100	100	100	95.7 (*S*)	30
411	$PhCH_2$	CO_2Et	NHAc	[Rh(COD)(1*R*,2*S*)-**7**]ClO_4	50	MeOH	–10	4	100	25	100	93.6 (*S*)	30
412	$PhCH_2$	CO_2Et	NHAc	[Rh(COD)(1*R*,2*S*)-**7**]ClO_4	50	MeOH	10	1	100	100	100	95.7 (*S*)	30
413	$PhCH_2$	CO_2Et	NHAc	[Rh(COD)(1*R*,2*S*)-**7**]ClO_4	50	MeOH	30	1	100	100	100	93.3 (*S*)	30
414	$PhCH_2$	CO_2Et	NHAc	[Rh(COD)(1*R*,2*S*)-**7**]ClO_4	50	MeOH	50	0.5	100	200	100	70.8 (*S*)	30
415	$PhCH_2$	CO_2Et	NHAc	[Rh(COD)(1*R*,2*S*)-**7**]ClO_4	50	MeOH	r.t.	1	19	19	19	85.0 (*S*)	30
416	$PhCH_2$	CO_2Et	NHBz	[Rh(COD)(1*R*,2*S*)-**7**]ClO_4	50	MeOH	r.t.	1	100	100	100	94.6 (*S*)	30
417	$PhCH_2$	CO_2Et	NHCbz	[Rh(COD)(1*R*,2*S*)-**7**]ClO_4	50	MeOH	r.t.	1	20	20	20	58.4 (*S*)	30
418	$PhCH_2$	CO_2Et	$NHCO_2CH_2$-$CH(CH_3)_2$	[Rh(COD)(1*R*,2*S*)-**7**]ClO_4	50	MeOH	r.t.	1	94	94	94	93.1 (*S*)	30

419	$PhCH_2$	CO_2Et	NHBoc	[Rh(COD)(1*R*,2*S*)-**7**]ClO_4	50	MeOH	r.t.	4	43	10.8	43	78.1 (*S*)	30
420	H	CO_2H	CH_2CO_2H	[Rh(COD)(*S*)-**1**]ClO_4	1	EtOH	20	–	–	–	–	10 (*R*)[a]	2a, b
421	H	CO_2H	CH_2CO_2H	[Rh(COD)(1*R*,2*S*)-**3**]BF_4	1	Dioxane	25	–	–	–	–	64 (*S*)	36
422	H	CO_2H	CH_2CO_2H	[Rh(COD)(1*R*,2*S*)-**3**]BF_4	1	MeOH	25	–	–	–	–	59 (*S*)	36
423	H	CO_2H	CH_2CO_2H	[Rh(COD)(1*R*)-**4**]BF_4	1	Dioxane	25	–	–	–	–	3 (*S*)	36
424	H	CO_2H	CH_2CO_2H	[Rh(COD)(1*R*)-**4**]BF_4	1	MeOH	25	–	–	–	–	0	36
425	H	CO_2H	CH_2CO_2H	[Rh(COD)(1*R*,2*R*)-**5**]BF_4	1	Dioxane	25	–	–	–	–	12 (*R*)	36
426	H	CO_2H	CH_2CO_2H	[Rh(COD)(1*R*,2*R*)-**5**]BF_4	1	MeOH	25	–	–	–	–	8 (*R*)	36
427	H	CO_2H	CH_2CO_2H	[Rh(COD)(2*R*)-**6**]BF_4	1	Dioxane	25	–	–	–	–	31 (*R*)	36
428	H	CO_2H	CH_2CO_2H	[Rh(COD)(2*R*)-**6**]BF_4	1	MeOH	25	–	–	–	–	14 (*R*)	36
429	H	CO_2Me	CH_2CO_2Me	[Rh(COD)(*R*)-**9**]BF_4	1	CD_3OD	25	–	–	–	–	70 (*S*)	13
430	H	CO_2Me	CH_2CO_2Me	[Rh(COD)(*R*)-**13**]BF_4	1	CD_3OD	25	–	–	–	–	40 (*S*)	13
431	H	CO_2Me	CH_2CO_2Me	[Rh(COD)(*R*)-**14**]BF_4	1	CD_3OD	25	–	–	–	–	78 (*S*)	13
432	H	CO_2Me	CH_2CO_2Me	[Rh(COD)(*R*)-**15**]BF_4	1	CD_3OD	25	–	–	–	–	80 (*S*)	13
433	H	CO_2Me	CH_2CO_2Me	[Rh(COD)(*R*)-**16**]BF_4	1	CD_3OD	25	–	–	–	–	25 (*S*)	13
434	H	CO_2H	CH_2CO_2H	[Rh(COD)(*S*)-**29**]ClO_4	1	EtOH	20	–	–	–	–	20 (*R*)[a]	2a, b

a) Optical yield.
b) t/2 for uptake 50% of theoretical hydrogen volume.
c) ee determination of the corresponding ester using diazomethane.
d) Addition of 1.5 equiv. HBF_4 .
e) ee determination after recrystallization.
f) Partial reaction with methanol to produce the corresponding ester.
g) The ee-values with respect to the α-carbon atom can be determined from the enantiomeric excesses of the diastereomer pairs of the ester.
h) Crude yield after evaporation of solvent.
i) Approx. reaction time = approx. time for uptake of half of the H_2 volume × 2.
j) Configuration (*S*) corresponds to the D-configuration of amino carboxylic acids.
k) Catalyst [RhCOD(*R*)-**9**]$^+$ – half-year exposure to air.
l) Preformed ligand-RhCl(Benzene).
m) Preformed complex.
n) Exposed to air.
o) Stirred for 1 h in 50% methanol/water.
p) Stock solution in benzene after 10 days (29 mL methanol + 1 mL stock solution).
q) Ligand stored for one month on air.
r) Catalyst solution agitated for 30 min with air.

Table 27.2 Asymmetric hydrogenation of other prochiral olefins.

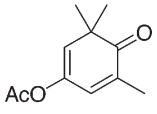

11

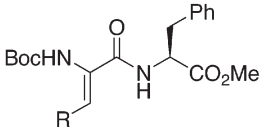

12

12a: R = Ph
12b: R = *p*-CH_3-Ph
12c: R = *p*-F-Ph
12d: R = *p*-CF_3-Ph

Entry	Catalyst	Substrate	Conditions				TON	TOF [h^{-1}]	Conv. [%]	ee [%]	Reference
			P[H_2] [bar]	Solvent	Temp. [°C]	Time h]					
1	[Rh(*R*)-**25**]BF_4	11	10	EtOAc	r.t.	18	100	5.6	100	71 (*S*)	34
2	[Rh(*S*)-**26**]BF_4	11	10	EtOAc	r.t.	18	100	5.6	100	71 (*R*)	34
3	[Rh(*S*)-**27**]BF_4	11	10	EtOAc	r.t.	18	100	5.6	100	5 (*S*)	34
4	[Rh(*S*)-**32**]BF_4	11	10	EtOAc	r.t.	18	100	5.6	100	30 (*R*)	34
5	[Rh(*S*)-**33**]BF_4	11	10	EtOAc	r.t.	18	100	5.6	100	95 (*R*)	34
6	[Rh(*S*)-**34**]BF_4	11	10	EtOAc	r.t.	18	100	5.6	100	31 (*R*)	34
7	[Rh(COD)(*R*)-**10**]BF_4	12a	1	MeOH	25	1	–	–	–	77 [a)]	7
8	[Rh(COD)(*R*)-**10**]BF_4	12b	1	MeOH	25	1.17	–	–	–	76 [a)]	7
9	[Rh(COD)(*R*)-**10**]BF_4	12c	1	MeOH	25	1.3	–	–	–	78 [a)]	7
10	[Rh(COD)(*R*)-**10**]BF_4	12d	1	MeOH	25	1.17	–	–	–	91 [a)]	7

a) The ee-values with respect to the *α*-carbon atom can be determined from the enantiomeric excesses of the diastereomer pairs of the ester (see [12]).

10 000 was completed within 16 h, giving the desired product in 97% ee (Table 27.1, entry 120; 98.3% ee at SCR 100, Table 27.1, entry 118). These results were comparable to those using phosphine and phosphinite ligands (e.g., DuPhos, 99% ee [20]; DIPAMP, 96% ee [21]; TRAP, 92% ee [22]; DIOP, 55% ee [23]; CAPP, 95.6% ee [24]; BPPFA, 21% ee [25]; Ph-β-Glup, 91.5% ee [26]; SpirOP, 95.7% ee [27]). Further application in the hydrogenation of methyl 2-acetamido-3-(3-methoxy-4-acetoxyphenyl)-acrylate (a crucial intermediate in the synthesis of L-dopa [28]) was successfully achieved in 97.4% ee (Table 27.1, entry 324). Similarly, the enantioselective hydrogenation of ethyl (*Z*)-2-acetamido-4-phenylcrotonate gave the homophenylalanine derivative in 92.5% ee (Table 27.1, entry 401). This product is a key component of (*S*,*S*)-benazepril, an angiotensin-converting enzyme inhibitor widely used as an antihypertensive agent [29]. Jiang studied the hydrogenation of *N*-protected (*Z*)-2-aminocrotonates and found that the enantioselectivity and activity were strongly dependent on the type of *N*-protecting group used (NHAc, 95.7% ee with 100% conv.; $NHCO_2Me$, 85% ee with 19% conv.; Table 27.1, entry 412 versus 415) [30]. The results from using Rh–DPAMPP compared favorably with many commonly used chiral Rh–diphosphine catalysts (e.g., Rh–BINAP, 21.8% ee with 100% conv.; Rh–DIPAMP, 50.8% ee with 100% conv.; Rh–BDPP, 69.4% ee with 100% conv.; Rh–PPM, 14.4% ee with 7.9% conv. under the same reaction conditions).

The introduction of extra stereogenicity at the phosphorus centers is one of the methods used to increase chiral induction. Indeed, replacement of the pro-*R* phenyl with an *o*-anisyl group on the ephedrine backbone of EPHOS **17** gave **19** which was highly effective in the hydrogenation of methyl α-acetamidocinnamate, giving the product in 99% ee (Table 27.1, entry 147). In contrast, the use of EPHOS **17** induced only 46% ee (Table 27.1, entry 144) under the same conditions [31]. Similarly, replacement of the phenyl group with 1-naphthyl gave ligand **20** which led to 95% ee in the same reaction (Table 27.1, entry 149). It is interesting to note that the structurally similar *o*-anisyl ligands **19** and **23** derived from (+) and (–)-ephedrine, respectively, both induce high ee-values with the same (*S*) configuration of the product amino ester. This clearly shows the predominance of the chiral P center over the carbon backbone effect. However, the poor result obtained in the case of **24** bearing *o*-anisyl (*S*p) aminophosphine and (*R*p) phosphinite groups might be due to the quasi-meso structure that did not give any asymmetric induction (Fig. 27.3 c) [1, 31].

Petit reported a close analogue to ProNOP lacking the rigid pyrrolidine ring, yet, the results with both ligands in the hydrogenation of (*E*)-acetamidocinnamic acid derivatives were similar (ProNOP, 61–86% ee; NETAlaNOP, 53–83% ee) [32]. With these substrates, it is important that the problem of *E*/*Z* isomerization (as highlighted by Noyori) should be considered [33]. Ligands **25** to **27** are the only type of amidophosphine-phosphinites applied in asymmetric hydrogenation [34]. Ligand **33** was found to be highly effective in the hydrogenation of 4-oxoisophorone enol acetate (100% conversion, 95% ee (*R*): Table 27.2, entry 5; Scheme 27.1). The product, (*S*)-phorenol acetate, is an intermediate in the synthesis of the natural pigment zeaxanthin [35]. The Rh complexes with **25** or **26**

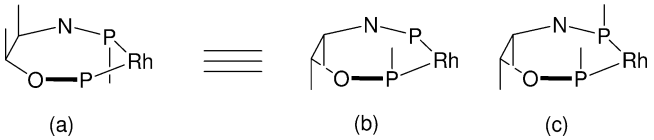

Fig. 27.3 Quasi-meso effect in asymmetric induction.

gave 71% ee in the same reaction (Table 27.2, entries 1 and 2). The other ephedrine-based ligands, including **1** and **3** to **6** [2, 36], afforded poor to moderate enantioselectivity in the rhodium-catalyzed hydrogenation of 2-acetamido-cinnamic acid derivatives. Structural variation leading to increased rigidity of the ligand backbone is one of the promising methods to enhance enantioselectivity. Cesarotti developed an aminophosphine-phosphinite based on the rigid pyrrolidine structure of prolinol [2]. However, results with this ligand in the enantiomeric hydrogenation of dehydroamino acid derivatives were only poor to moderate. Petit [32] improved the results and obtained up to 86% ee. Interestingly, when using [Rh(COD)(L)]ClO_4 as catalyst, both the *Z* and *E* isomeric substrates were converted to products with the same configuration (Table 27.1, entries 93 versus 200).

During the late 1980s, Döbler and Pracejus introduced the bicyclic [2.2.1] system to provide extra conformational rigidity to the ligand backbone [37]. The synthesis of these new chiral ligands was based on the resolution of the amino alcohol obtained from the aminolysis of *exo*-norbornane epoxide [38], followed by reaction with the corresponding chlorophosphine. Indeed, the *in-situ*-prepared cationic or neutral Rh catalysts based on ligand **35** resulted in better enantioselectivity in hydrogenation of 2-acetamido-acrylic acid (up to 89% ee: Table 27.1, entry 6).

The ease of preparation of (1*S*,2*R*)-1-hydroxylmethyl-2-amino-7,7-dimethylbicyclo [2.2.1] heptane from ketopinic acid prompted us to synthesize a new AMPP ligand (i.e., *exo*-**40**) [39]. The rhodium-catalyzed enantioselective hydrogenation of 2-acetamido-acrylic acid using this ligand gave the product in 77% ee with 95–100% conversion. Electron-withdrawing groups on the β-substituted phenyl ring of the substrate resulted in significant enantioselectivity enhancement (Ph, 77% ee; 4-MePh, 62% ee; 4-NO_2Ph, 90% ee). The effect of solvents on the enantioselectivity of the reaction was also quite significant, with acetone being found the best. Döbler performed the enantiomeric hydrogenation of standard dehydroamino acid and other heteroaryl derivatives using the rhodium complex based on bicyclo [3.3.0]-octane (i.e., **28**), resulting in moderate enantioselectivities (58–73% ee) [40]. More recently, ligands **36** to **39** based on the bicyclic

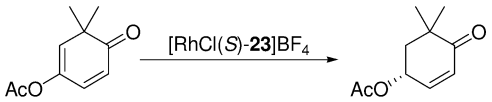

Scheme 27.1 95% ee

[2.2.1] system were prepared [41]. The effect of the additional *P*-stereogenic center(s) was also explored with these ligands. The application of these ligands in enantiomeric hydrogenation resulted in products with up to 91% ee and TOFs ranging from 600 to 4000 h^{-1}. The substitution of one or both P-phenyl groups by a *p*-tolyl group resulted in a slight decrease of the enantioselectivity, regardless of the heteroatom linker (N or O) [42].

27.3 Bisphosphinamidite Ligands

The early development of this type of ligand was concentrated during the late 1970s and early 1980s. In 1976, the first article published on this topic was written by Giongo and co-workers, who described the initial synthesis of a chiral bisphosphinamidite **41** and its application in the enantiomeric hydrogenation of a number of dehydroamino acid derivatives [43]. The resulting enantioselectivities were comparable to the state-of-the-art ligand DIOP. In pursuing the same line of research, the Pracejus group also prepared (*S*,*S*)-**41** and achieved similar results [44]. Subsequently, the Giongo group further introduced other C_2-symmetric, 1,2-diamine-tethered bisphosphinites **42–49** with ee-values reaching 94% in the hydrogenation of (*Z*)-2-acetamidoacrylic acid (Table 27.3) [45]. Interestingly, both Giongo and Onuma noticed that when the hydrogen atoms of the amino groups were replaced with methyl groups whilst keeping the backbone chirality unchanged (as in the cases of **45** versus **46** and **47** versus **48**), a reversal of product configuration was observed. The Onuma group rationalized this by proposing a model wherein the helicity of the edge-phenyl groups on the phosphorus atoms were of opposite sense in the presence and absence of the methyl groups, respectively, as a result of a change of chirality on the nitrogen atoms. Non-C_2-symmetric pyrrolidine-based ligands **50–52** were also tested in asymmetric hydrogenation [47], though the results obtained were unsatisfactory. The use of a 1,4-diamino bridged bisphosphinamidite **53** was described in a recent publication in which excellent selectivity was recorded for the hydrogenation of α-acylaminocinnamic acid [48].

Surprisingly, given that many *P*-chiral ligands are efficient chiral inducers, only one example has been reported of a C_2-symmetric, *P*-chiral bisphosphinamidite. Ligand **54** was prepared by Wills et al. and tested in the Rh-catalyzed enantioselective hydrogenation of α-acylaminoacrylate to give disappointingly low selectivity (33% ee) and low efficiency (TON = 20, TOF = 0.4) [49].

Bisphosphinamidites which are supported by an axially chiral framework are another important class of ligands. Although reported as early as 1980 [50], no reports on the use of binaphthyl-based bisphosphinamidite in asymmetric catalysis were published during the decade thereafter. As described above, the selectivity and substrate generality in these early attempts were very limited in scope. In 1998, we unveiled that by partially hydrogenating BINAM to H_8-BINAM and

Table 27.3 Bisphosphinamidite ligands.

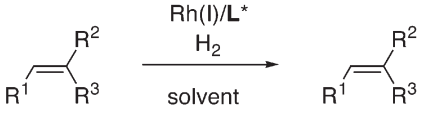

Entry	Substrate			Ligand (L)	P[H_2] [atm]	Solvent	Temp. [°C]	Time [h]	TON Sub:Rh	TOF [h^{-1}]	Conv. [%]	ee [%]	Reference(s)
	R^1	R^2	R^3										
1	H	Ph	NHAc	**55a**	1.0	THF	r.t.	0.5	200	100	100	93	51a, 52
2	H	Ph	NHAc	**55b**	2.0	THF	r.t.	0.17	200	1200	100	98	54
3	H	Ph	NHAc	**56a**	1.0	THF	r.t.	0.5	200	400	100	97	51b
4	H	Ph	NHAc	**56b**	2.0	THF	r.t.	0.17	200	1200	100	96	54
5	H	3-Cl-Ph	NHAc	**55b**	2.0	THF	r.t.	0.17	200	1200	100	98	54
6	H	3-Cl-Ph	NHAc	**56b**	2.0	THF	r.t.	0.17	200	1200	100	98	54
7	H	4-Cl-Ph	NHAc	**55a**	1.0	THF	r.t.	0.5	200	400	100	95	51a
8	H	4-Cl-Ph	NHAc	**56a**	1.0	THF	0	0.5	200	400	100	97	51a, b
9	H	3-Br-Ph	NHAc	**55b**	2.0	THF	r.t.	0.17	200	1200	100	98	54
10	H	3-Br-Ph	NHAc	**56b**	2.0	THF	r.t.	0.17	200	1200	100	97	54
11	H	4-Br-Ph	NHAc	**55b**	2.0	THF	r.t.	0.17	200	1200	100	98	54
12	H	4-Br-Ph	NHAc	**56b**	2.0	THF	r.t.	0.17	200	1200	100	95	54
13	H	4-F-Ph	NHAc	**55a**	1.0	THF	r.t.	0.5	172	344	86	90	51a
14	H	4-F-Ph	NHAc	**56a**	1.0	THF	0	0.5	200	400	100	96	51a, b
15	H	4-CF_3-Ph	NHAc	**55a**	1.0	THF	r.t.	0.5	500	400	100	95	51a, 52
16	H	4-CF_3-Ph	NHAc	**55b**	2.0	THF	r.t.	0.17	200	1200	100	99	54
17	H	4-CF_3-Ph	NHAc	**56a**	1.0	THF	0	0.5	200	400	100	99	51a, b
18	H	4-CF_3-Ph	NHAc	**56a**	1.0	THF	5	0.5	1000	2000	100	99	51a
19	H	4-CF_3-Ph	NHAc	**56b**	2.0	THF	r.t.	0.17	200	1200	100	97	54
20	H	3-CH_3O-Ph	NHAc	**55b**	2.0	THF	r.t.	0.17	200	1200	100	97	54

21	H	3-CH_3O-Ph	NHAc	**56b**	2.0	THF	r.t.	0.17	200	1200	100	97	54
22	H	3-CH_3-Ph	NHAc	**55a**	1.0	THF	r.t.	0.5	186	372	93	95	51b
23	H	3-CH_3-Ph	NHAc	**55b**	2.0	THF	r.t.	0.17	200	1200	100	98	54
24	H	3-CH_3-Ph	NHAc	**56a**	1.0	THF	0	0.5	200	400	100	98	51a, b
25	H	3-CH_3-Ph	NHAc	**56b**	2.0	THF	r.t.	0.17	200	1200	100	98	54
26	H	4-CH_3-Ph	NHAc	**55a**	1.0	THF	r.t.	0.5	500	1000	100	95	51a
27	H	4-CH_3-Ph	NHAc	**55b**	2.0	THF	r.t.	0.17	200	1200	100	96	54
28	H	4-CH_3-Ph	NHAc	**55b**	2.0	THF	r.t.	0.17	200	1200	100	94	54
29	H	4-CH_3-Ph	NHAc	**56a**	1.0	THF	0	0.5	200	400	100	97	51a, b
30	H	4-CH_3-Ph	NHAc	**56b**	2.0	THF	r.t.	0.17	200	1200	100	96	54
31	H	4-CH_3-Ph	NHAc	**56b**	2.0	THF	r.t.	0.17	200	1200	100	94	54
32	H	4-Et-Ph	NHAc	**55b**	2.0	THF	r.t.	0.17	200	1200	100	97	54
33	H	4-Et-Ph	NHAc	**56b**	2.0	THF	r.t.	0.17	200	1200	100	97	54
34	H	2-furyl	NHAc	**55a**	1.0	THF	r.t.	0.5	200	400	100	96	51a
35	H	2-furyl	NHAc	**55b**	2.0	THF	r.t.	0.17	200	1200	100	98	54
36	H	2-furyl	NHAc	**56a**	1.0	THF	0	0.5	200	400	100	98	51a, b
37	H	2-furyl	NHAc	**56b**	2.0	THF	r.t.	0.17	200	1200	100	96	54
38	Me	Ph	NHAc	**55b**	2.0	THF	r.t.	0.17	200	1200	100	93	54
39	Me	Ph	NHAc	**56b**	2.0	THF	r.t.	0.17	200	1200	100	94	54
40	Me	4-Cl-Ph	NHAc	**56a**	1	THF	0	2	200	100	100	80.3	51b
41	Me	4-CH_3-Ph	NHAc	**56a**	1	THF	0	2	193	97	97	77	51b
42	H	CO_2H	NHAc	**41a**	1	MeOH	25	–	570	–	95	73 [a)]	43
43	H	CO_2H	NHAc	**41a**	1	EtOH	25	–	–	–	90–100	76.7	45b (*R*)
44	H	CO_2H	NHAc	**41b**	1	EtOH	25	–	125	–	90–100	25.1	45b (*S*)
45	H	CO_2H	NHAc	**42**	25	EtOH	25	–	125	–	90–100	83 [a)]	45a
46	H	CO_2H	NHAc	**42**	5	EtOH	25	–	125	–	90–100	83.9 [a)]	45b
47	H	CO_2H	NHAc	**43**	1	EtOH	25	–	125	–	90–100	78.9 [a)]	45b
48	H	CO_2H	NHAc	**44**	1	EtOH	25	–	125	–	90–100	88.1	45b
49	H	CO_2H	NHAc	**45**	1	EtOH	25	–	125	–	90–100	89.5	45b

Table 27.3 (continued)

Entry	Substrate			Ligand (L)	P[H_2] [atm]	Solvent	Temp. [°C]	Time [h]	TON Sub:Rh	TOF [h^{-1}]	Conv. [%]	ee [%]	Reference(s)
	R^1	R^2	R^3										
50	H	CO_2H	NHAc	**46**	5	EtOH	25	–	125	–	90–100	86.2	45 b
51	H	CO_2H	NHAc	**47 a**	1	EtOH	25	–	125	–	90–100	24.0	45 b
52	H	CO_2H	NHAc	**48**	1	EtOH	25	–	125	–	90–100	90.9	45 b
53	H	CO_2H	NHAc	**49**	5	EtOH	25	–	125	–	90–100	12.0	45 b
54	H	CO_2H	NHAc	(*S*,*S*)-**50**	1	EtOH	25	–	125	–	–	33	47 a
55	H	CO_2H	NHAc	(*S*,*R*)-**50**	1	EtOH	25	–	125	–	–	61	47 a
56	H	CO_2H	NHAc	**51**	1	EtOH	25	–	125	–	–	68	47 a
57	H	CO_2H	NHAc	**53**	24	*i*PrOH	r.t.	24	77	32	77	68	48
58	H	CO_2H	NHAc	**55 a**	2.0	EtOH	r.t.	0.17	100	600	100	93.5	52
59	H	CO_2H	NHAc	**55 b**	3.4	MeOH	r.t.	0.17	500	3 000	100	98	53, 54
60	H	CO_2H	NHAc	**56 a**	2.0	EtOH	r.t.	0.17	100	600	100	99	51 b, 52
61	H	CO_2H	NHAc	**58**	1	EtOH	r.t.	1.5	74.5	50	15	78	55
62	Ph	CO_2H	NHAc	**41 a**	1	MeOH	25	–	300	–	95	84 [a)]	43, 45 a
63	Ph	CO_2H	NHBz	**41 a**	1	MeOH	25	–	50	–	70	68 [a)]	43
64	Ph	CO_2H	NHBz	**41 a**	1	EtOH	25	0.08–0.67	–	1 008	90–100	75	45 a
65	Ph	CO_2H	NHAc	**41 a**	1	MeOH	25	0.03	48	1 600	45	81.7 [a)]	44
66	Ph	CO_2H	NHAc	**41 a**	1	EtOH	25	–	125	–	90–100	77.3	45 b, 47 a
67	Ph	CO_2H	NHAc	**41 b**	1	EtOH	25	–	125	–	90–100	40.8	45 b, 47 a
68	Ph	CO_2H	NHAc	**42**	10	EtOH	0	–	125	–	90–100	93 [a)]	45 a
69	Ph	CO_2H	NHAc	**42**	5	EtOH	25	–	125	–	90–100	80.6 [a)]	45 b
70	Ph	CO_2H	NHAc	**43**	1	EtOH	25	–	125	–	90–100	74.8 [a)]	45 b
71	Ph	CO_2H	NHAc	**44**	1	EtOH	25	–	125	–	90–100	91.9	45 b
72	Ph	CO_2H	NHAc	**45**	2	EtOH	25	–	125	–	90–100	94.4	45 b,c, 47 a
73	Ph	CO_2H	NHAc	**46**	5	EtOH	25	–	125	–	90–100	68.4	45 b,c, 47 a

74	Ph	CO_2H	NHAc	**47a**	1	EtOH	25	–	125	–	90–100	47.0	45b, 47a
75	Ph	CO_2H	NHAc	**47a**	7.8	EtOH : PhH 1 : 1	r.t.	–	–	–	–	70	46
76	Ph	CO_2H	NHAc	**47b**	7.8	EtOH : PhH 1 : 1	r.t.	–	–	–	–	72	46
77	Ph	CO_2H	NHBz	**47a**	7.8	EtOH : PhH 1 : 1	r.t.	–	–	–	–	62	46
78	Ph	CO_2H	NHBz	**47b**	7.8	EtOH : PhH 1 : 1	r.t.	–	–	–	–	60	46
79	Ph	CO_2H	NHAc	**48**	1	EtOH	25	–	125	–	90–100	92.1	45b, 46, 47a
80	Ph	CO_2H	NHBz	**48**	7.8	EtOH	r.t.	–	–	–	–	92	46
81	Ph	CO_2H	NHAc	**49**	5	EtOH	25	–	125	–	90–100	rac	45b
82	Ph	CO_2H	NHAc	(*S*,*S*)-**50**	4.5	EtOH	25	–	125	–	–	35	47a
83	Ph	CO_2H	NHAc	(*S*,*R*)-**50**	4.5	EtOH	25	–	125	–	–	59	47a
84	Ph	CO_2H	NHAc	**51**	4.5	EtOH	25	–	125	–	–	69	47a
85	Ph	CO_2H	NHAc	**53**	1	*i*PrOH	r.t.	24	100	4.2	100	98	48
86	Ph	CO_2H	NHAc	**55a**	2.0	EtOH	r.t.	0.17	100	600	100	90.3	52
87	Ph	CO_2H	NHAc	**55b**	3.4	MeOH	r.t.	0.17	500	3 000	100	98	53, 54
88	Ph	CO_2H	NHAc	**56a**	2.0	EtOH	r.t.	0.17	100	600	100	94.2	52
89	Ph	CO_2H	NHAc	**57**	6.7	$(CH_3)_2CO$	25	5	100	20	100	79.6	56
90	Ph	CO_2H	NHAc	**58**	1	EtOH	r.t.	1.5	500	333	100	>98	55
91	Ph	CO_2Me	NHAc	**41a**	1	MeOH	25	–	450	–	100	49[a)]	43
92	Ph	CO_2Me	NHAc	**41a**	–	C_6H_6	25	0.03*	50	313	45	82.5[a)]	44
93	Ph	CO_2Me	NHAc	**41a**	1	EtOH	25	0.08–0.67	–	828	90–100	55	45a
94	Ph	CO_2Me	NHAc	**54**	1	MeOH	–	48	20	0.4	95	33	49
95	Ph	CO_2Me	NHAc	**55a**	2.0	THF	r.t.	0.17	100	600	100	90	52
96	Ph	CO_2Me	NHAc	**55a**	3.4	MeOH	r.t.	0.17	500	3 000	100	91	53, 54
97	Ph	CO_2Me	NHAc	**55b**	3.4	MeOH	r.t.	0.5	5000	10 000	100	98.6	53, 54
98	Ph	CO_2Me	NHAc	**55c**	3.4	MeOH	r.t.	0.5	500	1 000	100	13	53, 54
99	Ph	CO_2Me	NHAc	**56a**	2.0	THF	r.t.	0.17	100	600	100	96	51b, 52
100	Ph	CO_2Me	NHAc	**57**	6.7	$(CH_3)_2CO$	25	5	200	20	100	73.7	56

Table 27.3 (continued)

Entry	Substrate			Ligand (L)	P[H_2] [atm]	Solvent	Temp. [°C]	Time [h]	TON Sub:Rh	TOF [h^{-1}]	Conv. [%]	ee [%]	Reference(s)
	R^1	R^2	R^3										
101	Ph	CO_2Me	NHAc	**58**	1	$(CH_3)_2CO$	r.t.	1	500	500	100	>99	55
102	Ph	CO_2NH_2	NHAc	**47a**	7.8	EtOH:PhH 1:1	r.t.	–	–	–	–	92	46
103	Ph	CO_2NH_2	NHAc	**47b**	–	EtOH:PhH 1:1	r.t.	–	–	–	–	92	46
104	Ph	CO_2NH_2	NHAc	**47b**	–	EtOH:PhH 1:1	r.t.	–	–	–	–	70	46
105	2-Cl-Ph	CO_2H	NHAc	**55a**	2.0	EtOH	r.t.	0.17	100	600	100	90	52
106	2-Cl-Ph	CO_2H	NHAc	**56a**	2.0	THF	r.t.	0.17	100	600	100	94	51b, 52
107	2-Cl-Ph	CO_2H	NHAc	**57**	6.7	$(CH_3)_2CO$	25	5	100	20	100	78.1	56
108	2-Cl-Ph	CO_2H	NHAc	**58**	1	EtOH	r.t.	1.5	500	333	100	96	55
109	2-Cl-Ph	CO_2Me	NHAc	**55a**	2.0	THF	r.t.	0.17	100	600	100	90	52
110	2-Cl-Ph	CO_2Me	NHAc	**55b**	3.4	MeOH	r.t.	0.17	500	3000	100	97	53, 54
111	2-Cl-Ph	CO_2Me	NHAc	**56a**	2.0	THF	r.t.	0.17	100	600	100	97	52
112	2-Cl-Ph	CO_2Me	NHAc	**57**	6.7	$(CH_3)_2CO$	25	5	100	20	100	72.0	56
113	2-Cl-Ph	CO_2Me	NHAc	**58**	1	$(CH_3)_2CO$	r.t.	1	500	500	100	96	55
114	3-Cl-Ph	CO_2H	NHAc	**55a**	2.0	EtOH	r.t.	0.17	100	600	100	88	52
115	3-Cl-Ph	CO_2H	NHAc	**56a**	2.0	THF	r.t.	0.17	100	600	100	93	51b, 52
116	3-Cl-Ph	CO_2H	NHAc	**57**	6.7	$(CH_3)_2CO$	25	5	100	20	100	76.3	56
117	3-Cl-Ph	CO_2H	NHAc	**58**	1	EtOH	r.t.	1.5	500	333	100	95	55
118	3-Cl-Ph	CO_2Me	NHAc	**55a**	2.0	THF	r.t.	0.17	100	600	100	90	52
119	3-Cl-Ph	CO_2Me	NHAc	**55b**	3.4	MeOH	r.t.	0.17	500	3000	100	97	53, 54
120	3-Cl-Ph	CO_2Me	NHAc	**56a**	2.0	THF	r.t.	0.17	100	600	100	94	51b, 52
121	3-Cl-Ph	CO_2Me	NHAc	**57**	6.7	$(CH_3)_2CO$	25	5	100	20	100	72.1	56
122	3-Cl-Ph	CO_2Me	NHAc	**58**	1	$(CH_3)_2CO$	r.t.	1	500	500	100	>99	55
123	4-Cl-Ph	CO_2H	NHAc	**55a**	2.0	EtOH	r.t.	0.17	100	600	100	86	52
124	4-Cl-Ph	CO_2H	NHAc	**56a**	2.0	EtOH	r.t.	0.17	100	600	100	93	51b, 52

125	4-Cl-Ph	CO_2H	NHAc	**57**	6.7	$(CH_3)_2CO$	25	5	100	20	100	79.1	56
126	4-Cl-Ph	CO_2Me	NHAc	**55a**	2.0	THF	r.t.	0.17	100	600	100	88	52
127	4-Cl-Ph	CO_2Me	NHAc	**55b**	3.4	MeOH	r.t.	0.17	500	3000	100	98	53, 54
128	4-Cl-Ph	CO_2Me	NHAc	**56a**	2.0	THF	r.t.	0.17	100	600	100	94	51b, 52
129	4-Cl-Ph	CO_2Me	NHAc	**57**	6.7	$(CH_3)_2CO$	25	5	100	20	100	74.0	56
130	4-Cl-Ph	CO_2Me	NHAc	**58**	1	$(CH_3)_2CO$	r.t.	1	500	500	100	>99	55
131	4-Cl-Ph	CO_2Me	NHBz	**55b**	3.4	MeOH	r.t.	0.17	500	3000	100	99	53
132	4-Br-Ph	CO_2Me	NHAc	**55b**	3.4	MeOH	r.t.	0.17	500	3000	100	98	53
133	4-Br-Ph	CO_2Me	NHAc	**56a**	2.0	THF	r.t.	0.17	100	600	100	96	51b, 52
134	4-Br-Ph	CO_2Me	NHAc	**58**	1	$(CH_3)_2CO$	r.t.	1	500	500	100	>99	55
135	4-Br-Ph	CO_2Me	NHBz	**56a**	2.0	THF	r.t.	0.17	100	600	100	96	51b, 52
136	4-F-Ph	CO_2Me	NHAc	**55b**	3.4	MeOH	r.t.	0.17	500	3000	100	98	53, 54
137	4-F-Ph	CO_2Me	NHAc	**56a**	2.0	THF	r.t.	0.17	100	600	100	93	51b, 52
138	4-F-Ph	CO_2Me	NHAc	**57**	6.7	$(CH_3)_2CO$	25	5	100	20	100	73.0	56
139	4-F-Ph	CO_2Me	NHAc	**58**	1	$(CH_3)_2CO$	r.t.	1	500	500	100	>99	55
140	4-F-Ph	CO_2Me	NHBz	**56a**	2.0	THF	r.t.	0.17	100	600	100	94	51b, 52
141	4-F-Ph	CO_2Me	NHBz	**55b**	3.4	MeOH	r.t.	0.17	500	3000	100	99	53, 54
142	4-NO_2-Ph	CO_2H	NHAc	**56a**	2.0	EtOH	r.t.	0.17	100	600	100	90	51b, 52
143	4-NO_2-Ph	CO_2H	NHAc	**57**	6.7	$(CH_3)_2CO$	25	5	100	20	100	76.4	56
144	4-NO_2-Ph	CO_2Me	NHAc	**55a**	3.4	MeOH	r.t.	0.17	500	3000	100	82	53, 54
145	4-NO_2-Ph	CO_2Me	NHAc	**55b**	3.4	MeOH	r.t.	0.17	500	3000	100	96	53, 54
146	4-NO_2-Ph	CO_2Me	NHAc	**56a**	2.0	THF	r.t.	0.17	100	600	100	91	51b, 52
147	4-NO_2-Ph	CO_2Me	NHAc	**57**	6.7	$(CH_3)_2CO$	25	5	100	20	100	73.4	56
148	4-NO_2-Ph	CO_2Me	NHAc	**58**	1	$(CH_3)_2CO$	r.t.	1	500	500	100	94	55
149	4-CH_3-Ph	CO_2Me	NHAc	**55a**	3.4	MeOH	r.t.	0.17	500	3000	100	89	53, 54
150	4-CH_3-Ph	CO_2Me	NHAc	**55b**	3.4	MeOH	r.t.	0.17	500	3000	100	98	53, 54
151	4-CH_3-Ph	CO_2Me	NHAc	**56a**	2.0	THF	r.t.	0.17	100	600	100	94	51b, 52
152	4-CH_3-Ph	CO_2Me	NHAc	**57**	6.7	$(CH_3)_2CO$	25	5	200	20	100	71.2	56
153	4-CH_3-Ph	CO_2Me	NHAc	**58**	1	$(CH_3)_2CO$	r.t.	1	500	500	100	>98	55

Table 27.3 (continued)

Entry	Substrate			Ligand (L)	$P[H_2]$ [atm]	Solvent	Temp. [°C]	Time [h]	TON Sub:Rh	TOF [h^{-1}]	Conv. [%]	ee [%]	Reference(s)
	R^1	R^2	R^3										
154	4-CH_3-Ph	CO_2Me	NHBz	**56a**	2.0	THF	r.t.	0.17	100	600	100	95	51b, 52
155	2-CH_3O-Ph	CO_2H	NHAc	**56a**	2.0	EtOH	r.t.	0.17	100	600	100	93	51b, 52
156	2-CH_3O-Ph	CO_2H	NHAc	**57**	6.7	$(CH_3)_2CO$	25	5	100	20	100	79.0	56
157	2-CH_3O-Ph	CO_2H	NHAc	**58**	1	EtOH	r.t.	1.5	500	333	100	84	55
158	4-CH_3O-Ph	CO_2Me	NHAc	**53**	1	*i*PrOH	r.t.	24	100	4.2	100	91	48
159	4-CH_3O-Ph	CO_2Me	NHAc	**55a**	2.0	THF	r.t.	0.17	100	600	100	93	52
160	4-CH_3O-Ph	CO_2Me	NHAc	**55a**	3.4	MeOH	r.t.	0.17	500	3000	100	87	53, 54
161	4-CH_3O-Ph	CO_2Me	NHAc	**55b**	3.4	MeOH	r.t.	0.17	500	3000	100	98	53, 54
162	4-CH_3O-Ph	CO_2Me	NHAc	**56a**	2.0	THF	r.t.	0.17	100	600	100	93	51b, 52
163	4-CH_3O-Ph	CO_2Me	NHAc	**57**	6.7	$(CH_3)_2CO$	25	5	100	20	100	72.7	56
164	4-CH_3O-Ph	CO_2Me	NHAc	**58**	1	$(CH_3)_2CO$	r.t.	1	500	500	100	>99	55
165	4-CH_3O-Ph	CO_2Me	NHBz	**56a**	2.0	THF	r.t.	0.17	100	600	100	95	51b, 52
166	4-AcO-Ph	CO_2Me	NHAc	**55a**	3.4	MeOH	r.t.	0.17	500	3000	100	87	53,54
167	4-AcO-Ph	CO_2Me	NHAc	**55b**	3.4	MeOH	r.t.	0.17	500	3000	100	98	53, 54
168	4-HO-Ph	CO_2Me	NHAc	**57**	6.7	$(CH_3)_2CO$	25	5	100	20	100	74.6	56
169	3,4-(CH_2O_2)-Ph	CO_2H	NHAc	**41a**	1	MeOH	25		50		90	75 [a)]	43
170	3,4-(CH_2O_2)-Ph	CO_2H	NHAc	**41a**	1	EtOH	25		–	612	90–100	77	45a
171	3,4-(CH_2O_2)-Ph	CO_2H	NHAc	**55a**	2.0	EtOH	r.t.	0.17	100	600	100	77	52
172	3,4-(CH_2O_2)-Ph	CO_2H	NHAc	**56a**	2.0	EtOH	r.t.	0.17	100	600	100	91	51b, 52
173	3,4-(CH_2O_2)-Ph	CO_2H	NHAc	**57**	6.7	$(CH_3)_2CO$	25	5	100	20	100	80.3	56
174	3,4-(CH_2O_2)-Ph	CO_2H	NHAc	**58**	1	EtOH	r.t.	1.5	500	333	100	92	55
175	3,4-(CH_2O_2)-Ph	CO_2Me	NHAc	**55a**	3.4	MeOH	r.t.	0.17	500	3000	100	81	53
176	3,4-(CH_2O_2)-Ph	CO_2Me	NHAc	**55b**	3.4	MeOH	r.t.	0.17	500	3000	100	98	53, 54
177	3,4-(CH_2O_2)-Ph	CO_2Me	NHAc	**56a**	2.0	THF	r.t.	0.17	100	600	100	93	51b, 52
178	3,4-(CH_2O_2)-Ph	CO_2Me	NHAc	**57**	6.7	$(CH_3)_2CO$	25	5	100	20	100	76.2	56

179	3,4-(CH_2O_2)-Ph	CO_2Me	NHAc	**58**	1	$(CH_3)_2CO$	r.t.	1	500	500	100	>98	55
180	3-CH_3O,4-Ac-Ph	CO_2H	NHAc	**58**	1	EtOH	r.t.	1.5	500	333	100	94	55
181	3-CH_3O,4-AcO-Ph	CO_2H	NHAc	**41a**	1	EtOH	25	–	396	–	90–100	87	45a
182	2-furyl	CO_2Me	NHAc	**55a**	3.4	MeOH	r.t.	0.17	500	3000	100	84	53, 54
183	2-furyl	CO_2Me	NHAc	**55b**	3.4	MeOH	r.t.	0.17	500	3000	100	98	53, 54
184	2-furyl	CO_2Me	NHAc	**56a**	2.0	THF	r.t.	0.17	100	600	100	91	51b, 52
185	2-furyl	CO_2Me	NHAc	**58**	1	$(CH_3)_2CO$	r.t.	1.5	500	333	100	>99	55
186	2-furyl	CO_2H	NHBz	**56a**	2.0	THF	r.t.	0.17	100	600	100	94	51b, 52
187	2-furyl	CO_2Me	NHBz	**56a**	2.0	THF	r.t.	0.17	100	600	100	93	51b, 52
188	(*E*)-PhCH=CH	CO_2Me	NHAc	**56a**	2.0	THF	r.t.	0.17	100	600	100	90	51b, 52
189	H	CO_2Et	OC(O)Me	**58**	1	THF	r.t.	1.5	250	167	100	97	55
190	H	CO_2Me	NHAc	**53**	1	*i*PrOH	r.t.	24	77	3.2	77	68	48
191	H	CO_2Me	NHAc	**55a**	2.0	THF	r.t.	0.17	100	600	100	93	51, 52
192	H	CO_2Me	NHAc	**55b**	3.4	MeOH	r.t.	0.17	500	3000	100	97	53, 54
193	H	CO_2Me	NHAc	**56a**	2.0	THF	r.t.	0.17	100	600	100	97	52
194	H	CO_2Me	NHAc	**58**	1	$(CH_3)_2CO$	r.t.	1	500	500	100	95	55
195	*N*-Ac-3-indole	CO_2Me	NHBz	**56a**	2.0	THF	r.t.	0.17	100	600	100	93	52
196	H	CO_2H	CH_2CO_2H	**41a**	5	EtOH	25	–	50	–	90–100	12.3	45b
197	H	CO_2H	CH_2CO_2H	**41b**	5	EtOH	25	–	50	–	90–100	35.1	45b
198	H	CO_2H	CH_2CO_2H	**42**	5	EtOH	25	–	50	–	90–100	7.9	45b
199	H	CO_2H	CH_2CO_2H	**43**	5	EtOH	25	–	50	–	90–100	36.6	45b
200	H	CO_2H	CH_2CO_2H	**44**	5	EtOH	25	–	50	–	90–100	25.3	45b

Table 27.3 (continued)

Entry	Substrate			Ligand (L)	$P[H_2]$ [atm]	Solvent	Temp. [°C]	Time [h]	TON Sub:Rh	TOF [h^{-1}]	Conv. [%]	ee [%]	Reference(s)
	R^1	R^2	R^3										
201	H	CO_2H	CH_2CO_2H	**45**	5	EtOH	25	–	50	–	90–100	71.4	45 b, c
202	H	CO_2H	CH_2CO_2H	**46**	5	EtOH	25	–	50	–	90–100	5.8	45 b, c
203	H	CO_2H	CH_2CO_2H	**47 a**	5	EtOH	25	–	50	–	90–100	60.3	45 b
204	H	CO_2H	CH_2CO_2H	**48**	5	EtOH	25	–	50	–	90–100	8.2	45 b
205	H	CO_2H	CH_2CO_2H	**49**	5	EtOH	25	–	50	–	90–100	5.8	45 b
206	H	CO_2H	CH_2CO_2H	**58**	1	THF	r.t.	1.5	250	167	100	68	55
207	H	CO_2Me	CH_2CO_2Me	**58**	1	THF	r.t.	1.5	250	167	100	93	55
208	H	CO_2Me	OC(O)Me	**58**	1	THF	r.t.	1.5	250	167	100	96	55
209	CH_2OH	Me	$Me_2C{=}CH(CH_2)_2$	**52**	10	C_6H_6	r.t.	8	48	6.0	95	68	47 b
210	CH_2OH	$Me_2C{=}CH(CH_2)_2$	Me	**52**	10	C_6H_6	r.t.	8	49	6.1	97	61	47 b

a) Optical yield.

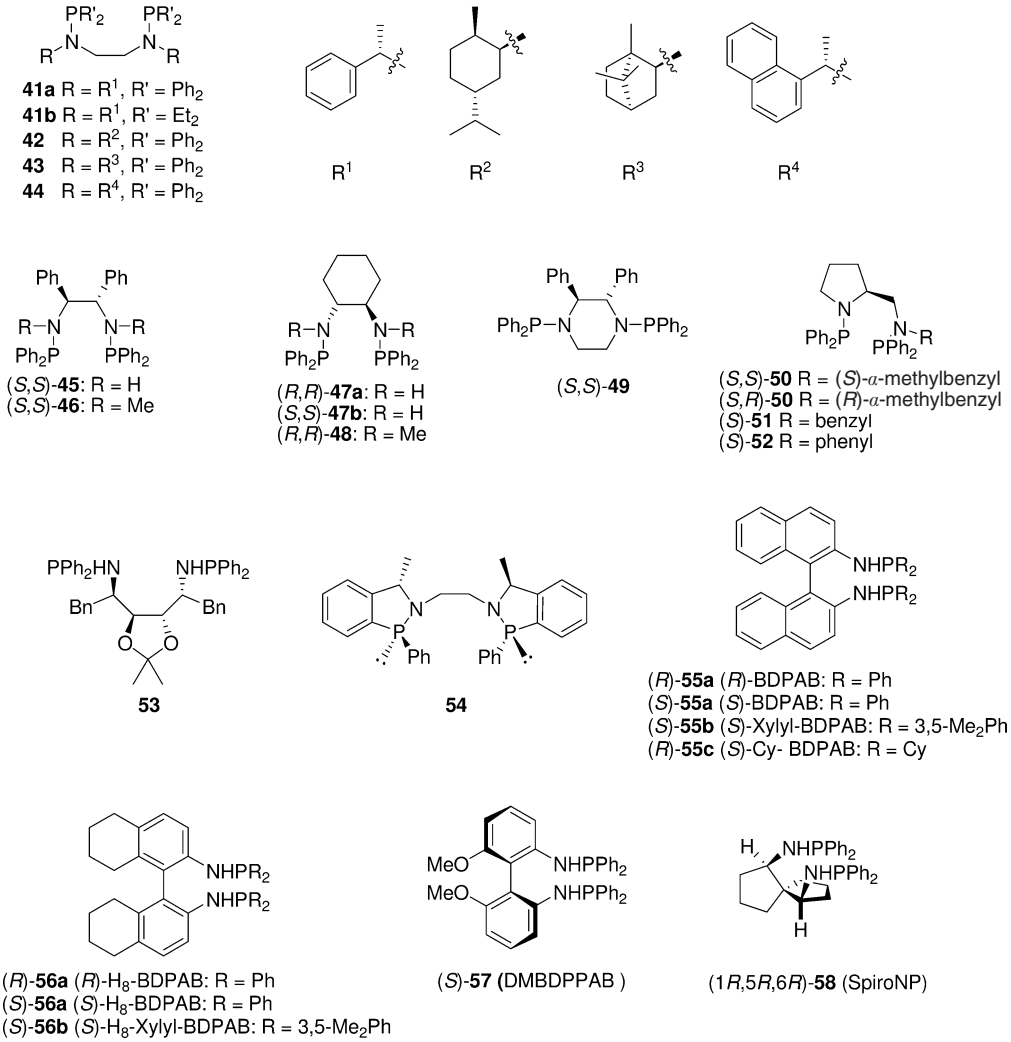

Fig. 27.4 Bisphosphinamidite ligands.

subsequently preparing the corresponding 2,2′-bis(diphenylphosphinoamino)-1,1′-binaphthyl (BDPABs), the enantioselectivities in the hydrogenation of enamides were significantly improved in the case of (*S*)-**55a** versus (*S*)-**56a** [51]. Similarly, in the asymmetric hydrogenation of (*Z*)-2-acetamido-3-arylacrylic acids, the same observation was noted [52]. A boost in ee-value was also induced by replacing Ph with 3,5-Me_2Ph (**55a** versus **55 b**) [53, 54]. A TOF as high as 3000 and a selectivity of up to 99% ee with the use of **55b** were observed, indicative of its high efficiency and effectiveness. In our recent findings, the conformationally rigid SpiroNP **58** also led to high enantioselectivities in the asym-

metric hydrogenation of dehydroamino acid derivatives [55]. An analogous biphenyl-based ligand **57**, however, was much less efficient than the binaphthyl-based or spiro-based counterparts [56].

27.4 Mixed Phosphine-Phosphoramidites and Phosphine-Aminophosphine Ligands

In contrast to the remarkable development of C_2-symmetrical ligands and C_1-nonsymmetrical ligands, the mixed bidentate ligands mentioned in the title were rather underdeveloped. The use of a ferrocene-based chiral backbone led to a promising class of new ligands having a wide scope and inducing good activity. Bophoz [57, 58] (Fig. 27.5, **68**) represented the first mixed phosphine-aminophosphine ligands for asymmetric catalysis with a wide scope of alkene substrates, including α,β-unsaturated acids, enamides, and acetamidocinnamic acid derivatives. The TON of these catalytic asymmetric hydrogenations was gener-

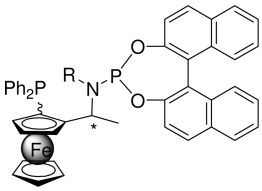

(*Rc*,*Sp*,*Sa*)-**59**: R = Me
(*Sc*,*Rp*,*Sa*)-**60**: R = Me
(*Sc*,*Rp*,*Ra*)-**61**: R = Me
(*Sc*,*Sp*,*Ra*)-**62**: R = Me
(*Sc*,*Sp*,*Sa*)-**63**: R = Me
(*Sc*,*Rp*,*Sa*)-**64**: R = H

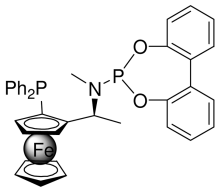

(*Sc*,*Rp*)-**65**

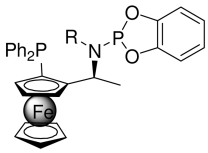

(*Sc*,*Rp*)-**66**

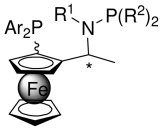

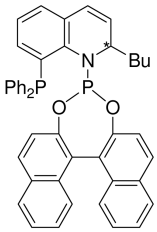

(*Sc*,*Ra*)-**83**
(*Rc*,*Ra*)-**84**

(*Rc*,*Sp*)-**67**: R^1 = H, R^2 = Ph, Ar = Ph
(*Rc*,*Sp*)-**68**: R^1 = Me, R^2 = Ph, Ar = Ph
(*Rc*,*Sp*)-**69**: R^1 = Et, R^2 = Ph, Ar = Ph
(*Rc*,*Sp*)-**70**: R^1 = Pr, R^2 = Ph, Ar = Ph
(*Rc*,*Sp*)-**71**: R^1 = Me, R^2 = ^{i}Pr, Ar = Ph
(*Rc*,*Sp*)-**72**: R^1 = Me, R^2 = Cy, Ar = Ph
(*Sc*,*Rp*)-**73**: R^1 = Me, R^2 = Ph, Ar = Ph
(*Sc*,*Rp*)-**74**: R^1 = Et, R^2 = Ph, Ar = Ph
(*Sc*,*Rp*)-**75**: R^1 = Pr, R^2 = Ph, Ar = Ph
(*Sc*,*Rp*)-**76**: R^1 = Me, R^2 = Et, Ar = Ph
(*Sc*,*Rp*)-**77**: R^1 = Me, R^2 = ^{i}Pr, Ar = Ph
(*Sc*,*Rp*)-**78**: R^1 = Me, R^2 = Ph, Ar = Ph
(*Rc*,*Sp*)-**79**: R^1 = Me, R^2 = 3,5-$(CH_3)_2C_6H_3$, Ar = Ph
(*Rc*,*Sp*)-**80**: R^1 = Me, R^2 = 3,5-$(CF_3)_2C_6H_3$, Ar = Ph
(*Rc*,*Sp*)-**81**: R^1 = Me, R^2 = Ph, Ar = 3,5-$(CF_3)_2C_6H_3$
(*Rc*,*Sp*)-**82**: R^1 = Me, R^2 = 3,5-$(CF_3)_2C_6H_3$, Ar = 3,5-$(CH_3)_2C_6H_3$

Fig. 27.5 Mixed phosphine-phosphoramidites and phosphine-aminophosphine ligands.

ally in the range of 15.8 to 100. The potential of industrial usage was increased by improving its SCR to 10 000 (Table 27.4, entry 53). The shelf stability is an attractive point of this type of ligand. Somewhat surprisingly, Maligres and Krska found that **73** was unable to induce enantioselectivity in the Ru(II)-catalyzed hydrogenation of (*Z*)-*α*-phenoxybutenoic acid (Table 27.4, entry 96) [59].

The introduction of a third chiral element onto the chiral backbone was of interest, and we constructed a modified PPFA [60] with extra axial chirality from BINOL (Fig. 27.5, **59**) [61]. This type of ligand contains three chirality elements. Indeed, the enantioselectivity and activity remained excellent in the enantiomeric hydrogenation of *α*-dehydroamino acid derivatives and enamides using these ligands (Table 27.4, entries 1, 52, 67, 69–71, 79), regardless of the electronic properties of the *para*-substituting group. A similar approach was taken by Zheng's group using different diastereomers [62]. The scope was further extended to dimethyl itaconate, which was hydrogenated with a higher TON and with excellent ee and activity (Table 27.4, entry 91).

Recently, we developed three new fluorinated ferrocenyl phosphine-aminophosphine ligands derived from *N*,*N*-dimethyl-1-ferrocenylethylamine (Ugi's amine) [63]. These ligands were efficiently applied in the Rh-catalyzed hydrogenation of various aryl enamides (92.1 to 99.7% ee) and *α*-dehydroamino acid derivatives (98.5 to 99.7% ee), with complete conversion. The Rh–complex based on **80** led to somewhat lower enantioselectivities in the hydrogenation of arylenamides with *para*-EDG; however, the enantioselectivities were almost equally high for substrates containing *para*-EDG or *para*-EWG (98.5 to 99.7% ee) at 5 °C. These ligands also showed a remarkable air- and water-stability.

The ferrocene-based ligands have proven to be promising in most aspects of asymmetric catalysis. The only drawback was, however, the laborious resolution of Ugi's amine [64] which is used as a starting material, although this problem was solved by the facile asymmetric hydrogenation of ferrocenyl ketones using (XylylP-Phos-Ru–DPEN)Cl_2 (with a nonoptimized SCR of up to 100 000 on a 150-g scale; Scheme 27.2) [65]. With this method in hand, it became more flexible and almost effortless to generate a large structural diversity of ferrocene-based chiral ligands.

Mixed phosphine-phosphoramidite ligands QUINAPHOS **83** and **84**, as developed by Leitner, worked well for the Rh-catalyzed hydrogenation of itaconic acid and *α*-dehydroamino acid derivatives. The ligand **84** also exerted extra reactivity, leading to an average TOF of 36 000 h^{-1} in the hydrogenation of dimethyl itaconate after the addition of a second batch of substrate with SCR 6000 : 1 [66]. In contrast to BINAPHOS-type ligands, the major asymmetric induction relied on the 2-position of the alkyl groups embedded in the fairly rigid heterocyclic skeleton.

Table 27.4 Mixed phosphine–phosphoramidites and phosphine–aminophosphine ligands.

Entry	Substrate			Catalyst	Conditions				TON	TOF [h^{-1}]	Conv. [%]	ee [%]	Reference(s)
	R^1	R^2	R^3		P[H_2] [bar]	Solvent	Temp. [°C]	Time [h]					
1	H	Ph	NHAc	Rh-(*Rc*,*Sp*,*Sa*)-**59**	20.7	THF	r.t.	7 [a)]	99	14.1	>99	87.5 (*S*)	61
2	H	Ph	NHAc	Rh-(*Sc*,*Rp*,*Sa*)-**60**	10	DCM	r.t.	1	5000	5000	100	99.3 (*R*)	62
3	H	Ph	NHAc	Rh-(*Sc*,*Rp*,*Ra*)-**61**	10	DCM	r.t.	1	100	100	100	10.6 (*S*)	62
4	H	Ph	NHAc	Rh-(*Sc*,*Sp*,*Ra*)-**62**	10	DCM	r.t.	1	100	100	100	99.6 (*S*)	62
5	H	Ph	NHAc	Rh-(*Sc*,*Sp*,*Sa*)-**63**	10	DCM	r.t.	1	100	100	100	82.6 (*R*)	62
6	H	Ph	NHAc	Rh-(*Sc*,*Rp*)-**65**	10	DCM	r.t.	1	100	100	100	81.5 (*S*)	62
7	H	Ph	NHAc	Rh-(*Sc*,*Rp*)-**66**	10	DCM	r.t.	1	100	100	100	78.1 (*R*)	62
8	H	Ph	NHAc	Rh-(*Sc*,*Rp*)-**73**	10	DCM	r.t.	1	100	100	100	61.8 (*R*)	62
9	H	Ph	NHAc	Rh-(*Rc*,*Sp*)-**67**	20.7	DCM	r.t.	10	100	10	100	70.0 (*S*)	63
10	H	Ph	NHAc	Rh-(*Rc*,*Sp*)-**68**	20.7	DCM	r.t.	8	100	12.5	100	80.6 (*S*)	63
11	H	Ph	NHAc	Rh-(*Rc*,*Sp*)-**80**	20.7	DCM	r.t.	16	100	6.25	100	94.6 (*S*)	63
12	H	Ph	NHAc	Rh-(*Rc*,*Sp*)-**81**	20.7	DCM	r.t.	10	100	10	100	35.0 (*S*)	63
13	H	Ph	NHAc	Rh-(*Rc*,*Sp*)-**82**	20.7	*i*-PrOH	r.t.	16	100	6.25	100	94.4 (*S*)	63
14	H	Ph	NHAc	Rh-(*Rc*,*Sp*)-**80**	20.7	Toluene	r.t.	16	100	6.25	100	93.5 (*S*)	63
15	H	Ph	NHAc	Rh-(*Rc*,*Sp*)-**80**	20.7	THF	r.t.	16	100	6.25	100	96.5 (*S*)	63
16	H	Ph	NHAc	Rh-(*Rc*,*Sp*)-**82**	20.7	THF	r.t.	8	100	12.5	100	96.2 (*S*)	63
17	H	Ph	NHAc	Rh-(*Rc*,*Sp*)-**80**	20.7	THF	r.t.	–	100	–	100	96.1 (*S*) [d)]	63
18	H	Ph	NHAc	Rh-(*Rc*,*Sp*)-**80**	20.7	THF	r.t.	–	500	–	100	95.8 (*S*) [d)]	63
19	H	Ph	NHAc	Rh-(*Rc*,*Sp*)-**80**	20.7	THF	r.t.	–	100	–	100	95.5 (*S*) [d)]	63
20	H	Ph	NHAc	Rh-(*Rc*,*Sp*)-**80**	20.7	THF	r.t.	–	100	–	100	95.2 (*S*) [d)]	63

21	H	Ph	NHAc	Rh-(*R*c,*S*p)-**80**	20.7	THF/H_2O 95/5	r.t.	–	100	–	100	95.1 (*S*) [d]	63
22	H	Ph	NHAc	Rh-(*R*c,*S*p)-**80**	20.7	THF/H_2O 70/30	r.t.	–	100	–	100	77.2 (*S*) [d]	63
23	H	Ph	NHAc	Rh-(*R*c,*S*p)-**80**	20.7	THF	r.t.	16	100	6.25	100	96.5 (*S*)	63
24	H	Ph	NHAc	Rh-(*R*c,*S*p)-**80**	20.7	THF	r.t.	16	200	12.5	100	95.8 (*S*)	63
25	H	Ph	NHAc	Rh-(*R*c,*S*p)-**80**	20.7	THF	r.t.	16	500	31.25	100	96.4 (*S*)	63
26	H	Ph	NHAc	Rh-(*R*c,*S*p)-**80**	20.7	THF	r.t.	16	1000	62.5	100	95.8 (*S*)	63
27	H	Ph	NHAc	Rh-(*R*c,*S*p)-**80**	20.7	THF	5	30	500	16.67	100	98.3 (*S*)	63
28	H	*p*-Cl-Ph	NHAc	Rh-(*S*c,*R*p,*S*a)-**60**	10	DCM	r.t.	1	1000	1000	100	98.8 (*R*)	62
29	H	*p*-Br-Ph	NHAc	Rh-(*S*c,*R*p,*S*a)-**60**	10	DCM	r.t.	1	1000	1000	100	99.0 (*R*)	62
30	H	*p*-Br-Ph	NHAc	Rh-(*R*c,*S*p)-**80**	20.7	THF	5	30	500	16.67	100	99.7 (*S*)	63
31	H	*p*-Br-Ph	NHAc	Rh-(*R*c,*S*p)-**80**	20.7	THF	r.t.	16	500	31.25	100	99.3 (*S*)	63
32	H	*p*-F-Ph	NHAc	Rh-(*S*c,*R*p,*S*a)-**60**	10	DCM	r.t.	1	1000	1000	100	98.7 (*R*)	62
33	H	*p*-CF_3-Ph	NHAc	Rh-(*R*c,*S*p)-**67**	20.7	DCM	r.t.	10	100	10	100	73.1 (*S*)	63
34	H	*p*-CF_3-Ph	NHAc	Rh-(*S*c,*R*p,*S*a)-**60**	10	DCM	r.t.	1	1000	1000	100	99.2 (*R*)	62
35	H	*p*-CF_3-Ph	NHAc	Rh-(*R*c,*S*p)-**68**	20.7	DCM	r.t.	8	100	12.5	100	79.6 (*S*)	63
36	H	*p*-CF_3-Ph	NHAc	Rh-(*R*c,*S*p)-**80**	20.7	THF	r.t.	16	500	31.25	100	97.1 (*S*)	63
37	H	*p*-CF_3-Ph	NHAc	Rh-(*R*c,*S*p)-**80**	20.7	THF	5	30	500	16.67	100	98.6 (*S*)	63
38	H	*m*-CH_3Ph	NHAc	Rh-(*R*c,*S*p)-**80**	20.7	THF	5	30	500	16.67	100	98.5 (*S*)	63
39	H	*p*-CH_3Ph	NHAc	Rh-(*R*c,*S*p)-**80**	20.7	THF	r.t.	16	500	31.25	100	92.1 (*S*)	63
40	H	*p*-CH_3Ph	NHAc	Rh-(*R*c,*S*p)-**80**	20.7	THF	5	30	500	16.67	100	99.4 (*S*)	63
41	H	*m*-CH_3OPh	NHAc	Rh-(*R*c,*S*p)-**80**	20.7	THF	5	30	500	16.67	100	99.0 (*S*)	63
42	H	*p*-CH_3OPh	NHAc	Rh-(*R*c,*S*p)-**80**	20.7	THF	r.t.	16	500	31.25	100	93.5 (*S*)	63
43	H	*p*-CH_3OPh	NHAc	Rh-(*R*c,*S*p)-**80**	20.7	THF	5	30	500	16.67	100	99.3 (*S*)	63
44	H	CO_2H	NHAc	Rh-(*R*c,*S*p)-**68**	0.7	THF	r.t.	1	95	95	>95	96 (*S*)	57
45	H	CO_2H	NHAc	Rh-(Sc,*R*p)-**73**	0.69–1.38	THF	25	24	100	4.2	100	96.1 (*R*) [b]	58
46	H	CO_2Me	NHAc	Rh-(*R*c,*S*p)-**68**	0.7	THF	r.t.	1	95	95	>95	98.5 (*S*)	57
47	H	CO_2Me	NHAc	Rh-(Sc,*R*p)-**73**	0.69–1.38	THF	25	1	40	40	100	98.4 (*R*)	58
48	H	CO_2Me	NHAc	Rh-(*R*c,*R*a)-**84**	30	DCM	r.t.	24	990	41.3	>99	97.8 (*S*)	62

Table 27.4 (continued)

Entry	Substrate			Catalyst	Conditions				TON	TOF [h^{-1}]	Conv. [%]	ee [%]	Reference(s)
	R^1	R^2	R^3		$P[H_2]$ [bar]	Solvent	Temp. [°C]	Time [h]					
49	H	CO_2Me	$NHCO_2Bn$	Rh-(*Rc*,*Sp*)-**68**	0.7	THF	r.t.	1	95	95	>95	98 (*S*)	57, 58
50	Me[c)]	CO_2Me	NHCO (2-oxopyrrolidin-1-yl)	Rh-(*Rc*,*Sp*)-**68**	2.8	THF	25	18	20.9	1.2	99	96.2 (*S*)	58
51	Ph	CO_2H	NHAc	Rh- (*Rc*,*Sp*)-**68**	0.69–1.38	THF	25	1	100	100	100	99.4 (*S*)[b)]	57, 58
52	Ph	CO_2Me	NHAc	Rh-(*Rc*,*Rp*,*Sa*)-**59**	20.7	THF	r.t.	7[a)]	99	14.1	>99	99.0 (*S*)	61
53	Ph	CO_2Me	NHAc	Rh-(*Sc*,*Rp*,*Sa*)-**60**	10	DCM	r.t.	1	10000	10000	100	99.0 (*R*)	62
54	Ph	CO_2Me	NHAc	Rh-(*Rc*,*Sp*)-**67**	0.7	THF	r.t.	1	95	95	95	97.2 (*S*)	57, 58
55	Ph	CO_2Me	NHAc	Rh- (*Rc*,*Sp*)-**68**	0.7	THF	r.t.	1	95	95	>95	99.1 (*S*)	57, 58
56	Ph	CO_2Me	NHAc	Rh-(*Rc*,*Sp*)-**68**	20.7	THF	r.t.	–	200	–	100	99.0 (*S*)	63
57	Ph	CO_2Me	NHAc	Rh- (*Rc*,*Sp*)-**68**	3.1	THF	r.t.	1.2	9630	8025	96.3	96.8 (*S*)	57, 58
58	Ph	CO_2Me	NHAc	Rh-(*Rc*,*Sp*)-**69**	0.7	THF	r.t.	1	95	95	95	94.3 (*S*)	57, 58
59	Ph	CO_2Me	NHAc	Rh-(*Rc*,*Sp*)-**70**	0.7	THF	r.t.	1	95	95	>95	93.3 (*S*)	57
60	Ph	CO_2Me	NHAc	Rh-(Sc,*Rp*)-**75**	0.69–1.38	THF	25	1	100	100	100	93.3 (*R*)	58
61	Ph	CO_2Me	NHAc	Rh-(*Rc*,*Sp*)-**80**	20.7	THF	r.t.	–	200	–	100	99.2 (*S*)	63
62	Ph	CO_2Me	NHAc	Rh-(*Rc*,*Sp*)-**81**	20.7	THF	r.t.	–	200	–	100	96.1 (*S*)	63
63	Ph	CO_2Me	NHAc	Rh-(*Rc*,*Sp*)-**82**	20.7	THF	r.t.	–	200	–	100	98.5 (*S*)	63
64	Ph	CO_2Me	NHBz	Rh-(*Rc*,*Sp*)-**68**	0.69–1.38	THF	25	6	100	16.7	100	98.4 (*S*)	58
65	Ph	CO_2Me	$NHCO_2$*t*-Bu	Rh-(*Rc*,*Sp*)-**68**	0.7	THF	r.t.	1	95	95	>95	99.5 (*S*)	57, 58
66	Bn	CO_2Et	$NHCO_2Bn$	Rh-(*Rc*,*Sp*)-**68**	0.69–1.38	THF	25	6	99	16.5	99	98.4 (*S*)	58
67	*p*-Cl-Ph	CO_2Me	NHAc	Rh-(*Rc*,*Sp*,*Sa*)-**59**	20.7	THF	r.t.	7[a)]	99	14.1	>99	99.0 (*S*)	61
68	*p*-Cl-Ph	CO_2Me	NHAc	Rh-(*Rc*,*Sp*)-**68**	0.69–1.38	THF	25	2	50	25	100	98.8 (*S*)	58
69	*p*-Br-Ph	CO_2Me	NHAc	Rh-(*Rc*,*Sp*,*Sa*)-**59**	20.7	THF	r.t.	7[a)]	99	14.1	>99	99.0 (*S*)	61
70	*p*-F-Ph	CO_2Me	NHAc	Rh-(*Rc*,*Sp*,*Sa*)-**59**	20.7	THF	r.t.	7[a)]	99	14.1	>99	99.0 (*S*)	61

71	*p*-NO_2-Ph	CO_2Me	NHAc	Rh-(*Rc*,*Sp*,*Sa*)-**59**	20.7	THF	r.t.	7 [a)]	99	14.1	>99	99.6 (*S*)	61
72	*p*-NO_2-Ph	CO_2Me	NHAc	Rh-(*Rc*,*Sp*)-**68**	0.69–1.38	THF	25	0.5	100	200	100	97.7 (*S*)	58
73	*p*-NO_2Ph	CO_2Me	NHAc	Rh-(*Rc*,*Sp*)-**68**	20.7	THF	r.t.	–	200	–	100	99.5 (*S*)	63
74	*p*-NO_2Ph	CO_2Me	NHAc	Rh-(*Rc*,*Sp*)-**80**	20.7	THF	r.t.	–	200	–	100	99.7 (*S*)	63
75	*p*-CN-Ph	CO_2Me	NHAc	Rh-(*Rc*,*Sp*)-**68**	0.69–1.38	THF	25	1	100	100	100	99.0 (*S*)	58
76	*o*-MeO-Ph	CO_2Me	NHAc	Rh-(*Rc*,*Sp*)-**68**	0.69–1.38	THF	25	2	49.8	24.9	99.5	97.7 (*S*)	58
77	*m*-MeO-Ph	CO_2Me	NHAc	Rh-(*Rc*,*Sp*)-**68**	0.69–1.38	THF	25	0.5	50	100	100	98.0 (*S*)	58
78	*p*-MeO-Ph	CO_2Me	NHAc	Rh-(*Rc*,*Sp*)-**68**	0.69–1.38	THF	25	0.5	45	90	90	97.9 (*S*)	58
79	*p*-Me-Ph	CO_2Me	NHAc	Rh-(*Rc*,*Sp*,*Sa*)-**59**	20.7	THF	r.t.	7 [a)]	99	14.1	>99	97.4 (*S*)	61
80	Cyclopropyl	CO_2Me	NHBz	Rh-(Sc,*Rp*)-**73**	0.69–1.38	THF	25	24	100	4.2	100	91.6 (*R*)	58
81	Cyclopropyl	CO_2Me	$NHCO_2$*t*-Bu	Rh-(*Rc*,*Sp*)-**68**	0.69–1.38	THF	25	6	90	15	90	98.6 (*S*)	58
82	Cyclopropyl	Bn	$NHCO_2$*t*-Bu	Rh-(*Rc*,*Sp*)-**68**	0.69–1.38	Acetone	25	1	94	94	94	>99 (*S*)	57, 58
83	1-Naphthyl	CO_2Me	NHAc	Rh-(*Rc*,*Sp*)-**68**	0.69–1.38	THF	25	6	95	15.8	>95	99.3 (*S*)	58
84	1-Naphthyl	CO_2Me	$NHCO_2$*t*-Bu	Rh-(*Rc*,*Sp*)-**68**	0.69–1.38	THF	25	6	95	15.8	>95	98.2 (*S*)	58
85	2-Naphthyl	CO_2Me	NHAc	Rh-(*Rc*,*Sp*)-**68**	0.69–1.38	THF	25	1	95	95	>95	98.1 (*S*)	58
86	2-Naphthyl	CO_2Me	$NHCO_2$*t*-Bu	Rh-(*Rc*,*Sp*)-**68**	0.69–1.38	THF	25	6	97	16.2	97	97.4 (*S*)	58
87	3-furyl	CO_2Me	NHCOPh	Rh-(Sc,*Rp*)-**73**	0.69–1.38	THF	25	6	100	16.7	100	96.6 (*R*)	58
88	3-furyl	CO_2Me	$NHCO_2$*t*-Bu	Rh-(*Rc*,*Sp*)-**68**	0.69–1.38	THF	25	6	98	16.3	98	97.2 (*S*)	58
89	H	CO_2H	CH_2CO_2H	Rh-(*Rc*,*Sp*)-**67**	20.7	MeOH	r.t.	6	95	15.8	>95	94.0 (*R*)	57
90	H	CO_2H	CH_2CO_2H	Rh-(*Rc*,*Sp*)-**68**	20.7	MeOH	r.t.	6	95	15.8	>95	97.4 (*R*)	57
91	H	CO_2Me	CH_2CO_2Me	Rh-(*Sc*,*Rp*,*Sa*)-**60**	10	DCM	r.t.	0.5	10 000	20 000	100	99.1 (*S*)	62
92	H	CO_2Me	CH_2CO_2Me	Rh-(*Rc*,*Sp*)-**67**	20.7	MeOH	r.t.	6	95	15.8	>95	91.6 (*R*)	57, 58
93	H	CO_2Me	CH_2CO_2Me	Rh-(*Rc*,*Sp*)-**68**	10	MeOH	r.t.	6	95	15.8	>95	94.0 (*R*)	57, 58
94	H	CO_2Me	CH_2CO_2Me	Rh-(*Sc*,*Ra*)-**83**	30	DCM	r.t.	24	990	41.3	>99	78.8 (*R*)	66
95	H	CO_2Me	CH_2CO_2Me	Rh-(*Rc*,*Ra*)-**84**	30	DCM	r.t.	24	990	41.3	>99	98.8 (*R*)	66
96	Me	CO_2H	OPh	Ru-(*Sc*,*Rp*)-**73**	6.2	MeOH/ EtOH/DCM 80/13/7	20–25	20	17.4	0.9	100	rac	59
97	Ph	CO_2H	CH_2CO_2H	Rh-(*Rc*,*Sp*)-**67**	20.7	MeOH	r.t.	6	95	15.8	>95	99.0 (*R*)	57
98	Ph	CO_2H	CH_2CO_2H	Rh-(*Rc*,*Sp*)-**68**	20.7	MeOH	r.t.	6	95	15.8	>95	89.0 (*R*)	57
99	Ph	CO_2Me	CH_2CO_2Me	Rh-(*Rc*,*Sp*)-**67**	20.7	MeOH	r.t.	6	95	15.8	>95	80.0 (*R*)	57

a) Average value.
b) The ee-value was determined by the corresponding methyl ester.
c) The ratio of *Z*/*E* is not provided.
d) The catalyst was prepared *in situ* in air.

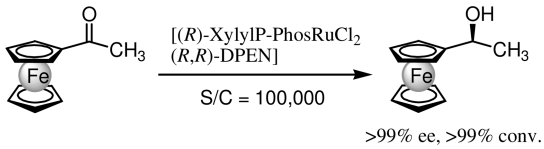

Scheme 27.2

27.5
Bisphosphinite Ligands (One P–O Bond)

A large number of bidentate phosphinites have been reported, with sugars being the most abundantly used backbone. *trans*-BDPCH **85** (Fig. 27.6) is the earliest example of a bisphosphinite used in the rhodium-catalyzed asymmetric hydrogenation of functionalized olefins inducing moderate ee-values (48.5–78.9%) [67]. A similar approach using a more rigid pentacyclic system as backbone (*trans*-BDPCP **86**) induced only poor to moderate ee-values. The best ee-value (78.9%) was obtained in the enantiomeric hydrogenation of α-acetamidoacrylic acid [68]. In 2000, Leitner developed a perfluorinated analogue **87** which induced 72% ee in the Rh-catalyzed hydrogenation of dimethyl methylsuccinate (Table 27.5, entry 934) in a supercritical CO_2 ($scCO_2$) and perfluorinated alcohol solvent [69]. An average TOF up to 40 000 h^{-1} was obtained with this system.

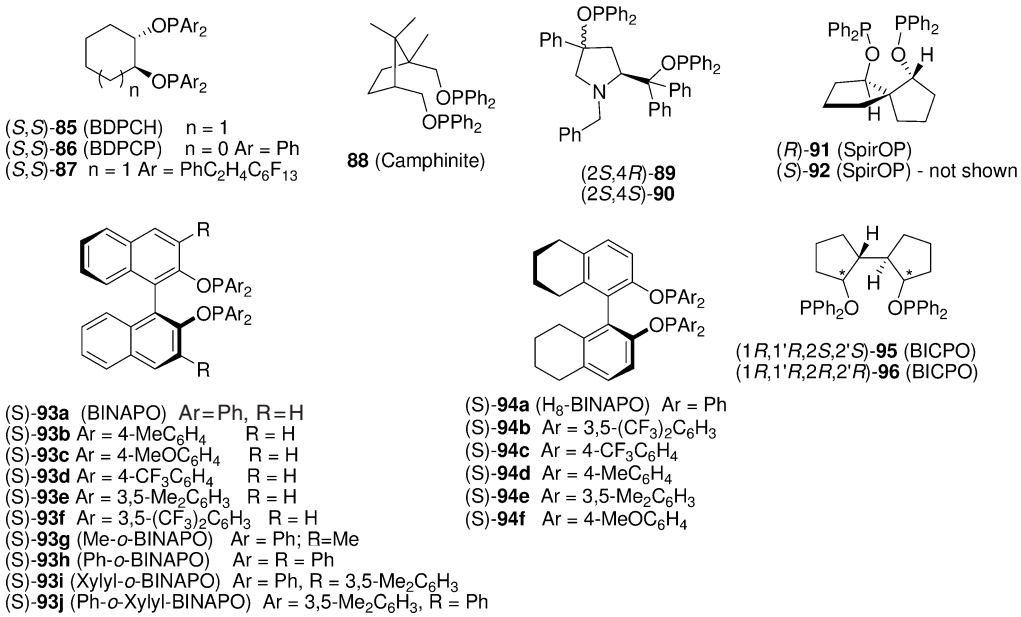

Fig. 27.6 Bisphosphinite ligands (one P–O bond).

The binaphthyl system has served as the basis of a several classes of ligands. It has been suggested that the highly skewed position of the naphthyl rings in BINAP is the determining factor in its effectiveness in asymmetric catalytic reactions [70]. In an early study by Grubbs, the use of atropisomeric BINAPO **93a** based on the binaphthol skeleton induced 6 to 76% ee in the Rh-catalyzed hydrogenation of α-dehydroamino acids and enamides [71]. Interestingly, we found that the partially hydrogenated H_8-BINAPO was more effective than BINAPO in the Rh-catalyzed hydrogenation of (*Z*)-acetamido-3-arylacrylic acids and their methyl esters (63.9–84% ee) [52]. In fact, recent research showed that chiral catalysts derived from the 5,5′,6,6′,7,7′,8,8′-octahydro-1,1′-bi-2,2′-naphthyl backbone (e.g., H_8-BINAP [72], H_8-BINOL [73, 74], H_8-BINAM [9], H_8-BDPAB [51], H_8-binaphthoxy [75], H_8-MAPs [76]) exhibited higher efficiency and enantioselectivity in asymmetric catalytic reactions than those prepared from the parent binaphthyl backbone, probably due to the steric and electronic modulation in the H_8-binaphthyl backbone [77]. A systematic quantification of the electronic and steric influences of these ligands were carried out by Bakos and Gergely [78]. A detrimental effect of *para*-electron-withdrawing substituents on the phenyl rings of this class of ligands was observed on enantioselectivity and activity in the hydrogenation of dimethyl itaconate (**94b** with 51.6% ee, Table 27.5, entry 939). In contrast, *para*-electron-donating groups (i.e., *p*-OMe group) enhanced the enantioselectivity (93.9% ee, Table 27.5, entry 944). Similarly, the use of **94f** (i.e., *p*-OMe group) in the hydrogenation of methyl (*Z*)-α-acetamido-cinnamate gave 98.6% ee. The 3,3′-disubstituted bisphosphinite ligand *o*-BINAPO (**93a, b)** reported by Zhang was successfully applied in the hydrogenation of enamides (67.2–96.3% ee) and α-dehydroamino acid derivatives (81.5–99.9% ee) [79]. The further demonstration of its application in the hydrogenation of β-aryl-substituted β-(acylamino)acrylates was also successful, leading to formation of the products with 80 to 99% ee (with **93i**) [80].

Chiral ligands **88** [81], **89** and **90** [82] with rigid backbones were found to be less effective in Rh-catalyzed hydrogenation reactions. In 1997, we introduced the novel ligand SpirOP (**91** and **92)** based on a rigid spiro backbone which mimics the binaphthyl rings in BINAP in its most effective state (skewed position), giving rise to an eight-membered chelate ring [27, 83]. Indeed, the desired hydrogenation product 2-acetamidopropionic acid was obtained in >99.9% ee, with complete conversion in 10 min using Rh–SpirOP. Similarly remarkable activity and enantioselectivity was found upon hydrogenation of the corresponding methyl ester using the same catalyst (99% ee, 99.9% conv.). The TOF of the hydrogenation of 2-acetamido-acrylic acid could be further increased to 10 000 h^{-1} at ambient temperature whilst retaining 96.8% ee. The substrate's scope was also excellent (>97% ee for (*Z*)-2-acetamido-3-arylacrylic acids and 94.2–97.2% ee for the corresponding methyl esters). It is of interest to note that the Rh–SpirOP complexes in methanol showed unexpected stability based on a ^{31}P-NMR study at ambient temperature for two days. It was further demonstrated that the use of SpirOP in the hydrogenation of α-phenylenamide gave rise to good to excellent enantioselectivities (85.6–97.4% ee) [84].

Table 27.5 Enantiomeric hydrogenation using bisphosphinite, bisphosphonite, or bisphosphite.

Entry	Substrate			Catalyst	Conditions				TON	TOF [h^{-1}]	Conv. [%]	ee [%]	Reference(s)
	R^1	R^2	R^3		$P[H_2]$ [bar]	Solvent	Temp. [°C]	Time [h]					
1	H	CO_2H	NHAc	[Rh(1,5-hexadiene) (+)-*trans*-**85**]Cl	50	–	–20	24	–	–	–	78.9 (*S*)	67
2	H	CO_2H	NHAc	[Rh(1,5-hexadiene) (+)-*trans*-**86**]Cl	50	–	–20	24	–	–	–	0	68a
3	H	CO_2H	NHAc	[Rh(COD)**91**]BF_4	1	MeOH	25	0.167	100	600	>99.9	>99.9 (*R*)	27
4	H	CO_2H	NHAc	[Rh(COD)**91**]BF_4	13.8	MeOH	25	1	10000	10000	>99.9	96.8 (*R*)	27
5	H	CO_2H	NHAc	[Rh(COD)**95**]BF_4	1	IPA	r.t.	24	100	4	100	94.8 (*S*)	85
6	H	CO_2H	NHAc	[Rh(COD)**97a**]BF_4	1	MeOH	25	0.0317 [f)]	50	1579	50	72.6	26
7	H	CO_2H	NHAc	[Rh(COD)**97a**]BF_4	1	MeOH	25	0.0167 [f)]	50	3000	50	97.7 (*S*)	91b
8	H	CO_2H	NHAc	[Rh(COD)**97c**]BF_4	1	MeOH	25	0.0167 [f)]	50	3000	50	96.5 (*S*)	91b
9	H	CO_2H	NHAc	[Rh(COD)**98a**]BF_4	1	MeOH	25	0.047 [f)]	50	1071	50	97.7 (*S*)	26
10	H	CO_2H	NHAc	[Rh(COD)**98a**]BF_4	1	MeOH	25	0.25	50	200	50	97.7 (*S*)	26
11	H	CO_2H	NHAc	[Rh(COD)**98a**]BF_4	100	MeOH	25	–	100 [c)]	–	–	93.9 (*S*)	26
12	H	CO_2H	NHAc	[Rh(COD)**98b**]BF_4	2.8	THF	r.t.	3	100	33	100	97 (*S*)	98
13	H	CO_2H	NHAc	[Rh(COD)**98b**]SbF_6	2–2.8	THF	r.t.	2–3	–	–	–	96.9	95b
14	H	CO_2H	NHAc	[Rh(COE)**93a**]Cl	102	Tol	25	24	25	1	50 [b)]	9 [a)]	71
15	H	CO_2H	NHAc	[Rh(COE)**93a**]Cl	95	Tol/acetone 1:1	0	24	50	2	100 [b)]	6 [a)]	71
16	H	CO_2H	NHAc	[Rh(NBD)**97a**]PF_6	1	EtOH	30	0.33	40	120	100 [b)]	67 (*S*)	88
17	H	CO_2H	NHAc	[Rh(NBD)**97a**]PF_6	1	EtOH	30	0.33	100	300	100 [b)]	68 (*S*)	88
18	H	CO_2H	NHAc	[Rh(NBD)**97a**]PF_6	1	EtOH	0	0.5	100	200	100 [b)]	74 (*S*)	88
19	H	CO_2H	NHAc	[Rh(NBD)**97a**]PF_6	1	EtOH	–20	1	100	100	100 [b)]	80 (*S*)	88

20	H	CO_2H	NHAc	[Rh(COD)**102a**]BF_4	2–2.8	THF	r.t.	2–3	–	–	–	95.0 (*S*)	95 b
21	H	CO_2H	NHAc	[Rh(COD)**103a**]SbF_6	2–2.8	THF	r.t.	2–3	–	–	–	90.8 (*R*)	95 b
22	H	CO_2H	NHAc	[Rh(COD)**114a**]BF_4	1	MeOH	25	0.017 [f]	50	2941	50	59 (*S*)	99
23	H	CO_2H	NHAc	[Rh(COD)**114a**]BF_4	1	PhH	25	6.67 [f]	50	8	50	48 (*S*)	99
24	H	CO_2H	NHAc	[Rh(COD)**114a**]BF_4	1	H_2O	25	7.58 [f]	50	7	50	14 (*S*)	99
25	H	CO_2H	NHAc	[Rh(COD)**114b**]BF_4	1	MeOH	25	0.017 [f]	50	2941	50	56 (*S*)	99
26	H	CO_2H	NHAc	[Rh(COD)**114b**]BF_4	1	PhH	25	8.08 [f]	50	6	50	71 (*S*)	99
27	H	CO_2H	NHAc	[Rh(COD)**114b**]BF_4	1	H_2O+Triton X-100 (0.1 mmol)	25	0.01 [f]	50	500	50	42 (*S*)	99
28	H	CO_2H	NHAc	[Rh(COD)**114b**]BF_4	1	H_2O+Triton X-100 (0.5 mmol)	25	0.05 [f]	50	1000	50	42 (*S*)	99
29	H	CO_2H	NHAc	[Rh(COD)**115a**]SbF_6	2.8	THF	r.t.	3	100	33	100	86 (*S*)	98
30	H	CO_2H	NHAc	[Rh(COD)**115a**]SbF_6	2.8	H_2O	r.t.	19	100	5	100	14 (*S*)	98
31	H	CO_2H	NHAc	[Rh(COD)**115b**]SbF_6	2.8	THF	r.t.	3	100	33	100	90 (*S*)	98
32	H	CO_2H	NHAc	[Rh(COD)**115c**]BF_4	2.8	THF	r.t.	–	150	–	100	87 (*S*)	98
33	H	CO_2H	NHAc	[Rh(COD)**115c**]BF_4	2.8	MeOH	r.t.	–	150	–	100	54 (*S*)	98
34	H	CO_2H	NHAc	[Rh(COD)**115c**]BF_4	2.8	H_2O	r.t.	–	150	–	100	53 (*S*)	98
35	H	CO_2H	NHAc	[Rh(COD)**115c**]BF_4	2.8	H_2O/EtOAc (1:1)	r.t.	–	100	–	100	6 (*S*)	98
36	H	CO_2H	NHAc	[Rh(COD)**115d**]BF_4	2.8	THF	r.t.	–	100	–	100	93 (*S*)	98
37	H	CO_2H	NHAc	[Rh(COD)**115d**]BF_4	2.8	MeOH	r.t.	–	100	–	100	37 (*S*)	98
38	H	CO_2H	NHAc	[Rh(COD)**115d**]BF_4	2.8	EtOH	r.t.	–	100	–	100	89 (*S*)	98
39	H	CO_2H	NHAc	[Rh(COD)**115d**]BF_4	2.8	H_2O	r.t.	–	100	–	100	2 (*S*)	98
40	H	CO_2H	NHAc	[Rh(COD)**115d**]BF_4	2.8	H_2O/EtOAc (1:1)	r.t.	–	100	–	100	2 (*S*)	98
41	H	CO_2H	NHAc	[Rh(COD)**115e**]BF_4	2.8	THF	r.t.	–	150	–	100	0	98
42	H	CO_2H	NHAc	[Rh(COD)**119d**]SbF_6	2.8	H_2O	r.t.	2	125	63	100	59 (*S*)	102
43	H	CO_2H	NHAc	[Rh(COD)**119e**]SbF_6	2.8	H_2O/EtOAc	r.t.	20	125	6	100	65 (*S*) [a]	102
44	H	CO_2H	NHAc	[Rh(COD)**128**]Cl	10	MeOH	r.t.	0.25	230	920	100	26 (*S*)	106
45	H	CO_2H	NHAc	[Rh(COD)**129**]Cl	56	MeOH	r.t.	1	260	260	100	14 (*R*)	106
46	H	CO_2H	NHAc	[Rh(COD)**132**]BF_4	34.5	Acetone	25	0.25	100	400	100	96.7 (*R*)	107
47	H	CO_2H	NHAc	[Rh(COD)**141b**]BF_4	3.5	MeOH	r.t.	0.5	1000	2000	>99	97 (*S*)	111
48	H	CO_2H	NHAc	[Rh(COD)**166**]BF_4	51	H_2O	r.t.	24	50	2	100	10 (*R*) [j]	129

Table 27.5 (continued)

Entry	Substrate			Catalyst	Conditions				TON	TOF [h^{-1}]	Conv. [%]	ee [%]	Reference(s)
	R^1	R^2	R^3		$P[H_2]$ [bar]	Solvent	Temp. [°C]	Time [h]					
49	H	CO_2Me	NHAc	[Rh(COD)**91**]BF_4	1	MeOH	25	0.167	100	600	>99.9	99.0 (*R*)	27
50	H	CO_2Me	NHAc	[Rh(COE)**93a**]Cl	99	Tol	0	53.5	30	0.6	60 [b)]	44 [a)]	71
51	H	CO_2Me	NHAc	[Rh(COE)**93a**]Cl	91	Tol/acetone 1:1	0	68.5	50	0.7	100 [b)]	76 [a)]	71
52	H	CO_2Me	NHAc	[Rh(COD)**93a**]PF_6	3	Tol	r.t.	12	100	8.3	100	73.2 (*S*)	79
53	H	CO_2Me	NHAc	[Rh(COD)**93g**]PF_6	3	Tol	r.t.	12	100	8.3	100	94.8 (*S*)	79
54	H	CO_2Me	NHAc	[Rh(COD)**93h**]PF_6	3	Tol	r.t.	12	100	8.3	100	99.9 (*S*)	79
55	H	CO_2Me	NHAc	[Rh(COD)**93i**]PF_6	3	Tol	r.t.	12	100	8.3	100	95.4 (*S*)	79
56	H	CO_2Me	NHAc	[Rh(COD)**93j**]PF_6	3	Tol	r.t.	12	100	8.3	100	93 (*S*)	79
57	H	CO_2Me	NHAc	[Rh(COD)**94a**]BF_4	6.9	DCM	r.t.	0.17	245	1441	49	81 (*S*)	52
58	H	CO_2Et	NHAc	[Rh(COD)**97a**]BF_4	1	MeOH	25	0.085 [f)]	50	588	50	58.2	26
59	H	CO_2Me	NHAc	[Rh(COD)**97a**]BF_4	1	MeOH	25	0.0267 [f)]	50	1875	50	73.4	26
60	H	CO_2Me	NHAc	[Rh(COD)**97a**]BF_4	1	MeOH	25	0.0167 [f)]	50	3000	50	90.9 (*S*)	91 b
61	H	CO_2Me	NHAc	[Rh(NBD)**97a**]PF_6	1	EtOH	30	0.167	100	600	100 [b)]	53 (*S*)	88
62	H	CO_2Me	NHAc	[Rh(NBD)**97a**]PF_6	1	EtOH	0	0.5	100	200	100 [b)]	78 (*S*)	88
63	H	CO_2Me	NHAc	[Rh(COD)**97b**]BF_4	1	H_2O	25	0.33	50	150	50	44 (S)	99
64	H	CO_2Me	NHAc	[Rh(COD)**97b**]BF_4	1	H_2O + 0.1 mmol $LiBF_4$	25	0.52	50	97	50	43 (S)	99
65	H	CO_2Me	NHAc	[Rh(COD)**97b**]BF_4	1	H_2O + 0.1 mmol $NaBF_4$	25	0.55	50	91	50	40 (S)	99
66	H	CO_2Me	NHAc	[Rh(COD)**97b**]BF_4	1	H_2O + 0.1 mmol KBF_4	25	0.53	50	94	50	42 (S)	99
67	H	CO_2Me	NHAc	[Rh(COD)**97b**]BF_4	1	H_2O + 0.1 mmol $RbBF_4$	25	0.62	50	81	50	42 (S)	99

68	H	CO_2Me	NHAc	[Rh(COD)**97b**]BF_4	1	H_2O+0.1 mmol $CsBF_4$	25	0.62	50	81	50	41 (S)	99
69	H	CO_2Me	NHAc	[Rh(COD)**97b**]BF_4	1	H_2O+Triton X100 (0.1 mmol)	25	0.067	50	750	50	69 (S)	99
70	H	CO_2Me	NHAc	[Rh(COD)**97b**]BF_4	1	H_2O+Triton X100+ 0.1 mmol $LiBF_4$	25	0.12	50	429	50	68 (S)	99
71	H	CO_2Me	NHAc	[Rh(COD)**97b**]BF_4	1	H_2O+Triton X100+ 0.1 mmol $NaBF_4$	25	0.1	50	500	50	68 (S)	99
72	H	CO_2Me	NHAc	[Rh(COD)**97b**]BF_4	1	H_2O+Triton X100+ 0.1 mmol KBF_4	25	0.1	50	500	50	68 (S)	99
73	H	CO_2Me	NHAc	[Rh(COD)**97b**]BF_4	1	H_2O+ Triton X100+0.1 mmol $RbBF_4$	25	0.15	50	333	50	68 (S)	99
74	H	CO_2Me	NHAc	[Rh(COD)**97b**]BF_4	1	H_2O+Triton X100+ 0.1 mmol $CsBF_4$	25	0.13	50	375	50	68 (S)	99
75	H	CO_2Me	NHAc	[Rh(COD)**97c**]BF_4	1	MeOH	25	0.0333 [f]	50	1500	50	95.2 (*S*)	91 b
76	H	CO_2Me	NHAc	[Rh(COD)**98a**]BF_4	1	MeOH	25	0.0217 [f]	50	2308	50	90.9	26
77	H	CO_2Et	NHAc	[Rh(COD)**98a**]BF_4	1	MeOH	25	0.0233 [f]	50	2143	50	83.0	26
78	H	CO_2Me	NHAc	[Rh(COD)**98a**]BF_4	1	MeOH	25	0.016 [f]	50	3333	50	90.6 (*S*)	91 e
79	H	CO_2Me	NHAc	[Rh(COD)**98i**]BF_4	1	MeOH	25	0.0333 [f]	50	1500	50	95 (*S*)	97
80	H	CO_2Me	NHAc	[Rh(COD)**98i**]BF_4	1	H_2O	25	0.467 [f]	50	107	50	79 (*S*)	97
81	H	CO_2Me	NHAc	[Rh(COD)**98i**]BF_4	1	H_2O+SDS, 0.035 [g]	25	0.133 [f]	50	375	50	93 (*S*)	97
82	H	CO_2Me	NHAc	[Rh(COD)**98i**]BF_4	1	H_2O+SDS, 0.173 [g]	25	0.0417 [f]	50	1200	50	97 (*S*)	97
83	H	CO_2Me	NHAc	[Rh(COD)**114a**]BF_4	1	PhH	25	0.017 [f]	50	2941	50	41 (*S*)	99
84	H	CO_2Me	NHAc	[Rh(COD)**114a**]BF_4	1	H_2O	25	1.22 [f]	50	41	50	34 (*S*)	99
85	H	CO_2Me	NHAc	[Rh(COD)**114a**]BF_4	1	MeOH	25	0.017 [f]	50	2941	50	75 (*S*)	99
86	H	CO_2Me	NHAc	[Rh(COD)**114b**]BF_4	1	MeOH	25	0.017 [f]	50	2941	50	71 (*S*)	99
87	H	CO_2Me	NHAc	[Rh(COD)**114b**]BF_4	1	PhH	25	0.017 [f]	50	2941	50	36 (*S*)	99
88	H	CO_2Me	NHAc	[Rh(COD)**114b**]BF_4	1	H_2O	25	0.33 [f]	50	152	50	44 (*S*)	99
89	H	CO_2Me	NHAc	[Rh(COD)**114b**]BF_4	1	H_2O+Triton X-100 (0.1 mmol)	25	0.067 [f]	50	746	50	69 (*S*)	99

Table 27.5 (continued)

Entry	Substrate			Catalyst	Conditions				TON	TOF [h^{-1}]	Conv. [%]	ee [%]	Reference(s)
	R^1	R^2	R^3		P[H_2] [bar]	Solvent	Temp. [°C]	Time [h]					
90	H	CO_2Me	NHAc	[Rh(COD)**114b**]BF_4	1	H_2O + Triton X-100 (0.5 mmol)	25	0.05 [f)]	50	1000	50	70 (*S*)	99
91	H	CO_2Me	NHAc	[Rh(COD)**115d**]BF_4	2.8	THF	r.t.	3	100	33	100	93 (*S*)	98
92	H	CO_2Me	NHAc	[Rh(COD)**115d**]BF_4	2.8	EtOH	r.t.	1	150	150	100	89 (*S*)	98
93	H	CO_2Me	NHAc	[Rh(COD)**115d**]BF_4	2.8	H_2O/THF (3:1)	r.t.	2	100	50	100	87 (*S*)	98
94	H	CO_2Me	NHAc	[Rh(COD)**115d**]BF_4	2.8	MeOH	r.t.	3	100	33	100	37 (*S*)	98
95	H	CO_2Me	NHAc	[Rh(COD)**115d**]BF_4	2.8	MeOH/H_2O (1:1)	r.t.	7	100	14	100	90 (*S*)	98
96	H	CO_2Me	NHAc	[Rh(COD)**115d**]BF_4	2.8	MeOH/H_2O (1:3)	r.t.	3	100	33	100	74 (*S*)	98
97	H	CO_2Me	NHAc	[Rh(COD)**115d**]BF_4	2.8	MeOH/H_2O (1:20)	r.t.	3	150	50	100	57 (*S*)	98
98	H	CO_2Me	NHAc	[Rh(COD)**115d**]BF_4	2.8	H_2O	r.t.	21	100	5	100	2 (*S*)	98
99	H	CO_2Me	NHAc	[Rh(COD)**115d**]BF_4	2.8	H_2O	r.t.	12	52.5	4	35	58 (*S*)	98
100	H	CO_2Me	NHAc	[Rh(COD)**115d**]BF_4	2.8	EtOH/H_2O (1:1)	r.t.	1	150	150	100	85 (*S*)	98
101	H	CO_2Me	NHAc	[Rh(COD)**115g**]SbF_6	2.8	H_2O	r.t.	1	150	150	100	61 (*S*)	98
102	H	CO_2Me	NHAc	[Rh(COD)**115g**]SbF_6	2.8	H_2O	r.t.	3	100	33	97	65 (*S*)	98
103	H	CO_2Me	NHAc	[Rh(COD)**115g**]SbF_6	2.8	THF	r.t.	1	150	150	100	86 (*S*)	98
104	H	CO_2Me	NHAc	[Rh(COD)**117**]BF_4	5	H_2O	r.t.	1.5	50	33	100	80 (*S*)	101
105	H	CO_2Me	NHAc	[Rh(COD)**119a**]SbF_6	2.07	THF	r.t.	–	–	–	~100	65 (*S*)	102
106	H	CO_2Me	NHAc	[Rh(COD)**119b**]SbF_6	2.07	THF	r.t.	–	–	–	~100	83 (*S*)	102
107	H	CO_2Me	NHAc	[Rh(COD)**119d**]SbF_6	2.8	H_2O	r.t.	2	125	63	100	55 (*S*)	102
108	H	CO_2Me	NHAc	[Rh(COD)**119e**]SbF_6	2.8	H_2O	r.t.	2	125	63	100	49 (*S*)	102
109	H	CO_2Me	NHAc	[Rh(COD)ent-**120**]BF_4	1	Acetone	r.t.	–	100	–	100	18 (*R*)	105
110	H	CO_2Me	NHAc	[Rh(COD)**121a**]BF_4	1	Acetone	r.t.	–	100	–	100	5 (*R*)	105
111	H	CO_2Me	NHAc	[Rh(COD)**121b**]BF_4	1	Acetone	r.t.	–	100	–	100	59 (*R*)	105

112	H	CO_2Me	NHAc	[Rh(COD)**121d**]BF_4	1	Acetone	r.t.	–	100	–	100	26 (*R*)	105
113	H	CO_2Me	NHAc	[Rh(COD)**122a**]BF_4	1	Acetone	r.t.	0.25	500	2000	100	76 (*R*)	105
114	H	CO_2Me	NHAc	[Rh(COD)**122b**]BF_4	1	Acetone/DCM 13:2	r.t.	–	100	–	100	85 (*R*)	105
115	H	CO_2Me	NHAc	[Rh(COD)**122b**]BF_4	1	Acetone/DCM 13:2	–25	0.33	100	303	100	91 (*R*)	105
116	H	CO_2Me	NHAc	[Rh(COD)**122c**]BF_4	1	Acetone	r.t.	–	100	–	100	80 (*R*)	105
117	H	CO_2Me	NHAc	[Rh(COD)**122d**]BF_4	1	Acetone/DCM 13:2	r.t.	–	100	–	100	78 (*R*)	105
118	H	CO_2Me	NHAc	[Rh(COD)**122e**]BF_4	1	Acetone	r.t.	–	100	–	100	87 (*R*)	105
119	H	CO_2Me	NHAc	[Rh(COD)**122e**]BF_4	1	Acetone	–25	0.5	100	200	100	93 (*R*)	105
120	H	CO_2Me	NHAc	[Ir(COD)**126**]BF_4	1	DCM	25	0.42	100	238	100	78 (*R*)	104
121	H	CO_2Me	NHAc	[Rh(COD)**126**]BF_4	1	DCM	25	0.25	100	400	100	8 (*R*)	104
122	H	CO_2Me	NHAc	[Ir(COD)**127**]BF_4	1	DCM	25	0.75	76	101	76	15 (*R*)	104
123	H	CO_2Me	NHAc	[Rh(COD)**127**]BF_4	1	DCM	25	0.02	100	5000	100	76 (*R*)	104
124	H	CO_2Me	NHAc	[Rh(COD)**127**]BF_4	1	DCM	25	0.75	96	128	96	81 (*R*)	104
125	H	CO_2Me	NHAc	[Rh(COD)**133a**]BF_4	1	IPA	r.t.	24	72	3	72	41	48
126	H	CO_2Me	NHAc	[Rh(COD)**133b**]BF_4	1	IPA	r.t.	24	77	2	77	46	48
127	H	CO_2Me	NHAc	[Rh(COD)**133c**]BF_4	1	IPA	r.t.	24	80	3	80	48	48
128	H	CO_2Me	NHAc	[Rh(COD)**136**]BF_4	1.3	DCM	r.t.	20	1000	50	100	90 (*R*)	109
129	H	CO_2Me	NHAc	[Rh(COD)**136**]BF_4	1.5	DCM	25	3	479	160	100	90 (*R*)	110
130	H	CO_2Me	NHAc	[Rh(COD)**138**]BF_4	1.3	DCM	r.t.	20	1000	50	100	99.5 (*R*)	109
131	H	CO_2Me	NHAc	[Rh(COD)**140**]BF_4	1.5	DCM	25	3	474	158	99	23 (*R*)	110
132	H	CO_2Me	NHAc	[Rh(COD)**141a**]BF_4	3.5	MeOH	r.t.	0.5	1000	2000	>99	96 (*S*)	111
133	H	CO_2Me	NHAc	[Rh(COD)**141a**]BF_4	3.5	MeOH/H_2O 9:1	r.t.	3	1000	333	>99	96 (*S*)	111
134	H	CO_2Me	NHAc	[Rh(COD)**141a**]BF_4	3.5	DCM	r.t.	1	1000	1000	>99	98 (*S*)	111
135	H	CO_2Me	NHAc	[Rh(COD)**141a**]BF_4	3.5	Tol	r.t.	0.5	1000	2000	>99	99 (*S*)	111
136	H	CO_2Me	NHAc	[Rh(COD)**141b**]BF_4	3.5	MeOH	r.t.	0.5	1000	2000	>99	99 (*S*)	111
137	H	CO_2Me	NHAc	[Rh(COD)**141c**]BF_4	3.5	MeOH	r.t.	1	50	50	5	–	111
138	H	CO_2Me	NHAc	[Rh(COD)**141c**]BF_4	3.5	MeOH	r.t.	16	980	61	98	74 (*S*)	111
139	H	CO_2Me	NHAc	[Rh(COD)**141d**]BF_4	3.5	MeOH	r.t.	21	250	12	25	46 (*S*)	111
140	H	CO_2Me	NHAc	[Ir(COD)**142a**]BF_4	5	DCM : MeOH 2:1	40	20	20	1	20	19 (*S*)	117 d

Table 27.5 (continued)

Entry	Substrate			Catalyst	Conditions				TON	TOF [h^{-1}]	Conv. [%]	ee [%]	Reference(s)
	R^1	R^2	R^3		$P[H_2]$ [bar]	Solvent	Temp. [°C]	Time [h]					
141	H	CO_2Me	NHAc	[Ir(COD)**142a**]BF_4	5	DCM : MeOH 2 : 1	40	20	9	0.45	9	7 (*S*)	117 d
142	H	CO_2Me	NHAc	[Ir(COD)**142a**]BF_4	1	DCM : MeOH 2 : 1	40	20	31	1.6	31	35 (*S*)	117 d
143	H	CO_2Me	NHAc	[Rh(COD)**142a**]BF_4	5	Tol : MeOH 2 : 1	40	20	94	4.7	94	33 (*S*)	117 d
144	H	CO_2Me	NHAc	[Ir(COD)**142b**]BF_4	5	DCM : MeOH 2 : 1	40	20	10	0.5	10	6 (*S*)	117 d
145	H	CO_2Me	NHAc	[Ir(COD)**142b**]BF_4	1	DCM : MeOH 2 : 1	40	20	22	1.1	22	24 (*S*)	117 d
146	H	CO_2Me	NHAc	[Rh(COD)**142b**]BF_4	5	Tol : MeOH 2 : 1	40	20	99	5	99	35 (*S*)	117 d
147	H	CO_2Me	NHAc	[Rh(COD)**142b**]BF_4	2	Tol : MeOH 2 : 1	40	20	100	5	100	21 (*S*)	117 d
148	H	CO_2Me	NHAc	[Rh(COD)**142b**]BF_4	5	DCM	40	20	100	5	100	10 (*S*)	117 d
149	H	CO_2Me	NHAc	[Ir(COD)**143a**]BF_4	1	DCM : MeOH 2 : 1	40	20	30	1.5	30	37 (*R*)	117c
150	H	CO_2Me	NHAc	[Rh(COD)**143a**]BF_4	5	Tol : MeOH 2 : 1	40	20	56	2.8	56	4 (*R*)	117 c
151	H	CO_2Me	NHAc	[Ir(COD)**143b**]BF_4	1	DCM : MeOH 2 : 1	40	20	24	1.2	24	28 (*R*)	117 c
152	H	CO_2Me	NHAc	[Rh(COD)**143b**]BF_4	5	Tol : MeOH 2 : 1	40	20	88	4.4	88	6 (*R*)	117 c
153	H	CO_2Me	NHAc	[Rh(COD)**144a**]BF_4	5	DCM	25	8	98	12.3	98	92 (*S*)	117 b
154	H	CO_2Me	NHAc	[Rh(COD)**144c**]BF_4	5	DCM	25	6	100	16.7	100	97 (*S*)	117 b
155	H	CO_2Me	NHAc	[Rh(COD)**144c**]BF_4	30	DCM	5	4	1000	250	100	>99 (*S*)	117 b
156	H	CO_2Me	NHAc	[Rh(COD)**145a**]BF_4	5	DCM	25	8	100	12.5	100	3 (*S*)	117 b
157	H	CO_2Me	NHAc	[Rh(COD)**146a**]BF_4	5	DCM	25	8	97	12.1	97	71 (*S*)	117 b
158	H	CO_2Me	NHAc	[Rh(COD)**146c**]BF_4	5	DCM	25	8	92	11.5	92	29 (*S*)	117 b
159	H	CO_2Me	NHAc	[Rh(COD)**149a**]BF_4	0.3	DCM	20	20	660	33	66	43.8 (*S*)	116
160	H	CO_2Me	NHAc	[Rh(COD)**149b**]BF_4	0.3	DCM	20	20	770	39	77	23.2 (*S*)	116
161	H	CO_2Me	NHAc	[Rh(COD)**149c**]BF_4	0.3	DCM	20	20	1000	50	>99	88.8 (*R*)	116
162	H	CO_2Me	NHAc	[Rh(COD)**149e**]BF_4	0.3	DCM	20	20	1000	50	>99	80.7 (*R*)	116
163	H	CO_2Me	NHAc	[Rh(COD)**159a**]BF_4	1	MeOH	r.t.	4	97	24.3	97	93 (*R*)	123
164	H	CO_2Me	NHAc	[Rh(COD)**159a**]BF_4	1	THF	r.t.	4	84	21	84	94 (*R*)	123

165	H	CO_2Me	NHAc	[Rh(COD)**159a**]BF_4	1	DCM/MeOH 9 : 1	r.t.	14	78	5.6	78	98 (*R*)	123
166	H	CO_2Me	NHAc	[Rh(COD)**159a**]BF_4	1	DCM	r.t.	14	77	5.5	77	99 (*R*)	123
167	H	CO_2Me	NHAc	[Rh(COD)**159b**]BF_4	1	DCM	r.t.	2.5	39	15.6	39	96 (*S*)	123
168	H	CO_2Me	NHAc	[Rh(COD)**159c**]BF_4	1	DCM	r.t.	14	100	7.1	100	4 (*S*)	123
169	H	CO_2Me	NHAc	[Rh(COD)**159d**]BF_4	1	DCM	r.t.	2.5	100	40	100	96 (*S*)	123
170	H	CO_2Me	NHAc	[Rh(COD)**159e**]BF_4	1	DCM	r.t.	2.5	100	40	100	95 (*R*)	123
171	H	CO_2Me	NHAc	[Rh(COD)**159f**]BF_4	1	DCM	r.t.	2.5	100	40	100	6 (*R*)	123
172	H	CO_2Me	NHAc	[Rh(COD)**159g**]BF_4	1	DCM	r.t.	2.5	100	40	100	95 (*S*)	123
173	H	CO_2Me	NHAc	[Rh(COD)**159h**]BF_4	1	DCM	r.t.	5	21	4.2	21	58 (*R*)	123
174	H	CO_2Me	NHAc	[Rh(COD)**160a**]BF_4	1	DCM	r.t.	2.5	32	12.8	32	61 (*S*)	123
175	H	CO_2Me	NHAc	[Rh(COD)**160b**]BF_4	1	DCM	r.t.	1	100	100	100	96 (*R*)	123
176	H	CO_2Me	NHAc	[Rh(COD)**163a**]PF_6	1	THF	r.t.	12	100	8.3	100	>99 (*S*)	128
177	H	CO_2Me	NHAc	[Rh(COD)**163b**]PF_6	1	THF	r.t.	12	100	8.3	100	96 (*S*)	128
178	H	CO_2Me	NHAc	[Rh(COD)**164a**]PF_6	1	THF	r.t.	12	100	8.3	100	>99 (*S*)	128
179	H	CO_2Me	NHAc	[Rh(COD)**164b**]PF_6	1	THF	r.t.	12	100	8.3	100	77 (*S*)	128
180	H	CO_2Me	NHAc	[Rh(COD)**166**]BF_4	51	H_2O/ EtOAc (1 : 1)	r.t.	24	50	2	100	18 (*R*)	129
181	H	CO_2Me	NHAc	[Rh(COD)**167a**]BF_4	1	DCM	r.t.	0.08	100	>1200	100	88.2 (*S*)	121 a, b
182	H	CO_2Me	NHAc	[Rh(COD)**167b**]BF_4	1	MeOH	25	1.3	100	77	100	91 (*R*)	121 b
183	H	CO_2Me	NHAc	[Rh(COD)**167b**]BF_4	1	DCM	25	2.5	100	40	100	>99 (*R*)	121 b
184	H	CO_2Me	NHAc	[Rh(COD)**167b**]BF_4	1	Tol	25	10	100	10	100	97 (*R*)	121 b
185	H	CO_2Me	NHAc	[Rh(COD)**167b**]BF_4	1	THF	25	2	100	50	100	92 (*R*)	121 b
186	H	CO_2Me	NHAc	[Rh(COD)**167b**]BF_4	1	DCM	25	2.5	100	40	100	>99 (*R*) [k)]	121 b
187	H	CO_2Me	NHAc	[Rh(COD)**167b**]BF_4	1	DCM	25	2.5	100	40	100	>99 (*R*) [l)]	121 a, b
188	H	CO_2Me	NHAc	[Rh(nbd)**167b**]BF_4	1	DCM	25	2.5	100	40	100	>99 (*R*) [l)]	121 b
189	H	CO_2Me	NHAc	[Rh(COD)**167c**]BF_4	1	DCM	r.t.	0.33	100	303	100	98.3 (*S*)	121 a, b
190	H	CO_2Me	NHAc	[Rh(COD)**167d**]BF_4	1	DCM	r.t.	0.33	100	303	100	97.6 (*R*)	121 a, b
191	H	CO_2Me	NHAc	[Rh(COD)**168a**]BF_4	5	DCM	25	8	100	13	100	92 (*S*)	126
192	H	CO_2Me	NHAc	[Rh(COD)**168a**]BF_4	30	DCM	25	12	100	8	100	98 (*S*)	126
193	H	CO_2Me	NHAc	[Rh(COD)**168b**]BF_4	5	DCM	25	8	71	9	71	82 (*S*)	126
194	H	CO_2Me	NHAc	[Rh(COD)**168c**]BF_4	5	DCM	25	8	46	6	46	15 (*S*)	126
195	H	CO_2Me	NHAc	[Rh(COD)**168d**]BF_4	5	DCM	25	8	33	4	33	12 (*S*)	126
196	H	Ph	NHAc	[Rh(COD)**91**]BF_4	6.9	MeOH	r.t.	0.167	100	600	100	83.3 (*R*)	84

Table 27.5 (continued)

Entry	Substrate			Catalyst	Conditions				TON	TOF [h^{-1}]	Conv. [%]	ee [%]	Reference(s)
	R^1	R^2	R^3		$P[H_2]$ [bar]	Solvent	Temp. [°C]	Time [h]					
197	H	Ph	NHAc	[Rh(COD)**91**]BF_4	6.9	IPA	r.t.	0.167	100	600	100	83.5 (*R*)	84
198	H	Ph	NHAc	[Rh(COD)**91**]BF_4	6.9	Acetone	r.t.	0.167	100	600	100	83.1 (*R*)	84
199	H	Ph	NHAc	[Rh(COD)**91**]BF_4	6.9	THF	r.t.	0.167	100	600	100	81.9 (*R*)	84
200	H	Ph	NHAc	[Rh(COD)**91**]BF_4	6.9	DCM	r.t.	0.167	100	600	100	82.5 (*R*)	84
201	H	Ph	NHAc	[Rh(COD)**91**]BF_4	6.9	Tol	r.t.	0.167	100	600	100	79.3 (*R*)	84
202	H	Ph	NHAc	[Rh(COD)**91**]ClO_4	1	IPA	0	0.167	100	600	100	89.0 (*R*)	84
203	H	4-Cl-Ph	NHAc	[Rh(COD)**91**]ClO_4	1	IPA	0	0.167	100	600	100	86.1 (*R*)	84
204	H	4-F-Ph	NHAc	[Rh(COD)**91**]ClO_4	1	IPA	0	0.167	100	600	100	87.9 (*R*)	84
205	H	4-CF_3-Ph	NHAc	[Rh(COD)**91**]ClO_4	1	IPA	0	0.167	100	600	100	90.0 (*R*)	84
206	H	3-Me-Ph	NHAc	[Rh(COD)**91**]ClO_4	1	IPA	0	0.167	100	600	100	85.6 (*R*)	84
207	H	4-Me-Ph	NHAc	[Rh(COD)**91**]ClO_4	1	IPA	0	0.167	100	600	100	86.5 (*R*)	84
208	*i*-Pr	CO_2H	NHAc	[Rh(COD)**95**]BF_4	1	IPA	r.t.	24	100	4	100	45.7 (*S*)	85
209	*i*-Pr	CO_2H	NHAc	[Rh(COD)**97a**]BF_4	1	MeOH	25	0.0316 [f]	50	1579	50	57.2	26
210	*i*-Pr	CO_2H	NHAc	[Rh(COD)**98a**]BF_4	1	MeOH	25	0.0133 [f]	50	3750	50	95.3	26
211	*i*-Pr	CO_2H	NHAc	[Rh(COD)**98a**]SbF_6	2–2.8	THF	r.t.	2–3	–	–	–	90.0 (*S*)	95 b
212	*i*-Pr	CO_2H	NHAc	[Rh(COD)**98b**]SbF_6	2–2.8	THF	r.t.	2–3	–	–	–	91.0 (*S*)	95 b
213	*i*-Pr	CO_2H	NHAc	[Rh(COD)**98c**]SbF_6	2–2.8	THF	r.t.	2–3	–	–	–	64.4	95 b
214	*i*-Pr	CO_2H	NHAc	[Rh(COD)**98d**]SbF_6	2–2.8	THF	r.t.	2–3	–	–	–	26.0	95 b
215	*i*-Pr	CO_2H	NHAc	[Rh(COD)**98g**]SbF_6	2–2.8	THF	r.t.	2–3	–	–	–	83.6	95 b
216	*i*-Pr	CO_2H	NHAc	[Rh(COD)**103a**]SbF_6	2–2.8	THF	r.t.	2–3	–	–	–	89.2 (*R*)	95 b
217	*i*-Pr	CO_2Me	NHAc	[Rh(COD)**98a**]BF_4	1	MeOH	25	0.02 [f]	50	2500	50	86.1	26
218	*i*-Pr (*Z*)	CO_2Me	NHAc	[Rh(COD)**98b**]SbF_6	2–2.8	THF	r.t.	2–3	–	–	–	92.0	95 b
219	*i*-Pr (*Z*/*E*)	CO_2Me	NHAc	[Rh(COD)**98b**]SbF_6	2–2.8	THF	r.t.	2–3	–	–	–	86.5	95 b
220	*i*-Pr	CO_2Me	NHAc	[[Rh(COD)**98d**]SbF_6	2–2.8	THF	r.t.	2–3	–	–	–	5.6 (*R*)	95 b

221	*i*-Pr	CO_2Me	NHAc	[Rh(COD)**98g**]SbF_6	2–2.8	THF	r.t.	2–3	–	–	–	87.2 (*S*)	95 b
222	*i*-Pr	CO_2Me	NHAc	[Rh(COD)**103a**]SbF_6	2–2.8	THF	r.t.	2–3	–	–	–	86.9 (*R*)	95 b
223	*i*-Pr	CO_2Me	NHAc	[Rh(COD)**103g**]SbF_6	2–2.8	THF	r.t.	2–3	–	–	–	86.5 (*R*)	95 b
224	*i*-Pr (*E*)	NHAc	CO_2Me	[Rh(COD)**98b**]SbF_6	2–2.8	THF	r.t.	2–3	–	–	–	73.3	95 b
225	Bn	CO_2Me	NHAc	[Rh(COD)**98b**]SbF_6	2–2.8	THF	r.t.	2–3	–	–	–	40.6 (*S*)	95 b
226	Bn	CO_2Me	NHAc	[Rh(COD)**103a**]SbF_6	2–2.8	THF	r.t.	2–3	–	–	–	67.0 (*R*)	95 b
227	Ph	CO_2H	NHAc	[Rh(1,5-hexadiene)(+)-*trans*-**85**]Cl	50	–	0	24	–	–	–	68.5 (*S*) [a]	67
228	Ph	CO_2H	NHAc	[Rh(1,5-hexadiene)d-*trans*-**86**]Cl	50	–	0	–	–	–	–	12 (*S*) [a]	68 a
229	Ph	CO_2H	NHAc	[Rh(COD)**88**]Cl	20.7	PhH/EtOH 1:1	60	24	50 [c]	2.1	100 [d]	4.3	81
230	Ph	CO_2H	NHAc	[Rh(COD)**91**]BF_4	1	MeOH	25	0.167	100	600	>99.9	97.9 (*R*)	27
231	Ph	CO_2H	NHAc	[Rh(COD)**93a**]BF_4	6.9	MeOH	r.t.	0.5	356	712	71.2	18 (*S*)	52
232	Ph	CO_2H	NHAc	[Rh(COD)**94a**]BF_4	6.9	MeOH	r.t.	0.5	410	820	81.9	74.2 (*S*)	52
233	Ph	CO_2H	NHAc	[Rh(COD)**95**]BF_4	1	DCE	r.t.	24	100	4	100	88.2 (*S*)	85
234	Ph	CO_2H	NHAc	[Rh(COD)**95**]BF_4	1	THF	r.t.	24	100	4	100	89.1 (*S*)	85
235	Ph	CO_2H	NHAc	[Rh(COD)**95**]BF_4	1	THF:Et_3N = 1:1	r.t.	24	30	1	30	30.9 (*S*)	85
236	Ph	CO_2H	NHAc	[Rh(COD)**95**]BF_4	1	MeOH	r.t.	24	100	4	100	92.4 (*S*)	85
237	Ph	CO_2H	NHAc	[Rh(COD)**95**]BF_4	1	MeOH : Et_3N = 1:1	r.t.	24	100	4	100	67.9 (*S*)	85
238	Ph	CO_2H	NHAc	[Rh(COD)**95**]BF_4	1	EtOH	r.t.	24	100	4	100	92.0 (*S*)	85
239	Ph	CO_2H	NHAc	[Rh(COD)**95**]BF_4	1	CF_3CH_2OH	r.t.	24	100	4	100	80.3 (*S*)	85
240	Ph	CO_2H	NHAc	[Rh(COD)**95**]BF_4	1	*t*-BuOH	r.t.	24	100	4	100	91.1 (*S*)	85
241	Ph	CO_2H	NHAc	[Rh(COD)**95**]BF_4	1	IPA	r.t.	24	100	4	100	94.7 (*S*)	85
242	Ph	CO_2H	NHAc	[Rh(COD)**95**]BF_4	1	IPA	0	24	100	4	100	96.1 (*S*)	85
243	Ph	CO_2H	NHAc	[Rh(COD)**95**]BF_4	1	IPA	r.t.	24	86.6	3.6	86.6	63.9 (*S*)	85
244	Ph	CO_2H	NHAc	[Rh(COD)**96**]BF_4	1	IPA	r.t.	24	100	4.2	100	83.5 (*R*)	85
245	Ph	CO_2H	NHAc	[Rh(COD)**97a**]BF_4	1	MeOH	25	0.11 [f]	50	455	50	73.2 (*S*)	26
246	Ph	CO_2H	NHAc	[Rh(COD)**97a**]BF_4	1	EtOH	25	0.1 [f]	50	500	50	71 (*S*) [a]	26
247	Ph	CO_2H	NHAc	$[Rh(COD)Cl]_2$ + **97a** (neutral)	1	EtOH	25	3	50	16.7	50	69 (*S*)	26

Table 27.5 (continued)

Entry	Substrate			Catalyst	Conditions				TON	TOF [h^{-1}]	Conv. [%]	ee [%]	Reference(s)
	R^1	R^2	R^3		$P[H_2]$ [bar]	Solvent	Temp. [°C]	Time [h]					
248	Ph	CO_2H	NHAc	[Rh(NBD)**97a**]PF_6	1	EtOH	30	1	100	100	100[b)]	61 (*S*)	88
249	Ph	CO_2H	NHAc	[Rh(NBD)**97a**]PF_6	1	EtOH	0	1.5	100	67	100[b)]	75 (*S*)	88
250	Ph	CO_2H	NHAc	[Rh(COD)**97a**]BF_4	1	MeOH	25	0.0333[f)]	50	1500	50	96.6 (*S*)	91b
251	Ph	CO_2H	NHAc	[Rh(COD)**97a**]BF_4	1	PhH	25	0.183[f)]	50	273	50	98.6 (*S*)	91b
252	Ph	CO_2H	NHAc	[Rh(COD)**97a**]BF_4	1	Tol	25	0.317[f)]	50	158	50	98.9 (*S*)	91b
253	Ph	CO_2H	NHAc	[Rh(COD)**97a**]BF_4	1	Tol	25	0.32	50	156	50	98.9 (*S*)	91b
254	Ph	CO_2H	NHAc	[Rh(COD)**97a**]Cl	50	–	25	8	100[c)]	–	–	46 (*S*)[a)]	89
255	Ph	CO_2H	NHAc	[Rh(COD)**97a**]ClO_4	1	EtOH	25	–	50	–	100	61 (*S*)	90
256	Ph	CO_2H	NHAc	[Rh(COD)**97b**]Cl	50	–	25	8	100[c)]	–	–	36 (*S*)[a)]	89
257	Ph	CO_2H	NHAc	[Rh(COD)**97b**]BF_4	1	H_2O	25	0.52	50	91	50	80 (S)	99
258	Ph	CO_2H	NHAc	[Rh(COD)**97b**]BF_4	1	H_2O + 0.1 mmol $LiBF_4$	25	0.5	50	100	50	64 (S)	99
259	Ph	CO_2H	NHAc	[Rh(COD)**97b**]BF_4	1	H_2O + 0.1 mmol $NaBF_4$	25	0.3	50	167	50	83 (S)	99
260	Ph	CO_2H	NHAc	[Rh(COD)**97b**]BF_4	1	H_2O + 0.1 mmol KBF_4	25	0.45	50	111	50	82 (S)	99
261	Ph	CO_2H	NHAc	[Rh(COD)**97b**]BF_4	1	H_2O + 0.1 mmol $RbBF_4$	25	0.33	50	150	50	82 (S)	99
262	Ph	CO_2H	NHAc	[Rh(COD)**97b**]BF_4	1	H_2O + 0.1 mmol $CsBF_4$	25	0.47	50	120	50	83 (S)	99
263	Ph	CO_2H	NHAc	[Rh(COD)**97c**]BF_4	1	MeOH	25	0.0667[f)]	50	750	50	95.1 (*S*)	91b
264	Ph	CO_2H	NHAc	[Rh(COD)**97c**]BF_4	1	PhH	25	0.467[f)]	50	107	50	85.5 (*S*)	91b
265	Ph	CO_2H	NHAc	[Rh(COD)**97c**]BF_4	1	Tol	25	8[f)]	50	6.25	50	82.3 (*S*)	91b
266	Ph	CO_2H	NHAc	[Rh(COD)**97d**]BF_4	1	MeOH	25	–	–	–	–	53.7 (*S*)	26

267	Ph	CO_2H	NHAc	[Rh(COD)**98a**]BF_4	1	MeOH	25	0.0233 [f]	50	2143	50	96.6 (*S*)	26
268	Ph	CO_2H	NHAc	[Rh(COD)**98a**]BF_4	1	MeOH	–27	–	–	–	–	99.3 (*S*)	26
269	Ph	CO_2H	NHAc	[Rh(COD)**98a**]BF_4	1	MeOH	–22.2	–	–	–	–	98.3 (*S*)	26
270	Ph	CO_2H	NHAc	[Rh(COD)**98a**]BF_4	1	MeOH	0.4	–	–	–	–	97.7 (*S*)	26
271	Ph	CO_2H	NHAc	[Rh(COD)**98a**]BF_4	1	MeOH	25	–	–	–	–	97.1 (*S*)	26
272	Ph	CO_2H	NHAc	[Rh(COD)**98a**]BF_4	1	MeOH	55.2	–	–	–	–	92.7 (*S*)	26
273	Ph	CO_2H	NHAc	[Rh(COD)**98a**]BF_4	1	EtOH	25	0.117 [f]	50	429	50	96 (*S*) [a]	26
274	Ph	CO_2H	NHAc	$[Rh(COD)Cl]_2$ + **98a** (neutral)	1	EtOH	25	1.67	50	30	50	87 (*S*) [a]	26
275	Ph	CO_2H	NHAc	[Rh(COD)**98a**]BF_4	1	MeOH	25	0.03	50	1667	50	96.5 (*S*)	91e
276	Ph	CO_2H	NHAc	[Rh(COD)**98a**]SbF_6	2–2.8	THF	r.t.	2–3	–	–	–	94.0	95a, b
277	Ph	CO_2H	NHAc	[Rh(COD)**98b**]SbF_6	2–2.8	THF	r.t.	2–3	–	–	–	99.0	95a, b
278	Ph	CO_2H	NHAc	[Rh(COD)**98c**]SbF_6	2–2.8	THF	r.t.	2–3	–	–	–	60.0	95a, b
279	Ph	CO_2H	NHAc	[Rh(COD)**98d**]SbF_6	2–2.8	THF	r.t.	–	–	–	–	71	95a
280	Ph	CO_2H	NHAc	[Rh(COD)**98f**]OTf	2–2.8	THF	r.t.	2–3	–	–	–	96.0	95b
281	Ph	CO_2H	NHAc	[Rh(COD)**98f**]SbF_6	2–2.8	THF	r.t.	2–3	–	–	–	93.0	95b
282	Ph	CO_2H	NHAc	[Rh(COD)**98g**]SbF_6	2–2.8	THF	r.t.	2–3	–	–	–	97.6	95b
283	Ph	CO_2H	NHAc	[Rh(COD)**98h**]SbF_6	2–2.8	THF	r.t.	2–3	–	–	–	91.0	95b
284	Ph	CO_2H	NHAc	[Rh(COD)**100**]Cl	50	–	25	8	100 [c]	–	–	80 (*S*) [a]	89
285	Ph	CO_2H	NHAc	[Rh(COD)**100b**]BF_4	1	MeOH	25	–	50	–	50	90 (*S*)	91e
286	Ph	CO_2H	NHAc	[Rh(COD)**101a**]BF_4	1	MeOH	25	0.0617 [f]	50	810	50	94.5 (*S*)	91c
287	Ph	CO_2H	NHAc	[Rh(COD)**101b**]BF_4	1	MeOH	25	0.0633 [f]	50	789	50	96.2 (*S*)	91c
288	Ph	CO_2H	NHAc	[Rh(COD)**101c**]BF_4	1	MeOH	25	0.0633 [f]	50	789	50	91.4 (*S*)	91c
289	Ph	CO_2H	NHAc	[Rh(COD)**101d**]BF_4	1	MeOH	25	0.0683 [f]	50	732	50	94.9 (*S*)	91c
290	Ph	CO_2H	NHAc	[Rh(COD)**101e**]BF_4	1	MeOH	25	0.0817 [f]	50	612	50	90.4 (*S*)	91c
291	Ph	CO_2H	NHAc	[Rh(COD)**101f**]BF_4	1	MeOH	25	0.142 [f]	50	353	50	93.6 (*S*)	91c
292	Ph	CO_2H	NHAc	[Rh(COD)**102a**]BF_4	2–2.8	THF	r.t.	2–3	–	–	–	94.5	95b
293	Ph	CO_2H	NHAc	[Rh(COD)**102a**]BF_4	2–2.8	THF	r.t.	–	–	–	–	98.3	95a
294	Ph	CO_2H	NHAc	[Rh(COD)**102b**]SbF_6	2–2.8	THF	r.t.	2–3	–	–	–	94.5	95b
295	Ph	CO_2H	NHAc	[Rh(COD)**103a**]BF_4	2–2.8	THF	r.t.	2–3	–	–	–	95.8	95b
296	Ph	CO_2H	NHAc	[Rh(COD)**103a**]SbF_6	2–2.8	THF	r.t.	2–3	–	–	–	97.0	95b

Table 27.5 (continued)

Entry	Substrate			Catalyst	Conditions				TON	TOF [h^{-1}]	Conv. [%]	ee [%]	Reference(s)
	R^1	R^2	R^3		$P[H_2]$ [bar]	Solvent	Temp. [°C]	Time [h]					
297	Ph	CO_2H	NHAc	[Rh(COD)**103a**]SbF_6	2–2.8	THF	r.t.	–	–	–	–	93	95 a
298	Ph	CO_2H	NHAc	[Rh(COD)**111**]ClO_4	1	EtOH	25	0.3	50	167	100	55 (*R*)	90
299	Ph	CO_2H	NHAc	[Rh(COD)**111**]ClO_4	1	EtOH	0	1	50	50	100	70 (*R*)	90
300	Ph	CO_2H	NHAc	[Rh(COD)**112b**]BF_4	1	MeOH	25	0.12	50	417	50	1 (*S*)	91 e
301	Ph	CO_2H	NHAc	[Rh(COD)**113a**]Cl	50	–	25	8	100 [c)]	–	–	0	89
302	Ph	CO_2H	NHAc	[Rh(COD)**113b**]Cl	50	–	25	8	100 [c)]	–	–	0	89
303	Ph	CO_2H	NHAc	[Rh(COD)**113c**]BF_4	1	MeOH	25	0.17	50	294	50	2 (*S*)	91 e
304	Ph	CO_2H	NHAc	[Rh(COD)**113d**]BF_4	1	MeOH	25	0.12	50	429	50	46 (*S*)	91 e
305	Ph	CO_2H	NHAc	[Rh(COD)**113e**]BF_4	1	MeOH	25	0.12	50	417	50	46 (*S*)	91 e
306	Ph	CO_2H	NHAc	[Rh(COD)**114a**]BF_4	1	MeOH	25	0.083 [f)]	50	602	50	55 (*S*)	99
307	Ph	CO_2H	NHAc	[Rh(COD)**114a**]BF_4	1	PhH	25	0.68 [f)]	50	74	50	58 (*S*)	99
308	Ph	CO_2H	NHAc	[Rh(COD)**114b**]BF_4	1	MeOH	25	0.05 [f)]	50	1000	50	52 (*S*)	99
309	Ph	CO_2H	NHAc	[Rh(COD)**114b**]BF_4	1	PhH	25	0.052 [f)]	50	97	50	80 (*S*)	99
310	Ph	CO_2H	NHAc	[Rh(COD)**115d**]BF_4	2.8	THF	r.t.	–	150	–	100	97 (*S*)	98
311	Ph	CO_2H	NHAc	[Rh(COD)**115d**]BF_4	2.8	H_2O/EtOAc (1:1)	r.t.	–	100	–	100	7 (*S*)	98
312	Ph	CO_2H	NHAc	[Rh(COD)**117**]BF_4	5	H_2O/MeOH/ EtOAc (0.6:0.4:2)	r.t.	3	100	33	100	96 (*S*)	101
313	Ph	CO_2H	NHAc	[Rh(COD)**117**]BF_4	5	H_2O/MeOH(3:2)	r.t.	1.5	100	67	100	95 (*S*)	101
314	Ph	CO_2H	NHAc	[Rh(COD)**119d**]SbF_6	2.8	H_2O/THF(1:1)	r.t.	24	15	0.6	12	65 (*S*)	102
315	Ph	CO_2H	NHAc	[Rh(COD)**119d**]SbF_6	2.8	THF	r.t.	2	125	63	100	70 (*S*)	102
316	Ph	CO_2H	NHAc	[Rh(COD)**124**]BF_4	1	EtOH	25	1	100	100	100	30 (*R*)	103
317	Ph	CO_2H	NHAc	[Rh(COD)**124**]BF_4	1	THF	25	1	100	100	100	40 (*R*)	103
318	Ph	CO_2H	NHAc	[Rh(COD)**124**]BF_4	1	THF	0	1	100	100	100	52 (*R*)	103

319	Ph	CO_2H	NHAc	[Rh(COD)**124**]BF_4	1	THF	–78	3	100	33	100	10 (*R*)	103
320	Ph	CO_2H	NHAc	[Rh(COD)**124**]BPh_4	1	THF	25	1	100	100	100	30 (*R*)	103
321	Ph	CO_2H	NHAc	[Rh(COD)**124**]BPh_4	1	EtOH	25	1	100	100	100	35 (*R*)	103
322	Ph	CO_2H	NHAc	[Rh(COD)**124**]Cl	20.4	PhH/EtOH 1:1	60	24	100	2	100	8.2 (*R*)	103
323	Ph	CO_2H	NHAc	[Rh(COD)**124**]ClO_4	1	THF	25	1	100	100	100	36 (*R*)	103
324	Ph	CO_2H	NHAc	[Rh(COD)**124**]ClO_4	1	EtOH	25	1	100	100	100	28 (*R*)	103
325	Ph	CO_2H	NHAc	[Rh(COD)**124**]PF_6	1	THF	25	1	100	100	100	32 (*R*)	103
326	Ph	CO_2H	NHAc	[Rh(COD)**124**]PF_6	1	EtOH	25	1	100	100	100	30 (*R*)	103
327	Ph	CO_2H	NHAc	[Rh(COD)**125**]BF_4	1	THF	25	1	100	100	100	54 (*S*)	103
328	Ph	CO_2H	NHAc	[Rh(COD)**126**]Cl	50	–	25	1	100 [c)]	100	100	62 (*R*) [a)]	89
329	Ph	CO_2H	NHAc	[Rh(COD)**128**]Cl	51	MeOH	r.t.	0.25	230	920	100	36 (*S*)	106
330	Ph	CO_2H	NHAc	[Rh(COD)**129**]Cl	51	MeOH	r.t.	1	270	270	100	15 (*R*)	106
331	Ph	CO_2H	NHAc	[Rh(COD)**131**]BF_4	1	PhH	25	6	89.5	15	89.5	40.8 (*R*)	108
332	Ph	CO_2H	NHAc	[Rh(COD)**132**]BF_4	1	Acetone	25	0.25–1	100	100–400	100	90.1 (*R*)	107
333	Ph	CO_2H	NHAc	[Rh(COD)**132**]BF_4	6.9	Acetone	25	0.25–1	100	100–400	100	92.8 (*R*)	107
334	Ph	CO_2H	NHAc	[Rh(COD)**132**]BF_4	34.5	Acetone	25	0.25–1	100	100–400	100	94.4 (*R*)	107
335	Ph	CO_2H	NHAc	[Rh(COD)**132**]BF_4	34.5	Acetone	–15	0.25–1	100	100–400	100	97.1 (*R*)	107
336	Ph	CO_2H	NHAc	[Rh(COD)**133a**]BF_4	1	IPA	r.t.	24	98	4	98	94 [j)]	48
337	Ph	CO_2H	NHAc	[Rh(COD)**133b**]BF_4	1	IPA	r.t.	24	94	4	94	89 [j)]	48
338	Ph	CO_2H	NHAc	[Rh(COD)**133c**]BF_4	1	IPA	r.t.	24	94	4	98	97 [j)]	48
339	Ph	CO_2H	NHAc	[Rh(COD)**134**]BF_4	1	PhH	25	5.0	85.6	17	85.6	25.6 (*R*)	108
340	Ph	CO_2H	NHAc	[Rh(COD)**135**]BF_4	1	PhH	25	7.5	93.4	12	93.4	57.1 (*R*)	108
341	Ph	CO_2H	NHAc	[Rh(COD)**141a**]BF_4	3.5	MeOH	r.t.	0.5	1000	2000	>99	93 (*S*)	111
342	Ph	CO_2H	NHAc	[Rh(COD)**141b**]BF_4	3.5	MeOH	r.t.	0.5	1000	2000	>99	99 (*S*)	111
343	Ph	CO_2H	NHAc	[Rh(COD)**142a**]BF_4	5	Tol:MeOH 2:1	40	20	100	5	100	31 (*S*)	117 d
344	Ph	CO_2H	NHAc	[Rh(COD)**142b**]BF_4	5	Tol:MeOH 2:1	40	20	100	5	100	30 (*S*)	117 d
345	Ph	CO_2H	NHAc	[Ir(COD)**142b**]BF_4	5	DCM:MeOH 2:1	40	20	18	0.9	18	15 (*S*)	117 d

Table 27.5 (continued)

Entry	Substrate			Catalyst	Conditions				TON	TOF [h^{-1}]	Conv. [%]	ee [%]	Reference(s)
	R^1	R^2	R^3		P[H_2] [bar]	Solvent	Temp. [°C]	Time [h]					
346	Ph	CO_2H	NHAc	[Rh(COD)**163a**]PF_6	1	THF	r.t.	12	99	8.3	100	99 (*S*)	128
347	Ph	CO_2H	NHAc	[Rh(COD)**164a**]PF_6	1	THF	r.t.	12	>99	8.3	100	>99 (*S*)	128
348	Ph	CO_2H	NHAc	[Rh(COD)**166**]BF_4	51	H_2O/EtOAc (1:1)	r.t.	24	50	2.1	100	50 (*R*) [j)]	129
349	Ph	CO_2H	NHAc	[Rh(NBD)**107**]ClO_4	1.48	PhH:EtOH=1:1	25	24	100	4	100	24.8 (*R*)	93
350	Ph	CO_2H	NHAc	[Rh(NBD)**107**]ClO_4	1.48	PhH:EtOH=1:1	25	24	47.5	2	95	31.0 (*R*)	93
351	Ph	CO_2H	NHAc	[Rh(NBD)**107**]ClO_4	1.48	PhH:EtOH=1:1	25	24	18.4	0.8	92	16.2 (*R*)	93
352	Ph	CO_2H	NHAc	[Rh(NBD)**107**]ClO_4	1.48	PhH:EtOH=1:1	40	24	95	4	95	14.9 (*R*)	93
353	Ph	CO_2H	NHAc	[Rh(NBD)**107**]ClO_4	1.48	PhH:EtOH=1:1	60	24	100	4	100	12.4 (*R*)	93
354	Ph	CO_2H	NHAc	[Rh(NBD)**107**]ClO_4	1.48	PhH:EtOH=1:1	80	24	96	4	96	5.3 (*R*)	93
355	Ph	CO_2H	NHAc	[Rh(NBD)**107**]ClO_4	1.48	PhH:EtOH=1:1	–15 to –20	7	53	8	53	62.7 (*R*)	93
356	Ph	CO_2H	NHAc	[Rh(NBD)**107**]ClO_4	1.48	PhH:EtOH=1:1	–15 to –20	7	18.8	3	94	27.7 (*R*)	93
357	Ph	CO_2H	NHAc	[Rh(NBD)**107**]ClO_4	1.97	PhH:EtOH=1:1	25	24	90	4	90	20.9 (*R*)	93
358	Ph	CO_2H	NHAc	[Rh(NBD)**108**]ClO_4	1.48	PhH:EtOH=1:1	25	24	100	4	100	63.4 (*S*)	93
359	Ph	CO_2H	NHAc	[Rh(NBD)**108**]ClO_4	1.48	PhH:EtOH=1:1	25	24	50	2	100	68.2 (*S*)	93
360	Ph	CO_2H	NHAc	[Rh(NBD)**108**]ClO_4	1.48	PhH:EtOH=1:1	25	24	20	0.9	100	44.1 (*S*)	93
361	Ph	CO_2H	NHAc	[Rh(NBD)**108**]ClO_4	1.48	PhH:EtOH=1:1	25	1	96	96	96	60.4 (*S*)	93
362	Ph	CO_2H	NHAc	[Rh(NBD)**108**]ClO_4	1.48	PhH:EtOH=1:1	25	2	100	50	100	66.9 (*S*)	93
363	Ph	CO_2H	NHAc	[Rh(NBD)**108**]ClO_4	1.48	PhH:EtOH=1:1	25	4	94	24	94	59.6 (*S*)	93
364	Ph	CO_2H	NHAc	[Rh(NBD)**108**]ClO_4	1.48	PhH:EtOH=1:1	40	24	100	4	100	45.9 (*S*)	93
365	Ph	CO_2H	NHAc	[Rh(NBD)**108**]ClO_4	1.48	PhH:EtOH=1:1	60	24	100	4	100	26.3 (*S*)	93
366	Ph	CO_2H	NHAc	[Rh(NBD)**108**]ClO_4	1.48	PhH:EtOH=1:1	80	24	100	4	100	12.9 (*S*)	93
367	Ph	CO_2H	NHAc	[Rh(NBD)**108**]ClO_4	1.48	PhH:EtOH=1:1	–15 to –20	6	20	3	20	80.1 (*S*)	93

368	Ph	CO_2H	NHAc	[Rh(NBD)**108**]ClO_4	1.48	PhH : EtOH = 1 : 1	–15 to –20	8	20	3	100	74.1 (*S*)	93
369	Ph	CO_2H	NHAc	[Rh(NBD)**108**]ClO_4	1.48	PhH : EtOH = 1 : 1	0	24	100	4	100	72.1 (*S*)	93
370	Ph	CO_2H	NHAc	[Rh(NBD)**108**]ClO_4	1.48	PhH : EtOH = 1 : 1	–5	24	93	4	93	78.4 (*S*)	93
371	Ph	CO_2H	NHAc	[Rh(NBD)**108**]ClO_4	1.48	PhH : EtOH = 1 : 1	–15	24	79	3	79	90.4 (*S*)	93
372	Ph	CO_2H	NHAc	[Rh(NBD)**108**]ClO_4	1.09	PhH : EtOH = 1 : 1	25	24	70	3	70	21.9 (*S*)	93
373	Ph	CO_2H	NHAc	[Rh(NBD)**108**]ClO_4	19.70	PhH : EtOH = 1 : 1	25	50	100	2	100	22.9 (*S*)	93
374	Ph	CO_2H	NHAc	[Rh(NBD)**109**]ClO_4 dimer	1.48	–	25	24	63	3	63 [b)]	13.8 (*R*)	94
375	Ph	CO_2H	NHAc	[Rh(NBD)**109**]ClO_4 dimer	1.48	–	25	24	50	2	100 [b)]	11.6 (*R*)	94
376	Ph	CO_2H	NHAc	[Rh(NBD)**109**]ClO_4 dimer	1.48	–	25	24	20	0.8	100 [b)]	14.9 (*R*)	94
377	Ph	CO_2H	NHAc	[Rh(NBD)**109**]ClO_4 dimer	1.48	–	40	24	100	4	100 [b)]	8.2 (*R*)	94
378	Ph	CO_2H	NHAc	[Rh(NBD)**109**]ClO_4 dimer	1.48	–	60	24	100	4	100 [b)]	1.6 (*S*)	94
379	Ph	CO_2H	NHAc	[Rh(NBD)**109**]ClO_4 dimer	1.48	–	80	24	100	4	100 [b)]	2.9 (*S*)	94
380	Ph	CO_2H	NHAc	[Rh(NBD)**109**]ClO_4 dimer	1.48	–	–15 to –20	7	93	13	93 [b)]	26.3 (*R*)	94
381	Ph	CO_2H	NHAc	[Rh(NBD)**109**]ClO_4 dimer	1.48	–	–15 to –20	7	20	3	100 [b)]	29.3 (*R*)	94
382	Ph	CO_2H	NHAc	[Rh(NBD)**110**]ClO_4 dimer	1.48	–	25	24	100	4	100 [b)]	4.8 (*R*)	94
383	Ph	CO_2H	NHAc	[Rh(NBD)**110**]ClO_4 dimer	1.48	–	25	24	50	2	100 [b)]	6.9 (*R*)	94

Table 27.5 (continued)

Entry	Substrate			Catalyst	Conditions				TON	TOF [h^{-1}]	Conv. [%]	ee [%]	Reference(s)
	R^1	R^2	R^3		P[H_2] [bar]	Solvent	Temp. [°C]	Time [h]					
384	Ph	CO_2H	NHAc	[Rh(NBD)**110**]ClO_4 dimer	1.48	–	25	24	19.4	0.8	97 [b)]	2.5 (*R*)	94
385	Ph	CO_2H	NHAc	[Rh(NBD)**110**]ClO_4 dimer	1.48	–	40	24	100	4	100 [b)]	3.1 (*R*)	94
386	Ph	CO_2H	NHAc	[Rh(NBD)**110**]ClO_4 dimer	1.48	–	60	24	100	4	100 [b)]	1.5 (*R*)	94
387	Ph	CO_2H	NHAc	[Rh(NBD)**110**]ClO_4 dimer	1.48	–	80	24	100	4	100 [b)]	2.1 (*R*)	94
388	Ph	CO_2H	NHAc	[Rh(NBD)**110**]ClO_4 dimer	1.48	–	–15 to –20	7	92	13	92 [b)]	12.1 (*R*)	94
389	Ph	CO_2H	NHAc	[Rh(NBD)**110**]ClO_4 dimer	1.48	–	–15 to –20	7	18.6	3	93 [b)]	9.5 (*R*)	94
390	Ph	CO_2H	NHAc	$[RhCl(COD)]_2$ + **165** + Et_3N	1	EtOH : PhH =1 : 1	r.t.	48	100	2	100	4.7 (*R*) [a)]	119
391	Ph	CO_2H	NHBz	[Rh(COD)**95**]BF_4	1	IPA	r.t.	24	100	4	100	89.2 (*S*)	85
392	Ph	CO_2H	NHBz	[Rh(COD)**97a**]BF_4	1	MeOH	25	0.0333	50	1500	50	95.0 (*S*)	91 b
393	Ph	CO_2H	NHBz	[Rh(COD)**97c**]BF_4	1	MeOH	25	0.05 [f)]	50	1000	50	93.7 (*S*)	91 b
394	Ph	CO_2H	NHBz	[Rh(COD)**98a**]BF_4	1	MeOH	25	0.117 [f)]	50	429	50	96 (*S*)	26
395	Ph	CO_2H	NHBz	[Rh(COD)**98a**]BF_4	50	MeOH	25		100 [b)]			95 (*S*)	26
396	Ph	CO_2H	NHBz	[Rh(COD)**128**]Cl	10	MeOH	r.t.	1	110	110	100	44 (*S*)	106
397	Ph	CO_2H	NHBz	[Rh(COD)**129**]Cl	51	MeOH	r.t.	1	100	100	100	17 (*R*)	106
398	Ph	CO_2H	NHBz	[Rh(COD)**163a**]PF_6	1	THF	r.t.	12	>99	8.3	100	>99 (*S*)	128
399	Ph	CO_2H	NHBz	[Rh(COD)**164a**]PF_6	1	THF	r.t.	12	>99	8.3	100	>99 (*S*)	128
400	Ph	CO_2Me	NHAc	[Rh(1,5-hexadiene)d-*trans*-**86**]Cl	50	–	50	–	–	–	–	43 (*S*) [a)]	68 a
401	Ph	CO_2Me	NHAc	[Rh(COD)**88**]Cl	69	PhH : EtOH =1 : 1	100	48	50 [c)]	–	[d)]	10.3	81
402	Ph	CO_2Me	NHAc	[Rh(COD)**91**]BF_4	1	MeOH	25	0.167	100	600	>99.9	95.7 (*R*)	27

403	Ph	CO_2Me	NHAc	[Rh(COD)**93a**]BF_4	6.9	DCM	r.t.	0.17	428	2518	85.5	64 (*S*)	52
404	Ph	CO_2Me	NHAc	[Rh(COE)**93a**]Cl	97	Tol/acetone 1:1	0	24	20.5	0.9	41 [b)]	76 [a)]	71
405	Ph	CO_2Me	NHAc	[Rh(COD)**94a**]BF_4	6.9	DCM	r.t.	0.17	500	2941	100	84 (*S*)	52
406	Ph	CO_2Me	NHAc	$[Rh(COD)Cl]_2$ + **97a** (cationic)	1	PhH	25	0.117 [f)]	50	429	50	6 (*S*) [a)]	26
407	Ph	CO_2Me	NHAc	$[Rh(COD)Cl]_2$ + **97a** (neutral)	1	EtOH	25	5.17 [f)]	50	10	50	63 (*S*) [a)]	26
408	Ph	CO_2Me	NHAc	$[Rh(COD)Cl]_2$ + **97a** (neutral)	1	PhH	25	>83.3 [f)]	50	0.6	50	14 (*S*) [a)]	26
409	Ph	CO_2Me	NHAc	[Rh(COD)**97a**]BF_4	1	MeOH	25	0.113 [f)]	50	441	50	72.2 (*S*)	26
410	Ph	CO_2Me	NHAc	[Rh(COD)**97a**]BF_4	1	MeOH	–21.3	–	–	–	–	82.3 (*S*)	26
411	Ph	CO_2Me	NHAc	[Rh(COD)**97a**]BF_4	1	MeOH	0.5	–	–	–	–	77.8 (*S*)	26
412	Ph	CO_2Me	NHAc	[Rh(COD)**97a**]BF_4	1	EtOH	25	0.1 [f)]	50	500	50	73 (*S*) [a)]	26, 91 e
413	Ph	CO_2Me	NHAc	[Rh(COD)**97a**]BF_4	1	MeOH	25	–	–	–	–	73 (*S*)	91 a
414	Ph	CO_2Me	NHAc	[Rh(COD)**97a**]BF_4	1	MeOH	25	0.1 [f)]	50	500	50	91.5 (*S*)	91 b
415	Ph	CO_2Me	NHAc	[Rh(COD)**97a**]BF_4	1	MeOH	25	0.12	50	417	50	72 (*S*)	91 e
416	Ph	CO_2Me	NHAc	[Rh(COD)**97a**]BF_4	1	PhH	25	0.08	50	625	50	6 (*R*)	91 e
417	Ph	CO_2Me	NHAc	[Rh(COD)**97a**]Cl	50	–	25	8	100 [c)]	–	–	8 (*S*) [a)]	89
418	Ph	CO_2Me	NHAc	[Rh(COD)**97a**]ClO_4	1	EtOH	25	–	50	–	100	60(*S*)	90
419	Ph	CO_2Me	NHAc	[Rh(NBD)**97a**]PF_6	1	EtOH	30	0.5	100	200	100 [b)]	60 (*S*)	88
420	Ph	CO_2Me	NHAc	[Rh(NBD)**97a**]PF_6	1	EtOH	0	3	100	33	100	65 (*S*)	88
421	Ph	CO_2Me	NHAc	[Rh(COD)**97b**]BF_4	1	H_2O + 0.1 mmol $LiBF_4$	25	0.033	50	1500	50	45 (S)	99
422	Ph	CO_2Me	NHAc	[Rh(COD)**97b**]BF_4	1	H_2O + 0.1 mmol $NaBF_4$	25	0.017	50	3000	50	41 (S)	99
423	Ph	CO_2Me	NHAc	[Rh(COD)**97b**]BF_4	1	H_2O + 0.1 mmol KBF_4	25	0.017	50	3000	50	41 (S)	99
424	Ph	CO_2Me	NHAc	[Rh(COD)**97b**]BF_4	1	H_2O + 0.1 mmol $RbBF_4$	25	0.033	50	1500	50	41 (S)	99
425	Ph	CO_2Me	NHAc	[Rh(COD)**97b**]BF_4	1	H_2O + 0.1 mmol $CsBF_4$	25	0.033	50	1500	50	41 (S)	99

Table 27.5 (continued)

Entry	Substrate			Catalyst	Conditions				TON	TOF [h^{-1}]	Conv. [%]	ee [%]	Reference(s)
	R^1	R^2	R^3		$P[H_2]$ [bar]	Solvent	Temp. [°C]	Time [h]					
426	Ph	CO_2Me	NHAc	[Rh(COD)**97b**]BF_4	1	H_2O	25	0.033	50	1500	50	41 (S)	99
427	Ph	CO_2Me	NHAc	[Rh(COD)**97b**]Cl	50	–	25	8	100 [c)]	–	–	10 (*S*) [a)]	89
428	Ph	CO_2Me	NHAc	[Rh(COD)**97c**]BF_4	1	MeOH	25	0.58	50	86	50	61 (*S*)	91a
429	Ph	CO_2Me	NHAc	[Rh(COD)**97c**]BF_4	1	MeOH + Triton X-100	25	0.07	50	714	50	87 (*S*)	91a
430	Ph	CO_2Me	NHAc	[Rh(COD)**97c**]BF_4	1	MeOH + Tween 20	25	0.12	50	417	50	86 (*S*)	91a
431	Ph	CO_2Me	NHAc	[Rh(COD)**97c**]BF_4	1	MeOH + Tween 40	25	0.1	50	500	50	86 (*S*)	91a
432	Ph	CO_2Me	NHAc	[Rh(COD)**97c**]BF_4	1	MeOH + Tween 60	25	0.12	50	417	50	85 (*S*)	91a
433	Ph	CO_2Me	NHAc	[Rh(COD)**97c**]BF_4	1	MeOH + Tween 80	25	0.13	50	385	50	87 (*S*)	91a
434	Ph	CO_2Me	NHAc	[Rh(COD)**97c**]BF_4	1	MeOH + Brij 56	25	0.1	50	500	50	83 (*S*)	91a
435	Ph	CO_2Me	NHAc	[Rh(COD)**97c**]BF_4	1	MeOH + Brij 58	25	0.08	50	625	50	85 (*S*)	91a
436	Ph	CO_2Me	NHAc	[Rh(COD)**97c**]BF_4	1	MeOH + Brij 76	25	0.12	50	417	50	83 (*S*)	91a
437	Ph	CO_2Me	NHAc	[Rh(COD)**97c**]BF_4	1	MeOH + Brij 78	25	0.1	50	500	50	82 (*S*)	91a
438	Ph	CO_2Me	NHAc	[Rh(COD)**97c**]BF_4	1	MeOH	25	0.05 [f)]	50	1000	50	94.8 (*S*)	91b
439	Ph	CO_2Me	NHAc	[Rh(COD)**97d**]BF_4	1	MeOH	25	–	–	–	–	17.2 (*S*)	26
440	Ph	CO_2Me	NHAc	[Rh(COD)**97d**]BF_4	1	MeOH	25	–	–	–	–	63 (*S*)	91a
441	Ph	CO_2Me	NHAc	$[Rh(COD)Cl]_2$ + **98a** (cationic)	1	PhH	25	0.117 [f)]	50	429	50	69 (*S*) [a)]	26
442	Ph	CO_2Me	NHAc	$[Rh(COD)Cl]_2$ + **98a** (neutral)	1	EtOH	25	10.7 [f)]	50	4.69	50	79 (*S*) [a)]	26
443	Ph	CO_2Me	NHAc	[Rh(COD)**98a**]BF_4	1	EtOH	25	0.117 [f)]	50	429	50	89 (*S*) [a)]	26
444	Ph	CO_2Me	NHAc	[Rh(COD)**98a**]BF_4	1	MeOH	25	0.103 [f)]	50	484	50	91.1 (*S*)	26
445	Ph	CO_2Me	NHAc	[Rh(COD)**98a**]BF_4	100	MeOH	25	0.00083 [f)]	50	60241	50	91.5 (*S*)	26
446	Ph	CO_2Me	NHAc	[Rh(COD)**98a**]BF_4	1	MeOH	–20	–	–	–	–	95.4 (*S*)	26

447	Ph	CO_2Me	NHAc	[Rh(COD)**98a**]BF_4	1	MeOH	–5.2	–	–	–	–	93.9 (*S*)	26
448	Ph	CO_2Me	NHAc	[Rh(COD)**98a**]BF_4	1	MeOH	10.1	–	–	–	–	93.2 (*S*)	26
449	Ph	CO_2Me	NHAc	[Rh(COD)**98a**]BF_4	1	MeOH	25	–	–	–	–	90.5 (*S*)	26
450	Ph	CO_2Me	NHAc	[Rh(COD)**98a**]BF_4	1	MeOH	40.6	–	–	–	–	88.0 (*S*)	26
451	Ph	CO_2Me	NHAc	[Rh(COD)**98a**]BF_4	1	MeOH	54.6	–	–	–	–	86.2 (*S*)	26
452	Ph	CO_2Me	NHAc	[Rh(COD)**98a**]BF_4	1	MeOH	25	–	–	–	–	91 (*S*)	91a
453	Ph	CO_2Me	NHAc	[Rh(COD)**98a**]BF_4	1	MeOH	25	0.1 [f]	50	500	50	91.5 (*S*)	91e
454	Ph	CO_2Me	NHAc	[Rh(COD)**98a**]BF_4	1	$ClCH_2CH_2Cl$	25	0.08	50	625	50	90 (*S*)	91e
455	Ph	CO_2Me	NHAc	[Rh(COD)**98a**]BF_4	1	CH_2Cl_2	25	0.17	50	294	50	89 (*S*)	91e
456	Ph	CO_2Me	NHAc	[Rh(COD)**98a**]BF_4	1	*o*-Xylene	25	0.03	50	1667	50	83 (*S*)	91e
457	Ph	CO_2Me	NHAc	[Rh(COD)**98a**]BF_4	1	*m*-Xylene	25	0.08	50	625	50	85 (*S*)	91e
458	Ph	CO_2Me	NHAc	[Rh(COD)**98a**]BF_4	1	*p*-Xylene	25	0.13	50	385	50	81 (*S*)	91e
459	Ph	CO_2Me	NHAc	[Rh(COD)**98a**]BF_4	1	EtOH	25	0.083 [f]	50	600	50	89 (*S*)	91e
460	Ph	CO_2Me	NHAc	[Rh(COD)**98a**]BF_4	1	THF	25	0.067 [f]	50	750	50	86.1 (*S*)	91e
461	Ph	CO_2Me	NHAc	[Rh(COD)**98a**]BF_4	1	PhH	25	0.117 [f]	50	429	50	81.0 (*S*)	91e
462	Ph	CO_2Me	NHAc	[Rh(COD)**98a**]BF_4	1	Tol	25	0.1 [f]	50	500	50	81.0 (*S*)	91e
463	Ph	CO_2Me	NHAc	[Rh(COD)**98a**]BF_4	2–2.8	THF	r.t.	2–3	–	–	–	84.7	95b
464	Ph	CO_2Me	NHAc	[Rh(COD)**98a**]SbF_6	2–2.8	THF	r.t.	2–3	–	–	–	90.2	95b
465	Ph	CO_2Me	NHAc	[Rh(COD)**98b**]BF_4	2–2.8	THF	r.t.	2–3	–	–	–	94.4	95b
466	Ph	CO_2Me	NHAc	[Rh(COD)**98b**]SbF_6	2–2.8	THF	r.t.	2–3	–	–	–	97.4	95b
467	Ph	CO_2Me	NHAc	[Rh(COD)**98c**]BF_4	2–2.8	THF	r.t.	2–3	–	–	–	6.2	95b
468	Ph	CO_2Me	NHAc	[Rh(COD)**98c**]SbF_6	2–2.8	THF	r.t.	2–3	–	–	–	2.0	95b
469	Ph	CO_2Me	NHAc	[Rh(COD)**98d**]BF_4	2–2.8	THF	r.t.	2–3	–	–	–	7.2	95b
470	Ph	CO_2Me	NHAc	[Rh(COD)**98e**]BF_4	2–2.8	THF	r.t.	2–3	–	–	–	9.8	95b
471	Ph	CO_2Me	NHAc	[Rh(COD)**98e**]SbF_6	2–2.8	THF	r.t.	2–3	–	–	–	2.0	95b
472	Ph	CO_2Me	NHAc	[Rh(COD)**98g**]BF_4	2–2.8	THF	r.t.	2–3	–	–	–	98.2	95b
473	Ph	CO_2Me	NHAc	[Rh(COD)**98g**]SbF_6	2–2.8	THF	r.t.	2–3	–	–	–	99.0	95b
474	Ph	CO_2Me	NHAc	[Rh(COD)**98h**]SbF_6	2–2.8	THF	r.t.	2–3	–	–	–	81.0	95b
475	Ph	CO_2Me	NHAc	[Rh(COD)**98i**]BF_4	1	MeOH	25	0.0567 [f]	50	882	50	95 (*S*)	97
476	Ph	CO_2Me	NHAc	[Rh(COD)**98i**]BF_4	1	H_2O	25	6 [f]	50	8	50	84 (*S*)	97
477	Ph	CO_2Me	NHAc	[Rh(COD)**98i**]BF_4	1	H_2O+SDS, 0.035 [g]	25	1.1 [f]	50	45	50	94 (*S*)	97

Table 27.5 (continued)

Entry	Substrate			Catalyst	Conditions				TON	TOF [h^{-1}]	Conv. [%]	ee [%]	Reference(s)
	R^1	R^2	R^3		P[H_2] [bar]	Solvent	Temp. [°C]	Time [h]					
478	Ph	CO_2Me	NHAc	[Rh(COD)**98i**]BF_4	1	H_2O+SDS, 0.173 [g)]	25	0.11 [f)]	50	469	50	97 (*S*)	97
479	Ph	CO_2Me	NHAc	[Rh(COD)**98i**]BF_4	1	H_2O+Triton X-100, 0.03 [g)]	25	1.083 [f)]	50	46	50	95 (*S*)	97
480	Ph	CO_2Me	NHAc	[Rh(COD)**98i**]BF_4	1	H_2O+Triton X-100, 0.1 [g)]	25	0.33 [f)]	50	150	50	95 (*S*)	97
481	Ph	CO_2Me	NHAc	[Rh(COD)**100**]Cl	50	–	25	8	100 [c)]	–	–	10 (*S*) [a)]	89
482	Ph	CO_2Me	NHAc	[Rh(COD)**100b**]BF_4	1	MeOH	25	–	–	–	–	89 (*S*)	91 a
483	Ph	CO_2Me	NHAc	[Rh(COD)**100b**]BF_4	1	MeOH	25	–	50	–	50	80 (*S*)	91 e
484	Ph	CO_2Me	NHAc	[Rh(COD)**101a**]BF_4	1	MeOH	25	0.09 [f)]	50	555	50	91.1 (*S*)	91 e
485	Ph	CO_2Me	NHAc	[Rh(COD)**101b**]BF_4	1	MeOH	25	0.093 [f)]	50	536	50	91.8 (*S*)	91 c
486	Ph	CO_2Me	NHAc	[Rh(COD)**101c**]BF_4	1	MeOH	25	0.11 [f)]	50	469	50	89.2 (*S*)	91 c
487	Ph	CO_2Me	NHAc	[Rh(COD)**101d**]BF_4	1	MeOH	25	0.15 [f)]	50	345	50	90.8 (*S*)	91 c
488	Ph	CO_2Me	NHAc	[Rh(COD)**101e**]BF_4	1	MeOH	25	0.12 [f)]	50	407	50	89.3 (*S*)	91 c
489	Ph	CO_2Me	NHAc	[Rh(COD)**101 f**]BF_4	1	MeOH	25	0.14 [f)]	50	361	50	83.8 (*S*)	91 c
490	Ph	CO_2Me	NHAc	[Rh(COD)**102a**]BF_4	2–2.8	THF	r.t.	2–3	–	–	–	98.3	95 b
491	Ph	CO_2Me	NHAc	[Rh(COD)**102a**]SbF_6	2–2.8	THF	r.t.	2–3	–	–	–	98.4	95 b
492	Ph	CO_2Me	NHAc	[Rh(COD)**102b**]SbF_6	2–2.8	THF	r.t.	2–3	–	–	–	94.9	95 b
493	Ph	CO_2Me	NHAc	[Rh(COD)**103a**]BF_4	2–2.8	THF	r.t.	2–3	–	–	–	93.0	95 b
494	Ph	CO_2Me	NHAc	[Rh(COD)**103a**]SbF_6	2–2.8	THF	r.t.	2–3	–	–	–	96.3	95 b
495	Ph	CO_2Me	NHAc	[Rh(COD)**103b**]BF_4	2–2.8	THF	r.t.	–	–	–	–	71.1	95 a
496	Ph	CO_2Me	NHAc	[Rh(COD)**103b**]BF_4	2–2.8	THF	r.t.	2–3	–	–	–	87.4	95 b
497	Ph	CO_2Me	NHAc	[Rh(COD)**103c**]BF_4	2–2.8	THF	r.t.	2–3	–	–	–	1.0	95 a, b
498	Ph	CO_2Me	NHAc	[Rh(COD)**103d**]BF_4	2–2.8	THF	r.t.	–	–	–	–	2.3	95 a, b
499	Ph	CO_2Me	NHAc	[Rh(COD)**103e**]BF_4	2–2.8	THF	r.t.	2–3	–	–	–	2.0	95 a, b

500	Ph	CO_2Me	NHAc	[Rh(COD)**103f**]BF_4	2–2.8	THF	r.t.	2–3	–	–	–	84.7	95 a, b
501	Ph	CO_2Me	NHAc	[Rh(COD)**104a**]BF_4	2–2.8	THF	r.t.	2–3	–	–	–	92.4	95 b
502	Ph	CO_2Me	NHAc	[Rh(COD)**104b**]BF_4	2–2.8	THF	r.t.	2–3	–	–	–	84.0	95 b
503	Ph	CO_2Me	NHAc	[Rh(COD)**104d**]BF_4	2–2.8	THF	r.t.	2–3	–	–	–	11.0	95 b
504	Ph	CO_2Me	NHAc	[Rh(COD)**105a**]BF_4	2–2.8	THF	r.t.	2–3	–	–	–	65.1	95 a, b
505	Ph	CO_2Me	NHAc	[Rh(COD)**106a**]SbF_6	2–2.8	THF	r.t.	2–3	–	–	–	83.2	95 b
506	Ph	CO_2Me	NHAc	[Rh(COD)**111**]ClO_4	1	EtOH	25	24	50	2	100	52 (*R*)	90
507	Ph	CO_2Me	NHAc	[Rh(COD)**112a**]BF_4	2–2.8	THF	r.t.	2–3	–	–	–	72.2	95 b
508	Ph	CO_2Me	NHAc	[Rh(COD)**112b**]BF_4	1	MeOH	25	0.07	50	714	50	1.5 (*S*)	91 e
509	Ph	CO_2Me	NHAc	[Rh(COD)**113a**]Cl	50	–	25	8	100 [c]	–	–	46 (*S*) [a]	89
510	Ph	CO_2Me	NHAc	[Rh(COD)**113b**]Cl	50	–	25	8	100 [c]	–	–	20 (*S*) [a]	89
511	Ph	CO_2Me	NHAc	[Rh(COD)**113c**]BF_4	1	MeOH	25	0.07	50	714	50	66 (*S*)	91 a, e
512	Ph	CO_2Me	NHAc	[Rh(COD)**113c**]BF_4	1	MeOH	25	0.067	50	750	50	66 (*S*)	91 e
513	Ph	CO_2Me	NHAc	[Rh(COD)**113d**]BF_4	1	MeOH	25	–	–	–	–	77 (*S*)	91 a
514	Ph	CO_2Me	NHAc	[Rh(COD)**113d**]BF_4	1	MeOH	25	0.13	50	750	50	83 (*S*)	91 e
515	Ph	CO_2Me	NHAc	[Rh(COD)**113e**]BF_4	1	MeOH	25	0.13	50	385	50	83 (*S*)	91 a, e
516	Ph	CO_2Me	NHAc	[Rh(COD)**113f**]BF_4	1	MeOH	25	–	–	–	–	59 (*S*)	91 a
517	Ph	CO_2Me	NHAc	[Rh(COD)**114a**]BF_4	1	MeOH	25	0.083 [f]	50	602	50	57 (*S*)	99
518	Ph	CO_2Me	NHAc	[Rh(COD)**114a**]BF_4	1	PhH	25	0.05 [f]	50	1000	50	43 (*S*)	99
519	Ph	CO_2Me	NHAc	[Rh(COD)**114b**]BF_4	1	MeOH	25	0.05 [f]	50	1000	50	53 (*S*)	99
520	Ph	CO_2Me	NHAc	[Rh(COD)**114b**]BF_4	1	PhH	25	0.033 [f]	50	1515	50	41 (*S*)	99
521	Ph	CO_2Me	NHAc	[Rh(COD)**116a**]SbF_6	2.07	THF	r.t.	–	–	–	–	35 (*R*)	102
522	Ph	CO_2Me	NHAc	[Rh(COD)**116b**]SbF_6	2.07	THF	r.t.	–	–	–	–	30 (*R*)	102
523	Ph	CO_2Me	NHAc	[Rh(COD)**117**]BF_4	5	H_2O	r.t.	6	20	3	100	88 (*S*)	101
524	Ph	CO_2Me	NHAc	[Rh(COD)**117**]BF_4	5	H_2O + 10 wt% SDS	r.t.	1	100	100	100	99.9 (*S*) [b]	101
525	Ph	CO_2Me	NHAc	[Rh(COD)**117**]BF_4	5	H_2O/EtOAc (1 : 1)	r.t.	1.5	50	33	100	87 (*S*)	101
526	Ph	CO_2Me	NHAc	[Rh(COD)**117**]BF_4	5	H_2O/MeOH/ EtOAc (0.6 : 0.4 : 1)	r.t.	3	100	33	100	98 (*S*)	101
527	Ph	CO_2Me	NHAc	[Rh(COD)**117**]BF_4	5	H_2O/MeOH (3 : 2)	r.t.	1.5	100	67	100	94 (*S*)	101
528	Ph	CO_2Me	NHAc	[Rh(COD)**118**]SbF_6	2.07	THF	r.t.	–	–	–	–	25 (*R*)	102
529	Ph	CO_2Me	NHAc	[Rh(COD)**119a**]SbF_6	2.07	THF	r.t.	–	–	–	~100	69 (*S*)	102

Table 27.5 (continued)

Entry	Substrate			Catalyst	Conditions				TON	TOF [h^{-1}]	Conv. [%]	ee [%]	Reference(s)
	R^1	R^2	R^3		P[H_2] [bar]	Solvent	Temp. [°C]	Time [h]					
530	Ph	CO_2Me	NHAc	[Rh(COD)**119b**]SbF_6	2.07	THF	r.t.	–	–	–	~100	87 (*S*)	102
531	Ph	CO_2Me	NHAc	[Rh(COD)**119c**]BF_4	5	H_2O/EtOAc (1:1)	r.t.	1.5	50	33	100	68 (*S*)	101
532	Ph	CO_2Me	NHAc	[Rh(COD)**119c**]BF_4	5	H_2O/MeOH/EtOAc (0.6:0.4:1)	r.t.	3	100	33	100	76 (*S*)	101
533	Ph	CO_2Me	NHAc	[Rh(COD)**119c**]BF_4	5	H_2O/MeOH (3:2)	r.t.	1.5	100	67	100	75 (*S*)	101
534	Ph	CO_2Me	NHAc	[Rh(COD)**119d**]BF_4	5	H_2O	r.t.	6	20	3	100	55 (*S*)	101
535	Ph	CO_2Me	NHAc	[Rh(COD)**119d**]BF_4	5	H_2O + 10 wt% SDS	r.t.	1	100	100	100	90 (*S*) [b]	101
536	Ph	CO_2Me	NHAc	[Rh(COD)ent-**120**]BF_4	1	Acetone	r.t.	0.08	100	1250	100	27 (*R*)	105
537	Ph	CO_2Me	NHAc	[Rh(COD)**121a**]BF_4	1	Acetone	r.t.	0.08	100	1250	100	18 (*R*)	105
538	Ph	CO_2Me	NHAc	[Rh(COD)**121b**]BF_4	1	Acetone	r.t.	0.08	100	1250	100	59 (*R*)	105
539	Ph	CO_2Me	NHAc	[Rh(COD)**121d**]BF_4	1	Acetone	r.t.	0.08	100	1250	100	32 (*R*)	105
540	Ph	CO_2Me	NHAc	[Rh(COD)**122a**]BF_4	1	Acetone	r.t.	0.08	95	1188	95	73 (*R*)	105
541	Ph	CO_2Me	NHAc	[Rh(COD)**122b**]BF_4	1	Acetone/DCM 13:2	r.t.	0.08	96	1200	96	81 (*R*)	105
542	Ph	CO_2Me	NHAc	[Rh(COD)**122c**]BF_4	1	Acetone	r.t.	0.08	100	1250	100	77 (*R*)	105
543	Ph	CO_2Me	NHAc	[Rh(COD)**122d**]BF_4	1	Acetone/DCM 13:2	r.t.	0.08	100	1250	100	75 (*R*)	105
544	Ph	CO_2Me	NHAc	[Rh(COD)**122e**]BF_4	1	Acetone	r.t.	0.08	100	1250	100	86 (*R*)	105
545	Ph	CO_2Me	NHAc	[Rh(COD)**123b**]SbF_6	2–2.8	THF	r.t.	2–3	–	–	–	49.0	95b
546	Ph	CO_2Me	NHAc	[Rh(COD)**124**]BF_4	1	THF	25	1	100	100	100	24 (*R*)	103
547	Ph	CO_2Me	NHAc	[Rh(COD)**124**]Cl	68	PhH:EtOH = 1:1	100	48	100	2.1	100	3.4 (*R*)	103
548	Ph	CO_2Me	NHAc	[Rh(COD)**125**]BF_4	1	THF	25	1	100	100	100	35 (*S*)	103
549	Ph	CO_2Me	NHAc	[Rh(COD)**126**]BF_4	1	DCM	25	0.02	100	5000	100	10 (*R*)	104
550	Ph	CO_2Me	NHAc	[Rh(COD)**126**]Cl	50	–	25	1	100 [c]	100	100	48 (*R*) [a]	89
551	Ph	CO_2Me	NHAc	[Ir(COD)**126**]BF_4	1	DCM	25	0.42	100	238	100	20 (*R*)	104
552	Ph	CO_2Me	NHAc	[Rh(COD)**127**]BF_4	1	DCM	25	0.02	100	5000	100	35 (*R*)	104

553	Ph	CO_2Me	NHAc	[Ir(COD)**127**]BF_4	1	DCM	25	0.75	100	133	100	10 (*R*)	104
554	Ph	CO_2Me	NHAc	[Rh(COD)**131**]BF_4	1	PhH	25	5.5	99.9	18	99.9	31.5 (*R*)	108
555	Ph	CO_2Me	NHAc	[Rh(COD)**132**]BF_4	34.5	Acetone	25	0.25	100	400	100	91.6 (*R*)	107
556	Ph	CO_2Me	NHAc	[Rh(COD)**132**]BF_4	34.5	MeOH	25	0.25	100	400	100	84 (*R*)	107
557	Ph	CO_2Me	NHAc	[Rh(COD)**132**]BF_4	34.5	IPA	25	0.25	100	400	100	89.4 (*R*)	107
558	Ph	CO_2Me	NHAc	[Rh(COD)**132**]BF_4	34.5	THF	25	0.25	100	400	100	86.3 (*R*)	107
559	Ph	CO_2Me	NHAc	[Rh(COD)**132**]BF_4	34.5	DCM	25	0.25	100	400	100	86.2 (*R*)	107
560	Ph	CO_2Me	NHAc	[Rh(COD)**132**]BF_4	34.5	PhH	25	0.25	100	400	100	82.9 (*R*)	107
561	Ph	CO_2Me	NHAc	[Rh(COD)**134**]BF_4	1	PhH	25	4.5	92.5	21	92.5	24.6 (*R*)	108
562	Ph	CO_2Me	NHAc	[Rh(COD)**135**]BF_4	1	PhH	25	7.5	96.6	13	96.6	46.2 (*R*)	108
563	Ph	CO_2Me	NHAc	[Rh(COD)**136**]BF_4	1.5	MeOH	25	20	388	19	81	19 (*R*)	110
564	Ph	CO_2Me	NHAc	[Rh(COD)**139**]BF_4	1.2	MeOH	–		100	–	100	54	113
565	Ph	CO_2Me	NHAc	[Rh(COD)**139**]BF_4	5	MeOH	–	2	94	47	94	47	113
566	Ph	CO_2Me	NHAc	[Rh(COD)**140**]BF_4	1.5	DCM	25	20	479	24	100	14 (*R*)	110
567	Ph	CO_2Me	NHAc	[Rh(COD)**141a**]BF_4	3.5	MeOH	r.t.	0.5	1000	2000	>99	95 (*S*)	111
568	Ph	CO_2Me	NHAc	[Rh(COD)**141a**]BF_4	5	MeOH	r.t.	2	5000	2500	>99	95 (*S*)	111
569	Ph	CO_2Me	NHAc	[Rh(COD)**141b**]BF_4	3.5	MeOH	r.t.	0.5	980	1960	98	97 (*S*)	111
570	Ph	CO_2Me	NHAc	[Rh(COD)**141b**]BF_4	3.5	Tol	r.t.	2	1000	500	>99	99 (*S*)	111
571	Ph	CO_2Me	NHAc	[Rh(COD)**141b**]BF_4	5	MeOH	r.t.	6	5000	833	>99	98.5 (*S*)	111
572	Ph	CO_2Me	NHAc	[Rh(COD)**144a**]BF_4	5	DCM	25	8	96	12	96	91 (*S*)	117 b
573	Ph	CO_2Me	NHAc	[Rh(COD)**144c**]BF_4	5	DCM	25	6	100	16.7	100	98 (*S*)	117 b
574	Ph	CO_2Me	NHAc	[Rh(COD)**144c**]BF_4	30	DCM	5	4	1000	250	100	>99 (*S*)	117 b
575	Ph	CO_2Me	NHAc	[Rh(COD)**145a**]BF_4	5	DCM	25	8	100	12.5	100	2 (*S*)	117 b
576	Ph	CO_2Me	NHAc	[Rh(COD)**146a**]BF_4	5	DCM	25	8	98	12.3	98	70 (*S*)	117 b
577	Ph	CO_2Me	NHAc	[Rh(COD)**146c**]BF_4	5	DCM	25	8	96	12	96	32 (*S*)	117 b
578	Ph	CO_2Me	NHAc	[Rh(COD)**147**]BF_4	1	THF	25	–	–	–	–	13	115
579	Ph	CO_2Me	NHAc	[Rh(COD)**150a**]BF_4	1	DCM	25	2.2	100	45.5	100	30 (*S*)	118
580	Ph	CO_2Me	NHAc	[Rh(COD)**150b**]BF_4	1	DCM	25	3.3	100	30.3	100	18 (*R*)	118
581	Ph	CO_2Me	NHAc	[Rh(COD)**150c**]BF_4	1	DCM	25	4.3	100	23.3	100	30 (*R*)	118
582	Ph	CO_2Me	NHAc	[Rh(COD)**150d**]BF_4	1	DCM	25	3	100	33.3	100	48 (*S*)	118

Table 27.5 (continued)

Entry	Substrate			Catalyst	Conditions				TON	TOF [h^{-1}]	Conv. [%]	ee [%]	Reference(s)
	R^1	R^2	R^3		P[H_2] [bar]	Solvent	Temp. [°C]	Time [h]					
583	Ph	CO_2Me	NHAc	[Rh(COD)**154a**]OTf	5	MeOH	r.t.	18	200	11.1	100	81 (*S*)	127
584	Ph	CO_2Me	NHAc	[Rh(COD)**154a**]OTf	5	Tol	r.t.	18	200	11.1	100	85 (*S*)	127
585	Ph	CO_2Me	NHAc	[Rh(COD)**154b**]OTf	5	Tol	r.t.	18	200	11.1	100	89 (*S*)	127
586	Ph	CO_2Me	NHAc	[Rh(COD)**154c**]OTf	5	Tol	r.t.	18	200	11.1	100	50 (*R*)	127
587	Ph	CO_2Me	NHAc	[Rh(COD)(*S*,*S*ax)-**155b**] BF_4	4.1	DCM	r.t.	24	450	18.8	90	70.3 (*R*)	124 a
588	Ph	CO_2Me	NHAc	[Rh(COD) (*S*,*R*ax)-**155b**]B F_4	4.1	DCM	r.t.	24	500	18.8	100	99.0 (*S*)	124 a
589	Ph	CO_2Me	NHAc	[Rh(COD)**155c**]BF_4	4.1	DCM	r.t.	24	225	9.4	45	22.0 (*S*)	124 a
590	Ph	CO_2Me	NHAc	[Rh(COD)**156a**]BF_4	4.1	DCM	r.t.	16	500	31.3	100	99.5 (*R*)	124 a
591	Ph	CO_2Me	NHAc	[Rh(COD)**156b**]BF_4	4.1	DCM	r.t.	16	500	31.3	100	56.1 (*R*)	124 a
592	Ph	CO_2Me	NHAc	[Rh(COD)**156c**]BF_4	4.1	DCM	r.t.	16	100	6.3	20	90.6 (*R*)	124 a
593	Ph	CO_2Me	NHAc	[Rh(COD)**159a**]BF_4	1	DCM	r.t.	24	100	4.2	100	97 (*R*)	123
594	Ph	CO_2Me	NHAc	[Rh(COD)**159b**]BF_4	1	DCM	r.t.	24	100	4.2	100	92 (*S*)	123
595	Ph	CO_2Me	NHAc	[Rh(COD)**159c**]BF_4	1	DCM	r.t.	24	50	2.1	100	6 (*S*)	123
596	Ph	CO_2Me	NHAc	[Rh(COD)**159d**]BF_4	1	DCM	r.t.	12	100	8.3	100	95 (*S*)	123
597	Ph	CO_2Me	NHAc	[Rh(COD)**159e**]BF_4	1	DCM	r.t.	12	100	8.3	100	95 (*R*)	123
598	Ph	CO_2Me	NHAc	[Rh(COD)**159f**]BF_4	1	DCM	r.t.	12	50	4.2	100	3 (*R*)	123
599	Ph	CO_2Me	NHAc	[Rh(COD)**159g**]BF_4	1	DCM	r.t.	12	50	4.2	100	89 (*S*)	123
600	Ph	CO_2Me	NHAc	[Rh(COD)**159h**]BF_4	1	DCM	r.t.	24	85	3.5	85	63 (*R*)	123
601	Ph	CO_2Me	NHAc	[Rh(COD)**160a**]BF_4	1	DCM	r.t.	12	50	4.2	100	65 (*S*)	123
602	Ph	CO_2Me	NHAc	[Rh(COD)**160b**]BF_4	1	DCM	r.t.	1	50	50	100	95 (*R*)	123
603	Ph	CO_2Me	NHAc	[Rh(COD)**163a**]PF_6	1	THF	r.t.	12	>99	8.3	100	>99 (*S*)	128
604	Ph	CO_2Me	NHAc	[Rh(COD)**164a**]PF_6	1	THF	r.t.	12	>99	8.3	100	>99 (*S*)	128

605	Ph	CO_2Me	NHAc	[Rh(COD)**166**]BF_4	1	DCM	r.t.	1	100	100	100	37 (*R*)	129
606	Ph	CO_2Me	NHAc	[Rh(COD)**166**]BF_4	1	DCE	r.t.	0.5	100	200	100	69 (*R*)	129
607	Ph	CO_2Me	NHAc	[Rh(COD)**166**]BF_4	50	DCE	r.t.	2	88	44	88	33 (*R*)	129
608	Ph	CO_2Me	NHAc	[Rh(COD)**166**]BF_4	30	H_2O	r.t.	24	40	1.7	100	13 (*R*)	129
609	Ph	CO_2Me	NHAc	[Rh(COD)**166**]BF_4	50	H_2O	r.t.	24	40	1.7	100	72 (*R*)	129
610	Ph	CO_2Me	NHAc	[Rh(COD)**166**]BF_4	70	H_2O	r.t.	24	40	1.7	100	62 (*R*)	129
611	Ph	CO_2Me	NHAc	[Rh(COD)**166**]BF_4	50	MeOH	r.t.	9	50	5.6	100	50 (*R*)	129
612	Ph	CO_2Me	NHAc	[Rh(COD)**166**]BF_4	50	H_2O/EtOAc (1:1)	r.t.	12(24) [h)]	50	4.2	100 (100) [i)]	73 (70) [i] (*R*)	129
613	Ph	CO_2Me	NHAc	[Rh(COD)**167a**]BF_4	1	DCM	25	0.17	100	588	100	84.1 (*S*)	121 a, b
614	Ph	CO_2Me	NHAc	[Rh(COD)**167b**]BF_4	1	DCM	25	3	100	33	100	98.8 (*R*)	121 a, b
615	Ph	CO_2Me	NHAc	[Rh(COD)**167c**]BF_4	1	DCM	r.t.	0.5	100	200	100	98.0 (*S*)	121 a
616	Ph	CO_2Me	NHAc	[Rh(COD)**167c**]BF_4	1	DCM	25	0.5	100	200	100	91 (*S*)	121 b
617	Ph	CO_2Me	NHAc	[Rh(COD)**167d**]BF_4	1	DCM	r.t.	0.5	100	200	100	94.3 (*R*)	121 a, b
618	Ph	CO_2Me	NHAc	[Rh(COD)**168a**]BF_4	5	DCM	25	8	77	6	77	94 (*S*)	126
619	Ph	CO_2Me	NHAc	[Rh(COD)**168a**]BF_4	30	DCM	25	12	72	6	72	98 (*S*)	126
620	Ph	CO_2Me	NHAc	[Rh(COD)**168b**]BF_4	5	DCM	25	8	53	7	53	85 (*S*)	126
621	Ph	CO_2Me	NHAc	[Rh(COD)**168c**]BF_4	5	DCM	25	8	29	4	29	18 (*S*)	126
622	Ph	CO_2Me	NHAc	[Rh(COD)**168d**]BF_4	5	DCM	25	8	35	4	35	17 (*S*)	126
623	Ph	CO_2Me	NHBz	[Rh(COD)**97a**]BF_4	1	MeOH	25	0.1 [f)]	50	500	50	87.3 (*S*)	91 b
624	Ph	CO_2Me	NHBz	[Rh(COD)**97c**]BF_4	1	MeOH	25	0.05 [f)]	50	1000	50	91.6 (*S*)	91 b
625	Ph	CO_2Me	NHBz	[Rh(COD)**98a**]BF_4	1	MeOH	25	0.117 [f)]	50	429	50	77 (*S*)	26
626	Ph	CO_2Me	NHBz	[Rh(COD)**98a**]BF_4	50	MeOH	25	–	100 [b)]	–	–	77 (*S*)	26
627	Ph	CO_2Me	NHBz	[Rh(COD)**117**]BF_4	5	H_2O/MeOH/ EtOAc (0.6:0.4:1)	r.t.	3	100	33	100	92 (*S*)	101
628	Ph	CO_2Me	NHBz	[Rh(COD)**117**]BF_4	5	H_2O/MeOH(3:2)	r.t.	1.5	100	67	100	90 (*S*)	101
629	Ph	CO_2Me	NHBz	[Rh(COD)**163a**]PF_6	1	THF	r.t.	12	>99	8.3	100	>99 (*S*)	128
630	Ph	CO_2Me	NHBz	[Rh(COD)**164a**]PF_6	1	THF	r.t.	12	>99	8.3	100	>99 (*S*)	128
631	Ph	CO_2Me	NHCbz	[Rh(COD)**98a**]BF_4	1	MeOH	25	–	–	–	–	57 (*S*) [a)]	10
632	Ph	CO_2Et	NHAc	[Rh(COD)**89**]PF_6	5	EtOH	60	7	90	13	90	7 (*S*)	82

Table 27.5 (continued)

Entry	Substrate			Catalyst	Conditions				TON	TOF [h^{-1}]	Conv. [%]	ee [%]	Reference(s)
	R^1	R^2	R^3		$P[H_2]$ [bar]	Solvent	Temp. [°C]	Time [h]					
633	Ph	CO_2Et	NHAc	[Rh(COD)**90**]PF_6	5	EtOH	60	3	85	28	85	12 (*S*)	82
634	Ph	CO_2Et	NHAc	[Rh(COD)**97a**]BF_4	1	MeOH	25	0.27 [f)]	50	187	50	58.3	26
635	Ph	CO_2Et	NHAc	[Rh(COD)**97a**]BF_4	1	MeOH	25	0.1 [f)]	50	500	50	90.6 (*S*)	91 b
636	Ph	CO_2Et	NHAc	[Rh(COD)**97c**]BF_4	1	MeOH	25	0.05 [f)]	50	1000	50	94.4 (*S*)	91 b
637	Ph	CO_2Et	NHAc	[Rh(COD)**98a**]BF_4	1	MeOH	25	0.08 [f)]	50	625	50	90.2	26
638	2-Cl-Ph	CO_2H	NHAc	[Rh(COD)**91**]BF_4	1	MeOH	25	0.167	100	600	>99.9	97.3 (*R*)	27
639	2-Cl-Ph	CO_2H	NHAc	[Rh(COD)**95**] BF_4	1	IPA	r.t.	24	100	4	100	92.9 (*S*)	85
640	2-Cl-Ph	CO_2H	NHAc	[Rh(COD)**132**]BF_4	34.5	Acetone	25	0.25–1	100	100–400	100	92.3 (*R*)	107
641	2-Cl-Ph	CO_2H	NHAc	[Rh(COD)**163a**]PF_6	1	THF	r.t.	12	>99	8.3	100	>99 (*S*)	128
642	2-Cl-Ph	CO_2H	NHAc	[Rh(COD)**164a**]PF_6	1	THF	r.t.	12	>99	8.3	100	>99 (*S*)	128
643	2-Cl-Ph	CO_2Me	NHAc	[Rh(COD)**94a**]BF_4	6.9	DCM	r.t.	0.17	500	2941	100	85 (*S*)	52
644	2-Cl-Ph	CO_2Me	NHAc	[Rh(COD)**93h**]PF_6	3	Tol	r.t.	12	100	8.3	100	81.5 (*S*)	79
645	2-Cl-Ph	CO_2Me	NHAc	[Rh(COD)**163a**]PF_6	1	THF	r.t.	12	>99	8.3	100	>99 (*S*)	128
646	2-Cl-Ph	CO_2Me	NHAc	[Rh(COD)**164a**]PF_6	1	THF	r.t.	12	>99	8.3	100	>99 (*S*)	128
647	3-Cl-Ph	CO_2H	NHAc	[Rh(COD)**91**]BF_4	1	MeOH	25	0.167	100	600	>99.9	97.4 (*R*)	27
648	3-Cl-Ph	CO_2H	NHAc	[Rh(COD)**93a**]BF_4	6.9	MeOH	r.t.	0.5	282	564	56.3	10.5 (*S*)	52
649	3-Cl-Ph	CO_2H	NHAc	[Rh(COD)**94a**]BF_4	6.9	MeOH	r.t.	0.5	440	880	87.9	37 (*S*)	52
650	3-Cl-Ph	CO_2H	NHAc	[Rh(COD)**132**]BF_4	34.5	Acetone	25	0.25–1	100	100–400	100	90.3 (*R*)	107
651	3-Cl-Ph	CO_2Me	NHAc	[Rh(COD)**93a**]BF_4	6.9	DCM	r.t.	0.17	352	2071	70.3	54.7 (*S*)	52
652	3-Cl-Ph	CO_2Me	NHAc	[Rh(COD)**94a**]BF_4	6.9	DCM	r.t.	0.17	500	2941	100	78.3 (*S*)	52
653	3-Cl-Ph	CO_2Me	NHAc	[Rh(COD)**166**]BF_4	51	H_2O/EtOAc (1:1)	r.t.	24	50	2	100	67 (*R*)	129
654	4-Cl-Ph	CO_2H	NHAc	[Rh(COD)**91**]BF_4	1	MeOH	25	0.167	100	600	>99.9	97.3 (*R*)	27
655	4-Cl-Ph	CO_2H	NHAc	[Rh(COD)**132**]BF_4	34.5	Acetone	25	0.25–1	100	100–400	100	93.3 (*R*)	107
656	4-Cl-Ph	CO_2H	NHAc	[Rh(COD)**132**]BF_4	34.5	Acetone	0–5	0.25–1	100	100–400	100	94.6 (*R*)	107

657	4-Cl-Ph	CO_2H	NHAc	[Rh(COD)**132**]BF_4	34.5	Acetone	–15	0.25–1	100	100–400	100	96.3 (*R*)	107
658	4-Cl-Ph	CO_2Me	NHAc	[Rh(COD)**91**]BF_4	1	MeOH	25	0.167	100	600	>99.9	94.2 (*R*)	27
659	4-Cl-Ph	CO_2Me	NHAc	[Rh(COD)**94a**]BF_4	6.9	DCM	r.t.	0.17	500	2941	100	80.8 (*S*)	52
660	4-Cl-Ph	CO_2Me	NHAc	[Rh(COD)**132**]BF_4	34.5	Acetone	25	0.25	100	400	100	91.3 (*R*)	107
661	3-Br-Ph	CO_2H	NHAc	[Rh(COD)**95**] BF_4	1	IPA	r.t.	24	100	4	100	93.5 (*S*)	85
662	3-Br-Ph	CO_2H	NHAc	[Rh(COD)**98a**]BF_4	2.8	THF	r.t.	3	100	33	100	89 (*S*)	98
663	3-Br-Ph	CO_2H	NHAc	[Rh(COD)**98b**]BF_4	2.8	THF	r.t.	3	100	33	100	97 (*S*)	98
664	3-Br-Ph	CO_2H	NHAc	[Rh(COD)**103a**]SbF_6	2–2.8	THF	r.t.	–	–	–	–	96.4	95 a
665	3-Br-Ph	CO_2H	NHAc	[Rh(COD)**115a**]SbF_6	2.8	THF	r.t.	3	100	33	100	74 (*S*)	98
666	3-Br-Ph	CO_2H	NHAc	[Rh(COD)**115b**]SbF_6	2.8	THF	r.t.	3	100	33	100	95 (*S*)	98
667	3-Br-Ph	CO_2H	NHAc	[Rh(COD)**115d**]BF_4	2.8	THF	r.t.	–	100	–	100	96 (*S*)	98
668	3-Br-Ph	CO_2H	NHAc	[Rh(COD)**163a**]PF_6	1	THF	r.t.	12	>99	8.3	100	>99 (*S*)	128
669	3-Br-Ph	CO_2H	NHAc	[Rh(COD)**164a**]PF_6	1	THF	r.t.	12	>99	8.3	100	>99 (*S*)	128
670	3-Br-Ph	CO_2Me	NHAc	[Rh(COD)**93h**]PF_6	3	Tol	r.t.	12	100	8.3	100	92.6 (*S*)	79
671	3-Br-Ph	CO_2Me	NHAc	[Rh(COD)**98a**]SbF_6	2–2.8	THF	r.t.	2–3	–	–	–	89.2	95 b
672	3-Br-Ph	CO_2Me	NHAc	[Rh(COD)**98b**]SbF_6	2–2.8	THF	r.t.	2–3	–	–	–	96.8	95 b
673	3-Br-Ph	CO_2Me	NHAc	[Rh(COD)**103a**]SbF_6	2–2.8	THF	r.t.	2–3	–	–	–	96.4	95 b
674	3-Br-Ph	CO_2Me	NHAc	[Rh(COD)**163a**]PF_6	1	THF	r.t.	12	>99	8.3	100	>99 (*S*)	128
675	3-Br-Ph	CO_2Me	NHAc	[Rh(COD)**164a**]PF_6	1	THF	r.t.	12	>99	8.3	100	>99 (*S*)	128
676	4-Br-Ph	CO_2H	NHAc	[Rh(COD)**98b**]SbF_6	2–2.8	THF	r.t.	2–3	–	–	–	98.0	95 b
677	4-Br-Ph	CO_2H	NHAc	[Rh(COD)**98c**]SbF_6	2–2.8	THF	r.t.	2–3				47.0	95 b
678	4-Br-Ph	CO_2H	NHAc	[Rh(COD)**103a**]SbF_6	2–2.8	THF	r.t.	2–3	–	–	–	96.4	95 b
679	4-Br-Ph	CO_2Me	NHAc	[Rh(COD)**91**]BF_4	1	MeOH	25	0.167	100	600	>99.9	96.3 (*R*)	27
680	4-Br-Ph	CO_2Me	NHAc	[Rh(COD)**132**]BF_4	34.5	Acetone	25	0.25	100	400	100	91.2 (*R*)	107
681	4-Br-Ph	CO_2Me	NHAc	[Rh(COD)**154a**]OTf	5	MeOH	r.t.	18	200	11.1	100	82 (*S*)	127
682	4-Br-Ph	CO_2Me	NHAc	[Rh(COD)**154a**]OTf	5	Tol	r.t.	18	200	11.1	100	87 (*S*)	127
683	4-Br-Ph	CO_2Me	NHAc	[Rh(COD)**154b**]OTf	5	Tol	r.t.	18	200	11.1	100	87 (*S*)	127
684	4-Br-Ph	CO_2Me	NHAc	[Rh(COD)**154c**]OTf	5	Tol	r.t.	18	196	10.9	98	29 (*R*)	127
685	2-F-Ph	CO_2H	NHAc	[Rh(COD)**98a**]BF_4	2.8	THF	r.t.	3	100	33	100	89 (*S*)	98
686	2-F-Ph	CO_2H	NHAc	[Rh(COD)**98b**]BF_4	2.8	THF	r.t.	3	100	33	100	97 (*S*)	98
687	2-F-Ph	CO_2H	NHAc	[Rh(COD)**115a**]SbF_6	2.8	THF	r.t.	3	100	33	100	63 (*S*)	98

Table 27.5 (continued)

Entry	Substrate			Catalyst	Conditions				TON	TOF [h^{-1}]	Conv. [%]	ee [%]	Reference(s)
	R^1	R^2	R^3		$P[H_2]$ [bar]	Solvent	Temp. [°C]	Time [h]					
688	2-F-Ph	CO_2H	NHAc	[Rh(COD)**115b**]SbF_6	2.8	THF	r.t.	3	100	33	100	96 (*S*)	98
689	2-F-Ph	CO_2Me	NHAc	[Rh(COD)**98a**]SbF_6	2–2.8	THF	r.t.	2–3	–	–	–	89.1	95 b
690	2-F-Ph	CO_2Me	NHAc	[Rh(COD)**98b**]SbF_6	2–2.8	THF	r.t.	2–3	–	–	–	96.8	95 b
691	2-F-Ph	CO_2Me	NHAc	[Rh(COD)**98g**]SbF_6	2–2.8	THF	r.t.	2–3	–	–	–	97.8	95 b
692	2-F-Ph	CO_2Me	NHAc	[Rh(COD)**103a**]SbF_6	2–2.8	THF	r.t.	2–3	–	–	–	95.6	95 b
693	2-F-Ph	CO_2Me	NHAc	[Rh(COD)**115a**]SbF_6	2.8	THF	r.t.	3	100	33	100	66 (*S*)	98
694	3-F-Ph	CO_2H	NHAc	[Rh(COD)**115d**]BF_4	2.8	THF	r.t.	–	100	–	100	95 (*S*)	98
695	3-F-Ph	CO_2H	NHAc	[Rh(COD)**115e**]BF_4	2.8	THF	r.t.	–	100	–	100	2 (*S*)	98
696	3-F-Ph	CO_2Me	NHAc	[Rh(COD)**98a**]SbF_6	2–2.8	THF	r.t.	2–3	–	–	–	88.9	95 b
697	3-F-Ph	CO_2Me	NHAc	[Rh(COD)**98b**]SbF_6	2–2.8	THF	r.t.	2–3	–	–	–	97.1	95 b
698	3-F-Ph	CO_2Me	NHAc	[Rh(COD)**103a**]SbF_6	2–2.8	THF	r.t.	2–3	–	–	–	96.3	95 b
699	4-F-Ph	CO_2H	NHAc	[Rh(COD)**95**] BF_4	1	IPA	r.t.	24	100	4	100	91.1 (*S*)	85
700	4-F-Ph	CO_2H	NHAc	[Rh(COD)**103a**]SbF_6	2–2.8	THF	r.t.	2–3	–	–	–	96.4	95 b
701	4-F-Ph	CO_2H	NHAc	[Rh(COD)**163a**]PF_6	1	THF	r.t.	12	99	8.3	100	99 (*S*)	128
702	4-F-Ph	CO_2H	NHAc	[Rh(COD)**164a**]PF_6	1	THF	r.t.	12	>99	8.3	100	>99 (*S*)	128
703	4-F-Ph	CO_2Me	NHAc	[Rh(COD)**91**]BF_4	1	MeOH	25	0.167	100	600	>99.9	95.5 (*R*)	27
704	4-F-Ph	CO_2Me	NHAc	[Rh(COD)**93h**]PF_6	3	Tol	r.t.	12	100	8.3	100	93.4 (*S*)	79
705	4-F-Ph	CO_2Me	NHAc	[Rh(COD)**98a**]BF_4	2–2.8	THF	r.t.	2–3	–	–	–	84.0	95b
706	4-F-Ph	CO_2Me	NHAc	[Rh(COD)**98a**]SbF_6	2–2.8	THF	r.t.	2–3	–	–	–	85.0	95 a, b
707	4-F-Ph	CO_2Me	NHAc	[Rh(COD)**98b**]SbF_6	2–2.8	THF	r.t.	2–3	–	–	–	97.2	95 a, b
708	4-F-Ph	CO_2Me	NHAc	[Rh(COD)**98c**]SbF_6	2–2.8	THF	r.t.	2–3	–	–	–	13.0	95 a, b
709	4-F-Ph	CO_2Me	NHAc	[Rh(COD)**98d**]SbF_6	2–2.8	THF	r.t.	2–3	–	–	–	9.0	95 a, b
710	4-F-Ph	CO_2Me	NHAc	[Rh(COD)**98f**]SbF_6	2–2.8	THF	r.t.	2–3	–	–	–	89.0	95 b
711	4-F-Ph	CO_2Me	NHAc	[Rh(COD)**98g**]SbF_6	2–2.8	THF	r.t.	2–3	–	–	–	98.7	95 b

712	4-F-Ph	CO_2Me	NHAc	[Rh(COD)**98h**]SbF_6	2–2.8	THF	r.t.	2–3	–	–	–	81.0	95 b
713	4-F-Ph	CO_2Me	NHAc	[Rh(COD)**102a**]BF_4	2–2.8	THF	r.t.	2–3	–	–	–	97.8	95 b
714	4-F-Ph	CO_2Me	NHAc	[Rh(COD)**103a**]SbF_6	2–2.8	THF	r.t.	2–3	–	–	–	96.2	95 b
715	4-F-Ph	CO_2Me	NHAc	[Rh(COD)**103b**]SbF_6	2–2.8	THF	r.t.	2–3	–	–	–	73.5	95 b
716	4-F-Ph	CO_2Me	NHAc	[Rh(COD)**103c**]SbF_6	2–2.8	THF	r.t.	2–3	–	–	–	<1	95 b
717	4-F-Ph	CO_2Me	NHAc	[Rh(COD)**103d**]SbF_6	2–2.8	THF	r.t.	2–3	–	–	–	11.0	95 b
718	4-F-Ph	CO_2Me	NHAc	[Rh(COD)**103e**]SbF_6	2–2.8	THF	r.t.	2–3	–	–	–	<1	95 b
719	4-F-Ph	CO_2Me	NHAc	[Rh(COD)**103f**]SbF_6	2–2.8	THF	r.t.	2–3	–	–	–	87.0	95 b
720	4-F-Ph	CO_2Me	NHAc	[Rh(COD)**104a**]BF_4	2–2.8	THF	r.t.	2–3	–	–	–	92.0	95 b
721	4-F-Ph	CO_2Me	NHAc	[Rh(COD)**132**]BF_4	34.5	Acetone	25	0.25	100	400	100	91.2 (*R*)	107
722	4-F-Ph	CO_2Me	NHAc	[Rh(COD)**163a**]PF_6	1	THF	r.t.	12	99	8.3	100	99 (*S*)	128
723	4-F-Ph	CO_2Me	NHAc	[Rh(COD)**164a**]PF_6	1	THF	r.t.	12	>99	8.3	100	>99 (*S*)	128
724	4-F-Ph	CO_2Me	NHCbz	[Rh(COD)**98a**]SbF_6	2–2.8	THF	r.t.	2–3	–	–	–	62.0	95 a, b
725	4-F-Ph	CO_2Me	NHCbz	[Rh(COD)**98b**]SbF_6	2–2.8	THF	r.t.	–	–	–	–	97	95 a
726	4-F-Ph	CO_2Me	NHCbz	[Rh(COD)**98b**]SbF_6	2–2.8	THF	r.t.	2–3	–	–	–	95.7	95 b
727	4-F-Ph	CO_2Me	NHCbz	[Rh(COD)**98c**]SbF_6	2–2.8	THF	r.t.	–	–	–	–	<1	95 a
728	4-F-Ph	CO_2Me	NHCbz	[Rh(COD)**98c**]SbF_6	2–2.8	THF	r.t.	2–3	–	–	–	<3	95 b
729	4-F-Ph	CO_2Me	NHCbz	[Rh(COD)**98d**]SbF_6	2–2.8	THF	r.t.	–	–	–	–	54	95 a
730	4-F-Ph	CO_2Me	NHCbz	[Rh(COD)**98d**]SbF_6	2–2.8	THF	r.t.	2–3	–	–	–	<5	95 b
731	4-F-Ph	CO_2Me	NHCbz	[Rh(COD)**98f**]SbF_6	2–2.8	THF	r.t.	2–3	–	–	–	85.0	95 b
732	4-F-Ph	CO_2Me	NHCbz	[Rh(COD)**102a**]BF_4	2–2.8	THF	r.t.	2–3	–	–	–	96.0	95 b
733	4-F-Ph	CO_2Me	NHCbz	[Rh(COD)**103a**]SbF_6	2–2.8	THF	r.t.	2–3	–	–	–	90.0	95 b
734	4-F-Ph	CO_2Me	NHCbz	[Rh(COD)**123a**]SbF_6	2–2.8	THF	r.t.	2–3	–	–	–	56.8	95 b
735	4-F-Ph	CO_2Me	NHCbz	[Rh(COD)**123b**]SbF_6	2–2.8	THF	r.t.	2–3	–	–	–	53.0	95 b
736	4-F-Ph	CO_2Me	NHCbz	[Rh(COD)**123f**]SbF_6	2–2.8	THF	r.t.	2–3	–	–	–	57.0	95 b
737	4-NO_2-Ph	CO_2H	NHAc	[Rh(COD)**91**]BF_4	1	MeOH	25	0.167	100	600	>99.9	97.0 (*R*)	27
738	4-NO_2-Ph	CO_2Me	NHAc	[Rh(COD)**132**]BF_4	34.5	Acetone	25	0.25	100	400	100	90.5 (*R*)	107
739	4-HO-Ph	CO_2H	NHAc	[Rh(1,5-hexadiene) (+)-*trans*-**85**]Cl	50	–	15	24	–	–	–	48.5 (S) [a]	67
740	4-HO-Ph	CO_2Me	NHAc	[Rh(COD)**132**]BF_4	34.5	Acetone	25	0.25	100	400	100	91.5 (*R*)	107
741	3-MeO-Ph	CO_2H	NHAc	[Rh(COD)**98a**]SbF_6	2–2.8	THF	r.t.	2–3	–	–	–	91.0	95 a, b

Table 27.5 (continued)

Entry	Substrate			Catalyst	Conditions				TON	TOF [h^{-1}]	Conv. [%]	ee [%]	Reference(s)
	R^1	R^2	R^3		P[H_2] [bar]	Solvent	Temp. [°C]	Time [h]					
742	3-MeO-Ph	CO_2H	NHAc	[Rh(COD)**98b**]SbF_6	2–2.8	THF	r.t.	2–3	–	–	–	97.0	95 a, b
743	3-MeO-Ph	CO_2H	NHAc	[Rh(COD)**98c**]SbF_6	2–2.8	THF	r.t.	2–3	–	–	–	53.0	95 a, b
744	3-MeO-Ph	CO_2H	NHAc	[Rh(COD)**98d**]SbF_6	2–2.8	THF	r.t.	2–3	–	–	–	5.0	95 a, b
745	3-MeO-Ph	CO_2H	NHAc	[Rh(COD)**103a**]SbF_6	2–2.8	THF	r.t.	2–3	–	–	–	95.9	95 b
746	3-MeO-Ph	CO_2H	NHAc	[Rh(COD)**103b**]SbF_6	2–2.8	THF	r.t.	2–3	–	–	–	73.4	95 b
747	3-MeO-Ph	CO_2H	NHAc	[Rh(COD)**103c**]SbF_6	2–2.8	THF	r.t.	2–3	–	–	–	<1	95 b
748	3-MeO-Ph	CO_2H	NHAc	[Rh(COD)**103d**]SbF_6	2–2.8	THF	r.t.	2–3	–	–	–	2.3	95 b
749	3-MeO-Ph	CO_2H	NHAc	[Rh(COD)**103e**]SbF_6	2–2.8	THF	r.t.	2–3	–	–	–	2.1	95 b
750	3-MeO-Ph	CO_2H	NHAc	[Rh(COD)**103f**]SbF_6	2–2.8	THF	r.t.	2–3	–	–	–	85.3	95 b
751	3-MeO-Ph	CO_2H	NHAc	[Rh(COD)**104a**]BF_4	2–2.8	THF	r.t.	2–3	–	–	–	93.1	95 b
752	3-MeO-Ph	CO_2H	NHAc	[Rh(COD)**132**]BF_4	34.5	Acetone	25	0.25–1	100	–	100	93.2 (*R*)	107
753	3-MeO-Ph	CO_2Me	NHAc	[Rh(COD)**98a**]SbF_6	2–2.8	THF	r.t.	2–3	–	–	–	88.0	95 b
754	3-MeO-Ph	CO_2Me	NHAc	[Rh(COD)**98b**]SbF_6	2–2.8	THF	r.t.	2–3	–	–	–	96.8	95 b
755	3-MeO-Ph	CO_2Me	NHAc	[Rh(COD)**98c**]SbF_6	2–2.8	THF	r.t.	2–3	–	–	–	21.0	95 b
756	3-MeO-Ph	CO_2Me	NHAc	[Rh(COD)**98g**]SbF_6	2–2.8	THF	r.t.	2–3	–	–	–	98.8	95 b
757	3-MeO-Ph	CO_2Me	NHAc	[Rh(COD)**116a**]SbF_6	2.07	THF	r.t.	–	–	–	–	70 (*R*)	1, 2
758	3-MeO-Ph	CO_2Me	NHAc	[Rh(COD)**116b**]SbF_6	2.07	THF	r.t.	–	–	–	–	40 (*R*)	102
759	3-MeO-Ph	CO_2Me	NHAc	[Rh(COD)**119a**]SbF_6	2.07	THF	r.t.	–	–	–	~100	70 (*S*)	102
760	3-MeO-Ph	CO_2Me	NHAc	[Rh(COD)**119b**]SbF_6	2.07	THF	r.t.	–	–	–	~100	92 (*S*)	102
761	4-MeO-Ph	CO_2H	NHAc	[Rh(COD)**95**]BF_4	1	IPA	r.t.	24	100	4	100	93.2 (*S*)	85
762	4-MeO-Ph	CO_2Me	NHAc	[Rh(COD)**91**]BF_4	1	MeOH	25	0.167	100	600	>99.9	96.2 (*R*)	27
763	4-MeO-Ph	CO_2Me	NHAc	[Rh(COD)**93h**]PF_6	3	Tol	r.t.	12	100	8.3	100	87.2 (*S*)	79
764	4-MeO-Ph	CO_2Me	NHAc	[Rh(COD)**94f**]BF_4	7	DCM	r.t.	0.1	500	5000	100	96.8 (*S*)	78
765	4-MeO-Ph	CO_2Me	NHAc	[Rh(COD)**94f**]BF_4	1	DCM	r.t.	0.42	488	1162	97.5	98.6 (*S*)	78
766	4-MeO-Ph	CO_2Me	NHAc	[Rh(COD)**117**]BF_4	5	H_2O/MeOH/EtOAc(0.6:0.4:1)	r.t.	3	100	33	100	98 (*S*)	101

767	4-MeO-Ph	CO_2Me	NHAc	[Rh(COD)**117**]BF_4	5	H_2O/MeOH (3:2)	r.t.	3	100	33	100	98 (*S*)	101
768	4-MeO-Ph	CO_2Me	NHAc	[Rh(COD)**132**]BF_4	34.5	Acetone	25	0.25	100	400	100	91.4 (*R*)	107
769	4-MeO-Ph	CO_2Me	NHAc	[Rh(COD)**133a**]BF_4	1	IPA	r.t.	24	97	4	97	90	48
770	3-Me-Ph	CO_2Me	NHAc	[Rh(COD)**93h**]SbF_6	3	THF	r.t.	12	100	8.3	100	96.3 (*S*)	79
771	4-Me-Ph	CO_2Me	NHAc	[Rh(COD)**91**]BF_4	1	MeOH	25	0.167	100	600	>99.9	95.6 (*R*)	27
772	4-Me-Ph	CO_2Me	NHAc	[Rh(COD)**94a**]BF_4	6.9	DCM	r.t.	0.17	500	2941	100	83.5 (*S*)	52
773	4-Me-Ph	CO_2Me	NHAc	[Rh(COD)**94d**]BF_4	7	DCM	r.t.	0.42	500	1190	100	92.5 (*S*)	78
774	4-Me-Ph	CO_2Me	NHAc	[Rh(COD)**132**]BF_4	34.5	Acetone	25	0.25	100	400	100	90.6 (*R*)	107
775	4-Me-Ph	CO_2Me	NHAc	[Rh(COD)**154a**]OTf	5	MeOH	r.t.	18	40	2.2	20	73 (*S*)	127
776	4-Me-Ph	CO_2Me	NHAc	[Rh(COD)**154a**]OTf	5	Tol	r.t.	18	120	6.7	60	85 (*S*)	127
777	4-Me-Ph	CO_2Me	NHAc	[Rh(COD)**154b**]OTf	5	Tol	r.t.	18	200	11.1	100	85 (*S*)	127
778	4-Me-Ph	CO_2Me	NHAc	[Rh(COD)**154c**]OTf	5	Tol	r.t.	18	186	10.3	93	34 (*R*)	127
779	4-Me-Ph	CO_2Me	NHBz	[Rh(COD)**94a**]BF_4	6.9	DCM	r.t.	0.17	479	2818	95.7	80 (*S*)	52
780	4-CF_3-Ph	CO_2Me	NHAc	[Rh(COD)**93h**]SbF_6	3	THF	r.t.	12	100	8.3	100	95.7 (*S*)	79
781	4-CF_3-Ph	CO_2Me	NHAc	[Rh(COD)**94c**]BF_4	7	DCM	r.t.	0.83	409	493	81.8	48.7 (*S*)	78
782	2-Naphthyl	CO_2H	NHAc	[Rh(COD)**95**]BF_4	1	IPA	r.t.	24	100	4	100	91.4 (*S*)	85
783	2-Naphthyl	CO_2H	NHAc	[Rh(COD)**98a**]SbF_6	2–2.8	THF	r.t.	2–3	–	–	–	94.0	95 b
784	2-Naphthyl	CO_2H	NHAc	[Rh(COD)**98b**]SbF_6	2–2.8	THF	r.t.	2–3	–	–	–	98.0	95 b
785	2-Naphthyl	CO_2H	NHAc	[Rh(COD)**98c**]SbF_6	2–2.8	THF	r.t.	2–3	–	–	–	22.0	95 b
786	2-Naphthyl	CO_2H	NHAc	[Rh(COD)**98d**]SbF_6	2–2.8	THF	r.t.	2–3	–	–	–	26.6	95 b
787	2-Naphthyl	CO_2H	NHAc	[Rh(COD)**103a**]SbF_6	2–2.8	THF	r.t.	–	–	–	–	96	95 a
788	2-Naphthyl	CO_2H	NHAc	[Rh(COD)**163a**]PF_6	1	THF	r.t.	12	>99	8.3	100	>99 (*S*)	128
789	2-Naphthyl	CO_2H	NHAc	[Rh(COD)**164a**]PF_6	1	THF	r.t.	12	>99	8.3	100	>99 (*S*)	128
790	2-Naphthyl	CO_2Me	NHAc	[Rh(COD)**93h**]PF_6	3	Tol	r.t.	12	100	8.3	100	97.3 (*S*)	79
791	2-Naphthyl	CO_2Me	NHAc	[Rh(COD)**93h**]SbF_6	3	THF	r.t.	12	100	8.3	100	94.1 (*S*)	79
792	2-Naphthyl	CO_2Me	NHAc	[Rh(COD)**98a**]SbF_6	2–2.8	THF	r.t.	2–3	–	–	–	86.5	95 b
793	2-Naphthyl	CO_2Me	NHAc	[Rh(COD)**98b**]SbF_6	2–2.8	THF	r.t.	2–3	–	–	–	97.1	95 b
794	2-Naphthyl	CO_2Me	NHAc	[Rh(COD)**98d**]SbF_6	2–2.8	THF	r.t.	2–3	–	–	–	10.8	95 b
795	2-Naphthyl	CO_2Me	NHAc	[Rh(COD)**103a**]SbF_6	2–2.8	THF	r.t.	2–3	–	–	–	96.0	95 b
796	2-Naphthyl	CO_2Me	NHAc	[Rh(COD)**104a**]BF_4	2–2.8	THF	r.t.	2–3	–	–	–	93.0	95 b

Table 27.5 (continued)

Entry	Substrate			Catalyst	Conditions				TON	TOF [h^{-1}]	Conv. [%]	ee [%]	Reference(s)
	R^1	R^2	R^3		$P[H_2]$ [bar]	Solvent	Temp. [°C]	Time [h]					
797	2-Naphthyl	CO_2Me	NHAc	[Rh(COD)**117**]BF_4	5	H_2O/MeOH/ EtOAc(0. 6:0.4 : 1)	r.t.	3	100	33	100	96 (*S*)	101
798	2-Naphthyl	CO_2Me	NHAc	[Rh(COD)**117**]BF_4	5	H_2O/MeOH (3:2)	r.t.	3	100	33	100	95 (*S*)	101
799	2-Naphthyl	CO_2Me	NHAc	[Rh(COD)**163a**]PF_6	1	THF	r.t.	12	>99	8.3	100	>99 (*S*)	128
800	2-Naphthyl	CO_2Me	NHAc	[Rh(COD)**164a**]PF_6	1	THF	r.t.	12	>99	8.3	100	>99 (*S*)	128
801	3,5-F_2-Ph	CO_2H	NHAc	[Rh(COD)**103a**]SbF_6	2–2.8	THF	r.t.	–	–	–	–	96.2	95 a, b
802	3,5-F_2-Ph	CO_2Me	NHAc	[Rh(COD)**98a**]SbF_6	2–2.8	THF	r.t.	2–3	–	–	–	88.3	95 b
803	3,5-F_2-Ph	CO_2Me	NHAc	[Rh(COD)**98b**]SbF_6	2–2.8	THF	r.t.	2–3	–	–	–	97.0	95 b
804	3,5-F_2-Ph	CO_2Me	NHAc	[Rh(COD)**98g**]SbF_6	2–2.8	THF	r.t.	2–3	–	–	–	98.4	95 b
805	3,5-F_2-Ph	CO_2Me	NHAc	[Rh(COD)**103b**]SbF_6	2–2.8	THF	r.t.	2–3	–	–	–	73.0	95 b
806	3,5-F_2-Ph	CO_2Me	NHAc	[Rh(COD)**103c**]SbF_6	2–2.8	THF	r.t.	2–3	–	–	–	3.0	95 b
807	3,5-F_2-Ph	CO_2Me	NHAc	[Rh(COD)**103d**]SbF_6	2–2.8	THF	r.t.	2–3	–	–	–	5.6	95 b
808	3,5-F_2-Ph	CO_2Me	NHAc	[Rh(COD)**103e**]SbF_6	2–2.8	THF	r.t.	2–3	–	–	–	2.7	95 b
809	3,5-F_2-Ph	CO_2Me	NHAc	[Rh(COD)**103f**]SbF_6	2–2.8	THF	r.t.	2–3	–	–	–	85.1	95 b
810	3,5-Me_2-P	CO_2Me	NHAc	[Rh(COD)**93e**]BF_4	7	DCM	r.t.	0.42	500	1190	100	93.9 (*S*)	78
811	3,5-Me_2-P	CO_2Me	NHAc	[Rh(COD)**94e**]BF_4	7	DCM	r.t.	0.22	500	2273	100	95.4 (*S*)	78
812	3,5-$(CF_3)_2$-Ph	CO_2Me	NHAc	[Rh(COD)**94b**]BF_4	7	DCM	r.t.	1.75	147	84	29.3	30.9 (*S*)	78
813	3,5-$(CF_3)_2$-Ph	CO_2Me	NHAc	[Rh(COD)**98b**]SbF_6	2–2.8	THF	r.t.	2–3	–	–	–	95.8	95b
814	3,5-$(CF_3)_2$-Ph	CO_2Me	NHAc	[Rh(NBD)**98b**]SbF_6	2.8	THF	r.t.	0.25	1000	4000	100	96.1 (*S*)	95 b
815	3,5-$(CF_3)_2$-Ph	CO_2Me	NHAc	[Rh(COD)**98a**]SbF_6	2–2.8	THF	r.t.	2–3	–	–	–	85.2	95 b
816	3,5-$(CF_3)_2$-Ph	CO_2Me	NHAc	[Rh(COD)**98g**]SbF_6	2–2.8	THF	r.t.	2–3	–	–	–	97.1	95 b
817	3,5-$(CF_3)_2$-Ph	CO_2Me	NHAc	[Rh(COD)**98g**]BF_4	2–2.8	THF	r.t.	2–3	–	–	–	96.9	95 b

818	3,5-$(CF_3)_2$-Ph	CO_2Me	NHAc	[Rh(COD)**102a**]BF_4	2–2.8	THF	r.t.	2–3	–	–	–	93.7	95 b
819	3,5-$(CF_3)_2$-Ph	CO_2Me	NHAc	[Rh(COD)**103a**]SbF_6	2–2.8	THF	r.t.	2–3	–	–	–	97.4	95 b
820	3,5-$(CF_3)_2$-Ph	CO_2Me	NHAc	[Rh(COD)**103b**]SbF_6	2–2.8	THF	r.t.	2–3	–	–	–	77.9	95 b
821	3,5-$(CF_3)_2$-Ph	CO_2Me	NHAc	[Rh(COD)**103c**]SbF_6	2–2.8	THF	r.t.	2–3	–	–	–	3.2	95 b
822	3,5-$(CF_3)_2$-Ph	CO_2Me	NHAc	[Rh(COD)**103d**]SbF_6	2–2.8	THF	r.t.	2–3	–	–	–	<1	95 b
823	3,5-$(CF_3)_2$-Ph	CO_2Me	NHAc	[Rh(COD)**103e**]SbF_6	2–2.8	THF	r.t.	2–3	–	–	–	<1	95 b
824	3,5-$(CF_3)_2$-Ph	CO_2Me	NHAc	[Rh(COD)**103f**]SbF_6	2–2.8	THF	r.t.	2–3	–	–	–	83.9	95 b
825	3,4-$(MeO)_2$-Ph	CO_2H	NHAc	[Rh(COD)**97a**]BF_4	1	MeOH	25	0.1 [f]	50	500	50	96.7 (*S*)	91 b
826	3,4-$(MeO)_2$-Ph	CO_2H	NHAc	[Rh(COD)**97c**]BF_4	1	MeOH	25	0.083 [f]	50	600	50	94.8 (*S*)	91 b
827	3,4-$(MeO)_2$-Ph	CO_2H	NHBz	[Rh(COD)**97a**]BF_4	1	MeOH	25	0.083 [f]	50	600	50	95.1 (*S*)	91 b
828	3,4-$(MeO)_2$-Ph	CO_2H	NHBz	[Rh(COD)**97c**]BF_4	1	MeOH	25	0.067 [f]	50	750	50	92.0 (*S*)	91 b
829	3,4-$(MeO)_2$-Ph	CO_2Me	NHAc	[Rh(COD)**97a**]BF_4	1	MeOH	25	0.37 [f]	50	136	50	92.4 (*S*)	91 b
830	3,4-$(MeO)_2$-Ph	CO_2Me	NHAc	[Rh(COD)**97c**]BF_4	1	MeOH	25	0.2 [f]	50	250	50	95.7 (*S*)	91 b
831	3,4-$(MeO)_2$-Ph	CO_2Me	NHBz	[Rh(COD)**97a**]BF_4	1	MeOH	25	0.13 [f]	50	375	50	87.7 (*S*)	91 b
832	3,4-$(MeO)_2$-Ph	CO_2Me	NHBz	[Rh(COD)**97c**]BF_4	1	MeOH	25	0.12 [f]	50	429	50	91.2 (*S*)	91 b
833	3,4-$(MeO)_2$-Ph	CO_2Et	NHAc	[Rh(COD)**97a**]BF_4	1	MeOH	25	0.13 [f]	50	375	50	90.6 (*S*)	91 b
834	3,4-$(MeO)_2$-Ph	CO_2Et	NHAc	[Rh(COD)**97c**]BF_4	1	MeOH	25	0.083 [f]	50	600	50	95.2 (*S*)	91 b
835	3,4-$(MeO)_2$-Ph	CO_2Et	NHBz	[Rh(COD)**97a**]BF_4	1	MeOH	25	0.17 [f]	50	300	50	88.9 (*S*)	91 b
836	3,4-$(MeO)_2$-Ph	CO_2Et	NHBz	[Rh(COD)**97c**]BF_4	1	MeOH	25	0.13 [f]	50	375	50	90.5 (*S*)	91 b
837	3,4-$(MeO)_2$-Ph	CO_2*i*-Pr	NHAc	[Rh(COD)**97a**]BF_4	1	MeOH	25	0.37 [f]	50	136	50	91.3 (*S*)	91 b
838	3,4-$(MeO)_2$-Ph	CO_2*i*-Pr	NHAc	[Rh(COD)**97c**]BF_4	1	MeOH	25	0.18 [f]	50	273	50	94.7 (*S*)	91 b
839	3,4-$(MeO)_2$-Ph	CO_2*i*-Pr	NHBz	[Rh(COD)**97a**]BF_4	1	MeOH	25	0.33 [f]	50	150	50	89.1 (*S*)	91 b
840	3,4-$(MeO)_2$-Ph	CO_2*i*-Pr	NHBz	[Rh(COD)**97c**]BF_4	1	MeOH	25	0.23 [f]	50	214	50	92.7 (*S*)	91 b
841	3,4-$(MeO)_2$-Ph	CO_2-C_2H_4OH	NHBz	[Rh(COD)**97a**]BF_4	1	MeOH	25	0.17 [f]	50	300	50	87.3 (*S*)	91 b
842	3,4-$(MeO)_2$-Ph	CO_2-C_2H_4OH	NHBz	[Rh(COD)**97c**]BF_4	1	MeOH	25	0.13 [f]	50	375	50	89.9 (*S*)	91 b
843	3-MeO-4-HO-Ph	CO_2H	NHBz	[Rh(COD)**97a**]BF_4	1	MeOH	25	0.067 [f]	50	750	50	96.9 (*S*)	91 b
844	3-MeO-4-HO-Ph	CO_2H	NHBz	[Rh(COD)**97c**]BF_4	1	MeOH	25	0.067 [f]	50	750	50	94.1 (*S*)	91 b

Table 27.5 (continued)

Entry	Substrate			Catalyst	Conditions				TON	TOF [h^{-1}]	Conv. [%]	ee [%]	Reference(s)
	R^1	R^2	R^3		P[H_2] [bar]	Solvent	Temp. [°C]	Time [h]					
845	3-MeO-4-HO-Ph	CO_2Me	NHAc	[Rh(COD)**97a**]BF_4	1	MeOH	25	0.2 [f)]	50	250	50	91.7 (*S*)	91b
846	3-MeO-4-HO-Ph	CO_2Me	NHAc	[Rh(COD)**97c**]BF_4	1	MeOH	25	0.083 [f)]	50	600	50	95.0 (*S*)	91b
847	3-MeO-4-HO-Ph	CO_2Me	NHAc	[Rh(COD)**132**]BF_4	34.5	Acetone	25	0.25	100	400	100	90.2 (*R*)	107
848	3-MeO-4-HO-Ph	CO_2Me	NHBz	[Rh(COD)**97a**]BF_4	1	MeOH	25	0.18 [f)]	50	273	50	89.0 (*S*)	91b
849	3-MeO-4-HO-Ph	CO_2Me	NHBz	[Rh(COD)**97c**]BF_4	1	MeOH	25	0.1 [f)]	50	500	50	92.1 (*S*)	91b
850	3-MeO-4-HO-Ph	$CO_2C_2H_4OH$	NHAc	[Rh(COD)**97a**]BF_4	1	MeOH	25	0.22 [f)]	50	231	50	91.7 (*S*)	91b
851	3-MeO-4-HO-Ph	$CO_2C_2H_4OH$	NHAc	[Rh(COD)**97c**]BF_4	1	MeOH	25	0.12 [f)]	50	429	50	95.5 (*S*)	91b
852	3-MeO-4-HO-Ph	$CO_2C_2H_4OH$	NHBz	[Rh(COD)**97a**]BF_4	1	MeOH	25	0.27 [f)]	50	188	50	88.4 (*S*)	91b
853	3-MeO-4-HO-Ph	$CO_2C_2H_4OH$	NHBz	[Rh(COD)**97c**]BF_4	1	MeOH	25	0.2 [f)]	50	250	50	90.2 (*S*)	91b
854	3-MeO-4-AcOPh	CO_2H	NHAc	[Rh(COD)**98a**]BF_4	1	MeOH	25	0.095 [f)]	50	526	50	94 (*S*)	26
855	3-MeO-4-AcOPh	CO_2H	NHAc	[Rh(COD)**97a**]BF_4	1	MeOH	25	0.08 [f)]	50	625	50	71 (*S*)	26
856	3-MeO-4-AcOPh	CO_2H	NHAc	[Rh(COD)**97a**]BF_4	1	MeOH	25	0.17 [f)]	50	300	50	96.0 (*S*)	91b
857	3-MeO-4-AcOPh	CO_2H	NHAc	[Rh(COD)**97c**]BF_4	1	MeOH	25	0.15 [f)]	50	333	50	95.2 (*S*)	91b
858	3-MeO-4-OAcPh	CO_2H	NHAc	[Rh(COD)**95**]BF_4	1	IPA	r.t.	24	100	4	100	95.0 (*S*)	85
859	3-MeO-4-AcOPh	CO_2H	NHAc	[Rh(COD)**124**]BF_4	1	THF	25	1	100	100	100	36 (*R*)	103
860	3-MeO-4-AcOPh	CO_2H	NHAc	[Rh(COD)**125**]BF_4	1	THF	25	1	100	100	100	65 (*S*)	103
861	3-MeO-4-AcOPh	CO_2Me	NHAc	[Rh(COD)**97a**]BF_4	1	MeOH	25	0.083 [f)]	50	600	50	92.4 (*S*)	91b
862	3-MeO-4-AcOPh	CO_2Me	NHAc	[Rh(COD)**97c**]BF_4	1	MeOH	25	0.05 [f)]	50	1000	50	95.6 (*S*)	91b
863	3-MeO-4-AcOPh	CO_2Me	NHAc	[Rh(COD)**98a**]BF_4	1	MeOH	25	0.15 [f)]	50	333	50	91 (*S*)	26
864	3-MeO-4-AcOPh	CO_2Me	NHBz	[Rh(COD)**97a**]BF_4	1	MeOH	25	0.083 [f)]	50	600	50	87.2 (*S*)	91b
865	3-MeO-4-AcOPh	CO_2Me	NHBz	[Rh(COD)**97c**]BF_4	1	MeOH	25	0.067 [f)]	50	750	50	91.3 (*S*)	91b
866	3-MeO-4-AcOPh	CO_2Et	NHAc	[Rh(COD)**98a**]BF_4	1	MeOH	25	0.14 [f)]	50	353	50	87 (*S*)	26
867	3-MeO-4-AcOPh	CO_2Et	NHBz	[Rh(COD)**97c**]BF_4	1	MeOH	25	0.083 [f)]	50	600	50	90.5 (*S*)	91b
868	3,4-(OCH_2O)-Ph	CO_2H	NHAc	[Rh(COD)**132**]BF_4	34.5	Acetone	25	0.25–1	100	100–400	100	94.2 (*R*)	107

869	3,4-(OCH_2O)-Ph	CO_2Me	NHAc	[Rh(COD)**91**]BF_4	1	MeOH	25	0.167	100	600	>99.9	94.9 (*R*)	27
870	3,4-(OCH_2O)-Ph	CO_2Me	NHAc	[Rh(COD)**132**]BF_4	34.5	Acetone	25	0.25	100	400	100	93.2 (*R*)	107
871	4-Ph-Ph	CO_2Me	NHAc	[Rh(COD)**93h**]SbF_6	3	THF	r.t.	12	100	8.3	100	94.2 (*S*)	79
872	2-Furyl	CO_2Me	NHAc	[Rh(COD)**91**]BF_4	1	MeOH	25	0.167	100	600	>99.9	97.2 (*R*)	27
873	2-Furyl	CO_2Me	NHBz	[Rh(COD)**94a**]BF_4	6.9	DCM	r.t.	0.17	500	2941	100	63.9 (*S*)	52
874	Thiophen-2-yl	CO_2H	NHAc	[Rh(COD)**95**]BF_4	1	IPA	r.t.	24	100	4	100	90.1 (*S*)	85
875	Thiophen-2-yl	CO_2H	NHAc	[Rh(COD)**98a**]BF_4	2.8	THF	r.t.	3	100	33	100	85 (*S*)	98
876	Thiophen-2-yl	CO_2H	NHAc	[Rh(COD)**98b**]BF_4	2.8	THF	r.t.	3	100	33	100	96 (*S*)	98
877	Thiophen-2-yl	CO_2H	NHAc	[Rh(COD)**115a**]SbF_6	2.8	THF	r.t.	3	91	30	91	26 (*S*)	98
878	Thiophen-2-yl	CO_2H	NHAc	[Rh(COD)**115b**]SbF_6	2.8	THF	r.t.	3	28	9	28	80 (*S*)	98
879	Thiophen-2-yl	CO_2Me	NHAc	[Rh(COD)**98a**]SbF_6	2–2.8	THF	r.t.	2–3	–	–	–	85.2	95 b
880	Thiophen-2-yl	CO_2Me	NHAc	[Rh(COD)**98b**]SbF_6	2–2.8	THF	r.t.	2–3	–	–	–	95.6	95 b
881	Thiophen-2-yl	CO_2Me	NHAc	[Rh(COD)**98g**]SbF_6	2–2.8	THF	r.t.	2–3	–	–	–	97.2	95 b
882	Thiophen-2-yl	CO_2Me	NHAc	[Rh(COD)**103a**]SbF_6	2–2.8	THF	r.t.	2–3	–	–	–	96	95 b
883	Thiophen-2-yl	CO_2Me	NHAc	[Rh(COD)**163a**]PF_6	1	THF	r.t.	12	95	7.9	100	95 (*S*)	128
884	Thiophen-2-yl	CO_2Me	NHAc	[Rh(COD)**164a**]PF_6	1	THF	r.t.	12	95	7.9	100	95 (*S*)	128
885	Thiophen-3-yl	CO_2H	NHAc	[Rh(COD)**98a**]BF_4	2.8	THF	r.t.	3	100	33	100	87 (*S*)	98
886	Thiophen-3-yl	CO_2H	NHAc	[Rh(COD)**98b**]BF_4	2.8	THF	r.t.	3	100	33	100	97 (*S*)	98
887	Thiophen-3-yl	CO_2H	NHAc	[Rh(COD)**115a**]SbF_6	2.8	THF	r.t.	3	86	29	86	28 (*S*)	98
888	Thiophen-3-yl	CO_2H	NHAc	[Rh(COD)**115b**]SbF_6	2.8	THF	r.t.	3	68	23	68	92 (*S*)	98
889	Thiophen-3-yl	CO_2Me	NHAc	[Rh(COD)**98a**]SbF_6	2–2.8	THF	r.t.	2–3	–	–	–	86.6	95 b
890	Thiophen-3-yl	CO_2Me	NHAc	[Rh(COD)**98b**]SbF_6	2–2.8	THF	r.t.	2–3	–	–	–	96.7	95 b
891	Thiophen-3-yl	CO_2Me	NHAc	[Rh(COD)**98g**]SbF_6	2–2.8	THF	r.t.	2–3	–	–	–	98.8	95 b
892	Thiophen-3-yl	CO_2Me	NHAc	[Rh(COD)**103a**]SbF_6	2–2.8	THF	r.t.	2–3	–	–	–	97.0	95 a, b
893	H	Ph	NHAc	[Rh(COD)**93a**]SbF_6	3	THF	r.t.	12	100	8.3	100	28.3 (*S*)	79
894	H	Ph	NHAc	[Rh(COD)**93g**]SbF_6	3	THF	r.t.	12	100	8.3	100	67.2 (*S*)	79
895	H	Ph	NHAc	[Rh(COD)**93h**]SbF_6	3	THF	r.t.	12	100	8.3	100	94.3 (*S*)	79
896	H	Ph	NHAc	[Rh(COD)**93i**]SbF_6	3	THF	r.t.	12	100	8.3	100	89.4 (*S*)	79
897	H	Ph	NHAc	[Rh(COD)**93j**]SbF_6	3	THF	r.t.	12	100	8.3	100	90.3 (*S*)	79
898	CO_2Me	Ph	NHAc	[Ru(*p*-cymene)**93a**]Cl	5.5	EtOH	50	20	25	1.25	100	2 (*S*)	80
899	CO_2Me	Ph	NHAc	[Ru(*p*-cymene)**93g**]Cl	5.5	EtOH	50	20	25	1.25	100	22 (*S*)	80

Table 27.5 (continued)

Entry	Substrate			Catalyst	Conditions				TON	TOF [h^{-1}]	Conv. [%]	ee [%]	Reference(s)
	R^1	R^2	R^3		$P[H_2]$ [bar]	Solvent	Temp. [°C]	Time [h]					
900	CO_2Me	Ph	NHAc	[Ru(*p*-cymene)**93h**]Cl	5.5	EtOH	50	20	25	1.25	100	98 (*S*)	80
901	CO_2Me	Ph	NHAc	[Ru(*p*-cymene)**93i**]Cl	5.5	EtOH	50	20	25	1.25	100	99 (*S*)	80
902	CO_2Me	Ph	NHAc	[Ru(*p*-cymene)**93j**]Cl	5.5	EtOH	50	20	25	1.25	100	97 (*S*)	80
903	CO_2Et	Ph	NHAc	[Ru(*p*-cymene)**93i**]Cl	5.5	EtOH	50	20	25	1.25	100	98 (*S*)	80
904	CO_2Me	2-MeO-Ph	NHAc	[Ru(*p*-cymene)**93i**]Cl	5.5	EtOH	50	20	25	1.25	100	80 (*S*)	80
905	CO_2Me	4-MeO-Ph	NHAc	[Ru(*p*-cymene)**93i**]Cl	5.5	EtOH	50	20	25	1.25	100	99 (*S*)	80
906	CO_2Me	2-Me-Ph	NHAc	[Ru(*p*-cymene)**93i**]Cl	5.5	EtOH	50	20	25	1.25	100	96 (*S*)	80
907	CO_2Me	4-Me-Ph	NHAc	[Ru(*p*-cymene)**93i**]Cl	5.5	EtOH	50	20	25	1.25	100	99 (*S*)	80
908	CO_2Me	4-Br-Ph	NHAc	[Ru(*p*-cymene)**93i**]Cl	5.5	EtOH	50	20	25	1.25	100	97 (*S*)	80
909	CO_2Me	4-Cl-Ph	NHAc	[Ru(*p*-cymene)**93i**]Cl	5.5	EtOH	50	20	25	1.25	100	97 (*S*)	80
910	CO_2Me	4-F-Ph	NHAc	[Ru(*p*-cymene)**93i**]Cl	5.5	EtOH	50	20	25	1.25	100	99 (*S*)	80
911	CO_2Et	4-Br-Ph	NHAc	[Ru(*p*-cymene)**93i**]Cl	5.5	EtOH	50	20	25	1.25	100	93 (*S*)	80
912	CO_2Et	4-Cl-Ph	NHAc	[Ru(*p*-cymene)**93i**]Cl	5.5	EtOH	50	20	25	1.25	100	95 (*S*)	80
913	CO_2Et	4-F-Ph	NHAc	[Ru(*p*-cymene)**93i**]Cl	5.5	EtOH	50	20	25	1.25	100	98 (*S*)	80
914	H	CO_2H	CH_2CO_2H	[Ir(COD)**142a**]BF_4	5	DCM : MeOH 2 : 1	40	4	100	25	100	35 (*R*)	117d
915	H	CO_2H	CH_2CO_2H	[Ir(COD)**142a**]BF_4	5	DCM : MeOH 2 : 1	25	12	70	5.8	70	34 (*R*)	117d
916	H	CO_2H	CH_2CO_2H	[Ir(COD)**142a**]BF_4	1	DCM : MeOH 2 : 1	40	4	100	25	100	54 (*R*)	117d
917	H	CO_2H	CH_2CO_2H	[Ir(COD)**142a**]BF_4	1	DCM : MeOH 2 : 1	25	8	50	6.3	50	40 (*R*)	117d
918	H	CO_2H	CH_2CO_2H	[Rh(COD)**142a**]BF_4	5	Tol : MeOH 2 : 1	40	6	70	11.7	70	45 (*R*)	117d

919	H	CO_2H	CH_2CO_2H	[Rh(COD)**142a**]BF_4	5	DCM : MeOH 2 : 1	40	6	13	2.2	13	–	117d
920	H	CO_2H	CH_2CO_2H	[Ir(COD)**142b**]BF_4	5	DCM : MeOH 2 : 1	40	4	100	25	100	29 (*R*)	117d
921	H	CO_2H	CH_2CO_2H	[Ir(COD)**142b**]BF_4	5	DCM : MeOH 2 : 1	25	12	68	5.7	68	32 (*R*)	117d
922	H	CO_2H	CH_2CO_2H	[Ir(COD)**142b**]BF_4	1	DCM : MeOH 2 : 1	40	4	87	21.8	87	47 (*R*)	117d
923	H	CO_2H	CH_2CO_2H	[Ir(COD)**142b**]BF_4	1	DCM : MeOH 2 : 1	25	8	70	8.8	70	26 (*R*)	117d
924	H	CO_2H	CH_2CO_2H	[Rh(COD)**142b**]BF_4	5	Tol : MeOH 2 : 1	40	6	99	16.5	99	49 (*R*)	117d
925	H	CO_2H	CH_2CO_2H	[Ir(COD)**142c**]BF_4	5	DCM : MeOH 2 : 1	40	20	100	5	100	13 (*R*)	117d
926	H	CO_2H	CH_2CO_2H	[Ir(COD)**142c**]BF_4	5	DCM : MeOH 2 : 1	25	12	44	3.7	44	11 (*R*)	117d
927	H	CO_2H	CH_2CO_2H	[Rh(COD)**142c**]BF_4	5	Tol : MeOH 2 : 1	40	20	20	1	20	20 (*R*)	117d
928	H	CO_2H	CH_2CO_2H	[Ir(COD)**143a**]BF_4	1	DCM : MeOH 2 : 1	40	6	100	16.7	100	15 (*S*)	117c
929	H	CO_2H	CH_2CO_2H	[Rh(COD)**143a**]BF_4	5	Tol : MeOH 2 : 1	40	20	100	5	100	11 (*R*)	117c
930	H	CO_2H	CH_2CO_2H	[Ir(COD)**143b**]BF_4	1	DCM : MeOH 2 : 1	40	6	100	16.7	100	13 (*S*)	117c
931	H	CO_2H	CH_2CO_2H	[Rh(COD)**143b**]BF_4	5	Tol : MeOH 2 : 1	40	20	100	5	100	10 (*R*)	117c
932	H	CO_2H	CH_2CO_2H	[Ir(COD)**143c**]BF_4	5	DCM : MeOH 2 : 1	40	20	47	2.4	47	8 (*R*)	117c
933	H	CO_2H	CH_2CO_2H	[Rh(COD)**143c**]BF_4	5	Tol : MeOH 2 : 1	40	20	100	5	100	50 (*R*)	117c
934	H	CO_2Me	CH_2CO_2Me	[Rh(COD)**87**]BARF	30–45	$scCO_2$	40–45	20	1000	50	100	73 (*R*)	69

Table 27.5 (continued)

Entry	Substrate			Catalyst	Conditions				TON	TOF [h^{-1}]	Conv. [%]	ee [%]	Reference(s)
	R^1	R^2	R^3		P[H_2] [bar]	Solvent	Temp. [°C]	Time [h]					
935	H	CO_2Me	CH_2CO_2Me	[Rh(COD)**93a**]BF_4	20	DCM	r.t.	0.28	500	1786	100	81.3 (*R*)	78
936	H	CO_2Me	CH_2CO_2Me	[Rh(COD)**93b**]BF_4	20	DCM	r.t.	0.17	500	2941	100	81.0 (*R*)	78
937	H	CO_2Me	CH_2CO_2Me	[Rh(COD)**93d**]BF_4	20	DCM	r.t.	0.5	500	1000	100	65.6 (*R*)	78
938	H	CO_2Me	CH_2CO_2Me	[Rh(COD)**93f**]BF_4	20	DCM	r.t.	1.5	412	275	82.3	50.9 (*R*)	78
939	H	CO_2Me	CH_2CO_2Me	[Rh(COD)**94b**]BF_4	20	DCM	r.t.	1.5	439	293	87.7	51.6 (*R*)	78
940	H	CO_2Me	CH_2CO_2Me	[Rh(COD)**94c**]BF_4	20	DCM	r.t.	0.33	500	1515	100	72.9 (*R*)	78
941	H	CO_2Me	CH_2CO_2Me	[Rh(COD)**94d**]BF_4	20	DCM	r.t.	0.12	500	4167	100	89.5 (*R*)	78
942	H	CO_2Me	CH_2CO_2Me	[Rh(COD)**94e**]BF_4	20	DCM	r.t.	0.15	500	3333	100	91.5 (*R*)	78
943	H	CO_2Me	CH_2CO_2Me	[Rh(COD)**94f**]BF_4	20	DCM	r.t.	0.083	500	6024	100	92.2 (*R*)	78
944	H	CO_2Me	CH_2CO_2Me	[Rh(COD)**94f**]BF_4	1	DCM	r.t.	0.42	500	1190	100	93.9 (*R*)	78
945	H	CO_2Me	CH_2CO_2Me	[Rh(COD)**97a**]ClO_4 + 0.1 Et_3N	1	EtOH	25	0.5	50	100	100	29 (*R*)	90
946	H	CO_2Me	CH_2CO_2Me	[Rh(COD)**97a**]ClO_4 + 0.2 Et_3N	1	EtOH	25	0.5	50	100	100	16 (*R*)	90
947	H	CO_2Me	CH_2CO_2Me	[Rh(COD)**111**]ClO_4	1	EtOH	25	0.5	50	100	100	45 (*R*)	90
948	H	CO_2Me	CH_2CO_2Me	[Rh(COD)**111**]ClO_4	1	EtOH	0	1	50	50	100	33 (*R*)	90
949	H	CO_2Me	CH_2CO_2Me	[Rh(COD)**111**]ClO_4	1	EtOH	25	0.3	50	167	100	31 (*S*)	90
950	H	CO_2Me	CH_2CO_2Me	[Rh(COD)**111**]ClO_4	1	EtOH	0	0.5	50	100	100	54 (*S*)	90
951	H	CO_2Me	CH_2CO_2Me	[Rh(COD)**111**]ClO_4 + 0.1 Et_3N	1	EtOH	25	0.1	50	500	100	51 (*S*)	90
952	H	CO_2Me	CH_2CO_2Me	[Rh(COD)**111**]ClO_4 + 0.2 Et_3N	1	EtOH	25	0.3	50	167	100	28 (*S*)	90
953	H	CO_2Me	CH_2CO_2Me	[Rh(COD)ent-**120**]BF_4	1	DCM	r.t.	0.08	100	1250	100	4 (*R*)	105

954	H	CO_2Me	CH_2CO_2Me	[Rh(COD)**121a**]BF_4	1	DCM	r.t.	0.08	100	1250	100	53 (*R*)	105
955	H	CO_2Me	CH_2CO_2Me	[Rh(COD)**121b**]BF_4	1	DCM	r.t.	0.08	100	1250	100	9 (*R*)	105
956	H	CO_2Me	CH_2CO_2Me	[Rh(COD)**121d**]BF_4	1	DCM	r.t.	0.08	100	1250	100	19 (*R*)	105
957	H	CO_2Me	CH_2CO_2Me	[Rh(COD)**122a**]BF_4	1	DCM	r.t.	0.08	100	1250	100	48 (*S*)	105
958	H	CO_2Me	CH_2CO_2Me	[Rh(COD)**122b**]BF_4	1	DCM	r.t.	0.08	100	1250	100	48 (*S*)	105
959	H	CO_2Me	CH_2CO_2Me	[Rh(COD)**122b**]BF_4	1	Acetone/DCM 13 : 2	r.t.	1.25	100	80	100	29 (*S*)	105
960	H	CO_2Me	CH_2CO_2Me	[Rh(COD)**122c**]BF_4	1	DCM	r.t.	0.08	100	1250	100	54 (*S*)	105
961	H	CO_2Me	CH_2CO_2Me	[Rh(COD)**122d**]BF_4	1	DCM	r.t.	0.08	100	1250	100	53 (*S*)	105
962	H	CO_2Me	CH_2CO_2Me	[Rh(COD)**122d**]BF_4	1	Acetone/DCM 13 : 2	r.t.	1	100	100	100	63 (*S*)	105
963	H	CO_2Me	CH_2CO_2Me	[Rh(COD)**122e**]BF_4	1	DCM	r.t.	0.08	100	1250	100	51 (*S*)	105
964	H	CO_2Me	CH_2CO_2Me	[Ir(COD)**126**]BF_4	1	DCM	25	5	2	0.4	2	3 (*R*)	104
965	H	CO_2Me	CH_2CO_2Me	[Rh(COD)**126**]BF_4	1	DCM	25	0.83	100	120	100	9 (*S*)	104
966	H	CO_2Me	CH_2CO_2Me	[Ir(COD)**127**]BF_4	1	DCM	25	28	100	3.6	100	24 (*S*)	104
967	H	CO_2Me	CH_2CO_2Me	[Rh(COD)**127**]BF_4	1	DCM	25	0.42	99	236	99	15 (*R*)	104
968	H	CO_2Me	CH_2CO_2Me	[Rh(COD)**136**]BF_4	1.3	DCM	r.t.	20	2000	100	100	97–99 (*R*)	109
969	H	CO_2Me	CH_2CO_2Me	[Rh(COD)**136**]BF_4	1.3	DCM	r.t.	20	1000	50	100	97–99 (*R*)	109
970	H	CO_2Me	CH_2CO_2Me	[Rh(COD)**137a**]BF_4	20	DCM	23	0.5	1000	2000	100	59.7 (*R*)	112
971	H	CO_2Me	CH_2CO_2Me	[Rh(COD)**137b**]BF_4	20	DCM	23	0.17	1000	5882	100	88.5 (*R*)	112
972	H	CO_2Me	CH_2CO_2Me	[Rh(COD)**138**]BF_4	1.3	DCM	r.t.	20	2000	100	100	>99.5 (*R*)	109
973	H	CO_2Me	CH_2CO_2Me	[Rh(COD)**138**]BF_4	1.3	DCM	r.t.	20	5380	269	100	>99.5 (*R*)	109
974	H	CO_2Me	CH_2CO_2Me	[Rh(COD)**138**]BF_4	1.3	DCM	r.t.	20	1000	500	100	>99.5 (*R*)	109
975	H	CO_2Me	CH_2CO_2Me	[Rh(COD)**142a**]BF_4	5	DCM	25	8	12	1.5	12	22 (*R*)	117b
976	H	CO_2Me	CH_2CO_2Me	[Rh(COD)**143a**]BF_4	5	DCM	25	8	28	3.5	28	64 (*R*)	117b
977	H	CO_2Me	CH_2CO_2Me	[Rh(COD)**144a**]BF_4	5	DCM	25	8	90	11.3	90	90 (*R*)	117a
978	H	CO_2Me	CH_2CO_2Me	[Rh(COD)**144a**]BF_4	5	Tol	25	8	16	2	16	2 (*S*)	117b
979	H	CO_2Me	CH_2CO_2Me	[Rh(COD)**144a**]BF_4	5	DCM	25	8	90	11.3	90	90 (*R*)	117b
980	H	CO_2Me	CH_2CO_2Me	[Rh(COD)**144a**]BF_4	5	AcOEt	25	8	8	1	8	2 (*R*)	117b
981	H	CO_2Me	CH_2CO_2Me	[Rh(COD)**144a**]BF_4	5	THF	25	8	99	12.4	99	12 (*R*)	117b
982	H	CO_2Me	CH_2CO_2Me	[Rh(COD)**144a**]BF_4	1	DCM	25	20	100	5	100	10 (*R*)	117b

Table 27.5 (continued)

Entry	Substrate			Catalyst	Conditions				TON	TOF [h^{-1}]	Conv. [%]	ee [%]	Reference(s)
	R^1	R^2	R^3		P[H_2] [bar]	Solvent	Temp. [°C]	Time [h]					
983	H	CO_2Me	CH_2CO_2Me	[Rh(COD)**144a**]BF_4	2	DCM	25	8	66	8.3	66	90 (*R*)	117b
984	H	CO_2Me	CH_2CO_2Me	[Rh(COD)**144a**]BF_4	10	DCM	25	3	90	30	90	90 (*R*)	117b
985	H	CO_2Me	CH_2CO_2Me	[Rh(COD)**144a**]BF_4	30	DCM	25	0.8	100	125	100	91 (*R*)	117b
986	H	CO_2Me	CH_2CO_2Me	[Rh(COD)**144a**]BF_4	5	DCM	25	8	90	11.3	90	90 (*R*)	117b
987	H	CO_2Me	CH_2CO_2Me	[Rh(COD)**144b**]BF_4	5	DCM	25	8	82	10.3	82	85 (*R*)	117a, b
988	H	CO_2Me	CH_2CO_2Me	[Rh(COD)**144c**]BF_4	5	DCM	25	6	100	16.7	100	97 (*R*)	117a, b
989	H	CO_2Me	CH_2CO_2Me	[Rh(COD)**144c**]BF_4	30	DCM	5	4	1000	250	100	>99 (*R*)	117b
990	H	CO_2Me	CH_2CO_2Me	[Rh(COD)**144d**]BF_4	5	DCM	25	8	50	6.3	50	50 (*S*)	117a, b
991	H	CO_2Me	CH_2CO_2Me	[Rh(COD)**144e**]BF_4	5	DCM	25	8	46	5.8	46	52 (*R*)	117a
992	H	CO_2Me	CH_2CO_2Me	[Rh(COD)**144e**]BF_4	5	DCM	25	8	46	5.8	46	52 (*R*)	117b
993	H	CO_2Me	CH_2CO_2Me	[Rh(COD)**144f**]BF_4	5	DCM	25	8	100	12.5	100	90 (*S*)	117b
994	H	CO_2Me	CH_2CO_2Me	[Rh(COD)**144g**]BF_4	5	DCM	25	8	100	12.5	100	92 (*R*)	117b
995	H	CO_2Me	CH_2CO_2Me	[Rh(COD)**145a**]BF_4	5	DCM	25	8	100	12.5	100	2 (*R*)	117a, b
996	H	CO_2Me	CH_2CO_2Me	[Rh(COD)**145b**]BF_4	5	DCM	25	8	98	12.3	98	2 (*R*)	117a, b
997	H	CO_2Me	CH_2CO_2Me	[Rh(COD)**145c**]BF_4	5	DCM	25	8	100	12.5	100	3 (*R*)	117a, b
998	H	CO_2Me	CH_2CO_2Me	[Rh(COD)**146a**]BF_4	5	DCM	25	8	87	10.9	87	67 (*R*)	117a, b
999	H	CO_2Me	CH_2CO_2Me	[Rh(COD)**146b**]BF_4	5	DCM	25	8	80	10	80	63 (*R*)	117a, b
1000	H	CO_2Me	CH_2CO_2Me	[Rh(COD)**146c**]BF_4	5	DCM	25	8	73	9.1	73	29 (*R*)	117a, b
1001	H	CO_2Me	CH_2CO_2Me	[Rh(COD)**146d**]BF_4	5	DCM	25	8	69	8.6	69	27 (*R*)	117a, b
1002	H	CO_2Me	CH_2CO_2Me	[Rh(COD)**149a**]BF_4	0.3	DCM	20	20	325	16	65	21.0 (*S*)	116
1003	H	CO_2Me	CH_2CO_2Me	[Rh(COD)**149b**]BF_4 [k)]	0.3	DCM	20	20	1000	50	>99	87.8 (*S*)	116
1004	H	CO_2Me	CH_2CO_2Me	[Rh(COD)**149c**]BF_4	0.3	DCM	–10	20	1000	50	>99	96.2 (*R*)	116
1005	H	CO_2Me	CH_2CO_2Me	[Rh(COD)**149c**]BF_4 [k)]	0.3	DCM	20	20	1000	50	>99	94.5 (*R*)	116
1006	H	CO_2Me	CH_2CO_2Me	[Rh(COD)**149d**]BF_4 [k)]	0.3	DCM	20	20	740	37	74	38.9 (*S*)	116

1007	H	CO_2Me	CH_2CO_2Me	[Rh(COD)**149e**]BF_4	0.3	DCM	20	20	1000	50	>99	96.8 (*R*)	116
1008	H	CO_2Me	CH_2CO_2Me	[Rh(COD)**149e**]BF_4	0.3	DCM	–10	20	1000	50	>99	98.2 (*R*)	116
1009	H	CO_2Me	CH_2CO_2Me	[Rh(COD)**149f**]BF_4	0.3	DCM	20	20	60	3	24	5.2 (*R*)	116
1010	H	CO_2Me	CH_2CO_2Me	[Rh(COD)**149g**]BF_4	0.3	DCM	20	20	1000	50	>99	49.3 (*R*)	116
1011	H	CO_2Me	CH_2CO_2Me	[Rh(COD)**150a**]BF_4	1	DCM	25	0.2	100	500	100	63 (*R*)	118
1012	H	CO_2Me	CH_2CO_2Me	[Rh(COD)**150b**]BF_4	1	DCM	25	3.3	100	30.3	100	66 (*R*)	118
1013	H	CO_2Me	CH_2CO_2Me	[Rh(COD)**150c**]BF_4	1	DCM	25	3.3	100	30.3	100	14 (*R*)	118
1014	H	CO_2Me	CH_2CO_2Me	[Rh(COD)**150d**]BF_4	1	DCM	25	0.25	100	400	100	70 (*R*)	118
1015	H	CO_2Me	CH_2CO_2Me	[Rh(COD)**151**]BF_4	1.3	DCM	22	2.5	1000	400	100	88 (*R*)	120
1016	H	CO_2Me	CH_2CO_2Me	[Rh(COD)**151**]BF_4	1.3	DCM	22	3.2	1860	581	93	87 (*R*)	120
1017	H	CO_2Me	CH_2CO_2Me	[Rh(COD)**152**]BF_4	1.3	DCM	22	1.5	1000	667	100	77 (*S*)	120
1018	H	CO_2Me	CH_2CO_2Me	[Rh(COD)**152**]BF_4	1.3	DCM	22	1.5	2000	1333	100	79 (*S*)	120
1019	H	CO_2Me	CH_2CO_2Me	[Rh(COD)**153**]BF_4	1.3	DCM	22	2.5	1000	400	100	52 (*S*)	120
1020	H	CO_2Me	CH_2CO_2Me	[Rh(COD)**153**]BF_4	1.3	DCM	22	2.8	1800	643	90	60 (*S*)	120
1021	H	CO_2Me	CH_2CO_2Me	[Rh(COD)**155c**]BF_4	4.1	DCM	r.t.	17	500	29.4	100	49.2 (*S*)	124b
1022	H	CO_2Me	CH_2CO_2Me	[Rh(COD)**156a**]BF_4	4.1	DCM	r.t.	17	500	29.4	100	99.3 (*S*)	124b
1023	H	CO_2Me	CH_2CO_2Me	[Rh(COD)**156a**]BF_4	5.1	DCM	r.t.	17	3000	176.5	100	99.8 (*S*)	124b
1024	H	CO_2Me	CH_2CO_2Me	[Rh(COD)**156a**]BF_4	4.1	DCM	r.t.	24	10000	416.7	100	99.6 (*S*)	124b
1025	H	CO_2Me	CH_2CO_2Me	[Rh(COD)**156b**]BF_4	4.1	DCM	r.t.	17	500	29.4	100	30.8 (*R*)	124b
1026	H	CO_2Me	CH_2CO_2Me	[Rh(COD)**156c**]BF_4	4.1	DCM	r.t.	17	500	29.4	100	1.8 (*R*)	124b
1027	H	CO_2H	Ph	[Rh(1,5-hexadiene)(+)-*trans*-**85**]Cl	50	–	50	–	–	–	–	0.7 (S) [a]	68a
1028	H	CO_2H	Ph	[Rh(1,5-hexadiene)d-*trans*-**86**]Cl	50	–	50	–	–	–	–	0	68a
1029	H	CO_2H	Ph	[Rh(COD)**88**]Cl	20.7	PhH : EtOH = 1 : 1	60	24	50 [c]	–	100 [d]	2	81
1030	H	CO_2H	Ph	[Rh(COD)**97a**]ClO_4	1	EtOH	25	1	50	50	100	2 (*S*)	90
1031	H	CO_2H	Ph	[Rh(COD)**97a**]ClO_4 + 0.1 Et_3N	1	EtOH	25	24	50	2	100	2 (*S*)	90
1032	H	CO_2H	Ph	[Rh(COD)**124**]BF_4	1	THF	25	1	100	100	100	27 (*R*)	103

Table 27.5 (continued)

Entry	Substrate			Catalyst	Conditions				TON	TOF [h^{-1}]	Conv. [%]	ee [%]	Reference(s)
	R^1	R^2	R^3		$P[H_2]$ [bar]	Solvent	Temp. [°C]	Time [h]					
1033	H	CO_2H	Ph	[Rh(COD)**124**]Cl	20.4	PhH : EtOH = 1 : 1	60	24	100	4	100	2.1 (*R*)	103
1034	H	CO_2H	Ph	[Rh(COD)**125**]BF_4	1	THF	25	1	100	100	100	17 (*S*)	103
1035	H	CO_2H	Ph	[Rh(COD)**148**]BF_4	1	Acetone	r.t.	2	–	–	>90	2–10	114
1036	H	CO_2Me	Ph	[Rh(1,5-hexadiene)(+)-*trans*-**85**]Cl	50	–	50	–	–	–	–	4.5 (*S*) [a)]	68a
1037	H	CO_2Me	Ph	[Rh(1,5-hexadiene)d-*trans*-**86**]Cl	50	–	50	–	–	–	–	20 (*S*) [a)]	68a
1038	H	CO_2Me	Ph	[Rh(COD)**88**]Cl	69	PhH : EtOH = 1 : 1	100	48	50 [c)]	–	[d)]	1.0	81
1039	H	CO_2Me	Ph	[Rh(COD)**98a**]BF_4	1	MeOH	25	9 [f)]	50	6	50	64 (*S*)	26
1040	H	CO_2Me	Ph	[Rh(COD)**98a**]BF_4	50	MeOH	25	–	100 [b)]			64 (*S*)	26
1041	H	CO_2Me	Ph	[Rh(COD)**124**]BF_4	1	THF	25	1	100	100	100	12 (*R*)	103
1042	H	CO_2Me	Ph	[Rh(COD)**124**]Cl	68	PhH : EtOH = 1 : 1	100	48	100	2	100	0	103
1043	H	CO_2Me	Ph	[Rh(COD)**125**]BF_4	1	THF	25	1	100	100	100	10 (*S*)	103
1044	Ph	CO_2H	Me	[Rh(COD)**88**]Cl	20.7	PhH : EtOH = 1 : 1	60	24	50 [c)]	–	100 [d)]	14.3	81
1045	Ph	CO_2H	Me	[Rh(COD)**124**]BF_4	1	THF	25	1	100	100	100	54 (*R*)	103
1046	Ph	CO_2H	Me	[Rh(COD)**124**]Cl	20.4	PhH : EtOH = 1 : 1	60	24	100	4	100	7.1 (*R*)	103
1047	Ph	CO_2H	Me	[Rh(COD)**125**]BF_4	1	THF	25	1	100	100	100	48 (*S*)	103
1048	CO_2H	Me	Ph	[Rh(COD)**97a**]ClO_4	1	EtOH	25	24	50	2	100	5 (*S*)	90
1049	CO_2H	Me	Ph	[Rh(COD)**97a**]ClO_4 +0.1 Et_3N	1	EtOH	25	24	50	2	100	5 (*S*)	90
1050	CO_2H	Ph	Me	[Rh(COD)**97a**]ClO_4	1	EtOH	25	24	50	2	100	5 (*S*)	90
1051	CO_2H	Ph	Me	[Rh(COD)**97a**]ClO_4 +0.1 Et_3N	1	EtOH	25	24	50	2	100	17 (*S*)	90

1052	Ph	CO_2Me	Me	[Rh(COD)**88**]Cl	20.7	PhH : EtOH = 1 : 1	100	48	50 [c)]	–	[d)]	4.3	81
1053	Ph	CO_2Me	Me	[Rh(COD)**124**]Cl	68	PhH : EtOH = 1 : 1	100	48	100	2	100	2.3 (*R*)	103
1054	Ph	CO_2H	Ph	[Rh(COD)**88**]Cl	20.7	PhH : EtOH = 1 : 1	60	24	50 [c)]	–	[d)]	12.0	81
1055	Ph	CO_2Me	Ph	[Rh(COD)**88**]Cl	20.7	PhH : EtOH = 1 : 1	100	48	50 [c)]	–	[d)]	4.6	81
1056	CO_2H	Me	CO_2H	[Rh(COD)**97a**]ClO_4	1	EtOH	25	24	50	2	100	23 (*S*)	90
1057	CO_2H	Me	CO_2H	[Rh(COD)**111**]ClO_4	1	EtOH	25	24	50	2	100	7 (*S*)	90
1058	CO_2H	Me	CO_2H	[Rh(**128**)Cl]$_2$	56	MeOH	r.t.	17	100	6	100	24 (*S*) [a)]	106
1059	CO_2H	Me	CO_2H	[Rh(COD)**128**]Cl	56	PhH	75	17	100	5.9	100	24 (*S*)	106
1060	CO_2H	Me	CO_2H	[Rh(COD)**129**]Cl	56	PhH	75	–	–	–	0	0	106
1076	H	Ph	C_2H_5	[Rh(**129**)Cl]$_2$	50	MeOH	r.t.	15	140	9	100	37 (*R*) [a)]	106
1077	Ph	H	Me	[Rh(COD)**97a**]BF_4	1	MeOH	25	0.03	50	1667	50	96.6 (*S*)	91 b
1078	Ph	H	Me	[Rh(COD)**97c**]BF_4	1	MeOH	25	0.07	50	714	50	95.1 (*S*)	91 b
1079	Ph	Me	Me	[Rh(COD)**97a**]BF_4	1	MeOH	25	0.1	50	500	50	91.5 (*S*)	91 b
1080	Ph	Me	Me	[Rh(COD)**97c**]BF_4	1	MeOH	25	0.05	50	1000	50	94.8 (*S*)	91 b
1081	Ph	Et	Me	[Rh(COD)**97a**]BF_4	1	MeOH	25	0.1	50	500	50	90.6 (*S*)	91 b
1082	Ph	Et	Me	[Rh(COD)**97c**]BF_4	1	MeOH	25	0.05	50	1000	50	94.4 (*S*)	91 b
1083	Ph	Et	Me	[Rh(COD)**97a**]BF_4	1	MeOH	25	0.1	50	500	50	90.6 (*S*)	91 b
1084	Ph	Et	Me	[Rh(COD)**97c**]BF_4	1	MeOH	25	0.05	50	1000	50	94.4 (*S*)	91 b
1085	Ph	H	Ph	[Rh(COD)**97a**]BF_4	1	MeOH	25	0.03	50	1667	50	95.0 (*S*)	91 b
1086	Ph	H	Ph	[Rh(COD)**97c**]BF_4	1	MeOH	25	0.05	50	1000	50	93.7 (*S*)	91 b
1087	Ph	Me	Ph	[Rh(COD)**97a**]BF_4	1	MeOH	25	0.1	50	500	50	87.3 (*S*)	91 b
1088	Ph	Me	Ph	[Rh(COD)**97c**]BF_4	1	MeOH	25	0.05	50	1000	50	91.6 (*S*)	91 b
1089													
1090	3,4-$(MeO)_2$-C_6H_3	H	Me	[Rh(COD)**97a**]BF_4	1	MeOH	25	0.1	50	500	50	96.7 (*S*)	91 b
1091	3,4-$(MeO)_2$-C_6H_3	H	Me	[Rh(COD)**97c**]BF_4	1	MeOH	25	0.08	50	625	50	94.8 (*S*)	91 b
1092	3-MeO-4-AcO-C_6H_3	H	Me	[Rh(COD)**97a**]BF_4	1	MeOH	25	0.05	50	1000	50	91.6 (*S*)	91 b
1093	3-MeO-4-AcO-C_6H_3	H	Me	[Rh(COD)**97c**]BF_4	1	MeOH	25	0.15	50	333	50	95.2 (*S*)	91 b

Table 27.5 (continued)

Entry	Substrate			Catalyst	Conditions				TON	TOF [h^{-1}]	Conv. [%]	ee [%]	Reference(s)
	R^1	R^2	R^3		$P[H_2]$ [bar]	Solvent	Temp. [°C]	Time [h]					
1094	3,4-$(MeO)_2$-C_6H_3	H	Ph	[Rh(COD)**97a**]BF_4	1	MeOH	25	0.08	50	625	50	95.1 (*S*)	91 b
1095	3,4-$(MeO)_2$-C_6H_3	H	Ph	[Rh(COD)**97c**]BF_4	1	MeOH	25	0.07	50	714	50	92.0 (*S*)	91 b
1096	3-MeO-4-HO-C_6H_3	H	Ph	[Rh(COD)**97a**]BF_4	1	MeOH	25	0.07	50	714	50	96.9 (*S*)	91 b
1097	3-MeO-4-HO-C_6H_3	H	Ph	[Rh(COD)**97c**]BF_4	1	MeOH	25	0.07	50	714	50	94.1 (*S*)	91 b
1098	3,4-$(MeO)_2$-C_6H_3	Et	Me	[Rh(COD)**97a**]BF_4	1	MeOH	25	0.13	50	385	50	90.6 (*S*)	91 b
1099	3,4-$(MeO)_2$-C_6H_3	Et	Me	[Rh(COD)**97c**]BF_4	1	MeOH	25	0.08	50	625	50	95.2 (*S*)	91 b
1100	3,4-$(MeO)_2$-C_6H_3	Et	Ph	[Rh(COD)**97a**]BF_4	1	MeOH	25	0.17	50	294	50	88.9 (*S*)	91 b
1101	3,4-$(MeO)_2$-C_6H_3	Et	Ph	[Rh(COD)**97c**]BF_4	1	MeOH	25	0.13	50	385	50	90.5 (*S*)	91 b
1102	3-MeO-4-AcO-C_6H_3	Et	Ph	[Rh(COD)**97a**]BF_4	1	MeOH	25	0.08	50	625	50	87.2 (*S*)	91 b
1103	3-MeO-4-AcO-C_6H_3	Et	Ph	[Rh(COD)**97c**]BF_4	1	MeOH	25	0.08	50	625	50	90.5 (*S*)	91 b
1104	3,4-$(MeO)_2$-C_6H_3	*i*-Pr	Me	[Rh(COD)**97a**]BF_4	1	MeOH	25	0.37	50	135	50	91.3 (*S*)	91 b
1105	3,4-$(MeO)_2$-C_6H_3	*i*-Pr	Me	[Rh(COD)**97c**]BF_4	1	MeOH	25	0.18	50	278	50	94.7 (*S*)	91 b
1106	3,4-$(MeO)_2$-C_6H_3	*i*-Pr	Ph	[Rh(COD)**97a**]BF_4	1	MeOH	25	0.33	50	152	50	89.1 (*S*)	91 b
1107	3,4-$(MeO)_2$-C_6H_3	*i*-Pr	Ph	[Rh(COD)**97c**]BF_4	1	MeOH	25	0.23	50	217	50	92.7 (*S*)	91 b
1108	3,4-$(MeO)_2$-C_6H_3	Me	Me	[Rh(COD)**97a**]BF_4	1	MeOH	25	0.37	50	135	50	92.4 (*S*)	91 b
1109	3,4-$(MeO)_2$-C_6H_3	Me	Me	[Rh(COD)**97c**]BF_4	1	MeOH	25	0.2	50	250	50	95.7 (*S*)	91 b
1110	3-MeO-4-AcO-C_6H_3	Me	Me	[Rh(COD)**97a**]BF_4	1	MeOH	25	0.08	50	625	50	92.4 (*S*)	91 b
1111	3-MeO-4-AcO-C_6H_3	Me	Me	[Rh(COD)**97c**]BF_4	1	MeOH	25	0.05	50	1000	50	95.6 (*S*)	91 b
1112	3-M3O-4AcO-C_6H_3	Me	Me	[Rh(COD)**97a**]BF_4	1	MeOH	25	0.2	50	250	50	91.7 (*S*)	91 b
1113	3-M3O-4AcO-C_6H_3	Me	Me	[Rh(COD)**97c**]BF_4	1	MeOH	25	0.08	50	625	50	95.0 (*S*)	91 b
1114	3,4-$(MeO)_2C_6H_3$	Me	Ph	[Rh(COD)**97a**]BF_4	1	MeOH	25	0.13	50	385	50	87.7 (*S*)	91 b
1115	3,4-$(MeO)_2C_6H_3$	Me	Ph	[Rh(COD)**97c**]BF_4	1	MeOH	25	0.12	50	417	50	91.2 (*S*)	91 b

1116	3-MeO-4-AcO-C_6H_3	Me	Ph	[Rh(COD)**97a**]BF_4	1	MeOH	25	0.08	50	625	50	87.2 (*S*)	91 b
1117	3-MeO-4-AcO-C_6H_3	Me	Ph	[Rh(COD)**97c**]BF_4	1	MeOH	25	0.07	50	714	50	91.3 (*S*)	91 b
1118	3-MeO-4-HO-C_6H_3	Me	Ph	[Rh(COD)**97a**]BF_4	1	MeOH	25	0.18	50	278	50	89.0 (*S*)	91 b
1119	3-MeO-4-HO-C_6H_3	Me	Ph	[Rh(COD)**97c**]BF_4	1	MeOH	25	0.1	50	500	50	92.1 (*S*)	91 b

a) Optical yield.
b) Estimated by proton NMR spectra.
c) Substrate : catalyst ratio.
d) Crude reaction yields were determined by ^{1}H-NMR and found to be quantitative.
f) t/2 for half-life time.
g) Surfactants.
h) Reaction time in the second cycle using recovered aqueous phase containing the catalyst.
i) Value obtained from the second cycle.
j) Determined as its methyl ester.
k) Catalysis carried out with preformed catalyst.
l) Ligand : metal ratio = 2

Table 27.6 Enantiomeric hydrogenation of tetrasubstituted substrates using bisphosphinite ligands.

Entry	Substrate				Catalyst	Conditions				TON	TOF [h^{-1}]	Conv. [%]	ee [%]	Reference
	R^1	R^2	R^3	R^4		$P(H_2)$ [bar]	Solvent	Temp [°C]	Time [h]					
1	Me	Me	CO_2H	NHAc	[Rh(COD)**98a**]BF_4	1	MeOH	25	16.7 [a)]	50	3	50	26.3 (*S*)	91 f
2	Me	Me	CO_2H	NHAc	[Rh(COD)**98a**]BF_4	100	MeOH	25	1.2 [a)]	50	42.9	50	21 (*S*)	91 f
3	Me	Me	CO_2H	NHAc	[Rh(COD)**98b**]SbF_6	2–2.8	THF	r.t.	2–3	–	–	–	15.5	95 b
4	Me	Me	CO_2Me	NHAc	[Rh(COD)**98b**]SbF_6	2–2.8	Propylene carbonate	r.t.	2–3	–	–	–	28.4 (S)	95 b
5	Me	Me	CO_2Me	NHAc	[[Rh(COD)**98d**]SbF_6	2–2.8	THF	r.t.	2–3	–	–	–	7.8 (R)	95 b
6	Me	Me	CO_2Me	NHAc	[Rh(COD)**103a**]SbF_6	2–2.8	THF	r.t.	2–3	–	–	–	10.1 (R)	95 b

a) t/2 for half-life time.

The enantioselectivities were found to be relatively independent of the solvent used. In 1998, Zhang reported a bisphosphinite based on a rigid bis-cyclopentyl ring system (BICPO, **95**, **96**) which induced 45.7 to 95% ee in the hydrogenation of *α*-dehydroamino acid derivatives [85].

Carbohydrate-based ligands represent an interesting area in the field of asymmetric catalysis (Tables 27.5 and 27.6). Apart from their unique biological properties, carbohydrates are highly functionalized inexpensive chiral-scaffolds. Various ligands derived from sugars, including glucose, galactose, mannitol, xylose, and trehalose, were synthesized and their effectiveness in asymmetric hydrogenation was differentiated by modulation of the steric and electronic properties. Claver and Diéguez summarized the application of carbohydrates in asymmetric catalysis in a recent review [86]. Other reviews relevant to this field also provided excellent information on their characterization and application [87]. Among these ligands, bidentate phosphorus donors were widely used in the form of phosphines, phosphinites, phosphites, or other mixed donor ligands.

Cullen [88], Thompson [89], Descotes [90] and Selke [91] were the early contributors to the use of a carbohydrate backbone in the Rh-catalyzed asymmetric hydrogenation of *α*-dehydroamino acid derivatives. A wide variety of 2,3-diphenylphosphinite pyranoside ligands (Fig. 27.7) were synthesized in order to probe the enantiodiscrimination from the stereocenters of the backbone. Among these, the best system was found by Selke to be based on *β*-glucopyranoside 2,3-diphosphinite ligand (i.e., **98a**), which provided up to 96% ee in the hydrogenation of 2-acetamidocinnamic acid [26, 91c]. The company VEB-ISIS produced L-DOPA in the former German Democratic Republic for many years based on an asymmetric olefin hydrogenation step using Selke's Ph -GLUP ligand [92].

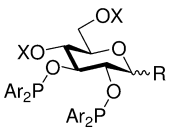

97a (Me-α-glup)	R = α–OMe, Ar = Ph, X-X = benzylidene
97b	R = α–OMe, Ar = Ph, X-X = ethylidene
97c	R = α–OMe, Ar = Ph, X = H
97d (Ph-α-glup)	R = α–OPh, Ar = Ph, X-X = benzylidene
98a (Ph-β-glup)	R = β–OPh, Ar = Ph, X-X = benzylidene
98b	R = β–OPh, Ar = 3,5-$(CH_3)_2C_6H_3$, X-X = benzylidene
98c	R = β–OPh, Ar = 3,5-$F_2C_6H_3$, X-X = benzylidene
98d	R = β–OPh, Ar = 3,5-$(CF_3)_2C_6H_3$, X-X=benzylidene
98e	R = β–OPh, Ar = 4-$CF_3C_6H_4$, X = H
98f	R = β–OPh, Ar = 4-$MeOC_6H_4$, X = H
98g	R = β–OPh, Ar = 3,5-$(Me_3Si)_2C_6H_3$, X = H
98h	R = β–OPh, Ar = 4-FC_6H_4, X = H
98i	R = β–OPh, Ar = Ph, X = H
98j	R = β–OPh, Ar = Ph, X-X = isopropylidene
99a	R = β–Ph, Ar = Ph, X = H
99b	R = β–Ph, Ar = Ph, X-X = isopropylidene
100a	R = β–OMe, Ar = Ph, X-X = isopropylidene
100b	R = β–OMe, Ar = Ph, X-X = benzylidene
101a	R = β–OBn, Ar = Ph, X-X = benzylidene
101b	R = β–*O*-2-Naphthyl, Ar = Ph, X-X = benzylidene
101c	R = β–*O*-(4-$MeOC_6H_4$), Ar = Ph, X-X = benzylidene
101d	R = β–*O*-(4-$NO_2C_6H_4$), Ar = Ph, X-X = benzylidene
101e	R = β–*O*-(2-$MeOC_6H_4$), Ar = Ph, X-X = benzylidene
101f	R = β–*O*-(2-$NO_2C_6H_4$), Ar = Ph, X-X = benzylidene

Fig. 27.7 2,3-Diphosphinite pyranoside ligands.

Šunjić [93] and Snatzke [94] systematically designed a series of pyranoside ligands **107–110** (see Fig. 27.10) for use in Rh-catalyzed hydrogenation. Ligand **108** proposed by Šunjić gave the highest ee-value (up to 90.4%). Thompson found poor results in the hydrogenation of (*Z*)-methyl *α*-acetamido-cinnamate (20–46% ee) using *β*-galactoside-based **113b** (see Fig. 27.10) [89]. Selke showed that *α*-galactose-based ligand **113a** induced higher enantioselectivity (86% ee) [91e].

In 1994, RajanBabu carried out systematic studies on the electronic and steric properties of the diphosphinite ligands (**102–106**) [95]. It was determined that, in the Rh-catalyzed hydrogenation of a wide variety of dehydroamino acid derivatives, high enantioselectivities (ee-values up to 99% in *S*-configuration) were obtained with **98b** and **98g** bearing electron-rich substituents, whereas poor selectivity was obtained using the electron-deficient ligands. These results raised the question of the preparation of products with the *R*-configuration. Preparing the other enantiomer of **98** from L-glucose would be prohibitively expensive. Nonetheless, RajanBabu developed *pseudo*-enantiomeric diphosphinite ligands based on the relationship of the 2,3-diphenylphosphinite and its corresponding 3,4-diphosphinite ligands (**98** and **103**; Fig. 27.8). Again, electron-rich phosphinites provided up to 99% ee of the products (dehydroamino acids) with the *R*-configuration. This might be the most convenient way to synthesize both enantiomers of aromatic and heteroaromatic alanines when using sugar-based diphosphinite ligands.

Two-phase catalysis has been established as a new field of study, and has achieved industrial-scale importance in olefin hydroformylation [96]. A significant advantage is the ease of separation of catalyst and product, which may have economic and environmental impact. Thus, removal of the 4,6-*O*-protecting group in 2,3-diphosphinite ligand **98** easily generated a water-soluble catalyst. The effectiveness of using Rh–complexes of diphosphinite **98a** in an aqueous system was proved successfully. Oehme reported that use of Ph-*β*-glup with free hydroxy groups (i.e., **98i** in Fig. 27.7) resulted in 84% ee with 100% conversion in the hydrogenation of (*Z*)-methyl *α*-acetamidocinnamate in water (95% ee in MeOH) [97]. The enantioselectivity was further improved (up to 97% ee) using a surfactant such as sodium dodecylsulfate (SDS) or Triton X-100. Similar results were obtained in the hydrogenation of methyl *α*-acetamidoacrylate. Selke reported more experimental results with **98i**. The enantioselectivities were similar to those obtained with protected 2,3-disphosphinite ligand **98** using metha-

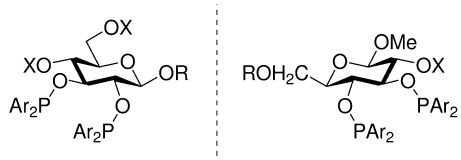

2,3-diphosphinite **98** 3,4-diphosphinite **103**, **104**, **112**

Fig. 27.8 *Pseudo*-enantiomeric diphosphinite pyranoside ligands.

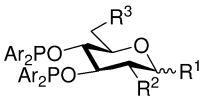

102a	R^1 = β–OMe, R^2 = NHAc, R^3 = OTBDMS, Ar = 3,5-$(CH_3)_2C_6H_3$
102b	R^1 = β–OMe, R^2 = NHAc, R^3 = OTBDMS, Ar = Ph
102c	R^1 = β–OMe, R^2 = NHAc, R^3 = OTBDMS, Ar = 3,5-$F_2C_6H_3$
102d	R^1 = β–OMe, R^2 = NHAc, R^3 = OTBDMS, Ar = 3,5-$(CF_3)_2C_6H_3$
102e	R^1 = β–OMe, R^2 = NHAc, R^3 = OTBDMS, Ar = 4-$CF_3C_6H_4$
102f	R^1 = β–OMe, R^2 = NHAc, R^3 = OTBDMS, Ar = 4-$MeOC_6H_4$
103a	R^1 = α–OMe, R^2 = R^3 = OBz, Ar = 3,5-$(CH_3)_2C_6H_3$
103b	R^1 = α–OMe, R^2 = R^3 = OBz, Ar = Ph
103c	R^1 = α–OMe, R^2 = R^3 = OBz, Ar = 3,5-$F_2C_6H_3$
103d	R^1 = α–OMe, R^2 = R^3 = OBz, Ar = 3,5-$(CF_3)_2C_6H_3$
103e	R^1 = α–OMe, R^2 = R^3 = OBz, Ar = 4-$CF_3C_6H_4$
103f	R^1 = α–OMe, R^2 = R^3 = OBz, Ar = 4-$MeOC_6H_4$
103g	R^1 = α–OMe, R^2 = R^3 = OBz, Ar = 3,5-$(Me_3Si)_2C_6H_3$
103h	R^1 = α–OMe, R^2 = R^3 = OBz, Ar = 4-FC_6H_4
104a	R^1 = α–OMe, R^2 = R^3 = OPiv, Ar = 3,5-$(CH_3)_2C_6H_3$
104b	R^1 = α–OMe, R^2 = R^3 = OPiv, Ar = Ph
104c	R^1 = α–OMe, R^2 = R^3 = OPiv, Ar = 3,5-$F_2C_6H_3$
104d	R^1 = α–OMe, R^2 = R^3 = OPiv, Ar = 3,5-$(CF_3)_2C_6H_3$
104e	R^1 = α–OMe, R^2 = R^3 = OPiv, Ar = 4-$CF_3C_6H_4$
104f	R^1 = α–OMe, R^2 = R^3 = OPiv, Ar = 4-$MeOC_6H_4$
104g	R^1 = α–OMe, R^2 = R^3 = OPiv, Ar = 3,5-$(Me_3Si)_2C_6H_3$
104h	R^1 = α–OMe, R^2 = R^3 = OPiv, Ar = 4-FC_6H_4
105a	R^1 = α–OMe, R^2 = H, R^3 = OTBDMS, Ar = 3,5-$(CH_3)_2C_6H_3$
105b	R^1 = α–OMe, R^2 = H, R^3 = OTBDMS, Ar = Ph
105c	R^1 = α–OMe, R^2 = H, R^3 = OTBDMS, Ar = 3,5-$F_2C_6H_3$
105d	R^1 = α–OMe, R^2 = H, R^3 = OTBDMS, Ar = 3,5-$(CF_3)_2C_6H_3$
105e	R^1 = α–OMe, R^2 = H, R^3 = OTBDMS, Ar = 4-$CF_3C_6H_4$
105f	R^1 = α–OMe, R^2 = H, R^3 = OTBDMS, Ar = 4-$MeOC_6H_4$
106a	R^1 = R^2 = H, R^3 = OTr, Ar = 3,5-$(CH_3)_2C_6H_3$
106b	R^1 = R^2 = H, R^3 = OTr, Ar = Ph
106c	R^1 = R^2 = H, R^3 = OTr, Ar = 3,5-$F_2C_6H_3$
106d	R^1 = R^2 = H, R^3 = OTr, Ar = 3,5-$(CF_3)_2C_6H_3$
106e	R^1 = R^2 = H, R^3 = OTr, Ar = 4-$CF_3C_6H_4$
106f	R^1 = R^2 = H, R^3 = OTr, Ar = 4-$MeOC_6H_4$

Fig. 27.9 Bisphosphinite–3,4-diphosphinite pyranoside ligands.

nol as solvent [91 a, b]. Attempts also were made by RajanBabu using modified D-salicin with pendant quaternary ammonium groups; however, the result in water (61% ee with **115 g** in the hydrogenation of methyl α-acetamidoacrylate) [98] was inferior to that obtained in organic solvents (up to 96% ee). Attempts were also made using mannoside-based 3,4-diphosphinite **112**, but only with moderate (72.2%) ee. Glucosamine-based 3,4-diphosphinite **102 a**, on the other hand, induced very high enantioselectivity (95–98.4%) in the Rh-catalyzed hydrogenation of various dehydroamino acids.

Recently, Miethchen modified diphosphinite **97 d** with a crown-ether linker in the 1,4-positions in order to study the effect on enantioselectivity in Rh-catalyzed asymmetric hydrogenation reactions [99]. Introduction of the crown ether in the 1,4-position of the carbohydrate allows the enantioselectivity to be tuned, based on a strong effect of the formation of cryptate species with alkali ions.

Unfortunately, the application of this new ligand **114** (Fig. 27.10) in the hydrogenation of various dehydroamino acid derivatives gave poorer results in comparison to the parent ligand **97d**.

In 1998, Uemura developed novel disaccharide diphosphinite ligands **119a** and **116a** (Fig. 27.10) from *α,α*-trehalose. Rh-catalyzed asymmetric hydrogenation of *α*-acetamidoacrylic and cinnamic acid derivatives afforded amino acids with up to 84% ee (*S*) (with ligand **119a**) and 72% ee (*R*) (with ligand **116a**), respectively [100]. The deprotected-hydroxyl diphosphinite ligand **119e** also enabled hydroge-

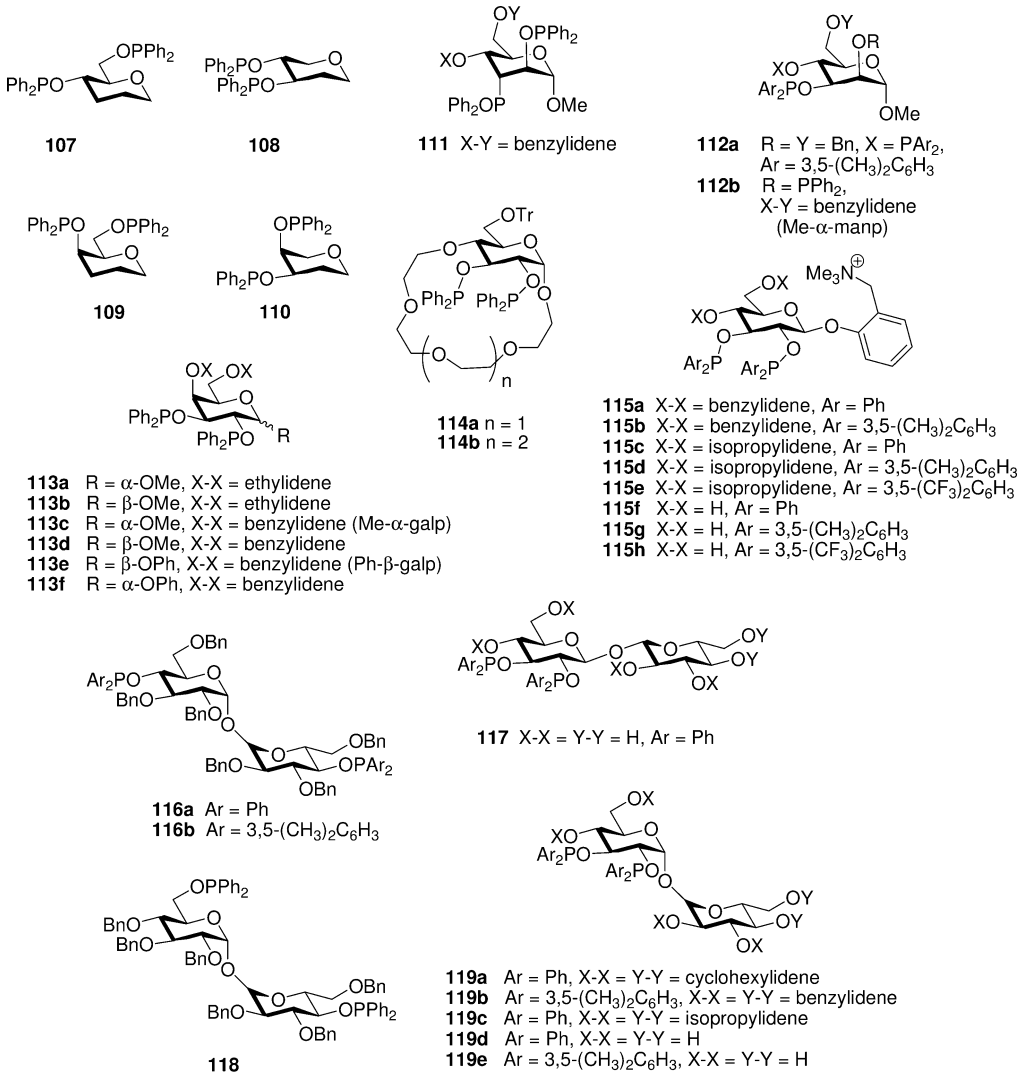

Fig. 27.10 Bisphosphinite–others pyranoside ligands.

nation of enamides and itaconic acid in aqueous solution with enhanced enantioselectivities (ee-values up to 99%) [101]. Similar reports by RajanBabu showed its application with moderate to good enantioselectivity [102].

In the light of the fruitful results obtained with the pyranoside-based bisphosphonites, RajanBabu also used a series of 3,4-diphosphinite ligands with a fructofuranoside backbone (i.e., **123**; Fig. 27.11) in the Rh-catalyzed hydrogenation of α-dehydroamino acids. However, the results were unsatisfactory (with only 49–57% ee) [95 b]. Similar results were found by Johnson with ligands based on α-D-glucofuranose (**124**) and α-L-idofuranose (**125**) with highest enantioselectivity (54% ee) obtained in the hydrogenation of α-methylcinnamic acid [103]. Diéguez and Ruiz described a facile synthesis of 3,4-diphosphinites **126** and **127** from D-(+)-xylose [104]. Application of these ligands in asymmetric hydrogenation showed that the enantioselectivity was strongly dependent on the absolute configuration of the C-3 stereocenter and the metal source. When ligand **126** was used in the rhodium-catalyzed hydrogenation of 2-acetamidoacrylic acid, the product was obtained with 76% ee. On the other hand, 78% ee was obtained using the Ir–**127** complex.

Díaz and Castillón reported new modular C_2 symmetric ligands prepared from D-glucosamine, D-glucitol and tartaric acid [105]. Ligand **122e** was found to induce the highest ee-value (93%), with full conversion in hydrogenation of methyl 2-acetamidoacrylate. In comparison to **ent-120**, the enantioselectivities of *N*-acetyl-L-alanine methyl ester induced by the catalysts based on **122** and **121** were strongly influenced by the stereocenters at positions 2 and 5 of the tetrahydrofuran ring and steric effect of the R groups. The configuration of the hydrogenation product (methyl 2-acetamidoacrylate and acetamidocinnamic acid ester) was influenced by the stereocenters at C-3 and C-4.

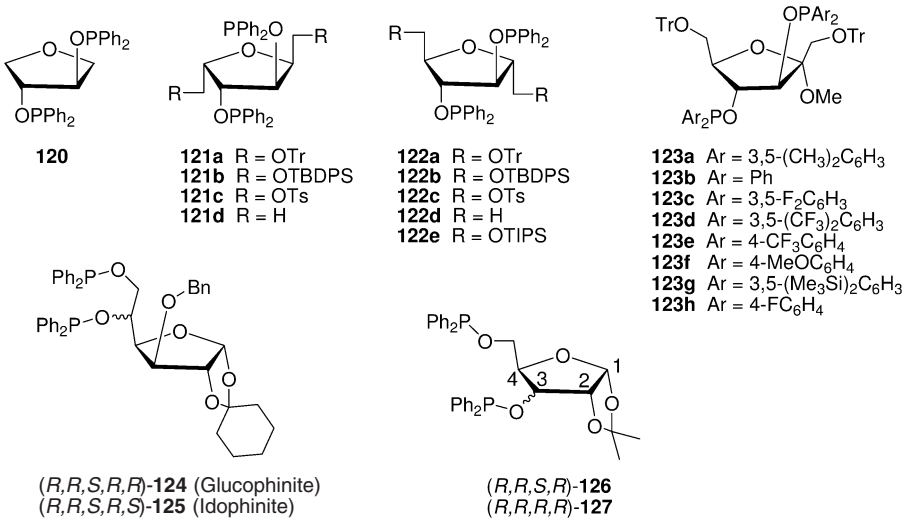

Fig. 27.11 Bisphosphinite–furanoside ligands.

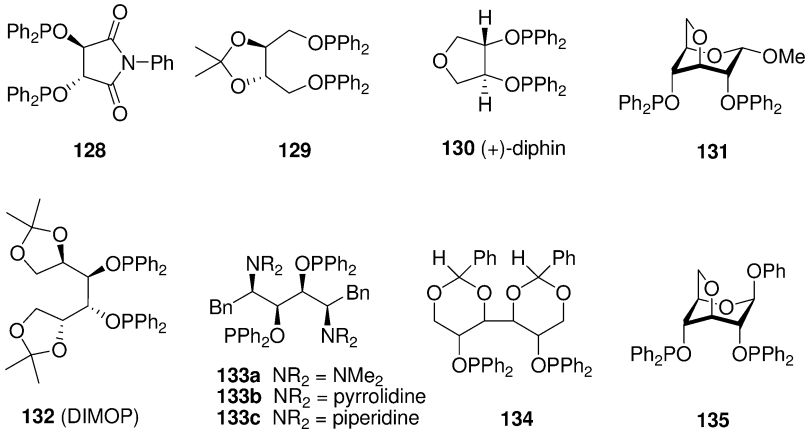

Fig. 27.12 Bisphosphinite–other carbohydrate-derived ligands.

Increasing the ligand rigidity provides one possibility of increasing enantioselectivity. Jackson and Lovel reported a ligand [(+)-Diphin **130**; Fig. 27.12] derived from natural L-tartaric acid [68 b], but use of this ligand containing a rigid tetrahydrofuran ring in the rhodium-catalyzed hydrogenation of α-acetamidocinnamic acid led to poor results (2% ee); in contrast, DIOP **129** induced 88% ee in the same reaction [68]. Bourson and Oliveros also developed a bisphosphonite ligand based on the *N*-phenylimide of natural L-tartaric acid **128** [106]. Unfortunately, the Rh-catalyzed hydrogenation of prochiral olefins gave unsatisfactory results with this ligand (1 to 44% ee). In 1999, we developed a new C_2 ligand (DIMOP **132**) from inexpensive D-mannitol, and found it to be highly effective in the Rh-catalyzed asymmetric hydrogenation of α-amidoacrylic acid and its derivatives [107]. For example, in the hydrogenation of 2-acetamidoacrylic acid, the product was obtained with full conversion in 15 min and 96.7% ee (SCR = 100). In all cases the desired products were found to have ee-values in excess of 90%. Lu and Jiang introduced three analogues based on D-mannitol and D-glucose, (**131**, **134**, and **135**). All ligands led to highly active catalysts with rhodium, but these were less enantioselective in the hydrogenation of α-acetamidocinnamic acid and its methyl ester (24.6–46.2% ee) [108]. Through structural modification of D-mannitol, Jiang and Zhang synthesized three bulky analogues (**133 a–133 c**), each of which induced moderate to excellent ee-values in the hydrogenation of dehydroamino acid derivatives (41–97% ee) [48].

27.6
Bisphosphonite Ligands (Two P–O Bonds)

In recent years, there is no doubt that BINOL is one of the most extensively studied motifs. Incorporating a chiral binol unit into the chiral or achiral backbone constitutes a straightforward way in which to generate new chiral ligands [109].

Both ligands **138** (ferrocene backbone; Fig. 27.13) and **136** (ethylene backbone) performed very well in the hydrogenation of itaconic acid dimethyl ester (97–99.5% ee) and 2-acetamido methyl acrylate (90–99.5% ee). Pringle and Orpen reported poor results in the hydrogenation of methyl 2-acetamido acrylate with the new modified ligand **140**, although the monodentate analogues performed surprisingly well [110]. An enhancement of enantioselectivity may be achieved by combining a chiral backbone with binol in a matching sense. Switching from an achiral backbone to chiral paracyclophane was successful, as reported by Zanotti-Gerosa [111]. Ligands **141 b** and **141 c** displayed a very strong matching/mismatching effect in the Rh-catalyzed hydrogenations of methyl 2-acetamido acrylate, inducing 99% ee and 0% ee, respectively, with the stereochemistry of the product being mainly controlled by the chirality of the backbone. Rh-**141 a** was a faster catalyst (TOF 2500 h^{-1}) than Rh-**141 b** (TOF 833 h^{-1}), albeit at the expense of a few percent lower ee. Bakos used (*S,S*)-pentane-2,3-diol as the chiral backbone leading to ligands **137 a** and **b** that induced moderate to good ee-values in the hydrogenation of dimethyl 2-methylsuccinate (59.7–88.5% ee) [112]. Vogt developed a new bisphosphonite based on 9,9-dimethylxanthene (**139**) and, by applying it to

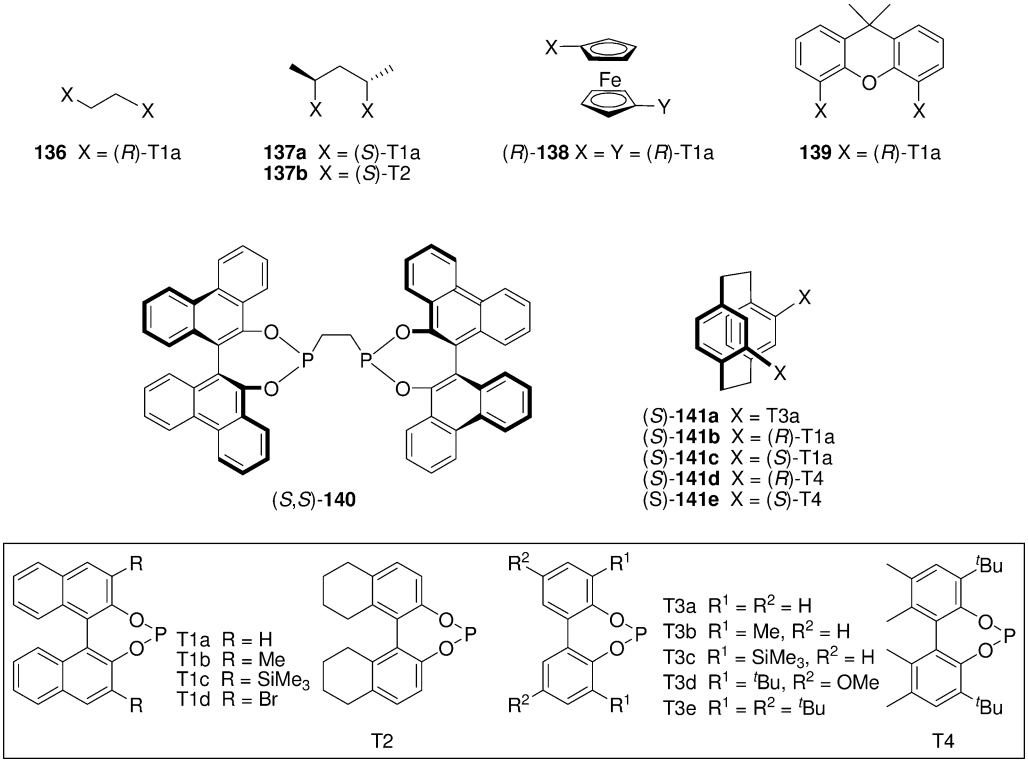

Fig. 27.13 Bisphosphonite ligands (two P–O bonds).

the rhodium-catalyzed hydrogenation of methyl (*Z*)-2-acetamidocinnamate, obtained 54% ee with full conversion [113].

27.7 Bisphosphite Ligands (Three P–O Bonds)

Wink reported the use of bisphosphite ligands in the asymmetric hydrogenation of enamides (2–10% ee) [114]. In 1998, Selke synthesized a series of analogues based on **98a**. Of these compounds, **147** (Fig. 27.14) was selected as ligand for the Rh-catalyzed hydrogenation of methyl (*Z*)-2-acetamidocinnamate, though it induced only low enantioselectivity (13% ee) [115].

In 1999, Reetz established a class of bidentate bisphosphite ligands **149** (Fig. 27.14) based on C_2-symmetric 1,4 : 3,6-dianhydro-D-mannite [116]. These ligands induced high enantioselectivity in the hydrogenation of dimethyl itaconate (98.2% ee) and methyl *N*-2-acetamidoacrylate (88.8% ee). The results also indicated a cooperative effect between the stereogenic centers of the ligand backbone and the axial chiral binaphthyl phosphite moieties, although the sense of enantioselectivity was predominantly controlled by the binaphthyl moieties (**149e** versus **149b** and **149c**). The use of biphenyl phosphite moieties led to ligands with better performance than those carrying binaphthyls, in spite of their easy epimerization.

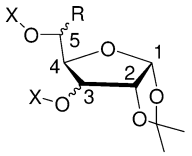

(*R*,*R*,*R*,*R*)-**142a** X = T3e, R = H
(*R*,*R*,*R*,*R*)-**142b** X = T3d, R = H
(*R*,*R*,*R*,*R*)-**142c** X = T3a, R = H
(*R*,*R*,*S*,*R*)-**143a** X = T3e, R = H
(*R*,*R*,*S*,*R*)-**143b** X = T3d, R = H
(*R*,*R*,*S*,*R*)-**143c** X = T3a, R = H
(*R*,*R*,*R*,*R*,*R*)-**144a** X = T3e, R = Me
(*R*,*R*,*R*,*R*,*R*)-**144b** X = T3d, R = Me
(*R*,*R*,*R*,*R*,*R*)-**144c** X = T3c, R = Me
(*R*,*R*,*R*,*R*,*R*)-**144d** X = (*S*)-T1a, R = Me
(*R*,*R*,*R*,*R*,*R*)-**144e** X = (*R*)-T1a, R = Me
(*R*,*R*,*R*,*R*,*R*)-**144f** X = (*S*)-T1c, R = Me
(*R*,*R*,*R*,*R*,*R*)-**144g** X = (*R*)-T1c, R = Me
(*R*,*R*,*S*,*R*,*R*)-**145a** X = T3e, R = Me
(*R*,*R*,*S*,*R*,*R*)-**145b** X = T3d, R = Me
(*R*,*R*,*S*,*R*,*R*)-**145c** X = T3c, R = Me
(*R*,*R*,*R*,*R*,*S*)-**146a** X = T3e, R = Me
(*R*,*R*,*R*,*R*,*S*)-**146b** X = T3d, R = Me
(*R*,*R*,*S*,*R*,*S*)-**146c** X = T3e, R = Me
(*R*,*R*,*S*,*R*,*S*)-**146d** X = T3d, R = Me

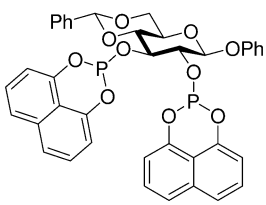

147

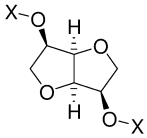

149a X = P(*O*-2-naphthyl)$_2$
149b X = (*S*)-T1a
149c X = (*R*)-T1a
149d X = T3a
149e X = T3b
149f X = T3e
149g X = T5

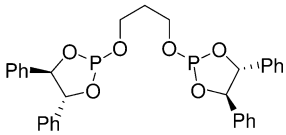

(*R*,*R*,*R*,*R*)-**148**

X–O–X

150a X = (*R*)-T1a
150b X = (*R*)-T1b
150c X = (*R*)-T1d
150d X = (*R*)-T2

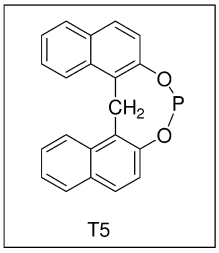

T5

Fig. 27.14 Bisphosphite ligands (three P–O bonds).

Recently, Claver and co-workers developed a series of highly effective modular C_1 diphosphite ligands **142–146** (Fig. 27.14) with a furanoside backbone [117]. Excellent enantioselectivities (ee-values up to >99%) and good activities were achieved in the Rh-catalyzed hydrogenation of dimethyl itaconate, methyl (*Z*)-2-acetamidocinnamate and methyl (*Z*)-2-acetamidoacrylate [117b]. Systematic variation of the stereocenters C-3 and C-5 at the ligand backbone showed that the enantiomeric excesses depended strongly on the absolute configuration of C-3 and only slightly on that of the stereocenter carbon C-5. Similar to Reetz's observation, the axially chiral binaphthyl substituent predominantly controlled the sense of the enantiodiscrimination. Bulky substituents at the *ortho*-positions of the achiral biaryl diphosphite moieties have a positive effect on enantioselectivity, especially with *o*-trimethylsilyl substituents in the biphenyl moieties of **144c**.

Börner reported the synthesis of pyrophosphites **149** with chiral binaphthyl substituents [118]. The results showed that the H_8-binaphthyl unit was the best for the Rh-catalyzed hydrogenation of methyl (*Z*)-2-acetamidocinnamate (48% ee) and dimethyl itaconate (70% ee).

27.8 Other Mixed-Donor Bidentate Ligands

In 1982, Yamashita reported the application of L-talopyranoside-based phosphine-phosphinite ligand **165** (Fig. 27.15), and found that it induced low enantioselectivity (4.7–13% ee) in the hydrogenation of *α*-acetamidocinnamic acid [119]. Reetz introduced the phosphine-phosphonite ligand (**151–153**), which led to moderate enantioselectivity (52–88% ee) in the Rh-catalyzed hydrogenation of dimethyl itaconate [120]. The binaphthyl unit remained an essential element in the system.

Claver and Ruiz reported excellent enantioselectivity (>99% ee) and good activities (TOF $>1200\,h^{-1}$) in the hydrogenation of methyl *N*-acetamidoacrylate and methyl *N*-acetamidocinnamate using phosphine–phosphite ligand **167** [121]. Again, ligands based on the biphenyl unit (especially with bulky *tert*-butyl groups in the *ortho* and *para positions*) showed a strong enantioinduction. Interestingly, **167** induced a higher activity and enantioselectivity than its corresponding diphosphine [122].

van Leeuwen and Claver designed a new class of chiral phosphine–phosphite ligands **159** and **160** with a stereogenic phosphine for the hydrogenation of methyl *N*-2-acetamidoacrylate and methyl *N*-2-acetamidocinnamate [123]. Up to 99% ee was achieved after systematically tuning the steric and electronic properties of the biaryl phosphite unit.

Pizzano and Suárez described a convenient preparation of a series of new chiral phosphine–phosphites based on the easy demethylation of *o*-anisyl phosphines [124]. Rh–**156a** complex was found to be the most effective catalyst for the hydrogenation of dimethyl itaconate (99.6% ee), whereas **155b** and **156a** induced >99% ee in the hydrogenation of methyl *N*-2-acetamidocinnamate. Reetz

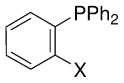

(*R*)-**151** X = (*R*)-T1a

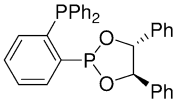

(*R*,*R*)-**152**

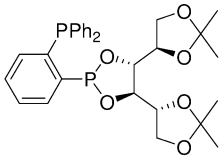

153

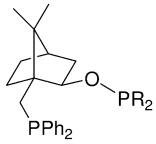

154a R = Ph
154b R = Mes
154c R = Cy

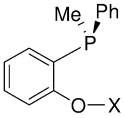

(*S*)-**155a** X = T3e
(*S*)-**155b** X = (*R*)-T4
(*S*)-**155c** X = (*S*)-T4

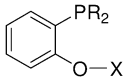

(*S*)-**156a** R = Ph, X = (*S*)-T4
(*S*)-**156b** R = Me, X = (*S*)-T4
(*S*)-**156c** R = ^{i}Pr, X = (*S*)-T4

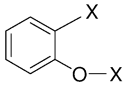

157 X = (*R*)-T1a

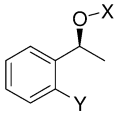

(*S*)-**158a** X = Y = (*S*)-T1a
(*S*)-**158b** X = (*R*)-T1a, Y = (*S*)-T1a
(*S*)-**158c** X = Y = (*R*)-T1a
(*S*)-**158d** X = (*S*)-T1a, Y = (*R*)-T1a

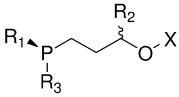

(*Sc*)-**159a** R^1, R^2, R^3 = Ph, X = T3e
(*Sc*)-**159b** R^1, R^3 = Ph, R^2 = Me, X = T3e
(*Sp*,*Sc*)-**159c** R^1 = 2-Anisyl, R^2, R^3 = Ph, X = T3e
(*Rp*,*Rc*)-**159d** R^1 = ^{t}Bu, R^2, R^3 = Ph, X = T3e
(*Rp*,*Sc*)-**159e** R^1 = ^{t}Bu, R^2, R^3 = Ph, X = T3e
(*Rp*,*racc*)-**159f** R^1 = ^{t}Bu, R^2, R^3 = Ph, X = T3e
(*Rp*,*Sc*)-**159g** R^1 = ^{t}Bu, R^2 = Me, R^3 = Ph, X = T3e
(*Sc*)-**159h** R^1, R^3 = ^{t}Bu, R^2 = Ph, X = T3e

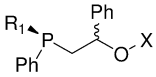

(*Rp*,*Sc*)-**160a** R^1 = ^{t}Bu, X = T3e
(*Rp*,*Rc*)-**160b** R^1 = ^{t}Bu, X = T3e

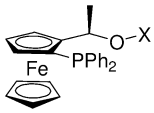

161 X = (*S*)-T1a

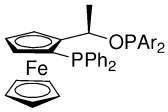

162a Ar = Ph
162b Ar = 3,5-$(CF_3)_2C_6H_3$

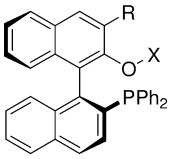

(*S*,*R*)-**163a** (*o*-BINAPHOS) X = (*R*)-T1a R = Ph
(*S*,*R*)-**163b** (BINAPHOS) X = (*R*)-T1a R = H

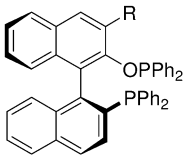

(*S*)-**164a** (*o*-BIPNITE) R = Ph
(*S*)-**164b** (BIPNITE) R = H

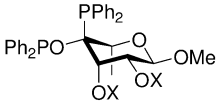

165 X-X = isopropylidene

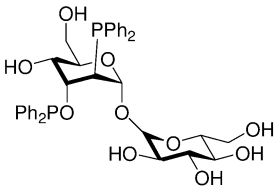

166

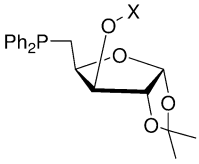

167a X = T3a
167b X = T3e
167c X = (*S*)-T1a
167d X = (*R*)-T1a

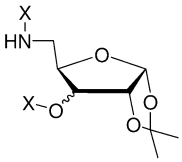

(*R*,*R*,*S*,*R*)-**168a** X=T3e
(*R*,*R*,*S*,*R*)-**168b** X=T3d
(*R*,*R*,*R*,*R*)-**168c** X=T3e
(*R*,*R*,*R*,*R*)-**168d** X=T3d

Fig. 27.15 Other mixed-donor bidentate ligands.

used (*S*)-1-(2-bromophenyl)ethanol together with binol to make ligands **158a–158d**. Use of these ligands in the Rh-catalyzed hydrogenation of itaconic acid dimethyl ester gave up to 79% ee [125].

The use of phosphite–phosphoramidite ligands **168a** and **b** provided up to 98% ee in the hydrogenation of methyl (*Z*)-*N*-2-acetylaminocinnamate, but the activities were rather low when compared to **167** or to the corresponding diphosphine ligand [126].

In contrast to the extensive studies on phosphine–phosphites, the corresponding phosphine–phosphinites are rarely exploited. Laschat introduced this design with a bicyclic chiral skeleton derived from (1*S*)-(+)-camphorsulfonic acid [127]. The Rh–complex based on dimesitylphosphinite **154b** was found to be the most reactive catalyst, and was used to produce methyl *N*-2-acetamidocinnamate, with 89% ee.

In 2004, we introduced new phosphine–phosphite ligands with a ferrocenyl scaffold derived from Ugi's amine [61]. Ligand **161** was found to exhibit good enantioselectivity in the hydrogenation of methyl *N*-2-acetamidocinnamate (85–89% ee). Ligand **162b** was also found to be highly effective in the hydrogenation of methyl *N*-2-acetamidocinnamate (95.3–99.6% ee) and *N*-acetyl-*α*-arylenamides (83–91% ee).

Zhang reported two new (*S*)-BINOL based ligands: phosphine–phosphite (*S,R*)-*o*-BINAPHOS **163** and phosphine–phosphinite (*S*)-*o*-BIPNITE **164** [128]. Applications of these ligands in the Rh-catalyzed hydrogenation of methyl *N*-2-acetamidocinnamate and methyl *N*-2-acetamidoacrylate induced very high enantioselectivities (>99% ee), and with a wide range of substrates.

Uemura developed a water-soluble phosphine–phosphinite ligand (derived from *α,α*-trehalose) (**166**) for the Rh-catalyzed hydrogenation of enamide derivatives; this induced only moderate enantioselectivity [129].

27.9 Ligands Containing Neutral S-Donors

Ligands containing thioethers are stereochemically very interesting, because upon coordination, the sulfur atom becomes a stereogenic center. In the absence of any stereocontrol, the *S*-center can be either (*R*)- or (*S*)-configured. However, if one imposes an efficient stereochemical control through judicious selection of the backbone chirality, it is possible to stabilize the configuration of the sulfur atom and thereby confer chiral information to the metal center. During the past few years, a number of reports have been disclosed describing attempts to harness this special property of thioethers in the asymmetric hydrogenation of a variety of prochiral olefins.

A number of dithioethers **169–173** (Fig. 27.16) based on the chiral skeleton of some well-known phosphines such as DIOP, Deguphos and BINAP, have been reported. The use of 1,4-dithioether ligands which lack contiguous chiral centers such as (+)-DiopsR_2 **169** [130], BINASR_2 **172** [131] and **173** [132] in the Ir- or

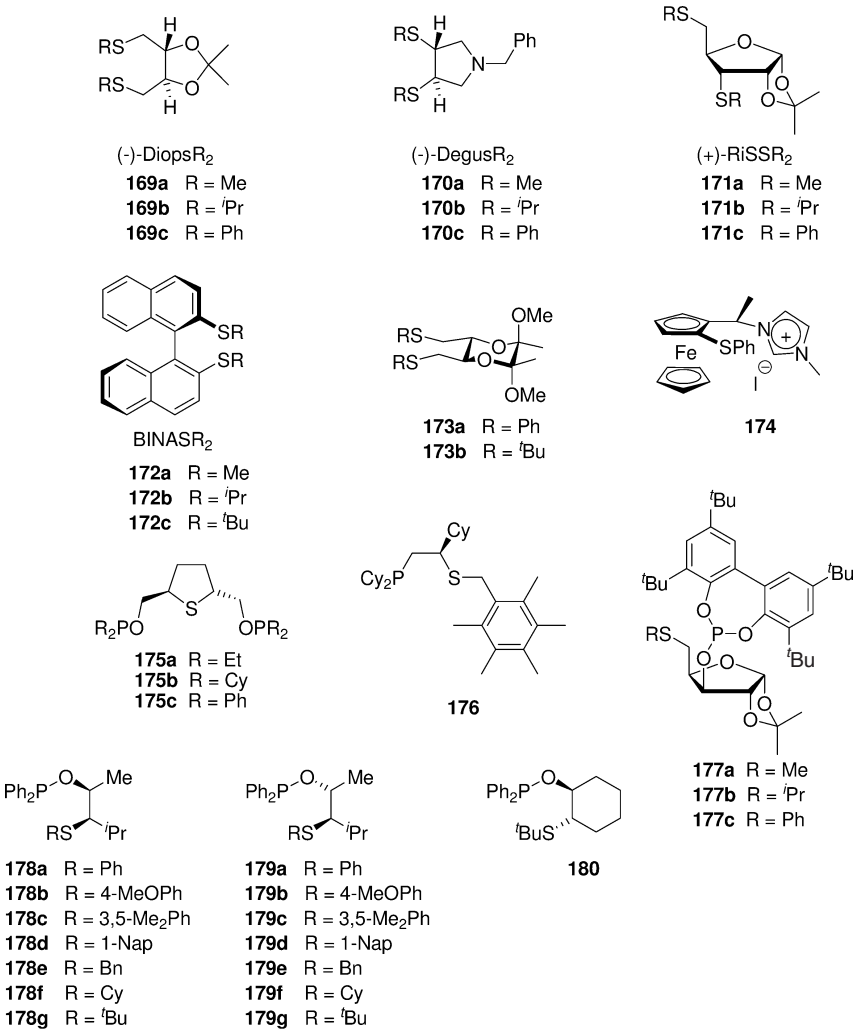

Fig. 27.16 Thioether-containing chiral ligands in asymmetric hydrogenation.

Rh-catalyzed asymmetric hydrogenation of itaconic acid and its derivatives, dehydroamino acid derivatives and enamides led to extremely poor to moderate enantioselectivities (Table 27.7). Although NMR spectroscopic studies of the iridium(I) cyclooctadiene complexes of **169** and **172** suggested that they possessed well-defined C_2-symmetry, implying that both sulfur atoms have the same configuration, their corresponding *cis*-dihydridoiridium(III) adducts appeared in the NMR spectrum as either a mixture of diastereomers or C_1-symmetric complexes, suggestive of the configurational lability of the ligated sulfur atom under remote chiral control in the octahedral complex, thus explaining the observed

Table 27.7 Enantiomeric hydrogenation using ligands containing a neutral S-donor.

Entry	Substrate			Catalyst	Conditions				TON	TOF [h^{-1}]	Conv. [%]	ee [%]	Reference
	R^1	R^2	R^3		$P(H_2)$ [bar]	Solvent	Temp [°C]	Time [h]					
1	H	Ph	NHAc	**179c** + $[Rh(COD)_2]SbF_6$	35.5	THF	r.t.	18	100	5.6	100	95	139
2	Me(*E*/*Z*)	Ph	NHAc	**173a** + $[Rh(NBD)_2]SbF_6$	3.1	CH_3OH	r.t.	24	100	4.0	95	21	132
3	Me(*E*/*Z*)	Ph	NHAc	**173b** + $[Rh(NBD)_2]SbF_6$	3.1	CH_3OH	r.t.	24	100	1.5	37	18	132
4	H	CO_2H	NHAc	**169c** + $[Ir(COD)_2]BF_4$	1	CH_2Cl_2	20	12	40	3.3	100	10	130
5	Me	CO_2Me	NHAc	**179c** vs. **180** + $[Rh(COD)_2]SbF_6$	7.9	THF	r.t.	18	100	5.6	100	97 vs. 98	139
6	Et	CO_2Me	NHAc	**179c** vs. **180** + $[Rh(COD)_2]SbF_6$	7.9	THF	r.t.	18	100	5.6	100	94 vs. 94	139
7	*i*Pr	CO_2Me	NHAc	**179c** vs. **180** + $[Rh(COD)_2]SbF_6$	7.9	THF	r.t.	18	100	5.6	100	89 vs. 36	139
8	Ph	CO_2H	NHAc	**169b** + $[Ir(COD)_2]BF_4$	1	CH_2Cl_2	20	16	40	2.4	96	37	130
9	Ph	CO_2H	NHAc	**170c** + $[Ir(COD)_2]BF_4$	1	CH_2Cl_2	20	2	40	20	100	27	133
10	Ph	CO_2Me	NHAc	**169c** + $[Ir(COD)_2]BF_4$	1	CH_2Cl_2	20	48	40	0.4	50	13	130
11	Ph	CO_2Me	NHAc	**172a–172c** + $[Ir(COD)_2]BF_4$	1	CH_3OH	25	0.5	100	–	–	–	131
12	Ph	CO_2Me	NHAc	**175b** + $[Rh(COD)_2]OTf$	4.1	CH_3OH	r.t.	O/N	50	–	100	55	134
13	Ph	CO_2Me	NHAc	**176** + $[Rh(COD)_2]OTf$	5.5	CH_3OH	r.t.	16	50	3.1	100	39	137
14	Ph	CO_2Me	NHAc	**178a** + $[Rh(COD)_2]SbF_6$	7.9	THF	r.t.	18	100	5.6	100	84	139
15	Ph	CO_2Me	NHAc	**179a** + $[Rh(COD)_2]SbF6$	7.9	THF	r.t.	18	100	5.6	100	95	139
16	Ph	CO_2Me	NHAc	**178c** + $[Rh(COD)_2]SbF_6$	7.9	THF	r.t.	18	100	5.6	100	81	139
17	Ph	CO_2Me	NHAc	**179c** + $[Rh(COD)_2]SbF_6$	7.9	THF	r.t.	18	100	5.6	100	97	139
18	Ph	CO_2Me	NHAc	**178f** + $[Rh(COD)_2]SbF_6$	7.9	THF	r.t.	18	100	5.6	100	84	139
19	Ph	CO_2Me	NHAc	**179f** + $[Rh(COD)_2]SbF_6$	7.9	THF	r.t.	18	100	5.6	NR		139
20	Ph	CO_2Me	NHAc	**178g** + $[Rh(COD)2]SbF_6$	7.9	THF	r.t.	18	100	5.6	100	82	139

Table 27.7 (continued)

Entry	Substrate			Catalyst	$P(H_2)$ [bar]	Conditions			TON	TOF [h^{-1}]	Conv. [%]	ee [%]	Reference
	R^1	R^2	R^3			Solvent	Temp [°C]	Time [h]					
21	Ph	CO_2Me	NHAc	**179g** + $[Rh(COD)_2]SbF_6$	7.9	THF	r.t.	18	100	5.6	20	68	139
22	Ph	CO_2Me	NHAc	**179c** vs. **180** + $[Rh(COD)_2]SbF_6$	7.9	THF	r.t.	18	100	5.6	100	97 vs. 97	139
23	3-Br-Ph	CO_2Me	NHAc	**179c** vs. **180** + $[Rh(COD)_2]SbF_6$	7.9	THF	r.t.	18	100	5.6	100	94 vs. 95	139
24	4-F,3-NO_2Ph	CO_2Me	NHAc	**179c** vs. **180** + $[Rh(COD)_2]SbF_6$	7.9	THF	r.t.	18	100	5.6	100	92 vs. 94	139
25	4-MeO-Ph	CO_2Me	NHAc	**179c** vs. **180** + $[Rh(COD)_2]SbF_6$	7.9	THF	r.t.	18	100	5.6	100	96 vs. 98	139
26	2-thienyl	CO_2Me	NHAc	**176** + $[Rh(COD)_2]OTf$	5.5	CH_3OH	r.t.	16	50	3.1	100	19	137
27	4-F,3-NO_2Ph	CO_2Me	NHAc	**176** + $[Rh(COD)_2]OTf$	5.5	CH_3OH	r.t.	16	50	3.1	100	51	137
28	H	CO_2H	CH_2CO_2H	**169b** + $[Ir(COD)_2]BF_4$	1	CH_2Cl_2	20	6	40	6.1	91	47	130
29	H	CO_2H	CH_2CO_2H	**170c** + $[Ir(COD_2]BF_4$	1	CH_2Cl_2	20	12	40	3.3	100	68	133
30	H	CO_2H	CH_2CO_2H	**171b** + $[Ir(COD_2]BF_4$	1	CH_2Cl_2	20	12	100	8.3	100	62	134
31	H	CO_2H	CH_2CO_2H	**172a172c** + $[Ir(COD_2]BF_4$	1	CH_3OH	25	0.5	100		b)	c)	131
32	H	CO_2H	CH_2CO_2H	**177b** + $[Ir(COD_2]BF_4$	1	N/A	40	12	50	4.2	100	51	138
33	H	CO_2Me	CH_2CO_2Me	**172a172c** + $[Ir(COD)_2]BF_4$	1	CH_3OH	25	0.5	100		b)	c)	131
34	H	CO_2Me	CH_2CO_2Me	**174** + $[Rh(COD_2]BF_4$	10.1	N/A	50	12	N/A		44	18	133

poor enantioselectivity [135, 136]. Slight improvements resulted when neighboring stereocenters were introduced, as in (–)-DegusR_2 **170** [133] and **171** [134] with S-substituents larger than a methyl group (Table 27.7, entries 29 and 30).

An unusual carbene-thioether hybrid ligand **174** was synthesized and applied in the rhodium-catalyzed asymmetric hydrogenation of dimethyl itaconate by Chung and co-workers; however, the selectivity and activity were low (Table 27.7, entry 34) [135].

Another major class of ligands containing a thioether functionality is the phosphorus–sulfur (P/S) mixed donor family. To date, only a few ligands of this type have been tested. The tridentate tetrahydrothiophene **175** flanked by two *trans-O*-methylene phosphinites was among the first P/S-ligands examined by Hauptman and co-workers, but only mediocre enantioselectivity was recorded in the hydrogenation of methyl α-acetamidoacrylate (Table 27.7, entry 12) [136]. Whilst the mode of coordination of **175** in the actual operating Rh-catalyst was unknown, the bidentate phosphine–thioethers **176**, prepared by the same team, also showed unsatisfactory results [137]. The xylofuranose-based phosphite–thioether **177** was also found to be inefficient (Table 27.7, entry 32) [138]. A breakthrough was unveiled by the Evans team [139], when Rh(I) complexes based on phosphinite–thioethers **178** and **179** were found to be highly efficient catalysts in the hydrogenation of a variety of enamide substrates. A side-by-side comparison revealed that skeleton **179** was generally more efficient than **178**, and sterically more encumbered *thio*-aryl substituents were generally superior than the less bulky ones or *thio*-alkyls. Remarkably, the meta-dialkyl effect, which was commonly noted in the phosphorus counterparts [140], also appeared to be operative here as **179** was found to be the optimal ligand (Table 27.7 entry 15). Moreover, the latter was found also to be effective in the enantioselective hydrogenation of β,β-disubstituted dehydroamino acids (Table 27.8, entries 1

Table 27.8 Enantiomeric hydrogenation of β,β-disubstituted dehydroamino acids and enamides.

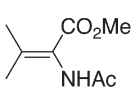

S1

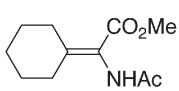

S2

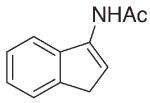

S3

Entry	Substrate			Catalyst]	Conditions				TON	TOF [h^{-1}]	Conv. [%]	ee [%]	Reference
	R^1	R^2	R^3		P(H_2 [bar]	Solvent	Temp [°C]	Time [h]					
1	S1			**179c** + [Rh(COD_2]SbF_6	7.9	THF	r.t.	18	100	5.6	100	93	139
2	S2			**179c** + [Rh(COD_2]SbF_6	1	THF	r.t.	18	100	5.6	100	95	139
3	S3			**179c** + [Rh(COD_2]SbF_6	7.9	THF	r.t.	18	100	5.6	100	92	139

and 2) and enamides (Table 27.7, entry 1; Table 27.8, entry 3). The more rigid ligand **180** also proved to be comparable to **179c**. In contrast to **178g** and **179g**, the *S*-*t*Bu group in **180** exerted a positive effect in the stereodifferentiating process and induced much better reactivity. The elegant investigations of Evans and co-workers recapitulated the fact that meticulous screening of the modifiable units – the *S*-substituents in this case – was the key to finding effective ligands [141, 142].

Acknowledgments

The authors thank the University Grants Committee Areas of Excellence Scheme in Hong Kong (AoE P/10-01) and the Hong Kong Polytechnic University Area of Strategic Development Fund for financial support of this study.

Abbreviations

AMPP	aminophosphine–phosphinite
DCE	dichloroethane
DCM	dichloromethane
IPA	isopropyl alcohol
r.t.	room temperature
$scCO_2$	supercritical CO_2
SCR	substrate:catalyst ratio
SDS	sodium dodecylsulfate
THF	tetrahydrofuran
TOF	turnover frequency
TON	turnover number

References

1 Agbossou, F., Suisse, I., *Coord. Chem. Rev.* **2003**, *242*, 145; Agbossou, F., Carpentier, J.-F., Hapiot, F., Suisse, I., *Coord. Chem. Rev.* **1998**, *178–180*, 1615.
1 (a) Cesarotti, E., Chiesa, A., D'Alfonso, G., *Tetrahedron Lett.*, **1982**, *23*, 2995; (b) Cesarotti, E., Chiesa, A., *J. Organomet. Chem.* **1983**, *251*, 79.
3 Pracejus, G., Pracejus, H., GDR Patent Appl. WPC07F/240486 (1982).
4 Döbler, C., Kreuzfeld, H.-J., Krause, H.W., Michalik, M., *Tetrahedron: Asymm.* **1993**, *4*, 1833.
5 Döbler, C., Kreuzfeld, H.-J., Michalik, M., Krause, H.W., *Tetrahedron: Asymm.* **1996**, *7*, 117.
6 Döbler, C., Kreuzfeld, H.-J., Krause, H.W. German Patent Appl. DE44344293 A1 (1996).
7 Kreuzfeld, H.-J., Döbler, C., Schmidt, U., Krause, H.W., *Chirality* **1998**, *10*, 535.
8 Krause, H.W., Schmidt, U., Taudien, S., Costisella, B., Michalik, M., *J. Mol. Cat. A: Chemical* **1995**, *104*, 147.

9 Kreuzfeld, H.-J., Schmidt, U., Döbler, C., Krause, H.W., *Tetrahedron: Asymm.* **1996**, *7*, 1011.
10 Kreuzfeld, H.-J., Döbler, Ch., Krause, H.W., Facklam, C., *Tetrahedron: Asymm.* **1993**, *4*, 2047.
11 Taudien, S., Schinkowski, K., *Tetrahedron: Asymm.* **1993**, *4*, 73.
12 Schmidt, U., Fisher, C., Grassert, I., Kempe, R., Fröhlich, R., Drauz, K., Oehme, G., *Angew. Chem. Int. Ed.* **1998**, *37*, 2851.
13 Heller, D., Kadyrov, R., *Tetrahedron: Asymm.* **1996**, *7*, 3025.
14 Krause, H.W., Oehme, G., Michalik, M., Fisher, C., *Chirality* **1998**, *10*, 564.
15 Krause, H.W., Foken, H., Pracejus, H., *New. J. Chem.* **1989**, *13*, 615.
16 Oehme, G., Dwars, T., Schmidt, U., Fisher, C., Krause, H.W., Drauz, K. German Patent Appl. DE19801952 C1 (1999).
17 Kreuzfeld, H.-J., Döbler, C., *J. Mol. Cat. A: Chemical* **1998**, *136*, 105.
18 Lou, R.L., Mi, A.Q., Jiang, Y.H., Qin, Y., Li, Z., Fu, F.M., Chan, A.S.C. *Tetrahedron* **2000**, *56*, 5857.
19 Mi, A.Q., Lou, R.L., Jiang, Y.H., Deng, J.G., Qin, Y., Fu, F.M., Li, Z., Hu, W.H., Chan, A.S.C., *Synlett* **1998**, 847.
20 Burk, M., *J. Am. Chem. Soc.* **1991**, *113*, 8518.
21 Knowles, W.S., *J. Chem. Edu.* **1986**, *63*, 222.
22 Sawamura, M., Kuwano, R., Ito, Y., *J. Am. Chem. Soc.* **1995**, *117*, 8602.
23 Kagan, H.B., Dang, T.P., *J. Am. Chem. Soc.* **1972**, *94*, 6429.
24 Ojima, I., Yoda, N., *Tetrahedron Lett.* **1980**, *21*, 1051.
25 Hayashi, T., Kumada, M., *Acc. Chem. Res.* **1982**, *15*, 395.
26 Selke, R., Pracejus, H., *J. Mol. Cat.* **1986**, *37*, 213.
27 Chan, A.S.C., Jiang, Y.Z., Hu, W.H., Mi, A.Q., Yan, M., Pai, C.C., Sun, J., Lau, C.P., Lou, R.L., Deng, J.G., *J. Am. Chem. Soc.* **1997**, *119*, 9570.
28 Knowles, W.S., *Acc. Chem. Res.* **1983**, *16*, 106.
29 Spindler, F. Pittelkow, U., Blaser, H.U., *Chirality* **1991**, *3*, 370.
30 Xie, Y.O., Lou, R.L., Li, Z., Mi, A.G., Jiang, Y.Z., *Tetrahedron: Asymm.* **2000**, *11*, 1487.
31 Moulin, D., Darcel, C., Jugé S., *Tetrahedron: Asymm.* **1999**, *10*, 4729.
32 Karim, A., Mortreux, A., Petit, F., *J. Organomet. Chem.* **1986**, *317*, 93.
33 Yasuda, A., Toriumi, K., Ito, T., Souchi, T., Noyori, R., *J. Am. Chem. Soc.* **1980**, *102*, 7932; Miyashita, A., Takaya, H., Souchi, T., Noyori, R., *Tetrahedron* **1984**, *40*, 1245.
34 Broger, E.A., Burkart, W., Henning, M., Scalone, M., Schmid, R., *Tetrahedron: Asymm.* **1998**, *9*, 4043.
35 Meyer, H., *Pure Appl. Chem.* **1979**, *51*, 300.
36 Pracejus, G., Pracejus, H., *J. Mol. Cat.* **1984**, *24*, 227.
37 Döbler, C., Kreuzfeld, H.-J; Pracejus, H., *J. Organomet. Chem.* **1988**, *344*, 89.
38 Arias, L.A., Adkins, S., Nagel, C.J., Bach, R.D., *J. Org. Chem.*, **1983**, *48*, 888.
39 Li, X.S., Lou, R.L., Yeung, C.H., Chan, A.S.C., Wong, W.K., *Tetrahedron: Asymm.* **2000**, *11*, 2077.
40 Döbler, C., Schmidt, U., Krause, H.W., Kreuzfeld, H.-J; Michalik, M., *Tetrahedron: Asymm.* **1995**, *6*, 385.
41 Dubrovina, N.V., Tararov, V.I., Kadyrova, Z., Monsees, A., Börner, A., *Synthesis* **2004**, 2047.
42 Krause, H.W., Kreuzfeld, H.-J; Döbler, C., *Tetrahedron: Asymm.* **1992**, *3*, 555.
43 Fiorini, M., Giongo, G.M., Marcati, F., Marconi, W., *J. Mol. Catal.* **1975/76**, *1*, 451.
44 Pracejus, G., Pracejus, H., *Tetrahedron Lett.* **1977**, *28*, 3497.
45 (a) Fiorini, M., Marcati, F., Giongo, G.M., *J. Mol. Catal.* **1978**, *4*, 125; (b) Fiorini, M., Giongo, G.M., *J. Mol. Catal.* **1979**, *5*, 303; (c) Fiorini, M., Giongo, G.M., *J. Mol. Catal.* **1980**, *7*, 411.
46 Onuma, K.-I., Ito, T., Nakamura, A., *Tetrahedron Lett.* **1979**, *30*, 3163.
47 (a) Valentini, C., Cernia, E., Fiorini, M., Giongo, G.M., *J. Mol. Catal.* **1984**, *23*, 81; (b) Ait Ali, M., Allaoud, S., Karim, A., Roucoux, A., Mortreux, A., *Tetrahedron: Asymm.* **1995**, *6*, 369.

48 Zhang, A., Jiang, B., *Tetrahedron Lett.* **2001**, *42*, 1761.
49 Brenchley, G., Fedouloff, M., Merrifield, E., Wills, M., *Tetrahedron: Asymm.* **1996**, *7*, 2809.
50 Miyano, S., Nawa, M., Hashimoto, H., *Chem. Lett.* **1980**, 729.
51 (a) Zhang, F.-Y., Pai, C.-C., Chan, A. S. C., *J. Am. Chem. Soc.* **1998**, *120*, 5808; (b) Chan, A. S. C., Zhang, F.-Y., US Patent Appl. US5919981 (1999).
52 Zhang, F.-Y., Kwok, W. H., Chan, A. S. C., *Tetrahedron: Asymm.* **2001**, *12*, 2337.
53 Guo, R., Li, X., Wu, J., Kwok, W. H., Chen, J., Choi, M. C. K., Chan, A. S. C., *Tetrahedron Lett.* **2002**, *43*, 6803.
54 Guo, R., Ph. D. Thesis, The Hong Kong Polytechnic University, **2003**.
55 Lin, C. W., Lin, C.-C., Lam, L. F.-L., Au-Yeung, T. T.-L., Chan, A. S. C., *Tetrahedron Lett.* **2004**, *45*, 7379.
56 Chen, Y.-X., Li, Y.-M., Lam, K.-H., Chan, A. S. C., *Chin. J. Chem.* **2003**, *21*, 66.
57 Boaz, N. W., Debenham, S. D., Mackenzie, E. B., Large, S. E., *Org. Lett.* **2002**, *4*, 2421.
58 Boaz, N. W., Patent Appl. WO 0226750 (2002).
59 Maligres, P. E., Krska, S. W., Humphrey, G. R., *Org. Lett.* **2004**, *6*, 3147.
60 PPFA: (*R*)-1-[(*S*)-2-(diphenylphosphino)-ferrocenyl]-*N*,*N*-Dimethylethylamine; Ref.: Hayashi, T., Mise, T., Fukushima, M., Kagotani, M., Nagashima, N., Hamada, Y., Matsumoto, A., Kawakami, S., Konishi, M., Yamamoto, K., Kumada, M., *Bull. Chem. Soc. Jpn.* **1980**, *53*, 1138.
61 Jia, X., Li, X., Lam, W. S., Kok, S. H. L., Xu, L., Lu, G., Yeung, C. H., Chan, A.S.C., *Tetrahedron: Asymm.* **2004**, *15*, 2273.
62 Hu, X. -P., Zheng, Z., *Org. Lett.* **2004**, *6*, 3585.
63 Li, X., Jia, X., Xu, L., Kok, S. H. L., Yip, C. W., Chan, A. S. C., *Adv. Synth. Catal.* **2005**, *347*, 1904.
64 Gokel, G. W., Ugi, I. K., *J. Chem. Ed.* **1972**, *49*, 294.
65 Lam, W. S., Kok, S. H. L., Au-Yeung, T. T.-L., Wu, J., Cheung, H. Y., Lam, F.-L., Yeung, C. H., Chan, A. S. C., *Adv. Synth. Catal.* **2006**, *348*, 370.
66 Franci, G., Faraone, F., Leitner, W., *Angew. Chem. Int. Ed.* **2000**, *39*, 1428.
67 Tanaka, M., Ogata, I., *J. S. C. Chem. Commun.* **1975**, 735.
68 (a) Hayashi, T., Tanaka, M., Ogata, I., *Tetrahedron Lett.* **1977**, *3*, 295; (b) Jackson, W. R., Lovel, C. G., *Aust. J. Chem.* **1982**, *35*, 2069.
69 Lange, S., Brinkmann, A., Trautner, P., Woelk, K., Bargon, J., Leitner, W., *Chirality* **2000**, *12*, 450.
70 Ohta, T., Takaya, H., Noyori, R., *Inorg. Chem.* **1988**, *27*, 566.
71 Grubbs, R. H., DeVries, R. A., *Tetrahedron Lett.* **1977**, *18*, 1879.
72 (a) Zhang, X., Taketomi, T., Yoshizumi, T., Kumobayashi, H., Akutagawa, S., Mashima, K., Takaya, H., *J. Am. Chem. Soc.* **1993**, *115*, 3318; (b) Zhang, X., Uemura, T., Matsumura, K., Kumobayashi, H., Sayo, N., Takaya, H., *Synlett* **1994**, *1*, 501; (c) Uemura, T., Zhang, X., Matsumura, K., Sayo, N., Kumobayashi, H., Ohta, T., Nozaki, K., Takaya, H., *J. Org. Chem.* **1996**, *61*, 5510.
73 (a) Zhang, F.-Y., Chan, A. S. C., *Tetrahedron: Asymm.* **1997**, *8*, 3651; (b) Chan, A.S.C., Zhang, F.-Y., Yip, C.-W., *J. Am. Chem. Soc.* **1997**, *119*, 4080.
74 Liu, G.-B., Tsukinoki, T., Kanda, T., Mitoma, Y., Tashiro, M., *Tetrahedron Lett.* **1998**, *39*, 5991.
75 Zhang, F.-Y., Chan, A. S. C., *Tetrahedron: Asymm.* **1998**, *9*, 1179.
76 Wang, Y., Guo, H., Ding, K., *Tetrahedron: Asymm.* **2000**, *11*, 4153.
77 Au-Yeung, T. T.-L., Chan, S.S., Chan, A. S. C., *Adv. Synth. Catal.* **2003**, *345*, 537.
78 Gergely, I., Hegedüs, C., Szöllösy, Á., Monsees, A., Riermeier, T., Bakos, J., *Tetrahedron Lett.* **2003**, *44*, 9025.
79 Zhou, Y.-G; Zhang, X., *Chem. Commun.* **2002**, *10*, 1124.
80 Zhou, Y.-G., Tang, W., Wang, W.-B., Li, W., Zhang, X., *J. Am. Chem. Soc.* **2002**, *124*, 4952.
81 Johnson, T. H., Pretzer, D. K., Thomen, S., Chaffin, V. J. K., Rangarajan, G., *J. Org. Chem.* **1979**, *44*, 1878.
82 Fuerte, A., Igesias, M., Sánchez, F., *J. Organomet. Chem.* **1999**, *588*, 186.

83 Chan, A. S. C., Hu, W., Pai, C.-C., Lau, C.P., Jiang, Y., Mi, A., Yan, M., Sun, J., Lou, R. L., Deng, J., *J. Am. Chem. Soc.* **1998**, *120*, 9975.

84 Hu, W., Yan, M., Lau, C.-P., Yang, S. M., Chan, A. S. C., *Tetrahedron Lett.* **1999**, *40*, 973.

85 Zhu, G., Zhang, X., *J. Org. Chem.* **1998**, *63*, 3133.

86 (a) Diéguez, M., Pámies, O., Claver, C., *Chem. Rev.* **2004**, *104*, 3189; (b) Diéguez, M., Pámies, O., Ruiz, A., Díaz, Y., Castillón, S., Claver, C., *Coord. Chem. Rev.* **2004**, *248*, 2165.

87 (a) RajanBabu, T. V., *Chem. Rev.* **2003**, *103*, 2645; (b) Ohe, K., Yonehara, K., Uemura, S., *Yuki Gosei Kagaku Kyokaishi* **2001**, *59*, 185; (c) Liu, X., Wang, Y., Miao, Q., Jin, Z., *Youji Huaxue* **2001**, *21*, 191; (d) Gyurcsik, B., Nagy, L., *Coord. Chem. Rev.* **2000**, *203*, 81; (e) Steinborn, D., Junicke, H., *Chem. Rev.* **2000**, *100*, 4283; (f) Chen, M., Lu, S., *Fenzi Cuihua* **2000**, *14*, 441; (g) Ayers, T. A., RajanBabu, T. V., in: Gadamasetti, K. G. (Ed.), *Process Chemistry in the Pharmaceutical Industry*. Dekker: New York, 1999; pp. 327–345; (h) RajanBabu, T. V., Casalnuovo, A. L., *Pure Appl. Chem.* **1994**, *66*, 1535; (i) Blaser, H.-U., *Chem. Rev.* **1992**, *92*, 935.

88 Cullen, W. R., Sugi, Y., *Tetrahedron Lett.* **1978**, *19*, 1635.

89 Jackson, R., Thompson, D. J., *J. Organomet. Chem.* **1978**, *159*, C29–C31.

90 Sinou, D., Descotes, G., *React. Kinet. Catal. Lett.* **1980**, *14*, 463.

91 (a) Selke, R., Ohff, M., Riepe, A., *Tetrahedron* **1996**, *52*, 15079; (b) Selke, R., Facklam, C., Foken, H., Heller, D., *Tetrahedron: Asymm.* **1993**, *4*, 369; (c) Selke, R., Schwarze, M., Baudisch, H., Grassert, I., Michalik, M., Oehme, G., Stoll, N., Costisella, B., *J. Mol. Catal.* **1993**, 84, 223; (d) Selke, R., *J. Organomet. Chem.* **1989**, *370*, 241; (e) Selke, R., *J. Prakt. Chem.* **1987**, *329*, 717; (f) Selke, R., *React. Kinet. Catal. Lett.* **1979**, *10*, 135.

92 Vocke, W., Hänel, R., Flöther, F.-U., *Chem. Techn.*, **1987**, *39*, 123.

93 Habŭs, I., Raza, Z., Šunjić, V., *J. Mol. Catal.* **1987**, *42*, 173.

94 Snatzke, G., Raza, Z., Habŭs, I., Šunjić, V., *J. Mol. Catal.* **1988**, *182*, 179.

95 (a) RajanBabu, T. V., Ayers, T. A., Cassalnuovo, A. L., *J. Am. Chem. Soc.* **1994**, *116*, 4101; (b) RajanBabu, T. V., Ayers, T. A., Halliday, G. A., You, K. K., Calabrese, J. C., *J. Org. Chem.* **1997**, *62*, 6012.

96 (a) Haggin, J., *Chem. Eng. News* **1994**, *72*, 28; (b) Cornils, B., *Nachr. Chem. Tech. Lab.* **1994**, *42*, 1136; (c) Cornils, B., *Angew. Chem.* **1995**, *107*, 1709; *Angew. Chem. Int. Ed. Engl.* **1995**, *34*, 1575; (d) Wiebus, E., Cornils, B., *Chem. Ing. Tech.* **1994**, *66*, 916; (e) Cornils, B., Wiebus, E., *Chemtech* **1995**, 25; (f) Trzeciak, A. M., Ziolkowski, J.J., *Coord. Chem. Rev.* **1999**, 883; (g) Lindner, E., Schneller, T., Auer, F., Mayer, H. A., *Angew. Chem. Int. Ed.* **1999**, *38*, 2154; (h) Herrmann, W. A., Elison, M., Fischer, J., Koecher, C., German Patent Appl. DE4447067 (1995); (i) Hermann, W., Elison, M., Fischer, J., Koecher, C., Oefele, K., German Patent Appl. DE4447066 (1995).

97 Oehme, G., Paetzold, E., Selke, R., *J. Mol. Catal.* **1992**, *71*, L1–L5.

98 Yan, Y. Y., RajanBabu, T. V., *J. Org. Chem.* **2001**, *66*, 3277.

99 Faltin, F., Fehring, V., Kadyrov, R., Arrieta, A., Schareina, T., Selke, R., Miethchen, R., *Synthesis* **2001**, 638.

100 Yonehara, K., Hashizume, T., Ohe, K., Uemura, S., *Bull. Chem. Soc. Jpn.* **1998**, *71*, 1967.

101 Yonehara, K., Hashizume, T., Mori, K., Ohe, K., Uemura, S., *J. Org. Chem.* **1999**, *64*, 5593.

102 Shin, S., RajanBabu, T. V., *Org. Lett.* **1999**, *1*, 1229.

103 Johnson, T. H., Rangarajan, G., *J. Org. Chem.* **1980**, *45*, 62.

104 Guimet, E., Diéguez, M., Ruiz, A., Claver, C., *Tetrahedron: Asymm.* **2004**, *15*, 2247.

105 Aghmiz, M., Aghmiz, A., Díaz, Y., Masdeu-Bultó, A., Claver, C., Castillón, S., *J. Org. Chem.* **2004**, *69*, 7502.

106 Bourson, J., Oliveros, L., *J. Organomet. Chem.* **1982**, *229*, 77.

107 Chen, Y., Li, X., Tong, S.-K., Choi, M.C.K., Chan, A.S.C., *Tetrahedron Lett.* **1999**, *40*, 957.

108 Jiang, P., Lu, S.J., *Chin. Chem. Lett.* **2000**, *11*, 587.

109 Reetz, M.T., Gosberg, A., Goddard, R., Kyung, S.-H., *Chem. Commun.* **1998**, 2077.

110 Claver, C., Fernandez, E., Gillon, A., Heslop, K., Hyett, D.J., Martorell, A., Orpen, A.G., Pringle, P.G., *Chem. Commun.* **2000**, 961.

111 Zanotti-Gerosa, A., Malan, C., Herzberg, D., *Org. Lett.* **2001**, *3*, 3687.

112 Gergely, I., Hegedüs, C., Gulyás, H., Szöllösy, Á., Monsees, A., Riermeier, T., Bakos, J., *Tetrahedron: Asymm.* **2003**, *14*, 1087.

113 Vlugt, J.I., Paulusse, J.M.J., Zijp, E.J., Tijmensen, J.A., Mills, A.M., Spek, A.L., Claver, C., Vogt, D., *Eur. J. Inorg. Chem.* **2004**, *21*, 4193.

114 Wink, D.J., Kwok, T.J., Yee, A., *Inorg. Chem.* **1990**, *29*, 5006.

115 Kadyrov, R., Heller, D., Selke, R., *Tetrahedron: Asymm.* **1998**, *9*, 329.

116 Reetz, M.T., Neugebauer, T., *Angew. Chem. Int. Ed.* **1999**, *38*, 179.

117 (a) Diéguez, M., Ruiz, A., Claver, C., *Dalton Trans.* **2003**, 2957; (b) Diéguez, M., Ruiz, A., Claver, C., *J. Org. Chem.* **2002**, *67*, 3796; (c) Pámies, O., Net, G., Ruiz, A., Claver, C., *Tetrahedron: Asymm.* **2000**, *11*, 1097; (d) Pámies, O., Net, G., Ruiz, A., Claver, C., *Eur. J. Inorg. Chem.* **2000**, 1287.

118 Korostylev, A., Selent, D., Monsees, A., Borgmann, C., Börner, A., *Tetrahedron: Asymm.* **2003**, *14*, 1905.

119 Yamashita, M., Hiramatsu, K., Yamada, M., Suzuki, N., Inokawa, S., *Bull. Chem. Soc. Jpn.* **1982**, *55*, 2917.

120 Reetz, M.T., Gosberg, A., *Tetrahedron: Asymm.* **1999**, *10*, 2129.

121 (a) Pámies, O., Diéguez, M., Net, G., Ruiz, A., Claver, C., *Chem. Comm.* **2000**, 2383; (b) Pámies, O., Diéguez, M., Net, G., Ruiz, A., Claver, C., *J. Org. Chem.* **2001**, *66*, 8364.

122 (a) Pámies, O., Net, G., Ruiz, A., Claver, C., *Eur. J. Inorg. Chem.* **2000**, 2011; (b) Diéguez, M., Pámies, O., Ruiz, A., Castillón, S., Claver, C., *Tetrahedron: Asymm.* **2000**, *11*, 4701.

123 Deerenberg, S., Pámies, O., Diéguez, M., Claver, C., Kamar, P.C.J., van Leeuwen, P.W.N.M., *J. Org. Chem.* **2001**, *66*, 7626.

124 (a) Suárez, A., Méndez-Rojas, M.A., Pizzano, A., *Organometallics* **2002**, *21*, 4611; (b) Suárez, A., Pizzano, A., *Tetrahedron: Asymm.* **2001**, *12*, 2501.

125 Reetz, M.T., Maiwald, P., *C. R. Chimie* **2002**, *5*, 341.

126 Diéguez, M., Ruiz, A., Claver, C., *Chem. Commun.* **2001**, 2702.

127 Monsees, A., Laschat, S., *Synlett* **2002**, *6*, 1011.

128 Yan, Y., Chi, Y., Zhang, X., *Tetrahedron: Asymm.* **2004**, *15*, 2173.

129 Ohe, K., Morioka, K., Yonehara, K., Uemura, S., *Tetrahedron: Asymm.* **2002**, *13*, 2155.

130 Diéguez, M., Orejón, A., Masdeu-Bultó, A.M., Echarri, R., Castillón, S., Claver, C., Ruiz, A., *J. Chem. Soc., Dalton Trans.* **1997**, 4611.

131 Diéguez, M., Ruiz, A., Claver, C., Doro, F., Sanna, M.G., Gladiali, S., *Inorg. Chim. Acta* **2004**, *357*, 2957.

132 Li, W., Waldkirch, J.P., Zhang, X., *J. Org. Chem.* **2002**, *67*, 7618.

133 Diéguez, M., Ruiz, A., Claver, C., Pereira, M.M., Rocha Gonsalves, A.M.d'A., *J. Chem. Soc., Dalton Trans.* **1998**, 3517.

134 Pámies, O., Diéguez, M., Net, G., Ruiz, A., Claver, C., *J. Chem. Soc., Dalton Trans.* **1999**, 3439.

135 Seo, H., Park, H.-J., Kim, B.Y., Lee, J.H., Son, S.U., Chung, Y.K., *Organometallics* **2003**, *22*, 618.

136 Hauptman, E., Shapiro, R., Marshall, W., *Organometallics* **1998**, *17*, 4976.

137 Hauptman, E., Fagan, P.J., Marshall, W., *Organometallics* **1999**, *18*, 2061.

138 Pámies, O., Diéguez, M., Net, G., Ruiz, A., Claver, C., *Organometallics* **2000**, *19*, 1488.

139 Evans, D.A., Michael, F.E., Tedrow, J.S., Campos, K.R., *J. Am. Chem. Soc.* **2003**, *125*, 3534.

140 For examples, see Guo, R., Au-Yeung, T. T.-L., Wu, J., Choi, M. C. K., Chan, A. S. C., *Tetrahedron: Asymm.* **2002**, *13*, 2519 and references therein.

141 Kawabata, Y., Tanaka, M., Ogata, I., *Chem. Lett.* **1976**, 1213.

142 Berens, U., Fischer, C., Selke, R., *Tetrahedron: Asymm.* **1995**, *6*, 1105.

28
Enantioselective Alkene Hydrogenation: Monodentate Ligands

Michel van den Berg, Ben L. Feringa, and Adriaan J. Minnaard

28.1
Introduction

In 1968, Knowles et al. [1] and Horner et al. [2] independently reported the use of a chiral, enantiomerically enriched, monodentate phosphine ligand in the rhodium-catalyzed homogeneous hydrogenation of a prochiral alkene (Scheme 28.1). Although enantioselectivities were low, this demonstrated the transformation of Wilkinson's catalyst, $Rh(PPh_3)_3Cl$ [3] into an enantioselective homogeneous hydrogenation catalyst [4].

In order to enhance enantioselective induction by preventing rotation around the rhodium–phosphorus bond, Dang and Kagan developed a chelating bidentate phosphine; DIOP [5]. By using tartaric acid as a starting material from the chiral pool, and by situating the chirality in the backbone, and not on phosphorus, synthesis of the ligand was simplified. In addition, it was the first example of a C_2 symmetric ligand, designed in this way to minimize the number of diastereomeric rhodium–ligand–substrate complexes. This strategy proved to be very effective, being confirmed several years later by Knowles et al. in the dimerization of PAMP to DIPAMP, which raised the enantioselectivity in the hydrogenation of methyl 2-acetamido-cinnamate from 55% to 95% [6].

The trend to develop chiral ligands devoid of chirality on phosphorus simplified the synthesis and led to the preparation of literally hundreds of chiral bi-

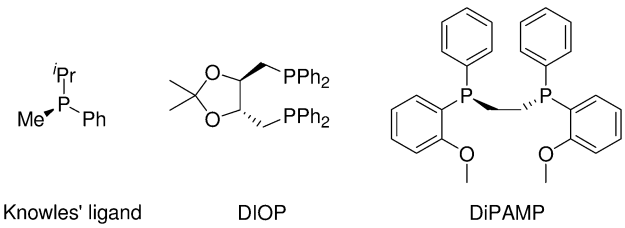

Scheme 28.1 Some of the first monodentate and bidentate ligands in enantioselective hydrogenation.

The Handbook of Homogeneous Hydrogenation.
Edited by J.G. de Vries and C.J. Elsevier
Copyright © 2007 WILEY-VCH Verlag GmbH & Co. KGaA, Weinheim
ISBN: 978-3-527-31161-3

sphosphines [7]. Together with the application of DIPAMP and Ph-β-Glup in commercial processes for L-DOPA [8], this established the use of bidentate phosphorus ligands as a *conditio sine qua non* for high ee-values in asymmetric hydrogenation. This was apparently underscored by the development of the very successful ligands BINAP, especially versatile with ruthenium, and DuPhos.

Knowles et al. had shown that the use of the P-chiral monodentate CAMP gave rise to an *e.e.* of 88% [9] in the formation of *N*-acyl-phenylalanine. However, due to the superior results obtained using bidentate ligands and the difficult preparation of P-chiral phosphines, this route was rarely followed for a long time [10, 11].

It thus came as a surprise that in the year 2000, three groups independently reported the use of three new classes of monodentate ligands (Scheme 28.2) [12]. The ligands induced remarkably high enantioselectivities, comparable to those obtained using the best bidentate phosphines, in the rhodium-catalyzed enantioselective alkene hydrogenation. All three being based on a BINOL backbone, and devoid of chirality on phosphorus, these monophosphonites [13], monophosphites [14] and monophosphoramidites [15] are very easy to prepare and are equipped with a variable alkyl, alkoxy, or amine functionality, respectively.

These reports announced the rapid development of a large variety of monodentate ligands for rhodium-catalyzed enantioselective hydrogenation. It was shown that the substrate scope for catalysts based on monodentate ligands is most probably at least as big as for their bidentate counterparts. Also, initial doubts about the activity and stability of the monodentate ligand-catalysts have been taken away. Several reports show that substrate : catalyst ratios (SCRs) of 10^3 or higher, essential for industrial application, are possible. In addition, reaction rates are in the studied cases comparable to those reached by catalysts based on state-of-the-art bidentate ligands [16].

The mechanism of the rhodium-catalyzed enantioselective hydrogenation has been thoroughly studied, and a wealth of information is now available. Logically, these studies have been performed using bidentate ligands. It will be very interesting to see whether catalytic cycles that have been proposed will also hold for catalysts equipped with monodentate ligands. Although a mechanistic study is still lacking [17], Zhou et al. performed a kinetic study of hydrogenations using the monodentate phosphoramidite SIPHOS [18]. As noticed earlier for MonoPhos,

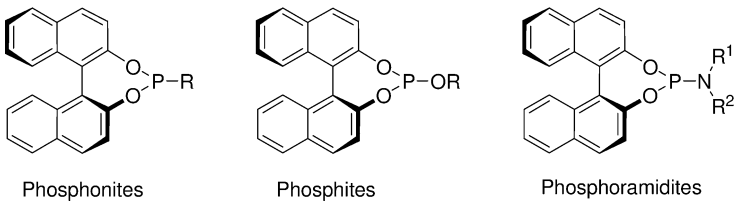

Scheme 28.2 New classes of monodentate ligands used in asymmetric hydrogenation. R = alkyl or aryl.

the enantioselectivity of the reactions was shown to be independent of the hydrogen pressure (e.g., hydrogen concentration) between 1 and 50 bar. This seems to be more general for monodentate ligands. In addition, the enantioselectivity decreases slightly with increasing temperature, and *vice versa*. Both observations disagree with the "major/minor" diastereomer part of the Halpern mechanism.

Both for MonoPhos and SIPHOS, a positive non-linear effect was observed with respect to the ee of the ligand. The observation that for several ligands a ligand:rhodium ratio of 1 : 1 gives a faster reaction than a L : Rh ratio of 2 : 1, with preservation of ee, tempted Zhou et al. to propose a mechanism with only one ligand on rhodium in the enantiodiscriminating step. This seems to contradict the recent results obtained using mixtures of ligands, a synergy that logically can only arise from a catalyst containing two different ligands. The application of these mixtures of monodentate ligands in catalysis, first shown by the group of Reetz and discussed in Chapter 36, in a number of cases affords higher ee-values than the corresponding pure ligands [19]. Very recent reports show that also the combination of chiral and achiral ligands can lead to unprecedented ee-values in enantioselective hydrogenation [20]. Combined with the modular construction of most monodentate ligands, and therefore the easy variation of their structure, this offers a tremendous opportunity for high throughput catalyst screening, as discussed in Chapter 36.

The present chapter provides a comprehensive overview of the literature relating to monodentate ligands in enantioselective hydrogenation until the end of 2004. Patent literature has not been covered. As the large majority of the ligands is available in both enantiomeric forms, the absolute configuration of the products has not been indicated. As most authors focus on the enantioselectivity of their catalysts, this will be reflected in this chapter. Whenever possible, attention will be given to turnover frequencies (TOF) and turnover numbers (TON). Parts of this chapter have been covered recently by a review of Jerphagnon, Renaud and Bruneau [21] and by De Vries and Ager [22].

28.2 Monodentate Phosphines

Although, in the past, most attention was paid to the use of bidentate phosphines, a number of monodentate phosphines has also been developed and applied in the rhodium-catalyzed hydrogenation of alkenes. These earlier-developed ligands are chiral on phosphorus (**1**) [9] and usually equipped with a phenyl and a methyl moiety (Scheme 28.3). The third substituent varies in size in order to maximize the chiral induction in the hydrogenation. The enantioselectivity in the hydrogenation of substrates such as the precursors of L-DOPA varies over a broad range, from 1% to 90% *e.e.* using ligands **1m** and **1l** (CAMP), respectively. The results of the other ligands fall between these values.

Ligands **2a**–**2d**, which are also chiral on phosphorus, and **3**, were used in the chemo- and enantioselective hydrogenation of (*E*)-3,7-dimethyl-2,6-dienoic acid

1a R^1 = Ph, R^2 = Me, R^3 = ^{n}Pr (mppp)
b R^1 = Ph, R^2 = Me, R^3 = ^{i}Pr
c R^1 = Ph, R^2 = Me, R^3 = ^{n}Bu
d R^1 = Ph, R^2 = Me, R^3 = ^{t}Bu
e R^1 = Ph, R^2 = Me, R^3 = 2-Me-4-Br-C_6H_3
f R^1 = Ph, R^2 = Me, R^3 = Bn (bmpp)
g R^1 = Ph, R^2 = Me, R^3 = Et
h R^1 = Ph, R^2 = Me, R^3 = *o*-anisyl (PAMP)
i R^1 = Ph, R^2 = Me, R^3 = *p*-anisyl
j R^1 = Ph, R^2 = Me, R^3 = 2-Et-C_6H_4
k R^1 = ^{n}Bu, R^2 = Me, R^3 = Bn
l R^1 = Cy, R^2 = Me, R^3 = *o*-anisyl (CAMP)
m R^1 = Me, R^2 = Ph, R^3 = *m*-anisyl
n R^1 = Me, R^2 = Ph, R^3 = Cy
o R^1 = Ph, R^2 = ^{i}Pr, R^3 = *o*-anisyl
p R^1 = Me, R^2 = ^{n}Pr, R^3 = *o*-anisyl
q R^1 = 2-Naphthyl, R^2 = Ph, R^3 = *p*-anisyl

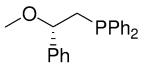

3

4a (1*R, 2R*) R^1 = (*l*)-Men, R^2 = Ph
b (1*S, 2R*) R^1 = (*l*)-Men, R^2 = Ph
c (1*S, 2S*) R^1 = (*l*)-Men, R^2 = Ph
d (1*R, 2S*) R^1 = (*l*)-Men, R^2 = Ph
e (1*R, 2R*) R^1 = ^{t}Bu, R^2 = Ph
f (1*S, 2R*) R^1 = ^{t}Bu, R^2 = Ph

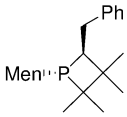

5

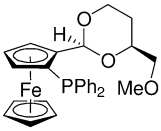

6

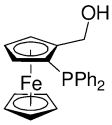

7

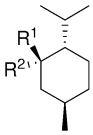

2a R^1 = (*S*)-PPh,Me, R^2 = H
b R^1 = (*R*)-PPh,Me, R^2 = H
c R^1 = H, R^2 = (*R*)-PPh,Me
d R^1 = H, R^2 = (*S*)-PPh,Me
e R^1 = PPh_2, R^2 = H (mdpp)
f R^1 = H, R^2 = PPh_2 (nmdpp)

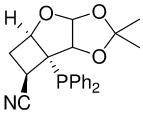

8

Scheme 28.3 Chiral monodentate phosphine ligands (men = menthyl, see **2**).

[23]. The *e.e.*-values were moderate, an improved result of 79% *e.e.* being obtained with nmdpp (**2f**) which is not chiral on phosphorus. The use of the other, non P-chiral, ligand mdpp (**2e**) gave low enantioselectivity. Ligand **2f** was also successfully used in the hydrogenation of 2-methylcinnamic and (*E*)-3-methylcinnamic acid [24].

Both ligands **4** [25] and **5** [26], in which phosphorus is part of a ring, were tested in the hydrogenation of *α*-acetamidocinnamic acid. Of these phosphirane ligands, only **4b** possessing a *trans*-configuration was able to induce reasonable enantioselectivities. Ferrocenyl-based monodentate phosphine **6**, used in a 4 : 1 ratio with $[Rh(COD)Cl]_2$, afforded an ee of 87% in this reaction, albeit with incomplete conversion [27]. Using ligand **7** under identical conditions, full conversion was reached, though with an *e.e.*-value of only 30%. Ligand **8**, derived from a carbohydrate, has also been applied with reasonable success [28].

Cyclic, C_2-symmetric monodentate phosphines with the phosphorus atom in a four-, five-, six-, or seven-membered ring have frequently been used in enantioselective hydrogenation (Scheme 28.4). The use of the six-membered oxaphosphiranes **9**, demonstrates that with these secondary phosphines high ee-values can be obtained in the hydrogenation of dehydroamino esters and methyl itaconate [29]. The atropisomeric ligands **10a–o** show a large effect of the size of the substituent on the enantioselectivity of the hydrogenation. Low ee-values in the hydrogenation of methyl *N*-acylcinnamate are obtained using ligand **10c** which

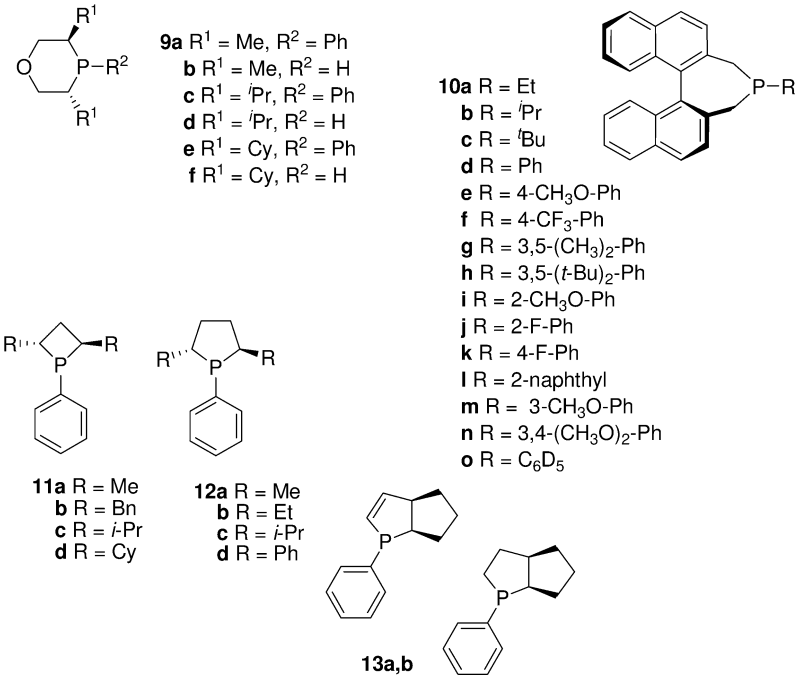

Scheme 28.4 Cyclic monodentate phosphine ligands.

contains a bulky *t*-Bu group [30]. When this group is replaced by a phenyl moiety, the *e.e.* obtained is 90%. After optimization by varying the substituent, excellent ee-values could be obtained [31]. Using these ligands, the first highly enantioselective ruthenium-catalyzed hydrogenation of β-ketoesters with monodentate ligands was also achieved [32].

As for ligands **11**, containing a four-membered ring [33, 34], ligands **12** which also contain a five-membered ring afford good enantioselectivities [35], especially **12d**. One could consider these ligands as monodentate analogues of DuPhos. The group of Fiaud [36] reported the existence of **12d** a year before the publication of the BINOL-based monodentate phosphonite, phosphite and phosphoramidite ligands.

Recently, two new P- and C-chiral monodentate phosphines **13** were reported. The ligands were applied in a number of transition metal-catalyzed reactions, though ee-values in the rhodium-catalyzed hydrogenation of *N*-acyl dehydrophenylalanine were only moderate [37].

28.3
Monodentate Phosphonites

Rhodium-catalyzed enantioselective hydrogenation using monodentate phosphonite ligands was first reported by the group of Pringle [13], followed by the group of Reetz (Scheme 28.5) [38]. The reported ligands are easily synthesized from an alkyl- or arylphosphorus dichloride and the appropriate BINOL or 9,9′-bisphenanthrol. The ligands are easily hydrolyzed in the presence of moisture, but are considerably more stable as their rhodium complexes [39].

Enantioselectivities obtained in the hydrogenation of methyl 2-acetamido-cinnamate, methyl 2-acetamido-acrylate and dimethyl itaconate are surprisingly high (up to 94% *e.e.*). The TOFs of the hydrogenation reactions using these monodentate phosphonites is fairly high, with most of the reactions with a SCR of 500 reaching TOFs of 250–300 mol $mol^{-1} \cdot h$ and full conversion at 1.5 bar. In addition, ligand **15d** has been studied in the rhodium- and iridium-catalyzed hydrogenation of a benzyl imine, but no chiral induction was observed [40].

The first – and until now only – case of ruthenium-catalyzed enantioselective ketone hydrogenation using monodentate ligands concerns phosphonite ligands [41]. In several cases, but especially with **15f**, excellent ee-values are obtained. The simple synthesis of these phosphonites makes them an interesting class of ligands for the synthesis of a ligand library for high-throughput experimentation (HTE). In addition, mixtures of ligands can be used (see Chapter 36).

28.4
Monodentate Phosphites

The chiral monodentate phosphites presented in Scheme 28.6 are easily prepared from a diol, phosphorus trichloride, and an alcohol. Usually, the diol is converted into the corresponding phosphoro chloridite, followed by reaction

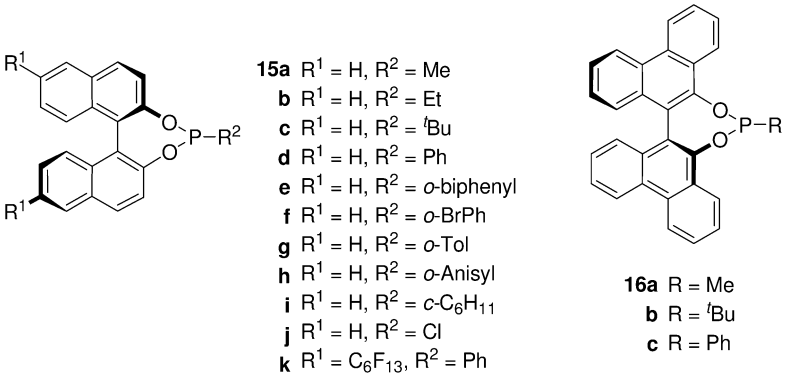

Scheme 28.5 Monodentate phosphonite ligands.

with the appropriate alcohol. The reversed approach – for example, reaction of a phosphoric dichloride with a diol – has also been used.

The application of monodentate phosphites as ligands in the rhodium-catalyzed enantioselective hydrogenation was first reported by the group of Reetz [14]. Initially, bidentate phosphites based on dianhydro-D-mannitol and two BINOL moieties were used, but it transpired that by substituting one of the BINOL moieties for methanol, leading to **17bh** and **17bi**, enantioselectivities in the rhodium-catalyzed hydrogenation were surprisingly high.

Based on a comparison of matched and mismatched ligands, it was shown that the BINOL moiety had the largest influence on the enantioselectivity of the reaction. Elaborating on this finding, a number of simple BINOL-based monodentate phosphite ligands was synthesized. The use of these ligands in the rhodium-catalyzed hydrogenation revealed their excellent behavior, resulting in high *e.e.*-values in the products. The group of Xiao reported monodentate phosphite ligands based on BINOL and L-menthol, **17bc** and **17bd** [42], while more recently Bakos et al. reported ligands derived from octahydro-BINOL, **18a** and **18b** [43] and the groups of Börner [44] and Helmchen [45] reported substituted BINOL-based phosphites. Large, helicene-like phosphites **19** have also been reported recently [46].

The initial report of Reetz describes the use of a Rh : L ratio of 1 : 1, although more recent experiments were conducted using a ratio of 1 : 2. Within this range, the enantioselectivities are unaffected. The combination of rhodium with ligands **17** used in the hydrogenation of methyl 2-acetamido cinnamate afforded enantioselectivities ranging from 2% to 99%. However, the majority of the results ranged from 75% to 99%. The use of ligands **17am** and **17an** gave the highest ee-values. Particularly striking was the influence of the BINOL moiety, which completely dominate the configuration of the product. The chiral alcohol present does not seem to have any influence. Similar to the use of monodentate phosphonites, the hydrogenations using monodentate phosphites are best performed in non-protic solvents. The rate of the reactions is high; even at a hydrogen pressure of 1.3 bar rates of 300 mol $mol^{-1} \cdot h$ were obtained. At an elevated pressure of 20 bar, TOFs up to 120 000 mol $mol^{-1} \cdot h$ were obtained in the hydrogenation of dimethyl itaconate with **18a**. This increase in pressure had only a marginal, if any, effect on the enantioselectivity. Recently, Reetz et al. reported the use of the "parent" phosphite ligand **17be** (a phosphoric acid diester) which led to *e.e.*-values of up to 85%. This was only slightly lower than the results obtained using ligand **17aa** [47]. The related phosphite **20**, based on TADDOL, was tested in an iridium-catalyzed imine hydrogenation but produced disappointing results [48].

Besides the phosphite ligands based on BINOL, phosphite ligands based on bisphenol are also used in rhodium-catalyzed hydrogenation. These ligands are shown in Scheme 28.7 and consist of a bisphenol with different substituents on the 3,3′,5,5′, and 6,6′-positions. The ligands without substituents on the 6,6′-positions are only fluxionally chiral. The use of readily available chiral alcohols (**21aa–21aj**) such as menthol in combination with bisphenol was thought to induce one of the bisphenol conformations in preponderant amounts [49]. The

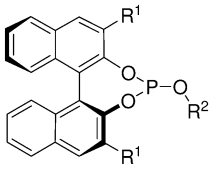

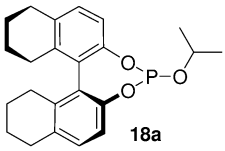

18a

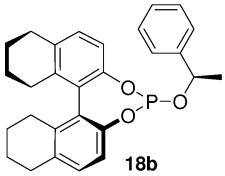

18b

17aa R^1 = H, R^2 = Me
ab R^1 = H, R^2 = Et
ac R^1 = H, R^2 = Ph
ad R^1 = H, R^2 = ^{i}Pr
ae R^1 = H, R^2 = *c*-C_5H_9
af R^1 = H, R^2 = *c*-C_6H_{11}
ag R^1 = H, R^2 = Bn
ah R^1 = H, R^2 = ^{t}Bu
ai R^1 = H, R^2 = ^{i}Bu [(*R*)-BINOL]
aj R^1 = H, R^2 = 9-Fluorenyl
ak R^1 = H, R^2 = $CH_2C(CH_3)_3$ [(*R*)-BINOL]
al R^1 = H, R^2 = $CH_2CH(C_2H_5)_2$ [(*R*)-BINOL]
am R^1 = H, R^2 = ^{i}Bu
an R^1 = H, R^2 = (*S*)-^{i}Bu [(*R*)-BINOL]
ao R^1 = H, R^2 = (*S*)-$CH_2CH(CH_3)C_2H_5$
ap R^1 = H, R^2 = (*S*)-$CH_2CH(CH_3)C_2H_5$ [(*R*)-BINOL]
aq R^1 = H, R^2 = (*R*)-$CH(CH_3)Ph$
ar R^1 = H, R^2 = (*S*)-$CH(CH_3)Ph$
as R^1 = H, R^2 = (*rac*)-$CH(CH_3)Ph$
at R^1 = H, R^2 = (*S*)-$CH(OCH_3)Ph$
au R^1 = H, R^2 = $CH_2CH_2N[CH(CH_3)_2]_2$
av R^1 = H, R^2 = $CH_2CH_2OCH_3$

17aw R^1 = H, R^2 = $CH_2CH_2OCH_3$ [(*R*)-BINOL]
ax R^1 = H, R^2 = CH_2CH_2Cl [(*R*)-BINOL]
ay R^1 = H, R^2 = CH_2CCl_3 [(*R*)-BINOL]
az R^1 = H, R^2 = 2-Br-Ph
ba R^1 = H, R^2 = 2,6-(CH_3)-Ph
bb R^1 = H, R^2 = 2,6-$(Ph)_2$-Ph
bc R^1 = H, R^2 = *L*-Menthyl
bd R^1 = H, R^2 = *L*-Menthyl [(*R*)-BINOL]
be R^1 = R^2 = H
bf R^1 = H, R^2 = $C(O)CH_3$ [(*R*)-BINOL]
bg R^1 = H, R^2 = C(O)Ph [(*R*)-BINOL]
bh R^1 = H, R^2 = see below [(*R*)-BINOL]
bi R^1 = H, R^2 = see below
bj R^1 = Br, R^2 = C(O)Ph [(*R*)-BINOL]
bk R^1 = Me, R^2 = C(O)Ph [(*R*)-BINOL]
bl R^1 = Ph, R^2 = C(O)Ph [(*R*)-BINOL]
bm R^1 = $SiMe_3$, R^2 = C(O)Ph [(*R*)-BINOL]

OR^2 in **17bh**, **17bi** =

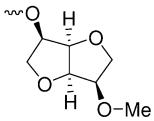

19a (*M*,*M*,*S*,*L*), R = *L*-Menthyl
b (*M*,*M*,*S*,*S*), R = 1-(*S*)-Phenylethyl
c (*M*,*M*,*S*,*R*), R = 1-(*R*)-Phenylethyl
d (*M*,*M*,*R*,*S*), R = 1-(*S*)-Phenylethyl
e (*M*,*M*,*R*,*R*), R = 1-(*R*)-Phenylethyl

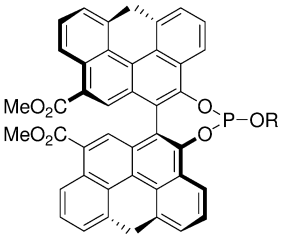

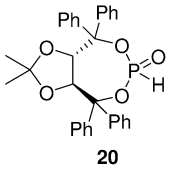

20

Scheme 28.6 Monodentate phosphite ligands derived from BINOL or related diols.

2 : 1 complexation of **21 ac** with rhodium resulted in a 5 : 1 diastereomeric mixture of $[Rh(\mathbf{21ac})_2COD]BF_4$. Within the two complexes, the bisphenol part of the ligands has the same conformation, and no complexes were found in which the two bisphenol parts have different conformations.

The axially chiral ligands **21 ak–21 ba** were recently reported by Ojima et al. [50]. In addition, the group of Driessen-Hölscher prepared a series of monodentate phosphites based on 5-Cl-6-MeO-bisphenol (**21 bb–21 bf**) [51]. Both series of ligands are successful. The use of phosphite ligand **22**, which has a chiral diol

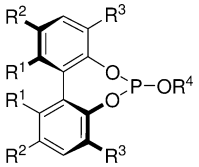

21aa-ad	$R^1 = R^2 = R^3 = H$, R^4 = see below
ae-ah	$R^1 = H$, $R^2 = R^3 = {}^t Bu$, R^4 = see below
ai	$R^1 = R^2 = R^3 = H$, R^4 = *L*-Menthyl
aj	$R^1 = H$, $R^2 = R^3 = {}^t Bu$, R^4 = *L*-Menthyl
ak	$R^1 = R^2 = Me$, $R^3 = H$, $R^4 = Ph$
al	$R^1 = R^2 = Me$, $R^3 = {}^t Bu$, $R^4 = Ph$
am	$R^1 = R^2 = Me$, $R^3 = H$, R^4 = 2-naphthyl
an	$R^1 = R^2 = Me$, $R^3 = {}^t Bu$, R^4 = 2-naphthyl
ao	$R^1 = R^2 = Me$, $R^3 = H$, R^4 = see below
ap	$R^1 = R^2 = Me$, $R^3 = {}^t Bu$, R^4 = see below
aq	$R^1 = R^2 = Me$, $R^3 = H$, R^4 = see below
ar	$R^1 = R^2 = R^3 = Me$, R^4 = see below
as	$R^1 = R^2 = Me$, $R^3 = Br$, R^4 = see below
at	$R^1 = R^2 = Me$, $R^3 = {}^t Bu$, R^4 = see below
au	$R^1 = R^2 = Me$, $R^3 = Ph$, R^4 = see below
av	$R^1 = R^2 = Me$, $R^3 = H$, R^4 = *L*-Menthyl
aw	$R^1 = R^2 = Me$, $R^3 = {}^t Bu$, R^4 = *L*-Menthyl
ax	$R^1 = R^2 = Me$, $R^3 = {}^t Bu$, R^4 = see below
ay	$R^1 = R^2 = Me$, $R^3 = H$, R^4 = *L*-Menthyl [(*R*)-biphenyl]
az	$R^1 = R^2 = Me$, $R^3 = {}^t Bu$, R^4 = *L*-Menthyl [(*R*)-biphenyl]
ba	$R^1 = R^2 = Me$, $R^3 = {}^t Bu$, R^4 = see below [(*R*)-biphenyl]
bb	$R^1 = OMe$, $R^2 = Cl$, $R^3 = H$, $R^4 = {}^i Pr$
bc	$R^1 = OMe$, $R^2 = Cl$, $R^3 = H$, $R^4 = Cy$
bd	$R^1 = OMe$, $R^2 = Cl$, $R^3 = H$, R^4 = (*R*)-Phenethyl
be	$R^1 = OMe$, $R^2 = Cl$, $R^3 = H$, $R^4 = Ph$
bf	$R^1 = OMe$, $R^2 = Cl$, $R^3 = H$, $R^4 = 2,6\text{-}(CH_3)_2\text{-}Ph$

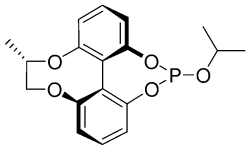

22

OR^4 in **21** =

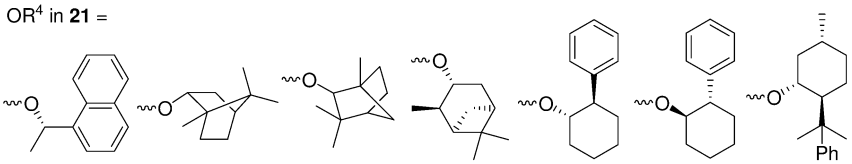

aa, ae **ab, af** **ac, ag** **ad, ah** **ao, ap** **aq - au** **ax, ba**

Scheme 28.7 Monodentate phosphite ligands derived from bisphenol.

bridging the 6,6′ position of the bisphenol backbone locking its conformation, was reported recently [52]. The use of **22** resulted in an excellent *e.e.* of 96% in the hydrogenation of dimethyl itaconic acid.

In general, the results obtained with monodentate ligands based on bisphenol are comparable to those obtained using ligands based on BINOL. Large substituents on the 3,3′-positions of the bisphenol results in lower ee-values. In some cases even the absolute configuration of the products is reversed. This is unfortunate, as bulky substituents on the 3,3′-positions increase the stability of the ligands towards hydrolysis, though the rate of the hydrogenation is not greatly influenced. The result of hydrogenations using these ligands is very solvent-dependent. The preferred solvents are dichloromethane and 1,2-dichloroethane, but when other solvents such as tetrahydrofuran, methanol, ethyl acetate or

chloroform are used, no enantioselectivity is observed. The factor determining the configuration of the product is, as in the case using BINOL-based ligands, the configuration of the biaryl moiety.

Rhodium-catalyzed hydrogenation of enamides has been successfully performed using monodentate phosphites **17**, with enantioselectivities of up to 95% being obtained [53]. The rate of hydrogenation is low; in order to reach full conversion with a SCR of 500, hydrogenation is performed at a pressure of 60 bar for 20 h. The use of ligand **17am** in the rhodium-catalyzed hydrogenation of aromatic enamides resulted in ee-values of up to 95%.

Monodentate phosphites have been used very successfully in the hydrogenation of enol-esters by the group of Reetz [54]. The use of ligands **17** which consist of a BINOL moiety and a simple alcohol gave only moderate results, from 21% to 65% *e.e.* Monodentate phosphite ligands derived from carbohydrates (**23** and **24**), however, afforded considerably higher enantioselectivities in the hydrogenation of enol esters derived from aliphatic alkynes (Scheme 28.8). Especially using an enol ester based on 2-furanoic acid, 90% ee was obtained. Performing the same reaction at –20 °C resulted in an ee of 94%. Thus far, the highest ee-value was obtained using (bidentate) Ru/PennPhos in the hydrogenation of the enol acetate based on 2-hexanone (75%) [55]. As for the *N*-acyl enamides, enol esters are hydrogenated at low rates. To reach full conversion, similar conditions were needed, with a SCR of 200 and a hydrogen pressure of 60 bar for 20 h.

The use of monodentate phosphite ligands in the hydrogenation of *β*-acylamino acrylates, affording derivatives of *β*-amino acids, has been demonstrated by Bruneau et al. [56]. Ligand **17bc** is clearly more effective in the hydrogenation of substrates with an *E*-configuration. In contrast, ligand **17bd**, a diastereomer of **17bc**, affords better results in the hydrogenation of substrates with the *Z*-configuration.

The carbohydrate ligands **23** and **24** were also applied in the hydrogenation of itaconate and enamides [57]. Also here, the configuration of the products is predominantly determined by the configuration of the BINOL moiety in the ligand. An extensive study, including the hydrogenation of *N*-acyl *β*-dehydroamino esters, using carbohydrate-derived monophosphites (also **25** and **26**) was recently reported by Zheng et al. [58].

Very recently, the group of Reetz published details of a monodentate phosphite ligand **27** (together with a large number of comparable phosphoramidite ligands) in which the BINOL unit bears a single *ortho*-substituent. This creates an additional stereocenter at phosphorus, which leads to mixtures of diastereomers. The ligand was found to be very successful in the hydrogenation of *N*-acyl dehydroalanine methyl ester [59].

As described for monodentate phosphonite ligands, monodentate phosphite ligands have also been used in a monodentate ligand combination approach.

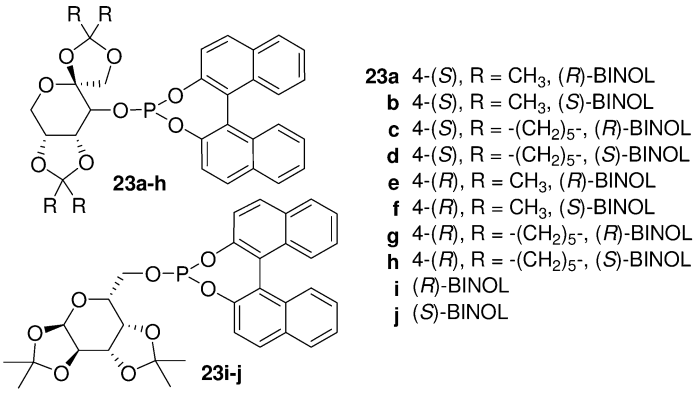

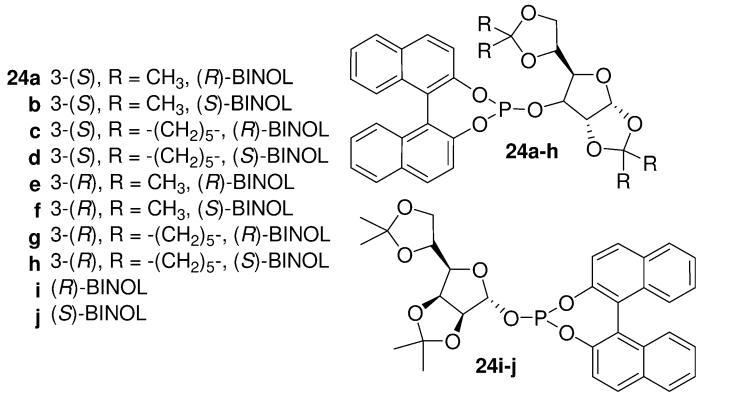

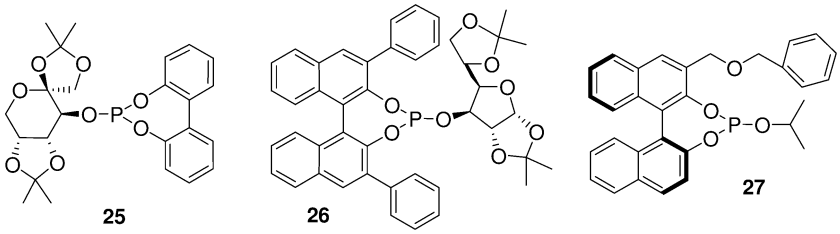

Scheme 28.8 Monodentate phosphite ligands based on carbohydrates.

28.5 Monodentate Phosphoramidites

The use of monodentate phosphoramidites in enantioselective hydrogenation was first reported in 2000, together with reports on the use of phosphites and phosphonites [15]. Phosphoramidites are prepared in a variety of ways, but the most common route is the treatment of a diol with PCl_3, followed by addition of an amine [60, 61]. MonoPhos (**29a**), the first reported phosphoramidite used as a ligand, is prepared from BINOL and HMPT in toluene [62]. Phosphoramidites, especially

those based on BINOL, have the distinct advantage of being resistant to water and oxygen (Scheme 28.9). Although sensitive to acidic conditions, this is hardly a handicap as their rhodium complexes are considerably less sensitive. This is revealed in the successful hydrogenation of dehydroamino acids. Together with their ease of preparation – mostly in one or two steps – this feature makes them very versatile, and has been employed successfully in HTE using ligands of phosphoramidites and in the use of ligand-mixtures (see Chapter 36).

The majority of the reported phosphoramidite ligands consist of BINOL and a diversity of readily available amines. Excellent enantioselectivities in the hydrogenation of α- and β-dehydroamino acids, itaconates and enamides [63, 64] have been reported. In a recent full report, the group of Minnaard, De Vries and Feringa noted that especially the BINOL-derived ligands containing a piperidine or

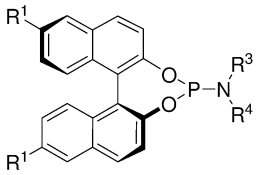

29a $R^1 = R^2 = H$, $R^3 = R^4 = Me$ (MonoPhos)
b $R^1 = R^2 = H$, $R^3 = R^4 = Et$
c $R^1 = R^2 = H$, $R^3 = R^4 = n$-Pr
d $R^1 = R^2 = H$, $R^3 = Me$, $R^4 = Bn$
e $R^1 = R^2 = H$, $R^3 = Me$, $R^4 = (R)$-$CH(CH_3)Ph$
f $R^1 = R^2 = H$, $R^3 = R^4 = (S)$-$CH(CH_3)Ph$
g $R^1 = R^2 = H$, $R^3 = H$, $R^4 = (R)$-$CH(CH_3)Ph$
h **ha - hl** $R^1 = R^2 = H$, R^3 - R^4 = see below
j $R^1 = Br$, $R^2 = H$, $R^3 = R^4 = Me$
k $R^1 = R^2 = R^3 = H$, R^4 = 4-vinylphenyl
l $R^1 = R^2 = R^3 = H$, R^4 = 8-quinoline
m $R^1 = R^2 = R^3 = H$, R^4 = 2-MeO-C_6H_4
n $R^1 = R^2 = H$, R^3 = 2-MeO-C_6H_4, R^4 = 4-vinylphenyl
o $R^1 = C_6F_{13}$, $R^2 = H$, $R^3 = Me$

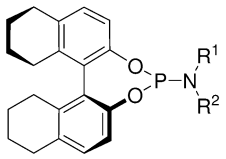

30a $R^1 = R^2 = Me$
b $R^1 = R^2 = Et$
c $R^1 = H$, $R^2 = (R)$-$CH(CH_3)Ph$
d $R^1 = Me$, $R^2 = (R)$-$CH(CH_3)Ph$
e **ea - ee** R^1 - R^2 = see below

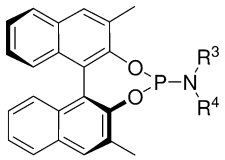

31a $R^1 = R^2 = Me$
b,c,d see below

NR^3R^4 in **29, 30** =

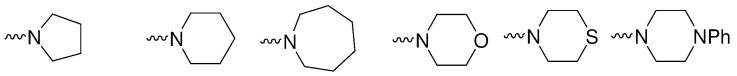

29ha **31b** | **29hb** (PipPhos) **30ea** **31c** | **29hc** **30eb** | **29hd** (MorfPhos) **30ec** **31d** | **29he** | **29hf** **30 ed**

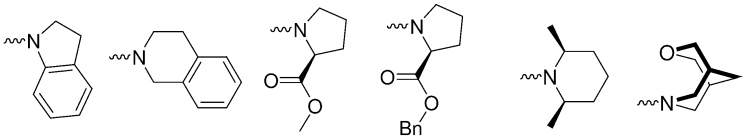

29hg | **29hh** **30ee** | **29hi** | **29hj** | **29hk** | **29hl**

Scheme 28.9 Monodentate phosphoramidites based on BINOL.

a morpholine substituent (PipPhos **29hb** and MorfPhos **29hd**, respectively) are the most privileged ligands [65]. Variations on this theme comprise the use of substituted BINOLs and octahydro-BINOL (H_8-BINOL) [17, 66]. In some cases these ligands afford higher ee-values. Very recently, it was shown that enol acetates and enol carbamates can also be hydrogenated, with excellent ee-values to the corresponding alcohol derivatives using PipPhos **29hb** [67]. Phosphoramidite ligand **29hl**, based on a combination of BINOL and oxa-bispidine, has been reported by the group of Waldmann [68].

Very recently, Reetz, Ma and Goddard reported phosphoramidites based on BINOL bearing a single *ortho*-substituent (Scheme 28.10) [69]. These ligands are also chiral on phosphorus, such that the synthesis results mostly in diastereomers which have to be separated. In several cases, however, one of the diastereomers was formed exclusively. Some of the ligands afford high ee-values in the hydrogenation of methyl *N*-acyl dehydroalanine and dimethyl itaconate.

Zhou et al. have reported extensively on the use of a spiro-biindanediol as the backbone in the ligands **35a–f** (Scheme 28.11, SIPHOS) [70]. Excellent results are obtained for a variety of substrates, and recently a full report has appeared on the use of these ligands [71]. Synthesis of the diol backbone requires a number of steps, including a resolution [72]. An additional and successful spiro-diol-derived phosphoramidite **39** has recently been disclosed by the group of Zhang [73].

Phosphoramidite ligands based on TADDOL (**36**) and on D-mannitol (**37**) [74] have also been used (Scheme 28.11). However, the enantioselectivities reported for the hydrogenation of α-dehydroamino acids and itaconates were generally lower compared to the ligands based on BINOL. A different strategy is the use of ligands **38a–g** based on the achiral diol catechol, and chiral amines [75].

The rate of hydrogenation of dehydroamino acids using $[Rh(MonoPhos)_2\text{-}COD]BF_4$ is not very high at 1 bar of hydrogen, though this can be overcome by applying higher pressure. Reactions performed with 5 bar reach TOFs of 200 to 600 mol $mol^{-1} \cdot h$. This increase in rate also allows for a reduction in the amount of catalyst needed to about 0.02–0.1 mol%. The increase in hydrogen pressure, up to 100 bar, does not affect the enantioselectivity; this is in contrast to the de-

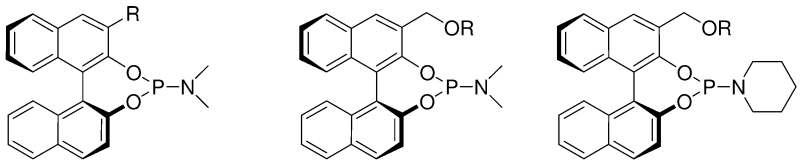

32a R = Me
b R = Ph
c R = SPh
d R = $SiMe_3$
e R = $SiPh_3$

33a R = C(O)Ph
b R = Me
c R = Bn

34a R = C(O)Ph
b R = Me
c R = Bn

Scheme 28.10 Monodentate phosphoramidites based on monosubstituted BINOL.

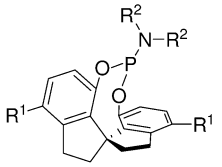

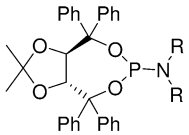

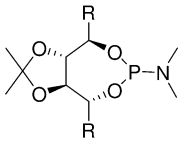

35a R^1 = H, R^2 = Me (SIPHOS)
b R^1 = H, R^2 = Et
c R^1 = H, R^2 = ^{i}Pr
d R^1 = H, R^2 = -$(CH_2)_4$-
e R^1 = Br, R^2 = Me
f R^1 = Ph, R^2 = Me
g R^1 = OMe, R^2 = Me

36a R = ^{i}Pr
b R = Bn

37a R = H
b R = Me
c R = Et
d R = ^{i}Bu
e R = Ph
f R = Me (*S*,*S*,*S*,*S*)
g R = Ph (*S*,*S*,*S*,*S*)

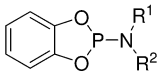

NR^1R^2 in **38g** =

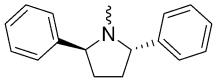

38a R^1 = (*S*)-$CH(CH_3)Ph$, R^2 = H
b R^1 = (*S*)-$CH(CH_3)Ph$, R^2 = Me
c R^1 = (*S*)-$CH(CH_3)Ph$, R^2 = Et
d R^1 = (*R*)-$CH(CH_3)Ph$, R^2 = ^{i}Pr
e R^1 = (*S*)-$CH(CH_3)Ph$, R^2 = Bn
f R^1 = (*S*)-$CH(CH_3)Ph$, R^2 = (*S*)-$CH(CH_3)Ph$
g R^1 - R^2 = see above

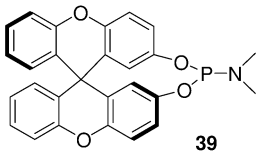

39

Scheme 28.11 Phosphoramidite ligands based on alternative backbones.

crease in *e.e.* which is seen upon increasing hydrogen pressure when using most bidentate ligands, and is a distinct advantage.

Initially, it was not clear whether monodentate ligands could, apart from enantioselectivity, compete with the established bidentate ligands. Activity and stability of the catalyst are also important parameters. Using MonoPhos **29a** and related phosphoramidites, it has been shown that monodentate ligands can (at least in a number of cases) keep up with the best bidentate ligands. Itaconic acid has been hydrogenated using $[Rh(MonoPhos)_2COD]BF_4$ at a SCR of 10 000 on 100-g scale. This reaction gave full conversion in 3 h, with 97.5% *e.e.* [76]. In the hydrogenation of β-dehydroamino esters, the reaction rates of MonoPhos **29a** and **29g** were compared with the bidentate ligands DuPhos, JosiPhos and PhanePhos; subsequently, the reactions with ligand **29g**, together with DuPhos, proved to be the fastest [16].

Monodentate phosphoramidite ligands were also employed in the rhodium-catalyzed hydrogenation of enamides. These hydrogenations generally require longer reaction times and higher hydrogen pressures (e.g., 1 to 20 h at 10 to 20 bar with 0.1–2 mol% catalyst). Good to excellent enantioselectivities are obtained using a variety of phosphoramidites. Very high enantioselectivities were reached using PipPhos **29hb**, MorfPhos **29hd** and members of the SIPHOS family.

Phosphoramidite ligands have also been very successful in the asymmetric hydrogenation of β-dehydroamino esters. As with bidentate ligands, there is a large difference in behavior during hydrogenation of the *E*- and *Z*-substrates. The *E*-isomer is generally hydrogenated more easily, and with a higher ee-value. However, by varying the ligand's structure and solvent, both *E*- and *Z*-β-dehydroamino esters could be hydrogenated with excellent ee-values using **29d** and **29g**, thereby surpassing – at that time – the bidentate ligands [77]. Recently, the SIPHOS ligands have also been shown as successful in the hydrogenation of *E*- and *Z*-β-dehydroamino esters.

Since monodentate phosphoramidites are so successful in asymmetric hydrogenation – both because of their performance and their ease of preparation – a logical extension is their application in recyclable systems. Doherty et al. were the first to prepare polymer-supported phosphoramidites by using the monomers **40** and **41** (Scheme 28.12); these led to high ee-values which fell somewhat upon polymerization [78]. The catalyst was shown to be capable of being recycled at least four times.

One highly successful approach was demonstrated by Ding et al., using self-supporting heterogeneous catalysts consisting of ligands such as **42** to create a polymer-type catalyst [79]. Both "dents" in the ligand coordinate to different rhodium ions. The results obtained using this self-supporting catalyst were comparable or better than those obtained using the analogous monomers. The reusability of the catalyst was at least seven cycles.

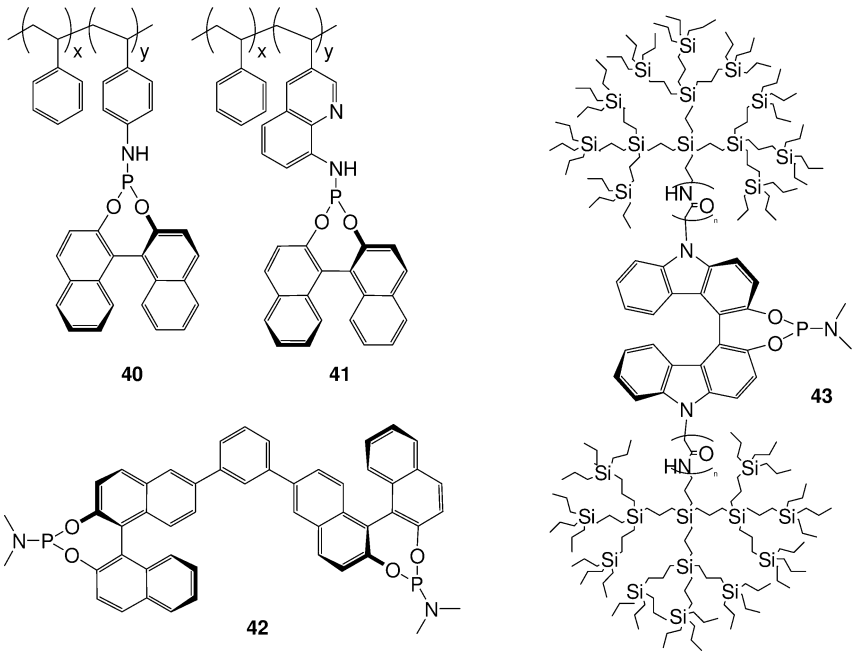

Scheme 28.12 Immobilized phosphoramidite ligands.

The immobilization of catalysts on a solid support is a well-known approach to render a system recycleable, and this has been performed recently by the immobilization of rhodium-MonoPhos **29a** on aluminosilicate AlTUD-1. The resultant system showed high efficiency in water, and could be recycled [80].

Another way of retaining the catalyst is to create dendrimer-supported ligands, thereby allowing separation of the product and catalyst by membranes. Based on the readily modified BICOL backbone, two dendrimer-ligands **43** were prepared that had performance comparable to that of MonoPhos **29a** in the hydrogenation of methyl *N*-acyl dehydrophenylalanine [81].

28.6 Monodentate Phosphinites, Aminophosphinites, Diazaphospholidines and Secondary Phosphine Oxides

In the quest for effective ligands in enantioselective hydrogenation, a number of groups have varied the atoms surrounding the phosphorus atom in order to develop new and hopefully successful ligands. An additional argument for ligand development is to circumvent existing patent literature. Next to phosphines, phosphonites, phosphites and phosphoramidites, attention has been paid to monodentate phosphinites. Surprisingly, as early as 1986 an excellent ee was reported in the hydrogenation of dimethyl itaconate using phosphinite **45** (Scheme 28.13) [82]. Most likely because ee-values were determined somewhat

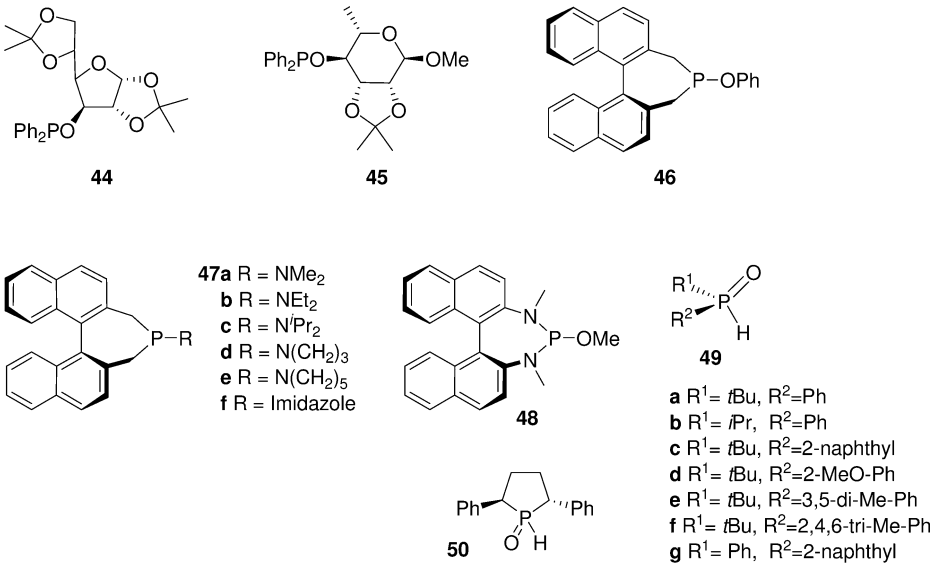

Scheme 28.13 Monodentate phosphinites, aminophosphinites, diazaphospholidines and secondary phosphine oxides.

inaccurately by measuring optical rotations, this result was generally overlooked. Nevertheless, it must be considered as an early example of a successful monodentate ligand. Other monodentate phosphinites, **44** and the recently reported **46** [83], were much less successful. Although phosphinites are rather stable in air, rapid hydrolysis takes place in the presence of moisture.

Monodentate aminophosphines **47** have been developed recently in analogy to the other BINOL-based ligands and related bidentate aminophosphines. Although the scope of these ligands has not been studied in depth, good ee-values can be obtained in rhodium-catalyzed enantioselective hydrogenation [84]. One recent study reports the preparation and use of diazaphospholidine **48** as a logical extension of the BINOL-based phosphites and phosphoramidites [85]. This ligand has not yet been studied in depth, mainly because the synthesis is rather laborious and the ligand is sensitive to hydrolysis.

Secondary phosphine oxides are known to be excellent ligands in palladium-catalyzed coupling reactions and platinum-catalyzed nitrile hydrolysis. A series of chiral enantiopure secondary phosphine oxides **49** and **50** has been prepared and studied in the iridium-catalyzed enantioselective hydrogenation of imines [48] and in the rhodium- and iridium-catalyzed hydrogenation functionalized olefins [86]. Especially in benzyl substituted imine-hydrogenation, **49a** ranks among the best ligands available in terms of *e.e.*

28.7
Hydrogenation of N-Acyl-α-Dehydroamino Acids and Esters

The hydrogenation of methyl *N*-acyl-dehydrophenylalanine **52a** and methyl *N*-acyl-dehydroalanine **53a** to their corresponding amino acid derivatives **54a** and **55a** are the benchmark reactions for rhodium-catalyzed enantioselective hydrogenation. Most newly developed ligands are tested in the hydrogenation of these substrates, and good enantioselectivities are often obtained. As the number of reports is overwhelming, a selection of the results is presented in Table 28.1. Only ligands that afford ee-values of 95% and higher have been included.

It transpires that most classes of monodentate ligands include members that are able to induce high enantioselectivity in the hydrogenation of the two benchmark substrates **52a** and **53a**. It is not clear whether their corresponding acids **52b** and **53b** have been studied or, alternatively, if the authors decided not to include (disappointing) ee-values. For phosphoramidite MonoPhos (**29a**), however, the ee-values are invariably excellent. Overall, the TOFs range from 50 to 170 h^{-1}, but have not been optimized in most cases. Unfortunately, with one exception [87], the hydrogenation of dehydroamino esters in which R^1 is a (functionalized) alkyl substituent has not been studied, probably because of their difficult accessibility.

As the hydrogenation of substituted dehydrophenylalanines is important from an industrial point of view, and the substrates are easily accessible, some phosphoramidites have been screened against a series of these substrates. According

Table 28.1 Enantioselective hydrogenation of *N*-acyl-dehydrophenylalanine and *N*-acyl-dehydroalanine.

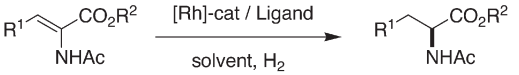

52a R^1 = Ph, R^2 = Me
52b R^1 = Ph, R^2 = H
53a R^1 = H, R^2 = Me
53b R^1 = H, R^2 = H

54a R^1 = Ph, R^2 = Me
54b R^1 = Ph, R^2 = H
55a R^1 = H, R^2 = Me
55b R^1 = H, R^2 = H

Entry	Ligand	54a (54b) ee [%]	55a (55b) ee [%]
1	**10d** [h)]	95	67
2	**10h** [h)]	95	94
3	**15b** [a)]	89	94
4	**17ac** [b)]		95
5	**17ae** [b)]		97
6	**17af** [b)]		95
7	**17ah** [b)]		95
8	**17am** [b)]		96
9	**17an** [b)]		96
10	**17aq** [b)]		96
11	**17at** [b)]		96
12	**29a** [c)]	97 (97)	>99 (>99)
13	**29b** [d)]	98	97
14	**29hb** [g)]	>99	>99
15	**29hc** [g)]	97	97
16	**29hd** [g)]	98	99
17	**29hf** [g)]	97	96
18	**29hh** [g)]	99	99
19	**30a** [e)]	94	>99
20	**30ea** [g)]	>99	97
21	**30eb** [g)]	96	
22	**30ec** [g)]	99	95
23	**30ed** [g)]	99	96
24	**30ee** [g)]	98	96
25	**35a** [f)]	98	97
26	**35d** [f)]	98	
27	**35e** [f)]	98	
28	**35f** [f)]	97	
29	**33a** [i)]		>98
30	**33b** [i)]		>98
31	**39** [j)]	98	98

a) Reactions carried out with SCR 500, in CH_2Cl_2, $p(H_2)=1.5$ bar, 25 °C, 3 h.
b) Reactions carried out with SCR 1000, in CH_2Cl_2 or $ClCH_2CH_2Cl$, $p(H_2)=1.3$ bar, 25 °C, 20 h.
c) Reactions carried out with SCR 100 or 1000, in CH_2Cl_2 or EtOAc, $p(H_2)=1$ bar, 25 °C, 1–3 h.
d) Reactions carried out in THF.
e) Reactions carried out in acetone.
f) Reactions carried out in toluene.
g) Reactions carried out with SCR 50, in CH_2Cl_2, $p(H_2)=5$ bar, 25 °C, 3 h.
h) Reactions carried out with SCR 100, in toluene + SDS, $p(H_2)=1$ bar, 25 °C, $t/2=0.5$–3 h.
i) Reactions carried out with pure diastereomers, SCR 200, in CH_2Cl_2, $p(H_2)=1.3$ bar, 20 h.
j) Reactions carried out with SCR 100, in CH_2Cl_2, $p(H_2)=1.3$ bar, r.t., 12 h.

to the data in Table 28.2, it is safe to assume that a large variety of sterically and electronically different substituents are tolerated without repercussions on the ee-value. This also leads to the assumption, for example, that the recently developed PipPhos **29hb** and MorfPhos **29hd**, being the second generation of MonoPhos **29a**, will perform very well. On average, TOFs using MonoPhos **29a** are around 500 h^{-1} at 5 bar, increasing to 1700 h^{-1} at 60 bar. In the case of a cyano substituent, a strongly decreased rate was observed, probably because of coordination of this group to rhodium. For SIPHOS **35** and **39**, the TOFs are about 50 to 100 h^{-1} at 1 bar.

Table 28.2 Enantiomeric hydrogenation of substituted methyl *N*-acyl-dehydrophenylalanine.

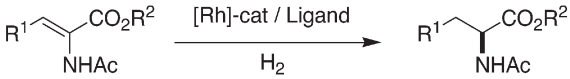

Entry	Substituent	29a	29b	30a	35a	39
1	R^1 = 3-MeO-Ph, R^2 = Me	97				
2	R^1 = 4-MeO-Ph, R^2 = Me	94	99	94	96	
3	R^1 = 3-MeO-4-AcO-Ph, R^2 = Me	96		96		
4	R^1 = 4-F-Ph, R^2 = Me	96	>99			>99
5	R^1 = 4-F-Ph, R^2 = H	93				
6	R^1 = 3-F-Ph, R^2 = Me	95				
7	R^1 = 3-F-Ph, R^2 = H	96				
8	R^1 = 2-F-Ph, R^2 = Me	95				
9	R^1 = 4-Cl-Ph, R^2 = Me	94	99	98	99	99
10	R^1 = 4-Cl-Ph, R^2 = H			83		
11	R^1 = 3,4-Cl_2-Ph, R^2 = H	97				
12	R^1 = 3,4-Cl_2-Ph, R^2 = Me	99				
13	R^1 = 3-NO_2-Ph, R^2 = Me	95			99	
14	R^1 = 4-NO_2-Ph, R^2 = Me	95	>99	96	99	
15	R^1 = 3-NO_2-4-F-Ph, R^2 = Me	95				
16	R^1 = 4-biphenyl, R^2 = Me	95				
17	R^1 = 3-F-4-biphenyl, R^2 = Me	93				
18	R^1 = 4-Ac-Ph, R^2 = Me	99	99			
19	R^1 = 4-Bz-Ph, R^2 = Me	94				
20	R^1 = 4-CN-Ph, R^2 = Me	92 [a)]				
21	R^1 = 1-naphthyl, R^2 = Me	93				
22	R^1 = 4-Br-Ph, R^2 = Me		99	91		
23	R^1 = 2-Cl-Ph, R^2 = Me		99	93	97	99
24	R^1 = 3-Cl-Ph, R^2 = Me		99			
25	R^1 = 3-Cl-Ph, R^2 = H			74		
26	R^1 = 4-Me-Ph, R^2 = Me		98		98	
27	R^1 = 3-Br-Ph, R^2 = Me					>99
28	R^1 = 2-naphthyl, R^2 = Me					>99

a) Very slow reaction was observed.

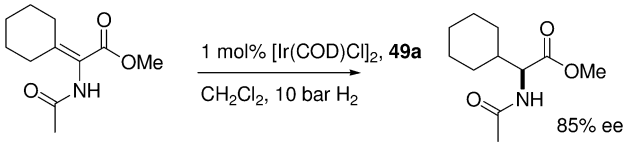

Scheme 28.14 Enantioselective hydrogenation of methyl *N*-acyl dehydrocyclohexylglycine.

Studies have been limited to substrates containing the *N*-acyl or *N*-benzoyl stereodirecting groups. On occasion, for further synthetic applications, a carbamate protecting group is preferred [88]. Substrates possessing two substituents at the β-position have also been ignored, with one exception (Scheme 28.14) [84]. In that report, secondary phosphine oxide **49a** induced 85% ee in the iridium-catalyzed hydrogenation of methyl *N*-acyl dehydrocyclohexylglycine, with a low TOF (1 h^{-1}). This (sub)class of substrates clearly deserves further investigation, as the number of bidentate ligands that induces excellent enantioselectivity is also limited.

28.8 Hydrogenation of Unsaturated Acids and Esters

Next to the hydrogenation of α-dehydroamino acids and esters, the hydrogenation of itaconic acid **56** and its corresponding dimethyl ester **57** is considered to be a benchmark reaction. In addition, the substrates are cheap and the products are valuable intermediates in natural product synthesis. A large number of monodentate ligands has been reported to give good and often excellent results in the hydrogenation of itaconic acid and its corresponding dimethyl ester; hence, only a selection is provided here.

All classes of ligands have members that perform well, although excellent ee-values are rare when phosphines are used, with the exception of ligand **9f** developed by the group of Helmchen. A large number of phosphite ligands has been explored, and both ligands based on BINOL and bisphenols give excellent ee-values. Only **57** has been used as a substrate, and not itaconic acid **56**. Phosphoramidites also perform extremely well, especially PipPhos **29hb**, MorfPhos **29hd**, and related ligands. One remarkable finding was the 100-g scale hydrogenation of itaconic acid **56** using a SCR of 10 000 (TOF 5000 h^{-1}) with MonoPhos **29a** at high pressure, giving quantitative yield and 97% ee [89] (Table 28.3). An even more impressive result was the hydrogenation of **57** with a S/C of 10 000 (TOF 40 000 at 20 bar, 98% ee) when applying phosphite **18a**. As mentioned previously, phosphinite **45** is an early example of a successful monodentate ligand in the hydrogenation of dimethyl itaconate. On average, TOFs range from 20 to 50 h^{-1} at 1 bar, and to 1300 h^{-1} at 10 bar.

Although some attention has been paid to the hydrogenation of β-substituted itaconates, that can be prepared by Stobbe condensation, this class of com-

Table 28.3 Enantioselective hydrogenation of itaconic acid and its dimethyl ester.

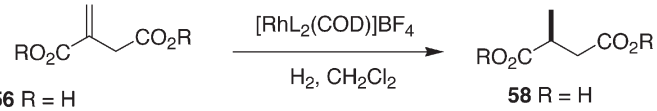

56 R = H
57 R = Me

58 R = H
59 R = Me

Entry	Ligand	58 [%]	59 [%]	Entry	Ligand	58	59
1	**9f**[a)]	96		25	**21bd**[d)]		99
2	**17ac**[b)]		98	26	**22**[d)]		96
3	**17ad**[b)]		99	27	**23e**[e)]		>99
4	**17ae**[b)]		99	28	**23f**[e)]		99
5	**17af**[b)]		97	29	**23g**[e)]		99
6	**17ai**[b)]		99	30	**24b**[e)]		99
7	**17aj**[b)]		96	31	**24d**[e)]		97
8	**17am**[b)]		99	32	**29a**[f)]	97	94
9	**17an**[b)]		99	33	**29hb**[g)]		99
10	**17ap**[b)]		97	34	**30ea**[g)]		99
11	**17aq**[b)]		99	35	**29hd**[g)]		98
12	**17ar**[b)]		99	36	**30ec**[g)]		98
13	**17as**[b)]		99	37	**30ed**[g)]		99
14	**17aw**[b)]		95	38	**29hh**[g)]		97
15	**17bc**[b)]		95	39	**30ee**[g)]		95
16	**17bh**[b)]		95	40	**33a**[h)]		96
17	**17bi**[b)]		98	41	**33b**[h)]		95
18	**18a**[b)]		99	42	**33c**[h)]		96
19	**18b**[b)]		98	43	**34a**[h)]		96
20	**21ak**[c)]		97	44	**34b**[h)]		96
21	**21am**[c)]		96	45	**34c**[h)]		97
22	**21as**[c)]		97	46	**45**		99
23	**21au**[c)]		98				
24	**21bb**[d)]		97				

a) Reactions carried out with SCR 500, in CH_2Cl_2, $p(H_2) = 1.1$ bar, 20 °C, 24 h.
b) Reactions carried out with SCR 1000, in CH_2Cl_2, $p(H_2) = 1.3$ bar, 20 °C, 20 h.
c) Reactions carried out with SCR 200, in CH_2Cl_2 or CH_2ClCH_2Cl, $p(H_2) = 7$ bar, 25 °C, 20 h. In some cases $[Rh(COD)_2]SbF_6$ was used instead of $[Rh(COD)_2]BF_4$ at 50 °C.
d) Reactions carried out with SCR 1000, in CH_2Cl_2, $p(H_2) = 3$ bar, 25 °C, 20 h. $[Rh(COD)_2]SbF_6$ was used instead of $[Rh(COD)_2]BF_4$ at 50 °C.
e) Reactions carried out with SCR 100, in CH_2Cl_2, $p(H_2) = 10$ bar, 25 °C, 12 h.
f) The reaction with itaconic acid was carried out on 100-g scale with SCR 10 000, in CH_2Cl_2, $p(H_2) = 100$ bar, 25 °C (at the start of the reaction), 2 h.
g) Reactions carried out with SCR 50, in CH_2Cl_2, $p(H_2) = 5$ bar, 25 °C, 4 h. For **29hb**, reaction carried out with SCR 1000, in CH_2Cl_2, $p(H_2) = 10$ bar, 25 °C, TOF 1300 h^{-1}.
h) Reactions carried out with SCR 200, in CH_2Cl_2, $p(H_2) = 1.3$ bar, 25 °C, 20 h.

pounds seems to have escaped attention in the hydrogenation using monodentate ligands, until now.

In general, unsaturated esters and acids have hardly been studied in rhodium-catalyzed hydrogenation. This is not surprising, as a carbonyl group at a suitable position is generally thought to be essential for obtaining high ee-values [90]. Using monodentate ligands, some studies were performed during the early years of asymmetric hydrogenation, with most providing low ee-values. An exception was the hydrogenation of (*E*)-3,7-dimethyl-2,6-dienoic acid that afforded the product in 79% ee using monophosphine **2f**. All the more surprising, therefore, was a recent study in which tiglic acid and a series of substituted cinnamic acids were hydrogenated using a combination of a monodentate phosphoramidite and a monodentate phosphine [91]. The rates were very high and excellent ee-values were obtained (details of this study are provided in Chapter 36).

28.9
Hydrogenation of *N*-Acyl Enamides, Enol Esters and Enol Carbamates

Rhodium-catalyzed enantioselective hydrogenation of *N*-acyl enamides provides access to enantioenriched amides which can be hydrolyzed to the free amines. The synthesis of the substrates is considerably less straightforward than that of *N*-acyl dehydroamino acids, which explains the smaller number of reports devoted to *N*-acyl enamides.

Nevertheless, a number of monodentate ligands have shown good performance in this hydrogenation. A selection of results for the hydrogenation of acyclic terminal enamides is listed in Table 28.4. Only the most successful ligands in terms of ee-value are reported, though both phosphites and phosphoramidites perform very well. The phosphite ligands are based on BINOL, and in particular **23c**, which contains a carbohydrate unit, provides excellent ee-values. As phosphoramidites, PipPhos **29hb**, SIPHOS **35a** and the phosphoramidite ligand based on catechol **38g** are excellent ligands. On average, the TOFs are approximately 25 h^{-1} at pressures of 10 to 25 bar, though PipPhos **29hb** is especially impressive, with a TOF of 250 h^{-1} at 25 bar.

N-Acyl enamides substituted at C2 and cyclic enamides have received considerably less attention. A selection of the results is listed in Table 28.5. Phosphite ligand **23c** appears to be the only ligand that gives excellent ee-values for both **62*Z*** and **62*E*** (the mixture was used). PipPhos **29hb** is the monodentate ligand of choice in the hydrogenation of cyclic enamides, and ranks between the best bidentate ligands that can handle these substrates. Clearly, **63** – and especially **67** – are substrates that escape selective hydrogenation with these ligands, until now. The TOFs generally range from 10 to 25 h^{-1}.

The rhodium-catalyzed enantioselective hydrogenation of enol esters is an alternative to the asymmetric reduction of ketones. Although enol esters are accessible both from ketones and alkynes, the number of studies reporting successful asymmetric hydrogenation has been limited. It appears that, compared

Table 28.4 Enantioselective hydrogenation of acyclic terminal *N*-acyl enamides.

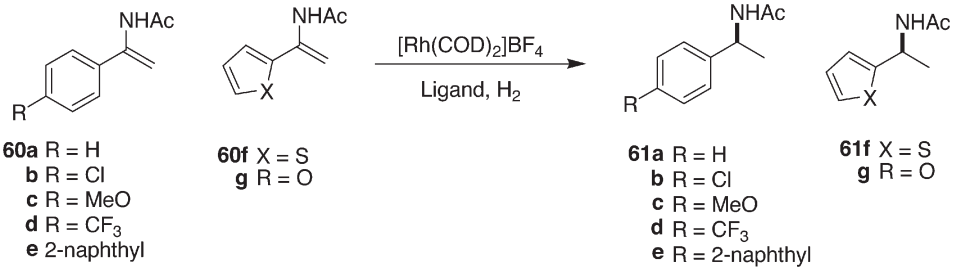

Entry	Ligand	61a [%]	61b [%]	61c [%]	61d [%]	61e [%]	61f [%]	61g [%]
1	**17ag**[a)]	95				94		
2	**17am**[a)]	95						
3	**23c**[f)]	95	98	96	98	97		
4	**29b**[b)]	97	90	98	99			
5	**29hb**[c)]	99	99	99				
6	**29hd**[c)]	99	99	99				
7	**29hf**[c)]	99	99	98				
8	**30a**[b)]	96	86	92	99			81
9	**30ea**[c)]	98	98	99				
10	**30ec**[c)]	97	97	98				
11	**35a**[d)]	98	99		99		96	99
12	**35d**[d)]	97	99					
13	**35e**[d)]	98	98					
14	**35f**[d)]	95	94					
15	**38g**[e)]	97	94	97				

a) Reactions carried out with SCR 500, in CH_2Cl_2, $p(H_2) = 60$ bar, 30 °C, 20 h.

b) Reactions carried out with SCR 200, in THF, $p(H_2) = 20$ bar, 5 °C, 8 h. More substrates were tested than shown in the table.

c) Reactions carried out with SCR 50, in CH_2Cl_2, $p(H_2) = 25$ bar, 25 °C, 20 h. One substrate was hydrogenated using **29hb** at SCR 1000 with an overall TOF of 250 h^{-1} giving the same ee and full conversion.

d) Reactions carried out with SCR 100, in toluene, $p(H_2) = 50$ bar, 5 °C, 12 h. More substrates were tested than shown in the table.

e) Reactions carried out with SCR 100, in EtOAc, $p(H_2) = 25$ bar, 25 °C, 16 h. More substrates were tested than shown in the table.

f) Reactions carried out with SCR 100, in CH_2Cl_2, $p(H_2) = 10$ bar, 25 °C, 12 h.

Table 28.5 Enantioselective hydrogenation of cyclic and substituted *N*-acyl enamides.

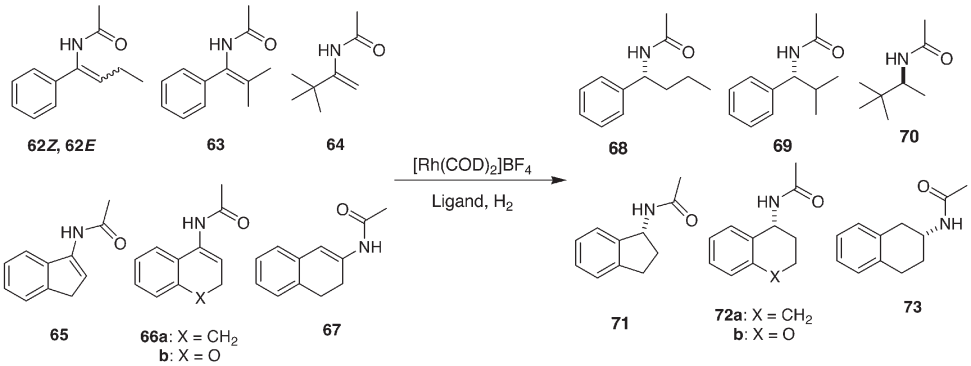

Entry	Ligand	**68** [**62*Z***]	**68** [**62*E***]	**69** [%]	**70** [%]	**71** [%]	**72a** [%]	**72b** [%]	**73** [%]
1	**17aq** a)	97	76						
2	**23c** b)	97	97						
3	**29hb** c)	96	3	–17	82*	98*	98	99	21
4	**30ea** c)	97	5	–1	44	82		99	28
5	**29hd** c)	98	23		27	97*	97*	99	13
6	**30ec** c)	99	26		13	89	88	99	15
7	**29hf** c)	98	17		21	87	82	99	8
8	**35a** d)					94			
9	**38g** e)	99	88		70		35		9

a) Reactions carried out with SCR 500, in CH_2Cl_2, $p(H_2) = 60$ bar, 30 °C, 20 h.
b) Reactions carried out with SCR 100, in CH_2Cl_2, $p(H_2) = 10$ bar, 25 °C, 12 h.
c) Reactions carried out with SCR 50, in CH_2Cl_2, $p(H_2) = 25$ bar, 25 °C, 20 h.
d) Reactions carried out at $p(H_2) = 100$ bar, 0 °C. The 5-bromo- and 6-methoxy-substituted compounds were obtained in 88% and 95% ee, respectively.
e) Reactions carried out with SCR 100, in CH_2Cl_2, $p(H_2) = 25$ bar, 25 °C, 16 h.
* Reactions carried out at –20 °C.

to the corresponding *N*-acyl enamides, the enantioselective hydrogenation of enol esters is considerably more difficult in terms of TOF and *e.e.*. An exception is the hydrogenation of enol esters derived from *α*-keto esters. Nevertheless, a limited number of bidentate ligands have been reported that afford *e.e.*-values >90% in aryl-, vinyl- or trifluoromethyl-substituted enol esters. For alkyl-substituted enol esters, the *e.e.*-values have only been moderate [92].

Reetz and Goossen et al. reported recently the asymmetric hydrogenation of a series of enol esters using monodentate phosphite ligands **17** and **24** based on a combination of BINOL and carbohydrates or simple alcohols; the results of these studies are shown in Table 28.6.

Unprecedented *e.e.*-values were obtained using ligand **24b** in the hydrogenation of aliphatic enol esters. A furyl substituent on the carboxylate is apparently

Table 28.6 Enantioselective hydrogenation of aliphatic enol esters.

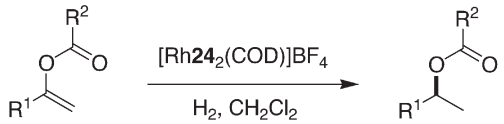

74a R^1 = ^{n}Bu, R^2 = Ph
b R^1 = ^{n}Bu, R^2 = Me
c R^1 = ^{n}Bu, R^2 = Et
d R^1 = ^{n}Bu, R^2 = ^{t}Bu
e R^1 = ^{n}Bu, R^2 = 2-Furyl
f R^1 = Et, R^2 = Ph
g R^1 = Et, R^2 = 2-*N*-Me-pyrrolyl
h R^1 = Et, R^2 = 2-Furyl

75a-h

Entry	Ligand	Product							
		75a	**75b**	**75c**	**75d**	**75e**	**75f**	**75g**	**75h**
1	**24b**[a)]	86	74	74	42	90*	80	72	84
2	**24f**[a), b)]	13	32	6	10	22	11	5	34

a) Reactions carried out with SCR 200, in CH_2Cl_2, $p(H_2) = 60$ bar, 30 °C, 20 h (TOF = 5 h^{-1}).
b) Using ligand **24f** the conversion was between 76% and 100%.
* At –20 °C, 94% ee was obtained.

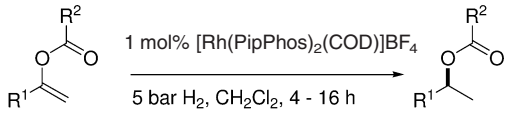

		ee%
74i	R^1 = Ph, R^2 = Me	**75i** 90
j	R^1 = Ph, R^2 = NEt_2	**j** 96
k	R^1 = 4-Cl-Ph, R^2 = Me	**k** 90
l	R^1 = 4-NO_2-Ph, R^2 = Me	**l** 98
m	R^1 = 4-NO_2-Ph, R^2 = NEt_2	**m** 98
n	R^1 = ^{n}Bu, R^2 = NEt_2	**n** 63
o	R^1 = Bn, R^2 = NEt_2	**o** 73
p	R^1 = Me_3Si, R^2 = NEt_2	**p** 43
q	R^1 = 1*E*-heptenyl, R^2 = NEt_2	**q** 97
r	R^1 = styryl, R^2 = NEt_2	**r** 76

Scheme 28.15 Enantioselective hydrogenation of enol acetates and enol carbamates.

beneficial for the enantioselectivity. The reactions are most likely not very fast, which is also the case using bidentate ligands.

In order to mimic the electronic properties of the corresponding *N*-acyl enamide, enol carbamate **74j** (Scheme 28.15) has been introduced in the enantioselective hydrogenation using rhodium and a series of secondary phosphinoxide ligands **49**. The use of 2 mol% of Rh/L and 1 bar of hydrogen gave full conversion and 81% *e.e.* in a slow reaction. Unfortunately, the *e.e.*-values fell upon increasing the hydrogen pressure.

Very recently, however, the use of Rh/PipPhos **29hb** was reported as an excellent catalyst for the hydrogenation of both enol acetates and enol carbamates (Scheme 28.15). The carbamate group induced higher enantioselectivities compared to the corresponding acyl group, and the hydrogenations were faster (TOFs up to 25 h^{-1} at 5 bar). Remarkably, dienol carbamates **74q** and **74r** were hydrogenated to the corresponding allylic carbamate, leaving the additional double bond intact.

28.10
Hydrogenation of *N*-Acyl-*β*-Dehydroamino Acid Esters

Enantiopure *β*-amino acids can efficiently be obtained using rhodium-catalyzed asymmetric hydrogenation. The substrates are synthesized by reacting the *β*-keto esters with NH_4OAc and subsequent acylation with acetic anhydride. This reaction generally results in a mixture of double bond isomers [93]. Compared to the corresponding *α*-dehydroamino acids and esters, their *β*-analogues are considerably more challenging. There is a large difference in behavior of the hydrogenation of the *E*- and *Z*-stereoisomers. The *E*-isomer is generally hydrogenated at higher rate and with considerably higher ee than the *Z*-isomer. A few monodentate ligands have been studied for the rhodium-catalyzed hydrogenation of this class of compounds. Phosphites **17bc** and **24c** induce high ee-values but require a high catalyst loading and long reaction times. In addition, for **24c** the conversion is incomplete. Better results have been obtained using phosphoramidites; for example, it has been shown that using BINOL-based phosphoramidites, different ligands and different solvents were necessary to hydrogenate the different double bond isomers. Excellent ee-values were obtained, however. In particular for the Z-isomers, **29g** was the best ligand available at the time, also taking into account the bidentate ligands. SIPHOS ligand **35a** also provides high ee-values, with the advantage that mixtures of *E* and *Z* substrates can be used (Table 28.7). The reactions are slow (TOF 1 h^{-1} at 100 bar), however. In general, the TOFs vary considerable among the ligands, ranging from 3 h^{-1} at 15 bar to 200 h^{-1} at 10 bar.

Table 28.7 Enantioselective hydrogenation of *N*-Acyl-*β*-dehydroamino acid esters.

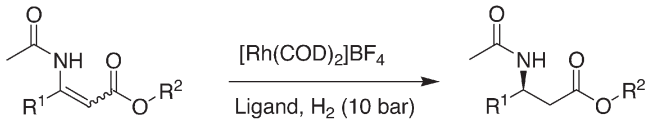

78a R^1 = Me, R^2 = Me
b R^1 = Me, R^2 = Et
d R^1 = Ph, R^2 = Et
e R^1 = Et, R^2 = Me
f R^1 = ^{i}Pr, R^2 = Et
g R^1 = *p*-F-Ph, R^2 = Me
h R^1 = *o*-Br-Ph, R^2 = Me
i R^1 = *m*-Br-Ph, R^2 = Me
j R^1 = *p*-Br-Ph, R^2 = Me
k R^1 = *p*-Cl-Ph, R^2 = Me
l R^1 = *p*-Me-Ph, R^2 = Me
m R^1 = *p*-MeO-Ph, R^2 = Me

79a-m

	Ligand	79a *E/Z*	79b *E/Z*	79d *Z*	79e *E/Z*	79f *E/Z*	79g *Z*	79h	79i	79j	79k	79l	79m
1	**17bc**[a)]	91/55	94/38	52									
2	**24c**[b)]	96/–	96/–	93	98/–								
3	**29a**[c)]	91/–											
4	**29d**[c)]	99/–	98/–		99/–	99/–							
5	**29g**[d)]	–/95	–/94	92	–/94	–/92	94						
6	**35**[e)]	89	87	90				91	92	94	91	91	93

a) Reactions carried out with SCR 100, in CH_2Cl_2, $p(H_2)$ = 15 bar, 30 h.
b) Reactions carried out with SCR 50, in CH_2Cl_2, $p(H_2)$ = 30 bar, 12–48 h. Conversions were incomplete.
c) Reactions carried out with SCR 50, in CH_2Cl_2, $p(H_2)$ = 10 bar, 4 h or SCR of 200, in CH_2Cl_2, $p(H_2)$ = 25 bar, 6 h.
d) Reactions carried out with SCR 50, in *i*-PrOH, $p(H_2)$ = 10 bar, 0.3 h or with SCR 200, in *i*-PrOH, $p(H_2)$ = 10 bar, 1 h.
e) Reactions carried out with SCR 50, in CH_2Cl_2, $p(H_2)$ = 100 bar, 48 h. Mixtures of *Z* and *E* were used.

28.11 Hydrogenation of Ketones and Imines

Although this chapter is devoted to the hydrogenation of alkenes, it is interesting to include the studies that have appeared on the hydrogenation of imines and ketones. Surprisingly, the enantioselective imine hydrogenation using monodentate ligands has been reported in only a few studies. BINOL-based monodentate phosphonite ligand **15d** has been studied in the rhodium- and iridium-catalyzed hydrogenation of benzyl imine **80** (Scheme 28.16) [40]. No chiral

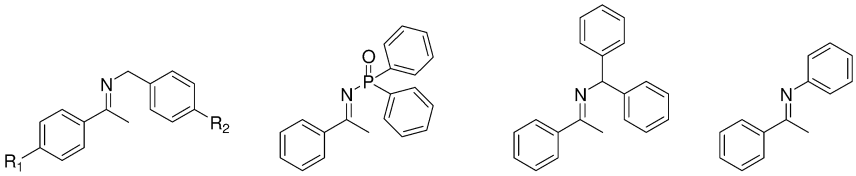

80 $R_1 = R_2 = H$
81 $R_1 = OMe$, $R_2 = H$
82 $R_1 = H$, $R_2 = OMe$
83 $R_1 = H$, $R_2 = Cl$
84 $R_1 = Cl$, $R_2 = H$

85 **86** **87**

Scheme 28.16 Imines for enantioselective hydrogenation.

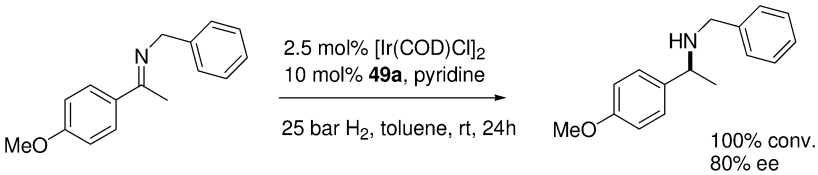

Scheme 28.17 Enantioselective hydrogenation of benzyl imines using iridium/secondary phosphinoxide ligands.

induction was observed. In a thorough study, secondary phosphine oxide ligands **49** and **50** were used in the iridium-catalyzed hydrogenation of a series of imines [48]. Enantioselectivities up to 80% and full conversion were reached with Ir/**49a** in the hydrogenation of benzyl imine **81** in toluene, adding pyridine as a co-ligand (Scheme 28.17). This places the catalyst among the best catalysts

Table 28.8 Enantioselective hydrogenation of β-keto esters using monodentate phosphine ligands.

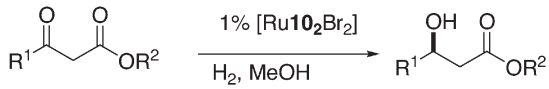

88a $R^1 = Me$, $R^2 = Me$
88b $R^1 = Et$, $R^2 = Me$
88c $R^1 = CH_2Cl$, $R^2 = Et$
88d $R^1 = Ph$, $R^2 = Et$

89a $R^1 = Me$, $R^2 = Me$
89b $R^1 = Et$, $R^2 = Me$
89c $R^1 = CH_2Cl$, $R^2 = Et$
89d $R^1 = Ph$, $R^2 = Et$

Entry	Ligand	Substrate	Yield [%]	ee [%]
1	**10d**[a)]	**88a**	95	84
2	**10e**[a)]	**88a**	97	92
3	**10e**[a)]	**88b**	99	94
4	**10e**[a)]	**88c**	77	38
5	**10e**[a)]	**88d**	99	95
6	**10o**[a)]	**88a**	98	64

a) Reactions carried out with SCR 1000, in MeOH, $p(H_2) = 40–80$ bar, at 50 °C, 16 h.

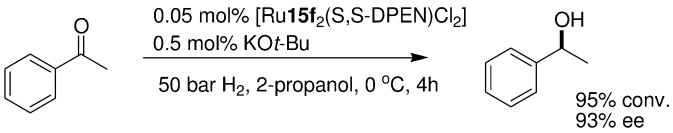

Scheme 28.18 Enantioselective hydrogenation of aryl-methyl ketones.

known for benzyl imine hydrogenation in terms of enantioselectivity, although the reactions are slow. Low *e.e.*-values were obtained with *N*-diphenylphosphinoyl ketimine **85**, benzhydryl imine **86** and aryl imine **87**. A chiral phosphoric acid diester **20**, based on TADDOL was also tested, but gave very low *e.e.*-values.

At the same time, however, the iridium-catalyzed hydrogenation of **80** was reported using chiral phosphoric acid diester **17be** based on BINOL [47a]. Full conversion and a maximum *e.e.* of 50% was observed, again in a slow reaction. Interestingly, a catalyst based on palladium and **17be** afforded 39% *e.e.* and full conversion in the hydrogenation of aryl imine **87**.

In an early report, the *β*-keto ester methyl acetylacetate was hydrogenated with 71% ee using Rh/CAMP [94]. In a thorough study, the group of Beller reported excellent results in the ruthenium-catalyzed hydrogenation of *β*-keto esters using monodentate phosphines based on the binaphthyl skeleton. The phosphoramidite MonoPhos **29a** and a related phosphonite gave only low ee-values in this reaction. A selection of the results is presented in Table 28.8. One remarkable point was the difference between the non-deuterated ligand **10d** and its deuterated analogue **10o**.

Recently, the first report was made on the ruthenium-catalyzed enantioselective hydrogenation of aryl-methyl ketones using monodentate phosphonites (Scheme 28.18). In particular, ligand **15f** induced excellent ee-values. One very early report on rhodium-catalyzed hydrogenation of ketones using the monophosphine bmpp **1f** met with a low *e.e.* [95].

28.12 Conclusions

It is safe to state that monodentate ligands have rapidly found their place in rhodium-catalyzed enantioselective hydrogenation, and the high speed at which new ligands appear continuously is the best illustration of their versatility. On the one hand, the straightforward preparation and the use of ligand libraries (see Chapter 36) makes the rapid development of tailor-made ligands possible. On the other hand, it clear from the information provided in this chapter that certain ligands, such as PipPhos **29hb**, SIPHOS **35a**, and some BINOL and biphenol-based phosphites, are so-called privileged ligands with a large scope.

Nevertheless, there remains a plethora of substrates that have not yet been studied using the monodentate ligand approach. In the application of asymmetric hydrogenation, it is very important to go beyond the benchmark substrates, and several studies have already shown that the scope of enantioselective hydrogenation might be much broader than was originally assumed.

One especially underexposed aspect in most reports is that of the TOF and TON of the catalyst. Not only from a scientific point of view, but also because of the costs of the precious metals used, this must be an important characteristic of catalytic systems.

Abbreviations

HTE high-throughput experimentation
TOF turnover frequency
TON turnover number

References

1 (a) W.S. Knowles, M.J. Sabacky, *J. Chem. Soc. Chem. Commun.* **1968**, 1445; (b) W.S. Knowles, *Acc. Chem. Res.* **1983**, *16*, 106.
2 L. Horner, H. Siegel, H. Büthe, *Angew. Chem. Int. Ed. Engl.* **1968**, *7*, 942.
3 J.A. Osborn, F.H. Jardine, J.F. Young, G. Wilkinson, *J. Chem. Soc. A* **1966**, 1711.
4 For an excellent overview of the field of enantioselective hydrogenation, see: J.M. Brown, in: E.N. Jacobsen, A. Pfaltz, H. Yamamoto (Eds.), *Comprehensive Asymmetric Catalysis*, Springer, Berlin, **1999**, Vol. 1, Chapter 5.1.
5 (a) T.P. Dang, H.B. Kagan, *J. Chem. Soc. Chem. Commun.* **1971**, 481; (b) H.B. Kagan, T.P. Dang, *J. Am. Chem. Soc.* **1972**, *94*, 6429.
6 B.D. Vineyard, W.S. Knowles, M.J. Sabacky, G.L. Bachman, D.J. Weinkauff, *J. Am. Chem. Soc.* **1977**, *99*, 5946.
7 (a) H. Brunner, W. Zettlmeier, *Handbook of Enantioselective Catalysis*, VCH, Weinheim, **1993**; (b) R. Noyori, *Asymmetric Catalysis in Organic Synthesis*, Wiley, New York, **1993**; (c) H.B. Kagan, in: J.D. Morrison (Ed.), *Asymmetric Synthesis*, Academic Press, Inc., Orlando, **1985**, Volume 5; (d) H. Brunner, *Top. Stereochem.* **1988**, *18*, 129; (e) H.-U. Blaser, C. Malan, B. Pugin, F. Spindler, H. Steiner, M. Studer, *Adv. Synth. Catal.* **2003**, *345*, 103.
8 H.U. Blaser, E. Schmidt (Eds.), *Asymmetric Catalysis on Industrial Scale: Challenges, Approaches and Solutions*, Wiley-VCH, **2004**.
9 (a) W.S. Knowles, M.J. Sabacky, B.D. Vineyard, *J. Chem. Soc. Chem. Commun.* **1972**, 10; (b) J. Solodar, *J. Org. Chem.* **1978**, *43*, 1787.
10 For a discussion on this topic, see: X. Zhang, *Enantiomer* **1999**, *4*, 541.
11 For a review on the use of chiral monodentate phosphines in asymmetric catalysis, see: F. Lagasse, H.B. Kagan, *Chem. Pharm. Bull.* **2000**, *48*, 315.
12 For a perspective on the use of chiral monodentate phosphorus ligands in enantioselective olefin hydrogenations see: I.V. Komarov, A. Börner, *Angew. Chem. Int. Ed.* **2001**, *40*, 1197. As a forerunner, the development of a new, though less enantioselective, monodentate phosphine ligand was reported; F. Guillen, J.-C. Fiaud, *Tetrahedron Lett.* **1999**, *40*, 2939.
13 C. Claver, E. Fernandez, A. Gillon, K. Heslop, D.J. Hyett, A. Martorell, A.G. Orpen, P.G. Pringle, *Chem. Commun.* **2000**, 961.
14 M.T. Reetz, G. Mehler, *Angew. Chem. Int. Ed.* **2000**, *39*, 3889.
15 M. van den Berg, A.J. Minnaard, E.P. Schudde, J. van Esch, A.H.M. de Vries, J.G. de Vries, B.L. Feringa, *J. Am. Chem. Soc.* **2000**, *122*, 11539.
16 D. Peña, A.J. Minnaard, A.H.M. de Vries, J.G. de Vries, B.L. Feringa, *Org. Lett.* **2003**, *5*, 475.
17 For an initial study using the phosphoramidite MonoPhos, see: M. van den Berg, A.J. Minnaard, R.M. Haak, M. Leeman, E.P. Schudde, A. Meetsma, B.L. Feringa,

A. H. M. de Vries, C. E. P. Maljaars, C. E. Willans, D. Hyett, J. A. F. Boogers, H. J. W. Henderickx, J. G. de Vries, *Adv. Synth. Catal.* **2003**, *345*, 308.
18 Y. Fu, X. X. Guo, S. F. Zhu, A. G. Hu, J. H. Xie, Q. L. Zhou, *J. Org. Chem.* **2004**, *69*, 4648.
19 M. T. Reetz, T. Sell, A. Meiswinkel, G. Mehler, *Angew. Chem. Int. Ed.* **2003**, *42*, 790.
20 (a) M. T. Reetz, X. Li, *Angew. Chem. Int. Ed.* **2005**, *44*, 2959; (b) see Ref. 91.
21 T. Jerphagnon, J.-L. Renaud, C. Bruneau, *Tetrahedron; Asymm.* **2004**, *15*, 2101.
22 J. G. de Vries, in: D. Ager (Ed.), *Handbook of Chiral Chemicals*, M. Dekker, **2004**.
23 D. Valentine, Jr., K. K. Johnson, W. Priester, R. C. Sun, K. Toth, G. Saucy, *J. Org. Chem.* **1980**, *45*, 3698.
24 (a) J. D. Morrison, R. E. Burnett, A. M. Aguiar, C. J. Morrow, C. Phillips, *J. Am. Chem. Soc.* **1971**, *93*, 1301; (b) J. D. Morrison, W. F. Masler, *J. Org. Chem.* **1974**, *39*, 270.
25 A. Marinetti, F. Mathey, L. Ricard, *Organometallics* **1993**, *12*, 1207.
26 A. Marinetti, L. Ricard, *Organometallics* **1994**, *13*, 3956.
27 O. Riant, O. Samuel, T. Flessner, S. Taudien, H. B. Kagan, *J. Org. Chem.* **1997**, *62*, 6733.
28 S. Saito, Y. Nakamura, Y. Morita, *Chem. Pharm. Bull.* **1985**, *33*, 5284.
29 M. Ostermeier, J. Priess, G. Helmchen, *Angew. Chem. Int. Ed.* **2002**, *41*, 612.
30 K. Junge, G. Oehme, A. Monsees, T. Riermeier, U. Dingerdissen, M. Beller, *Tetrahedron Lett.* **2002**, 43, 4977.
31 K. Junge, B. Hagemann, S. Enthaler, A. Spannenberg, M. Michalik, G. Oehme, A. Monsees, T. Riermeier, M. Beller, *Tetrahedron; Asymm.* **2004**, *15*, 2621.
32 K. Junge, B. Hagemann, S. Enthaler, G. Oehme, M. Michalik, A. Monsees, T. Riermeier, U. Dingerdissen, M. Beller, *Angew. Chem. Int. Ed.* **2004**, *43*, 5066.
33 A. Marinetti, J.-P. Gent, *C. R. Chimie* **2003**, *6*, 507.
34 A. Marinetti, S. Jus, F. Labrue, A. Lemarchand, J.-P. Gent, L. Ricard, *Synthesis*, **2001**, 2091.
35 M. J. Burk, J. E. Feaster, R. L. Harlow, *Tetrahedron; Asymm.* **1991**, *2*, 569. Ligands **12b** and **12c** have not been tested in asymmetric hydrogenation.
36 (a) F. Guillen, M. Rivard, M. Toffano, J. Y. Legros, J. C. Daran, J. C. Fiaud, *Tetrahedron* **2002**, *58*, 5895; (b) see Ref. 12; (c) C. Dobrota, M. Toffano, J. C. Fiaud, *Tetrahedron Lett.* **2004**, *45*, 8153.
37 Z. Pakulski, O. M. Demchuk, J. Frelek, R. Luboradzki, K. M. Pietrusiewicz, *Eur. J. Org. Chem.* **2004**, 3913.
38 M. T. Reetz, T. Sell, *Tetrahedron Lett.* **2000**, *41*, 6333.
39 S. Trinkhaus, R. Kadyrov, R. Selke, J. Holz, L. Götze, A. Borner, *J. Mol. Cat. A. Chem.* **1999**, *144*, 15.
40 A. Martorell, C. Claver, E. Fernandez, *Inorg. Chem. Comm.* **2000**, *3*, 132.
41 Y. Xu, N. W. Alcock, G. J. Clarkson, G. Docherty, G. Woodward, M. Wills, *Org. Lett.* **2004**, *6*, 4105.
42 W. Chen, J. Xiao, *Tetrahedron Lett.* **2001**, *42*, 2897.
43 I. Gergely, C. Hegedüs, H. Gulyás, Á. Szöllösy, A. Monsees, T. Riermeier, J. Bakos, *Tetrahedron: Asymmetry* **2003**, *14*, 1087.
44 A. Korostylev, A. Monsees, C. Fischer, A. Börner, *Tetrahedron: Asymmetry* **2004**, *15*, 1001.
45 M. Ostermeier, B. Brunner, C. Korff, G. Helmchen, *Eur. J. Org. Chem.* **2003**, 3453.
46 D. Nakano, M. Yamaguchi, *Tetrahedron Lett.* **2003**, *44*, 4969.
47 (a) M. T. Reetz, T. Sell, R. Goddard, *Chimia* **2003**, *57*, 290; (b) M. T. Reetz, *Russ. J. Org. Chem.* **2003**, *39*, 392.
48 X.-B. Jiang, A. J. Minnaard, B. Hessen, B. L. Feringa, A. L. L. Duchateau, J. G. O. Andrien, J. A. F. Boogers, J. G. de Vries, *Org. Lett.* **2003**, *5*, 1503.
49 W. Chen, J. Xiao, *Tetrahedron Lett.* **2001**, *42*, 8737.
50 Z. Hua, V. C. Vassar, I. Ojima, *Org. Lett.* **2003**, *5*, 3831.
51 B. Meseguer, T. Prinz, U. Scholz, H.-C. Militzer, F. Agel, B. Driessen-Hölscher EP 1 298 136, 2003, to Bayer AG.
52 P. Hannen, H.-C. Millitzer, E. M. Vogl, F. A. Rampf, *Chem. Commun.* **2003**, 2210.

53 M.T. Reetz, G. Mehler, A. Meiswinkel, T. Sell, *Tetrahedron Lett.* **2002**, *43*, 7941.

54 M.T. Reetz, L.J. Goossen, A. Meiswinkel, J. Paetzold, J. Feldthusen Jensen, *Org. Lett.* **2003**, *5*, 3099.

55 Q. Jiang. D. Xiao, P. Cao, X. Zhang, *Angew. Chem. Int. Ed.* **1998**, *37*, 1100.

56 T. Jerphagnon, J.-L. Renaud, P. Demonchaux, A. Ferreira, C. Bruneau, *Adv. Synth. Catal.* **2004**, *346*, 33.

57 H. Huang, Z. Zheng, H. Luo, C. Bai, X. Hu, H. Chen, *Org. Lett.* **2003**, *5*, 4137.

58 (a) H. Huang, X. Liu, S. Chen, H. Chen, Z. Zheng *Tetrahedron: Asymm.* **2004**, *15*, 2011; (b) Note added in proof: a new class of monodentate phosphites based on a combination of D-mannitol and BINOL or bisphenols affords excellent ee s in the hydrogenation of *α*-and *β*-*α*-acyl-dehydroamino esters, *N*-acyl enamides and itaconates, see: H. Huang, Z. Zheng, H. Luo, C. Bai, X. Hu, H. Chen, *J. Org. Chem.* **2004**, *69*, 2355.

59 M.T. Reetz, J.-A. Ma, R. Goddard, *Angew. Chem. Int. Ed.* **2005**, *44*, 412.

60 (a) K. Nozaki, N. Sakai, T. Nanno, T. Higashijima, S. Mano, T. Horiuchi, H. Takaya, *J. Am. Chem. Soc.* **1997**, *119*, 4413; (b) A. Duursma, J.-G. Boiteau, L. Lefort, J.A.F. Boogers, A.H.M. de Vries, J.G. de Vries, A.J. Minnaard, B.L. Feringa, *J. Org. Chem.* **2004**, *69*, 8045.

61 For alternative routes, see: (a) Ref. 17; (b) A. van Rooy, D. Burgers, P.C.J. Kamer, P.W.N.M. van Leeuwen, *Recl. Trav. Chim. Pays-Bas* **1996**, *115*, 492.

62 R. Hulst, N.K. de Vries, B.L. Feringa, *Tetrahedron: Asymmetry* **1994**, *5*, 699.

63 M. Van den Berg, R.M. Haak, A.J. Minnaard, A.H.M. de Vries, J.G. de Vries, B.L. Feringa, *Adv. Synth. Catal.* **2002**, *344*, 1003.

64 (a) X. Jia, X. Li, L. Xu, Q. Chi, X. Yao, A.S.C. Chan, *J. Org. Chem.* **2003**, *68*, 4539; (b) X. Jia, R. Guo, X. Li, X. Yao, A.S.C. Chan, *Tetrahedron Lett.* **2002**, *43*, 5541.

65 H. Bernsmann, M. van den Berg, R. Hoen, A.J. Minnaard, G. Mehler, M.T. Reetz, J.G. de Vries, B.L. Feringa, *J. Org. Chem.* **2005**, *70*, 943.

66 (a) Q. Zeng, H. Liu, X. Cui, A. Mi, Y. Jiang, X. Li, M.C.K. Choi, A.S.C. Chan, *Tetrahedron: Asymmetry* **2002**, *13*, 115; (b) Q. Zeng, H. Liu, A. Mi, Y. Jiang, X. Li, M.C.K. Choi, A.S.C. Chan, *Tetrahedron* **2002**, *58*, 8799; (c) X. Li, X. Jia, G. Lu, T.T.-L. Au-Yeung, K.-H. Lam, T.W.H. Lo, A.S.C. Chan, *Tetrahedron: Asymmetry* **2003**, *14*, 2687.

67 L. Panella, B.L. Feringa, J.G. de Vries, A.J. Minnaard, *Org. Lett.* **2005**, *7*, 4177.

68 O. Huttenloch, J. Spieler, H. Waldmann, *Chem. Eur. J.* **2000**, *6*, 671.

69 M.T. Reetz, J.-A. Ma, R. Goddard, *Angew. Chem. Int. Ed.* **2005**, *44*, 412.

70 (a) A.-G. Hu, Y. Fu, J.-H. Xie, H. Zhou, L.-X. Wang, Q.-L. Zhou, *Angew. Chem. Int. Ed.* **2002**, *41*, 2348; (b) Y. Fu, J.-H. Xie, A.-G. Hu, H. Zhou, L.-X. Wang, Q.-L. Zhou, *Chem. Commun.* **2002**, 480; (c) S.-F. Zhu, Y. Fu, J.-H. Xie, B. Liu, L. Xing, Q.-L. Zhou, *Tetrahedron: Asymmetry* **2003**, *14*, 3219.

71 Y. Fu, X.-X. Guo, S.-F. Zhu, A.-G. Hu, J.-H. Xie, Q.-L. Zhou, *J. Org. Chem.* **2004**, *69*, 4648.

72 V.B. Birman, A.L. Rheingold, K.-C. Lam, *Tetrahedron: Asymmetry* **1999**, *10*, 125.

73 S. Wu, W. Zhang, Z. Zhang, X. Zhang, *Org. Lett.* **2004**, *6*, 3565.

74 A. Bayer, P. Murszat, U. Thewalt, B. Rieger, *Eur. J. Inorg. Chem.* **2002**, 2614.

75 R. Hoen, M. van den Berg, H. Bernsmann, A.J. Minnaard, J.G. de Vries, B.L. Feringa, *Org. Lett.* **2004**, *6*, 1433.

76 M. van den Berg, PhD. Thesis **2005**, University of Groningen, The Netherlands.

77 D. Peña, A.J. Minnaard, J.G. de Vries, B.L. Feringa, *J. Am. Chem. Soc.* **2002**, *124*, 14552.

78 S. Doherty, E.G. Robins, I. Pál, C.R. Newman, C. Hardacre, D. Rooney, D.A. Mooney, *Tetrahedron: Asymmetry* **2003**, *14*, 1517. Of course, once polymerized the ligands are no longer monodentate.

79 X. Wang, K. Ding, *J. Am. Chem. Soc.* **2004**, *126*, 10524.

80 C. Simons, U. Hanefeld, I.W.C.E. Arends, A.J. Minnaard, T. Maschmeyer, R.A. Sheldon, *Chem. Comm.* **2004**, 2830.

81 P.N.M. Botman, A. Amore, R. van Heerbeek, J.W. Back, H. Hiemstra, J.N.H. Reek, J.H. van Maarseveen *Tetrahedron Lett.* **2004**, *45*, 5999.

82 M. Yamashita, M. Kobayashi, M. Sugiura, K. Tsunekawa, T. Oshikawa, S. Inokawa, H. Yamamoto, *Bull. Chem. Soc. Jpn.* **1986**, *59*, 175.

83 Y. Chi, X. Zhang, *Tetrahedron Lett.* **2002**, *43*, 4849.

84 K. Junge, G. Oehme, A. Monsees, T. Riermeier, U. Dingerdissen, M. Beller, *J. Organomet. Chem.* **2003**, *675*, 91.

85 M.T. Reetz, H. Oka, R. Goddard, *Synthesis* **2003**, 1809.

86 X.-B., Jiang, M. van den Berg, A.J. Minnaard, B.L. Feringa, J.G. de Vries, *Tetrahedron: Asymmetry* **2004**, *15*, 2223.

87 The methyl-substituted substrate has been hydrogenated with SIPHOS in excellent ee; see: Ref. [68b].

88 MonoPhos **29a** has shown to give the same ee-values for *N*-acyl, *N*-BOC and *N*-Z protection (unpublished results).

89 M. van den Berg, E.P. Schudde, A.J. Minnaard, B.L. Feringa, J. G. de Vries (unpublished results).

90 (a) E. Farrington, M.C. Franchini, J.M. Brown, *Chem. Comm.* **1998**, 277; (b) J.M. Brown, *Angew. Chem. Int. Ed. Engl.* **1987**, *26*, 191.

91 R. Hoen, J.A.F. Boogers, H. Bernsmann, A.J. Minnaard, A. Meetsma, T.D. Tiemersma-Wegman, A.H.M. de Vries, J.G. de Vries, B.L. Feringa, *Angew. Chem. Int. Ed.* **2005**, *44*, 4209.

92 N.W. Boaz, *Tetrahedron Lett.* **1998**, *39*, 5505.

93 See, however J. You, H.-J. Drexler, S. Zhang, C. Fischer, D. Heller, *Angew. Chem. Int. Ed.* **2003**, *42*, 913 for an in-depth study of the synthesis of these stereoisomers.

94 (a) J. Solodar, *Chemtech* **1975**, 421. For the enantioselective hydrogenation of cyclopenta-1,3,4,-trione using Rh/CAMP, see (b) C.J. Sih, J.B. Heather, G.P. Peruzzotti, P. Price, R. Sood, L.-F.H. Lee, *J. Am. Chem. Soc.* **1973**, *95*, 1676.

95 P. Bonvicini, A. Levi, G. Modena, G. Scorrano, *J. Chem. Soc., Chem. Comm.* **1972**, 1188.

29
P,N and Non-Phosphorus Ligands

Andreas Pfaltz and Sharon Bell

29.1
Introduction

The first homogeneous enantioselective hydrogenation catalysts were developed during the 1960s [1, 2]. Since then the range and scope of chiral hydrogenation catalysts has expanded to the point where many functionalized substrates can be hydrogenated in good enantiomeric excess. This breakthrough is largely due to the C_2-symmetric diphosphine catalysts such as DIOP [3], the first such diphosphine, and DIPAMP [4], used in the first industrial-scale enantioselective homogeneous hydrogenation to produce L-DOPA. Since that time, numerous other phosphorus ligands have been introduced, which have considerably expanded the scope of enantioselective hydrogenation.

More recently, there has been increasing interest in the synthesis of hydrogenation catalysts with ligands other than the diphosphines. The initial success of titanocene catalysts in the hydrogenation of unfunctionalized alkenes (see Section 29.5) led to a great deal of research into metallocene catalysts. Iridium complexes with ligands bearing a coordinating phosphorus (P) and nitrogen (N) atoms have shown considerable success in recent years.

P,N and non-phosphorus ligands have been most successful in the enantiomeric iridium-catalyzed hydrogenation of unfunctionalized alkenes [5], and for this reason this chapter necessarily overlaps with Chapter 30. Here, the emphasis is on ligand synthesis and structure, whereas Chapter 30 expands on substrates, reaction conditions and reaction optimization. However, a number of specific substrates are mentioned in the comparison of catalysts, and their structures are illustrated in Figure 29.1.

The Handbook of Homogeneous Hydrogenation.
Edited by J.G. de Vries and C.J. Elsevier
Copyright © 2007 WILEY-VCH Verlag GmbH & Co. KGaA, Weinheim
ISBN: 978-3-527-31161-3

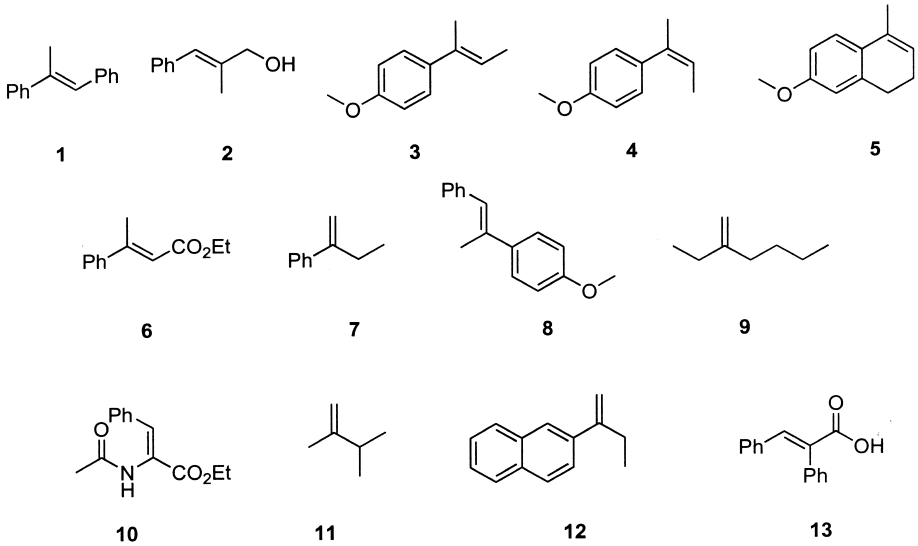

Fig. 29.1 Substrates discussed in this chapter.

29.2 Oxazoline-Derived P,N Ligands

The Crabtree catalyst ($[Ir(PCy_3)(py)(COD)]PF_6$) [6] shows remarkable activity in the hydrogenation of alkenes, particularly sterically hindered tri- and even tetra-substituted alkenes. Its structure has inspired a great deal of research into chiral P,N ligands for enantioselective hydrogenation, producing a variety of useful catalysts. The largest and most successful group of chiral analogues of the Crabtree catalyst are iridium complexes with oxazoline-derived P,N ligands.

The oxazoline-derived P,N ligands can be classified into four groups according to structure: phosphino-oxazolines; phosphite- and phosphinite-oxazolines; catalysts containing a P–N bond; and structurally related non-oxazoline catalysts.

29.2.1 Phosphino-oxazolines

The most extensively studied of these systems are the phosphino-oxazoline (PHOX) catalysts **14** (Fig. 29.2). Good enantioselectivity has been achieved with these catalysts over a broad range of substrates [7].

The highest enantioselectivity in the hydrogenation of unfunctionalized tri-substituted alkenes has been achieved with catalyst **14a**. The same catalyst was also used to hydrogenate α,β-unsaturated phosphonates with enantiomeric excesses (ee) of 70 to 94% [8].

The PHOX ligands have a modular structure (Scheme 29.1). They are synthesized from chiral amino alcohols and benzonitrile or bromobenzonitrile: the

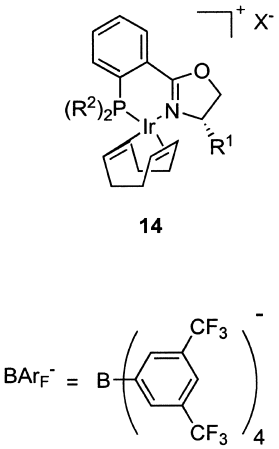

	R^1	R^2	X
a)	*t*Bu	*o*-tol	BAr_F^-
b)	*t*Bu	*o*-tol	PF_6^-
c)	CH_2*t*Bu	Ph	BAr_F^-
d)	*t*Bu	Cy	BAr_F^-
e)	*i*Pr	Ph	PF_6^-
f)	*i*Pr	Ph	BAr_F^-
g)	*t*Bu	Ph	PF_6^-
h)	*i*Pr	*o*-tol	PF_6^-

Fig. 29.2 PHOX catalyst **14**.

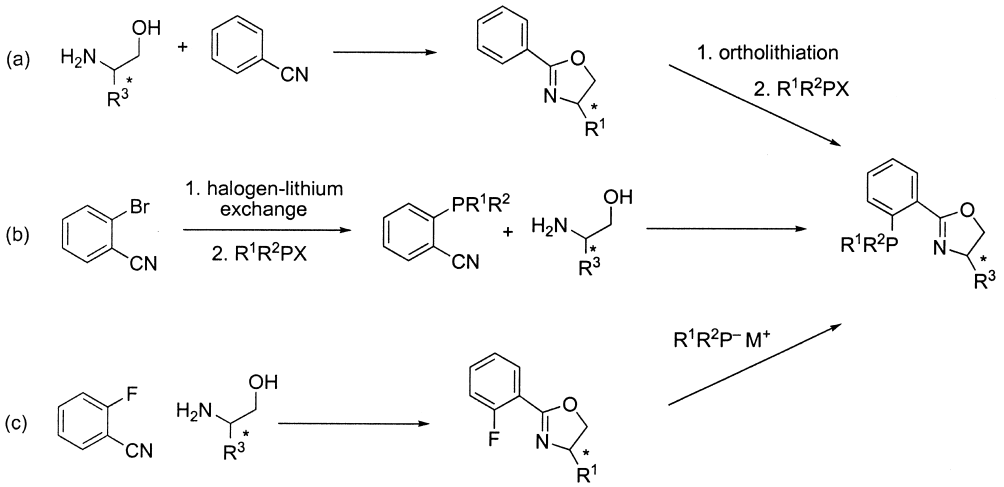

Scheme 29.1 Synthesis routes to the PHOX ligand.

phosphine is introduced *via* ortholithiation [9, 10] or lithium–halogen exchange as the first step [10–12] in ligand synthesis. Alternatively, the phosphine moiety can be introduced by nucleophilic substitution using an *ortho*-fluorophenyloxazoline as precursor (Scheme 29.1, route c) [13].

The stability of the PHOX catalysts containing the BAr_F counterion was found to be higher than that of those containing a PF_6^- counterion. The catalysts were more stable to air and moisture and, during hydrogenation, were deactivated more slowly than the corresponding PF_6^- catalysts, giving full conversion at >0.02 mol% catalyst loading [10].

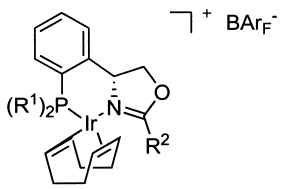

15

	R^1	R^2
a)	Ph	*t*Bu
b)	Ph	$CHPh_2$
c)	Ph	3,5-*t*$Bu_2C_6H_3$
d)	Ph	adamantyl
e)	Cy	*t*Bu

Fig. 29.3 PHOX catalysts **15**.

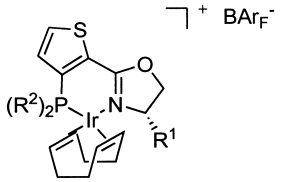

16

26a-d

	R^1	R^2
a)	*i*Pr	Ph
b)	*t*Bu	Ph
c)	*t*Bu	*o*-tol
d)	*t*Bu	Cy

Fig. 29.4 HetPHOX catalyst **6**.

A series of analogues of the original PHOX catalyst, in which the phenyl bridge is attached to C(4) instead of C(2) of the oxazoline ring (**15**, Fig. 29.3), were recently synthesized [14]. These catalysts were used to hydrogenate a number of substrates, including a range of 1-phenylbutenoic acids, with >90% ee.

Another PHOX analogue has the aryl ring of the PHOX catalyst replaced by a thiophene unit **16** (Fig. 29.4) [15]. The synthesis is similar to that of the PHOX catalysts, starting with *ortho*-metallation of the thiophene. The catalysts showed similar selectivity to PHOX, and were used to hydrogenate substrates **1** and **2** with maximum enantioselectivities of 99% and 94%, respectively.

JM-Phos, a PHOX analogue with an alkyl backbone (**17**, Fig. 29.5) has been used to hydrogenate a number of substrates with moderate to good enantioselectivity [16].

Another alkyl-bridged PHOX (**18**, Fig. 29.6) was recently synthesized [17], and used to hydrogenate a series of substituted methylstilbenes in 75–95% ee, and β-methylcinnamic esters in 80–99% ee. The hydrogenation results suggest that the selectivity of these catalysts is mainly derived from the substitution at the stereogenic center on the oxazoline ring, with the other stereocenter having a relatively minor effect on the ee-value.

The ligand synthesis is straightforward, using amino alcohols as the source of chirality in the oxazoline ring, whereas the stereochemistry in the phospholane ring is controlled by an enantioselective deprotonation using sparteine (Scheme 29.2).

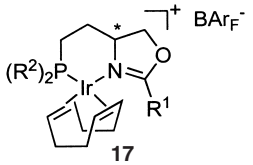

	R^1	R^2		R^1	R^2
	a) Me	Ph		f) CH(Ph)$_2$	Ph
	b) *t*Bu	Ph		g) CH(Ph)$_2$	*o*-tol
	c) *t*Bu	*o*-tol		h) C(Ph)$_2$Me	*o*-tol
	d) 1-Ad	Ph		i) Ph	Ph
1-Ad = 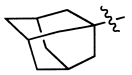	e) C(Ph)$_3$	Ph		j) 3,5-*t*Bu$_2$C$_6$H$_3$	Ph

Fig. 29.5 JM-PHOS catalyst **17**.

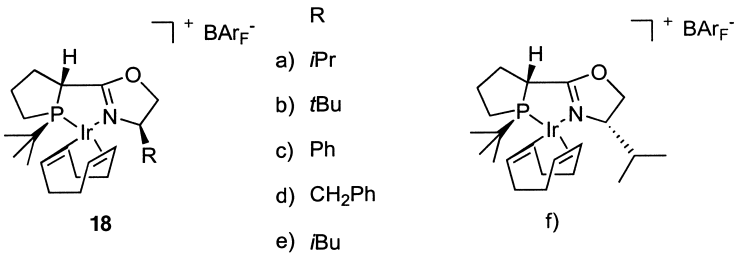

Fig. 29.6 Phospholane-oxazoline catalyst **18**.

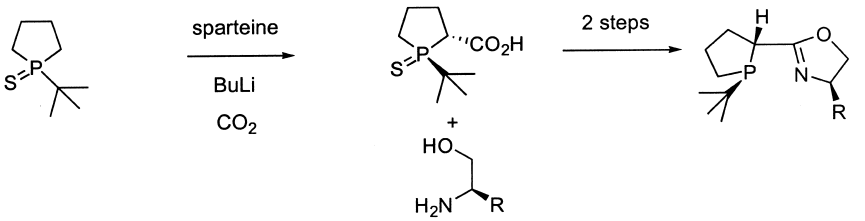

Scheme 29.2 Synthesis of ligands for catalyst **18**.

The ferrocene-oxazoline catalyst **19** (Fig. 29.7) has recently been used to hydrogenate substituted quinolines [18]. The ligand synthesis is again similar to that of the original PHOX ligand, with introduction of phosphorus *via* orthometallation.

29.2.2
Phosphite and Phosphinite Oxazolines

A PHOX analogue containing a P–O bond, the TADDOL-derived phosphite oxazoline catalyst **20a** (Fig. 29.8) has been used in the hydrogenation of a number of substituted styrenes, as well as in asymmetric allylic alkylation [19]. However,

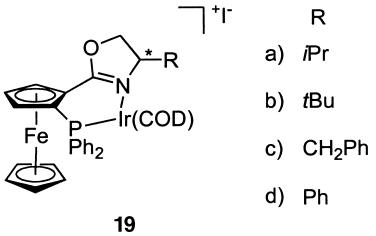

Fig. 29.7 Ferrocene-oxazoline catalyst **19**.

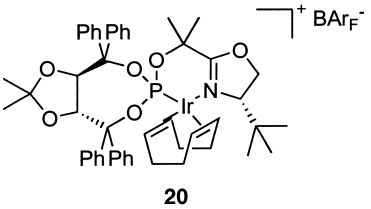

Fig. 29.8 Catalyst **20**.

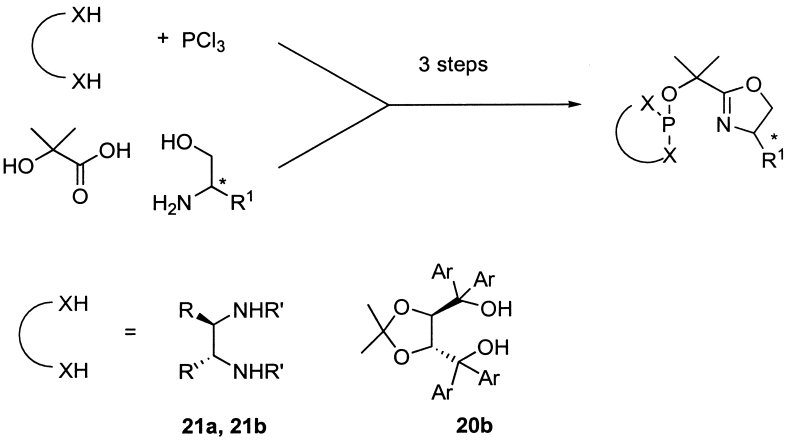

Scheme 29.3 Synthesis of aminophosphine and phosphinite catalysts **20b**, **21a** and **21b**.

the enantioselectivities were only moderate and catalytic activity was low, requiring 4 mol% catalyst.

The synthesis strategy is shown in Scheme 29.3. The incorporation of a diol or diamine gives ligand **20b** or ligands **21a** and **21b**, respectively.

More recent developments are the SerPHOX catalyst **22** [20] and the ThrePHOX catalyst **23** [21] (Fig. 29.9), derived from serine or threonine, respectively (Scheme 29.4).

In many cases, these catalysts proved to be superior to the PHOX complexes **14**. Complexes **23a** and **23g** are among the most efficient catalysts (and are

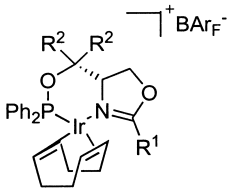

22

R^1	R^2
a) ferrocenyl	*i*Pr
b) ferrocenyl	*i*Bu
c) ferrocenyl	CH_2Ph
d) 3,5-*t*$Bu_2C_6H_3$	CH_2Ph

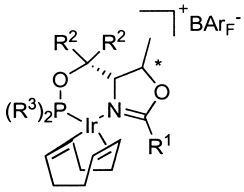

23

	R^1	R^2	R^3	
a)	Ph	CH_2Ph	Ph	(4*S*, 5*S*)
b)	Ph	CH_2Ph	Ph	(4*S*, 5*R*)
c)	Ph	CH_2Ph	*o*-tol	
d)	Ph	Me	Ph	
e)	3,5-$Me_2C_6H_3$	CH_2Ph	Ph	
f)	3,5-*t*$Bu_2C_6H_3$	CH_2Ph	Ph	
g)	Ph	CH_2Ph	Cy	

Fig. 29.9 SerPHOX and ThrePHOX catalysts **22** and **23**.

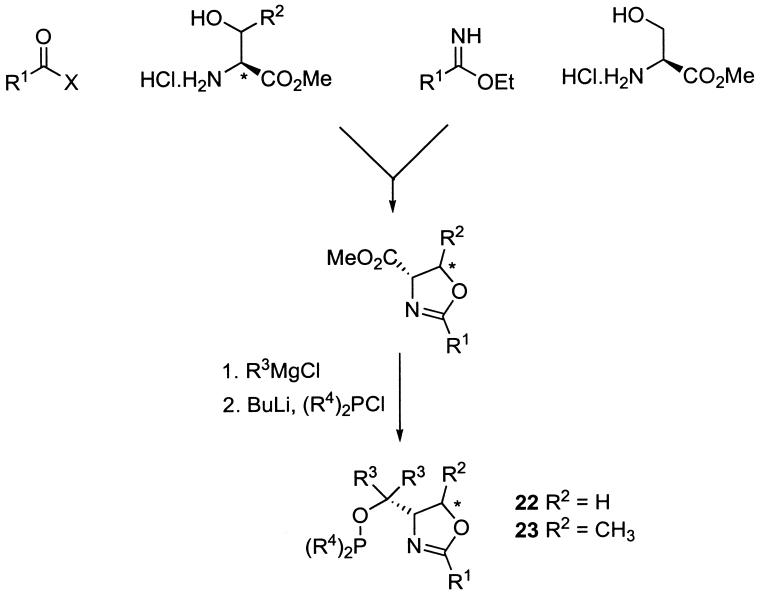

Scheme 29.4 Synthesis of SerPHOX (**22**) and ThrePHOX (**23**) catalysts.

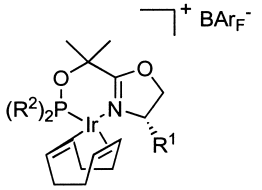

	R^1	R^2
a)	*t*Bu	Ph
b)	*t*Bu	*o*-tol
c)	*i*Pr	Ph
d)	*i*Pr	*o*-tol

24

Fig. 29.10 SimplePHOX catalyst **24**.

Scheme 29.5 Synthesis of SimplePHOX catalysts.

now commercially available [22]), giving high enantioselectivities and turnover numbers (TONs) for a range of trisubstituted and 1,1-disubstituted alkenes. The additional methyl group on the oxazoline ring of ThrePHOX ligands led to greater selectivity in the hydrogenation of substrates **1**, **3**, and **4** [21]. The synthesis is again modular (Scheme 29.4).

Another efficient, readily available catalyst is the SimplePHOX complex (**24**, Fig. 29.10) [23].

The ligand synthesis requires only two steps from simple starting materials. As with the PHOX type catalysts, chirality is built in through the use of a chiral amino alcohol (Scheme 29.5).

Complex **24a** proved to be a particularly efficient catalyst for the hydrogenation of the cyclic substrate **5**, affording 95% ee, which currently is the highest ee-value obtained with any catalyst for this substrate. High enantioselectivities were also obtained with α,β-unsaturated substrate **6**. Catalyst **24a** also gave higher selectivity than the ThrePHOX catalysts **23** in the hydrogenation of substrates **2** and **4**.

29.2.3
Oxazoline-Derived Ligands Containing a P–N Bond

The first oxazoline-derived catalysts containing P–N bonds to be synthesized were the diaminophosphines **21** (Fig. 29.11) (details of the synthesis are shown in Scheme 29.3). This class of catalysts gave good enantiomeric excesses in the hydrogenations of some unfunctionalized olefins, albeit with low conversions and high catalyst loading (4 mol%) [19, 24]. Analogous complexes with N-aryl-

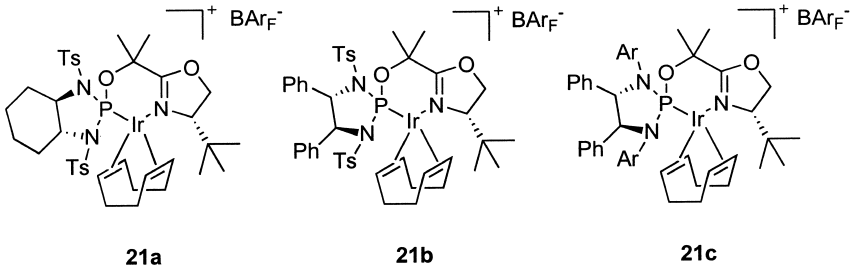

Fig. 29.11 Diaminophosphine catalysts **21**.

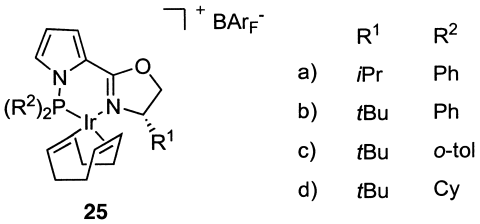

	R^1	R^2
a)	*i*Pr	Ph
b)	*t*Bu	Ph
c)	*t*Bu	*o*-tol
d)	*t*Bu	Cy

Fig. 29.12 PyrPHOX catalyst **25**.

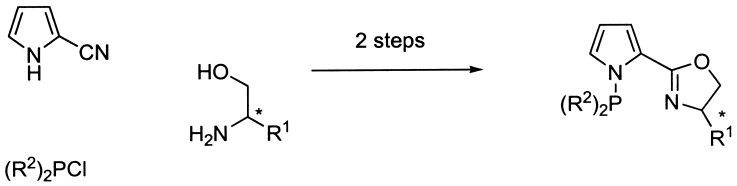

Scheme 29.6 Synthesis of PyrPHOX catalysts.

substituted ligands **21c** demonstrate much higher reactivity, and have been shown to be particularly efficient catalysts for the hydrogenation of α,β-unsaturated carboxylic esters [5].

PyrPHOX catalysts **25** (Fig. 29.12) [25], with a pyrrole instead of a phenyl bridge, showed selectivity which was comparable to – and in some cases better than – that of the PHOX catalysts **14**.

The synthesis is similar to that of the PHOX catalysts (Scheme 29.6), starting with oxazoline formation from the pyrrole nitrile and an amino alcohol, followed by introduction of the phosphine group.

The pyrrolidine-oxazoline catalysts **26** (Fig. 29.13) can be conveniently synthesized from proline in five steps, and have been used to hydrogenate the methylstilbenes **1** and **8** in 92% ee and 94% ee, respectively [26].

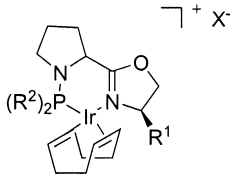

26

	R^1	R^2	X^-
a)	*i*Pr	Ph	PF_6^-
b)	*i*Pr	Ph	BAr_F^-
c)	*t*Bu	Ph	BAr_F^-
d)	*t*Bu	*o*-tol	PF_6^-
e)	*t*Bu	*o*-tol	BAr_F^-
f)	*t*Bu	2-Ethylphenyl	BAr_F^-
g)	*t*Bu	2,3-$Me_2C_6H_3$	BAr_F^-
h)	*t*Bu	2,4-$Me_2C_6H_3$	BAr_F^-

Fig. 29.13 Pyrrolidine-oxazoline catalyst **26**.

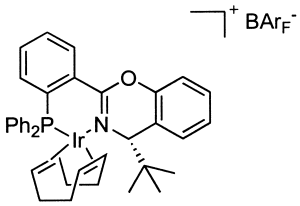

27

Fig. 29.14 Phosphino-benzoxazine catalyst **27**.

29.2.4
Structurally Related Ligands

A number of ligands have been synthesized which have structural similarities to the oxazoline-derived ligands.

The first of these was the phosphino-benzoxazine catalyst **27** (Fig. 29.14) [27]. This catalyst contains a six-membered benzoxazine ring in place of the five-membered oxazoline ring in the PHOX catalysts. It was hoped that this change would bring the chiral center on the ring into closer contact with the metal, resulting in higher enantioselectivities. However, enantiomeric excesses were only modest with the substrates chosen.

The phosphino-imidazoline catalyst **28** (Fig. 29.15) is a close analogue of the original PHOX ligand.

Phosphino-imidazoline ligands of this type were originally synthesized by Busacca and coworkers and used in an enantioselective Heck reaction [28].

The additional nitrogen atom in the ring gives another site for substitution (Scheme 29.7), and thus for steric and electronic tuning of the ligand structure. A range of catalysts were prepared and used in the hydrogenation of unfunctionalized alkenes. These outperformed the original PHOX catalyst in the hydrogenation of substrates **3**, **4**, and **5** [29]. They have also been successfully applied to the hydrogenation of terpenoid dienes and trienes [30].

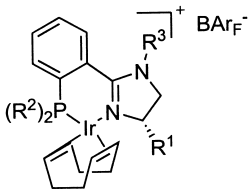

28

	R^1	R^2	R^3
a)	*i*Pr	Ph	*i*Pr
b)	*i*Pr	Ph	Cy
c)	*i*Pr	Ph	CH_2Ph
d)	*i*Pr	Ph	Ph
e)	*t*Bu	Ph	Ph
f)	*t*Bu	Ph	*p*-$MeOC_6H_4$
g)	*t*Bu	Ph	*p*-$CF_3C_6H_4$
h)	*t*Bu	Ph	*p*-tol
i)	*t*Bu	*o*-tol	Ph
j)	*t*Bu	*o*-tol	CH_2Ph

Fig. 29.15 Phosphino-imidazoline catalysts **28**.

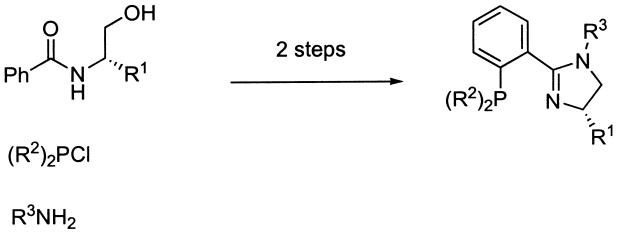

Scheme 29.7 Synthesis of phosphino-imidazoline ligands.

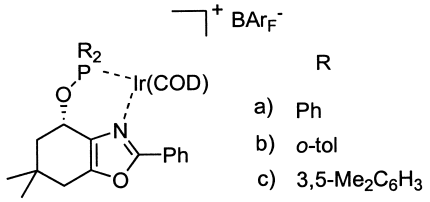

29

Fig. 29.16 Phosphinite-oxazole catalyst **29**.

Finally, the phosphinite-oxazole catalyst **29** (Fig. 29.16) was recently reported and used to hydrogenate a series of functionalized and unfunctionalized alkenes [31]. It was anticipated that the planar oxazole unit and the fused ring system would improve the enantioselectivity compared to the PHOX catalyst by increasing rigidity in the six-membered chelating ring [32]. Indeed, these catalysts

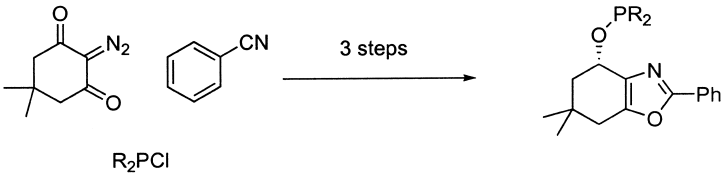

Scheme 29.8 Synthesis of phosphinite-oxazole catalysts.

proved to be highly selective, rivaling the most selective oxazoline-based catalysts in the hydrogenation of a range of substrates.

The ligands are synthesized from achiral starting materials using a ketocarbene-nitrile cycloaddition as the key step (Scheme 29.8). The stereogenic center is introduced by enantioselective reduction of the carbonyl group in the cycloaddition product.

29.3
Pyridine and Quinoline-Derived P,N Ligands

Knochel and coworkers synthesized a series of camphor-derived pyridine and quinoline P,N ligands. The catalysts **30** (Fig. 29.17) were used to hydrogenate substrates **1** and **2** in up to 95% and 96% ee, respectively [33]. The selectivities were moderate for other unfunctionalized alkenes; however, a high enantioselectivity was reported for the hydrogenation of ethyl acetamidocinnamate **10** [34].

The ligands derive their chirality from the ring bearing the phosphorus atom, synthesized from (+)-camphor (R = H) or (+)-nopinone (R = CH_3) (Scheme 29.9).

Recently, a series of pyridine- and quinoline-derived catalysts **31** (Fig. 29.18) have been developed. Ligands **31 a–k** were obtained by reduction of pyridyl ke-

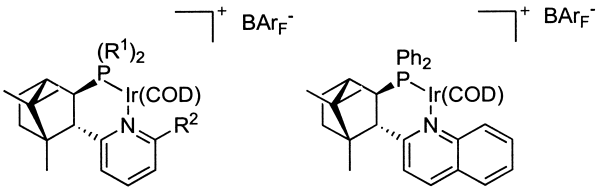

30a-c **30d**

	R^1	R^2
a)	Ph	H
b)	Ph	Ph
c)	Cy	H

Fig. 29.17 Catalyst **30**.

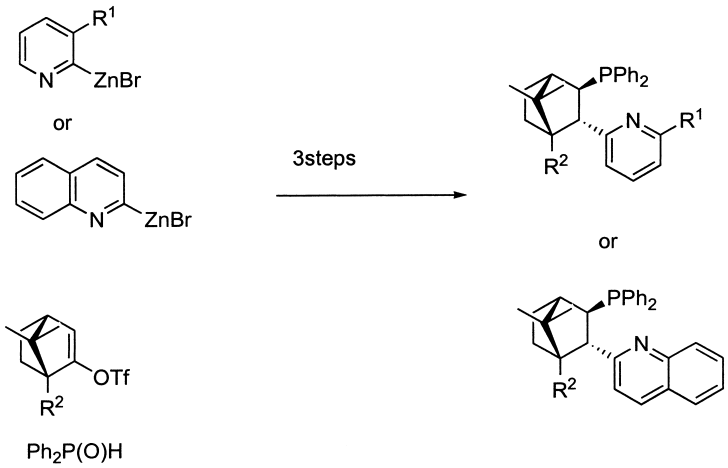

Scheme 29.9 Synthesis of pyridine-derived ligands for catalysts **30**.

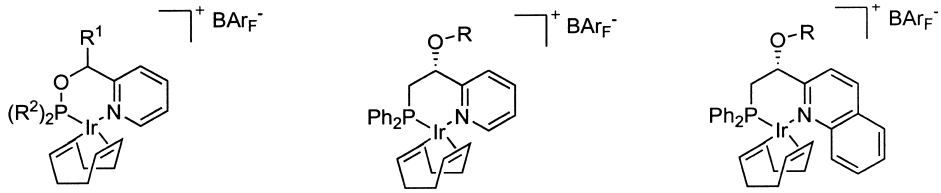

31 a-k

	R^1	R^2
a)	Me	Ph
b)	Me	*o*-tol
c)	Ph	Ph
d)	Ph	*o*-tol
e)	Ph	Cy
f)	Ph	*t*Bu
g)	*t*Bu	Ph
h)	*t*Bu	*o*-tol
i)	*t*Bu	Cy
j)	*t*Bu	*t*Bu
k)	trityl	Ph

31 l-n

	R
l)	Si(*t*Bu)Me_2
m)	Si(*i*Pr)$_3$
n)	Si(*t*Bu)Ph_2

31 o-r

	R
o)	Si(*t*Bu)Me_2
p)	Si(*i*Pr)$_3$
q)	Si(*t*Bu)Ph_2

Fig. 29.18 Pyridine-based catalysts **31**.

tones and resolution of the resulting alcohols. Ligands **31 l–n** were synthesized *via* enantioselective reduction of pyridyl ketones and protection as silyl ethers, and ligands **31 o–q** were accessed through Sharpless dihydroxylation of a quinolyl alkene, followed by tosylation and introduction of the phosphine group.

In the hydrogenation of **1**, catalysts **31 a–j** gave 87–97% ee, whereas catalyst **31 k**, with the very bulky trityl substituent on the alkyl backbone, only gave 38% ee. The silyl substituent was found to have a significant effect on selectivity: catalyst **31 l** gave 88% ee, while catalyst **31 n** gave only 4% ee with substrate **1** [35]. This remarkable effect was rationalized based on X-ray structural data.

29.4 Carbenoid Imidazolylidene Ligands

The first application of a heterocyclic carbenoid achiral ligand for hydrogenation of alkenes was reported in 2001 by Nolan and coworkers. Both ruthenium [36] and iridium [37] complexes proved to be active catalysts. Turnover frequency (TOF) values of up to 24 000 h^{-1} (at 373 K) were measured for a ruthenium catalyst in the hydrogenation of 1-hexene.

Another series of achiral iridium catalysts containing phosphine and heterocyclic carbenes have also been tested in the hydrogenation of unfunctionalized alkenes [38]. These showed similar activity to the Crabtree catalyst, with one analogue giving improved conversion in the hydrogenation of **11**.

Subsequently, Burgess and coworkers developed the chiral carbenoid ligands **32** (Scheme 29.10), which were structurally related to the JM-PHOS ligand [39, 40].

The most selective catalyst in this series, complex **32 c**, with very bulky substituents at the oxazoline and the imidazolylidene moiety, was used to hydrogenate a range of trisubstituted alkenes with enantiomeric excesses of greater than

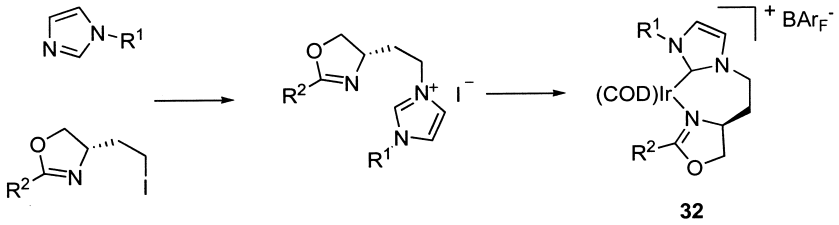

32

	R^1	R^2
a)	Ph	2,6-(*i*Pr)$_2$C$_6$H$_3$
b)	*t*Bu	2,6-(*i*Pr)$_2$C$_6$H$_3$
c)	1-Ad	2,6-(*i*Pr)$_2$C$_6$H$_3$
d)	CHPh$_2$	2,6-(*i*Pr)$_2$C$_6$H$_3$
e)	1-Ad	2,5-(Et)$_2$C$_6$H$_3$

Scheme 29.10 Carbenoid imidazolylidene ligands based on the JM-PHOS ligand (**32**).

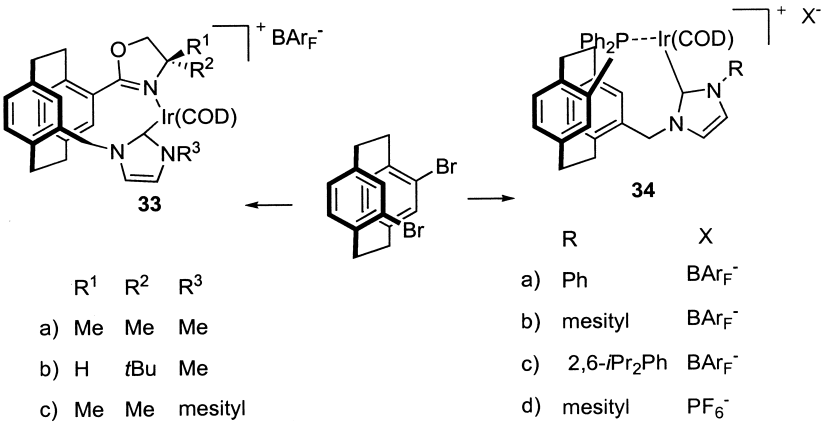

Fig. 29.19 Paracyclophane catalysts.

90%. It was found that the R^1 substituent on the carbenoid ring had a greater effect on selectivity than the R^2 substituent on the oxazoline. All the other catalysts **32a**, **32b**, **32d** and **32e** gave distinctly lower enantioselectivities.

Recently, carbene-oxazoline catalysts **33** and carbene-phosphine catalysts **34** (Fig. 29.19) with a chiral paracyclophane backbone have been synthesized and used to hydrogenate a variety of alkenes, with modest selectivity [41].

29.5 Metallocenes

The metallocenes are described in greater detail in Chapter 30.

Catalyst **35b** was used by Buchwald and coworkers with $[PhMe_2NH]^+$-$[(BC_6F_5)_4]^-$ to hydrogenate tetrasubstituted unfunctionalized cyclic olefins with up to 97% ee [42].

The enantiopure catalyst **35b** was synthesized from **35c** [43] *via* the binaphtholate **35a** [44, 45].

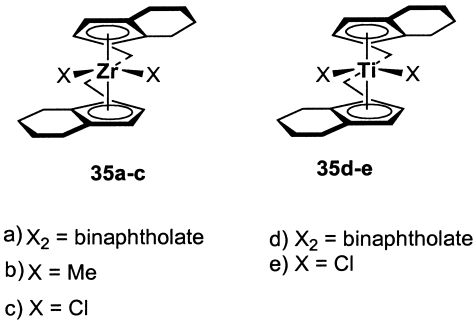

Fig. 29.20 EBTHI catalysts **35**.

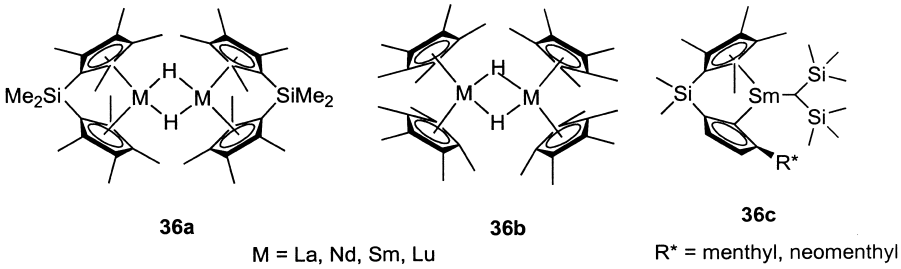

Fig. 29.21 Cyclopentadienyl lanthanide catalysts **36**.

The most selective – and also most general – titanocene catalyst is complex **35d**, also studied by Buchwald and coworkers. This catalyst was used to hydrogenate a variety of functionalized and unfunctionalized cyclic and acyclic alkenes with excellent ee-values in most cases [46]. Enamines could also be hydrogenated with enantiomeric excesses of 80–90% [47]. However, high catalyst loadings (5–8 mol%) and long reaction times were required to drive the reactions to completion.

Marks and coworkers developed a series of cyclopentadienyl-lanthanide complexes. In the initial investigations on achiral catalysts **36a** and **36b** (Fig. 29.21), TOFs greater than 100 000 h^{-1} were observed in the hydrogenation of 1,2-disubstituted unfunctionalized alkenes [48].

Chiral analogue **36c** was then synthesized [49]. Catalyst **36c** (R = menthyl) hydrogenated 2-phenyl-1-butene **7** with 96% ee at 195 K, with enantioselectivity being found to be highly temperature-dependent.

29.6 Other Ligands

The cobalt complex **37** was used in combination with quinine as a chiral coordinating base to hydrogenate 1,2-diphenyl-2-propene-1-one in 49% ee (Fig. 29.22) [50]. However, no further studies of this type of catalyst were reported.

Corma and coworkers tested a number of rhodium and other transition metal complexes with ligands based on proline (Fig. 29.23). These authors reported ee-values of 54–90% for the hydrogenation of dehydroamino acid derivatives with a catalyst prepared from ligand **38** [51]. With ligand **39**, an ee-value of 34% was recorded for the hydrogenation of ethyl acetamidocinnamate **10** [52].

Brauer and coworkers also prepared a rhodium catalyst, using an amino-phospholane ligand, catalyst **40** (Fig. 29.24). This was used to hydrogenate ethyl acetamidocinnamate **10** in 60% ee [53].

Catalyst **41** (Fig. 29.29) is based on a sulfinyl imine, with the stereogenic center at the sulfinamide group. The best catalyst in this series, **41a**, gave 94% ee in the hydrogenation of substrate **1** [54]. The catalyst has low activity, with 5 mol% catalyst being required.

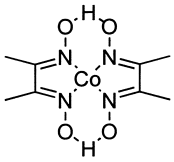

37

Fig. 29.22 Cobalt catalyst **37**.

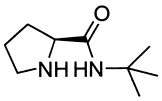

38

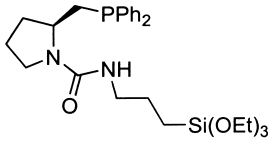

39

Fig. 29.23 Ligands **38** and **39**.

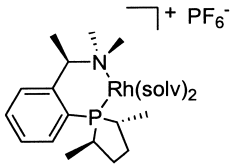

40

Fig. 29.24 Catalyst **40**.

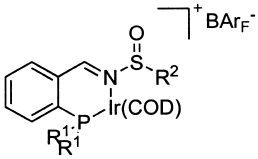

41

	R^1	R^2
a)	*o*-tol	*t*Bu
b)	*o*-tol	1-Ad
c)	*o*-tol	3-ethylpentyl
d)	*o*-tol	*p*-tol
e)	*o*-tol	mesityl
f)	3,5-$Me_2C_6H_3$	*t*Bu
g)	Ph	*t*Bu

Fig. 29.25 Sulfinyl imine catalyst **41**.

Finally, another group of rhodium catalysts based on ligands **42** to **45** (Fig. 29.26) has recently been synthesized and tested on the enantiomeric hydrogenation of α-phenylcinnamic acid **13**, giving 59 to 84% ee [55, 56]. The same complexes, when immobilized on mesoporous silica, were found to be even more enantioselective. The results obtained with rhodium complexes based on ligands such as **38**, **43**, **44**, or **45** are in contrast to the general experience that catalysts containing only nitrogen ligands are catalytically inactive and show a tendency to decompose under hydrogen pressure to give metallic rhodium.

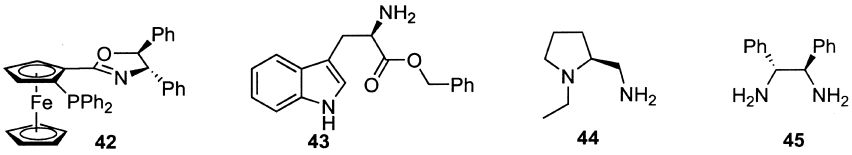

42-45 $[Rh(COD)L]^{+}CF_3SO_3^{-}$

Fig. 29.26 Catalysts **42** to **45**.

Further studies will be necessary to confirm these results and to establish the potential of catalysts of this type.

29.7 Conclusions

The development of chiral P,N and non-phosphorus ligands for the asymmetric hydrogenation of C=C bonds remains a young and rapidly developing field of research. The application range of these ligands is largely complementary to chiral phosphines. While chiral phosphines form efficient catalysts in combination with Rh and Ru, the primary domain of P,N ligands is Ir-catalyzed hydrogenation (see Chapter 30). Iridium complexes with chiral P,N ligands have considerably expanded the application range of asymmetric hydrogenation to unfunctionalized alkenes as well as various functionalized olefins, which give poor results with Rh or Ru catalysts. The most efficient P,N ligands developed to date have been oxazoline derivatives such as ThrePHOX 23 or SimplePHOX 24, and the bicyclic oxazole derivative **29**. Promising results have also been obtained with the carbenoid P,C ligand **32**. Metallocene catalysts have also been successfully applied for asymmetric hydrogenation of unfunctionalized alkenes, though as yet this class of catalysts has found only limited use.

Abbreviations

ee	enantiomeric excess
PHOX	phosphino-oxazoline
TOF	turnover frequency
TON	turnover number

References

1 L. Horner, H. Siegel, H. Büthe, *Angew. Chem.* **1968**, 1034.
2 W.S. Knowles, M.J. Sabacky, *J. Chem. Soc. Chem. Commun.* **1968**, 1445.
3 T.P. Dang, H.B. Kagan, *J. Chem. Soc. Chem. Commun.* **1971**, 481.
4 B.D. Vineyard, W.S. Knowles, M.J. Sabacky, G.L. Bachman, D.J. Weinkauff, *J. Am. Chem. Soc.* **1977**, *99*, 5946.
5 A. Pfaltz, J. Blankenstein, R. Hilgraf, E. Hörmann, S. McIntyre, F. Menges, M. Schönleber, S.P. Smidt, B. Wüstenberg, N. Zimmermann, *Adv. Synth. Catal.* **2003**, *345*, 33.
6 R. Crabtree, *Acc. Chem. Res.* **1979**, *12*, 331.
7 A. Lightfoot, P. Schnider, A. Pfaltz, *Angew. Chem. Int. Ed.* **1998**, *37*, 2897.
8 N.S. Goulioukina, M. Dolgina, G.N. Bondarenko, I.P. Beletskaya, M.M. Ilyin, V.A. Davankov, A. Pfaltz, *Tetrahedron Asymm.* **2003**, *14*, 1397.
9 D.G. Blackmond, A. Lightfoot, A. Pfaltz, T. Rosner, P. Schnider, N. Zimmermann, *Chirality* **2000**, *12*, 442.
10 G. Koch, G.C. Lloyd-Jones, O. Loiseleur, A. Pfaltz, R. Pretot, S. Schaffner, P. Schnider, P. von Matt, *Rec. Trav. Chim. Pays-Bas* **1995**, *114*, 206.
11 P. Von Matt, A. Pfaltz, *Angew. Chem. Int. Ed. Engl.* **1993**, *32*, 556.
12 J.V. Allen, G.J. Dawson, C.G. Frost, J.M.J. Williams, *Tetrahedron* **1994**, *50*, 799.
13 M. Peer, J.C. de Jong, M. Kiefer, T. Langer, H. Rieck, H. Schell, P. Sennhenn, J. Sprinz, H. Steinhagen, B. Wiese, G. Helmchen, *Tetrahedron* **1996**, *52*, 7547.
14 D. Liu, W. Tang, X. Zhang, *Org. Lett.* **2004**, *6*, 513.
15 P.G. Cozzi, F. Menges, S. Kaiser, *Synlett* **2003**, *6*, 829.
16 D.R. Hou, J.H. Reibenspies, T.J. Colacot, K. Burgess, *Chem. Eur. J.* **2001**, *7*, 5391.
17 W. Tang, W. Wang, X. Zhang, *Angew. Chem. Int. Ed.* **2003**, *42*, 943.
18 S. Lu, X. Han, Y. Zhou, *Adv. Synth. Catal.* **2004**, *346*, 909.
19 R. Hilgraf, A. Pfaltz, *Synlett* **1999**, *11*, 1814.
20 J. Blankenstein, A. Pfaltz, *Angew. Chem. Int. Ed.* **2001**, *40*, 4445.
21 F. Menges, A. Pfaltz, *Adv. Synth. Catal.* **2002**, *344*, 40.
22 Available from STREM: complex **23a** catalog number 77-5020, complex **23g** catalog number 77-5010.
23 S.P. Smidt, F. Menges, A. Pfaltz, *Org. Lett.* **2004**, *6*, 2023.
24 R. Hilgraf, A. Pfaltz, *Adv. Synth. Catal.* **2005**, *347*, 61.
25 P.G. Cozzi, N. Zimmermann, R. Hilgraf, S. Schaffner, A. Pfaltz, *Adv. Synth. Catal.* **2001**, *343*, 450.
26 G. Xu, S.R. Gilbertson, *Tetrahedron Lett.* **2003**, *44*, 953.
27 G.H. Bernardinelli, E.P. Kündig, P. Meier, A. Pfaltz, K. Radkowski, N. Zimmermann, M. Neuburger-Zehnder, *Helv. Chim. Acta* **2001**, *84*, 3233.
28 C. Busacca, WO2001018012, **2001**.
29 F. Menges, M. Neuburger, A. Pfaltz, *Org. Lett.* **2002**, *4*, 4173.
30 Patent application: B. Wüstenberg, F. Menges, T. Netscher, A. Pfaltz, (DSM), 22. 12. 2004.
31 K. Källstrom, C. Hedberg, P. Brandt, A. Bayer, P.G. Andersson, *J. Am. Chem. Soc.* **2004**, *126*, 14308.
32 P. Brandt, C. Hedberg, P.G. Andersson, *Chem. Eur. J.* **2003**, *9*, 339.
33 T. Bunlaksananusorn, K. Polborn, P. Knochel, *Angew. Chem.* **2003**, *42*, 3941.
34 T. Bunlaksananusorn, P. Knochel, *J. Org. Chem.* **2004**, *69*, 4595.
35 W.J. Drury, N. Zimmermann, M. Keenan, M. Hayashi, S, Kaiser, R. Goddard, A. Pfaltz, *Angew. Chem. Int. Ed.* **2004**, *43*, 70.
36 H.M. Lee, D.C. Smith, Z. He, E.D. Stevens, C.S. Yi, S.P. Nolan, *Organometallics* **2001**, *20*, 794.
37 H.M. Lee, T. Jiang, E.D. Stevens, S.P. Nolan, *Organometallics* **2001**, *20*, 1255.
38 L.D. Vázquez-Serrano, B.T. Owens, J.M. Buriak, *J. Chem. Soc. Chem. Commun.* **2002**, 2518.
39 M.T. Powell, D.R. Hou, M.C. Perry, X. Cui, K. Burgess, *J. Am. Chem. Soc.* **2001**, *123*, 8878.

40 M.C. Perry, X. Cui, M.T. Powell, D.R. Hou, J.H. Riebenspies, K. Burgess, *J. Am. Chem. Soc.* **2003**, *125*, 113.

41 C. Bolm, T. Focken, G. Raabe, *Tetrahedron Asymm.* **2003**, *14*, 1733.

42 M.V. Troutman, D.H. Appella, S.L. Buchwald, *J. Am. Chem. Soc.* **1999**, *121*, 4916.

43 F.R.W.P. Wild, L. Zsolnai, G. Huttner, H.H. Brintzinger, *J. Organomet. Chem.* **1985**, *232*, 233.

44 R.B. Grossman, W.M. Davis, S.L. Buchwald, *J. Am. Chem. Soc.* **1991**, *113*, 2321.

45 R.M. Waymouth, F. Bangerter, P. Pino, *Inorg. Chem.* **1988**, *27*, 758.

46 R.D. Broene, S.L. Buchwald, *J. Am. Chem. Soc.* **1993**, *115*, 12569.

47 N.E. Lee, S.L. Buchwald, *J. Am. Chem. Soc.* **1994**, *116*, 5985.

48 G. Jeske, H. Lauke, H. Mauermann, H. Schumann, T.J. Marks, *J. Am. Chem. Soc.* **1985**, *107*, 8111.

49 V.P. Conticello, L. Brard, M.A. Giardello, Y. Tsuji, M. Sabat, C.L Stern, T.J. Marks, *J. Am. Chem. Soc.* **1992**, *114*, 2761.

50 Y. Ohgo, S. Takeuchi, Y. Natori, J. Yoshimura, *Bull. Chem. Soc. Jpn.* **1981**, *54*, 2124.

51 A. Corma, M. Iglesias, C. Del Pino, F. Sánchez, *J. Chem. Soc. Chem. Commun.* **1991**, *1252*, 1253.

52 A. Carmona, A. Corma, M. Iglesias, A. San José, F. Sánchez, *J. Organomet. Chem.* **1995**, *492*, 11.

53 D.J. Brauer, K.W. Kottsieper, S. Rossenbach, O. Stelzer, *Eur. J. Inorg. Chem.* **2003**, 1748.

54 L.B. Schenkel, J.A. Ellman, *J. Org. Chem.* **2003**, *69*, 1800.

55 J. Rouzaud, M.D. Jones, R. Raja, B.F.G. Johnson, J.M. Thomas, M.J. Duer, *Helv. Chim. Acta* **2003**, *86*, 1753.

56 M.D. Jones, R. Raja, J.M. Thomas, B.F.G. Johnson, D.W. Lewis, J. Rouzaud, K.D.M. Harris, *Angew. Chem. Int. Ed.* **2003**, *42*, 4326.

30
Enantioselective Hydrogenation of Unfunctionalized Alkenes

Andreas Pfaltz and Sharon Bell

30.1
Introduction

Enantioselective hydrogenation of functionalized alkenes is a well-developed field. A wide variety of rhodium and ruthenium catalysts and substrates are available for this purpose (see Chapters 23 to 28), and the reaction is widely used as a common synthetic tool in both academia and industry.

Unfunctionalized alkenes have posed more of a problem, as they have no polar moiety which can coordinate to the catalyst. Such an additional metal binding site next to the C=C bond has proven to be crucial for directing coordination to the catalyst and, therefore, rhodium and ruthenium complexes, which are highly selective for functionalized alkenes, generally provide only low enantioselectivity for this class of substrates.

Initially, progress in this area was hampered by the lack of suitable analytical methods for chiral hydrocarbons. Early studies relied on optical rotation to determine enantiomeric excess (ee) values, but with the development of chiral gas chromatography (GC) and high-performance liquid chromatography (HPLC) columns, chromatographic methods have become more common.

Aided by these developments, the past five years has seen a rapid growth in this area. A breakthrough was the introduction of iridium catalysts with chiral P,N ligands. A large number of new P,N and other ligands have been synthesized and applied to the hydrogenation of unfunctionalized alkenes. This chapter details the catalysts, conditions and substrates used in the enantiomeric hydrogenation of unfunctionalized alkenes.

The Handbook of Homogeneous Hydrogenation.
Edited by J.G. de Vries and C.J. Elsevier
Copyright © 2007 WILEY-VCH Verlag GmbH & Co. KGaA, Weinheim
ISBN: 978-3-527-31161-3

30.2
Terminal Alkenes

30.2.1
2-Aryl-1-Butenes

The enantioselective hydrogenation of terminal 1,1-disubstituted olefins presents a particular challenge. Enantioface differentiation in the compounds relies on the different interactions of the catalyst with the two substituents which, as in the case of **1** and **2** (Fig. 30.1), are sterically quite similar.

Initially, research focused on the use of C_2-symmetric rhodium and ruthenium-phosphine and phosphinite complexes: a rhodium–phosphine complex **3** (Fig. 30.2) was used in the first reported enantioselective hydrogenation of substrate **1** (Table 30.1, entry 1) [1].

With most rhodium and ruthenium catalysts **4** and **5** (Fig. 30.2), only low enantioselectivities were obtained (Table 30.1, entries 1–6) [2–6]. However, good results were reported by Noyori and coworkers, who used DuPHOS with potassium *tert*-butoxide activation to hydrogenate substrate **1** in 86% ee (Table 30.1, entry 6) [6], as well as hydrogenating a range of other 1,1-disubstituted alkenes (see Section 30.2.2).

However, the best-researched group of catalysts for these substrates is the metallocenes (Fig. 30.3; Table 30.1, entries 7–13) [7–14]. The highest ee-value was obtained with the chiral samarium metallocene **10a**. Hydrogenation of **1** at –78 °C gave 2-phenylbutane in 96% ee (Table 30.1, entry 12) [12]. Turnover frequencies (TOFs) as high as 1210 h^{-1} have been recorded for these catalysts [14]. Catalyst **10b**, the titanocene analogue of **10a**, has been synthesized and used to hydrogenate **1** in 60% ee (Table 30.1, entry 13) [13].

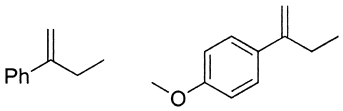

1 **2**

Fig. 30.1 Alkenes discussed in Section 30.2.1.

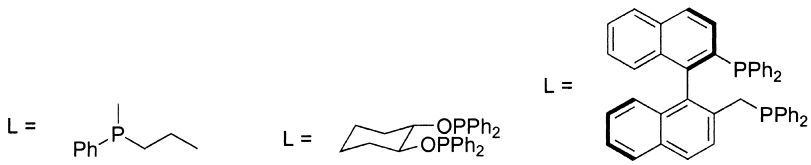

3 **4** **5**

[Rh(1,5-hexadiene)L_2]$^+$Cl$^-$ [Rh(1,5-hexadiene)L]$^+$Cl$^-$ [Rh(COD)L]$^+$Cl

Fig. 30.2 Rhodium catalysts **3**, **4** and **5**.

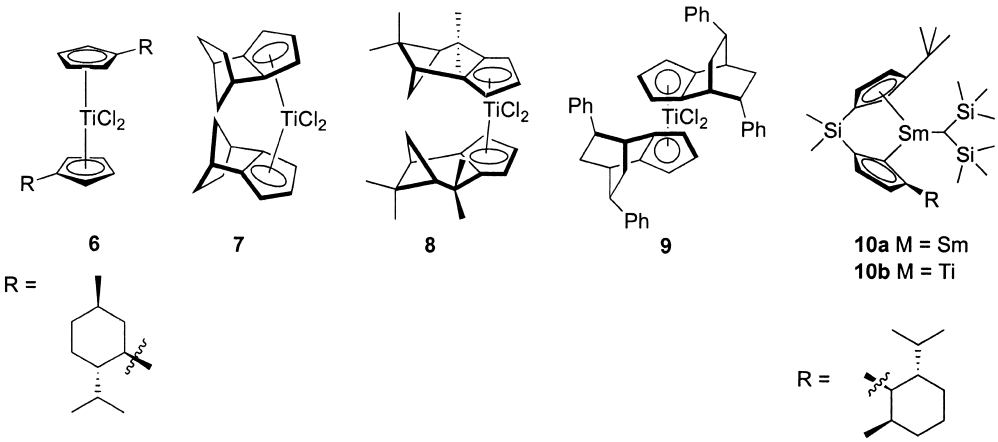

Fig. 30.3 Selected catalysts for the hydrogenation of substrate **1**.

More recently, Ir-JM-Phos **11** (Fig. 30.4) was used to hydrogenate **1** in a moderate 40% ee (Table 30.1, entry 14) [15]. This catalyst was found to be more selective in the hydrogenation of trisubstituted alkenes (see Section 30.3).

Substrate **2** has also been used as a test substrate: HPLC separation methods exist for **2**, while ee-value determination of **1** is more difficult [6, 17]. Reflecting the general recent interest in the hydrogenation of unfunctionalized olefins, the past few years have seen the publication of a number of results for this substrate [15, 18–26]. The highest enantioselectivities were achieved using catalysts **12b** [22] and **14a** [26].

Pressure effects have been found to have a significant effect on the enantioselectivity of hydrogenation of terminal olefins with ThrePHOX catalysts, in contrast to trisubstituted olefins [17, 25]. For example, in the hydrogenation of **2** with catalyst **12b**, 94% ee was obtained at 1 bar H_2, compared to 58% ee at 50 bar H_2 (Table 30.2).

The ThrePHOX catalyst was also used to hydrogenate a wider range of 2-aryl-1-butenes. Substrates **15–18**, **20** and **21** (Fig. 30.6) were hydrogenated in high yield and ee (Table 30.3).

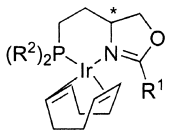

11a R^1 = ^{t}Bu R^2 = Ph

11b R^1 = Bn R^2 = *o*-tol

11c R^1 = *t*-Bu R^2 = *o*-tol

Fig. 30.4 Catalyst **11**.

Table 30.1 Hydrogenation of substrate **1**.

Entry	Catalyst	Loading [mol%]	Solvent	Temp. [°C]	Pressure [bar]	ee [%]	TOF [h^{-1}] (TON)[a)]	Reference
1	**3**	0.5	Benzene	r.t.	1	8 (*S*)		1
2	**4**			50	50	33 (*R*)		2
3	Ru–DIOP	0.1	No solvent	20	100	1.9 (*S*)		3
4	BINAP	1.5	DCM	30	25	29 (*S*)	4	4
5	**5**	1	Benzene/ methanol	30	25	65 (*R*)	1	5
6	DuPHOS + *t*BuOK	0.5	2-Propanol	r.t.	8	74 (*R*)	13 (200)	6
7	**6**	1	Toluene	20	1	11.2[b)] (*S*)		7
8	**6**	1	Hexane/ THF	5	1	28 (*S*)		8
9	**7**			–20		27[b)] (*R*)		9
10	**8**	0.02–0.04	Toluene	r.t.	1	69 (*S*)		10
11	**9**	1	Toluene	–75	1	77[b)] (*R*)	10	11
12	**10a**	0.2–1		–78		96 (*S*)	(500)	12
13	**10b**	1	Hexane/ THF	20	1	48 (*S*)	2 (100)	14
14	**11**	0.3	DCM	25	50	40 (*R*)	165	15

a) TOF data given where available; TON data given where reactions were complete after a standard reaction time, or where no time data were available.
b) Values corrected from the original papers, where ee calculations were based on an incorrect $[\alpha]_D$ value for 2-phenylbutane (22.7 rather than 28.4 [16]).

The DuPHOS/potassium *tert*-butoxide system was also used to hydrogenate these substrates, in addition to substrates **19** and **22** (Fig. 30.6; Table 30.4) [6]. Under normal conditions, ruthenium–diphosphine catalysts are known to be unreactive with styrenes: however, in the presence of potassium *tert*-butoxide, the substrates **15–22** were hydrogenated with high conversion.

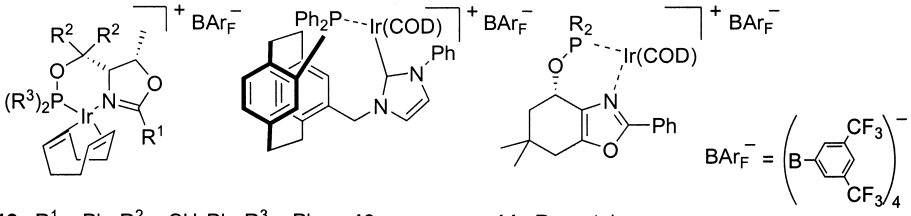

12a R^1 = Ph, R^2 = CH_2Ph, R^3 = Ph **13a**
12b R^1 = Ph, R^2 = CH_2Ph, R^3 = Cy
12c R^1 = 3,5-(*t*Bu)$_2C_6H_3$, R^2 = CH_2Ph, R^3 = Ph
12d R^1 = 3,5-$Me_2C_6H_3$, R^2 = CH_2Ph, R^3 = Ph

14a R = *o*-tol
14b R = Ph
14c R = 3,5-$Me_2C_6H_3$

Fig. 30.5 Selected catalysts for the hydrogenation of substrate **2**.

Table 30.2 Most selective hydrogenations of substrate **2**.

Entry	Catalyst	Loading [mol%]	Solvent	Temp. [°C]	Pressure [bar]	ee [%]	TOF [h^{-1}] (TON)[a)]	Reference
1	**12a**	1	DCM	0	1	89 (*R*)	50 (100)	22
2	**12b**	1	DCM	25	1	94	200 (100)	25
3	**13a**	1	DCM	25	1	79 (*S*)	(100)	23
4	**14a**	0.5	DCM	r.t.	50	97 (*S*)	100 (200)	26

a) TON data given where reactions were complete after a standard reaction time, or where no time data were available.

Table 30.3 Hydrogenation of substrates **15**–**18**, **20** and **21** with ThrePHOX catalyst **12b**.

Substrate	ee [%]	Conversion [%]	Pressure [bar]	Catalyst loading [mol%]	TOF [h^{-1}] (TON)[a)]
15	91	>99	1	1	200 (100)
16	88	>99	1	1	200 (100)
17	89	>99	1	1	200 (100)
18	93	>99	1	1	200 (100)
20	92	>99	1	1	200 (100)
21	94	>99	1	1	200 (100)

a) All reactions were complete after standard reaction time of 30 min: the calculated TOF is a lower limit of the true TOF.

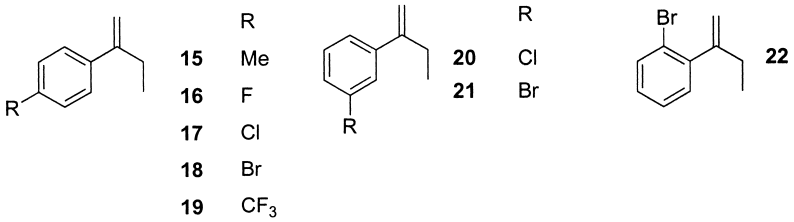

Fig. 30.6 Substrates **15**–**22**.

Table 30.4 Hydrogenation of substrates **15**–**22** with $RuCl_2[(R,R)\text{-MeDuPHOS}](DMF)_n$.[a)]

Substrate	ee [%]	Absolute configuration	Conversion [%]	Catalyst loading [mol%]	TOF [h^{-1}] (TON)[b)]
15	87	*R*	87	0.3	20
16	82	*R*	97	0.15	40
17	85	*R*	94	0.07	80
18	83	*R*	100	0.15	40 (660)
19	81	*R*	99.5	0.04	160
20	89	*R*	87	0.2	30
21	86	*R*	100	0.2	30 (520)
22	69	*R*	33	0.26	8

a) Hydrogenations carried out in 2-propanol at 30 °C using 8 bar H_2.
b) TON data given where reactions were complete after a standard reaction time, or where no time data were available.

30.2.2
Other Terminal Alkenes

A range of other terminal alkenes has been hydrogenated with ruthenium–diphosphine catalysts. The first set of substrates (Fig. 30.7; Table 30.5) was hydrogenated with Ru–BINAP in dichloromethane (DCM) at 30 °C. Products of double bond migration were also detected [5].

The modified BINAP catalyst **5** has been used for the hydrogenation of a number of analogues of substrate **1** (substrates **32**–**35**, Fig. 30.8; Table 30.6), though again, enantioselectivities were modest [4]. Substrate **31** has also been hydrogenated with a ruthenium–BINAP-hydride cluster with low selectivity (11% ee) [27].

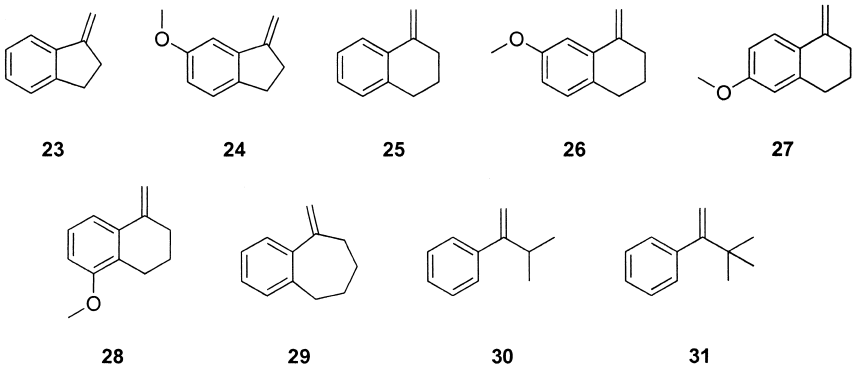

Fig. 30.7 Substrates **23**–**31**.

Table 30.5 Hydrogenation of substrates **23**–**31** with $[Rh(BINAP)(COD)]^{+}X^{-}$.[a)]

Substrate	ee [%]	Absolute configuration	Conversion [%]	Pressure [bar]	Catalyst loading [mol%]	TOF [h^{-1}]
23[b)]	78	*S*	100	100	4	1
24[b)]	45	–	100	100	4	1
25	80	*S*	81	25	1.5	15
26	71	(+)	85	25	1.5	16
27[b)]	75	–	100	100	4	0.6
28[b)]	61	(+)	100	100	4	0.6
29	44	(–)	56	25	1.5	1.6
30	35	*R*	100	25	1.5	0.8
31	40	–	87	25	1.5	1

a) Hydrogenations carried out in DCM at 30 °C.
b) Isomerization products also detected.

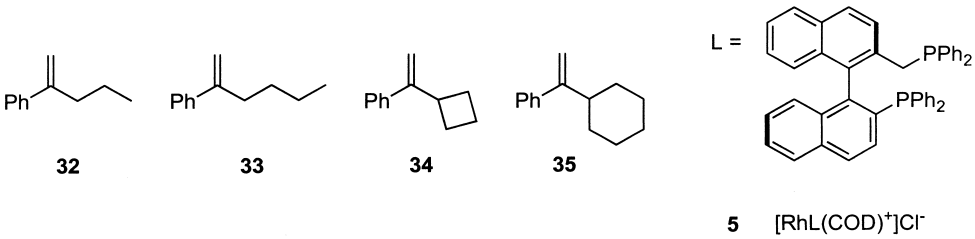

Fig. 30.8 Substrates **32**–**35** and catalyst **5**.

Table 30.6 Hydrogenation of substrates **30**–**35** with catalyst **5**.[a)]

Substrate	ee [%]	Absolute configuration	Conversion [%]	TOF [h^{-1}] (TON)[b)]
30	17	*R*	100	4 (100)
31	31	*R*	75	3
32	77	*R*	100	2
33	55	*R*	100	4 (100)
34	16	(–)	100	4 (100)
35	2	*R*	100	2

a) Hydrogenations performed in 1:1 benzene:methanol at 30 °C using 25 bar H_2 and 1 mol% catalyst.
b) TON data given where reactions were complete after a standard reaction time, or where no time data were available.

30.3 Trisubstituted Alkenes

30.3.1 Introduction

Substrates **36** to **40** (Fig. 30.9) have become standard test substrates, and many catalysts have been evaluated with this set of alkenes. For that reason the hydrogenation of these test substrates is discussed in one section. Some catalysts have also been used to hydrogenate a wider variety of alkenes (see Section 30.3.2).

Initially, the benchmark for the enantioselective hydrogenation of trisubstituted unfunctionalized alkenes was set very high, with the titanocene catalyst **41** (Fig. 30.10) being used to hydrogenate test substrates **36**, **38** and **40**, as well as some others (see Section 30.3.2) in very high selectivity [28]. However, the catalysts were not very active, requiring high catalyst loadings (4 mol%) and long reaction times. Phosphino-oxazoline-derived iridium catalysts (Ir–PHOX, **42**; Fig. 30.10), which were introduced later, gave very high ee-values with diaryl alkenes **36** and **37** and moderate to good enantioselectivities with substrates **38**, **36**, and **39** [29, 30]. The turnover number (TON) and TOF were clearly superior compared with the titanocene **41**. Substrate **43** was also hydrogenated with this catalyst in 95% ee.

Subsequently, further investigations were focused on this catalyst class.

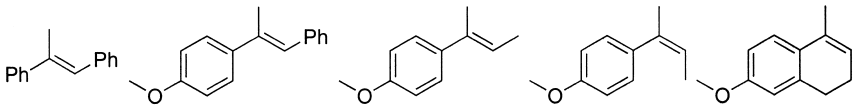

36 **37** **38** **39** **40**

Fig. 30.9 Trisubstituted alkenes used as test substrates.

30.3.2
Ir Catalysts

As discussed below, Ir complexes derived from chiral P,N ligands have become the catalysts of choice for the enantiomeric hydrogenation of unfunctionalized trisubstituted olefins. Therefore, the most important characteristics of these catalysts are briefly summarized here [30–32].

The catalyst precursors (cationic Ir–COD complexes with weakly coordinating anions such as BAr_F) are air- and moisture-stable, and are therefore easy to handle. It is possible to store them for several months under air. Two of the most versatile catalysts (ThrePHOX catalysts, **12a** and **12b**) recently became commercially available [33].

The catalysts are highly reactive: maximum TOFs of $>5000\ h^{-1}$ at 277 K were measured for the hydrogenation of substrate **2** with catalysts of type **42**. The reaction is mass transfer-limited at room temperature and, therefore, a value of $5000\ h^{-1}$ represents a lower limit for the possible maximum TOF [31]. Full conversion was achieved with catalyst loadings as low as 0.01 mol% (substrate **2**, catalyst **12a**).

Reactions are typically run at 10 to 100 bar H_2, though pressure has a minimal effect on enantioselectivity.

Common solvents used are DCM, 1,2-dichloroethane, and toluene. More strongly coordinating solvents such as tetrahydrofuran (THF), acetonitrile or alcohols deactivate the catalyst.

The anion plays a crucial role. BAr_F and other bulky fluorinated tetra-arylborates or tetraalkoxyaluminates are the most suitable anions. Hexafluorophosphate-containing catalysts display high reactivity in the initial phase of the reaction, but suffer deactivation before the reaction reaches completion. Tetrafluoroborate, triflate or other more strongly coordinating anions inhibit the catalyst.

In contrast to the hydrogenation of imines, where addition of acids and/or iodine often has a beneficial effect, here additives of this type were found to deactivate the catalyst.

30.3.3
Standard Test Substrates

The promising results obtained with Ir–PHOX complexes prompted an extensive search for related, more selective catalysts with broader substrate scope.

The diamine and TADDOL-derived catalysts **44** were tested on substrates **36**–**39**, giving good enantioselectivities; however, high catalyst loadings of 4 mol% were required for full conversion [34].

SimplePHOX complex **45** (Fig. 30.10) was used to hydrogenate substrates **36** and **38**–**40**, and proved to be one of the most selective catalysts for the hydrogenation of substrate **40** [24].

A new group of PHOX catalysts was developed, based on the attachment of the oxazoline at the 2-position rather than the 5-position as in the original

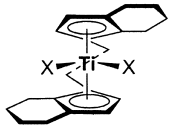

41
X = 1,1'-binaph-2,2'-diolate

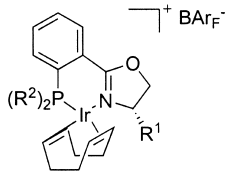

42a R^1 = *t*Bu, R^2 = Cy
42b R^1 = *t*Bu, R^2 = *o*-tol

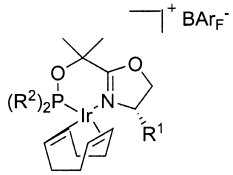

45a R^1 = Ph, R^2 = Bn
45b R^1 = *t*Bu, R^2 = *o*-tol
45c R^1 = *i*Pr, R^2 = Ph

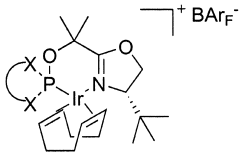

44

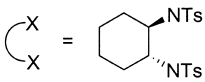

44a

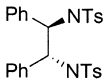

44b

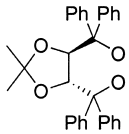

44c

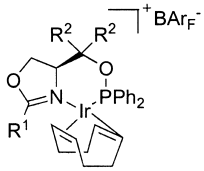

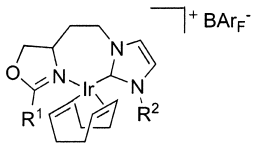

46a R^1 = Ph, R^2 = 2,6-(*i*Pr)$_2$C$_6$H$_3$
46b R^1 = 1-adamantyl, R^2 = 2,6-(*i*Pr)$_2$C$_6$H$_3$
46c R^1 = 1-adamantyl, R^2 = 2,6-(Et)$_2$C$_6$H$_3$

47a R^1 = Ph, R^2 = 2,6(*i*Pr)$_2$C$_6$H$_3$
47b R^1 = 1-adamantyl, R^2 = 2,6-(*i*Pr)$_2$C$_6$H$_3$
47c = R^1 = 1-adamantyl, R^2 = 2,6-(*i*Pr)$_2$C$_6$H$_3$

Fig. 30.10 Selected catalysts for the hydrogenation of trisubstituted alkenes.

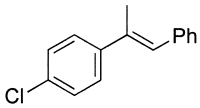

43

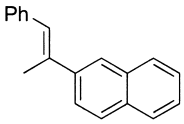

48

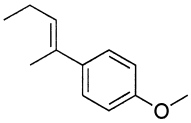

49

Fig. 30.11 Substrates **43**, **48** and **49**.

PHOX catalysts. While the first generation of these catalysts (SerPHOX **46**, Fig. 30.10) hydrogenated substrates **36** and **38–40** in good yield and ee [19], significant progress was made with the second generation of catalysts [22]. With an additional chiral center, ThrePHOX catalysts **12** (Fig. 30.5) gave very high enantioselectivities, particularly for substrates **38** (Table 30.9, entry 7) and **39** (Table 30.10, entry 7). Complexes **12** are also efficient catalysts for the hydrogenation of 1,1-disubstituted substrates (see Section 30.2.1).

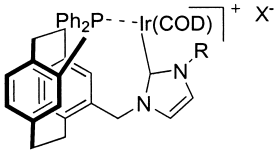

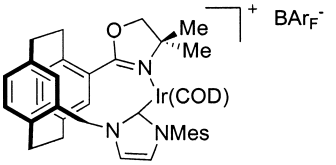

13a R = Ph, X^- = BAr_F^-
13b R = 2,4,6-Me_3Ph, X^- = BAr_F^-
13c R = 2,6-*i*-Pr_2Ph, X^- = BAr_F^-
13d R = 2,4,6-Me_3Ph, X^- = PF_6^-

50

Fig. 30.12 Catalysts **13** and **50**.

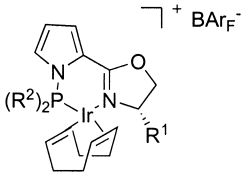

51 [37]
R^1 = *i*Pr, *t*Bu; R^2 = aryl, Cy

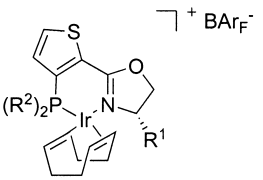

52a [38]
R^1 = *i*Pr, *t*Bu; R^2 = aryl, Cy

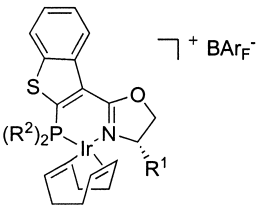

52b [38]
R^1 = *i*Pr, *t*Bu; R^2 = aryl

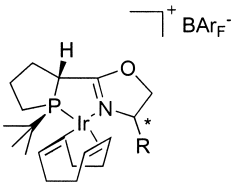

R = *i*Pr, *t*Bu, Ph, Bn, *i*Bu
54 [39]

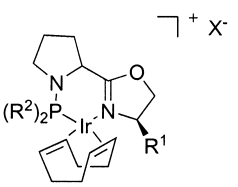

R = aryl, X = BAr_F, PF_6
55 [40]

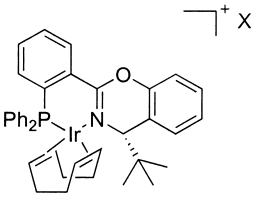

56a X = BAr_F^- [18]
56b X = PF_6^-

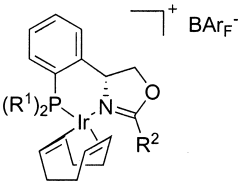

R^1 = Ph, Cy;
R^2 = bulky aryl, alkyl

57 [41]

Fig. 30.13 Catalysts **51**–**57**.

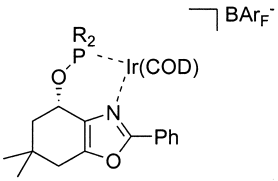

14a R = *o*-tol
14b R = Ph
14c R = 3,5-Me$_2$Ph

Fig. 30.14 Oxazole–phosphinite complex **14**.

The structurally related JM-Phos catalyst **11** (Fig. 30.10) gave generally lower selectivity for substrates **36–40** [15]. Deuteration studies using D_2 with these catalysts showed substantial deuterium incorporation into the allylic positions of substrates **39** and **2**. Deuterium incorporation has also been observed with Ir–PHOX catalysts [35], which implies that reversible H abstraction at the allylic position occurs during the hydrogenation reaction.

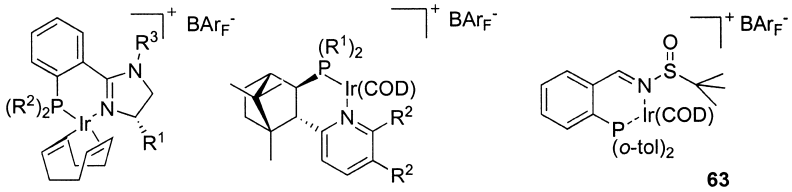

58a R^1 = *t*Bu, R^2 = *o*-tol, R^3 = Ph
58b R^1 = *t*Bu, R^2 = *o*-tol, R^3 = Bn

59a R^1 = Ph, R^2 = H
59b R^1 = Ph, R^2 = -CH$_2$CH=CHCH$_2$-

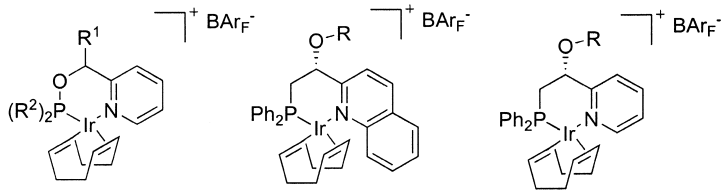

60

a R^1 = *t*Bu, R^2 = *t*Bu (*S*)
b R^1 = Ph, R^2 = Ph
c R^1 = *t*Bu, R^2 = Ph (*S*)
d R^1 = *t*Bu, R^2 = *o*-tol (*R*)
e R^1 = *t*Bu, R^2 = Cy (*S*)
f R^1 = trityl, R^2 = Ph (*R*)

61

a R = Si(*t*Bu)Me$_2$
b R = Si(*i*Pr)$_3$
c R = Si(*t*Bu)Ph$_2$

62

a R = Si(*t*Bu)Me$_2$
b R = Si(*i*Pr)$_3$
c R = Si(*t*Bu)Ph$_2$

Fig. 30.15 Catalysts **58–63**.

Table 30.7 Hydrogenation of substrate **36**.

Entry	Catalyst	Loading [mol%]	Solvent	Temp. [°C]	Pressure [bar]	ee [%]	TOF [h^{-1}] (TON)[a)]	Reference
1	**41**	5	THF	65	5	>99 (*S*)	2	28
2	**42a**	1	DCM	25	50	99 (*R*)	50 (100)	30
3	**44a**	4	DCM	r.t.	100	94 (*R*)	2	34
4	**47a**	0.2–0.6	DCM	25	50	98 (*S*)	250	21
5	**45a**	1	DCM	r.t.	50	99 (*R*)	50 (100)	24
6	**46a**	0.4	DCM	23	50	98 (*R*)	125 (250)	19
7	**12a**	0.02	DCM	r.t.	50	99 (*R*)	2500 (5000)	22
8	**11b**	0.2	DCM	25	50	95 (*S*)	250	15
9	**58a**	1	DCM	r.t.	50	94 (*R*)	50 (100)	42
10	**14b**	0.5	DCM	r.t.	30	>99 (*S*)	100 (200)	26
11	**59a**	0.5	toluene	25	50	95 (*S*)	8 (100)	43
12	**50**	1	DCM	25	50	28 (*R*)		36
13	**13a**	1	DCM	25	50	82 (*R*)	4	23
14	**60a**	1	DCM	r.t.	50	97 (*R*)	50 (100)	44
15	**63**	5	DCM	r.t.	50	94 (*R*)	20	45

a) TON data given where reactions were complete after a standard reaction time, or where no time data were available.

In addition to P,N ligands, the carbenoid-oxazoline catalysts **47** (Fig. 30.10) were used to hydrogenate test substrates **36**–**39**, as well as substrates **48** and **49**, which were hydrogenated in 93% ee and 84% ee, respectively [21]. These catalysts were also used to hydrogenate 1,1-disubstituted alkenes (see Section 30.2.1).

In recent years, many related ligands have been produced. Bolm and co-workers have produced new carbenoid catalysts **13** and **50** (Fig. 30.12) based on a paracyclophane backbone [23, 36]. To date, however, enantioselectivities have been modest with these catalysts.

Table 30.8 Hydrogenation of substrate **37**.

Entry	Catalyst	Loading [mol%]	Solvent	Temp. [°C]	Pressure [bar]	ee [%]	TOF [h^{-1}] (TON)[a)]	Reference
1	**42a**	1	DCM	25	50	99 (*R*)	50 (100)	30
2	**44b**	4	DCM	r.t.	100	92 (*R*)	7	34
3	**47a**	0.6	DCM	25	50	97 (*S*)	80	21
4	**11c**	0.2	DCM	–5	70	94 (*S*)	150	15
5	**59b**	1	toluene	25	50	95 (*S*)	40	43

a) TON data given where reactions were complete after a standard reaction time, or where no time data were available.

Table 30.9 Hydrogenation of substrate **38**.

Entry	Catalyst	Loading [mol%]	Solvent	Temp. [°C]	Pressure [bar]	ee [%]	TOF [h^{-1}] (TON)[a)]	Reference
1	**41**	5	THF	65	133	95 (*R*)	0.3	28
2	**42b**	0.1	DCM	r.t.	50	61 (*R*)	(330)	29
3	**44b**	4	DCM	r.t.	100	85 (*R*)	10 (25)	34
4	**47a**	0.6	DCM	25	50	91 (*S*)	80 (165)	21
5	**45b**	1	DCM	r.t.	50	91 (*R*)	50 (100)	24
6	**46b**	0.1	DCM	23	50	96 (*R*)	500 (1000)	19
7	**12c**	0.1	DCM	r.t.	50	99 (*R*)	500 (1000)	22
8	**11a**	0.6	DCM	25	50	80 (*S*)	75	15
9	**14a**	0.5	DCM	r.t.	50	96 (*S*)	100 (200)	26
10	**58b**	1	DCM	r.t.	50	90 (*R*)	50 (100)	42
11	**13a**	1	DCM	25	50	37 (*R*)	(100)	23
12	**60b**	1	DCM	r.t.	50	87	(100)	44

a) TON data given where reactions were complete after a standard reaction time, or where no time data were available.

A number of ligands have been prepared in which the PHOX aryl bridge has been replaced by heterocyclic rings, as shown in Figure 30.13. A phosphino-oxazoline complex **56** and a PHOX analogue **57**, in which the phenyl bridge is attached to C(5) of the oxazoline ring, have also been reported. None of these catalysts had any particular advantages compared to the best PHOX or SerPHOX/

Table 30.10 Hydrogenation of substrate **39**.

Entry	Catalyst	Loading [mol%]	Solvent	Temp. [°C]	Pressure [bar]	ee [%]	TOF [h^{-1}] (TON)[a)]	Reference
1	**41**	5	THF	65	133	31	0.1	28
2	**45c**	1	DCM	r.t.	50	89 (*R*)	50 (100)	24
3	**42b**	1	DCM	r.t.	50	42	(97)	29
4	**44c**	4	DCM	r.t.	100	90 (*S*)	10 (25)	34
5	**47a**	0.6	DCM	25	50	80 (*R*)	50	21
6	**49c**	0.4	DCM	23	50	85 (*S*)	125 (250)	19
7	**12d**	1	DCM	r.t.	50	92 (*S*)	50 (100)	22
8	**11a**	0.6	DCM	25	50	75 (*R*)	60	15
9	**58a**	1	DCM	r.t.	50	88 (*S*)	50 (100)	42
10	**13a**	1	DCM	25	50	79 (*R*)	(100)	23
11	**60b**	1	DCM	r.t.	50	90	(100)	44

a) TON data given where reactions were complete after a standard reaction time, or where no time data were available.

Table 30.11 Hydrogenation of substrate **40**.

Entry	Catalyst	Loading [mol%]	Solvent	Temp. [°C]	Pressure [bar]	ee [%]	TOF [h^{-1}] (TON)[a)]	Reference
1	**41**	5	THF	65	120	93	0.1	28
2	**45b**	0.2	DCM	r.t.	50	95 (*S*)	50 (100)	24
3	**46c**	0.5	DCM	23	50	85 (*S*)	100 (200)	19
4	**12a**	0.1	DCM	r.t.	50	85 (*S*)	50 (100)	22
5	**14a**	0.5	DCM	r.t.	50	94 (*R*)	100 (200)	26
6	**58a**	1	DCM	r.t.	50	91 (*S*)	50 (100)	42

a) TON data given where reactions were complete after a standard reaction time, or where no time data were available.

ThrePHOX complexes. The phospholane **54** and catalyst **57**, however, gave promising results for the hydrogenation of α,β-unsaturated carboxylic esters.

The oxazole–phosphinite complexes **14** (Fig. 30.14) proved to be highly selective catalysts, comparable to the best catalysts developed so far (see entries in Tables 30.9 and 30.11–30.13) [26].

Catalyst **58**, in which the oxazoline ring has been replaced with an imidazoline, gave ee-values in the low 90% region for substrates **36** and **38–40** [42]. However, for certain substrates (see Section 30.5), replacement of the oxazoline by an imidazoline has resulted in significantly higher enantioselectivity. Recently, a number of pyridine- and quinoline-derived iridium complexes **59–62** have been developed, which gave promising enantioselectivities with substrates **36–39** [43, 44]. However, these catalysts cannot yet compete with the most efficient oxazoline-based complexes and complex **14**.

The sulfinyl imine catalyst **63**, which has a stereogenic sulfur atom, hydrogenated substrate **36** in 94% ee; however, high catalyst loadings were used [45].

The full results for substrates **36–40** are detailed in Tables 30.7 to 30.11.

In summary, the most efficient catalysts for substrates **36–40** are the SerPHOX and ThrePHOX complexes **46** and **12**, as well as the recently reported oxazole–phosphinite complexes **14**.

30.3.4
Other Substrates

The titanocene catalyst **41** was used to hydrogenate a range of aryl-substituted alkenes (Fig. 30.16, Table 30.12) [28].

Styrene derivatives **68–71** (Fig. 30.17; Table 30.13) were hydrogenated with moderate to high selectivity using carbene complexes **13a** and **13b** [20].

Recently, a breakthrough in the hydrogenation of unfunctionalized olefins was made [51]. For the first time, high enantioselectivities with purely alkyl-substituted alkenes such as **72–74** could be achieved using pyridine–phosphinite catalysts **75** and **76**.

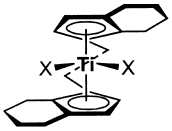

41

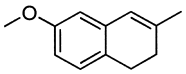

64

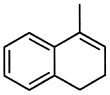

65

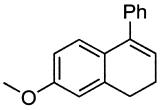

66

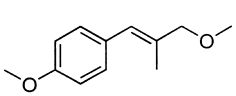

67

X_2 = 1,1'-binaphth-2,2'-diolate

Fig. 30.16 Catalyst **41** and substrates **64–67**.

Table 30.12 Hydrogenation of substrates **64–67**. [a)]

Substrate	ee [%]	Conversion [%]	Catalyst	TOF [h^{-1}]
64	92	77	**40**	0.4
65	83	70	**40**	0.1
66	83	87	**40**	0.05
67	94	86	**40**	0.4

a) Hydrogenations carried out in THF at 65 °C using 133 bar H_2 and 5 mol% of **41**.

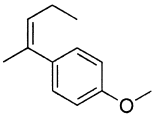

68

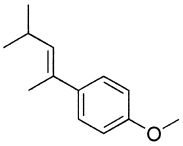

69

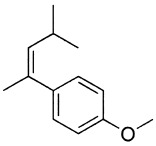

70

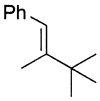

71

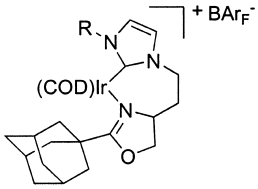

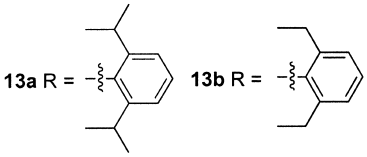

Fig. 30.17 Substrates **68–71** and catalyst **13**.

Table 30.13 Hydrogenation of substrates **68**–**71** with catalyst **13**.[a)]

Substrate	ee [%]	Conversion [%]	Pressure [bar]	TOF [h^{-1}] (TON)[b)]
68	49	58	50	50
69	97	100	2	80 (167)
70	89	92	2	80
71	86	18	1	15

a) Hydrogenations performed in DCM at 25 °C using 0.6 mol% of catalyst **13**.
a) TON data given where the reaction was complete after a standard reaction time.

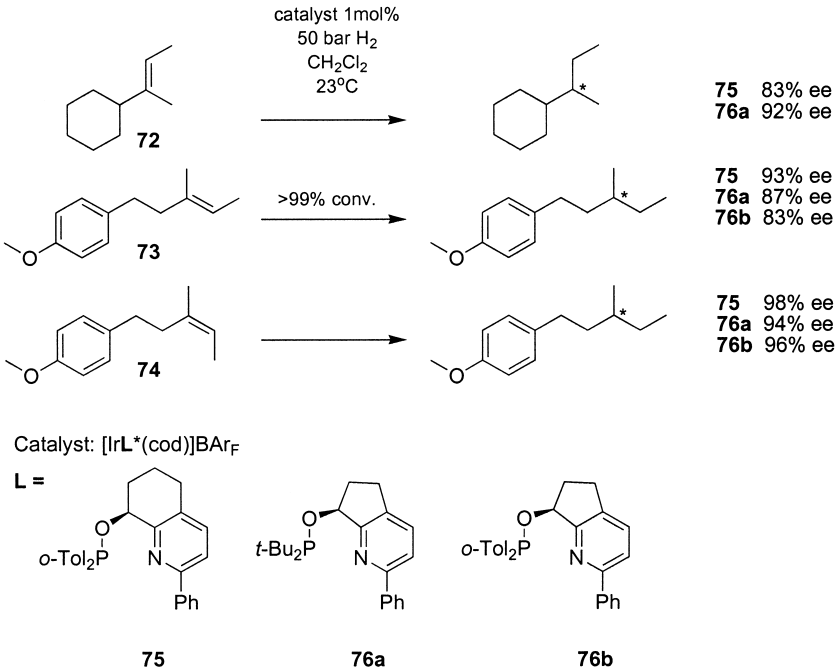

Fig. 30.18 Substrates **72**–**74** and catalysts **75** and **76**.

30.4 Tetrasubstituted Alkenes

30.4.1 Substrates

Tetrasubstituted alkenes are challenging substrates for enantioselective hydrogenation because of their inherently low reactivity. Crabtree showed that it was possible to hydrogenate unfunctionalized tetrasubstituted alkenes with iridium catalysts [46]. Among the iridium catalysts described in the previous section, several were found to be sufficiently reactive to achieve full conversion with alkene **77** (Table 30.14). However, the enantioselectivities were significantly lower than with trisubstituted olefins, and higher catalyst loadings were necessary.

The highest ee-values were obtained with the PHOX catalyst **42** and the pyridine-derived catalyst **60a** (Table 30.14, entries 1 and 2).

The metallocenes are the most selective catalysts developed to date for the hydrogenation of tetrasubstituted alkenes. However, the required catalyst loadings are relatively high (5–8 mol%). Catalyst **78** was activated with $[PhMe_2NH]^+[(BC_6F_5)_4]^-$ and used to hydrogenate a number of tetrasubstituted alkenes [47] (Fig. 30.20; Table 30.15). The ratios of *cis* to *trans* products obtained from cyclic substrates **80** to **86** were generally high (>95 : 5).

Table 30.14 Enantioselective hydrogenation of **77**.

Entry	Catalyst	Loading [mol%]	Solvent	Temp. [°C]	Pressure [bar]	ee [%]	Absolute config.	TOF [h^{-1}] (TON)[a)]	Reference
1	**42c**	2	DCM	r.t.	50	81	–	(50)	29
2	**60a**	1	DCM	r.t.	50	81	–	(100)	44
3	**56b**	1	DCM	r.t.	50	31	*S*	12	18
4	**14b**	1	DCM	r.t.	100	15	*S*	2	26

a) TON data given where no time data were available.

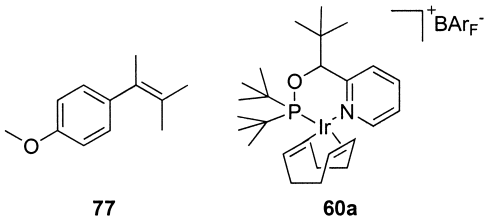

Fig. 30.19 Substrate **77** and catalyst **60a**.

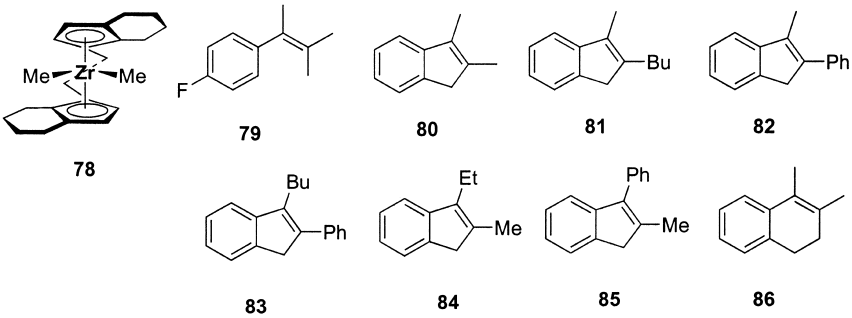

Fig. 30.20 Substrates **79**–**86** and catalyst **78**.

Table 30.15 Hydrogenation of tetrasubstituted alkenes with catalyst **78**. [a)]

Substrate	Absolute configuration	ee [%]	Yield [%]	Pressure [bar]	TON [b)]
79	(+)	96	77	117	10
80	(+)	93	87	117	11
81	(+)	92	96	5	12
82	(–)	99	89	69	18
83	(–)	98	94	103	12
84	–	52	95	117	12
85	(–)	78	94	138	12
86	–	92	91	138	16

a) Hydrogenations performed in benzene at 65 °C using 5–8 mol% catalyst.
b) Reaction times quoted as "between 13 h and 21 h" (30 h for **82**) [47].

30.5 Dienes and Trienes

Burgess and coworkers investigated the hydrogenation of the conjugated diene **87** (Scheme 30.1) [48]. Kinetic studies showed that the reaction occurred mostly stepwise *via* 2,3-diphenyl-1-butene, while only a small part of the diene was converted directly to 2,3-diphenylbutane, without dissociation of the catalyst from the intermediate mono-alkene. The first hydrogenation step was found to proceed with low enantioselectivity, whereas the second step was characterized by strong catalyst and strong substrate control.

In a more recent study [49], a number of similar substrates were hydrogenated. Varying amounts of the *meso* products were detected, and ee-values of 24% to 99% were recorded. With substrates **88**, significant amounts of double bond migration products were formed (Scheme 30.2).

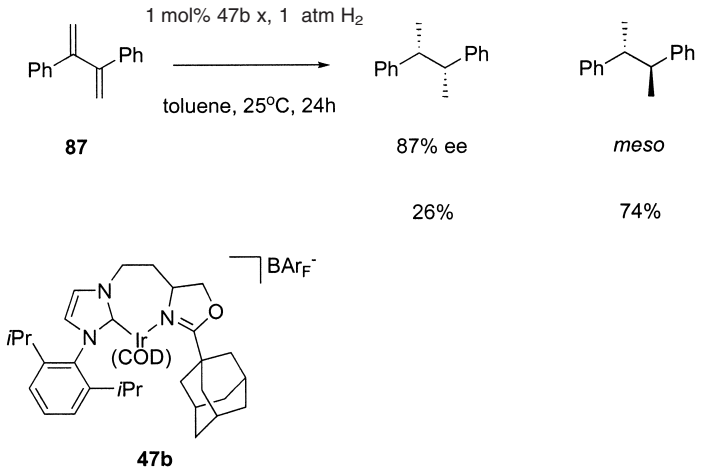

Scheme 30.1 Hydrogenation of substrate **87**.

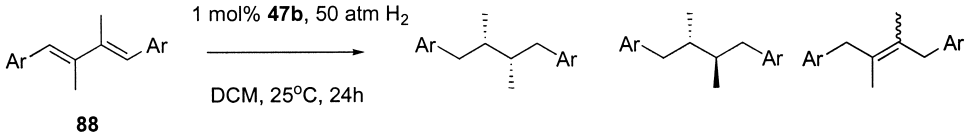

Scheme 30.2 Hydrogenation and double bond migration with dienes **88**.

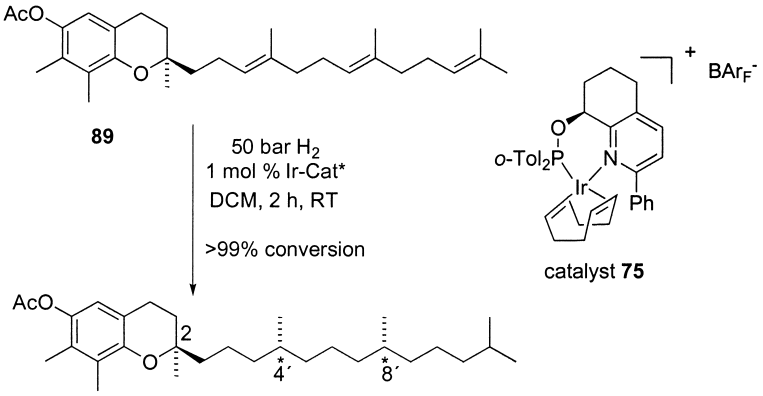

Scheme 30.3 Hydrogenation of vitamin E precursor **89**.

The development of chiral hydrogenation catalysts for unfunctionalized alkenes also allows enantioselective hydrogenation of functionalized olefins where the functionality in the molecule is remote from the double bond. A series of oxazoline-, imidazoline- and pyridine-derived catalysts have been screened for the hydrogenation of unsaturated derivatives of vitamin E (Scheme 30.3). Hy-

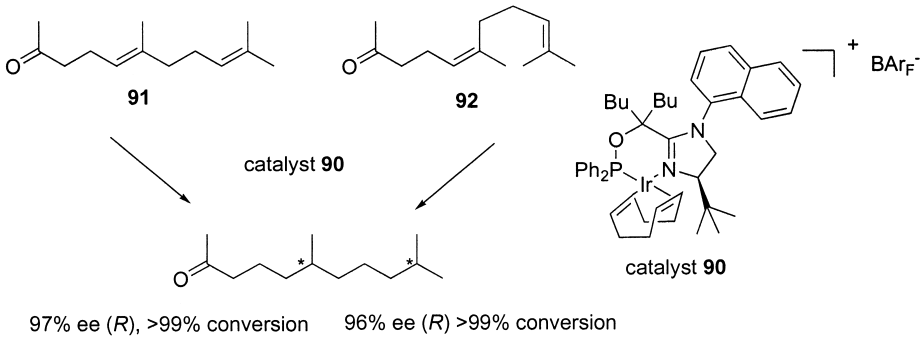

Scheme 30.4 Hydrogenation of dienes **91** and **92**.

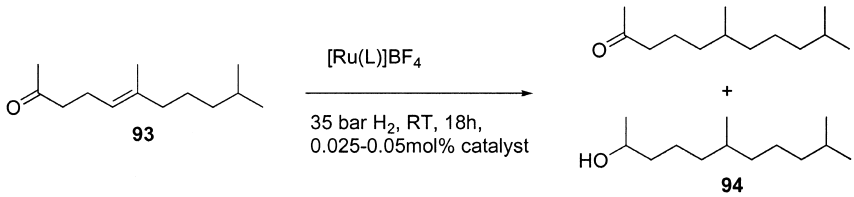

Scheme 30.5 Hydrogenation of substrate **93**.

drogenation of γ-tocotrienyl acetate **89** with catalyst **75** gave the natural (*R*,*R*,*R*)-isomer in 98% yield (the remaining 2% being the other three isomers) [50, 51] (Scheme 30.3). Catalyst **90** (Scheme 30.4) was also identified as a very selective catalyst, producing the (*R*,*R*,*R*)-isomer with >90% selectivity (<5% *RRS*, <4% *RSR*, <1% *RSS*).

In addition, a number of related dienes and trienes (Scheme 30.4) were hydrogenated with catalyst **90**, with promising results.

Substrate **91** was also hydrogenated in 75% ee using a ruthenium catalyst, $[Ru(MeOBIPHEP)](BF_4)_2$ (Scheme 30.4). A similar substrate (**93**, Scheme 30.5) was hydrogenated with a series of ruthenium catalysts: the fully reduced alcohol **94** was a side product. The best result (93% ee, 97 : 3 ketone : alcohol) was obtained with $[Ru(MeOBIPHEP)](BF_4)_2$ [52].

30.6 Conclusions

During recent years, substantial progress has been made in the hydrogenation of unfunctionalized alkenes. With iridium complexes derived from chiral phosphino-oxazolines and related ligands, excellent enantioselectivities and high TON/TOF values can now be obtained for a wide range of unfunctionalized olefins. Most substrates studied to date have at least one aryl substituent at the

double bond. However, recent results (see Section 30.5) have demonstrated that, even for purely alkyl-substituted alkenes, high enantioselectivities can be achieved. Most of the ligands developed so far are modular, allowing optimization of the catalyst structure for a particular substrate.

Tetrasubstituted alkenes remain a challenge. Here, the highest enantioselectivities were obtained with zirconocene catalysts, though the high catalyst loadings required and low TOFs reduce the practicality of these catalysts.

The mechanism of iridium-catalyzed hydrogenation remains unclear. Although several experimental [31, 53, 54] and computational [53, 55, 56] studies have been reported recently, further investigations will be necessary to establish a coherent mechanistic model. Until now, most studies have dealt with simple test substrates; hence, it will be important to explore more complex and also industrially important substrates, in order to determine the full scope and limitations of iridium catalysis.

Abbreviations

DCM	dichloromethane
PHOX	phosphino-oxazoline
r.t.	room temperature
THF	tetrahydrofuran
TOF	turnover frequency
TON	turnover number

References

1 L. Horner, H. Siegel, H. Büthe, *Angew. Chem.* **1968**, 1034.
2 M. Tanaka, I. Ogata, *J. Chem. Soc. Chem. Commun.* **1975**, 735.
3 M. Bianchi, U. Matteoli, P. Frediani, G. Menchi, F. Piacenti, C. Botteghi, M. Marchetti, *J. Organomet. Chem.* **1983**, *252*, 317.
4 K. Inagaki, T. Ohta, K. Nozaki, H. Takaya, *J. Organomet. Chem.* **1997**, *531*, 159.
5 T. Ohta, H. Ikegami, T. Miyake, H. Takaya, *J. Organomet. Chem.* **1995**, *502*, 169.
6 G. S. Forman, T. Ohkuma, W. P. Hems, R. Noyori, *Tetrahedron Lett.* **2000**, *41*, 9471.
7 E. Cesarotti, R. Ugo, H. B. Kagan, *Angew. Chem.* **1979**, *91*, 842.
8 E. Cesarotti, R. Ugo, R. Vitiello, *J. Mol. Catal. Sect. A* **1981**, *12*, 63.
9 L. A. Paquette, J. A. McKinney, M. L. McLaughlin, A. L. Rheingold, *Tetrahedron Lett.* **1986**, *27*, 5599.
10 L. A. Paquette, M. R. Sivik, E. I. Bzowej, K. J. Stanton, *Organometallics* **1995**, *14*, 4865.
11 R. L. Halterman, K. P. C. Vollhardt, M. E. Welker, *J. Am. Chem. Soc.* **1987**, *109*, 8105.
12 V. P. Conticello, L. Brard, M. A. Giardello, Y. Tsuji, M. Sabat, C. L. Stern, T. J. Marks, *J. Am. Chem. Soc.* **1992**, *114*, 2761.
13 C. M. Haar, C. L. Stern, T. J. Marks, *Organometallics* **1996**, *15*, 1765.
14 P. Beagley, P. J. Davies, A. J. Blacker, C. White, *Organometallics* **2002**, *21*, 5852.

15 D.R. Hou, J.H. Reibenspies, T.J. Colacot, K. Burgess, *Chem. Eur. J.* **2001**, *7*, 5391.
16 M.A. Giardello, V.P. Conticello, L. Brard, M.R. Gagné, T.J. Marks, *J. Am. Chem. Soc.* **1994**, *116*, 10241.
17 R. Schmid, E.A. Broger, M. Cereghetti, Y. Crameri, J. Foricher, M. Lalonde, R.K. Müller, M. Scalone, G. Schoettel, U. Zutter, *Pure Appl. Chem.* **1996**, *68*, 131.
18 G.H. Bernardinelli, E.P. Kündig, P. Meier, A. Pfaltz, K. Radkowski, N. Zimmermann, M. Neuburger-Zehnder, *Helv. Chim. Acta* **2001**, *84*, 3233.
19 J. Blankenstein, A. Pfaltz, *Angew. Chem. Int. Ed.* **2001**, *40*, 4445.
20 M.C. Perry, X. Cui, M.T. Powell, D.R. Hou, J.H. Riebenspies, K. Burgess, *J. Am. Chem. Soc.* **2003**, *125*, 113.
21 M.T. Powell, D.R. Hou, M.C. Perry, X. Cui, K. Burgess, *J. Am. Chem. Soc.* **2001**, *123*, 8878.
22 F. Menges, A. Pfaltz, *Adv. Synth. Catal.* **2002**, *344*, 40.
23 T. Focken, G. Raabe, C. Bolm, *Tetrahedron Asymm.* **2004**, *15*, 1693.
24 S.P. Smidt, F. Menges, A. Pfaltz, *Org. Lett.* **2004**, *6*, 2023.
25 S. McIntyre, E. Hörmann, F. Menges, S.P. Smidt, A. Pfaltz, *Adv. Synth. Catal.* **2005**, *347*, 1.
26 K. Källstrom, C. Hedberg, P. Brandt, A. Bayer, P.G. Andersson, *J. Am. Chem. Soc.* **2004**, *126*, 14308.
27 U. Matteoli, V. Beghetto, A. Scrivanti, *J. Mol. Cat. A: Chemical* **1996**, *109*, 45.
28 R.D. Broene, S.L. Buchwald, *J. Am. Chem. Soc.* **1993**, *115*, 12569.
29 A. Lightfoot, P. Schnider, A. Pfaltz, *Angew. Chem. Int. Ed.* **1998**, *37*, 2897.
30 D.G. Blackmond, A. Lightfoot, A. Pfaltz, T. Rosner, P. Schnider, N. Zimmermann, *Chirality* **2000**, *12*, 442.
31 S. Smidt, N. Zimmermann, M. Studer, A. Pfaltz, *Chem. Eur. J.* **2004**, *10*, 4685.
32 A. Pfaltz, J. Blankenstein, R. Hilgraf, E. Hörmann, S. McIntyre, F. Menges, M. Schönleber, S.P. Smidt, B. Wüstenberg, N. Zimmermann, *Adv. Synth. Catal.* **2003**, *345*, 33.
33 Available from Strem: ((4*S*,5*S*)-(–)-*O*-[1-Benzyl-1-(5-methyl-2-phenyl-4,5-dihydrooxazol-4-yl)-2-phenylethyl]-dicyclohexylphosphinite)(1,5-COD)iridium (I) tetrakis(3,5-bis(trifluoromethyl)phenylborate, CAS number 583844-38-6, catalog number 77-5010 and ((4*S*,5*S*)-(+)-*O*-[1-Benzyl-1-(5-methyl-2-phenyl-4,5-dihydrooxazol-4-yl)-2-phenylethyl]-diphenylphosphinite)(1,5-COD)iridium (I) tetrakis(3,5-bis(trifluoromethyl)phenylborate, CAS number 405235-55-4, catalog number 77-5020.
34 R. Hilgraf, A. Pfaltz, *Synlett* **1999**, *11*, 1814.
35 P. Schnider, Ph.D. Dissertation, University of Basel, Basel, **1996**.
36 C. Bolm, T. Focken, G. Raabe, *Tetrahedron Asymm.* **2003**, *14*, 1733.
37 P.G. Cozzi, N. Zimmermann, R. Hilgraf, S. Schaffner, A. Pfaltz, *Adv. Synth. Catal.* **2001**, *343*, 450.
38 P.G. Cozzi, F. Menges, S. Kaiser, *Synlett* **2003**, *6*, 829.
39 W. Tang, W. Wang, X. Zhang, *Angew. Chem. Int. Ed.* **2003**, *42*, 943.
40 G. Xu, S.R. Gilbertson, *Tetrahedron Lett.* **2003**, *44*, 953.
41 D. Liu, W. Tang, X. Zhang, *Org. Lett.* **2004**, *6*, 513.
42 F. Menges, M. Neuburger, A. Pfaltz, *Org. Lett.* **2002**, *4*, 4173.
43 T. Bunlaksananusorn, K. Polborn, P. Knochel, *Angew. Chem.* **2003**, *42*, 3941.
44 W.J. Drury, N. Zimmermann, M. Keenan, M. Hayashi, S. Kaiser, R. Goddard, A. Pfaltz, *Angew. Chem. Int. Ed.* **2004**, *43*, 70.
45 L.B. Schenkel, J.A. Ellman, *J. Org. Chem.* **2003**, *69*, 1800.
46 R. Crabtree, *Acc. Chem. Res.* **1979**, *12*, 331.
47 M. Troutman, D.H. Apella, S.L. Buchwald, *J. Am. Chem. Soc.* **1999**, *121*, 4916.
48 X. Cui, K. Burgess, *J. Am. Chem. Soc.* **2003**, *125*, 14212.
49 X. Cui, J.W. Ogle, K. Burgess, *J. Chem. Soc. Chem. Commun.* **2005**, 672.
50 B. Wüstenberg, Ph.D. Dissertation, University of Basel, Basel, **2003**.
51 S. Bell, B. Wüstenberg, S. Kaiser, F. Menges, T. Netscher, A. Pfaltz, *Science* **2006**, *311*, 642.
52 Patent: EP Appl. 92905551 (1992), USP Appl. 5274125 (1992), E. Broger, J. Foricher, B. Helser, R. Schmid, F. Hoffmann-La Roche AG.

53 C. Mazet, S. P. Smidt, M. Meuwly, A. Pfaltz, *J. Am. Chem. Soc.* **2004**, *126*, 14176.
54 R. Dietiker, P. Chen, *Angew. Chem. Int. Ed.* **2004**, *43*, 5513.
55 P. Brandt, C. Hedberg, P. G. Andersson, *Chem. Eur. J.* **2003**, *9*, 339.
56 Y. Fan, X. Cui, K. Burgess, M. B. Hall, *J. Am. Chem. Soc.* **2004**, *126*, 16688.

31
Mechanism of Enantioselective Hydrogenation

John M. Brown

31.1
Introduction

The discovery of the first practical catalyst for homogeneous hydrogenation by Wilkinson, Osborn, Jardine and Young in 1965 [1] occurred at around the same time that others, especially Mislow and Horner [2], were demonstrating that chiral trivalent phosphorus compounds were capable of existing as stable, non-interconverting enantiomers. With suitable adaptation of Wilkinson's catalyst, a prostereogenic alkene could be hydrogenated with preferential formation of one enantiomer of the reduced product. The possibility of such enantioselective hydrogenation was recognized by both Horner [3] and Knowles [4], but it was Knowles who won the race to demonstrate the first example in 1968. This led rapidly to a period of seminal discoveries: the application of chelate biphosphine ligands came from Kagan [5], and the development of a full-scale enantioselective hydrogenation of a dehydroamino acid to provide a rhodium-complex-based catalytic synthesis of L-Dopa by Knowles' team at Monsanto [6]. For many years this provided a substantial part of the supply of the main drug active in the control of Parkinson's disease. Kagan was also the first to demonstrate, in his synthesis and application of DIOP (derived very simply from *RR*- or *SS*-tartaric acid), that the difficult synthesis of enantiomerically pure phosphines was unnecessary for effective enantioselective hydrogenation, since a suitable chelate backbone could provide the necessary level of stereochemical control. For many years the development of enantioselective hydrogenation converged on the preparation of enantiomerically pure chelate diphosphines and the application of their rhodium complexes to the hydrogenation of dehydroamino acids, enamides and closely related reactants [7]. Although both ruthenium [8] and iridium catalysts [9] for homogeneous hydrogenation were known at an early stage, the development of effective enantioselective hydrogenation in these two spheres occurred much later. For ruthenium enantioselective hydrogenation, the spectacular efficiency of BINAP catalysts [10] developed by Noyori's group was first demonstrated for alkenes, and then in rather greater depth for ketones [11]. The high efficiency of iridium complexes in hydrogenation had been demonstrated

The Handbook of Homogeneous Hydrogenation.
Edited by J.G. de Vries and C.J. Elsevier
Copyright © 2007 WILEY-VCH Verlag GmbH & Co. KGaA, Weinheim
ISBN: 978-3-527-31161-3

in **1976** by Crabtree and Morris [9], but it was 20 years later before Pfaltz and Lightfoot developed the first asymmetric variant [12]. Whilst initially rather slow to recognize the potential of asymmetric hydrogenation, and enantioselective catalysis in general for industrial scale-up, the pharmaceutical and fine chemical industries are in the forefront of current developments [13]. The ease of operation of homogeneous catalytic hydrogenation, the high stereochemical efficiency and the wide range of reactants which are currently amenable to the procedures make this a versatile synthetic method at all scales.

31.2 Rhodium-Catalyzed Hydrogenations

31.2.1 Background

The mechanism of enantioselective hydrogenation by rhodium complexes has been reviewed on several occasions, including a recent detailed publication by the present author [14]. In addition, much of the contemporary work by Gridnev and Imamoto has been reviewed, as described below. Consequently, details of the older studies will be cited only briefly to provide the necessary context, after which the post-1998 developments will be discussed in detail. For a mature field, it is surprising how much new and significant information has been reported during the past five years.

Older studies into the mechanism of enantioselective hydrogenation were characterized by two main approaches: (i) the measurement and detailed analysis of reaction kinetics by Halpern and coworkers [15]; and (ii) the characterization of reactive intermediates in solution by NMR [16], augmented by X-ray analyses and other physico-chemical techniques. The rhodium catalyst is frequently introduced as a cationic diphosphine dialkene complex which requires an initial hydrogenation of the dialkene before an active catalyst is formed. Heller and coworkers have studied this process in some depth [17]. Hydrogenation of the first double bond *in situ* may be followed by a sequential hydrogenation of the now freely dissociating mono-alkene. With a high [Rh]/[substrate] ratio (typical of small-scale work), precatalyst reduction can influence the rate of hydrogenation of the substrate, and the reactivity of norbornadiene and cycloocta-1,5-diene precatalysts is distinct. Overall, the accumulated mechanistic evidence indicates several key features of the reaction mechanism, which made it distinct from the simple Wilkinson's hydrogenation pathway:

- In the absence of reactant, (cationic) biphosphine rhodium complexes exist in methanol, the generally preferred reaction medium, as a *bis*-solvate. The affinity for dihydrogen is low.
- In the presence of the dehydroamino acid reactant, bidentate complexation as an enamide occurs. With a chiral diphosphine ligand, two diastereomeric forms of the enamide complex are observed in equilibrium that differ in the

prostereogenic face of the alkene bound to rhodium. The major species in solution corresponds with the isomer characterized by X-ray crystallography. The association constant for enamide formation varies widely with the ligand, with smaller bite angles tending to give stronger binding.

- At low temperatures, only the disfavored enamide complex reacts with dihydrogen, forming an alkylhydride complex that decomposes to form the hydrogenation product above –50 °C. No evidence for an intermediate dihydride could be established, although its involvement was assumed. All of the described intermediates give well-defined and distinctive NMR spectra in which ^{1}H, ^{31}P and ^{13}C (with enrichment) are all informative.
- Dihydrogen addition to the enamide complex is rate-limiting and irreversible. With *para*-enriched hydrogen, there is no *ortho-para* equilibration in a dehydroamino acid turnover system until hydrogenation is complete [18] (this last precept has come under recent close scrutiny).

These observations and results can be expressed in the "hour-glass" double catalytic cycle first briefly introduced by Brown and coworkers [19], but indelibly associated with the detailed kinetic study of Clark and Landis (Fig. 31.1) [15 a]. For this study, the Monsanto ligand DIPAMP was selected and this proved to be especially revealing. Because the enamide complexes are formed here with a particularly strong association complex, the enantiomer excess in hydrogenation is very sensitive to the temperature and dihydrogen pressure. Access to the "minor enamide" pathway is controlled by the depth of the ground-state energy-well associated with the major enamide complex. This influences the extent to which the minor enamide pathway dominates catalysis, and permits the direct testing of the model over a wide range of conditions, with excellent correlation between experiment and theory.

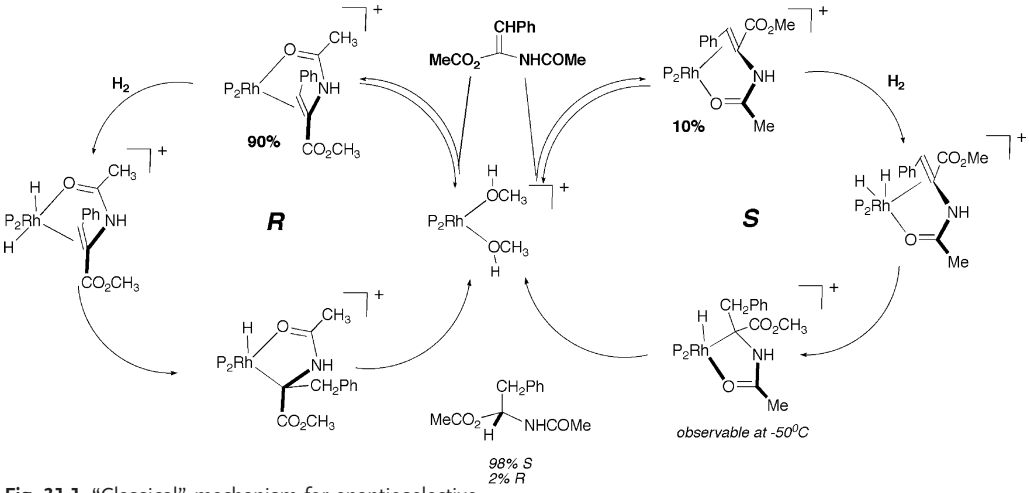

Fig. 31.1 "Classical" mechanism for enantioselective hydrogenation [15a,b, 19]; P_2 = (*R*,*R*)-DIPAMP.

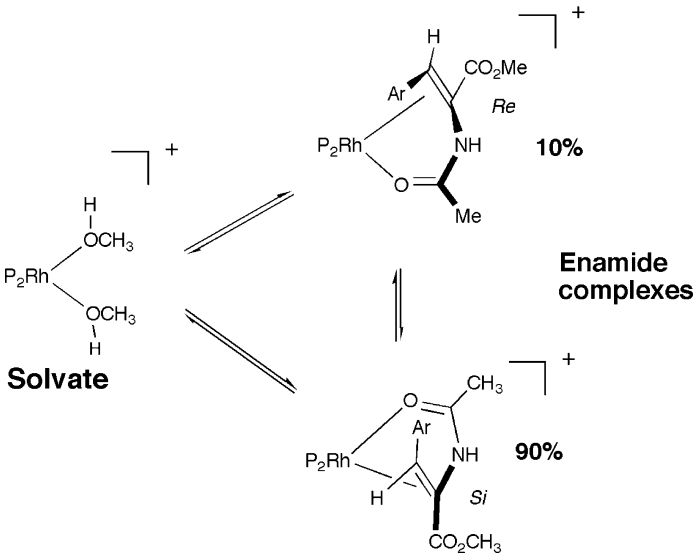

Fig. 31.2 Typically (DIPAMP, CHIRAPHOS), the intramolecular exchange of *Re* and *Si* complexes is several times faster than the dissociation to reform the solvate complex.

In this kinetic study, the interconversion of the two diastereomeric enamide complexes was treated as a dissociative process, proceeding through the solvate complex. This is not the main pathway, as clearly revealed by spin-saturation ^{31}P-NMR experiments that demonstrate the retention of identity of the two separate phosphorus nuclei during the exchange process; a solvate has equivalent ^{31}P sites [20]. The recognition that this intramolecular process is occurring requires some modification of the rate constants, but not the fundamental mechanistic principles enshrined in the model. It is a general and fundamentally important fact that the processes of Figure 31.2 are fast relative to catalytic turnover.

31.2.2
More Recent Developments

Mechanistic studies carried out up to the late 1990s served to reinforce rather than to overturn the mechanistic models then in place. During that period there had also been significant developments in ligand design that greatly enhanced the utility and range of rhodium enantioselective hydrogenation. The first major contribution came from Dupont, where Burk and coworkers synthesized the DUPHOS ligand family and showed how their rhodium complexes were significantly superior to any previous examples, and made enantioselective hydrogenation a far more general synthetic reaction [21]. A key factor was the phospholane structure; part of the culture of the subject had been built around the idea that arylphosphine

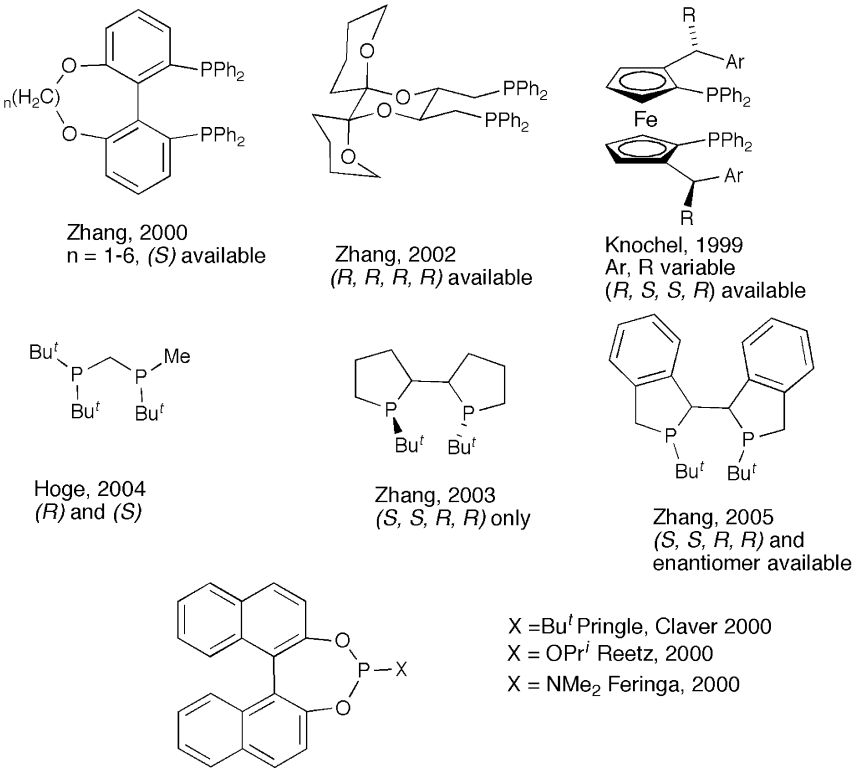

Fig. 31.3 Examples of second- and third-generation phosphine and diphosphine ligands.

moieties played a crucial part in enantioselection. With alkylphosphines now also seen to be important, Evans and coworkers demonstrated a neat synthesis of enantiomerically enriched variants by the sparteine-promoted deprotonation of one of the diastereotopic methyl groups of $H_3B \cdot PBu^t(CH_3)_2$ [22]. This discovery enabled Imamoto's group to synthesize a range of diphosphines based on the general motif $R_LR_SP(X)PR_SR_L$, where R_S and R_L are small and large alkyl groups respectively and (X) represents the chelate backbone [23]. Other notable successes have been obtained with electron-rich diphosphines such as the PHANEPHOS ligand based on [2.2]-paracyclophane [24]. The design of effective electron-rich ligands for enantioselective catalysis based on these and related themes, has been a trademark of Zhang's studies [25]. In parallel with these developments of new families of chelate diphosphines, new investigations – most effectively developed by Feringa's group after three near-concurrent reports [26] – have demonstrated the comparable utility of appropriately designed monophosphines or other P(III) compounds (Fig. 31.3). In considering the practical applications of a particular ligand, it is important to determine whether the required enantiomer is easily available. In several cases, especially where phosphorus chirality is involved, only one of the two may be accessed readily.

The enhanced synthetic potential of rhodium-complex-catalyzed enantioselective hydrogenation provided by these advances in ligand design has led to renewed interest in the reaction mechanism, and here we highlight four recent topics: (i) the extended base of reactive intermediates; (ii) an improved quadrant model for ligand–substrate interactions; (iii) computational approaches to mechanism; and (iv) (*bis*)-monophosphine rhodium complexes in enantioselective hydrogenation. These are discussed in turn.

31.2.3
Transient and Reactive Intermediates in Rhodium Enantioselective Hydrogenation

The status quo provided by the early mechanistic studies described above was incomplete in several respects. Although the affinity of the solvate complex for dihydrogen was known to be low, the addition product remained uncharacterized. Likewise, the putative H_2 addition intermediate between the enamide complex and the transient, but observable, alkylhydride had not been characterized.

A common characteristic of the "second generation" of ligands for enantioselective hydrogenation is the electron-rich nature of the diphosphine. The electronic character of the ligand will of course affect the relative stability of different states in the catalytic cycle and influence their accessibility. In the "classical" biarylphosphine-based chemistry, formation of a stable dihydride from the initial 16-electron Rh solvate complex had never been demonstrated. The fleeting existence of a hydridic intermediate could be inferred from the reversible *ortho-para* equilibration of dihydrogen by the solvate complex [17]. In a thorough study of observable intermediates in the catalytic cycle of dehydroamino acid hydrogenation by the C_2-symmetric ligand BisP* (see Fig. 31.4), a solvate dihydride was characterized for the first time at low temperatures [27]. The complex, present to the extent of ca. 20% at –90 °C under ambient hydrogen pressure, existed as an unequal pair of rapidly equilibrating diastereoisomers. When hydrogen deuteride (HD) was employed, the D-*trans*-solvent isomers predominated by 1.3 : 1. The derived equilibrium constant at 20 °C implies that the dihydride is present to only a minor extent at $[H_2] = 4$ mM, the ambient equilibrium concentration. Within the same family of alkylphosphine chelates, the larger bite angle of the xylylene-bridged complex permits the exclusive formation of a pair of diastereomeric solvate dihydrides at –70 °C, persistent to –20 °C [28]. With the lower homologue of the bis-P* ligand (Miniphos), the isolated complexes tend to be of the general structure $(P_2)_2Rh^+$. Reaction with dihydrogen provides NMR-characterizable complexes of the form $(P_2)_2RhH_2^+$, and hydrogenation can proceed from this state by complete dissociation of one diphosphine moiety [29]. At ambient temperature this is transformed into a bridged dihydride complex. A further example of a stable solvate dihydride was obtained during a study of the reaction of PHANEPHOS rhodium complexes with *para*-enriched dihydrogen. In the presence of a dehydroamino ester, a diastereomeric pair of spin-excited solvate dihydride complexes could be identified, structurally related to the examples described above [30].

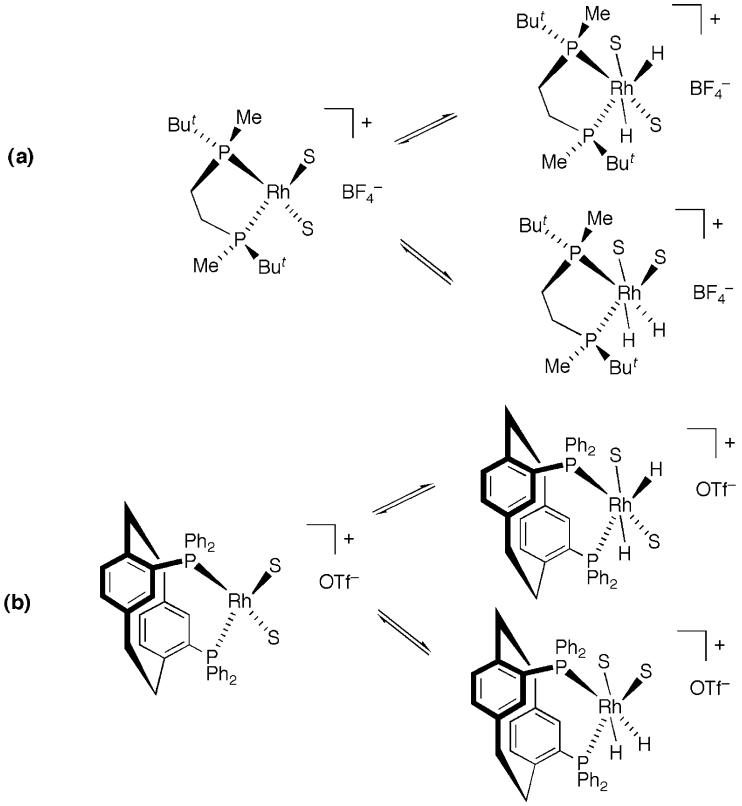

Fig. 31.4 Solvate dihydrides characterized at low temperature [S=CH_3OH or CD_3OD]. Dihydrides formed *in situ* react rapidly with the common substrates of enantioselective hydrogenation, and the reduced product is formed with high enantioselectivity. At ambient pressure, the proportion of dihydrides is 45% at –100 °C for (a) with a 10:1 diastereomer ratio, and 40% for (b) at –40 °C, with a 2:1 diastereomer ratio.

The accepted mechanism for hydrogenation of alkenes by Wilkinson's catalyst involves the addition of dihydrogen prior to coordination of the alkene, followed by migratory insertion [31]. The new demonstrations of the existence of solvate dihydride complexes inevitably raise the question as to whether the same mechanism can apply in rhodium enantioselective hydrogenation. The evidence in support of this possibility is analyzed in more detail later.

Whatever the route to a rhodium dihydride alkene complex, the hydrogen must be transferred sequentially to the double bond. It had always been assumed that the first C–H bond is formed β to the amido-group, so that the more stable Rh–substrate chelate is formed. This is the alkylhydride isomer observed in stoichiometric NMR studies at low temperatures, and is supported by studies under catalytic turnover conditions, assuming a normal isotope effect.

Thus, earlier studies by Brown and Parker [32] had shown that the isotope partitioning in catalyzed HD addition to dehydroamino esters indicated predominant prior migration of H to the β-position of the ensuing amino acid derivative so that the α-position was relatively rich in D. This sequence is not invariably observed, however. A key experiment was based on a prior observation by Burk's group that the stereochemical course of enantioselective hydrogenation of two closely related enamides was diametrically opposite [33]. In order to confirm that a fundamental change in mechanism is responsible, an HD isotope partitioning experiment was carried out for these substrates (Fig. 31.5) [34]. In this investigation, the pattern of D-substitution was as expected in the product derived from the Ph-substituted enamide, but it was reversed for the Bu^t-substituted enamide. Only the Bu^t-compound gave informative results in NMR studies; the intermediate alkylhydride indicated alkene-only coordination with a non-participating amide, in consequence of the steric bulk of the Bu^t-group. It was assumed that the alkylhydride complex was formed directly from the solvate dihydride and alkene. In examining the same problem, a computational study of the difference between enamides with bulky (Bu^t) and small (CN) substituents predicted opposite product configurations, although chelated substrates were employed in the computational model which contrast with the experimental NMR evidence described above [35].

The enamide dihydride intermediate that precedes migratory insertion has proved elusive, despite one earlier claim where the evidence is incomplete and possibly not correctly interpreted [36]. Hydrogenation by rhodium complexes of

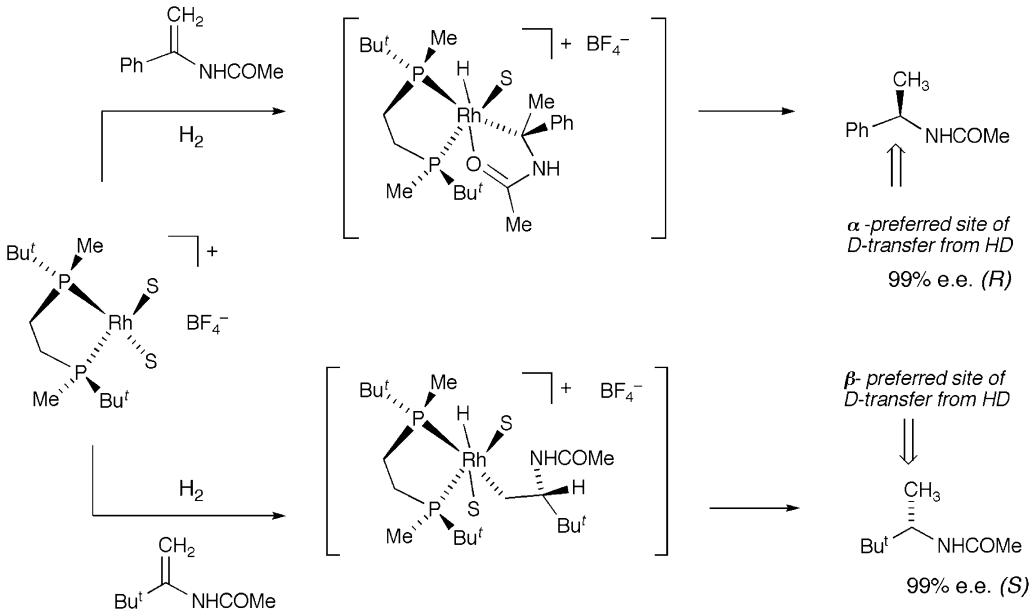

Fig. 31.5 Normal and anomalous pathways for the hydrogenation of alkylenamides.

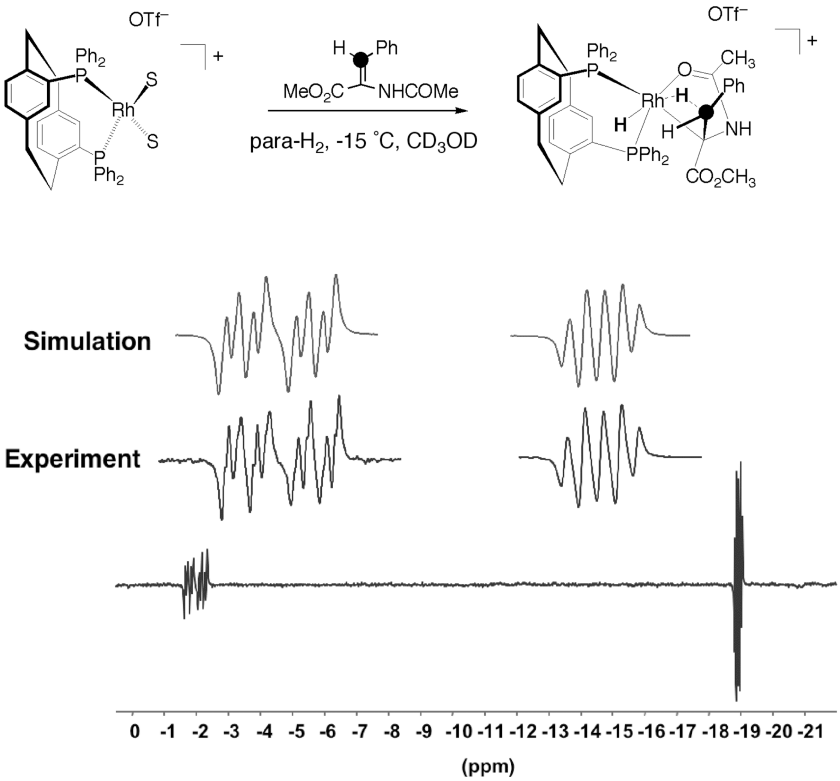

Fig. 31.6 ^{1}H-NMR spectrum of the initial reaction product of β-^{13}C-labeled enamide with *para*-enriched H_2 at –15 °C in CD_3OD; the agostic C–H is at –2 ppm.

the ligand PHANEPHOS occurs under quite unusual conditions (H_2 bubbling through substrate solution at –40 °C), and is applicable to some otherwise sluggish reactions [23]. This suggests a highly reactive catalyst, which could reveal the structure of pre-insertion intermediates. When dehydroamino acid hydrogenation was carried out with *para*-enriched H_2, and the ^{1}H-PHIP-NMR monitored, a new transient dihydride was observed with intact substrate [37] (Fig. 31.6). The transient possessed unusual chemical shifts, and full analysis showed that it was indeed the desired dihydride, but one where a single hydrogen has been captured in agostic flight from rhodium to carbon. Tracking the process of spin excitation indicates that this transient is linked to the hydrogenation product and the $P_2RhS_2^+$ solvate, but not to the reactant. An intrinsic advantage of the PHIP procedure is that the characteristic absorption-emission (AE) spectra are only observed whilst there is spin coupling of the hydrogens of the original *para*-H_2 molecule so that artifacts remain invisible. This is the only example of a dihydride intermediate on the pathway, and may be a special case that demonstrates the unusual properties of this particular ligand.

31.2.4
Mnemonics for the Sense of Enantioselective Hydrogenation

Very early on in the development of enantioselective hydrogenation it was recognized that a simple rule that linked the stereochemical course of the reaction to the structure of the ligand would be exceedingly valuable. Several efforts were made in this direction: Kagan linked the chelate twist (λ or δ) to the predominant enantiomer [38], while Kyba considered the sense of twist of the dialkene precursor of the catalyst [39] and Knowles introduced the Quadrant Rule [40]. The last of these was potentially more useful than the others, since it specifically considered the binding of substrate. The C_2-symmetrical ligand was considered as $R_LR_SP(X)PR_SR_L$ with the bulky R_L ligands disposed to equatorial positions in the chelate ring and R_S to axial positions. That was consistent with X-ray crystallographic evidence available at the time, which also indicated that in a square-planar complex the equatorial groups have closer contact to the bound substrate than the axial groups. The rule was incomplete in its predictive power in its original form, however, and needed correction. With the advent of a new generation of electron-rich alkylphosphine ligands it was first realized in a report by Marinetti and coworkers that even Knowle's modified Quadrant Rule failed

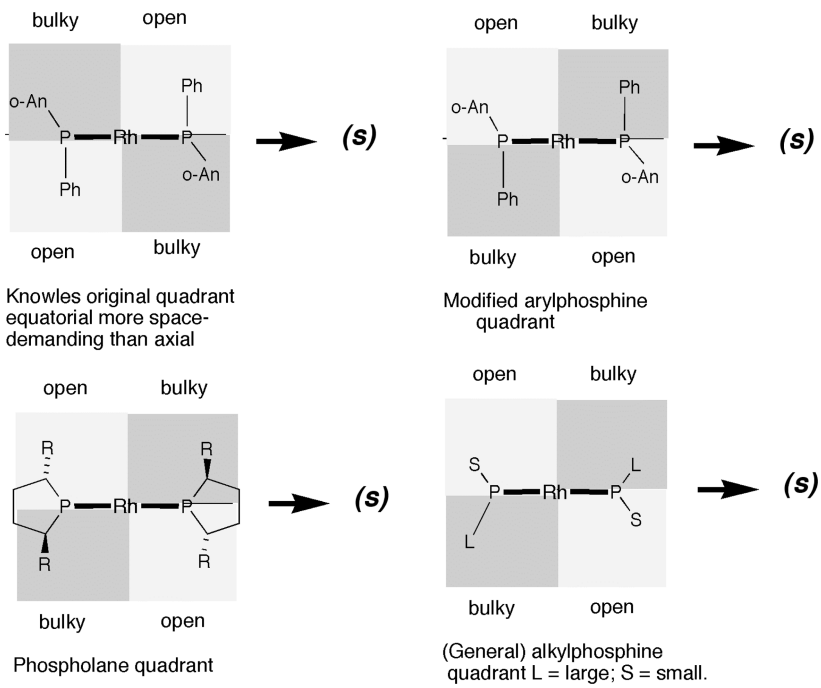

Fig. 31.7 Modern presentations of the Quadrant Rule for predicting the course of enamide hydrogenation, following the original work of Knowles.

to make the correct predictions [41]. The reasons for this become clear when the basis of the rule is considered; it analyzes the steric interactions that exist in a four-coordinate square-planar intermediate. It remained for Gridnev and Imamoto to reassess the analysis and present an alternative that may have far more general applicability [42]. In their modified model, the important stereodetermining step is six-coordinate and located at the point where both dihydrogen and the chelating reactant are bound. With this modification, the bulky groups in a diarylphosphine chelate are defined as the axial rather than the equatorial phenyls, the opposite of the original indications of Knowles. The current status of the Quadrant Rule and its relationship to the original form, now applicable to a much broader range of ligands, is shown in Figure 31.7. Formulation of this Rule in specific cases is aided by a thorough analysis of the X-ray structures of the "precatalyst" diolefin complex, with respect to the bite angle and coordination geometry of the dialkene [43].

31.2.5
Status of the Computational Study of Rhodium-Complex-Catalyzed Enantioselective Hydrogenation

The development of density function theory (DFT), together with the rapid increase in computational power experienced during the last decade, has made real homogeneous catalytic systems accessible to quantum mechanical calculations. In the study of enantioselective hydrogenation, one sequence of investigations stands out, however. The studies of Feldgus and Landis address the "classical" model of enantioselective hydrogenation without considering more recent investigations into solvate dihydride pathways, but consider the possible routes for that in a high degree of detail [44]. Their first report is concerned with achiral models (Fig. 31.8). Starting with the square-planar enamide complex, the computational analysis centers on the successive formation of a dihydrogen complex, dihydride, alkylhydride and reduced but coordinated product, as well as the intervening transition states. At each stage there are several geometrical isomers to be considered, and the computational process treats the intermediate species as non-interconverting, save for the dihydride. Although the computation was carried out with $(PH_3)_2$ as model ligand, only species with *cis*-phosphine geometry were considered. With these constraints, the energy surface was constructed for four possible pathways defined by the four possible approach trajectories of H_2 towards the square-planar enamide complex (above and below the two linear axes), each of which flows through a sequence of distinct geometrical isomers. The interconversion of isomers at the dihydride level was analyzed independently by an alkene dissociation pathway, the only one that was energetically viable. These results demonstrate the feasibility of interconversion with a computed barrier of 14.1 kcal mol^{-1}. The kinetic isotope effects for the steps affected by isotope substitution and the consequences of reduction of the substrate by HD are also studied. When addition of $H_2(D_2)$ is turnover-limiting, a significant isotope effect should be observed (1.4–1.7). For the case that insertion is turnover-

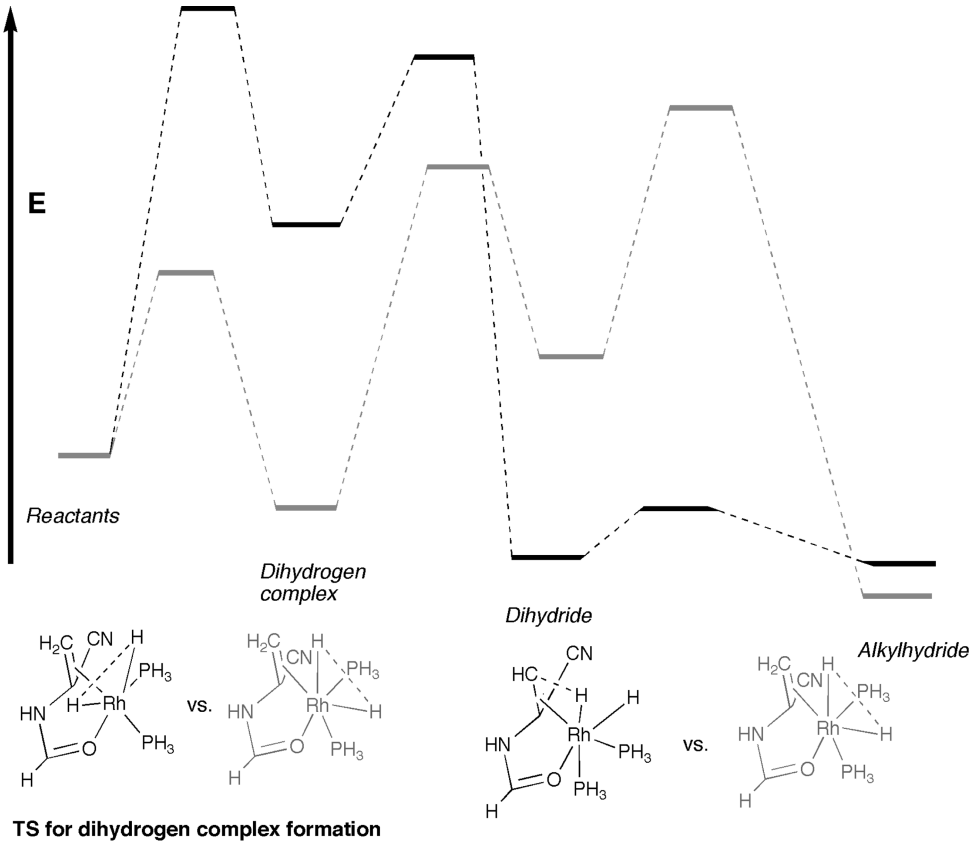

Fig. 31.8 Two of the four possible pathways in the hydrogenation of the model complex shown; schematic energies derived from DFT calculations. The alternative routes are associated with higher barriers. The absolute energies, but not the main conclusions, are unaltered when $2\times PH_3$ is replaced by $Me_2P(CH_2)_2PMe_2$.

limiting, the kinetic isotope effect is small and in keeping with experimental results (1.0–1.15). The experimental result for HD addition to the dehydroamino ester places the D-atom predominantly at the α-position of the reduced product. This is replicated only by the turnover-limiting insertion mechanism, and not the alternative oxidative addition. The conclusions of course assume comparability between the simple model phosphines and the "real" ligand.

The success in a simple model system encouraged Feldgus and Landis to study the fuller DUPHOS-based system for enantioselective hydrogenation (as defined in Fig. 31.9) [45]. ONIOM methods were required because of the level of complexity; a core of the rhodium-complexed atoms was treated by DFT at B3LYP level, the core organic atoms at Hartree-Fock level, and the remainder by

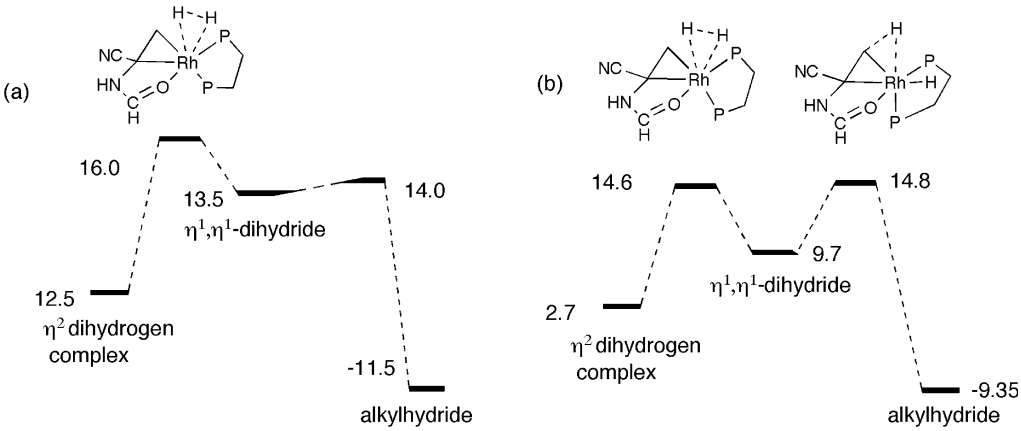

Fig. 31.9 Turnover-limiting transition states for enantioselective hydrogenation derived from DFT calculations. (a) ONIOM calculations, PP = Me-DUPHOS [45]. (b) Full computation on all atoms, PP = *bis*-PP* with a rigid Et group to simulate Bu^t [47]. Numbers refer to the energy in kcal mol^{-1} of the states relative to the resting state.

molecular mechanics (MM), employing Landis' universal force field (UFF) method. The same steps were carried out in the computation as before, but now two diastereoisomeric pathways can be considered. It was assumed that the two possible enamide complexes do not interconvert other than through the solvate, at variance with experimental observation [46], and that there is no other crossover possible between the two pathways. Nevertheless, the computation correctly predicts the difference in ground-state energy favoring the major diastereomer of enamide complex, and the lower energy pathway for hydrogenation that is available to the minor diastereomer. Of the four stereochemically distinct pathways considered in the earlier report, the same one (Feldgus and Landis' path **A**) is found to be most favorable here. The most interesting difference found in the full model is that H_2 addition rather than migratory insertion is turnover-limiting. These observations inspire confidence that the transition-state structures being considered in the turnover-limiting region make accurate predictions about the outcome of asymmetric hydrogenation. Much still remains to be considered and evaluated at a level of detail.

In a later approach, using B3LYP, DFT with the same basis sets as above was applied to all atom computation for the pathway in enantioselective hydrogenation by bisP*Rh^+. At this higher level of theory, the turnover-limiting transition state was at a similar position on the energy profile for both diastereomeric pathways [47]. This involved the early part of the H_2 addition to form an η^2-complex, which then goes on to form the dihydride, but by (reversibly) traversing a low energy barrier. The two transition states relevant to limiting turnover here are the initial H_2 addition and the conversion of the η^2-dihydrogen complex into a η^1,η^1-dihydride; the second of these is very slightly higher in energy

than the first. The same conclusions as before were drawn concerning the energetic preference for reaction via the minor diastereomer, and by a clear margin. The general comment needs to be made that increasing computer power, and increasing sophistication of the theoretical model, will lead to alteration of the detailed energy surface for enantioselective hydrogenation without altering the fundamental conclusions.

31.2.6
Monophosphines in Rhodium-Complex-Catalyzed Enantioselective Hydrogenation

A significant success was achieved by Knowles and his colleagues using the monophosphine CAMP, describing work that paved the way to practical applications of asymmetric hydrogenation [48]. Largely because of difficulties in obtaining the ligand enantiomerically pure, attention soon switched to C_2-symmetrical diphosphines (DIPAMP, DIOP) where the problem was averted or controlled. It has only been during the past few years that monoligating phosphanes have reasserted prominence (Fig. 31.10). An initial report by Guillen and Fiaud on the efficacy of monophospholanes [49] was rapidly followed by several further reports [25]. Among these, the studies of Feringa, de Vries and colleagues on BINOL-derived phosphoramidites have been developed most vigorously [50]. The observed reactivity of phosphoramidites as ligands in the Rh-catalyzed hydrogenation of both α- and β-dehydroaminoacids is comparable to that of the commonly employed diphosphines [51]. It is very likely that two molecules of the monophosphane are involved in coordination to rhodium throughout the catalytic cycle. There is a pronounced positive non-linear effect when scalemic phosphoramidite is employed. Solutions containing less than 2 equiv. of the monodentate ligand per rhodium provide for reactive catalysis. There is a rate dependence on the L/Rh ratio, but the *ee* remains constant over the L/Rh range of 1 to 2. This result was attributed to the tendency of *bis*(monophosphane)-rhodium complexes to disproportionate, unlike their diphosphane-rhodium analogues. Electrospray-mass spectrometry (ES-MS) analysis of the reacting solution revealed the presence of P_1Rh^+, P_2Rh^+, P_3Rh^+ and P_4Rh^+ at different times, and also that the initial $[P_2Rh(norbornadiene)]^+$ complex persists for long periods after the initiation of hydrogenation [52]. With two different phosphorus ligands in combination, the *ee* in hydrogenation may be enhanced over their separate use, indicating that the catalytic intermediate leading to enantiodifferentiation incorporates both ligands. This is reinforced by the observation that a combination of enantiopure and achiral ligands leads to different results from the enantiopure ligand alone; in some cases the incorporation of the achiral partner leads to reversal of the sense of enantioselectivity. Excellent results may be obtained in the rhodium-complex-catalyzed hydrogenation of a simple dehydroamino ester with a 1:1 mixture of an atropisomerically stable BINOL-derived phosphite and a related configurationally labile 2,2′-biphenol-derived phosphite. It proved difficult to put these observations on a more quantitative footing because the catalyst system is complex under turnover conditions [53].

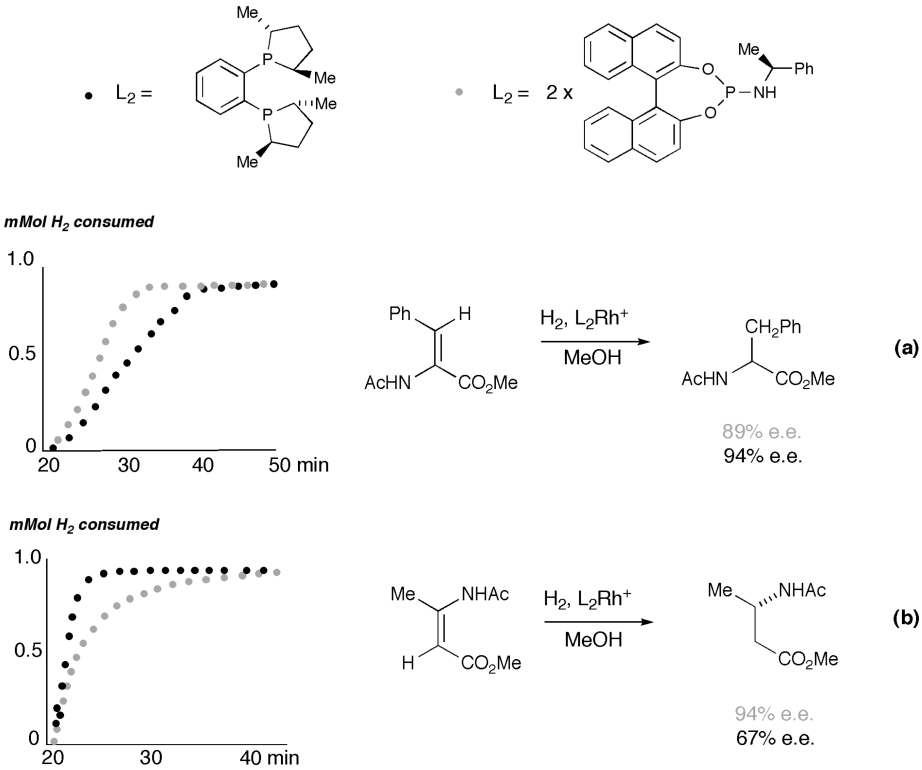

Fig. 31.10 Comparison of rate (schematic) and enantioselectivity for mono- and bidentate phosphorus ligands on 1 mM scale. (a) α-Dehydroamino ester, 2 bar H_2; (b) β-dehydroamino ester, 10 bar H_2.

31.2.7
Mechanism of Hydrogenation of β-Dehydroamino Acid Precursors

As the range of rhodium enantioselective hydrogenation has been extended, new types of reactant have been involved in reduction, and with high enantioselectivity. The synthesis of β-amino acids falls within this compass, and recent examples have demonstrated successful hydrogenation of both (*E*)- and (*Z*)-precursors [54]. This raises the question as to whether the mechanism is the same as has been defined in the α-dehydroamino acid case. The reduction of simple reactants indicated a dramatic difference between the diastereomers, which is part of a generally observed pattern; the (*E*)-isomer gave the better *ee*-values, but only the (*Z*)-isomer showed substantial diminution of enantioselectivity at higher pressures [55]. There is a difference in the enamide association constant from the two reactant diastereomers, with the (*Z*)-isomer the more strongly bound. This can lead to zero-order kinetics for its hydrogenation using DIPAMPRh$^+$, whereas the corresponding (*E*)-isomer hydrogenates with first-order kinetics and

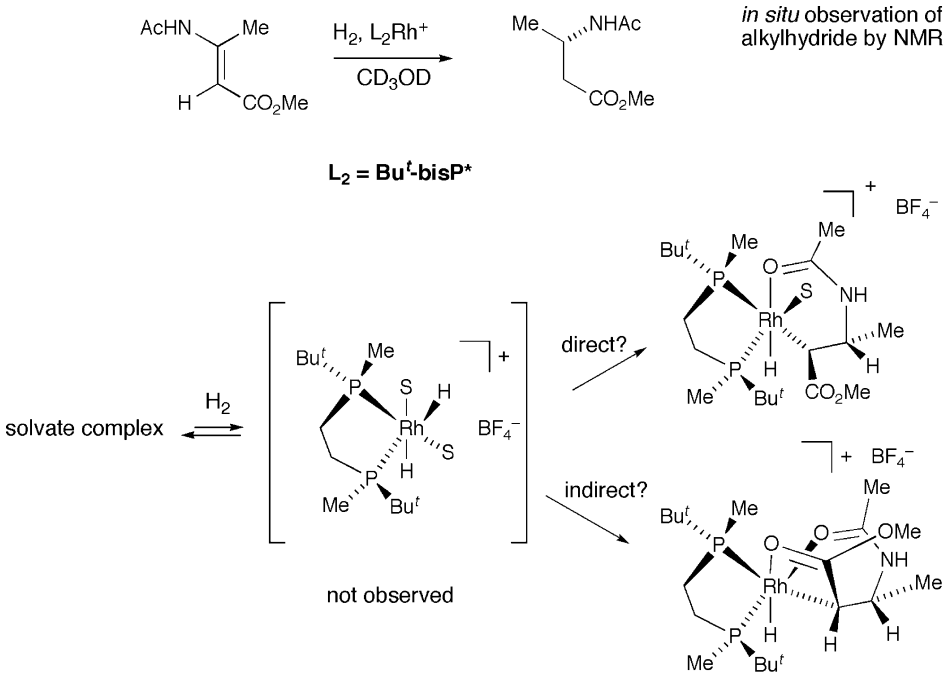

Fig. 31.11 Intermediates in the enantioselective hydrogenation of β-amino ester precursors.

higher *ee*. The accessibility of stable intermediates in this chemistry has led to a different correlation between the configuration of the enamide complexes and the reaction course than for the α-dehydroamino ester case. For two examples, the configuration of the enamide complex established by X-ray corresponds with that of the main hydrogenation product. The authors conclude that there are only slight differences between the hydrogenation activities of the *re*- and *si*-bound diastereomers [56]. *In-situ* study of the intermediates in the hydrogenation of β-dehydroamino esters reveals the formation of several alkylhydrides at low temperatures from the (*E*)-isomer, although only one enantiomer of reduced product is formed [57]. Because the carboxyl group better stabilizes the β-C–Rh bond, the intermediates are formed by hydride delivery to the enamide-bearing carbon, in contrast to the normal α-dehydroamino ester case. This partly explains the absence of the anticipated correlation between enamide configuration and the stereochemical outcome of hydrogenation (Fig. 31.11).

31.2.8
Current Status of Rhodium Hydrogenations

Although the main features of the mechanism have been in place for almost 20 years, recent results have provided considerable refinement. It is becoming clear that a single pathway cannot fit all ligands and all reactants, although there are

common principles, which apply quite generally. Even the paradigm that the configuration of the product is stereochemically related to the less-favored form of the complexed substrate is violable. Evans and coworkers investigated the synthesis and catalytic reactivity of a series of easily prepared P–S chelate ligands in enantioselective catalysis [58]. For hydrogenation, high enantioselectivity was observed in dehydroamino acid reduction (Fig. 31.12). Most significantly, an X-ray structure of the derived enamide complex (shown to be the exclusive diastereomer in solution by NMR) indicated that the alkene was bound to rhodium through the face to which H_2 is delivered during hydrogenation. This of course undermines any absolute rule linking the minor diastereomer with the stereochemical outcome of enantioselective hydrogenation. It does not, however, violate the new statement of the Quadrant Rule, where the geometry of the turnover-limiting reaction transition state is cryptically taken into consideration, so that the correct steric interactions between ligand and bound substrate are properly considered.

The combination of recent studies on reactive intermediates and computation provides a more incisive insight into the reaction mechanism. In particular, the role of the solvate dihydride, now characterized, needs to be readdressed, as does the older idea that dihydrogen addition rather than migratory insertion is the turnover-limiting step. The first of these points needs to be analyzed in terms of known, and accepted, kinetic models. By deriving the formal rate equation, Heller has demonstrated that a catalytic cycle based solely on the initial formation of a solvate dihydride would not show any pressure dependence of *ee* [59]. This is at variance with the original studies of Halpern and Landis, among others. From the careful studies of Imamoto and Gridnev, there is no doubt that the observed solvate dihydride (SH_2) complex reacts rapidly and quantitatively at low temperature with the alkene substrate, giving product with the expected enantioselectivity. Even at the lowest temperatures, SH_2 is only a minor component of the equilibrium mixture. Based on the published equation for the equilibrium thermodynamics, there is substantially less than 0.1% of the dihydride complex present in equilibrium with the solvate complex under ambient conditions. The alkene normally binds strongly to the solvate, displacing the equilibrium and further attenuating the possibility of reaction through that pathway. (In unpublished calculations based on measured equilibrium constants in the DIPHOS-Rh^+-catalyzed hydrogenation of (*Z*)-*α*-methyl acetamidocinnamate and Halpern's kinetic data, an unrealistically high rate constant for the reaction between $Rh(dppe)(MeOH)_2$ and H_2 is required to accommodate the dihydride route; U. Sharma, P.J. Guiry and J.M. Brown, unpublished results.) The observation of SH_2 complexes is in any event limited to the highly electron-rich ligand families synthesized recently. Several of these ligands have shown exceptional promise in the enantioselective hydrogenation of tetrasubstituted alkenes, specifically *β,β*-disubstituted dehydroamino acids [60]. These are precisely the cases where reactant binding to the solvate complex would be expected to be weakened relative to the conventional substrates, and provide the most opportunity for intervention of the SH_2 pathway. This possibility merits further experimental investigation.

Both the recent computational studies of Feldgus and Landis, and the experimental contributions of Imamoto and Gridnev, have revived the possibility that the turnover-limiting step in enantioselective hydrogenation is migratory insertion rather than dihydrogen addition. Either fits in with the modified Quadrant Rule. The lack of extensive experimental evidence on dihydride intermediates (the only characterized case being some way towards the alkylhydride state because of an agostic Rh–H–C_α linkage) makes generalization difficult. At the same time, it is abundantly clear that the stereochemical course of very large numbers of rhodium-catalyzed enantioselective hydrogenations are governed by factors that permit accurate predictions based on the geometrical model (see Fig. 31.12). There is a good case for the conclusion that different catalyst/substrate systems operate by the same pathway, and with the same factors controlling enantioselectivity, which is defined at the stage of migratory insertion. The relative heights of energy barriers in the H_2 addition, Rh–H insertion steps will vary from case to case.

Since there are unresolved issues in the fine detail of reaction mechanism, it is worth recalling an earlier publication on reactive intermediates in iridium hydrogenation [61]. In general, conventional Ir diphosphine complexes turnover slowly or not at all when enantioselective hydrogenation of standard substrates is attempted, and essentially all the practical and useful recent synthetic contri-

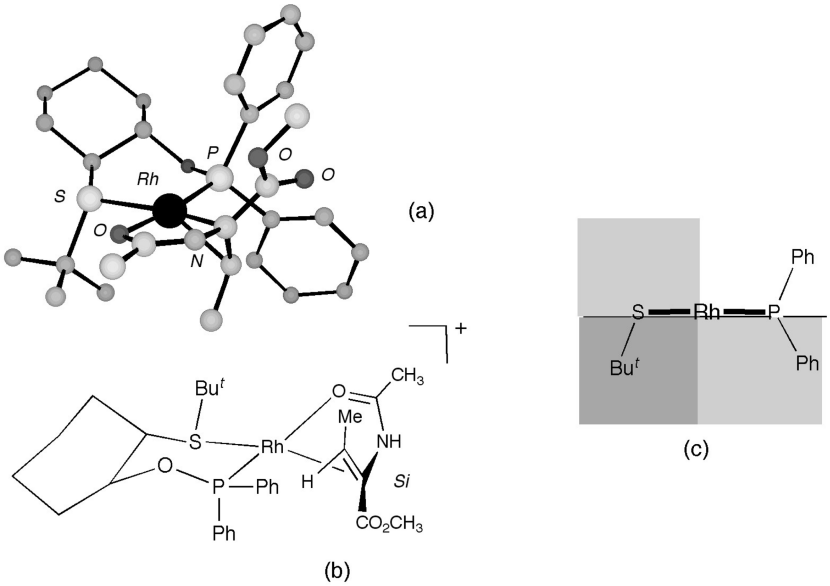

Fig. 31.12 (a) X-ray structure of the enamide complex that corresponds to the "correct" hand of product (from [58]). Solvent hydrogens and counterion are omitted for clarity. (b) Structure of the cation in (a). (c) Application of the Quadrant Rule by these authors.

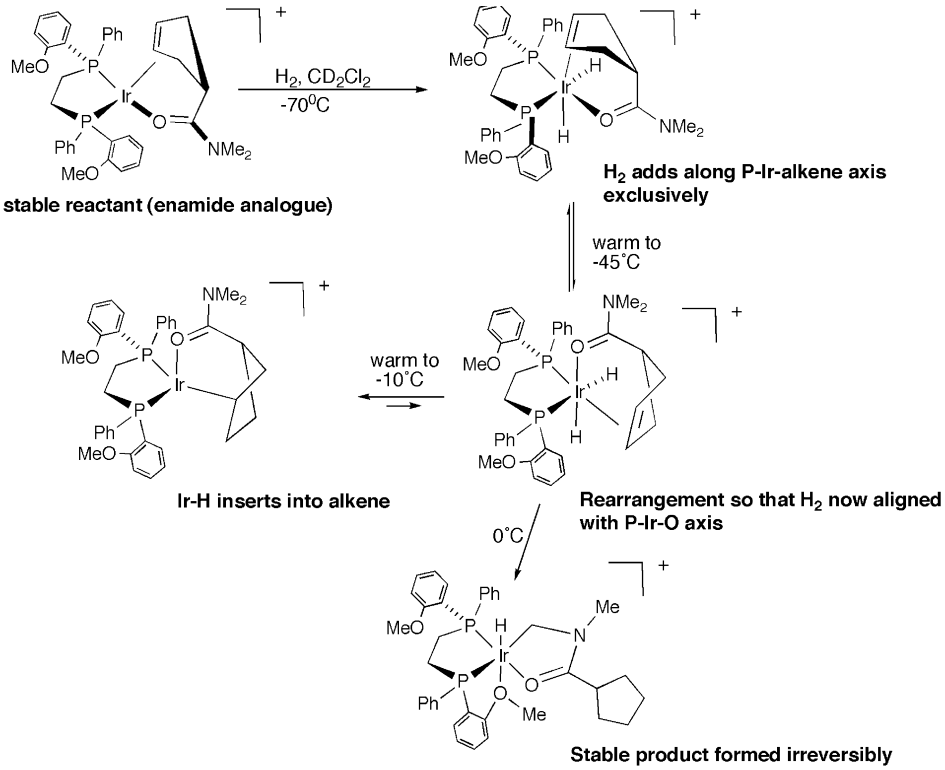

Fig. 31.13 An iridium analogue for the stereochemical course of dihydrogen addition in enantioselective hydrogenation.

butions stem from the use of phosphinamine, phosphinocarbene or aminocarbene chelates. The dihydride intermediates on the P_2Ir^+ reaction pathway are more accessible than in the rhodium case, and reveal features that must surely be relevant to the current debate. Consider the sequence of NMR-characterized species shown in Figure 31.13. The initial addition of dihydrogen to the enamide complex occurs in parallel to the C–Rh–P axis, giving a diastereomeric pair of dihydride complexes that are stable at –70 °C. At higher temperatures complete rearrangement to a pair of H–Rh–O diastereomers occurs, and on further warming thence to an alkylhydride that is stable at ambient temperature. These observations have a clear relevance to the discussion on Rh hydrogenation; they define the likely course of dihydrogen addition and the existence of a low-energy pathway for internal rearrangements of the dihydride intermediate. In terms of the detailed stereochemical pathways defined by Feldgus and Landis, they indicate the strong possibility of easy interconversion mechanisms at each stage, whether or not these pathways have been identified computationally.

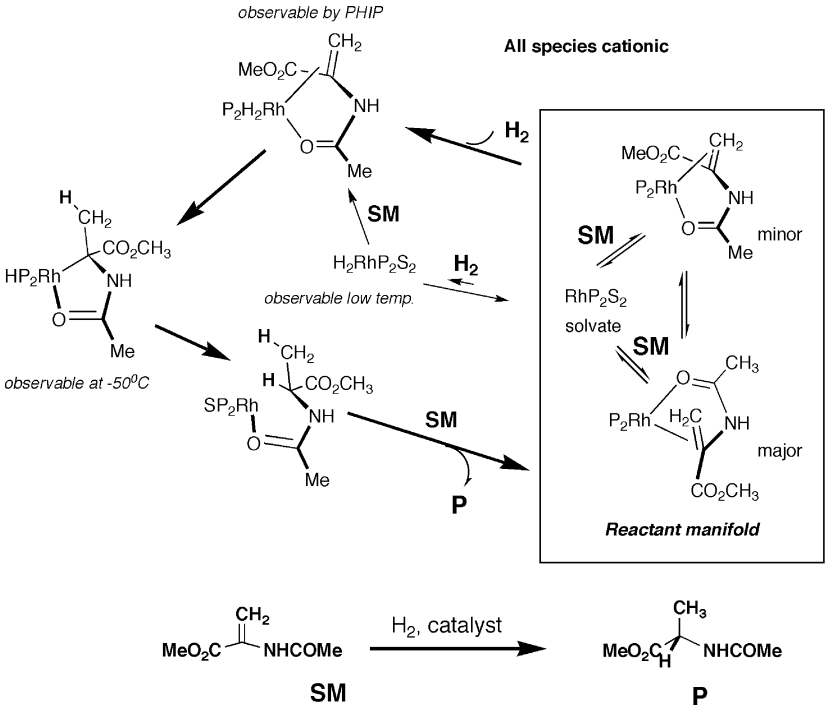

Fig. 31.14 The present state of knowledge on rhodium-complex-catalyzed enantioselective hydrogenation. The H_2 addition stage in the main cycle is predicted to be two-step in DFT calculations; whether that or migratory insertion is turnover-limiting remains debatable.

A summary of the status quo might state that current models can accurately predict the stereochemical sense of dehydroamino acid hydrogenation for a given ligand. There is still some uncertainty over the nature of the turnover-limiting transition state, which could be either H_2 addition or migratory insertion, depending on specific factors for the particular reaction. The predicted stereochemical sense is the same, however, based on analysis of a modified six-coordinate quadrant model arising from the most sterically favorable enamide dihydride. The alternative "hydrogen-first, then alkene" model proposed by Gridnev and Imamoto leads to the same conclusions, but the relative binding constants for hydrogen and dehydroamino acid militate against this pathway in most cases. It could well be important in those examples where the substrate is intrinsically weakly binding, as is found in the hydrogenation of β,β-disubstituted dehydroamino acids. The state of current knowledge on intermediates in rhodium-complex-catalyzed enantioselective hydrogenation is summarized in Figure 31.14, specifying the route for production of the favored enantiomer [62].

31.3
Ruthenium-Complex-Catalyzed Hydrogenations

Far more ruthenium-complex-catalyzed enantioselective hydrogenation has been directed towards ketone reduction rather than alkene reduction. Recent studies carried out on the mechanism of C=C hydrogenation has been rather limited. One reason for this has been the contrast between the ease of access of the active hydrogenation catalyst in rhodium chemistry and ruthenium chemistry. For rhodium, the cationic complex L_2Rh^+(alkene), where (alkene) is cycloocta-1,5-diene or norbornadiene, is readily and almost universally available; otherwise the active catalyst can be prepared *in situ* directly from the ligand. Generating the catalyst has always been more challenging in ruthenium hydrogenations, and a variety of protocols have been published over the years. Recent publications have provided access to cationic L_2Ru^+HX species where X represents a labile ligand or solvent molecules [63]. The additional hydride compared to the corresponding rhodium species serves to emphasize differences in reaction mechanisms between the two catalyst families.

31.3.1
Reactive Intermediates in Ruthenium-Complex-Catalyzed Hydrogenations

The most successful attempt to capture reactive intermediates stems from the NMR-based studies of Bergens and Wiles [64]. The accessibility of a BINAP Ru–H complex with labile ligands permits the solution characterization of an enamide complex from (*Z*)-*α*-methyl acetamidocinnamate (MAC) with a single solvent molecule in place, *trans*- to the hydride. The configuration of the bound alkene is identical to that of the final hydrogenation product (i.e., the major diastereomer is the precursor of product). On warming from –40 °C to –20 °C, this is converted into a Ru alkyl, itself stable until the addition of dihydrogen, which promotes the formation of the hydrogenated product. The coordination geometry of both intermediates was established by HETCOR and other techniques. Theses experiments provide a simple model for ruthenium-catalyzed hydrogenation of dehydroamino acids, and may be relevant to other bidentate reactants. These investigations are summarized in more detail in [14].

31.3.2
Kinetic Analysis of Ruthenium-Complex-Catalyzed Hydrogenations

There is only one detailed kinetic study of ruthenium enantioselective hydrogenation, in this case involving (BINAP)$Ru(OAc)_2$, and MAC [65]. The extensive study involved reaction kinetics, isotopic analysis of reaction components and products, and *in-situ* NMR. The derived catalytic cycle is shown in Figure 31.15, differing from the Bergens' studies described above in that the intermediates – both observed and assumed – are neutral rather than cationic. Right up to the formation of the alkylruthenium intermediate, the individual steps are revers-

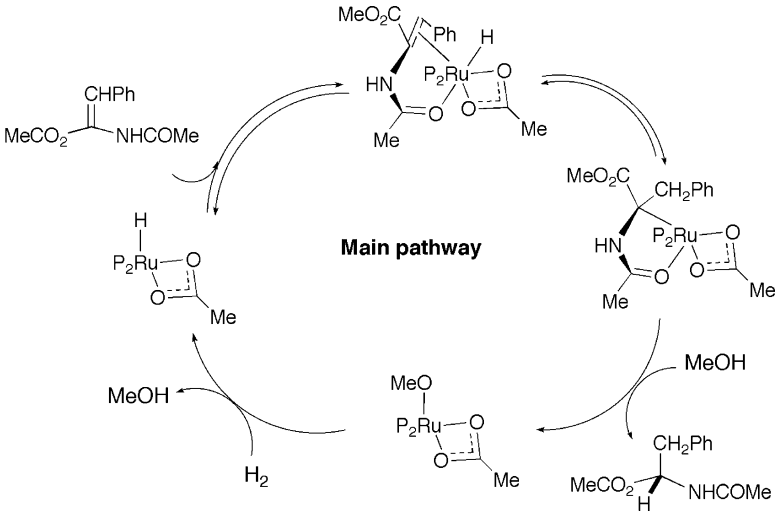

Fig. 31.15 Mechanism of the enantioselective hydrogenation of enamides by Ru BINAP, giving the opposite stereochemical course to the corresponding Rh catalyst. Note the heterolytic nature of the addition process with one of the two hydrogens arising from solvent.

ible. Formally, the second hydrogen comes from the solvent MeOH as well as molecular hydrogen, as had been seen in earlier studies from the same laboratory in α,β-unsaturated acid reductions [66]. In the kinetic studies, a first-order response to both [H_2] and [catalyst] was observed, but a more complex relationship with [substrate] was seen, close to inverse first-order. Individual runs follow first-order kinetics at [H_2] <7 bar, that do not reflect this inhibition by substrate, and this is interpreted to reflect the (irreversible) formation of an enamide-derived inert byproduct $P_2RuH(OAc)S$ (S = substrate), with a geometry that is unfavorable for H-transfer. This supposed byproduct was observed by NMR, under conditions that simulate catalytic hydrogenation at –60 °C. It is the [P_2RuH (OAc)] species that is the true catalyst precursor.

31.4 Iridium-Complex-Catalyzed Hydrogenations

31.4.1 Background

The classical notion has been that iridium complexes can be effective hydrogenation catalysts, with defined limitations. In this respect, Crabtree and Morris made the key breakthroughs [9], and their catalyst (Fig. 31.16) has been widely employed for the reduction of simple alkenes. It was widely successful in the di-

rected (diastereoselective) hydrogenation of alkenes carrying an adjacent polar group [67], but application to enantioselective hydrogenation was lacking. This situation changed with the demonstration by Lightfoot and Pfaltz that chelate P-N-ligated Ir complexes were successful catalysts for enantioselective hydrogenation. The publication has stimulated several parallel developments by other groups as well as improvements in the original Pfaltz ligand, resulting in the present capability to achieve high enantioselectivity in a wide range of cases with readily accessible catalyst systems [68].

31.4.2
Mechanistic and Computational Studies

The mechanistic basis of iridium-complex-catalyzed enantioselective hydrogenation is less secure than in the rhodium case. It is well known that square-planar iridium complexes exhibit a stronger affinity for dihydrogen than their rhodium counterparts. In earlier studies, Crabtree et al. investigated the addition of H_2 to their complex and observed two stereoisomeric intermediate dihydrides in the hydrogenation of the coordinated cycloocta-1,5-diene. The observations were in contrast to the course of H_2 addition to *bis*-phosphine iridium complexes [69].

This formed a basis for the study of the H_2 addition step in a precatalyst for Ir enantioselective hydrogenation [70]. By NMR, it proved possible to characterize a single diastereomer of the initial addition product at –40 °C in THF, the configuration of which was defined by nOe methods. This was converted into a mixture of two diastereomers of the disolvate dihydride with release of cyclooctane at 0 °C. In all cases, H *trans*-N is preferred over H *trans*-P, as was originally observed by Crabtree. The investigations were completed by DFT computational studies on the initial steps of the reaction sequence as a model for the stereose-

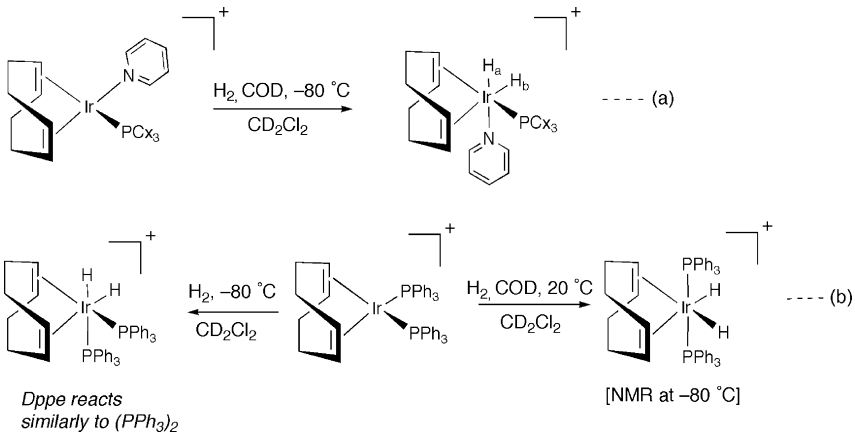

Fig. 31.16 Stable hydrides formed from (a) amine/phosphine iridium cations and (b) *bis*-phosphine or diphosphine iridium cations.

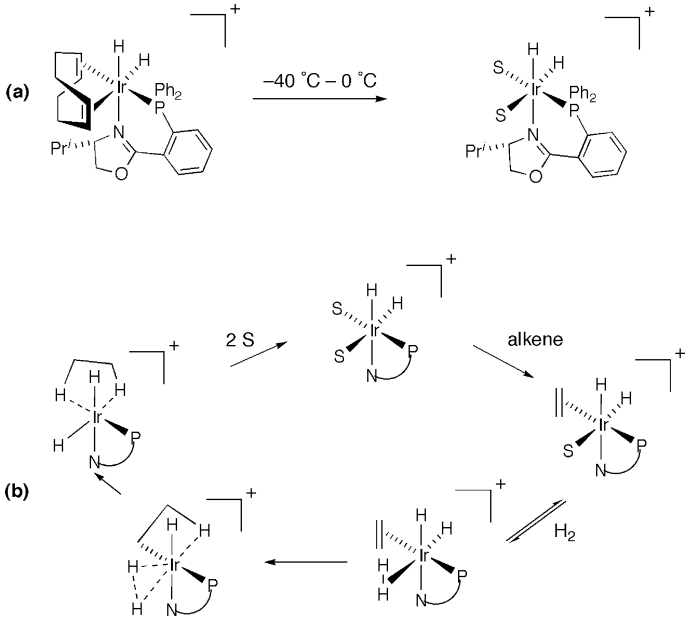

Fig. 31.17 (a) Experimental observation of dihydrides in the PHOXIr$^+$ system by NMR (S=THF). (b) The DFT-derived mechanism for Ir-catalyzed enantioselective hydrogenation involving the sequential addition of two molecules of dihydrogen, with a single H-atom transfer from each one (S=CH_2Cl_2).

lectivity of the initial step in iridium-complex-catalyzed asymmetric hydrogenation. This defines the relative energies of the cycloocta-1,5-diene dihydride diastereomers and the solvate (methanol) dihydride diastereomers. The lowest energy structures at these two levels are shown in Figure 31.17.

An informative set of calculations was carried out by Brandt et al., coupled to experimental studies that demonstrated first-order dependence of the turnover rate on both catalyst and H_2, and zero-order dependence on alkene (α-methyl-(*E*)-stilbene) concentration [71]. The incentive for this investigation was the absence of any characterized advanced intermediates on the catalytic pathway. As a result of the computation, a catalytic cycle (for ethene) was proposed in which H_2 addition to iridium was followed by alkene coordination and migratory insertion. The critical difference in this study was the proposal that a second molecule of H_2 is involved that facilitates formation of the Ir alkylhydride intermediate. In addition, the reductive elimination of R–H and re-addition of H_2 are concerted. This postulate was subsequently challenged. For hydrogenation of styrene by the "standard" Pfaltz catalyst, ES-MS analysis of the intermediates formed at different stages in the catalytic cycle revealed only Ir(I) and Ir(III) species, supporting a cycle (at least under low-pressure conditions in the gas

phase) for which a dihydridoalkene complex is assembled and undergoes successive migratory insertion and reductive elimination [72].

31.4.3
Counter-Ion Effects

A remarkable feature of iridium enantioselective hydrogenation is the promotion of the reaction by large non-coordinating anions [73]. This has been the subject of considerable activity (anticipated in an earlier study by Osborn and coworkers) on the effects of the counterion in Rh enantioselective hydrogenation [74]. The iridium chemistry was motivated by initial synthetic limitations. With PF_6^- as counterion to the ligated Ir cation, the reaction ceases after a limited number of turnovers because of catalyst deactivation. The mechanism of

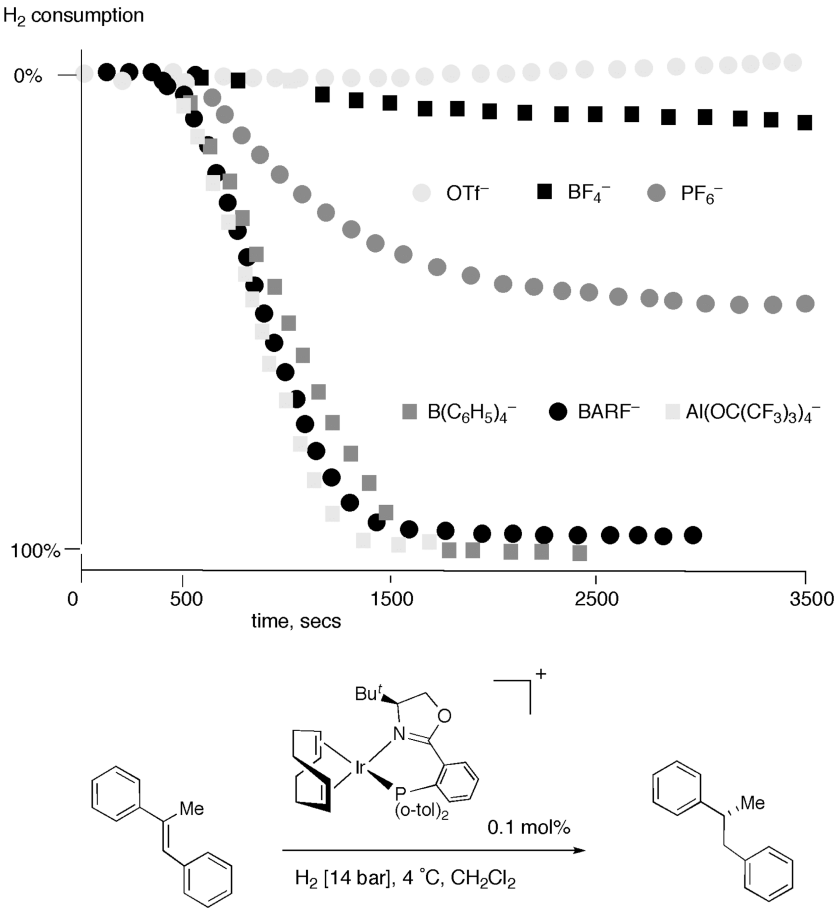

Fig. 31.18 Anion effects on the enantioselective hydrogenation shown (adapted from [77]).

deactivation is similar to that originally observed with Crabtree's catalyst, in that an inactive dimeric trihydride is formed irreversibly [75]. When the large anion BARf is employed, the reaction is considerably faster, and not subject to inhibition. This observation stimulated a body of physico-chemical studies on the nature of ion-pair effects in these and related complexes [76]. In a detailed kinetic study of hydrogenation, the large effect of counter-ion on reaction rate was not reflected in any influence on the *ee* of the reaction, which was the same (within experimental error) for a series of three bulky and three small anions (Fig. 31.18). In the course of these studies it was found that: (i) CH_2Cl_2 is the best solvent; (ii) the catalytic reaction is inhibited by water at very low concentrations, and success therefore requires careful drying of the reaction components; (iii) there is a first-order dependence on [H_2], and on [catalyst] at low loading; and (iv) the reaction rate decreased slightly with increasing [alkene], but only when the bulky non-coordinating anions were employed [77].

In recent studies, Burgess and coworkers noted that examples of the enantioselective hydrogenation of conjugated dienes are fairly sparse in the literature [78]. They demonstrated that the diene binds strongly to their iminocarbene Ir^+ catalyst under hydrogenation conditions, and the course of reaction changed when the reactant was consumed. This was subsequently controlled by the superior rate of hydrogenation of the monoene enantiomer that is stereochemically the better matched to the configuration of the catalyst. The overall reaction was biphasic, with hydrogenation of the coordinated diene dominant until it was consumed.

31.5 Summary and Conclusions

Since the first demonstration of enantioselective hydrogenation by Knowles and colleagues at Monsanto, and the important early contributions of Kagan, enantioselective hydrogenation has consistently been central to the development of enantioselective catalysis. The present chapter concentrates on the hydrogenation of alkenes, though since the mid-1980s the hydrogenation of ketones has been pursued with equal vigor. Part of the reason for this is the sheer simplicity of the procedure, and the versatility of the outcome. Equally, the ability to carry out enantioselective hydrogenation on an industrial scale has provided a strong impetus for catalyst discovery and development, with several important recent developments having arisen from industrial laboratories. The first wave of development exclusively involved rhodium catalysts, and these dominated up to 1985. However, with the advent of ruthenium BINAP catalysts, introduced by Noyori and Takaya, the emphasis changed dramatically. The increased versatility and the productive involvement of both C=C and C=O functionalities made this the focal point of enantioselective hydrogenation for a decade, and led to the award of the Nobel Prize (of course equally shared with Sharpless for enantioselective oxidation) jointly to Knowles and Noyori. The recent upsurge of interest

has had several drivers. A new generation of ligands has increased the scope of the rhodium-complex-catalyzed reaction and further improved enantioselectivity. The discovery and development of iridium enantioselective hydrogenation by Pfaltz and coworkers has extended the substrate scope. The reintroduction of monophosphine catalysts for enantioselective hydrogenation, and especially the recognition that two different phosphine ligands (only one need be chiral) can operate cooperatively, offers exciting new prospects. As the synthetic utility is extended, it is equally necessary to address the mechanistic aspects and to provide a complete picture of this centrally important reaction.

Acknowledgments

The author thanks Dr. Monika Mayr, Dr. Linnea Soler and Jeremy Taylor for their helpful comments made on the draft of this chapter.

Abbreviations

AE	absorption-emission
DFT	density function theory
ES-MS	electrospray-mass spectrometry
MAC	(*Z*)-*a*-methyl acetamidocinnamate
MM	molecular mechanics
UFF	universal force field

References

1 Osborn, J.A., Jardine, F.H., Young, G.W., Wilkinson, G., *J. Chem. Soc. A*, **1966**, 1711.
2 Horner, L., Winkler, H., *Annalen*, **1965**, *685*, 1; Horner, L., Balzer, W.D., Peterson, D.J., *Tetrahedron Lett.*, **1966**, 3315; Korpiun, O., Mislow, K., *J. Am. Chem. Soc.*, **1967**, *89*, 4784; Korpiun, O., Lewis, R.A., Chickos, J., Mislow, K., *J. Am. Chem. Soc.*, **1968**, *90*, 4842; Naumann, K., Zon, G., Mislow, K., *J. Am. Chem. Soc.*, **1969**, *91*, 7012.
3 Horner, L., Siegel, H., Buethe, H., *Angew. Chem., Int. Ed.*, **1968**, *7*, 942.
4 Knowles, W.S., Sabacky, M.J., *Chem. Commun.*, **1968**, 1445.
5 Kagan, H.B., Dang, T.P., *J. Am. Chem. Soc.*, **1972**, *94*, 6429.
6 Vineyard, B.D., Knowles, W.S., Sabacky, M.J., Bachman, G.L., Weinkauff, D.J., *J. Am. Chem. Soc.*, **1977**, *99*, 5946.
7 Chaloner, P.A., Esteruelas, M.A., Joo, F., Oro, L.A., *Homogeneous Hydrogenation*, Kluwer, Dordrecht, **1994**; Noyori, R., *Asymmetric Catalysis in Organic Synthesis* (especially Chapter 2), John Wiley & Sons, Inc., New York, **1994**; Ojima, I. (Ed.), *Catalytic Asymmetric Synthesis*, John Wiley & Sons, Inc., New York, **2000**.
8 Hallman, P.S., Evans, D., Osborn, J.A., Wilkinson, G., *Chem. Commun.*, **1967**, 305; Hallman, P.S., McGarvey, B.R., Wilkinson, G., *J. Chem. Soc. A*, **1968**, 3143; Rose, D., Gilbert, J.D., Richardson, R.P., Wilkinson, G., *J. Chem. Soc. A*, **1969**, 2610.

9 Crabtree, R. H., Felkin, H., Morris, G. E., *Chem. Commun.*, **1976**, 716; Crabtree, R. H., Felkin, H., Morris, G. E., *J. Organomet. Chem.*, **1977**, *141*, 205.

10 Noyori, R., Ohta, M., Hsiao, Y., Kitamura, M., Ohta, T., Takaya, H., *J. Am. Chem. Soc.*, **1986**, *108*, 7117; Takaya, H., Ohta, T., Sayo, N., Kumobayashi, H., Akutagawa, S., Inoue, S., Kasahara, I., Noyori, R., *J. Am. Chem. Soc.*, **1987**, *109*, 1596; Ohta, T., Takaya, H., Kitamura, M., Nagai, K., Noyori, R., *J. Org. Chem.*, **1987**, *52*, 3174.

11 Kitamura, M., Ohkuma, T., Inoue, S., Sayo, N., Kumobayashi, H., Akutagawa, S., Ohta, T., Takaya, H., Noyori, R., *J. Am. Chem. Soc.*, **1988**, *110*, 629; Noyori, R., Ohkuma, T., Kitamura, M., Takaya, H., Sayo, N., Kumobayashi, H., Akutagawa, S., *J. Am. Chem. Soc.*, **1987**, *109*, 5856.

12 Lightfoot, A., Schnider, P., Pfaltz, A., *Angew. Chem., Int. Ed.*, **1998**, *37*, 2897.

13 Blaser, H.-U., Schmidt, E. (Eds.), *Asymmetric Catalysis on an Industrial Scale; Challenges, Approaches and Solutions.* Wiley-VCH, New York, **2004**.

14 Brown, J. M., in: Jacobsen, E. N., Pfaltz, A., Yamamoto, H. (Eds.), *Comprehensive Asymmetric Catalysis*, Volume I, Chapter 5.1. Springer, Berlin, **1999**, pp. 121.

15 (a) Landis, C. R., Halpern, J., *J. Am. Chem. Soc.*, **1987**, *109*, 1746; (b) Halpern, J., *Science*, **1982**, *217*, 401; (c) Halpern, J., Chan, A. S. C., *J. Am. Chem. Soc.*, **1980**, *102*, 838; (d) Chan, A. S. C., Pluth, J. J., Halpern, J., *J. Am. Chem. Soc.*, **1980**, *102*, 5952; (e) Sun, Y. K., Landau, R. N., Wang, J., Leblond, C., Blackmond, D. G., *J. Am. Chem. Soc.*, **1996**, *118*, 1348.

16 Brown, J. M., Chaloner, P. A., Nicholson, P. N., *J. Chem. Soc., Chem. Commun.*, **1978**, 646; Brown, J. M., Chaloner, P. A., *Tetrahedron Lett.*, **1978**, 1877; Brown, J. M., Chaloner, P. A., *J. Chem. Soc., Chem. Commun.*, **1978**, 321; Brown, J. M., Chaloner, P. A., Descotes, G., Glaser, R., Lafont, D., Sinou, D., *J. Chem. Soc., Chem. Commun.*, **1979**, 611; Brown, J. M., Chaloner, P. A., *J. Chem. Soc., Chem. Commun.*, **1979**, 613; Brown, J. M., Chaloner, P. A., *J. Chem. Soc., Chem. Commun.*, **1980**, 344; Brown, J. M., Chaloner, P. A., Glaser, R., Geresh, S., *Tetrahedron*, **1980**, *36*, 815; Descotes, G., Lafont, D., Sinou, D., Brown, J. M., Chaloner, P. A., Parker, D., *New J. Chem.*, **1981**, *5*, 167.

17 Drexler, H.-J., Baumann, W., Spannenberg, A., Fischer, C., Heller, D., *J. Organometal. Chem.*, **2001**, *621*, 89; Borner, A., Heller, D., *Tetrahedron Lett.*, **2001**, *42*, 223; Braun, W., Salzer, A., Drexler, H.-J., Spannenberg, A., Heller, D., *Dalton Trans.* **2003**, 1606.

18 Brown, J. M., Canning, L. R., Downs, A. J., Forster, A. M., *J. Organomet. Chem.*, **1983**, *255*, 103.

19 Brown, J. M., Chaloner, P. A., Parker, D., *Adv. Chem. Ser.*, **1982**, *196*, 355.

20 Brown, J. M., Chaloner, P. A., Morris, G. A., *J. Chem. Soc. Chem. Commun.*, **1983**, 664; Brown, J. M., Chaloner, P. A., Morris, G. A., *J. Chem. Soc. Perkin Trans. 2*, **1987**, 1583; Ramsden, J. A., Claridge, T. D. W., Brown, J. M., *J. Chem. Soc. Chem. Commun.*, **1995**, 2469.

21 Burk, M. J., Feaster, J. E., Nugent, W. A., Harlow, R. L., *J. Am. Chem. Soc.*, **1993**, *115*, 10125.

22 Muci, A. R., Campos, K. R., Evans, D. A., *J. Am. Chem. Soc.*, **1995**, *117*, 9075.

23 Imamoto, T., Watanabe, J., Wada, Y., Masuda, H., Yamada, H., Tsuruta, H., Matsukawa, S., Yamaguchi, K., *J. Am. Chem. Soc.*, **1998**, *120*, 1635; Miura, T., Imamoto, T., *Tetrahedron Lett.*, **1999**, *40*, 4833; Gridnev, I. D., Yamanoi, Y., Higashi, N., Tsuruta, H., Yasutake, M., Imamoto, T., *Adv. Synth. Catal.*, **2001**, *343*, 118; Gridnev, I. D., Yasutake, M., Higashi, N., Imamoto, T., *J. Am. Chem. Soc.*, **2001**, *123*, 5268; Imamoto, T., *Pure Appl. Chem.*, **2001**, *73*, 373; Ohashi, A., Imamoto, T., *Tetrahedron Lett.*, **2001**, *42*, 1099; Yasutake, M., Gridnev, I. D., Higashi, N., Imamoto, T., *Org. Lett.*, **2001**, *3*, 1701; Ohashi, A., Kikuchi, S., Yasutake, M., Imamoto, T., *Eur. J. Org. Chem.*, **2002**, 2535; Crepy, K. V. L., Imamoto, T., *Adv. Synth. Catal.*, **2003**, *345*, 79; Oohara, N., Katagiri, K., Imamoto, T., *Tetrahedron: Asymmetry*, **2003**, *14*, 2171.

24 Pye, P. J., Rossen, K., Reamer, R. A., Tsou, N. N., Volante, R. P., Reider, P. J., *J. Am. Chem. Soc.*, **1997**, *119*, 6207; Ros-

sen, K., Pye, P.J., DiMichele, L.M., Volante, R.P., Reider, P.J., *Tetrahedron Lett.*, **1998**, *39*, 6823.
25 Tang, W.J., Zhang, X.M., *Chem. Rev.*, **2003**, *103*, 3029.
26 Claver, C., Fernandez, E., Gillon, A., Heslop, K., Hyett, D.J., Martorell, A., Orpen, A.G., Pringle, P.G., *Chem. Commun.*, **2000**, 961; Reetz, M.T., Sell, T., *Tetrahedron Lett.*, **2000**, *41*, 6333; van den Berg, M., Minnaard, A.J., Schudde, E.P., van Esch, J., de Vries, A.H.M., de Vries, J.G., Feringa, B.L., *J. Am. Chem. Soc.*, **2000**, *122*, 11539; van den Berg, M., Haak, R.M., Minnaard, A.J., De Vries, A.H.M., De Vries, J.G., Feringa, B.L., *Adv. Synth. Catal.*, **2002**, *344*, 1003.
27 Gridnev, I.D., Higashi, N., Asakura, K., Imamoto, T., *J. Am. Chem. Soc.*, **2000**, *122*, 7183.
28 Gridnev, I.D., Higashi, N., Imamoto, T., *Organometallics*, **2001**, *20*, 4542.
29 Gridnev, I.D., Yamanoi, Y., Higashi, N., Tsuruta, H., Yasutake, M., Imamoto, T., *Adv. Synth. Catal.*, **2001**, *343*, 118; Gridnev, I.D., Imamoto, T., *Organometallics*, **2001**, *20*, 545.
30 Heinrich, H., Giernoth, R., Bargon, J., Brown, J.M., *Chem. Commun.*, **2001**, 1296.
31 Halpern, J., Wong, C.S., *J. Chem. Soc., Chem. Commun.*, **1973**, 629.
32 Brown, J.M., Parker, D., *Organometallics*, **1982**, *1*, 950.
33 Burk, M.J., Casy, G., Johnson, N.B., *J. Org. Chem.*, **1998**, *63*, 6084.
34 Gridnev, I.D., Higashi, N., Imamoto, T., *J. Am. Chem. Soc.*, **2000**, *122*, 10486.
35 Feldgus, S., Landis, C.R., *Organometallics*, **2001**, *20*, 2374.
36 Harthun, A., Kadyrov, R., Selke, R., Bargon, J., *Angew. Chem., Int. Ed. Engl.*, **1997**, *36*, 1103.
37 Giernoth, R., Heinrich, H., Adams, N.J., Deeth, R.J., Bargon, J., Brown, J.M., *J. Am. Chem. Soc.*, **2000**, *122*, 12381.
38 Samuel, O., Couffignal, R., Lauer, M., Zhang, S.Y., Kagan, H.B., *Nouv. J. Chim.*, **1981**, *5*, 15, see also: Fryzuk, M.D., Bosnich, B., *J. Am. Chem. Soc.*, **1977**, *99*, 6262; Pavlov, V.A., Klabunovskii, E.I., Struchkov, Y.T., Voloboev, A.A., Yanovsky, A.I., *J. Mol. Catal.*, **1988**, *44*, 217.
39 Kyba, E.P., Davis, R.E., Juri, P.N., Shirley, K.R., *Inorg. Chem.* **1981**, *20*, 3616.
40 Knowles, W.S., *Accounts Chem. Res.*, **1983**, *16*, 106.
41 Marinetti, A., Jus, S., Genet, J.P., *Tetrahedron Lett.*, **1999**, *40*, 8365.
42 Gridnev, I.D., Imamoto, T., *Accounts Chem. Res.*, **2004**, *37*, 633.
43 Drexler, H.J., Zhang, S.L., Sun, A.L., Spannenberg, A., Arrieta, A., Preetz, A., Heller, D., *Tetrahedron: Asymmetry*, **2004**, *15*, 2139.
44 Landis, C.R., Hilfenhaus, P., Feldgus, S., *J. Am. Chem. Soc.*, **1999**, *121*, 8741.
45 Feldgus, S., Landis, C.R., *J. Am. Chem. Soc.*, **2000**, *122*, 12714.
46 Ramsden, J.A., Claridge, T., Brown, J.M., *J. Chem. Soc. Chem. Commun.*, **1995**, 2469, and references therein.
47 Li, M., Tang, D., Luo, X., Shen, W., *Int. J. Quantum Chem.*, **2005**, *102*, 53.
48 Knowles, W.S., Sabacky, M.J., Vineyard, B.D., *J. Chem. Soc. Chem. Commun.*, **1972**, 10.
49 Guillen, F., Fiaud, J.-C., *Tetrahedron Lett.*, **1999**, *40*, 2939; Guillen, F., Rivard, M., Toffano, M., Legros, J.-Y., Daran, J.-C., *Tetrahedron*, **2002**, *58*, 5895; Fiaud, J.-C., Dobrota, C., Toffano, M., Fiaud, J.-C., *Tetrahedron Lett.*, **2004**, *45*, 8153.
50 Bernsmann, H., van den Berg, M., Hoen, R., Minnaard, A.J., Mehler, G., Reetz, M.T., De Vries, J.G., Feringa, B.L., *J. Org. Chem.*, **2005**, *70*, 943.
51 Hoen, R., van den Berg, M., Bernsmann, H., Minnaard, A.J., de Vries, J.G., Feringa, B.L., *Org. Lett.*, **2004**, *6*, 1433, and references therein.
52 van den Berg, M., et al., *Adv. Synth. Catal.*, **2003**, *345*, 308.
53 Reetz, M.T., Mehler, G., *Tetrahedron Lett.*, **2003**, *44*, 4593; Reetz, M.T., Mehler, G., Melswinkel, A., Sell, T., *Tetrahedron: Asymmetry*, **2004**, *15*, 3483; Reetz, M.T., Li, X., *Angew. Chem., Int. Ed.*, **2005**, *44*, 2959.
54 Wu, H.P., Hoge, G., *Org. Lett.*, **2004**, *6*, 3645; Reetz, M.T., Li, X.G., *Tetrahedron*, **2004**, *60*, 9709; Jerphagnon, T., Renaud, J.L., Demonchaux, P., Ferreira, A., Bruneau, C., *Adv. Synth. Catal.*, **2004**, *346*, 33;

Huang, H.M., Liu, X.C., Chen, S., Chen, H.L., Zheng, Z., *Tetrahedron: Asymmetry*, **2004**, *15*, 2011; Hsiao, Y., et al., *J. Am. Chem. Soc.*, **2004**, *126*, 9918; Hoge, G., Samas, B., *Tetrahedron: Asymmetry*, **2004**, *15*, 2155; Tang, W., Wu, S., Zhang, X., *J. Am. Chem. Soc.*, **2003**, *125*, 9570; Tang, W., Wang, W., Chi, Y., Zhang, X., *Angew. Chem.-Int. Ed.*, **2003**, *42*, 3509; Tang, W., Zhang, X., *Org. Lett.*, **2002**, *4*, 4159; Pena, D., Minnaard, A.J., de Vries, J.G., Feringa, B.L., *J. Am. Chem. Soc.*, **2002**, *124*, 14552; Yasutake, M., Gridnev, I.D., Higashi, N., Imamoto, T., *Org. Lett.*, **2001**, *3*, 1701; Zhu, G., Chen, Z., Zhang, X., *J. Org. Chem.*, **1999**, *64*, 6907; Zhu, G., Casalnuovo, A.L., Zhang, X., *J. Org. Chem.*, **1998**, *63*, 8100.

55 Heller, D., Holz, J., Komarov, I., Drexler, H.-J., You, J., Drauz, K., Borner, A., *Tetrahedron: Asymmetry*, **2002**, *13*, 2735; Heller, D., Drexler, H.-J., You, J., Baumann, W., Drauz, K., Krimmer, H.-P., Borner, A., *Chem. Eur. J.*, **2002**, *8*, 5196.

56 Drexler, H.-J., Baumann, W., Schmidt, T., Zhang, S., Sun, A., Spannenberg, A., Fischer, C., Buschmann, H., Heller, D., *Angew. Chem., Int. Ed.*, **2005**, *44*, 1184.

57 Yasutake, M., Gridnev, I.D., Higashi, N., Imamoto, T., *Org. Lett.*, **2001**, *3*, 1701.

58 Evans, D.A., Michael, F.E., Tedrow, J.S., Campos, K.R., *J. Am. Chem. Soc.*, **2003**, *125*, 3534.

59 Drexler, H.J., You, J.S., Zhang, S.L., Fischer, C., Baumann, W., Spannenberg, A., Heller, D., *Org. Process Res. Dev.*, **2003**, *7*, 355.

60 Tang, W.J., Wu, S.L., Zhang, X.M., *J. Am. Chem. Soc.*, **2003**, *125*, 9570.

61 Brown, J.M., Maddox, P.J., *Chem. Commun.*, **1987**, 1278.

62 Brown, J.M., *J. Organomet. Chem.*, **2004**, *689*, 4006.

63 Wiles, J.A., Bergens, S.H., Vanhessche, K.P.M., Dobbs, D.A., Rautenstrauch, V., *Angew. Chem.-Int. Ed.*, **2001**, *40*, 914; Wiles, J.A., Daley, C.J.A., Hamilton, R.J., Leong, C.G., Bergens, S.H., *Organometallics*, **2004**, *23*, 4564.

64 Wiles, J.A., Bergens, S.H., *Organometallics*, **1999**, *18*, 3709; Wiles, J.A., Bergens, S.H., *Organometallics*, **1998**, *17*, 2228; Wiles, J.A., Bergens, S.H., Young, V.G., *J. Am. Chem. Soc.*, **1997**, *119*, 2940.

65 Kitamura, M., Tsukamoto, M., Bessho, Y., Yoshimura, M., Kobs, U., Widhalm, M., Noyori, R., *J. Am. Chem. Soc.*, **2002**, *124*, 6649.

66 Ohta, T., Takaya, H., Noyori, R., *Tetrahedron Lett.*, **1990**, *31*, 7189.

67 Crabtree, R.H., Davis, M.W., *Organometallics*, **1983**, *2*, 681; Crabtree, R.H., Davis, M.W., *J. Org. Chem.*, **1986**, *51*, 2655.

68 Examples include: Kaellstroem, K., Hedberg, C., Brandt, P., Bayer, A., Andersson, P.G., *J. Am. Chem. Soc.*, **2004**, *126*, 14308; Trifonova, A., Diesen, J.S., Chapman, C.J., Andersson, P.G., *Org. Lett.*, **2004**, *6*, 3825; Smidt, S.P., Menges, F., Pfaltz, A., *Org. Lett.*, **2004**, *6*, 2023; Liu, D., Tang, W., Zhang, X., *Org. Lett.*, **2004**, *6*, 513; Schenkel, L.B., Ellman, J.A., *J. Org. Chem.*, **2004**, *69*, 1800–1802; Drury, W.J., Zimmermann, N., Keenan, M., Hayashi, M., Kaiser, S., Goddard, R., Pfaltz, A., *Angew. Chem.-Int. Ed.*, **2004**, *43*, 70; Mazet, C., Smidt, S.P., Meuwly, M., Pfaltz, A., *J. Am. Chem. Soc.*, **2004**, *126*, 14176; Perry, M.C., Cui, X.H., Powell, M.T., Hou, D.R., Reibenspies, J.H., Burgess, K., *J. Am. Chem. Soc.*, **2003**, *125*, 113; Menges, F., Pfaltz, A., *Adv. Synth. Catal.*, **2002**, *344*, 40–44; Cozzi, P.G., Zimmermann, N., Hilgraf, R., Schaffner, S., Pfaltz, A., *Adv. Synth. Catal.*, **2001**, *343*, 450; Blankenstein, J., Pfaltz, A., *Angew. Chem.-Int. Ed.*, **2001**, *40*, 4445.

69 Crabtree, R.H., Felkin, H., Morris, G.E., *J. Organomet. Chem.*, **1977**, *141*, 205; Crabtree, R.H., Felkin, H., Khan, T., Morris, G.E., *J. Organomet. Chem.*, **1978**, *144*, C15; Crabtree, R.H., Felkin, H., Fillebeen-Khan, T., Morris, G.E., *J. Organomet. Chem.*, **1979**, *168*, 183.

70 Mazet, C., Smidt, S.P., Meuwly, M., Pfaltz, A., *J. Am. Chem. Soc.*, **2004**, *126*, 14176.

71 Brandt, P., Hedberg, C., Andersson, P.G., *Chem.-Eur. J.*, **2003**, *9*, 339.

72 Dietiker, R., Chen, P., *Angew. Chem., Int. Ed.*, **2004**, *43*, 5513.

73 Blackmond, D.G., Lightfoot, A., Pfaltz, A., Rosner, T., Schnider, P., Zimmerman, N., *Chirality*, **2000**, *12*, 442.

74 Buriak, J.M., Klein, J.C., Herrington, D.G., Osborn, J.A., *Chem. Eur. J.*, **2000**, *6*, 139.

75 Smidt, S.P., Pfaltz, A., Martinez-Viviente, E., Pregosin, P.S., Albinati, A., *Organometallics*, **2003**, *22*, 1000.

76 Macchioni, A., *Eur. J. Inorg. Chem.*, **2003**, 195; Macchioni, A., *Chem. Rev.*, **2005**, *105*, 2039; Drago, D., Pregosin, P.S., Pfaltz, A., *Chem. Commun.*, **2002**, 286; Martinez-Viviente, E., Pregosin, P.S., *Inorg. Chem.*, **2003**, *42*, 2209; Martinez-Viviente, E., Pregosin, P.S., Vial, L., Herse, C., Lacour, J., *Chem. Eur. J.*, **2004**, *10*, 2912; Pregosin, P.S., Martinez-Viviente, E., Kumar, P.G.A., *J. Chem. Soc. Dalton Trans.*, **2003**, 4007.

77 Smidt, S.P., Zimmermann, N., Studer, M., Pfaltz, A., *Chem.-Eur. J.*, **2004**, *10*, 4685.

78 Cui, X., Ogle, J.W., Burgess, K., *Chem. Commun.*, **2005**, 672; Cui, X., Burgess, K., *J. Am. Chem. Soc.*, **2003**, *125*, 14212.

32
Enantioselective Ketone and β-Keto Ester Hydrogenations (Including Mechanisms)

Takeshi Ohkuma and Ryoji Noyori

Enantioselective hydrogenation of β-keto esters is a well-established procedure to produce chiral β-hydroxy esters in high optical purity [1–4]. Many important biologically active compounds have been synthesized through this procedure, even on a commercial scale [1–4]. Ru complexes [5] bearing appropriate chiral phosphine ligands [6–8] provide excellent catalytic efficiency for this reaction. Certain chiral Rh catalysts [3, 4] and heterogeneous Ni catalysts [9] are also utilized. The recent development of the chiral diphosphine/diamine–Ru catalyst enables rapid and stereoselective hydrogenation of simple ketones without a hetero-atom functionality close to the carbonyl group [2, 4]. These enantioselective transformations are summarized in the present chapter.

32.1
Chiral Ligands

In enantioselective hydrogenation of ketonic substrates, the excellent catalytic performance such as high turnover number (TON), turnover frequency (TOF = TON h^{-1} or s^{-1}), and enantioselectivity is achievable only when (pre)catalysts are prepared by the appropriate combination of metal species and chiral ligands [6–8, 10, 11]. Stereo-repulsive interaction between substituents of ligands and substrates is normally utilized for the regulation of stereochemistry. The metal and ligand must be carefully selected because of the diversity of substrate structures [1–5]. Chiral diphosphine ligands with a C_2 symmetry (see Fig. 32.1) have played a main role in this respect. Recently, however, various effective C_1 phosphine ligands as well as phosphinite ligands have been developed, the structures of which are illustrated in Figures 32.2 and 32.3, respectively. Chiral amine and imine ligands (Fig. 32.4) are also useful, particularly when they are coupled with a chiral diphosphine ligand in the hydrogenation of simple ketones [2, 4, 5]. Immobilized BINAPs are detailed in Figure 32.5.

The Handbook of Homogeneous Hydrogenation.
Edited by J.G. de Vries and C.J. Elsevier
Copyright © 2007 WILEY-VCH Verlag GmbH & Co. KGaA, Weinheim
ISBN: 978-3-527-31161-3

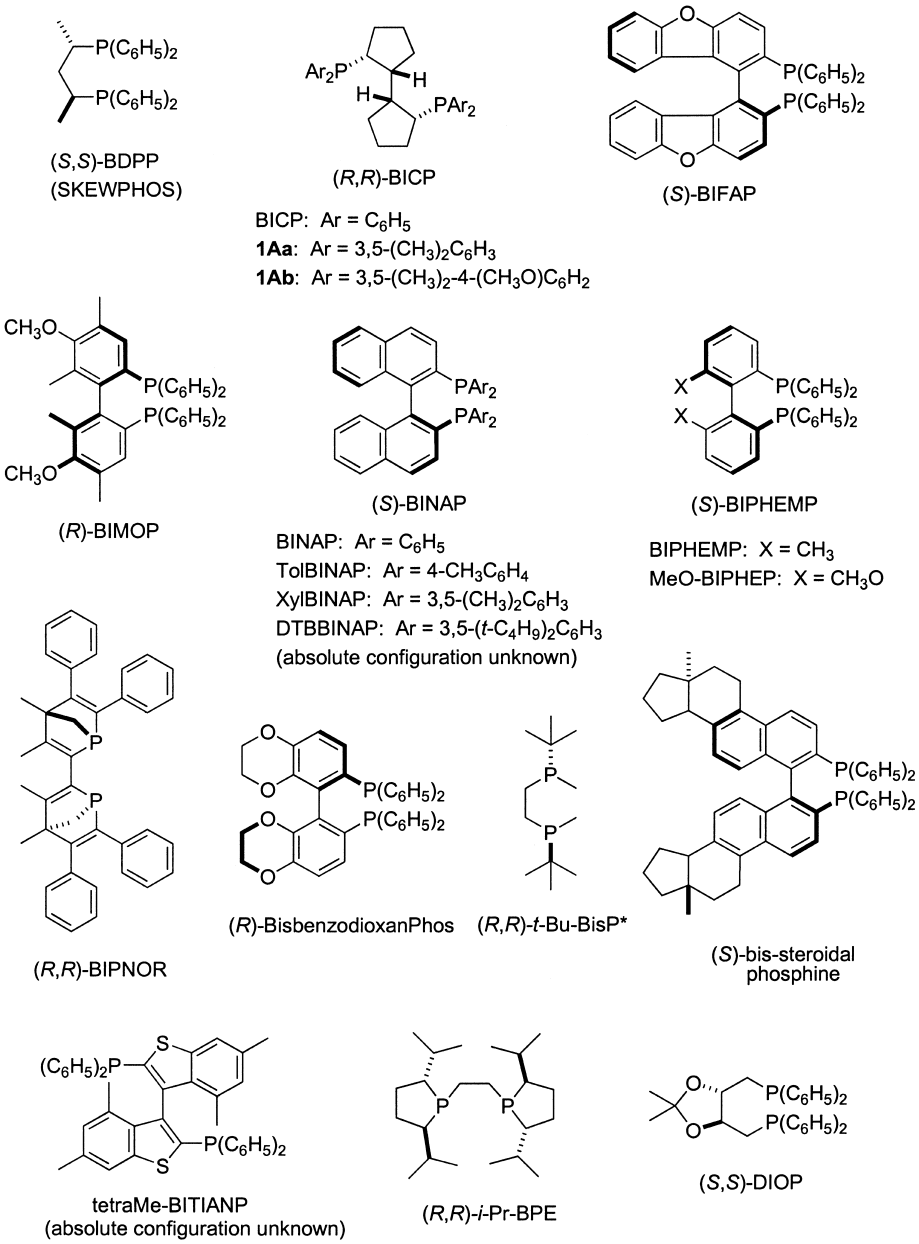

Fig. 32.1 C_2-chiral phosphine ligands.

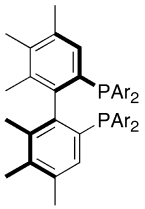

(*R*)-Xyl-HexaPHEMP
Ar = 3,5-$(CH_3)_2C_6H_3$

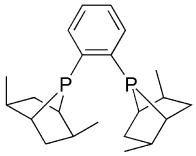

(*R*,*S*,*R*,*S*)-Me-PennPhos

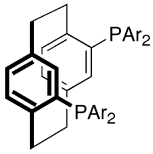

(*S*)-[2.2]PHANEPHOS
PHANEPHOS: Ar = C_6H_5
xylyl-PHANEPHOS: Ar = 3,5-$(CH_3)_2C_6H_3$

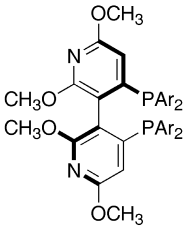

(*R*)-P-Phos
P-Phos: Ar = C_6H_5
Tol-P-Phos: Ar = 4-$CH_3C_6H_4$
Xyl-P-Phos: Ar = 3,5-$(CH_3)_2C_6H_3$

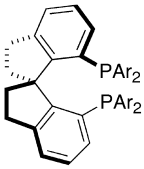

(*S*)-Xyl-SDP
Ar = 3,5-$(CH_3)_2C_6H_3$

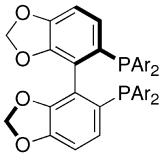

(*R*)-SEGPHOS
SEGPHOS: Ar = C_6H_5
DTBM-SEGPHOS:
Ar = 4-CH_3O-3,5-(*t*-$C_4H_9)_2C_6H_2$
(absolute configuration unknown)

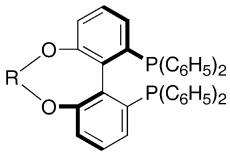

(*R*)-TunaPhos
C3TunaPhos: R = $(CH_2)_3$
C4TunaPhos: R = $(CH_2)_4$

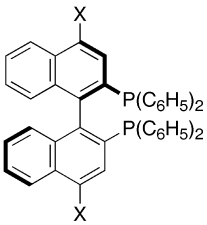

(*R*)-**1B**
1Ba: X = $BrNH_3CH_2$
1Bb: X = $(CH_3)_3Si$

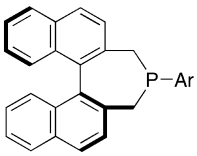

(*S*)-**1C**
Ar = 4-$CH_3OC_6H_4$

Fig. 32.1 (continued)

32.2 β-Keto Esters and Analogues

32.2.1 β-Keto Esters

The enantioselective hydrogenation of β-keto esters is important, because the resulting optically active β-hydroxy esters are converted to useful chiral building blocks [1–4]. The development of BINAP–Ru(II) catalysts allowed the highly enantioselective hydrogenation of β-keto esters. As shown in Figure 32.6, methyl-

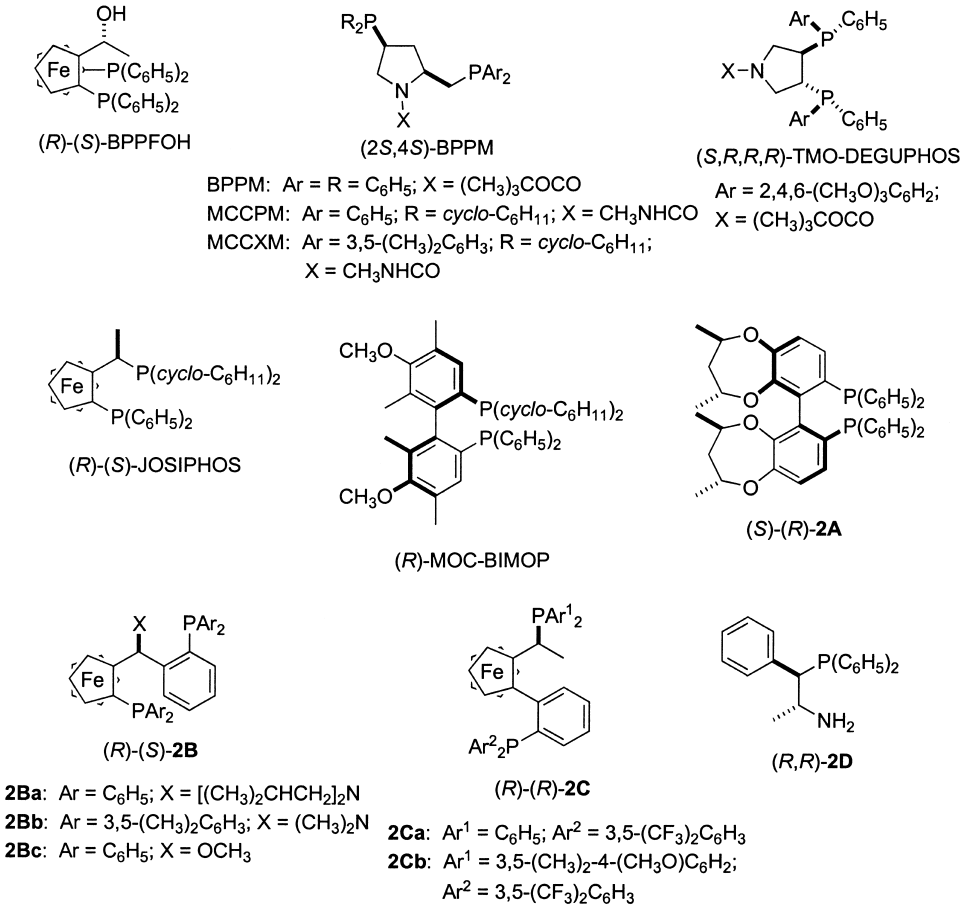

Fig. 32.2 Phosphine ligands with C_1 chirality.

3-oxobutanoate was hydrogenated in methanol containing an (*R*)-BINAP–Ru(II) complex to give (*R*)-methyl-3-hydroxybutanoate in >99% ee quantitatively [1, 2, 12]. The anionic halogen ligands on the Ru center are crucial to achieve high catalytic activity. Ru complexes with a formula of RuX_2(binap) (X = Cl, Br, or I; empirical formula with a polymeric form) [12] or $RuCl_2$(binap)$(dmf)_n$ (oligomeric form) [13] catalyze the hydrogenation of a wide variety of *β*-keto esters with a substrate : catalyst molar ratio (SCR) as high as 10 000. Several isolated or *in-situ*-prepared BINAP–Ru complexes show a similar performance [14]. The hydrogenation is accelerated by an addition of strong acid [14b, d, 15]. The use of more sterically demanding XylBINAP as a chiral ligand gives 99.9% ee [16]. Even a racemic XylBINAP–Ru complex can be used for this reaction in the presence of 0.5 equiv. of (*S*)-DM-DABN, a chiral aromatic diamine, as a poisoning compound [16]. Here, the *R* alcohol is obtained in 99.3% ee due to the selective

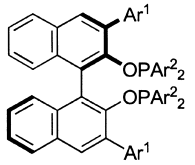

(*R*)-BINAPO

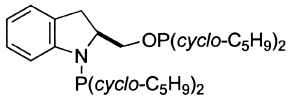

(*S*)-Cp,Cp-IndoNOP

Ph-*o*-xylyl-BINAPO: $Ar^1 = C_6H_5$, $Ar^2 = 3,5\text{-}(CH_3)_2C_6H_3$

Xylyl-*o*-BINAPO: $Ar^1 = 3,5\text{-}(CH_3)_2C_6H_3$, $Ar^2 = C_6H_5$

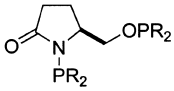

(*S*)-oxoProNOP

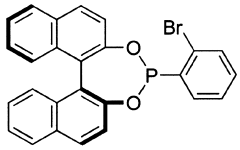

(*S*)-**3A**

Ph,Ph-oxoProNOP: $R = C_6H_5$

Cy,Cy-oxoProNOP: R = *cyclo*-C_6H_{11}

Fig. 32.3 Phosphinite ligands.

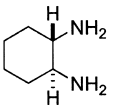

(*S*,*S*)-CYDN

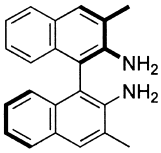

(*R*)-DM-DABN

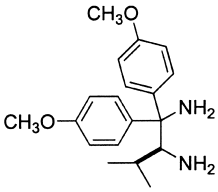

(*S*)-DAIPEN

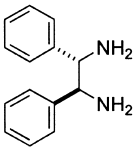

(*S*,*S*)-DPEN

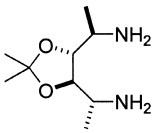

(*R*)-IPHAN

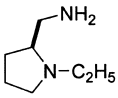

(*S*)-**4A**

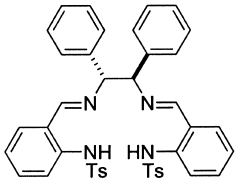

(*R*,*R*)-**4B**

Fig. 32.4 Amine and imine ligands.

formation of a feebly active (*S*)-XylBINAP/(*S*)-DM-DABN–Ru complex. Other useful biaryl diphosphines include BIPHEMP [14m], BIMOP [17], MeO-BIPHEP [18], C4TunaPhos [19], BIFAP [20], BisbenzodioxanPhos [21], P-phos [22], tetraMe-BITIANP [23], bis-steroidal phosphine [24], and **2A** [25]. The reaction can be run in aqueous phase by use of a BINAP derivative with ammonium functions **1Ba** [11b, 26, 27]. Hydrogenation catalyzed by a Ru complex bearing *i*-Pr-BPE, proceeds smoothly under a low pressure of H_2, probably due to the

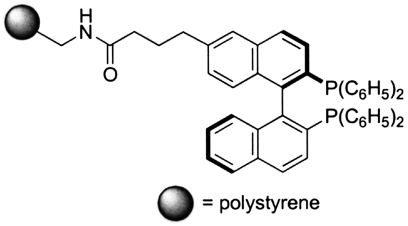

(*R*)-APBBINAP

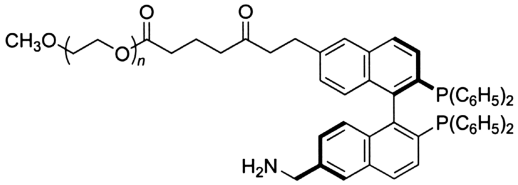

PEG-(*R*)-Am-BINAP

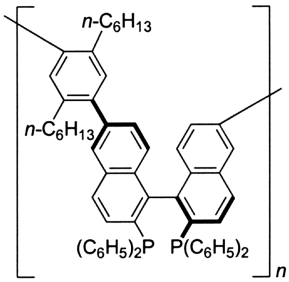

(*R*)-poly(BINAP)

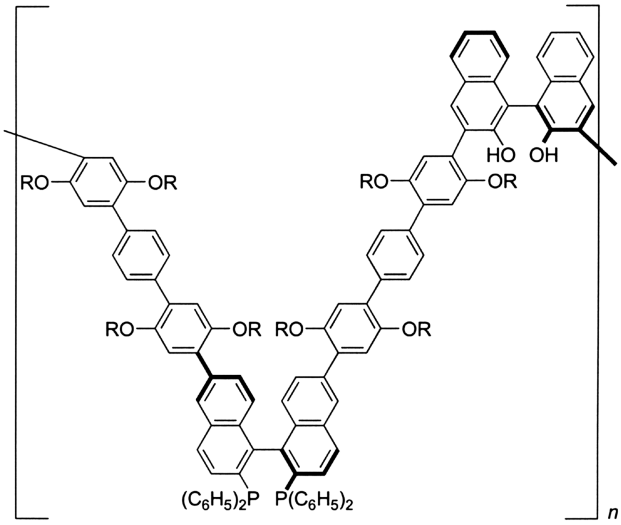

R = *n*-C_6H_{13}

(*R*,*R*)-poly(BINOL-BINAP)

Fig. 32.5 Polymer-bound BINAPs.

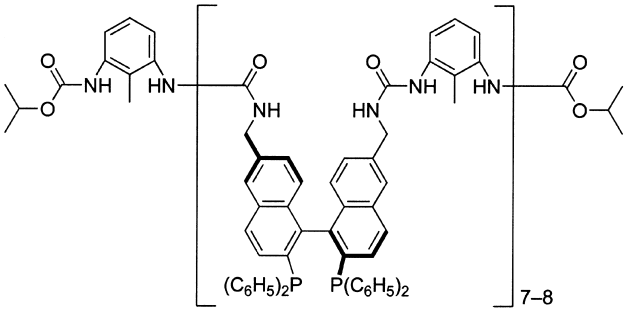

(*R*)-poly-NAP

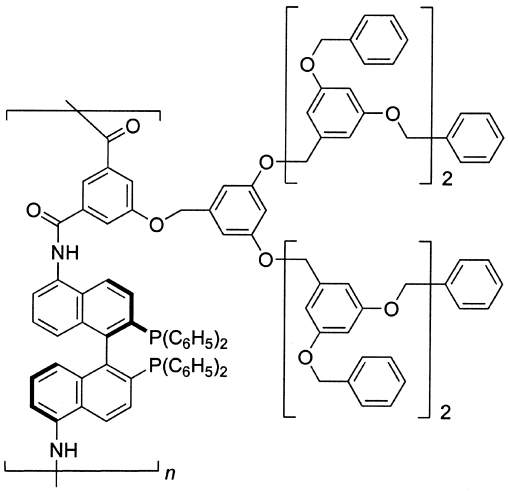

(*R*)-**5A**

Fig. 32.5 (continued)

electron-donating ability of the aliphatic diphosphine ligand [28]. A Ru complex with *t*-Bu-BisP* having chiral centers on the phosphorus atoms also shows high enantioselectivity [7a, 29]. $Ru(OCOCF_3)_2$([2.2]-phanephos) in the presence of $(n\text{-}C_4H_9)_4NI$ catalyzes the reaction of β-keto esters at a low temperature and under a low H_2 pressure, without the addition of a strong acid [30]. A Ru complex prepared from $Ru[\eta^3\text{-}CH_2C(CH_3)CH_2](cod)$, 2 equiv. of chiral monophosphine **1C**, and HBr catalyzes the hydrogenation of methyl-3-oxobutanoate with an optical yield of 95% [31]. C_1-chiral ferrocenyl ligands [8] are also useful. Ru complexes with **2Ba** [32] and **2Cb** [33], and a JOSIPHOS–Rh complex [34] yield chiral alcohols in 98.6, 95, and 97% ee, respectively. A C_2-symmetric bisphosphinite ligand, Ph-*o*-xylyl-BINAPO, is also useful in the Ru-catalyzed reaction [35]. Some

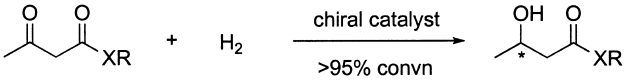

Fig. 32.6 Enantioselective hydrogenation of β-keto carboxylic acid derivatives.

XR	Chiral catalyst (SCR) [a)]	Solvent	H_2 [atm]	Temp. [°C]	ee [%]	Con-fig.	TON	TOF [h^{-1}]
OCH_3	$RuCl_2$[(*R*)-binap] (2000)	CH_3OH	100	23	>99	*R*	1980	55
OCH_3	$RuCl_2$[(*R*)-binap](dmf)$_n$ (1960)	CH_3OH	100	25	99	*R*	1960	49
OCH_3	$RuCl_2$[(*R*)-binap](dmf)$_n$ (2330)	CH_3OH	4	100	98	*R*	2330	388
OCH_3	$[NH_2(C_2H_5)]_2[\{RuCl[(R)\text{-binap}]\}_2(\mu\text{-}Cl)_3]$ (1410)	CH_3OH	100	25	>99	*R*	1340	33
OCH_3	$[RuI\{(S)\text{-binap}\}C_6H_6]I$ (2380)	CH_3OH	100	20	99	*R*	2380	99
OCH_3	$Ru[\eta^3\text{-}CH_2C(CH_3)CH_2]_2$-[(*S*)-binap] + HBr (50)	CH_3OH	1	rt	97 [b)]	*S*	40	0.8
OCH_3	*trans*-$RuCl_2$[(*R*)-binap]py_2 + HCl (1000)	CH_3OH	3.7	60	99.9	*R*	1000	42
OCH_3	$[RuCl_2(cod)]_n$–(*R*)-BINAP (100)	CH_3OH	4	rt	99	*R*	100	4
OCH_3	$RuCl_2$[(*R*)-xylbinap](dmf)$_n$ (1500)	CH_3OH	100	rt	99.9	*R*	1500	94
OCH_3	$RuCl_2$[(±)-xylbinap](dmf)$_n$ –0.5 (*S*)-DM-DABN (750)	CH_3OH	100	rt	99.3	*R*	750	47
OCH_3	$RuCl_2$[(*S*)-bis-steroidal phosphine](dmf)$_n$ (1270)	CH_3OH	100	100	99	*S*	1270	1270
OCH_3	$RuBr_2$[(*S*)-biphemp] (200)	CH_3OH	5	50	>99	*S*	200	3
OCH_3	$[RuI_2(p\text{-cymene})]_2$–(*R*)-BIMOP (2000)	1:1 CH_3OH–CH_2Cl_2	10	30–40	100	*R*	2000	100
OCH_3	$RuCl_3$–(*S*)-MeO-BIPHEP (100)	CH_3OH	4	50	99	*S*	100	25
OCH_3	$RuCl_2$[(*R*)-c4tunaphos]-(dmf)$_n$ (100)	CH_3OH	51	60	99.1	*R*	100	5
OCH_3	$RuCl_2$[(*S*)-(*R*)-**2A**](dmf)$_n$ (667)	79:1 CH_3OH–CH_2Cl_2	3.4	70	99.4	*S*	667	28
OCH_3	$RuCl_2$[(*S*)-bifap](dmf)$_n$ (1000)	CH_3OH	100	70	100	*S*	1000	500
OCH_3	$Ru[\eta^3\text{-}CH_2C(CH_3)CH_2]_2$-[(*R,R*)-*i*-pr-bpe] + HBr (500)	9:1 CH_3OH–H_2O	4	35	99.3	*S*	500	25
OCH_3	$Ru[\eta^3\text{-}CH_2C(CH_3)CH_2]_2$-[(*S,S*)-*t*-bu-bisp*] + HBr (200)	10:1 CH_3OH–H_2O	6	70	97 [c)]	*R*	172	17
OCH_3	$Ru(OCOCF_3)_2$[(*S*)-[2.2]-phanephos] + $(n\text{-}C_4H_9)_4NI$ (125–250)	10:1 CH_3OH–H_2O	3	–5	96	*R*	<250	<14
OCH_3 [d)]	$[RuI_2(p\text{-cymene})]_2$–(*R*)-(*R*)-**2Cb** + HCl (1000)	CH_3OH	5	80	95	*S*	>990	>62

XR	Chiral catalyst (SCR) [a)]	Solvent	H_2 [atm]	Temp. [°C]	ee [%]	Con-fig.	TON	TOF [h^{-1}]
OCH_3 [d)]	Ru[η^3-$CH_2C(CH_3)CH_2$]$_2$-(cod)–(*S*)-**1B** + HBr (100)	CH_3OH	60	100	95	*R*	99	12
OCH_3	[$RuCl_2$(*p*-cymene)]$_2$–(*S*)-Ph-*o*-Xylyl-BINAPO (100)	3:1 C_2H_5OH–CH_2Cl_2	5.4	50	96	*S*	100	5
OCH_3	$RuCl_2$[(*R*)-poly-nap](dmf)$_n$ (1000)	CH_3OH	40	50	99	*R*	1000	71
OCH_3	Ru[η^3-$CH_2C(CH_3)CH_2$]$_2$-[peg-(*R*)-am-binap] + HBr (10 000)	CH_3OH	100	50	99	*R*	10 000	208
OC_2H_5	Ru[η^3-$CH_2C(CH_3)CH_2$]$_2$-(cod)–(*S*)-BINAP + HBr (3000)	C_2H_5OH [e)]	4	50	99	*S*	>2970	>165
OC_2H_5	$RuCl_2$[(*R*)-bisbenzodiox-anephos](dmf)$_n$ (1000)	C_2H_5OH	3.4	80–90	99.5	*R*	1000	<42
OC_2H_5	$RuCl_2$[(*S*)-p-phos](dmf)$_n$ (400)	10:1 C_2H_5OH–CH_2Cl_2	3.4	70	98.6	–	400	<33
OC_2H_5	$RuCl_2$[(–)-tetrame-bitianp] (1000)	CH_3OH	100	70	99	*R*	950	475
OC_2H_5	Ru[η^3-$CH_2C(CH_3)CH_2$]$_2$-(cod)–(*R*)-(*S*)-**2Ba** + HBr (200)	C_2H_5OH	50	50	98.6	*S*	200	11
OC_2H_5	Ru[η^3-$CH_2C(CH_3)CH_2$]$_2$-(cod)–(*R*)-**1Aa** + HBr (1000)	H_2O	40	50	98	*R*	1000	67
OC_2H_5	[Rh(nbd)$_2$]BF_4–(*R*)-(*S*)-JOSIPHOS (100)	CH_3OH	20	rt	97	*S*	100	7
$OC(CH_3)_3$	[$NH_2(C_2H_5)$]$_2$[{RuCl[(*R*)-binap]}$_2$(μ-Cl)$_3$] + HCl (2170)	CH_3OH	3	40	>97	*R*	2170	271
NH_2	Ru[η^3-$CH_2C(CH_3)CH_2$]$_2$-[(*S*,*S*)-*t*-bu-bisp*] + HBr (71)	10:1 CH_3OH–H_2O	6	50	89	*R*	71	7
NHC_6H_5	[$NH_2(C_2H_5)$]$_2$[{RuCl[(*R*)-binap]}$_2$(μ-Cl)$_3$] (500)	CH_3OH	30	60	>95	*R*	495	10
$N(CH_3)_2$	$RuBr_2$[(*S*)-binap] (680)	C_2H_5OH	63	27	96	*S*	680	8
SC_2H_5	$RuCl_2$[(*R*)-binap] (530)	C_2H_5OH	95	27	93 [f)]	*R*	218	3

a) SCR = substrate : catalyst molar ratio.
b) 80% yield.
c) 86% yield.
d) Methyl-3-oxopentanoate.
e) 0.3 equiv. to substrate.
f) 42% yield.

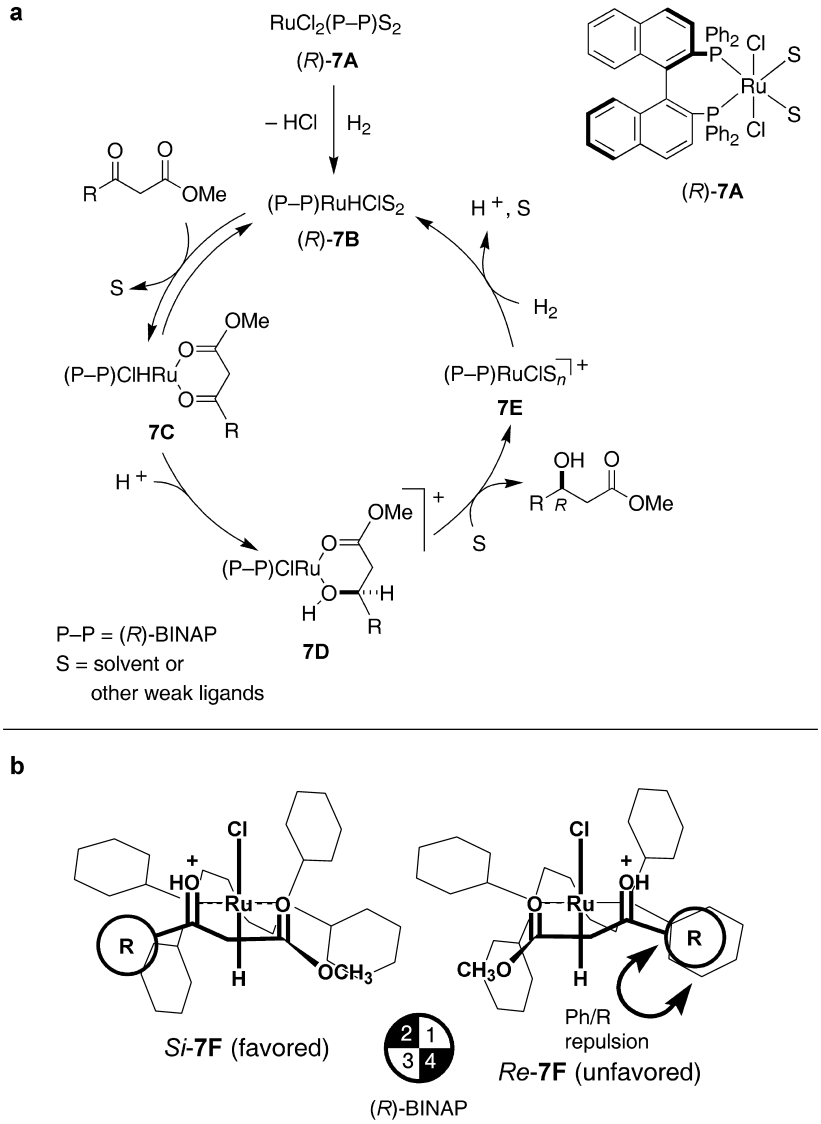

Fig. 32.7 (*R*)-BINAP–Ru-catalyzed hydrogenation of β-keto esters. (a) Catalytic cycle. (b) Transition-state models.

reusable catalysts have been developed for this reaction. An oligomeric Poly-NAP–Ru catalyst can be used five times in the hydrogenation, with an SCR of 1000 [36]. A Ru complex with PEG-Am-BINAP is applicable to the reaction with an SCR of 10 000 in methanol [37]. This complex can be separated as a precipitate by addition of ether to the reaction mixture. It is reusable four times, with an SCR of 100 per batch. A Ru complex of APBBINAP which is a BINAP li-

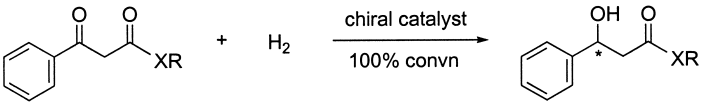

Fig. 32.8 Hydrogenation of benzoylacetic acid derivatives.

XR	Chiral catalyst (SCR) [a)]	Solvent	H_2 [atm]	Temp. [°C]	ee [%]	Con-fig.	TON	TOF [h^{-1}]
OC_2H_5	Ru[η^3-$CH_2C(CH_3)CH_2]_2$-(cod)–(*S*)-Meo-BIPHEP + HBr (50)	C_2H_5OH	1	50	97 [b)]	*R*	45	3
OC_2H_5	$[NH_2(C_2H_5)]_2[\{RuCl[(R)$-segphos]$\}_2(\mu$-Cl$)_3]$ (10 000)	C_2H_5OH	30	80	97.6	*S*	10 000	1667
OC_2H_5	$RuCl_2[(S)$-tol-p-phos]$(dmf)_n$ (800)	1 : 1 C_2H_5OH–CH_2Cl_2	20	90	96.4	*R*	800	400
OC_2H_5	$RuCl_2[(S)$-(*R*)-**2A**]$(dmf)_n$ (667)	79 : 1 CH_3OH–CH_2Cl_2	3.4	70	97.7	*R*	667	28
OC_2H_5	Ru[η^3-$CH_2C(CH_3)CH_2]_2$-(cod)–(*R*)-(*S*)-**2Bc** + HBr (200)	C_2H_5OH	50	50	98	*R*	200	–
OC_2H_5	Ru[η^3-$CH_2C(CH_3)CH_2]_2$-(cod)–(*S*)-**1C** + HBr (100)	C_2H_5OH	60	100	95	*S*	99	12
OC_2H_5	$[RuCl_2(p$-cymene$)]_2$–(*S*)-Xylyl-*o*-BINAPO (100)	3 : 1 C_2H_5OH–CH_2Cl_2	5.4	50	99	*R*	100	5
$NHCH_3$	$RuCl_2[(R)$-binap]$(dmf)_n$ (1800)	CH_3OH	14	100	>99.9 [c)]	*S*	900	50

a) SCR = substrate : catalyst molar ratio.
b) 90% yield.
c) 50% yield.

gand bound on polystyrene [38], and an immobilized BINAP–Ru complex in a polydimethylsiloxane membrane [39] are also usable for this transformation. β-Keto dimethylcarboxamides and thioesters are also hydrogenated with BINAP–Ru complexes enantioselectively [40, 41]. A Ru complex with a *t*-Bu-BisP* is useful for the reaction of a β-keto amide [7 a, 29].

A mechanistic model for the asymmetric hydrogenation of β-keto esters catalyzed by (*R*)-BINAP–Ru complex is shown in Figure 32.7. The $RuCl_2$ precatalyst (*R*)-**7A** reacts with H_2 to give the active RuHCl (*R*)-**7B** with removal of HCl [2]. The substrate and **7B** reversibly form the σ-chelate complex **7C**, whose geometry is unfavorable for metal-to-carbonyl hydride transfer. Protonation at carbonyl-oxygen then increases the electrophilicity of the carbonyl-carbon, with conversion of σ-coordination to π-interaction causing facile hydride migration onto the carbonyl

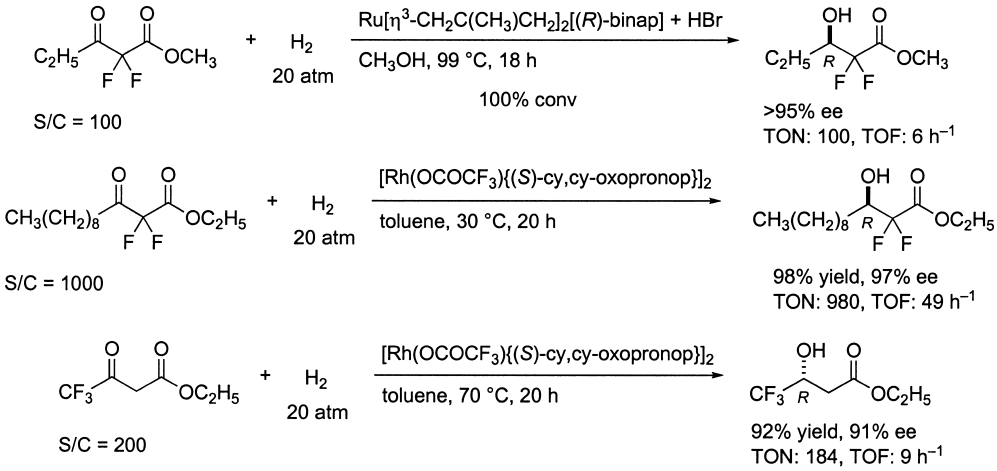

Fig. 32.9 Hydrogenation of fluorinated β-keto esters.

carbon. The hydroxy ester ligand of **7D** is replaced by solvent molecules, giving **7E**. Regeneration of **7B** by heterolysis of H_2 with **7E** completes the catalytic cycle.

The high level of enantiofacial selection is made in the hydride transfer step **7C** → **7D** [2]. The chelating geometry in the transition state **7F** decreases the activation energy. The chiral environment derived from (*R*)-BINAP clearly differentiates diastereomeric *Si*-**7F** and *Re*-**7F** (Fig. 32.7b). The *Si* structure affording the *R* alcohol is much more favored than the *Re* structure, which suffers from the Ph/R repulsion.

Figure 32.8 shows examples of enantioselective hydrogenation of benzoylacetic acid derivatives. The ethyl ester is hydrogenated in the presence of an (*R*)-SEGPHOS–Ru complex with an SCR of 10 000 under 30 atm of H_2 to afford the *S* alcohol in 97.6% ee quantitatively [42]. The small dihedral angle of the SEGPHOS–Ru complex (65°) may have a major influence on the high enantioselectivity. MeO-BIPHEP [14q, 18], Tol-P-Phos [43], **2A** [25], ferrocenyl diphosphine **2Bc** [44], and the monodentate phosphine **1C** [31] also show high enantioselectivity. A Ru complex with the diphosphinite ligand Xylyl-*o*-BINAPO gives the hydroxy ester in 99% ee [35]. Reaction of *N*-methylbenzoylacetamide with an (*R*)-BINAP–Ru catalyst gives the *S* alcohol in an enantiomerically pure form, albeit in 50% yield [45].

α,α-Difluoro-*β*-keto esters are hydrogenated with an (*R*)-BINAP–Ru complex to yield the (*R*)-hydroxy esters in >95% ee (Fig. 32.9) [46]. The sense of enantioselection is consistent with that of reaction of nonfluorinated substrates. A Cy,Cy-OxoProNOP–Rh complex also shows high enantioselectivity for the hydrogenation of fluorinated *β*-keto esters [47]. The sense of enantioface-selection depends heavily on the fluorinated position. Reaction of ethyl-2,2-difluoro-3-oxododecanoate catalyzed by an (*S*)-Cy,Cy-OxoProNOP–Rh complex gives the *R* (*β*) alcohol in 97% ee. By contrast, ethyl-4,4,4-trifluoro-3-oxobutanoate is converted to the *R* (*α*) alcohol in 91% ee with the same catalyst.

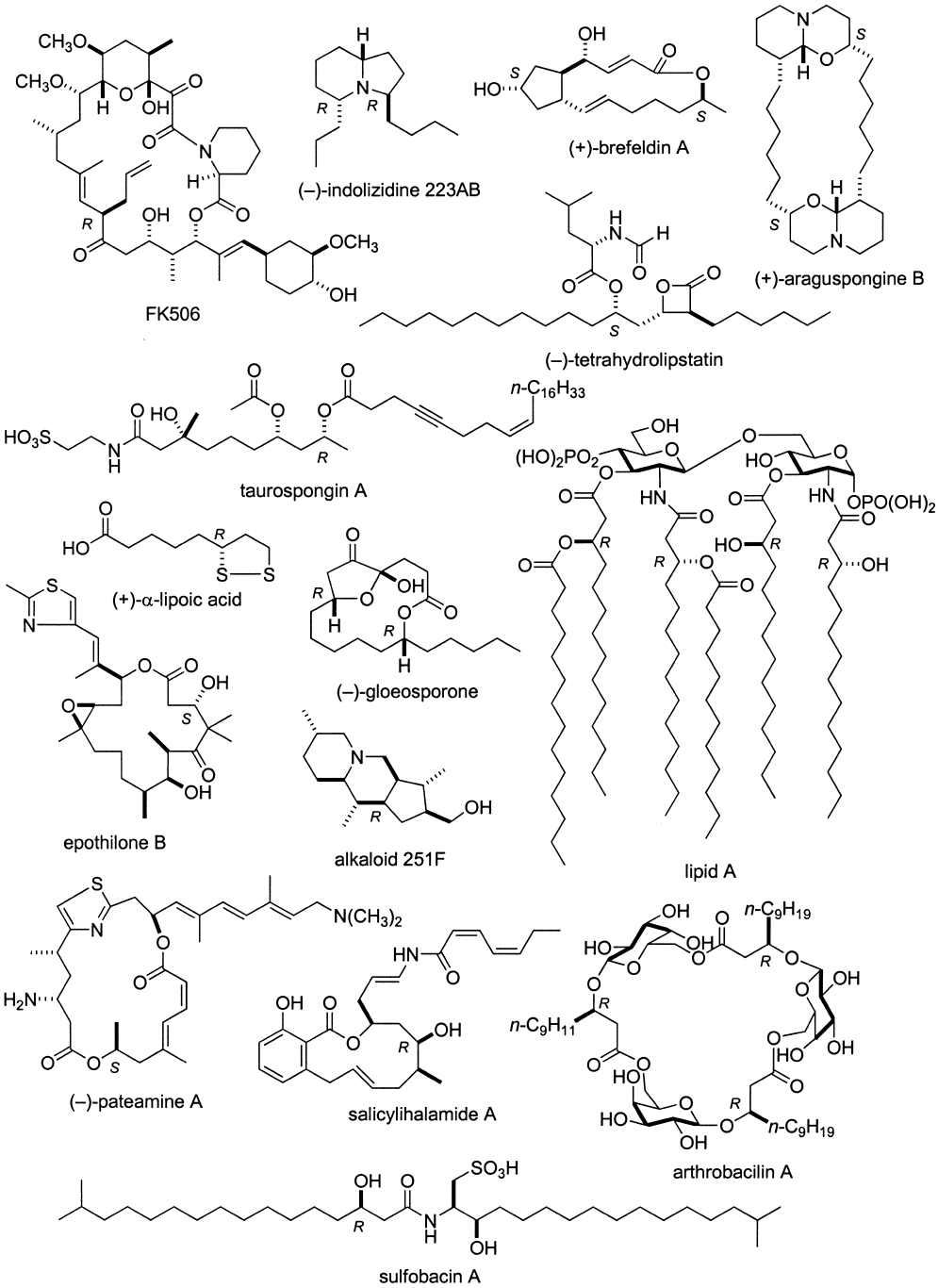

Fig. 32.10 Examples of biologically active compounds obtainable through BINAP–Ru-catalyzed hydrogenation of β-keto esters.

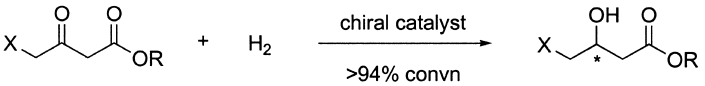

Fig. 32.11 Hydrogenation of difunctionalized ketones.

X	R	Chiral catalyst (SCR) [a)]	H_2 [atm]	Temp. [°C]	ee [%]	Con-fig.	TON	TOF [h^{-1}]
$C_6H_5CH_2OCH_2$	CH_3	$RuBr_2$[(*S*)-binap] (370)	50	26	99	*S*	148	0.8
CH_3O	CH_3	Ru[η^3-$CH_2C(CH_3)CH_2]_2$-[(*R*,*R*)-*i*-pr-bpe] + HBr (500)	4	35	95.5	*R*	500	25
$C_6H_5CH_2O$	C_2H_5	$RuBr_2$[(*S*)-binap] (560)	100	28	78	*R*	543	12
$C_6H_5CH_2O$	C_2H_5	$RuBr_2$[(*S*)-binap] (560)	100	100	98	*R*	554	111
$C_6H_5CH_2O$	C_2H_5	Ru[η^3-$CH_2C(CH_3)CH_2]_2$-(cod)–(*R*)-Meo-BIPHEP + HBr (3000)	8	80	98	*S*	3000	63
$[(CH_3)_2CH]_3SiO$	C_2H_5	$RuBr_2$[(*S*)-binap] (290)	100	27	95	*R*	290	3
Cl	C_2H_5	$RuBr_2$[(*S*)-binap] (1080)	77	24	56	*R*	1080	26
Cl	C_2H_5	$RuBr_2$[(*S*)-binap] (1300)	100	100	97	*R*	1300	19 500
Cl	C_2H_5	Ru[η^3-$CH_2C(CH_3)CH_2]_2$-[(*R*,*R*)-*i*-pr-bpe] + HBr (500)	4	35	76	*R*	500	25
Cl	C_2H_5	$RuCl_3$–(*S*)-MeO-BIPHEP (100)	4	120	92	*R*	100	17
Cl	C_2H_5	$[NH_2(C_2H_5)]_2[\{RuCl[(R)$-segphos]$\}_2(\mu$-Cl$)_3]$ (2500)	30	90	98.5	*S*	2500	1250
Cl	C_2H_5	$RuCl_2$[(*R*)-bisbenzodioxanephos](dmf)$_n$ (1000)	3.4	80–90	97	*S*	1000	<83
Cl	C_2H_5	$RuCl_2$[(*S*)-p-phos](dmf)$_n$ (2780)	3.4	80	98	–	2780	<232
Cl	C_2H_5	$[RuCl_2(p$-cymene$)]_2$–(*S*)-Ph-*o*-Xylyl-BINAPO (100)	5.4	50	98	*R*	100	5
$Cl(CH_3)_2NH$	C_2H_5	$[RhCl(cod)]_2$–(2*S*,4*S*)-MCCXM (100)	20	50	85	*S*	100	5
$Cl(CH_3)_3N$	C_2H_5	$[NH_2(C_2H_5)]_2[\{RuCl[(R)$-binap$]\}_2(\mu$-Cl$)_3]$ (–)	100	25	96 [b)]	*S*	–	–

a) SCR = substrate : catalyst molar ratio.
b) 75% yield.

The BINAP–Ru(II)-catalyzed enantioselective hydrogenation of β-keto esters is used for the synthesis of a wide range of important natural and man-made compounds [1–4, 48]; some examples of these are listed in Figure 32.10, wherein chiral centers created by the enantioselective reaction are labeled with *R* or *S*.

The enantioselective hydrogenation of ketones which have two heteroatoms on both sides of the carbonyl group tends to give lower enantioselectivity due to the competitive interaction of the functionalities with the catalyst. The extent depends

on the electronic and steric properties of the coordinating groups. Methyl-5-benzyloxy-3-oxopentanoate is hydrogenated with the (*S*)-BINAP–Ru catalyst to afford the *S* alcohol in 99% ee (Fig. 32.11) [40]. The sense and degree of enantioselection is the same as that in the reaction of methyl-3-oxobutanoate, but the situation is changed when 4-benzyloxy- and 4-chloro-3-oxobutanoate are employed as substrates, with only moderate optical yields (78% and 56%, respectively) being obtained by reaction at room temperature. However, the optical yield is increased to 98% and 97%, respectively, when the reactions are conducted at 100 °C [49]. The analogous substrate connecting a bulky triisopropylsilyloxy group at the C4 position is reduced with high enantioselectivity even at room temperature [49]. β-Keto ester possessing a chlorotrimethylammonium function is also reduced with a high optical yield [14m]. Ru catalysts with other C_2-chiral biaryl diphosphines [14q, 18, 21, 22, 42] and Ph-*o*-Xylyl-BINAPO [35], a bisphosphinite, show similar enantioselectivity. Methyl-4-methoxy-3-oxobutanoate is hydrogenated with an *i*-Pr-BPE–Ru complex to afford the hydroxy ester in 95.5% ee even at 35 °C, whereas the ee-value obtained by the reaction of 4-chloro ketone is 76% [28]. An MCCXM–Rh complex catalyzes hydrogenation of the 4-chlorodimethylammonium derivative to yield the alcohol in 85% ee [50].

The BINAP–Ru-catalyzed hydrogenation of difunctional ketones has been applied to the asymmetric synthesis of several bioactive compounds (see Fig. 32.12) [1, 49–51]. Stereocenters derived from the BINAP–Ru are labeled by *R* or *S*.

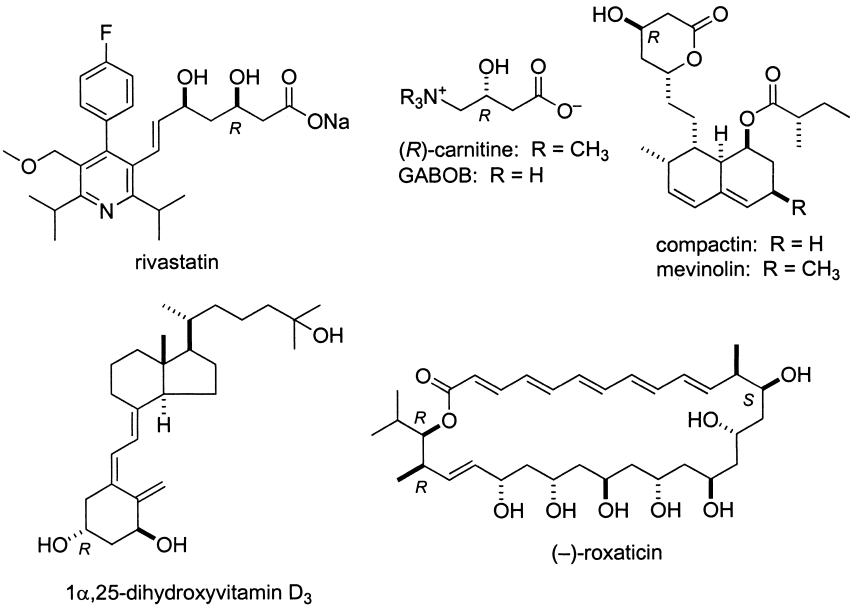

Fig. 32.12 Examples of biologically active compounds obtainable through BINAP–Ru-catalyzed hydrogenation of difunctionalized ketones.

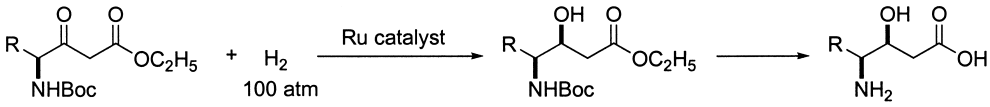

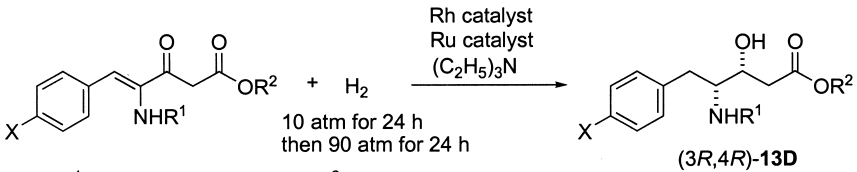

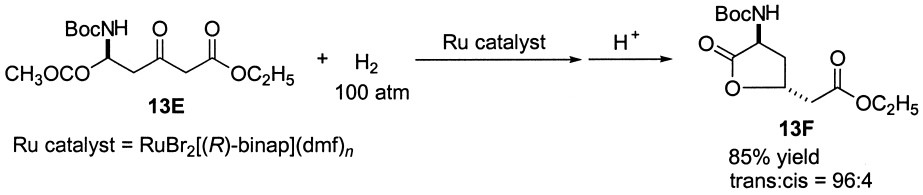

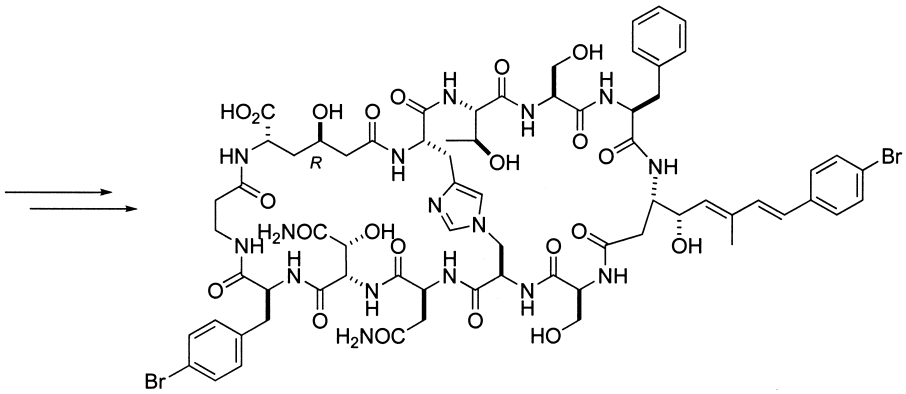

theonellamide F

Fig. 32.13 Diastereoselective hydrogenation of chiral β-keto esters.

BINAP–Ru is effective for the diastereoselective hydrogenation of some chiral β-keto esters (Fig. 32.13). Reaction of *N*-Boc-protected (*S*)-γ-amino β-keto esters **13A** catalyzed by the (*R*)-BINAP–Ru complex results in the *syn* alcohols **13B** exclusively [52]. The stereocenter at the β-position is controlled by the chirality of the catalyst; therefore, use of the *S* catalyst affords the *anti* isomer, as predicted. Derivatives of statine, a key component of the aspartic proteinase inhibitor pep-

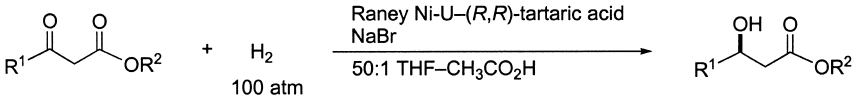

Raney Ni-U = ultrasonic irradiated Raney Ni

Fig. 32.14 Hydrogenation of β-keto esters catalyzed by modified Raney Ni.

R^1	R^2	Temperature [°C]	Time [h]	ee [%]
CH_3	CH_3	100	4	86
C_2H_5	CH_3	60	34	94
n-C_6H_{13}	CH_3	60	52	90
$(CH_3)_2CH$	CH_3	60	71	96
cyclo-C_3H_5	CH_3	60	48	98.6
CH_3	$(CH_3)_2CH$	60	45	87
CH_3	$(CH_3)_3C$	60	40	88

statine, are efficiently synthesized by this method [1, 52]. Tandem hydrogenation of *N*-acetyl- or *N*-Boc-protected γ-amino γ,δ-unsaturated β-keto esters **13C** in the presence of an (*S*)-BINAP–Rh and –Ru catalyst gives (3*R*,4*R*)-**13D** exclusively [53]. First, enantioselective reduction of the olefinic moiety catalyzed by the BINAP–Rh complex occurs preferentially at low H_2 pressure, after which the carbonyl group is reduced with the BINAP–Ru catalyst under high pressure of H_2. The hydrogenation of an *N*-Boc-protected (*S*)-δ-amino β-keto ester **13E** in the presence of the (*R*)-BINAP–Ru complex followed by an acid-catalyzed cyclization affords selectively the *trans* lactone **13F**, which is a useful intermediate for the synthesis of theonellamide F, an antifungal agent [54].

Highly enantioselective hydrogenation of β-keto esters is achieved by using a Raney Ni catalyst modified by tartaric acid and NaBr (Fig. 32.14) [9, 55]. The catalyst should be prepared under controlled conditions including suitable pH (3–4), temperature (100 °C), and concentration of the modifier (1%) to achieve an optimum stereoselectivity. The addition of NaBr, an achiral modifier, is important. Furthermore, ultrasonic irradiation of the catalyst tends to increase the activity and enantioselectivity [9f,g]. Ultrasonication may remove nonselective sites of the catalyst surface.

Enantioselective hydrogenation of β-keto esters catalyzed by the modified Raney Ni is useful for the synthesis of biologically active compounds, as shown in Figure 32.15 [56–58]. A large-scale synthesis of (–)-tetrahydrolipstatin (orlistat), a pancreatic lipase inhibitor (F. Hoffmann-La Roche AG), is carried out using this method [58].

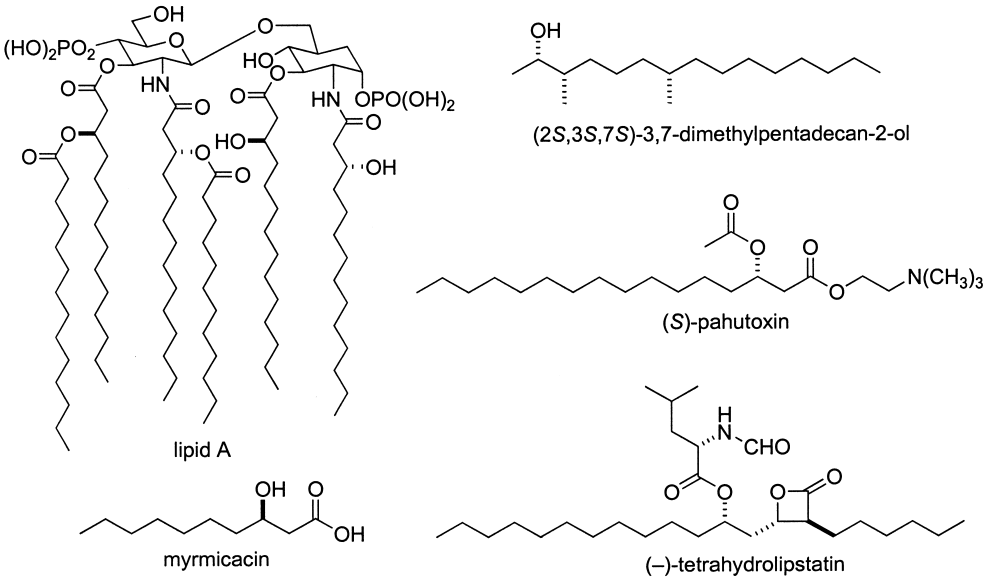

Fig. 32.15 Examples of biologically active compounds obtainable through asymmetric hydrogenation of β-keto esters catalyzed by modified Raney Ni.

32.2.2
1,3-Diketones

Double hydrogenation of 1,3-diketones in the presence of an appropriate chiral catalyst yields the chiral 1,3-diols with an excellent diastereo- and enantioselectivity (Fig. 32.16). When 2,4-pentanedione is hydrogenated with an (*R*)-BINAP–Ru catalyst, enantiomerically pure (*R*,*R*)-2,4-pentanediol (*anti*:*syn* = 99:1) is obtained quantitatively [40, 59]. Dissymmetric 5-methyl-2,4-hexanedione and 1-phenyl-1,3-butanedione are also reduced stereoselectively to give the chiral *anti* diols. Ru complexes bearing other ligands such as C_2-chiral BIPHEMP [60] and BDPP [61] as well as C_1-symmetric **2Ca** [33] show similar stereoselectivity. The hydrogenation of methyl-3,5-dioxohexanoate catalyzed by a BINAP–Ru complex gives an 81:19 mixture of the *anti* (78% ee) and *syn* dihydroxy esters [62]. The stereoselective outcome shows that the C3 carbonyl group is preferentially reduced over the C5 carbonyl function. Hydrogenation of ethyl-2,4-dioxopentanoate with an (*S*)-MeO-BIPHEP–Ru catalyst followed by *in-situ* cyclization affords an 84:16 mixture of (3*R*,5*S*)-3-hydroxy-5-methyltetrahydrofuran-2-one in 98% ee and the 3*R*,5*R* isomer in 87% ee [63]. A Ru complex bearing a chiral ferrocenyl diphosphine (*S*)-(*R*)-2Bc catalyzes the hydrogenation of 1,3-diphenyl-1,3-propanedione with almost perfect diastereo- and enantioselectivity [44]. A BIPHEMP–Ru complex is also usable [64]. The BINAP–Ru-catalyzed hydrogenation of 1,5-dichloro-2,4-pentanedione results in the chiral *anti* diol in 92–94%

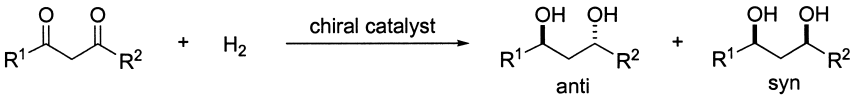

Fig. 32.16 Hydrogenation of 1,3-diketones to give the chiral 1,3-diols.

R^1	R^2	Catalyst (SCR) [a)]	H_2 [atm]	Temp. [°C]	Yield [%]	dr [b)]	ee [%] [c)]	TON	TOF [h^{-1}]
CH_3	CH_3	$RuCl_2$[(*R*)-binap] (2000)	72	30	100	99:1	100	2000	22
CH_3	CH_3	RuHCl[(*R*)-biphemp]-[$P(C_6H_5)_3$] + HCl (2000)	100	50	100	99:1	>99.9	2000	83
CH_3	CH_3	$[RuCl_2(C_6H_6)]_2$–(*R*,*R*)-BDPP (1695)	80	80	100	75:25	97	1695	106
CH_3	CH_3	$[RuI_2(p\text{-cymene})]_2$–(*R*)-(*R*)-**2Ca** + HCl (1000)	100	80	>99	>99:1	97	>990	>58
CH_3	$(CH_3)_2CH$	$[NH_2(C_2H_5)_2][\{RuCl[(R)\text{-binap}]\}_2(\mu\text{-Cl})_3]$ (500)	50	50	92	97:3	98	460	23
CH_3	C_6H_5	$RuBr_2$[(*R*)-binap] (360)	83	26	98	94:6	94	360	6
CH_3	CH_3O-$COCH_2$	$[NH_2(C_2H_5)_2][\{RuCl[(R)\text{-binap}]\}_2(\mu\text{-Cl})_3]$ (– [d)])	100	50	100 [e)]	81:19	78	–	–
CH_3	C_2H_5OCO	$RuBr_2$[(*S*)-meo-biphep] (200)	100	80	>99 [f)]	84:16	98	>198	5
C_6H_5	C_6H_5	$RuCl_2$[(*R*)-biphemp] (170)	100	40	70	94:6	87	119	2
C_6H_5	C_6H_5	$Ru[\eta^3\text{-}CH_2C(CH_3)CH_2]_2$-(cod)–(*S*)-(*R*)-**2Bc** + HBr (200)	50	50	100	>99.5:0.5	>99	200	–
$ClCH_2$	$ClCH_2$	$[NH_2(C_2H_5)_2][\{RuCl[(R)\text{-binap}]\}_2(\mu\text{-Cl})_3]$ (– [d)])	85	102	– [d)]	– [d)]	92–94	–	–

a) SCR = substrate : catalyst molar ratio.
b) *Anti* : *syn* diastereomeric ratio.
c) % ee of the *anti* diol.
d) Not reported.
e) A mixture of diol and δ-lactone.
f) (3*R*,5*S*)-3-Hydroxy-5-methyltetrahydrofuran-2-one.

ee, which is a synthetically useful chiral polyfunctionalized compound [65]. Under appropriate conditions, mono-hydrogenation of 1-phenyl-1,3-butanedione catalyzed by $[NH_2(C_2H_5)_2][\{RuCl[(R)\text{-binap}]\}_2(\mu\text{-Cl})_3]$ occurs selectively to give (*R*)-1-phenyl-3-hydroxybutan-1-one (Fig. 32.17) [59]. As shown in Figure 32.18, the asymmetric hydrogenation of 1,3-diketones catalyzed by a BINAP–Ru complex is used for the synthesis of bioactive compounds with contiguous polyhydroxy groups [66].

A chirally modified Raney Ni catalyzes the hydrogenation of 1,3-diketones selectively to give the *anti* 1,3-diols in about 90% ee (Fig. 32.19) [67]. Natural compounds such as africanol and ngaione are synthesized via this method [68].

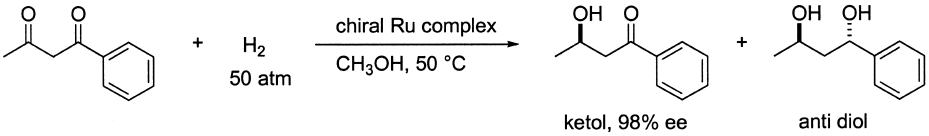

chiral Ru complex = $[NH_2(C_2H_5)_2][\{RuCl[(R)\text{-binap}]\}_2(\mu\text{-}Cl)_3]$ 89% yield, ketol:diol = 98:2
S/C = 500 TON = 445, TOF: 22 h^{-1}

Fig. 32.17 Mono-hydrogenation of 1-phenyl-1,3-butanedione catalyzed by a BINAP–Ru complex.

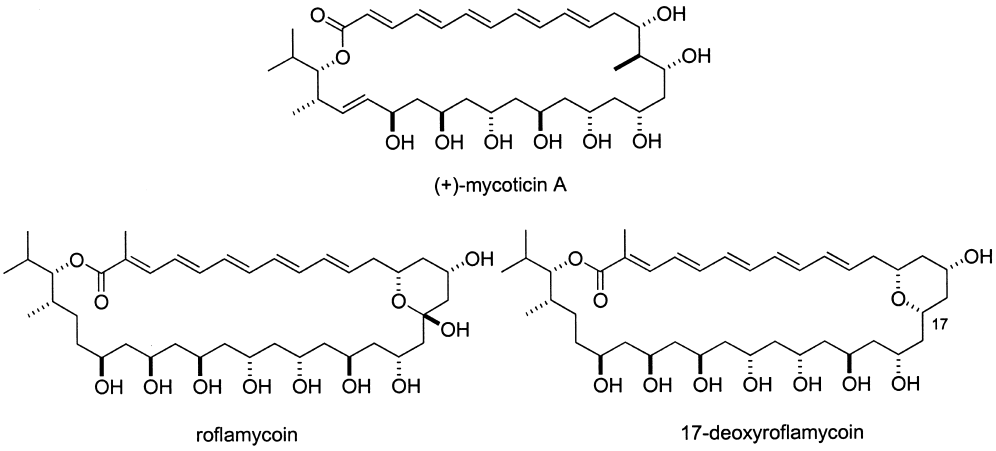

Fig. 32.18 Examples of biologically active compounds obtainable through BINAP–Ru-catalyzed hydrogenation of 1,3-diketones.

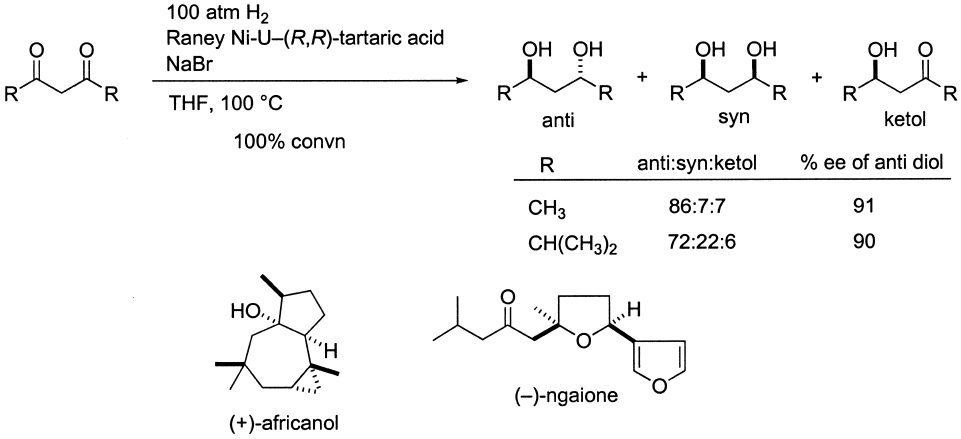

R	anti:syn:ketol	% ee of anti diol
CH_3	86:7:7	91
$CH(CH_3)_2$	72:22:6	90

Fig. 32.19 Hydrogenation of 1,3-diketones catalyzed by modified Raney Ni.

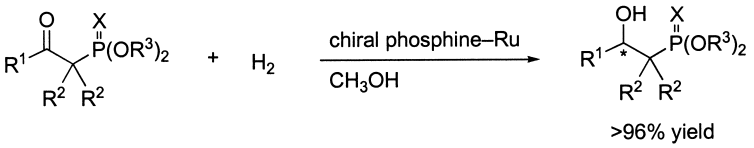

Fig. 32.20 Hydrogenation of β-keto phosphonates.

R^1	R^2	R^3	X	Chiral phosphine (SCR) [a]	H_2 [atm]	Temp. [°C]	ee [%]	Con-fig.	TON	TOF [h^{-1}]
CH_3	H	CH_3	O	(*R*)-BINAP (1220)	4	25	98	*R*	1208	17
CH_3	H	C_2H_5	O	(*S*)-BINAP (50)	1	50	99	*S*	50	1
CH_3	H	C_2H_5	O	(*R*,*R*)-BDPP (50–100)	30	rt	95	*R*	<100	<2
CH_3	CH_3	CH_3	O	(*R*)-BINAP (370–530)	4	50	98	*R*	<514	<9
n-C_5H_{11}	H	CH_3	O	(*S*)-BINAP (100)	100	rt	98	*S*	100	1
$(CH_3)_2CH$	H	CH_3	O	(*S*)-BINAP (370–530)	4	80	96	*S*	<509	<32
C_6H_5	H	CH_3	O	(*R*)-BINAP (370–530)	4	60	95	*R*	<509	<3
n-C_5H_{11}	H	CH_3	S	(*S*)-MeO-BIPHEP (100)	100	rt	94	*S*	100	1
$(CH_3)_2CH$	H	CH_3	S	(*S*)-MeO-BIPHEP (100)	10	rt	93	*S*	100	1

a) SCR = Substrate : catalyst molar ratio.

32.2.3
β-Keto Phosphonates, Sulfonates, and Sulfones

Enantioselective hydrogenation of β-keto phosphonates in the presence of an (*R*)-BINAP–Ru complex under 1–4 atm H_2 and at room temperature provides the (*R*)-β-hydroxy phosphonates in up to 99% ee (Fig. 32.20) [69]. The sense of enantioface selection is the same as that observed in the reaction of β-keto carboxylic esters (see Fig. 32.14). A BDPP–Ru catalyst is also usable [70]. Similarly, β-keto thiophosphonates are hydrogenated with a MeO-BIPHEP–Ru catalyst with up to 94% optical yield [69 b].

BINAP–Ru catalysts also show high enantioselectivity in the hydrogenation of β-keto sulfonates. Reaction of sodium β-keto sulfonates with (*R*)-BINAP–Ru catalyst quantitatively gives the (*R*)-β-hydroxy sulfonates in up to 97% ee (Fig. 32.21) [15]. In the same manner, hydrogenation of β-keto sulfones in the presence of an (*R*)-MeO-BIPHEP–Ru catalyst affords the (*R*)-hydroxy sulfones in >95% ee [71].

Figure 32.22 shows the diastereoselective hydrogenation of (*R*)-β-keto sulfoxides with Meo-BIPHEP–Ru catalysts [72]. The *R* chiral center of the substrate matches with the *S* catalyst, giving the *S*,*R* alcohols in >99 : 1 selectivity, whereas reactions with the *R* catalyst affords a 6 : 94 to 10 : 90 mixture of the *S*,*R* and *R*,*R* diastereomeric alcohols. The diastereoselection is controlled mainly by the configuration of the catalyst.

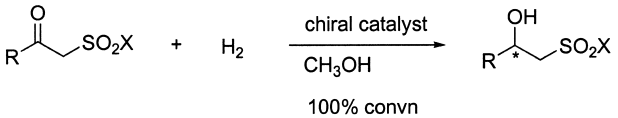

Fig. 32.21 Hydrogenation of β-keto sulfonates.

R	X	Chiral catalyst (SCR) [a)]	H_2 [atm]	Temp. [°C]	ee [%]	Con-fig.	TON	TOF [h^{-1}]
CH_3	ONa	$RuCl_2$[(*R*)-binap](dmf)$_n$ + HCl (200)	1	50	97	*R*	200	8
n-$C_{15}H_{31}$	ONa	$RuCl_2$[(*R*)-binap](dmf)$_n$ + HCl (200)	1	50	96	*R*	200	8
$(CH_3)_2CH$	ONa	$RuCl_2$[(*R*)-binap](dmf)$_n$ + HCl (200)	1	50	97	*R*	200	8
C_6H_5	ONa	$RuCl_2$[(*R*)-binap](dmf)$_n$ + HCl (200)	1	50	96	*R*	200	67
CH_3	C_6H_5	$RuBr_2$[(*R*)-meo-biphep] (100)	1	65	>95	*R*	100	4
n-C_5H_{11}	C_6H_5	$RuBr_2$[(*R*)-meo-biphep] (100)	1	65	>95	*R*	100	4
cyclo-C_6H_{11}	C_6H_5	$RuBr_2$[(*R*)-meo-biphep] (100)	1	65	>95	*R*	100	4
C_6H_5	C_6H_5	$RuBr_2$[(*S*)-meo-biphep] (100)	75	40	>95	*S*	100	4

a) SCR = Substrate : catalyst molar ratio.

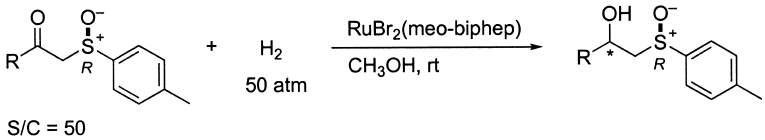

Fig. 32.22 Diastereoselective hydrogenation of β-keto sulfoxides.

R	MeO-BIPHEP	Time [h]	Yield [%]	*S,R*:*R,R*	TON	TOF [h^{-1}]
n-C_6H_{13}	*S*	25	82	>99:1	41	2
n-C_6H_{13}	*R*	25	74	6:94	37	2
C_6H_5	*S*	63	70	>99:1	35	0.6
C_6H_5	*R*	63	95	10:90	48	0.8

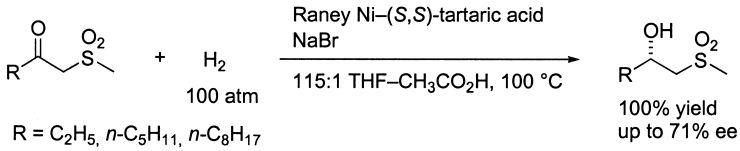

Fig. 32.23 Hydrogenation of β-keto sulfones catalyzed by modified Raney Ni.

Enantioselective hydrogenation of β-keto sulfones in the presence of (*S*,*S*)-tartaric acid modified Raney Ni gives the *S* alcohols in up to 71% ee (Fig. 32.23) [73].

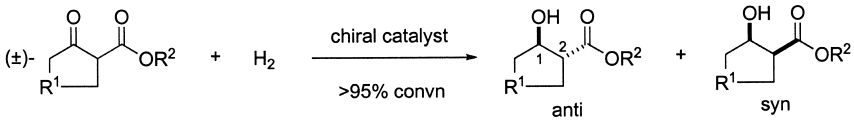

Fig. 32.24 Hydrogenation of racemic 2-alkoxycarbonyl cycloalkanones via dynamic kinetic resolution.

R^1	R^2	Catalyst (SCR) [a)]	Solvent	H_2 [atm]	dr [b)]	*Anti* alcohol		TON	TOF [h^{-1}]
						ee [%]	Con-fig.		
CH_2	CH_3	[RuCl{(*R*)-binap}C_6H_6]Cl (1820)	CH_2Cl_2	100	99:1	92	1*R*,2*R*	1820	30
CH_2	CH_3	[RuI{(*S*)-binap}(*p*-cymene)]I (1370)	CH_2Cl_2 [c)]	100	99:1	95	1*S*,2*S*	1302	33
CH_2	CH_3	Ru[η^3-$CH_2C(CH_3)CH_2]_2$-[(*R*,*R*)-*i*-pr-bpe] + HBr (500)	9:1 CH_3OH–H_2O	4	96:4	98.3	1*S*,2*S*	500	25
CH_2	CH_3	Ru[η^3-$CH_2C(CH_3)CH_2]_2$-[(*S*,*S*)-*t*-bu-bisp*] + HBr (200)	10:1 CH_3OH–H_2O	6	84:16	96	– [d)]	200	20
CH_2	CH_3	$RuCl_2$[(+)-tetrame-bitianp] (1000)	CH_3OH	100	93:7	99	1*R*,2*R*	1000	500
CH_2	C_2H_5	Ru[η^3-$CH_2C(CH_3)CH_2]_2$-(cod)–(*R*)-BINAP + HBr (100)	CH_3OH	20	97:3 [e)]	94	1*R*,2*R*	50	25
$(CH_2)_2$	C_2H_5	[RuCl{(*R*)-binap}C_6H_6]Cl (530)	CH_2Cl_2	100	95:5	90	1*R*,2*R*	530	9
$(CH_2)_2$	C_2H_5	Ru[η^3-$CH_2C(CH_3)CH_2]_2$-(cod)–(*S*)-BINAP + HBr (100)	CH_2Cl_2	20	74:26	91	1*S*,2*S*	100	33
$(CH_2)_2$	C_2H_5	Ru[η^3-$CH_2C(CH_3)CH_2]_2$-(cod)–(*R*)-(*S*)-**2Bb** + HBr (200)	C_2H_5OH	50	92:8	>99	1*R*,2*R*	<200	<3
$(CH_2)_3$	CH_3	[RuCl{(*R*)-binap}C_6H_6]Cl (910)	CH_2Cl_2	100	93:7	93	1*R*,2*R*	910	11

a) SCR = substrate : catalyst molar ratio.
b) *Anti* : *syn* diastereomeric ratio.
c) Contaminated with <1% of water.
d) Not determined.
e) 50% conversion.

32.2.4
Dynamic Kinetic Resolution

It is possible that hydrogenation of racemic α-mono-substituted β-keto esters provides four stereoisomers of the corresponding hydroxy esters. Fortunately, enantioselective hydrogenation of such racemic compounds can selectively yield

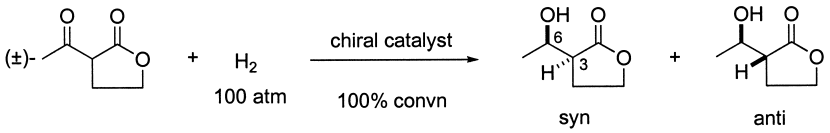

Fig. 32.25 Hydrogenation of 3-acetyltetrahydrofuran-2-one via dynamic kinetic resolution.

Catalyst (SCR) [a)]	Solvent	dr [b)]	*Syn* alcohol		TON	TOF [h^{-1}]
			ee [%]	Config.		
[RuCl{(*R*)-binap}C_6H_6]Cl (1350)	C_2H_5OH	98:2	94	3*S*,6*R*	1350	18
[RuI_2(*p*-cymene)]$_2$–(*S*)-BINAP (770)	3:1 CH_3OH–CH_2Cl_2	99:1	97	3*R*,6*S*	770	19
$RuCl_2$[(+)-tetrame-bitianp] (1000)	CH_3OH	96:4	91	3*S*,6*R*	1000	20

a) SCR = substrate : catalyst molar ratio.
a) *Syn* : *anti* diastereomeric ratio.

a single stereoisomer of products through the *in-situ* racemization under appropriate conditions, because the α position of β-keto esters is configurationally labile [1]. In fact, as shown in Figure 32.24, racemic 2-methoxycarbonylcyclopentanone is hydrogenated with [RuCl{(*R*)-binap}C_6H_6]Cl in CH_2Cl_2 instead of conventional methanol and ethanol to afford the 1*R*,2*R* hydroxy-ester in 92% ee with a 99:1 *anti*-selectivity [74, 75]. The diastereoselectivity decreases to some extent with increasing ring-size of the substrate, while the enantioselectivity is not affected. High stereoselectivity is obtainable by hydrogenation with Ru catalysts bearing *i*-Pr-BPE [28], *t*-Bu-BisP* [29], tetraMe-BITIANP [23], and a chiral ferrocenyl diphosphine **2Bb** [32] in alcoholic solvents. The enantioselective hydrogenation through dynamic kinetic resolution is the result of catalyst-based intermolecular enantioselective induction and substrate-based intramolecular enantioselective induction, as well as suitable kinetic parameters [76]. The computer-aided analysis of (*R*)-BINAP–Ru-catalyzed hydrogenation of racemic 2-ethoxycarbonylcycloheptanone in CH_2Cl_2 reveals that the *R* keto ester is hydrogenated 9.8-fold faster than the *S* isomer, and that equilibration between both enantiomers of the substrate occurs 4.4-fold faster than hydrogenation of the slow-reacting *S* substrate. Hydrogenation of racemic 3-acetyltetrahydrofuran-2-one catalyzed by the (*R*)-BINAP–Ru complex gives the 3*S*,6*R* (*syn*) product exclusively (Fig. 32.25) [14n, 74b]. A tetraMe-BITIANP–Ru catalyst is also usable [23].

This chemistry is applicable to the hydrogenation of acyclic compounds such as α-acylamino-, α-ammonio-, α-amidomethyl-, and α-chloro-substituted β-keto esters (Fig. 32.26) [14n, 74a, 77–79]. The (*R*)-BINAP–Ru-catalyzed hydrogenation of the α-acylamino and α-amidomethyl ketones in CH_2Cl_2 leads to the 2*S*,3*R* (*syn*) alcohols in up to 98% ee [14n, 74a]. The use of sterically hindered

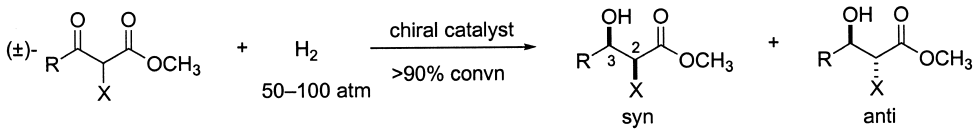

Fig. 32.26 Hydrogenation of acyclic α-substituted β-keto esters via dynamic kinetic resolution.

R	X	Catalyst (SCR) [a)]	Solvent	dr [b)]	Major diastereomer		TON	TOF [h^{-1}]
					ee [%]	Config.		
CH_3	CH_3CO-NH	$RuBr_2$[(*R*)-binap] (270)	CH_2Cl_2	99:1	98	2*S*,3*R*	270	5
CH_3	CH_3CO-NH	Ru[η^3-$CH_2C(CH_3)CH_2]_2$ [(*R*)-binap] + HCl (100)	CH_3OH	76:24	95	2*S*,3*R*	90	<2
CH_3	$(CH_3)_2C$-HCONH	Ru[η^3-$CH_2C(CH_3)CH_2]_2$ [(*R*)-binap] + HBr (100)	CH_3OH	77:23	92	2*S*,3*R*	90	<2
$(CH_3)_2$-CH	C_6H_5CO-NH [c)]	Ru[η^3-$CH_2C(CH_3)CH_2]_2$ [(*R*)-bisbenzodioxanphos] + HBr (50)	CH_2Cl_2 [d)]	>99:1	98	2*S*,3*R*	45	2
$(CH_3)_2$-CH	$ClNH_3$ [e)]	$RuCl_2$[(*S*)-binap]$(dmf)_n$ (26)	CH_2Cl_2	1:>99 [f)]	98	2*S*,3*S*	21	4
$(CH_3)_2$-CH	$ClNH_3$ [c)]	Ru[η^3-$CH_2C(CH_3)CH_2]_2$ [(*S*)-bisbenzodioxanphos] + HBr (50)	1:10 C_2H_5OH–CH_2Cl_2 [g)]	1:99	97	2*S*,3*S*	45	2
Ar [h)]	$ClNH_3$	$[IrCl(cod)]_2$–(*R*)-MeO-BIPHEP + NaI + $NaOCOCH_3$ (33)	CH_3CO_2H	1:>99 [i)]	95	2*R*,3*R*	29	0.3
Ar [j)]	CH_3CO-NH	$RuBr_2$[(*R*)-binap] (265)	CH_2Cl_2	99:1	94	2*S*,3*R*	265	2
CH_3	phthalimide	$[NH_2(C_2H_5)_2][\{RuCl[(R)$-c3tunaphos$]\}_2(\mu\text{-}Cl)_3]$ (– [k)])	CH_3OH	3:97	>99	2*R*,3*R*	–	–
CH_3	C_6H_5CO-$NHCH_2$	$[NH_2(C_2H_5)_2][\{RuCl[(R)$-binap$]\}_2(\mu\text{-}Cl)_3]$ (100)	CH_2Cl_2	94:6	98	2*S*,3*R*	100	5
CH_3	C_6H_5CO-$NHCH_2$	[RuI{(*S*)-binap}-(*p*-cymene)]I (100)	99.5:0.5 CH_2Cl_2–H_2O	94:6	97	2*R*,3*R*	98	2
CH_3	C_6H_5CO-$NHCH_2$	$[RuI_2(p\text{-cymene})]_2$–(+)-DTBBINAP (1000)	1:7 CH_3OH–CH_2Cl_2	99:1 [l)]	99	2*S*,3*R*	550	14
CH_3	C_6H_5CO-$NHCH_2$	$[NH_2(C_2H_5)_2][\{RuCl[(-)$-dtbm-segphos$]\}_2(\mu\text{-}Cl)_3]$ (– [k)])	– [k)]	99.3:0.7	99.4	2*S*,3*R*	–	–
CH_3	Cl [c)]	Ru[η^3-$CH_2C(CH_3)CH_2]_2$-(cod)–(*R*)-BINAP (200)	CH_2Cl_2	1:99	99	2*R*,3*R*	200	40

R	X	Catalyst (SCR) [a)]	Solvent	dr [b)]	Major diastereomer		TON	TOF [h^{-1}]
					ee [%]	Config.		
CH_3	CH_3	Ru[η^3-$CH_2C(CH_3)CH_2$]$_2$-[(*R*,*R*)-*i*-pr-bpe] + HBr (500)	9:1 CH_3OH–H_2O [m)]	58:42	96	2*R*,3*R*	500	25
CH_3	CH_3	[RuCl{(*R*)-binap}C_6H_6]Cl (625)	CH_2Cl_2	32:68	94 [n)]	2*R*,3*R* [n)]	625	10

a) SCR = substrate : catalyst molar ratio.
b) *Syn* : *anti* diastereomeric ratio.
c) Ethyl ester.
d) 130 atm H_2.
e) Benzyl ester.
f) 82% yield after conversion to the benzyl amide.
g) 12 atm H_2.
h) 4-Benzyloxyphenyl.
i) 88% yield after conversion to the benzyloxycarbonyl amide.
j) 3,4-Methylenedioxyphenyl.
k) Not reported.
l) 55% conversion.
m) 4 atm H_2.
n) Value of the *syn* alcohol.

ligands, DTBBINAP and DTBM-SEGPHOS, results in excellent stereoselectivity, affording the almost pure *syn* α-amidomethyl β-hydroxy ester [14n, 42]. BisbenzodioxanPhos also induces high stereoselectivity [78b]. Highly *anti*-selective hydrogenation with the BINAP– or BisbenzodioxanPhos–Ru complex is achieved by using α-amino β-keto ester hydrochlorides (R = alkyl) instead of the acylamino compounds in CH_2Cl_2 or a 1:10 mixture of ethanol and CH_2Cl_2 [78, 79]. An (*R*)-MeO-BIPHEP–Ir complex catalyzes the hydrogenation of methyl α-amino benzoylacetate hydrochlorides in acetic acid to afford the 2*R*,3*R* (*anti*) products selectively [80]. Addition of $NaOCOCH_3$ and NaI is essential to attain high enantioselectivity. Hydrogenation of an α-phthalimide β-keto ester catalyzed by the (*R*)-C3TunaPhos–Ru complex in methanol selectively gives the 2*R*,3*R* (*anti*) product in >99% ee [81]. An α-chloro β-keto ester is hydrogenated with a BINAP–Ru dimethallyl complex to give predominantly the *anti* chloro alcohol in 99% ee [77b]. Hydrogenation of a simple α-methyl β-keto ester gives low diastereoselectivity, while the ee-value of the product remains high [28, 74]. Similarly, the BINAP–Ru-catalyzed hydrogenation of α-acylamino- or α-bromo-substituted β-keto phosphonates affords selectively the corresponding *syn* alcohols in up to >98% ee (Fig. 32.27) [69a, 82]. The mode of stereoselection is the same as that observed in the reaction of α-substituted β-keto carboxylic esters.

The stereoselective hydrogenation of α-substituted β-keto carboxylates and phosphonates via dynamic kinetic resolution catalyzed by a BINAP–Ru com-

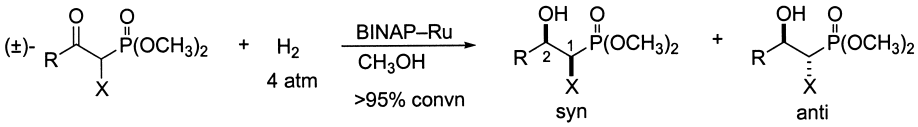

BINAP–Ru = $RuCl_2$(binap)(dmf)$_n$

Fig. 32.27 Hydrogenation of α-substituted β-keto phosphonates via dynamic kinetic resolution.

R	X	BINAP (SCR) [a]	Temp. [°C]	dr [b]	*Syn* alcohol		TON	TOF [h^{-1}]
					ee [%]	Config.		
CH_3	CH_3CONH	*R* (590)	25	97:3	>98	1*R*,2*R*	590	9
C_6H_5	CH_3CONH	*R* (100)	45	98:2	95	1*R*,2*R*	100	0.8
CH_3	Br	*S* (590)	25	90:10 [c]	98	1*R*,2*S*	561	6

a) SCR = substrate : catalyst molar ratio.
b) *Syn* : *anti* diastereomeric ratio.
c) Contaminated with 15% of a debrominated compound.

plexes is now widely used for the synthesis of important bioactive compounds, as well as some chiral diphosphines [1–4, 69a, 74, 83]. Some examples are listed in Figure 32.28. The stereocenter according to the BINAP–Ru chemistry is labeled by *R* or *S*. The chiral 2-acetoxyazetidinone, a key intermediate in the synthesis of carbapenems, is synthesized through the BINAP–Ru-catalyzed hydrogenation of methyl-2-benzamidomethyl-3-oxobutanoate via dynamic kinetic resolution on an industrial scale at Takasago International Corporation (Fig. 32.29) [1, 2, 84].

32.3 Simple Ketones

32.3.1 Alkyl Aryl Ketones

The hydrogenation of simple ketones was difficult. Because of the absence of hetero-atoms near the carbonyl function, these ketones cannot form a stable cyclic transition state, as shown in the reaction of β-keto esters (see Fig. 32.7) [2]. Most neutral or cationic metal-catalysts bearing monodentate or bidentate chiral phosphine ligands produced unsatisfactory results [4]. A breakthrough in this field was achieved by the development of Ru catalysts bearing both BINAP and a chiral 1,2-diamine on the center metal [2, 85]. Hydrogenation of 601 g acetophenone with only 2.2 mg *trans*-$RuCl_2$[(*S*)-tolbinap][(*S*,*S*)-dpen] in alkaline-base containing 2-propanol at 30 °C, under 45 atm of H_2 completes in 48 h, resulting

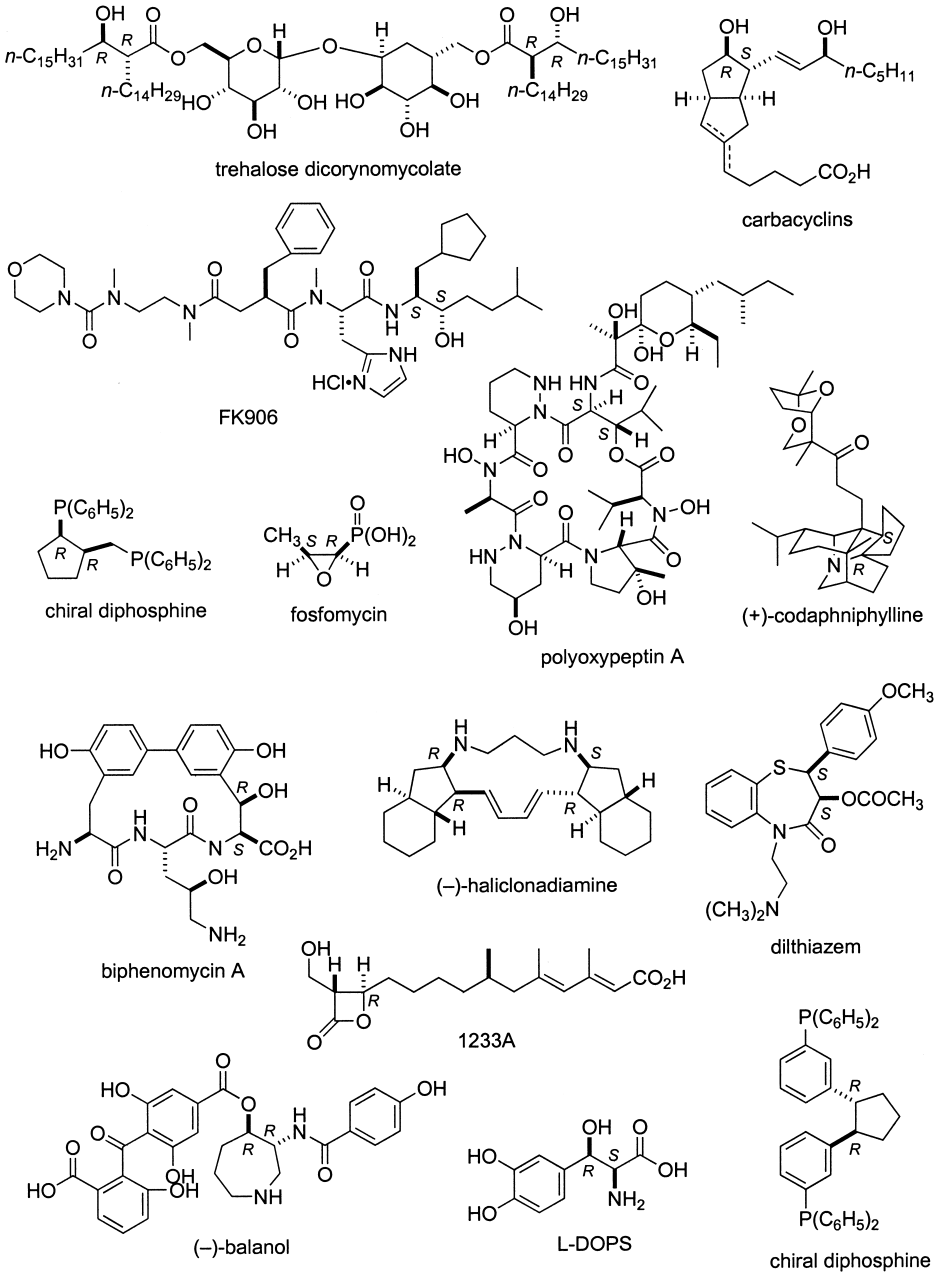

Fig. 32.28 Examples of bioactive compounds and chiral diphosphines obtainable by BINAP–Ru-catalyzed hydrogenation via dynamic kinetic resolution.

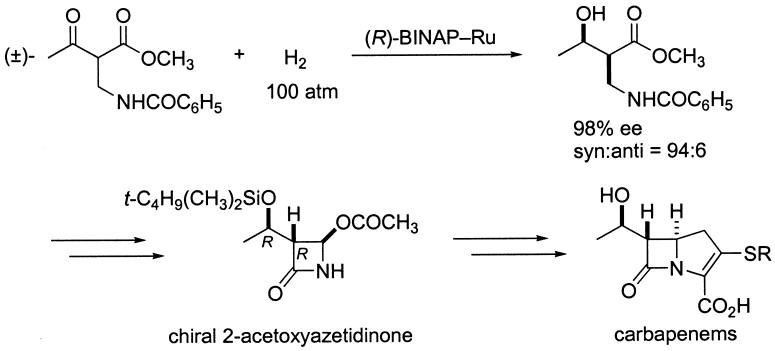

Fig. 32.29 Industrial synthesis of a carbapenem intermediate by BINAP–Ru-catalyzed hydrogenation.

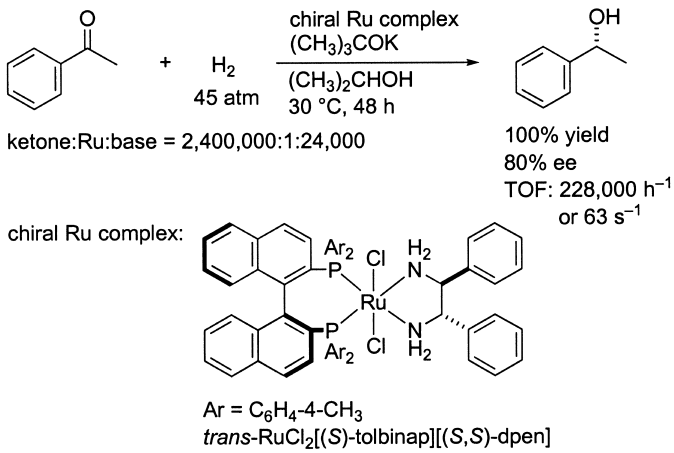

Fig. 32.30 Rapid hydrogenation of acetophenone catalyzed by the TolBINAP/DPEN–Ru complex.

in (*R*)-1-phenylethanol in 80% ee (Fig. 32.30) [86]. The TON reaches 2 400 000, while the TOF at 30% conversion was calculated as 228 000 h^{-1} or 63 s^{-1}.

Highly enantioselective hydrogenation of simple ketones has been achieved by the use of the catalyst consisting of *trans*-$RuCl_2$[(*S*)-xylbinap][(*S*)-daipen] (or the *R*/*R* combination) and $(CH_3)_3COK$ [(*S*,*S*)- or (*R*,*R*)-**31D**] in 2-propanol (Fig. 32.31) [87]. For example, hydrogenation of acetophenone catalyzed by (*S*,*S*)-**31D** with an SCR of 100 000 under 8 atm H_2 quantitatively gives (*R*)-1-phenylethanol in 99% ee. The combination of XylBINAP and DPEN (**31E**) also shows excellent enantioselectivity. This reaction tolerates many functionalities on the aryl ring such as F, Cl, Br, I, CF_3, OCH_3, $CO_2CH(CH_3)_2$, NO_2, and NH_2 [87]. The electronic and steric properties of the substituents hardly affect the enantioselection. Propiophenone, isobutyrophenone, cyclopropyl phenyl ketone, and 1′- and 2′-acetonaphthone are converted to the corresponding chiral alcohols in ex-

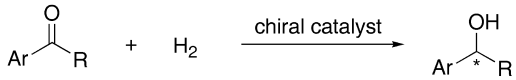

chiral catalyst:

trans-$RuCl_2$[(*S*)-tolbinap][(*S*)-daipen] + $(CH_3)_3COK$; (*S*,*S*)-**31A**
trans-$RuCl_2$[(*S*)-tolbinap][(*S*,*S*)-dpen] + $(CH_3)_3COK$; (*S*,*SS*)-**31B**
$RuCl_2$[(*S*)-tolbinap](pica) + $(CH_3)_3COK$; (*S*)-**31C**
trans-$RuCl_2$[(*S*)-xylbinap][(*S*)-daipen] + $(CH_3)_3COK$; (*S*,*S*)-**31D**
trans-$RuCl_2$[(*S*)-xylbinap][(*S*,*S*)-dpen] + $(CH_3)_3COK$; (*S*,*SS*)-**31E**
trans-RuHCl[(*S*)-binap][(*S*,*S*)-cydn] + $(CH_3)_2CHOK$; (*S*,*SS*)-**31F**
trans-RuH(η^1-BH_4)[(*S*)-xylbinap][(*S*,*S*)-dpen]; (*S*,*SS*)-**31G**
trans-RuH(η^1-BH_4)[(*S*)-xylbinap][(*S*,*S*)-dpen] + $(CH_3)_3COK$; (*S*,*SS*)-**31H**
trans-$RuCl_2$[(*S*)-xyl-hexaphemp][(*S*)-daipen] + $(CH_3)_3COK$; (*S*,*S*)-**31I**
trans-$RuCl_2$[(*R*)-xyl-p-phos][(*R*,*R*)-dpen] + $(CH_3)_3COK$; (*R*,*RR*)-**31J**
trans-$RuCl_2$[(*R*)-xylyl-phanephos][(*S*,*S*)-dpen] + $(CH_3)_3COK$; (*R*,*SS*)-**31K**
trans-$RuCl_2$[(*R*)-**1Bb**][(*R*)-daipen] + $(CH_3)_3COK$; (*R*,*R*)-**31L**
trans-$RuCl_2$[(*S*)-xyl-sdp][(*R*,*R*)-dpen] + $(CH_3)_3COK$; (*S*,*RR*)-**31M**
trans-$RuCl_2$[(*S*)-**3A**]$_2$[(*S*,*S*)-dpen] + $(CH_3)_3COK$; (*S*,*SS*)-**31N**
$RuCl_2$[(*S*,*S*)-bdpp][(*S*,*S*)-dpen] + $(CH_3)_3COK$; (*SS*,*SS*)-**31O**
$RuBr_2$[(*R*,*R*)-bipnor]–(*S*,*S*)-DPEN + KOH; (*RR*,*SS*)-**31P**
$RuCl_2$[(*S*,*S*)-**1Aa**](dmf)$_n$–2-(*n*-propyl)aniline + $(CH_3)_3CONa$; (*SS*)-**31Q**
$[NH_2(C_2H_5)_2][\{RuCl[(S)\text{-tolbinap}]\}_2(\mu\text{-}Cl)_3]$; (*S*)-**31R**
$RuClCp^*$(cod)–(*S*)-**4A** + KOH; (*S*)-**31S**
trans-RuHCl[(*S*)-binap][(*R*,*R*)-**2D**] + $(CH_3)_3COK$; (*S*,*RR*)-**31T**
$RuCl_2[P(C_6H_5)_3]_3$ + (*R*,*R*)-**4B** + $(CH_3)_3COK$; (*R*,*R*)-**31U**
$[RhCl(nbd)]_2$–(*S*,*S*)-DIOP + $(C_2H_5)_3N$; (*S*,*S*)-**31V**
$[RhCl(nbd)]_2$–(*S*,*S*)-BDPP + $(C_2H_5)_3N$; (*S*,*S*)-**31W**
$[RhCl(cod)]_2$–(*R*,*S*,*R*,*S*)-Me-PennPhos + 2,6-lutidine + KBr; (*R*,*S*,*R*,*S*)-**31X**
$[Ir\{(S)\text{-binap}\}(cod)]BF_4$–$P[2\text{-}N(CH_3)_2C_6H_4]_2C_6H_5$; (*S*)-**31Y**

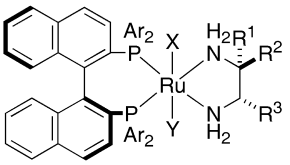

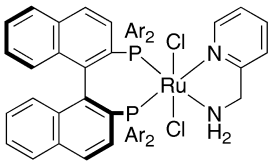

trans-$RuCl_2$[(*S*)-tolbinap][(*S*)-daipen]: X = Y = Cl,
Ar = 4-$CH_3C_6H_4$, R^1 = R^2 = 4-$CH_3OC_6H_4$, R^3 = $(CH_3)_2CH$
trans-$RuCl_2$[(*S*)-tolbinap][(*S*,*S*)-dpen]: X = Y = Cl,
Ar = 4-$CH_3C_6H_4$, R^1 = H, R^2 = R^3 = C_6H_5
trans-$RuCl_2$[(*S*)-xylbinap][(*S*)-daipen]: X = Y = Cl,
Ar = 3,5-$(CH_3)_2C_6H_3$, R^1 = R^2 = 4-$CH_3OC_6H_4$, R^3 = $(CH_3)_2CH$
trans-$RuCl_2$[(*S*)-xylbinap][(*S*,*S*)-dpen]: X = Y = Cl,
Ar = 3,5-$(CH_3)_2C_6H_3$, R^1 = H, R^2 = R^3 = C_6H_5
trans-RuH(η^1-BH_4)[(*S*)-xylbinap][(*S*,*S*)-dpen]: X = H, Y = η^1-BH_4,
Ar = 3,5-$(CH_3)_2C_6H_3$, R^1 = H, R^2 = R^3 = C_6H_5

$RuCl_2$[(*S*)-tolbinap](pica): Ar = 4-CH_3(
diastereomeric mixture

Fig. 32.31 Hydrogenation of alkyl aryl ketones.

R	Ar	Catalyst	SCR[a)]	H_2 [atm]	Temp. [°C]	Yield [%]	ee [%]	Con-fig.	TON	TOF [h^{-1}]
CH_3	C_6H_5	(*S*,*S*)-**31E**	100 000	8	45	100	99	*R*	100 000	40 000
CH_3	C_6H_5	(*S*,*SS*)-**31F**	5000	3	20	100	88	*R*	5 000	>417
CH_3	C_6H_5	(*S*,*SS*)-**31G**	100 000	8	45	100	99	*R*	100 000	14 286
CH_3	C_6H_5	(*S*,*SS*)-**31H**	100 000	8	45	100	99	*R*	100 000	133 333
CH_3	C_6H_5	(*S*,*S*)-**31I**	3000	8	rt	>99	99	*R*	>2 970	>6 364
CH_3	C_6H_5	(*R*,*RR*)-**31J**	100 000	34	25–28	99.7	99	*S*	99 700	2 764
CH_3	C_6H_5	(*R*,*SS*)-**31K**	20 000	8	18–20	>99	99	*R*	>19 800	>13 200
CH_3	C_6H_5	(*R*,*R*)-**31L**	1 000 000	48	rt	100	98.6	*S*	1 000 000	20 000
CH_3	C_6H_5	(*S*,*RR*)-**31M**	100 000	50	40	98	98	*S*	98 000	1 361
CH_3	C_6H_5	(*S*,*SS*)-**31N**	2000	50	0	95	93	*R*	1900	475
CH_3	C_6H_5	(*SS*,*SS*)-**31O**	500	2	rt	100	84	*R*	500	10
CH_3	C_6H_5	(*S*,*RR*)-**31T**	2000	2	5	>99	71	*S*	>1 980	>495
CH_3	C_6H_5	(*R*,*R*)-**31U**	100	30	rt	100	76	*S*	100	6
CH_3	C_6H_5	(*S*,*S*)-**31V**	200	69	50	64	80	–	128	21
CH_3	C_6H_5	(*S*,*S*)-**31W**	100	69	50	72	82	*S*	72	3
CH_3	C_6H_5	(*R*,*S*,*R*,*S*)-**31X**	100[b)]	30	rt	97	95	*S*	97	4
CH_3	C_6H_5	(*S*)-**31Y**	100	54–61	60	63	54	*S*	63	0.5
CH_3	2-$CH_3C_6H_4$	(*S*,*S*)-**31A**	100 000	10	28	94	99	*R*	94 000	1 958
CH_3	3-$CH_3C_6H_4$	(*S*,*S*)-**31D**	10 000	10	28	98	100	*R*	9 800	204
CH_3	3-$CH_3C_6H_4$	(*SS*)-**31Q**	500	7	rt	>99	93	*S*	>495	>33
CH_3	4-$CH_3C_6H_4$	(*R*,*RR*)-**31E**	2000	4	28	100	98	*S*	2 000	286
CH_3	4-*n*-$C_4H_9C_6H_4$	(*R*,*RR*)-**31E**	2000	4	28	100	98	*S*	2 000	400
CH_3	2,4-$(CH_3)_2C_6H_3$	(*R*,*R*)-**31D**	2000	4	28	99	99	*S*	1 980	248
CH_3	2-FC_6H_4	(*S*,*S*)-**31D**	2000	8	28	100	97	*R*	2 000	154
CH_3	2-FC_6H_4	(*S*)-**31R**	1300	85	35	21	>99	–	273	6
CH_3	3-FC_6H_4	(*R*,*RR*)-**31E**	2000	4	28	99	98	*S*	1 980	330
CH_3	4-FC_6H_4	(*R*,*R*)-**31D**	2000	4	28	100	97	*S*	2 000	333
CH_3	2-ClC_6H_4	(*R*,*RR*)-**31E**	2000	4	28	99.5	98	*S*	1 980	110
CH_3	2-BrC_6H_4	(*R*,*R*)-**31A**	10 000	10	28	100	98	*S*	10 000	1 667
CH_3	2-BrC_6H_4	(*R*,*R*)-**31D**	2000	4	28	99	96	*S*	1 980	660
CH_3	2-BrC_6H_4	(*S*)-**31R**	950	85	35	95	97	*S*	903	19
CH_3	3-BrC_6H_4	(*R*,*R*)-**31D**	2000	4	28	100	99.5	*S*	2 000	667
CH_3	4-BrC_6H_4	(*S*,*S*)-**31D**	20 000	8	28	99.9	99.6	*R*	19 980	3 996
CH_3	4-BrC_6H_4	(*S*,*S*)-**31D**	500	1	28	99.7	99.6	*R*	499	166
CH_3	4-BrC_6H_4	(*R*,*SS*)-**31K**	3000	8	18–20	>99	99	*R*	>2970	>2 970
CH_3	4-IC_6H_4	(*S*,*S*)-**31D**	2000	8	28	99.7	99	*R*	1 994	499
CH_3	2-$CF_3C_6H_4$	(*R*,*R*)-**31D**	2000	4	28	99	99	*S*	1 980	660
CH_3	3-$CF_3C_6H_4$	(*R*,*R*)-**31D**	2000	4	28	100	99	*S*	2 000	500
CH_3	3-$CF_3C_6H_4$	(*R*,*SS*)-**31K**	3000	8	18–20	>99	99	*R*	>2970	>5 940
CH_3	4-$CF_3C_6H_4$	(*S*,*S*)-**31D**	10 000	10	28	100	99.6	*R*	10 000	500
CH_3	2-$CH_3OC_6H_4$	(*R*,*R*)-**31D**	2 000	4	28	100	92	*S*	2 000	200
CH_3	3-$CH_3OC_6H_4$	(*R*,*R*)-**31D**	2 000	4	28	99	99	*S*	1 980	495
CH_3	4-$CH_3OC_6H_4$	(*S*,*S*)-**31D**	2 000	10	28	100	100	*R*	2 000	2 000
CH_3	4-$CH_3OC_6H_4$	(*R*,*S*,*R*,*S*)-**31X**	100	30	rt	83	94	*S*	83	2
CH_3	3-(*R*)-glycidyl-oxyphenyl	(*S*,*SS*)-**31G**	2 000	8	25	99	99	*R*,*R*	1 980	141
CH_3	4-(C_2H_5OCO)-C_6H_4	(*S*,*SS*)-**31G**	4 000	8	25	100	99	*R*	4 000	267

R	Ar	Catalyst	SCR[a)]	H_2 [atm]	Temp. [°C]	Yield [%]	ee [%]	Con-fig.	TON	TOF [h^{-1}]
CH_3	4-[$(CH_3)_2CH$-OCO]C_6H_4	(*S*,*S*)-**31D**	2000	8	28	100	99	*R*	2000	667
CH_3	4-$NO_2C_6H_4$	(*S*,*S*)-**31D**	2000	8	28	100	99.8	*R*	2000	133
CH_3	4-$NH_2C_6H_4$	(*S*,*S*)-**31D**	2000	8	28	100	99	*R*	2000	500
CH_3	1-naphthyl	(*S*,*SS*)-**31B**	100000	10	28	99.5	98	*R*	99500	2488
CH_3	1-naphthyl	(*R*,*RR*)-**31E**	2000	4	28	99	99	*S*	1980	495
CH_3	1-naphthyl	(*S*,*S*)-**31V**	200	69	50	100	84	–	200	40
CH_3	2-naphthyl	(*R*,*RR*)-**31E**	2000	4	28	99	98	*S*	1980	495
CH_3	2-naphthyl	(*RR*,*SS*)-**31P**	500	5	28	65	81	*R*	325	33
C_2H_5	C_6H_5	(*R*,*RR*)-**31E**	2000	4	28	100	99	*S*	2000	133
C_2H_5	C_6H_5	(*S*,*RR*)-**31K**	3000	5.5	18–20	>99	98	*S*	>2970	>1980
C_2H_5	C_6H_5	(*R*,*S*,*R*,*S*)-**31X**	100	30	rt	95	93	*S*	95	1
C_2H_5	4-FC_6H_4	(*R*,*RR*)-**31E**	2000	4	28	99	99	*S*	1980	248
C_2H_5	4-ClC_6H_4	(*S*,*S*)-**31D**	20000	8	28	99.9	99	*R*	19980	1249
$(CH_3)_2CH$	C_6H_5	(*R*,*R*)-**31D**	10000	8	28	99.7	99	*S*	9970	712
$(CH_3)_2CH$	C_6H_5	(*S*)-**31Y**	200	54–61	90	78	84	*R*	156	1
cyclo-C_3H_5	C_6H_5	(*S*,*S*)-**31D**	2000	8	28	99.7	96	*R*	1994	142
$(CH_3)_2CH$-CH_2	C_6H_5	(*S*)-**31S**	100	10	30	98	95	*R*	98	<16
$(CH_3)_3C$	C_6H_5	(*S*)-**31C**	2000	5	25	100	97	*R*	2000	167
$(CH_3)_3C$	C_6H_5	(*S*)-**31S**	100	10	30	99	81	*R*	99	<17

a) SCR = substrate : catalyst molar ratio.
b) Without addition of KBr.

cellent ee. *trans*-RuHCl[(*S*)-binap][(*S*,*S*)-cydn] with $(CH_3)_3COK$ (**31F**) also exhibits high catalytic activity [88]. In a similar manner, Ru catalysts bearing biaryl diphosphines, Xyl-HexaPHEMP (**31I**) [89], Xyl-P-Phos (**31J**) [90], and **1Bb** (**31L**) [91], show high enantioselectivity. The use of planar-chiral Xylyl-Phanephos (**31K**) [92] or chiral spiro diphosphine Xyl-SDP (**31M**) [93] gives excellent results. A Ru complex with a chiral monodentate phosphinite **3A** and DPEN in a 2:1 ratio (**31N**) shows high selectivity [94]. BDPP/DPEN–Ru (**31O**) [14p] or BIPNOR/DPEN–Ru catalysts (**31P**) [95] results in a good enantioselectivity. An *in-situ*-prepared catalyst from $RuCl_2$(**1Aa**)$(dmf)_n$, achiral 2-(*n*-propylthio)aniline, and $(CH_3)_3CONa$ (**31Q**) shows high enantioselectivity in ethanol [96]. Selection of alcoholic solvent notably affects the stereoselection. Ru catalyst bearing BINAP and a chiral amino phosphine **2D** (**31T**) [97] or a nitrogen-based tetradentate ligand **4B** (**31U**) [98] are also usable. Sterically hindered pivalophenone is smoothly hydrogenated with $RuCl_2$[(*S*)-tolbinap](pica) (PICA = *α*-picolylamine) and $(CH_3)_3COK$ [(*S*)-**31C**] to yield the *R* alcohol in 97% ee [99]. The best enantioselectivity is achievable in ethanol. A ternary catalyst system consisting of RuClCp*(cod) (Cp* = pentamethylcyclopentadienyl), a chiral diamine **4A**, and KOH (**31S**) is also usable [100]. Halogen-substituted acetophenones at the C2′

position are hydrogenated in the presence of $[NH_2(C_2H_5)_2][\{RuCl(tolbinap)\}_2(\mu\text{-}Cl)_3]$ (**31R**) to afford the chiral alcohols in up to >99% ee [101].

The BINAP/1,2-diamine–$RuCl_2$ complexes require the addition of alkaline base to form reactive RuH_2 species for the hydrogenation of simple ketones to neutralize releasing HCl. *trans*-$RuH(\eta^1\text{-}BH_4)$(xylbinap)(dpen) (**31G**) produces the active species without an additional base, while an even higher rate is obtainable in the presence of an alkaline base (Fig. 32.31) [102]. The base-free procedure can be applied to the hydrogenation of several base-sensitive ketones. For example, the reaction of ethyl-4-acetylbenzoate catalyzed by (*S*,*SS*)-**31G** quantitatively yields ethyl (*R*)-4-(1-hydroxyethyl)benzoate in 99% ee [102]. No transesterification is observed.

Enantioselective hydrogenation of alkyl aryl ketones catalyzed by chiral diphosphine–Rh complexes has also been reported. A catalyst system consisting of $[RhCl(nbd)]_2$, DIOP, and $(C_2H_5)_3N$ (**31V**) promotes the hydrogenation of acetophenone and 1′-acetonaphthone with high enantioselectivity (Fig. 32.31) [103, 104]. Hydrogenation of acetophenone with a BDPP–Rh catalyst (**31W**) gives 82% optical yield [105]. A Me-PennPhos–Rh complex with 2,6-lutidine and KBr (**31X**) catalyzed the hydrogenation of several aromatic ketones in up to 95% ee [106]. A cationic BINAP–Ir(I) complex with an achiral aminophosphine (**31Y**) is also usable [107].

Figure 32.32 shows a proposed mechanism for the hydrogenation of simple ketones catalyzed by TolBINAP/DPEN–Ru complexes [2, 108–110]. Under the hydrogenation conditions, the precatalyst **32A** is converted to the cationic RuH species **32B**, which equilibrates with the neutral complex **32E**. The 16-electron species **32B** reacts reversibly with an H_2 molecule to form **32C**, followed by a base- or solvent-assisted deprotonation resulting in the active RuH_2 species **32D**. A ketone is immediately reduced by **32D** to give the alcohol product and the 16-electron species **32E**, which is spontaneously protonated by alcoholic solvent, generating **32B**. Under highly basic or aprotic conditions, **32D** is reproduced by the reaction of **32E** and H_2. The six-membered pericyclic transition state **32F**, in which carbonyl moiety of the ketone does not interact with the Ru center, results in a low energy barrier at the reducing step, **32D** → **32E** [2, 108, 109]. The H–Ru–N–H 1,4-dipole function fits well with the carbonyl dipole. The hydride on the Ru center migrates to the electrophilic carbonyl carbon, while the amino-proton is delivered to the carbonyl oxygen simultaneously. Therefore, the presence of the NH_2 (or NH) end is crucial to achieve high catalytic activity.

As shown in Figure 32.30, the hydrogenation of acetophenone catalyzed by the (*S*)-TolBINAP/(*S*,*S*)-DPEN–Ru complex gives (*R*)-1-phenylethanol. The sense of enantioselection is general for various simple aromatic ketones. According to the "metal–ligand bifunctional mechanism" described above, the absolute configuration of alcohol products is kinetically determined at the stage of **32D**→**32E** (Fig. 32.32) [2, 108, 109]. Both possible diastereomeric transition states, *Si*-**33A** and *Re*-**33A** (Fig. 32.33), utilize the NH_{ax} (not NH_{eq}) proton for formation of the pericyclic ring due to the smaller H–Ru–N–H_{ax} dihedral angle. The *R* alcohol is selectively produced through *Si*-**33A**, because the *Re*-**33A** lead-

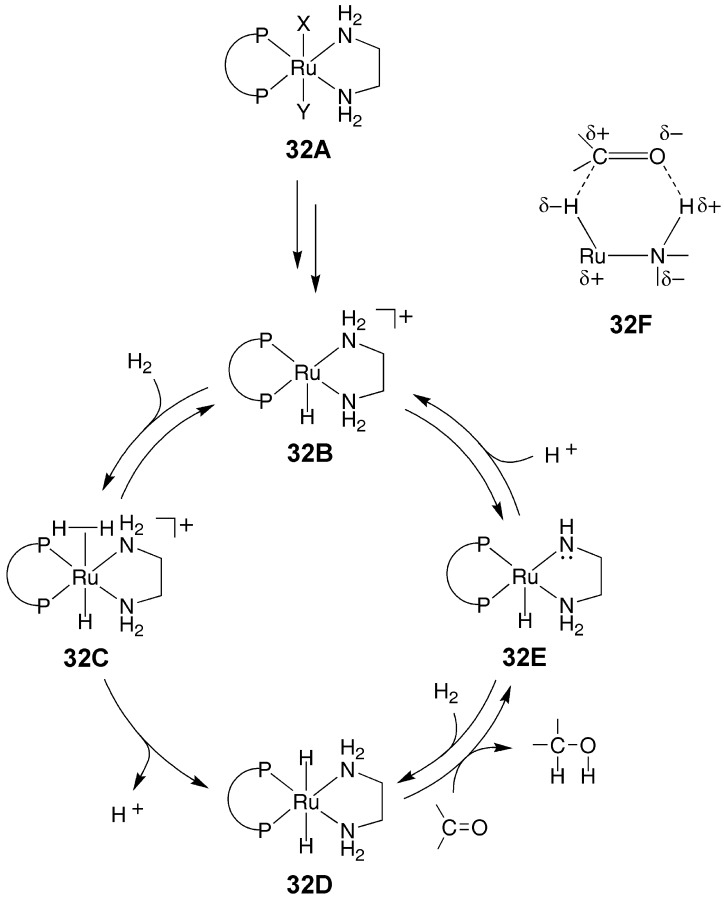

Fig. 32.32 Proposed catalytic cycle of hydrogenation of simple ketones with the TolBINAP/DPEN–Ru catalyst.

ing to the *S* alcohol suffers from significant nonbonded repulsion between the *P*-tolyl group and the phenyl ring of acetophenone. This explanation is consistent with the result that the use of the bulkier XylBINAP achieves higher optical yield (99% versus 80%).

The BINAP/1,2-diamine–Ru catalysts achieve rapid and enantioselective hydrogenation of simple aromatic ketones. However, enantioselective hydrogenation of 1-tetralones is difficult with these catalysts. This problem is solved by the use of IPHAN (Fig. 32.4), a chiral 1,4-diamine [111]. Hydrogenation of 1-tetralone with an (*S*)-XylBINAP/(*R*)-IPHAN–Ru complex and $(CH_3)_3COK$ [(*S*,*R*)-**34C**] in 2-propanol gives (*R*)-1-tetralol in 99% ee (Fig. 32.34). Tetralones substituted by CH_3O and F at the C7 position are reduced with **34C** in 99% and 98% optical yield, respectively. The use of an (*S*)-TolBINAP/(*R*)-IPHAN–Ru catalyst

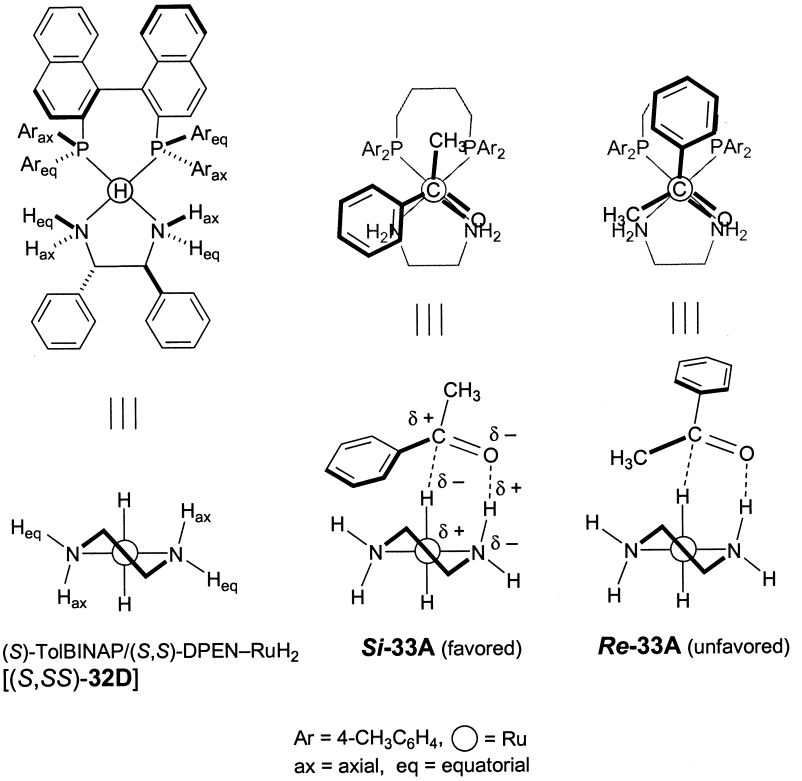

Fig. 32.33 Schematic view of the RuH_2 species and diastereomeric transition states in the hydrogenation of acetophenone. The equatorially oriented phenyl groups in the DPEN are omitted in **33A**.

[(*S*,*R*)-**34B**] or the *R*,*S* combination gives the best results for the hydrogenation of 4-, 5-, and 6-substituted ketones. 5,7-Disubstituted ketones are stereoselectively reduced with an (*S*)-BINAP/(*R*)-IPHAN catalyst. A cationic BINAP–Ir(I) complex with an addition of achiral aminophosphine (**31Y**) effects for hydrogenation of a series of cyclic aromatic ketones (Fig. 32.34) [112]. 1-Tetralones and their analogues are hydrogenated in up to 95% optical yield, while the reaction requires H_2 pressure up to 57 atm and temperature of 90 °C. The hydrogenation of 1-indanone under the same conditions gives 1-indanol in 86% ee [112].

Immobilized catalysts on solid supports inherently have benefits because of their easy separation from the products and the possibility of recycling. They are also expected to be useful for combinatorial chemistry and high-throughput experimentation. The polystyrene-bound BINAP/DPEN–Ru complex (beads) in the presence of $(CH_3)_3COK$ catalyzes the hydrogenation of 1′-acetonaphthone with an SCR of 12 300 in a 2-propanol–DMF mixture (1 : 1, v/v) to afford the chiral alcohol in 97% ee (Fig. 32.35) [113]. This supported complex is separable

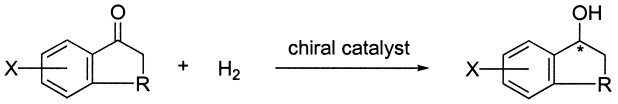

chiral catalyst:

trans-$RuCl_2$[(*S*)-binap][(*R*)-iphan] + $(CH_3)_3COK$; (*S*,*R*)-**34A**
trans-$RuCl_2$[(*S*)-tolbinap][(*R*)-iphan] + $(CH_3)_3COK$; (*S*,*R*)-**34B**
trans-$RuCl_2$[(*S*)-xylbinap][(*R*)-iphan] + $(CH_3)_3COK$; (*S*,*R*)-**34C**

Fig. 32.34 Hydrogenation of cyclic aromatic ketones.

R	X	Catalyst	SCR[a)]	H_2 [atm]	Temp. [°C]	Yield [%]	ee [%]	Con-fig.	TON	TOF [h^{-1}]
CH_2	H	(*S*)-**31Y**	190–230	50–57	90	72	86	*S*	<166	<8
CH_2	5-Cl	(*R*)-**31Y**	190–230	50–57	90	81	84	–[b)]	<186	<10
$(CH_2)_2$	H	(*R*)-**31Y**	190–230	50–57	90	88	95	*R*	<202	<3
$(CH_2)_2$	H	(*S*,*R*)-**34C**	3000	9	25	99.6	99	*R*	2988	374
$(CH_2)_2$	5-CH_3O	(*S*,*R*)-**34B**	55000	9	25	100	98	*R*	55000	3929
$(CH_2)_2$	6-CH_3O	(*S*,*R*)-**34B**	1000	9	25	98	92	*R*	980	75
$(CH_2)_2$	7-CH_3O	(*R*)-**31Y**	190–230	50–57	90	74	95	–[b)]	<170	<3
$(CH_2)_2$	7-CH_3O	(*S*,*R*)-**34C**	3300	9	25	100	99	*R*	3300	413
$(CH_2)_2$	7-NO_2	(*R*)-**31Y**	190–230	50–57	90	64	94	–[b)]	<147	<2
$(CH_2)_2$	7-F	(*S*,*R*)-**34C**	3000	9	25	100	98	*R*	3000	375
$(CH_2)_2$	5,7-$(CH_3)_2$	(*R*)-**31Y**	190–230	50–57	90	78	95	–[b)]	<179	<3
$(CH_2)_2$	5,7-$(CH_3)_2$	(*S*,*R*)-**34A**	3300	9	25	99.9	95	*R*	3297	1648
$(CH_3)_2$-CCH_2	H	(*R*,*R*)-**34B**	12000	9	25	99.9	93	*R*	11988	666
OCH_2	H	(*R*)-**31Y**	190–230	50–57	90	89	93	*R*	<205	<3
SCH_2	H	(*S*)-**31Y**	190–230	50–57	90	87	84	*S*	<200	<5

a) SCR = substrate : catalyst molar ratio.
b) Not reported.

by a simple filtration, and is reusable as a catalyst. The reaction with SCR of 2470 per batch can be conducted 14 times without loss of enantioselectivity (total TON = 33000). Some heterogenized BINAP/DPEN–Ru catalysts have also been used for this purpose. Poly-NAP [114], poly(BINOL–BINAP) [115], poly(BINAP) [116], or dendritic BINAP **5A** [117] show a high performance. Ru catalysts with poly-NAP [114] or **5A** [117] can be reused four times, with SCR of 1000 per batch and 500 per batch, respectively.

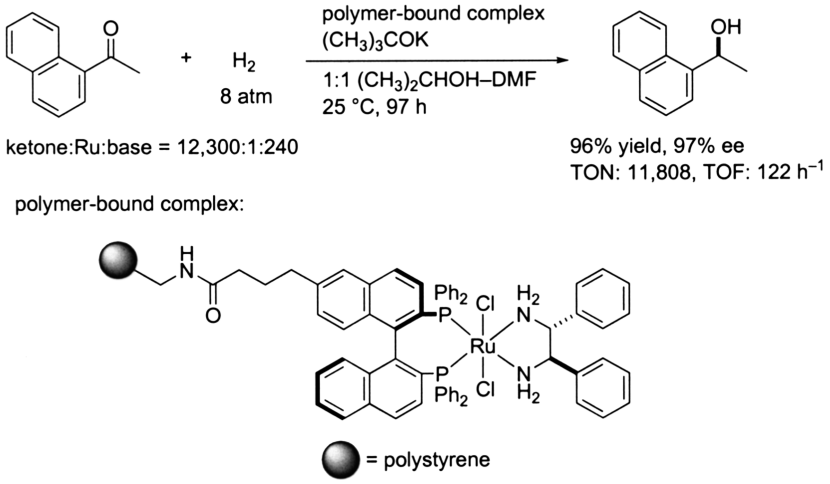

Fig. 32.35 Hydrogenation of 1′-acetonaphthone with the polymer-bound BINAP/DPEN–Ru catalyst.

32.3.2
Hetero-Substituted Aromatic Ketones

Enantioselective hydrogenation of α-, β-, and γ-amino-substituted ketones yields the corresponding chiral amino alcohols directly. Several chirally modified Rh and Ru catalysts have been applied in this reaction. Hydrogenation of 2-aminoacetophenone hydrochloride catalyzed by MOC-BIMOP–$[Rh(nbd)_2]ClO_4$ [118] or $[RhX(cy,cy\text{-}oxopronop)]_2$ (X = Cl, $OCOCF_3$) [119] provides the corresponding amino alcohol in 93% ee (Fig. 32.36). 2-(Dimethylamino)acetophenone hydrochloride is hydrogenated to the chiral amino alcohol in 96% ee with an MCCPM–Rh catalyst at an SCR of 100 000 [120, 121]. Epinephrine hydrochloride is produced in 95% ee by hydrogenation in the presence of $[Rh(nbd)(bppfoh)]ClO_4$ and $(C_2H_5)_3N$ [122]. 2-Dialkylamino ketones in their neutral form are reduced with BINAP–Ru [14n, 40] and DIOP–Rh [123] catalysts in high optical yield. The MCCPM–Rh-catalyzed hydrogenation of β- and γ-amino ketone hydrochlorides gives the corresponding chiral amino alcohols in up to 91% ee [124]. Hydrogenation of 2-(dimethylamino)acetophenones with Cy,Cy-oxoProNOP–Rh [125] and Cp,Cp-IndoNOP–Rh [126] catalysts affords the chiral alcohols in up to >99% ee. This reaction is applied to the synthesis of an atypical β-adrenergic phenylethanolaminotetraline agonist SR58611A [127].

A chiral catalyst consisting of *trans*-$RuCl_2$(xylbinap)(daipen) and $(CH_3)_3COK$ in 2-propanol effects asymmetric hydrogenation of α-, β-, and γ-amino aromatic ketones [128]. Hydrogenation of 2-(dimethylamino)acetophenone catalyzed by the (*R*)-XylBINAP/(*R*)-DAIPEN–Ru complex [(*R*,*R*)-**31D**] gives the *R* amino alcohol in 93% ee (Fig. 32.36). The optical yield is increased up to 99.8%, when

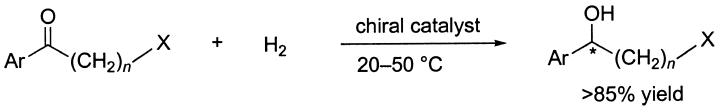

Fig. 32.36 Hydrogenation of α-, β-, or γ-heterosubstituted aromatic ketones.

Ar	*n*	X	Catalyst (SCR) [a)]	H_2 [atm]	ee [%]	Con-fig.	TON	TOF [h^{-1}]
C_6H_5	1	$ClNH_3$	$[Rh(nbd)_2]ClO_4$–(*R*)-MOC-BIMOP + $(C_2H_5)_3N$ (1000)	90	93	*R*	1000	6
C_6H_5	1	$ClNH_3$	[Rh{(*S*)-cy,cy-oxo-pronop}-(cod)]BF_4 (200)	50	93	*S*	200	100
C_6H_5	1	$ClC_6H_5CH_2NH_2$	$[RhCl(cod)]_2$–(2*S*,4*S*)-MCCPM + $(C_2H_5)_3N$ (1000)	20	93	*S*	1000	50
3,4-$(OH)_2C_6H_3$	1	$ClCH_3NH_2$	[Rh{(*R*)-(*S*)-bppfoh}(nbd)]-ClO_4 + $(C_2H_5)_3N$ (100)	50	95	*R*	100	0.6
C_6H_5	1	$(CH_3)_2N$	$RuBr_2$[(*S*)-binap] (500)	100	95	*S*	425	18
C_6H_5	1	$(CH_3)_2N$	(*R*,*R*)-**31D** (2000)	8	93	*R*	2000	167
2-naphthyl	1	$(C_2H_5)_2N$	$[RhCl(nbd)]_2$–(*S*,*S*)-DIOP (200)	70	95	+	186	9
C_6H_5	1	$Cl(CH_3)_2NH$	$[Rh(OCOCF_3)\{(S)\text{-cp,cp-indonop}\}]_2$ (200)	50	>99	*S*	200	11
3-ClC_6H_4	1	$Cl(CH_3)_2NH$	[Rh{(*R*)-cy,cy-oxo-pronop}-(cod)]BF_4 (200)	1	96	*R*	200	11
C_6H_5	1	$Cl(C_2H_5)_2NH$	$[RhCl(cod)]_2$–(2*S*,4*S*)-MCCPM + $(C_2H_5)_3N$ (100000)	20	97	*S*	100000	5000
3-ClC_6H_4	1	C_6H_5CONH	$RuCl_2$[(*S*,*S*)-**1Ab**]$(dmf)_n$–$(CH_3)_3CSCH_2CH_2NH_2$ + $(CH_3)_3CONa$ (500)	7	93	*R*	>495	>33
C_6H_5	1	$C_6H_5CO(CH_3)N$	(*R*,*R*)-**31D** (2000)	8	99.8	*R*	2000	250
4-C_6H_5-$CH_2OC_6H_4$	1	$C_6H_5CO[3,4\text{-}(CH_3O)_2\text{-}C_6H_3(CH_2)_2]N$	(*R*,*R*)-**31D** (2000)	8	97	*R*	2000	83
C_6H_5	2	$ClCH_3NH_2$	$[RhCl(cod)]_2$–(2*S*,4*S*)-MCCPM + $(C_2H_5)_3N$ (1000)	30	79.8	*R*	1000	21
C_6H_5	2	$(CH_3)_2N$	(*S*,*S*)-**31D** (10,000) [b)]	8	97.5	*R*	10000	2000
C_6H_5	2	$(CH_3)_2N$	(*S*,*SS*)-**31G** (4000)	8	97	*R*	4000	333
2-thienyl	2	$(CH_3)_2N$	(*R*,*R*)-**31D** (2000) [b)]	8	92	*S*	2000	286
2-thienyl	2	$(CH_3)_2N$	$RuCl_2$[(*R*,*R*)-bicp]$(dmf)_n$–$NH_2C(CH_3)_2CH_2NH_2$ + $(CH_3)_3CONa$ (2000)	7	96	*S*	1800	120
C_6H_5	2	$Cl(CH_3)_2NH$	[Rh{(*S*)-cy,cy-oxo-pronop}-(cod)]BF_4 (200)	50	93 [c)]	*R*	180	4
C_6H_5	2	$ClC_6H_5CH_2(CH_3)$-NH_2	$[RhCl(cod)]_2$–(2*S*,4*S*)-MCCPM + $(C_2H_5)_3N$ (1000)	30	90.8	*R*	1000	21
4-FC_6H_4	3	R′ [d)]	(*S*,*S*)-**31D** (10000)	8	99	*R*	10000	313

Ar	*n*	X	Catalyst (SCR) [a)]	H_2 [atm]	ee [%]	Config.	TON	TOF [h^{-1}]
C_6H_5	3	$Cl(CH_3)_2NH$	[Rh{(*S*)-cy,cy-oxo-pronop}-(cod)]BF_4 (200)	50 [e)]	92	*R*	192	5
C_6H_5	3	$ClC_6H_5CH_2(CH_3)$-NH_2	$[RhCl(cod)]_2$–(2*S*,4*S*)-MCCPM + $(C_2H_5)_3N$ (250)	50	88.4	*R*	250	4
C_6H_5	1	CH_3O	(*R*,*R*)-**31D** (2000)	8	95	*R*	2000	400
4-$CF_3C_6H_4$	1	CH_3O	$RuCl_2$[(*S*,*S*)-**1Ab**](dmf)$_n$–$(CH_3)_3CSCH_2CH_2NH_2$ + $(CH_3)_3CONa$ (500)	7 [f)]	97	*R*	>495	>33

a) SCR = substrate : catalyst molar ratio.
b) *trans*-$RuCl_2$(xylbinap)(daipen) is treated with $(CH_3)_3COK$ in 2-propanol prior to hydrogenation.
c) Contaminated with 5% propiophenone.
d) R' = 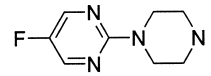
e) At 80 °C.
f) At –10 °C.

acetophenone derivatives with an amido group at the *α* position are hydrogenated with the same catalyst [128]. This method is applied to the synthesis of (*R*)-denopamine, a β_1-receptor agonist used for treating congestive heart failure (the structure is shown in Fig. 32.44) [128]. When 3-(dimethylamino)propiophenone, a base-labile *β*-amino ketone, is reduced under controlled conditions using an (*S*)-XylBINAP/(*S*)-DAIPEN–Ru catalyst prepared from the $RuCl_2$ complex and a minimum amount of $(CH_3)_3COK$, the *R* amino alcohol is obtained in 97.5% ee and in 96% yield, contaminated with 2% of 1-phenyl-1-propanol, a deamination-derived byproduct [128]. The desired product is obtained quantitatively by reaction with *trans*-$RuH(\eta^1\text{-}BH_4)$[(*S*)-xylbinap][(*S*,*S*)-dpen] [(*S*,*SS*)-**31G**] under base-free conditions [102]. Similarly, a 2-thienyl derivative is also reduced selectively [129]. The chiral *β*-amino alcohols are key intermediates for the synthesis of antidepressants (*R*)-fluoxetine and (*S*)-duloxetine (see Fig. 32.44). The *γ*-amino ketone shown in Figure 32.36 is hydrogenated with (*S*,*S*)-**31D** in basic 2-propanol, giving the *R* alcohol in 99% ee, which is a potent antipsychotic, BMS 181100 (see Fig. 32.44) [128]. Hydrogenation of 2-methoxyacetophenone catalyzed by (*R*,*R*)-**31D** affords the *R* *α*-methoxy alcohol in 95% ee (Fig. 32.36) [85 a]. A Ru catalyst consisting of $RuCl_2$(**1Ab**)(dmf)$_n$, achiral $(CH_3)_3CSCH_2CH_2$-NH_2, and $(CH_3)_3CONa$ effects enantioselective hydrogenation of 2-benzyloxy-amino- and 2-methoxyacetophenone derivatives (Fig. 32.36) [96]. Hydrogenation of 3-dimethylamino-1-(2-thienyl)-1-propanone, a *β*-amino ketone, with a BICP/$NH_2C(CH_3)_2CH_2NH_2$–Ru catalyst gives the *β*-amino alcohol in 96% ee [96].

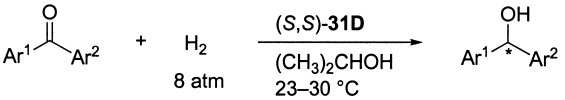

Fig. 32.37 Hydrogenation of diaryl ketones.

Ar^1	Ar^2	SCR[a)]	Yield [%]	ee [%]	Config.	TON	TOF [h^{-1}]
2-$CH_3C_6H_4$	C_6H_5	2000	99	93	*S*	1980	180
2-$CH_3OC_6H_4$	C_6H_5	2000	100	99	*S*	2000	133
2-FC_6H_4	C_6H_5	2000	99	97	*S*	1980	141
2-ClC_6H_4	C_6H_5	20000	99	97	*S*	19800	360
2-BrC_6H_4	C_6H_5	2000	99	96	*S*	1980	152
2-BrC_6H_4	4-$CH_3C_6H_4$	2000	99	98	*S*	1980	132
4-$CH_3OC_6H_4$	C_6H_5	2000	95	35	*R*	1900	146
4-$CF_3C_6H_4$	C_6H_5	2000	99	47	*S*	1980	165
4-$CH_3OC_6H_4$	4-$CF_3C_6H_4$	2000	97	61	–	1940	162
Ferrocenyl[b)]	C_6H_5	2000	100	95	*S*	2000	154

a) SCR = substrate : catalyst molar ratio.
b) (*S*,*S*)-**31A** is used as a catalyst.

32.3.3
Diaryl Ketones

Enantioselective hydrogenation of pro-chiral diaryl ketones requires the electronic or steric differentiation of two otherwise similar aromatic functions. Furthermore, hydrogenolysis of the produced diarylmethanols is to be avoided. Hydrogenation of 2-substituted benzophenones in the presence of an (*S*)-XylBINAP/(*S*)-DAIPEN–Ru complex and $(CH_3)_3COK$ [(*S*,*S*)-**31D**] in 2-propanol provides the diarylmethanol in up to 99% ee (Fig. 32.37) [130]. No detectable diarylmethane is produced under such basic conditions. 2-Substitution of electron-donating and -attracting groups such as CH_3, CH_3O, F, Cl, and Br has a minimal effect on enantioselectivity. Chiral alcohols obtained from 2-methyl- and 2-bromo-4′-methylbenzophenones are easily converted to antihistaminic (*S*)-orphenadrine and (*R*)-neobenodine, respectively (see Fig. 32.44) [130]. Substrates with a substituent at the C3 or C4 positions are hydrogenated with only moderate enantioselectivity. Benzoylferrocene is hydrogenated with an (*S*)-TolBINAP/(*S*)-DAIPEN–Ru catalyst [(*S*,*S*)-**31A**] to afford the *S* alcohol in 95% ee [130].

32.3.4
Heteroaromatic Ketones

General enantioselective hydrogenation of heteroaromatic ketones is achieved by means of the XylBINAP/DAIPEN–Ru complexes and $(CH_3)_3COK$ in 2-propanol. A variety of substrates with an electron-rich and -deficient heteroaromatic func-

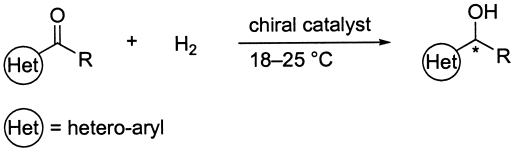

Fig. 32.38 Hydrogenation of heteroaromatic ketones.

Het	R	Catalyst (SCR)[a]	H_2 [atm]	Yield [%]	ee [%]	Con-fig.	TON	TOF [h^{-1}]
2-furyl	CH_3	(*R*,*R*)-**31D** (40 000)	50	96	99	*S*	38 400	3 200
2-furyl	CH_3	(*R*,*SS*)-**31K** (3000)	5.5	>99	96	*R*	>2 970	>1 188
2-furyl	CH_3	(*S*,*RR*)-**31M** (5000)	50	99	98	*S*	4 950	990
2-furyl	CH_3	(*R*,*S*,*R*,*S*)-**31X** (100)	30[b]	83	96	*S*	99	10
2-furyl	n-C_5H_{11}	(*R*,*R*)-**31D** (2000)	8	100	98	*S*	2 000	167
2-furyl	$(CH_3)_3C$	(*S*)-**31C** (2400)	8	99	97	*R*	2 376	475
2-thienyl	CH_3	(*R*,*R*)-**31D** (5000)	8	100	99	*S*	5 000	417
2-thienyl	CH_3	(*S*,*S*)-**31D** (1000)	1	100	99	*R*	1 000	59
2-thienyl	CH_3	$RuCl_2$[(*R*,*R*)-bicp]-(tmeda)–(*R*,*R*)-DPEN + KOH (500)	4[c]	100	93	*S*	500	10
2-thienyl	CH_3	(*S*,*RR*)-**31M** (5000)	50	98	98	*S*	4 900	980
2-thienyl	$(CH_3)_3C$	(*S*)-**31C** (2100)	8	100	98	*R*	2 100	420
2-(5-chloro)-thienyl	CH_3	$RuCl_2$[(*R*,*R*)-bicp](dmf)$_n$–$NH_2C(CH_3)_2CH_2NH_2$ + $(CH_3)_3CONa$ (500)	7	>99	94	*S*	>198	>13
3-thienyl	CH_3	(*R*,*R*)-**31D** (5000)	8	100	99.7	*S*	5 000	1 000
3-thienyl	CH_3	(*S*,*RR*)-**31K** (3000)	5.5	>99	98	*S*	22 970	2 990
2-(1-methyl)-pyrrolyl	CH_3	(*S*,*S*)-**31D** (1000)	8	61	97	–	610	31
2-[1-(4-toluene-sulfonyl)]-pyrrolyl	CH_3	(*R*,*R*)-**31D** (1000)	8[d]	93	98	*S*	1 000	56
2-thiazolyl	CH_3	(*R*,*R*)-**31D** (2000)[e]	8	100	96	*S*	2 000	167
2-pyridyl	CH_3	(*R*,*R*)-**31D** (2000)[e]	8	99.7	96	*S*	1 994	665
2-pyridyl	$(CH_3)_2CH$	(*R*,*R*)-**31D** (2000)	8	100	94	*S*	2 000	167
3-pyridyl	CH_3	(*R*,*R*)-**31D** (5000)	8	100	99.6	*S*	5 000	417
3-pyridyl	CH_3	(*R*,*SS*)-**31K** (1500)	8	>99	99	*R*	>1485	>495
4-pyridyl	CH_3	(*R*,*R*)-**31D** (5000)	8	100	99.8	*S*	5 000	417
2,6-diacetyl-pyridine		(*R*,*R*)-**31D** (10 000)	8	99.9	100	*S*,*S*	9 990	588

a) SCR = substrate : catalyst molar ratio.
b) Reaction in methanol.
c) At –30 °C.
d) Reaction in 1 : 10 DMF : 2-propanol.
e) $B[OCH(CH_3)_2]_3$ is added. Ketone/B = 100.

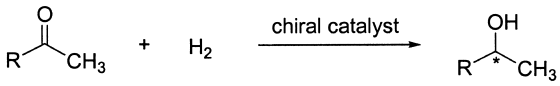

catalyst:
RuH(η^1-BH_4)[(*S*)-tolbinap](pica); (*S*)-**39A**

Fig. 32.39 Hydrogenation of alkyl methyl ketones.

R	Catalyst	SCR[a)]	Solvent	H_2 [atm]	Yield [%]	ee [%]	Con-fig.	TON	TOF [h^{-1}]
n-C_4H_9	(*R,S,R,S*)-**31X**	100	CH_3OH	30	96	75	*S*	96	2
$(CH_3)_2$-$CHCH_2$	(*R,S,R,S*)-**31X**	100	CH_3OH	30	66	85	*S*	66	0.9
$(CH_3)_2CH$	(*R,S,R,S*)-**31X**	100	CH_3OH	30	99	84	*S*	99	1
cyclo-C_3H_5	(*S,S*)-**31D**	11 000	$(CH_3)_2CHOH$	10	96	95	*R*	10 560	880
cyclo-C_6H_{11}	(*R,S,R,S*)-**31X**	100	CH_3OH	30	90	92	*S*	90	0.9
cyclo-C_6H_{11}	(*S,S*)-**31D**	10 000	$(CH_3)_2CHOH$	8	99	85	*R*	9 900	990
$(CH_3)_3C$	(*S*)-**31C**	100 000	C_2H_5OH	20	100	98	*S*	100 000	4 167
$(CH_3)_3C$	(*S*)-**39A**	2 000	C_2H_5OH	4	100	97	*S*	2 000	400
$(CH_3)_3C$[b)]	(*R*)-**31C**	2 300	C_2H_5OH	5	100	97	*R*	2 300	460
$(CH_3)_3C$	(*R,S,R,S*)-**31X**	100	CH_3OH	30	51	94	*S*	51	0.5
$(CH_3)_3C$	[Rh{(*S,R,R,R*)-tmo-deguphos}-(cod)]BF_4	1 000	$(CH_3)_2CHOH$	73	30	84	*S*	300	288
1-methyl-cyclopropyl	(*S,S*)-**31D**	500	$(CH_3)_2CHOH$	4	96	98	–	480	160
1-adamantyl	(*S*)-**31C**	2 000	C_2H_5OH	5	100	98	*S*	2 000	400

a) SCR = substrate : catalyst molar ratio.
b) 2,2-Dimethyl-3-undecanone.

tion are converted to the chiral alcohols in high ee (Fig. 32.38) [129]. Hydrogenation of 2-acetylfuran with (*R,R*)-**31D** gives (*S*)-1-(2-furyl)ethanol in 99% ee, leaving the furan ring intact. With the same catalyst, 2- and 3-acetylthiophene are reduced in >99% optical yield. Sterically congested 2-pivaloylfuran and 2-pivaloylthiophene are enantioselectively reduced with the TolBINAP/PICA–Ru complex and $(CH_3)_3COK$ (**31C**) in ethanol [99]. Reaction of the substrates with 2-(1-methyl)pyrrolyl or 2-[1-(4-toluenesulfonyl)]pyrrolyl group also gives high enantioselectivity. Under the regular conditions, reaction of 2-acetylthiazol and 2-acetylpyridine do not go to completion, probably due to the high binding ability of the alcoholic products to the catalyst metal center. This problem is solved when $B[OCH(CH_3)_2]_3$ (ketone : Ru : borate = 2000 : 1 : 20) is added as a co-catalyst [129]. The hydrogenation of 3- and 4-acetylpyridine under standard conditions yields the pyridyl alcohols in excellent ee. Double hydrogenation of 2,6-diacetylpyridine in the presence of (*R,R*)-**31D** gives the *S,S* diol in 100% yield out of three possi-

ble stereoisomers. The (*R*)-Xylyl-Phanephos/(*S*,*S*)-DPEN–Ru catalyst [(*R*,*SS*)-**31K**] [92] and (*R*)-Xyl-SDP/(*R*,*R*)-DPEN–Ru catalyst [(*R*,*RR*)-**31M**] [93] also show excellent performance in this reaction. The *in-situ*-prepared catalyst from $RuCl_2$[(*R*,*R*)-bicp](tmeda), (*R*,*R*)-DPEN, and KOH is also usable [131]. A BICP/$NH_2C(CH_3)_2CH_2NH_2$–Ru catalyst promotes hydrogenation of 2-acetyl-5-chlorothiophene to afford the chiral alcohol in 94% ee [96]. Reaction of 2-acetylfuran with the Me-PennPhos–Rh catalyst (**31X**) gives 96% optical yield [106].

32.3.5
Dialkyl Ketones

The enantioselective hydrogenation of simple aliphatic ketones remains difficult because of the lack of general chemistry to differentiate two alkyl groups. The Me-PennPhos–Rh catalyst (**31X**) attains a good optical yield in the hydrogenation of *n*-alkyl methyl ketones (Fig. 32.39) [106]. 2-Hexanone is reduced with (*R*,*S*,*R*,*S*)-**31X** to afford (*S*)-2-hexanol in 75% ee. Sterically demanded pinacolone is reduced with 94% optical yield [106]. The (*S*)-XylBINAP/(*S*)-DAIPEN–Ru complex [(*S*,*S*)-**31D**] catalyzes the hydrogenation of cyclopropyl methyl ketone and cyclohexyl methyl ketone in basic 2-propanol to give the *R* alcohols in 95% and 85% ee, respectively (Fig. 32.39) [85 a, 87]. Pinacolone is efficiently hydrogenated with the (*S*)-TolBINAP/PICA–Ru complex and $(CH_3)_3COK$ [(*S*)-**31C**] in ethanol to afford the *S* alcohol in 98% ee [99]. The reaction completes with an SCR of 100 000. 2,2-Dimethyl-3-undecanone and 1-adamantyl methyl ketone are also hydrogenated enantioselectively. $RuH(\eta^1\text{-}BH_4)$(tolbinap)(pica) (**39A**) reduces pinacolone under base-free conditions [99]. The TMO-DEGUPHOS–Rh catalyzes hydrogenation of pinacolone in 84% optical yield [132].

Heterogeneous Ni catalysts modified by tartaric acid and NaBr show relatively high enantioselectivity for the hydrogenation of simple aliphatic ketones (Fig. 32.40) [133]. In the presence of an excess amount of pivalic acid, 2-alka-

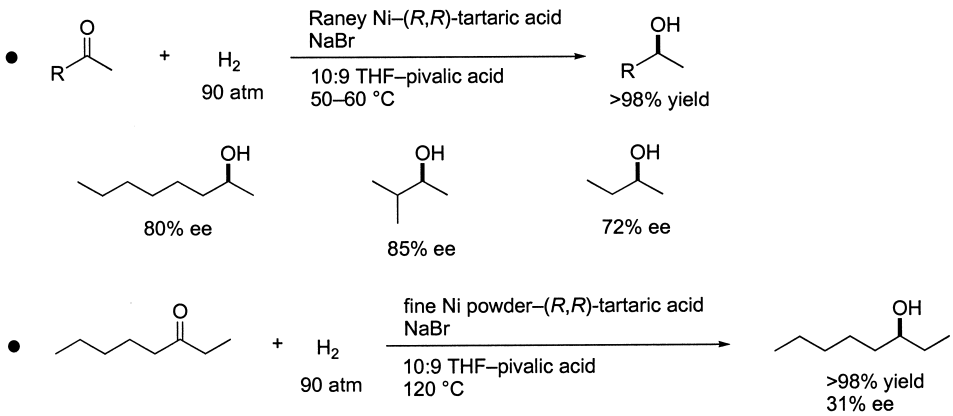

Fig. 32.40 Hydrogenation of aliphatic ketones with the modified Raney Ni.

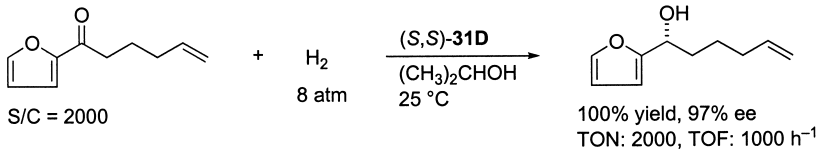

Fig. 32.41 Hydrogenation of an unconjugated enone to the chiral enol.

nones are reduced with the modified Raney Ni catalyst to give the 2-alkanols in up to 85% ee. Even 3-octanone is reduced with 31% optical yield, when the chirally modified fine Ni powder is used as a catalyst in place of a chiral Raney Ni [133 c].

32.3.6
Unsaturated Ketones

The enantioselective hydrogenation of unsaturated ketones to chiral unsaturated alcohols is a difficult subject, because most existing hydrogenation catalysts preferentially reduce olefinic bonds over carbonyl functions. This long-standing problem has been solved by the use of BINAP/chiral 1,2-diamine–Ru catalysts in base-containing 2-propanol [86, 87, 102, 129, 134–136]. As shown in Figure 32.41, 1-(2-furyl)-4-penten-1-one, an unconjugated enone, is hydrogenated with (*S*)-XylBINAP/(*S*)-DAIPEN–Ru and $(CH_3)_3COK$ [(*S*,*S*)-**31D**] in 2-propanol, yielding the *R* enol in 100% yield and in 97% ee [129]. The olefinic bond is left intact.

Enantioselective hydrogenation of *α*,*β*-unsaturated ketones affording chiral allylic alcohol is also achieved with the BINAP/1,2-diamine–Ru catalyst system. A variety of allylic alcohols in high optical purity are obtained by reaction with *trans*-$RuCl_2$[(*S*)-xylbinap][(*S*)-daipen] (or the *R*/*R* combination) and K_2CO_3 (**42A**) in 2-propanol (Fig. 32.42) [87]. The use of a relatively weak base, K_2CO_3, effectively prevents the formation of undesired polymeric byproducts. Hydrogenation of benzalacetone (**a**) catalyzed by (*S*,*S*)-**42A** gives (*R*)-(*E*)-4-phenyl-3-buten-2-ol in 97% ee. No saturation of the olefinic bond was observed. Hydrogenation of (*E*)-6-methyl-2-hepten-4-one (**g**) with (*R*,*R*)-**42A** affords the *S* allylic alcohol in 90% ee [87], which is a synthetic intermediate of the *α*-tocopherol (vitamin E) side chain (see Fig. 32.44). Reaction of 1-acetylcycloalkenes (**i**–**k**) results in the allylic alcohols in >99% ee. Highly base-sensitive 3-nonene-2-one (**e**) is hydrogenated with (*S*,*S*)-**42A** in basic 2-propanol under high dilution conditions ([ketone]= 0.1 M) to give (*R*)-3-none-2-ol in high yield [87]. When the reaction is conducted with *trans*-$RuH(\eta^1\text{-}BH_4)$[(*S*)-xylbinap][(*S*,*S*)-dpen] [(*S*,*SS*)-**31G**] without addition of base, the desired *R* allylic alcohol is quantitatively obtained, even with a 2.0 M substrate concentration [102]. (*R*)-Xylyl-PhanePhos/(*S*,*S*)-DPEN–Ru catalyst [(*R*,*SS*)-**31K**] [92] and (*S*)-Xyl-SDP/(*R*,*R*)-DPEN–Ru catalyst [(*S*,*RR*)-**31M**] [93] are also useful for this reaction. The olefinic *t*-butyl ketones (**c** and **f**) are smoothly hydrogenated with the TolBINAP/PICA–Ru complex (**31C**) in basic ethanol [99].

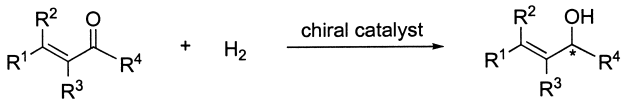

a: $R^1 = C_6H_5$; $R^2 = R^3 = H$; $R^4 = CH_3$
b: $R^1 = C_6H_5$; $R^2 = R^3 = H$; $R^4 = (CH_3)_2CH$
c: $R^1 = C_6H_5$; $R^2 = R^3 = H$; $R^4 = (CH_3)_3C$
d: R^1 = 2-thienyl; $R^2 = R^3 = H$; $R^4 = CH_3$
e: $R^1 = n\text{-}C_5H_{11}$; $R^2 = R^3 = H$; $R^4 = CH_3$
f: $R^1 = n\text{-}C_6H_{13}$; $R^2 = R^3 = H$; $R^4 = (CH_3)_3C$
g: $R^1 = CH_3$; $R^2 = R^3 = H$; $R^4 = (CH_3)_2CHCH_2$
h: $R^1 = R^2 = R^4 = CH_3$; $R^3 = H$
i: R^1–$R^3 = (CH_2)_4$; $R^2 = H$; $R^4 = CH_3$
j: R^1–$R^3 = (CH_2)_5$; $R^2 = H$; $R^4 = CH_3$
k: R^1–$R^3 = (CH_2)_3$; $R^2 = R^4 = CH_3$
l: R^1 = 2,6,6-trimethylcyclohexenyl; $R^2 = R^3 = H$; $R^4 = CH_3$ (β-ionone)

catalyst:
trans-$RuCl_2$[(*S*)-xylbinap][(*S*)-daipen] + K_2CO_3; (*S*,*S*)-**42A**
trans-$RuCl_2$[(*S*)-xylbinap][(*S*,*S*)-dpen] + K_2CO_3; (*S*,*SS*)-**42B**

Fig. 32.42 Hydrogenation of α,β-unsaturated ketones.

Substrate	Catalyst	SCR [a)]	H_2 [atm]	Yield [%]	ee [%]	Config.	TON	TOF [h^{-1}]
a	(*S*,*S*)-**42A**	100 000	80	100	97	*R*	100 000	2500
a	(*S*,*S*)-**42A**	10 000	10	100	96	*R*	10 000	667
a	(*R*,*SS*)-**31K**	3 000	5.5	> 99	97	*R*	>2970	>2970
a	(*S*,*RR*)-**31M**	5 000	50	100	96	*S*	5 000	1667
b	(*S*,*S*)-**42A**	2 000	8	100	86	*R*	2 000	100
c	(*S*)-**31C**	2 050	5	100	97	*S*	2 050	410
d	(*R*,*R*)-**42A**	5 000	8	100	91	*S*	5 000	714
e	(*S*,*S*)-**31D**	2 000	8	98	97	*R*	1 960	131
e	(*S*,*SS*)-**31G**	4 000	8	95	99	*R*	3 800	238
f [b]	(*R*)-**31C**	2 040	8	99.6 [b)]	98 [c)]	*R* [c)]	2 032	406
g	(*R*,*R*)-**42A**	2 000	10	100	90	*S*	2 000	54
h	(*S*,*SS*)-**42B**	10 000	8	100	93	*R*	10 000	625
i	(*S*,*S*)-**31D**	10 000	10	99	100	*R*	9 900	619
j	(*S*,*S*)-**31D**	2 000	8	99.9	99	*R*	1 998	285
k	(*S*,*S*)-**31D**	13 000	10	100	99	*R*	13 000	867
l	(*S*,*S*)-**42A**	10 000	8	99	94	*R*	9 900	450

a) SCR = substrate : catalyst molar ratio.
b) A 5 : 1 *E*/*Z* mixture.
c) Data of the *E* alcohol.

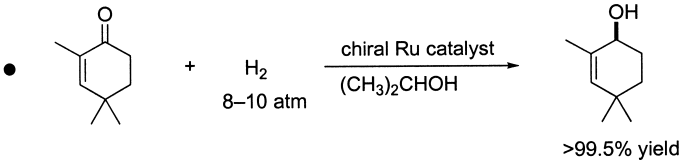

Ru catalyst	S/C	temp, °C	% ee	confign	TON	TOF, h^{-1}
(*R*,*SS*)-**31B**	500	0	96	*S*	500	83
(*R*,*SS*)-**31B**	10,000	28	94	*S*	10,000	208
(*S*,*R*)-**34B**	10,000	25	96	*R*	9,950	1421

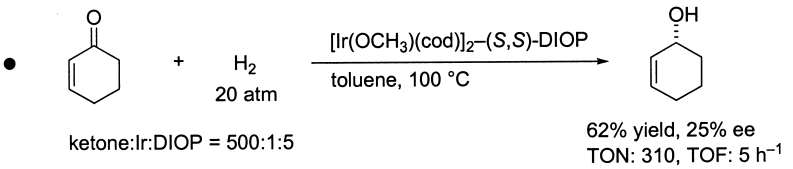

Fig. 32.43 Hydrogenation of 2-cyclohexenones.

Hydrogenation of 2,4,4-trimethyl-2-cyclohexenone, a cyclic enone, with (*R*)-TolBINAP/(*S*,*S*)-DPEN–Ru [(*R*,*SS*)-**31B**] (not (*R*,*RR*)-**31B**) in basic 2-propanol affords the *S* allylic alcohol in 96% ee (Fig. 32.43) [135, 136]. (*R*,*RR*)- or (*S*,*SS*)-**31B** gives lower reactivity and enantioselectivity. The (*S*)-TolBINAP/(*R*)-IPHAN–Ru complex and $(CH_3)_3COK$ [(*S*,*R*)-**34B**] is also an excellent catalyst for hydrogenation of the cyclic enone [111]. The allylic alcohol product is a useful intermediate for the synthesis of carotenoid-derived odorants and other bioactive terpenes. Hydrogenation of 2-cyclohexenone in the presence of the (*S*,*S*)-DIOP–Ir catalyst gives (*R*)-2-cyclohexenol in 25% ee (Fig. 32.43) [137].

Enantioselective hydrogenation of simple ketones catalyzed by BINAP/chiral diamine–Ru complexes is applied to the synthesis of biologically active compounds and a chiral phosphine ligand. Some examples are shown in Figure 32.44 [85 a, 87, 102, 128, 130, 135].

32.3.7
Kinetic Resolution and Dynamic Kinetic Resolution

Hydrogenation of racemic 2-isopropylcyclohexanone with *trans*-RuH(η^1-BH_4)[(*S*)-xylbinap][(*R*,*R*)-dpen] [(*S*,*RR*)-**31G**] in 2-propanol selectively consumes the *R* ketone, resulting in the *S* substrate in 91% ee and (1*R*,2*R*)-2-isopropylcyclohexanol in 85% ee (*cis*:*trans*=100:0) at 53% conversion (Fig. 32.45) [102]. The k_{fast}/k_{slow} reaches 28. Similarly, racemic 2-methoxycyclohexanone is hydrogenated with (*S*,*SS*)-**31G** to give the unreacted *R* ketone in 94% ee and the 1*R*,2*S* alcohol in 91% ee (*cis*:*trans*=100:0) at 53% conversion [102]. The k_{fast}/k_{slow} is 38.

Enantiomers of 2-monosubstituted cycloalkanones equilibrate in base-containing alcoholic media. When one of the two isomers is preferably hydrogenated

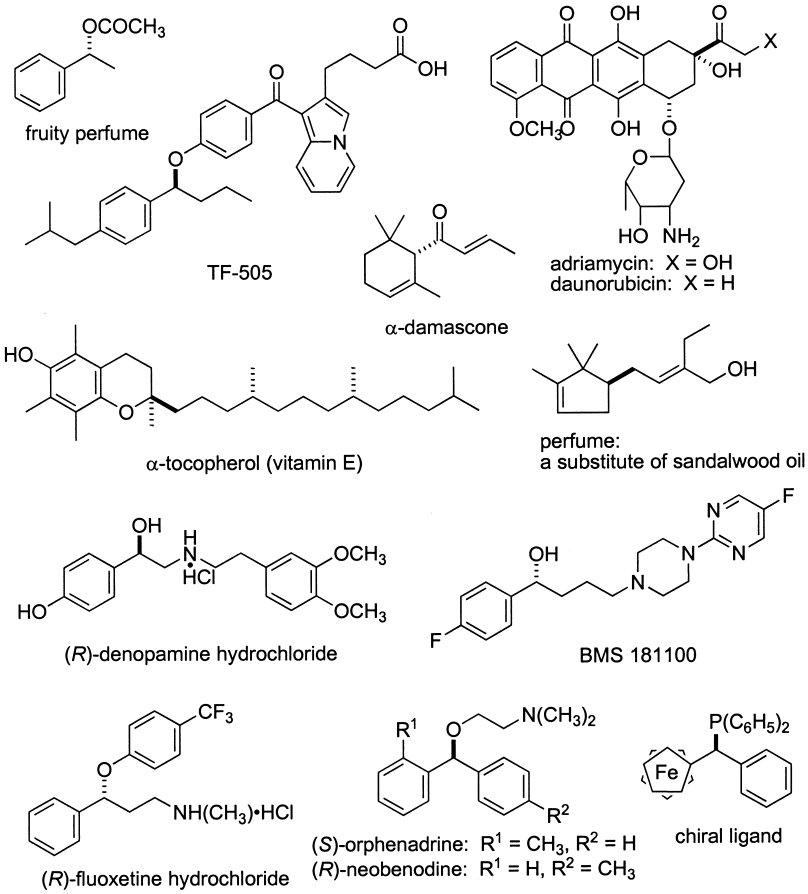

Fig. 32.44 Examples of biologically active compounds and a chiral ligand obtainable through hydrogenation of simple ketones catalyzed by BINAP/chiral diamine–Ru complexes.

over the other one with high diastereoselectivity, single isomeric alcohols among four possible stereoisomers are obtained through dynamic kinetic resolution (see Section 32.2.4). Indeed, hydrogenation of racemic 2-phenylcyclohexanone (**c**) with *trans*-$RuCl_2$[(*R*)-tolbinap][(*R*,*R*)-dpen] and $(CH_3)_3COK$ [(*R*,*RR*)-**31B**] ([$(CH_3)_3COK$] = 18 mM) in 2-propanol gives (1*S*,2*S*)-2-phenylcyclohexanol (*cis*: *trans* = 100 : 0) in 99.6% ee and in 100% yield (Fig. 32.46) [138]. The electronic property of aryl substituents has only a minimal effect on the stereoselectivity. With the same catalyst, 1-naphthyl- and 2-naphthyl-substituted cyclohexanones (**f** and **g**) are selectively converted to the 1*S*,2*S* alcohols. When (*S*)-BINAP/(*R*,*R*)-DPEN–Ru catalyst ([KOH] = 32 mM) is used for hydrogenation of 2-isopropylcyclohexanone (**b**), the 1*R*,2*R* alcohol (*cis*: *trans* = 99.8 : 0.2) with 93% ee is obtained [139]. Reaction of 2-methoxycyclohexanone (**h**) with (*S*)-XylBINAP/(*S*,*S*)-DPEN–Ru cata-

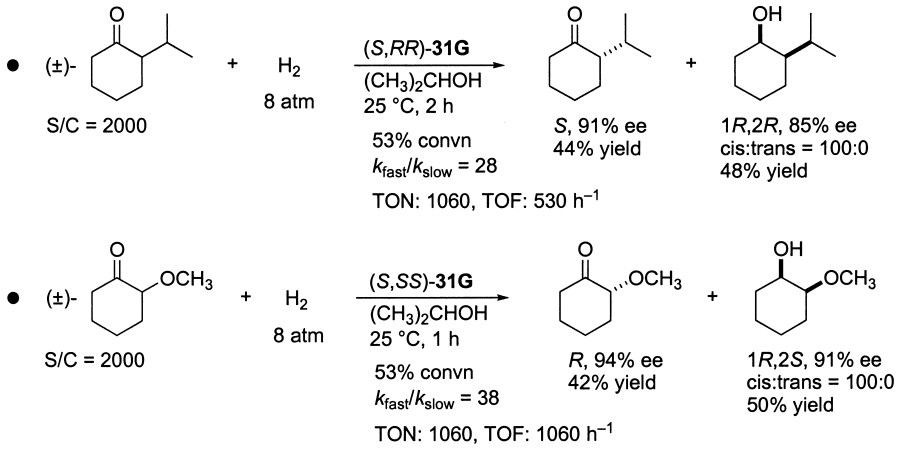

Fig. 32.45 Kinetic resolution of racemic 2-substituted cyclohexanones via hydrogenation with RuH(η^1-BH_4)(xylbinap)(d-pen).

lyst in basic 2-propanol at 5 °C gives the 1*R*,2*S* alcohol in 99% ee (*cis*:*trans*=99.5:0.5) [140]. The chiral alcohol is a key intermediate for the synthesis of the potent antibacterial sanfetrinem and its analogues (Fig. 32.47) [140]. In the presence of (*S*)-XylBINAP/(*R*)-DAIPEN–Ru, 2-(*tert*-butoxycarbonylamino)cyclohexanone (**i**) is also converted to the 1*S*,2*R* amino alcohol in 82% ee (*cis*:*trans*=99:1) (Fig. 32.46) [87]. Hydrogenation of 2-phenylcyclopentanone (**a**), a lower homologue, catalyzed by (*R*)-XylBINAP/(*R*)-DAIPEN–Ru complex and $(CH_3)_3COK$ [(*R*,*R*)-**31D**] ([$(CH_3)_3COK$]=50 mM) affords (1*S*,2*S*)-2-phenylcyclopentanol (*cis*:*trans*=100:0) in 98% ee [138]. Reaction of 2-phenylcycloheptanone (**j**) with the (*R*)-TolBINAP/(*S*,*S*)-DPEN combined catalyst (*R*,*SS*)-**31B** gives (1*S*,2*S*)-2-phenylcycloheptanol (*cis*:*trans*=100:0) in 95% ee [138]. When (*R*,*RR*)-**31B** is used for this reaction, the 1*R*,2*S* alcohol is obtained in only 84% ee (*cis*:*trans*=100:0). The hydrogenation catalyzed by **31B** is applicable to the azacyclohexanone derivatives, **k** and **l** (Fig. 32.46). Reaction of **k** with the *R*,*RR* catalyst gives the 2*S*,3*S* product (*cis*:*trans*=96:4) in 96% ee. This chiral compound can be used for the synthesis of hNK_1 antagonist L-733,060 (Fig. 32.47) [138]. The 3-methoxyphenyl ketone **l** is reduced with the *S*,*SS* catalyst to yield the 3*S*,4*R* alcohol (*cis*:*trans*=>99:1) in 97% ee. This product serves as a synthetic intermediate of (–)-precramol, a D_2/D_3-auto and sigma receptor agonist (Fig. 32.47) [138].

Hydrogenation of racemic 2-phenylpropiophenone, an acyclic chiral ketone, with the (*S*)-XylBINAP/(*S*)-DAIPEN–Ru complex and $(CH_3)_3COK$ [(*S*,*S*)-**31D**] ([$(CH_3)_3COK$]=2 mM) in 2-propanol gives the 1*R*,2*R* alcohol (*syn*:*anti*=99:1) in 96% ee (Fig. 32.48) [85 a].

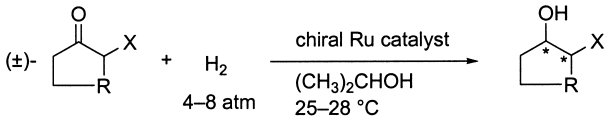

a: R = CH_2; X = C_6H_5
b: R = $(CH_2)_2$; X = $(CH_3)_2CH$
c: R = $(CH_2)_2$; X = C_6H_5
d: R = $(CH_2)_2$; X = 4-$CH_3OC_6H_4$
e: R = $(CH_2)_2$; X = 4-$CF_3C_6H_4$
f: R = $(CH_2)_2$; X = 1-naphthyl
g: R = $(CH_2)_2$; X = 2-naphthyl
h: R = $(CH_2)_2$; X = CH_3O
i: R = $(CH_2)_2$; X = $(CH_3)_3COCONH$
j: R = $(CH_2)_3$; X = C_6H_5
k: R = $CH_2N(CH_2C_6H_5)$; X = C_6H_5
l: R = $N(n\text{-}C_3H_7)CH_2$; X = 3-$CH_3OC_6H_4$

Fig. 32.46 Hydrogenation of racemic 2-substituted cyclohexanones through dynamic kinetic resolution catalyzed by BINAP/chiral diamine–Ru complexes with base.

Ketone [M] a)	Catalyst (SCR) b)	Base [mM]	Yield [%]	dr c)	*cis* alcohol		TON	TOF [h^{-1}]
					ee [%]	Config.		
a (0.5)	(*R*,*R*)-**31D** (2000)	50	100	100:0	98	1*S*,2*S*	2000	21
b (0.8)	$RuCl_2$[(*S*)-binap](dmf)$_n$–(*R*,*R*)-DPEN + KOH (500)	32	100	99.8:0.2	93	1*R*,2*R*	500	45
c (0.5)	(*R*,*RR*)-**31B** (100000)	18	100	100:0	99.6	1*S*,2*S*	100000	2083
d (0.5)	(*R*,*RR*)-**31B** (2000)	5	100	100:0	99.5	1*S*,2*S*	2000	500
e (0.5)	(*R*,*RR*)-**31B** (2000)	6	99.9	99.9:0.1	98	1*S*,2*S*	1998	500
f (0.5)	(*R*,*RR*)-**31B** (2000)	9	>99	98:2	93	1*S*,2*S*	>1980	>124
g (0.5)	(*R*,*RR*)-**31B** (2000)	10	>99	>99:1	>99	1*S*,2*S*	>1980	>495
h (– d))	$[NH_2(C_2H_5)_2][\{RuCl[(S)\text{-xylbinap}]_2(\mu\text{-}Cl)_3\}$–(*S*,*S*)-DPEN + KOH (1000) e)	– d)	>99.9	99.5:0.5	99	1*R*,2*S*	>999	50
i (0.2)	*trans*-$RuCl_2$[(*S*)-xylbinap]-[(*R*)-daipen] + KOH (300)	133	98	99:1	82	1*S*,2*R*	294	59
j (0.5)	(*R*,*SS*)-**31B** (2000)	25	100	100:0	95	1*S*,2*S*	2000	83
k (0.125)	(*R*,*RR*)-**31B** (500)	19	100	96:4	96	2*S*,3*S*	500	25
l (0.125)	(*S*,*SS*)-**31B** (500)	25	100	>99:1	97	3*S*,4*R*	500	21

a) Concentration of substrate.
b) SCR = substrate : catalyst molar ratio.
c) *Cis* : *trans* diastereomeric ratio.
d) Not reported.
e) Under 50 atm H_2 at 5 °C.

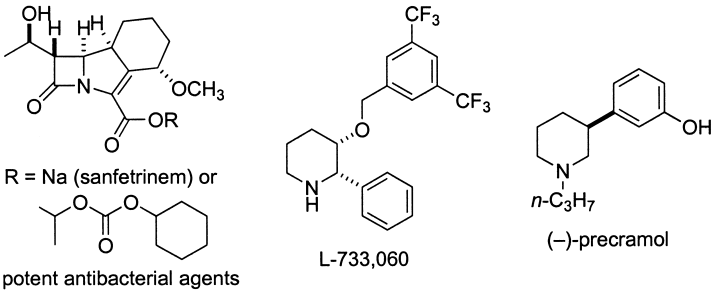

Fig. 32.47 Biologically active compounds achievable by BINAP/1,2-diamine–Ru-catalyzed hydrogenation of 2-substituted cyclohexanones through dynamic kinetic resolution.

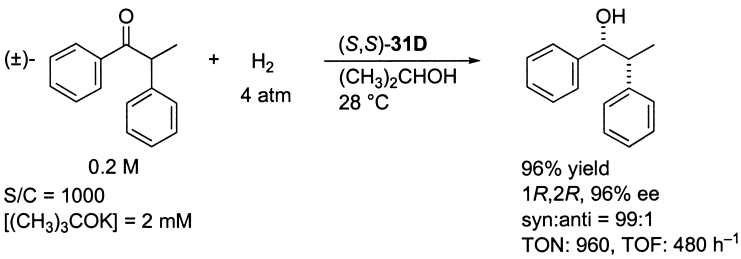

Fig. 32.48 Hydrogenation of racemic 2-phenylpropiophenone through dynamic kinetic resolution.

32.3.8
Enantioselective Activation and Deactivation

Although the hydrogenation of prochiral ketones with racemic catalysts gives racemic alcohols, the reactivity of two enantiomeric catalysts differs in a non-racemic environment. Thus, the addition of an appropriate chiral activator to a racemic metal complex can provide an enantioselective catalyst. A racemic $RuCl_2$(tolbinap)$(dmf)_n$ is a poor catalyst for the hydrogenation of 2,4,4-trimethyl-2-cyclohexenone. The addition of an equimolar amount of (*S*,*S*)-DPEN to the Ru complex promotes the reaction in a 7 : 1 2-propanol : toluene mixture containing KOH to give (*S*)-2,4,4-trimethyl-2-cyclohexenol in 95% ee (Fig. 32.49) [136]. This high ee-value, close to 96%, is obtainable in the hydrogenation catalyzed by an optically pure (*R*)-TolBINAP/(*S*,*S*)-DPEN–Ru complex under otherwise identical conditions [135, 136]. On the other hand, the *R*,*RR* combination gives the *R* alcohol in only 26% ee. The stereoselective outcome depends heavily on the structures of the diphosphine, diamine, and ketonic substrates. The (±)-TolBINAP/(*S*,*S*)-DPEN–Ru-catalyzed hydrogenation of 2′-methylacetophenone, an acyclic aromatic ketone, gives the *R* alcohol in 90% ee (Fig. 32.49) [136].

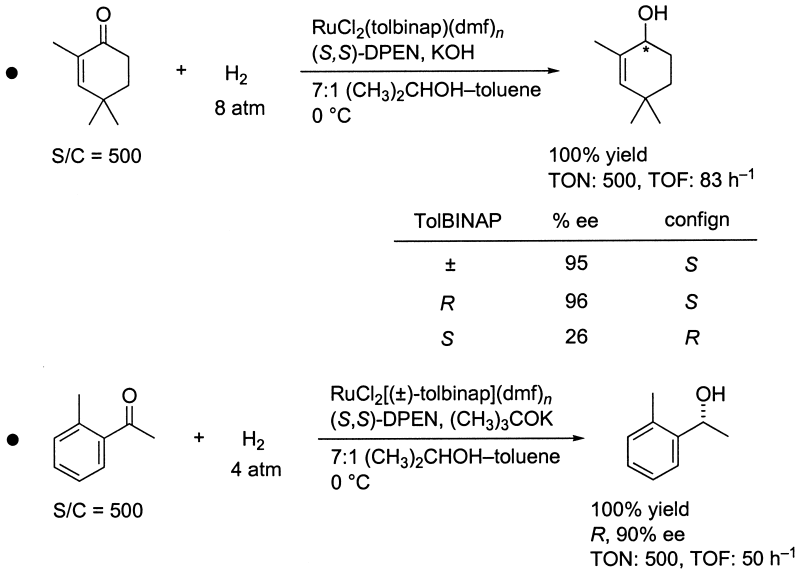

Fig. 32.49 Hydrogenation of ketones catalyzed by racemic BINAP–Ru complexes and (*S*,*S*)-DPEN: asymmetric activation.

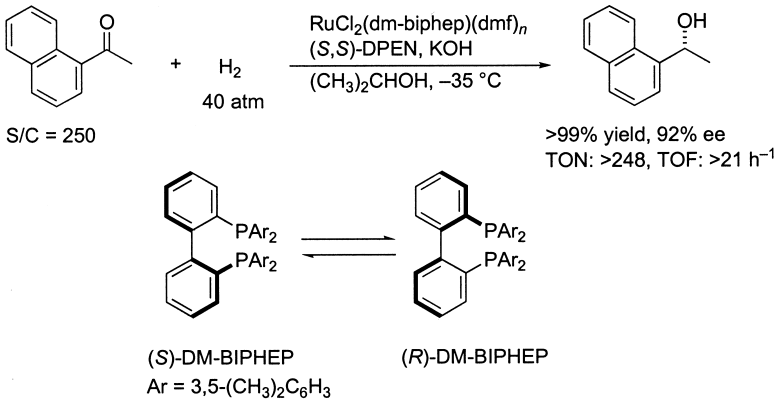

Fig. 32.50 Hydrogenation of 1-acetonaphthone with a DM-BIPHEP/(*S*,*S*)-DPEN–Ru catalyst.

DM-BIPHEP, a conformationally flexible diphosphine, exists as an equilibrium mixture of the *R* and *S* isomers (Fig. 32.50) [141]. Addition of an equimolar amount of (*S*,*S*)-DPEN to $RuCl_2$(dm-biphep)$(dmf)_n$ forms a 3:1 mixture of (*S*)-DM-BIPHEP/(*S*,*S*)-DPEN–$RuCl_2$ complex and the *R*,*SS* diastereoisomer. The major *S*,*SS* complex gives a more active and enantioselective catalyst for the hydro-

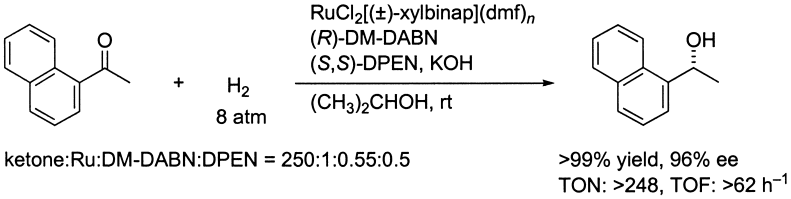

Fig. 32.51 Hydrogenation of 1-acetonaphthone with a (±)-Xyl-BINAP/(*R*)-DM-DABN/(*S*,*S*)-DPEN–Ru catalyst.

genation of acyclic aromatic ketones. Hydrogenation of 1-acetonaphthone with the DM-BIPHEP/(S,S)-DPEN–Ru complex and KOH in 2-propanol at –35 °C gives the *R* alcohol in 92% ee.

(*R*)-DM-DABN, a chiral aromatic diamine, interacts preferentially with $RuCl_2$[(*R*)-xylbinap](dmf)$_n$ over the *S* isomer affording the less-reactive $RuCl_2$[(*R*)-xylbinap][(*R*)-dm-dabn] for hydrogenation of aromatic ketones [142]. Combined use of the enantiomer-selective deactivation and the asymmetric activation described above (see Fig. 32.49) results in a highly enantioselective hydrogenation of aromatic ketones using a racemic XylBINAP–$RuCl_2$ complex. 1′-Acetonaphthone is hydrogenated with a catalyst consisting of $RuCl_2$[(±)-xylbinap](dmf)$_n$, (*R*)-DM-DABN, (*S*,*S*)-DPEN, and KOH in a 1 : 0.55 : 0.5 : 2 ratio to give the *R* alcohol in 96% ee.

Abbreviations

ee enantiomeric excess
TOF turnover frequency
TON turnover number

References

1 R. Noyori, *Asymmetric Catalysis in Organic Synthesis*, Wiley, New York, **1994**, Chapter 2.

2 (a) R. Noyori, *Angew. Chem. Int. Ed.* **2002**, *41*, 2008; (b) R. Noyori, *Adv. Synth. Catal.* **2003**, *345*, 15; (c) R. Noyori, M. Kitamura, T. Ohkuma, *Proc. Natl. Acad. Sci. USA* **2004**, *101*, 5356.

3 Reviews: (a) R. Noyori, M. Kitamura, in: *Modern Synthetic Methods* (Ed. R. Scheffold), Springer, Berlin, **1989**, Vol. 5, p. 115; (b) H. Takaya, T. Ohta, R. Noyori, in: *Catalytic Asymmetric Synthesis* (Ed. I. Ojima), VCH, New York, **1993**, Chapter 1; (c) I. Ojima, M. Eguchi, M. Tzamarioudaki, in: *Comprehensive Organometallic Chemistry II* (Eds. E.W. Abel, F.G.A. Stone, G. Wilkinson), Pergamon, Oxford, **1995**, Vol. 12, Chapter 2; (d) H. Brunner, *Methods of Organic Chemistry* (Houben-Weyl) 4th edn. **1995**, Vol. E21d, Chapter 2.3.1; (e) J.P. Genêt, in: *Reductions in Organic Synthesis* (Ed. A.F. Abdel-Magid), American Chemical Society, Washington, DC, **1996**, Chapter 2; (f) D.J. Ager, S.A. Laneman, *Tetrahedron: Asymmetry* **1997**, *8*, 3327.

4 Recent reviews: (a) T. Ohkuma, R. Noyori, in: *Transition Metals for Organic Synthesis* (Eds. M. Beller, C. Bolm), Wiley-VCH, Weinheim, **1998**, Vol. 2, p. 25; (b) T. Ohkuma, R. Noyori, in: *Comprehensive Asymmetric Catalysis* (Eds. E. N. Jacobsen, A. Pfaltz, H. Yamamoto), Springer, Berlin, **1999**, Vol. 1, Chapter 6.1; (c) T. Ohkuma, M. Kitamura, R. Noyori, in: *Catalytic Asymmetric Synthesis*, 2nd ed. (Ed. I. Ojima), Wiley-VCH, New York, **2000**, Chapter 1; (d) H.-U. Blaser, C. Malan, B. Pugin, F. Spindler, H. Steiner, M. Studer, *Adv. Synth. Catal.* **2003**, *345*, 103; (e) T. Ohkuma, R. Noyori, in: *Comprehensive Asymmetric Catalysis Supplement 1* (Eds. E. N. Jacobsen, A. Pfaltz, H. Yamamoto), Springer, Berlin Heidelberg, **2004**, Chapter 6.1.

5 Reviews on Ru-catalyzed hydrogenation: (a) T. Naota, H. Takaya, S. Murahashi, *Chem. Rev.* **1998**, *98*, 2599; (b) M. Kitamura, R. Noyori, in: *Ruthenium in Organic Synthesis* (Ed. S. Murahashi), Wiley-VCH, New York, **2004**, Chapter 2.

6 General reviews on chiral ligands: (a) H. B. Kagan, in: *Asymmetric Synthesis* (Ed. J. D. Morrison), Academic Press, Orlando, **1985**, Vol. 5, Chapter 1; (b) H. Brunner, *Topics in Stereochemistry* **1988**, *18*, 129; (c) H.-U. Blaser, *Chem. Rev.* **1992**, *92*, 935; (d) H. Brunner, W. Zettlmeier, *Handbook of Enantioselective Catalysis*, VCH, Weinheim, **1993**; (e) J. Seyden-Penne, *Chiral Auxiliaries and Ligands in Asymmetric Synthesis*, Wiley, New York, **1995**.

7 Reviews on chiral diphosphine ligands: (a) K. V. L. Crépy, T. Imamoto, *Adv. Synth. Catal.* **2003**, *345*, 79; (b) T. T.-L. Au-Yeung, S.-S. Chan, A. S. C. Chan, *Adv. Synth. Catal.* **2003**, *345*, 537; (c) W. Tang, X. Zhang, *Chem. Rev.* **2003**, *103*, 3029.

8 Reviews on ferrocenyl ligands: (a) L. Schwink, P. Knochel, *Chem. Eur. J.* **1998**, *4*, 950; (b) C. J. Richards, A. J. Locke, *Tetrahedron: Asymmetry* **1998**, *9*, 2377; (c) P. Barbaro, C. Bianchini, G. Giambastiani, S. L. Parisel, *Coord. Chem. Rev.* **2004**, *248*, 2131.

9 (a) Y. Izumi, *Adv. Catal.* **1983**, *32*, 215; (b) A. Tai, T. Harada, in: *Tailored Metal Catalysts* (Ed. Y. Iwasawa), Reidel, Dordrecht, **1986**, pp. 265; (c) T. Osawa, T. Harada, A. Tai, *J. Catal.* **1990**, *121*, 7; (d) A. Tai, T. Kikukawa, T. Sugimura, Y. Inoue, S. Abe, T. Osawa, T. Harada, *Bull. Chem. Soc. Jpn.* **1994**, *67*, 2473; (e) T. Sugimura, T. Osawa, S. Nakagawa, T. Harada, A. Tai, *Stud. Surf. Sci. Catal.* **1996**, *101*, 231; (f) A. Tai, T. Sugimura, in: *Chiral Catalyst Immobilization and Recycling* (Eds. D. E. De Vos, I. F. J. Vankelecom, P. A. Jacobs), Wiley-VCH, Weinheim, **2000**, Chapter 8; (g) T. Sugimura, S. Nakagawa, A. Tai, *Bull. Chem. Soc. Jpn.* **2002**, *75*, 355.

10 Other nitrogen- or sulfur-based ligands: (a) D. Lucet, T. Le Gall, C. Mioskowski, *Angew. Chem. Int. Ed.* **1998**, *37*, 2580; (b) G. Chelucci, R. P. Thummel, *Chem. Rev.* **2002**, *102*, 3129; (c) F. Agbossou-Niedercorn, I. Suisse, *Coord. Chem. Rev.* **2003**, *242*, 145; (d) A. M. Masdeu-Bultó, M. Diéguez, E. Martin, M. Gómez, *Coord. Chem. Rev.* **2003**, *242*, 159; (e) G. Chelucci, G. Orrú, G. A. Pinna, *Tetrahedron* **2003**, *59*, 9471.

11 Supported ligands on solid or polymer: (a) D. J. Bayston, M. E. C. Polywka, in: *Chiral Catalyst Immobilization and Recycling* (Eds. D. E. De Vos, I. F. J. Vankelecom, P. A. Jacobs), Wiley-VCH, Weinheim, **2000**, Chapter 9; (b) C. Saluzzo, M. Lemaire, *Adv. Synth. Catal.* **2002**, *344*, 915.

12 R. Noyori, T. Ohkuma, M. Kitamura, H. Takaya, N. Sayo, H. Kumobayashi, S. Akutagawa, *J. Am. Chem. Soc.* **1987**, *109*, 5856.

13 (a) M. Kitamura, M. Tokunaga, T. Ohkuma, R. Noyori, *Tetrahedron Lett.* **1991**, *32*, 4163; (b) M. Kitamura, M. Tokunaga, T. Ohkuma, R. Noyori, *Org. Synth.* **1993**, *71*, 1.

14 (a) T. Ikariya, Y. Ishii, H. Kawano, T. Arai, M. Saburi, S. Yoshikawa, S. Akutagawa, *J. Chem. Soc. Chem. Commun.* **1985**, 922; (b) D. F. Taber, L. J. Silverberg, *Tetrahedron Lett.* **1991**, *32*, 4227; (c) B. Heiser, E. A. Broger, Y. Crameri, *Tetrahedron: Asymmetry* **1991**, *2*, 51; (d) S. A. King, A. S. Thompson, A. O. King, T. R. Verhoeven, *J. Org. Chem.* **1992**, *57*, 6689; (e) J. B. Hoke, L. S. Hollis, E. W. Stern, *J. Organomet. Chem.*

1993, *455*, 193; (f) J.P. Genêt, V. Ratovelomanana-Vidal, M.C. Cano de Andrade, X. Pfister, P. Guerreiro, J.Y. Lenoir, *Tetrahedron Lett.* **1995**, *36*, 4801; (g) H. Doucet, P.L. Gendre, C. Bruneau, P.H. Dixneuf, J.-C. Souvie, *Tetrahedron: Asymmetry* **1996**, *7*, 525; (h) S.A. King, L. DiMichele, in: *Catalysis of Organic Reactions* (Eds. M.G. Scaros, M.L. Prunier), Dekker, New York, **1995**, p. 157; (i) T. Ohta, Y. Tonomura, K. Nozaki, H. Takaya, K. Mashima, *Organometallics* **1996**, *15*, 1521; (j) L. Shao, K. Takeuchi, M. Ikemoto, T. Kawai, M. Ogasawara, H. Takeuchi, H. Kawano, M. Saburi, *J. Organomet. Chem.* **1992**, *435*, 133; (k) K. Mashima, T. Hino, H. Takaya, *J. Chem. Soc. Dalton Trans.* **1992**, 2099; (l) D.D. Pathak, H. Adams, N.A. Bailey, P.J. King, C. White, *J. Organomet. Chem.* **1994**, *479*, 237; (m) J.P. Genêt, C. Pinel, V. Ratovelomanana-Vidal, S. Mallart, X. Pfister, L. Bischoff, M.C. Cano de Andrade, S. Darses, C. Galopin, J.A. Laffitte, *Tetrahedron: Asymmetry* **1994**, *5*, 675; (n) K. Mashima, K. Kusano, N. Sato, Y. Matsumura, K. Nozaki, H. Kumobayashi, N. Sayo, Y. Hori, T. Ishizaki, S. Akutagawa, H. Takaya, *J. Org. Chem.* **1994**, *59*, 3064; (o) P. Guerreiro, M.-C. Cano de Andrade, J.-C. Henry, J.-P. Tranchier, P. Phansavath, V. Ratovelamanana-Vidal, J.-P. Genêt, T. Homri, A.R. Touati, B.B. Hassine, *C.R. Acad. Paris* **1999**, 175; (p) O.M. Akotsi, K. Metera, R.D. Reid, R. Mcdonald, S.H. Bergens, *Chirality* **2000**, *12*, 514; (q) V. Ratovelomanana-Vidal, C. Girard, R. Touai, J.P. Tranchier, B.B. Hassine, J.P. Genêt. *Adv. Synth. Catal.* **2003**, *345*, 261.

15 M. Kitamura, M. Yoshimura, N. Kanda, R. Noyori, *Tetrahedron* **1999**, *55*, 8769.

16 (a) K. Mikami, Y. Yusa, T. Korenaga, *Org. Lett.* **2002**, *4*, 1643; (b) K. Mikami, T. Korenaga, Y. Yusa, M. Yamanaka, *Adv. Synth. Catal.* **2003**, *345*, 246.

17 M. Murata, T. Morimoto, K. Achiwa, *Synlett* **1991**, 827.

18 J. Madec, X. Pfister, P. Phansavath, V. Ratovelomanana-Vidal, J.-P. Genêt, *Tetrahedron* **2001**, *57*, 2563.

19 Z. Zhang, H. Qian, J. Longmire, X. Zhang, *J. Org. Chem.* **2000**, *65*, 6223.

20 A.E. Sollewjin Gelpke, H. Kooijman, A.L. Spek, H. Hiemstra, *Chem. Eur. J.* **1999**, *5*, 2472.

21 C.-C. Pai, Y.-M. Li, Z.-Y. Zhou, A.S.C. Chan, *Tetrahedron Lett.* **2002**, *43*, 2789.

22 C.-C. Pai, C.-W. Lin, C.-C. Lin, C.-C. Chen, A.S.C. Chan, W.T. Wong, *J. Am. Chem. Soc.* **2000**, *122*, 11513.

23 T. Benincori, E. Brenna, F. Sannicolò, L. Trimarco, P. Antognazza, E. Cesarotti, F. Demartin, T. Pilati, *J. Org. Chem.* **1996**, *61*, 6244.

24 V. Enev, C.L.J. Ewers, M. Harre, K. Nickisch, J.T. Mohr, *J. Org. Chem.* **1997**, *62*, 7092.

25 L. Qiu, J. Qi, C.-C. Pai, S. Chan, Z. Zhou, M.C.K. Choi, A.S.C. Chan, *Org. Lett.* **2002**, *4*, 4599.

26 T. Lamouille, C. Saluzzo, R. ter Halle, F. Le Guyader, M. Lemaire, *Tetrahedron Lett.* **2001**, *42*, 663.

27 T. Dwars, G. Oehme, *Adv. Synth. Catal.* **2002**, *344*, 239.

28 M.J. Burk, T.G.P. Harper, C.S. Kalberg, *J. Am. Chem. Soc.* **1995**, *117*, 4423.

29 T. Yamano, N. Taya, M. Kawada, T. Huang, T. Imamoto, *Tetrahedron Lett.* **1999**, *40*, 2577.

30 P.J. Pye, K. Rossen, R.A. Reamer, R.P. Volante, P.J. Reider, *Tetrahedron Lett.* **1998**, *39*, 4441.

31 K. Junge, B. Hagemann, S. Enthaler, G. Oehme, M. Michalik, A. Monsees, T. Riermeier, U. Dingerdissen, M. Beller, *Angew. Chem. Int. Ed.* **2004**, *43*, 5066.

32 T. Ireland, K. Tappe, G. Grossheimann, P. Knochel, *Chem. Eur. J.* **2002**, *8*, 843.

33 T. Sturm, W. Weissensteiner, F. Spindler, *Adv. Synth. Catal.* **2003**, *345*, 160.

34 A. Togni, C. Breutel, A. Schnyder, F. Spindler, H. Landert, A. Tijani, *J. Am. Chem. Soc.* **1994**, *116*, 4062.

35 Y.-G. Zhou, W. Tang, W.-B. Wang, W. Li, X. Zhang, *J. Am. Chem. Soc.* **2002**, *124*, 4952.

36 R. ter Halle, B. Colasson, E. Schulz, M. Spagnol, M. Lemaire, *Tetrahedron Lett.* **2000**, *41*, 643.

37 P. Guerreiro, V. Ratovelomanana-Vidal, J.-P. Genêt, P. Dellis, *Tetrahedron Lett.* **2001**, *42*, 3423.

38 D.J. Bayston, J.L. Fraser, M.R. Ashton, A.D. Baxter, M.E.C. Polywka, E. Moses, *J. Org. Chem.* **1998**, *63*, 3137.

39 (a) D. Tas, C. Thoelen, I.F.J. Vankelecom, P.A. Jacobs, *Chem. Commun.* **1997**, 2323; (b) I. Vankelecom, A. Wolfson, S. Geresh, M. Landau, M. Gottlieb, M. Hershkovitz, *Chem. Commun.* **1999**, 2407.

40 M. Kitamura, T. Ohkuma, S. Inoue, N. Sayo, H. Kumobayashi, S. Akutagawa, T. Ohta, H. Takaya, R. Noyori, *J. Am. Chem. Soc.* **1988**, *110*, 629.

41 P.L. Gendre, M. Offenbecher, C. Bruneau, P.H. Dixneuf, *Tetrahedron: Asymmetry* **1998**, *9*, 2279.

42 T. Saito, T. Yokozawa, T. Ishizaki, T. Moroi, N. Sayo, T. Miura, H. Kumobayashi, *Adv. Synth. Catal.* **2001**, *343*, 264.

43 J. Wu, H. Chen, Z.-Y. Zhou, C.H. Yeung, A.S.C. Chan, *Synlett* **2001**, 1050.

44 M. Lotz, K. Polborn, P. Knochel, *Angew. Chem. Int. Ed.* **2002**, *41*, 4708.

45 H.-L. Huang, L.T. Liu, S.-F. Chen, H. Ku, *Tetrahedron: Asymmetry* **1998**, *9*, 1637.

46 D. Blanc, V. Ratovelomanana-Vidal, J.-P. Gillet, J.-P. Genêt, *J. Organomet. Chem.* **2000**, *603*, 128.

47 Y. Kuroi, D. Asada, K. Iseki, *Tetrahedron Lett.* **2000**, *41*, 9853.

48 (a) S.L. Schreiber, S.E. Kelly, J.A. Porco, Jr., T. Sammakia, E.M. Suh, *J. Am. Chem. Soc.* **1988**, *110*, 6210; (b) M. Nakatsuka, J.A. Ragan, T. Sammakia, D.B. Smith, D.E. Uehling, S.L. Schreiber, *J. Am. Chem. Soc.* **1990**, *112*, 5583; (c) S.C. Case-Green, S.G. Davies, C.J.R. Hedgecock, *Synlett* **1991**, 781; (d) D.F. Taber, L.J. Silverberg, E.D. Robinson, *J. Am. Chem. Soc.* **1991**, *113*, 6639; (e) J.E. Boldwin, R.M. Adlington, S.H. Ramcharitar, *Synlett* **1992**, 875; (f) D.F. Taber, P.B. Deker, L.J. Silverberg, *J. Org. Chem.* **1992**, *57*, 5990; (g) K. Nozaki, N. Sato, H. Takaya, *Tetrahedron: Asymmetry* **1993**, *4*, 2179; (h) S.D. Rychnovsky, R.C. Hoye, *J. Am. Chem. Soc.* **1994**, *116*, 1753; (i) D.M. Garcia, H. Yamada, S. Hatakeyama, M. Nishizawa, *Tetrahedron Lett.* **1994**, *35*, 3325; (j) D.F. Taber, K.K. You, *J. Am. Chem. Soc.* **1995**, *117*, 5757; (k) D.S. Keegan, S.R. Hagen, D.A. Johnson, *Tetrahedron: Asymmetry* **1996**, *7*, 3559; (l) C. Spino, N. Mayes, H. Desfossés, *Tetrahedron Lett.* **1996**, *37*, 6503; (m) A. Balog, C. Harris, K. Savin, X.-G. Zhang, T.C. Chou, S.J. Danishefsky, *Angew. Chem. Int. Ed.* **1998**, *37*, 2675; (n) N. Irako, T. Shioiri, *Tetrahedron Lett.* **1998**, *39*, 5793; (o) J.E. Boldwin, A. Melman, V. Lee, C.R. Firkin, R.C. Whitehead, *J. Am. Chem. Soc.* **1998**, *120*, 8559; (p) H. Lebel, E.N. Jacobsen, *J. Org. Chem.* **1998**, *63*, 9624; (q) D. Romo, R.M. Rzasa, H.A. Shea, K. Park, J.M. Langenhan, L. Sun, A. Akhiezer, J.O. Liu, *J. Am. Chem. Soc.* **1998**, *120*, 12237; (r) T.T. Upadhya, M.D. Nikalje, A. Sudalai, *Tetrahedron Lett.* **2001**, *42*, 4891; (s) A. Fürstner, T. Dierkes, O.R. Thiel, G. Blanda, *Chem. Eur. J.* **2001**, *7*, 5286.

49 M. Kitamura, T. Ohkuma, H. Takaya, R. Noyori, *Tetrahedron Lett.* **1988**, *29*, 1555.

50 H. Takeda, S. Hosokawa, M. Aburatani, K. Achiwa, *Synlett* **1991**, 193.

51 (a) S.D. Rychnovsky, R.C. Hoye, *J. Am. Chem. Soc.* **1994**, *116*, 1753; (b) B.M. Trost, P.R. Hanson, *Tetrahedron Lett.* **1994**, *35*, 8119; (c) G. Beck, H. Jendralla, K. Kesseler, *Synthesis* **1995**, 1014.

52 T. Nishi, M. Kitamura, T. Ohkuma, R. Noyori, *Tetrahedron Lett.* **1988**, *29*, 6327.

53 T. Doi, M. Kokubo, K. Yamamoto, T. Takahashi, *J. Org. Chem.* **1998**, *63*, 428.

54 K. Tohdo, Y. Hamada, T. Shioiri, *Synlett* **1994**, 105.

55 (a) Y.I. Petrov, E.I. Klabunovskii, A.A. Balandin, *Kinet. Katal.* **1967**, *8*, 814; (b) Y. Nitta, T. Utsumi, T. Imanaka, S. Teranishi, *J. Catal.* **1986**, *101*, 376; (c) L. Fu, H.H. Kung, W.M.H. Sachtler, *J. Mol. Catal.* **1987**, *42*, 29; (d) G. Wittmann, G.B. Bartók, M. Bartók, G.V. Smith, *J. Mol. Catal.* **1990**, *60*, 1; (e) H. Brunner, M. Muschiol, T. Wischert, *Tetrahedron: Asymmetry* **1990**, *3*, 159; (f) G. Webb, P.B. Wells, *Catal. Today* **1992**, *12*, 319; (g) G. Webb, in: *Chiral Reactions in Heterogeneous Catalysis* (Eds. G. Jannes, V. Dubois), Plenum, New York, **1995**, p. 61.

56 Reviews: (a) H.-U. Blaser, M. Müller, in: *Heterogeneous Catalysis and Fine Chemicals II* (Eds. M. Guisnet, et al.), Elsevier,

Amsterdam, **1991**, p. 73; (b) H.-U. Blaser, B. Pugin, in: *Chiral Reactions in Heterogeneous Catalysis* (Eds. G. Jannes, V. Dubois), Plenum, New York, **1995**, p. 33.

57 (a) H. Schildknecht, K. Koob, *Angew. Chem.* **1971**, *83*, 110; (b) T. Shiba, S. Kusumoto, *J. Synth. Org. Chem. Jpn.* **1988**, *46*, 501; (c) M. Yoshikawa, T. Sugimura, A. Tai, *Agric. Biol. Chem.* **1989**, *53*, 37; (d) A. Tai, N. Morimoto, M. Yoshikawa, K. Uehara, T. Sugimura, T. Kikukawa, *Agric. Biol. Chem.* **1990**, *54*, 1753; (e) T. Kikukawa, A. Tai, *Shokubai*, **1992**, *34*, 182.

58 R. Schmid, M. Scalone, in: *Comprehensive Asymmetric Catalysis* (Eds. E. N. Jacobsen, A. Pfaltz, H. Yamamoto), Springer, Berlin, **1999**, Vol. 3, Chapter 41.2.

59 H. Kawano, Y. Ishii, M. Saburi, Y. Uchida, *J. Chem. Soc. Chem. Commun.* **1988**, 87.

60 A. Mezzetti, A. Tschumper, G. Consiglio, *J. Chem. Soc. Dalton Trans.* **1995**, 49.

61 H. Brunner, A. Terfort, *Tetrahedron: Asymmetry* **1995**, *6*, 919.

62 L. Shao, H. Kawano, M. Saburi, Y. Uchida, *Tetrahedron* **1993**, *49*, 1997.

63 V. Blandin, J.-F. Carpentier, A. Mortreux, *Tetrahedron: Asymmetry* **1998**, *9*, 2765.

64 D. Pini, A. Mandoli, A. Iuliano, P. Salvadori, *Tetrahedron: Asymmetry* **1995**, *6*, 1031.

65 S. D. Rychnovsky, G. Griesgraber, S. Zeller, D. J. Skalitzky, *J. Org. Chem.* **1991**, *56*, 5161.

66 (a) C. S. Poss, S. D. Rychnovsky, S. L. Schreiber, *J. Am. Chem. Soc.* **1993**, *115*, 3360; (b) S. D. Rychnovsky, U. R. Khire, G. Yang, *J. Am. Chem. Soc.* **1997**, *119*, 2058; (c) S. D. Rychnovsky, G. Yang, Y. Hu, U. R. Khire, *J. Org. Chem.* **1997**, *62*, 3022.

67 (a) A. Tai, T. Kikukawa, T. Sugimura, Y. Inoue, T. Osawa, S. Fujii, *J. Chem. Soc. Chem. Commun.* **1991**, 795; (b) H. Brunner, K. Amberger, J. Wiehl, *Bull. Soc. Chim. Belg.* **1991**, *100*, 571.

68 (a) T. Sugimura, T. Futagawa, A. Tai, *Chem. Lett.* **1990**, 2295; (b) T. Sugimura, A. Tai, K. Koguro, *Tetrahedron* **1994**, *50*, 11647.

69 (a) M. Kitamura, M. Tokunaga, R. Noyori, *J. Am. Chem. Soc.* **1995**, *117*, 2931; (b) I. Gautier, V. Ratovelomanana-Vidal, P. Savignac, J.-P. Genêt, *Tetrahedron Lett.* **1996**, *37*, 7721.

70 D. Blanc, J.-C. Henry, V. Ratovelomanana-Vidal, J.-P. Genêt, *Tetrahedron Lett.* **1997**, *38*, 6603.

71 P. Bertus, P. Phansavath, V. Ratovelomanana-Vidal, J.-P. Genêt, A. R. Touati, T. Homri, B. B. Hassine, *Tetrahedron: Asymmetry* **1999**, *10*, 1369.

72 S. D. De Paule, L. Piombo, V. Ratovelomanana-Vidal, C. Greck, J.-P. Genêt, *Eur. J. Org. Chem.* **2000**, 1535.

73 Y. Hiraki, K. Ito, T. Harada, A. Tai, *Chem. Lett.* **1981**, 131.

74 (a) R. Noyori, T. Ikeda, T. Ohkuma, M. Widhalm, M. Kitamura, H. Takaya, S. Akutagawa, N. Sayo, T. Saito, T. Taketomi, H. Kumobayashi, *J. Am. Chem. Soc.* **1989**, *111*, 9134; (b) M. Kitamura, T. Ohkuma, M. Tokunaga, R. Noyori, *Tetrahedron: Asymmetry* **1990**, *1*, 1.

75 J.-P. Genêt, X. Pfister, V. Ratovelomanana-Vidal, C. Pinel, J.-A. Laffitte, *Tetrahedron Lett.* **1994**, *35*, 4559.

76 (a) M. Kitamura, M. Tokunaga, R. Noyori, *J. Am. Chem. Soc.* **1993**, *115*, 144; (b) M. Kitamura, M. Tokunaga, R. Noyori, *Tetrahedron* **1993**, *49*, 1853; (c) R. Noyori, M. Tokunaga, M. Kitamura, *Bull. Chem. Soc. Jpn.* **1995**, *68*, 36.

77 (a) J.-P. Genêt, C. Pinel, S. Mallart, S. Juge, S. Thorimbert, J.-A. Laffitte, *Tetrahedron: Asymmetry* **1991**, *2*, 555; (b) J.-P. Genêt, M. C. Cano de Andrade, V. Ratovelomanana-Vidal, *Tetrahedron Lett.* **1995**, *36*, 2063.

78 (a) C. Mordant, P. Dünkelmann, V. Ratovelomanana-Vidal, J.-P. Genêt, *Chem. Commun.* **2004**, 1296; (b) C. Mordant, P. Dünkelmann, V. Ratovelomanana-Vidal, J.-P. Genêt, *Eur. J. Org. Chem.* **2004**, 3017.

79 K. Makino, T. Goto, Y. Hiroki, Y. Hamada, *Angew. Chem. Int. Ed.* **2004**, *43*, 882.

80 K. Makino, Y. Hiroki, Y. Hamada, *J. Am. Chem. Soc.* **2005**, *127*, 5784.

81 A. Lei, S. Wu, M. He, X. Zhang, *J. Am. Chem. Soc.* **2004**, *126*, 1626.

82 M. Kitamura, M. Tokunaga, T. Pham, W.D. Lubell, R. Noyori, *Tetrahedron Lett.* **1995**, *36*, 5769.

83 (a) N. Fukuda, K. Mashima, Y. Matsumura, H. Takaya, *Tetrahedron Lett.* **1990**, *31*, 7185; (b) K. Inoguchi, K. Achiwa, *Synlett* **1991**, 49; (c) U. Schmidt, V. Leitenberger, H. Griesser, J. Schmidt, R. Meyer, *Synthesis* **1992**, 1248; (d) S. Akutagawa, in: *Chirality in Industry* (Eds. A.N. Collins, G.N. Sheldrake, J. Crosby), Wiley, Chichester, **1992**, Chapter 17; (e) P.M. Wovkulich, K. Shankaran, J. Kiegiel, M.R. Uskokovic, *J. Org. Chem.* **1993**, *58*, 832; (f) C.H. Heathcock, J.C. Kath, R.B. Ruggeri, *J. Org. Chem.* **1995**, *60*, 1120; (g) H. Ohtake, S. Yonishi, H, Tsutsumi, M. Murata, *Abstracts of Papers, 69th National Meeting of the Chemical Society of Japan*, Kyoto, Chemical Society of Japan, Tokyo, **1995**, p. 1030, 1H107; (h) J.-P. Genêt, M.C. Caño de Andrade, V. Ratovelomanana-Vidal, *Tetrahedron Lett.* **1995**, *36*, 2063; (i) M. Nishizawa, D.M. García, R. Minagawa, Y. Noguchi, H. Imagawa, H. Yamada, R. Watanabe, Y.C. Yoo, I. Azuma, *Synlett* **1996**, 452; (j) D.F. Taber, Y. Wang, *J. Am. Chem. Soc.* **1997**, *119*, 22; (k) E. Coulon, M. Cristina, Caño de Andrade, V. Ratovelomanana-Vidal, J.-P. Genêt, *Tetrahedron Lett.* **1998**, *39*, 6467; (l) K. Makino, N. Okamoto, O. Hara, Y. Hamada, *Tetrahedron: Asymmetry* **2001**, *12*, 1757.

84 R. Noyori, S. Hashiguchi, T. Yamano, in: *Applied Homogeneous Catalysis with Organometallic Compounds*, 2nd ed. (Eds. B. Cornils, W.A. Herrmann), Wiley-VCH, Weinheim, **2002**, Vol. 1, Chapter 2.9.

85 (a) R. Noyori, T. Ohkuma, *Angew. Chem. Int. Ed.* **2001**, *40*, 40; (b) R. Noyori, M. Koizumi, D. Ishii, T. Ohkuma, *Pure Appl. Chem.* **2001**, *73*, 227; (c) R. Noyori, *Angew. Chem. Int. Ed.* **2002**, *41*, 2008; (d) R. Noyori, *Adv. Synth. Catal.* **2003**, *345*, 15; (e) R. Noyori, T. Ohkuma, *Pure Appl. Chem.* **1999**, *71*, 1493.

86 (a) H. Doucet, T. Ohkuma, K. Murata, T. Yokozawa, M. Kozawa, E. Katayama, A.F. England, T. Ikariya, R. Noyori, *Angew. Chem. Int. Ed.* **1998**, *37*, 1703; (b) T. Ohkuma, H. Ooka, S. Hashiguchi, T. Ikariya, R. Noyori, *J. Am. Chem. Soc.* **1995**, *117*, 2675.

87 T. Ohkuma, M. Koizumi, H. Doucet, T. Pham, M. Kozawa, K. Murata, E. Katayama, T. Yokozawa, T. Ikariya, R. Noyori, *J. Am. Chem. Soc.* **1998**, *120*, 13529.

88 K. Abdur-Rashid, A.J. Lough, R.H. Morris, *Organometallics* **2001**, *20*, 1047.

89 J.P. Henschke, M.J. Burk, C.G. Malan, D. Herzberg, J.A. Peterson, A.J. Wildsmith, C.J. Cobley, G. Casy, *Adv. Synth. Catal.* **2003**, *345*, 300.

90 J. Wu, H. Chen, W. Kwok, R. Guo, Z. Zhou, C. Yeung, A.S.C. Chan, *J. Org. Chem.* **2002**, *67*, 7908.

91 A. Hu, H.L. Ngo, W. Lin, *Org. Lett.* **2004**, *6*, 2937.

92 M.J. Burk, W. Hems, D. Herzberg, C. Malan, A. Zanotti-Gerosa, *Org. Lett.* **2000**, *2*, 4173.

93 J.-H. Xie, L.-X. Wang, Y. Fu, S.-F. Zhu, B.-M. Fan, H.-F. Duan, Q.-L. Zhou, *J. Am. Chem. Soc.* **2003**, *125*, 4404.

94 Y. Xu, N.W. Alcock, G.J. Clarkson, G. Docherty, G. Woodward, M. Wills, *Org. Lett.* **2004**, *6*, 4105.

95 F. Robin, F. Mercier, L. Ricard, F. Mathey, M. Spagnol, *Chem. Eur. J.* **1997**, *3*, 1365.

96 D.G. Genov, D.J. Ager, *Angew. Chem. Int. Ed.* **2004**, *43*, 2816.

97 R. Guo, A.J. Lough, R.H. Morris, D. Song, *Organometallics* **2004**, *23*, 5524.

98 I. Karamé, M. Jahjah, A. Messaoudi, M.L. Tommasino, M. Lemaire, *Tetrahedron: Asymmetry* **2004**, *15*, 1569.

99 T. Ohkuma, C.A. Sandoval, R. Srinivasan, Q. Lin, Y. Wei, K. Muñiz, R. Noyori, *J. Am. Chem. Soc.* **2005**, *127*, 8288.

100 M. Ito, M. Hirakawa, K. Murata, T. Ikariya, *Organometallics* **2001**, *20*, 379.

101 R.-X. Li, P.-M. Cheng, D.-W. Li, H. Chen, X.-J. Li, C. Wessman, N.-B. Wong, K.-C. Tin, *J. Mol. Catal. A: Chemical* **2000**, *159*, 179.

102 T. Ohkuma, M. Koizumi, K. Muñiz, G. Hilt, C. Kabuto, R. Noyori, *J. Am. Chem. Soc.* **2002**, *124*, 6508.

103 B. Heil, S. Torös, J. Bakos, L. Markó, *J. Organomet. Chem.* **1979**, *175*, 229.

104 S. Torös, B. Heil, L. Kollár, L. Markó, *J. Organomet. Chem.* **1980**, *197*, 85.

105 J. Bakos, I. Tóth, B. Heil, L. Markó, *J. Organomet. Chem.* **1985**, *279*, 23.

106 Q. Jiang, Y. Jiang, D. Xiao, P. Cao, X. Zhang, *Angew. Chem. Int. Ed.* **1998**, *37*, 1100.

107 X. Zhang, H. Kumobayashi, H. Takaya, *Tetrahedron: Asymmetry* **1994**, *5*, 1179.

108 R. Noyori, C.A. Sandoval, K. Muñiz, T. Ohkuma, *Proc. R. Soc. Lond. A* **2005**, *363*, 901.

109 C.A. Sandoval, T. Ohkuma, K. Muñiz, R. Noyori, *J. Am. Chem. Soc.* **2003**, *125*, 13490.

110 K. Abdur-Rashid, S.E. Clapham, A. Hadzovic, J.N. Harvey, A.J. Lough, R.H. Morris, *J. Am. Chem. Soc.* **2002**, *124*, 15104.

111 T. Ohkuma, T. Hattori, H. Ooka, T. Inoue, R. Noyori, *Org. Lett.* **2004**, *6*, 2681.

112 X. Zhang, T. Taketomi, T. Yoshizumi, H. Kumobayashi, S. Akutagawa, K. Mashima, H. Takaya, *J. Am. Chem. Soc.* **1993**, *115*, 3318.

113 T. Ohkuma, H. Takeno, R. Noyori, *Adv. Synth. Catal.* **2001**, *343*, 369.

114 R. ter Halle, E. Schulz, M. Spagnol, M. Lemaire, *Synlett* **2000**, 680.

115 H.-B. Yu, Q.-S. Hu, L. Pu, *J. Am. Chem. Soc.* **2000**, *122*, 6500.

116 H.-B. Yu, Q.-S. Hu, L. Pu, *Tetrahedron Lett.* **2000**, *41*, 1681.

117 G.-J. Deng, B. Yi, Y.-Y. Huang, W.-J. Tang, Y.-M. He, Q.-H. Fan, *Adv. Synth. Catal.* **2004**, *346*, 1440.

118 K. Yoshikawa, N. Yamamoto, M. Murata, K. Awano, T. Morimoto, K. Achiwa, *Tetrahedron: Asymmetry* **1992**, *3*, 13.

119 A. Roucoux, M. Devocelle, J.-F. Carpentier, F. Agbossou, A. Mortreux, *Synlett* **1995**, 358.

120 S. Sakuraba, H. Takahashi, H. Takeda, K. Achiwa, *Chem. Pharm. Bull.* **1995**, *43*, 738.

121 H. Takeda, T. Tachinami, M. Aburatani, H. Takahashi, T. Morimoto, K. Achiwa, *Tetrahedron Lett.* **1989**, *30*, 363.

122 T. Hayashi, A. Katsumura, M. Konishi, M. Kumada, *Tetrahedron Lett.* **1979**, 425.

123 S. Torös, L. Kollár, B. Heil, L. Markó, *J. Organomet. Chem.* **1982**, *232*, C17.

124 (a) S. Sakuraba, K. Achiwa, *Synlett* **1991**, 689; (b) S. Sakuraba, N. Nakajima, K. Achiwa, *Synlett* **1992**, 829; (c) S. Sakuraba, K. Achiwa, *Chem. Pharm. Bull.* **1995**, *43*, 748.

125 M. Devocelle, F. Agbossou, A. Mortreux, *Synlett* **1997**, 1306.

126 C. Pasquier, S. Naili, L. Pelinski, J. Brocard, A. Mortreux, F. Agbossou, *Tetrahedron: Asymmetry* **1998**, *9*, 193.

127 M. Devocelle, A. Mortreux, F. Agbossou, J.-R. Dormoy, *Tetrahedron Lett.* **1999**, *40*, 4551.

128 T. Ohkuma, D. Ishii, H. Takeno, R. Noyori, *J. Am. Chem. Soc.* **2000**, *122*, 6510.

129 T. Ohkuma, M. Koizumi, M. Yoshida, R. Noyori, *Org. Lett.* **2000**, *2*, 1749.

130 T. Ohkuma, M. Koizumi, H. Ikehira, T. Yokozawa, R. Noyori, *Org. Lett.* **2000**, *2*, 659.

131 P. Cao, X. Zhang, *J. Org. Chem.* **1999**, *64*, 2127.

132 U. Nagel, C. Roller, *Z. Naturforsch. Ser. B* **1998**, *53*, 267.

133 (a) T. Osawa, *Chem. Lett.* **1985**, 1609; (b) T. Osawa, T. Harada, A. Tai, *J. Mol. Catal.* **1994**, *87*, 333; (c) T. Osawa, A. Tai, Y. Imachi, S. Takasaki, in: *Chiral Reactions in Heterogeneous Catalysis* (Eds. G. Jannes, V. Dubois), Plenum, New York, **1995**, pp. 75; (d) T. Harada, T. Osawa, in: *Chiral Reactions in Heterogeneous Catalysis* (Eds. G. Jannes, V. Dubois), Plenum, New York, **1995**, p. 83.

134 T. Ohkuma, H. Ooka, T. Ikariya, R. Noyori, *J. Am. Chem. Soc.* **1995**, *117*, 10417.

135 T. Ohkuma, H. Ikehira, T. Ikariya, R. Noyori, *Synlett* **1997**, 467.

136 T. Ohkuma, H. Doucet, T. Pham, K. Mikami, T. Korenaga, M. Terada, R. Noyori, *J. Am. Chem. Soc.* **1998**, *120*, 1086.

137 R. Spogliarich, S. Vidotto, E. Farnetti, M. Graziani, N.V. Gulati, *Tetrahedron: Asymmetry* **1992**, *3*, 1001.

138 T. Ohkuma, J. Li, R. Noyori, *Synlett* **2004**, 1383.

139 T. Ohkuma, H. Ooka, M. Yamakawa, T. Ikariya, R. Noyori, *J. Org. Chem.* **1996**, *61*, 4872.

140 T. Matsumoto, T. Murayama, S. Mitsuhashi, T. Miura, *Tetrahedron Lett.* **1999**, *40*, 5043.

141 K. Mikami, T. Korenaga, M. Terada, T. Ohkuma, T. Pham, R. Noyori, *Angew. Chem. Int. Ed.* **1999**, *38*, 495.

142 K. Mikami, T. Korenaga, T. Ohkuma, R. Noyori, *Angew. Chem. Int. Ed.* **2000**, *39*, 3707.

33
Rhodium-Catalyzed Enantioselective Hydrogenation of Functionalized Ketones

André Mortreux and Abdallah Karim

This chapter is dedicated to the memory of Professors Francis Petit and Hidemasa Takaya, two friends who have been pioneers in the field of homogeneous catalysis and enantioselective catalysis.

33.1
Introduction

Enantioselective hydrogenation, using molecular hydrogen to reduce prochiral olefins, ketones, and imines, has become one of the most efficient, practical, and atom-economical methods for the construction of chiral compounds [1–3]. Since the early 1970s, significant attention has been devoted to the discovery of new asymmetric catalysts, in which transition metal complexes modified by chiral phosphorous ligands have emerged as preferential catalysts for asymmetric hydrogenation. Thousands of efficient chiral phosphorous ligands with diverse structures have been developed for their application to asymmetric hydrogenation. Indeed, many represent the key step in industrial processes for the preparation of enantiomerically pure compounds. Consequently, numerous reviews have been devoted to the application of enantioselective catalysis in that context [4, 5].

In this chapter, we will focus on the rhodium-catalyzed hydrogenation of functionalized ketones and the development of chiral phosphorous ligands for this process. Although there are other chiral phosphorous ligands which are effective for ruthenium-, iridium-, platinum-, titanium-, zirconium-, and palladium-catalyzed hydrogenation, they will not be discussed here. For details of these chemistries, the reader should refer to other chapters of this book.

The Handbook of Homogeneous Hydrogenation.
Edited by J.G. de Vries and C.J. Elsevier
Copyright © 2007 WILEY-VCH Verlag GmbH & Co. KGaA, Weinheim
ISBN: 978-3-527-31161-3

33.2
Basic Principles of Ketone Hydrogenation on Rhodium Catalysts

In contrast to olefins, the hydrogenation of ketones on rhodium–phosphine complexes requires the presence of rather basic ligands, where either the classical aromatic groups in PPh_2 moieties have been changed or hydrogenated into PCy_2, or via synthesis involving the introduction of phosphorous–alkyl functions at some stage of the chiral ligand synthesis. This was first recognized by Schrock and Osborn, who found that the *cationic* catalytic precursors $[RhH_2\{P(C_6H_5)(CH_3)_2\}_2L_2]X$ (L = solvent, X = PF_6^- or ClO_4^-) reduce acetone under 1 atm of H_2 in the presence of a small amount of water [6]. The same trend was observed later by Fujitsu, where the carbonyl group of *α,β*-unsaturated ketones was chemoselectively reduced on peralkyl-phosphine cationic rhodium system at 30 °C and atmospheric hydrogen pressure [7]. Tani and Otsuka achieved hydrogenation of ketonic substrates using a cationic rhodium complex with a fully alkylated bidentate diphosphane [8a]. In each of these cases, the high basicity of the ligands [9] increases the electron density of the rhodium center so that the overall reaction rate is accelerated [8a]. The same is true when using *covalent* catalytic precursors such as $HRh(PCy_3)_3$ [7].

As a consequence of these preliminary results obtained with achiral ligands (and even when aryl-phosphorous chiral ligands were used in early studies), the objectives of many research groups have been to develop chiral ligands bearing alkyl substituents at phosphorus. In general, this allows the provision of a high reactivity at room temperature, which is often a prerequisite to obtaining and/or to improving enantioselectivities. In this chapter, an attempt will be made to describe most of the investigations conducted in this field, and the text will be devoted to ketoesters, -amides and -amines, most of which are suitable for the synthesis of chiral alcohols that can be used either directly as biologically active compounds or as chiral synthons valuable in the pharmaceutical industry.

33.3
Enantioselective Hydrogenation of Ketoesters

33.3.1
Enantioselective Hydrogenation of Ketopantoyllactone (KPL)

Among ketoesters, tremendous efforts have been devoted to the hydrogenation of dihydro-4,4-dimethyl-2,3-furandione (KPL), not only as a model reaction but also because the product *R*(–)-pantolactone is a key intermediate in the synthesis of vitamin B_5 and coenzyme A (Scheme 33.1).

One of the first investigations related to this chemistry reported the use of a ligand which was developed by Achiwa and Ojima during the late 1970s, and was derived from L-hydroxyproline, a natural amino acid, However, for hydrogenation using this diphenylphosphino-substituted bidentate ligand, BPPM (**1**),

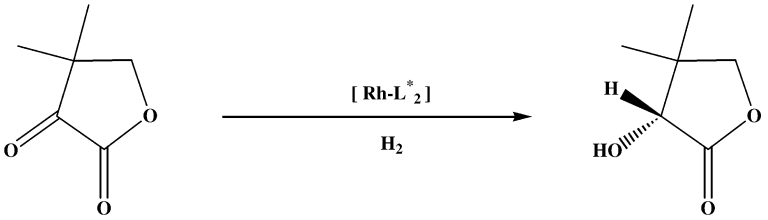

Scheme 33.1 Hydrogenation of ketopantoyllactone.

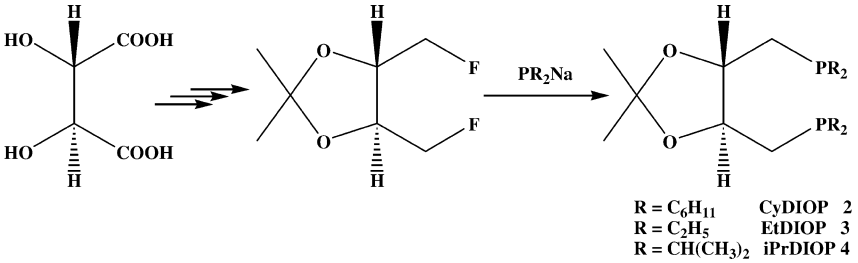

Scheme 33.2 DIOP-derived peralkyl ligands.

rather harsh reaction conditions (50 °C, 50 bar) were required, and the product was obtained with 87% ee [10].

Earlier studies conducted by Tani had confirmed the role of the basicity of the ligand in terms of activity, upon using dicyclohexyl, diethyl and diisopropyl modified DIOP **2**, **3**, and **4** (Scheme 33.2) for ketone hydrogenation [11]. Details of their use in KPL hydrogenation were published initially by Yamamoto, but the ee-values obtained were not very high (e.g., 45% with **2**) [12].

These investigations were followed by the synthesis of a series of new ligands derived again from L-hydroxyproline. Within this series, a fine tuning of electronic and steric effects was made by variation of the substituents on both phosphorus atoms, using the same ligand backbone (Scheme 33.3). BCCP **5** was synthesized and applied by Tani [11c], and also used by Achiwa, who prepared mixed alkyl-aryl diphosphine ligands, leading to highly dissymmetric bidentates giving rise either to highly suitable ligands in terms of activity *and* enantioselectivity, or to others which are clearly of minimal use for this reaction (e.g., compare BCPM and BCPP in Table 33.1) [13].

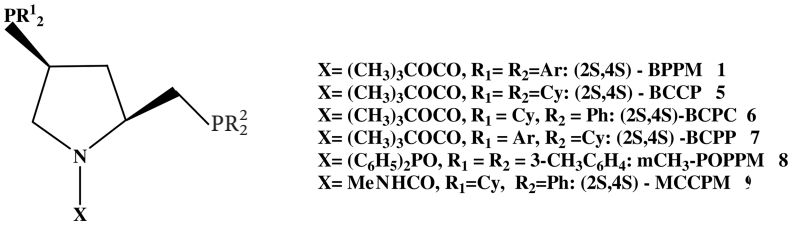

Scheme 33.3 L-Hydroxyproline-derived bidentate ligands.

Table 33.1 Catalytic results on rhodium-catalyzed ketopantoyllactone hydrogenation.[a)]

Catalyst/ligand	SCR[b)]	Reaction conditions [Solvent; temp., H_2 pressure, time]	ee [%] (config.)	Reference
[RhCl(2*S*,4*S*)-BPPM]$_2$/**1**	100	C_6H_6, 30 °C, 50 atm, 45 h	87 (*R*)	10b
[RhCl(*R*)-Cy-DIOP]$_2$/**2**	50	C_6H_6-EtOH(3/1), r.t., 15 atm, 15 h	45 (*R*)	12
[Rh(*R*)-*i*Pr-DIOP(NBD)]$^+$ClO4$^-$/**4**	200	EtOH, r.t., 1 atm, 1 h	7 (*S*)	11
[RhCl(*R*)-*i*Pr-DIOP]$_2$/**4**	200	C_6H_6, 35 °C, 1 atm, 1 h	54 (*R*)	11
[RhCl(2*S*,4*S*)-BCCP]$_2$/**5**	200	THF, 50 °C, 50 atm, 45 h	66 (*S*)	10
[RhCl(2*S*,4*S*)-BCCP]$_2$/**5**	10000	THF, 50 °C, 50 atm, 45 h	61 (*S*)	13
[RhCl(2*S*,4*S*)-BCPM]$_2$/**6**	10000	THF, 50 °C, 50 atm, 45 h	90 (*R*)	13
[RhCl(2*S*,4*S*)-BCPP]$_2$/**7**	1000	THF, 50 °C, 50 atm, 45 h	9 (*R*)	13
[RhCl(2*S*,4*S*)-*m*-MePOPPM]/**8**	150000	PhMe, 40 °C, 12 atm	95 (*R*)	14
[RhCl(*S*)-Ph,Ph-ProNOP]$_2$/**10**	200	PhMe, 50 °C, 50 atm, 18 h	60 (*R*)	15a
[RhCl(*S*)-Cy,Cy-ProNOP]$_2$/**11**	200	PhMe, 20 °C, 1 atm, 1 h,	47 (*R*)	15b
[RhCl(*S*)-Cp,Cp-ProNOP]$_2$/**12**	200	PhMe, 20 °C, 1 atm, 1 h	76 (*R*)	15b
[RhCl(*S*)-Cp,Cp-ProNOP]$_2$/**12**	10000	PhMe, 70 °C, 50 atm, 3 h	77 (*R*)	15b
[RhCl(*S*)-Cp,Cp-isoAlaNOP]$_2$/**13**	200	PhMe, 20 °C, 1 atm, 20 min	89 (*S*)	15e
[RhCl(*S*)-Ph,Cp-isoAlaNOP]$_2$/**14**	200	PhMe, 20 °C, 1 atm, 12 h	81 (*R*)	15e
[RhCl(*S*)-Cy,Cy-oxoProNOP]$_2$/**15**	200	PhMe, 20 °C, 1 atm, 2 h	96.6 (*R*)	15e
[Rh(CF_3CO_2)(*S*)Cy,Cy-oxoProNOP]$_2$/**15**	200	PhMe, 20 °C, 1 atm, 5 min	97.7 (*R*)	15e
[RhI(*S*)-Cp,Cp-oxoProNOP]$_2$/**16**	200	PhMe, 20 °C, 1 atm, 1 h	98 (*R*)	15e
[Rh(CF_3CO_2)(*S*)Cp,Cp-oxoProNOP]$_2$/**16**	200	PhMe, 20 °C, 1 atm, 5 min	98.7 (*R*)	15e
[Rh(CF_3CO_2)(*S*)Cp,Cp-oxoProNOP]$_2$/**16**	70000	PhMe, 40 °C, 40 atm, 24 h	96 (*R*)	15e
[Rh(CF_3CO_2)(*S*)-Cp,Cp-IndoNOP]$_2$/**18**	200	PhMe, 20 °C, 1 atm, 45 min	>99 (*R*)	15o
[Rh(CF_3CO_2)(*S*)-Cp,Cp-IndoNOP]$_2$/**18**	5000	PhMe, 20 °C, 1 atm, 5 h	97 (*R*)	15o
[Rh(CF_3CO_2)*syn*-(*S*,*S*)-Cr(CO)$_3$-Cp, Cp-IndoNOP]$_2$/**19**	200	PhMe, 20 °C, 1 atm, 1 h	>99 (*R*)	15o
[Rh(CF_3CO_2)*anti*-(*R*,*S*)-Cr(CO)$_3$-Cp, Cp-IndoNOP]$_2$/**20**	200	PhMe, 20 °C, 1 atm, 90 min	84 (*R*)	15o
[Rh(CF_3CO_2)(*S*)-Cp,Cp-QuinoNOP]$_2$/**21**	200	PhMe, 20 °C, 50 atm, 20 min	95 (*R*)	15p
[Rh(CF_3CO_2)*syn*-(*S*,*S*)-Cr(CO)$_3$-Cp, Cp-QuinoNOP]$_2$/**22**	200	PhMe, 20 °C, 50 atm, 30 min	85 (*R*)	15p
[Rh(CF_3CO_2)*anti*-(*R*,*S*)-Cr(CO)$_3$-Cp, Cp-QuinoNOP]$_2$/**23**	200	PhMe, 20 °C, 50 atm, 30 min	87 (*R*)	15p
[Rh(CF_3CO_2)Ph-MannOP]$_2$/**24**	200	PhMe, 50 °C, 50 atm, 19 h	44 (*S*)	18
[Rh(CF_3CO_2)Cp-MannOP]$_2$/**25**	200	PhMe, 20 °C, 50 atm, 4 h	80 (*R*)	18
[Rh(CF_3CO_2)Cy MannOP]$_2$/**26**	200	PhMe, 20 °C, 1 atm, 2 h	84 (*R*)	18
[RhCl(*S*)-Ph,Ph-ProNN′P]$_2$/**27**	200	PhMe, 50 °C, 50 atm, 18 h	33 (*R*)	15h
[RhCl(*S*)-Cp,Cp-ProNN′P]$_2$/**29**	200	PhMe, 20 °C, 1 atm, 12 min	70 (*S*)	15h
[RhCl(*S*)-Cy,Cy-ProNN′P]$_2$/**29**	200	PhMe, 20 °C, 1 atm, 7 h	69 (*S*)	15h
[RhCl(*S*)-Cp,Ph-ProNN′P]$_2$/**30**	200	PhMe, 20 °C, 1 atm, 8 h	80 (*S*)	15h
[RhCl(*S*)-Cp,Ph-ProNN′P]$_2$/**30**	200	PhMe, 20 °C, 1 atm, 24 min	83 (*S*)	15h
[Rh(CF_3CO_2)(*S*)-Cy,Ph-ProNN′P]$_2$/**31**	200	PhMe, 20 °C, 1 atm, 48 h	62 (*S*)	15h
[RhCl(*S*)-Cp,Ph-ProNN′P]$_2$/**30**	200	PhMe, 50 °C, 1 atm, 2 h	78 (*S*)	15h
[RhCl(*S*)-Cp,Ph-ProNN′P]$_2$/**30**	200	PhMe, 70 °C, 1 atm, 4 h	64 (*S*)	15h
[Rh(CF_3SO_3)BoPHOZ]$_2$/**32**	100	THF, 20 °C, 20 atm, 6 h	97.2 (*R*)	19

a) Catalysts were used either as isolated dimer complexes or, in the case of preformed *in situ* from addition of 2 equiv. bidentate ligand to the rhodium dimers [Rh(COD)X]$_2$ (X = Cl, $OCOCF_3$). Both techniques gave almost identical results, as exemplified by several authors.

b) SCR = substrate:catalyst ratio.

It must be recognized, however, that the preparation of such ligands requires synthetic schemes composed sometimes of 13 to 15 steps. This, from an industrial viewpoint, is an obvious drawback which would probably preclude any application.

The present authors began studying this reaction during the early 1980s, using chiral, natural amino acids and amino alcohols as starting materials to synthesize the so-called AMPP ligands (*AM*ino *P*hosphine *P*hosphinites) via a simple procedure by which the phosphino moieties are introduced via phosphinylation of the OH and NH functions of the amino alcohols using dialkylchlorophosphines (Scheme 33.4).

As expected, whereas hydrogenation using the previously reported ligand Ph,Ph-ProNOP **10** required higher temperatures and pressures to achieve conversion, the catalysts based on the peralkyl Cy,Cy-ProNOP **11** and Cp,Cp-ProNOP **12** ligands proved to be active and selective at room temperature and at 1 bar H_2. Furthermore, a one-pot, two-step procedure allowed the synthesis of mixed alkyl-aryl or alkyl-alkyl ligands via addition of 1 equiv. of chlorodialkylphosphine followed by 1 equiv. of another phosphinylating reagent (Scheme 33.5).

Using this procedure, a new series of AMPP ligands could be rapidly synthesized according to the starting amino alcohol and the phosphinylation reagents (Scheme 33.6) [15 a–h]. Of particular interest in the corresponding series of ligands arising from isoalaninol is the fact that changing the substituents at phosphorus could lead to a complete reversal of the asymmetric induction, using the same ligand backbone (see ligands **13** and **14**).

Following these early investigations, the major breakthrough in this field has been the change in both the structure of the ligand frame and that of the anion in the starting rhodium catalytic precursor. The [Rh(TFA){(S)-(Cp,Cp)oxoPro-

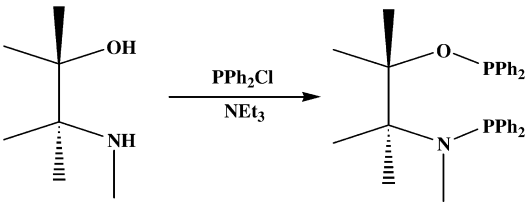

Scheme 33.4 One-step synthesis of aminophosphine phosphinite bidentate ligands.

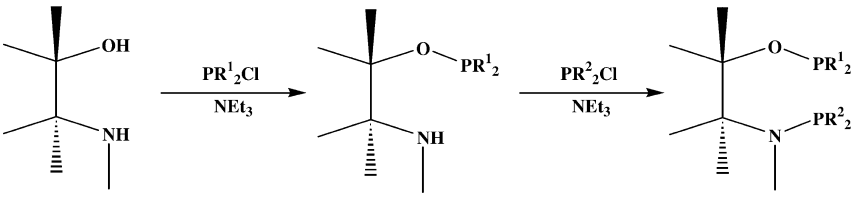

Scheme 33.5 One-pot, two-step procedure for the synthesis of mixed AMPP ligands.

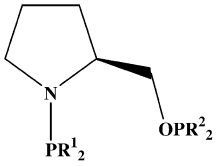

$R_1 = R_2 = Ph$ (S)-Ph,Ph-ProNOP 9
$R_1 = R_2 = Cy$ (S)-Cy,Cy-ProNOP 10
$R_1 = R_2 = Cp$ (S)-Cp,Cp-ProNOP 11

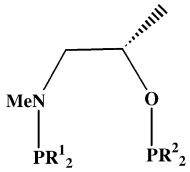

$R^1 = R^2 = Cp$ (S)-Cp,Cp-isoAlaNOP 13
$R^1 = Ph, R^2 = Cp$ (S)-Ph,Cp-isoAlaNOP 14

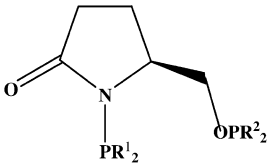

$R^1 = R^2 = Cy$ (S)-Cy,Cy-oxoProNOP 15
$R^1 = R^2 = Cp$ (S)-Cp,Cp-oxoProNOP 16
$R^1 = R^2 = iPr$ (S)-i-Pr,i-Pr-oxoProNOP 17

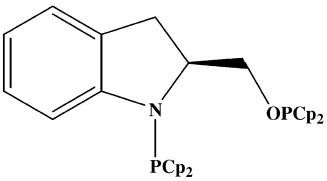

(S)-Cp,Cp-IndoNOP 18

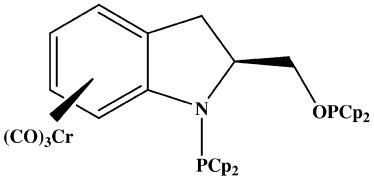

syn-(S,2S)-Cr(CO)$_3$-Cp,Cp-IndoNOP 19

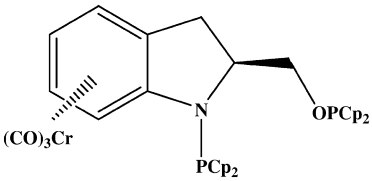

anti-(R,2S)-Cr(CO)$_3$-Cp,Cp-IndoNOP 20

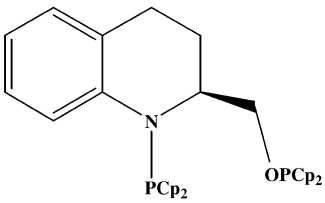

(S)-Cp,Cp-QuinoNOP 21

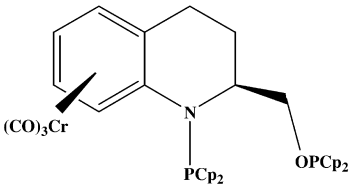

syn-(S,2S)-Cr(CO)$_3$-Cp,Cp-QuinoNOP 22

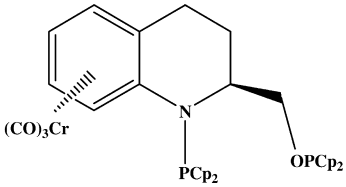

anti-(R,2S)-Cr(CO)$_3$-Cp,Cp-QuinoNOP 23

Scheme 33.6 AMPP ligands synthesized from amino alcohols.

NOP}]$_2$ amidophosphinite **15** complex catalyzes hydrogenation of the ketopantoyllactone, with ee-values up to 97% under very straightforward experimental conditions (20 °C, 1 bar H_2). The change of anion from chlorine to trifluoroacetate in the dimer complex allowed an enhancement of the reactivity of one order of magnitude, together with an increase in ee-values. In fact, ee-values of 96% have been obtained in a pilot plant using a substrate:catalyst ratio of 70 000 [15 e]. Other related ligands that fulfill these two key points – namely an increased rigidity of the ligand framework and electron-donating phosphorus atoms – have been synthesized from (*S*)-indoline carboxylic acid and (*S*)-1,2,3,4-tetrahydroisoquinoline carboxylic acid, and this led to similar (or even better) results in terms of enantioselectivity [15 o, p]. Ligands formed by chromium tricarbonyl complexation on the aromatic part of the ligand framework gave almost perfect enantioselectivity due to a beneficial effect of the matching chiralities in the *syn* form, even with the chloro dimer as the rhodium precursor.

The use of sugars as the chiral source of the corresponding C2-symmetrical basic diphosphanes has been successfully explored. Aryldiphosphinites based on sugars have also been used successfully in the enantioselective hydrogenation of enamides [16, 17], and their behavior in the stereoselective hydrogenation of ketones has also been reported [17 c]. In this context, the 1,3–4,6-di-*O*-benzylidene-D-mannitol carbohydrate derivative can be readily prepared to provide, by further diphosphinylation, the C2-symmetric diphosphinites Ph,Ph-MannOP **24** Cp,Cp-MannOP **25** and Cy,Cy-MannOP **26** ligands, the latter being the more enantioselective (Scheme 33.7) [18].

Another series of bisaminophosphine (BAMP) ligands (Scheme 33.8) obtained by phosphinylation of diamines has also been synthesized and applied successfully, giving rise to better activities and selectivities using cyclohexyl-substituted phosphorus moieties [15 h].

Interestingly, the use of phosphino-ferrocenylaminophosphine ligand **32** of the BOPHOZ series has also given good results for that reaction, indicating that dissymmetry of the ligand associated with the presence of a PN function may result in improved reactivities and selectivities, as observed with AMPP ligands.

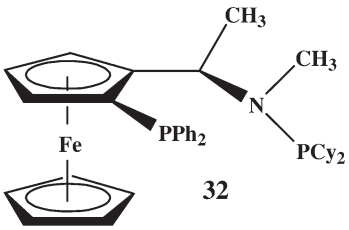

32

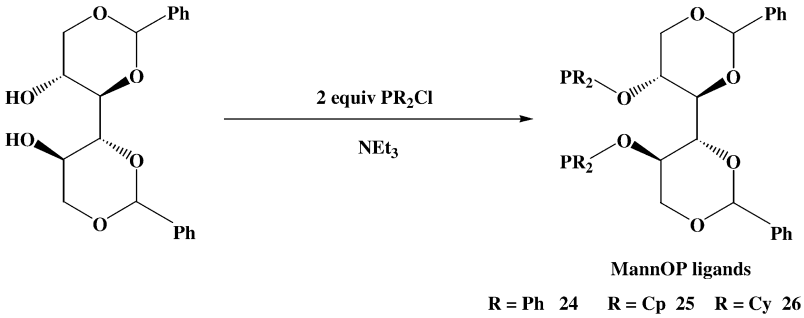

Scheme 33.7 MannOP ligands synthesized from D-mannitol.

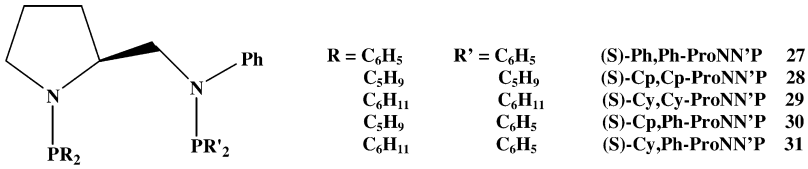

Scheme 33.8 BAMP ligands synthesized from diamines.

33.3.2 Hydrogenation of Ketoesters and Ketoamides

33.3.2.1 *α*-Ketoesters and Ketoamides

Some neutral rhodium catalysts with chiral ligands, such as MCCPM **9** (see Scheme 33.3) [20c], Cy,Cy-oxoProNOP **15**, and Cp,Cp-IndoNOP **18**, demonstrate excellent enantioselectivities and reactivities in the hydrogenation of *α*-ketoesters and ketoamides; indeed, they compare well with ruthenium-based catalysts (Table 33.2). Togni et al. have successfully used the Josiphos **47** ligand for the hydrogenation of ethyl acetoacetate [27], while the use of MannOPs has led to somewhat high enantioselectivities [18].

The enantioselective hydrogenation of isatine derivatives has also been performed with high ee-values (up to 94%) using the alkyl-substituted oxoProNOP ligands (15j).

Some developments have been carried out for the enantioselective synthesis of biologically active compounds. One such example is the synthesis of ethyl (*R*)-2-hydroxy-4-phenylbutyrate, an important intermediate for the angiotensin-converting enzyme (ACE) inhibitor benazepril, or for coenzyme A, using the NORPHOS ligand (Scheme 33.9) [21].

Substituted mandelamides such as **34** (Scheme 33.10) constitute a new class of agrochemical fungicides, acting specifically against the oomycetes family of phytopathogenic fungi such as *Phytophthora infestans* (potato late blight) and *Plasmopara viticola* (grape downy mildew) [34, 35]. Novel concise approaches to

Table 33.2 Enantioselective hydrogenation of α-ketoesters and ketoamides.

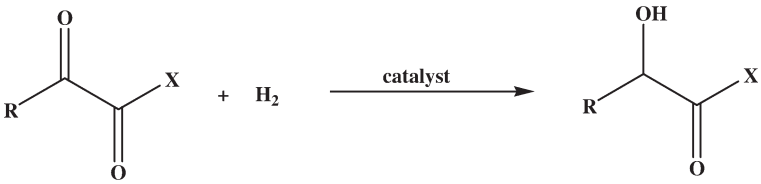

R	X	Catalyst	Reaction conditions [Solvent, temp, H_2 pressure, S:Rh, time][a)]	ee [%] (config.)	Reference
CH_3	CH_3O	[RhCl(2*S*,4*S*)-MCCPM]$_2$/**9**	THF, 20 °C, 20 atm, 1000, 24 h	87 (*R*)	20c–24
CH_3	CH_3O	[RhClPh-MannOP]$_2$/**24**	Toluene, 20 °C, 50 atm, 56 h	48 (*R*)	18
CH_3	CH_3O	[RhClCp-MannOP]$_2$/**25**	Toluene, 20 °C, 50 atm, 3 h	76 (*R*)	18
CH_3	CH_3O	[Rh(TFA)Cp-MannOP]$_2$/**25**	Toluene, 20 °C, 50 atm, 3 h	78 (*R*)	18
CH_3	CH_3O	[Rh(Cl)Cy-MannOP]$_2$/**26**	Toluene, 20 °C, 50 atm, 3 h	82 (*R*)	18
CH_3	CH_3O	[Rh(TFA)Cy-MannOP]$_2$/**26**	Toluene, 20 °C, 50 atm, 3 h	86 (*R*)	18
CH_3	CH_3O	[RhCl(*S*)-Cy,Cy-oxoProNOP]$_2$/**15**	Toluene, 20 °C, 20 atm, 3 h	95 (*R*)	15j
CH_3	CH_3O	[Rh(CF_3CO_2)(*S*,*S*)-Cr(CO)$_3$-Cp, Cp-IndoNOP]$_2$/**19**	MeOH, 20 °C, 50 atm, 6 h	95 (*R*)	15l
CH_3	C_2H_5O	[RhCl(2*S*,3*S*)-NORPHOS]$_2$/**33**	Toluene/MeOH, 25 °C, 20 atm, 50, 3 h	89 (*S*)	21
CH_3	C_2H_5O	[RhCl (2*S*,3*S*)-NORPHOS]$_2$/**33**	Toluene, 20 °C, 50 atm, 18 h	96 (*S*)	21
CH_3	C_2H_5O	[Rh(CF_3SO_3)BOPHOZ]$_2$/**32**	CH_3OH, 25 °C, 100 atm, 50, 3 h	92.4(*R*)	19
Ph(CH_2)$_2$	C_2H_5O	[RhClPh-MannNOP]$_2$/**24**	THF, 20 °C, 20 atm, 100, 6 h	43 (*S*)	18
Ph(CH_2)$_2$-	C_2H_5O	[RhClCp-MannOP]$_2$/**25**	Toluene, 50 °C, 50 atm, 200, 48 h	65 (*S*)	18
Ph	$PhCH_2NH$	[Rh(TFA)Cp-MannOP]$_2$/**25**	Toluene, 20 °C, 1 atm, 18 h	50 (*S*)	18
Ph	$PhCH_2NH$	[Rh(Cl)Cy-MannOP]$_2$/**26**	Toluene, 20 °C, 50 atm, 18 h	76 (*S*)	18
Ph	$PhCH_2NH$	[Rh(TFA)Cy-MannOP]$_2$/**26**	Toluene, 20 °C, 50 atm, 18 h	65 (*S*)	18
Ph	$PhCH_2NH$	[RhCl(*S*)-Ph,Cp-isoAlaNOP]$_2$/**14**	Toluene, 20 °C, 50 atm, 18 h	88 (*S*)	15e
Ph	$PhCH_2NH$	[RhCl(*S*)-Cy,Cy-oxoProNOP]$_2$/**15**	Toluene, 20 °C, 1 atm, 24 h	95 (*S*)	15j
Ph	$PhCH_2NH$	[RhCl(*S*)-Cp,Cp-IndoNOP]$_2$/**18**	Toluene, 20 °C, 1 atm, 24 h	91 (*S*)	15o
Ph	$PhCH_2NH$	[RhCl(*S*,*S*)-Cr(CO)$_3$-Cp, Cp-IndoNOP]$_2$/**19**	Toluene, 20 °C, 1 atm, 24 h	97 (*S*)	15o
Ph	$PhCH_2NH$	[RhCl(*S*)-Cp,CpQuinoNOP]$_2$/**21**	Toluene, 20 °C, 1 atm, 3 h	99 (*S*)	15p
Ph	$PhCH_2NH$	[RhCl-*syn*-(*S*,*S*)-Cr(CO)$_3$Cp, Cp-QuinoNOP]$_2$/**22**	Toluene, 20 °C, 50 atm, 19 h	94 (*S*)	15p
Ph	$PhCH_2NH$	[RhCl-*anti*-(*S*,*S*)-Cr(CO)$_3$-Cp, Cp-QuinoNOP]$_2$/**23**	Toluene, 20 °C, 50 atm, 18 h	99 (*S*)	15p

a) S:Rh = substrate:catalyst ratio = 200, unless otherwise stated. Catalysts were generally prepared *in situ* by reacting [Rh(COD)Cl]$_2$ or[Rh(COD)(OCOCF$_3$)]$_2$ with 2 equiv. ligand in the solvent used for the catalytic reaction.

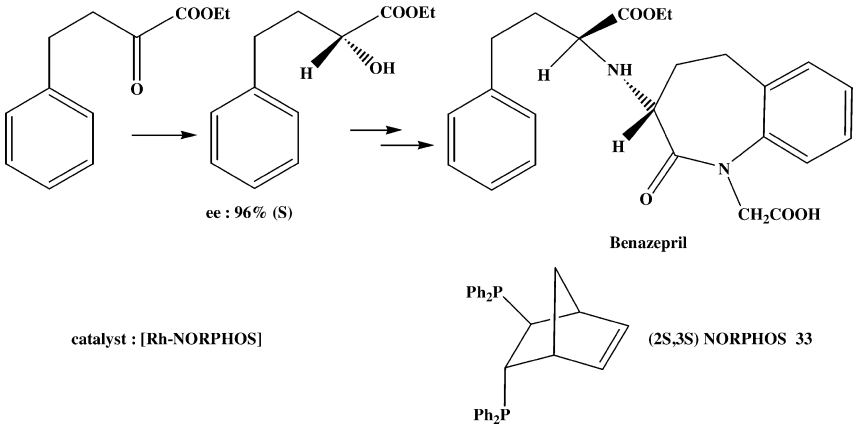

Scheme 33.9 Enantioselective hydrogenation with Rh–NORPHOS complex as a key step in the synthesis of the ACE inhibitor benazepril (see Table 33.2).

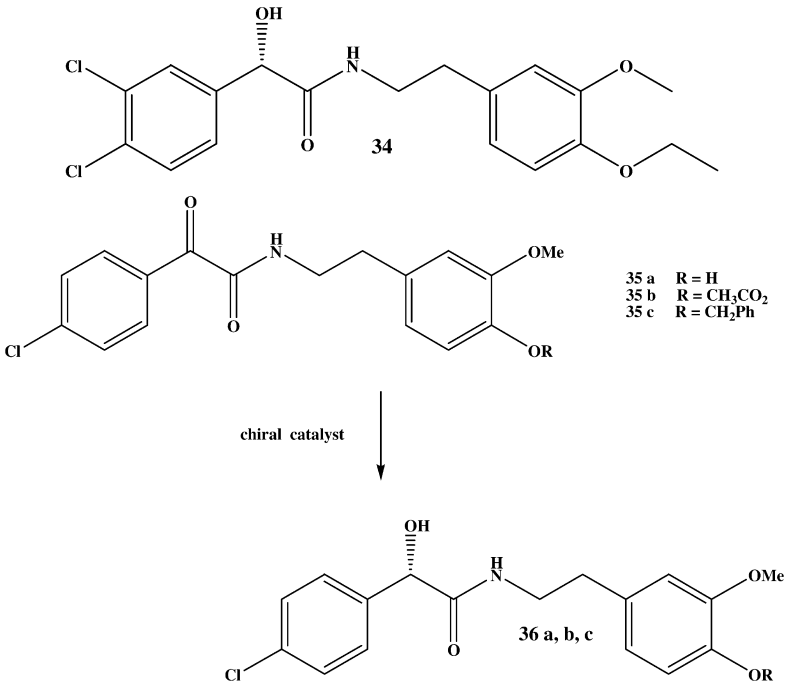

Scheme 33.10 Synthesis of substituted mandelic amides via enantioselective reduction of a phenylglyoxylic acid derivative.

Table 33.3 Hydrogenation of phenylglyoxylic derivatives.

Substrate	Catalyst	Reaction conditions [a] [Solvent, temp, H_2 pressure]	TON/TOF [h^{-1}]	ee [%] (config.)
35a	[RhCl(*R*)-Cy,Cy-oxoProNOP]$_2$/**15**	CH_2Cl_2, 0 °C, 20 bar	100/5	87 (*R*)
35a	[RhCl(2*S*,4*S*)-BCPM]$_2$/**6**	THF, 20 °C, 10 bar	100/5	74 (*S*)
35a	[RhCl(*S*)-MeOBIPHEP]$_2$/**41**	CH_2Cl_2, 40 °C, 20 bar	100/5	65 (*S*)
35a	[RhCl(*R*)-BICHEP]$_2$/**40**	CH_2Cl_2, 40 °C, 20 bar	100/5	47 (*R*)
35a	[RhCl(2*S*,4*S*)-Ar*-BPPM]$_2$/**39**	THF, 20 °C,10 bar	89/5	47 (*S*)
35a	[RhCl(*R*,*R*)-Ar*-DIOP]$_2$/**38**	CH_2Cl_2, 40 °C, 20 bar	37/2	44 (*S*)
35b	[RhCl(*S*)-*i*-Pr-MeOBIPHEP]$_2$/**42**	CH_2Cl_2, 40 °C, 20 bar	96/5	62 (*S*)
35c	[RhCl(2*S*,4*S*)-BCPM]$_2$/**6**	THF, 20 °C, 10 bar	93/2	64 (*S*)
35c	[RhCl(*S*)-*i*-Pr-MeOBIPHEP]$_2$/**42**	CH_2Cl_2, 40 °C, 20 bar	95/2	54 (*S*)
35c	[RhCl(Mandyphos)]$_2$/**37**	THF, 25 °C, 60 bar	25/1	40 (*R*)

a) Substrate : Rh ratio = 100. Catalysts were prepared *in situ* by addition of the bidentate ligand to [Rh(norbornadiene)Cl]$_2$.

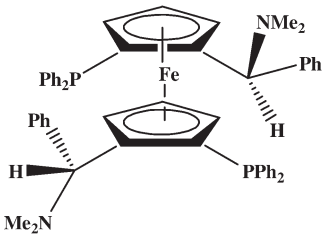

Mandiphos 37

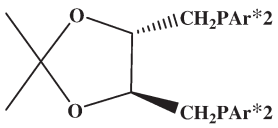

(R,R)-Ar*-DIOP 38
Ar = 3,5-*t*Bu$_2$-4-MeO-C$_6$H$_2$

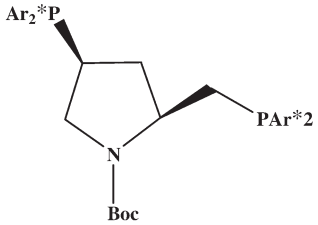

(2S,4S)-Ar*-BPPM 39
Ar = 3,5-*t*Bu$_2$-4-MeO-C$_6$H$_2$

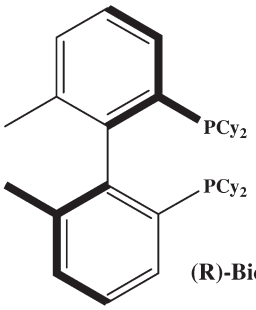

(R)-Bichep 40

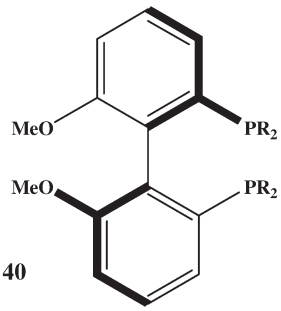

R = Ph **MeOBiphep 41**

R = CH(CH$_3$)$_2$ ***i*Pr-MeOBiphep 42**

.

enantiopure mandelamides have been checked, and one of these involves the enantioselective reduction of a ketamide to produce directly the mandelamide, in which case the Cy,Cy-oxoProNOP ligand **15** was found to be the most efficient (Table 33.3) [28].

33.3.2.2 α,γ-Diketoesters

In recent years, much effort has been devoted to the enantioselective hydrogenation of β-ketoesters, essentially using ruthenium-based catalysts. The aim of these reactions is to produce selectively enantiopure *syn* diols which are the key building blocks for the synthesis of inhibitors of HMG-coenzyme A reductase. Due to the availability of the AMPP ligands, and the reactivity of the rhodium catalysts based on them (notably the alkyl-substituted ones) towards ketonic sub-

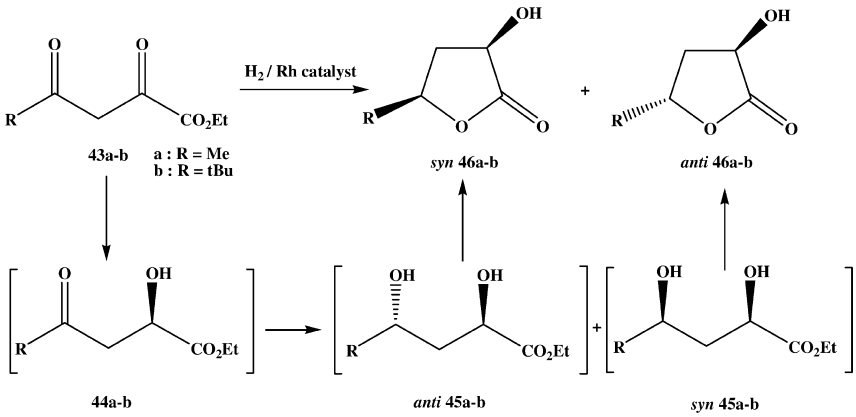

Scheme 33.11 Asymmetric hydrogenation of α,γ-diketoesters.

Table 33.4 Enantioselective hydrogenation of α,γ-diketoesters using rhodium catalysts [15m].[a)]

Substrate	Catalyst	Time [h]	4 select.	6 select.	*syn*:*anti*	ee [*syn*/*anti*]
43a	[RhCl(2*S*,4*S*)-BPPM]$_2$/**1**	67	63	26	54:46	58/64
	[RhCl(*S*)-MeO-BIPHEP]$_2$/**36**	138	82	18	54/46	79/53
	[RhCl(*S*)-Cy,Cy-oxoProNOP]/**15**	84	81	18	65:35	80/60
	[Rh(TFA) (*S*)-Cy,Cy-oxoProNOP]$_2$/**15**	86	45	47	48:52	80/86
	[RhCl(*S*)-Cp,Cp-oxoProNOP]$_2$/**16**	19	64	23	42:58	73/86
	[RhCl(*S*)-Cp,Cp-oxoProNOP]$_2$/**16**	70	3	91	44:56	73/86
	[Rh(TFA) (*S*)-Cp,Cp-oxoProNOP]$_2$/**16**	26	39	56	45:55	72/87
	[Rh((*R*)-MTPA)(*S*)-Cp,Cp-oxoProNOP]$_2$/**16**	44	42	49	49:51	73/81
43b	[RhCl(*S*)-Cy,Cy-oxoProNOP]$_2$/**15**	17	>99	0	–	88 (–)
	[RhCl(*R*)-Cp,Cp-oxoProNOP]$_2$/**16(R)**	25	78	22	31/69	97 (–)
	[RhCl(*S*)-Cp,Cp-oxoProNOP]$_2$/**16**	88	88	12	32:68	97 (+)
	[Rh(TFA)(*S*)-Cp,Cp-oxoProNOP]$_2$/**16**	38	>99	0	–	48 (+)
	[Rh((*R*)-MTPA)(*S*)-Cp,Cp-oxoProNOP]$_2$/**16**	140	4	92	49:51	73/81

a) Reaction conditions: for **43a** substrate: toluene, 60 °C, 50 atm H_2, [**43a**]/[P]/[Rh] = 200:2.2:1, [Rh] = 0.6–1.4 mmol L^{-1}; for **43b** substrate: toluene, 60 °C, 50 atm H_2, [**43b**]/[Rh] = 50:1, [Rh] = 0.5–4.0 mmol L^{-1}. Catalysts were prepared *in situ* from the appropriate precursor [Rh(COD)X]$_2$ (X = Cl, TFA or MTPA) and 2.2 equiv. ligand.

strates, some investigations have been made into the synthesis of 2-hydroxy-4-butyrolactones in a one-pot hydrogenation process (Scheme 33.11) [15 m] (see also Table 33.4).

The Rh complex of the chiral C_1 symmetry Josiphos **47** is also effective for the enantioselective hydrogenation of ethyl 3-oxobutanoate [27].

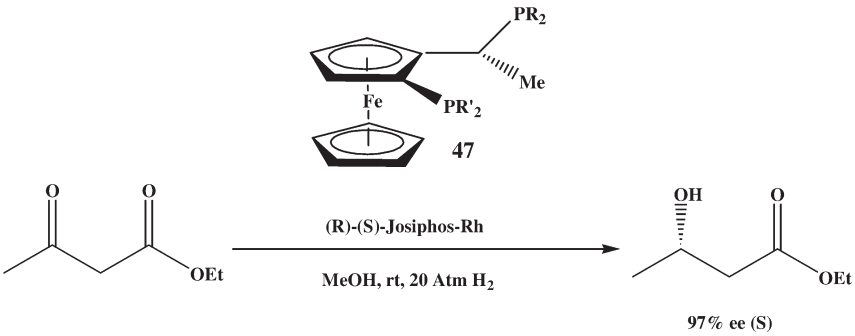

33.3.3 Hydrogenation of Amino Ketones

33.3.3.1 *α*-Amino Ketones

Amino ketones and their hydrochloride salts can be effectively hydrogenated with chiral rhodium catalysts (Table 33.5). The rhodium precatalysts, when combined with chiral phosphorus ligands such as BPPFOH **4** [20 b], hydroxyproline derivatives ligands [20–24], Cy,Cy-oxo-ProNOP **15**, Cp,Cp-oxoProNOP **16**, and

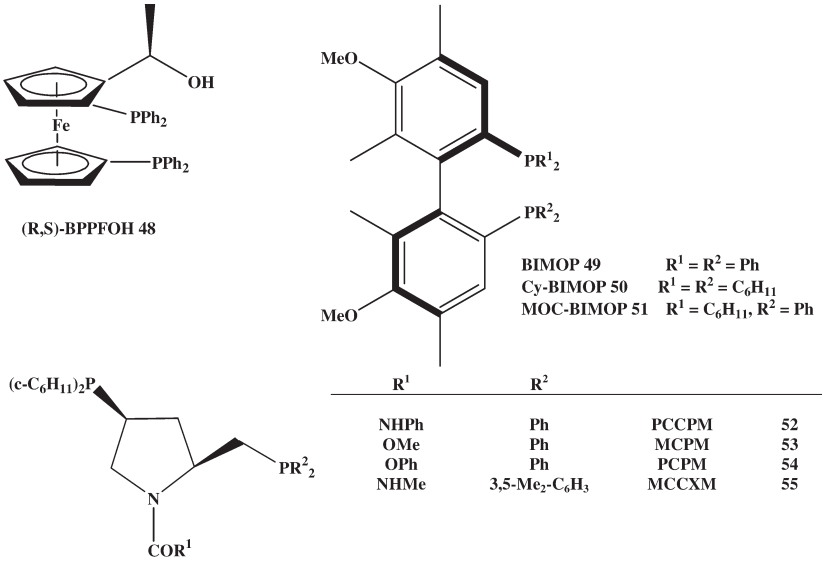

Table 33.5 Enantioselective hydrogenation of α-amino ketones catalyzed by rhodium (I) complexes.[a)]

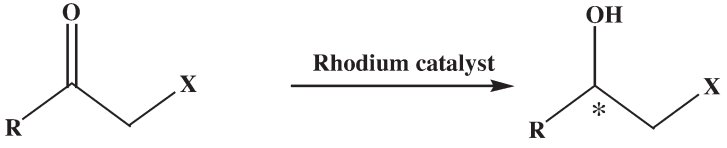

Chiral ligand	R	X	Reaction conditions [Solvent, temp., H_2 pressure, S:Rh]	ee [%] (config.)	Reference
(*R*,*S*)-BPPFOH/**48**	$(3,4)(OH)_2Ph$	NHMe.HCl	NEt_3, MeOH, r·t., 50 bar, 100	95 (*R*)	20b
(*S*)-Cy,Cy-oxoProNOP/**15**	Ph	$NH_2 \cdot HCl$	MeOH, 20 °C, 50 bar, 200	93 (*S*)	15i
(*S*)-Cy,Cy-oxoProNOP/**15**	Ph	$NMe_2 \cdot HCl$	MeOH, 20 °C, 50 bar, 200	96 (*S*)	15i
(*S*)-Cp,Cp-IndoNOP/**18**	Ph	$NMe_2 \cdot HCl$	Toluene, 20 °C, 50 bar, 200	99 (*S*)	15p
(*S*)-Cp,Cp-oxoProNOP/**16**	Ph	$NMe_2 \cdot HCl$	MeOH, 20 °C, 20 bar, 200	93 (*S*)	15i
(2*S*,4*S*)-MCCPM/**9**	Ph	$N(Me)CH_2Ph \cdot HCl$	MeOH, 50 °C, 30 bar, 1000	91 (*R*)	23a
(*S*)-Cp,Cp-oxoProNOP/**16**	Me	$NMe_2 \cdot HCl$	Toluene, 80 °C, 50 bar, 200	97 (*S*)	15p
(2*S*,4*S*)-MCCPM/**9**	Me	$NMe_2 \cdot HCl$	NEt_3, MeOH, 50 °C, 20 bar, 10^3	86 (*S*)	21
(2*S*,4*S*)-BCPM/**6**	CH_2Ph	$NEt_2 \cdot HCl$	NEt_3, MeOH, 50 °C, 20 bar, 10^3	91 (*S*)	20
(2*S*,4*S*)-BCPM/**6**	Ph	$NH_2 \cdot HCl$	NEt_3, MeOH, 50 °C, 20 bar, 10^3	81 (*R*)	23a
(2*S*,4*S*)-BCPM/**6**	Ph	NHMe · HCl	NEt_3, MeOH, 50 °C, 20 bar, 10^3	81 (*R*)	23a
(2*S*,4*S*)-BCPM/**6**	Ph	$NHCH_2Ph \cdot HCl$	NEt_3, MeOH, 50 °C, 20 bar, 10^3	87 (*S*)	23a
(2*S*,4*S*)-MCCPM/**9**	Ph	$NHCH_2Ph \cdot HCl$	NEt_3, MeOH, 50 °C, 20 bar, 10^3	93 (*S*)	23a
(*R*,*R*)DIOP	Ph	NEt_2	Benzene, NEt_3, 50 °C, 70 bar, 200	93 (+)	25
(2*S*,4*S*)-MCCPM/**9**	Ph	$NEt_2 \cdot HCl$	NEt_3, MeOH, 50 °C, 20 bar, 10^5	97 (*S*)	23a
(2*S*,4*S*)-BCPM/**6**	Ph	$NEt_2 \cdot HCl$	NEt_3, MeOH, 50 °C, 20 bar, 10^3	93 (*S*)	23a
(2*S*,4*S*)-BCPM/**6**	Ph	$NHCH_2Ph \cdot HCl$	NEt_3, MeOH, 50 °C, 20 bar, 10^3	85 (*S*)	23a

(*R*,*S*)-BPPFOH/**48**	3,4-$(OH)_2$Ph	NHMe · HCl	MeOH, NEt_3, 40 °C, 50 bar, 100	95 (*R*)	20b
(2*S*,4*S*)-MCCPM/**9**	3-(OCH_2Ph)Ph	N(Me)CH_2Ph · HCl	NEt_3, MeOH, 50 °C, 20 bar, 10^3	85 (*S*)	23b
(2*S*,4*S*)-MCPM/**53**	3-(OCH_2Ph)Ph	N(Me)CH_2Ph · HCl	NEt_3, MeOH, 50 °C, 20 bar, 10^3	85 (*S*)	23b
(*R*,*R*)DIOP	2-Naphthyl	NEt_2	Benzene, NE_{t3}, 50 °C,70 bar, 200	95 (*S*)	25
(2*S*,4*S*)-MCCPM/**9**	CH_2OPh	$NHCHMe_2$ · HCl	NEt_3, MeOH, 50 °C, 20 bar, 10^3	87 (*S*)	21
(2*S*,4*S*)-MCCPM/**9**	CH_2OPh	$NHCH_2$Ph · HCl	NEt_3, MeOH, 50 °C, 20 bar, 10^3	97 (*S*)	21
(2*S*,4*S*)-MCCPM/**9**	CH_2O-(C_6H_3-3,5-Me_2)	$NHCH_2$Ph · HCl	NEt_3, MeOH, 50 °C, 20 bar, 10^3	95 (*S*)	21
(2*S*,4*S*)-MCCPM/**9**	$CH_2OC_6H_4(CH_2)$OMe	NH-*i*-Pr · HCl	NEt_3, MeOH, 50 °C, 20 bar, 10^3	93 (*S*)	21
(2*S*,4*S*)-MCCPM/**9**	CH_2O(1-Naphthyl)	NH-*i*-Pr · HCl	NEt_3, MeOH, 50 °C, 20 bar, 10^3	91 (*S*)	21
(2*S*,4*S*)-MCCXM/**55**	CH_2COOEt	NMe_2 · HCl	NEt_3, MeOH, 50 °C, 20 bar, 10^3	85 (*S*)	22a
(2*S*,4*S*)-MCCPM/**9**	CH_2COOEt	NMe_2 · HCl	NEt_3, MeOH, 50 °C, 20 bar, 10^3	83 (*S*)	22a
(2*S*,4*S*)-MCCPM/**9**	Ph	N(Me)CH_2Ph · HCl	NEt_3, MeOH, 50 °C, 20 bar, 10^3	91 (*R*)	22b
(2*S*,4*S*)-MCCXM/**55**	Ph	N(Me)CH_2Ph · HCl	NEt_3, MeOH, 50 °C, 20 bar, 10^3	82 (*R*)	22b
(2*S*,4*S*)-BCPM/**6**	Ph	N(Me)CH_2Ph · HCl	NEt_3, MeOH, 50 °C, 20 bar, 10^3	83 (*R*)	22b
MannNOP/**25**	Ph	NMe_2 · HCl	EtOH, 50 °C, 50 bar, 200	58 (*S*)	18
MannNOP/**26**	Ph	NMe_2 · HCl	EtOH, 50 °C, 50 bar, 200	78 (*S*)	18
BIMOP/**49**	Ph	NH_2 · HCl	NEt_3, MeOH, 50 °C, 50 bar, 500	8 (*S*)	31
CY-BIMOP/**50**	Ph	NH_2 · HCl	NEt_3, MeOH, 50 °C, 50 bar, 500	55 (*R*)	31
MOC-BIMOP/**51**	Ph	NH_2 · HCl	NEt_3, MeOH, 50 °C, 50 bar, 10^3	93 (*R*)	31

a) Catalysts were generally preformed *in situ* upon addition of the ligands to the $[Rh(COD)Cl]_2$ dimer, except for the reactions described in [15i], where the *in-situ* procedure used the mononuclear $Rh(COD)_2BF_4$ complex with 1.1 equiv. ligand. The reactions were conducted to completion after 5 to 24 h.

Cp,Cp-IndoNOP **18** [15p], have provided excellent enantioselectivity and reactivity for the enantioselective hydrogenation of α-, β-, and γ-alkyl amino ketone hydrochloride salts.

The enantioselective hydrogenation of α-amino ketones has been applied extensively to the synthesis of chiral drugs such as the β-agonist SR 58611 (Sanofi Cie). *m*-Chlorstyreneoxide was obtained via carbene-induced ring closure of the amino alcohol. Epoxide-opening by a chiral amine obtained via a ruthenium-catalyzed hydrogenation of an enamide has led to the desired compound where

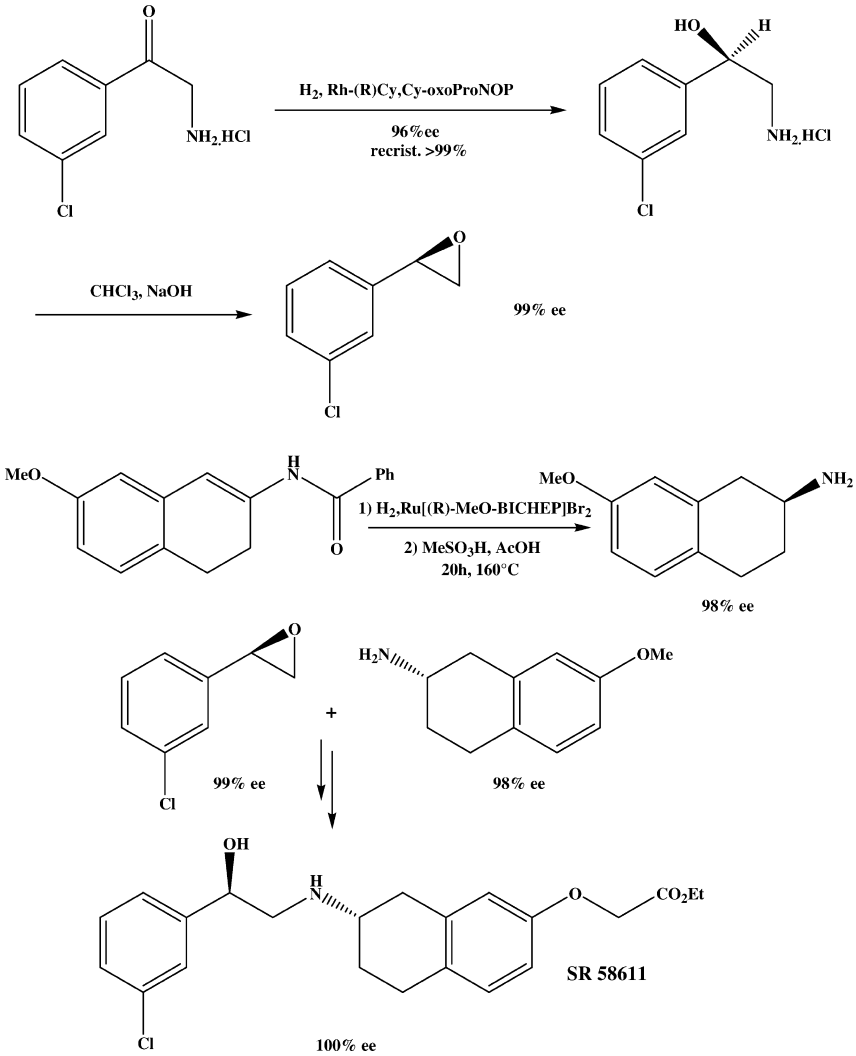

Scheme 33.12 Enantioselective synthesis of the β-agonist SR 58611 using two enantioselective hydrogenations processes [15n].

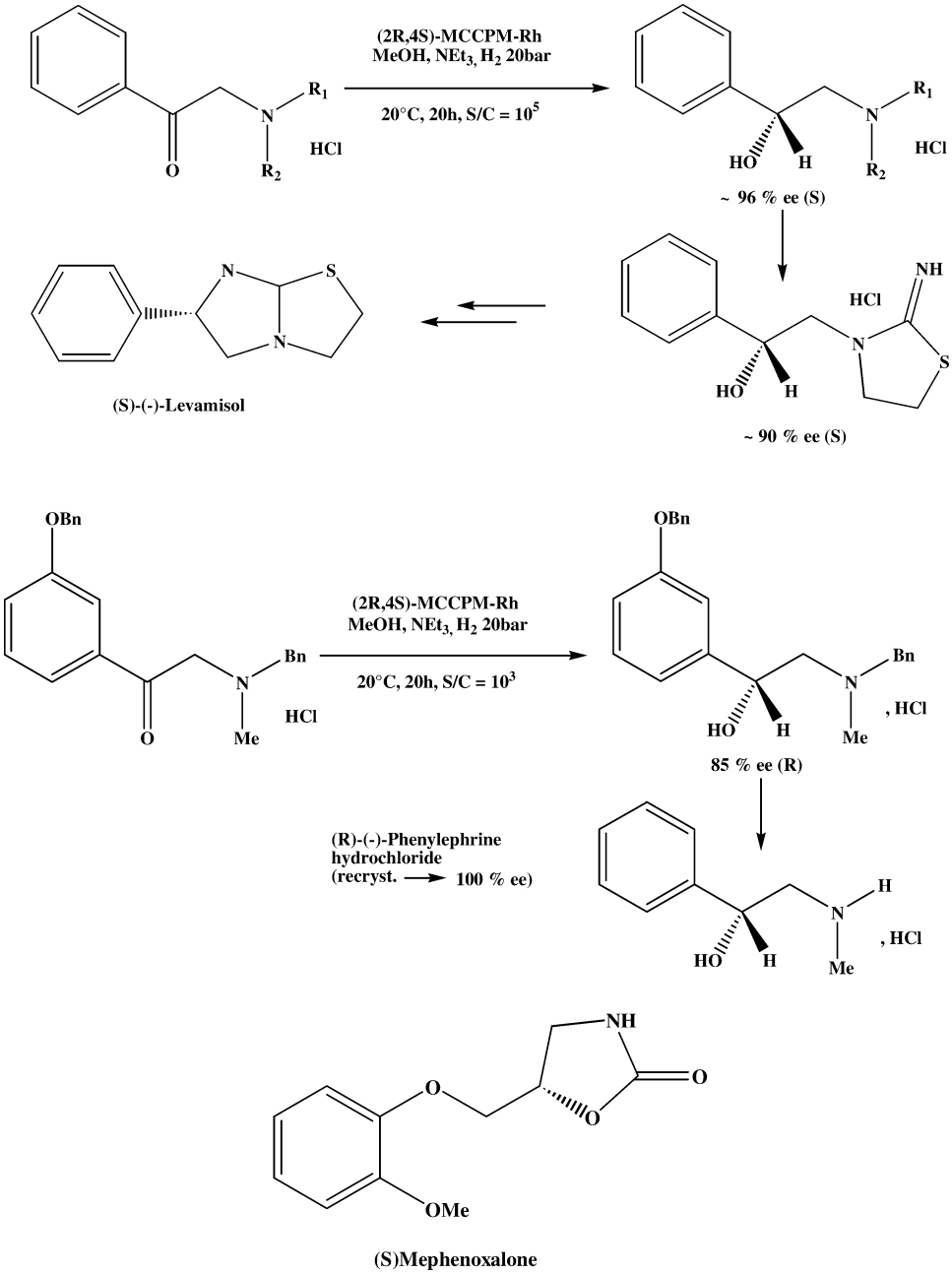

Scheme 33.13 Some applications of the enantioselective hydrogenation of α-amino ketones.

the two enantioselective centers have been obtained by asymmetric hydrogenation (Scheme 33.12) [15 n].

The neutral (2*S*,4*S*)-MCCPM **9**–rhodium complex was also found to be an efficient catalyst for the enantioselective hydrogenation of other *α*-aminoacetophenone derivatives. A practical enantioselective synthesis of (*S*)-(–)-levamisole [23 a], phenylephrine [23 b], and mephenoxalone [23] was realized by using this hydrogenation as a key reaction (Scheme 33.13).

The enantioselective hydrogenation of 3-aryloxy-2-oxo-1-propylamine derivatives leads directly to 1-amino-3-aryloxy-2-propanol derivatives, which serve as *α*-adrenergic blocking agents. (*S*)-Propranolol is obtained in 90.8% ee from the corresponding *α*-amino ketone, using 0.01 mol.% of the neutral (*S*,*S*)-MCCPM **9**–Rh complex [21], and from norcarnitine using the MCCXM **54** ligand [22 a].

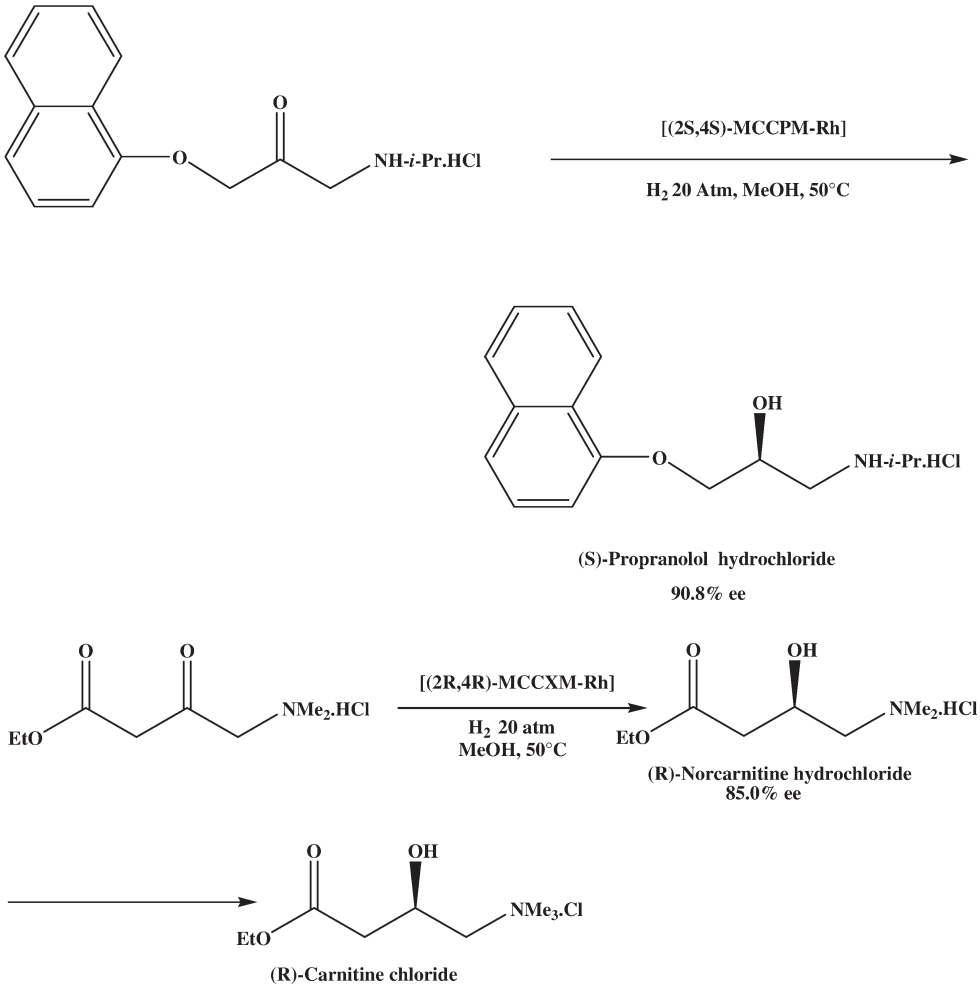

Epinephrine derivatives have also been synthesized using the (*R*,*S*)-BPPFOH ligand **48** [20a, b].

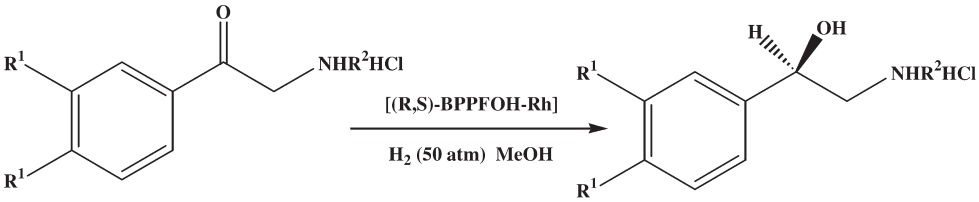

a: R^1 = OH R^2=Me 95% ee (R)- Epinephrine hydrochloride
b: R^1 = OMe R^2=H 92% ee

(*R*)-Salbutamol (levosalbutamol) was prepared in 90% yield and 70% ee by enantioselective hydrogenation of salbutamon using BCPPM **6** as ligand [29].

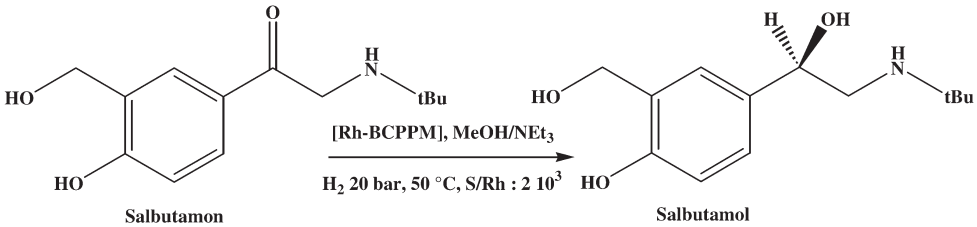

A synthetic route to optically active eprozinol, an anti-asthmatic compound, has been developed by efficient enantioselective hydrogenations of *α*- and *β*-amino ketone hydrochloride derivatives with a MCCPM–rhodium catalyst [30].

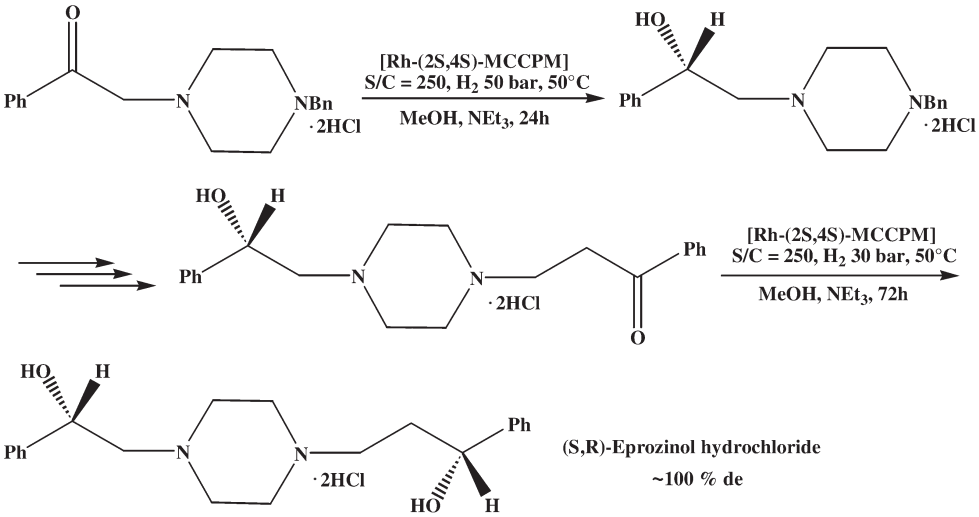

The (*R*)-amino ketone is hydrogenated enantioselectively by a neutral complex $[\{(S)\text{-}(R)\text{-BPPFOH}\}RhCl]_2$ to give the (*R*,*R*)-isoproterenol analogue, a compound which has been shown to possess very potent *β*-adrenoreceptor agonistic activity [33].

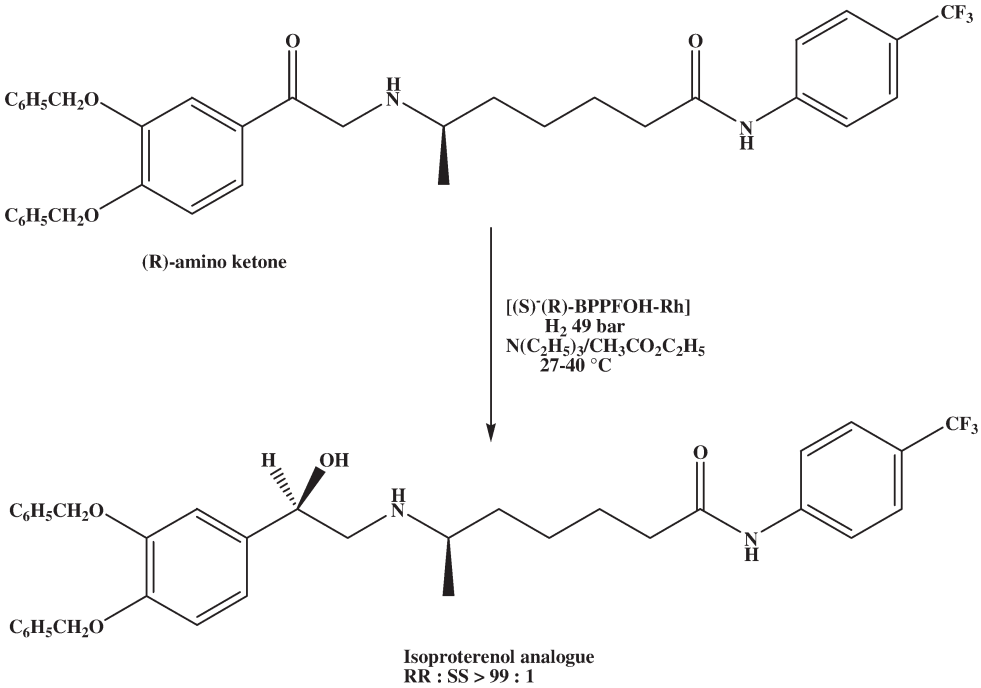

33.3.3.2 *β*- and *γ*-Amino Ketones

The (2*S*,4*S*)-MCCPM–Rh(I) complex was found previously by Achiwa and colleagues to be an efficient catalyst for the enantioselective hydrogenation of *β*-amino ketone derivatives, leading to a practical enantioselective synthesis of (*R*)-fluoxetine [*N*-methyl-3-(4-trifluoromethylphenoxy)-3-phenylpropylamine] hydrochloride [22 b]. Moreover, the use of AMPP ligands again proved to be efficient for these substrates, as exemplified in Table 33.6 [15 i].

Zhang and colleagues [26] synthesized the Duanphos enantiomers **57** and **58**, and reported on the Rh–Duanphos-catalyzed highly efficient hydrogenation of a series of *β*-secondary-amino ketones with ee-values of up to >99%, and with turnover numbers (TONs) of more than 4500 (Table 33.7). This hydrogenation provides a potentially practical synthesis for key pharmaceutical intermediates. The *γ*-secondary amino alcohols are of particular interest to synthetic chemists as they are key intermediates for the synthesis of an important class of antidepressants, **59–62** [32].

Table 33.6 Hydrogenation of a series of aromatic β-and γ-amino ketones **55a–b** and **56** with [Rh–AMPP] catalysts.

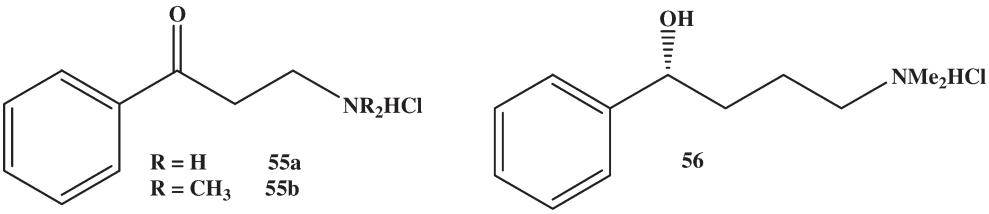

Substrate	Chiral ligand	Reaction conditions [temp, time (h)][a)]	ee [%] (config.)
55a	(*S*)-Cy,Cy-oxoProNOP/**15**	50 °C, 21	85 (*R*)
55b	(*S*)-Cy,Cy-oxoProNOP/**15**	20 °C, 45	93 (*R*)
55b	(*S*)-Cy,Cy-oxoProNOP/**15**	50 °C, 22	89 (*R*)
55b	(*S*)-Cy,Cy-oxoProNOP/**15**	50 °C, 18	87 (*R*)
55b	(*S*)-Cp,Cp-oxoProNOP/**16**	20 °C, 26	85 (*R*)
55b	(*S*)-Cy,Cy-ProNOP/**11**	20 °C, 44	77 (*R*)
55b	(*S*)-Cy,Cy-ProNOP/**11**	50 °C, 16	62 (*R*)
56	(*S*)-Cy,Cy-oxoProNOP/**15**	80 °C, 40	92 (*R*)

Solvent: MeOH; H_2 pressure: 50 atm., S:Rh ratio = 200; NEt_3:Rh = 5:1. TOFs are in the range 4.5 to 12.5 h^{-1}.
Catalysts were prepared *in situ* from the $[Rh(COD)_2]BF_4$ and 1.1 equiv. ligand.

Table 33.7 Hydrogenation of a series of β-secondary-amino ketones with Rh(Sc,Rp)-Duanphos catalyst.[a)]

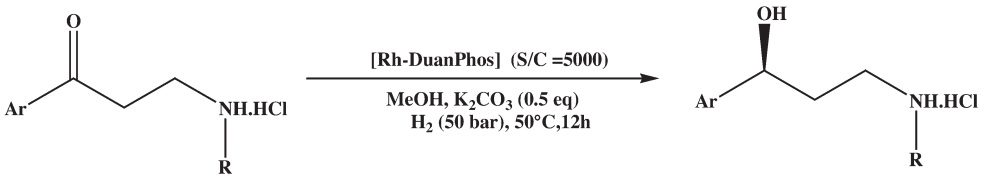

Substrate	Yield [%]	ee [%]	Configuration
Ar = 2-Me-Ph, R = Me	92	99	*S*
Ar = Ph, R = Me	90	98	*S*
Ar = 3-Br-Ph, R = Me	90	96	*S*
Ar = 4-Br-Ph, R = Me	93	99	*S*
Ar = 2-OMe-Ph, R = Me	93	93	*S*
Ar = 4-OMe-Ph, R = Me	93	99	*S*
Ar = 2-Naphthyl, R = Me	92	99	*S*
Ar = 2-Phenyl, R = CH_2-Ph	90	96	*S*
Ar = 2-Thienyl, R = Me	93	>99	*S*

a) The catalyst was the isolated $[Rh(Duanphos)(NBD)]SbF_6$ complex.

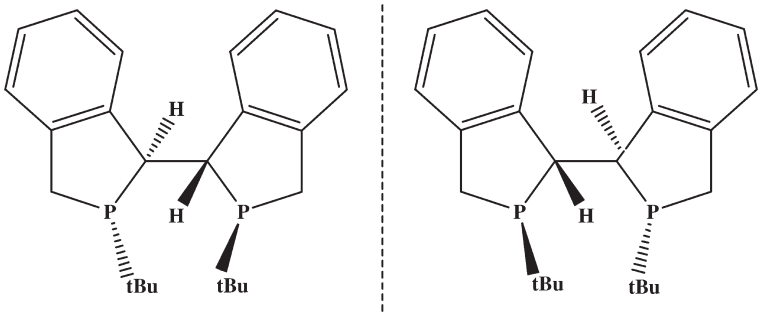

(Sc,Rp)-Duanphos 57 (Rc,Sp)-Duanphos 58

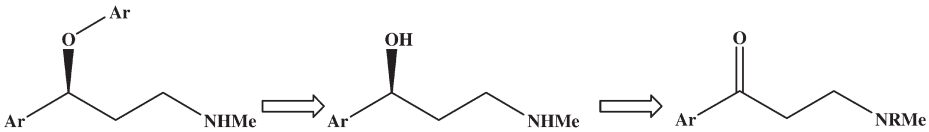

59 Ar = Ph, Ar = 4-CF_3-Ph Fluoxetine
60 Ar = Ph, Ar = 2-CH_3-Ph Tomoxetine
61 Ar = Ph, Ar = 2-OMe-4-CF_3-Ph Nisoxetine
62 Ar = thiophenyl, Ar = 1-naphtyl Fluoxetine

(93-99 % ee, up to >4500 TON)

R = CH_2Ph, Me or H

33.4 Enantioselective Hydrogenation of Fluoroketones

The catalytic enantioselective synthesis of chiral organofluorine compounds has played an important role in the development of medicines and materials based on the influence of fluorine's unique properties. Moreover, homochiral *R*-trifluoromethyl alcohols are versatile intermediates for the synthesis of anti-ferroelectric liquid crystalline molecules. Recently, Kuroki et al. found that chiral rhodium-(amidophosphinephosphinite) complexes, prepared from [Rh(COD)O-$COCF_3]_2$ and oxoProNOP ligands, catalyze the hydrogenation of 2,2-difluoro-3-oxocarboxylates and 4,4,4-trifluoroacetoacetate to give the corresponding β-hydroxy esters with good to excellent enantioselectivity (Table 33.8) [36, 37]. The stereochemical outcome from the latter β-ketoester indicated that the trifluoromethyl group has a significant influence on the enantiotopic face selection. An interesting feature that should be highlighted here is the fact that, although ruthenium-based catalysts are generally superior to rhodium, the results obtained with fluoroketones show that use of the latter catalysts, combined with the proper ligands (where the electronic properties have been tuned using alkyl substituents) are much more efficient, as when using ketopantoyllactone and ketoamide substrates.

Table 33.8 Enantioselective hydrogenation of α-fluoro-substituted β-ketoesters.

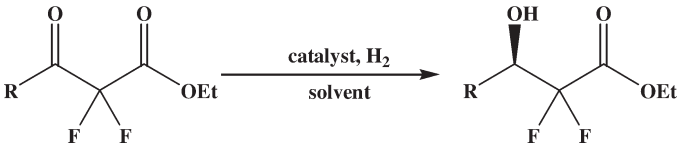

R	Catalyst [a)]	Reaction conditions [Solvent, temp., H_2 pressure, t (h)]	Yield [%]	ee [%] (con-fig.)
c-C_6H_{11}	[$RuBr_2$(*R*)BINAP]	EtOH, 100 °C, 100 atm, 24	96	77 (*R*)
$CH_3(CH_2)_8$	[RuCl((*R*)-Biphemp)(*p*-cymene)] Cl	EtOH, 100 °C, 100 atm, 24	100	81 (*R*)
CH_3	[Rh((*S*)-Cy,Cy-oxoProNOP)$OCOCF_3]_2$/**15**	Toluene, 30 °C 20 atm, 20	93	96 (*R*)
$(CH_3)_2CHCH_2$	[Rh((*S*)-Cy,Cy-oxoProNOP)$OCOCF_3]_2$/**15**	Toluene, 70 °C 20 atm, 20	95	92 (*R*)
Ph	[Rh((*S*)-Cy,Cy-oxoProNOP)$OCOCF_3]_2$/**15**	Toluene, 30 °C 20 atm, 20	97	84 (*R*)
$PhCH_2$	[Rh((*S*)-Cy,Cy-oxoProNOP)$OCOCF_3]_2$/**51**	Toluene, 30 °C 20 atm, 20	63	94 (*R*)
$PhCH_2CH_2$	[Rh((*S*)-Cy,Cy-oxoProNOP)$OCOCF_3]_2$/**15**	Toluene, 30 °C 20 atm, 20	100	96 (*R*)
$PhCH_2OCH_2$	[Rh((*S*)-Cy,Cy-oxoProNOP)$OCOCF_3]_2$/**15**	Toluene, 30 °C 20 atm, 20	95	95 (*R*)
c-C_6H_{11}	[Rh((*S*)-Cy,Cy-oxoProNOP)$OCOCF_3]_2$/**15**	Toluene, 70 °C 20 atm, 20	81	94 (*R*)
c-C_6H_{11}	[Rh((*S*)-Cp,Cp-oxoProNOP)$OCOCF_3]_2$/**16**	Toluene, 70 °C, 20 atm, 20	99	94 (*R*)
$CH_3(CH_2)_8$	[Rh((*S*)-Cy,Cy-oxoProNOP)$OCOCF_3]_2$/**15**	Toluene, 30 °C, 20 atm, 20	98	97 (*R*)
$CH_3(CH_2)_8$	[Rh((*S*)-Cy,Cy-oxoProNOP)$Cl]_2$/**15**	Toluene, 30 °C, 50 atm, 18	43	90 (*R*)
$CH_3(CH_2)_8$	[Rh((*S*)-*i*-Pr,*i*-Pr-oxoProNOP)$OCOCF_3]_2$/**17**	Toluene, 30 °C, 10 atm, 20	99	97 (*R*)

a) Catalysts were prepared and isolated before use; 0.1–0.5 mol.% of catalyst was used.

Table 33.9 Enantioselective hydrogenation of α-fluoroalkyl-substituted ketones.[a)]

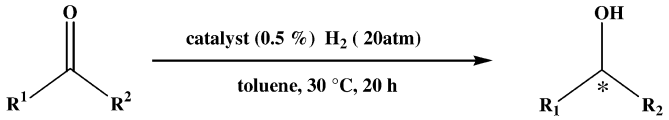

R^1	R^2	Catalyst	Yield [%]	ee [%] (config.)
CF_3	C_8H_{17}	[Rh((*S*)-Cy,Cy-oxoProNOP)$OCOCF_3]_2$/**15**	99	97 (*R*)
CF_3	C_8H_{17}	[Rh((*S*)-*i*-Pr,*i*-Pr-oxoProNOP)$OCOCF_3]_2$/**17**	100	97 (*S*)
CHF_2	C_8H_{17}	[Rh((*S*)-Cp,Cp-oxoProNOP)$OCOCF_3]_2$/**16**	100	27
CH_2F	C_8H_{17}	[Rh((*S*)-Cy,Cy-oxoProNOP)$OCOCF_3]_2$/**15**	100	15
CH_3	C_8H_{17}	[Rh((*S*)-Cy,Cy-oxoProNOP)$OCOCF_3]_2$/**15**	<1	–
CH_3	Ph	[Rh((*S*)-Cy,Cy-oxoProNOP)$OCOCF_3]_2$/**15**	2	8
CF_3	Ph	[Rh((*S*)-Cy,Cy-oxoProNOP)$OCOCF_3]_2$/**15**	93	73 (*R*)
C_2F_5	C_9H_{19}	[Rh((*S*)-Cy,Cy-oxoProNOP)$OCOCF_3]_2$/**15**	100	97 (*R*)

a) Catalysts were prepared and isolated before their use in catalysis.

Table 33.10 Enantioselective hydrogenation of α-trifluoromethyl-substituted ketones.[a)]

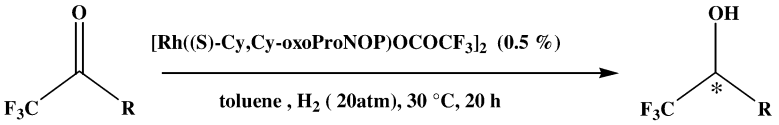

R	Yield [%]	ee [%] (config.)
C_6H_{13}	98	97 (*R*)
c-C_6H_{11}	90	97 (*S*)
c-$C_6H_{11}CH_2$	97	98 –
$PhCH_2$	97	97 –
$PhCH_2CH_2$	99	96 –
$PhCH_2OCH_2$	100	86 –
p-ClPh	8	38 –
p-CH_3OPh	100	83 –

a) The catalyst was prepared and isolated before use.

Another series of experiments has been performed using simple ketones substituted by fluoroalkyl groups. In this way it is clearly shown that the presence of a perfluorine group adjacent to the carbonyl to be hydrogenated is essential in order to provide both excellent activities and enantioselectivities (Table 33.9).

The direct substitution by a trifluoromethyl group led in most cases to excellent results, as detailed in Table 33.10.

33.5 Conclusions

Enantioselective catalytic hydrogenation is unquestionably one of the most significant transformations for use in both laboratory- and industrial-scale syntheses. The development of tunable chiral phosphorous ligands, and their ability to control enantioselectivity and reactivity, has allowed enantioselective catalytic hydrogenation to achieve unprecedented versatility and synthetic utility. This is exemplified in the preparation of enantiomerically enriched intermediates from prochiral ketones, notably in the synthesis of drugs and fine chemicals. Despite these excellent results, problems persist with regard to practical applications, notably the very high cost of some ligands, often in excess of that of the rhodium catalyst. In addition, TON values will also need to be increased. Whilst the nature of the chiral ligand is important, and fine tuning of the electronic properties may enhance the reaction's rate-limiting steps, reactivity and enantioselectivity may also be improved by changing the anion. Overall, rhodium-

based catalysts compare well with their ruthenium counterparts, while the use of chiral and/or highly dissymmetric mixed ligands has also proved successful. One major breakthrough in hydroformylation has been the use of a phosphine-phosphinite ligand [38] (also seen with the AMPP EPHOS ligand [39]), though future research must take into account the fact that asymmetric *and* dissymmetric ligands may lead to excellent enantioselectivities. It is essential that this point is considered in any future studies aimed at synthesizing new ligands from starting materials available in the chiral pool.

Abbreviations and Acronyms

AMPP *am*ino *p*hosphine *p*hosphinite
BAMP bisaminophosphine
KPL ketopantoyllactone
TON turnover number

References

1 (a) B.R. James, *Homogeneous Hydrogenation*, Wiley, New York, **1973**; (b) A.P.G. Kieboom, F. van Rantwijk, H. van Bekkum, *Hydrogenation and Hydrogenolysis in Synthetic Organic Chemistry*, Delft University Press, Rotterdam, **1977**; (c) A.J. Birch, D.H. Williamson, *Organic Reactions*, New York, **1976**, Vol. 24, p. 1; (d) B.R. James, *Adv. Organomet. Chem.* **1979**, *17*, 319; (e) R. Noyori, M. Kitamura, in: R. Scheffold (Ed.), *Modern Synthetic Methods*. Springer, Berlin **1989**, Vol. 5, p. 115; (f) H. Takaya, R. Noyori, in: B.M. Trost, I. Fleming (Eds.), *Comprehensive Organic Synthesis*, Vol. 8. Pergamon, Oxford, **1991**, p. 443; (g) H. Takaya, T. Ohta, R. Noyori, in: I. Ojima (Ed.), *Catalytic Asymmetric Synthesis*. VCH, New York, **1993**, Chapter 1; (h) P.A. Chaloner, M.A. Esteruelas, F. Joo , L.A. Oro, *Homogeneous Hydrogenation*, Kluwer, Dordrecht, **1994**; (i) R. Noyori, *Asymmetric Catalysis in Organic Synthesis*, Wiley, New York, **1994**, Chapter 2; (j) H. Brunner, in: G. Helmchen, R.W. Hoffman, J. Mulzer, E. Schaumann (Eds.), *Methods of Organic Chemistry* (Houben-Weyl), 4th edn. Thieme, Stuttgart, **1995**, Vol. E21d, p. 3945; (k) V. Fehring, R. Selke, *Angew. Chem. Int. Ed.*, **1998**, *37*, 1827.

2 (a) P. Rylander, *Catalytic Hydrogenation in Organic Syntheses*, Academic Press, New York, **1979**; (b) P.N. Rylander, *Hydrogenation Methods*, Academic Press, London, **1985**; (c) K. Harada, T. Munegumi, in: B.M. Trost, I. Fleming (Eds.), *Comprehensive Organic Synthesis*, Vol. 8. Pergamon, Oxford, **1991**, p. 139; (d) S. Siegel, in: B.M. Trost, I. Fleming (Eds.), *Comprehensive Organic Synthesis*, Vol. 8. Pergamon, Oxford, **1991**, p. 417.

3 (a) T. Ohkuma, R. Noyori, in: M. Beller, C. Bolm (Eds.), *Transition Metals for Organic Synthesis: Building Blocks and Fine Chemicals*, Vol. 2. Wiley-VCH, Weinheim, **1998**, p. 25; (b) T. Ohkuma, R. Noyori, in: E.N. Jacobsen, A. Pfaltz, H. Yamamoto (Eds.), *Comprehensive Asymmetric Catalysis*. Springer, Berlin, **1999**, Vol. 1, p. 199; (c) T. Ohkuma, M. Kitamura, R. Noyori, in: I. Ojima (Ed.), *Catalytic Asymmetric Synthesis*, 2nd edn. Wiley-VCH, New York, **2000**, p. 1.

4 (a) Y. Izumi, A. Tai, *Stereo-Differentiating Reactions: The Nature of Asymmetric Reactions*; Academic Press, New York, **1977**; (b) B. Bosnich (Ed.), *Asymmetric Cataly-*

sis. Martinus Nijhoff, New York, **1986**; (c) I. Ojima (Ed.), *Catalytic Asymmetric Synthesis*. VCH, New York, **1993**; (d) H. Brunner, W. Zettlmeier, *Handbook of Enantioselective Catalysis*. VCH, Weinheim, **1993**; (e) R. Noyori, *Asymmetric Catalysis in Organic Synthesis*. Wiley, New York, **1994**; (f) G. Jannes, V. Dubois (Eds.), *Chiral Reactions in Heterogeneous Catalysis*; Plenum, New York, **1995**; (g) B. Cornils, W.A. Herrmann (Eds.), *Applied Homogeneous Catalysis with Organometallic Compounds*. VCH, Weinheim, **1996**; Vols. 1 and 2; (h) M. Beller, C. Bolm (Eds.), *Transition Metals for Organic Synthesis: Building Blocks and Fine Chemicals*. Wiley-VCH, Weinheim, **1998**; Vols. 1 and 2; (i) E.N. Jacobsen, A. Pfaltz, H. Yamamoto (Eds.), *Comprehensive Asymmetric Catalysis*. Springer, Berlin, **1999**; Vols. 1–3; (j) I. Ojima (Ed.), *Catalytic Asymmetric Synthesis*. Wiley-VCH, New York, **2000**.

5 (a) G.M.R. Tombo, D. Bellus, *Angew. Chem., Int. Ed. Engl.* **1991**, *30*, 1193; (b) B. Cornils, W.A Herrmann, M. Rasch, *Angew. Chem., Int. Ed. Engl.* **1994**, *33*, 2144; (c) H.-U. Blaser, B. Pugin, in: G. Jannes, V. Dubois (Eds.), *Chiral Reactions in Heterogeneous Catalysis*. Plenum, New York, **1995**, p. 33; (d) R. Noyori, S. Hashiguchi, in: B. Cornils, W.A. Herrmann (Eds.), *Applied Homogeneous Catalysis with Organometallic Compounds* VCH, Weinheim, **1996**; Vol. 1, p. 552; (e) H.-U. Blaser, B. Pugin, F. Spindler, in: B. Cornils, W.A. Herrmann (Eds.), *Applied Homogeneous Catalysis with Organometallic Compounds*. VCH, Weinheim, **1996**; Vol. 2, p. 992; (f), W.A. Herrmann, B. Cornils, *Angew. Chem., Int. Ed. Engl.* **1997**, *36*, 1049; (g) W. Keim, in: M. Beller, C. Bolm (Eds.), *Transition Metals for Organic Synthesis: Building Blocks and Fine Chemicals*. Wiley-VCH, Weinheim, **1998**; Vol. 1, p. 14; (h) H.-U. Blaser, F. Spindler, in: E.N. Jacobsen, A. Pfaltz, H. Yamamoto (Eds.), *Comprehensive Asymmetric Catalysis*. Springer, Berlin, **1999**; Vol. 3, p. 1427; (i) R. Schmid, M. Scalone, in: E.N. Jacobsen, A. Pfaltz, H. Yamamoto (Eds.), *Comprehensive Asymmetric Catalysis*. Springer, Berlin, **1999**, Vol. 3, p. 1440; (j) T. Aratani, in: E.N. Jacobsen, A. Pfaltz, H. Yamamoto (Eds.), *Comprehensive Asymmetric Catalysis*. Springer, Berlin, **1999**; Vol. 3, p. 1451; (k) S. Akutagawa, in: E.N. Jacobsen, A. Pfaltz, H. Yamamoto (Eds.), *Comprehensive Asymmetric Catalysis*. Springer, Berlin, **1999**; Vol. 3, p. 1461; (l) H.U. Blaser, F. Spindler, M. Studer, *Applied Catalysis A: General* **2001**, *221*, 119; (m) G. Beck, *Synlett* **2002**, 837.

6 R.R. Schrock, J.A. Osborn, *J. Chem. Soc. Chem. Commun.* **1970**, 567.

7 H. Fujitsu, E.Matsumura, K. Takeshita, L. Mochida, *J. Chem. Soc. Perkin Trans I* **1981**, 2650.

8 (a) M.J. Burk, T.G.P. Harper, J.R. Lee, C. Kalberg, *Tetrahedron Lett.* **1994**, 35, 4963; (b) I.M. Lorkovic, R.R. Duff, Jr., M.S. Wrighton, *J. Am. Chem. Soc.* **1995**, *117*, 3617.

9 C.A. Tolman, *Chem. Rev.* **1977**, *77*, 313.

10 (a) K. Achiwa, T. Kogure, I. Ojima, *Chem. Lett.* **1977**, 4431; (b) I. Ojima, T. Kogure, T. Terasaki, K. Achiwa, *J. Org. Chem.* **1978**, *43*, 3444; (c) I. Ojima, T. Kogure, Y. Yoda *Org. Synth.* **1985**, *63*, 18.

11 (a) K. Tani, K. Suwa, E. Tanigawa, T. Yoshida, T. Okano, S. Otsuka, *Chem. Lett.* **1982**, 261; (b) K. Tani, K. Suwa, T. Yamagata, S. Otsuka, *Chem. Lett.* **1982**, 265; (c) K. Tani, T. Ise, Y. Tatsuno, T. Saito, *J. Chem. Soc. Chem. Commun.* **1984**, 1641; (d) K. Tani, E. Tanigawa, Y. Tatsuno, S. Otsuka, *J. Organomet. Chem.* **1985**, *279*, 87; (e) K. Tani, K. Suwa, E. Tanigawa, T. Ise, T. Yamagata, Y. Tatsuno, S. Otsuka, *J. Organomet. Chem.* **1989**, *370*, 203.

12 K. Yamamoto, Saeed-ur-Rehman, *Chem. Lett.* **1984**, 1603.

13 T. Morimoto, H. Takahashi, K. Fujii, M. Chiba, K. Achiwa, *Tetrahedron Lett.* **1986**, *27*, 4477; T. Morimoto, H. Takahashi, K. Fujii, M. Chiba, K. Achiwa, *Chem. Lett.* **1986**, 2061.

14 A. Broger, Y. Crameri, *EP 0218970* **1987**; R. Schmid, *Chimia* **1996**, 50, 110.

15 (a) A. Karim, A. Mortreux, F. Petit, G. Buono, G. Peiffer, C. Siv, *J. Organomet. Chem.* **1986**, *317*, 93; (b) C. Hatat, A. Karim, N. Kokel, A.Mortreux, F. Petit, *Tetrahedron Lett.* **1988**, 29, 3675; (c) C. Hatat, A. Karim, N. Kokel, A. Mor-

treux, F. Petit, *New J. Chem.* **1990**, *14*, 141; (d) A. Roucoux, F. Agbossou, A. Mortreux, F. Petit, *Tetrahedron: Asymm.* **1993**, *4*, 2279; (e) F. Agbossou, J.-F. Carpentier, C. Hatat, N. Kokel, A. Mortreux, P. Betz, R. Goddart, C. Krüger, *Organometallics* **1995**, *14*, 2480; (f) A. Roucoux, M. Devocelle, J.-F. Carpentier, F. Agbossou, A. Mortreux, *Synlett* **1995**, 358; (g) A. Roucoux, L. Thieffry, J.-F. Carpentier, M. Devocelle, C. Méliet, F. Agbossou, A. Mortreux, A. J. Welch, *Organometallics* **1996**, *15*, 2440; (h) A. Roucoux, I. Suisse, M. Devocelle, J.-F. Carpentier, F. Agbossou, A. Mortreux, *Tetrahedron: Asymm.* **1996**, *2*, 379; (i) M. Devocelle, F. Agbossou, A. Mortreux, *Synlett* **1997**, 1306; (j) J.-F. Carpentier, A. Mortreux, *Tetrahedron: Asymm.* **1997**, *8*, 1083; (k) C. Pasquier, S. Naili, L. Pelinski, J. Brocard, A. Mortreux, F. Agbossou, *Tetrahedron: Asymm.* **1998**, *9*, 193; (l) F. Agbossou, J.-F. Carpentier, F. Hapiot, I. Suisse, A. Mortreux, *Coord. Chem. Rev.* **1998**, *178*, 1615; (m) V. Blandin, J. F. Carpentier, A. Mortreux, *Eur. J. Org. Chem.* **1999**, 1787; (n) M. Devocelle, A. Mortreux, F. Agbossou, J.-R. Dormoy, *Tetrahedron Lett.*, **1999**, *40*, 4551; (o) C. Pasquier, S. Naili, A. Mortreux, F. Agbossou, L. Pélinski, J. Brocard, J. Eilers, I. Reiners, V. Peper, J. Martens, *Organometallics* **2000**, *19*, 5723; (p) C. Pasquier, S. Naili, L. Pelinski, J. Brocard, A. Mortreux, F. Agbossou, *Tetrahedron Lett.* **2001**, *42*, 2809.

16 Examples of carbohydrate diphosphinites: (a) R. Selke, H. Pracejus, *J. Mol. Catal.* **1986**, *37*, 213 and references cited therein; (b) R. Selke, *J. Mol. Catal.* **1986**, *37*, 227; (c) R. Selke, M. Schwarze, H. Baudish, I. Grassert, M. Michalik, G. Oehme, N. Stoll, B. Costisella, *J. Mol. Catal.* **1993**, *84*, 223; (d) R. J. Selke, *Organomet. Chem.* **1989**, *370*, 241; (e) W. R. Cullen, Y. Sugi, *Tetrahedron Lett.* **1978**, *19*, 1635; (f) H.-J. Kreutzfeld, C. Döbler, H. W. Krause, B. Facklam, *Tetrahedron: Asymm.* **1993**, *4*, 2047; (g) T. V. RajanBabu, T. A. Ayers, A. L. Casalnuovo, *J. Am. Chem. Soc.* **1994**, *62*, 6012; (h) T. V. RajanBabu, B. Radetich, K. K. You, T. A. Ayers, A. L. Casalnuovo, J. C. Calabrese, *J. Org. Chem.* **1999**, *64*, 3429.

17 For examples of open-chain sugar-based diphosphanes: (a) M. Yamashita, M. Naoi, H. Imoto, T. Oshikawa, *Bull. Soc. Chem. Jpn.* **1989**, *62*, 942; (b) Y. Chen, Li, X., S. K. Tong, M. C. K. Choi, A. S. C. Chan, *Tetrahedron Lett.* **1999**, *40*, 957; (c) A. Bendaya, H. Masotti, G. Peiffer, C. Siv, A. Archalvis, *J. Organomet. Chem.* **1993**, *444*, 41; (d) B.M. Choudary, M. Ravichandra Sarma, A. Dyurga Prasad, N. Narender, *Indian J. Chem.* **1994**, *33B*, 152.

18 (a) S. Naili, I. Suisse A. Mortreux, F. Agbossou, M. Ait Ali, A. Karim, *Tetrahedron Lett.* **2000**, *41*, 2867.

19 N. W. Boaz, S. D. Debenham, E. B. Mackenzie, S. E. Large, *Org. Lett.* **2002**, *14*, 2421.

20 (a) T. Hayashi, M. Mise, M. Kumada, *Tetrahedron Lett.* **1976**, 4351; (b) T. Hayashi, A. Katsumura, M. Konishi, M. Kumada, *Tetrahedron Lett.* **1979**, 425; (c) K. Inoguchi, S. Sakuraba, K. Achiwa, *Synlett*, **1992**, 169.

21 H. Takahashi, S. Sakuraba, H. Takeda, K. Achiwa, *J. Am. Chem. Soc.* **1990**, *112*, 5876.

22 (a) H. Takeda, S. Hosokawa, M. Aburatani, K. Achiwa, *Synlett* **1991**, 193; (b) S. Sakuraba, K. Achiwa, *Synlett* **1991**, 689.

23 (a) H. Takeda, T. Tachinami, M. Aburatani, H. Takahashi, T. Motimoto, K. Achiwa, *Tetrahedron Lett.* **1989**, *30*, 363; (b) H. Takeda, T. Tachinami, M. Aburatani, H. Takahashi, T. Motimoto, K. Achiwa, *Tetrahedron Lett.* **1989**, *30*, 367.

24 H. Takahashi, T. Morimoto, K. Achiwa *Chem. Lett.* **1987**, 855.

25 S. Törös, B. Heil, L. Kollár, L. Markó *J. Organomet. Chem.* **1982**, *232*, C17.

26 D. Liu, W. Gao, C. Wang, X. Zhang, *Angew. Chem. Int. Ed.* **2005**, *44*, 1687.

27 A. Togni, C. Breutel, A. Schnyder, F. Spindler, H. Landert, A. Tijani, *J. Am. Chem. Soc.* **1994**, *116*, 4062.

28 F. Cederbaum, C. Lamberth, C. Malan, F. Naud, F. Spindler, M. Studer, H. U. Blaser, *Adv. Synth. Catal.* **2004**, *346*, 842.

29 P. Kreye, A. Lehnhart, F. D. Klingler, Boehringer Ingelheim Pharma GmbH & Co. K.-G., (Germany). German Patent (2004), 6 pp. DE 10249576 B3 20040408.

30 S. Sakuraba, N. Nakajima, K. Achiwa *Tetrahedron: Asymm.* **1993**, (4), 1457.

31 T. Morimoto, K. Yoshikawa, M. Murata, N. Yamamoto, K. Achiwa. *Chem. Pharm. Bull.* **2004**, 52, 1445.

32 For enantioselective synthesis of compounds **55a**, **55b** and **56**, see: (a) V. Ratovelomanana-Vidal, C. Girard, R. Touati, J.P. Tranchier, B.B. Hassine, J.P. Genêt, *Adv. Synth. Catal.* **2003**, *345*, 261, and references therein. For enantioselective synthesis of **62**, see: (a); for **59**: J. Deeter, J. Frazier, G. Staten, M. Staszak, L. Weigel, *Tetrahedron Lett.* **1990**, *31*, 7101; **60**: H. Liu, B.H. Hoff, T. Anthonsen, *Chirality* **2000**, *12*, 26; **61**: A. Kamal, G.B.R. Khanna, R. Ramu, T. Krishnaji, *Tetrahedron Lett.* **2003**, *44*, 4783.

33 H.P. Märki, Y. Crameri, R. Eigenmann, A. Krasso, H. Ramuz, K. Bernauer, M. Goodman, K.L. Melmon, *Helv. Chim. Acta* **1988**, *71*, 320.

34 R.G. Griffiths, J. Dancer, E. O'Neill, J.L. Harwood, *New Phytologist* **2003**, *158*, 345.

35 O. Ort, U. Döller, W. Reissel, S.D. Lindell, T.L. Hough, D.J. Simpson, J.P. Chung, *Pesticide Sci.* **1997**, *50*, 331.

36 Y. Kuroki, Y. Sakamaki, K. Iseki, *Org. Lett.* **2001**, *3*, 457.

37 Y. Kuroki, D. Asada, K. Iseki, *Tetrahedron. Lett.* **2000**, *41*, 9853.

38 N. Sakai, S. Mano, K. Nozaki, H. Takaya, *J. Am. Chem. Soc.* **1993**, *115*, 7033.

39 Y. Pottier, A. Mortreux, F. Petit, *J. Organomet. Chem.* **1989**, *370*, 333.

34
Enantioselective Hydrogenation of C=N Functions and Enamines

Felix Spindler and Hans-Ulrich Blaser

34.1
Introduction

Chiral amines were always considered important targets for synthetic chemists, and attempts to prepare such compounds enantioselectively date back to quite early times. Selected milestones for the development of enantioselective catalysts for the reduction of C=N functions are listed in Table 34.1. At first, only heterogeneous hydrogenation catalysts such as Pt black, Pd/C or Raney nickel were applied. These were modified with chiral auxiliaries in the hope that some induction – that is, transfer of chirality from the auxiliary to the reactant – might occur. These efforts were undertaken on a purely empirical basis, without any understanding of what might influence the desired selectivity. Only very few substrate types were studied and, not surprisingly, enantioselectivities were

Table 34.1 Selected milestones for the enantioselective hydrogenation of C=N functions.

Year	Substrate	Catalyst	Chiral auxiliary [a)]	ee [%]	Comment	Reference
1941	oxime	Pt black	Menthoxyacetic acid	3	First reported experiment	1
1958	dioxime	Pd	Silk fibroin	15	Chiral support	2
1975	oxime	Ru complex	diop	15	Homogeneous Ru catalyst	3
1975	imine	Rh complex	diop	22	Homogeneous Rh catalyst	4
1984	C=N–Alk	Rh complex	bdpp	72	First useful ee	5
1989	C=N–Alk	Rh complex	$bdpp_{sulf}$	94	First very high ee	6
1990	C=N–Ar	Ir complex	bdpp	84	Homogeneous Ir catalyst	7
1992	cycl. imine	Ti complex	ebthi	99	Homogeneous Ti catalyst	8
1992	C=N–X	Rh complex	duphos	96	Acyl hydrazone	9
1996	C=N–X	Ru complex	N′N ligand	97	Transfer hydrogenation	10
1996	MEA imine	Ir complex	josiphos	80	First industrial application	11

a) For structures of ligands, see Figs. 34.1 and 34.3.

The Handbook of Homogeneous Hydrogenation.
Edited by J.G. de Vries and C.J. Elsevier
Copyright © 2007 WILEY-VCH Verlag GmbH & Co. KGaA, Weinheim
ISBN: 978-3-527-31161-3

low and could not always be reproduced. The first reports on homogeneous Ru and Rh catalysts appeared in 1975, but useful enantioselectivities were only reported in 1984 by the Marko group. Remarkable progress has been made during the 1990s, however, and today several very selective catalysts are available for different types of C=N functions, with the first industrial process being announced in 1996.

Despite this significant progress, the enantioselective hydrogenation of prochiral C=N groups (imines, oximes, hydrazones, etc.) and enamines to obtain the corresponding chiral amines still represents a major challenge. Whereas many highly enantioselective chiral catalysts have been developed for the asymmetric hydrogenation of alkenes and ketones bearing various functional groups, much fewer catalysts are effective for the hydrogenation of substrates with a C=N function (for pertinent recent reviews, see [12–17]). There are several reasons that might explain this situation. On the one hand, the enantioselective hydrogenation of enamides and other C=C groups (and later also of C=O compounds) was so successful that most attention was directed to these substrates [12]. On the other hand, C=N compounds have some chemical peculiarities that make their stereoselective reduction more complex than that of C=O and C=C compounds. Even though the preparation starting from the corresponding amine derivative and carbonyl compound is relatively simple, complete conversion is not always possible and formation of trimers or oligomers can occur. Both the starting amine (e.g., [6 a]) and the oligomers can be catalyst poisons. In addition, the resulting C=N compounds are often sensitive to hydrolysis and the presence of *syn*/*anti* as well as enamine isomers can be a problem for selective hydrogenation.

Generally, the imine substrates are prepared from the corresponding ketone and amine and are hydrogenated as isolated (and purified) compounds. However, reductive amination where the C=N function is prepared *in situ* is attractive from an industrial point of view, and indeed there are some successful examples reported below [18, 19]. It is reasonably certain that most catalysts described in this chapter catalyze the addition of H_2 directly to the C=N bond and not to the tautomeric enamine C=C bond, even though enamines can also be hydrogenated enantioselectively.

The nature of the substituent directly attached to the N-atom influences the properties (basicity, reduction potential, etc.) of the C=N function more than the substituents at the carbon atom. For example, it was found that Ir-diphosphine catalysts that are very active for N-aryl imines are deactivated rapidly when applied for aliphatic imines [7], or that titanocene-based catalysts are active only for *N*-alkyl imines but not for *N*-aryl imines [8, 20, 21]. Oximes and other C=N–X compounds show even more pronounced differences in reactivity.

The following sections provide an overview on the state of the art for the enantioselective hydrogenation (including transfer hydrogenation) of various classes of C=N groups, together with a short, critical assessment of the presently known catalytic systems. Only selective (ee >80%) or otherwise interesting catalysts are included and, furthermore, other reduction methods for C=N functions (hydride reduction, hydrosilylation) are only covered summarily.

34.2
Chiral Ligands

The catalytic properties of an enantioselective homogeneous catalyst are determined by the choice of the metal, the chiral ligand, and the anion. Since the choice of metals is limited – only Ir, Rh, Ru and Ti have proved to be effective – and the anion is usually either coordinating or non-coordinating (leading to cationic catalysts), the chiral ligand is the most important parameter controlling catalyst performance. For the reduction of the various C=N functions, several ligand types have been shown to give satisfactory to very good catalytic properties

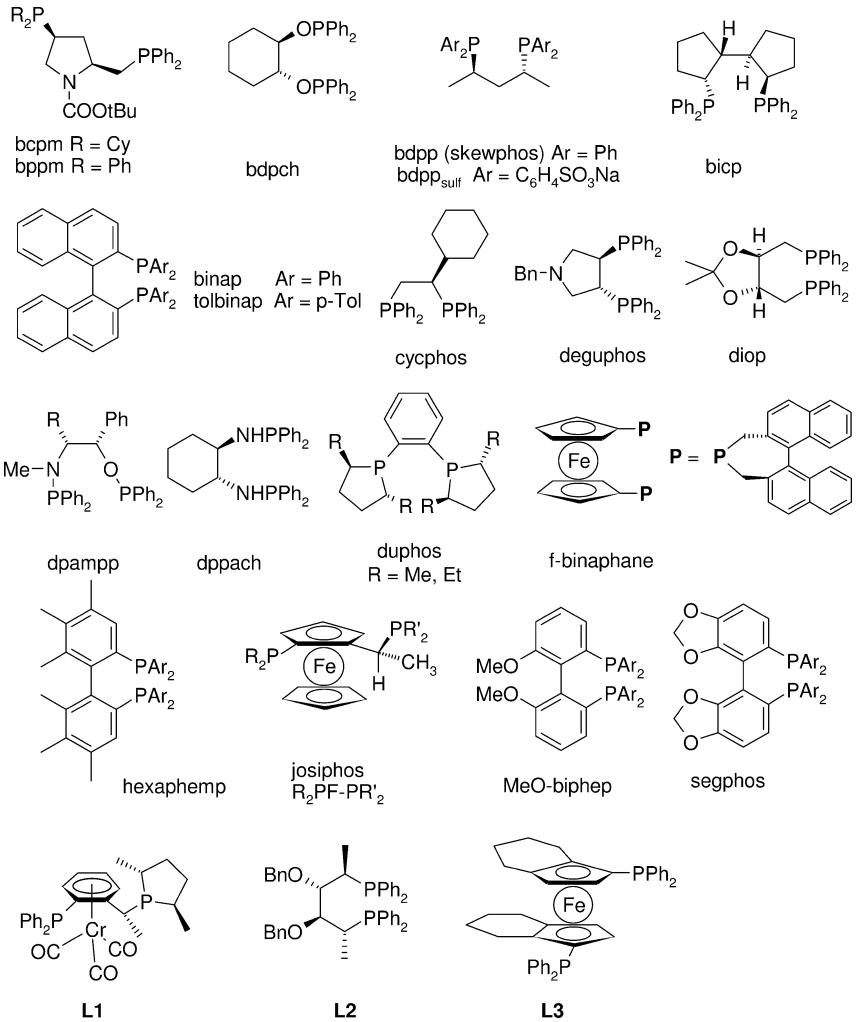

Fig. 34.1 Structures and abbreviations/numbers for diphosphine ligands.

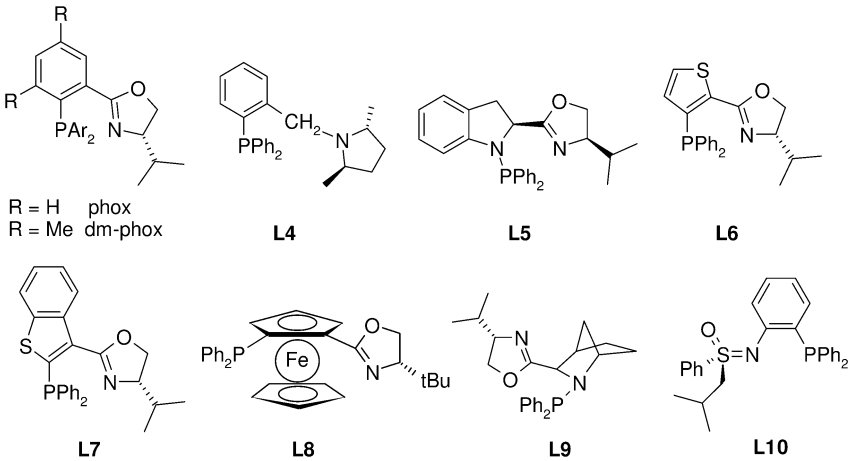

Fig. 34.2 Structures and abbreviations/numbers for PN ligands.

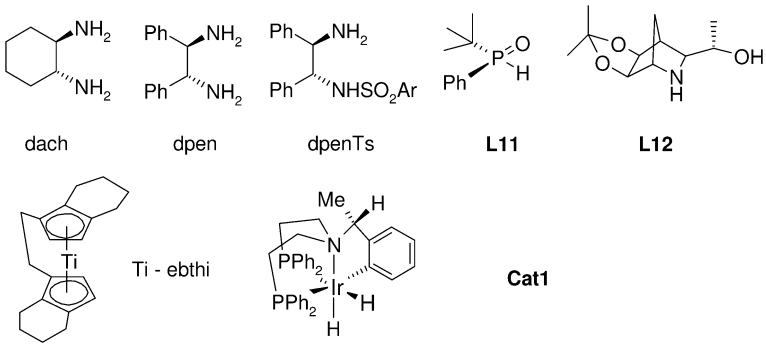

Fig. 34.3 Structures and abbreviations/numbers for miscellaneous ligands and catalysts.

– that is, enantioselectivity (ee, %), productivity (turnover number; TON) or substrate:catalyst ratio (SCR) and activity (turnover frequency; TOF; h^{-1}). We have depicted the most important ligands in Figs. 34.1 to 34.3, arranged either alphabetically for those with a name, or numbered as **Lx**. A cursory investigation of the depicted ligands shows a bewildering diversity of structural elements. Most ligands have actually been prepared not with the reduction of C=N compounds in mind, but have first been tested on C=C or C=O groups and later shown also to be viable for C=N functions. Most ligands are not (yet) available commercially, which diminishes their attractiveness for synthetic applications.

34.3
N-Aryl Imines

With the exception of the (*S*)-metolachlor process, no C=N hydrogenation has been commercialized and most investigations described in this chapter have been carried out with a few model substrates. Much effort has been devoted in identifying catalysts which are able to hydrogenate substrates of the type **1** (see Fig. 34.4), since *N*-alkyl-2,6-disubstituted anilines with a stereogenic C-atom in the *α*-position are intermediates for a number of important acylanilide pesticides, the most important example being the herbicide Metolachlor® (Fig. 34.5) [11, 22]. Since not all stereoisomers are biologically active, the stereoselective synthesis of the most effective ones is of industrial interest. Hence, the enantioselective hydrogenation of the imine **1a** will be discussed in somewhat more detail.

Hydrogenation of the imines **1a** and **1b** was investigated extensively by several research groups [28]. Whilst, initially, useful results were obtained with chiral Rh diphosphine catalysts [29], an important step towards a technically feasible catalyst was made with newly developed Ir diphosphine complexes [7]. Despite a significant tendency for deactivation, SCR values of ≥10 000 and reasonable reaction rates were achieved for the hydrogenation of MEA-imine with an Ir–diop complex in the presence of iodide ions (Table 34.2; entry 2.1). The hydrogenation of other *N*-aryl imines with similar structural elements showed that both the 2,6-alkyl substituents of the *N*-phenyl group as well as the methoxy-substituent contribute to the high enantioselectivity. Replacing the methoxy group of the DMA-imine **1b** by an ethyl group led to a decrease in ee from 69% to 52%, while further replacement of the 2,6-dimethyl phenyl by a phenyl group reduced the ee to 18% [7]. Despite these good results, both catalyst activity as well as productivity were insufficient for a technical application for a high-volume product.

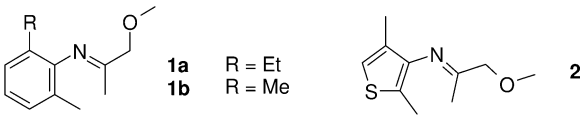

Fig. 34.4 Structures of *N*-aryl imines.

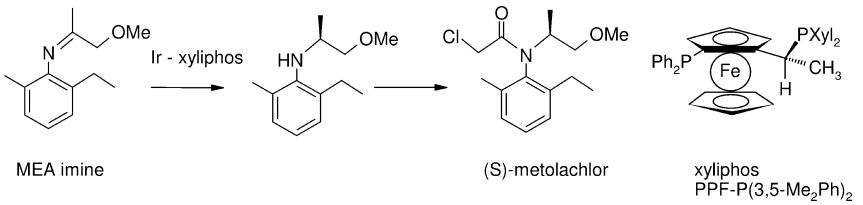

Fig. 34.5 Synthesis of *S*-metolachlor.

Table 34.2 Selected results for the enantioselective hydrogenation of *N*-aryl imines **1** and **2** (for structures, see Fig. 34.4): Catalytic system, reaction conditions, enantioselectivity, productivity and activity.

Entry	Substrate	Catalyst	p [bar]	ee [%]	SCR	TOF [h^{-1}]	Reference
2.1	**1a**	Ir–diop/I^-	100	62	10 000	200	7
2.2	**1a**	Ir–PPF-$PXyl_2$/I^-/H^+	80	78	1 000 000	350 000	23
2.3	**1a**	Ir–PPF-PAr_2 [a)]/I^-/H^+	80	87	5 000	31	23
2.4	**2**	Ir–PPF-$Pxyl_2$/ I^-/H^+	60	80	100	200	23
2.5	**1b**	[Ir(diop)$(OCOCF_3)_3$]	40	90	500	3	24
2.6	**1a** [b)]	Ir–PPF-$PXyl_2$/I^-/H^+	80	78	10 000	>600	25
2.7	**1a**	Ir–PPF-$PXyl_2$ [c)]/I^-/H^+	80	78	120 000	12 000	26
2.8	**1a**	Ir–**L1**	80	82	100	~6	27

Reactions carried out between r.t. and 50 °C, unless otherwise noted.
a) Ar = 3,5-Me_2-4-NPr_2-Ph.
b) Formed *in situ* from 2-methyl-6-ethyl-aniline + methoxyacetone.
c) Immobilized on SiO_2.
SCR: Substrate:catalyst ratio.

The final breakthrough on the way to a production process for the metolachlor herbicide came in 1993. A new class of Ir–ferrocenyl diphosphine complexes turned out to be stable and, in the presence of both acetic acid and iodide, provided extraordinarily active and productive catalysts which also did not deactivate [30]. An extensive ligand optimization led to the choice of $[Ir(cod)Cl]_2$-PPF-$PXyl_2$ (xyliphos) as the optimal catalyst. At a hydrogen pressure of 80 bar, a temperature of 50 °C, and using an SCR of >10 000, complete conversion could be reached within 3–4 h with an enantiomeric excess of around 80% (Table 34.2; entry 2.2). The best enantioselectivities of 87% were obtained with N-substituted xyliphos ligands, albeit with much lower activity (e.g., see entry 2.3). It is noteworthy, that the 2,6-disubstituted phenyl group in **1** could be replaced by a 2,4-disubstituted thien-3-yl group (imine **2**) without loss in catalyst activity (entry 2.4). Scale-up presented no major problems, and the production plant was opened officially in November 1996. At present, there is no convincing explanation for the remarkable effect of iodide and acid and, interestingly, Osborn and Sablong reported that completely halogen-free catalysts can also give very good enantioselectivities (e.g., 90% ee with imine **1b**) (entry 2.5). The Ir-xyliphos catalyst was also tested for the reductive amination where the MEA imine is prepared *in situ* [25], as well in an immobilized version [26]. However, while for both variants the ee-values were satisfactory, catalyst productivity was not sufficient for a commercial application (Table 34.2; entries 2.6 and 2.7). Even though the scope of this new catalytic system has not yet been fully determined, it was successfully applied to the hydrogenation of imines **2** (entry 2.4), **3a** and **9** (see below). Recently, Salzer reported very good ee-values

with an interesting josiphos analogue **L1** based on an arene chromium tricarbonyl scaffold, but the TON and TOF were both very low (entry 2.8).

As can be seen from the data in Table 34.3, there are today a number of catalysts achieving medium to very high ee-values for the model substrates of the type **3**. Most of the successful catalyst systems are Ir-diphosphines, inspired by the catalysts described above for the metolachlor production and Ir-phosphinooxazoline complexes originally developed by Pfaltz [31].

Ir–josiphos and the Ir–f-binaphane catalyst developed by Zhang and coworkers achieved ee-values of 94 to >99% with several imines of the type **3** (Table 34.3; entries 3.1, 3.2, 3.8) and in presence of 1.5 equiv. Ti(*Oi*Pr)$_4$. Ir–f-binaphane was also able to catalyze the reductive amination of aromatic ketones with a variety of substituted anilines with high ee-values but relatively low catalyst activity (entry 3.9). Claver and coworkers achieved ee-values of up to 57% for the Ir-catalyzed hydrogenation of **3b** using sugar-derived bisphosphinite and bisphosphite ligands [39], while Vargas et al. [40] reported 84% ee with an Ir-phosphine-phosphite catalyst.

Several new PN ligands were developed and tested using model substrates **3**. The Ir-phox catalyst originally developed by Pfaltz achieved ee-values of up to 89% with reasonable TONs which could be increased up to 6800 in supercritical CO_2 (scCO_2), albeit with some loss in enantioselectivity (Table 34.3; entries 3.3, 3.4). Ir catalysts with similar P-N ligands also achieved respectable catalyst performances (see entries 3.5, 3.6, 3.10). It was also shown that various Ir-phosphinooxazoline catalysts work well in sCO_2-ionic liquid systems, allowing easy separation and recycling of the catalyst with similar catalyst performance [31b]. Very recently, Moessner and Bolm [41] reported phosphinosulfoximines such as **L10** as a new, very efficient ligand class for the Ir-catalyzed hydrogenation of selected *N*-aryl imines. The best enantioselectivities (90–98% ee) were obtained for imines with an *N*-(*p*-MeO)-phenyl group, with TONs up to 1000 (e.g., see entry 3.11). The addition of iodine is required in order to produce an active catalyst.

Ru–diphosphine–diamine complexes developed originally by Noyori for the hydrogenation of aryl ketones are also suitable for the hydrogenation of imines. The best results are obtained for *N*-aryl imines where a Ru–duphos–diamine complex achieved up to 94% ee, albeit with relatively low activity and productivity (entry 3.7) (for data relating to cyclic imines, see Table 34.5).

Besides these results, we registered with interest the first example of a Pd–binap-catalyzed hydrogenation of a fluorinated α-imino ester in the presence of trifluoroacetic acid in fluorinated alcohols (with ee-values up to 91%, but very low TON and TOF) [42].

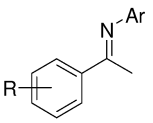

3a	Ar = Ph	R = 3,5-Me$_2$
3b	Ar = Ph	R = H
3c	Ar = o-Xyl	var. R
3d	Ar = p-An	var. R
3e	var. Ar	var. R

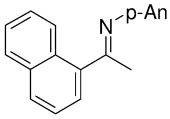

3f

Fig. 34.6 Structure of *N*-aryl imines.

Table 34.3 Selected results for the enantioselective hydrogenation of the model *N*-aryl imines **3** (for structures, see Fig. 34.6): Catalytic system, reaction conditions, enantioselectivity, productivity and activity.

Entry	Substrate	Catalyst	p [bar]	ee [%]	SCR	TOF [h^{-1}]	Reference(s)
3.1	**3a**	Ir–PPF-P(4-CF_3Ph)$_2$/I^-/H^+	80	96	200	n.a.	23
3.2	**3a**	Ir–f-binaphane	~70	>99	100	2–4	32
3.3	**3b**	Ir–dm-phox	100	89 [a)]	1000	~100	31a
3.4	**3b**	Ir–phox (scCO_2)	30	74	6800	2800	33
3.5	**3b**	Ir–**L5**	20	90	50	4	34a
3.6	**3b**	Ir–**L6** or **L7**	50	83–86	1000	250	34b
3.7	**3b**	Ru–Et-duphos–diamine [b)]/ *t*BuOK	15	92–94	100	≤5	35, 36
3.8	**3c**	Ir–f-binaphane/I_2	~70	94–95	100	2–4	32
3.9	**3d** [c)]	Ir–f-binaphane/I_2/Ti(*O*iPr)$_4$	~70	90–96	100	10	37
3.10	**3e**	Ir–**L9**	20	80–90	200	~100	38
3.11	**3f**	Ir–**L10**/I_2	20	98	200 [d)]	50	41

Reactions carried out between r.t. and 50 °C, unless otherwise noted.
a) At 5 °C.
b) dach or dpen.
c) Formed *in situ* from the corresponding acetophenones and anilines.
d) At SCR 1000, a pressure of 50 bar is required for full conversion.
n.a.: data not available.

34.4 *N*-Alkyl Imines

Until now, few acyclic *N*-alkyl imines or the corresponding amines have been found to be of practical industrial importance. Most studies reported herein were carried out with model substrates, especially with the *N*-benzyl imine of acetophenone **5a** and some analogues thereof (Fig. 34.7). One reason for this choice could be the easy preparation of a pure crystalline starting material, and another reason might be that the chiral primary amines can be obtained by hydrogenolysis of the benzyl group. As can be seen in Table 34.4, there are several catalyst systems with fair to good ee-values and activities.

Enantioselectivities >90% were reported for a Ti–ebthi catalyst (Table 34.4; entry 4.1) and for some Rh–diphosphine complexes (entries 4.2–4.4). Interestingly, the highest ee-values were obtained using sulfonated diphosphines (bdpp$_{sulf}$) in an aqueous biphasic medium (entry 4.3). The degree of sulfonation strongly affected the enantioselectivity: the Rh–mono-sulfonated bdpp gave 94% ee, compared to 65% ee with Rh–bdpp in MeOH, and almost racemic product with bis- or tris-sulfonated ligands. In addition, the activity of the mono-sulfonated cata-

Table 34.4 Selected results for the enantioselective hydrogenation of *N*-alkyl imines and enamines (for structures, see Fig. 34.7): Catalytic system, reaction conditions, enantioselectivity, productivity and activity.

Entry	Substrate	Catalyst	p [bar]	ee [%]	SCR	TOF [h^{-1}]	Reference
4.1	**4**	Ti–ebthi	5	92	20	4	21
4.2	**5a**	Rh–cycphos	100	91	100	0.7	43
4.3	**5a**	Rh–$bdpp_{sulf}$	70	96	100	16	6b
4.4	**5b**	Rh–bdpp/AOT micelles	70	92	100	4.6	44
4.5	**5a**	Ir–**L4**	100	46	100	>36 000	45
4.6	**5a**	Ir–**L5**	50	82	50	4	34
4.7	**5a**	Ru–dppach–dach	3	92	1500	23	47
4.8	**5**	Ir–**L11**/pyridine	25	80–83	20	<1	46
4.9	a)	Rh–deguphos	60	98	200	~60	48

Reactions carried out between r.t. and 50 °C, unless otherwise noted.

a) Reductive amination of PhCOCOOH or $PhCH_2COCOOH$ with $BnNH_2$.

lyst was higher by a factor of 5 compared to bdpp [6b]. A similar positive effect for the presence of a sulfo group was described by Buriak and Osborn (entry 4.4). *N*-Alkyl imines of cyclic ketones can be reduced with moderate to good enantioselectivities using a Ru–diamine complex and formate as transfer reducing agent, but the catalytic activities and productivities for all of these catalysts ranged from very low to modest [10].

Ir–PN catalysts which are quite effective for *N*-aryl imines also show some promise for *N*-alkyl derivatives. Of special interest were the high TOF claimed for the Ir–**L4** system, but unfortunately the ee is very low (entry 4.5). Several other Ir–PN were described with moderate to good ee-values, but again the TON and TOF were modest, as shown (Table 34.4; entry 4.6 (see also [49]).

Imine **5a** is also hydrogenated with good ee and TON using a Ru–diphosphine–diamine complex originally developed by Noyori (entry 4.7). An unusual

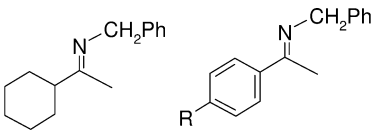

4 **5a** R = H
5b R = OMe

Fig. 34.7 Structures of *N*-alkyl imines.

catalyst was developed by Feringa and de Vries, who applied secondary phosphine oxides of the type **L11** for the Ir-catalyzed hydrogenation of various benzyl imines **5**. While the enantioselectivities were surprisingly good, activity and productivity were very low (e.g., see entry 4.8).

Recently, Börner and coworkers described an efficient Rh–deguphos catalyst for the reductive amination of α-keto acids with benzyl amine. *E.e.*-values up to 98% were obtained for the reaction of phenyl pyruvic acid and $PhCH_2COCOOH$ (entry 4.9), albeit with often incomplete conversion and low TOFs. Similar results were also obtained for several other α-keto acids, and also with ligands such as norphos and chiraphos. An interesting variant for the preparation of α-amino acid derivatives is the one-pot preparation of aromatic α-(*N*-cyclohexylamino) amides from the corresponding aryl iodide, cyclohexylamine under a H_2/CO atmosphere catalyzed by Pd–duphos or Pd–Trost ligands [50]. Yields and ee-values were in the order of 30–50% and 90>99%, respectively, and a catalyst loading of around 4% was necessary.

Besides these results, we registered with interest the claim by Magee and Norton [51] that (Cp)W–diphosphine complexes are able to hydrogenate imines via a novel ionic mechanism, albeit with low ee and TOF.

34.5 Cyclic Imines and Heteraromatic Substrates

Cyclic imines do not have the problem of *syn*/*anti* isomerism and therefore, in principle, higher enantioselectivities can be expected (Fig. 34.8). Several cyclic model substrates **6** were hydrogenated using the Ti–ebthi catalyst, with ee-values up to 99% (Table 34.5; entry 5.1), whereas enantioselectivities for acyclic imines were ≤90% [20, 21]. Unfortunately, these very selective catalysts operate at low SCRs and exhibit TOFs $<3\ h^{-1}$. In this respect, iridium–diphosphine catalysts, in the presence of various additives, seem more promising because they show higher activities. With several different ligands such as josiphos, bicp, bi-

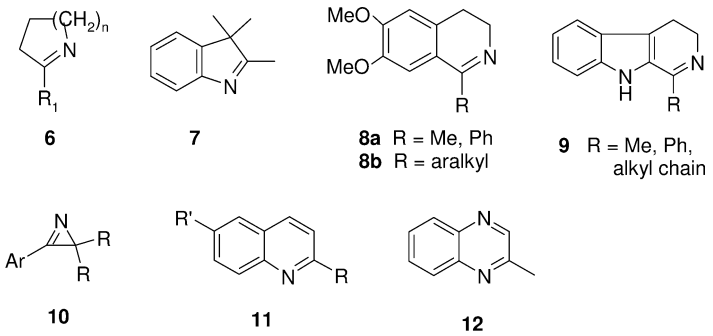

Fig. 34.8 Structures of cyclic imines and heteroaromatic substrates.

Table 34.5 Selected results for the enantioselective hydrogenation of cyclic imines (for structures, see Fig. 34.8): Catalytic system, reaction conditions, enantioselectivity, productivity and activity.

Entry	Substrate	Catalyst	p [bar]	ee [%]	SCR	TOF [h^{-1}]	Reference
5.1	**6**	Ti–ebthi	5	99	100	up to 2	8
5.2	**7**	Ir–bicp/phthalimide	70	95	200	2	52
5.3	**7**	Ir–Xyl_2PF-$PXyl_2/I^-/H^+$	40	93	250	56	23
5.4	**7**	Ir–Tol-binap/$PhCH_2NH_2$	60	90	100	6	53
5.5	**7**	Ir–**L2**/I_2	~70	82–85	100	~4	54
5.6	**7**	Ir–**L3**	65	79	100	~5	55
5.7	**8a**	Ti–ebthi	5	96	20	<1	8
5.8	**8a**	Ru–dpenTs	F[a)]	84	200	6–30	10
5.9	**8b**	Ir–bcpm or binap/ F_4-phthalimide	100	86–88	100	5	56
5.10	**8b**	Ru–dpenTs	F[a)]	92–95	200	15–30	10
5.11	**9**	Ru–dpenTs	F[a)]	96–97	1000	35–83	10
5.12	**9**	Ru–dpenTs	F[a)]	>98	~2000	~800	57
5.13	**10**	Ru–**L12**/*i*PrOH	IP[a)]	44–78	100	up to 3000	58
5.14	**11**	Ir–**L7**/I_2	~40	90–92	1000	~80	59
5.15	**11**[b)]	Ir–MeO-biphep/I_2	50	90–96	100	~6	60
5.16	**11**[b)]	Ir–P-phos	50	88–92	100	~6	61
5.17	**12**	**Cat1** (see Fig. 34.3)	5[c)]	90	100	~4	62

Reactions carried out between r.t. and 50 °C, unless otherwise noted.
a) Reducing agent ammonium formate (F) or *i*PrOH (IP).
b) With a wide variety of R and R' substituents.
c) At 100 °C, yield 54%.

nap or the diop analogue **L2**, model compound **7** was reduced with ee-values of 79–94% Only moderate TONs and, with the exception of Ir–josiphos, also very low TOFs were observed (entries 5.2–5.6). Interestingly, the best enantioselectivities were achieved in the presence of a variety of additives with unknown function. Recently, Giernoth demonstrated that the reaction with an Ir–josiphos catalyst could also be carried out in ionic liquids, with slightly lower enantioselectivities but similar catalyst activities [63].

Cyclic imines **8** and **9** are intermediates or models of biologically active compounds and can be reduced with ee-values of 88 to 96% using Ti–ebthi, Ir–bcpm or Ir–binap in the presence of additives (entries 5.7, 5.9), as well as with the transfer hydrogenation catalyst Ru–dpenTs (entries 5.8, 5.10–5.12). As pointed out earlier, Ru–diphosphine–diamine complexes are also effective for imines, and the best results for **7** and **8a** were 88% and 79% ee, respectively [36]. Azirines **10** are unusual substrates which could be transfer-hydrogenated with a catalyst prepared *in situ* from $[RuCl_2(p\text{-cymene})]_2$ and amino alcohol **L12**, with ee-values of 44 to 78% and respectable TOFs of up to 3000 (entry 5.13).

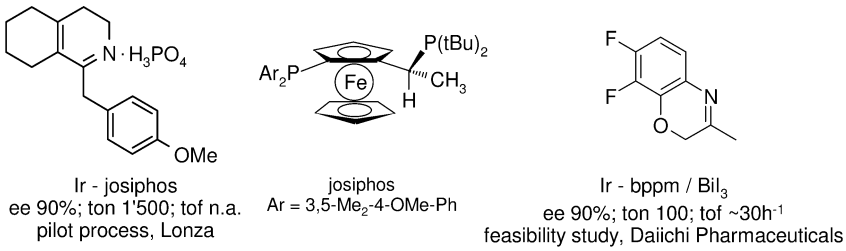

Fig. 34.9 Hydrogenation of a dextromethorphan and levofloxacin intermediate.

The hydrogenation of substituted heteroaromatic substrates such as pyridines, pyrazines or quinolines also allows access to a variety of cyclic amines. Until now, the results with pyridines have been disappointing (ee-values < 30% [64]) except for a report claiming the hydrogenation of *N*-iminium pyridine ylides using Ir–phox catalysts with ee-values up to 90% (TON 50, TOF ~6 h^{-1}) [65]. A patent described the Ir–josiphos-catalyzed hydrogenation of a pyrazine amide with ee-values up to 77% but very low catalyst activity (TON ~20, TOF 1 h^{-1}) [66]. Better results were obtained for the Ir-catalyzed hydrogenation of quinoline derivatives **11** (various R and R′ substituents) using ferrocene-based PN ligand **L7** (entry 5.14), MeO-biphep (entry 5.15) and P-phos (entry 5.16). In the best cases, ee-values of 90–96% were obtained with SCRs up to 1000, leading to full conversion after 12 h. Similarly, quinoxaline **12** was hydrogenated with **Cat1** containing a tridentate PNN ligand (entry 5.17). Quinoxaline **12** serves a model substrate for the diastereoselective reduction of folic acid for which high selectivity was claimed for an Ir–bppm complex adsorbed onto silica, a claim which later had to be retracted [67]. At present, the best stereoselectivities for folic acid derivatives are about 50% diastereomeric excess (d.e.) using water-soluble Rh–josiphos or Rh–biphep catalysts [68, 69].

A technical process was developed by Lonza for the Ir-catalyzed hydrogenation of an intermediate of dextromethorphan (Fig. 34.9) which was carried out on a >100-kg scale [70]. Important success factors were ligand fine tuning and the use of a biphasic system; chemoselectivity with respect to C=C hydrogenation was high, but catalyst productivity rather low for an economical technical application. Satoh et al. reported up to 90% ee for the hydrogenation of an intermediate of the antibiotic levofloxacin using Ir–diphosphine complexes. Best results were obtained with bppm and a modified diop in the presence of bismuth iodide at low temperature [71].

34.6 Miscellaneous C=N–X Systems

Less-common types of C=N derivatives can also be reduced enantioselectively. An interesting example is the hydrogenation of the aromatic *N*-acyl hydrazones **13** with the Rh–duphos catalyst (Table 34.6; entry 6.1). This reaction was devel-

Table 34.6 Selected results for the enantioselective hydrogenation of miscellaneous C=N–X compounds (for structures, see Fig. 34.10): Catalytic system, reaction conditions, enantioselectivity, productivity and activity.

Entry	Substrate	Catalyst	p [bar]	ee [%]	SCR	TOF [h^{-1}]	Reference
6.1	**13**	Rh–duphos	4	88–96	500	14–42	9
6.2	**14**	Ru–binap	4	99	90	6	72
6.3	**15**	Ir–dpampp/I^-	48	93	100[a)]	0.5	73
6.4	**16**	Rh–josiphos, Cy_2PF-PCy_2	70	99	500	500	74

Reactions carried out between r.t. and 50 °C, unless otherwise noted.
a) Conversion 22%.

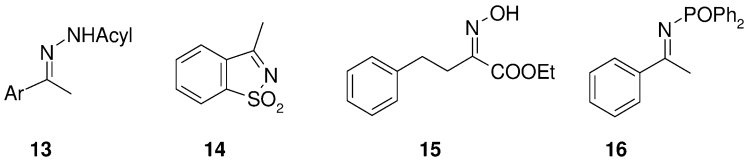

Fig. 34.10 Structures of miscellaneous C=N–X substrates.

oped by Burk et al. [9] in analogy to the well-known hydrogenation of enamides. The results confirm that the presence of a second group in the substrate molecule that is able to bind to the metal is beneficial for achieving high enantioselectivity. The resulting *N*-acyl hydrazines can be reduced to the primary amine using SmI_2, but an effective technical solution for cleavage of the N–N bond to obtain the primary amine without racemization is still lacking. A cyclic *N*-sulfonyl-imine **14** can be hydrogenated with Ru–binap with good to very good enantioselectives (entry 6.2), whereas acyclic analogues are reduced with lower ee-values [75]. Oximes can be hydrogenated with very good enantioselectivity (but low activity) with the novel Ir–dpampp complex (entry 6.3), while Ru–binap [76a] or Rh–binap [76b] were also active but with modest ee-values. Phosphinyl imines

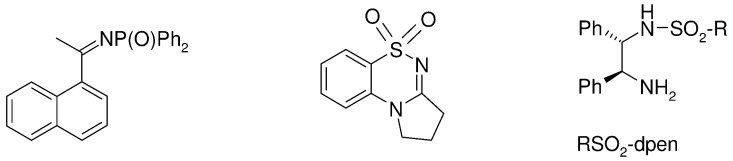

Me5cpRh - RSO2dpen
ee 99%; ton ~1'000; tof 1000h-1
pilot process?, Avecia

Ru - binap - dpen
ee 87%; ton 2'500; tof ~400h-1
bench scale, Dow Chirotech

Fig. 34.11 Industrial processes with C=N–X substrates.

16 are highly suitable substrates for Rh–josiphos catalysts, with ee-values up to 99% (entry 6.4) (Fig. 34.10).

Two technical applications of C=N–X substrates have been reported. Noyori's Ru–PP–NN catalyst system was successfully applied in a feasibility study by Dow Chirotech for the hydrogenation of a sulfonyl amidine [77], while Avecia showed the commercial viability of its CATHy catalyst based on a pentamethyl cyclopentadienyl Rh complex for the reduction of phosphinyl imines [78] (Fig. 34.11).

34.7 Enamines

Until recently, the hydrogenation of enamines has scarcely been investigated. Results have been reported for model substrates **17** and **18**, indicating that such transformations are possible in principle (Fig. 34.12). Substrate **17** was hydrogenated with Ir–diop with ee-values of 60–64% and with Rh–bdpch with 72% ee

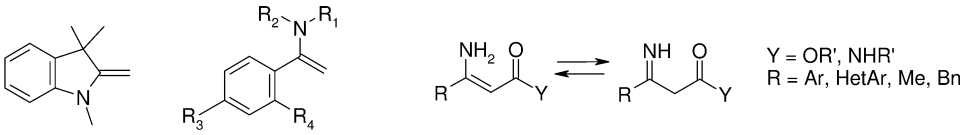

17 **18** **19**

Fig. 34.12 Structures of enamines.

Table 34.7 Selected results for the enantioselective hydrogenation of enamines (for structures, see Fig. 34.12): Catalytic system, reaction conditions, enantioselectivity, productivity and activity.

Entry	Substrate	Catalyst	p [bar]	ee [%]	SCR	TOF [h^{-1}]	Reference
7.1	**17**	Ir–diop/iodide	20	60–64	50	n.a.	79
7.2	**17**	Rh–bdpch	20	60–72	50	n.a.	80
7.3	**18**	Ti–ebthi	1–5	89–98	20	<1	81
7.4	**19**	Rh–josiphos	~6	93–97	330	20–30	82
7.5	**19** [a)]	Ru–tol-binap or segphos	30	94–97	100 [b)]	1–5	83a
7.6	**20**	Rh–josiphos, $(4\text{-}CF_3Ph)_2PF\text{-}PtBu_2$	~6	94	350	50	84

Reactions carried out between r.t. and 50 °C, unless otherwise noted.
a) Y=RO.
b) In some cases SCR 1000, conversions 10–85%.
n.a.: data not available.

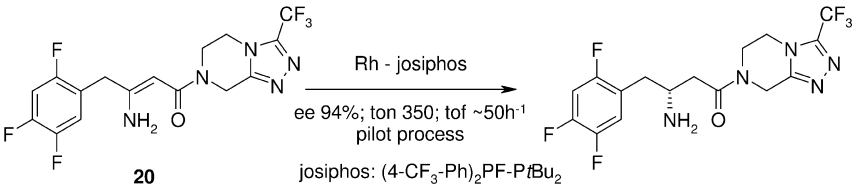

Fig. 34.13 Hydrogenation of the β-dehydro amino acid amide intermediate for MK-0431.

(Table 34.7; entries 7.1 and 7.2). Enamines of the type **18** were reduced in presence of Ti–ebthi with high enantioselectivities of 89–98% (entry 7.3), while Rh–diop achieved only 39% ee [80]. In both cases, catalyst activities and productivities are too low for practical purposes.

This has changed recently with the development of the hydrogenation of primary enamines/imines **19** leading to β-amino acid derivatives, a reaction with considerable synthetic and industrial potential. While the hydrogenation of analogous acylated derivatives is a well-known transformation, it was quite unexpected that the unprotected substrate is amenable to enantioselective hydrogenation. Indeed, two catalysts, Rh–josiphos and Ru–binap (and analogues) were found by Merck [82] and Takasago [83], respectively, at almost the same time. With both catalysts, very good ee-values are achieved for several different derivatives of **19** (Table 34.7; entries 7.4 and 7.5), but for both activity is an issue. While the Rh–josiphos gives high conversion at an SCR of 330 after 6 to 20 h, the Ru–binap catalysts at an SCR of 100 (in some cases 1000) do not give full conversion even after 15 to 88 h. Interestingly, deuteration experiments performed by Merck indicate that it is not the enamine C=C bond which is reduced, but the tautomeric primary imine.

Merck has developed a pilot process for the hydrogenation of an intermediate **20** for MK-0431 (Fig. 34.13) and carried out the reduction on a >50-kg scale with ee-values up to 98%, albeit with low to medium TONs and TOFs [84]. Takasago has developed a reductive amination version where the corresponding β-keto ester is hydrogenated in the presence of amines, giving directly the corresponding β-amino ester, though as yet no details are available of this process [83].

34.8 Mechanistic Aspects

Only a few detailed studies of the reaction mechanism of the homogeneous hydrogenation of imines have been published until now. A generalization seems to be very difficult for two reasons. First, rather different catalyst types are effective and probably act by different mechanisms. Second, the effect of certain additives (especially iodide or iodine and acid/base) is often decisive for ee and rate, but a promoter in one case can be a deactivator in another case.

For Rh and Ir diphosphine-based catalysts there exist some indications on reactive species and also on hydrogen activation. James and coworkers [43, 85] investigated the Rh-catalyzed DMA-imine hydrogenation and concluded that the imine is η^1-coordinated to the Rh center via the nitrogen lone pair, and not via the π-system of the C=N bond. They also suggested that the hydrogen activation occurs after the imine is coordinated.

Osborn and Chan [86] isolated and characterized Ir^{III} complexes of the type: $[Ir(diphosphine)I_4]^-$, $[Ir(diphosphine)I_2]_2$ and $[Ir(diphosphine)I_3]_2$. All three Ir complexes were found to be catalytically active for the hydrogenation of DMA imine **1b**, suggesting the formation of the same active monomeric Ir species as for the *in-situ*-formed catalyst by splitting of the iodo-bridge. Based on these results, the catalytic cycle depicted in Figure 34.14 can be postulated: The starting species is an Ir^{III}–H species that coordinates the imine via the lone pair in a η^1-manner (as proposed for the Rh-catalyzed reaction). A η^1,η^2-migration leads to two diastereomeric adducts with a π-coordinated imine that then inserts into the Ir–H bond to give the corresponding Ir amide complexes. The last step is a simultaneous hydrogenolysis of the Ir–N and the formation of an Ir–H bond, presumably via heterolytic splitting of the dihydrogen bond. In contrast to the Rh diphosphine-catalyzed hydrogenation of C=C bonds that most likely occurs via Rh^I and Rh^{III} species, the cycle in Figure 34.14 consists exclusively of Ir^{III} species. It is clear, that this basic catalytic cycles neither explains the mode of enantioselection nor the sometimes dramatic effects of additives – for example, the strong rate enhancement by acids observed for the Ir–xyliphos-catalyzed MEA imine hydrogenation.

A similar mechanism was postulated for the Ti-catalyzed reactions by Buchwald [21, 87]. The active catalyst was proposed to be the monohydride species ebthi-Ti-H, produced by reacting ebthi-TiR_2 with *n*-BuLi followed by phenylsi-

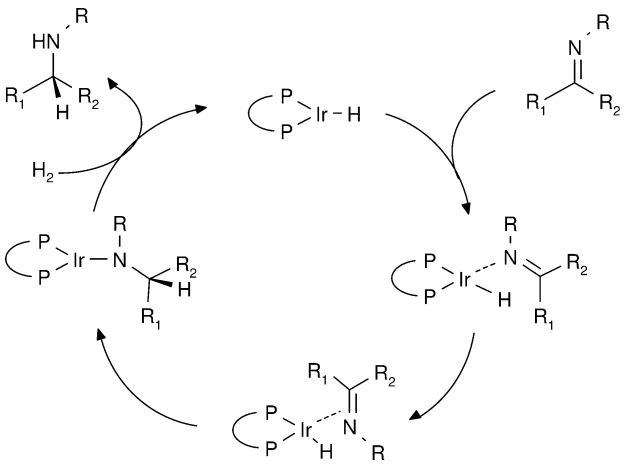

Fig. 34.14 Schematic catalytic cycle postulated for the Ir diphosphine-catalyzed hydrogenation of *N*-aryl imines. For clarity, the halide ligands are not shown.

lane. Kinetic and deuterium-labeling studies are in agreement with the following reaction sequence: Ebthi-Ti-H reacts with the imine via 1,2 insertion reaction to form two diastereomeric Ti amide complexes which react via σ bond metathesis with dihydrogen to regenerate the titanium hydride and to form the two product enantiomers. The reaction of the titanium amide complex with molecular hydrogen is proposed to be the rate-determining step. The discrimination of the catalyst is due only to the size difference of the imine substituents, thereby explaining the potential detrimental effect of the presence of *syn* and *anti* isomers. The absolute configuration of the major enantiomer can be predicted by simple steric arguments, assuming that the 1,2-insertion is the product-determining step.

34.9 Alternative Reduction Systems

Hydride reductions of C=N groups are well known in organic chemistry. It was therefore obvious to try to use chiral auxiliaries in order to render the reducing agent enantioselective [88]. The chiral catalyst is prepared by addition of a chiral diol or amino alcohol, and the active species is formed by reaction of OH or NH groups of the chiral auxiliary with the metal hydride. A major drawback of most hydride reduction methods is the fact that stoichiometric or higher amounts of chiral material are needed and that the hydrolyzed borates and aluminates must be disposed of, which leads to increased costs for the reduction step.

Several stoichiometric chiral reducing agents starting from BH_3, $LiAlH_4$ or $NaBH_4$ and relatively cheap amino alcohols or diols have been developed for the reduction of imines and oxime derivatives [89, 90]. The ee-values are medium to very high. The most effective chiral auxiliaries can be prepared in one or two steps from rather cheap starting materials such as amino acids, tartaric acid or sugars, and they can probably be recycled. As an overall assessment, chiral hydrides are at present useful on a laboratory scale, but their potential for technical applications is medium to low.

The situation for the hydrosilylation of C=N functions with regard to ecology and economy is somewhat similar as for the hydride reduction, except that fewer effective catalytic systems have been developed [91]. Despite some recent progress with highly selective Ti-based [92] and Cu-based [93] catalysts using cheap polymethylhydrosiloxane as reducing agent, hydrosilylation will see its major applications in small-scale laboratory synthesis.

Chiral amines can also be produced using aminotransferases, either by kinetic resolution of the racemic amine or by asymmetric synthesis from the corresponding prochiral ketone. The reaction involves the transfer of an amino group, a proton and two electrons from a primary amine to a ketone, and proceeds via an intermediate imine adduct. A variety of chiral amines can be obtained with high to very high ee-values. Several transformations have been developed and can be carried out on a 100-kg scale [94].

34.10
Assessment of Catalysts and Conclusions

Different criteria are important for assessing the applicability of a catalyst, either for preparative purposes or for the technical manufacture of chiral fine and specialty chemicals [95]. In both cases, enantioselectivity is of course the decisive prerequisite. For preparative use, easy availability and handling of the catalyst will probably play a major role. For technical applications, catalyst activity (TOF), productivity (TON), availability on a large scale and of course cost, also play important roles. In general, ee's should be >90%, unless a further enrichment is straightforward. The minimal activity and productivity required is less predictable. Consider an example of this situation. For an SCR of 1000 and a TOF of 10 h^{-1}, the reaction will take 100 h for completion – certainly not an acceptable reaction time for a large-volume chemical. However, for preparative small-scale applications, the SCR could be lowered to 100 and the reaction time would be an acceptable 10 h. A summary of the range of reaction conditions, ee-values, SCRs and TOF for important chiral catalysts and substrates is provided in Table 34.8. An overall assessment for the different systems takes into consideration not only the catalytic properties of a catalyst for a given transformation but also its ecological and economical aspects.

34.10.1
Iridium Complexes

Among the various catalyst types investigated in recent years for the hydrogenation of imines, Ir–diphosphine complexes have proved to be most versatile catalysts. The first catalyst of this type generated *in situ* from $[Ir(cod)Cl]_2$, a chiral diphosphine and iodide was developed by the Ciba-Geigy catalysis group in 1985. Ir ferrocenyl diphosphines (josiphos) complexes in presence of iodide and acid

Table 34.8 Typical ranges of reaction conditions, optical yields, turnover frequencies (TOF) and substrate:catalyst ratios (SCR) for the hydrogenation of C=N functions using various chiral catalytic systems.

Catalyst	Substrate type	p [bar]	T [°C]	ee [%]	SCR	TOF [h^{-1}]
Ir–PP	N-aryl imines	20–80	0–30	70–99	100–>1 000 000	2–>350 000
	Cyclic imines	40–70	20–30	80–97	100–1000	5–50
Ir–PN	Imines	100	r.t.	75–90	25–>1000	4–250
Rh–PP	Imines	60–100	<0–30	80–96	40–1000	0.1–50
	N-acyl hydrazones	4	<0–20	70–96	500–1000	10–1000
	Phosphinylimines	70	60	90–99	100–500	100–500
Ru–PP–NN	Acyclic imines	3–20	30	60–94	500–1500	20–50
Ru–NN	Imines	Formate	30	85–97	100–1000	6–83
Ti–ebthi	Cyclic imines	5–33	45–65	98–99	20–100	0.4–2.4

are the most active and productive enantioselective catalysts for the hydrogenation of the *N*-aryl-imines. The josiphos ligands are quite stable, easy to tune to the special needs of the imine structure, and a large variety is commercially available in technical quantities. Most other Ir complexes have not been studied in great detail, and many require the presence of additives such as iodine or phthalimide for good performance. Ligands such as f-binaphane, bicp or the tol-binap are patent-protected but are available commercially. The Ir–phox catalysts developed by Pfaltz and related Ir–PN complexes have some potential for C=N hydrogenation but, curiously, it seems that there is a limit to their enantioselectivity at ca. 90% ee.

34.10.2
Rhodium Complexes

Rhodium diphosphine catalysts can be easily prepared from $[Rh(nbd)Cl]_2$ and a chiral diphosphine, and are suitable for the hydrogenation of imines and *N*-acyl hydrazones. However, with most imine substrates they exhibit lower activities than the analogous Ir catalysts. The most selective diphosphine ligand is $bdpp_{sulf}$, which is not easily available. Rh–duphos is very selective for the hydrogenation of *N*-acyl hydrazones and with TOFs up to 1000 h^{-1} would be active enough for a technical application. Rh–josiphos complexes are the catalysts of choice for the hydrogenation of phosphinyl imines. Recently developed (pentamethylcyclopentyl)Rh–tosylated diamine or amino alcohol complexes are active for the transfer hydrogenation for a variety of C=N functions, and can be an attractive alternative for specific applications.

34.10.3
Ruthenium Complexes

In contrast to the wide scope of Ru–binap for the hydrogenation of substituted alkenes and ketones, their use in the hydrogenation C=N groups is limited due to the tendency to deactivate in presence of bases. Of more interest, though not yet fully explored, are Ru complexes containing both a diphosphine and a diamine. (Arene)Ru complexes in the presence of tosylated diamines are also able to reduce imines under transfer hydrogenation conditions with high activities and high to very high enantioselectivities.

34.10.4
Titanium Complexes

Despite the remarkable enantioselectivities observed with the Ti–ebthi catalyst for the imine and enamine hydrogenation, we consider its technical potential rather low. The ligand is difficult to prepare, the activation of the catalyst precursor is tricky, for the moment the catalytic activity is far too low for preparative purposes, and last – but not least – its tolerance for other functional groups is low.

A summary of the present state of the art for the enantioselective hydrogenation organized according to catalyst type is provided in Table 34.8. While an increasing number of catalysts with high ee-values are reported, progress concerning activity and productivity is much slower. Compared to the situation for the analogous C=C and C=O hydrogenation, there are still many areas where minimal systematic information is available. The most visible success stories such as the (*S*)-metolachlor case are rather "anecdotal" in nature. Nevertheless, they are proof that it is possible to hydrogenate C=N functions with not only adequate enantioselectivity but also high activity and productivity.

Abbreviations

d.e. diastereomeric excess
ee enantiomeric excess
SCR substrate:catalyst ratio
TOF turnover frequency
TON turnover number

References

1 Y. Nakamura, *Bull. Chem. Soc. Jpn.* **1941**, *16*, 367.
2 T. Yoshida, K. Harada, *Bull. Chem. Soc. Jpn.* **1971**, *44*, 1062.
3 C. Botteghi, M. Bianchi, E. Benedetti, U. Matteoli, *Chimia* **1975**, *29*, 256.
4 H.B. Kagan, N. Langlois, T.P. Dang, *J. Organomet. Chem.* **1975**, *90*, 353.
5 S. Vastag, J. Bakos, S. Torös, N.E. Takach, R.B. King, B. Heil, L. Marko, *J. Mol. Catal.* **1984**, *22*, 283.
6 (a) J. Bakos, A. Drosz, B. Heil, M. Laghmari, P. Lhoste, D. Sinon, *Chem. Commun.* **1991**, 1684; (b) C. Lensink, E. Rijnberg, J.G. de Vries, *J. Mol. Catal. A: Chemical* **1997**, *116*, 199; (c) C. Lensink, J.G. de Vries, *Tetrahedron: Asymmetry*, **1992**, *3*, 235.
7 F. Spindler, B. Pugin, H.U. Blaser, *Angew. Chem. Int. Ed.* **1990**, *29*, 558, and F. Spindler, B. Pugin, unpublished results.
8 C.A. Willoughby, S.L. Buchwald, *J. Org. Chem.* **1993**, *58*, 7627.
9 M.J. Burk, J.E. Feaster, *J. Am. Chem. Soc.* **1992**, *114*, 6266; M.J. Burk, J.P. Martinez, J.E. Feaster, N. Cosford, *Tetrahedron* **1994**, *50*, 4399.
10 N. Uematsu, A. Fujii, S. Hashiguchi, T. Ikariya, R. Noyori, *J. Am. Chem. Soc.* **1996**, *118*, 4916.
11 H.U. Blaser, H.P. Buser, K. Coers, R. Hanreich, H.P. Jalett, E. Jelsch, B. Pugin, H.D. Schneider, F. Spindler, A. Wegmann, *Chimia* **1999**, *53*, 275.
12 T. Ohkuma, M. Kitamura, R. Noyori, in: I. Ojima (Ed.), *Catalytic Asymmetric Synthesis*, 2nd edition. Wiley-VCH, Weinheim, **2000**, p. 1.
13 H.U. Blaser, F. Spindler, in: E.N. Jacobsen, A. Pfaltz, H. Yamamoto (Eds.), *Comprehensive Asymmetric Catalysis*. Springer, Berlin, **1999**, p. 247.
14 H.U. Blaser, B. Pugin, F. Spindler, in: B. Cornils, W.A. Herrmann (Eds.), *Applied Homogeneous Catalysis by Organometallic Complexes*, 2nd edition. Wiley-VCH, Weinheim, **2002**, p. 1131.
15 H.U. Blaser, F. Spindler, *ChimicaOggi* **1995**, *13*(6), 11.
16 J.M. Brunel, *Recent Res. Devel. Organic Chem.* **2003**, *7*, 155.
17 W. Tang. X. Zhang, *Chem. Rev.* **2003**, *103*, 3029.

18 V. I. Tararov, R. Kadyrov, T. H. Riermeier, C. Fischer, A. Börner, *Adv. Synth. Catal.* **2004**, *346*, 561.
19 V. I. Tararov, A. Börner, *Synlett* **2005**, 203.
20 C. A. Willoughby, S. L. Buchwald, *J. Am. Chem. Soc.* **1992**, *114*, 7562.
21 C. A. Willoughby, S. L. Buchwald, *J. Am. Chem. Soc.* **1994**, *116*, 8952.
22 H. U. Blaser, F. Spindler, *Topics Catal.* **1997**, *4*, 275
23 H. U. Blaser, H. P. Buser, R. Häusel, H. P. Jalett, F. Spindler, *J. Organomet. Chem.* **2001**, *621*, 34.
24 R. Sablong, J. A. Osborn, *Tetrahedron: Asymmetry* **1996**, *7*, 3059.
25 H. U. Blaser, H. P. Buser, H. P. Jalett, B. Pugin, F. Spindler, *Synlett* **1999**, 867.
26 B. Pugin, H. Landert, F. Spindler, H. U. Blaser, *Adv. Synth. Catal.* **2002**, *344*, 974.
27 W. Braun, A. Salzer, F. Spindler, E. Alberico, *Appl. Catal. A: General* **2004**, *274*, 191.
28 H. U. Blaser, *Adv. Synth. Catal.* **2002**, *344*, 17 and references therein.
29 W. R. Cullen, M. D. Fryzuk, B. R. James, J. P. Kutney, G.-J. Kang, G. Herb, I. S. Thorburn, R. Spogliarich., *J. Mol. Catal.* **1990**, *62*, 243.
30 H. U. Blaser, B. Pugin, F. Spindler, A. Togni, *C.R. Chimie* **2002**, *5*, 1.
31 (a) P. Schnider, G. Koch, R. Prétt, G. Wang, F. M. Bohnen, C. Krüger, A. Pfaltz, *Chem Eur. J.* **1997**, *3*, 887; (b) M. Solinas, A. Pfaltz, P. G. Cozzi, W. Leitner, *J. Am. Chem. Soc.* **2004**, *126*, 16142.
32 D. Xiao, X. Zhang, *Angew. Chem. Int. Ed.* **2001**, *40*, 3425.
33 S. Kainz, A. Brinkmann, W. Leitner, A. Pfaltz, *J. Am. Chem. Soc.* **1999**, *121*, 6421.
34 (a) C. Blanc, F. Agbossou-Niedercorn, G. Nowogrocki, *Tetrahedron: Asymmetry* **2004**, *15*, 2159; (b) P. G. Cozzi, F. Menges, S. Kaiser, *Synlett* **2003**, 833.
35 C. J. Cobley, J. P. Henschke, J. Ramschen, WO 02/8169, **2001**, (assigned to ChiroTech).
36 C. J. Cobley, J. P. Henschke, *Adv. Synth. Catal.* **2003**, *345*, 195.
37 Y. Chi, Y-Z. Zhou, X. Zhang, *J. Org. Chem.* **2003**, *68*, 4121.
38 A. Trifonova, J. S. Diesen, C. J. Chapman, P. G. Andersson, *Org. Lett.* **2004**, *6*, 3825.
39 E. Guiu, B. Munoz, S. Castillon, C. Claver, *Adv. Synth. Catal.* **2003**, *345*, 169.
40 S. Vargas, M. Rubio, A. Suarez, A. Pizzano, *Tetrahedron Lett.* **2005**, *46*, 2049.
41 C. Moessner, C. Bolm, *Angew. Chem. Int. Ed.* **2005**, *44*, 7564.
42 H. Abe, H. Amii, K. Uneyama, *Org. Lett.* **2001**, *3*, 313.
43 A. G. Becalski, W. R. Cullen, M. D. Fryzuk, B. R. James, G.-J. Kang, S. J. Rettig, *Inorg. Chem.* **1991**, *30*, 5002.
44 J. Buriak, J. A. Osborn, *Organometallics* **1996**, *15*, 3161.
45 J. P. Cahill, A. P. Lightfoot, R. Goddard, J. Dust, P.J. Guiry, *Tetrahedron: Asymmetry* **1998**, *9*, 4307.
46 X.-B. Jiang, A. J. Minnaard, B. Hessen, B. L. Feringa, A. L. L. Duchateau, J. G. O. Andrien, J. A. F. Boogers, J. G. de Vries, *Org. Lett.* **2003**, *5*, 1503.
47 K. Abdur-Rashid, A. J. Lough, R. H. Morris, *Organometallics* **2001**, *20*, 1047.
48 R. Kadyrov, T. H. Riermeier, U. Dingerdissen, V. I. Tararov, A. Börner, *J. Org. Chem.* **2003**, *68*, 4067.
49 M. B. Ezhova, B. O. Patrick, B. R. James, F. J. Waller, M. E. Ford, *J. Mol. Catal. A: Chemical* **2004**, *224*, 71.
50 P. Nanayakkara, H. Alper, *Chem. Commun.* **2003**, 2384.
51 M. P. Magee, J. R. Norton, *J. Am. Chem. Soc.* **2001**, *123*, 1779.
52 G. Zhu, X. Zhang, *Tetrahedron: Asymmetry* **1998**, 9, 2415.
53 K. Tani, J. Onouchi, T. Yamagata, Y. Kataoka, *Chem. Lett.* **1995**, 955.
54 D. Liu, W. Li, X. Zhang, *Tetrahedron: Asymmetry* **2004**, *15*, 2177.
55 M. T. Reetz, E. W. Beuttenmüller, R. Goddard, M. Pasto, *Tetrahedron Lett.* **1999**, *40*, 4977.
56 T. Morimoto, N. Suzuki, K. Achiwa, *Heterocycles* **1996**, *43*, 2557.
57 P. Roszkowski, K. Wojtasiewicz, A. Leniewski, J. K. Maurin, T. Lis, Z. Czarnocki, *J. Mol. Catal. A: Chemical* **2005**, *232*, 143.
58 P. Roth, P. G. Andersson, P. Somfai, *Chem. Commun.* **2002**, 1752,
59 S.-M. Lu, X.-W. Han, Y.-G. Zhou, *Adv. Synth. Catal.* **2004**, *346*, 905.
60 W.-B. Wang, S.-M. Lu, P.-Y. Yang, X.-W. Han, Y.-G. Zhou, *J. Am. Chem. Soc.* **2003**, *125*, 10536.

61 L. Xu, K.H. Lam, J. Ji, J. Wu, Q.-H. Fan, W.-H. Lo, A.S.C. Chan, *Chem. Commun.* **2005**, 1390.

62 C. Bianchini, P. Barbaro, G. Scapacci, E. Farnetti, M. Graziani, *Organometallics* **1998**, *17*, 3308.

63 R. Giernoth, M.S. Krumm, *Adv. Synth. Catal.* **2004**, *346*, 989.

64 H.U. Blaser, Ch. Malan, B. Pugin, F. Spindler, H. Steiner, M. Studer, *Adv. Synth. Catal.* **2003**, *345*, 103.

65 C.Y. Legault, A.B. Charette, *J. Am. Chem. Soc.* **2005**, *127*, 8966.

66 R. Fuchs, EP 0803502 A2, **1997**, assigned to Lonza AG.

67 H. Brunner, S. Rosenboem, *Monatshefte für Chemie* **2000**, *131*, 1371.

68 H.U. Blaser, W. Brieden, B. Pugin, F. Spindler, M. Studer, A. Togni, *Topics in Catalysis* **2002**, *19*, 3 and information on commercial ligands in http://www.solvias.com/english/products-and-services/chemicals/ligands/index.html

69 V. Groehn, R. Moser, B. Pugin, *Adv. Synth. Catal.* **2005**, *347*, 1855.

70 J.F. McGarrity, W. Brieden, R. Fuchs, H-P. Mettler, B. Schmidt, O. Werbitzky, in: H.U. Blaser, E. Schmidt (Eds.), *Large Scale Asymmetric Catalysis.* Wiley-VCH, Weinheim, **2003**, p. 283.

71 K. Satoh, M. Inenaga, K. Kanai, *Tetrahedron: Asymmetry* **1998**, *9*, 2657.

72 W. Oppolzer, M. Wills, C. Starkemann, G. Bernardinelli, *Tetrahedron Lett.* **1990**, *31*, 4117.

73 Y. Xie, A. Mi, Y. Jiang, H. Liu, *Synth. Commun.* **2001**, *31*, 2767.

74 F. Spindler, H.U. Blaser, *Adv. Synth. Catal.* **2001**, *343*, 68.

75 A.B. Charette, A. Giroux, *Tetrahedron Lett.*, **1996**, *37*, 6669.

76 (a) P. Krasik, H. Alper, *Tetrahedron: Asymmetry* **1992**, *3*, 1283; (b) A.S.C. Chan, C.-C. Chen, C.-W. Lin, Y.-C. Lin, M.-C. Cheng, S.-M. Peng, *Chem. Commun.* **1995**, 1767.

77 C.J. Cobley, E. Foucher, J.-P. Lecouve, I.C. Lennon, J.A. Ramsden, G. Thominot, *Tetrahedron: Asymmetry* **2003**, *14*, 3431.

78 J. Blacker, J. Martin, in: H.U. Blaser, E. Schmidt (Eds.), *Large Scale Asymmetric Catalysis.* Wiley-VCH, Weinheim, **2003**, p. 201.

79 B. Pugin, Solvias AG, unpublished results.

80 V.I. Tararov, R. Kadyrov, T.H. Riermeier, J. Holz, A. Börner, *Tetrahedron Lett.* **2000**, *41*, 2351.

81 N. Lee, S.L. Buchwald, *J. Am. Chem. Soc.* **1994**, *116*, 5985.

82 Y. Hsiao, N.L. Rivera, T. Rosner, S.N. Krska, E. Njolito, F. Wang, Y. Sun, J.D. Armstrong, E.J.J. Grabowski, R.D. Tillyer, F. Spindler, C. Malan, *J. Am. Chem. Soc.* **2004**, *126*, 9918.

83 (a) K. Matsumura, X. Zhang, Xiaoyong, T. Saito, Eur. Pat. Appl. **2004**; EP 1386901; (b) M. Sodeoka, Y. Hamashima, PCT Int. Appl. **2005**, WO 2005016866 A2.

84 M. Rouhi, *Chem. Eng. News* **2004**, *82*(24), 47.

85 B.R. James, *Catalysis Today* **1997**, *37*, 209.

86 Y. Ng. Cheong Chan, J.A. Osborn, *J. Am. Chem. Soc.* **1990**, *112*, 9400

87 J. Campora, S.L. Buchwald, E. Gutiérrez-Puebla, A. Monge, *Organometallics* **1995**, *14*, 2039, and references cited therein.

88 S. Wallbaum, J. Martens, *Tetrahedron: Asymmetry* **1992**, *3*, 1475.

89 L. Deloux, M. Srebnik, *Chem. Rev.* **1993**, *93*, 763.

90 For a recent publication, see T. Yamada, T. Nagata, K.D. Sugi, K. Yorozu, T. Ikeno, Y. Ohtsuka, D. Miyazaki, T. Mukaiyama, *Chem. Eur. J.* **2003**, *9*, 4485.

91 For a review, see J.F. Carpentier, V. Bette, *Curr. Org. Chem.* **2002**, *6*, 913.

92 M.C. Hansen, S.L. Buchwald, *Org. Lett.* **2000**, 2, 713 and references cited therein.

93 B.H. Lipshutz, H. Shimizu, *Angew. Chem. Int. Ed.* **2004**, *43*, 2228.

94 (a) D.I. Stirling, in: A.N. Collins, G.N. Sheldrake, J. Crosby, (Eds.), *Chirality in Industry.* John Wiley & Sons, Chichester, **1992**, p. 209; (b) A.S. Bommarius, in: K. Drauz, H. Waldmann (Eds.), *Enzyme Catalysis in Organic Synthesis,* 2nd edition. Wiley-VCH Verlag GmbH, Weinheim, **2002**, 3, 1047

95 H.U. Blaser, B. Pugin, F. Spindler, *J. Mol. Catal. A: Chemical* **2005**, *231*, 1.

35
Enantioselective Transfer Hydrogenation

A. John Blacker

35.1
Introduction

Transfer hydrogenation is the movement of a hydride ion and proton (or two protons and two electrons) from a hydrogen donor to a substrate acceptor, effectively a disproportionation. In the case of hydrogenation, molecular hydrogen is the donor, and this topic is considered elsewhere in this Handbook. The substrate acceptor is unsaturated and can be, for example, a ketone, imine or alkene. The hydrogen donor is a good reductant and is often an alcohol, alkane or formate. The reaction is mediated by a catalyst that helps in the hydride transfer. When applied to ketones using isopropanol as the hydrogen donor and a Lewis acid to catalyze the reaction, the non-asymmetric transformation is known as the Meerwein–Pondorf–Verley reaction. Transfer dehydrogenation is the movement of a hydride ion and proton in the opposite direction. For alcohol substrates yielding ketone products, it is also known as the Oppenauer oxidation.

If the catalyst is chiral, it can transfer hydride selectively to one prochiral face of an acceptor to provide an optically active product (Fig. 35.1).

A number of excellent reviews have recently been published [1]; consequently, this chapter will consider mainly the practical aspects of asymmetric transfer hydrogenation by reviewing each of the components of the reaction, namely catalyst, hydrogen donor, substrate, product and other elements such as solvent, reaction conditions and scale-up.

In broad terms there are three types of catalyst for transfer hydrogenation: dehydrogenases; heterogeneous; and homogenous metal catalysts. Here, the first two are mentioned for completeness, and the main focus of this chapter will be asymmetric transfer hydrogenation with homogenous metal catalysts.

Nature uses enantioselective transfer hydrogenation to reduce metabolites, for example pyruvate to give (*S*)-lactic acid and 2-ketoglutarate to give (*S*)-2-hydroxyglutarate. The reaction is reversible and the equilibrium position depends on the concentration of the species. The enzyme catalysts are named dehydrogenases, and they employ a soluble cofactor or hydride acceptor called NAD(P) in its oxi-

The Handbook of Homogeneous Hydrogenation.
Edited by J.G. de Vries and C.J. Elsevier
Copyright © 2007 WILEY-VCH Verlag GmbH & Co. KGaA, Weinheim
ISBN: 978-3-527-31161-3

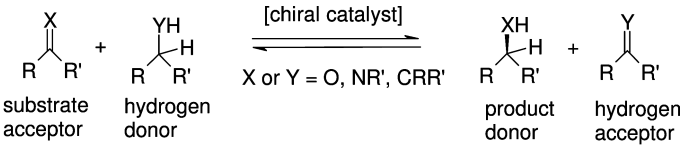

Fig. 35.1 The asymmetric transfer hydrogenation reaction.

dized form, and NAD(P)H in the reduced form [2 a]. NAD(P) can be reduced to NAD(P)H, if the concentration of hydride donor is high relative to the hydride acceptor. The similarity of enantioselective transfer hydrogenation and dehydrogenase-catalyzed reactions has been recognized in a number of studies [2 b–e].

Chemical catalysts for transfer hydrogenation have been known for many decades [2 e]. The most commonly used are heterogeneous catalysts such as Pd/C, or Raney Ni, which are able to mediate for example the reduction of alkenes by dehydrogenation of an alkane present in high concentration. Cyclohexene, cyclohexadiene and dihydronaphthalene are commonly used as hydrogen donors since the byproducts are aromatic and therefore more difficult to reduce. The heterogeneous reaction is useful for simple non-chiral reductions, but attempts at the enantioselective reaction have failed because the mechanism seems to occur via a radical (two-proton and two-electron) mechanism that makes it unsuitable for enantioselective reactions [2 c].

35.2 Homogenous Metal Catalysts

35.2.1 Early studies

Transfer hydrogenation of ketones, aldehydes, and alkenes using homogenous catalysts was successfully realized by Henbest et al. [3 a] and furthered by Colonna et al. [3 b] using iridium(III) phosphite or sulfoxide complexes and the hydrogen donor isopropanol (IPA system). In some seminal studies, Mestroni et al. reported the achiral transfer hydrogenation of carbonyl, azomethine and nitrogroups using iridium and rhodium bipyridine and similar complexes [3 c]. These authors went on to develop the first enantioselective transfer hydrogenation using iridium Schiff base complexes with the hydrogen donor IPA, noting the fall in enantiomeric excess with conversion that occurs as a result of the reverse dehydrogenation [3 d]. Bäckvall reported the transfer hydrogenation of ketones and imines using IPA and catalyzed by a ruthenium complex [4 a, b], while Mestroni's group then reported the use of rhodium phenanthroline catalysts in diastereoselective reductions [4 c].

One of the earliest reports of enantioselective transfer hydrogenation was by Alper et al., who used chiral Schiff bases and a dichlororuthenium(II)benzene complex employing the IPA system [5]. In another report, Lemaire et al. utilized

chiral diamines complexed with rhodium [6]. Mestroni and Gladiali have reported extensive investigations aimed at improving the catalysts and optimizing the system [7]. Despite these efforts, the product optical purities remained modest at around 65% enantiomeric excess (ee), and this failed to generate much interest – especially as enantioselective hydrogenation was giving outstanding performances. Evans reported the transfer hydrogenation of acetophenone in high enantiomeric excess using a chiral samarium(III) aminoalcohol complex, although low turnover numbers (TON) make the use of this catalyst impractical [8]. Shvo invented a very promising catalyst which was based on ruthenium cyclopentadienes [9], while Bäckvall and others have studied this elegant and effective system further [10]. Noyori et al. provided the step-change improvement required with their report of a catalyst based on a complex between chiral 1,2-aminoalcohols and dichlororuthenium(II)arene able to enantioselectively reduce ketones in 98% ee using the IPA system [11, 12]. The problem with this system is the reversibility of the reaction, which leads to poor conversions and falling optical purities. The development of *N*-tosyldiamine ligands with rutheniumarene complexes enabled use of the irreversible hydrogen donor formic acid when used as a mixture with triethylamine (TEAF) [13].

The reports by Noyori sparked intense academic and industrial interest in this area, and these studies led ultimately to a plethora of reports describing investigations into new catalysts [1]. In this respect, a variety of metals have been employed, including cobalt, nickel, palladium, platinum and zinc, though the best catalysts have employed ruthenium [11], rhodium [14, 15] and iridium [14, 16, 17].

35.2.2
Group VIII Metal Catalysts

The Group VIII metals are able to cycle between the d6 and d8 electronic states, and are used in their +2 or +3 oxidation states. Particularly effective has been the use of ruthenium arenes and the isoelectronic rhodium or iridium cyclopentadienes [11–16]. These ligands remain coordinated to the metal, and are important in defining the electronics, sterics, stability, and asymmetry around the metal. Alkylation of the arene or cyclopentadiene affects each of these factors, and it is difficult to draw conclusions or to predict the best catalyst. A number of ruthenium arenes have been prepared and their activities and selectivities compared [12], although the ruthenium cymene is most often used, mainly for its generally good performance and commercial availability. Likewise, a number of rhodium or iridium cyclopentadienes have been prepared which, when complexed with a chiral ligand, have been named CATHy^{TM} catalysts. The present author's studies have shown that the extra stability and steric bulk imparted by the pentamethylcyclopentadiene (cp*) make this consistently the best ligand. The cyclopentadiene (cp) ligand seems to provide lower ee-values, most likely because of it size, and it is also less stable and less soluble. The tetraphenyl analogue appears to be too large, as it produces only moderate optical inductions. The use of a chiral cyclopentadiene such as neomenthylcyclopentadiene pro-

vided disappointing results, although tethered cyclopentadienyls are currently showing more promise [18].

The dichlororuthenium arene dimers are conveniently prepared by refluxing ethanolic ruthenium trichloride in the appropriate cyclohexadiene [19]. The dichloro(pentamethylcyclopentadienyl) rhodium dimer is prepared by refluxing Dewar benzene and rhodium trichloride, whilst the dichloro(pentamethylcyclopentadienyl)iridium dimer is prepared by reaction of the cyclopentadiene with iridium trichloride [20]. Alternatively, the complexes can be purchased from most precious-metal suppliers. It should be noted that these ruthenium, rhodium and iridium arenes are all fine, dusty, solids and are potential respiratory sensitizers. Hence, the materials should be handled with great care, especially when weighing or charging operations are being carried out. Appropriate protective clothing and air extraction facilities should be used at all times.

Since most transfer hydrogenation catalysts employ precious metals, a high number of turnovers are required in order to make their use economic. As the ligands are simply made they are generally of low cost. In our experience, for the average pharmaceutical intermediate, a substrate : catalyst ratio (SCR) of about 1000:1 is sufficient for the catalyst's contribution to the product cost to be minor. These SCRs are regularly achieved, and so from an economic standpoint there has been little incentive to recover and recycle the catalyst, unless a low-cost product is required. The recovery of precious metals from waste streams provides another way in which costs can be minimized.

35.2.3
Chiral Ligands

The ligands are usually bidentate, and are based on diamines or aminoalcohols, though some reports exist of 1,2-aminothiols, aminosulfoxides, aminophosphines, aminophosphine oxides, biscarbenes and alpha amino acids being used as ligands. Diols do not appear to function as ligands. Other ligands that have been found to be effective include tridentate diaminoalcohols and tetradentate diaminodiphosphines, diaminodiphenols or diaminodialcohols. As has often occurred in studies of asymmetry, there are many types of ligand available but few studies have compared the designs, enabling conclusions to be drawn about their activity and selectivity. The best ligand–metal combinations should provide catalysts that, above all, show high activity, high selectivity, broad scope and have low cost, as well as being easily prepared. Moreover, they should be available in both antipodes, be stable, pure, non-toxic, recyclable, and easily separated from the product. From an industrial perspective, the ownership of intellectual property is also an important consideration. Based on these criteria it is not surprising that diamines and aminoalcohol ligands with ruthenium, rhodium and iridium metals have emerged as widely useful catalysts for enantioselective transfer hydrogenation.

The most successful ligands are unsymmetrical chiral diamines or aminoalcohols, perhaps because they influence the configuration of the ligated metal chir-

al center. Although such chiral centers are not stable they may lie sufficiently within the timescale of a rapidly turning-over catalyst.

The backbone of the bidentate ligand is usually an ethylene bridge so that a 1,2 relationship between the heteroatoms provides a stable five-membered ring with the metal. As the ring becomes enlarged the association with the metal is weakened and these ligands give lower optical inductions. The other substituents that form the chiral centers are essential in inducing optical activity in the product. Their main role is thought to be in providing the steric bulk that stabilizes a twisted conformation. A 1,2-*trans* stereochemistry in the ligand is generally more effective than a 1,2-*cis* geometry, an exception being *cis*-1,2-aminoindanol. The diphenylethylenediamine (DPEN) ligands are especially useful as they are relatively inexpensive and easily made on the kilogram scale. The diamines are used in either the IPA or TEAF system and have been N-substituted with aryl, alkyl, acetoyl, thioacetoyl and sulfonyl groups. The latter are preferred as they lower the pK_a of the amine allowing an ionic bond with the metal. In general, arylsulfonyl groups have been used, the most prevalent being tosyl (TsDPEN) [11, 21], although alkyl groups including trifluoromethylsulfonyl (TfDPEN) [22] and camphorsulfonyl (CsDPEN) [23] have also been used. The latter is very useful, providing generally very high ee-values, perhaps as a result of the additional steric bulk and remote functionality. The (1*R*)-camphor sulfonyl group has been found to give the same optical inductions as the (1*S*) group, implying that the chirality around the camphor has little effect on the enantiomeric excess of the product. One interesting observation, however, is that the ee-values sometimes increase slightly after the start of a reaction, and this has been shown to be a result of the enantioselective reduction of the ketone group on the camphor, giving an even better ligand. A library of *N*′-arylsulfonylethylenediamines has been synthesized (Fig. 35.2), though studies have shown little correlation between the electronic or steric nature of the arylsulfonyl group and the activity or selectivity of the catalyst. Indeed, only minor changes in the enantiomeric excess of selected products were observed, making this a fine-tuning tool.

The *N*-arylsulfonyl ligands are synthesized by reaction of mole equivalents of the optically active diamine and sulfonyl chloride, followed by recrystallization [21].

The aminoalcohol ligands are combined with the metal to produce catalysts that are used most effectively in the IPA system. Here, very high turnover numbers (TONs) have been achieved with a variety of ligands. The most frequently used are based on commercially available norephedrine and *cis*-1,2-aminoindanol as these are inexpensive, available in both enantiomers, and can be used unmodified [12, 24, 25] (see Fig. 35.2). Other simple and highly active ligands that have been prepared are based on azanorbornanemethanol [26] and benzylthio-1,2-diphenylethanol [16]. Gladiali and Elberico have recently reviewed the ligands that have been used in enantioselective transfer hydrogenation [1 a].

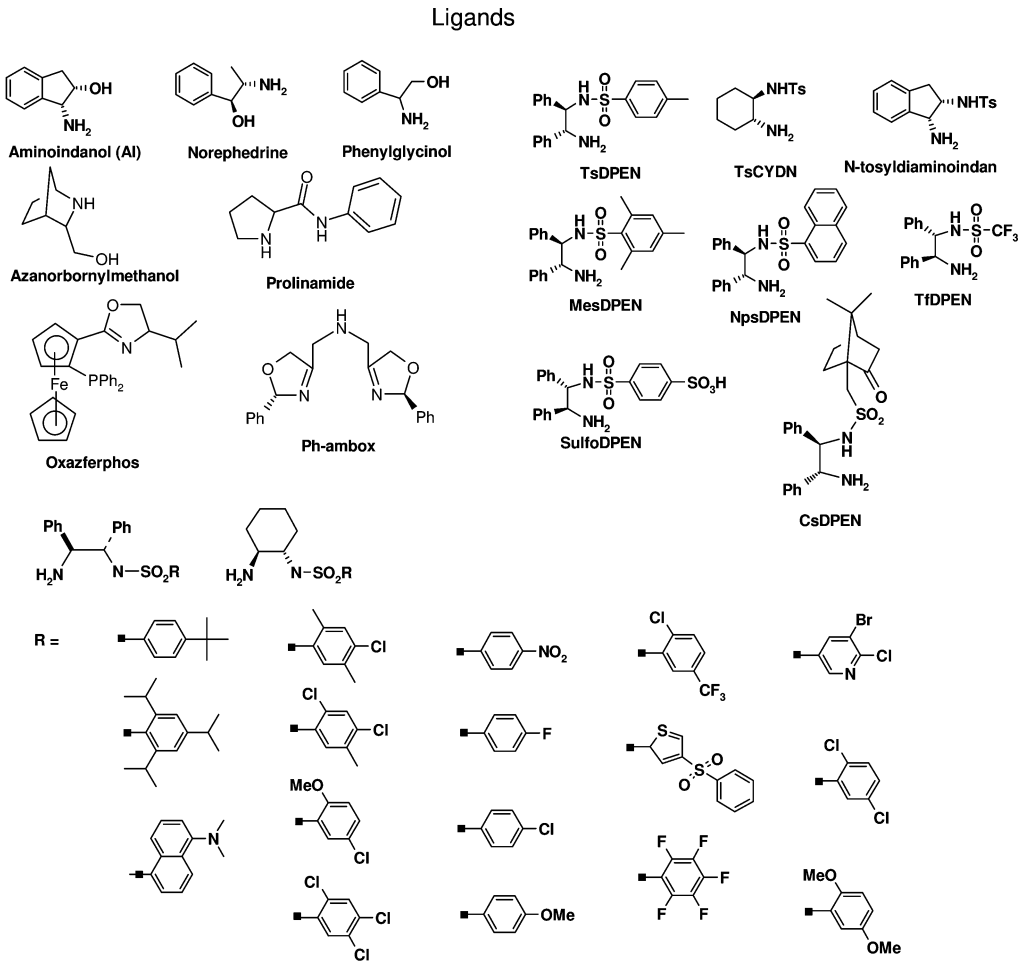

Fig. 35.2 Some examples of 1,2-aminoalcohol and 1,2-diamine ligands and a readily prepared library of *N*-sulfonyldiamine ligands.

35.2.4
Immobilized Ligands

The advantages that heterogeneous catalysts have is that they are easily separable from the product, and can be recycled. A number of studies have been conducted in which ligands have been attached or bound to polymeric material to provide an immobilized ligand, and these include polyacrylate and silica [27], polyurea [28], polythiourea [29], polyether [30, 31] and dendritic [32] systems. Upon metal coordination, the immobilized catalysts have retained most of the activity and selectivity, but they now provide the advantage of simple separation and recycling. For exam-

ple, Tu et al. have used a modified phenylsulfonylchloride and attached this to diphenylethylenediamine to produce an analogue of TsDPEN [33]. This is then linked to a silica gel polymer to produce the immobilized ligand. The ruthenium cymene complex actively catalyzes the enantioselective transfer hydrogenation of acetophenone, with the same selectivity and activity as the soluble catalyst. However, after multiple recycling the activity falls off somewhat, presumably due to metal leaching, though the selectivity remains high. Xiao has overcome this problem by using a polyethylene glycol-immobilized ligand and carrying out the reaction in water; the catalyst is then precipitated by changing the solvent polarity [31]. In this way, twenty recycles of the catalyst could be achieved, without any adverse effects.

35.2.5
Water-Soluble Ligands

The standard ruthenium arene and CATHy™ catalysts are insoluble in water, but are nevertheless stable in the presence of water. Reactions in the IPA system can be carried out in mixtures of isopropanol and water; the net effect is a lower rate due to dilution of the hydrogen donor. The use of formate salts in water, with CATHy™ or other transfer hydrogenation catalysts dissolved in a second immiscible phase was shown to work well with a number of substrates and in some cases to improved reaction rates [34]. The use of water as reaction solvent will be discussed in more detail in Section 35.5.

In some cases it is useful to have the catalyst soluble in water: some substrates are only soluble in water, others give higher ee-values in this solvent, and there may be benefits in separating the catalyst from product that is soluble in an organic phase. Ligands have been prepared that provide solubility in water. Typically, these involve a sulfonated ligand, and two approaches have been reported: (i) the use of a sulfonate group on the *N*-arylsulfonamide of the diamine [35]; and (ii) use of a sulfonate on the phenyl groups of diphenylethylenediamine [36]. Both ligands are reasonably easily prepared.

35.2.6
Catalyst Selection

The catalysts involved in enantioselective transfer hydrogenation are simply prepared by mixing equimolar amounts of the ligand and metal complex *in situ*, so that different ligands and metal complexes can be combined in different ways to generate a library of catalysts. Since the reactions do not involve molecular hydrogen, it is a simple matter to set up an experiment to screen catalysts to find the most active and enantioselective for a substrate (sadly, this is not true for the ruthenium catalysts, most of which are sensitive towards oxygen, while the catalysts based on aminoalcohols are extremely sensitive towards oxygen). A SCR of 100:1 is often used to ensure a rapid and successful reaction.

As mentioned earlier, ruthenium cymene, rhodium and iridium pentamethylcyclopentadiene are good metal complexes, to start with, in a screen. It is diffi-

cult to predict which metal will give the best enantiomeric excess for a particular substrate. In general, ruthenium gives lower rates than rhodium or iridium CATHy™ catalysts, but the selectivities can be quite different. The IPA and TEAF systems are screened, and a range of aminoalcohol and diamine ligands are tested; aminoalcohols are usually only successful in the IPA system. Either enantiomer of *cis*-1,2-aminoindanol, TsDPEN and CsDPEN are good starting points in a screen, and these are usually tested in a range of solvents, as this can have more bearing on the optical induction than a large ligand screen.

When making pharmaceuticals, one critical issue is to control and minimize metal impurities in the product, often to less than 10 ppm. Each product requires a different work-up and purification protocol, and it is difficult to describe a general solution. On some occasions washing removes the catalyst, but at other times the product is crystallized and the catalyst remains in the mother liquors; occasionally, the product is volatile and can be distilled. Sometimes the catalyst is carried forward to the next stage and is removed at this point. In our experience, residual metal has not been problematic, but if it is then either immobilized or water-soluble catalysts, as described in this chapter, can be employed.

35.2.7
Catalyst Preparation

The catalysts are best prepared *in situ* by mixing a half-equivalent of the dichloro-metal aromatic dimer with an equivalent of the ligand in a suitable solvent such as acetonitrile, dichloromethane or isopropanol. A base is used to remove the hydrochloric acid formed (Fig. 35.3). If 1 equiv. of base is used, the inactive pre-catalyst is prepared, and further addition of base activates the catalyst to the 16-electron species. In the IPA system the base is conveniently aqueous sodium hydroxide or sodium isopropoxide in isopropanol, whereas in the TEAF system, triethylamine activates the catalyst. In practice, since the amount of catalyst is tiny, any residual acid in the solvent can neutralize the added base, so a small excess is often used. To prevent the active 16-electron species sitting around, the catalyst is often activated in the presence of the hydrogen donor. The amount of catalyst required for a transformation depends on the desired reaction rate. Typically, it is desirable to achieve complete conversion of the substrate within several hours, and to this extent the catalyst is often used at 0.1 mol.% (with SCR 1000:1). Some substrate–catalyst combinations are less active, requiring more catalyst (e.g., up to 1 mol.%; SCR 100:1), in other reactions catalyst TONs of 10 000 (SCR 10 000:1) have been realized.

The ruthenium [37] and rhodium [38] pre-catalysts have been prepared and isolated; likewise, the 16- and 18-electron hydride species have been prepared and characterized [38–40]. There is little practical advantage in using the catalysts in this form, other than for mechanistic studies or when special circumstances are required (e.g., neutral reaction conditions).

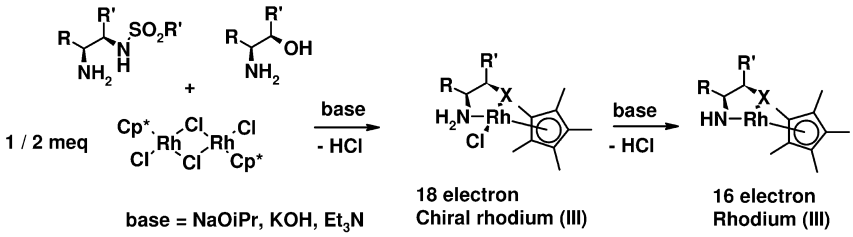

Fig. 35.3 Catalyst preparation.

35.2.8
The Reaction Mechanism

The mechanism of the Meerwein–Pondorf–Verley reaction is by coordination of a Lewis acid to isopropanol and the substrate ketone, followed by intermolecular hydride transfer, by beta elimination [41]. Initially, the mechanism of catalytic asymmetric transfer hydrogenation was thought to follow a similar course. Indeed, Bäckvall et al. have proposed this with the Shvo catalyst [42], though Casey et al. found evidence for a non-metal-activation of the carbonyl (i.e., concerted proton and hydride transfer [43]). This follows a similar mechanism to that proposed by Noyori [44] and Andersson [45], for the ruthenium arene-based catalysts. By the use of deuterium-labeling studies, Bäckvall has shown that different catalysts seem to be involved in different reaction mechanisms [46].

For the ruthenium arene and CATHy^{TM} catalysts, the mechanism has been studied in some detail. An outline mechanism for the reaction is illustrated in Figure 35.4.

The primary amine on the ligand is essential in allowing elimination of hydrogen chloride to generate the active 16-electron metal. This indicates why 1,2-aminoalcohols and diamines are good ligands, but 1,2-diols are not. After complexing with the metal, the amide thus formed is basic (the basicity of this is intriguing, the implication being that the metal is able to lower the pK_a by many orders of magnitude). In either the IPA or TEAF system the amide should readily reprotonate. The nitrogen–metal bond changes from one that is covalent to one that is dative. At this point in the cycle, the metal is likely to become more oxidative and be reduced to the metal–hydride intermediate. The 18-electron metal hydrides of the ruthenium, rhodium and iridium catalysts have been characterized and shown to be active [37–40]. The metal is now a chiral center and appears to be configurationally stable and optically active. Indeed, when the substrate binds the hydride is delivered selectively to one prochiral face. It seems likely that the ligand NH protons are involved in hydrogen bonding with the substrate. Substitution of the primary amine results in a dramatic loss of activity, for example $NH_2 > NHMe \gg NMe_2$. Noyori's studies on the analogous ruthenium arene catalysts also indicate that the ruthenium is optically active and that the substrate interacts by hydrogen bonding [44].

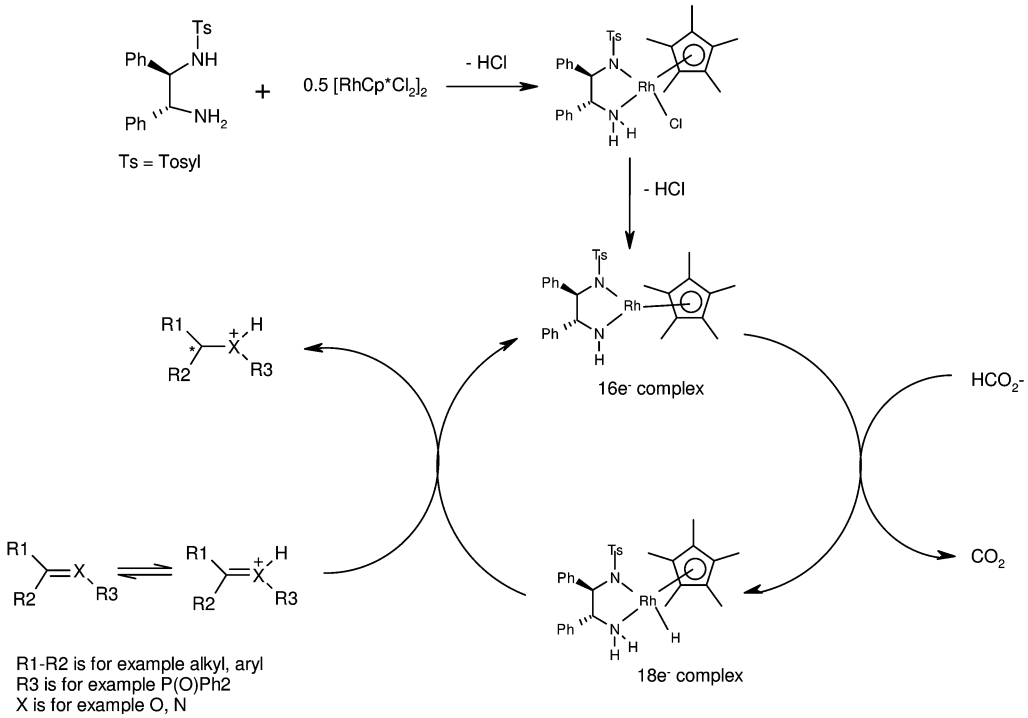

Fig. 35.4 Outline mechanism for the rhodium-catalyzed enantioselective transfer hydrogenation reaction.

35.3 Hydrogen Donors

35.3.1 The IPA System

Alcohols will serve as hydrogen donors for the reduction of ketones and iminium salts, but not imines. Isopropanol is frequently used, and during the process is oxidized into acetone. The reaction is reversible and the products are in equilibrium with the starting materials. To enhance formation of the product, isopropanol is used in large excess and conveniently becomes the solvent. Initially, the reaction is controlled kinetically and the selectivity is high. As the concentration of the product and acetone increase, the rate of the reverse reaction also increases, and the ratio of enantiomers comes under thermodynamic control, with the result that the optical purity of the product falls. The rhodium and iridium CATHy^{TM} catalysts are more active than the ruthenium arenes not only in the forward transfer hydrogenation but also in the reverse dehydrogenation. As a consequence, the optical purity of the product can fall faster with the

former than with the latter catalysts. In order to obtain high yields and to avoid the slow racemization of the product, it was initially necessary to work under dilute conditions. However, this limitation was overcome by continuous removal of the acetone as it was formed by distillation [47]. As the CATHy™ catalysts are less stable at higher temperatures, this distillation is best performed under reduced pressure at below 40 °C.

The reversibility of the reaction can be used to good effect in asymmetric dehydrogenation and dynamic kinetic resolutions (see later for discussion).

Other alcohols such as methanol and ethanol will also react, but are typically less effective as the aldehyde byproducts can interfere in the reaction. Isobutanol is an effective hydrogen donor, and others such as glucose will also react but cannot be used in such high concentrations. Isopropanol can be mixed with an inert solvent, including water, but the rates of reaction fall linearly, as expected.

Avecia and others have successfully scaled-up the IPA process to prepare a number of products in high optical purity in a simple and efficient reaction [1c, 48].

35.3.2
The TEAF System

Formic acid has long been recognized as a good and irreversible hydrogen donor, and used in both heterogeneous and homogenous transfer hydrogenations [49a]. The reagent keeps the reaction under kinetic control since CO_2 generated as a byproduct is gassed out of the system, thereby preventing the reverse reaction that is, in any case, thermodynamically unfavorable. Consequently, there is no fall in product optical purity as the reaction proceeds. The use of formic acid, either neat or diluted with a solvent, is effective in some transfer hydrogenations, but results can be inconsistent. The combination with triethylamine has been very effective [49b]. The reagent is known as TEAF, and can be used in different ratios of formic acid and triethylamine. The most commonly used mixture is a 5:2 molar ratio of formic acid to triethylamine, which is the azeotrope of these two liquids [50]). Practically speaking, it is easier to prepare the 5:2 TEAF by mixing the correct amounts of the components, than by distillation. The addition of triethylamine to formic acid is considerably exothermic, and is best done by slow addition of one of the reagents with good mixing. Making TEAF *in situ* during the transfer hydrogenation is disadvantageous as the heat evolution makes the reaction difficult to control. The 5:2 TEAF is a single phase at ambient temperature and remains so when diluted with most solvents; however, other ratios of formic acid and triethylamine can form biphasic solutions.

Xiao has recently published reports showing that mixtures of triethylamine and formic acid can be used in water, and this greatly simplifies measurement of pH. The ruthenium catalyst is active when the pH is >4; this corresponds with the aqueous pK_a of formic acid 3.6 [52].

With the rhodium catalyst, and using TEAF in organic media, the situation is more complex. An example in which a series of formic acid : triethylamine ratios

Table 35.1 The effect of the triethylamine : formic acid ratio (TEAF) on reaction rate.

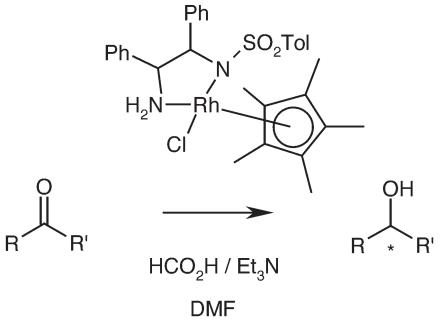

Mole ratio $HCO_2H:Et_3N$ (1 M)	Time [h]	Conversion [%]
1:0	4	2
	15	26
3:1	4	50
	15	89
2.5:1	4	80
	15	100
2:1	4	50
	15	73
1.5:1	4	30
	15	73
1:1	4	50
	15	100
0.67:1	4	50
	15	95
0.5:1	4	50
	15	97
0.4:1	4	48
	15	100

has been evaluated under identical conditions with a ketone in DMF is shown in Table 35.1.

As can be seen from the data in Table 35.1, the maximum reaction rate is achieved at the 5:2 formic acid : triethylamine ratio that is the commonly used azeotropic mixture known as TEAF. When more acid is present, the catalyst may be less active, but equally there may be less formate anion (i.e., the active reagent). The concentration of the latter also depends upon the solvent being used. When there is more triethylamine present the reaction rate also decreases, and there are some indications that triethylamine may deactivate the catalyst. However, the use of formic acid mixtures with ammonia, ethylamine or diethylamine is less effective than triethylamine.

Table 35.2 The pK_a-values of formic acid and triethylamine in different solvents.

Solvent	HCOOH	Et_3NH^+
Water	3.7	10.7
MeOH	8.4	10.9
EtOH	9.1	8.1
Aqueous EtOH	5.4	8.4
DMSO	10.3	9.0
NMP	11.0	8.7
DMF	11.5	9.2

The 5:2 TEAF reagent is acidic, with the extent of the acidity depending upon the solvent in which the reagent is used. Variations of triethylamine and formic acid pK_a-values with solvent are listed in Table 35.2. The pK_a of formic acid in many of the common solvents used is much higher than water, so there would appear to be little free formate in the reaction; thus, it becomes difficult to explain the reaction in such conditions (e.g., those in Table 35.1).

Triethylamine may act to buffer the pH, which changes as formic acid is consumed during the reaction. An excess of formic acid over substrate is often used. Though not essential (as will be discussed later), it is sometimes preferable to charge TEAF during the reaction in order to ensure a high yield of product.

Other salts of formic acid have been used with good results. For example, sodium and preferably potassium formate salts have been used in a water/organic biphasic system [36, 52], or with the water-soluble catalysts discussed above. The aqueous system makes the pH much easier to control; minimal CO_2 is generated during the reaction as it is trapped as bicarbonate, and often better reaction rates are observed. The use of hydrazinium monoformate salts as hydrogen donors with heterogeneous catalysts has also been reported [53].

The TEAF system can be used to reduce ketones, certain alkenes and imines. With regard to the latter substrate, during our studies it was realized that 5:2 TEAF in some solvents was sufficiently acidic to protonate the imine (pK_a ca. 6 in water). Iminium salts are much more reactive than imines due to inductive effects (cf. the Strecker reaction), and it was thus considered likely that an iminium salt was being reduced to an ammonium salt [54]. This explains why imines are not reduced in the IPA system which is neutral, and not acidic. When an iminium salt was pre-prepared by mixing equal amounts of an imine and acid, and used in the IPA system, the iminium was reduced, albeit with lower rate and moderate enantioselectivity. Quaternary iminium salts were also reduced to tertiary amines. Nevertheless, as other kinetic studies have indicated a pre-equilibrium with imine, it is possible that the proton formally sits on the catalyst and the iminium is formed during the catalytic cycle. It is, of course, possible that the mechanism of imine transfer hydrogenation is different to that of ketone reduction, and a metal-coordinated imine may be involved [55].

Table 35.3 Examples of the effect of solvent on enantioselectivity with two different ketones.

Solvent	ee [%]	Conversion [%]
Ketone 1		
Methanol	58	>90
Dimethylsulfoxide	72	>90
Dimethylformamide	52	>90
Acetonitrile	4	>90
Ethyl acetate	46	>90
Tetrahydrofuran	60	>90
Dichloromethane	16	>90
Toluene	0	>90
Ketone 2		
Neat	74	17
Methanol	78	14
Isopropanol	79	19
Dimethylformamide	80	100
Dimethylacetamide	79	98
1,4-Dioxane	82	52
Ethyl acetate	80	74
tert-Butyl acetate	77	50
Tetrahydrofuran	80	71
Glyme	74	59
Diglyme	74	18
Methoxyethanol	74	21
tert-Butylmethyl ether	73	30
Dichloromethane	80	51
Triethylamine	78	82
2-Pentanone	77	30
Toluene	63	13

Ketone 1: an electron-rich aryl alkyl ketone. For the screening studies, 1 mol.% catalyst was used and the reactions were analyzed after 1 h.
Ketone 2: an electron-deficient aryl alkyl ketone. For the screening studies, 1 mol.% catalyst was used and the reactions were analyzed after 1 h.

In many cases the solvent was observed to have a large effect on the optical purity of the product. Examples of this, with a ketone and the rhodium cp* TsDPEN catalyst, are shown in Table 35.3. Further optimization of this reaction improved the enantiomeric excess to 98%. A second example involved the reduction of 4-fluoroacetophenone; in this case the enantioselectivity was largely unaffected, but the rate of reduction changed markedly with solvent. Development of this process improved the optical purity to 98.5% ee.

A rationale for these results is that the catalyst interacts with the substrate through weak intermolecular association, and that the strength and nature of

this are sensitive to the solvent. Since it is difficult to predict the best solvent, the best approach is to screen a suitable range of those available.

35.3.3
Other Hydrogen Donors

Hydrogen will not reduce ketones or imines using CATHy™ or related catalysts. Inorganic hydrogen donors that have been used include dithionite and dihydrogenphosphite salts, metal hydrides such as sodium borohydride, and sodium cyanoborohydride. Recently, amines have been shown to function as hydrogen donors with some catalysts. The enzymic cofactor NADH can be used stoichiometrically, and the potential exists to use this catalytically [56].

Hydrogen donors that function poorly with homogenous catalysts include hydrazine hydrate, alkenes (e.g., cyclohexene), and ascorbic acid. This is somewhat surprising as they can be very effective in heterogeneous transfer hydrogenation.

35.4
Substrates and Products

A successful chemical technology is one that can be applied to any situation arising. Enantioselective transfer hydrogenation catalysts are rapidly gaining acceptance as a means of easily preparing optically active alcohols and amines. In our laboratory, we have tested more than 200 substrates, amongst which very few failed to give any reaction, and most give a high enantiomeric excess.

35.4.1
Aldehydes

Transfer hydrogenation is a mild and efficient means of reducing aldehydes, and can be advantageous over other reagents such as sodium borohydride. Clearly, the product is a primary alcohol and therefore not chiral, but a chiral center might be alpha to the aldehyde, in which case a resolution can be effected. Indeed, under the appropriate conditions the chiral center can be racemized and a dynamic kinetic resolution effected [57].

35.4.2
Ketones

The easiest substrates to test are acetophenones, as many substituted analogues are commercially available from laboratory suppliers. A large range of results have been reported; the best enantiomeric excesses achieved and relevant literature reference are detailed in Tables 35.4 and 35.5. The range of ketones that can be reduced includes substituted diaryl, dialkyl and arylalkyl ketones, alpha-,

Table 35.4 Optical purities realized with various substituted acetophenones.

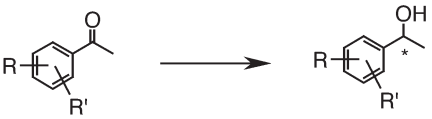

R	R′	ee [%]	Reductant	Catalyst	TOF [h^{-1}]	Reference
H	H	99	TEAF	RuCl(mes)TsDPEN	10	37 b
4-F	H	98.5	TEAF	RhClcp*CsDPEN	75	1 c
2-Cl	H	97	IPA	$RuCl_2PPh_3$(phambox)	1200	61
3-Cl	H	99.7	IPA	$RuCl_2PPh_3$(oxazferrphos)	100	58
4-Cl	H	98.7	IPA	$RuCl_2PPh_3$(oxazferrphos)	100	58
2-Br	H	99	TEAF	RuCl(cym)prolinamide	<16.7	60
3-Br	H	99.7	IPA	RuCl(cym)prolinamide	100	58
4-Br	H	99.3	IPA	RuCl(cym)prolinamide	100	58
2-OMe	H	95	TEAF	RuCl(cym)prolinamide	16.7	60
3-OMe	H	98	IPA	RuCl(hmb)azanorbornylmethanol	3000	59 b
4-OMe	H	97	TEAF	RuCl(mes)TsDPEN	10	37 b
3-NO_2	H	91	IPA	RuCl(hmb)azanorbornylmethanol	3000	59 b
4-NO_2	H	89	IPA	RuCl(cym)azanorbornylmethanol	200	59 a
3-NH_2	H	99	IPA	RuCl(hmb)azanorbornylmethanol	3000	59 b
2-Me	H	>99	IPA	$RuCl_2PPh_3$(oxazferrphos)	100	58
3-Me	H	>99	IPA	$RuCl_2PPh_3$(oxazferrphos)	100	58
4-Me	H	>99	IPA	$RuCl_2PPh_3$(oxazferrphos)	100	58
2-CF_3	H	96	IPA	RhClcp*TsDPEN	16.7	63
3-CF_3	H	97	IPA	RhClcp*TsDPEN	16.7	63
4-CF_3	H	88	IPA	RuCl(cym)azanorbornylmethanol	200	59 a
3-CF_3	5-CF_3	92	IPA	RhClcp*TsCYDN	65	64

For ligand acronyms, see Figure 35.2.
Arene acronyms are as follows: mes = 2,4,6-mesitylene; hmb = hexamethylbenzene; cym = 1,4-cymene; cp* = pentamethylcyclopentadienyl.
TOF: Turnover frequency.

beta-unsaturated, alpha-substituted, cyclic, heterocyclic and alicyclic ketones. The substrates may bear functional groups including halides, ethers, thioethers, alkenes, amines, alcohols, amides, acids, esters and nitriles, yet selective reduction of the ketone is still achieved. The range of chiral alcohols that has been produced by asymmetric transfer hydrogenation, together with best values of enantiomeric excess, is illustrated in Figure 35.5. Of particular note are some unusual examples, for example the use of transfer hydrogenation to form optically active phthalides [73], pyridyl alcohols [78], diols [72] and drug intermediates such as isophorone [76], L-699,392 (an LTD_4 antagonist) and MK0417 (a carbonic anhydrase inhibitor) [49 e]. This is only a small selection of such reactions, as many examples from industry are confidential and cannot be reported here.

Table 35.5 Optical purities realized with various acylbenzenes.

R	ee [%]	Reductant	Catalyst	TOF [h^{-1}]	Reference
Me	99	TEAF	RuCl(mes)TsDPEN	10	37b
Et	99.7	IPA	$RuCl_2PPh_3$(oxazferrphos)	25	58
*n*Pr	92	IPA	RuCl(cym)azanorbornylmethanol	100	59a
*i*Pr	90	IPA	RuCl(cym)azanorbornylmethanol	<13	59a
*n*Bu	98.7	IPA	$RuCl_2PPh_3$(oxazferrphos)	50	58
*t*Bu	93	IPA	$RuCl_2PPh_3$(oxazferrphos)	12.5	65
*n*Hx	95	IPA	RuCl(cym)azanorbornylmethanol	100	59a
CH_2Cl	97	TEAF	RhClcp*TsDPEN	1000	66
CH_2OH	94	TEAF	RhClcp*TsDPEN	<16.7	67
CH_2OTs	93	TEAF	RhClcp*TsDPEN	<16.7	67
CH_2CN	98	TEAF	RuCl(cym)TsDPEN	42	68
CH_2N_3	92	TEAF	RuCl(cym)TsDPEN	4	68
CH_2NO_2	98	TEAF	RuCl(cym)TsDPEN	12.5	68
CH_2NMeCO_2tBu	99	TEAF	RuCl(cym)aminoindanol	<8	69
TMS	98	IPA	RuCl(cym)TsDPEN	–	70
COEt	99	TEAF	RuCl(cym)TsDPEN	12.5	71

For ligand acronyms, see Figure 35.2.
Arene acronyms are as follows: mes = 2, 4, 6-mesitylene; cym = 1,4-cymene; cp* = pentamethylcyclopentadienyl.
TOF: Turnover frequency.

In general, dialkyl ketones are reduced with lower ee than aryl alkyl ketones. In the case of rhodium-based catalysts, strongly electron-withdrawing substituents on aryl ketones tend to give lower enantiomeric excesses, whilst in the case of ruthenium the trend seems to be reversed. Coordinating groups alpha to the ketone can give variable results since the product can act as a ligand and either enhance or interfere with the catalyst. Most substrates are reduced with excellent enantioselectivity and with good catalyst turnover frequencies (TOFs).

35.4.3
Aldimines

The transfer hydrogenation of aldimines has not been reported. In our own studies we have tested the simple Schiff base adduct between benzylamine and benzaldehyde and shown this to be reduced in straightforward manner.

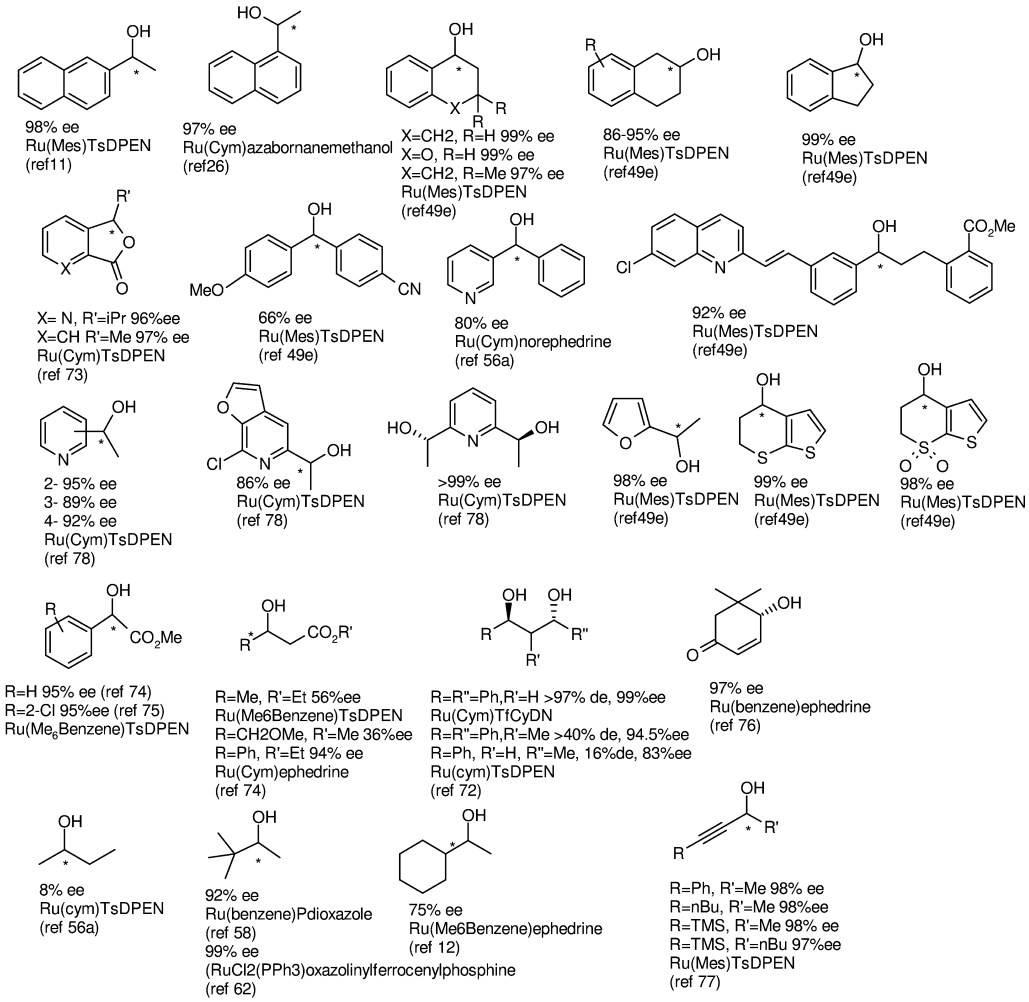

Fig. 35.5 Examples of alcohols produced, and their optical purities.

35.4.4
Ketimines

The reduction of imines and iminium salts present a particular difficulty in that those which are N-substituted can exist in different geometrical isomers that are reduced at different rates and with different selectivities. One way to overcome this problem is to use cyclic imines that can exist only as *cis* isomers. Although these are good substrates, this is not a general solution. The cyclic amines produced by transfer hydrogenation, together with best reported enantiomeric excesses, are listed in Table 35.6. Primary amines are difficult to pre-

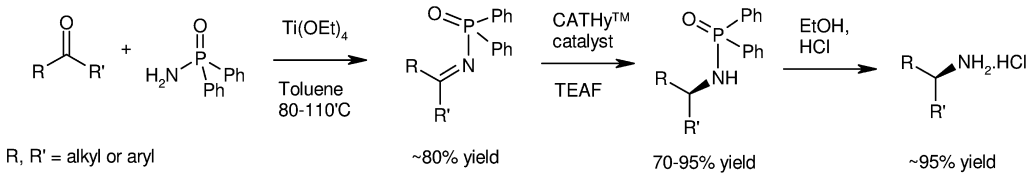

Fig. 35.6 Synthesis of chiral amines by an improved procedure for making diphenylphosphinylimines, followed by asymmetric transfer hydrogenation.

Table 35.6 Optical purities realized with various cyclic imines.

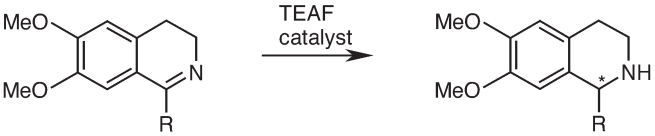

R	ee [%]	Reductant	Catalyst	TOF [h^{-1}]	Reference
methyl	95	TEAF	RuCl(cym)TsDPEN	67	1k
ethyl	83	TEAF	RhClcp*TsDPEN	1200	15b
isopropyl	99	TEAF	RhClcp*TsDPEN	1200	15b
cyclohexyl	97	TEAF	RhClcp*TsDPEN	1200	15b
phenyl	84	TEAF	RuCl(bnz)NpsDPEN	25	1k
2-bromophenyl	98	TEAF	RuCl(bnz)NpsDPEN	<7	84
3,4-dimethoxyphenyl	84	TEAF	RuCl(bnz)NpsDPEN	8.3	1k
3,4-dimethoxybenzyl	95	TEAF	RuCl(cym)MesDPEN	<28	1k
3,4-dimethoxyhomophenyl	92	TEAF	RuCl(cym)MesDPEN	16.7	1k

For ligand acronyms, see Figure 35.2.
Arene acronyms are as follows: bnz = benzene; cym = 1,4-cymene; cp* = pentamethylcyclopentadienyl.

pare directly as the imines are unstable in TEAF; consequently, N-substitution is required. *N*-benzyl and *N*-alkyl imines are often reduced, but with moderate ee-values due to the geometrical isomer problem [1k, 15b, 37b]. Some *N*-acyl, *N*-sulfonyl, oximes and hydrazones are reduced, but the reaction appears to be substrate-specific. Diphenylphosphinylimines are particularly good substrates [79], as the large steric size of the diphenylphosphinyl group may cause the imine to exist in predominantly one geometrical isomer, and this leads to high optical activities. The published method for preparing diphenylphosphinylimines involves reacting diphenylphosphinylchloride with the primary imine [83], though in our experience this leads to low yields. An improved method for their preparation involves reacting diphenylphosphonylamide with the ketone and dehydrating with titanium tetraisopropoxide (Fig. 35.6).

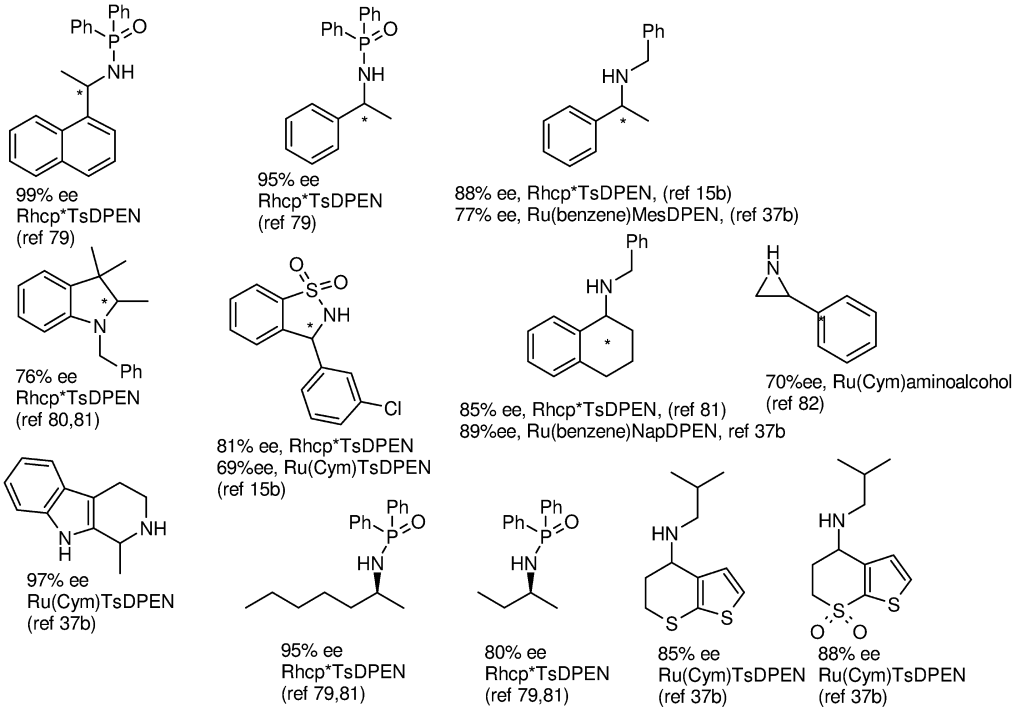

Fig. 35.7 Examples of amines produced, and their optical purities.

The imine may be isolated in good yield, or more conveniently the transfer hydrogenation can be carried out directly on this mixture. The diphenylphosphonylamine product is hydrolyzed with acidic ethanol to yield the primary amine. Alternatively, the diphenylphosphonylamine can be alkylated and the protecting group then removed to yield a secondary amine. Most imines that have been reduced are arylalkyl, though excellent results have been obtained with the phosphinylimines of dialkyl substrates (e.g., 2-butanone, 2-hexanone and 2-octanone substrates). The enantiomeric excesses achieved with a variety of imine substrates are illustrated in Figure 35.7.

The synthesis of amines by the *in-situ* reductive amination of ketones is termed the Leuckart–Wallach reaction. Recently, an asymmetric transfer hydrogenation version of this reaction has been realized [85]. Whilst many catalysts tested give significant amounts of the alcohol, a few produced almost quantitative levels of the chiral amine, in high enantiomeric excess.

A recent development is the transfer hydrogenation of heterocyclic systems such as pyrrole, pyridinium and quinoline systems. Whilst at present the yields and enantioselectivities are modest, further development may improve this situation. For example, 1-methyl-isoquinoline has been reduced to the tetrahydro species and 1-picoline has been reduced to 1-methylpiperidine [86]. Interestingly, these reductions involve alkene as well as imine reduction.

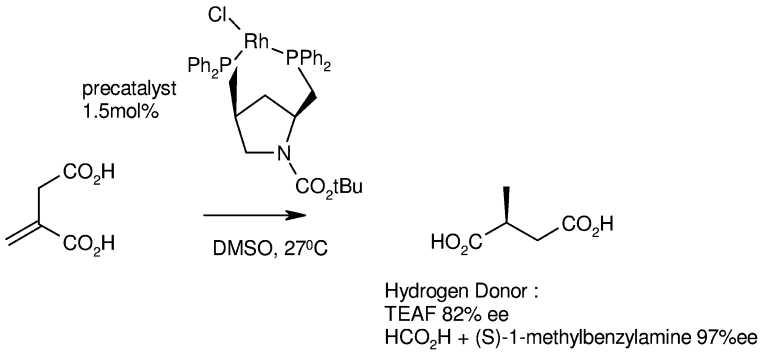

Fig. 35.8 Optical activities achieved by enantioselective transfer hydrogenation of alkenes.

35.4.5
Alkenes

Brunner, Leitner and others have reported the enantioselective transfer hydrogenation of alpha-, beta-unsaturated alkenes of the acrylate type [50]. The catalysts are usually rhodium phosphine-based and the reductant is formic acid or salts. The rates of reduction of alkenes using rhodium and iridium diamine complexes is modest [87]. An example of this reaction is shown in Figure 35.8. Williams has shown the transfer hydrogenation of alkenes such as indene and styrene using IPA [88].

Enantioselective Michael reactions have been achieved using both the Rh-based CATHy catalysts [89 a] and the Ru-based Noyori catalysts [89 b].

35.5
Solvents

The IPA system does not require a co-solvent, but one can be used if this proves advantageous. In the TEAF system a solvent is normally used, though neat TEAF or formic acid can be used if required. The solvent can have a large effect on the reaction rate and optical purity of the product; this may in part be because the substrate seems to bind by weak electrostatic interactions with the catalyst, and is also partly due to the pH of the system. Solvents have a dramatic effect on the ionization of formic acid; for example, in water the pK_a is 3.7, but in DMF it is 11.5. This is because formation of the formate anion becomes less favorable with less polar solvents (see Table 35.2). The pK_a of triethylamine is far less sensitive. As a consequence, formic acid and triethylamine may remain unreacted and not form a salt. The variation in formic acid pK_a can also have a significant impact on the catalyst and substrate, particularly when this is an imine.

Typically, solvents are screened to identify one that gives optimal results. Assuming that the substrate and catalyst are soluble, solvent polarities varying from alkanes, aromatics, halogenated, ethers, acetonitrile, esters, alcohols, dipolar aprotic to water have been used. An example of this, using a ketone and the rhodium cp* TsDPEN catalyst, is shown in Table 35.3. Further optimization of this reaction improved the enantiomeric excess to 98%. A second example involved the reduction of 4-fluoroacetophenone; in this case the enantioselectivity was largely unaffected but the rate of reduction changed markedly with solvent. Development of this process improved the optical purity to 98.5% *e.e.*

Water has been shown to enhance the activity of ruthenium and rhodium catalysts in both the TEAF and potassium formate systems [34, 36, 52]. The aqueous systems enable much simpler control of pH; this is important, as Xiao has found that a low pH markedly slows the reaction [52]. The pH at which this occurs corresponds with the pK_a of formic acid (i.e., 3.7), implying that the formate anion is required for complexation with the catalyst. Xiao has proposed two possible catalytic cycles – one that provides poor ee-values at low pH as a result of ligand decomplexation, and another that gives high ee-values at high pH.

35.6 Reaction Conditions, Optimization, and Scale-Up

The transfer hydrogenation methods described above are sufficient to carry out laboratory-scale studies, but it is unlikely that a direct scale-up of these processes would result in identical yields and selectivities. This is because the reaction mixtures are biphasic liquid, gas. The gas which is distilled off is acetone from the IPA system, and carbon dioxide from the TEAF system. The rate of gas disengagement is related to the superficial surface area. As the process is scaled-up, or the height of the liquid increases, the ratio of surface area to volume decreases. In order to improve de-gassing, parameters such as stirring rates, reactor design and temperature are important, and these will be discussed along with other factors found important in process scale-up.

35.6.1 Temperature

Typically, heterogeneous transfer hydrogenations are carried out at higher temperatures. The Noyori–Ikariya ruthenium arene catalysts are stable up to temperatures around 80 °C, whilst the rhodium and iridium CATHy™ catalysts are best used below 40 °C.

In the IPA system, prevention of the back-reaction depends on how efficiently the acetone is distilled off. Normally, this would be best carried out at the boiling point of isopropanol (80 °C), but for optimal performance of the catalyst this was best done at ambient temperature, and under reduced pressure. Whilst acetone

Table 35.7 The effect of temperature on rate and optical purity in enantiomeric transfer hydrogenation of 4-fluoroacetophenone.

Temperature [°C]	e.e [%]	Relative rate
20	95.7	1.00
5	97.8	0.60
0	98.4	0.37
–5	98.4	0.26

Catalyst = RhClcp*CsDPEN; Reductant = TEAF; TOF = 75 h^{-1}.

can be fractionally distilled, it is simpler to distil the mixture with isopropanol and to maintain constant volume by continuously charging fresh solvent. In the TEAF system, the reaction is normally operated at ambient temperature. Operating at lower temperatures can improve the enantiomeric excess slightly, but this generally results in lower reaction rates. An example of the results achieved, for 4-fluoroacetophenone and Rhcp*TsDPEN, is detailed in Table 35.7.

35.6.2 Productivity

The optimization of any industrial process involves trying to improve productivity. This is the amount of product produced in a given time per unit of volume, and relates to the yield, the reaction concentration and the cycle time. The yields in transfer hydrogenations are usually quantitative as there are no side reactions, though in some systems the catalyst activity may change and thus the reaction profile will be altered (see later for a discussion of this). Originally, concentrations used in the IPA system were low and reaction times quite long in order to prevent any back-reaction, but these have now been considerably improved using methods for the efficient removal of acetone. Essentially, this is a problem of engineering a system to give high rates of liquid-vapor mass transfer. One simple solution is to use a vacuum distillation process, though efficient agitation and gas sparging can also help. Depending upon the efficiency with which the acetone is removed, concentrations up to several molar and short cycle times have been achieved at low catalyst loadings, whilst retaining the enantiopurity of the product. It is interesting to note that the batch process is clearly not the best means of achieving such an improvement; rather, a reactor which provides much larger surface areas (e.g., a thin film evaporator) is better suited. Currently, a number of such reactor designs are under evaluation.

In the TEAF system there is no problem with any back-reaction, and concentrations up to 10 M are possible. Although neat TEAF has been used satisfactorily, it is quite viscous and so it is preferable to use a diluent. As mentioned above, the solvent may have a marked effect on both reaction rate and enantioselectivity.

35.6.3 Reaction Control

The IPA system is convenient in being almost thermo-neutral. All of the components can be mixed safely at the start of the reaction, and the reaction is initiated with small amounts of potassium hydroxide, or isopropoxide. The reaction is clean and no side reactions seem to occur. There is no apparent formation of hydrogen.

The TEAF system is usually only slightly exothermic, and so again all components can be mixed together (TEAF is prepared separately as this process is exothermic). In this case the triethylamine in the TEAF is sufficient to activate the catalyst. In the laboratory high conversions are seen, but on scale-up some substrates fail to be completely converted.

Extensive investigations in our laboratories on the deactivation of rhodium and iridium catalysts has shown there to be a number of different mechanisms involved. Both, rhodium and iridium catalysts are generally less stable at higher temperatures, and have more labile ligands than their ruthenium counterparts. All of the catalysts are affected by pH, but the ruthenium catalysts seem to be more readily deactivated by acid. Indeed, these reactions are often quenched with acetic acid, whilst stronger acids are used to quench the rhodium reactions. Each of the catalysts can be deactivated by product inhibition, the ruthenium catalyst with aromatic substrates such as phenylethanol, and the rhodium and iridium ones by bidentate chelating products.

Ruthenium catalysts are much more sensitive to oxygen [11, 13, 37]. By contrast, the rhodium catalysts are not particularly sensitive to oxygen, but this does depend upon the system. In fact, in the TEAF system small amounts of oxygen are beneficial in maintaining the oxidized metal [91]. The mechanism of rhodium reduction appears to be complex, and is in part due to poisoning by carbon monoxide. Catalyst poisoning of rhodium can occur as a result of the low-level catalyzed decomposition of TEAF (Fig. 35.9) [90]. The side reactions can be minimized by keeping a low concentration of TEAF, and this is achieved by controlled addition of the reagent. Another technique is to sweep away the carbon monoxide and to keep its solution concentration low; this is achieved sim-

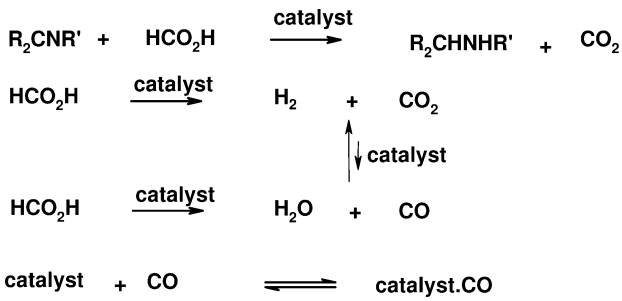

Fig. 35.9 Pathways for the catalyzed decomposition of formic acid.

ply by sparging the reaction solution with nitrogen gas. Good mixing and a high gas flow enable complete conversion of most ketones, including acetophenone. One byproduct of TEAF decomposition is hydrogen, and analysis of the off-gas has shown hydrogen to be produced when the substrate runs out. This decomposition is a slow reaction compared to the desired asymmetric transfer hydrogenation. A high gas flow can help to dilute the hydrogen below the flammable limit, and the incorporation of low levels of oxygen into the nitrogen can improve catalyst activity.

The second cause of catalyst deactivation is reduction of the metal; this is usually observed by darkening of the reaction mass. It has been found that rhodium and iridium CATHy^{TM} catalysts can be retained in their active oxidation state by including an oxidant in the reaction medium. This is most conveniently performed by including a low level of oxygen in the nitrogen gas, typically between 0.5 and 2.0 vol.% (i.e., below the combustion point of hydrogen and the solvents). When this is carried out, the yellow/orange coloring of the reaction solution remains throughout the process [91].

35.6.4
Large-Scale Processes

Numerous enantioselective transfer hydrogenation processes have now been developed and operated at commercial scale to give consistent, high-quality products, economically. These include variously substituted aryl alcohols, styrene oxides and alicyclic and aliphatic amines. Those discussed in the public domain include (*S*)-3-trifluoromethylphenylethanol [48], (*R*)-3,5-bistrifluorophenylethanol [64], 3-nitrophenylethanol [92], (*S*)-4-fluorophenylethanol [1c], (*R*)-1-tetralol [1c], and (*R*)-1-methylnaphthylamine [1c].

35.7
Discussion

It is useful to compare asymmetric hydrogenation and enantioselective transfer hydrogenation so that the appropriate technique can be used when required. Hydrogen gas is a cheap and clean source of reducing power that is widely used in industry, though its use has some drawbacks. For example, it is difficult to handle, being volatile and flammable, and it is poorly soluble in most reaction media such that the use of pressure is required to increase its solvated concentration. The result is that the commercial use of hydrogen requires complex and often expensive equipment. This is especially true in the fine-chemical industry, where batch reactions are normally operated. A further drawback is that hydrogenations are exothermic, and at large-scale the temperature in such reactions is usually controlled by the slow addition of one reagent. However this is often not possible because the catalyst and hydrogen are present at low concentrations, yet for reasonable reaction rates the substrate is required at high con-

centration. The only option is efficient heat removal, which becomes more difficult as the scale increases. Nevertheless, hydrogenations are so useful that many companies see great benefits in possessing a hydrogenation capability. Asymmetric hydrogenation with Ru and Rh phosphine catalysts are most successful, with electron-deficient alkenes having a carbonyl to coordinate to. Asymmetric transfer hydrogenation is less effective in this type of reaction, although ketones and imines are reduced efficiently using this process. The same reaction is generally more difficult with asymmetric hydrogenation. As many more studies have been performed on asymmetric hydrogenation than transfer hydrogenation, the former reaction is better understood. In this respect a large number of catalysts have been prepared, though it is generally true to say that syntheses of the diphosphine ligands are more complex and the costs therefore higher. On the other hand, the TONs achieved with asymmetric hydrogenation catalysts are several orders of magnitude higher than those for transfer hydrogenation. As might be expected, both systems are useful, and a judicious choice of the appropriate technology during route selection will ensure the best manufacturing solution.

As will be appreciated from this review of enantioselective transfer hydrogenation, a remarkable understanding has been achieved in only a few years, and the technology is undergoing rapid development on a number of fronts, including: aqueous reactions [52], dynamic kinetic resolutions [42], cascade or coupled reactions [78], immobilized catalysts [27–32] and, importantly, the introduction of new, more active catalysts [93] and reaction conditions [94]. The primary reasons for the growing use of asymmetric transfer hydrogenation are the simplicity with which these reactions can be carried out, and the high yields and selectivities usually observed. Consequently, the broad reaction scope and favorable economics of this technology is being increasingly adopted in industrial syntheses, notably in the preparation of pharmaceutical intermediates.

Abbreviations

CsDPEN	camphorsulfonyl diphenylethylenediamine
DPEN	diphenylethylenediamine
IPA	isopropanol
NAD(P)	nicotinamide adenine dinucleotide (phosphate)
TEAF	triethylamine: formic acid (5:2 molar mixture)
TfDPEN	trifluoromethylsulfonyl diphenylethylenediamine
TOF	turnover frequency
TON	turnover number
TsDPEN	tosyl diphenylethylenediamine

References

1 (a) S. Gladiali, E. Alberico, *Chem. Soc. Rev.* **2006**, *35*, 226; (b) S. Gladiali, E. Alberico, in: M. Beller, C. Bolm (Eds.), *Transition Metals for Organic Synthesis*, 2nd edn. Wiley-VCH, **2004**, p. 145; (c) *Transition Metals for Organic Synthesis*, 1st ed. **1998**, p. 97; (d) A. J. Blacker, J. Martin, in: H.-U. Blaser, E. Schmidt (Eds.), *Asymmetric Catalysis on Industrial Scale*. Wiley-VCH **2003**, p. 201; (e) T. Naota, H. Takaya, S.-I. Murahashi, *Chem. Rev.* **1998**, *98*, 2599; (f) V. Fehring, R. Selke, *Angew. Chem. Int. Ed.* **1998**, *37*, 1827; (g) M. Palmer, M. Wills, *Tetrahedron: Asymmetry* **1999**, *10*, 2045; (h) M. Wills, M. Palmer, A. Smith, J. Kenny, T. Walsgrove, *Molecules* **2000**, *5*, 4; (i) J. Bäckvall, *J. Organomet. Chem.* **2002**, *652*, 105; (j) D. Carmona, M. Lamata, L. Oro, *Eur. J. Inorg. Chem.* **2002**, 2239; (k) K. Everaere, A. Mortreux, J.-F. Carpentier, *Adv. Synth. Catal.* **2003**, *345*, 67; (l) R. Noyori, S. Hashiguchi, *Acc. Chem. Res.* **1997**, *30*, 97.

2 (a) J. Jones, *Tetrahedron* **1986**, *42*, 3351; E. Schoffers, E. Golebiowski, C. Johnson, *Tetrahedron* **1996**, *52*, 3769; (b) A. Hage, D. Petra, J. Field, D. Schipper, J. Wijnberg, P. Kamer, J. Reek, P. van Leeuwen, R. Wever, H. Schoemaker, *Tetrahedron: Asymmetry* **2001**, *12*, 1025; (c) R. Ruppert, E. Steckhahn, *Chem. Commun.* **1988**, *17*, 1150; (d) E. Steckhahn, S. Herrmann, R. Ruppert, J. Thõmmes, C. Wandrey, *Angew. Chem. Int. Ed.* **1990**, *29*, 388; (e) P. Rylander, *Best Synthetic Methods: Hydrogenation Methods*, Academic Press, **1985**.

3 (a) Y. Haddad, H. Henbest, J. Husbands, T. Mitchell, *Proc. Chem. Soc.* **1964**, 361; (b) M. Gullotti, R. Ugo, S. Colonna, *J. Chem. Soc. (C)*, **1971**, 2652; (c) G. Zassinovich, G. Mestroni, A. Camus, *J. Mol. Catal.* **1977**, *2*(1), 63; G. Zassinovich, G. Mestroni, A. Camus, *J. Organomet. Chem.* **1979**, *168*(2), C37; G. Mestroni, A. Camus, G. Zassinovich, *Aspects of Homogenous Catalysis* **1981**, *4*, 71; (d) G. Zassinovich, A. Camus, G. Mestroni, *J. Mol. Catal.* **1980**, *9*(3), 345; G. Zassinovich, G. Mestroni, *J. Mol. Catal.* **1987**, 42(1), 81.

4 (a) R. Chowdhury, J.-E. Bäckvall, *Chem. Commun.* **1991**, 1063; (b) G. Wang, J. Bãckvall, *Chem. Commun* **1992**, 980; (c) G. Mestroni, G. Zassinovich, E. Alessio, M. Tornatore, *J. Mol. Catal.* **1989**, *49*(2), 175.

5 P. Krasik, H. Alper. *Tetrahedron* **1994**, 50(15), 4347.

6 P. Gamez, F. Fache, P. Mangeney, M. Lemaire, *Tetrahedron Lett.* **1993**, *34*(43), 6897.

7 G. Zassinovich, G. Mestroni, S. Gladiali, *Chem. Rev.* **1992**, *92*, 1051.

8 D. Evans, S. Nelson, M. Gagne, A. Muci, *J. Am. Chem. Soc.* **1993**, *115*, 9800.

9 Y. Shvo, D. Czarkie, Y. Rahamin, *J. Am. Chem. Soc.* **1986**, *108*, 7400.

10 M. Almeida, M. Beller, G.-Z. Wang, J.-E. Bäckvall, *Chem. Eur. J.* **1996**, *2*, 1533.

11 S. Hashiguchi, A. Fujii, J. Takehara, T. Ikariya, R. Noyori, *J. Am. Chem. Soc.* **1995**, *117*, 7562.

12 J. Takehara, S. Hashiguchi, A. Fujii, S. Inoue, T. Ikariya, R. Noyori, *Chem. Commun.* **1996**, 233.

13 A. Fujii, S. Hashiguchi, N. Uematsu, T. Ikariya, R. Noyori, *Chem. Commun.* **1996**, 233.

14 A. J. Blacker, B. Mellor, WO9842643B1, Avecia Ltd, filed 26/03/97.

15 (a) K. Mashima, T. Abe, K. Tani, *Chem. Lett.* **1998**, 1199; (b) J. Mao, D. Baker, *Org. Lett.* **1999**, *1*(6), 841; (c) K. Murata, T. Ikariya, *J. Org. Chem.* **1999**, 64, 2186.

16 D. Petra, P. Kamer, A. Speck, H. Schoemaker, P. van Leeuwen, *J. Org. Chem.* **2000**, *65*, 3010.

17 S. Inoue, K. Nomura, S. Hashiguchi, R. Noyori, Y. Izawa, *Chem. Lett.* **1997**, 957.

18 J. Hannedouche, G. Clarkson, M. Wills, *J. Am. Chem. Soc.* **2004**, *126*, 986; F. Cheung, A. Hayes, J. Hannedouche, A. Yim, M. Wills, *J. Org. Chem.* **2005**, *70*, 3188.

19 M. Bennett, A. Smith, *J. Chem. Soc., Dalton Trans.* **1974**, 233.

20 I. Ojima, A. Vu, D. Bonafoux, Organometallic complexes of rhodium, in: *Houben-Weyl Science of Synthesis*, Thieme, **2003**, Chapter 1.5.3.2, p. 540; J. O'Connor, Organometallic complexes of rhodium,

in: *Houben-Weyl Science of Synthesis*, Thieme, **2003**, Chapter 1.6.2.1, p. 635.
21 T. Oda, R. Irie, T. Katsuki, H. Okawa, *SynLett.* **1992**, 641.
22 B. Mohar, A. Valleix, J.-R. Desmurs, M. Felemez, A. Wagner, C. Mioskowski, *Chem. Commun.* **2001**, 2572.
23 I. Houson, Avecia Ltd WO04024708.
24 M. Wills, M. Gamble, M. Palmer, A. Smith, J. Studley, J. Kenny, *J. Mol. Catal. A, Chemistry* **1999**, *146*, 139; M. Palmer, J. Kenny, T. Walsgrove, A. Kawamoto, M. Wills, *J. Chem. Soc., Perkin Trans. 1* **2002**, 416.
25 C. Frost, P. Mendonca, *Tetrahedron: Asymmetry* **2000**, *11*, 1845.
26 D. Alonso, D. Guijarro, P. Pinho, O. Temme, P. Andersson, *J. Org. Chem.* **1998**, *63*, 2749; D. Alonso, S. Nordin, P. Roth, T. Tarnai, P. Anderson, *J. Org. Chem.* **2000**, *65*, 3116.
27 R. ter Halle, E. Schulz, M. Lemaire, *SynLett.* **1997**, 1257; D. Bayston, C. Travers, M. Polwka, *Tetrahedron: Asymmetry* **1998**, *9*, 2015; A. Sandee, D. Petra, J. Reek, P. Kamer, P. van Leeuwen, *Chem. Eur. J.* **2001**, *7*, 1202; A. Rolland, D. Herault, F. Touchard, C. Saluzzo, R. Duval, M. Lemaire, *Tetrahedron: Asymmetry* **2001**, *12*, 811; J.-X. Gao, X. Yi, C. Tang, P.-P. Xu, H.-L. Wan, *Polym. Adv. Technol.* **2001**, *12*, 716.
28 D. Pears, J. Blacker, EnCat™ system, unpublished results.
29 F. Touchard, F. Fache, M. Lemaire, *Eur. J. Org. Chem.* **2000**, 3787.
30 S. Bastin, R. Eaves, C. Edwards, O. Ichihara, M. Whittaker, M. Wills, *J. Org. Chem.* **2004**, *69*, 5405.
31 X. Li, W. Chen, W. Hems, F. King, J. Xiao, *Tetrahedron Lett.* **2004**, *45*, 951; X. Li, W. Chen, W. Hems, F. King, J. Xiao, *Org. Lett.* **2003**, *5*, 4559.
32 Y.-C. Chen, T.-F. Wu, J.-G. Deng, H. Liu, Y.-Z. Jiang, M. Choi, A. Chan, *Chem. Commun.* **2001**, 1488; Y.-C. Chen, T.-F. Wu, J.-G. Deng, H. Liu, H. Cui, J. Zhu, Y.-Z. Jiang, M. Choi, A. Chan, *J. Org. Chem.* **2002**, *67*, 5301.
33 P. Liu, P. Gu, F. Wang, Y. Tu, *Org. Lett.* **2004**, *6*, 169.
34 J. Martin, J. Blacker, unpublished results; X. Wu, X. Li, W. Hems, F. King, J. Xiao, *Org. Biomol. Chem.* **2004**, *2*, 1818.
35 T. Thorpe, J. Blacker, S. Brown, C. Bubert, J. Crosby, S. Fitzjohn, J. Muxworthy, J. Williams, *Tetrahedron Lett.* **2001**, *42*, 4037; T. Thorpe, J. Blacker, S. Brown, C. Bubert, J. Crosby, S. Fitzjohn, J. Muxworthy, J. Williams, *Tetrahedron Lett.* **2001**, *42*, 4041.
36 H. Rhyoo, H.-J. Park, Y. Chung, *Chem. Commun.* **2001**, 2064; H. Rhyoo, H.-J. Park, W. Suh, Y. Chung, *Tetrahedron Lett.* **2002**, *43*, 269.
37 (a) S. Hashiguchi, A. Fujii, J. Takehara, T. Ikariya, R. Noyori, *J. Am. Chem. Soc.* **1995**, *117*, 7562; (b) N. Uematsu, A. Fujii, S. Hashiguchi, T. Ikariya, R. Noyori, *J. Am. Chem. Soc.* **1996**, *118*, 4916.
38 K. Mashima, T. Abe, K. Tani, *Chem. Lett.* **1998**, 1201.
39 K. Haack, S. Hashiguchi, A. Fujii, T. Ikariya, R. Noyori, *Angew. Chem. Int. Ed. Engl.* **1997**, *36*, 285.
40 T. Koike, T. Ikariya, *Adv. Synth. Catal.* **2004**, *37*, 346; J. Grace, R. Perrutz, G. Hodges, unpublished results.
41 H. Meerwein, R. Schmidt, *Justus Liebigs Ann. Chem.* **1925**, *444*, 221; A. Verley. *Bull. Soc. Chim. Fr.* **1937**, *37*, 537; W. Ponndorf, *Angew. Chem.* **1926**, *39*, 138.
42 M. Almeida, M. Beller, G. Wang, J.E. Bãckvall, *Chem. Eur. J.* **1996**, *2*, 1533; O. Pamies, J.-E. Bäckvall, *Chem. Eur. J.* **2001**, *7*(23), 5052.
43 C. Casey, S. Singer, D. Powell, R. Hayashi, M. Kavana, *J. Am. Chem. Soc.* **2001**, *123*, 1090.
44 R. Noyori, M. Yamakawa, S. Hashiguchi, *J. Org. Chem.* **2001**, *66*, 7931, 66.
45 D. Alonso, P. Brandt, S. Nordin, P. Andersson, *J. Am. Chem. Soc.* **1999**, *121*, 9580.
46 Y. Laxmi, J.-E. Bãckvall, *Chem. Commun.* **2000**, 611.
47 X. Sun, G. Manos, J. Blacker, J. Martin, A. Gavriilidis, *Org. Proc. Res. Dev.* **2004**, *8*, 909.
48 M. Miyagi, J. Takehara, S. Collet, K. Okano, *Org. Proc. Res. Dev.* **2000**, *4*(5), 346; K. Tanaka, M. Katsurada, F. Ohno, Y. Shiga, M. Oda, M. Miyagi, J. Takehara, K. Okano, *J. Org. Chem.* **2000**, *65*, 432.
49 (a) Y. Watanabe, T. Ohta, Y. Tsuji, *Bull. Chem. Soc. Jpn.* **1982**, *55*, 2441; (b) B. Khai, A. Arcelli, *Tetrahedron Lett.* **1985**,

26, 3365; (c) S. Ram, R. Ehrenkaufer, *Synthesis* **1988**, 91; (d) R. Johnstone, A. Willby, I. Entwhistle, *Chem. Rev.* **1985**, *85*, 129; (e) A. Fujii, S. Hashiguchi, N. Uematsu, T. Ikariya, R. Noyori, *J. Am. Chem. Soc.* **1996**, *118*, 2521.

50 (a) H. Brunner, W. Leitner, *Angew. Chem. Int. Ed. Engl.* **1988**, *27*, 1180; (b) H. Brunner, E. Graf, W. Leitner, K. Wutz, *Syn. Comm.* **1989**, 743; (c) K. Wagner, *Angew. Chem. Int. Ed. Engl.* **1970**, *9*, 50; (d) K. Narita, M. Sekiya, *Chem. Pharm. Bull.* **1977**, *25*, 135.

51 (a) C. Ritchie, *J. Am. Chem. Soc.* **1969**, *91*, 6749; (b) V. Belskii, *Bull. Acad. Sci. USSR Div. Chem. Soc.* **1981**, *30*(5), 736; (c) M. Schulbach, *Chem. Ber.* **1923**, *56*, 1895; (d) D.A. Evans unpublished results; K. Izutsu, IUPAC Analytical Chemistry Div. Commission on Electroanalytical Chemistry. Acid-Base Dissociation Constants in Dipolar Aprotic Solvents. Chemical Data Series No. 35, Blackwell Scientific Publications **1990**; (e) E. Grunwald, B. Berkowitz, *J. Am. Chem. Soc.* **1951**, *73*, 4939; (f) H. Sigel, R. Malini-Balakrishnan, U. Haering, *J. Am. Chem. Soc.* **1985**, *107*, 5137; (g) Z. Pawlak, *J. Chem. Thermo.* **1991**, *23*, 135.

52 X. Wu, X. Li, F. King, J. Xiao, *Angew. Chem. Int. Ed.* **2005**, *44*, 3407.

53 S. Gowda, D. Gowda, *Tetrahedron* **2002**, *58*, 2211.

54 J. Blacker, L. Campbell, Avecia Ltd, EP1117627; M. Magee, J. Norton, *J. Am. Chem. Soc.* **2001**, *123*, 1778.

55 C. Longley, T. Goodwin, G. Wilkinson, *Polyhedron* **1986**, *5*(10), 1625; S. Nyburg, A. Parkins, M. Sidi-Boumedine, *Polyhedron* **1993**, *12*(10), 1119.

56 (a) J. Blacker, J. Martin, unpublished results; (b) B. Khai, A. Arcelli, *J. Org. Chem.* **1989**, *54*, 949; B. Khai, A. Arcelli, *Tetrahedron Lett.* **1996**, *37*(36), 6599; (c) J. Blacker, M. Stirling, M. Page, unpublished results (Patent pending).

57 S. Bull, J. Blacker, F. Feuillet, unpublished results.

58 (a) Y. Nishibayashi, I. Takei, S. Uemura, M. Hidai, *Organometallics* **1999**, *18*, 2291; (b) D. Alonso, S. Nordin, P. Roth, T. Tarnai, P. Anderson, *J. Org. Chem.* **2000**, *65*, 3116; (c) S. Nordin, P. Roth, T. Tarnai, D. Alonso, P. Brandt, P. Anderson, *Chem. Eur. J.* **2001**, *7*, 1431.

60 H. Rhyoo, Y. Yoon, H.-J. Park, Y. Chung, *Tetrahedron Lett.* **2001**, *42*, 5045.

61 Y. Jiang, Q. Jiang, X. Zhang, *J. Am. Chem. Soc.* **1998**, *120*, 3817.

62 Y. Jiang, Q. Jiang, G. Zhu, X. Zhang, *Tetrahedron Lett.* **1997**, *38*, 215.

63 K. Murata, T. Ikariya, R. Noyori, *J. Org. Chem.* **1999**, *64*, 2186.

64 P. Devine, H. Karl, Merck and Co., Inc., US6777580.

65 Y. Arikawa, M. Ueoka, K. Matoba, Y. Nishibashi, M. Hidai, S. Uemura, *J. Organomet. Chem.* **1999**, *163*, 572.

66 T. Hamada, T. Torii, K. Izawa, R. Noyori, T. Ikariya, *Org. Lett.* **2002**, *4*, 4373.

67 D. Cross, J. Kenny, I. Houson, L. Campbell, T. Walsgrove, M. Wills, *Tetrahedron: Asymmetry* **2001**, *12*, 1801.

68 M. Watanabe, K. Murata, T. Ikariya, *J. Org. Chem.* **2002**, *67*, 1712.

69 A. Kawamoto, M. Wills, *J. Chem. Soc., Perkin Trans.I* **2001**, 1916.

70 J. Cossrow, S. Rychnovsky, *Org. Lett.* **2002**, *4*, 147.

71 T. Koike, K. Murata, T. Ikariya, *Org. Lett.* **2000**, *2*, 3833.

72 J. Cossy, F. Eustache, P.I. Dalko, *Tetrahedron Lett.* **2001**, *42*, 5005.

73 K. Everaere, J.-L. Scheffler, A. Mortreux, J.-F. Carpentier, *Tetrahedron Lett.* **2001**, *42*, 1899.

74 K. Everaere, J.-F. Carpentier, A. Mortreux, M. Bulliard, *Tetrahedron: Asymmetry* **1998**, *9*, 2971.

75 P. Wolsenholme-Hogg, J. Blacker, J. Martin, unpublished results.

76 M. Hennig, K. Püntener, M. Scalone, *Tetrahedron: Asymmetry* **2000**, *11*, 1849.

77 K. Matsumura, S. Hashiguchi, T. Ikariya, R. Noyori, *J. Am. Chem. Soc.* **1997**, *119*, 8738.

78 K. Okano, K. Murata, T. Ikariya, *Tetrahedron Lett.* **2000**, *41*, 9277.

79 L. Campbell, J. Martin, Avecia Ltd, EP1210305.

80 J. Blacker, L. Campbell, Avecia Ltd US6,509,467.

81 L. Campbell, J. Martin, unpublished results.

82 P. Roth, P.G. Andersson, P. Somfai, *Chem. Commun.* **2002**, *1752*, 16.

83 B. Krzyzanowska, W. Stec, *Synthesis* **1978**, 521; B. Krzyzanowska, W. Stec, *Synth. Commun.* **1982**, 270.

84 E. Vedejs, P. Trapencieris, E. Suna, *J. Org. Chem.* **1999**, *64*, 6724.

85 R. Kadyrov, T. Riermeier, *Angew. Chem. Int. Ed.* **2003**, *42*, 5472.

86 B. Baragana, J. Martin, unpublished results.

87 D. Xue, Y.-C. Chen, X. Cui, Q.-W. Wang, J. Zhu, J.-G. Deng, *J. Org. Chem.* **2005**, *70*(9), 3584.

88 J.M.J. Williams, personal communication.

89 (a) T. Suzuki, T. Torii, *Tetrahedron: Asymmetry* **2001**, *12*, 1077; (b) M. Watanabe, K. Murata, T. Ikariya, *J. Am. Chem. Soc.* **2003**, *125*, 7508.

90 (a) W. Leitner, *Angew. Chem. Int. Ed.* **1995**, *34*, 2207; (b) H. Ishida, K. Tanaka, M. Morimoto, T. Tanaka, *Organometallics* **1986**, *5*(4), 724; (c) J.-P. Collin, R. Ruppert, J.-P. Sauvage, *Nouv. J. Chim.* **1985**, *9*(6), 395; (d) J. Shin, D. Churchill, G. Parkin, *J. Organomet. Chem.* **2002**, *642*, 9.

91 G. Hodges, N. Powles, Avecia Ltd UK Patent App. 0424004.

92 A.M. Rouhi, *Chem. Eng. News*, June 14, **2004**, 51.

93 H. Matsunga, N. Yoshioka, T. Kunieda, *Tetrahedron Lett.* **2001**, *42*, 8857.

94 S. Lutsenko, C. Moberg, *Tetrahedron: Asymmetry* **2001**, *12*, 2529.

36
High-Throughput Experimentation and Ligand Libraries

Johannes G. de Vries and Laurent Lefort

36.1
Introduction

Following Knowles' initial success in enantioselective hydrogenation, there was a growing expectation that from now on it would be possible to produce all enantiopure chiral compounds by enantioselective catalysis [1]. Indeed, Kagan's finding of chiral bisphosphine ligands with chirality residing in the backbone made the challenge of developing new chiral ligands highly attractive to synthetic organic chemists [2]. This resulted in an avalanche of papers – which continues to the present day – describing the development of new chiral ligands which were tested in well-known reactions; an example is the enantioselective hydrogenation of methyl-2-acetamido-cinnamate [3]. Some of these developments, such as Noyori's BINAP, were highly successful and have resulted in industrial applications [4]. Yet, in retrospect, after what must have been an astonishingly massive research effort, the impact of enantioselective hydrogenation – and indeed of enantioselective catalysis using transition-metal complexes – is perhaps not as large as one might have expected. This is due to a number of factors. Scientifically, it soon became evident that the prediction of ligand structure required to affect the desired high enantioselectivity of a new substrate was an impossible affair, thereby making it necessary to test – and probably to invent – new ligands for every new substrate. In addition, the scope of the successful chiral catalysts was found to be limited to special classes of substrates, decorated either with an extra functionality in a position allowing additional ligation to the metal, or with extra π-orbitals near the functionality that needs to be reduced.

When examining more closely the impact that this technology had on the production of fine chemicals, the picture is even bleaker [4, 5]. Even today, the majority of enantiopure chemicals (most of which are intermediates for drugs) is produced either by fermentation or by classical resolution – that is, the separation of diastereomeric salts. There are a number of reasons for this, which can be summarized as follows [6]:

- Short development time. Time-to-market pressure does not leave sufficient time to identify the correct catalyst and develop a robust process. As every

The Handbook of Homogeneous Hydrogenation.
Edited by J.G. de Vries and C.J. Elsevier
Copyright © 2007 WILEY-VCH Verlag GmbH & Co. KGaA, Weinheim
ISBN: 978-3-527-31161-3

month of delay in launch of the new drug can mean a substantial loss of revenue, the choice is often made for reliable, readily implemented and well-known chemistry; in this case classical resolution.

- Cost of the catalyst. The transition metals used, such as rhodium, ruthenium, iridium or palladium, are extremely expensive. The same holds for complicated chiral ligands that often take six to ten synthetic steps for their production. An excellent way to beat these costs is to develop a highly active catalyst. A substrate : catalyst ratio (SCR) of 1000 is often quoted as a minimum requirement. In the celebrated Metolachlor process, a SCR of over 100 000 is possible. Factors determining the rate of reaction are numerous and often poorly understood. Deactivation of the catalyst also has a profound effect on the overall rate of the reaction.
- Fit of the catalytic step in the overall total synthesis. Many cases are known where the catalytic step proceeded beautifully, but the number of synthetic steps was much higher than in the racemic route. Ultimately, the number of steps and costs of the starting materials are the determining factors in production costs.
- Availability of ligands, both on small scale for testing and on production scale. The synthesis and purification of a ligand is a long and cumbersome affair. Thus, until recently, most research groups did not possess more than a handful of ligands. If none of these worked for the customer substrate, then the company would lose the bid for the production, as insufficient time would be available to synthesize new ligands. Even worse is the situation regarding the availability of the kilogram quantities. These are produced in a manner akin to proper large-scale productions and require expensive process development, which will take a considerable amount of time. Few companies were willing to invest upfront in the production of kilogram amounts of ligands, and this forms a major barrier for implementation of the technology in first-generation processes.
- Robustness of the process. Many transition metal-catalyzed reactions function well at the laboratory scale, but on scaling up substrate and product inhibition may be an issue, and sensitivity to impurities may also become apparent. Increasing the SCR, which is often necessary for the economics of the process, also increases the impurity : catalyst ratio. It is also very important to keep the number of components to a minimum, as extraction, crystallization and distillation are the only economic means of purification. Ligands can be a nuisance in this respect, particularly if they are used in amounts over 5 mol%. Reproducibility also is a stringent requirement. Thus, possible inhibition mechanisms should be recognized in order to avoid unwanted surprises during production.

It is not surprising that in this frustrating situation many workers in the field – and in particular in industry – eyed with envy the developments in the area of combinatorial chemistry, and wondered if the same tricks such as split-and-mix [7] and high-throughput screening could be applied to the field of enantioselec-

tive catalysis [8]. Most people assumed that screening mixtures of ligands would provide meaningless results and, indeed, this is rarely a useful enterprise. However, the implementation of high-throughput screening techniques was much more appealing [6, 8, 9]. Even before the advent of combinatorial chemistry, research teams had engaged in the practice of performing multiple reactions at the same time, or even using a number of punctured vials containing different catalysts or substrates in a single autoclave. Indeed, apart from the desire to test as many ligands as possible, most people investigating homogeneous catalysis are well aware of the need to screen other variables of the reaction. We have recently compiled a list of parameters that we consider important both for screening as well as for optimizing reactions (Table 36.1) [6]. It is clear that, in the past, not many of these variables were tested in view of the repetitive nature of the experiments.

Apart from enantioselective catalysis, there is a more general need to perform large numbers of experiments. As most reactions catalyzed by transition metal catalysts proceed through a number of intermediates in a multistep sequence, it is often impossible to identify good structure–activity relationships. Although there are many parameters that affect the outcome of the overall reaction, the effect they have on the discrete steps may differ widely and may even be opposing, which makes it impossible to obtain linear correlations. This thwarts most attempts to direct the optimization approach with a rational choice of parameters based on analogies, which is the common approach in synthetic research. Thus, a slow and painful step-by-step approach in finding "leads" and optimization was common practice. Thus, also for nonchiral reactions, it will usually be impossible to predict what the best catalyst will look like, although there is of

Table 36.1 Parameters for HTS of homogeneous transition metal-catalyzed reactions.

1	Metal	
2	Counterion	
3	Ligand	Catalyst tuning
4	Ancillary ligand	
5	Metal : ligand ratio	
6	Method of catalyst preparation	
7	Substrate : catalyst ratio	
8	Reactant	
9	Solvent	
10	Temperature	Optimizing
11	Pressure	the reaction
12	Ratio of substrate to reactants	conditions
13	Concentration of catalyst, substrate and reactants	
14	Order of mixing catalyst and reactants	
15	Rate of addition of one or more reactants	
16	pH	
17	Additives such as acids, bases or tetra-alkylammonium salts	

course a very large body of literature available that will provide a number of starting points for the search. Nevertheless, extensive screening of metal precursors, ligands and solvents will be necessary in both the lead finding and the optimization phase.

In addition, the large number of experiments and the higher diversity space that can be accessed also greatly improve the quality of the data obtained. Trends are more easily observed as the correlation becomes more reliable with the increasing number of experiments.

In conclusion, it seems likely that high-throughput experimentation (HTE) will not only be a tremendous methodology to solve the time-to-market problem, but will also enhance the scope as well as the quality of academic research to a large extent.

36.2 High-Throughput Experimentation

What is the essence of HTE? It is the ability to perform a larger number of experiments than is manually possible. In the search for a new or improved hydrogenation catalysts, one necessarily needs to go through the following consecutive experimental steps:

- Synthesis of ligands/catalysts.
- Testing of the catalyst in the reaction of interest (including optimization following the parameters listed in Table 36.1).
- Analysis of the products formed during the catalytic reaction.

Consequently, any techniques leading to an acceleration (in terms of the number of experiments performed per unit of time) of one or several of these three experimental steps is sufficient to qualify the research endeavor as being part of an HTE effort. Several strategies can be envisaged to speed up the experiments, as follows.

36.2.1 Serial Mode

In a serial mode (Fig. 36.1), one experimental step (in catalysis research this is usually the preparation of the ligand or the catalyst) is repeated *n* times before moving on to the next step. The only difference with traditional research is that the complete experiment (synthesis/testing/analysis) is carried out for a set of catalysts rather than for an individual species. For example, a library of ligands from the same class can be assembled via traditional organic synthesis prior to its testing in catalysis. (A "library" of compounds is a rather large collection of different compounds with some common features and usually the same function, for example triarylphosphines or imidazolidinones.) Ideally, the compounds in the library can be structurally varied in at least two positions to cre-

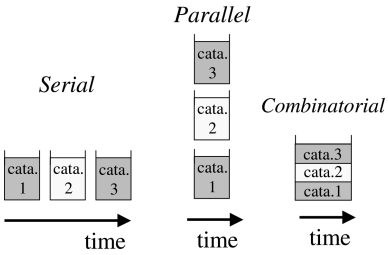

Fig. 36.1 Different modes to perform experiments.

ate a large diversity. No significant time reduction is expected unless rapid testing and/or analysis can be coupled to it.

36.2.2
Parallel Experimentation

A second strategy relies on parallel experimentation. In this case, the same experimental step is performed over *n* samples in *n* separated vessels at the same time. Robotic equipment such as automated liquid-handlers, multi-well reactors and auto-samplers for the analysis are used to perform the repetitive tasks in parallel. This automated equipment often works in a serial fashion as, for example, a liquid handler with a single dispensing syringe filling the wells of a microtiter plate, one after another. However, the chemical formation of the catalyst or the catalytic reaction are run at the same time, assuming that their rate is slow compared to the time needed to add all the components. The whole process appears parallel for the human user whose intervention is reduced.

36.2.3
Combinatorial Protocols

In combinatorial protocols, *n* experiments are performed at the same time in the same vessel. This methodology is the most efficient in terms of time and resources, but can only be applied in discrete cases in homogeneous catalysis. Indeed, the efficiency of a catalyst can only be measured when it is submitted to the reactants. Testing a mixture of catalysts in solution would give the overall efficiency of the mixture, without any indications about individual performances.

To date, only living polymerization catalysts have been tested in a combinatorial fashion, using electrospray mass spectrometry (EMS) to discover the best-performing catalyst [10]. This protocol would seem less-suited for hydrogenation. Elaborate techniques have nevertheless been designed to test pooled catalysts. They involve immobilization of the catalysts on polymer beads and testing these in a reaction with a chromogenic substrate in a viscous medium, which limits the diffusion of the colored products to the neighborhood of the active bead [11]. In the extreme case of an entirely new reaction where the expectation is that most of the catalytic species will not be active, such a combinatorial testing

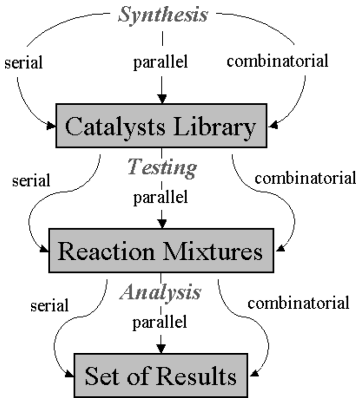

Fig. 36.2 Steps for the development of new or improved catalysts and HTE modes.

could nevertheless be used. Deconvolution strategies such as those used for libraries of small organic molecules would allow identification of the active catalyst by performing a minimum number of experiments. For example, using the so-called deconvolution by orthogonal libraries, the active species among n catalysts could be identified by performing only 3.3 logn experiments [12].

The ideal HTE set-up should be composed of accelerated procedures for each step of the experiment (Fig. 36.2). The reason for this is that in a set of consecutive steps, the slower step is rate-determining. Ideally, the most efficient set-up would combine a combinatorial synthesis of a diverse library of catalysts with a one-pot catalytic testing coupled to identification of the best candidate. Unfortunately, such a protocol has not been implemented yet for the discovery of new hydrogenation catalysts, and most HTE protocols involve at best a succession of steps involving parallel procedures. As can be seen from Fig. 36.2, there can be no HTE without a library of catalysts. In homogeneous hydrogenation, this is usually synonymous to a library of ligands. Methodologies to prepare libraries of ligands/catalysts are described in Section 36.3. Following the advent of parallel pressure reactors, parallel catalytic testing has become possible, and its application in hydrogenation – as well as new methodologies for fast catalytic testing – will be discussed in Section 36.4. Details of fast analysis will be outlined in Section 36.5.

36.3
Generating and Testing Libraries of Catalysts and Ligands

36.3.1
Libraries of Individually Synthesized Ligands

It is clear that the high-throughput approach is only possible if there are sufficient catalysts available. Fortunately, in hydrogenation it is usually possible to form the pre-catalyst simply by mixing a metal precursor and the ligand in a

suitable solvent. Several groups have taken advantage of the commercial availability of numerous metal precursors and ligands to set up high-throughput protocols.

Nugent prepared a library of 256 catalysts by combining 32 commercially available chiral phosphines with eight metal precursors based on Rh, Ir and Ru [13]. All the catalysts were generated *in situ* simply by mixing stock solutions of the metal sources and stock solutions of the ligands. The catalysts were tested in the enantioselective hydrogenation of 3-alkylidene-2-piperidones. The best result was obtained with 2,4-bis(diphenylphosphino)pentane (BDPP) in combination with $[Ir(COD)_2]BF_4$; this was quite surprising as this system was known to be unselective in related reactions due to its high degree of flexibility.

Jessop et al. used 29 metal salts and five ligands to identify a catalyst for the hydrogenation of CO_2 [14]. These authors were able to identify a highly active catalyst outside the platinum group. Indeed, the known $NiCl_2$(dcpe) (dcpe = $Cy_2PCH_2CH_2PCy_2$) was found to be able to catalyze the formation of formic acid in up to 4400 TON.

Researchers at Chirotech focused on the use of Noyori's Ru(II) dichloride(diphosphine)(diamine) complexes for the enantioselective hydrogenation of non-olefinic compounds [15]. Taking advantage of the large libraries of structurally diverse bisphosphines and diamines they had at their disposal, they were able to generate an array of catalysts with very different stereoelectronic properties (Scheme 36.1). The pre-catalyst preparation required nothing more than boiling $[RuCl_2C_6H_6]_2$ and the diphosphine in DMF, followed by treatment with the diamine at room temperature. In the case of ketone hydrogenation, the research team discovered that Phanephos was the best-performing diphosphine. In combination with DPEN or DACH, it forms a highly efficient catalyst for the enantioselective hydrogenation of simple aromatic, heteroaromatic, and α,β-unsaturated ketones [15 c]. By testing the hydrogenation of imines, the combination of Et-Duphos and DACH was found to give the best results for *N*-(phenylethylidene)aniline (up to 94% ee after optimization). Overall, these authors observed that the best diphosphine/diamine combination was different for each substrate [15 a].

Blaser et al. carried out an extensive screening of homogeneous catalysts for the enantioselective hydrogenation of *p*-chlorophenylglyoxylic acid derivatives [16]. A broad range of chiral electron-rich bisphosphines combined with Rh or Ru was used. While no satisfying catalyst was found for phenylglyoxylic amides, Ru/MeO-BiPhep achieved ee-values of 90–93%, with TONs up to 4000 and TOFs up to 210 h^{-1} for the methyl ester (Scheme 36.2).

After some mechanistic studies showing that the reduction of *N,O*-acetals proceeds via a prochiral iminium cation, Börner et al. aimed at finding an enantioselective catalyst for this transformation by preparing a library of 144 catalysts [17]. Pre-catalysts were generated *in situ* by mixing one ligand out of a library of 48 members with either $[Rh(COD)_2]BF_4$, $[Rh(COD)_2]OTf$, or $[Rh(COD)Cl]_2$. The best catalyst obtained was a combination of $[Rh(COD)_2]BF_4$ and Norphos, which gave up to 80% ee (Scheme 36.3).

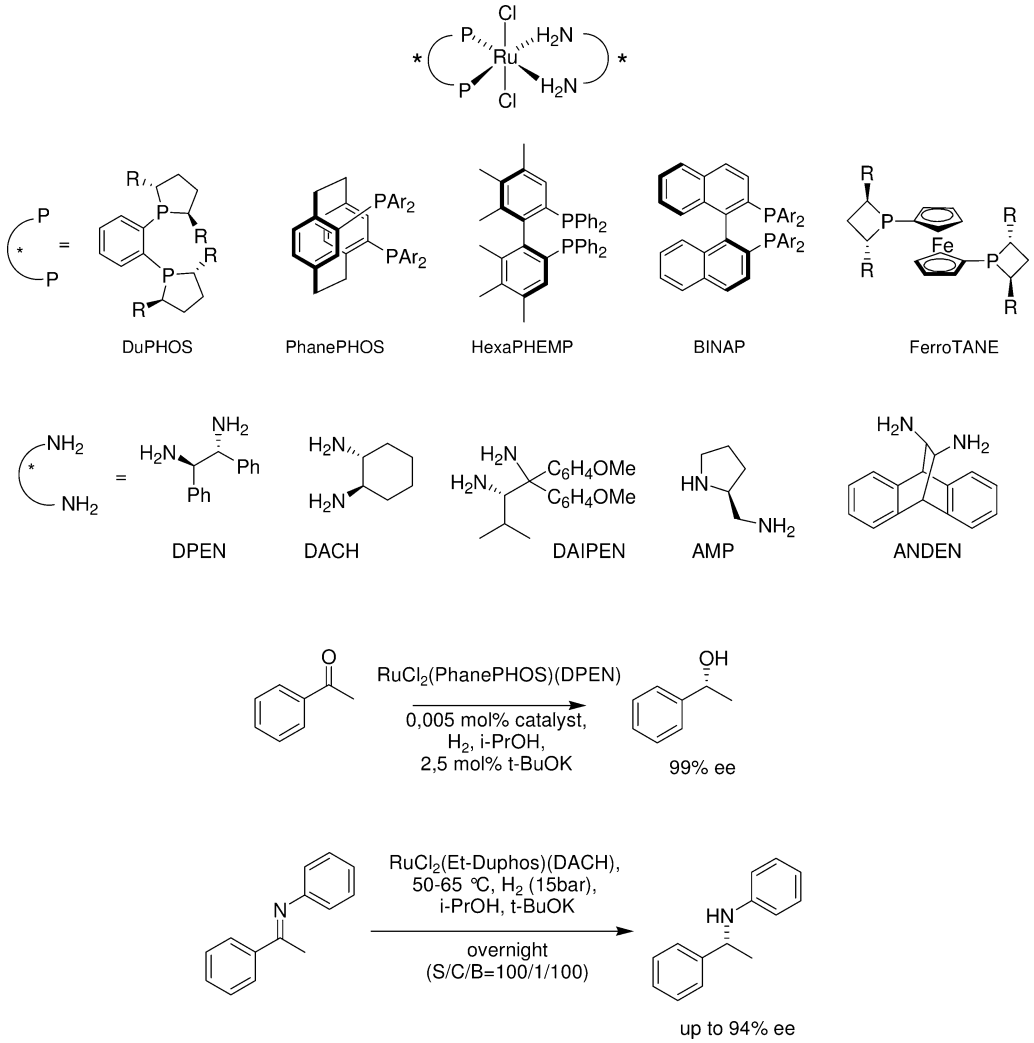

Scheme 36.1 Library approach in enantioselective ketone hydrogenation.

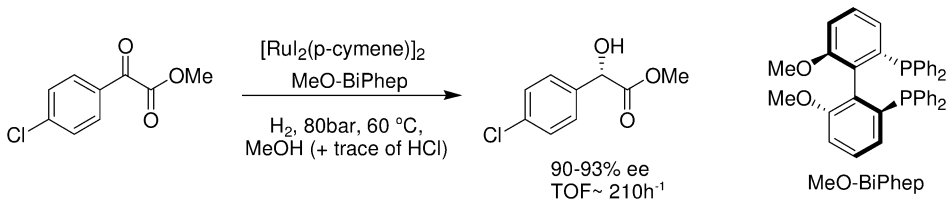

Scheme 36.2 Enantioselective hydrogenation of methyl *p*-chlorophenylglyoxylate.

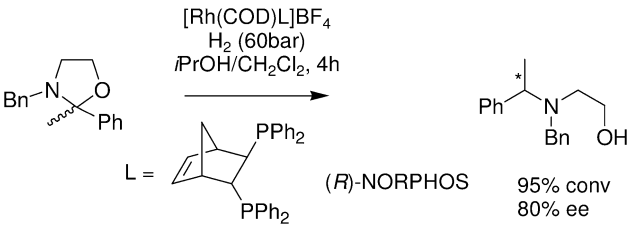

Scheme 36.3 Enantioselective hydrogenation of *N,O*-acetals.

The solvent plays an important role in the outcome of a homogeneous hydrogenation reaction. Consequently, variation of the solvent can be seen as another, highly relevant means of generating a library of catalytic systems. Feng et al. used ionic liquids (IL) as solvent, and studied their influence on the enantioselective hydrogenation of the traditional benchmark substrates (MAA, MAC) catalyzed by various diphosphine/Rh systems [18]. In their screening endeavor, these authors included seven classes of chiral bisphosphines and four different ILs. The ILs were tested pure and mixed with water (wet ILs), which can generate triphasic mixtures depending on the water:IL ratio. The wet ILs were superior to the usual organic solvent in terms of enantioselectivity. This, however, was true only for the ferrocene-based chiral bisphosphines. It was also shown that recycling of the catalyst was possible, since the Rh complex remained almost entirely in the IL phase.

Using traditional synthetic methods, other groups aimed at preparing their own library of ligands from the same family. Each ligand is synthesized and purified individually, thus limiting the size of the library to, at the most, a few dozen members. Diversity is introduced along the way via divergent synthesis. In this approach, a key advanced intermediate (enantiopure in the case of enantioselective hydrogenation) is prepared on a large scale and used to synthesize many different ligands [19a].

Burgess et al. prepared libraries of phosphine-oxazoline and *N*-heterocyclic carbene-oxazoline ligands for the enantioselective hydrogenation of arylalkenes (Scheme 36.4) [19]. The chiral P,N-ligands, initially introduced by Pfaltz, allow the formation of enantioselective versions of the Crabtree catalyst, $[Ir(COD)(Pyridine)PCy_3]^+PF_6^-$ [20]. Ten phosphine-oxazoline ligands (**2**) were prepared from the common intermediate (**1**) by three different routes [19a] and tested in the enantioselective hydrogenation of several arylalkenes [19b]. The best results (full conversion, 95% ee) were obtained with $R_1 = CHPh_2$ and $R_2 = 2\text{-}MeC_6H_4$ in the hydrogenation of *E*-1,2-diphenylpropene. The nature of the R_1 substituent was observed to be crucial, since changing from $R_1 = CHPh_2$ to $R_1 = CMePh_2$ led to poor results (12% conversion, 14% ee), thus validating the necessity to screen a set of related ligands. For the *N*-heterocyclic carbene-oxazoline, a larger library was prepared by reacting two small libraries of synthetic constituents (i.e., oxazoline electrophiles and imidazole nucleophiles) with each other [19c]. Up to 108 ligands could be generated from six oxazolines and 18 imidazoles, prepared

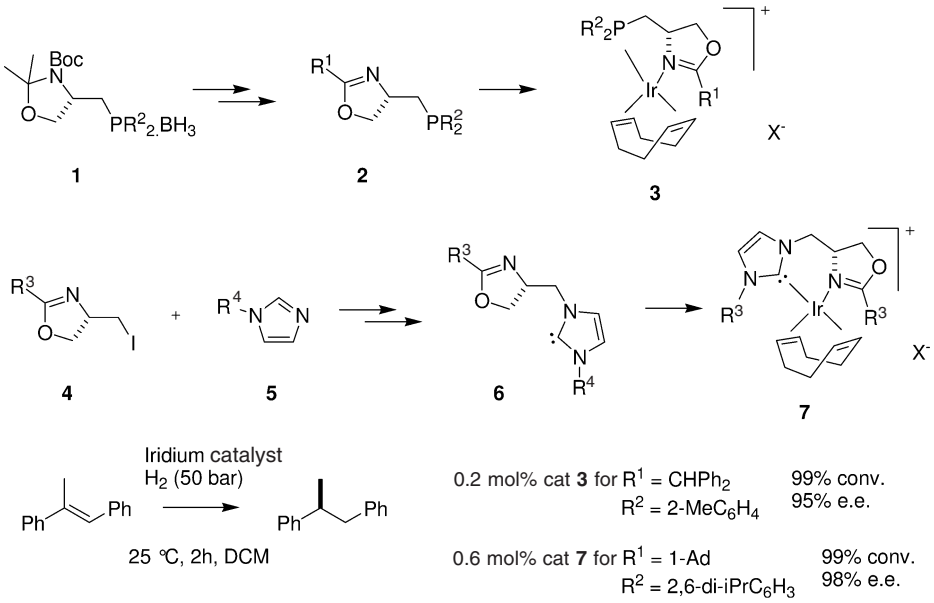

Scheme 36.4 Libraries of P,N- and C,N-ligands in the Ir-catalyzed enantioselective hydrogenation of unfunctionalized olefins.

via three different routes. Several ligands appeared to be quite efficient in the enantioselective hydrogenation of a range of arylalkenes. Again, the high sensitivity of the catalysis to both substituents, R^3 and R^4, was demonstrated. The carbene-oxazoline ligands appeared to be superior to their phosphine-oxazoline counterparts as they are not sensitive to air/moisture and they allow the hydrogenation to be performed under milder conditions.

Salzer et al. prepared a set of planar-chiral diphosphine ligands based on the arene chromium tricarbonyl backbone (Fig. 36.3) [21]. The straightforward four-step synthetic route allowed the preparation of 20 ligands of this family. These ligands were tested in Ru- and Rh-catalyzed enantioselective hydrogenation of various substrates, including the standard C=C substrates (dimethyl itaconate, methyl-2-acetamidocinnamate, methyl-2-acetamidoacrylate) as well as MEA-imine (1-(methoxymethyl)ethylidene-methylethylaniline) and ethyl pyruvate. Moderate conversions and ee-values were obtained.

A small library of ten chiral amino-alcohol ligands was assembled by Pericàs et al. [22]. The synthesis involved a three-step route starting from enantiomerically pure phenylglycidol obtained by Sharpless epoxidation. Diversity can be introduced in two positions, by varying the protecting group of the primary alcohol or the alkylating reagent of the amino group (Scheme 36.5). These ligands were tested in the Ru-catalyzed transfer hydrogenation of aromatic ketones, leading to an ee-value of up to 76% in the case of acetophenone.

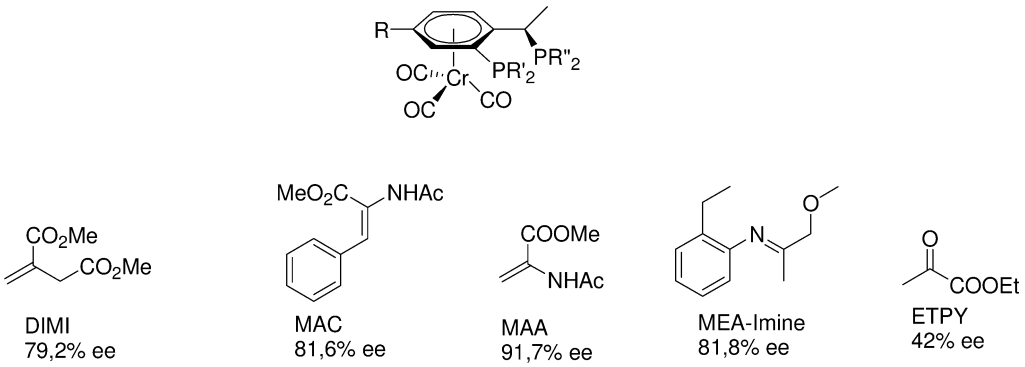

Fig. 36.3 Library of planar-chiral diphosphine ligands.

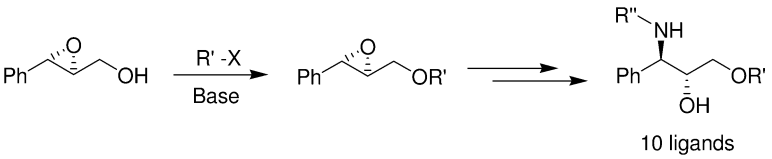

Scheme 36.5 Library of aminoalcohol ligands.

Adolfsson et al. prepared a library of modular dipeptide-analogue ligands [23]. The 45 members of this library were synthesized manually, via a two-step straightforward synthesis, by combining nine amino acids with five amino alcohols (Scheme 36.6). The library was tested in the Ru-catalyzed transfer hydrogenation of aromatic ketones with isopropanol as the hydrogen source. With few exceptions, all the ligands gave good enantioselectivities (>85% ee), whilst the catalytic activity varied significantly within the library. Steric hindrance appeared to be the most important parameter influencing the activity. The influence of

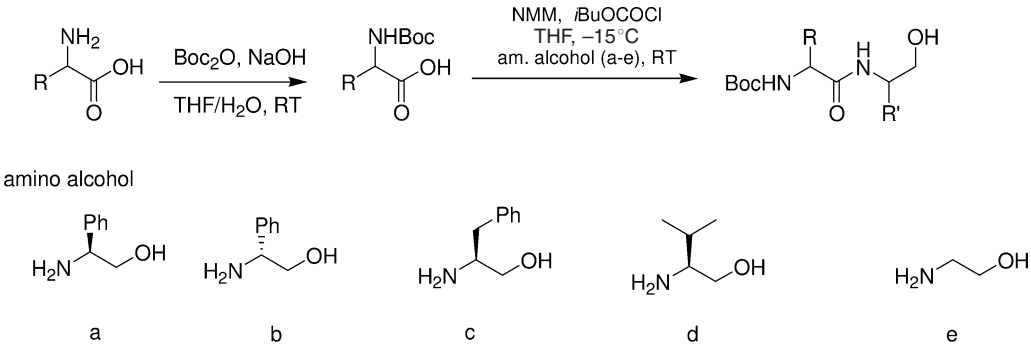

Scheme 36.6 Library of ligands for transfer hydrogenation.

the *N*-terminal protecting group on the ee-value was also investigated, with ligands based on N-Boc-protected alanine and phenylglycinol proving superior.

Pfeffer, de Vries and coworkers developed the use of ruthenacycles, based on chiral aromatic amines as enantioselective transfer hydrogenation catalysts. These authors were able to develop an automated protocol to produce these catalysts by reacting ligand and metal precursor in the presence of base, KPF_6 in CH_3CN. After removal of the solvent, isopropanol was added followed by the substrate, acetophenone, and KO*t*Bu. In this way, a library of eight chiral

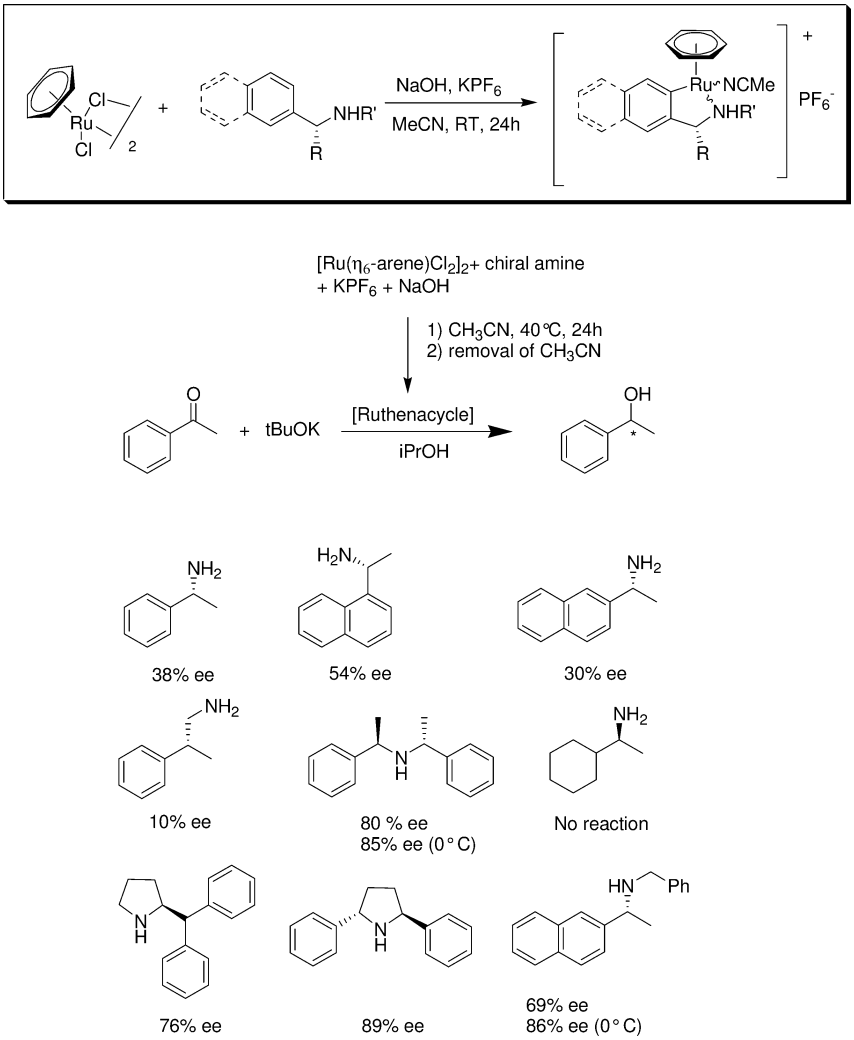

Scheme 36.7 Parallel ruthenacycle preparation and screening in asymmetric transfer hydrogenation.

amines and two metal precursors was screened in a single run. The best results were obtained with 2,5-diphenylpyrrolidine as ligand and $[Ru(benzene)Cl_2]_2$ as metal precursor (Scheme 36.7) [24].

One limiting factor in all approaches towards ligand libraries is the limited availability of chiral starting materials. Thus, several groups have turned towards Nature to obtain a boundless supply of chiral materials. In a seminal approach, Whitesides et al. attached a nonchiral rhodium–bisphosphine complex to biotin. This conjugate was subsequently complexed to the protein avidin. Enantioselective hydrogenation of 2-acetamido-acrylate using this superstructure proceeded with 44% ee [25]. Ward has subsequently refined this concept by using genetically modified forms of avidin, which resulted in a catalyst that could hydrogenate the same substrate with 96% ee [26]. In order to broaden this concept, several groups have developed approaches to covalently modify enzymes with metal catalysts. It is clear that with current capabilities for the genetic modification of proteins, very large libraries of enzymes could, in principle, become available. Reetz has reported the attachment of catalysts and ligands to papain using a maleimide linker [27]; the catalysts proved to be active, but the enantioselectivity in these reactions remained at very low levels. Reetz also reported the attachment of a bisphosphine ligand, though without further catalytic use.

De Vries and coworkers managed to attach a bulky phosphite ligand to Cys25 in papain via a phenacyl bromide linker (Scheme 36.8). Treatment of this modified enzyme with $[Rh(COD)_2]BF_4$ followed by purification gave an enzyme containing exactly one rhodium atom (ES-MS). This construct was an active hydrogenation catalyst capable of completely hydrogenating methyl 2-acetamidoacrylate in an aqueous phosphate buffer at 12 bar overnight at a SCR of 800. However, the hydrogenation product was racemic [28].

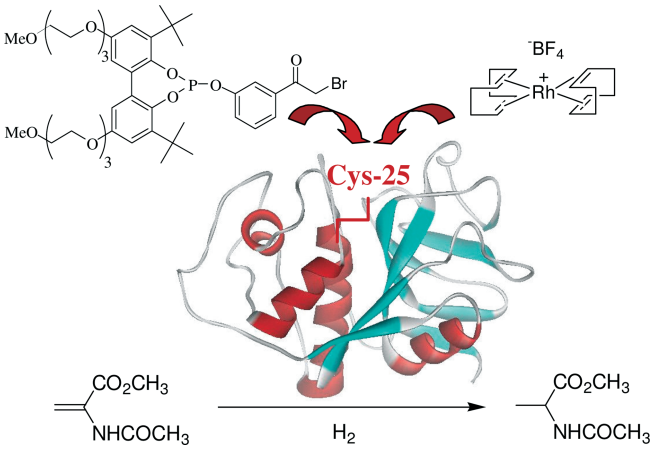

Scheme 36.8 Papain-bound rhodium complex as a hydrogenation catalyst.

36.3.2
Automated Synthesis of Ligand Libraries

In all of the previous examples, the library of ligands was assembled by synthesizing one ligand at a time using traditional synthetic methods. This tedious approach constitutes a major bottleneck for the application of HTE in homogeneous hydrogenation. Drawing inspiration from the techniques used in combinatorial chemistry for the automated synthesis of large libraries of small organic molecules, a few groups have developed a number of new solutions based on solid-phase synthesis to prepare libraries of ligands.

Gilbertson used the diversity available from the use of the 20 natural amino acids in peptides by creating two new phosphine-containing amino acids **9a** and **b**; these were incorporated in the form of their thiooxides **8** into random peptide sequences (Fig. 36.4) [29].

Using the Multipin method, Gilbertson then synthesized 27 undecapeptides on solid phase, which were presumed to have a helical conformation. This was induced by frequent use of the α-alkylated amino acid aminoisobutyric acid. The phosphine-thiooxide-containing residues were positioned in the i and $i + 4$ positions, which would lead to the two phosphines being adjacent in the helical peptide chain. In addition, Gilbertson synthesized 36 peptides containing phosphines in the i and $i + 1$ positions.

When the peptide synthesis was complete, the phosphines were deprotected by sequential treatment with MeOTf and HMPT (Scheme 36.9). Addition of the rhodium precursor then created the catalyst library, which was screened, on the pin in the enantioselective hydrogenation of methyl-2-acetamidoacrylate (see Scheme 36.10). Unfortunately, this beautiful concept was poorly rewarded with rather low enantioselectivities.

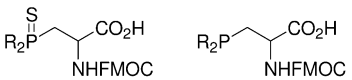

8a R = Ph
8b R = Cy

9a R = Ph
9b R = Cy

Fig. 36.4 Phosphorus-containing amino acids.

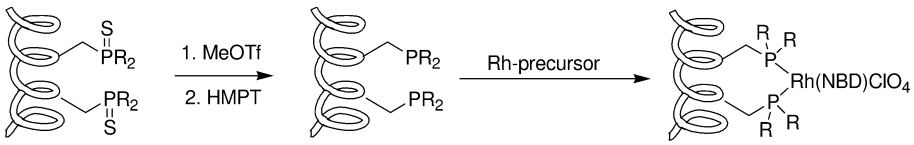

Scheme 36.9 Libraries of phosphine-containing helical undecapeptides.

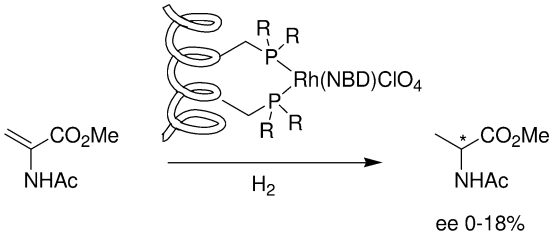

Scheme 36.10 Enantioselective hydrogenation using libraries of peptide-based rhodium catalysts.

There is one more report on the synthesis of a library of phosphorus ligands on solid phase. Waldmann et al. prepared a library of phosphoramidites on beads (Fig. 36.5), but these were only applied in enantioselective C–C-bond formation. In fact, as two ligands need to be bound to the catalyst, the use of an immobilized monodentate ligands should most likely be avoided unless the proximity between the ligands is sufficiently close. In addition, crosslinking by the metal may have a negative impact on the permeability of the polymer for the substrate.

The screening of catalysts attached to beads is not a straightforward task [30]. The presence of the polymeric support in the vicinity of the catalytic site can have a significant influence on its activity and selectivity. If, ultimately, the goal is to prepare homogeneous catalysts, important discrepancies can be faced between the performances obtained with the supported catalysts and those obtained with its soluble counterpart, which places in doubt the validity of screening ligands on supports [31]. There is also the problem of slow diffusion of the reagents into and products out of the beads affecting the outcome of the catalysis. De Bellefon believes that mass-transport limitation was indeed the main reason for the low ee-values obtained by Gilbertson [32]. Ranking the catalysts attached to a polymer can also be problematic. A rigorous comparison of the activity of two catalysts is possible only if both have the same number of active sites. For supported catalysts, this quantity is difficult to evaluate as most of the solution-phase analytical techniques can no longer be applied. In order to avoid these difficulties, it would be highly desirable to design a rapid, automated protocol for the synthesis of libraries

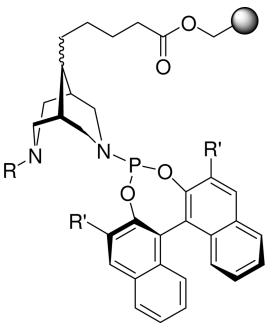

Fig. 36.5 Library of immobilized phosphoramidite ligands.

of ligands in solution. This can be accomplished either via solid-phase synthesis, with the ultimate step being cleavage of the ligand from the bead, or directly via solution-phase synthesis. If examples of libraries of ligands in solution can be found in the literature [33], almost none is related to hydrogenation, for the simple reason that most of the ligands used in hydrogenation are phosphorus-based and involve lengthy syntheses, which are difficult to adapt to automation. Not surprisingly, only two examples have been identified for the rapid automated synthesis of large libraries of phosphorus ligands in solution.

While the first synthesis does not pertain to hydrogenation, it is worthy of mention as it involves a three-component condensation reaction leading directly to the formation of ligands with a purity (wt%) ranging from 79 to 95%. Lapointe prepared a library of 96 aminomethylphosphines by condensation of a secondary phosphine, an arylaldehyde and a primary or secondary amine (2 phosphines×6 aldehydes×8 amines) (Scheme 36.11) [34]. The reaction is high-yielding, obviating the need for purification. One ligand prepared via the library protocol was used successfully to synthesize a Pd complex, with the yield being only slightly lower than for a pure ligand. No examples of the use of this library of ligands in catalysis have been reported.

The second example of rapid automated synthesis of large libraries of phosphorus ligands in solution was reported by DSM. Feringa/Minnaard/De Vries developed the use of simple BINOL-based monodentate phosphoramidites as ligands for enantioselective hydrogenation (see Chapter 28) [35]. Since these ligands are easily prepared, a protocol for their automated synthesis in solution became an attainable goal. The first step of the most common phosphoramidite synthesis – the formation of the phosphochloridite from the BINOL or diol and PCl_3 – proceeds essentially quantitatively, and purification is effected by distilling off excess PCl_3. The robotic synthesis can thus begin with stock solutions of the stable phosphochloridites, leaving only a single synthetic step. This last step usually yields the ligands in a purity with respect to phosphorus of 90–95%, the main contaminant being triethylammonium chloride. Thus, it is clear that the final purification is the only hurdle that needs to be taken in order to effect this robotic ligand synthesis. Although parallel column chromatography is feasible, this solution is not very appealing. To verify if purification is really necessary, a known phosphoramidite (derived from (*R*)-2,2′-binaphthol and diethylamine) was synthesized and tested without purification in the Rh-catalyzed hydrogenation of methyl-2-acetamidocinnamate. This led to very poor results: both conversion and enantioselectivity were substantially lower than with

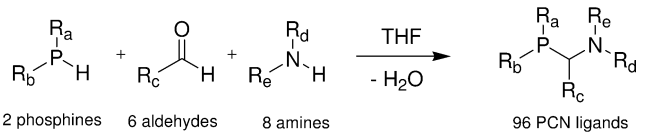

Scheme 36.11 Parallel synthesis of a library of aminophosphine ligands.

the purified ligand. Since the main culprit is the presence of soluble chloride (a known catalyst inhibitor), the solvent for the ligand synthesis was switched to toluene, allowing complete removal of the chloride salt by filtration. Remarkably, the ligand purified in this manner had a very similar performance in the hydrogenation reaction as the purified ligand. This simple finding opened the door to automation. The coupling reactions between phosphochloridite and amine were performed in a 96-well microtiter plate equipped with an oleophobic filter. After 2 h of reaction, the microplate was placed on a manifold, vacuum was applied, and the filtered ligand solutions were collected in another 96-well plate. This protocol was initially tested on a set of 32 ligands, which were subsequently screened in the Rh-catalyzed enantioselective hydrogenation of two model substrates (see Fig. 36.6) [36].

Scheme 36.12 shows the results of this library of 32 phosphoramidites in the enantioselective hydrogenation at 6 bar H_2 of methyl-2-acetamido-cinnamate and methyl-*Z*-3-acetamido-2-butenoate. For the first substrate, almost all members of the library led to full conversions, indicating that most ligands were formed with an acceptable degree of purity. ^{31}P-NMR revealed the presence of trace amounts of other phosphorus species that remarkably did not affect the performance of the catalyst. Best results are obtained with ligands based on piperidines, such as Pipphos (B7) and A8; in addition, two other good ligands based on secondary amines were found (A7 and C7). The enantioselectivities are on average 5% lower than with the purified ligands.

The hydrogenation of methyl-*Z*-3-acetamido-2-butenoate resulted in more surprises. Although ligand D7 based on a primary amine was known to give good results with these substrates [37], the library shows that in general all BINOL-based phosphoramidites that contain a primary amine with branching in the α-

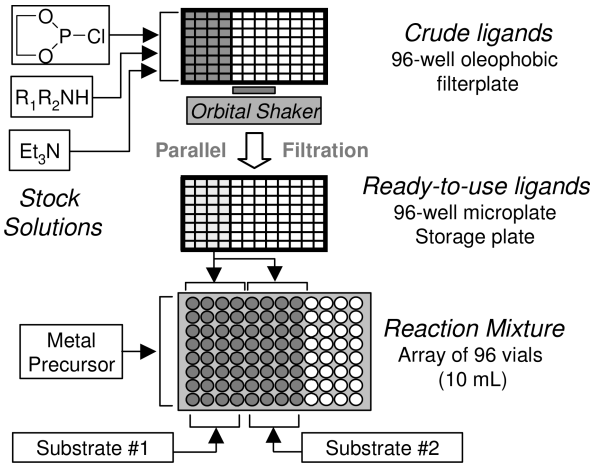

Fig. 36.6 Phosphoramidite library synthesis and screening protocol. (Reproduced by permission of the American Chemical Society from [36].)

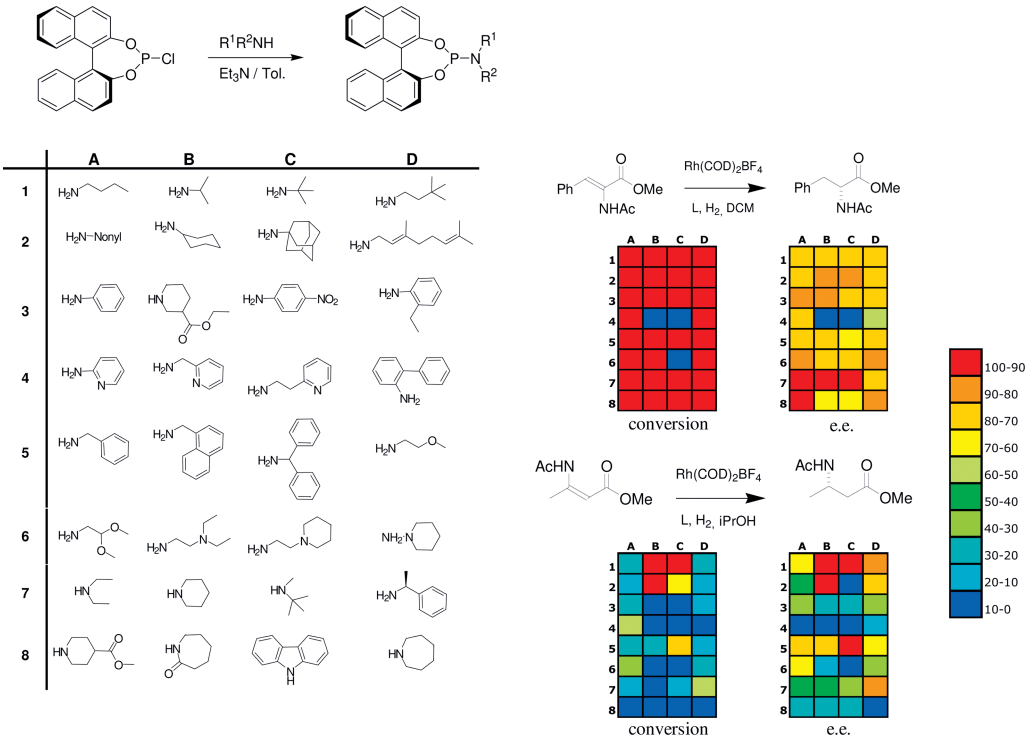

Scheme 36.12 Parallel synthesis and screening of monodentate phosphoramidites in enantioselective hydrogenation.

Table 36.2 Comparison of library ligands with purified ligands.

Ligand	Purified ligands		Library ligands	
	Conversion [%]	ee [%]	Conversion [%]	ee [%]
A7	8	46	11	41
B1	100	95	95	92
B7	11	55	7	43
D7	96	94	51	88

position give excellent results (B1, C1, B2). A comparison of four ligands from this library with the results obtained with the purified ligands clearly shows that there is some erosion of rate and enantioselectivity due to the impurities present in the library ligands (Table 36.2). However, the relative order remains the same, and the results therefore have an excellent predictive value.

This "Instant Ligand Library" concept is now routinely used by DSM Pharma Chemicals for customer's requests.

Clearly, the method can also be used for other monodentate ligands such as phosphites. The application of this library approach to copper-catalyzed enantioselective C–C-bond formation has also been reported [38].

36.3.3
Mixtures of Chiral Monodentate Ligands

It has been established that usually two monodentate ligands (phosphoramidites, phosphites or phosphonites) are present in their rhodium-based hydrogenation catalysts. This would allow the possibility of testing catalysts based on two different monodentate ligands. Initially, this does not seem very appealing, as the suspected outcome would be the formation of a mixture of the heterocatalyst and the two homocatalysts (Scheme 36.13).

However, it is possible that the heterocatalyst becomes the dominant one, either if it is more stable and thus formed in large excess, or if it is a more active, kinetically dominant catalyst. Recently, both Reetz et al. and Feringa/Minnaard/de Vries et al. have shown that this approach can be beneficial. Earlier attempts by Chen and Xiao using mixtures of monodentate phosphites based on bisphenol and a chiral alcohol were not successful [39]. In our experience, the majority of catalysts based on mixtures of monodentate ligands show a poorer performance than the individual homo-catalysts. However, in a few instances there is a positive effect.

In the studies conducted by Reetz, rhodium catalysts based on mixtures of monodentate phosphites, monodentate phosphonites and combinations of the two were screened in the enantioselective hydrogenation of α- and β-*N*-acetyl-dehydroamino acid esters, enamides and dimethyl itaconate [40], and a number of the more striking positive results are listed in Table 36.3. An enhanced ee-value was found mostly with combinations of two phosphonites, or one phosphonite and one phosphite, in particular when one of the ligands carries a bulky substituent and the other a small one.

The DSM group simultaneously developed this approach using the monodentate phosphoramidites. In this research, mixtures of two phosphoramidite ligands were screened using ligands **10a–f** in the enantioselective hydrogenation of an aliphatic and an aromatic *Z*-β-dehydroamino acid ester (**11a** and **b**; Fig. 36.7). The results of the screening are displayed in Fig. 36.7; entries 1–6 show the results with the homo catalysts. Upon screening mixtures of these ligands, most combinations of two different ligands induced lower enantioselectivity. However, there was one marked exception: all combinations including the NH ligand **10f** led to better results (Fig. 36.7, entries 7–11) [41]. Particularly striking is the combination of ligand **10c**, which was the worst performer in the homo catalyst series in combination with **10f** (entry 9).

$$RhL^1L^2 \rightleftharpoons RhL^1L^1 + RhL^2L^2$$

Scheme 36.13 Mixture of catalytic complexes obtained when using mixtures of ligands.

Table 36.3 Use of mixtures of monodentate phosphonites and or phosphites in the rhodium-catalyzed hydrogenation of substituted olefins.[a)]

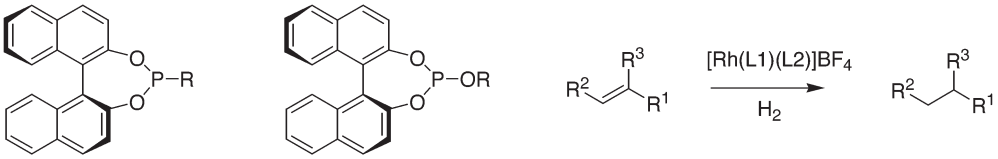

La R = CH_3
Lb R = *c*-C_6H_{11}
Lc R = $C(CH_3)_3$

Lp R = CH_3
Lq R = 2,6-diMeC_6H_3
Lr R = 9-fluorenyl

	R^1 = CO_2Me, R^2 = H, R^3 = NHAc	R^1 = CO_2Me, R^2 = Ph, R^3 = NHAc	R^1 = Ar, R^2 = H, R^3 = NHAc	R^1 = CH_2CO_2Me, R^2 = H, R^3 = CO_2Me	R^1 = Me, R^2 = CO_2Me, R^3 = NHAc
La	92	90%	76%	90%	95%
Lb	92			22%	66%
Lc	93	69%	13%	57%	45%
Lp	77				75%
Lq	32				
Lr	94				
La/Lb	98	97%		89%	
La/Lc	98	99%	96%	96%	
Lp/Lq	85				
Lb/Lp	96				92%
Lc/Lp	98				99%
Lc/Lr	97				
Lb/Lr	96				

a) All hydrogenations performed in CH_2Cl_2. Hydrogen pressure 1.3–1.5 bar, except for *β*-dehydro amino acid esters (60 bar).
L/Rh = 2; SCR = 500 (aromatic enamides), 50 (*β*-dehydro amino acid esters) and 1000 for the other substrates.

Gennari and Piarulli created a library of 16 phosphite and phosphoramidite ligands made from bisphenol and chiral alcohols and chiral amines, respectively. In addition to the homocatalysts, these authors tested 115 mixed combinations in the rhodium-catalyzed hydrogenation of methyl-2-acetamido-acrylate. Here, the picture is even more obscure, as the bisphenol can occur in two atropisomeric forms, which are not stable in the ligand, but tend to be fixed in the complex [39]. They found lower enantioselectivities using combinations of two different phosphites, or combinations of two different phosphoramidites. However, 16 combinations of phosphites with phosphoramidites were found that induced higher enantioselectivity than the "homocatalysts", whilst retaining the high rate induced by the phosphite ligands [42].

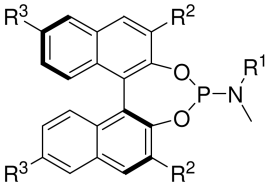

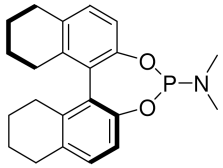

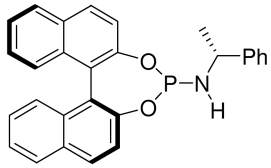

(*S*)-**10a** R^1 = Me, R^2 = R^3 = H, MonoPhos (*S*)-**10b** (*S*,*R*)-**10f**
(*S*)-**10c** R^1 = R^2 = Me, R^3 = H
(*S*)-**10d** R^1 = Me, R^2 = H, R^3 = Br
(*S*)-**10e** R^1 = Bn, R^2 = R^3 = H

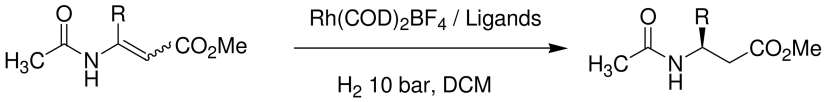

11a R = Me
b R = Ph

12a, **b**

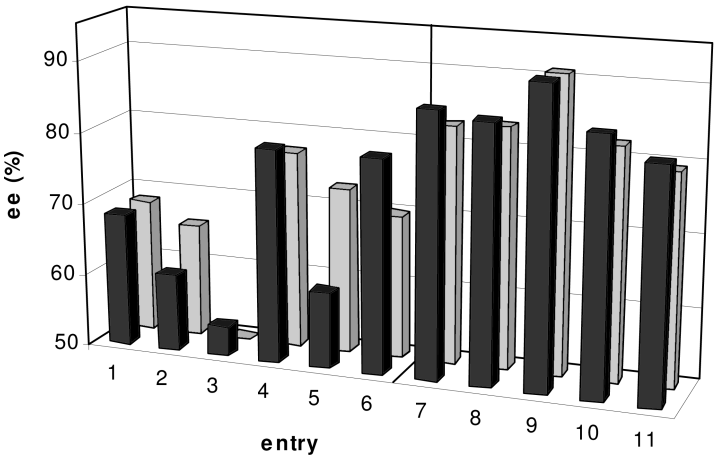

Fig. 36.7 Rh/phosphoramidite-catalyzed hydrogenations using homo (entries 1–6) and hetero (entries 7–11) catalysts (black bars: results with **11a**, light grey bars: results with **11b**; 1=**10a**, 2=**10b**, 3=**10c**, 4=**10d**, 5=**10e**, 6=**10f**, 7=**10f+10a**, 8=**10f+10b**, 9=**10f+10c**, 10=**10f+10d**, 11=**10f+10e**). (Reprinted by permission of the RSC from [41].)

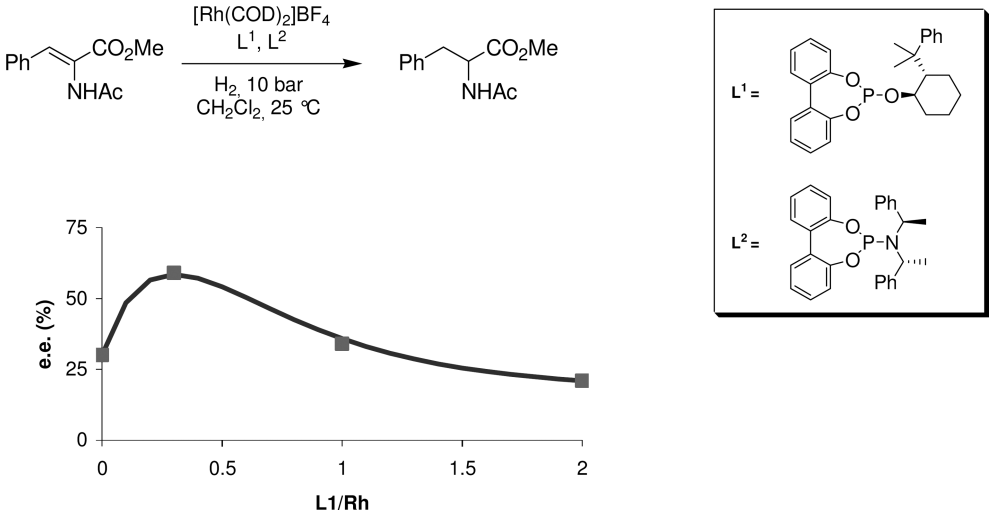

Fig. 36.8 ee-values obtained in the Rh-catalyzed hydrogenation of methyl-2-acetamidocinnamate, plotted against the ligand ratio (the ratio (L^1 + L^2)/Rh always remains 2).

The simple concept of mixtures of monodentate ligand allows one to generate large libraries of catalysts. For instance, 10 ligands can lead to 55 possible combinations, and a library of 96 ligands to 4656 combinations. Such as finding greatly increases the chance of identifying a catalyst that will induce high enantioselectivity in the hydrogenation of the substrate of choice [43].

In a collaboration between the Gennari/Piarulli group and the DSM group, another parameter in the ligand mixture concept – namely the ratio between the two ligands – was explored [44]. These groups were able to show that a 1:1 mixture of the two monodentate ligands L^1 and L^2 (whilst keeping the (L^1+L^2)/Rh ratio equal to 2) was not necessarily the best ratio. The best ee-value for the hydrogenation of methyl-2-acetamidocinnamate was obtained for a ratio L^1:L^2 equal to 0.25:1.75 (59% ee instead of the 34% ee obtained with the 1:1 mixture; Fig. 36.4). This finding can be explained by the different activities of the less enantioselective homo complexes RhL^1L^1 and RhL^2L^2, under the assumption that the hetero complex is more enantioselective than the homo complexes (i.e., a beneficial effect of the ligand mixture). In this case, RhL^1L^1 is a fast catalyst and RhL^2L^2 is slow, both relatively to the hetero complex. Thus, using an excess of L^2 strongly minimizes the amount of the faster RhL^1L^1. Although the homo complex RhL^2L^2 is the major complex present in solution, this is inconsequential as it has a low activity. The observed enantioselectivity is thus mainly due to the catalytic action of the hetero complex – that is, the most enantioselective catalyst. The ratio L^1:L^2 in the case of mixtures of ligands must, therefore, be considered as an important parameter that needs to be fine-tuned.

36.3.4
Mixtures of Chiral Monodentate Ligands and Nonchiral Ligands

In addition to complexes based on the combination of two different chiral monodentate ligands, combinations of a single chiral monodentate ligand with other nonchiral ligands are also possible. Reetz et al. have reported this approach using mixtures of chiral monodentate phosphites or phosphonites with nonchiral phosphines in enantioselective hydrogenations. This led to large changes in the enantioselectivity of the reaction; in one case, a reversal of enantioselectivity was observed from 92% (*S*) to 59% (*R*) [40b]. In a more recent finding, Reetz and Li describe the use of mixtures of chiral phosphonites and a biphenyl-based phosphite in the rhodium-catalyzed enantioselective hydrogenation of aliphatic *β*-dehydroamino acid esters. These biphenyl-based ligands are fluxionally atropisomeric. Here, the enantioselectivity increases from 45% to 98% upon switching from the homocatalyst based on phosphonites **13a** to a 1:1 mixture of **13a** and **14a** or a 1:1 mixture of **13a** and **14b** (Scheme 36.14). In addition, it was found that in several cases the enantioselectivity could be improved by using mixtures of either **13a** or **13b** with an achiral monodentate phosphine or phosphite [45].

Similar mixed-ligand hydrogenations, based upon the combination of nonchiral phosphines (e.g., PPh_3) and chiral phosphoramidites were independently developed by DSM in search of an effective and economic catalyst for the enantioselective hydrogenation of an *α*-alkylated cinnamic acid derivative (Scheme 36.15). The product is a key intermediate in the synthesis of the renin inhibitor Aliskiren [46]. The enantioselective hydrogenation of this class of substrate has been investigated only minimally, although more recently Walphos (a ferrocene-based bisphosphine) was found to provide good results with this particular substrate, whereas other well-known bisphosphine ligands were not suitable [47].

The use of 2 equiv. of MonoPhos (**10a**) in the rhodium-catalyzed enantioselective hydrogenation of the key cinnamic acid derivative **15** resulted in the formation of **16** in 50% conversion and 20% ee after 5 h in isopropanol at 60 °C and 25 bar of hydrogen. Other phosphoramidites, such as the sterically demanding ligand **10c**, resulted in slightly better activity and enantioselectivity. In seeking a

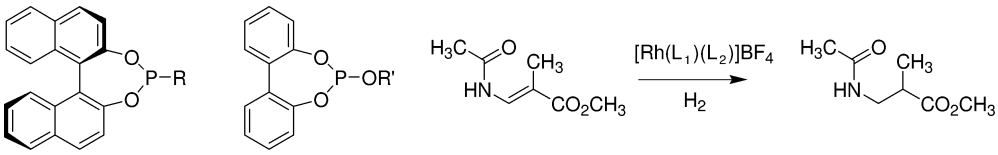

13a R = *t*Bu
13b R = OMe

14a R = Me
14b R = CH_2Ph

Scheme 36.14 Use of mixtures of ligands improves enantioselectivity (Rh : L^1;L^2 : S = 1 : 1 : 1 : 50, 60 bar H_2, CH_2Cl_2, r.t., 20 h).

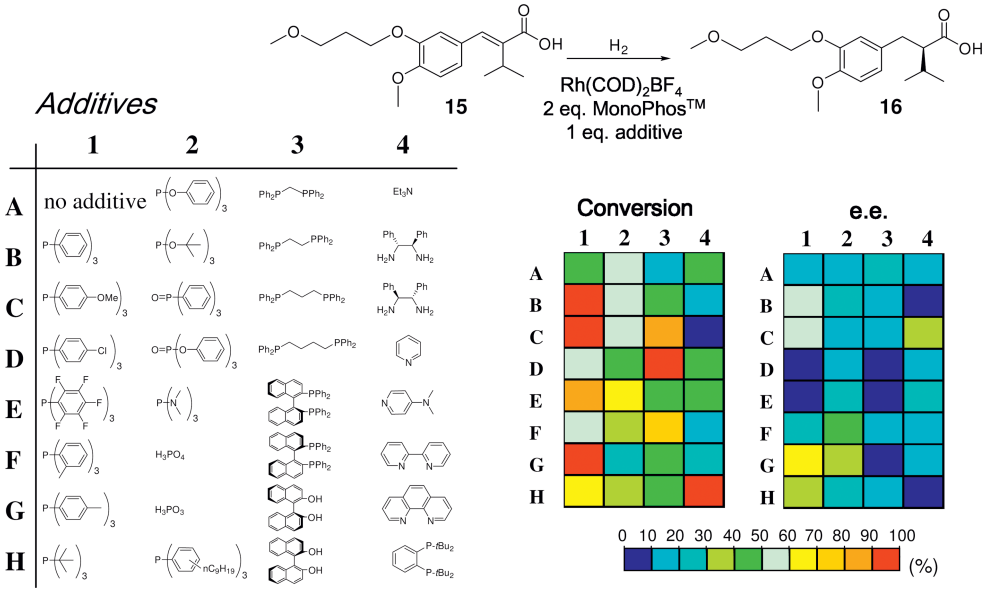

Scheme 36.15 Screening additives for the enantioselective hydrogenation of α-alkylcinnamic acids.

method to increase the reaction rate, a range of additives was tested, largely with a view to increasing electron density on rhodium, as this is known to be the main parameter affecting the rate of oxidative addition of hydrogen, the rate-determining step [48].

The effect of a range of additives on enantioselective hydrogenation of the cinnamic acid precursor is shown in Scheme 36.15. One trend that emerges from this screen is the positive effect of the monodentate phosphines, in particular, tri-*p*-tolylphosphine.

Further library screening resulted in finding an even better-performing 3,3′-dimethyl-substituted ligand **10g** (Scheme 36.16). The reaction temperature is a compromise between rate and enantioselectivity. In a solvent screen, a mixture of isopropanol and water was found to give the best results. At 55 °C, the reaction is fast, allowing an economic SCR of 5000. The enantioselectivity of the product is 90% (Scheme 36.16) [49]. In this case, the use of an achiral phosphine as additive increased not only the enantioselectivity rather drastically, but also the rate of hydrogenation 100-fold. This is a clear example where the power of HTE and random screening led to remarkable results that, otherwise, would never have been found. This reaction is now performed on ton-scale by DSM Pharma Chemicals.

The Feringa/Minnaard/de Vries group has further extended the scope of this cinnamate hydrogenation (Table 36.4) [50]. In all cases, a pronounced effect of the added triarylphosphine was found; usually, the best results were obtained with a combination of ligands **10g** or **10h** in combination with tri-*ortho*-tolyl-

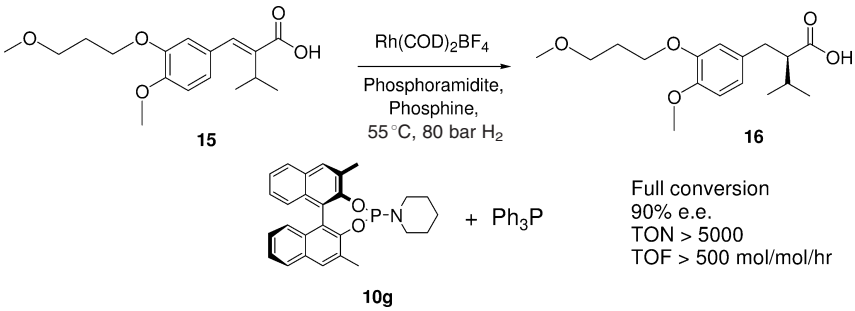

Scheme 36.16 Enantioselective hydrogenation of the Aliskiren intermediate.

Table 36.4 Asymmetric hydrogenation of acrylates and cinnamates [a, b)]

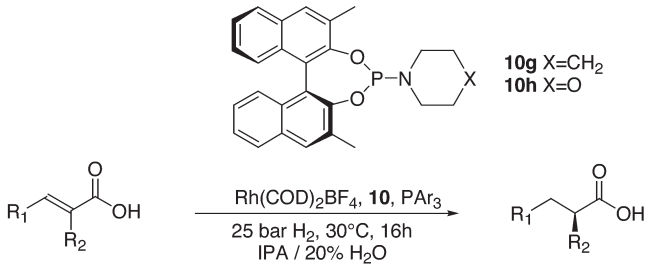

17 R_1=Me, R_2=Me
18 R_1=Ph, R_2=Me
19 R_1=Ph, R_2=*i*-Pr
20 R_1=3,4-MeOPh, R_2=*i*-Pr
21 R_1=4-CF_3Ph, R_2=*i*-Pr
22 R_1=Ph, R_2=Ph

23 R_1=Me, R_2=Me
24 R_1=Ph, R_2=Me
25 R_1=Ph, R_2=*i*-Pr
26 R_1=3,4-MeOPh, R_2=*i*-Pr
27 R_1=4-CF_3Ph, R_2=*i*-Pr
28 R_1=Ph, R_2=Ph

Entry	Substrate	Product	Ligand	Ar	ee [c)]
1	**17**	**23**	**10h**	*m*-Tol	87%
2	**18**	**24**	**10g**	–	2% [d)]
3	**18**	**24**	**10g**	Ph	88%
4	**19**	**24**	**10g**	*o*-Tol	97%
2	**19**	**25**	**10g**	*o*-Tol	99 [%e)]
3	**20**	**26**	**10g**	Ph	92%
4	**21**	**27**	**10g**	*m*-Tol	95%
5 [f)]	**22**	**28**	**10g**	*o*-Tol	95%

a) Reaction conditions: 1 mmol substrate in 4 mL solvent with 0.01 mmol $Rh(COD)_2BF_4$, 0.02 mmol phosphoramidite and 0.01 mmol PR_3.
b) Reactions run for 16 h.
c) In all cases the *R* enantiomer of ligand gave the *S* enantiomer of product.
d) 34% conversion.
e) 98% conversion.
f) Reaction performed at 60 °C.

phosphine. In practice, the ratio Rh : phosphoramidite : Ar_3P = 1 : 2 : 1 gives the best results. NMR studies revealed that under these conditions the mixed complex [Rh(Phosphoramidite)(PAr_3)(COD)]BF_4 plus a substantial amount of [Rh(Phosphoramidite)$_2$(COD)]BF_4 is present. However, this latter complex leads to a catalyst, which is 100-fold slower than the mixed complex, and hence it has no effect. If, on the contrary, a ratio of 1 : 1 : 1 is used, the NMR shows substantial amounts of [Rh(PAr_3)$_2$(COD)]BF_4, a fast catalyst leading to racemic product.

36.3.5
Supramolecular Approaches to Ligand Libraries

Having a modular ligand structure is a prerequisite for the preparation of libraries. This means that it should be possible to introduce the diversity at a late stage of the synthesis. For bidentate ligands, the preference would be to have two highly diverse building blocks that can be joined in the last stage of the synthesis. This coupling does not necessarily have to be through a covalent bond. Two research groups have developed this supramolecular concept quite successfully. Reek et al. have introduced the Supraphos concept, in which a library of bidentate phosphine phosphite ligands can be made from two building blocks: a zinc tetraphenylporphyrine, substituted with a phosphite group on one of the arene rings; and a phosphine (or phosphite) containing a pyridine group

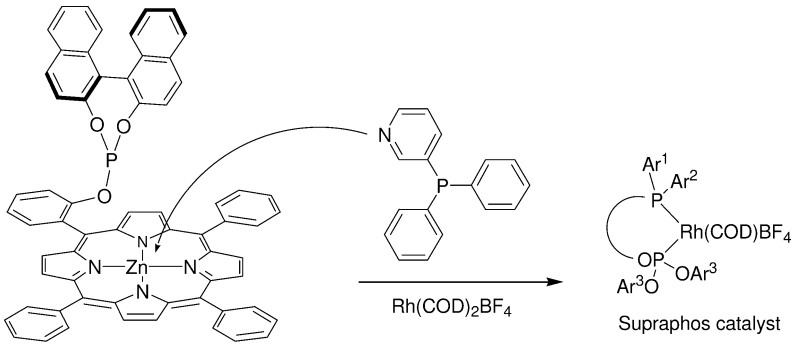

Scheme 36.17 The Supraphos concept for ligand libraries.

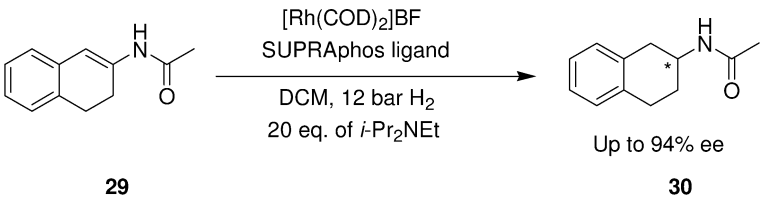

Scheme 36.18 Use of a supramolecular ligand library in enantioselective hydrogenation.

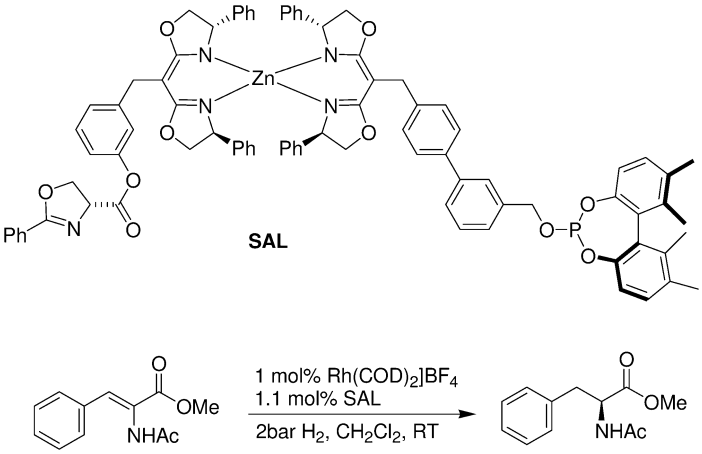

Scheme 36.19 Use of self-assembled ligands in enantioselective hydrogenation.

capable of binding to the zinc of the porphyrine. In this way, the two building blocks can self-assemble *in situ* to form a bidentate ligand (Scheme 36.17) [51].

In collaboration with the DSM group, this concept was applied in enantioselective hydrogenation. Using a library of seven different phosphite-containing zinc porphyrines and 14 different nitrogen base-containing phosphines, a single hit was found in the rhodium-catalyzed enantioselective hydrogenation of 2-acetamido-3,4-dihydro-naphthalene. With the combination made from the (*S*)-BINOL-based porphyrine-phosphite and 3-pyridyldiphenylphosphine, the product was obtained in 94% ee, whereas the other ligands induced ee-values up to 56% [52]. Previous results with rhodium catalysts led to only 72% ee in the hydrogenation of this substrate, although with ruthenium catalysts 90% ee was obtained.

A similar approach has been reported by Takacs et al., who used the principle of self-assembly of two bifunctional units around a metal, typically zinc [53]. Each unit contains a ligating group, such as a phosphine, a phosphite or an oxazoline, that may or may not be chiral, which is linked via an aryl group or a biphenyl group onto a chiral bisoxazoline. The coordination of the two bisoxazoline units to the metal creates a bidentate ligand. In this way, these authors created a library of $10 \times 11 = 110$ different bidentate ligands that were tested in the enantioselective hydrogenation of methyl-2-acetamidocinnamate at 2 bar hydrogen pressure (an example is shown in Scheme 36.19). Enantioselectivities of up to 82% were obtained.

The use of supramolecular ligand libraries in homogeneous catalysis was reviewed by Breit [54].

36.4 Methodology for Testing Catalysts

Once a library has been produced, it must be screened for the desired properties. In catalysis, this property is of course the ability of the catalyst to catalyze a given transformation. Consequently, the screen consists of submitting all members of the catalyst library to a set of reagents and observing whether the desired products are selectively formed at an acceptable rate. As mentioned previously, the screening of pooled catalysts is rare, and high-throughput screening mostly involves the use of parallel reactors where each vessel of the reactor is filled with one single catalytic species. At an early stage, major chemical companies such as DuPont, Shell and DSM had begun the development of reactors for multiple reactions to speed up catalysis research for bulk chemicals and polymers, often in cooperation with fine-mechanical companies. Later, companies which specialized in combinatorial chemistry and catalysis (e.g., Symyx, Avantium and HTE) developed their own machinery, and some of this equipment is now commercially available. For hydrogenation reactions, these HTE reactors may consist of between eight and 348 high-pressure vessels. The equipment capable of handling these high numbers is often based on the use of a titer well-plate, confined in a pressure chamber. The following machines are useful for batch hydrogenations [55]:

- Parr MRS Series 5000: six vessels, independent P (up to 200 bar) and T (up to 300 °C), magnetic stirring.
- Argonaut Endeavor™: eight vessels, independent P (up to 30 bar) and T (up to 200 °C), overhead stirring.
- Amtec SPR16: 16 vessels, independent P (up to 150 bar) and T (up to 250 °C), overhead stirring.
- Chemspeed Autoplant A100: 40 vessels, independent P (up to 100 bar) and T (–20 to 250 °C), overhead stirring.
- Premex A96: custom-made for DSM, now commercially available, 96 vessels, same P (up to 100 bar) and T (up to 200 °C), magnetic stirring.

This list is not exhaustive, as it is beyond the scope of this chapter to review all the hardware available. Here, we would rather focus on original approaches to accelerate the testing of catalysts as, for example, that followed by de Bellefon [32, 56]. This group designed two systems for the fast serial testing of hydrogenation catalysts. While all the commercially available parallel reactors are batch reactors, de Bellefon uses a continuous flow-through, high-pressure reactor. The various catalyst/substrate/H_2 mixtures to be tested are injected by pulses into the reactor. The pulses are carried by a continuous liquid flow through the reactor, and the products collected at the outlet for analysis. In this set-up, a micromixer is used to insure the formation of a stable foam (H_2/aqueous solution of water-soluble catalyst) with small gas bubbles (ca. 200 μm average diameter), thus avoiding any mass-transport limitations [32]. By using this system, de Bellefon et al. were able very quickly to collect large amounts of kinetic data for

the enantioselective hydrogenation of methyl-2-acetamido-cinnamate by Rh/(*S,S*)-BDPPTS [the sulfonated analogue of the well-known BDPP (2,3-bis-diphenylphosphinobutane)]. A total of 214 experiments was carried out with a throughput testing frequency (i.e., the number of experiment carried out per unit of time) of 15 per day [56b]. In a subsequent set-up, de Bellefon used a mesh flow micro-reactor for the fast screening of a library of 20 hydrogenation catalysts [56a]. The main part of the reactor is a micro-contactor that ensures good contact between the two phases (liquid–gas), without agitation. The reactor can be fed continuously with mixtures of catalyst (as little as 10 nmol) and substrate under H_2 pressure, thus allowing a rapid screening of the catalyst library. In case of catalysts with low activities, the reaction time is increased by reducing the flow rate of the carrier solvent, or eventually by reducing to 0. Up to 20 chiral diphosphine/Rh complexes have been evaluated for the enantioselective hydrogenation of methyl-2-acetamido-cinnamate, and a fairly good agreement between the published and measured ee-values was obtained.

Another concept related to accelerated testing was introduced by Kagan in 1998 [57]. Instead of testing a large number of different catalysts, this procedure allows the rapid estimation of the scope of a given catalyst. The idea was to test a catalytic system with a set of different substrates in one single pot. The method is valid if the products do not interfere with the catalyst (i.e., there is no autoinduction). Otherwise, the only requirement is an analytical method capable of distinguishing between all species (including enantiomers in case of enantioselective catalysis) eventually present in the reaction mixture. Kagan applied this method to the enantioselective diborane reduction of ketones, catalyzed by oxazaborolidine, and was able to test five substrates at once. Later, Feringa/Minnaard/de Vries et al. used the same idea in enantioselective hydrogenation, and were able to test up to eight *N*-acyl enamides with Rh/monodentate phosphoramidites in one pot [58]. This method is rather simple to put in place, and permits rapid assessment of the substrate scope of a catalyst.

36.5 High-Throughput Analysis

As we have seen so far, libraries of hydrogenation catalysts are never composed of more than a few dozen members, up to 100 to 200 at the most. Consequently, modern analytical equipment such as gas chromatography (GC) or high-performance liquid chromatography (HPLC) equipped with an auto-sampler or even flow-through NMR systems are sufficient to handle the analysis of the entire library. Nevertheless, a few groups have initiated research towards the development of fast, sometimes parallel, analytical procedures. A few reviews have appeared on this subject [59]. Here, we will concentrate on the methods developed to analyze hydrogenation reactions, or methods that could likely be applied.

Crabtree et al. investigated the use of reactive dyes that change color upon undergoing catalytic reaction [60]. Two new dyes containing a C=C or C=N bond were

synthesized so that, upon reduction of the double bond, they would lose their coloration. The two dyes were used as substrate for the screening of a small library of hydrosilylation catalysts, and allowed rapid visual identification of the fastest catalyst. Clearly, these dyes may also be used in hydrogenation reactions.

Mioskowski et al. used immunoassays for the high-throughput analysis of a library of 88 catalysts for the enantioselective transfer hydrogenation of benzoyl formic acid (BF) [61]. The library was prepared by combining a set of 22 chiral diamine ligands with four metal precursors. Yields and ee-values were determined by competitive enzyme immunoassays (EIA), using two solid-supported monoclonal antibodies: mAb-15, which binds both enantiomers; and m-Ab-8, which exhibits high stereoselectivity towards (*S*)-mandelic acid (MA). After automated sample preparation, the activity and enantioselectivity of all library members could be measured in parallel with a plate absorbance reader. A total of 42 representative samples was also analyzed by HPLC. A good correlation between HPLC and EIA was obtained (average error in ee-value ca. ±9%). The best catalyst identified allowed quantitative reduction of BF to MA with an enantiomeric excess of 81%.

Morken et al. used high-throughput ^{13}C-NMR measurements to rapidly screen for the activity and enantioselectivity of a library of 30 catalysts in the enantioselective transfer hydrogenation of dialkyl ketones [62]. The idea was based on the fact that enantiotopic groups are rendered diastereotopic upon formation of a neighboring chiral center and consequently can be distinguished by NMR. The group prepared a ^{13}C-enriched ketone containing the requisite enantiotopic group attached to a stable stereocenter, and tested it as a substrate in Ru-catalyzed enantioselective transfer hydrogenation. The results obtained by NMR compared well with those obtained by GC (±3% variation in ee-value). The best catalyst was based on hexamethylbenzene-$RuCl_2$ dimer and simple phenylglycinol.

Van Leeuwen et al. designed a high-throughput screening method based on IR spectroscopy to rapidly identify enantioselective hydrogen-transfer catalysts for acetophenone [63]. The idea was to screen for the reverse reaction – that is, the dehydrogenation of 1-phenylethanol. The difference in reaction rate between the (*R*)- or the (*S*)-alcohol is a measure of the enantioselectivity, and can be determined rapidly by infra-red monitoring of the CO group of both the reagent (acetone) and the product (acetophenone). The method was tested with two known catalysts, and appeared to provide quite accurate measurements of the ee-values.

36.6 Conclusions

The use of combinatorial and HTE methods in homogeneous hydrogenation has blossomed over the past five years. This has been fuelled first by the urgent need to identify useful catalysts for the production of fine chemicals, in particular enantiopure pharma intermediates. The second impetus came from academia, where many investigators realized that, with regard to enantioselective cat-

alysis, ligand design is a highly elusive concept. Thus, those workers in academia began to seek ways of increasing the chances of hitting the "right" ligand, inspired by the successes of combinatorial chemistry.

Although the introduction of automation in the laboratory created the possibility for high-throughput screening, this itself was not enough. The need to create large ligand libraries has induced many breakthroughs, such as the concept of modularity, monodentate chiral ligands, mixtures of ligands, supramolecular ligand libraries, and enzyme–metal conjugates. Moreover, new concepts for rapid testing have evolved, such as the flow systems.

HTE should never be considered as a mindless exercise to identify a catalyst. Rather, the design of a set of experiments requires a good overview of what really determines the diversity space for this particular reaction. For this reason, HTE will always remain linked with areas of more classical research, such as mechanistic studies.

Future challenges of major interest will be the creation of new catalysts and ligand types, and the identification of new catalytic reactions. While HTE can clearly be used to speed up this research, the large number of experiments associated with HTE has led in the past – and will continue to lead in the future – to totally unexpected findings. Ultimately, further applications outside the area of enantioselective catalysis are also expected.

Abbreviations

BF	benzoyl formic acid
EIA	enzyme immunoassay
EMS	electrospray mass spectrometry
GC	gas chromatography
HPLC	high-performance liquid chromatography
HTE	high-throughput experimentation
MA	mandelic acid
mAb	monoclonal antibody
SCR	substrate : catalyst ratio

References

1 (a) W. S. Knowles, M. J. Sabacky, *J. Chem. Soc. Chem. Commun.* **1968**, 1445; (b) W. S. Knowles, *Acc. Chem. Res.* **1983**, *16*, 106.

2 (a) T. P. Dang, H. B. Kagan, *J. Chem. Soc. Chem. Commun.* **1971**, 481; (b) H. B. Kagan, T. P. Dang, *J. Am. Chem. Soc.* **1972**, *94*, 6429.

3 (a) H. Brunner, W. Zettlmeier, *Handbook of Enantioselective Catalysis*, VCH, Weinheim, **1993**; (b) R. Noyori, *Asymmetric Catalysis in Organic Synthesis*, Wiley, New York, **1993**; (c) H. B. Kagan, in: J. D. Morrison (Ed.), *Asymmetric Synthesis*, Academic Press, Inc., Orlando, **1985**, Vol. 5, p. 1; (d) H. Brunner, *Top. Stereochem.* **1988**, *18*, 129.

4 (a) H. U. Blaser, E. Schmidt (Eds.), *Asymmetric Catalysis on Industrial Scale: Challenges, Approaches and Solutions*, Wiley-VCH, Weinheim, **2004**; (b) J. G. de Vries, in: I. T. Horvath (Ed.), *Encyclopedia of Catalysis*, John Wiley & Sons, New York, **2003**, Vol. 3, p. 295; (c) H. Kumobayashi, *Recl. Trav. Chim. Pays-bas* **1996**, *115*, 201.

5 (a) H. U. Blaser, F. Spindler, M. Studer, *Appl. Catal. A Gen.* **2001**, *221*, 119; (b) J. M. Hawkins, T. J. N. Watson, *Angew. Chem. Int. Ed.* **2004**, *43*, 3224.

6 J. G. de Vries, A. H. M. de Vries, *Eur. J. Org. Chem.* **2003**, 799.

7 A. Furka, W. D. Bennett, *Comb. Chem. High Throughput Screen.* **1999**, *2*, 105.

8 K. C. Nicolaou, R. Hanko, W. Hartwig (Eds.), *Handbook of Combinatorial Chemistry*, Wiley-VCH, Weinheim, **2002**.

9 (a) A. Hagemeyer, B. Jandeleit, Y. Liu, D. M. Poojary, H. W. Turner, A. F. Volpe Jr., W. H. Weinberg, *Appl. Catal. A. Gen.* **2001**, *221*(1/2), 23; (b) M. Reetz, *Angew. Chem. Int. Ed.* **2001**, *40*, 284; (c) S. Dahmen, S. Bräse, *Synthesis* **2001**, 1431; (d) A. Hoveyda, in: K. C. Nicolaou, R. Hanko, W. Hartwig (Eds.), *Handbook of Combinatorial Chemistry*, Wiley-VCH, Weinheim, **2002**, Vol. 2, p. 991; (e) K. Ding, H. Du, Y. Yuan, J. Long, *Chem. Eur. J.* **2004**, *10*, 2872; (f) C. Gennari, U. Piarulli, *Chem. Rev.* **2003**, *103*, 3071.

10 P. Chen, *Angew. Chem. Int. Ed.* **2003**, *42*, 2832.

11 K.-J. Johansson, M. R. M. Andreae, A. Berkessel, A. P. Davis, *Tetrahedron Lett.* **2005**, *46*, 3923.

12 D. Tiebes, in: G. Jung (Ed.), *Combinatorial Chemistry: Synthesis, Analysis, Screening*, Wiley-VCH, Weinheim, **1999**, p. 16.

13 T. Y. Yue, W. A. Nugent, *J. Am. Chem. Soc.* **2002**, *124*, 13692.

14 C. C. Tai, C. Tangel, B. Roller, P. G. Jessop, *Inorg. Chem.* **2003**, *42*, 73410.

15 (a) C. J. Cobley, J. P. Henschke, *Adv. Synth. Cat.* **2003**, *345*, 195; (b) R. McCague, *Spec. Chem. Mag.* **2002**, 26; (c) M. J. Burk, W. Hems, D. Herzberg, C. Malan, A. Zanotti-Gerosa, *Org. Lett.* **2000**, *4*, 4173.

16 F. Cederbaum, C. Lamberth, C. Malan, F. Naud, F. Spindler, M. Studer, H.-U. Blaser, *Adv. Synth. Catal.* **2004**, *346*, 842.

17 V. I. Tararov, R. Kadyrov, A. Monsees, T. H. Riermeier, A. Börner, *Adv. Synth. Catal.* **2003**, *345*, 239.

18 B. Pugin, M. Studer, E. Kuesters, G. Sedelmeier, X. Feng, *Adv. Synth. Catal.* **2004**, *346*, 1481.

19 (a) A. M. Porte, J. Reibenspies, K. J. Burgess, *J. Am. Chem. Soc.* **1998**, *120*, 9180; (b) D. R. Hou, J. Reibenspies, T. J. Colacot, K. Burgess, *Chem. Eur. J.* **2001**, *7*, 5391; (c) M. C. Perry, X. Cui, M. T. Powell, D. R. Hou, J. H. Reibenspies, K. Burgess, *J. Am. Chem. Soc.* **2003**, *125*, 113.

20 See Chapter 2.

21 W. Braun, A. Salzer, F. Spindler, E. Alberico, *Appl. Cat. A Gen.* **2004**, *274*, 191.

22 M. Pastó, A. Riera, M. A. Pericàs, *Eur. J. Org. Chem.* **2002**, 2337.

23 I. M. Pastor, P. Västilä, H. Adolfsson, *Chem. Eur. J.* **2003**, *9*, 4031.

24 J.-B. Sortais, V. Ritleng, A. Voelklin, A. Holuigue, H. Smail, L. Barloy, C. Sirlin, G. K. M. Verzijl, J. A. F. Boogers, A. H. M. de Vries, J. G. de Vries, M. Pfeffer, *Org. Lett.* **2005**, *7*, 1247.

25 M. E. Wilson, G. M. Whitesides, *J. Am. Chem. Soc.* **1978**, *100*, 306.

26 (a) M. Skander, N. Humbert, J. Collot, J. Gradinaru, G. Klein, A. Loosli, J. Sauser, A. Zocchi, F. Gilardoni, T. R. Ward, *J. Am. Chem. Soc.* **2004**, *126*, 14411; (b) C. Letondor, N. Humbert, T. R. Ward, *Proc. Natl. Acad. Sci. USA* **2005**, *102*, 4683; (c) T. R. Ward, *Chem. Eur. J.* **2005**, *13*, 3798.

27 (a) M. T. Reetz, *Tetrahedron* **2002**, *58*, 6595; (b) M. T. Reetz, M. Rentzsch, A. Pletsch, M. Maywald, *Chimia* **2002**, *56*, 721.

28 L. Panella, J. Broos, J. Jin, M. W. Fraaije, D. B. Janssen, M. Jeronimus-Stratingh, B. L. Feringa, A. J. Minnaard, J. G. de Vries, *Chem. Commun.* **2005**, 5656.

29 S. R. Gilbertson, X. Wang, *Tetrahedron* **1999**, *55*, 11609.

30 R. H. Crabtree, *Chem. Commun.* **1999**, 1611.

31 Cases have been reported where the immobilized catalyst was actually faster than its homogenous counterpart. This is probably due to the prevention of dimerization and/or cluster formation,

common causes of deactivation. See for example: (a) B. Pugin, *J. Mol. Cat. A: Chemical* **1996**, *107*, 273–279; (b) H.-U. Blaser, B. Pugin, F. Spindler, A. Togni, *C. R. Chimie* **2002**, *5*, 379–385.

32 C. De Bellefon, N. Tanchoux, S. Caravieilhes, P. Grenouillet, V. Hessel, *Angew. Chem. Int. Ed.* **2000**, *39*, 3442.

33 C. Gennari, U. Piarulli, *Chem. Rev.* **2003**, *103*, 3071.

34 A. M. Lapointe, *J. Comb. Chem.* **1999**, *1*, 101.

35 (a) M. van den Berg, A. J. Minnaard, E. P. Schudde, J. van Esch, A. H. M. de Vries, J. G. de Vries, B. L. Feringa, *J. Am. Chem. Soc.* **2000**, *122*, 11539; (b) M. van den Berg, A. J. Minnaard, R. M. Haak, M. Leeman, E. P. Schudde, A. Meetsma, B. L. Feringa, A. H. M. de Vries, C. E. P. Maljaars, C. E. Willans, D. J. Hyett, J. A. F. Boogers, H. J. W. Henderickx, J. G. de Vries, *Adv. Synth. Catal.* **2003**, *345*, 308–322.

36 L. Lefort, J. A. F. Boogers, A. H. M. de Vries, J. G. de Vries, *Org. Lett.* **2004**, *6*, 1733.

37 D. Peña, A. J. Minnaard, J. G. de Vries, B. L. Feringa, *J. Am. Chem. Soc.* **2002**, *124*, 14552–14553.

38 A. Duursma, L. Lefort, J. A. F. Boogers, A. H. M. de Vries, J. G. de Vries, A. J. Minnaard, B. L. Feringa, *Org. Biomol. Chem.* **2004**, *2*, 1682.

39 W. Chen, J. Xiao, *Tetrahedron Lett.* **2001**, *42*, 8737.

40 (a) M. T. Reetz, T. Sell, A. Meiswinkel, G. Mehler, *Angew. Chem. Int. Ed.* **2003**, *42*, 790; (b) M. T. Reetz, G. Mehler, *Tetrahedron Lett.* **2003**, *44*, 4593; (c) M. T. Reetz, T. Sell, G. Mehler, A. Meiswinkel, *Tetrahedron Asymm.* **2004**, *15*, 2165; (d) M. T. Reetz, X. Li, *Tetrahedron* **2004**, *60*, 9709.

41 D. Peña, A. J. Minnaard, J. A. F. Boogers, A. H. M. de Vries, J. G. de Vries, B. L. Feringa, *Org. Biomol. Chem.* **2003**, *1*, 1087.

42 C. Monti, C. Gennari, U. Piarulli, *Tetrahedron Lett.* **2004**, *45*, 6859.

43 For n ligands the total number of combinations (hetero and homo) is given by the formula: n(n+1)/2.

44 C. Monti, C. Gennari, U. Piarulli, J. G. de Vries, A. H. M. de Vries, L. Lefort, *Chem. Eur. J.* **2005**, *11*, 6701.

45 M. T. Reetz, X. Li, *Angew. Chem. Int. Ed.* **2005**, *44*, 2959.

46 (a) J. M. Wood, J. Maibaum, J. Rahuel, M. G. Grutter, N. C. Cohen, V. Rasetti, H. Ruger, R. Goschke, S. Stutz, W. Fuhrer, W. Schilling, P. Rigollier, Y. Yamaguchi, F. Cumin, H. P. Baum, C. R. Schnell, P. Herold, R. Mah, C. Jensen, E. O'Brien, A. Stanton, M. P. Bedigian, *Biochem. Biophys. Res. Commun.* **2005**, *308*, 698; (b) P. Herold, S. Stutz, T. Sturm, W. Weissensteiner, F. Spindler, WO 02/02500.

47 T. Sturm, W. Weissensteiner, F. Spindler, *Adv. Synth. Cat.* **2003**, *345*, 160.

48 T. Benincori, E. Cesarotti, O. Piccolo, F. Sannicòlo, *J. Org. Chem.* **2000**, *65*, 2043, and references contained therein.

49 A. H. M. de Vries, L. Lefort, J. A. F. Boogers, J. G. de Vries, D. J. Ager, *Chimica Oggi* **2005**, *23*(2), Supplement on Chiral Technologies, 18.

50 R. Hoen, J. A. F. Boogers, H. Bernsmann, A. J. Minnaard, A. Meetsma, T. D. Tiemersma-Wegman, A. H. M. de Vries, J. G. de Vries, B. L. Feringa, *Angew. Chem. Int. Ed.* **2005**, *44*, 4209.

51 (a) V. F. Slagt, M. Röder, P. C. J. Kamer, P. W. N. M. Van Leeuwen, J. N. H. Reek, *J. Am. Chem. Soc.* **2004**, *126*, 4056; (b) M. J. Wilkinson, P. W. N. M. van Leeuwen, J. N. H. Reek, *Org. Biomol. Chem.* **2005**, *3*, 2371.

52 X.-B. Jiang, L. Lefort, P. E. Goudriaan, A. H. M. de Vries, P. W. N. M. van Leeuwen, J. G. de Vries, J. N. H. Reek, *Angew. Chem. Int. Ed.* **2006**, *45*, 1223.

53 (a) J. M. Takacs, K. Chaiseeda, S. A. Moteki, D. Sahadeva Reddy, D. Wu, K. Chandra, *Pure Appl. Chem.* **2005**, accepted for publication; (b) J. M. Takacs, D. Sahadeva Reddy, S. A. Moteki, D. Wu, H. Palencia, *J. Am. Chem. Soc.* **2004**, *126*, 4494.

54 B. Breit, *Angew. Chem. Int. Ed.* **2005**, *44*, 6816.

55 More information can be found on the websites of the companies: www.parrinst.com; www.argotech.com; www.amtec-chemnitz.de; www.chemspeed.com; www.premex-reactorag.ch/e/spezialloesungen/produkteneuheiten/.

56 (a) R. Abdallah, V. Meille, J. Shaw, D. Wenn, C. de Bellefon, *Chem. Commun.*

2004, 372; (b) C. de Bellefon, N. Pester, T. Lamouille, P. Grenouillet, V. Hessel, *Adv. Synth. Catal.* **2003**, *345*, 190; (c) C. de Bellefon, R. Abdallah, T. Lamouille, N. Pestre, S. Caravieilhes, P. Grenouillet, *Chimia* **2002**, *56*, 621.

57 H. B. Kagan, *J. Organomet. Chem.* **1998**, *567*, 3.

58 H. Bernsmann, M. van den Berg, R. Hoen, A. J. Minnaard, G. Mehler, M. T. Reetz, J. G. de Vries, B. L. Feringa, *J. Org. Chem.* **2005**, *70*, 943.

59 (a) B. Jandeleit, D. J. Schaefer, T. S. Powers, H. W. Turner, W. H. Weinberg, *Angew. Chem. Int. Ed.* **1999**, *38*, 2494; (b) M. T. Reetz, *Angew. Chem. Int. Ed.* **2001**, *40*, 284; (c) M. T. Reetz, *Angew. Chem. Int. Ed.* **2002**, *41*, 1335.

60 (a) A. C. Cooper, L. H. McAlexander, D. H. Lee, M. T. Torres, R. H. Crabtree, *J. Am. Chem. Soc.* **1998**, *120*, 9971; (b) J. A. Loch, R. H. Crabtree, *Pure Appl. Chem.* **2001**, *73*, 119.

61 F. Taran, C. Gauchet, B. Mohar, S. Meunier, A. Valleix, P. Y. Renard, C. Crémin-non, J. Grassi, A. Wagner, C. Miokowski, *Angew. Chem. Int. Ed.* **2002**, *41*, 124.

62 M. E. Evans, J. P. Morken, *J. Am. Chem. Soc.* **2002**, *124*, 9020.

63 D. G. I. Petra, J. N. H. Reek, P. C. J. Kamer, H. E. Schoemaker, P. W. N. M. van Leeuwen, *Chem. Commun.* **2000**, 683.

37
Industrial Applications

Hans-Ulrich Blaser, Felix Spindler, and Marc Thommen

37.1
Introduction and Scope of the Chapter

While hydrogenation is without doubt the most important catalytic methodology for the manufacture of fine chemicals, until now most reactions have been carried out with heterogeneous catalysts. Heterogeneous hydrogenation catalysts have an exceptionally broad applicability for the chemo- and diastereoselective reduction of various functional groups, are convenient to handle, and catalyst separation is usually straightforward [1]. Homogeneous catalysts have found application for a number of special selectivity problems, the most important of which is enantioselective hydrogenation. While this will be the dominant topic of this chapter, a few scattered reports have been made where achiral complexes such as the Wilkinson catalyst, $RhCl(Ph_3P)_3$, or Ru–phosphine complexes have been applied on an industrial scale. In this regard, we will mention three examples [2]: (i) the chemoselective hydrogenation of α,β-unsaturated aldehydes; (ii) the diastereoselective hydrogenation of a tetracycline antibiotic; and (iii) the chemoselective hydrogenation of avermectin derivatives.

As already mentioned, the most important industrial application of homogeneous hydrogenation catalysts is for the enantioselective synthesis of chiral compounds. Today, not only pharmaceuticals and vitamins [3], agrochemicals [4], flavors and fragrances [5] but also functional materials [6, 7] are increasingly produced as enantiomerically pure compounds. The reason for this development is the often superior performance of the pure enantiomers and/or that regulations demand the evaluation of both enantiomers of a biologically active compound before its approval. This trend has made the economical enantioselective synthesis of chiral performance chemicals a very important topic.

Industrial interest in the application of enantioselective catalysts began in earnest during the mid-1960s when the first reports of successful enantioselective transformations with homogeneous metal complexes were published. Within a surprisingly short period, production processes for two small-scale products, L-dopa (hydrogenation) and cilostatin (cyclopropanation) were developed and implemented by

The Handbook of Homogeneous Hydrogenation.
Edited by J.G. de Vries and C.J. Elsevier
Copyright © 2007 WILEY-VCH Verlag GmbH & Co. KGaA, Weinheim
ISBN: 978-3-527-31161-3

Monsanto and Sumitomo, respectively. For quite some time it was not really clear whether these applications were mere curiosities or whether this would be the beginning of a new area where chiral compounds would be produced predominantly by asymmetric catalysis. One reason for this state of affairs was that both companies were reluctant to disclose information on the new technology.

Very soon, other chemical and pharmaceutical companies entered the field with appreciable manpower, examples being Roche, Ciba-Geigy, Takasago, Enichem and VEB-Isis. Some companies worked in collaboration with academic laboratories, while others relied on strong in-house research efforts. During the past few years, a new type of player has appeared, however – smaller companies which are more or less dedicated exclusively to the development and application of enantioselective processes for the manufacture of chiral intermediates and products. Many of these enterprises are either start-ups, for example Chiral Quest or Chirotech (now part of the Dow Chemical Company), concentrating on a few promising technologies. Alternatively, they are spin-offs from large corporations, examples being our own company, Solvias (a spin-off from Ciba-Geigy/Novartis), NSC Technologies (a spin-off from Monsanto, now part of Great Lakes Chemicals) or Degussa Homogeneous Catalysts, and these usually have a broader technology base.

A very good overview on the scientific state of the art of enantioselective catalysis can be found in two recent monographs, *Comprehensive Asymmetric Catalysis* (edited by Jacobsen, Yamamoto and Pfaltz) [8], and *Catalytic Asymmetric Synthesis* (edited by Ojima) [9]. Progress in enantioselective hydrogenation has been summarized in several recent reviews [10–13]. For the compilation of industrial applications, we have relied on a recent study [14], a monograph on large-scale asymmetric catalysis [15], and several excellent up-to-date overviews [16–21] describing the applications of enantioselective hydrogenation technology, mainly in the pharmaceutical industry. Since it is notoriously difficult to obtain precise information on industrial processes, many references relate to rather informal sources such as *Chemical and Engineering News* reports, proceedings of commercial meetings, and personal communications. This chapter describes the state of the art for the application of homogeneous hydrogenation for the industrial production of enantiomerically enriched chiral compounds. Within the chapter, the subjects covered include the enantioselective hydrogenation processes that have been and/or are presently used for commercial manufacture, pilot- and bench-scale processes not (yet) used in actual production, as well as some feasibility studies and optimized hydrogenations of model substrates.

37.2 Requirements for Technical-Scale Applications

Pharmaceuticals or agrochemicals usually have complex, multifunctional structures and are produced via multistep syntheses. Compared to basic chemicals, they are relatively small-scale but high-value products with short product lives,

traditionally produced in multipurpose batch equipment. The time for development of the production process is often very short since the "time to market" affects the profitability of the product.

Despite dramatic progress in the scientific domain, relatively few enantioselective catalytic reactions are used on an industrial scale today [14, 15]. A major reason for this is that the application of enantioselective catalysts on a large scale presents some very special challenges and problems [22, 23]. Some of these problems are due to the special situation for manufacturing chiral products, while others are due to the nature of the (enantioselective) catalytic process. Whether a synthetic route containing an enantioselective catalytic step can be considered for a particular product is usually determined by the answer to two questions [23, 24]:

- Can the costs for the overall manufacturing process compete with alternative routes?
- Can the catalytic step be developed in the given time frame?

Several critical factors determine the technical feasibility of an enantioselective process step, but it must be stressed that even if all these criteria are met there is no guarantee that it is actually used!

37.2.1
Catalyst Performance

The *enantioselectivity*, expressed as enantiomeric excess (ee, %) of a catalyst should be >99% for pharmaceuticals if no purification is possible. This case is quite rare, and ee-values >90% are often acceptable. *Chemoselectivity* (or functional group tolerance) will be very important when multifunctional substrates are involved. The *catalyst productivity*, given as turnover number (TON: mol product per mol catalyst) or as substrate : catalyst ratio (SCR), determines catalyst costs. For hydrogenation reactions, TONs should be >1000 for high-value products and >50 000 for large-scale or less-expensive products (catalyst re-use increases the productivity).

The *catalyst activity*, given as average turnover frequency (TOF: mol product per mol catalyst per reaction time; units h^{-1}), affects the production capacity. For hydrogenations, TOFs should be $>200\ h^{-1}$ for small-scale products, and $>10\,000\ h^{-1}$ for large-scale products. Due to lower catalyst costs and often higher added values, lower TON and TOF values are acceptable for enantioselective oxidation and C–C bond-forming reactions.

37.2.2
Availability and Cost of the Catalyst

Chiral ligands and many metal precursors are expensive and/or not easily available. Typical costs for chiral diphosphines are 100 to 500 $ per gram for laboratory quantities, and 2000 to >100 000 $ per kg on a larger scale. Chiral ligands

such as salen or amino alcohols used for early transition metals are usually much cheaper. At this time, only relatively few chiral ligands are available commercially on a technical scale, and many of these are patent protected and therefore a license is need for their commercial application.

37.2.3 Development Time

The development time can be a hurdle, especially when the optimal catalyst has yet to be developed or no commercial catalyst is available for a particular substrate (substrate specificity), and/or when not much is known on the desired catalytic transformation (technological maturity). When developing a process for a new chemical entity (NCE) in the pharmaceutical or agrochemical industry, the time restraints can be severe (Fig. 37.1). In these cases it is more important to find a competitive process on time than an optimal process too late. So-called second-generation processes – for example, for chiral switches, generic pharmaceuticals or for the manufacture of other fine chemicals – have different requirements. Here, the time factor is usually not so important, but a high-performance process is necessary. The increasing time pressure has led to the development and implementation of high-throughput systems (HTS) for catalyst testing with the help of robots and multi-parallel high-pressure equipment allowing the screening of up to 100 samples per day [25, 26].

In addition, many other aspects must be considered when developing a catalytic reaction for industrial use; these include catalyst separation, stability and poisoning, handling problems, space-time yield, process sensitivity and robustness, toxicity of metals and reagent, and safety aspects, as well as the need for high-pressure equipment.

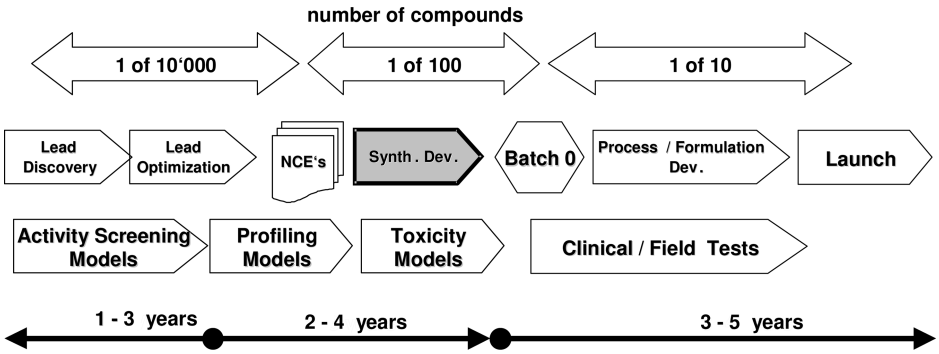

Fig. 37.1 Development process for a new chemical entity in the pharmaceutical industry.

37.3
Process Development and Equipment

The choice of a development strategy that promises the best answer in the shortest time is the first decision to be made at the start of every process development [27]. This strategy will depend on a number of considerations, including the goal of the development, the know-how of the investigators, the time frame, the available manpower and equipment, and so on. In process development, there is usually a hierarchy of goals (or criteria) to be met. It is simply not possible to reach all the requirements for a technically useful process in one step. The catalyst selectivity (combined of course with an acceptable activity) is the first criterion – just as in academic research. However, when a reasonable selectivity has been obtained, other criteria will become important: catalyst activity, productivity and stability, catalyst separation (and maybe recycling). Then, questions such as the effect of substrate quality and last but not least the cost and availability of the chiral catalyst and other materials must be addressed. The final process is a compromise, since quite often not all of these requirements can be fulfilled maximally. It is useful to divide the development of a manufacturing process into different phases, although it is rarely possible to proceed in a linear fashion and very often one has to go back to an earlier phase in order to answer additional question before it is possible to go on.

Most chiral chemicals are relatively small-scale products (1 to 1000 tonnes per year for pharmaceuticals, 500 to 10 000 tonnes per year for agrochemicals) that are usually produced in multipurpose batch equipment. This is probably the case for most catalytic reactions described in this chapter; however, as a rule very little information on process technology is provided by the manufacturers. Here, we will discuss only briefly the reactor choices for hydrogenation reaction typically carried out in the liquid phase. For a successful implementation the following demands must be met:

- Very good dispersion of the hydrogen gas (and a suspended catalyst for heterogeneous systems) in the reaction solution (efficient gas-liquid mixing and stirring).
- Very effective heat removal (reaction control), as well as safe handling of the sometimes pyrophoric and/or air-sensitive catalysts.

In practice, two reactor types have proven to be capable of meeting these requirements as well as the need for high reliability in operation and ease of control: the stirred autoclave and the loop reactor (see Table 37.1).

- The loop reactor provides very efficient hydrogen dispersion, with the heat exchanger surface being almost unlimited. It is especially useful when the space-time yield is very high (fast reaction, high substrate concentration) or when a low reaction temperature is required.
- The stirred autoclave is probably more versatile; it has an advantage when substrate slurries or viscous media are to be used, or when the starting material is added continuously. In addition, it is usually easier to clean and less space and lower investment costs are required.

Table 37.1 Comparison of the loop reactor and the stirred autoclave.

Reactor type	Loop reactor	Stirred autoclave
	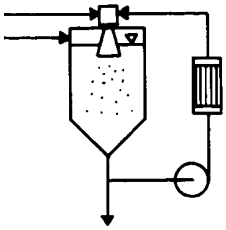	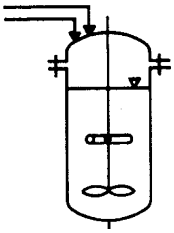
Gas-dispersion	Mixing nozzle (Venturi principle)	Mechanical agitator (hollow–shaft turbine)
Efficiency	High	Medium to high
Heat removal	>1300 W m^{-2} K, very high exchange area	~900 W m^{-2} K, limited exchange area
Problem areas	Circulating pump (viscous slurries) continuous feed addition	Heat exchange capacity
Recommended	High performance, dedicated plant	Multi-purpose plant

37.4 Industrial Processes: General Comments

In a recent study [14] we have collected and tabulated information on chemocatalytic asymmetric processes operated in regular production, as well as on those in the pilot- and bench-scale state; a statistical summary of this information is presented in Table 37.2. The following definitions were used:

- *Production processes* are operated on a more or less regular basis – that is, all relevant problems concerning catalyst performance and separation, supply of materials, product isolation and purification, noble metal recovery, etc. have been solved.
- *Pilot processes* are technically on a similar level especially with regard to catalyst performance; they have been carried out on multi kilogram to tonne scale, but have not (yet) been applied on a regular basis.
- *Bench-scale processes* have an optimized catalyst performance and have been carried out a few times on a small scale, but are for some reason not yet ready for production purposes.
- *Feasibility studies* very often demonstrate proof of principle without much optimization.

An analysis of the processes listed in Table 37.2 shows that asymmetric hydrogenation of C=C and C=O functions is by far the predominant transition metal-catalyzed transformation applied for industrial processes, followed by epoxidation and dihydroxylation reactions. On the one hand, this is due to the broad scope of catalytic hydrogenation, and on the other hand it could be attributed to

Table 37.2 Statistics for the industrial application of chemocatalytic enantioselective processes [14].

Transformation	Production		Pilot		Bench scale
	>5 t y^{-1}	<5 t y^{-1}	>50 kg	<50 kg	
Hydrogenation of enamides	1	1	2	6	4
Hydrogenation of C=C-COOR and C=C–CH–OH	2	0	3	4	6
Hydrogenation of other C=C systems	1	0	1	1	2
Hydrogenation of α and β functionalized ketones	2	3	3	2	4
Hydrogenation/reduction of other keto groups	0	0	2	2	4
Hydrogenation of C=N	1	0	1	0	0
Dihydroxylation of C=C	0	1	0	0	4
Epoxidation of C=C, oxidation of sulfide	2	2	1	0	2
Isomerization, epoxide opening, addition reactions	2	4	2	0	1
Total	11	11	15	15	27

the early success of Knowles with the L-dopa process, because for many years, most academic and industrial research was focused on this transformation. The success with epoxidation and dihydroxylation can essentially be attributed to the efforts of Sharpless, Katsuki and Jacobsen. If one analyzes the structures of the starting materials, it is quite clear that many of these compounds are complex and multifunctional – that is, the successful catalytic systems are not only enantioselective but also tolerate many functional groups.

The most common chiral auxiliaries are diphosphines (biphep, binap and analogues, DuPhos, ferrocenyl-based ligands, etc.) and cinchona and tartaric acid-derived compounds. It is clear that the optimal chiral auxiliary is determined not only by the chiral backbone (type or family) but also by the substituents of the coordinating groups. Therefore, modular ligands with substituents that can easily be varied and tuned to the needs of a specific transformation have an inherent advantage (principle of modularity).

The most often cited *success factor* by industrial developers was the choice of the right ligand – that is, the desired transformation was possible because either a new ligand type was found (or claimed to be designed) or because an existing ligand could be optimized by adapting the coordinating groups to the needs of the reaction (electronic and/or steric tuning). However, the choice of the right metal precursor (especially for Ru-catalyzed reactions) and/or anion as well as the addition of promoters were also reported to be decisive for high catalyst activity and productivity. Careful optimization of the reaction conditions (temperature, pressure, solvent, concentrations, etc.) and the ability to crystallize the product directly from the reaction solution with very high ee were also mentioned several times to have been important for a successful commercial process.

The following *critical factors* often made process development difficult. The sensitivity of the catalyst towards impurities (byproducts in the starting material, oxygen, water, etc.) usually could be controlled with a strict purification protocol, but in some cases a change of the overall synthetic route of the substrate was necessary. Sometimes, the stability of the ligand or catalyst and its productivity (given as TON) or its activity (given as TOF) were critical; careful optimization was often successful to overcome this problem. Other critical issues mentioned included the need for high pressures or very low temperatures (expensive equipment), a lack of commercial availability, difficult preparation of the ligand or catalyst, and/or problems with a patented ligand system. Surprisingly, despite the fact that homogeneous catalysts were used in most applications, catalyst separation was mentioned only once to have been a major obstacle. More of an issue were residual metals in the product, especially for pharmaceutical applications and when the homogeneous catalyst was used late in the synthesis.

Besides the already cited study, we have relied on the overviews mentioned earlier [16–21] describing the application of enantioselective hydrogenation technology mainly in the pharma industry, and also on a literature search.

37.5 Chemo- and Diastereoselective Hydrogenations

Unsaturated alcohols are important intermediates for aroma chemicals and vitamins, with one interesting access being hydrogenation of the corresponding unsaturated aldehyde, which is very difficult to achieve with heterogeneous catalysts. Rhone-Poulenc has developed a water-soluble Ru catalyst with sulfonated triphenylphosphine ligands (TPPTS) for the hydrogenation of cinnamaldehyde (Fig. 37.2; $R_1 = H$, $R_2 = Ph$) to cinnamyl alcohol and of 3-methyl-2-buten-1-al (Fig. 37.2; R_1, $R_2 = Me$) to 3-methyl-2-buten-1-ol (prenol) with very high chemoselectivities at high conversion [2a]. The reaction was preformed in a two-phase aqueous organic system allowing easy recycle of the catalyst by phase separation, but it appears that the economics of the catalytic system was still insufficient for commercial application.

While diastereoselective reactions are well known with heterogeneous catalysts, in many cases a homogeneous catalyst will give a higher selectivity. For hydrogenation of the exocyclic C=C bond in methacycline, Hovione has developed a modified form of Wilkinson's catalyst which produces the desired 6-α epimer in >99% yield. According to De Vries [2a], the reaction is performed on a scale of several tens of tons per year. The catalyst is not recycled, but the Ph_3P is oxidized to $Ph_3P{=}O$ which is recovered as is the rhodium salt.

The final example shown in Figure 37.2 is the highly chemoselective hydrogenation of the C_{22}–C_{23} double bond in avermectin derivatives to give ivermectin, used against river blindness in many African countries. This drug, which originally was developed by Merck as an antiparasitic agent, was shown to be highly effective also for human treatment, and in 1987 Merck decided to donate the

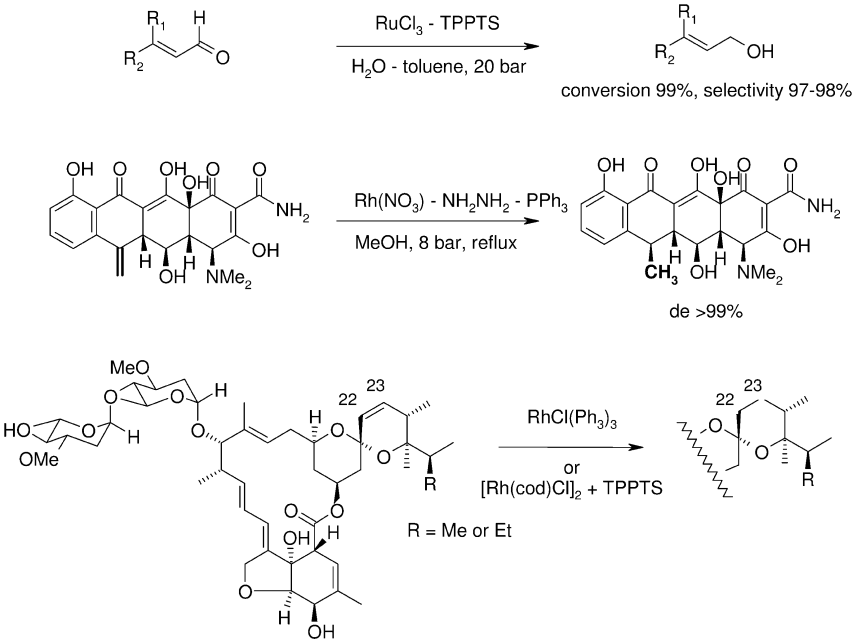

Fig. 37.2 Chemo- and diastereoselective hydrogenations of complex molecules with homogeneous catalysts.

drug to all affected persons [2b]. Avermectin is a fermentation product, and Merck chemists developed a very selective hydrogenation process using the classical Wilkinson catalyst in toluene at 3 bar hydrogen pressure which is probably still used for the manufacture of ivermectin [2c]. Since a major problem is the complete removal of Rh, Antibioticos developed a two-phase process (toluene/water/nBu$_4$NBr) using a catalyst formed *in situ* from [Rh(cod)Cl]$_2$ and TPPTS which gave yields of >98% with all the rhodium in the aqueous phase [2d].

37.6 Enantioselective Hydrogenation of C=C Bonds

37.6.1 Dehydro α-Amino Acid Derivatives

There is little doubt that the hydrogenation of dehydro α-amino acids is the best-studied enantioselective catalytic reaction. This was initiated by the successful development of the L-dopa process by Knowles (see below) and for many years, acetylated aminocinnamic acid derivatives were the model substrates to test most newly developed ligands. As can be seen below, this is the transformation most often used for the stereoselective synthesis of a variety of pharma and

agro targets, even though the difficult and expensive preparation of the dehydro amino acids derivatives precluded the manufacture of large-volume α-amino acids. Because of their importance for the development of industrial enantioselective catalysis, we will discuss several early applications in some detail, but will only summarize the results obtained in other cases.

37.6.1.1 L-Dopa (Monsanto, VEB Isis-Chemie)

According to Knowles [28], Monsanto has been producing L-dopa, a drug to relieve Parkinson's disease, on the scale of ca. 1 t y^{-1} for many years. A few years after Monsanto, the East-German company VEB Isis-Chemie also carried out this process on a similar scale but terminated the production after a few years [29]. The key step in the synthesis is the enantioselective hydrogenation of an enamide intermediate (Fig. 37.3).

Monsanto carried out the reaction in a water/isopropanol mixture at relatively low temperature and pressure. Because the free ligand racemizes slowly, an isolated $[Rh(dipamp)(diene)]^+BF_4^-$ complex was used as the catalyst, showing a very good performance: an ee of 95%, TON 10 000–20 000, TOF 1000 h^{-1}. Today, ee-values of 95% are no longer exceptional for the hydrogenation of enamides, but this was certainly not the case at the time the process was developed. It is therefore not surprising that for many years enamide hydrogenation was *the* standard test reaction for new ligands. One of the key factors for success was of course the dipamp ligand developed by Knowles and his team within an amazingly short time. Figure 37.4 shows the concept of the Monsanto scientists: (i) stereogenic phosphorus atom; and (ii) bidentate structure with C_2-symmetry. The VEB Isis team chose a different

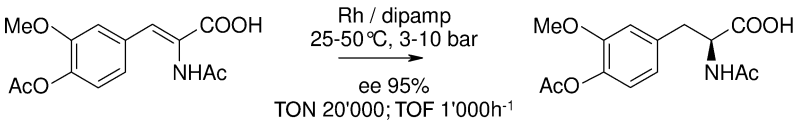

Fig. 37.3 Monsanto's L-dopa process.

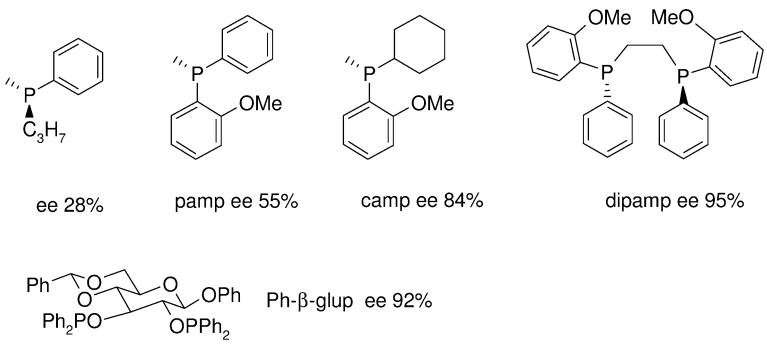

Fig. 37.4 Ligands developed for the manufacture of L-dopa.

approach by starting with a (cheap) chiral pool molecule for the construction of the Ph-β-glup ligand, also with two coordinating P atoms. The Rh/Ph-β-glup sulfate complex functioned at 40 °C/1 bar; however, with ee-values of 91–92%, TONs of 2000 and TOFs of $\sim$330 h^{-1} it did not quite reach the performance of Rh–dipamp.

One very important feature of the Monsanto process was the fact that the reaction was started with a slurry of reactants and ended with a slurry of the pure product with close to 100% ee, allowing easy separation of both the catalyst and the undesired racemate in one step. Critical issues for both the Monsanto and the VEB Isis processes were the quality of the starting material (enamide syntheses are often problematic) and especially the concentration of oxygen and peroxides in the reaction solution.

A Rh–dipamp complex was later applied by NSC Technologies for the manufacture of several unnatural amino acids with good catalyst performances (ee 95–98%, TON 5000–20 000) [30] and was also very selective but with low activity (ee 98%, TON 20) in a feasibility study for a synthesis of acromelobic acid by Abbott Laboratories [31].

37.6.1.2 **Aspartame (Enichem/Anic, Degussa)**

Phenylalanine is an intermediate for the aspartame sweetener and, for a short time, it was produced by Enichem/Anic [32] on a scale of ca. 15 t, using a variant of the L-dopa procedure as summarized in Figure 37.5. The Rh–eniphos catalyst was considerably less selective than Rh–dipamp, but easier to prepare and much cheaper. Traces of Rh were removed by treatment with a thiol-containing resin, and crystallization of the ammonium salt gave a product of >99% ee [33]. Due to the low stability of the ligand (P–N bond cleavage) reaction conditions had to be carefully controlled. A few years later, Degussa developed a pilot process with a Rh–deguphos catalyst which operated at 50 °C/15 bar and achieved ee-values up to 99% (TON 10 000, TOF 3000 h^{-1}) [34].

37.6.1.3 **Various Pilot- and Bench-Scale Processes for α-Amino Acid Derivatives**

Processes for several α-amino acid derivatives with a variety of structural elements were developed and carried out on a scale of up to multi hundred kilograms by

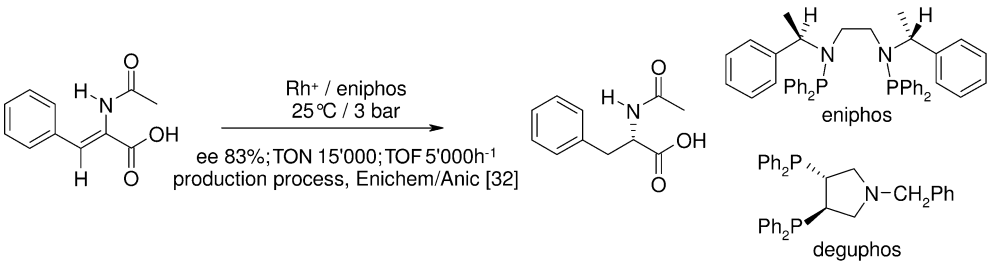

Fig. 37.5 The phenylalanine process.

Dow/Chirotech [35, 36], Topcro Pharma [37] as well as by Solvias [38] using Rh–DuPhos catalysts (Fig. 37.6). Besides these successful examples, a process using Rh–DuPhos was abandoned because of reproducibility problems due to impurities carried over from the preceding step, and because of concerns about the toxicity of 2-nitropropane, even though ee-values of 99% were achieved [39].

Tunable ferrocene-based diphosphines lead to effective catalysts for the production of α-amino acid derivatives with unusual structural elements. 2-Piperazinecarboxylic acid derivatives are interesting intermediates – for example, for Crixivan, the well-known HIV protease inhibitor produced by Merck. The hydrogenation of an unusually substituted cyclic enamide was used by Lonza [40–42] to produce >200 kg of the piperazine intermediate depicted in Figure 37.7 using an optimized Rh–Josiphos catalyst. Important for good catalyst performance were the choice of the ligand as well as the substituents at the tetrahydropyrazine. Surprisingly, the same catalyst was also able to hydrogenate a corresponding pyrazine amide with ee-values up to 77%, but much lower activity [43].

A Ru–Josiphos catalyst was highly selective for the hydrogenation of an intermediate for an anthrax lethal factor inhibitor with a tetra-substituted C=C bond, as depicted in Figure 37.8 (Merck [44]). Rh–Josiphos (Lonza [42]) and Rh–BoPhoz (Eastman [45]) catalysts were effective for the hydrogenation of an exocyclic and a cyclopropyl-substituted C=C bond.

Earlier examples of pilot- and bench-scale processes are summarized in [14]. Several cases with high ee-values and medium activity using Rh–bpm ligands were reported by Hoechst (now Sanofi Aventis) [46]; Ru–binap and Ru–biphep

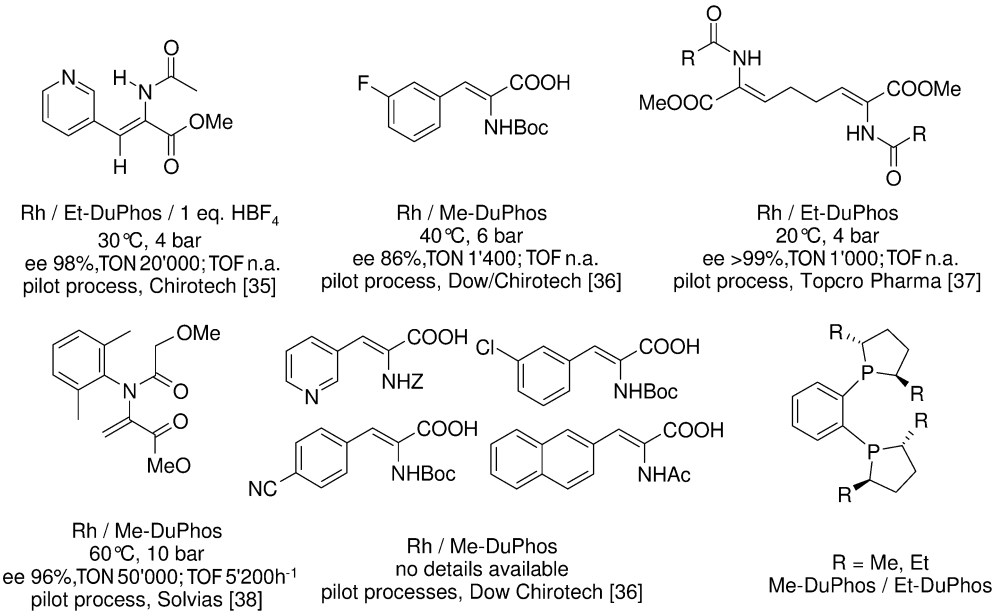

Fig. 37.6 Substrates and ligands for the synthesis of various α-amino acid derivatives.

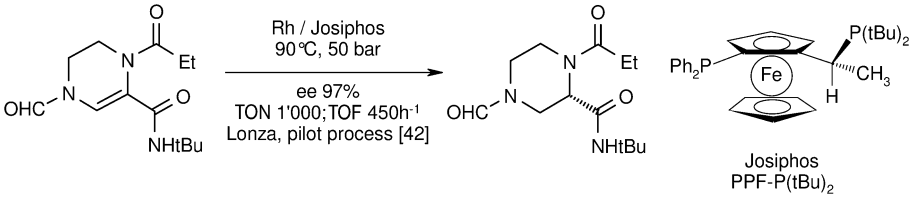

Fig. 37.7 Process for a 2-piperazinecarboxylic acid derivative.

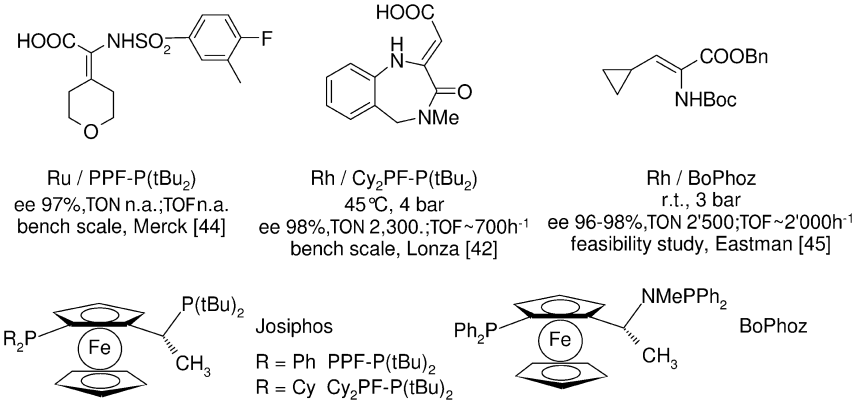

Fig. 37.8 Substrates and ligands for the synthesis of various α-amino acid derivatives.

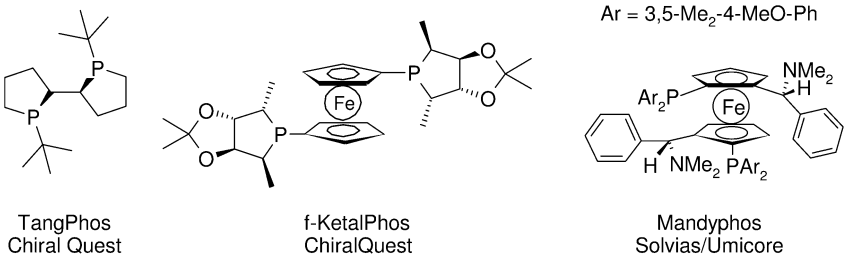

Fig. 37.9 Structures of TangPhos, f-KetalPhos and Mandyphos.

complexes were also effective catalysts for cyclic and exocyclic dehydro amino acid derivatives.

Recent results have shown that a number of other commercially available ligands can be expected to have industrial potential for the hydrogenation of dehydro α-amino acid derivatives. However, it must be pointed out that in most cases model substrates and not industrially relevant targets have been investigated until now. Chiral Quest has shown that Rh–TangPhos as well as Rh–f-KetalPhos (for structures, see Fig. 37.9) were able to hydrogenate a variety of α-dehydro amino acid derivatives with ee-values of 98–>99%, TONs of up to 10 000

and TOFs of >100 h^{-1} under mild conditions (r.t., 2–3 bar) [47]. A Rh–Mandyphos catalyst of Solvias/Umicore (see Fig. 37.9) achieved ee-values >98% with TONs >20000 and TOF up to 7700 h^{-1} (25 °C, 1 bar) for the model substrate MAC [48]. Finally, Eastman's Rh–BoPhoz also achieved ee-values of 97–>99% for a variety of α-dehydro amino acid derivatives, in some cases with TONs up to 10000 and very high activities at r.t./~1 bar [49].

37.6.2
Dehydro β-Amino Acid Derivatives

In contrast to dehydro α-amino acids, the hydrogenation of acetylated β-dehydroamino acid derivatives has only recently been of industrial interest and, accordingly, no applications on a larger scale have yet been reported. Several ligands such as certain phospholanes or phosphoramidites might have industrial potential, but until now these have only been tested on model substrates under standard conditions [50]. Chiral Quest's TangPhos and Binapine (Fig. 37.10) have been shown to hydrogenate several acetylated dehydro β-amino acid derivatives with ee-values of 98–99% and TONs of 10000 at r.t., 1 bar [3, 47].

With this background, the finding by Merck chemists [51] that unprotected dehydro β-amino acids are good substrates for the Rh-catalyzed hydrogenations was both very unexpected and very exciting. Interestingly, deuteration experiments indicate that it is not the enamine C=C bond which is reduced but the tautomeric imine! Not only simple derivatives but also the complex intermediate for MK-0431 (see Fig. 37.10) can be hydrogenated successfully, and the latter has been pro-

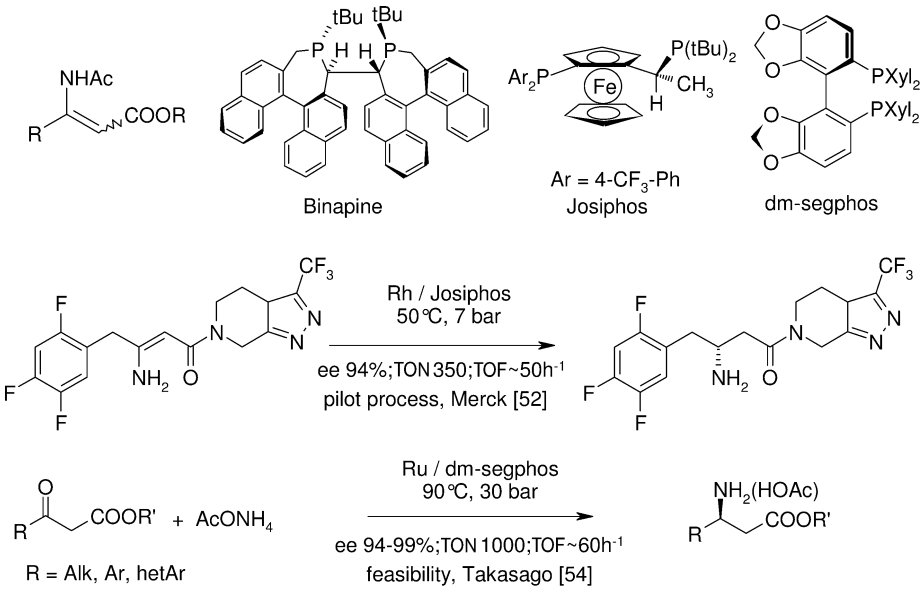

Fig. 37.10 Hydrogenation of β-dehydro amino acid derivatives; substrate and ligand structures.

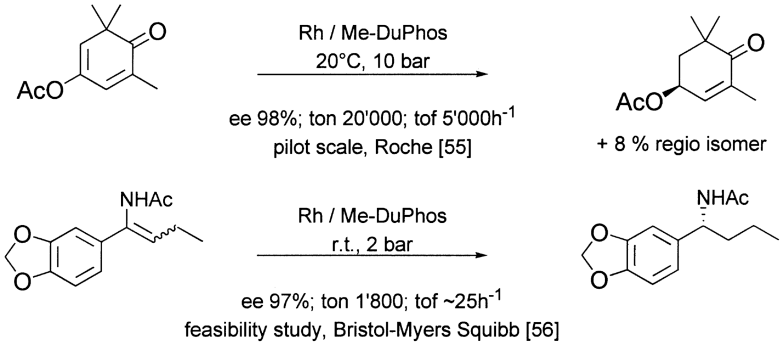

Fig. 37.11 Hydrogenation of enamides and enol acetates.

duced on a >50-kg scale with ee-values up to 98%, albeit with low to medium TONs and TOFs [52]. At almost the same time, Takasago [53, 54] reported that a Ru–segphos catalyst could hydrogenate unprotected dehydro β-amino esters with ee-values of 94–97%. Of special industrial relevance is the fact that the Ru–segphos catalysts also work very well for the reductive amination of a variety of β-keto esters to give the corresponding β-amino ester in one step, with ee-values up to 99% at an SCR of 1000 with TOFs of $\sim 60\ h^{-1}$ (Fig. 37.10 [53c, 54]).

37.6.3
Simple Enamides and Enol Acetates

The hydrogenation of enamides and enol acetates without acid function is often more demanding, and at present is not applied widely. Besides a bench-scale application by Roche with a Ru–biphep catalyst [55], two examples are of interest: a pilot process for a cyclic enol acetate by Roche [55], and a feasibility study by Bristol-Myers Squibb [56], both using Rh–DuPhos catalysts (Fig. 37.11). In the latter case, despite very good ee-values, a chiral pool route was finally chosen. Chiral Quest's Rh–f-KetalPhos (see Fig. 37.9) has been shown to hydrogenate a variety of substituted aryl enamide model substrates at r.t., 1 bar, with very promising catalyst performance (ee 98–99%, TON 10 000) [47].

37.6.4
Itaconic Acid Derivatives

Even though it was realized early on that, in analogy to enamides, itaconic acid derivatives are also preferred substrates due to the presence of a second coordinating group, industrial applications are still rare. Just as dehydro amino acids, substituted itaconic derivatives exist as *E* and *Z* isomers, but several phospholane type ligands are able to accept *E*/*Z* mixtures. Two early examples using a Rh–deguphos and Rh–bpm catalyst, respectively, were reported by Hoechst (now Sanofi Aventis) with good to high ee-values but low TONs (for details see [14, 46]).

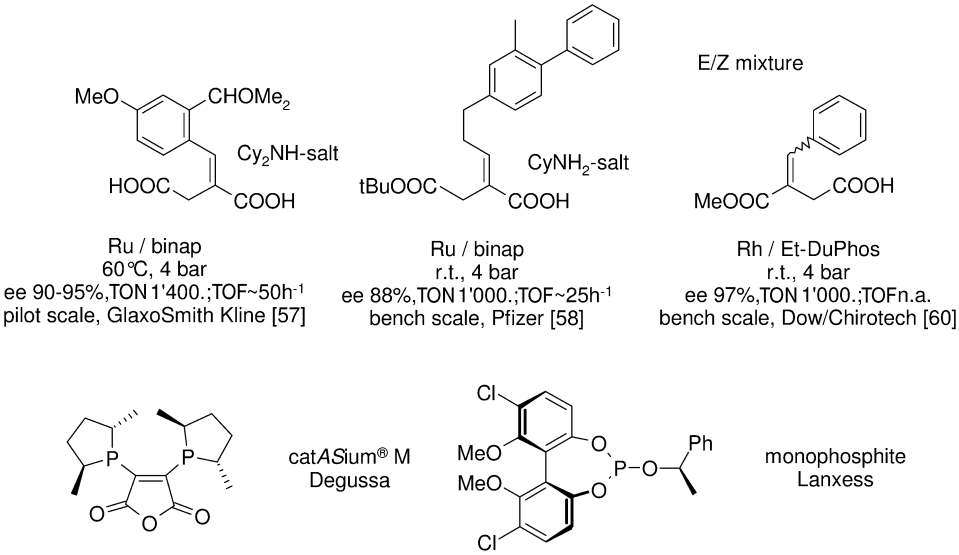

Fig. 37.12 Hydrogenation of itaconic acid derivatives; substrate and ligand structures.

During the past few years, several applications on the pilot and bench scale have been reported (Fig. 37.12). Interestingly, in two cases it was not the otherwise very effective Rh–phospholane complexes that was selected for preparative purposes but rather a Ru–binap catalyst. As described by GlaxoSmithKline, Rh–DuPhos actually gave higher ee-values in the ligand screening, but the results were not always reproducible and the Ru–binap catalyst was cheaper [57]. Pfizer obtained good results for the Rh–FerroTANE-catalyzed hydrogenation of the free acid (ee 94%, TON 1000), but ultimately chose a Ru–binap catalyst for scale-up [58].

Optimized procedures were developed for the hydrogenation of several model substrates, with very promising results for future industrial applications. Rh–DuPhos was used for itaconic amides by Dow/Chirotech [59, 60] and gave ee-values of 96–97%, TON 100 000, TOF 13 000 h^{-1} at 45 °C, 10 bar. For dimethyl itaconates, Chiral Quest reported ee-values up to 99%, TON 5000, at r.t./1.5 bar using TangPhos [47], while Rh–cat*A*Sium® M (Degussa [61]) achieved ee-values up to 99%, TON 10 000, TOFs up to 40 000 h^{-1} at 25 °C/4 bar, and Rh–monophosphite (Lanxess [62]) gave ee-values up to 99%, TON 10 000, TOFs up to 5 000 h^{-1} at 0 °C/0.5 bar (ligand structures see Fig. 37.12).

37.6.5
Allylic Alcohols and α,β-Unsaturated Acids

The hydrogenation of allylic alcohols and α,β-unsaturated acids leads to products with a very high synthetic potential, and both transformations were used quite early for industrial applications. In both cases Ru complexes with axially chiral biaryl ligands (binap analogues) are the catalysts of choice. Here, we will dis-

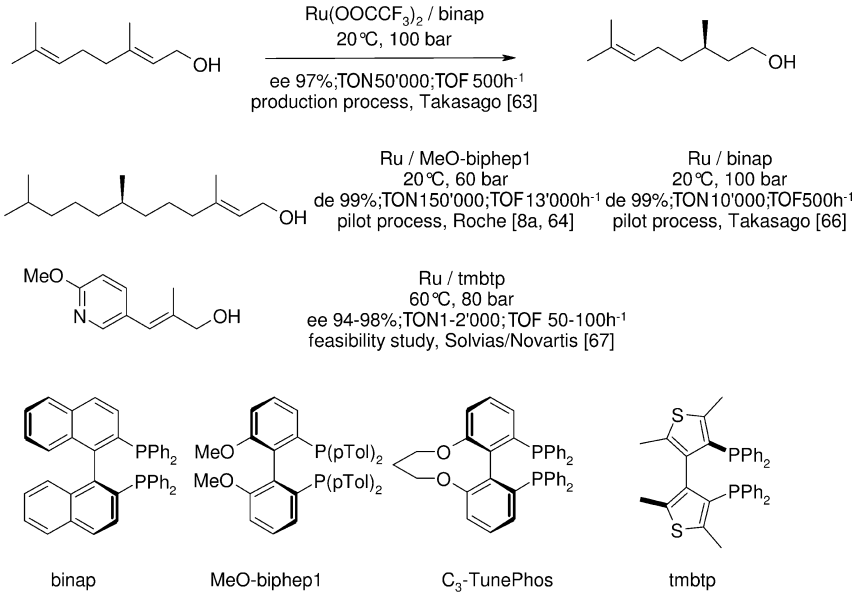

Fig. 37.13 Hydrogenation of various allylic alcohols.

cuss two examples in some detail and summarize the results for other processes.

37.6.5.1 **Allylic Alcohols** (Fig. 37.13)

Citronellol, a fragrance as well as an intermediate for vitamin E, can be prepared starting with geraniol. This transformation requires a specific Ru precursor and is highly chemoselective. It is carried out by Takasago on a 300 t y^{-1} scale [63]. Roche has reported a similar pilot process which works at 20 °C and 60 bar using the same Ru precursor with MeO-biphep as ligand; the ee is 99%, TON 30 000, and TOF 1500 h^{-1} [8a, 64]. In a recent feasibility study, Chiral Quest [65] has reached 98% ee and 100 000 turnovers with a Ru–TunePhos catalyst. Pilot processes with similar catalyst performances were developed by Roche [8a, 64] as well as by Takasago [66] for the longer-chain vitamin E intermediate. Clearly, the existing stereogenic center does not affect the enantioselectivity of the catalysts. Bench-scale processes for the hydrogenation of allylic alcohols using a Ru–binap and Ru–biphep catalyst, respectively, were reported by Roche earlier (summarized in [14]), and a recent feasibility study showed that heterobiaryl ligands can also be effective ligands for this transformation [67].

The hydrogenation of a racemic homoallylic alcohol is the key reaction for a new synthetic route for producing paroxetine, and recently reported by Ricordati [68] (Fig. 37.14). The best results (>99% ee for both *cis* and *trans* products) were

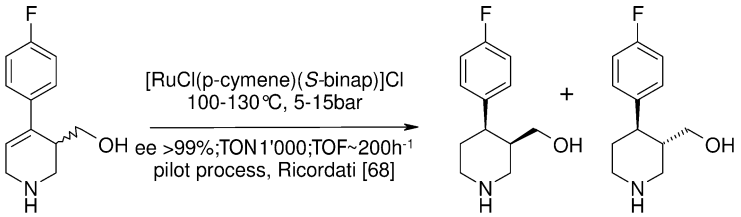

Fig. 37.14 Hydrogenation of a homoallylic alcohol.

obtained with a recrystallized [RuCl(*p*-cymene)(binap)]Cl complex in isopropanol. The reaction was carried out on a 100-kg batch size.

37.6.5.2 *α,β*-Unsaturated Acids

One of the first applications of the then newly developed Ru–binap catalysts for *α,β*-unsaturated acids was an alternative process to produce (*S*)-naproxen. (*S*)-Naproxen is a large-scale anti-inflammatory drug and is actually produced via the resolution of a racemate. For some time it was considered to be one of the most attractive goals for asymmetric catalysis. Indeed, several catalytic syntheses have been developed for the synthesis of (*S*)-naproxen intermediates in recent years (for a summary see [14]). The best results for the hydrogenation route were obtained by Takasago [69] (Fig. 37.15), who recently reported that a Ru–H_8-binap catalyst achieved even higher activities (TON 5000, TOF 600 h^{-1} at 15 °C, 50 bar) [16].

However, despite some quite good catalytic results it has become clear that the original resolution variant will be the optimal process for quite some time [70]. Several reasons are responsible for this situation, illustrating some of the issues when developing industrial processes as discussed earlier:

- The resolution process developed by Syntex is almost ideal (Pope Peachy resolution), with an efficient racemization and recycling of the unwanted (*R*)-enantiomer (yield >95% of (*S*)-naproxen from the racemate) and the chiral auxiliary (recovery >98%).
- The starting materials used for the catalytic versions are much more expensive; US$ 20–25 kg^{-1} for the vinyl and >>US$ 50 kg^{-1} for the acrylic acid derivative, compared to ca. US$ 10 kg^{-1} for methoxybromonaphthalene used in the Syntex process.

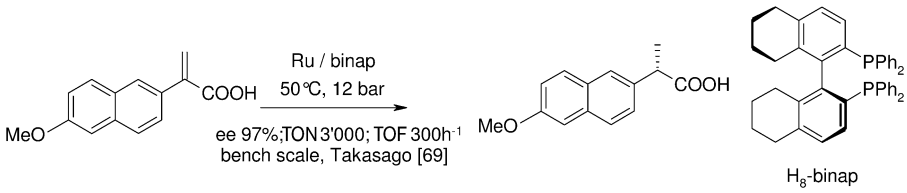

Fig. 37.15 Naproxen via enantioselective hydrogenation.

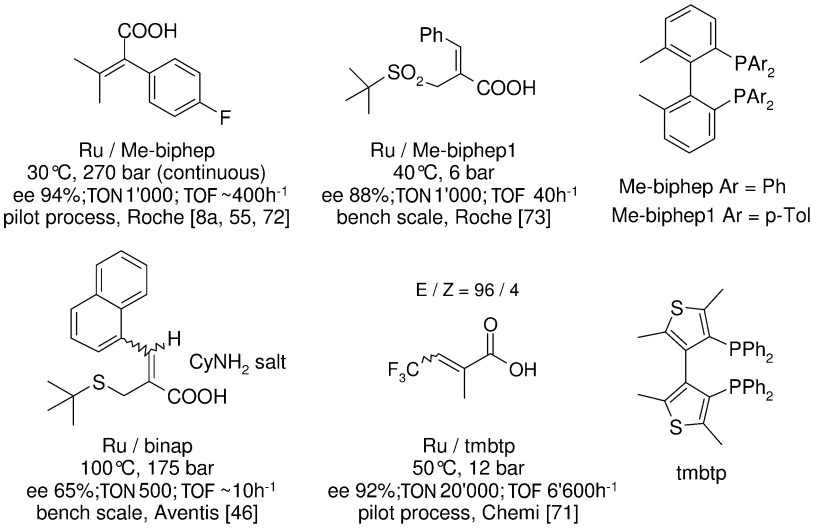

Fig. 37.16 Ru-catalyzed hydrogenation of α,β-unsaturated acids.

- Some of the developed catalytic transformations are not (yet) very effective, and in all cases further enrichment would be necessary, which can only be done by making a salt derivative.

Ru complexes containing biaryl-type ligands are the catalysts of choice for most α,β-unsaturated acids, and pertinent examples are depicted in Figure 37.16. The substrate range from tetrasubstituted C=C bonds to substrates with sulfur-containing substituents, even though in the latter case catalyst performance is as yet insufficient for technical application. A trifluoromethyl-substituted unsaturated acid (*E*/*Z* mixture) was hydrogenated by Chemi in a 4000-L reactor on a 340-kg scale with tmbtp, a hetero binap analogue [33, 71].

Interestingly, Rh complexes can also be used effectively for sterically hindered α,β-unsaturated acids or salts, as evidenced by the processes depicted in Figure 37.17. Few details have been released for the pilot process developed by Solvias for Speedel/Novartis [74, 75], but the hydrogenation has been carried out on a multi-hundred-kilogram scale. Recently, DSM has divulged bench-scale results for the same transformation with a novel Rh–phosphoramidite–PPh_3 catalyst with somewhat lower enantioselectivity [76], and seemingly has applied the process on a production scale. While the catalytic performance of these two catalysts is adequate for manufacture, this is not (yet) the case for the examples of SmithKline Beecham [77] and Takeda Chemical Industries [78]; indeed, Takeda has developed an alternative technical process for the active ingredient.

The α,β-unsaturated ester shown in Figure 37.18, with a rather unusual substitution pattern, was hydrogenated successfully for the synthesis of candoxatril.

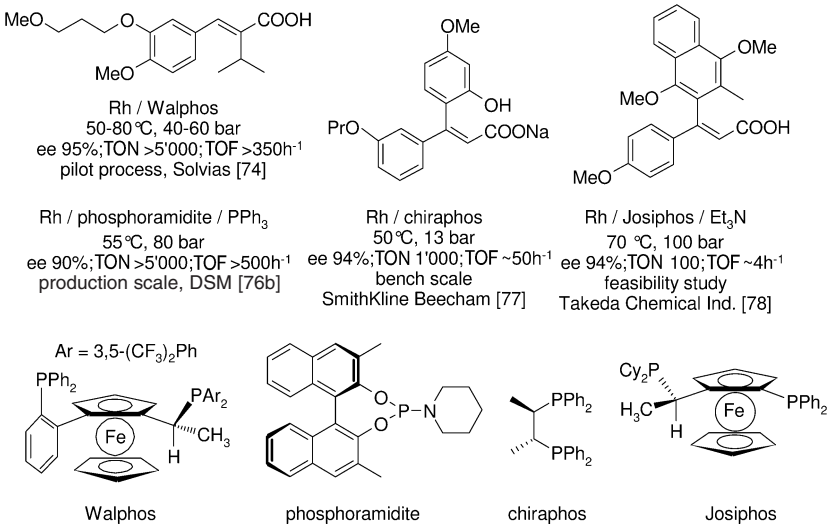

Fig. 37.17 Rh-catalyzed hydrogenation of α,β-unsaturated acids.

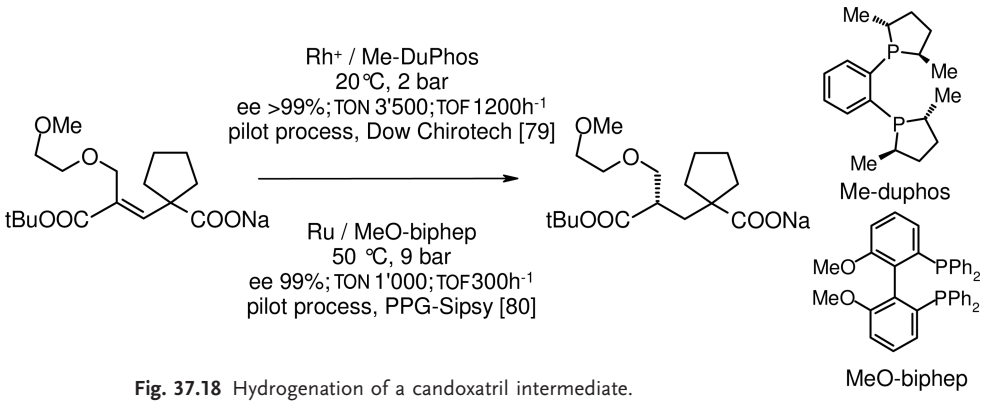

Fig. 37.18 Hydrogenation of a candoxatril intermediate.

The hydrogenation was carried out on 12-kg scale for Pfizer by Dow/Chirotech, using a cationic Rh–DuPhos catalyst [79] and on 250-kg scale by PPG-Sipsy with a Ru–biphep complex [80]. Both catalysts achieved very high enantioselectivities and medium activities.

37.6.6
Miscellaneous C=C Systems

Besides the olefins with privileged substitution patterns, several complex C=C substrates were hydrogenated on a production scale with good to excellent suc-

cess. Here, we describe several processes in some detail and summarize others, with minimal comment.

37.6.6.1 Hydrogenation of a Biotin Intermediate (Lonza)

During the course of the development of a new technical synthesis at Lonza for biotin (a water-soluble vitamin), the Rh–Josiphos-catalyzed diastereoselective hydrogenation of a tetrasubstituted C=C bond turned out to be a key step [40, 42, 81] (Fig. 37.19).

Selected results of the process development are summarized in Table 37.3. It is remarkable that homogeneous catalysts with most ligand classes gave even lower diastereomeric excess (de)-values than the achiral heterogeneous Rh–Al_2O_3 catalyst, and Rh–Josiphos complexes with aromatic R′ groups were inactive. The high effectiveness of catalysts with PPF-$PtBu_2$ as ligand was therefore even more surprising. While the feasibility study was carried out with SCR of 50 to 100, optimization of the reaction resulted in TONs of 2000. The enantioselective hydrogenation (*N*-benzyl instead of *N*-(*R*)-phenethyl) with Rh–PPF-$PtBu_2$ afforded the desired enantiomer with up to 90% *ee*. For the production process the diastereoselective variant was chosen and for a few years several tons were manufactured annually.

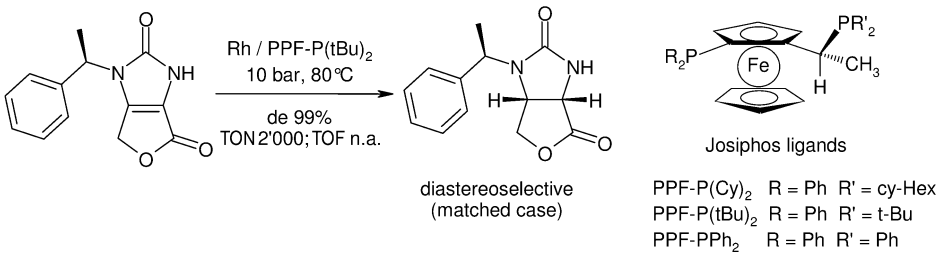

Fig. 37.19 Hydrogenation of a biotin intermediate.

Table 37.3 Selected results for the hydrogenation of the biotin intermediate.

Catalyst	de [%]	Comments/ligand structures
Rh–Al_2O_3	40	Heterogeneous
Rh–bdpp	50	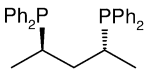 bdpp
Rh–moddiop	66	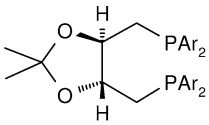 moddiop Ar = 3,5-Me_2-4-(OMe)Ph
Rh–PPF-PPh_2	No reaction	
Rh–PPF-PCy_2	88	
Rh–PPF-P(*t*Bu)$_2$	99	

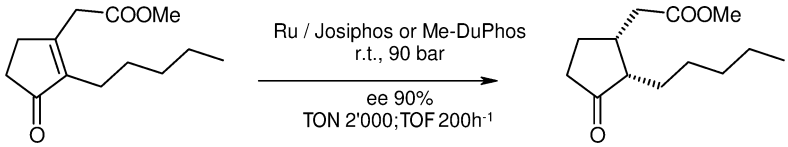

Fig. 37.20 Hydrogenation of a dihydrojasmonate intermediate.

Table 37.4 Ligand effect on activity and selectivity.

Ligand	SCR	TOF [h^{-1}]	*cis/trans*	ee *cis* [%]
Me-DuPhos	300	5	99/1	69
Josiphos	500	250	98/2	86
Me–DuPhos	2000	120	>97/3	60
Josiphos	2000	200	>97/3	90

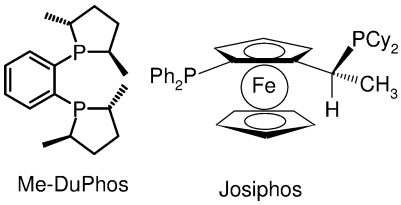

Catalyst: [Ru(H)(cyclooctatriene)(ligand)]BF_4.
SCR: Substrate : catalyst ratio.

37.6.6.2 Synthesis of (+)-Methyl *cis*-Dihydrojasmonate (Firmenich)

Dihydrojasmonates are ubiquitous and cheap perfume ingredients. Firmenich established that (+)-*cis*-methyl dihydrojasmonate (Fig. 37.20) is the preferred stereoisomer, and subsequently developed an enantioselective process and began production on a multi-ton per year scale [82, 83].

A novel Ru precursor and a new reaction system had to be found because the classical Ru complexes and conditions for the hydrogenation of C=C bonds did not work. Besides the enantioselectivity, chemo- and *cis*-selectivity and activity problems (tetrasubstituted C=C) were solved on a very good level. A broad screening of Ru catalysts (partly in collaboration with Solvias) showed that selected Josiphos ligands and DuPhos satisfied the prerequisites (see Table 37.4).

37.6.6.3 Intermediate for Tipranavir (Chirotech)

The diastereoselective process depicted in Figure 37.21 was developed by Chirotech [18, 36, 84] for Pharmacia and Upjohn [85], and is being carried out on a "production" scale. Essential was the addition of Na_2CO_3 as co-catalyst. The catalyst tolerates an *E*/*Z* mixture of substrate, and shows high chemoselectivity with respect to reduction of the nitro group, which can be a problem. An alternative pilot process was recently described by Boehringer-Ingelheim using a Rh–cat*A*-*S*ium® M catalyst which achieved selectivities of >98% de and a TOF of ca. 40 h^{-1} with an SCR of 1000 at 60 °C/10 bar [86].

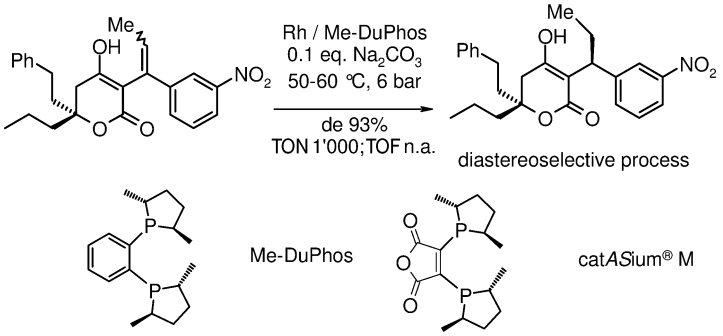

Fig. 37.21 Hydrogenation of a tipranavir intermediate.

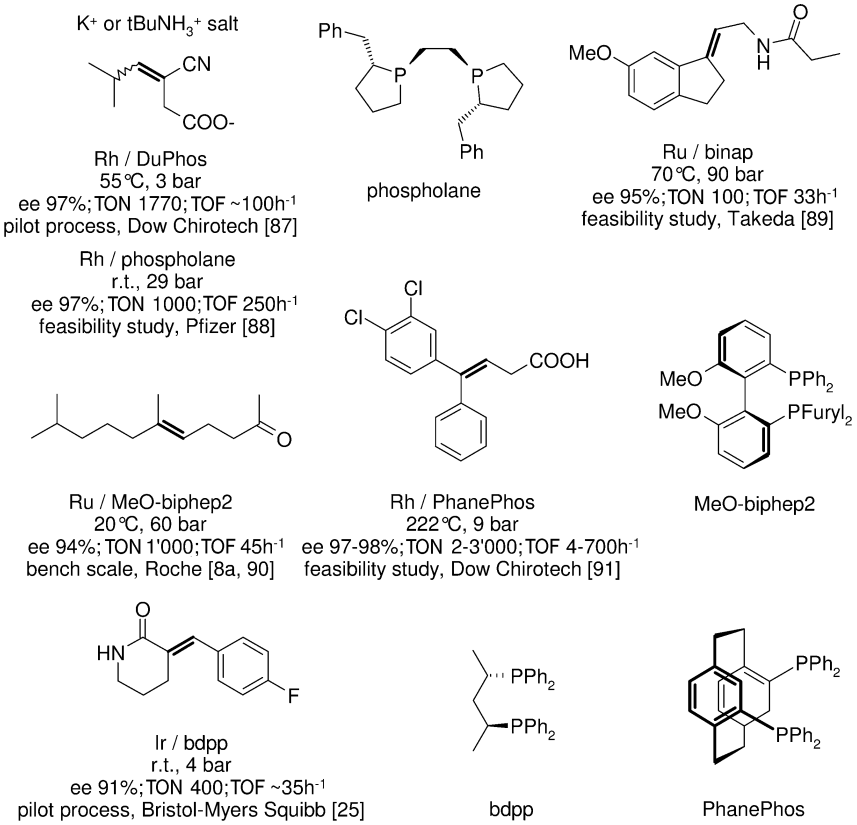

Fig. 37.22 Hydrogenation of various functionalized alkenes.

37.6.6.4 Various C=C Substrates

Further hydrogenations of a variety of C=C substrates depicted in Figure 37.22 range from a pilot process to several feasibility studies. Of special interest are PhanePhos, originally reported by Merck, an unsymmetrically substituted phospholane developed by Pfizer, and the rare case of an Ir–diphosphine complex active for the hydrogenation of a C=C bond. Nevertheless, the catalyst performances of most processes summarized in Figure 37.22 are probably not (yet) sufficient for manufacturing purposes. Indeed, several of the reports explicitly mention that further development was stopped, either because another route proved to be superior or because the compound was abandoned.

37.7 Enantioselective Hydrogenation of C=O Bonds

Most catalysts originally developed for C=C bonds show a rather poor performance for the hydrogenation of many ketones. However, this situation changed dramatically when it was found that selected Ru–binap and later Ru–binap–diamine complexes achieve excellent enantioselectivities, as well as very high TONs and TOFs, for a variety of ketones [92]. Since then, it has been demonstrated that many α- and β-functionalized, as well as aromatic ketones, are suitable substrates for hydrogenation with industrially viable catalytic results. For the reduction of various ketones biocatalytic methods are an industrially viable alternative to chemocatalysts [15].

37.7.1 α-Functionalized Ketones

(*R*)-1,2-Propanediol is an intermediate for (*S*)-oxafloxazin, a bactericide which until recently was sold as a racemate. The (*R*)-diol is now produced by Takasago via hydrogenation of hydroxyacetone (see Fig. 37.23) using a Ru–Tol–binap catalyst on a 50 t y^{-1} scale [92 b]. Recently, it was reported that segphos – a newly developed biaryl diphosphine – shows even better results, achieving >98% ee and TON and TOF of 10 000 and $\sim$1400 h^{-1}, respectively [16, 93].

The two production processes using α-amino ketone substrates depicted in Figure 37.24 were developed by Boehringer-Ingelheim to improve on existing resolution syntheses for adrenaline and phenylephrine [94]. Unfortunately, few details are available but both processes are carried out with a Rh–mccpm catalyst with very high TONs and TOFs, albeit with medium ee-values of 88% which increase to >99% after precipitation of the free base.

The hydrogenation of α-amino ketones was also a key step for the synthesis of three more pharma actives (Fig. 37.25). Roche [95] divulged a pilot process involving the hydrogenation/dynamic kinetic resolution of a cyclic α-amino ketone using an optimized MeO–biphep ligand. The Ru-catalyzed reaction was carried out on a 9-kg scale with excellent enantio- and diastereoselectivities, and very

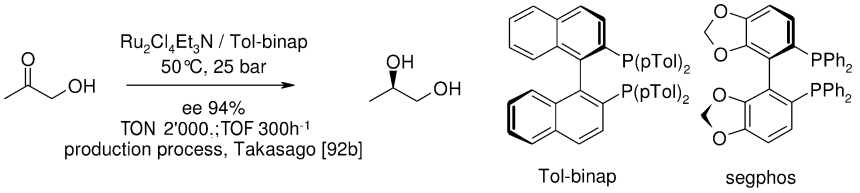

Fig. 37.23 Hydrogenation of hydroxyacetone.

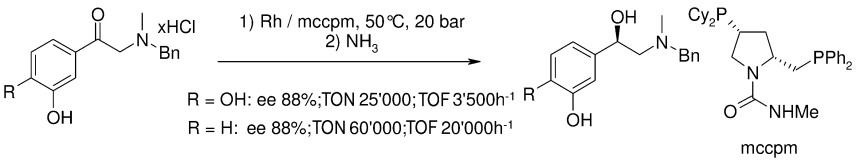

Fig. 37.24 Production processes for adrenaline (R=OH) and phenylephrine (R=H) intermediates.

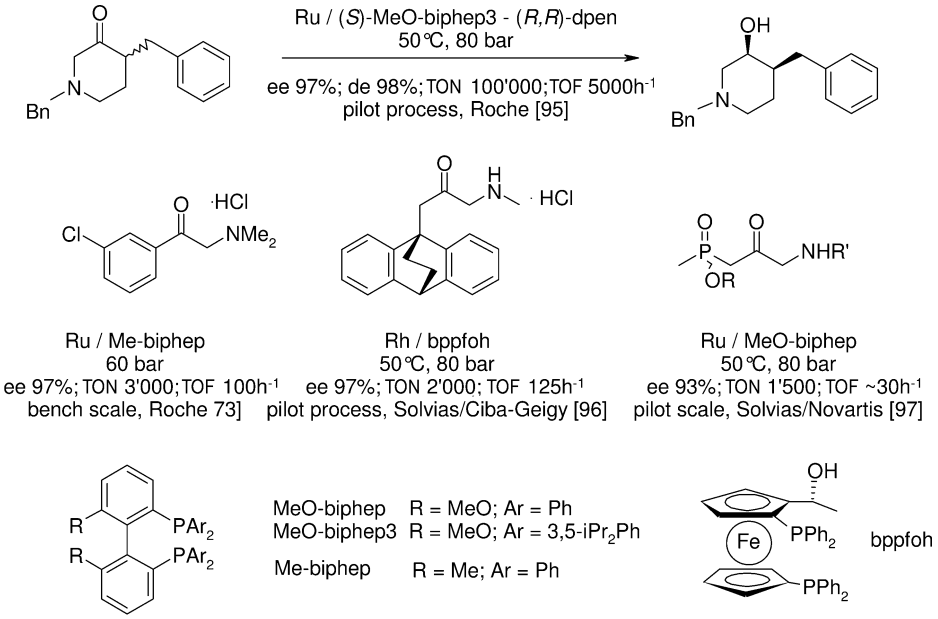

Fig. 37.25 Hydrogenation of various α-amino ketones.

high TON and TOF. A bench-scale process for the reduction of an aromatic ketone reported earlier relied on a Ru–Me-biphep catalyst [73]. A pilot process was reported by Solvias/Ciba-Geigy which was operated on a multi-10-kg scale involving a Rh–bppfoh-catalyzed hydrogenation of an intermediate for the antide-

pressant levoprotiline [96]. Important for success was the fact that crystallization of the product both enhanced ee-values and allowed separation of the catalyst from the product. A pilot process was developed by Solvias for Novartis for the hydrogenation of an α-amino-α'-phosphinate ester with moderate catalyst performance using a Ru–MeO–biphep catalyst [97]. Clearly, this substrate could also be considered to be an analogue of a β-keto ester (see below). Recently, the application of Ru/C_3-TunePhos to the hydrogenation of aromatic α-phthalimide ketones was reported as having excellent catalyst performance but requiring relatively high temperatures and pressures (60–80 °C, 100 bar, ee up to >99%, TON up to 10 000, TOF 140 h^{-1}), thus opening up a viable route for the synthesis of a variety of amino alcohols [98].

The hydrogenation of α-keto acid derivatives is a promising route to a variety of α-hydroxy and α-amino acids. Until now, homogeneous catalysts have achieved good ee-values but only insufficient TONs and TOFs and, indeed, heterogeneous cinchona-modified Pt catalysts are a viable alternative [10, 99, 100]. The hydrogenation of an α-ketolactone (Fig. 37.26) was the key step for the enantioselective synthesis of pantothenic acid. A pilot process was developed by Roche [8a], and (*R*)-pantolactone was produced in multi-100-kg quantities. A Rh–bpm catalyst proved to be highly active with satisfactory selectivity. Important were the fine tuning of the ligand and the choice of anion; critical for the very good catalyst performance were the purity of substrate and solvent, as well as of hydrogen. For the production of kilogram quantities of (*S*)-*p*-chloro mandelic acid, a Ru–MeO–biphep catalyst achieved 90–93% ee with acceptable TONs and TOFs, indicating that this hydrogenation might be feasible for the production of an agrochemical intermediate, both from a technical and an economical point of view [100]. The hydrogenation of two other α-keto esters was less successful as the catalyst activities were relatively low [73].

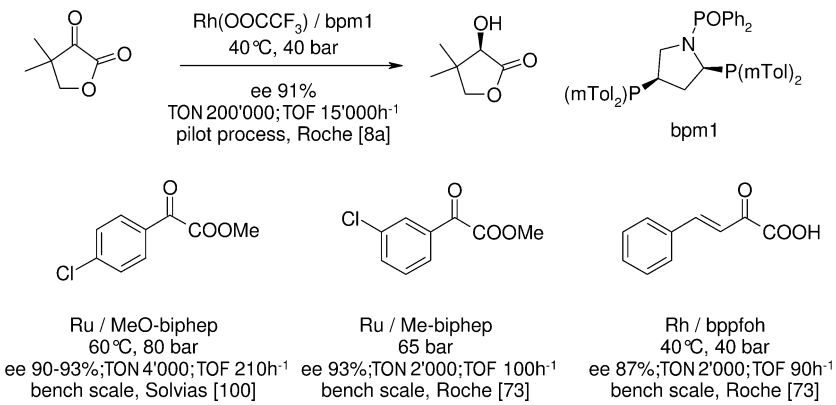

Fig. 37.26 Hydrogenation of α-keto acid derivatives.

37.7.2
β-Functionalized Ketones

β-Ketone esters are certainly privileged substrates, and several industrial processes rely on their enantioselective hydrogenation. The most important is the hydrogenation/dynamic kinetic resolution shown in Figure 37.27 for the production of an intermediate for carbapenem antibiotics carried out by Takasago on a scale of 50 to 120 t y^{-1} [66, 92b, 101]. Similar results (ee 98–99%, de 94%, TON 200, TOF ~600 h^{-1} at 50 °C/100 bar) were obtained by Chemi with a Ru–tmbtp catalyst [33, 102]. It was also recently reported that an optimized segphos ligand can achieve even higher stereoselectivities with >99% ee and 99% de (TON and TOF not specified) [16, 93].

Several processes using simple β-keto ester substrates were developed to various stages. Some early examples of bench-scale processes using Ru–binap were described by Takasago and Aventis (for more information, see [14]). NSC Technologies [103] manufactures three β-hydroxy esters building blocks; one of these is produced on the scale of 100s of kilograms, while two other are in the pilot stage. Lanxess has developed similar technology for the hydrogenation of several substrates on the basis of its ClMeO–biphep ligand which is applied on technical scale [3, 104] (Fig. 37.28). Also depicted in Figure 37.28 is the hydrogenation of a chlorinated β-keto ester developed to the pilot stage and applied on a multi-100-kg scale by Chemi, using its proprietary tmbtp ligand [71]. Chiral Quest has claimed a technical process for this substrate as well as for other keto esters using Ru–TunePhos catalysts [3, 47]. Acetyl acetone can be reduced to 2,4-pentane diol with >99% ee and >98% de using Ru–ClMeO–biphep, the reaction having been carried out by Lanxess on a scale of several kilograms, though few details are available [3, 104, 105] and Roche has described a pilot process for a long-chain β-keto ester, an intermediate for Orlistat (see Fig. 37.28) [8a, 73]. More complex substrates can also be hydrogenated successfully, as demonstrated by the two last examples shown in Figure 37.28. A bench-scale process

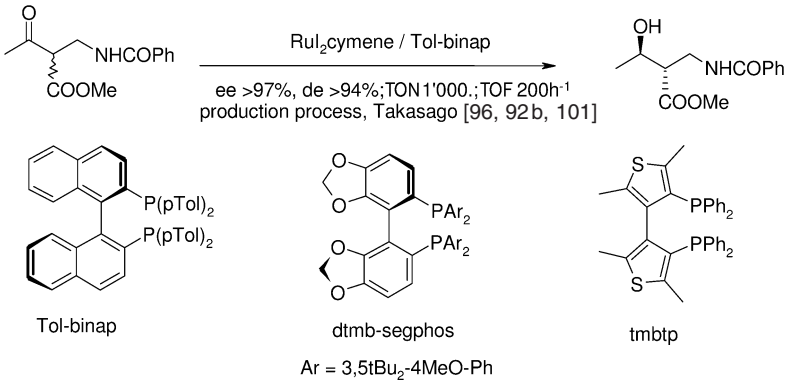

Fig. 37.27 Hydrogenation/dynamic kinetic resolution of a penem intermediate.

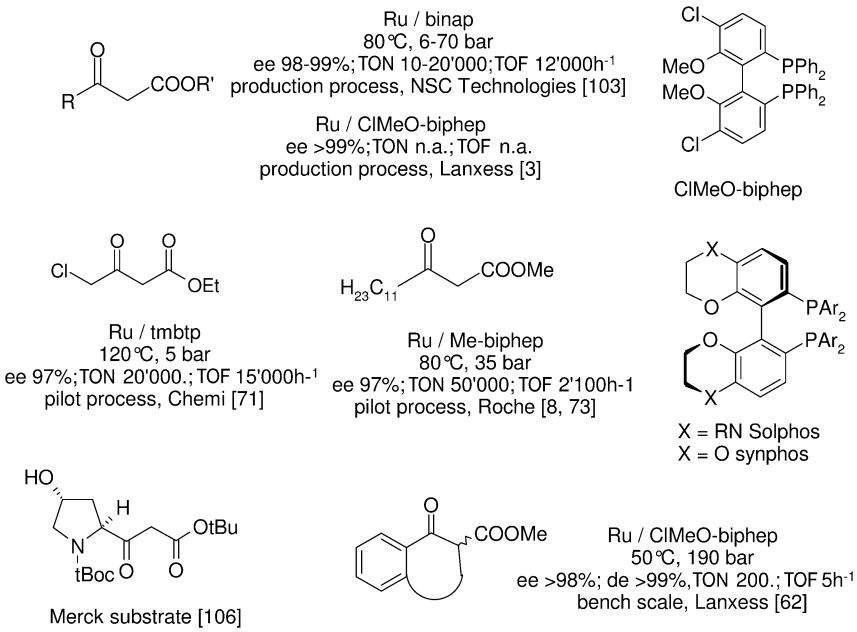

Fig. 37.28 Hydrogenation of β-keto acid derivatives.

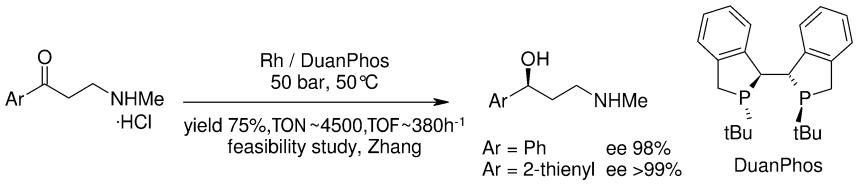

Fig. 37.29 Hydrogenation of γ-amino ketones.

has been reported by Lanxess for a cyclic keto ester (exact structure unknown) with high stereoselectivities but low catalyst activity [62], and Ru–Tol–binap was used by Merck to hydrogenate a hydroxyproline derivative, albeit with modest stereoselectivity of 76% de on a kilogram scale [106].

Based on hydrogenations of model substrates, several new ligands promise to have a similar potential as those described above. For example, Ru–Solphos (Solvias) catalysts have been shown to hydrogenate various β-keto esters and β-diketones with ee-values up to >99% and TONs of up to 100 000 (for ethyl-3-oxobutanoate) [75], while Ru–Synphos (Synkem) [107] catalysts achieved 99.4% ee at an SCR of 7000 for the hydrogenation of ethyl acetoacetate (for ligand structures, see Fig. 37.28).

Recently, Zhang and coworkers [108] showed Rh–DuanPhos to be a very effective catalyst for the hydrogenation of a variety of aromatic γ-amino ketones. In a

feasibility study, the hydrogenation of the intermediates of (*S*)-fluoxetine and (*S*)-duloxetine was achieved with ee-values of 89% and >99%, respectively, at an impressive SCR of 6000, albeit with a relatively low chemical yield of 75% (Fig. 37.29).

37.7.3
Aromatic Ketones

The effective hydrogenation of ketones without *α*- or *β*-functionality has only recently developed to be an important methodology with Noyori's discovery of the Ru-based transfer hydrogenation catalysts on the one hand, and the very active Ru–diphosphine–diamine systems on the other hand [92a]. Both methodologies rely on the presence of an N–H bond allowing an effective outer sphere reduction mechanism. The technology has been licensed by several companies using various diphosphines [16, 109–112], but it is not clear whether it is already used for specific manufacturing purposes.

The hydrogenation of a number of aromatic ketones is shown in Figure 37.30. Noyori's very effective Ru–diphosphine–diamine technology was developed by several companies. It is not clear on which scale the processes developed by Takasago (dm-binap = 3,5-xylyl-binap) [16] and Dow/Chirotech [109–111] for the reduction of substituted acetophenones are actually applied commercially. Using the Xyl-PhanePhos–dpen catalyst, a highly efficient bench-scale process was developed for the hydrogenation of *p*-fluoroacetophenone (ee 98%, TON 100 000, TOF 50 000 h^{-1} at r.t., 8 bar) [109]. Ru–P-Phos (licensed to Johnson Matthey [112]) achieved ee-values >99.9% and TON up to 100 000 for sev-

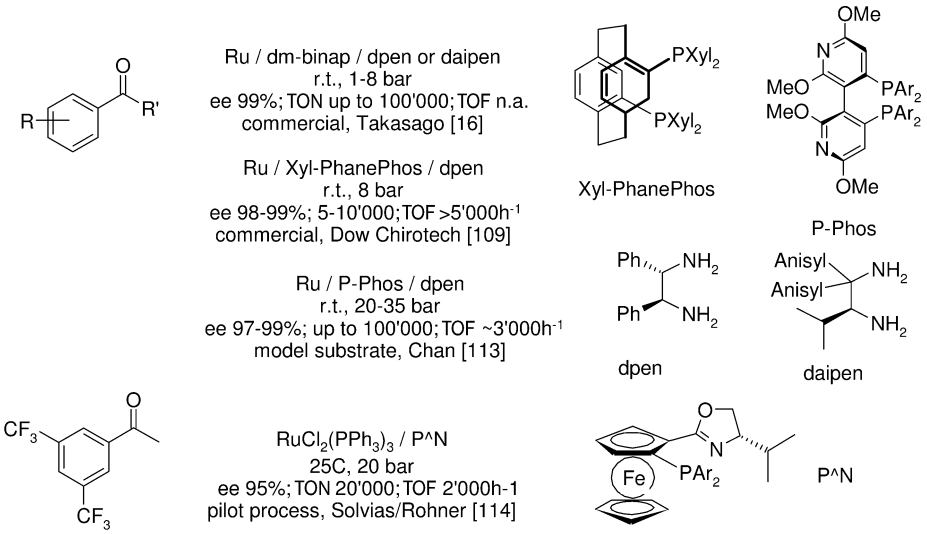

Fig. 37.30 Hydrogenation of aromatic ketones.

eral model substrates [113]. A pilot process was developed by Solvias for the production of 3,5-$(CF_3)_2$-phenyl ethanol using a newly developed Ru–(phosphinoferrocenyl)oxazoline complex [114] which, though not containing an N–H bond, showed very high activity for the hydrogenation of a variety of aryl ketones.

Several Ru-catalyzed transfer hydrogenations have been developed and applied up to the multi-10-kg scale. Two variants are applied, one based on Ru–amino alcohol complexes with *i*PrOH/base, and the other based on Ru–Ts–dpen complexes with $HCOOH/NEt_3$ as reducing system, respectively. As shown in Figure 37.31, excellent enantioselectivities have been obtained for several aryl ketones, but with lower activities than for comparable hydrogenation reactions described above (see, for example, the results for *bis*-trifluoromethyl-acetophenone in Fig. 37.30). Avecia has developed transfer hydrogenation technology under the term CATHy using Me_5cp–Ru catalysts, and claims several applications on the multi-100-kg scale [3, 115], while Lanxess has applied Noyori's Ru–Ts–dpen system to the reduction of aryl keto esters on a scale of >2 tons [62, 104]. Of special interest are the chemoselectivity in the case of nitro-acetophenone [3] and the ability to reduce rather complex molecules, as illustrated by the Otsuka feasibility study [116].

Finally, hydride reduction using BH_3 in presence of 1,2-amino alcohols (CBS reduction) can be run catalytically, albeit with very low TONs and TOFs. Nevertheless, several processes based on this technology have been developed and run on a scale of up to 50 kg. Three such cases are shown in Figure 37.32 (more can be found in [14]). Lonza used a proline-derived catalyst to manufacture 50 kg of an intermediate for Josiphos ligands [119]. Merck used the same catalyst to reduce bistrifluoro-acetophenone on kilogram scale but, compared to the results for the (transfer) hydrogenation processes described above, the TON (20–50) and TOF ($\sim 20\ h^{-1}$) were much lower [117, 120]. Sepracor also developed this technology for an aryl-γ-keto ester with respectable ee-values but, again, low activity [121], while Merck reported a pilot process for the reduction of a more complex intermediate using the aminoindanol ligand N^O (see Fig. 37.31) [122]. Finally, a Co-salen-catalyzed borohydride reduction was developed by Mitsui for a heteroaryl ketone, albeit with relatively low ee-values [123].

37.8
Enantioselective Hydrogenation of C=N Bonds

The enantioselective hydrogenation of C=N bonds is the least-developed hydrogenation reaction, even though many active ingredients contain chiral amine moieties. The main reason for this situation is that effective catalysts – mainly Ir–diphosphine complexes – have been developed only during the past 10 years [124]. A major incentive for the development of more active catalysts was the chiral switch of metolachlor made in 1997 by Ciba-Geigy [125, 126].

Metolachlor is the active ingredient of Dual, one of the most important grass herbicides for use in maize and a number of other crops. In 1996, after years of intensive research, Dual Magnum with a content of approximately 90% (*S*)-diaste-

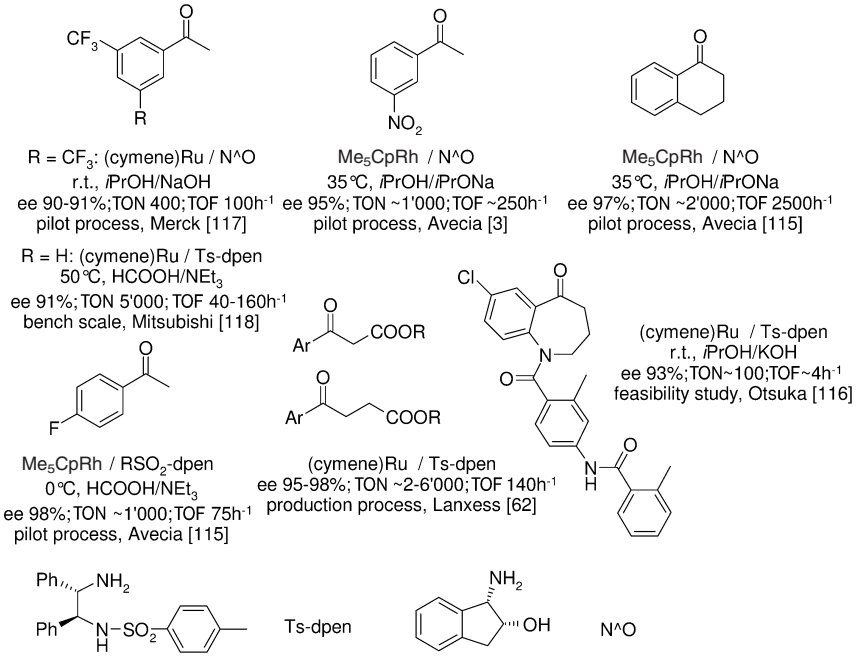

Fig. 37.31 Transfer hydrogenation of aromatic ketones.

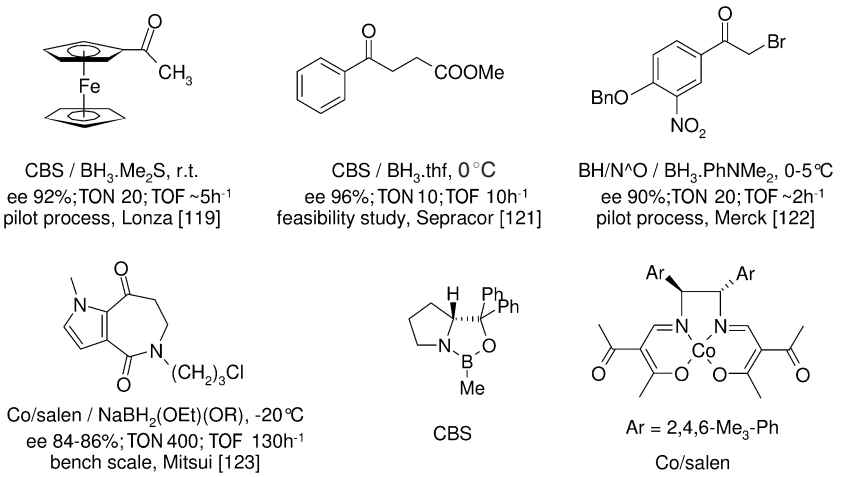

Fig. 37.32 Hydride reductions of aromatic ketones.

reomers and with the same biological effect at about 65% of the use rate, was introduced onto the market. This "chiral switch" was made possible by the new technical process that is briefly described below. The key step of this new synthesis is the enantioselective hydrogenation of the isolated MEA imine (Fig. 37.33).

The search for a commercially viable process took many years [126]. Several approaches with Rh or Ir complexes using commercially available diphosphine ligands were not successful. A critical breakthrough was achieved when Ir complexes with a new class of ferrocenyl-based ligands (now called Solvias Josiphos) were used. Extremely active and productive catalysts were obtained, especially in the presence of acid and iodide ions. Different Josiphos ligands were tested and a selection of the best results obtained is shown in Table 37.5.

The optimized process operates at 80 bar hydrogen and 50 °C with a catalyst generated *in situ* from $[Ir(cod)Cl]_2$ and the Josiphos ligand PPF-$PXyl_2$ (short name Xyliphos) at a SCR of >1 000 000. Complete conversion is reached within 3–4 h, the initial TOFs exceed 1 800 000 h^{-1}, and the ee is about 80%. This process is now operated by Syngenta on a scale of >10 000 t y^{-1} [127].

Following this success, a number of technical C=N hydrogenation processes were developed (Fig. 37.34). While enantioselectivities are good to excellent, catalytic activities and productivities are far behind the metolachlor process. An Ir-catalyzed hydrogenation developed by Lonza for an intermediate of dextromethorphan was carried out on a >100-kg scale [41, 42, 81]. Important success factors were the ligand fine tuning and use of a biphasic system. Chemoselectivity is high, but catalyst productivity rather low, for an economical technical application. Satoh et al. reported up to 90% ee for the hydrogenation of an intermediate of the antibiotic levofloxacin using Ir–diphosphine complexes. The best

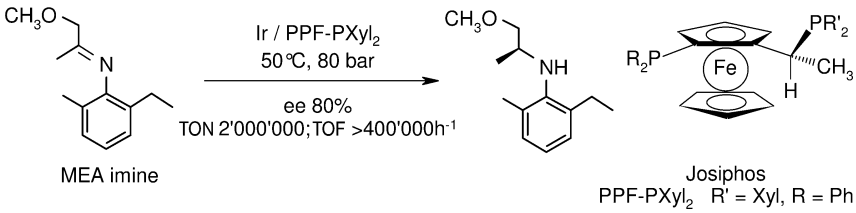

Fig. 37.33 Metolachlor hydrogenation process.

Table 37.5 Most successful ligands for the hydrogenation of MEA imine (for ligand structures, see Fig. 37.33).

R	R′	TON	TOF [h^{-1}]	ee [%]	Comments
Ph	3,5-xylyl	1 000 000	> 300 000	79	Production process
p-CF_3Ph	3,5-xylyl	800	400	82	Ligand screening
Ph	4-*t*Bu-C_6H_4	5000	80	87	Low temperature
Ph	4-(^{n}Pr)$_2$N-3,5-xyl	100 000	28 000	83	Optimized conditions

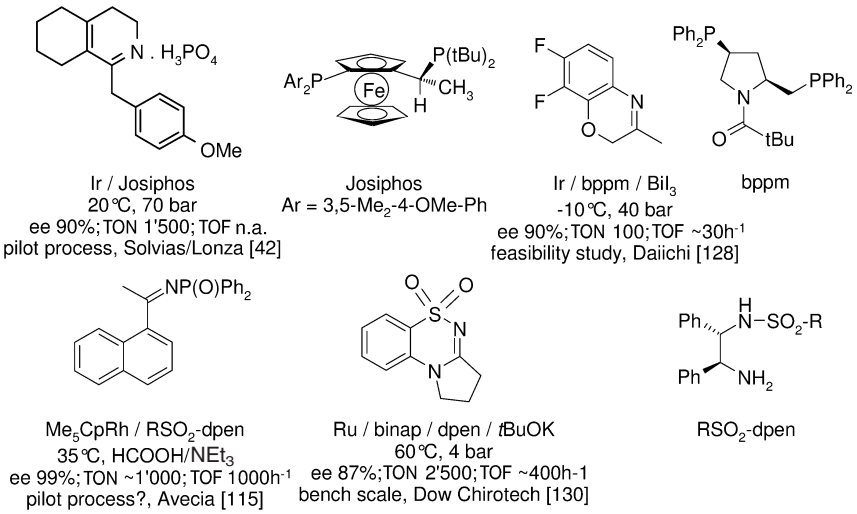

Fig. 37.34 Hydrogenation of a various C=N bonds.

results were obtained with bppm and modified diop ligands in the presence of bismuth iodide at low temperature [128].

Besides Ir–diphosphines, two more catalyst systems have shown promise for industrial application. As mentioned in Section 37.5.2, the Rh–Josiphos-catalyzed hydrogenation of unprotected β-dehydro amino acid derivatives by Merck actually involves the hydrogenation of a C=N and not a C=C bond (see Fig. 37.10) [3, 51]. Noyori's Ru–PP–NN catalyst system seems also suitable for C=N hydrogenation [129], and was successfully applied in a feasibility study by Dow/Chirotech for the hydrogenation of a sulfonyl amidine [130]. Avecia also showed the viability of its CATHy catalyst for the transfer hydrogenation of phosphinyl imines [115] (see Fig. 37.34).

37.9
Ligands and Metal Complexes for Large-Scale Applications

There is no doubt that the chiral ligand is at the heart of any enantioselective homogeneous process. As explained above, it is of course crucial to apply the correct metal (the correct choice of metal precursor or anion can be decisive), as well as a suitable solvent and reaction conditions. However, since there are much fewer metal precursors, anions or solvents than there are potential ligands, process research and development (R&D) is very much centered around finding the optimal ligand. Accordingly, most patents of hydrogenation processes are focused on the structure, the synthesis and/or the application of chiral ligands and the availability of the ligands in the required quantity at the right time is one of the central issues of process development.

In the past, when an enantioselective catalytic process was developed and scaled up for the production of a chiral intermediate, the preparation of the chiral ligand in the amounts required for each phase was very much part of process development. This is well described in Knowles' Nobel Lecture for the L-dopa process [28a]. While the design of the dipamp ligand was an extraordinary achievement, without a technical synthesis the manufacture of L-dopa would still not have been possible. The same was also true for the Josiphos ligands developed by the former Ciba-Geigy (now Solvias/Syngenta) for the manufacture of (*S*)-metolachlor which, with an annual volume of >10 000 tonnes is today's largest catalytic process for a chiral intermediate [127]. The need to develop the actual manufacturing process not only for the intermediate but also for the chiral ligand places additional pressure on the application of chiral catalysts which had (and will have even more) to compete with alternative technologies such as resolution processes (simulated moving bed, crystallization, etc.), chiral pool approaches or biocatalysis.

During the past few years the situation has changed considerably as several companies have developed technology and ligand portfolios which are available for applications on a technical scale [47, 111, 112, 131–135, 141]. In the following sections we have compiled: (i) a list of companies offering technology and various services in the field of homogeneous hydrogenation; (ii) ligands which have been used on a technical scale as described in Sections 37.6 to 37.8, and/or which are available on scale and have a confirmed potential for technical applications; (iii) information on metal complexes; and (iv) information on intellectual property (IP) issues.

37.9.1
Companies Offering Services, Technology, Ligands and Catalysts

- *Chemi:* Proprietary diphosphine ligands, process R&D, custom manufacturing. Some pilot and bench scale processes.
- *Chiral Quest Inc.*: Proprietary chiral ligands, process R&D [47].
- *Degussa Homogeneous Catalysts*: Proprietary chiral ligands, process R&D, custom manufacturing. Various bench-scale and pilot applications [135].
- *Digital Specialty Chemicals*: Supply of phosphine ligands on kilogram scale, especially patent-free ligands [136].
- *Dow/Chirotech*: Proprietary chiral ligands, process R&D, custom manufacturing. Several production processes, many pilot- and bench-scale processes [111].
- *DSM Pharma Chemicals*: Proprietary technology, process R&D, custom manufacturing. Production process [137].
- *Great Lakes Fine Chemicals*: Know-how from NSC Technologies/Monsanto, several production and pilot processes [30].
- *Japan Science and Technology Corporation:* Licensing Noyori technology.

- *Johnson Matthey, Catalysis and Chiral Technologies (Synetix)*: In licensed chiral ligands, process R&D. Metal precursors and M-L complexes in technical quantities; recovery of noble metals [112].
- *Lanxess (Bayer)*: Proprietary ligands, process R&D, custom manufacturing [62].
- *Lonza*: Process R&D, custom manufacturing. One production process, several pilot- and bench-scale processes [42].
- *NPIL Pharma (Avecia):* Proprietary technology, process R&D, custom manufacturing. Some pilot and bench scale processes [115].
- *Rhodia*: Expertise in phosphorus chemistry, manufacture of binap [138].
- *PPG-Sipsy*: License for selected catalyst systems, process R&D, custom manufacturing. Several processes [139].
- *Synkem*: Proprietary ligands, process R&D, custom manufacturing [140].
- *Solvias* (spin-off from Ciba-Geigy/Novartis): Proprietary chiral ligands, process R&D. Several production processes, many pilot- and bench-scale applications [141].
- *Takasago*: Early and strong efforts in developing the potential of the binap ligand for isomerization and hydrogenation. Proprietary ligand families, process R&D, custom manufacturing. Several production and pilot processes [142].
- *Umicore AG* (formerly OMG, dmc^2, Degussa): Proprietary chiral ligands (collaboration with Solvias). Metal precursors and M-L complexes in technical quantities; recovery of noble metals [143].

37.9.2
Chiral Ligands with Established Industrial Performance

Here, we list only those ligands which have either been used successfully on industrially relevant target substrates or have demonstrated excellent overall catalyst performance (ee >98%, TON >5000, TOF >1000 h^{-1}) for the hydrogenation of model substrates. Comments and references can be found in the preceding sections. It must be stressed that, in addition to the ligands compiled in Figures 37.35 to 37.38, the ligand suppliers listed above offer many more ligands with industrial potential which, however, has not (yet) been documented adequately.

The following classes of ligands with often similar performance profiles are distinguished: biaryl diphosphines, phospholanes, ferrocenyl-based diphosphines and miscellaneous phosphorus-based ligands. Only one enantiomer of each ligand is depicted, but in general both enantiomers are available, even though in a few cases the prices might vary if the ligand is prepared from chiral pool material.

37.9.3
Metal Complexes and Anions

Once the optimal metal/ligand/anion combination has been determined, the choice of the metal complex which is actually put into the reaction solution will become of importance. Active hydrogenation catalysts are metal–ligand complexes which can either be prepared *in situ* simply by mixing a suitable precur-

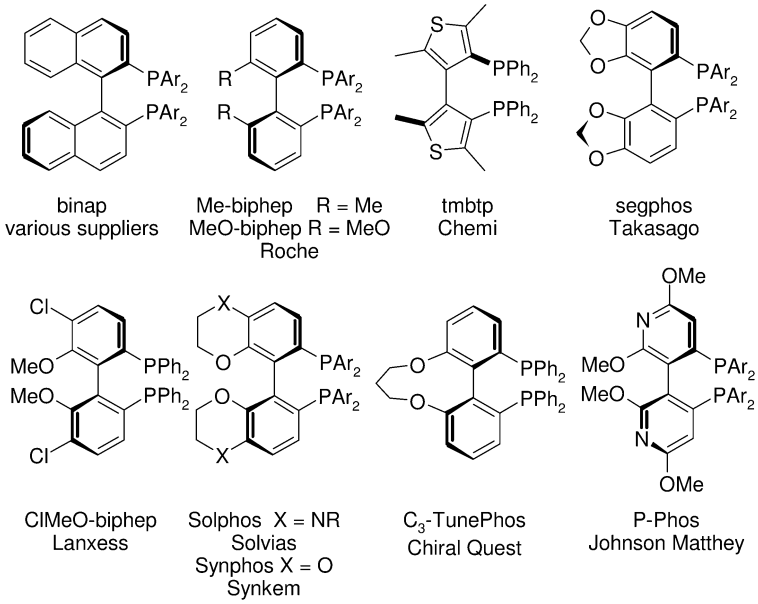

Fig. 37.35 Biaryl diphosphines; (*R*)-enantiomers are shown.

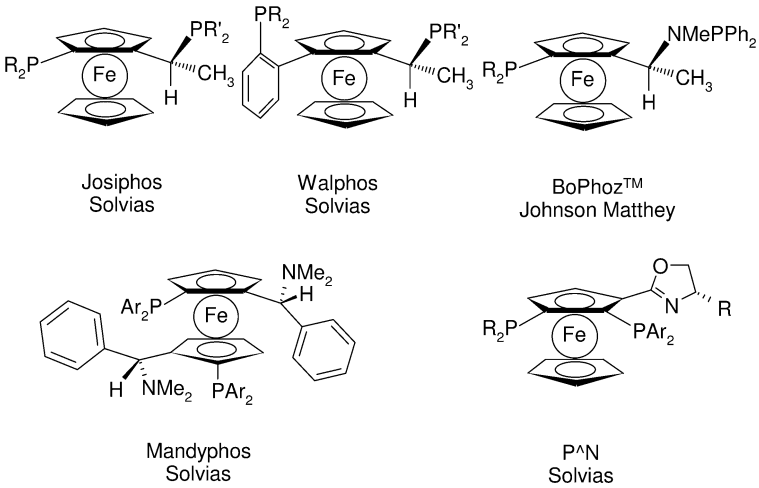

Fig. 37.36 Ferrocenyl phosphines.

sor and the ligand, or by using a single component, "ready-to-use" metal–ligand (M–L) system which is prepared in an extra step and isolated before use (selected examples are depicted in Fig. 37.39) [143, 144].

While there are cases where only one of the two methods works, very often both approaches give a similar catalyst performance, and consequently the de-

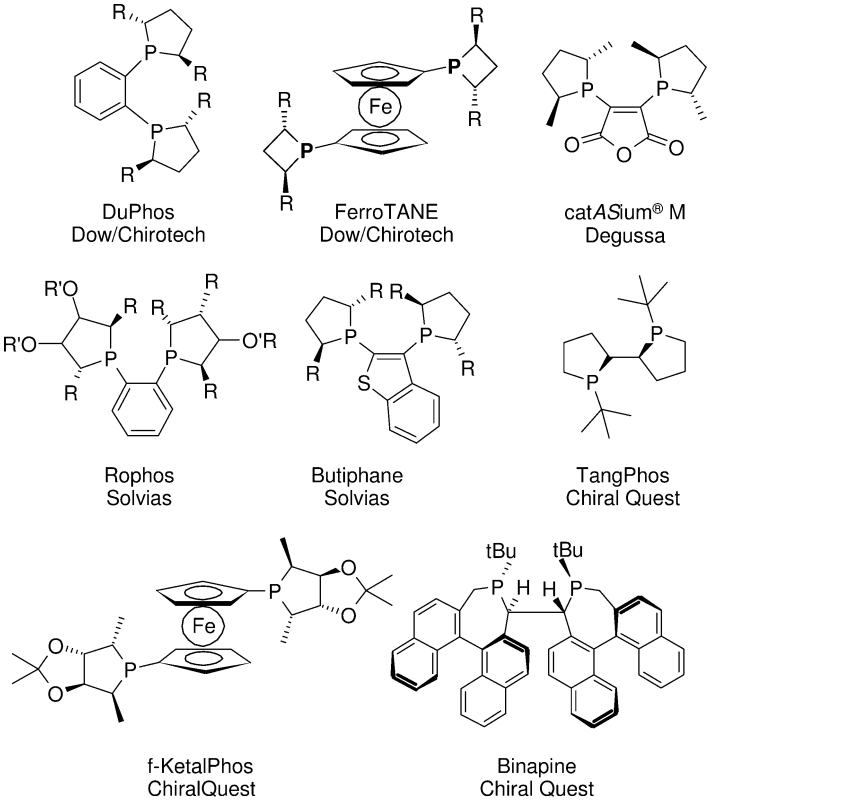

Fig. 37.37 Phospholane-type ligands and analogues.

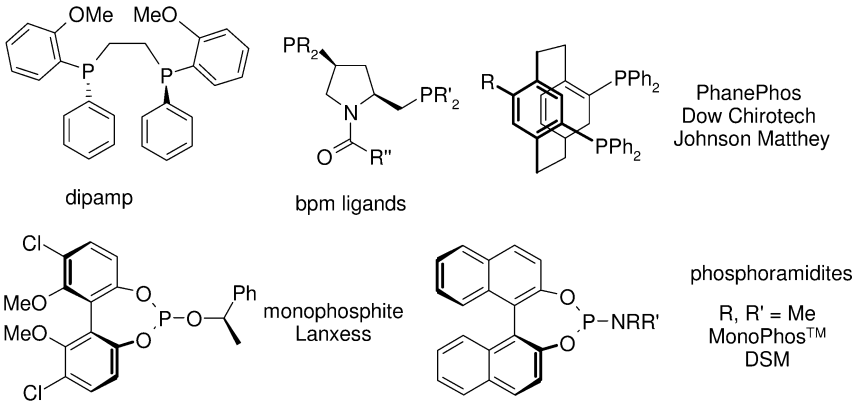

Fig. 37.38 Miscellaneous ligands.

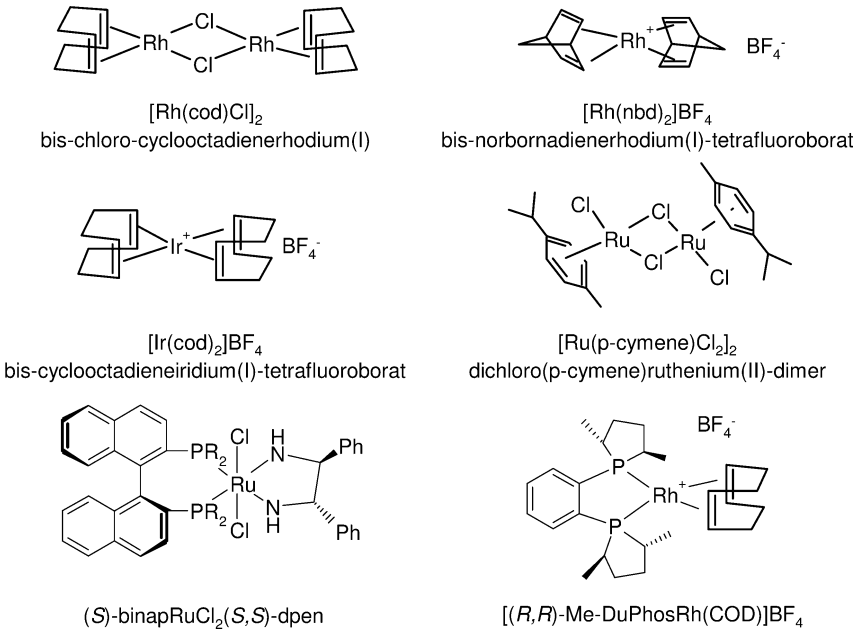

Fig. 37.39 Important metal precursors and selected M-L-complexes.

velopment chemist has a choice. The *in-situ* method is very flexible and allows the use of standard metal precursor complexes which are offered by all major catalyst suppliers. Since several of the most effective ligands are air-sensitive, handling and ligand stability can be a problem. Single-component catalysts require an additional preparation step, but in many cases, the metal–phosphine complexes are more stable, less air-sensitive and therefore easier to handle than the free ligands. Furthermore, the reaction set-up is simplified because the initial step of premixing the precursor and the ligand is no longer required. As a drawback, the preparation of M–L complexes on a technical scale requires specific know-how for each individual complex and might therefore restrict the choice of the metal supplier.

As a general rule, most phospholanes are relatively air-sensitive and usually sold as rhodium–diene complexes. The ferrocene-based ligands, as well as phosphoramidites and phosphites, are relatively easy to handle, and the corresponding Rh, Ir and Ru complexes are usually prepared *in situ*. Even though most biaryl type ligands are quite insensitive, most of them are applied as preformed Ru complexes.

37.9.4
Intellectual Property Aspects

Not surprisingly, most of the versatile privileged ligands are patent-protected. If the licensing policy of the patent owner is very restrictive, or if the royalties are too high, many potential users will not use a patented technology [24]. On the other hand, a technology-providing company must finance its R&D efforts, and licensing fees are an important consideration in this context. In the chiral ligand business, two basic IP models are being used and most companies providing chiral ligands have adopted some variation thereof [132, 133, 145]:

- The classical royalty model, where the license fee is based on the added value of the new technology for the customer. As a rule, the royalties depend on the production volume and/or value of the chiral compound produced with the proprietary ligand, and are usually a percentage of product sales or a similar reference number. Also accepted are volume-independent royalties such as up-front or milestone payments.
- The "all-inclusive" model, where the price of the chiral ligand includes not only the manufacturing but also the IP license costs.

The classical royalty model has long been the norm, and is still well accepted for the manufacture of fine chemicals or commodities where the production costs are a very significant part of the final price of the product. However, our experience is that this model is not well accepted in the Life Science Industry and often presents a real hurdle for the application of proprietary technology for the production of new chemical entities. The "all-inclusive" model takes care of these concerns, and allows the customer to compare competing solutions on the basis of actual costs as well as of their potential for improvement. The same is true for volume-independent payments, and for both methods all process improvements totally benefit the customer's bottom line and are not reduced by increasing royalty fees.

37.10
Conclusions and Future Developments

Is homogeneous asymmetric hydrogenation a mature manufacturing technology? The answer is clearly "NOT YET" – with, perhaps, the exception of a few privileged substrate types. Our definition of a mature manufacturing technology can be summarized as follows:

- Well-defined and widely known scope and limitations (selectivity, activity, productivity, functional group tolerance).
- Many existing technical applications; required equipment widely available.
- Routinely considered in route design during process R&D.

- Relevant catalysts and auxiliaries are commercially available (including well-defined handling of IP issues), both in large numbers for screening as well as in technical quantities for production.

The results summarized in the preceding sections show, even for asymmetric hydrogenation, the most advanced catalytic methodology, that some of these points must be answered by "not quite" or "not yet satisfactory". However, we have the impression that during the past few years technical progress has accelerated, with one of the most significant signs of this development being the growing number of companies active in this exciting area of chemical technology. The visibility of enantioselective hydrogenation as a superb manufacturing tool for chiral intermediates and active products will certainly be enhanced not only by these companies scientific/technical publications but also by their considerable marketing efforts.

Since the first production processes were implemented by Monsanto and Sumitomo in the early 1970s, the number of production processes has grown rather slowly and comprises today (only) about 15 to 20 entries. Of these, 11 are medium to large scale, while all of the others are applied on a scale of 1 t y^{-1} or less, and several of them are no longer in operation. On the positive side, many more processes developed to the pilot or bench scale are, in principle, ready for technical application.

There are several reasons for this rather slow progress. Perhaps the most important reason is the fact that many development chemists are not familiar with the progress made in enantioselective catalysis. In many cases, catalytic methods would be competitive or even superior to classical methods, but they are not considered during synthesis planning. Because it takes more time (and money!) to identify and develop a suitable catalyst, the very tight time schedule and the very high attrition rate for new chemical entities in the pharmaceutical industry also is an obstacle. Another reason is the unfortunate fact that many reports on catalytic chemistry deal only with monofunctional model substrates, and often do not provide information on TON and TOF values. And last but not least, with the exception of the monodentate ligands based on binol and analogues thereof, many of the chiral ligands are not trivial to prepare. Furthermore, several very effective ligands have not been readily available in large quantities.

We are convinced that in the near future the industrial application of enantioselective hydrogenation technology will accelerate further, and there are several points to strengthen this view. There is the usual time lag for any new technology to be used in actual production – we think (or hope!) that we are at present on the flat part of the classical S-shaped curve. As the compilation in Section 37.9.1 shows, an increasing number of medium- and small-sized companies now have expertise in developing catalytic syntheses and offer their services to those companies which cannot – or do not want to – develop such processes in-house. In addition, several companies now offer chiral ligands or catalysts in the quantities required for large-scale processes.

On the chemical side, there is no doubt that new and more selective and active catalysts will be developed for ever-more types of transformations. Hopefully, some

of these will belong to the small elite group of privileged catalysts, able to tolerate significant structural variations without loss in catalyst performance. In addition, high-throughput experimentation will in many cases allow more tests to be carried out, thereby shortening the time needed to identify the correct catalyst.

Acknowledgments

The authors thank their many colleagues and friends in the industrial catalytic community for their willingness to give advice and to share the invaluable information cited as personal comments in the references.

Abbreviations

de	diastereomeric excess
ee	enantiomeric excess
HTS	high-throughput system
NCE	new chemical entity
r.t.	room temperature
SCR	substrate : catalyst ratio
TOF	turnover frequency
TON	turnover number
TPPTS	sulfonated triphenylphosphine

References

1 For a short overview, see H. U. Blaser, H. Steiner, M. Studer, in: C. Bolm, M. Beller (Eds.), *Transition Metals for Organic Synthesis*, 2nd edition. Wiley-VCH, Weinheim, **2004**, Vol. 2, p. 125.

2 (a) For details, see J.G. de Vries, in: I. T. Horvath (Ed.), *Encyclopedia of Catalysis*. Wiley, New York, **2003**, Vol. 3, p. 295; (b) *Chem. Eng. News* **2005**, *83*(25), Special issue on pharmaceuticals; http://pubs.acs. org/cen/coverstory/83/8325/8325ivermectin.html; (c) J. C. Chabala, M. H. Fisher, US 4199569, **1978** (assigned to Merck); (d) W. Cabri, Antibioticos, personal communication.

3 For an update, see M. Rouhi, *Chem. Eng. News* **2004**, *82*(24), 47.

4 G. M. Ramos Tombo, H. U. Blaser, in: G. T. Brooks, T. R. Roberts (Eds.), *Pesticide Chemistry and Bioscience*. Royal Society of Chemistry, Cambridge, **1999**, p. 33 and references cited therein.

5 R. Noyori, *Chemtech* **1992**, *22*, 366.

6 E. Polastro, in: G. Jannes, V. Dubois (Eds.), *Chiral Reactions in Heterogeneous Catalysis*. Plenum Press, New York, **1995**, p. 5.

7 D. Pauluth, A. E. F. Wächter, in: A. N. Collins, G. N. Sheldrake, J. Crosby (Eds.), *Chirality in Industry II*. John Wiley, **1997**, p. 263.

8 E. N. Jacobsen, H. Yamamoto, A. Pfaltz (Eds.), *Comprehensive Asymmetric Catalysis*. Springer, Berlin, **1999**, p. 1309. (a) R. Schmid, M. Scalone, *ibid*, p. 1439.

9 I. Ojima (Ed.), *Catalytic Asymmetric Synthesis*. Wiley-VCH, New York, **2000**.

10 H. U. Blaser, Ch. Malan, B. Pugin, F. Spindler, H. Steiner, M. Studer, *Adv. Synth. Catal.* **2003**, *345*, 103.

11 T.T.-L. Au-Yeung, A.S.C. Chan, *Coord. Chem. Rev.* **2004**, *248*, 2151.
12 W. Tang, X. Zhang, *Chem. Rev.* **2003**, *103*, 3029.
13 P. Barbaro, C. Bianchini, G. Giambastiani, S.L. Parisel, *Coord. Chem. Rev.* **2004**, *248*, 2131.
14 H.U. Blaser, F. Spindler, M. Studer, *Applied Catalysis A: General* **2001**, *221*, 119.
15 H.U. Blaser, E. Schmidt (Eds.), *Large Scale Asymmetric Catalysis.* Wiley-VCH, Weinheim, **2003**.
16 H. Kumobayashi, T. Miura, N. Sayo, T. Saito, X. Zhang, *Synlett* **2001**, 1055.
17 I.C. Lennon, P.H. Moran, *Curr. Opin. Drug Discovery Dev.* **2003**, *6*, 855.
18 I.C. Lennon, C.J. Pilkington, *Synthesis* **2003**, 1639.
19 T. Iida, T. Mase, *Curr. Opin. Drug Discovery Dev.* **2002**, *5*, 834.
20 M. Ikunaka, *Chem. Eur. J.* **2003**, *9*, 379.
21 M. Breuer, K. Ditrich, T. Habicher, B. Hauer, M. Kessler, R. Stürmer, T. Zelinski, *Angew. Chem. Int. Ed.* **2004**, *43*, 788.
22 R.A. Sheldon, *Chirotechnology.* Marcel Decker, Inc., New York, **1993**.
23 H.U. Blaser, B. Pugin, F. Spindler, *J. Mol. Catal. A: Chemical* **2005**, *231*, 1.
24 A very restrictive policy is described in J.M. Hawkins, T.J.N. Watson, *Angew. Chem. Int. Ed.* **2004**, *43*, 3224.
25 T.-Y. Yue, W.A. Nugent, *J. Am. Chem. Soc.* **2002**, *124*, 13692.
26 J.G. de Vries, A.H.M. de Vries, *Eur. J. Org. Chem.* **2003**, 799; C. Gennari, U. Piarulli, *Chem. Rev.* **2003**, *103*, 3071.
27 For a detailed discussion see F. Spindler, H.U. Blaser, *Enantiomer* **1999**, *4*, 557.
28 (a) W.S. Knowles, *Angew. Chem. Int. Ed.* **2002**, *41*, 1998. Earlier publications: W.S. Knowles, *Chem. Ind. (Dekker) (Catal. Org. React.)* **1996**, *68*, 141; *Acc. Chem. Res.* **1983**, *16*, 106 and *J. Chem. Ed.* **1986**, *63*, 222.
29 R. Selke, in: H.U. Blaser, E. Schmidt (Eds.), *Large Scale Asymmetric Catalysis.* Wiley-VCH, Weinheim, **2003**, p. 39.
30 D.J. Ager, S.A. Lanemann, in: H.U. Blaser, E. Schmidt (Eds.), *Large Scale Asymmetric Catalysis.* Wiley-VCH, Weinheim, **2003**, p. 259.
31 M. Adamczyk, S.R. Akireddy, R.E. Reddy, *Org. Lett.* **2000**, *2*, 3421.
32 M. Fiorini, M. Riocci, M. Giongo, EP 077 099, assigned to Anic S.p.A. (1982). Described in Ref. 40 and in I. Ojima, N. Clos, C. Bastos, *Tetrahedron* **1989**, *45*, 6901.
33 O. Piccolo, personal communication.
34 J.G. Andrade, G. Prescher, *Chem. Ind. (Dekker) (Catal. Org. React.)* **1989**, *40*, 33.
35 M.J. Burk, Chirotech, personal communication.
36 C.J. Cobley, N.B. Johnson, I.C. Lennon, R. McCague, J.A. Ramsden, A. Zenotti-Gerosa, in: H.U. Blaser, E. Schmidt (Eds.), *Large Scale Asymmetric Catalysis.* Wiley-VCH, Weinheim, **2003**, p. 269.
37 J. Hiebl, H. Kollmann, F. Rovenszky, K. Winkler, *J. Org. Chem.* **1999**, *64*, 1947
38 H.U. Blaser, F. Spindler, *Topics in Catalysis* **1997**, *4*, 275.
39 J. Singh, D.R. Kronenthal, M. Schwinden, J.D. Godfrey, R. Fox, E.J. Vawter, B. Zhang, T.P. Kissick, B. Patel, O. Mneimne, M. Humora, C.G. Papaloannou, W. Szymanski, M.K.Y. Wong, C.K. Chen, J.E. Helkes, J.D. DiMarco, J. Qiu, R.P. Deshpande, J.Z. Gougoutas, R.H. Mueller, *Org. Lett.* **2003**, *5*, 3155.
40 W. Brieden, in: *Proceedings of the Chiral USA '97 Symposium*, Spring Innovation, Stockport UK, **1997**, p. 45.
41 W. Brieden, in: *Proceedings of the ChiraSource '99 Symposium.* The Catalyst Group, Spring House, USA, **1999**.
42 J.F. McGarrity, W. Brieden, R. Fuchs, H.-P. Mettler, B. Schmidt, O. Werbitzky, in: H.U. Blaser, E. Schmidt (Eds.), *Large Scale Asymmetric Catalysis.* Wiley-VCH, Weinheim, **2003**, p. 283.
43 R. Fuchs, EP 803502, **1996** (assigned to Lonza AG).
44 C.S. Shultz, S.D. Dreher, N. Ikemoto, J.M. Williams, E.J.J. Grabowski, S.W. Krska, Y. Sun, P.G. Dormer, L. DiMichele, *Org. Lett.* **2005**, *7*, 3405.
45 N.W. Boaz, S.D. Debenham, S.E. Large, M.K. Moore, *Tetrahedron: Asymmetry* **2003**, *14*, 3575.
46 G. Beck, Synlett, **2002**, 837.
47 X. Zhang, *Chim. Oggi/Chem. Today* **2004**, *22*(5), Supplement on Chiral Catalysis, 10.
48 F. Spindler, C. Malan, M. Lotz, M. Kesselgruber, U. Pittelkow, A. Rivas-Nass,

O. Briel, H. U. Blaser, *Tetrahedron: Asymmetry* **2004**, *15*, 2299.
49 N. W. Boaz, E. B. Mackenzie, S. D. Debenham, S. E. Large, J. A. Ponasik, *J. Org. Chem.* **2005**, *70*, 1872.
50 H.-J. Drexler, J. You, S. Zhang, C. Fischer, W. Baumann, A. Spanneberg, D. Heller, *Org. Process Res. Develop.* **2003**, *7*, 355 and references cited therein. D. Peña, A. J. Minnaard, J. G. de Vries, B.L. Feringa, *J. Am. Chem. Soc.*, **2002**, *124*, 14552.
51 Y. Hsiao, N. R. Rivera, T. Rosner, S. W. Krska, E. Njolito, F. Wang, Y. Sun, J. D. Armstrong, E. J. J. Grabowski, R. D. Tillyer, F. Spindler, C. Malan, *J. Am. Chem. Soc.* **2004**, *126*, 9918.
52 M. Rouhi, *Chem. Eng. News* **2004**, *82*(37), 28.
53 (a) K. Matsumura, X. Zhang, Xiaoyong, T. Saito, EP 1386901, **2005** (assigned to Takasago); (b) M. Sodeoka, Y. Hamashima, WO 2005016866 A2, **2005** (assigned to Takasago); (c) K. Matsumura, X. Zhang, Xiaoyong, T. Saito, US 0023344 A1, **2004** (assigned to Takasago).
54 T. Saito, Takasago, presentation at the 19th NACS meeting, Philadelphia, **2005** and personal communication.
55 M. Scalone, R. Schmid, E. A. Broger, W. Burkart, M. Cereghetti, Y. Crameri, J. Foricher, M. Henning, F. Kienzle, F. Montavon, G. Schoettel, D. Tesauro, S. Wang, R. Zell, U. Zutter, in: *Proceedings of the ChiraTech '97 Symposium*, **1997**.
56 L. Storace, L. Anzalone, P.N. Confalone, W. P. Davies, J. M. Fortunak, M. Giangiordano, J. J. Haley, K. Kamholz, H.-Y. Li, P. Ma, W. A. Nugent, R. L. Parson, P. J. Sheeran, C. E. Silverman, R. E. Waltermire, C. C. Wood, *Org. Process Res. Dev.* **2002**, *6*, 54.
57 M. D. Wallace, M. A. McGuire, M. S. Yu, L. Goldfinger, L. Liu, W. Dai, S. Shilcrat, *Org. Process Res. Dev.* **2004**, *8*, 738.
58 C. P. Ashcroft, S. Challenger, A. M. Derrick, R. Storey, N. M. Thomson, *Org. Process Res. Dev.* **2003**, *7*, 362.
59 C. J. Cobley, I. C. Lennon, C. Praquin, A. Zenotti-Gerosa, R. B. Appell, C.T. Goralski, A. C. Sutterer, *Org. Process Res. Dev.* **2003**, *7*, 407.
60 M. J. Burk, F. Bienewald, M. Harris, A. Zanotti-Gerosa, *Angew. Chem. Int. Ed.* **1998**, *37*, 1931.
61 J. Almena, A. Monsees, R. Kadyrov, T. H. Riermeier, B. Gotov, J. Holz, A. Börner, *Adv. Synth. Catal.* **2004**, *346*, 1263.
62 F. Rampf, *Proceedings Chiral USA* **2004**, Scientific Update, Mayfield, UK.
63 S. Akutagawa, *Topics in Catal.* **1997**, *4*, 271. S. Akutagawa, Takasago, personal communication.
64 T. Netscher, M. Scalone, R. Schmid, in: H. U. Blaser, E. Schmidt (Eds.), *Large Scale Asymmetric Catalysis*. Wiley-VCH, Weinheim, **2003**, p. 71.
65 X. Zhang, Proceedings Chiral USA **2004**, Scientific Update, Mayfield, UK.
66 S. Akutagawa, *Appl. Catal.* **1995**, *128*, 171.
67 M. Bänziger, J. Cercus, H. Hirt, K. Laumen, C. Malan, F. Spindler, F. Struber, T. Troxler, *Tetrahedron: Asymmetry* **2003**, *14*, 3469.
68 F. Bonifacio, D. Macinetti, C. Crescenti, G. De Iasi, M. Donnarumma, C. Mastrangeli, *PharmaChem* **2003**, *2*(11/12), 13.
69 H. Kumobayashi, *Recl. Trav. Chim. Pays-Bas* **1996**, *115*, 201.
70 P. J. Harrington, E. Lodewijk, *Org. Process Res. Dev.* **1997**, *1*, 72.
71 T. Benincori, S. Rizzo, F. Sannicolò, O. Piccolo, in: *Proceedings of the ChiraSource 2000 Symposium*, **2000**, The Catalyst Group, Spring House, USA.
72 Y. Crameri, J. Foricher, U. Hengartner, C. J. Jenny, F. Kienzle, H. Ramuz, M. Scalone, M. Schlageter, R. Schmid, S. Wang, *Chimia* **1997**, *51*, 303.
73 R. Schmid, E. A. Broger, in: *Proceedings of the ChiralEurope '94 Symposium*, **1994**, Spring Innovation, Stockport, UK, p. 79.
74 T. Sturm, W. Weissensteiner, F. Spindler, *Adv. Synth. Catal.* **2003**, *345*, 160.
75 F. Spindler, Solvias AG, unpublished results.
76 (a) R. Hoen, J. A. F. Boogers, H. Bernsmann, A. J. Minnaard, A. Meetsma, T. D. Tiemersma-Wegman, A. H. M. de Vries, J. G. de Vries, B. L. Feringa, *Angew. Chem. Int. Ed.* **2005**, *44*, 4209; (b) A. H. M. de Vries, L. Lefort, J. A. F. Boogers, J. G. de Vries, D. J. Ager, *Chim. Oggi/Chem. Today* **2005**, *23*(3), Supplement on Chiral Technologies, 18.

77 M.A. McGuire, S.C. Shilcrat, E. Sorenson, *Tetrahedron Lett.* **1999**, *40*, 3293.
78 T. Ikemoto, T. Nagata, M. Yamano, T. Ito, Y. Mizuno, K. Tomimatsu, *Tetrahedron Lett.* **2004**, *45*, 7757. T. Yamano, Takeda Chemical Ind., personal communication.
79 M. Burk, F. Bienewald, S. Challenger, A. Derrick, J.A. Ramsden, *J. Org. Chem.* **1999**, *64*, 3290.
80 M. Bulliard, B. Laboue, J. Lastennet, S. Roussiane, *Org. Process Res. Dev.* **2001**, *5*, 438.
81 R. Imwinkelried, *Chimia* **1997**, *51*, 300.
82 V. Rautenstrauch, in: *Proceedings of the International Symposium on Chirality*, September 5–7, **1999**, Cambridge. Spring Innovation, Stockport, UK, p. 204.
83 D.A. Dobbs, K.P.M. Vanhessche, E. Brazi, V. Rautenstrauch, J.-Y. Lenoir, J.-P. Genêt, J. Wiles, S.H. Bergens, *Angew. Chem. Int. Ed.* **2000**, *39*, 1992. D. Dobbs, K. Vanhessche, V. Rautenstrauch, WO 98/52 687, **1997** (assigned to Firmenich).
84 M.J. Burk, *Acc. Chem. Res.* **2000**, *33*, 363.
85 B.D. Hewitt, Pharmacia & Upjohn. *Chem. Eng. News* **1999**, *77*(44), 35.
86 F.D. Klingler (Boehringer-Ingelheim) and A. Börner (University of Rostock), personal communication. F.D. Klingler, M. Steigerwald, R. Ehlenz, DE 103 13 118 A1, **2003** (assigned to Boehringer-Ingelheim).
87 M.J. Burk, P.D. de Koning, T.M. Grote, M.S. Hoekstra, G. Hoge, R.A. Jennings, W.S. Kissel, T.V. Le, I.C. Lennon, T.A. Mulhern, J.A. Ramsden, R.A. Wade, *J. Org. Chem.* **2003**, *68*, 5731.
88 G. Hoge, *J. Am. Chem. Soc.* **2003**, *125*, 10219.
89 K. Fukatsu, O. Uchikawa, M. Kawada, T. Yamano, M. Yamashita, K. Kato, K. Hirai, S. Hinuma, M. Miyamoto, S. Ohkawa, *J. Med. Chem.* **2002**, *45*, 4212.
90 E. Broger, Y. Crameri, P. Jones, WO 99/01 453, **1997** (assigned to Hoffmann-La Roche).
91 L.T. Boulton, I.C. Lennon, R. McCague, *Org. Biomol. Chem.* **2003**, *1*, 1094.
92 (a) For a recent account, see R. Noyori, M. Kitamura, T. Ohkuma, *Proc. Natl. Acad. Sci. USA* **2004**, *101*, 5356; (b) H. Kumobayashi, *Recl. Trav. Chim. Pays-Bas* **1996**, *115*, 201.
93 M. Saito, T. Yokozawa, T. Ishizaki, T. Moroi, N. Sayo, T. Miura, H. Kumobayashi, *Adv. Synth. Catal.* **2001**, *343*, 264.
94 F.D. Klingler (Boehringer-Ingelheim) personal communication. F.D. Klingler, L. Wolter, W. Dietrich, EP 1 147 075, **1999** (assigned to Boehringer-Ingelheim); F.D. Klingler, L. Wolter, EP 1 210 318, **1999** (assigned to Boehringer-Ingelheim).
95 M. Scalone, P. Waldmeier, *Org. Process Res. Dev.* **2003**, *7*, 418.
96 H.U. Blaser, R. Gamboni, G. Rihs, G. Sedelmeier, E. Schaub, E. Schmidt, B. Schmitz, F. Spindler, H.-J. Wetter, in: K.G. Gadamasetti (Ed.), *Process Chemistry in the Pharmaceutical Industry*. Marcel Dekker, Inc., New York, **1999**, p. 189.
97 G. Penn (Novartis), F. Spindler (Solvias), unpublished.
98 A. Lei, S. Wu, M. He, X. Zhang, *J. Am. Chem. Soc.* **2004**, *126*, 1626.
99 H.U. Blaser, M. Eissen, P.F. Fauquex, K. Hungerbühler, E. Schmidt, G. Sedelmeier, M. Studer, in: H.U. Blaser, E. Schmidt (Eds.), *Large Scale Asymmetric Catalysis*. Wiley-VCH, Weinheim, **2003**, p. 91.
100 F. Cederbaum, C. Lamberth, C. Malan, F. Naud, F. Spindler, M. Studer, H.U. Blaser, *Adv. Synth. Catal.* **2004**, *346*, 842.
101 R. Noyori, M. Tokunago, M. Kitamura, *Bull. Chem. Soc. Jpn.* **1995**, *68*, 36.
102 T. Benincori, E. Cesarotti, O. Piccolo, A. Sannicolò, *J. Org. Chem.* **2000**, *65*, 2043.
103 D. Ager, S. Lanemann, NSC Technologies, personal communication.
104 H. Hugl, Lanxess, personal communication.
105 A. Gerlach, U. Scholz, *Specialty Chemicals Magazine* **2004**, *24*(4), 37.
106 J.D. Armstrong, in: *Proceedings of the ChiraTech '96 Symposium*, **1996**, The Catalyst Group, Spring House, USA.
107 V. Vidal, J.P. Genêt, personal communication. S. Jenlin, N. Champion, P. Dellis, V. Ratovelomanana-Vidal, J.-P. Genêt, *Synthesis*, **2005**, 3666.
108 D. Liu, W. Gao, C. Wang, X. Zhang, *Angew. Chem. Int. Ed.* **2005**, *44*, 1687.

109 D. Chaplin, P. Harrington, J.P. Henschke, I.C. Lennon, G. Meck, P. Moran, C.J. Pilkington, J.A. Ramsden, S. Warkins, A. Zenotti-Gerosa, *Org. Process Res. Dev.* **2003**, *7*, 89.

110 I.C. Lennon, C.J. Pilkington, *Synthesis* **2003**, 1639.

111 I.C. Lennon, P. Moran, *Chim. Oggi/Chem. Today* **2004**, *22*(5), Supplement on Chiral Catalysis, 37.

112 D. Geffroy, F. Hancock, W.P. Hems, A. Zanotti-Gerosa, *Chim. Oggi/Chem. Today* **2004**, *22*(5), Supplement on Chiral Catalysis, 41. A. Zanotti-Gerosa, M. Groarke, W.P. Hems, *Chem. Spec. Mag.* **2004**, December p. 42.

113 J. Wu, H. Chen, W. Kwok, R. Guo, Z. Zhou, C-H. Yeung, A.S.C. Chan, *J. Org. Chem.* **2002**, *67*, 7908. J. Wu, J.-X. Ji, R. Guo, C.-H. Yeung, A.S.C. Chan, *Eur. J. Chem.* **2003**, *9*, 2963.

114 F. Naud, C. Malan, F. Spindler, C. Rüggeberg, A.T. Schmidt, H.U. Blaser, *Adv. Synth. Catal.* **2006**, *348*, 47.

115 J. Blacker, J. Martin, in: H.U. Blaser, E. Schmidt (Eds.), *Large Scale Asymmetric Catalysis*. Wiley-VCH, Weinheim, **2003**, p. 201.

116 H. Yamashita, T. Ohtani, S. Morita, K. Otsubo, K. Kan, J. Matsubara, K. Kitano, Y. Kawano, M. Uchida, F. Tabusa, *Heterocycles* **2002**, *56*, 123.

117 K.B. Hansen, J.R. Chilenski, R. Desmond, P.N. Devine, E.J.J. Grabowski, R. Heid, M. Kubryk, D.J. Mathre, R. Varsolona, *Tetrahedron: Asymmetry* **2003**, *14*, 3581.

118 M. Miyaga, J. Takehara, S. Collet, K. Okano, *Org. Process Res. Dev.* **2000**, *4*, 346.

119 W. Brieden, WO 9616971, **1994** (assigned to Lonza AG). W. Brieden, Lonza, personal communication.

120 K.M.J. Brands, J.F. Payack, J.D. Rosen, T.D. Nelson, A. Candelario, M.A. Huffman, M.M. Zhao, J. Li, B. Craig, Z.J. Song, D.M. Tschaen, K. Hansen, P.N. Devine, P.J. Pye, K. Rossen, P.G. Dormer, R.A. Raemer, C.J. Welch, D.J. Mathre, N.N. Tsou, J.M. McNamara, P.J. Reider, *J. Am. Chem. Soc.* **2003**, *125*, 2129.

121 J.W. Hilborn, Z.-H. Lu, A.R. Jurgens, Q.K. Fang, P. Byers, S.A. Wald, C.H. Senanayake, *Tetrahedron Lett.* **2001**, *42*, 8919.

122 H.S. Wilkinson, G.J. Tanoury, S.A. Wald, C.H. Senanayake, *Org. Process Res. Dev.* **2002**, *6*, 146.

123 T. Nagata, *Specialty Chemicals Magazine*, **2002**, *22*(6), 34.

124 F. Spindler, H.U. Blaser, in: C. Bolm, M. Beller (Eds.), *Transition Metals for Organic Synthesis*. Wiley-VCH, Weinheim, 2nd edition, Vol. 2, **2004**, p. 113.

125 H.U. Blaser, H.P. Buser, K. Coers, R. Hanreich, H.P. Jalett, E. Jelsch, B. Pugin, H.D. Schneider, F. Spindler, A. Wegmann, *Chimia* **1999**, *53*, 275.

126 H.U. Blaser, *Adv. Synth. Catal.* **2002**, *344*, 17.

127 H.U. Blaser, R. Hanreich, H.-D. Schneider, F. Spindler, B. Steinacher, in: H.U. Blaser, E. Schmidt (Eds.), *Large Scale Asymmetric Catalysis*. Wiley-VCH, Weinheim, **2003**, p. 55.

128 K. Satoh, M. Inenaga, K. Kanai, *Tetrahedron: Asymmetry* **1998**, *9*, 2657.

129 C.J. Cobley, J.P. Henschke, *Adv. Synth. Catal.* **2003**, *345*, 195.

130 C.J. Cobley, E. Foucher, J.-P. Lecouve, I.C. Lennon, J.A. Ramsden, G. Thominot, *Tetrahedron: Asymmetry* **2003**, *14*, 3431.

131 H.U. Blaser, *Chim. Oggi/Chem. Today* **2004**, *22*(5), Supplement on Chiral Catalysis, 4.

132 G. Casey, N.B. Johnson, I.C. Lennon, *Chim. Oggi/Chem. Today* **2003**, *21*(12), 63.

133 M. Thommen, H.U. Blaser, *Chim. Oggi/Chem. Today* **2003**, *21*(12), 6.

134 M. Thommen, H.U. Blaser, *Chim. Oggi/Chem. Today* **2003**, *21*(12), 27.

135 T.H. Riermeier, A. Monsees, J. Holz, A. Börner, *Chim. Oggi/Chem. Today* **2004**, *22*(5), Supplement on Chiral Catalysis, 22. www.catallium.com.

136 see www.digitalchem.com.

137 M. van den Berg, D. Peña, A.J. Minnaard, L. Lefort, J.A.F. Boogers, A.H.M. de Vries, J.G. de Vries, *Chim. Oggi/Chem. Today* **2004**, *22*(5), Supplement on Chiral Catalysis, 18.

138 J. G. Strong, *PharmaChem* **2003**, *2*(6), 20.
139 L. Pinchard, *PharmaChem* **2003**, *2*(6), 23.
140 M. Buillard, *Specialty Chemicals Magazine* **2004**, *24*(9), 20.
141 H. U. Blaser, M. Thommen, *Chim. Oggi/Chem. Today* **2004**, *22*(5), Supplement on Chiral Catalysis, 6.
142 H. Shimizu, I. Nagasaki, T. Saito, *Tetrahedron* **2005**, *61*, 5405.
143 C. Le Ret, O. Briel, *Chim. Oggi/Chem. Today* **2004**, *22*(5), Supplement on Chiral Catalysis, 29.
144 A. Rivas-Nass, O. Briel, *Chim. Oggi* **2003**, *21*(12), 58.
145 *Chim. Oggi/Chem. Today* **2004**, *22*(5), Supplement on Chiral Catalysis.

Part V
Phase Separation in Homogeneous Hydrogenation

The Handbook of Homogeneous Hydrogenation.
Edited by J.G. de Vries and C.J. Elsevier
Copyright © 2007 WILEY-VCH Verlag GmbH & Co. KGaA, Weinheim
ISBN: 978-3-527-31161-3

38
Two-Phase Aqueous Hydrogenations

Ferenc Joó and Ágnes Kathó

38.1
Introduction

When a catalytic reaction is carried out in a mixture of two immiscible liquids it is often possible to separate the catalyst and the products (together with the unreacted starting materials) into the two liquid phases formed when stirring is stopped. Such two-phase catalytic processes retain all of the advantages of homogeneous catalysis (efficient use of the molecularly dispersed catalyst, high selectivity, possibility of tailoring the catalyst to the particular substrate by modification of the ligand environment) and combine those with the ease of recovery of a heterogeneous catalyst [1–4]. There are several organic solvents, which have limited miscibility with water and – in principle – these are suitable for two-phase catalysis. (Similarly, there are also water-immiscible ionic liquids (ILs) and supercritical fluids (SCFs), but in the general discussion aqueous-organic biphasic mixtures are used as examples.) Liquid organic substrates may form separate phases themselves. For an efficient recovery, the catalyst must be insoluble in one of the phases which, in turn, should preferentially dissolve the substrates and products. In general – though not always – the substrates and products of a catalyzed reaction are not especially soluble in water and partition to the organic phase (Scheme 38.1, A). In such cases, strongly hydrophilic catalysts are used, while for water-soluble substrates the catalyst should be dissolved in a water-immiscible organic solvent (Scheme 38.1, B). Ideally, the interaction of the catalyst with the substrates and products will not change its solubility properties and no leaching of the catalyst to the other phase takes place.

Water is a highly polar – and hence protic – solvent, the presence of which may strongly influence the chemistry of two-phase aqueous processes. Of course, all components of the reaction mixture should be stable to water, and to this end care must be taken with the choice of catalyst. Today, aqueous organometallic catalysis has become a mature field of chemistry, and a very wide choice of water-soluble and water-stable hydrogenation catalysts is available. It should also be borne in mind that water is a reactive solvent and may take part

The Handbook of Homogeneous Hydrogenation.
Edited by J.G. de Vries and C.J. Elsevier
Copyright © 2006 WILEY-VCH Verlag GmbH & Co. KGaA, Weinheim
ISBN: 3-527-31161-0

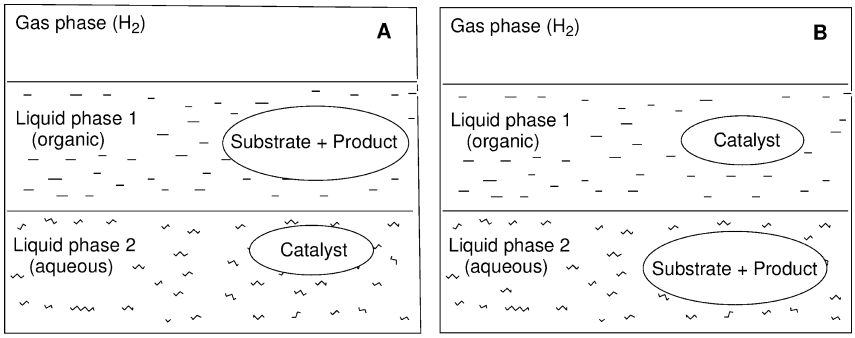

Scheme 38.1 General arrangements in aqueous two-phase hydrogenations.

in proton exchange, hydration, telomerization and so forth as side reactions to hydrogenation. Engineering aspects are also important. In practice, the two liquids are not completely "immiscible" but have limited miscibility in each other. For example, the solubility of ethyl acetate in water at 20 °C is 6.1 wt.%, while that of water in EtOAc is 3.3 wt.%. Very similar numbers were determined for Et_2O in H_2O (6.9 wt.%) and H_2O in Et_2O (3.3 wt.%). (For other mutual miscibility data with water as one of the phases, see [5] and for general solvent properties [6].) Usually, saturation of both liquids with the other component of the biphasic mixture does not lead to appreciable volume changes when the catalyzed reaction takes place in a batch reactor. However, in a flow system the mobile phase (the solution of the substrates and products) may gradually carry away the solvent of the catalyst-containing stationary phase. The solubility of hydrogen in water (0.81 mM at 20 °C) is somewhat less than in the common organic solvents (e.g., in methanol 3.75 mM, benzene 2.94 mM, toluene 3.50 mM; all data at 20 °C) [7]. Lower concentrations of dissolved H_2 usually lead to lower reaction rates, but it has also been shown [8] that the selectivity of a catalytic hydrogenation may be strongly influenced by the hydrogen pressure – that is, by the concentration of dissolved hydrogen.

Since the overwhelming majority of the important substrates of hydrogenation are insoluble in water, it is the catalyst that should be applied in the aqueous phase. Some of the catalysts are water-soluble due to their ionic nature, such as $[Co(CN)_5]^{3-}$, or the chloro-aqua complexes of ruthenium(III) or rhodium (III) obtained by dissolution of $RuCl_3 \cdot aq$ or $RhCl_3 \cdot aq$ in aqueous hydrochloric acid. However, by far the most common approach is the solubilization of well-known transition metal-based hydrogenation catalysts by substitution of their tertiary phosphine (or other) ligands with analogous but highly water-soluble ligands. The best-known examples are the mono- and trisulfonated triphenylphosphines (3-diphenylphosphinobenzenesulfonic acid, *m*tppms, and 3,3′,3″-phosphinetriylbenzenesulfonic acid, *m*tppts, respectively) (Scheme 38.2). Functionalization with alkylene sulfate, phosphonate, carboxylate, ammonium, and phosphonium groups is also used for making phosphine ligands water-soluble.

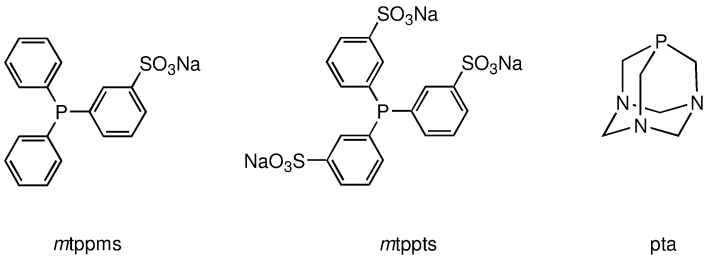

Scheme 38.2 Frequently used water-soluble tertiary phosphines.

Some phosphines are easily soluble in water due to their strong hydrogen-bonding capacity. Representatives of these ligands are 1,3,5-triaza-7-phosphaadamantane (pta), the polyoxyethylene-substituted and the carbohydrate-derived phosphines. A detailed compilation of water-soluble phosphines (together with the known solubilities) can be found in [4].

Catalytic hydrogenation is an important synthetic process, but studies on such reactions of simple olefins were frequently performed with the aim of characterizing new catalysts. Many of these investigations were carried out in homogeneous aqueous solutions and therefore fall outside the scope of this chapter. Nevertheless, important conclusions could be drawn with regard to the mechanisms of hydrogenations catalyzed by transition metal complexes in water. Water, as a polar solvent, may stabilize polar transition states and in doing so may facilitate the activation of dihydrogen. Strong hydration of H^+ makes the energetics of heterolytic splitting of H_2 comparable to that of its homolytic activation [9]. The balance of these two processes – that is, the formation of monohydrido- or/and dihydrido-complexes – is strongly influenced by the pH of the aqueous solutions [10, 11]. These mechanistic features of dihydrogen activation have their consequences in the reaction rates and selectivities of the catalyzed hydrogenations.

Several books [1–4, 12] and reviews [13–20] are available on transition metal complex-catalyzed hydrogenations in aqueous systems, but only a few cover biphasic aqueous processes specifically. In the following sections of this chapter, only two-phase reactions are described, which have been arranged according to the functional groups involved in the hydrogenation. Most of the results are compiled into tables and are not discussed individually in the text. The catalytic activities are expressed as *turnover frequencies* (TOF, h^{-1}) defined as mole reacted substrate (mol catalyst · h)$^{-1}$. In most cases, TOF values were calculated from the experimental conditions (conversion, reaction times, concentrations) given in the original paper, and often represent the lowest limit of the catalytic activity.

Table 38.1 Aqueous-organic two-phase achiral hydrogenation of alkenes.

Entry	Catalyst	Substrate	TOF [h^{-1}]	Solvent, conditions and remarks	Reference
1	[RhCl(*m*tppms)$_3$][a)]	1-hexene	38.1	H_2O, 25 °C, 3 bar H_2	21
		cyclohexene	9.1		
2	$RhCl_3$ + *m*tppms, 1:3	1-octene	85	H_2O/benzene, 35 °C, P_{tot} = 1 bar	22
3	$RhCl_3$ + *m*tppms, 1:6	cyclohexene	50	H_2O, 50 °C, P_{tot} = 1 bar, co-solvents	23
4	[{RhCl(COD)}$_2$] + DSPrPE,[b),c)] 1:1.5	1-hexene	up to 25	H_2O/THF 6/1, 60 °C, 3.5 bar H_2	24
5	[{RhCl(COD)}$_2$] + DHPrPE,[d)] 1:1.5	1-hexene	up to 25	H_2O/THF 6/1, 60 °C, 3.5 bar H_2	24
6	[{RhCl(COD)}$_2$]	1-hexene	220	H_2O, r.t., P_{tot} = 1 bar	25
	+ $Ph_2P(CH_2)_2CONHC(CH_3)_2CH_2SO_3Li$	1-octene	76		
		cyclopentene	48		
		cyclohexene	60		
		cyclooctene	40		
		carvone	36	both double bonds are hydrogenated	
		limonene	21	both double bonds are hydrogenated	
7	[RhCl(pta)$_3$][e)]	allylbenzene		H_2O, 50 °C, P_{tot} = 1 bar	26
		cinnamaldehyde			
8	[Rh(NO)(*m*tppts)$_3$][f)]	cyclohexene	2.8	H_2O, 25 °C, 1 bar H_2	27
		cyclohexene	1.0	H_2O/*i*PrOH, 25 °C, 1 bar H_2	
		cyclooctene	2.7	H_2O, 25 °C, 1 bar H_2	
9	[Rh(acac)(CO)(PR_3)][g)]	1-hexene		H_2O, 30 °C, 1 bar H_2	28
	PR_3 = *m*tppts, pta, cyep[h)]	cyclohexene			
10	[Rh(amphos)(MeOH)$_2$]$^{3+}$ [i)]	1-hexene		H_2O/CH_2Cl_2, Et_2O,or *n*-pentane	29
		styrene		r.t., P_{tot} = 1 bar	
11	[Rh(NBD)(n-phophos)]$^{3+}$ [j), k)]	1-hexene	up to 150	H_2O/CH_2Cl_2 or Et_2O, 25 °C, 3 bar H_2	30
	n = 2, 3, 6, 10				

12	$[Rh(COD)_2][BF_4] + Na_2[Ph_2P(CH_2)_{12})PO_3]$, 1 : 3	1-decene		H_2O, r.t., P_{tot}=1 bar, metal deposition with 1-hexene and cyclohexene	31
13	$[RuHCl(m\text{tppms})_3]$	1-hexene	18.9	H_2O, 25 °C, 3 bar H_2	21
		cyclohexene	8.9		
14	$[RuCl_2(m\text{tppms})_2]$	1-hexene	18.0	H_2O, 30 °C, P_{tot}=1 bar	32
15	$[RuHCl(m\text{tppms})_3]$	styrene	10.8	H_2O, 60 °C, P_{tot}=1 bar	32
16	$[RuH(OAc)(m\text{tppms})_3]$	styrene	25.0	H_2O, 60 °C, P_{tot}=1 bar	32
17	$[RuHCl(CO)(m\text{tppms})_3]$	styrene	3.0	H_2O/decalin 1/1 100 °C, 70 bar H_2	33
		cyclohexene	1.1		
18	$[RuH(CO)(m\text{tppms})_3(CH_3CN)]^+$	1-hexene	10.5	H_2O/*n*-heptane 1/1, 80 °C, 28 bar H_2	34
		1-decene	3.0		
		cyclohexene	3.3		
		styrene	5.5		
19	$[Ru(H)_2(CO)(m\text{tppms})_3]$	1-hexene	6.8	H_2O/*n*-heptane 1/1, 100 °C, 28 bar H_2	35
		1-decene	5.1		
		cyclohexene	1.6		
		styrene	4.0		
20	$[Ru(CO)_3(m\text{tppms})_2]$	1-hexene	7.0	H_2O/*n*-heptane 1/1, 100 °C, 28 bar H_2	35
		1-decene	5.4		
		cyclohexene	1.8		
		styrene	4.0		
21	$[RuCl(Cp)(m\text{tppms})_2]$ [l)]	1-hexene	85	H_2O/toluene 1/1, 100 °C, 35 bar H_2	36
22	$[RuCl_2(m\text{tppms})_3(DMSO)]$ [m)]	1-hexene	98	H_2O/toluene 1/1, 80–100 °C, 35 bar H_2	37
		cyclohexene	64		
23	$[RuCl_2(DMSO)_4]$	1-hexene	82	H_2O, 80 °C, 28 bar H_2	38

Table 38.1 (continued)

Entry	Catalyst	Substrate	TOF [h^{-1}]	Solvent, conditions and remarks	Reference
24	$[RuCl(CO)(Cp^*)(PR_3)]$ [n)]	sorbic acid	up to 16	H_2O/*n*-heptane, 80 °C, 50 bar H_2	39
	$[Ru(CO)(Cp^*)(PR_3)][CF_3SO_3]$				
	$R=CH_2OH$, $(CH_2)_3OH$, C_6H_4-3-SO_3Na				
25	$[\{RuCl_2(PR_3)\}_2]$, $R=(CH_2)_3OH$	sorbic acid	192	H_2O/ethyl acetate, 80 °C, 50 bar H_2	40
26	$[Ru_3(CO)_{12-x}(m\text{tppms})_x]$, x = 1, 2, 3	1-octene	45–95	H_2O, 60 °C, 60 bar H_2	41
		1-decene	32		
		cyclohexene	39–252		
		styrene	490		
27	$[Ru(\eta^6\text{-}C_6H_6)(CH_3CN)_3]^{2+}$	1-octene	min. 250	H_2O/benzene, 110 °C, 40 bar H_2	42
		1-decene	min. 250		
		1-dodecene	min. 250		
		styrene	min. 250		
28	$[Ru(6,6'\text{-}Cl_2bipy)_2(H_2O)_2][CF_3SO_3]_2$ [o)]	1-octene	min. 500	H_2O, 130 °C, 40 bar H_2	43
		1-decene	min. 500		
		cyclohexene	430		
		styrene	min. 500		
29	$[RuCl(Cp)(pta)_2]$	benzylidene-acetone	9.5	H_2O/*n*-octane, 80 °C, 32 bar H_2, selective hydrogenation to 4-phenyl-butan-2-one	44
	$[RuCl(Cp^*)(pta)_2]$		2.6		45
	$[Ru\{Cp(CH_2)_2NEt_2\}(pta)_2][PF_6]$		2.4		
	$[Ru\{Cp(CH_2)_2NEt_2\}(pta)_2(MeCN)][PF_6]$		3.3		
	$[Ru(Cp)(pta)(CH_3CN)_2][PF_6]$		9.5		
	$[Ru(Cp)(pta)_2(CH_3CN)][PF_6]$		6.2		
	$[Ru(Cp^*)(pta)_2(CH_3CN)][PF_6]$		6.4		

30	$Na_3[RuCl(\eta^6\text{-arene})(dppbts)]$ [p)]	styrene		H_2O/substrate, 100 °C, 45 bar H_2	46
	arene = *p*-cymene [q)]		1100		
	arene = [2.2]-paracyclophane		2000		
31	$[Co_2(CO)_8(m\text{tppts})_2]$	cyclohexene	1.8	H_2O, 20 °C, 30 bar H_2	27
		1-decene	11.9	H_2O, 100 °C, 70 bar H_2/CO 1/1, no aldehyde formation	
32	$[W(CO)_3(m\text{tppms})_2(CH_3CN)]$	styrene	10	H_2O/*n*-heptane, 140 °C, 70 bar H_2, Et_2NH	47

a) *m*tppms = monosulfonated triphenylphosphine.
b) COD = 1,5-cyclooctadiene.
c) DSPrPE = C_2H_4-1,2-$[P(CH_2CH_2CH_2SO_3Na)_2]_2$.
d) DHPrPE = C_2H_4-1,2-$[P(CH_2CH_2CH_2OH)_2]_2$.
e) pta = 1,3,5-triaza-7-phosphaadamantane.
f) *m*tppts = trisulfonated triphenylphosphine.
g) acac = 2,4-pentanedionate.
h) cyep = $P(CH_2CH_2CN)_3$.
i) amphos = $[Ph_2PCH_2CH_2NMe_3][NO_3]$.
j) n-phophos = $[Ph_2P(CH_2CH_2)_nPMe_3][NO_3]$.
k) NBD = bicyclo[2.2.1]hepta-2,5-diene.
l) Cp = η^5-C_5H_5.
m) DMSO = $(CH_3)_2SO$.
n) Cp* = η^5-$C_5(CH_3)_5$.
o) bipy = 2,2′-bipyridine.
p) dppbts = C_6H_4-1,2-$[P(C_6H_4\text{-}4\text{-}SO_3)_2]_2$.
q) *p*-cymene = 4-isopropyltoluene.

38.2
Two-Phase Hydrogenation of Alkenes, Alkynes, and Arenes

Several copper, silver, ruthenium, rhodium, and cobalt compounds (e.g., $RuCl_3 \cdot aq$, $[RuCl_4(bipy)]^{2-}$ (bipy = 2,2′-bipyridine), $RhCl_3 \cdot aq$, *bis*(dimethylglyoximato)cobalt derivatives (cobaloximes), etc.) have been found to catalyze hydrogenations in aqueous solutions [9]. Although important for the early research into homogeneous catalysis, these catalysts did not gain synthetic significance.

Several examples of achiral biphasic hydrogenations are shown in Table 38.1. It can be seen, that the activity of the various phosphine complexes of precious metals rarely exceeds 100 h^{-1} under mild conditions. In many cases hydrogenation is accompanied by isomerization of the olefinic substrates.

$[CoH(CN)_5]^{3-}$ is readily formed under mild conditions from $Co(CN)_2$, KCN and H_2; [Eqs. (1) and (2)]. It is an active catalyst for the hydrogenation of a variety of unsaturated substrates, and in fact in the first documented examples of two-phase hydrogenations this catalyst was used [48, 49]. The catalysis suffers from several drawbacks such as rapid "aging" with a loss of activity, and the need to use highly basic aqueous solutions.

$$Co(CN)_2 + 3\,KCN \rightleftharpoons K_3[Co(CN)_5] \tag{1}$$

$$2\,K_3[Co(CN_5] + H_2 = 2\,K_3[CoH(CN)_5] \tag{2}$$

Conjugated dienes (such as 1,3-cyclohexadiene, cyclopentadiene, 2,4-hexadienoic-sorbic-acid) and polyenes can be selectively hydrogenated to monoenes; unactivated alkenes are totally unreactive [20]. Unfortunately, the possibilities for modification of the catalyst by ligand alteration or by the use of additives are very limited [50, 51].

The various isomeric hexenoic acids are useful starting materials for the production of fine chemicals, and the stereoselective hydrogenation of sorbic acid has attracted considerable interest. It was shown recently that this reaction could be catalyzed by $[Ru(CO)(Cp^*)(m\text{tppts})][CF_3SO_3]$ ($Cp^* = \eta^5\text{-}C_5Me_5$) in a water:*n*-heptane biphasic mixture to yield *trans*-3-hexenoic acid with up to 85% selectivity [39] (Scheme 38.3). Conversely, the use of $[\{RuCl_2(PR_3)_2\}_2]$ ($R = CH_2CH_2CH_2OH$) as catalyst precursor led to the selective formation of 4-hexenoic acid [40].

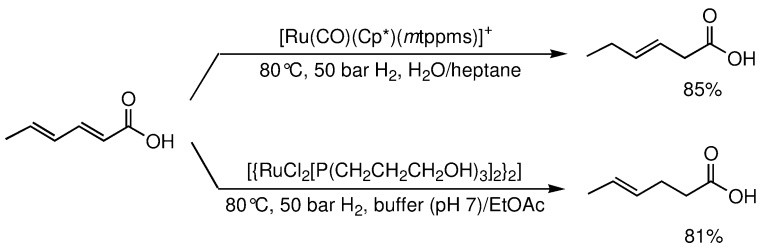

Scheme 38.3

Such selectivity changes were also observed on the effect of water. For example, the hydrogenation of 3,8-nonadienoic acid catalyzed by $[RhCl\{P(p\text{-tolyl})_3\}_3]$ in benzene (30 °C, 1 bar H_2, one phase) afforded 3-nonenoic acid (up to 75% selectivity), whereas in the presence of a separate aqueous phase 8-nonenoic acid was obtained with 98% selectivity [52]. It should be noted that, in this reaction, the catalyst was dissolved in the organic phase (see Scheme 38.1, B); in fact, the first report of aqueous two-phase catalysis with tertiary phosphine complexes of Rh(I) [23] also described the hydrogenation of butenediol (in the aqueous phase) catalyzed by $[RhCl(PPh_3)_3]$ dissolved in benzene. The organic solvent can also be replaced by a supercritical fluid dissolving the catalyst. Itaconic acid (in the aqueous phase) was hydrogenated with $[Rh(COD)_2][BF_4] + P(C_6H_4\text{-}3\text{-}CH_2CH_2C_6F_{13})_3$ dissolved in supercritical CO_2 ($scCO_2$) [53] (COD = 1,5-cycloctadiene). Since the catalyst is insoluble in water, there is no leaching when the aqueous phase is removed from the reactor and replaced by a fresh solution of the substrate.

In two-phase aqueous hydrogenations the catalyst and the substrates are found in the separate liquid phases, and the reaction rate depends on the solubility of the substrates in the catalyst-containing phase (or on the size of the interfacial area in case the reaction takes place at the phase boundaries). Mass transfer between the phases and interaction of the catalyst with the substrates can be facilitated by proper modification of the ligands, for example by attaching crown ether [54] or cyclodextrin [55] moieties to the tertiary phosphine ligands. $[\{RhCl(COD)\}_2]$ combined with 3n-diphenylphosphinobenzo-[3n-crown-n] ethers (n = 4, 5, 6, and 7; Scheme 38.4 a) showed high catalytic activities towards the catalytic hydrogenation of potassium and lithium cinnamates in water : benzene biphasic mixtures. At 30 °C, under 1 bar H_2 pressure, TOFs as high as 720 to 4440 h^{-1} were determined. The latter value is 50 times higher than that observed with $[\{RhCl(COD)\}_2] + PPh_3$ + benzo-[18-crown-6], and the catalytic activity varied in parallel with the ability of the crown-modified phosphine ligand to extract K- and Li-cinnamate from the aqueous into the benzene phase. Both observations relate to the active role of the crown-ether unit built into the ligand in bringing together the Rh(I) center of the catalyst and the substrate [54]. Similarly, β-cyclodextrin was attached to bis(2-diphenylphosphinoethyl)amine [55]. The reaction of the resulting bidentate phosphine (Scheme 38.4 b) with $[Rh(COD)_2][BF_4]$ afforded a highly water-soluble catalyst which showed enhanced activity (factor of 3 to 6) in the hydrogenation of higher olefins compared to $PhN(CH_2PPh_2)_2/[Rh(COD)_2][BF_4]$ in

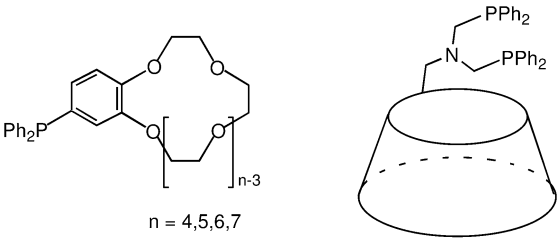

a b

Scheme 38.4

water:substrate biphasic systems. Moreover, in a 1:1 mixture of Ph-$(CH_2)_2$-$CH=CH_2$ and C_8H_{17}-$CH=CH_2$, the β-cyclodextrin-modified catalyst was selective in favor of the phenyl-substituted olefin which interacts strongly with the cyclodextrin unit. Indeed, the substrate selectivity decreased drastically on addition of *p*-xylene, which competes for the β-cyclodextrin cavity [52].

The hydrogenation of polymers results in improved thermal and oxidative stability, reduced gas permeability, and greater resistance to oils and fluids. Aqueous emulsions of acrylonitrile-butadiene-styrene (ABS) co-polymers (as obtained in the polymerization process) were hydrogenated at 70–100 °C and 15 bar (r.t.) H_2 with $[RhCl(PPh_3)_3]$, $[RhH(CO)(PPh_3)_3]$, or $[Rh(COD)(PPh_3)_2][BF_4]$ catalysts dissolved in acetone:toluene mixtures, and this resulted in the saturation of up to 70% of the double bonds. Neither the nitrile nor the aromatic functionalities were hydrogenated. The recovery of the catalyst in the organic phase was also claimed [56, 57]. Several carboxylatoalkyl-diphenylphosphines, Ph_2P-$(CH_2)_n$-CO_2Na (n = 1, 2, 4, 5, 7) together with *p*- or *m*-Ph_2P-C_6H_4-CO_2Na and their rhodium complexes were synthetized and used for the hydrogenation of various polymers (polybutadiene, PBD; nitrile-butadiene rubber, NBR; and styrene-butadiene rubber, SBR) in water:toluene biphasic media. With $[\{RhCl[Ph_2P\text{-}(CH_2)_5\text{-}CO_2Na]_2\}_2]$ and $[\{RhCl[Ph_2P\text{-}(CH_2)_7\text{-}CO_2Na]_2\}_2]$ as catalysts, the pendant (terminal) vinyl units of the polymers were hydrogenated preferentially over the internal double bonds. At 100 °C and 15 bar H_2 total conversions as high as 84% (PBD), 62% (NBR), and 50% (SBR) were obtained [58, 59]. Exceptionally high catalytic activities (TOF > 840 h^{-1}) were achieved in the hydrogenation of polybutadiene-1,4-*block*-poly(ethylene oxide) with an *in-situ*-prepared Rh/*m*tppts catalyst in the presence of the micelle-forming agent dodecyltrimethylammonium chloride [60]. In the presence of a non-ionic surfactant Triton X-305, NBR latexes were only slowly hydrogenated by $[RhCl(m\text{tppms})_3]$ (TOF = 4.0–9.3 h^{-1}) [61].

Aqueous two-phase hydrogenations are dominated by platinum group metal catalysts containing water-soluble tertiary phosphine ligands. The extremely stable and versatile N-heterocyclic carbene complexes attracted only limited interest, despite the fact that such complexes were described in the literature [62–65]. Recently, it was reported that the water-soluble [RuXY(1-butyl-3-methylimidazol-2-ylidene) (η^6-*p*-cymene)]$^{n+}$ (X = Cl^-, H_2O; Y = Cl^-, H_2O, pta) complexes preferentially hydrogenated cinnamaldehyde and benzylideneacetone at the C=C double bond (Scheme 38.5) with TOF values of 30 to 60 h^{-1} in water:substrate biphasic mixtures (80 °C, 10 bar H_2) [66].

The catalytic modification of lipid dispersions (liposomes) or the lipid membranes of living cells [4, 67] is a special application of the homogeneous hydrogenation of alkenes in aqueous biphasic (microheterogeneous) media. An ideal catalyst efficiently reduces the unsaturated fatty acid units in the polar lipids at low temperatures (0–40 °C) in an aqueous environment, does not effect transformations other than hydrogenation, can be totally removed from the cell after the reaction is completed, and has no "self-effect", such as toxicity. To date, the most investigated homogeneous catalyst for biomembrane hydrogenation is $[Pd(QS)_2]$, QS = 1,2-dioxy-9,10-anthraquinone-3-sulfonic acid (Alizarin red) [68].

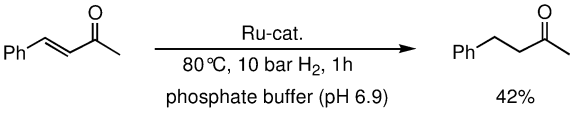

Scheme 38.5

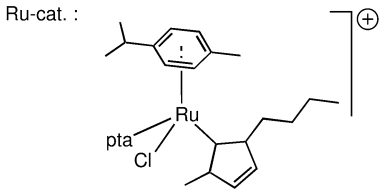

The hydrogenation of alkynes in aqueous systems has been much less studied than that of alkenes. Interestingly, *mer*-[Ir(H)(H)Cl(PMe_3)$_3$] was found to be water-soluble and to catalyze the hydrogenation of various terminal and internal alkynes to alkanes (TOFs in the range of 1–2 h^{-1} at 60 °C, 28 bar H_2). However, this catalytic activity was displayed only in aqueous mixtures, there being no activity in organic solvents [69]. Although the detailed mechanism of the reaction was not elucidated, ^{1}H-NMR spectra showed – in addition to the neutral *mer*-[Ir(H)(H)Cl(PMe_3)$_3$] complex – the presence of the cationic *mer*-[Ir(H)(H)(H_2O)(PMe_3)$_3$]$^+$ species in which the H_2O ligand may be easily replaced by the substrate alkyne. In aqueous solutions, chloride dissociation from the neutral catalysts or their precursors is facilitated (compared to the dissociation of a phosphine ligand) by the strong solvation of the resulting ions, and may lead to the alteration of the catalytic properties [70].

Diphenylacetylene and 1-phenyl-1-propyne were hydrogenated to the corresponding 1,2-disubstituted alkenes in aqueous organic biphasic media using [{$RuCl_2$(*m*tppms)$_2$}$_2$] and an excess of *m*tppms (80 °C, 1 bar H_2, TOFs up to 25 h^{-1}). The stereoselectivity of the reaction depended heavily on the pH of the catalyst-containing aqueous phase (Fig. 38.1) and, under acidic conditions, *Z*-alkenes could be obtained with a selectivity close to 100% [71].

The hydrogenation of benzene to cyclohexane is a large-scale industrial process applying heterogeneous ruthenium catalysts in the presence of water and zinc-based additives. Several attempts were made to develop homogeneous catalysts for the hydrogenation of arenes. It has been reported that benzene and monosubstituted benzenes can be efficiently hydrogenated in aqueous biphasic systems with hydridoareneruthenium cluster catalysts, such as [Ru_3(μ_2-H)$_2$(μ_2-OH)(μ_3-O)(η^6-C_6H_6)(η^6-C_6Me_6)$_2$]$^+$ [72–75] and with phosphine-containing areneruthenium compounds such as [$RuCl_2$(η^6-*p*-cymene)(pta)], [$RuCl_2$(η^6-*p*-cymene)(*m*tppts)] and related complexes [76, 77]. It was reported, that the well-known alkene hydrogenation catalyst, [$RuCl_2$(*m*tppts)$_2$], also catalyzed the hydrogenation of benzene to cyclohexane, whereas in the presence of $ZnCl_2$ the major product (91%) was cyclohexene [78]. Lignin phenols were hydrogenated to the corresponding cyclohexanols with Ru(II)/*m*tppms or *m*tppts catalysts, resulting

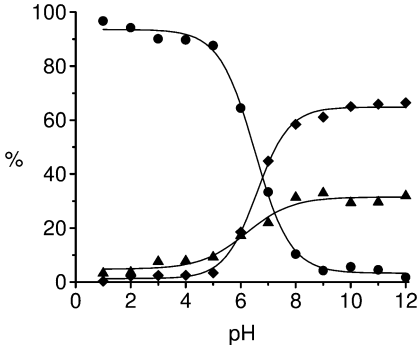

Fig. 38.1 Product distribution in the hydrogenation of diphenylacetylene as a function of the pH. [{$RuCl_2$(*m*tppms)$_2$}$_2$]=6.6 mg (6.79×10^{-3} mmol ruthenium), *m*tppms=8.1 mg (2.03×10^{-2} mmol), diphenylacetylene=89.1 mg (0.5 mmol), 1 bar H_2, 1 mL chlorobenzene, 2 mL phosphate buffer, 50 °C, 3 h. ●, *Z*-stilbene; ▲, *E*-stilbene; ◆, 1,2-diphenylethane. (Reproduced with permission from H. H. Horváth, F. Joó, *React. Kinet. Catal. Lett.* **2005**, *85*, 355–360.)

in inhibition of the light-induced yellowing of lignin and lignin-rich wood pulps [79]. While the mentioned catalysts can be useful for synthetic purposes, recent studies [80, 81] called attention to the possible formation of metal colloids in such aqueous arene hydrogenations. A very thorough analysis of the two-phase hydrogenation of benzene with $[Ru_3(\mu_2\text{-}H)_3(\eta^6\text{-}C_6H_6)(\eta^6\text{-}C_6Me_6)_2(\mu_3\text{-}O)]^+$ has revealed, that indeed the reduction was catalyzed by trace Ru(0) derived from the water-soluble cluster under the reaction conditions [82].

38.3
Enantioselective Hydrogenation of Alkenes in Two-Phase Aqueous Systems

Examples of enantioselective hydrogenations of alkenes in aqueous biphasic systems are listed in Table 38.2. Of course, the original references contain much more information; in order to compile Table 38.2, only those reactions with the highest enantiomeric excess were selected. In most of these investigations the activity and selectivity of the catalysts were characterized in reduction of the standard substrates of enantioselective hydrogenations (dehydroaminoacid derivatives, dimethyl itaconate; Scheme 38.6); however, in a few cases substrates of more practical significance (isobutylatropic acid, geraniol) were also used. Not surprisingly, this field of catalysis is dominated by rhodium complexes of the most diverse tertiary phosphine ligands (Scheme 38.7), although a few ruthenium and iridium complexes have also been studied. In the quest of catalysts with increasingly greater stereoselectivities, the catalytic activity was often of secondary significance. In most cases the reactions were run until complete hydrogenation, and the TOFs derived from the reaction times required (or greatly exceeding the time needed) for full conversions were not particularly well defined.

Table 38.2 Enantioselective hydrogenation of alkenes in aqueous-organic two-phase systems.

Entry	Catalyst	Substrate	ee [%]	TOF [h^{-1}]	Solvent	Conditions	Reference
1	$[\{RhCl(COD)\}_2]$ + (*S*,*S*)-**A**	BzACH	86 (*R*)	≥8.3	H_2O/EtOAC (1/1)	25 °C, 10 bar	83
2	$[\{RhCl(COD)\}_2]$ + (*S*,*S*)-**A**	AACMe	88 (*R*)	≥8.3	H_2O/EtOAC (1/1)	25 °C, 10 bar	84
3	$[\{RhCl(COD)\}_2]$ + (*S*,*S*)-**C**	$ITAMe_2$	43 (*S*)	≥8.3	H_2O/EtOAC (1/1)	25 °C, 10 bar	84
4	$[Rh(NBD)(B)]^{5+}$	AACMe	77	50	H_2O/EtOAc/benzene (2/1/1)	20 °C, 14 bar	85
5	$[Rh(NBD)\{(S,S)\text{-}\mathbf{E}\}]^+$	AACMe	50	n.d.	H_2O/EtOAC + HBF_4	20 °C, 14 bar	86
6	$[Rh(NBD)\{(S,S)\text{-}\mathbf{E}\}]^+$	AACH	67 (*R*)	16.7	H_2O/EtOAc/benzene (2/1/1)	20 °C, 14 bar	87
7	$[\{RhCl(COD)\}_2]$ + **G**	AACMe	69	67	H_2O/EtOAC (1/1)	25 °C, 1 bar	88
8	$[Rh(NBD)\{(R,R\text{-}H\}]$	$ITAMe_2$	66	0.9	H_2O/MeOH/*n*-heptane (1/1/2)	r.t., 5 bar	89
9	$[Ir(NBD)\{(R,R\text{-}\mathbf{H}\}]$	$ITAMe_2$	76	0.9	H_2O/MeOH/*n*-heptane (1/1/2)	r.t., 5 bar	89
10	$[\{RhCl(COD)\}_2]$ + **F** ($n=1$)	AACH	87	≥12.5	H_2O/EtOAC (1/1)	r.t., 10 bar	90
11	$[\{RhCl(COD)\}_2]$ + **F** ($n=1$)	AACMe	74	≥12.5	H_2O/EtOAC (1/1)	r.t., 10 bar	90
12	$[\{RhCl(COD)\}_2]$ + **F** ($n=1$)	$ITAMe_2$	28	≥12.5	H_2O/EtOAC (1/1)	r.t., 10 bar	90
13	$[Rh(COD)(I)][BF_4]$	AACMe	22 (*R*)	115	H_2O/EtOAC (1/1)	25 °C, 1 bar	91
14	$[Rh(NBD)(J)][CF_3SO_3]$	AACH	74 (*R*)	≥97	H_2O/EtOAC (1/1) (pH = 7.0)	r.t., 1 bar, [P] = 4.0%	92
15	$[Rh(NBD)(J)][CF_3SO_3]$	AACH	89 (*R*)	20	H_2O/EtOAC (1/1)	r.t., 1 bar, [P] = 1.0%	93
16	$[Rh(COD)(\alpha,\alpha\text{-}\mathbf{K})][BF_4]$	AACMe	76 (*S*)	≥34	H_2O/MeOH/EtOAc (3/2/5)	r.t., 5 bar	94
17	$[Rh(COD)(\beta,\beta\text{-}\mathbf{K})][BF_4]$	AACMe	98 (*S*)	≥34	H_2O/MeOH/EtOAc (3/2/5)	r.t., 5 bar	94
18	$[Rh(COD)(L)][BF_4]$	AACMe	73 (*R*)	≥4.2	H_2O/EtOAC (1/1)	r.t., 50 bar	95
19	$[\{RhCl(COD)\}_2]$ + **F** (mixt.)[a]	dehydropeptides	87	≥1.0	H_2O/CH_2Cl_2 (1/2)	25 °C, 10 bar	96
20	$[Rh(NBD)_2][BF_4]$ + **M**	AAMe	79 (*R*)	77	H_2O/EtOAC (10/7)	25 °C, 1 bar	97
21	$[\{RhCl(COD)\}_2]$ + (*R*,*R*)-**N**	AACA-Na	60–80	≥1.1	H_2O/toluene (AAC-Na in the aq. phase, catalyst in the toluene phase!)	r.t., 1 bar	98
22	$[\{RuCl_2(\eta^6\text{-}p\text{-cymene})\}_2]$ + **P**	isobutyl atropica.	64	51	H_2O/EtOAC, Et_3N	24–30 °C, 60 bar	99

Table 38.2 (continued)

Entry	Catalyst	Substrate	ee [%]	TOF [h^{-1}]	Solvent	Conditions	Reference
23	$[RuCl(\eta^6\text{-}C_6H_6)\{(R)\text{-}(+)\text{-}\mathbf{R}\}]Cl$	AACH	72 (*R*)	0.3	H_2O/EtOAC (1/1)	r.t., 4 bar	100
24	Ru(II)/**Q**	geraniol	98	n.d.	H_2O/EtOAC	n.d.	101
25	$[Ru(OAc)_2(tolBINAP)]$	tiglic acid	92	2.2	H_2O/[bmim][PF_6]/$scCO_2$	25 °C, 5 bar	102
26	$[Ru(OAc)_2(tolBINAP)]$	isobutyl atropica.	"poor"	2.2	H_2O/[bmim][PF_6]/$scCO_2$	25 °C, 60 bar	102

For ligands **A**–**R**, see Scheme 38.7.
a) Mixture of mono- (25%), di- (70%), and trisulfonated (5%) BDPP.
n.d. = no data.

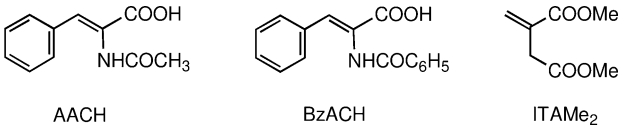

Scheme 38.6 Standard substrates for enantioselective hydrogenations.

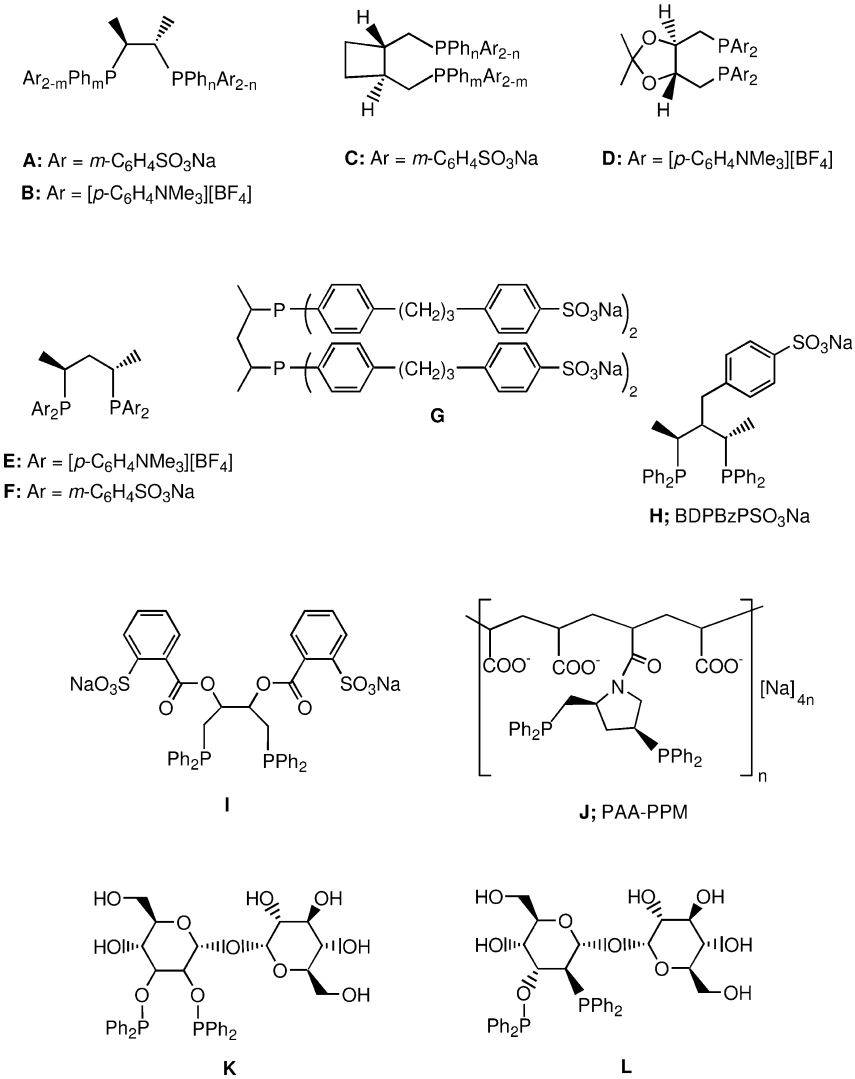

Scheme 38.7

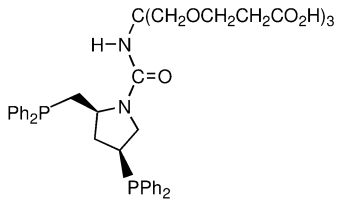

M

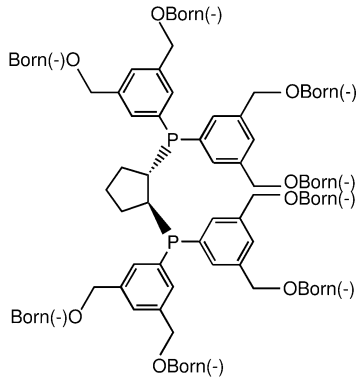

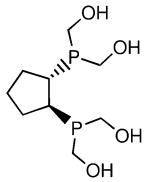

O

N; OBorn(-):

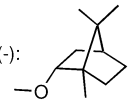

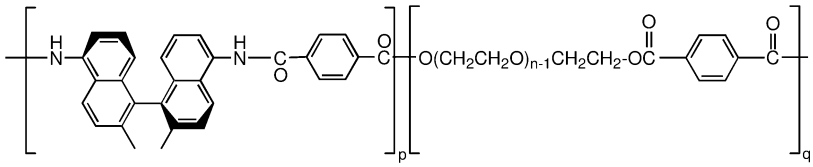

P; PEG-BINAP

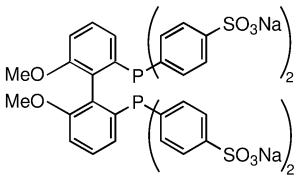

Q; MeOBIPHEP-TS

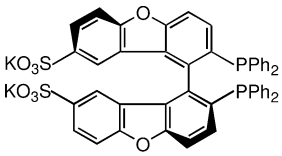

R; BIFAPS

Scheme 38.7 (continued)

In general, the chiral ligands are water-soluble variants of those already studied in purely organic solvents (e.g., the sulfonated chiraphos, A, cyclobutane-diop, C, BDPP, F, MeOBIPHEP-TS, Q, BIFAPS, R and the quaternary ammonium derivatives of diop, D, BDPP, E). Solubility in water could also be achieved by attaching the parent phosphine molecule to a water-soluble polymer (J, M, P). The chiral phosphinites and phosphines derived from carbohydrates (e.g., K and L) have intrinsic solubility in water. During studies of one-phase

systems it was found that in several cases the catalytic activity and selectivity of an asymmetric hydrogenation was substantially decreased when it was performed in water instead of an organic solvent [4]; however, both the activity and selectivity could be restored by the addition of surfactants [103–106]. Based on these observations, a chiral *and* surfactant phosphine, G was synthetized and used as ligand in the Rh(I) complex-catalyzed hydrogenation of methyl α-acetamidocinnamate in MeOH and in H_2O : EtOAc. Indeed, with this ligand only a slight decrease in the catalytic activity and in the enantioselectivity was observed in the aqueous two-phase system compared to the reactions in methanol (69% versus 75% ee), while with the tetrasulfonated BDPP (F) the reaction was slowed considerably and the enantioselectivity fell from 72% to 20% upon the same solvent change [88]. Similar observations were made in water : ethyl acetate biphasic systems with the Ru(II)-catalysts containing the surfactant PEG-BINAP ligand (Scheme 38.7) – that is, the catalytic activity was found to be higher than in homogeneous solutions made either with ethyl acetate or with methanol : water (1 : 1) mixtures [99]. The latter catalyst was used for the synthesis of the anti-inflammatory drugs ibuprofen and naproxen by hydrogenation of the corresponding 2-arylacrylic acids (Scheme 38.8) [99].

Whether asymmetric hydrogenations in aqueous two-phase systems will develop into practically significant procedures remains to be seen. Nevertheless, it is clear from the above investigations, that aqueous biphases are suitable media for asymmetric hydrogenations, and with the proper choice of the catalyst and the reaction conditions, very high selectivities and good catalytic activities can be achieved (see for example entry 17 in Table 38.2). High-throughput screening of catalysts and conditions with specifically designed microdevices [107] may also accelerate the advancement of this area of catalysis.

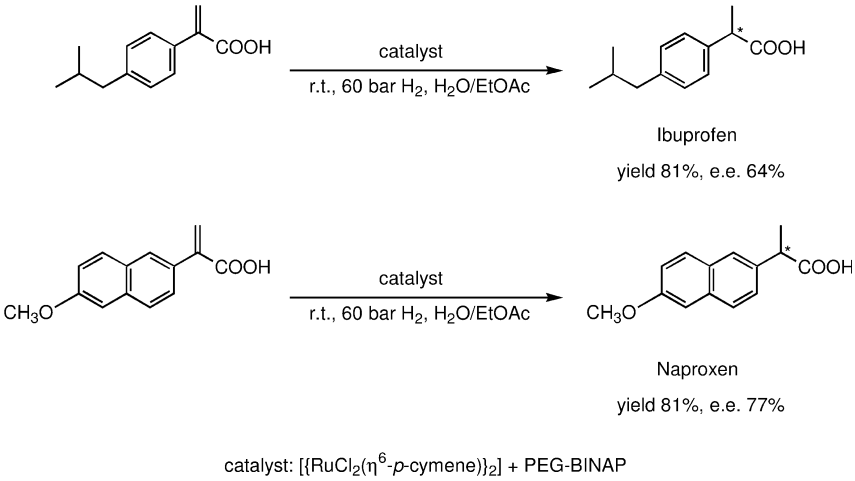

Scheme 38.8

38.4
Aqueous Two-Phase Hydrogenation of Aldehydes and Ketones

Hydrogenation of the carbonyl function can be achieved in aqueous biphasic systems (Table 38.3) using catalysts with water-soluble chiral ligands (Scheme 38.9). Most of these catalysts contain ruthenium [108, 109], although a few rhodium, iridium, osmium, and palladium complexes have also been found useful for this type of catalytic conversion. By far the greatest attention was devoted to the selective hydrogenation of *α,β*-unsaturated aldehydes, since the resulting allylic alcohols are important fine chemicals and synthetic intermediates for the flavor and fragrance industries.

Details of the hydrogenation of cinnamaldehyde (Scheme 38.10) and other *α,β*-unsaturated aldehydes were very thoroughly studied by several groups [10, 11, 110–120]. The general conclusion was that Ru(II)-phosphine complexes are suitable for the synthesis of allylic alcohols (selective C=O hydrogenation), while Rh(I)–phosphine complexes catalyze the selective hydrogenation of C=C bonds and yield saturated aldehydes. The reaction mechanisms behind this plain statement are certainly more complex, since it has been reported that, with the proper choice of pH of the aqueous phase, *either* cinnamyl alcohol (pH ≥ 8) *or* 3-phenylpropionaldehyde (pH ≤ 5) can be *selectively* obtained by hydrogenation of cinnamaldehyde with the same catalyst precursor, $[\{RuCl_2(m\text{tppms})_2\}_2]$, in the presence of excess *m*tppms (Fig. 38.2) [10, 11].

This finding is the consequence of the distribution of various ruthenium(II) hydrides in aqueous solutions as a function of pH; $[RuHCl(m\text{tppms})_3]$ is stable in acidic solutions, while under basic conditions the dominant species is $[RuH_2(m\text{tppms})_4]$ [10, 11]. A similar distribution of the Ru(II) hydrido-species as a function of the pH was observed with complexes of the related *p*-monosulfonated triphenylphosphine, *p*tppms, too [116]. Nevertheless, the picture is even more complicated, since the unsaturated alcohol : saturated aldehyde ratio depends also on the hydrogen pressure, and selective formation of the allylic alcohol product can be observed in acidic solutions (e.g., at pH 3) at elevated pressures of H_2 (10–40 bar; [117, 120]). (The effects of pH on the reaction rate of C=O hydrogenation were also studied in detail with the $[IrCp^*(H_2O)_3]^{2+}$ and $[RuCpH(pta)_2]$ catalyst precursors [118, 128].)

As elsewhere in the various fields of hydrogenation, the number of catalysts with ligands other than tertiary phosphines is rather limited. Bis-phosphonic acid derivatives of 2,2′-bipyridine and 1,2-cyclohexanediamines were used as ligands in iridium complexes which catalyzed the hydrogenation of acetophenone and several substituted acetophenones [130]. $[Ru(6,6'\text{-}Cl_2bipy)_2(H_2O)_2][CF_3SO_3]_2$ was also active in the biphasic hydrogenation of aldehydes and ketones [43]. The Ru(II)-N-heterocyclic carbene complex (see Scheme 38.5) catalyzed the hydrogenation of aldehydes and ketones; besides, in addition, the redox isomerization of allylic alcohol was also observed and part of this substrate was hydrogenated to propanol via prior isomerization to propionaldehyde [66].

Table 38.3 Hydrogenation of aldehydes and ketones in aqueous-organic two-phase systems.

Entry	Catalyst	Substrate	TOF [h^{-1}]	Selectivity [%][a)]	Solvent and conditions	Reference
1	$RuCl_3$/3–5 *m*tppts	crotonaldehyde	48	99	H_2O/toluene 1/1, 35–50 °C, 20–50 bar H_2	110
		prenal	400	97		111
		cinnamaldehyde	66	98		112
		citral	13	98		113
2	$[\{RhCl(COD)\}_2]$/5 *m*tppts	crotonaldehyde	625	99[b)]	H_2O/toluene 1/1, or H_2O/hexane 1/1, 30–80 °C, 20–40 bar H_2	111
		prenal	600	95[b)]		114
		cinnamaldehyde	124	96[b)]		
		citral	13	95[b)]		
3	$[RhCl(mtppts)_3]$	cinnamaldehyde	140	95	H_2O/toluene 1/1, 50–90 °C, 10–40 bar H_2	115
4	$[\{RuCl_2(mtppms)_2\}_2]$/*m*tppms	cinnamaldehyde	≤15	93 (pH 8) varies with pH	aq. buffer of various pH/chlorobenzene 3/5, 80 °C, 1 bar H_2	10, 11
5	$[\{RuCl_2(ptppms)_2\}_2]$/*p*tppms	cinnamaldehyde	≤13	95 (pH 13) varies with pH	aq. buffer of various pH/chlorobenzene 3/5, 80 °C, 1 bar H_2	116
6	$[\{RuCl_2(mtppms)_2\}_2]$/*m*tppms	cinnamaldehyde	≤14	93 (pH 3) varies with H_2 pressure	aq. buffer of various pH/chlorobenzene 3/3, 80 °C, 1–11 bar H_2	117

Table 38.3 (continued)

Entry	Catalyst	Substrate	TOF [h^{-1}]	Selectivity [%] [a)]	Solvent and conditions	Reference
7	$RuCl_3$/6 *m*tppms, $RuCl_3$/6 *m*tppts	cinnamaldehyde	≤25	≤95	H_2O/toluene 1/1, 100 °C, 30 bar H_2	119
	[{$RuCl_2$(*m*tppms)$_2$}$_2$], [{RuHCl(*m*tppms)$_2$}$_2$]					
	$OsCl_3$/6 *m*tppms, $OsCl_3$/6 *m*tppts		≤20	≤90		
	[OsH_4(*m*tppms)$_3$], [OsHCl(CO)(*m*tppms)$_2$]					
	[{$OsCl_2$(*m*tppms)$_2$}$_2$]		0.4	100		
8	$RuCl_3$/ 5 *m*tppts	cinnamaldehyde	≤95	≤96	H_2O/toluene 1/1, 40 °C, 20 bar H_2	120
	[{$RuCl_2$(*m*tppts)$_2$}$_2$], [RuH_2(*m*tppts)$_4$]					
	[RuH(OAc)(*m*tppts)$_3$], [RuHCl(*m*tppts)$_3$]					
	[RuH(η^6-$C_6H_5CH_3$)(*m*tppts)$_2$]Cl		0		H_2O/Et_2O, 40 °C, 20 bar H_2	
	$RuCl_3$/5 *m*tppts	crotonaldehyde	116	99	H_2O/toluene 1/1, 40 °C, 20 bar H_2	
	[RuHCl(*m*tppts)$_3$]		342	93		
	[RuH_2(*m*tppts)$_4$]		140	93		
	[{$RuCl_2$(*m*tppts)$_2$}$_2$]		13	32		
	[{$RuCl_2$(*m*tppts)$_2$}$_2$]		16	46	H_2O/Et_2O, 40 °C, 20 bar H_2	
	[RuHCl(*m*tppts)$_3$]	prenal	400	100	H_2O/toluene 1/1, 20 °C, 20 bar H_2, 23% over-reduction to 3-methyl-butanol	
9	[{RhCl(COD)}$_2$]/*m*tppts	benzaldehyde	33		aq. buffer (pH 7)/EtOAc 1/1, 65 °C, 20 bar (r.t.) H_2	121
	[{RhCl(COD)}$_2$]/T(p-A)PTS	benzaldehyde	16			
	[{RhCl(COD)}$_2$]/T(p-A)PTS	hexanal	19			
	[{Ir(COD)Cl}$_2$]/*m*tppts	benzaldehyde	3			
	[{Ir(COD)Cl}$_2$]/T(p-A)PTS	benzaldehyde	3			
	[{Ir(COD)Cl}$_2$]/T(2,4-X)PTS	benzaldehyde	40			

10	$[RuCl_2(pta)_4]$	benzaldehyde	7.2		aq. buffer (pH 8)/chlorobenzene 1/1	122
11	$[Ir(COD)\{P(CH_2OH)_3\}_3]Cl$	cinnamaldehyde	20	≤97	H_2O/benzene 1/1, 100–125 °C, 30–100 bar H_2	123
12	$[RhI_4(mtpa)_2]I$ [d]	cinnamaldehyde	190	88 [b]	H_2O/toluene 1/1, 60 °C, 35 bar H_2	124
	$[RuI_4(mtpa)_2] \cdot 2H_2O$		40	94		
	$[RuI_2(mpta)_3(H_2O)]I_3 \cdot 2H_2O$		183	80		
13	$[RhI(CO)(mpta)_3]I_3 \cdot 4H_2O$	pentanal	108	80 [c]	H_2O/substrate, 80 °C, 80 bar H_2	125
		hexanal	108	84 [c]		
		heptanal	106	78 [c]		
14	$[PdCl_2(m\text{tppts})_2]$	crotonaldehyde	3750	100 [b]	H_2O/benzene 30/5, 10–60 °C, 1–50 bar H_2	126
		cinnamaldehyde	1250	≤58		
		citral	307	≤97 [b]	main product: citronellal	127
15	$[RuCpCl(pta)_2]$	benzylideneacetone	10–35	75–89 [b]	H_2O/*n*-octane 1/2, 130 °C, 31.5 bar H_2	44
	$RuCp^*Cl(pta)_2]$		6–11	81–94		
16	$[RuCpH(pta)_2]$	benzylideneacetone	3.3	99 (pH 4.5) [b]	aq. phosphate buffer/substrate, 25 °C, 4 bar H_2	128
17	$[\{Ir(COD)Cl\}_2]$/**L1**, **L2** or **L3**	various ketones	1	100 [c]	H_2O/substrate, or H_2O/EtOAc, r.t., 40 bar H_2	129
	$[\{RhCl(COD)\}_2]$/**L1**, **L2** or **L3**					
18	$[Ru(\eta^6\text{-}C_6H_6)(CH_3CN)_3]^{2+}$	cyclohexen-2-one	178	96 [b]	H_2O/benzene, 90–110 °C, 40 bar H_2	42
		mesityl oxide	118	100 [b]		
		benzylideneacetone	245	98 [b]		

Table 38.3 (continued)

Entry	Catalyst	Substrate	TOF [h^{-1}]	Selectivity [%] [a]	Solvent and conditions	Reference
19	$[Ru(6,6'\text{-}Cl_2bipy)_2(H_2O)_2][CF_3SO_3]_2$	cinnamaldehyde	120	71	H_2O/toluene 8/5, or H_2O/cyclohexane 8/5, 130 °C, 40 bar H_2	43
		mesityl oxide	233	100 [b]		
		benzylideneacetone	220	98 [b]		
		acetophenone	213			
20	$[\{RuCl_2(m\text{tppts})_2\}_2]$	benzylideneacetone	3	98 [b]	H_2O/benzene 5/2, 80 °C, 35 bar H_2	120
	$[\{RuCl_2(m\text{tppts})_2\}_2]$	benzylideneacetone	5	95 [b]	H_2O/CH_2Cl_2 5/2, 80 °C, 35 bar H_2	
	$[RuH_2(m\text{tppts})_4]$	benzylideneacetone	9	78 [b]	H_2O/benzene 5/2, 80 °C, 35 bar H_2	
21	$[Ir(COD)_2][BF_4]$/ **L4**	acetophenone	18	52 (ee)	H_2O/MeOH/substrate, 50 °C, 45 bar H_2	130
		4-MeO-acetophenone	≥9.5	50 (ee)		
		2-MeO-acetophenone	≥9.5	70 (ee)		
		t-butylphenylketone	≥9.5	72 (ee)		
22	$[RuBr_2(6,6'\text{-diamBINAP.2HBr})]$	ethyl acetoacetate	≥63	94 (ee)	H_2O/substrate, 50 °C, 40 bar H_2	131
	$[RuBr_2(4,4'\text{-diamBINAP.2HBr})]$	ethyl acetoacetate	≥67	99 (ee)	H_2O/substrate, 50 °C, 40 bar H_2	132
	$[RuBr_2(5,5'\text{-diamBINAP.2HBr})]$	ethyl acetoacetate	≥67	99 (ee)	H_2O/substrate, 50 °C, 40 bar H_2	132
23	$[RuCl_2(\eta^6\text{-}p\text{-cymene})(\mathbf{L5})]$	cinnamaldehyde	39 [b]		aq. phosphate buffer (pH 6.9)/substrate, 80 °C, 10 bar H_2	66
		acetophenone	40			
		benzylideneacetone	29 [b]			
	$[RuCl(\eta^6\text{-}p\text{-cymene})(\text{pta})(\mathbf{L5})]^+$	cinnamaldehyde	59 [b]			
		acetophenone	65			
		benzylideneacetone	60 [b]			

24	$[\{RhCl(COD)\}_2]$/chiral diphenyl-phosphinoacetamides	acetophenone	7	22 (ee)	H_2O/benzene 1/4, 50 °C, 1 bar H_2	133
25	$RuCl_3$/8 *m*tppts	cinnamaldehyde	36	92	H_2O/toluene 1/50, 40 °C, 40 bar H_2	135
	$RuCl_3$/8 *m*tppts	cinnamaldehyde	124	99	H_2O/sc CO_2 (140 bar), 40 °C, 40 bar H_2	
	$RhCl_3$/8 *m*tppts	cinnamaldehyde	114	100 [b)]	H_2O/sc CO_2 (140 bar), 40 °C, 40 bar H_2	
	$Pd(OAc)_2$/8 *m*tppts	cinnamaldehyde	72	100 [b)]	H_2O/sc CO_2 (140 bar), 40 °C, 40 bar H_2	

a) Unsaturated alcohol.
b) Saturated aldehyde or ketone.
c) Alkanol.
d) mpta = N-methyl-pta.
For the ligands *m*tppms, *m*tppts and pta, see Scheme 38.2; for T(p-A)PTS, T(2,4-X)PTS, diamBINAP.2HBr, and **L1–L5**, see Scheme 38.9.

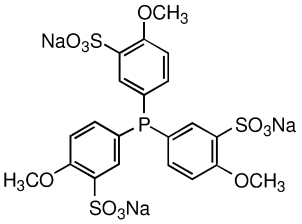

t(*p*-A)pts

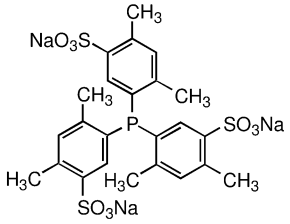

t(2,4-X)pts

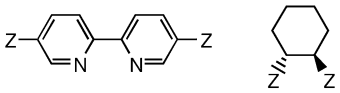

L1 : Z = -C(O)NHC$_3$H$_6$PO$_3$H$_2$
L2 : Z = -PO$_3$H$_2$
L3 : Z = -NHC(O)NHC$_6$H$_4$PO$_3$H$_2$

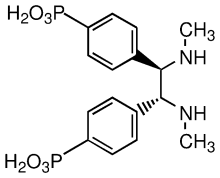

L4

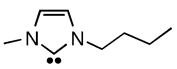

L5

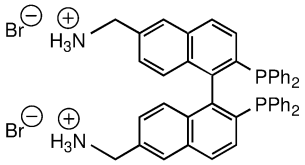

6'6'-diamBINAP

Scheme 38.9

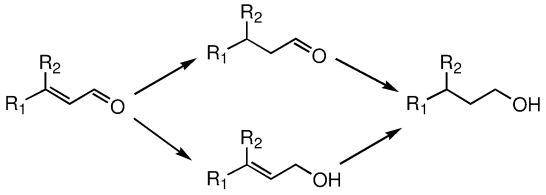

R_1 = Ph, R_2 = H : cinnamaldehyde
R_1 = CH$_3$, R_2 = H : crotonaldehyde
R_1 = R_2 = CH$_3$: prenal

Scheme 38.10

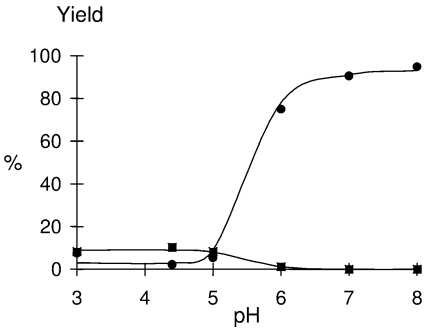

Fig. 38.2 Effect of pH on the yield of products in hydrogenation of *trans*-cinnamaldehyde with [{$RuCl_2$(*m*tppms)$_2$}$_2$] and *m*tppms as catalyst precursors. ●, cinnamyl alcohol; ■, dihydrocinnamaldehyde. [cinnamaldehyde]=80 mM in chlorobenzene (5 mL); [Ru]=3.4 mM; [*m*tppms]=10.3 mM; [KCl]=0.2 M in 0.2 M phosphate buffer (3 mL), 80 °C, H_2, P_{total}=1 bar. (Reproduced with permission from F. Joó, J. Kovács, A. Cs. Bényei, Á. Kathó, *Catal. Today* **1998**, *42*, 441–448.)

Enantioselective hydrogenation of prochiral ketones has rarely been studied in aqueous biphasic media. In addition to the chiral bisphosphonic acid derivatives of 1,2-cyclohexanediamine [130], the protonated 4,4′-, 5,5′-, and 6,6′-aminomethyl-substituted BINAP (diamBINAP · 2HBr) ligands (Scheme 38.7) served as constituents of the Ru(II)-based catalysts in the biphasic hydrogenations of ethyl acetoacetate [131, 132]. These catalysts were recovered in the aqueous phase and used in at least four cycles, with only a marginal loss of activity and enantioselectivity.

Besides the "conventional" aqueous : organic two-phase systems making use of hydrosoluble catalysts (i.e., version A in Scheme 38.1), reports have also been made on other approaches. Acetophenone dissolved in the benzene phase was hydrogenated with the unmodified Wilkinson's catalyst, [$RhCl(PPh_3)_3$] or its analogs containing chiral diphenylphosphinoacetamides (prepared from α-amino-acids) in the presence of an aqueous phase (and triethylamine) [133]. In this case, the role of the two phases is not in the separation of the catalyst and the substrate (products), but rather in facilitating the formation of the catalytically active Rh(I)-monohydride species by extracting the HCl byproduct into the aqueous phase [Eq. (4)].

$$[RhCl(P)_3 + H_2 \rightleftharpoons [RhH_2Cl(P)_3] \quad (3)$$

$$[RhH_2Cl(P)_3] \rightleftharpoons [RhH(P)_3] + H^+ + Cl^- \quad (4)$$

In another example, undecanal was hydrogenated to undecanol with a water-soluble catalyst in the presence of chemically modified β-cyclodextrins, which facilitated the mass transfer between the aqueous and the organic phase [134]. Hydrogenation of cinnamaldehyde with very high (99%) selectivity to cinnamyl alcohol was also performed in water : $scCO_2$ biphasic systems [135] which al-

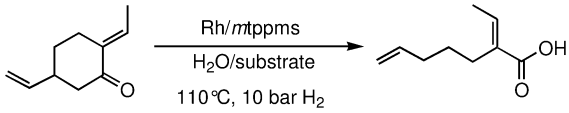

Scheme 38.11

lowed an efficient mass transfer between the substrate-containing and the catalyst-containing phases.

The δ-lactone (Scheme 38.11) can be efficiently obtained by the telomerization of butadiene and CO_2. Its biphasic hydrogenation with an *in-situ*-prepared Rh/*m*tppts catalyst yields 2-ethylidene-6-heptenoic acid (and its isomers) [136]. Note, that the catalyst is selective for the hydrogenolysis of the lactone in the presence of two olefinic double bonds; this is probably due to the relatively large [P]:[Rh] ratio (10 : 1) which is known to inhibit C=C hydrogenations with [RhCl(*m*tppms)$_3$]. The mixture of heptenoic acids can further be hydrogenated on Pd/C and Mo/Rh catalysts to 2-ethylheptanol which finds several applications in lubricants, solvents, and plasticizers. This is one of the rare examples of using CO_2 as a C1 building block in a transition metal-catalyzed synthetic process.

38.5
Aqueous Two-Phase Hydrogenations of Nitro-Compounds, Imines, Nitriles, Oximes, and Heteroaromatics

Although amines are very important intermediates or targets of synthesis, relatively few studies have been conducted on their catalytic production in aqueous-organic biphasic systems. It has long been known that $[CoH(CN)_5]^{3-}$ is capable of hydrogenating nitro-, azoxy- and azo-compounds under mild conditions [49]. Both the C=C and -NO_2 groups in 2-nitro-(2,5-dimethoxyphenyl)nitroethene were hydrogenated with an *in-situ*-prepared $RuCl_3$/*m*tppms catalyst in a two-phase reaction (90 °C, 40 bar H_2) to yield 2-(2,5-dimethoxyphenyl)ethylamine [137].

The catalytic hydrogenation of chloro-nitroaromatics is usually accompanied by dehalogenation. However, choloranilines could be obtained with very high selectivities (Scheme 38.12) on the catalytic action of rhodium(I) catalysts having β-cyclodextrin-modified chelating bisphosphine ligands [138, 139]. Nitrobenzene and several substituted nitroaromatics were selectively hydrogenated to the corresponding anilines in biphasic systems composed of water and the substrates with a water-soluble catalyst *in situ* prepared from $FeSO_4 \cdot 7H_2O$ and $EDTANa_2$ (Fe : ligand = 1 : 5) [140]. Chloronitrobenzenes were hydrogenated to chloroanilines with ≥99.0% selectivity. Although somewhat harsh conditions had to be used (150 °C, 28 bar H_2), the TOF values were very high (430 to 1300 h^{-1}) and the catalyst could be recycled with no loss of activity or selectivity (tested in five cycles). Traditionally, Fe(0) is used in the stoichiometric (Béchamp-) reduction of nitrobenzene and in the heterogeneous catalytic hydrogenation of nitro compounds; however, this method is a rare example of the efficient use of soluble Fe-complexes in homogeneous catalytic hydrogenations.

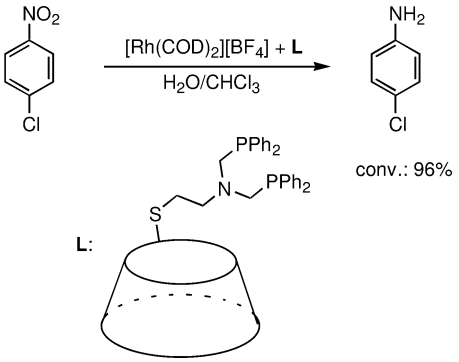

Scheme 38.12

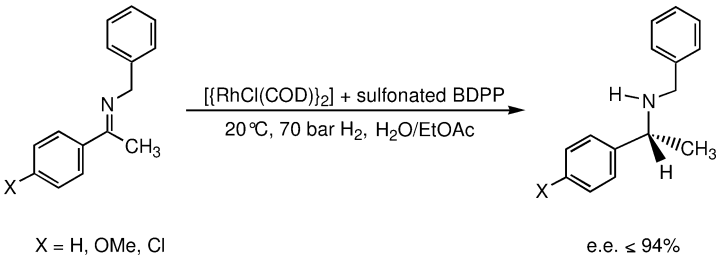

Scheme 38.13

Certain benzylimines are sufficiently resistant to hydrolysis, and their hydrogenation can also be studied in aqueous biphasic systems. The hydrogenation of acetophenone benzylimines (Scheme 38.13), catalyzed by $[\{RhCl(COD)\}_2]$ + sulfonated BDPP (Scheme 38.7, F) afforded the corresponding amines with enantioselectivities up to 96%, provided that the degree of sulfonation of BDPP was close to 1 (in fact it was 1.41–1.65) [141]. When more than one of the BDPP phenyl rings was sulfonated the enantioselectivity decreased sharply. The "monosulfonation effect" was studied in detail with well-characterized complexes of sulfonated BDPP with N = 1, 2, 3, or 4 sulfonate groups [142]. Indeed, it was confirmed that by far the highest enantioselectivity was obtained with the monosulfonated ligand (N = 1, ee 94%; N = 2, ee 2%; N = 3, ee 3%; N = 4, ee 63%). With the monosulfonated BDPP ligand, the resulting rhodium(I) complex is very soluble in ethyl acetate and moves completely to the organic phase during hydrogenation. It is assumed, that the sulfonate group of the ligand coordinates to the cationic rhodium center and the resulting zwitterionic product dissolves in the organic solvent. In a related study, acetophenone benzylimine was hydrogenated with a $[Rh\{(-)\text{-BDPP}\}(NBD)][ClO_4]$ catalyst in reverse micellar systems [143]. In the presence of the bis(2-ethylhexyl)sulfosuccinate (AOT) surfactant, as well as with various RSO_3Na salts, the enantioselectivity was appreciably

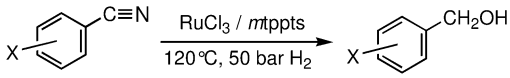

Scheme 38.14

X = H, 3-Me, 4-Me, 4-Br

higher then in their absence, showing again the selectivity-promoting effect of the possible coordination of the sulfonate anion to the cationic catalyst.

The hydrogenation of aliphatic and aromatic nitriles was catalyzed by *in-situ*-prepared Ru/*m*tppts catalysts in two-phase systems with close to quantitative conversion to the corresponding benzylalcohols (Scheme 38.14) [144]. Interestingly, the reactions were facilitated at high [P]:[Ru] ratios, and benzonitrile was completely converted to benzyl alcohol at [P]:[Ru] ≥20. It is assumed that, in the first step of the reaction, the nitriles are hydrogenated to imines, which undergo rapid hydrolysis to aldehydes at the reaction temperature (120 °C), after which the aldehydes are further hydrogenated to alcohols (this latter reaction is indeed promoted by high phosphine concentrations [145]).

Ketoximes and oximes of 2-oxo-acids are hydrogenated to amines by $[CoH(CN)_5]^{3-}$. The latter reaction allows the preparation of *α*-amino-acids by reductive amination of 2-oxo-acids in aqueous ammonia. At 40–50 °C and 70 bar H_2 the yields are ca. 90% [146].

The removal of sulfur and nitrogen from petroleum has enormous significance. Industrially, this is carried out by heterogeneous hydrogenation (hydrotreating). Several attempts were made to hydrogenate thiophene, benzo[*b*]thiophene, and quinoline in aqueous biphases using rhodium(I) and ruthenium(II) complexes of sulfonated phosphines and nitrogen-containing ligands [147–150], not only in model systems but also with naphthas of various origin. Indeed, 78% of the benzo[*b*]thiophene in a naphtha containing 4500 ppm sulfur was hydrogenated (TOF = 6.5 h^{-1}) to dihydrobenzo[*b*]thiophene at 130 °C and 70 bar H_2 with a catalyst prepared *in situ* from $RuCl_3$ and *m*tppms [151–153]. The same catalyst was even more active in the hydrogenation of quinoline to tetrahydroquinoline, while linear or cyclic olefins were reduced only to a small extent and other aromatics (e.g., benzene, toluene, naphthalene) were not hydrogenated at all.

38.6 Conclusions

Aqueous two-phase hydrogenation may be a method of choice for synthetic purposes when no incompatibility problems between water and the substrates, products, or catalyst arise. It has already been proven by the success of the Ruhrchemie-Rhône-Poulenc hydroformylation process, that the catalyst can be retained in the aqueous phase with very high efficiency, and that aqueous-organic biphasic processes using organometallic catalysts are suitable for indus-

trial applications. Whether a new, large-scale biphasic hydrogenation process will emerge remains to be seen. The many interesting synthetic examples of aqueous biphasic hydrogenations discussed in this chapter serve as a solid ground for such developments, and the combination of water with suitable supercritical fluids or ionic liquids may further widen the synthetic possibilities offered by aqueous two-phase hydrogenations.

Abbreviations

ABS acrylonitrile-butadiene-styrene
IL ionic liquid
NBR nitrile-butadiene rubber
PBD polybutadiene
SBR styrene-butadiene rubber
SCF supercritical fluid
TOF turnover frequency

References

1 D.J. Adams, P.J. Dyson, S.J. Tavener, *Chemistry in Alternative Reaction Media*. Wiley, Chichester, **2004**.
2 F. Joó, Á. Kathó, in: *Aqueous Phase Organometallic Catalysis* (Eds. B. Cornils, W.A. Herrmann), 2nd edn. Wiley-VCH, Weinheim, **2004**, p. 429.
3 F. Joó, in: *Encyclopedia of Catalysis* (Ed. I.T. Horváth). Wiley, New York, **2002**, Vol. I. p. 737.
4 F. Joó, *Aqueous Organometallic Catalysis*. Kluwer, Dordrecht, **2001**.
5 D. Stoye, in: *Ullmann's Encyclopedia of Industrial Chemistry* (Eds. B. Elvers, S. Hawkins, W. Russey, G. Schulz), 5th edn. VCH, Weinheim, **1993**, p. 437.
6 C. Reichardt, *Solvents and Solvent Effects in Organic Chemistry*, 3rd edn. Wiley-VCH, Weinheim, **2003**.
7 W.F. Linke, A. Seidell, *Solubilities of Inorganic and Metal-Organic Compounds*. American Chemical Society, Washington, DC, **1958**.
8 Y. Sun, R.N. Landau, J. Wang, C. LeBlond, D.G. Blackmond, *J. Am. Chem. Soc.* **1996**, *118*, 1348.
9 B.R. James, *Homogeneous Hydrogenation*. Wiley, New York, **1973**.
10 F. Joó, J. Kovács, A.C. Bényei, Á. Kathó, *Angew. Chem.* **1998**, *110*, 1024–1026; *Angew. Chem. Int. Ed. Engl.* **1998**, *37*, 969.
11 F. Joó, J. Kovács, A.Cs. Bényei, Á. Kathó, *Catal. Today* **1998**, *42*, 441.
12 P.A. Chaloner, M.A. Esteruelas, F. Joó, L.A. Oro, *Homogeneous Hydrogenation*. Kluwer, Dordrecht, **1994**.
13 T. Dwars, G. Oehme, *Adv. Synth. Catal.* **2002**, *344*, 239.
14 F. Joó, *Acc. Chem. Res.* **2002**, *35*, 738.
15 F. Joó, É. Papp, Á. Kathó, *Top. Catal.* **1998**, *5*, 113.
16 N. Pinault, D.W. Bruce, *Coord. Chem. Rev.* **2003**, *241*, 1.
17 B. Drießen-Hölscher, *Adv. Catal.* **1998**, *42*, 473.
18 T.V. RajanBabu, Y.-Y. Yan, S. Shin, *Curr. Org. Chem.* **2003**, *7*, 1759.
19 F. Joó, Á. Kathó, *J. Mol. Catal. A.: Chemical* **1997**, *116*, 3.
20 J. Kwiatek, *Catal. Rev.* **1967**, *1*, 37.
21 A.F. Borowski, D.J. Cole-Hamilton, G. Wilkinson, *Nouv. J. Chim.* **1978**, *2*, 13.
22 V.R. Parameswaran, S. Vancheesan, *Proc. Indian Acad. Sci.* **1991**, *103*, 1.
23 Y. Dror, J. Manassen, *J. Mol. Catal.* **1977**, *2*, 219.

24 G.T. Baxley, T.J.R. Weakley, W.K. Miller, D.K. Lyon, D.R. Tyler, *J. Mol. Catal. A.: Chemical* **1997**, *116*, 191.
25 R. Grzybek, *React. Kinet. Catal. Lett.* **1996**, *58*, 315.
26 D.J. Darensbourg, F. Joó, M. Kannisto, Á. Kathó, J.H. Reibenspies, *Organometallics* **1992**, *11*, 1990.
27 W.A. Herrmann, J. Kulpe, J. Kellner, H. Riepl, *DE 3840600* to Hoechst AG, **1990**.
28 F.P. Pruchnik, P. Smolenskí, K. Wajda-Hermanowicz, *J. Organomet. Chem.* **1998**, *570*, 63.
29 R.T. Smith, R.K. Ungar, M.C. Baird, *Transition Met. Chem.* **1982**, *7*, 288.
30 E. Renaud, R.B. Russell, S. Fortier, S.J. Brown, M.C. Baird, *J. Organomet. Chem.* **1991**, *419*, 403.
31 T.L. Schull, L.R. Olano, D.A. Knight, *Tetrahedron* **2000**, *56*, 7093.
32 Z. Tóth, F. Joó, M.T. Beck, *Inorg. Chim. Acta* **1980**, *42*, 153.
33 A. Andriollo, A. Bolívar, F.A. López, D.E. Páez, *Inorg. Chim. Acta* **1995**, *238*, 187.
34 P.J. Baricelli, L. Izaguirre, J. López, E. Lujano, F. López-Linares, *J. Mol. Catal. A.: Chemical* **2004**, *208*, 67.
35 P.J. Baricelli, G. Rodríguez, M. Rodríguez, E. Lujano, F. López-Linares, *Appl. Catal. A.: General* **2003**, *239*, 25.
36 T. Suárez, B. Fontal, M. Reyes, F. Bellandi, R.R. Contreras, G. León, P. Cancines, *React. Kinet. Catal. Lett.* **2002**, *76*, 161.
37 T. Suárez, B. Fontal, M. Reyes, F. Bellandi, R.R. Contreras, A. Bahsas, G. León, P. Cancines, B. Castillo, *React. Kinet. Catal. Lett.* **2004**, *82*, 317.
38 B. Fontal, A. Anzelotti, M. Reyes, F. Bellandi, T. Suárez, *Catal. Lett.* **1999**, *59*, 187.
39 B. Drießen-Hölscher, J. Heinen, *J. Organomet. Chem.* **1998**, *570*, 141.
40 J. Heinen, M.S. Tupayachi, B. Drießen-Hölscher, *Catal. Today* **1999**, *48*, 273.
41 D.J. Ellis, P.J. Dyson, D.G. Parker, T. Welton, *J. Mol. Catal. A.: Chemical* **1999**, *150*, 71.
42 W.-C. Chang, C.-P. Lau, L. Cheng, Y.-S. Leung, *J. Organomet. Chem.* **1994**, *464*, 103.
43 C.-P. Lau, L. Cheng, *J. Mol. Catal.* **1993**, *84*, 39.
44 D.N. Akbayeva, L. Gonsalvi, W. Oberhauser, M. Peruzzini, F. Vizza, P. Brüggeller, A. Romerosa, G. Sava, A. Bergamo, *Chem. Commun.* **2003**, 264.
45 S. Bolaño, L. Gonsalvi, F. Zanobini, F. Vizza, V. Bertolasi, A. Romerosa, M. Peruzzini, *J. Mol. Catal. A.: Chemical* **2004**, *224*, 61.
46 C. Daguenet, R. Scopelliti, P.J. Dyson, *Organometallics* **2004**, *23*, 4849.
47 P. Baricelli, G. Morfes, D.E. Páez, *J. Mol. Catal. A.: Chemical* **2001**, *176*, 1.
48 M.S. Spencer, D.A. Dowden, *DBP 1114183* to Imperial Chemical Industries Ltd., **1962**.
49 J. Kwiatek, I.L. Mador, J.K. Seyler, *J. Am. Chem. Soc.* **1962**, *84*, 304.
50 D.L. Reger, M.M. Habib, D.J. Fauth, *J. Org. Chem.* **1980**, *45*, 3860.
51 J.-T. Lee, H. Alper, *J. Org. Chem.* **1990**, *55*, 1854.
52 T. Okano, M. Kaji, S. Isotani, J. Kiji, *Tetrahedron Lett.* **1992**, *33*, 5547.
53 K. Burgemeister, W. Leitner, 14th Int. Symp. Hom. Catal., Munich, **2004**, P 0203, *Book of Abstracts*, p. 214.
54 T. Okano, M. Iwahara, H. Konishi, J. Kiji, *J. Organomet. Chem.* **1988**, *346*, 267.
55 M.T. Reetz, S.R. Waldvogel, *Angew. Chem. Int. Ed. Engl.* **1997**, *36*, 865. *Angew. Chem.* **1997**, *109*, 870.
56 B.A. Murrer, J.W. Jenkins, *GB 2070023* to Johnson Matthey & Co. Ltd., **1981**.
57 B.A. Murrer, J.W. Jenkins, *USP 4,469,849* to Johnson Matthey & Co. Ltd., **1984**.
58 D.C. Mudalige, G.L. Rempel, *J. Mol. Catal. A.: Chemical* **1997**, *116*, 309.
59 D.C. Mudalige, G.L. Rempel, *J. Mol. Catal. A.: Chemical* **1997**, *123*, 15.
60 V. Kotzabasakis, E. Georgopoulou, M. Pitsikalis, N. Hadjichristidis, G. Papadogianakis, *J. Mol. Catal. A.: Chemical* **2005**, *231*, 93.
61 N.K. Singha, S. Sivaram, S.S. Talwar, *Rubber Chem. Technol.* **1995**, *68*, 281.
62 W.A. Herrmann, L.J. Goossen, M.J. Spiegler, *J. Organomet. Chem.* **1997**, *547*, 357.
63 W.A. Herrmann, M. Elison, J. Fischer, C. Köcher, *USP 5,663,451* to Hoechst AG, **1997**.

64 W.A. Herrmann, M. Elison, J. Fischer, C. Köcher, K. Öfele, *USP 5,728,839* to Hoechst AG, **1998**.
65 J.C. Garrison, R.S. Simons, C.A. Tessier, W.J. Youngs, *J. Organomet. Chem.* **2003**, *673*, 1.
66 P. Csabai, F. Joó, *Organometallics* **2004**, *23*, 5640.
67 L. Vígh, F. Joó, in: *Applied Homogeneous Catalysis with Organometallic Compounds* (Eds. B. Cornils, W.A. Herrmann), VCH, Weinheim, **1996**, Chapter 3.3.10.2.
68 F. Joó, N. Balogh, L.I. Horváth, G. Filep, I. Horváth, L. Vígh, *Anal. Biochem.* **1991**, *194*, 34.
69 T.X. Le, J.S. Merola, *Organometallics* **1993**, *12*, 3798.
70 G. Papp, H. Horváth, Á. Kathó, F. Joó, *Helv. Chim. Acta* **2005**, *88*, 566.
71 H.H. Horváth, F. Joó, *React. Kinet. Catal. Lett.* **2005**, *85*, 355.
72 L. Plasseraud, G. Süss-Fink, *J. Organomet. Chem.* **1997**, *539*, 163.
73 E.G. Fidalgo, L. Plasseraud, G. Süss-Fink, *J. Mol. Catal. A.: Chemical* **1998**, *132*, 5.
74 M. Faure, A. Tesouro Vallina, H. Stoeckli-Evans, G. Süss-Fink, *J. Organomet. Chem.* **2001**, *621*, 103.
75 G. Süss-Fink, M. Faure, T.R. Ward, *Angew. Chem. Int. Ed.* **2002**, *41*, 99.
76 P.J. Dyson, D.J. Ellis, G. Laurenczy, *Adv. Synth. Catal.* **2003**, *345*, 211.
77 P.J. Dyson, D.J. Ellis, W. Henderson, G. Laurenczy, *Adv. Synth. Catal.* **2003**, *345*, 216.
78 D.U. Parmar, S.D. Bhatt, H.C. Bajaj, R.V. Jasra, *J. Mol. Catal. A.: Chemical* **2003**, *202*, 9.
79 T.Q. Hu, M. Ezhova, T.Y.H. Wong, A.Z. Lu, B.R. James, 13th Int. Symp. Hom. Catal., Tarragona, **2002**, P. 016, *Book of Abstracts*, p. 66.
80 C. Daguenet, P.J. Dyson, *Catal. Commun.* **2003**, *4*, 153.
81 J.A. Widegren, M.A. Bennett, R.G. Finke, *J. Am. Chem. Soc.* **2003**, *125*, 10301.
82 C.M. Hagen, L. Vieille-Petit, G. Laurenczy, G. Süss-Fink, R.G. Finke, *Organometallics* **2005**, *24*, 1819.
83 F. Alario, Y. Amrani, Y. Colleuille, T.P. Dang, J. Jenck, D. Morel, D. Sinou, *J. Chem. Soc., Chem. Commun.* **1986**, 202.
84 Y. Amrani, L. Lecomte, D. Sinou, J. Bakos, I. Tóth, B. Heil, *Organometallics* **1989**, *8*, 542.
85 I. Tóth, B.E. Hanson, M.E. Davis, *Tetrahedron: Asymmetry* **1990**, *1*, 913.
86 I. Tóth, B.E. Hanson, M.E. Davis, *J. Organomet. Chem.* **1990**, *396*, 363.
87 I. Tóth, B.E. Hanson, M.E. Davis, *Catal. Lett.* **1990**, *5*, 183.
88 H. Ding, B.E. Hanson, J. Bakos, *Angew. Chem. Int. Ed. Engl.* **1995**, *34*, 1645; *Angew. Chem.* **1995**, *107*, 1728.
89 C. Bianchini, P. Barbaro, G. Scapacci, *J. Organomet. Chem.* **2001**, *621*, 26.
90 C. Lensink, E. Rijnberg, J.G. de Vries, *J. Mol. Catal. A: Chem.* **1997**, *116*, 199.
91 S. Trinkhaus, R. Kadyrov, R. Selke, J. Holz, L. Götze, A. Börner, *J. Mol. Catal. A.: Chemical* **1999**, *144*, 15.
92 T. Malström, C. Andersson, *Chem. Commun.* **1996**, 1135.
93 T. Malström, C. Andersson, *J. Mol. Catal. A.: Chemical* **1999**, *139*, 259.
94 K. Yonehara, T. Hashizume, K. Mori, K. Ohe, S. Uemura, *J. Org. Chem.* **1999**, *64*, 5593.
95 K. Ohe, K. Morioka, K. Yonehara, S. Uemura, *Tetrahedron: Asymmetry* **2002**, *13*, 2155.
96 M. Laghmari, D. Sinou, A. Masdeu, C. Claver, *J. Organomet. Chem.* **1992**, *438*, 213.
97 B. Pugin, *PCT Int. Appl. WO 01 04,131 (EP1194437)* to Solvias AG, **2001**.
98 H. Brunner, S. Stefaniak, M. Zabel, *Synthesis* **1999**, 1776.
99 Q.-H. Fan, G.-J. Deng, X.-M. Chen, W.-C. Xie, D.-Z. Jiang, D.-S. Liu, A.S.C. Chan, *J Mol. Catal. A.: Chemical* **2000**, *159*, 37.
100 A.E. Sollewijn Gelpke, H. Kooijman, A.L. Spek, H. Hiemstra, *Chem. Eur. J.* **1999**, *5*, 2472.
101 R. Schmid, E.A. Broger, M. Cereghetti, Y. Crameri, J. Foricher, M. Lalonde, R.K. Müller, M. Scalone, G. Schoettel, U. Zutter, *Pure Appl. Chem.* **1996**, *68*, 131.
102 R.A. Brown, P. Pollet, E. McKoon, C.A. Eckert, C.L. Liotta, P.G. Jessop, *J. Am. Chem. Soc.* **2001**, *123*, 1254.
103 G. Oehme, E. Paetzold, R. Selke, *J. Mol. Catal.* **1992**, *71*, L1.

104 G. Oehme, I. Grassert, E. Paetzold, R. Meisel, K. Drexler, H. Fuhrmann, *Coord. Chem. Rev.* **1999**, *185–186*, 585.

105 F. Robert, G. Oehme, I. Grassert, D. Sinou, *J. Mol. Catal. A.: Chemical* **2000**, *156*, 127.

106 I. Grassert, J. Kovács, H. Fuhrmann, G. Oehme, *Adv. Synth. Catal.* **2002**, *344*, 312.

107 C. de Bellefon, N. Pestre, T. Lamouille, P. Grenouillet, V. Hessel, *Adv. Synth. Catal.* **2003**, *345*, 190.

108 E. Fache, F. Senocq, C. Santini, J.-M. Basset, *J. Chem. Soc., Chem. Commun.* **1990**, 1776.

109 E. Fache, F. Senocq, C. Santini, J.M. Basset, *J. Mol. Catal.* **1992**, *72*, 337.

110 J.M. Grosselin, C. Mercier, *J. Mol. Catal.* **1990**, *63*, L25.

111 J.M. Grosselin, C. Mercier, G. Allmang, F. Grass, *Organometallics* **1991**, *10*, 2126.

112 J.M. Grosselin, C. Mercier, *USP 4,925,990* to Rhone-Poulenc Sante, **1990**.

113 C. Mercier, P. Chabardes, *Pure Appl. Chem.* **1994**, *7*, 1509.

114 J.M. Grosselin, *EP 0 362037* to Rhone-Poulenc Sante, **1990**.

115 K. Nuithitikul, M. Winterbottom, *Chem. Eng. Sci.* **2004**, *59*, 5439.

116 G. Papp, J. Kovács, A.Cs. Bényei, G. Laurenczy, L. Nádasdi, F. Joó, *Can. J. Chem.* **2001**, *79*, 635.

117 G. Papp, J. Elek, L. Nádasdi, G. Laurenczy, F. Joó, *Adv. Synth. Catal.* **2003**, *345*, 172.

118 N. Makihara, S. Ogo, Y. Watanabe, *Organometallics* **2001**, *20*, 497.

119 R.A. Sánchez-Delgado, M. Medina, F. López-Linares, A. Fuentes, *J. Mol. Catal. A.: Chemical* **1997**, *116*, 167.

120 M. Hernandez, P. Kalck, *J. Mol. Catal. A.: Chemical* **1997**, *116*, 131.

121 H. Gulyás, A.C. Bényei, J. Bakos, *Inorg. Chim. Acta* **2004**, *357*, 3094.

122 D.J. Darensbourg, F. Joó, M. Kannisto, Á. Kathó, J.H. Reibenspies, D.J. Daigle, *Inorg. Chem.* **1994**, *33*, 200.

123 A. Fukuoka, W. Kosugi, F. Morishita, M. Hirano, L. McCaffrey, W. Henderson, S. Komiya, *Chem. Commun.* **1999**, 489.

124 P. Smolenski, F.P. Pruchnik, Z. Ciunik, T. Lis, *Inorg. Chem.* **2003**, *42*, 3318.

125 F.P. Pruchnik, P. Smolenski, E,. Galdecka, Z. Galdecki, *New J. Chem.* **1998**, 1395.

126 K.-C. Tin, N.-B. Wong, R.-X. Li, Y.-Z. Li, J.-Y. Hu, X.-J. Li, *J. Mol. Catal. A.: Chemical* **1999**, *137*, 121.

127 K.-C. Tin, N.-B. Wong, R.-X. Li, Y.-Z. Li, X.-J. Li, *J. Mol. Catal. A.: Chemical* **1999**, *137*, 113.

128 C.A. Mebi, B.J. Frost, *Organometallics* **2005**, *24*, 2339.

129 V. Penicaud, C. Maillet, P. Janvier, M. Pipelier, B. Bujoli, *Eur. J. Org. Chem.* **1999**, 1745.

130 C. Maillet, T. Praveen, P. Janvier, S. Minguet, M. Evain, C. Saluzzo, M. Lorraine Tommasino, B. Bujoli, *J. Org. Chem.* **2002**, *67*, 8191.

131 T. Lamouille, C. Saluzzo, R. ter Halle, F. Le Guyader, M. Lemaire, *Tetrahedron Lett.* **2001**, *42*, 663.

132 M. Berthod, C. Saluzzo, G. Mignani, M. Lemaire, *Tetrahedron: Asymmetry* **2004**, *15*, 639.

133 F. Joó, E. Trócsányi, *J. Organomet. Chem.* **1982**, *231*, 63.

134 E. Monflier, *Recent Res. Dev. Org. Chem.* **1998**, *2*, 623.

135 B.M. Bhanage, Y. Ikushima, M. Shirai, M. Arai, *Chem. Commun.* **1999**, 1277.

136 A. Behr, M. Urschey, V.A. Brehme, *Green Chem.* **2003**, *5*, 198.

137 Y. Shi, X. Du, H. Chen, X.-J. Li, J.-Y. Hu, *Shiyou Huagong* **2003**, *32*, 1051. *C.A.* 140:289167.

138 M.T. Reetz, C. Frömbgen, *Synthesis* **1999**, 1555.

139 M.T. Reetz, *J. Heterocyc. Chem.* **1998**, *35*, 1065.

140 R.M. Deshpande, A.N. Mahajan, M.M. Diwakar, P.S. Ozarde, R.V. Chaudhari, *J. Org. Chem.* **2004**, *69*, 4835.

141 J. Bakos, Á. Orosz, B. Heil, M. Laghmari, P. Lhoste, D. Sinou, *J. Chem. Soc., Chem. Commun.* **1991**, 1684.

142 C. Lensink, J.G. de Vries, *Tetrahedron: Asymmetry* **1992**, *3*, 235.

143 J.M. Buriak, J.A. Osborn, *Organometallics* **1996**, *15*, 3161.

144 Y. P. Xie, J. Men, Y. Z. Li, H. Chen, P. M. Cheng, X. J. Li, *Catal. Commun.* **2004**, *5*, 237.

145 A. Bényei, F. Joó, *J. Mol. Catal.* **1990**, *58*, 151.

146 M. Murakami, R. Kawai, K. Suzuki, *J. Chem. Soc. Japan* **1963**, *84*, 669.

147 R. A. Sánchez-Delgado, *Organometallic Modeling of the Hydrodesulfurization and Hydrodenitrogenation Reactions.* Kluwer, Dordrecht, **2002**.

148 C. Bianchini, A. Meli, *Acc. Chem. Res.* **1998**, *31*, 109.

149 I. Rojas, F. Lopez-Linares, N. Valencia, C. Bianchini, *J. Mol. Catal. A.: Chemical* **1999**, *144*, 1.

150 M. A. Busolo, F. Lopez-Linares, A. Andriollo, D. E. Paez, *J. Mol. Catal. A.: Chemical* **2002**, *189*, 211.

151 D. E. Paez, A. Andriollo, R. A. Sanchez-Delgado, N. Valencia, R. E. Galiasso, F. A. Lopez, *USP 5,753,584* to Intevep S. A., **1998**.

152 D. E. Paez, A. Andriollo, R. A. Sanchez-Delgado, N. Valencia, R. E. Galiasso, F. A. Lopez, *USP 5,958,223* to Intevep S. A., **1999**.

153 D. E. Paez, A. Andriollo, R. A. Sanchez-Delgado, N. Valencia, R. E. Galiasso, F. A. Lopez, *USP 5,981,421* to Intevep S. A., **1999**

39
Supercritical and Compressed Carbon Dioxide as Reaction Medium and Mass Separating Agent for Hydrogenation Reactions using Organometallic Catalysts

Walter Leitner

39.1
Introduction

Compressed and (in particular) supercritical carbon dioxide ($scCO_2$) is finding increasing interest as alternative solvent system to replace classical volatile organic chemicals (VOC) in chemical processes [1]. During the past decade, research with this medium and other supercritical fluids (SCFs) has shown that the potential of these "green solvents" reaches far beyond the substitution of potentially harmful substances and offers new opportunities for the control of chemical reactions on both molecular and engineering levels. This chapter will summarize recent advances in this field for the specific example of hydrogenation reactions using organometallic complex catalysts.

Hydrogenation using SCFs has already found considerable industrial interest and application using typical heterogeneous catalysts. Hoffmann LaRoche has operated $scCO_2$ technology for a key step in a vitamin synthesis [2]. Likewise, research teams at Degussa [3] and in Scandinavia [4] have conducted intensive investigations into the hydrogenation of fatty acid esters in $scCO_2$ and sc-propane, respectively, including the recent development of a demonstration plant [5]. The multipurpose plant opened by Thomas Swan in the UK in 2002, based on their collaboration with the group of Poliakoff at the University of Nottingham, is probably the most advanced example for hydrogenation with $scCO_2$ at present, allowing an annual production capacity of up to 1000 tonnes [6]. These examples demonstrate that SCF technology is a viable option for hydrogenation reactions in the fine chemical and pharmaceutical industries. The combination of the advanced reaction engineering of compressed CO_2 and other SCFs with the molecular design of organometallic complex catalysis seems therefore highly attractive.

The fundamental properties of SCFs and their relation to organometallic catalysis have been reviewed extensively in recent years, and will not be re-iterated here [1, 7]. The term "supercritical" indicates that the substance used as reaction medium or solvent is heated and compressed beyond its critical temperature and pressure. For CO_2, which is the most widely used SCF in hydrogenation reactions, these values are $T_c = 31.04\,^{\circ}C$ and $p_c = 73.83$ bar. Owing to the complex

The Handbook of Homogeneous Hydrogenation.
Edited by J.G. de Vries and C.J. Elsevier
Copyright © 2007 WILEY-VCH Verlag GmbH & Co. KGaA, Weinheim
ISBN: 978-3-527-31161-3

phase behavior of multicomponent reaction mixtures as encountered in hydrogenation processes, this notation includes truly monophasic as well as multiphasic systems. For simplicity, we will use the term "supercritical" for general discussions in this chapter, and specify the nature of mixtures if necessary. We will furthermore refer to "homogeneous catalysts" in this chapter only for truly monophasic systems, whereas we will use "organometallic catalysts" as notation for the active species in general.

One of the most attractive features of using novel solvent systems for organometallic hydrogenation is the development of new separation and immobilization concepts. A number of interesting approaches has been investigated very recently by exploiting the physico-chemical properties of compressed (supercritical *or* subcritical) CO_2. We will extend the discussion in this chapter to these systems, and highlight similarities and differences between the various methods. Clearly, many of these techniques are still in their very early stages of development and have been demonstrated often for singular examples only. With this chapter, we hope to stimulate further research in the area in order to validate the individual techniques for potential applications.

39.2
The Molecular and Reaction Engineering Basis of Organometallic-Catalyzed Hydrogenations using Compressed and $scCO_2$

39.2.1
Control of Hydrogen Availability

Hydrogenation reactions carried out with soluble organometallic catalysts are often very sensitive to the availability of H_2 in the catalyst phase. The availability of the gaseous reagent at the active center is limited by the maximum solubility of H_2 and the rate of its diffusion into the catalyst phase. This may affect reaction rates as well as selectivities in hydrogenation reactions [8, 9]. Both, solubility and mass transfer are strongly influenced by compressed and $scCO_2$-based media, offering an additional control parameter in hydrogenation reactions. Figure 39.1 depicts the situation for a conventional hydrogenation set-up, for a biphasic $scCO_2$/liquid system, and for a single-phase reaction mixture, assuming that all components (including the catalyst) are sufficiently soluble in $scCO_2$ to reach a single phase.

Organic liquids often show very high solubilities for CO_2, associated with a very significant volume expansion (Fig. 39.1, center). Such "expanded liquids" [10] are formed in the presence of $scCO_2$ from solutions or also from neat liquid substrates. The physico-chemical properties of these phases can differ significantly from those of the non-expanded liquids. Viscosity and surface tension are reduced, increasing therefore the rate of mass transfer between the liquid and the supercritical phase. The solubility of H_2 in the expanded liquid phase is also increased. Under single-phase conditions (Fig. 39.1, right), all mass transfer barriers (gas/liquid) have disappeared completely and the reactive gas is fully mis-

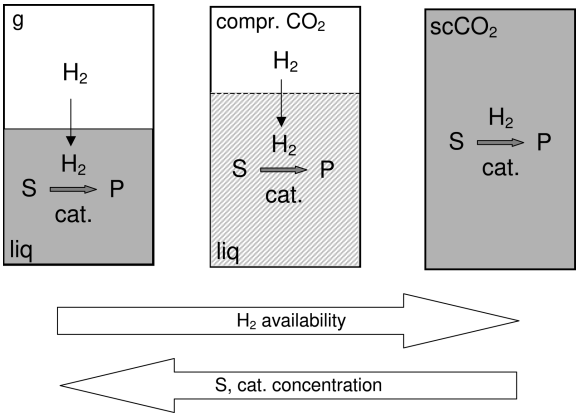

Fig. 39.1 Organometallic complex-catalyzed hydrogenation under conventional conditions, in liquids expanded with compressed (super- or subcritical) CO_2 and under monophasic supercritical conditions.

cible with the reactive phase. This situation ensures the maximum availability of H_2 for the reaction. However, as the liquid phase expands and finally dissolves completely in the SCF phase, the catalyst and substrate become distributed over a larger volume. Depending on the reaction order of each component in the rate law of the reaction, the overall rate and selectivity can therefore have a fairly complex dependence on the phase behavior of such systems [11, 12].

Other liquid phases such as ionic liquids (ILs) or poly(ethyleneglycol) (PEG) also show very high CO_2 affinities, albeit the volume expansion is generally less pronounced. Hydrogen solubility in ILs as a function of additional CO_2 has been measured using high-pressure ^{1}H-NMR spectroscopy, and an increase by a factor of three to five has been noted at typical operating pressures. These data could be corroborated with the preparative results of the iridium-catalyzed imine hydrogenation in IL/scCO_2 mixtures (see Section 39.2.3), where reactions were often sluggish in the pure ionic liquid, but occurred smoothly in the biphasic system at identical H_2 partial pressure [13]. Such systems are of particular interest as they allow for continuous-flow operation of organometallic hydrogenation without the use of any additional organic solvent (*vide infra*).

39.2.2
Catalyst Recycling and Immobilization

Owing to the large synthetic importance of hydrogenation reactions, many individual techniques have been developed to address the fundamental problem of catalyst recycling and immobilization by using compressed gases and SCFs. The following general pattern emerges from these investigations to date [14], and will be reflected also in the examples to be discussed in detail in Section 39.2.3.

39.2.2.1 Solubility Control for Separation

Compressed CO_2 can be used to control the solubility of suitably modified organometallic complexes in reaction mixtures, thus allowing selective separation processes. Three different scenarios can be envisaged for hydrogenation reactions:

- CO_2 as anti-solvent: The introduction of CO_2 to a reaction mixture selectively precipitates the organometallic hydrogenation catalysts, followed by SCF extraction of the products and recovery of the catalyst in active form.
- CO_2 as adjustable-solvent: In this case, the reaction is carried out in $scCO_2$ under truly monophasic conditions and the catalyst is selectively precipitated through a change in temperature and/or pressure. Again, product isolation is achieved by SCF extraction.
- CO_2 as co-solvent: Here, CO_2 is used to solubilize a catalyst, which is insoluble in the pure organic liquid, in an expanded organic phase. Once the CO_2 is removed at the end of the reaction, the catalyst precipitates and can be removed by filtration.

39.2.2.2 Membrane Separation

CO_2-philic catalysts that allow operation under fully homogeneous supercritical conditions are usually much larger than typical organic products, and can be retained by suitably size-selective membranes.

39.2.2.3 Biphasic Liquid/Supercritical Systems

As with classical multiphase catalysis, the organometallic catalyst is retained here in a liquid phase that is immiscible with the second phase containing substrates and/or products. For hydrogenation, the liquid/SCF system is always biphasic, whereas conventional systems are usually triphasic (liquid-1/liquid-2/H_2). The liquid phase must provide a stable environment for the organometallic catalyst and should be insoluble in the SCF phase. Water, ILs and PEG have been used successfully for this purpose, together with $scCO_2$ as the mobile phase. Again, the products must not be too polar in order to be effectively extracted if CO_2 is used as the SCF.

39.2.2.4 Inverted Biphasic Systems

Biphasic systems that contain the catalyst in the supercritical phase and the substrates/products in a second liquid phase can also be implemented. With water as the polar phase, these "inverted" systems are particularly attractive for the conversion of highly polar and/or low-volatile hydrophilic substrates with limited solubility in typical SCFs such as $scCO_2$.

39.2.2.5 **Solid-Supported Catalysts**

The heterogenization of organometallic catalysts on inorganic or organic solids has been extensively studied with traditional organic solvents. Mass transfer limitations and metal leaching have been identified as major obstacles for the practical use of this approach. Both factors might be reduced if an SCF is used as the mobile phase, albeit systematic studies are currently not yet available.

39.2.3 **Catalytic Systems for Hydrogenation using SCFs, and their Synthetic Applications**

The area of organometallic-catalyzed hydrogenation in SCFs was pioneered during the mid-1990s by studies on the hydrogenation of CO_2 itself to yield formic acid or derivatives such as formamides [15, 16]. Although the phase behavior of the multicomponent reaction mixtures is probably more complex than anticipated in these early studies, these investigations showed that the high availability of hydrogen under supercritical conditions can be exploited to achieve very high turnover frequencies (TOFs) with sufficiently CO_2-soluble metal catalysts. The generally low solubility of organometallic catalysts in $scCO_2$ was identified as a major limitation upon attempts to extend this methodology to asymmetric hydrogenation of C=C double bonds. For example, a ruthenium catalyst containing partly hydrogenated BINAP **2** as ligand required the presence of a co-solvent in the hydrogenation of dehydroamino acids in $scCO_2$ (Scheme 39.1) [17]. The cationic rhodium catalyst based on Et-DuPHOS (**5**) was rendered sufficiently CO_2-soluble in combination with the perfluoroalkyl substituted anion tetrakis[3,5-bis(trifluoromethyl)phenyl]borate (BARF) [18].

The most general approach to generate highly CO_2-soluble catalysts is the attachment of a "CO_2-philic" [19] side group at the periphery of a ligand in the organometallic catalyst [20]. Until now, fluor-containing groups have been used most widely to generate hydrogenation catalysts. Fluorinated aryl phosphines have been investigated for Ru-catalyzed chemoselective hydrogenation of α,β-unsaturated aldehydes in $scCO_2$ [21]. CO_2-soluble hydrogenation catalysts bearing a large number of perfluoroalkyl group [22] or extended fluorous polymers [23] are extremely soluble, and they reach a size where they can be efficiently retained by membrane

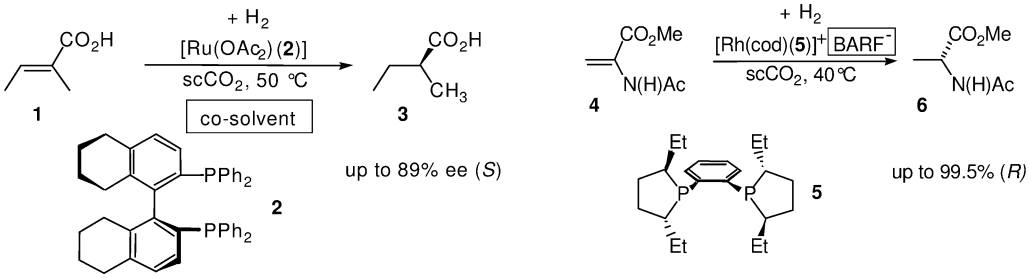

Scheme 39.1 Early examples for enantioselective hydrogenation in $scCO_2$.

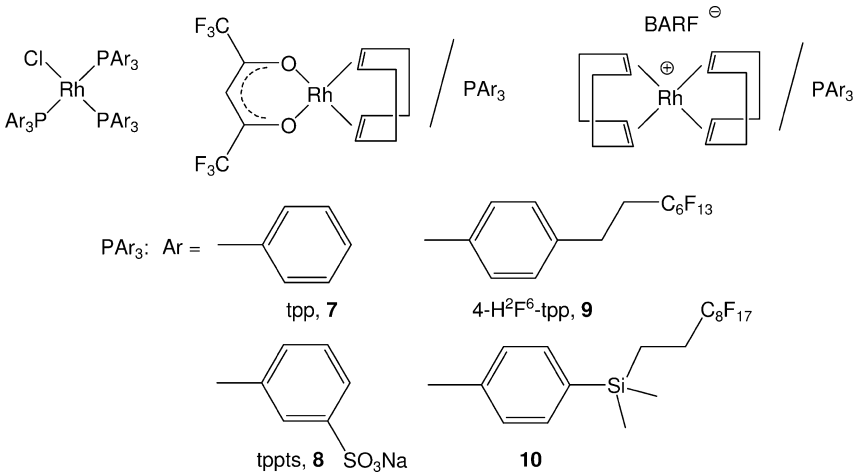

Scheme 39.2 Examples of typical rhodium-based catalyst systems and modified derivatives of triphenylphosphine as used to control their solubility with $scCO_2$ in homogeneous or multiphase systems (BARF = tetrakis[3,5-bis (trifluoromethyl)phenyl]borate).

filtration. For example, the rhodium-catalyzed hydrogenation of butene as a model reaction has been carried out successfully in a continuous membrane reactor using the perfluoroalkyl-substituted derivative of triphenylphosphine **10** (Scheme 39.2) to generate an analogue of Wilkinson's catalyst [22].

The reaction sequence of hydroformylation and reductive amination (hydroaminomethylation) of the allylamine **11** provides an illustrative example for additional reaction control in $scCO_2$ (Scheme 39.3). Under conventional conditions, path B is preferred, leading to pyrrolidone **12** as the major product. In $scCO_2$, however, the secondary amine is temporarily protected as the corresponding carbamic acid and the hydrogen availability is strongly increased. Therefore, path A prevails, leading first to the hydroformylation product **13** and finally to the saturated heterocycle **14** as the major product. The application of the rhodium-based catalytic system for this reaction under $scCO_2$ conditions was made possible by the use of the CO_2-philic derivative of triphenylphosphine **9** [24].

Chiral ligand frameworks that have been modified with perfluoroalkyl groups and applied to asymmetric hydrogenation include chelating ligands such as BINAP [25–27], BINAPHOS [28–30], phosphino-oxazolines [31], and phosphonites [32], as well as monodentate phosphoramidites and phosphites [27, 33]. The application of 3-H^2F^6-(*R,S*)-BINAPHOS (**16**) in the asymmetric hydrogenation of α,β-unsaturated carboxylic acid derivatives is shown in Scheme 39.4. Owing to the relatively high molecular weight of the chiral framework, ligand **16** has a fairly low fluorine content of only 34%. This is sufficient, however, to render the ligand highly CO_2-philic, allowing for example investigation of the reactivity of its rhodium complexes in $scCO_2$ by high-pressure multinuclear NMR spec-

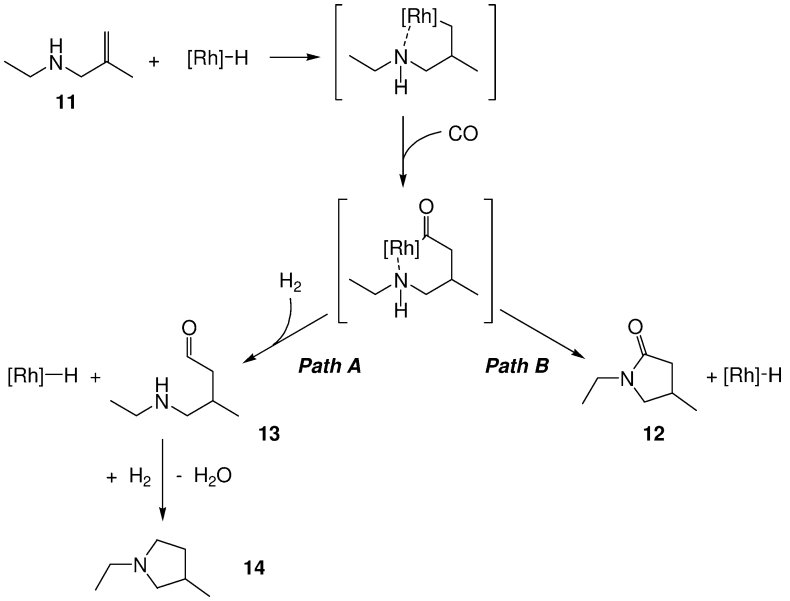

Scheme 39.3 Product control by affecting the relative rates of competing reaction pathways in $scCO_2$. Path A is preferred in $scCO_2$, whereas path B prevails in conventional solvents.

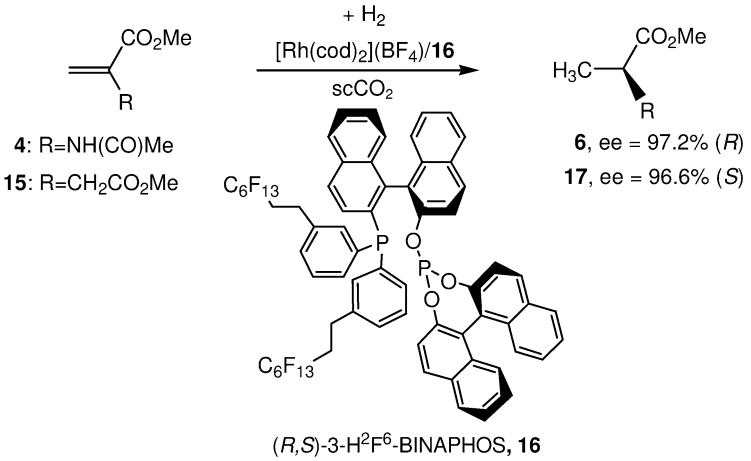

Scheme 39.4 Enantioselective hydrogenation in $scCO_2$ using a CO_2-philic derivative of BINAPHOS.

troscopy [28b]. In combination with the cationic precursor $[Rh(cod)_2][BF_4]$, high conversion and excellent ee-values were obtained for substrates **4** and **15**. Visual inspection of the reaction mixture indicated that fully homogeneous conditions could be achieved with **15**, whereas small amounts of substrate **4** remained al-

ways undissolved under the used conditions. The catalytic active species was, however, contained predominantly in the $scCO_2$ phase, as indicated by the typical yellow-orange color.

It is apparent from these prototypical results that the solubility of both catalysts and substrates can place certain constraints on the hydrogenation in $scCO_2$ under truly homogeneous conditions. Co-solvents such as methanol or trifluorotoluene (benzotrifluoromethane, BTF) can be used to overcome these limitations, but they partly offset the purpose of using a VOC-free system. Most recently, supercritical hydrofluorocarbons such as 1,1,1,2-tetrafluoroethane have been suggested as possible alternatives to $scCO_2$, with an improved solubility profile for polar substrates and catalysts [34]. A very attractive approach utilizing a combination of two benign solvents is the application of an inverted $scCO_2$/H_2O biphasic system, where the limited solubility of the polar substrates and products is turned into an advantage allowing simple and efficient separation and recycling of the catalyst [30].

The principle of the inverted system is depicted in Figure 39.2, together with typical results. The CO_2-philic catalyst, which is generated in the same way as above, is contained in the $scCO_2$ phase, whereas the polar product partitions preferentially into the aqueous phase. Using a rhodium catalyst formed with the chiral BINAPHOS-derivative **16**, reasonable reaction rates and excellent ee-values were observed with substrate **4**. The catalyst was recycled without loss of activity or selectivity, leading to an average value of 98.4 ± 0.6% ee in five consecutive runs. Metal and phosphorus leaching into the aqueous phase was below the detection limit of 1 ppm, and recovery of product **6** was nearly quantitative. Similar results were obtained with itaconic acid (**18**) as another prototypical substrate [30].

Continuous-flow hydrogenation processes using $scCO_2$ as the mobile substrate/product phase can be envisaged also in systems where the catalyst is immobilized in the liquid phase. The hydrogenation of styrene (Scheme 39.5) is often used as a first benchmark reaction to evaluate such immobilization methods. Water is only sparingly soluble in $scCO_2$ and can be applied as a catalyst compartment with typical sulfonated water-soluble phosphine ligands such as tppts (**8**) [35]. Despite the use of a SCF as the substrate/product phase, the system seems to be operating under mass transfer limitations, and surfactants have been used to generate emulsion- and microemulsion-type reaction mix-

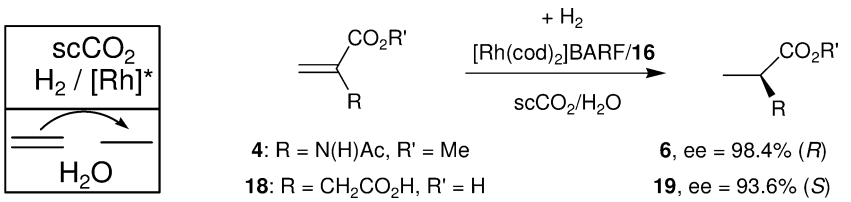

Fig. 39.2 Enantioselective hydrogenation of polar substrates in an inverted $scCO_2$/water biphasic system.

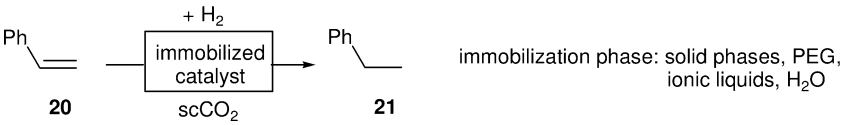

Scheme 39.5 Hydrogenation of styrene as a test reaction for immobilization methods, using $scCO_2$ as the mobile phase.

tures for enhanced performance in these systems [36]. High molecular-weight PEG has been demonstrated as a catalyst immobilization phase for organometallic hydrogenation with the same test reaction [37]. Although this catalyst phase would be a solid at the reaction temperature, it melts in the presence of $scCO_2$ as the compressed gas dissolves in the polymer. An attractive feature of this system is that no catalyst modification is necessary with triphenylphosphine (**7**)-based catalysts, suggesting that many chiral catalysts might also operate under the same conditions.

Ionic liquids (ILs) form also biphasic mixtures with $scCO_2$, and can serve as catalyst reservoirs for hydrogenation processes. The hydrogenation of supercritical CO_2 to formamides was used to investigate the possibility of controlling consecutive reaction pathways in such biphasic mixtures [38]. Asymmetric hydrogenation with ruthenium–BINAP catalysts similar to **2** in ILs allowed recycling of the chiral catalyst after extraction of the product with $scCO_2$ [39]. The iridium-catalyzed asymmetric hydrogenation of imines revealed a synergistic effect of the use of both media in this combination as compared to the individual solvent systems (Scheme 39.6) [13].

The secondary aryl amine **24** is far less basic than primary or secondary alkyl amines, and does not form the carbamic acid to any detectable extent in the presence of $scCO_2$ [31]. Therefore, **24** is extracted readily from the catalyst-containing IL phase, which can be recycled without noticeable loss of activity and selectivity [13]. In fact, it transpires that the active species is more stable towards oxygen in the IL than in organic solvents. Furthermore, the choice of anion of the IL largely controls the performance of the active cationic species, allowing even the use of an otherwise inactive iridium chloride precursor [{Ir(cod)Cl}$_2$] to form *in-situ* catalysts

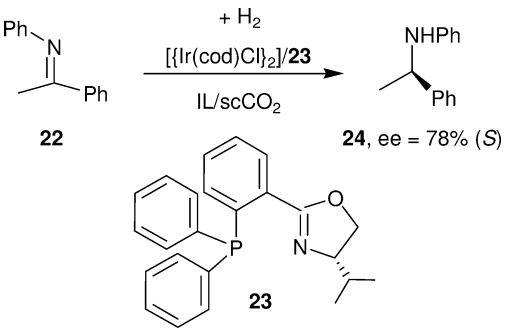

Scheme 39.6 Enantiomeric hydrogenation of imine **22** in an IL/$scCO_2$ biphasic system using an *in-situ*-activated iridium catalyst.

in such media. This allows a rapid variation and screening of ligands with alternative structures to **23**. As mentioned in Section 39.2.1, the inherent problems of low H_2 solubility and low viscosity of some ILs is overcome in the biphasic system through the beneficial effects of $scCO_2$.

The presence of compressed CO_2 can also enhance the mass transport properties in liquid/supercritical reaction mixtures where the catalyst resides in the neat substrate. A striking example is the hydrogenation of vinyl arenes using Wilkinson's catalyst [RhCl(**7**)$_3$] at temperatures below the melting point of the solid substrates, where the presence of even subcritical CO_2 induces a significant melting point depression [40]. High rates and enantioselectivities were reported also for a ruthenium-catalyzed hydrogenation of β-keto esters [41] and a rhodium-catalyzed cascade reaction sequence involving hydrogenation as a key step under conditions where a liquid substrate/$scCO_2$ biphasic system is likely to be present [42].

The effects of added CO_2 on mass transfer properties and solubility were assessed in some detail for the catalytic asymmetric hydrogenation of 2-(6′-methoxy-2′-naphthyl) acrylic acid to (*S*)-naproxen using Ru–(*S*)-BINAP-type catalysts in methanolic solution. The catalytic studies showed that a higher reaction rate was observed under a total CO_2/H_2 pressure of ca. 100 bar ($pH_2 = 50$ bar) than under a pressure of 50 bar H_2 alone. Upon further increase of the CO_2 pressure, the catalyst could be precipitated and solvent and product were removed, at least partly by supercritical extraction. Unfortunately, attempts to re-use the catalyst were hampered by its deactivation during the recycling process [11].

Most recently, a catalyst system based on PEG-modified phosphine ligands was reported to allow for a highly effective CO_2-induced separation procedure. In this case, the $scCO_2$ was used only at the separation stage to precipitate the catalyst and extract the products. The hydrogenation of styrene to ethyl benzene was used as a benchmark reaction, and it was shown that the catalytic active species could be recovered and not only re-used for another hydrogenation but also be subjected as a "cartridge" to a series of different transformations [43].

It should be noted, however, that CO_2 cannot be used only to precipitate, but also to solubilize catalysts in organic solvents. Not surprisingly, this method again relies on the application of CO_2-philic catalysts. As outlined above, these complexes are often highly fluorinated and hence, in certain cases, are immiscible with organic solvents. When expanded with CO_2, the liquid phase becomes increasingly "fluorophilic" until the catalyst finally dissolves. Release of CO_2 reverses the process and leads to precipitation of the catalyst. This method was demonstrated again for the hydrogenation of styrene to ethylbenzene using [RhCl(**9**)$_3$] as the catalyst precursor and cyclohexane as solvent. To facilitate the handling of the dissolved and re-precipitated catalyst, fluorous silica gel was used as a catalyst "sponge". In recycling experiments employing this system, the fluorous Wilkinson's catalyst showed only marginal activity decrease over five cycles [44].

Control of product solubility by compressed CO_2 is also possible. Primary and secondary alkylamines form carbamic acids or ammonium carbamates in the

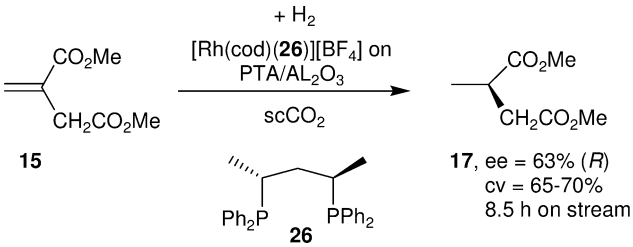

Scheme 39.7 Continuous-flow hydrogenation of dimethyl itaconate (**15**) using a solid-supported chiral catalyst and $scCO_2$ as the mobile phase ($PTA = H_3P_{40}PW_{12}$).

presence of compressed CO_2. It has been shown that this reaction can be used to modulate the reactivity of such species in $scCO_2$ solution in reductive amination reactions (cf. Scheme 39.3) [24]. Depending on their substitution pattern and the exact solvent system, however, these compounds may also precipitate from the reaction mixture upon their formation by hydrogenation of the corresponding imines [31] or nitriles [45]. In favorable cases, this can be used for a simple catalyst separation scheme with organometallic catalysts in expanded solvent systems [45].

Finally, SCFs and $scCO_2$ allow for continuous-flow fixed-bed hydrogenations with heterogenized solid-supported catalysts. The application of ruthenium complexes that were linked covalently to solid supports was demonstrated early on in CO_2 hydrogenation [46, 47]. Ruthenium complexes were also supported on silica in combination with ligand **8** using the supported-aqueous-phase (SAP) approach [35]. Application of $scCO_2$ yielded better conversions for the hydrogenation of cinnamaldehyde than using toluene with the same method. A silica-adsorbed Wilkinson catalyst [RhCl(**7**)$_3$]/SBA-15 was investigated recently for the hydrogenation of simple olefins, as shown in Scheme 39.5 [48]. For asymmetric hydrogenation, true continuous-flow operation was demonstrated most recently with a Skewphos (**26**)-based cationic rhodium catalyst that was anchored to alumina by electrostatic interaction via a polyoxometallate anion. Steady-state conversion and enantioselectivity was observed for the hydrogenation of dimethyl itaconate (**15**) over a period of more than 8 h (Scheme 39.7) [49].

39.2.4
Mechanistic Aspects

The large body of examples discussed in the previous section indicates that SCFs, and in particular $scCO_2$, offer a broad potential for applications in hydrogenation reactions. Very little is known, however, about possible interactions between the catalytically active species and the reaction medium in such systems. In particular, two possible transformations of CO_2 in the presence of hydrogen must be considered, which are also transition metal-catalyzed (Scheme 39.8). The water gas shift (WGS) reaction can lead to the formation of CO, and has

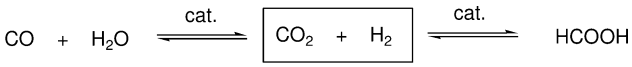

Scheme 39.8 Possible reactions of CO_2 in the presence of H_2 under transition metal-catalyzed hydrogenation conditions.

been observed as a major deactivation and poisoning pathway with heterogeneous catalysts in a number of cases [50]. Successful hydroformylation/hydrogenation sequences, such as that shown in Scheme 39.3, indicate that organometallic transition metal hydrogenation catalysts can tolerate CO in certain cases. Nevertheless, activities and selectivities might be expected to be altered in the presence of this additional ligand, though to date no such cases have been reported.

The second reaction to be considered is the formation of formic acid from H_2 and CO_2. This reaction is very effectively catalyzed by rhodium and ruthenium hydride complexes similar to those involved in C=C or C=O hydrogenation reactions. As formic acid itself is a widely used hydrogen transfer reagent, a hydrogenation carried out in $scCO_2$ may actually follow a transfer hydrogenation pathway involving formate intermediates rather than the classical hydride route. The hydrogenation of dimethyl itaconate **15** using a cationic CO_2-philic rhodium catalyst formed with ligand **27** was used as a probe reaction to distinguish between these two possibilities (Scheme 39.9) [32].

The distribution of isotopomers **17**-d_n obtained from the reaction of **15** with D_2 in $scCO_2$ and other media was used as a diagnostic tool. In particular, the 2,3- and 1,3-pattern in the dideutero products **17**-d_2 differs significantly from the classical hydrogenation and the transfer hydrogenation pathway owing to a shift in relative rates between rearrangement and hydrogen transfer processes [51]. The 2,3-addition is largely preferred in the hydrogenation pathway, whereas the 1,3-isomer is the major product obtained from transfer hydrogenation. The

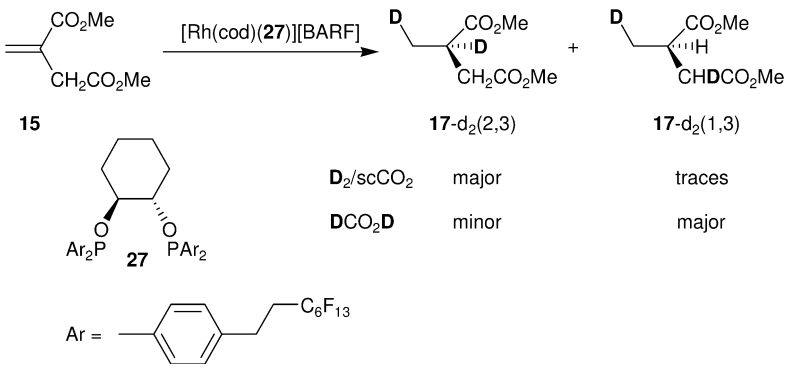

Scheme 39.9 Deuterium labeling as a mechanistic probe for hydrogenation pathways in $scCO_2$.

pattern observed in $scCO_2$ was largely identical to that observed with D_2 in hexane or sc-ethane, revealing a preferred 2,3-addition mode with no significant incorporation at C-1. It was therefore concluded that formate intermediates are unlikely to play a major role in the productive catalytic cycle. This was further supported by parahydrogen-induced polarization (PHIP)-NMR measurements indicating that the two H atoms are transferred pairways without significant scrambling which would be unlikely for a formic acid pathway.

Interestingly, the enantioselectivity of the hydrogenation shown in Scheme 39.9 exhibited a large dependence on the partial pressure of hydrogen in conventional solvents, whereas it was almost independent of this parameter in $scCO_2$. As fundamental differences in the hydrogenation pathways were ruled out by the above-mentioned experiments, it seems most likely that the availability of hydrogen (see Section 39.2.1) is the controlling factor for this observation.

39.3 Conclusions and Outlook

Compressed and, in particular, supercritical CO_2 offers great potential as reaction medium and/or mass-separating agent for organometallic hydrogenation reactions. Especially, the design of integrated reaction and separation processes represents a highly attractive development for the future. There is increasing evidence that flexible and small-scale engineering solutions are possible that would allow the advantages of molecular catalyst design to be combined with continuous-flow operation. Indeed, such modular "cartridge" systems offer an interesting alternative to the classical batch-wise processing of the fine chemical and pharmaceutical industries, especially for the high-pressure reactions often encountered with hydrogenation.

As the factors that control the reaction rates and selectivities of these systems become better understood, the design of highly effective catalytic systems may also become increasingly rational. At present, the control of hydrogen availability and chemical interactions with amine groups in substrates and products are emerging as general themes. However, many additional options to regulate the structure, solubility, phase behavior, and chemical interactions on all levels can undoubtedly be discovered through interdisciplinary efforts by molecular scientists and engineers in this field.

Finally, it should be stressed that CO_2 is not the only SCF to demonstrate potential use in hydrogenation reactions. While the established technology platform and largely benign character of $scCO_2$ make it the current preferred choice, other SCFs may possess complementary properties in terms of polarity, solvation, and reactivities. In future, it is possible that alkanes (e.g., ethane and propane), fluorohydrocarbons and more reactive SCFs such as N_2O – or even water – may also be envisaged for this purpose.

Abbreviations

BTF	benzotrifluoromethane
IL	ionic liquid
PEG	poly(ethyleneglycol)
SAP	supported-aqueous-phase
$scCO_2$	supercritical carbon dioxide
SCF	supercritical fluid
VOC	volatile organic chemical

References

1 P.G. Jessop, W. Leitner (Eds.), *Chemical Synthesis Using Supercritical Fluids*. Wiley-VCH, Weinheim, **1999**.

2 *Roche Magazin* **1992** (41, May), 2.

3 T. Tacke, S. Wieland, P. Panster, *Process Technol. Proc.* **1996**, *12*, 17.

4 M. Härröd, P. Møller, in: P. Rudolph von Rohr, C. Trepp (Eds.), *High Pressure Chemical Engineering*. Elsevier. Netherlands, **1996**.

5 M. Härröd, S. Van der Hark, A. Holmqvist, *Chemical Engineering Transactions* **2002**, *2*, 537.

6 (a) P. Licence, J. Ke, M. Sokolova, S.K. Ross, M. Poliakoff, *Green Chem.* **2003**, *5*, 99; (b) http://www.thomas-swan.co.uk.

7 For selected reviews, see: (a) P.G. Jessop, T. Ikariya, R. Noyori, *Chem. Rev.* **1999**, *99*, 475; (b) W. Leitner, *Acc. Chem. Res.* **2002**, *35*, 746; (c) D.J. Cole-Hamilton, *Science* **2003**, *299*, 1702.

8 Y. Sun, R.N. Landau, J. Wang, C. LeBlond, D.G. Blackmond, *J. Am. Chem. Soc.* **1996**, *118*, 1348.

9 (a) D. Heller, H.-J. Drexler, C. Fischer, H. Buschmann, W. Baumann, B. Heller, *Angew. Chem. Int. Ed. Engl.* **2000**, *39*, 495; (b) See also Chapter 10 of this book.

10 M. Wei, G.T. Musie, D.H. Busch, B. Subramanian, *J. Am. Chem. Soc.* **2001**, *124*, 2513.

11 G.B. Coombes, F. Dehghani, F.P. Lucien, A.K. Dillow, N.R. Foster, in: M.A. Abraham, R.P. Hesketh (Eds.), *Reaction Engineering for Pollution Prevention*. Elsevier. Amsterdam, **2000**.

12 M. Nunes da Ponte, A. Milewska, D. Gourgouillon, D. Chouchi, I. Fonseca, *Proceeding of the 8th Meeting on Supercritical Fluids*, Bordeaux, France, **2002**, p. 129.

13 M. Solinas, A. Pfaltz, P.G. Cozzi, W. Leitner, *J. Am. Chem. Soc.* **2004**, *126*, 16142.

14 C.M. Gordon, W. Leitner, *Homogeneous Catalysis in Supercritical Solvents as a Special Unit Operation*, in:, B. Cornils, W.A. Herrmann, D. Vogt, I. Horvath, H. Olivier-Bourbigon, W. Leitner, S. Mecking (Eds.), *Multiphase Homogeneous Catalysis*. Wiley-VCH, **2005**.

15 For general reviews of this area, see: (a) Leitner, W., *Angew. Chem. Int. Ed.* **1995**, *34*, 2207; (b) P.G. Jessop, T. Ikariya, R. Noyori, *Chem. Rev.* **1995**, *95*, 259.

16 P.G. Jessop, Y. Hsiao, T. Ikariya, R. Noyori, *J. Am. Chem. Soc.* **1994**, *116*, 8851.

17 J. Xiao, S.C.A. Nefkens, P.G. Jessop, T. Ikariya, R. Noyori, *Tetrahedron Lett.* **1996**, *37*, 2813.

18 M.J. Burk, S. Feng, M.F. Gross, W. Tumas, *J. Am. Chem. Soc.* **1995**, *117*, 8277.

19 W. Leitner, *Nature* **2000**, *405*, 129.

20 S. Kainz, D. Koch, W. Baumann, W. Leitner, *Angew. Chem. Int. Ed.* **1997**, *36*, 1628.

21 F. Zhao, Y. Ikushima, M. Chatterjee, O. Sato, M. Arai, *J. Supercrit. Fluids* **2003**, *27*, 65.

22 (a) L.J.P. van den Broeke, E.L.V. Goetheer, A.W. Verkerk, E. de Wolf, B.-J. Deelman, G. van Koten, J.T.F. Keurentjes, *Angew. Chem. Int. Ed.* **2001**, *40*, 4473;

(b) E. L. V. Goetheer, A. W. Verkerk, L. J. P. van den Broeke, E. de Wolf, B.-J. Deelman, G. van Koten, J. T. F. Keurentjes, *J. Catalysis* **2003**, *219*, 126.

23 (a) Z. K. Lopez-Castillo, R. Flores, I. Kani, J. P. Fackler, A. Akgerman, *Ind. Eng. Chem. Res.* **2002**, *41*, 3075; (b) I. Kani, M. A. Omary, M. A. Rawashdeh-Omary, Z. K. Lopez-Castillo, R. Flores, A. Akgerman, J. P. Fackler, *Tetrahedron* **2002**, *58*, 3923; (c) Z. K. Lopez-Castillo, R. Flores, I. Kani, J. P. Fackler, A. Akgerman, *Ind. Eng. Chem. Res.* **2003**, *42*, 6720.

24 K. Wittmann, W. Wisniewski, R. Mynott, W. Leitner, C.L. Kranemann, T. Rische, P. Eilbracht, S. Kluwer, J. M. Ernsting, C.J. Elsevier, *Chem. Eur. J.* **2001**, *7*, 4584.

25 X. Dong, C. Erkey, *J. Mol. Catal. A: Chem.* **2004**, *211*, 73.

26 M. Berthod, G. Minami, M. Lemaire, *Tetrahedron: Asymm.* **2004**, *15*, 1121.

27 Y. Hu, D. J. Birdsall, A. M. Stuart, E. G. Hope, J. Xiao, *J. Mol. Catal. A: Chem.* **2004**, *219*, 57.

28 (a) G. Franciò, W. Leitner, *Chem. Commun.* **1999**, 1663; (b) G. Franciò, K. Wittmann, W. Leitner, *J. Organomet. Chem.* **2001**, *621*, 130.

29 D. Bonafoux, Z. H. Hua, B. H. Wang, I. Ojima, *J. Fluor. Chem.* **2001**, *112*, 101.

30 K. Burgemeister, G. Franciò, H. Hugl, W. Leitner, *Chem. Commun.* **2005**, 6026.

31 S. Kainz, A. Brinkmann, W. Leitner, A. Pfaltz, *J. Am. Chem. Soc.* **1999**, *121*, 6421.

32 S. Lange, A. Brinkmann, P. Trautner, K. Woelk, J. Bargon, W. Leitner, *Chirality* **2000**, *12*, 450.

33 D. J. Adams, W. P. Chen, E. G. Hope, S. Lange, A. M. Stuart, A. West, J. L. Xiao, *Green Chem.* **2003**, *5*, 118.

34 A. P. Abbott, W. Eltrinhgam, E. G. Hope, M. Nicola, *Green Chem.* **2005**, *7*, 721.

35 B. M. Bhanage, M. Shirai, M. Arai, Y. Ikushima, *Chem. Commun.* **1999**, 1277.

36 G. B. Jacobson, C. T. Lee, K. P. Johnston, W. Tumas, *J. Am. Chem. Soc.* **1999**, *121*, 11902.

37 D. J. Heldebrant, P. G. Jessop, *J. Am. Chem. Soc.* **2003**, *125*, 5600.

38 F. C. Liu, M. B. Abrams, R. T. Baker, W. Tumas, *Chem. Commun.* **2001**, 433.

39 R. A. Brown, P. Pollet, E. McKoon, C. A. Eckert, C. L. Liotta, P. G. Jessop, *J. Am. Chem. Soc.* **2001**, *123*, 1254.

40 P. G. Jessop, D. C. Wynne, S. DeHaai, D. Nakawatase, *Chem. Commun.* **2000**, 693.

41 S. Wang, F. Kienzle, *Ind. Eng. Chem. Res.* **2000**, *39*, 4487.

42 E. Teoh, W. R. Jackson, A. J. Robinson, *Aust. J. Chem.* **2005**, *58*, 63.

43 M. Solinas, J. Jiang, O. Stelzer, W. Leitner, *Angew. Chem. Int. Ed. Engl.* **2005**, *44*, 2291.

44 C. D. Ablan, J. P. Hallett, K. N. West, R. S. Jones, C. A. Eckert, C. L. Liotta, P. G. Jessop, *Chem. Commun.* **2003**, 2972.

45 X. Xiaofeng, C. L. Liotta, C. A. Eckert, *Ind. Eng. Chem. Res.* **2004**, *43*, 7907.

46 L. Schmid, O. Krocher, R. A. Koppel, A. Baiker, *Micropor. Mesopor. Mater.* **2000**, *35–36*, 181.

47 Y. Kayaki, Y. Shimokawatoko, T. Ikariya, *Adv. Synth. Catal.* **2003**, *345*, 175.

48 J. Huang, T. Jiang, B. Han, T. Mu, Y. Wang, X. Li, H. Chen, *Catal. Lett.* **2004**, *98*, 225.

49 P. Stephenson, P. Licence, S. K. Ross, M. Poliakoff, *Green Chem.* **2004**, *6*, 521.

50 M. Burgener, D. Ferri, J.-D. Grunwaldt, T. Mallat, A. Baiker, *J. Phys. Chem. B.* **2005** and references therein.

51 S. Lange, W. Leitner, *J. Chem. Soc. Dalton Trans.* **2002**, 752.

40
Fluorous Catalysts and Fluorous Phase Catalyst Separation for Hydrogenation Catalysis

Elwin de Wolf and Berth-Jan Deelman

40.1
Introduction

Since the first demonstration of the technique of fluorous biphasic catalyst separation by Horváth and Rábai in 1994 [1], this separation technique has been extensively studied and is maturing into a good alternative next to other catalyst recycling methods. Several reviews have appeared within a relatively short period, underlining the growth of interest in this field [2]. This chapter focuses on the application of fluorous techniques for the separation and recycling of soluble hydrogenation catalysts. Soluble or homogeneous hydrogenation catalysts are mostly employed for the selective hydrogenation of fine chemicals where high chemoselectivity, regioselectivity and, in some cases, even enantioselectivity is required. The resulting products are usually of reasonably high-added value and, from an economical perspective, it is not always necessary to recycle the catalyst or its components. However, a high selectivity is often only obtained at the cost of activity, and consequently high catalyst loadings are needed in some cases. In addition, catalyst residues in the end product are often undesirable because of their toxicity profile or unwanted side effects in subsequent synthetic transformations. In those cases, fluorous biphasic separation can have advantages over other separation and recycling techniques:

- Because of the thermomorphic properties of fluorous organic biphasic systems, homogeneous single-phase reaction conditions are still possible, preventing the risk of liquid–liquid or liquid–solid mass transport limitations that may influence the activity or selectivity of the catalyst. Above its consolute temperature, the mixed fluorous-organic phase has generally enough "solvent power" for organic substrates and products to dissolve completely.
- The fluorocarbon component of the solvent system, preferably high-boiling to limit emission to the atmosphere, is usually inert and not reactive towards the catalyst.
- Finally – and perhaps most importantly – the fluorous tagging of the catalyst that introduces affinity for the fluorous phase can be a very mild immobilization technique, as there is no direct covalent link with a support and the sepa-

The Handbook of Homogeneous Hydrogenation.
Edited by J.G. de Vries and C.J. Elsevier
Copyright © 2007 WILEY-VCH Verlag GmbH & Co. KGaA, Weinheim
ISBN: 978-3-527-31161-3

ration itself does not impose additional thermal stress on the catalyst. (Recycling of a homogeneous catalyst by distillation of the more volatile solvent and products is often not possible due to thermal degradation of the catalyst.) In this chapter it will be shown that, by using certain specific spacers between the fluorous tags and the active site of the catalyst, it is possible to leave the selectivity and activity of the catalyst intact.

To be fair, it should be realized that if a catalyst must be recycled for economic reasons, the recycling efficiency compared to the nonfunctionalized catalyst must be higher in order to compensate for the increased price of the fluorous catalyst itself. However, every recycling technique has its own cost that must be evaluated for each specific case.

Apart from applications in catalysis, fluorous biphasic separation strategies are also being developed for application in (high-throughput) organic synthesis schemes [3], and even in bioorganic synthesis [4]. In some cases, the fluorous solvent has been used advantageously for its "green" properties [5] or to enhance the rate of specific reactions [6].

In the following sections, an overview is provided of fluorous hydrogenation catalysts that have been developed for fluorous biphasic separation strategies, along with a discussion of their performance in hydrogenation reactions and the recycling efficiencies attained. The chapter does not include fluorous hydrogenation catalysts for application in supercritical carbon dioxide ($scCO_2$), which have been described in Chapter 39.

A wide range of fluorous phosphorus ligands have become available that are based on different spacer-units between the perfluoroalkyl tails and the remainder of the ligand. Alkylphosphines having a $-(CH_2)_n-$ moiety, triarylphosphines with a perfluoroalkyl tail directly connected to the aryl ring, and triaryl phosphines with an additional spacer unit between the perfluoroalkyl group and the aryl ring, are the most commonly applied. Additional spacers among the latter class of phosphines are $-(CH_2)_n-$, $-SiMe_{3-b}(CH_2CH_2)_b-$, and $-OCH_2-$ moieties.

40.2
Catalysts Based on Fluorous Alkylphosphines, -Phosphinites, -Phosphonites, and -Phosphites

The first fluorous phosphine ligands for application in fluorous phase catalysis were fluorous trialkylphosphines **1** [7–9].

Ligands **1a** (C_6F_{13}-tail) and **1b** (C_8F_{17}-tail) were applied in the fluorous hydrogenation of internal and terminal alkenes [10] and styrenes [10, 11]. The Wilkinson-type complexes [RhCl(**1a–b**)$_3$] displayed lower activities compared to [RhCl(PPh_3)$_3$]. Catalyst recycling resulted on average in a 1.5% lower yield after each cycle [10]. Although Rh-leaching was not measured, it is most probably comparable to the values obtained for hydroboration with the same catalyst (ca. 0.2% per cycle). The loss of yield which does not appear to match with the loss

of rhodium could be indicative of loss of dissociated ligand, which leads to the formation of less active species (*vide infra*).

$P((CH_2)_mC_xF_{2x+1})_2((CH_2)_nC_xF_{2x+1})$

1

a: $m = n = 2$; $x = 6$
b: $m = n = 2$; $x = 8$
c: $m = n = 2$; $x = 10$
d: $m = 2$; $n = 3$; $x = 8$
e: $m = 3$; $n = 2$; $x = 8$
f: $m = n = 3$; $x = 8$
g: $m = 3$; $n = 4$; $x = 8$
h: $m = 4$; $n = 3$; $x = 8$
i: $m = n = 4$; $x = 8$
j: $m = n = 5$; $x = 8$

The fluorous alkylphosphines **2** [8, 12] and **3** [8, 13], containing one or two perfluoroalkyl tails, respectively, have also been prepared. Partition coefficients of the chiral fluorous monophosphines **3a–b** were found to be lower than the values measured for the corresponding phosphines **1**, which contain one extra perfluoroalkyl tail [13]. In addition, fluorous phosphinites, phosphonites and phosphites **4a–e** and diphosphonite **5** have become available [8, 14].

$R_2P(CH_2CH_2C_xF_{2x+1})$

2

a: R = Cy; $x = 6$
b: R = ^{i}Pr; $x = 6$
c: R = Ph; $x = 6$

$RP(CH_2CH_2C_xF_{2x+1})_2$

3

a: R = menthyl; $x = 6$
b: R = menthyl; $x = 8$
c: R = Ph; $x = 6$

$R_{3-a}P(OCH_2CH_2C_6F_{13})_a$

4

a: $a = 3$
b: $a = 2$; R = Ph
c: $a = 1$; R = Ph
d: $a = 1$, R = ^{i}Pr
e: $a = 1$, R = Cy

$(C_6F_{13}CH_2CH_2O)_2P$–$P(OCH_2CH_2C_6F_{13})_2$

5

The ligands **2a**, **2c** and **4d–e** were used for the rhodium-catalyzed hydrogenation of 1-hexene under homogeneous conditions, using the 1-hexene itself as solvent [12, 14]. The catalysts were synthesized *in situ* by reacting $[RhCl(COD)]_2$ with 6 equiv. of the ligand. As for fluorous trialkylphosphines **1**, lower activities were found compared to the catalyst based on PPh_3. Turnover numbers (TONs) after 24 h were found to increase in the order **2a**<**4d**<**4e** ≈ **2c**<PPh_3.

In a similar fashion, **2a**, **2c**, **4a** and **4c** were also tested in the hydrogenation of 1-hexene under fluorous biphasic conditions (1-hexene/PFMCH = 1:2 (v:v)) [12, 14]. Relatively low activities were found for all catalysts, with activities increasing in the order **4a**<**4c**<**2a**<**2c**.

A cationic complex, formed *in situ* from **5** and $[Rh(COD)_2]OTf$, was also active in biphasic hydrogenation [14]. No preference for the fluorous phase was found for ligands containing only one perfluoroalkyl tail, but neutral and cationic complexes, containing mono- and bidentate **4a** or **5**, respectively, were selectively dissolved in the fluorous phase. No leaching and recycling studies were performed.

In general, the fluorous catalysts containing fluorous alkylphosphines display good recycling efficiency, but their activity is lower compared to existing systems containing PPh_3 as ligand.

40.3
Catalysts Based on Perfluoroalkyl-Substituted Arylphosphines

A large variety of fluorous triarylphosphines that differ in the type of isolating group between the perfluoroalkyl tail and the aryl ring, has been reported. The simplest ones are arylphosphines **6–9**, with the perfluoroalkyl tail directly connected to the aryl ring. The electron-withdrawing effect of the perfluoroalkyl tails was clearly noticeable upon application of some of these fluorous compounds in homogeneous catalysis. The reaction rates that were found in fluorous hydrogenation of styrene using $[RhCl(L)_3]$ (L = **6**, **7c** [8, 15, 16] or **8** [16, 17]) or $[Rh(\mu\text{-}Cl)(\mathbf{9})]_2$ [8] as catalyst were all lower compared to that of the nonfluorous analogues (based on PPh_3, $EtPPh_2$, or DPPE (DPPE = 1,2-bis(diphenylphosphino)ethane)) [11]. However, the activities observed were similar to catalysts containing $P(3\text{-}C_6H_4CF_3)_3$ or $P(4\text{-}C_6H_4CF_3)_3$ as ligand, indicating that the strong electron-withdrawing character of the perfluoroalkyl tails was responsible. The reaction rates were unaffected upon recycling of the catalysts in all cases, and essentially no rhodium (i.e., < 1 ppm) or free ligand could be detected in the toluene layer by inductively coupled plasma-atomic absorption spectroscopy (ICP-AAS) analysis [11].

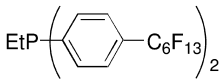

6

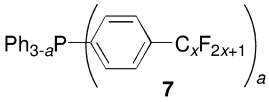

7

a: $a = 1$, $x = 6$
b: $a = 2$, $x = 6$
c: $a = 3$, $x = 6$
d: $a = 3$, $x = 8$

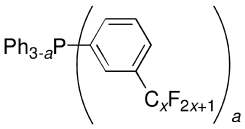

8

a: $a = 1$, $x = 6$
b: $a = 2$, $x = 6$
c: $a = 3$, $x = 6$
d: $a = 3$, $x = 8$

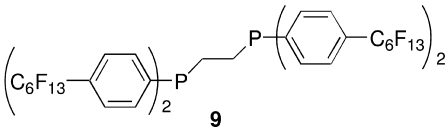

9

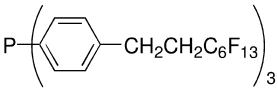

10

To overcome the electron-withdrawing effect of the perfluoroalkyl tail exerted on the phosphorus atom when the tail is directly coupled to the aryl ring, extra spacers have been introduced, the most frequently used one being $-(CH_2)_n-$ units. Compound **10** was used to demonstrate in the context of styrene hydrogenation how the use of a volatile fluorous solvent can be eliminated [18]. The fluorous solvent was replaced by fluorous silica, and the fluorophilicity of the remaining organic solvent was increased by expansion with CO_2 to allow the fluorous Wilkinson-type catalyst to dissolve. Release of the CO_2 pressure causes the catalyst to re-precipitate on the fluorous silica, facilitating the recycling of the catalyst. The catalyst was recycled four times with essentially no drop in activity, and Rh leaching was below the detection limit (<0.5%), although phosphine leaching was not measured.

Another solution to insulate the phosphorus donor-atom from the electron-withdrawing perfluoroalkyl tail, and to simultaneously provide easy synthetic access to the introduction of more tails to one aryl ring, is the use of the $-Si(Me)_{3-b}(CH_2CH_2-)_b$ spacer. Here, the silicon atom acts as an additional insulator for the electron-withdrawing effect of the perfluoroalkyl tail, while it can simultaneously be used as a branching point for the attachment of up to three tails per aryl ring. Using this principle, phosphines **11** were prepared [19]. Similarly, highly fluorous derivatives of DPPE **12** were obtained [20].

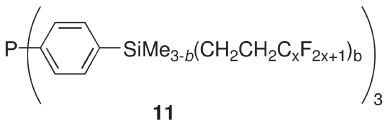

11

a: $b = 0$
b: $b = 1$; $x = 6$
c: $b = 1$; $x = 8$
d: $b = 2$; $x = 6$
e: $b = 2$; $x = 8$
f: $b = 3$; $x = 6$
g: $b = 3$; $x = 8$

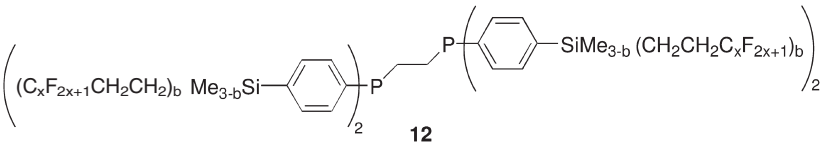

12

a: $R_f = C_6F_{13}$, $b = 1$
b: $R_f = C_6F_{13}$, $b = 2$
c: $R_f = C_6F_{13}$, $b = 3$
d: $R_f = C_8F_{17}$, $b = 1$
e: $b = 0$

The possible electronic influence of a fluorous *para*-silyl-substituent was studied in detail using a wide range of physico-chemical techniques [19–23], sug-

gesting that the electron-withdrawing effect of the perfluoroalkyl group is effectively cancelled by the ethylsilyl spacer. The partition coefficients measured for **11 b–g**, in general, are higher than values obtained for fluorous triphenylphosphine **10**, despite the larger organic part of the former [19 b]. Partition coefficients in *n*-pentane/PFMCH behaved as described above for fluorous trialkyl- and triaryl-phosphines – that is, more tails as well as longer tails give higher partition coefficients. Similar behavior was observed in *n*-octane/PFMCH for **11 b–e**. Surprisingly, upon attachment of another tail ($b=3$, **11 f–g**), the partition coefficient decreased, with **12 g** ($x=8$) having a higher value than **12** ($x=6$). Even more unexpected partitioning behavior was found in toluene/PFMCH; that is, upon lengthening the tail from $x=6$ to $x=8$, the partition coefficient increased for $b=1$, remained unchanged for $b=2$, and decreased for $b=3$. Furthermore, maximum values were found for $b=2$. Interestingly, this unexpected behavior was not observed for fluorous diphosphines **13** – that is, the partition coefficient increased upon increasing the number of tails, resulting in a maximum value ($P=92$) for **13 c** containing 12 tails.

The unexpected behavior observed for fluorous, silyl-substituted monophosphines **12** was studied in further detail, using combinatorial techniques and statistical design of experiments [24]. A library of phosphines **11** (*a*, *b*, *x*, *pos*) was prepared by parallel synthesis, with *a* (1–3) being the number of silyl-substituted phenyl groups, *b* (1–3) the number of tails per Si-atom, *x* (4, 6, 8, 10) the length of the tail, and *pos* (*meta* (C3), *para* (C4) or 3,5-substituted (C3C5)) the position of the Si-atom on the aryl ring. Using this approach, the highest partition coefficient was observed for **11** (2, 3, 6, C3C5) ($P=236$).

Complexes $[RhCl(L)_3]$ (L=**11 a–c**) were applied in the fluorous hydrogenation of 1-octene in a fluorous biphasic system, as well as in benzotrifluoride (BTF) [22]. The activities measured in the hybrid solvent BTF were comparable with that of Wilkinson's catalyst, $[RhCl(PPh_3)_3]$, with activities increasing in the order **11 c** < PPh_3 ≈ **11 b** < **11 a**. This was the first example of a fluorous hydrogenation catalyst with similar activity compared to the nonfluorous analogue. $[RhCl(\mathbf{12c})_3]$ was tested for its hydrogenation activity upon recycling in a fluorous biphasic solvent system. Nine cycles were performed, with an average Rh leaching of 0.1% per cycle. The extent of rhodium leaching, as studied by ICP-AAS, turned out to be small (0.1% Rh detected), whereas leaching of dissociated ligand was substantial (2% per cycle for L=**11 c**). These studies demonstrated that, when recycling of catalysts with fluorous biphasic separation techniques is applied, both leaching of the transition metal, leaching of (expensive) fluorous solvent and of free fluorous ligand should be considered.

Some of the improved fluorous arylsilylphosphines in the library **11** (***a***, ***b***, ***x***, ***pos***) were tested in the context of hydrosilylation catalysis [24]. Rh and phosphine leaching were driven down further to non-detectable levels (< 0.1%) and 0.8%, respectively, and it can be expected that even better results are possible for hydrogenation catalysis.

Fluorous diphosphine complexes $[Rh(COD)(\mathbf{12})]BF_4$ showed amphiphilic behavior, resulting in the formation of aggregates with a size of several hundreds

of nanometers in acetone solutions [23]. When these fluorous diphosphine rhodium complexes were applied in the hydrogenation of 1-octene and 4-octyne [23], interesting differences in catalytic performance were observed between fluorous and nonfluorous derivatives of $[Rh(COD)(DPPE)]BF_4$ – that is, the fluorous catalyst displayed lower isomerization rate constants, resulting in higher hydrogenation activity and selectivity. This phenomenon was explained by the unique aggregation behavior of the fluorous catalyst that was not previously observed.

Fluorous biphasic recycling of [Rh(COD)(**12c**)]BF_4 was studied in two fluorous solvent systems (acetone/PFMCH and hexane/FC-75). Recycling was possible in both systems without loss of conversion. ICP-AAS-measurements on the organic phase showed the presence of rhodium and phosphorus in a 1:2 molar ratio, indicating that diphosphines can be used to prevent leaching of free fluorous ligand. Interestingly, no rhodium (<0.08%) could be detected in the organic phase when hexane/FC-75 was used as solvent system.

Another spacer which was used to insulate the phosphorus atom from the electron-withdrawing effect of the perfluoroalkyl tail is the $–O-(CH_2)_n–$ spacer that contains an electron-donating oxygen atom directly attached to the aryl ring [25]. Fluorous derivatives of triphenylphosphine containing this ether spacer (**13a–c**) were prepared, though the lower $^1J_{PtP}$ coupling constant of *cis*-$[PtCl_2(\mathbf{13a})_2]$ and higher ν_{CO} of *trans*-$[MCl(CO)(\mathbf{13a})_2]$ (M = Rh, Ir) compared to *cis*-$[PtCl_2\{P(C_6H_4\text{-}p\text{-}OMe)_3\}_2]$ and *trans*-$[MCl(CO)\{P(C_6H_4\text{-}p\text{-}OMe)_3\}_2]$, respectively, indicates that the oxygen atom does not fully insulate the electron-withdrawing effect [26]. Ligands **13a–c** were found to be soluble in organic solvents (Et_2O, $CHCl_3$) as well as fluorous solvents (C_8F_{18}) [25].

The oxygen-spaced derivative **13a** (along with related derivatives) was successfully employed in the Rh-catalyzed hydrogenation of (*E*)-cinnamate and 2-cyclohexen-1-one, with activities comparable to that of the corresponding PPh_3 derivative [27]. Recycling efficiency studies demonstrated a two- to three-fold drop in activity over three cycles, while leaching values were in the range 0.37 to 0.56% (Rh) and 0.94 to 0.95% (phosphine) for the last two cycles. The highly fluorous derivative **14** displayed the lowest leaching: 0.12 to 0.23% (Rh) and 0.46 to 0.63% (phosphine), but the presence of two perfluoroalkyl tails induce an eight-fold drop in activity compared to PPh_3.

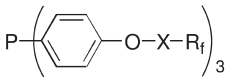

13

a: X = CH_2; R_f = C_7F_{15}
b: X = $(CH_2)_3$; R_f = C_8F_{17}
c: X = $CH_2O(CH_2)_2$; R_f = $CF_2(O(CF_3)CFCF_2)_{3.38}(OCF_2)_{0.11}OCF_3$

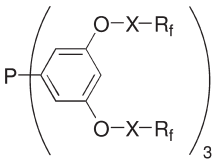

14 X = CH_2, R_f = C_7F_{15}

To solve the issue of ligand leaching that was encountered in some of the examples above, fluorous polymeric phosphine ligands **15a–c** [28] were developed. The rhodium complexes prepared from **15a–c** using a 3:1 ratio of P:Rh [28b, 29] displayed good turnover frequencies (TOFs) in the case of **15a**, but reaction rates for **15b,c** were lower. The catalyst derived from **15a** was recycled seven times without loss of activity, although leaching was not studied quantitatively.

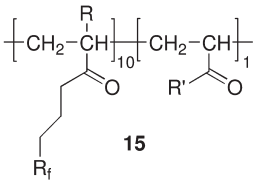

15

a: $R_f = C_8F_{17}$; R = H; R' = $-NH(CH_2)_3PPh_2$
b: $R_f = C_8F_{17}$; R = Me; R' = $-NH(CH_2)_3PPh_2$
c: $R_f = -NEtSO_2(CF_2)_{3\text{-}7}CF_3$; R = Me; R' = $-NH(CH_2)_3PPh_2$

Remarkably, the use of a fluorous biphasic solvent system in combination with a $[Rh(NBD)(DPPE)]^+$-type catalyst (NBD = norbornadiene) copolymerized into a porous nonfluorous ethylene dimethacrylate polymer, resulted in an increased activity of the catalyst relative to a situation when only toluene was used as solvent [30]. The results were explained by assuming that fluorophobicity of the substrate (methyl-*trans*-cinnamate) leads to a relatively higher local substrate concentration inside the cavities of the polymer when the fluorous solvent is used. That is, the polymer could be viewed as a better solvent than the fluorous solvent system. This interpretation was supported by the observations that: (i) the increase in activity correlates linearly with the volume fraction of fluorous solvent (PFMCH); and (ii) the porous ethylene dimethacrylate polymer by itself lowers the concentration of decane in PFMCH from 75 mM to 50 mM, corresponding to a 600 mM local concentration of decane in the polymer. Gas to liquid mass transport limitation of dihydrogen could be ruled out as a possible cause.

40.4
Fluorous Anions for the Separation of Cationic Hydrogenation Catalysts

Rendering the catalyst preferentially soluble in the fluorous phase by functionalization of the ligand(s) has certain disadvantages. For each ligand, the fluorous analogue must be prepared separately. Furthermore, as shown above, the perfluoroalkyl tail can influence the catalytically active metal center electronically. For cationic catalysts, this problem can be overcome by functionalization of the anion. Also, because of their ionic character, these complexes are less fluorophilic by nature, and fluorination of the ligand system is often insufficient to obtain high fluorophilicity.

Today, many fluorinated borate anions are recognized [31], the most well-known being $[B(C_6F_5)_4]^-_4$ and $[B(3,5\text{-}C_6H_3(CF_3)_2]^-_4$ (BARF). Furthermore, it is known that the attachment of (short) perfluoroalkyl groups increases the lipophilicity of these anions [32]. With these considerations in mind, fluorous derivatives of tetraphenylborate containing $-C_6F_{13}$ or $-SiMe_2CH_2CH_2C_6F_{13}$ groups were prepared [33]. It was found that attachment of a long (1*H*,1*H*,2*H*,2*H*-perfluoroalkyl)dimethylsilyl group to the anion in complex **16** considerably increases the solubility in apolar solvents. The sodium salt **17** of a fluorous derivative of tetraphenylborate containing eight tails even dissolved in a fluorous solvent [34]. The fluorous borate anions were successfully used to boost the fluorophilicity of complexes of the type $[Rh(COD)(Ar_2PCH_2CH_2PAr_2)]X$ (Ar = aryl, X = weakly coordinating anion) that were previously shown to be not sufficiently fluorophilic for fluorous biphasic separation protocols unless the aryl groups were very heavily perfluoroalkylated. By employing highly fluorous borate anions resulting in complexes **18a,b**, only lightly fluorous diphosphines were needed to obtain good recycling efficiencies [35]. In addition, the use of these fluorous anions as counterions in butane-bridged $[Rh(COD)(Ph_2PCH_2CH_2CH_2CH_2PPh_2)]X$ (X = BF_4, or fluorous tetraarylborate) led to significantly enhanced reaction rates under nonfluorous conditions.

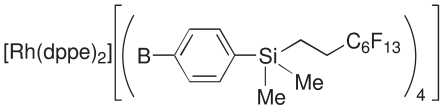

16

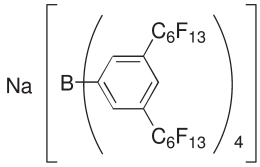

17

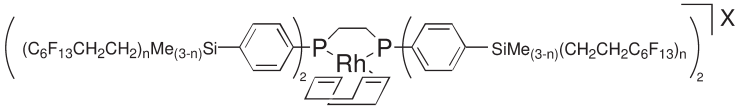

18a: n = 1, X =

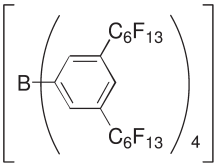

18b: n = 2, X =

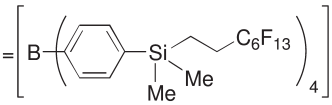

40.5
Catalysts Based on Nonphosphorus Ligands

To date, fluorous hydrogenation catalysts have been mainly based on phosphorus ligands with one exception. This is a system consisting of fluorous dendrimer-encapsulated Pd(0) nanoparticles that is active for the hydrogenation of alkenes and conjugated alkenes, and can be recovered by fluorous biphasic separation [36]. Recently, the same system was demonstrated in CO_2-induced phase switching of a fluorous biphasic solvent system, offering an alternative to temperature-induced mixing and demixing strategies [37].

40.6
Enantioselective Hydrogenation Catalysts

Although fluorous derivatives of DPPE were successfully employed in catalytic hydrogenation (*vide supra*), chiral fluorous diphosphines have had limited success in enantioselective hydrogenation. For example, ethylene-spaced and nonethylene-spaced 6,6′-perfluoroalkylated BINAP-type phosphines based on the 1,1′-binaphthyl unit have been investigated in Ru-mediated hydrogenation [38]. Enantioselectivities obtained in methanol and dichloromethane were comparable with that of the nonfunctionalized Ru-BINAP system, with the nonethylene-spaced ligand showing the lowest activity [38, 39]. Recycling became possible only by chromatography over fluorous silica gel. The challenge remains to render the large organic core – that is often needed to induce enantioselectivity – sufficiently fluorophilic for preferential solubility in perfluorocarbon solvents.

40.7
Conclusions

Based on the content of this chapter, it can be concluded that several phosphorus ligand systems are now available for the efficient fluorous biphasic recovery of hydrogenation catalysts. In most cases, the perfluoroalkyl tail exerts an electron-withdrawing effect on the ligand system and the catalytically active metal center. This leads to lower activity in hydrogenation reactions, though selectivity is usually not an issue. Only fluorous catalysts containing the $–SiMe_{3-b}(CH_2CH_2)_b–$ and $–OCH_2–$ spacers display similar or higher activity in hydrogenation catalysis compared to their nonfluorous analogues. For hydrogenations by cationic metal complexes that are difficult to render fluorophilic by perfluoroalkylation of the ligand system alone, highly fluorous borate counterions have been developed.

Recently, the fluorous biphasic separation technique has been enriched with two new developments, both of which were demonstrated in hydrogenation. The need for a fluorous solvent can be eliminated by using fluorous silica as a fluorous catalyst scavenger. In liquid–liquid biphasic systems, reversible expan-

sion with CO_2, as an alternative to temperature shuttling, has been employed to switch between biphasic and monophasic conditions. Asymmetric hydrogenation combined with fluorous biphasic separation strategies remains a field that is relatively underdeveloped, and represents a clear challenge for future studies.

Abbreviations

BTF	benzotrifluoride (α,α,α-trifluorotoluene)
FC-75	perfluoro-2-butyltetrahydrofuran
ICP-AAS	inductively coupled plasma-atomic absorption spectroscopy
NBD	norbornadiene
PFMCH	perfluoromethylcyclohexane
$scCO_2$	supercritical carbon dioxide
TON	turnover number

References and Notes

1 Horváth, I.T., Rábai, J., *Science* **1994**, *266*, 72.

2 (a) Gladysz, J.A., Curran, D.P., Horváth, I. (Eds.), *Handbook of Fluorous Chemistry*. Wiley-VCH, Weinheim, Germany, **2004**; (b) de Wolf, E., van Koten, G., Deelman, B.-J., *Chem. Soc. Rev.* **1999**, *28*, 37; (c) Hope, E.G., Stuart, A.M., *J. Fluorine Chem.* **1999**, *100*, 75; (d) Horváth, I.T., *Acc. Chem. Res.* **1998**, *31*, 641; (e) Curran, D.P., *Angew. Chem., Int. Ed.* **1998**, *37*, 1174; (f) Cornils, B., *Angew. Chem., Int. Ed. Engl.* **1997**, *36*, 2057.

3 Curran, D.P., in: Gladysz, J.A., Curran, D.P., Horváth, I. (Eds.), *Handbook of Fluorous Chemistry*. Wiley-VCH, Weinheim, Germany, **2004**, p. 101.

4 Hungerhoff, B., Sonnenschein, H., Theil, F., *Angew. Chem. Int. Ed.* **2001**, *40*, 2492.

5 Nakano, H., Kitazume, T., *Green Chemistry* **1999**, *1*, 179.

6 Myers, K.E., Kumar, K., *J. Am. Chem. Soc.* **2000**, *122*, 12025.

7 Alvey, L.J., Rutherford, D., Juliette, J.J.J., Gladysz, J.A., *J. Org. Chem.* **1998**, *63*, 6302.

8 Bhattacharyya, P., Gudmunsen, D., Hope, E.G., Kemmitt, R.D.W., Paige, D.R., Stuart, A.M., *J. Chem. Soc., Perkin Trans. 1* **1997**, 3609.

9 (a) Benefice-Malouet, S., Blancou, H., Commeyras, A., *J. Fluorine Chem.* **1985**, *30*, 171; (b) Langer, F., Püntener, K., Stürmer, R., Knochel, P., *Tetrahedron Asym.* **1997**, *8*, 715.

10 Rutherford, D., Juliette, J.J.J., Rocaboy, C., Horváth, I.T., Gladysz, J.A., *Catal. Today* **1998**, *42*, 381.

11 Hope, E.G., Kemmitt, R.D.W., Paige, D.R., Stuart, A.M., *J. Fluorine Chem.* **1999**, *99*, 197.

12 Smith, D.C., Stevens, E.D., Nolan, S.P., *Inorg. Chem.* **1999**, *38*, 5277.

13 Klose, A., Gladysz, J.A., *Tetrahedron: Asymm.* **1999**, *10*, 2665.

14 Haar, C.M., Huang, J., Nolan, S.P., Petersen, J.L., *Organometallics* **1998**, *17*, 5018.

15 Chen, W., Xiao, J., *Tetrahedron Lett.* **2000**, *41*, 3697.

16 Schneider, S., Bannwarth, W., *Angew. Chem. Int. Ed.* **2000**, *39*, 4142.

17 Hope, E.G., Kemmitt, R.D.W., Paige, D.R., Stuart, A.M., Wood, D.R.W., *Polyhedron* **1999**, *18*, 2913.

18 Ablan, C.D., Hallett, J.P., West, K.N., Jones, R.S., Eckert, C.A., Liotta, C.L., Jessop, P.G., *Chem. Commun.* **2003**, 2972.

19 (a) Richter, B., van Koten, G., Deelman, B.-J., *J. Mol. Catal. (A), Chem.* **1999**, *145*, 317; (b) Richter, B., de Wolf, E., van Ko-

ten, G., Deelman, B.-J., *J. Org. Chem.* **2000**, *65*, 3885.
20 de Wolf, E., Richter, B., Deelman, B.-J., van Koten, G., *J. Org. Chem.* **2000**, *65*, 5424.
21 de Wolf, E., Mens, A. J. M., Gijzeman, O. L. J., van Lenthe, J., Jenneskens, L. W., Deelman, B.-J., van Koten, G., *Inorg. Chem.* **2003**, *42*, 2115.
22 (a) Richter, B., Spek, A. L., van Koten, G., Deelman, B.-J., *J. Am. Chem. Soc.* **2000**, *122*, 3945; (b) Richter, B., de Wolf, E., Deelman, B.-J., van Koten, G. PCT Int. Appl. WO 0018444, **2000**.
23 de Wolf, E., Spek, A. L., Kuipers, B. W. M., Philipse, A. P., Meeldijk, J. D., Bomans, P. H. H., Frederik, P. M., Deelman, B.-J., van Koten, G., *Tetrahedron* **2002**, *58*, 3911.
24 (a) de Wolf, A. C. A., *Fluorous Phosphines as Green Ligands for Homogeneous Catalysis; Solving Problems in Fluorous Catalysis.* PhD Thesis, Utrecht University, Dept. of Metal-Mediated Synthesis, **2002**.
(b) de Wolf, E., Riccomagno, E., de Pater, J. J. M., Deelman, B.-J., van Koten, G. *J. Comb. Chem.* **2004**, *6*, 363.
25 Sinou, D., Pozzi, G., Hope, E. G., Stuart, A. M., *Tetrahedron Lett.* **1999**, *40*, 849.
26 Bhattacharyya, P., Croxtall, B., Fawcett, J., Fawcett, J., Gudmunsen, D., Hope, E. G., Kemmitt, R. D. W., Paige, D. R., Russell, D. R., Stuart, A. M., Wood, D. R. W., *J. Fluorine Chem.* **2000**, *101*, 247.
27 Sinou, D., Maillard, D., Aghmiz, A., Masdeu i-Bultó, A. M., *Adv. Synth. Catal.* **2003**, *345*, 603.
28 (a) Bergbreiter, D. E., Franchina, J. G., *Chem. Commun.* **1997**, 1531; (b) Bergbreiter, D. E., Franchina, J. G., Case, B. L., Williams, L. K., Frels, J. D., Koshti, N., *Comb. Chem. High Throughput Screening* **2000**, *3*, 153.
29 Bergbreiter, D. E., Franchina, J. G., Case, B. L., *Org. Lett.* **2000**, *2*, 393.
30 Vinson, S. L., Gagné, M. R., *Chem. Commun.* **2001**, 1130.
31 Pawelke, G., Bürger, H., *Coord. Chem. Rev.* **2001**, *215*, 243.
32 Fujiki, K., Ichikawa, J., Kobayashi, H., Sonoda, A., Sonoda, T., *J. Fluorine Chem.* **2000**, *102*, 293.
33 van den Broeke, J., Lutz, M., Kooijman, H., Spek, A. L., Deelman, B.-J., van Koten, G., *Organometallics* **2001**, *20*, 2114.
34 van den Broeke, J., Deelman, B.-J., van Koten, G., *Tetrahedron Lett.* **2001**, *42*, 8085.
35 van den Broeke, J., de Wolf, E., Deelman, B.-J., van Koten, G., *Adv. Synth. Catal.* **2003**, *345*, 625.
36 Chechik, V., Crooks, R. M., *J. Am. Chem. Soc.* **2000**, *122*, 1243.
37 West, K. N., Hallett, J. P., Jones, R. S., Bush, D., Liotta, C. L., Eckert, C. A., *Ind. Eng. Chem. Res.* **2004**, *43*, 4827.
38 Birdsall, D. J., Hope, E. G., Stuart, A. M., Chen, W., Hu, Y., Xiao, J., *Tetrahedron Lett.* **2001**, *42*, 8551.
39 Hope, E. G., Stuart, A. M., West, A. J., *Green Chem.* **2004**, *6*, 345.

41
Catalytic Hydrogenation using Ionic Liquids as Catalyst Phase

Peter Wasserscheid and Peter Schulz

41.1
Introduction to Ionic Liquids

Ionic liquids are characterized by the following three definition criteria:
- they consist entirely of ions;
- they have melting points below 100 °C; and
- they exhibit no detectable vapor pressure below the temperature of their thermal decomposition.

As a consequence of these properties, most ions forming ionic liquids display low charge densities resulting in low intermolecular interaction. Some of the most common ions used to date for the formation of ionic liquids are shown in Figure 41.1.

Ionic liquids can be classified according to the different classes of cations, namely as imidazolium, pyridinium, ammonium, and phosphonium salts. These cations form low-temperature melting salts in combination with many different anions. Low-melting chloroaluminate salts can be regarded as the first ionic liquids to be studied in detail, and in the modern literature they are often referred to as "first-generation ionic liquids". They were described as early as in 1948 by Hurley and Wier at the Rice Institute in Texas as bath solutions for the electroplating of aluminum [1, 2]. Later, during the 1970s and 1980s, these systems were intensively studied by the groups of Osteryoung [3, 4], Wilkes [5], Hussey [6–8], and Seddon [9].

In 1992, ionic liquid methodology received a substantial boost when Wilkes and Zaworotko described the synthesis of non-chloroaluminate, room-temperature liquid melts (e.g., low-melting tetrafluoroborate melts) which may be regarded as "second-generation ionic liquids" [10]. Nowadays, tetrafluoroborate and (the slightly later published [11]) hexafluorophosphate ionic liquids are still widely used in ionic liquid research. However, their use in many technical applications will be clearly limited by their slight – but clearly existing – tendency to hydrolyze. Consequently, the technical application of tetrafluoroborate and

The Handbook of Homogeneous Hydrogenation.
Edited by J.G. de Vries and C.J. Elsevier
Copyright © 2007 WILEY-VCH Verlag GmbH & Co. KGaA, Weinheim
ISBN: 978-3-527-31161-3

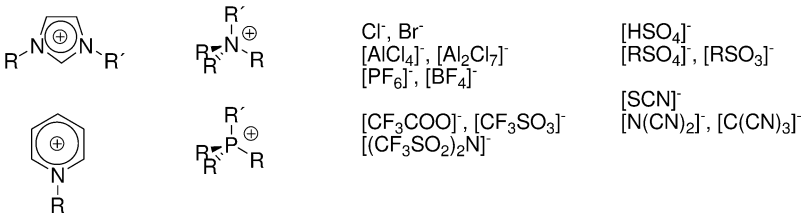

Fig. 41.1 Typical cations and anions used for the formation of ionic liquids.

hexafluorophosphate ionic liquids will be restricted to those applications where water-free conditions can be realized at acceptable costs.

In 1996, Grätzel, Bonhôte and coworkers published the synthesis and properties of ionic liquids with anions containing CF_3- and other fluorinated alkyl groups [12]. These are usually highly hydrophobic melts with high stability (even under acidic conditions) against hydrolysis.

In recent times, the development of new ionic liquids has made great progress. Important developments include a range of new halogen-free ionic liquids (e.g., benzenesulfonates [13], toluenesulfonates, alkylsulfates [14], hydrogensulfate [15, 16], dicyanamides [17], thiocyanates [18], etc.), as well as functionalized (task-specific) [19–23], fluorinated [24], deuterated [25] and chiral ionic liquids [26–30].

Moreover, ionic liquids are readily commercial available today, with a number of commercial suppliers [31] offering ionic liquids, and some imidazolium-based systems being available even in ton-scale quantities. For example, Solvent Innovation offers the ionic liquid 1-ethyl-3-methylimidazolium ethylsulfate on a ton-scale; a full set of toxicological data is also available for this specific ionic liquids (for more details, see www.solvent-innovation.com). The quality of commercial ionic liquid samples has clearly improved in recent years. The fact that small amounts of impurities significantly influence the properties of the ionic liquid, and especially its usefulness for catalytic reactions [32], makes the quality of an ionic liquid an important consideration. Among the potential impurities in ionic liquids, water, halide ions and organic starting material are of great importance for transition-metal chemistry, while the color of an ionic liquid is not a critical parameter in most applications. Without any doubt, the improved commercial availability of ionic liquids is a key factor for the strongly increasing interest in this new class of liquid materials.

Due to the large number of available ionic liquids, it becomes increasingly important to understand structure–property relationships in a way that allows a specific ionic liquid to be selected or designed for a given application. In this respect, a conclusive general understanding is yet to be determined. However, during the past three years, the availability of reliable thermodynamic data has increased exponentially, providing a much better base for predictive modeling. Some key properties of well-investigated ionic liquids that may also be relevant for applications in liquid–liquid biphasic hydrogenation reactions are displayed in Table 41.1.

Table 41.1 Comparison of some properties of well-established ionic liquid systems with the 1-ethyl-3-methylimidazolium [EMIM] and 1-butyl-3-methylimidazolium [BMIM] ions.

Ionic liquid	M.p./g.p. [°C]	Viscosity [cP]	Density[a)] [g mL^{-1}]	Tendency for hydrolysis[c)]	Reference(s)
[EMIM][$AlCl_4$]	7 (mp)	18[a)]	1.240	very high	5, 33
[EMIM][BF_4]	6 (gp)	34[a)]	1.240	existent	34
[EMIM][CF_3SO_3]	–3 (mp)	45[a)]	1.390	very low	12
[EMIM][$(CF_3SO_2)_2N$]	–9 (mp)	31[a)]	1.518	very low	35
[BMIM][PF_6]	6 (mp)	207[a)]	1.363	existent	36–38
[BMIM][CF_3SO_3]	16 (mp)	90[b)]	1.290	very low	12
[BMIM][$(CF_3SO_2)_2N$]	–4 (mp)	52[b)]	1.429	very low	12
[BMIM][*n*-$C_8H_{17}OSO_4$]	35 (mp)	875[b)]	1.060	low	14

g.p. = glass point; m.p. = melting point.
a) At 25 °C.
b) At 20 °C.
c) Very high = immediate hydrolysis, even with traces of water; existent = slow hydrolysis with water accelerated at higher temperature; low = slow hydrolysis only in acidic solutions at elevated temperature; very low = no hydrolysis even at higher temperature in acidic solutions.
n.d. = not determined.

In this chapter we will deal only with a small selection of ionic liquids, which have been successfully used in the context of hydrogenation reactions. These ion combinations, together with the abbreviations used in the following text, are displayed in Figure 41.2.

Furthermore, it is far beyond the scope of this chapter to provide any detailed insight into the materials science aspects of ionic liquids. However, it should be clearly stated that at least some understanding of the ionic liquid material is a prerequisite for its successful use as a catalyst layer in hydrogenation reactions. Therefore, the interested reader is strongly encouraged to explore the more specialized literature [39].

A significant part of the ballooning number of publications on ionic liquid chemistry (more than 1100 during 2004 according to SciFinder) deals with transition-metal catalysis in these unusual liquid materials. This intense publication activity has been documented in a number of comprehensive review articles and book chapters [39–44]. There are many good reasons for applying ionic liquids as alternative solvents in transition metal-catalyzed reactions. Besides their very low vapor pressure and their good thermal stability [45, 46], an important advantage is the possibility of tuning their solubility [47] and acidity/coordination properties [48] by varying the nature of the anions and cations systematically.

Depending on the acidity/coordination properties of the anion and on the reactivity of the cation (the possibility of carbene ligand formation from 1,3-dialkylimidazolium salts is of particular importance here [49–56]), the ionic liquid

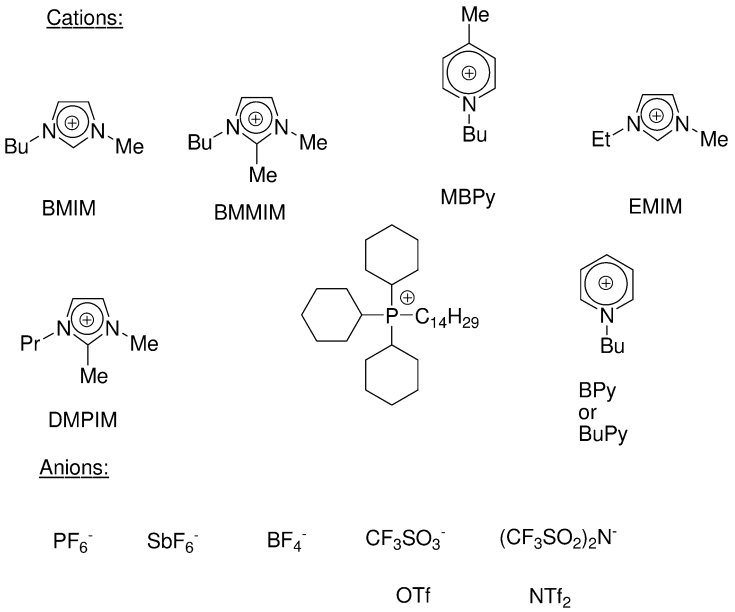

Fig. 41.2 Ionic liquids referred to in the text, and their abbreviations.

can be regarded as an "innocent" solvent, as a ligand precursor, as a co-catalyst or as the catalyst itself.

Ionic liquids with weakly coordinating, inert anions (e.g., $[(CF_3SO_2)_2N]^-$, $[BF_4]^-$ or $[PF_6]^-$ under anhydrous conditions) and inert cations (cations that do not coordinate to the catalyst themselves and that do not form species under the reaction conditions that coordinate to the catalyst) can be considered as "innocent" solvents in transition-metal catalysis. In these cases, the role of the ionic liquid is solely to provide a more or less polar, more or less weakly coordinating medium for the transition-metal catalyst that additionally offers special solubility for the feedstock and products.

However, unlike most conventional solvents, many ionic liquids combine high solvating power for polar catalyst complexes (polarity) with weak coordination (nucleophilicity) [57]. It is this combination that enables a biphasic reaction mode with these ionic liquids even for catalyst systems which are deactivated by water or polar organic solvents. Most interestingly, the biphasic reaction mode allows, in principle, the recycling of the ionic catalyst solution and thus a significant enhancement of the efficiency of the catalyst complex applied. This option is especially interesting for biphasic hydrogenation reactions, since the polarity of the reactants decreases during the reaction so that the less-polar products show lower solubility in the ionic catalyst phase than the substrate. Therefore, product isolation can be carried out by simple decantation in most cases and the catalyst containing ionic liquid can be reused immediately.

Table 41.2 Solubility of H_2 in water, organic solvents and ionic liquids, at 0.101 MPa (1 atm) [59].

Solvent	Henry's constant [k_h Mpa^{-1}][a)]	10^3 [H_2] [M]	Density [g mL^{-1}]	Viscosity [cP]	Reference(s)
Benzene [b)]	4.47×10^2 (4.39×10^2)	2.54 (2.57)	0.878	0.60 [c)]	61, 62
Cyclohexane [b)]	2.57×10^2 (2.55×10^2)	3.63 (3.66)	0.777	1.62 [b)]	61, 62
[BMIM][BF_4] [b)]	5.8×10^2 (1.63×10^2)	0.86 [d)] (3.0)	1.12	219 [c)]	63
[BMIM][PF_6] [b, c)]	6.6×10^2 (5.38×10^2)	0.73 [d)] (0.88)	1.363	450 [c)]	63
[BMIM]Tf_2N] [c)]	4.5×10^2	0.77 [d)]	1.433	69 [c)]	63
[BMMIM][Tf_2N] [c, e)]	3.8×10^2	0.86 [d)]	1.421	97.1 [c)]	64
[BuPy][Tf_2N] [c, f)]	3.9×10^2	0.89 [d)]	1.449	57 [c)]	35
[BMPy][Tf_2N] [c, g)]	3.7×10^2	0.90 [d)]	1.387	85 [c)]	65
[BMIM][SbF_6] [c)]	4.9×10^2	0.93 [d)]	1.699	95	–
[BMIM][CF_3COO] [c)]	4.9×10^2	0.98 [d)]	1.198	73 [b)]	12
[HMIM][BF_4] [c, h)]	5.7×10^2	0.79 [d)]	1.14	314.0 [b)]	31, 66
[OMIM][BF_4] [c)]	6.4×10^2	0.62 [d)]	1.106	135.0 [b)]	66
[BMIM][CF_3SO_3] [c)]	4.6×10^2	0.97 [d)]	1.290	90 [b)]	12
[$P(C_6H_{13})_3(C_{14}H_{29})$][$PF_3(C_2F_5)_3$] [c)]	0.7×10^2	1.84 [d)]	1.196	498 [b)]	31

a) $k_H = P_{H2}/X_{H2}$, the partial pressure of hydrogen is expressed in MPa.
b 293 K.
c) 298 K.
d) Calculated from the solubility under 10.1 MPa, supposing that solubility changes linearly with the partial pressure.
e) $[BMMIM]^+$ = 1,2-dimethyl-3-butylimidazolium.
f) $[BuPy]^+$ = *N*-butylpyridinium.
g) $[BMPy]^+$ = *N*-butyl-*N*-methylpyrrolidinium.
h) $[HMIM]^+$ = 1-hexyl-3-methylimidazolium.

In this chapter we will focus uniquely on the application of ionic liquids in transition metal-catalyzed hydrogenation reactions. In this context, the hydrogen solubility in ionic liquids is an important issue. However, very few publications deal with this matter so far [58–60]. For the ionic liquid [BMIM][PF_6], the solubility of hydrogen has been found to be very low [58]. With the gravimetric microbalance method used by Brennecke et al. the solubility was even undetectable due to uncertainties in density measurement of the ionic liquid. This led, in the case of low-solubility gases, to large uncertainty (up to 75%) in determination of Henry's constant. In fact, these authors reported that the solubility of hydrogen in [BMIM][PF_6] is lower than in all conventional organic solvents.

In another publication, Dyson et al. [59] reported on hydrogen solubilities in several ionic liquids obtained by the use of ^{1}H-NMR technique. The results are summarized in Table 41.2.

Since the solubility of hydrogen in ionic liquids is very low, hydrogenation in ionic liquids takes place at low hydrogen concentrations. This is a disadvantage as higher pressures may be required in some cases. However, the diffusivity of hydrogen into ionic liquids can be expected to be high. According to Scovazzo and coworkers, the diffusivities of gases in ionic liquids depend strongly on the solute size as well as on the viscosity of the ionic liquid and the temperature [67]. The

high diffusivity of hydrogen results in high hydrogen transfer rates into the catalyst layer so that – during a hydrogenation reaction – the consumed hydrogen can be replenished rapidly. This fact explains the many successful hydrogenation reactions that have been reported in ionic liquids (see below), despite the low hydrogen solubility in these media. Indeed, hydrogenation reactions in ionic liquids proceed in many examples in comparable rates to those in conventional organic solvents, even though on occasion longer reaction times have been reported.

41.2
Homogeneous Catalyzed Hydrogenation in Biphasic Liquid–Liquid Systems

41.2.1
Hydrogenation of Olefins

The first investigations of biphasic hydrogenation reactions with ionic catalyst phases were reported by Chauvin et al. [68]. In general, the correct immobilization of a transition-metal catalyst in an ionic liquid requires either the use of an ionic catalyst complex or a polar or ionic modified ligand. Chauvin et al. studied the ionic Osborne complex $[Rh(nbd)(PPh_3)_2][PF_6]$ (nbd = norbornadiene) for the hydrogenation of pent-1-ene in several ionic liquids (Table 41.3). The authors reported the hydrogenation in ionic liquid to be almost five-fold faster in $[BMIM][SbF_6]$ than the conventional homogeneous reaction in acetone. However, the reaction was found to occur much more slowly using a hexafluorophosphate ionic liquid. This effect was attributed to the better solubility of pen-

Table 41.3 Rh-catalyzed hydrogenation of pent-1-ene [68].

No.	Solvent	Conversion [%]			
		Pent-1-ene	Yield [a)]		TOF [min^{-1}] [b)]
			Pentane	Pent-2-ene	
1 [c)]	Acetone	99	38	61	0.55
2	$[BMIM][SbF_6]$	96	83	13	2.54
3	$[BMIM][PF_6]$	97	56	41	1.72
4	$[BMIM][BF_4]$	10	5	5	0.15
5 [d)]	[BMIM][Cl] : CuCl	18	0	18 (98% *cis*)	0
6 [e)]	$[BMIM][PF_6]$	99	25	74	0.73

a) Catalyst 0.05 mmol; pent-1-ene: 8.4 mmol; solvent: 4 mL, T = 30 °C, $p(H_2) = 0.1$ MPa; t = 2 h.
b) TOF = mol (pentane) per mol (rhodium) and time [min].
c) 10 mL acetone, 9.2 mmol pent-1-ene.
d) The molten salt was synthesized from 1.5 equiv. CuCl and 1 equiv. [BMIM][Cl].
e) In the presence of 2 mL acetone.

tene in the hexafluoroantimonate ionic liquid. The very poor yield in [BMIM][BF_4], however, was due to a high level of residual Cl^- ions in the used ionic liquid, leading to catalyst deactivation. At that time the preparation of this tetrafluoroborate ionic liquid in chloride-free quality was clearly a problem.

To date, several reports have been published dealing with the non-stereoselective hydrogenation of olefins in a liquid–liquid biphasic system containing ionic liquids [69–72].

The immobilization of $Pd(acac)_2$ as hydrogenation catalyst in the ionic liquids [BMIM][BF_4] and [BMIM][PF_6] was reported by Dupont et al. in 2000 [70]. These authors compared the biphasic hydrogenation of butadiene with the homogeneous system with all reactants being dissolved in CH_2Cl_2, with the reaction in neat butadiene and with a heterogeneous system using Pd on carbon as catalyst. The report showed that, for 1,3-butadiene hydrogenation, the selectivities achieved with $Pd(acac)_2$ dissolved in ionic liquids were similar to those observed under homogeneous conditions and were higher than under heterogeneous conditions (using Pd on carbon as the catalyst) or in neat 1,3-butadiene (Table 41.4).

The authors extended their investigations to a series of functionalized dienes such as sorbic acid, methyl sorbate, 1-nitro-1,3-butadiene, and cyclic dienes.

The group of Dupont also studied the catalytic activity of $RuCl_2(PPh_3)_3$ and $K_3Co(CN)_5$ in [BMIM][BF_4] for the hydrogenation of a number of unfunctionalized, unsaturated hydrocarbon compounds [69]. It was found that, in case of the ruthenium complex being the catalyst, the interaction of $RuCl_2(PPh_3)_3$ with the ionic liquid led to a stable, ionic purple solution, and no leaching of the Ru-complex could be detected by extraction with hydrocarbon solvents. Compared to the classical water-soluble catalysts (based on transition-metal complexes modified with water-soluble phosphane ligands [73, 74]), relatively high turnover frequencies (TOFs) of up to 537 h^{-1} were achieved. It is also noteworthy that the hydrogenation in ionic liquid required less drastic conditions (temperature

Table 41.4 Comparison of the hydrogenation of 1,3-butadiene to butenes in different solvents [70].

Entry	Solvent	Time [h]	Conversion [%]	Selectivity [%]				TON
				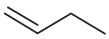	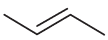			
1	[BMIM][BF_4]	12	98.2	55.5	5.1	35.2	4.2	982
2	[BMIM][PF_6]	13	88.5	46.2	8.5	38.2	7.1	885
3	CH_2Cl_2	13	93.0	44.2	6.3	47.3	2.2	930
4	a) ———	13	82.4	46.8	4.7	35.4	13.1	824
5	b) ———	1	61.9	24.2	7.2	30.8	37.8	619

Conditions: 50 °C, $p(H_2) = 20$ bar; 0.08 mmol $Pd(acac)_2$; diene/Pd = 1000.
TON = Turnover number = mol hydrogenated substrate per mol catalyst precursor.
a) In liquid 1,3-butadiene.
b) In liquid 1,3-butadiene using Pd/C as catalyst.

Table 41.5 Hydrogenation of several olefins with $RuCl_2(PPh_3)_3$ in [BMIM][BF_4] [69].

Entry	Olefin	Conversion [a] [%]	[Ru] [mmol]	Time [h]	Selectivity [%]			TOF [b] [h^{-1}]
					But-1-ene	But-2-enes	*n*-Butane	
1	Hex-1-ene	100	0.041	6				328
2	Hex-1-ene	84 [c]	0.041	3				537
3	Cyclohexene	30	0.041	4.5				170
4	Cyclohexene	100 [d]	0.065	20				73
5	Butadiene	18	0.041	1	22	33	45	543
6	Butadiene	68	0.041	4.5	29	42	29	493
7	Butadiene	100 [e]	0.041	8	20	67	13	377

Conditions: T = 30 °C; $p(H_2)$ = 25 bar.

a) Conversion of butadiene was calculated for the hydrogenation of only one double bond.

b) Turnover frequency = mol (product) × mol $(Ru)^{-1}$ h^{-1}.

c) Only *n*-hexane and hex-1-ene were detected.

d) At 60 °C.

e) 40 atm H_2.

and hydrogen pressure) compared to the hydrogenation in the aqueous medium using the water-soluble catalyst. Selected results of the Ru-catalyzed hydrogenation in [BMIM][BF_4] are shown in Table 41.5.

Hydrogenation of butadiene with $K_3Co(CN)_5$, which is known to hydrogenate selectively conjugated dienes [75], was possible with 100% conversion and selectivity and a TOF up to 72 h^{-1} in the ionic liquid [BMIM][BF_4], but the catalyst was deactivated after the first run and the inactive complex $(BMIM)_3Co(CN)_5$ was formed [69].

Many low-oxidation state transition-metal (carbonyl) clusters are salts and can be stabilized in ionic liquids due to their ionic character. Interestingly, Dyson et al. revealed that the activity of certain clusters in the hydrogenation of alkene substrates is up to 3.6-fold faster when these clusters were immobilized in ionic liquids, compared to their activity observed in organic solvents [72]. These authors evaluated the clusters $[HFe(CO)_{11}]^-$, $[HWOs_3(CO)_{14}]^-$, $[H_3Os_4(CO)_{12}]^-$ and $[Ru_6C(CO)_{16}]^{2-}$ as catalysts/precatalysts in the hydrogenation of styrene to ethylbenzene in [BMIM][BF_4], octane and methanol, respectively. Using $[Ru_6C(CO)_{16}]^{2-}$ as catalyst precursor in [BMIM][BF_4], the same research group also obtained good results for the partial reduction of cyclohexadienes to cyclohexene. However, by poisoning the catalytic phase with mercury and by means of high-pressure ^{1}H-NMR experiments, they showed that under the reaction conditions Ru-colloids/Ru-nanoparticles were formed and the latter acted as the catalyst in these reactions. These studies represent therefore examples of heterogeneous catalysis with nanoparticles in ionic liquids. In this context it should be mentioned that several other reports have been made about the formation, stabilization and immobilization of nanoparticles in ionic liquids. Several of these suspensions have been successfully applied in different hydrogenation reactions [40, 71, 76–85], but as these reactions are clearly

Table 41.6 Hydrogenation of styrene to ethylbenzene using $[H_3Os_4(CO)_{12}]^-$ as a catalyst precursor in various ionic liquids [72].

Ionic liquid	TOF [mol mol^{-1} h^{-1}]
[BMIM][BF_4]	587
[BMIM][PF_6]	522
[BMIM][$(CF_3SO_2)_2N$]	587
[BMMIM][PF_6]	392
[BMMIM][BF_4]	413
[BMMIM][$(CF_3SO_2)_2N$]	457
[OMPy][BF_4]	718

Conditions: $p(H_2) = 50.7$ bar, 100 °C, 4 h; cluster concentration 5×10^{-4} M, ionic liquid (1 mL), styrene (1 mL), total reactor volume (30 mL).
TOF calculated as average value over 4 h.

examples of heterogeneous hydrogenation in ionic liquids they will not be discussed here in more detail. In contrast to the ruthenium-containing cluster, a homogeneous hydride complex was characterized under reaction conditions when the osmium-containing clusters were dissolved in ionic liquids. A comparison of the TOFs of the $[H_3Os_4(CO)_{12}]^-$-catalyzed hydrogenation of styrene to ethylbenzene in various ionic liquids is presented in Table 41.6.

The TOFs in all ionic liquids are quite similar, although the values are somewhat lower in [BMMIM][PF_6], [BMMIM][BF_4] and [BMMIM][$(CF_3SO_2)_2N$] than in the [BMIM]-containing ionic liquids. The highest activity was found when [OMPy][BF_4] was used as the ionic liquid. An explanation for this could be the fact that [BMMIM]-containing ionic liquids possess the highest viscosities and therefore have the lowest mass transfer rates for hydrogen. The experiment with [OMPy][BF_4] (OMPy = 1-octyl-3-methylpyridinium cation) is special in that only for this ionic liquid can the reaction mixture form a single phase, thus preventing any liquid–liquid mass transport resistance. On the other hand, catalyst recycling by a simple decantation process is not possible in that latter case.

41.2.2
Hydrogenation of Arenes

The hydrogenation of arenes is industrially important, but so far has been dominated by the use of heterogeneous catalysts. In principle, ionic liquids offer the chance to use a liquid–liquid biphasic system where the homogeneous catalyst is immobilized and the ionic catalyst solution is reusable.

An unusual arene hydrogenation in ionic liquids was published by Seddon et al. in 1999 [86]. These authors reported a new means of hydrogenating aromatic compounds by dissolving electropositive metals in ionic liquids with HCl as the

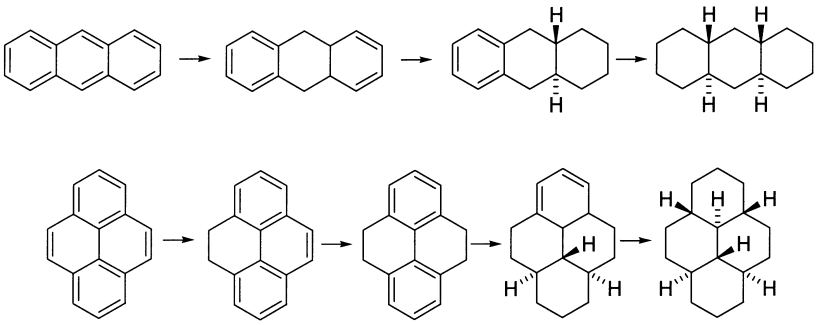

Scheme 41.1 Reduction of anthracene and pyrene using electropositive metals in ionic liquids with HCl as the proton source.

proton source. As the metals aluminum, zinc and lithium were used as bulk (and were converted to metal chlorides by reaction with HCl during the hydrogenation reaction), it may be a point of discussion whether the reaction can really be considered as being homogeneous. However, the authors found that the best system for hydrogenation was [EMIM][HCl_2], with additional anhydrous HCl gas as a proton source in the presence of aluminum, where the aluminum-(III)-chloride as byproduct of the reaction precipitated and the composition of the ionic liquid remained largely unaffected. In this way the complete reduction of anthracene and pyrene was carried out (Scheme 41.1).

The partial reduction of 9,10-dimethylanthracene gave rise to two isomers in a 6 : 1 ratio. The major product was the *cis*-isomer, and the minor product the *trans*-isomer. The system is not suitable for the reduction of simple aromatics such as benzene or naphthalene. The yields there were quite low with 2% and 15%, respectively.

Dyson et al. [87, 88] applied ruthenium clusters as a catalyst for the hydrogenation of benzene, toluene, cymene, ethylbenzene, and chlorobenzene. A direct comparison of the two biphasic systems, water/organic solvent and ionic liquid/organic solvent, showed that the TOFs obtained in the ionic liquid and the aqueous media were similar [88]. The results of the hydrogenation in the two biphasic systems are listed in Table 41.7. The authors proposed that the catalytically active species was $[H_6Ru_4(\eta_6\text{-}C_6H_6)_4]^{2+}$ in the ionic liquid-containing system, as was shown for the water-containing system [89]. Again, the advantage of the ionic liquid-containing biphasic system was the easy separation of products and the possibility of reusing the catalytic active phase.

Dyson et al. also showed that it is important to account for the chloride concentration in the ionic liquid [87]. These authors proved that chloride impurities, resulting from the synthesis of the ionic liquid, have a strong influence on hydrogenation activity. This was demonstrated by a comparison of hydrogenation activity in [BMIM][BF_4] which was made via the classical ion-exchange reaction (metathesis route, Scheme 41.2 (1)), with a chloride concentration of 0.2 mol kg^{-1}, and the same ionic liquid which was made by direct conversion of

Table 41.7 Comparative studies of the biphasic hydrogenation reactions of arenes in [BMIM][BF_4] and water with [$H_4Ru_4(\eta_6$-$C_6H_6)_4$][BF_4]$_2$ as the catalyst precursor [88].

Substrate	Reaction system	Reaction conditions	Conversion [%]	Catalytic turnover[a)] [mol mol^{-1} h^{-1}]
Benzene	Ionic liquid	60 atm H_2, 90 °C, 2.5 h	91	364
	Water	60 atm H_2, 90 °C, 2.5 h	88	352
Toluene	Ionic liquid	60 atm H_2, 90 °C, 3 h	72	240
	Water	60 atm H_2, 90 °C, 3 h	78	261
Cumene	Ionic liquid	60 atm H_2, 90 °C, 2.5 h	34	136
	Water	60 atm H_2, 90 °C, 2.5 h	31	124

a) Catalytic turnover calculated on the assumption that the tetraruthenium catalyst does not break down into monoruthenium fragments, which is entirely consistent with the data.

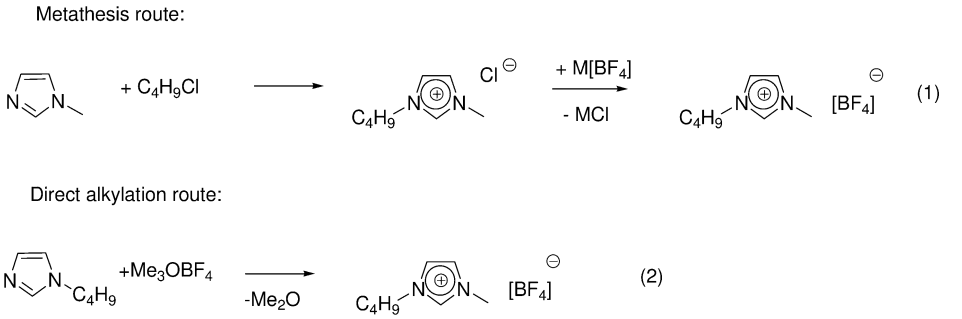

Scheme 41.2 Metathesis route and direct alkylation route for the synthesis of [BMIM][BF_4].

butylimidazole and trimethyloxonium tetrafluoroborate (direct methylation route, Scheme 41.2 (2)), which was essentially chloride-free. The data relating to this study are presented in Table 41.8.

Based on the results of these studies it is quite evident that the reaction with ionic liquid as immobilization phase requires a chloride-free catalyst phase in order to achieve any advantage over the reaction with water as the immobilizing phase.

Very interesting results were obtained by using [Ru(η^6-*p*-cymene)(η^2-triphos)Cl][PF_6] in a biphasic system with [BMIM][BF_4] as catalyst phase [90]. The hydrogenation of benzene, toluene and ethylbenzene in this ionic liquid proved to proceed with higher yields and accordingly with higher TOFs than in the monophasic system with CH_2Cl_2 as solvent. The TOF (yield) of benzene hydrogenation was found to increase from 242 (52%) in CH_2Cl_2 to 476 mol mol^{-1} h^{-1} (82%) in the ionic liquid, for toluene from 74 (19%) to 205 mol mol^{-1} h^{-1} (42%), and for ethylbenzene from 57 (17%) to 127 mol mol^{-1} h^{-1} (30%), respec-

Table 41.8 The hydrogenation of various arene substrates using $Ru(\eta^6\text{-}C_{10}H_{14})(pta)Cl_2$ immobilized in water and in $[BMIM][BF_4]$ of different Cl^- contents [87].

Substrate	Reaction conditions	TOF[a] [mol mol^{-1} h^{-1}]
Toluene	Water	130
Toluene	$[BMIM][BF_4]$[b]	54
Toluene	$[BMIM][BF_4]$[c]	136
Ethylbenzene	Water	122
Ethylbenzene	$[BMIM][BF_4]$[b]	53
Ethylbenzene	$[BMIM][BF_4]$[c]	145
Chlorobenzene	Water	11
Chlorobenzene	$[BMIM][BF_4]$[b]	6
Chlorobenzene	$[BMIM][BF_4]$[c]	18

Reaction conditions: catalyst (30 mg) in solvent (10 mL), substrate (1 mL), H_2 (60 atm) 90 °C, 1 h. Products formed were completely hydrogenated cyclohexane or alkane analogues of substrate.
a) Turnovers in mol substrate converted mol^{-1} catalyst h^{-1}.
b) Made via metathesis route, $[Cl]^-$ 0.2 mol kg^{-1}.
c) Made via methylation of alkylimidazole, chloride content zero.

tively. With allylbenzene as the substrate the authors observed selective hydrogenation of the benzyl group so that the unsaturated alkyl chain remained intact. The hydrogenation yielded allylcyclohexane with a quite high TOF of 329 mol mol^{-1} h^{-1} (84% yield), whereas the system was inactive toward arenes with *R*-alkene substituents such as styrene and 1,3-divinylbenzene.

41.2.3 Hydrogenation of Polymers

The hydrogenation in a liquid–liquid system with ionic liquids as the catalyst phase was also applied to the hydrogenation of polymers. The first studies were presented by the group of Rosso et al. [91], who investigated the rhodium-catalyzed hydrogenation of polybutadiene (PBD), nitrile-butadiene rubber (NBR) and styrene-butadiene rubber (SBR) in a $[BMIM][BF_4]$/toluene and a $[BMIM][BF_4]$/toluene/water system. The activity of the catalyst followed the trend PBD > NBR > SBR, which is the same order as the solubility of the polymers in the ionic liquid. The values in percentage total hydrogenation after 4 h reaction time were 94% for PBD and 43% for NBR, and after a reaction time of 3 h was 19% for SBR.

For the hydrogenation of polystyrene-*b*-polybutadiene-*b*-polystyrene (SBS) block co-polymer with Ru–TPPTS complex as catalyst, Jang et al. [92] applied a polyether-modified ammonium salt ionic liquid/organic biphasic system (Fig. 41.3).

Hydrogenation conditions were optimized by addition of triphenylphosphine as promoter ligand, and the hydrogenation degree of SBS was up to 89%. Hy-

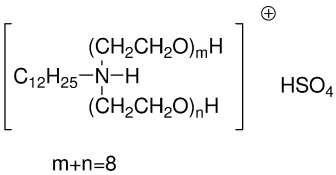

Fig. 41.3 The structure of the polyether-modified ammonium salt ionic liquid.

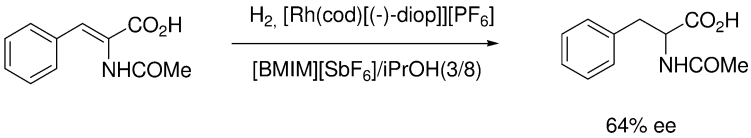

Fig. 41.4 Rhodium-catalyzed enantiomeric hydrogenation of α-acetamidocinnamic acid in the system [BMIM][SbF_6]/isopropanol system.

drogenation of the benzene ring and gel formation has not been observed. The active catalyst obviously remained in the ionic liquid and was reused three times without significant loss in catalytic activity.

41.2.4
Stereoselective Hydrogenation

Details of the first stereoselective hydrogenation in ionic liquids were published by the group of Chauvin [68], who reported the enantioselective hydrogenation of the enamide α-acetamidocinnamic acid in the biphasic system [BMIM][SbF_6]/*i*PrOH (ratio 3 : 8) catalyzed by [Rh(cod){(–)-diop}][PF_6]. The reaction afforded (*S*)-*N*-acetylphenylalanine in 64% enantiomeric excess (ee) (Fig. 41.4). The product was easily and quantitatively separated and the ionic liquid could be recovered, while the loss of rhodium was less than 0.02%.

Dupont et al. [60] studied the same reaction, but used [BMIM][PF_6] and [BMIM][BF_4] as ionic liquids. A special focus of their investigations was on the influence of H_2-pressure on conversion. The Henry coefficient solubility constant was determined by pressure drop experiment in a reactor, which is a known procedure to measure gas solubilities [93]. The values reported by these authors were $K = 3.0 \times 10^{-3}$ mol L^{-1} atm^{-1} for [BMIM][BF_4]/H_2 and 8.8×10^{-4} mol L^{-1} atm^{-1} for [BMIM][PF_6]/H_2 at room temperature, which differ significantly from those determined by the ^{1}H-NMR technique (see Table 41.2) [59]. However, their values indicated that molecular hydrogen is almost four times more soluble in [BMIM][BF_4] than in [BMIM][PF_6] under the same pressure. According to the authors, this is reflected by the values of conversion (ee), which were 73% (93% ee) for [BMIM][BF_4] and 26% (81% ee) for [BMIM][PF_6] at 50 bar H_2 pressure (Table 41.9, entries 2 and 4).

The variation of hydrogen pressure in the experiments using [BMIM][PF_6] as the ionic liquid (Table 41.9, entries 1–3) also showed that conversion and enan-

Table 41.9 The enantiomeric hydrogenation of (*Z*)-α-acetamido cinnamic acid: the effect of hydrogen concentration in the liquid phase on the conversion and the enantioselectivity.

Entry	Catalyst phase	$p(H_2)$ [atm]	Solubility H_2 [mol L^{-1}]	Conversion [%]	ee [b)] [%]
1	[BMIM][PF_6]	5	4.4×10^{-3}	7	66
2	[BMIM][PF_6]	50	4.4×10^{-2}	26	81
3	[BMIM][PF_6]	100	8.9×10^{-1}	41	90
4	[BMIM][BF_4]	50	1.5×10^{-1}	73	93
5	^{i}PrOH	50	129.3 [c)]	99	94

Reaction conditions: room temperature, 24 h, 950 rpm, 3 mL ionic liquid and 9 mL isopropanol, substrate/[Rh] = 100.
b) Determined by chiral GC.
c) Calculated from data reported by Frölich [94].

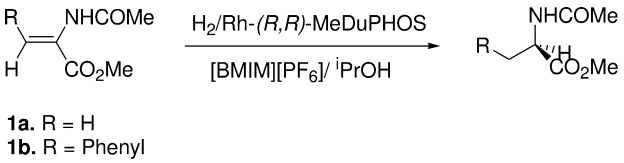

1a. R = H
1b. R = Phenyl

Fig. 41.5 Enantiomeric hydrogenation of enamides catalyzed by Rh–MeDuPHOS complex heterogenized in [BMIM][PF_6].

tioselectivity increased with the higher hydrogen availability (higher pressure, higher solubility) within the ionic liquid.

Another type of chiral rhodium complex [Rh–MeDuPHOS] was also immobilized in [BMIM][PF_6] and used in the enantiomeric hydrogenation of related enamides [95] (Fig. 41.5). Geresh et al. focused their research on the stabilization of the air-sensitive catalyst in the air-stable ionic liquid, so that the complex was protected from attack by atmospheric oxygen and recycling was possible.

The results are comparable to those of homogeneous reaction conditions (Table 41.10), and recycling of the catalyst was successful with constant ee-values over five cycles, even though conversion decreased. Amazingly, the catalyst was still active, despite being stored under atmospheric conditions for 24 h (Table 41.10, entry 7).

A special example for a regioselective hydrogenation in ionic liquids was reported by our group and by Drießen-Hölscher [96, 97]. Based on investigations in the biphasic system water/*n*-heptane, the ruthenium-catalyzed hydrogenation of sorbic acid to *cis*-3-hexenoic acid according to Scheme 41.3 in the system [BMIM][PF_6]/MTBE was studied [98].

In comparison to polar organic solvents (e.g., glycol), a more than threefold increase in activity with comparable selectivity to *cis*-3-hexenoic acid was ob-

Table 41.10 Enantiomeric hydrogenation of enamides with Rh–MeDuPHOS in [BMIM][PF_6]–*i*PrOH [95].

Entry		1a Conversion		1b Conversion	
		[%]	ee [%]	[%]	ee [%]
1	Homogeneous [a)]	100	97 (*R*)	100	99 (*R*)
2	Homogeneous [b)]	5	57 (*R*)	–	–
3	Heterogeneous; first cycle	100	93 (*R*)	83	96 (*R*)
4	Heterogeneous; second cycle	100	80 (*R*)	64	96 (*R*)
5	Heterogeneous; third cycle			62	95 (*R*)
6	Heterogeneous; fourth cycle			60	94 (*R*)
7	Heterogeneous; fifth cycle [c)]			58	94 (*R*)

Reaction conditions for homogeneous catalyst: 25 °C, 2 atm H_2, 7 g *i*PrOH; reaction time = 5 min. In the heterogeneous system, 5 g ionic liquid was added; reaction time = 20 min.

a) Preparation of the catalyst and of feeding into the reactor were performed under nitrogen.

b) Catalyst prepared in an inert atmosphere and exposed to air for a few minutes during feeding into the reactor. For cycles 3 to 7, all manipulations were performed in air.

c) Left to stand in air for 24 h.

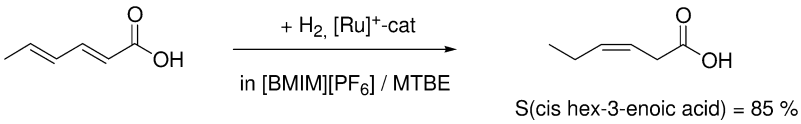

Scheme 41.3 Regioselective hydrogenation of sorbic acid in the biphasic system [BMIM][PF_6]/MTBE.

served in the ionic liquid. This is explained by a part deactivation (through complexation) of the catalytic active center in those polar organic solvents that are able to dissolve the cationic Ru-catalyst. In contrast, the ionic liquid [BMIM][PF_6] is known to combine high solvation power for ionic metal complexes with relatively weak coordination strength. In this way, the catalyst can be dissolved in a "more innocent" environment than is the case if polar organic solvents are used. After the biphasic hydrogenation of sorbic acid, the ionic catalyst solution could be recovered by phase separation and reused four times with no significant loss of selectivity, but with a decreasing conversion from 74.0 and 77.4%, to 59.6 and 35.8% in the third and forth runs, where the autoclave containing the catalyst phase was left to stand overnight between the second and the third runs.

A comparison of hydrogenation activity in a biphasic ionic liquid-containing system and a homogeneous media was carried out by Dupont et al. [99]. These authors used a [$RuCl_2$-(*S*)-BINAP]$_2$ NEt_3 catalyst precursor dissolved in [BMIM][BF_4]. This

system hydrogenates 2-arylacrylic acids (Fig. 41.6) (aryl = Ph or 6-MeO-naphthyl) with enantioselectivities similar to or higher than those obtained in homogeneous media. After reaction, the product was completely dissolved in the isopropanol-containing phase and separated by simple decantation. The ionic catalyst solution was recycled three times, without significant changes in activity and selectivity (Table 41.11).

In enantioselective hydrogenation the substrates can be divided in two classes (Fig. 41.7):

- Class I are components which require low H_2-pressure to obtain good enantioselectivities (e.g., tiglic acid).
- Class II components require high H_2-pressure (e.g., atropic acid) [100, 101].

Under this aspect, the group of Jessop [102] investigated the influence of the ionic liquid used on enantioselectivity in the hydrogenation of atropic acid as an example

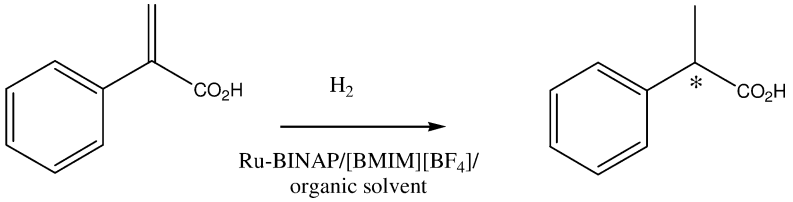

Fig. 41.6 Hydrogenation of 2-phenylacrylic acid in the system [BMIM][BF_4]/organic.

Table 41.11 Enantiomeric hydrogenation of 2-phenylacrylic acid giving 2-phenylpropionic acid. Reaction conditions: [Ru] = 0.034 mmol; ROH = 30 mL; [BMIM][BF_4] = 3 mL; time = 20 h [99].

Entry	Catalyst	Co-solvents	SCR	P [atm]	Conversion [%]	ee [%] (conf.)
1	*in situ* Ru-(*S*)-BINAP	MeOH	40	35	100	62 (*S*)
2	[Ru-Cl_2-(*S*)-BINAP]$_2$ · NEt_3	MeOH	80	25	100	83 (*S*)
3	[Ru-Cl_2-(*S*)-BINAP]$_2$ · NEt_4	*i*-PrOH	80	25	100	64 (*S*)
4	*in situ* Ru-(*R*)-BINAP	MeOH/[BMIM][BF_4]	40	25	100	86 (*R*)
5	*in situ* Ru-(*R*)-BINAP	*i*-PrOH/[BMIM][BF_4]	80	35	99	69 (*R*)
6	Recycle of entry 5	*i*-PrOH/[BMIM][BF_4]	80	22	99	72 (*R*)
7	Recycle of entry 6	*i*-PrOH/[BMIM][BF_4]	80	25	99	77 (*R*)
8	Recycle of entry 7	*i*-PrOH/[BMIM][BF_4]	80	25	99	70 (*R*)
9	[Ru-Cl_2-(*S*)-BINAP]$_2$ · NEt_3	*i*-PrOH/[BMIM][BF_4]	20	50	100	78 (*S*)
10	Recycle of entry 8	*i*-PrOH/[BMIM][BF_4]	20	75	100	84 (*S*)
11	Recycle of entry 9	*i*-PrOH/[BMIM][BF_4]	20	25	90	79 (*S*)
12	Recycle of entry 10	*i*-PrOH/[BMIM][BF_4]	20	100	95	67 (*S*)
13	[Ru-Cl_2-(*S*)-BINAP]$_2$ · NEt_3	*i*-PrOH/[BMIM][BF_4]	400	25	100	72 (*S*)

SCR = substrate : catalyst ratio.

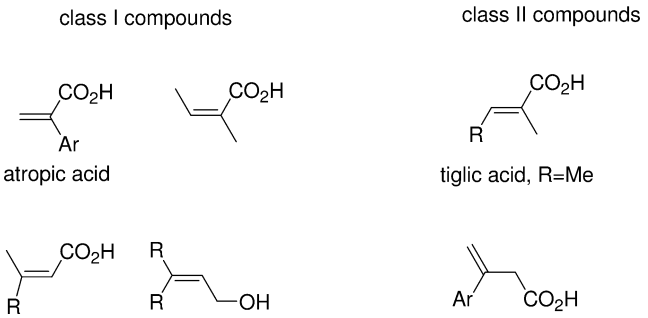

Fig. 41.7 Classification of substrates for enantioselective hydrogenation.

for Class I compounds, and of tiglic acid as an example for Class II compounds. These authors found a strong dependency of ee on the used solvent for the hydrogenation of atropic acid. The ee-values varied in the range of 72 to 95%, and increased in the following order: MeOH < [EMIM][CF_3SO_3] < [BMIM][BF_4] = [MBPy][BF_4] < [BMIM][PF_6] = [DMPIM] [$(CF_3SO_2)_2N$)] < [EMIM][$(CF_3SO_2)_2N$)].

For Class II components, the enantioselectivity for asymmetric hydrogenation in ionic liquids (without co-solvent) was low. The best enantioselectivities were obtained with methanol as co-solvent as the viscosity was much lower (i.e., the mass transfer was higher), and hydrogen solubility was presumably higher compared to the pure ionic liquids. For the reactions in neat ionic liquids, the selectivity was again dependent upon the choice of ionic liquid, increasing in the order: [BMIM][BF_4] < [EMIM][O_3SCF_3] < [BMIM][PF_6] = [EMIM][N(OTf)$_2$] < [DMPIM][N(OTf)$_2$].

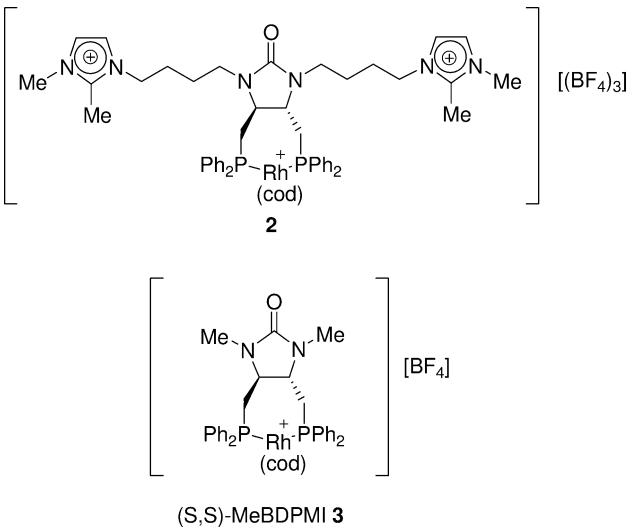

Fig. 41.8 Rh-complex with a bisphosphine-containing cation as ligand.

Table 41.12 Rh-catalyzed enantiomeric hydrogenation of *N*-acetylphenylethenamine using Rh-complex **2** and Me-BDPMI **3** in a [BMIM][SbF_6]/*i*PrOH two-phase solvent systems [103].[a)]

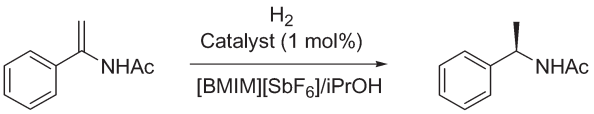

Entry	Catalyst	Run	Time [h]	Conversion [%][b)]	ee [%][c)]
1	2	1	1	100	97.0
2		2	1	100	96.6
3		3	1	100	96.2
4		4	1	82	95.4
5		4	8	100	95.4
6	3	1	1	100	95.8
7		2	1	100	95.1
8		3	1	78	94.2
9		4	1	51	91.4
10		4	12	85	88.0
11[d)]	3	1	1	100	95.6

a) Reaction conditions: Catalyst : substrate ratio = 0.01 : 1; [BMIM][SbF_6]/*i*PrOH = 1/2 (v/v); reaction temperature: 20 °C; p(H_2) = 1 atm.
b) Determined by NMR and GC.
c) Determined by chiral GC using CP-Chirasil Dex CB column.
d) Reaction carried out in the presence of 0.5 mol% **3**.

These results demonstrate that the effectiveness of hydrogenation in ionic liquids is not only a parameter of H_2 availability. Indeed, many solvent parameters – including polarity, coordinating ability and hydrophobicity – should be taken into account, though these have not yet been studied.

Lee et al. [103] synthesized a chiral Rh-complex with a bisphosphine-containing cation as ligand (Fig. 41.8, **2**) to improve the immobilization of the transition-metal complex within the ionic liquid.

Immobilization of this complex in the biphasic system [BMIM][SbF_6]/*i*PrOH showed better results compared to the non-modified complex Me-BDPMI (Fig. 41.8, **3**). The ionic catalyst solution was reused three times without loss of activity (Table 41.12). At the fourth run the conversion decreased, though high conversions could be still realized by increasing the reaction time.

A broad screening of ligands and ionic liquids was carried out by Feng et al. [104]. For rhodium-catalyzed hydrogenation of enamides the best catalysts were found to be the rhodium–ferrocenyl–diphosphine complexes with taniaphos, josiphos, walphos and mandyphos as ligands (Fig. 41.9).

Screening of the reaction media showed that, with the use of an ionic liquid/water mixture (a so-called "wet ionic liquid"), recycling of the catalyst could be improved compared to the reaction in ionic liquid without co-solvent. The com-

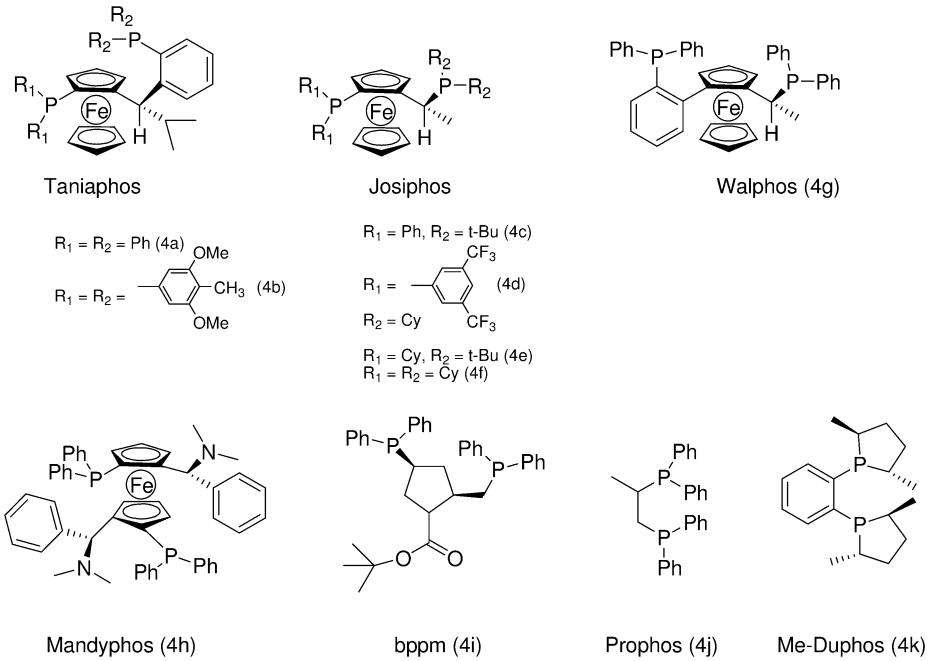

Fig. 41.9 Structures of the ligands used for enantioselective hydrogenation in the study of Feng et al. [104].

parative study with methyl-α-acetamidoacrylate hydrogenation showed that the ionic liquid/water media gave good results with regard to conversion, enantioselectivity, and catalyst separation (Table 41.13).

41.2.5
Ketone and Imine Hydrogenation in Ionic Liquids

Only one report exists on ketone hydrogenation in ionic liquids which applies Rh-complexes as catalysts [105]. The groups of Yinghuai, Ke and Hawthorne synthesized a new carborane-based room-temperature ionic liquid consisting of an *N*-*n*-butylpyridinium cation and a $[CB_{11}H_{12}]^-$ anion, and used this ionic liquid as reaction medium in the asymmetric hydrogenation of unsymmetrical aryl ketones in the presence of the chelating ligand (*R*)-BINAP and a rhodacarborane catalyst (Table 41.14). Compared to hydrogenation in tetrahydrofuran and in "classical" ionic liquids, the best results were achieved with the carborane-based ionic liquid.

Lin et al. [106] studied the hydrogenation of β-aryl ketoester using a ruthenium BINAP system with different substituents at the 4,4′-position of the BINAP ligand. The best enantioselectivities were achieved with steric demanding and electron-donating 4,4′-substituents. For example, ee-values of 97.2% and 99.5% were obtained for the hydrogenation of ethyl benzoylacetate with R = trimethylsilane (**5**,

Table 41.13 Enantioselective hydrogenation of enamides catalyzed by Rh-Taniaphos in various ionic liquids/water combinations and in conventional solvents [104].

Entry	Reaction medium	Conversion [%]	ee [%]	Catalyst separation	No. of phases
1	MeOH-H_2O [a)]	100	98	–	1
2	MeOH	100	97	–	1
3	*i*-PrOH	92	95	–	1
4	Toluene	47	28	–	1
5	[BMIM]BF_4	32	>99	–	1
6	[BMIM]PF_6	6	91	–	1
7	[BMIM]BF_4/*i*-PrOH	64	96	+	2
8	[BMIM]PF_6/*i*-PrOH	12	93	+	2
9	[OMIM]BF_4/H_2O	100	>99	++	2
10	[BMIM]Tf_2N/H_2O	97	>99	++	2
11	[BMIM]BF_4-H_2O [b)]/Toluene	100	>99	++	2
Reaction using ligand **4b**, substrate: methyl-*α*-acetamidoacrylate					
12	MeOH	53	97	–	1
13	*i*-PrOH	84	95	–	1
14	[BMIM]BF_4	17	98	–	1
15	[BMIM]BF_4/*i*-PrOH	43	99	++	2
16	[OMIM]PF_6/*i*-PrOH	47	98	++	2
17	[OMIM]BF_4/H_2O	70	>99	++ *)	2
18	[BMIM]Tf_2N/H_2O	90	>99	++	2
19	[BMIM]BF_4-H_2O [b)]/Toluene	100	>99	++	2
Reaction using ligand **4a**, substrate: methyl-*α*-acetamidocinnamate					
20	*i*-PrOH	100	94	–	1
21	[BMIM]BF_4	52	93	–	1
22	[BMIM]BF_4/*i*-PrOH	100	93	+	2
23	[OMIM]BF_4/H_2O	100	95	++	2
24	[BMIM]BF_4-H_2O [b)]/Toluene	100	94	++	2
25	[OMIM]BF_4/H_2O [c)]/Toluene	100	95	++	3
Reaction using ligand **4b**, substrate: methyl-*α*-acetamidocinnamate					
26	*i*-PrOH	100	99	–	2
27	[OMIM]BF_4/H_2O	100	>99	++	2

ILs: ca. 2 mL, co-solvents: ca. 2–3 mL, SCR = 200, [S] = 0.25 M in co-solvent, room temperature, $P(H_2) = 1$ bar, t = 20 min.
"–" no, "+" good (some leaching), "++" excellent (no leaching).
a) v:v = 4:1.
b) v:v = 6:1.
c) v:v = 3:1.
*) ICP-MS: 0.9 ppm Rh content in co-solvent.

Table 41.14 Rhodium-catalyzed hydrogenation of acetophenone (A) and ethyl benzoylformate (B) [105].

Solvent	Conversion [%] [b)]	ee [%] [c)]	TOF [h^{-1}] [d)]
[OMIM][BF_4]	100 (A, B)	97.3 (A), 99.3 (B)	194 (A), 201 (B)
[BMIM][BF_6]	100 (A, B)	97.8 (A), 98.2 (B)	207 (A), 213 (B)
[BPy][$CB_{10}H_{12}$]	100 (A, B)	99.1 (A), 99.5 (B)	239 (A), 306 (B)
Tetrahydrofuran	82 (A), 87 (B)	91.3 (A), 85.7 (B)	96 (A), 107 (B)

Molar ratio of catalyst/(*R*)-BINAP/acetophenone = 1 : 1.5 : 1000;
reaction conditions: H_2 (12 atm), 50 °C, 12 h; [cat.] = 8.1×10^{-4} M.
b) Determined by GC.
c) Determined by GC on a Chirasil DEX CB column.
d) TOF = (mol hydrogenation product mol Rh h^{-1}), determined after 3 h.

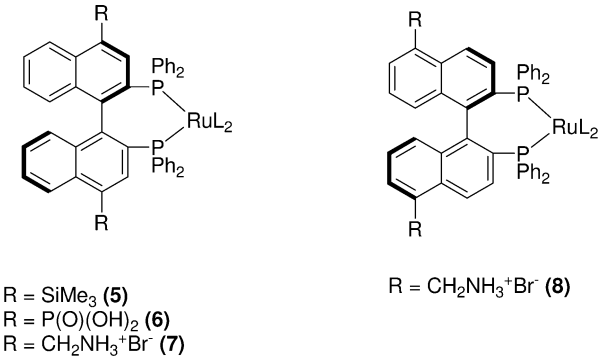

Fig. 41.10 Ru-complexes as used by Lin et al. in the hydrogenation of β-aryl ketoester in several ionic liquids.

Fig. 41.10), and R = bisphosphonic acid (**6**, Fig. 41.10), respectively, as substituents. By immobilization of these catalysts in [BMIM][BF_4], a slight deterioration in ee-values (reduction by 1%) was observed for the trimethylsilane-substituted catalyst, while an increase (by up to 2.6%) was observed for the bisphosphonic acid-substituted catalyst. Both catalysts were recycled and reused four times and the ee (conversion) decreased from 97.3% (>98) to 95.1% (62%) in the case of trimethylsilane as substituent, and from 97.5% (98) to 74.7% (44%) for the bisphosphonic acid-substituted catalyst. In both cases no significant leaching was detected. Higher conversion rates with comparable ee-values were achieved by using [MMPIM] [$(CF_3SO_2)_2N$] as ionic liquid [107]. These findings can be explained by an absence of the anions [BF_4] and [PF_6] (with their potential to liberate the catalyst poison F^- in a hydrolysis reaction) and substitution of the acidic proton at the 2-position of the imidazolium cation by a methyl group, which safely prevents carbene formation with the transition metal.

The same catalyst was used in the asymmetric hydrogenation of β-keto esters in [BMIM][PF_6], [BMIM][BF_4] and [MMPIM][$(CF_3SO_2)_2N$] with complete conversions and ee-values of up to 99.3% [108].

Another substituted derivative of BINAP was used by Lemaire et al. [109]. The ammonium salt catalysts (**7** and **8**, Fig. 41.10) were prepared *in situ* from the bromohydrates and [Ru(η^3-2-methylallyl)$_2$(η^2-COD)], and immobilized in several ionic liquids. By comparative studies of the hydrogenation of ethyl acetoacetate, the best results were obtained with imidazolium- and pyridinium-containing ionic liquids. No significant ee was observed with the phosphonium salt. This observation was attributed to problems of solubility and to the ability of complexation for the phosphonium ion. From the anionic side, use of the $[BF_4]^-$ anion appeared superior compared to $[PF_6]^-$ and $[(CF_3SO_2)_2N]^-$.

Due to chloride impurities of the ionic liquids in use, all selectivities were lower than the selectivities in pure water. Surprisingly, the selectivity increased from 76 to 90% and from 85 to 90% with reuse of the ionic catalyst solution based on [BMIM][BF_4] and [BPy][NTf_2], respectively.

Ionic liquids have also been applied in transfer hydrogenation. Ohta et al. [110] examined the transfer hydrogenation of acetophenone derivatives with a formic acid–triethylamine azeotropic mixture in the ionic liquids [BMIM][PF_6] and [BMIM][BF_4]. These authors compared the TsDPEN-coordinated Ru(II) complexes (**9**, Fig. 41.11) with the ionic catalyst synthesized with the task-specific ionic liquid (**10**, Fig. 41.11) as ligand in the presence of [$RuCl_2$(benzene)]$_2$. The enantioselectivities of the catalyst immobilized by the task-specific ionic liquid **10** in [BMIM][PF_6] were comparable with those of the TsDPEN-coordinated Ru(II) catalyst **9**, and the loss of activities occurred one cycle later than with catalyst **9**.

Table 41.15 Recycling of **9**- and **10**-Ru in the asymmetric transfer hydrogenation of acetophenone with the azeotrope in [BMIM][PF_6] [110].

Cycle	Catalyst 9-Ru Conversion		Catalyst 10-Ru[a] Conversion	
	[%][b]	ee [%][b]	[%][b]	ee [%][b]
1	96	93	98	92
2	99	92	>99	93
3	95	92	99	93
4	88	92	92	93
5	63	93	75	90

Reaction conditions: room temperature, 24 h, SCR = 100.
a) A mixture of **10** and [$RuCl_2$(benzene)]$_2$ was used.
b) Determined by capillary GLC analysis using a chiral Cyclodex-B column.

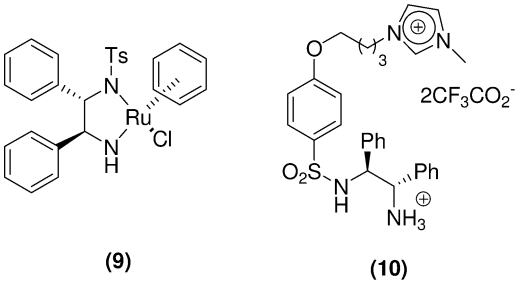

Fig. 41.11 Ru-complex and task-specific ionic liquid for the hydrogenation of acetophenone derivatives.

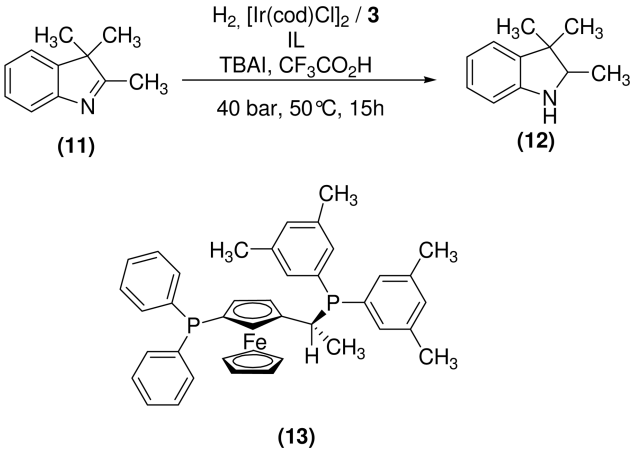

Fig. 41.12 Enantioselective hydrogenation of trimethylindolenine.

41.2.6
Imine Hydrogenation

Very few examples describe the hydrogenation of imines in ionic liquids. Giernoth et al. [111] performed a screening of eight different ionic liquids (the cations were $[BMIM]^+$, $[C_{10}MIM]^+$, $[BMPy]^+$ and $[C_{10}MPy]^+$ combined with the anions $[BF_4]^-$ and $[(CF_3SO_2)_2N]^-$), and compared them with toluene as solvent in the hydrogenation of trimethylindolenine (**11**, Fig. 41.12) with Ir-xyliphos as catalyst (**13**, Fig. 41.12).

Besides immobilization of the catalyst, the benefit of the ionic liquids is in this case a reduction of the reaction time from 23 h in toluene to less than 15 h in $[C_{10}MIM][BF_4]$ with no loss of selectivity, although the ionic media require slightly higher reaction temperatures (Table 41.16). Furthermore, a stabilization of the ionic catalyst solution against atmospheric oxygen is observed. This stabilization ef-

Table 41.16 Enantioselective hydrogenation of **11** [111].

Entry	Solvent	Conversion [%]	ee [%] [a)]
1 [d)]	Toluene [b)]	100	90
2 [d)]	Toluene [c)]	98	86
3 [d)]	[BMIM][BF_4]	100	56
4 [d)]	[BMIM][BF_4]	45	56
5 [d)]	[BMIM][NTf_2]	100	70
6 [d)]	[BMIM][NTf_2]	91	68
7 [d)]	[C_{10}MIM][NTf_2]	100	76
8 [d)]	[C_{10}MIM][NTf_2]	100	72
9 [e)]	[C_{10}MIM][BF_4]	98	84
10 [e)]	[C_{10}MIM][NTf_2]	92	76

Reaction conditions: 0.4% catalyst loading, $p(H_2) = 40$ bar, 50 °C, 15 h.
a) (*S*)-enantiomer.
b) 23-h reaction time, 30 °C.
c) 15-h reaction time, 50 °C.
d) Under strictly anaerobic conditions.
e) After 8-h reaction time and transfer through air.

fect facilitates the transfer of freshly prepared catalyst to the autoclave through air making the handling of the ionic liquid/catalyst-system much easier.

41.3 Homogeneous Catalyzed Hydrogenation in Biphasic Ionic Liquid/Supercritical (sc)CO_2 System

A very interesting way of performing homogeneous hydrogenation reactions in an ionic catalyst phase is to combine them with a compressed CO_2 extraction phase. The significant solubility of CO_2 in the ionic liquid enhances the availability of hydrogen in the ionic liquid in two ways. First, hydrogen solubility in the ionic liquid phase is greatly increased by the "co-solvent" CO_2. Second, the viscosity of the ionic liquid is drastically reduced by the presence of CO_2, thus enhancing the mass transport of hydrogen into the ionic liquid phase.

The fact that no ionic liquid is soluble in a pure compressed CO_2 phase makes the combination of both solvent systems – which are at the extreme ends of the polarity and volatility scales – especially attractive for continuous processes [102, 112–114].

41.4
Supported Ionic Liquid Phase Catalysis

A rather new concept for biphasic reactions with ionic liquids is the supported ionic liquid phase (SILP) concept [115]. The SILP catalyst consists of a dissolved homogeneous catalyst in ionic liquid, which covers a highly porous support material (Fig. 41.13). Based on the surface area of the solid support and the amount of the ionic liquid medium, an average ionic liquid layer thickness of between 2 and 10 Å can be estimated. This means that the mass transfer limitations in the fluid/ionic liquid system are greatly reduced. Furthermore, the amount of ionic liquid required in these systems is very small, and the reaction can be carried in classical fixed-bed reactors.

The SILP concept has been successfully applied to homogeneous hydrogenation by Mehnert et al. [116]. In these investigations, the hydrogenation of 1-hexene, cyclohexene and 2,3-dimethylbutene was carried out with the complex $[Rh(nbd)(PPh_3)_2][PF_6]$ (nbd = norbornadiene, PPh_3 = triphenylphosphine). In comparison to the classical homogeneous and to the biphasic reaction systems, the catalyst showed enhanced activity by using the SILP concept (see Table 41.7). For example, the reaction rate for the hydrogenation of 1-hexene increased from $k_0 = 0.4\ min^{-1}$ at 50 °C for the homogeneous phase to $k_0 = 11.2\ min^{-1}$ at 30 °C for the SILP catalyst. This corresponded to an increase in TOF from 46 mol mol^{-1} min^{-1} for the biphasic hydrogenation of 1-hexene to 447 mol mol^{-1} min^{-1} (Table 41.17, entries 5 and 10).

The same catalyst was reused for 18 batch runs, without any significant loss of activity. The level of rhodium leaching remained below the detection limit, and the isolated organic phases did not exhibit any further reactivity, which additionally verified full retention of the active species.

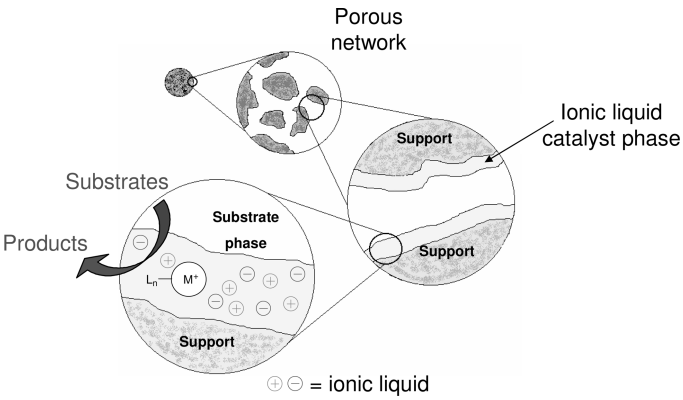

Fig. 41.13 Supported ionic liquid phase (SILP) catalyst. The ionic liquid phase containing a rhodium complex is immobilized on the surface of a silica gel support material.

Table 41.17 Comparative hydrogenation studies using supported ionic liquid catalysts, biphasic catalyst systems and the classical homogeneous catalyst systems [116]. [a)]

Entry	Substrate	Substrate [mol]	Solvent [b)] [mol]	Pressure [psig]	Temperature [c)] [°C]	Time [min]	Conversion [%]	Yield [d)] [%]	TOF_{ave} [e)] [min^{-1}]	k_h [f)] [min^{-1}]	Comments
1	1-C_6=	0.12	0.94	15	23 (25)	120	100	68	28	0.4	
2	1-C_6=	0.12	0.96	72	22 (28)	45	100	91	135	2.1	
3	1-C_6=	0.14	0.95	150	23 (29)	23	98	86	291	3.6	
4	1-C_6=	0.13	0.97	300	23 (30)	20	99	91	329	6.5	
5 [g)]	1-C_6=	0.13	0.96	600	25 (34)	16	100	99	447	11.2	
6	1-C_6=	0.11	0.83	900	23 (33)	7	97	94	821	21.7	
7 [h)]	c-C_6=	0.13	0.99	600	24 (31)	20	95	91	329	9	
8 [i)]	DMB	0.13	0.96	600	22 (23)	120	34	29	17	0.6	
9 [j)]	1-C_6=	0.04	0.2	600	30 (30)	120	44	20	4	–	Biphasic
10 [k)]	1-C_6=	1.2	1.5	600	50 (50)	120	96	29	46	0.4	Acetone

a) All runs conducted at stirring speed of 2200 rpm in a 300-mL autoclave equipped with a basket insert (Robinson-Mahoney reactor) and a catalyst charge of $c(Rh) = 0.018 \times 10^{-3}$ mol.
b) Heptane used as solvent.
c) Values in parentheses give maximum reaction temperature due to exotherm (small impact on k_h for entries 1–8; comparison with entry 10 will not be influenced).
d) Yield of hydrogenated product 2 reaction byproducts consisted of isomerized olefins (for hexene-1: c,t-hexene-2 and c,t-hexene-3).
e) TOF_{ave} defined as mol (hydrogenated product) per mol (rhodium) per min (full reaction time); reactions were stopped after 120 min or > 95% conversion.
f) k_h is initial rate constant for the appearance of hydrogenated product.
g) No transport limitation was apparent under the applied reaction conditions; the reaction was also investigated at 1800 rpm with no change of k_h.
h) Substrate: c-C6 = cyclohexene.
i) Substrate: DMB = 2,3-dimethyl-2-butene.
j) Liquid–liquid biphasic reaction was carried out in a 70-mL autoclave at a stirring speed of 1600 rpm with a catalyst charge of $c(Rh) = 0.018 \times 10^{-3}$ mol in 4 mL ionic liquid.
k) Homogeneous catalysis carried out in 300-mL autoclave at stirring speed of 2200 rpm in acetone solution with a catalyst concentration $c(Rh) = 0.06 \times 10^{-3}$ mol.

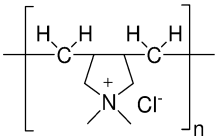

Fig. 41.14 Poly(diallyl-dimethylammoniumchloride).

Table 41.18 Homogeneous, biphasic and heterogeneous enantioselective hydrogenations of methyl acetoacetate with Ru-BINAP [117].

Entry	Reaction	Solvent	TOF [h^{-1}] (re-use)	ee [%]	Selectivity [a)]
1	Homogeneous	Methanol	103	99	85
2		Isopropanol	74	99	93
3		Methanol [b)]	88	99	91
4	Biphasic	Isopropanol	16 (15)	97	83
5	SILP	Isopropanol	29 (29)	97	87

Reaction conditions: 2 μmol complex, SCR = 140, 40 bar H_2, 60 °C, 1 h. Homogeneous: 4 mL solvent. Biphasic: 1 g [BMIM][PF_6], 4 mL solvent. Heterogeneous: 0.2 g polymer, 1 g [BMIM][PF_6], 4 mL solvent.

a) Selectivity to methyl hydroxybutyrate due to the formation of the corresponding acetal.

b) Addition of 0.2 g polymer.

To our knowledge, there is to date only one report concerning asymmetric hydrogenation using a SILP catalyst [117]. Methyl acetoacetate was hydrogenated using Ru-BINAP dissolved in [BMIM][PF_6] and immobilized on the poly(diallyl-dimethylammonium chloride) support (Fig. 41.14).

This polymeric phase simultaneously heterogenizes the transition-metal complex and the ionic liquid, so that the catalyst is fully recyclable. The SILP-catalyst was less active than the homogeneous reference system, but clearly more active than the biphasic system (Table 41.18).

Beside SILP experiments with silica as support material, reports have also been made on the use of membranes coated with ionic liquid catalyst solution for the hydrogenation reaction of propene and ethene. The membranes were obtained by supporting various ionic liquids, each containing 16 to 23 mmol Rh(I) complex Rh(nbd)$(PPh_3)_2^+$ (nbd = norbornadiene), in the pores of poly(vinylidene fluoride) filter membranes [118].

41.5 Conclusion

The use of ionic liquids has been successfully studied in many transition metal-catalyzed hydrogenation reactions, ranging from simple alkene hydrogenation to asymmetric examples. To date, almost all applications have included procedures of multiphase catalysis with the transition-metal complex being immobilized in the ionic liquid by its ionic nature or by means of an ionic (or highly polar) ligand.

A large part of the research has been dedicated to liquid–liquid-biphasic hydrogenation reactions. Hydrogenation, in principle, is very well suited for a biphasic reaction mode using ionic liquids. Many hydrogenation catalysts are ionic or polar and – most importantly – the polarity of the product is lower than the polarity of the substrate. This allows easy product separation after the reaction with low product solubility in the catalyst phase. Moreover, the formation of heavy, polar side products that would accumulate in the catalyst phase during recycling is not very likely in hydrogenation chemistry. Consequently, many of the research projects published to date have focused on aspects of recycling. Regarding the fact that not only the metal complex but also the ionic liquid itself is a valuable part of the reaction mixture, the concept aims for full and intact recovery of the ionic catalyst solution and its reuse.

Many of the examples presented in this chapter have shown much promise in this respect. It was seen that in many cases the activity and selectivity of known transition-metal complexes does not change too much in the ionic environment, indicating weak interaction of the ionic liquid ions and the complex in most cases. Selectivity optimization based on ligand design – which is especially important in asymmetric catalysis – is also possible in an ionic liquid environment. However, some important differences to the homogeneous reactions in organic solvents must be taken into account. Hydrogen solubility in ionic liquids is low compared to that in traditional solvents, and consequently the hydrogen concentration is low at the catalytic center. The mass transfer of hydrogen into the catalyst layer is affected by the viscosity of the ionic liquid (with low viscosities enhancing mass transfer), but has been found to be sufficiently rapid in most cases to reach acceptable reaction rates comparable to those obtained in organic media.

Specifically interesting variations of the hydrogenation using ionic liquids are the transition metal-catalyzed hydrogenations in the system ionic liquid/compressed CO_2 and the SILP concept. In both cases the advantages of a molecular defined, homogeneous, selective and recyclable hydrogenation catalyst are combined with very efficient, continuous catalyst recovery and recycling. Both concepts offer new approaches for process intensification in homogeneous hydrogenation catalysis.

Abbreviations

BMIM	1-butyl-3-methylimidazolium
EMIM	1-ethyl-3-methylimidazolium
NBR	nitrile-butadiene rubber
PBD	polybutadiene
SBR	styrene-butadiene rubber
$scCO_2$	supercritical CO_2
SCR	substrate : catalyst ratio
SILP	supported ionic liquid phase
TOF	turnover frequency
TON	turnover number

References

1 F. H. Hurley, US Patent **1948**, 2.
2 F. H. Hurley, T. P. Wier, Jr., *J. Electrochem. Soc.* **1951**, *98*, 207.
3 H. L. Chum, V. R. Koch, L. L. Miller, R. A. Osteryoung, *J. Am. Chem. Soc.* **1975**, *97*, 3264.
4 J. Robinson, R. A. Osteryoung, *J. Am. Chem. Soc.* **1979**, *101*, 323.
5 J. S. Wilkes, J. A. Levisky, R. A. Wilson, C. L. Hussey, *Inorg. Chem.* **1982**, *21*, 1263.
6 T. M. Laher, C. L. Hussey, *Inorg. Chem.* **1983**, *22*.
7 T. B. Scheffler, C. L. Hussey, *Inorg. Chem.* **1984**, *23*, 1926.
8 B. Appleby, C. L. Hussey, K. Seddon, J. E. Turp, *Nature* **1986**, *323*, 614.
9 P. B. Hitchcock, T. J. Mohammed, K. Seddon, J. A. Zora, C. L. Hussey, E. H. Ward, *Inorg. Chim. Acta* **1986**, *113*, L25.
10 J. S. Wilkes, M. J. J. Zarowotko, *J. Chem. Soc., Chem. Commun.* **1992**, 965.
11 J. Fuller, R. T. Carlin, H. C. de Long, D. J. Haworth, *J. Chem. Soc., Chem. Commun.* **1994**, 299.
12 P. Bonhôte, A. P. Dias, N. Papagergiou, K. Kalyanasumdaram, M. Grätzel, *Inorg. Chem.* **1996**, *35*, 1168.
13 H. Waffenschmidt, PhD thesis, RWTH Aachen, **2000**.
14 P. Wasserscheid, R. van Hal, A. Boesmann, *Green Chemistry* **2002**, *4*, 400.
15 W. Keim, W. Korth, P. Wasserscheid, World Patent 2000 0016902 **2000** (to BP Chemicals Limited).
16 P. Wasserscheid, M. Sesing, W. Korth, *Green Chemistry* **2002**, *4*, 134.
17 Y. Yoshida, K. Muroi, A. Otsuka, G. Saito, M. Takahashi, T. Yoko, *Inorg. Chem.* **2004**, *43*, 1458.
18 P. Wang, S. M. Kakeeruddin, R. Humphry-Baker, M. Grätzel, *Chem. Mater.* **2004**, *16*, 2694.
19 A. E. Visser, R. P. Swatlowski, M. W. Reichert, J. H. Davis, R. D. Rogers, R. Mayton, S. Sheff, A. Wiezbicki, *Chem. Commun.* **2001**, 135.
20 A. E. Visser, R. P. Swatlowski, M. W. Reichert, R. Mayton, S. Sheff, A. Wiezbicki, J. H. Davis, Jr., R. D. Rogers, *Environ. Sci. Technol.* **2002**, *36*, 2523.
21 S. Anjaiha, S. Chandrasekhar, R. Gree, *Tetrahedron Lett.* **2004**, *45*, 569.
22 P. Wasserscheid, B. Driessen-Hoelscher, R. Van Hal, C. H. Steffens, J. Zimmermann, *Chem. Commun.* **2003**, 2038.
23 J. H. Davis, Jr., *Chem. Lett.* **2004**, *33*, 1072.
24 T. L. Merrigan, E. D. Bates, S. C. Dorman, J. H. Davis, Jr., *Chem. Commun.* **2000**, 2051.
25 C. Hardacre, J. D. Holbrey, S. E. J. McMath, *Chem. Commun.* **2001**, 367.
26 B. Pegot, G. Vo-Thanh, D. Gori, A. Loupy, *Tetrahedron Lett.* **2004**, *45*, 6425.
27 M. J. Earle, P. B. McCormac, K. Seddon, *Green Chemistry* **1999**, *1*, 23.
28 J. Ding, T. Welton, D. W. Armstrong, *Anal. Chem.* **2004**, *76*, 6819.

29 Z. Wang, Q. Wang, Y. Zhang, W. Bao, *Tetrahedron Lett.* **2005**, *46*, 4657.
30 P. Wasserscheid, A. Bösmann, C. Bolm, *Chem. Commun.* **2002**, 200.
31 Solvent Innovation (www.solvent-innovation.com); Fluka (www.Fluka.com); Merck (www.merck.de); Acros Organics (www.acros.com); Wako (www.wako-chem.co.jp); Iolitec (www.iolitec.com).
32 K. Seddon, A. Stark, M. J. Torres, *Pure Appl. Chem.* **2000**, *72*, 2275.
33 A. A. Fannin, Jr., D. A. Floreani, L. A. King, J. S. Landers, B. J. Piersma, D. J. Stech, R. J. Vaughn, J. S. Wilkes, J. L. William, *J. Phys. Chem.* **1984**, *88*, 2614.
34 J. Fuller, R. T. Carlin, R. A. Osteryoung, *J. Electrochem. Soc.* **1997**, *144*, 3881.
35 A. Noda, K. Hayamizu, M. Watanabe, *Chem. Phys. Chem. B* **2001**, *105*, 4603.
36 Melting point: J. D. Holbrey, R. D. Rogers, Melting Points and Phase Diagram, in: P. Wasserscheid, T. Welton (Eds.), *Ionic Liquids in Synthesis*, Wiley VCH, Weinheim **2003**, p. 41.
37 Viscosity: S. N. Baker, G. A. Baker, G. A. Kane, F. V. Bright, *J. Phys. Chem. B* **2001**, *105*, 9663.
38 Density: S. Chun, S. V. Dzyuba, R. A. Bartsch, *Anal. Chem.* **2001**, *73*, 3737.
39 P. Wasserscheid, T. Welton (Eds.), *Ionic Liquids in Synthesis* **2003**, p. 213.
40 T. Welton, *Coord. Chem. Rev.* **2004**, *248*, 2459.
41 H. Olivier-Bourbigou, L. Magna, *J. Mol. Catal. A-Chemical* **2002**, *182/183*, 419.
42 R. Sheldon, *Chem. Commun.* **2001**, 2399
43 C. M. Gordon, *Appl. Catal. A (General)* **2001**, *222*, 101.
44 P. Wasserscheid, W. Keim, *Angew. Chem. Int. Ed. Engl.* **2000**, *39*, 3772.
45 K. J. Baranyai, G. B. Deacon, D. R. MacFarlane, J. M. Pringle, *Aust. J. Chem.* **2004**, *57*, 145.
46 M. Kosmulski, J. Gustafson, J. B. Rosenholm, *Thermochim. Acta* **2004**, *412*, 47.
47 J. D. Holbrey, R. D. Rogers, A. E. Visser, Solubility and solvation, in: P. Wasserscheid, T. Welton (Eds.), *Ionic Liquids in Synthesis*, Wiley-VCH, Weinheim **2003**, p. 68.
48 T. Welton, Polarity, in: P. Wasserscheid, T. Welton (Eds.), *Ionic Liquids in Synthesis*, Wiley-VCH, Weinheim **2003**, p. 94.
49 D. Bourissou, O. Guerret, F. P. Gabbai, G. Bertrand, *Chem. Rev.* **2000**, *100*, 39.
50 L. Xu, W. Chen, J. Xiao, *Organometallics* **2000**, *19*, 1123.
51 A. J. Arduengo, R. L. Harlow, M. Kline, *J. Am. Chem. Soc.* **1991**, *113*, 361.
52 A. J. Arduengo, H. V. R. Dias, R. L. Harlow, *J. Am. Chem. Soc.* **1992**, *114*, 5530.
53 W. A. Herrmann, M. Elison, J. Fischer, C. Koecher, G. R. J. Artus, *Angew. Chem. Int. Ed. Engl.* **1995**, *34*, 2371.
54 C. J. Mathews, P. J. Smith, T. Welton, A. J. P. White, *Organometallics* **2001**, *20*, 3848.
55 D. S. McGuinness, K. J. Cavell, B. F. Yates, *Chem. Commun.* **2001**, 355.
56 M. Hasan, I. V. Kozhevnikov, M. R. H. Siddiqui, C. Femoni, A. Steiner, N. Winterton, *Inorg. Chem.* **2001**, *40*, 795.
57 P. Wasserscheid, C. M. Gordon, C. Hilgers, M. J. Maldoon, *Chem. Commun.* **2001**, 1186.
58 J. L. Anthony, E. J. Maginn, J. F. Brennecke, *J. Phys. Chem. B* **2002**, *106*, 7315.
59 P. J. Dyson, G. Laurenczy, C. A. Ohlin, J. Vallance, T. Welton, *Chem. Commun.* **2003**, 2418.
60 A. Berger, R. F. de Souza, M. R. Delgado, J. Dupont, *Tetrahedron: Asymmetry* **2001**, *12*, 1825.
61 R. C. Weast (Ed.), *CRC Handbook of Chemistry and Physics 1972–1973*, 53rd edn. CER, Ohio.
62 ACS, *Physical Properties of Chemical Compounds*, **1955**.
63 J. G. Huddleston, A. E. Visser, W. M. Reichert, H. D. Willauer, A. G. Broker, R. D. Rogers, *Green Chemistry* **2001**, *3*, 156.
64 A. J. Mc Lean, M. J. Muldoon, C. M. Gordon, I. R. Dunkin, *Chem. Commun.* **2002**, 1880.
65 M. R. MacFarlane, P. Meakin, J. Sun, N. Amini, M. Forsyth, *J. Phys. Chem. B* **1999**, *103*, 4164.
66 L.C. Branco, J. N. Rosa, J. J. Moura Ramos, C. A. M. Afonso, *Chem. Eur. J.* **2002**, *8*, 3671.
67 D. Morgan, L. Ferguson, P. Scovazuzo, *Indust. Eng. Chem. Res.* **2005**, *44*, 4815
68 Y. Chauvin, L. Mussmann, H. Olivier, *Angew. Chem. Int. Ed. Engl.* **1996**, *34*, 2698.

69 P. A. Z. Suarez, J. E. L. Dullius, S. Einloft, R. F. de Souza, J. Dupont, *Inorg. Chim. Acta* **1997**, *255*, 207.
70 J. Dupont, P. A. Z. Suarez, A. P. Umpierre, R. F. De Souza, *J. Braz. Chem. Soc.* **2000**, *11*, 293.
71 L. M. Rossi, G. Machado, P. F. P. Fichtner, S. R. Teixeira, J. Dupont, *Catal. Lett.* **2004**, *92*, 149.
72 D. Zhao, P. J. Dyson, G. Laurenczy, J. S. McIndoe, *J. Mol. Catal. A: Chemical* **2004**, *214*, 19.
73 W. A. Herrmann, C. W. Kohlpaintner, *Angew. Chem. Int. Ed. Engl.* **1993**, *32*, 1524.
74 B. Cornils, *Angew. Chem. Int. Ed. Engl.* **1995**, *34*, 1575.
75 J. Kwiatek, J. K. Seyler, *Adv. Chem. Ser.* **1968**, *70*, 207.
76 K. Anderson, S. Cortinas Fernandez, C. Hardacre, P. C. Marr, *Inorg. Chem. Communications* **2004**, *7*, 73.
77 J. Dupont, G. S. Fonseca, A. P. Umpierre, P. F. P. Fichtner, S. R. Teixeira, *J. Am. Chem. Soc.* **2002**, *124*, 4228.
78 G. S. Fonseca, A. P. Umpierre, P. F. P. Fichtner, S. R. Teixeira, J. Dupont, *Chem. Eur. J.* **2003**, *9*, 3263.
79 G. S. Fonseca, J. D. Scholten, J. Dupont, *Synlett* **2004**, 1525.
80 J. Huang, T. Jiang, B. Han, H. Gao, Y. Chang, G. Zhao, W. Wu, *Chem. Commun.* **2003**, 1654.
81 J. Huang, T. Jiang, H. Gao, B. Han, Z. Liu, W. Wu, Y. Chang, G. Zhao, *Angew. Chem. Int. Ed. Engl.* **2004**, *43*, 1397.
82 L. M. Rossi, J. Dupont, G. Machado, P. F. P. Fichtner, C. Radtke, I. J. R. Baumvol, S. R. Teixeira, *J. Braz. Chem. Soc.* **2004**, *15*, 904.
83 C. W. Scheeren, G. Machado, J. Dupont, P. F. P. Fichtner, S. R. Teixeira, *Inorg. Chem.* **2003**, *42*, 4738.
84 E. T. Silveira, A. P. Umpierre, L. M. Rossi, G. Machado, J. Morais, G. V. Soares, I. J. R. Baumvol, S. R. Teixeira, P. F. P. Fichtner, J. Dupont, *Chemistry (Weinheim, Germany)* **2004**, *10*, 3734.
85 R. Tatumi, H. Fujihara, *Chem. Commun.* **2005**, 83.
86 C. J. Adams, M. J. Earle, K.R. Seddon, *Chem. Commun.* **1999**, 1043.
87 P. J. Dyson, D. J. Ellis, W. Henderson, G. Laurenczy, *Adv. Synth. Catal.* **2003**, *345*, 216.
88 P. J. Dyson, D. J. Ellis, T. Welton, D. G. Parker, *Chem. Commun.* **1999**, 25.
89 L. Plasseraud, G. Süss-Fink, *J. Organometal. Chem.* **1997**, *539*, 163.
90 C. J. Boxwell, P. J. Dyson, D. J. Ellis, T. Welton, *J. Am. Chem. Soc.* **2002**, *124*, 9334.
91 S. MacLeod, R. J. Rosso, *Adv. Synth. Catal.* **2003**, *345*, 568.
92 L. Wei, J. Y. Jiang, Y. H. Wang, Z. L. Jin, *J. Mol. Catal. A-Chemical* **2004**, *221*, 47.
93 A. Deimling, B. M. Karandikar, Y. T. Shah, N. L. Carr, *Chem. Eng. J.* **1984**, *29*, 140.
94 P. K. Frölich, E. J. Tauch, J. J. Hogan, A. A. Peer, *Ind. Eng. Chem.* **1931**, *23*, 548.
95 S. Guernik, A. Wolfson, M. Herskowitz, N. Greenspoon, S. Geresh, *Chem. Commun.* **2001**, 2314.
96 J. Heinen, M. Sandoval Tupayachi, B. Driessen-Hölscher, *Catalysis Today* **1999**, *48*, 273.
97 B. Driessen-Hölscher, J. Heinen, *J. Organometal. Chem.* **1998**, *570*, 141.
98 S. Steines, P. Wasserscheid, B. Driessen-Hölscher, *J. Prak. Chem. (Weinheim, Germany)* **2000**, *342*, 348.
99 A. L. Monteiro, F. K. Zinn, R. F. de Souza, J. Dupont, *Tetrahedron: Asymmetry* **1997**, *8*, 177.
100 Y. Sun, R. N. Landau, J. Wang, C. LeBlond, D. G. Blackmond, *J. Am. Chem. Soc.* **1996**, *118*, 1348.
101 R. Noyori, *Asymmetric Catalysis in Organic Synthesis.* John Wiley & Sons, **1994**.
102 P. G. Jessop, R. R. Stanley, R. A. Brown, C. A. Eckert, C. L. Liotta, T. T. Ngo, P. Pollet, *Green Chemistry* **2003**, *5*, 123.
103 S. G. Lee, Y. J. Zhang, J. Y. Piao, H. Yoon, C. E. Song, J.H. Choi, J. Hong, *Chem. Commun.* **2003**, 2624.
104 B. Pugin, M. Studer, E. Kuesters, G. Sedelmeier, X. Feng, *Adv. Synth. Catal.* **2004**, *346*, 1481.
105 Y. Zhu, K. Carpenter, C. C. Bun, S. Bahnmueller, C. P. Ke, V. S. Srid, L.W. Kee, M. F. Hawthorne, *Angew. Chem. Int. Ed. Engl.* **2003**, *42*, 3792.

106 A. Hu, H.L. Ngo, W. Lin, *Angew. Chem. Int. Ed. Engl.* **2004**, *43*, 2501.

107 H.L. Ngo, A.G. Hu, W.B. Lin, *Tetrahedron Lett.* **2005**, *46*, 595.

108 H.L. Ngo, A. Hu, W. Lin, *Chem. Commun.* **2003**, 1912.

109 M. Berthod, J.-M. Jörger, G. Mignani, M. Vaultier, M. Lemaire, *Tetrahedron: Asymmetry* **2004**, *15*, 2219.

110 I. Kawasaki, K. Tsunoda, T. Tsuji, T. Yamaguchi, H. Shibuta, N. Uchida, M. Yamashita, S. Ohta, *Chem. Commun.* **2005**, 2134.

111 R. Giernoth, M.S. Krumm, *Adv. Synth. Catal.* **2004**, *346*, 989.

112 R.A. Brown, P. Pollet, E. McKoon, C.A. Eckert, C.L. Liotta, P.G. Jessop, *J. Am. Chem. Soc.* **2001**, *123*, 1254.

113 F. Liu, M.B. Abrams, R.T. Baker, W. Tumas, *Chem. Commun.* **2001**, 433.

114 M. Solinas, A. Pfaltz, P.G. Cozzi, W. Leitner, *J. Am. Chem. Soc.* **2004**, *126*, 16142.

115 C.P. Mehnert, *Chem. Eur. J.* **2004**, *11*, 50.

116 C.P. Mehnert, E.J. Mozeleski, R.A. Cook, *Chem. Commun.* **2002**, 3010.

117 A. Wolfson, I.F.J. Vankelecom, P.A. Jacobs, *Tetrahedron Lett.* **2003**, *44*, 1195.

118 T.H. Cho, J. Fuller, R.T. Carlin, *High Temperature Material Processes (New York)* **1998**, *2*, 543.

42
Immobilization Techniques

Imre Tóth and Paul C. van Geem

42.1
Introduction

The immobilization of homogeneous catalysts remains an intensively developing research area, despite some doubts about its universal value for industrial application. Many books and reviews have been devoted to this topic over the past 40 years [1–13]. Hydrogenation with homogeneous catalysts is an important synthetic tool because of its regio- and enantioselectivity and its tolerance of functional groups. Therefore, homogeneous hydrogenation catalysts are among the most frequently targeted systems for immobilization. The majority of efforts for the immobilization of homogeneous hydrogenation catalysts are directed towards asymmetric hydrogenation. This is understandable, as enantioselective hydrogenation utilizes expensive precious metals and chiral ligands. Immobilization offers the possibility of ready separation and re-use of these catalysts. In this way – especially when a relatively cheap substrate is hydrogenated – a significant saving can be made in catalyst costs, making enantioselective hydrogenation eventually competitive with other routes such as optical resolution, chiral pool, biological approach, and so forth. As discussed below, various methods and support materials are used for immobilization. In truly ideal cases, some additional benefits are obtained by the immobilization, such as synergetic effects with the support giving enhanced activity and/or selectivity for the supported catalyst. Immobilization can also increase the stability of the supported complex against dimerization or cluster formation, which otherwise can be reasons for deactivation. Naturally, immobilization requires additional synthetic routes and procedures for making the complexes and supports suitable for immobilization, and this can increase the catalyst costs significantly. For this reason, an immobilized catalyst generally should possess several times higher turnover number (TON) or higher activity than its homogeneous counterpart. Blaser and coworkers [14] have recommended minimal turnover frequencies (TOFs) of 500 and 10 000 h^{-1}, or minimal TONs of 1000 and 50 000 for small- and large-scale production of fine chemicals, respectively. These conditions are

The Handbook of Homogeneous Hydrogenation.
Edited by J.G. de Vries and C.J. Elsevier
Copyright © 2007 WILEY-VCH Verlag GmbH & Co. KGaA, Weinheim
ISBN: 978-3-527-31161-3

not easily met in practice because of eventual deactivation or degradation of the catalyst.

Catalyst loss during separation of the homogeneous catalyst from the product can be an important issue, especially when using precious metal complexes, not only for economical but also for toxicological (environmental) reasons. The former is more characteristic for large-scale production, while the latter is seen more for small-scale fine chemicals or pharmaceuticals. Immobilization offers a solution not only for easy catalyst recovery, but also for the problems of product contamination. However, the development of an active and stable immobilized analogue of a homogeneous catalyst, which does not leach the metal component, is quite a laborious task. Too often, the time frame given to develop a synthetic route is so tight that an industrial research team can barely deal with these challenges. It is perhaps due to the latter issue – together with the relatively few homogeneous applications – that has so far prevented the broad spread of supported homogeneous hydrogenation catalysts within the chemical industry.

42.2 Engineering and Experimental Aspects

Heterogeneously catalyzed hydrogenation is a three-phase gas–liquid–solid reaction. Hydrogen from the gas phase dissolves in the liquid phase and reacts with the substrate on the external and internal surfaces of the solid catalyst. Mass transfer can influence the observed reaction rate, depending on the rate of the surface reaction [15]. Three mass transfer resistances may be present in this system (Fig. 42.1):

- at the gas–liquid interface for hydrogen;
- at the liquid–solid interface;
- by diffusion in the pore system of the catalyst.

Mass transfer can disguise the intrinsic kinetics severely [15]. For example, suppose the intrinsic kinetics is given by a power rate law:

$$r = k_0 \exp(-E_a/RT)[S]^m[H_2]^n[cat] \quad (M\,s^{-1})$$

The observed rate in the pore diffusion regime would then be (hydrogen diffusion limiting):

$$r_{obs} = k_0 \exp(-{}^1/_2 E_a/RT)[S]^m[H_2]^{(n+1)/2}[cat] \quad (M\,s^{-1})$$

Hydrogen transfer from the gas phase to the liquid phase becomes rate limiting with very fast hydrogenations (or with insufficient agitation). The observed reaction rate is then equal to the rate of gas–liquid mass transfer of hydrogen and becomes first order in hydrogen and independent of substrate concentration. The activation energy decreases to that of a diffusion process.

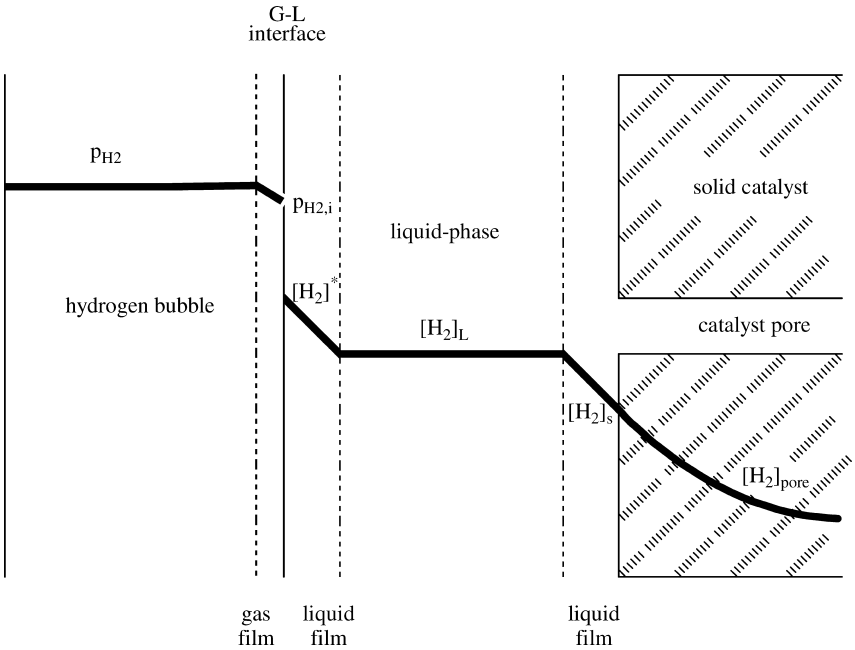

Fig. 42.1 Mass transfer resistances for hydrogen in heterogeneous catalytic hydrogenation.

$$r_{obs} = k_{GL}[H_2]^* = k_{GL} He\, p_{H2}[cat] \quad (M\,s^{-1})$$

In this formula, $[H_2]^*$ is the concentration of hydrogen in the liquid in equilibrium with the gas phase, related by the Henry coefficient.

It is clear from above that it is by no means easy to obtain intrinsic kinetics. However, comparison of different catalysts makes no sense when mass transfer effects disguise the intrinsic kinetics. Kinetic data are also hardly available from the TOF values, which are typically used for the characterization of the catalysts. These values are very convenient for a fast comparison of catalyst activities by measuring under the same reaction conditions (reaction temperature and time; catalyst, substrate and hydrogen concentration, etc.). However, different research groups seldom use the same reaction conditions, making comparison in activity difficult solely on the basis of TOF. Some notion of the intrinsic kinetics, either in the form of a power rate law or more sophisticated Langmuir-Hinshelwood type expressions, would help the chemical engineer greatly in scale-up and reactor design.

One could even think of taking advantage of pore diffusion limitation in enantioselective hydrogenation. The enantiomeric excess (ee) is in many homogeneously catalyzed cases dependent on the hydrogen concentration in solution, and increases with decreasing hydrogen pressure in some cases. The origin of this effect was explained by Landis and Halpern [16] in terms of the different

responses of the major and minor catalyst–substrate diastereomers to the hydrogen pressure. Blackmond and coworkers [17] showed later the importance of gas–liquid hydrogen transfer in this respect, and emphasized the role of the actual hydrogen concentration in solution, which was the decisive factor in determining the enantioselectivity. Anchoring of the catalyst in small pores would offer the opportunity to reduce the hydrogen concentration in the pore system below that of the bulk liquid phase and might help to increase enantioselectivity. Perhaps this mechanism is playing a role in the enantioselective hydrogenations using mesoporous silica supports. The difference with conventional silica supports may not stem from enhanced confinement in the mesoporous environment as was proposed [18], but from different diffusional regimes instead.

The reader should also be aware of some experimental pitfalls, which were not fully recognized in the early days of immobilization.

1. The leached metal can be catalytically active, either in the homogeneous phase or in the form of small metallic particles, suspended in the solution or deposited on the reactor wall or internals.
2. When no traces of metal are observed in the products of a batch experiment, one cannot exclude the possibility that metal went into solution under reaction conditions. Then, the dissolved metal could catalyze the reaction homogeneously with re-adsorption on cooling down at the end of the experiment.
3. The metal may be reduced to its zerovalent state and form small metallic particles on the support. These metal particles may take part in the reaction, especially in catalytic hydrogenation.

Therefore, it is advised to perform a "filtrate test" by taking a sample of the reaction solution under reaction conditions by hot filtering, and testing this solution for catalytic activity immediately, before any leached species can transform into an inactive one [19]. Furthermore, used catalysts should be checked on the presence of metallic particles. These are certainly not easily detected in small amounts and/or when they are of nanometer size. However, peculiar selectivity changes in time could give an indication of metal formation. Hydrogenation activity for aromatic rings is especially suspicious, because unlike most metals of Groups 8 to 10 of the Periodic Table, homogeneous catalysts are generally inactive for this reaction.

42.3 Immobilization Methods

Homogeneous catalysts can be immobilized on solid inorganic supports, such as silica, alumina and active carbon, or on solid polymers, often in the form of cross-linked polystyrene [1–5]. The inorganic supports have the advantages of a dimensionally stable pore system, generally better transport of reactants, higher mechanical strength and higher temperature stability. The polymeric supports

on the other hand are chemically more stable and offer more possibilities for fine-tuning of their structure during synthesis.

One can distinguish between physical and chemical methods of immobilization (Fig. 42.2). The former makes use of weak interactions between the metal

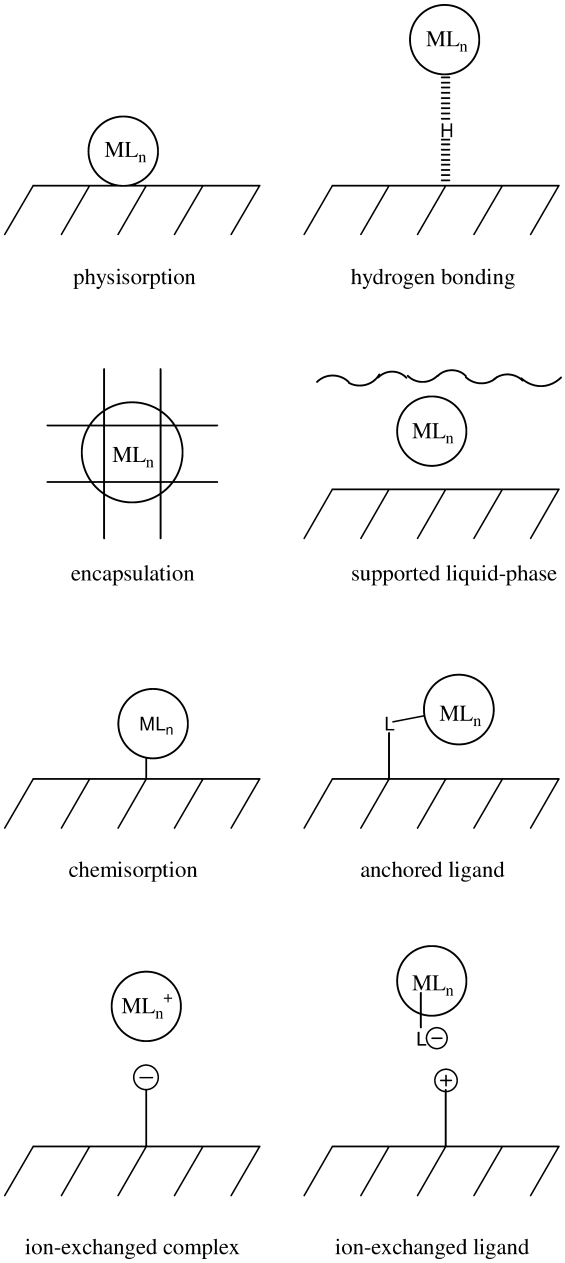

Fig. 42.2 Immobilization methods.

complex and the support: van der Waals forces, dipole–dipole interaction, π-π-stacking, and hydrogen bonding. Examples are physical adsorption, encapsulation of metal complexes in zeolites or entanglement in a polymer matrix, supported liquid phase catalysts, and hydrogen-bonded catalysts. The latter leads to the formation of a covalent or ionic chemical bond between the complex and the support. Examples are chemisorption of the metal complex on the support (usually through a metal–surface bond), covalent bonding of the ligand to the support, ionic bonding of the complex to the support (where the charge may reside on the metal or on a functional group of the ligand).

Immobilization on a soluble support is a special case with the clear advantage of avoiding mass transfer resistances inherent to a heterogeneous catalyst. However, separation of the catalyst from the products being in the same phase is less straightforward. Separation can be done by precipitation of the catalyst by changing the solvent polarity, but a more favored method is membrane filtration. The latter method is possible when the homogeneous catalyst is attached to a polymeric chain or to a dendrimer; its size becomes then large enough for a feasible ultrafiltration. Catalysis in two immiscible liquid phases, with the homogeneous catalyst being dissolved (immobilized) in a separate liquid phase, is discussed in Chapters 38 and 40.

42.3.1
Physical Methods of Immobilization

The simplest method of immobilization is physical adsorption of the metal complex onto a porous inorganic support material. However, the catalytic complexes are easily re-dissolved in the reaction medium because of the relatively weak interaction of the metal complex with the support by only physical forces. Therefore, application of this type of physisorbed homogeneous catalysts is limited to gas-phase reactions or to reactions in liquid media, in which the complexes are insoluble [2, 20]. Although physisorption is only a weak interaction, the catalytic properties may change, as the relative energies of the species in the catalytic cycle may have different degrees of interaction with the surface. One cannot define a sharp borderline between physisorption and chemisorption of the metal complex, because supports will always contain surface groups, which can form a coordinative bond with the metal atom (see Section 42.3.5) or which can form hydrogen bonds to a part of the metal complex (Section 42.3.1.2).

Another physical method of immobilization is occlusion of the homogeneous catalyst into the voids of an inorganic or organic matrix, which contain pore systems small enough to prevent escaping of the metal complex [1]. Occluded metal complexes in the cages of zeolites are most appealing in this respect because of their well-defined structure. The entanglement of metal complexes in a cross-linked inorganic or organic polymer is also a powerful method.

Table 42.1 Enantioselective hydrogenations using (*R*)-$RuCl_2$(*p*-cymene)(BINAP) adsorbed on zeolite Beta [22].

Substrate	Substrate: Ru ratio	Temp. [K]	P_{H_2} [MPa]	Time [h]	Conversion [%]	TOF [h^{-1}]	ee [%]
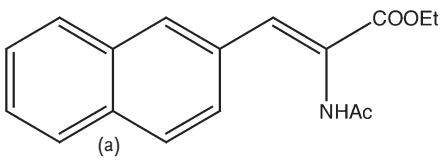	100	293	0.69	3	100	60	82.3
	100	293	0.69	22	99	6	80

Reactions carried out in methanol or ethylene glycol solvent. (a) Homogeneous catalyst.

42.3.1.1 **Physisorption of Metal Complexes**

Liquid-phase application of rhodium complexes adsorbed on zeolite VPI-5 proved to be possible for hydrogenation of sodium 4-styrenesulfonate in aqueous solution. The catalytic complexes are hardly soluble in water, and these immobilized catalysts could be recycled with low loss of rhodium and reactivity [20]. Adsorption of chiral rhodium and ruthenium complexes in hexagonal mesoporous silica, with a pore size of 26 Å for a tight fit, yielded catalysts with low leaching by using water or aqueous methanol as solvent. However, only moderate enantioselectivities (11–62% ee) were obtained [21]. More success was achieved with the adsorption of BINAP complexes on zeolite BETA. The chloro-Ru–BINAP catalyst system was adsorbed strongly on the acid form of zeolite BETA. The adsorbed catalyst system provided significantly higher activities and enantioselectivities in the enantiomeric hydrogenation of prochiral dehydroamino acids than the homogeneous analogue (Table 42.1). [22]. Furthermore, the heterogenized catalyst showed no leaching. Clearly, the heterogeneous system proved to be superior to the homogeneous counterpart. The exact nature of binding of the chiral chloro-Ru–BINAP system is not known. However, among a variety of zeolites and silicas tested, only the acid form of zeolite BETA proved to be a suitable support material. This led to the conclusion that the chiral Ru complex is immobilized by another means than ion exchange and/or hydrogen bonding. Molecular modeling studies indicated a very good fitting of the π-electron-rich aryl groups of the chiral ligand in the surface pores of zeolite BETA. Thus, a "key–lock" effect might be responsible for the success of this particular system.

42.3.1.2 **Weak Chemisorption: Supported Hydrogen-Bonded (SHB) Catalysts**

Most immobilization methods require modification of the ligands for anchoring to the support by introducing functional groups such as vinyl, trialkoxysilyl, sulfonic acid, and amino groups. The consequence is often a more elaborate synthesis of the ligand, which adds to the costs of an immobilized catalyst. However, two interesting approaches were developed in recent years, when unmodi-

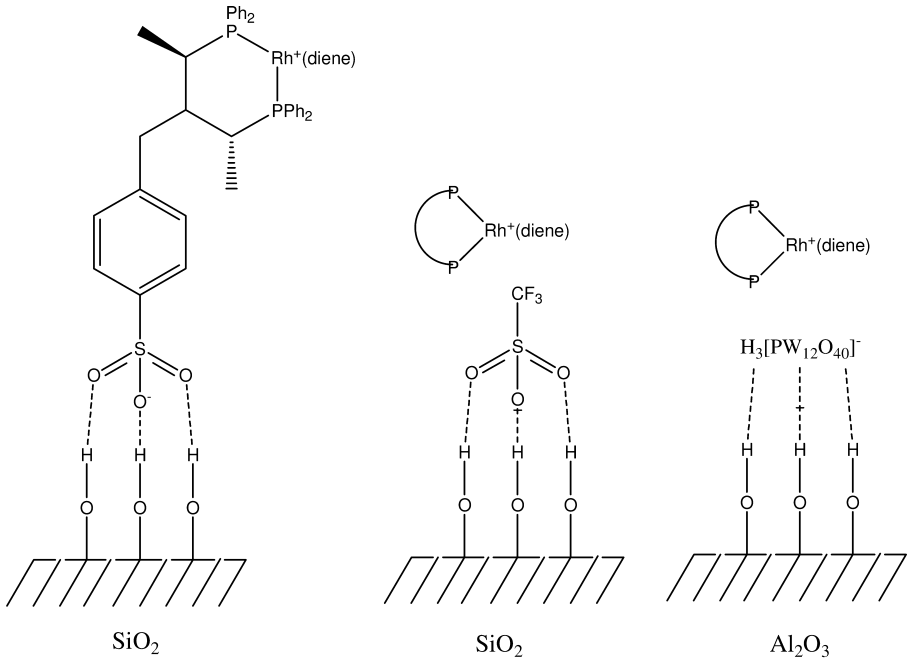

diene: norbornadiene, cyclooctadiene
P-P: bidentate (chiral) phosphorus ligand

Fig. 42.3 Hydrogen bonding in the adsorption of metal complexes [25, 32].

fied homogeneous catalysts were immobilized, using hydrogen-bonding interactions with the support.

The first example is a Rh complex of a tripodal sulfonated phosphine, where the sulfonic acid group forms hydrogen bonds to the silanol groups of the silica support (Fig. 42.3 a). Because of hydrogen bonding, the catalyst resembles supported aqueous-phase catalysts (these are discussed in Section 42.3.4). The adsorption strength of the complex is highly dependent on the coverage with silanol groups, which depends on the temperature pretreatment of the silica. The adsorbed catalyst was tested in the hydrogenation of styrene in liquid phase showing no loss of activity and Rh-leaching during recycle runs [23].

Analogous to the attachment of sulfonate groups in the previous example, other highly polar anionic groups such as non-coordinating trifluoromethylsulfonate (triflate) anions will also bind to silica or zeolites. Thus, it is possible to attach the anions of a positively charged metal complex by hydrogen bonding to the silica. In this way, cationic Ru or Rh complexes containing an achiral or a chiral bisphosphine, respectively, were successfully immobilized to silicas for hydrogenation reactions [24–28]. The triflate anions are thought to be hydrogen-bonded to the surface silanol groups of silica, immobilizing the metal complex by electrostatic forces (Fig. 42.3 b). In both cases, the heterogenized catalysts

provided higher selectivity than the homogeneous counterparts (Table 42.2). In an attempt to rationalize the high selectivity of the SHB catalyst, various model studies were carried out in different phases with the Ru system. The obtained results led to the conclusion that, in contrast to the homogeneous system in solution, no heterolytic splitting of H_2 at Ru occurs in the heterogeneous phase. Another possible explanation for the enhanced selectivity with the SHB systems is that of site isolation. Both systems showed no metal leaching upon several consecutive uses, and the activity of the chiral SHB Rh system was even higher than that of the homogeneous analogue.

Augustine [29–31] has discovered an anchoring method for cationic complexes by using heteropoly acids (HPA: $H_xAB_{12}O_{40}$, A = P, Si; B = Mo, W, V) modified oxidic supports. The heteropoly acid probably binds through hydrogen bonds to the support and acts as a linker to the metal complex. Thus, these systems are probably analogous to the SHB catalysts, which are described above. The nature of the binding of the complex to the HPA is not yet clear; it could be a weak coordinate bonding of the HPA oxygen atoms to the metal or an ionic bond between a cationic metal complex and a negatively charged HPA (Fig. 42.3 c). Researchers at Engelhard Corporation have actively investigated this new type of immobilized catalysts in cooperation with Chirotech Technology Ltd. [32–35], while Johnson Matthey – another catalyst producer – has obtained a license for this Cataxa technology from Seton Hall University [36].

The preparation of this type of catalyst is quite simple. HPAs such as phosphotungstic acid were adsorbed onto inorganic supports such as clays, alumina, and active carbon. Subsequently, the metal complex was added to form the immobilized catalyst. If necessary, the catalyst can be pre-reduced. These types of catalysts were developed mainly for enantioselective hydrogenations. For instance, a supported chiral catalyst that was based on a cationic Rh(DIPAMP) complex, phosphotungstic acid and alumina showed an ee-value of 93% with a TOF of about 100 h^{-1} in the hydrogenation of 2-acetamidoacrylic acid methyl ester (Fig. 42.4; Table 42.2).

As shown in Table 42.2, the immobilized catalysts showed higher activity than their homogeneous counterparts. Furthermore, the enantioselectivity of the supported Rh–dipamp system was also higher than that of the homogeneous analogue. Leaching was hardly observed, and the catalysts could be recycled many times, when appropriate reaction conditions and solvent polarity were chosen. Because of the negative charge of heteropoly acids, this immobilization method is also suited for supporting other cationic hydrogenation catalysts.

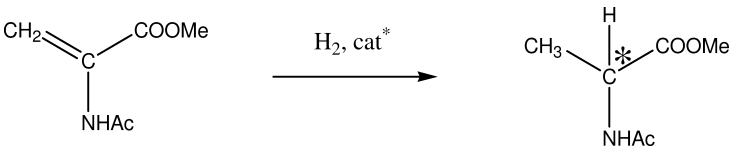

Fig. 42.4 Enantioselective hydrogenation of 2-acetamidoacrylic acid methyl ester.

Table 42.2 Enantioselective hydrogenation of methyl-2-acetamidoacrylate with $[RhL^*\{COD\}]^+$ SHB catalyst at 298 K in ethanol.

Ligand	Anion	Support	Substrate: Rh ratio	P_{H_2} [MPa]	Cycle number	TOF [h^{-1}]	ee [%]	Reference
dipamp	BF_4	None	40		homog.	15	76	31
	PTA	Al_2O_3		0.1	1	19	90	31
	PTA	Al_2O_3			3	100	95	31
Me-Duphos		None	40		homog.	198	96	31
	PTA	Al_2O_3		0.1	3	264	95	31
	OTf	None[a]		0.055	homog.	x > 99%	87	27
	OTf	MCM-41[a]			4	x > 99%	99	27

PTA = phosphotungstic acid; x = conversion.
a) Solvent = hexane.

The latter and above-described SHB catalysts represent some of the few examples when an immobilized system is superior to its homogeneous counterpart. Naturally, the use of these catalyst systems is limited to reactions, where the metal keeps its positive charges in all intermediates of the catalytic cycle (see further in Section 42.3.7).

The studies of Thomas and Raja [28] showed a remarkable effect of pore size on enantioselectivity (Table 42.3). The immobilized catalysts were more active than the homogeneous ones, but their enantioselectivity increased dramatically on supports which had smaller-diameter pores. This effect was ascribed to more steric confinement of the catalyst–substrate complex in the narrower pores. This confinement will lead to a larger influence of the chiral directing group on the orientation of the substrate. Although pore diffusion limitation can lead to lower hydrogen concentrations in narrow pores with a possible effect on enantioselectivity (see Section 42.2), this seems not to be the case here, because the immobilized catalyst with the smallest pores is the most active one.

Some of these catalysts with non-chiral ligands showed interesting regioselectivity in the hydrogenation of the carbon–carbon double bond of unsaturated ketones [24] and of the aldehyde group of 4-nitro-benzaldehyde (the nitro group was not affected). Furthermore, a remarkable tolerance was observed to sulfur in the hydrogenation of sulfur-containing aldehydes [32, 33].

42.3.2
Encapsulated Homogeneous Catalysts

Zeolites are crystalline porous solids with pore dimensions at the molecular level. Some zeolite types, such as the faujasites (zeolite X and Y or their hexagonal isomer EMT), possess large supercages with an internal diameter of approximately 1.2 nm, connected by pores with a diameter of approximately 0.75 nm. A metal complex will be confined in the supercage, when its size exceeds 0.8 nm.

Table 42.3 Enantioselective hydrogenation of methyl benzoylformate using [Rh(COD)(L-L)][OTf] SHB catalysts supported on Davison silicas of different pore sizes [28].

Ligand	Pore diameter [nm]	Conversion [%]	TOF [h^{-1}]	ee [%]
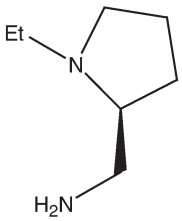	Homogeneous	62	46	0
	3.8	93.3	153	77
	6	93.9	154	61
	25	86.1	141	0
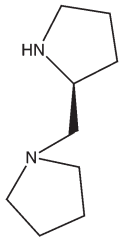	Homogeneous	46.2	145	53
	3.8	95.8	166	94
	6	91.5	159	78
	25	86.9	151	59

Reaction conditions: Substrate = 0.5 g; solvent = 30 mL; H_2 pressure = 2 MPa; temperature = 313 K; reaction time = 2 h.

Although zeolite-encapsulated metal complexes were known for some time, the principle that such complexes could act as a new type of immobilized homogeneous catalysts was probably first demonstrated only in 1985 [37]. This achievement opened a new and fruitful area of research in immobilizing homogeneous catalysts. These catalysts are named appropriately ship-in-the-bottle (SIB) catalysts (see Fig. 42.5). General overviews of zeolite-encapsulated metal complexes were given [38, 39].

42.3.2.1 **Synthesis of SIB Catalysts**

Three methods can be followed for the synthesis of a SIB catalyst: (i) zeolite synthesis around the metal complex; (ii) template synthesis; and (iii) the flexible ligand method.

Zeolite synthesis around a metal complex was introduced by Balkus [40]. The metal complex is added to the zeolite synthesis mixture and is incorporated into the zeolite structure during the zeolite synthesis. Of course, this procedure is only applicable when the metal complex is soluble in the synthesis mixture and can withstand the hydrothermal synthesis conditions. Another requirement is that the zeolite structure-directing agent added must be removable by a milder

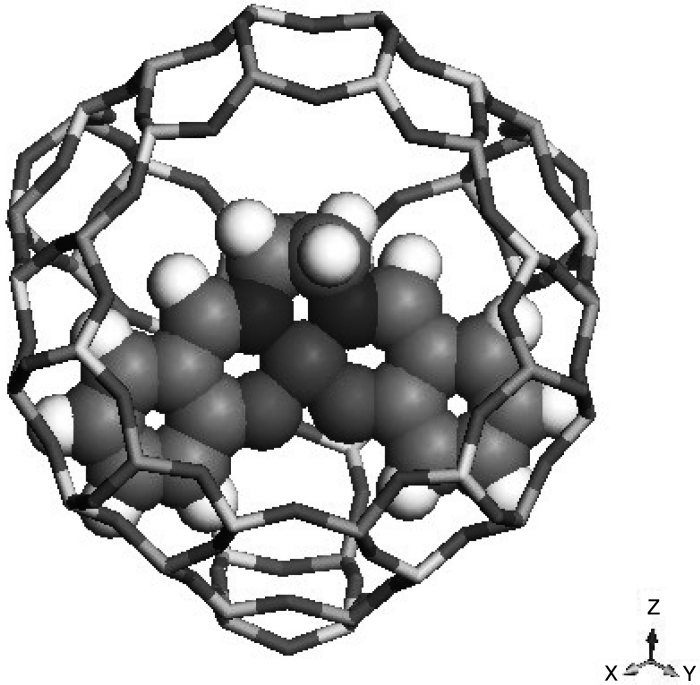

Fig. 42.5 Schematic view of Pd–salen complex in the supercage of faujasites.

procedure than calcination, which would also destroy the occluded metal complexes.

Metal ions are introduced first in the zeolite by ion exchange in the other two methods. These metal ions act as a template for small, coordinating molecules in the template method. Finally, these small ligands react with each other to form a large multidentate ligand around the metal atom. In this way, the metal complex becomes too large for escaping from the zeolite cage. Fine examples are the formation of metal phthalocyanine complexes from 1,2-dicyanobenzene and the formation of salen complexes from salicylaldehyde and diamines.

Subsequent to an exchange with metal ions, the zeolite is treated with a solution or a melt of the ligand in the flexible ligand method. It is required that the ligand can diffuse through the zeolite pores in a stretched conformation. When the ligand encounters a metal ion, it will form a metal complex by folding itself around the metal ion. The final complex is then confined to the zeolite cage. An example is the synthesis of salen-type complexes in faujasites. This method works quite well with nitrogen ligands, when they are not too bulky. In all three methods, any excess ligand or metal complexes adsorbed on the exterior surface of the zeolite must be removed by thorough extraction procedures to obtain the final catalyst.

Phosphine ligands cause problems in SIB catalyst synthesis because of their size and of their chemical reactivity. The commonly used bidentate phosphine

ligands are too bulky to pass the window of the faujasite supercage. It is difficult to obtain well-defined products, even with small monodentate phosphines such as PMe_3, PMe_2Ph or $PMePh_2$ as shown with $[Rh(CO)_2Cl]_2$ inside dealuminated zeolite Y [41].

The diffusion of reactants inside zeolite pores is slow (Knudsen diffusion). Access to the catalytic species would become even more difficult, when the zeolite has a too-high loading with metal complexes. Too many occupied supercages would block the zeolite pore system and make most of the metal complexes inaccessible for reactants. An unrestricted diffusion through the zeolite crystal is only guaranteed when an occupied supercage is surrounded by empty ones; a rule of thumb is to aim at a loading of one metal complex per every 10 supercages. In that case, real SIB catalytic systems are obtained, as was shown by the work of Jacobs and many others.

42.3.2.2 **Application of SIB Catalysts**

The zeolite types that can be used as a host for SIB catalysts are rather limited. They must possess large cages that are accessible through at least 10-ring windows for the ligands or the precursors to pass. Obvious choices are the faujasite zeolites X and Y and their hexagonal isomer, zeolite EMT (diameter supercage approximately 1.2 nm and window 0.74×0.65 nm), or the more recently discovered cloverite [42] that possesses far larger cages (3 nm diameter). A new approach by Hölderich and coworkers [43] enlarges the void space in the zeolite structure by dealumination and steaming. This method allows the introduction of larger ligands than the original faujasite supercage.

The metal complexes in an SIB catalyst are confined to separate supercages. Consequently, the formation of inactive dimers is no longer possible. Shape-selectivity is another feature of SIB catalysts that follows from the restricted space inside the zeolite pore system. This can be simply due to discrimination in size of the reactant molecules (a large reactant molecule is excluded from the zeolite) or to a constrained orientation of the reactant at the catalytic site (transition state selectivity).

The few examples of SIB hydrogenation catalysts consist mainly of encapsulated Group 8 to 10 metal complexes of the salen ligand (Fig. 42.5). Pd(salen) complex encaged in zeolite Y is a more selective catalyst than PdY or Pd/carbon in the hydrogenation of octene-1 and cyclooctadiene at 333 K under 1.5 MPa of H_2 pressure [44]. Salen-type complexes with other metals such as Ru, Ni, and Rh were also effective catalysts for alkene hydrogenation [45–47]. These SIB catalysts were more active than the homogeneous catalysts due to the prevention of dimer formation, and showed shape-selective behavior in some studies. More bulky alkenes were hydrogenated less rapidly. There are very few examples of asymmetric hydrogenations with SIB catalysts; enantioselectivities are comparable with or lower than those of the homogeneous catalysts [46, 48].

42.3.3
Catalysts Entangled in a Polymer

Free motion of organic molecules in a polymer gel becomes impossible when their size is too large with respect to the pore dimensions of the polymer network. Thus, a large homogeneous metal complex catalyst can be entrapped in a polymer network, which is the amorphous equivalent of encaging the catalytic complex in the crystalline structure of a zeolite. Flexibility in the polymer network can be advantageous in order to keep the conformation of the metal complex similar to that in the liquid phase. On the other hand, too much flexibility leads to swelling in certain solvents with leaching of the complex as a consequence.

The same entrapment can be obtained in a silica matrix by sol–gel polymerization of tetramethoxysilane (for more detail, see Section 42.3.6.2) in the presence of dissolved metal complex [49]. A number of phosphine complexes of Ru, Rh, and Ir were immobilized by this method and tested for the isomerization of allylbenzene. It turned out that a good solubility of the complexes in the aqueous sol–gel mixture is important to achieve a high loading. The water-soluble TPPTS complexes are therefore more suitable precursors than the lipophilic triphenylphosphine complexes. Avnir and Blum [50,51] used the same method to obtain leach-proof, recyclable catalysts for hydrodehalogenation and alkene hydrogenation, respectively. Enantioselectivities of these catalysts were comparable to those of the corresponding homogeneous catalysts in the hydrogenation of itaconic acid (Table 42.4). Metal leaching was below the detection limit of 1 ppm. Some deactivation occurred, probably because of pore blocking by the product. The catalyst could be fully regenerated by washing with dichloromethane.

Table 42.4 Enantioselective hydrogenation of itaconic acid using sol–gel-entrapped Rh complexes [51].

Catalyst	Cycle number	Yield [%]	ee [%]
Ru(BINAP)Cl_2(*p*-cymene)/SiO_2 [a)]	1	100	52
	2	98	50
	3	95	46
	4	90	41
Rh(diop)(COD)Cl/SiO_2 [b)]	1	100	34
	2	55	32
	3	39	25
	4 [c)]	100	30
Rh(diop)(COD)Cl [b)] homogeneous	n.a.	100	41

a) Substrate : Ru ratio = 30; solvent = water; reaction time = 24 h; temperature = 353 K; H_2 pressure = 1.01 MPa.
b) Substrate : Ru ratio = 50; solvent = ethanol; reaction time = 16 h; temperature = 348 K; H_2 pressure = 1.32 MPa.
c) After washing with CH_2Cl_2.

Table 42.5 Enantioselective hydrogenation of methyl-2-acetamidoacrylate with [Rh(MeDuphos)(COD)][CF_3SO_3] entangled in a polymer network.

Matrix	Solvent	T [K]	P_{H_2} [MPa]	Time [h]	TOF [h^{-1}]	ee [%]	Reference
Homogeneous	MeOH	333	4	2	482	99	55a
PDMS	MeOH	333	4	24	28	90	55a
PDMS	Water	298	0.2	6	12.6	96.9	55b
PVA-1	Water	298	0.2	6	12.9	96.1	55b
PVA-2	Water	298	0.2	6	12.4	95.7	55b

Patchornik and coworkers [52] have introduced [Rh(norbornadiene)(dppe)][PF_6] inside the polymer matrix of a cross-linked polystyrene gel using tetrahydrofuran (THF) as a solvent. This medium resulted in a high degree of swelling of the polymer. Shrinkage of the gel occurred after evaporation of THF, and the complex remained encapsulated in the polymer matrix. This catalyst hydrogenated hexene-1 in methanol as solvent, which caused no swelling of the polymer. The catalyst was stable upon repeated use and no indication of homogeneous catalytic activity was found. These findings show that the metal complex is confined in the polymer matrix as long as no swelling of the polymer occurs.

A metal complex can also be incorporated in a polymer matrix by creating the polymer network *in situ*. A fine example of this is the cross-linking of polydimethylsiloxane (PDMS) pre-polymer in the presence of the dissolved metal complex and a cross-linker. The metal complex becomes entangled in the polymer network, giving no leaching into solution unless swelling of the polymer occurs. FePc, Ru–BINAP and Jacobsen's catalyst were each immobilized in this way [53]. Chiral hydrogenation with Ru–BINAP/PDMS showed catalytic activity and enantioselectivity approaching those of the homogeneous catalyst. The PDMS is more than a carrier for the complex. It also plays an active role in the transport of reactants to the catalytic site. This field was reviewed in 2000 [54], though some more recent investigations have described the encapsulation of [Rh(MeDuPHOS)(COD)][CF_3SO_3] in PDMS and cross-linked polyvinylalcohol (PVA) for the asymmetric hydrogenation of methyl-2-acetamidoacrylate [55]. Excellent enantioselectivities were obtained, but the catalytic activity was significantly lower than that of the homogeneous catalyst (Table 42.5).

42.3.4
Catalyst Dissolved in a Supported Liquid-Phase

As mentioned in Section 42.2, mass transfer can be rate-limiting in the case of very active homogeneous systems. Since mass transfer from gas to liquid or from liquid to liquid is dependent on the contacting area, this problem can be circumvented by adsorbing the catalyst solution onto an inert porous support

(e.g., silica, alumina, kieselguhr) which has a very large (inert) surface area. The supported liquid-phase catalyst (SLPC) system obtained is also advantageous for eliminating corrosion problems, as most of the supported solution is not in direct contact with the reactor material. Since the liquid phase containing the catalyst must remain supported throughout the reaction, the term SLPC also refers to stationary liquid-phase catalysis. It follows that by the original concept, SLP catalysts are most suited for gas-phase processes, as soluble liquid reactants or products would cause dilution or leaching of the catalyst. However, gas-phase hydrogenation is not sensible due to the readily available choice of reliable heterogeneous catalysts and to the low volatility of the most interesting substrates. Thus, understandably, most of the studies on conventional SLP system were performed for other reactions, such as hydration of ethylene or hydroformylation of small olefins by using concentrated acids or Rh-compounds in molten PPh_3, respectively, as supported catalysts.

42.3.4.1 **Supported Aqueous-Phase Catalysis**

Parallel with the development of two-(liquid)-phase catalysis, the concept of SLPC has been extended to liquid-phase processes. For this purpose, also two immiscible solutions are required. One of these contains the catalyst and is supported on an appropriate porous carrier, while the other serves as a mobile phase for the transport of substrate and products. Arhancet et al. have demonstrated the concept first by adsorbing an aqueous solution of the highly water-soluble Rh-complex of trisulfonated triphenylphosphine, TPPTS, on a hydrophilic support (controlled-pore silicate glass) [56]. The supported aqueous-phase catalyst (SAPC) obtained showed no Rh-leaching in continuous hydroformylation of olefins in apolar solvents [19a]. By the most likely model (except when the pores are completely flooded with the aqueous solution or not too-water-soluble substrates are used), the highly hydrophilic substituents on the ligands of SAPC are strongly associated with the adsorbed water and surface hydroxyl groups. Meanwhile, the metal center (M), which is in a relatively hydrophobic local environment, is pushed into the non-aqueous phase (see Fig. 42.6) [12, 57]. In this manner, SAPC resembles analogous silica-anchored, SHB or ion-exchanged catalyst.

By the development of two-phase catalysis a large number of water-soluble ligands including chiral ligands have been synthesized, which could make an excellent basis for SAPC. Unfortunately, this opportunity is not yet fully exploited for hydrogenation, perhaps partly due to some problems in the continuous use or recycling of these catalysts. For example, Ru-TPPTS catalysts showed excellent results in the first use for the selective hydrogenation of some α,β-unsaturated aldehydes [58]. Hydrogenation of 3-methyl-2-butenal to 3-methyl-butenol was carried out at 323 K under 100 bar H_2 pressure with 88.5% selectivity and 100% conversion (TON $\sim$490). However, upon recycling the activity of the catalyst decreased dramatically without losses of metal or selectivity. The catalysts showed the same characteristic for other aldehydes. Based on infra-red measurements and by the increased carbon content on the silica after use, it was reasoned that adsorption

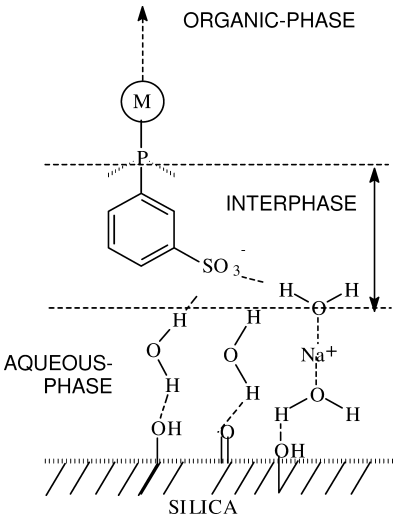

Fig. 42.6 Working model for SAP Rh-TPPTS catalyst.

of the substrate and products was the primary cause of deactivation. Several water-soluble ligands such as BDPP and Chiraphos derivatives were also tested in SAP for the hydrogenation of dehydroamino acids [57]. These catalysts also showed deactivation upon reuse, without detectable metal leaching. Because the enantioselectivity of these catalysts was lower than that of the homogeneous analogues (organic or two-phase), these catalysts were not investigated further.

42.3.4.2 **Hybrid SLP Systems**

Clearly, a two-phase system can also be created between two organic phases. Many water-soluble (polar) ligands are also soluble in a polar organic solvent directly or after further functionalization. The obtained polar phase with the catalysts can be supported on the silica, analogous to SLPC above. When the reaction product is (partly) soluble in a second immiscible apolar organic solvent (and the catalyst is not), an anhydrous analogue of SAPC is created. The elimination of water content can be advantageous for the selectivity, as proven by Davis and Wan by using chiral Ru-sulfonated BINAP systems for enantioselective hydrogenation of double bonds using glycols as solvents for the supported phase [59]. The use of this hybrid catalyst is also advantageous for the minimization of supported-liquid loss, which is a typical problem of SAP or SLP catalysts. Another successful hybrid SLPC system was reported by Horváth using $PtCl_2(CH_3CN)_2$ dissolved in $BF_3 \cdot H_2O$ as stationary phase [60]. The solution was supported on silica-glass and used in a trickle-bed reactor for the continuous hydrogenation of aromatic hydrocarbons at room temperature under 27–55 bar H_2 pressure. It was shown that no metal leaching took place upon a one-day test, but the catalyst showed a slight deactivation after 48 h, possibly due to loss of

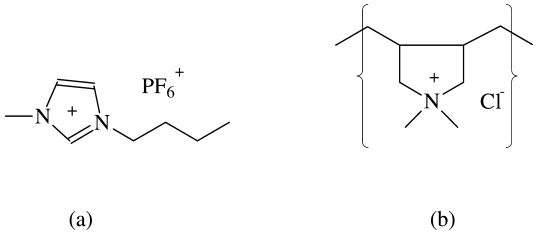

Fig. 42.7 Ionic liquid and its support used for making SILP catalyst [63].

the $BF_3 \cdot H_2O$ (acid) component. Some metallic particles were also found, indicating that heterogeneous contribution could not be excluded.

Until now, SLPC catalysts have remained difficult to control in the plant due to loss of supported liquids, adsorption of substrates/products, or changes in the pore structure [61]. Some recent developments to overcome these problems have included chemical bonding of the stationary phase by the analogy of gas chromatography (GC) practice. For example, polyglycols can be bound to the silica after appropriate functionalization [62]. Another interesting approach has been developed by Vankelecom and coworkers, by supporting transition-metal complexes in ionic liquid solvents on poly(diallyldimethylammonium) chloride (Fig. 42.7) [63]. The supported ionic-liquid phase (SILP) Wilkinson catalyst obtained showed similar performance to its homogeneous counterpart in the hydrogenation of alkenes. The SILP variant of Ru-BINAP catalyst was somewhat slower (TOF 29 h^{-1}, at 333 K, under 40 bar H_2 pressure) in the hydrogenation of methylacetoacetate to the monoalcohol derivative than its homogeneous variant giving yet similarly high (97% ee) enantioselectivity. However, none of these SILP catalysts contained traces of metals in the mobile phases (toluene, ether, methanol, isopropanol).

42.3.5
Covalently Bound Metal Centers

Here, only chemisorbed metal complexes with a direct bond between the metal and the surface will be discussed. Immobilized complexes, where the organic ligand forms a covalent bond with the support, are treated separately in Section 42.3.6. Reactions of organometallic compounds with the surface of carriers have evolved into a new branch of chemistry, frequently termed Surface Organometallic Chemistry. The reaction of organometallic species with surface hydroxyls produces isolated alkyl- or hydrido-metal species that are grafted to the surface and show very interesting catalytic properties. Usually, the proton reacts with the organic ligand or an anionic ligand under elimination of a hydrocarbon or HX. For example, neopentyl (Np) complexes of Ti, Zr, Hf and Ta were immobilized and the catalytic properties of these new materials were explored [64–66]. The surface bound tris(isopropyloxy) species of Zr, Hf and Nd (Table 42.6) are among the best heterogeneous catalysts for the Meerwein-Ponndorf-Verley hydrogen transfer reduction of ketones (Fig. 42.8) [67, 68].

Table 42.6 Transfer hydrogenation using grafted metal alkoxide catalysts.

Substrate	Catalyst	Support	S : M	T [K]	Time [h]	Conversion [%]	*trans*/*cis*	Reference
4-*t*-Butyl-cyclo-hexanone	Al(O*i*Pr)$_3$	–	20	298	5	<1	7	68
	Nd(O*t*Bu)$_3$	–	7	298	5	95	2.7	68
	=Nd(O*i*Pr)	MCM-41	52	298	5	90	3.3	68
	=Nd(O*t*Bu)	MCM-41	59	298	5	96	3.3	68
Cyclohexanone	-Zr(O*i*Pr)$_3$	Silica	77	353	23	73		67
	-Hf(O*i*Pr)$_3$	Silica	77	353	23	50		67

S : M = substrate : metal ratio.

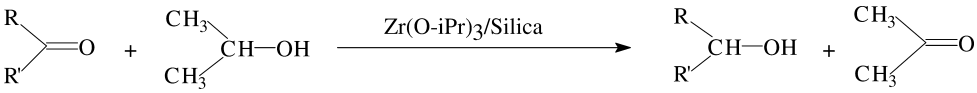

Fig. 42.8 Meerwein-Ponndorf-Verley reaction.

42.3.6
Covalent Attachment of Ligands

Anchoring of one or more ligands of a homogeneous catalyst to the support is preferred over chemisorption of the metal, because the coordination shell around the metal is kept as close as possible to the homogeneous case. In fact, the distance between the complex and the surface can be controlled by choosing an appropriate spacer, which links the ligand to the support. Covalent anchoring of the ligand is by far the most intensively investigated method, despite the laborious synthetic efforts involved. Some general remarks about this method are:

1. When using monodentate ligands, it is better to anchor the complex instead of the ligand to preserve the conformation of the catalyst.
2. The metal is usually stronger bound by anchored bi- or multidentate ligands than by monodentate ones.
3. Higher loading should lead to more active catalysts. However, complexes on neighboring sites frequently form inactive dimers. Site isolation is therefore desirable, which can be performed by several methods: (i) decreasing the density of hydroxyl groups on the support; (ii) dilution of the reactive ligand with another reagent for hydroxyl groups; or (iii) incorporation of the functionalized ligand during synthesis of the support.
4. Degradation of the ligand or the linker to the support must be avoided, as this results in metal leaching and catalyst deactivation. For example, phosphorus ligands are sensitive to oxidizing impurities in the feed (peroxides).
5. Recovery of the metal from a spent catalyst is possible, but the recovery of the ligand is not.

42.3.6.1 Grafting to Oxide Supports

Functionalized trialkoxysilanes are most widely used for grafting of ligands to inorganic supports. They have been used for a long time in other areas such as the preparation of stationary phases for chromatography and the improvement of adhesion between polymers and metal surfaces [69–72]. Trialkoxysilanes react with the surface hydroxyl groups to form from one to three Si–O bridges to the surface. Silica is the preferred oxide because of its high temperature stability and chemical resistance except under alkaline conditions. Today, ordered mesoporous silicas of the MCM-41 type are quite popular, because they have tunable uniform cylindrical pores in the range of 2 to 10 nm.

The surface density of hydroxyl groups depends on the thermal pretreatment of the silica [73, 74]. Drying at 473 K results in a high density (ca. 4–5 OH nm^{-2}), while a pretreatment temperature of 973 K is recommended to obtain isolated silanol groups (1.5 OH nm^{-2}) [75].

Solid-state NMR studies have provided important information on the grafting process and the mobility of anchored metal complexes; in this respect, reference is made to investigations by the groups of Fyfe [76], Blümel [77], Lindner [78], and others [79].

Some examples will illustrate the versatility of the covalent anchoring of catalytic complexes to silica. At Solvias/Ciba-Geigy [80–84], Pugin and Blaser and coworkers grafted many chiral ligands to silica through amide and carbamate bonds (Fig. 42.9). Commercially available 3-amino and 3-isocyanatopropyltrialkoxysilanes proved very useful for anchoring a range of carboxylic acid, sulfonic acid, and amino- and hydroxy-substituted ligands. The immobilized catalysts retained high activity and enantioselectivity in the asymmetric hydrogenation of dehydroamino acid derivatives without leaching of metal.

The immobilized catalysts attained similar enantioselectivities as the homogeneous catalysts, but the latter were still more active (Table 42.7). An astonishing high turnover frequency was obtained with the immobilized xyliphos catalyst (Fig. 42.9 c) on silica for the hydrogenation of the so-called MEA-imine, a precursor of the herbicide *S*-metolachlor [83]. The polystyrene-supported variant was significantly slower, most likely due to slower mass transport. Variation in ligand loading had only a small effect on catalytic activity of cationic metal complexes, whereas activity was decreased substantially on increased loading of neutral complexes. This effect was ascribed to the formation of inactive dimers in the latter case, while electrostatic repulsion effectively inhibited dimer formation from cationic complexes [81, 82].

The cyclopentadienyl group is another interesting ligand for immobilization. Its titanium complexes can be transformed by reduction with butyl lithium into highly active alkene hydrogenation catalysts having a TOF of about 7000 h^{-1} at 60 °C [85]. Similar metallocene catalysts have also been extensively studied on polymer supports, as shown in the following section.

Alcohols react with surface hydroxyl group to form C–O–Si bonds. Because this type of bond is not very stable, trialkoxysilanes are preferred for anchoring. Exceptions to this rule are polyhydric alcohols, such as tris(hydroxymethyl)phosphine [86], which forms multiple bonds with the surface.

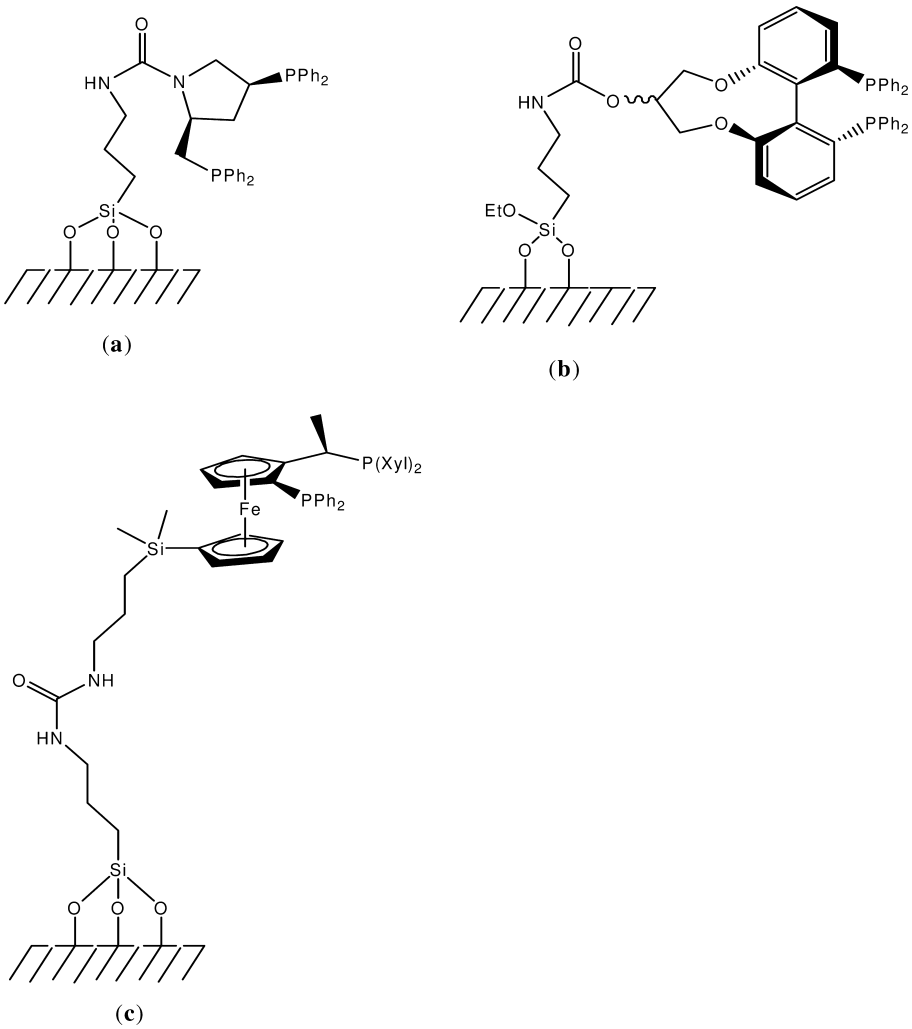

Fig. 42.9 Examples of covalently bound ligands on silica.

42.3.6.2 **Sol–Gel Method**

An alternative approach to using a preformed support material is the sol–gel method, which utilizes trialkoxysilyl-modified ligands or metal complexes in co-condensation with tetraethoxysilane (tetraethoxy orthosilicate, TEOS) under hydrolytic conditions. Multinuclear solid-state NMR studies showed that a more homogeneous dispersion was obtained in the final silica structure than by using preformed supports [87]. Furthermore, the ligand is bound more strongly through more Si–O–Si bonds and a higher loading can be achieved. It is also claimed that less metal leaching occurs with these sol–gel catalysts than is ob-

Table 42.7 Examples of enantioselective hydrogenations with silica-grafted catalysts.

Substrate	Ligand	Metal precursor	Substrate: Rh ratio	T [K]	P_{H_2} [MPa]	TOF [h^{-1}]	ee [%]	Reference
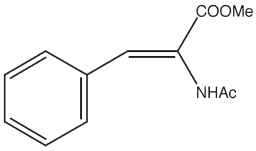	bppm (Fig. 42.9a)	$[Rh(COD)_2]$ $[BF_4]$	200	298	0.1	1080	94.8	82
			200	298	0.1	780	93.5	
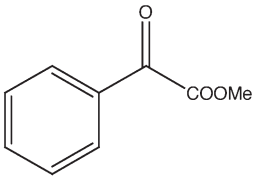	MeO-biphep (Fig. 42.9b)	$[Rh(COD)_2]$ $[BF_4]$		313	8	32	90	84
				313	8	21	82	
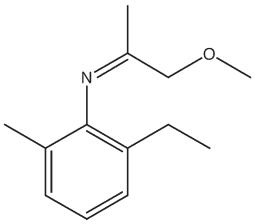	Xyliphos (Fig. 42.9c)	$[Ir(COD)Cl]_2$	120 000	298–303	8	55 400	80	83
			120 000	298–303	8	12 000	78	

tainable by attachments to a silica surface. On the other hand, part of the active material may not be accessible to reactants, as was shown for a sol–gel-immobilized cyclopentadienyl titanium hydrogenation catalyst [88]. The activity of the immobilized catalyst depends on the purity of the TEOS used; more active catalysts are obtained using commercial TEOS than with freshly distilled TEOS. The commercial TEOS contained more condensed silicates by ageing and led to a product with six times more titanium species in the surface layer. Fine-tuning of the pore system of the silica structure can also be carried out by using organic cross-linkers, such as 1,4-bis(triethoxysilyl)benzene. The sol–gel method was used by Degussa to manufacture commercially available immobilized homogeneous catalysts, known under their trade name Deloxan (Table 42.8) [89].

42.3.6.3 **Anchoring with Organic Phosphonates**

Organic phosphonates represent another class of anchoring agents, which react with zirconium hydroxide to form pillared structures. These are also referred to as molecularly engineered layered structures (MELS). Layered compounds of organic phosphonates of zirconium with the formula of $Zr(RPO_3)_2$ have been rec-

Table 42.8 Deloxan hydrogenation catalysts.

Catalyst code	Immobilized functionality	Particle size [mm]	BET [$m^2 g^{-1}$]
HK I/Rh	RhCl $[PhP[(CH_2)_3\text{-}SiO_{3/2}]_2]_3$	0.4–1.8 0.1–0.4	550–750
AP II/PM	$PdCl_2$ $[N[(CH_2)_3\text{-}SiO_{3/2}]_3]_2$	0.3–2.0 0.02–0.2	400–800

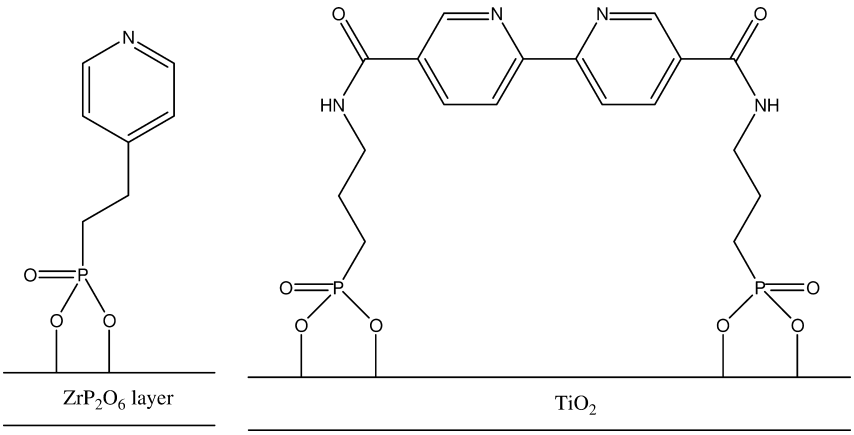

Fig. 42.10 Ligands anchored to zirconium phosphonate-layered structures or titanium dioxide particles.

ognized for 30 years. The size of the organic R group determines the spacing between the ZrP_2O_6 layers, while the presence of a functional group in R may give acidic or basic properties to the material, or it may serve as a ligand for the immobilization of homogeneous catalysts. This field was pioneered by DiGiacomo, and Dines and Callahan at Occidental Research Corporation [90], who developed (among others) supported catalysts for hydrogenation. These catalysts were attached through pyridine ligands (Fig. 42.10). Pillaring with bisphosphonic acids, which have a large rigid spacer between the two phosphonic acid functions, can further optimize the pore system of the layered material.

A selective hydrogenation catalyst for alkynes was obtained with the $PdCl_2$ complex of such immobilized pyridine. Diphenylacetylene was hydrogenated under 0.44 MPa H_2 in ethanolic solution. At full conversion, the following selectivities were observed: *cis*-stilbene 80.7%, *trans*-stilbene 16.1%, and only 3.2% 1,2-diphenylethane [90].

A similar type of immobilization was obtained by reacting the phosphonylated 2,2′-bipyridine ligand depicted in Figure 42.10 with excess titanium alkoxide. Rhodium and iridium complexes of this immobilized ligand showed activity for

the hydrogenation of olefinic double and triple bonds and for the hydrogenation of ketones. This catalyst showed very little leaching, and could be recycled at least for four times with no loss of activity [91].

42.3.6.4 **Attachment to Polymer Supports**

Merrifield was the first to use polymer supports, such as functionalized polystyrenes, in a reaction other than simple acid–base catalysis. His group has synthesized polypeptides by the stepwise addition of amino acids to a growing peptide chain, which was covalently bound to the resin [92]. Because Merrifield's discovery coincided with the rapid development of homogeneous catalysis, the idea was quickly and extensively adapted for polymer-supported transition metal catalysis. Today, virtually all homogeneous catalytic reactions have been tested on polymer supports, and a large variety of functional groups have been introduced to polymers. Furthermore, various polymeric composites – including natural products and enzymes – have been employed as carrier. Here, because of the limited space, only a few examples will be provided, but for a broad overview of the subject the reader is referred to references [1–5]. Covalently bound polymer-supported catalysts are synthesized using either of the three following methods: (i) by attachment to functionalized polymers; (ii) by attachment to a functionalized monomer unit followed by polymerization; or (iii) by grafting to another polymer after introduction of the ligands.

42.3.6.4.1 **Functionalized Polymers as Supports**

Grubbs, Collman, and Pittman, Jr. have developed methods for the phosphination and subsequent catalytic use of Merrifield and other styrene–divinylbenzene resins [1–5]. For example, the $P(C_6H_5)_2$-group was attached to Merrifield resins by reaction with $LiP(C_6H_5)_2$. The phosphine functionality can be introduced to polystyrenes by alternative approaches, such as lithiation (e.g., with butyllithium) followed by a reaction with $ClP(C_6H_5)_2$. Lithiation offers also an alternative route to the introduction of other functional groups. It was found that the distribution of relatively bulky phosphine groups in the resin was strongly affected by the degree of cross-linking. In spite of this, the phosphinated resins obtained provided active polymer-supported Wilkinson catalysts after treatment with Rh-precursors [93]. It was shown that by using solvents, which caused swelling, Rh–phosphine complexes were formed inside the resin. Subsequently, after removing the solvent, only the surface species could be destroyed by oxidative treatment. By re-swelling the beads, the locked catalytic sites inside the micro channels became active, while the catalyst could be readily separated after each use by simple filtration. Furthermore, the supported Wilkinson catalyst showed shape selectivity for the hydrogenation of small olefins. Encouraged by this success, various phosphines were immobilized on Merrifield and other resins and tested for other systems as homogeneous catalysis evolved [1–5]. Today, phosphinated styrene–divinylbenzene resins are commercially available with varying amounts of cross-links. One disadvantage

with regard to the use of phosphinated Merrifield resins is their low thermal stability due to ready quaternization of the supported phosphine groups by neighboring residual benzyl chloride groups above 353 K. Another potential problem, which is generally associated wtih monodentate ligands (see also other sections), is to control the coordination chemistry in reactions with metal complexes. For example, six different supported Rh–phosphine complexes were identified using NMR spectroscopy in the reaction of phosphinated polystyrene with an Rh-precursor [94]. In order to achieve a regular distribution of two or more monodentate ligands in the supported complex, it is preferable to immobilize the ligands after complexation. This can be achieved by using alternative polymerization methods, as discussed in the following two sections.

Alternatively, bi- or multidentate ligands can also be used for support. As an additional benefit, the latter offer greater stability for the coordinatively bound metal center against leaching through ligand dissociation and substitution reactions. The first, somewhat remarkable, approach to this is shown in Figure 42.11, based on numerous examples of the support of bidentate phosphines on polymers [1–5].

The supported DIOP derivative above represents one of the first attempts for supported enantioselective catalysis [95]. The immobilized ligand was used in the presence of Rh-precursors for asymmetric hydrogenation of prochiral olefins. Dehydroamino acids require polar solvents for dissolution, which cause shrinking of the polystyrene resins. For this reason, the supported Rh–DIOP complex gave no activity for such substrates. By using apolar systems such as α-ethylstyrene in benzene some activity could be detected, albeit with very low enantioselectivity (1.5% ee). The resin-supported DIOP catalyst proved to be a much better suited catalyst for the enantioselective hydrosilylation of ketones in apolar solvents, giving up to 58% ee to the appropriate chiral alcohols, and similar to that obtained with the homogeneous analogue.

Another interesting example is the supportation of Noyori's catalyst family containing Ru-chiral BINAP and chiral 1,2-diphenylethylenediamine [96]. These catalysts are suitable for the enantioselective hydrogenation of a variety of sub-

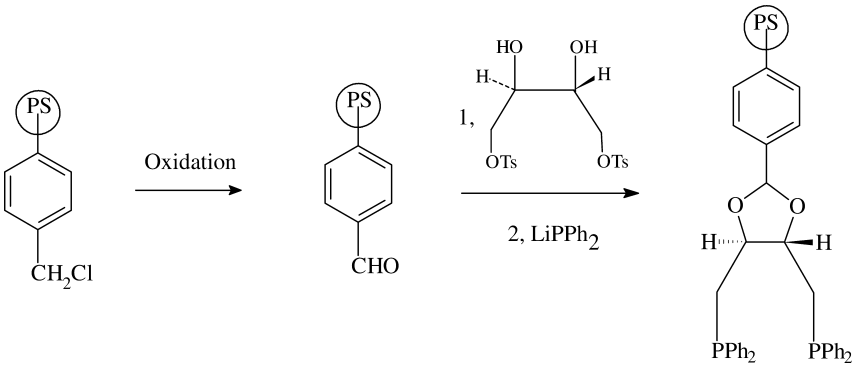

Fig. 42.11 Immobilization of chiral DIOP to Merrifield resin.

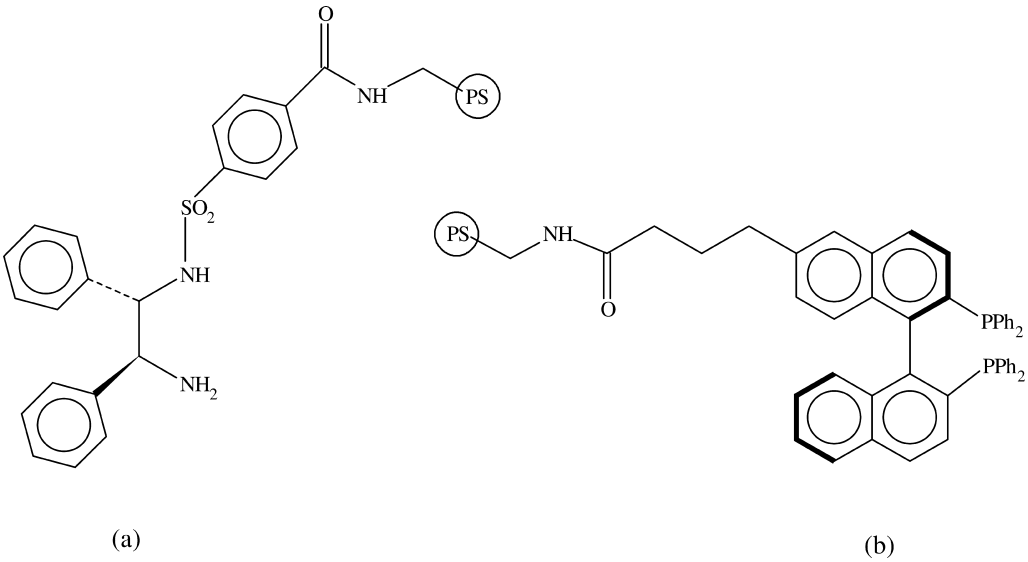

Fig. 42.12 Immobilization of Noyori's catalyst components on functionalized polystyrene.

strates and for chiral transfer hydrogenation of ketones. By using two different approaches, either the chiral amine component (Fig. 42.12 a) [97] or the chiral diphosphine component (Fig. 42.12 b) [98, 99] was supported on aminomethylated polystyrenes. After adding the Ru-precursor and the other component, the obtained catalysts were used in enantioselective transfer or direct hydrogenation of various ketones at 303 K, 1 bar or 298–323 K under 8–40 bar H_2 (including also itaconic acid derivatives as substrates), respectively. Most of these catalysts gave >95% ee, albeit with relatively low rates (the homogeneous system also gives relatively low activity). Nevertheless, because of the very slight extent of deactivation, up to 33 000 TON could be achieved upon repeated recycling [99]. These catalyst systems were also immobilized to other resins, including polyethylene glycol (PEG), and yielding similarly good results [100, 101].

In addition to phosphine ligands, a variety of other monodentate and chelating ligands have been introduced to functionalized polymers [1–5]. For example, cyclopentadiene was immobilized to Merrifield resins to obtain titanocene complexes (Fig. 42.13) [102]. The immobilization of anionic cyclopentadiene ligands represents a transition between chemisorption and the presently discussed coordinative attachment of ligands. The depicted immobilization method can also be adopted for other metallocenes. The titanocene derivatives are mostly known for their high hydrogenation and isomerization activity (see also Section 42.3.6.1) [103].

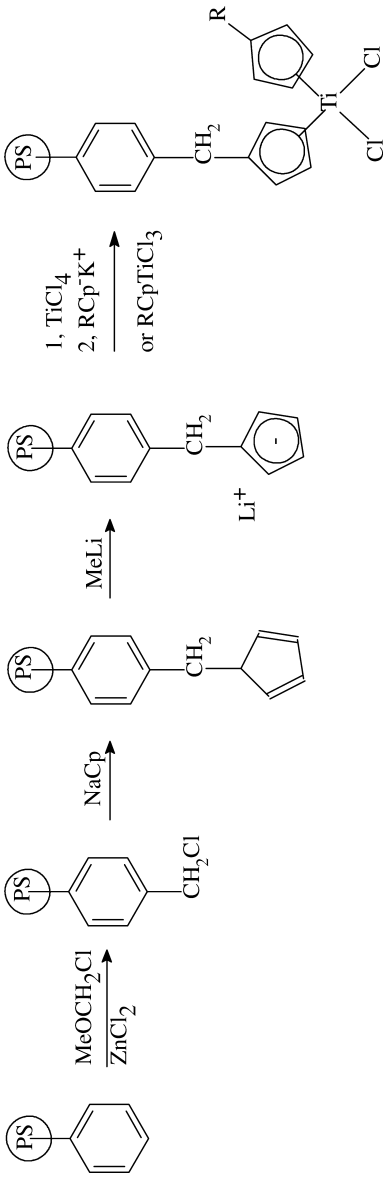

Fig. 42.13 Immobilization of cyclopentadiene for the preparation of polymer-supported titanocene complex.

42.3.6.4.2 **Enzymes as Support**

Natural polymers can also be used as carriers for immobilized catalyst. Enzymes can be immobilized to polymers or to other supports and, interestingly, can also be used to support homogeneous catalysts to provide real biomimetic systems [104]. It was reasoned that enzymes such as avidin have asymmetric sites, and this could induce chirality. Thus, in principle, the immobilization of an achiral complex into a chiral enzyme could give an asymmetric catalyst. Biotin as a substrate was known to bind strongly with the enzyme avidin, and it was for this reason that biotin was selected as spacer between an achiral bidentate aminophosphine and the active site of the enzyme (Fig. 42.14). The biotin-functionalized phosphine was coordinated to a Rh(I)-precursor and attached to the enzyme; the enzyme-supported catalyst gave optical induction in the hydrogenation of a dehydroamino acid derivative. A maximum of 41% ee was achieved, which indicated significant chiral induction by the enzyme support. A similar effect was noted by supporting the achiral Wilkinson complex to optically active cellulose for similar reactions [105].

42.3.6.4.3 **Functionalized Monomers**

Polystyrene or other polymer carriers are tunable in terms of properties such as swelling and pore size by varying the degree of cross-linking, or by introducing copolymer units. However, pre-made polymers provide an intrinsically inhomogeneous structure due to the limited accessibility of the polymer-pores for functionalization. This problem can be circumvented by attaching the ligand or catalyst complex to a monomer unit. Subsequently, the functionalized monomer can be polymerized or copolymerized with an appropriate choice of other units to obtain the desired supported catalyst. One potential disadvantage of this method is that the physical properties of the designed polymer are not always known beforehand, and this might lead to laborious fine-tuning. In copolymerization of the ligand-substituted monomer, it is also important to match the activity of different monomer units for a random polymerization.

For example, a proline-based chiral ligand was attached to a vinyl-substituted monomer (Fig. 42.15) by reacting vinylbenzoyl chloride with the amine functionality of the ligand [106]. As mentioned previously, the apolar Merrifield resin as a support is not swollen in polar solvents. Hence, in order to match the polarity of the resin with that of the typically used substrates in enantioselective hydrogenation, the functionalized monomer was copolymerized with polar units of methacrylic acid 2-hydroxyethyl ester.

The polymer-supported chiral phosphine obtained (Fig. 42.15) was treated with an Rh precursor and used for the enantioselective hydrogenation of dehydroamino acid derivatives. The obtained catalyst gave up to 82% ee, albeit with still low activity. Stille has developed this immobilization technique further by even more careful tuning of the polarity of the support with that of the reaction medium. For example, he introduced DIOP to a monomer vinylbenzaldehyde in reactions analogous to those shown for the polymer in Figure 42.11.

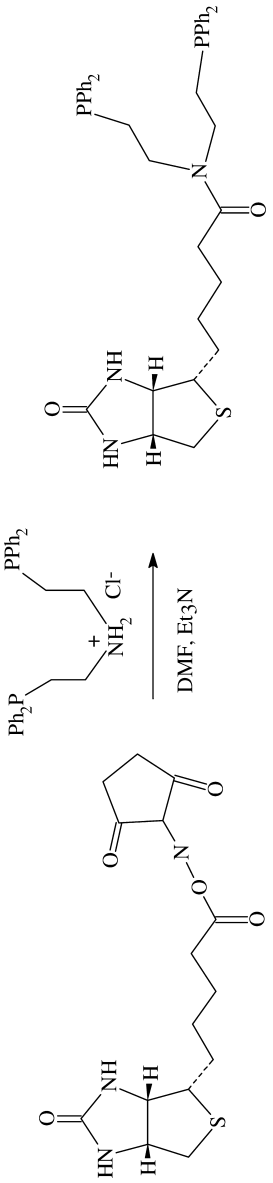

Fig. 42.14 Immobilization of an achiral phosphine derivative via enzyme-bound biotin.

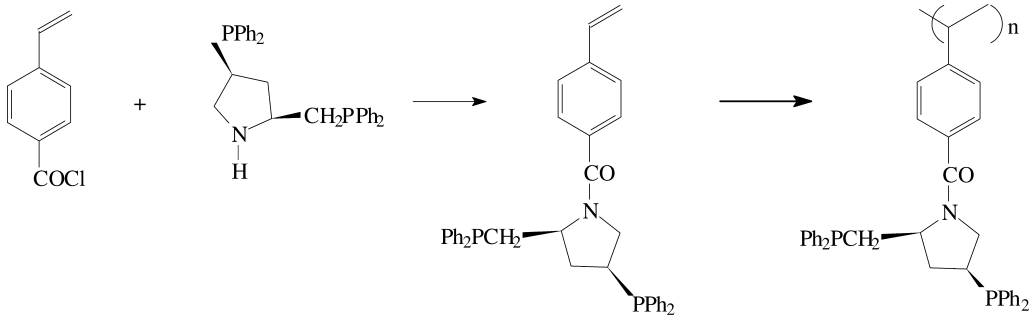

Fig. 42.15 Immobilization via functionalization of the monomer unit.

The monomer was copolymerized with methacrylates to obtain various composites with the supported ligand [107]. The obtained catalysts showed similar enantioselectivities in the hydrogenation of dehydroamino acids to their homogeneous counterparts, but with reduced rates. Nevertheless, the immobilized catalysts could be recycled by simple filtration without loss of Rh or enantioselectivity. By using an interesting approach, the styrene derivative of the DIOP ditosylate precursor was copolymerized with methylvinyl ketone. The carbonyl groups of the polymer-supported chiral ditosylate obtained were then hydrogenated enantioselectively by using homogeneous DIOP complexes [108]. Thus, supported chiral alcohol functionalities were obtained on the polymer. Subsequently, the supported ditosylate groups, which remained intact upon hydrogenation, were converted into supported chiral Rh–DIOP complexes. By using this approach, the role of chiral supports could be studied in asymmetric induction.

Using another interesting approach, the attachment of chiral BINAP was carried out by polycondensation of an amino-BINAP derivative with terephthaloyl chloride in the presence of optically pure 2,4-pentanediol (Fig. 42.16), which resulted in the formation of a chiral polyamide–polyester composite [109]. In fact, a similar material was obtained to that described above by Stille in an elegant and simple manner. The chiral polymer-bound ligand was then used in Ru-catalyzed hydrogenation of the Naproxen® precursor, with excellent optical purities. Because BINAP as a chiral ligand is so effective in similar reactions, it is difficult to estimate whether the chiral support contributed to the improvement in enantioselectivity. However, the support had a positive effect on the rates, which were significantly higher with the immobilized catalyst than with the homogeneous Ru–BINAP. The concept of this immobilization method can clearly be adopted for other enantioselective catalytic reactions.

Ultimately, the ligand itself can be polymerized and used as both ligand and support in one [110]. Pu and coworkers have prepared the rigid chiral poly-BINAP ligand below (Fig. 42.17) and used it after treatment with Rh and Ru in asymmetric hydrogenations. The supported catalysts showed similar activities and enantioselectivities to their homogeneous analogues, with the benefit of

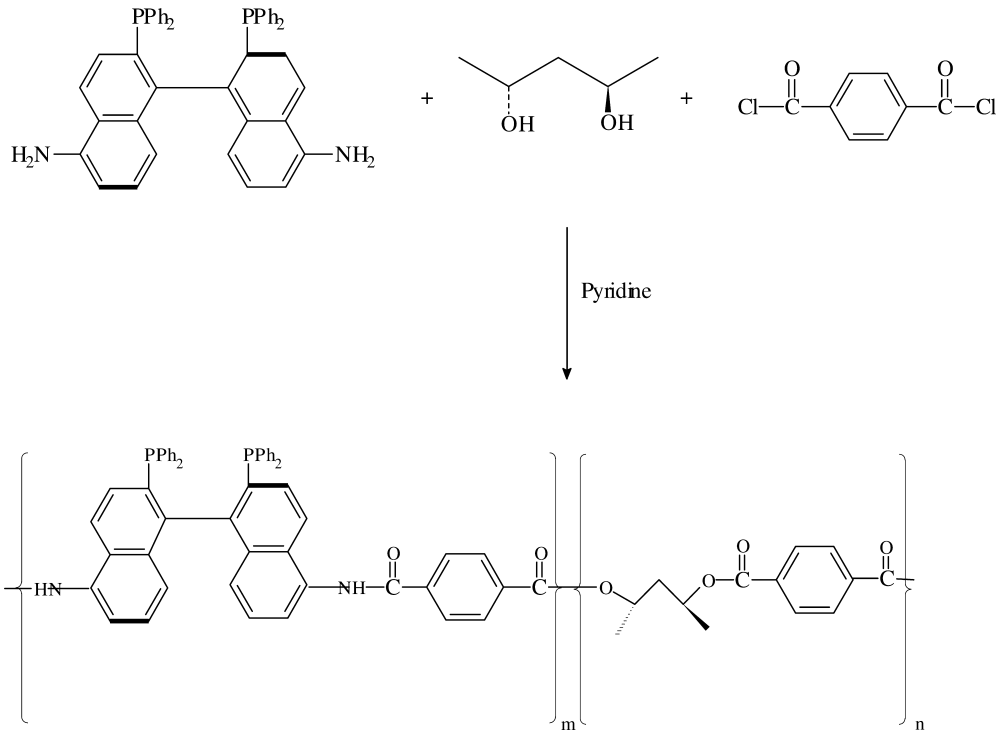

Fig. 42.16 Chiral polyester–polyamide composite containing supported BINAP.

easy separation by simple filtration. The recovered catalyst showed identical rate and ee upon re-use.

Chiral catalysts remain primary targets for immobilization by using similar methods. Since the steric arrangement of bulky aromatic groups of chiral ligands is the primary source of optical induction, most approaches use the chelate backbone of ligands for functionalization in order to minimize interference with the chelate (aryl) conformation.

Instead of monomers, the ligands and catalyst can also be attached to organic, fluorocarbon-, or water-soluble oligomers. Bergbreiter has pioneered the synthesis and use of these systems [111]. Thus, by varying the properties of the oligomeric chain, supported catalysts can be designed, which dissolve at high temperature and separate at lower temperature, thereby facilitating catalyst–product separation. Alternatively, oligomeric supports are also available which have reverse solubility parameters, separating at high temperatures.

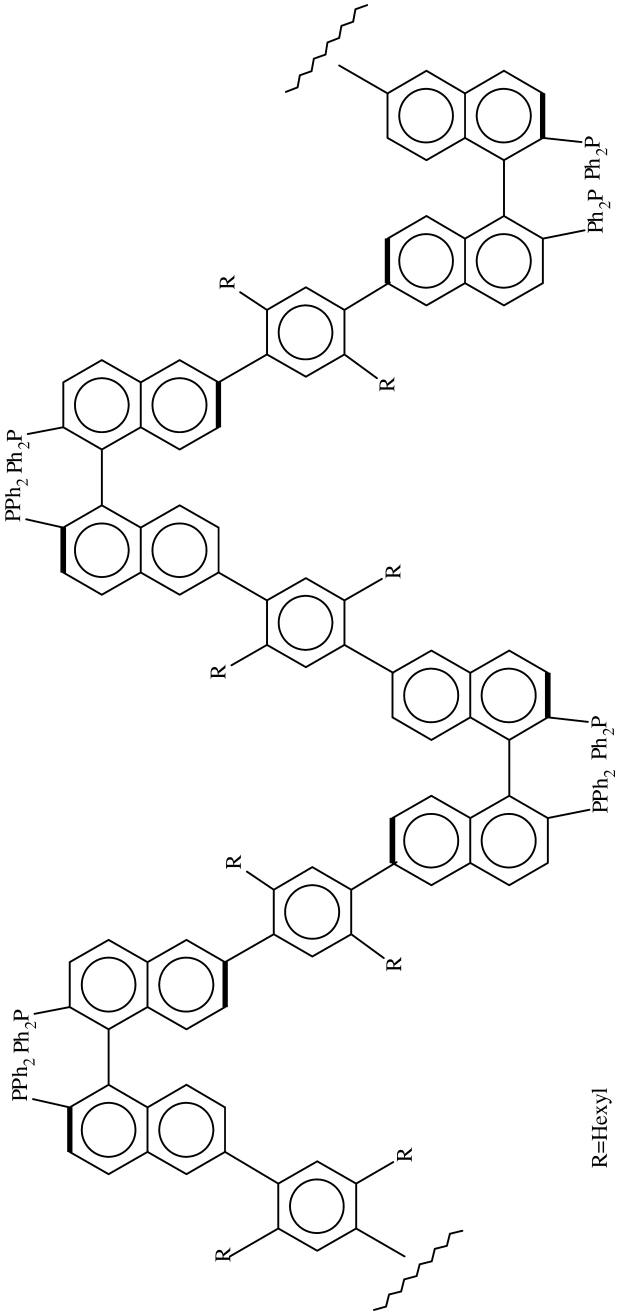

Fig. 42.17 Rigid poly-BINAP ligand.

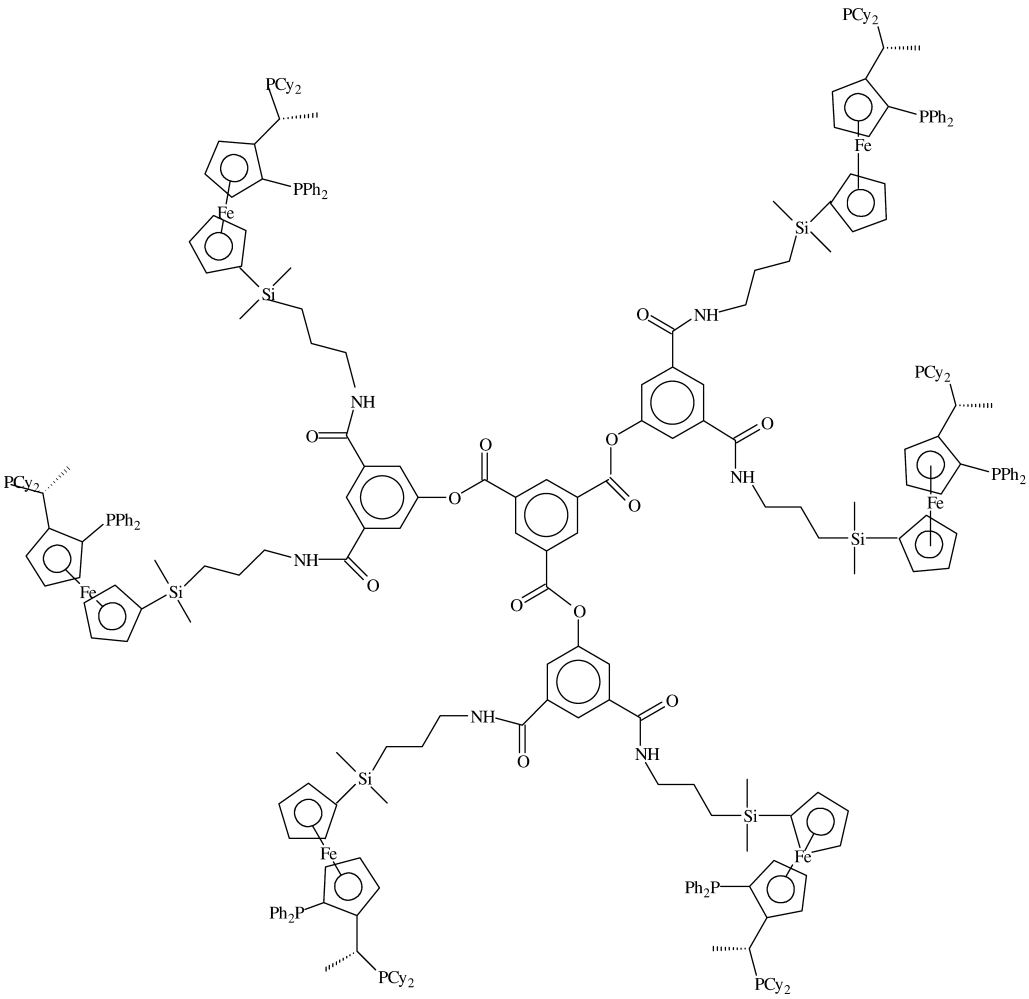

Fig. 42.18 Dendrimer-supported Josiphos.

42.3.6.4.4 **Dendrimers as Supports: Membrane Filtration**

By using a somewhat analogous approach, the catalysts can also be attached to soluble dendrimers, long fluorocarbons, cyclodextrins or crown ethers and used conveniently in membrane filtration for catalyst-product separation. For example, a chiral ferrocenyl ligand, Josiphos, was attached to some different dendrimers containing benzene-1,3,5-tricarboxylic acid (three arms) (Fig. 42.18) and adamantane-1,3,5,7-tetracarboxylic acid cores (four arms) [112]. After treating with Rh-precursors, the soluble dendrimer-supported catalyst obtained showed similar activity and enantioselectivity (>98% ee) in the hydrogenation of dimethyl itaconate as their homogeneous analogue, albeit with a slight decrease

in ee-value due to an increase in dendrimer size. All of the dendrimers were retained by a commercial nanofiltration membrane [112].

Membrane filtration can also be achieved by attaching carbosilane dendrimers to a single bidentate ligand [113]. In this case, the ligand itself serves as core for the dendrimer, and the size and polarity can be tuned as desired. Another way of performing membrane filtration is to introduce long fluorous ponytails to phosphine ligands [114]. The subsequently obtained Rh-complex is then soluble in supercritical CO_2 and can be used, amongst other things, for the hydrogenation of 1-butene at 353 K, 200 bar. The catalyst can be used with slight deactivation in either batch or continuous mode by using a simple microporous silica membrane for filtration.

42.3.6.4.5 **Grafting to Polymers**

The internal space of polymers is generally not accessible to molecules of unmatched polarity. Furthermore, the attachment of very large catalyst complexes might even be sterically hindered at the surface. By using functionalized monomers as support (see Section 42.3.6.4.3), the attached ligand (catalyst) might be locked in the formed copolymer. An alternative solution to this problem is to graft the functionalized monomer or oligomer to a carrier polymer. One advantage of this approach is that the properties of the core are irrelevant and the desired monomer/oligomer structure can be introduced as a surfactant and spacer. The grafting can be carried out by using either irradiation, electrochemical or/and chemical methods [12]. In addition to silica carriers, the grafting of phosphine-substituted styrene on phosphinated Merrifield resins was also studied [115].

Grafted catalysts are commercially available on fibrous polyethylene supports; for example, Johnson Matthey has developed the FibreCat™ catalyst family for a variety of reactions [116]. By using this approach, diphenylphosphino groups could be grafted to the fiber via phenyl or benzyl linkers, followed by complexation to transition-metal compounds. For example, the Rh FibreCat catalysts obtained (Fig. 42.19) showed similar selectivity to their homogeneous counterparts in reactions such as hydrogenation of geraniol to citronellol or carvone to 7,8-dihydrocarvone. Because hydrogenation of the least-hindered double bond in these substrates occurs more rapidly with homogeneous and FibreCat catalysts than with other double bonds in the molecule, selective hydrogenation can be achieved [116]. However, this is generally not the case when using conventional heterogeneous catalyst.

In conclusion, the covalent attachment of ligands to a support material is a widely investigated and still expanding field, and includes many examples of recyclable catalysts with activity and (enantio-) selectivity which is comparable to that of the corresponding homogeneous catalyst. However, this method requires the inclusion of extra synthetic steps in order to attach the ligand to the support, while stability of the ligand/linker combination is a prerequisite to prevent metal leaching.

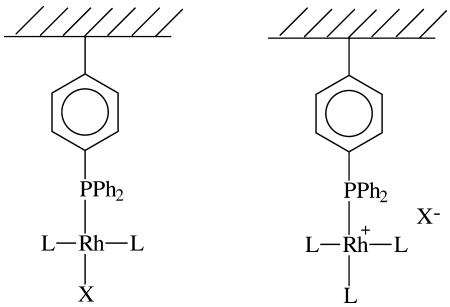

Fig. 42.19 Rh-FibreCat™ family.

42.3.7
Ionic Bonding of Metals to Supports

As an alternative to covalent attachment, the metal centers of catalyst complexes can also be supported by ion exchange. Clearly, a condition of this approach is that both the metal complex and the support are appropriate ionic compounds. By using multiply charged metal complexes, multiply bound supported complexes can be obtained, and this can minimize the chance of leaching. Furthermore, it should be considered that most homogeneous catalytic reactions proceed through changes in the oxidation state of the metal. Thus, before starting immobilization, it is important to consider whether the metal center retains at least one of its charges in each of the possible intermediates of the whole catalytic cycle.

As described below, ionic catalyst complexes can be supported to both inorganic and polymer (dendrimer) carriers. The efficiency of the support is determined by the general rules of ion exchange and, for this reason, in order to achieve a successful approach it is important to exclude the formation or presence of other ionic compounds, which might compete for (liberate) the catalyst ion from the support.

42.3.7.1 **Ionically Bound Metal Centers on Inorganic Supports**

The most significant class of inorganic supports, which is used for the direct ion exchange of positively charged transition-metal complexes, are smectite clays. Pinnavaia has introduced the use of these swelling, layered silicate clays for catalysis. Other clays include montmorillonite, bentonite, and laponite. As shown by Pinnavaia, cationic transition-metal complexes can be readily exchanged (intercalated) into the solvated interlayers of these silicates (Eq. (1)) [117]:

$$\overline{\underline{Na^+(solv)}} + ML_n^+ \xrightleftharpoons{solvent} \overline{\underline{ML_n^+(solv)}} + Na^+ \qquad (1)$$

When using appropriate solvents for swelling of the interlayers, the intercalated metal ions are accessible to both substrates and catalysis. One of the first such demonstrations was also carried out with the Wilkinson complex for hydrogena-

tion reactions [118]. The intercalated Rh–PPh_3 complexes showed similar activities in the hydrogenation of several olefins and alkynes (298 K, 1 bar H_2) to their homogeneous counterparts, albeit with some extent of deactivation. The deactivation was attributed to the formation of the monohydrido compound, which is in equilibrium with the cationic dihydrido species (Eq. (2)) [119]. (The formation of monohydride is especially favored in the presence of bases).

$$H_2Rh^+(PPh_3)_3 \rightleftharpoons H^+ + HRh(PPh_3)_3 \qquad (2)$$

Other than catalyst stability, shape selectivity is an additional important aspect that is associated with the use of intercalated complexes. For this reason, many studies have concentrated on demonstrating shape- and size-selective catalysis by influencing the interlayer space with swelling solvents rather than carrying out leaching tests. Some of these attempts were successful, and with several types of intercalated catalyst, including the Wilkinson analogues. For example, it has been shown that a chiral Rh^+–DIOP complex, when intercalated into sodium hectorite, is highly sensitive to the size of the ester group in terms of activity and enantioselectivity in the enantioselective hydrogenation of itaconic ester derivatives [120].

Naturally, other inorganic supports were also studied, one example being the immobilization of the Wilkinson complex on bentonite [121]. In this case, only surface-supported complexes were obtained, which were significantly faster than the homogeneous analogues (at 308 K, 1 bar) for several different alkenes such as 1-octene, cyclohexene, norbornadiene, and cyclohexen-1-one. This effect was explained by site isolation which prevented dimer formation. These complexes also showed some deactivation, most likely for the same reason as outlined above (see Eq. (2)). Other silicates such as mesoporous MCM-41 can also be used as supports for ionic complexes. Hölderich et al. immobilized cationic Rh-complexes of chiral ligands in the pores of this support [122] and, by using Me-Duphos complexes, were able to achieve TON values exceeding 4000 and 92% ee in the hydrogenation of itaconate by maintaining the catalyst configuration. The activity of the complexes was less high, most likely due to the limited accessibility of the intercalated catalysts.

42.3.7.2 **Ionically Bound Metal Centers on Polymer Supports**

Ion-exchange resins are the most obvious choices for supporting ionic complexes on polymer carriers. Cation-exchange resins are synthesized by introducing strong or weak acid groups, most frequently -SO_3H or -COOH, to polymer supports. Anion-exchange resins contain quaternary and/or tertiary amines as functional groups. Because of the easy functionalization, polystyrene–divinylbenzene and (meth)acrylic acid–divinylbenzene polymers are the dominant materials for used ion-exchange resins. Most commercially available ion-exchange resins are designed to function in aqueous media, and are usually gel-type polymers with a low degree of cross-linking and high polarity in the functional

groups. These resins are hygroscopic materials, and can barely tolerate organic solvents. Macroreticular forms with a lower degree of functional groups are better suited for use in organic media, and several of the latter type are available commercially. The traditional polystyrene- or acrylate-based ion-exchange resins have relatively low thermal stability, with a maximum recommended reaction temperatures of 80 to 100 °C. Several new resins offer some improvement in thermal stability; these include Nafion (DuPont) as cation and polyvinylpyridine (and other cyclic nitrogen base) derivatives as anion exchange resins. The structure of Nafion, which consists of a perfluorinated polymeric backbone with side chains containing $CF_2CF_2SO_3H$ groups, can be considered as particularly unique. The sulfonate groups are clustered together to give the resin an inverse micellar structure. Nafion can be used in either protic or polar solvents and, since the H-form is a very strong heterogeneous acid (superacid), the resin has found use in a variety of synthetic applications. Nafion resins are also available in solutions, as membrane foils, and as layers supported on silica.

Cation-exchange resins have been exploited mainly for the immobilization of monocationic Rh-phosphine complexes for hydrogenation reactions. According to Eq. (2), formation of the monohydride can be suppressed by using an excess of acidic resin. However, the presence of an acid can catalyze undesirable side reactions in the case of sensitive alkenes. Bidentate phosphines are somewhat less sensitive for the formation of monohydrido complexes, especially in the absence of strong bases. It has been shown that supported cationic Rh complexes of several chiral bisphosphinites on sulfonated polystyrenes maintained their high enantioselectivity over 15 consecutive uses in the enantioselective hydrogenation of dehydroamino acids [123]. However, the activity of the supported complexes slowly decreased, and some Rh-leaching occurred. This was ascribed to a slow decomposition through oxidation of the ligand rather than to monohydride formation. It was also shown that free acid functionality gave a higher supportation efficiency than either Li- or ammonium salts, though the latter gave a higher activity in the reaction. The use of the salt form was required with one phosphinite ligand, which was sensitive to acid-catalyzed hydrolysis. The swelling properties of the resins had only a slight effect on the enantioselectivity, but greatly influenced the hydrogenation rates.

42.3.8
Attachment of Ligands via Ion Exchange

As described in Section 42.3.7, ion-exchanged metal ions are often vulnerable to leaching through the formation of a neutral or zerovalent species. In similar manner to the situation in Section 42.3.6, this problem can be circumvented by ion exchanging the metal complexes via the ligands rather than the metal itself. As in covalent immobilization in general, two approaches can be followed: the ligands can be exchanged either prior to or after complexation to the metal centers. In particular, when the presence of several coordinated monodentate ligands is required, the latter method is advised as it provides better control on

the coordination chemistry and immobilization efficiency. As discussed earlier, many homogeneous catalyst complexes contain electronic charges at the metal center. However, when ion exchange of the metal center is not desirable, it can be avoided by choosing the opposite electronic charge for the functional groups of the ligand. As with the support, the same materials can be used as described in Section 42.3.6. However, to date predominantly ion-exchange resins (see Section 42.3.7.2) have been used, as the ion exchange of large ligands into the restricted interlayer space of smectite clays or other silicates (see Section 42.3.7.1) is a much more difficult task.

The first attempts at immobilizing ligands onto ion-exchange resins were also carried out by using Wilkinson analogues. For example, acid forms of macroporous cation-exchange resins were treated with a *p*-amino-substituted triphenylphosphine derivative $P[(4\text{-}C_6H_4)N(CH_3)_2]_3$ [124]. Tang and coworkers found that the phosphine functionality was protonated more easily by the resin than the amino group and, in this manner, in subsequent treatments with Co, Rh, or precursors, predominantly amine complexes were obtained. Presumably, because of the relatively weak coordinative binding of amine ligands, these catalyst systems showed leaching in the hydroformylation test reaction. Protonation or quaternization of the phosphorus groups of similar aminophosphines can be avoided by protecting them. Since the phosphorus atoms of these aminophosphines coordinate much more strongly than the amino groups, the phosphorus atoms can be most conveniently protected by coordination to the desired metal precursor before immobilization. This was demonstrated by using similar amino derivatives of several chiral bidentate phosphines such as Chiraphos and BDPP in the Rh-catalyzed enantioselective hydrogenation of dehydroamino acid derivatives [125]. For example, the reaction of *S,S*-Chiraphos-*p*-$(N(CH_3)_2)_4$ with Rh^+-precursors resulted in the formation of bidentate phosphine complexes, which could subsequently be protonated at the free amine functionalities with acid forms of ion-exchange resins. Thus the complex, including the charge at Rh, could be bound with five ion pairs to the resin (Fig. 42.20). Presumably due to this strong bonding, the catalysts showed no leaching in subsequent catalytic tests. Furthermore, it was found that the addition of amines stronger than *N,N*-dimethylaniline removed the complex completely from the resin by simple acid–base chemistry. Such easy liberation of the catalyst would be very useful in the regeneration of fouled (spent) catalyst, which is a clear advance compared to covalently bound catalysts.

The size and swelling of the resin beads was found to have a dramatic influence on the reaction rate and enantioselectivity. When using large beads of gel-type resins – which swell well – the rates with ion-exchange catalysts were several orders of magnitude less than those of the homogeneous counterpart. However, by using finely dispersed gel-type resins (with an increased surface area), and Nafion-based resins in particular (Fig. 42.20), the rates were significantly improved and approached those of the homogeneous analogues [125].

In general, the reaction rates can be increased by introducing longer spacer groups to the (covalently or ionically) bound ligands, by detaching the metal

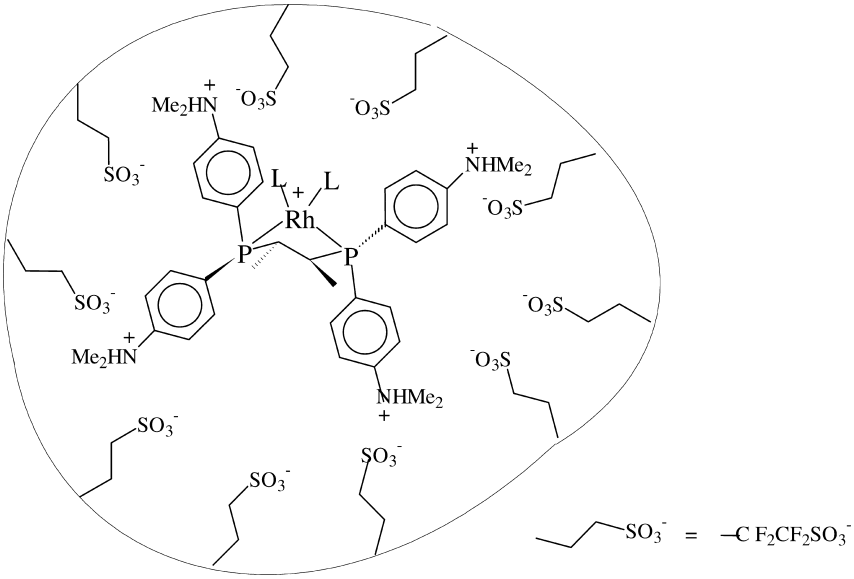

Fig. 42.20 Nafion-supported [Rh^+-(*S*,*S*)-Chiraphos-(*p*-N$(CH_3)_2)_4$].

center from the proximity of the surface. For example, it was shown that by using $Rh^+(NBD)[Ph_2P(CH_2)_nPMe_3^+]_2$ complexes, which were supported on cation-exchange resins in hydrogenation reactions, the rates generally increased by increasing the alkyl chain from n = 2 to n = 10 [126]. However, the effect was not shared by each alkene tested. One possible reason for this might be that Rh as a monocation is also exchanged to the resin, thus disturbing the trend. As mentioned above, ion exchange with the metal can be avoided by choosing the opposite charge for the ionic groups of the ligands. For this goal, and by assuming a typically cationic metal center as example, negatively charged ligands should be used with anion-exchange resins. Most water-soluble ligands developed for two-phase catalysis contain anionic sulfonate (SO_3^-) groups (see Chapter 39), and these could be readily used for immobilization by ion exchange. Despite the large number of available sulfonated ligands and the convenience of immobilization, this option has not yet been fully exploited. However, several examples are known which utilize sulfonated chiral BINAP on layered double hydroxides and sulfonated triphenylphosphine on anion-exchange resin in hydrogenation reactions [127, 128].

One special case is the combination of immobilization by entanglement and ionic bonding. A negatively charged phosphonated BINAP ruthenium complex and a phosphonic acid spacer reacted with a positively charged polymer to give a polymer network, which is held together by ionic bonding [129]; the structure of this is depicted in Figure 42.21.

This catalyst showed high enantioselectivity in the hydrogenation of dimethyl itaconate. The best enantioselectivities (83–89% ee) were obtained in ethanol as

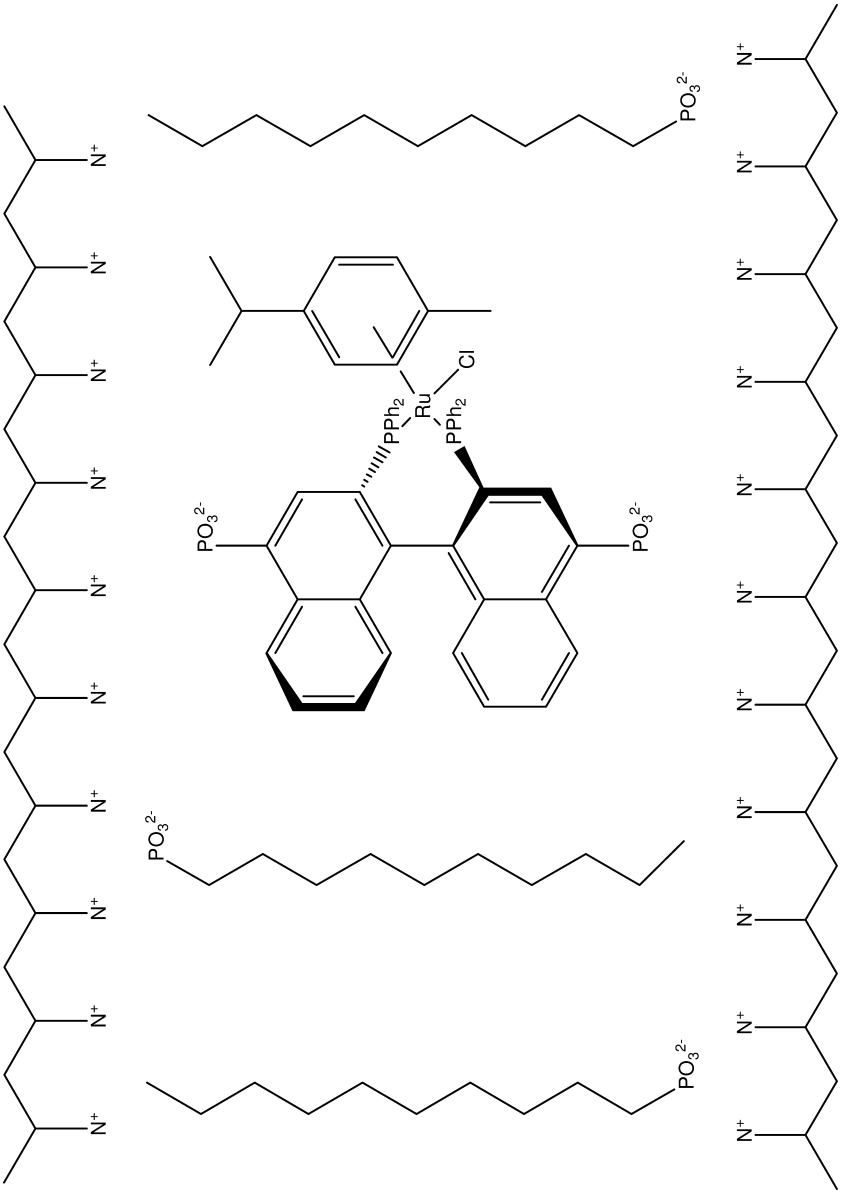

Fig. 42.21 Schematic drawing of the polyelectrolyte-entrapped ruthenium complex.

solvent, and approached the value obtained with a homogeneous Ru–BINAP catalyst (91% ee). The partial dissolution or swelling of these catalysts in ethanol may be responsible for the observed high enantioselectivities. Remarkably, much lower – and even opposite – enantioselectivities were found in less-polar solvents, such as toluene. It appears that the conformation of the network – and probably also the structure of the complex – depend heavily on the solvent used.

42.4 Catalyst Deactivation

Every catalyst is susceptible to catalyst deactivation, and immobilized catalysts form no exception to this rule. A number of observed deactivation mechanisms are listed below (see also Chapter 44):

- Loss of metal by ligand degradation. The oxidation of phosphorus ligands by peroxide impurities in the feed is an example. Purification of the feed is an obvious remedy. It is much more difficult to find a solution when ligand degradation is inherent to the catalytic reaction mechanism (e.g., phosphonium salt formation).
- Loss of metal by ligand substitution. Reactants or products can form soluble complexes with the metal by replacing the original ligands. In particular, weakly coordinating ligands such as amines, imines and O-based ligands are susceptible for replacement.
- Loss of catalytic complex by dissolution from the support. This can either occur to physically bound catalysts (physisorbed, entangled in a polymer, hydrogen-bonded), when the reaction medium has too-good solvent properties. The catalyst complex can also be dissolved from ionically bound species by ion exchange with electrolytes in the reaction mixture, or when the covalent bond to the support is broken (e.g., by hydrolysis). In the case of SIB catalysts, a good solvent such as ethanol can displace a salen-type ligand from the metal.
- Formation of inactive dimeric species. Site isolation is the solution to this problem, which is not possible using homogeneous catalyst.
- Reaction of the active species with functional groups (hydroxyls) on the support. Protection (end-capping) of the functional groups is the proposed remedy, but it is difficult to protect them all, for steric reasons.
- Deposition of insoluble material in the pores of the catalyst by polymerization or condensation reactions, for instance. Sometimes a washing procedure regenerates the catalyst.
- Deactivation may also be inherent to the catalytic system and similar to deactivation of the homogeneous catalyst. An example is the formation of a stable *ortho*-metalated species.
- Deactivation or loss of selectivity can also occur when the ligands are not able to protect the metal against reduction to metallic particles. In this case, one must avoid high hydrogen pressures.

The regeneration of deactivated immobilized catalysts is not as easy as with conventional supported metal catalysts, where combustion of the deposited material is frequently used. Because such a procedure would destroy the organic ligands, one must resort to washing procedures. However, when this method fails, attempts must be made to recover the metal and the ligand, and to prepare a fresh catalyst. In principle, it is possible to recover the metal complexes from physically and ionically immobilized catalysts. This can also be done from covalently bound catalysts by using an easily hydrolyzable linker.

42.5 Conclusions

The selectivity of homogeneous hydrogenation catalysts often surpasses that of conventional heterogeneous catalysts. The application of homogeneous hydrogenation catalysts in the fine chemical industry is steadily increasing, though process economics dictate the recovery and re-use of the catalyst in order to arrive at acceptable catalyst costs, unless the catalyst is extremely active. Since the separation and recovery of a homogeneous catalyst from a product mixture is not always possible without destroying the catalyst, homogeneous catalysts were modified to alleviate the separation problem. One direction of research is to immobilize homogeneous catalysts on a solid support in order to obtain a heterogeneous catalyst with at least similar catalytic activity and selectivity as the original homogeneous catalyst. However, the application of such an immobilized catalyst always introduces the possibility of mass-transfer limitations from the liquid phase to the exterior catalyst surface, or within the catalyst pore system. More detailed knowledge of the reaction kinetics is needed to evaluate the performance of this type of catalyst, and for scale-up and reactor design.

42.6 Outlook

The most promising immobilization methods are in our view:
- Physical entrapment in a polymer matrix.
- Surface hydrogen-bonding.
- Ionic bonding of the ligand to an ion exchanger.
- Covalent bonding of the ligand to the support.

The first two methods have the advantage that no modification of the homogeneous catalyst is needed. Surface hydrogen-bonded catalysts are limited to cationic complexes, while physical entrapment is more widely applicable. However, both methods are very sensitive to the solvent properties of the reaction medium. The chemical methods of immobilization require modification of the ligand, and this may be quite laborious. In the case of irreversible catalyst deacti-

vation, recovery of the metal is possible for all four types of immobilized catalysts. Recovery of the ligand or the entire complex is possible in all cases, except for the covalently bound ligands. Attachment of the homogeneous catalyst to a soluble polymer or dendrimer permits its use as a homogeneous catalyst with a size which is large enough for separation by membrane filtration. However, although this approach is very popular nowadays in academia, it is likely that industrial applications will have to wait until the stability of membranes has been proven.

Abbreviations

HPA	heteropoly acid
MELS	molecularly engineered layered structures
PDMS	polydimethylsiloxane
PVA	polyvinylalcohol
SAPC	supported aqueous-phase catalysis
SHB	supported hydrogen-bonded
SIB	ship-in-the-bottle
SILP	supported ionic-liquid phase
SLPC	supported liquid-phase catalyst
TEOS	tetraethoxy orthosilicate
THF	tetrahydrofuran
TOF	turnover frequency
TON	turnover number
TPPTS	trisulfonated triphenylphosphine

References

1 Yu. I. Yermakov, B. N. Kuznetsov, V. A. Zakharov, *Catalysis by Supported Complexes, Studies in Surface Science Catalysis, Vol. 8*, Elsevier, Amsterdam, **1981**.

2 F. R. Hartley, *Supported Metal Complexes*, D. Reidel, Dordrecht, **1985**.

3 A. Syamal, M.M. Syngh, *Asian J. Chem. Rev.* **1993**, *4*, 89.

4 P. Panster, S. Wieland, in: B. Cornils, W. A. Herrmann (Eds.), *Applied Homogeneous Catalysis with Organometallic Compounds*. Wiley-VCH, Weinheim, **1996**, p. 605.

5 A. D. Pomogailo, *Catalysis by Polymer-Immobilized Complexes*. Gordon & Breach, Australia, **1998**.

6 K. Fodor, S. G. A. Kolmschot, R. A. Sheldon, *Enantiomer* **1999**, *4*, 497.

7 B. Pugin, H.-U. Blaser, in: E. N. Jacobsen, A. Pfaltz, H. Yamamoto (Eds.), *Comprehensive Asymmetric Catalysis I–III, Vol. 3*. Springer, Berlin, **1999**, p. 1367.

8 G. G. Hlatky, *Chem. Rev.* **2000**, *100*, 1347.

9 K. Shu, *Curr. Opin. Chem. Biol.* **2000**, *4*, 338.

10 I. W. C. E. Arends, R. A. Sheldon, *Appl. Catal., A* **2001**, *212*, 175.

11 D. E. de Vos, B. F. Sels, P. A. Jacobs, *Adv. Catal.* **2001**, *46*, 1.

12 I. Tóth, P.C. van Geem, in: I. T. Horváth (Ed. in chief), *Encyclopedia of Catalysis*. Wiley, New York, **2003**, Volume 4, p. 164.

13 D. E. De Vos, I. F. J. Vankelecom, P. A. Jacobs, *Chiral Catalyst Immobilization and Recycling*. Wiley-VCH, Weinheim, **2000**.

14 H. U. Blaser, F. Spindler, M. Studer, *Appl. Catal. A, General* **2001**, *221*, 119.

15 (a) C. N. Satterfield, *Mass Transfer in Heterogeneous Catalysis*. Krieger, 1970, reprinted **1981**; (b) C. N. Satterfield, T. K. Sherwood, *The Role of Diffusion in Catalysis*. Addison Wesley Publishing Company, Inc., **1963**; (c) J. J. Carberry, *Chemical and Catalytic Reaction Engineering*. McGraw-Hill, **1976**.

16 C. R. Landis, J. Halpern, *J. Am. Chem. Soc.* **1987**, *109*, 1746.

17 Y. Sun, R. N. Landau, J. Wang, C. LeBlond, D. G. Blackmond, *J. Am. Chem. Soc.* **1996**, *118*, 1348.

18 J. M. Thomas, T. Maschmeyer, B. F. G. Johnson, D. S. Shephard, *J. Mol. Catal. A: Chemical* **1999**, *141*, 139.

19 See for example: (a) I. T. Horváth, *Catal. Lett.* **1990**, *6*, 43; (b) R. A. Sheldon, M. Wallau, I. W. C. E. Arends, U. Schuchardt, *Acc. Chem. Res.* **1998**, *31*, 485; (c) M. Dams, L. Drijkoningen, D. De Vos, P. Jacobs, *Chem. Commun.* **2002**, 1062.

20 J. R. Anderson, E. M. Campi, W. R. Jackson, Z. P. Yang, *J. Mol. Catal., A: Chem.* **1997**, *116*, 109.

21 J. Jamis, J. R. Anderson, R. S. Dickson, E. M. Campi, W. R. Jackson, *J. Organomet. Chem.* **2000**, *603*, 80.

22 World Patent *WO 97/14500* (April 24, 1997), W. Van Brussel, M. Renard, D. Tas, V. H. Rane, R. Parton, P. A. Jacobs (to KU Leuven Research & Development).

23 C. Bianchini, D. G. Burnaby, J. Evans, P. Frediani, A. Meli, W. Oberhauser, R. Psaro, L. Sordelli, F. Vizza, *J. Am. Chem. Soc.* **1999**, *121*, 5961.

24 C. Bianchini, V. Dal Santo, A. Meli, W. Oberhauser, R. Psaro, F. Vizza, *Organometallics* **2000**, *19*, 2433.

25 C. Bianchini, P. Barbaro, V. Dal Santo, R. Gobetto, A. Meli, W. Oberhauser, R. Psaro, F. Vizza, *Adv. Synth. Catal.* **2001**, *313*, 41.

26 F. M. de Rege, D. K. Morita, K. C. Ott, W. Tumas, R. D. Broene, *Chem. Commun.* **2000**, 1797.

27 F. M. de Rege, D. K. Morita, K. C. Ott, W. Tumas, R. D. Broene, *Chemical Industries (Dekker) 82 (Catalysis of Organic Reactions)*, **2001**, p. 439.

28 J. M. Thomas, R. Raja, *J. Organometal. Chem.* **2004**, *689*, 4110.

29 US Patent 6,025,295 (February 15, 2000), S. K. Tanielyan, R. L. Augustine (to Seton Hall University).

30 R. Augustine, S. Tanielyan, S. Anderson, H. Yang, *Chem. Commun.* **1999**, 1257.

31 R. L. Augustine, S. K. Tanielyan, S. Anderson, H. Yang, Y. Gao, in: *Chemical Industries (Dekker) 82 (Catalysis of Organic Reactions)*, **2001**, p. 497; *Stud. Surface Sci. Catal.* **2000**, *130*, 3351.

32 J. A. M. Brandts, J. G. Donkervoort, C. Ansems, P. H. Berben, A. Gerlach, M. J. Burk, in: M. E. Ford (Ed.), *Chemical Industries (Dekker) 82 (Catalysis of Organic Reactions)*, **2001**, p. 573.

33 M. J. Burk, A. Gerlach, D. Semmeril, *J. Org. Chem.* **2000**, *65*, 8933.

34 J. A. M. Brandts, E. G. M. Kuijpers, P. H. Berben, *Studies Surface Sci. Catal.* **2003**, *145*, 451.

35 J. A. M. Brandts, P. H. Berben, *Org. Process Res. Dev.* **2003**, *7*, 393.

36 D. Geffroy, F. Hancock, W. P. Hems, A. Zanotti-Gerosa, *Chimica Oggi Suppl.* **2004**, 38.

37 B. V. Romanovsky, *Acta Phys. Chem.* **1985**, *31*, 215.

38 G. Schulz-Ekloff, S. Ernst, in: G. Ertl, H. Knoezinger, J. Weitkamp (Eds.), *Handbook of Heterogeneous Catalysis*, Vol. 1. Wiley-VCH, Weinheim, **1997**, p. 374.

39 D. E. de Vos, F. Thibault-Starzyk, P. P. Knops-Gerrits, R. F. Parton, P. A. Jacobs, *Macromol. Symp.* **1994**, *80*, 157.

40 S. Kowalak, K. J. Balkus, Jr., *Collect. Czech. Chem. Commun.* **1992**, *57*, 774.

41 A. Janssen, J. P. M. Niederer, W. F. Hölderich, *Catal. Lett.* **1997**, *48*, 165.

42 M. Estermann, L. B. M. McCusker, C. Baerlocher, A. Merrouche, H. Kessler, *Nature* **1991**, *352*, 320.

43 W. Hölderich, H. H. Wagner, in: G. Centi et al. (Eds.), *Catalysis by Unique Metal Ion Structures in Solid Matrices*. Kluwer Academic Publishers, **2001**, p. 279.

44 D. E. de Vos, P. A. Jacobs, in: R. von Ballmoos, J. B. Higgins, M. M. J. Treacy (Eds.), *Proceedings, 9th International Zeolite Conference, Montreal 1992*. Butterworth-Heinemann, **1993**, p. 615.

45 (a) S. Ernst, O. Batréau, *Stud. Surface Sci. Catal.* **1995**, *94*, 479; (b) S. Ernst, S. Ost, K. Yang, in: *DGMK Tagungsbericht (C_4 Chemistry-Manufacture and Use of C_4-hydrocarbons, Aachen)*, **1997**, *9705*, 279.

46 D. Chatterjee, H.C. Bajaj, A. Das, K. Bhatt, *J. Mol. Catal.* **1994**, *92*, L235.

47 A. Zsigmond, K. Bogár, F. Notheisz, *Catal. Lett.* **2002**, *83*, 55; *J. Catal.* **2003**, *213*, 103.

48 E. Möllmann, P. Tomlinson, W.F. Hölderich, *J. Mol. Catal. A: Chemical* **2003**, *206*, 253.

49 H. Sertchook, D. Avnir, J. Blum, F. Joó, Á. Kathó, H. Schumann, R. Weimann, S. Wernik, *J. Mol. Catal., A: Chemical* **1996**, *108*, 153.

50 J. Blum, A. Rosenfeld, F. Gelman, H. Schumann, D. Avnir, *J. Mol. Catal. A: Chemical* **1999**, *146*, 117.

51 F. Gelman, D. Avnir, H. Schumann, J. Blum, *J. Mol. Catal. A: Chemical* **1999**, *146*, 123.

52 A. Patchornik, Y. Ben-David, D. Milstein, *J. Chem. Soc., Chem. Commun.* **1990**, 1090.

53 (a) R.F. Parton, I.F.J. Vankelecom, D. Tas, K.B.M. Janssen, P.P. Knops-Gerrits, P.A. Jacobs, *J. Mol. Catal., A: Chemical* **1996**, *113*, 283; (b) I.F.J. Vankelecom, D. Tas, R.F. Parton, V. van de Vyver, P.A. Jacobs, *Angew. Chem., Int. Ed. Engl.* **1996**, *35*, 1346.

54 I.F.J. Vankelecom, P.A. Jacobs, *Catal. Today* **2000**, *56*, 147.

55 (a) I.F.J. Vankelecom, A. Wolfson, S. Geresh, M. Landau, M. Gottlieb, M. Hershkovitz, *Chem. Commun.* **1999**, 2407; (b) A. Wolfson, S. Geresh, M. Gottlieb, M. Hershkowitz, *Tetrahedron Asymm.* **2002**, *13*, 465.

56 J.P. Arhancet, M.E. Davis, J.S. Merola, B.E. Hanson, *Nature* **1989**, *339*, 454.

57 I. Tóth, I. Guo, B.E. Hanson, *J. Mol. Catal., A, Chemical* **1997**, *116*, 217.

58 E. Fache, C. Mercier, N. Pagnier, B. Despeyroux, P. Panster, *J. Mol. Catal.* **1993**, *79*, 117.

59 K.T. Wan, M.E. Davis, *Nature* **1994**, *370*, 449.

60 I.T. Horváth, *Angew. Chem., Int. Ed. Engl.* **1991**, *30*, 1009.

61 M. Hoffmeister, D. Hesse, *Chem. Eng. Sci.* **1990**, *45*, 2575.

62 R. Neumann, M. Cohen, *Angew. Chem., Int. Ed. Engl.* **1997**, *36*, 1738.

63 A. Wolfson, I.F.J. Vankelecom, P.A. Jacobs, *Tetrahedron Lett.* **2003**, *44*, 1195.

64 S.L. Scott, J.-M. Basset, *J. Mol. Catal.* **1994**, *86*, 5.

65 G.P. Niccolai, J.-M. Basset, in: E.G. Derouane et al. (Eds.), *Catalytic Activation and Functionalisation of Light Alkanes.* Kluwer Academic Publisher, Boston, Mass., **1998**, p. 111.

66 F. Lefebvre, J. Thivolle-Cazat, V. Dufaud, G.P. Niccolai, J.-M. Basset, *Appl. Catal., A: General* **1999**, *182*, 1.

67 F. Quignard, O. Graziani, A. Choplin, *Appl. Catal., A: General* **1999**, *182*, 29.

68 R. Anwander, C. Palm, *Stud. Surface Sci. Catal.* **1998**, *117*, 413.

69 D.E. Leyden (Ed.), *Silanes, Surfaces and Interfaces.* Gordon & Breach, New York, **1986**.

70 D.E. Leyden, W.T. Collins, *Chemically Modified Surfaces in Science and Industry.* Gordon & Breach, New York, **1988**.

71 H.A. Mottola, J.R. Steinmetz (Eds.), *Chemically Modified Surfaces.* Elsevier, New York, **1992**.

72 L.N.H. Arakaki, C. Airoldi, *Quim. Nova* **1999**, *22*, 246.

73 R.K. Iler, *The Chemistry of Silica*, 2nd edn. Wiley-Interscience, New York, **1981**.

74 K.K. Unger, *Porous Silica.* Elsevier, New York, **1979**.

75 P. van der Voort, E.F. Vansant, *J. Liq. Chromatogr. Rel. Technol.* **1996**, *19*, 2723.

76 L. Bemi, H.C. Clark, J.A. Davies, C.A. Fyfe, R.E. Wasylishen, *J. Am. Chem. Soc.* **1982**, *104*, 438.

77 C. Merckle, J. Blümel, *J. Organometal. Chem.* **2001**, *627*, 44; *Adv. Synth. Catal.* **2003**, *345*, 584, and references therein.

78 E. Lindner, T. Salesch, S. Brugger, S. Steinbrecher, E. Plies, M. Seiler, H. Bertagnolli, H.A. Mayer, *Eur. J. Inorg. Chem.* **2002**, 1998, and references therein.

79 W.E. Rudzinski, T.L. Montgomery, J.S. Frye, B.L. Hawkins, G.E. Maciel, *J. Catal.* **1986**, *98*, 444.

80 European Patent 0496699 A1 and 0496700 A1 (January 16, 1992), B. Pugin, M. Müller, F. Spindler (to Ciba-Geigy AG).

81 B. Pugin, M. Müller, *Stud. Surface Sci. Catal.* **1993**, *78*, 107.
82 B. Pugin, *J. Mol. Catal. A, Chemical* **1996**, *107*, 273.
83 B. Pugin, H. Landert, F. Spindler, H.-U. Blaser, *Adv. Synth. Catal.* **2002**, *344*, 974.
84 I. Steiner, R. Aufdenblatten, A. Togni, H.-U. Blaser, B. Pugin, *Tetrahedron Asymmetry* **2004**, *15*, 2307.
85 M. Čapka, A. Reissová, *Collect. Czech. Chem. Commun.* **1989**, *54*, 1760.
86 T. Shido, T. Okazaki, M. Ichikawa, *J. Catal.* **1995**, *157*, 436.
87 (a) U. Schubert, *New J. Chem.* **1994**, *18*, 1049; (b) J. J. Yang, I. M. El-Nahal, I.-S. Chuang, G. E. Maciel, *J. Non-Cryst. Solids* **1997**, *209*, 19; (c) E. Lindner, M. Kemmler, H. A. Mayer, P. Wegner, *J. Am. Chem. Soc.* **1994**, *116*, 348.
88 J. Čermák, M. Kvičalová, V. Blechta, M. Čapka, Z. Bastl, *J. Organomet. Chem.* **1996**, *509*, 77.
89 S. Wieland, P. Panster, *Chemistry and Industry* (Dekker), **1995**, *62*, 383.
90 US Patent 4,384,981 (May 24, 1983), M. B. Dines, P. M. DiGiacomo, K. P. Callahan, (to Occidental Research Corp.).
91 (a) C. Maillet, P. Janvier, M. Pipelier, T. Praveen, Y. Andres, B. Bujoli, *Chem. Mater.* **2001**, *13*, 2879; (b) C. Maillet, P. Janvier, M.-J. Bertrand, T. Praveen, B. Bujoli, *Eur. J. Org. Chem.* **2002**, 1685.
92 R. B. Merrifield, *Science* **1965**, *150*, 178.
93 R. H. Grubbs, L.C. Kroll, *J. Am. Chem. Soc.* **1971**, *93*, 3062.
94 A. J. Naaktgeboren, R. J. M. Nolte, W. Drenth, *J. Am. Chem. Soc.* **1980**, *102*, 3350.
95 W. Dumont, J. C. Poulin, D. T. Phat, H. B. Kagan, *J. Am. Chem. Soc.* **1973**, *95*, 8295.
96 T. Ohkuma, H. Ooka, S. Hashiguchi, T. Ikariya, R. Noyori, *J. Am. Chem. Soc.* **1995**, *117*, 2675.
97 D. J. Bayston, C. B. Travers, M. E. C. Polywka, *Tetrahedron Asymmetry* **1998**, *9*, 2015.
98 D. J. Bayston, J. L. Fraser, M. R. Ashton, A. D. Baxter, M. E. C. Polywka, E. Moses, *J. Org. Chem.* **1998**, *63*, 3137.
99 T. Ohkuma, H. Takeno, Y. Honda, R. Noyori, *Adv. Synth. Catal.* **2001**, *343*, 369.
100 C. Saluzzo, T. Lamouille, D. Hérault, M. Lemaire, *Bioorg. & Med. Chem. Lett.* **2002**, *12*, 1841.
101 P. Guerreiro, V. Ratovelomanana-Vidal, J.-P. Genêt, P. Dellis, *Tetrahedron Lett.* **2001**, *42*, 3423.
102 R. H. Grubbs, C. Gibbons, L. C. Kroll, W. D. Bonds, C. H. Brubaker, *J. Am. Chem. Soc.* **1973**, *95*, 2373.
103 Y. Qian, K. Hong, H. Zong, J. Huang, *Polym. Adv. Technol.* **1996**, *7*, 619.
104 M. E. Wilson, G. M. Whitesides, *J. Am. Chem. Soc.* **1978**, *100*, 306.
105 H. Pracejus, M. Bursian, East German Patent 92031, **1972**.
106 K. Achiwa, *Chem. Lett.* **1978**, 905.
107 N. Takaishi, H. Imai, C. A. Bertelo, J. K. Stille, *J. Am. Chem. Soc.* **1978**, *100*, 264.
108 T. Masuda, J. K. Stille, *J. Am. Chem. Soc.* **1978**, *100*, 268.
109 Q. Fan, C. Ren, C. Yeung, W. Hu, A. S. C. Chan, *J. Am. Chem. Soc.* **1999**, *121*, 7407.
110 H.-B. Yu, Q.-S. Hu, L. Pu, *Tetrahedron Lett.* **2000**, *41*, 1681.
111 D. E. Bergbreiter, *Catal. Today* **1998**, *42*, 389.
112 C. Köllner, B. Pugin, A. Togni, *J. Am. Chem. Soc.* **1998**, *120*, 10274.
113 J. N. H. Reek, D. de Groot, G. E. Oosterom, P. C. J. Kamer, P. W. N. M. van Leeuwen, *Compt. Rend. Chimie* **2003**, *6*, 1061.
114 L. J. P. van den Broeke, E. L. V. Goetheer, A. W. Verkerk, E. de Wolf, B.-J. Deelman, G. van Koten, J. T. F. Keurentjes, *Angew. Chem. Int. Ed.* **2001**, *40*, 4473.
115 E. Ruckenstein, L. Hong, *Chem. Mater.* **1992**, *4*, 122.
116 World Patent WO02/36648 A1 (May 10, 2002), K. Ekman, R. Peltonen, M. Sundell (to Johnson Matthey); see also www.chemicals.matthey.com.
117 F. Farzaneh, T. J. Pinnavaia, *Inorg. Chem.* **1983**, *22*, 2216.
118 T. J. Pinnavaia, R. Raythatha, J. G.-S. Lee, L. J. Halloran, J. F. Hoffman, *J. Am. Chem. Soc.* **1979**, *101*, 6891.
119 R. R. Schrock, J. A. Osborn, *J. Am. Chem. Soc.* **1976**, *98*, 2134.
120 T. Sento, S. Shimazu, N. Ichikuni, T. Uematsu, *J. Mol. Catal. A, Chemial* **1999**, *137*, 263.

121 M. Bartók, Gy. Szöllösi, Á. Mastalir, L. Dékány, *J. Mol. Cat., A, Chemical* **1999**, *139*, 227.

122 W.F. Hölderich, H.H. Wagner, in: G. Centi et al. (Eds.), *Catalysis by Unique Metal Ion Structures in Solid Matrices*. Kluwer, **2001**, p. 279.

123 R. Selke, K. Häupke, H.W. Krause, *J. Mol. Catal.* **1989**, *56*, 315.

124 S.C. Tang, T.E. Paxson, L. Kim, *J. Mol. Catal.* **1980**, *9*, 313.

125 (a) I. Tóth, B.E. Hanson, M.E. Davis, *J. Organomet. Chem.* **1990**, *397*, 109; (b) I. Tóth, B.E. Hanson, *J. Mol. Catal.* **1992**, *71*, 365.

126 E. Renaud, M.C. Baird, *J. Chem. Soc., Dalton Trans.* **1992**, 2905.

127 D. Tas, D. Jeanmart, R.F. Parton, P.A. Jacobs, in: H.-U. Blaser, A. Baiker, R. Prins (Eds.), *Stud. Surface. Sci. Catal.*, (*Heterogeneous Catalysis and Fine Chemicals IV*), Elsevier, Amsterdam, **1997**, *108*, p. 493.

128 F. Joó, M.T. Beck, *J. Mol. Catal.* **1984**, *24*, 135.

129 A. Köckritz, S. Bischoff, V. Morawsky, U. Prüsse, K.-D. Vorlop, *J. Mol. Catal. A: Chemical* **2002**, *180*, 231.

Part VI
Miscellaneous Topics in Homogeneous Hydrogenation

The Handbook of Homogeneous Hydrogenation.
Edited by J.G. de Vries and C.J. Elsevier
Copyright © 2007 WILEY-VCH Verlag GmbH & Co. KGaA, Weinheim
ISBN: 978-3-527-31161-3

43
Transition Metal-Catalyzed Regeneration of Nicotinamide Cofactors

Stephan Lütz

This chapter is dedicated to the memory of Prof. Dr. E. Steckhan (1943–2000).

43.1
Introduction

Among the many reactions that biocatalysts can bring about [1, 2], redox reactions are of special interest for the synthesis of chiral compounds, including hydroxy acids [3], amino acids [4, 5], steroids [6] or alcohols [7–12] from prochiral precursors. The biocatalysts involved in these reactions belong to the class of oxidoreductases (E.C.1) and are dependent on so-called coenzymes or cofactors [13]. These cofactors can act as hydrogen, oxygen or electron-delivery systems. Nature has developed an amazing molecular machinery for this transfer of redox equivalents, using enzyme-bound (e.g., FMN, FAD or PQQ) or freely dissociated (e.g., NAD/H, NADP/H) molecules (Fig. 43.1).

The most important coenzymes in synthetic organic chemistry [14] and industrially applied biotransformations [15] are the nicotinamide cofactors NAD/H (**3a/8a**, Scheme 43.1) and NAD(P)/H (**3b/8b**, Scheme 43.1). These pyridine nucleotides are essential components of the cell [16]. In all the reactions where they are involved, they serve solely as hydride donors or acceptors. The oxidized and reduced form of the molecules are shown in Scheme 43.1, the redox reaction taking place at the C-4 atom of the nicotinamide moiety.

Formally, in its oxidized state the cofactor NAD^+ is charged negatively due to the two phosphate groups; the positive charge denotes quaternization of the nitrogen. It is noteworthy that from the reduced form only the 1,4-NAD(P)H instead of the 1,6-NAD(P)H is enzyme-active, which imposes some restrictions on the regeneration systems in terms of the selectivity.

Cofactor regeneration is a necessary prerequisite for an *in-vitro* application of oxidoreductase enzymes, as the cofactors are too expensive to be used in stoichiometric amounts (Fig. 43.2) [17, 18].

Furthermore, too-high levels of cofactors can even act as inhibitors for the production enzyme; thus, a low level of the coenzyme and constant regenera-

The Handbook of Homogeneous Hydrogenation.
Edited by J.G. de Vries and C.J. Elsevier
Copyright © 2007 WILEY-VCH Verlag GmbH & Co. KGaA, Weinheim
ISBN: 978-3-527-31161-3

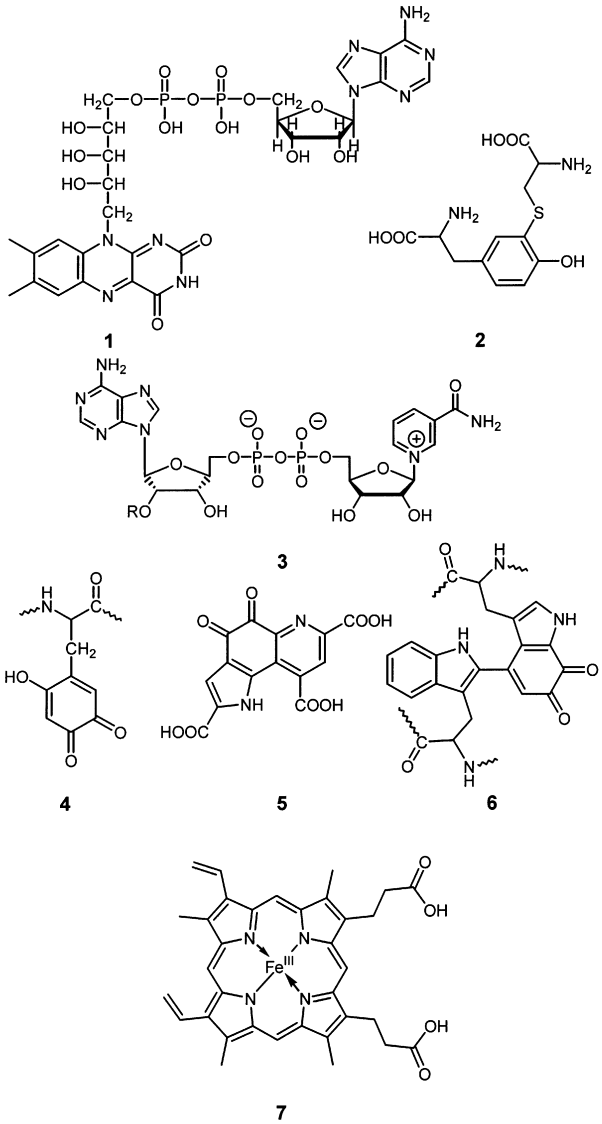

Fig. 43.1 Prosthetic groups in oxidoreductases (**1**: flavin adenine dinucleotide (FAD); **2**: thio-tyrosine; **3 a** (R = H): nicotinamide adenine dinucleotide; **3 b** (R = PO_3^{2-}): nicotinamide adenine dinucleotide phosphate ($NADP^+$); **4**: 6-hydroxy-DOPA; **5**: methoxanthine (pyrroloquinoline quinine; PQQ); **6**: tryptophan-tryptophan quinine).

tion of the desired oxidation state is necessary. In principle, both reactions which are implied in Scheme 43.1 – reduction and oxidation – are of interest in synthetic applications, but this chapter will focus only on the reduction reaction. The most important enzymatic reactions, in which regeneration of the nicotinamide cofactors are used, are alcohol dehydrogenase (ADH)-catalyzed [19], in

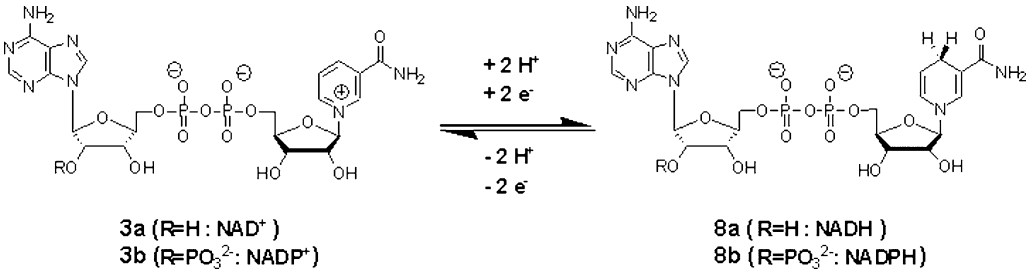

Scheme 43.1 Oxidized (left, NAD(P)$^+$, **3a**/**3b**) and reduced (right, NAD(P)H, **8a**/**8b**) forms of nicotinamide cofactors.

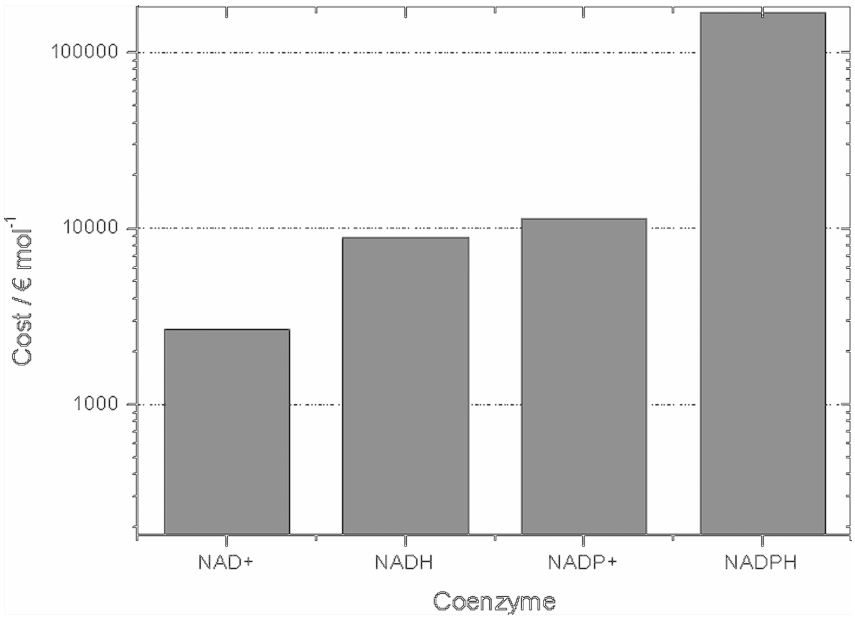

Fig. 43.2 Costs of nicotinamide cofactors (Source: Jülich Fine Chemicals, 2003).

which the reduced cofactor is the direct hydride source to convert a ketone into an alcohol, and monooxygenase-catalyzed biotransformations [20], where molecular oxygen is the final electron acceptor: one oxygen atom is selectively transferred to the substrate while the other is reduced by the cofactor to form water. Here, only ADH-catalyzed reactions will be shown as examples, but the regeneration systems also apply to monooxygenases.

The principal strategies of cofactor regeneration – namely the enzymatic, chemical and electrochemical approach – are presented in Scheme 43.2 and have been reviewed recently [17, 21–23]. This chapter does not intend to be exhaustive; rather, it focuses on the systems where a transition-metal complex and

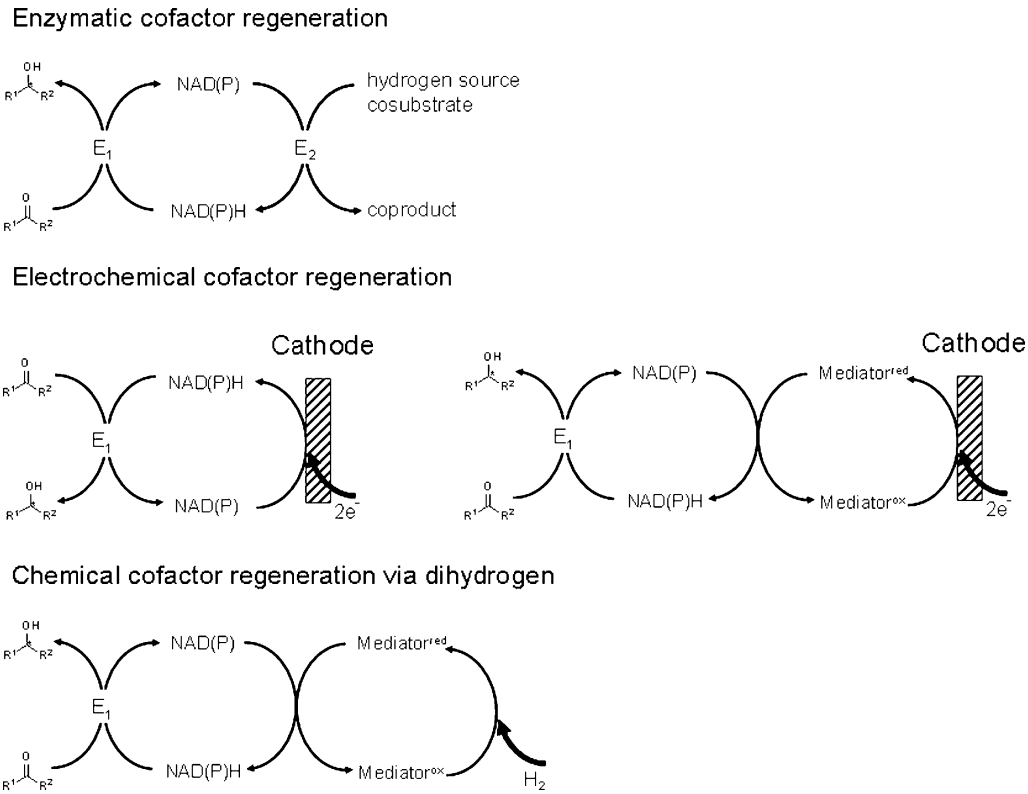

Scheme 43.2 Principal strategies of cofactor regeneration (E_1: production enzyme; E_2: regeneration enzyme).

molecular hydrogen are involved, and includes a brief overview of enzymatic systems for comparison.

43.2 Enzymatic Cofactor Regeneration

Enzymatic cofactor regeneration can be subdivided into two categories: the enzyme-coupled approach, where two different enzymes are used (one for the production reaction, and one for the regeneration reaction); and the substrate-coupled approach, where one and the same enzyme is used for both production and regeneration ($E_1 = E_2$). The most convenient and commonly used enzymatic regeneration systems are summarized in Table 43.1.

A recently developed method uses a hydrogenase from *Pyrococcus furiosus* to regenerate reduced cofactors, using molecular hydrogen as reducing agent. This very promising approach is the first example of a biocatalytic hydrogenation of

Table 43.1 Enzymatic cofactor regeneration.

Regeneration reaction	Cofactor	Regeneration enzyme
$HCOOH/CO_2$	NAD	Formate dehydrogenase
Isopropanol/Acetone	NADP	ADH
Glucose/Gluconic acid	NAD/NADP	Glucose dehydrogenase

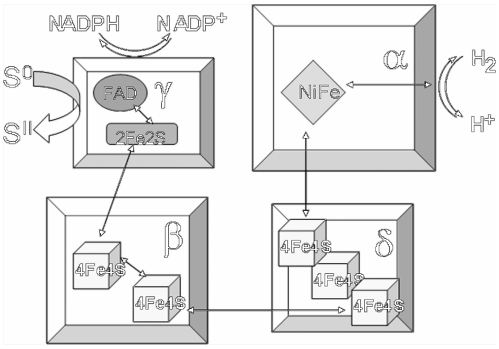

Fig. 43.3 The four subunits of *Pyrococcus furiosus* hydrogenase I involved in cofactor hydrogenation.

cofactors, and has been applied practically on a laboratory scale [24, 25]. Turnover frequencies (TOF) of 28 to 44 h^{-1} have been achieved for this reaction.

The active center of the enzyme consists of four subunits (Fig. 43.3) [26, 27], and the heterolytic cleavage of molecular hydrogen takes place at the α-subunit containing a nickel-iron center. The electrons are then channeled via several iron-sulfur-clusters to the γ-subunit, where either sulfur or cofactor reduction can occur.

To circumvent the cofactor regeneration problem, redox biotransformations are also carried out in whole cells – for example, baker's yeast [28, 29] or engineered *Escherichia coli* cells [30] – using the intracellular cofactor pool and inherent or recombinant regeneration systems.

43.3 Electrochemical Cofactor Regeneration

Electrochemical cofactor reduction can be achieved by direct reduction of the cofactor at the electrode surface, or indirectly by using a mediator molecule to shuttle electrons between the electrode and the cofactor. For details on the direct approach the reader is referred elsewhere [31, 32], since here no transition-metal complexes are involved. One point to be considered in the direct approach is the issue of selectivity. Whereas direct cofactor oxidation can be successfully achieved, special care must be taken to produce enzyme active reduced cofactors by direct electrolysis.

Several dyes or transition-metal complexes can be used as redox mediators in indirect electrolyses. Pentamethylcyclopentadienyl-rhodium(bipyridine) complexes $[Cp^*Rh^{III}(bpy)(H_2O)]^{2+}$ **9** [33], which were pioneered and intensively studied by Steckhan et al. [34–36], are very versatile catalysts for the reduction of cofactors.

Complex **9** (Scheme 43.3) can be reduced by different redox equivalents to the active rhodium(I) species **10**; namely, by electrons, formate [37, 38], and hydrogen. This hydrido complex then transfers the hydride ion onto the nicotinamide. In electrochemical applications, TOFs in the range of 5 to 11 h^{-1} have been reported [31, 39]. It is noteworthy that this complex accepts NAD^+ and $NADP^+$ as substrates with the same efficiency and almost exclusively produces the 1,4-reduced cofactor (selectivity >99%).

For application in an electrochemical enzyme membrane reactor, polymer-supported derivatives of **9** have been synthesized, which could be retained by ultrafiltration membranes and were thus retained within the electroenzymatic reactor [31, 40].

The unmodified complex can be applied in very dilute concentrations allowing total turnover numbers (TONs), or a substrate (NAD(P)) to catalyst (rhodium complex) ratio of up to 400 [41]. This efficiency was due to the design of a three-dimensional electrode, which also resulted in an extraordinary space-time yield of the reduced cofactor of up to 1 kg L^{-1} per day.

Several successful examples of coupling this regeneration system to synthesis reactions with different electrochemical reactors have been reported, including ADH and monooxygenase reactions [39, 42, 43].

Recently, the use of pentamethylcyclopentadienyl(1,10-phenanthroline-5,6-dione)chloro rhodium(III) hexafluorophosphate $[(Cp^*)Rh^{III}(phend)Cl]PF_6$, **11** (Fig. 43.4) has been reported for the electrochemical NAD^+ reduction. TONs between 7 and 453 h^{-1} have been achieved by varying pH, temperature and the complex concentrations [44]. This study reveals only preliminary results, so the mechanism of cofactor reduction is not explained; however, due to the structural

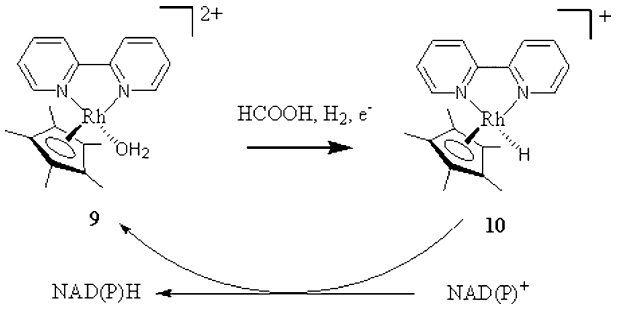

Scheme 43.3 Cofactor reduction using the pentamethylcyclopentadienyl rhodium(bipyridine) complex (**9**/**10**).

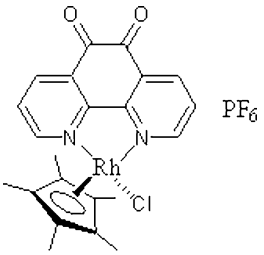

11

Fig. 43.4 Pentamethylcyclopentadienyl(1,10-phenanthroline-5,6-dione)chloro rhodium(III) hexafluorophosphate (**11**).

resemblance to the bipyridine complex (see Scheme 43.3), the same mechanism can be assumed.

Considering that these two transition-metal complexes are the only ones reported for the electrochemical cofactor reduction, the results are quite promising and show the need for further research in this field to identify new catalysts. In addition to the use of soluble redox mediators in electrochemical cofactor regeneration, modified electrodes have also been used. Details on these systems can also be found in the above-mentioned reviews [31, 32].

43.4 Chemical Cofactor Regeneration

The first example of a chemical cofactor reduction utilizing hydrogen dates back to the 1980s, and is a hybrid approach [45].

Using two types of specially synthesized rhodium-complexes (**12a**/**12b**), pyruvate is chemically hydrogenated to produce racemic lactate. Within the mixture, both a D- and L-specific lactate dehydrogenase (D-/L-LDH) are co-immobilized, which oxidize the lactate back to pyruvate while reducing NAD^+ to NADH (Scheme 43.4). The reduced cofactor is then used by the producing enzyme (ADH from horse liver, HL-ADH), to reduce a ketone to an alcohol. Two examples have been examined. The first example is the reduction of cyclohexanone to cyclohexanol, which proceeded to 100% conversion after 8 days, resulting in total TONs (TTNs) of 1500 for the Rh-complexes **12** and 50 for NAD. The second example concerns the reduction of (±)-2-norbornanone to 72% *endo*-norbornanol (38% ee) and 28% *exo*-norbornanol (>99% ee), which was also completed in 8 days, and resulted in the same TTNs as for the first case.

Besides the electrochemical application, the (Cp*)Rh(bpy)-complex **9** can also be used to reduce cofactors with hydrogen. In a recent study it was compared with ruthenium complex **13** $[RuCl_2(TPPTS)_2]_2$ (TPPTS: tris(*m*-sulfonatophenyl)-phosphine; Scheme 43.5). Both complexes were used to regenerate the cofactors in the reduction of 2-heptanone to (*S*)-2-heptanol, catalyzed by an ADH from *Thermoanaerobium brockii* (*Tb*ADH) [46, 47]. The TON for both catalysts was 18.

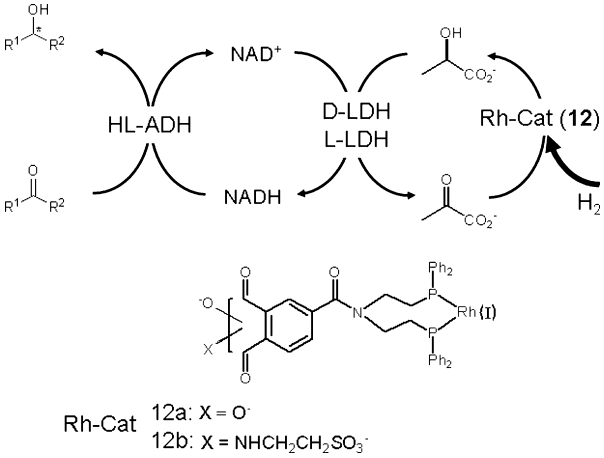

Scheme 43.4 The first hybrid organometallic/enzymatic cofactor regeneration using hydrogen.

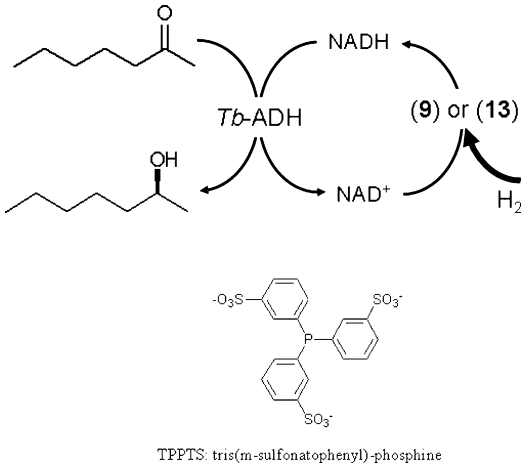

Scheme 43.5 Direct hydrogenation of cofactors with transition-metal complexes in an enzymatic synthesis.

A different approach is the combination of a Pt-carbonyl-cluster with a special dye, Safranine O (Saf^+; 3,7-diamino-2,8-dimethyl-5-phenylphenazinium) in an aqueous/organic two-phase system [48]. The dye is reduced in the organic phase and subsequently, in a type of phase-transfer catalysis, it reduced the cofactor in the aqueous phase. In this example L-LDH is used as a production enzyme, reducing pyruvate to L-lactate (Scheme 43.6). Complete conversion was obtained within 48 h, the mixture containing pyruvate, NAD^+ and the Pt-cluster catalyst in a 600 : 10 : 1 molar ratio. The TOF for NAD^+ was 15 h^{-1}.

These three systems are the only ones reported in the literature for achieving cofactor reduction utilizing molecular hydrogen and transition-metal complexes.

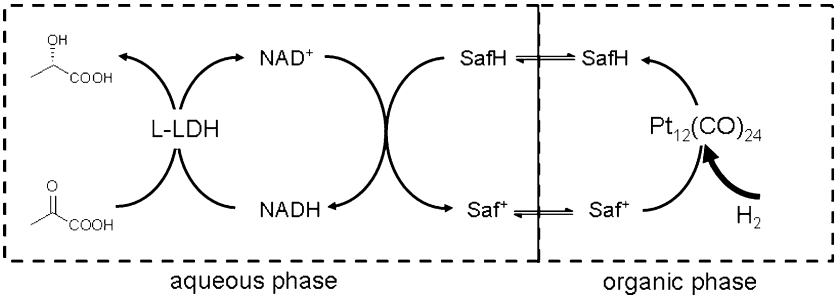

Scheme 43.6 Cofactor reduction using a Pt-carbonyl-cluster/dye system.

43.5
Other Chemical Cofactor Regeneration Procedures

Regeneration of the oxidized form of the cofactors, while not within the frame of this chapter, is needed for several biotransformations (e.g., oxidative kinetic resolution of diols). In these procedures, transition-metal complexes have also been applied. For this task, $Ru(phend)_3$ complex and derivatives thereof can be used, either with oxygen or in an electrochemical procedure [49–51].

A number of photochemically or photoelectrochemically activated transition-metal complexes have also been used, both for oxidation and reduction of the nicotinamide cofactors. Among these complexes is the aforementioned Cp*Rh(bpy)-complex **9** [52, 53]. For details of these systems or other regeneration procedures using special dyes, the reader is referred to other reviews on coenzyme regeneration [17, 21–23].

43.6
Conclusions and Outlook

Until now, only a few versatile, selective and effective transition-metal complexes have been applied in nicotinamide cofactor reduction. The TOFs are well within the same order of magnitude for all systems studied, and are within the same range as reported for the hydrogenase enzyme; thus, the catalytic efficiency is comparable. The most versatile complex Cp*Rh(bpy) (**9**) stands out due to its acceptance of NAD^+ and $NADP^+$, acceptance of various redox equivalents (formate, hydrogen and electrons), and its high selectivity towards enzymatically active 1,4-NAD(P)H.

With biocatalysis becoming increasingly accepted in synthetic organic chemistry on both the laboratory and industrial scale, there is a huge need for new complexes that can utilize electrons or hydrogen as redox equivalents in cofactor reduction. These redox equivalents are very inexpensive, readily available, and produce no side products, which in turn significantly facilitates the downstream processing of products.

Nevertheless, today enzymatic regeneration procedures are more conveniently applied. The enzymes are available commercially (e.g., [18]). Although more expensive than hydrogen or electrons, the redox equivalents for the enzymatic regeneration procedures (formic acid, glucose or isopropanol) are – in view of the very high cofactor prices – economically as feasible as hydrogen and electrons, and the side products are volatile (CO_2, acetone) or highly polar (gluconate) and can be easily separated from the desired product of the biotransformation.

Depending on the development of new regeneration systems, the choice of the ideal system might well depend on the specific synthetic application.

Acknowledgments

The author thanks Prof. C. Wandrey and Prof. A. Liese for their ongoing support and fruitful discussions, Dr. N. Rao for proofreading the manuscript, and R. Mertens, H. Offermann and D. Hahn for help in drawing the figures.

Abbreviations

ADH	alcohol dehydrogenase
FAD	flavin adenine dinucleotide
FMN	flavin mononucleotide
LDH	lactate dehydrogenase
NAD(P)	nicotinamide adenine dinucleotide (phosphate)
PQQ	pyrroloquinoline quinone
TOF	turnover frequency
TON	turnover number
TTN	total turnover number

References

1 Liese, A., Lütz, S, in: *Ullmann's Encyclopedia of Industrial Chemistry*, Electronic Release; 7th edn. Wiley-VCH, Weinheim, **2004**.
2 Straathof, A. J. J., Panke, S., Schmid, A., *Curr. Opin. Biotechnol.* **2002**, *13*, 548.
3 Vasic-Racki, D., Jonas, M., Wandrey, C., Hummel, W., Kula, M. R., *Appl. Microbiol. Biotechnol.* **1989**, *31*, 215.
4 Kragl, U., Vasic-Racki, D., Wandrey, C., *Ind. J. Chem.* **1993**, *32*, 103.
5 Bommarius, A. S., Schwarm, M., Drauz, K., *J. Mol. Catal. B-Enzym.* **1998**, *5*, 1.
6 Crocq, V., Masson, C., Winter, J., Richard, C., Lemaitre, Q., Lenay, J., Vivat, M., Buendia, J., Prat, D., *Organic Process Res. & Dev.* **1997**, *1*, 2.
7 Findrik, Z., Vasic-Racki, D., Lütz, S., Daussmann, T., Wandrey, C., *Biotechnol. Lett.* **2005**, *27*(15), 1087.
8 Kruse, W., Hummel, W., Kragl, U., *Recl. Trav. Chim. Pays-B* **1996**, *115*, 239.

9 Liese, A., Karutz, M., Kamphuis, J., Wandrey, C., Kragl, U., *Biotechnol. Bioeng.* **1996**, *51*, 544.
10 Liese, A., Zelinski, T., Kula, M.R., Kierkels, H., Karutz, M., Kragl, U., Wandrey, C., *J. Mol. Catal. B-Enzym.* **1998**, *4*, 91.
11 Rissom, S., Beliczey, J., Giffels, G., Kragl, U., Wandrey, C., *Tetrahedron Asymmetry* **1999**, *10*, 923.
12 Röthig, T.R., Kulbe, K.D., Buckmann, F., Carrea, G., *Biotechnol. Lett.* **1990**, *12*, 353.
13 Fang, J.M., Lin, C.H., Bradshaw, C.W., Wong, C.H., *J. Chem. Soc., Perkin Trans. 1* **1995**, 967.
14 Roberts, S.M., *J. Chem. Soc., Perkin Trans. 1* **2000**, 611.
15 Liese, A., Seelbach, K., Wandrey, C., *Industrial Biotransformations*, 1st edn. VCH, Weinheim, **2000**.
16 Voet, D., Voet, J., *Biochemistry*, 3rd edn. Wiley, New York, **2004**.
17 Wichmann, R., Vasic-Racki, D., in: *Advances in Biochemical Engineering/Biotechnology: Technology Transfer in Biotechnology: From Lab to Industry to Production*, **2005**; Vol. 92, p. 225.
18 www.juelich-chemicals.de.
19 Kula, M.R., Kragl, U., in: Patel, R.N. (Ed.), *Stereoselective Biocatalysis*. Marcel Dekker, New York, **2000**, p. 839.
20 Stewart, J.D., *Curr. Org. Chem.* **1998**, *2*, 195.
21 Whitesides, G.M., Wong, C.H., Pollak, A., *ACS Symposium Series* **1982**, *185*, 205.
22 Wichmann, R., Wandrey, C., Buckmann, A.F., Kula, M.R., *Biotechnol. Bioeng.* **2000**, *67*, 791.
23 Adlercreutz, P., *Biocatal. Biotransform.* **1996**, *14*, 1.
24 Mertens, R., Liese, A., *Curr. Opin. Biotechnol.* **2004**, *15*, 343.
25 Mertens, R., Greiner, L., van den Ban, E.C.D., Haaker, H., Liese, A., *J. Mol. Catal. B-Enzym.* **2003**, *24-5*, 39.
26 Rakhely, G., Zhou, Z.H., Adams, M.W.W., Kovacs, K.L., *Eur. J. Biochem.* **1999**, *266*, 1158.
27 Silva, P.J., de Castro, B., Hagen, W.R., *J. Biol. Inorganic Chem.* **1999**, *4*, 284.
28 Rodriguez, S., Schroeder, K.T., Kayser, M.M., Stewart, J.D., *J. Org. Chem.* **2000**, *65*, 2586.
29 Stewart, J.D., *Curr. Opin. Biotechnol.* **2000**, *11*, 363.
30 Ernst, M., Kaup, B., Muller, M., Bringer-Meyer, S., Sahm, H., *Appl. Microbiol. Biotechnol.* **2005**, *66*, 629.
31 Steckhan, E., *Top. Curr. Chem.* **1994**, *170*, 83.
32 Hollmann, F., Schmid, A., *Biocatal. Biotransform.* **2004**, *22*, 63.
33 Hollmann, F., Witholt, B., Schmid, A., *J. Mol. Catal. B-Enzym.* **2002**, *19*, 167.
34 Ruppert, R., Herrmann, S., Steckhan, E., *J. Chem. Soc. Chem. Commun.* **1988**, 1150.
35 Steckhan, E., Herrmann, S., Ruppert, R., Dietz, E., Frede, M., Spika, E., *Organometallics* **1991**, *10*, 1568.
36 Steckhan, E., Herrmann, S., Ruppert, R., Thommes, J., Wandrey, C., *Angew. Chem.-Int. Ed. Engl.* **1990**, *29*, 388.
37 Lo, H.C., Fish, R.H., *Angew. Chem. Int. Ed.* **2002**, *41*, 478.
38 Lo, H.C., Leiva, C., Buriez, O., Kerr, J.B., Olmstead, M.M., Fish, R.H., *Inorg. Chem.* **2001**, *40*, 6705.
39 Hollmann, F., Schmid, A., Steckhan, E., *Angew. Chem. Int. Ed.* **2001**, *40*, 169.
40 Steckhan, E., Arns, T., Heineman, W.R., Hilt, G., Hoormann, D., Jorissen, J., Kroner, L., Lewall, B., Pütter, H., *Chemosphere* **2001**, *43*, 63.
41 Vuorilehto, K., Lütz, S., Wandrey, C., *Bioelectrochemistry* **2004**, *65*, 1.
42 Delecouls-Servat, K., Basseguy, R., Bergel, A., *Chem. Eng. Sci.* **2002**, *57*, 4633.
43 Delecouls-Servat, K., Basseguy, R., Bergel, A., *Bioelectrochemistry* **2002**, *55*, 93.
44 Morera, S., Guadalupe, A.R., *Abstracts Papers Am. Chem. Soc.* **2002**, *223*, U197.
45 Abril, O., Whitesides, G.M., *J. Am. Chem. Soc.* **1982**, *104*, 1552.
46 Hembre, R.T., Wagenknecht, P.S., Penney, J.M., patent application US6599723, **2003**.
47 Wagenknecht, P.S., Penney, J.M., Hembre, R.T., *Organometallics* **2003**, *22*, 1180.
48 Bhaduri, S., Mathur, P., Payra, P., Sharma, K., *J. Am. Chem. Soc.* **1998**, *120*, 12127.

49 Hilt, G., Lewall, B., Montero, G., Utley, J. H. P., Steckhan, E., *Liebigs Ann.-Recl.* **1997**, 2289.
50 Hilt, G., Steckhan, E., *J. Chem. Soc. Chem. Commun.* **1993**, 1706.
51 Hilt, G., Jarbawi, T., Heineman, W. R., Steckhan, E., *Chem. Eur. J.* **1997**, *3*, 79.
52 Willner, I., Maidan, R., Shapira, M., *J. Chem. Soc. Perkin Trans. 2* **1990**, 559.
53 Wienkamp, R., Steckhan, E., *Angew. Chem. Int. Ed. Engl.* **1983**, *22*, 497.

44
Catalyst Inhibition and Deactivation in Homogeneous Hydrogenation

Detlef Heller, André H. M. de Vries, and Johannes G. de Vries

44.1
Introduction

The cost of the catalysts represents a major hurdle on the road to the industrial application of homogeneous catalysis, and in particular for the production of fine chemicals [1, 2]. This is particularly true for chiral catalysts that are based on expensive metals, such as rhodium, iridium, ruthenium and palladium, and on chiral ligands that are prepared by lengthy total syntheses, which often makes them more expensive than the metals. In spite of this, the number of large-scale applications for these catalysts is growing. Clearly, these can only be economic if the substrate : catalyst ratio (SCR) can be very high, often between 10^3 and 10^5.

Unfortunately, systematic knowledge on how to increase the rate of a certain catalytic reaction is lacking. In each case, it will be necessary to conduct research related to the kinetics of the reaction in order to determine the identity of the rate-determining step. Once this is known, it may be possible to speed up the catalysts by making directed changes. Nevertheless, a few handles are known in homogeneous hydrogenation based on kinetic considerations (see, for example, Chapter 10). In most hydrogenation reactions the reaction is first order in hydrogen, which means that the oxidative addition of hydrogen is the rate-determining step. Since the metal oxidation state increases in this step, it may be possible to accelerate it by increasing electron density on the catalysts, for example by changing from aryl to the more electron-donating alkyl-substituted phosphine ligands. The anion effect may also be profound: for example cationic complexes of rhodium are faster than neutral ones in most cases [3]. Other parameters which influence the reaction rate include: solvent, hydrogen pressure, and steric factors, which may require fine-tuning of the ligand for each particular reaction.

Arguably the best way to accelerate the rate of a reaction catalyzed by a soluble transition metal catalyst is by preventing deactivation of the catalyst. Most chemists who have investigated the kinetics of transition metal-catalyzed reactions are familiar with kinetic curves that shoot off with dazzling speed during

The Handbook of Homogeneous Hydrogenation.
Edited by J. G. de Vries and C. J. Elsevier
Copyright © 2007 WILEY-VCH Verlag GmbH & Co. KGaA, Weinheim
ISBN: 978-3-527-31161-3

the first few minutes, but rapidly curve off to reach a steady speed that is may be only a fraction of the initial rate. If only it were possible to maintain this initial speed. What is happening to these catalysts? In this chapter we will attempt to answer this question for homogeneous hydrogenation reactions, by describing in some detail all known causes of catalyst inhibition and deactivation.

44.2 Mechanisms of Catalyst Inhibition

All known inhibition phenomena are related to some change at the level of the metal complex structure. In this respect, a number of different general phenomena can be discerned:

- Induction periods. In most hydrogenation reactions the chemist will either start with a preformed complex or with a catalyst that is prepared *in situ* from a metal precursor and the ligand. Usually, both types of catalysts need to undergo further change before they can enter the catalytic cycle. In hydrogenation it is often a diene ligand that needs to be removed by hydrogenation, but this may be a surprisingly slow step (as will be discussed later).
- Substrate and product inhibition. Few academic researchers are familiar with this phenomenon as they usually run their hydrogenations at low substrate concentrations and low SCR. However, for industrial applications the space–time yield of a reaction – the amount of product per unit reactor volume per time unit – is quite important. Clearly, the higher the substrate concentration the higher the space–time yield and the more economic the process. More often than not, either substrate or product inhibition becomes a problem when the substrate concentration is increased to 10 wt% or more.
- Reversible inhibition caused by materials that can function as ligand. Many compounds will bind to a metal; this might be the solvent or impurities in the substrate or the solvent. It can also be a functional group in the substrate or the product, such as a nitrile. Too many ligands bound to the metal complex may lead to inhibition of one of the steps in the catalytic cycle. Likely candidates are formation of the substrate–catalyst complex or the oxidative addition of hydrogen. Removal of the contaminant will usually restore the catalytic activity.
- Irreversible inhibition or deactivation of the catalyst. There may be many reasons for this. A very common one is formation of dimers, trimers or higher clusters that are much less active than the original catalyst. This can be precipitated by ligand loss or by the presence of bridging ligands, such as water, halide, or acetate. Other causes may be oxidants or just thermal decomposition. The end point of this process may be bulk metal, which is still an active hydrogenation catalyst, although it may be less active than the homogeneous complex where every metal atom participates in the reaction. In many processes, a lack of substrate may lead to catalyst decomposition; for this reason catalyst recycling is not always possible.

Usually, the inhibition is detected by kinetic measurements. Substrate and product inhibition are easily detected by measuring the rate as function of substrate concentration, or by carrying out the hydrogenation in the presence of varying amounts of product. Suspected poisons can be added and their effect on the rate measured. Extensive purification of substrate, ligand, catalysts precursor and solvent, and comparing rates between pure and impure reactants will also help to pinpoint the culprit. In industrial productions the number of purifications is usually kept to a minimum to save costs. Nevertheless, it is best to plan the total synthesis in such a way that purification can be executed before the hydrogenation step. Spectroscopic investigation of the catalyst at the end or even during the reaction can be extremely helpful to determine the cause of deactivation. Increasingly, modern mass spectroscopy techniques such as MALDI and electrospray mass spectrometry (EMS) are used for this purpose.

44.3 Induction Periods

44.3.1 Introduction

The "active species" mediating a catalytic process usually are highly reactive as a result of the presence of labile ligands or free coordination sites. Due to this high reactivity, the "active species" are generally difficult to handle and thus are not directly applicable as catalysts. Thus, the actual catalyst is often employed in a modified form, the precatalyst. This can in many cases be accomplished by the use of a stabilizing ligand. Such ligands include dienes such as 1,5-cyclooctadiene (COD) or 2,5-norbornadiene (NBD) [4], ethylene, but also α,ω-dienes such as 1,5-hexadiene [5] and 1,6-heptadiene [6], and CO.

Various methods have been used to convert precatalysts into the active species [7]. Ethylene can be easily displaced from the central atom of the corresponding complexes in solution, even at room temperature. CO-ligands in carbonyl complexes can conveniently be removed photochemically [8]. Increasing the temperature is a further common method used to labilize precatalysts with respect to stabilizing ligands [9].

However, these stabilizing ligands are not always kinetically innocent. The influence of the diene ligands of cationic Rh-complexes on catalytic activity in asymmetric hydrogenation was quantitatively investigated by Heller et al. [10]. These results will be discussed in more detail in view of the ubiquity of the use of catalyst precursors containing diene ligands in enantioselective hydrogenation [11].

44.3.2
Induction Period Caused by Slow Hydrogenation of COD or NBD

In enantioselective hydrogenation, complexes of the type [Rh(PP*)(diene)]anion (PP* = chelating chiral ligand; e.g., a bisphosphine) are often employed as the precatalyst. In addition, the so-called "in-situ" technique, whereby the hydrogenation is simply carried out by applying hydrogen pressure to a solution containing a catalyst precursor such as $[Rh(diene)_2]$anion, a chiral ligand and the substrate, is also conventional. Sometimes, catalyst precursor and ligand are stirred for a while before addition of substrate. Evaporation of this solution will remove one equivalent of the diene. According to Brunner, approximately half of the investigations of enantioselective hydrogenations with the model substrate (*Z*)-*N*-2-acetamido-cinnamic acid are accomplished with catalysts prepared *in situ* [12].

The comparison of hydrogen consumption in the rhodium-catalyzed enantiomeric hydrogenation of a *β*-dehydroamino acid using Et-Duphos (Et-DuPHOS = 1,2-bis(2,5-diethyl-phospholanyl)benzene)) as the chiral ligand shows the huge differences in rate, depending on the manner in which the catalyst was prepared (Fig. 44.1) [10b, c].

In spite of equal product enantioselectivities of 86.5%, the three methods clearly differ in rate. Noticeable *induction periods* are apparent upon the use of

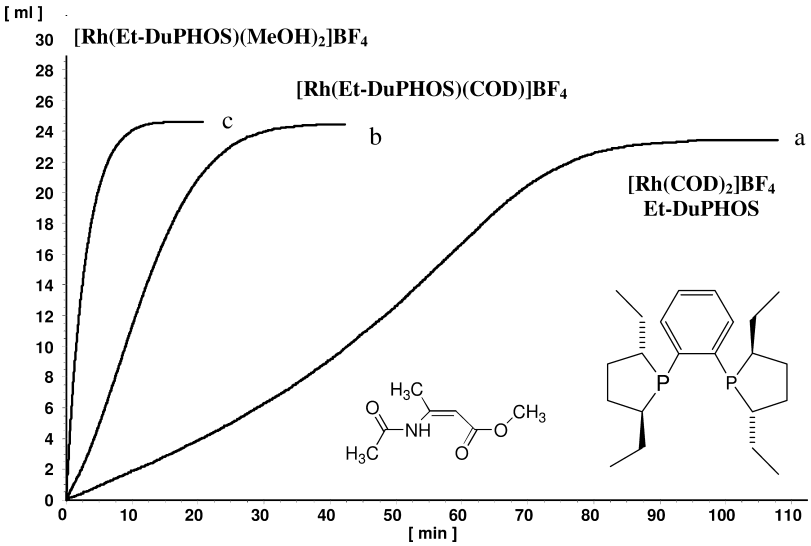

Fig. 44.1 Different methods for the hydrogenation of methyl-3-acetamido butenoate with Et-DuPHOS. Curve a: in-situ technique ($[Rh(COD)_2]BF_4$ + Et-DuPHOS). Curve b: application of the commercial COD precatalyst ($[Rh(Et\text{-}DuPHOS)(COD)]BF_4$). Curve c: as the solvent complex ($[Rh(Et\text{-}DuPHOS)(MeOH)_2]BF_4$). Reaction conditions for each case: 0.01 mmol catalyst, 1.0 mmol substrate, 15.0 mL MeOH, 1.0 bar total pressure, 25.0 °C.

[Rh(Et-DuPHOS)(COD)]BF_4, and even more when applying the in-situ technique. In both cases, there is still COD detectable in solution even after hydrogenation of the substrate has gone to completion. These induction periods have now been shown to occur with various substrates, chiral ligands (several chelate ring sizes were investigated), dienes, and also solvents [10]. The end of the induction period is rather clearly indicated as a maximum in the rate profile. For the right curve of Fig. 44.1 (*in-situ* catalyst), this is shown in Fig. 44.2.

In the literature it has been generally assumed that hydrogenation of the "spectator" dienes with cationic Rh(I)-complexes [13] proceeds rapidly before the hydrogenation of the prochiral alkene. These induction periods, which were found in many hydrogenation reactions, however, prove without doubt the slower hydrogenation of the dienes.

The two most frequently applied dienes COD and NBD differ significantly with regard to the observed induction periods. In Fig. 44.3, the hydrogen uptake curves are shown for the enantioselective hydrogenation of methyl (*Z*)-2-acetamido-cinnamate using Et-Duphos as ligand employing the two different diene complexes in comparison with the solvent complex. Clearly, the norbornadiene is hydrogenated off much faster in this case.

These induction periods, which have also been described qualitatively by others [14], considerably complicate a comparison of the activity of various catalysts and a kinetic analysis of the hydrogen consumption curve.

Further proof for the fact that these induction periods are caused by slow hydrogenation of the diene ligand was obtained by NMR-spectroscopic measurements under hydrogenation conditions [10f, 15]. The registration of ^{31}P- *and* ^{1}H-spectra allows the simultaneous monitoring of changes in the bisphosphine complexes and substrate conversion. The results of the hydrogenation of methyl-

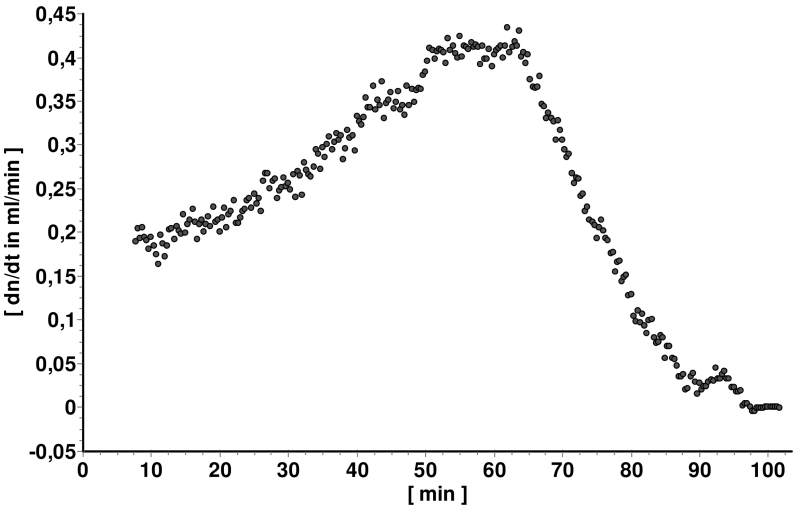

Fig. 44.2 Rate profile for the right curve of Fig. 44.1.

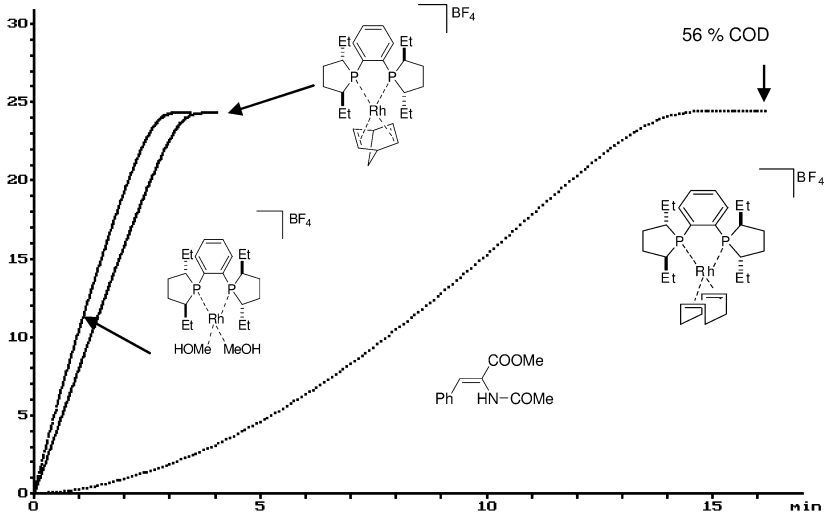

Fig. 44.3 Comparison of hydrogenation rates using various Rh–DuPhos-complexes containing different "spectator" ligands.

(*Z*)-2-acetamido cinnamate with a five-membered ring chelate catalyst based on DIPAMP are illustrated graphically in Fig. 44.4 (see also [10d]).

The results of this experiment prove unequivocally that, in addition to the substrate complex, the diene complex is present throughout the hydrogenation reaction. Even after 500 turnovers of the prochiral alkene, unchanged COD precatalyst is still present in solution.

In order to circumvent these induction periods and to allow full utilization of the "intrinsic activity" of a catalyst, one can best use the corresponding solvent complexes, as was practiced previously by Halpern et al. [16]. This invokes the practical problem of for how long the precatalyst must be prehydrogenated to remove all diene. To answer this question, the rate constants for hydrogenation of the diene in the diene complexes have been determined with various ligands, dienes, and solvents. As a result of the generally high stability constants of the diene complexes, the diene hydrogenation under isobaric conditions can be described as a pseudo-first-order reaction. This highly selective hydrogenation can be analyzed both in the presence of an excess of diene – Michaelis-Menten kinetics in the saturation range – and as stoichiometric hydrogenation of the precatalysts. For the latter hydrogenation, NMR spectroscopy is the most suitable analysis tool [10a]. In order to determine the rate constants for the diene hydrogenation, use of the first method was found to be best.

In Table 44.1 selected rate constants for the hydrogenation of the dienes COD and NBD for various ligands (chiral and achiral) are summarized. As expected, for all systems investigated, the hydrogenation of NBD was faster than the hydrogenation of COD [13a,c, 17].

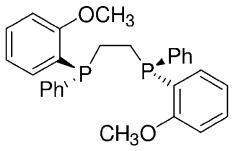

DIPAMP

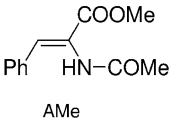

AMe

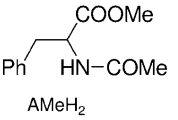

$AMeH_2$

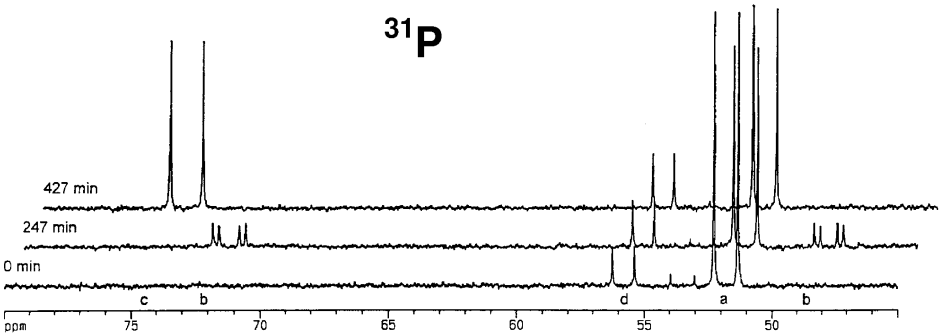

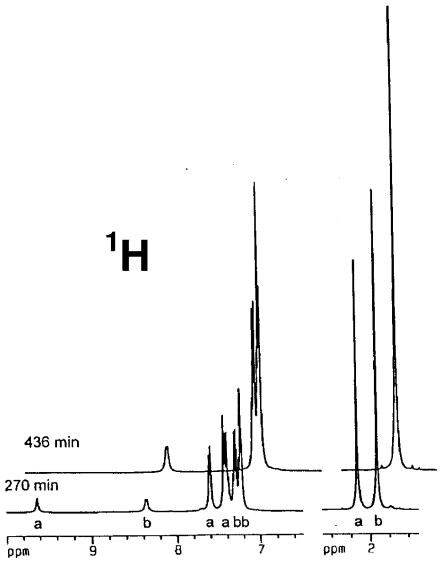

Fig. 44.4 NMR-spectroscopic monitoring of the enantioselective hydrogenation of (*Z*)-*N*-acetylamino methyl cinnamate using [Rh((*R*,*R*)-DIPAMP)(COD)]BF_4 as catalyst under stationary conditions (reaction conditions: 0.01 mmol Rh-complex, 5.0 mmol prochiral alkene; 5.0 mL methanol-methanol-d_4 (1:1); details can be found in [10f]). Legend for ^{31}P-NMR: a: [Rh(DIPAMP)(COD)]BF_4; b: [Rh(DIPAMP)(AMe)]BF_4; c: [Rh(DIPAMP)$(MeOH)_2$]BF_4; d: [Rh$(DIPAMP)_2$]BF_4. Legend for ^{1}H-NMR: a: AMe; b: $AMeH_2$.

Table 44.1 Rate constants (k_{2j}) (for the hydrogenation of the dienes COD and NBD for different ring chelates of the type [Rh(ligand)(diene)]BF_4. (Reaction conditions: 25.0 °C; 1.013 bar total pressure. Values were obtained in MeOH as solvent unless stated otherwise.)

Ligand	$k_{2\,COD}$ [1 min^{-1}]	$k_{2\,NBD}$ [1 min^{-1}]	$k_{2\,NBD}/k_{2\,COD}$	Reference
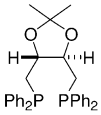	0.23 0.22 [a)] 0.25 [e)]	1.29	5.6	10g
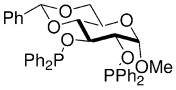	0.37 0.37 [a)]	13.40	36.2	10g
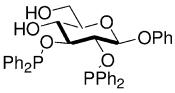	0.20 0.19 [a)]	9.52 47.6		10g
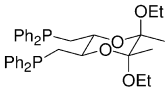	0.14	1.11	7.9	10g
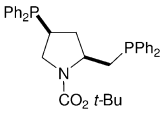	0.22	1.20	5.5	10g
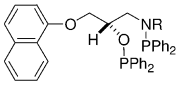				
R = cyclohexyl	5.44 2.63 [e)]	20.17	3.7	10g
R = 3-pentyl	4.09	21.48	5.3	
R = 2-propyl	3.77	21.96	5.8	
R = cyclopentyl	2.94	18.40	6.3	
R = methyl	0.53	8.20	15.5	

Table 44.1 (continued)

Ligand	$k_{2\ COD}$ [l min^{-1}]	$k_{2\ NBD}$ [l min^{-1}]	$k_{2\ NBD}/k_{2\ COD}$	Reference
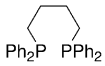	0.16	1.25	7.8	10g
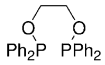	0.25	16.6	66	10d
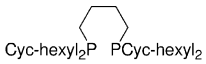	7.15	230	32	10d
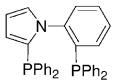	0.33	33.7	98	10d
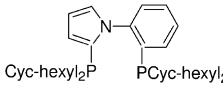	1.1	at least 700[b)]	at least 630[b)]	10d
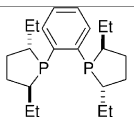	≈ 0.014[c)]	52	≈ 3700	10d
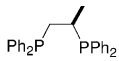	≈ 0.003[c)]	9.2	≈ 3000	10d
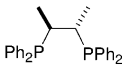	≈ 0.0018[c)]	3	≈ 1700	10d
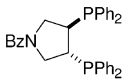	≈ 0.0017[d)]	–	–	18
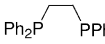	≈ 0.002–0.0035[c)]	17.3	≈ 4800	10d
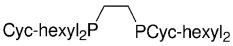	0.075	48.8	650	10d
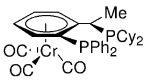	≈ 0.03	3.6 4.8[e)]	≈ 120	10a

Table 44.1 (continued)

Ligand	$k_{2\ COD}$ [l min^{-1}]	$k_{2\ NBD}$ [l min^{-1}]	$k_{2\ NBD}/k_{2\ COD}$	Reference
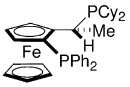	–	≈ 33	–	10a
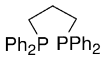	0.024	1.55	65	10d

a) From the initial rate of the stoichiometric catalyst hydrogenation.
b) In view of the high activity at the chosen catalyst concentration, mass transfer limitations cannot be excluded.
c) Values were determined in an autoclave under pseudoisobaric conditions and standardized to 1.013 bar total pressure. Thus, these are indicative values only. For that reason, the ratios $k_{2\,NBD}/k_{2\,COD}$ are only guide values.
d) From a parameter optimization of experimental hydrogenations at 10 bar H_2 pressure, standardized to 1.013 bar.
e) Value obtained in THF.

With NBD as diene, the rate constants for the listed ligands may differ by a factor of 600. For COD, the analogue difference approximately amounts to three orders of magnitude. A comparison of the reactivities of the respective NBD and COD complexes of five-membered chelates in diene hydrogenation clearly reveals higher differences than are found for the six- and seven-membered chelates. The reasons behind these differences are unclear, although when examining the published X-ray structures it would seem that the generally less active COD complexes all have a larger tetrahedral distortion from the expected square–planar structure than the structures of the corresponding NBD complexes [19].

Few data are available for rhodium complexes based on monodentate ligands. In a recent study, the rate of COD hydrogenation in $Rh(MonoPhos)_2(COD)BF_4$ was determined as 0.071 min^{-1}, which is somewhat slower than the corresponding DuPhos complex [20].

An interesting methodology to evaluate whether different diene catalyst precursors vary in their diene hydrogenation activity was reported by McCague et al. [21]. Two diene complexes based on different dienes are simply mixed in the ratio 1 : 1, though each complex contains the chiral ligand with the opposite configuration. The higher the ee-value of the resulting hydrogenations, the more the employed dienes differ in their hydrogenation activity. However, obtaining a racemate does not exclude the possibility that dienes do not interfere with the enantioselective hydrogenation; it merely proves that the dienes behave in an analogous manner.

Blackmond and Reetz have reported a case where two rhodium-containing diastereomeric bisphosphite ligands were compared [22]. In spite of the great

similarity of the two catalysts, huge differences in rate profile were observed, which were largely due to slow hydrogenation of the COD in one of the two complexes when compared to the other (Fig. 44.5).

In summary, the induction period observed in the enantioselective hydrogenation of prochiral alkenes is caused by a slow hydrogenation of the diene introduced into the system as part of the precatalyst. This interfering parallel hydrogenation of the dienes is influenced by several factors: the pseudo-rate constants $k_{2\,COD}$ and $k_{2\,NBD}$, the Michaelis constant of the diene complex, the Michaelis constant of the prochiral alkene, and the precatalyst : substrate ratio. The method of catalyst formation also plays an important role; the amount of interfering diene is doubled compared to the preformed complex if the catalytic solutions are prepared *in situ*. It should be stressed, however, that these induction periods are particularly important at 1 bar hydrogen pressure. At higher pressures the diene hydrogenation tends to be very fast and the induction periods become less pronounced.

The published quantification of the rate of hydrogenation of the dienes COD and NBD of a large number of cationic rhodium(I) chelate complexes allows a good estimation of expected effects on the rate of enantioselective hydrogenation of prochiral alkenes. From the first-order pseudo-rate constants the time needed for complete hydrogenation of the diene introduced as part of the rhodium precursor can be easily calculated as six- to seven-fold the half life. It is recommended that the transfer into the solvent complex be followed by NMR spectroscopy.

It should be noted that dienes and polyenes in general are well known to be catalyst poisons. Apart from the catalyst, the source of these inhibitors may stem from the solvent or, more frequently, from the substrate [23].

Crabtree described the use of dibenzo[a,e]cyclooctatetraene, a potent selective poison of homogeneous hydrogenation catalysts, as a tool to distinguish between homogeneous and heterogeneous catalysis in the hydrogenation of hexene with a range of catalysts [24].

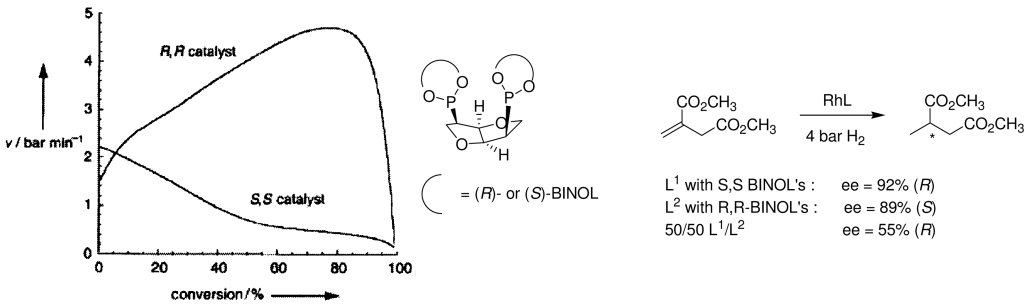

Fig. 44.5 Differences in rate profile between diastereomeric catalysts are caused by differences in the COD hydrogenation rate.

If an induction period is observed in hydrogenation reactions due to slow hydrogenation of the diene, a number of solutions are available. First, it is wise to preform the catalyst by adding the ligands to a solution of the catalyst precursor. By doing this the first equivalent of diene is displaced from the metal by the ligand(s). Evaporation of this solution will remove the first equivalent of diene. Pre-hydrogenation of the catalyst before addition of the substrate will remove the second diene. However, sometimes the solvent-stabilized complex formed by doing this is less stable. With rhodium catalysts based on monodentate ligands that function best in the poorly coordinating solvent dichloromethane, this procedure is not recommended. Finally, increasing the pressure usually minimizes the induction period to a large extent.

44.4 Substrate and Product Inhibition

For hydrogenation to take place, the substrate usually needs to bind to the metal complex, although exceptions are known to this rule [25]. Substrate inhibition can occur in a number of ways, for example if more than one molecule of substrate binds to the metal complex. At low concentration this may be a minor species, whereas at high substrate concentration this may be the only species. One example of this is the hydrogenation of allyl alcohol using Wilkinson's catalyst. Here, the rate dependence on the substrate concentration went through a maximum at 1.2 mmol L^{-1}. The authors propose that this is caused by formation of a complex containing two molecules of allyl alcohol (Scheme 44.1) [26].

However, it should be noted that the authors did not isolate or characterize any intermediates. It is unclear as to whether this would be the case if highly stable π-allyl complexes were to have been involved.

Vedejs et al. reported catalyst inhibition during a study on the enantioselective transfer hydrogenation of dihydro-isoquinolines using Noyori's catalyst (Scheme 44.2) [27]. Here, the problem is caused by the bidentate nature of the substrate. Whereas the bromo compound **1a** could be rapidly reduced, the tosylamide-substituted compound **1b** could not be reduced, and although the problem could be alleviated somewhat by alkylation of the sulfinamide to **1c**, hydrogenation of this was still sluggish. Although the authors propose this to be a case of product

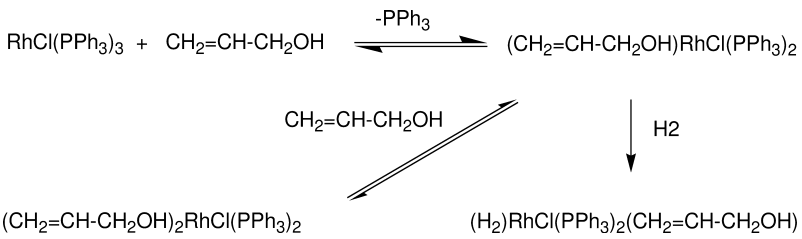

Scheme 44.1 Substrate inhibition in the hydrogenation of allyl alcohol.

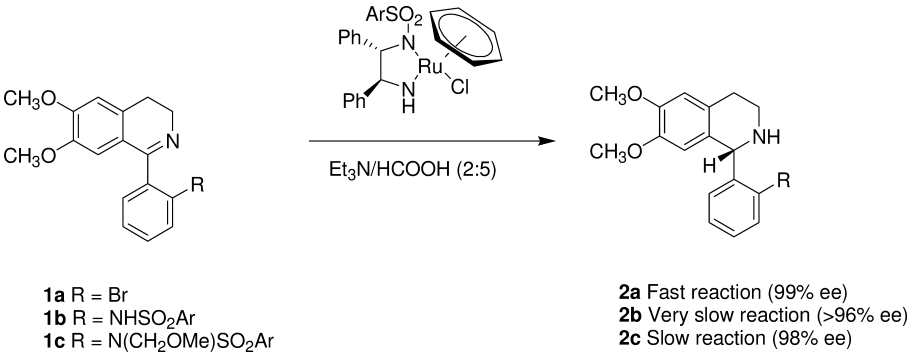

Scheme 44.2 Catalyst inhibition caused by functional groups in the substrate.

inhibition, both substrate and product could be possible inhibitors in the case of **1b** and **1c**.

Carpentier and coworkers studied the asymmetric transfer hydrogenation of β-ketoesters using chiral ruthenium complexes prepared from $[(\eta^6\text{-}p\text{-cymene})\text{-}RuCl_2]_2$ and chiral aminoalcohols based on norephedrine. During this study, these authors became aware of substrate inhibition when ketoesters carrying 4-halo-substituents were used. It transpired that this was caused by formation of a complex between the substrate and the catalyst [28].

Since analogous ketoesters not containing halide could be hydrogenated in good yield, the acidity of the enolate seems to be the main reason for the replacement of the aminoalcohol ligand by the halogenated acetoacetate. Indeed,

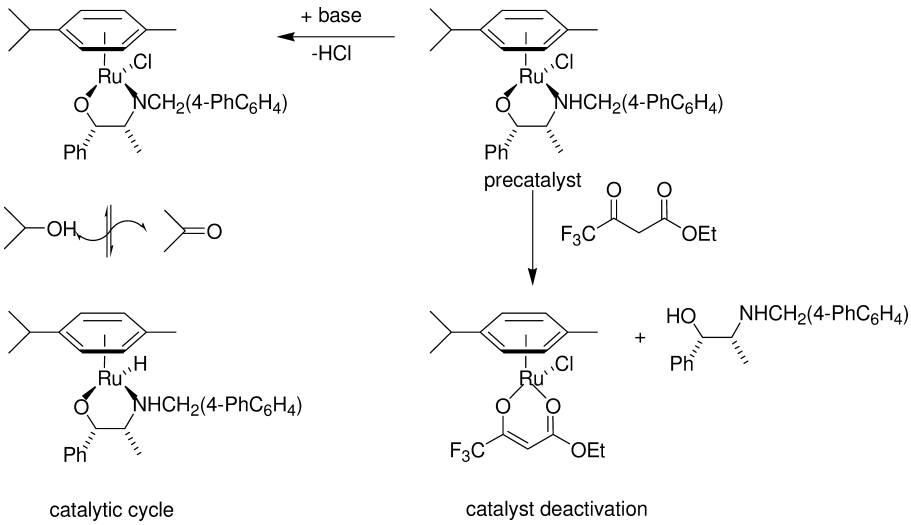

Scheme 44.3 Substrate inhibition in enantioselective transfer hydrogenation.

it is our own experience that Ru-catalyzed transfer hydrogenation reactions are easily inhibited by the addition of acid.

The use of $RuCl_3$ with the water-soluble ligand tris-sulfonated triphenylphosphine (TPPTS) made it possible to selectively hydrogenate cinnamaldehyde to cinnamyl alcohol in a two-phase aqueous organic system (Fig. 44.6, upper). This not only allowed easy recycling of the catalyst by phase separation; it also resulted in extremely high selectivity to the desired unsaturated alcohol [29]. Unfortunately, the cinnamaldehyde hydrogenation was not sufficiently economic as product inhibition occurred at higher concentrations of cinnamaldehyde (Fig. 44.6, lower) [30].

The fate of the catalyst in these reactions was determined by Kalck and coworkers using ^{31}P-NMR [31]. In addition to $[RuH(TPPTS)_3Cl]$, which is the

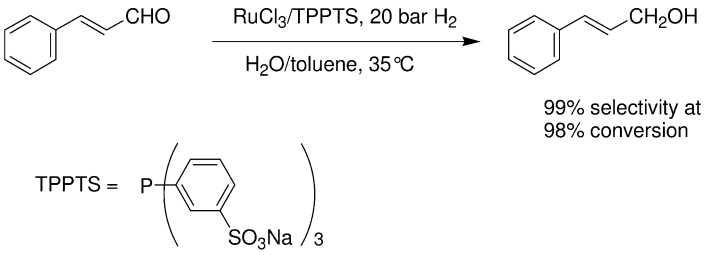

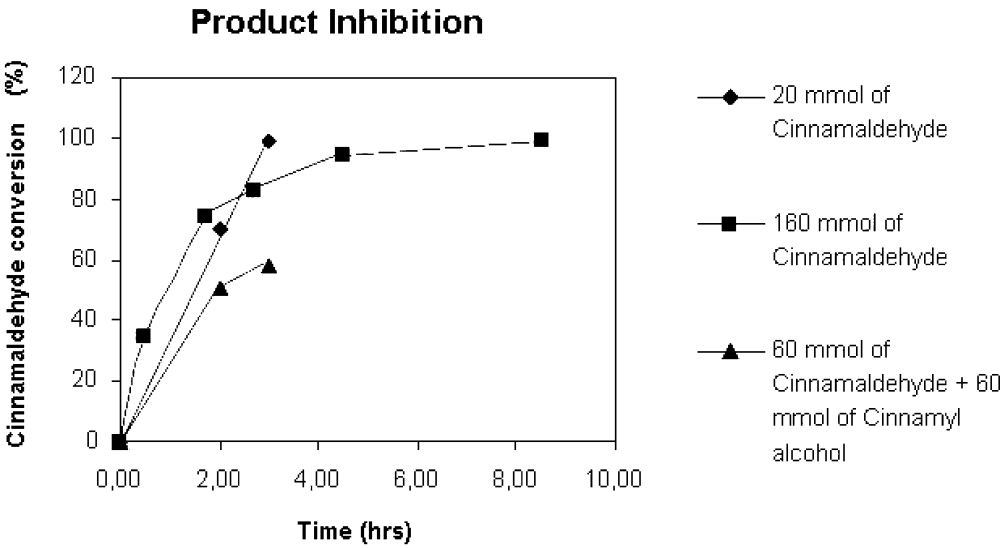

Fig. 44.6 Product inhibition in the ruthenium-catalyzed hydrogenation of cinnamaldehyde. Reaction conditions: 0.1 mmol $RuCl_3$, 0.5 mmol TPPTS, H_2O:toluene ratio 5 mL:5 mL.

probable catalyst, these authors identified three species with the general structure $[RuH(\eta^6\text{-}R\text{-}C_6H_5)(TPPTS)_2]Cl$ that were not catalytically active. A species with $R = CH_3$ obviously stems from the solvent. The other two species with $R = cis\text{-}PhCH{=}CHCH_2OH$ and $PhCH_2CH_2CH_2OH$ stem from isomerized starting material and over-hydrogenated product. The fact that no complex containing *trans*-cinnamyl alcohol was found probably means that the two aromatic fragments are bound in a bidentate fashion through η^6 coordination with the aromatic ring and with the oxygen atom, which is impossible with the *trans*-substrate.

Joó found substrate inhibition in the transfer hydrogenation of aliphatic and aromatic aldehydes with NaO_2CH if the reaction was catalyzed by $[RuCl_2(PPh_3)_3]$ in the presence of a phase-transfer catalyst (PTC) in an organic solvent. Joó found that the reaction became much less sensitive to the substrate concentration if it was carried out under genuine biphasic conditions, without PTC using the water-soluble $[RuCl_2(m\text{-}TPPMS)_2]_2$ as catalyst. Here, the concentration of substrate in the aqueous phase is limited by its solubility, preventing the occurrence of substrate inhibition [32].

Substrates containing aromatics such as phenyl groups as a structural element may form relatively stable arene complexes with Rh-species. Using NMR spectroscopy, Gridnev and Imamoto determined that rhodium-η^6-complexes can form with the phenyl substituent of the hydrogenation product methyl-(*Z*)-2-acetamidocinnamate [33]. Bargon et al. described interesting complexes with styrene derivatives by means of the parahydrogen-induced polarization (PHIP) method [34].

Researchers at Merck & Co. [35] who, together with scientists from Solvias, had developed the enantioselective hydrogenation of unprotected enamine amides and esters [36], reported a more recent example of product inhibition. The product amine amide or ester was found to be an inhibitor of the catalyst, and indeed instances of catalyst poisoning by amines have been reported several times (see later). The authors also found an excellent solution to this problem: the addition of BOC-anhydride to the hydrogenation reaction neatly reacts away all the amine to form the BOC-protected amine, whereas the enamine was left unreacted (Scheme 44.4). This addition resulted in a remarkable rate enhancement [35].

James et al. reported a case of product inhibition in the Rh-catalyzed enantioselective hydrogenation of *N*-phenyl benzaldehyde imine [37]. These authors were able to isolate the deactivated catalyst, and to obtain its X-ray structure, which showed, surprisingly, that it was a rhodium complex with the product bound through a η^4-π-arene interaction (Scheme 44.5). More cases of inhibition via formation of metal arene complexes will be detailed in Section 44.5.

If substrates contain nitrogen bases capable of complexing to the metal, this usually has an adverse effect on the hydrogenation reaction. Döbler and coworkers found that enantioselective hydrogenation of (*Z*)-2-acylamino-3- and 4-pyridylacrylic acids using Rh/Propraphos did not proceed at room temperature and 1 bar H_2 pressure [38]. Drawing the obvious conclusion that this may be a

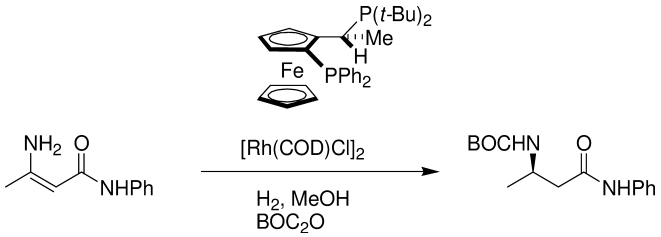

Scheme 44.4 Prevention of product inhibition via a secondary reaction.

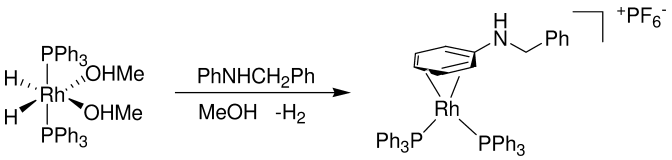

Scheme 44.5 Catalyst inhibition through formation of stable arene complex.

case of substrate inhibition caused by interaction between the pyridine and the rhodium complex, these authors performed the hydrogenation in the presence of excess HBF_4, which fully protonates the pyridine nitrogen. This had the desired effect, as now the hydrogenation of these substrates proceeded at very high rates at SCR = 1000. Similar findings were reported by Laneman et al., who used Rh/DuPHOS as a catalyst for these substrates. Here, the hydrogenation proceeded without protonation of the pyridine, but the rate of the reaction and the ee-value of the product were very low [39].

Nitrile groups in the substrate may also cause problems. Minnaard, Feringa and de Vries reported the enantioselective hydrogenation of a range of substituted 2-acetamido-cinnamates at 5 bar pressure using Rh/MonoPhos. Whereas most substrates could be hydrogenated with turnover frequencies (TOFs) of between 200 h^{-1} and 600 h^{-1}, the 4-cyano-substituted substrate was hydrogenated very slowly at this pressure with a TOF of only 4 h^{-1} [40].

A similar problem was noted by researchers from Pfizer and Dowpharma in their synthesis of (*S*)-3-aminomethyl-5-methylhexanoic acid (Pregabalin, **5**) via the enantioselective hydrogenation of an acrylonitrile-type substrate **3** (Scheme 44.6) [41].

The attempted hydrogenation of ester **3a** was problematic, as the reaction proceeded slowly at room temperature and although the rate could be increased by performing the reaction at 55 °C, the ee-value of the product remained low with a range of catalysts. The problem arises through the fact that the nitrile coordinates to the metal in a linear fashion with Rh–N–C aligned; this precludes the alkene from binding to the metal centrum in a bidentate fashion. The problem could be solved by instead using the carboxylate **3b** as its *tert*-butylammonium salt. The carboxylate binds to the metal allowing the alkene to coordinate also. Thus, **3b** could be hydrogenated at SCR = 2700 and 45 °C in 4 h. The product was isolated in 99% yield and 97.7% ee. Hydrogenation of the nitrile to the

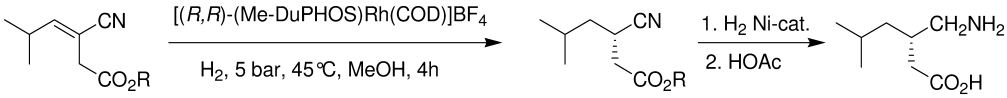

3 a R = Et
3 b R = *t*BuNH$_3$

4a 19 % ee
4b 97.7 % ee

5

Scheme 44.6 Overcoming inhibition by nitrile in enantioselective hydrogenation.

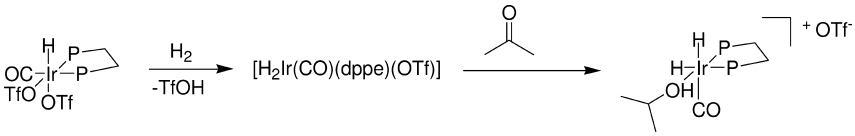

Scheme 44.7 Product inhibition in iridium-catalyzed acetone hydrogenation.

amine and neutralization with acetic acid gave Pregabalin in 61% yield and 99.8% ee.

Eisenberg reported product inhibition in the hydrogenation of acetone with a cationic iridium complex [42]. Apparently, the bond between iridium and isopropanol is too strong on account of the cationic nature of the complex (Scheme 44.7).

It may be concluded that substrate and product inhibition are the rule rather than the exception in scaled-up hydrogenation processes. Nevertheless, there are a number of ways to circumvent this problem. Two-phase catalysis may decrease the substrate and product concentration in the phase containing the catalyst to a large extent. Using a solvent in which substrate and product do not dissolve very well is an equally good solution. In case the substrate and product are solids, we speak of a "slurry hydrogenation". This has the added advantage that often the product crystallizes in a very pure form during the hydrogenation reaction. It may also be possible to slowly dose the substrate. Finally, if the problem is caused by a functional group in the substrate there are a number of ways to circumvent it by making changes either to the functional group in question or at positions nearby in the substrate.

44.5
Reversible Inhibition Caused by Materials that can Function as Ligand

Many compounds or materials are capable of binding in a reversible fashion to a transition metal complex. If the binding is very strong, or if a large excess of the compound is present, then inhibition is likely to result. Although many examples of this phenomenon have been reported in the literature, only a few have been studied systematically.

44.5.1
Catalyst Deactivation Caused by Solvents

Common solvents for homogeneous hydrogenations are simple alcohols, aromatic solvents such as toluene, THF, EtOAc, CH_2Cl_2, and also water. In some cases the solvent can become an inhibitor. In the preceding section, the formation of catalytically inactive complexes through the formation of a η^6-toluene complex with a ruthenium catalyst and a η^4-arene complex with a rhodium catalyst was described. Earlier, Halpern et al. highlighted the stability of Rh^I-η^6-aromatic complexes with chelating bisphosphines [43]. Likewise, Burk et al. recently showed that the hydrogenation of ethyl-α-benzoyloxycrotonate with the highly active Rh-Et-DuPHOS system does not proceed in benzene, although it does so in other solvents with high selectivity and activity. This inhibition is caused by formation of the inactive $[Rh(Et\text{-}DuPHOS)(benzene)]^+$-complex, which was characterized by ^{31}P-NMR spectroscopy [44, 45].

Crystal structures of stable arene complexes are also known, for example the benzene complex of (1*R*,2*R*)-*trans*-1,2-bis((diphenylphosphino)-methyl)cyclobutane-Rh^I [46], [Rh((*R*,*R*)-Et-DuPHOS)(benzene)]BF_4 (Fig. 44.7), and [Rh((*S*,*S*)-Me-DuPHOS)(toluene)]BF_4 [47].

These η^6-aromatic complexes are not easily spotted by routine NMR measurements, as ^{31}P-NMR data for aromatic and methanol complexes are very similar (Table 44.2). However, the two types of complexes can be distinguished unequivocally by using ^{103}Rh-NMR spectroscopy [48,49].

Due to the relative stability of such η^6-arene complexes there is a strong likelihood that in aromatic solvents only parts of the employed Rh-catalyst are available for catalysis. As seen earlier, substrates and products with aromatic substituents can also lead to catalyst deactivation.

In the hydrogenation of methyl-(*Z*)-β-(*N*-acetyl)-aminocrotonate with [Rh(DIPAMP)$(MeOH)_2$]BF_4, the decrease in activity due to addition of traces of aromatics to the solvent MeOH could be proven quantitatively. The concentration of the arene complex during the hydrogenation (as estimated from kinetic analyses) could be confirmed by NMR-spectroscopy (^{31}P and ^{103}Rh) (Figs. 44.8 and

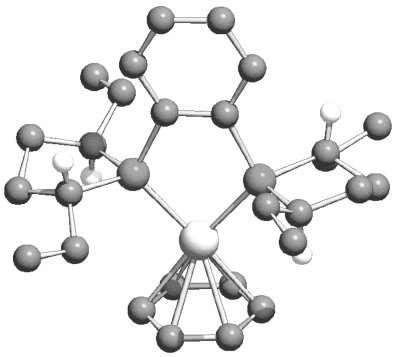

Fig. 44.7 The molecular structure of [Rh((*R*,*R*)-Et-DuPHOS)(benzene)].

Table 44.2 ^{31}P- and ^{103}Rh-NMR data for solvent-stabilized cations of the type [Rh(P-P)(solvent)]BF_4 in [D_4]methanol at 298 K [47].

Ligand (P-P)	Solvent	$\delta(^{31}P)$ [ppm]	$^1J(^{31}P,^{103}Rh)$ [Hz]	$\delta(^{103}Rh)$ [ppm]
Et-DuPHOS	η^6-benzene	93.0	202	–1116
	methanol	95.7	205	–149
Me-DuPHOS	η^6-toluene	99.3	202	–1139
	methanol	101.8	205	–218 [a)]
DIPAMP	η^6-benzene	72.2	207	–1006
	η^6-*p*-xylene	75.7	207	–956
	methanol	81.2	208	–38
Ph-*β*-glup-OH	η^6-toluene	136.4 and 134.8	228 and 228	–762
	methanol	147.6 and 142.9	229 and 226	–28

a) Value from Ref. [50].

44.9) [47]. From the ratio of initial rates (Fig. 44.8), the amount of inactive *p*-xylene complex present at the start of the hydrogenation was determined as 47%, while the corresponding NMR-spectrum (Fig. 44.9) gave a value of 50%.

Nevertheless, it should be pointed out that enantioselective hydrogenations also proceed in aromatic solvents. After all, the concentrations and ratios of stability constants of all complexes in solution decide the decrease in activity.

Another clear example is the hydrogenation of methyl-(*Z*)-*β*-(*N*-acetyl)-aminocrotonate with the Me-DuPHOS system in toluene as solvent: at 20 bar hydrogen pres-

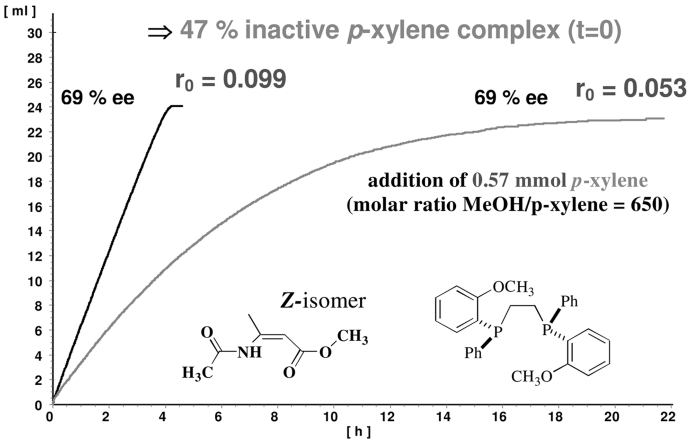

Fig. 44.8 Hydrogenation of methyl-(*Z*)-2-acetamidocrotonate in pure methanol (black) and after addition of 0.57 mmol *p*-xylene (gray). Reaction conditions: 0.01 mmol [Rh(DIPAMP)$(MeOH)_2$]BF_4, 1.0 mmol prochiral alkene, 1.0 bar overall pressure in 15.0 mL methanol at 25.0 °C; r_0 = initial rate (mL min^{-1}).

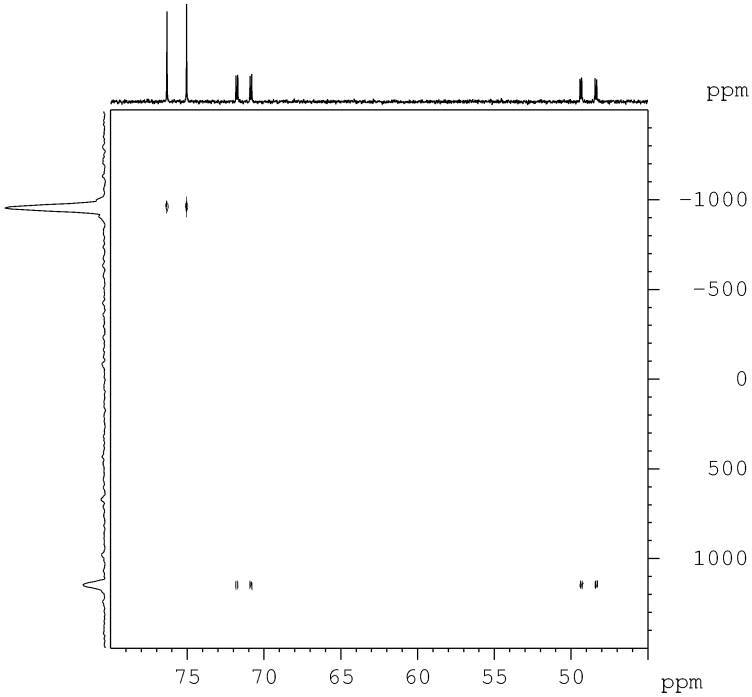

Fig. 44.9 $^{31}P,^{103}Rh\{^{1}H\}$ HMQC NMR spectrum of a methanolic solution of $[Rh(DIPAMP)]^{+}$ solvent complex (0.01 mmol), which was treated with 1 mmol methyl-(*Z*)-*β*-(*N*-acetyl)-aminocrotonate and 0.57 mmol *p*-xylene (molar ratio xylene complex: substrate complex = 1.0). The Rh shifts are –956 (xylene complex) and 1148 ppm (substrate complex).

sure this reaction results in an ee-value of 64% after 24 h at room temperature [51]. On the other hand, using $[Rh(Me\text{-}DuPHOS)(MeOH)_2]BF_4$ in methanol as solvent gives a complete conversion after a hydrogenation of only 4 min under normal pressure and at 25.0 °C, with an ee-value of 87.8% [52]. The reason for this distinct increase in activity lies not only in the avoidance of "induction periods" [53], but undoubtedly also in the exclusion of the stable arene complex [Rh((*S*,*S*)-Me-DuPHOS)(toluene)]BF_4, which is unable to catalyze the enantioselective hydrogenation. The crystal structure of the arene complex can be found in [47].

In recent studies on hydrogenation catalyzed by soluble iron-diimine complexes, Chirik and coworkers noted that the major deactivation pathway of these complexes occurs via formation of η^6-arene complexes [54].

Acetonitrile is another solvent that may retard the reaction. Although no cases of inhibition by acetonitrile have been described in the literature, we usually find no hydrogenation activity at all when using rhodium/MonoPhos catalysts in this solvent. Presumably, this is true for most transition metal catalysts.

Horner noted inhibition by ethers, $MeNO_2$, malonate esters and DMF in the hydrogenation of cyclohexene with Wilkinson's catalyst. Almost complete inhibi-

tion was observed upon use of DMSO, acetonitrile, chloroform, chlorobenzene, and acetic acid [55].

Eshova et al. studied the hydrogenation of CO_2 to formic acid in several solvents in the presence of an equivalent of Et_3N using Wilkinson's catalyst. These authors conducted an extensive NMR study into the various decomposition pathways of the catalyst [56]. Apparently, DMSO is capable of rapidly displacing one equivalent of PPh_3 on the catalyst; a second equivalent is slowly displaced. The dissolved phosphine can be easily oxidized, the oxidant in this case being shown as CO_2. Triethylamine was also capable of displacing PPh_3, though the resulting complex, $RhCl(PPh_3)_2(Et_3N)$, is extremely sensitive towards oxidation.

In conclusion, in general it is best to avoid aromatic solvents and strongly coordinating solvents such as acetonitrile when conducting homogeneous hydrogenation reactions.

44.5.2
Catalyst Inhibition Caused by Compounds Containing Heteroatoms

Almost all phosphorus(III) compounds, such as phosphines, phosphites, phosphonites and phosphoramidites, are excellent ligands for late transition metals. Having excess ligand present, beyond the amount necessary to stabilize the complex, will retard or completely inhibit the catalysis [57]. This can be highly relevant if the purities of metal precursors and ligands are not exactly known. Bergbreiter showed that inhibition by excess PPh_3 can be reversed by the addition of silver salts, which form complexes with phosphines having a high complex constant [58].

Mixed results have been reported with sulfur compounds. There is no doubt that thiols and thioethers are ligands for transition metals; thioethers tend to be fairly weak ligands, and occasionally have been used in chiral ligands for hydrogenation and transfer hydrogenation. Substrates may contain thioether groups, although hydrogenation will be somewhat slower [59]. Homogeneous alkene hydrogenation catalyzed by the Wilkinson catalyst was not inhibited by trace amounts of PhSH, but the addition of 42 equiv. with respect to rhodium caused complete inhibition [59].

Whereas most hydrogenation catalysts function very well in water (see for example Chapter 38 for two-phase aqueous catalysis), scattered instances are known of inhibition by water. Laue et al. attached Noyori's transfer hydrogenation catalyst to a soluble polymer and used this in a continuous device in which the catalyst was separated from the product by a membrane. The catalyst was found to be inhibited by the presence of traces of water in the feed stream, though this could be reversed by continuously feeding a small amount of potassium isopropoxide [60]. A case of water inhibition in iridium-catalyzed hydrogenation is described in Section 44.6.2.

In the Rh-BINAP-catalyzed allyl amine isomerization step used in Takasago's Menthol process, the catalyst is inhibited by water through the formation of a hydroxyl-bridged rhodium trinuclear complex $[\{Rh(BINAP)\}_3(\mu_2\text{-}OH)_2]ClO_4$ [61].

However, it is unclear whether this complex can also form during hydrogenation reactions.

Two groups have reported the inhibition of hydrogenation catalysts by primary amines. Rijnberg, Lensink and de Vries studied the biphasic asymmetric hydrogenation of *N*-benzyl imines using Rh–BDPP complexes in which the ligand was mono-, di-, tri- or tetra-sulfonated [62]. It was found that, in particular, the monosulfonated ligand led to a catalyst which induced very high enantioselectivity. The rate of the reaction was also seen to depend heavily on the purity of the substrate. Since the imine can hydrolyze under these reaction conditions, the effect of added acetophenone as well as benzylamine was studied. Whereas the added acetophenone showed no effect, the addition of benzylamine was found to lead to complete inhibition of the catalyst.

James and coworkers found that one benzylamine is actually bound to the rhodium in the active catalyst in hydrogenations of $PhCH{=}NRCH_2Ph$ using $[Rh(COD)(PPh_3)_2]PF_6$ as catalyst precursor. However, the addition of more than two equivalents of benzylamine inhibited the catalysis [63].

Great care must be taken not to generalize these effects, as the addition of primary diamines to ruthenium bisphosphine complexes generates a very active catalyst for ketone hydrogenation after the addition of base (see Chapter 32).

44.5.3
Inhibition by CO and Sources of CO

As described in the preceding section, the presence of excess ligand leads to reversible catalyst inhibition. If the ligand binds very strongly, the effect may be irreversible. Carbon monoxide (CO) is a ligand that binds fairly strongly to most transition metals, and many reports have been made concerning its inhibitory effects in homogeneous hydrogenation.

In a study on the hydrogenation of aromatic substrates, Fish and coworkers noted a major difference in rate between $Ru_3(CO)_{12}$ and $H_4Ru_4(CO)_{12}$. This difference was attributed to the fact that, upon formation of the second catalyst from the first when pressurizing the reaction with hydrogen, some excess CO would form, which inhibits binding of the substrate [64]. Markó reported CO inhibition in the $Cr(CO)_6$/NaOMe-catalyzed hydrogenation of ketones [65], while Kliger and coworkers studied the hydrogenation of unsaturated hydrocarbons with a catalyst which was prepared by the addition of primary, secondary, or tertiary octylamines to $Pt(OAc)_4$ [66]. These authors identified a linear inverse relationship between the rate of hydrogenation and the amount of CO added, with full inhibition being obtained at $Pt/CO = 5$. Although the authors did not draw any structural conclusions, this result would seem rather typical for the formation of Pt colloids (see Chapter 9).

Many authors have noted that aldehydes may function as a source of CO via a decarbonylation process [67]. Wilkinson and coworkers noted that $[RhCl(PPh_3)_3]$ is capable of decarbonylating 90% of *n*-heptanal within 24 h at room temperature [68]. The complex formed, $[RhCl(CO)(PPh_3)_2]$, is completely

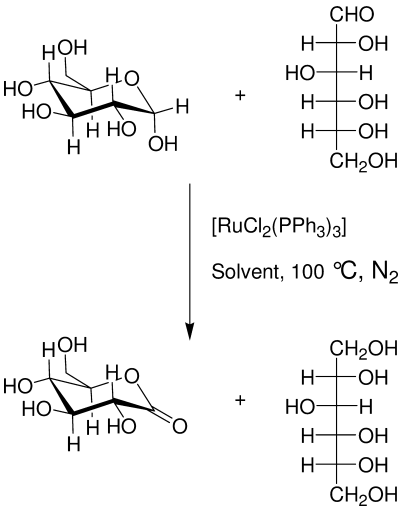

Scheme 44.8 Catalytic disproportionation of glucose.

inactive as a hydrogenation catalyst [69]. This is a severe drawback of aldehyde hydrogenations both with soluble transition metal catalysts as well as with heterogeneous catalysts.

Rajagopal et al. studied the disproportionation of D-glucose using $[RuCl_2(PPh_3)_3]$ in several solvents such as DMF or dimethylacetamide (DMA) (Scheme 44.8). These authors noted deactivation of the catalyst, which was caused by the formation of inactive CO-complexes such as $[RuCl_2(CO)(PPh_3)_2(DMF)]$, $[RuCl_2(CO)(PPh_3)_2(DMA)]$ and *cis*-$[RuCl_2(CO)_2(PPh_3)_2]$ [70].

In some cases primary alcohols can be catalytically dehydrogenated under hydrogenation conditions, leading to the formation of aldehydes, which can in turn decarbonylate leading to inactive metal carbonyl complexes. In a typical example, Chaudhari reported that during the hydrogenation of allyl alcohol using Wilkinson's catalyst, the catalyst was deactivated by the formation of $[RhCl(CO)(PPh_3)_2]$ [26]. Similarly, in hydrogenations using $[RuCl_2(PPh_3)_3]$ which were performed in primary alcohols such as 2-methoxy-ethanol or tetrahydrofurfurol, $[RuClH(CO)(PPh_3)_3]$ was formed, which is inactive as hydrogenation catalyst but still showed activity in the transfer hydrogenation reaction of Scheme 44.8 [71].

44.5.4
Inhibition by Acids and Bases

Many publications report on the effect that acids and bases can have on catalysis by transition metal complexes, and in most cases positive effects are reported.

When homogeneous catalysis is carried out under aqueous conditions, the pH of the solution becomes an issue, and very often different rates are obtained at different pH-values. A striking example was reported by Xiao and coworkers

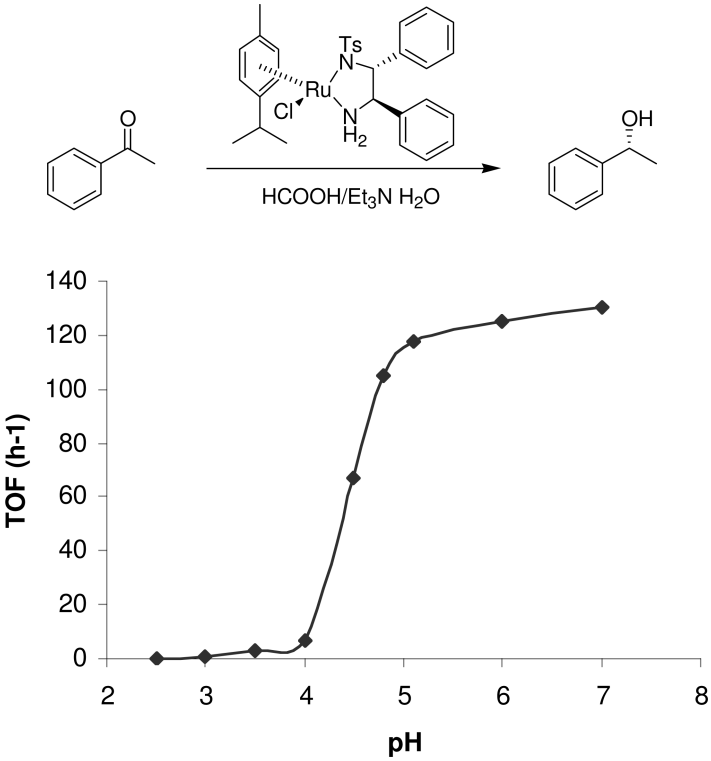

Fig. 44.10 Relationship between the rate of enantiomeric transfer hydrogenation and pH-value.

[72] while examining the enantioselective transfer hydrogenation of acetophenone. While using the Noyori-Ikariya enantioselective transfer hydrogenation catalyst Ru-Ts-dpen with the Et_3N/HCOOH azeotrope in water, these authors noticed that the reaction had a very long induction period. Since the reaction with NaOOCH started instantaneously, the question arose as to whether the pH of the solution was an important parameter, in view of the fact that the azeotrope is a 2:5 Et_3N:HCOOOH mixture. Carrying out the reaction at different pH-values immediately proved this point, whereby only at pH >4 did the reaction take off immediately (Fig. 44.10). The inhibition at low pH is caused by protonation of the ligand at the sulfonamide position.

44.6
Irreversible Deactivation

44.6.1
Inhibition by Anions

One sure way of inhibiting metal catalysts is by the addition of metal cyanides. Cyanide has a strong binding affinity to most transition metals, the result usually being complete inactivation of the catalyst [73].

Halides are also a frequent source of inhibition. In general, halides bind very well to transition metals, although the bond can be weakened by the use of polar solvents. Thus, not all cases of inhibition by halides are irreversible. Inhibition may be caused not only by reversible binding to the metal, but also through the formation of halide-bridged bimetallic complexes, which generally exhibit much lower activity in hydrogenation reactions. In a study on the use of carboranes as counterion for rhodium phosphine hydrogenation catalysts, inhibition was found to occur through the formation of dimeric $[(PPh_3)_2HRh(\mu\text{-}Cl)_2(\mu\text{-}H)RhH(PPh_3)_2][CB_{11}H_{12}]$ [74]. An extensive study of dimeric halide-bridged rhodium species observed in solution using PHIP was recently published by Duckett et al. [75].

Halide impurities may have a negative effect on the rate of a hydrogenation reaction, as was observed by Cobley et al. These authors studied the asymmetric hydrogenation of 2-methylenesuccinamic acid using [(*S,S*)-(Et-DuPHOS)Rh-(COD)]BF_4 as catalyst [76]. They were able to obtain a 30-fold acceleration upon removal of a chloride impurity from the substrate (Scheme 44.9).

Dyson recently warned that chloride impurities present in ionic liquids prepared by the classical metathesis reaction may cause severe catalyst inhibition. This may be aggravated by the fact that metal-chloride dissociation is disfavored in ionic liquids, in spite of their polar nature [77].

44.6.2
Inhibition by Oxidation and by Ligand Modification

Nindakova and Shainyan studied the decomposition pathways of Rh–DIOP complexes. Even upon prolonged exposure to hydrogen, the catalyst decomposed in the absence of substrate with, according to these authors, the Rh-bis-

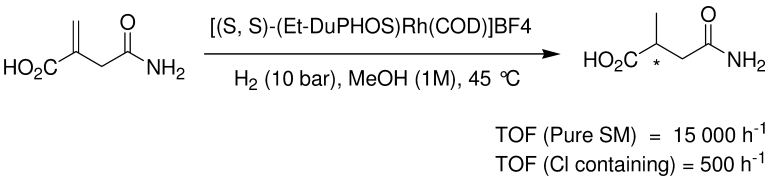

Scheme 44.9 Chloride inhibition in the enantioselective hydrogenation of 2-methylenesuccinamic acid.

phosphine oxide being a major decomposition product. The oxygen presumably stems from very small (ppm) amounts present in the hydrogen supply. Other products were η^6-Arene-Rh–DIOP complexes if the catalyst was stirred in aromatic solvents, and a binuclear compound was also detected. The assignment of structures was based exclusively on ^{31}P-NMR findings [78].

Ruiz and coworkers developed a new phosphine–phosphite ligand, which was tested in the enantioselective hydrogenation of methyl-2-acetamidoacrylate and methyl-2-acetamido-cinnamate [79]. These authors obtained the highest enantioselectivities in CH_2Cl_2, whereas in MeOH not only was the ee-value lower, but it also slowly declined during the hydrogenation reaction (Scheme 44.10). This was interpreted as slow decomposition of the phosphite part of the ligand, presumably through hydrolysis, and was confirmed by ^{31}P-NMR measurements.

In a kinetic study on the enantioselective hydrogenation of methyl-2-acetamido-acrylate with Rh/MonoPhos in *i*-PrOH, Heeres and coworkers identified an impurity in the solvent that destroyed part of the catalyst, leading to a dependence of the rate on catalyst concentration that did not pass through zero (Fig. 44.11) [80]. Closer inspection revealed the impurity to be a peroxide (positive test on peroxide strip), and the problem was solved by purifying the solvent by distillation. In fact, this is a very general phenomenon, as peroxides may be present not only in solvents but also in substrates. In general, it is worthwhile purifying both substrate and solvent before the hydrogenation reaction.

Inhibition by oxygen is also a problem in transfer hydrogenation, though the degree of inhibition may differ strongly, depending on the nature of the catalyst. In our own experience, the Noyori/Ikariya ruthenium catalysts based on amino-alcohols are extremely sensitive to oxygen. One possible reason for this might be the dehydrogenation of the ligand alcohol function to an aldehyde, although insertion of oxygen into the ruthenium–hydride bond also seems possible. Gavrilidis et al. tested the sensitivity of [RhCp*((1*R*, 2*S*)-aminoindanolate)Cl] to oxy-

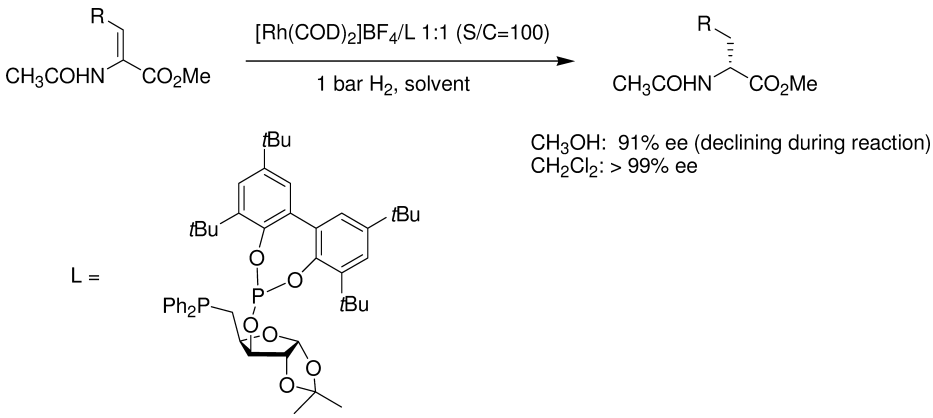

Scheme 44.10 Phosphine–phosphite ligand in enantioselective hydrogenation.

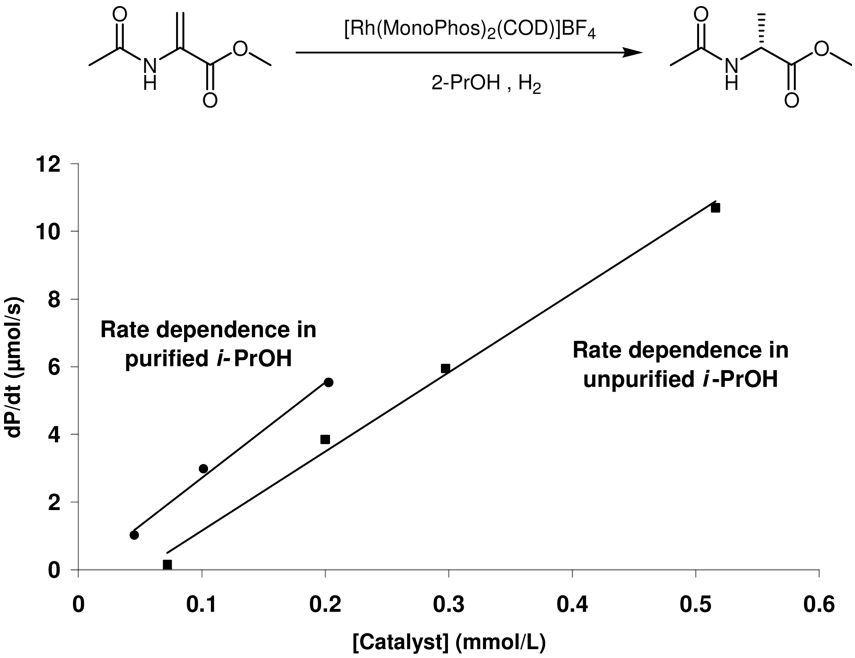

Fig. 44.11 Inhibition by peroxide in the solvent leads to a lower rate of reaction.

gen in the transfer hydrogenation of acetophenone with *i*-PrOH, and noted that after 60 min only 25% conversion was reached, as opposed to 95% under N_2 [81].

44.6.3
Formation of Dimers, Trimers, Clusters, Colloids, and Solids

The events described in the previous section are not necessarily sufficient to deactivate the catalyst. The real deactivation presumably occurs through formation of dimers or polynuclear species that have lower reactivity. These higher-order species usually do not revert back to the more active monomeric species.

In hydrogenations with Wilkinson's catalyst, ligand dissociation precedes substrate binding. Bergbreiter, in an attempt to speed up hydrogenation by aiding ligand dissociation through the addition of silver salts that bind to triphenylphosphine, found that this had the reverse effect [58]. The lower rates were caused by the formation of the dimer, which is much less soluble and exhibits only one-tenth the catalytic activity of the monomer [82].

Eisenberg and coworkers studied intermediates in the hydrogenation of alkenes using Wilkinson's catalyst and PHIP (see Chapter 12). These authors identified a range of dimers, and found that the stability of $[H_2Rh(PPh_3)_2(\mu\text{-}Cl)_2Rh(PPh_3)(\text{alkene})]$ depends strongly on the electron-withdrawing properties of the alkene [83].

The formation of dimers and trimers is a major issue in hydrogenations with iridium catalysts. In the context of developing an industrial process to produce (*S*)-metolachlor via an enantioselective imine hydrogenation (see Chapters 34 and 37), Blaser et al. investigated the causes of catalyst deactivation in the iridium/bisphosphine-catalyzed hydrogenation of DMA imine (Scheme 44.11) [84].

Blaser and colleagues made the following observations regarding catalyst deactivation:

- Most tested Ir-catalysts had very high initial activity, but then slowed significantly.
- The degree of deactivation is strongly dependent on ligand structure, solvent and temperature.
- With Ir/BDPP/iodide as catalyst, productivity was higher at –5 °C than at room temperature.
- Even with the most productive catalysts, reactions did not go to completion at SCR = 15 000.
- The purity of the substrate was important. The presence of dimethylaniline is detrimental.
- No inhibition was observed upon the addition of product.

All of these observations were interpreted as signs of catalyst deactivation through the irreversible formation of inactive or less-active species. Indeed, the formation of trihydride-bridged iridium dimers had already been described by Crabtree (see Chapter 2) (Scheme 44.12) [85].

Several strategies were developed to prevent the formation of unreactive dimers [86], with one of the more successful methods being immobilization of the catalyst on solid support. Whereas normally, most immobilized catalysts lose activity in comparison to their soluble analogues, in this case the rate increased, due to the prevention of deactivation by dimerization. Even more convincing, there was a negative correlation between the loading on the resin and the rate of the reaction (Fig. 44.12).

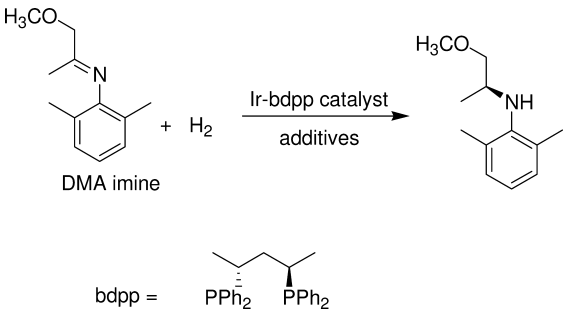

Scheme 44.11 Iridium-catalyzed enantioselective imine hydrogenation.

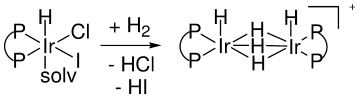

Scheme 44.12 Formation of inactive iridium dimers in hydrogenation reactions.

Pfaltz and coworkers have conducted extensive studies on how the anion affects the rate of hydrogenation in the Ir–PHOX-catalyzed hydrogenation of (*E*)-1,2-diphenyl-1-propene (Table 44.3) [87].

These authors assumed that the lack of reactivity with the triflate complex is caused by strong binding of the triflate to iridium. Clearly, the tetra-arylborate and the tetra-alkoxyaluminate anions induce the highest rate. When more substrate was added after the reaction had completed and was vented with Ar, the reaction resumed at the same rate with catalysts containing one of the last three anions, whereas the PF_6-catalyst had lost all activity. The authors also noted a large difference in the sensitivity to added water. Whereas all catalysts lost some activity upon the addition of 0.05% (v/v) water, the PF_6 catalyst completely lost activity. The authors had shown previously that the PF_6 catalyst easily forms an inactive trimeric hydride-bridged iridium cluster [88], and it does indeed seem likely that the deactivation proceeds via these clusters.

Pregosin studied the interaction between iridium and the counterions by measuring diffusion using ^1H and ^{19}F pulsed gradient spin echo (PGSE), as well as the ^1H ^{19}F heteronuclear Overhauser effect (HOESY) [89]. Whereas in CD_3OD all complexes were completely cationic with freely moving anions, in CH_2Cl_2 (the solvent used for hydrogenation) there is a difference between the OTf, PF_6 and BF_4 complexes on the one hand and the two tetra-arylborate complexes on the other hand. Whereas the first three complexes are again fully cationic, the latter two show a much stronger cation–anion interaction. In view of the size of the anions, it is clear that the stronger cation–anion interaction can

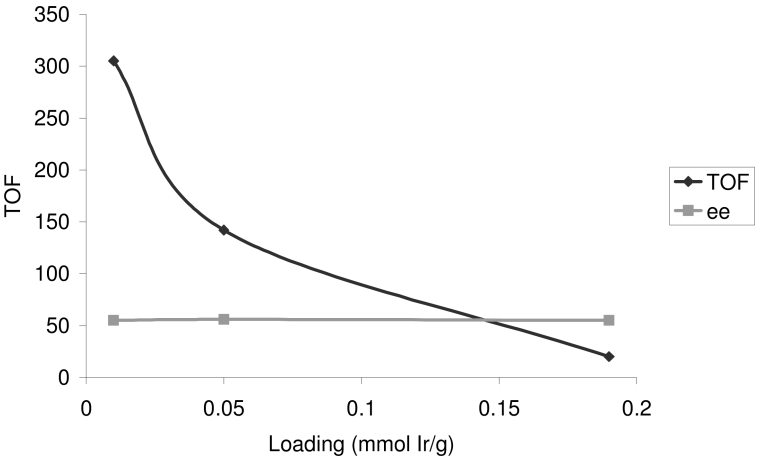

Fig. 44.12 Dependence of rate of imine hydrogenation on catalyst loading on the support.

Table 44.3 Anion effect on the rate of iridium-catalyzed alkene hydrogenation.

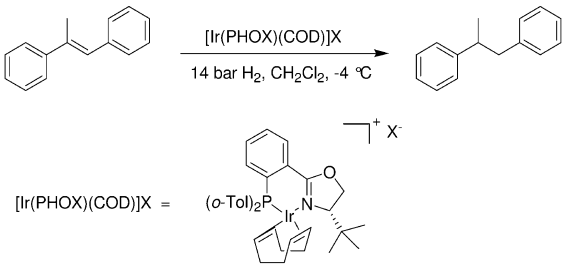

X	Rate of hydrogenation [mol L^{-1} h^{-1}]	ee-value
PF_6	0.63	97.3
BF_4	0.12	97.9
OTf	0	–
$B(3,5\text{-di-}CF_3\text{-}C_6H_3)_4$ ($BarF^-$)	1.70	96.9
$B(C_6F_5)_4$	1.42	97.2
$Al(OC(CF_3)_3)_4$	1.86	97.3

retard formation of the clusters, which involves the bringing together of two relatively large species.

Dervisi recently reported similar findings: upon treatment of an iridium bisphosphine catalyst containing a PF_6-anion with H_2, hydride-bridged dimers and trimers were isolated [90].

44.7 Conclusions

It is clear from the above discussions that many mechanisms exist that may deactivate or completely inhibit a transition metal catalyst. However, danger lurks in every corner! The metal precursor, the ligand, the solvent, the substrate and the reagents may all contain functional groups or impurities that might interact adversely with the metal complex. Under the influence of external agents, or simply by heat or by light, the complex may loose a ligand; however, the now underligated complex will usually dimerize or trimerize to form less-active complexes. Fortunately, once the mechanism of inhibition has been established, it is very often possible to effect changes that counteract the inhibition mechanism. Synthetic chemists can usually circumvent 95% of the problems by using very low SCRs, though for economic reasons this is not an option in ton-scale production. Inhibition is, therefore, a very important part of process development for a homogeneous transition metal-catalyzed reaction, and in almost all cases low-cost solutions can be found. Nevertheless, when planning a multi-step syn-

thesis on the ton-scale, it may be wise to introduce a purification step preceding the hydrogenation reaction.

Abbreviations

COD	1,5-cyclooctadiene
DMA	dimethylacetamide
DMF	dimethylformamide
DMSO	dimethyl sulfoxide
EMS	electrospray mass spectrometry
NBD	2,5-norbornadiene
PGSE	pulsed gradient spin echo
PHIP	parahydrogen-induced polarization
PTC	phase-transfer catalyst
SCR	substrate : catalyst ratio
THF	tetrahydrofuran
TPPTS	tris-sulfonated triphenylphosphine
TOF	turnover frequency
TON	turnover number

References

1 (a) J.G. de Vries, in: I.T. Horvath (Ed.), *Encyclopedia of Catalysis*. John Wiley & Sons, New York, **2003**, Vol. 3, p. 295; (b) J.G. de Vries, A.H.M. de Vries, *Eur. J. Org. Chem.* **2003**, 799.

2 H.-U. Blaser, E. Schmidt (Eds.), *Asymmetric Catalysis on Industrial Scale: Challenges, Approaches and Solutions*. Wiley-VCH, Weinheim, **2004**.

3 B.R. James, *Homogeneous Hydrogenation*. John Wiley & Sons, New York, **1973**.

4 (a) M. Green, T.A. Kuc, S.H. Taylor, *J. Chem. Soc., Chem. Commun.* **1970**, 1553.

5 (a) C. Winkhous, H. Singer, *Chem. Ber.* **1967**, *99*, 3602; (b) L. Horner, H. Siegel, H. Buth, *Angew. Chem. Int. Ed.* **1968**, *7*, 942.

6 W. Bonrath, K.R. Pörschke, S. Michaelis, *Angew. Chem. Int. Ed.* **1990**, *29*, 298–300.

7 C. Elschenbroich, A. Salzer (Eds.), *Organometallchemie*, 3rd edn. B.G. Teubner, Stuttgart, **1993**, p. 304.

8 L. Moggi, A. Juris, D. Sandrini, M.F. Manfrin, *Rev. Chem. Inter.* **1981**, *4*, 171.

9 H. Bönnemann, *Angew. Chem. Int. Ed.* **1985**, *24*, 248.

10 (a) W. Braun, A. Salzer, H.-J. Drexler, A. Spannenberg, D. Heller, *Dalton Trans.* **2003**, 1606; (b) H.-J. Drexler, J. You, S. Zhang, C. Fischer, W. Baumann, A. Spannenberg, D. Heller, *Org. Proc. Res. Dev.* **2003**, 355; (c) D. Heller, H.-J. Drexler, J. You, W. Baumann, K. Drauz, H.-P. Krimmer, A. Börner, *Chem. Eur. J.* **2002**, *8*, 5196; d) H.-J. Drexler, W. Baumann, A. Spannenberg, C. Fischer, D. Heller, *J. Organomet. Chem.* **2001**, *621*, 89; (e) A. Börner, D. Heller, *Tetrahedron Lett.* **2001**, *42*, 223; (f) W. Baumann, S. Mansel, D. Heller, S. Borns, *Mag. Res. Chem.* **1997**, *35*, 701; (g) D. Heller, S. Borns, W. Baumann, R. Selke, *Chem. Ber.* **1996**, *129*, 85; (h) D. Heller, K. Kortus, R. Selke, *Liebigs Ann.* **1995**, 575.

11 Recently, the mechanism of the hydrogenation of NBD with $[Rh(NBD)(PPh_3)_2]BF_4$ in CH_2Cl_2 has been extensively investigated. For details, see: M.E. Esterulas, J. Herrero, M. Mar-

tin, L.A. Oro, V.M. Real, *J. Organomet. Chem.* **2000**, *599*, 178.
12 H. Brunner, Hydrogenation, in: B. Cornils, W.A. Herrmann (Eds.), *Applied Homogeneous Catalysis with Organometallic Compounds*, Vols. I–III, Ch. 2.2, p. 195 and cited references. Wiley-VCH, Weinheim, **2002**.
13 (a) J.R. Shapley, R.R. Schrock, J.A. Osborn, *J. Am. Chem. Soc.* **1969**, *91*, 2816; (b) R.R. Schrock, J.A. Osborn, *J. Am. Chem. Soc.* **1971**, *93*, 3089; (c) R.R. Schrock, J.A. Osborn, *J. Am. Chem. Soc.* **1976**, *98*, 2134; (d) R.R. Schrock, J.A. Osborn, *J. Am. Chem. Soc.* **1976**, *98*, 4450.
14 (a) U. Nagel, T. Krink, *Angew. Chem. Int. Ed.* **1993**, *32*, 1052; (b) U. Nagel, A. Bublewitz, *Chem. Ber.* **1992**, *125*, 1061; (c) U. Nagel, E. Kinzel, J. Andrade, G. Prescher, *Chem. Ber.* **1986**, *119*, 3326.
15 D. Heller, W. Baumann, DE 10202173 C2, **2003**.
16 C.R. Landis, J. Halpern, *J. Am. Chem. Soc.* **1987**, *109*, 1746.
17 G. Strukul, P. D'Olimpio, M. Bonivento, F. Pinna, M. Graziani, *J. Mol. Catal.* **1977**, *2*, 179.
18 L. Greiner, M.B. Ternbach, *Adv. Synth. Catal.* **2004**, *346*, 1392.
19 H.-J. Drexler, S. Zhang, A. Sun, A. Spannenberg, A. Arrietta, A. Preetz, D. Heller, *Tetrahedron: Asymm.* **2004**, *15*, 2139.
20 M. van den Berg, Dissertation, University of Groningen, **2006**.
21 C.J. Cobley, I.C. Lennon, R. McCague, J.A. Ramsden, A. Zanotti-Gerosa, *Tetrahedron Lett.* **2001**, *42*, 7481.
22 (a) D.G. Blackmond, *Acc. Chem. Res.* **2000**, *33*, 402; (b) D.G. Blackmond, T. Rosner, T. Neugebauer, M.T. Reetz, *Angew. Chem. Int. Ed.* **1999**, *38*, 2196.
23 (a) R.W. Adams, G.E. Batley, J.C. Bailar, Jr., *J. Am. Chem. Soc.* **1968**, *90*, 6051; (b) E.N. Frankel, T.L. Mounts, R.O. Butterfields, H.J. Dutton, *Adv. Chem. Ser.* **1968**, *70*, 177; (c) J.A. Heldal, E.N. Frankel, *J. Am. Oil Chem. Soc.* **1985**, *62*, 1117.
24 D.R. Anton, R.H. Crabtree, *Organometallics* **1983**, *2*, 855.
25 (a) R. Noyori, M. Yamakawa, S. Hashiguchi, *J. Org. Chem.* **2001**, *66*, 7932; (b) K. Abdur-Rashid, S.E. Clapham, A. Hadzovic, J.N. Harvey, A.J. Lough, R.H. Morris, *J. Am. Chem. Soc.* **2002**, *124*, 15104.
26 J.G. Wadkar, R.V. Chaudhari, *J. Mol. Catal.* **1983**, *22*, 103.
27 E. Vedejs, P. Trapencieris, E. Suna, *J. Org. Chem.* **1999**, *64*, 6724.
28 K. Everaere, A. Mortreux, M. Bulliard, J. Brussee, A. van der Gen, G. Nowogrocki, J.-F. Carpentier, *Eur. J. Org. Chem.* **2001**, 275.
29 J.M. Grosselin, C. Mercier, G. Allmang, F. Grass, *Organometallics* **1991**, *10*, 2126.
30 J.G. de Vries, unpublished results.
31 M. Hernandez, P. Kalck, *J. Mol. Catal. A Chem.* **1997**, *116*, 131–146.
32 F. Joó, *Acc. Chem. Res.* **2002**, *35*, 738 and references cited therein.
33 (a) I.D. Gridnev, N. Higashi, K. Asakura, T. Imamoto, *J. Am. Chem. Soc.* **2000**, *122*, 7183; (b) I.D. Gridnev, M. Yasutake, N. Higashi, T. Imamoto, *J. Am. Chem. Soc.* **2001**, *123*, 5268.
34 (a) P. Hübler, J. Bargon, *Angew. Chem. Int. Ed.* **2000**, *39*, 3701; (b) P. Hübler, R. Giernoth, G. Kummerle, J. Bargon, *J. Am. Chem. Soc.* **1999**, *121*, 5311; (c) R. Giernoth, P. Hübler, J. Bargon, *Angew. Chem. Int. Ed.* **1998**, *37*, 2473.
35 K.B. Hansen, T. Rosner, M. Kubryk, P.G. Dormer, J.D. Armstrong, III, *Org. Lett.* **2005**, *7*, 4935.
36 Y. Hsiao, N.R. Rivera, T. Rosner, S.W. Krska, E. Njolito, F. Wang, Y. Sun, J.D. Armstrong, III, E.J.J. Grabowski, R.D. Tillyer, F. Spindler, C. Malan, *J. Am. Chem. Soc.* **2004**, *126*, 9918.
37 P. Marcazzan, B.O. Patrick, B.R. James, *Organometallics* **2003**, *22*, 1177.
38 C. Döbler, H.-J. Kreuzfeld, M. Michalik, H.W. Krause, *Tetrahedron Asymm.* **1996**, *7*, 117.
39 S.A. Laneman, D.E. Froen, D.J. Ager, *Chem. Ind. (Dekker)* **1998**, *75 (Catalysis of Organic Reactions)*, 525.
40 M. van den Berg, A.J. Minnaard, R.M. Haak, M. Leeman, E.P. Schudde, A. Meetsma, B.L. Feringa, A.H.M. de Vries, C.E.P. Maljaars, C.E. Willans, D.J. Hyett, J.A.F. Boogers, H.J.W. Henderickx, J.G. de Vries, *Adv. Synth. Catal.* **2003**, *345*, 308.

41 M.J. Burk, P.D. de Koning, T.M. Grote, M.S. Hoekstra, G. Hoge, R.A. Jennings, W.S. Kissel, T.V. Le, I.C. Lennon, T.A. Mulhern, J.A. Ramsden, R.A. Wade, *J. Org. Chem.* **2003**, *68*, 5731.

42 B.P. Cleary, R. Eisenberg, *Inorg. Chim. Acta* **1995**, *240*, 135.

43 (a) J. Halpern, D.P. Riley, A.S.C. Chan, J.S. Pluth, *J. Am. Chem. Soc.* **1977**, *99*, 8055; (b) C.R. Landis, J. Halpern, *Organometallics* **1983**, *2*, 840.

44 M.J. Burk, C.S. Kalberg, A. Pizzano, *J. Am. Chem. Soc.* **1998**, *120*, 4345.

45 M.J. Burk, F. Bienewald, S. Challenger, A. Derrick, J.A. Ramsden, *J. Org. Chem.* **1999**, *64*, 3290.

46 M. Townsend, J.F. Blount, *Inorg. Chem.* **1981**, *20*, 269.

47 D. Heller, H.-J. Drexler, A. Spannenberg, B. Heller, J. You, W. Baumann, *Angew. Chem. Int. Ed.* **2002**, *41*, 777.

48 (a) R. Benn, A. Rufińska, *Angew. Chem. Int. Ed.* **1986**, *25*, 861; (b) W. von Philipsborn, *Chem. Soc. Rev.* **1999**, *28*, 95. (c) J.M.Ernsting, S. Gaemers, C.J. Elsevier, *Magn. Reson. Chem.* **2004**, *42*, 721.

49 (a) J.M. Ernsting, C.J. Elsevier, W.G.J. de Lange, K. Timmer, *Magn. Reson. Chem.* **1991**, *29*, 118–124; (b) W. Leitner, M. Bühl, R. Fornika, C. Six, W. Baumann, E. Dinjus, M. Kessler, C. Krüger, A. Rufińska, *Organometallics* **1999**, *18*, 1196.

50 W. Baumann, *Adv. Synth. Catal,* submitted.

51 G. Zhu, Z. Chen, X. Zhang, *J. Org. Chem.* **1999**, *64*, 6907.

52 D. Heller, J. Holz, H.-J. Drexler, J. Lang, K. Drauz, H.-P. Krimmer, A. Börner, *J. Org. Chem.* **2001**, *66*, 6816.

53 By hydrogenation of the diene, the cyclooctadiene precatalyst can easily be transformed into the solvent complex. (a) H.-J. Drexler, W. Baumann, A. Spannenberg, C. Fischer, D. Heller, *J. Organomet. Chem.* **2001**, *621*, 89. Analogue findings for seven-ring-chelates can be found in: (b) D. Heller, S. Borns, W. Baumann, R. Selke, *Chem. Ber.* **1996**, *129*, 85.

54 S.C. Bart, E.J. Hawrelak, E. Lobkovsky, P.J. Chirik, *Organometallics* **2005**, *24*, 5518.

55 L. Horner, H. Buethe, H. Sigel, *Tetrahedron Lett.* **1968**, *37*, 4023.

56 N.N. Ezhova, N.V. Kolesnichenko, A.V. Bulygin, E.V. Slivinskii, S. Han, *Russ. Chem. Bull. Int. Ed.* **2002**, *51*, 2165.

57 (a) P.S. Hallmann, D. Evans, J.A. Osborn, G. Wilkinson, *Chem. Commun.* **1967**, 305; (b) R. Bonnaire, L. Horner, F. Schumacher, *J. Organomet. Chem.* **1978**, *161*, C41; (c) M.A. Esteruelas, J. Herrero, M. Martin, L.A. Oro, V.M. Real, *J. Organomet. Chem.* **2000**, *599*, 178.

58 D.E. Bergbreiter, M.S. Bursten, *J. Macromol. Sci.-Chem.* **1981**, *A16*, 369.

59 A.J. Birch, K.A.M. Walker, *Tetrahedron Lett.* **1967**, 1935.

60 S. Laue, L. Greiner, J. Woltinger, A. Liese, *Adv. Synth. Catal.* **2001**, *343*, 711.

61 T. Yamagata, K. Tani, Y. Tatsuno, T. Saito, *J. Chem. Soc. Chem. Commun.* **1988**, 466.

62 C. Lensink, E. Rijnberg, J.G. de Vries, *J. Mol. Catal. A: Chem.* **1997**, *116*, 199.

63 P. Marcazzan, B. O'Patrick, B.R. James, *Inorg. Chem.* **2004**, *43*, 6838.

64 R.H. Fish, A.D. Thormodsen, G.A. Cremer, *J. Am. Chem. Soc.* **1982**, *104*, 5234.

65 L. Markó, Z. Nagy-Magos, *J. Organomet. Chem.* **1985**, *285*, 193.

66 E.G. Kliger, L.P. Shuikina, V.M. Frolov, *Kinet. Catal.* **1996**, *37*, 218.

67 S. Kolarić, V. Šunjić, *J. Mol. Catal. A: Chem.* **1996**, *111*, 239.

68 M.C. Baird, C.J. Nyman, G. Wilkinson, *J. Chem. Soc. A* **1968**, 348.

69 J.A. Osborn, F.M. Jardine, J.F. Young, G. Wilkinson, *J. Chem. Soc. A* **1966**, 1711.

70 S. Rajagopal, S. Vancheesan, J. Rajaram, J.C. Kuriacose, *J. Mol. Catal.* **1983**, *22*, 131.

71 S. Rajagopal, S. Vancheesan, J. Rajaram, J.C. Kuriacose, *J. Mol. Catal.* **1983**, *22*, 137.

72 X. Wu, X. Li, F. King, J. Xiao, *Angew. Chem. Int. Ed.* **2005**, *44*, 3407.

73 Surprisingly, no direct references to cyanide inhibition of hydrogenation catalysts could be found. For a general reaction showing the swift reaction of a transition metal complex with cyanide as a means to isolate the ligand, see for ex-

ample: D.P. Riley, R.E. Shumate, *J. Org. Chem.* **1980**, *45*, 5187.
74 A. Rifat, N.J. Patmore, M.F. Mahon, A.S. Weller, *Organometallics* **2002**, *21*, 2856.
75 S.A. Colebrooke, S.B. Duckett, J.A.B. Lohman, R. Eisenberg, *Chem. Eur. J.* **2004**, *10*, 2459.
76 C.J. Cobley, I.C. Lennon, C. Praquin, A. Zanotti-Gerosa, *Org. Proc. Res. Dev.* **2003**, *7*, 407.
77 C. Daguenet, P. Dyson, *Organometallics* **2004**, *23*, 6080.
78 L.O. Nindakova, B.A. Shainyan, *Russ. Chem. Bull. Int. Ed.* **2001**, *50*, 1855.
79 O. Pàmies, M. Diéguez, G. Net, A. Ruiz, C. Claver, *J. Org. Chem.* **2001**, *66*, 8364.
80 N. van Vegten, M. van den Berg, A.J. Minnaard, B.L. Feringa, J.G. de Vries, H.J. Heeres, unpublished results. For a preliminary publication, see: M. van den Berg, Dissertation, University of Groningen, **2006**.
81 X. Sun, G. Manos, J. Blacker, J. Martin, A. Gavrilidis, *Org. Proc. Res. Dev.* **2004**, *8*, 909.
82 J. Halpern, C.S. Wong, *J. Chem. Soc. Chem. Commun.* **1973**, 629.
83 S.B. Duckett, C.L. Newell, R. Eisenberg, *J. Am. Chem. Soc.* **1994**, *116*, 10548.
84 B. Pugin, H. Landert, F. Spindler, H.-U. Blaser, *Adv. Synth. Catal.* **2002**, *344*, 974.
85 R. Crabtree, *Acc. Chem. Res.* **1979**, *12*, 331.
86 H.-U. Blaser, B. Pugin, F. Spindler, A. Togni, *C.R. Chim.* **2002**, *5*, 379.
87 S.P. Schmidt, N. Zimmerman, M. Studer, A. Pfaltz, *Chem. Eur. J.* **2004**, *10*, 4685.
88 S.P. Schmidt, A. Pfaltz, E. Martínez-Viviente, P.S. Pregosin, A. Albinati, *Organometallics* **2003**, *22*, 1000.
89 E. Martínez-Viviente, P.S. Pregosin, *Inorg. Chem.* **2003**, *42*, 2209.
90 A. Dervisi, C. Carcedo, L. Ooi, *Adv. Synth. Catal.* **2006**, *348*, 175.

45
Chemical Reaction Engineering Aspects of Homogeneous Hydrogenations

Claude de Bellefon and Nathalie Pestre

45.1
Introduction

The proper design of a reactor should lead to processes where the intrinsic kinetics would play the dominant role, leading to the maximum allowable conversion and yield. In many practical reactors, however, physical processes limit the production or throughput of the system. Thus, the basic problem in chemical reactor design and scale-up is to distribute and control the reactants, products and catalyst concentrations, as well as the heat or other energy sources in specific cases (photochemistry, microwave-assisted reactions, etc.), throughout the reactor. Ideally, such a control would allow the maximization of conversion and yield without the formation of side-products, in addition to operating safely away from runaway zones. Therefore, chemical reactor design involves a knowledge not only of the intrinsic kinetics of the target synthesis, related thermodynamic data (e.g., solubilities, heat of reaction), reactor characteristics in terms of mass and heat transfer, flow pattern, phases hold up, but also their interactions.

For single liquid-phase reactors, knowledge of mixing in the reactor is generally sufficient to account for mass and heat distribution over the reactor volume. Furthermore, when the reaction is not too rapid compared to the mixing times, and there is no large exo- or endothermicity, knowledge of the intrinsic kinetics is the only information required for reactor scale-up, and this allows predictions to be made of reactor performance in a relatively straightforward manner. Scale-up issues are discussed elsewhere in details [1–4]. This is the case for homogeneous single-phase hydrogenations – that is, those conducted with a hydrogen transfer reagent such as isopropanol and which are carried out in one liquid phase with a soluble molecular catalyst and in the absence of a gas or an immiscible liquid. Such hydrogenations can be analyzed and treated like any other homogeneous reaction. In such a case – and because H-transfer catalytic hydrogenations are not very fast – scale-up is easily achieved.

Most hydrogenations are carried out using dihydrogen, a molecular catalyst, and the substrate dissolved in a liquid layer, leading to a gas–liquid process.

The Handbook of Homogeneous Hydrogenation.
Edited by J.G. de Vries and C.J. Elsevier
Copyright © 2007 WILEY-VCH Verlag GmbH & Co. KGaA, Weinheim
ISBN: 978-3-527-31161-3

Among the chemical industries, gas–liquid reactors are very common. Indeed, they are used for a wide variety of applications, such as the production of chemicals by oxidation, hydrogenation, halogenation, sulfation, polymerization, for gas scrubbing of CO_2, H_2S, SO_2, NO_x, HF, Cl_2, and also in bioprocesses such as aerobic fermentation and biological waste treatments [4]. Many types of gas–liquid reactors have been reported that are presently used in industry [5]; these include bubble columns, spray columns, multistage sieve plate bubble columns, falling film reactors, stirred-tank reactors and loop reactors [3]. In such reactors, in addition to mixing each phase, it is important to recognize other properties before a meaningful design can be proposed. The extent of the gas–liquid interface is one of the most important properties, as it governs mass transfer between the gas and liquid phases. Liquid phase hold-up is also important, since when catalytic hydrogenations take place in the liquid phase the phase hold-up will influence reactor productivity and heat transfer.

The aim of this chapter is to define the general requirements typical of gas–liquid hydrogenations – that is, the main problems of hydrogenations related to chemical engineering – and to analyze the influences of limiting physical phenomena on productivity and selectivity. Whilst the chapter may help chemical engineers, the main intention is to provide chemists with a degree of understanding to help in the design and choice of laboratory reactors, and to become more familiar with the scale-up of homogeneous hydrogenation processes. A preliminary, more generalized text – *Chemical Reaction Engineering Aspects of Homogeneous Catalyzed Processes* – has already been published [6], while other aspects such as catalyst separation are detailed elsewhere in this book. Multiphase hydrogenations (e.g., gas–liquid–liquid hydrogenations) are not detailed here, and similar multiphase hydroformylations have been analyzed elsewhere [7]. Other biphasic liquid–liquid hydrogenations using H-transfer reagents (sodium or ammonium formate, formic acid, etc.) are known, but are not used extensively on an industrial scale and will not be described here.

45.2 Fundamentals

45.2.1 Basics of Mass Transfer in Gas–Liquid Systems

First, we must consider a gas–liquid system separated by an interface. When the thermodynamic equilibrium concentration is not reached for a transferable solute A in the gas phase, a concentration gradient is established between the two phases, and this will create a mass transfer flow of A from the gas phase to the liquid phase. This is described by the "two-film" model proposed by W. G. Whitman, where interphase mass transfer is ensured by diffusion of the solute through two stagnant layers of thickness δ_G and δ_L on both sides of the interface (Fig. 45.1) [1–4].

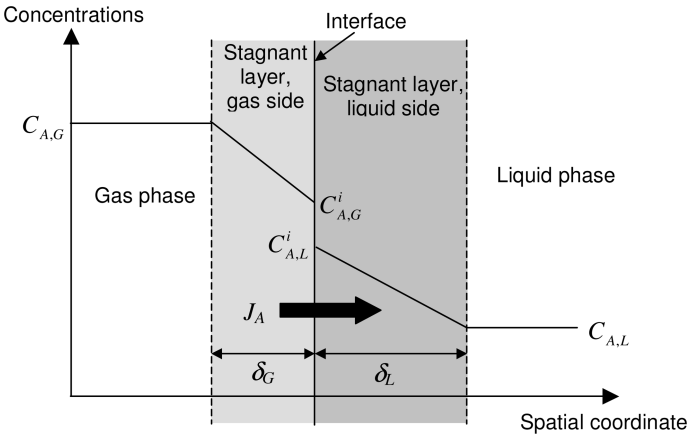

Fig. 45.1 Schematic presentation of the two stagnant films theory applied to gas–liquid systems, indicating the concentration profiles on both sides of the interface.

The application of Fick's law leads to the following description of mass transfer (Eq. (1)):

$$J_A = \frac{D_{A,G}}{\delta_G}(C_{A,G} - C^i_{A,G}) = \frac{D_{A,L}}{\delta_L}(C^i_{A,L} - C_{A,L}) \tag{1}$$

where J_A is the molar rate of mass transfer per unit of interfacial area (mol s^{-1} m^{-2}) between the phases, $D_{A,G}$ and $D_{A,L}$ are the molecular diffusion coefficients ($m^2 \cdot s^{-1}$), $C_{A,G}$ and $C_{A,L}$ are the actual concentrations (mol m^{-3}) in the bulk of the liquid $C^i_{A,G}$ and $C^i_{A,L}$ are the concentrations of solute A at the interface in the gas and the liquid phase, respectively.

The molar transfer rate coefficient k_G (gas side) or k_L (liquid side) (m s^{-1}) can be defined as the ratio between the intrinsic molecular diffusivity of the solute gas A in the gas or liquid matrix and the diffusion lengths δ_G or δ_L (Eqs. (2) and (3)). The diffusion lengths depend on the reactor flow and mixing properties.

$$\frac{D_{A,G}}{\delta_G} = k_G \tag{2}$$

$$\frac{D_{A,L}}{\delta_L} = k_L \tag{3}$$

Note that Eq. (3) (respectively Eq. (2)) is in fact the definition of the liquid (gas) film thickness δ_L (δ_G), which cannot be measured because it does not really exist. The advantage of this model is its simplicity, its teaching power, and its ability to describe the coupling of mass transfer with chemical reactions sufficiently accurately for most practical cases.

Using these definitions, Eq. (1) can be rewritten as Eq. (4):

$$J_A = k_G(C_{A,G} - C^i_{A,G}) = k_L(C^i_{A,L} - C_{A,L}) \tag{4}$$

It can be assumed for almost all practical cases that equilibrium exists at the interface between the two phases. The concentrations of solute A at the interface, $C^i_{A,G}$ and $C^i_{A,L}$, are related by the equilibrium relation of Eq. (5) and which, for gases in general and hydrogen in particular, is often described using simplified Henry's law applied at the interface (Eq. (6)).

$$C^i_{A,L} = m_A C^i_{A,G} \tag{5}$$

$$C^i_{A,L} = \frac{P^i_{pA}}{H_A} \tag{6}$$

Taking the Henry's coefficient H_A as constant, and with the definitions of the molar transfer coefficients k_G and k_L (m s^{-1}), the concentrations at the interface, that cannot be measured, can be eliminated and Eq. (4) applied to the solute A rearranges to:

$$J_A = \left(\frac{RT}{k_G H_A} + \frac{1}{k_L}\right)^{-1}\left(\frac{P_{pA}}{H_A} - C_{A,L}\right) \tag{7}$$

Note that the groups $\frac{RT}{k_G H_A}$ and $\frac{1}{k_L}$ represent the mass transfer resistances on the gas and liquid sides, respectively.

In most of hydrogenation processes, the gas phase is mainly composed of hydrogen used in a pure form, often in a high gas phase concentration (H_2 pressure >0.1 MPa). The other component is the solvent at the saturated vapor pressure, which can be often neglected since hydrogenations with molecular catalysts are performed at rather low temperatures (20–100 °C). Furthermore, the diffusion coefficient of hydrogen is high, leading to large values of k_G. Finally, hydrogen is poorly soluble in liquids, and this reflects in high values of H_A. All of these considerations support the assumption that gas-phase resistance against mass transfer is negligible for hydrogenations. Thus in practice, Eq. (7) reduces to:

$$J_H = k_L\left(\frac{P_{pH}}{H_H} - C_{H,L}\right) \quad \text{or} \quad J_H = k_L(C^{eq}_{H,L} - C_{H,L}) \tag{8}$$

Knowing the interfacial or contact area A (m^2) between the gas and the liquid phase, the total molar flow Φ_H (mol s^{-1}) of transferred hydrogen is:

$$\Phi_H = k_L A\left(\frac{P_{pH}}{H_H} - C_{H,L}\right) \tag{9}$$

Of course, when designing reactors it is interesting to refer to the specific contact area a (m^2 m$_{G+L}$$^{-3}$) – that is, the interfacial area per unit volume of gas–

liquid emulsion $V_R = V_G + V_L$. The contact area A and the specific contact area a are related by Eq. (10):

$$A = aV_R \tag{10}$$

In some cases, it can be useful to use other definitions for the specific contact area. For example, some authors use a_L, which is the interfacial area per unit volume of liquid ($m^2\ m_L^{-3}$) or a_G, the interfacial area per unit volume of gas ($m^2\ m_G^{-3}$). Note that the nomenclature a, a_L or a_G is not always specified. The specific contact areas are related by:

$$A = aV_R = a_L V_L = a_G V_G = a_L \varepsilon_L V_R = a_G \varepsilon_G V_R = a_G(1 - \varepsilon_L) V_R \tag{11}$$

where ε_L is the liquid hold-up of the gas–liquid emulsion. Using the definition, the total molar flow Φ_H becomes:

$$\Phi_H = k_L a \left(\frac{P_{pH}}{H_H} - C_{H,L} \right) V_R \tag{12}$$

Note that the ratio $r_{obs} = \Phi_H / V_R$ (mol $s^{-1}\ m^{-3}$) is the observed rate of hydrogen consumption from the gas phase.

This simplified description of molecular transfer of hydrogen from the gas phase into the bulk of the liquid phase will be used extensively to describe the coupling of mass transfer with the catalytic reaction. Beside the Henry coefficient (which will be described in Section 45.2.2.2 and is a thermodynamic constant independent of the reactor used), the key parameters governing the mass transfer process are the mass transfer coefficient k_L and the specific contact area a. Correlations used for the estimation of these parameters or their product (i.e., the volumetric mass transfer coefficient $k_L a$) will be presented in Section 45.3 on industrial reactors and scale-up issues. Note that the reciprocal of the latter coefficient has a dimension of time and is the characteristic time for the diffusion mass transfer process $t_{diffGL} = 1/k_L a$ (s).

45.2.2
Physical and Chemical Data for Hydrogenations

The design of gas–liquid reactors requires the consideration of four sets of basic data:

(i) the heat of reaction;
(ii) distribution of the reagents between the phases at thermodynamic equilibrium – that is, hydrogen solubility in the liquid and the vapor pressure of the solvent in the gas phase;
(iii) the physical rate at which hydrogen transfers from the gas phase to the liquid phase – that is, mainly driven by the hydrogen diffusivity in the liquid (see above) and the interfacial surface area; and
(iv) the chemical rate of transformation that is the intrinsic kinetic; this last point is dealt with in Chapter 10, and will not be reviewed here.

Although a comprehensive review of the data cited in points (i), (ii) and (iii) is beyond the scope of this chapter, this section presents a selected collection of data specific to hydrogen. For a more extensive discussion on the topic, the reader is directed to textbooks in the field [8, 9].

45.2.2.1 **Heat of Reaction**

Hydrogenation reactions are mild to highly exothermic (Table 45.1). The highly exothermic nitro-aromatic hydrogenations are generally performed with heterogeneous catalysts. Homogeneous hydrogenations concern almost exclusively the reduction of carbon–carbon double bonds, carbonyls and imines which are mildly exothermic. Furthermore, they are very selective so that in the case of large molecules featuring several chemical functions, only one is generally hydrogenated, with the corresponding exotherm.

The Benson group contribution method, and more recent methodologies, allow the computation of heat of hydrogenation reactions, even for large molecules (note that Benson method gives the reaction enthalpy assuming each species to be a perfect gas!). Software and database (e.g., NIST) are also available.

45.2.2.2 **Solubility**

Many definitions are used to express the solubility of gases in liquids, but usually the equilibrium law is defined as:

$$H_A^x = \frac{P_{pA}}{x_A} \tag{13}$$

where x_A is the mole fraction of gas A dissolved in the liquid, and P_{pA} (MPa) is the partial pressure of the gas A.

This equilibrium can also be expressed by Eq. (14) using the concentration of A at the equilibrium in the liquid phase $C_{A,L}^{eq}$ (mol m^{-3}):

$$H_A = \frac{P_{pA}}{C_{A,L}^{eq}} \tag{14}$$

Table 45.1 Heat of reaction for selected hydrogenations.

Reaction	Example	ΔH [kJ mol^{-1}]
Alkenes to alkanes	RCH=CHR → RCH_2-CH_2R	–117
	Cyclopentene → cyclopentane	–113
Nitriles to amines	RC≡N → RCH_2-NH_2	–120
Alkynes to alkenes	RC≡CR → RCH=CHR	–155
Aromatics to cycloalkanes	Benzene → cyclohexane	–208
Alkynes to alkanes	RC≡CR → RCH_2-CH_2R	–274
Nitro-aromatics to amines	Ph-NO_2 → Ph-NH_2	–493

Table 45.2 Examples of experimental correlations for hydrogen solubility.

Solvent	Range/Units	$C^{eq}_{H,l}$ or H^x_H	Reference
Ethanol	293–333 K	$C^{eq}_{H,L} = 0.0099 \exp\left(-\frac{2640}{RT}\right) P_{pH}$	10
Cyclohexane	283–323 K	$C^{eq}_{H,L} = 0.00529 \exp\left(-\frac{3775}{RT}\right) P_{pH}$	10
α-Methylstyrene		$C^{eq}_{H,L} = (0.145T–16.985)\ P_{pH}$	11
Toluene/ethyl pyruvate	C_{Etpy} (mol m^{-3}) 2–10 MPa 293–343 K	$C^{eq}_{H,L} = (357.2–10173\ C_{Etpy}) \exp\left(-\frac{6352}{RT}\right) P_{pH}$	12
Rapeseed oil	0.03–1 MPa 413–473 K	$C^{eq}_{H,L} = 0.203 \exp\left(-\frac{5900}{RT}\right) P_{pH}$	13
Methanol	H^x_H (MPa) P_{pH} (Pa) 0.1–1.6 MPa 20–140 °C	$H^x_H = \exp\left(-122.3 + \frac{4815.6}{T} + 17.5 \ln(T) - 1.4 \times 10^{-7} P_{pH}\right)$	14

All correlations adapted to SI units: $C^{eq}_{H,L}$ (mol m^{-3}), T(K), P_{pH} (MPa) unless otherwise stated.

H^x_A (MPa) (Eq. (13)) and H_A (MPa m^3 mol^{-1}) (Eq. (14)) are often referred to as "Henry's constant", but they are in fact definitions which can be used for any composition of the phases. They reduce to Henry's law for an ideal gas phase (low pressure) and for infinitely dilute solution, and are "Henry's constant" as they are the limit when $C^{eq}_{A,L}$ (or x_A) goes to zero. When both phases behave ideally, H depends on temperature only; for a dilute dissolving gas, H depends also on pressure when the gas phase deviates from a perfect gas; finally, for a non-ideal solution (gas or liquid), H depends on the composition. This clearly shows that H is not a "classical" thermodynamic constant and it should be called "Henry's coefficient".

For hydrogen, and within the temperature range used for homogeneous hydrogenations, H decreases when temperature increases and is only slightly dependent on pressure and composition when an excess of solvent is used (Table 45.2). Although it is rarely encountered in homogeneous hydrogenations, examples of the pressure dependence on hydrogen solubility are also provided.

H_A and H^x_A are related by the expression:

$$H_A = \frac{H^x_A}{C_L} \tag{15}$$

where C_L (mol m^{-3}) is the total concentration of the liquid phase. Often, only H^x_A is available. In order to compute $C^{eq}_{A,L}$, C_L must be calculated or estimated which can be difficult for mixed solvents and/or for real liquid phase containing high concentrated reaction species for hydrogenation reaction. For example, the calculation of C_L, H_A then $C^{eq}_{A,L}$ requires a knowledge of the liquid density at the working temperature.

As discussed above, the hydrogen concentration increases with temperature, and that contributes to the overall activation energy up to 6.4 kJ mol^{-1}, far from

being negligible. It is thus advisable to correct the measured activation energy from that of hydrogen dissolution in order to obtain the true chemical activation energy of the catalytic process.

No comprehensive compilation of published hydrogen solubility data is available. However, useful data sources can be found elsewhere [7, 8, 15, 16]. As a well-known general trend for mono- or di-atomic non-polar gases, the solubility

Table 45.3 Examples of H_2 solubility at 25 °C and <0.1 MPa.[a)]

Type	Solvent	$C^{eq}_{H,L}$ [mol m^{-3}]	Reference
Ionic liquids	Various	0.62 to 0.98	17
Water	Water	0.81	14
Alcohols	Methanol	3.40 to 3.70	17, 18
	Ethanol	3.00 to 3.50	17–20
	2-Propanol	3.27	18
	1-Butanol	2.90	18
	Cyclohexanol	1.60	19
Ethers	1,4-Dioxane	2.06	18
Esters	Ethylacetate	3.45	18
	n-Butylacetate	3.55	18
Ketones	Acetone	3.15 to 4.10	15, 19, 20
	Cyclohexanone	2.17	21
Alkanes	*n*-Hexane	4.83	19
	n-Heptane	4.60 to 4.70	15, 19, 20
	n-Octane	4.21	19
	n-Nonane	3.87	19
	Cyclohexane	3.40 to 3.80	17–20
	2,2,4-Trimethylpentane	4.74	19
Alkenes	1-Tetradecene	2.81	18
	Cyclohexene	3.27	21
Aromatics	Aniline	1.08	18
	Nitrobenzene	1.40	18
	Chlorobenzene	2.56	19
	Benzene	2.54 to 2.98	17–20
	1,2,4-Trimethylbenzene	2.59	18
	α-Methylstyrene	2.65	22
	Ethylbenzene	2.69	18
	Toluene	2.81 to 3.50	17, 18
	m-Xylene	2.91 to 3.40	18, 19
Chloroalkanes	1,2-Dichloroethane	2.25	18
	Tetrachloromethane	3.14 to 3.47	15, 18
	1,1,2,2-Tetrachloroethane	3.84	19
Fluorous	1,1,2-Trichloro-1,2,2-trifluoroethane	5.51	19
	n-Perfluoroheptane	6.30 to 6.31	15, 19
Others	Carbon disulfide	2.48	15, 19
	Dimethyl sulfoxide	1.07	19

a) Some values computed from published correlations.

of hydrogen is very small in liquids exhibiting strong cohesion forces such as water and ionic liquids, but it increases in organic solvent and reaches high solubility for fluorous media (Table 45.3).

Gas solubility in mixed solvents (and, therefore, Henry's constant) varies with solvent composition. The simplest approximation for this is given in Eq. (16) [23]:

$$\ln(H_A^{x,mix}) = \sum_{j=\text{solvents}} x_j^{mix} \ln(H_A^{x,j}) \tag{16}$$

where x_j^{mix} is the molar fraction of solvent j in the mixture.

Good approximate values could be obtained using Eq. (16). For a 1 : 1 mixture of methanol and methyl formate, calculated ($H_H^{x,calc} = 520$ MPa) and measured ($H_H^{x,exp} = 495$ MPa) Henry coefficients only differ by less than 5% [24].

Very often, solubility and/or Henry's coefficients are determined for each application, preferentially using a liquid phase as close as possible to the real liquid composition, and under the actual operating conditions. Details of experimental methods have been published [16, 25]. Direct measurement of the hydrogen concentration in the liquid phase is also possible using specific probes. Whereas several sensors and techniques have been developed in the past, they cannot generally be applied to processes that may involve high temperature and pressure (up to 500 K and 10 MPa) and corrosive environments. These problems seem to be solved with a new development, albeit the response time is still an issue for very fast processes [26]. Note that solubility could vary during the course of reaction since the composition of the liquid changes [27].

45.2.2.3 **Diffusivity**

The gas A must transfer from the gas phase to the liquid phase. Equation (1) describes the specific (per m^2) molar flow (J_A) of A through the gas–liquid interface. Considering only limitations in the liquid phase, this molar flow notably depends on the liquid molecular diffusion coefficient $D_{A,L}$ ($m^2\,s^{-1}$). Based on the liquid state theories, $D_{A,L}$ can be calculated using the Stokes-Einstein expression, and many correlations have been developed in order to estimate the liquid diffusion coefficients. The best-known example is the Wilke and Chang (W-C) relationship, but many others have been established and compared (Table 45.4) [28–33].

The coefficients are defined for infinitely dilute solution of solute in the solvent L. However, they are assumed to be valid even for concentrations of solute of 5 to 10 mol.%. The relationships are available for pure solvent, and could be used for mixture of solvents composed of molecules of close size and shape. They all refer to the solvent viscosity which can be estimated or measured. Pressure has a negligible influence on liquid viscosity, which decreases with temperature. As a consequence, pressure has a weak influence on liquid diffusion coefficient; conversely, diffusivity increases significantly with temperature (Table 45.4). For mixtures of liquids, an averaged value for the viscosity should be employed.

Table 45.4 Estimation of the diffusion coefficient in liquid phase.

1	Stokes-Einstein	$D_{A,L} = \frac{kT}{3\pi\mu_L\sigma_A}$	
2	Wilke and Chang	$D_{A,L} = 5.8810^{-17}\frac{T\sqrt{\varphi M_L}}{\mu_L v_A^{0.6}}$	$\varphi=1$, non-associated liquid $\varphi=2.6$, water $\varphi=1$–2, liquid with hydrogen bonding
3	Diaz et al.	$D_{A,L}(25°C) = 1.8610^{-12}\frac{v_L^{0.36}}{v_A^{0.64}\mu_L^{0.61}}$	$273<T<338$ K
		$\frac{D_{A,L}(T)}{D_{A,L}(25°C)} = 4996\, e^{\frac{-2539}{T}}$	$a=1$, $b=-1.15$, water
4	Sovová	$D_{A,L} = 1.3210^{-15}\frac{a\mu_L^b}{v_A^{0.6}}$	$a=1.8$, $b=-1.15$, spherical molecule $a=203.2$, $b=-0.5$, alkane, *n*-alcohol

Generally, diffusion coefficients at infinite dilution are in the range 5×10^{-10} and 3×10^{-9} $m^2\,s^{-1}$ [29, 35, 36]. Since hydrogen is a very small molecule, it diffuses faster than most other dissolved gas. As a result, correlation-based estimates are often underestimated, as shown in Table 45.5.

A wide range of values (one decade!) could be obtained using correlations as well as using different experimental methods [34, 38, 43]. As for solubility, diffusion coefficient at infinite dilution should be determined experimentally using the real liquid phase. Experimental methods are, however, more complex to carry out and correlations are widely used.

45.2.3
Coupling Between Mass Transfer and a Single Homogeneous Irreversible Reaction

For a simple hydrogenation reaction between H_2 transferred from the gas phase with the substrate S present in the bulk liquid phase ($S+H_2\rightarrow P$), considering no mass transfer resistance on the gas side and a gradientless concentration of the molecular catalyst in the liquid phase, various concentration profiles in the liquid boundary layer, or film, exist (Fig. 45.2).

Case 1 in Figure 45.2 refers to a case where the reaction between S and H_2 is very slow. In that case, the rate of hydrogen consumed by the reaction (i.e., the rate of the reaction) is small compared to the maximum rate of mass transfer. Thus, mass transfer feeds the liquid phase easily with dissolved hydrogen. The liquid-phase hydrogen concentration is very close to that at equilibrium given by the Henry's law:

$$C_{H,L} \cong C_{H,L}^{eq} = \frac{P_{pH}}{H_H} \tag{17}$$

Table 45.5 Experimental value of the diffusion coefficient of H_2 ($D_{H\,L}$ $m^2\,s^{-1}$) in some usual liquids and estimates.

Solvent/Reference	T [K]	$D_{H,L}$ [$m^2\,s^{-1}$]		W-C [a] [$m^2\,s^{-1}$]	e [b] [%]	Sovová [a] [$m^2\,s^{-1}$]	e [b] [%]	Diaz [a] [$m^2\,s^{-1}$]	e [b] [%]
Water [37]	294	5.10×10^{-9}		2.92×10^{-9}	43	3.13×10^{-9}	39	3.23×10^{-9}	37
Methanol [37, 38]	293	1.65×10^{-8}	1.72×10^{-8}	5.74×10^{-9}	65	8.86×10^{-9}	46	5.51×10^{-9}	67
Ethanol [37, 38]	293	1.49×10^{-8}	1.51×10^{-8}	3.04×10^{-9}	80	6.25×10^{-9}	58	4.26×10^{-9}	71
1-Propanol [37, 38]	298	1.19×10^{-8}	1.28×10^{-8}	1.81×10^{-9}	85	4.55×10^{-9}	62	3.25×10^{-9}	73
2-Methyl-1-propanol [37, 38]	293	7.90×10^{-9}	7.93×10^{-9}						
1-Pentanol [37, 38]	293	1.64×10^{-8}	2.04×10^{-8}						
Acetone [38]	298	4.17×10^{-8}		1.08×10^{-8}	74	2.03×10^{-8}	51	1.04×10^{-8}	75
Benzene [38]	298	2.00×10^{-8}		6.48×10^{-9}	68	9.55×10^{-9}	52	7.67×10^{-9}	62
Cyclohexane [38]	298	1.73×10^{-8}		4.55×10^{-9}	74	6.10×10^{-9}	65	6.52×10^{-9}	62
Cyclohexene [38]	298	2.24×10^{-8}		6.13×10^{-9}	73	8.71×10^{-9}	61	7.70×10^{-9}	66
a-Methylstyrene [39]	298	1.10×10^{-8}							
Cumene [39]	298	1.30×10^{-8}							
n-Hexane [38]	298	6.24×10^{-8}		1.41×10^{-8}	77	1.26×10^{-8}	80	1.37×10^{-8}	78
n-Heptane [38]	298	5.01×10^{-8}		1.16×10^{-8}	77	1.10×10^{-8}	78	1.23×10^{-8}	76
n-Octane [38]	298	4.49×10^{-8}		8.84×10^{-9}	80	9.31×10^{-9}	79	1.05×10^{-8}	77
Tetrachloromethane [37, 38, 40]	298	9.75×10^{-9}	1.05×10^{-8}	5.78×10^{-9}	41	5.66×10^{-9}	42	6.17×10^{-9}	37
Triperfluorobutylamine [41, 42]	298	6.52×10^{-9}	8.25×10^{-8}						

a) See Table 45.4 for expression (W-C: Wilke and Chang).
b) e = 100×(experimental value–calculated value)/experimental value.

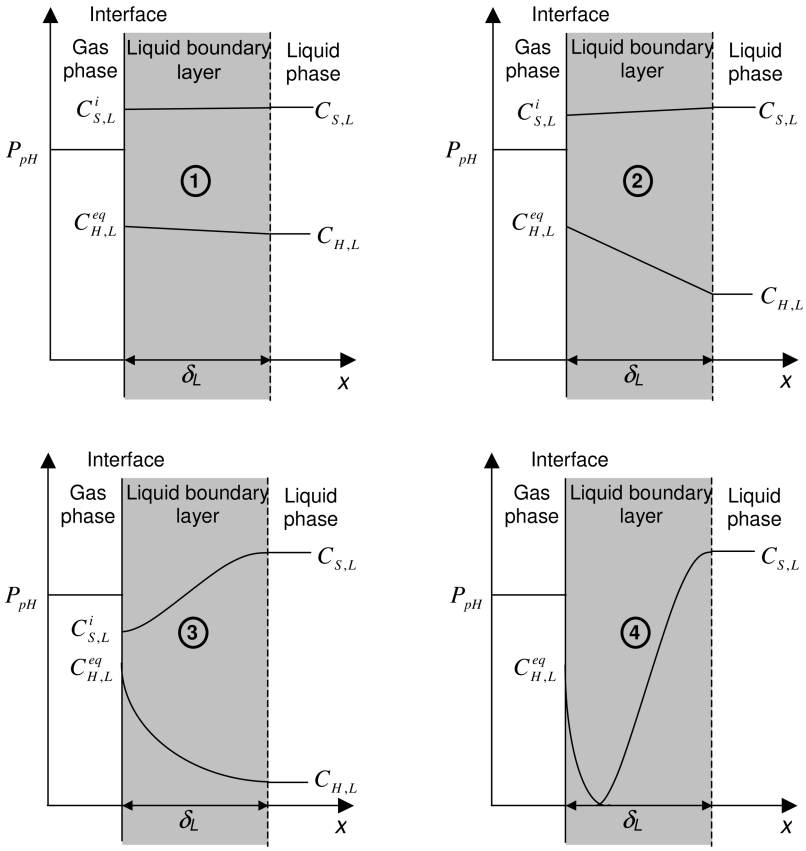

Fig. 45.2 Possible qualitative concentration profiles in the liquid boundary layer for homogeneous hydrogenations with molecular catalysts.

The concentration of the substrate S is also uniform throughout the boundary layer. This case is often called "chemical regime", because the limiting phenomenon is the chemical reaction and not the physical process of mass transfer. In that case, the gas–liquid contact area (A, a, a_L...) is not a crucial parameter; conversely, the liquid retention (ε_L) must be high to promote the reaction.

Curve 2 in Figure 45.2 depicts the case where the hydrogenation reaction is not that slow. Most of the conversion still takes place in the bulk of the liquid, so that the concentration of S in the film is almost that in the bulk of the liquid; the fall in hydrogen concentration across the film is mainly due to the diffusional resistance coupled to the "pumping" effect of the reaction in the bulk liquid. In that case an efficient reactor must have a high liquid retention, ε_L, for the reaction to take place in the bulk, and a high surface area, a, for hydrogen transfer through the film.

In case 3 in Figure 45.2, the curves give qualitatively the concentrations distributions for a moderately fast reaction. Here, a significant fraction of the gas that dissolves, is converted within the boundary layer before reaching the bulk liquid. Correspondingly, S is also converted in the film and its concentration is lower than in the bulk of liquid phase. Since a significant part of the conversion takes place in the film, the interface area becomes even more important than in the previous cases, and reactors developing a larger specific contact area will drive to higher conversion rates. Finally, in case 4, the reaction is so fast that it occurs completely in the film. No reaction takes place in the bulk liquid phase ($C_{H,L}=0$) and the observed rate of conversion is proportional to the contact area. The liquid retention ε_L is of no importance.

The above general qualitative discussion points that at least three important parameters play a role in the coupling of mass transfer with the chemical reaction:

- the ratio between the intrinsic reaction rate and the maximum transfer rate;
- the specific contact area (or interface/volume ratio) of the gas–liquid phases; and
- the concentration ratio $C_{H,L}^{eq}/C_{S,L}$.

Although more fundamental approaches are used in the science of chemical reaction engineering to account for the diffusion/reaction coupling, we rather propose the explanation restricted to rate laws of first order with respect to hydrogen and based on intuition.

The exact composition of the liquid with respect to hydrogen cannot be guessed. Consequently, we can only estimate either transfer or reaction maximum rates and fluxes. From Eq. (12), the maximum mass transfer rate Φ_H^{max} (mol s^{-1}) is obtained when the reaction is so "fast" that the bulk concentration of dissolved hydrogen is zero ($C_{H,L}= 0$), as given in Eq. (18).

$$\Phi_H^{max} = k_L a V_R \frac{P_{pH}}{H_H} = k_L a V_R C_{H,L}^{eq} \tag{18}$$

Assuming a first-order rate law with respect to hydrogen, with a kinetic constant k_c, the maximum rate of chemical reaction (mol s^{-1} m$_L^{-3}$) is obtained when the hydrogen concentration reaches equilibrium ($C_{H,L}=C_{H,L}^{eq}$) and the corresponding maximum reaction flux Φ_{Chem}^{max}(mol s^{-1}) results in Eq. (19).

$\Phi_{Chem}=rV_R=k_c C_{H,L} V_R$ with $C_{H,L}=C_{H,L}^{eq}$ affords:

$$\Phi_{Chem}^{max} = rV_R = k_c C_{H,L}^{eq} V_R \tag{19}$$

If ϕ^2 is the ratio of these maximal fluxes, this is rewritten as (Eq. (20)):

$$\phi^2 = \frac{rV_L}{k_L a V_R}\left(\frac{P_{pH}}{H_H} - C_{H,L}\right)^{-1} = \frac{r}{k_L a_L C_{H,L}^{eq}} = \frac{k_c}{k_L a_L} = \frac{k_c \varepsilon_L}{k_L a} \tag{20}$$

Three situations arise:

- $k_L a \gg k_c \varepsilon_L \Leftrightarrow \phi^2 \ll 1$. The mass transfer is very easy compared to the chemical reaction. The latter is thus the limiting process, and the reacting system is described as operating in the "chemical regime" as depicted in Figure 45.2 a.
- $k_L a \ll k_c \varepsilon_L \Leftrightarrow \phi^2 \gg 1$. The mass transfer is difficult compared to the chemical reaction. The mass transfer is the limiting process, and the system is described as operating in the "diffusion controlled regime" (Fig. 45.2, cases 1 to 4).
- $k_L a$ and $k_c \varepsilon_L$ are close $\Leftrightarrow \phi^2$ is close to unity. Both the chemical and physical processes are important and contribute to the overall hydrogenation rate.

The reasoning was built using the constants describing the physical and chemical processes. It is often more convenient to compare the characteristic times of the processes involved. Equation (20) transforms into Eq. (21):

$$\phi^2 = \frac{k_c}{k_L a_L} = \frac{t_{\mathrm{diffGL}}}{t_c} \tag{21}$$

where t_{diffGL} is the characteristic diffusional gas–liquid mass transfer time ($t_{\mathrm{diffGL}} = 1/k_L a_L$) and t_c is the characteristic chemical reaction time which, for a first-order reaction, is the reciprocal of the kinetic constant ($t_c = 1/k_c$). Many other physical phenomena that can interfere with the chemical reaction are described by their characteristic times. These include macro- and micro-mixing, mass transport by convection, and heat exchange. Often, a simple comparison of these characteristic times offers a simple and convenient tool to identify the dominant process in the reactor.

The *qualitative* results above are obtained for *first-order* kinetics. The proper quantitative dimensionless criterion describing reaction/diffusion coupling for kinetic laws *n*th order with respect to the gas solute and *m*th order with respect to the substrate has been derived using more complex mathematics, following the pioneering investigations of Hatta. For homogeneous hydrogenations $S + H_2 \rightarrow P$, the rate laws write $r = k_c (C_{H,L})^n (C_{S,L})^m$ leading to the Hatta number (Eq. (22)).

$$Ha = \frac{1}{k_L} \sqrt{\frac{2}{n+1} D_{H,L} k_c C_{H,L}^{i\,(n-1)} C_{S,L}^{m}} \tag{22}$$

where $D_{H,L}$ is the diffusion coefficient of hydrogen in the liquid and $C_{H,L}^{i}$ is the hydrogen concentration at the interface (see Fig. 45.1). It can be easily recognized that both numbers *Ha* and ϕ compare the rate of chemical reaction and that of diffusion.

In order to compute *Ha*, the first problem is the knowledge of $C_{H,L}^{i}$. It was noted earlier that the resistance to mass transfer on the gas side is negligible, but this assumption is valid only when the gas phase is composed of pure hydrogen – that is, the vapor pressure of the solvent and substrate are negligible and it must be checked. Under this assumption, Eq. (17) applies and Eq. (22) becomes:

$$Ha = \frac{1}{k_L}\sqrt{\frac{2}{n+1} D_{H,L} k_c C_{H,L}^{eq\,(n-1)} C_{S,L}^{m}} \tag{23}$$

In general, the intrinsic kinetics, the diffusion, mass transfer and Henry coefficients are either known or can be estimated, while the Hatta number can be determined. This is the first step in assessing the working regime of the reactor.

The Hatta criterion compares the rates of the mass transfer (diffusion) process and that of the chemical reaction. In gas–liquid reactions, a further complication arises because the chemical reaction can lead to an increase of the rate of mass transfer. Intuition provides an explanation for this. Some of the reaction will proceed within the liquid boundary layer, and consequently some hydrogen will be consumed already within the boundary layer. As a result, the molar transfer rate J_H with reaction will be higher than that without reaction. One can now feel the impact of the rate of reaction not only on the transfer rate but also, as a second-order effect, on the *enhancement* of the transfer rate. In the case of a slow reaction (see case 2 in Fig. 45.2), the enhancement is negligible. For a faster reaction, however, a large part of the conversion occurs in the boundary layer, and this results in an overall increase of mass transfer (cases 3 and 4 in Fig. 45.2).

For a more general and quantitative description of the mass transfer rate and in the absence of mass transfer limitations on the gas side, the enhancement factor $E \geq 1$ is defined as:

$$J_H = E k_L (C_{H,L}^{eq} - C_{H,L}) \tag{24}$$

Since E depends itself on $C_{H,L}$, which in turn depends on the intrinsic kinetics, its value is not obvious to compute. For first-order reactions, the system formed with Eqs. (24) to (26), and with the given boundary conditions and corresponding to the qualitative profiles of Figure 45.2, must be solved.

$$\text{Mass balance of hydrogen:} \quad D_{H,L}\frac{d^2 C_H}{dx^2} = k_c C_H C_S \tag{25}$$

$$\text{Mass balance of the substrate:} \quad D_{S,L}\frac{d^2 C_S}{dx^2} = k_c C_H C_S \tag{26}$$

Boundary conditions: $x=0$, $C_H = C_{H,L}^{i}$ and $dC_S/dx = 0$
$x=\delta_L$, $C_H = C_{H,L}$ and $C_S = C_{S,L}$

The boundary conditions require knowledge of the interface concentration of hydrogen $C_{H,L}^{i}$ to compute E (see below). For hydrogenations, the equilibrium concentration ($C_{H,L}^{i} = C_{H,L}^{eq}$) can be used, albeit with the assumption of no mass transfer resistance on the gas side. Otherwise, it must be determined using Eq. (4). The boundary conditions for the substrate S state that it is not transferred to the gas phase – that is, S is not vaporized. This assumption is most often

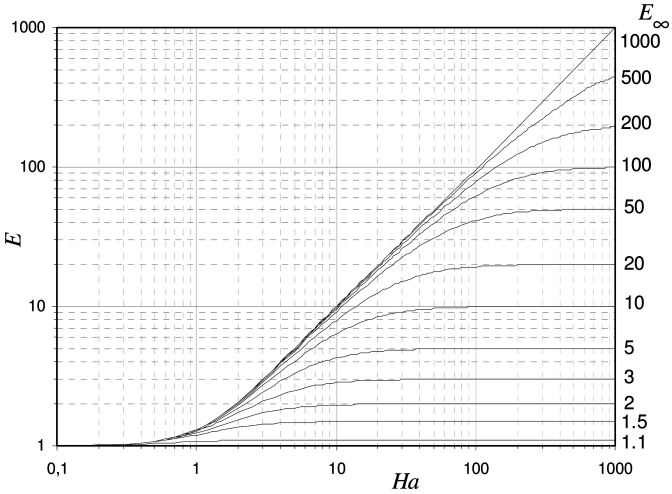

Fig. 45.3 The Van Krevelen and Hoftijzer diagram.

valid since substrates involved in homogeneous hydrogenations are rather large molecules of molecular weight ≥120 and with high boiling points (≥150 °C). Key values k_L, $D_{H,L}$, $D_{S,L}$, k_c are of the same type as those required to compute the Hatta number (see above).

An approximate analytical solution to this system has been proposed by van Krevelen and Hoftijzer (Eq. (27) and Fig. 45.3)):

$$E = \frac{Ha'}{th(Ha')}, \quad Ha' = Ha\sqrt{\frac{E_\infty - E}{E_\infty - 1}}, \quad E_\infty = 1 + \frac{D_{S,L}C_{S,L}}{D_{H,L}C^{i}_{H,L}} \tag{27}$$

where E_∞ is the limiting enhancement factor.

From Eq. (27), the enhancement factor E, and hence J_H, is obtained by trial and error. Using the two numbers Ha and E, the four situations in Figure 45.2 can be now quantitatively described:

- Situation 1: very slow reaction, $Ha \to 0$, $C_{H,L} \cong C^{i}_{H,L} \cong C^{eq}_{H,L}$ diffusion processes are not limiting, the reactor performances are readily estimated using the intrinsic chemical kinetics.
- Situation 2: slow chemical reaction, $Ha < 0.3$, $E \cong 1$. The Hatta number is small, and thus the chemical reaction does not modify the mass transfer process and consequently, $E \cong 1$. However, the chemical reaction is not so slow compared to the mass transfer rate. The hydrogen concentration in the bulk is smaller than the equilibrium concentration. The substrate concentration A is constant in the film and is almost that in the bulk. The consumption of H_2 and A is negligible in the film and takes place in the bulk of the liquid. The reactor performances are obtained straightforwardly (see below). The mass transfer rate is obtained by $J_H = k_L(C^{eq}_{H,L} - C_{H,L})$.

- Situation 3: fast reaction, $0.3 < Ha < 3$, $E > 1$. The reaction occurs in the boundary layer to a large extent so that the hydrogen concentration in the bulk of the liquid is very low. The mass transfer rate is obtained by $J_H = Ek_L(C_{H,L}^{eq} - C_{H,L})$ with $E \cong \sqrt{1 + Ha^2}$, $E < E_\infty$.
- Situation 4: very fast reaction, $Ha > 3$ and $E < E_\infty$, $E \cong Ha$. All the conversion occurs in the boundary layer. The hydrogen concentration in the bulk of the liquid falls to zero. Thus, all the catalyst in the bulk is useless. For instantaneous reactions, $Ha \gg 3$, $E = E_\infty$ and the reaction takes place in a narrow plane located somewhere in the boundary layer; the larger E_∞ the closer to the interface the reaction plane. If the limiting enhancement factor E_∞ is very high, it is said that the reaction takes place at the gas–liquid interface. Such a case is referred to as "surface reaction".

In situations 3 and 4, as much interface area as possible with a minimum volume of bulk liquid is required. However, hydrogenations are not very fast reactions and, in most cases, situations 1 or 2 prevail.

In this section, we have examined how the coupling between mass transfer and the chemical reaction defines the concentration profile of the limiting reagent (i.e., hydrogen), and how the mass or molar flow between the gas and the liquid phase can be computed. In the next section, the estimation of the overall rate of reaction (i.e., the reactor productivity) will be reviewed for different gas–liquid reactors.

45.2.4
Coupling of Reaction and Mass Transfer in Ideal Reactors

On a theoretical basis, when considering two fluid phases and the three basic ideal reactors (i.e., a closed stirred tank (batch), continuous stirred tank (CSTR) and plug flow), six ideal reactor types can be listed. Applying the specificity of homogeneous hydrogenations reduces the number to only four cases. Indeed, when considering a gas phase composed of pure hydrogen, perfectly mixed or plug flow considerations for the gas phase are equivalent. Second, as hydrogen is poorly soluble, hydrogenation reactors are conducted under constant hydrogen pressure to achieve high substrate conversion. Thus, the three ideal reactors investigated here are:

- stirred tank reactor, closed to liquid, open to gas feed (batch or B)
- stirred tank reactor, open to the liquid and the gas (CSTR)
- plug flow reactor, open to the liquid and the gas (PF).

(Note here that the term "batch" refers to the liquid phase – that is, to the dissolved reagents.)

Last but not least, the following simplifications and/or assumptions are generally valid and/or can be achieved and checked:

1. The gas phase is pure hydrogen at constant pressure (no need to write gas phase mass balance).

2. The hydrogenation corresponds to a single reaction $S+\nu H_2 \rightarrow P$ with very high chemo- or regio-selectivity; thus, negligible side reactions and with $\nu=1$ generally, the ubiquitous case of asymmetric hydrogenations has been investigated [43].
3. The liquid phase volume can be considered as constant (except for the semi-batch!), since the change in molar volume going from the reagent to product is minimal, especially in the case of the rather large molecules used in pharmaceutical applications and/or the reagent is diluted with a solvent.
4. Isothermal conditions prevail.

In the following, the mass balance for substrate S and hydrogen in the liquid phase are written, considering that assumptions 1 to 4 hold. For a more illustrative view, mass balance is proposed with the concentrations as variables. In general, if the reaction stoichiometry is known, then the conversion number is used as the unified single variable.

45.2.4.1 Mass Balance for a Batch Reactor

For substrate S: $$\frac{dC_{S,L}}{dt} = -r(C_{H,L}, C_{S,L}) \tag{28}$$

For hydrogen: $$\frac{dC_{H,L}}{dt} = \underbrace{-\nu r(C_{H,L}, C_{S,L})}_{\text{Reaction}} + \underbrace{Ek_L a(C_{H,L}^{eq} - C_{H,L})}_{\text{Mass transfer}} \tag{29}$$

Clearly, for a very slow reaction ($Ha<0.3$), the gas to liquid mass transfer is not limiting, which translates into $C_{H,L} \cong C_{H,L}^{eq}$ (see above), thus making the contribution of mass transfer negligible. Equation (29) can be discarded as $C_{H,L} \cong C_{H,L}^{eq}$ can be used in Eq. (28).

From a production viewpoint, the operating parameter is the time required to achieve a given conversion of S. It is obtained by solving the set of differential Eqs. (28) and (29). This requires knowledge of the intrinsic rate law $r(C_S, C_H)$, the volumetric mass transfer coefficient $k_L a$, the boundary conditions (initial and final concentrations of hydrogen and substrate S, i.e., $C_{H,L}^{in}$, $C_{H,L}^{out}$, $C_{S,L}^{in}$, and $C_{S,L}^{out}$, the two latter being related by the conversion), and a good estimate of the enhancement factor E. The latter factor is estimated with Eq. (27), and requires knowledge of the hydrogen and substrate S diffusion coefficients in the liquid phase and the Hatta number.

Very often, the quasi steady-state assumption for the hydrogen liquid phase concentration is proposed (Eq. (30)):

$$\frac{dC_{H,L}}{dt} = -\nu r(C_{H,L}, C_{S,L}) + Ek_L a(C_{H,L}^{eq} - C_{H,L}) \cong 0 \tag{30}$$

This generally leads to a much simpler integration of Eq. (28). Even under a constant hydrogen pressure, this assumption is not valid in the early stages of

the reaction, nor when complete conversion is achieved as hydrogen will still be transferred as long as the hydrogen liquid phase concentration does not reach the equilibrium concentration. However, it is generally valid for most of the reaction course.

When applying, the simplified following expressions are obtained:

$$\text{For substrate S:} \quad t_{\text{Batch}} = \int_{C_{\text{S,L}}^{\text{in}}}^{C_{\text{S,L}}^{\text{out}}} \frac{dC_{\text{S,L}}}{r(C_{\text{H,L}}, C_{\text{S,L}})} \tag{31}$$

$$\text{For hydrogen:} \quad Ek_{\text{L}}a(C_{\text{H,L}}^{\text{eq}} - C_{\text{H,L}}) = vr(C_{\text{H,L}}, C_{\text{S,L}}) \tag{32}$$

45.2.4.2 **Mass Balance for a CSTR Reactor**

$$\text{For substrate S:} \quad \underbrace{\frac{Q}{V_{\text{L}}} C_{\text{S,L}}^{\text{in}}}_{\text{Inlet}} - \underbrace{r(C_{\text{H,L}}, C_{\text{S,L}})}_{\text{Reaction}} = \underbrace{\frac{Q}{V_{\text{L}}} C_{\text{S,L}}^{\text{out}}}_{\text{Outlet}} + \underbrace{\frac{dC_{\text{S,L}}}{dt}}_{\text{Accumulation}} \tag{33}$$

$$\text{For hydrogen:} \quad \frac{Q}{V_{\text{L}}} C_{\text{H,L}}^{\text{in}} - vr(C_{\text{H,L}}, C_{\text{S,L}}) + \underbrace{Ek_{\text{L}}a(C_{\text{H,L}}^{\text{eq}} - C_{\text{H,L}})}_{\text{Mass transfer}} = \frac{Q}{V_{\text{L}}} C_{\text{H,L}}^{\text{out}} + \frac{dC_{\text{H,L}}}{dt} \tag{34}$$

Similar to the case of the batch reactor, $C_{\text{H,L}} \cong C_{\text{H,L}}^{\text{eq}}$ (for $Ha < 0.3$) and Eq. (34) is eliminated.

The operating parameter for the CSTR reactor is the liquid flow rate Q, which sets the residence time of the liquid through the ratio Q/V_{L} and finally the conversion. From a production viewpoint, the (residence) time required to achieve a given conversion of S (or outlet concentration of S) is obtained by solving the set of Eqs. (33) and (34). The characteristics of the reactor $k_{\text{L}}a$ and V_{L} must be known. In general, whereas V_{L} is easily determined in a batch reactor, it is not in a CSTR. Rather, $V_{\text{L}} = \varepsilon_{\text{L}} V_{\text{R}}$ will be used, which requires knowledge of the liquid hold-up ε_{L}. Correlations provide $k_{\text{L}}a$ (see below) and ε_{L} characteristics for the different reactor types [3].

45.2.4.2.1 **Simplified Mass Balances**

In most continuous hydrogenations, hydrogen is fed through the gas inlet only ($C_{\text{H,L}}^{\text{in}} = 0$). As hydrogen is poorly soluble in liquids, the outlet molar flow of hydrogen in the liquid can be neglected ($QC_{\text{H,L}}^{\text{out}}/V_{\text{L}} \cong 0$) compared to the mass transfer flow and the reaction flow. Because the reactor is perfectly mixed, the outlet concentration of S is that in the reactor ($C_{\text{S,L}}^{\text{out}} = C_{\text{S,L}}$). Finally, CSTRs are operated over production times much longer than the residence time (otherwise there is no point in working with a continuous reactor!); thus, steady-state conditions stand for most of the production, which translate into:

$$\frac{dC_{S,L}}{dt} \cong 0 \quad \text{and} \quad \frac{dC_{H,L}}{dt} \cong 0$$

With these simplifications, Eqs. (33) and (34) reduce to a set of algebraic Eqs. (35) and (36), which can easily be solved.

$$\text{For reagent A:} \quad \frac{Q}{\varepsilon V_R}(C_{S,L}^{in} - C_{S,L}) = r(C_{H,L}, C_{S,L}) \tag{35}$$

$$\text{For hydrogen:} \quad Ek_L a(C_{H,L}^{eq} - C_{H,L}) = \nu r(C_{H,L}, C_{S,L}) \tag{36}$$

Note that these equations allow the residence time and conversion to be computed, but other process issues are neglected. For example, although assumption 1 is considered, any solvent exhibits some vapor pressure and thus can be extracted by the outlet hydrogen feed.

45.2.4.3 **Mass Balance for a Plug Flow Reactor**

Beside assumptions 1 to 4, a further operating condition is required (and is most often valid!) which simplifies the analysis. The hydrogen flow rate is large compared to the hydrogen consumption by the chemical reaction, and this translates into assuming the liquid hold-up ε_L constant over the reactor length. Under these conditions, and considering the simplifications ($C_{H,L}^{in}=0$, $QC_{H,L}^{out}/V_L=0$ and steady state) proposed in Section 45.2.4.2 on CSTR, the simplified mass balances for S and hydrogen in the liquid phase become:

$$\text{For substrate S:} \quad \frac{\varepsilon_L V_R}{Q} = \int_{C_{S,L}^{in}}^{C_{S,L}^{out}} \frac{dC_{S,L}}{r(C_{H,L}, C_{S,L})} \tag{37}$$

$$\text{For hydrogen:} \quad Ek_L a(C_{H,L}^{eq} - C_{H,L}) = \nu r(C_{H,L}, C_{S,L}) \tag{38}$$

45.3 Industrial Reactor and Scale-Up Issues

Many types of reactor may be used for gas–liquid reactions, including bubble columns, mechanically stirred tanks, plate columns, counter- or co-current packed bed columns, falling films, venturi ejectors, and spray columns. These types of equipment differ in properties such as shape, size, arrangement of internal components used to promote gas–liquid contact and heat removal. They also cover a wide variety of fields, including chemistry, biochemistry, refining, petro-chemistry, food processing, environment, and pharmaceuticals [3, 5]. Selective hydrogenation processes are generally carried out in stirred tank batch reactors ("Batch"), with some examples using CSTRs [44 a] or jet-loop venturi re-

actors [44 b]. Loop reactors are suited to the efficient removal of heat while maintaining good gas to liquid mass transfer capabilities.

Stirred tank reactors are mostly used because they provide a rapid means of obtaining a uniform composition and temperature throughout the reaction mixture; they also offer the flexibility required for the small-scale production of many different molecules. Companies such as Biazzi, Davy Process Technology (Buss loop technology), DeDietrich and others provide technology adapted to hydrogenations (i.e., pressures up to 100 bar and temperatures up to 200 °C) [45–47]. Here, some scale-up issues related to stirred tank reactors are described.

Mechanically stirred gas–liquid reactor performances are affected by the degree of mixing, apparatus geometry, stirring power, flow rate, discharge and feed locations for the gas and liquid. For a correct design, the following requirements must be satisfied:

- satisfactory reactants and catalyst homogeneity in the liquid phase;
- satisfactory dissipation of the reaction heat to insure reactor stability and a reasonable uniform reactor temperature; and
- optimal gas hold-up and sufficient bubble break up to guarantee adequate gas–liquid mass transfer.

Quantitative design correlations to meet these requirements are available in the literature [1–3].

The scale-up of mechanically stirred gas–liquid reactors mainly involves reactor size and stirrer size, and is generally based on homothetic designs from pilot tests. The similitude in the scale-up means that the following parameters are – or at least should be – kept constant:

(i) power dissipation of the stirrer per unit volume (or mass) of liquid;
(ii) heat transfer capability per unit reactor volume; and
(iii) gas–liquid volumetric mass transfer coefficient.

Point (i) only requires the assumption that the power input per unit volume is constant. Items (ii) and (iii) are further discussed below. Most often, these three conditions are difficult to satisfy simultaneously, and a choice must be made between them.

For most homogeneous hydrogenations, heat transfer is generally not an issue. With heat of reactions in the range 100 to 150 kJ mol^{-1} (see above), and considering that dilute (0.5 to 2 kmol m^{-3}) solutions of the substrate are most often used, the maximum adiabatic temperature rise can be estimated (Eq. (39)):

$$\Delta T_{\mathrm{adiab}}^{\max} = \frac{C_{\mathrm{A,L}}^{\mathrm{in}}(-\Delta H)}{\rho_{\mathrm{L}} c_{\mathrm{pm}}} \tag{39}$$

For organic liquids, ρ_L and c_{pm} are in the range 800 to 1100 kg m^{-3} and 2000 to 3000 J kg^{-1} K^{-1}, respectively; this leads to maximum adiabatic temperature rises of 15 to 150 K. Conventional mechanically agitated tank reactors can deal with $\Delta T_{\mathrm{adiab}}^{\max}$ in the range 0 to 20 K, but from $20 < \Delta T_{\mathrm{adiab}}^{\max} < 50$, the boiling tem-

perature of the solvent must be checked for safety as a rise of the total pressure may be large depending on the solvent. A pressure-resistant liquid condenser may be used as a simple heat exchanger. From $50 < \Delta T_{adiab}^{max} < 150$, specifically designed reactors displaying good to excellent heat transfer capacity must be used. Two technologies are available for this: (i) stirred tanks equipped with high surface internals to improve heat exchange (Biazzi); or (ii) loop reactors equipped with an external heat exchanger (Buss loop reactor) [45–47]. While most hydrogenators are stirred tanks, loop reactors are also used for asymmetric hydrogenations [48, 49]. It should be noted, however, that the mass transfer capability of such loop reactors was questioned [50].

The schematic illustration in Figure 45.4 shows that, beside the gas injection, the gas–liquid stirred tank is very similar to devices used for single liquid-phase operations. However, both good mixing and good mass transfer between the gas and the liquid phase are required. Thus, high-shear impellers are preferred to propellers, which are less efficient for promoting a large interfacial area. Rushton-type turbines satisfy these requirements, and are largely used in industry. Typical aspect ratios are given in the figure for the tank, equipped with internals (three to four baffles, gas-sparger) and for the widely used six flat-blades turbine (Rushton-type). Similar turbines equipped with hollow shaft and impellers – the so-called "self-inducing gas effect turbines" such as the Cavitator® – allow better gas–liquid mass transfer.

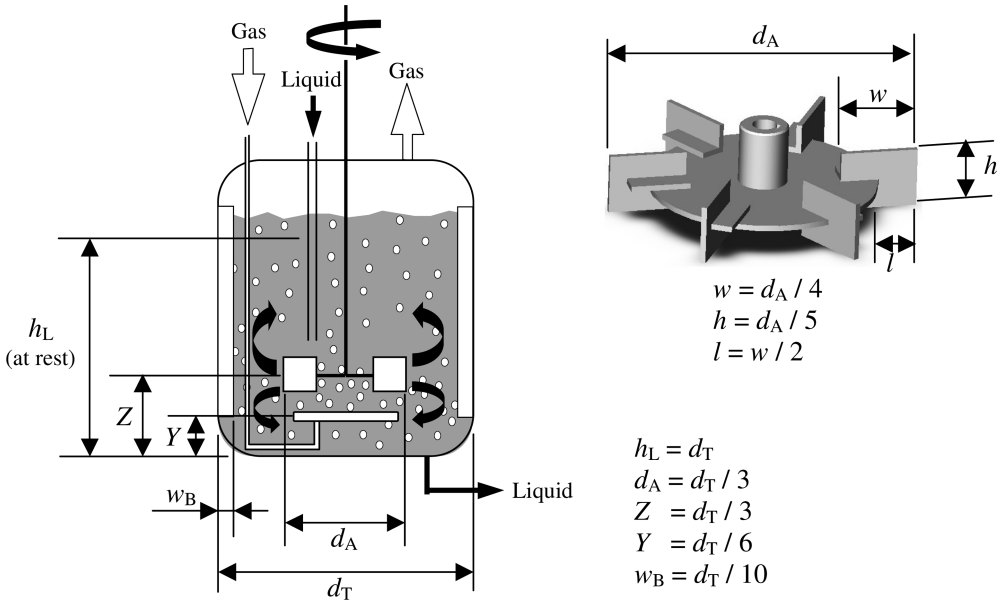

Fig. 45.4 Left: Schematic diagram of a continuous stirred tank reactor with gas and liquid inlet and outlet. Right: A Rushton-type turbine (adapted from [3]).

Batch operations are usually performed in a similar vessel without liquid and gas outlet. In such a set-up (batch) the hydrogen is still fed to the tank, at a flow rate corresponding to the chemical consumption, and possibly to heat removal capability.

Many correlations allow estimation of the gas–liquid volumetric mass transfer coefficient $k_L a$ in mechanically stirred tank reactors. The following intends not to provide a comprehensive review but rather a critical evaluation of selected correlations adapted to hydrogenations [Eqs. (40) to (43)] [25, 51–53].

$$k_L a = 0.06\left(\frac{D_{A,L}}{d_A^2}\right)\left(\frac{N_R d_A^2 \rho_L}{\mu_L}\right)^{1.5}\left(\frac{N_R^2 d_A}{g}\right)^{0.19}\left(\frac{\mu_L}{\rho_L D_{H,L}}\right)^{0.5}\left(\frac{\mu_L V_{SG}}{\sigma_L}\right)^{0.6}\left(\frac{N_R d_A}{V_{SG}}\right)^{0.32} \tag{40}$$

$$k_L a = 0.026\left(\frac{P}{V_L}\right)^{0.4} V_{SG}^{0.5} \tag{41}$$

$$k_L a = 55.2\left(\frac{D_{A,L}}{d_A^2}\right)\left(\frac{N_R^2 d_A}{g}\right)^{2.07}\left(\frac{N_R d_A^2 \rho_L}{\mu_L}\right)^{1.2}\left(\frac{N_R^2 d_A^3 \rho_L}{\sigma_L}\right)^{-1.34} \tag{42}$$

$$k_L a = 0.0003\left(\frac{D_{A,L}}{d_A^2}\right)\left(\frac{\mu_L}{\rho_L D_{A,L}}\right)^{0.5}\left(\frac{N_R d_A^2 \rho_L}{\mu_L}\right)^{1.45}\left(\frac{N_R^2 d_A^3 \rho_L}{\sigma_L}\right)^{0.5} \tag{43}$$

All correlations exhibit a dependence of the volumetric mass transfer coefficient $k_l a$ towards: (i) the properties of the fluids such as those of the liquid (μ_L, ρ_L, σ_L) and of the gas ($D_{A,L}$); (ii) the vessel geometry (d_A thus d_T and others; see Fig. 45.4); and (iii) the agitation speed (N_R). All of these data are easy to collect, and the determination of $k_L a$ should not be problematic.

However, correlations have been established using some experimental investigations, and thus are checked for a restricted range of operating conditions (reactor volume, nature of the liquid, of the gas, pressure and temperature range) and reactor set-up.

For example, the first and second correlations [Eqs. (40) and (41)] were established using a continuous flow of air/oxygen in an open-end gas set-up which resulted in an important contribution of the superficial gas velocity (V_{SG}) to the

Table 45.6 Reactor and experimental conditions used for the correlations.

	V_R	Turbine	Baffles	Gas "A"	Liquid	Temp. [°C]	P [MPa]	Reference
Eq. (40)	12′L	6×Rushton	4	O_2	glycerol-water mixtures	30	0.1	51
Eq. (42)	2.25′L	6×Rushton	2	H_2	propylene	24–60	1.1–5.5	53
Eq. (43)	0.5′L	6×Rushton gas-effect	4	H_2 N_2	water ethanol	20–80	1–5	25

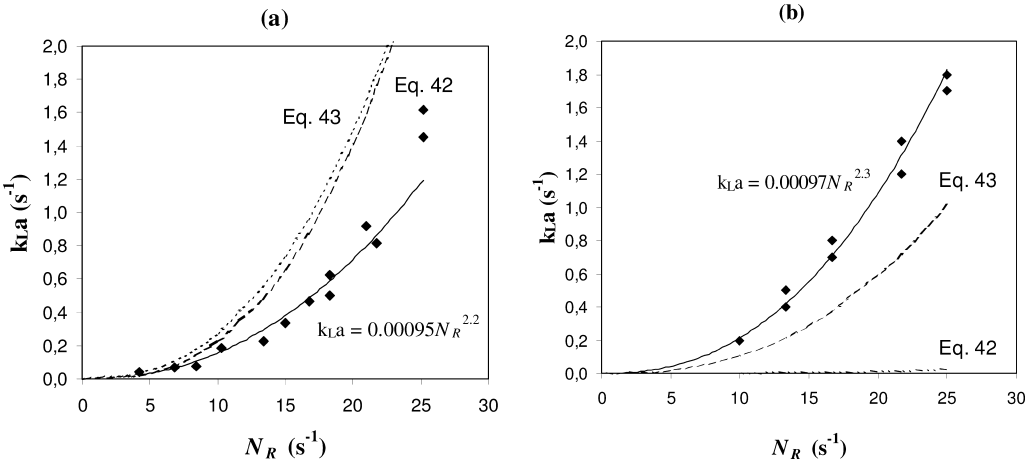

Fig. 45.5 Dependence of the volumetric mass transfer coefficient with the speed of agitation for correlations of Eqs. (42) and (43) and comparison with experimental data for: (a) a 25-cm^3 tank reactor equipped with a four-blade impeller; and (b) a 300-cm^3 tank reactor equipped with a four-blade gas-inducing turbine.

mass transfer process. A correlation close to that in Eq. (41) has been used for the scale-up of Jacobsen hydrolytic kinetic resolution [54]. However, such correlations cannot be used for batch reactors equipped with a hydrogen delivery system, a set-up often encountered in batch production for fine chemicals. Consequently, before any further investigations are made it is highly advisable to check the numerical values obtained, using the three proposed correlations.

A comparison between the two last correlations and experimental data for small laboratory reactors (25 to 300 cm^3) equipped with a magnetic stirrer or a traditional six-blade impeller (not Rushton-type) and using a catalytic hydrogenation in organic solvent has been published (Fig. 45.5) [55].

Three conclusions can be made:

- The two correlations can yield very similar predictions when used inappropriately (i.e., without consideration of the very small size of the reactor, Fig. 45.5 a), but they give different results when larger tank dimensions are reached (Fig. 45.5 b).
- The experimental data are not well fitted by the correlations, thus demonstrating the importance of the stirrer shape and dimensions.
- In the case where no correlations are available (i.e., the application involves an exotic fluid, a non-traditional stirrer or a very small reactor), experimental measurements of k_La must be performed to afford power law correlations valid for very similar reactor, turbines and fluids. Several techniques for k_La determination have been published [56].

45.4
Future Developments

In the future, it is possible that homogeneous hydrogenations will develop to a point where continuous processes are required [44 b]. This will not necessarily be due to large-scale production but, rather, to technological pressures from the pharmaceutical industry. The driving force behind this will be the need for a more rational use of expensive catalysts (asymmetric hydrogenations), for homogeneous catalyst recovery (ionic liquids, other bi-phase systems), or supported catalyst technology. The CSTR might not represent the best choice when switching to continuous processes.

Batch or semi-batch reactors are used in fine chemical and pharmaceutical productions because the production rates are small enough to allow quenching of the reaction, and because a single reactor system may be used for many products. In some cases, continuous operation may be mandatory for reasons dictated by the scale of production, economics, kinetics and safety. For asymmetric hydrogenations, expensive molecular catalysts are often used in gas–liquid systems for which precise control of reaction conditions is necessary. Capital costs in term of occupancy might also be an issue. Some hydrogenations display strong exotherms, such as the hydrogenation of nitro-derivatives, and this requires specific scale-up design that is not easy to achieve with traditional reactor technology. Last – and by no means least – hydrogen is considered to be a dangerous reagent, and any design aiming at reducing the hydrogen inventory inside the reaction medium would be beneficial.

New reactor technologies are currently under development, and these include meso- and micro-structured reactors or the use of membranes. Among meso-structured reactors, monolithic catalysts play a pre-eminent role in environmental applications, initially in the cleaning of automotive exhaust gases. Beside this gas–solid application, other meso-structures such as membranes [57, 58], corrugated plate or other "arranged catalysts" and, of course, monoliths can be used as multiphase reactors [59, 60]. These reactors also offer a real potential for process intensification, which has already been demonstrated in commercial applications such as the production of hydrogen peroxide.

In recent years, micro-structured reactors have attracted considerable attention for a variety of applications [61, 62]. Such micro devices are characterized by a laminar flow, and the very high surface-to-volume ratio they provide leads to increased mass and heat transfer, offering the potential for process intensification. It has also been recognized that micro-structured components, because of their low mass and thermal inertia, are able to offer short response times for unsteady state periodic operations. Micro-reactors have been used successfully for fluorination, oxidations and both heterogeneous [63–65] and homogeneous hydrogenations [66]. A review on gas–liquid micro-structured reactors has been published [67]. The very small material inventory when using micro devices offers another advantage, notably as a laboratory tool for screening applications, kinetics determination and process data acquisition, where the main concern is

to gain as much information as possible with minimal reagent inventory [66, 68].

While batch reactors remain the "workhorse" in fine chemical production, the need to switch to continuous processes will increase the use of meso- and micro-structured reactors both at the laboratory scale (for discovery, process data determination, demonstration, small-scale production) and at the production level.

Nomenclature

Symbol	Definition	Unit
A	Interfacial area	m^2
a	Specific interfacial area per volume of gas–liquid emulsion	$m^2\ m_{G+L}^{-3}$
a_L	Specific interfacial area per volume of liquid	$m^2\ m_L^{-3}$
$C_{A,G}$	Concentration of gas A in the gas phase	$mol\ m_G^{-3}$
$C_{A,L}$	Concentration of gas A in the bulk of the liquid	$mol\ m_L^{-3}$
$C_{A,G}^{i}$	Concentration of gas A at the interface, gas side	$mol\ m_G^{-3}$
$C_{A,L}^{i}$	Concentration of gas A at the interface, liquid side	$mol\ m_L^{-3}$
$C_{A,L}^{eq}$	Concentration of gas A in the liquid at equilibrium	$ml\ m_L^{-3}$
$C_{H,L}$	Concentration of hydrogen dissolved in the bulk of the liquid	$ml\ m_L^{-3}$
$C_{H,L}^{eq}$	Concentration of hydrogen in the liquid at equilibrium	$mol\ m_L^{-3}$
$C_{S,L}$	Concentration of substrate S in the bulk of the liquid	$mol\ m_L^{-3}$
$C_{S,L}^{i}$	Concentration of substrate S at the interface, liquid side	$mol\ m_L^{-3}$
C_H	Hydrogen concentration in the intrinsic kinetic law	$mol\ m_L^{-3}$
C_S	Substrate concentration in the intrinsic kinetic law	$mol\ m_L^{-3}$
C_L	Total concentration of the liquid	$mol\ m_L^{-3}$
c_{pm}	Global specific heat of the liquid	$J\ kg^{-1}\ K^{-1}$
d_A	Diameter of the turbine, of the agitation device	m
$D_{A,G}$	Diffusion coefficient of gas A in the gas phase	$m^2\ s^{-1}$
$D_{A,L}$	Diffusion coefficient of dissolved gas A in the liquid phase	$m^2\ s^{-1}$
$D_{H,L}$	Diffusion coefficient of hydrogen in the liquid phase	$m^2\ s^{-1}$
$D_{S,L}$	Diffusion coefficient of substrate S in the liquid phase	$m^2\ s^{-1}$

Symbol	Definition	Unit
E	Enhancement factor	–
g	Acceleration due to gravity	9.81 m s^{-2}
H_A or H_H	Henry constant for gas A or hydrogen related to concentration	MPa m^3 mol^{-1}
H_A^x or H_H^x	Henry constant for gas A or hydrogen related to molar fraction	MPa
in	Superscript related to initial (Batch) or inlet (CSTR, PF) concentration	–
J_A, J_H	Mass transfer rate of gas A, of hydrogen	mol s^{-1} m_L^{-3}
k_c	Reaction rate constant	variable
k_L	Mass transfer coefficient of the gas being transferred, liquid side	m s^{-1}
$k_L a$	Volumetric mass transfer coefficient of the gas being transferred	s^{-1}
M_L	Molar weight of the liquid (in Table 45.3)	kg mol^{-1}
n, m	Reaction order in intrinsic kinetic law	–
N_R	Rotational speed of turbine, of agitation device	s^{-1}
out	Superscript related to final (Batch) or outlet (CSTR, PF) concentration	–
P	Power dissipated in reactor	W
P_{pA}, P_{pH}	Partial pressure of gas A, or hydrogen, in the gas phase	MPa or Pa
Q	Volumetric liquid flow rate	m_L^3 s^{-1}
r	Intrinsic rate of reaction	mol m_L^{-3} s^{-1}
V_G	Volume of gas in the gas–liquid emulsion	m_G^3
V_L	Volume of liquid in the gas–liquid emulsion	m_L^3
V_R	Volume of the gas–liquid emulsion in the reactor	m_{G+L}^3
V_{SG}	Superficial gas velocity	m s^{-1}
x	Spatial coordinate	m
x_A	Molar fraction of dissolved gas A in the liquid phase	–
x_i	Molar fraction of compound i in the liquid phase (general)	–
x_j^{mix}	Molar fraction of solvent j in the liquid mixture	–
ΔH	Heat of reaction (unit to be used in equations)	J mol^{-1} K^{-1}
ε_L	Volume fraction of the gas–liquid emulsion occupied by the gas	–
μ_L	Dynamic viscosity of the liquid	Pa s
v_A	Molar volume of dissolved gas A at its normal boiling temperature	m^3 mol^{-1}
v_L	Molar volume of the liquid L at its normal boiling temperature	m^3 mol^{-1}

Symbol	Definition	Unit
ν	Stoichiometric coefficient	–
ρ_L	Density of the liquid phase	kg m_L^{-3}
σ_A	Spherical diameter of dissolved A molecule	m
σ_L	Superficial or interfacial tension of the liquid	N m^{-1}

Abbreviations

CSTR continuous stirred tank reactor
PFR plug flow reactor
STR stirred tank reactor (batch reactor)

References

1 K. R. Westerterp, W. P. M. van Swaaij, A. A. C. M. Beenackers, *Chemical Reactor Design and Operation*. John Wiley, New York, **1984**.
2 O. Levenspiel, *Chemical Reaction Engineering*, 2nd edn. John Wiley, New York, **1972**.
3 P. Trambouze, J.-P. Euzen, R. Bononno, *Chemical Reactors: From Design to Operation*. Technip, Paris, **2004**.
4 A. Giannetto, P. L. Silveston, *Multiphase Catalytic Reactors: Theory, Design, Scale-up*. Hemisphere Publishing Corp., **1986**.
5 P. Mills, R. V. Chaudhari, *Catal. Today* **1997**, *37*, 367.
6 M. Baerns, P. Claus, in: B. Cornils, W. A. Herrmann (Eds.), *Applied Homogeneous Catalysis with Organometallic Compounds*. VCH, Weinheim, **1996**, vol. 2.
7 O. Wachsena, K. Himmlerb, B. Cornils, *Catal. Today* **1998**, *42*, 373.
8 J. C. Charpentier, Solubility and diffusivity of gases in liquids, in: A. Giannetto, P. L. Silveston, *Multiphase Catalytic Reactors: Theory, Design, Scale-up*. Hemisphere Publishing Corp., **1986**, p. 81.
9 B. E. Poling, J. M. Prausnitz, J. P. O'Connell, *The Properties of Gases and Liquids*, 5th edn. McGraw-Hill, New York, **2000**.
10 E. D. Snijder, G. F. Versteeg, W. P. M. van Swaaij, *J. Chem. Eng. Data* **1994**, *39*, 405.
11 V. Meille, C. de Bellefon, D. Schweich, *Ind. Eng. Chem. Res.* **2002**, *41*, 1711.
12 H. U. Blaser, H.-P. Jalett, M. Garland, M. Studer, H. Thies, A. Wirth-Tijani, *J. Catal.* **1998**, *173*, 282.
13 B. Fillion, B. I. Morsi, *Ind. Eng. Chem. Res.* **2000**, *39*, 2157.
14 Q. Liu, F. Takemura, A. Yabe, *J. Chem. Eng. Data* **1996**, *41*, 1141.
15 C. L. Young (Ed.), *IUPAC Solubility Data Series*. Pergamon Press, Oxford, UK, **1981**, Vols. 5–6.
16 G. T. Hefter, R. P. T. Tomkins, *The Experimental Determination of Solubilities – IUPAC*. Wiley & Sons, **2003**.
17 P. J. Dyson, G. Laurenczy, C. A. Ohlin, J. Vallance, T. Welton, *Chem. Commun.* **2003**, *19*, 2418.
18 E. Wilhelm, R. Battino, *Chem. Rev.* **1973**, *73*, 1.
19 P. Luhring, A. Schumpe, *J. Chem. Eng. Data* **1989**, *34*, 250.
20 J. L. Anthony, E. J. Maginn, J. F. Brennecke, *J. Phys. Chem. B* **2002**, *106*, 7315.
21 M. Herskowitz, J. Wisniak, L. Skiadman, *J. Chem. Eng. Data* **1983**, *28*, 164.
22 M. Herskowitz, S. Morita, J. M. Smith, *J. Chem. Eng. Data* **1978**, *23*, 227.
23 J. M. Prausnitz, R. N. Lichtenthaler, E. G. Azevedo, *Molecular Thermodynamics of Fluid-Phase Equilibria*, 3rd edn. Prentice-

Hall PTR, Upper Saddle River, New Jersey, USA, **1999**.
24 M. S. Wainwright, T. Ahn, D. L. Trimm, N. W. Cant, *J. Chem. Eng. Data* **1987**, *32*, 22.
25 E. Dietrich, C. Mathieu, H. Delmas, J. Jenck, *Chem. Eng. Sci.* **1992**, *47*, 3597.
26 M. Meyberg, F. Roessler, *Ind. Eng. Chem. Res.* **2005**, *44*, 9705–9711. See also www.fugatron.com.
27 V. R. Choudhary, M. G. Sane, H. Vadgaonkar, *J. Chem. Eng. Data* **1986**, *31*, 294.
28 C. R. Wilke, P. Chang, *AIChE J.* **1955**, *1*, 264.
29 E. L. Cussler, *Diffusion, Mass Transfer in Fluid Systems*, 2nd edn. Cambridge University Press, **1997**.
30 D. L. Wise, G. Houghton, *Chem. Eng. Sci.* **1966**, *21*, 999.
31 M. Diaz, A. Vega, J. Coca, *Chem. Eng. Commun.* **1987**, *52*, 271.
32 H. Sovova, *Coll. Czech. Chem. Commun.* **1976**, *41*, 3715.
33 D. M. Himmelblau, *Chem. Rev.* **1964**, *64*, 527.
34 D. Schweich, *Génie de la réaction chimique*. Tec&Doc, Paris, **2001**.
35 J. Lieto, *Le génie chimique à l'usage des chimistes*, **1998**.
36 K. Sporka, J. Hanika, V. Ruzicka, *Coll. Czech. Chem. Commun.* **1969**, *34*, 3145.
37 K. Sporka, J. Hanika, V. Ruzicka, M. Halousek, *Coll. Czech. Chem. Commun.* **1971**, *36*, 2130.
38 C. N. Satterfield, Y. H. Ma, T. K. Sherwood, *Inst. Chem. Eng. Symp. Ser.* **1968**, *28*, 22.
39 M. Ross, J. H. Hildebrand, *J. Chem. Physics* **1964**, *40*, 2397.
40 K. Nakanishi, E. M. Voigt, J. H. Hildebrand, *J. Chem. Physics* **1965**, *42*, 1860.
41 R. J. Powell, J. H. Hildebrand, *J. Chem. Physics* **1971**, *55*, 4715.
42 G. Wild, J. C. Charpentier, *Techniques de l'ingénieur* **1987**, *P*, 605.
43 (a) C. de Bellefon, in: E. Derouane, et al. (Eds.), *Principles and Methods for Accelerated Catalyst Design*. NATO ASI, Kluwer, **2002**, p. 71. (b) N. Pestre, V. Meille, C. de Bellefon, *J. Mol. Catal. A*: **2006**.
44 (a) S. Wang, F. Kienzle, *Org. Proc. Res. Dev.* **1998**, *2*, 226; (b) B. Chen, U. Dingerdissen, J. G. E. Krauter, H. G. J. Lansink Rotgerink, K. Möbus, D. J. Ostgard, P. Panster, T. H. Riermeier, S. Seebald, T. Tacke, H. Trauthwein, *Appl. Catal.* **2005**, *280*, 17.
45 J.-P. Landert, T. Scubla, *Chem. Eng. (New York)* **1995**, *102*, 118.
46 P. Cramers, C. Selinger, *PharmaChem* **2002**, *1*, 7.
47 See on the internet: www.biazzi.ch, www.davyprotech.com, www.dedietrichddz.com.
48 J. F. McGarrity, W. Brieden, R. Fuchs, H.-P. Mettler, B. Schmidt, O. Werbitzky, in: H.-U. Blaser, E. Schmidt (Eds.), *Asymmetric Catalysis on Industrial Scale*. Wiley-VCH, **2004**, p. 283.
49 H.-U. Blaser, R. Hanreich, H.-D. Schneider, F. Spindler, B. Steinacher, in: H.-U. Blaser, E. Schmidt (Eds.), *Asymmetric Catalysis on Industrial Scale*. Wiley-VCH, **2004**, p. 55.
50 R. Imwinkelried, *Chimia* **1997**, *51*, 300.
51 H. Yagi, F. Yoshida, *Ind. Eng. Chem., Process Des. Dev.* **1975**, *14*, 488.
52 S. Y. Lee, Y. P. Tsui, *Chem. Eng. Prog.* **1999**, 23.
53 T. I. Mizan, J. Li, B. I. Morsi, M.-Y. Chang, *Chem. Eng. Sci.* **1994**, *49*, 821.
54 L. Aouni, K. E. Hemberger, S. Jasmin, H. Kabir, J. F. Larrow, I. Le-Fur, Ph. Morel, T. Schlama, in: H.-U. Blaser, E. Schmidt (Eds.), *Asymmetric Catalysis on Industrial Scale*. Wiley-VCH, **2004**, p. 165.
55 V. Meille, N. Pestre, P. Fongarland, C. de Bellefon, *Ind. Chem. Eng. Res.* **2004**, *43*, 924.
56 A. L. Màrques, G. Wild, N. Midoux, *Chem. Eng. Sci.* **1994**, *33*, 247.
57 L. Greiner, D. H. Mueller, E. C. D. van den Ban, J. Woeltinger, C. Wandrey, A. Liese, *Adv. Synth. Catal.* **2003**, *345*, 679.
58 V. Diakov, A. Varma, *AIChE J.* **2003**, *49*, 2933.
59 A. Cybulski, J. A. Moulijn, *Structured Catalysts and Reactors*. Dekker, New York, **1998**.
60 S. Roy, T. Bauer, M. Al-Dahhan, P. Lehner, T. Turek, *AIChE J.* **2004**, *50*, 2918.
61 K. Jähnisch, V. Hessel, H. Löwe, M. Baerns, *Angew. Chem. Int. Ed.* **2004**, *43*, 406.
62 (a) V. Hessel, S. Hardt, H. Löwe, *Chemical Micro Process Engineering (Fundamen-*

tals, Modelling and reactions). Wiley-VCH, **2004**; (b) V. Hessel, H. Löwe, A. Müller, G. Kolb, *Micro Chemical Process Engineering (Processing and Plants)*. Wiley-VCH, **2005**.

63 K. K. Yeong, A. Gavriilidis, R. Zapf, V. Hessel, *Chem. Eng. Sci.* **2004**, *59*, 3491.

64 R. Abdallah, V. Meille, J. Shaw, D. Wenn, C. de Bellefon, *Chem. Commun.* **2004**, 372.

65 J. Kobayashi, Y. Mori, K. Okamoto, R. Akiyama, M. Ueno, T. Kitamori, S. Kobayashi, *Science* **2004**, *304*, 1305.

66 (a) C. de Bellefon, N. Tanchoux, S. Caravieilhes, P. Grenouillet, V. Hessel, *Angew. Chem. Int. Ed.* **2000**, *39*, 3442; (b) R. Abdallah, V. Meille, J. Shaw, D. Wenn, C. de Bellefon, *Chem. Commun.* **2004**, 372; (c) C. de Bellefon, T. Lamouille, N. Pestre, F. Bornette, F. Neumann, V. Hessel, *Catal. Today* **2005**, *110*, 179.

67 V. Hessel, P. Angeli, A. Gavriilidis, H. Löwe, *Ind. Eng. Chem. Res.* **2005**, *44*, 9750.

68 (a) C. de Bellefon, N. Pestre, T. Lamouille, P. Grenouillet, V. Hessel, *Adv. Synth. Cat.* **2003**, *345*, 190; (b) C. de Bellefon, R. Abdallah, T. Lamouille, N. Pestre, S. Caravieilhes, P. Grenouillet, *Chimia* **2002**, *56*, 621.

Subject Index

a

absorption coefficient 266 ff
acetamidocinnamate 1040, 1044
acetamidocinnamic acid 1401
acetoacetate 248
acetophenone 248
acids and anhydrides 442 ff
acids, unsaturated 872 ff
acridine 474 ff
acryl chloride 171
acryl hydrazones 75
acyclic allyl alcohols 655
actinide 111
activation of the C-X bond 533 ff
– 1,2-insertion 538
– by σ-bond metathesis 537
– by oxidative addition 538
– by S_N2 attack of the hydride ligand 538
activation, heterolytic 378, 389, 392
acyl-hydrazones 75
adiabatic temperature, maximum 1535
1,2-addition 402
1,4-additon 402, 718 f
agglomeration 218, 219
aggregate, fluorous 1383
aggregation 218
agostic 36
alcohol 1230
– as promoter 492, 506
– homologation 506
– two-phase hydrogenation 1344
– unsaturated 875
alcohol with exocyclic double bonds 646
aldehyde 51, 60 ff, 167, 168, 229, 413 ff, 437 ff, 1229, 1344
– α,β-unsaturated 1365
– benzaldehyde 171, 187
– cinnamaldehyde 415, 416
– diamine-modified Ru catalysts 422
– reductive amination 437 ff
aldimine 1231
aldol cycloreduction 716
aldol reaction 609
aldolization 717
aliphatic 229
alicyclic olefins 229
aliphatic carbonyl 248
alkane, dehydrogenation 137
alkene 3, 46, 51, 58, 65, 111, 113 ff, 119, 132, 134 ff, 136, 155, 164, 174, 201, 220, 226, 229 ff, 233 f, 237 f, 338, 375, 389, 390, 853 ff, 1234, 1334, 1386, 1394
– acrylate 868
– acrylonitrile 78
– α-acylaminoacrylic 17
– association 22
– butadiene rubbers 99
– metylcinnamic acids 15
– 2-*cis*-hexene 85
– 3-*cis*-hexene 85
– cluster 201
– complex formation 87
– conjugated 87
– coordination 7
– crotonitrile 78
– cyclohexene 75, 99
– cyclooctene 73, 99
– β-dehydroamino acid 18
– electron-deficient 77
– electron-poor 388, 389
– enamides 866 ff
– enol ester 870
– ethylene 85
– α-ethylstyrene 87
– fatty acid 87
– 1-hexene 85
– hydrogenation 202, 205, 632
– insertion 79, 88
– isomerization 8, 71 ff

The Handbook of Homogeneous Hydrogenation.
Edited by J. G. de Vries and C. J. Elsevier
Copyright © 2007 WILEY-VCH Verlag GmbH & Co. KGaA, Weinheim
ISBN: 978-3-527-31161-3

– methacrylonitrile 78
– 1-octene 103
– pentene 75
– α-phenylacryl acid 14
– polyunsaturated 87
– rotation 97
– styrene 80
– terminal 1050, 1054
– tetrasubsituted 1056 ff, 1066
– 2-trans-hexene 85
– trisubstituted 117
– two-phase hydrogenation 1327 ff, 1334
– unfunctionalized 1038, 1042, 1044
– vegetable oils 99
alkoxide 590, 601
alkyl
– carbonate 502
– halides 502
alkyl halides 515 ff, 520, 527 ff, 532 ff
α-alkylated cinnamic acid 1267
alkylhydride complex 1080
alkylphosphines 1078
alkyl-substituted 1063
alkyne 41, 54, 65, 72, 111, 114, 129, 208, 229, 341, 343, 347, 375, 377, 390 f, 1334, 1337, 1386
– acetylene 85
– 1-alkyne 380, 385
– diphenylethyne 74
– electron-poor 375
– 1-heptyne 79
– hydrogenation 206, 377
– internal 379, 381, 389
– 1-octyne 87
– 2-pentyne 79
– phenylacetylene 74, 166
– 1-phenyl-1-propyne 74
– semihydrogenation 75, 375, 376, 378, 391
– terminal 377, 379
– two-phase hydrogenation 1334
allene 73
allyl amine 230
allyl alcohol 222 f, 225, 640
allylbenzene 1400
allylcyclohexane 1400
allyl halides 527
aryl halides 514 ff, 527 ff, 539
alternative solvents 1391
aluminum 1398
aluminum (III) 588
– isopropoxide 602, 603
amide 61
amidophosphinite 1171
amido phosphine-phosphinite ligands 1170 f
amido-directive hydrogenation 654
amido-itaconates 814
amine 1232
amino acid precursors 16
amino alcohol 1219, 1254
amino ketones 1177 ff
amino phosphines 1095
amino phosphines-phosphinite ligands 1170
aminocarbene chelate 1091
amino phosphine-phosphinites (AMPPs) 883
aminophosphinites 1010 ff
aminophospholane 1044
amphiphile, fluorous 1383
androsterone 608
aniline 506
anion
– coordinating 42
– non-coordinating 42
– weakly-coordinating 384, 1385
anisole 242, 244
anthracene 138, 1398
anthracenes 457 ff
anti-selectivity 698, 701
APB 1114
arenes 111, 138 ff, 234, 241, 456 ff, 460, 1334, 1397
– η^2-arene 539
– naphthalenes 138
– phenanthrene 138
– parahydrogen 326 ff
– phosphines 325
– radical 532, 535 ff
– stereochemistry 334
– two-phase hydrogenation 1334, 1352
– unsaturated 37
– vinyl 54
η^6-arene 1502
aromatic alkenes 229
aromatic compounds 244
aromatics 55
2-arylacrylic acids 1404
aryl bromides 517, 520 ff, 526 ff, 533
aryl chlorides 517 ff, 526 ff, 532
aryl fluorides 518 ff
arylphosphines 1077
aqueous systems 462, 480
atomic absorption spectroscopy (AAS) 1380
atropic acids 1404

atropisomeric 854
– BIHEP 857
– diphosphines 676, 698
– system 756
automated synthesis 1258
avidin 1257

b
BAMP ligands, from diamines 1172
BAr_F 1031, 1057
– sensibility in $scCo_2$ 1365
base 193
basic chelating phosphines 526 ff, 535 ff
BasPhos 759
BCCP 5 1167
BCPC 6 1167
BCPM 1167
BCPP 1167
BDPAP 761
BDPMI 751, 868
BDPP 751, 876
BeePHOS 792
(S,S)-benazepril 905
bench-scale process 1284
benzaldehyde 246
benzene 241, 244, 457 ff, 1337
benzene derivatives 241
benzo[b]thiophene 471
benzofuran 479
benzothiophene 470 ff
biomembrane 1336
biphasic hydrogenation 1327 ff
benzotrifluoride (BTF) 1382
benzyl halides 517, 526 ff
biaryl bisphosphine 853 ff
bicarbonate hydrogenation 499
BICHEP 757, 864
BICP 867 ff
– arylenamides 752
– α-dehydroamino acids 752
– β-dehydroamino acids 752
– MOM-protected β-hydroxy enamides 752
bidentate phosphonites 924
bidentate phosphorus ligands 883
BIFAB 758
bifunctional catalysis 61
BIHEP 867
BIHEMP 817, 854, 872
BIMOP 757
BINAP 17, 469, 757, 817 ff, 864, 1073, 1386, 1407
– immobilized 1105
– Ru-H complex 1093
BINAPHOS 1366, 1368
BINAPO 760, 925
BINOL 762
BINOL-derived 1086
BIPNOR 864
BITIOP 872, 876
biocatalyst 1471
– alcohol dehydrogenase (ADH) 1472
– hydrogenase 1474
– oxidoreductase 1471 f
biological approach 1421
biotin 1257
biphase catalysts 457 ff
biphasic conditions 473
biphasic system
– IL/$scCO_2$ 1369
– inverted 1364, 1368
– liquid-liquid 242, 244, 250, 1386, 1394 ff
– liquid/supercritical 1364
– PEG/scCO2 1369
– water/scCO2 1368
BIPHEP 757, 854
BIPNOR 747
bisdehydropeptine 676
bis(diphenylphosphino)ethane (DPPE) 101, 1380 f, 1383, 1386
2,4-bis(diphenylphosphino)pentane (BDPP) 1251
bisphosphinamidite 907
bisphosphinite 924, 978, 980
bis(phospholanyl)benzenes (DuPHOS) 17, 758, 774, 823, 1050, 1052, 1054
– α-amino acid derivatives 759
– – β-branched 759
– enamides 759
– enol acetates 759
– itaconic acids 759
bis(phosphopholanyl)ethanes (BPE) 17, 758 f, 774, 782, 806 f, 809
– BPE-4 760
– family 823
BisbenzodioxanPhos 758
BisP* 867
bisphosphine rhodium complexes 1074
bisphosphonic acid substituted 1409
bite angle 161, 186
BITIANP 758, 872, 876
BNAP 756
Bodenstein principle 259 ff
bond dissociation energies 364
bonding, hydrogen 52
BoPhoz 755, 762

BPPFA 753
BPPFOH 1177
– analogue, α,β-unsaturated acids 753
BPPM 19, 750, 1167
butadiene 73, 224, 395, 1395
1,4-butanediol 442
2,3-butanedione 250
1-butenyl(trimethyl)ammonium bromide 231
Butiphane 789
2-butyne-1,4-diol 239
γ-butyrolactone 442

C

calorimetry 275 ff
CAMP 16, 746
– dehydroamino acids 746
Cannizzaro reaction 609
carbamate 504, 505
carbamic acid 1366
carbene 1253
carbenium ion 155
carbon dioxide 489 ff, 1365, 1372, 1381, 1386 f
– expansion with 1387
– symmetric phospholane ligands (DuPhos and BPE) 773
carbon dioxide hydrogenation
– alcohol as promoter 492, 495, 506
– base as promoter 490, 492
– CO_2 499
– formate esters 500 ff
– formic acid 490 ff
– to formaldehyde 506
– to formamides 504 ff
– to formate esters 507
– to methane 506
– to methanol 489, 506
– to oxalic acid 499 f
– water as promoter 495, 506
carbon monoxide, synthesis of 489, 503
carbonate esters 503
carbon-halogen bond 514
– reactivity of 513, 530, 532, 534
carbon tetrachloride 516, 519, 524, 528 ff, 534 ff
carbonylation
– of alcohol 500
– of amines 504
CarboPhos 760
carboxylic acid 413 ff.
– α,β-unsaturated 1366
– from alkyl halides and CO_2 507
carboxylic acids 650
– unsaturated 650
cartridge catalyst 1370, 1373
catalyst
– actinide 126 ff, 132 ff
– activation 389
– air sensitivity 1402
– availability 1281
– η^4-anthracene 460
– cationic 379
– chiral 336
– chromium 376, 397
– cobalt 402, 475
– colloidal 342
– control 671, 691
– cost 1281
– Crabtree 1042
– deactivation 39
– development time 1282
– dihydride 3 f
– divalent palladium 392
– DuPhos-Rh 797
– fluorous 385, 1377 ff, 1380, 1383, 1386
– heterogeneous 140 ff, 388, 456, 463, 467, 484
– – surface organometallic chemistry 141 ff
– immobilization 1010
– immobilized 388
– iridium, see iridium catalyst
– iron 377
– isomerization 384
– lanthanide 126 ff, 129 ff, 131 ff, 632, 638
– lanthanocene 131
– Lindlar 375, 388
– Meerwein-Ponndorf-Verley-Oppenauer (MPVO) 601, 602, 603, 613
– metallocene 113
– monohydride 3, 4, 380
– nanoparticles 406
– nickel 1105
– osmium 382
– palladium 375, 388, 406
– – cluster 388
– – zerovalent 391
– performance 1281
– phospholane 808, 815, 820
– platinum 86, 406
– polymer-supported 141
– recycling of 248, 1377, 1382, 1383, 1384, 1415
– $[Rh_2(OAc)_4]$ 26

– rhodium, see rhodium catalyst
– ruthenium, see ruthenium catalyst
– ship-in-the bottle (SIB) 1431, 1432, 1433
– Shvo 594, 595, 603, 1217
– silica support 141
– silica-grafted 467 ff
– solid supported, see solid supported catalyst
– substrate complex 260 ff
– supported aqueous-phase (SAPC) 1436
– supported hydrogen-bonded (SHB) 1427, 1429 f
– supported liquid-phase catalyst (SLPC) system 1436
– supported palladium 467
– thermal degradation of 1378
– titanocene catalyst 694, 1063
– transfer hydrogenation, see transfer hydrogenation, catalyst
– biphasic conditions 473
– water-soluble 462, 472 ff, 478
– Wilkinson's catalyst 5, 551
– Wilkinson's type 1378, 1381, 1382
– Ziegler-type 107
– zirconium 395
catalyst deactivation 1395, 1461
catalyst inhibition 1483
– decomposition 1508
– mechanism 1484
– of the ligand phrase 1508
– peroxide 1508
catalyst poisoning 1238
– in $scCO_2$ 1371
catalyst recovery 236, 574, 1415
catalyst recycling 233, 480
catalyst scavenger, fluorous 1386
catalysts separation, fluorous biphasic 1377
catalytic cycle 1115
catalytic reductive coupling 727
CatASium 759, 779
– $[Ir(PCy_3)(py)(nbd)]^+$: Crabtree's catalyst 639
cationic ligand, immobilization 1406
CBD 750
C-C bond formation 713, 736
cell, flow-through 274 ff
C-H activation 113
chelate twist 1082
chemical reduction 217
chemical shift 299
– ^1H 300
– ^{31}P 300, 301
chemisorption 1425, 1426, 1427, 447
chemoselective hydrogenation 389, 1286
– vinyl epoxides 74
– α,β-unsaturated compounds 74, 77
chemoselectivity 414
chemospecific 6
chiral alcohols 1230
chiral amine 1234
chiral pool 1421
CHIRAPHOS 750
chloride impurities 1398
chlorobenzene 514, 517, 520
cinchona alkaloids 249
cinchonidine 249, 250
cinnamaldehyde 245, 415, 1350
(E)-cinnamate 1383
cis-addition 12
cis-1,2-aminoindanol 1219
cis hydrogen addition 456, 474
cis-1,3-pentadiene 73
cis-1,4-polyisoprene 570
cis-3-hexenoic acid 1402
cis stereospecificity 463 ff
citronella 246
cluster 89, 199 ff
– aggregation 200
– anionic 202
– aromatic 207
– biphasic catalysts 205
– chiral 201
– fragmentation 200, 203, 212
– heteronuclear 209
– high-nuclearity 212
– hydrosilylation 211
– inhomogeneous diene hydrogenation 205
– ionic liquids 205, 206
– layer-segregated 209
– silica-supported 202
– transfer hydrogenation, α,β-unsaturated ketone 211
CNRPhos 759
CO_2, see carbon dioxide
cod (cyclooctadiene) 36
cofactor 1471 ff
colloids 217
– aqueous colloidal solutions 226
– suspension 251
– zerovalent transition-metal colloids 217
combinatorial 1246 ff, 1382
complex
– allyl 73

– cationic rhodium 6
– 5-coordinate 48
– dihydride 86, 397
– dihydrogen 52, 157
– dinuclear 395, 397
– divalent 400
– hydride 87
– intermediate 367
– palladium (II) 407
– platinum (II) 407
– product catalyst 335
– rhodium 3
– – cationic 21
– ruthenium, divalent 401
– solvento 366
– unsaturated 48, 366
– zerovalent 400
complexation of acceptor 593
compressed CO_2, see supercritical carbon dioxide ($scCO_2$))
concentration gradient 266 ff
concentration-time data 263 ff
cone angle 54
conjugated aromatic alkenes 224
consecutive hydrogenation
– alpha diketones 685
– bis(dehydroamino acids) 691
– symmetrical dienes 691
continous racemization 612
continuous-flow process, using $scCO_2$ 1368, 1371
coordinative attachment 1447
copper 435 ff
– chemoselectivity 425
– phenyldimethylphosphine-stabilized copper (I) hydrides 425
co-solvents, for use with CO_2 1368
counterion 35, 1098
p-cresol 466
cresol derivatives 242
crotonaldehyde 1350
crystal structure analysis 287 ff
C_s-symmetry 16
cumene 242
cyanations 590
cyclic homoallyl 643, 673, 679
cyclic hydrogenation 395
cyclic ketone 248
cyclic BETA-keto esters 697
cyclic unsaturated alcohols 649
2-cyclohexen-1-one 1383
cycloalkanones 1150
cycloalkyl halides 520 ff, 525, 530, 534
β-cyclodextrin 1335, 1351 f
1,3-cyclohexadiene 73
cyclohexanone 247
cyclohexene 221 f, 227, 229, 1413
cycloisomerization 733, 734
1,3-cyclooctadiene 72, 222, 226, 395 f
1,5-cyclooctadiene 72
cyclooctene 221 f, 224
cyclopentadiene (cp) 1217
cyclopentadienyl 463

d

DAIPEN 1133
DBI 506
DBPE 95
DBU 491
DCPE 101
DCPP 101
DDT 520, 532, 534
deactivation 1483
– η^6-arene complexes 1502
– deiodination 520, 524, 526, 533, 536
– electrochemical 532 ff, 536 ff
– heterocyclic halides 517 ff, 520 ff, 527, 532 ff
– heterogeneous 520
– microwave-enhanced 527
– phase-transfer 518, 528, 533
– product forming step of 538
– regioselective 522, 524, 534
– stereoselective 518, 531
1,9-decadiene 73
decarbonylation 610
degradation 513 ff
DeguPHOS 751
dehalogenation 527
– by miscellaneous methods 533 ff
– chemoselective 518 ff, 525 ff, 532
– debromination 517, 520 ff, 933
– dechlorination 519, 524 f, 530
– defluorination 514 ff
– deiodination 520, 524, 526, 533, 536
– electrochemical 532 ff, 536 ff
– heterocyclic halides 517 ff, 520 ff, 527, 532 ff
– heterogeneous 520
– microwave-enhanced 527
– phase-transfer 518, 528, 533
– photocatalytic 534
– product forming step of 538
– regioselective 522, 524, 534
– stereoselective 518, 531
– under carbonylation conditions 533

dehydroamino acid 638, 883, 1073 ff, 1081, 1087, 1445
– in sCO_2 1365
dehydroamino acid derivatives 754, 756, 918, 1448
α-dehydroamino acid derivatives 788
β-dehydroamino acid derivatives 801, 805
dehydroamino ester 1078, 1080
dehydrodipeptides 671 f
α-dehydroamino ester 1088
dehydrogenation 35, 41
– alkane 137
dendrimers 225, 1386, 1453
density function theory (DFT) 1082, 1095
Derjaguin-Landau-Verway-Overbeek (DLVO) theory 218
deuteration 368
deuterium transfer 588
Dewar-Chatt-Duncanson model 726, 731
diamine 1105
diaminophosphine 1036
diastereoselective hydrogenation 1286
– dehydrodepsipeptide 673, 679
diastereoselective 1120
diastereoselectivity 1122
diazaphospholidines 1010 ff
diene 12, 112, 114, 129, 131 f, 136, 375, 395, 397, 1067
– $[HRuCl(CO)(PR_3)_{3]}$ 553
– $[(CH_3)_3CH)Al]$ 563
– $[(CH_3(CH_2)_3CH(C_2H_5)CO_2)_2Ni]$ 555, 563
– $[Ir(COD)L_2]PF_6$ 563
– $[Ir(COD)(PMePh_2)_2]PF_6$ 563
– $[RhH(PPh_3)_4]$ 552
– $[RhHCO(PPh_3)_3]$ 552
– $[RuCl_2(PPh_3)_3]$ 553
– $[RuCl_2(PPh_3)_4]$ 553
– $[RuHCl(PPh_3)_3]$ 552
– alkylaluminum 556
– alkylalumoxane 555
– amine 553
– based polymers 547
– bimetallic complexes 554
– butadiene 73, 1395
– cobalt or nickelbenzolhydroxamic acid 554
– conjugated 394, 402, 404
– cyclic 404
– cyclohexadienes 99
– 2-ethylhexanoic acid nickel 555
– metallocene 557 ff
– nickel acetylacetonate 554 f
– non-conjugated 394, 402
– rare earth (Sm) metallocene 558
– selective 404
– titanium compounds 556
diffusion 298, 309
diffusion control 267 ff
diffusivity
– correlation 1526
– estimation 1526
– experimental value 1527
dihydride 49, 1079, 1095
dihydride complex 1089
dihydrofuran derivatives 650
dihydrogen 36, 380
dihydrogen complex 48, 52, 65, 1084 f
diketo ester 684
α,γ-diketoester 1176 ff
1,3-diketone 1122
diketone 684
α-diketone 250
DIMAP 1086
3,3-dimethyl-1-butyne 241
dimethylformamide 504 ff
DIMOP 760
DIOP 15, 469, 483, 746, 749, 867, 907, 995, 1086, 1450
DIOP-derived peralkyl ligands 1167
DIOP modifications 860
DIPAMP 16, 746, 864, 871, 995 ff, 1075
diphenylehtylendiamine (DPEN) 1219
diphos 457, 459, 469
diphosphines 22, 95, 107, 672, 783
diphosphinite 672, 1105
diphosphonite 974
dipole-dipole interaction 1426
DIPPE 95
DIPPP 95
directive hydrogenation 668
directivity 667 ff
– amide 653
– carbamate group 653, 667
– carboxylate 650
– ether linkage 649
– hydroxyl 649
disproportionation
– 1,3-cyclohexadiene 468
– palladium 468
dissociation 6, 31, 36, 327
– collision-induced 363
– reversible 377
disubstituted benzene 242
β,β-disubstituted dehydroamino 1092

divalent 400
domino-hydroformylation-reduction 436 ff
– cobalt catalysts 436
– rhodium catalysts 437
double hydrogenation 1122
double eniantioselective induction 670
double bond, migration 87
double stereodifferentiation 691
DPAMPP 761
DPCP 751
drug candidates 35
DuanPhos 784, 793, 807, 809, 1184
DuPHAMIN 784
DuPHOS 17, 758, 779, 823, 1050, 1052, 1054
dynamic kinetic resolution 612
– 2-alkyl-β-keto esters 701
– α-amido-β-keto ester 698
– effect of N-protecting groups 702
– β-keto ester 698 f
– α-substituted β-keto esters 697 f
dynamic stereomutation 697

e
Eadie-Hofstee 262
early transition metal 111
effective hydrogen concentration 270 ff
electrochemical reduction of CO_2 499
electron diffraction (EDX) 220, 227, 234
electron-rich diphosphines 1077, 1078
electropositive metals 1397
electrospray ionization (ESI) 359
– tandem ESI-MS 359
electrostatic interaction 672, 676
elemental analysis 227
elementary reactions 359
elementary steps 277
β-elimination 97
enamide 756, 1044, 1080, 1401
enantiomeric excess 15, 249
enantioselective catalysis 1245 ff
enantioselective hydrogenation 17, 19, 34, 39, 58 ff, 249, 404, 481, 1029, 1096, 1245 ff, 1386 f
– activation 1156
– deactivation 1156
– of C=C bonds 1287
– – allylic alcohols 1295
– – dehydro α-amino acid derivatives 1287
– – hydro β-amino acid derivatives 1292
– – itaconic acid derivatives 1293
– – miscellaneous C=C systems 1298
– – simple enamides and enol acetate 1293
– – α,β- unsaturated acids 1296
– of C=O bonds 1302
– – aromatic ketones 1306
– – alkene 1338
– – – Josiphos 839
– – – Mandyphos 836
– – – Taniaphos 842
– – – Bppfa 836
– – – ferrocene-based ligands 833
– – – Ferri Phos 836
– – alternative reduction system 1209
– – catalyst precursor 1490
– – cyclic imines 1202
– – dienes 1491
– – enamines 1206
– – α-functionalized ketones 1302
– – β-functionalized ketones 1304
– – heteraromatic substrates 1202
– – iridium complexes 1210
– – mechanistic aspects 1207
– – miscellaneous C=N-X systems 1204
– – N-alkyl imines 1200
– – N-aryl imines 1197
– – NMR spectroscopic monitoring 1489
– – rhodium complexes 1211
– – ruthenium complexes 1211
– – substrates 1341
– – titanium complexes 1211
– of C=N bonds 1309
– transfer hydrogenation 1215
enantioselectivity 116, 134 ff, 185, 1105, 1377
– cyclic imine 123
– cyclopentadienyl 117
– enanime 120 f, 124
– imine 120 ff
– metallocene 116
encapsulated homogeneous catalyst 1430
encapsulation 1425
energy dispersive spectroscopy 227
engineering by catylsis 577
1,5-enantioselective induction 667
enol carbamates 1016 ff
enol ester 1016 ff
enzyme inhibition 261
enzyme membrane reactor, electrochemical 1476
epinephrine 1183
eprozinol 1183
equilibrium approximation 259 ff

Eschweiler-Clarke reaction 610
esters 55, 445 ff
– dimethyl oxalate 446
– multidentate ligands 449
– ruthenium 449
– unsaturated 872 ff
esters and carboxyl acids 651
Et-DuPHOS 1251
ethene 1415
ethyl acetoacetate 1410
ethyl nicotinate 484
ethyl pyruvate 248, 249, 250
1-ethyl-3-methylimidazolim ethylsulfate 1390
exchange processes, intramolecular 277 ff
exo hydroxyl group 650
expanded liquids 1362
extended X-ray absorption fine structure (EXAFS) 220, 229
extinction 275 ff
extrusion 218

f
FAD 1471
FMN 1471
faujasite supercage 1433
feasibility studies 1284
FerriPhos 754, 836
ferrocene 753
ferrocene-based diphosphines
– enantioselective hydrogenation 833
– hydrogenation of C=O function 848
– hydrogenation of C=N function 848
– hydrogenation of substituted alkenes 848
– major applications 847
ferrocene hybrids 756, 760
ferrocene oxazoline 1033
ferrocenyl phosphine 76
– dehydroamino acid derivatives 756
– itaconates 756
FerroPhos 754
FerroTANE 756, 760
FerroTANE family 813
fiber-optical probes 274
five-membered phosphacycles 785
fixed-bed reactors 1413
flow rate measurements 265
fluorinated phosphines 1365, 1370
– for use in CO_2 1365
fluorocarbon 1377
fluorination 1384
fluoroketones 1186 ff
fluoroacetophenone 250
fluorophilicity 1384, 1386
fluorous 1378
fluorous biphasic 1377 ff
fluorphobicity 1384
formamide 504 ff
formate complexes 494 ff
formate esters 500 ff, 507
formation of M-H bond 538 ff
formic acid 489 ff, 1225, 1372
fragmentation 360 ff
functional group 42
functional group tolerance 518, 524, 526 ff
functionalized ketones 1165 ff
FUPMOP 757

g
gas effect turbines 1538
gas hold-up 1537
gas solubility 265 ff
global warming 489
gravimetric microbalance 1393
gross-activities 283
gross-kinetics 283
– measurements 280 ff

h
half-life 263
haloarene, see aryl halide
halocarbon 36
halogen/hydrogen exchange, see dehalogenation
Hatta number 1530
HCFC's 519 ff
H-D exchange 368
heat of reaction 1522
heat transfer 1537
hemilabile 392, 525
Henbest system 599
Henry coefficient 1423
heteroaromatics 470, 1352
heteroaromatic compounds
heterobimetallic complexes 201
N-heterocyclic carbene 36, 182, 531 ff, 1336
heterocyclic carbenes 1042, 1253
heterogeneous catalyst 549, 1422 f
– acids and anhydride 441
heterogenization of catalysts 519, 522
heterolytic activation 714
heterolytic hydrogenation 61
heterotopic 50

1,5-hexadiene 73
3,4-hexanedione 250
1-hexene 1413
2-hexene 12
1-hexyne 241
hex-2-yne 238
hex-3-yn-1-ol 239
– cyclodextrin 230
high-throughput analysis 1273
high-throughput ^{13}C-NMR 1274
high-throughput experimentation (HTE) 1246 ff, 1248, 1378
– combinatorial 1249
– parallel 1249
– serial 1248
hold-up, liquid 1518
homoallyl alcohols 643
homolytic hydrogen activation 714, 737
H-transfer catalytic 1517
hybrid (SLP) system 1437
hydride cluster 38
hydride complex 1397
hydride donor 164, 167 ff
hydride transfer 154, 162, 172, 176 ff, 179 ff, 184 ff, 190
– direct 588
– kinetic hydricity 179
hydride-proton transfer 593
– mechanism 593
(α-hydroxyalkyl)acrylate 653
hydrogen addition 458, 463 ff
– biphasic liquid-liquid 227
hydroaminomethylation 1366
– domino isomerization hydroaminomethylation 441
– fenpiprane 440
– linear selective hydroaminomethylation of propene 440
hydroboration 35
hydrofluorocarbons 1368
hydroformylation 6, 713, 1372
– in $scCO_2$ 1366
hydrogen 79
– adduct 32
– coordination, solvent-assisted 82
– ionic liquids 1392
– oxidative addition 79
– para 313 ff, 381
– partial pressure 269 ff
– pressure drop experiment 1401
– solubility 269 ff, 1405
hydrogen activation 97
– heterolytic 79
hydrogen bond
– stabilizing transition states 495 f
– unconventional 498
hydrogenase, nickel 93
hydrogen bonding 52 169, 697, 1426
hydrogen consumption 264 ff
hydrogen donor 588, 597 f, 600, 1215, 1224
– cyclohexene 1229
– dithionite 1229
– hydrazine hydrate 1229
– hydrogen 1229
– hydrogenphosphite 1229
– IPA system 1224
– sodium borohydride 1229
– sodium cyanoborohydride 1229
– TEAF system 1225
hydrogen transfer 35, 518, 522, 526 ff, 533, 597, 603, 613
1,4-hydrogenation 376, 397 ff
hydrogenation curves 280 ff
hydrogenolysis 48, 113, 127, 129 ff, 135 ff, 496, 1352
– of the C-X bond, see dehalogenation
– thiophenes 471
hydrometallation 729, 734
hydrosilane 155
β-hydroxy ester 1105
hydroxy-directive hydrogenation 653
– of acyclic homoallyl alcohols 664
hydroxyketones 685
L-hydroxyproline 1166
– derived bidentate ligands 1167

i

ibuprofen 1343
ICP-ASS (inductively coupled plasma – atomic absorption spectroscopy 1383
ICP-leaching 1382
ideal gas law 264
imine 20, 35, 41, 49, 111, 131, 189, 413 ff, 635, 754, 1021 ff, 1232, 1352 f, 1411
– formation of carbamates 1371
– in IL/$scCO_2$ 1363
– two-phase hydrogenation 1352 f
iminium 1232
iminium compounds 184
iminocarbene 1098
immersion probes 274
immobilization 1394
– cationic catalyst 469
– of organometallic catalysts 1363 ff
– see heterogenization

– technique 1377
immobilized 1220
immobilized catalyst 466 ff, 479 ff, 484 ff
immunoassays 1274
impeller 1538
indole 475, 478, 481
indole, hydrogenation 475, 478
IndoNOP 761
induced fitting 676
induction periods, 280 ff, 1484 f, 1502
– catalyst precursor 1486
– diene complex 1487
– diene ligands 1485, 1488, 1490
– in-situ technique 1486 f
– precatalyst 1485 f
– solvent complex 1486, 1488
– spectator ligands 1488
– stabilizing ligand 1485
inductively coupled plasma atomic absorption spectroscopy (ICP-AAS) 1380, 1382
industrial applications 1279
– of chemocatalytic eniantioselective processes 1285
– – critical factor 1285
– – success factor 1285
industrial processes, general comments 1284
inhibition by oxidation 1507
inhibition by oxygen 1508
initial rate method 261 ff
inorganic supports 1424
in-situ monitoring 264 ff
instant ligand library 1262
intellectual property aspects 1316
interfacial area 266 ff
intermediate 40, 326, 329, 536 ff
intramolecular chiral induction 670
ion, organometallic 365
ion-exchange complex 1325
ion-exchange reaction 1398
ion-exchange resins 1456
ionic bonding 1455
ionic catalyst complex 1394
ionic hydrogenation 153 ff, 497 f
ionic liquids 233, 243, 506, 1253, 1327, 1363, 1368, 1389 ff, 1438
– properties 1391
IR spectroscopy 236, 275 ff
iridium 31, 483, 1029, 1030, 1042, 1049, 1056, 1066, 1217, 1383
iridium alkylhydride intermediate 1096
iridium catalyst 608, 638, 651
– $[Ir(PCy_3)(py)(nbd)]^+$ 633, 639 f, 651, 654 ff, 664, 691
– aldehyde 414
– carbene 691
– transfer hydrogenation 427
iridium-catalyzed hydrogenation 1014
iridium complex 599, 1090, 1094 f
– Vaska's complex 31
iridium-JM-Phos 1051
Iridium-xyliphos 1411
irreversible deactivation 1507 ff
– anion 1507, 1509 f
– clusters 1509
– formation of dimers 1509 f
irreversible inhibition 1484
isatine derivatives 1172
isobaric conditions 259 ff
isomerization 6, 48, 378
– hydrogen-assisted 390
– substrate 408
isopropanol 1224
isopropoxide 590
(R,R)-isoproterenol 1184
isoproylbenzene 242
isotope effect 1079
isotopic label 273
isotopic labeling 364, 367
itaconic acid 754, 813
itaconate derivatives 667

j

JM-Phos 482, 762, 1060
JosiPhos 754, 816, 1177, 1453

k

Kephos 779
ketamine 1231
ketoamides 1172
ketoesters 1166
– α-keto esters 249, 1172
– β-keto ester 249, 1105
– – hydrogenation, with scCO2 1370
ketone 19, 23, 35, 49, 51, 55, 60, 66, 153 ff, 167 f, 170 ff, 174, 183, 193, 229, 297, 367, 413 ff, 426 ff, 437, 635, 874, 1021, 1229, 1344, 1407
– acetone 171, 177
– acyclic 248
– acetophenone 170 ff, 177
– aliphatic 1147
– alkyl aryl 1137
– amino 1141

– aromatic 1137
– benzophenone 156
– copper, chemoselectivity 435
– cyclic aromatic 1139
– cyclohexanone 175
– diaryl 1144
– dysfunctional 119
– heteroaromatic 1144
– mechanism 498
– two-phase hydrogenation 1344
ketopantoyllactone (KPL) 1166
β-keto phosphonates 1125
β-keto sulfonate 1125
β-keto sulfones 1125
kinetic 23, 56, 101, 189, 257
kinetic chemical resolution 691
kinetic control 267 ff
kinetic energy 363
kinetic isotope effect 1084
kinetic discrimination 573
kinetic parameters 567, 672
kinetic resolution 125, 586, 613, 691
– acrylic acid derivatives 693
– (α-acylaminoethyl)acrylate 692
– (α-carbamoylethyl)acrylate 692
– cyclic ketones 694
– disubstituted 1-pyrrolines 694
– dynamic 1128
– imine 694, 695
– keto esters 694
– ketone 694, 695
– (α-methoxyethyl)acrylates 692
kinetics
– 1-octene 105
– enantio-determining step 23
– first-order 380, 383, 389
– isotope effect 188, 190
– Michaelis-Menten 257 ff
– rate 105
– rate-determining step 9
– second-order 380
kinetic study 459, 471, 476, 477
Knudsen diffusion 1433
Kolbe coupling 775
K_R;K_S ratio 692

l

labeling 191
lanthanide 111
lanthanide alkoxides 601 f
lanthanide complexes 1044
Lanxess Inc. 578
leaching 1383
Leuckart-Wallach reaction 610
(S)-(–)-levamisole 1182
library 1248 ff
– amidophosphinite, ketopantoyllactone 1171
– bidentate phosphines 101 ff
– chiral bisphosphine
– water-soluble 473, 1221
ligand screening large-scale 1311
limiting case 263 ff
linear 395
Lineweaver-Burk 262
lipophilicity 1385
liposomes, hydrogenation 1336
liquid melts 1389 ff
lithium 1398
lock-and-key 288

m

macrocyclic 531 ff
maleic acid 237
MalPhos, β-acylaminoacrylate 760
mandelamides, synthesis 1172 ff
MandyPhos 754
– electrospray 361
– – ionization(ESI) 359
– ionic complex, isotopomers 359
– mass spectrometry 359 ff
– m/z ratio 361 ff
– quadrupole 364
– tandem ESI-MS 359
– octopole 363
ManNOP ligands 171 ff, 1172
mass transfer 1362, 1397, 1405, 1413, 1435, 1518, 1539
– Fick's law 1519
– interfacial area 1519
– resistance 1423, 1520
mass transport limitations 1377, 1384
matched point 670
Maxwell-Boltzmann statistics 363
MCCPM 751, 1167
MCCXM 1177
MCPM 1177
mechanism 40 ff, 46, 56, 313, 377 f, 383, 387, 391 ff, 458, 462, 471, 565
– associative pathway 9
– deuterium labeling 471, 477
– – experiment 474
– diastereomer 23
– dihydride 25, 384, 405
– dissociative pathway 9
– β- elimination 7

– β-H elimination 128, 135 ff
– heterolytic 93
– hydrogen activation 97
– hydrolytic 53 ff
– insertion 112, 135 ff
– kinetic studies 471, 477
– metal-ligand bifunctional 1137
– model 1115
– monohydride 384
– oxidative addition 7, 112
– palladium complexes 572
– reductive elimination 7, 112
– rhodium-based catalysts 565
– ruthenium-based catalysts 568
mediator 518 ff, 524, 1475 ff
Meerwein-Ponndorf-Verley (MPV) reduction 588, 598, 1215, 1438
melting point depression, by compressed CO_2 1369, 1370
membrane separation 1364, 1365
menthol 757, 872, 876
menthol process 1503
MeO-BIPHEP 757, 1251
MeO-BIPHEP-Cl 757
MeO-NAPhePhos 758
mephenoxalone 1182
Merrifield resins 1446
mesoporous silica 1045
metal atom 217
metal hydride 48, 153 ff, 158, 161
– acidity 157, 159
– bimetallic 186
– dihydride 159 ff
– dihydrogen complex 164, 169, 179
– hydricity 159 ff, 194
– hydride donors 159
– hydride transfer 168
– insertion of CO_2 492, 494 ff, 506
– kinetic hydricity 160, 163
– reaction with alkyl halides 503
– thermodynamic hydricity 160
metallo-aldehyde enolates 720
metallocene 1043, 1050, 1066
methanol, synthesis of 489 f
4-methoxy-cinamic 237
2-methoxy-4-propylephenol 242
methyl acetoacetate 1415
methylacrylate 221
methylanisole 242
3-methyl-1-pentyne-3-ol 241
2-methyl quinoxaline 483
methylstilbene 1032, 1037
methyl-trans-cinnamate 1384
metolachlor 34, 39, 753
(S)-metolachlor 1510
– *N*-aryl imines for 1197
– process 1197
methyl glycolate 446
methyl trans-cinnamate 237
methyl trifluoroacetate 445
Michaelis constant (K_M) 260 ff
Michaelis-Menten equation 259 ff
Michael-type addition mechanism 562
microemulsions 237
migratory insertion 1092, 1096
MiniPhos 747
miscibility, liquids 1328
mismatched pair 670
mixing, gas-liquid
MOC-BIMOP 757, 854
MOD-BCPM 751
MOD-DIOP 749, 751, 875
model discrimination 258 ff
model, enzyme hydrogenase 76
mole fraction 269 ff
molecular engineered layer structures (MELS) 1442
molecular mechanism 1085
monocycle arenes 245
monodentate ligand 995 ff, 1259 ff
mononuclear 379
MonoPhos 763, 996 ff
monophosphine CAMP 1086
monophosphite 996 ff
monophosphonite 996 ff
monophosphoramidite 996 ff
MorfPhos 1007 ff
Morita-Baylis-Hillman cyclization 717
MPV alkynylation 590
mtppms 1328, 1329
mtppts 1328
mutation of stereogenic center 701

n

N-aryl imines for 1197
N-acylhydrazones 20
NAD/H 1471
NADP/H 1471
Nafion 1457, 1459
N-alkylimines 20
nanocatalyst 228, 244
nanocluster 227
nanomaterials 220
nanoparticles 217, 1396
– colloidal 238
– soluble noble metal nanoparticles 217

N-acryl-*α*-dehydroamino acids and esters 1011 ff
naphthalene 457 ff
1-naphtyl Fluoxetine 1186
Naproxen 1343
N-arylsulfonyl ligands 1219
Nasulphos 473
NBR (acrylonitrile-butadieme rubber) hydrogenation 571
neodymium isopropoxide 600
N-heteroaromatics 474
nickel 93 ff, 99 ff, 101 ff, 105
– bridging hydrides 95
– colloidal 107
– coordination chemistry 94
– dihydride 96
– dinuclear 96
– hydride bridging 96
– mononuclear 107
nicotinamide 1471
– regeneration 1471
NIMAP, in scCO2 1365
NIMSP, in scCO2 1365
Nippon Zeon 578
Nisoxetine 1186
nitrile 55, 1352
– two-phase hydrogenation 1352
nitrile-butadiene rubber (NBR) 1400
nitroaromatics 1352
nitrogen 76
NMR spectroscopy 102, 201, 229, 231, 236, 297 ff, 315, 1487
– COSY 297, 302 f, 306, 309
– coupling constant 299 ff, 306
– 2D 299, 300, 302, 306
– deuterium 403
– DYPAS 338 ff
– enrichment 319
– EXSY 299, 303, 305 f
– flow cell 272
– FT 297
– ^{1}H, ^{19}F heteronuclear Overhausen effect (HOESY) 1511
– heteronuclear multiple quantum correlation (HMQC) 302 ff
– ^{1}H-NMR technique 1393
– high pressure 474, 1373, 1366
– – experiments 477
– – in scCO2 1366
– – operando 471, 483
– hydride 94 ff
– magnetic resonance imaging 353
– NOESY 303, 306
– orthohydrogen 322
– paradeuterium 323
– parahydrogen 313 ff, 319
– – apparatus 320
– PASADENA 314, 338
– PHIP 10, 23, 207, 298, 299, 314 ff, 324, 338, 342 ff, 381, 389, 401, 403
– – applications 324
– – ALTADENA 349
– – ^{13}C 344, 346, 348
– – ^{19}F 352
– – heteronuclei 344 ff
– – ^{15}N 352
– – ^{31}P 300, 307, 308, 345
– – procedure 1081
– – ^{29}Si 345
– satellites 335
– probe heads 272
– ^{103}Rh 298, 300, 1498, 1500
– storage 319
– technique 1373
– variable temperature 299
N-(*α*-ketoacyl)*α*-amino 676
N-acyl enamides 1016 ff
N-acyl-*β*-dehydroamino acid and esters 1020 ff
N-heteroaromatics 476
N-isopropylacrylamide 225
N-ligand 1029, 1030
nitrile 568
non-linear fit 262 ff
norbornadiene 73
NORPHOS 751, 1172, 1251
Noyori's catalyst family 1445

o

octane 227
oct-1-ene 221 f, 224
o-EtO-DPPE 105
o-MeO-DPPP 101, 104
o-MeO-DPPPP 104
Oppenauer oxidation 588, 1215
optical resolution 1421
orthometalation 591
Osborne complex 1394
osmium 45, 64 ff, 425
– alkenyl 382
– five-coordinate 65
oxalic acid, synthesis 499
oxazoline 602, 1253
oxime
– two-phase/hydrogenation 1352
oxoProNOP 761

p
palladium 71 ff, 480, 1386
– catalyst 72
– arenes 467
– benzenes 468
– cluster 74
– orthometallated 80
– nanoparticles 1386
– particles 468
– $Pd(acac)_2$ 1395
– Pd(O) nanoparticles 1386
– polymer 75
PAMP 995 ff
papain 1257
parahydrogen 313 ff
parallel reactors
– Amtec SPR16 1272
– Argonaut Endeavor 1272
– Chemspeed Autoplant A100 1272
– Parr MRS 1272
– Premex A96 1272
Parkinson's disease 1073
partial hydrogenation 225, 245
– 2-butyne-1,4-diol 239
– dienes 220
partial pressure, hydrogen 269 ff
partition coefficient 1382
PCB's 515, 521, 523, 532
PCCPM 1177
P-chiral 747, 996 ff
P-chiral compounds, *N*-methyl enamides 756
PCPM 1177
PennPhos 759, 784
– cyclic enamide 760
– enol acetates 760
1,4-pentadiene 73
pent-1-ene 1394
pentamethylcyclopentadiene (cp*) 1217
pentamethylcyclopentadienyl-rhodium (bipyridine) 1476
peralkyl-phosphine 1166
perfluoroalkyl 1378 ff, 1380, 1382 ff
perfluoromethylcyclohexane (PFMCH) 1382 ff
PhanePhos 19, 753, 1077 f, 1081, 1251
PHANEPHOS 24, 864
phase behavior 1362
phase behavior of acid 1365
PHEMP 870
phenol 467
phenylacetylene 239, 241, 383 ff, 385, 387
1-phenyl 1-cyclohexene 237
1-phenyl-1-propyne, semihydrogenation 391
1-phenyl 3-propyne 241
Phenyl-b-Glup 760
phenylephrine 1182
phenylglyoxylic derivatives, hydrogenation 1175
P-heterocyclic ligands 787
σ-Ph-HexaMeO-BIPHEP 758
PHIP 212
PHIM 762
polyaromatics 457 ff
porphyrin complexes 530
phosphetanes 810
phosphinamine 1091
phosphinane 810
phosphine 6, 36, 72, 77, 84, 87, 95, 327, 377, 458, 463, 470, 475, 1105, 1328
phosphines 10, 72, 1378 ff, 1380, 1381, 1382
– (S,S)-BDPPTS 1273
– (S,S)-BPPM 19
– 2,3-bis-dipenylphosphinoburane 1273
– aminomethylphosphines 1260
– chiral 14, 16, 1379, 1386
– diphosphines, electron rich 24
– fluorous 1378 ff, 1382
– monodentate 15, 997 ff
– solubility 1329
– surfactant 1343
– Walphos 1267
– water-soluble 1329
phosphine oxide, secondary 1010 ff
– aminophosphine 918
phosphinite 983
– amino alcohol 1169 ff
– fluorous 1378 ff
phosphinocarbene 1091
phosphino-imidazoline 1038
phosphino-oxazoline (PHOX) 1030 ff, 1051 ff, 1066
– alkenes 762
phosphite, fluorous 1378 ff
phosphites 762, 983, 1086, 1263 ff
– monodentate 1000
– solubility in $scCO_2$ 1366
phospholane 783, 808, 815, 820, 1076
phosphonites 1263 ff
– fluorous 1378 ff
– mixed-alkyl-aryl or alkyl-alkyl 1169
– monodentate 1000 ff
phosphonium ion 1410

phosphoramidites 918, 1259 ff, 1260
– monodentate 1005 ff
– MonoPhos 1267
– NMR studies 1270
– polymer-supported 1009
– solubility in $scCO_2$ 1366
phosphorous ligand 1029 f, 1378, 1386
phthalic anhydrides 442
PYRPHOS 864 ff
physisorption 1425, 1426, 1427
pilot process 1284
PipPhos 1007 ff, 1261
platinum (Pt) 71 ff, 84, 1383
– arene 456
– complexes, Tin 84
P,N ligands 1049, 1057, 1253
PNNP 761
polybutadiene (PBD) 1400
polychloroalkanes 520, 524, 526, 533
polychlorobenzenes 518, 520 ff, 527, 531 ff
poly(ethylenglycol) (PEG) 1363, 1369
POLYDIPHOS 480
polyenes, soybean oil 72
polyfluorinated arenes 518, 524, 528, 533 ff
polymers 1336, 1400 f
polyoxoanions 244
pore diffusion limitation 1430
powder X-ray diffraction (XRD) 220
power input 1537
P-P bond formation 776
PPCP 751
PPFA 753
P-Phos 757, 872
PPPM
– D-amino acids 751
– itaconic acid derivates 751
^{i}Pr-BeePhos 747
precatalyst 284
pre-equilibria 277 ff
Pregabalin 1498
prenal 1350
pressure 73, 1057
pressure effects 1051
– on enantioselectivity 1373
primary phosphines 779
process for
– aspartame (Enichem/Anic, Degussa) 1289
– Biotin intermediate (LONZA) 1299
– L-Dopa (Monsanto, VEB Isis-Chemie) 1288
– (+) methyl *cis*-dihydrojasmonate (Firmenich) 1299
– (R)-pantolactone 1304
– penem intermediate (Takasago) 1305
– Tipranavir intermediate (Chirotech) 1300
prochiral heteroaromatics 481
prochiral substances 249
production of fine chemicals 1245
production process 1284
product-proportional concentration 264 ff
(S)-Propranolol 1182
propene 1415
PROPHOS 750
porphyrine 1271
protective agent see stabilizer
proton donor 157, 167 ff
proton transfer 154, 165 ff, 180, 190
π-π-stacking 1426
P-S chelate 1089
pta 1329 ff
pyrene 466, 1398
pyridine 474, 481
pyrone 638
PYRPHOS 751, 762

q
quadrant model 775
quadrant rule 1082, 1083, 1090
QuinaPhos 762, 919
quinine 1044
quinoline 474, 1033, 1354
– two-phase hydrogenation 1354

r
racemization 612
– keto esters 697
rate 40
– rate-determining step 1483
rate constant 333, 338, 1490
– observed (k_{obs}) 263 ff
reaction mechanism 258 ff
– activation of dihydrogen 324
– CIDNP 318
– PHIP 318
reaction probability 364
reaction progress kinetic analysis 261
reaction rate 40, 1413, 1483
– effect of phase behavior 1370
– influence of phase behavior 1363
– measurements 264
reactor technology 577
reactor
– batch 1533
– Biazzi 1537
– continous stirred tank (CSTR) 1533

– Davy Process Technology 1537
– DeDietrich 1537
– industrial 1536
– membranes 1541
– micro-structured reactor 1541
– monolithic 1541
– plug flow reactor 1533
– stirred tank 1533
recovery of catalysts, see recycling
recycling 227, 236, 251, 518 ff, 524, 1363 ff
recycling process 243, 248
reducing agent 513, 516 ff, 534 ff
– complex metal hydrides 520 ff, 531, 539
– cysteine 530, 535
– dithiothreitol 530
– hydrogen donors other than hydrides 526 ff
– – alcoholates 526, 539
– – cyclic amines 526
– – formates 526 ff, 539
– – metal alkyls 521, 526, 528, 539
– hydrosilanes 524 ff, 538
– hydrostasnnanes 524 ff, 539
– molecular hydrogen 517 ff, 538
– simple metal hydrides 520 ff ,539
– sulfides 530, 535
– Ti(III) citrate 530, 533
– zero-valent metals 530 ff, 533
reductive acetylation of ketones 610
reductive aldol coupling 714, 721
reductive aldol cyclization 719
reductive aldolization 716
reductive animation 1202
– of ketones and aldehydes
– – enamine 438
– – imine 438
– – carbinolamine 438
– – aqueous ammonia 439
reductive coupling 725, 726, 732
– catalytic 727
reductive cyclization 733
regioselection 727
regression analysis, least-squares 280
(–)-reserpine 603, 608
retroaldolization 717
reversible inhibition 1484, 1499
– acetonitrile 1502
– acids 1505
– aldehydes 1504
– allyl alcohol 1505
– aromatic solvents 1500 f
– bases 1505
– benzylamine 1504
– carbon monoxide (CO) 1504
– CO-complexes 1505
– compounds containing heteroatoms 1503
– DMF 1502
– DMSO 1503
– ethers 1502
– malonate esters 1502
– $MeNO_2$ 1502
– pH-value 1505
– primary amines 1504
– sulfur compounds 1503
– toluene 1501
– triethylamine 1503
– water 1503
rhenium complex 756
rhodacarborane 1407
rhodium 364 ff, 641, 647, 651, 655, 662, 731 ff, 774, 1044, 1045, 1049, 1165, 1217, 1378, 1381, 1382, 1383, 1385
– as grafted catalyst 468, 480
– hydrogenation, of arenes 456
– hydrogenation of benzenes 468
– Rh-BINAP, asymmetric isomerizations 756
– $^{103}Rh(^{1}H)$HMQC NMR 1502
– Rh-MeDuPhos 1402
rhodium catalyst 3, 384 ff, 386 ff, 402, 428 ff, 638
– $[Rh((–)\text{-}(diop))]^+$ 673
– [Rh((–)-binap)]+ 665, 670
– $[Rh((–)\text{-}bppm))]^+$ 675
– $[Rh((–)\text{-}diop))]^+$ 675, 679
– [Rh((+)-binap)]+ 665, 670
– $[Rh((+)\text{-}bppm))]^+$ 674, 679
– $[Rh((+)\text{-}diop))]^+$ 673
– $[Rh(–)\text{-}((R,R)\text{-}dipamp))]^+$ 673
– $[Rh(+)\text{-}(R,R)\text{-}diop]^+$ 677
– $[Rh(C_5Me_5)Cl_2]_2$ 26
– $[Rh(chiraphos)]^+$ 668
– [RhCl((–)-Cydiop)] 679
– [RhCl((+)-Cydiop)] 679
– $[RhCl(PPh_3)_3]$ 5, 8, 639, 641, 647, 652, 661, 670, 679
– [RhCl((S)-Cy,Cy-oxoProNOP)] 686
– [RhCl((S)-MeO-BIPHEP)] 686
– [RhCl((S,S)-Cy-POP-AE)] 679
– $[Rh(cod)((S,S)\text{-}Et\text{-}Duphos))]^+$ 678
– $[Rh(cod)((S,S)\text{-}Me\text{-}Duphos))]^+$ 677 f
– $[Rh(cod)((R,R)\text{-}chiraphos))]^+$ 678
– $[Rh(cod)((R,R)\text{-}dipamp))]^+$ 678

– [Rh(DIOXOP)]$^+$ 674
– [Rh(dipamp)]$^+$ 692
– [Rh(diphos-2)]$^+$ 662, 668
– [Rh(diphos-3)]$^+$ 675
– [Rh(diphos-4)(cod)]$^+$ 640, 651, 655 ff, 668
– [Rh(diphos-4)(nbd)]$^+$ 649, 653
– [Rh(diphos-4)]$^+$ 633 f, 662, 673 f
– [Rh(DPP-AE)]$^+$ 674 f
– [RhH(CO)(PPh$_3$)$_3$] 5, 551, 552
– [Rh(nbd)((R,R)-dipamp)]$^+$ 693
– [Rh(nbd)(diphos-4)]$^+$ 649
– [Rh(OAc)$_2$((R)-binap)] 656
– [Rh(OAc)$_2$((S)-binap)] 656
– [Rh(Ph-CAPP)]$^+$ 661, 674
– [Rh((R)-binap)]$^+$ 668
– [Rh((R)-phanephos)]$^+$ 664
– [Rh((R,R)-dimap)]$^+$ 658
– [Rh((R,R)-dipamp)]+ 661, 674, 676 f
– [Rh((R,R)-Et-Duphos)]$^+$ 634, 664, 673 f
– [Rh((R,R)-Me-Duphos)]$^+$ 633, 664, 686
– [Rh((R,R)-Pr-Duphos)]$^+$ 633 f
– [Rh((S)-Pindophos)]$^+$ 674
– [Rh((S)-skewphos)]$^+$ 668
– [Rh((S,S)-bppm)]$^+$ 677, 686
– [Rh((S,S)-chiraphos)]$^+$ 674
– [Rh((S,S)-Cy-POP-AE)]$^+$ 679
– [Rh(S,S)-dipamp]$^+$ 661
– [Rh((S,S)-Et-Duphos)]$^+$ 664, 673 f
– [Rh((S,S)-Me-Duphos)]$^+$ 655
– [Rh((S,S)-MeO-POP-AE)]$^+$ 672, 674 f
– [Rh((S,S)-POP-AE)]$^+$ 675
– [RhCl(diphos-3)]Cl 636
– [RhCl((S)-bdpp)]Cl 636
– [RhCl((S,S)-bdpp)]Cl 637, 695
– addition of triethylamine 428
– aldehydes hydrogenation 417
– asymmetric 14
– cationic 21
– cinnamaldehyde 417
– decarbonylation 417
– dihydride 24
– dinuclear 26
– immobilized 419
– precursor, Rh(TFA)) 1169
– Rhodium-diene 12, 17
– transfer hydrogenation 419
– water-soluble 419, 430
– Wilkinson's catalyst 649, 650
– zerovalent 400
rhodium(dihydride) 405
rhodium(I) complexes 714, 1074
rhodium-catalyzed 174, 731, 774, 779
– mechanism 21
rhodium-ferrocenyl-diphosphine 1406
Rh-Propraphos 884
RoPhos 759
ruthenacycles 1256
ruthenium 45 ff, 49, 53 ff, 56 ff, 60, 405, 1023, 1049 ff, 1069, 1105, 1217, 1386
– BINAP 815, 1098, 1415
– hydrogenation of arenes 456
– hydrogenation of N-heterocycles 478
– monohydride 380
– phosphines 380
– Ru(η^6-p-cymene)(η^2-triphos)Cl [PF$_6$] 1399
– synthesis 50
ruthenium catalyst 378, 400, 420, 422, 431, 461, 475, 638
– [Ru(allyl)$_2$((R)-binap)] 700
– [Ru(allyl)$_2$((S)-binap)] 700
– [RuBr$_2$((–)-chiraphos)] 703
– [RuBr$_2$(diphos-4)] 681
– [Rh(Br-Ph-CAPP)] 673
– [RuBr$_2$(PPh$_3$)$_3$] 681
– [RuBr$_2$((R)-binap)] 699, 703 f
– [RuBr((R)-binap(benzene))]Br 704
– [RuBr$_2$((R)-binap)1/2NEt$_3$] 682 ff
– [RuBr$_2$((R)-MeO-BIPHEP)] 661, 681, 686, 699, 703, 705
– [RuBr$_2$((R)-synphos)] 705
– [RuBr$_2$((R,R)-Meduphos)] 689
– [RuBr$_2$((S)-binap)] 682 ff, 685
– [RuBr$_2$((S)-binap)1/2NEt$_3$] 682 ff
– [RuBr$_2$((S)-MeO-BIPHEP)] 681, 685 ff, 690, 699, 705
– [RuBr$_2$((S)-synphos)] 703, 705
– [RuBr$_2$((S)-tol-binap)] 684
– [Ru$_2$(CO)$_4$(OAc)$_2$(PPh$_3$)$_2$] 633
– [RuCl(C$_6$H$_6$)((R)-binap)]Cl 699
– [RuCl$_2$((R)-binap)]$_2$NEt$_3$ 686, 704
– [RuCl((R)-3,5-di-*t*-Bu-binap) (p-cymene)] 704
– [RuCl$_2$(P(C$_6$H$_4$-p-Me)$_3$)$_3$-EN-KOH] 637
– [RuCl$_2$(P(C$_6$H$_4$-p-OMe)$_3$)$_3$-EN-KOH] 637
– [RuCl$_2$(PPh)$_3$-EN-KOH] 635
– [RuCl$_2$(PPh$_3$)((S)-BIPHEP)] 689
– [RuCl$_2$(PPh$_3$)$_3$] 686, 1395
– [Ru$_2$Cl$_2$((R)-binap)] 685, 689
– [RuCl$_2$((R)-binap) Et$_2$NH] 682
– [RuCl$_2$((R)-binap(dmf)$_m$-(S,S)-DPEN-KOH)] 706
– [RuCl$_2$((R)-tol-binap)(dmf)$_m$-(S,S-DPEN-^{t}BuOK)] 706
– [RuCl$_2$((R)-tol-binap)(dmf)$_m$-(R,R)-DPEN-^{t}BuOK)] 706
– [RuCl$_4$((R)-binap)$_2$(NEt$_3$)] 687

– [$RuCl_4$((R)binap)$_2$(NEt_3)] 685
– [$RuCl_2$((S)-binap)] 689, 695
– [$RuCl_2$((S)-binap)(dmf)$_m$] 703
– [$RuCl_2$((S)-binap)(dmf)$_m$-(R,R)-DPEN-KOH] 636, 706
– [$RuCl_2$((S)-binap Et_2NH)] 682
– [$RuCl_2$((S)-binap)$_2NEt_3$] 1403
– [Ru_2Cl_4((R)-binap)$_2$(NEt_3)] 689
– [Ru_2Cl_4((S)-binap)$_2$(NEt_3)] 687
– [Ru(OAc)$_2$((R)-binap)] 692
– [Ru(OAc)$_2$((S)-binap)] 692
– [Ru(OAc)$_2$((R)-tol-binap)] 661
– [Ru(OAc)$_2$((S)-tol-binap)] 661
– [Ru(OAc)$_2$((S)-3,5-xylil-BIPHEP)] 634
– [Ru(O_2CCF_3)$_2$((R)-binap)] 703
– [Ru((R)-MeO-BIPHEP)Br_2] 702
– [Ru((Ru)-MeO-BIPHEP)] 700
– [Ru((S)-AMPP)(methallyl)$_2$] 688
– [Ru((S)-AMPP)(TFA)$_2$] 688
– [Ru((S)-AMPP)(R)-MTPA)$_2$] 688
– [Ru((S)-binap)] 700
– [RuCl((S)-binap)(*p*-cymene)]Cl 686
– [$RuCl_2$(S)-binap](dmf)$_n$ 704, 705
– [$RuCl_2$((S)-binap)]$_2$(NEt_3)-(S,S)-DPEN-KOH 706
– [Ru(S)-C_3-Tunephos] 705
– [Ru((S)-MeO-BIPHEP)] 700
– [Ru((S)-MeO-BIPHEP)Br_2] 702
– [$RuCl_2$((S)-3,5-xylyl-binap)]$_2$(NEt_3)-(S,S)-DPEN-KOH 706
– [Ru(TFA)$_2$((R)-MeO-BIPHEP)] 687
– [Ru(TFA)$_2$(PPh_3)$_2$] 668
– [Ru(TFA)$_2$((R)-tol-binap)] 687
– aldehydes 420
– chemoselectivity 422
– diamine-modified 433
– phosphines 431 ff
– unsaturated ketone 433
ruthenium complexes, 16 electron 593

S

(R)-Salbutamol 1183
samarium 1050
scale-up 1236
SegPhos 758, 872
selective hydrogenation 391, 394
selective, see chemoselective
selectivity 41
– solvent 400
– stereo- and chemo- 389
self-assembly 1271
separation
– fluorous biphasic 1377, 1386, 1387
S-heteroaromatics 470
silica, fluorous 1381, 1386
SiPhos 763, 996 ff
SkewPHOS 751
skimmer potential 361
SK-Phos 867
– enamides 749
– MOM protected β hydroxy enamide 749
smectite clays 1455
sol-gel method 1441
sol-gel polymerization 1434
solid polymers 1424
solid-phase synthesis 1258 ff
solid-supported catalyst
– supercritical carbon dioxide ($scCO_2$) 1365
solubility 1522
– correlation 1523
– gas 1328
– Henry's coefficient 1520, 1523
– Henry's law 1520
– hydrogen 1523
– in water 1328
– organometallic catalyst in $scCO_2$ 1365
– temperature 1523
solvent 35, 361, 365 f
– complex 277 ff
– coordinating 32, 384
– dissociation 31
– effects 360, 491 ff
– evaporation enthalpy 271
– fluorous 1378, 1381, 1383, 1384
– – biphasic 1382, 1384
– free 181 ff, 187
– non-coordinating 33
– recycling 576
– weakly-coordinating 42
sorbic acid 1334, 1402
spacer 1378, 1383
stabilization 218, 219
– biomaterial as a protective material 232
– coulombic repulsion 218
– electrostatic 218
– electrosteric 219
– surfactants 242
– osmotic repulsion 219
– steric 218, 219
– supercritical microemulsions 236
– with solvents 220
– with traditional ligands 220
stabilizer 217 f, 228, 251
– cellulose derivatives 219

– chitosan 223
– cyclodextrin 219
– dendrimers 225
– non-usual polymers 221
– oligomer 219
– polymer 219, 220
– polyoxoanions 227
– surfactants 226
– thiolated β-cyclodextrin 229
stationary conditions 283
steady-state approach 259 ff
stereochemistry 34, 46
stereocontrolled, see stereoselective
stereoselective 375, 382, 388
stirring speed 267 ff
stoichiometric 190
styrene 229
styrene hydration, in $scCO_2$ 1370
styrene-butadiene polymer 568
styrene-butadiene rubber (SBR) 1400
styrene-butadiene-styrene polymer 568
substrate and product inhibition 1484, 1494 ff
– allyl alcohol 1494
– amines 1497
– biphasic conditions 1497
– cinnamyl alcohol 1496
– dihydro-isoquinolines 1494
– enamide amides 1497
– isopropanol 1499
– ketoesters 1495
– nitrile 1498
– pyridine 1498
substrate atalyst ratio (SCR) 1246 ff
substrate-control 670, 685, 691
substrate-directive hydrogenation
– keto-compounds 681
– β-keto ester derivatives 681
substrate-metal complex 667
succinic anhydride 442
sulfinyl imine 1044
sulphonated phosphines 527, 1328
sulphos 457, 478 ff
supercritical carbon dioxide ($scCO_2$) 234, 236 f, 491, 800, 1361, 1366, 1378, 1412
– as adjustable-solvent 1364
– as anti- solvent 1364, 1370
– as co-solvent 1364
– as temporary protecting group 1366
– industrial application 1361
supercritical fluids 236, 245, 1327, 1335
supported aqueous-phase catalyst (SAPC) 1436
supported catalysts 140
supported hydrogen-bonded (SHB) catalyst 467, 1427, 1429, 1430
supported ionic liquid phase (SLIP) 1413
supported liquid-phase catalyst (SLPC) system 1436
supramolecular, Supraphos 1270
surface organometallic 469
1,2-syn 376
syn-diastereoselectivity 697
SynPhos 758
syn-selectivity 698
synthesis 42
systems 472

t

tag, fluorous 1377 ff
tail, perfluoroalkyl 1381
tandem enantiomeric hydrogenation, didehydrodipeptides 677
tandem catalyst 796
TangPhos 784, 793, 806, 807
– unsymmetrical 747
– dehydroamino acid derivates 754
TaniaPhos, enol acetate 754
tantalum
– hydrogenation of benzene 464
– hydrogenation of naphthalene 464
task-specific ionic liquid 1410
TCSM 466, 479
TEAF 1225
technical-scale applications 1280
– equipment 1283
– process development 1283
tethered single-site catalysts 457 ff
tetraalkoxyaluminates 1057
Tetra-BITIANP 758
tetralin 466
TetraMe-BITIOP 758
tetraphenylborate, fluorous 1385
TGA 228
theory, density functional 389
thermalization 363
thermodynamic conditions 273 ff
thiobenzolhydrazone 78
thiophene 470 ff, 479
thiosemicarbazone 78
tiglic acids 1405
time-to-market 1245
Tishchenko reaction 609

Tishchenko-type processes 721
titanocene 696, 1044, 1050, 1056
TolBINAP 757
Tol-P-Phos 758
Tomoxetine 1186
T-Phos 867
total pressure 269 ff
transfer 175, 585, 595, 599, 1215, 1255 ff, 1274, 1275, 1410
transfer hydrogenation 175, 427, 585, 595, 599, 1215, 1255 ff, 1274, 1275, 1410
transfer hydrogenation catalyst 585, 603, 612
– enantioselective 63
– in $scCO_2$ 1372
– mechanism 63
transfer mechanism, direct 587
transfer, pair-wise 381
transition metal alkoxide 591
transition metal (carbonyl)clusters 1396
transition state 1116
transmission electronic microscopy (TEM) 220 f, 227 f, 231, 234 ff, 242, 245 f
– high resolution 247
transport phenomena 265 ff
trans-1,3-pentadiene 73
trans-stilbene 237
TRAP
– dehydroamino ester 755
– indoles 755
trichickenfootphos
– dehydroamino acids 747
– enamides 747
– α,β-unsaturated nitrile 747
triene 136, 1067
– 1,5,9-cyclododecatriene 86
triethyl silane 155 ff
triethylamine 1225
triflic acid 155
trifluoroacetate 155
trifluoroacetic acid 155
trimethylindolenine 1411
trimethylsilane-substituted 1409
triphenylphosphine monosulfonate 472
triphenylphosphine trisulfonate 472
triphos 457 ff, 470 ff, 475 ff, 477
TunaPhos 758
TunePhos 870, 871
turbines 1538
two-phase hydrogenation 1354
two-phase, see two-phase hydrogenation

u

UCAPs 760
Ugi amine 753
UlluPHOS 779, 789, 819
unfunctionalized olefins 1049
unsaturated acids and esters 1014
unsaturated alcohols 229
α,β-unsaturated aldehydes, in $scCO_2$ 1365
a,β-unsaturated carbonyl substrates 754
α,β-unsaturated carboxylic acid derivatives, in $scCO_2$ 1366
α,β-unsaturated carboxylic ester 1037
β,γ-unsaturated esters 650
unsaturated route 12
UV-visible spectroscopy 220, 227 f, 231, 237

v

Van der Waals forces 1426
Van Krevelen and Hoftijzer 1532
vapor pressure 265 ff, 270 ff
variable pressure 307, 308
variable temperature 307
variables of reaction 1247
vinyl acetate 227
vinyl epoxides 74
vinyl halides 525, 530, 538
virial coefficients 265
vitamin B12 528 ff
vitamin E 1068
volatile organic chemicals (VOC) 1361, 1368

w

WalPhos,
– dehydroamino acid derivatives 755
– itaconic acid derivatives 755
– α,β-unsaturated carboxylic acids 755
water gas shift (WGS) reaction 1371
water
– as promoter 492, 506
– as reaction solvent, 490 f
water-soluble 10
wet-ionic liquid 1406
wide angle X-ray scattering 222
Wilkinson catalyst 586, 590, 591, 714, 731, 1073, 1079, 1444
– in CO_2 1370
– silica support 1371
– solubility in $scCO_2$ 1366

X
X-ray photoelectron spectroscopy (XPS) 220, 229, 234, 246
XRD 227, 228, 234, 245
Xyl-BDPAB 761
Xyl-BINAP 757
Xyl-PHANEPHOS 753
Xyl-P-Phos 758

Z
zeolites 1430, 1431, 1432
– NaA 609
β-zeolites 1427
Zimmerman-Traxler-type transition state 716
zinc 1398
zirconium (IV) isopropoxide 611